Scientific and Technical Aerospace Reports

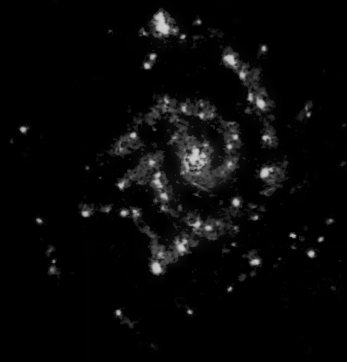

An Abstract Journal

Volume 32, Number 3
March 1994
N94-14908 to N94-17677

The NASA STI Program ... in Profile

Since its founding, NASA has been dedicated to the advancement of aeronautics and space science. The NASA Scientific and Technical Information (STI) Program plays a key part in helping NASA maintain this important role.

The NASA STI Program provides access to the NASA STI Database, the largest collection of aeronautical and space science STI in the world. The Program is also NASA's institutional mechanism for disseminating the results of its research and development activities.

Specialized services that help round out the Program's diverse offerings include creating custom thesauri, translating material to or from 34 foreign languages, building customized databases, organizing and publishing research results ... even providing videos.

For more information about the NASA STI Program, you can:

- **Phone** the NASA Access Help Desk at (301) 621-0390
- **Fax** your question to the NASA Access Help Desk at (301) 621-0134
- **E-mail** your question via the **Internet** to help@sti.nasa.gov
- **Write** to:

  NASA Access Help Desk
  NASA Center for AeroSpace Information
  800 Elkridge Landing Road
  Linthicum Heights, MD 21090-2934

Scientific and Technical Aerospace Reports

Scientific and Technical Aerospace Reports (STAR), is published each month as a major product of the International Aerospace Database, managed by the NASA Scientific and Technical Information (STI) Program.

Inside this issue you will find:

Front Matter
A typical citation and abstract sample explaining the standard format, which includes codes for ordering reports.

An Abstract Section
Citations and abstracts of reports and publications that provide comprehensive coverage of worldwide aerospace-related topics including aeronautics and space science technology. *STAR* lists published and publicly available reports entered into the NASA STI Database during the four weeks preceding publication of this issue. These citations and abstracts are listed by subject categories.

An Index Section
- Subject
- Personal author
- Corporate source
- Contract number
- Report number.

Appendix
A guide for ordering cited reports, registering with the NASA STI Program, and using the available products and services. Additionally, price schedules, phone numbers, and addresses are included in this information packed section.

NASA also sponsors companion journals, *International Aerospace Abstracts (IAA)*, and *NASA Open Volumes on Aerospace (NOVA)*. They list abstracts of the open literature on aerospace subjects available worldwide. IAA is available from the American Institute of Aeronautics and Astronautics (AIAA), and *NOVA* is for internal NASA use only, available from the NASA Center for AeroSpace Information (CASI).

Reports found in *STAR* are also available through the NASA online retrieval service, RECON, and the Aerospace Database through DIALOG.

The NASA STI Program gathers information through national and international agreements and exchanges and makes this information available to the NASA community and to the public in many forms through various outlets.

For additional information on the NASA STI Program, call the NASA Access Help Desk at (301) 621-0390, or write to:

NASA Center for AeroSpace Information
800 Elkridge Landing Road
Linthicum Heights, Maryland 21090-2934

US ISSN 0036-8741

This publication was prepared by the NASA Center for AeroSpace Information,
800 Elkridge Landing Road, Linthicum Heights, MD 21090-2934, (301) 621-0390.

Volume 32 Number 3 / March 1994

TABLE OF CONTENTS

AERONAUTICS For related information see also *Astronautics.*

01 AERONAUTICS (GENERAL) **853**

02 AERODYNAMICS **855**
Includes aerodynamics of bodies, combinations, wings, rotors, and control surfaces; and internal flow in ducts and turbomachinery. For related information see also *34 Fluid Mechanics and Heat Transfer.*

03 AIR TRANSPORTATION AND SAFETY **862**
Includes passenger and cargo air transport operations; and aircraft accidents. For related information see also *16 Space Transportation* and *85 Urban Technology and Transportation.*

04 AIRCRAFT COMMUNICATIONS AND NAVIGATION **863**
Includes digital and voice communication with aircraft; air navigation systems (satellite and ground based); and air traffic control. For related information see also *17 Space Communications, Spacecraft Communications, Command and Tracking* and *32 Communications and Radar.*

05 AIRCRAFT DESIGN, TESTING AND PERFORMANCE **865**
Includes aircraft simulation technology. For related information see also *18 Spacecraft Design, Testing and Performance* and *39 Structural Mechanics.* For land transportation vehicles see *85 Urban Technology and Transportation.*

06 AIRCRAFT INSTRUMENTATION **868**
Includes cockpit and cabin display devices; and flight instruments. For related information see also *19 Spacecraft Instrumentation* and *35 Instrumentation and Photography.*

07 AIRCRAFT PROPULSION AND POWER **868**
Includes prime propulsion systems and systems components, e.g., gas turbine engines and compressors; and onboard auxiliary power plants for aircraft. For related information see also *20 Spacecraft Propulsion and Power, 28 Propellants and Fuels,* and *44 Energy Production and Conversion.*

08 AIRCRAFT STABILITY AND CONTROL **870**
Includes aircraft handling qualities; piloting; flight controls; and autopilots. For related information see also *05 Aircraft Design, Testing and Performance.*

09 RESEARCH AND SUPPORT FACILITIES (AIR) **871**
Includes airports, hangars and runways; aircraft repair and overhaul facilities; wind tunnels; shock tubes; and aircraft engine test stands. For related information see also *14 Ground Support Systems and Facilities (Space).*

ASTRONAUTICS For related information see also *Aeronautics.*

12 ASTRONAUTICS (GENERAL) **873**
For extraterrestrial exploration see *91 Lunar and Planetary Exploration.*

13 ASTRODYNAMICS **874**
Includes powered and free-flight trajectories; and orbital and launching dynamics.

14 GROUND SUPPORT SYSTEMS AND FACILITIES (SPACE) **875**
Includes launch complexes, research and production facilities; ground support equipment, e.g., mobile transporters; and simulators. For related information see also *09 Research and Support Facilities (Air).*

15 LAUNCH VEHICLES AND SPACE VEHICLES **878**
Includes boosters; operating problems of launch/space vehicle systems; and reusable vehicles. For related information see also *20 Spacecraft Propulsion and Power.*

16 SPACE TRANSPORTATION **879**
Includes passenger and cargo space transportation, e.g., shuttle operations; and space rescue techniques. For related information see also *03 Air Transportation and Safety* and *18 Spacecraft Design, Testing and Performance.* For space suits see *54 Man/System Technology and Life Support.*

17 SPACE COMMUNICATIONS, SPACECRAFT COMMUNICATIONS, COMMAND AND TRACKING **883**
Includes telemetry; space communications networks; astronavigation and guidance; and radio blackout. For related information see also *04 Aircraft Communications and Navigation* and *32 Communications and Radar.*

N.A.—No abstracts were assigned to this category for this issue.

18 SPACECRAFT DESIGN, TESTING AND PERFORMANCE **884**
Includes satellites; space platforms; space stations; spacecraft systems and components such as thermal and environmental controls; and attitude controls. For life support systems see *54 Man/System Technology and Life Support.* For related information see also *05 Aircraft Design, Testing and Performance, 39 Structural Mechanics,* and *16 Space Transportation.*

19 SPACECRAFT INSTRUMENTATION **899**
For related information see also *06 Aircraft Instrumentation* and *35 Instrumentation and Photography.*

20 SPACECRAFT PROPULSION AND POWER **923**
Includes main propulsion systems and components, e.g., rocket engines; and spacecraft auxiliary power sources. For related information see also *07 Aircraft Propulsion and Power, 28 Propellants and Fuels, 44 Energy Production and Conversion,* and *15 Launch Vehicles and Space Vehicles.*

CHEMISTRY AND MATERIALS

23 CHEMISTRY AND MATERIALS (GENERAL) **929**

24 COMPOSITE MATERIALS **930**
Includes physical, chemical, and mechanical properties of laminates and other composite materials. For ceramic materials see *27 Nonmetallic Materials.*

25 INORGANIC AND PHYSICAL CHEMISTRY **942**
Includes chemical analysis, e.g., chromatography; combustion theory; electrochemistry; and photochemistry. For related information see also *77 Thermodynamics and Statistical Physics.*

26 METALLIC MATERIALS **954**
Includes physical, chemical, and mechanical properties of metals, e.g., corrosion; and metallurgy.

27 NONMETALLIC MATERIALS **962**
Includes physical, chemical, and mechanical properties of plastics, elastomers, lubricants, polymers, textiles, adhesives, and ceramic materials. For composite materials see *24 Composite Materials.*

28 PROPELLANTS AND FUELS **975**
Includes rocket propellants, igniters and oxidizers; their storage and handling procedures; and aircraft fuels. For related information see also *07 Aircraft Propulsion and Power, 20 Spacecraft Propulsion and Power,* and *44 Energy Production and Conversion.*

29 MATERIALS PROCESSING **976**
Includes space-based development of products and processes for commercial application. For biological materials see *55 Space Biology:*

ENGINEERING For related information see also *Physics.*

31 ENGINEERING (GENERAL) **983**
Includes vacuum technology; control engineering; display engineering; cryogenics; and fire prevention.

32 COMMUNICATIONS AND RADAR **986**
Includes radar; land and global communications; communications theory; and optical communications. For related information see also *04 Aircraft Communications and Navigation* and *17 Space Communications, Spacecraft Communications, Command and Tracking.* For search and rescue see *03 Air Transportation and Safety,* and *16 Space Transportation.*

33 ELECTRONICS AND ELECTRICAL ENGINEERING **1007**
Includes test equipment and maintainability; components, e.g., tunnel diodes and transistors; microminiaturization; and integrated circuitry. For related information see also *60 Computer Operations and Hardware* and *76 Solid-State Physics.*

34 FLUID MECHANICS AND HEAT TRANSFER **1016**
Includes boundary layers; hydrodynamics; fluidics; mass transfer and ablation cooling. For related information see also *02 Aerodynamics* and *77 Thermodynamics and Statistical Physics.*

35 INSTRUMENTATION AND PHOTOGRAPHY **1031**
Includes remote sensors; measuring instruments and gauges; detectors; cameras and photographic supplies; and holography. For aerial photography see *43 Earth Resources and Remote Sensing.* For related information see also *06 Aircraft Instrumentation* and *19 Spacecraft Instrumentation.*

36 LASERS AND MASERS **1037**
Includes parametric amplifiers. For related information see also *76 Solid-State Physics.*

37 MECHANICAL ENGINEERING **1045**
Includes auxiliary systems (nonpower); machine elements and processes; and mechanical equipment.

38 QUALITY ASSURANCE AND RELIABILITY **1049**
Includes product sampling procedures and techniques; and quality control.

39 STRUCTURAL MECHANICS **1056**
Includes structural element design and weight analysis; fatigue; and thermal stress. For applications see *05 Aircraft Design, Testing and Performance* and *18 Spacecraft Design, Testing and Performance.*

GEOSCIENCES For related information see also *Space Sciences.*

42 GEOSCIENCES (GENERAL) **1063**

43 EARTH RESOURCES AND REMOTE SENSING **1081**
Includes remote sensing of earth resources by aircraft and spacecraft; photogrammetry; and aerial photography. For instrumentation see *35 Instrumentation and Photography.*

44 ENERGY PRODUCTION AND CONVERSION **1091**
Includes specific energy conversion systems, e.g., fuel cells; global sources of energy; geophysical conversion; and windpower. For related information see also *07 Aircraft Propulsion and Power, 20 Spacecraft Propulsion and Power,* and *28 Propellants and Fuels.*

45 ENVIRONMENT POLLUTION **1094**
Includes atmospheric, noise, thermal, and water pollution.

46 GEOPHYSICS **1097**
Includes aeronomy; upper and lower atmosphere studies; ionospheric and magnetospheric physics; and geomagnetism. For space radiation see *93 Space Radiation.*

47 METEOROLOGY AND CLIMATOLOGY **1105**
Includes weather forecasting and modification.

48 OCEANOGRAPHY **1111**
Includes biological, dynamic, and physical oceanography; and marine resources. For related information see also *43 Earth Resources and Remote Sensing.*

LIFE SCIENCES

51 LIFE SCIENCES (GENERAL) **1115**

52 AEROSPACE MEDICINE **1119**
Includes physiological factors; biological effects of radiation; and effects of weightlessness on man and animals.

53 BEHAVIORAL SCIENCES **1131**
Includes psychological factors; individual and group behavior; crew training and evaluation; and psychiatric research.

54 MAN/SYSTEM TECHNOLOGY AND LIFE SUPPORT **1134**
Includes human engineering; biotechnology; and space suits and protective clothing. For related information see also *16 Space Transportation.*

55 SPACE BIOLOGY **1139**
Includes exobiology; planetary biology; and extraterrestrial life.

MATHEMATICAL AND COMPUTER SCIENCES

59 MATHEMATICAL AND COMPUTER SCIENCES (GENERAL) **1140**

60 COMPUTER OPERATIONS AND HARDWARE **1140**
Includes hardware for computer graphics, firmware, and data processing. For components see *33 Electronics and Electrical Engineering.*

61 COMPUTER PROGRAMMING AND SOFTWARE **1141**
Includes computer programs, routines, algorithms, and specific applications, e.g., CAD/CAM.

62 COMPUTER SYSTEMS **1157**
Includes computer networks and special application computer systems.

63 CYBERNETICS **1163**
Includes feedback and control theory, artificial intelligence, robotics and expert systems. For related information see also *54 Man/System Technology and Life Support.*

64 NUMERICAL ANALYSIS **1168**
Includes iteration, difference equations, and numerical approximation.

65 STATISTICS AND PROBABILITY **1172**
Includes data sampling and smoothing; Monte Carlo method; and stochastic processes.

66 SYSTEMS ANALYSIS **1174**
Includes mathematical modeling; network analysis; and operations research.

67 THEORETICAL MATHEMATICS **1174**
Includes topology and number theory.

PHYSICS For related information see also *Engineering.*

70 PHYSICS (GENERAL) **1175**
For precision time and time interval (PTTI) see *35 Instrumentation and Photography*; for geophysics, astrophysics or solar physics see *46 Geophysics, 90 Astrophysics*, or *92 Solar Physics.*

71 ACOUSTICS **1176**
Includes sound generation, transmission, and attenuation. For noise pollution see *45 Environment Pollution.*

72 ATOMIC AND MOLECULAR PHYSICS **1179**
Includes atomic structure, electron properties, and molecular spectra.

73 NUCLEAR AND HIGH-ENERGY PHYSICS **1187**
Includes elementary and nuclear particles; and reactor theory. For space radiation see *93 Space Radiation.*

74 OPTICS **1189**
Includes light phenomena and optical devices. For lasers see *36 Lasers and Masers.*

75 PLASMA PHYSICS **1200**
Includes magnetohydrodynamics and plasma fusion. For ionospheric plasmas see *46 Geophysics.* For space plasmas see *90 Astrophysics.*

76 SOLID-STATE PHYSICS **1205**
Includes superconductivity. For related information see also *33 Electronics and Electrical Engineering* and *36 Lasers and Masers.*

77 THERMODYNAMICS AND STATISTICAL PHYSICS **1219**
Includes quantum mechanics; theoretical physics; and Bose and Fermi statistics. For related information see also *25 Inorganic and Physical Chemistry* and *34 Fluid Mechanics and Heat Transfer.*

SOCIAL SCIENCES

80 SOCIAL SCIENCES (GENERAL) **1221**
Includes educational matters.

81 ADMINISTRATION AND MANAGEMENT **1222**
Includes management planning and research.

82 DOCUMENTATION AND INFORMATION SCIENCE **1226**
Includes information management; information storage and retrieval technology; technical writing; graphic arts; and micrography. For computer documentation see *61 Computer Programming and Software.*

83 ECONOMICS AND COST ANALYSIS **1235**
Includes cost effectiveness studies.

84 LAW, POLITICAL SCIENCE AND SPACE POLICY **1235**
Includes NASA appropriation hearings; aviation law; space law and policy; international law; international cooperation; and patent policy.

85 URBAN TECHNOLOGY AND TRANSPORTATION **1235**
Includes applications of space technology to urban problems; technology transfer; technology assessment; and surface and mass transportation. For related information see *03 Air Transportation and Safety, 16 Space Transportation,* and *44 Energy Production and Conversion.*

SPACE SCIENCES For related information see also *Geosciences.*

88 SPACE SCIENCES (GENERAL) ..... **N.A.**

89 ASTRONOMY **1236**
Includes radio, gamma-ray, and infrared astronomy; and astrometry.

90 ASTROPHYSICS **1239**
Includes cosmology; celestial mechanics; space plasmas; and interstellar and interplanetary gases and dust. For related information see also *75 Plasma Physics.*

91 LUNAR AND PLANETARY EXPLORATION **1246**
Includes planetology; and manned and unmanned flights. For spacecraft design or space stations see *18 Spacecraft Design, Testing and Performance.*

92 SOLAR PHYSICS **1298**
Includes solar activity, solar flares, solar radiation and sunspots. For related information see also *93 Space Radiation.*

93 SPACE RADIATION **1300**
Includes cosmic radiation; and inner and outer earth's radiation belts. For biological effects of radiation see *52 Aerospace Medicine.* For theory see *73 Nuclear and High-Energy Physics.*

GENERAL

Includes aeronautical, astronautical, and space science related histories, biographies, and pertinent reports too broad for categorization; histories or broad overviews of NASA programs.

99 GENERAL **1301**

SUBJECT INDEX **I-1**

PERSONAL AUTHOR INDEX **I-185**

CORPORATE SOURCE INDEX **I-207**

CONTRACT NUMBER INDEX **I-237**

REPORT NUMBER INDEX **I-243**

APPENDIX **A-1**

TYPICAL CITATION AND ABSTRACT

NASA SPONSORED
ON MICROFICHE

ACCESSION NUMBER → **N94-12270*#** United Technologies Corp., West Palm Beach, FL. ← CORPORATE SOURCE
Pratt and Whitney.

TITLE → **ADVANCED CONTROL FOR AIRBREATHING ENGINES, VOLUME 1: PRATT AND WHITNEY**

AUTHOR → J. A. Ralph Jul. 1993 83 p ← PUBLICATION DATE

CONTRACT OR GRANT → (Contract NAS3-25952; RTOP 505-62-61)

REPORT NUMBERS → (NASA-CR-189203; E-8006; NAS 1.26:189203) Avail: CASI HC A05/MF A01 ← AVAILABILITY SOURCE AND PRICE CODE

The application of advanced control concepts to air breathing engines may yield significant improvements in aircraft/engine performance and operability. Screening studies of advanced control concepts for air breathing engines were conducted by three major domestic aircraft engine manufacturers to determine the potential impact of concepts on turbine engine performance and operability. The purpose of the studies was to identify concepts which offered high potential yet may incur high research and development risk. A target suite of proposed advanced control concepts was formulated and evaluated in a two phase study to quantify each concept's impact on desired engine characteristics. To aid in the evaluation specific aircraft/engine combinations were considered: a Military High Performance Fighter mission, a High Speed Civil Transport mission, and a Civil Tiltrotor mission. Each of the advanced control concepts considered in the study are defined and described. The concept potential impact on engine performance was determined. Relevant figures of merit on which to evaluate the concepts are determined. Finally, the concepts are ranked with respect to the target aircraft/engine missions. A final report describing the screening studies was prepared by each engine manufacturer. Volume 1 of these reports describes the studies performed by Pratt & Whitney. Author (revised)

VOLUME 32 NUMBER 3 / March 1994

Scientific and Technical Aerospace Reports

A Monthly Publication of the National Aeronautics and Space Administration

01 AERONAUTICS (GENERAL)

N94-14965# Federal Aviation Administration, Washington, DC. Office of Aviation Policy and Plans.
US CIVIL AIRMEN STATISTICS: CALENDAR YEAR 1992
Jun. 1993 156 p
(AD-A267708; FAA-APO-93-6) Avail: CASI HC A08/MF A02

This report contains calendar year statistics on pilots and nonpilots and the number of certificates issued. It also contains a count of pilots and nonpilots by state and county. DTIC

N94-15120# National Aerospace Lab., Amsterdam (Netherlands).
SYMPOSIUM ON THE FUTURE OF AERONAUTICS IN THE NETHERLANDS [DE TOEKOMST VAN NEDERLAND IN DE LUCHTVAART]
1991 167 p In DUTCH Symposium held in Delft, Netherlands, 26 Apr. 1991
(ETN-93-93780) Avail: CASI HC A08/MF A02

The history of fifty years of the Netherlands Association of Aeronautical Engineers, and the predicted and real developments in the aviation in the period 1961-1991 are depicted. The future of the Schiphol airport and the developments in the European air traffic control are presented. The tasks and prospects of aviation inspection are discussed. The expectations for the future KLM, Fokker the National Aerospace Laboratory, and military aviation in The Netherlands are treated. Developments in the Higher Technical Aerospace Education in the Netherlands and at the Faculty of Aeronautics and Astronautics of the Technical University of Delft are described. For individual titles, see N94-15121 through N94-15131.

N94-15121# Netherlands Association of Aeronautical Engineers, Amsterdam.
FIFTY YEARS OF THE NETHERLANDS ASSOCIATION OF AERONAUTICAL ENGINEERS [VIJFTIG JAAR NVVL: EEN TERUGBLIK]
F. J. Sterk *In* NAL, Symposium on the Future of Aeronautics in the Netherlands 1991 7 p In DUTCH (For primary document see N94-15120 03-01)
Avail: CASI HC A02/MF A02

The history of fifty years of the Netherlands Association of Aeronautical Engineers is depicted. The guidelines for the foundation of the Association are given. The main activity of the Association was and still is the organization of lectures, symposia, and conferences. ESA

N94-15122# Technische Univ., Delft (Netherlands). Faculteit der Luchtvaart- en Ruimtevaarttechniek.
PREDICTED AND REAL DEVELOPMENT IN THE AVIATION IN THE PERIOD 1961-1991 [VOORSPELDE EN WERKELIJKE ONTWIKKELINGEN IN DE VERKEERSLUCHTVAART (1961-1991)]
H. Wittenberg *In* NAL, Symposium on the Future of Aeronautics in the Netherlands 1991 43 p In DUTCH (For primary document see N94-15120 03-01)
Avail: CASI HC A03/MF A02

The predictions in developments in aeronautical techniques and aviation given at a symposium in 1966 are taken in a retrospective view and compared with the real developments in the period 1961-1991. It is concluded that the expectations run too high. With respect to technical developments this could be due to the belief in the 'technology push' rather then in the 'market demand'. In general, predictions have to consider social factors ('scenario techniques'). The development of aviation is influenced by many factors, and many efforts are still required to allow predictions based on models. ESA

N94-15123# Netherlands Association of Aeronautical Engineers, Amsterdam.
THE FUTURE OF SCHIPHOL: GROWTH WITHIN BOUNDARIES [DE TOEKOMST VAN SCHIPHOL: GROEIEN BINNEN GRENZEN] **c09**
R. denBesten *In* NAL, Symposium on the Future of Aeronautics in the Netherlands 1991 16 p In DUTCH (For primary document see N94-15120 03-01)
Avail: CASI HC A03/MF A02

The planned, controlled growth of the Schipol airport considering clear environmental boundary conditions is discussed. Within the tendency of concentration in the European aviation, Schipol tries to become one of the mainports ('hubs') on which intercontinental air traffic concentrates. The planned expansions of the airport and the consequences for the employment and the environment are outlined. ESA

N94-15124# Rijksluchtvaartdienst, The Hague (Netherlands).
DEVELOPMENTS IN THE EUROPEAN AIR TRAFFIC CONTROL [ONTWIKKELINGEN IN DE EUROPESE LUCHTVERKEERSBEVEILIGING] **c04**
J. P. F. deKoning *In* NAL, Symposium on the Future of Aeronautics in the Netherlands 1991 16 p In DUTCH (For primary document see N94-15120 03-01)
Avail: CASI HC A03/MF A02

Present and future developments in the Air Traffic Control (ATC) are presented. The integrated Eurocontrol ATC operational concept is outlined. The future air traffic control services are presented. The integrated concept includes the combination of civil and military systems. The different system functions have to be compared and possibly adapted. ESA

N94-15125# Rijksluchtvaartdienst, Schiphol (Netherlands).
AVIATION INSPECTION PROSPECTS [TOEKOMSTVERWACHTING RLD, LUCHTVAARTINSPECTIE] **c03**
H. N. Wolleswinkel *In* NAL, Symposium on the Future of Aeronautics in the Netherlands 1991 22 p In DUTCH (For primary document see N94-15120 03-01)
Avail: CASI HC A03/MF A02

The main tasks of aviation inspection, namely guaranteeing safety and minimizing the environment effects of civil aviation as well as the expectations, are discussed. The activities and methods are strongly changing due to increasing internationalization and environment consciousness. The establishment and application of international rules are outlined. ESA

N94-15126# KLM Aerocarto, Schiphol (Netherlands).
AVIATION AND THE KLM: PAST AND FUTURE [DE LUCHTVAART EN DE KLM: VERLEDEN EN TOEKOMST] **c99**
C. denHartog *In* NAL, Symposium on the Future of Aeronautics in the Netherlands 1991 7 p In DUTCH (For primary document see N94-15120 03-01)
Avail: CASI HC A02/MF A02

Some aspects of the seventy years of history and of the future of KLM are discussed. Some examples are given to illustrate that the history of KLM is a good reflection of civil aviation as a whole. The expected technological innovations, international strategic airline alliances, and the significance of civil aviation for the Netherlands are outlined. ESA

N94-15127# Fokker B.V., Amsterdam (Netherlands).
EXPECTATIONS FOR THE FUTURE OF FOKKER [TOEKOMSTVERWACHTINGEN FOKKER]
M. vanderVeen *In* NAL, Symposium on the Future of Aeronautics in the Netherlands 1991 3 p In DUTCH (For primary document see N94-15120 03-01)
Avail: CASI HC A01/MF A02

The perspectives of the Fokker Aircraft Company are outlined. The main emphasis is on civil regional airlines for 50 to 130 passengers; although, participation in Dutch military projects remains important. Until the year 2000 the emphasis is on the extension of the Fo50 and Fo100 aircraft. After 2000 the emphasis will be on aviation deregulation, environmental issues, integrated flight management, and integrated transportation systems. ESA

N94-15128# Ministry of Defence, The Hague (Netherlands).
EXPECTATIONS FOR THE FUTURE OF MILITARY AVIATION [TOEKOMSTVERWACHTINGEN MILITAIRE LUCHTVAART]
Rudolf J. W. Merison *In* NAL, Symposium on the Future of Aeronautics in the Netherlands 1991 12 p In DUTCH (For primary document see N94-15120 03-01)
Avail: CASI HC A03/MF A02

An overview is given of the existing possibilities in the Netherlands in the field of defense oriented aeronautics and astronautics research and development, with emphasis on the Royal Air Force. From a national military strategic point of view there is a growing need for a European defense industry in which The Netherlands can contribute. The program EUCLID (European Cooperation for the Long term in Defense) was started to integrate the defense developments in Europe. ESA

N94-15129# National Aerospace Lab., Amsterdam (Netherlands).
EXPECTATIONS FOR THE FUTURE OF THE NATIONAL AEROSPACE LABORATORY [TOEKOMSTVERWACHTINGEN NATIONAAL LUCHT- EN RUIMTEVAARTLABORATORIUM] **c09**
B. M. Spee *In its* Symposium on the Future of Aeronautics in the Netherlands 1991 17 p In DUTCH (For primary document see N94-15120 03-01)
Avail: CASI HC A03/MF A02

The perspectives of the National Aerospace Laboratories (NLR) in the field of aeronautics are depicted. The new required civil and military technologies to which NLR is planning to contribute are overviewed. The required research will take place in an international framework. The important role of the large NLR research facilities is described. ESA

N94-15130# Haarlem Univ. (Netherlands).
DEVELOPMENTS IN THE HIGHER TECHNICAL AEROSPACE EDUCATION [ONTWIKKELINGEN IN HET VLIEGTUIGBOUWKUNDIG HOGER TECHNISCH ONDERWIJS] **c80**
P. J. L. M. vanderZanden *In* NAL, Symposium on the Future of Aeronautics in the Netherlands 1991 12 p In DUTCH (For primary document see N94-15120 03-01)
Avail: CASI HC A03/MF A02

Developments in the Higher Technical Aerospace Education in the Netherlands since 1986 are described. The tasks of high schools in general and of higher aerospace technical education in particular are depicted. The developments in the speciality and in the execution of the profession of the higher aerospace technical engineer is described. The developments in the education process are outlined. The profession of teacher at a higher technical school is sketched. The developments in the relations between higher technical schools on the one hand and universities and industry on the other hand are described including the international dimension. ESA

N94-15131# Technische Univ., Delft (Netherlands). Faculteit der Luchtvaart- en Ruimtevaarttechniek.
EXPECTATIONS FOR THE FUTURE OF THE FACULTY OF AERONAUTICS AND ASTRONAUTICS OF THE TECHNICAL UNIVERSITY OF DELFT [TOEKOMSTVERWACHTINGEN FACULTEIT DER LUCHTVAART- EN RUIMTEVAARTTECHNIEK TU-DELFT] **c80**
T. deJong *In* NAL, Symposium on the Future of Aeronautics in the Netherlands 1991 9 p In DUTCH (For primary document see N94-15120 03-01)
Avail: CASI HC A02/MF A02

The developments at the Faculty of Aeronautics and Astronautics of the TU Delft are described. The purpose of the Faculty is the education of engineers in all the fields of aeronautics and astronautics. The structure of the education and the important role of postdoctoral education are outlined. The intensive international cooperation in the fields of education and research is very important for the future, and the faculty has to maintain its position which is unique in the Netherlands. ESA

N94-15798*# National Aeronautics and Space Administration. Ames Research Center, Moffett Field, CA.
NAS TECHNICAL SUMMARIES: NUMERICAL AERODYNAMIC SIMULATION PROGRAM, MARCH 1991 - FEBRUARY 1992
1992 266 p Original contains color illustrations
(NASA-TM-109335; NAS 1.15:109335) Avail: CASI HC A12/MF A03; 176 functional color pages

NASA created the Numerical Aerodynamic Simulation (NAS) Program in 1987 to focus resources on solving critical problems in aeroscience and related disciplines by utilizing the power of the most advanced supercomputers available. The NAS Program provides scientists with the necessary computing power to solve today's most demanding computational fluid dynamics problems and serves as a pathfinder in integrating leading-edge supercomputing technologies, thus benefiting other supercomputer centers in Government and industry. This report contains selected scientific results from the 1991-92 NAS Operational Year, March 4, 1991 to March 3, 1992, which is the fifth year of operation. During this year, the scientific community was given access to a Cray-2 and a Cray Y-MP. The Cray-2, the first generation supercomputer, has four processors, 256 megawords of central memory, and a total sustained speed of 250 million floating point operations per second. The Cray Y-MP, the second generation supercomputer, has eight processors and a total sustained speed of one billion floating point operations per second. Additional memory was installed this year, doubling capacity from 128 to 256 megawords of solid-state storage-device memory. Because of its higher performance, the Cray Y-MP delivered approximately 77 percent of the total number of supercomputer hours used during this year. Author (revised)

N94-16480* National Aeronautics and Space Administration, Washington, DC.
AERONAUTICAL ENGINEERING: A CONTINUING BIBLIOGRAPHY WITH INDEXES (SUPPLEMENT 295)
Sep. 1993 168 p
(NASA-SP-7037(295); NAS 1.21:7037(295)) Avail: CASI HC A08

This bibliography lists 581 reports, articles, and other documents introduced into the NASA Scientific and Technical Information System in Sep. 1993. Subject coverage includes: design, construction and testing of aircraft and aircraft engines; aircraft components, equipment, and systems; ground support systems; and theoretical and applied aspects of aerodynamics and general fluid dynamics. Author

N94-16481* National Aeronautics and Space Administration, Washington, DC.
COMMONWEALTH OF INDEPENDENT STATES AEROSPACE SCIENCE AND TECHNOLOGY, 1992: A BIBLIOGRAPHY WITH INDEXES
Aug. 1993 313 p
(NASA-SP-7106; NAS 1.21:7106) Avail: CASI HC A14

This bibliography contains 1237 annotated references to reports and journal articles of Commonwealth of Independent States (CIS) intellectual origin entered into the NASA Scientific and Technical Information System during 1992. Representative subject areas include the following: aeronautics, astronautics, chemistry and materials, engineering, geosciences, life sciences, mathematical and computer sciences, physics, social sciences, and space sciences. Author

N94-17614 National Aerospace Lab., Emmeloord (Netherlands). Structures and Materials Div.
OVERVIEW OF THE FAA/DCA/NLR PROGRAMS RELATED TO AGEING AIRCRAFT
Harold H. Ottens and J. Ben deJonge 16 Mar. 1993 24 p Presented at International Workshop on Structural Integrity of Ageing Airplanes, Atlanta,

GA, 31 Mar. - 3 Apr. 1992 Limited Reproducibility: More than 20% of this document may be affected by microfiche quality
(NLR-TR-92119-U; ETN-93-94786) Avail: CASI HC A03

An overview of the research currently carried out at the National Aerospace Laboratory (NLR) (The Netherlands), with regard to the problems of ageing aircraft, is given. This research is primarily directed towards the prevention of ageing aircraft problems in future aircraft and is concentrated in two areas: prevention of multiple site damage in lap joints; improved knowledge in operational load experience. The major part of this research is carried out in some form of international cooperation. The Memorandum of Cooperation between Federal Aviation Administration and the Netherlands Civil Aviation Department in the area of aviation safety provides an effective framework for the coordination of research efforts related to ageing aircraft problems. NLR experiences with this cooperation and support from FAA are very stimulating. ESA

02 AERODYNAMICS

Includes aerodynamics of bodies, combinations, wings, rotors, and control surfaces; and internal flow in ducts and turbomachinery.

For related information see also *34 Fluid Mechanics and Heat Transfer.*

N94-14942# Air Force Systems Command, Wright-Patterson AFB, OH. Foreign Aerospace Science and Technology Center.
THE EFFECT OF THE NOSE SHAPE AND WING LOCATION TOWARD THE WING VORTEX BREAKDOWN
Feng Yanan, Xia Xuejian, and Liu Rizhi 16 Jul. 1993 14 p Transl. into ENGLISH from Hangkong Xuebao (China), v. 11, no. 12, 1990 p 588-591
(AD-A267724; FASTC-ID(RS)T-0735-92) Avail: CASI HC A03/MF A01

The variation of the wing vortex breakdown vs. the angle of attack for a missile with a cruciform set of wings was investigated through experiments. The tests were carried out by conducting the flow pattern visualization in the water channel at BUAA. The model had two nose shapes - pointed and blunted nose. The wing was set at fore or aft location along the axis of the body. The experimental results indicate that for the configuration with the same nose, the location of the vortex breakdown for the wing with aft location is closer to the wing trailing edge than that of the wing with fore location. While for the configuration with the wing at an aft location, the wing vortex breakdown for the blunt nose is delayed compared to that for the pointed nose. DTIC

N94-14959# Colorado Univ., Boulder. Dept. of Aerospace Engineering Sciences.
UNSTEADY SEPARATED FLOWS: EMPIRICAL MODEL AND CONTROL Final Report, 1 Aug. 1988 - 31 Dec. 1992
Marvin Luttges and Michael Robinson 7 Jun. 1993 29 p
(Grant AF-AFOSR-0272-88)
(AD-A267282; AFOSR-93-0466TR) Avail: CASI HC A03/MF A01

Research examined the similarity behavior between forced unsteady separated flows elicited by airfoils and delta wings. For the first time, all of the existing unsteady separation data reported in open literature was assembled and contrasted directly. A vortex model which predicted vortex development and shedding characteristics from first principles was developed. Preliminary work was also initiated in using neural network techniques to model and predict these nonlinear unsteady flows. DTIC

N94-14963 Arizona Univ., Tucson. Dept. of Aerospace and Mechanical Engineering.
THE TURBULENT WALL JET Final Report, Nov. 1991 - 1992
I. Wygnanski and M. D. Zhou 18 May 1993 7 p Limited Reproducibility: More than 20% of this document may be affected by microfiche quality
(Grant AF-AFOSR-0176-88)
(AD-A267675; AFOSR-93-0485TR) Avail: Issuing Activity (Defense Technical Information Center (DTIC))

The flow of a wall jet embedded in an external stream or in a quiescent surrounding fluid was investigated experimentally. It was determined that the flow scales with the excess momentum injected into the stream and the viscosity of the fluid rather than the jet efflux velocity and the dimension of the nozzle. In the presence of an external stream, a velocity ratio parameter R = (Ui - U)/(Uj + U) had to be added in order to obtain a universal scaling of this flow. Low-amplitude external excitation of the wall jet resulted in a reduction of skin friction and drag. The only possible cause for this behavior observed is the enhancement of the two-dimensionality of the large eddies as expressed by spanwise coherence and correlation measurements. DTIC

N94-14973# Naval Postgraduate School, Monterey, CA.
LASER DOPPLER VELOCIMETRY MEASUREMENTS ACROSS A NORMAL SHOCK IN TRANSONIC FLOW M.S. Thesis
David A. Perretta 25 Mar. 1993 117 p
(AD-A267240) Avail: CASI HC A06/MF A02

One-dimensional laser-Doppler velocimetry measurements were taken with standard optics in back scatter mode across a normal shock at a Mach number of 1.35. Back pressure on a blow-down supersonic tunnel was controlled to place a normal shock in a 4 by 4 inch test section and schlieren visualization techniques were used to verify and record shock position and behavior. Velocity surveys were taken across the shock, using various filtering techniques, in an attempt to quantify shock unsteadiness. Additional surveys were performed to further characterize the flow in the test section. The velocity surveys upstream and downstream of the shock compared favorably with pressure and temperature data and normal shock relations. Surveys across the shock indicated distinct and repeatable velocity patterns, and the measured location of the shock matched schlieren photographs. DTIC

N94-15105# Aeronautical Systems Div., Wright-Patterson AFB, OH.
AN UNCERTAINTY ANALYSIS OF INLET DYNAMIC FLOW DISTORTION USING AN ANALOG/DIGITAL HYBRID EDITING SYSTEM Final Report, Feb. 1991 - Dec. 1992
Maryann Zelenak Mar. 1993 337 p
(AD-A266924; ASC-TR-93-5005) Avail: CASI HC A15/MF A03

The objectives of this analysis were to establish precision and bias errors for an analog/digital hybrid computer system (DYNADEC) used in the dynamic data editing phase of inlet wind tunnel testing. An uncertainty analysis was initiated to evaluate the system using inlet data from the Aeronautical Systems Center (ASC)/Arnold Engineering Development Center (AEDC) Freejet Development program. Three test points from a subscale freejet test and three test points from a wind tunnel test of the same F-15 inlet model were selected to cover a wide range of test conditions and turbulence levels. Precision errors of the 40 total pressure probes at the location of the engine face were 1-2% of the 40 total pressure recovery magnitudes. Precision errors of the Pratt and Whitney K a2 distortion index, the parameter used to edit the data on DYNADEC, were also investigated. These results indicated that K a2 precision errors decreased with higher turbulence levels. Static bias errors were also computed by sending known signal through the DYNADEC system and measuring the output quantity. Static bias errors were much smaller in comparison to the precision error magnitudes and may be considered negligible. DTIC

N94-15655*# Eidetics International, Inc., Torrance, CA.
AERODYNAMIC CONTROL OF NASP-TYPE VEHICLES THROUGH VORTEX MANIPULATION. VOLUME 1: STATIC WATER TUNNEL TESTS
Carlos J. Suarez, T. Terry Ng, Lih-Yenn Ong, and Gerald N. Malcolm Sep. 1993 88 p Sponsored by NASA, Washington
(Contract NAS2-13196)
(NASA-CR-177626-Vol-1; A-93138-Vol-1; NAS 1.26:177626-Vol-1) Avail: CASI HC A05/MF A01

Water tunnel tests were conducted on a NASP-type configuration to evaluate different pneumatic Forebody Vortex Control (FVC) methods. Flow visualization and yawing moment measurements were performed at angles of attack from 0 deg to 30 deg. The pneumatic techniques tested included jet and slot blowing. In general, blowing can be used efficiently to manipulate the forebody vortices at angles of attack greater than 20 deg. These vortices are naturally symmetric up to alpha = 25 deg and asymmetric between 25 deg and 30 deg angle of attack. Results indicate that tangential aft jet blowing is the most promising method for this configuration. Aft jet blowing produces a yawing moment towards the blowing side and the trends with blowing rate are well behaved. The size of the nozzle is not the dominant factor in the blowing process; the change in the blowing 'momentum,' i.e., the product of the mass flow rate and the velocity of the jet, appears to be the important parameter in the water tunnel (incompressible

and unchoked flow at the nozzle exit). Forward jet blowing is very unpredictable and sensitive to mass flow rate changes. Slot blowing (with the exception of very low blowing rates) acts as a flow 'separator'; it promotes early separation on the blow side, producing a yawing moment toward the non-blowing side for the C(sub mu) range investigated.
Author (revised)

N94-15657*# National Aeronautics and Space Administration. Ames Research Center, Moffett Field, CA.
SUPPRESSION OF DYNAMIC STALL WITH A LEADING-EDGE SLAT ON A VR-7 AIRFOIL
K. W. McAlister and C. Tung Mar. 1993 71 p
(RTOP 505-61-51)
(NASA-TP-3357; ATCOM-TR-92-A-013; A-93006; NAS 1.60:3357) Avail: CASI HC A04/MF A01

The VR-7 airfoil was experimentally studied with and without a leading-edge slat at fixed angles of attack from 0 deg to 30 deg at Re = 200,000 and for unsteady pitching motions described by alpha equals alpha(sub m) + 10 deg(sin(wt)). The models were two dimensional, and the test was performed in a water tunnel at Ames Research Center. The unsteady conditions ranged over Re equals 100,000 to 250,000, k equals 0.001 to 0.2, and alpha(sub m) = 10 deg to 20 deg. Unsteady lift, drag, and pitching-moment measurements were obtained along with fluorescent-dye flow visualizations. The addition of the slat was found to delay the static-drag and static-moment stall by about 5 degrees and to eliminate completely the development of a dynamic-stall vortex during unsteady motions that reached angles as high as 25 degrees. In all of the unsteady cases studied, the slat caused a significant reduction in the force and moment hysteresis amplitudes. The reduced frequency was found to have the greatest effect on the results, whereas the Reynolds number had little effect on the behavior of either the basic or the slatted airfoil. The slat caused a slight drag penalty at low angles of attack, but generally increased the lift/drag ratio when averaged over the full cycle of oscillation. Author (revised)

N94-15677*# Eidetics International, Inc., Torrance, CA.
AERODYNAMIC CONTROL OF NASP-TYPE VEHICLES THROUGH VORTEX MANIPULATION. VOLUME 2: STATIC WIND TUNNEL TESTS
Carlos J. Suarez, Brian R. Kramer, Brooke C. Smith, and Gerald N. Malcolm Sep. 1993 144 p Sponsored by NASA, Washington
(Contract NAS2-13196)
(NASA-CR-177626-Vol-2; A-93138-Vol-2; NAS 1.26:177626-Vol-2) Avail: CASI HC A07/MF A02

Forebody Vortex Control (FVC) was explored in this research program for potential application to a NASP-type configuration. Wind tunnel tests were conducted to evaluate a number of jet blowing schemes. The configuration tested has a slender forebody and a 78 deg swept delta wing. Blowing jets were implemented on the leeward side of the forebody with small circular tubes tangential to the surface that could be directed aft, forward, or at angles in between. The effects of blowing are observed primarily in the yawing and rolling moments and are highly dependent on the jet configuration and the angle of attack. Results show that the baseline flow field, without blowing activated, is quite sensitive to the geometry differences of the various protruding jets, as well as being sensitive to the blowing, particularly in the angle of attack range where the forebody vortices are naturally asymmetric. The time lag of the flow field response to the initiation of blowing was also measured. The time response was very short, on the order of the time required for the flow disturbance to travel the distance from the nozzle to the specific airframe location of interest at the free stream velocity. Overall, results indicate that sizable yawing and rolling moments can be induced with modest blowing levels. However, direct application of this technique on a very slender forebody would require thorough wind tunnel testing to optimize the jet location and configuration.
Author (revised)

N94-15678*# Eloret Corp., Sunnyvale, CA. Thermosciences Div.
PARTICLE KINETIC SIMULATION OF HIGH ALTITUDE HYPERVELOCITY FLIGHT Report, 1 Jan. - 31 Aug. 1993
Brian L. Haas 12 Oct. 1993 58 p
(Contract NCC2-582)
(NASA-CR-194599; NAS 1.26:194599) Avail: CASI HC A04/MF A01

In this grant period, the focus has been on enhancement and application of the direct simulation Monte Carlo (DSMC) particle method for computing hypersonic flows of re-entry vehicles. Enhancement efforts dealt with modeling gas-gas interactions for thermal non-equilibrium relaxation processes and gas-surface interactions for prediction of vehicle surface temperatures. Both are important for application to problems of engineering interest. The code was employed in a parametric study to improve future applications, and in simulations of aeropass maneuvers in support of the Magellan mission. Detailed comparisons between continuum models for internal energy relaxation and DSMC models reveals that several discrepancies exist. These include definitions of relaxation parameters and the methodologies for implementing them in DSMC codes. These issues were clarified and all differences were rectified in a paper (Appendix A) submitted to Physics of Fluids A, featuring several key figures in the DSMC community as co-authors and B. Haas as first author. This material will be presented at the Fluid Dynamics meeting of the American Physical Society on November 21, 1993. The aerodynamics of space vehicles in highly rarefied flows are very sensitive to the vehicle surface temperatures. Rather than require prescribed temperature estimates for spacecraft as is typically done in DSMC methods, a new technique was developed which couples the dynamic surface heat transfer characteristics into the DSMC flow simulation code to compute surface temperatures directly. This model, when applied to thin planar bodies such as solar panels, was described in AIAA Paper No. 93-2765 (Appendix B) and was presented at the Thermophysics Conference in July 1993. The paper has been submitted to the Journal of Thermophysics and Heat Transfer. Application of the DSMC method to problems of practical interest requires a trade off between solution accuracy and computational expense and limitations. A parametric study was performed and reported in AIAA Paper No. 93-2806 (Appendix C) which assessed the accuracy penalties associated with simulations of varying grid resolution and flow domain size. The paper was also presented at the Thermophysics Conference and will be submitted to the journal shortly. Finally, the DSMC code was employed to assess the pitch, yaw, and roll aerodynamics of the Magellan spacecraft during entry into the Venus atmosphere at off-design attitudes. This work was in support of the Magellan aerobraking maneuver of May 25-Aug. 3, 1993. Furthermore, analysis of the roll characteristics of the configuration with canted solar panels was performed in support of the proposed 'Windmill' experiment. Results were reported in AIAA Paper No. 93-3676 (Appendix D) presented at the Atmospheric Flight Mechanics Conference in August 1993, and were submitted to Journal of Spacecraft and Rockets. Author

N94-15681*# National Aeronautics and Space Administration. Langley Research Center, Hampton, VA.
WIND TUNNEL INVESTIGATION OF THREE AXISYMMETRIC COWLS OF DIFFERENT LENGTHS AT MACH NUMBERS FROM 0.60 TO 0.92
Richard J. Re and William K. Abeyounis Sep. 1993 285 p Sponsored by NASA, Washington
(RTOP 535-03-10-01)
(NASA-TM-4488; L-17191; NAS 1.15:4488) Avail: CASI HC A13/MF A03

Pressure distributions on three inlets having different cowl lengths were obtained in the Langley 16-Foot Transonic Tunnel. The cowl diameter ratio (highlight diameter to maximum diameter) was 0.85 and the cowl length ratios (cowl length to maximum diameter) were 0.337, 0.439, and 0.547. The cowls had identical nondimensionalized (with respect to cowl length) external geometry and identical internal geometry. The internal contraction ratio (highlight area to throat area) was 1.250. The inlets had longitudinal rows of static pressure orifices on the top and bottom (external) surfaces and on the contraction (internal) and diffuser surfaces. The afterbody was cylindrical in shape, and its diameter was equal to the maximum diameter of the cowl. Depending on the cowl configuration and free-stream Mach number, the mass-flow ratio varied between 0.27 and 0.87 during the tests. Angle of attack varied from 0 to 4.1 deg at selected Mach numbers and mass-flow ratios, and the Reynolds number varied with the Mach number from 3.2x10(exp 6) to 4.2x10(exp 6) per foot. Author (revised)

N94-15696# Royal Aerospace Establishment, Farnborough (England). Aerodynamics and Propulsion Dept.
HEAT TRANSFER AND AERODYNAMICS OF A 3D DESIGN NOZZLE GUIDE VANE TESTED IN THE PYESTOCK ISENTROPIC LIGHT PISTON FACILITY
K. S. Chana 17 Dec. 1992 15 p Presented at the AGARD 80th

Symposium of the Propulsion and Energetics Panel on Heat Transfer and Cooling in Gas Turbines, Antalaya, Turkey, 12-16 Oct. 1992 Original contains color illustrations
(RAE-TM-Aero/Prop-19; BR316026; ETN-93-94495) Copyright Avail: CASI HC A03/MF A01

The prediction of the heat transfer to the blade and endwalls in high pressure turbines, which is particularly important for an accurate assessment of turbine component life is addressed. On the endwalls, there are often complex three dimensional (3D) (secondary) flows present which make predictions of heat transfer particularly difficult. A detailed investigation of this area was carried out on a fully annular cascade of highly 3D nozzle guide vanes. Measurements were made on the vane and endwalls to determine heat transfer and aerodynamic characteristics. Testing was conducted in a short duration isentropic light piston test facility, at engine representative Reynolds number, Mach number, and gas to wall temperature ratio. Interpreted test data are compared with computations obtained at test conditions. ESA

N94-15720*# Eidetics International, Inc., Torrance, CA.
AERODYNAMIC CONTROL OF NASP-TYPE VEHICLES THROUGH VORTEX MANIPULATION, VOLUME 4
Brooke C. Smith, Carlos J. Suarez, William M. Porada, and Gerald N. Malcolm Sep. 1993 151 p Sponsored by NASA, Washington
(Contract NAS2-13196)
(NASA-CR-177626-Vol-4; A-93138; NAS 1.26:177626-Vol-4) Avail: CASI HC A08/MF A02

Forebody Vortex Control (FVC) is an emerging technology that has received widespread and concentrated attention by many researchers for application on fighter aircraft to enhance aerodynamic controllability at high angles of attack. This research explores potential application of FVC to a NASP-type configuration. The configuration investigated is characterized by a slender, circular cross-section forebody and a 78 deg swept delta wing. A man-in-the-loop, six-degress-of-freedom, high-fidelity simulation was developed that demonstrates the implementation and advantages of pneumatic forebody vortex control. Static wind tunnel tests were used as the basis for the aerodynamic characteristics modeled in the simulation. Dynamic free-to-roll wind tunnel tests were analyzed and the wing rock motion investigated. A non-linear model of the dynamic effects of the bare airframe and the forebody vortex control system were developed that closely represented the observed behavior. Multiple state-of-the-art digital flight control systems were developed that included different utilizations of pneumatic vortex control. These were evaluated through manned simulation. Design parameters for a pneumatic forebody vortex control system were based on data collected regarding the use of blowing and the mass flow required during realistic flight maneuvers. Author (revised)

N94-15780*# Eidetics International, Inc., Torrance, CA.
AERODYNAMIC CONTROL OF NASP-TYPE VEHICLES THROUGH VORTEX MANIPULATION. VOLUME 3: WING ROCK EXPERIMENTS
Carlos J. Suarez, Brooke C. Smith, Brian R. Kramer, T. Terry Ng, Lih-Yenn Ong, and Gerald N. Malcolm Sep. 1993 130 p
(Contract NAS2-13196)
(NASA-CR-177626; A-93138; NAS 1.26:177626) Avail: CASI HC A07/MF A02

Free-to-roll tests were conducted in water and wind tunnels in an effort to investigate the mechanisms of wing rock on a NASP-type vehicle. The configuration tested consisted of a highly-slender forebody and a 78 deg swept delta wing. In the water tunnel test, extensive flow visualization was performed and roll angle histories were obtained. In the wind tunnel test, the roll angle, forces and moments, and limited forebody and wing surface pressures were measured during the wing rock motion. A limit cycle oscillation was observed for angles of attack between 22 deg and 30 deg. In general, the experiments confirmed that the main flow phenomena responsible for the wing-body-tail wing rock are the interactions between the forebody and the wing vortices. The variation of roll acceleration (determined from the second derivative of the roll angle time history) with roll angle clearly slowed the energy balance necessary to sustain the limit cycle oscillation. Different means of suppressing wing rock by controlling the forebody vortices using small blowing jets were also explored. Steady blowing was found to be capable of suppressing wing rock, but significant vortex asymmetrices are created, causing the model to stop at a non-zero roll angle. On the other hand, alternating pulsed blowing on the left and right sides of the fore body was demonstrated to be a potentially effective means of suppressing wing rock and eliminating large asymmetric moments at high angles of attack. Author (revised)

N94-15787# Stanford Univ., CA. Dept. of Aeronautics and Astronautics.
PARTICLE SIMULATION OF HYPERSONIC FLOW Final Report, 1 Apr. 1990 - 31 Mar. 1993
Donald Baganoff 26 May 1993 40 p
(Grant AF-AFOSR-0232-90)
(AD-A267185; AFOSR-93-0457TR) Avail: CASI HC A03/MF A01

A particle code for simulating a rarefied hypersonic flow is developed which accounts for a multiple species gas in thermochemical nonequilibrium and which takes advantage of the parallel architecture of the Intel iPSC/860 supercomputer. Various tests were conducted using a generic blunt body consisting of a hemispherically blunted 60-degree half-angle cone at angle of attack. The different tests conducted show that the performance of the parallel code using 512 nodes exceeds by an order of magnitude the performance obtained for a highly vectorized code run on a single processor of the Cray YMP, that scaleup is found to be nearly linear with the number of processors used, that run time can be greatly reduced by employing a large number of particles, and that runs with 67.5 million particles can be carried out when employing the large memory of the Intel iPSC/860. Other results relate to different applications of the code for studying the near-continuum state of a gas near a cold solid boundary. DTIC

N94-15824# Dayton Univ., OH. Dept. of Chemistry.
CENTER FOR ROTORCRAFT EDUCATION AND RESEARCH PROGRESS REPORT, 1987 - 1992 Final Report, 1 Jan. 1988 - 31 Dec. 1992
Inderjit Chopra Jun. 1993 133 p
(Contract DAAL03-88-C-0002)
(AD-A266760; ARO-25467.74-EG-RW) Avail: CASI HC A07/MF A02

Established in 1981, the Center for Rotorcraft Education and Research at the University of Maryland has achieved international recognition as a center of excellence in rotorcraft engineering based on the quality and quantity of its research output and advanced-degree recipients. In the process of growth, it has built an integrated team of rotorcraft dedicated research faculty and staff, a pipeline of high quality graduate students, and a group of specialized rotorcraft research facilities and instrumentation unmatched by any other university. The center carried out interdisciplinary research program built around four interrelated areas that advanced understanding and predictive capability in: Aerodynamics-unsteady aerodynamics, dynamic stall, and rotor/airframe interaction tests and analyses; Dynamics and Aeroelasticity-bearingless and composite rotor tests and analyses, and minimization of rotor/body vibrations by optimization techniques; Flight Dynamics and Control-control of the dynamic behavior of highly coupled rotor-fuselage configurations; and Structures and Materials-structural integrity, energy absorption, and modeling of composite blades. Author (revised)

N94-16471 Naval Postgraduate School, Monterey, CA.
A RAPID COMPUTATIONAL MODEL FOR ESTIMATING THE PERFORMANCE OF COMPLIANT AIRFOILS IN CASCADES Technical Report, Jan. - Jun. 1992
F. Sisto and M. Avila 1 Jul. 1992 21 p Limited Reproducibility: More than 20% of this document may be affected by microfiche quality
(AD-A266275; NPS-AA-93-001) Avail: Issuing Activity (Defense Technical Information Center (DTIC))

We consider the problem of designing the blades in a turbomachine to have a specific schedule of structural stiffness in order to achieve more favorable aerothermodynamic performance characteristics than is possible with rigid blades. This problem of 'aerothermodynamic tailoring' is extremely complex because of the need to couple the flow computation over a deformable surface with the structural dynamics computation. In this report an analysis is presented which accomplishes this objective by means of a two-dimensional incompressible potential flow model using vortex sheet representation of the blades. Details of the analysis and of the resulting computer program together with representative results are described. DTIC

N94-16510*# MCAT Inst., San Jose, CA.
COMPUTATION OF THE FLUID AND OPTICAL FIELDS ABOUT THE STRATOSPHERIC OBSERVATORY FOR INFRARED ASTRONOMY (SOFIA) AND THE COUPLING OF FLUIDS, DYNAMICS, AND CONTROL LAWS ON PARALLEL COMPUTERS Final Report
Christopher A. Atwood May 1993 185 p
(Contract NCC2-677)
(NASA-CR-193168; NAS 1.26:193168; MCAT-93-09) Avail: CASI HC A09/MF A02

The June 1992 to May 1993 grant NCC-2-677 provided for the continued demonstration of Computational Fluid Dynamics (CFD) as applied to the Stratospheric Observatory for Infrared Astronomy (SOFIA). While earlier grant years allowed validation of CFD through comparison against experiments, this year a new design proposal was evaluated. The new configuration would place the cavity aft of the wing, as opposed to the earlier baseline which was located immediately aft of the cockpit. This aft cavity placement allows for simplified structural and aircraft modification requirements, thus lowering the program cost of this national astronomy resource. Three appendices concerning this subject are presented. For individual titles, see N94-16511 through N94-16513.

N94-16511*# MCAT Inst., San Jose, CA.
SELECTED COMPUTATIONS OF TRANSONIC CAVITY FLOWS
Christopher A. Atwood *In its* Computation of the Fluid and Optical Fields About the Stratospheric Observatory for Infrared Astronomy (SOFIA) and the Coupling of Fluids, Dynamics, and Control Laws on Parallel Computers May 1993 13 p The 1993 ASME Fluids Engineering Conference of the Forum on Computational Aero- and Hydro-Acoustics held in Washington, DC, 20-24 Jun. 1993 (For primary document see N94-16510 03-02)
Avail: CASI HC A03/MF A02

An efficient diagonal scheme implemented in an overset mesh framework has permitted the analysis of geometrically complex cavity flows via the Reynolds averaged Navier-Stokes equations. Use of rapid hyperbolic and algebraic grid methods has allowed simple specification of critical turbulent regions with an algebraic turbulence model. Comparisons between numerical and experimental results are made in two dimensions for the following problems: a backward-facing step; a resonating cavity; and two quieted cavity configurations. In three-dimensions the flow about three early concepts of the stratospheric Observatory For Infrared Astronomy (SOFIA) are compared to wind-tunnel data. Shedding frequencies of resolved shear layer structures are compared against experiment for the quieted cavities. The results demonstrate the progress of computational assessment of configuration safety and performance. Author (revised)

N94-16512*# MCAT Inst., San Jose, CA.
UNSTEADY FLUID AND OPTICAL SIMULATION OF TRANSONIC AERO-WINDOWS
Christopher A. Atwood *In its* Computation of the Fluid and Optical Fields About the Stratospheric Observatory for Infrared Astronomy (SOFIA) and the Coupling of Fluids, Dynamics, and Control Laws on Parallel Computers May 1993 12 p Conference of the AIAA 24th Fluid Dynamics, PlasmaDynamics, and Lasers held in Orlando, FL, 6-9 Jul. 1993 (For primary document see N94-16510 03-02)
(AIAA Paper 93-3017) Avail: CASI HC A03/MF A02

The time-varying fluid and optical fields of several cavity configurations have been computed on overset mesh systems using the Reynolds-averaged Navier-Stokes equations and geometric optics. Comparisons between numerical results and Airborne Optical Adjunct (AOA) flight data are made in two-dimensions for a quieted cavity geometry with two lip-blowing rates. In three-dimensions, two proposed aero-window locations for the Stratospheric Observatory For Infrared Astronomy (SOFIA) are discussed. The simulations indicate that convection of large shear layer structures across the aperture cause the blur circle diameter to be three times the diffraction-limited diameter in the near-infrared band. Author

N94-16513*# MCAT Inst., San Jose, CA.
COMPUTATION OF A CONTROLLED STORE SEPARATION FROM A CAVITY
Christopher A. Atwood *In its* Computation of the Fluid and Optical Fields About the Stratospheric Observatory for Infrared Astronomy (SOFIA) and the Coupling of Fluids, Dynamics, and Control Laws on Parallel Computers May 1993 17 p Proposed for presentation at the AIAA 32nd Aerospace Sciences Meeting and Exhibit, Reno, NV, 10-13 Jan. 1994 (For primary document see N94-16510 03-02)
Avail: CASI HC A03/MF A02

Coupling of the Reynolds-averaged Navier-Stokes equations, rigid-body dynamics, and a pitch attitude control law is demonstrated in two- and three-dimensions. The application problem was the separation of a canard-controlled store from an open-flow rectangular cavity bay at a freestream Mach number of 1.2. The transient flowfield was computed using a diagonal scheme in an overset mesh framework, with the resultant aerodynamic loads used as the forcing functions in the nonlinear dynamics equations. The proportional and rate gyro sensitivities were computed a priori using pole placement techniques for the linearized dynamical equations. These fixed gain values were used in the controller for the nonlinear simulation. Reasonable comparison between the full and linearized equations for a perturbed two-dimensional missile was found. Also in two-dimensions, a controlled store was found to possess improved separation characteristics over a canard-fixed store. In three-dimensions, trajectory comparisons with wind-tunnel data for the canard-fixed case will be made. In addition, it will be determined if a canard-controlled store is an effective means of improving cavity store separation characteristics. Author (revised)

N94-16571*# National Aeronautics and Space Administration. Lewis Research Center, Cleveland, OH.
FLOW ANALYSIS FOR THE NACELLE OF AN ADVANCED DUCTED PROPELLER AT HIGH ANGLE-OF-ATTACK AND AT CRUISE WITH BOUNDARY LAYER CONTROL
D. P. Hwang, D. R. Boldman, and C. E. Hughes Jan. 1994 9 p Proposed for presentation at the 32nd Aerospace Sciences Meeting and Exhibit, Reno, NV, 10-13 Jan. 1994; sponsored by AIAA
(RTOP 535-03-10)
(NASA-TM-106371; AIAA Paper 94-0391; E-8181; NAS 1.15:106371)
Copyright Avail: CASI HC A02/MF A01

An axisymmetric panel code and a three dimensional Navier-Stokes code (used as an inviscid Euler code) were verified for low speed, high angle of attack flow conditions. A three dimensional Navier-Stokes code (used as an inviscid code), and an axisymmetric Navier-Stokes code (used as both viscous and inviscid code) were also assessed for high Mach number cruise conditions. The boundary layer calculations were made by using the results from the panel code or Euler calculation. The panel method can predict the internal surface pressure distributions very well if no shock exists. However, only Euler and Navier-Stokes calculations can provide a good prediction of the surface static pressure distribution including the pressure rise across the shock. Because of the high CPU time required for a three dimensional Navier-Stokes calculation, only the axisymmetric Navier-Stokes calculation was considered at cruise conditions. The use of suction and tangential blowing boundary layer control to eliminate the flow separation on the internal surface was demonstrated for low free stream Mach number and high angle of attack cases. The calculation also shows that transition from laminar flow to turbulent flow on the external cowl surface can be delayed by using suction boundary layer control at cruise flow conditions. The results were compared with experimental data where possible. Author

N94-16572*# National Aeronautics and Space Administration. Langley Research Center, Hampton, VA.
EFFECTS OF INTERNAL YAW-VECTORING DEVICES ON THE STATIC PERFORMANCE OF A PITCH-VECTORING NONAXISYMMETRIC CONVERGENT-DIVERGENT NOZZLE
Scott C. Asbury Washington NASA. Washington Sep. 1993 109 p
(RTOP 505-68-70-06)
(NASA-TP-3369; L-17229; NAS 1.60:3369) Avail: CASI HC A06/MF A02

An investigation was conducted in the static test facility of the Langley 16-Foot Transonic Tunnel to evaluate the internal performance of a nonaxisymmetric convergent divergent nozzle designed to have simultaneous pitch and yaw thrust vectoring capability. This concept utilized divergent flap deflection for thrust vectoring in the pitch plane and flow-turning deflectors installed within the divergent flaps for yaw thrust vectoring. Modifications consisting of reducing the sidewall length and deflecting the sidewall outboard were investigated as means to increase yaw-vectoring performance. This investigation studied the effects of multiaxis (pitch and

yaw) thrust vectoring on nozzle internal performance characteristics. All tests were conducted with no external flow, and nozzle pressure ratio was varied from 2.0 to approximately 13.0. The results indicate that this nozzle concept can successfully generate multiaxis thrust vectoring. Deflection of the divergent flaps produced resultant pitch vector angles that, although dependent on nozzle pressure ratio, were nearly equal to the geometric pitch vector angle. Losses in resultant thrust due to pitch vectoring were small or negligible. The yaw deflectors produced resultant yaw vector angles up to 21 degrees that were controllable by varying yaw deflector rotation. However, yaw deflector rotation resulted in significant losses in thrust ratios and, in some cases, nozzle discharge coefficient. Either of the sidewall modifications generally reduced these losses and increased maximum resultant yaw vector angle. During multiaxis (simultaneous pitch and yaw) thrust vectoring, little or no cross coupling between the thrust vectoring processes was observed. Author (revised)

N94-16573*# National Aeronautics and Space Administration. Langley Research Center, Hampton, VA.

WIND TUNNEL INVESTIGATIONS OF FOREBODY STRAKES FOR YAW CONTROL ON F/A-18 MODEL AT SUBSONIC AND TRANSONIC SPEEDS

Gary E. Erickson and Daniel G. Murri Washington NASA. Washington Sep. 1993 101 p
(RTOP 505-68-30-03)
(NASA-TP-3360; L-17197; NAS 1.60:3360) Avail: CASI HC A06/MF A02

Wind tunnel investigations have been conducted of forebody strakes for yaw control on 0.06-scale models of the F/A-18 aircraft at free-stream Mach numbers of 0.20 to 0.90. The testing was conducted in the 7- by 10-Foot Transonic Tunnel at the David Taylor Research Center and the Langley 7- by 10-Foot High-Speed Tunnel. The principal objectives of the testing were to determine the effects of the Mach number and the strake plan form on the strake yaw control effectiveness and the corresponding strake vortex induced flow field. The wind tunnel model configurations simulated an actuated conformal strake deployed for maximum yaw control at high angles of attack. The test data included six-component forces and moments on the complete model, surface static pressure distributions on the forebody and wing leading-edge extensions, and on-surface and off-surface flow visualizations. The results from these studies show that the strake produces large yaw control increments at high angles of attack that exceed the effect of conventional rudders at low angles of attack. The strake yaw control increments diminish with increasing Mach number but continue to exceed the effect of rudder deflection at angles of attack greater than 30 degrees. The character of the strake vortex induced flow field is similar at subsonic and transonic speeds. Cropping the strake planform to account for geometric and structural constraints on the F-18 aircraft has a small effect on the yaw control increments at subsonic speeds and no effect at transonic speeds. Author (revised)

N94-16574*# National Aeronautics and Space Administration. Langley Research Center, Hampton, VA.

WIND-TUNNEL INVESTIGATION OF AERODYNAMIC EFFICIENCY OF THREE PLANAR ELLIPTICAL WINGS WITH CURVATURE OF QUARTER-CHORD LINE

Raymond E. Mineck and Paul M. H. W. Vijgen (High Technology Corp., Hampton, VA.) Washington NASA. Washington Oct. 1993 80 p
(RTOP 505-59-10-03)
(NASA-TP-3359; L-17185; NAS 1.60:3359) Avail: CASI HC A05/MF A01

Three planar, untwisted wings with the same elliptical chord distribution but with different curvatures of the quarter-chord line were tested in the Langley 8-Foot Transonic Pressure Tunnel (8-ft TPT) and the Langley 7- by 10-Foot High-Speed Tunnel (7 x 10 HST). A fourth wing with a rectangular planform and the same projected area and span was also tested. Force and moment measurements from the 8-ft TPT tests are presented for Mach numbers from 0.3 to 0.5 and angles of attack from -4 degrees to 7 degrees. Sketches of the oil-flow patterns on the upper surfaces of the wings and some force and moment measurements from the 7 x 10 HST tests are presented at a Mach number of 0.5. Increasing the curvature of the quarter-chord line makes the angle of zero lift more negative but has little effect on the drag coefficient at zero lift. The changes in lift-curve slope and in the Oswald efficiency factor with the change in curvature of the quarter-chord line (wingtip location) indicate that the elliptical wing with the unswept quarter-chord line has the lowest lifting efficiency and the elliptical wing with the unswept trailing edge has the highest lifting efficiency; the crescent-shaped planform wing has an efficiency in between. Author

N94-16583# Royal Aircraft Establishment, Farnborough (England).

DETERMINATION OF THE EFFECT OF THE WALLS OF A WIND-TUNNEL FROM THE PARAMETERS OF FLOW NEAR THEM [OPREDELENIE VLIYANIYA STENOK AERODINAMICHESKOI TRUBY PO PARAMETRAM POTOKA VBLIZI NIKH]

S. A. Glaskov Jan. 1993 19 p Transl. into ENGLISH from Uchenye Zapiski TsAGI, XIX (Russia), no. 3, 1988 p 34-35 In RUSSIAN
(RAE-Lib-Trans-2201) Copyright Avail: CASI HC A03/MF A01

This paper describes a method based on the use of two flow variables measured at a boundary close to the tunnel wall to calculate wall interference. It is similar to earlier work in the West although the author was probably unaware of this work. Derived from text

N94-16798# Air Force Inst. of Tech., Wright-Patterson AFB, OH. School of Engineering.

HOPH BIFURCATION IN VISCOUS, LOW SPEED FLOWS ABOUT AN AIRFOIL WITH STRUCTURAL COUPLING Ph.D. Thesis

Mark J. Lutton Mar. 1993 152 p
(AD-A266542; AFIT/DS/AA/93-1) Avail: CASI HC A08/MF A02

The locations of Hopf bifurcation points associated with the viscous, incompressible flow about a NACA 0012 airfoil with structural coupling are computed for very low Reynolds numbers (less than 2000). A semi-implicit, first-order-accurate time-integration algorithm is employed to solve the stream-function-vorticity form of the Navier-Stokes equations. The formulation models the inclusion of simple structural elements affixed to the airfoil and captures the resulting airfoil motion. The equations describing the airfoil motion are integrated in time using a fourth-order Runge-Kutta algorithm. The dissertation is divided into two parts. In part one, numerical experiments are performed in the laminar regime to determine if the structural model of the airfoil has an effect upon the location of the Hopf bifurcation point when compared with the fixed airfoil. Results are reported for a variety of structural characteristics including variations of torsional and linear spring constants, inertial properties, structural coupling, and structural damping. The structure of the solution space is explored by means of phase plots. In part two, the Baldwin-Lomax turbulence model is implemented to model turbulent flow. A numerical effort is made to predict the onset of unsteady flow. DTIC

N94-16913# Naval Postgraduate School, Monterey, CA.

DETERMINING THE EFFECT OF ENDWALL BOUNDARY LAYER SUCTION IN A LARGE SCALE SUBSONIC COMPRESSOR CASCADE M.S. Thesis

Matthew A. Webber 31 Mar. 1993 140 p
(AD-A267208) Avail: CASI HC A07/MF A02

An arrangement of suction slots was installed in the Naval Postgraduate School's subsonic cascade wind tunnel. The aim was to improve flow two dimensionality to enable flow separation of the installed controlled diffusion blades at high incidence. The slots were located 17.25 inches upstream of the test section. Pressure and laser Doppler velocimetry measurements were made, for a Reynolds number of 711000 and an inlet flow angle of 44.4 deg, upstream and downstream of the test section to determine the effects of varying suction. The set of baseline inlet flow field measurements was to be used for comparison purposes in future tunnel modifications. The results showed that the tunnel endwall boundary layers were asymmetric for the baseline configuration. Uniform suction was not achieved in both the pitchwise and spanwise directions. However, the axial velocity ratio was reduced by 1.9 percent and the blade loading increased slightly with increased suction. DTIC

N94-17021# University of Southern California, Los Angeles. Dept. of Aerospace Engineering.

TO EXTEND THE THIRTEEN-MOMENT THEORY AND ITS APPLICATION TO PROBLEMS IN RAREFIED HYPERSONIC FLOW Final Report, 1 Dec. 1990 - 31 May 1993

H. K. Cheng 18 May 1993 33 p
(Grant AF-AFOSR-0104-91)
(AD-A267384; AFOSR-93-0477TR) Avail: CASI HC A03/MF A01

The theoretical development and supporting particle-simulation (DMSC) and other computational studies carried out during the past two years have strengthened the principle for correlating a flow far from translational equilibrium with the Navier-Stokes (NS) solutions. The work also expands the scope of its application demonstrating its applicability in the correlation/prediction of velocity and enthalpy profiles as well as distribution functions for monatomic gas. DTIC

N94-17074# Air Force Inst. of Tech., Wright-Patterson AFB, OH.
COMPUTATIONAL AERODYNAMICS WITH ICING EFFECTS Ph.D. Thesis
Thomas N. Mouch May 1993 160 p
(AD-A267509; AFIT/CI/CIA-93-007D) Avail: CASI HC A08/MF A02

A quick, inexpensive technique has been developed for the analysis of a full aircraft configuration with iced surfaces. A comprehensive literature search of icing analysis methods is presented. Viscous effects for the flow field about an airfoil with an iced leading edge are accounted for in a thin-layer Navier-Stokes code (ARC2D). A panel code (PMARC) solves the flow field away from the body. The results of the airfoil analysis represent the near-field solutions and are used to modify the boundary conditions in the three-dimensional calculations with the panel code by matching the local circulation. This process is repeated until the total lift coefficient between successive iterations differs by less than a specified value. Comparison with viscous experimental data shows excellent results for lift coefficient and a strong improvement over the basic PMARC for drag and pitching moment coefficients. For the full configuration considered, with ice simulated on the horizontal tail, pitching moment data predicts a very sudden unstable pitch break above angle of attack = 8 deg. This tendency models the pitch tendency described in the literature for similar configurations with an iced horizontal tail. Thus, a quick method has been developed to handle a full configuration with viscous effects. DTIC

N94-17081*# MCAT Inst., San Jose, CA.
PROGRESS IN COMPUTATIONAL UNSTEADY AERODYNAMICS
Shigeru Obayashi Nov. 1993 20 p
(Contract NCC2-605)
(NASA-CR-177630; A-94021; NAS 1.26:177630) Avail: CASI HC A03/MF A01

After vigorous development for over twenty years, Computational Fluid Dynamics (CFD) in the field of aerospace engineering has arrived at a turning point toward maturity. This paper discusses issues related to algorithm development for the Euler/Navier Stokes equations, code validation and recent applications of CFD for unsteady aerodynamics. Algorithm development is a fundamental element for a good CFD program. Code validation tries to bridge the reliability gap between CFD and experiment. Many of the recent applications also take a multidisciplinary approach, which is a future trend for CFD applications. As computers become more affordable, CFD is expected to be a better scientific and engineering tool. Author

N94-17099# Yale Univ., New Haven, CT. Mason Lab.
STRUCTURE OF HIGH REYNOLDS NUMBER TURBULENT BOUNDARY LAYER Final Technical Report, 1 Jan. 1990 - 31 Dec. 1992
K. R. Sreenivasan 6 Jun. 1993 16 p
(Grant AF-AFOSR-0120-90)
(AD-A267476; AFOSR-93-0471TR) Avail: CASI HC A03/MF A01

A brief summary of the work done at Yale in the collaborative research program between Yale, Princeton, and Penn State is given. One of the findings of the work is that there is a second-order 'transition' between the low-Reynolds-number boundary layer and the high Reynolds-number boundary layer. The nature of this transition and the elucidation of this mechanism is one of the topics of this research. Other aspects concern the self-similar scaling aspects of the Reynolds shear stress, scaling of the probability density of velocity increments, and the scaling of the multiplier distributions for the energy dissipation. DTIC

N94-17221# Air Force Inst. of Tech., Wright-Patterson AFB, OH.
AN EXPERIMENTAL INVESTIGATION OF THE EFFECTS OF LEADING EDGE GEOMETRY ON THE DYNAMICS OF BLUNT FIN-INDUCED SHOCK WAVE TURBULENT BOUNDARY LAYER INTERACTION M.S. Thesis
Kelly Kleifges May 1993 99 p
(AD-A267656; AFIT/CI/CIA-93-093) Avail: CASI HC A05/MF A02

Fluctuating wall pressure measurements have been made on the centerline upstream of blunt fins in a Mach 5 flow. Standard time series analysis and conditional sampling algorithms have been used to examine the effects of leading edge sweep, leading edge shape, and fin root modifications on the RMS level and spectral content of fluctuating pressures. Results show that the fluctuating loads can be reduced significantly by appropriate modification of the fin leading edge. Leading edge sweep considerably reduces the mean and RMS pressure loading at the fin root, the extent of the region of unsteady separation shock motion (i.e. the intermittent region), and the separation length. The spectral content of pressure fluctuations in the intermittent region shifts to higher frequencies with leading edge sweep, while the spectral content of pressure fluctuations in the separated region is virtually unchanged by leading edge sweep. Of the different fin leading edge geometries which induce the same size interaction, the 'blunter' configurations produce smaller intermittent regions and larger separated regions. While the use of a strake at the fin leading edge root has virtually no effect, a swept hemicylindrically blunted root fillet reduces the centerline upstream influence and intermittent region length by 50% and reduces the mean and RMS pressure loading at the fin root by 75% and 95% respectively. DTIC

N94-17222# Air Force Inst. of Tech., Wright-Patterson AFB, OH. Foreign Aerospace Science and Technology Center.
NUMERICAL SOLUTION OF SUPG FINITE-ELEMENT METHOD FOR SUPERSONIC VISCOUS FLOW
Guo-Qun Xu and Guo-Fu Zhang 20 Jul. 1993 22 p Transl. into ENGLISH from Lixue Xuebao (China), v. 23, no. 5, 1991 p 533-541
(AD-A267762; FASTC-ID(RS)T-0932-92) Avail: CASI HC A03/MF A01

A streamline upwind/Petrov-Galerkin (SUPG) weighted residual formalism was developed in the paper for the quasi-simplified Navier-Stokes equations. Numerical computations were made for Burger's equation, the nonviscous shock wave reflection problem, as well as supersonic laminar flow over a flat plate and compression corner flow by using the method. The results of the computations show that this method is accurate, convergent, and stable. DTIC

N94-17260*# Wichita State Univ., KS. National Inst. for Aviation.
SUPERSONIC FLOW VISUALIZATION OF A NACELLE IN CLOSE PROXIMITY TO A SIMULATED WING Final Technical Report
Kasim Biber and David R. Ellis Jul. 1993 43 p
(NASA Order A-24888-D)
(NASA-CR-194675; NAS 1.26:194675; NIAR-93-18) Avail: CASI HC A03/MF A01

A flow visualization study was made in the 9 x 9 inch supersonic wind tunnel at Wichita State University to examine shock and boundary layer flow interaction for a nacelle in close proximity to the lower surface of a simulated wing. The test matrix included variations of angle of attack from -2 degrees to +4 degrees, nacelle-wing gap from 0.5 to 3-nacelle inlet diameter (0.12 inch), and Reynolds number based on nacelle length (1.164 inch) from 1.16 x 10(exp 6) to 1.45 x 10(exp 6) at a nominal Mach number of 2. Schlieren pictures of wing and nacelle flowfield were recorded by a video camera during each tunnel run. Results show that the nacelle inlet shock wave remains attached to the inlet lip and its impingement does not significantly affect the wing boundary layer. At the nacelle trailing edge location, the wing boundary layer thickness is approximately one nacelle inlet diameter at alpha = 0 degrees and it decreases with increase of angle of attack. Author (revised)

N94-17274# Air Force Systems Command, Wright-Patterson AFB, OH. Foreign Aerospace Science and Technology Center.
EXPERIMENTAL STUDY OF VORTEX AND AERODYNAMIC CHARACTERISTICS OF STACK WINGS WITH SIDESLIP
Bao Guohua 20 Jul. 1993 15 p Transl. into ENGLISH from Kongqidonglixue Xuebao (China), v. 7, no. 2, Jun. 1989 p 215-219
(AD-A267722; FASTC-ID(RS)T-0034-93) Avail: CASI HC A03/MF A01

This paper reports on an experimental study of stack wings with small aspect ratio, and describes the variation of detached vortex system at the aircraft wing leading edge with different aspect ratios. The influence on aerodynamic characteristics due to vortex twisting and bursting is analyzed. As revealed in the study, sideslip delays the vortex twisting at the upstream

side of the aircraft wing. The vortex bursts early. At the downward side, the phenomena are exactly in reverse. During sideslip, bursting of an asymmetrical vortex has an obvious influence on the aerodynamic characteristics. DTIC

N94-17284*# National Aeronautics and Space Administration. Langley Research Center, Hampton, VA.
SUBSONIC AERODYNAMIC CHARACTERISTICS OF THE HL-20 LIFTING-BODY CONFIGURATION
George M. Ware and Christopher I. Cruz Nov. 1993 29 p
(RTOP 505-40-61-01)
(NASA-TM-4515; L-17261; NAS 1.15:4515) Avail: CASI HC A03/MF A01

The HL-20 is proposed as a possible future manned spacecraft. The configuration consists of a low-aspect-ratio body with a flat undersurface. Three fins (a small centerline fin and two outboard (tip) fins set at a dihedral angle of 50 deg) are mounted on the aft body. The control system consists of elevon surfaces on the outboard fins, a set of four body flaps on the upper and lower aft body, and an all-movable center fin. Both the elevons and body flaps were capable of trimming the model to angles of attack from -2 deg to above 20 deg. The maximum trimmed lift-drag ratio was 3.6. Replacing the flat-plate tip fins with airfoil tip fins increased the maximum trimmed lift-drag ratio to 4.2. The elevons were effective as a roll control, but they produced about as much yawing moment as rolling moment because of the tip-fin dihedral angle. The body flaps produced less rolling moment than the elevons and only small values of yawing moment. A limited investigation of the effect of varying tip-fin dihedral angle indicated that a dihedral angle of 50 deg was a reasonable compromise for longitudinal and lateral stability, longitudinal trim, and performance at subsonic speeds. Author (revised)

N94-17461 Wright Lab., Wright-Patterson AFB, OH.
AN EXPERIMENTAL STUDY OF FLUCTUATING WALL PRESSURES IN A HIGHLY SWEPT, SHARP FIN-INDUCED, MACH 5 SHOCK WAVE/TURBULENT BOUNDARY LAYER INTERACTION Final Report, Aug. 1990 - May 1992
J. D. Schmisseur Jan. 1993 158 p Limited Reproducibility: More than 20% of this document may be affected by microfiche quality
(AF Proj. 2404)
(AD-A268394; WL-TR-93-3058) Avail: CASI HC A08

Fluctuating wall pressure measurements have been made beneath the shock wave/turbulent boundary layer interaction generated by a sharp, unswept fin at angle of attack. Tests were conducted at Mach 5 with a freestream unit Reynolds number of 47.88 x 106 /m. The boundary layer developed naturally on the tunnel floor under approximately adiabatic temperature conditions. From visual inspection and standard time series analysis of fluctuating wall pressure signals, it has been shown that the separation shock wave undergoes a translating, intermittent type motion for fin angles between 16 and 28 degrees. Both the mean wall pressures and higher order moments are quasi-conically symmetric when collapsed in a conical coordinate system. Finally, the maximum wall pressure standard deviation in the intermittent region has been shown to scale with the sweep of the interaction and not with the inviscid pressure rise as has been previously suggested in the literature. DTIC

N94-17558*# Sverdrup Technology, Inc., Brook Park, OH.
THIN-LAYER AND FULL NAVIER-STOKES CALCULATIONS FOR TURBULENT SUPERSONIC FLOW OVER A CONE AT AN ANGLE OF ATTACK Final Report
Crawford F. Smith and Steve D. Podleski Nov. 1993 102 p
(Contract NAS3-25266; RTOP 533-02-35)
(NASA-CR-189103; E-8197; NAS 1.26:189103) Avail: CASI HC A06/MF A02

The proper use of a computational fluid dynamics code requires a good understanding of the particular code being applied. In this report the application of CFL3D, a thin-layer Navier-Stokes code, is compared with the results obtained from PARC3D, a full Navier-Stokes code. In order to gain an understanding of the use of this code, a simple problem was chosen in which several key features of the code could be exercised. The problem chosen is a cone in supersonic flow at an angle of attack. The issues of grid resolution, grid blocking, and multigridding with CFL3D are explored. The use of multigridding resulted in a significant reduction in the computational time required to solve the problem. Solutions obtained are compared with the results using the full Navier-Stokes equations solver PARC3D. The results obtained with the CFL3D code compared well with the PARC3D solutions. Author

N94-17574# Cincinnati Univ., OH. Dept. of Aerospace Engineering and Engineering Mechanics.
AN INVESTIGATION OF OBLIQUE SHOCK/BOUNDARY LAYER INTERACTION CONTROL Final Report, 1 Dec. 1990 - 31 Mar. 1993
A. Hamed 30 Jun. 1993 14 p
(Grant AF-AFOSR-0101-91)
(AD-A268106; AFOSR-93-0613TR) Avail: CASI HC A03/MF A01

The objective of this work is to provide a basic understanding of the flow in the shock boundary layer interactions and of the mechanisms of their control. A parametric investigation was conducted to determine the effect of bleed configuration on the flow in the interaction region of an incident oblique shock with a turbulent boundary layer. Results of the numerical flow simulations were obtained for different slot widths, depths and slat angles over a bleed mass flow range between zero and choked conditions. The bleed results reveal a complex structure of compression expansion wave system over the bleed port entrance, and different levels of flow operation inside the slot. Code development for the implicit numerical solution of the two dimensional compressible Navier-Stokes and K-Epsilon equations was completed. The code was used in the simulation of unsteady supersonic cavity flow and the results compared with experimental data. DTIC

N94-17580# California Inst. of Tech., Pasadena. Graduate Aeronautical Labs.
CHEMICAL REACTIONS IN TURBULENT MIXING FLOWS Final Report, 15 May - 30 Dec. 1992
Paul E. Dimotakis, James E. Broadwell, and Anthony Leonard 30 Jun. 1993 9 p
(Grant AF-AFOSR-0304-90)
(AD-A268287; AFOSR-93-0568TR) Avail: CASI HC A02/MF A01

This is a supplement to the Final Annual Report for this Grant. It documents: (1) an upgrade/modification to the Supersonic Shear Layer (S3L) combustion facility, and (2) progress and developments in digital-image-data systems and acquisition, realized during the extension period, ending 30 June 1992. DTIC

N94-17609# Wright Lab., Wright-Patterson AFB, OH.
LASER VELOCIMETRY MEASUREMENTS OF VORTEX FLOWS ON A DELTA WING AT MACH 1.9 Final Report, Aug. 1990 - Sep. 1992
Linda G. Smith, Mark S. Maurice, Charles Tyler, George L. Seibert, and C. D. Miller Jan. 1993 115 p
(AF Proj. 2404)
(AD-A268596; WL-TR-93-3059) Avail: CASI HC A06/MF A02

Off-body flow visualizations and fluid velocity measurements are conducted in a supersonic vortex flow. Three-dimensional laser velocimetry measurements are made in the leeward flowfield over a simple sharp-edged delta wing with 75 degree sweep angle. Tests are conducted at Mach 1.9 and Reynolds number of 2.4 x 10(exp 6) based on model root chord. Measurements are made at 40% and 80% chord positions for 20 and 30 degree angles of attack and at 40% chord for 35 degrees. Mean velocities and turbulence intensities are measured on the five planes. Measurement accuracy is discussed in detail. The measurements define the location of the vortex core and provide the flowfield velocities surrounding the vortex. The difficulties inherent with seeding high velocity vortex flows are discussed. DTIC

N94-17639*# National Aeronautics and Space Administration. Langley Research Center, Hampton, VA.
USER'S MANUAL FOR THE LANGLEY RESEARCH CENTER 14- BY 22-FOOT SUBSONIC TUNNEL STATIC DATA ACQUISITION SYSTEM
Nettie M. Orie and P. Frank Quinto Nov. 1993 108 p
(RTOP 535-03-10-02)
(NASA-TM-109027; NAS 1.15:109027) Avail: CASI HC A06/MF A02

The Static Data Acquisition System (SDAS) components primarily responsible for acquiring data at the 14- by 22-Foot Subsonic Tunnel are the NEFF 620/600 Data Acquisition Unit (DAU) and the PSI 780B electronically scanned pressure (ESP) measurement system. A 9250

Modcomp computer is used to process the signal, to do all aerodynamic calculation, and to control the output of data. All of the tasks required to support a wind tunnel investigation are menu driven. The purpose of this report is to acquaint users of this system with the wide range of capabilities that exist with the available hardware and software and provide them with the proper procedures to follow when setting up or running individual tests. Author

03 AIR TRANSPORTATION AND SAFETY

Includes passenger and cargo air transport operations; and aircraft accidents.

For related information see also *16 Space Transportation* and *85 Urban Technology and Transportation.*

N94-15336* National Aeronautics and Space Administration. Lewis Research Center, Cleveland, OH.

NASA IMAGES 6 (Videotape)

Jan. 1988 Videotape: 28 min. 30 sec. playing time, in color, with sound (NASA-TM-109437; NONP-VT-93-190234) Avail: CASI VHS A01/BETA A22

The videotape is comprised of clips regarding aircraft safety and development through NASA research at its various centers. CASI

N94-15426* National Aeronautics and Space Administration, Washington, DC.

LIFE SAVING SATELLITES (Videotape)

Aug. 1985 Videotape: 6 min. 16 sec. playing time, in color, with sound (NASA-TM-109616; NONP-VT-93-190414) Avail: CASI VHS A01/BETA A22

Details of COSPAS/SARSAT, the international search and rescue project, are covered. CASI

N94-15444*# Clemson Univ., SC. Dept. of Electrical and Computer Engineering.

DESIGNING CLUTTER REJECTION FILTERS WITH COMPLEX COEFFICIENTS FOR AIRBORNE PULSED DOPPLER WEATHER RADAR Final Technical Report No. 16

Dennis A. Jamora Washington NASA, Washington Oct. 1993 82 p (Grant NAG1-928; RTOP 505-64-12-02)

(NASA-CR-4550; NAS 1.26:4550; DOT/FAA/RD-93/24) Avail: CASI HC A05/MF A01

Ground clutter interference is a major problem for airborne pulse Doppler radar operating at low altitudes in a look-down mode. With Doppler zero set at the aircraft ground speed, ground clutter rejection filtering is typically accomplished using a high-pass filter with real valued coefficients and a stopband notch centered at zero Doppler. Clutter spectra from the NASA Wind Shear Flight Experiments of 1991-1992 show that the dominant clutter mode can be located away from zero Doppler, particularly at short ranges dominated by sidelobe returns. Use of digital notch filters with complex valued coefficients so that the stopband notch can be located at any Doppler frequency is investigated. Several clutter mode tracking algorithms are considered to estimate the Doppler frequency location of the dominant clutter mode. From the examination of night data, when a dominant clutter mode away from zero Doppler is present, complex filtering is able to significantly increase clutter rejection over use of a notch filter centered at zero Doppler. Author (revised)

N94-15542# Aeronautical Research Labs., Melbourne (Australia).

AIRCRAFT ACCIDENT INVESTIGATION AT ARL: THE FIRST 50 YEARS General Document

J. L. Kepert Mar. 1993 107 p

(AD-A267086; ARL-GD-37; DODA-AR-007-134) Avail: CASI HC A06/MF A02

Early Australian experience with the investigation of aircraft accidents is covered briefly as a prelude to the foundation of the Aeronautical Research Laboratory. With its foundation, a more scientific approach was possible. ARL was quickly involved with accident investigation, an activity which has been maintained throughout its fifty year history. This report examines ARL experiences during those fifty years with the idea of providing some useful guidelines for the next half-century. DTIC

N94-15550*# National Aeronautics and Space Administration. Ames Research Center, Moffett Field, CA.

ALTITUDE DEVIATIONS: BREAKDOWNS OF AN ERROR-TOLERANT SYSTEM

Everett A. Palmer, Edwin L. Hutchins (California Univ., San Diego.), Richard D. Ritter, and Inge VanCleemput (Wellesley Coll., MA.) Oct. 1993 44 p Sponsored by NASA and FAA, Washington

(RTOP 505-64-13)

(NASA-TM-108788; A-93119; NAS 1.15:108788) Avail: CASI HC A03/MF A01

Pilot reports of aviation incidents to the Aviation Safety Reporting System (ASRS) provide a window on the problems occurring in today's airline cockpits. The narratives of 10 pilot reports of errors made in the automation-assisted altitude-change task are used to illustrate some of the issues of pilots interacting with automatic systems. These narratives are then used to construct a description of the cockpit as an information processing system. The analysis concentrates on the error-tolerant properties of the system and on how breakdowns can occasionally occur. An error-tolerant system can detect and correct its internal processing errors. The cockpit system consists of two or three pilots supported by autoflight, flight-management, and alerting systems. These humans and machines have distributed access to clearance information and perform redundant processing of information. Errors can be detected as deviations from either expected behavior or as deviations from expected information. Breakdowns in this system can occur when the checking and cross-checking tasks that give the system its error-tolerant properties are not performed because of distractions or other task demands. Recommendations based on the analysis for improving the error tolerance of the cockpit system are given.

Author (revised)

N94-15637# Army Aeromedical Research Lab., Fort Rucker, AL.

BASIC PRINCIPLES OF HELICOPTER CRASHWORTHINESS Final Report

Dennis F. Shanahan Feb. 1993 36 p

(DA Proj. 3M1-62787-A-878)

(AD-A267099; USAARL-93-15) Avail: CASI HC A03/MF A01

Crashworthiness can be defined as the ability of an aircraft and its internal systems to protect occupants from injury in the event of a crash. In general, injury in aircraft crashes can be considered to arise from three distinct sources: (1) excessive acceleration forces; (2) direct trauma from contact with hard surfaces; and (3) exposure to environmental factors such as fire, smoke, water, and chemicals resulting in burns, drowning, or asphyxiation. Consequently, effective crashworthiness designs must consider all possible sources of injury and eliminate or mitigate as many as practical for a given design impact limit. This involves considerations of the following: (1) strength of the container (cockpit and cabin); (2) the adequacy of seats and restraint systems; (3) energy attenuation; (4) elimination of injurious objects in occupants local environment; and (5) post-crash factors, principally fire prevention and adequacy of escape routes. The U.S. Army UH-60 Black Hawk and AH-64 Apache helicopters were the first helicopters built to modern crashworthiness specifications. This paper uses data gained from the investigation of crashes of these helicopters to illustrate basic crashworthiness principles and to demonstrate their effectiveness when systematically incorporated into helicopter designs. DTIC

N94-16438# Army Engineer Waterways Experiment Station, Vicksburg, MS. Geotechnical Lab.

TECHNICAL URBAN SEARCH AND RESCUE, SYSTEM TO LOCATE SURVIVORS (STOLS) UNITS: OPERATOR'S MANUAL Final Report

May 1993 56 p

(AD-A266317; WES/IR/GL-93-1) Avail: CASI HC A04/MF A01

The U.S. Army Corps of Engineers disaster response can be classified into three phases: (1) Initial; (2) Sustained; and (3) Recovery. The Initial phase is described as the Corps' response in the first 72 hours after the disaster. The Sustained phase may continue for days to weeks depending upon the severity and location of the disaster. The Recovery and final effort continues until the completion of the task. The technical urban search effort for survivors by the Corps of Engineers is categorized in the Initial phase. For effective survivor location, it is necessary to mobilize, deploy, and initialize the search effort in less than 24 hours. It is also necessary for technical search teams to be in a constant state of readiness for the mission. DTIC

N94-16464# National Transportation Safety Board, Washington, DC.
NATIONAL TRANSPORTATION SAFETY BOARD ANNUAL REVIEW OF AIRCRAFT ACCIDENT DATA, US GENERAL AVIATION, CALENDAR YEAR 1989
1993 88 p
(PB93-160687; NTSB/ARG-93/01) Avail: CASI HC A05/MF A01

The report presents a statistical compilation and review of general aviation accidents which occurred in 1989 in the United States, its territories and possessions, and in international waters. The accidents reported are all those involving U.S. registered aircraft not conducting operations under 14 CFR 121, 14 CFR 125, 14 CFR 127, or 14 CFR 135. The report is divided into five sections: All Accidents; Fatal Accidents; Serious Injury Accidents; Property Damage Accidents and Midair Collision Accidents. Several tables present accident parameters for 1989 accidents only, and each section includes tabulations which present comparative statistics for 1989 and for the five-year period 1984-1988. NTIS

N94-16520*# National Aeronautics and Space Administration. Lewis Research Center, Cleveland, OH.
DEVELOPMENT OF A PROPOSED INTERNATIONAL STANDARD FOR CERTIFICATION OF AIRCRAFT TO HIGH INTENSITY RADIATED FIELDS (HIRF)
Noel B. Sargent Oct. 1993 7 p Proposed for presentation at the 1994 International Pacific Air and Space Technology Conference, Singapore, China, 14-18 Feb. 1994; sponsored by SIAE and SAE
(RTOP 940-30-09-21)
(NASA-TM-106357; E-8141; NAS 1.15:106357) Avail: CASI HC A02/MF A01

Avionic systems performing critical functions in modern aircraft are potentially susceptible to the hazards of electromagnetic radiation from ground and airborne transmitters. The Federal Aviation Administration (FAA) requested that the Society of Automotive Engineers (SAE) coordinate the development of procedures and guidance material which can be used during the aircraft certification process to ensure adequate protection against high intensity radiated fields (HIRF). This paper addresses both the technical challenge of drafting a certification procedure and guidance standard as well as the management process used by the SAE subcommittee AE4R to converge a diverse range of opinions by its international membership in the shortest possible time. Author (revised)

N94-17262# Wichita State Univ., KS. National Inst. for Aviation Research.
THE AIRLINE QUALITY REPORT 1993
Brent D. Bowen (Nebraska Univ., Omaha.) and Dean E. Headly 1993 48 p
(NIAR-93-11) Avail: CASI HC A03/MF A01

The Airline Quality Rating was developed and first announced in early 1991 as an objective method of comparing airline performance on combined multiple factors important to consumers. The Airline Quality Rating 1993 (NIAR Report 93-11) is a summary of month-by-month quality ratings for the nine major domestic U.S. airlines operating during 1992. Using the Airline Quality Rating (AQR) system and monthly performance data for each airline for the calendar year of 1992, individual and comparative ratings are reported. This research monograph contains a brief summary of the AQR methodology, detailed data and charts that track comparative quality for major domestic airlines across the 12 month period of 1992, and results reflecting industry averages. Also, comparative Airline Quality Rating data for 1991 is included to provide a longer term view of quality in the industry. Author (revised)

N94-17471# National Transportation Safety Board, Washington, DC.
ANNUAL REVIEW OF AIRCRAFT ACCIDENT DATA. US AIR CARRIER OPERATIONS, CALENDAR YEAR 1990
4 Oct. 1993 74 p
(PB94-102787; NTSB/ARC-93/02) Avail: CASI HC A04/MF A01

This publication presents the record of aviation accidents involving revenue operations of U.S. Air Carriers including Commuter Air Carriers and On Demand Air Taxis for calendar year 1990. The report is divided into three major sections according to the federal regulations under which the flight was conducted - 14 CFR 121, 125, 127, Scheduled 14 CFR 135, or Nonscheduled 14 CFR 135. In each section of the report tables are presented to describe the losses and characteristics of 1990 accidents to enable comparison with prior years. Author

N94-17586 Federal Aviation Administration, Washington, DC. Office of Civil Aviation Security.
CRIMINAL ACTS AGAINST CIVIL AVIATION, FISCAL YEAR 1992
1992 90 p Limited Reproducibility: More than 20% of this document may be affected by microfiche quality
(AD-A268014) Avail: CASI HC A05

Civil aviation overall continued to be the object of numerous criminal acts in 1992, but, in those instances where attacks resulted from factors other than personal motivation, the factors tended to be regional, rather than global, in nature. Accordingly, the geographical distribution of incidents varied widely: from a high of 34 in Europe to a low of 4 in North America. Most criminal acts against civil aviation in Asia were the result of internal ethnic or religious confrontations. These included rocket attacks against airports and aircraft by Afghan guerrillas as well as violence against Air India offices in both Bangladesh and Pakistan by Muslims protesting Hindus' destruction of the mosque in Ayodhya, India. For the first year since 1986, there were no projectile attacks against Narita Airport in Japan, the site of attacks and protests since before its construction even began in 1969. Although contractors and politicians associated with the airport continue to be the targets of leftist radicals, Narita Airport has been eclipsed as an issue by the military, the monarchy, and what the leftists term Japanese economic imperialism. The most significant aviation incident in Asia, the hijacking of a Vietnam Airlines aircraft by a former South Vietnamese Air Force pilot living in the U.S., may not bode well for the future as Vietnamese expatriates attempt to frustrate moves by both U.S. companies and the U.S. government to do business with the regime in Hanoi. DTIC

N94-15125# Rijksluchtvaartdienst, Schiphol (Netherlands).
AVIATION INSPECTION PROSPECTS [TOEKOMSTVERWACHTING RLD, LUCHTVAARTINSPECTIE]
H. N. Wolleswinkel *In* NAL, Symposium on the Future of Aeronautics in the Netherlands 1991 22 p In DUTCH (For primary document see N94-15120 03-01)
Avail: CASI HC A03/MF A02

04 AIRCRAFT COMMUNICATIONS AND NAVIGATION

Includes digital and voice communication with aircraft; air navigation systems (satellite and ground based); and air traffic control.

For related information see also *17 Space Communications, Spacecraft Communications, Command and Tracking* and *Communications and Radar.*

N94-14919# Carnegie-Mellon Univ., Pittsburgh, PA. Robotics Inst.
PERCEPTION FOR OUTDOOR NAVIGATION Annual Report No. 3, 16 Aug. 1991 - 15 Aug. 1992
Charles Thorpe, Takeo Kanade, Martial Hebert, and Dean Pomerleau Sep. 1992 71 p
(Contract DACA76-89-C-0014)
(AD-A266867; CMU-RI-TR-92-16) Avail: CASI HC A04/MF A01

This report reviews progress at Carnegie Mellon from August 16, 1991 to August 15, 1992 on research sponsored by DARPA, DoD, monitored by the U.S. Army Topographic Engineering Center under contract DACA 76-89-C-0014, titled Perception for Outdoor Navigation. Research supported by this contract includes perception for road following, terrain mapping for off-road navigation, and systems software for building integrated mobile robots. We overview our efforts for the year, and list our publications and personnel, then provide further detail on several of our subprojects. DTIC

N94-14971# Carnegie-Mellon Univ., Pittsburgh, PA. Robotics Inst.
RACCOON: A REAL-TIME AUTONOMOUS CAR CHASER OPERATING OPTIMALLY AT NIGHT
Rahul Sukthankar Oct. 1992 18 p
(Contracts DACA76-89-C-0014; DAAE07-90-C-R059)
(AD-A266963; CMU-RI-TR-92-13) Avail: CASI HC A03/MF A01

RACCOON is a vision system that tracks car taillights at night. It builds

a global map in real time of the lead vehicle's position based on the location and separation of the taillights in a sequence of video images. RACCOON has been integrated into a car following experiment on the CMU Navlab II, a computer-controlled HMMWV testbed. The Navlab II safely followed a lead vehicle on a winding road in light traffic at 32 km/h. DTIC

N94-14972# Carnegie-Mellon Univ., Pittsburgh, PA. Robotics Inst.
PANACEA: AN ACTIVE SENSOR CONTROLLER FOR THE ALVINN AUTONOMOUS DRIVING SYSTEM
Rahul Sukthankar, Dean Pomerleau, and Charles Thorpe Apr. 1993 13 p
(Contracts DACA76-89-C-0014; DAAE07-90-C-R059)
(AD-A266964; CMU-RI-TR-93-09) Avail: CASI HC A03/MF A01

Panacea is a modular system which incorporates a steerable sensor into an existing neural network driving system, ALVINN. A fixed camera cannot see the road when it makes sharp bends. For a vision system that builds a map of the road, it is straightforward to point the camera down the road; but ALVINN directly outputs a steering command without generating an intermediate road representation. Insight from the training scheme used in ALVINN, however, provides an interpretation of the steering command in terms of the road geometry and appropriate camera pointing strategies. Tests on the Carnegie Mellon Navlab II with a steerable camera have shown that the system significantly improves ALVINN's performance, particularly in situations requiring sharp turns and quick responses. DTIC

N94-15498# Carnegie-Mellon Univ., Pittsburgh, PA. Robotics Inst.
MASSIVELY PARALLEL, ADAPTIVE, COLOR IMAGE PROCESSING FOR AUTONOMOUS ROAD FOLLOWING
Todd Jochem and Shumeet Baluja May 1993 29 p
(Contracts DACA76-89-C-0014; DAAE07-90-C-R059)
(AD-A266988; CMU-RI-TR-93-10) Avail: CASI HC A03/MF A01

In recent years, significant progress has been made towards achieving autonomous roadway navigation using video images. None of these systems take full advantage of all the information in the 512x512 pixel frame, 30 frame/second color image sequence. This can be attributed to the large amount of data which is present in the color video image stream (22.5 Mbytes/sec) as well as the limited amount of computing resources available to the systems. We have increased the available computing power by using a parallel computer. Specifically, a single instruction, multiple data (SIMD) machine was used to develop simple and efficient parallel algorithms, largely based on connectionist techniques, which can process every pixel in the incoming 30 frame/second, color video image stream. The system uses substantially larger frames and processes them at faster rates than other color road following systems. This is achievable through the use of algorithms specifically designed for a fine-grained parallel machine as opposed to ones ported from existing systems to parallel architectures. The algorithms presented here were tested on 4k and 16k processor MasPar MP-1 and on 4K, 8K, and 16K processor MasPar MP-2 parallel machines and were used to drive Carnegie Mellon's testbed vehicle, the Navlab I, on paved roads near campus. DTIC

N94-16439# Massachusetts Inst. of Tech., Lexington. Lincoln Lab.
ATCRBS REPLY ENVIRONMENT AT MEMPHIS INTERNATIONAL AIRPORT Project Report
Arnold D. Kaminsky, Katherine M. Hollister, and Martin J. Brennan 28 May 1993 37 p
(Contracts F19628-90-C-0002; DTFA01-93-Z-02012)
(AD-A266322; DOT/FAA/NR-93/3) Avail: CASI HC A03/MF A01

This report demonstrates, through data and analysis, how the airport environment can affect ATCRBS surveillance. The Lincoln Laboratory ATCRBS Monopulse Processing Subsystem was used to collect reply data at Memphis International Airport during Mar. 1991. These data show a correlation between aircraft density, potential reflectors, and ATCRBS reply integrity. The number of replies has been shown to be directly related to multipath from reflecting surfaces including taxiing aircraft. Additionally, it is shown that conditions can exist during which not all of the replies from ATCRBS equipped aircraft can be processed when forming target report measurements. Finally, it is shown that the bunching of replies in both time and space can introduce reply decoder overloading. DTIC

N94-16457 Defence Research Establishment, Ottawa (Ontario).
INTERFEROMETRIC GPS ATTITUDE: A STOCHASTIC ERROR MODEL, DREO REPORT
J. C. McMillan Feb. 1993 80 p Limited Reproducibility: More than 20% of this document may be affected by microfiche quality
(AD-A266411; DREO-1168) Avail: CASI HC A05

During the August 1992 sea trial off the west coast of Vancouver Island, onboard the CFAV Endeavour, data was collected from a relatively new type of GPS (Global Positioning System) receiver which measures attitude (heading, pitch and roll) as well as the usual GPS measurements of position and velocity. GPS attitude has the potential to provide rapid and precise attitude for a relatively low cost. Attitude is conventionally determined using inertial equipment, which for precise work is very expensive, large and requires a long settling time after turn-on. The receiver being evaluated on this sea trial was an Ashtech Three-Dimensional Direction Finding System (3DF). This report provides some general background on GPS attitude technology, presents the attitude errors observed during this sea trial and characterizes these errors as stochastic processes. DTIC

N94-16835# Mitre Corp., McLean, VA.
CATEGORY (CAT) 3B LEVEL 1 TEST PLAN FOR GLOBAL POSITIONING SYSTEM (GPS) Final Report
P. A. ODonnell, R. Braff, and C. A. Shively Sep. 1993 41 p
(Contract DTFA01-93-C-00001)
(DOT/FAA/RD-93/21; MTR-93W0000102) Avail: CASI HC A03/MF A01

The FAA has established a program to demonstrate the feasibility of differential GPS (DGPS) based technology for Category (CAT) IIIb precision approach and landing applications. DGPS includes code corrections and phase differencing or phase correction (real-time kinematic) techniques. Contractors will provide complete systems including ground reference and signal monitor equipment, ground-air data link, and an aircraft instrumented with DGPS receiver/processor driving a flight director/autopilot. Several contractor systems are expected to undergo flight testing and optional satellite simulator testing. This Level 1 plan describes the test concepts and objectives, and also outlines the preparation of Level 2 and Level 3 Test Plans. The primary objective of the flight test is to demonstrate whether a contractor's DGPS system meets either sensor accuracy requirements for CAT IIIb approaches or the total system error requirements of the new tunnel-in-space concept. Additional objectives are to demonstrate adequate integrity and continuity of service. This plan describes specific objectives, guidelines and measures of success (MOS's) for the flight tests. The primary objective of the optional satellite simulator testing is to determine the robustness and integrity characteristics of a contractor's system in response to variations in satellite signals that cannot readily be produced during flight testing. This plan describes specific characteristics to be measured by the satellite simulator testing. Author

N94-16906# Mitre Corp., McLean, VA.
WIDE-AREA DIFFERENTIAL GLOBAL POSITIONING SYSTEM (WDGPS)/WIDE-AREA INTEGRITY BROADCAST (WIB) ALTERNATIVES ANALYSIS Final Report
Chris Hegarty, Kelly Markin, and Dan OLaughlin Sep. 1993 44 p
(Contract DTFA01-93-C-00001)
(DOT/FAA/SE-93/3; MTR-93W0000059) Avail: CASI HC A03/MF A01

A study was conducted by MITRE to determine alternative concepts for Wide-area Differential Global Positioning System (WDGPS) for the national airspace system (NAS). The study was undertaken in support of the concept exploration phase analyses required by the Transportation System Acquisition Review Council (TSARC). The results of the study are documented in this paper. The paper provides a description of alternatives to WDGPS, various alternative implementations of WDGPS, advantages and disadvantages of each alternative, and risk areas which were identified. Two WDGPS architecture end-states are recommended. The preferred end-state will depend on the results of required trade-off studies which are identified in this paper. A plan for the transition from the Wide-area Integrity Broadcast (WIB) to the selected WDGPS end-state architecture is also presented. Author

N94-17458 Federal Aviation Administration, Washington, DC. Office of Airport Planning and Programming.
THE 11TH ANNUAL REPORT OF ACCOMPLISHMENTS UNDER THE AIRPORT IMPROVEMENT PROGRAM: FISCAL YEAR 1992 Annual Report
1992 128 p Limited Reproducibility: More than 20% of this document may be affected by microfiche quality
(AD-A268328; DOT/FAA/PP-93-2) Avail: CASI HC A07

The Airport and Airway Safety, Capacity, Noise Improvement, and Intermodal Transportation Act of 1992 authorized the extension of AIP at a funding level of $2.05 billion through FY 1993. This Act included provisions resulting in a number of changes in AIP. The primary changes include the expanded eligibility of items under the Military Airport Program; eligibility for the relocation of air traffic control towers and navigational aids (including radar) if they impede other projects funded under the AIP; the eligibility of land, paving, drainage, aircraft deicing equipment, and structures for centralized aircraft deicing areas; and projects to comply with the Americans with Disabilities Act of 1990, Clean Air Act, and Federal Water Pollution Control Act. The Act also increases from three to seven the number of states which may participate in the State Block Grant Program and extends the program through FY 1996. DTIC

N94-15124# Rijksluchtvaartdienst, The Hague (Netherlands).
DEVELOPMENTS IN THE EUROPEAN AIR TRAFFIC CONTROL [ONTWIKKELINGEN IN DE EUROPESE LUCHTVERKEERSBEVEILIGING]
J. P. F. deKoning *In* NAL, Symposium on the Future of Aeronautics in the Netherlands 1991 16 p In DUTCH (For primary document see N94-15120 03-01)
Avail: CASI HC A03/MF A02

05 AIRCRAFT DESIGN, TESTING AND PERFORMANCE

Includes aircraft simulation technology.

For related information see also *18 Spacecraft Design, Testing and Performance* and *39 Structural Mechanics*.For land transportation vehicles see *85 Urban Technology and Transportation.*

N94-14951# Army Research Lab., Aberdeen Proving Ground, MD.
STATIC AEROELASTIC RESPONSE OF AN AIRCRAFT WITH ASYMMETRIC WING PLANFORMS REPRESENTATIVE OF COMBAT DAMAGE Final Report, Oct. 1991 - Oct. 1992
Jong-Ho Woo Jun. 1993 65 p
(DA Proj. 1L1-62618-AH-80)
(AD-A266890; ARL-TR-153) Avail: CASI HC A04/MF A01

An analysis of the static aeroelastic response of an aircraft with asymmetrical wing planforms representing combat damage is described. The analysis was performed using the MSC/NASTRAN Aeroelastic Code. Structural and aerodynamic models are based on the finite element approach and are created independently for both the damaged and undamaged cases. Fuselage, wings (with aileron), stabilators, and vertical wings (with rudders) are considered as lifting and control surfaces in the aerodynamic model. Five different wings structural models, one undamaged and four damaged, are examined. Doublet-Lattice subsonic theory is used to account for interference effects among multiple lifting surfaces and bodies. The stability and control derivatives, airloads, and trim values are obtained for the damaged-wing aircraft. Effects of damage, including the influence of wing-body interference, on the aircraft's flight dynamics are discussed. DTIC

N94-14976# Naval Postgraduate School, Monterey, CA.
PARAMETRIC STUDY OF A FINITE ELEMENT MODEL OF THE SIDEWINDER MISSILE M.S. Thesis
Gregory G. VanDyke Mar. 1993 59 p
(AD-A267245) Avail: CASI HC A04/MF A01

The long range Maritime Patrol mission has evolved and expanded such that the U.S. Navy's maritime patrol aircraft (P-3C Orion) has become an attractive platform from which to employ a wide variety of air launched weapons. Specifically the need for a stand alone air-to-air defensive capability was identified. In 1989 the Naval Air Test Center at Patuxent River, Maryland began investigations for this through the P-3C/AIM-9 integration program. Naval Postgraduate School responded to this with the construction of a ground vibration test stand and the conduction of a preliminary vibrational characterization of the AIM-9 missile. From these tests a two degree of freedom lumped mass model was developed along with the determination of the primary and secondary missile resonate modes in pitch. In addition, a mathematical model of the AIM-9 missile was developed using finite element techniques. This model was used to analytically determine the modal parameters of the missile and set up a model test system to experimentally verify the model parameters in view of natural frequencies, mode shapes and transient response. This investigation extends the finite element model utility by refining the model structural code to incorporate an improved mass distribution geometry, thus providing more accurate correspondence between observed natural frequencies and model generated modes and performing a parametric study on the model to discover its sensitivity conformation and material changes. This would anticipate any future missile block upgrades, provide further verification of the finite element model and provide model refinement to more accurately represent the physical structure and behavior. These techniques are inherently missile generic and could, with proper calibration be applied to any weapon to be loaded on any platform. This would provide the Navy with an accurate and cost effective methodology for identifying a potential wing flutter problem prior to ever loading and flying a weapon. DTIC

N94-15321* National Aeronautics and Space Administration, Washington, DC.
MISSION ADAPTIVE WING (Videotape)
Oct. 1986 Videotape: 3 min. 7 sec. playing time, in color, with sound
(NASA-TM-109448; NONP-VT-93-190245) Avail: CASI VHS A01/BETA A22

This document looks at an aircraft wing that can change shape in flights from a flat to curved surface according to the necessary flight mode. CASI

N94-15323* National Aeronautics and Space Administration, Washington, DC.
NATIONAL AERO-SPACE PLANE (Videotape)
Jul. 1990 Videotape: 3 min. 3 sec. playing time, in color, with sound
(NASA-TM-109450; NONP-VT-93-190247) Avail: CASI VHS A01/BETA A22

This document presents updated model photography of 'old' NASP design. CASI

N94-15324* National Aeronautics and Space Administration, Washington, DC.
NATIONAL AERO-SPACE PLANE RESOURCE REEL (Videotape)
Aug. 1991 Videotape: 22 min. playing time, in color, with sound
(NASA-TM-109451; NONP-VT-93-190248) Avail: CASI VHS A01/BETA A22

This document presents a series of takes and sequences of model photography of the 1991 NASP design. CASI

N94-15327* National Aeronautics and Space Administration, Washington, DC.
X-29: EXPERIMENT IN FLIGHT (Videotape)
Jan. 1991 Videotape: 2 min. 51 sec. playing time, in color, with sound
(NASA-TM-109454; NONP-VT-93-190251) Avail: CASI VHS A01/BETA A22

This document examines the goals and accomplishments of the forward sweep-winged X-29. CASI

N94-15328* National Aeronautics and Space Administration, Washington, DC.
XV-15: TILTROTOR (Videotape)
Jan. 1991 Videotape: 2 min. 35 sec. playing time, in color, with sound
(NASA-TM-109455; NONP-VT-93-190252) Avail: CASI VHS A01/BETA A22

This document explains the technology of the XV-15 aircraft that takes off and lands like a helicopter and flies like a jet. CASI

N94-15396* National Aeronautics and Space Administration, Washington, DC.
BETTER WAY TO FLY (Videotape)
Feb. 1988 Videotape: 3 min. 31 sec. playing time, in color, with sound
(NASA-TM-109447; NONP-VT-93-190244) Avail: CASI VHS A01/BETA A22

This document shows the advanced cockpit making piloting more efficient and flying safer. CASI

N94-15429*# North Dakota Univ., Grand Forks. Dept. of Atmospheric Sciences.
PRELIMINARY ANALYSIS OF UNIVERSITY OF NORTH DAKOTA AIRCRAFT DATA FROM THE FIRE CIRRUS IFO-2 Semiannual Status Report, 15 Oct. 1992 - 14 Apr. 1993
Michael R. Poellot 1993 10 p
(Grant NAG1-1351)
(NASA-CR-193357; NAS 1.26:193357) Avail: CASI HC A02/MF A01

This report describes the progress and performance by the University of North Dakota under NASA Research Award NAG-1-1351, 'Preliminary Analysis of University of North Dakota Aircraft Data from the FIRE Cirrus IFO-II,' for the period October 15, 1992 to April 14, 1993. Included is a summary of the data archival status and preliminary analysis efforts. During this reporting period, data archival efforts were directed toward providing reduced data for the FIRE data archive and fulfilling special requests for reduced and valued and value-added data. Derived from text

N94-15651# Aeronautical Research Labs., Melbourne (Australia).
HELICOPTER STRUCTURES: A REVIEW OF LOADS, FATIGUE DESIGN TECHNIQUES, AND USAGE MONITORING
D. C. Lombardo May 1993 71 p
(AD-A267115; ARL-TR-15; DODA-AR-007-137) Avail: CASI HC A04/MF A01

This report is a review of traditional practice with respect to helicopter structural integrity. Aspects covered are: significant fatigue loads for the airframe and rotor system, the methods used in the fatigue design of current and previous generation rotorcraft, fatigue test requirements, and health and usage monitoring methods. DTIC

N94-15692# Army Test and Evaluation Command, Aberdeen Proving Ground, MD.
NON-LETHAL UNMANNED AERIAL VEHICLES (UAVs) Final Test Operations Procedure
15 Jun. 1993 43 p Supersedes AD-871331; X70-17501
(AD-A267139; TOP-6-2-040; AD-871331) Avail: CASI HC A03/MF A01

This TOP describes testing methods for determining the technical characteristics of Non-Lethal Unmanned Aerial Vehicles (UAV's). It provides a general description of facilities, instrumentation, and tasks required. It also specifies the documentation required including safety, environmental, and frequency authorization documentation. In details methodology for measuring Center of Gravity, developing flight profiles, performing flight tests, and performing transportability tests. This TOP discusses in general Electromagnetic Environmental, Manpower Integration/Reliability, Availability, Maintainability (MANPRINT/RAM), and Aural/Visual/Acoustic testing. DTIC

N94-15718*# National Aeronautics and Space Administration. Ames Research Center, Moffett Field, CA.
THE LIFT-FAN POWERED-LIFT AIRCRAFT CONCEPT: LESSONS LEARNED
Wallace H. Deckert Sep. 1993 79 p Sponsored by NASA, Washington
(NASA Order A-25364-D)
(NASA-CR-177616; A-93107; NAS 1.26:177616) Avail: CASI HC A05/MF A01

This is one of a series of reports on the lessons learned from past research related to lift-fan aircraft concepts. An extensive review is presented of the many lift-fan aircraft design studies conducted by both government and industry over the past 45 years. Mission applications and design integration including discussions on manifolding hot gas generators, hot gas dusting, and energy transfer control are addressed. Past lift-fan evaluations of the Avrocar are discussed. Lessons learned from these past efforts are identified. Author (revised)

N94-15722*# National Aeronautics and Space Administration. Langley Research Center, Hampton, VA.
PHYSICAL PROPERTIES OF THE BENCHMARK MODELS PROGRAM SUPERCRITICAL WING
Bryan E. Dansberry, Michael H. Durham, Robert M. Bennett, David L. Turnock (Lockheed Engineering and Sciences Co., Hampton, VA.), Walter A. Silva, and Jose A. Rivera, Jr. Washington Sep. 1993 62 p
(RTOP 505-63-50-16)
(NASA-TM-4457; L-17177; NAS 1.15:4457) Avail: CASI HC A04/MF A01

The goal of the Benchmark Models Program is to provide data useful in the development and evaluation of aeroelastic computational fluid dynamics (CFD) codes. To that end, a series of three similar wing models are being flutter tested in the Langley Transonic Dynamics Tunnel. These models are designed to simultaneously acquire model response data and unsteady surface pressure data during wing flutter conditions. The supercritical wing is the second model of this series. It is a rigid semispan model with a rectangular planform and a NASA SC(2)-0414 supercritical airfoil shape. The supercritical wing model was flutter tested on a flexible mount, called the Pitch and Plunge Apparatus, that provides a well-defined, two-degree-of-freedom dynamic system. The supercritical wing model and associated flutter test apparatus is described and experimentally determined wind-off structural dynamic characteristics of the combined rigid model and flexible mount system are included. Author (revised)

N94-15731# Air Force Inst. of Tech., Wright-Patterson AFB, OH. School of Engineering.
AN ANALYSIS OF TACTICAL AIRLIFTER CHARACTERISTICS AND THEIR IMPACT ON THEATER AIRLIFT SYSTEM PERFORMANCE M.S. Thesis
John J. Koger Mar. 1993 124 p
(AD-A266719; AFIT/GST/ENS/93M-05) Avail: CASI HC A06/MF A02

This study used computer simulation and Response Surface Technology to determine what tactical airlifter characteristics most impact theater airlift system performance in a Southwest Asia (SWA) scenario. Some Aircraft characteristics were grouped into functional sets, while others were considered individually. After screening one characteristic, reliability, with a two-level factorial experiment, a Box-Behnken design was used to estimate second-order metamodels. A stepwise regression procedure indicated that, if attrition rates are ignored, airlift system performance is most impacted by the aircraft's size, survivability, cruise speed, and ability to operate on short fields. The SWA scenario used in this study covers a large geographical area and varying threat levels and types. The results of this study were compared with those of an earlier study that used the much smaller, low threat Central American scenario. It was determined that across a range of scenarios airlift system performance is most affected by the aircraft's size, survivability, cruise speed, ability to operate on short fields, and ability to operate on unprepared surfaces. DTIC

N94-15761 Sundstrand Corp., Rockford, IL.
ADVANCED COOLING FOR HIGH POWER ELECTRIC ACTUATORS Interim Report, Jan. - Sep. 1992
Michael G. Schneider and Timothy J. Bland Jan. 1993 154 p Limited Reproducibility: More than 20% of this document may be affected by microfiche quality
(Contract F33615-91-C-2139)
(AD-A266984; WL-TR-93-2047) Avail: Issuing Activity (Defense Technical Information Center (DTIC))

The development of more electric technologies for future military aircraft promises to provide significant redundancy, reliability, maintainability, and performance benefits. Advanced Cooling For High Power Electric Actuators particularly address the use electro-mechanical actuators (EMA's), and an approach for cooling EMA's using the combined concepts of passive reflux cooling and phase change materials (PCM's) for energy storage. The planned program involves four Phases: Phase 1 Requirements and Trade Studies; Phase 2 Detailed Design; Phase 3 Fabrication and Test Plans; and Phase 4 Test/Data Correlation. During Phase 1 Sundstrand identified actuator cooling requirements and evaluated the effects of several critical parameters on the use of passive reflux cooling in combination with PCM. DTIC

N94-15783*# National Aeronautics and Space Administration. Hugh L. Dryden Flight Research Facility, Edwards, CA.

IN-FLIGHT INVESTIGATION OF A ROTATING CYLINDER-BASED STRUCTURAL EXCITATION SYSTEM FOR FLUTTER TESTING

Lura Vernon Washington Jun. 1993 22 p See also A93-34074

(RTOP 505-63-50)

(NASA-TM-4512; H-1883; NAS 1.15:4512) Avail: CASI HC A03/MF A01

A research excitation system was test flown at the NASA Dryden Flight Research Facility on the two-seat F-16XL aircraft. The excitation system is a wingtip-mounted vane with a rotating slotted cylinder at the trailing edge. As the cylinder rotates during flight, the flow is alternately deflected upward and downward through the slot, resulting in a periodic lift force at twice the cylinder's rotational frequency. Flight testing was conducted to determine the excitation system's effectiveness in the subsonic, transonic, and supersonic flight regimes. Primary research objectives were to determine the system's ability to develop adequate force levels to excite the aircraft's structure and to determine the frequency range over which the system could excite structural modes of the aircraft. In addition, studies were conducted to determine optimal excitation parameters, such as sweep duration, sweep type, and energy levels. The results from the exciter were compared with results from atmospheric turbulence excitation at the same flight conditions. The comparison indicated that the vane with a rotating slotted cylinder provides superior results. The results from the forced excitation were of higher quality and had less variation than the results from atmospheric turbulence. The forced excitation data also invariably yielded higher structural damping values than those from the atmospheric turbulence data. Author

N94-15950*# National Aeronautics and Space Administration. Ames Research Center, Moffett Field, CA.

LIFT-FAN AIRCRAFT: LESSONS LEARNED-THE PILOT'S PERSPECTIVE

Ronald M. Gerdes Aug. 1993 33 p

(NASA Order A-24364-D)

(NASA-CR-177620; A-93114; NAS 1.26:177620) Avail: CASI HC A03/MF A01

This paper is written from an engineering test pilot's point of view. Its purpose is to present lift-fan 'lessons learned' from the perspective of first-hand experience accumulated during the period 1962 through 1988 while flight testing vertical/short take-off and landing (V/STOL) experimental aircraft and evaluating piloted engineering simulations of promising V/STOL concepts. Specifically, the scope of the discussions to follow is primarily based upon a critical review of the writer's personal accounts of 30 hours of XV-5A/B and 2 hours of X-14A flight testing as well as a limited simulator evaluation of the Grumman Design 755 lift-fan aircraft. Opinions of other test pilots who flew these aircraft and the aircraft simulator are also included and supplement the writer's comments. Furthermore, the lessons learned are presented from the perspective of the writer's flying experience: 10,000 hours in 100 fixed- and rotary-wing aircraft including 330 hours in 5 experimental V/STOL research aircraft. The paper is organized to present to the reader a clear picture of lift-fan lessons learned from three distinct points of view in order to facilitate application of the lesson principles to future designs. Lessons learned are first discussed with respect to case histories of specific flight and simulator investigations. These principles are then organized and restated with respect to four selected design criteria categories in Appendix I. Lastly, Appendix II is a discussion of the design of a hypothetical supersonic short take-off vertical landing (STOVL) fighter/attack aircraft. Author

N94-16122# Texas Univ., Austin. Dept. of Aerospace Engineering and Engineering Mechanics.

ADAPTIVE ALGORITHM FOR AIRCRAFT CONFIGURATION IN TURBULENT FLOW Final Report, 10 Jan. 1991 - 30 Sep. 1992

John Kallinderis 25 Nov. 1992 57 p

(Grant AF-AFOSR-0022-91)

(AD-A266188; CAR-92-8; AFOSR-93-0433TR) Avail: CASI HC A04/MF A01

The flow around aircraft configurations has been simulated. A code for numerical simulation and study of 3-D aircraft flowfields has been developed. The code consists of a hybrid scheme which solves the Navier-Stokes equations within the viscous regions around the aircraft while the simple Euler system is solved everywhere else. Efficient resolution of local flow physics such as shear layers, shock waves, and vortices is achieved by a specially developed adaptive grid algorithm. The method employs division and/or deletion of grid cells, as well as redistribution of points in order to resolve local flow features more accurately and efficiently. A hybrid grid consisting of prisms and tetrahedra grid-cells is employed. The first type is appropriate for the viscous regions, while the second type is suitable for the inviscid regions. A grid generator of prisms around an F-16-type aircraft was developed. Flow visualization is greatly enhanced with a developed computer graphics code. DTIC

N94-16498*# Iowa State Univ. of Science and Technology, Ames. Dept. of Aerospace Engineering and Engineering Mechanics.

TRAJECTORY OPTIMIZATION FOR THE NATIONAL AEROSPACE PLANE Final Report, 13 Jun. 1992 - 30 Oct. 1993

Ping Lu Nov. 1993 28 p

(Grant NAG1-1255)

(NASA-CR-194618; NAS 1.26:194618) Avail: CASI HC A03/MF A01

The objective of this second phase research is to investigate the optimal ascent trajectory for the National Aerospace Plane (NASP) from runway take-off to orbital insertion and address the unique problems associated with the hypersonic flight trajectory optimization. The trajectory optimization problem for an aerospace plane is a highly challenging problem because of the complexity involved. Previous work has been successful in obtaining sub-optimal trajectories by using energy-state approximation and time-scale decomposition techniques. But it is known that the energy-state approximation is not valid in certain portions of the trajectory. This research aims at employing full dynamics of the aerospace plane and emphasizing direct trajectory optimization methods. The major accomplishments of this research include the first-time development of an inverse dynamics approach in trajectory optimization which enables us to generate optimal trajectories for the aerospace plane efficiently and reliably, and general analytical solutions to constrained hypersonic trajectories that has wide application in trajectory optimization as well as in guidance and flight dynamics. Optimal trajectories in abort landing and ascent augmented with rocket propulsion and thrust vectoring control were also investigated. Motivated by this study, a new global trajectory optimization tool using continuous simulated annealing and a nonlinear predictive feedback guidance law have been under investigation and some promising results have been obtained, which may well lead to more significant development and application in the near future. Author (revised)

N94-17055*# National Aeronautics and Space Administration. Langley Research Center, Hampton, VA.

AEROTHERMOELASTIC ANALYSIS OF A NASP DEMONSTRATOR MODEL

Jennifer Heeg, Thomas A. Zeiler (Lockheed Engineering and Sciences Co., Hampton, VA.), Anthony S. Pototzky (Lockheed Engineering and Sciences Co., Hampton, VA.), Charles V. Spain (Lockheed Engineering and Sciences Co., Hampton, VA.), and Walter C. Engelund Oct. 1993 13 p See also A93-33933

(RTOP 505-63-50-15)

(NASA-TM-109007; NAS 1.15:109007) Avail: CASI HC A03/MF A01

The proposed National Aerospace Plane (NASP) is designed to travel at speeds up to Mach 25. Because aerodynamic heating during high-speed flight through the atmosphere could destiffen a structure, significant couplings between the elastic and rigid body modes could result in lower flutter speeds and more pronounced aeroelastic response characteristics. These speeds will also generate thermal loads on the structure. The purpose of this research is to develop methodologies applicable to the NASP and to apply them to a representative model to determine its aerothermoelastic characteristics when subjected to these thermal loads. This paper describes an aerothermoelastic analysis of the generic hypersonic vehicle configuration. The steps involved in this analysis were: generating vehicle surface temperatures at the appropriate flight conditions; applying these temperatures to the vehicle's structure to predict changes in the stiffness resulting from material property degradation; predicting the vibration characteristics of the heated structure at the various temperature conditions; performing aerodynamic analyses; and conducting flutter analysis of the heated vehicle. Results of these analyses and conclusions representative of a NASP vehicle are provided in this paper. Author

N94-17117 Aeronautical Research Labs., Melbourne (Australia).
A REVIEW OF AUSTRALIAN AND NEW ZEALAND INVESTIGATIONS ON AERONAUTICAL FATIGUE DURING THE PERIOD APRIL 1991 TO MARCH 1993 Technical Note
J. M. Grandage Apr. 1993 40 p Limited Reproducibility: More than 20% of this document may be affected by microfiche quality
(AD-A267532; ARL-TN-32; DODA-AR-008-351) Avail: CASI HC A03

This document was prepared for presentation to the 23rd Conference of the International Committee on Aeronautical Fatigue scheduled to be held in Stockholm, Sweden on June 7 and 8, 1993. A review is given of the aircraft fatigue research and associated activities which form part of the programs of the Aeronautical Research Laboratory, Universities, the Civil Aviation Authority, the Australia aircraft industry and the Defence Scientific Establish, New Zealand. The review summarizes fatigue-related research programs as well as fatigue investigations on specific military and civil aircraft. DTIC

N94-17425 Logicon Technical Services, Inc., Dayton, OH.
DEFINITIONS OF TERMS RELATING TO AIRCRAFT WINDSCREENS, CANOPIES, AND TRANSPARENCIES Final Report, Oct. 1990 - Nov. 1992
Maryann H. Barbato, William N. Kama, Harry L. Task, Martha A. Hausmann, and John C. Bridenbaugh Mar. 1993 45 p Limited Reproducibility: More than 20% of this document may be affected by microfiche quality
(Contract F33615-89-C-0532)
(AD-A268403; AL-TR-1993-0036) Avail: Issuing Activity (Defense Technical Information Center (DTIC))

This report presents a glossary of terms relating to aircraft windscreens, canopies, and transparencies. It addresses the need to have a single reference source which provides a common vocabulary for use by designers, materials engineers, manufacturers, evaluators, maintenance personnel, and user agencies concerned with aircraft transparencies. Its intent is to facilitate and enhance communication between these disciplines by clarifying and defining terms used within the aircraft transparency industry. DTIC

N94-17435 Naval Air Warfare Center, China Lake, CA. Weapons Div.
EQUATIONS OF MOTION OF A HINGED BODY OVER A SPHERICAL EARTH Final Report, May 1990 - 1992
Megaera C. Halter Aug. 1993 41 p Limited Reproducibility: More than 20% of this document may be affected by microfiche quality
(AD-A268408; NAWCWPNS-TP-8134) Avail: CASI HC A03

The six-degree-of-freedom (6-DOF) equations of motion are derived in vector form for a hinged vehicle flying over a spherical Earth. Initially, the most general form of the equations is developed assuming that the combustor may roll with respect to the body, as well as deflect in pitch and yaw. Next, the primary case is developed in which the combustor cannot roll with respect to the body. Finally, these equations are specialized to dime simpler cases. The motivation for deriving this set of equations is to support feasibility studies of the low drag ramjet (LDR), which is streamlined by deleting all aerodynamic surfaces. AH directional control comes from thrust vectoring, which is accomplished by deflecting the entire motor rather than just the exhaust nozzle, as in more conventional designs. Since the motor is a large fraction of the total vehicle mass, its inertia has a significant effect on the dynamics of the overall vehicle. Sufficient detail is included to serve as a tutorial. DTIC

N94-17472 General Accounting Office, Washington, DC. National Security and International Affairs Div.
NAVAL AVIATION: THE NAVY IS TAKING ACTIONS TO IMPROVE THE COMBAT CAPABILITIES OF ITS TACTICAL AIRCRAFT. REPORT TO CONGRESSIONAL REQUESTERS
Jul. 1993 32 p Limited Reproducibility: More than 20% of this document may be affected by microfiche quality
(AD-A268002; GAO/NSIAD-93-204) Avail: Issuing Activity (Defense Technical Information Center (DTIC))

The Chairman of the Legislation and National Security Subcommittee of the House Committee on Government Operations and the Chairman of the Oversight of Government Management Subcommittee of the Senate Committee on Governmental Affairs asked the General Accounting Office to determine whether certain aircraft had the capabilities needed to perform their assigned missions during Operation Desert Storm. This report focuses on several Navy and Marine Corps aircraft. Several factors contributed to the Gulf War victory by creating favorable conditions under which to plan and fight the war, and these should be considered when assessing the effectiveness of U.S. weapons in the war. Commanders had nearly 6 months to plan and develop an air campaign that when initiated, quickly gained air superiority and effectively neutralized much of Iraq's air defense system. In addition, Iraq's forces remained in a primarily defensive posture throughout the war. These factors helped enable the Coalition to determine its tactics and decide when and where offensive air and ground actions would occur. DTIC

N94-16090 National Research Council of Canada, Ottawa (Ontario).
KC-135 ACCELERATION MONITORING AND DATA ACQUISITION SYSTEM
Bjarni V. Tryggvason and Patrick J. Sullivan *In its* Proceedings of the Second Workshop on Microgravity Experimentation 1990 3 p (For primary document see N94-16071 03-29)
Avail: Issuing Activity (National Research Council, Publication Sales and Distribution, Montreal Road, Ottawa, Ontario, K1A OR6 Canada)

N94-16865*# North Carolina State Univ., Raleigh. Dept. of Textile Engineering, Chemistry and Science.
AEROELASTIC AIRFOIL SMART SPAR
Skott Greenhalgh, Christopher M. Pastore, and Moishe Garfinkle (Drexel Univ., Philadelphia, PA.) *In* NASA. Langley Research Center, FIBER-TEX 1992: The Sixth Conference on Advanced Engineering Fibers and Textile Structures for Composites Aug. 1993 p 343-351 (For primary document see N94-16845 03-24)
Avail: CASI HC A02/MF A03

06 AIRCRAFT INSTRUMENTATION

Includes cockpit and cabin display devices; and flight instruments.

For related information see also *19 Spacecraft Instrumentation* and *35 Instrumentation and Photography.*

N94-15187*# Alabama Univ., Huntsville. Coll. of Science.
TESTING AND MANAGEMENT OF FLIGHT INSTRUMENTS AND THEIR DATA Final Report, 1 Dec. 1988 - 30 Nov. 1991
Richard H. Comfort Dec. 1991 4 p
(Grant NAG8-122)
(NASA-CR-194332; NAS 1.26:194332) Avail: CASI HC A01/MF A01

Hardware activities were concentrated on the Low Energy Ion Facility (LEIF), which is used for testing and calibration of most of the flight instruments for near-Earth observations. The ion beam generated by the ion source in the LEIF has been required for the proper testing and calibration of the primary components of the Thermal Ion Dynamics Experiment (TIDE) to be flown on the POLAR spacecraft of the Global Geospace Science (GGS) flight program. Additional work has been done on equipment and techniques for diagnosing and testing microchannel plates. These plates are used in the imager as well as the flight instruments. CASI

07 AIRCRAFT PROPULSION AND POWER

Includes prime propulsion systems and systems components, e.g., gas turbine engines and compressors; and onboard auxilliary power plants for aircraft.

For related information see also *20 Spacecraft Propulsion and Power, 28 Propellants and Fuels,* and *44 Energy Production and Conversion.*

N94-14964 Air Force Inst. of Tech., Wright-Patterson AFB, OH.
TURBINE BLADE TIP FILM COOLING MEASUREMENTS M.S. Thesis
Dean A. Ward Dec. 1992 186 p Limited Reproducibility: More than 20% of this document may be affected by microfiche quality
(AD-A267686; AFIT/CI/CIA-93-011) Avail: Issuing Activity (Defense Technical Information Center (DTIC))

In the design of gas turbine engines, the need to accurately know the heat transfer characteristics of the turbine blade tip is of extreme importance.

The pressure differential between the pressure and suction side of the blade induces a strong secondary flow of hot combustion gases through the clearance gap between the turbine blade tip and shroud. This leakage flow is detrimental to the tip of the blade. In order to minimize this leakage flow, designers need to accurately know the heat transfer characteristics of the blade and blade tip so that dimensional changes may be accurately predicted. If dimensional changes are accurately known, the clearance gap and the secondary flow may be minimized and the overall thermal efficiency of the gas turbine engine increased. In addition, increased blade life is often achieved by cooling of the blade and blade tip. DTIC

N94-15141*# National Aeronautics and Space Administration. Hugh L. Dryden Flight Research Facility, Edwards, CA.

FLIGHT-DETERMINED ENGINE EXHAUST CHARACTERISTICS OF AN F404 ENGINE IN AN F-18 AIRPLANE

Kimberly A. Ennix, Frank W. Burcham, Jr., and Lannie D. Webb Oct. 1993 15 p Presented at the AIAA/SAE/ASME/ASEE 29th Joint Propulsion Conference and Exhibit, Monterey, CA, 28-30 Jun. 1993 See also A93-50267

(RTOP 537-03-20)

(NASA-TM-4538; H-1910; NAS 1.15:4538; AIAA Paper 93-2543)

Copyright Avail: CASI HC A03/MF A01

Personnel at the NASA Langley Research Center (NASA-Langley) and the NASA Dryden Flight Research Facility (NASA-Dryden) recently completed a joint acoustic flight test program. Several types of aircraft with high nozzle pressure ratio engines were flown to satisfy a twofold objective. First, assessments were made of subsonic climb-to-cruise noise from flights conducted at varying altitudes in a Mach 0.30 to 0.90 range. Second, using data from flights conducted at constant altitude in a Mach 0.30 to 0.95 range, engineers obtained a high quality noise database. This database was desired to validate the Aircraft Noise Prediction Program and other system noise prediction codes. NASA-Dryden personnel analyzed the engine data from several aircraft that were flown in the test program to determine the exhaust characteristics. The analysis of the exhaust characteristics from the F-18 aircraft are reported. An overview of the flight test planning, instrumentation, test procedures, data analysis, engine modeling codes, and results are presented. Author (revised)

N94-15192*# Sverdrup Technology, Inc., Brook Park, OH. Lewis Research Center Group.

ROTARY ENGINE PERFORMANCE COMPUTER PROGRAM (RCEMAP AND RCEMAPPC): USER'S GUIDE Final Report

Timothy A. Bartrand and Edward A. Willis Oct. 1993 240 p

(Contract NAS3-25266; RTOP 505-62-11)

(NASA-CR-191192; E-8133; NAS 1.26:191192) Avail: CASI HC A11/MF A03

This report is a user's guide for a computer code that simulates the performance of several rotary combustion engine configurations. It is intended to assist prospective users in getting started with RCEMAP and/or RCEMAPPC. RCEMAP (Rotary Combustion Engine performance MAP generating code) is the mainframe version, while RCEMAPPC is a simplified subset designed for the personal computer, or PC, environment. Both versions are based on an open, zero-dimensional combustion system model for the prediction of instantaneous pressures, temperature, chemical composition and other in-chamber thermodynamic properties. Both versions predict overall engine performance and thermal characteristics, including bmep, bsfc, exhaust gas temperature, average material temperatures, and turbocharger operating conditions. Required inputs include engine geometry, materials, constants for use in the combustion heat release model, and turbomachinery maps. Illustrative examples and sample input files for both versions are included. Author (revised)

N94-15338* National Aeronautics and Space Administration. Lewis Research Center, Cleveland, OH.

FUTUREPATH 1 (Videotape)

Apr. 1988 Videotape: 8 min. 30 sec. playing time, in color, with sound (NASA-TM-109439; NONP-VT-93-190236) Avail: CASI VHS A01/BETA A22

The videotape presents material concerning Advanced Turboprop programs. Additionally, material covering the development of power systems for Freedom is shown. CASI

N94-15344* National Aeronautics and Space Administration, Washington, DC.

BACK TO PROPELLERS (Videotape)

Jun. 1987 Videotape: 2 min. 50 sec. playing time, in color, with sound (NASA-TM-109445; NONP-VT-93-190242) Avail: CASI VHS A01/BETA A22

The videotape shows the unique propfan design. The propfan is designed to achieve the speeds and altitudes of jets while only using half the normal amount of fuel. CASI

N94-15866*# National Aeronautics and Space Administration. Lewis Research Center, Cleveland, OH.

EFFECT OF WIND TUNNEL ACOUSTIC MODES ON LINEAR OSCILLATING CASCADE AERODYNAMICS

Daniel H. Buffum and Sanford Fleeter (Purdue Univ., West Lafayette, IN.) May 1993 43 p Presented at the 38th ASME International Gas Turbine and Aeroengine Congress and Exposition, Cincinnati, OH, 24-27 May 1993; sponsored by ASME

(RTOP 505-62-10)

(NASA-TM-106367; E-8171; NAS 1.15:106367) Avail: CASI HC A03/MF A01

The aerodynamics of a biconvex airfoil cascade oscillating in torsion is investigated using the unsteady aerodynamic influence coefficient technique. For subsonic flow and reduced frequencies as large as 0.9, airfoil surface unsteady pressures resulting from oscillation of one of the airfoils are measured using flush-mounted high-frequency-response pressure transducers. The influence coefficient data are examined in detail and then used to predict the unsteady aerodynamics of a cascade oscillating at various interblade phase angles. These results are correlated with experimental data obtained in the traveling-wave mode of oscillation and linearized analysis predictions. It is found that the unsteady pressure disturbances created by an oscillating airfoil excite wind tunnel acoustic modes which have detrimental effects on the experimental data. Acoustic treatment is proposed to rectify this problem. Author

N94-16516# Coordinating Research Council, Inc., Atlanta, GA.

EFFECTS OF RVP, T(50), AND OXYGENATES ON HOT-START AND DRIVEABILITY PERFORMANCE AT HIGH AND LOW ALTITUDE

May 1993 99 p

(AD-A266382; CRC-584) Avail: CASI HC A05/MF A02

A two-phase test program was conducted during July and August 1992 in Longmont, Colorado, and Phoenix, Arizona. The program was designed to investigate the effects of Reid vapor pressure, T(50), and oxygenates on hot-start and driveability performance of vehicles operated at high and low altitude in high and intermediate ambient temperature ranges. The temperature ranges had means of 70 F and 84 F in Longmont and 99 F in Phoenix. Twenty 1983 - 1992 model-year vehicles were tested on a set of eighteen fuels which included six hydrocarbon only fuels, six gasoline ethanol blends, and six gasoline-MTBE blends. Fuel-injected vehicles produced only about one-third the demerits of the carbureted vehicles and were insensitive, in most cases, to T(50) and the other fuel variables studied. For carbureted vehicles, decreasing T(50) had no effect with high-RVP fuels, but reduced T(50) fuels degraded driveability with low-RVP fuels. In carbureted vehicles, gasoline oxygenate blends showed generally improved driveability at high altitude with high-RVP fuels. An alternative driveability procedure that emphasized stop-and-go driving showed no significant fuel effects. DTIC

N94-17386*# National Aeronautics and Space Administration. Lewis Research Center, Cleveland, OH.

EXPERIMENTAL AND COMPUTATIONAL INVESTIGATION OF THE NASA LOW-SPEED CENTRIFUGAL COMPRESSOR FLOW FIELD

Michael D. Hathaway, Randall M. Chriss, Jerry R. Wood, and Anthony J. Strazisar Washington Sep. 1993 21 p Presented at the 37th International Gas Turbine and Aero Engine Congress and Exposition, Cologne, Germany, 1-4 Jun. 1992; sponsored by ASME See also A93-19436 Prepared in cooperation with Army Research Lab., Cleveland, OH

(RTOP 505-62-52)

(NASA-TM-4481; E-7651; NAS 1.15:4481; AVSCOM-TR-91-C-052) Avail: CASI HC A03/MF A01

An experimental and computational investigation of the NASA Lewis

Research Center's low-speed centrifugal compressor (LSCC) flow field was conducted using laser anemometry and Dawes' three-dimensional viscous code. The experimental configuration consisted of a backswept impeller followed by a vaneless diffuser. Measurements of the three-dimensional velocity field were acquired at several measurement planes through the compressor. The measurements describe both the throughflow and secondary velocity field along each measurement plane. In several cases the measurements provide details of the flow within the blade boundary layers. Insight into the complex flow physics within centrifugal compressors is provided by the computational fluid dynamics analysis (CFD), and assessment of the CFD predictions is provided by comparison with the measurements. Five-hole probe and hot-wire surveys at the inlet and exit to the impeller as well as surface flow visualization along the impeller blade surfaces provided independent confirmation of the laser measurement technique. The results clearly document the development of the throughflow velocity wake that is characteristic of unshrouded centrifugal compressors. Derived from text

N94-17470*# National Aeronautics and Space Administration. Lewis Research Center, Cleveland, OH.
JET ENGINE PERFORMANCE ENHANCEMENT THROUGH USE OF A WAVE-ROTOR TOPPING CYCLE
Jack Wilson (Sverdrup Technology, Inc., Brook Park, OH.) and Daniel E. Paxson Washington Oct. 1993 12 p
(RTOP 505-62-10)
(NASA-TM-4486; E-7836; NAS 1.15:4486) Avail: CASI HC A03/MF A01

A simple model is used to calculate the thermal efficiency and specific power of simple jet engines and jet engines with a wave-rotor topping cycle. The performance of the wave rotor is based on measurements from a previous experiment. Applied to the case of an aircraft flying at Mach 0.8, the calculations show that an engine with a wave rotor topping cycle may have gains in thermal efficiency of approximately 1 to 2 percent and gains in specific power of approximately 10 to 16 percent over a simple jet engine with the same overall compression ratio. Even greater gains are possible if the wave rotor's performance can be improved. Author

N94-16157# Army Missile Command, Redstone Arsenal, AL.
WIND TUNNEL INVESTIGATION WITH AN OPERATIONAL TURBOJET ENGINE
Lamar M. Auman *In* Huntsville Association of Technical Societies, TABES 1993: 9th Annual Technical and Business Exhibition and Symposium 1993 6 p (For primary document see N94-16129 03-38)
(TABES Paper 93-662) Avail: CASI HC A02/MF A03

08 AIRCRAFT STABILITY AND CONTROL

Includes aircraft handling qualities; piloting; flight controls; and autopilots.

For related information see also *05 Aircraft Design, Testing and Performance.*

N94-15279* National Aeronautics and Space Administration. Lyndon B. Johnson Space Center, Houston, TX.
STS-26 STA TRAINING (HAUCK) (Videotape)
May 1988 Videotape: 3 min. 50 sec. playing time, in color, with sound
(NASA-TM-109555; NONP-VT-93-190353) Avail: CASI VHS A01/BETA A22

This video shows astronaut Rick Hauck at the Shuttle Training Aircraft (STA), CU's of the heads-up display, and air-to-air exercises. CASI

N94-15416*# Georgia Inst. of Tech., Atlanta. School of Aerospace Engineering.
RESEARCH IN ROBUST CONTROL FOR HYPERSONIC AIRCRAFT Progress Report No. 2, 1 Dec. 1992 - 31 Aug. 1993
A. J. Calise Oct. 1993 24 p
(Grant NAG1-1451)
(NASA-CR-194106; NAS 1.26:194106) Avail: CASI HC A03/MF A01

The research during the second reporting period has focused on robust control design for hypersonic vehicles. An already existing design for the Hypersonic Winged-Cone Configuration has been enhanced. Uncertainty models for the effects of propulsion system perturbations due to angle of attack variations, structural vibrations, and uncertainty in control effectiveness were developed. Using H(sub infinity) and mu-synthesis techniques, various control designs were performed in order to investigate the impact of these effects on achievable robust performance. Derived from text

N94-15532*# Auburn Univ., AL. Dept. of Aerospace Engineering.
AERODYNAMIC FLIGHT CONTROL TO INCREASE PAYLOAD CAPABILITY OF FUTURE LAUNCH VEHICLES Final Report, 14 Dec. 1992 - 31 Aug. 1993
John E. Cochran, Jr., Y.-M. Cheng, Todd Leleux, Scott Bigelow, and William Hasbrook 31 Aug. 1993 89 p
(Contract NAS8-39131)
(NASA-CR-193850; NAS 1.26:193850) Avail: CASI HC A05/MF A01

In this report, we provide some examples of French, Russian, Chinese, and Japanese launch vehicles that have utilized fins in their designs. Next, the aerodynamic design of the fins is considered in Section 3. Some comments on basic static stability and control theory are followed by a brief description of an aerodynamic characteristics prediction code that was used to estimate the characteristics of a modified NLS 1.5 Stage vehicle. Alternative fin designs are proposed and some estimated aerodynamic characteristics presented and discussed. Also included in Section 3 is a discussion of possible methods of enhancement of the aerodynamic efficiency of fins, such as vortex generators and jet flaps. We consider the construction of fins for launch vehicles in Section 4 and offer an assessment of the state-of-the-art in the use of composites for aerodynamic control surfaces on high speed vehicles. We also comment on the use of smart materials for launch vehicle fins. The dynamic stability and control of a launch vehicle that utilizes both thrust vector control (engine nozzle gimballing) and movable fins is the subject addressed in Section 5. We give a short derivation of equations of motion for a launch vehicle moving in a vertical plane above a spherical earth, discuss the use of a gravity-turn nominal trajectory, and give the form of the period equations linearized about such a nominal. We then consider feedback control of vehicle attitude using both engine gimballing and fin deflection. Conclusions are stated and recommendations made in Section 6. An appendix contains aerodynamic data in tabular and graphical formats. Author (revised)

N94-15730# Air Force Inst. of Tech., Wright-Patterson AFB, OH. School of Engineering.
DEVELOPMENT OF AN AIR-TO-AIR REFUELING AUTOMATIC FLIGHT CONTROL SYSTEM USING QUANTITATIVE FEEDBACK THEORY M.S. Thesis
Dennis W. Trosen Jun. 1993 127 p
(AD-A266718; AFIT/GE/ENG/93J-03) Avail: CASI HC A07/MF A02

Quantitative Feedback Theory and the improved method Quantitative Feedback Theory are enhanced to include the rejection of disturbance at the system output. The enhanced Quantitative Feedback Theory and improved method Quantitative Feedback Theory processes are applied to the design of an automatic flight control system to regulate position of the C-135B fuel receiving aircraft relative to the tanker during air-to-air refueling. A simple feedback control system is developed that will achieve stable position regulation. State-space aircraft models are generated. An inner loop autopilot is designed to reduce the plant cutoff frequency and provide the system inputs for the Quantitative Feedback Theory compensators. Disturbance models representing disturbance due to wind gusts and refueling are developed. The flight control system is designed using the enhanced Quantitative Feedback Theory equations. Linear simulations are performed on MATRIX, and nonlinear simulations are run on EASY5x. The results of the simulations show excellent results. The simulation results indicate that air-to-air automatic flight control system are technically achievable, and that implementation in USAF aircraft is possible. DTIC

N94-15793*# National Aeronautics and Space Administration. Ames Research Center, Moffett Field, CA.
FIDELITY ASSESSMENT OF A UH-60A SIMULATION ON THE NASA AMES VERTICAL MOTION SIMULATOR
Adolph Atencio, Jr. Sep. 1993 318 p Sponsored by NASA, Washington
(RTOP 505-59-52)
(NASA-TM-104016; A-93071; NAS 1.15:104016; USAATC-TR-93-A-005) Avail: CASI HC A14/MF A03

Helicopter handling qualities research requires that a ground-based simulation be a high-fidelity representation of the actual helicopter, especially over the frequency range of the investigation. This experiment was performed to assess the current capability to simulate the UH-60A Black Hawk helicopter on the Vertical Motion Simulator (VMS) at NASA Ames, to develop a methodology for assessing the fidelity of a simulation, and to find the causes for lack of fidelity. The approach used was to compare the simulation to the flight vehicle for a series of tasks performed in flight and in the simulator. The results show that subjective handling qualities ratings from flight to simulator overlap, and the mathematical model matches the UH-60A helicopter very well over the range of frequencies critical to handling qualities evaluation. Pilot comments, however, indicate a need for improvement in the perceptual fidelity of the simulation in the areas of motion and visual cuing. The methodology used to make the fidelity assessment proved useful in showing differences in pilot work load and strategy, but additional work is needed to refine objective methods for determining causes of lack of fidelity. Author

N94-16107# Virginia Polytechnic Inst. and State Univ., Blacksburg. Dept. of Engineering Science and Mechanics.

AERODYNAMIC/DYNAMIC/CONTROL INTERACTION Final Report, 15 Oct. 1989 - 14 Oct. 1992

Dean T. Mook and Ali H. Nayfeh 22 Dec. 1992 22 p

(Grant AF-AFOSR-0032-90)

(AD-A266187; AFOSR-93-0443TR) Avail: CASI HC A03/MF A01

The present report attempts to present a comprehensive review of achievements made under the support of a continuing series of related AFOSR grants. The essence of all the work was to develop numerical simulations that capture the interactions among aerodynamics, rigid-body dynamics, structural dynamics, and control systems. All of these components of a flying airplane were viewed simply as elements of a single dynamic system. All the work led toward an end result in which a maneuvering aircraft could be simulated without resorting to wind-tunnel or flight tests. A major obstacle to this development is the fact that one must know the motion of the aircraft and its control-surface deflections in order to calculate the flowfield, and one must know the flowfield in order to calculate the aerodynamic forces and, from them, the motions. One cannot determine the flowfield unless one knows the motion of the airplane and one cannot determine the motion unless one knows the flowfield. In this work the PI's have made significant advances in the development of the needed methodology. By expanding the structural deflections in terms of the free-vibration modes, the principal investigators were able to covert the governing partial-differential equations of the structure into a system of ordinary-differential equations. The aerodynamic loads were obtained by refining and extending the vortex-lattice concept. However, it must be noted that both the aerodynamic model and the structural models used in the examples can be changed, by simply changing subroutines in the general code, without changing the general approach. DTIC

N94-17412# Air Force Inst. of Tech., Wright-Patterson AFB, OH.

A COMPARATIVE STUDY OF ANALOG AND DIGITAL CONTROL LAWS FOR THE UMCSL TRUSS M.S. Thesis

Anthony M. Mitchell 1992 157 p

(AD-A267980; AFIT/CI/CIA-93-008) Avail: CASI HC A08/MF A02

This thesis is based on research conducted at the University of Washington Department of Aeronautics and Astronautics Control Systems Laboratory (UWCSL). The UWCSL 20-bay planar truss is a replica of an experimental testbed at the United States Air Force Academy. Validation and modification of existing finite element models of the truss and the two primary means of structurally-borne actuation, the air jet thrusters and the reaction mass actuators, was accomplished and is discussed. Verification of classical analog controllers to actively suppress vibration of the planar bending modes of the truss using the air jet thruster and reaction mass actuators in independent and in hybrid configurations is reported in this thesis. The discretization and digitization of the classical control law was accomplished and the results of computer simulation, linear and non-linear, and experimental testing are reported. A comparison of the performance of the analog and the digital control laws is reported. The design of an optimal controller for the reaction mass actuators utilizing Linear Quadratic (LQ) techniques is reported, and includes non-linear simulation. Simulation of hybrid actuation utilizing the optimal reaction mass actuator control law and the classical air jet thruster controllers is also reported. Recommendations for future study based upon both the hardware implementation and the computer simulation are suggested in the conclusions of this thesis. DTIC

09 RESEARCH AND SUPPORT FACILITIES (AIR)

Includes airports, hangars and runways; aircraft repair and overhaul facilities; wind tunnels; shock tubes; and aircraft engine test stands.

For related information see also *14 Ground Support Systems and Facilities (Space).*

N94-14908# Army Construction Engineering Research Lab., Champaign, IL.

VIBRO-ACOUSTIC ANALYSIS OF AN AIRCRAFT MAINTENANCE DOCK Final Report

James Wilcoski and Louis Sutherland Aug. 1992 253 p

(Contract MIPR-ENM9486)

(AD-A266778; CERL-TR-FM-92/03) Avail: CASI HC A12/MF A03

This report documents an analysis of the effects of high-level acoustic environments on an Aircraft Maintenance Dock (AMD) designed for the U.S. Air Force by the U.S. Army Corps of Engineers. The analysis includes detailed estimation of the maximum sound levels inside the facility, identification of facility components that are potentially sensitive to high-level vibro-acoustic loads, and a summary of design considerations appropriate for this environment. Several critical components of the AMD were analyzed. Design modifications have been recommended as a result of this analysis for this facility, including increases in ductwork thickness, a new ductwork joint design, and vibration isolation for ductwork, exhaust fans, pipe systems, light fixtures, and wind truss supports. A summary of recommended design practices to minimize potential structural damage or equipment malfunction due to the high vibro-acoustic environments was developed. The type of steel construction to be employed for this facility is not normally exposed to high-intensity vibro-acoustic loading. However, if proper consideration is given to the vibro-acoustic loads specified here for building design and qualifications of internal equipment, the planned use of the facility should not be significantly impaired. DTIC

N94-15117*# MCAT Inst., San Jose, CA.

DEVELOPMENT OF A QUIET SUPERSONIC WIND TUNNEL WITH A CRYOGENIC ADAPTIVE NOZZLE Progress Report

Stephen W. D. Wolf Oct. 1993 138 p Original contains color illustrations

(Contract NCC2-604)

(NASA-CR-194548; NAS 1.26:194548; MCAT-93-19) Avail: CASI HC A07/MF A02; 6 functional color pages

The main objective of this work is to develop an interim Quiet (low-disturbance) supersonic wind tunnel for the NASA-Ames Fluid Mechanics Laboratory (FML). The main emphasis is to bring on-line a full-scale Mach 1.6 tunnel as rapidly as possible to impact the NASA High Speed Research Program (HSRP). The development of a cryogenic adaptive nozzle and other sophisticated features of the tunnel will now happen later, after the full scale wind tunnel is in operation. The work under this contract for the period of this report can be summarized as follows: provide aerodynamic design requirements for the NASA-Ames Fluid Mechanics Laboratory (FML) Laminar Flow Supersonic Wind Tunnel (LFSWT); research design parameters for a unique Mach 1.6 drive system for the LFSWT using an 1/8th-scale Proof-of-Concept (PoC) supersonic wind tunnel; carry out boundary layer transition studies in PoC to aid the design of critical components of the LFSWT; appraise the State of the Art in quiet supersonic wind tunnel design; and help develop a supersonic research capability within the FML particularly in the areas of high speed transition measurements and schlieren techniques. The body of this annual report summarizes the work of the Principal Investigator. Derived from text

N94-15325* National Aeronautics and Space Administration, Washington, DC.

ROTORCRAFT RESEARCH (Videotape)

Jun. 1986 Videotape: 2 min. 40 sec. playing time, in color, with sound

(NASA-TM-109452; NONP-VT-93-190249) Avail: CASI VHS A01/BETA A22

This document describes wind tunnel testing and computer modeling done on the rotorcraft prior to building the final aircraft. CASI

N94-15543# Aeronautical Research Labs., Melbourne (Australia).
A MICROPROCESSOR CONTROLLER FOR A TOWING TANK DRIVE AND FLOW VISUALISATION SYSTEM
C. W. Sutton, D. T. Hourigan, and P. S. Woods Mar. 1993 34 p
(AD-A267087; ARL-TN-24; DODA-AR-007-087) Avail: CASI HC A03/MF A01

This paper describes a microprocessor controlled system. The system enables test models to be towed at a predetermined constant velocity through water in a towing tank and provides camera trigger control for recording flow visualization. DTIC

N94-15794*# National Aeronautics and Space Administration. Langley Research Center, Hampton, VA.
WALL INTERFERENCE AND BOUNDARY SIMULATION IN A TRANSONIC WIND TUNNEL WITH A DISCRETELY SLOTTED TEST SECTION
Jassim A. Al-Saadi Washington Sep. 1993 75 p
(RTOP 505-59-54-01)
(NASA-TP-3334; L-16973; NAS 1.60:3334) Avail: CASI HC A04/MF A01

A computational simulation of a transonic wind tunnel test section with longitudinally slotted walls is developed and described herein. The nonlinear slot model includes dynamic pressure effects and a plenum pressure constraint, and each slot is treated individually. The solution is performed using a finite-difference method that solves an extended transonic small disturbance equation. The walls serve as the outer boundary conditions in the relaxation technique, and an interaction procedure is used at the slotted walls. Measured boundary pressures are not required to establish the wall conditions but are currently used to assess the accuracy of the simulation. This method can also calculate a free-air solution as well as solutions that employ the classical homogeneous wall conditions. The simulation is used to examine two commercial transport aircraft models at a supercritical Mach number for zero-lift and cruise conditions. Good agreement between measured and calculated wall pressures is obtained for the model geometries and flow conditions examined herein. Some localized disagreement is noted, which is attributed to improper simulation of viscous effects in the slots. Author

N94-15819*# National Aeronautics and Space Administration. Lewis Research Center, Cleveland, OH.
NASA LEWIS 9- BY 15-FOOT LOW-SPEED WIND TUNNEL USER MANUAL
Ronald H. Soeder Jul. 1993 50 p
(RTOP 505-62-84)
(NASA-TM-106247; E-7968; NAS 1.15:106247) Avail: CASI HC A03/MF A01

This manual describes the 9- by 15-Foot Low-Speed Wind Tunnel at the Lewis Research Center and provides information for users who wish to conduct experiments in this atmospheric facility. Tunnel variables such as pressures, temperatures, available tests section area, and Mach number ranges (0.05 to 0.20) are discussed. In addition, general support systems such as air systems, hydraulic system, hydrogen system, laser system, flow visualization system, and model support systems are described. Instrumentation and data processing and acquisition systems are also discussed. Author

N94-15847 Wright Lab., Wright-Patterson AFB, OH.
DESIGN OF ROUND-TO-SQUARE TRANSITION SECTION; ANALYSIS AND COMPUTER CODE Interim Report, 1 Dec. 1992 - 31 Jan. 1993
Tzong H. Chen and Abdollah S. Nejad Jan. 1993 19 p Limited Reproducibility: More than 20% of this document may be affected by microfiche quality
(AF Proj. 2308)
(AD-A267173; WL-TR-93-2054) Avail: Issuing Activity (Defense Technical Information Center (DTIC))

A generalized analytical form of the surface of a transition section which interfaces round and square cross sections of a wind tunnel is presented. Also included is a listing of the computer code which generates the surface coordinates in the format required by the vax computer at the Air Force Machine Shop at Wright-Patterson Air Force Base. DTIC

N94-15856 Aeronautical Research Labs., Melbourne (Australia).
FLIGHT INSTRUMENT SOFTWARE FOR THE F/A-18 RESEARCH SIMULATOR
Y. Y. Link Mar. 1993 26 p Limited Reproducibility: More than 20% of this document may be affected by microfiche quality
(AD-A267170; ARL-TN-17; DODA-AR-006-680) Avail: Issuing Activity (Defense Technical Information Center (DTIC))

The standby flight instruments are replicated on two high resolution raster displays for the F/A-18 research simulator. A software package was developed using NOVA*CG1, an implementation of the CGI graphics standard, to control a MVME393 multi-channel graphics controller. The software is written in C for the Motorola MVME147 single board computer under the UNIX System V/68 operating system. Increased performance is achieved by decomposing the instrument dial pointers into a number of trapezoids, and storing these as device level command lists. DTIC

N94-17263# Wichita State Univ., KS. National Inst. for Aviation Research.
DESIGN OF NON-SLED SETUP TO MEASURE HEAD INJURY CRITERIA
Hamid M. Lankarani and Sanjeev Aravinthan 1993 117 p
(NIAR-92-20) Avail: CASI HC A06/MF A02

Injury assessment measurements for important body regions are critical issues in the evaluation of occupant protection systems. In this project a new method is designed and developed to evaluate the head injury criteria. Various methods are prevalent in analyzing a head injury. However, these methods are found to be more complex, time consuming, and expensive. A typical method is the 'sled test' which is followed universally to mimic occupant kinematics in frontal crash. In this study, three methods of 'non-sled' test setup were designed to measure head injury criteria in a more simple, reliable, and cost-effective way. In addition to the above, we firmly believe these methods are more versatile and can deliver more accurate results. Author (revised)

N94-17403# Aerospace Medical Research Labs., Brooks AFB, TX. Human Resources Directorate.
THEORETICAL IMPLICATIONS AND EMPIRICAL FINDINGS ON INSTRUCTIONAL CONTROL AND PART-WHOLE-TASK TRAINING Final Report, Jan. 1992 - Apr. 1993
Joseph S. Mattoon and Bernell J. Edwards Jun. 1993 35 p
(AF Proj. 1123)
(AD-A267826; AL/HR-TR-1993-0089) Avail: CASI HC A03/MF A01

A review of the literature and two experiments were conducted to examine instructional control and part-whole-task training methods applied to simulation training. The literature and results of the experiments indicate that learner-controlled systems are probably less effective than those that use computer programming to automatically adjust instructional support according to the learners' progress during practice activities Also, part-task training methods may facilitate the effectiveness of instructional control by reducing the complexity of performance measures and en route learning tasks. DTIC

N94-17405# Naval Civil Engineering Lab., Port Hueneme, CA.
STRUCTURED FINITE VOLUME MODELING OF US NAVY AIRCRAFT ENGINE TEST CELLS TASK 2: TURBOPROP ENGINE, VOLUME 1 Final Report, 1990 - Sep. 1992
P. L. Daley and W. A. Mahaffey Jun. 1993 59 p
(Contract N47408-91-C-1228)
(AD-A267833; NCEL-CR-93-003-Vol-1) Avail: CASI HC A04/MF A01

This report presents results of the numerical simulation of a U.S. Naval turboprop test cell facility. The ultimate purpose of this simulation was to provide the Navy with a numerical model to be used for the evaluation of the aerothermal performance of test cells. This simulation was performed using the structured finite volume (SFV) computer code. A description of the physical model, mathematical details, boundary conditions, and results of the study are presented and covered in Volume 1. Volume 2, Code Documentation and Listings, provides a copy of the input files developed for the modeling of turboprop test cells. DTIC

N94-17432# Adaptive Research Corp., Huntsville, AL.
STRUCTURED FINITE VOLUME MODELING OF US NAVY AIRCRAFT ENGINE TEST CELLS. TASK 1: TURBOSHAFT ENGINE, VOLUME 1 Final Report, Dec. 1990 - Sep. 1992
P.L. Daley and W.A. Mahaffey Jun. 1993 59 p
(Contract N47408-91-C-1228)
(AD-A268176; NCEL-CR-93-002-Vol-1) Avail: CASI HC A04/MF A01

This report presents results of the numerical simulation of a U.S. Naval turboshaft test cell facility. The ultimate purpose of this simulation was to provide the Navy with a numerical model to be used for the evaluation of the aerothermal performance of test cells. This simulation was performed using the structured finite volume (SFV) computer code. A description of the physical model, mathematical details, boundary conditions, and results of the study are presented and covered in Volume 1. Volume 2, Code Documentation and Listings, provides a copy of the input files developed for the modeling of turboshaft test cells. DTIC

N94-17508# Adaptive Research Corp., Huntsville, AL.
STRUCTURED FINITE VOLUME MODELING OF US NAVY AIRCRAFT ENGINE TEST CELLS. TASK 1: TURBOSHAFT ENGINE-CODE DOCUMENTATION AND LISTINGS, VOLUME 2 Final Report, Dec. 1990 - Sep. 1992
P.L. Daley and W.A. Mahaffey Jun. 1993 147 p
(Contract N47408-91-C-1228)
(AD-A268177; NCEL-CR-93-002-Vol-2) Avail: CASI HC A07/MF A02

This report presents results of the numerical simulation of a U.S. Naval turboshaft test cell facility. The ultimate purpose of this simulation was to provide the Navy with a numerical model to be used for the evaluation of the aerothermal performance of test cells. This simulation was performed using the structured finite volume (SFV) computer code. A description of the physical model, mathematical details, boundary conditions, and results of the study are presented and covered in Volume 1. Volume 2, Code Documentation and Listings, provides a copy of the input files developed for the modeling of turboshaft test cells. DTIC

N94-17569# Adaptive Research Corp., Huntsville, AL.
STRUCTURED FINITE VOLUME MODELING OF US NAVY AIRCRAFT ENGINE TEST CELLS. TASK 2: TURBOPROP ENGINE. VOLUME 2: CODE DOCUMENTATION AND LISTINGS Final Report, Dec. 1990 - Sep. 1992
P. L. Daley and W. A. Mahaffey Jun. 1993 135 p
(Contract N47408-91-C-1228)
(AD-A268386; NCEL-CR-93-003-Vol-2) Avail: CASI HC A07/MF A02

This report presents results of the numerical simulation of a U.S. Naval turboprop test cell facility. The ultimate purpose of this simulation was to provide the Navy with a numerical model to be used for the evaluation of the aerothermal performance of test cells. This simulation was performed using the structured finite volume (SFV) computer code. A description of the physical model, mathematical details, boundary conditions, and results of the study are presented and covered in Volume 1. Volume 2, Code Documentation and Listings, provides a copy of the input files developed for the modeling of turboprop test cells. DTIC

N94-15062# Catania Astrophysical Observatory (Italy).
A TEST FACILITY TO CALIBRATE EUV DETECTORS
Giovanni Bonanno, Giampiero Naletto (Padua Univ., Italy.), and Giuseppe Tondello (Padua Univ., Italy.) *In* ESA, Proceedings of an ESA Symposium on Photon Detectors for Space Instrumentation Dec. 1992 p 233-236
(For primary document see N94-15025 03-19)
Copyright Avail: CASI HC A01/MF A04

N94-15123# Netherlands Association of Aeronautical Engineers, Amsterdam.
THE FUTURE OF SCHIPHOL: GROWTH WITHIN BOUNDARIES [DE TOEKOMST VAN SCHIPHOL: GROEIEN BINNEN GRENZEN]
R. denBesten *In* NAL, Symposium on the Future of Aeronautics in the Netherlands 1991 16 p In DUTCH (For primary document see N94-15120 03-01)
Avail: CASI HC A03/MF A02

N94-15129# National Aerospace Lab., Amsterdam (Netherlands).
EXPECTATIONS FOR THE FUTURE OF THE NATIONAL AEROSPACE LABORATORY [TOEKOMSTVERWACHTINGEN NATIONAAL LUCHT- EN RUIMTEVAARTLABORATORIUM]
B. M. Spee *In its* Symposium on the Future of Aeronautics in the Netherlands 1991 17 p In DUTCH (For primary document see N94-15120 03-01)
Avail: CASI HC A03/MF A02

12 ASTRONAUTICS (GENERAL)

For extraterrestrial exploration see *91 Lunar and Planetary Exploration.*

N94-15000# National Space Development Agency, Ibaraki (Japan). Launch Vehicle and Satellite System Lab.
PRE-PHASE A STUDY REPORT OF LUNAR POLAR ORBITER [TSUKI SHUUKAI KANSOKU EISEI NO SHISUTEMU KENTOU]
Takeshi Wazoe Nov. 1992 91 p In Japanese
(NASDA-TK-SS0440; JTN-93-80450) Avail: CASI HC A05/MF A01

An overview is presented of a conceptual study of a lunar revolving satellite whose missions are to conduct the following: topographical, geological, and crust explorations of the moon; water resource explorations at lunar polar region; and a lunar surface landing experiment. The study was conducted for two cases: a two ton observation satellite and an observation satellite plus landing experiment vehicle. It was concluded that transfer to a development phase was feasible in both cases. The topics covered include the following: mission study; mission analysis, system study, and analysis of lunar revolving observation satellite; subsystem study of lunar revolving observation satellite; study, analysis, and subsystem study of landing experiment system; and study of the development program.
Author (NASDA)

N94-15308* National Aeronautics and Space Administration. Goddard Space Flight Center, Greenbelt, MD.
GAS HIGHLIGHTS, 1988 (Videotape)
Feb. 1989 Videotape: 30 min. playing time, in color, with sound
(NASA-TM-109600; NONP-VT-93-190398) Avail: CASI VHS A01/BETA A22

The videotape shows highlights of GSFC's involvement in the Get Away Special program during the 1988 calendar year. CASI

N94-15469* National Aeronautics and Space Administration. Lyndon B. Johnson Space Center, Houston, TX.
STS-26 CREW PARTICIPATION IN MEETINGS (Videotape)
Aug. 1988 Videotape: 13 min. playing time, in color, with sound
(NASA-TM-109519; NONP-VT-93-190316) Avail: CASI VHS A01/BETA A22

This videotape shows the crew attending and participating in a Payloads Operation Working Group (POWG) meeting, a Flight Rules meeting, and a Flight Operation Review (FOR) meeting. CASI

N94-15471* National Aeronautics and Space Administration. Lyndon B. Johnson Space Center, Houston, TX.
MARS ROVER SAMPLE RETURN MISSION (Videotape)
Sep. 1988 Videotape: 5 min. playing time, in color, with sound
(NASA-TM-109521; NONP-VT-93-190318) Avail: CASI VHS A01/BETA A22

This videotape was created by NASA JSC's Missions Planning Division to depict a future unmanned Mars mission. CASI

N94-15500* National Aeronautics and Space Administration. Lewis Research Center, Cleveland, OH.
ASTRONAUTS NUMBER 2 (Videotape)
Sep. 1988 Videotape: 29 min. playing time, in color, with sound
(NASA-TM-109429; NONP-VT-93-190226) Avail: CASI VHS A01/BETA A22

The story of Alan Shepard's May 1961 suborbital flight is presented. This is a re-release of 'The Flight of Freedom 7'. CASI

N94-15501* National Aeronautics and Space Administration. Lewis Research Center, Cleveland, OH.
ASTRONAUTS NUMBER 3 (Videotape)
Sep. 1988 Videotape: 28 min. 30 sec. playing time, in color, with sound (NASA-TM-109430; NONP-VT-93-190227) Avail: CASI VHS A01/BETA A22

John Glenn's flight into space is reviewed. This is a re-release of 'The Flight of Friendship 7'. CASI

N94-16584# European Space Agency. European Space Research and Technology Center, ESTEC, Noordwijk (Netherlands).
LOOKING AT SCIENCE ON BOARD EURECA
Olivier Minster, Louisa Innocenti, Dick Mesland, and Stefan Heerd, ed. May 1993 39 p LIMITED REPRODUCIBILITY: More than 20% of this document may be affected by color photographs Original contains color illustrations
(ESA-BR-80; ISBN-92-9092-099-8) Copyright Avail: CASI HC A03/MF A01

The European Retrievable Carrier (Eureca) is the first platform designed to be retrieved from orbit and possibly to be relaunched with a different payload. For its first mission in July 1992, Eureca was deployed from the Space Shuttle Atlantis (flight STS 46) by ESA astronaut and mission specialist, Claude Nicollier. It then used its own propulsion system to transfer to its operational orbit at 508 km where, after commissioning, payload operation started. Since Eureca has been specially designed for investigations in the microgravity environment, this publication concentrates mainly on this aspect of the mission. Microgravity research is a newcomer to the scientific disciplines and is perhaps not very well known to, or understood by, those not directly involved. An explanation of the microgravity environment is presented. This is followed by an explanation of the interest microgravity holds for researchers, and a review of the different scientific fields, Material Sciences, Fluid Physics, Life Sciences, for which investigations have been carried out during the Eureca mission, together with a brief description of the on-board facilities and their flight performances. The last two chapters describe the Space Science and technology experiments carried out during the mission. Derived from text

N94-17306# Air Force Inst. of Tech., Wright-Patterson AFB, OH.
MILITARY SPACE PROGRAMS IN THE PRESS: AN ANALYSIS FOR CHANGE M.S. Thesis
John Kennedy 1993 79 p
(AD-A267799) Avail: CASI HC A05/MF A01

The military space program is not known in any great detail by the general American public. The reasons for this lie in the heavily classified nature of the majority of military space programs. This, in turn, brings the media into conflict with the military. It is a conflict derived from the media's desire to have freedom of access to information vs. national security requirements. DTIC

N94-16362*# National Aeronautics and Space Administration. Lyndon B. Johnson Space Center, Houston, TX.
THE FIRST LUNAR OUTPOST: THE DESIGN REFERENCE MISSION AND A NEW ERA IN LUNAR SCIENCE Abstract Only
Gary E. Lofgren *In* Lunar and Planetary Inst., Twenty-Fourth Lunar and Planetary Science Conference. Part 2: G-M 1993 p 891-892 (For primary document see N94-16173 03-91)
Avail: CASI HC A01/MF A06

N94-17142 European Space Agency. European Space Research and Technology Center, ESTEC, Noordwijk (Netherlands).
SMALL MISSIONS FOR SPACE SCIENCE Abstract Only
H. Olthof *In* CNES, Small Satellites Systems and Services Jan. 1993 p 165 (For primary document see N94-17131 03-18)
Copyright Avail: Issuing Activity (CEPADUES-Editions, 111 rue Nicolas-Vaquelin, 31100 Toulouse, France)

N94-17143 Dornier System G.m.b.H., Friedrichshafen (Germany).
STRATEGY FOR A SMALL SATELLITE PROGRAM AND A PROPOSAL FOR A FIRST MISSION
N. Pailer, G. Hampel, E. Bachor, G. Lippner, and H. Kunow (Kiel Univ., Germany.) *In* CNES, Small Satellites Systems and Services Jan. 1993 p 167-180 (For primary document see N94-17131 03-18)
Copyright Avail: Issuing Activity (CEPADUES-Editions, 111 rue Nicolas-Vaquelin, 31100 Toulouse, France)

N94-17144 Telespazio S.p.A., Rome (Italy).
SMALL SATELLITE MISSIONS TO LONG-PERIOD COMETS
Ettore Perozzi and Eduard M. Pittich (Slovak Academy of Sciences, Bratislava, Czechoslovakia.) *In* CNES, Small Satellites Systems and Services Jan. 1993 p 181-184 (For primary document see N94-17131 03-18)
Copyright Avail: Issuing Activity (CEPADUES-Editions, 111 rue Nicolas-Vaquelin, 31100 Toulouse, France)

N94-17145* Jet Propulsion Lab., California Inst. of Tech., Pasadena.
SMALL SPACECRAFT FOR PLANETARY EXPLORATION
Ross M. Jones *In* CNES, Small Satellites Systems and Services Jan. 1993 p 185-195 (For primary document see N94-17131 03-18)
Copyright Avail: Issuing Activity (CEPADUES-Editions, 111 rue Nicolas-Vaquelin, 31100 Toulouse, France)

13 ASTRODYNAMICS

Includes powered and free-flight trajectories; and orbital and launching dynamics.

N94-15493* National Aeronautics and Space Administration, Washington, DC.
SPACE FLIGHT: THE APPLICATION OF ORBITAL MECHANICS (Videotape)
Dec. 1989 Videotape: 35 min. 30 sec. playing time, in color, with sound (NASA-TM-109424; NONP-VT-93-190221) Avail: CASI VHS A01/BETA A22

This is a primer on orbital mechanics originally intended for college-level physics students. CASI

N94-17010 Air Force Inst. of Tech., Wright-Patterson AFB, OH.
NEIGHBORING EXTREMAL GUIDANCE FOR SYSTEMS WITH PIECEWISE LINEAR CONTROL USING TIME AS THE REFERENCE VARIABLE M.S. Thesis
William A. Libby May 1993 58 p Limited Reproducibility: More than 20% of this document may be affected by microfiche quality
(AD-A267942; AFIT/CI/CIA-93-113) Avail: Issuing Activity (Defense Technical Information Center (DTIC))

A guidance law for the control of a system in the neighborhood of a nominal suboptimal trajectory is developed. The guidance law is demonstrated using a lunar launch problem with constraints at orbit entry. A set of precomputed gains is used by the guidance law to operate on an extremal path in the neighborhood of the suboptimal trajectory. The guidance law and gains are designed to minimize the change in the desired performance index while still satisfying the final path constraints. In the lunar launch problem, the nominal suboptimal trajectory minimizes the final time using piecewise linear control. This trajectory is obtained to provide a nominal control history. The guidance law is found by minimizing the second variation of the suboptimal trajectory performance index subject to the final constraints being satisfied. For the lunar launch problem, the guidance law leads to a set of gains that relates deviations from the suboptimal trajectory to required changes in the nominal control history. The deviations from the suboptimal trajectory, used together with the precomputed gains, determines the change in the nominal control history required to meet the final constraints while minimizing the change in the final time. DTIC

N94-15589*# Deutsches Geodaetisches Forschungsinst., Munich (Germany).
ON THE ACCURACY OF ERS-1 ORBIT PREDICTIONS
Rolf Koenig, H. Li, Franz-Heinrich Massmann, J. C. Raimondo, C. Rajasenan, and C. Reigber *In* NASA. Goddard Space Flight Center, Eighth International Workshop on Laser Ranging Instrumentation Jun. 1993 8 p Prepared in cooperation with Deutsche Geodaetische Kommission, Munich, Germany (For primary document see N94-15552 03-19)
Avail: CASI HC A02/MF A06

N94-15591*# Satellite Laser Ranger Group, Hailsham (England).
TIMEBIAS CORRECTIONS TO PREDICTIONS
Roger Wood and Philip Gibbs *In* NASA. Goddard Space Flight Center, Eighth International Workshop on Laser Ranging Instrumentation Jun. 1993 6 p (For primary document see N94-15552 03-19)
Avail: CASI HC A02/MF A06

N94-17134 Dassault Aviation, Istres (France). Centre Spatiale.
LOW EARTH ORBIT CONSTELLATIONS: ORBIT CONTROL OR NOT
Jose Radzik and Gerard Maral (Ecole Nationale Superieure des Telecommunications, Toulouse, France.) *In* CNES, Small Satellites Systems and Services Jan. 1993 p 61-70 (For primary document see N94-17131 03-18)
Copyright Avail: Issuing Activity (CEPADUES-Editions, 111 rue Nicolas-Vaquelin, 31100 Toulouse, France)

14 GROUND SUPPORT SYSTEMS AND FACILITIES (SPACE)

Includes launch complexes, research and production facilities; ground support equipment, e.g., mobile transporters; and simulators.

For related information see also *09 Research and Support Facilities (Air).*

N94-15236* National Aeronautics and Space Administration, Washington, DC.
HUMAN FACTOR STUDIES (Videotape)
Aug. 1985 Videotape: 2 min. 55 sec. playing time, in color, with sound (NASA-TM-109665; NONP-VT-93-190463) Avail: CASI VHS A01/BETA A22

This video tape looks at research done in the Manned Vehicle Systems Research Facility at ARC to investigate issues related to aircraft pilot and crew performance. CASI

N94-15265* National Aeronautics and Space Administration. Lyndon B. Johnson Space Center, Houston, TX.
STS-30 SUITED ASCENT TRAINING IN FIXED BASE SMS (Videotape)
Apr. 1989 Videotape: 10 min. 59 sec. playing time, in color, with sound (NASA-TM-109581; NONP-VT-93-190379) Avail: CASI VHS A01/BETA A22

The Space Shuttle crew is shown training for the ascent portion of the mission in the fixed base/SMS. CASI

N94-15270* National Aeronautics and Space Administration. Goddard Space Flight Center, Greenbelt, MD.
GFSC-TV DEMO TAPE (Videotape)
Jan. 1989 Videotape: 8 min. 20 sec. playing time, in color, with sound (NASA-TM-109586; NONP-VT-93-190384) Avail: CASI VHS A01/BETA A22

This demonstration tape produced by and for the Goddard Space Flight Center Television facility shows some of the capabilities of this state of the art facility that are available to projects at Goddard. CASI

N94-15273* National Aeronautics and Space Administration. Goddard Space Flight Center, Greenbelt, MD.
STOCK FOOTAGE OF GODDARD SPACE FLIGHT CENTER AND HEADQUARTERS (Videotape)
Jun. 1989 Videotape: 25 min. playing time, in color, with sound (NASA-TM-109589; NONP-VT-93-190387) Avail: CASI VHS A01/BETA A22

Produced for Century Teleproductions in Boston, MA this video is a camera master showing various views, with natural sound, of the space flight center during the late spring. This finished footage is used in an interactive laser disc presentation that is used at Kennedy Space Center Visitor Center. CASI

N94-15299* National Aeronautics and Space Administration. Lyndon B. Johnson Space Center, Houston, TX.
THE 61-M LONG DURATION SIM VIDEO HIGHLIGHTS RESOURCE TAPE (Videotape)
Jan. 1988 Videotape: 37 min. playing time, in color, with sound (NASA-TM-109569; NONP-VT-93-190367) Avail: CASI VHS A01/BETA A22

This video shows the crew on the middeck mockup during the long duration sim. The video also shows the FCR during the sim. CASI

N94-15301* National Aeronautics and Space Administration. Lyndon B. Johnson Space Center, Houston, TX.
STS-30 MAGELLAN DEPLOY SIM IN SMS AND MOCR (Videotape)
Feb. 1989 Videotape: 9 min. playing time, in color, with sound (NASA-TM-109571; NONP-VT-93-190369) Avail: CASI VHS A01/BETA A22

The Space Shuttle crew is shown in SMS training for the Magellan spacecraft deploy. Intercuts of the MOCR are included. CASI

N94-15318* National Aeronautics and Space Administration. Ames Research Center, Moffett Field, CA.
MANNED VEHICLE SYSTEMS RESEARCH FACILITY (Videotape)
Mar. 1989 Videotape: 8 min. playing time, in color, with sound (NASA-TM-109650; NONP-VT-93-190448) Avail: CASI VHS A01/BETA A22

This videotape presents a guided tour of the Manned Vehicle Systems Research Facility (MVSRF) at ARC. CASI

N94-15331* National Aeronautics and Space Administration. Lyndon B. Johnson Space Center, Houston, TX.
STS-26 IUS AND LATCH CONTINGENCY TRAINING (Videotape)
Mar. 1988 Videotape: 16 min. 53 sec. playing time, in color, with sound (NASA-TM-109561; NONP-VT-93-190359) Avail: CASI VHS A01/BETA A22

Astronauts Nelson and Lounge are shown in the WETF while astronauts Covey and Hilmer observe topside. CASI

N94-15332* National Aeronautics and Space Administration. Lyndon B. Johnson Space Center, Houston, TX.
STS-26 GENERIC INTEGRATED IUS DEPLOY SIMULATION (Videotape)
Feb. 1988 Videotape: 16 min. 10 sec. playing time, in color, with sound (NASA-TM-109562; NONP-VT-93-190360) Avail: CASI VHS A01/BETA A22

The crew is shown in the SMS during TDRS deploy training. It includes intercuts of the MOCR. CASI

N94-15333* National Aeronautics and Space Administration. Lyndon B. Johnson Space Center, Houston, TX.
STS-26 EVA RESCUE TRAINING (Videotape)
Jul. 1988 Videotape: 15 min. playing time, in color, with sound (NASA-TM-109563; NONP-VT-93-190361) Avail: CASI VHS A01/BETA A22

This video shows astronauts Covey, Hilmers, and Hauck training in SES. It involves a simulated EVA rescue using the RMS. A computer-generated image is used to simulate the movement of a free-floating astronaut for grapple with the arm. CASI

N94-15386* National Aeronautics and Space Administration. Lyndon B. Johnson Space Center, Houston, TX.
BUILDING 46 GRAND OPENING (Videotape)
Feb. 1989 Videotape: 5 min. playing time, in color, with sound (NASA-TM-109524; NONP-VT-93-190321) Avail: CASI VHS A01/BETA A22

This video tape shows the grand opening ceremonies of Building 46 Central Computer Facility at the NASA Johnson Space Center. CASI

N94-15393* National Aeronautics and Space Administration. Lyndon B. Johnson Space Center, Houston, TX.
LUNAR CURATORIAL FACILITY RESOURCE (Videotape)
Jul. 1989 Videotape: 6 min. 46 sec. playing time, in color, with sound (NASA-TM-109531; NONP-VT-93-190328) Avail: CASI VHS A01/BETA A22

This video tape shows daily activities in the Lunar Curatorial Facility. The video covers the various studies being conducted on lunar dust, rock, and core samples brought back by Apollo crews. CASI

N94-15442* National Aeronautics and Space Administration. Lyndon B. Johnson Space Center, Houston, TX.
STS-31 HUBBLE SPACE TELESCOPE DEPLOY: TRAINING AT MDF WITH HAWLEY (Videotape)
Apr. 1990 Videotape: 7 min. 30 sec. playing time, in color, with sound (NASA-TM-109481; NONP-VT-93-190278) Avail: CASI VHS A01/BETA A22

Astronaut Steve Hawley is shown working with the Hubble Space Telescope mockup on the Remote Manipulator System mockup above the Manipulator Development Facility (MDF). CASI

N94-15449* National Aeronautics and Space Administration. Lyndon B. Johnson Space Center, Houston, TX.
STS-31 HST DEPLOY SIM IN SMS AND MOCR (Videotape)
Apr. 1990 Videotape: 15 min. playing time, in color, with sound (NASA-TM-109482; NONP-VT-93-190279) Avail: CASI VHS A01/BETA A22

This video shows the crew on a simulated middeck during the Hubble Space Telescope (HTS) deploy simulation. Intercut from the MOCR is included. CASI

N94-15450* National Aeronautics and Space Administration. Lyndon B. Johnson Space Center, Houston, TX.
STS-31 CREW TRAINING INFLIGHT MAINTENANCE AND BAILOUT EXERCISES IN CCT AND WFTF (Videotape)
Mar. 1990 Videotape: 19 min. playing time, in color, with sound (NASA-TM-109483; NONP-VT-93-190280) Avail: CASI VHS A01/BETA A22

The crew is shown in the CCT practicing on orbit maintenance tasks, along with bailout procedures. The crew is also shown practicing water survival techniques in the Weightless Environment Training Facility (WETF). CASI

N94-15451* National Aeronautics and Space Administration. Lyndon B. Johnson Space Center, Houston, TX.
STS-31 CREW TRAINING: FIREFIGHTING, FOOD TASTING, EVA PREP AND POST (Videotape)
Mar. 1990 Videotape: 17 min. 35 sec. playing time, in color, with sound (NASA-TM-109484; NONP-VT-93-190281) Avail: CASI VHS A01/BETA A22

The Space Shuttle crew is shown lighting a pond of gasoline and then performing firefighting tasks. The crew is also shown tasting food including lemonade, chicken casserole, and tortillas, and performing extravehicular activity (EVA) equipment checkouts in the CCT middeck and airlock. CASI

N94-15452* National Aeronautics and Space Administration. Lyndon B. Johnson Space Center, Houston, TX.
STS-40 CREW DURING SPACELAB SIM (Videotape)
Aug. 1990 Videotape: 12 min. 50 sec. playing time, in color, with sound (NASA-TM-109493; NONP-VT-93-190290) Avail: CASI VHS A01/BETA A22

Crew members working in the SLS-1 simulator are shown. Activities in the module mockup include work with the cardiovascular equipment, Body Mass Measurement Device, and Jellyfish experiment. Author (revised)

N94-15467* National Aeronautics and Space Administration. Lyndon B. Johnson Space Center, Houston, TX.
RICHARDS, DICK: TRAINING CLIP (Videotape)
Jul. 1989 Videotape: 12 min. playing time, in color, with sound (NASA-TM-109503; NONP-VT-93-190300) Avail: CASI VHS A01/BETA A22

Astronaut Richards is shown during his ASCAN training, including weightless environment training facility (WETF) training and various simulations. CASI

N94-15473* National Aeronautics and Space Administration. Lyndon B. Johnson Space Center, Houston, TX.
COMMITMENT TO CHALLENGE (Videotape)
May 1988 Videotape: 13 min. playing time, in color, with sound (NASA-TM-109523; NONP-VT-93-190320) Avail: CASI VHS A01/BETA A22

This videotape gives a brief overview of the NASA JSC including the following: mission control, mission operations, and mission planning; new scientific and technologies developments; and educational programs. CASI

N94-15474* National Aeronautics and Space Administration. Lyndon B. Johnson Space Center, Houston, TX.
STS-26 LONG DURATION SIMULATION: CREW ENTERING SMS (Videotape)
Sep. 1988 Videotape: 2 min. 45 sec. playing time, in color, with sound (NASA-TM-109560; NONP-VT-93-190358) Avail: CASI VHS A01/BETA A22

This video shows the crew entering the SMS for the long-duration SIM in preparation for their flight. CASI

N94-15517* National Aeronautics and Space Administration. Lyndon B. Johnson Space Center, Houston, TX.
STS-41 CREW TRAINING BAILOUT IN CCT, 16mm CAMERA CLASS EVA PREP, HABITATION EQUIPMENT PROCEDURES, AND FOOD TASTING (Videotape)
Sep. 1990 Videotape: 17 min. 27 sec. playing time, in color, with sound (NASA-TM-109517; NONP-VT-93-190314) Avail: CASI VHS A01/BETA A22

This videotape shows the crew during several training exercises including work in the CCT, photography class, and food tasting. CASI

N94-16025# Mitre Corp., McLean, VA. Center for Advanced Aviation System Development.
TEST PLAN FOR THE EVALUATION OF THE INITIAL CAPABILITY OF THE NATIONAL SATELLITE TEST BED: PHASE 1D Final Report
Daniel G. OLaughlin Aug. 1993 48 p
(Contract DTFA01-93-C-00001)
(DOT/FAA/RD-93/20; MTR-93W0000075) Avail: CASI HC A03/MF A01

This document contains a plan for testing Wide-area Differential GPS (WDGPS) and Wide-area Integrity Broadcast (Wig) concepts in the National Satellite Test Bed (NSTB). This report documents the test plan for the next test subphase (ID), and covers the flight test definition, data collection, reduction and analysis, organizational responsibilities, and schedule. The specific objectives of the testing during this subphase are to: obtain data on the time to detect, transmit, process, and receive an integrity alarm using a satellite broadcast relay of the alarm from the ground to the test aircraft; obtain preliminary data on the performance of WDGPS, and specifically of ionospheric corrections for WDGPS using a satellite broadcast of the differential corrections; and compare the performance achieved with WDGPS with that of Local-Area Differential GPS (LDGPS). Author (revised)

N94-17548# Deutsche Forschungsanstalt fuer Luft- und Raumfahrt, Cologne (Germany). Abt. Biophysik.
DESIGN OF AN EXPERIMENT HARDWARE FOR THE ESA SPACE FACILITY BIOPAN Thesis - Fachhochschule Aachen [DAS DESIGN EINER FLUGHARDWARE FUR EIN WELTRAUMEXPERIMENT AUF DER ESA-EINRICHTUNG BIOPAN]
Rene Delonge Dec. 1992 106 p In GERMAN
(DLR-FB-93-06; ETN-93-94621) Avail: CASI HC A06/MF A02

The design of sample carriers, for an experiment concerning the exposure of biological systems to the space environment, which will be part of the multiuser experiment facility called BIOPAN (Biological Pan), is described. BIOPAN is a circular, pan shaped container, which will be mounted on the sphere shaped descent module of the BION satellite assembly. The lid of this container will be opened after attaining the proper orbit to expose all accommodated experiments. The single sample carriers described are of a regular hexagonal shape and were designed in respect to the available area on the experiment platform of the container. A quartz disc on top and a circular membrane inside with corresponding horizontal and vertical air shafts ensure the exposure to the characteristic space environment. ESA

N94-15600*# Institut fuer Angewandte Geodaesie, Koetzing (Germany). Forschungseinrichtung Satellitengeodaesie.
LLR: ACTIVITIES IN WETTZELL

Ulrich Schreiber, J. Mueller (Technische Univ., Munich, Germany.), Reiner Dassing, N. Brandl, K. H. Haufe, G. Herold, R. Kahn, K. Roettcher, and R. Stoeger *In* NASA. Goddard Space Flight Center, Eighth International Workshop on Laser Ranging Instrumentation Jun. 1993 3 p (For primary document see N94-15552 03-19)
Avail: CASI HC A01/MF A06

N94-15601*# Bendix Field Engineering Corp., Seabrook, MD.
MATERA LASER RANGING OBSERVATORY (MLRO): AN OVERVIEW
Thomas K. Varghese, Winfield M. Decker, Henry A. Crooks, and Giuseppe Bianco (Italian Space Agency, Matera.) *In* NASA. Goddard Space Flight Center, Eighth International Workshop on Laser Ranging Instrumentation Jun. 1993 5 p (For primary document see N94-15552 03-19)
Avail: CASI HC A01/MF A06

N94-15602*# Department of Administrative Services, Canberra (Australia). Orroral Geodetic Observatory.
PERFORMANCE OF THE UPGRADED ORRORAL LASER RANGING SYSTEM
John M. Luck *In* NASA. Goddard Space Flight Center, Eighth International Workshop on Laser Ranging Instrumentation Jun. 1993 25 p (For primary document see N94-15552 03-19)
Avail: CASI HC A03/MF A06

N94-15604*# Polish Academy of Sciences, Kornik. Space Research Center.
UPGRADING OF THE BOROWIEC LASER STATION
Stanislaw Schillak, E. Butkiewicz, and J. Wiktorowski *In* NASA. Goddard Space Flight Center, Eighth International Workshop on Laser Ranging Instrumentation Jun. 1993 7 p (For primary document see N94-15552 03-19)
Avail: CASI HC A02/MF A06

N94-15605*# Shanghai Observatory (China).
DEVELOPMENT OF SHANGHAI SATELLITE LASER RANGING STATION
Fu-Min Yang, De-Tong Tan, Chi-Kun Xiao, Wan-Zhen Chen, J.-H. Zhang, Z.-P. Zhang, Wen-Hu Lu, Z.-Q. Hu, W.-F. Tang, and J.-P. Chen *In* NASA. Goddard Space Flight Center, Eighth International Workshop on Laser Ranging Instrumentation Jun. 1993 7 p Sponsored in part by Chinese National Science Foundation and Chinese Astronomical Committee (For primary document see N94-15552 03-19)
Avail: CASI HC A02/MF A06

N94-15606*# Institut fuer Angewandte Geodaesie, Koetzing (Germany). Fundamentalstation Wettzell.
WLRS Status Report
Reiner Dassing, W. Schlueter, and Ulrich Schreiber (Technische Univ., Munich, Germany.) *In* NASA. Goddard Space Flight Center, Eighth International Workshop on Laser Ranging Instrumentation Jun. 1993 3 p (For primary document see N94-15552 03-19)
Avail: CASI HC A01/MF A06

N94-15608*# State Seismological Bureau of China, Beijing. Inst. of Seismology.
NEW PROGRESS OF RANGING TECHNOLOGY AT WUHAN SATELLITE LASER RANGING STATION
Zhiz-Hong Xia, Wen-Wei Ye, and Qing-Fu Cai *In* NASA. Goddard Space Flight Center, Eighth International Workshop on Laser Ranging Instrumentation Jun. 1993 8 p (For primary document see N94-15552 03-19)
Avail: CASI HC A02/MF A06

N94-15609*# Bendix Field Engineering Corp., Seabrook, MD.
TLRS-3 SYSTEM UPGRADES
Richard Eichinger, Grace Cheng, William Crawford, Don Cresswell, Henry A. Crooks, Howard Donovan, David R. Edge, Kenneth S. Emenheiser, William P. Hanrahan, III, and J. Michael Heinick et al *In* NASA. Goddard Space Flight Center, Eighth International Workshop on Laser Ranging Instrumentation Jun. 1993 16 p (For primary document see N94-15552 03-19)
Avail: CASI HC A03/MF A06

N94-15610*# Institut fuer Angewandte Geodaesie, Koetzing (Germany). Fundamentalstation Wettzell der Forschungsgruppe Satellitengeodaesie.
RESULTS OF THE MTLRS-1 UPGRADE
Peter Sperber, L. Amberg, G. Blenski, W. Etling, U. Hessels, R. Motz, and L. Beyer *In* NASA. Goddard Space Flight Center, Eighth International Workshop on Laser Ranging Instrumentation Jun. 1993 9 p (For primary document see N94-15552 03-19)
Avail: CASI HC A02/MF A06

N94-15611*# Institut fuer Angewandte Geodaesie, Koetzing (Germany). Fundamentalstation Wettzell der Forschungsgruppe Satellitengeodaesie.
THE NEW MTLRS-1 RECEIVING SYSTEM
Peter Sperber, U. Hessels, R. Motz, and H.-M. Guether (Hoechst A.G., Frankfurt am Main, Germany.) *In* NASA. Goddard Space Flight Center, Eighth International Workshop on Laser Ranging Instrumentation Jun. 1993 7 p (For primary document see N94-15552 03-19)
Avail: CASI HC A02/MF A06

N94-15612*# Institut fuer Angewandte Geodaesie, Koetzing (Germany). Fundamentalstation Wettzell.
THE NEW MTLRS TRANSMITTING SYSTEM
Peter Sperber, U. Hessels, R. Motz, Wiard Beek (Technische Hogeschool, Delft, Netherlands.), Jacek W. Offierski (Technische Hogeschool, Delft, Netherlands.), and C. VanEs (Technische Hogeschool, Delft, Netherlands.) *In* NASA. Goddard Space Flight Center, Eighth International Workshop on Laser Ranging Instrumentation Jun. 1993 7 p (For primary document see N94-15552 03-19)
Avail: CASI HC A01/MF A06

N94-15613*# Technische Hogeschool, Delft (Netherlands). Observatory for Satellite Geodesy.
TRANSPUTER BASED CONTROL SYSTEM FOR MTLRS
Erik Vermaat, Jacek W. Offierski, Klaus H. Otten, Wiard Beek, C. vanEs, and Peter Sperber (Institut fuer Angewandte Geodaesie, Koetzing, Germany.) *In* NASA. Goddard Space Flight Center, Eighth International Workshop on Laser Ranging Instrumentation Jun. 1993 9 p (For primary document see N94-15552 03-19)
Avail: CASI HC A02/MF A06

N94-15621*# Czech Technical Univ., Prague. Faculty of Nuclear Science.
SATELLITE LASER STATION HELWAN STATUS 1992 Abstract Only
M. Cech, Karel Hamal, Helena Jelinkova, Antonin Novotny, Ivan Prochazka, B. B. Baghos (National Research Inst. of Astronomy and Geophysics, Helwan, Egypt.), Y. Helali (National Research Inst. of Astronomy and Geophysics, Helwan, Egypt.), and M. J. Tawadros (National Research Inst. of Astronomy and Geophysics, Helwan, Egypt.) *In* NASA. Goddard Space Flight Center, Eighth International Workshop on Laser Ranging Instrumentation Jun. 1993 1 p Sponsored in part by Smithsonian Astrophysical Observatory (For primary document see N94-15552 03-19)
(Contracts ERS-1/7831/91; ERS-1/7831/92)
Avail: CASI HC A01/MF A06

N94-15623*# Academy of Sciences, Potsdam (German D.R.).
THE THIRD GENERATION SLR STATION POTSDAM NO. 7836
H. Fischer, Ludwig Grunwaldt, and Reinhart Neubert *In* NASA. Goddard Space Flight Center, Eighth International Workshop on Laser Ranging Instrumentation Jun. 1993 6 p (For primary document see N94-15552 03-19)
Avail: CASI HC A02/MF A06

N94-16150*# McDonnell-Douglas Corp., Huntsville, AL. Spacelab Design Engineering.
THE SPACELAB IPS STAR SIMULATOR
Francis C. Wessling, III *In* Huntsville Association of Technical Societies, TABES 1993: 9th Annual Technical and Business Exhibition and Symposium 1993 4 p (For primary document see N94-16129 03-38)
(Contract NAS8-39400)
(TABES Paper 93-650) Avail: CASI HC A01/MF A03

N94-17154 VEGA Space Systems Engineering Ltd., Harpenden (England).
A PROPOSED GROUND SEGMENT DESIGN FOR SMALL SATELLITES
R. S. Thompson, C. J. Ashton, and A. N. Pidgeon *In* CNES, Small Satellites Systems and Services Jan. 1993 p 321-329 (For primary document see N94-17131 03-18)
Copyright Avail: Issuing Activity (CEPADUES-Editions, 111 rue Nicolas-Vaquelin, 31100 Toulouse, France)

N94-17155 INISEL, Torrejon de Ardoz (Spain).
GROUND SEGMENT DEFINITION FOR THE SPANISH SMALL SATELLITE PROGRAM (MINISAT)
F. Cancillo, L. Guzman, and L. A. SanJose *In* CNES, Small Satellites Systems and Services Jan. 1993 p 331-338 (For primary document see N94-17131 03-18)
Copyright Avail: Issuing Activity (CEPADUES-Editions, 111 rue Nicolas-Vaquelin, 31100 Toulouse, France)

N94-17156 Centre National d'Etudes Spatiales, Toulouse (France).
OREMUS: PROTOTYPE OF AN ORBIT DETERMINATION CENTER DEDICATED TO MINI-SATELLITE CONTROL [OREMUS: PROTOTYPE DE CENTRE D'ORBITOGRAPHIE POUR LE CONTROLE DE MINISATELLITES]
Francois Laporte, Genevieve Campan, and Huguette Conessa * *In its* Small Satellites Systems and Services Jan. 1993 p 339-347 In FRENCH (For primary document see N94-17131 03-18)
Copyright Avail: Issuing Activity (CEPADUES-Editions, 111 rue Nicolas-Vaquelin, 31100 Toulouse, France)

N94-17157 Ecole Nationale Superieure de l'Aeronautique et de l'Espace, Toulouse (France). Lab. d'Automatique.
DATA PROCESSING SYSTEM FOR ARSENE GROUND STATION: A TOOL FOR SMALL SATELLITE CONTROL AND DEVELOPMENT [LE SYSTEME INFORMATIQUE DE LA STATION SOL ARSENE: OUTIL DE CONTROLE ET DE DEVELOPPEMENT POUR PETITS SATELLITES]
Jacques Lamaison and Jean-Henri Llareus *In* CNES, Small Satellites Systems and Services Jan. 1993 p 349-359 In FRENCH (For primary document see N94-17131 03-18)
Copyright Avail: Issuing Activity (CEPADUES-Editions, 111 rue Nicolas-Vaquelin, 31100 Toulouse, France)

N94-17158 European Space Agency. European Space Research and Technology Center, ESTEC, Noordwijk (Netherlands).
SATELLITE CONTROL: A COMPREHENSIVE APPROACH
J. T. Garner *In* CNES, Small Satellites Systems and Services Jan. 1993 p 361-371 (For primary document see N94-17131 03-18)
Copyright Avail: Issuing Activity (CEPADUES-Editions, 111 rue Nicolas-Vaquelin, 31100 Toulouse, France)

15 LAUNCH VEHICLES AND SPACE VEHICLES

Includes boosters; operating problems of launch/space vehicle systems; and reusable vehicles.

For related information see also *20 Spacecraft Propulsion and Power.*

N94-15341* National Aeronautics and Space Administration, Washington, DC.
MISSION SAN MARCO (Videotape)
Nov. 1988 Videotape: 3 min. 14 sec. playing time, in color, with sound (NASA-TM-109442; NONP-VT-93-190239) Avail: CASI VHS A01/BETA A22
The videotape shows a satellite launch from San Marco, Africa. CASI

N94-16552# Naval Research Lab., Washington, DC.
NUMERICAL MODELING OF THE TEMPERATURE GRADIENTS AND SPECTRA OF THE PLASMA ARMATURE ON THUNDERBOLT
Memorandum Report
Paul C. Kepple and Robert W. Clark 14 Jun. 1993 42 p (AD-A266414; NRL/MR/6721-93-7317) Avail: CASI HC A03/MF A01
Numerical simulations of the spectra recorded on Thunderbolt shots 26 and 27 are presented. The calculations proceed via multifrequency radiation transport and are based on the assumptions that the plasma armature is cylindrically symmetric, the atomic constituents are homogeneously mixed and in pressure equilibrium, and the temperature gradient is specified. For the case of shot 27, the simulation is in excellent agreement with experiment and leads to a specific inference of a temperature gradient. For the case of shot 26, (where one capacitor bank fired early) the simulations indicate that the plasma armature for this shot did not satisfy some or all of the assumptions above. Since the aluminum absorption feature on shot 26 is too narrow relative to the B 2 and Cu 1 features there probably was a 'blob' of aluminum near the wall. DTIC

N94-16148# General Dynamics Corp., Huntsville, AL. Space Systems Div.
THE CLOSING WINDOW OF OPPORTUNITY: ADDRESSING THE US SPACE LAUNCH VEHICLE CRISIS
Todd Mosher *In* Huntsville Association of Technical Societies, TABES 1993: 9th Annual Technical and Business Exhibition and Symposium 1993 9 p (For primary document see N94-16129 03-38)
(TABES Paper 93-640) Avail: CASI HC A02/MF A03

N94-17137 European Space Agency, Paris (France).
SMALL LAUNCHERS (CURRENT AND FUTURE PROJECTS IN THE WORLD) [LES PETITS LANCEURS (PROJETS ACTUELS ET FUTURS DANS LE MONDE)]
W. G. Naumann *In* CNES, Small Satellites Systems and Services Jan. 1993 p 103-119 In FRENCH (For primary document see N94-17131 03-18)
Copyright Avail: Issuing Activity (CEPADUES-Editions, 111 rue Nicolas-Vaquelin, 31100 Toulouse, France)

N94-17138 Telespazio S.p.A., Rome (Italy).
SMALL SATELLITE CONSTELLATION DEPLOYMENT STRATEGIES
Giuseppe Rondinelli and Enrico Masci *In* CNES, Small Satellites Systems and Services Jan. 1993 p 121-130 (For primary document see N94-17131 03-18)
Copyright Avail: Issuing Activity (CEPADUES-Editions, 111 rue Nicolas-Vaquelin, 31100 Toulouse, France)

N94-17139 McDonnell-Douglas Space Systems Co., Huntington Beach, CA. Delta Launch Vehicle Div.
DELTA LAUNCH VEHICLE: ACCOMMODATIONS FOR SMALL SATELLITES
K. R. Know *In* CNES, Small Satellites Systems and Services Jan. 1993 p 131-138 (For primary document see N94-17131 03-18)
Copyright Avail: Issuing Activity (CEPADUES-Editions, 111 rue Nicolas-Vaquelin, 31100 Toulouse, France)

N94-17140 Centre National d'Etudes Spatiales, Paris (France). Direction des Lanceurs.
ARIANE 5 LIGHT DERIVATIVES [LES DERIVES LEGERS D'ARIANE 5]
Jean-Marc Astorg *In its* Small Satellites Systems and Services Jan. 1993 p 139-149 In FRENCH (For primary document see N94-17131 03-18)
Copyright Avail: Issuing Activity (CEPADUES-Editions, 111 rue Nicolas-Vaquelin, 31100 Toulouse, France)

N94-17141 Israel Aircraft Industries Ltd., Tel-Aviv. Electronic Div.
NEXT LAUNCH SYSTEM
C. Oiknine *In* CNES, Small Satellites Systems and Services Jan. 1993 p 151-160 (For primary document see N94-17131 03-18)
Copyright Avail: Issuing Activity (CEPADUES-Editions, 111 rue Nicolas-Vaquelin, 31100 Toulouse, France)

16 SPACE TRANSPORTATION

Includes passenger and cargo space transportation, e.g., shuttle operations; and space rescue techniques.

For related information see also *03 Air Transportation and Safety* and *18 Spacecraft Design, Testing and Performance.* For space suits see *54 Man/System Technology and Life Support.*

N94-14941# Air Force Systems Command, Wright-Patterson AFB, OH. Foreign Aerospace Science and Technology Center.
VERTICAL-TAIL AERODYNAMIC CONFIGURATION OF SPACE SHUTTLE ORBITER
Zhu Yikun 16 Jul. 1993 23 p Transl. into ENGLISH from unidentified Chinese language periodical, p 115-123
(AD-A267723; FASTC-ID(RS)T-0731-92) Avail: CASI HC A03/MF A01

From a discussion of the principle of the vertical-tail aerodynamic configuration of the Space Shuttle Orbiter in the preliminary design stage and analysis of the vertical-tail aerodynamic configuration (including layout) of the present-day Space Shuttle Orbiter, the author clarified three possible modes of vertical-tail aerodynamic configuration of the Space Shuttle Orbiter. The principal measures for the lateral-direction aerodynamic characteristics for an improved Space Shuttle Orbiter are also clarified. These results have direct reference value on the aerodynamic configuration and the preliminary design on the exterior shape of the Space Shuttle Orbiter. DTIC

N94-14969# Carnegie-Mellon Univ., Pittsburgh, PA. Robotics Inst.
SERPENTINE MANIPULATOR PLANNING AND CONTROL FOR NASA SPACE-SHUTTLE PAYLOAD SERVICING
Herman Herman and Hagen Schempf Oct. 1992 37 p
(AD-A266961; CMU-RI-TR-92-10) Avail: CASI HC A03/MF A01

The use of a highly-redundant manipulator, so-called 'serpentine' manipulator, is proposed as a solution for servicing space-payloads during the payload installation process before launch on the Space-Shuttle. The staging of the system would be inside a large cleanroom area, the Payload Changeout Room (PCR), which sits on the Rotating Service Structure (RSS), allowing it to be swung into mated contact with the Space-Shuttle as it sits on the launchpad at the John F. Kennedy Space Center in Cape Canaveral, Florida. This report is not so much concerned with the design and implementation issues associated with a serpentine manipulator, but rather with the planning, control and user-interface issues. We thus present a brief introduction to the actual application environment and its restrictions, followed by the theoretical background and implementation issues of planning and control algorithms developed specifically for a serpentine manipulator operating within the confined spaces of the PCR and the Space-Shuttle cargo-bay. The approach used to generate a continuous path is to develop and use a minimizing continuous energy curve for the manipulator, and then fit the discretized link-sections to that curve. The operator is then able to modify this curve directly, allowing for shaping of the serpentine, and for the placement of obstacles that can then be avoided. This algorithm can be implemented in real-time, and curve-parameters can also be adjusted such as flexibility and curvature of the curve. An A* method is used to search for the shortest distance between two goal points in order to construct the curve. In order to avoid obstacles (real and artificial), available from a database or which can be placed by the operator using the operator interface display, we use an obstacle potential field FIRAS function. DTIC

N94-15191*# Lockheed Missiles and Space Co., Huntsville, AL.
SPACE STATION THERMAL STORAGE/REFRIGERATION SYSTEM RESEARCH AND DEVELOPMENT Final Report
W. G. Dean and Z. S. Karu 26 Feb. 1993 345 p
(Contract NAS8-36401)
(NASA-CR-193841; NAS 1.26:193841; LMSC-HSV-TR-P037989) Avail: CASI HC A15/MF A03

Space Station thermal loading conditions represent an order of magnitude increase over current and previous spacecraft such as Skylab, Apollo, Pegasus III, Lunar Rover Vehicle, and Lockheed TRIDENT missiles. Thermal storage units (TSU's) were successfully used on these as well as many applications for ground based solar energy storage applications. It is desirable to store thermal energy during peak loading conditions as an alternative to providing increased radiator surface area which adds to the weight of the system. Basically, TSU's store heat by melting a phase change material (PCM) such as a paraffin. The physical property data for the PCM's used in the design of these TSU's is well defined in the literature. Design techniques are generally well established for the TSU's. However, the Space Station provides a new challenge in the application of these data and techniques because of three factors: the large size of the TSU required, the integration of the TSU for the Space Station thermal management concept with its diverse opportunities for storage application, and the TSU's interface with a two-phase (liquid/vapor) thermal bus/central heat rejection system. The objective in the thermal storage research and development task was to design, fabricate, and test a demonstration unit. One test article was to be a passive thermal storage unit capable of storing frozen food at -20 F for a minimum of 90 days. A second unit was to be capable of storing frozen biological samples at -94 F, again for a minimum of 90 days. The articles developed were compatible with shuttle mission conditions, including safety and handling by astronauts. Further, storage rack concepts were presented so that these units can be integrated into Space Station logistics module storage racks. The extreme sensitivity of spacecraft radiator systems design-to-heat rejection temperature requirements is well known. A large radiator area penalty is incurred if low temperatures are accommodated via a single centralized radiator system. As per the scope of work of this task, the applicability of refrigeration system tailored to meet the specialized requirements of storage of food and biological samples was investigated. The issues addressed were the anticipated power consumption and feasible designs and cycles for meeting specific storage requirements. Further, development issues were assessed related to the operation of vapor compression systems in micro-gravity addressing separation of vapor and liquid phases (via capillary systems). Author (revised)

N94-15225* National Aeronautics and Space Administration. Lyndon B. Johnson Space Center, Houston, TX.
ASTRO SMILE (Videotape)
Mar. 1989 Videotape: 20 min. 3 sec. playing time, in color, with sound
(NASA-TM-109506; NONP-VT-93-190303) Avail: CASI VHS A01/BETA A22

This is a humorous look at life aboard the Space Shuttle. CASI

N94-15261* National Aeronautics and Space Administration. Lyndon B. Johnson Space Center, Houston, TX.
STS-26 POST-FLIGHT PRESS CONFERENCE (Videotape)
Oct. 1988 Videotape: 15 min. playing time, in color, with sound
(NASA-TM-109557; NONP-VT-93-190355) Avail: CASI VHS A01/BETA A22

This video tape contains footage selected and narrated by the STS-26 crew including launch, TDRS-C/IUS (Tracking and Data Relay Satellite C / Inertial Upper Stage) deployment, onboard activities, and landing. CASI

N94-15262* National Aeronautics and Space Administration. Lyndon B. Johnson Space Center, Houston, TX.
STS-26 ONBOARD 16mm PHOTOGRAPHY QUICK RELEASE (Videotape)
Oct. 1988 Videotape: 23 min. playing time, in color, with sound
(NASA-TM-109558; NONP-VT-93-190356) Avail: CASI VHS A01/BETA A22

This video tape features scenes shot by the crew of onboard activities including the TDRS (Tracking and Data Relay Satellite) deploy, Earth views, and middeck experiments. CASI

N94-15264* National Aeronautics and Space Administration. Lyndon B. Johnson Space Center, Houston, TX.
STS-30 POST-FLIGHT PRESS CONFERENCE (Videotape)
May 1989 Videotape: 16 min. 30 sec. playing time, in color, with sound
(NASA-TM-109580; NONP-VT-93-190378) Avail: CASI VHS A01/BETA A22

This video contains footage selected and narrated by the Commander and Space Shuttle crew including launch, Magellan/IUS deployment, onboard crew activities, and landing. CASI

N94-15266* National Aeronautics and Space Administration. Lyndon B. Johnson Space Center, Houston, TX.
STS-30 MISSION TAPE (Videotape)

May 1989 Videotape: 59 min. playing time, in color, with sound (NASA-TM-109582; NONP-VT-93-190380) Avail: CASI VHS A01/BETA A22

This video contains important visual events including launch, Magellan/IUS Highlights Resource onboard crew activities, and landing. Air-to-ground transmission between the crew and Mission control is also included. CASI

N94-15306* National Aeronautics and Space Administration. Lyndon B. Johnson Space Center, Houston, TX.

STS-29 POST-FLIGHT PRESS CONFERENCE (Videotape)

Apr. 1989 Videotape: 22 min. playing time, in color, with sound (NASA-TM-109575; NONP-VT-93-190373) Avail: CASI VHS A01/BETA A22

This video contains footage selected and narrated by the Commander and the Space Shuttle crew including launch, TDRS-D/IUS deployment, onboard crew activities, and landing. CASI

N94-15307* National Aeronautics and Space Administration. Lyndon B. Johnson Space Center, Houston, TX.

STS-29 ONBOARD 16mm PHOTOGRAPHY QUICK RELEASE (Videotape)

Mar. 1989 Videotape: 24 min. 20 sec. playing time, in color, with sound (NASA-TM-109576; NONP-VT-93-190374) Avail: CASI VHS A01/BETA A22

This video features scenes shot by the crew of onboard activities including Earth shots, middeck experiments, TDRS deploy, and other mission objectives. CASI

N94-15314* National Aeronautics and Space Administration, Washington, DC.

SPACE SHUTTLE HIGHLIGHTS (Videotape)

Jan. 1985 Videotape: 3 min. 20 sec. playing time, in color, with sound (NASA-TM-109606; NONP-VT-93-190404) Avail: CASI VHS A01/BETA A22

This videotape recaps the space shuttle successes of 1984: STS 41-B, STS 41-C, STS 41-G, and 51-A. CASI

N94-15317* National Aeronautics and Space Administration. Lyndon B. Johnson Space Center, Houston, TX.

RETURN TO SPACE MISSION: THE STS-26 CREW REPORT (Videotape)

Feb. 1989 Videotape: 17 min. 30 sec. playing time, in color, with sound (NASA-TM-109568; NONP-VT-93-190366) Avail: CASI VHS A01/BETA A22

This videotape features footage from NASA's return to space flight after the 51-L accident. The videotape is narrated by the crew, and it includes the following: launch, landing, and the TDRS/IUS deployment. CASI

N94-15346* National Aeronautics and Space Administration, Washington, DC.

GEARING UP FOR 1988 (Videotape)

Dec. 1986 Videotape: 4 min. 59 sec. playing time, in color, with sound (NASA-TM-109617; NONP-VT-93-190415) Avail: CASI VHS A01/BETA A22

This video explains all engineering efforts to ensure safety and reliability for the next Shuttle mission, STS-26. CASI

N94-15353* National Aeronautics and Space Administration. Lyndon B. Johnson Space Center, Houston, TX.

STS-34 SPACE SHUTTLE PORTABLE ONBOARD COMPUTER (SPOC) BRIEFING (Videotape)

Aug. 1989 Videotape: 7 min. 10 sec. playing time, in color, with sound (NASA-TM-109458; NONP-VT-93-190255) Avail: CASI VHS A01/BETA A22

The Space Shuttle crew is shown learning how to operate the Shuttle Portable Onboard Computer (SPOC). CASI

N94-15354* National Aeronautics and Space Administration. Lyndon B. Johnson Space Center, Houston, TX.

STS-34 POST-FLIGHT PRESS CONFERENCE (Videotape)

Nov. 1989 Videotape: 8 min. 54 sec. playing time, in color, with sound (NASA-TM-109459; NONP-VT-93-190256) Avail: CASI VHS A01/BETA A22

This video tape contains footage selected and narrated by crew including launch, Galileo/IUS deployment, onboard crew activities, and landing. CASI

N94-15355* National Aeronautics and Space Administration. Lyndon B. Johnson Space Center, Houston, TX.

STS-34 ONBOARD 16mm PHOTOGRAPHY QUICK RELEASE (Videotape)

Oct. 1989 Videotape: 23 min. 50 sec. playing time, in color, with sound (NASA-TM-109460; NONP-VT-93-190257) Avail: CASI VHS A01/BETA A22

This video tape features scenes shot by the crew of onboard activities including Galileo deploy, Shuttle Solar Backscatter Ultraviolet (SSBUV) student experiments, other activities on the flight deck and middeck, and Earth and payload bay views. CASI

N94-15356* National Aeronautics and Space Administration. Lyndon B. Johnson Space Center, Houston, TX.

STS-34 MISSION HIGHLIGHTS RESOURCE TAPE, PART 1 (Videotape)

Nov. 1989 Videotape: 53 min. 21 sec. playing time, in color, with sound (NASA-TM-109461; NONP-VT-93-190258) Avail: CASI VHS A01/BETA A22

This video tape contains important visual events including launch Galileo/IUS deployment, onboard crew activities, and landing. Also included is air-to-ground transmission between the crew and Mission Control. CASI

N94-15357* National Aeronautics and Space Administration. Lyndon B. Johnson Space Center, Houston, TX.

STS-34 MCCULLY AND BAKER DURING IFM TRAINING (Videotape)

Aug. 1989 Videotape: 10 min. 20 sec. playing time, in color, with sound (NASA-TM-109462; NONP-VT-93-190259) Avail: CASI VHS A01/BETA A22

Astronauts McCully and Baker are shown learning how to use various tools that will be aboard the Space Shuttle. They are also seen cleaning air filters and checking wires. CASI

N94-15358* National Aeronautics and Space Administration. Lyndon B. Johnson Space Center, Houston, TX.

STS-34 GALILEO INTEGRATED DEPLOY SIM (Videotape)

Sep. 1989 Videotape: 12 min. 23 sec. playing time, in color, with sound (NASA-TM-109463; NONP-VT-93-190260) Avail: CASI VHS A01/BETA A22

The Space Shuttle crew practices Galileo deploy from the SMS. Intercuts of the MOCR are included. CASI

N94-15373* National Aeronautics and Space Administration. Lyndon B. Johnson Space Center, Houston, TX.

STS-29 MISSION HIGHLIGHTS RESOURCE TAPE (Videotape)

Apr. 1989 Videotape: 58 min. playing time, in color, with sound (NASA-TM-109542; NONP-VT-93-190339) Avail: CASI VHS A01/BETA A22

This video contains important visual events including launch, TDRS-D/IUS deployment, onboard crew activities, and landing. Also included are air-to-ground transmission between the crew and Mission Control. CASI

N94-15376* National Aeronautics and Space Administration. Lyndon B. Johnson Space Center, Houston, TX.

STS-32 ONBOARD 16mm PHOTOGRAPHY QUICK RELEASE (Videotape)

Jan. 1990 Videotape: 21 min. 50 sec. playing time, in color, with sound (NASA-TM-109472; NONP-VT-93-190269) Avail: CASI VHS A01/BETA A22

This video tape features scenes, shot by the crew, of onboard activities including Syncom deploy, Long Duration Exposure Facility retrieval, various middeck experiments, and Earth and payload bay views. CASI

N94-15379* National Aeronautics and Space Administration. Lyndon B. Johnson Space Center, Houston, TX.

STS-32 LDEF APPROACH IN SES (Videotape)

Nov. 1989 Videotape: 9 min. 50 sec. playing time, in color, with sound (NASA-TM-109474; NONP-VT-93-190271) Avail: CASI VHS A01/BETA A22

Astronauts Wetherbee, Dunbar, and Low are shown in the Shuttle Engineering Simulator (SES) practicing techniques for approaching the Long Duration Exposure Facility on orbit. CASI

N94-15384* National Aeronautics and Space Administration. Lyndon B. Johnson Space Center, Houston, TX.
STS-31 POST-FLIGHT CONFERENCE (Videotape)
May 1990 Videotape: 22 min. 10 sec. playing time, in color, with sound (NASA-TM-109477; NONP-VT-93-190274) Avail: CASI VHS A01/BETA A22

This video tape contains footage selected and narrated by the STS-31 Commander and crew including launch, Hubble Space Telescope deployment, onboard activities, and landing. CASI

N94-15389* National Aeronautics and Space Administration. Lyndon B. Johnson Space Center, Houston, TX.
MOVEMENT IN MICROGRAVITY (Videotape)
May 1988 Videotape: 8 min. 50 sec. playing time, in color, with sound (NASA-TM-109526; NONP-VT-93-190323) Avail: CASI VHS A01/BETA A22

This video takes a serious and humorous look at life in the low gravity environment of space flight. The video also includes onboard activities from Skylab to Space Shuttle missions. CASI

N94-15398* National Aeronautics and Space Administration. Lyndon B. Johnson Space Center, Houston, TX.
STS-33 EVA PREP AND POST WITH GREGORY, BLAHA, CARTER, THORTON, AND MUSGRAVE IN FFT (Videotape)
Oct. 1989 Videotape: 9 min. 5 sec. playing time, in color, with sound (NASA-TM-109469; NONP-VT-93-190266) Avail: CASI VHS A01/BETA A22

This video tape shows the crew in the airlock of the FFT, talking with technicians about the extravehicular activity (EVA) equipment. Thornton and Carter put on EVA suits and enter the airlock as the other crew members help with checklists. CASI

N94-15400* National Aeronautics and Space Administration. Lyndon B. Johnson Space Center, Houston, TX.
STS-33 CREW POST FLIGHT FILM (Videotape)
Feb. 1990 Videotape: 20 min. playing time, in color, with sound (NASA-TM-109470; NONP-VT-93-190267) Avail: CASI VHS A01/BETA A22

This video tape contains footage selected by the Commander and crew of the STS-33 DoD mission, including launch, limited onboard activities, and landing. CASI

N94-15403* National Aeronautics and Space Administration. Lyndon B. Johnson Space Center, Houston, TX.
STS-27 CREW PRESENTATION CLIP (Videotape)
Jan. 1989 Videotape: 14 min. 15 sec. playing time, in color, with sound (NASA-TM-109551; NONP-VT-93-190349) Avail: CASI VHS A01/BETA A22

This video features scenes from this Department of Defense Space Shuttle Mission. Included are launch, landing, the crew playing weightless football and exercising, and food preparation on middeck. CASI

N94-15407* National Aeronautics and Space Administration. Lyndon B. Johnson Space Center, Houston, TX.
STS-26 MISSIONS HIGHLIGHT RESOURCE TAPE (Videotape)
Oct. 1988 Videotape: 57 min. playing time, in color, with sound (NASA-TM-109559; NONP-VT-93-190357) Avail: CASI VHS A01/BETA A22

This video contains important visual events including launch, TDRS-C/IUS onboard crew activities and landing. Also includes air-to-ground transmission between ground and Mission Control. CASI

N94-15423* National Aeronautics and Space Administration. Lyndon B. Johnson Space Center, Houston, TX.
STS-30 ONBOARD 16mm PHOTOGRAPHY QUICK RELEASE (Videotape)
May 1989 Videotape: 21 min. 35 sec. playing time, in color, with sound (NASA-TM-109579; NONP-VT-93-190377) Avail: CASI VHS A01/BETA A22

This video features scenes shot by the Space Shuttle crew of onboard activities including Magellan deploy, Earth views, payload bay views, and middeck views. CASI

N94-15438* National Aeronautics and Space Administration. Lyndon B. Johnson Space Center, Houston, TX.
STS-31 ONBOARD 16mm PHOTOGRAPHY QUICK RELEASE (Videotape)
May 1990 Videotape: 30 min. playing time, in color, with sound (NASA-TM-109478; NONP-VT-93-190275) Avail: CASI VHS A01/BETA A22

This video features scenes shot by the crew of onboard activities including Hubble Space Telescope deploy, remote manipulator system (RMS) checkout, flight deck and middeck experiments, and Earth and payload bay views. CASI

N94-15440* National Aeronautics and Space Administration. Lyndon B. Johnson Space Center, Houston, TX.
STS-31 MISSION HIGHLIGHTS RESOURCE TAPE (Videotape)
Jun. 1990 Videotape: 56 min. playing time, in color, with sound (NASA-TM-109479; NONP-VT-93-190276) Avail: CASI VHS A01/BETA A22

This video contains important visual events including launch, Hubble Space Telescope deployment, onboard crew activities, and landing. Air-to-ground transmission between crew and Mission Control is also included. CASI

N94-15461* National Aeronautics and Space Administration. Lyndon B. Johnson Space Center, Houston, TX.
STS-36 CREW PRESENTATION CLIP (Videotape)
Jul. 1990 Videotape: 20 min. playing time, in color, with sound (NASA-TM-109497; NONP-VT-93-190294) Avail: CASI VHS A01/BETA A22

This video features scenes from this Department of Defense Shuttle mission showing crew onboard activities. CASI

N94-15464* National Aeronautics and Space Administration. Lyndon B. Johnson Space Center, Houston, TX.
STS-35 ONBOARD PHOTOGRAPHY QUICK RELEASE (Videotape)
Dec. 1990 Videotape: 25 min. playing time, in color, with sound (NASA-TM-109500; NONP-VT-93-190297) Avail: CASI VHS A01/BETA A22

This video features scenes shot by the crew of onboard activities including ASTRO-1 operation, middeck experiments, flight deck views, and earth and payload bay views. CASI

N94-15465* National Aeronautics and Space Administration. Lyndon B. Johnson Space Center, Houston, TX.
STS-35 MISSION HIGHLIGHTS RESOURCE TAPE (Videotape)
Feb. 1991 Videotape: 59 min. 27 sec. playing time, in color, with sound (NASA-TM-109501; NONP-VT-93-190298) Avail: CASI VHS A01/BETA A22

This document contains video on launch, ASTRO-1 operations, onboard operations, crew activities, and landing. It also includes air-to-ground transmission between crew and Mission Control. CASI

N94-15466* National Aeronautics and Space Administration. Lyndon B. Johnson Space Center, Houston, TX.
SCIENCE OPERATION IN SPACE: LESSONS (Videotape)
1988 Videotape: 32 min. playing time, in color, with sound (NASA-TM-109502; NONP-VT-93-190299) Avail: CASI VHS A01/BETA A22

This program (conceived by a group of veteran Shuttle astronauts) shows prospective experimenters how they can better design their

experiments for operation onboard Shuttle flights. Shuttle astronauts Dunbar, Seddon, Hoffman, Cleave, Ross, and ChangDiaz also show how crews live and work in space. CASI

N94-15468* National Aeronautics and Space Administration. Lyndon B. Johnson Space Center, Houston, TX.
STS-27 CREW DEORBIT PREP IN SMS WITH GIBSON, SHEPARD, MULLANE, ROSS, AND G. GARDNER (Videotape)
May 1988 Videotape: 5 min. playing time, in color, with sound
(NASA-TM-109518; NONP-VT-93-190315) Avail: CASI VHS A01/BETA A22

This videotape shows the crew training. Forward and aft flight deck views are provided. CASI

N94-15516* National Aeronautics and Space Administration. Lyndon B. Johnson Space Center, Houston, TX.
STS-41 POST-FLIGHT PRESS PRESENTATION (Videotape)
Nov. 1990 Videotape: 21 min. 36 sec. playing time, in color, with sound
(NASA-TM-109514; NONP-VT-93-190311) Avail: CASI VHS A01/BETA A22

This videotape contains footage selected and narrated by the crew. The footage covers the launch, the deployment of Ulysses, onboard crew activities, and the landing. CASI

N94-15518* National Aeronautics and Space Administration. Lyndon B. Johnson Space Center, Houston, TX.
STS-41 ONBOARD 16mm PHOTOGRAPHY QUICK RELEASE (Videotape)
Oct. 1990 Videotape: 17 min. 34 sec. playing time, in color, with sound
(NASA-TM-109515; NONP-VT-93-190312) Avail: CASI VHS A01/BETA A22

This videotape features scenes of onboard activities. The videotape was shot by the crew. The scenes include the following: Ulysses' deployment, middeck experiments, computer workstations, and Earth payload bay views. CASI

N94-15521* National Aeronautics and Space Administration. Lyndon B. Johnson Space Center, Houston, TX.
STS-41 MISSION HIGHLIGHTS RESOURCE TAPE (Videotape)
Jan. 1991 Videotape: 54 min. 44 sec. playing time, in color, with sound
(NASA-TM-109516; NONP-VT-93-190313) Avail: CASI VHS A01/BETA A22

This videotape contains important visual events including launch, Ulysses' deployment, onboard crew activities, and landing. The videotape also includes air-to-ground transmission between the crew and Mission Control. CASI

N94-15831*# Boeing Defense and Space Group, Huntsville, AL. Advanced Civil Space Systems.
SPACE TRANSFER CONCEPTS AND ANALYSES FOR EXPLORATION MISSIONS, PHASE 4 Final Report, Jan. - Aug. 1993
Gordon R. Woodcock Sep. 1993 141 p
(Contract NAS8-37857)
(NASA-CR-193849; NAS 1.26:193849; D615-10070) Avail: CASI HC A07/MF A02

Earlier studies carried out under this contract covered a wide range of lunar and Mars transportation options, and lunar rove concepts and technology needs. The current report discusses the activities conducted under Technical Directives 16 and 17. Mars transportation was addressed as well as a review and update of architectures and propulsion systems. Author

N94-16468# RADEX, Inc., Bedford, MA.
POLAR 2 MODEL OF THE WAKE SHIELD EXPERIMENT
M. F. Tautz 16 Dec. 1992 43 p
(Contract F19628-89-C-0068)
(AD-A266243; RXR-92121; PL-TR-92-2343; SR-12) Avail: CASI HC A03/MF A01

The current-voltage characteristic of a charged probe in the wake of a shielding disk is calculated using the POLAR code. The current-voltage curves are parameterized with respect to the tilt angle of the shielding disk. Estimates of the magnitude of probe current for conditions simulating the CHAWS space shuttle experiment are given. DTIC

N94-16530# Amptek, Inc., Bedford, MA.
PROTOTYPE INSTRUMENTATION AND DESIGN STUDIES Final Report, 4 Sep. 1987 - 31 Mar. 1993
Alan C. Huber, John O. McGarity, John A. Pantazis, A. W. Everest, and David J. Sperry 31 Mar. 1993 35 p
(Contract F19628-87-C-0094)
(AD-A266402; PL-TR-93-2080) Avail: CASI HC A03/MF A01

The Shuttle Potential and Return Electron Experiment (SPREE) was flown as part of the Tethered Satellite System (TSS-1) on STS-46 launched on 31 Jul. 1992. A significant portion of this contract has been spent on the design and development of the SPREE analyzer system. The successful launch and operation of the SPREE during the TSS-1 and EOIM mission were the culmination of the past five years' work. This final report details the SPREE system as flown and some of the preliminary results. These successes include a real-time charging detection algorithm that correctly and accurately diagnosed the potential of the Shuttle with respect to the ambient plasma, a particle correlator system that was able to accurately detect and analyze wave/particle interactions triggered by electron beam operations, a pair of digital data recorders that archived 5 Gigabytes of data, two sets of triquadraspherical electrostatic analyzers that measured the flux of electrons and ions from 10 eV to 10 KeV and from 10000 to 1 x 10(exp 14) particles/sq cm-ster-sec., and occasional operating pressures that exceeded 0.0001 Torr. DTIC

N94-17320*# National Aeronautics and Space Administration. Lyndon B. Johnson Space Center, Houston, TX.
HUMAN TRANSPORTATION SYSTEM (HTS) STUDY, VOLUME 2 Final Report
N. Lance, M. S. Geyer, and M. T. Gaunce Oct. 1993 560 p
(RTOP 906-11-01-01)
(NASA-TM-104779-Vol-2; S-739; NAS 1.15:104779-Vol-2) Avail: CASI HC A24/MF A04

This report summarizes work completed under the Human Transportation System Study. This study was conducted by the New Initiatives Office at JSC with the technical support of Boeing, General Dynamics, Lockheed, McDonnell-Douglas, Martin Marietta, and Rockwell. The study was designed to generate information on determining the appropriate path to follow for new system development to meet the Nation's space transportation needs. The study evaluates 18 transportation architecture options using a parametric set of mission requirements. These options include use of current systems (e.g., Shuttle, Titan, etc.) as well as proposed systems (e.g., PLS, Single-Stage-to-Orbit, etc.) to assess the impact of various considerations, such as the cost of alternate access, or the benefit of separating people and cargo. The architecture options are compared to each other with six measurable evaluation criteria or attributes. They are: funding profile, human safety, probability of mission success, architecture cost risk, launch schedule confidence, and environmental impact. Values for these attributes are presented for the architecture options, with pertinent conclusions and recommendations. Derived from text

N94-17656*# Thiokol Corp., Brigham City, UT.
POSTFLIGHT HARDWARE EVALUATION 360T026 (RSRM-26, STS-47) Final Report
Greg Nielson May 1993 279 p
(Contract NAS8-38100)
(NASA-CR-192559; NAS 1.26:192559; TWR-64204) Avail: CASI HC A13/MF A03

The final report for the Clearfield disassembly evaluation and a continuation of the KSC postflight assessment for the 360T026 (STS-47) Redesigned Solid Rocket Motor (RSRM) flight set is provided. All observed hardware conditions were documented on PFOR's and are included in Appendices A, B, and C. Appendices D and E contain the measurements and safety factor data for the nozzle and insulation components. This report, along with the KSC Ten-Day Postflight Hardware Evaluation Report (TWR-64203), represents a summary of the 360T026 hardware evaluation. The as-flown hardware configuration is documented in TWR-60472. Disassembly evaluation photograph numbers are logged in TWA-1987. The 360T026 flight set disassembly evaluations described were performed at the RSRM Refurbishment Facility in Clearfield, Utah. The final factory joint

demate occurred on 12 April 1993. Detailed evaluations were performed in accordance with the Clearfield Postflight Engineering Evaluation Plan (PEEP), TWR-50051, Revision A. All observations were compared against limits that are also defined in the PEEP. These limits outline the criteria for categorizing the observations as acceptable, reportable, or critical. Hardware conditions that were unexpected and/or determined to be reportable or critical were evaluated by the applicable CPT and tracked through the PFAR system. Author (revised)

N94-16151*# National Aeronautics and Space Administration. Marshall Space Flight Center, Huntsville, AL.
COST-EFFECTIVE TEST METHODS FOR SHUTTLE PAYLOADS
Michael L. Tinker *In* Huntsville Association of Technical Societies, TABES 1993: 9th Annual Technical and Business Exhibition and Symposium 1993 6 p (For primary document see N94-16129 03-38)
(TABES Paper 93-651) Avail: CASI HC A02/MF A03

17 SPACE COMM., SPACECRAFT COMM., COMMAND & TRACKING

Includes telemetry; space communications networks; astronavigation and guidance; and radio blackout.

For related information see also *04 Aircraft Communications and Navigation* and *32 Communications and Radar.*

N94-15648*# National Aeronautics and Space Administration. Ames Research Center, Moffett Field, CA.
BANDWIDTH CHARACTERISTICS OF MULTIMEDIA DATA TRAFFIC ON A LOCAL AREA NETWORK
Shery L. Chuang, Sharon Doubek (RECOM Software, Inc., San Jose, CA.), and Richard F. Haines Sep. 1993 11 p
(RTOP 476-14-03)
(NASA-TM-104026; A-93088; NAS 1.15:104026) Avail: CASI HC A03/MF A01

Limited spacecraft communication links call for users to investigate the potential use of video compression and multimedia technologies to optimize bandwidth allocations. The objective was to determine the transmission characteristics of multimedia data - motion video, text or bitmap graphics, and files transmitted independently and simultaneously over an ethernet local area network. Commercial desktop video teleconferencing hardware and software and Intel's proprietary Digital Video Interactive (DVI) video compression algorithm were used, and typical task scenarios were selected. The transmission time, packet size, number of packets, and network utilization of the data were recorded. Each data type - compressed motion video, text and/or bitmapped graphics, and a compressed image file - was first transmitted independently and its characteristics recorded. The results showed that an average bandwidth of 7.4 kilobits per second (kbps) was used to transmit graphics; an average bandwidth of 86.8 kbps was used to transmit an 18.9-kilobyte (kB) image file; a bandwidth of 728.9 kbps was used to transmit compressed motion video at 15 frames per second (fps); and a bandwidth of 75.9 kbps was used to transmit compressed motion video at 1.5 fps. Average packet sizes were 933 bytes for graphics, 498.5 bytes for the image file, 345.8 bytes for motion video at 15 fps, and 341.9 bytes for motion video at 1.5 fps. Simultaneous transmission of multimedia data types was also characterized. The multimedia packets used transmission bandwidths of 341.4 kbps and 105.8kbps. Bandwidth utilization varied according to the frame rate (frames per second) setting for the transmission of motion video. Packet size did not vary significantly between the data types. When these characteristics are applied to Space Station Freedom (SSF), the packet sizes fall within the maximum specified by the Consultative Committee for Space Data Systems (CCSDS). The uplink of imagery to SSF may be performed at minimal frame rates and/or within seconds of delay, depending on the user's allocated bandwidth. Further research to identify the acceptable delay interval and its impact on human performance is required. Additional studies in network performance using various video compression algorithms and integrated multimedia techniques are needed to determine the optimal design approach for utilizing SSF's data communications system. Author (revised)

N94-16056# Sandia National Labs., Albuquerque, NM.
EVALUATION OF MIDBAND ANALOG FIBER OPTIC TELEMETRY LINKS
G. J. Hansen May 1993 46 p
(Contract DE-AC04-76DP-00789)
(DE93-015128; SAND-93-0910) Avail: CASI HC A03/MF A01

Midband (1 KHz-500 MHz) analog fiber optic data links were purchased for evaluation from three suppliers. Ortel Corp., Alhambra, CA, provided units built to the specifications. Kaman Sciences Corp, Colorado Springs, CO, and Laser Diode Inc., Princeton, NJ, provided units similar to the specification but with significant differences. The final version of the Ortel units met the specification but were marginal in dynamic range. The other units failed to meet the specification but showed promise for future application. DOE

N94-17111*# Communications Satellite Corp., Clarksburg, MD.
ON-BOARD B-ISDN FAST PACKET SWITCHING ARCHITECTURES. PHASE 1: STUDY Final Report
Faris Faris, Thomas Inukai, Fred Lee, Dilip Paul, and Dong-Jye Shyy Oct. 1993 499 p
(Contract NASw-4528; RTOP 506-72-21)
(NASA-CR-191143; E-8137; NAS 1.26:191143) Avail: CASI HC A21/MF A04

The broadband integrate services digital network (B-ISDN) is an emerging telecommunications technology that will meet most of the telecommunications networking needs in the mid-1990's to early next century. The satellite-based system is well positioned for providing B-ISDN service with its inherent capabilities of point-to-multipoint and broadcast transmission, virtually unlimited connectivity between any two points within a beam coverage, short deployment time of communications facility, flexible and dynamic reallocation of space segment capacity, and distance insensitive cost. On-board processing satellites, particularly in a multiple spot beam environment, will provide enhanced connectivity, better performance, optimized access and transmission link design, and lower user service cost. The following are described: the user and network aspects of broadband services; the current development status in broadband services; various satellite network architectures including system design issues; and various fast packet switch architectures and their detail designs. Author (revised)

N94-17487*# National Aeronautics and Space Administration. Lewis Research Center, Cleveland, OH.
NASA LEWIS MESHED VSAT WORKSHOP MEETING SUMMARY
William Ivancic Nov. 1993 7 p Proposed for presentation at the 15th International Communications Satellite Conference, San Diego, CA, 28 Feb. - 3 Mar. 1994; sponsored by AIAA
(RTOP 506-72-21)
(NASA-TM-106332; E-8093; NAS 1.15:106332; AIAA Paper 94-0993)
Avail: CASI HC A02/MF A01

NASA Lewis Research Center's Space Electronics Division (SED) hosted a workshop to address specific topics related to future meshed very small-aperture terminal (VSAT) satellite communications networks. The ideas generated by this workshop will help to identify potential markets and focus technology development within the commercial satellite communications industry and NASA. The workshop resulted in recommendations concerning these principal points of interest: the window of opportunity for a meshed VSAT system; system availability; ground terminal antenna sizes; recommended multifrequency for time division multiple access (TDMA) uplink; a packet switch design concept for narrowband; and fault tolerance design concepts. This report presents a summary of group presentations and discussion associated with the technological, economic, and operational issues of meshed VSAT architectures that utilize processing satellites. Author

N94-17488*# National Aeronautics and Space Administration. Lewis Research Center, Cleveland, OH.
ON-BOARD PACKET SWITCH ARCHITECTURES FOR COMMUNICATION SATELLITES
Mary Jo Shalkhauser and Jorge A. Quintana Sep. 1993 11 p
(RTOP 506-72-21)
(NASA-TM-106328; E-8087; NAS 1.15:106328) Avail: CASI HC A03/MF A01

NASA Lewis Research Center is developing an on-board information switching processor for a multichannel communications signal processing satellite. The information switching processor is a flexible, high-throughput, fault tolerant, on-board baseband packet switch used to route user data among user ground terminals. Through industry study contracts and in-house investigations, several packet switching architectures were examined for possible implementation. Three contention-free switching architectures were studied in detail, namely the shared memory approach, the shared bus approach, and the shared memory per beam approach. These three switching architectures are discussed and the advantages and disadvantages of each approach are examined. Author (revised)

18 SPACECRAFT DESIGN, TESTING AND PERFORMANCE

Includes satellites; space platforms; space stations; spacecraft systems and components such as thermal and environmental controls; and attitude controls.

For life support systems see *54 Man/System Technology and Life Support.* For related information see also *05 Aircraft Design, Testing and Performance, 39 Structural Mechanics,* and *16 Space Transportation.*

N94-15001# National Space Development Agency, Tokyo (Japan).
DEVELOPMENT OF JAPANESE EARTH RESOURCES SATELLITE-1 (JERS-1; FUYO-1) AND IT'S OPERATIONAL RESULTS [CHIKYUU SHIGEN EISEI 1 GOU (JERS-1) NO KAIHATSU OYOBI SONO SEIKA]
31 Mar. 1993 734 p
(NASDA-SPP-930001; JTN-93-80476) Avail: CASI HC A99/MF A06

Various aspects of development progress from the policy decision to the launch and early orbit phase operation of the JERS-I (Japanese Earth Resources Satellite-I) are presented. The items presented are as follows: the fundamental development policy, related organizations, and the system for the development; the master schedule and the progress of the development; the outline of JERS-I including its missions, the structure and characteristics of the system, and the operation plan; satellite mission and the system design analyses; the system development, including that of subsystems and components, production and test of the system development model, the integration and test of the system PFM (Proto-Flight Model), and the modification and post-modification test of the PFM; interfaces with other programs; program control; satellite operation in the launch and early orbit operation phase and the analysis and evaluation of the operation results; and the initial examination on on-orbit failures. Author (NASDA)

N94-15007*# National Aeronautics and Space Administration. Marshall Space Flight Center, Huntsville, AL.
RESULTS OF AN ELECTRICAL POWER SYSTEM FAULT STUDY (CDDF) Final Report No. N06
N. R. Dugal-Whitehead and Y. B. Johnson Washington Sep. 1993 44 p
(NASA-TP-3413; M-731; NAS 1.60:3413) Avail: CASI HC A03/MF A01

This report gives the results of an electrical power system fault study which has been conducted over the last 2 and one-half years. First, the results of the literature search into electrical power system faults in space and terrestrial power system applications are reported. A description of the intended implementations of the power system faults into the Large Autonomous Spacecraft Electrical Power System (LASEPS) breadboard is then presented. Then, the actual implementation of the faults into the breadboard is discussed along with a discussion describing the LASEPS breadboard. Finally, the results of the injected faults and breadboard failures are discussed. Author (revised)

N94-15147# Naval War Coll., Newport, RI. Dept. of Operations.
SPACE COUNTERSURVEILLANCE: A REQUISITE FOR THEATER DEFENSE PLANNING Final Report
Donald A. Meyer 17 May 1993 37 p
(AD-A266871) Avail: CASI HC A03/MF A01

The first space war has been successfully fought hundreds of miles above the sands of the Middle East, and U.S. space warriors are now contemplating future conflicts and how space can better contribute to operational success on the battlefield. However, the lessons of U.S. space dominance during Desert Storm also received much attention from other nations -- many of which U.S. forces may someday face in a future skirmish. These nations have learned the value of space assets and are busily seeking to acquire a space surveillance capability of their own. The U.S. national military strategy calls for its forces to exercise space control and deny potential enemies use of the space medium when necessary -- but does the U.S. possess the weapons and plans to successfully accomplish this task? This paper examines both U.S. and enemy capabilities in the space warfare realm. Further, it suggests that the U.S. can better organize its space warfare personnel under a Space Component Commander concept to successfully accomplish the space countersurveillance mission at the theater level of operational warfare. DTIC

N94-15193*# National Aeronautics and Space Administration. Goddard Space Flight Center, Greenbelt, MD.
PRELAUNCH OPTICAL CHARACTERIZATION OF THE LASER GEODYNAMIC SATELLITE (LAGEOS 2)
Peter O. Minott, Thomas W. Zagwodzki, Thomas Varghese (Allied-Signal Aerospace Co., Seabrook, MD.), and Michael Seldon (Allied-Signal Aerospace Co., Seabrook, MD.) Sep. 1993 343 p
(NASA-TP-3400; NAS 1.60:3400; Rept-93B00102) Avail: CASI HC A15/MF A03

The optical range correction (the distance between the apparent retroreflective skin of the satellite and the center of mass) of the LAGEOS 2 was determined using computer analysis of theoretical and experimentally measured far field diffraction patterns, and with short pulse lasers using both streak camera-based range receivers and more conventional PMT-based range receivers. The three measurement techniques yielded range correction values from 248 to 253 millimeters dependent on laser wavelength, pulsewidth, and polarization, location of the receiver in the far field diffraction pattern and detection technique (peak, half maximum, centroid, or constant fraction). The Lidar cross section of LAGEOS 2 was measured at 4 to 10 million square meters, comparable to the LAGEOS 1. Author

N94-15227* National Aeronautics and Space Administration. Marshall Space Flight Center, Huntsville, AL.
LONG DURATION EXPOSURE FACILITY IS COMING HOME (Videotape)
Nov. 1989 Videotape: 2 min. 8 sec. playing time, in color, with sound
(NASA-TM-109656; NONP-VT-93-190454) Avail: CASI VHS A01/BETA A22

This video tape describes how the Long Duration Exposure Facility will provide knowledge of the effects of space on various materials over a long period of time. CASI

N94-15267* National Aeronautics and Space Administration. Goddard Space Flight Center, Greenbelt, MD.
ORBITING SOLAR OPERATIONS (Videotape)
Jul. 1988 Videotape: 10 min. playing time, in color, with sound
(NASA-TM-109583; NONP-VT-93-190381) Avail: CASI VHS A01/BETA A22

A short video presentation about the capabilities, accomplishments, and limitations of the Orbiting Solar Operations is presented. CASI

N94-15269* National Aeronautics and Space Administration. Goddard Space Flight Center, Greenbelt, MD.
TDRS VIDEO CLIP (Videotape)
Jan. 1989 Videotape: 57 sec. playing time, in color, with sound
(NASA-TM-109585; NONP-VT-93-190383) Avail: CASI VHS A01/BETA A22

This video presents Tracking and Data Relay Satellite and Goddard Space Flight Center involvement. CASI

N94-15274* National Aeronautics and Space Administration. Marshall Space Flight Center, Huntsville, AL.
SPACE STATION: THE LINK TO AMERICA'S FUTURE (Videotape)
Feb. 1989 Videotape: 5 min. 41 sec. playing time, in color, with sound
(NASA-TM-109653; NONP-VT-93-190451) Avail: CASI VHS A01/BETA A22

This video tape documents the planned design and development of the Space Station. CASI

N94-15278* National Aeronautics and Space Administration. Marshall Space Flight Center, Huntsville, AL.
INERTIAL UPPER STAGE (Videotape)
Feb. 1989 Videotape: 5 min. playing time, in color, with sound
(NASA-TM-109654; NONP-VT-93-190452) Avail: CASI VHS A01/BETA A22

This video tape details the importance of the Inertial Upper Stage in projecting various satellites from the Shuttle's cargo bay. CASI

N94-15296* National Aeronautics and Space Administration, Washington, DC.
COMET HALLEY RETURNS (Videotape)
Dec. 1985 Videotape: 3 min. 5 sec. playing time, in color, with sound
(NASA-TM-109608; NONP-VT-93-190406) Avail: CASI VHS A01/BETA A22

This videotape shows the five exploratory spacecraft, representing several countries, that will study Comet Halley: Giotto, Vega 1 and 2, Planet A, and Sakigaki. CASI

N94-15436* National Aeronautics and Space Administration, Washington, DC.
FIRST US MARS LANDING (Videotape)
Jun. 1976 Videotape: 4 min. 30 sec. playing time, in color, with sound
(NASA-TM-109669; NONP-VT-93-190467) Avail: CASI VHS A01/BETA A22

This video shows the launches of Viking 1 and 2 and discusses objectives of the first mission to Mars. CASI

N94-15446*# National Aeronautics and Space Administration. Langley Research Center, Hampton, VA.
MINIMUM ACCOMMODATION FOR AEROBRAKE ASSEMBLY. PHASE 2: STRUCTURAL CONCEPTS FOR A LUNAR TRANSFER VEHICLE AEROBRAKE WHICH CAN BE ASSEMBLED ON ORBIT Final Report
John T. Dorsey, Judith J. Watson, and Robin D. Tutterow Oct. 1993 38 p
(RTOP 506-43-41-02)
(NASA-TM-107610; NAS 1.15:107610) Avail: CASI HC A03/MF A01

A multidisciplinary conceptual study was conducted to define a reusable lunar transfer vehicle (LTV) aerobrake which could be launched on a Space Shuttle of Titan 4 and assembled on orbit at Space Station Freedom. A major objective was to design an aerobrake, with integrated structure and thermal protection systems, which has a mass less than 20 percent (9040 lb) of the LTV lunar return mass. The aerobrake segmentation concepts, the structural concepts, a joint concept for assembly, and a structural design with analysis of the aerobrake are described. Results show that a 50-foot diameter LTV aerobrake can be designed for on-orbit assembly which will achieve the 20 percent mass budget.
Author (revised)

N94-15458* National Aeronautics and Space Administration. Lyndon B. Johnson Space Center, Houston, TX.
DARE TO DREAM (Videotape)
Jun. 1989 Videotape: 5 min. 52 sec. playing time, in color, with sound
(NASA-TM-109512; NONP-VT-93-190309) Avail: CASI VHS A01/BETA A22

This video describes the Space Station Freedom and discusses the purpose of this international project. CASI

N94-15496* National Aeronautics and Space Administration. Langley Research Center, Hampton, VA.
LONG DURATION EXPOSURE FACILITY RETRIEVAL ANIMATION (Videotape)
Nov. 1989 Videotape: 4 min. 15 sec. playing time, in color, with sound
(NASA-TM-109426; NONP-VT-93-190223) Avail: CASI VHS A01/BETA A22

This video is a computer animation of a Long Duration Exposure Facility (LDEF) retrieval. CASI

N94-15497* National Aeronautics and Space Administration. Langley Research Center, Hampton, VA.
LONG DURATION EXPOSURE FACILITY (Videotape)
Jun. 1989 Videotape: 4 min. 15 sec. playing time, in color, with sound
(NASA-TM-109427; NONP-VT-93-190224) Avail: CASI VHS A01/BETA A22

A summary of the Long Duration Exposure Facility from launch through plans for the retrieval is presented. CASI

N94-15510* National Aeronautics and Space Administration, Washington, DC.
SPACE STATION RESOURCE REEL (Videotape)
Jul. 1990 Videotape: 24 min. playing time, in color, with sound
(NASA-TM-109673; NONP-VT-93-190471) Avail: CASI VHS A01/BETA A22

This video presents a series of takes and sequences with model photography of 1990 Space Station design. CASI

N94-15666# Rome Lab., Griffiss AFB, NY.
ANALYSIS OF LEADING EDGE AND TRAILING EDGE COVER GLASS SAMPLES BEFORE AND AFTER TREATMENT WITH ADVANCED SATELLITE CONTAMINATION REMOVAL TECHNIQUES Report, Oct. 1991 - Jun. 1992
S. P. Hotaling Apr. 1993 38 p
(AD-A267055; RL-TR-93-51) Avail: CASI HC A03/MF A01

Two samples from LDEF experiment M0003-4 were analyzed for molecular and particulate contamination prior to and following treatment with advanced satellite contamination removal techniques (CO2 Gas/Solid Jet Spray and Oxygen Ion Beam). The pre- and post-cleaning measurements and analyses will be presented. The Jet Spray removed particulates in seconds. The low energy reactive oxygen ion beam removed 5000 A of photo-polymerized organic hydrocarbon contamination in less than 1 hour. Spectroscopic analytical techniques were applied to the analysis of cleaning efficiency including: Fourier Transform Infrared, Auger, X-ray Photoemission, Energy Dispersive X-ray, and Ultraviolet/Visible. The results of this work suggest that the contamination studied here was due to spacecraft self contamination enhanced by atomic oxygen plasma dynamics and solar UV radiation. These results also suggest the efficacy for the Jet Spray and Ion Beam contamination control technologies for spacecraft optical surfaces. DTIC

N94-15712*# National Aeronautics and Space Administration. Goddard Space Flight Center, Greenbelt, MD.
SATELLITE SITUATION REPORT, VOLUME 33, NO. 3
30 Sep. 1993 100 p
(NASA-TM-109278; NAS 1.15:109278) Avail: CASI HC A05/MF A02

This report consists of data computed at the U.S. Space Command, GSFC, or provided by satellite owners. A space objects box score table is presented with data under the following headings: source/organization, objects in orbit, and decayed objects. The objects in orbit and decayed objects headings have payload, debris, and total as subheadings. The bulk of the document is objects-in-orbit tables with data under the following headings: international designation, name, catalog number, source, launch date, period minutes, inclination, apogee (km), perigee (km), and notes.
CASI

N94-15749# Aerospace Corp., El Segundo, CA.
LONG DURATION EXPOSURE FACILITY EXPERIMENT M0003 DEINTEGRATION/FINDINGS AND IMPACTS
M. J. Meshishnek, S. R. Gyetvay, and C. H. Jaggers 15 Dec. 1992 41 p
(Contract F04701-88-C-0089)
(AD-A267140; TR-92(2935)-17; SMC-TR-93-21) Avail: CASI HC A03/MF A01

The Aerospace Corporation Long Duration Exposure Facility (LDEF) Experiment M0003 consists of 19 subexperiments from the Aerospace Laboratories, DOD Laboratories, and contractor organizations. It was designed to study the effects of the space environment on a large variety of spacecraft materials and components, both current and developmental. The experiment was housed in four LDEF trays and contained over 1250 specimens, two data systems, and two environment exposure control canisters. Nearly identical pairs of trays were located on the leading and

trailing edges of LDEF. The materials in these trays span nearly all generic functions in spacecraft such as optics, thermal control, composites, solar power, and electronics. Effects of the space environment such as vacuum, ultraviolet, atomic oxygen, meteoroid and debris, thermal cycling, and synergistic effects on various samples are described. Summaries of the on-board data are presented DTIC

N94-15753*# National Aeronautics and Space Administration. Hugh L. Dryden Flight Research Facility, Edwards, CA.

FLIGHT TESTING OF AIRBREATHING HYPERSONIC VEHICLES

John W. Hicks Oct. 1993 37 p Presented at Space Course 1993, Munich, Germany, 11-12 Oct. 1993 Sponsored by NASA, Washington (RTOP 505-70-00)

(NASA-TM-4524; Paper-37; H-1934; NAS 1.15:4524) Avail: CASI HC A03/MF A01

Using the scramjet engine as the prime example of a hypersonic airbreathing concept, this paper reviews the history of and addresses the need for hypersonic flight tests. It also describes how such tests can contribute to the development of airbreathing technology. Aspects of captive-carry and free-flight concepts are compared. An incremental flight envelope expansion technique for manned flight vehicles is also described. Such critical issues as required instrumentation technology and proper scaling of experimental devices are addressed. Lastly, examples of international flight test approaches, existing programs, or concepts currently under study, development, or both, are given. Author (revised)

N94-15857# Arnold Engineering Development Center, Arnold AFS, TN.

SOLAR ABSORPTANCE OF OPTICAL SURFACES CONTAMINATED WITH SPACECRAFT MATERIAL OUTGASSING PRODUCTS Final Report, 8-27 Jul. 1992

W. T. Bertrand and B. E. Wood Jul. 1993 23 p

(AD-A267202; AEDC-TR-93-7) Avail: CASI HC A03/MF A01

As satellite applications become more sophisticated and satellite lifetimes are extended, the roles of contamination prediction and control become increasingly important. Contamination can alter the spectral characteristics of cryogenically cooled optical systems, increase the solar absorptance of thermal control surfaces causing the spacecraft to overheat, or degrade the power output of solar cells. The Solar Absorptance Measurements Chamber was developed to measure the change in integrated solar absorptance of aluminum coated mirrors by condensed outgassing contaminants irradiated by a solar simulator under vacuum. In previous tests, the location of the solar simulator did not allow irradiation of the sample mirror during the contamination phase. The test chamber was modified, and measurements were made to compare the solar absorptance change for samples irradiated during contamination to samples with no irradiation during contamination. Sources of the contaminants were two spacecraft materials, Furane Products Uralane 5753-AB (LV) encapsulant and Dow Corning 93-500 encapsulant. DTIC

N94-15864*# George Washington Univ., Hampton, VA. Joint Inst. for Advancement of Flight Sciences.

A FEASIBILITY STUDY OF A MICROGRAVITY ENHANCEMENT SYSTEM FOR SPACE STATION FREEDOM

Preston S. Diamond and Robert H. Tolson Oct. 1993 120 p See also A93-52902

(Contract NCC1-104; RTOP 476-14-06-01)

(NASA-CR-191550; NAS 1.26:191550) Avail: CASI HC A06/MF A02

The current low frequency microgravity requirements for Space Station Freedom (SSF) call for a level of less than 1 micro-g over 50 percent of all the laboratory racks for continuous periods of 30 days for at least 180 days per year. While this requirement is attainable for some of the laboratory modules for the Permanently Manned Configuration (PMC), it can not be met for the Man-Tended Configuration (MTC). In addition, many experiments would prefer even lower acceleration levels. To improve the microgravity environment, the Microgravity Enhancement System (MESYS) will apply a continuous thrust to SSF, to negate the disturbing gravity gradient and drag forces. The MESYS consists of a sensor, throttle-able thrusters and a control system. Both a proof mass system and accelerometer were evaluated for use as the sensor. The net result of the MESYS will be to shift the microgravity contours from the center of mass to a chosen location. Results indicate the MESYS is not feasible for MTC since it will require 5,073 kg of hydrazine fuel and 7,660 watts of power for 30 days of operation during average atmospheric conditions. For PMC, the MESYS is much more practical since only 4,008 kg of fuel and 5,640 watts of power are required. Author (revised)

N94-15935*# National Aeronautics and Space Administration. Lyndon B. Johnson Space Center, Houston, TX.

APPARATUS AND METHOD FOR PRODUCING AN ARTIFICIAL GRAVITATIONAL FIELD Patent Application

Jason McCanna, inventor (to NASA) 3 Jun. 1993 24 p

(NASA-Case-MSC-22021-1; NAS 1.71:MSC-22021-1;

US-Patent-Appl-SN-073847) Avail: CASI HC A03/MF A01

An apparatus and method is disclosed for producing an artificial gravitational field in a spacecraft by rotating the same around a spin axis. The centrifugal force thereby created acts as an artificial gravitational force. The apparatus includes an engine which produces a drive force offset from the spin axis to drive the spacecraft towards a destination. The engine is also used as a counterbalance for a crew cabin for rotation of the spacecraft. Mass of the spacecraft, which may include either the engine or crew cabin, is shifted such that the centrifugal force acting on that mass is no longer directed through the center of mass of the craft. This off-center centrifugal force creates a moment that counterbalances the moment produced by the off-center drive force to eliminate unwanted rotation which would otherwise be precipitated by the offset drive force. NASA

N94-15951*# National Aeronautics and Space Administration. Lyndon B. Johnson Space Center, Houston, TX.

TETRAHEDRAL LANDER Patent Application

Karen L. Nyberg, inventor (to NASA) 3 Feb. 1993 18 p

(NASA-Case-MSC-22082-1; NAS 1.71:MSC-22082-1;

US-Patent-Appl-SN-012893) Avail: CASI HC A03/MF A01

An apparatus and method is disclosed for decelerating and absorbing impact of a re-entry vehicle suitable for payloads that are relatively light as well as payloads weighing several tons or more. The apparatus includes four inflatable legs displaced equidistantly from each other around a capsule or housing which contains a payload. The legs are inflated at a designated altitude after entering Earth's atmosphere to slow the descent of the re-entry vehicle. Connected between each of the four legs are drag inducing surfaces that deploy as the legs inflate. The drag inducing surfaces are triangularly shaped with one such surface being connected between each pair of legs for a total of six drag inducing surfaces. The legs have drag inducing outer surfaces which act to slow the descent of the re-entry vehicle. NASA

N94-16455# Texas Univ., Austin. Dept. of Aerospace Engineering and Engineering Mechanics.

PULSE RESPONSE BASED CONTROL FOR MINIMUM TIME MANEUVER OF FLEXIBLE SPACECRAFT Final Report, 1 Jul. - 30 Nov. 1992

Jeffrey K. Bennighof 10 May 1993 98 p

(Grant AF-AFOSR-0297-90)

(AD-A266186; AFOSR-93-0429TR) Avail: CASI HC A05/MF A02

The pulse response based control method for minimum time maneuver of flexible spacecraft is described. This method makes it possible to obtain minimum time control profiles for linear systems solely on the basis of measured response to pulses in control inputs and gross inertial properties of the system, such as total mass or total mass moment of inertia. The accuracy with which the final state of the system can be specified is shown to be related to the observability of the system with the given outputs. A special algorithm is developed for solving the numerical optimization problem arising in this approach. For maneuver problems, nonlinear behavior is handled by explicitly modeling the deviation from linear behavior in those few modes in which it is significant. A feedback control scheme to complement pulse response based control, which is stable in the presence of nonlinear rotational stiffening effects and input bounds, is presented. Also, a near minimum time method which requires virtually no real time computation is described. Numerical examples illustrate the method and its features and extensions. DTIC

N94-16501# European Space Agency. European Space Research and Technology Center, ESTEC, Noordwijk (Netherlands).

THE LAUNCH OF ELDO
John Krige Mar. 1993 38 p
(ESA-HSR-7) Avail: CASI HC A03/MF A01

The intergovernmental negotiations which led to the signature of a convention in April 1962 establishing ELDO, the European Space Vehicle Launcher Development Organization, are described. The initial program of this organization foresaw the construction of a three stage rocket capped by a satellite test vehicle, with the work on each component spread between the four major western European states. After describing the British military origins of the first stage, called Blue Streak, we shall go on to explore how the UK managed to persuade first France, then Germany, and finally Italy to participate in the program. Author (revised)

N94-16502*# Teledyne Brown Engineering, Colorado Springs, CO.
HISTORY OF ON-ORBIT SATELLITE FRAGMENTATIONS
David J. Nauer Jul. 1992 266 p
(Contract NAS9-18209)
(NASA-CR-191644; NAS 1.26:191644; CS92-TR-JSC-007) Avail: CASI HC A12/MF A03

Since the first serious satellite fragmentation occurred in Jun. 1961, and instantaneously increased the total Earth satellite population by more than 400 percent, the issue of space operations within the finite region of space around the Earth has been the subject of increasing interest and concern. The prolific satellite fragmentations of the 1970's and the marked increase in the number of fragmentations in the 1980's served to widen international research into the characteristics and consequences of such events. Plans for large, manned space stations in the next decade and beyond demand a better understanding of the hazards of the dynamic Earth satellite population. The contribution of satellite fragmentations to the growth of the Earth satellite population is complex and varied. The majority of detectable fragmentation debris have already fallen out of orbit, and the effects of 40 percent of all fragmentations have completely disappeared. In this volume, satellite fragmentations are categorized by their assessed nature and to a lesser degree by their effect on the near-Earth space environment. A satellite breakup is the usually destructive disassociation of an orbital payload, rocket body, or structure, often with a wide range of ejecta velocities. A satellite breakup may be accidental or the result of intentional actions, e.g., due to a propulsion system malfunction or a space weapons test, respectively. An anomalous event is the unplanned separation, usually at low velocity, of one or more detectable objects from a satellite which remains essentially intact. Anomalous events can be caused by material deterioration of items such as thermal blankets, protective shields, or solar panels. As a general rule, a satellite breakup will produce considerably more debris, both trackable and non-trackable, than an anomalous event. From one perspective, satellite breakups may be viewed as a measure of the effects of man's activity on the environment, while anomalous events may be a measure of the environment on man-made objects. Author

N94-16503*# Teledyne Brown Engineering, Colorado Springs, CO.
THE FRAGMENTATION OF KOSMOS 2163
Jan. 1992 14 p
(Contract NAS9-18209)
(NASA-CR-191643; NAS 1.26:191643; CS92-TR-JSC-002) Avail: CASI HC A03/MF A01

On 6 Dec. 1991 Kosmos 2163, a maneuverable Soviet spacecraft which had been in orbit for 58 days, experienced a major breakup at an altitude of approximately 210 km. Although numerous pieces of debris were created, the fragments decayed rapidly leaving no long-term impact on the near-Earth environment. The assessed cause of the event is the deliberate detonation of an explosive device. Details of this event are presented.
Author (revised)

N94-16523# European Space Agency. European Space Research and Technology Center, ESTEC, Noordwijk (Netherlands).
CHOOSING ESRO'S FIRST SCIENTIFIC SATELLITES
Arturo Russo Nov. 1992 53 p
(ESA-HSR-3) Avail: CASI HC A04/MF A01

The choice of the scientific payloads of the European Space Research Organization's (ESRO's) first generation of satellites is analyzed. Concentration is on those aspects of the decision process that involved more directly the scientific community and that emerged as major issues in the discussion of the Launching Program Advisory Committee (LPAC). The main theme was the growing competition between the various fields of space science within the progressive retrenching of the Organization's financial resources available for the satellite program. A general overview of the status of the program by the end of 1966 is presented. The choice of the first small satellites' payloads (ESRO 1 and 2, and HEOS-A) and the difficult definition of the TD satellite program are discussed. This part covers a time span going from early 1963 to the spring of 1966. In the second part, the narrative starts from the spring of 1967, when the decision to recommend a second HEOS-type satellite was taken, and then analyzes the complex situation determined by the crisis of the TD program in 1968, and the debates which eventually led to the abandonment of TD-2 and the start of the far less ambitious ESRO 5 project. Derived from text

N94-16525# European Space Agency. European Space Research and Technology Center, ESTEC, Noordwijk (Netherlands).
THE EARLY DEVELOPMENT OF THE TELECOMMUNICATIONS SATELLITE PROGRAMME IN ESRO (1965-1971)
Arturo Russo May 1993 86 p
(ESA-HSR-9) Avail: CASI HC A05/MF A01

The European Space Research Organization (ESRO) was created in the early 1960's as an organization solely devoted to space science. At the end of 1966, however, after a request from the European Conference on Satellite Communications, the ESRO Council accepted to undertake a six-month study to evaluate the technical and financial implications involved in the development and launching of a few experimental communications satellites and to indicate other developments of interest in the field of application satellites. The analysis of the difficult beginning of ESRO's telecommunications program is discussed. The actual implementation of this program up to 1978 when the first experimental satellite (OTS-2) was successfully launched is discussed. Derived from text

N94-16905*# Florida Univ., Gainesville. Center for Intelligent Machines and Robotics.
DEVELOPMENT OF A PROTOTYPE KINESTATIC PLATFORM FOR APPLICATION TO SPACE AND GROUND SERVICING TASKS. PHASE 1: CONCEPT MODELING Final Report
J. Duffy and C. Crane Sep. 1993 53 p Original contains color illustrations
(Grant NAG10-0109)
(NASA-CR-194036; NAS 1.26:194036) Avail: CASI HC A04/MF A01; 2 functional color pages

The Center for Intelligent Machines and Robotics (CIMAR) of the University of Florida, in conjunction with Rockwell International is developing an electro-mechanical device called a Kinestatic Platform (KP) for aerospace applications. The goal of the current project is to develop a prototype KP which is capable of manipulating a 50 lb. payload. This prototype will demonstrate the feasibility of implementing a scaled up version to perform high precision manipulation of distributed systems and to control contact forces and allowable motions (rotations and translations), which is defined here as Kinestatic Control, in a six dimensional, partially constrained environment, simultaneously and independently. The objectives of the Phase 1 effort were as follows: (1) Identify specific NASA applications where the KP technology can be applied. (2) Select one application for development. (3) Develop a conceptual design of the KP specifically for the selected application. This includes the steps of developing a set of detailed performance criteria, establishing and making selection of the mechanism design parameters, and evaluating the expected system response. (4) Develop a computer graphics animation of the KP as it performs the selected application. This report will proceed by providing a technical description of the KP followed by how each of these objectives was addressed. Derived from text

N94-16909# Aerospace Corp., El Segundo, CA. Mechanics and Materials Technology Center.
PERFORMANCE OF SILVERED TEFLON THERMAL CONTROL BLANKETS ON SPACECRAFT
G. Pippin, W. K. Stuckey, and C. S. Hemminger 15 Mar. 1993 15 p
(Contract F04701-88-C-0089)
(AD-A266284; TR-93(3935)-9) Avail: CASI HC A03/MF A01

Silver-backed fluorinated ethylene propylene Teflon (Ag/FEP) thin film material was used for thermal control in many locations on the Long

Duration Exposure Facility (LDEF). The Ag/FEP registered the effects of atomic oxygen, solar ultraviolet radiation, meteoroid and debris impacts, thermal cycling, and contamination. This report summarizes the post-flight condition of the Ag/FEP, compares the results with performance on other spacecraft, and presents lifetime estimates for use under a variety of environmental exposures. Measurements of optical property and mechanical property and surface chemistry changes with exposure conditions, and their significance for design considerations and expected performance lifetimes, are reported for material flown on LDEF. The LDEF based data provides detailed information performance of Ag/FEP under relatively long term exposure in low Earth orbit. Comparison of this data with results from short term shuttle flights, Solar Max, SCATHA, other satellites, and ground based measurements is made to present a comprehensive summary of the use of this material for spacecraft applications. DTIC

N94-16990# Boston Coll., Chestnut Hill, MA. Inst. for Space Research.
L-SHELL BINNING AND DISPLAY OF SENSOR DATA FROM THE CRRES SPACECRAFT Scientific Report No. 1, 31 Dec. 1991 - 30 Dec. 1992
Dennis E. Delorey, John Palys, Paul N. Pruneau, and Daniel Madden 29 Mar. 1993 14 p
(Contract F19628-92-K-0003)
(AD-A267256; BC-ISR-93-02; PL-TR-93-2074) Avail: CASI HC A03/MF A01

A computerized analysis system is being developed for the CRRES spacecraft to facilitate L-shell studies of the instrument parameters over the lifetime of the vehicle. A PC-hosted graphics display system is being developed for the analysis of this data. DTIC

N94-17072*# National Aeronautics and Space Administration. Langley Research Center, Hampton, VA.
SOYUZ/ACRV ACCOMMODATION STUDY
Jonathan Cruz, Marston J. Gould, and Eric Dahlstrom (Lockheed Engineering and Sciences Co., Hampton, VA.) Nov. 1993 152 p
(RTOP 476-14-06)
(NASA-TM-107733; NAS 1.15:107733) Avail: CASI HC A08/MF A02

Included is a set of viewgraphs that present the results of a study conducted at the LaRC Space Station Freedom Office at the request of the Space Station Freedom Level 1 Program Office and the JSC ACRV Project Office to determine the implications of accommodating two Soyuz TM spacecraft as Assured Crew Return Vehicles (ACRV) on the Space Station Freedom (SSF) at the Permanently Crewed Capability (PCC) stage. The study examined operational as well as system issues associated with the accommodation of the Soyuz for several potential configuration options. Operational issues considered include physical hardware clearances, worst case Soyuz departure paths, and impacts to baseline operations such as Pressurized Logistics Module (PLM) exchange, Space Station Remote Manipulator System (SSRMS) attachment, Extravehicular Activity (EVA), and automatic rendezvous and docking (AR&D). Systems impact analysis included determining differences between Soyuz interface requirements and SSF capabilities for the Electrical Power System (EPS), Thermal Control System (TCS), Communications and Tracking (C&T), Audio-Video Subsystem (A/V), Data Management System (DMS), and Environmental Control and Life Support System (ECLSS). Significant findings of this study have indicated that the current AV capability of the Soyuz will need to be increased to provide adequate departure clearances for a worst case escape from an uncontrolled SSF and that an interface element will be required to mate the Soyuz vehicles to station, provide for AR&D structural loads, and to house Soyuz-to-SSF system interfaces. Author (revised)

N94-17103# Air Force Inst. of Tech., Wright-Patterson AFB, OH.
IMPLEMENTING A 50X50 GRAVITY FIELD MODEL IN AN ORBIT DETERMINATION SYSTEM M.S. Thesis
Daniel J. Fonte, Jr. Jun. 1993 328 p
(AD-A267548; AFIT/CI/CIA-93-089) Avail: CASI HC A15/MF A03

The Kepler problem treats the earth as if it is a spherical body of uniform density. In actuality, the earth's shape deviates from a sphere in terms of latitude (described by zonal harmonics), longitude (sectorial harmonics), and combinations of both latitude and longitude (tesseral harmonics). Operational Orbit Determination (OD) systems in the 1960's focused on the effects of the first few zonal harmonics since they represented the dominant terms of the geopotential perturbation, they were well known, and the use of a limited number of harmonics greatly simplified the perturbation theory used. The demand for increasingly accurate modeling of a satellite's motion, combined with an increase in knowledge of the geopotential and an advancement in computer technology, led to the inclusion of tesseral harmonics. The Draper Laboratory version of the Goddard Trajectory Determination System (R&D GTDS), one operational OD system, can currently implement up to a 21x21 gravity field model in its Cowell and Semianalytic Satellite Theory (SST) orbit generators. This thesis investigates the extension of R&D GTDS to include a 50x50 gravity field model in the Cowell and SST orbit generators. This extension would require code modifications in the following environments to support the various operational versions of R&D GTDS: IBM, VAX, Sun Workstation, and Silicon Graphics. DTIC

N94-17131 Centre National d'Etudes Spatiales, Toulouse (France).
SMALL SATELLITES SYSTEMS AND SERVICES [SYSTEMES ET SERVICES A PETITS SATELLITES]
Jan. 1993 731 p In ENGLISH and FRENCH Colloquium held in Arcachon, France, Jun. 1992
(ISBN-2-85-428327-9; ETN-93-94440) Copyright Avail: Issuing Activity (CEPADUES-Editions, 111 rue Nicolas-Vaquelin, 31100 Toulouse, France)

The various documents provided at the first 'Small Satellite Systems and Services' symposium are incorporated in the present work and classified according to the themes of the symposium sessions. A synthesis by the session leaders is given at the end of each theme. Eleven sessions were held, with the following headings: system analysis and simulations, launch facilities, sciences of the Universe, Earth observation, ground facilities, radiocommunication systems and their applications, satellite architecture, subsystem technology, access to space technology, and economic aspects. The last one is a poster session. All the documents indicate a strong and active interest in small satellites, as regards ground infrastructures, radiocommunication systems, satellite architecture, and subsystem technology in particular. For individual titles, see N94-17132 through N94-17191.

N94-17132 Telespazio S.p.A., Rome (Italy).
SMALL SATELLITE CONSTELLATION SYSTEM: OPTIMIZATION CRITERIA
B. Pavesi and P. Palmucci *In* CNES, Small Satellites Systems and Services Jan. 1993 p 39-50 (For primary document see N94-17131 03-18)
Copyright Avail: Issuing Activity (CEPADUES-Editions, 111 rue Nicolas-Vaquelin, 31100 Toulouse, France)

The systematic approach adopted to implement an optimal network architecture design as conditioned by the service requirements is discussed. The methodology is outlined and key parameters are identified: service and traffic requirements, constellation parameters, system parameters such as access and modulation techniques, link budgets, channellization, signalling, and antenna configuration. The best compromise solution is derived; the system's efficiency and availability are quantified. The economic aspects are also taken into account in the evaluation of the system feasibility. ESA

N94-17133 Centre National d'Etudes Spatiales, Toulouse (France).
AMIGAU: A PROTOTYPE TOOL AIMED AT MISSION ANALYSIS FOR SATELLITES AND SATELLITE CONSTELLATIONS [AMIGAU: PROTOTYPE D'OUTIL D'ANALYSE DE MISSION POUR SATELLITES ET CONSTELLATIONS DE SATELLITES]
Jacques Foliard, Alain Lamy, and Stephane Pascal (Societe d'Economie et de Mathematique Appliquees, Paris, France.) *In its* Small Satellites Systems and Services Jan. 1993 p 51-59 In FRENCH (For primary document see N94-17131 03-18)
Copyright Avail: Issuing Activity (CEPADUES-Editions, 111 rue Nicolas-Vaquelin, 31100 Toulouse, France)

From current spatial mechanics studies related to orbiting mini-satellites or mini-satellite constellations, it is demonstrated that the various problems related to mission analysis are similar (i.e., phase, Sun synchronization, fuel budget, maneuvering strategies, and position locating). In order to facilitate mission analysis, a single easy-to-use tool is necessary. The AMIGAU (French acronym for mission analysis by graphics, diagrams, and tools), which includes calculation modules based on spatial mechanics formerly developed for mission analyses or operations, is described. Typical

problems of mission analysis, its context and environment, as well as AMIGAU components are discussed. Two application examples which demonstrate the interest of simulations are detailed: determination of the altitude and local hour of the phased Sun synchronized orbit of an observation satellite; and a stationkeeping study of an orbiting satellite in a phased Sun synchronized orbit. ESA

N94-17134 Dassault Aviation, Istres (France). Centre Spatiale.
LOW EARTH ORBIT CONSTELLATIONS: ORBIT CONTROL OR NOT **c13**

Jose Radzik and Gerard Maral (Ecole Nationale Superieure des Telecommunications, Toulouse, France.) *In* CNES, Small Satellites Systems and Services Jan. 1993 p 61-70 (For primary document see N94-17131 03-18)

Copyright Avail: Issuing Activity (CEPADUES-Editions, 111 rue Nicolas-Vaquelin, 31100 Toulouse, France)

The aim of the study is to list the arguments for and against the adoption of orbit control. The first section is a semi-analytical calculation of the probability of visibility with minimum elevation angle of a single satellite, to be used for altitudes less than 2000 km. Section two evaluates the number of noncontrolled satellites needed to guarantee a given probability of visibility for the whole constellation. Section three gives a comparison between noncontrolled and controlled constellations in the case of very low altitudes (less than 800 km). The main problem is the effect of atmospheric drag which reduces significantly the coverage performance of the satellite at its end of life. Evaluating the semi-major-axis contraction and eccentricity evolution with time allows us to define the noncontrolled satellite constellations. ESA

N94-17135 Ecole Nationale Superieure des Telecommunications, Toulouse (France).
IMPACT OF LAUNCHING UNCERTAINTIES ON THE VISIBILITY OF COMMUNICATION SATELLITE CONSTELLATIONS WITHOUT ORBIT CONTROL [IMPACT DES INCERTITUDES DE LANCEMENT SUR LES PERFORMANCES DE VISIBILITE DE CONSTELLATIONS DE SATELLITES DE TELECOMMUNICATIONS SANS CONTROLE D'ORBITE]

Jean Jacques DeRidder, Gerard Maral, and Chantal Tamise (Toulouse Univ., France.) *In* CNES, Small Satellites Systems and Services Jan. 1993 p 71-83 In FRENCH (For primary document see N94-17131 03-18)

Copyright Avail: Issuing Activity (CEPADUES-Editions, 111 rue Nicolas-Vaquelin, 31100 Toulouse, France)

A statistical analysis and modeling of satellite constellations without orbit control is proposed. After definition, the visibility of a satellite is calculated. Satellite displacement and launching uncertainty modeling allows statistical calculations of visibility performance criteria, which is determined by means of a numerical method. Visibility performance evolution for a constellation without orbit control is dicussed: simulating conditions, variance influence on altitude, and latitude influence are studied. Results enable the system designer to decide in favor of orbit control or not according to the service and economical constraints of the mission. ESA

N94-17136 Centre National d'Etudes Spatiales, Toulouse (France).
RADIOCOMMUNICATION PROBLEMS OF A POSITION REPORTING AND BIDIRECTIONAL MESSAGERY SYSTEM USING VHF/UHF WITH LOW-EARTH ORBIT SATELLITES [ASPECTS RADIOCOMMUNICATIONS DANS UN SYSTEME DE LOCALISATION ET MESSAGERIE BIDIRECTIONNELLE EN VHF/UHF PAR SATELLITES EN ORBITE BASSE] **c32**

G. Lesthievent and M. Margery *In its* Small Satellites Systems and Services Jan. 1993 p 85-99 In FRENCH (For primary document see N94-17131 03-18)

Copyright Avail: Issuing Activity (CEPADUES-Editions, 111 rue Nicolas-Vaquelin, 31100 Toulouse, France)

Low Earth orbit minisatellite constellations are used for VHF/UHF links between mission centers and mobile terminals for the development of position reporting and telemetry services. Due to the nature of this task, specific constraints are imposed on the radiocommunication system. The constraints are reviewed, as well as the additive and multiplicative perturbations of the transmission channel that result in thermal and galactic noise, interferences and jammings, and ionospheric scintillation. System parameters and architecture are discussed using a 'downwards' approach to determine link performance. An analysis of the forward and return link is presented as well as computer simulation models which allow a statistical estimation of the performance in terms of acquisition ratio. ESA

N94-17137 European Space Agency, Paris (France).
SMALL LAUNCHERS (CURRENT AND FUTURE PROJECTS IN THE WORLD) [LES PETITS LANCEURS (PROJETS ACTUELS ET FUTURS DANS LE MONDE)] **c15**

W. G. Naumann *In* CNES, Small Satellites Systems and Services Jan. 1993 p 103-119 In FRENCH (For primary document see N94-17131 03-18)

Copyright Avail: Issuing Activity (CEPADUES-Editions, 111 rue Nicolas-Vaquelin, 31100 Toulouse, France)

Small satellites need launching services using small launchers capable of injecting 100 to 1000 kg into a polar orbit at an altitude of 1000 km. Operational small launchers are reviewed as well as developing and planned ones. Launcher characteristics, constraints, performance, and status are detailed. Few technical problems are encountered, as most launcher projects call for existing components and well known technologies. Most of the difficulties have come from launch site availability and from financial considerations. ESA

N94-17138 Telespazio S.p.A., Rome (Italy).
SMALL SATELLITE CONSTELLATION DEPLOYMENT STRATEGIES **c15**

Giuseppe Rondinelli and Enrico Masci *In* CNES, Small Satellites Systems and Services Jan. 1993 p 121-130 (For primary document see N94-17131 03-18)

Copyright Avail: Issuing Activity (CEPADUES-Editions, 111 rue Nicolas-Vaquelin, 31100 Toulouse, France)

Some optimization criteria for deployment policies of small satellite constellations are shown. The planned system (from an orbital point of view), the launcher role, and small launcher and conventional launcher characteristics are reviewed. Additionally, trade off considerations are addressed: launchers/orbit type, launcher capability/constellation implementation, launcher/launch base selection, launcher availability/constellation deployment time, launch strategy/orbit and constellation deployment time, and launch strategy/orbit and constellation requirements. Considering all the factors involved in the process, a mixed technique performed both logically and analytically allows minimization of the selected objective functions. Two primary objective functions are as follows: cost/kg on orbit and time of deployment. ESA

N94-17139 McDonnell-Douglas Space Systems Co., Huntington Beach, CA. Delta Launch Vehicle Div.
DELTA LAUNCH VEHICLE: ACCOMMODATIONS FOR SMALL SATELLITES **c15**

K. R. Know *In* CNES, Small Satellites Systems and Services Jan. 1993 p 131-138 (For primary document see N94-17131 03-18)

Copyright Avail: Issuing Activity (CEPADUES-Editions, 111 rue Nicolas-Vaquelin, 31100 Toulouse, France)

The possibility of comanifesting small satellites of different sizes and masses into low Earth orbits with the Delta launch vehicle is examined. Several benefits are offered: (1) the variety of vehicle configurations (number of strap-on solid motors and fairing diameter options) and launch sites allows more flexibility in accommodating desired physical shapes and mission orbit parameters; (2) the individual satellite launch service will be significantly less than a dedicated single launcher; and (3) the long and successful launch record of the Delta program provides the added confidence in achieving a successful program. ESA

N94-17140 Centre National d'Etudes Spatiales, Paris (France). Direction des Lanceurs.
ARIANE 5 LIGHT DERIVATIVES [LES DERIVES LEGERS D'ARIANE 5] **c15**

Jean-Marc Astorg *In its* Small Satellites Systems and Services Jan. 1993 p 139-149 In FRENCH (For primary document see N94-17131 03-18)

Copyright Avail: Issuing Activity (CEPADUES-Editions, 111 rue Nicolas-Vaquelin, 31100 Toulouse, France)

The Ariane 5 light derivatives are studied in order to complete Ariane 5

launch services with regard to medium size Sun synchronous spacecrafts (S derivative) and small satellites (P derivative). The P derivative is a three stage launcher with two solid propellant motors and a bipropellant upper stage. It is capable of placing 1 ton in a 1000 km circular polar orbit or two 450 kg payloads in the same orbit. The light derivatives are mainly derived from the Ariane 5 solid propellant booster and upper stage. The payload volume is particulary large (2.8 m internal maximal diameter, 6 m height). The light derivatives will be launched from the Ariane spaceport in Guyana. They will use Ariane 5 facilities for payload preparation and launch operation with a specific building for launcher integration. The first flight of the P derivative is scheduled for 1998. ESA

N94-17141 Israel Aircraft Industries Ltd., Tel-Aviv. Electronic Div.
NEXT LAUNCH SYSTEM **c15**
C. Oiknine *In* CNES, Small Satellites Systems and Services Jan. 1993 p 151-160 (For primary document see N94-17131 03-18)
Copyright Avail: Issuing Activity (CEPADUES-Editions, 111 rue Nicolas-Vaquelin, 31100 Toulouse, France)

The NEXT launch system is proposed by Israel Aircraft Industries to provide a low cost launch service capability for small satellites. It is an adaptation of the existing Shavit 1 launcher vehicle system. The NEXT launch system incorporates modern flight proven components and has three major elements: the launcher vehicle which consists of a three stage solid rocket motor booster with a liquid bipropellant system at the upper stage; the launcher erector transporter; and the launch operations support equipment. A new approach for launch service operations allows low cost launch service and use of proven technology insures reliability. Performances and orbital accuracy are specified. ESA

N94-17142 European Space Agency. European Space Research and Technology Center, ESTEC, Noordwijk (Netherlands).
SMALL MISSIONS FOR SPACE SCIENCE Abstract Only **c12**
H. Olthof *In* CNES, Small Satellites Systems and Services Jan. 1993 p 165 (For primary document see N94-17131 03-18)
Copyright Avail: Issuing Activity (CEPADUES-Editions, 111 rue Nicolas-Vaquelin, 31100 Toulouse, France)

According to the recommendations of the ESA program review panel, an analysis of the interest in small missions within the European scientific community was initiated. Three actions were undertaken: a call for ideas for small missions; a workshop on 'design approaches and development philosophies of small satellites'; and a technical assessment of two examples of small satellites. From the results, a meeting of the Science Program Committee concluded that ESA should continue fostering small satellite programs and should offer limited support to the member states on a case by case basis. ESA

N94-17143 Dornier System G.m.b.H., Friedrichshafen (Germany).
STRATEGY FOR A SMALL SATELLITE PROGRAM AND A PROPOSAL FOR A FIRST MISSION **c12**
N. Pailer, G. Hampel, E. Bachor, G. Lippner, and H. Kunow (Kiel Univ., Germany.) *In* CNES, Small Satellites Systems and Services Jan. 1993 p 167-180 (For primary document see N94-17131 03-18)
Copyright Avail: Issuing Activity (CEPADUES-Editions, 111 rue Nicolas-Vaquelin, 31100 Toulouse, France)

The Ulysses Reference Mission (URM) was initiated after NASA cancelled its contribution to the International Solar Polar Mission. A small satellite was designed to carry the five main Ulysses instruments on board and to perform scientific baseline measurements. A feasibility study was undertaken to specify the requirements for a small satellite bus, to design a modular bus unit system--the characteristics of which are reviewed, and to plan the URM mission objectives. Finally a new system of adaptable components was established as a basis for future programs. ESA

N94-17144 Telespazio S.p.A., Rome (Italy).
SMALL SATELLITE MISSIONS TO LONG-PERIOD COMETS **c12**
Ettore Perozzi and Eduard M. Pittich (Slovak Academy of Sciences, Bratislava, Czechoslovakia.) *In* CNES, Small Satellites Systems and Services Jan. 1993 p 181-184 (For primary document see N94-17131 03-18)
Copyright Avail: Issuing Activity (CEPADUES-Editions, 111 rue Nicolas-Vaquelin, 31100 Toulouse, France)

Advantages which are expected from space missions towards long period comets and the difficulties of planning such a mission are explained. Conventional missions cannot be planned due to the long waiting time for the comet to appear and the limited time span from discovery to launch. As interplanetary missions with small satellites are now feasible (Giotto experiment) the development of small launchers may solve the major difficulties regarding missions to long period comets, the only objects of the solar system that cannot be reached at present by other means. ESA

N94-17145* Jet Propulsion Lab., California Inst. of Tech., Pasadena.
SMALL SPACECRAFT FOR PLANETARY EXPLORATION **c12**
Ross M. Jones *In* CNES, Small Satellites Systems and Services Jan. 1993 p 185-195 (For primary document see N94-17131 03-18)
Copyright Avail: Issuing Activity (CEPADUES-Editions, 111 rue Nicolas-Vaquelin, 31100 Toulouse, France)

There is need for lower cost, more frequent planetary science missions to compliment the 'once a decade' large multidisciplinary missions. The Solar System Exploration Division of NASA's Office of Space Science and Applications has initiated a program of planetary missions using small spacecraft. This program is called Discovery. Conceptual designs of small spacecraft (100 to 500 kg) for potential Discovery missions to near Earth asteroids are summarized. Another class of spacecraft that could be used for Discovery missions are called microspacecraft. Microspacecraft would be compatible with small launch vehicles such as Pegasus. The term 'microspacecraft' is used here for spacecraft concepts whose mass is about 10 kg. A study of a microspacecraft for a mission to near Earth asteroids is also summarized. ESA

N94-17146 Ecole Nationale Superieure de l'Aeronautique et de l'Espace, Toulouse (France).
BRIDGE: A SMALL SCIENTIFIC SATELLITE FOR GEODESY [BRIDGE: UN PETIT SATELLITE SCIENTIFIQUE POUR LA GEODESIE]
Benedicte Escudier, Michel Bousquet, Francois Barlier (Centre National d'Etudes Spatiales, Toulouse, France.), Georges Balmino (Centre National d'Etudes Spatiales, Toulouse, France.), Maryline Ranc (THARSYS, France.), and Reinhold Bertrand (Stuttgart Univ., Germany.) *In* CNES, Small Satellites Systems and Services Jan. 1993 p 197-207 In FRENCH (For primary document see N94-17131 03-18)
Copyright Avail: Issuing Activity (CEPADUES-Editions, 111 rue Nicolas-Vaquelin, 31100 Toulouse, France)

The results obtained from a preliminary scientific mission study realized by a small satellite in low Earth orbit and using DORIS (Doppler Orbitography and Radiopositioning Integrated from Space) is summarized. Scientific objectives are exposed: Earth gravity field, satellite orbit analysis, ionosphere, and thermosphere density variations are to be studied. The principle of the DORIS system is explained and DORIS is described in detail as well as measurement processing. The BRIDGE mission analysis involves the orbit selection from the on-orbit lifetime, the orbit characteristics, launching, satellite visibilities, constraints due to the payload and to the platform. Finally one circular and two elliptical orbits are selected. Platform predimensioning is discussed. Linking and mass budgets are presented as well as the BRIDGE platform stabilization system. ESA

N94-17147 Bremen Univ. (Germany). Center of Applied Space Technology and Microgravity.
COSMIC DUST AND SPACE DEBRIS MEASUREMENTS ON BOARD THE SMALL SATELLITES HITEN AND BREM-SAT **c90**
H. Iglseder *In* CNES, Small Satellites Systems and Services Jan. 1993 p 209-217 (For primary document see N94-17131 03-18)
Copyright Avail: Issuing Activity (CEPADUES-Editions, 111 rue Nicolas-Vaquelin, 31100 Toulouse, France)

Primary goals of the MUSES-A HITEN mission are to verify technologies and techniques required for lunar and planetary missions in the near future. One of the objectives was an experiment related with the detection and the measurement of mass, velocity and crude flight direction of micrometeroid particles with a Miniaturized Dust Detector (MDC). The experiment set up, the measuring principle and the results of two year operation are discussed; preliminary results show the cosmic dust flux versus time, particle velocity and mass; the spatial and directional distributions are presented as well as the orbital flight velocities of the particles. Space debris measurements are planned with the MDC on board of the microsatellite BREM-SAT. The two main objectives of this future mission are outlined. ESA

N94-17148 Institute for Space Science and Technology, Inc., Gainesville, FL.

SYNMOD: A LOW-RESOURCE, LOW-COST MEANS OF MONITORING THE NEAR-EARTH SPACE DEBRIS ENVIRONMENT

J. Derral Mulholland (Observatoire de la Cote d'Azur, Nice, France.) *In* CNES, Small Satellites Systems and Services Jan. 1993 p 219-227 Prepared in cooperation with Institute for Space Science and Technology, Inc., Magagnose, France (For primary document see N94-17131 03-18)

Copyright Avail: Issuing Activity (CEPADUES-Editions, 111 rue Nicolas-Vaquelin, 31100 Toulouse, France)

Synoptic Monitoring of Orbital Debris (SYNMOD) is a concept that envisions a network of satellites equipped with high time resolution orbital debris impact detectors based on those of the LDEF Interplanetary Dust Experiment (IDE). The ideal network consists of such devices orbiting at a wide variety of altitudes and inclinations with continuous temporal coverage. Modest downlink telemetry requirements permit rapid evaluation of the local debris environment at each spacecraft and by simultaneous analysis of the data from the entire network of the global debris environment. Installing the detectors on the solar panel backsides insures that the system can be adapted in a uniform way to a variety of large and small spacecrafts. IDE provided the first mapping of the angular distribution of small particulates in the near Earth environment, which was shown extremely nonisotropic and time variant. Most of the orbital debris is contained in clouds, some of them in eccentric orbits and/or exceeding 2000 km in extent. Their knowledge can be obtained by continual monitoring on a global network, for which SYNMOD is proposed as a basis. ESA

N94-17149 Max-Planck-Inst. fuer Extraterrestrische Physik, Garching (Germany).

ROLE AND DEVELOPMENT OF SMALL SATELLITE MISSIONS IN SPACE PLASMA PHYSICS **c75**

A. Valenzuela *In* CNES, Small Satellites Systems and Services Jan. 1993 p 229-254 (For primary document see N94-17131 03-18)

Copyright Avail: Issuing Activity (CEPADUES-Editions, 111 rue Nicolas-Vaquelin, 31100 Toulouse, France)

Main space missions from the beginning of the space research are reviewed. Statistical tables give number and percentage of launches, scientific objectives, characteristics of spacecrafts and plasma-physics satellites such as Firewheel, AMPTE/IRM, Viking, Freja, Equator-S, IMPACT, including experiments and instruments. Various design principles, common elements, mission essential requirements and benefits are explained. ESA

N94-17150 MATRA Marconi Space, Toulouse (France).

EARTH OBSERVATION FROM SMALL SATELLITES [OBSERVATION DE LA TERRE A PARTIR DE MINISATELLITE] **c43**

C. Vialet *In* CNES, Small Satellites Systems and Services Jan. 1993 p 259-277 (For primary document see N94-17131 03-18)

Copyright Avail: Issuing Activity (CEPADUES-Editions, 111 rue Nicolas-Vaquelin, 31100 Toulouse, France)

A variety of valuable Earth observation missions can be performed on the basis of existing instrument designs and with the MSS/Fairchild class 2 bus. A general description of the multimission platform and the development status is given. Optical and microwave instruments for Earth observation, ground segment, mission and control center, and payload user center are considered. Instruments were selected for their modest mass and power requirements. The multimission platform is of a modular design; the satellite is compatible with the Pegasus or Taurus launcher and can use SPOT, ERS, and LANDSAT ground stations. Satellite characteristics for along track optical stereo and for altimetry are given as an example. ESA

N94-17151 Lockheed Aircraft Corp., Palo Alto, CA.

SMALL IMAGING SATELLITE FOR EARTH OBSERVING SYSTEM ADJUNCT **c43**

Steven Kilston, Vera Kilston, and Thomas F. Utsch (Air Force Space Div., Los Angeles, CA.) *In* CNES, Small Satellites Systems and Services Jan. 1993 p 279-290 (For primary document see N94-17131 03-18)

Copyright Avail: Issuing Activity (CEPADUES-Editions, 111 rue Nicolas-Vaquelin, 31100 Toulouse, France)

A small multi-mission imaging satellite was developed as an adjunct to the Earth observing system constellation of moderate sized, long life sensing platforms to complement and improve support to the data collection. The satellite's electrooptical sensing payload is designed to operate in many different data collection modes; an operations mode allowing quick changes in the swath width, spatial resolution, and spectral bands being collected can optimize the system coverage. Characteristics of the reliable camera, sensor subsystem design, and sensor parameters are specified. The system, designed for 3 to 5 years lifetime, may find various applications, and could be used to support military data needs in event of a military operation. ESA

N94-17152 Centre National d'Etudes Spatiales, Toulouse (France).

ADEQUATION OF MINI SATELLITES TO OCEANIC ALTIMETRY MISSIONS [MINISATELLITES ET ALTIMETRIE OCEANIQUE OPERATIONNELLE: L'ADEQUATION]

G. Bellaieche and J. P. Aguttes *In its* Small Satellites Systems and Services Jan. 1993 p 291-302 In FRENCH (For primary document see N94-17131 03-18)

Copyright Avail: Issuing Activity (CEPADUES-Editions, 111 rue Nicolas-Vaquelin, 31100 Toulouse, France)

Association of the mini satellite concept and oceanic altimetry missions is discussed. Mission definition and most constraining requirements (mesoscale for example) demonstrate mini satellites to be quite adequate for such missions. Progress in altimeter characteristics, orbit determination, and position reporting allow consideration of oceanic altimetry missions using low Earth orbit satellites. Satellite constellation, trace keeping and orbital period, and required payload characteristics are exposed. The mission requirements covering Sun synchronous orbit, service area, ground system, and launcher characteristics as well as constellation maintenance strategy are specified. Two options for the satellite, orbital mechanics, propulsion, onboard power and stabilizing subsystems, onboard management, satellite ground linkings, mechanical and thermal subsystems, budgets, and planning are discussed. ESA

N94-17153 Societe Anonyme d'Etudes et Realisations Nucleaires, Limeil-Brevannes (France).

SYDONI: AN INTENSIFIED SYSTEM FOR NIGHT OBSERVATION [SYDONI: SYSTEME D'OBSERVATION NOCTURNE INTENSIFIE]

A. Colmon, M. Tissot, and P. Turon *In* CNES, Small Satellites Systems and Services Jan. 1993 p 303-315 In FRENCH (For primary document see N94-17131 03-18)

Copyright Avail: Issuing Activity (CEPADUES-Editions, 111 rue Nicolas-Vaquelin, 31100 Toulouse, France)

An onboard observation device for small satellites is proposed. Called SYDONI, it uses image intensification techniques. Advantages of the night imagery, photometric magnitudes, intensifier characteristics parameters and performance, and signal to noise ratio are discussed. Possible applications are listed. A meteorological mission is selected as a qualification mission; it uses microsatellites and allows demonstration of intensified observation interest and possible use in space. Performances required for the instruments, the camera, the attitude control, and the signal processing as well as platform characteristics are discussed. Possible improvements concern higher signal to noise ratio, larger observation field and higher resolution, improved attitude control, and higher shooting frequency; possible solutions are outlined. ESA

N94-17154 VEGA Space Systems Engineering Ltd., Harpenden (England).

A PROPOSED GROUND SEGMENT DESIGN FOR SMALL SATELLITES **c14**

R. S. Thompson, C. J. Ashton, and A. N. Pidgeon *In* CNES, Small Satellites Systems and Services Jan. 1993 p 321-329 (For primary document see N94-17131 03-18)

Copyright Avail: Issuing Activity (CEPADUES-Editions, 111 rue Nicolas-Vaquelin, 31100 Toulouse, France)

For missions involving small low cost satellites under development, a low cost ground segment comprising an integrated spacecraft control system and ground station based on commercial hardware, making use of modern software technology, and collocating and integrating both the ground station and mission control system, is proposed. A reduced cost antenna system and low cost solid state amplifiers are used as ground station components. The spacecraft control system makes use of standard workstations, configurable software, graphical user interfaces, and automated procedure execution. The cost of the system is still further reduced by collocating

both the spacecraft control system and the ground station, thus simplifying the interfaces. The separation of these components is still possible for missions such as polar orbiting ones. ESA

N94-17155 INISEL, Torrejon de Ardoz (Spain).
GROUND SEGMENT DEFINITION FOR THE SPANISH SMALL SATELLITE PROGRAM (MINISAT) **c14**
F. Cancillo, L. Guzman, and L. A. SanJose *In* CNES, Small Satellites Systems and Services Jan. 1993 p 331-338 (For primary document see N94-17131 03-18)
Copyright Avail: Issuing Activity (CEPADUES-Editions, 111 rue Nicolas-Vaquelin, 31100 Toulouse, France)

The ground segment approach considered for the Spanish program of small satellites (MINISAT), aimed at the development of a general purpose platform to cover a wide range of missions from digital communications to astronomy and Earth observation, is addressed. Mission scenario and general requirements on the ground segment are specified. Architecture of the ground station, the Earth station structure, and control center design are discussed. The payload control center is described in detail. ESA

N94-17156 Centre National d'Etudes Spatiales, Toulouse (France).
OREMUS: PROTOTYPE OF AN ORBIT DETERMINATION CENTER DEDICATED TO MINI-SATELLITE CONTROL [OREMUS: PROTOTYPE DE CENTRE D'ORBITOGRAPHIE POUR LE CONTROLE DE MINISATELLITES] **c14**
Francois Laporte, Genevieve Campan, and Huguette Conessa *In its* Small Satellites Systems and Services Jan. 1993 p 339-347 In FRENCH (For primary document see N94-17131 03-18)
Copyright Avail: Issuing Activity (CEPADUES-Editions, 111 rue Nicolas-Vaquelin, 31100 Toulouse, France)

The OREMUS project aims to achieve at moderate cost a ground segment prototype for the purposes of orbiting satellite operations. In order to demonstrate the feasibility of a general system capable of satisfying the requirements of various users, main functions to be improved are data acquisition, orbit restitution, orbital maneuver calculations, and orbit linked expected operations. MERCATOR system architecture, components, capabilities, interest, and performance are recalled as well as the OOC (Operational Orbit determination Center) needs as regards the software. Characteristics and advantages of a new man machine interface called SISSI are presented. The OREMUS general system is based on MERCATOR and SISSI functions, and on the recovery of former modulus used in spatial mechanics. Descriptor files are documented by the users. Prototype main functions, data acquisition, orbit restitution, attitude restitution, orbital maneuver calculations, orbit linked expected operations, file management, and parameters graphic visualization are available in a control ground segment. These functions are performed by means of modulus; the linking and interfaces of which are managed by the man machine interface. ESA

N94-17157 Ecole Nationale Superieure de l'Aeronautique et de l'Espace, Toulouse (France). Lab. d'Automatique.
DATA PROCESSING SYSTEM FOR ARSENE GROUND STATION: A TOOL FOR SMALL SATELLITE CONTROL AND DEVELOPMENT [LE SYSTEME INFORMATIQUE DE LA STATION SOL ARSENE: OUTIL DE CONTROLE ET DE DEVELOPPEMENT POUR PETITS SATELLITES] **c14**
Jacques Lamaison and Jean-Henri Llareus *In* CNES, Small Satellites Systems and Services Jan. 1993 p 349-359 In FRENCH (For primary document see N94-17131 03-18)
Copyright Avail: Issuing Activity (CEPADUES-Editions, 111 rue Nicolas-Vaquelin, 31100 Toulouse, France)

The ARSENE project history is recalled as well as the ARSENE minisatellite design: mass less than 150 kg, spin stabilization, attitude control through cold gas jets and Galileo sensor, apogee motor. ARSENE is aimed at radio amateur telecommunications. The data processing system of ARSENE ground station is fully described: specifications, operational requirements, performances, ground segment architecture, control system, main operational stations (control, expert, synoptic command and monitoring stations, orbit tracking, reduced telemetry beacon, and simulation/test stations), basic production resources, telemetry decoder, and software. The satellite control system configuration of the ARSENE ground station is discussed as well as the successive developments of the data processing system: telemetry new decoder, status and alarm display control, and ground station telemonitoring. ESA

N94-17158 European Space Agency. European Space Research and Technology Center, ESTEC, Noordwijk (Netherlands).
SATELLITE CONTROL: A COMPREHENSIVE APPROACH **c14**
J. T. Garner *In* CNES, Small Satellites Systems and Services Jan. 1993 p 361-371 (For primary document see N94-17131 03-18)
Copyright Avail: Issuing Activity (CEPADUES-Editions, 111 rue Nicolas-Vaquelin, 31100 Toulouse, France)

The prelaunch and post launch controls undertaken by the Telemetry Tracking and Telecommand (TTC) systems operated under the executive control of the Earth Segment using the European Test and Operations Language (ETOL) are discussed. The condition and status of the European Space Agency communication satellites that are in orbit are also monitored through ETOL. To employ common equipment and methodology throughout the complete life cycle of the satellite, prelaunch activities must be a simulation of expected post launch conditions. Such a comprehensive approach gives opportunities for reusing equipment and methodologies; it was applied to small satellites with industrial partners under direct ESA control using the CSMF (Communication Satellite Monitoring Facility) stand alone workstations and presents a cost effective solution enhancing safety of system operations. ESA

N94-17159 Department of Trade and Industry, Stevenage (England). Radiocommunications Agency.
REGULATION OF LOW EARTH ORBIT SATELLITES
Don Jayasuriya *In* CNES, Small Satellites Systems and Services Jan. 1993 p 377-384 (For primary document see N94-17131 03-18)
Copyright Avail: Issuing Activity (CEPADUES-Editions, 111 rue Nicolas-Vaquelin, 31100 Toulouse, France)

Allocation of a number of frequency bands within which low Earth systems could operate was made to the mobile satellite service by the WARC-92 conference. These allocations and their associated inter and intra-service frequency sharing difficulties are described. Former radio regulations have served adequately for the satellite systems operated from the Geostationary Satellite Orbit (GSO); WARC-92 adopted an interim regulatory system for non-GSO satellite networks. The operation of Low Earth Orbit (LEO) systems are subjected to a number of provisos relating to the protection of planned or existing services; prior to their implementation in LEO, they have to show the possibility of operating within these provisos. A way to resolve difficulties arising from the use of certain frequencies and the approval of terminals are prerequisites for paneuropean operations. ESA

N94-17160 Ministry of Posts and Telecommunications, Tokyo (Japan).
A STUDY ON AN EXPERIMENTAL COMMUNICATION SYSTEM USING MICROSATELLITES **c32**
R. Suzuki, Y. Hashimoto, R. Miura, M. Tanaka, T. Obuchi (Nippon Electric Co. Ltd., Tokyo, Japan.), K. Miyazaki (Nippon Electric Co. Ltd., Tokyo, Japan.), O. Nakagawa (Nippon Electric Co. Ltd., Tokyo, Japan.), M. Matsui (Nippon Electric Co. Ltd., Tokyo, Japan.), and N. Muranaka (Nippon Electric Co. Ltd., Tokyo, Japan.) *In* CNES, Small Satellites Systems and Services Jan. 1993 p 385-391 (For primary document see N94-17131 03-18)
Copyright Avail: Issuing Activity (CEPADUES-Editions, 111 rue Nicolas-Vaquelin, 31100 Toulouse, France)

An experimental communication network using microsatellites is studied to solve the problems inherent in the use of geostationary satellites. A few microsatellites pick up and deliver voice and digital information from/to ground stations, and/or from/to satellites. A microsatellite features twin structures of twenty six hedron connected to each other by an expanded mast; it is 50 kg of dumbbell shape. A total of 9.6 kbps and 1.2 kbps are used for the ground link and the intersatellite link respectively with onboard digital processing techniques. The formation of the microsatellites in one orbit is used tc widen the real time communication area. A possibility of a delay time reduction for package message communication is expected using the intersatellite link. ESA

N94-17161 Italspazio, Rome (Italy).
LEOCOM-SPES: LOW COST MESSAGE COMMUNICATIONS **c32**
G. Barresi, L. Caporicci, R. DelRicco, S. DiGirolamo, B. Pavesi, and G.

Rondinelli *In* CNES, Small Satellites Systems and Services Jan. 1993 p 393-404 (For primary document see N94-17131 03-18)
Copyright Avail: Issuing Activity (CEPADUES-Editions, 111 rue Nicolas-Vaquelin, 31100 Toulouse, France)

For the user categories which do not need real time connections, LEOCOM-SPES (Space Pony Express) is an economic and attractive personal communications system based on a sparse constellation applicable to message/data communications. The system architecture, the major system elements, the orbit and constellation selection, the system implementation, the ground segment, the user terminal, the network operation, and traffic scenario and requirements are outlined. Satellite and launch costs, investment costs for the central control station, and user charges are also discussed. To conclude, the Leostar spacecraft performances are summerized: Leostar is a stabilized satellite designed for operation in low altitude Earth orbits. ESA

N94-17162 Centre National d'Etudes Spatiales, Toulouse (France).
TAOS (S80): A (LEO-MSS) SYSTEM FOR POSITION REPORTING AND TELEMANAGEMENT SERVICES [TAOS (S80): UN SYSTEME LEO-MSS POUR DES SERVICES DE LOCALISATION ET DE TELEGESTION] c32
A. Gautier and P. Dumont *In its* Small Satellites Systems and Services Jan. 1993 p 405-415 In FRENCH (For primary document see N94-17131 03-18)
Copyright Avail: Issuing Activity (CEPADUES-Editions, 111 rue Nicolas-Vaquelin, 31100 Toulouse, France)

A position reporting and telemanagement system based on the use of minisatellites (mass less than 150 kg) with limited investment and operation costs is presented. The system is designed from an analyses of market study results. The space segment is composed of a LEO-MSS (Low Earth Orbit Mini Satellite System) constellation: solution advantages are reviewed. Frequency band regulations and frequency allotment are specified. The space segment (constellation, satellite platforms), ground segment (mission and control), mobile terminal stations (connecting links, position reporting through Doppler/distance or external measurements) are described. Forward and return link budgets and communication protocols are presented. The system performances as regards capacity, response time, availability, and reliability are specified. A feasibility study using S80T, a meteorological satellite, investigates the two critical points underlined in the preliminary study. ESA

N94-17163 Orbital Sciences Corp., Fairfax, VA.
THE ORBCOMM SYSTEM c32
Martin Deckett *In* CNES, Small Satellites Systems and Services Jan. 1993 p 417-426 (For primary document see N94-17131 03-18)
Copyright Avail: Issuing Activity (CEPADUES-Editions, 111 rue Nicolas-Vaquelin, 31100 Toulouse, France)

The objectives, architecture, characteristics, performance, and costs of the ORBCOMM data communications and position determination system designed to bring low cost mobile communications to every country throughout the world are outlined. The system uses a constellation of small satellites in low Earth orbits, operating at VHF, as relays for the ORBCOMM network. On the ground, a simple Network Control Center (NCC) is connected to gateway Earth stations. The user needs a desk top computer at central office, connected to the NCC computer, and pocket size remote terminals. Three generic services can be provided: SecurNet for emergency alerts, MapNet for position reports, and DataNet for two way data transmission. Coverage, outage periods, choices made for ORBCOMM and capital and operating costs are also discussed. ESA

N94-17164 European Space Agency. European Space Research and Technology Center, ESTEC, Noordwijk (Netherlands). Radiofrequency Systems Div.
MAGSS-14: MEDIUM ALTITUDE GLOBAL MOBILE SATELLITE SYSTEM WITH ENHANCED REGIONAL COVERAGE c32
J. Benedicto, J. Fortuny, and P. Rastrilla *In* CNES, Small Satellites Systems and Services Jan. 1993 p 427-436 (For primary document see N94-17131 03-18)
Copyright Avail: Issuing Activity (CEPADUES-Editions, 111 rue Nicolas-Vaquelin, 31100 Toulouse, France)

The basic parameters and performance of a Medium Altitude Global Satellite System (MAGSS-14) considered as an effective way to provide voice communications services to users equipped with handheld and portable terminals are described. MAGSS-14 is based on 14 medium size satellites in a Medium Earth Orbit (MEO) constellation, and offers significant advantages in terms of gradual buildup and global coverage. The constellation parameters are optimized to enhance the coverage in terms of minimum elevation angle in the regions contained between 30 and 60 deg latitude. Network topology, payload design, link budgets, and system capacity are also discussed. ESA

N94-17165 Italspazio, Rome (Italy).
FEASIBILITY STUDY OF A PERSONAL COMMUNICATIONS SYSTEM IRIDIUM-LIKE c32
L. Caporicci, R. DelRicco, S. DiGirolamo, C. Soddu, and G. Pondinelli *In* CNES, Small Satellites Systems and Services Jan. 1993 p 437-449 (For primary document see N94-17131 03-18)
Copyright Avail: Issuing Activity (CEPADUES-Editions, 111 rue Nicolas-Vaquelin, 31100 Toulouse, France)

A candidate architecture applicable to personal communications systems, via Low Earth Orbit (LEO) satellites is outlined. The concept of the IRIDIUM Motorola system has been adopted as derived from the available public documentation. The following topics are covered: system architecture (IRIDIUM like concept) and scenario; constellation characteristics, user links, coverage and frequency reuse; Leostar-E spacecraft and payload architecture definition; traffic management (access, routing, networking); and organization aspects and manufacturing strategies. Additional efforts are required in order to assess a convenient cost/technology tradeoff. ESA

N94-17166 Centre National d'Etudes Spatiales, Toulouse (France).
S 80/T: A MICRO SATELLITE SYSTEM COMBINING HIGH PERFORMANCES AND LIMITED RESOURCES [S 80/T: UN MICRO-SATELLITE SYSTEME QUI COMBINE HAUTES PERFORMANCES ET RESSOURCES LIMITEES]
Jean-Claude Llorens *In its* Small Satellites Systems and Services Jan. 1993 p 451-458 In FRENCH (For primary document see N94-17131 03-18)
Copyright Avail: Issuing Activity (CEPADUES-Editions, 111 rue Nicolas-Vaquelin, 31100 Toulouse, France)

The mission of the experimental technological microsatellite S80T is specified: 148 to 149.9 MHz frequency band analysis and modulation experiments. The system is described: platform, payload, data acquisition, satellite control, and user ground station. The spectral analysis of the frequency band is performed by means of statistical treatments of the noise at the satellite repeater entry, short duration event treatment, and treatments using time signals; calibration strategy, measurement connections between the real power at the repeater entry and the noise power picked up by the antenna, measurement sequencing, and exploitation are described. Characteristics of the main elements of the user ground station are specified: telecommand, telecontrol, tracking, interfacing computer, measuring equipment and techniques. Project development, management, quality and reliability are also outlined. ESA

N94-17167 Ellipsat Corp., Washington, DC.
THE ELLIPSO (TM) SYSTEM: ELLIPTICAL LOW ORBITS FOR MOBILE COMMUNICATIONS
David Castiel *In* CNES, Small Satellites Systems and Services Jan. 1993 p 459-463 (For primary document see N94-17131 03-18)
Copyright Avail: Issuing Activity (CEPADUES-Editions, 111 rue Nicolas-Vaquelin, 31100 Toulouse, France)

The ELLIPSO system is aimed at providing mobile voice services via satellites located in low Earth elliptical orbits and operating in the 1610 to 1625.5 MHz and 2483.5 to 2500 MHz bands. Orbital characteristics and time coverage over northern and southern latitudes are outlined. ELLIPSO uses Code Division Multiple Access (CDMA) within frequency segments to achieve an efficient FDMA (Frequency Division MA)/CDMA scheme. ELLIPSO satellites and ground control station equipment are also described. ELLIPSO also supports position determination embedded in the overall system, according to a concept called the Geobeacon system: position detection is obtained through measurements of time difference of arrivals and of frequency difference of arrivals. ESA

N94-17168 Starsys Research Corp., Boulder, CO.
STARSYS: A VIEW AFTER WARC-92 c32
Ashok Kaveeshwar and Raul Rodriguez *In* CNES, Small Satellites

Systems and Services Jan. 1993 p 465-472 (For primary document see N94-17131 03-18)
Copyright Avail: Issuing Activity (CEPADUES-Editions, 111 rue Nicolas-Vaquelin, 31100 Toulouse, France)

The STARSYS system is aimed at providing low cost global positioning and messaging by satellite. STARSYS is a data only system using very brief message transmission times. Code Division Multiple Access (CDMA) is used for frequency sharing; it enables transmitted data to be coded for unique user identification and also to employ Doppler and radio ranging to determine the geographical location of a transmitting terminal. The STARSYS system is composed of the field receiver/transmitter, the Low Earth Orbit (LEO) satellite constellation and the ground station elements. Each message transmission is able to contain up to thirty two digital characters. Market applications are numerous: theft control, vehicle and logistic tracking and messaging, personal communications, utility and environmental data acquisition and transfer. Co-primary frequency allocation at WARC-92 accelerated interest for potential customers and investors, although the amount of frequency allocation (less than 1 GHz) is small. ESA

N94-17169 Surrey Satellite Technology Ltd., Guildford (England).
UoSAT: A DECADE OF EXPERIENCE PIONEERING MICROSATELLITES
J. M. Radbone (Surrey Univ., London, England.) and M. N. Sweeting (Surrey Univ., London, England.) *In* CNES, Small Satellites Systems and Services Jan. 1993 p 477-487 Prepared in cooperation with Surrey Univ., Guildford, England (For primary document see N94-17131 03-18)
Copyright Avail: Issuing Activity (CEPADUES-Editions, 111 rue Nicolas-Vaquelin, 31100 Toulouse, France)

Two satellites constructed as examples of low cost missions are examined and the technical and management techniques employed are described. Following first UoSAT missions, KITSAT-A is an experimental mission, S80/T a demonstration mission to evaluate the use of VHF frequencies for future low Earth orbit systems and CERISE, a modified microsatellite platform, will carry a classified payload. All these satellites are based on UoSAT-5 platform. Key technical and management issues for successful microsatellite missions are reviewed: simple interfaces, flexible design, control of requirements and modularity, quality and product assurance for the technical aspect, contract conditions, project length, efficient communications, integrated and co-located team, flexibility of organization and personnel for the management conditions. ESA

N94-17170 Alcatel Espace, Toulouse (France).
CERISE MICROSATELLITE SYSTEM [LE SYSTEME MICROSATELLITE CERISE]
J. Kaced *In* CNES, Small Satellites Systems and Services Jan. 1993 p 489-496 In FRENCH (For primary document see N94-17131 03-18)
Copyright Avail: Issuing Activity (CEPADUES-Editions, 111 rue Nicolas-Vaquelin, 31100 Toulouse, France)

The main CERISE objective is measurement and characterization of the radioelectrical environment onboard a low orbit satellite in a wide frequency band. It involves a microsatellite with a mass less than 50 kg, microsatellite command/control, a ground station for telemetry scientific exploitation. Mission design and constraints are reviewed: satellite orbit in terms of the launch opportunity, no orbit control, simplified attitude control, onboard data storage capacity, short life time, low cost, launch opportunities. CERISE system is built from the UoSAT-5 concept improved as regards electrical power, flight software, telemetry/telecommand frequency modifications. Details of the CERISE payload (computer, hyperfrequency sensor, onboard testing and qualification) and groundstation (microsatellite position acquisition, orbital acceptance, telemetry exploiting unit) are dealt with. ESA

N94-17171 European Space Agency. European Space Research and Technology Center, ESTEC, Noordwijk (Netherlands).
IMPACT OF ADVANCES IN TECHNOLOGY ON FUTURE SPACECRAFT DESIGN
F. Gampe and G. Lippner (Dornier System G.m.b.H., Friedrichshafen, Germany.) *In* CNES, Small Satellites Systems and Services Jan. 1993 p 497-514 (For primary document see N94-17131 03-18)
Copyright Avail: Issuing Activity (CEPADUES-Editions, 111 rue Nicolas-Vaquelin, 31100 Toulouse, France)

The status of the ESTEC study of the title is presented. The role of the study within the small satellite systems and services is shown, main topics, objectives and approach are summarized. Advances in technology are surveyed, followed by recommendations for an advanced engineering approach including a survey of launchers and of application fields, by a pool of potential model missions. Three of them were selected for a detailed analysis: model missions and advanced technology, advanced design, launch opportunities, the ground segment approach and the commercial approach are discussed. Potential new services are identified and payload characteristics analyzed for the reference missions. A set of reference mission requirements is established for case studies. ESA

N94-17172 Aerospatiale, Cannes (France).
S-80: A SATELLITE FOR LESS THAN 50 MF [S-80: UN SATELLITE A MOINS DE 50 MF]
A. Lamothe *In* CNES, Small Satellites Systems and Services Jan. 1993 p 515-520 In FRENCH (For primary document see N94-17131 03-18)
Copyright Avail: Issuing Activity (CEPADUES-Editions, 111 rue Nicolas-Vaquelin, 31100 Toulouse, France)

The S-80 is a localization system for mobiles using a constellation of small low Earth orbiting satellites. The main objective of the definition study of the space segment is the design of the S-80 satellite for a cost less than 50 MF. The objective was achieved by a specific technical approach; furthermore the satellite offers a wide mission capacity. Main specifications of the S-80 system are recalled: constellation characteristics, payload, schedule, launch opportunities. The ways to achieve the cost objective are addressed: simple technology, adequate electronics, integrated colocated teams, adequate quality policy. Expertise inherited from former projects such as EOLE or ARESENE is recalled. S-80 satellite elements, characteristics and performance are specified. ESA

N94-17173 Ministry of Aeronautics and Astronautics, Shanghai (China). Bureau of Astronautics.
SMALL SATELLITE MODULAR DESIGN AND APPLICATION PROSPECT
Jie Yuan and Jin-Jun Chen *In* CNES, Small Satellites Systems and Services Jan. 1993 p 521-531 (For primary document see N94-17131 03-18)
Copyright Avail: Issuing Activity (CEPADUES-Editions, 111 rue Nicolas-Vaquelin, 31100 Toulouse, France)

A small satellite modular architecture is introduced, which is based on systematically analyzing the subsystem functions of small satellites. A whole spacecraft is divided into three modules: the payload module, the attitude control module and the common service module. The payload module offers three versions to select according to payload mass; the attitude control module offers gravity gradient modules, spin stabilized modules and two types of three axis stabilization module; common service module is the small satellite control center including control system, power system and TTC (Telemetry, Tracking and Control) system. Several basic module configurations are possible: gravity gradient model, spin stabilized model, the payload module mass varying between 50 to 150 kg. The use of a Chinese launch vehicle to launch these modular small satellites is possible. Small satellite applications in the military, civil and scientific fields are prospected. ESA

N94-17174 Fabrica Italiana Apparecchiature Radioelettriche S.p.A., Milan. **c44**
ARSENE GaAs SOLAR ARRAY
L. Brambilla, A. Caon, R. Contini, G. DAccolti, E. Rossi, G. Verzeni, B. Bollani (Centro Informazioni Studi Esperienze, Milan, Italy.), C. Flores (Centro Informazioni Studi Esperienze, Milan, Italy.), F. Paletta (Centro Informazioni Studi Esperienze, Milan, Italy.), and D. Passoni (Centro Informazioni Studi Esperienze, Milan, Italy.) et al *In* CNES, Small Satellites Systems and Services Jan. 1993 p 537-546 (For primary document see N94-17131 03-18)
Copyright Avail: Issuing Activity (CEPADUES-Editions, 111 rue Nicolas-Vaquelin, 31100 Toulouse, France)

The GaAs solar array of ARSENE, a radioamateur spin stabilized spacecraft, is presented. The solar array uses typical Liquid Phase Epitaxy (LPE) solar cells and consists of six body mounted solar panels; each panel comprises an aluminum honeycomb substrate with aluminum skins insulated on the active area. For the qualification and acceptance of the ARSENE solar array, an engineering solar panel was submitted to the qualification tests including thermal vacuum, thermal shocks. The flight units are submitted to the thermal vacuum test. The final acceptance tests

include rotational, acoustic and vibration tests performed at satellite level. Predicted power output, GaAs solar cell manufacturing, solar panel assembly and testing are discussed. ESA

N94-17175 Eagle-Picher Industries, Inc., Joplin, MO.
SMALL SATELLITE NICKEL-HYDROGEN AND NICKEL-METAL HYDRIDE POWER APPLICATIONS **c20**
William Dean Cook and Dwaine Coates *In* CNES, Small Satellites Systems and Services Jan. 1993 p 547-556 (For primary document see N94-17131 03-18)
Copyright Avail: Issuing Activity (CEPADUES-Editions, 111 rue Nicolas-Vaquelin, 31100 Toulouse, France)

Nickel and silver-metal hydride batteries are being developed for aerospace applications. Metal hydride batteries offer a number of advantages over other aerospace battery systems. Nickel-metal hydride batteries have twice the gravimetric energy density of nickel-cadmium and twice the volumetric energy density of nickel-hydrogen. Silver-metal hydride batteries have the potential of three times the energy density of nickel-metal hydride and exhibit superior charge retention characteristics. Aerospace metal hydride batteries are hermetically sealed, operate at low pressure and are prismatic in geometry. They exhibit excellent overcharge and overdischarge capability. Preliminary calorimetry data indicates superior thermal performance as compared to nickel-cadmium and nickel-hydrogen batteries. Some initial AC impedance spectroscopy work has been completed on both metal-hydrogen and metal-hydride battery systems. The objective of current programs is to develop high energy density, long cycle life metal-hydride batteries for the aerospace market and to establish a testing database to support future applications. ESA

N94-17176 European Space Agency. European Space Research and Technology Center, ESTEC, Noordwijk (Netherlands). Power Conditioning Section.
A POWER SYSTEM FOR A MICROSATELLITE **c20**
Dan Olsson *In* CNES, Small Satellites Systems and Services Jan. 1993 p 557-566 (For primary document see N94-17131 03-18)
Copyright Avail: Issuing Activity (CEPADUES-Editions, 111 rue Nicolas-Vaquelin, 31100 Toulouse, France)

A power system for a microsatellite was designed for the Space Technology Research Vehicle (STRV-1) mainly aimed at technology demonstration experiments and studies of radiation effects and planned to be launched into geostationary transfer orbit. The low average solar array power (25 W) and the small volume allocation of the power system electronics (2.8 dm cubed) became a challenge when trying to produce a failure tolerant power system. The power system elements: shunt regulator, battery discharge regulator, power distribution, solar array, battery, and their management and protection are described. Power system performance and growth potential are also discussed. After several simplification iteractions, a modular power electronics system with a high degree of failure tolerance, with a mass less than 2.5 kg and an internal power consumption less than 3 W was developed. ESA

N94-17177 INISEL, Torrejon de Ardoz (Spain).
DATA HANDLING STRATEGY FOR THE SPANISH SMALL SATELLITE PROGRAM (MINISAT) **c82**
X. Lobao and L. Pina *In* CNES, Small Satellites Systems and Services Jan. 1993 p 567-575 (For primary document see N94-17131 03-18)
Copyright Avail: Issuing Activity (CEPADUES-Editions, 111 rue Nicolas-Vaquelin, 31100 Toulouse, France)

The data handling approach considered for the Spanish program of small satellites, aimed at the development of a general purpose platform to cover missions varying from digital communications to astronomy and Earth observations is described. It consists of the centralization of the platform intelligence in the data handling computer; as a result, the computer is devoted to several mission dependent functions besides its normal data handling functions: attitude determination and control, thermal control, power distribution control, processing of payload mission data. Data handling system, subsystems, basic characteristics, connection to the data handling users, onboard computer structure are discussed. Solid state memory devices are used to allow the required high data capacity while keeping reasonable mass, size and power budgets. ESA

N94-17178 Centre National d'Etudes Spatiales, Toulouse (France).
THE STRV ON BOARD DATA HANDLING (OBDH) SYSTEM: AN INTRODUCTION **c82**
H. G. Andrews *In its* Small Satellites Systems and Services Jan. 1993 p 577-578 (For primary document see N94-17131 03-18)
Copyright Avail: Issuing Activity (CEPADUES-Editions, 111 rue Nicolas-Vaquelin, 31100 Toulouse, France)

The operation of the Space Technology Research Vehicle (STRV) On Board Data Handling (OBDH) system is outlined. STRV is a 50 kg satellite designed to research and demonstrate new and improved technologies. OBDH system consists of six functionally separate units: the uplink unit, two on-board computers, the command distribution unit, the data acquisition unit, the downlink unit. They are described and their function is outlined. The OBDH system supports the data processing and control requirements of each STRV equipment. ESA

N94-17179 Aerospatiale, Cannes (France).
A MINI SATELLITE CALLED ARSENE: THE WAY TO MAKE IT AT A MINIMUM COST [UN MINISATELLITE NOMME ARSENE: COMMENT LE REALISER A COUT MINIMUM]
Jean-Paul Rihet and Jean-Pierre Redon (Centre National d'Etudes Spatiales, Toulouse, France.) *In* CNES, Small Satellites Systems and Services Jan. 1993 p 583-600 In FRENCH (For primary document see N94-17131 03-18)
Copyright Avail: Issuing Activity (CEPADUES-Editions, 111 rue Nicolas-Vaquelin, 31100 Toulouse, France)

The context of the radioamateur ARSENE project is recalled. The ARSENE idea, concept, specifications, mechanical and electrical architecture, placement in final orbit and station keeping as well as financing are discussed. The ways used to achieve ARSENE at minimal cost are explained: solutions for mechanics, integration methods, project management by industry, precision, quality, costs and the acquired expertise as regards industry and project management are dealt with. ESA

N94-17180 Technische Univ., Berlin (Germany).
TUBSAT: LOW COST ACCESS TO SPACE TECHNOLOGY
U. Renner, B. Luebke-Ossenbeck, and P. Butz *In* CNES, Small Satellites Systems and Services Jan. 1993 p 601-610 (For primary document see N94-17131 03-18)
Copyright Avail: Issuing Activity (CEPADUES-Editions, 111 rue Nicolas-Vaquelin, 31100 Toulouse, France)

The TUBSAT design philosophy, that provides at affordable cost conditions all necessary services to the customer, is based on the balance between low cost experiments, low cost launch opportunities (secondary payloads), and low cost space platforms. Design concept, launch opportunity, volume, mass, electrical power supply, thermal control, TTC (Telemetry, Tracking and Control), data handling, and attitude control are discussed. A high attitude control accuracy to any desired direction is required. Using TUBSAT-A prototype, the design concept was verified, data handling and the three axis sensor were qualified. ESA

N94-17181 Etude et Realisation de Micro-Satellites, Paris (France).
STANDARD PLATFORMS FOR SMALL SATELLITES [PLATES-FORMES STANDARDS POUR PETITS SATELLITES]
Marc Schaefer *In* CNES, Small Satellites Systems and Services Jan. 1993 p 611-616 In FRENCH (For primary document see N94-17131 03-18)
Copyright Avail: Issuing Activity (CEPADUES-Editions, 111 rue Nicolas-Vaquelin, 31100 Toulouse, France)

Platforms usable for various scientific or civil missions are proposed by the team responsible for the SARA (French acronym for satellite amateur radio astronomy) project. Classical solutions are studied to be adapted to launcher special interfaces. A three axis stabilized platform is selected as an example of the low cost microsatellite possibilities: the frame, the precision of the attitude control, the pitch, roll and yaw stabilization through gravity gradient, the payload mass and possibilities, and the characteristics of the equipment are discussed. Possible applications are outlined: orbital component tests, Earth observations, and electronic mailsystems. Low costs, short development duration, and launch possibilities are mentioned. Achievement of advanced platforms with high pointing and attitude control performance is possible. ESA

N94-17182 Instituto Nacional de Tecnica Aeroespacial, Madrid (Spain).
MINISAT PROGRAMME
Jose M. Dorado *In* CNES, Small Satellites Systems and Services Jan. 1993 p 617-623 (For primary document see N94-17131 03-18)
Copyright Avail: Issuing Activity (CEPADUES-Editions, 111 rue Nicolas-Vaquelin, 31100 Toulouse, France)

The objective of the MINISAT program is to obtain the necessary elements to perform space missions in a way that offers payload support capabilities similar to those of a 'normal' mission, shorter delays and lower costs. A system including a space platform and a ground segment for orbit and mission control, both with a high degree of standardization is a first objective. Concept of the MINISAT platform is discussed; program status is outlined. Main characteristics of the MINISAT platform are specified: orbit, launchers, applications, dimensions, mass, electrical power, payload data, stabilization, and propulsion. ESA

N94-17183 Defence Research Agency, Farnborough (England). Space Sector.
THE SPACE TECHNOLOGY RESEARCH VEHICLE: DEVELOPMENT STATUS
K. A. Ryden *In* CNES, Small Satellites Systems and Services Jan. 1993 p 625-630 (For primary document see N94-17131 03-18)
Copyright Avail: Issuing Activity (CEPADUES-Editions, 111 rue Nicolas-Vaquelin, 31100 Toulouse, France)

The Space Technology Research Vehicles (STRV's) under development are described and the up to date technical status is detailed. The two vehicles are to carry into orbit a range of new technology which requires in-orbit evaluation prior to much larger and more expensive missions. Structure power system, radio frequency system, onboard data handling system, attitude control system, experiments and ground segment are discussed. The new technologies include radiation-resistant microelectronics, radiation monitoring instruments, advanced structural materials, electrostatic hazard measuring instruments, alleviation techniques, and new power system components. ESA

N94-17184 Technion - Israel Inst. of Tech., Haifa. Space Research Inst.
ON-BOARD SPATIAL SCIENTIFIC EXPERIMENT PROJECT ON SMALL SATELLITES [PROJET D'EXPERIENCE SCIENTIFIQUE SPATIALE EMBARQUEE SUR PETIT SATELLITE]
I. H. Keroub *In* CNES, Small Satellites Systems and Services Jan. 1993 p 631-637 In FRENCH (For primary document see N94-17131 03-18)
Copyright Avail: Issuing Activity (CEPADUES-Editions, 111 rue Nicolas-Vaquelin, 31100 Toulouse, France)

An experiment using small satellites for geophysical exploration is proposed: modeling the longitudinal variance of the total electronic content latidudinal gradients. The various segments for the implementation satellite segment, receiving segment (antenna, receiver, filtering and detection, and recorder), exploitation segment (use of new methods for calculating the total electronic content, scientific interest such as transhorizon propagation of radiowaves, adequate modeling of the total electronic content) are described. Expected results are a contribution to ionospheric modeling in real and delayed time, progress in knowledge of the ionospheric transversal propagation, and a contribution to the transhorizon transionospheric propagation fields. ESA

N94-17185 AeroAstro, Inc., Herndon, VA.
ALEXIS AND HETE: TWO SMALL, LOW COST, SCIENTIFIC SATELLITE SYSTEMS
Francois Martel and Rick Fleeter *In* CNES, Small Satellites Systems and Services Jan. 1993 p 639-649 (For primary document see N94-17131 03-18)
Copyright Avail: Issuing Activity (CEPADUES-Editions, 111 rue Nicolas-Vaquelin, 31100 Toulouse, France)

ALEXIS and HETE are two examples of integrated space and ground station system designed for independent use by research institutions. ALEXIS was designed as a space platform carrying telescopes for technology testing and astrophysical observations. It is schematically presented; specifications are summarized and the ground station design is outlined. The HETE principal mission is the detection and precise location of the sources of gamma ray bursts, using an array of gamma detectors, an imaging x ray telescope and four telescopes. General specifications are given; improvements compared to ALEXIS system are detailed, in particular the structure and specific objectives of the twenty ground stations. Some information is given concerning planning and development budget. ESA

N94-17186 THARSYS (France).
TITUS: A MICRO-SATELLITE FOR TECHNOLOGY DEMONSTRATION
M. Moreliere and R. Bertrand *In* CNES, Small Satellites Systems and Services Jan. 1993 p 651-657 (For primary document see N94-17131 03-18)
Copyright Avail: Issuing Activity (CEPADUES-Editions, 111 rue Nicolas-Vaquelin, 31100 Toulouse, France)

TITUS, the first representative of a small satellite family is designed as a microsatellite (50 kg) to be launched by Ariane-4 or Pegasus to offer opportunities for technology demonstration in Earth orbit. TITUS is to be injected into geostationary transfer orbits or into Sun synchronous orbits in order to cross the Polar Horn, the South Atlantic Anomaly or the Van Allen Belts with each revolution; both orbits allow to demonstrate or to qualify space equipment such as electrical and electronic components, solar cells, batteries, sensors, microwave components, and mechanical equiment. TITUS system specifications, mission aspects and modular bus design are discussed. An example of a gravity gradient stabilized platform is detailed. TITUS project characteristics are summarized. ESA

N94-17187 Orbital Sciences Corp., Fairfax, VA.
BIG RESULTS WITH SMALL SPACE SYSTEMS: WHAT SMALL SYSTEMS ARE DOING TODAY
Gilbert D. Rye and Henry F. LeMieux *In* CNES, Small Satellites Systems and Services Jan. 1993 p 665-684 (For primary document see N94-17131 03-18)
Copyright Avail: Issuing Activity (CEPADUES-Editions, 111 rue Nicolas-Vaquelin, 31100 Toulouse, France)

Emerging customer needs in small space systems and the capabilities that evolved in response to these needs are reviewed. The benefits realized in communications, observation and remote sensing, space research and experimentation are described; space system designs and mission objectives, instrumentation requirements, and spacecraft characteristics are detailed. Examples of space products and services are discussed: Pegasus, Taurus and PegaStar characteristics and capabilities, turnkey and space based services. Trends for the future are outlined: increasing capabilities, system sophistication, spacecraft mass, and bus performance. ESA

N94-17188 Bureau Veritas, Courbevoie (France).
SMALL SATELLITE PRODUCT ASSURANCE [L'ASSURANCE PRODUIT DES PETITS SATELLITES] **c38**
J. DeMontlivault and Jacques Cadelec (Calireal, Palaiseau, France.) *In* CNES, Small Satellites Systems and Services Jan. 1993 p 685-694 In FRENCH (For primary document see N94-17131 03-18)
Copyright Avail: Issuing Activity (CEPADUES-Editions, 111 rue Nicolas-Vaquelin, 31100 Toulouse, France)

In order to increase the interest in small satellites, their cost must be reduced; reducing product assurance costs induced by quality requirements is a major objective. For a logical approach, small satellites are classified in three main categories: satellites for experimental operations with a short lifetime, operational satellites manufactured in small mass with long lifetime requirements, operational satellites (long lifetime required), of which only a few models are produced. The various requirements as regards the product assurance are examined for each satellite category: general requirements for space approach, reliability, electronic components, materials and processes, quality assurance, documentation, tests, and management. Ideal product assurance system integrates quality teams and engineering teams. ESA

N94-17189 Intespace, Toulouse (France).
ENVIRONMENT TESTS FOR MINI SATELLITES [ESSAIS D'ENVIRONNEMENT DES MINI SATELLITES]
Gerard Boures and Joseph Merlet *In* CNES, Small Satellites Systems and Services Jan. 1993 p 695-701 In FRENCH (For primary document see N94-17131 03-18)
Copyright Avail: Issuing Activity (CEPADUES-Editions, 111 rue Nicolas-Vaquelin, 31100 Toulouse, France)

A global approach integrating from the design test methods and equipment and measuring sensors for lower test costs and duration is

proposed: defining first the test program through a customized logical analysis; improving the global process by minimized acceptance tests (especially mechanical tests); using qualification tests for the first model and acceptance of the recurrent models through a comparison with the first model; reinforcing design test links by improving data processing and data communications; and simplifying and optimizing tasks. Simpler thermal tests, fewer measurement points, and use of 'lost' sensors are examples. These could speed up the satellite achievement and lower the corresponding costs. ESA

N94-17190 Smith System Engineering Ltd., Guildford (England).
COST DRIVERS: WHY DO CONVENTIONAL SATELLITES COST SO MUCH? c83
Chris Elliott *In* CNES, Small Satellites Systems and Services Jan. 1993 p 703-708 (For primary document see N94-17131 03-18)
Copyright Avail: Issuing Activity (CEPADUES-Editions, 111 rue Nicolas-Vaquelin, 31100 Toulouse, France)

From discussions with U.S. and European specialists, it was concluded that a positive feedback mechanism systematically forces space missions to become more expensive, to take longer time to execute, while they do not satisfy their user needs. The mechanism is analyzed and consequences for the conduct of the projects are explained. In spite of reasonable decisions at each stage of the project design and planning the costs are mounting in a 'vicious' spiral. Five major changes needed to put the costs onto a down spiral are discussed: users to determine needs, failures are tolerated, appropriate technology is used (maximum use of already existing devices), missions dedicated to fewer payloads, viticus, short project duration with small teams involved, preferably collocated. As a result, costs come down: the 'virtuous' spiral. ESA

N94-17191 Euroconsult, Paris (France).
KEY TRENDS OF THE SMALL SATELLITE MARKET c83
Stephane Chenard *In* CNES, Small Satellites Systems and Services Jan. 1993 p 709-722 (For primary document see N94-17131 03-18)
Copyright Avail: Issuing Activity (CEPADUES-Editions, 111 rue Nicolas-Vaquelin, 31100 Toulouse, France)

Characteristics of the small satellite families (minisatellites, microsatellites, nanosatellites plus the Delta class) are given. In spite of some adverse technology trends, the financial and operational advantages of the small satellites are solid: downsizing of programs such as the Earth observation system, new available launch options, progressive build-up of the satellite constellations, and progress at equipment level (onboard data processing capacity, solar array specific specific power). The five families of applications (in orbit technology demonstration, gap fillers, overlays and 'augmentsats', niche applications, start-up entrepreneurs, use of more expensive and sophisticated systems) are discussed, as well as their impact on the satellite industry and on the launch industry. Possible market development is outlined. ESA

N94-17240# Amptek, Inc., Bedford, MA.
SPACE SYSTEMS ENVIRONMENTAL INTERACTION STUDIES
M. A. Morgan, Alan C. Huber, John O. McGarity, David J. Sperry, and Scott J. Moran 12 Jan. 1993 36 p
(Contract F19628-91-C-0112)
(AD-A267280; PL-TR-93-2006; SR-1) Avail: CASI HC A03/MF A01

Under Task 1, the Photovoltaic Array Space Power Plus Diagnostics (PASP Plus) experiment, encompassing most of Amptek's effort in the report period, Amptek has done the following: (1) designed and built the experiment controller; (2) provided an electrostatic analyzer (ESA), two QCM's, and three calorimeters (CAL's); (3) worked with PL/GPSP on testing and integrating PASP Plus into the APEX satellite; and (4) provided ground support equipment for spacecraft integration and mission operation. The controller is comprised of a central processing unit, an array biasing and electrometer unit, an array 1-5 curve measurement unit, a power conversion unit, and interfaces to the 16 array modules, ten PASP Plus instruments (not including the Dosimeter), and the APEX spacecraft. The PASP Plus Controller and the ten other instruments it controls (Sun Sensor, Langmuir Probe, ESA, Transient Pulse Monitor, Electron Emitter, 2 QCM's, 3 CAL's) are described in detail, giving size (dimensions), weight, data rates and outputs, and input power requirements. On Tasks 2 and 3, at a much lower level of effort, Amptek supported PL/GPSP's work on the Charge Hazards and Wake Studies (CHAWS) experiment (O to -5000 V sweep power supply and engineering assistance) and on the Space Wave Interactions with Plasmas Experiment (SWIPE). DTIC

N94-17246# Air Force Inst. of Tech., Wright-Patterson AFB, OH.
DESIGN OF A FLUID ELASTIC ACTUATOR WITH APPLICATION TO STRUCTURE CONTROL M.S. Thesis
Mark K. Ciero May 1993 152 p
(AD-A267649) Avail: CASI HC A08/MF A02

An elastically deformable pressure vessel is used as an actuator. The internal pressure is controlled hydraulically via force applied to an external bellows. The resulting elongation of the vessel is a linear function of the input force, and depends on the physical properties of the vessel, fluid, and bellows. The design includes an orifice through which fluid flows adding damping to the actuator. Mathematical models of the actuator are developed which relate performance of the actuator to its geometry and material properties. A static analysis yields the linear relationship between the commanded input force and the resulting elongation of the vessel. A model of the passive (no input force) response of the actuator indicates it will act as a passive damper. The active response (application of a dynamic input force yielding a dynamic elongation) is limited in frequency by the orifice damping. Strategies for optimizing the actuator size and material properties are developed from the models. Actuators manufactured with differing materials and fluids were tested. The static results are linear and matched the analysis. The passive results and the model predictions confirm that the configuration of the actuators, as built, is poor for passive damping. The correlation between the model and active experiments is excellent. Actuation bandwidth is shown to be selectable by selecting orifice size. Tailoring the material properties of the vessel by the use of optimally designed composite laminates results in a factor of two improvement in the performance. The actuator is useful for structural control. Its performance is comparable to other available actuators, it is constructed of off-the-shelf hardware, and it has the advantages of a built-in frequency limit and easily customizable performance characteristics. DTIC

N94-17266# Massachusetts Inst. of Tech., Cambridge. Dept. of Aeronautics and Astronautics.
HIGH VOLTAGE CONDUCTORS IN SPACECRAFT Final Report, Aug. 1992 - Jul. 1993
Daniel Hastings 7 May 1993 90 p
(Grant AF-AFOSR-0340-87)
(AD-A267268; AFOSR-93-0462TR) Avail: CASI HC A05/MF A01

Future solar arrays are being designed for much higher voltages in order to meet high power demands at low currents. Unfortunately, negatively biased high voltage solar cells have been observed to arc when exposed to the low earth orbit plasma environment. Analytical and numerical models of this arcing phenomenon on conventional solar cells have been developed which show excellent agreement with experimental data. With an understanding of a mechanism for arcing, it is possible to determine methods of arc rate mitigation and to predict arc rates for experiments. Using the previously developed models, it was determined that the arcing rate can be decreased by the following means: (1) increasing the interconnector work function; (2) increasing the thickness of the coverglass and adhesive; (3) decreasing the secondary electron yield of the coverglass and adhesive; (4) decreasing the ratio of the coverglass/adhesive dielectric constants; and (5) overhanging the coverglass. Of these, methods (4) and (5) show the most promise in reducing or even eliminating arcing. In addition, arcing rates were predicted for the high voltage biased arrays of the Air Force's Photovoltaic and Space Power Plus Diagnostics experiment (PASP Plus) and NASA's Solar Array Module Plasma Interactions Experiment (SAMPIE). These predictions provide both expectations for the missions and a means to test the numerical and analytical models in the space environment for different solar cell technologies. Finally, a numerical model of the arc initiation process was also developed for wrap-through-contact cells, but experimental data is not available for comparison. DTIC

N94-17280*# Rensselaer Polytechnic Inst., Troy, NY. Electrical, Computer, and Systems Engineering Dept.
PATH PLANNING FOR ROBOTIC TRUSS ASSEMBLY Final Report, 21 Mar. 1992 - 22 Sep. 1993
Arthur C. Sanderson 22 Sep. 1993 314 p

(Grant NAG1-1413)
(NASA-CR-194652; NAS 1.26:194652) Avail: CASI HC A14/MF A03

A new Potential Fields approach to the robotic path planning problem is proposed and implemented. Our approach, which is based on one originally proposed by Munger, computes an incremental joint vector based upon attraction to a goal and repulsion from obstacles. By repetitively adding and computing these 'steps', it is hoped (but not guaranteed) that the robot will reach its goal. An attractive force exerted by the goal is found by solving for the the minimum norm solution to the linear Jacobian equation. A repulsive force between obstacles and the robot's links is used to avoid collisions. Its magnitude is inversely proportional to the distance. Together, these forces make the goal the global minimum potential point, but local minima can stop the robot from ever reaching that point. Our approach improves on a basic, potential field paradigm developed by Munger by using an active, adaptive field - what we will call a 'flexible' potential field. Active fields are stronger when objects move towards one another and weaker when they move apart. An adaptive field's strength is individually tailored to be just strong enough to avoid any collision. In addition to the local planner, a global planning algorithm helps the planner to avoid local field minima by providing subgoals. These subgoals are based on the obstacles which caused the local planner to fail. A best-first search algorithm A* is used for graph search. Author (revised)

N94-17368# Air Force Inst. of Tech., Wright-Patterson AFB, OH.
A GUIDANCE AND NAVIGATION SYSTEM FOR TWO SPACECRAFT RENDEZVOUS IN TRANSLUNAR HALO ORBIT Ph.D. Thesis
Brian L. Jones May 1993 189 p
(AD-A267498; AFIT/CI/CIA-93-011D) Avail: CASI HC A09/MF A02

This research considers the design of a representative end-to-end guidance and navigation system for the terminal phase rendezvous of two spacecraft in the circular restricted three-body problem. It assumes the target vehicle is in a small radius translunar halo orbit; the target vehicle remains passive with respect to the rendezvous profile. The chaser vehicle is in an independent small radius translunar halo orbit and executes all rendezvous maneuvers. First, the halo orbit guidance problem is formulated in the frequency-domain from which an output feedback guidance law is developed using H2 control theory. Linear simulation results validate the guidance law and provide data which quantify the effect of control inputs, noise characteristics and halo orbit characteristics on the steady state halo orbit station-keeping costs. Secondly, a two spacecraft terminal phase rendezvous targeting law is derived; nonlinear simulation results validate the targeting law. DTIC

N94-17388# Assistant Secretary of Defense (Production and Logistics), Washington, DC.
MODEL DESIGNATION OF MILITARY AEROSPACE VEHICLES
H. Covington 19 Feb. 1993 157 p
(AD-A267852; DOD-4120.15-L) Avail: CASI HC A08/MF A02

This list is reissued under the authority of DoD Directive 4120.15, 'Designing and Naming Military Aerospace Vehicles,' 2 May 1985. Its purpose is to prescribe uniform procedures for designating and naming aerospace vehicles and to list approved designators and names. DTIC

N94-17584*# National Aeronautics and Space Administration. Goddard Space Flight Center, Greenbelt, MD.
SATELLITE SITUATION REPORT, VOLUME 31, NUMBER 1
31 Mar. 1991 96 p
(NASA-TM-105088; NAS 1.15:105088) Avail: CASI HC A05/MF A01

Data computed at GSFC, NORAD, or provided by satellite owners is reported. A space objects box score is presented of objects in orbit and decayed objects. Data of objects in orbit is presented in tabular form and the table headings include name of the object, catalog number, source, launch date, period minutes, inclination, apogee KM., perigee KM., and transmitting frequency. Author

N94-17669# Los Alamos National Lab., NM.
DETECTING SMALL DEBRIS USING A GROUND-BASED PHOTON COUNTING DETECTOR
C. Ho, W. C. Priedhorsky, and M. H. Baron 1993 10 p Presented at the Society of Photo-Optical Instrumentation Engineers (SPIE) OE/Aerospace Science and Sensing Meeting, Orlando, FL, 11-16 Apr. 1993
(Contract W-7405-eng-36)
(DE93-012623; LA-UR-93-1199; CONF-930445-10) Avail: CASI HC A02/MF A01

We describe a sensitive technique for detecting small space debris that exploits a fast photon-counting imager. Microchannel plate detectors using crossed delay-line readout can achieve a resolution of 2048 x 2048 spatial pixels and a maximum count rate of about 10(sup 6) photons per second. A baseline debris-tracking system might couple this detector to a 16-cm aperture telescope. The detector yields x, y, and time information for each detected photon. When visualized in (x, y, t) space, photons from a fast-moving orbital object appear on a straight line. They can be distinguished from diffuse background photons, randomly scattered in the space, and star photons, which fall on a line with sidereal velocity. By searching for this unique signature, we can detect and track small debris objects. At dawn and dusk, a spherical object of 1.3 cm diameter at 400 km will reflect sunlight for an apparent magnitude of V approximately = 16. The baseline system would detect about 16 photons from this object as it crosses a 1 degree field of view in about 1 second. The line in (x, y, t) space will be significant in a diffuse background of approximately 10(sup 6) photons. We discuss the data processing scheme and line detection algorithm. The advantages of this technique are that one can (1) detect cm-size debris objects with a small telescope, and (2) detect debris moving with any direction and velocity. In this paper, we describe the progress in the development of detector and data acquisition system, the preparation for a field test for such a system, and the development and optimization of the data analysis algorithm. Detection sensitivity would currently be constrained by the capability of the data acquisition and the data processing systems, but further improvements could alleviate these bottlenecks. DOE

N94-15558*# Technische Univ., Graz (Austria). Inst. for Space Research.
WORK AT GRAZ ON SATELLITE SIGNATURES
Georg Kirchner and Franz Koidl *In* NASA. Goddard Space Flight Center, Eighth International Workshop on Laser Ranging Instrumentation Jun. 1993 8 p (For primary document see N94-15552 03-19)
Avail: CASI HC A02/MF A06

N94-15889*# Nauchno-Proizvodstvennoe Obedinenie Radio, Moscow (USSR).
ALMAZ
V. Viter *In* JPL, Proceedings of the Third Spaceborne Imaging Radar Symposium 28 May 1993 p 53-58 (For primary document see N94-15886 03-32)
Avail: CASI HC A02/MF A04

N94-15892*# European Space Research Lab., Noordwijk (Netherlands).
ENVISAT ASAR
Jacques Louet *In* JPL, Proceedings of the Third Spaceborne Imaging Radar Symposium 28 May 1993 p 75-97 (For primary document see N94-15886 03-32)
Avail: CASI HC A03/MF A04

N94-15893*# Canadian Space Agency, Ottawa (Ontario).
RADARSAT PROGRAM
J. McNally and S. Parashar *In* JPL, Proceedings of the Third Spaceborne Imaging Radar Symposium 28 May 1993 p 99-117 (For primary document see N94-15886 03-32)
Avail: CASI HC A03/MF A04

N94-15903*# National Aeronautics and Space Administration, Washington, DC.
SIR-C/X-SAR FREE FLYER CONCEPT
R. Monson *In* JPL, Proceedings of the Third Spaceborne Imaging Radar Symposium 28 May 1993 p 233-249 (For primary document see N94-15886 03-32)
Avail: CASI HC A03/MF A04

N94-16084 Canadian Space Agency, Ottawa (Ontario).
THE CANADIAN SPACE STATION USER DEVELOPMENT PROGRAM. WHERE DO WE GO FROM HERE?
Parvez Kumar *In* National Research Council Canada, Proceedings of the Second Workshop on Microgravity Experimentation 1990 3 p

(For primary document see N94-16071 03-29)
Avail: Issuing Activity (National Research Council, Publication Sales and Distribution, Montreal Road, Ottawa, Ontario, K1A OR6 Canada)

N94-16101 Saskatchewan Univ., Saskatoon. Dept. of Mechanical Engineering.
THE DESIGN AND ANALYSIS OF A MODULAR MICROGRAVITY TEST PLATFORM FOR USE ABOARD THE NASA KC-135 AIRCRAFT
Alain Durand, Roger Hertz, Darren Mitchell, and Kamiel S. Rezkallah *In* National Research Council Canada, Proceedings of the Second Workshop on Microgravity Experimentation 1990 7 p (For primary document see N94-16071 03-29)
Avail: Issuing Activity (National Research Council, Publication Sales and Distribution, Montreal Road, Ottawa, Ontario, K1A OR6 Canada)

N94-16152# McDonnell-Douglas Corp., Huntsville, AL. Manned Space System.
GROUND INTEGRATED ET-DERIVED SPACE PLATFORMS FOR ONORBIT APPLICATIONS
A. R. Pagano, Jr. and E. M. Enright *In* Huntsville Association of Technical Societies, TABES 1993: 9th Annual Technical and Business Exhibition and Symposium 1993 11 p (For primary document see N94-16129 03-38)
(TABES Paper 93-652) Avail: CASI HC A03/MF A03

N94-16154# Alabama Univ., Huntsville. Dept. of Civil and Environmental Engineering.
AN ANALYSIS OF THE DYNAMIC RESPONSE OF THE SPACE STATION FREEDOM DUE TO A MODULE PERFORATION BY AN ORBITAL DEBRIS PARTICLE IMPACT
William P. Schonberg and John P. Celestian *In* Huntsville Association of Technical Societies, TABES 1993: 9th Annual Technical and Business Exhibition and Symposium 1993 6 p (For primary document see N94-16129 03-38)
(TABES Paper 93-653) Avail: CASI HC A02/MF A03

N94-16374*# Science Applications International Corp., Glendora, CA.
THE EFFECT OF AN ON-ORBIT NEAR ENCOUNTER ON THE NUMBER FLUX DENSITY OF MICRON SIZED PARTICLES Abstract Only
Carl R. Maag, William G. Tanner (Baylor Univ., Waco, TX.), Tim J. Stevenson (Kent Univ., Canterbury, England.), Janet Borg (Institut d'Astrophysique, Paris, France.), Jean-Pierre Bibring (Institut d'Astrophysique, Paris, France.), W. Merle Alexander (Baylor Univ., Waco, TX.), and Andrew J. Maag (Stanford Univ., CA.) *In* Lunar and Planetary Inst., Twenty-Fourth Lunar and Planetary Science Conference. Part 2: G-M 1993 p 915 (For primary document see N94-16173 03-91)
Avail: CASI HC A01/MF A06

19 SPACECRAFT INSTRUMENTATION

For related information see also *06 Aircraft Instrumentation* and *35 Instrumentation and Photography.*

N94-15025# European Space Agency, Paris (France).
PROCEEDINGS OF AN ESA SYMPOSIUM ON PHOTON DETECTORS FOR SPACE INSTRUMENTATION
T. D. Guyenne, ed. and J. J. Hunt, ed. Dec. 1992 415 p Symposium held in Noordwijk, Netherlands, 10-12 Nov. 1992
(ESA-SP-356; ISBN-9-29-092266-4; ETN-93-93952) Copyright Avail: CASI HC A18/MF A04

Papers presented at a symposium to assess the status of research in photon detectors and to define a policy to achieve coherence in European detector research are presented. A photon detector is the heart of many space experiments; its characteristics and performance determine the size of the photon collection area and, consequently, directly influence the size and cost of the spacecraft. Given the access to technology previously classified, new perspectives are opened for photon detection in some ranges of the electromagnetic spectrum, particularly in the infrared and at submillimeter wavelengths. For individual titles, see N94-15026 through N94-15103.

N94-15026*# National Aeronautics and Space Administration. Goddard Space Flight Center, Greenbelt, MD.
BACKGROUND SUPPRESSION TECHNIQUES IN GERMANIUM DETECTORS
Neil Gehrels and Cynthia Cheung *In* ESA, Proceedings of an ESA Symposium on Photon Detectors for Space Instrumentation Dec. 1992 p 5-11 (For primary document see N94-15025 03-19)
Copyright Avail: CASI HC A02/MF A04

A new generation of astrophysical gamma ray spectrometers employing germanium solid state detectors for precise energy measurement are currently being planned for spaceflight in the late 1990's and the early 21st century. Because the observations of weak celestial sources are carried out in an intense radiation environment, the key objective of instrument design is to find ways to reduce the background. The current state of the knowledge in this field is reviewed and the new hardware techniques under design and test are discussed. Many of these techniques have already been flight tested on balloon platforms. Recent results from some of these tests are presented. By carefully applying these techniques it should be possible to achieve sensitivities that are factors of 3 to 10 better than would be obtained for a conventional instrument of similar weight. ESA

N94-15027*# National Aeronautics and Space Administration. Goddard Space Flight Center, Greenbelt, MD.
X RAY MICROCALORIMETERS: PRINCIPLES AND PERFORMANCE **c35**
S. H. Moseley, M. Juda (Wisconsin Univ., Madison.), R. L. Kelley, D. McCammon (Wisconsin Univ., Madison.), C. K. Stahle (National Academy of Sciences - National Research Council, Greenbelt, MD.), A. E. Szymkowiak, and J. Zhang (Wisconsin Univ., Madison.) *In* ESA, Proceedings of an ESA Symposium on Photon Detectors for Space Instrumentation Dec. 1992 p 13-19 (For primary document see N94-15025 03-19)
Copyright Avail: CASI HC A02/MF A04

Microcalorimeters operating at cryogenic temperatures can be excellent X-ray spectrometers. They simultaneously offer very high spectral resolving power and high efficiency. These attributes are important for X-ray astronomy where most sources have low fluxes and where high spectral resolution is essential for understanding the physics of the emitting regions. The principles of operation of these detectors, limits to their sensitivity, design considerations, techniques of fabrication, and their performance as X-ray spectrometers, are reviewed. ESA

N94-15028# European Space Agency. European Space Research and Technology Center, ESTEC, Noordwijk (Netherlands). Astrophysics Div.
A NEW APPROACH TO OPTICAL PHOTON DETECTION **c35**
M. A. C. Perryman, C. L. Foden, and A. Peacock *In its* Proceedings of an ESA Symposium on Photon Detectors for Space Instrumentation Dec. 1992 p 21-26 (For primary document see N94-15025 03-19)
Copyright Avail: CASI HC A02/MF A04

Considerable theoretical and experimental effort is being devoted to the development of superconducting tunnel junction X-ray photon counting detectors, with the goal of providing good quantum efficiency combined with high energy resolution. The fundamental physical processes underlying the use of such detectors (the partial destruction of the superconducting state leading to free charge carriers which can be detected through quantum mechanical tunneling at the junctions) are equally applicable at longer wavelengths. Optical photon counting should be possible using an array of closely packed junctions, or with an array of widely spaced junctions fabricated on a superconducting substrate of higher energy gap, employing the principle of quasi-particle trapping. Such a device should combine most of the advantages of CCD's (Charge Coupled Devices) and present photon counting systems; as a specific example, the combination of Al junctions with a Nb or Sn substrate provides the basis for a large area detector with very high sensitivity to individual optical and UV photons, high intrinsic time resolution, and moderate energy resolution. Some key astronomical applications of such a device are noted. ESA

N94-15029# Consiglio Nazionale delle Ricerche, Bologna (Italy). Ist. di Tecnologie e Studio sulle Radiazioni Extraterrestri.
CdTe ARRAY DETECTORS FOR HIGH ENERGY ASTRONOMY **c89**
E. Caroli, G. Baldazzi (Bologna Univ., Italy.), G. DiCocco, A. Donati, W. Dusi, G. Malaguti (Bologna Univ., Italy.), J. B. Stephen, and M. Trifoglio

In ESA, Proceedings of an ESA Symposium on Photon Detectors for Space Instrumentation Dec. 1992 p 27-31 (For primary document see N94-15025 03-19)

Copyright Avail: CASI HC A01/MF A04

The results of missions such as SIGMA and CGRO have convincingly demonstrated the need for fine spectroscopy and imaging in high energy astronomy. A possible answer to these requirements could be offered by Position Sensitive Detectors (PSD) based on modular arrays of Cadmium Telluride (CdTe) micro-spectrometers. CdTe is a room temperature compound semiconductor with high Z that can be formed into small devices acting as X and gamma ray spectrometers. PSD's based on CdTe would offer fine intrinsic spatial resolution (down to a few millimeters), good spectroscopic performance (less than 2% FWHM energy resolution at 511 keV) and high efficiency in the 10 keV to 5 MeV range. Experimental results obtained on CdTe micro-detectors with different geometrical shapes and size and on a sample of 5 by 5 units packed in a bidimensional array are presented. A design for assembling CdTe units in arrays of large detection area is suggested together with an evaluation of the achievable efficiency. ESA

N94-15030# Danish Space Research Inst., Lyngby.

THE IMAGING MICROSTRIP PROPORTIONAL COUNTER: FEATURES OF A PRACTICAL DESIGN **c35**

C. Budtz-Jorgensen, A. Bahnsen, M. MohlMadsen, and H. W. Schnopper *In* ESA, Proceedings of an ESA Symposium on Photon Detectors for Space Instrumentation Dec. 1992 p 33-38 (For primary document see N94-15025 03-19)

Copyright Avail: CASI HC A02/MF A04

An investigation of the LEPC (Low Energy Proportional Counter) is presented. A set of four imaging Microstrip Proportional Counters (MSPC) are to be provided as part of XSPECT, a contribution to the SODART telescopes. A High EPC (HEPC) and an LEPC will be provided for each of the SODART telescopes. The design is fixed and a prototype of LEPC is under construction. The properties of this detector are described. The detector has an excellent energy resolution of delta(E)(sub FWHM) = 0.33 (E/1 keV)(exp 1/2) keV. The inherent position resolution is less than 0.2 mm around 6 keV, and positional nonlinearities are less than 0.1 mm. The measured point spread function shows the capability for studying weak objects in the vicinity of strong ones. The gas gain is independent of position to better than 0.5 percent. The efficiency of charged particle rejection was measured. ESA

N94-15031# Space Research Organization Netherlands, Utrecht. Space Research Lab.

SUPERCONDUCTIVE X RAY PHOTON DETECTORS **c76**

P. A. J. deKorte *In* ESA, Proceedings of an ESA Symposium on Photon Detectors for Space Instrumentation Dec. 1992 p 41-50 Sponsored by Netherlands Technology Foundation (For primary document see N94-15025 03-19)

Copyright Avail: CASI HC A02/MF A04

The status and developments in the area of superconductive photon detectors are reviewed with emphasis on superconductive tunnel junctions. An introduction to the basics of superconductive tunnel junctions for radiation is given together with the requirements on the read out electronics. Special attention is devoted to the influence of the various quasi-particle and phonon loss processes on the detector performance. The process of quasi-particle trapping, depending on the proximity effect, and the results obtained in the various experimental structures are addressed. This process also plays a central role in the read out of absorbers of a size substantially larger than the junctions themselves. Results of another way to increase detector size by the use of detector arrays are presented. ESA

N94-15032# Paris VI Univ. (France).

METASTABLE SUPERCONDUCTORS AS PHOTON DETECTORS **c76**

T. Girard, V. Jeudy, D. Limagne, V. Pagesy, A. Pagesy, and G. Waysand *In* ESA, Proceedings of an ESA Symposium on Photon Detectors for Space Instrumentation Dec. 1992 p 51-55 Prepared in cooperation with Paris VII Univ., Fra nce (For primary document see N94-15025 03-19)

Copyright Avail: CASI HC A01/MF A04

The operational principles of superheated superconducting spheres are reviewed, and results of significance to their application in radiation detection are discussed. Metastable superconductors are found in either intrinsic or geometric states, naively characterized by microspheres and strips, respectively. With spheres, prototype matrix detectors have been built and provide the basis for potential imaging systems as well as specific particle detection systems. Recent results demonstrate that with rather large microspheres not selected in size, energy resolution can be achieved. Strips, recently studied with an induction readout technique, indicate a possible new form of detector with an enhanced capacity for energy resolution. ESA

N94-15033# GEC Hirst Research Centre, Wembley (England).

DEVELOPMENT OF X RAY CCDS **c89**

D. J. Burt *In* ESA, Proceedings of an ESA Symposium on Photon Detectors for Space Instrumentation Dec. 1992 p 57-67 Prepared in cooperation with English Electric Valve Co. Ltd., Chelmsford, England (For primary document see N94-15025 03-19)

Copyright Avail: CASI HC A03/MF A04

The basic technology and development of X-ray CCD's (Charge Coupled Devices) for astronomical applications are described. The optimizations necessary to maximize the energy resolution and detection efficiency of devices over a wide range of X-ray energies are included. Practical results are reported. ESA

N94-15034# Max-Planck-Inst. fuer Extraterrestrische Physik, Garching (Germany).

THE XMM pn-CCD DETECTOR SYSTEM: FIRST RESULTS **c76**

H. Braeuninger, R. Danner, N. Findeis (KETEK G.m.b.H., Haimhausen, Germany.), D. Hauff, P. Holl (KETEK G.m.b.H., Haimhausen, Germany.), J. Kemmer (KETEK G.m.b.H., Haimhausen, Germany.), E. Kendziorra (Tuebingen Univ., Germany.), J. Kraemer (Tuebingen Univ., Germany.), P. Lechner, and G. Lutz et al *In* ESA, Proceedings of an ESA Symposium on Photon Detectors for Space Instrumentation Dec. 1992 p 69-73 (For primary document see N94-15025 03-19)

(Contract BMFT-50-OX-90020/XMM-EPIC)

Copyright Avail: CASI HC A01/MF A04

The pn-CCD (Charge Coupled Device) is a novel type of CCD developed for fast X-ray imaging and spectroscopy for the X-ray Multi Mirror (XMM) satellite mission. Each 200 by 64 pixel large pn-CCD unit with a sensitive area of 3 by 1 sq cm is a fully depleted detector. With the use of the CMOS Amplifier and Multiplexing chip (CAMEX64B) it is possible to read out the 64 CCD channels in parallel before they are multiplexed and sent to an ADC. For the first time the system of a 64 channel pn-CCD together with CAMEX64B readout, ADC conversion, and data acquisition and storage has been brought into operation. First images of an Fe-55 X-ray source are presented and discussed. ESA

N94-15035# Space Research Organization Netherlands, Utrecht. Space Research Lab.

THE DEVELOPMENT OF BACK-ILLUMINATED CCD'S FOR XMM **c76**

P. W. A. M. Verhoeve, F. A. Jansen (Space Research Organization Netherlands, Leiden.), P. A. J. deKorte, A. J. F. denBoggende, A. C. Brinkman, H. J. M. Aarts (Space Research Organization Netherlands, Leiden.), D. Burt (GEC Hirst Research Centre, Wembley, England.), and P. Pool (English Electric Valve Co. Ltd., Chelmsford, England.) *In* ESA, Proceedings of an ESA Symposium on Photon Detectors for Space Instrumentation Dec. 1992 p 75-80 (For primary document see N94-15025 03-19)

Copyright Avail: CASI HC A02/MF A04

The Reflection Grating Spectrometer (RGS) on ESA's X-ray Multi Mirror mission (XMM) will perform spectroscopy in the energy range of 0.3 to 2.5 keV. For optimum photon detection efficiency, the RGS will be equipped with fully depleted, back illuminated large area CCD's (Charge Coupled Devices) as detectors. The backside accumulation layer is produced by ion implantation and subsequent pulsed laser annealing and should not be thicker than 0.05 micrometers. So far, the CCD development program has resulted in a large area CCD with good performance with respect to read noise, charge transfer efficiency, and radiation hardening. Back illuminated CCD's have been fabricated with very shallow activated p+ layers (0.06 micrometers, from spreading resistance profiles). X-ray measurements, however, indicate that there is a 0.22 micrometer thick layer with charge collection less than unity. This may be due to a layer of implanted boron and associated lattice damage, which is left unanealed. Anodic etching,

ultralow energy implantation, and gas immersed laser doping are being studied as improvements and alternatives. ESA

N94-15036# Interuniversity Micro-Electronics Center, Leuven (Belgium).
THINNED, BACKSIDE ILLUMINATED, AREA CCD IMAGER FOR ELECTRON DETECTION **c76**
I. Debusschere, I. Born, C. Claeys, K. DeBackker, A. Verbist, J. Adema (Delft Electronic Products, Roden, Netherlands.), and L. Bosch (Delft Electronic Products, Roden, Netherlands.) *In* ESA, Proceedings of an ESA Symposium on Photon Detectors for Space Instrumentation Dec. 1992 p 81-85 (For primary document see N94-15025 03-19)
(Contract HV-CCD-N88/20/21/22)
Copyright Avail: CASI HC A01/MF A04

A thinned, backside illuminated, two dimensional Charge Coupled Device (CCD) realized for incorporation into an image intensifier is reported. The detection of electrons of moderate energy (5 to 15 keV) by means of a CCD requires backside irradiation of devices whose sensitive region is thinned down to about 10 micrometers, such that the electrons are absorbed in the sensitive volume of the CCD. After thinning and packaging, the CCD's are subjected to a high temperature vacuum bake-out cycle, which poses severe requirements on both the die and wire bonding. The CCD's are finally incorporated into the image intensifier. ESA

N94-15037*# California Univ., Berkeley. Experimental Astrophysics Group.
MICROCHANNEL PLATE IMAGING DETECTORS FOR THE ULTRAVIOLET **c35**
O. H. W. Siegmund, M. A. Gummin, J. Stock, and D. Marsh *In* ESA, Proceedings of an ESA Symposium on Photon Detectors for Space Instrumentation Dec. 1992 p 89-96 (For primary document see N94-15025 03-19)
(Grants NAGw-1290; NAGw-2640; NAGw-1879; NAGw-2032)
Copyright Avail: CASI HC A02/MF A04

There has been significant progress over the last few years in the development of technologies for microchannel plate imaging detectors in the Ultraviolet (UV). Areas where significant developments have occurred include enhancements of quantum detection efficiency through improved photocathodes, advances in microchannel plate performance characteristics, and development of high performance image readout techniques. The current developments in these areas are summarized, with their applications in astrophysical instrumentation. ESA

N94-15038# Leicester Univ. (England). X Ray Astronomy Group.
MICROCHANNEL PLATE DETECTORS FOR SPACE ASTRONOMY **c89**
G. W. Fraser *In* ESA, Proceedings of an ESA Symposium on Photon Detectors for Space Instrumentation Dec. 1992 p 97-102 (For primary document see N94-15025 03-19)
Copyright Avail: CASI HC A02/MF A04

Open window Microchannel Plates (MCP's) are currently the detectors of choice for space astronomy in the Extreme Ultraviolet (EUV) and Far Ultraviolet (FUV) bands. MCP's are also commonly used in soft X-ray astronomy and, in sealed tubes, for optical photon counting. Work in a number of important development areas is described: MCP and MCP image readout operation at high count rates; the testing of 'low noise' MCP's fabricated from radioisotope free lead glass; and the construction and operation of large format (approximately 100 sq cm) channel plate detectors. The effects of in vacuo contaminants on an MCP bearing a CsI photocathode are also discussed. ESA

N94-15039# University Coll., London (England). Dept. of Physics and Astronomy.
THE MIC PHOTON COUNTING DETECTOR **c89**
J. L. A. Fordham, D. A. Bone, M. K. Oldfield, J. G. Bellis, and T. J. Norton (Imperial Coll. of Science and Technology, London, England.) *In* ESA, Proceedings of an ESA Symposium on Photon Detectors for Space Instrumentation Dec. 1992 p 103-106 (For primary document see N94-15025 03-19)
(Contract ESA-8819/90/NL/US(SC))
Copyright Avail: CASI HC A01/MF A04

The MIC (Microchannel plate Intensified CCD (Charge Coupled Device)) detector is an advanced performance Micro Channel Plate (MCP) intensified CCD photon counting detector developed for high resolution, high dynamic range, astronomical applications. The heart of the detector is an MCP intensifier developed specifically for photon counting applications. The maximum detector format is 3072 by 2304 pixels. The measured resolution of the detector system is 18 micrometers FWHM at 490 nm. The detector is linear to approximately 1,000,000 events/detector area/sec on a flat field and linear to count rates up to 200 events/object/s on star images. Two versions of the system have been developed. The first for ground based astronomical applications based around a 40 mm diameter intensifier, was proven in trials at a number of large optical telescopes. The second, specifically for the ESA X-Ray Multi Mirror Mission (XMM), where the MIC has been accepted as the blue detector for the incorporated Optical Monitor (OM). For the XMM-OM, the system is based around a 25 mm diameter intensifier. At present, under development, is a 75 mm diameter version of the detector which will have a maximum format of 6144 by 4608 pixels. Details of the MIC detector and its performance are presented. ESA

N94-15040*# California Univ., Berkeley. Space Sciences Lab.
PROSPECTS FOR HIGH PRESSURE IMAGING GAS SCINTILLATION DRIFT CHAMBERS **c35**
T. K. Edberg, A. Parsons, B. Sadoulet, S. Weiss, J. Wilkerson, and G. Smith (California Univ., Berkeley. Lawrence Berkeley Lab.) *In* ESA, Proceedings of an ESA Symposium on Photon Detectors for Space Instrumentation Dec. 1992 p 107-110 (For primary document see N94-15025 03-19)
(Grants NAGw-2115; NGT-50462)
Copyright Avail: CASI HC A01/MF A04

The current developmental status and future potential of a promising hard X-ray and gamma ray detector are presented: the high pressure xenon gas scintillation imaging drift chamber. A scheme for reading out the scintillation light waveshifting fibers, which allows operation at pressures at least as high as 20 atmospheres, is used. This technique combines excellent spatial resolution (approximately 200 rms allowing 1.5 arcminute mapping resolution), very good energy resolution (within a factor of three of Ge detectors), good time resolution (approximately 100 ns), and extremely high sensitivity because of excellent background rejection capabilities; it also offers possibilities for extrapolation to large area detectors. Results from tests with a prototype chamber are presented. The design of a scientific instrument for a balloon flight planned in 1995 is described. This instrument, the Scintillation Imaging Gas filled Hard X-ray Telescope (SIGHT), is optimized for detecting 30 to 300 keV X-rays. It has an active area of 1140 sq cm, with a stopping power of between 2.0 and 2.7 g/sq cm of xenon at 20 atmospheres. Possible future evolutionary tracks of the technology leading to innovative satellite applications are discussed. ESA

N94-15041*# Ball Aerospace Systems Div., Boulder, CO.
CCDS AND PHOTON COUNTING DEVICES: APPLICATIONS IN SPACE AND FROM THE GROUND **c76**
W. A. Delamere, M. M. Blouke (Tektronix, Inc., Beaverton, OR.), J. S. Flores, and W. W. Frame *In* ESA, Proceedings of an ESA Symposium on Photon Detectors for Space Instrumentation Dec. 1992 p 111-113 Sponsored by NASA. Langley Research Center and Tektronix, Inc. (For primary document see N94-15025 03-19)
Copyright Avail: CASI HC A01/MF A04

The development of the 2048 by 2048 CCD (Charge Coupled Device) for a second generation space telescope instrument has resulted in devices with very few defects, dark currents of less than 12 electrons/pixel/hour at -80 deg, readout noise levels of less than 4 electrons rms, and excellent charge transfer efficiency at signal levels of less than 10 electrons. A second generation of devices that capitalize on these characteristics have been produced and are currently in test. Faster frame transfer devices that preserve these characteristics have been designed that include tridirectional taps in the serial register. The state of the art in CCD's as photon counting detectors is reviewed. ESA

N94-15042# Linde A.G., Munich (Germany). Process Engineering and Contracting Div.
FUTURE DEVELOPMENT IN CRYOGENIC TECHNIQUES FOR SPACE
M. Wanner *In* ESA, Proceedings of an ESA Symposium on Photon Detectors for Space Instrumentation Dec. 1992 p 115-122 (For primary document see N94-15025 03-19)
Copyright Avail: CASI HC A02/MF A04

The detection of faint electromagnetic radiation in space astronomy

and astrophysics requires very low temperatures to improve the signal to noise ratio of the very sensitive detectors in order to reduce the electronic noise of the detector amplifiers and finally to suppress the self emission of infrared radiation of the telescope itself. To provide such a cryogenic environment in space, both open and closed loop cooling systems using different cryogens are in use, thereby covering the whole temperature range from about 80K down to 1.8K. Future applications such as highly sensitive bolometers or SQUID's will ask for temperatures down to the subKelvin range. Such temperatures can be achieved by sophisticated low temperature cooling stages. Cryogenic cooling in space basically relies on the same cooling principles as in the laboratory. However the systems in general have to be specifically designed and new components have to be developed to match the cryogenic infrastructure to the specific demands of the optical instrument, the requirements from the satellite and the constraints imposed by the space environment. ESA

N94-15043# Rockwell International Science Center, Anaheim, CA.
VISIBLE LIGHT PHOTON COUNTERS FOR ASTRONOMY c89
M. G. Stapelbroek, M. D. Petroff, and R. Bharat *In* ESA, Proceedings of an ESA Symposium on Photon Detectors for Space Instrumentation Dec. 1992 p 125-128 (For primary document see N94-15025 03-19)
Copyright Avail: CASI HC A01/MF A04

The demonstration of Visible Light Photon Counters (VLPCs) with a counting quantum efficiency of 60% is reported. A quantum efficiency in excess of 85% should be achievable with optimization. With such high photon detection efficiencies, the VLPC can have many applications in astronomy. Performance characteristics of this type of device are described and compared with other types of existing photon counters. Present devices operate best at a temperature of 6 to 7K. Due to the high and fast internal gain in the VLPC, the signal from a single detected photon is well above noise and can be monitored through simple readout circuitry. Compact multichannel cassettes which provide convenient optical inputs to line arrays of VLPCs and ease electrical readout from the arrays were designed. By inserting these cassettes into an efficient cryostat of simple design, the cassette could be cooled down rapidly to operating temperatures to evaluate VLPCs for various applications. Operation of the cassette and cryostat is described. ESA

N94-15044# National Optical Astronomy Lab. Tucson, AZ.
LARGE SCIENTIFIC 2-D ARRAYS FOR THE 1-5 MICRON REGION c74
A. M. Fowler *In* ESA, Proceedings of an ESA Symposium on Photon Detectors for Space Instrumentation Dec. 1992 p 129-135 Sponsored by NSF (For primary document see N94-15025 03-19)
Copyright Avail: CASI HC A02/MF A04

The performances, advantages, and disadvantages of three detector technologies, which have produced devices of interest to astronomy and other scientific users, are compared: platinum silicide (PtSi), mercury cadmium telluride (MCT), and indium antimonide (InSb). All high performance arrays use a Source Follower per Detector (SFD) type of multiplexer readout because CCDs (Charge Coupled Devices) do not perform well at low operating temperatures. In addition, hybrid indium bump technology is used by all arrays for fabrication, yield, and performance reasons. The evolution of the present focal planes and where the technology is headed are discussed, covering the operation of the various technologies, and data on the performance of several of the new 256 by 256 focal planes is presented. Evaluation procedures used for astronomy applications and techniques for low noise operation are also discussed. The future trends in even larger focal planes and the requirements for the next generation of arrays are discussed. ESA

N94-15045# Max-Planck-Inst. fuer Astronomie, Heidelberg (Germany).
PHOTOCONDUCTORS AND ARRAYS FOR THE FAR-INFRARED c74
J. Wolf *In* ESA, Proceedings of an ESA Symposium on Photon Detectors for Space Instrumentation Dec. 1992 p 137-146 Sponsored in part by Deutsche Agentur fuer Raumfahrtangelegenheite G.m.b.H. (For primary document see N94-15025 03-19)
Copyright Avail: CASI HC A02/MF A04

Doped silicon and germanium are used as extrinisic photoconductors for infrared astronomy from ground based, balloon and airborne observatories, and from space platforms. The detectors of the Infrared Space Observatory (ISO) will be capable of observing at the sensitivity limits imposed by natural sky background radiation. For the first time, ISO will use stressed Ge:Ga detectors on a satellite covering the wavelength range out to 240 micrometers. Preflight testing has shown that ISO's calibration will have to correct high energy radiation effects and delayed flux response of detectors. For future far infrared projects, these problems might be solved by blocked impurityband detectors. Several other difficulties in today's detector assembly production and readout technology also deserve improvements. ESA

N94-15046# Battelle Inst., Frankfurt am Main (Germany).
IMPURITY CONDUCTION PHOTOCONDUCTOR DETECTORS
D. Engemann, R. Faymonville, R. Felten, O. Frenzl, and D. Haschberger *In* ESA, Proceedings of an ESA Symposium on Photon Detectors for Space Instrumentation Dec. 1992 p 147-152 Sponsored by ESTEC (For primary document see N94-15025 03-19)
Copyright Avail: CASI HC A02/MF A04

A radiation hardening of photoconductive infrared detectors for the application in space instrumentation is under development on the basis of the blocked impurity band concept. These detectors are Impurity Conduction Band (ICB) detectors based on thin epitaxial layers. Both linear and two dimensional arrays have been fabricated out of this material. Their internal structure and layout and their photoconductive performance are outlined. Current responsivities between 5 A/W and 10 A/W and noise equivalent power values in the order of 10 to the minus 17th power W/square root of Hz are obtained. ESA

N94-15047# Institut National des Sciences Appliquees, Toulouse (France). Lab. de Physique des Solides.
BIB PHOTODETECTORS BASED ON ANTIMONY DOPED SILICON
G. Sirmain, P. Etieve (Tekelec-Systemes, Les Ulis, France.), W. Knap, C. Meny, S. Pasquier, P. Adet (Tekelec-Systemes, Les Ulis, France.), N. Fabre (Laboratoire d'Automatique et d'Analyse des Systemes, Toulouse, France.), A. Murray (London Univ., England.), M. Griffin (London Univ., England.), and J. Leotin *In* ESA, Proceedings of an ESA Symposium on Photon Detectors for Space Instrumentation Dec. 1992 p 153-158 Sponsored by Region Midi-Pyrenees; Direction des Recherches, Etudes et Techniques; CNES; and CNRS (For primary document see N94-15025 03-19)
Copyright Avail: CASI HC A02/MF A04

Preliminary results on a developed Blocked Impurity Band (BIB) photodetector based on antimony silicon and processed by chemical vapor deposition growth technique are presented. The device displays a significant spectral responsivity in the 30 micrometer wavelength region where photoconductors based on Ge:Be have bad performances because of lattice modes absorption. This development aims at implementing the focal plane of the spaceborne atmosphere probe SAFIRE (Spectroscopy of the Atmosphere using Far InfraRed Emission) instrument. ESA

N94-15048# London Univ. (England). Dept. of Physics.
OPTIMISATION OF FIR PHOTOCONDUCTORS FOR ATMOSPHERIC SPECTROSCOPY
A. G. Murray, M. J. Griffin, P. A. R. Ade, J. Leotin (Institut National des Sciences Appliquees, Toulouse, France.), C. Meny (Institut National des Sciences Appliquees, Toulouse, France.), and G. Sirmain (Institut National des Sciences Appliquees, Toulouse, France.) *In* ESA, Proceedings of an ESA Symposium on Photon Detectors for Space Instrumentation Dec. 1992 p 159-163 Sponsored by Science Research Council (For primary document see N94-15025 03-19)
Copyright Avail: CASI HC A01/MF A04

The optimization of far infrared photoconductive detectors for use in balloon-borne or satellite-borne limb sounding atmospheric spectrometers was investigated. Instruments of this kind find important applications in the study of stratospheric chemistry, and the influence of anthropogenic pollutants. The choice of detector type for a given spectral region, and the optimization of the operational parameters (temperature, bias voltage, readout electronics) to achieve the best detector performance (detective quantum efficiency, speed of response) are considered. Results are presented for Ge:Ga, Ge:Sb, Ge:Be, Ge:Zn, bulk photoconductors, and for Si:Sb BIB detectors. ESA

N94-15049# Academy of Sciences (USSR), Moscow. Inst. of Radioengineering and Electronics.
NONSTATIONARY BEHAVIOUR OF LOW BACKGROUND PHOTON DETECTORS c35

B. I. Fouks *In* ESA, Proceedings of an ESA Symposium on Photon Detectors for Space Instrumentation Dec. 1992 p 167-174 (For primary document see N94-15025 03-19)
Copyright Avail: CASI HC A02/MF A04

Principles and results of the theory of nonstationary processes in extrinsic detectors are presented. The low resistive detector contacts, being ohmic during DC flowing, are well injecting extra carriers during flowing of AC even if the AC changes are very slow. At a low temperature and background, a free carrier charge does not limit AC value and the latter is confined by contact nonstationary injection ability. As a result, the current response on an illumination change is the long term one; it depends on the background value and contact parameter; it is completed by the long term oscillations. The theory explains all photoresponse peculiarities, including incomprehensible ones before. It describes well any nonstationary processes in various high resistivity semiconductors. The data of a number of extrinsic detector arrays are presented. ESA

N94-15050# Universidad Politecnica de Barcelona (Spain).
SCHOTTKY BARRIER FOCAL PLANE ARRAYS FOR SWIR AND MWIR **c76**

E. Roca, J. Vermeiren (Interuniversity Micro-Electronics Center, Leuven, Belgium.), W. Platz (Messerschmitt-Boelkow-Blohm G.m.b.H., Munich, Germany.), G. Marangoni (Elettronica S.R.L., Rome, Italy.), and M. Fabbricotti (European Space Agency. European Space Research and Technology Center, ESTEC, Noordwijk, Netherlands.) *In* ESA, Proceedings of an ESA Symposium on Photon Detectors for Space Instrumentation Dec. 1992 p 175-179 (For primary document see N94-15025 03-19)
(Contract ESA-6044/84/NL/PB)
Copyright Avail: CASI HC A01/MF A04

A 1536 pixels butted array consisting of three truly linear CCD (Charge Coupled Device) submodules was developed for infrared imaging. The pixel gap at the butting edges is nominally one and maximum two pixels and the alignment accuracy is better than 5 micrometers within the detector plane and better than 50 micrometers in the Z direction. Schottky barrier sensors were used as IR detectors incorporating three different silicides working in the front-side illumination mode. The main differences between these silicides are the cut-off wavelength and the operating temperature. CoSi2 and NiSi show a cut-off wavelength of about 2.8 micrometers allowing an operating temperature of 150 K and passive cooling, whereas PtSi has a cut-off wavelength of about 6 micrometers working at 77 K. All three devices present a good photoresponse uniformity along the sensor row and also a good noise behavior. ESA

N94-15051# Philips Components Ltd., Southampton (England).
ADVANCED HIGH PERFORMANCE CdHgTe MULTIPLEXED ARRAYS **c76**

I. M. Baker, D. E. Charlton, C. Arthurs, and G. Crimes *In* ESA, Proceedings of an ESA Symposium on Photon Detectors for Space Instrumentation Dec. 1992 p 181-185 Sponsored by Ministry of Defence (For primary document see N94-15025 03-19)
Copyright Avail: CASI HC A01/MF A04

Very sensitive CdHgTe-silicon hybrid focal plane arrays for infrared applications were demonstrated in linear formats up to 1024 elements and in two dimensional arrays of up to 128 by 128 elements. The hybrid technology is based on photovoltaic, CdHgTe diode arrays coupled to full custom, CMOS, silicon multiplexing circuitry. The technology used for the next generation of advanced linear and two dimensional infrared arrays is described. The use of optical concentration for special applications is described and current progress on the 2.5 micrometer two dimensional focal plane for the HRIS (High Resolution Imaging Spectrometer) program is outlined. ESA

N94-15052# Commissariat a l'Energie Atomique, Grenoble (France). Technologies Avancees.
A 12.5 MICRON INFRARED DETECTOR FOR EARTH OBSERVATION

J. P. Chamonal, P. Audebert, I. Bischoff, J. Y. Laurent, J. P. Belle, F. Marion, and L. P. Angebault (Societe Francaise d'Aerothermodynamique, Veurey-Voroize.) *In* ESA, Proceedings of an ESA Symposium on Photon Detectors for Space Instrumentation Dec. 1992 p 187-190 Sponsored by Ministry of Defence; CNES; and ESTEC (For primary document see N94-15025 03-19)
Copyright Avail: CASI HC A01/MF A04

Results obtained on 12.5 micrometer HgCdTe (mercury cadmium telluride) infrared detectors are presented and information on the first butted IRCCD (Infrared Charge Coupled Device) prototype to be fabricated within the frame of an ESA contract is given. The objective of these programs is to develop future long buttable linear arrays of a few thousand pixels for Earth observation from satellites. ESA

N94-15053# Academy of Sciences (USSR), Saint Petersburg. National Research Inst.
LEAD CHALCOGENIDES BASED IR PHOTOSENSITIVE ARRAY DETECTORS WITH COORDINATE ADDRESSING **c76**

G. A. Agranov, S. K. Novoselov, R. M. Stepanov, A. Z. Doon, A. V. Pashkevich, A. I. Ivanov, I. K. Nemchuk, V. K. Nesterov, and V. E. Skoriukin *In* ESA, Proceedings of an ESA Symposium on Photon Detectors for Space Instrumentation Dec. 1992 p 191-195 (For primary document see N94-15025 03-19)
Copyright Avail: CASI HC A01/MF A04

Coordinate addressed photodetector arrays based on thin films of lead chalcogenides and operating in different wavebands of the infrared spectral regions are described. The arrays feature high sensitivity, close to BLIP mode, wide dynamic range, and low heat dissipation. Their advantages include random access, element block selection, image scaling, and on chip data encoding. Different design configurations with elements from 128 by 128 to 512 by 512 are discussed and experimental parameters and characteristics of the experimental arrays are presented. ESA

N94-15054# Space Research Organization Netherlands, Groningen.
SUBMILLIMETERWAVE SIS MIXER DEVELOPMENTS **c76**

H. vandeStadt, T. deGraauw, C. E. Honingh, R. A. Panhuyzen, H. H. A. Schaeffer, E. Armandillo (European Space Agency. European Space Research and Technology Center, ESTEC, Noordwijk, Netherlands.), M. M. T. M. Dierichs (Groningen Rijksuniv., Netherlands.), T. M. Klapwijk (Groningen Rijksuniv., Netherlands.), G. deLange (Groningen Rijksuniv., Netherlands.), and A. Skalare (Chalmers Univ. of Technology, Goeteborg, Sweden.) *In* ESA, Proceedings of an ESA Symposium on Photon Detectors for Space Instrumentation Dec. 1992 p 197-200 Sponsored in part by Science Research Council (For primary document see N94-15025 03-19)
(Contract ESA-7898/88/NL/PB(SC))
Copyright Avail: CASI HC A01/MF A04

The use of SIS tunnel junctions as mixers in submillimeterwave heterodyne receivers provides the best possible sensitivities up to frequencies as high as 500 GHz. Several laboratories have now demonstrated that SIS receivers in that regime have better sensitivity than the more traditional Schottky instruments. In addition, the low level of local oscillator power required for SIS receivers makes further development especially attractive for the high frequencies, possibly up into the THz regime. A fabrication process of niobium tunnel junctions and their application in waveguide mixers for the 330 to 380 GHz as well as the 410 to 490 GHz bands are described. The use of SIS detectors in planar antennas is especially promising for applications in imaging array receivers. The use of planar double dipole antennas in combination with ellipsoidal lenses is described. ESA

N94-15055# Chalmers Univ. of Technology, Goeteborg (Sweden).
HOT ELECTRON MIXERS, THE POTENTIAL COMPETITION **c89**

Erik L. Kollberg, E. Gershenzon (Academy of Pedagogical Sciences of the USSR, Moscow.), G. Goltsman (Academy of Pedagogical Sciences of the USSR, Moscow.), and K. S. Yngvesson (Massachusetts Univ., Amherst.) *In* ESA, Proceedings of an ESA Symposium on Photon Detectors for Space Instrumentation Dec. 1992 p 201-206 (For primary document see N94-15025 03-19)
Copyright Avail: CASI HC A02/MF A04

The urgent need in radio astronomy for low noise heterodyne receivers for frequencies above about 500 GHz is discussed. It is not certain that mixers based on superconducting quasiparticle tunneling (SIS mixers) may turn out to be the answer to this need. In order to try to find an alternative way for realizing low noise heterodyne receivers for submillimeter waves, so called hot electron bolometric effects for mixing are now being investigated. Two basically different approaches are tried, one based on semiconductors and one on superconductors. Both methods are discussed. Experimental evidence so far shows that with semiconductor heterostructures, two Dimensional Gas (2DEG) 18 dB conversion loss has

been obtained, and of the order of 5 dB using superconductors. Noise has as yet not been experimentally determined. Calculations suggest that the 2DEG mixers may offer of the order of 500 K (or less) DSB at 1 THz, while for superconductor devices still lower noise temperatures are predicted. ESA

N94-15056# Max-Planck-Inst. fuer Radioastronomie, Bonn (Germany).
SUBMM/FIR BOLOMETERS **c35**
E. Kreysa *In* ESA, Proceedings of an ESA Symposium on Photon Detectors for Space Instrumentation Dec. 1992 p 207-210 (For primary document see N94-15025 03-19)
Copyright Avail: CASI HC A01/MF A04

The theory of operation of submm/FIR bolometers and their technology are described. Bolometers are detectors that work by recording the temperature rise due to the absorption of radiation with the aid of a resistance thermometer. Photons of any wavelength can be detected as long as an efficient absorbing structure for that wavelength can be designed. In fact, even particle radiation can be detected by the same mechanism. While thoughout much of the electromagnetic spectrum other types of detectors are superior, bolometers are still the most sensitive detectors for continuum radiation in the mm/submm range. Therefore, all large ground based mm/submm telescopes are equipped with bolometers for continuum studies. In principle, the performance of a bolometer can be improved without limits by lowering the operating temperature. At temperatures below 300 mK, bolometers have the potential to operate near the fundamental background limit in most environments. Combining them into arrays is relatively easy because of the basic simplicity of the detectors and the associated electronics. Therefore bolometers seem to be able to stand up to the challenge of competing detector technologies in the near future. ESA

N94-15057# Danish Space Research Inst., Lyngby.
OUTLOOK FOR HARD X RAY AND GAMMA RAY ASTRONOMY **c89**
Niels Lund *In* ESA, Proceedings of an ESA Symposium on Photon Detectors for Space Instrumentation Dec. 1992 p 213-216 (For primary document see N94-15025 03-19)
Copyright Avail: CASI HC A01/MF A04

Some future prospects for astronomy in the hard x-ray and gamma ray band are discussed. In this region, no dramatic breakthroughs in detector technology appeared over recent years, although performance improvements have been reported in many areas. It is suggested that the potentially most important future development for hard X-ray astronomy may be flux concentrating telescopes working above 20 keV. ESA

N94-15058# European Space Agency. European Space Research and Technology Center, ESTEC, Noordwijk (Netherlands). Space Science Dept.
DEVELOPMENTS IN EXTREME ULTRAVIOLET AND X RAY INSTRUMENTATION **c74**
A. Peacock and J. A. M. Bleeker (Space Research Organization Netherlands, Utrecht.) *In its* Proceedings of an ESA Symposium on Photon Detectors for Space Instrumentation Dec. 1992 p 217-218 (For primary document see N94-15025 03-19)
Copyright Avail: CASI HC A01/MF A04

An overview of the symposium to review the future photon detector needs for ESA's long term science program 'Horizon 2000' and beyond is presented. Once future requirements for detector instrumentation are determined it will be possible to focus the agency's technological research program on the key areas requiring further development and support. In the region covering extreme ultraviolet (EUV) and x-ray wavelengths, a number of papers demonstrated the current limitations of various detector systems and highlighted possible future developments and trends. A resume of the principle issues, raised at the symposium specifically for EUV and x-ray photon detectors, is provided. ESA

N94-15059# Max-Planck-Inst. fuer Astronomie, Heidelberg (Germany).
INFRARED DETECTORS AND COOLERS FOR SPACE INSTRUMENTATION: SUMMARY AND CONCLUDING REMARKS
D. Lemke *In* ESA, Proceedings of an ESA Symposium on Photon Detectors for Space Instrumentation Dec. 1992 p 219-220 (For primary document see N94-15025 03-19)
Copyright Avail: CASI HC A01/MF A04

Remarks on posters and oral presentations addressing the application of infrared detectors and coolers as space instrumentation are presented. Achievements and status in this area are summarized: a comparison of the IRAS (Infrared Astronomy Satellite) mission with the ISO (Infrared Space Observatory); transient effects in extrinsic photoconductors; block impurity band detectors; and bolometers. Future developments are discussed: coverage of the far IR by even larger arrays; cooling of the new generation IR mission by closed cycle coolers; and definition of the next mission. The progress in IR astronomy is outlined in conclusion. ESA

N94-15060# Delft Electronic Products, Roden (Netherlands).
DEVELOPMENT OF AN ULTRA VIOLET AURORAL IMAGER FOR THE FREJA PROJECT
J. Adema, R. A. King (Calgary Univ., Alberta.), and R. Wlochowicz (National Research Council of Canada, Ottawa, Ontario.) *In* ESA, Proceedings of an ESA Symposium on Photon Detectors for Space Instrumentation Dec. 1992 p 223-226 (For primary document see N94-15025 03-19)
Copyright Avail: CASI HC A01/MF A04

A long term program for the research of the aurora and the interaction of the solar wind plasma with the Earth's magnetic field and atmosphere is discussed. The Freja satellite is part of that program. Among several other experiments, the Freja satellite carries two UV sensitive cameras which will make images of the aurora. The cameras contain special types of UV image intensifiers. The satellite was launched on 5 Oct. 1992 and first images have already been received. ESA

N94-15061# Stanford Linear Accelerator Center, CA.
GAMMA LARGE AREA SILICON TELESCOPE: APPLYING SI STRIP DETECTOR TECHNOLOGY TO THE DETECTION OF GAMMA RAYS IN SPACE **c89**
W. B. Atwood, E. D. Bloom, G. L. Godfrey, P. L. Hertz (Naval Research Lab., Washington, DC.), Ying-Chi Lin (Stanford Univ., CA.), P. L. Nolan (Stanford Univ., CA.), A. E. Snyder (Stanford Univ., CA.), R. E. Taylor, K. S. Wood (Naval Research Lab., Washington, DC.), and P. F. Michelson (Stanford Univ., CA.) *In* ESA, Proceedings of an ESA Symposium on Photon Detectors for Space Instrumentation Dec. 1992 p 227-232 (For primary document see N94-15025 03-19)
Copyright Avail: CASI HC A02/MF A04

The recent discoveries and excitement generated by EGRET (Energetic Gamma Ray Experiment Telescope) (presently operating on CGRO (Compton Gamma Ray Observatory)) has prompted an investigation into modern technologies ultimately leading to the next generation space based gamma ray telescope. The goal is to design a detector that would increase the data acquisition rate by almost two orders of magnitude beyond EGRET, while at the same time improving on the angular resolution, the energy measurement of reconstructed gamma rays and the triggering capability of the instrument. The proposed GLAST (Gamma Ray Large Area Silicon Telescope) instrument is based on silicon particle detectors that offer the advantages of no consumables, no gas volume, robust (versus fragile), long lived, and self triggering. The GLAST detector is roughly modeled after EGRET in that a tracking module precedes a calorimeter. The GLAST tracker has planes of cross strip (x, y) 300 micrometer match silicon detectors coupled to a thin radiator to measure the coordinates of converted electron-positron pairs. An angular resolution of 0.1 deg at high energy is possible (the low energy angular resolution 100 MeV would be about 2 deg, limited by multiple scattering). The increased depth of the GLAST calorimeter over EGRET's extends the energy range to about 300 GeV. ESA

N94-15062# Catania Astrophysical Observatory (Italy).
A TEST FACILITY TO CALIBRATE EUV DETECTORS **c09**
Giovanni Bonanno, Giampiero Naletto (Padua Univ., Italy.), and Giuseppe Tondello (Padua Univ., Italy.) *In* ESA, Proceedings of an ESA Symposium on Photon Detectors for Space Instrumentation Dec. 1992 p 233-236 (For primary document see N94-15025 03-19)
Copyright Avail: CASI HC A01/MF A04

A test facility to calibrate detectors in the ultraviolet region between 300 A and 2500 A is described. It consists of a vacuum normal incidence Johnson-Onaka monochromator with a set of interchangeable gratings and several UV lamps to optimally cover the whole spectral range. A pair of NIST calibrated photodiodes allows an absolute measurement of the photon flux outcoming from the monochromator, and thus it is possible to evaluate

the quantum efficiency of the detectors under test. Moreover, other characteristic parameters of UV detectors can be evaluated, like for example the spatial resolution and the uniformity response. The results of the quantum efficiency measurements of an EEV ion implanted CCD (Charge Coupled Device) are shown. The possible improvements necessary to optimize this test facility are discussed. ESA

N94-15063# Mullard Space Science Lab., Dorking (England).
THE GRAZING INCIDENCE DETECTORS FOR THE SOHO CORONAL DIAGNOSTIC SPECTROMETER
A. A. Breeveld and P. D. Thomas *In* ESA, Proceedings of an ESA Symposium on Photon Detectors for Space Instrumentation Dec. 1992 p 237-241 (For primary document see N94-15025 03-19)
Copyright Avail: CASI HC A01/MF A04

The Grazing Incidence Spectrometer (GIS) forms part of the Coronal Diagnostic Spectrometer (CDS) on SOHO (Solar and Heliospheric Observatory). Ultraviolet light is focused onto a Rowland circle, where four detectors image the spectra of chosen wavelength ranges, between 15 and 80 nm. Since the detectors are tangential to the circle, the incoming light meets the surfaces at grazing incidence. The detector design is a microchannel plate 'z-stack', backed by a SPAN anode, position sensitive in one dimension. The detectors are required to work at a high speed (100,000 counts/sec) and to have a resolution of better than 47 micrometers over the 50 mm length. The design, construction and performance testing of the GIS detectors and associated electronics are examined in the context of the resolution and throughout requirements. The special requirements needed for a space application and for running an anode at high voltage are described. ESA

N94-15064# Wise Observatory, Tel Aviv (Israel).
THE TAUVEX EXPERIMENT
Noah Brosch (Tel-Aviv Univ., Israel.), Amotz Shemi (Tel-Aviv Univ., Israel.), Jeremy Topaz (Electro-Optical Industries Ltd., Rehovot, Israel.), and Ofer Braun (Electro-Optical Industries Ltd., Rehovot, Israel.) *In* ESA, Proceedings of an ESA Symposium on Photon Detectors for Space Instrumentation Dec. 1992 p 243-247 (For primary document see N94-15025 03-19)
Copyright Avail: CASI HC A01/MF A04

The TAUVEX (Tel Aviv University UV Explorer) payload will be launched in 1995 onboard the spectrum X-gamma spacecraft, as part of the SODART (Soviet-Danish X-ray Telescope) high energy experiment. It consists of three 20 cm diameter coaligned telescopes imaging the same 0 deg .9 diameter sky area onto photon counting detectors in the 1400 to 2800 A band. The expected lifetime of the platform of at least three years will permit coverage of approximately 8% of the sky with a sensitivity of approximately 21 mag for point sources. The entire design of the payload depends strongly on the availability of imaging photon counting detectors in the desired spectral range. ESA

N94-15065# Philips Components Ltd., Southampton (England).
DISCRETE CMT INFRARED DETECTORS FOR SPACE APPLICATION, FROM ISSR TO SECOND GENERATION METEOSAT AND MIPAS
D. E. Charlton, L. G. Moore, and W. I. McMillan (MATRA Marconi Space, England.) *In* ESA, Proceedings of an ESA Symposium on Photon Detectors for Space Instrumentation Dec. 1992 p 249-254 (For primary document see N94-15025 03-19)
Copyright Avail: CASI HC A02/MF A04

Design constraints, electronic requirements, and housing requirements for space application of CMT detectors are described. The CMT detector was used in the thermal band of the Infrared Spin Scan Radiometer (ISSR) flown on the U.S. Synchronous Meteorological Satellite in the 1970's. Space application calls for high performance, often in low background flux, and with a diversity of wavelength. This presents design constraints often more demanding than terrestrial applications. However, there is considerable freedom to optimize temperature of operation. Verification of performance requirements calls for both practical demonstrations and modeling. CMT photodiodes are generally best at shorter wavelengths, while photoconductive detectors are generally better at long wavelengths. The diffference in approach and the design trades required in detectors for space application are compared with terrestrial thermal imaging. This is illustrated by consideration of the design trades for the MIPAS (Michelson Interferometer for Passive Atmospheric Sounding) detectors and preamplifiers. ESA

N94-15066# London Univ. (England). Dept. of Physics.
PERFORMANCE TESTING OF DOPED-GERMANIUM PHOTOCONDUCTORS FOR THE ISO LONG WAVELENGTH SPECTROMETER
S. E. Church, M. J. Griffin, P. A. R. Ade, M. C. Price, R. J. Emery (Rutherford Appleton Lab., Chilton, England.), and B. M. Swinyard (Rutherford Appleton Lab., Chilton, England.) *In* ESA, Proceedings of an ESA Symposium on Photon Detectors for Space Instrumentation Dec. 1992 p 255-260 Sponsored in part by Science Research Council (For primary document see N94-15025 03-19)
Copyright Avail: CASI HC A02/MF A04

The ISO (Infrared Space Observatory) Long Wavelength Spectrometer (LWS) uses an array of ten doped germanium photoconductors to cover the wavelength range 45 to 200 micrometers. The performance of the detectors was characterized, optimized, and calibrated, both individually and in the flight instrument. The detector test techniques and calibration methods are described and results for the spectral response, dark current, responsivity, and noise equivalent power are presented. The dependence of these parameters on operating conditions was explored and optimum values established for the flight instrument. Calibration of the flight instrument demonstrated that the sensitivity of the LWS is within specifications. ESA

N94-15067# London Univ. (England). Dept. of Physics.
NON-LINEAR EFFECTS IN DOPED-GERMANIUM PHOTOCONDUCTORS FOR THE ISO LONG WAVELENGTH SPECTROMETER
S. E. Church, M. C. Price, M. J. Griffin, P. A. R. Ade, R. J. Emery (Rutherford Appleton Lab., Chilton, England.), and B. M. Swinyard (Rutherford Appleton Lab., Chilton, England.) *In* ESA, Proceedings of an ESA Symposium on Photon Detectors for Space Instrumentation Dec. 1992 p 261-264 Sponsored in part by Science Research Council (For primary document see N94-15025 03-19)
Copyright Avail: CASI HC A01/MF A04

The ISO (Infrared Space Observatory) Long Wavelength Spectrometer (LWS) uses an array of ten doped Ge photoconductors to cover the wavelength range 45 to 200 micrometers. Under the low background conditions appropriate to the LWS, these devices are know to exhibit a number of memory effects, such as spontaneous spiking at high signal levels and slow relaxation after a step change in illumination. This type of nonlinear behavior can cause degradation of the excellent instantaneous sensitivity of the LWS detectors, and other calibration problems. These effects were studied and the implications of operation and calibration of the LWS are considered. ESA

N94-15068# Consiglio Nazionale delle Ricerche, Naples (Italy). Ist. di Cibernetica.
Nb-BASED SJTJ FOR NUCLEAR DETECTION: PRELIMINARY RESULTS WITH ALPHA RADIATION **c76**
R. Cristiano, E. Esposito, L. Frunzio, S. Pagano, A. Barone (Naples Univ., Italy.), G. Peluso (Naples Univ., Italy.), G. Pepe (Naples Univ., Italy.), H. Akoh (Tsukuba Univ., Ibaraki, Japan.), H. Nakagawa (Tsukuba Univ., Ibaraki, Japan.), and S. Takada (Tsukuba Univ., Ibaraki, Japan.) *In* ESA, Proceedings of an ESA Symposium on Photon Detectors for Space Instrumentation Dec. 1992 p 265-268 Sponsored by CNR and ETL (For primary document see N94-15025 03-19)
Copyright Avail: CASI HC A01/MF A04

High quality Nb based Superconducting Josephson Tunnel Junctions (SJTJ) are promising devices as detectors of nuclear radiation because of the low energy threshold, fast response, and good thermal cyclability. The samples utilized were fabricated with underlayer technique and a self aligned insulation process in silicon substrates. A 5 by 5 sq mm chip containing as many as 240 SJTJ's was designed with various junction configurations oriented toward energy and time sensitive detection. The chip was irradiated with alpha particles from an Am-241 source located 5 mm above the junction and separated by a mechanically controlled shutter. Pulse height and risetime spectra of both 'island' type and series connected SJTJ's are reported. Signals generated by nuclear radiation were observed at temperatures up to 2K, where a reduction of the collected charge occurs because of the enhancement of the recombination rate. ESA

N94-15069*# National Aeronautics and Space Administration. Goddard Space Flight Center, Greenbelt, MD.
THE STIS MAMA STATUS: CURRENT DETECTOR PERFORMANCE

A. C. Danks (Hughes STX, Inc., Greenbelt, MD.), C. Joseph (Wisconsin Univ., Madison.), R. Bybee (Ball Aerospace Systems Div., Boulder, CO.), V. Argebright (Ball Aerospace Systems Div., Boulder, CO.), J. Abraham (Ball Aerospace Systems Div., Boulder, CO.), R. Kimble, and B. Woodgate *In* ESA, Proceedings of an ESA Symposium on Photon Detectors for Space Instrumentation Dec. 1992 p 269-274 (For primary document see N94-15025 03-19)

Copyright Avail: CASI HC A02/MF A04

The STIS (Space Telescope Imaging Spectrograph) is a second generation Hubble instrument scheduled to fly in 1997. Through a variety of modes, the instrument will provide spectral resolutions from R approximately 50 in the objective spectroscopy mode to 100,000 in the high resolution echelle mode in the wavelength region from 115 to 1000 nm. In the UV the instrument employs two MAMA (Multimode Anode Microchannel plate Arrays) 1024 by 1024 pixel detectors, which provide high DQE (Detective Quantum Efficiency), and good dynamic range and resolution. The current progress and performance of these detectors are reported, illustrating that the technology is mature and that the performance is very close to flight requirements. ESA

N94-15070# Mullard Space Science Lab., Dorking (England).
AN ADIABATIC DEMAGNETISATION REFRIGERATOR WITH A MECHANICAL PRE-COOLER FOR SPACE APPLICATIONS

I. J. Davenport, A. Smith, I. Hepburn (London Univ., England.), P. A. R. Ade (London Univ., England.), and T. J. Sumner (Imperial Coll. of Science and Technology, London, England.) *In* ESA, Proceedings of an ESA Symposium on Photon Detectors for Space Instrumentation Dec. 1992 p 275-279 Sponsored in part by Science Research Council (For primary document see N94-15025 03-19)

Copyright Avail: CASI HC A01/MF A04

An Adiabatic Demagnetization Refrigerator (ADR) suitable for use in space would have applications in the fields of mm/submm and x-ray astronomy. Since ADR's operate in the absence of gravity without the need for highly complex modifications from established laboratory designs, they could offer a considerable advantage over He-3 refrigerators. The concept of an ADR backed by a mechanical pre-cooler is evaluated. Either a second ADR or a recycling Helium bath is used between the ADR and the mechanical cooler. This has the potential for both high reliability and very long operations. A system design which is related to the present development status of mechanical coolers is presented. The performance of such a system is evaluated. The operational parameters addressed include: achievable temperature and stability; hold and recycle times; and residual magnetic field strength. ESA

N94-15071# Interuniversity Micro-Electronics Center, Leuven (Belgium).
RADIATION HARDENING OF A CCD TECHNOLOGY THROUGH PROCESS AND DESIGN MODIFICATIONS **c76**

I. Debusschere, A. Simone, A. Alaerts, and C. Claeys *In* ESA, Proceedings of an ESA Symposium on Photon Detectors for Space Instrumentation Dec. 1992 p 281-284 (For primary document see N94-15025 03-19)

(Contract ESTEC-8615/90/NL/PM(SC))

Copyright Avail: CASI HC A01/MF A04

A three level polysilicon, buried channel Charge Coupled Device (CCD) technology was tested for Co-60 ionizing radiation damage. Both CCD image sensors and test structures were evaluated. This allows a better understanding of the degradation phenomena and of the countermeasures needed for a radiation hardened technology. In a first phase the radiation hardness of the standard process was assessed. The results obtained led to the implementation of process and design modifications. Devices of the modified technology were evaluated up to a total dose of 90 Krad(Si) and showed a tangible improvement in the radiation hardness. ESA

N94-15072*# National Aeronautics and Space Administration. Goddard Space Flight Center, Greenbelt, MD.
X-RAY SPECTROSCOPY WITH SILICON PIN AND AVALANCHE PHOTO DIODES **c74**

U. D. Desai *In* ESA, Proceedings of an ESA Symposium on Photon Detectors for Space Instrumentation Dec. 1992 p 285-287 (For primary document see N94-15025 03-19)

Copyright Avail: CASI HC A01/MF A04

Results of an evaluation of silicon P-Intrinsic-N (PIN) photodiodes and Avalanche Photodiodes (APD) for the direct detection of soft x rays from 1 to 20 keV and for the detection of scintillation light output from CsI(Tl) for higher x ray energies (30 to 1000 keV) are presented. About one keV resolution was achieved at room temperature for both the PIN and APD detectors for soft x rays (1 to 20 keV). Commercially available, low power (18 mV), low noise, hybrid preamplifiers, were used. These photodiodes were also coupled to CsI(Tl) scintillator and obtained about 6 resolution at 662 keV. The photodiode frequency response matches well with the emission spectrum of the CsI(Tl) scintillator providing good spectral resolution and a higher signal than NaI(Tl) when viewed by conventional photomultipliers. A PIN-CsI(Tl) combination provides a low energy threshold of around 60 keV while for the APD-CsI(Tl) it is 15 keV. ESA

N94-15073# Battelle Inst., Frankfurt am Main (Germany).
EXTRINSIC PHOTOCONDUCTOR DETECTORS FOR THE WAVELENGTH RANGE 2 MICRONS TO 240 MICRONS **c76**

D. Engemann, R. Faymonville, R. Felten, O. Frenzl, M. Overhamm, M. Griffin (London Univ., England.), P. Ade (London Univ., England.), S. Church (London Univ., England.), and A. Murray (London Univ., England.) *In* ESA, Proceedings of an ESA Symposium on Photon Detectors for Space Instrumentation Dec. 1992 p 289-292 Sponsored by DLR and ESTEC (For primary document see N94-15025 03-19)

Copyright Avail: CASI HC A01/MF A04

Extrinsic photoconductors are favored detectors for infrared photon detection in astronomical instruments of cooled space telescopes which provide low background flux conditions. Elementary silicon and germanium host crystal detectors doped by shallow impurities cover the infrared spectral range from 2 to 120 micrometers, and up to 240 micrometers by application of high uniaxial stress to germanium. The instruments of ISO (Infrared Space Observatory) are equipped with extrinsic photoconductors. The physical background and the status of the detector technology of the ISO detectors is described. The designs and the mounts are given. The measurement method of the spectral response used is presented. ESA

N94-15074# Battelle Inst., Frankfurt am Main (Germany).
THE DETECTOR ASSEMBLIES OF ISOPHOT AND THE SPECTROMETERS ISO-SWS AND ISO-LWS

D. Engemann, R. Faymonville, R. Felten, O. Frenzl, and M. Overhamm *In* ESA, Proceedings of an ESA Symposium on Photon Detectors for Space Instrumentation Dec. 1992 p 293-298 (For primary document see N94-15025 03-19)

Copyright Avail: CASI HC A02/MF A04

The development, qualification, and testing of the detector assemblies of three instruments for the European satellite Infrared Space Observatory (ISO) are reported: ISOPHOT (photometer, polarimeter, spectrometer); ISO SWS (Short Wavelength Spectrometer); and ISO LWS (Long Wavelength Spectrometer). For each instrument three models were developed: engineering qualification models, flight models, and flight space models. The different assemblies are described and the applied radiometric test methods are presented together with the performance data. ESA

N94-15075# National Physical Lab., Teddington (England). Quantum Metrology Div.
IMPROVED OPTICAL RADIATION DETECTORS AND THEIR CALIBRATION: 200 nm - 30 MICRONS **c76**

Nigel Fox *In* ESA, Proceedings of an ESA Symposium on Photon Detectors for Space Instrumentation Dec. 1992 p 299-301 (For primary document see N94-15025 03-19)

Copyright Avail: CASI HC A01/MF A04

The establishment of a spectral responsivity scale for the spectral region 200 nm to 30 micrometers is reported. This required the construction of a range of facilities to evaluate detectors of different types and where necessary the development of special detectors with a higher performance than commercial devices. Significant improvements in the accuracy of optical radiation measurements in the visible and near infrared was achieved and work to develop detectors of improved performance for the ultraviolet and infrared spectral regions continues. Calibration services are offered using the facilities developed for this work. ESA

N94-15076# Consiglio Nazionale delle Ricerche, Palermo (Italy). Ist. di Fisica Cosmica ed Applicazioni dell'Informatica.
THE HIGH PRESSURE GAS SCINTILLATION PROPORTIONAL COUNTER FOR SAX

A. Bonura, S. Giarrusso, L. Lombardo, G. Manzo, S. Re, G. LaRosa, F. Celi, R. DiRaffaele, and G. Fazio *In* ESA, Proceedings of an ESA Symposium on Photon Detectors for Space Instrumentation Dec. 1992 p 303-307 (For primary document see N94-15025 03-19)
Copyright Avail: CASI HC A01/MF A04

The High Pressure Gas Scintillation Proportional Counter (HPGSPC), one of the experiments on board the Italian X-ray Astronomy Satellite SAX, is described. The experiment has a field of view of about 1 deg, an energy bandpass from less than 4 to 120 keV, a demonstrated energy resolution of about 5 keV at 60 keV and an extrapolated resolution (at 60 keV) of less than 2 keV. This is obtained with an entrance area of 450 sq cm and an absorption-pressure of 50 cm.atm. ESA

N94-15077# London Univ. (England). Dept. of Physics.
IONISING RADIATION-INDUCED EFFECTS IN DOPED GERMANIUM FIR PHOTOCONDUCTORS **c76**
M. C. Price, M. J. Griffin, S. E. Church, A. G. Murray, and P. A. R. Ade *In* ESA, Proceedings of an ESA Symposium on Photon Detectors for Space Instrumentation Dec. 1992 p 309-312 (For primary document see N94-15025 03-19)
Copyright Avail: CASI HC A01/MF A04

Bulk Ge:Be and Ge:Ga photoconductive devices with a typical crystal size of about 1 mm, are currently the most sensitive detectors for FIR satellite instruments in the wavelength range 40 to 200 micrometers. Due to their high sensitivity and relatively large volume, the performance of these detectors is strongly influenced by ionizing radiation in space. Individual absorption events cause glitches in the data stream which must be rejected; and changes in detector dark current, responsivity and noise arise due to the accumulated ionizing radiation exposure. It is essential to characterize and minimize these effects in order to attain the best overall performance of satellite-borne detectors. Radiation tests in Ge:Be and Ge:Ga (stressed and unstressed) detectors for the ISO (Infrared Space Observatory) Long Wavelength Spectrometer (LWS), a low background FIR astronomical instrument, and SAFIRE (Spectroscopy of an Atmosphere using Far Infrared Emission), a higher background Earth looking instrument, were carried out. The effects of ionizing radiation on the performance parameters of the different detectors types are described and discussed. The effectiveness of curing the detectors by bias boosting is considered, and the implications of the ionizing environment for operation of FIR satellite instruments are outlined. ESA

N94-15078# Institut de Radio Astronomie Millimetrique, Grenoble (France).
PREPARATION AND PROPERTIES OF Nb/Al SIS AND SIN JUNCTIONS FOR MILLIMETER AND SUBMILLIMETER RADIOASTRONOMICAL RECEIVERS **c76**
K. H. Gundlach, T. Lehnert, D. Billon-Pierron, M. Voss, and P. Pasturel *In* ESA, Proceedings of an ESA Symposium on Photon Detectors for Space Instrumentation Dec. 1992 p 313-316 (For primary document see N94-15025 03-19)
Copyright Avail: CASI HC A01/MF A04

The sharp onset of the quasiparticle current in Superconductor Insulator Superconductor (SIS) tunnel junctions is used for frequency mixing in radioastronomical receivers. Efforts to develop and routinely produce various Nb based devices for frequencies up to 690 GHz are outlined. The fabrication and properties of single (SIS) and double barrier (SISIS) devices, anodization spectroscopy, thermal annealing, a method to prepare submicron junctions using optical lithography and on Nb based SIN junctions, are reported. The latter type has no Josephson effects which can interfere with low noise quasiparticle mixing. ESA

N94-15079# London Univ. (England). Dept. of Physics.
IN ORBIT ADIABATIC DEMAGNETIZATION REFRIGERATION FOR BOLOMETRIC AND MICROCALORIMETRIC DETECTORS
I. D. Hepburn, P. A. R. Ade, I. Davenport (Mullard Space Science Lab., Dorking, England.), A. Smith (Mullard Space Science Lab., Dorking, England.), and T. J. Sumner (Imperial Coll. of Science and Technology, London, England.) *In* ESA, Proceedings of an ESA Symposium on Photon Detectors for Space Instrumentation Dec. 1992 p 317-320 (For primary document see N94-15025 03-19)
Copyright Avail: CASI HC A01/MF A04

The new generation of photon detectors for satellite based mm/submm and X-ray astronomical observations require cooling to temperatures in the range 60 to 300 mK. At present Adiabatic Demagnetization Refrigeration (ADR) is the best proposed technique for producing these temperatures in orbit due to its inherent simplicity and gravity independent operation. For the efficient utilization of an ADR it is important to realize long operational times at base temperature with short recycle times. These criteria are dependent on several parameters; the required operating temperature, the cryogen bath temperature, the amount of heat leakage to the paramagnetic salt, the volume and type of salt and the maximum obtainable magnetic field. For space application these parameters are restricted by the limitations imposed on the physical size, the mass, the available electrical power and the cooling power available. The design considerations required in order to match these parameters are described and test data from a working laboratory system is presented. ESA

N94-15080# Leicester Univ. (England). X Ray Astronomy Group.
CCD'S ON HIGH RESISTIVITY BULK SILICON FOR X RAY SPECTROSCOPY ON XMM **c76**
A. D. Holland, M. J. L. Turner, A. A. Wells, and D. J. Burt (GEC Hirst Research Centre, Wembley, England.) *In* ESA, Proceedings of an ESA Symposium on Photon Detectors for Space Instrumentation Dec. 1992 p 321-324 Sponsored by Science Research Council (For primary document see N94-15025 03-19)
Copyright Avail: CASI HC A01/MF A04

CCD's (Charge Coupled Devices) were chosen as the X-ray imaging spectrometers on ESA's cornerstone mission XMM (X-ray astronomy Multi Mirror). The CCD's being developed for the nondispersive imaging spectrometer (EPIC), operating in the 0.1 to 15 keV band and which require high quantum efficiency with Fano limited energy resolution are described. The CCD's are manufactured on bulk silicon with resistivity greater than 8000 Omega cm. This produces a depletion depth approaching 90 micrometers which yields good X-ray spectroscopy with high efficiency (90 percent at 6.4 keV). The developments described are sufficient to satisfy the high energy requirements of the EPIC imaging spectrometer. ESA

N94-15081# Bergen Univ. (Norway). Dept. of Physics.
A NEW DETECTOR CONCEPT FOR ENERGETIC AURORAL X RAY IMAGING
G. A. Johansen and J. Stadsnes *In* ESA, Proceedings of an ESA Symposium on Photon Detectors for Space Instrumentation Dec. 1992 p 325-328 Sponsored by Royal Norwegian Council for Scientific and Industrial Research and Norwegian Research Council for Science and the Humanities (For primary document see N94-15025 03-19)
Copyright Avail: CASI HC A01/MF A04

Energetic electrons being precipitated from the Earth's magnetosphere into the upper atmosphere in the auroral regions, emit bremsstrahlung X-rays. From a satellite an X-ray camera can be used for remote mapping of this electron precipitation. In connection with projects like Aurio (Auroral Imaging Observatory), selected for flight in ESA's polar platform program, it is desirable to develop new and better imaging detectors to cover especially the high energy range (about 10 to 150 keV). Scintillation crystals provide sufficient stopping efficiency at high X-ray energies. A scintillation readout device, the Electron bombarded silicon Diode Photo Multiplier Tube (EDPMT) is described with the first experimental results. Some ideas on how the EDPMT can be made position sensitive to be used together with a scintillating plate as a rugged and simple X-ray camera are presented. ESA

N94-15082# Max-Planck-Inst. fuer Astronomie, Heidelberg (Germany).
CHARACTERIZATION OF DETECTORS AND CALIBRATION OF THE ISOPHOT EXPERIMENT
U. Groezinger, S. Kirches, D. Lemke, J. Schubert, B. Schulz, and J. Wolf *In* ESA, Proceedings of an ESA Symposium on Photon Detectors for Space Instrumentation Dec. 1992 p 329-333 (For primary document see N94-15025 03-19)
Copyright Avail: CASI HC A01/MF A04

The test facilities, test strategy and some example results of the calibration of ISOPHOT, one of the four focal plane experiments on ISO (Infrared Space Observatory), are described. Sophisticated test equipment is required in order to exploit the full potential of low background infrared photodetectors. The laboratory test set up described is flexible enough to deal with different types of sensitive detectors and arrays under a large

variety of test conditions such as photon background, flux sequences, temperatures, high energy radiation, etc. The calibration facility for testing the complete ISOPHOT experiment simulates the optical and cryogenic environment of ISO and allows accurate performance measurements under very low background conditions combined with near real time data evaluation. The performance of the Si:Ga, Si:B, Ge:Ga and stressed Ge:Ga detector assemblies is reported. ESA

N94-15083# Tuebingen Univ. (Germany). Physikalisches Inst.
SUBSTRATE EFFECTS IN SUPERCONDUCTING TUNNEL JUNCTION DETECTORS **c76**
S. Lemke, F. Hebrank, R. Gross, R. P. Huebener, T. Weimann (Physikalisch-Technische Bundesanstalt, Brunswick, Germany.), R. Poepel (Physikalisch-Technische Bundesanstalt, Brunswick, Germany.), J. Niemeyer (Physikalisch-Technische Bundesanstalt, Brunswick, Germany.), U. Schnakenberg (Fraunhofer-Inst. fuer Mikrostrukturtechnik, Berlin, Germany.), and W. Benecke (Bremen Univ., Germany.) *In* ESA, Proceedings of an ESA Symposium on Photon Detectors for Space Instrumentation Dec. 1992 p 335-338 Sponsored by DFG (For primary document see N94-15025 03-19)
Copyright Avail: CASI HC A01/MF A04

Superconducting Nb/AlOx/Nb tunnel junction detectors on bulk Si substrates show a spatially inhomogeneous detector response when part of the energy of an ionizing particle is deposited in the substrate. Nb/AlOx/Nb tunnel junctions with V(sub m) = 24 mV were prepared on 1 to 2 micrometer thick Si membranes. The spatial homogeneity of the response signal for the detection of 35 keV electrons improves significantly for junctions on Si membranes as compared to junctions on bulk silicon. The signal decay time for the membrane detector is about 450 microseconds at T = 5K, reducing the minimum energy (e) required to generate and count a single excess quasiparticle to (e) less than 6 meV. Constraints for the spectroscopy of X-rays with high energy resolution in superconducting tunnel junction detectors are discussed. ESA

N94-15084# Space Research Organization Netherlands, Groningen.
CHARACTERISTICS OF THE ISO SHORT WAVELENGTH SPECTROMETER DETECTORS
J. W. Wensink, W. Luinge, D. Beintema, E. A. Valentijn, T. deGraauw, R. Katterloher (Max-Planck-Inst. fuer Physik und Astrophysik, Garching, Germany.), L. Barl (Max-Planck-Inst. fuer Physik und Astrophysik, Garching, Germany.), and E. T. Young (Arizona Univ., Tucson.) *In* ESA, Proceedings of an ESA Symposium on Photon Detectors for Space Instrumentation Dec. 1992 p 339-344 (For primary document see N94-15025 03-19)
Copyright Avail: CASI HC A02/MF A04

The ISO (Infrared Space Observatory) Short Wavelength Spectrometer (SWS) employs four different types of detectors, which will all be operated at a low flux. Preliminary results of an extensive characterization of these detectors, both in the flight instrument and in a laboratory setup, are presented. In general, the performance of the instrument is as expected and quite low instrument noise equivalent powers are achieved (approximately 10 to the minus 17th power W/square root of Hz). However, the behavior of at least one of the detector types, Si:Sb, is troublesome. Characteristic features of this behavior are presented: long time transient response, memory effects, hook effects and excess noise. The Si:Sb transient responses can be described by two time constants. In contrast with the amplitude of the transient responses, these time constants depend only weakly on illumination power, temperature and bias voltage. This anomalous detector behavior implies specific designs of the observation strategies, which have to avoid 'flat-fielding' difficulties. ESA

N94-15085# National Physical Lab., Teddington (England). Quantum Metrology Div.
ABSOLUTE RADIOMETRIC MEASUREMENTS IN SPACE: ARMS
J. E. Martin and N. P. Fox *In* ESA, Proceedings of an ESA Symposium on Photon Detectors for Space Instrumentation Dec. 1992 p 345-348 (For primary document see N94-15025 03-19)
Copyright Avail: CASI HC A01/MF A04

The Absolute Radiometric Measurements in Space (ARMS) project proposes the development of a new primary radiometric standard for use in space traceable to the SI system of units. The standard, the Cryogenic Solar Absolute Radiometer (CSAR) will be capable of measuring the total irradiance of the Sun with an uncertainty of 0.01 percent, and a resolution of 0.001 percent, more than a factor ten improvement over existing instruments. ARMS was submitted to ESA in response to a call for opportunities for Columbus precursor flights and CSAR is currently on the provisional payload of Eureca 3. ESA

N94-15086# Mullard Space Science Lab., Dorking (England).
DATA PROCESSING SYSTEM FOR FLIGHT SPECTROMETER
A. J. McCalden *In* ESA, Proceedings of an ESA Symposium on Photon Detectors for Space Instrumentation Dec. 1992 p 349-352 Sponsored by Science Research Council (For primary document see N94-15025 03-19)
Copyright Avail: CASI HC A01/MF A04

An outline of the Grazing Incidence detector Spectrometer (GIS) for the Soho (Solar and Heliospheric Laboratory) Coronal Diagnostic Spectrometer (CDS) is presented and the design of the transputer based data processor and control system, is described. The GIS uses four detector heads each having a microchannel plate EUV sensor with one dimensional progressive geometry readout. They are arranged around the Rowland circle of a grating and cover four separate wavelength ranges over 150 to 800 A. The sensor information is decoded to provide 2048 positions for each detector head which map directly as wavelength. The science information processing and the command and housekeeping system is described, including an appreciation of the important tradeoffs necessary for a practical design for space applications. ESA

N94-15087# Institut National des Sciences Appliquees, Toulouse (France). Lab. de Physique des Solides.
SILICON GALLIUM DOPED PHOTOCONDUCTOR DEVELOPMENT FOR THE AROME BALLOON BORNE INSTRUMENT **c89**
C. Meny, I. Ristorcelli (Centre d'Etude Spatiale des Rayonnements, Toulouse, France.), M. Giard (Centre d'Etude Spatiale des Rayonnements, Toulouse, France.), G. Sirmain, G. Serra (Centre d'Etude Spatiale des Rayonnements, Toulouse, France.), G. Lucas (Commissariat a l'Energie Atomique, Grenoble, France.), and J. Leotin *In* ESA, Proceedings of an ESA Symposium on Photon Detectors for Space Instrumentation Dec. 1992 p 353-356 (For primary document see N94-15025 03-19)
Copyright Avail: CASI HC A01/MF A04

The measurement of IR emission features in extended sources originating from PAH's (Polycyclic Aromatic Molecules) material is addressed by the AROME instrument, a balloon borne telescope. For this purpose four Si:Ga photoconductors were developed. They operate at 1.6K inside an integrating cavity. A cold FET based TIA preamplifier provides low noise photocurrent measurement. The estimated noise equivalent power (blip) is 8 times 10 to the minus 14th power W/square root of Hz. ESA

N94-15088# Rutherford Appleton Lab., Chilton (England).
THE LABORATORY PERFORMANCE OF THE SHORT WAVELENGTH INSTRUMENT FOR THE ALONG TRACK SCANNING RADIOMETER ATSR-2 (INITIAL RESULTS)
P. D. Read, D. Field, A. L. Hardie, K. A. Lidiard, J. E. Magraw, H. S. Taylor, I. A. J. Tosh, M. A. Trower, and D. J. White *In* ESA, Proceedings of an ESA Symposium on Photon Detectors for Space Instrumentation Dec. 1992 p 357-360 (For primary document see N94-15025 03-19)
Copyright Avail: CASI HC A01/MF A04

ATSR-2 is a follow up instrument to ATSR due to be launched in 1994 as part of the ERS-2 payload, and the unit level testing is proceeding as the instrument nears completion. In addition to the identical four channel sea surface temperature measuring radiometer, used on ATSR, there is an additional three channel short wavelength (visible) radiometer, for land and vegetation sensing using selected wavelengths of 555, 659 and 865 nm. The arrangement of the instrument is shown and some performance data from the visible radiometer currently under test is given. ESA

N94-15089*# Northwestern Univ., Evanston, IL. Dept. of Physics and Astronomy.
A MULTILAYERED APPROACH TO SUPERCONDUCTING TUNNEL JUNCTION X RAY DETECTORS **c76**
E. D. Rippert, S. N. Song, J. B. Ketterson, S. R. Maglic, S. Lomatch, C. Thomas, M. A. Cheida, and M. P. Ulmer *In* ESA, Proceedings of an ESA Symposium on Photon Detectors for Space Instrumentation Dec. 1992 p 361-363 (For primary document see N94-15025 03-19)

(Grants NAGw-2859; NSF DMR-88-09864)
Copyright Avail: CASI HC A01/MF A04

'First generation' superconducting tunnel junction X-ray detectors (characterized by a single tunnel junction in direct contact with its substrate, with totally external amplification) remain more than an order of magnitude away from their theoretical energy resolutions which are in the order of eV's. The difficulties that first generation devices are encountering are being attacked by a 'second generation' of superconducting X-ray detector designs including quasiparticle trapping configurations and Josephson junction arrays. A second generation design concept, the multilayered superconducting tunnel junction X-ray detector, consisting of tens to hundreds of tunnel junctions stacked on top of one another (a superlattice), is presented. Some of the possibilities of this engineered materials approach include the tuning of phonon transmission characteristics of the material, suppression of parasitic quasiparticle trapping and intrinsic amplification. ESA

N94-15090# Imperial Coll. of Science and Technology, London (England). Blackett Lab.

APPLICATIONS FOR LARGE AREA SILICON DRIFT DETECTORS ON X RAY AND GAMMA RAY ASTRONOMY **c89**

G. K. Rochester, T. J. Sumner, R. J. Wheadon, G. Hall, B. Swinyard (Rutherford Appleton Lab., Chilton, England.), and P. Seller (Rutherford Appleton Lab., Chilton, England.) *In* ESA, Proceedings of an ESA Symposium on Photon Detectors for Space Instrumentation Dec. 1992 p 365-368 (For primary document see N94-15025 03-19)
Copyright Avail: CASI HC A01/MF A04

The energy resolution of a conventional silicon spectrometer is limited by the noise associated with leakage currents and capacitance. The noise can be reduced by cooling and by using detectors which have a small capacitance. In principle, silicon devices using drift technology should in some respects be superior to CCD's (Charge Coupled Devices). Measurements were made on both position sensitive spectrometers and large area photodiodes at low temperatures. Timing resolutions of a few microseconds, position resolutions of the order a fraction of a millimeter, and FWHM energy resolutions of 1 keV at 20 keV were obtained for single photon events in a 1 sq cm detector. As scintillator readout devices the photodiodes give a resolution comparable with that of conventional diodes when coupled to CsI(Tl) at room temperature, and superior to that of conventional diodes when coupled to BGO at low temperature. ESA

N94-15091# Societe Anonyme de Telecommunications, Paris (France). Div. Astronomique et Defense.

IR DETECTORS AND SUBSYSTEMS FOR SPACE APPLICATIONS

Michel Royer, Dominique Lorans, Bruno Flaux, and Robert Picault *In* ESA, Proceedings of an ESA Symposium on Photon Detectors for Space Instrumentation Dec. 1992 p 369-372 (For primary document see N94-15025 03-19)
Copyright Avail: CASI HC A01/MF A04

A review of IR detection modules for space application with an emphasis on three new programs is presented. The first two belong to the spectrometry application and the third to lidar technology. The first program called Omega consists of arrays of detectors for Mars '94 spacecraft to be implemented in the Meudon Observatory (France) IR spectrometer, named Omega, with the purpose to observe mineralogy, water, ice and atmosphere in the IR spectrum. The flight models, each having two arrays and IR filters in a dedicated housing, are under development. The second consists of IR detectors for the IASI (Improved Atmospheric Sounding Infrared) instrument of which the aim is: IR observation of clouds for the Globsat program. The feasibility of long wavelength IR photoconductor with LPE HgCdTe material was studied. The last application is HF heterodyne detectors for lidar application (wind speed measurement projects). The instruments are laser wind sounder (wind speed lidar) and the purpose is the global change from tropics atmosphere in case of a satellite (or airborne) onboard instrument. A subsystem for heteorodyne detector including a high stability (100 kHz) CO2 laser at lambda = 9.11 micrometers and a HgCdTe photovoltaic detector T = 140 K fc = 1000 MHz, is under development. These two last instruments are candidates as payload to be integrated into the ESA polar platforms. ESA

N94-15092# Fraunhofer Inst. fuer Physikalische Messtechnik, Freiburg (Germany).

INFRARED DETECTOR ANNEALING AND CALIBRATION WITH IR-LASER DIODES **c36**

U. Schiessl, M. Tacke, and D. Lemke (Max-Planck-Inst. fuer Astronomie, Heidelberg, Germany.) *In* ESA, Proceedings of an ESA Symposium on Photon Detectors for Space Instrumentation Dec. 1992 p 373-377 (For primary document see N94-15025 03-19)
(Grant BMFT-511/DARA-01-RS-89376)
Copyright Avail: CASI HC A01/MF A04

High sensitivity infrared detectors made from extrinsic semiconductors are of considerable importance for astronomical missions on satellites in Earth orbit. High energy radiation changes their sensitivity and their calibration. The photoconductors therefore necessitate onboard annealing and frequent recalibrations. Mid infrared diode lasers with low power dissipation are used for both applications, annealing with the stimulated, and recalibration with the spontaneous emission mode. ESA

N94-15093# Swedish Inst. of Space Physics, Kiruna.

REQUIREMENTS ON CCD-DETECTORS FOR GROUND-BASED AURORAL IMAGING **c89**

A. Steen and U. Braendstroem *In* ESA, Proceedings of an ESA Symposium on Photon Detectors for Space Instrumentation Dec. 1992 p 379-382 (For primary document see N94-15025 03-19)
Copyright Avail: CASI HC A01/MF A04

The aurora is a three dimensional time dependent signal with additional information in the spectral regime. The large dynamic range of the auroral signal raises rigorous requirements on the imaging detector. A new system for ground based auroral imaging, ALIS (Auroral Large Imaging System), is being constructed in the northern part of Sweden, using up to 14 stations with CCD (Charge Coupled Device) cameras. The stations are separated with about 50 km and are connected to a control center. Tomographic conversion techniques are applied to derive the three dimensional auroral signal. The key component of the ALIS system is the imaging detector. Unfortunately it is not possible to acquire an ideal auroral imaging detector; instead several compromises are necessary and shortcomings need to be overcome. The important aspects of the design of a ground based auroral imaging system are discussed. ESA

N94-15094# Mullard Space Science Lab., Dorking (England).

PERFORMANCE OF THE POSITION-SENSITIVE PROPORTIONAL COUNTERS OF THE YOHKOH BRAGG CRYSTAL SPECTROMETER

M. W. Trow *In* ESA, Proceedings of an ESA Symposium on Photon Detectors for Space Instrumentation Dec. 1992 p 383-387 Sponsored by Science Research Council (For primary document see N94-15025 03-19)
Copyright Avail: CASI HC A01/MF A04

The position sensitive proportional counter used in the Bragg Crystal Spectrometer (BCS) on the Yohkoh spacecraft (formerly known as Solar-A) is described. The BCS provides time resolved spectra of solar flares in soft X-rays (2.4 to 7.0 keV) with improved sensitivity over previous studies. This sealed detector, filled with a Xe-Ar-CO2 gas mixture, uses thin (15 micrometers) anodes, and a backgammon cathode board to provide one dimensional imaging along the dispersion axis of the spectrometer. The performance and calibration procedures for the detectors are discussed, and the use of the calibrations in interpreting BCS data is illustrated. ESA

N94-15095# Center for Industrial Research, Oslo (Norway).

SILICON RADIATION SENSOR SYSTEMS FOR GAMMA AND X RAY DETECTION AT SI **c76**

Svein Tunheim, Einar Nygaard, Arne Kjensmo, Lars Evensen, Fin Serck-Hanssen, and Per Ohlckers *In* ESA, Proceedings of an ESA Symposium on Photon Detectors for Space Instrumentation Dec. 1992 p 389-391 (For primary document see N94-15025 03-19)
Copyright Avail: CASI HC A01/MF A04

An ongoing research and development program in the field of silicon radiation sensor systems for gamma and X-ray detection is presented. In particular, the activities on double sided/single sided silicon radiation sensors and in front end electronics ASIC's (Application Specific Integrated Circuits) are described. ESA

N94-15096# Dunsink Observatory, Dublin (Ireland). School of Cosmic Physics.

THE RUTHERFORD APPLETON LABORATORY PHOTON COUNTING DETECTOR **c35**

I. G. vanBreda, M. K. Carter (Rutherford Appleton Lab., Chilton, England.), B. E. Patchett (Rutherford Appleton Lab., Chilton, England.), and P. D. Read (Rutherford Appleton Lab., Chilton, England.) *In* ESA, Proceedings of an ESA Symposium on Photon Detectors for Space Instrumentation Dec. 1992 p 393-396 (For primary document see N94-15025 03-19)

Copyright Avail: CASI HC A01/MF A04

The Rutherford Appleton Laboratory Photon Counting Detector is a two dimensional area detector having a wide range of applications at optical, UV and X-ray wavelengths, both ground based and in space. It makes use of a microchannel plate intensifier and 'software centroiding' to derive the coordinates for photon events. The intensifier is coupled by means of a fiber optic taper either to a frame transfer CCD (Charge Coupled Device) or a CID camera running at video rates. Readout data frames are passed to a transputer array for analysis, where the event centroids are first calculated using an approximate numerical algorithm, then corrected using a lookup table. The current characteristics of the detector and some possible future developments are discussed. ESA

N94-15097# Technische Physische Dienst TNO-TH, Delft (Netherlands).

ASSESSMENT OF TDI OPERATION OF A FRAME TRANSFER CCD FOR HIGH RESOLUTION IMAGING FROM A FAST SPINNING SPACECRAFT

Peter Verhoeff and P. Gondoin (European Space Agency. European Space Research and Technology Center, ESTEC, Noordwijk, Netherlands.) *In* ESA, Proceedings of an ESA Symposium on Photon Detectors for Space Instrumentation Dec. 1992 p 397-400 Sponsored in part by Netherlands Agency for Aerospace Programs (For primary document see N94-15025 03-19)

(Contract ESA-9180/90/NL/PR)

Copyright Avail: CASI HC A01/MF A04

A simulation setup, radiometrically representative of Earth observation condition from a geosynchronous spinning spacecraft, was built. This simulation set up is used to verify the performance of a commercially matrix CCD (Charge Coupled Device) when operating in Time Delay and Integration (TDI) mode. The results from a measurement program using representative scene illumination and image speed conditions are described. The measurement results obtained with CCD operating in TDI mode were compared to results obtained in a conventional staring mode of CCD operation. In addition, the results of the performed MTF measurements were compared with results obtained from a simulation model. ESA

N94-15098# Interuniversity Micro-Electronics Center, Leuven (Belgium).

A LINEAR MONOLITHIC 4-6 ON SILICON IR DETECTOR ARRAY **c76**

J. VanDamme, J. Vermeiren, H. Zogg (Eidgenoessische Technische Hochschule, Zurich, Switzerland.), J. Masek (Eidgenoessische Technische Hochschule, Zurich, Switzerland.), and M. Fabbricotti (European Space Agency. European Space Research and Technology Center, ESTEC, Noordwijk, Netherlands.) *In* ESA, Proceedings of an ESA Symposium on Photon Detectors for Space Instrumentation Dec. 1992 p 401-404 Sponsored by Gruppe fuer Ruestungsdienste and Swiss NSF (For primary document see N94-15025 03-19)

(Contract ESA-7085/87/NL/PB)

Copyright Avail: CASI HC A01/MF A04

A linear array of monolithically grown PbTe and PbSnSe detectors on (111)-Si for MWIR and TIR imaging applications was designed and processed. The array consists of a staggered row of 2 by 128 detectors on a 100 micrometers pitch. The readout circuitry, integrated on the Si substrate consists of a COS multiplexer with a direct injection input stage, a charge reduction stage and charge to voltage conversion stage for each individual detector. This XDI (MultipeXed Direct Injection) circuit also allows for on-chip nonuniformity compensation with a switched capacitor network. ESA

N94-15099# Interuniversity Micro-Electronics Center, Leuven (Belgium).

CRYOGENIC READOUT ELECTRONICS FOR ASTRONOMICAL APPLICATIONS **c89**

B. Dierickx, J. Vermeiren, S. Cos, R. Faymonville (Battelle Inst., Frankfurt am Main, Germany.), and D. Lemke (Max-Planck-Inst. fuer Astronomie, Heidelberg, Germany.) *In* ESA, Proceedings of an ESA Symposium on Photon Detectors for Space Instrumentation Dec. 1992 p 405-408 Sponsored by Deutsche Agentur fuer Raumfahrtangelegenheiten G.m.b.H. (For primary document see N94-15025 03-19)

Copyright Avail: CASI HC A01/MF A04

The development of the cold readout electronics for the ISOPHOT focal plane experiment on the ISO (Infrared Space Observatory) is reported. For this low background application, custom designed highly sensitive integrating charge amplifiers are used for the readout of the extrinsic IR detectors. The use of CMOS circuits allows the multiplexing and readout of a large number of detectors at the detector temperature, with a very low power dissipation. The CMOS readout amplifier/multiplexer for deep cryogenic operation is discussed. The device is able to interface directly with extrinsic photoconductive detectors cooled down to the 1.8 to 10K range. In order to observe faint objects under low light level conditions the integration capacitor is 80 fF, featuring a saturation at 1 million charge carriers for an output voltage swing of 2 V and a noise level of 0.5 mV root mean square in nondestructive readout mode. With this circuit coupled to detectors with a responsivity of around 5 to 10 A/W, it is possible to reach noise equivalent power values of 10 to the minus 17th power W/square root of Hz. The multiplexer can be operated with only 10 wires for the supplies, and the clocking of the circuits. ESA

N94-15100# Interuniversity Micro-Electronics Center, Leuven (Belgium).

A MONOLITHIC PbTeCCD FOCAL PLANE ARRAY FOR MWIR IMAGING **c76**

J. VanDamme, J. Vermeiren, G. Marangoni (Elettronica S.R.L., Rome, Italy.), M. DAntoni (Elettronica S.R.L., Rome, Italy.), W. Platz (Messerschmitt-Boelkow-Blohm G.m.b.H., Munich, Germany.), and M. Fabbricotti (European Space Agency. European Space Research and Technology Center, ESTEC, Noordwijk, Netherlands.) *In* ESA, Proceedings of an ESA Symposium on Photon Detectors for Space Instrumentation Dec. 1992 p 409-412 (For primary document see N94-15025 03-19)

(Contract ESA-6044/84/NL/PB)

Copyright Avail: CASI HC A01/MF A04

A 1536 pixels butted array consisting of three CCD (Charge Coupled Device) modules with a truly linear sensor row and with a bilinear readout organization was developed for infrared imaging. The pixel gap at the butting edges is nominally 1 and maximum 2 pixels and the alignment accuracy is better than 5 micrometers within the detector plane and better than 50 micrometers in the Z direction. Photoconductive polycrystalline PbTe detectors were deposited directly on top of a CCD multiplexer circuit, resulting in most probably a lead salt detector array with the highest degree of integration, reported so far. The devices are operated in the 77 to 120K range and are showing a peak responsivity of 240 GV/J and a minimum noise equivalent power of 130 fW/square root of Hz. ESA

N94-15101# Cambridge Univ. (England). Dept. of Materials Science and Metallurgy.

QUASIPARTICLE TRAPPING IN DISTRIBUTED SUPERCONDUCTING THREE-TERMINAL TUNNEL JUNCTION DEVICES **c76**

P. A. Warburton and M. G. Blamire *In* ESA, Proceedings of an ESA Symposium on Photon Detectors for Space Instrumentation Dec. 1992 p 413-416 Sponsored in part Science Research Council; Royal Society; and NRL (For primary document see N94-15025 03-19)

Copyright Avail: CASI HC A01/MF A04

In order to investigate quasiparticle trapping effects, three-terminal superconducting double tunnel junctions in which quasdiparticles are injected into a base bilayer Nb-Mo heterostructure were fabricated. The Mo layer thickness is variable. Quasiparticle multiplication has been observed in devices with sufficiently low Mo gap energy. By injecting quasiparticles at varying energies, nonequilibrium phonons created by the inelastic scattering of trapped quasiparticles are shown to be of significance in the trapping process. ESA

N94-15102*# National Aeronautics and Space Administration, Washington, DC.

NASA'S ULTRAVIOLET ASTROPHYSICS BRANCH: PRESENT AND FUTURE DETECTOR PROGRAM

Barry Y. Welsh (Jet Propulsion Lab., California Inst. of Tech., Pasadena.) *In* ESA, Proceedings of an ESA Symposium on Photon Detectors for

Space Instrumentation Dec. 1992 p 417-421 (For primary document see N94-15025 03-19)
Copyright Avail: CASI HC A01/MF A04

The various concepts in ultraviolet detector technology currently being funded by NASA's Astrophysics Division to carry out observations in the 100 to 3000 A region are reviewed. In order to match the science objectives of future space missions with new observational techniques, critical detector technology needs in the ultraviolet regime have been identified. The attempt by NASA's Astrophysics Division Advanced Programs Branch to formulate an integrated detector technology plan as part of the ongoing 'Astrotech 21' program in order to provide the technology base for these astrophysics missions of the 21st century is described. ESA

N94-15103# Imperial Coll. of Science and Technology, London (England).

THE EPITAXIAL Si X RAY BOLOMETER AN ALTERNATIVE TO ION IMPLANTED DEVICES **c76**

C. C. Zammit, T. J. Sumner, I. D. Hepburn (London Univ., England.), P. A. R. Ade (London Univ., England.), P. Hutchin (Southampton Univ., England.), and G. Ensell (Southampton Univ., England.) *In* ESA, Proceedings of an ESA Symposium on Photon Detectors for Space Instrumentation Dec. 1992 p 423-425 (For primary document see N94-15025 03-19)
Copyright Avail: CASI HC A01/MF A04

The ion implanted Si bolometer has unequaled performance as a high resolution X-ray detector. The superconducting tunnel junction detector has to date, been unable to provide such performance. A new form of Si bolometer using single crystal epitaxial growth to replace ion implantation for better power handling, good uniformity and low excess noise, is under development. The use of epitaxial growth allows the production of single crystal layers with a thickness of up to 40 micrometers with simultaneous doping from a secondary dopant gas stream. In addition, the layer can be capped with an undoped layer to minimize excess noise and further improve performance. ESA

N94-15552*# National Aeronautics and Space Administration. Goddard Space Flight Center, Greenbelt, MD.

EIGHTH INTERNATIONAL WORKSHOP ON LASER RANGING INSTRUMENTATION

John J. Degnan, comp. Washington Jun. 1993 741 p Workshop held in Annapolis, MD, 18-22 May 1992
(NASA-CP-3214; Rept-93B00079; NAS 1.55:3214) Avail: CASI HC A99/MF A06

The Eighth International Workshop for Laser Ranging Instrumentation was held in Annapolis, Maryland in May 1992, and was sponsored by the NASA Goddard Space Flight Center in Greenbelt, Maryland. The workshop is held once every 2 to 3 years under differing institutional sponsorship and provides a forum for participants to exchange information on the latest developments in satellite and lunar laser ranging hardware, software, science applications, and data analysis techniques. The satellite laser ranging (SLR) technique provides sub-centimeter precision range measurements to artificial satellites and the Moon. The data has application to a wide range of Earth and lunar science issues including precise orbit determination, terrestrial reference frames, geodesy, geodynamics, oceanography, time transfer, lunar dynamics, gravity and relativity. For individual titles, see N94-15553 through N94-15625.

N94-15553*# National Aeronautics and Space Administration. Goddard Space Flight Center, Greenbelt, MD.

LASER TRACKING FOR VERTICAL CONTROL **c36**

Peter Dunn (Hughes STX, Inc., Lanham, MD.), Mark Torrence (Hughes STX, Inc., Lanham, MD.), Erricos Pavlis (Maryland Univ., College Park.), Ron Kolenkiewicz, and David Smith *In its* Eighth International Workshop on Laser Ranging Instrumentation Jun. 1993 18 p (For primary document see N94-15552 03-19)
Avail: CASI HC A03/MF A06

The Global Laser Tracking Network has provided LAGEOS ranging data of high accuracy since the first MERIT campaign in late 1983 and we can now resolve centimeter-level three dimensional positions of participating observatories at monthly intervals. In this analysis, the station height estimates have been considered separately from the horizontal components, and can be determined by the strongest stations with a formal standard error of 2 mm using eight years of continuous observations. The rate of change in the vertical can be resolved to a few mm/year, which is at the expected level of several geophysical effects. In comparing the behavior of the stations to that predicted by recent models of post-glacial rebound, we find no correlation in this very small effect. Particular attention must be applied to data and survey quality control when measuring the vertical component, and the survey observations are critical components of the geodynamic results. Seasonal patterns are observed in the heights of most stations, and the possibility of secular motion at the level of several millimeters per year cannot be excluded. Any such motion must be considered in the interpretation of horizontal inter-site measurements, and can help to identify mechanisms which can cause variations which occur linearly with time, seasonally, or abruptly. Author

N94-15554*# Deutsches Geodaetisches Forschungsinst., Munich (Germany).

LASER RANGING NETWORK PERFORMANCE AND ROUTINE ORBIT DETERMINATION AT D-PAF **c36**

Franz-Heinrich Massmann, C. Reigber, H. Li, Rolf Koenig, J. C. Raimondo, C. Rajasenan, and M. Vei *In* NASA. Goddard Space Flight Center, Eighth International Workshop on Laser Ranging Instrumentation Jun. 1993 15 p Prepared in cooperation with Deutsche Geodaetische Kommission, Munich, Germany (For primary document see N94-15552 03-19)
Avail: CASI HC A03/MF A06

ERS-1 is now about 8 months in orbit and has been tracked by the global laser network from the very beginning of the mission. The German processing and archiving facility for ERS-1 (D-PAF) is coordinating and supporting the network and performing the different routine orbit determination tasks. This paper presents details about the global network status, the communication to D-PAF and the tracking data and orbit processing system at D-PAF. The quality of the preliminary and precise orbits are shown and some problem areas are identified. Author

N94-15555*# Ministry of Posts and Telecommunications, Tokyo (Japan). Communications Research Lab.

LASER RANGING APPLICATION TO TIME TRANSFER USING GEODETIC SATELLITE AND TO OTHER JAPANESE SPACE PROGRAMS **c36**

Hiroo Kunimori, Fujinobu Takahashi, Toshikazu Itabe, and Atsushi Yamamoto (Maritime Safety Agency, Tokyo, Japan.) *In* NASA. Goddard Space Flight Center, Eighth International Workshop on Laser Ranging Instrumentation Jun. 1993 9 p (For primary document see N94-15552 03-19)
Avail: CASI HC A02/MF A06

Communications Research Laboratory (CRL) has been developing a laser time transfer system using a satellite laser ranging (SLR) system. We propose Japanese geodetic satellite 'AJISAI', launched in 1986 as a target satellite. The surface is covered not only with corner cube reflectors but also with mirrors. The mirrors are originally designed for observation of flushing solar light reflected by the separate mirrors while the satellite is spinning. In the experiment, synchronized laser pulses are transferred via specified mirror from one station to another while the satellite is up on the horizon to both stations. The system is based on the epoch timing ranging system with 40 ps ranging precision, connected together with UTC(CRL). Simulation study indicates that two stations at thousands of km distance from each other can be linked with signal strength of more than 10 photons and the distributed images of laser beam from AJISAI mirrors give many chances for two stations to link each other during a single AJISAI pass. Retro-reflector In Space for Advanced Earth Observation Satellite (ADEOS) and RendDezVous docking mission of Experimental Technology Satellite-7 (ETS-7) are briefly presented. Author (revised)

N94-15556*# Texas Univ., Austin. Center for Space Research.

APPLICATIONS OF SLR **c36**

Bob E. Schutz *In* NASA. Goddard Space Flight Center, Eighth International Workshop on Laser Ranging Instrumentation Jun. 1993 4 p (For primary document see N94-15552 03-19)
Avail: CASI HC A01/MF A06

Satellite Laser Ranging (SLR) has a rich history of development which began in the 1960s with 10 meter-level first generation systems. These systems evolved with order of magnitude improvements to the systems that now produce several millimeter single shot range precisions. What

began, in part, as an interesting application of the new laser technology has become an essential component of modern, precision space geodesy, which in turn enables contributions to a variety of science areas. Modern space geodesy is the beneficiary of technological developments which have enabled precision geodetic measurements. Aside from SLR and its closely related technique, Lunar Laser Ranging (LLR), Very Long Baseline Interferometry (VLBI) has made prominent science contributions also. In recent years, the Global Positioning System (GPS) has demonstrated a rapidly growing popularity as the result of demonstrated low cost with high precision instrumentation. Other modern techniques such as DORIS have demonstrated the ability to make significant science contributions; furthermore, PRARE can be expected to contribute in its own right. An appropriate question is 'why should several techniques be financially supported'? While there are several answers, I offer the opinion that, in consideration of the broad science areas that are the benefactors of space geodesy, no single technique can meet all the requirements and/or expectations of the science areas in which space geodesy contributes or has the potential for contributing. The more well-known science areas include plate tectonics, earthquake processes, Earth rotation/orientation, gravity (static and temporal), ocean circulation, land, and ice topography, to name a few applications. It is unfortunate that the modern space geodesy techniques are often viewed as competitive, but this view is usually encouraged by funding competition, especially in an era of growing needs but diminishing budgets. The techniques are, for the most part, complementary and the ability to reduce the data to geodetic parameters from several techniques promotes confidence in the geophysical interpretations. In the following sections, the current SLR applications are reviewed in the context of the other techniques. The strengths and limitations of SLR are reviewed and speculation about the future prospects are offered. Author

N94-15557*# Royal Greenwich Observatory, Cambridge (England).
SATELLITE SIGNATURES IN SLR OBSERVATIONS **c36**
G. M. Appleby *In* NASA. Goddard Space Flight Center, Eighth International Workshop on Laser Ranging Instrumentation Jun. 1993 14 p (For primary document see N94-15552 03-19)
Avail: CASI HC A03/MF A06

We examine the evidence for the detection of satellite-dependent signatures in the laser range observations obtained by the UK single-photon Satellite Laser Ranging (SLR) System models of the expected observation distributions from Ajisai and Lageos are developed from the published satellite spread functions and from the characteristics of the SLR System and compared with the observations. The effects of varying return strengths are discussed using the models and by experimental observations of Ajisai, during which a range of return levels from single to multiple photons is achieved. The implications of these results for system-dependent center for mass corrections are discussed. Author (revised)

N94-15558*# Technische Univ., Graz (Austria). Inst. for Space Research.
WORK AT GRAZ ON SATELLITE SIGNATURES **c18**
Georg Kirchner and Franz Koidl *In* NASA. Goddard Space Flight Center, Eighth International Workshop on Laser Ranging Instrumentation Jun. 1993 8 p (For primary document see N94-15552 03-19)
Avail: CASI HC A02/MF A06

The size and shape of the satellites retroreflector arrays have a major impact on the distribution and scatter of the return signal; this can be seen clearly when reaching sub-cm ranging accuracies and when using Single-Photon Detectors with single- or multi-photon returns; for other receiver systems (using MCP's), it should be checked also. As a consequence, the necessary center-of-mass correction for some satellites will differ, depending on the receiver systems. While this effect is not yet visible on small satellites or small retro-reflector arrays (like STARLETTE, ERS1), it can be in the order of centimeters on AJISAI or ETALON. Author (revised)

N94-15559*# Hughes STX, Inc., Lanham, MD.
THE PRECISION OF TODAY'S SATELLITE LASER RANGING SYSTEMS
Peter J. Dunn, Mark H. Torrence, Van S. Hussen (Bendix Field Engineering Corp., Greenbelt, MD.), and Michael R. Pearlman (Smithsonian Astrophysical Observatory, Cambridge, MA.) *In* NASA. Goddard Space Flight Center, Eighth International Workshop on Laser Ranging Instrumentation Jun. 1993 11 p (For primary document see N94-15552 03-19)
Avail: CASI HC A03/MF A06

Recent improvements in the accuracy of modern satellite laser ranging (SLR) systems are strengthened by the new capability of many instruments to track an increasing number of geodetic satellite targets without significant scheduling conflict. This will allow the refinement of some geophysical parameters, such as solid Earth tidal effects and GM, and the improved temporal resolution of others, such as Earth orientation and station position. Better time resolution for the locations of fixed observatories will allow us to monitor more subtle motions at the stations, and transportable systems will be able to provide indicators of long term trends with shorter occupations. If we are to take advantage of these improvements, care must be taken to preserve the essential accuracy of an increasing volume of range observations at each stage of the data reduction process. Derived from text

N94-15560*# Royal Greenwich Observatory, Cambridge (England).
SLR DATA SCREENING; LOCATION OF PEAK OF DATA DISTRIBUTION **c82**
Andrew T. Sinclair *In* NASA. Goddard Space Flight Center, Eighth International Workshop on Laser Ranging Instrumentation Jun. 1993 10 p (For primary document see N94-15552 03-19)
Avail: CASI HC A02/MF A06

At the 5th Laser Ranging Instrumentation Workshop held at Herstmonceux in 1984, consideration was given to the formation of on-site normal points by laser stations, and an algorithm was formulated. The algorithm included a recommendation that an iterated 3.0 x rms rejection criterion should be used to screen the data, and that arithmetic means should be formed within the normal point bins of the retained data. From Sept. 1990 onwards, this algorithm and screening criterion have been brought into effect by various laser stations for forming on-site normal points, and small variants of the algorithm are used by most analysis centers for forming normal points from full-rate data, although the data screening criterion they use ranges from about 2.5 to 3.0 x rms. At the CSTG Satellite Laser Ranging (SLR) Subcommission, a working group was set up in Mar. 1991 to review the recommended screening procedure. This paper has been influenced by the discussions of this working group, although the views expressed are primarily those of this author. The main thrust of this paper is that, particularly for single photon systems, a more important issue than data screening is the determination of the peak of a data distribution and hence, the determination of the bias of the peak from the mean. Several methods of determining the peak are discussed. Author (revised)

N94-15561*# Geodetic Inst., Helsinki (Finland).
ADAPTIVE MEDIAN FILTERING FOR PREPROCESSING OF TIME SERIES MEASUREMENTS **c65**
Matti Paunonen *In* NASA. Goddard Space Flight Center, Eighth International Workshop on Laser Ranging Instrumentation Jun. 1993 7 p (For primary document see N94-15552 03-19)
Avail: CASI HC A02/MF A06

A median (L1-norm) filtering program using polynomials was developed. This program was used in automatic recycling data screening. Additionally, a special adaptive program to work with asymmetric distributions was developed. Examples of adaptive median filtering of satellite laser range observations and TV satellite time measurements are given. The program proved to be versatile and time saving in data screening of time series measurements. Author (revised)

N94-15562*# Bendix Field Engineering Corp., Seabrook, MD.
SATCOP MISSION PLANNING SOFTWARE PACKAGE **c61**
Steve Bucey *In* NASA. Goddard Space Flight Center, Eighth International Workshop on Laser Ranging Instrumentation Jun. 1993 13 p (For primary document see N94-15552 03-19)
Avail: CASI HC A03/MF A06

As the CDSLR Network grows into the 1990's, it is undergoing many changes in both its capabilities and requirements. On the one hand, great progress has been made in terms of increasing the SLR systems' performance. Upgrades to the onsite computer and improved laser ranging hardware have greatly increased the number of satellite passes which can be acquired during an operating shift by reducing the amount of time

needed for operations other than actual ranging. On the other hand, more requirements have been placed on the systems. Many more satellites have become available, with more scheduled for launch, thus, increasing the likelihood of simultaneous satellite visibility. In addition, the possible scenarios required for ranging these many satellites are changing frequently, with conflicting priorities and needs. It became apparent that some tools needed to be developed to assist the planners in determining Network ranging priorities. Such tools have been developed at Bendix under the direction of NASA's Dynamics of the Solid Earth Project (DOSE) for both long range planning and routine operations to maximize the amount of data collected. This paper reviews some of these tools and describe their uses. Derived from text

N94-15563*# National Aeronautics and Space Administration. Goddard Space Flight Center, Greenbelt, MD.

Nd:YLF LASER FOR AIRBORNE/SPACEBORNE LASER RANGING c36

Joseph L. Dallas and Mark D. Selker *In its* Eighth International Workshop on Laser Ranging Instrumentation Jun. 1993 6 p (For primary document see N94-15552 03-19)

Avail: CASI HC A02/MF A06

In order to meet the need for light weight, long lifetime, efficient, short pulse lasers, a diode-pumped, Nd:YLF oscillator and regenerative amplifier is being developed. The anticipated output is 20 mJ per 10 picosecond pulse, running at a repetition rate of 40 Hz. The fundamental wavelength is at 1047 nm. The oscillator is pumped by a single laser diode bar and mode locked using an electro-optic, intra-cavity phase modulator. The output from the oscillator is injected as a seed into the regenerative amplifier. The regenerative amplifier laser crystal is optically pumped by two 60W quasi-cw laser diode bars. Each diode is collimated using a custom designed micro-lens bar. The injected 10 ps pulse from the oscillator is kept circulating within the regenerative amplifier until this nanojoule level seed pulse is amplified to 2-3 millijoules. At this point the pulse is ejected and sent on to a more standard single pass amplifier where the energy is boosted to 20 mJ. The footprint of the entire laser (oscillator-regenerative amplifier-amplifier) will fit on a 3 by 4 ft. optical pallet. Author (revised)

N94-15564*# Czech Technical Univ., Prague. Faculty of Nuclear Science and Physical Engineering.

ALTERNATIVE WAVELENGTHS FOR LASER RANGING c36

Karel Hamal *In* NASA. Goddard Space Flight Center, Eighth International Workshop on Laser Ranging Instrumentation Jun. 1993 2 p (For primary document see N94-15552 03-19)

Avail: CASI HC A01/MF A06

The following are considered to be necessary to accomplish multicolor laser ranging: the nature of the atmospheric dispersion and absorption, the satellite/lunar/ground retro-array characteristics, and ground/satellite ranging machine performance. The energy balance and jitter budget have to be considered as well. It is concluded that the existing satellite/laser retroreflectors seem inadequate for future experiments. The Raman Stokes/Anti-Stokes (0.68/0.43 micron) plus solid state detector appear to be promising instrumentation that satisfy the ground/satellite and satellite/ground ranging machine requirements on the precision, compactness, and data processing. Derived from text

N94-15565*# Czech Technical Univ., Prague. Faculty of Nuclear Science and Physical Engineering.

NEW METHODS OF GENERATION OF ULTRASHORT LASER PULSES FOR RANGING c36

Helena Jelinkova, Karel Hamal, V. Kubecek, and Ivan Prochazka *In* NASA. Goddard Space Flight Center, Eighth International Workshop on Laser Ranging Instrumentation Jun. 1993 6 p (For primary document see N94-15552 03-19)

Avail: CASI HC A02/MF A06

To reach the millimeter satellite laser ranging accuracy, the goal for nineties, new laser ranging techniques have to be applied. To increase the laser ranging precision, the application of the ultrashort laser pulses in connection with the new signal detection and processing techniques, is inevitable. The two wavelength laser ranging is one of the ways to measure the atmospheric dispersion to improve the existing atmospheric correction models and hence, to increase the overall system ranging accuracy to the desired value. We are presenting a review of several nonstandard techniques of ultrashort laser pulses generation, which may be utilized for laser ranging: compression of the nanosecond pulses using stimulated Brillouin and Raman backscattering; compression of the mode-locked pulses using Raman backscattering; passive mode-locking technique with nonlinear mirror; and passive mode-locking technique with the negative feedback. Derived from text

N94-15566*# Academia Sinica, Shanghai (China). Lab. of Laser Technology.

SIMULTANEOUS COMPRESSION OF THE PASSIVELY MODE-LOCKED PULSEWIDTH AND PULSE TRAIN c32

Xiang-Chun Yang, Xiao-Lei Zhu, Zhao-Qing Wu, Zhan-Ao Sun, Fu-Min Yang (Shanghai Observatory, China.), De-Tong Tan (Shanghai Observatory, China.), Wan-Zhen Chen (Shanghai Observatory, China.), Wen-Hu Lu (Shanghai Observatory, China.), and Chi-Kun Xiao (Shanghai Observatory, China.) *In* NASA. Goddard Space Flight Center, Eighth International Workshop on Laser Ranging Instrumentation Jun. 1993 4 p (For primary document see N94-15552 03-19)

Avail: CASI HC A01/MF A06

Simultaneous compression of the passively mode-locked pulse width and pulse train have been achieved by using a plano-convex unstable resonator hybrided by a nonlinear Sagnac ring interferometer. The greater than 30 mJ single pulse energy of a lone oscillator and less than or equal to 10 ps pulsewidth have been obtained. Using this system, the LAGEOS and ETALON satellites' laser ranging have been performed successfully. Author (revised)

N94-15567*# Czech Technical Univ., Prague. Faculty of Nuclear Science and Physical Engineering.

AN IMPROVED LIGHT SOURCE FOR LASER RANGING c36

Karel Hamal and Martin Richardson (University of Central Florida, Orlando.) *In* NASA. Goddard Space Flight Center, Eighth International Workshop on Laser Ranging Instrumentation Jun. 1993 2 p (For primary document see N94-15552 03-19)

Avail: CASI HC A01/MF A06

The development of a new laser material, Cr-doped LiSAF, makes possible the development of a laser source for satellite ranging systems that is more superior in performance capabilities than current Nd:YAG-based laser sources. This new material offers the potential of shorter pulses and more preferable wavelengths (850 and 425 nm) than multiwavelength Nd:YAG systems, leading to superior ranging resolution and greater detection sensitivity. We are embarking on a feasibility study of a two-wavelength, mode-locked laser system based on Cr:LiSAF, providing shorter pulses for improved ranging resolution. Derived from text

N94-15568*# Bendix Field Engineering Corp., Seabrook, MD.

PRELIMINARY RESULTS FROM THE PORTABLE STANDARD SATELLITE LASER RANGING INTERCOMPARISON WITH MOBLAS-7

Michael Selden, Thomas K. Varghese, Michael Heinick, and Thomas Oldham *In* NASA. Goddard Space Flight Center, Eighth International Workshop on Laser Ranging Instrumentation Jun. 1993 8 p (For primary document see N94-15552 03-19)

Avail: CASI HC A02/MF A06

Conventional Satellite Laser Ranging (SLR) instrumentation has been configured and successfully used to provide high-accuracy laboratory measurements on the LAGEOS-2 and TOPEX cube-corner arrays. The instrumentation, referred to as the Portable Standard, has also been used for field measurements of satellite ranges in tandem with MOBLAS-7. Preliminary results of the SLR measurements suggest that improved range accuracy can be achieved using this system. Results are discussed. Author

N94-15569*# Politecnico di Milano (Italy). Dipt. di Elettronica e Informazione.

PERFORMANCE OPTIMIZATION OF DETECTOR ELECTRONICS FOR MILLIMETER LASER RANGING c36

Sergio Cova, A. Lacaita, and Giancarlo Ripamonti (Milan Univ., Italy.) *In* NASA. Goddard Space Flight Center, Eighth International Workshop on Laser Ranging Instrumentation Jun. 1993 18 p Sponsored in part by Italian Space Agency; CNR; and Italian Ministry of University and Research (For primary document see N94-15552 03-19)

Avail: CASI HC A03/MF A06

The front-end electronic circuitry plays a fundamental role in determining

the performance actually obtained from ultrafast and highly sensitive photodetectors. We deal here with electronic problems met working with microchannel plate photomultipliers (MCP-PMTs) and single photon avalanche diodes (SPADs) for detecting single optical photons and measuring their arrival time with picosecond resolution. The performance of available fast circuits is critically analyzed. Criteria for selecting the most suitable electronics are derived and solutions for exploiting the detector performance are presented and discussed. Author (revised)

N94-15570*# Politecnico di Milano (Italy). Dipt. di Elettronica e Informazione.

TRACKING CAPABILITIES OF SPADS FOR LASER RANGING **c36**

F. Zappa, Giancarlo Ripamonti (Milan Univ., Italy.), A. Lacaita, Sergio Cova, and C. Samori *In* NASA. Goddard Space Flight Center, Eighth International Workshop on Laser Ranging Instrumentation Jun. 1993 6 p Sponsored in part by Italian Space Agency; CNR; and Italian Ministry of University and Research (For primary document see N94-15552 03-19)

Avail: CASI HC A02/MF A06

The spatial sensitivity of Single-Photon Avalanche Diodes (SPADs) can be exploited in laser ranging measurements to finely tune the laser spot in the center of the detector sensitive area. We report the performance of a SPAD with 100 micron diameter. It features a time resolution better than 80 ps rms when operated 4V above V(b) at minus 30 C, and a spatial sensitivity better than 20 microns to radial displacements of the laser spot. New SPAD structures with auxiliary delay detectors are proposed. These improved devices could allow a two dimensional sensitivity, that could be employed for the design of pointing servos. Author (revised)

N94-15571*# Politecnico di Milano (Italy). Dipt. di Elettronica e Informazione.

HOW TO SQUEEZE HIGH QUANTUM EFFICIENCY AND HIGH TIME RESOLUTION OUT OF A SPAD **c36**

A. Lacaita, F. Zappa, Sergio Cova, Giancarlo Ripamonti (Milan Univ., Italy.), and A. Spinelli *In* NASA. Goddard Space Flight Center, Eighth International Workshop on Laser Ranging Instrumentation Jun. 1993 6 p Sponsored in part by Italian Space Agency; CNR; and Italian Ministry of University and Research (For primary document see N94-15552 03-19)

Avail: CASI HC A02/MF A06

We address the issue whether Single-Photon Avalanche Diodes (SPADs) can be suitably designed to achieve a trade-off between quantum efficiency and time resolution performance. We briefly recall the physical mechanisms setting the time resolution of avalanche photodiodes operated in single-photon counting, and we give some criteria for the design of SPADs with a quantum efficiency better than 10 percent at 1064 nm together with a time resolution below 50 ps rms. Author (revised)

N94-15572*# Czech Technical Univ., Prague. Faculty of Nuclear Science and Physical Engineering.

THE SOLID STATE DETECTOR TECHNOLOGY FOR PICOSECOND LASER RANGING **c76**

Ivan Prochazka *In* NASA. Goddard Space Flight Center, Eighth International Workshop on Laser Ranging Instrumentation Jun. 1993 5 p (For primary document see N94-15552 03-19)

Avail: CASI HC A01/MF A06

We developed an all solid state laser ranging detector technology, which makes the goal of millimeter accuracy achievable. Our design and construction philosophy is to combine the techniques of single photon ranging, ultrashort laser pulses, and fast fixed threshold discrimination while avoiding any analog signal processing within the laser ranging chain. The all solid state laser ranging detector package consists of the START detector and the STOP solid state photon counting module. Both the detectors are working in an optically triggered avalanche switching regime. The optical signal is triggering an avalanche current buildup which results in the generation of a uniform, fast risetime output pulse. Derived from text

N94-15573*# Bendix Field Engineering Corp., Seabrook, MD.

STREAK CAMERA BASED SLR RECEIVER FOR TWO COLOR ATMOSPHERIC MEASUREMENTS **c35**

Thomas K. Varghese, Christopher Clarke, Thomas Oldham, and Michael Selden *In* NASA. Goddard Space Flight Center, Eighth International Workshop on Laser Ranging Instrumentation Jun. 1993 11 p (For primary document see N94-15552 03-19)

Avail: CASI HC A03/MF A06

To realize accurate two-color differential measurements, an image digitizing system with variable spatial resolution was designed, built, and integrated to a photon-counting picosecond streak camera, yielding a temporal scan resolution better than 300 femtosecond/pixel. The streak camera is configured to operate with 3 spatial channels; two of these support green (532 nm) and uv (355 nm) while the third accommodates reference pulses (764 nm) for real-time calibration. Critical parameters affecting differential timing accuracy such as pulse width and shape, number of received photons, streak camera/imaging system nonlinearities, dynamic range, and noise characteristics were investigated to optimize the system for accurate differential delay measurements. The streak camera output image consists of three image fields, each field is 1024 pixels along the time axis and 16 pixels across the spatial axis. Each of the image fields may be independently positioned across the spatial axis. Two of the image fields are used for the two wavelengths used in the experiment; the third window measures the temporal separation of a pair of diode laser pulses which verify the streak camera sweep speed for each data frame. The sum of the 16 pixel intensities across each of the 1024 temporal positions for the three data windows is used to extract the three waveforms. The waveform data is processed using an iterative three-point running average filter (10 to 30 iterations are used) to remove high-frequency structure. The pulse pair separations are determined using the half-max and centroid type analysis. Rigorous experimental verification has demonstrated that this simplified process provides the best measurement accuracy. To calibrate the receiver system sweep, two laser pulses with precisely known temporal separation are scanned along the full length of the sweep axis. The experimental measurements are then modeled using polynomial regression to obtain a best fit to the data. Data aggregation using normal point approach has provided accurate data fitting techniques and is found to be much more convenient than using the full rate single shot data. The systematic errors from this model have been found to be less than 3 ps for normal points. Author (revised)

N94-15574*# Czech Technical Univ., Prague. Faculty of Nuclear Science and Physical Engineering.

THE FIRST SATELLITE LASER ECHOES RECORDED ON THE STREAK CAMERA **c36**

Karel Hamal, Ivan Prochazka, Georg Kirchner (Technische Univ., Graz, Austria.), and F. Koidl (Technische Univ., Graz, Austria.) *In* NASA. Goddard Space Flight Center, Eighth International Workshop on Laser Ranging Instrumentation Jun. 1993 7 p (For primary document see N94-15552 03-19)

Avail: CASI HC A02/MF A06

The application of the streak camera with the circular sweep for the satellite laser ranging is described. The Modular Streak Camera system employing the circular sweep option was integrated into the conventional Satellite Laser System. The experimental satellite tracking and ranging has been performed. The first satellite laser echo streak camera records are presented. Author (revised)

N94-15575*# Institut fuer Angewandte Geodaesie, Koetzing (Germany). Fundamentalstation Wettzell der Forschungsgruppe Satellitengeodaesie.

EXPERIENCE AND RESULTS OF THE 1991 MTLRS-1 USSR CAMPAIGN **c36**

Peter Sperber and H. Hauck (Institut fuer Angewandte Geodaesie, Frankfurt am Main, Germany.) *In* NASA. Goddard Space Flight Center, Eighth International Workshop on Laser Ranging Instrumentation Jun. 1993 8 p (For primary document see N94-15552 03-19)

Avail: CASI HC A02/MF A06

The year 1991 was a special year for the mobile laser ranging systems. Due to the scheduled upgrades of the Modular Transportable Laser Ranging Systems, MTLRS#1 and MTLRS#2, neither a WEGENER MEDLAS nor a Crustal Dynamics Project campaign was carried out in 1991. After the successful upgrade of MTLRS#1 in the first half of 1991 the system departed from Wettzell in August to make measurements at two sites in the USSR. In Riga/Latvia, we operated close to the fixed SLR system. In Simeiz/Ucrainea, the place for MTLRS#1 pad was choosen to collocate the two fixed SLR stations in Simeiz (300 m distance to MTLRS#1) and Kazivelli (about 3 km distance). Author (revised)

N94-15576*# Main Astronomical Observatory, Kiev (Ukraine).
ETALON-1,-2 CENTER OF MASS CORRECTION AND ARRAY REFLECTIVITY **c36**
N. T. Mironov, A. I. Emetz, A. N. Zaharov (United Space Device Corp., Moscow, Russia.), and V. E. Tchebotarev (United Space Device Corp., Moscow, Russia.) *In* NASA. Goddard Space Flight Center, Eighth International Workshop on Laser Ranging Instrumentation Jun. 1993 24 p (For primary document see N94-15552 03-19)
Avail: CASI HC A03/MF A06

Center of mass correction to be applied to measured ranges to the ETALON 1 and 2 satellites is considered. Numerical values of the correction and reflectivity from the retroreflector array are computed. The variations of these values with satellite orientation are investigated. Author

N94-15577*# National Aeronautics and Space Administration. Goddard Space Flight Center, Greenbelt, MD.
TEST RESULTS FROM LAGEOS-2 OPTICAL CHARACTERIZATION USING PULSED LASERS **c36**
Thomas K. Varghese (Bendix Field Engineering Corp., Seabrook, MD.), Michael Selden (Bendix Field Engineering Corp., Seabrook, MD.), Thomas Oldham (Bendix Field Engineering Corp., Seabrook, MD.), Christopher Clarke (Bendix Field Engineering Corp., Seabrook, MD.), and Thomas Zagwodzki *In its* Eighth International Workshop on Laser Ranging Instrumentation Jun. 1993 14 p (For primary document see N94-15552 03-19)
Avail: CASI HC A03/MF A06

The Laser Geodynamic Satellite-2 (LAGEOS-2) has undergone extensive optical testing at NASA Goddard Space Flight Center during 1989. The techniques included measuring the far field diffraction pattern using cw and pulsed lasers. In the pulsed measurement technique, response of the satellite was studied by measuring the far-field diffraction pattern (FFDP) as a function of pulsewidth, wavelength, polarization, position in the FFDP, detector/processing techniques, and satellite orientation. The purpose of the pulsed laser testing was two-fold: (1) to characterize the satellite optical response with the detector and signal processing electronics currently used in most SLR stations using the portable laser ranging standard, and (2) to characterize the satellite response for various conditions using the highest bandwidth optical detector (streak camera) available for the next generation of satellite laser ranging (SLR) technology. The portable ranging standard employed multiple measurement devices and an optical calibration scheme to eliminate range-dependent and amplitude-dependent systematics. These precautions were taken to eliminate/minimize instrumental errors and provide maximum accuracy. For LAGEOS orbit (6000 Km), ground stations are located 34 to 38 Mu radians off the axis of the return signal from the satellite; therefore, an optical mask was used to restrict the field of view (FOV) of detection to this annular region of the FFDP. The two measurement techniques were implemented using an aperture sharing scheme and complemented each other by providing mutual verification.
Author (revised)

N94-15578*# Bendix Field Engineering Corp., Seabrook, MD.
ANALYSIS OF TOPEX LASER RETROREFLECTOR ARRAY CHARACTERISTICS
Thomas K. Varghese *In* NASA. Goddard Space Flight Center, Eighth International Workshop on Laser Ranging Instrumentation Jun. 1993 12 p (For primary document see N94-15552 03-19)
Avail: CASI HC A03/MF A06

The joint U.S./French TOPEX/POSEIDON mission was successfully launched on August 10, 1992 for the study of ocean height variation using microwave altimetry. Accurate determination of the satellite orbit is paramount to the determination of the above phenomenon. To accomplish this, using laser ranging, the satellite is equipped with a laser retroreflector array (LRA) around the altimeter antennae. The goal of laser ranging is to obtain precision orbits with a radial accuracy of 13 cm to the center of mass of the satellite. This requires the laser range correction to the LRA reference be known at the sub-cm level and is quite a challenge considering the geometry of the LRA. Detailed studies were initiated by the TOPEX project office (Christensen) under the auspices of the CDP/DOSE project (Degnan) at Goddard Space Flight Center. Author (revised)

N94-15579*# Bendix Field Engineering Corp., Seabrook, MD.
HISTORICAL MOBLAS SYSTEM CHARACTERIZATION **c36**
Van S. Husson *In* NASA. Goddard Space Flight Center, Eighth International Workshop on Laser Ranging Instrumentation Jun. 1993 23 p (For primary document see N94-15552 03-19)
Avail: CASI HC A03/MF A06

This paper is written as a direct response to the published NASA Laser Geodynamic Satellite (LAGEOS) orbital solution SL7.1, in order to close the data information loop with an emphasis on the NASA Mobile Laser Ranging System's (MOBLAS) LAGEOS full rate data since November 1, 1983. A preliminary analysis of the supporting information (i.e. satellite laser ranging system eccentricities and system dependent range and time bias corrections) contained in SL7.1 indicated centimeter (cm) level discrepancies. In addition, a preliminary analysis of the computed monthly MOBLAS range biases from SL7.1 appear to show cm level systematic trends, some of which appear to be 'real', particularly in the 1984 to 1987 time period. This paper is intended to be a reference document for known MOBLAS systematic errors (magnitude and direction) and for supporting MOBLAS information (eccentricities, hardware configurations, and potential data problem periods). Therefore, this report is different than your typical system characterization report, but will be more valuable to the user. The MOBLAS error models and supporting information contained in this paper will be easily accessible from the Crustal Dynamics Data Information System (CDDIS). Author (revised)

N94-15580*# National Aeronautics and Space Administration. Goddard Space Flight Center, Greenbelt, MD.
OPTIMUM WAVELENGTHS FOR TWO COLOR RANGING **c32**
John J. Degnan *In its* Eighth International Workshop on Laser Ranging Instrumentation Jun. 1993 14 p (For primary document see N94-15552 03-19)
Avail: CASI HC A03/MF A06

The range uncertainties associated with the refractive atmosphere can be mitigated by the technique of two color, or dual wavelength, ranging. The precision of the differential time of flight (DTOF) measurement depends on the atmospheric dispersion between the two wavelengths, the received pulsewidths and photoelectron counts, and on the amount of temporal averaging. In general, the transmitted wavelengths are not independently chosen but instead are generated via nonlinear optics techniques (harmonic crystals, Raman scattering, etc.) which also determine their relative pulsewidths. The mean received photoelectrons at each wavelength are calculated via the familiar radar link equation which contains several wavelength dependent parameters. By collecting the various wavelength dependent terms, one can define a wavelength figure of merit for a two color laser ranging system. In this paper, we apply the wavelength figure of merit to the case of an extremely clear atmosphere and draw several conclusions regarding the relative merits of fundamental-second harmonic, fundamental-third harmonic, second-third harmonic, and Raman two color systems. We find that, in spite of the larger dispersion between wavelengths, fundamental-third harmonic systems have the lowest figure of merit due to a combination of poor detector performance at the fundamental and poor atmospheric transmission at the third harmonic. The fundamental-second harmonic systems (approximately 700 nm and 350 nm) have the highest figure of merit, but second-third harmonic systems, using fundamental transmitters near 1000 nm, are a close second. Raman-shifted transmitters appear to offer no advantage over harmonic systems because of the relatively small wavelength separation that can be achieved in light gases such as hydrogen and the lack of good ultrashort pulse transmitters with an optimum fundamental wavelength near 400 nm. Author (revised)

N94-15581*# National Aeronautics and Space Administration. Goddard Space Flight Center, Greenbelt, MD.
TWO COLOR SATELLITE LASER RANGING UPGRADES AT GODDARD'S 1.2m TELESCOPE FACILITY **c35**
Thomas W. Zagwodzki, Jan F. McGarry, John J. Degnan, and Thomas K. Varghese (Bendix Field Engineering Corp., Seabrook, MD.) *In its* Eighth International Workshop on Laser Ranging Instrumentation Jun. 1993 13 p (For primary document see N94-15552 03-19)
Avail: CASI HC A03/MF A06

The ranging laboratory at Goddard's 1.2 m telescope tracking facility has recently been upgraded to include a single photoelectron sensitive Hamamatsu streak camera-based range receiver which uses doubled and tripled Nd:YAG frequencies for satellite laser ranging. Other ranging system upgrades include a new continuum laser, which will deliver up to 30 millijoules (mJ) at both 532 and 355 nm at a pulsewidth of 30 picoseconds (FWHM),

and replacement of both ranging and tracking computers with COMPAQ 386 based systems. Preliminary results using a photomultiplier-tube based receiver and waveform digitizer indicate agreement within the accuracy of the measurement with the theoretical Marini and Murray model for atmospheric refraction. Two color streak camera measurements are used to further analyze the accuracy of these and other atmospheric refraction models. Author (revised)

N94-15582*# Institut fuer Angewandte Geodaesie, Koetzing (Germany). Forschungseinrichtung Satellitengeodaesie Fundamentalstation Wettzell.

MEASURING ATMOSPHERIC DISPERSION WITH WLRS IN MULTIPLE WAVELENGTH MODE **c32**

Ulrich Schreiber, K. H. Haufe (Institut fuer Angewandte Geodaesie, Koetzing, Germany.), and Reiner Dassing (Institut fuer Angewandte Geodaesie, Koetzing, Germany.) *In* NASA. Goddard Space Flight Center, Eighth International Workshop on Laser Ranging Instrumentation Jun. 1993 8 p (For primary document see N94-15552 03-19)

Avail: CASI HC A02/MF A06

The WLRS (Wettzell Laser Ranging System) allows the simultaneous tracking of satellites on two different wavelengths. These are the fundamental frequency of Nd:YAG at 1.064 microns and the second harmonic at 532 nm. Range measurements to the satellite LAGEOS were carried out with different experimental set-ups, after developing a detector unit based on a silicon avalanche photodiode in Geiger mode, which is sufficiently sensitive in the infrared domain. An approach towards a quantitative interpretation of the data is suggested and discussed briefly. Author (revised)

N94-15583*# National Aeronautics and Space Administration. Goddard Space Flight Center, Greenbelt, MD.

MILLIMETER ACCURACY SATELLITES FOR TWO COLOR RANGING **c32**

John J. Degnan *In its* Eighth International Workshop on Laser Ranging Instrumentation Jun. 1993 16 p (For primary document see N94-15552 03-19)

Avail: CASI HC A03/MF A06

The principal technical challenge in designing a millimeter accuracy satellite to support two color observations at high altitudes is to provide high optical cross-section simultaneously with minimal pulse spreading. In order to address this issue, we provide, a brief review of some fundamental properties of optical retroreflectors when used in spacecraft target arrays, develop a simple model for a spherical geodetic satellite, and use the model to determine some basic design criteria for a new generation of geodetic satellites capable of supporting millimeter accuracy two color laser ranging. We find that increasing the satellite diameter provides: a larger surface area for additional cube mounting thereby leading to higher cross-sections; and makes the satellite surface a better match for the incoming planar phasefront of the laser beam. Restricting the retroreflector field of view (e.g. by recessing it in its holder) limits the target response to the fraction of the satellite surface which best matches the optical phasefront thereby controlling the amount of pulse spreading. In surveying the arrays carried by existing satellites, we find that European STARLETTE and ERS-1 satellites appear to be the best candidates for supporting near term two color experiments in space. Author (revised)

N94-15584*# Czech Technical Univ., Prague. Faculty of Nuclear Science and Physical Engineering.

TWO WAVELENGTH SATELLITE LASER RANGING USING SPAD **c36**

Ivan Prochazka, Karel Hamal, Helena Jelinkova, Georg Kirchner (Technische Univ., Graz, Austria.), and F. Koidl (Technische Univ., Graz, Austria.) *In* NASA. Goddard Space Flight Center, Eighth International Workshop on Laser Ranging Instrumentation Jun. 1993 4 p (For primary document see N94-15552 03-19)

Avail: CASI HC A01/MF A06

When ranging to satellites with lasers, there are several principal contributions to the error budget: from the laser ranging system on the ground, from the satellite retroarray geometry, and from the atmosphere. Using a single wavelength, we have routinely achieved a ranging precision of 8 millimeters when ranging to the ERS-1 and Starlette satellites. The systematic error of the atmosphere, assuming the existing dispersion models, is expected to be of the order of 1 cm. Multiple wavelengths ranging might contribute to the refinement of the existing models. Taking into account the energy balance, the existing picosecond lasers and the existing receiver and detection technology, several pairs or multiple wavelengths may be considered. To be able to improve the atmospheric models to the subcentimeter accuracy level, the differential time interval (DTI) has to be determined within a few picoseconds depending on the selected wavelength pair. There exist several projects based on picosecond lasers as transmitters and on two types of detection techniques: one is based on photodetectors, like photomultipliers or photodiodes connected to the time interval meters. Another technique is based on the use of a streak camera as an echo signal detector, temporal analyzer, and time interval vernier. The temporal analysis at a single wavelength using the streak camera showed the complexity of the problem. Derived from text

N94-15585*# Aerospatiale, Cannes (France). Optical Dept.

NEW PERSPECTIVES FOR HIGH ACCURACY SLR WITH SECOND GENERATION GEODESIC SATELLITES

Glenn Lund *In* NASA. Goddard Space Flight Center, Eighth International Workshop on Laser Ranging Instrumentation Jun. 1993 9 p (For primary document see N94-15552 03-19)

Avail: CASI HC A02/MF A06

This paper reports on the accuracy limitations imposed by geodesic satellite signatures, and on the potential for achieving millimetric performances by means of alternative satellite concepts and an optimized 2-color system tradeoff. Long distance laser ranging, when performed between a ground (emitter/receiver) station and a distant geodesic satellite, is now reputed to enable short arc trajectory determinations to be achieved with an accuracy of 1 to 2 centimeters. This state-of-the-art accuracy is limited principally by the uncertainties inherent to single-color atmospheric path length correction. Motivated by the study of phenomena such as postglacial rebound, and the detailed analysis of small-scale volcanic and strain deformations, the drive towards millimetric accuracies will inevitably be felt. With the advent of short pulse (less than 50 ps) dual wavelength ranging, combined with adequate detection equipment (such as a fast-scanning streak camera or ultra-fast solid-state detectors) the atmospheric uncertainty could potentially be reduced to the level of a few millimeters, thus, exposing other less significant error contributions, of which by far the most significant will then be the morphology of the retroreflector satellites themselves. Existing geodesic satellites are simply dense spheres, several 10's of cm in diameter, encrusted with a large number (426 in the case of LAGEOS) of small cube-corner reflectors. A single incident pulse, thus, results in a significant number of randomly phased, quasi-simultaneous return pulses. These combine coherently at the receiver to produce a convolved interference waveform which cannot, on a shot to shot basis, be accurately and unambiguously correlated to the satellite center of mass. This paper proposes alternative geodesic satellite concepts, based on the use of a very small number of cube-corner retroreflectors, in which the above difficulties are eliminated while ensuring, for a given emitted pulse, the return of a single clean pulse with an adequate cross-section.

Author (revised)

N94-15586*# National Aeronautics and Space Administration. Goddard Space Flight Center, Greenbelt, MD.

STATE-OF-THE-ART SATELLITE LASER RANGE MODELING FOR GEODETIC AND OCEANOGRAPHIC APPLICATIONS **c36**

Steve M. Klosko (Hughes STX, Inc., Lanham, MD.) and David E. Smith *In its* Eighth International Workshop on Laser Ranging Instrumentation Jun. 1993 14 p (For primary document see N94-15552 03-19)

Avail: CASI HC A03/MF A06

Significant improvements have been made in the modeling and accuracy of Satellite Laser Range (SLR) data since the launch of LAGEOS in 1976. Some of these include: improved models of the static geopotential, solid-Earth and ocean tides, more advanced atmospheric drag models, and the adoption of the J2000 reference system with improved nutation and precession. Site positioning using SLR systems currently yield approximately 2 cm static and 5 mm/y kinematic descriptions of the geocentric location of these sites. Incorporation of a large set of observations from advanced Satellite Laser Ranging (SLR) tracking systems have directly made major contributions to the gravitational fields and in advancing the state-of-the-art in precision orbit determination. SLR is the baseline tracking system for the altimeter bearing TOPEX/Poseidon and ERS-1 satellites and thus, will play an important role in providing the Conventional Terrestrial Reference Frame for instantaneously locating the geocentric position of the ocean surface over time, in providing an unchanging range standard

for altimeter range calibration, and for improving the geoid models to separate gravitational from ocean circulation signals seen in the sea surface. Nevertheless, despite the unprecedented improvements in the accuracy of the models used to support orbit reduction of laser observations, there still remain systematic unmodeled effects which limit the full exploitation of modern SLR data. Author (revised)

N94-15587*# National Aeronautics and Space Administration. Goddard Space Flight Center, Greenbelt, MD.
GEOMETRIC ANALYSIS OF SATELLITE LASER RANGING DATA c82
Brion Conklin (Bendix Field Engineering Corp., Seabrook, MD.), Steven Bucey (Bendix Field Engineering Corp., Seabrook, MD.), Van S. Husson (Bendix Field Engineering Corp., Seabrook, MD.), Winfield M. Decker (Bendix Field Engineering Corp., Seabrook, MD.), and John J. Degnan *In its* Eighth International Workshop on Laser Ranging Instrumentation Jun. 1993 8 p (For primary document see N94-15552 03-19)
Avail: CASI HC A02/MF A06

The analysis of simultaneous laser data is investigated using the method of trilateration. Analysis of data from 1987 to 1992 is presented with selected baseline rates and station positions. The use of simultaneous Etalon data is simulated to demonstrate the additional global coverage these satellites provide. Trilateration has a great potential for regional deformation studies with monthly LAGEOS American solutions between 3-12 millimeters. Author (revised)

N94-15588*# Ecole Superieure des Geometres et Topographes, Evry (France).
IMPROVEMENT OF SLR ACCURACY, A POSSIBLE NEW STEP
Michel Kasser *In* NASA. Goddard Space Flight Center, Eighth International Workshop on Laser Ranging Instrumentation Jun. 1993 7 p (For primary document see N94-15552 03-19)
Avail: CASI HC A02/MF A06

The satellite laser ranging (SLR) technology experienced a large number of technical improvements since the early 1970's, leading now to a millimetric instrumental accuracy. Presently, it appears as useless to increase these instrumental performances as long as the atmospheric propagation delay suffers its actual imprecision. It has been proposed for many years to work in multiwavelength mode, but up to now the considerable technological difficulties of subpicosecond timing have seriously delayed such an approach. Then a new possibility is proposed, using a device which is not optimized now for SLR but has already given good results in the lower troposphere for wind measurement: the association of a radar and a sodar. While waiting for the 2-lambda methodology, this one could provide an atmospheric propagation delay at the millimeter level during a few years with only little technological investment. Author (revised)

N94-15589*# Deutsches Geodaetisches Forschungsinst., Munich (Germany).
ON THE ACCURACY OF ERS-1 ORBIT PREDICTIONS c13
Rolf Koenig, H. Li, Franz-Heinrich Massmann, J. C. Raimondo, C. Rajasenan, and C. Reigber *In* NASA. Goddard Space Flight Center, Eighth International Workshop on Laser Ranging Instrumentation Jun. 1993 8 p Prepared in cooperation with Deutsche Geodaetische Kommission, Munich, Germany (For primary document see N94-15552 03-19)
Avail: CASI HC A02/MF A06

Since the launch of ERS-1, the D-PAF (German Processing and Archiving Facility) provides regularly orbit predictions for the worldwide SLR (Satellite Laser Ranging) tracking network. The weekly distributed orbital elements are so called tuned IRV's and tuned SAO-elements. The tuning procedure, designed to improve the accuracy of the recovery of the orbit at the stations, is discussed based on numerical results. This shows that tuning of elements is essential for ERS-1 with the currently applied tracking procedures. The orbital elements are updated by daily distributed time bias functions. The generation of the time bias function is explained. Problems and numerical results are presented. The time bias function increases the prediction accuracy considerably. Finally, the quality assessment of ERS-1 orbit predictions is described. The accuracy is compiled for about 250 days since launch. The average accuracy lies in the range of 50-100 ms and has considerably improved. Derived from text

N94-15590*# Geodetic Inst., Helsinki (Finland).
COMPENSATION FOR THE DISTORTION IN SATELLITE LASER RANGE PREDICTIONS DUE TO VARYING PULSE TRAVEL TIMES c36
Matti Paunonen *In* NASA. Goddard Space Flight Center, Eighth International Workshop on Laser Ranging Instrumentation Jun. 1993 4 p (For primary document see N94-15552 03-19)
Avail: CASI HC A01/MF A06

A method for compensating for the effect of the varying travel time of a transmitted laser pulse to a satellite is described. The 'observed minus predicted' range differences then appear to be linear, which makes data screening or use in range gating more effective. Author (revised)

N94-15591*# Satellite Laser Ranger Group, Hailsham (England).
TIMEBIAS CORRECTIONS TO PREDICTIONS c13
Roger Wood and Philip Gibbs *In* NASA. Goddard Space Flight Center, Eighth International Workshop on Laser Ranging Instrumentation Jun. 1993 6 p (For primary document see N94-15552 03-19)
Avail: CASI HC A02/MF A06

The importance of an accurate knowledge of the time bias corrections to predicted orbits to a satellite laser ranging (SLR) observer, especially for low satellites, is highlighted. Sources of time bias values and the optimum strategy for extrapolation are discussed from the viewpoint of the observer wishing to maximize the chances of getting returns from the next pass. What is said may be seen as a commercial encouraging wider and speedier use of existing data centers for mutually beneficial exchange of time bias data. Author (revised)

N94-15592*# Royal Greenwich Observatory, Cambridge (England).
FORMATION OF ON-SITE NORMAL POINTS c64
G. M. Appleby and Andrew T. Sinclair *In* NASA. Goddard Space Flight Center, Eighth International Workshop on Laser Ranging Instrumentation Jun. 1993 7 p (For primary document see N94-15552 03-19)
Avail: CASI HC A02/MF A06

We describe our methods of fitting a smoothing function to observational range differences from a predicted orbit, by deducing corrections to the orbit in the radial and along-track directions. The method has been used on observations of a variety of satellites, and using predicted orbits computed both by numerical integration using IRV's as starting values and analytically from orbital elements. The along-track corrections to the predicted orbit have been successfully used in the form of time biases to improve subsequent predictions, and a statistical test has been devised to ensure that the range residuals may be used to form unbiased quick look normal points. Author (revised)

N94-15593*# McDonald Observatory, Austin, TX.
POISSON FILTERING OF LASER RANGING DATA c36
Randall L. Ricklefs and Peter J. Shelus *In* NASA. Goddard Space Flight Center, Eighth International Workshop on Laser Ranging Instrumentation Jun. 1993 7 p (For primary document see N94-15552 03-19)
Avail: CASI HC A02/MF A06

The filtering of data in a high noise, low signal strength environment is a situation encountered routinely in lunar laser ranging (LLR) and, to a lesser extent, in artificial satellite laser ranging (SLR). The use of Poisson statistics as one of the tools for filtering LLR data is described first in a historical context. The more recent application of this statistical technique to noisy SLR data is also described. Author (revised)

N94-15594*# Czech Technical Univ., Prague.
COMPUTER NETWORKING AT SLR STATIONS c32
Antonin Novotny *In* NASA. Goddard Space Flight Center, Eighth International Workshop on Laser Ranging Instrumentation Jun. 1993 10 p (For primary document see N94-15552 03-19)
Avail: CASI HC A02/MF A06

There are several existing communication methods to deliver data from the satellite laser ranging (SLR) station to the SLR data center and back: telephonmodem, telex, and computer networks. The SLR scientific community has been exploiting mainly INTERNET, BITNET/EARN, and SPAN. The total of 56 countries are connected to INTERNET and the number of nodes is exponentially growing. The computer networks mentioned above and others are connected through E-mail protocol. The scientific progress of SLR requires the increase of communication speed and the amount of the transmitted data. The TOPEX/POSEIDON test campaign

required to deliver Quick Look data (1.7 kB/pass) from a SLR site to SLR data center within 8 hours and full rate data (up to 500 kB/pass) within 24 hours. We developed networking for the remote SLR station in Helwan, Egypt. The reliable scheme for data delivery consists of: compression of MERIT2 format (up to 89 percent), encoding to ASCII Me (files); and e-mail sending from SLR station--e-mail receiving, decoding, and decompression at the center. We do propose to use the ZIP method for compression/decompression and the UUCODE method for ASCII encoding/decoding. This method will be useful for stations connected via telephonemodems or commercial networks. The electronics delivery could solve the problem of the too late receiving of the FR data by SLR data center. Author (revised)

N94-15595*# National Aeronautics and Space Administration. Goddard Space Flight Center, Greenbelt, MD.

UPGRADING NASA/DOSE LASER RANGING SYSTEM CONTROL COMPUTERS **c60**

Randall L. Ricklefs (McDonald Observatory, Austin, TX.), Jack Cheek (Hughes STX, Inc., Lanham, MD.), Paul J. Seery (Bendix Field Engineering Corp., Seabrook, MD.), Kenneth S. Emenheiser (Bendix Field Engineering Corp., Seabrook, MD.), William P. Hanrahan, III (Bendix Field Engineering Corp., Seabrook, MD.), and Jan F. McGarry *In its* Eighth International Workshop on Laser Ranging Instrumentation Jun. 1993 6 p (For primary document see N94-15552 03-19)

Avail: CASI HC A02/MF A06

Laser ranging systems now managed by the NASA Dynamics of the Solid Earth (DOSE) and operated by the Bendix Field Engineering Corporation, the University of Hawaii, and the University of Texas have produced a wealth on interdisciplinary scientific data over the last three decades. Despite upgrades to the most of the ranging station subsystems, the control computers remain a mix of 1970's vintage minicomputers. These encompass a wide range of vendors, operating systems, and languages, making hardware and software support increasingly difficult. Current technology allows replacement of controller computers at a relatively low cost while maintaining excellent processing power and a friendly operating environment. The new controller systems are now being designed using IBM-PC-compatible 80486-based microcomputers, a real-time Unix operating system (LynxOS), and X-windows/Motif IB, and serial interfaces have been chosen. This design supports minimizing short and long term costs by relying on proven standards for both hardware and software components. Currently, the project is in the design and prototyping stage with the first systems targeted for production in mid-1993. Author (revised)

N94-15596*# Bendix Field Engineering Corp., Seabrook, MD.

HP UPGRADE OPERATIONAL STREAMLINING **c60**

David R. Edge, Kenneth S. Emenheiser, William P. Hanrahan, III, D. McCollums, Paul J. Seery, and Randall L. Ricklefs (McDonald Observatory, Austin, TX.) *In* NASA. Goddard Space Flight Center, Eighth International Workshop on Laser Ranging Instrumentation Jun. 1993 8 p (For primary document see N94-15552 03-19)

Avail: CASI HC A02/MF A06

New computer technology and resources must be successfully integrated into CDSLR station operations to manage new complex operational tracking requirements, support the on site production of new data products, support ongoing station performance improvements, and to support new station communication requirements. The NASA CDSLR Network is in the process of upgrading station computer resources with HP UNIX workstations, designed to automate a wide range of operational station requirements. The primary HP upgrade objective was to relocate computer intensive data system tasks from the controller computer to a new advanced computer environment designed to meet the new data system requirements. The HP UNIX environment supports fully automated real time data communications, data management, data processing, and data quality control. Automated data compression procedures are used to improve the efficiency of station data communications. In addition, the UNIX environment supports a number of semi-automated technical and administrative operational station tasks. The x window user interface generates multiple simultaneous color graphics displays, providing direct operator visibility and control over a wide range of operational station functions. Author (revised)

N94-15597*# Shanghai Observatory (China).

APPLICATION OF THE ROBUST ESTIMATE IN SLR DATA PREPROCESSING **c62**

De-Tong Tan, Zhong-Ping Zhang, Hua-Guan Xu, and Peiz-Hang Jia (Academia Sinica, Shanghai, China.) *In* NASA. Goddard Space Flight Center, Eighth International Workshop on Laser Ranging Instrumentation Jun. 1993 9 p (For primary document see N94-15552 03-19)

Avail: CASI HC A02/MF A06

An M-estimator, one kind of a robust estimator, has been used in satellite laser ranging (SLR) data preprocessing. It has been shown that the M-estimator has a 50 percent or more breakdown point.

Author (revised)

N94-15598*# McDonald Observatory, Austin, TX.

A COMPUTER-CONTROLLED x-y OFFSET GUIDING STAGE FOR THE MLRS **c35**

Peter J. Shelus, A. L. Whipple, J. R. Wiant, Randall L. Ricklefs, and Frank M. Melsheimer (DFM Engineering, Inc., Longmont, CA.) *In* NASA. Goddard Space Flight Center, Eighth International Workshop on Laser Ranging Instrumentation Jun. 1993 5 p (For primary document see N94-15552 03-19)

Avail: CASI HC A01/MF A06

The MLRS has experienced excellent success in its lunar and artificial satellite laser ranging operations during its many years of operation, in spite of its relatively small 'receive' aperture. We continue to strive, however, for a greater volume of data, together with better accuracy and precision. We have just now completed the design, construction, and implementation of a computer controlled x-y offset guiding stage for the MLRS, analogous to the manual one that had been a part of the original 2.7-m lunar laser ranging system on Mt. Locke at McDonald Observatory. In the past, we had been hampered by the lack of a satisfactory hardware design which could fit within the very cramped quarters of the MLRS telescope's tail piece. Recently, with funding support from the U.S. Naval Observatory and the design and construction expertise of DFM Engineering, Inc., a satisfactory instrument has been specified, designed, built, and installed. This instrument will greatly expand MLRS observational opportunities by allowing the observing crews to actively guide on visible off axis lunar surface features or background stars while the on-axis lunar surface retroreflector targets are in the dark. This paper describes this instrument and its present implementation at the MLRS. Author (revised)

N94-15599*# McDonald Observatory, Austin, TX.

LUNAR LASER RANGING DATA PROCESSING IN A UNIX/X WINDOWS ENVIRONMENT **c36**

Randall L. Ricklefs and Judit G. Ries *In* NASA. Goddard Space Flight Center, Eighth International Workshop on Laser Ranging Instrumentation Jun. 1993 8 p (For primary document see N94-15552 03-19)

Avail: CASI HC A02/MF A06

In cooperation with the NASA Crustal Dynamics Project initiative placing workstation computers at each of its laser ranging stations to handle data filtering and normalpointing, MLRS personnel have developed a new generation of software to provide the same services for the lunar laser ranging data type. The Unix operating system and X windows/Motif provides an environment for both batch and interactive filtering and normalpointing as well as prediction calculations. The goal is to provide a transportable and maintainable data reduction environment. This software and some sample displays are presented. that the lunar (or satellite) datacould be processed on one computer while data was taken on the other. The reduction of the data was totally interactive and in no way automated. In addition, lunar predictions were produced on-site, another first in the effort to down-size historically mainframe-based applications. Extraction of earth rotation parameters was at one time attempted on site in near-realtime. In 1988, the Crustal Dynamics Project SLR Computer Panel mandated the installation of Hewlett-Packard 9000/360 Unix workstations at each NASA-operated laser ranging station to relieve the aging controller computers of much of their data and communications handling responsibility and to provide on-site data filtering and normal pointing for a growing list of artificial satellite targets. This was seen by MLRS staff as an opportunity to provide a better lunar data processing environment as well.

Author (revised)

N94-15600*# Institut fuer Angewandte Geodaesie, Koetzing (Germany). Forschungseinrichtung Satellitengeodaesie.
LLR: ACTIVITIES IN WETTZELL **c14**
Ulrich Schreiber, J. Mueller (Technische Univ., Munich, Germany.), Reiner Dassing, N. Brandl, K. H. Haufe, G. Herold, R. Kahn, K. Roettcher, and R. Stoeger *In* NASA. Goddard Space Flight Center, Eighth International Workshop on Laser Ranging Instrumentation Jun. 1993 3 p (For primary document see N94-15552 03-19)
Avail: CASI HC A01/MF A06

Following the idea of a fundamental station, the Wettzell Laser Ranging Station was designed to range to all types of satellites and to the moon. After obtaining the first lunar echos in October 1990, the system's operation was improved. A short report of lunar ranging activities is given.
Author (revised)

N94-15601*# Bendix Field Engineering Corp., Seabrook, MD.
MATERA LASER RANGING OBSERVATORY (MLRO): AN OVERVIEW **c14**
Thomas K. Varghese, Winfield M. Decker, Henry A. Crooks, and Giuseppe Bianco (Italian Space Agency, Matera.) *In* NASA. Goddard Space Flight Center, Eighth International Workshop on Laser Ranging Instrumentation Jun. 1993 5 p (For primary document see N94-15552 03-19)
Avail: CASI HC A01/MF A06

The Agenzia Spaziale Italiana (ASI) is currently under negotiation with the Bendix Field Engineering Corporation (BFEC) of the Allied Signal Aerospace Company (ASAC) to build a state-of-the-art laser ranging observatory for the Centro di Geodesia Spaziale, in Matera, Italy. The contract calls for the delivery of a system based on a 1.5 meter afocal Cassegrain astronomical quality telescope with multiple ports to support a variety of experiments for the future, with primary emphasis on laser ranging. Three focal planes, viz. Cassegrain, Coude, and Nasmyth will be available for these experiments. The open telescope system will be protected from dust and turbulence using a specialized dome which will be part of the building facilities to be provided by ASI. The fixed observatory facility will be partitioned into four areas for locating the following: laser, transmit/receive optics, telescope/dome enclosure, and the operations console. The optical tables and mount rest on a common concrete pad for added mechanical stability. Provisions will be in place for minimizing the effects of EMI, for obtaining maximum cleanliness for high power laser and transmit optics, and for providing an ergonomic environment fitting to a state-of-the-art multipurpose laboratory. The system is currently designed to be highly modular and adaptable for scaling or changes in technology. It is conceived to be a highly automated system with superior performance specifications to any currently operational system. Provisions are also made to adapt and accommodate changes that are of significance during the course of design and integration.
Author (revised)

N94-15602*# Department of Administrative Services, Canberra (Australia). Orroral Geodetic Observatory.
PERFORMANCE OF THE UPGRADED ORRORAL LASER RANGING SYSTEM **c14**
John M. Luck *In* NASA. Goddard Space Flight Center, Eighth International Workshop on Laser Ranging Instrumentation Jun. 1993 25 p (For primary document see N94-15552 03-19)
Avail: CASI HC A03/MF A06

The topics discussed include the following: upgrade arrangements, system prior to 1991, elements of the upgrade, laser performance, timing system performance, pass productivity, system precision, system accuracy, telescope pointing and future upgrades and extensions.
CASI

N94-15603*# Technische Univ., Graz (Austria). Inst. for Space Research.
SUB-cm RANGING AND OTHER IMPROVEMENTS IN GRAZ **c36**
Georg Kirchner and Franz Koidl *In* NASA. Goddard Space Flight Center, Eighth International Workshop on Laser Ranging Instrumentation Jun. 1993 6 p (For primary document see N94-15552 03-19)
Avail: CASI HC A02/MF A06

A lot of tests and experiments have been made in Graz during the last 2 years to increase performance and accuracy; using the SPAD from the Prag group as receiver, we have reached now about 5 mm RMS from the calibration target, and about 8 mm RMS from ERS1 and STARLETTE. In addition, by routinely using the semitrain, the number of returns has been increased significantly for most satellites.
Derived from text

N94-15604*# Polish Academy of Sciences, Kornik. Space Research Center.
UPGRADING OF THE BOROWIEC LASER STATION **c14**
Stanislaw Schillak, E. Butkiewicz, and J. Wiktorowski *In* NASA. Goddard Space Flight Center, Eighth International Workshop on Laser Ranging Instrumentation Jun. 1993 7 p (For primary document see N94-15552 03-19)
Avail: CASI HC A02/MF A06

The major upgrade at the Borowiec satellite laser ranging (SLR) station since the last workshop is the new third generation laser, which has been installed in September 1991. Short description of the new CONTINUUM laser and first results of satellites observations are presented. The results confirm expected increase in accuracy (3-5 cm) and in the number of measurements per satellite pass (several hundred). In addition, information about second Borowiec SLR system is presented. Borowiec No 2 is designated for Tunisia in the next year. The system is not yet operational.
Author (revised)

N94-15605*# Shanghai Observatory (China).
DEVELOPMENT OF SHANGHAI SATELLITE LASER RANGING STATION **c14**
Fu-Min Yang, De-Tong Tan, Chi-Kun Xiao, Wan-Zhen Chen, J.-H. Zhang, Z.-P. Zhang, Wen-Hu Lu, Z.-Q. Hu, W.-F. Tang, and J.-P. Chen *In* NASA. Goddard Space Flight Center, Eighth International Workshop on Laser Ranging Instrumentation Jun. 1993 7 p Sponsored in part by Chinese National Science Foundation and Chinese Astronomical Committee (For primary document see N94-15552 03-19)
Avail: CASI HC A02/MF A06

The topics covered include the following: improvement of the system hardware; upgrading of the software; the observation status; preliminary daylight tracking capability; testing the new type of laser; and future plans.
CASI

N94-15606*# Institut fuer Angewandte Geodaesie, Koetzing (Germany). Fundamentalstation Wettzell.
WLRS Status Report **c14**
Reiner Dassing, W. Schlueter, and Ulrich Schreiber (Technische Univ., Munich, Germany.) *In* NASA. Goddard Space Flight Center, Eighth International Workshop on Laser Ranging Instrumentation Jun. 1993 3 p (For primary document see N94-15552 03-19)
Avail: CASI HC A01/MF A06

This status-report of the Wettzell Laser Ranging System (WLRS) gives an overview of its set up and the developments necessary to make the system operational.
Author (revised)

N94-15607*# Naval Research Lab., Washington, DC. Optical Systems Section.
GROUND BASED LASER RANGING FOR SATELLITE LOCATION **c36**
G. C. Gilbreath and Harold D. Newby (Phillips Labs., Malabar, FL.) *In* NASA. Goddard Space Flight Center, Eighth International Workshop on Laser Ranging Instrumentation Jun. 1993 6 p (For primary document see N94-15552 03-19)
Avail: CASI HC A02/MF A06

In this article, we describe a new satellite laser ranging capability which is a joint effort between the Naval Research Laboratory and Air Force Optical Tracking Facility at Malabar, Florida. Initial measurements off LAGEOS indicate that uncorrected radial range rms values of 8 mm are readily achievable. The number of photoelectron counts are on the order of 180 which are off by an order of magnitude from predicted values.
Author (revised)

N94-15608*# State Seismological Bureau of China, Beijing. Inst. of Seismology.
NEW PROGRESS OF RANGING TECHNOLOGY AT WUHAN SATELLITE LASER RANGING STATION **c14**
Zhiz-Hong Xia, Wen-Wei Ye, and Qing-Fu Cai *In* NASA. Goddard Space Flight Center, Eighth International Workshop on Laser Ranging Instrumentation Jun. 1993 8 p (For primary document see N94-15552

03-19)
Avail: CASI HC A02/MF A06

A satellite laser ranging system with an accuracy of the level of centimeter has been successfully developed at the Institute of Seismology, State Seismological Bureau with the cooperation of the Institute of Geodesy and Geophysics, Chinese Academy of Science. With significant improvements on the base of the second generation SLR system developed in 1985, ranging accuracy of the new system has been upgraded from 15 cm to 3-4 cm. Measuring range has also been expanded, so that the ETALON satellite with an orbit height of 20,000 km launched by the former U.S.S.R. can now be tracked. Compared with the 2nd generation SLR system, the newly developed system has the following improvements. A Q modulated laser is replaced by a mode-locked YAG laser. The new device has a pulse width of 150 ps and a repetition rate of 1-4 pps. A quick response photomultiplier has been adopted as the receiver for echo; for example, the adoption of the MCP tube has obviously reduced the jitter error of the transit time and has improved the ranging accuracy. The whole system is controlled by an IBM PC/XT Computer to guide automatic tracking and measurement. It can carry out these functions for satellite orbit calculation, real-time tracking and adjusting, data acquisition and the preprocessed of observing data, etc. The automatization level and reliability of the observation have obviously improved. Author (revised)

N94-15609*# Bendix Field Engineering Corp., Seabrook, MD.
TLRS-3 SYSTEM UPGRADES **c14**
Richard Eichinger, Grace Cheng, William Crawford, Don Cresswell, Henry A. Crooks, Howard Donovan, David R. Edge, Kenneth S. Emenheiser, William P. Hanrahan, III, and J. Michael Heinick et al *In* NASA. Goddard Space Flight Center, Eighth International Workshop on Laser Ranging Instrumentation Jun. 1993 16 p (For primary document see N94-15552 03-19)
Avail: CASI HC A03/MF A06

This presentation describes the upgrades to the Transportable Laser Ranging Systems serial number three (TLRS-3), and the impact that these upgrades will have on the TLRS-3 performance in the field. The four major areas of system upgrades are the HP-380 computer, the Optical Attenuation Mechanism (OAM), the upgraded spatial, spectral and temporal filtering for improved daylight ranging capability, and the software upgrade to enable the system to track the Etalon satellites. The TLRS-3 was returned to the Goddard Geophysical and Astronomical Observatory (GGAO) in December 1991 for system upgrades in preparation of the TOPEX/POSEIDON campaign scheduled to begin in the summer of 1992. Many system upgrades were incorporated into the system while interleaving planned facility maintenance making TLRS-3 a more versatile and more dependable laser ranging system. The TLRS-3 was initially baselined with the MOBLAS-7 via simultaneous satellite ranging on the LAGEOS, Ajisai, Starlette, and ERS-I satellites. During the upgrades and following completion of the system upgrades intercomparisons with the MOBLAS-7 were made to verify the integrity and accuracy of the system changes. Several other groups of personnel participated in the TLRS-3 upgrade and they are: the Survey Section, the Precision Measurement Equipment Laboratory, the Architectural and Engineering Services Department, the Precision Timing Section, and the station personnel at TLRS-3 and MOBLAS-7.
Author (revised)

N94-15610*# Institut fuer Angewandte Geodaesie, Koetzing (Germany). Fundamentalstation Wettzell der Forschungsgruppe Satellitengeodaesie.
RESULTS OF THE MTLRS-1 UPGRADE **c14**
Peter Sperber, L. Amberg, G. Blenski, W. Etling, U. Hessels, R. Motz, and L. Beyer *In* NASA. Goddard Space Flight Center, Eighth International Workshop on Laser Ranging Instrumentation Jun. 1993 9 p (For primary document see N94-15552 03-19)
Avail: CASI HC A02/MF A06

In this report, the results of the upgrade of the German Modular Transportable Laser Ranging System MTLRS-1 are summarized. A short description of the new components and their influence on the system accuracy is given. It is shown, that the single shot accuracy of the MTLRS-1 has been improved from 5 cm to 1 cm. Author (revised)

N94-15611*# Institut fuer Angewandte Geodaesie, Koetzing (Germany). Fundamentalstation Wettzell der Forschungsgruppe Satellitengeodaesie.
THE NEW MTLRS-1 RECEIVING SYSTEM **c14**
Peter Sperber, U. Hessels, R. Motz, and H.-M. Guether (Hoechst A.G., Frankfurt am Main, Germany.) *In* NASA. Goddard Space Flight Center, Eighth International Workshop on Laser Ranging Instrumentation Jun. 1993 7 p (For primary document see N94-15552 03-19)
Avail: CASI HC A02/MF A06

In this report, we are giving a detailed description of the new receiving system of the German Modular Transportable Laser Ranging System MTLRS-1, consisting of a spectral time and field of view filter and a Single Photon Avalanche Diode (SPAD) as a single photon detector. The system gives full day and night ranging capability to all satellites with cm accuracy. Author (revised)

N94-15612*# Institut fuer Angewandte Geodaesie, Koetzing (Germany). Fundamentalstation Wettzell.
THE NEW MTLRS TRANSMITTING SYSTEM **c14**
Peter Sperber, U. Hessels, R. Motz, Wiard Beek (Technische Hogeschool, Delft, Netherlands.), Jacek W. Offierski (Technische Hogeschool, Delft, Netherlands.), and C. VanEs (Technische Hogeschool, Delft, Netherlands.) *In* NASA. Goddard Space Flight Center, Eighth International Workshop on Laser Ranging Instrumentation Jun. 1993 7 p (For primary document see N94-15552 03-19)
Avail: CASI HC A01/MF A06

This paper presents a detailed description about the new transmitting system of the Modular Transportable Laser Ranging Systems MTLRS-1/2. A simplified theory of the Self Filtering Unstable Resonator (SFUR) is explained. Laser design details are discussed concerning the extreme environmental conditions in which these mobile systems are operating. Details are given concerning the new avalanche START detector. The new SFUR laser and START detector are necessary parts in order to bring both mobile systems towards 1 cm ranging accuracy. Author (revised)

N94-15613*# Technische Hogeschool, Delft (Netherlands). Observatory for Satellite Geodesy.
TRANSPUTER BASED CONTROL SYSTEM FOR MTLRS **c14**
Erik Vermaat, Jacek W. Offierski, Klaus H. Otten, Wiard Beek, C. vanEs, and Peter Sperber (Institut fuer Angewandte Geodaesie, Koetzing, Germany.) *In* NASA. Goddard Space Flight Center, Eighth International Workshop on Laser Ranging Instrumentation Jun. 1993 9 p (For primary document see N94-15552 03-19)
Avail: CASI HC A02/MF A06

The Modular Transportable Laser Ranging Systems (MTLRS-1 and MTLRS-2) have been designed in the early eighties and have been in operation very successfully since 1984. The original design of the electronic control system was based on the philosophy of parallel processing, but these ideas could at that time only be implemented to a very limited extent. This present system utilizes two MOTOROLA 6800 8-bit processors slaved to a HP A-600 micro-computer. These processors support the telescope tracking system and the data-acquisition/formatting, respectively. Nevertheless, the overall design still is largely hardware oriented. Because the system is now some nine years old, aging of components increases the risk of malfunctioning and some components or units are outdated and not available anymore. The control system for MTLRS is now being re-designed completely, based on the original philosophy of parallel processing, making use of contemporary advanced electronics and processor technology. The new design aims at the requirements for Satellite Laser Ranging (SLR) in the nineties, making use of the extensive operational experience obtained with the two transportable systems.
Derived from text

N94-15614*# National Aeronautics and Space Administration. Goddard Space Flight Center, Greenbelt, MD.
AIRBORNE 2 COLOR RANGING EXPERIMENT **c32**
Pamela S. Millar, James B. Abshire, Jan F. McGarry, Thomas W. Zagwodzki, and Linda K. Pacini *In its* Eighth International Workshop on Laser Ranging Instrumentation Jun. 1993 16 p (For primary document see N94-15552 03-19)
Avail: CASI HC A03/MF A06

Horizontal variations in the atmospheric refractivity are a limiting error source for many precise laser and radio space geodetic techniques. This experiment was designed to directly measure horizontal variations in atmospheric refractivity, for the first time, by using 2 color laser ranging measurements to an aircraft. The 2 color laser system at the Goddard

Optical Research Facility (GORF) ranged to a cooperative laser target package on a T-39 aircraft. Circular patterns which extended from the southern edge of the Washington D.C. Beltway to the southern edge of Baltimore, MD were flown counter clockwise around Greenbelt, MD. Successful acquisition, tracking, and ranging for 21 circular paths were achieved on three flights in August 1992, resulting in over 20,000 two color ranging measurements. Author (revised)

N94-15615*# Aerospatiale, Cannes (France). Optical Dept.
GLRS-R 2-COLOUR RETROREFLECTOR TARGET DESIGN AND PREDICTED PERFORMANCE **c36**
Glenn Lund *In* NASA. Goddard Space Flight Center, Eighth International Workshop on Laser Ranging Instrumentation Jun. 1993 16 p (For primary document see N94-15552 03-19)
Avail: CASI HC A03/MF A06

This paper reports on the retroreflector ground-target design for the GLRS-R spaceborne dual-wavelength laser ranging system. The described passive design flows down from the requirements of high station autonomy, high global FOV (up to 60 degrees zenith angle), little or no multiple pulse returns, and adequate optical cross section for most ranging geometries. The proposed solution makes use of 5 hollow cube-corner retroreflectors of which one points to the zenith and the remaining four are inclined from the vertical at uniform azimuthal spacings. The need for fairly large (is approximately 10 cm) retroreflectors is expected (within turbulence limitations) to generate quite narrow diffraction lobes, thus placing non-trivial requirements on the vectorial accuracy of velocity aberration corrections. A good compromise solution is found by appropriately spoiling just one of the retroreflector dihedral angles from 90 degrees, thus generating two symmetrically oriented diffraction lobes in the return beam. The required spoil angles are found to have little dependence on ground target latitude. Various link budget analyses are presented, showing the influence of such factors as point-ahead optimization, turbulence, ranging angle, atmospheric visibility and ground target thermal deformations. Author (revised)

N94-15616*# National Oceanic and Atmospheric Administration, Boulder, CO. Wave Propagation Lab.
EFFECTS ON THE GEODYNAMIC LASER RANGING SYSTEM **c36**
James H. Churnside *In* NASA. Goddard Space Flight Center, Eighth International Workshop on Laser Ranging Instrumentation Jun. 1993 16 p (For primary document see N94-15552 03-19)
Avail: CASI HC A03/MF A06

The Geodynamic Laser Ranging System (GLRS) is one of several instruments being developed by the National Aeronautics and Space Administration (NASA) for implementation as part of the Earth Observing System in the mid-1990s (Cohen et al., 1987; Bruno et al., 1988). It consists of a laser transmitter and receiver in space and an array of retroreflectors on the ground. The transmitter produces short (100 ps) pulses of light at two harmonics (0.532 and 0.355 microns) of the Nd:YAG laser. These propagate to a retroreflector on the ground and return. The receiver collects the reflected light and measures the round-trip transit time. Ranging from several angles accurately determines the position of the retroreflector, and changes in position caused by geophysical processes can be monitored. Derived from text

N94-15617*# National Aeronautics and Space Administration. Goddard Space Flight Center, Greenbelt, MD.
DEVELOPMENT OF THE MARS OBSERVER LASER ALTIMETER (MOLA) **c36**
Bertrand L. Johnson, Jr et al *In its* Eighth International Workshop on Laser Ranging Instrumentation Jun. 1993 3 p (For primary document see N94-15552 03-19)
Avail: CASI HC A01/MF A06

The Mars Observer (MO) spacecraft payload scientific mission is to gather data on Martian global topography, gravity, weather, magnetic field and its interaction with the solar flux, surface chemistry, and mineralogy over one Mars year. In mid-1988 the need for a replacement altimeter as part of the payload complement arose. The Mars Observer Laser Altimeter (MOLA) was proposed by GSFC as an in-house effort and shortly afterward was 'conditionally' accepted. Constraints on funding, schedule, power, and mass were imposed with periodic reviews during the instrument development to authorize continuation. MOLA was designed, tested, and delivered in less than 36 months and integrated with the spacecraft. During spacecraft payload testing, the laser failed due to contamination in the laser cavity. In only 6 months, the laser was removed, rebuilt from spare parts, retested, and the instrument reassembled, realigned, requalified, and again delivered for spacecraft integration. Other aspects of the development of the MOLA are presented. Derived from text

N94-15618*# National Aeronautics and Space Administration. Goddard Space Flight Center, Greenbelt, MD.
BENCH CHECKOUT EQUIPMENT FOR SPACEBORNE LASER ALTIMETER SYSTEMS **c35**
James C. Smith, Gregory C. Elman (Ressler Associates, Inc., Laurel, MD.), Kent D. Christian (Bendix Field Engineering Corp., Columbia, MD.), John F. Cavanaugh, Luis Ramos-Izquierdo, and Dan E. Hopf (Science Systems and Applications, Inc., Lanham, MD.) *In its* Eighth International Workshop on Laser Ranging Instrumentation Jun. 1993 22 p (For primary document see N94-15552 03-19)
Avail: CASI HC A03/MF A06

This paper addresses the requirements for testing and characterizing spaceborne laser altimeter systems. The Bench Checkout Equipment (BCE) system, test requirements, and flow-down traceability from the instrument system's functional requirements will also be presented. Mars Observer Laser Altimeter (MOLA) and the MOLA BCE are presented as representative of a 'typical' laser altimeter and its corresponding test system. The testing requirements of other or future laser altimeter systems may vary slightly due to the specific spacecraft interface and project requirements. MOLA, the first solid-state interplanetary laser altimeter, was designed to be operational in Mars orbit for two Earth years. MOLA transmits a 7.5 ns pulse at a wavelength of 1.064 microns with a 0.25 mr beam divergence and a pulse repetition rate of 10 Hz. The output energy is specified at 45 mj at the beginning of mapping orbit and 30 mj at the end of one Martian year. MOLA will measure the laser pulse transit time from the spacecraft to the Mars surface and return to a resolution of 1.5 meters. Derived from text

N94-15619*# Czech Technical Univ., Prague. Faculty of Nuclear Science and Physical Engineering.
MARS LASER ALTIMETER BASED ON A SINGLE PHOTON RANGING TECHNIQUE **c36**
Ivan Prochazka, Karel Hamal, B. Sopko, and S. Pershin (Academy of Sciences, USSR, Moscow.) *In* NASA. Goddard Space Flight Center, Eighth International Workshop on Laser Ranging Instrumentation Jun. 1993 4 p (For primary document see N94-15552 03-19)
Avail: CASI HC A01/MF A06

The Mars 94/96 Mission will carry, among others things, the balloon probe experiment. The balloon with the scientific cargo in the gondola underneath will drift in the Mars atmosphere, its altitude will range from zero, in the night, up to 5 km at noon. The accurate gondola altitude will be determined by an altimeter. As the Balloon gondola mass is strictly limited, the altimeter total mass and power consumption are critical; maximum allowed is a few hundred grams a few tens of mWatts of average power consumption. We did propose, design, and construct the laser altimeter based on the single photon ranging technique. Topics covered include the following: principle of operation, altimeter construction, and ground tests. Derived from text

N94-15620*# National Aeronautics and Space Administration. Goddard Space Flight Center, Greenbelt, MD.
MULTI-BEAM LASER ALTIMETER **c36**
Jack L. Bufton, David J. Harding, and Luis Ramos-Izquierdo *In its* Eighth International Workshop on Laser Ranging Instrumentation Jun. 1993 9 p (For primary document see N94-15552 03-19)
Avail: CASI HC A02/MF A06

Laser altimetry provides a high-resolution, high-accuracy method for measurement of the elevation and horizontal variability of Earth-surface topography. The basis of the measurement is the timing of the round-trip propagation of short-duration pulses of laser radiation between a spacecraft and the Earth's surface. Vertical resolution of the altimetry measurement is determined primarily by laser pulsewidth, surface-induced spreading in time of the reflected pulse, and the timing precision of the altimeter electronics. With conventional gain-switched pulses from solid-state lasers and sub-nsec resolution electronics, sub-meter vertical range resolution is possible from

orbital attitudes of several hundred kilometers. Horizontal resolution is a function of laser beam footprint size at the surface and the spacing between successive laser pulses. Laser divergence angle and altimeter platform height above the surface determine the laser footprint size at the surface, while laser pulse repetition-rate, laser transmitter beam configuration, and altimeter platform velocity determine the space between successive laser pulses. Multiple laser transitters in a singlaltimeter instrument provide across-track and along-track coverage that can be used to construct a range image of the Earth's surface. Other aspects of the multi-beam laser altimeter are discussed. Derived from text

N94-15621*# Czech Technical Univ., Prague. Faculty of Nuclear Science.

SATELLITE LASER STATION HELWAN STATUS 1992 Abstract Only **c14**

M. Cech, Karel Hamal, Helena Jelinkova, Antonin Novotny, Ivan Prochazka, B. B. Baghos (National Research Inst. of Astronomy and Geophysics, Helwan, Egypt.), Y. Helali (National Research Inst. of Astronomy and Geophysics, Helwan, Egypt.), and M. J. Tawadros (National Research Inst. of Astronomy and Geophysics, Helwan, Egypt.) *In* NASA. Goddard Space Flight Center, Eighth International Workshop on Laser Ranging Instrumentation Jun. 1993 1 p Sponsored in part by Smithsonian Astrophysical Observatory (For primary document see N94-15552 03-19)
(Contracts ERS-1/7831/91; ERS-1/7831/92)
Avail: CASI HC A01/MF A06

The Satellite Laser Station Helwan has been operated jointly by the National Research Institute of Astronomy and Geophysics in Helwan, Egypt and the Czech Technical University in Prague, Czechslovakia. The station components have been carefully tuned to increase the systems overall stability and reliability critical for the remote location. The mount correction model based on the Gaussian smoothing has been implemented to simplify the blind satellite acquisition and tracking. The on-site normal points generation algorithm has been implemented, the station has been connected to the international information network. The ERS-1 satellite has been included into the tracking schedule. The station range capability has been verified by experimental Etalon 1 ranging by April 1992. The ranging precision of 2-3 centimeters is obtained when ranging to ERS-1, Starlette, and Lageos satellites. Derived from text

N94-15622*# Bendix Field Engineering Corp., Seabrook, MD.

OPTICAL ATTENUATION MECHANISM UPGRADES, MOBLAS, AND TLRS SYSTEMS

Richard Eichinger, Toni Johnson, Paul Malitson, Thomas Oldham, and Loyal Stewart *In* NASA. Goddard Space Flight Center, Eighth International Workshop on Laser Ranging Instrumentation Jun. 1993 12 p (For primary document see N94-15552 03-19)
Avail: CASI HC A03/MF A06

This poster presentation describes the Optical Attenuation Mechanism (OAM) Upgrades to the MOBLAS and TLRS Crustal Dynamics Satellite Laser Ranging (CDSLR) systems. The upgrades were for the purposes of preparing these systems to laser range to the TOPEX/POSEIDON spacecraft when it will be launched in the summer of 1992. The OAM permits the laser receiver to operate over the expected large signal dynamic range from TOPEX/POSEIDON and it reduces the number of pre- and post-calibrations for each satellite during multi-satellite tracking operations. It further simplifies the calibration bias corrections that had been made due to the pass-to-pass variation of the photomultiplier supply voltage and the transmit filter glass thickness. The upgrade incorporated improvements to the optical alignment capability of each CDSLR system through the addition of a CCD camera into the MOBLAS receive telescope and an alignment telescope onto the TLRS optical table. The OAM is stepper motor and microprocessor based; and the system can be controlled either manually by a control switch panel or computer controlled via an EIA RS-232C serial interface. The OAM has a neutral density (ND) range of 0.0 to 4.0 and the positioning is absolute referenced in steps of 0.1 ND. Both the fixed transmit filter and the daylight filter are solenoid actuated with digital inputs and outputs to and from the OAM microprocessor. During automated operation, the operator has the option to overide the remote control and control the OAM system via a local control switch panel.
Author (revised)

N94-15623*# Academy of Sciences, Potsdam (German D.R.).

THE THIRD GENERATION SLR STATION POTSDAM NO. 7836 **c14**

H. Fischer, Ludwig Grunwaldt, and Reinhart Neubert *In* NASA. Goddard Space Flight Center, Eighth International Workshop on Laser Ranging Instrumentation Jun. 1993 6 p (For primary document see N94-15552 03-19)
Avail: CASI HC A02/MF A06

The new satellite laser ranging (SLR) station Potsdam has been installed during the winter of 1991/1992 in an existing dome near the old ruby laser at Helmert Tower. It has been built around a one-meter-Coude telescope and is equipped by a 50 ps Nd:YAG laser and a SPAD receiver. The first successful Lageos passes were obtained in May 1992 demonstrating 2-3 cm rms at the single photon level. The new station will be used for experimental work and selected campaigns as well. Author (revised)

N94-15624*# Bendix Field Engineering Corp., Seabrook, MD.

PERFORMANCE COMPARISON OF HIGH SPEED MICROCHANNEL PLATE PHOTOMULTIPLIER TUBES **c33**

Thomas Varghese, Michael Selden, and Thomas Oldham *In* NASA. Goddard Space Flight Center, Eighth International Workshop on Laser Ranging Instrumentation Jun. 1993 9 p (For primary document see N94-15552 03-19)
Avail: CASI HC A02/MF A06

The transit time spread characteristics of high speed microchannel photomultipliers has improved since the upgrade of the NASA CDSLR network to MCP-PMT's in the mid-1980's. The improvement comes from the incorporation of 6 micron (pore size) microchannels and offers significant improvement to the satellite ranging precision. To examine the impact on ranging precision, two microchannel plate photomultiplier tubes (MCP-PMT) were evaluated for output pulse characteristics and temporal jitter. These were a Hamamatsu R 2566 U-7 MCP-PMT (6 micron) and an ITT 4129f MCP-PMT (12 micron). Derived from text

N94-15625*# National Aeronautics and Space Administration. Goddard Space Flight Center, Greenbelt, MD.

STATION REPORT ON THE GODDARD SPACE FLIGHT CENTER (GSFC) 1.2 METER TELESCOPE FACILITY **c89**

Jan F. McGarry, Thomas W. Zagwodzki, Arnold Abbott, John J. Degnan, Jack W. Cheek (Hughes STX, Inc., Lanham, MD.), Richard S. Chabot (Bendix Field Engineering Corp., Seabrook, MD.), David A. Grolemund (Bendix Field Engineering Corp., Seabrook, MD.), and Jim D. Fitzgerald (Bendix Field Engineering Corp., Seabrook, MD.) *In its* Eighth International Workshop on Laser Ranging Instrumentation Jun. 1993 8 p (For primary document see N94-15552 03-19)
Avail: CASI HC A02/MF A06

The 1.2 meter telescope system was built for the Goddard Space Flight Center (GSFC) in 1973-74 by the Kollmorgen Corporation as a highly accurate tracking telescope. The telescope is an azimuth-elevation mounted six mirror Coude system. The facility has been used for a wide range of experimentation including helioseismology, two color refractometry, lunar laser ranging, satellite laser ranging, visual tracking of rocket launches, and most recently satellite and aircraft streak camera work. The telescope is a multi-user facility housed in a two story dome with the telescope located on the second floor above the experimenter's area. Up to six experiments can be accommodated at a given time, with actual use of the telescope being determined by the location of the final Coude mirror. The telescope facility is currently one of the primary test sites for the Crustal Dynamics Network's new UNIX based telescope controller software, and is also the site of the joint Crustal Dynamics Project / Photonics Branch two color research into atmospheric refraction. Author (revised)

N94-17083*# Electromagnetic Sciences, Inc., Norcross, GA.

MICROWAVE REFLECTOMETER IONIZATION SENSOR

Joseph Seals, Jeffrey A. Fordham, Robert G. Pauley (Georgia Tech Research Inst., Atlanta.), and Mario D. Simonutti (Millitech Corp., South Deerfield, MA.) Oct. 1993 402 p
(Contract NAS1-19063; RTOP 505-64-12-04)
(NASA-CR-191464; NAS 1.26:191464) Avail: CASI HC A18/MF A04

The development of the Microwave Reflectometer Ionization Sensor (MRIS) Instrument for use on the Aeroassist Flight Experiment (AFE) spacecraft is described. The instrument contract was terminated, due to cancellation of the AFE program, subsequent to testing of an engineering

development model. The MRIS, a four-frequency reflectometer, was designed for the detection and location of critical electron density levels in spacecraft reentry plasmas. The instrument would sample the relative magnitude and phase of reflected signals at discrete frequency steps across 4 GHz bandwidths centered at four frequencies: 20, 44, 95, and 140 GHz. The sampled data would be stored for later processing to calculate the distance from the spacecraft surface to the critical electron densities versus time. Four stepped PM CW transmitter receivers were located behind the thermal protection system of the spacecraft with horn antennas radiating and receiving through an insulating tile. Techniques were developed to deal with interference, including multiple reflections and resonance effects, resulting from the antenna configuration and operating environment.

Author (revised)

N94-17126*# Southwest Research Inst., Houston, TX.

PRINCIPAL INVESTIGATORS DATA PACKAGE FOR PROJECT INITIATION CONFERENCE (PIC): EUVS SOUNDING ROCKET NO. 36.117CL. TARGET: VENUS

S. Alan Stern 16 Nov. 1993 34 p

(Grant NAG5-5006)

(NASA-CR-194663; NAS 1.26:194663) Avail: CASI HC A03/MF A01

The region of the UV between 500 and 1200 A is a rich one for the study of planetary and astrophysical targets. EUV atmospheric spectroscopy opens up an important window on ion and neutral nitrogen, oxygen, and noble gas emissions. In this document we describe the specific scientific background and motivations for this Venus EUV rocket observation along with experiment design and mission parameters. Author

N94-17592 Institut d'Aeronomie Spatiale de Belgique, Brussels.

SECOND FLIGHT OF THE SPACELAB GRILLE SPECTROMETER DURING THE ATLAS-1 MISSION

M. deMaziere, C. Muller, C. Lippens, J. Vercheval, D. Fonteyn, R. Armante (Office National d'Etudes et de Recherches Aerospatiales, Paris, France.), C. Camy-Peyret (Office National d'Etudes et de Recherches Aerospatiales, Paris, France.), V. Achard (Office National d'Etudes et de Recherches Aerospatiales, Paris, France.), J. Besson (Office National d'Etudes et de Recherches Aerospatiales, Paris, France.), and J. Marcault (Office National d'Etudes et de Recherches Aerospatiales, Paris, France.) et al 1992 18 p Submitted for publication Sponsored by CNES; Ministere de l'Environnement et du Cadre de Vie, Neuilly, France, and Ministry of Science Policy, Belgium

(Aeronautica-Acta-A-367-1992; ETN-93-94627) Copyright Avail: Institut d'Aeronomie Spatiale de Belgique, 3 Avenue Circulaire, B-1180 Brussels, Belgium

The second flight of the Spacelab grille spectrometer, which took advantage of the favorable timeline and of the extra day to perform more than 65 successful solar occultation runs, is addressed. The purpose of the Atlas mission, flown onboard the American Space Shuttle, was to study the evolution of atmospheric properties over an entire solar cycle. The grille spectrometer measured the vertical concentration profiles of trace gases. It succeeded in obtaining spectra pertinent to its ten target molecules in the full range of altitudes available to the solar infrared occultation technique. These ten molecules are H2O, CO, CO2, CH4, NO, NO2, N2O, HCl, HF, and O3. A preliminary analysis of an HCl observation is presented showing no significant change of upper atmospheric hydrogen chloride in comparison with previous data. ESA

N94-16100 Laval Univ. (Quebec).

PRECISE MEASUREMENT AND UTILIZATION OF ACCELERATION DATA

L. Potvin, C. Rioux, and R. J. Slobodrian *In* National Research Council Canada, Proceedings of the Second Workshop on Microgravity Experimentation 1990 5 p (For primary document see N94-16071 03-29)

Avail: Issuing Activity (National Research Council, Publication Sales and Distribution, Montreal Road, Ottawa, Ontario, K1A OR6 Canada)

20 SPACECRAFT PROPULSION AND POWER

Includes main propulsion systems and components, e.g., rocket engines; and spacecraft auxilliary power sources.

For related information see also *07 Aircraft Propulsion and Power, 28 Propellants and Fuels, 44 Energy Production and Conversion,* and *15 Launch Vehicles and Space Vehicles.*

N94-15118*# National Aeronautics and Space Administration. Lewis Research Center, Cleveland, OH.

SPACE EXPLORATION INITIATIVE FUELS, MATERIALS AND RELATED NUCLEAR PROPULSION TECHNOLOGIES PANEL Final Report

S. K. Bhattacharyya (Argonne National Lab., IL.), C. Olsen (Idaho National Engineering Lab., Idaho Falls.), R. Cooper (Oak Ridge National Lab., TN.), R. B. Matthews (Los Alamos National Lab., NM.), C. Walter (Lawrence Livermore National Lab., CA.), and R. J. Titran Sep. 1993 314 p

(RTOP 593-71-00)

(NASA-TM-105706; E-8100; NAS 1.15:105706) Avail: CASI HC A14/MF A03

This report was prepared by members of the Fuels, Materials and Related Technologies Panel, with assistance from a number of industry observers as well as laboratory colleagues of the panel members. It represents a consensus view of the panel members. This report was not subjected to a thorough review by DOE, NASA or DoD, and the opinions expressed should not be construed to represent the official position of these organizations, individually or jointly. Topics addressed include: requirement for fuels and materials development for nuclear thermal propulsion (NTP) and nuclear electric propulsion (NEP); overview of proposed concepts; fuels technology development plan; materials technology development plan; other reactor technology development; and fuels and materials requirements for advanced propulsion concepts.

Author (revised)

N94-15217# Advisory Group for Aerospace Research and Development, Neuilly-Sur-Seine (France). Propulsion and Energetics Panel.

ROCKET MOTOR PLUME TECHNOLOGY [L'ETUDE DES JETS DES MOTEURS-FUSEES]

Jun. 1993 196 p In ENGLISH and FRENCH Lecture series held in Neubiberg, Germany, 7-8 Jun. 1993 and in Ankara, Turkey, 10-11 Jun. 1993

(AGARD-LS-188; ISBN-92-835-0713-4) Copyright Avail: CASI HC A09/MF A03

Requirements for missile guidance and stealth properties are changing and becoming more stringent. There is no up-to-date synthesis relating rocket motor plume properties to these new requirements. The work performed and recently finished within PEP WG 21 formed the basis for this Lecture Series. The scope of the Lecture Series will be rocket motor exhaust products and plumes in all their aspects. Plume properties are addressed and methods of numerical simulation and experimental assessment described. Specifically, plume structure, after-burning phenomena, primary and secondary smoke, plume radiation signatures, and plume microwave interactions are described in detail. Operational aspects linked to these topics discuss how rocket plumes influence missile detection, guidance, and tracking. Ways in which plumes may be modified to reduce or eliminate this influence are suggested. For individual titles, see N94-15218 through N94-15223.

N94-15218# Societe Nationale des Poudres et Explosifs, Vert-Le-Petit (France).

PLUME PRIMARY SMOKE

J. C. Chastenet *In* AGARD, Rocket Motor Plume Technology Jun. 1993 19 p (For primary document see N94-15217 03-20)

Copyright Avail: CASI HC A03/MF A03

The exhaust from a solid propellant rocket motor usually contains condensed species. These particles, also called 'Primary Smoke', are often prejudicial to missile detectability and to the guidance system. To avoid operational problems it is necessary to know and quantify the effects of particles on all aspects of missile deployment. A brief description of the origin of the primary smoke is given. It continues with details of the interaction between particles and light as function of both particles and light properties (nature, size, wavelength, etc). The effects of particles on plume visibility, attenuation of an optical beam propagated through the

plume and the contribution of particles on optical signatures of the plume are also described. Finally, various methods used in NATO countries to quantify the primary smoke effects are discussed. Author (revised)

N94-15219# Royal Ordnance PLC, Kidderminster (England). Rocket Motors Div.
PROPULSION
P. K. Smith *In* AGARD, Rocket Motor Plume Technology Jun. 1993 24 p (For primary document see N94-15217 03-20)
Copyright Avail: CASI HC A03/MF A03

Current requirements for missile systems increasingly stress the need for stealth capability. For the majority of missile systems and missions, the exhaust plume is likely to be the major contributor to overall missile signature, especially considering the recent developments in low emission and low Radar Cross Section coatings for motor bodies. This implies the need for the lowest possible rocket exhaust signature over a wide range of frequencies from the UV through visible and IR to microwave and radio frequencies. The choice of propellant type, Double Base; Composite etc, plays a significant part in determining the exhaust signature of the rocket motor as does the selection of inert materials for liners, inhibitors, and nozzles. It is also possible with certain propellants to incorporate additives which reduce exhaust signature either by modifying the chemistry or the afterburning plume or more significantly by suppressing secondary combustion and hence dramatically reducing plume temperature. The feasibility of plume signature control on the various missions envisaged by the missile designer is considered. The choice of propellant type and hardware components to give low signature is discussed together with performance implications. Signature reduction results obtained over a wide range of frequencies are also presented. Author (revised)

N94-15220# Phillips Lab., Edwards AFB, CA. Propulsion Directorate.
SECONDARY SMOKE
P. A. Kessel *In* AGARD, Rocket Motor Plume Technology Jun. 1993 10 p (For primary document see N94-15217 03-20)
Copyright Avail: CASI HC A02/MF A03

The open literature on secondary smoke formation, prediction, and classification is briefly reviewed. This review was limited to the open literature in order to promote the widest possible discussion within the AGARD engineering community. The recently completed PEP WG 21 proposal for smoke classification is presented. Secondary smoke is defined and the physics of condensation of vapor onto droplets is reviewed. The basis for the existing droplet condensation models is discussed and the existing methodology for predicting secondary smoke light attenuation and scattering is presented. Test data taken to establish the initial conditions for heterogeneous nucleation in rocket plumes is presented. Comparisons between secondary smoke predictions and flight data are presented. The state of the art of secondary smoke modeling is discussed and suggestions are made for improvements. Author

N94-15221# Science Applications International Corp., Fort Washington, PA. Propulsive Sciences Div.
ROCKET MOTOR PLUME FLOWFIELDS: PHENOMENOLOGY AND SIMULATION
Sanford M. Dash *In* AGARD, Rocket Motor Plume Technology Jun. 1993 30 p (For primary document see N94-15217 03-20)
Copyright Avail: CASI HC A03/MF A03

The varied processes occurring in rocket motor exhaust plumes and methodology for simulating these processes are described. Rocket motor plumes contain shock waves due to under/overexpansion; the exhaust mixes with the external stream in a highly compressible turbulent environment; unburnt products of combustion after-burn strongly at lower altitudes; and solid propellant plumes contain particulates which are generally out of equilibrium with the gas-phase exhaust. Earlier methodology simulated the varied processes using boundary layer type coupling. Current methods implement solutions of the full or reduced (parabolized) Navier-Stokes equations where all fluid dynamic and thermochemical processes are strongly coupled. Earlier methodology are reviewed briefly while the status of current methods is addressed in greater detail. Author (revised)

N94-15222# Royal Ordnance PLC, Aylesbury (England).
MICROWAVE PROPERTIES AND SYSTEMS OVERVIEW **c32**
Ronald Lawrence *In* AGARD, Rocket Motor Plume Technology Jun. 1993 35 p (For primary document see N94-15217 03-20)
Copyright Avail: CASI HC A03/MF A03

Of particular significance to the operational success of a missile using microwave communications is the interference introduced by the rocket exhaust plume. As a hot and turbulent gas stream the exhaust has electrical properties that can seriously degrade guidance and tracking. Also present is the potential for missile detection offered by energy scattered from microwave signals impinging upon the plume to present a radar cross section, and an exhaust signature from inherent emission sources within the plume. This paper presented in AGARD Lecture Series 188, follows from AGARD Advisory Report 287 submitted by Propulsion and Energetics Panel Working Group 21 entitled 'Terminology and Assessment Methods of Solid Propellant Rocket Exhaust Signatures.' It provides a description of microwave propagation through a rocket exhaust, the cause of signal attenuation, and the generation of phase and amplitude sideband noise. Consideration is given to the effects of missile flight velocity and altitude. Diffraction and refraction processes are discussed, particularly in relation to plumes containing high density concentrations of free electrons. Radiation sources, mainly at millimetric wavelengths, are included together with signature implications. The effects of exhaust interference with communications is examined from a system point of view and some methods of relief from the interference are considered. Author (revised)

N94-15223# Deutsche Aerospace A.G., Munich (Germany). Dynamics Systems.
PLUME RADIATION **c32**
R. Dirscherl *In* AGARD, Rocket Motor Plume Technology Jun. 1993 47 p (For primary document see N94-15217 03-20)
Copyright Avail: CASI HC A03/MF A03

The electromagnetic radiation originating from the exhaust plume of tactical missile motors is of outstanding importance for military system designers. Both missile- and countermeasure engineer rely on the knowledge of plume radiation properties, be it for guidance/interference control or for passive detection of adversary missiles. To allow access to plume radiation properties, they are characterized with respect to the radiation producing mechanisms like afterburning, its chemical constituents, and reactions as well as particle radiation. A classification of plume spectral emissivity regions is given due to the constraints imposed by available sensor technology and atmospheric propagation windows. Additionally assessment methods are presented that allow a common and general grouping of rocket motor properties into various categories. These methods describe state of the art experimental evaluation techniques as well as calculation codes that are most commonly used by developers of NATO countries. Dominant aspects influencing plume radiation are discussed and a standardized test technique is proposed for the assessment of plume radiation properties that include prediction procedures. These recommendations on terminology and assessment methods should be common to all employers of plume radiation. Special emphasis is put on the omnipresent need for self-protection by the passive detection of plume radiation in the ultraviolet (UV) and infrared (IR) spectral band. Author

N94-15229* National Aeronautics and Space Administration. Marshall Space Flight Center, Huntsville, AL.
ADVANCED SOLID ROCKET MOTOR (Videotape)
Mar. 1989 Videotape: 2 min. 1 sec. playing time, in color, with sound (NASA-TM-109658; NONP-VT-93-190456) Avail: CASI VHS A01/BETA A22

This video tape describes the redesign and construction of the Advanced Solid Rocket Motor. CASI

N94-15351* National Aeronautics and Space Administration. Lewis Research Center, Cleveland, OH.
NASA IMAGES 10 (Videotape)
Mar. 1988 Videotape: 29 min. playing time, in color, with sound (NASA-TM-109419; NONP-VT-93-190216) Avail: CASI VHS A01/BETA A22

Electric propulsion engine research from the 1960's is looked at. CASI

N94-15482*# Mechanical Technology, Inc., Latham, NY.
SPDE/SPRE FINAL SUMMARY REPORT

George Dochat Sep. 1993 98 p
(Contract NAS3-23883; RTOP 590-13-11)
(NASA-CR-187086; E-8126; NAS 1.26:187086) Avail: CASI HC A05/MF A02

Mechanical Technology Incorporated (MTI) performed acceptance testing on the Space Power Research Engine (SPRE), which demonstrated satisfactory operation and sufficient reliability for delivery to NASA Lewis Research Center. The unit produced 13.5 kW PV power with an efficiency of 22 percent versus design goals of 28.8 kW PV power and efficiency of 28 percent. Maximum electric power was only 8 kWe due to lower alternator efficiency. One of the major shortcomings of the SPRE was linear alternator efficiency, which was only 70 percent compared to a design value of 90 percent. It was determined from static tests that the major cause for the efficiency shortfall was the location of the magnetic structure surrounding the linear alternator. Testing of an alternator configuration without a surrounding magnetic structure on a linear dynamometer confirmed earlier static test results. Linear alternator efficiency improved from 70 percent to over 90 percent. Testing of the MTI SPRE was also performed with hydrodynamic bearings and achieved full-stroke, stable operation. This testing indicated that hydrodynamic bearings may be useful in free piston Stirling engines. An important factor in achieving stable operation at design stroke was isolating a portion of the bearing length from the engine pressure variations. In addition, the heat pipe heater head design indicates that integration of a Stirling engine with a heat source can be performed via heat pipes. This design provides a baseline against which alternative designs can be measured. Author (revised)

N94-15503* National Aeronautics and Space Administration. Lewis Research Center, Cleveland, OH.
FUTUREPATH 1 (Videotape)
Apr. 1988 Videotape: 27 min. 15 sec. playing time, in color, with sound
(NASA-TM-109431; NONP-VT-93-190228) Avail: CASI VHS A01/BETA A22

This video looks at the photovoltaic and solar dynamic power systems being developed for Freedom and the Advanced Turboprop Program. CASI

N94-15837 Massachusetts Inst. of Tech., Cambridge. Dept. of Aeronautics and Astronautics.
NUCLEAR ROCKET PLUME STUDIES Final Report, Aug. 1991 - Jul. 1993
Daniel Hastings 5 May 1993 92 p Limited Reproducibility: More than 20% of this document may be affected by microfiche quality
(Grant AF-AFOSR-0415-91)
(AD-A267154; AFOSR-93-0461TR) Avail: Issuing Activity (Defense Technical Information Center (DTIC))

A description and detailed computational analysis of a vortex cleaning system designed to remove radioactive material from the plumes of nuclear rockets is included. The proposed system is designed to remove both particulates and radioactive gaseous material from the plume. A two part computational model is used to examine the system's ability to remove particulates, and the results indicate that under some conditions, the system can remove over 99% of the particles in the flow. Two critical parameters which govern the effectiveness of the system are identified and the information necessary to estimate cleaning efficiencies for particles of known sizes and densities is provided. A simple steady analytical solution is also developed to examine the system's ability to remove gaseous radioactive material. This analysis, while inconclusive, suggests that the swirl rates necessary to achieve useful efficiencies are too high to be achieved in any practical manner. Therefore, this system is probably not suitable for use, with gaseous radioactive material. It was concluded that the system can cause negligible specific impulse losses, though there may be a substantial mass penalty associated with its use. DTIC

N94-15876*# National Aeronautics and Space Administration. Pasadena Office, CA.
CARBON-CARBON GRID FOR ION ENGINES Patent Application
Charles E. Garner, inventor (to NASA) (Jet Propulsion Lab., California Inst. of Tech., Pasadena.) 1 Jul. 1993 23 p
(Contract NAS7-918)
(NASA-Case-NPO-19174-1-CU; NAS 1.71:NPO-19174-1-CU; US-Patent-Appl-SN-089064) Avail: CASI HC A03/MF A01

A method and apparatus of manufacturing a grid member for use in an ion discharge apparatus provides a woven carbon fiber in a matrix of carbon. The carbon fibers are orientated to provide a negatibe coefficient of thermal expansion for at least a portion of the grid member's operative range of use. NASA

N94-15927*# National Aeronautics and Space Administration. Pasadena Office, CA.
SEGMENTED ION THRUSTER Patent Application
John R. Brophy, inventor (to NASA) (Jet Propulsion Lab., California Inst. of Tech., Pasadena.) 25 Aug. 1992 27 p
(Contract NAS7-918)
(NASA-Case-NPO-18192-1-CU; NAS 1.71:NPO-18192-1-CU; US-Patent-Appl-SN-934988) Avail: CASI HC A03/MF A01

Apparatus and methods for large-area, high-power ion engines comprise dividing a single engine into a combination of smaller discharge chambers (or segments) configured to operate as a single large-area engine. This segmented ion thruster (SIT) approach enables the development of 100-kW class argon ion engines for operation at a specific impulse of 10,000 s. A combination of six 30-cm diameter ion chambers operating as a single engine can process over 100 kW. Such a segmented ion engine can be operated from a single power processor unit. NASA

N94-15947*# National Aeronautics and Space Administration. Langley Research Center, Hampton, VA.
SHOCK-FREE SUPERSONIC ELLIPTIC NOZZLES AND METHOD OF FORMING SAME Patent Application
John M. Seiner, inventor (to NASA) and Roy S. Baty, inventor (to NASA) 19 Jul. 1993 20 p
(NASA-Case-LAR-14054-1; NAS 1.71:LAR-14054-1; US-Patent-Appl-SN-095563) Avail: CASI HC A03/MF A01

A method of forming a shock-free supersonic elliptic nozzle, in which the nozzle to be designed is divided into three sections, a circular-to-elliptic section which begins at a circular nozzle inlet, an elliptic subsonic section downstream from the circular-to-elliptic section, and a supersonic section downstream from the elliptic subsonic section is described. The maximum and minimum radii for each axial point in the circular-to-elliptic section and the elliptic subsonic section are then separately determined, the maximum and minimum radii being the radii for the widest part of an elliptic cross-section and the narrowest part of the elliptic cross-section, respectively. The maximum and minimum radii for each axial point in the supersonic section are determined based on the Method of Characteristics. Then, each of the three sections are based on the maximum and minimum radii for each axial point in the section. The resulting nozzle is acoustically superior. NASA

N94-16482# Colorado Univ., Boulder. Center for Combustion Research.
FUNDAMENTAL STUDIES OF ROCKET COMBUSTION CHEMISTRY AND COMBUSTION INSTABILITY Final Technical Report, 1989 - 1992
Melvyn C. Branch, John W. Daily, Shankar Mahalingam, and Gregory J. Fiechtner Feb. 1993 34 p
(Grant AF-AFOSR-0121-90)
(AD-A266248; CCR-93-01; AFOSR-93-0432TR) Avail: CASI HC A03/MF A01

This report provides a summary of results obtained over the past year in fundamental studies of the chemistry of solid rocket combustion and of combustion instability in liquid rocket combustion. A coordinated research program has been initiated to study separate aspects of the complex multidimensional, multiphase, and multicomponent reacting flow characteristic of rocket combustion. The focus of the combustion chemistry studies is on flame reactions of gas phase species formed as decomposition products near the surface of the propellant. These flames typically involve a variety of fuel species and nitrogen oxides as oxidizers. The focus of the combustion instability studies is the effect of atomization and vaporization processes on the oscillatory conditions characteristic of combustion instability. The research objectives, progress, and research in progress in each of these areas are summarized in the report. DTIC

N94-16496*# National Aeronautics and Space Administration. Lyndon B. Johnson Space Center, Houston, TX.
LUNAR LANDER AND RETURN PROPULSION SYSTEM TRADE STUDY

Eric A. Hurlbert, Robert Moreland, Gerald B. Sanders, Edward A. Robertson, David Amidei, and John Mulholland et al Aug. 1993 202 p
(NASA-TP-3388; S-728; NAS 1.60:3388) Avail: CASI HC A10/MF A03

This trade study was initiated at NASA/JSC in May 1992 to develop and evaluate main propulsion system alternatives to the reference First Lunar Outpost (FLO) lander and return-stage transportation system concept. Thirteen alternative configurations were developed to explore the impacts of various combinations of return stage propellants, using either pressure or pump-fed propulsion systems and various staging options. Besides two-stage vehicle concepts, the merits of single-stage and stage-and-a-half options were also assessed in combination with high-performance liquid oxygen and liquid hydrogen propellants. Configurations using an integrated modular cryogenic engine were developed to assess potential improvements in packaging efficiency, mass performance, and system reliability compared to non-modular cryogenic designs. The selection process to evaluate the various designs was the analytic hierarchy process. The trade study showed that a pressure-fed MMH/N2O4 return stage and RL10-based lander stage is the best option for a 1999 launch. While results of this study are tailored to FLO needs, the design date, criteria, and selection methodology are applicable to the design of other crewed lunar landing and return vehicles. Author

N94-16504*# Teledyne Brown Engineering, Colorado Springs, CO.
THE FRAGMENTATION OF THE NIMBUS 6 ROCKET BODY
David J. Nauer and Nicholas L. Johnson Nov. 1991 46 p Original contains color illustrations
(Contract NAS9-18209)
(NASA-CR-191645; NAS 1.26:191645; CS91-TR-JSC-017) Avail: CASI HC A03/MF A01; 5 functional color pages

On 1 May 1991, the Nimbus 6 second stage Delta Rocket Body experienced a major breakup at an altitude of approximately 1,100 km. There were numerous pieces left in long-lived orbits, adding to the long-term hazard in this orbital regime already present from previous Delta Rocket Body explosions. The assessed cause of the event is an accidental explosion of the Delta second stage by documented processes experienced by other similar Delta second stages. Various aspects of the event are discussed. Author

N94-16590*# Aerojet-General Corp., Sacramento, CA. Propulsion Div.
ALS ENGINE PROPELLANT EFFECTOR SYSTEM Final Summary Report
Colin Faulkner and Roger Payne 15 Nov. 1993 59 p
(Contract NAS8-38073)
(NASA-CR-194650; NAS 1.26:194650) Avail: CASI HC A04/MF A01

This report summarizes analysis, design, and experimental testing done on the propellant effector (valve plus electromechanical actuator) for the Advanced Launch System (ALS) main engine. Author

N94-16654*# Aerojet-General Corp., Sacramento, CA. Propulsion Div.
ALS ENGINE CONTROLLER SYSTEM Final Summary Report
Roger Payne 15 Nov. 1993 52 p
(Contract NAS8-38074)
(NASA-CR-194647; NAS 1.26:194647) Avail: CASI HC A04/MF A01

This report summarizes analysis and design done on the controller system for the Advanced Launch System (ALS) main engine. Author

N94-16773# Department of Energy, Idaho Falls, ID.
SPACE NUCLEAR FACILITY TEST CAPABILITY AT THE BAIKAL-1 AND IGR SITES SEMIPALATINSK-21, KAZAKHSTAN
T. J. Hill, M. L. Stanley, and J. S. Martinell Jan. 1993 85 p Presented at the Nuclear Power Engineering in Space Nuclear Rocket Engines, Kazakhstan, Russia, 22-26 Sep. 1992
(Contract DE-AC07-76ID-01570)
(DE93-011662; DOE/FTR-93011662; CONF-9209177-Summ) Avail: CASI HC A05/MF A01 (US Sales Only)

The International Space Technology Assessment Program was established 1/19/92 to take advantage of the availability of Russian space technology and hardware. DOE had two delegations visit CIS and assess its space nuclear power and propulsion technologies. The visit coincided with the Conference on Nuclear Power Engineering in Space Nuclear Rocket Engines at Semipalatinsk-21 (Kurchatov, Kazakhstan) on Sept. 22-25, 1992. Reactor facilities assessed in Semipalatinski-21 included the IVG-1 reactor (a nuclear furnace, which has been modified and now called IVG-1M), the RA reactor, and the Impulse Graphite Reactor (IGR), the CIS version of TREAT. Although the reactor facilities are being maintained satisfactorily, the support infrastructure appears to be degrading. The group assessment is based on two half-day tours of the Baikals-1 test facility and a brief (2 hr) tour of IGR; because of limited time and the large size of the tour group, it was impossible to obtain answers to all prepared questions. Potential benefit is that CIS fuels and facilities may permit USA to conduct a lower priced space nuclear propulsion program while achieving higher performance capability faster, and immediate access to test facilities that cannot be available in this country for 5 years. Information needs to be obtained about available data acquisition capability, accuracy, frequency response, and number of channels. Potential areas of interest with broad application in the U.S. nuclear industry are listed. DOE

N94-16834# General Accounting Office, Washington, DC. National Security and International Affairs Div.
SPACE SHUTTLE MAIN ENGINE. NASA HAS NOT EVALUATED THE ALTERNATE FUEL TURBOPUMP COSTS AND BENEFITS. REPORT TO THE ADMINISTRATOR OF THE NATIONAL AERONAUTICS AND SPACE ADMINISTRATION
Oct. 1993 15 p
(GAO/NSIAD-94-54; B-255456) Avail: CASI HC A03/MF A01; GAO, PO Box 6015, Gaithersburg, MD 20877 HC

NASA's plans to develop an alternate high pressure fuel turbopump for the Space Shuttle's main engines were assessed by the General Accounting Office as a part of the evaluation of the Space Shuttle Safety and Obsolescence Upgrade program. The objective was to determine whether NASA has adequately analyzed cost, performance, and benefits that are expected to result from this program in comparison to other alternatives before resuming development of the alternate pump, which was suspended in 1992. The alternate fuel pump is one of five improvements being developed or planned to significantly enhance safety margins of the engines. Derived from text

N94-16880*# Sverdrup Technology, Inc., Brook Park, OH. Lewis Research Center Group.
HOLLOW CATHODE HEATER DEVELOPMENT FOR THE SPACE STATION PLASMA CONTACTOR Final Report
George C. Soulas Oct. 1993 14 p Presented at the 23rd International Electric Propulsion Conference, Seattle, WA, 13-16 Sep. 1993; sponsored by AIAA, DGLR, and JSASS
(Contract NAS3-25266; RTOP 474-46-10)
(NASA-CR-191131; E-7846; NAS 1.26:191131) Avail: CASI HC A03/MF A01

A hollow cathode-based plasma contactor has been selected for use on the Space Station. During the operation of the plasma contactor, the hollow cathode heater will endure approximately 12000 thermal cycles. Since a hollow cathode heater failure would result in a plasma contactor failure, a hollow cathode heater development program was established to produce a reliable heater design. The development program includes the heater design, process documents for both heater fabrication and assembly, and heater testing. The heater design was a modification of a sheathed ion thruster cathode heater. Three heaters have been tested to date using direct current power supplies. Performance testing was conducted to determine input current and power requirements for achieving activation and ignition temperatures, single unit operational repeatability, and unit-to-unit operational repeatability. Comparisons of performance testing data at the ignition input current level for the three heaters show the unit-to-unit repeatability of input power and tube temperature near the cathode tip to be within 3.5 W and 44 degrees C, respectively. Cyclic testing was then conducted to evaluate reliability under thermal cycling. The first heater, although damaged during assembly, completed 5985 ignition cycles before failing. Two additional heaters were subsequently fabricated and have completed 3178 cycles to date in an on-going test. Author

N94-16922*# Ball Aerospace Systems Div., Boulder, CO. Electro-Optics and Cryogenics Div.
POWER REACTANT STORAGE ASSEMBLY (PRSA) (SPACE SHUTTLE). PRSA HYDROGEN AND OXYGEN DVT TANK REFURBISHMENT Final Report
15 Jul. 1993 31 p

(Contract NAS9-18398)
(NASA-CR-188262; NAS 1.26:188262; CR0009-1039) Avail: CASI HC A03/MF A01

The Power Reactant Storage Assembly (PRSA) liquid hydrogen Development Verification Test (H2 DVT) tank assembly (Beech Aircraft Corporation P/N 15548-0116-1, S/N 07399000SHT0001) and liquid oxygen (O2) DVT tank assembly (Beech Aircraft Corporation P/N 15548-0115-1, S/N 07399000SXT0001) were refurbished by Ball Electro-Optics and Cryogenics Division to provide NASA JSC, Propulsion and Power Division, the capability of performing engineering tests. The refurbishments incorporated the latest flight configuration hardware and avionics changes necessary to make the tanks function like flight articles. This final report summarizes these refurbishment activities. Also included are up-to-date records of the pressure time and cycle histories. Author (revised)

N94-17016*# Aerojet-General Corp., Sacramento, CA. Propulsion Div.
ALS LIQUID HYDROGEN TURBOPUMP Final Summary Report
Deborah K. Rickman 15 Nov. 1993 59 p
(Contract NAS8-37593)
(NASA-CR-194646; NAS 1.26:194646) Avail: CASI HC A04/MF A01

This report summarized analysis, design, and experimental work done on the liquid hydrogen turbopump for the ALS main engine. Author

N94-17053 Air Force Inst. of Tech., Wright-Patterson AFB, OH.
DEVELOPMENT AND ANALYSIS OF STARTUP STRATEGIES FOR PARTICLE BED NUCLEAR ROCKET ENGINE M.S. Thesis
David E. Suzuki Jun. 1993 104 p Limited Reproducibility: More than 20% of this document may be affected by microfiche quality
(AD-A267949; AFIT/CI/CIA-93-088) Avail: Issuing Activity (Defense Technical Information Center (DTIC))

The particle bed reactor (PBR) nuclear thermal propulsion rocket engine concept is the focus of the Air Force's Space Nuclear Thermal Propulsion program. While much progress has been made in developing the concept, several technical issues remain. Perhaps foremost among these concerns is the issue of flow stability through the porous, heated bed of fuel particles. There are two complementary technical issues associated with this concern: the identification of the flow stability boundary and the design of the engine controller to maintain stable operation. This thesis examines a portion of the latter issue which has yet to be addressed in detail. Specifically, it develops and analyzes general engine system startup strategies which maintain stable flow through the PBR fuel elements while reaching the design conditions as quickly as possible. The PBR engine studies are conducted using a computer model of a representative particle bed reactor and engine system. The computer program utilized is an augmented version of SAFSIM, an existing nuclear thermal propulsion modeling code; the augmentation, dubbed SAFSIM+, was developed by the author and provides a more complete engine system modeling tool. DTIC

N94-17080*# Thiokol Corp., Brigham City, UT.
RSRM NOZZLE ACTUATOR BRACKET/LUG FRACTURE MECHANICS QUALIFICATION TEST Final Report
Peggy Kelley Jul. 1993 53 p
(Contract NAS8-30490)
(NASA-CR-193859; TRW-18168; NAS 1.26:193859) Avail: CASI HC A04/MF A01

This is the final report for the actuator bracket/lug fracture mechanics qualification test. The test plan (CTP-0071) outlined a two-phase test program designed to answer questions about the fracture criticality of the redesigned solid rocket motor (RSRM) nozzle actuator bracket. An analysis conducted using the NASA/FLAGRO fracture mechanics computer program indicated that the actuator bracket might be a fracture critical component. In the NASA/FLAGRO analysis, a simple lug model was used to represent the actuator bracket. It was calculated that the bracket would fracture if subjected to an actuator stall load in the presence of a 0.10 in. corner crack at the actuator attachment hole. The 0.10 in. crack size corresponds to the nondestructive inspection detectability limit for the actuator bracket. The inspection method used is the dye penetrant method. The actuator stall load (103,424 lb) is the maximum load which the actuator bracket is required to withstand during motor operation. This testing was designed to establish the accuracy of the analytical model and to directly determine whether the actuator bracket is capable of meeting fracture mechanics safe-life requirements. Author

N94-17096*# Rockwell International Corp., Canoga Park, CA. Rocketdyne Div.
ADVANCED TRANSPORTATION SYSTEM STUDIES TECHNICAL AREA 3: ALTERNATE PROPULSION SUBSYSTEM CONCEPTS, VOLUME 2 Interim Final Report, 6 Apr. 1992 - 5 Apr. 1993
Daniel Levak Apr. 1993 15 p
(Contract NAS8-39210)
(NASA-CR-193863; NAS 1.26:193863; RI/RD93-123-2) Avail: CASI HC A03/MF A01

The Alternate Propulsion Subsystem Concepts contract had five tasks defined for the first year. The tasks were: F-1A Restart Study, J-2S Restart Study, Propulsion Database Development, Space Shuttle Main Engine (SSME) Upper Stage Use, and CER's for Liquid Propellant Rocket Engines. The detailed study results, with the data to support the conclusions from various analyses, are being reported as a series of five separate Final Task Reports. Consequently, this volume only reports the required programmatic information concerning Computer Aided Design Documentation, and New Technology Reports. A detailed Executive Summary, covering all the tasks, is also available as Volume 1.
Author (revised)

N94-17097*# Rockwell International Corp., Canoga Park, CA. Rocketdyne Div.
ADVANCED TRANSPORTATION SYSTEM STUDIES TECHNICAL AREA 3: ALTERNATE PROPULSION SUBSYSTEM CONCEPTS, VOLUME 3 Interim Final Report, 6 Apr. 1992 - 5 Apr. 1993
Daniel Levak Apr. 1993 40 p
(Contract NAS8-39210)
(NASA-CR-193864; NAS 1.26:193864; RI/RD93-123-3) Avail: CASI HC A03/MF A01

The objective of this contract was to provide definition of alternate propulsion systems for both earth-to-orbit (ETO) and in-space vehicles (upper stages and space transfer vehicles). For such propulsion systems, technical data to describe performance, weight, dimensions, etc. was provided along with programmatic information such as cost, schedule, needed facilities, etc. Advanced technology and advanced development needs were determined and provided. This volume separately presents the various program cost estimates that were generated under three tasks: the F-1A Restart Task, the J-2S Restart Task, and the SSME Upper Stage Use Task. The conclusions, technical results, and the program cost estimates are described in more detail in Volume 1 - Executive Summary and in individual Final Task Reports. Author

N94-17098*# Rockwell International Corp., Canoga Park, CA. Rocketdtne Div.
ADVANCED TRANSPORTATION SYSTEM STUDIES TECHNICAL AREA 3: ALTERNATE PROPULSION SYSTEM CONCEPTS. SSME UPPER STAGE USE Task Final Report, May 1992 - Apr. 1993
Eric Strangeland and Daniel Levak Apr. 1993 145 p
(Contract NAS8-39210)
(NASA-CR-193865; NAS 1.26:193865) Avail: CASI HC A07/MF A02

The main objective was to determine viable methods for starting the Space Shuttle Main Engine (SSME) in an altitude environment and restarting it in an orbit environment with minimum changes in utilization of the engine system or hardware. The study concluded that the use of the SSME in an upper stage is feasible with minimal changes to the engine systems. The altitude start case requires only a change in the valve sequencing during start and reorificing of the ASI lines. Inlet pressures can be moderately low at 40 psia for the LOX and 32 psia for the H2. The orbital restart case adds the need to recirculate propellant and thermal control paint (to keep the turbomachinery inlets cold to minimize the tank pressures needed), and the need to heat two small components (to maintain acceptable mixture ratios during the early part of the start). These actions allow start anytime after approximately 120 minutes. Earlier starts (approximately one hour) are also possible but would require additional component heating for mixture ratio control during the early portion of the start sequence.
Author (revised)

N94-17123*# Southern Research Inst., Birmingham, AL.
SRB THERMAL CURTAIN DESIGN SUPPORT Final Report
Carl A. Dixon Dec. 1991 42 p Sponsored by U.S. Polymeric B.P. Chemicals, Santa Anna, CA

(Contract NAS8-38261)
(NASA-CR-193857; SRI-MME-92-564-7079; NAS 1.26:193857) Avail: CASI HC A03/MF A01

The objective of the program during this time period was to evaluate candidate materials that could be used to design an improved Solid Rocket Motor (SRM) Aft Skirt Thermal Curtain (ASTC). The ASTC is a flexible, high temperature, cloth and insulation composite that is used to protect the hardware located inside the aft skirt of the shuttle solid rocket booster. The current ASTC consists of nine layers of insulating materials and is 2.58 inches thick. The ASTC is made up of twenty four segments. The segments are hand sewn together during installation on the aft skirt. The weight of the current ASTC is approximated at about six hundred pounds. This weight does not include the weight of the mounting hardware and ties required to install the twenty four ASTC segments (which is significant). The current effort entailed measuring the thermophysical properties of six candidate materials (quartz, S glass, and Kevlar woven into nominal 0.25 inch thick layers by angle interlock and polar-weave) and then using these properties in a computer program to predict the thermal performance of various curtain configurations subjected to an SRM heat flux.

Author (revised)

N94-17124*# Southern Research Inst., Birmingham, AL.
SRB THERMAL CURTAIN DESIGN SUPPORT Final Report, 16 Feb. 1990 - 28 Feb. 1993
Carl A. Dixon, Wayne E. Lundblad, and John R. Koenig Nov. 1992 161 p Sponsored by BP Chemicals (Hitco) Inc., Birmingham, AL
(Contract NAS8-38261)
(NASA-CR-193858; SRI-MME-92-564-7079; NAS 1.26:193858) Avail: CASI HC A08/MF A02

Improvements in SRB Thermal Curtain were identified by thermal design featuring: selection of materials capable of thermal protection and service temperatures by tri-layering quartz, S2 glass, and Kevlar in thinner cross section; weaving in single piece (instead of 24 sections) to achieve improved strength; and weaving to reduce manufacturing cost with angle interlock construction.

Author (revised)

N94-17213*# Thiokol Corp., Brigham City, UT. Space Operations.
FLIGHT 20 (STS-45) POLYSULFIDE GAS PATH INVESTIGATION Final Report
Rey C. Bjorkman, Charles W. Bown, Scott D. Smith, Jerry L. Walters, Suresh B. Kulkarni, Roger V. Cook, David A. Sebahar, Craig S. Walker, M. Reed Haddock, and Robert E. Lindstrom Jul. 1992 182 p
(Contract NAS8-38100)
(NASA-CR-193861; TRW-63941; NAS 1.26:193861; Publ-922023) Avail: CASI HC A09/MF A02

This report documents the results of the investigation into causes of gas paths on the 20A and 20B case-to-nozzle joints on STS-42. The investigation was conducted by the Investigation Board appointed by the senior vice president and general manager of Space Operations, Mr. R. E. Lindstrom, on 7 Feb. 1992. The probability of gas path occurrence in the nozzle-to-case-joint polysulfide had been identified during joint redesign. However, actual flight gas path incidence has been limited to RSRM-11 and the 20A and 20B segments. The blow-by condition on the 20A segment was a first time occurrence which was a special concern. The investigation covered all technical aspects associated with the gas path and blow-by conditions: materials and processing history, design requirements and as-built compliance to the design, thermal and structural analyses, computer modeling, and laboratory experimentation with the materials involved. The investigation was coordinated with Mr. Ken Jones at NASA Marshall in bi-weekly teleconferences. The Board also supported Dr. James C. Blair's independent NASA investigation team by providing copies of collected data, conducting requested analyses, and supporting several all-day teleconferences to provide understanding and resolve issues. The Dr. Blair support requirement was successfully concluded on 4 Mar. 1992.

Derived from text

N94-17256*# National Aeronautics and Space Administration. Lewis Research Center, Cleveland, OH.
OVERVIEW OF THE SOLAR DYNAMIC GROUND TEST DEMONSTRATION PROGRAM
Richard K. Shaltens and Robert V. Boyle (Allied-Signal Aerospace Co., Tempe, AZ.) Aug. 1993 8 p Presented at the 28th Intersociety Energy Conversion Engineering Conference, Atlanta, GA, 8-13 Aug. 1993; sponsored by ACS
(RTOP 585-03-21)
(NASA-TM-106296; E-8034; NAS 1.15:106296) Avail: CASI HC A02/MF A01

The Solar Dynamic (SD) Ground Test Demonstration (GTD) program demonstrates the availability of SD technologies in a simulated space environment at the NASA Lewis Research Center (LeRC) vacuum facility. An aerospace industry/ government team is working together to design, fabricate, build, and test a complete SD system. This paper reviews the goals and status of the SD GTD program. A description of the SD system includes key design features of the system, subsystems, and components as reported at the Critical Design Review (CDR).

Author

N94-17277*# Aerotherm Corp., Huntsville, AL.
ASRM NOZZLE THERMAL ANALYSIS Final Report
Forrest Strobel and Belinda King Nov. 1993 101 p
(Contract NAS8-39611)
(NASA-CR-194672; NAS 1.26:194672; AEROTHERM-FR-7186-93-15)
Avail: CASI HC A06/MF A02

This report describes results from the nozzle thermal analysis contract which has been performed to support NASA/Marshall Space Flight Center in the development of the Advanced Solid Rocket Motor (ASRM). The emphasis of this study has been directed to four potential problem areas of the nozzle. These areas are the submerged nozzle region containing the flex seal, the nozzle entrance region, the material interface region in the nozzle exit cone, and the aft region of the exit cone. This study was limited throughout by inadequate material response models, especially for the polyisoprene flex seal and the low density carbon phenolic used in the exit cone. Thermal response and particle erosion calculations were performed for each of the potential problem areas. Results from these studies showed excessive erosion (large negative safety margins) to occur in the flex seal and nozzle entrance regions. The exit cone was found to be marginally adequate (near zero safety margins) and the material interface region was found not to be a problem.

Author

N94-17308 Stuttgart Univ. (Germany). Inst. fuer Raumfahrtsysteme.
HIGH POWER STEADY STATE MPD THRUSTERS Final Report, Sep. 1989 - Aug. 1991
Monika Auweter-Kurtz, Harald Habiger, Helmut Kurtz, Herbert Schrade, and Cristian Sleziona Apr. 1993 56 p Limited Reproducibility: More than 20% of this document may be affected by microfiche quality
(Grant AF-AFOSR-0535-89)
(AD-A267277; PL-TR-92-3054) Avail: CASI HC A04

At the Institut fuer Raumfahrtsysteme (IRS) rotation symmetric magnetoplasmadynamic thrusters with self induced magnetic fields are investigated at high current levels in a steady state operation mode. MPD thrusters with different geometrics were compared, and the influence of mass flow rate and power input on the operating conditions of the thrusters explored. By optical and probe measurements, a systematic investigation of the plasma plume has been started. The investigation of the various instabilities of the arc and the plasma flow appearing at high power levels was continued. The computer code development for the geometry optimization of continuous self-field MPD thrusters, running with argon, was modified by considering higher degrees of ionization, which showed better agreement with the experiment.

DTIC

N94-17442*# Computational Fluid Dynamics Research Corp., Huntsville, AL.
COMPUTATIONAL ANALYSIS OF VARIABLE THRUST ENGINE (VTE) PERFORMANCE Final Report, 21 Apr. 1989 - Jan. 1993
M. G. Giridharan, A. Krishnan, and A. J. Przekwas Feb. 1993 95 p
(Contract NAS8-37196)
(NASA-CR-193852; CFDRC-4075/3; NAS 1.26:193852) Avail: CASI HC A05/MF A01

The Variable Thrust Engine (VTE) of the Orbital Maneuvering Vehicle (OMV) uses a hypergolic propellant combination of Monomethyl Hydrazine (MMH) and Nitrogen Tetroxide (NTO) as fuel and oxidizer, respectively. The performance of the VTE depends on a number of complex interacting phenomena such as atomization, spray dynamics, vaporization, turbulent mixing, convective/radiative heat transfer, and hypergolic combustion. This study involved the development of a comprehensive numerical methodology

to facilitate detailed analysis of the VTE. An existing Computational Fluid Dynamics (CFD) code was extensively modified to include the following models: a two-liquid, two-phase Eulerian-Lagrangian spray model; a chemical equilibrium model; and a discrete ordinate radiation heat transfer model. The modified code was used to conduct a series of simulations to assess the effects of various physical phenomena and boundary conditions on the VTE performance. The details of the models and the results of the simulations are presented. Author (revised)

N94-17474# Air Force Inst. of Tech., Wright-Patterson AFB, OH. School of Engineering.
FLOW INSTABILITY TESTS FOR A PARTICLE BED REACTOR NUCLEAR THERMAL ROCKET FUEL ELEMENT M.S. Thesis
Timothy J. Lawrence May 1993 345 p
(AD-A268012; AFIT/CI/CIA-93-079) Avail: CASI HC A15/MF A03

Recent analyses have focused on the flow stability characteristics of a particle bed reactor (PBR). These laminar flow instabilities may exist in reactors with parallel paths and are caused by the heating of the gas at low Reynolds numbers. This phenomena can be described as follows: several parallel channels are connected at the plenum regions and are stabilized by some inlet temperature and pressure; a perturbation in one channel causes the temperature to rise and increases the gas viscosity and reduces the gas density; the pressure drop is fixed by the plenum regions, therefore, the mass flow rate in the channel would decrease; the decrease in flow reduces the ability to remove the energy added and the temperature increases; and finally, this process could continue until the fuel element fails. Several analyses based on different methods have derived similar curves to show that these instabilities may exist at low Reynolds numbers and high phi's ((Tfinal Tinitial)/Tinitial). These analyses need to be experimentally verified. DTIC

N94-17483*# National Aeronautics and Space Administration. Lewis Research Center, Cleveland, OH.
SPACE STATION FREEDOM ELECTRICAL PERFORMANCE MODEL
Jeffrey S. Hojnicki, Robert D. Green, Thomas W. Kerslake, David B. McKissock, and Jeffrey J. Trudell Nov. 1993 9 p Presented at the 28th Intersociety Energy Conversion Engineering Conference, Atlanta, GA, 8-13 Aug. 1993; sponsored by American Chemical Society
(RTOP 474-12-10)
(NASA-TM-106395; E-8220; NAS 1.15:106395) Avail: CASI HC A02/MF A01

The baseline Space Station Freedom electric power system (EPS) employs photovoltaic (PV) arrays and nickel hydrogen (NiH2) batteries to supply power to housekeeping and user electrical loads via a direct current (dc) distribution system. The EPS was originally designed for an operating life of 30 years through orbital replacement of components. As the design and development of the EPS continues, accurate EPS performance predictions are needed to assess design options, operating scenarios, and resource allocations. To meet these needs, NASA Lewis Research Center (LeRC) has, over a 10 year period, developed SPACE (Station Power Analysis for Capability Evaluation), a computer code designed to predict EPS performance. This paper describes SPACE, its functionality, and its capabilities. Author (revised)

N94-17543# Naval Postgraduate School, Monterey, CA.
HEAT TRANSFER PARAMETRIC SYSTEM IDENTIFICATION M.S. Thesis
Gregory K. Parker Jun. 1993 116 p
(AD-A268525) Avail: CASI HC A06/MF A02

This work describes the development of a computer based model that would allow for determination of the transient thermal response characteristics of jet vanes of any size. The model used a thermal lump approach method, considering only conductive and convective heat transfer properties. A constrained optimizer was used to adjust the unknown variables until an adequate match was achieved between the calculated values of the energy balance equations and the experimental data obtained from test firings of a rocket motor. The full scale modeling results were compared to previous quarter scale models in an attempt to determine the applicability of the quarter scale results to full scale vanes. It was determined that the quarter scale model did not provide an accurate representation of the heat transfer process in larger scale vanes, although the full scale model provided a sufficient representation of the thermal response of the jet vane. DTIC

N94-17587 Air Force Inst. of Tech., Wright-Patterson AFB, OH.
APPLICATION OF A NEPTUNE PROPULSION CONCEPT TO A MANNED MARS EXCURSION M.S. Thesis
Charles J. Finley Apr. 1993 135 p Limited Reproducibility: More than 20% of this document may be affected by microfiche quality
(AD-A268053; AFIT/CI/CIA-93-111) Avail: CASI HC A07

NEPTUNE is a multimegawatt electric propulsion system. It uses a proven compact nuclear thermal rocket, NERVA, in a closed cycle with a magnetohydrodynamic (MHD) generator to power a magnetoplasmadynamic (MPD) thruster. This thesis defines constraints on an externally sourced propulsion system intended to carry out a manned Martian excursion. It assesses NEPTUNE's ability to conform to these constraints. Because an unmodified NEPTUNE system is too large, the thesis develops modifications to the system which reduce its size. The result is a far less proven, but more useful derivative of the unmodified NEPTUNE system. DTIC

N94-17589 Johns Hopkins Univ., Columbia, MD. Chemical Propulsion Information Agency.
CPIA/M5 LIQUID PROPELLANT ENGINE MANUAL
27 Jul. 1993 12 p Limited Reproducibility: More than 20% of this document may be affected by microfiche quality
(AD-A268062; CPIA-LBP/MJP-06-93) Avail: Issuing Activity (Defense Technical Information Center (DTIC))

The F-1A is an uprated version of the F-1. It is a step-thrust bipropellant engine which uses liquid oxygen as the oxidizer and RP-1 as the fuel. The engine operates on a gas generator cycle. Nominal sea level thrust is 1,800,000 lb(sub f) with step-thrust down to 75%. The step-thrust is obtained by oxidizer flow control on the gas generator. DTIC

N94-16149# Martin Marietta Corp., New Orleans, LA. Manned Space Systems.
SPACE PROPULSION SYNERGY GROUP ETO TECHNOLOGY ASSESSMENTS
James Bray *In* Huntsville Association of Technical Societies, TABES 1993: 9th Annual Technical and Business Exhibition and Symposium 1993 9 p (For primary document see N94-16129 03-38)
(TABES Paper 93-641) Avail: CASI HC A02/MF A03

N94-17175 Eagle-Picher Industries, Inc., Joplin, MO.
SMALL SATELLITE NICKEL-HYDROGEN AND NICKEL-METAL HYDRIDE POWER APPLICATIONS
William Dean Cook and Dwaine Coates *In* CNES, Small Satellites Systems and Services Jan. 1993 p 547-556 (For primary document see N94-17131 03-18)
Copyright Avail: Issuing Activity (CEPADUES-Editions, 111 rue Nicolas-Vaquelin, 31100 Toulouse, France)

N94-17176 European Space Agency. European Space Research and Technology Center, ESTEC, Noordwijk (Netherlands). Power Conditioning Section.
A POWER SYSTEM FOR A MICROSATELLITE
Dan Olsson *In* CNES, Small Satellites Systems and Services Jan. 1993 p 557-566 (For primary document see N94-17131 03-18)
Copyright Avail: Issuing Activity (CEPADUES-Editions, 111 rue Nicolas-Vaquelin, 31100 Toulouse, France)

23 CHEMISTRY AND MATERIALS (GENERAL)

N94-15734# Dartmouth Coll., Hanover, NH.
SYNTHESIS AND CHEMISTRY OF NOVEL CYCLIC FLUOROCARBONS Final Report, 1 Nov. 1989 - 31 Oct. 1992
David M. Lemal 27 May 1993 10 p
(Grant AF-AFOSR-0015-90)
(AD-A267148; AFOSR-93-0469TR) Avail: CASI HC A02/MF A01

New, unusual perfluorinated organic molecules have been synthesized and their chemistry has been examined. Reaction mechanisms of fluorocarbon derivatives have been investigated, and new synthetic methodology has been developed. The nature and chemistry of excited states as well as ground states have been explored. DTIC

N94-15769*# National Aeronautics and Space Administration. Lewis Research Center, Cleveland, OH.
THE FRICTION AND WEAR OF CERAMIC/CERAMIC AND CERAMIC/METAL COMBINATIONS IN SLIDING CONTACT
Harold E. Sliney and Christopher DellaCorte Oct. 1993 13 p Presented at the STLE-ASME Tribology Conference, New Orleans, LA, 24-27 Oct. 1993; sponsored by STLE Prepared for DOE, Office of Vehicle and Engine R&D
(RTOP 505-63-5A)
(NASA-TM-106348; DOE/NASA/50306-3; E-8121; NAS 1.15:106348)
Avail: CASI HC A03/MF A01

The tribological characteristics of ceramics sliding on ceramics are compared to those of ceramics sliding on a nickel based turbine alloy. The friction and wear of oxide ceramics and silicon-based ceramics in air at temperatures from room ambient to 900 C (in a few cases to 1200 C) were measured for a hemispherically-tipped pin on a flat sliding contact geometry. In general, especially at high temperature, friction and wear were lower for ceramic/metal combinations than for ceramic/ceramic combinations. The better tribological performance for ceramic/metal combinations is attributed primarily to the lubricious nature of the oxidized surface of the metal. Author (revised)

N94-17192 Air Force Inst. of Tech., Wright-Patterson AFB, OH.
SYNTHESIS, REACTIVITY, AND CHARACTERIZATION OF (-HEXACARBOCYCLIC) MANGANESE DICARBONYL COMPLEXES WITH SULFUR AND PHOSPHORUS LIGANDS Ph.D. Thesis
Jeffrey L. Moler May 1993 271 p Limited Reproducibility: More than 20% of this document may be affected by microfiche quality
(AD-A267592; AFIT/CI/CIA-93-012D) Avail: Issuing Activity (Defense Technical Information Center (DTIC))

A series of (eta(exp 5) pentamethyl benzyl) manganese dicarbonyl phosphite complexes have been synthesized. Manganese coordinated phosphites react with the exocyclic methylene of the coordinated pentamethyl benzyl ligand generating either benzyne or a carbene, an eta(exp 6) hexaalkyl benzene, and dialkyl- or diaryl phosphonate complexes. Their decomposition to phosphonates was observed under reduced pressure or in the presence of olefins. Benzyne, from the triphenyl phosphite complexes was observed indirectly through the formation of diphenylene. The production of methylene carbenes was observed by the formation of ethene and cyclopropanes. The generation of olefins or cyclopropanes indicated that ethylidene was produced. DTIC

N94-16144*# National Aeronautics and Space Administration. Marshall Space Flight Center, Huntsville, AL.
EMERGING TECHNOLOGIES FOR THE CHANGING GLOBAL MARKET
Wendy Cruit, Scott Schutzenhofer, Ben Goldberg, and Kurt Everhart (Sverdrup Technology, Inc., Huntsville, AL.) *In* Huntsville Association of Technical Societies, TABES 1993: 9th Annual Technical and Business Exhibition and Symposium 1993 11 p (For primary document see N94-16129 03-38)
(TABES Paper 93-612) Avail: CASI HC A03/MF A03

N94-16325*# Academy of Sciences (USSR), Moscow.
TERRESTRIAL BITUMEN ANALOGUE OF ORGUEIL ORGANIC MATERIAL DEMONSTRATES HIGH SENSITIVITY TO USUAL HF-HCl TREATMENT Abstract Only
A. V. Korochantsev and O. V. Nikolaeva *In* Lunar and Planetary Inst., Twenty-Fourth Lunar and Planetary Science Conference. Part 2: G-M 1993 p 817-818 (For primary document see N94-16173 03-91)
Avail: CASI HC A01/MF A06

24 COMPOSITE MATERIALS

Includes physical, chemical, and mechanical properties of laminates and other composite materials.

For ceramic materials see *27 Nonmetallic Materials*.

N94-14975# Naval Postgraduate School, Monterey, CA.
THERMAL STRESSES OF A TRIMATERIAL MEDIUM IN A NONUNIFORM TEMPERATURE FIELD M.S. Thesis
Michael J. Neibert Mar. 1993 108 p
(AD-A267243) Avail: CASI HC A06/MF A02

The objective of this investigation was to conduct a parametric study of the effect of a nonuniform temperature field on the system behavior of a trilayered medium. In particular, the resulting shear and normal stresses along the media interfaces are analyzed. A finite element model utilizing a recently developed element which provides for both axial and lateral displacement continuity is employed. First, the effect of the material properties, that is, Young's Modulus and coefficient of thermal expansion, is examined. Then, the effect of the geometric properties, that is, length and thickness dimensions of the midlayer, is analyzed. Finally, a study of the effect of a nonuniform temperature field on the trimaterial medium is conducted. DTIC

N94-14999# Army Research Lab., Watertown, MA.
THE EFFECT OF PLASMA TREATMENT ON INTERFACIAL BOND CHARACTERISTICS OF KEVLAR/EPOXY LAMINATES AS MEASURED BY T-PEEL TESTS Final Report
Rachel A. Michaud and Joey L. Mead May 1993 13 p
(AD-A266920; ARL-TR-141) Avail: CASI HC A03/MF A01

Composite materials are used in a wide variety of applications where their anisotropic properties allow the material to be tailored for each application. Unfortunately, aramid fiber composites may have limited applications due to poor transverse properties. These poor transverse properties are the result of weak interfacial bonding. Improvement of the interfacial bond strength has been an area of active research. Plasma treatment is one method that can be used to modify the surface of a fiber in an effort to improve the fiber-matrix adhesion. Kevlar/epoxy laminates were peel-tested (T-peel) to study the effect of plasma treatment on the interfacial properties. The T-peel results indicate that ammonia plasma treatment improves the interfacial bond strength of Kevlar/epoxy composites, increasing the T-peel strengths by approximately 30%. DTIC

N94-15106*# Virginia Univ., Charlottesville. School of Engineering and Applied Science.
INELASTIC DEFORMATION OF METAL MATRIX COMPOSITES Final Report
C. J. Lissenden, C. T. Herakovich, and M-J. Pindera Sep. 1993 109 p
(Grant NAG1-745; RTOP 506-73-43-03)
(NASA-CR-191522; AM-93-03; NAS 1.26:191522) Avail: CASI HC A06/MF A02

A theoretical model capable of predicting the thermomechanical response of continuously reinforced metal matrix composite laminates subjected to multiaxial loading was developed. A micromechanical model is used in conjunction with nonlinear lamination theory to determine inelastic laminae response. Matrix viscoplasticity, residual stresses, and damage to the fiber/matrix interfacial zone are explicitly included in the model. The representative cell of the micromechanical model is considered to be in a state of generalized plane strain, enabling a quasi two-dimensional analysis to be performed. Constant strain finite elements are formulated with elastic-viscoplastic constitutive equations. Interfacial debonding is incorporated into the model through interface elements based on the interfacial debonding theory originally presented by Needleman, and modified by Tvergaard. Nonlinear interfacial constitutive equations relate interfacial tractions to displacement discontinuities at the interface. Theoretical predictions are compared with the results of an experimental program conducted on silicon carbide/titanium (SiC/Ti) unidirectional, (O4), and angle-ply, (+34)(sub s), tubular specimens. Multiaxial loading included increments of axial tension, compression, torque, and internal pressure. Loadings were chosen in an effort to distinguish inelastic deformation due to damage from matrix plasticity and separate time-dependent effects from time-independent effects. Results show that fiber/matrix debonding is nonuniform throughout the composite and is a major factor in the effective response. Also, significant creep behavior occurs at relatively low applied stress levels at room temperature. Author (revised)

N94-15143# Colorado Univ., Boulder. Dept. of Mechanical Engineering.
DYNAMIC BEHAVIOR OF FIBER AND PARTICLE REINFORCED COMPOSITES Final Report
Subhendu K. Datta 12 Mar. 1993 12 p
(Contract N00014-91-J-1297)
(AD-A266905) Avail: CASI HC A03/MF A01

Models were developed for wave propagation in a particle or fiber reinforced composite material in order to describe its dynamic anisotropic and dispersive properties. Model predictions were compared with experimental results for inversion of anisotropic properties of the constituents. Measured properties were related to the microstructure. The effects of interface/interphase on the effective properties were studied by the modeling technique in order to characterize interface/interphase. The characteristics of guided waves in fiber reinforced laminated plates and shells were analyzed to the characterization of anisotropic properties of a lamina. We also investigated the effect of the properties of the interface material layers (bond layers) between the laminae on the dispersion and dynamic response of guided waves. In addition, for thick laminated composites, it is of interest to investigate the dispersion of guided waves in order to model them as homogeneous anisotropic media. The transient response of laminated composite plates due to impact was studied. Of particular interest is the dependence of the response on the duration of impact. The maximum interlaminar stresses for damage development were analyzed. DTIC

N94-15184*# Analytical Services and Materials, Inc., Hampton, VA.
CRACK-TIP-OPENING ANGLE MEASUREMENTS AND CRACK TUNNELING UNDER STABLE TEARING IN THIN SHEET 2024-T3 ALUMINUM ALLOY Final Report
D. S. Dawicke and M. A. Sutton (South Carolina Univ., Columbia.) Sep. 1993 33 p
(Contract NAS1-19399; NAG1-1489; RTOP 538-02-10-01)
(NASA-CR-191523; NAS 1.26:191523) Avail: CASI HC A03/MF A01

The stable tearing behavior of thin sheets 2024-T3 aluminum alloy was studied for middle crack tension specimens having initial cracks that were: flat cracks (low fatigue stress) and 45 degrees through-thickness slant cracks (high fatigue stress). The critical crack-tip-opening angle (CTOA) values during stable tearing were measured by two independent methods, optical microscopy and digital image correlation. Results from the two methods agreed well. The CTOA measurements and observations of the fracture surfaces showed that the initial stable tearing behavior of low and high fatigue stress tests is significantly different. The cracks in the low fatigue stress tests underwent a transition from flat-to-slant crack growth, during which the CTOA values were high and significant crack tunneling occurred. After crack growth equal to about the thickness, CTOA reached a constant value of 6 deg and after crack growth equal to about twice the thickness, crack tunneling stabilized. The initial high CTOA values, in the low fatigue crack tests, coincided with large three-dimensional crack front shape changes due to a variation in the through-thickness crack tip constraint. The cracks in the high fatigue stress tests reach the same constant CTOA value after crack growth equal to about the thickness, but produced only a slightly higher CTOA value during initial crack growth. For crack growth on the 45 degree slant, the crack front and local field variables are still highly three-dimensional. However, the constant CTOA values and stable crack front shape may allow the process to be approximated with two-dimensional models. Author (revised)

N94-15190*# Washington Univ., Saint Louis, MO. Dept. of Physics.
PHYSICAL INTERPRETATION AND DEVELOPMENT OF ULTRASONIC NONDESTRUCTIVE EVALUATION TECHNIQUES APPLIED TO THE QUANTITATIVE CHARACTERIZATION OF TEXTILE COMPOSITE MATERIALS Semiannual Progress Report, 15 Mar. - 14 Sep. 1993
James G. Miller 1993 15 p
(Grant NsG-1601)
(NASA-CR-194549; NAS 1.26:194549) Avail: CASI HC A03/MF A01

In this Progress Report, we describe our current research activities concerning the development and implementation of advanced ultrasonic nondestructive evaluation methods applied to the characterization of stitched composite materials and bonded aluminum plate specimens. One purpose of this investigation is to identify and characterize specific features of polar backscatter interrogation which enhance the ability of ultrasound to detect flaws in a stitched composite laminate. Another focus is to explore the feasibility of implementing medical linear array imaging technology as a viable ultrasonic-based nondestructive evaluation method to inspect and characterize bonded aluminum lap joints. As an approach to implementing quantitative ultrasonic inspection methods to both of these materials, we focus on the physics that underlies the detection of flaws in such materials. Derived from text

N94-15254# Technische Hochschule, Aachen (Germany). Sonderforschungsbereich 332.
PRODUCTION TECHNOLOGY FOR COMPONENTS FROM NONMETALLIC FIBER REINFORCED MATERIALS [PRODUKTIONSTECHNIK FUER BAUTEILE AUS NICHTMETALLISCHEN FASERVERBUNDWERKSTOFFEN]
1992 231 p In GERMAN
(ETN-93-94607) Avail: CASI HC A11/MF A03

Properties of fiber reinforced composite materials for aerospatial applications are examined from an economic and technological point of view with focus on automation and flexibility of manufacturing processes. The following topics were included: construction, testing and representation of resins and fibers; construction and calculation; production processes; machine development; component testing and quality assurance; and construction of a computer aided equipment for economic planning and evaluation of production facilities for fiber reinforced composite components. For individual titles, see N94-15255 through N94-15260.

N94-15255# Technische Hochschule, Aachen (Germany).
CONSTRUCTION, TESTING, AND REPRESENTATION OF RESIN AND FIBER REINFORCED MATERIALS [AUFBAU, PRUEFUNG, UND AUFMACHUNG DER HARZE UND FASERN]
R. Kaldenhoff *In its* Production Technology for Components from Nonmetallic Fiber Reinforced Materials 1992 p 4-41 In GERMAN (For primary document see N94-15254 03-24)
Avail: CASI HC A03/MF A03

Specific mechanical and chemical properties and material adapted treatments of raw materials for fiber reinforced composites fabrication are investigated. Systematic acquisition and evaluation of data such as modulus of elasticity were performed for each experiment. Surface examinations of glass, carbon and aramid fibers were carried out using electron and infrared spectroscopy, and electron and transmission electron microscopy. A fiber bundle pull-out test was performed for estimation of fiber matrix adhesion. Creep behavior of filaments and laminates from textile glass threads was investigated under constant loading. The influence of cooling velocity on crystallization temperature and enthalpy was characterized in carbon fiber reinforced polyether ether ketone. Thermochemical properties such as failure strength of high temperature thermoplastics and matrix material for fiber reinforced composites were studied. Delaminations with and without cracks, compression damages and failure behavior were observed in several textile reinforced composites with epoxy matrix subjected to tensile stress. ESA

N94-15256# Technische Hochschule, Aachen (Germany).
CONSTRUCTION AND CALCULATION [KONSTRUKTION UND BERECHNUNG]
J. Grittner *In its* Production Technology for Components from Nonmetallic Fiber Reinforced Materials 1992 p 42-78 In GERMAN (For primary document see N94-15254 03-24)
Avail: CASI HC A03/MF A03

Finite element, transfer, matrix, Fourier series, and finite difference methods are used for optimization of structure of fiber composite reinforced materials. A hybrid process was used with combination of transfer matrix and finite elements methods, for condensation of elastic node structures. The Southwell method, which is based on evaluation of load deformation behavior, was employed for stability studies of composite plates. Transfer matrices were developed for elastic, spatial node, and frame structures using Maxwell-Mohr methods. Delaminations and interlaminar stresses in multilayer composites were calculated for analytic characterization of matrix plastic behavior with consideration of hygrothermal boundary conditions. An articulation was modeled using beam theory for estimation of flexion and shear stresses. A program based on the combination of transfer matrix and finite differences methods was developed for stability, stiffness and strength problems in plates, and allowed the buckling critical load to be determined. Characteristic functions, deduced from short duration tractions tests under temperature and deformation rate variations, were calculated for consideration of temperature and humidity. The hybrid method is found to allow computation time to be significantly reduced. ESA

N94-15257# Technische Hochschule, Aachen (Germany).
PRODUCTION PROCESS [FERTIGUNGSPROZESS]
M. Goedel *In its* Production Technology for Components from Nonmetallic

Fiber Reinforced Materials 1992 p 80-128 In GERMAN (For primary document see N94-15254 03-24)
Avail: CASI HC A03/MF A03

Processes for development, production, and completion of components, with strong curvature and concave or convex contours, made of fiber reinforced composites with plastic matrix, are described. The focus is on the development of a mathematical model for description of the draping ability of textile surfaces. A multilayer multiaxial stacking of fibers was constructed so that a half finished fabric was obtained in which fiber orientation was fixed by a filament system. A quadratic draping ability tester was designed, in order to obtain a characteristic value for description of fabrics deformation behavior with consideration of roving and filament fineness. Immersion tests were carried out taking into account several laminates stackings and wrapping processes. Draping ability tests were performed with a facility integrated in a computer aided design system. Fiber orientation was defined so that test reproductibility was guaranteed. Draping ability was examined as a function of filament fineness and fabrics construction for a carbon material. It is concluded that fiber reinforced composites have a great usability potential despite their high production costs. ESA

N94-15258# Technische Hochschule, Aachen (Germany).
MACHINE DEVELOPMENT [MASCHINENENTWICKLUNG]
T. Baeumer *In its* Production Technology for Components from Nonmetallic Fiber Reinforced Materials 1992 p 130-167 In GERMAN (For primary document see N94-15254 03-24)
Avail: CASI HC A03/MF A03

A wrapping process with the perspective of an automated production and tape layering process is developed for manufacturing long fiber reinforced components whose contours have spherical curvature. A production facility was built. The facility was based on a portal robot particularly adapted to fabrication process integration because of its motions and measurement capabilities. It is noticed that wrapping process must be carefully implemented in order to avoid fiber damaging (spool departure and roll up on the wrapping core); eletromagnetic and capacitive sensors must be installed for short term recognition of perturbations such as fiber friction and failure and a strongly oscillating thread tension on a roving spool. The following studies are identified as necessary for tape layering: optimization of the tape layering head and transposition of properties of duroplastic prepreg systems, such as bonding mechanisms; and fiber orientation and viscosity influence, into practical treatment technologies. For heating of thermoplastic rovings, Nd:YAG laser was chosen because its wavelength allows the ray to be coupled in a fiber; alternative processes were examined, such as hot air heating of glass fiber/polyproyle and infrared and CO2 laser heating of carbon fiber/polyether ether ketone system. ESA

N94-15259# Technische Hochschule, Aachen (Germany).
COMPONENT TESTING AND QUALITY ASSURANCE [BAUTEILPRUEFUNG UND QUALITAETSSICHERUNG]
S. Ruemenapp *In its* Production Technology for Components from Nonmetallic Fiber Reinforced Materials 1992 p 168-206 In GERMAN (For primary document see N94-15254 03-24)
Avail: CASI HC A03/MF A03

A quality assurance system based on results of nondestructive tests, damage studies, and stiffness calculations is developed for fiber reinforced composites. All available material inspection processes were systematically compiled and analyzed in terms of computer integration, automation possibilities, and integrability in the production course. Detection capabilities of ultrasonic and X-ray inspection were qualitatively and quantitatively compared for flaw and delamination examination. Ultrasonic technology was studied in terms of frequency behavior and acoustic field, evaluating the reflected echo of the sound pulse at a glass plate with a frequency analyzer. Flaw recognition capabilities of holographic interferometry were investigated under thermal loading and internal failures were detected at material surface. Adhesion monitoring in autoclave was performed by dielectrometry; it is shown that electric conductivity increases with temperature and the process, combined with one line control of adhesion, is adequate for bonding cycle optimization. Impact behavior of sandwich structures was examined in order to understand damage initiation in fiber reinforced composites. A quality data base, which provides requirements of computer aided quality assurance and fiber technology, was developed. It is concluded that ultrasonic evaluation has the best potential for automation. ESA

N94-15260# Technische Hochschule, Aachen (Germany).
DEVELOPMENT OF A COMPUTER SUPPORTED INSTRUMENTATION FOR ECONOMIC PLANNING AND EVALUATION OF PRODUCTION FACILITIES FOR FIBER REINFORCED COMPOSITES ELEMENTS [ERSTELLUNG EINES RECHNERUNTERSTUETZTEN INSTRUMENTARIUMS ZUR WIRTSCHAFTLICHEN PLANUNG UND BEWERTUNG VON PRODUKTIONSANLAGEN FUER BAUTEILE AUS FASERVERBUNDWERKSTSTOFF]
C. Ullmann *In its* Production Technology for Components from Nonmetallic Fiber Reinforced Materials 1992 p 208-229 In GERMAN (For primary document see N94-15254 03-24)
Avail: CASI HC A03/MF A03

Classification and structuring of technological knowledge specific to fiber reinforced composites are performed and an object oriented depiction of planning relevant knowledge for wrapping, layup, and postprocessing technologies is included in an expert system. The influence factors on economy of composites facilities were determined for evaluation of investment alternatives. The evaluation module about the dynamic investment calculation was extended using developed prototypes for alternative solution concepts. Well known knowledge acquisition methods were analyzed, modified, and implemented considering their usability for fiber reinforced composites technology. Rapid prototyping was used for ascertaining fundamental properties of the expert system considering composite production facility configurations. ESA

N94-15275*# Old Dominion Univ., Norfolk, VA. Dept. of Civil Engineering.
POLYMER INFILTRATION STUDIES Progress Report, 1 Apr. - 30 Jun. 1993
Joseph M. Marchello Jun. 1993 42 p
(Grant NAG1-1067)
(NASA-CR-194494; NAS 1.26:194494) Avail: CASI HC A03/MF A01

Significant progress has been made on the preparation of carbon fiber composites using advanced polymer resins during the past three months. Current and ongoing research activities reported herein include: (1) Prepregger Hot Sled Operation; (2) Ribbonizing Powder-Impregnated Towpreg; (3) Textile Composites from Powder-Coated Towpreg: Role of Bulk Factor; and (4) Powder Curtain Prepreg Process. During the coming months research will be directed toward further development of the new powder curtain prepregging method and on ways to customize dry powder towpreg for textile and robotic applications in aircraft part fabrication. Studies of multi-tow powder prepregging and ribbon preparation will be conducted in conjunction with continued development of prepegging technology and the various aspects of composite part fabrication using customized towpreg. Also, work will continue on the analysis of the new solution prepegger. For individual titles, see N94-15276 through N94-15277.

N94-15276*# National Aeronautics and Space Administration. Langley Research Center, Hampton, VA.
A NEW NASA LaRC MULTI-PURPOSE PREPREGGING UNIT
S. P. Wilkinson (College of William and Mary, Williamsburg, VA.), J. M. Marchello (Old Dominion Univ., Norfolk, VA.), D. Dixon (Applied Poleramic, Inc., Benicia, CA.), and N. J. Johnston *In* Old Dominion Univ., Polymer Infiltration Studies Jun. 1993 8 p Reprinted from 38th International SAMPE Symposium, 1993 p 1-15 Symposium held 10-13 May 1993 (For primary document see N94-15275 03-24)
Avail: CASI HC A02/MF A01

A multi-purpose prepregging machine has been designed and built for NASA Langley Research Center. The machine has numerous advantages over existing units due to its various modular components. Each of these can be used individually or simultaneously depending on the required prepregging method. A reverse roll coater provides the ability to prepare thin films from typical hot-melt thermoset formulations. Also, if necessary, the design allows direct fiber impregnation within the reverse roll coater gap. Included in the impregnation module is a solution dip tank allowing the fabrication of thermoplastic prepregs from solution. The proceeding modules within the unit consist of four nip stations, two hot-plates, a hot-sled option and a high temperature oven. This paper describes the

advantages of such a modular construction and discusses the various processing combinations available to the prepregger. A variety of high performance prepreg material systems were produced on IM7 (Hercules) carbon fiber. These included LaRC RP46, a PMR-type resin processed from methanol and two polyamide acids, LaRC IA and LaRC ITPI, prpregged from N-methyl pyrrolidinone (NMP). Parameters involved in the production of these prepreg materials are presented as are the mechanical properties of the resulting good quality laminates. A brief introduction into the existing prepregging science is presented. Topics relating to solution prepregging are identified with a focus on the current research effort and its future development. Author

N94-15277*# National Aeronautics and Space Administration. Langley Research Center, Hampton, VA.
PROCESSING, PROPERTIES AND APPLICATIONS OF COMPOSITES USING POWDER-COATED EPOXY TOWPREG TECHNOLOGY
T. D. Bayha (Lockheed Aeronautical Systems Co., Marietta, GA.), P. P. Osborne (Lockheed Aeronautical Systems Co., Marietta, GA.), T. P. Thrasher (Lockheed Aeronautical Systems Co., Marietta, GA.), J. T. Hartness (BASF Structural Materials, Inc., Anaheim, CA.), N. J. Johnston, J. M. Marchello (Old Dominion Univ., Norfolk, VA.), and M. K. Hugh (Old Dominion Univ., Norfolk, VA.) *In* Old Dominion Univ., Polymer Infiltration Studies Jun. 1993 21 p Presented at NASA's Fourth Advanced Composites Technology Conference, Salt Lake City, UT, Jun. 1993 (For primary document see N94-15275 03-24)
Avail: CASI HC A03/MF A01

Composite manufacturing using the current prepregging technology of impregnating liquid resin into three-dimensionally reinforced textile preforms can be a costly and difficult operation. Alternatively, using polymer in the solid form, grinding it into a powder, and then depositing it onto a carbon fiber tow prior to making a textile preform is a viable method for the production of complex textile shapes. The powder-coated towpreg yarn is stable, needs no refrigeration, contains no solvents and is easy to process into various woven and braided preforms for later consolidation into composite structures. NASA's Advanced Composites Technology (ACT) program has provided an avenue for developing the technology by which advanced resins and their powder-coated preforms may be used in aircraft structures. Two-dimensional braiding and weaving studies using powder-coated towpreg have been conducted to determine the effect of resin content, towpreg size and twist on textile composite properties. Studies have been made to customize the towpreg to reduce friction and bulk factor. Processing parameters have been determined for three epoxy resin systems on eight-harness satin fabric, and on more advanced 3-D preform architectures for the downselected resin system. Processing effects and the resultant mechanical properties of these textile composites will be presented and compared. Author

N94-15345* National Aeronautics and Space Administration, Washington, DC.
BETTER AIRPLANE WINGS (Videotape)
Nov. 1989 Videotape: 3 min. 23 sec. playing time, in color, with sound (NASA-TM-109446; NONP-VT-93-190243) Avail: CASI VHS A01/BETA A22

The videotape discusses the new composites that will be used to create lighter yet stronger aircraft wings. CASI

N94-15484*# North Carolina State Univ., Raleigh. Dept. of Textile Engineering, Chemistry and Science.
ILLUSTRATED GLOSSARY OF TEXTILE TERMS FOR COMPOSITES
Christopher M. Pastore Sep. 1993 32 p
(NASA Order L-18543-D; RTOP 510-02-11-08)
(NASA-CR-191539; NAS 1.26:191539) Avail: CASI HC A03/MF A01

A glossary was developed to define textile terminology applicable to the manufacture of composites. Terms describing fabric structure were illustrated for clarity. Descriptive terms for defects from both textile and composites industry were included. Author (revised)

N94-15528# Rensselaer Polytechnic Inst., Troy, NY.
HIGH TEMPERATURE ADVANCED STRUCTURAL COMPOSITES. VOLUME 2: CERAMIC MATRIX COMPOSITES, FIBER PROCESSIING AND PROPERTIES, AND INTERFACES Final Report, 1 Oct. 1986 - 13 Jun. 1992
George J. Dvorak and R. J. Diefendorf 2 Apr. 1993 335 p
(Contract N00014-86-K-0770)
(AD-A267023) Avail: CASI HC A15/MF A03

Final results obtained on the High Temperature Advanced Structural Composites Program at Rensselaer Polytechnic Institute are described in three volumes. Volume one contains the Executive Summary and reprints of papers on Intermetallic Compounds. Volume two contains reprints of papers on Ceramic Matrix Composites, Fiber Processing and Properties, and on Interfaces. The third volume contains reprints of papers on Mechanics. DTIC

N94-15626# Rensselaer Polytechnic Inst., Troy, NY.
HIGH TEMPERATURE ADVANCED STRUCTURAL COMPOSITES. VOLUME 3: MECHANICS Final Report, 1 Oct. 1986 - 13 Jun. 1992
George J. Dvorak and R. J. Diefendorf 2 Apr. 1993 455 p
(Contract N000014-86-K-0770)
(AD-A267024) Avail: CASI HC A20/MF A04

The final results obtained on the High Temperature Advanced Structural Composites Program at Rensselaer Polytechnic Institute are described in three volumes. Volume one contains the Executive Summary and reprints of papers on Intermetallic Compounds. Volume two contains reprints of papers on Ceramic Matrix Composites, Fiber Processing and Properties and on Interfaces. The third volume contains reprints of papers on Mechanics. DTIC

N94-15699# Admiralty Research Establishment, Gosport (England).
SOUND RADIATION FROM INFINITE LAMINATED COMPOSITE SHELL WITH PERIODIC RIB STIFFENING
J. H. James Oct. 1992 29 p
(DRA/TM(USGR)92326; BR315174; ETN-93-94502) Avail: CASI HC A03/MF A01

A theory of sound radiation from an infinite cylindrical shell which is stiffened periodically by ribs is given. Both shell and ribs are laminated composites. The shell is modeled by the differential equations of a thin shell theory. The flexible ribs, which exert both forces and moments on the shell's surface, are modeled by thin conical shell finite elements; degrees of freedom other than those at the shell's surface are removed by receptance methods. Excitations are time harmonic mechanical forces at arbitrary points on the shell's surface and ribs, and acoustic monopoles in the exterior and interior fluids. ESA

N94-15835 Rensselaer Polytechnic Inst., Troy, NY.
HIGH TEMPERATURE ADVANCED STRUCTURAL COMPOSITES. VOLUME 1: EXECUTIVE SUMMARY AND INTERMETALLIC COMPOUNDS Final Report, 1 Oct. 1986 - 13 Jun. 1992
George J. Dvorak and R. J. Diefendorf 2 Apr. 1993 335 p Limited Reproducibility: More than 20% of this document may be affected by microfiche quality
(Contract N00014-86-K-0770)
(AD-A267022) Avail: CASI HC A15

Final results obtained on the High Temperature Advanced Structural Composites Program at Rensselaer Polytechnic Institute are described in three volumes. Volume one contains the Executive Summary and reprints of papers on Intermetallic Compounds. Volume two contains reprints of papers on Ceramic Matrix Composites, Fiber Processing and Properties, and on Interfaces. The third volume contains reprints of papers on Mechanics. DTIC

N94-15878*# National Aeronautics and Space Administration. Langley Research Center, Hampton, VA.
METHOD AND APPARATUS FOR NON-DESTRUCTIVE EVALUATION OF COMPOSITE MATERIALS WITH CLOTH SURFACE IMPRESSIONS Patent Application
Eric Irvine Madaras, inventor (to NASA) 16 Aug. 1993 36 p
(NASA-Case-LAR-14535-1; NAS 1.71:LAR-14535-1;
US-Patent-Appl-SN-110278) Avail: CASI HC A03/MF A01

A method and related apparatus for non-destructive evaluation of composite materials by determination of the quantity known as Integrated Polar Backscatter, which avoids errors caused by surface texture left by cloth impressions by identifying frequency ranges associated with peaks in a power spectrum for the backscattered signal, and removing such frequency

ranges from the calculation of Integrated Polar Backscatter for all scan sites on the composite material is presented. NASA

N94-15926*# National Aeronautics and Space Administration. Ames Research Center, Moffett Field, CA.
IMPROVED COMPOSITE FLEXIBLE BLANKET INSULATION Patent Application
Demetrius A. Kourtides, inventor (to NASA) and David M. Lowe, inventor (to NASA) (San Jose State Univ., Moffett Field, CA.) 1 Aug. 1991 53 p
(NASA-Case-ARC-11955-1-CU; NAS 1.71:ARC-11955-1-CU;
US-Patent-Appl-SN-739026) Avail: CASI HC A04/MF A01

An improved composite flexible blanket insulation is presented comprising top silicon carbide having an interlock design, wherein the reflective shield is composed of single or double aluminized polyimide and wherein the polyimide film has a honeycomb pattern. NASA

N94-15929*# National Aeronautics and Space Administration. Lewis Research Center, Cleveland, OH.
METHOD OF PRODUCING A SILICON CARBIDE FIBER REINFORCED STRONTIUM ALUMINOSILICATE GLASS-CERAMIC MATRIX COMPOSITE Patent Application
Narottam P. Bansal, inventor (to NASA) 16 Sep. 1993 9 p
(NASA-Case-LEW-15263-2; NAS 1.71:LEW-15263-2;
US-Patent-Appl-SN-128007) Avail: CASI HC A02/MF A01

A SrO-Al2O3 - 2SrO2 (SAS) glass ceramic matrix is reinforced with CVD SiC continuous fibers. This material is prepared by casting a slurry of SAS glass powder into tapes. Mats of continuous CVD-SiC fibers are alternately stacked with the matrix tapes. This tape-mat stack is warm-pressed to produce a 'green' composite. Organic constituents are burned out of the 'green' composite, and the remaining interim material is hot pressed. NASA

N94-16008# Oak Ridge National Lab., TN.
NEXTEL(TRADEMARK)/SiC COMPOSITES USING FORCED CHEMICAL VAPOR INFILTRATION
B. L. Weaver (Minnesota Mining and Mfg. Co., Saint Paul.), R. A. Lowden, J. C. McLaughlin, D. P. Stinton, T. M. Besmann, and O. J. Schwarz 1993 9 p Presented at the HTCMC Meeting, France, 20-23 Sep. 1993
(Contract DE-AC05-84OR-21400)
(DE93-013532; CONF-9309149-1) Avail: CASI HC A02/MF A01

Oxide fiber-reinforced silicon carbide matrix composites were fabricated employing the forced-flow, thermal gradient chemical vapor infiltration (FCVI) process. Composites using Nextel(trademark) fibers of varying composition were prepared to investigate the effectiveness of each Nextel(trademark) fiber as a reinforcement for the given matrix. A carbon interface coating was used for the baseline materials, however, alternate interlayers with improved oxidation resistance were also explored. Room-temperature flexure strengths of as-fabricated composites and specimens heated in air at 1273 K were measured and compared to results for other SiC-matrix composites. DOE

N94-16017# Oak Ridge National Lab., TN.
MODELING THE THERMAL CONDUCTIVITY OF FIBER-REINFORCED CERAMIC COMPOSITES
S. C. Beecher and R. B. Dinwiddie 1993 9 p Presented at the 17th Annual Conference on Composites and Advanced Ceramics, Cocoa Beach, FL, 11-15 Jan. 1993
(Contract DE-AC05-84OR-21400)
(DE93-015340; CONF-930164-12) Avail: CASI HC A02/MF A01

A review of models for the prediction of the thermal conductivity of uni-directional fiber-reinforced composites will be presented. The ability of these models to give an accurate prediction of the composite thermal conductivity depends on the amount of information known about the constituent phase properties under the assumption that these properties do not change as a result of processing. Also presented are models that take into account the effects of fiber coatings. DOE

N94-16057# Argonne National Lab., IL. Materials and Components Technology Div.
MECHANICAL PROPERTIES OF MAGNESIUM AMMONIUM PHOSPHATE CEMENTS AND THEIR ZEOLITE COMPOSITES
A. S. Wagh, D. Singh, W. Subhan, and N. Chawla Apr. 1993 23 p Presented at the 95th Annual Meeting of the American Ceramic Society, Cincinnati, OH, 18-22 Apr. 1993
(Contract W-31-109-eng-38)
(DE93-015155; ANL/MCT/CP-78063; CONF-930438-21) Avail: CASI HC A03/MF A01

Phosphate-bonded cements have been proposed as candidates for solidification and stabilization of mixed wastes. Magnesium ammonium phosphate (MAP) has been investigated as a candidate material. Detailed physical and mechanical properties of MAP cement are reported. It is synthesized by the route of reaction of calcined MgO and ammonium phosphate solution. Samples are made by setting the cement at room temperature and slight pressure. The porosity is reduced to approximately 11% by impregnation of ammonium phosphate solution. Detailed mechanical properties such as flexural strength, fracture toughness, and compression strength are reported and fracture mechanical analyses supported with scanning electron microscopy are provided. Properties of composites of these cements with zeolites, which may be used for containment of radioactive as well as chemical waste are studied. We demonstrate that the strengths of these composites compare well with portland cement even after 50% loading of zeolites. Fracture mechanical implications of such loadings are given. DOE

N94-16065# Oak Ridge National Lab., TN.
OVERVIEW OF CHEMICAL VAPOR INFILTRATION
T. M. Besmann, D. P. Stinton, and R. A. Lowden 1993 16 p Presented at the International Conference on High Temperature Ceramic Matrix Composites, Bordeaux, France, 20-25 Sep. 1993
(Contract DE-AC05-84OR-21400)
(DE93-015440; CONF-930961-2) Avail: CASI HC A03/MF A01

Chemical vapor infiltration (CVI) is developing into a commercially important method for the fabrication of continuous filament ceramic composites. Current efforts are focused on the development of an improved understanding of the various processes in CVI and its modeling. New approaches to CVI are being explored, including pressure pulse infiltration and microwave heating. Material development is also proceeding with emphasis on improving the oxidation resistance of the interfacial layer between the fiber and matrix. This paper briefly reviews these subjects, indicating the current state of the science and technology. DOE

N94-16158# Pacific Northwest Lab., Richland, WA.
ENVIRONMENTAL EFFECTS ON ELEVATED TEMPERATURE SUBCRITICAL CRACK GROWTH OF SiC/SiC COMPOSITES
C. H. Henager, Jr. and R. H. Jones 1993 10 p Presented at the Conference on Critical Issues in the Development of High Temperature Structural Materials, Kona, HI, 7-12 Mar. 1993
(Contract DE-AC06-76RL-01830)
(DE93-015688; PNL-SA-21693; CONF-930317-1) Avail: CASI HC A02/MF A01

Time-dependent crack growth measurements of ceramic composites in varying environments were conducted on materials consisting of chemical vapor infiltrated SiC reinforced with Nicalon fibers having C-interfaces. Crack velocities are determined as a function of applied stress intensity and time for varying O2 levels. Results are presented for crack velocity/stress intensity relationships in pure Ar and in Ar plus 2000-, 5000-, 10,000-, and 20,000-ppM O2 atmospheres at 1100C. A 2D micromechanics model is used to represent the time-dependence of observed crack bridging events and to rationalize the observed phenomena. DOE

N94-16440# Louisiana State Univ., Baton Rouge. Dept. of Civil Engineering.
ANISOTROPIC DAMAGE MECHANICS MODELING IN METAL MATRIX COMPOSITES Final Report, 1 Apr. 1992 - 31 Mar. 1993
George Z. Voyiadjis, Peter I. Kattan, Anthony R. Venson, and Taehyo Park 15 May 1993 142 p
(Grant AF-AFOSR-0227-90)
(AD-A266328; AFOSR-93-0431TR) Avail: CASI HC A07/MF A02

A consistent and systematic theory is developed for the analysis of damage mechanisms in metal matrix composites (MMC's). The theory involves both analytical and experimental procedures for the quantification of certain types of damage in MMC's. The analytical model involves both overall and local approaches to characterize damage in these materials. A series of experiments are conducted for micro- and macro-structural

characterization of the MMC. Experiments were conducted on a titanium aluminide SiC-reinforced metal matrix composite. Center-cracked plates with laminate layups of (0/90)s, and (+/-45)s were tested under uniaxial tension. In order to investigate and model damage evolution, each of the specimens is loaded to different load levels ranging from fracture load down to 70% of the fracture load. Scanning electron microscopy (SEM) is performed on representative cross-sections of the damaged specimens. The measured crack densities are then used to define the damage parameters that are used in the theoretical model. DTIC

N94-16461# Oak Ridge National Lab., TN.
EVALUATION OF THE INTERFACIAL MECHANICAL PROPERTIES IN FIBER-REINFORCED CERAMIC COMPOSITES
M. K. Ferber, A. A. Wereszczak, L. Riester, R. A. Lowden, and K. K. Chawla (New Mexico Inst. of Mining and Technology, Socorro.) 1993 40 p Presented at the 17th Annual Conference on Composites and Advanced Ceramics, Cocoa Beach, FL, 11-15 Jan. 1993
(Contract DE-AC05-84OR-21400)
(DE93-015494; CONF-930164-10) Avail: CASI HC A03/MF A01

The application of a micro-indentation technique to the measurement of interfacial properties in fiber reinforced ceramic composites is examined. Specific fiber/matrix systems included SiC/glass, SiC/macro-defect-free (MDF) cement, SiC/SiC, and mullite/glass. The effect of fiber coatings upon the interfacial properties was also investigated. These properties which included the debond strength, interfacial shear stress, and residual axial fiber stress were evaluated by measuring the force-displacement curves generated during load-unload cycles. Estimates of these three stress values were obtained by matching the experimental force-displacement curves with data predicted from an existing model. In general the SiC/glass composites exhibited the lowest values of the interfacial shear and debond stresses. The sliding characteristics of the SiC/MDF cement and SiC/SiC composites were strongly influenced by the residual axial stress and the nature of the fiber coating. In the case of the mullite/glass composite, the high values of the interfacial shear and debond stresses reduced the measurement sensitivity, thereby increasing the uncertainty in the estimates of the interfacial properties. DOE

N94-16483# California Univ., Santa Barbara. Materials Dept.
THE PROCESSING AND MECHANICAL PROPERTIES OF HIGH TEMPERATURE/HIGH PERFORMANCE COMPOSITES. BOOK 1: COONSTITUENT PROPERTIES OF COMPOSITES Annual Report, Mar. 1992 - Apr. 1993
Anthony G. Evans and Frederick A. Leckie 28 Feb. 1993 336 p
(Contract N00014-92-J-1808)
(AD-A266394) Avail: CASI HC A15/MF A03

The partial contents are as follows: a microcomposite test procedure for evaluating the constituent properties of ceramic matrix composites; design, analysis, and application of an improved push-through test for the measurement of interface properties in composites; fiber bundle push-out: a technique for the measurement of interfacial sliding properties; mechanics of the fiber pushout test; effects of fiber roughness on interface sliding in composites; fiber coating concepts for brittle matrix composites; preliminary assessment of mica as high-temperature fiber coating for SiC composites; models for metal/ceramic interface fracture; mode 2 fracture toughness of a brittle adhesive layer; and cracking of thin bonded films in residual tension. DTIC

N94-16484# California Univ., Santa Barbara. Materials Dept.
THE PROCESSING AND MECHANICAL PROPERTIES OF HIGH TEMPERATURE/HIGH PERFORMANCE COMPOSITES. BOOK 2: COONSTITUENT PROPERTIES AND MACROSCOPIC PERFORMANCE Annual Report, Mar. 1992 - Apr. 1993
Anthony G. Evans and Frederick A. Leckie Apr. 1993 541 p
(Contract N00014-92-J-1808)
(AD-A266395) Avail: CASI HC A23/MF A04

The partial contents are as follows: a methodology for relating the tensile constitutive behavior of ceramic matrix composites to constituent properties; damage and failure in unidirectional ceramic-matrix composites; a self-consistent model for multi-fiber crack bridging; damage mechanisms and the mechanical properties of a laminated 0/90 ceramic/matrix composite; mechanical properties of continuous-fiber-reinforced carbon matrix composites and relationships to constituent properties; notch effects in carbon matrix composites; the mechanics of failure of silicon carbide fiber-reinforced glass-matrix composites; stochastic aspects of matrix cracking in brittle matrix composites; and the role of fiber bridging in the delamination resistance of fiber-reinforced composites. DTIC

N94-16485# California Univ., Santa Barbara. Materials Dept.
THE PROCESSING AND MECHANICAL PROPERTIES OF HIGH TEMPERATURE/HIGH PERFORMANCE COMPOSITES. BOOK 3: COONSTITUENT PROPERTIES AND MACROSCOPIC PERFORMANCE Annual Report, Mar. 1992 - Apr. 1993
Anthony G. Evans and Frederick A. Leckie Apr. 1993 475 p
(Contract N00014-92-J-1808)
(AD-A266396) Avail: CASI HC A20/MF A04

The partial contents are as follows: mode 1 fatigue cracking in a fiber reinforced metal matrix composite; fatigue crack growth in fiber-reinforced metal-matrix composites; the anisotropic mechanical properties of a Ti matrix composite reinforced with SiC fibers; models for the creep of ceramic matrix composite materials; the creep and fracture resistance of gamma-TiAl reinforced with Al2O3 fibers; the mechanical properties of Al alloys reinforced with continuous Al2O3 fibers; the mode fracture resistance of unidirectional fiber-reinforced aluminum matrix composites; the ultimate tensile strength of metal and ceramic-matrix composites; cracking and damage mechanisms in ceramic/metal multilayers. DTIC

N94-16528# California Univ., Santa Barbara. Materials Dept.
THE PROCESSING AND MECHANICAL PROPERTIES OF HIGH TEMPERATURE/HIGH PERFORMANCE COMPOSITES. BOOK 4: COONSTITUTIVE LAWS AND DESIGN Annual Report, Mar. 1992 - Apr. 1993
Anthony G. Evans and Frederick A. Leckie Apr. 1993 483 p
(Contract N00014-92-J-1808)
(AD-A266397) Avail: CASI HC A21/MF A04

The partial contents are as follows: remarks on crack-bridging concepts; notch ductile-to-brittle transition due to localized inelastic band; on the tensile strength of a fiber-reinforced ceramic composite containing a crack-like flaw; mechanical behavior of a continuous fiber-reinforced aluminum matrix composite subjected to transverse and thermal loading; modeling of anisotropic behavior of weakly bonded fiber reinforced MMC's; transverse ductility of metal matrix composites; localization due to damage in two direction fiber reinforced composites; on the notch-sensitivity and toughness of a ceramic composite; thermal, mechanical, and creep behavior of metal matrix composite; and the treatment of fatigue and damage accumulation in composite design. DTIC

N94-16529# California Univ., Santa Barbara. Materials Dept.
THE PROCESSING AND MECHANICAL PROPERTIES OF HIGH TEMPERATURE/HIGH PERFORMANCE COMPOSITES. BOOK 5: PROCESSING AND MISCELLANEOUS PROPERTIES Annual Report, Mar. 1992 - Apr. 1993
Anthony G. Evans and Frederick A. Leckie Apr. 1993 501 p
(Contract N00014-92-J-1808)
(AD-A266398) Avail: CASI HC A22/MF A04

The partial contents are as follows: computer aided manufacturing through selective material deposition; environmentally compatible double coating concepts for sapphire fiber reinforced y-TiAl; modeling the fracture of fibers during metal matrix composite consolidation; the effect of processing on the interface structure/property relationship in a Ti 24Al 11 Nb (at%) composite; the evolution of metastable Bf borides in a Ti-Al-B alloy; measurement of residual stresses in sapphire fiber composites using optical fluorescence; compressive failure of fiber composites; compressive failure of fiber composite: The roles of multi-axial loading and creep; and mechanical properties of partially dense alumina produced from powder compacts. DTIC

N94-16534 Department of the Navy, Washington, DC.
PROCESS FOR SHAPING ARTICLES FROM ELECTROSETTING COMPOSITIONS Patent
Ronald P. Reitz, inventor (to Navy) 16 Mar. 1993 10 p Filed 11 Sep. 1989
(AD-D015787; US-Patent-5,194,181; US-Patent-Appl-SN-405178; US-Patent-Class-252-500) Avail: US Patent and Trademark Office

This invention is a phase changing composition for making articles that

can be influenced as to shape and cure time by the application of an electric field. Also disclosed are apparatus and processes for using the material. The composition is characterized in that under the influence of an electrostatic field, the cure time of the composition is significantly shorter. DTIC

N94-16537 Department of the Navy, Washington, DC.
ELECTROSTATIC FIBER SPREADER INCLUDING A CORONA DISCHARGE DEVICE Patent
Jonathan M. Peritt, inventor (to Navy), Richard Everett, inventor (to Navy), and Alan Edelstein, inventor (to Navy) 6 Apr. 1993 6 p Filed 5 Nov. 1991
(AD-D015793; US-Patent-5,200,620; US-Patent-Appl-SN-788018; US-Patent-Class-250-324) Avail: US Patent and Trademark Office

A fiber spreader is provided which reduces fiber damage that occurs during spreading. The fiber spreader includes a thin electrically grounded support sheet for supporting a layer of fibers on one surface thereof. The fibers supported on the support sheet are guided by a plurality of guide rollers past at least one corona discharge region at which the fibers are spread substantially uniformly. A motor driven spool advances the support sheet past the corona discharge region. The fibers are attached to the support sheet by an electrostatic attraction. The guide rollers are positioned so as to provide at least one region in which the sheet and the fibers are physically separated to allow for the uniform spreading of the fibers. After the fibers are spread, the fibers and the support sheet are united again and collected on a motor-driven spool. DTIC

N94-16569# Georgia Inst. of Tech., Atlanta.
CONTINUOUS FABRICATION OF SiC FIBER TOWS BY CHEMICAL VAPOR DEPOSITION Final Report, 1 Sep. 1991 - 31 Dec. 1992
W. J. Lackey, J. A. Hanigofsky, G. B. Freeman, R. D. Hardin, and B. N. Beckloff 1 Jan. 1993 106 p
(AD-A266460; GIT-A-9056; WL-TR-93-4013) Avail: CASI HC A06/MF A02

The objective of this 15-month effort was to determine the feasibility of preparing small diameter SiC fiber tows by chemical vapor deposition for use as reinforcing fibers in ceramic and metal matrix composites. The proposed goal of codepositing SiC + Si3N4 was modified 2 months into the project in order to concentrate on fiber coating technology for SiC fiber development only. Our approach was to develop spreading techniques for filaments of the substrate tow so that SiC could be rapidly deposited without bonding the filaments together. Following some initial experiments, a statistical processing study was completed to define processing conditions where the desired 5 micrometers SiC coating thickness would be achieved. Processing-property correlations were determined using multiple regression analysis. Stress calculations were used to aide in substrate selection--the carbon fiber which had the minimal fiber/coating stress due to thermal expansion mismatch was determined to be the Amoco T-300, unsized, and untwisted fiber. Several fiber spreading techniques were evaluated to minimize fiber agglomeration. Cyclic tension, in conjunction with gas jets or stationary and moving rollers was determined to be ineffective for spreading the fiber tow. The most promising results, however, were obtained from electromagnetic spreading of the fiber tow. DTIC

N94-16795 Universal Technology Corp., Dayton, OH.
STRESS ANALYSIS OF LAMINATED COMPOSITES WITH PREFORMED HOLES. PART 1: SINGLE PLIES WITH EMBEDDED MATERIAL DISCONTINUITIES Final Report, 26 May - 30 Sep. 1992
Endel V. Iarve 30 Sep. 1992 28 p Limited Reproducibility: More than 20% of this document may be affected by microfiche quality
(Contract F33615-89-C-5609)
(AD-A266524; WL-TR-93-4063-Pt-1) Avail: Issuing Activity (Defense Technical Information Center (DTIC))

An analytical and experimental study was conducted to develop a computational model adequate for stress analyses of AS4/3501-6 composite plates containing preformed 1/4 diameter holes, which were found in previous and parallel experimental studies to possess superior open-hole tension and compression strengths relative to composites with drilled holes of equal diameter. The preformed-hole composites contain embedded material discontinuities resulting from the interpenetration of adjacent composite layers in the actual, laminated systems. The effort reported addresses the initial development of the model for single layers containing the material discontinuities present in laminates. The analytical method is suitable for adaptation to problems involving smart materials, electronic packaging, micro-electromechanical systems, and joining/fastening. The proposed computational model is based on spline approximations of the displacement components. Solutions were obtained relative to curvilinear coordinates that mapped the preformed hole region onto a rectangular region and the embedded material boundaries into coordinate lines. DTIC

N94-16836*# Texas Univ., San Antonio. Div. of Engineering.
EFFECT OF IMPACT DAMAGE AND OPEN HOLE ON COMPRESSIVE STRENGTH OF HYBRID COMPOSITE LAMINATES Final Report, 1 Jun. 1992 - 31 May 1993
Clement Hiel (National Aeronautics and Space Administration. Ames Research Center, Moffett Field, CA.) and H. F. Brinson 31 May 1993 77 p
(Contract NCC2-724)
(NASA-CR-194603; NAS 1.26:194603) Avail: CASI HC A05/MF A01

Impact damage tolerance is a frequently listed design requirement for composites hardware. The effect of impact damage and open hole size on laminate compressive strength was studied on sandwich beam specimens which combine CFRP-GFRP hybrid skins and a syntactic foam core. Three test specimen configurations have been investigated for this study. The first two were sandwich beams which were loaded in pure bending (by four point flexure). One series had a skin damaged by impact, and the second series had a circular hole machined through one of the skins. The reduction of compressive strength with increasing damage (hole) size was compared. Additionally a third series of uniaxially loaded open hole compression coupons were tested to generate baseline data for comparison with both series of sandwich beams. For individual titles, see N94-16837 through N94-16837.

N94-16837*# National Aeronautics and Space Administration. Ames Research Center, Moffett Field, CA.
LOW AND HIGH VELOCITY IMPACT RESPONSE OF THICK HYBRID COMPOSITES
Clement Hiel and Ori Ishai *In* Texas Univ., Effect of Impact Damage and Open Hole on Compressive Strength of Hybrid Composite Laminates 31 May 1993 p 1149-1159 (For primary document see N94-16836 03-24)
Avail: CASI HC A03/MF A01

The effects of low and high velocity impact on thick hybrid composites (THC's) were experimentally compared. Test Beams consisted of CFRP skins which were bonded onto an interleaved syntactic foam core and cured at 177 C (350 F). The impactor tip for both cases was a 16 mm (0.625 inch) steel hemisphere. In spite of the order of magnitude difference in velocity ranges and impactor weights, similar relationships between impact energy, damage size, and residual strength were found. The dependence of the skin compressive strength on damage size agree well with analytical open hole models for composite laminates and may enable the prediction of ultimate performance for the damaged composite, based on visual inspection. Author

N94-16845*# National Aeronautics and Space Administration. Langley Research Center, Hampton, VA.
FIBER-TEX 1992: THE SIXTH CONFERENCE ON ADVANCED ENGINEERING FIBERS AND TEXTILE STRUCTURES FOR COMPOSITES
John D. Buckley, ed. Washington Aug. 1993 357 p Conference held in Philadelphia, PA, 27-29 Oct. 1992 Sponsored by DOD; Drexel Univ.; Clemson Univ.; and North Carolina State Univ.
(RTOP 505-63-50-05)
(NASA-CP-3211; L-17266; NAS 1.55:3211) Avail: CASI HC A16/MF A03

The FIBER-TEX 1992 proceedings contain the papers presented at the conference held on 27-29 Oct. 1992 at Drexel University. The conference was held to create a forum to encourage an interrelationship of the various disciplines involved in the fabrication of materials, the types of equipment, and the processes used in the production of advanced composite structures. Topics discussed were advanced engineering fibers, textile processes and structures, structural fabric production, mechanics and characteristics of woven composites, and the latest requirements for the use of textiles in

the production of composite materials and structures as related to global activities focused on textile structural composites. For individual titles, see N94-16846 through N94-16865.

N94-16846*# National Aeronautics and Space Administration. Langley Research Center, Hampton, VA.

AN OVERVIEW OF THE NASA TEXTILE COMPOSITES PROGRAM

H. Benson Dexter *In its* FIBER-TEX 1992: The Sixth Conference on Advanced Engineering Fibers and Textile Structures for Composites Aug. 1993 p 1-31 (For primary document see N94-16845 03-24)

Avail: CASI HC A03/MF A03

The NASA Langley Research Center is conducting and sponsoring research to explore the benefits of textile reinforced composites for civil transport aircraft primary structures. The objective of this program is to develop and demonstrate the potential of affordable textile reinforced composite materials to meet design properties and damage tolerance requirements of advanced aircraft structures. In addition to in-house research, the program includes major participation by the aircraft industry and aerospace textile companies. The major program elements include development of textile preforms, processing science, mechanics of materials, experimental characterization of materials, and development and evaluation of textile reinforced composite structural elements and subcomponents. The NASA Langley in-house research is focused on science-based understanding of resin transfer molding (RTM), development of powder-coated towpreg processes, analysis methodology, and development of a performance database on textile reinforced composites. The focus of the textile industry participation is on development of multidirectional, damage-tolerant preforms, and the aircraft industry participation is in the areas of innovative design concepts, cost-effective fabrication, and testing of textile reinforced composite structural elements and subcomponents. Textile processes such as 3-D weaving, 2-D and 3-D braiding, and knitting/stitching are being compared with conventional laminated tape processes for improved damage tolerance. Through-the-thickness reinforcements offer significant damage tolerance improvements. However, these gains must be weighed against potential loss in in-plane properties such as strength and stiffness. Analytical trade studies are underway to establish design guidelines for the application of textile material forms to meet specific loading requirements. Fabrication and testing of large structural components are required to establish the full potential of textile reinforced composite materials. The goals of the NASA Langley-sponsored research program are to demonstrate technology readiness with subscale composite components by 1995 and to verify the performance of full-scale composite primary aircraft structural components by 1997. The status of textile reinforced composite structural elements under development by Boeing, Douglas, Lockheed, and Grumman are presented. Included are braided frames and woven/stitched wing and fuselage panels. Author

N94-16847*# Ford Motor Co., Dearborn, MI. Materials Science Dept.

TECHNO-ECONOMIC REQUIREMENTS FOR AUTOMOTIVE COMPOSITES

Scot Arnold *In* NASA. Langley Research Center, FIBER-TEX 1992: The Sixth Conference on Advanced Engineering Fibers and Textile Structures for Composites Aug. 1993 p 33-48 (For primary document see N94-16845 03-24)

Avail: CASI HC A03/MF A03

New technology generally serves two main goals of the automotive industry: one is to enable vehicles to comply with various governmental regulations and the other is to provide a competitive edge in the market. The latter goal can either be served through improved manufacturing and design capabilities, such as computer aided design and computer aided manufacturing, or through improved product performance, such as anti-lock braking (ABS). Although safety features are sometimes customer driven, such as the increasing use of airbags and ABS, most are determined by regulations as outlined by the Federal Motor Vehicle Safety Standards (FMVSS). Other standards, set by the Environmental Protection Agency, determine acceptable levels of emissions and fuel consumption. State governments, such as in California, are also setting precedent standards, such as requiring manufacturers to offer zero-emission vehicles as a certain fraction of their sales in the state. The drive to apply new materials in the automobile stems from the need to reduce weight and improve fuel efficiency. Topics discussed include: new lightweight materials; types of automotive materials; automotive composite applications; the role for composite materials in automotive applications; advantages and disadvantages of composite materials; material substitution economics; economic perspective; production economics; and composite materials production economics.

Author (revised)

N94-16848*# Katholieke Univ. te Leuven (Belgium). Dept. of Metallurgy and Materials Engineering.

RESEARCH IN TEXTILE COMPOSITES AT KU, LEUVEN

Ignaas Verpoest, Jan Ivens, Aart WillemvanVuure, and Vassilios Efstratiou *In* NASA. Langley Research Center, FIBER-TEX 1992: The Sixth Conference on Advanced Engineering Fibers and Textile Structures for Composites Aug. 1993 p 49-68 (For primary document see N94-16845 03-24)

Avail: CASI HC A03/MF A03

An overview is presented of the research on textile composites at Katholieke Universiteit Leuven. Three dimensionally woven sandwich fabric preforms are investigated for delamination resistant sandwich structures, velvet woven 2.5 dimensional fabrics for delamination resistant laminates, and knitted fabrics with good drapability for laminates of complex shape.

Author (revised)

N94-16849*# ICI Fiberite, Greenville, TX.

DESIGN AND COST DRIVERS IN 2-D BRAIDING

Alberto Morales *In* NASA. Langley Research Center, FIBER-TEX 1992: The Sixth Conference on Advanced Engineering Fibers and Textile Structures for Composites Aug. 1993 p 69-77 (For primary document see N94-16845 03-24)

Avail: CASI HC A02/MF A03

Fundamentally, the braiding process is a highly efficient, low cost method for combining single yarns into circumferential shapes, as evidenced by the number of applications for continuous sleeving. However, this braiding approach cannot fully demonstrate that it can drastically reduce the cost of complex shape structural preforms. Factors such as part geometry, machine design and configuration, materials used, and operating parameters are described as key cost drivers and what is needed to minimize their effect on elevating the cost of structural braided preforms.

Author (revised)

N94-16850*# Ulster Coll., Newtownabbey (North Ireland). Engineering Composites Research Centre.

WEAVING MULTI-LAYER FABRICS FOR REINFORCEMENT OF ENGINEERING COMPONENTS

B. J. Hill, R. McIlhagger, and P. McLaughlin *In* NASA. Langley Research Center, FIBER-TEX 1992: The Sixth Conference on Advanced Engineering Fibers and Textile Structures for Composites Aug. 1993 p 79-96 (For primary document see N94-16845 03-24)

Avail: CASI HC A03/MF A03

The performance of interlinked, multi-layer fabrics and near net shape preforms for engineering applications, woven on a 48 shaft dobby loom using glass, aramid, and carbon continuous filament yarns is assessed. The interlinking was formed using the warp yarns. Two basic types of structure were used. The first used a single warp beam and hence each of the warp yarns followed a similar path to form four layer interlinked reinforcements and preforms. In the second two warp beams were used, one for the interlinking yarns which pass from the top to the bottom layer through-the-thickness of the fabric and vice versa, and the other to provide 'straight' yarns in the body of the structure to carry the axial loading. Fabrics up to 15mm in thickness were constructed with varying amounts of through-the-thickness reinforcement. Tapered T and I sections were also woven, with the shaping produced by progressive removal of ends during construction. These fabrics and preforms were impregnated with resin and cured to form composite samples for testing. Using these two basic types of construction, the influence of reinforcement construction and the proportion and type of interlinking yarn on the performance of the composite was assessed. Author (revised)

N94-16851*# West Virginia Univ., Morgantown. Dept. of Mechanical and Aerospace Engineering.

EFFECT OF TOW ALIGNMENT ON THE MECHANICAL PERFORMANCE OF 3D WOVEN TEXTILE COMPOSITES

Timothy L. Norman, Patti Allison (General Electric Co., Cincinnati, OH.), Jack W. Baldwin (General Electric Co., Cincinnati, OH.), Brian K. Gracias (General Electric Co., Cincinnati, OH.), and Dave Seesdorf (Westinghouse

Electric Corp., Pittsburgh, PA.) *In* NASA. Langley Research Center, FIBER-TEX 1992: The Sixth Conference on Advanced Engineering Fibers and Textile Structures for Composites Aug. 1993 p 97-113 Sponsored by GE (For primary document see N94-16845 03-24)
Avail: CASI HC A03/MF A03

Three-dimensional (3D) woven preforms are currently being considered for use as primary structural components. Lack of technology to properly manufacture, characterize and predict mechanical properties, and predict damage mechanisms leading to failure are problems facing designers of textile composite materials. Two material systems with identical specifications but different manufacturing approaches are investigated. One manufacturing approach resulted in an irregular (nonuniform) preform geometry. The other approach yielded the expected preform geometry (uniform). The objectives are to compare the mechanical properties of the uniform and nonuniform angle interlock 3D weave constructions. The effect of adding layers of laminated tape to the outer surfaces of the textile preform is also examined. Damage mechanisms are investigated and test methods are evaluated.
Author (revised)

N94-16852*# General Electric Co., Cincinnati, OH. Aircraft Engines.
AN ENGINEERING APPROACH FOR THE APPLICATION OF TEXTILE COMPOSITES TO A STRUCTURAL COMPONENT
Jack W. Baldwin, Brian K. Gracias, and Steven R. Clark (ICI Fiberite, Tempe, AZ.) *In* NASA. Langley Research Center, FIBER-TEX 1992: The Sixth Conference on Advanced Engineering Fibers and Textile Structures for Composites Aug. 1993 p 115-124 (For primary document see N94-16845 03-24)
Avail: CASI HC A02/MF A03

An engineering approach for the application of textile composites to a structural component is addressed. The main objective is to improve impact resistance of composite blades by using some form of 3-D reinforcement. Project goals, results, and conclusions are discussed. CASI

N94-16853*# Saint Petersburg Scientific Research Inst. of Chemical Fibers and Composite Materials (Russia).
NEW TEXTILE COMPOSITE MATERIALS DEVELOPMENT, PRODUCTION, APPLICATION
Petr Y. Mikhailov *In* NASA. Langley Research Center, FIBER-TEX 1992: The Sixth Conference on Advanced Engineering Fibers and Textile Structures for Composites Aug. 1993 p 125-138 (For primary document see N94-16845 03-24)
Avail: CASI HC A03/MF A03

New textile composite materials development, production, and application are discussed. Topics covered include: super-high-strength, super-high-modulus fibers, filaments, and materials manufactured on their basis; heat-resistant and nonflammable fibers, filaments, and textile fabrics; fibers and textile fabrics based on fluorocarbon poylmers; antifriction textile fabrics based on polyfen filaments; development of new types of textile combines and composite materials; and carbon filament-based fabrics.
CASI

N94-16854*# Saint Petersburg Scientific Research Inst. of Chemical Fibers and Composite Materials (Russia).
PRODUCTION AND APPLICATION OF CHEMICAL FIBERS WITH SPECIAL PROPERTIES FOR MANUFACTURING COMPOSITE MATERIALS AND GOODS OF DIFFERENT USAGE
R. Levit *In* NASA. Langley Research Center, FIBER-TEX 1992: The Sixth Conference on Advanced Engineering Fibers and Textile Structures for Composites Aug. 1993 p 139-145 (For primary document see N94-16845 03-24)
Avail: CASI HC A02/MF A03

The development of modern technologies demands the creation of new nonmetallic, fibrous materials with specific properties. The fibers and materials developed by NII 'Chimvolokno', St. Petersburg, can be divided into two groups. The first group includes heat-resistant fibers, fire-resistant fibers, thermotropic fibers, fibers for medical application, and textile structures. The second group contains refractory fibers, chemoresistant and antifriction fibers, fibers on the basis of polyvinyl alcohol, microfiltering films, and paperlike and nonwoven materials. In cooperation with NPO 'Chimvolokno' MYTITSHI, we developed and started producing heat-resistant high-strength fibers on the base of polyhetarearilin and aromatic polyimides (SVM and terlon); heat-resistant fibers on the base of polyemede (aramid); fire-retardant fibers (togilen); chemoresistant and antifriction fibers on the basis of homo and copolymers of polytetrafluoroethylene (polyfen and ftorin); and water soluble, acetylated, and high-modulus fibers from polyvinyl alcohol (vylen). Separate reports will deal with textile structures and thermotropic fibers, as well as with medical fibers. One of the groups of refractory fibers carbon fibers (CF) and the corresponding paperlike nonwoven materials are discussed in detail. Also, composite materials (CM) and their base, which is the subject of the author's research since 1968, is discussed.
Author (revised)

N94-16855*# Saint Petersburg Scientific Research Inst. of Chemical Fibers and Composite Materials (Russia).
FIBERS AND MATERIALS OF MEDICAL APPLICATION
L. I. Fridman *In* NASA. Langley Research Center, FIBER-TEX 1992: The Sixth Conference on Advanced Engineering Fibers and Textile Structures for Composites Aug. 1993 p 147-150 (For primary document see N94-16845 03-24)
Avail: CASI HC A01/MF A03

Efferent sorption methods of organism detoxication (by medical trend) are presented. Recently, specialists have shown their keen interest in the problem of treating exogenous and endogenous intoxications. This was stipulated by the growing production and accumulation of chemical products for industrial, agricultural, and domestic needs. To solve this problem the industrial production of carbon fibrous adsorbents was developed and implemented at NII Chimvolokno in St. Petersburg. A description of the carbon fibers is given. Also, application of modern composite materials for manufacturing compression-distraction apparatus used for setting fractured bones is described. Derived from text

N94-16856*# Virginia Polytechnic Inst. and State Univ., Blacksburg. Dept. of Engineering Science and Mechanics.
TEXTILE COMPOSITE PROCESSING SCIENCE
Alfred C. Loos, Vincent H. Hammond, David E. Kranbuehl (College of William and Mary, Williamsburg, VA.), and Gregory H. Hasko (Lockheed Engineering and Sciences Co., Hampton, VA.) *In* NASA. Langley Research Center, FIBER-TEX 1992: The Sixth Conference on Advanced Engineering Fibers and Textile Structures for Composites Aug. 1993 p 151-166 (For primary document see N94-16845 03-24)
(Grants NAG1-343; NAG1-237)
Avail: CASI HC A03/MF A03

A multi-dimensional model of the Resin Transfer Molding (RTM) process was developed for the prediction of the infiltration behavior of a resin into an anisotropic fiber preform. Frequency dependent electromagnetic sensing (FDEMS) was developed for in-situ monitoring of the RTM process. Flow visualization and mold filling experiments were conducted to verify sensor measurements and model predictions. Test results indicated good agreement between model predictions, sensor readings, and experimental data.
Author (revised)

N94-16857*# Drexel Univ., Philadelphia, PA.
INFLUENCE OF FIBER PACKING STRUCTURE ON PERMEABILITY
Zhong Cai and Alexander L. Berdichevsky (CR Industries, Elgin, IL.) *In* NASA. Langley Research Center, FIBER-TEX 1992: The Sixth Conference on Advanced Engineering Fibers and Textile Structures for Composites Aug. 1993 p 167-181 (For primary document see N94-16845 03-24)
Avail: CASI HC A03/MF A03

The study on the permeability of an aligned fiber bundle is the key building block in modeling the permeability of advanced woven and braided preforms. Available results on the permeability of fiber bundles in the literature show that a substantial difference exists between numerical and analytical calculations on idealized fiber packing structures, such as square and hexagonal packing, and experimental measurements on practical fiber bundles. The present study focuses on the variation of the permeability of a fiber bundle under practical process conditions. Fiber bundles are considered as containing openings and fiber clusters within the bundle. Numerical simulations on the influence of various openings on the permeability were conducted. Idealized packing structures are used, but with introduced openings distributed in different patterns. Both longitudinal and transverse flow are considered. The results show that openings within the fiber bundle have substantial effect on the permeability. In the longitudinal flow case, the openings become the dominant flow path. In the transverse flow case, the fiber clusters reduce the gap sizes among fibers. Therefore

the permeability is greatly influenced by these openings and clusters, respectively. In addition to the porosity or fiber volume fraction, which is commonly used in the permeability expression, another fiber bundle status parameter, the ultimate fiber volume fraction, is introduced to capture the disturbance within a fiber bundle. Author (revised)

N94-16858*# Textile Research Inst., Princeton, NJ.
CHARACTERIZATION OF VOIDS FORMED DURING LIQUID IMPREGNATION OF NONWOVEN MULTIFILAMENT GLASS NETWORKS AS RELATED TO COMPOSITE PROCESSING
Anant D. Mahale, Robert K. Prudhomme, and Ludwig Rebenfeld *In* NASA. Langley Research Center, FIBER-TEX 1992: The Sixth Conference on Advanced Engineering Fibers and Textile Structures for Composites Aug. 1993 p 183-202 Prepared in cooperation with Princeton Univ., NJ (For primary document see N94-16845 03-24)
Avail: CASI HC A03/MF A03

A technique based on matching the refractive index of an invading liquid to that of a fiber mat was used to study entrapment of air ('voids') that occurs during forced in-plane radial flow into nonwoven multifilament glass networks. The usefulness of this technique is demonstrated in quantifying and mapping the air pockets. Experiments with a series of fluids with surface tensions varying from 28 x 10(exp -3) to 36 x 10(exp -3) N/m, viscosities from 45 x 10(exp -3) to 290 x 10(exp -3) Pa.s, and inlet flow rates from 0.15 x 10(exp -6) to 0.75 x 10(exp -6) m(exp 3)/s, showed that void content is a function of the capillary number characterizing the flow process. A critical value of capillary number, Ca = 2.5 x 10(exp -3), identifies a zone below which void content increases exponentially with decreasing capillary number. Above this critical value, negligible entrapment of voids is observed. Similar experiments carried out on surface treated nonwoven mats spanning a range of equilibrium contact angles from 20 deg to 78 deg showed that there is a critical contact angle above which negligible entrapment is observed. Below this value, there is no apparent effect of contact angle on the void fraction - capillary number relationship described earlier. Studies on the effect of filament wettability, and fluid velocity and viscosity on the size of the entrapment (voids) were also carried out. These indicate that larger sized entrapments which envelop more than one pore are favored by a low capillary number in comparison to smaller, pore level bubbles. Experiments were carried out on deformed mats - imposing high permeability spots at regular intervals on a background of low permeability. The effect of these spatial fluctuations in heterogeneity of the mat on entrapment is currently being studied. Author (revised)

N94-16859*# National Aeronautics and Space Administration. Lewis Research Center, Cleveland, OH.
DEVELOPMENT OF BRAIDED FIBER SEALS FOR ENGINE APPLICATIONS
Zhong Cai (Drexel Univ., Philadelphia, PA.), Rajakkannu Mutharasan (Drexel Univ., Philadelphia, PA.), Frank K. Ko (Drexel Univ., Philadelphia, PA.), Guang-Wu Du (Drexel Univ., Philadelphia, PA.), and Bruce M. Steinetz *In* NASA. Langley Research Center, FIBER-TEX 1992: The Sixth Conference on Advanced Engineering Fibers and Textile Structures for Composites Aug. 1993 p 203-214 (For primary document see N94-16845 03-24)
Avail: CASI HC A03/MF A03

A new type of braided fiber seal was developed for high temperature engine applications. Development work performed includes seal design, fabrication, leakage flow testing, and flow resistance modeling. This new type of seal utilizes the high flow resistance of tightly packed fibers and the conformability of textile structures. The seal contains a core part with aligned fibers, and a sheath with braided fiber layers. Seal samples are made by using the conventional braiding process. Leakage flow measurements are then performed. Mass flow rate versus the simulated engine pressure and preload pressure is recorded. The flow resistance of the seal is analyzed using the Ergun equation for flow through porous media, including both laminar and turbulent effects. The two constants in the Ergun equation are evaluated for the seal structures. Leakage flow of the seal under the test condition is found to be in the transition flow region. The analysis is used to predict the leakage flow performance of the seal with the determined design parameters. Author (revised)

N94-16860*# North Carolina State Univ., Raleigh. Coll. of Textiles.
QUANTIFICATION OF PROCESSING ARTIFACTS IN TEXTILE COMPOSITES
Christopher M. Pastore *In* NASA. Langley Research Center, FIBER-TEX 1992: The Sixth Conference on Advanced Engineering Fibers and Textile Structures for Composites Aug. 1993 p 215-234 Sponsored in part by North Carolina Supercomputing Association (For primary document see N94-16845 03-24)
Avail: CASI HC A03/MF A03

One of the greatest difficulties in developing detailed models of the mechanical response of textile reinforced composites is an accurate model of the reinforcing elements. In the case of elastic property prediction, the variation of fiber position may not have a critical role in performance. However, when considering highly localized stress events, such as those associated with cracks and holes, the exact position of the reinforcement probably dominates the failure mode. Models were developed for idealized reinforcements which provide an insight into the local behavior. However, even casual observations of micrographical images reveals that the actual material deviates strongly from the idealized models. Some of the deviations and causes are presented for triaxially braided and three dimensionally woven textile composites. The necessary modeling steps to accommodate these variations are presented with some examples. Some of the ramifications of not accounting for these discrepencies are also addressed. Author (revised)

N94-16861*# Texas Univ., Arlington. Center for Composite Materials.
STOCHASTIC DAMAGE EVOLUTION IN TEXTILE LAMINATES
Yuris A. Dzenis, Alexander E. Bogdanovich (North Carolina State Univ., Raleigh.), and Christopher M. Pastore (North Carolina State Univ., Raleigh.) *In* NASA. Langley Research Center, FIBER-TEX 1992: The Sixth Conference on Advanced Engineering Fibers and Textile Structures for Composites Aug. 1993 p 235-248 (For primary document see N94-16845 03-24)
Avail: CASI HC A03/MF A03

A probabilistic model utilizing random material characteristics to predict damage evolution in textile laminates is presented. Model is based on a division of each ply into two sublaminas consisting of cells. The probability of cell failure is calculated using stochastic function theory and maximal strain failure criterion. Three modes of failure, i.e. fiber breakage, matrix failure in transverse direction, as well as matrix or interface shear cracking, are taken into account. Computed failure probabilities are utilized in reducing cell stiffness based on the mesovolume concept. A numerical algorithm is developed predicting the damage evolution and deformation history of textile laminates. Effect of scatter of fiber orientation on cell properties is discussed. Weave influence on damage accumulation is illustrated with the help of an example of a Kevlar/epoxy laminate. Author (revised)

N94-16862*# Lockheed Engineering and Sciences Co., Hampton, VA.
DEVELOPMENT OF TEST METHODS FOR TEXTILE COMPOSITES
John E. Masters, Peter G. Ifju (Virginia Polytechnic Inst., Blacksburg.), and Mark J. Fedro (Boeing Defense and Space Group, Philadelphia, PA.) *In* NASA. Langley Research Center, FIBER-TEX 1992: The Sixth Conference on Advanced Engineering Fibers and Textile Structures for Composites Aug. 1993 p 249-269 (For primary document see N94-16845 03-24)
Avail: CASI HC A03/MF A03

NASA's Advanced Composite Technology (ACT) Program was initiated in 1990 with the purpose of developing less costly composite aircraft structures. A number of innovative materials and processes were evaluated as a part of this effort. Chief among them are composite materials reinforced with textile preforms. These new forms of composite materials bring with them potential testing problems. Methods currently in practice were developed over the years for composite materials made from prepreg tape or simple 2-D woven fabrics. A wide variety of 2-D and 3-D braided, woven, stitched, and knit preforms were suggested for application in the ACT program. The applicability of existing test methods to the wide range of emerging materials bears investigation. The overriding concern is that the values measured are accurate representations of the true material response. The ultimate objective of this work is to establish a set of test methods to evaluate the textile composites developed for the ACT Program. Author (revised)

N94-16863*# North Carolina State Univ., Raleigh. Coll. of Textiles.
THREE-DIMENSIONAL ANALYSIS OF ANISOTROPIC SPATIALLY REINFORCED STRUCTURES
Alexander E. Bogdanovich (Latvian P. Stuchka State Univ., Riga.) *In*

NASA. Langley Research Center, FIBER-TEX 1992: The Sixth Conference on Advanced Engineering Fibers and Textile Structures for Composites Aug. 1993 p 271-304 (For primary document see N94-16845 03-24)
Avail: CASI HC A03/MF A03

The material-adaptive three-dimensional analysis of inhomogeneous structures based on the meso-volume concept and application of deficient spline functions for displacement approximations is proposed. The general methodology is demonstrated on the example of a brick-type mosaic parallelepiped arbitrarily composed of anisotropic meso-volumes. A partition of each meso-volume into sub-elements, application of deficient spline functions for a local approximation of displacements and, finally, the use of the variational principle allows one to obtain displacements, strains, and stresses at anypoint within the structural part. All of the necessary external and internal boundary conditions (including the conditions of continuity of transverse stresses at interfaces between adjacent meso-volumes) can be satisfied with requisite accuracy by increasing the density of the sub-element mesh. The application of the methodology to textile composite materials is described. Several numerical examples for woven and braided rectangular composite plates and stiffened panels under transverse bending are considered. Some typical effects of stress concentrations due to the material inhomogeneities are demonstrated. Author (revised)

N94-16864*# Douglas Aircraft Co., Inc., Long Beach, CA.
TECHNO-ECONOMIC REQUIREMENTS FOR COMPOSITE AIRCRAFT COMPONENTS
Ray Palmer *In* NASA. Langley Research Center, FIBER-TEX 1992: The Sixth Conference on Advanced Engineering Fibers and Textile Structures for Composites Aug. 1993 p 305-341 (For primary document see N94-16845 03-24)
(Contract NAS1-18862)
Avail: CASI HC A03/MF A03

The primary reason for use of composites is to save structural weight. A well designed composite aircraft structure will usually save 25-30 percent of a well designed metal structure. The weight savings then translates into improved performance of the aircraft in measures of greater payload, increased flying range or improved efficiency - less use of fuel. Composite materials offer technical advantages. Key technical advantages that composites offer are high stiffness, tailored strength capability, fatigue resistance, and corrosion resistance. Low thermal expansion properties produce dimensionally stable structures over a wide range of temperature. Specialty resin 'char' forming characteristics in a fire environment offer potential fire barrier application and safer aircraft. The materials and processes of composite fabrication offer the potential for lower cost structures in the near future. The application of composite materials to aircraft are discussed. Author (revised)

N94-16865*# North Carolina State Univ., Raleigh. Dept. of Textile Engineering, Chemistry and Science.
AEROELASTIC AIRFOIL SMART SPAR **c05**
Skott Greenhalgh, Christopher M. Pastore, and Moishe Garfinkle (Drexel Univ., Philadelphia, PA.) *In* NASA. Langley Research Center, FIBER-TEX 1992: The Sixth Conference on Advanced Engineering Fibers and Textile Structures for Composites Aug. 1993 p 343-351 (For primary document see N94-16845 03-24)
Avail: CASI HC A02/MF A03

Aircraft wings and rotor-blades are subject to undesirable bending and twisting excursions that arise from unsteady aerodynamic forces during high speed flight, abrupt maneuvers, or hard landings. These bending excursions can range in amplitude from wing-tip flutter to failure. A continuous-filament construction 'smart' laminated composite box-beam spar is described which corrects itself when subject to undesirable bending excursions or flutter. The load-bearing spar is constructed so that any tendency for the wing or rotor-blade to bend from its normal position is met by opposite twisting of the spar to restore the wing to its normal position. Experimental and theoretical characterization of these spars was made to evaluate the torsion-flexure coupling associated with symmetric lay-ups. The materials used were uniweave AS-4 graphite and a matrix comprised of Shell 8132 resin and U-40 hardener. Experimental tests were conducted on five spars to determine spar twist and bend as a function of load for 0, 17, 30, 45 and 60 deg fiber angle lay-ups. Symmetric fiber lay-ups do exhibit torsion-flexure couplings. Predictions of the twist and bend versus load were made for different fiber orientations in laminated spars using a spline function structural analysis. The analytical results were compared with experimental results for validation. Excellent correlation between experimental and analytical values was found. Author (revised)

N94-16933 Department of the Navy, Washington, DC.
TECHNIQUES FOR PREPARATION OF INGOT METALLURGICAL DISCONTINUOUS COMPOSITES Patent
Amarnath P. Divecha, inventor (to Navy), Subhash D. Karmarkar, inventor (to Navy), William A. Ferrando, inventor (to Navy), Scott M. Hoover, inventor (to Navy), and James M. Kerr, inventor (to Navy) 16 Mar. 1993 6 p Filed 4 Nov. 91
(AD-D015748; US-Patent-5,193,605; US-Patent-Appl-SN-787807) Avail: US Patent and Trademark Office

This is a process for the production of ingots of castable discontinuous metal matrix composites by encapsulating particulate refractory material of the B4C or SiC in a matrix metal of Li or Al to form a solid master alloy, and introducing the master alloy into molten Mg or an alloy thereof, mixing and then cooling to solidify the resultant mixture and form an ingot with the refractory material-substantially dispersed in the ingot. DTIC

N94-17013# Carnegie-Mellon Univ., Pittsburgh, PA.
STRUCTURAL CHARACTERIZATION OF EPITAXIAL LAYERS FOR INFRARED DETECTORS Annual Technical Report, 1 Jun. 1992 - 31 May 1993
D. W. Greve 22 Jun. 1993 9 p
(Contract F49620-92-J-0285)
(AD-A267875; AFOSR-93-0597TR) Avail: CASI HC A02/MF A01

Initial structural characterization of germanium-silicon epitaxial layers for heterojunction internal photoemission and multiple quantum well infrared detectors has been performed. Cross sectional TEM of multiple quantum wells has been used to confirm period and well thickness measurements performed by other techniques. No defects were observed by TEM in these layers. A variety of other layers including multiple quantum wells on relaxed buffers and heterojunction internal photoemission detector structures have been characterized by defect etching and X-ray diffraction. DTIC

N94-17235# Pacific Northwest Lab., Richland, WA.
CHARACTERIZATION OF NANOSCALE OXIDE AND OXYHYDROXIDE POWDERS USING EXAFS SPECTROSCOPY
J. G. Darab, J. C. Linehan, D. W. Matson, and Y. Ma (Washington Univ., Seattle.) Jun. 1993 7 p Presented at the Spring Meeting of the Materials Research Society, San Francisco, CA, 12-16 Apr. 1993
(Contract DE-AC06-76RL-01830)
(DE93-015683; PNL-SA-21667; CONF-930405-23) Avail: CASI HC A02/MF A01

Extended x-ray absorption fine structure (EXAFS) spectroscopy has been used to determine the structural environment local to iron(3) and zircorium(4) cations in respectively, nanoscale iron oxyhydroxide, and nanoscale zirconium oxide powders. The iron oxyhydroxide powder, produced by the modified reverse micelle (MRM) technology, was found to have a short-range structure most similar to that of goethite (alpha-FeOOH). The short-range structure of the zirconium oxide powder, produced using the rapid thermal decomposition of solutes (RTDS) technology, was found to be a mixture of monoclinic zirconia and cubic zirconia environments. DOE

N94-17271 Aerospace Corp., El Segundo, CA. Engineering and Technology Group.
FIBER STRENGTH UTILIZATION IN CARBON/CARBON COMPOSITES Technical Report
R. J. Zaldivar, Gerry S. Rellick, and J. M. Yang 15 May 1993 34 p
Limited Reproducibility: More than 20% of this document may be affected by microfiche quality
(Contract F04701-88-C-0089)
(AD-A267713; TR-92(2935)-1; SMC-TR-93-33) Avail: Issuing Activity (Defense Technical Information Center (DTIC))

The utilization of tensile strength of carbon fibers in unidirectional carbon/carbon (C/C) composites was studied for a series of four mesophase-pitch-based carbon fibers in a carbon matrix derived from a polyarylacetylene (PAA) resin. The fibers had moduli of 35, 75, and 130 Mpsi. Composite processing conditions ranged from the cured-resin state to various heat-treatment temperatures (HTTs) from 1100 to 1750 deg C for the C/Cs. Room-temperature tensile strength and modulus were

measured for the various processing conditions, and were correlated with SEM observations of fracture surfaces, fiber and matrix microstructures, and fiber/matrix interphase structures. Fiber tensile strength utilization (FSU) is defined as the ratio of apparent fiber strength in the C/C to the fiber strength in an epoxy-resin-matrix composite. Carbonization heat treatment to 1100 deg C results in a battle carbon matrix that bonds strongly with the three lower modulus fibers, resulting in matrix-dominated failure at FSU values of 24 to 35%. However, the composite with the 130-Mpsi modulus filament had an FSU of 79%. It is attributed to a combination of tough fracture within the filament itself and a weaker fiber/matrix interface. Both factors lead to crack deflection and blunting rather than to crack propagation. The presence of a weakened interface is inferred from observations of fiber pullout. Much of the FSU of the three lower modulus fibers is recovered by HIT to 2100 or 2400 deg C, principally as a result of interface weakening, which works to prevent matrix-dominated fracture. With HTT to 2750 deg C, there is a drop in FSU for all the composites; it is apparently the result of a combination of fiber degradation and reduced matrix stress-transfer capability. DTIC

N94-17295*# Massachusetts Inst. of Tech., Cambridge. Technical Lab. for Advanced Composites.

PREDICTION OF THERMAL CYCLING INDUCED CRACKING IN POLYMER MATRIX COMPOSITES Semiannual Report, Feb. - Jul. 1993

Hugh L. McManus Nov. 1993 36 p

(Grant NAG1-1493)

(NASA-CR-194677; NAS 1.26:194677) Avail: CASI HC A03/MF A01

This report summarizes the work done in the period February 1993 through July 1993 on the 'Prediction of Thermal Cycling Induced Cracking In Polymer Matrix Composites' program. An oral presentation of this work was given to Langley personnel in September of 1993. This document was prepared for archival purposes. Progress studies have been performed on the effects of spatial variations in material strength. Qualitative agreement was found with observed patterns of crack distribution. These results were presented to NASA Langley personnel in November 1992. The analytical methodology developed by Prof. McManus in the summer of 1992 (under an ASEE fellowship) has been generalized. A method for predicting matrix cracking due to decreasing temperatures and/or thermal cycling in all plies of an arbitrary laminate has been implemented as a computer code. The code also predicts changes in properties due to the cracking. Experimental progressive cracking studies on a variety of laminates were carried out at Langley Research Center. Results were correlated to predictions using the new methods. Results were initially mixed. This motivated an exploration of the configuration of cracks within laminates. A crack configuration study was carried out by cutting and/or sanding specimens in order to examine the distribution of cracks within the specimens. These investigations were supplemented by dye-penetrant enhanced X-ray photographs. The behavior of thin plies was found to be different from the behavior of thicker plies (or ply groups) on which existing theories are based. Significant edge effects were also noted, which caused the traditional metric of microcracking (count of cracks on a polished edge) to be very inaccurate in some cases. With edge and configuration taken into account, rough agreement with predictions was achieved. All results to date were reviewed with NASA Langley personnel in September 1993. Derived from text

N94-17379# Rhode Island Univ., Kingston. Dept. of Mechanical Engineering and Applied Mechanics.

ASPECTS OF HIGH TEMPERATURE DAMAGE IN FIBER REINFORCED TITANIUM METAL MATRIX COMPOSITES Annual Report, Jun. 1992 - Jun. 1993

H. Ghonem, D. Zheng, M. Tamin, Y. Win, and M. Thompson (United Technologies Corp., East Hartford, CT.) Jul. 1993 153 p

(Contract F49620-92-J-0291)

(AD-A267907; URI-MSL-93-10; AFOSR-93-0599TR) Avail: CASI HC A08/MF A02

Aspects associated with high temperature damage in fiber reinforced Metal Matrix Composites (MMC) were investigated and are presented in this report in the form of five separate sections. In the first section, the fatigue and fatigue crack growth characteristics in neat laminates made of Timetal 21S were studied in relation to both temperature and loading frequency effects. The second section deals with the evolution of the thermal residual stresses in the composite when cooling from consolidation temperature or subjecting the composite to then-nal cycles. A new mechanical simulation method capable of measuring the induced residual stress on real; time basis has been developed in this study. The third section extends this issue to the time-dependent internal stress and strain states of MMC's under the thermomechanical loading conditions. Here, a new micromechanical model employing the four-phase concentric cylinder configuration has been proposed. Based on this model, the time-dependent behavior of continuous fiber reinforced metal matrix composites has been evaluated for the SCS-6/Timetal 21S composite. These results are presented in the fourth section. The last section of this report deals with the high temperature fatigue crack growth characteristics of the continuous fiber reinforced titanium metal matrix composite sigma l240/Timetal 12lS. The time-dependent features of the crack growth was examined in relation to the variation of both testing temperature and loading frequency. The principal damage mechanism of this composite under the load condition employed was identified to be the crack bridging and fiber/matrix debonding confined to regions near the crack surfaces. DTIC

N94-17457 Cambridge Univ. (England). Dept. of Engineering.

DIRECT OBSERVATION OF FRACTURE OF CAS-GLASS/SiC COMPOSITES AND PROCESSING OF TOUGHENED ALUMINA Final Report, 1 Apr. 1991 - 31 Mar. 1992

H. R. Shercliff, G. Vekinis, M. F. Ashby, and P. W. Beaumont Sep. 1992 99 p Limited Reproducibility: More than 20% of this document may be affected by microfiche quality

(Grant AF-AFOSR-0221-91)

(AD-A268275; CUED/C-MATS/TR203; AFOSR-93-0582TR) Avail: Issuing Activity (Defense Technical Information Center (DTIC))

The first part of the report describes the continuation of a test series which has been undertaken on the laminated CAS-glass SiC fiber reinforced material provided by the USAF Materials Laboratory, Dayton, Ohio. Fracture mechanisms have been studied in four-point bend and in two geometries - double cantilever beam and double edge-notched tension. Dynamic in-situ scanning electron microscopy has enabled a clear characterization of sub-critical damage, and crack interactions prior to final failure, both of which have a strong influence on the material failure strength. The second part of the report describes preliminary studies on the fracture behavior of alumina toughened with ductile metal reinforcements. Specimens of alumina reinforced with discrete particles (mainly cobalt) have been produced by pretreating metal powders and mixing them with alumina powder followed by sintering under protective atmospheres. Processing conditions have been developed, and fracture surfaces studied in the scanning electron microscope. Crack bridging by metal ligaments has been observed. The ligaments fail by necking and/or shearing. The materials and processing route appear to be promising, especially in terms of controlling the interfacial reactions and strength. DTIC

N94-17473 Air Force Inst. of Tech., Wright-Patterson AFB, OH.

EVALUATION OF HYBRID REINFORCEMENT (FIBER-REINFORCED-PLASTIC ROD WITH STEEL CORE) M.S. Thesis

Markus J. Henneke Aug. 1993 175 p Limited Reproducibility: More than 20% of this document may be affected by microfiche quality

(AD-A268009; AFIT/CI/CIA-93-114) Avail: CASI HC A08

The corrosion of concrete reinforcement is a problem that seriously affects structures exposed to harsh environments (parking garages, marine structures, chemical plants, etc.). Currently the most popular method of corrosion protection is epoxy-coating for steel rebars and tendons. As an alternative to epoxy-coating, this project presents an initial evaluation of hybrid reinforcement. Hybrid reinforcement consists of a FRP (fiber-reinforced-plastic) skin with a steel core. The FRP skin (fully-bonded) is made of braided, epoxy-impregnated aramid or vinylon fiber. Besides protecting the steel core from corrosion, the FRP skin provides a structural function. Hybrid reinforcement allows specifying a reinforcement behavior by changing the core-to-skin cross-sectional ratios and by combining different core and skin materials. Uniaxial tensile test results are presented to show the characteristics of different hybrid rods. Results from beams reinforced with hybrid rods are presented to demonstrate the flexural behavior of concrete members reinforced with hybrid rods. DTIC

N94-17597 Materials Sciences Corp., Blue Bell, PA.

THERMO-MECHANICAL ANALYSIS OF OXIDATION PROTECTED CARBON-CARBON COMPOSITES Annual Report, Feb. 1992 - Feb. 1993

Zvi Hashin, Mark Jones, and Thomas Cassin Jun. 1993 25 p Limited Reproducibility: More than 20% of this document may be affected by microfiche quality
(Contract F49620-92-C-0024)
(AD-A268191; MSC-TPR-3318/1507; AFOSR-93-0591TR) Avail: Issuing Activity (Defense Technical Information Center (DTIC))

The AFOSR oxidation-protected C-C composite program is focused on developing and verifying mathematical models predicting the thermomechanical properties of exposed carbon-carbon composites. These models will be utilized to make judgements on the merits of both current and future materials concepts for oxidation resistance. These efforts are focused on the understanding of the formation and growth of damage within these materials and on the influence of oxidation protection constituents on the overall carbon-carbon material system. Models will be used to investigate the effects of inhibitors, microcrack patterns, fiber coatings, surface coatings, and matrix replacements on effective thermomechanical properties of carbon-carbon materials. The result of these models will allow the quantification of effective crack management strategies to improve the overall performance of these materials. Parallel efforts in this program include an experimental portion for the quantification of microcracks within the material and a variety of thermomechanical tests on specimens with and without coatings and inhibitors. Different material systems will allow a full range of constituent and processing variables to be studied. Results of these experiments will be compared to the predictions of the mathematical models in order to suggest improved design methods for carbon. DTIC

N94-17638*# Virginia Univ., Charlottesville. School of Engineering and Applied Science.
ENVIRONMENT ENHANCED FATIGUE CRACK PROPAGATION IN METALS: INPUTS TO FRACTURE MECHANICS LIFE PREDICTION MODELS Final Report
Richard P. Gangloff and Sang-Shik Kim Sep. 1993 224 p
(Grant NAG1-745; RTOP 510-02-12-10)
(NASA-CR-191538; NAS 1.26:191538) Avail: CASI HC A10/MF A03

This report is a critical review of both environment-enhanced fatigue crack propagation data and the predictive capabilities of crack growth rate models. This information provides the necessary foundation for incorporating environmental effects in NASA FLAGRO and will better enable predictions of aerospace component fatigue lives. The review presents extensive literature data on 'stress corrosion cracking and corrosion fatigue.' The linear elastic fracture mechanics approach, based on stress intensity range (Delta(K)) similitude with microscopic crack propagation threshold and growth rates, provides a basis for these data. Results are presented showing enhanced growth rates for gases (viz., H2 and H2O) and electrolytes (e.g. NaCl and H2O) in aerospace alloys including: C-Mn and heat treated alloy steels, aluminum alloys, nickel-based superalloys, and titanium alloys. Environment causes purely time-dependent accelerated fatigue crack growth above the monotonic load cracking threshold (KIEAC) and promotes cycle-time dependent cracking below (KIEAC). These phenomenon are discussed in terms of hydrogen embrittlement, dissolution, and film rupture crack tip damage mechanisms. Author (revised)

25 INORGANIC AND PHYSICAL CHEMISTRY

Includes chemical analysis, e.g., chromatography; combustion theory; electrochemistry; and photochemistry.

For related information see also *77 Thermodynamics and Statistical Physics.*.

N94-14909# Cornell Univ., Ithaca, NY. Dept. of Chemistry.
STRUCTURAL AND DYNAMICAL ASPECTS OF ELECTRODEPOSITION Final Report, 26 Feb. 1990 - 15 Feb. 1993
Hector D. Abruna May 1993 6 p
(Contract DAAL03-90-G-0048)
(AD-A266786; ARO-27502.4-CH) Avail: CASI HC A02/MF A01

The basic aim of this contract was to investigate structural and dynamical aspects of electrochemical phase formation. In these investigations we have emphasized the underpotential deposition of metal mono and multilayers employing electrochemical, x-ray based and ultra high vacuum surface spectroscopic techniques. We have been able to study: (1) The underpotential deposition of silver on a Pt(111) electrode as function of concentration, potential sweep rate, the presence of co-adsorbates. From these studies we have been able to determine that two monolayers of silver are deposited at underpotentials and that the stability of the second layer is a strong function of the concentration of silver in solution and the potential sweep rate. The presence of co-adsorbates can have a profound influence in the deposition and the magnitude of this effect(s) is strongly dependent on the type of adsorbate employed. (2) The underpotential deposition of copper on an iodine covered platinum surface by x-ray based techniques with emphasis on: isotherms derived from electrochemical and x-ray based measurements, mode of deposition, structure of the copper layer. We have found that isotherms derived from x-ray based measurements consistently yield a significantly higher coverage (relative to electrochemically derived isotherms) that we ascribe to copper species weakly associated with the interface. We have also found that the deposition appears to obey a mechanism where sites deeper in the platinum surface are occupied first and that sites further up are the progressively occupied. The structure of the copper appears to be strongly influenced by the chemisorbed iodine. The copper atoms appear to occupy bridge sites on the surface. DTIC

N94-14911# Dayton Univ., OH. Research Inst.
SCHOLARLY RESEARCH PROGRAM IN FUEL ANALYSIS AND COMBUSTION RESEARCH Final Report, Sep. 1987 - Sep. 1992
R. C. Striebich Feb. 1993 88 p
(Contract F33615-87-C-2714)
(AD-A266789; WL-TR-93-2033) Avail: CASI HC A05/MF A01

A total of 40 individually funded tasks were performed under this effort. These tasks were concerned with many fuel analysis and combustion research, conducted for the Fuels Branch (WL/POSF), Lubrications Branch (WL/POSL) and other Aero Propulsion and Power Directorate Laboratories. This report is a compilation of 1-2 page summaries from each of the tasks. More information on each task is available in the technical reports, journal articles, letter reports or informal information listed for the project. Although the subjects covered under this contract are too varied to list here, the most often addressed areas were research topics in gas chromatography and related instrumentation, thermal stability testing and methods development, lubrications research and combustion studies. DTIC

N94-14946# Army Research Lab., Aberdeen Proving Ground, MD.
ELECTRONIC SPECTROSCOPY OF THE GAS-PHASE OH-Kr VAN DER WAALS COMPLEX Final Report, Nov. 1991 - Jan. 1993
Rosario C. Sausa and George W. Lemire Jul. 1993 27 p
(DA Proj. 1L1-61102-AH-43)
(AD-A266891; ARL-TR-161) Avail: CASI HC A03/MF A01

The van der Waals complex OH-Kr was detected in a free jet expansion by laser-induced fluorescence (LIF) near the (1,0) band of the A(sup 2)Sigma(+) reverse yields X(sup 2)Pi(sub i) transition of uncomplexed OH. The excitation spectrum reveals a progression of vibrational bands which were assigned to the stretching motion of the complex. A Birge-Sponer plot at this progression yields a fundamental frequency of omega(sup prime)(sub c) = 196 +/- 8 cm(sup -1) and an anharmonicity constant of omega(sup prime)(sub c)Xi(sup prime)(sub c) = 7.4 +/- 0.7 cm(sup -1) for the A(sup 2)Sigma(+) excited state. The lower limit of the binding energy of the complex is measured as D(sup prime)(sub o)(nu(sup prime) = 1) is greater than or equal to 1,131 cm(sup -1). These results are compared to those obtained from recent gas-phase LIF studies on the OH-Ne and OH-Ar complexes near the A(sup 2)Sigma(+) reverse yields X(sup 2) Pi(sub i) (0,0) and (1,0) bands of OH, respectively, and those from a matrix LIF study on the OH-Kr complex near the (2,0) band of OH. DTIC

N94-14956# Emory Univ., Atlanta, GA. Dept. of Chemistry.
THE THERMAL DISSOCIATION OF NH2CHO(ND2CHO) ON Si(100)-2X1 Technical Report No. 20
Y. Bu and M. C. Lin 21 Jul. 1993 27 p Submitted for publication
(Contract N00014-89-J-1235)
(AD-A266903) Avail: CASI HC A03/MF A01

The interaction between NH2CHO(ND2CHO) and Si(100)-2x1 was investigated using HREELS, UPS, and XPS. At 100 K, formamide molecules randomly adsorbed on the surface, but became ordered, likely with the O-atom attached to the surface, as the 2 L NH2CHO dosed Si(100) surface

was warmed to 220 K. At this temperature, the formation of some Si-H species is indicated by the appearance of the 256 meV peak due to Si-H stretching vibration in HREELS. When the sample was annealed at 450 K, the OH and more H species were formed. In addition, a peak at 172(160) meV appeared in HREELS, which could be attributed to the HN=C (DN=C) and/or HNCO (DNCO) species. The latter species is more clearly evident in the UP spectrum. At 550 K, the breaking of CH, NH, and probably some OH bonds continued and the OH and H dominated the adspecies. Further annealing the sample at higher temperatures caused the formation of Si-O-Si complex as indicated by the 129 meV peak in HREELS due to the asymmetric stretching mode of the Si-O-Si species. Above 800 K, the Si-H stretching mode at 260 meV decreased dramatically because of the desorption of the H-species. DTIC

N94-14962 Wright Lab., Wright-Patterson AFB, OH.
SUPERSONIC COMBUSTION RESEARCH LABORATORY. VOLUME 1: DESIGN AND FABRICATION Interim Report, Jan. 1992 - 1993
Mark R. Gruber and Abdollah S. Nejad Jan. 1993 54 p Limited Reproducibility: More than 20% of this document may be affected by microfiche quality
(AF Proj. 2308)
(AD-A267667; WL-TR-93-2052-Vol-1) Avail: Issuing Activity (Defense Technical Information Center (DTIC))

The Experimental Research Branch of the Advanced Propulsion Division at Wright-Patterson Air Force Base began taking steps toward the development and installation of a supersonic combustion research facility during FY-90. A large-scale in-house research facility devoted to the study of supersonic fuel air mixing and combustion has been designed, fabricated, and installed. The purpose of the report that follows is to present documentation of the features of the air supply system, the design details and the characteristics of the actual supersonic combustion tunnel, and a description of the control system and instrumentation. DTIC

N94-15111# Pennsylvania Univ., Philadelphia.
THEORETICAL PREDICTION OF THE UV ADSORPTION AND FLUORESCENCE SPECTRA OF TYROSINE AND PHENYLALANINE Final Report, May - Aug. 1992
Hendrik F. Hameka and James O. Jensen May 1993 22 p
(Contract DAAL03-91-C-0034)
(AD-A266970; ERDEC-TR-059) Avail: CASI HC A03/MF A01

This report presents a theoretical study of the ground state and of the first excited state of phenylalanine and tyrosine to interpret the excitation absorption and the fluorescence emission spectra of the two molecules. The computations are performed with the Gaussian 90 Program Package using 3-21G basis sets. The ground state is computed with the HF option and the excited state with the Configuration Interaction, Single (CIS) Excitations option only. This report optimized the molecular geometries of both the ground and excited states and computed the excitation energies at both geometries. In conclusion, the excited state is due to a superposition of excitations from bonding orbitals in the alanine chain to a pi orbital in the benzene ring and to an orbital in the C-C bond attached to the ring. DTIC

N94-15146# Cornell Univ., Ithaca, NY.
REACTION AND DIFFUSION IN TURBULENT COMBUSTION
S. B. Pope 18 Jun. 1993 37 p
(Contract DE-FG02-90ER-14128)
(DE93-017085; DOE/ER-14128/T1) Avail: CASI HC A03/MF A01

A class of turbulent combustion models known as PDF methods has been developed. These methods have the important virtue that both convection and reaction can be treated without turbulence-modelling assumptions. However, a mixing model is required to account for the effects of molecular diffusion. Currently, the available mixing models are known to have some significant defects. Motivation of the project is to seek a better understanding of molecular diffusion in turbulent reactive flows; and thereby to provide guidance to the development of improved mixing models. Principal approach taken in the research is to use Direct Numerical Simulations (DNS) to study the coupled processes of reaction and molecular mixing in turbulent combustion. Because of inevitable computational limitations, it is impossible to simulate turbulent combustion in the parameter range of practical interest. Instead, our approach is to study very simple turbulent reactive flows that contain qualitatively some of the same phenomena as real flames. Statistical models will be developed that are applicable to practical combustion devices. The DNS studies related to non-premixed combustion are described. An additional topic studied, was mixing from the viewpoint of relative molecular motion. DOE

N94-15157# European Space Agency, Paris (France).
SOUNDING ROCKET EXPERIMENTS IN FLUID SCIENCE AND MATERIALS SCIENCES: TEXUS 25 TO 27 AND MASER 4, VOLUME 3 Final Reports
Olivier Minster and Brigitte Kaldeich, ed. Feb. 1993 133 p Original contains color illustrations
(ESA-SP-1132-Vol-3; ISBN-9-29-092104-8; ETN-93-94426) Copyright Avail: CASI HC A07/MF A02; ESA, EPD, ESTEC, Noordwijk, Netherlands, HC

Experiments in materials and fluid sciences carried out during the flights of the sounding rocket TEXUS 25, 26, and 27 and MASER 4, all in 1990, are reported. The following topics are discussed: Measurement of Interfacial Tension (MITE); the onset and flow pattern of magnetic Benard convection; pool boiling heat transfer; ultrasound absorption in molten salts; orientation of DNA during free solution electrophoresis; electrophoresis visualization; density and temperature relaxation near the critical point of CO2; temperature propagation in near critical fluids prior to and during separation; pressures of supercritical salt solutions; unidirectional solidification of liquid crystal material; partial melting of Y-Ba-Cu oxide; remelting of Fe-C-Si alloy in a ceramic mold; separation behavior of monotectic alloys; liquid phase sintering of tungsten composites; and the behavior of the energy storage material, LiF. For individual titles, see N94-15158 through N94-15172.

N94-15158# Consiglio Nazionale delle Ricerche, Genoa (Italy). Ist. di Chimica Fisica Applicata dei Materiali.
MEASUREMENTS OF INTERFACIAL TENSION: MITE
L. Liggieri, F. Ravera, E. Ricci, and A. Passerone *In* ESA, Sounding Rocket Experiments in Fluid Science and Materials Sciences: TEXUS 25 to 27 and MASER 4, Volume 3 Feb. 1993 p 9-15 (For primary document see N94-15157 03-25)
Copyright Avail: CASI HC A02/MF A02; ESA, EPD, ESTEC, Noordwijk, Netherlands, HC

The MITE experiment was flown on MASER 4 in Mar. 1990. The aim of the experiment was to test in microgravity a new method called the Pressure Derivative (PD) method. The PD method was developed to measure interfacial tension of couples of liquids and is applicable in conditions where the Bond number (Bo) equals zero. The methodology of the PD method is outlined. The flight experiment is described and results and conclusions are given. It was found that the behavior of the module was satisfactory, and it allowed us to measure values of the interfacial tension of the water/alpha-BromoNaphtalene couple which are in good agreement with values found on ground for the same materials. It is pointed out that the experimental signal recorded in space is much smoother and less disturbed than the ones recorded on ground. ESA

N94-15159# Technische Univ., Munich (Germany). Sektion Physik.
BENARD CONVECTION OF MAGNETIC COLLOIDS UNDER MICROGRAVITY c29
S. Odenbach *In* ESA, Sounding Rocket Experiments in Fluid Science and Materials Sciences: TEXUS 25 to 27 and MASER 4, Volume 3 Feb. 1993 p 16-23 (For primary document see N94-15157 03-25)
Copyright Avail: CASI HC A02/MF A02; ESA, EPD, ESTEC, Noordwijk, Netherlands, HC

The onset and the flow pattern of magnetic Benard convection under reduced gravity were investigated. This Benard convection is a form of thermal convection which can be induced in a magnetizable fluid even without gravity. This is possible when suitable magnetic fields are applied. The experiment consists of two concentric hollow cylindrical containers. The cylindrical gap between the containers is filled with ferrofluid (a suspension of small magnetite particles in an appropriate solute). The gap is heated from its inner wall and cooled on the outer surface. This special geometry establishes periodic boundary conditions. Those boundary conditions are not feasible in a ground based experiment, but they are very important for theoretical investigations. The flow profile was investigated as a function of the strength of the applied magnetic fields. Magnetic convection was clearly observed in a microgravity experiment flown with a TEXUS sounding rocket flight in Spring 1990. ESA

N94-15160# Technische Univ., Munich (Germany). Lab. fuer Angewandte Thermodynamik und Technologie unter Mikrogravitation.

POOL BOILING: SINGLE BUBBLE EXPERIMENT **c29**

B. Vogel and J. Straub *In* ESA, Sounding Rocket Experiments in Fluid Science and Materials Sciences: TEXUS 25 to 27 and MASER 4, Volume 3 Feb. 1993 p 24-34 Sponsored by BMFT (For primary document see N94-15157 03-25)

Copyright Avail: CASI HC A03/MF A02; ESA, EPD, ESTEC, Noordwijk, Netherlands, HC

To gain new knowledge about pool boiling heat transfer in microgravity and on Earth, single bubble experiments were made in the frame of the TEXUS program. By combining conventional and optical measuring techniques, the governing heat transport mechanisms should be detected. Data about bubble growth, heater temperatures, and temperature profiles close to the bubble, show that for subcooled boiling in microgravity, evaporation is the primary heat transport mechanism, and establishes together with the secondary mechanisms condensation and Marangoni flow, a steady state heat transfer. ESA

N94-15161# Technische Hochschule, Aachen (Germany). Zentrum fuer Physikalische Chemie unter Mikrogravitation.

ULTRASOUND ABSORPTION IN MOLTEN SALTS **c71**

E. P. Rejek, J. Richter, L. Schoester, and M. Vogt *In* ESA, Sounding Rocket Experiments in Fluid Science and Materials Sciences: TEXUS 25 to 27 and MASER 4, Volume 3 Feb. 1993 p 36-41 (For primary document see N94-15157 03-25)

Copyright Avail: CASI HC A02/MF A02; ESA, EPD, ESTEC, Noordwijk, Netherlands, HC

Measurements of ultrasound absorption in liquids show values that exceed the classical values calculated from viscosity and heat conduction by one order of magnitude. In terrestrial experiments, absorption in binary nitrate melts as a function of composition, temperature, and frequency was investigated with the pulse transmission method and the Debye-Sears method. The disturbances caused by convection led to this experiment under microgravity conditions, in order to perform precise reference measurements. The results of three TEXUS experiments showed, however, that the absorption was 20 percent, respectively 15 percent higher. In this third microgravity experiment (TEXUS 25) no significant difference between microgravity and terrestrial values could be found, whereas lower absorption was expected. This new microgravity effect is to be confirmed in further experiments. ESA

N94-15162# Chalmers Univ. of Technology, Goeteborg (Sweden). Dept. of Physical Chemistry.

ORIENTATION OF DNA DURING FREE-SOLUTION ELECTROPHORESIS **c29**

Mats Jonsson, Ulf Jacobsson, Bengt Norden, and Tore Eriksson *In* ESA, Sounding Rocket Experiments in Fluid Science and Materials Sciences: TEXUS 25 to 27 and MASER 4, Volume 3 Feb. 1993 p 42-52 Sponsored by Swedish Board for Space Activities (For primary document see N94-15157 03-25)

Copyright Avail: CASI HC A03/MF A02; ESA, EPD, ESTEC, Noordwijk, Netherlands, HC

The orientation of deoxyribonucleic acid (DNA) during electrophoresis in a free solution under microgravity conditions was studied in a sounding rocket flight with a microgravity time of about 7 minutes. The orientation was detected by Linear Dichroism (LD) spectroscopy utilizing a phase modulation technique. The aim of the experiment was to determine whether microgravity conditions, as an effect of absence of gravity induced convection, would lead to results different from those on the ground regarding the orientational response to electrophoresis in a solution. Duplex T2 DNA (170,000 basepairs) was subjected to rectangular pulses of field strengths between 10 and 100 V/cm. Each pulse has a duration of 30 seconds and the field free time between the pulses was 20 seconds. At the higher field strengths the rise profile of the DNA orientation displays a pronounced overshoot before it reaches a steady state, a behavior which confirms observations in experiments on the ground that the build up of the orientation occurs via a state of high orientational order. The degree of steady state orientation and the amplitude of the orientation overshoot both increase with field strength. However, the orientation is low (S about 0.006 at 100 V/cm). The orientational decay in the absence of field appears to be somewhat slower the higher the field strength of the pulse. However, the signal to noise ratio of the measurement was low, and the LD baseline also varied during the flight, which obviated safe conclusions about the detailed behavior of the DNA and a reliable comparison with ground experiments. Therefore, further experiments with improved equipment are necessary before a final assessment of the relevance of microgravity for the study of electrophoretic orientation of DNA can be made. ESA

N94-15163# Toulouse Univ. (France). Lab. de Genie Chimique et Electrochimie.

ELECTROPHORESIS VISUALISATION

Helene Roux-deBalmann and Victor Sanchez *In* ESA, Sounding Rocket Experiments in Fluid Science and Materials Sciences: TEXUS 25 to 27 and MASER 4, Volume 3 Feb. 1993 p 54-62 Original contains color illustrations (For primary document see N94-15157 03-25)

Copyright Avail: CASI HC A02/MF A02; ESA, EPD, ESTEC, Noordwijk, Netherlands, HC

An experiment based on Continuous Flow Electrophoresis (CFE), a process that permits purifying or separating products, such as proteins or cells, flown in TEXUS 27 in 1990, is reported. TEXUS provides only about 6 minutes of microgravity conditions, and specific equipment was used to get relevant information. During the CFE process certain phenomena are observed which can modify the originally cylindrical shape of the injected stream that contains the species to be separated, thus resulting in a loss of resolution. Such phenomena are Poiseuille flow, electroosmosis, and electrohydrodynamics. The experiment described was aimed at studying different kinds of transport phenomena. It was found that by working with alternating current the electrohydrodynamic phenomena could be studied without any inference with the other ones. With a direct current, the coupling of electrohydrodynamic with all other phenomena could be assessed. The experimental design is described and results and conclusions given. ESA

N94-15164# Commissariat a l'Energie Atomique, Gif-sur-Yvette (France). Service de Physique de l'Etat Condense.

DENSITY AND TEMPERATURE RELAXATION NEAR THE CRITICAL POINT OF CARBON DIOXIDE UNDER REDUCED GRAVITY **c29**

D. Beysens, Y. Garrabos (Centre National de la Recherche Scientifique, Villetaneuse, France.), P. Guenoun, B. Khalil, and B. LeNeindre (Centre National de la Recherche Scientifique, Villetaneuse, France.) *In* ESA, Sounding Rocket Experiments in Fluid Science and Materials Sciences: TEXUS 25 to 27 and MASER 4, Volume 3 Feb. 1993 p 64-78 Sponsored in part by CNES (For primary document see N94-15157 03-25)

Copyright Avail: CASI HC A03/MF A02; ESA, EPD, ESTEC, Noordwijk, Netherlands, HC

In order to investigate the different aspects of the transport of heat and mass in the absence of gravity, a thermal cycle was performed close to and around the critical point of CO2 at critical density. A cell was designed which allows surface and bulk phenomena to be distinguished. Special optical devices were used to observe the sample and measure locally temperature and density. Experiments under Earth's gravity a few mK close to the critical temperature (T(sub C)) are first presented. They enable convection patterns to be observed and a Grashof number as large as 100,000 to be measured. The thermal cycle of the experiment in weightlessness starts at T(sub C) + 2 mK, where the relaxation of the perturbations caused by liftoff are studied: fluid flows, density and temperature gradients. The effect of a quench from T(sub C) + 2 mK to T(sub C) + 1 mK then at T(sub C) - 1 mK and then again at T(sub C) + 2 mK were performed and observations given. ESA

N94-15165# Deutsche Forschungsanstalt fuer Luft- und Raumfahrt, Cologne (Germany). Inst. fuer Raumsimulation.

TEMPERATURE PROPAGATION IN NEAR-CRITICAL FLUIDS PRIOR TO AND DURING SEPARATION **c29**

H. Klein, G. Schmitz, and D. Woermann (Cologne Univ., Germany.) *In* ESA, Sounding Rocket Experiments in Fluid Science and Materials Sciences: TEXUS 25 to 27 and MASER 4, Volume 3 Feb. 1993 p 80-83 Repr. from Physical Review A, v. 43, no. 8, 1991 Sponsored in part by Deutsche Agentur fuer Raumfahrtangelegenheiten G.m.b.H. (For primary document see N94-15157 03-25)

Copyright Avail: CASI HC A01/MF A02; ESA, EPD, ESTEC, Noordwijk, Netherlands, HC

Temperature propagation in a near critical fluid sample (SF6) was

experimentally studied under reduced gravity in space. The experiment was carried out in the TEXUS sounding rocket and light scattering was used to observe the beginning of the gas liquid phase separation and to follow its development. The separation was recorded by video. Onset of phase separation was indicated by the appearance of a spinodal scattering ring. Critical speeding up of temperature equilibration prior to phase separation and markedly slowed down temperature equilibration during phase separation were observed. ESA

N94-15166# Bristol Univ. (England). Interface Analysis Center.
PRESSURES OF SUPERCRITICAL SALT SOLUTIONS
D. J. Turner *In* ESA, Sounding Rocket Experiments in Fluid Science and Materials Sciences: TEXUS 25 to 27 and MASER 4, Volume 3 Feb. 1993 p 84-90 (For primary document see N94-15157 03-25)
Copyright Avail: CASI HC A02/MF A02; ESA, EPD, ESTEC, Noordwijk, Netherlands, HC

It is hypothesized that the gravitational field of the Earth results in such severe sedimentation of sodium chloride solutions that the apparent critical temperatures are increased above their true, zero g, values. If this is true, then gravitational effects offer an explanation for the apparent violation of universality in the critical behavior of sodium chloride solutions. Experiments, designed to test this hypothesis in an independent manner using a technique which is easier to interpret than inductance and which has a direct bearing on the rather uncertain p, V, T properties, are addressed. The concept of the experiment was quite simple. If a solution is just above its true, zero g, critical point and the Earth's gravitational field is sufficient to induce a phase separation, then this change must cause a transfer of particles from the 'vapor' to the liquid phase with a consequent reduction in the pressure. The experiment was designed to look for an increase in pressure as a consequence of the reverse procedure of going from the Earth's gravity to microgravity. With a solution 0.001 M in sodium chloride at a density of 0.313 and a temperature of 377.5 C there was no detectable increase in pressure in going to microgravity. Under the conditions of the experiment, the detection limit would have been 3 bar. Potentially, the system is much more sensitive but to achieve its potential, the temperature overshoot would have to be much reduced and a longer period for thermal equilibration probably allowed. Also, heat flows would probably need to be more carefully controlled. If the experiment were to be repeated, it would almost certainly be desirable to use a cell temperature nearer to 375 C, a larger concentration and a lower mean density. ESA

N94-15167# Electrotechnical Lab., Tsukuba (Japan).
UNIDIRECTIONAL SOLIDIFICATION OF LIQUID-CRYSTAL MATERIAL **c29**
A. Iwasaki, S. Hosokawa, I. Kudo, M. Tanimoto, H. Sakurai (Ishikawajima-Harima Heavy Industries Co. Ltd., Tokyo, Japan.), Y. Arai (Ishikawajima-Harima Heavy Industries Co. Ltd., Tokyo, Japan.), T. Watanabe (Ishikawajima-Harima Heavy Industries Co. Ltd., Tokyo, Japan.), S. Kawai (Ishikawajima-Harima Heavy Industries Co. Ltd., Tokyo, Japan.), M. Ishikawa (Mitsubishi Research Inst., Inc., Tokyo, Japan.), and S. Kamei (Mitsubishi Research Inst., Inc., Tokyo, Japan.) *In* ESA, Sounding Rocket Experiments in Fluid Science and Materials Sciences: TEXUS 25 to 27 and MASER 4, Volume 3 Feb. 1993 p 92-99 Sponsored by Mechanical Social Systems Foundation and Society of Japanese Aerospace Co., Inc. Original contains color illustrations (For primary document see N94-15157 03-25)
Copyright Avail: CASI HC A02/MF A02; ESA, EPD, ESTEC, Noordwijk, Netherlands, HC

The process of the advancing interface and the adjacent region of the fluid during unidirectional solidification of liquid crystal material was investigated using polarization microscopy and interferometry. In the isotropic-nematic interface, some wavy patterns were observed and the existence of different mechanisms at different gravity levels was identified. In front of the nematic-solid interface, microconvection, which was recognized on the ground, disappeared under microgravity conditions. The effect of gravity on thermal transport and phase transition using a liquid crystal material as a unique model material is discussed. ESA

N94-15168# Hitachi Ltd., Tokyo (Japan). Research Lab.
PARTIAL MELTING EXPERIMENT OF Y-Ba-Cu OXIDE **c29**
Akira Yoshinari, Akira Okayama, H. Kodama, and N. Hamano *In* ESA, Sounding Rocket Experiments in Fluid Science and Materials Sciences: TEXUS 25 to 27 and MASER 4, Volume 3 Feb. 1993 p 100-109 (For primary document see N94-15157 03-25)
Copyright Avail: CASI HC A02/MF A02; ESA, EPD, ESTEC, Noordwijk, Netherlands, HC

The samples A (Y rich) and the samples B (Cu rich), made of two different compositions of Y-Ba-Cu-O high temperature superconducting alloy, were partially melted either under microgravity in the sounding rocket MASER or on the ground for reference. After partial melting and solidification in microgravity, Y-Ba-Cu-O samples require heat treatment on the ground. Whether a possible effect of microgravity remains after this heat treatment was studied to give a guideline for the selection of materials for future microgravity experiments. The properties of the samples were therfore investigated again after heat treatment. A comparison between samples A and B was made and results concerning the following properties are given: microstructure, superconductive transition temperature, specific resistance, critical current density, and phase distribution. While the samples A partially melted on Earth and in microgravity showed the same microstruture, the samples B had clearly different structures. The sample B partially melted on Earth showed a structure difference between its top and its bottom as Y2O3 and YBa2CuO6 phases segregated towards the bottom, and BaCu2O2 towards the top. In contrast, after melting under microgravity, Y2O3, YBa2Cu3O6, and BaCuO2 phases are distributed uniformly on the sample. After heat treatment, all samples had the same superconductive transition temperature. However, above the transition temperature, the samples A and B had smaller specific resistance when processed on Earth. After sintering at 1213 or 1238 K, the ground reference sample A exhibits a larger critical current density than the flight sample A. The same holds for samples B, but only after heat treatment at 1238 K. Critical current densities in samples B after heat treatment at 1213 K are comparable. ESA

N94-15169# Maschinenfabrik Augsburg-Nuernberg A.G., Munich (Germany). Centre de Geophysique Interne.
REMELTING OF Fe-C-SI-ALLOY IN A CERAMIC MOLD SKIN **c29**
W. Amende, P. Harmathy, and G. Vael *In* ESA, Sounding Rocket Experiments in Fluid Science and Materials Sciences: TEXUS 25 to 27 and MASER 4, Volume 3 Feb. 1993 p 110-119 Sponsored by BMFT (For primary document see N94-15157 03-25)
Copyright Avail: CASI HC A02/MF A02; ESA, EPD, ESTEC, Noordwijk, Netherlands, HC

An experiment prepared for the flight TEXUS 27 in which rod shaped samples made of Fe-C-Si alloys with different amount of silicon were remelted is presented. The aim of the experiment was to clarify the following points: the reliability of the mold skin during the processing of polymorphous alloys with an abrupt change in volume and in thermal expansion; the behavior of brazed joints in the sample; the processing of samples consisting of segments with a different composition connected by brazing; and the formation of gaseous products by chemical reaction between carbon rich melts and the oxide ceramic coating. ESA

N94-15170# Hamburg Univ. (Germany).
SEPARATION BEHAVIOUR OF MONOTECTIC ALLOYS **c29**
H. Ahlborn and K. Loehberg (Technische Univ., Berlin, Germany.) *In* ESA, Sounding Rocket Experiments in Fluid Science and Materials Sciences: TEXUS 25 to 27 and MASER 4, Volume 3 Feb. 1993 p 120-124 (For primary document see N94-15157 03-25)
Copyright Avail: CASI HC A01/MF A02; ESA, EPD, ESTEC, Noordwijk, Netherlands, HC

A TEXUS experiment to study the impact of wetting the crucible material on the separation process in monotectic alloys is presented. Al-Ir alloys with a critical composition were cooled through the miscibility gap during the TEXUS flight in crucibles wetted by the alloy phases in a different way. Whether the higher melting component gets sucked to the crucible wall (if it is wetting the crucible wall better than the lower melting In rich component) was investigated. In such a case, it would form the outer layer, contrary to earlier space results. Results and conclusions are given. ESA

N94-15171# Royal Inst. of Tech., Stockholm (Sweden). Dept. of Casting Metals.
LIQUID PHASE SINTERING OF TUNGSTEN COMPOSITES UNDER MICROGRAVITY. EFFECT OF MATRIX COMPOSITION **c29**
L. B. Ekbom and A. Eliasson *In* ESA, Sounding Rocket Experiments in

Fluid Science and Materials Sciences: TEXUS 25 to 27 and MASER 4, Volume 3 Feb. 1993 p 126-134 Sponsored in part by Swedish Board for Space Activities (For primary document see N94-15157 03-25)
Copyright Avail: CASI HC A02/MF A02; ESA, EPD, ESTEC, Noordwijk, Netherlands, HC

Liquid phase sintering of tungsten heavy metals, which are composites consisting of tungsten particles in a Ni-Fe-W matrix, was investigated under microgravity in TEXUS sounding rockets. Tungsten heavy metals are fabricated from powders by liquid phase sintering, during which the tungsten particles grow in the liquid matrix phase. Experiments were performed in which the surface tension between the molten matrix and the tungsten particles was varied. The heavy metal matrix composition is optimized to a Ni/Fe ratio at which tunsgten particles are effectively separated from each other by the liquid phase during sintering. By using other matrix compositions, the separation and growth processes can be influenced. The addition of a small amount of sulphur to the matrix will decrease the surface tension while a nickel matrix increases the tension. Such matrix compositions were used for the study of liquid phase sintering under microgravity. TEXUS flight experiments were used to achieve up to 5 minutes of liquid phase sintering under microgravity. To study the effect of surface tension between the molten matrix and the tungsten particles, short time tests of these systems during parabolic flights were performed. The results of the parabolic flight and TEXUS 26 and 27 experiments are evaluated. ESA

N94-15172# Deutsche Forschungsanstalt fuer Luft- und Raumfahrt, Stuttgart (Germany). Inst. fuer Technische Thermodynamik.
HEAT STORAGE MODULE **c44**
H. J. Staehle and F. Lindner *In* ESA, Sounding Rocket Experiments in Fluid Science and Materials Sciences: TEXUS 25 to 27 and MASER 4, Volume 3 Feb. 1993 p 136-141 (For primary document see N94-15157 03-25)
Copyright Avail: CASI HC A02/MF A02; ESA, EPD, ESTEC, Noordwijk, Netherlands, HC

Experiments performed on TEXUS 27 sounding rocket to investigate the thermal energy storage module of solar dynamic systems are reported. One of the most suitable energy storage materials for the desired temperature range of 800 to 900 C is lithium fluoride (LiF). Due to the large volume increase during melting of approximately 22% and the corrosivity in the molten state, a canister made of graphite or glass carbon was developed for space use. The heat exchanging wall is equipped with channels and the canister is filled in such a way that molten LiF occupies the whole volume except the channels. In the discharge model, the crystallization of LiF starts at the outer wall and continues towards the center of the canister. There, a void forms due to the volume contraction. The next melting cycle starts again at the heat exchanging wall, and the surplus of volume, due to the pressure of the central void, is able to penetrate the channels against the capillary forces. As soon as the melting front reaches the void, the capillary forces drive the melt out of the channels and a new cycle can start. Tests under terrestrial conditions revealed that the melt did not penetrate the channels as long as the gravity dependent pressure did not exceed the capillary pressure. The TEXUS experiments reported were performed to clarify the following points under microgravity: the melting/freezing behavior of LiF; the formation of the void(s) (Does one void form or several voids? Where is the void located? If several voids are generated, how is their distribution?); and the predicted function of the volume compensation. ESA

N94-15684# North Carolina Central Univ., Durham. Dept. of Physics.
THE PRESSURE BROADENING OF HDO BY O2, N2, H2, AND He BETWEEN 100 K AND 600 K
Thomas M. Goyette, David W. Ferguson, Frank C. DeLucia, Jyotsna M. Dutta, and Charles R. Jones 30 Jun. 1993 26 p
(Contract F49620-89-C-0080)
(AD-A267118; AFOSR-93-0540TR) Avail: CASI HC A03/MF A01

Microwave transitions of HDO pressure-broadened by H2, O2, N2, and He were studied in the temperature region between 100 and 600 K. Measurements below 250 K were made in a collisionally cooled cell. Above this temperature a conventional equilibrium cell was used in the region where the HDO has non-negligible vapor pressure. Significant variations in both the pressure broadening parameter and its temperature dependence were observed among the studied transitions. Ordinarily, a power law is used to describe this temperature dependence. Deviations from this were observed below 150K. DTIC

N94-15685# Army Research Lab., Aberdeen Proving Ground, MD.
SPECTRAL STUDIES OF SOLID PROPELLANT COMBUSTION 4: ABSORPTION AND BURN RATE RESULTS FOR M43, XM39, AND M10 PROPELLANTS Final Report, 1 Jun. - 31 Dec. 1992
M. W. Teague, Gurbax Singh, and John A. Vanderhoff Aug. 1993 28 p
(DA Proj. 1L1-61102-AH-43)
(AD-A267119; ARL-TR-180) Avail: CASI HC A03/MF A01

An optical absorption experiment coupled to a windowed strand burner has been used to obtain dark zone temperatures and nitric oxide concentrations for two nitramine propellants (M43 and XM39) and a single base propellant (M10). Moreover, burn rates as a function of pressure were determined from the video record of the propellant burns. These measurements were taken over a pressure range from 0.8 to 2 MPa. DTIC

N94-15713*# Princeton Univ., NJ. Dept. of Mechanical and Aerospace Engineering.
MECHANISMS OF COMBUSTION LIMITS IN PREMIXED GAS FLAMES AT MICROGRAVITY Final Report, 15 Dec. 1988 - 17 Dec. 1991
Paul D. Ronney (University of Southern California, Los Angeles.) 1991 22 p
(Grant NAG3-965)
(NASA-CR-194557; NAS 1.26:194557) Avail: CASI HC A03/MF A01

A three-year experimental and theoretical research program on the mechanisms of combustion limits of premixed gasflames at microgravity was conducted. Progress during this program is identified and avenues for future studies are discussed. Derived from text

N94-15760 Washington Univ., Seattle. Dept. of Biochemistry.
STUDY OF PROTEIN-H2O INTERACTIONS BY MULTIDIMENSIONAL NMR SPECTROSCOPY Report, 1 Apr. 1991 - 31 Mar. 1993
Rachel E. Klevit Jul. 1993 8 p Limited Reproducibility: More than 20% of this document may be affected by microfiche quality
(Contract N00014-91-J-1766)
(AD-A266955) Avail: CASI HC A02

Water has been shown to play an integral role in both structural and catalytic aspects of protein function. Strongly-bound water molecules are observed in high-resolution protein structures by x-ray diffraction studies of single crystals of protein molecules. The pilot studies described here were aimed at ascertaining the feasibility of detecting strongly-bound water molecules in solution using multidimensional heteronuclear NMR spectroscopy. Three dimensional -(1H, 15N)-HMQC-ROESY spectroscopy was implemented on a Bruker AM-500 spectrometer and spectra were collected on a series of related HPr protein molecules. Interactions involving both H20 and -OH groups were reproducibly detected in the spectra. The results indicate that this approach is capable of yielding a limited amount of information concerning protein-water interactions and is not likely to become a generally-used technique. DTIC

N94-15766*# Vanderbilt Univ., Nashville, TN. Dept. of Physics and Astronomy.
ANALYTICAL AND EXPERIMENTAL INVESTIGATION OF THE FEASIBILITY OF ACCELERATED LIFETIME TESTING OF MATERIALS EXPOSED TO AN ATOMIC OXYGEN BEAM Final Report
Royal Albridge, Alan Barnes, and Norman Tolk 11 Jun. 1993 48 p
(Contract NAS8-37744)
(NASA-CR-193851; NAS 1.26:193851) Avail: CASI HC A03/MF A01

The interaction of atomic particles with surfaces is of both scientific and technological interest. Past work emphasizes the measurement of high-energy sputtering yields. Very little work utilized low-energy beams for which chemical and electronic effects can be important. Even less work has been carried out using well-defined low-energy projectiles. The use of low-energy, reactive projectiles permits one to investigate surface processes that have not been well characterized. As the energy of the projectile decreases, the collisional cascades and spikes, that are common for high-energy projectiles, become less important, and chemical and electronic effects can play a significant role. Aspects of particle-surface interactions are of concern in several areas of technology. For example, the erosion, desorption, and glow of surfaces of spacecraft in orbit are important in the

arena of space technology. The materials studied under this contract are of possible use on the exterior portions of the power generation system of Space Station Freedom. Under the original designs, Space Station Freedom's power generation system would generate potential differences on the surface as high as 200 volts. Ions in the plasma that often surround orbiting vehicles would be accelerated by these potentials leading to bombardment and erosion of the exposed surfaces. The major constituent of the atmosphere, approximately 90 percent, in the low earth orbit region is atomic oxygen. Since atomic oxygen is extremely reactive with most materials, chemical effects can arise in addition to the physical sputtering caused by the acceleration of the oxygen ions. Furthermore, the incident oxygen ions can remain embedded in the exposed surfaces, altering the chemical composition of the surfaces. Since the effective binding energy of a chemically altered surface can be quite different from that of the pure substrate, the sputtering yield of a chemically altered surface is usually different also. The low-energy O+ sputtering yield measurements, reported here, will help quantify the erosion rates for materials exposed to the low-earth orbit environment. These measurements are of technological importance in another respect. In most surface analysis techniques, a surface is bombarded with ions, electrons or photons. Information concerning the structure of the surface and near-surface bulk, abundance of impurities and defects, as well as other surface properties are obtained either from the desorbed species or from the scattered projectiles. Because of their low penetration depth, low-energy ions provide an advantage over other techniques because they provide information that is more indicative of conditions on the surface rather than integrated effects arising from deeper in the bulk. A better understanding of the microscopic processes involved in these interactions is not only of basic scientific interest, but will also aid the scientific community by increasing the accuracy and usefulness of these surface analysis techniques. Derived from text

N94-15861# Aluminum Co. of America, Alcoa Center, PA.
GAS SEPARATIONS USING CERAMIC MEMBRANES
C. L. Lin, J. C. S. Wu, G. R. Gallaher, G. W. Smith, D. L. Flowers, T. E. Gerdes, and P. K. T. Liu Feb. 1993 203 p
(Contract DE-AC21-88MC-25135)
(DE93-000278; DOE/MC-25135/3341) Avail: CASI HC A10/MF A03

This study covers a comprehensive evaluation of existing ceramic membranes for high temperature gas separations. A methodology has been established for microporous characterization stability and gas separation efficiency. A mathematical model was developed to predict gas separations with existing membranes. Silica and zeolitic modifications of existing membranes were pursued to enhance its separation efficiency. Some of the membrane modifications demonstrate unique separation properties. Use of the dense-silica membranes for hydrogen enrichment was identified as a promising candidate for future development. In addition, the decomposition of trace ammonia contaminant via a catalytic membrane reactor appears feasible. A further economic analysis is required to assess its commercial viability. DOE

N94-15977# United Technologies Research Center, East Hartford, CT.
A PROPOSED MECHANISM FOR THE PYROLYSIS OF DIBORANE
M. B. Colket and J. A. Montgomery, Jr. 1993 4 p Presented at the 1993 Joint Central States and Eastern Sections of the Combustion Institute Conference, New Orleans, LA, 15-17 Mar. 1993
(Contract DE-FG02-86ER-13560)
(DE93-014275; CONF-930392-2) Avail: CASI HC A01/MF A01

We examined the technique used by Fridman and Fehlner. The products B3H7 and B3H9 were trace species observed over the mass range 34-38 amu. Additional reactions were included to form the tetraborane and pentaborane; the five-step reaction is tabulated along with rate and reverse rate constants. Predictions are compared to decomposition data of Clarke and Pease. DOE

N94-16011# Brookhaven National Lab., Upton, NY.
IN SITU STUDIES OF PASSIVE FILM CHEMISTRY USING X RAY ABSORPTION SPECTROSCOPY
A. J. Davenport, H. S. Isaacs, J. A. Bardwell (National Research Council of Canada, Ottawa, Ontario.), and B. MacDougall (National Research Council of Canada, Ottawa, Ontario.) 1993 8 p Presented at the 12th International Corrosion Congress, Houston, TX, 19-24 Sep. 1993
(Contract DE-AC02-76CH-00016)
(DE93-014023; BNL-48665; CONF-9309150-1) Avail: CASI HC A02/MF A01

The passive film on sputter-deposited thin film Fe and Fe-26Cr electrodes has been examined using in situ X-ray Absorption Near Edge Spectroscopy (XANES). During the x-ray spectroscopic measurements, samples were maintained under potentiostatic control in pH 8.4 borate buffer. The passive film on both Fe and Fe-26Cr is formed from the metal without any detectable losses due to dissolution. Cathodic reduction leads to a loss of Fe from the film in both cases, but substantially less Fe is lost in the case of Fe-26Cr. Transpassive dissolution of Cr from Fe-26Cr only occurred on the second potential cycle after the film had been enriched in Cr due to the reductive dissolution of Fe. Simultaneous collection of both the Fe and Cr x-ray absorption edges provides quantitative information on the relative amounts of material lost during passivation and reduction. DOE

N94-16014# Oak Ridge National Lab., TN.
APPLICATION OF Z-CONTRAST IMAGING TO OBTAIN COLUMN-BY-COLUMN SPECTROSCOPIC ANALYSIS OF MATERIALS
N. D. Browning and S. J. Pennycook Jan. 1993 7 p Presented at the 16th Material Research Society International Symposium on the Scientific Basis for Nuclear Waste Management Fall Meeting, Boston, MA, 30 Nov. - 5 Dec. 1992
(Contract DE-AC05-84OR-21400)
(DE93-015333; CONF-921101-125) Avail: CASI HC A02/MF A01

Z-contrast imaging has been shown to be an effective method for obtaining a high-resolution image from a scanning transmission electron microscope (STEM). The incoherent nature of the high-angle scattering makes image interpretation straightforward and intuitive with the resolution limited only by the 2.2 A electron probe. The optimum experimental conditions for Z-contrast imaging also coincide with those used for analytical microscopy, enabling microanalysis to be performed with the same spatial resolution as the image. The detection limits afforded by a parallel detection system for electron energy loss spectroscopy (EELS) allows column-by-column core-loss spectroscopy to be performed using the Z-contrast image to position the electron probe. Preliminary results from the study of YBa2Cu3O(7-delta) illustrate the spatial resolution available with this technique and the potential applications for materials science. DOE

N94-16060# California Univ., Berkeley. Lawrence Berkeley Lab.
A COMPARISON OF ONE AND TWO DIMENSIONAL FLAME QUENCHING: HEAT TRANSFER RESULTS
O. A. Ezekoye and R. Greif Mar. 1993 10 p Presented at the National Conference and Exposition on Heat Transfer, Atlanta, GA, 8-11 Aug. 1993
(Contract DE-AC03-76SF-00098)
(DE93-015196; LBL-33817; CONF-930830-22) Avail: CASI HC A02/MF A01

A theoretical investigation of laminar premixed flame quenching is carried out. Two orientations in which a flame may contact a cold wall are compared and contrasted by solving the conservation equations of mass, energy, and species utilizing a finite difference methodology. A one-step mechanism is used to specify the reaction rates. A simple analytical model, which is in qualitative agreement with the numerical results, is also presented. The results show that the heat transfer histories for one and two dimensional laminar flame quenching are similar. DOE

N94-16105# Oak Ridge National Lab., TN.
CORROSION KINETICS AND MECHANISMS FOR NUCLEAR GRADE GRAPHITES
L. E. Fuller, Jr., O. C. Kopp, and A. D. Underwood 1993 17 p Presented at the NACE Annual Corrosion Conference and Materials Performance and Corrosion Show, New Orleans, LA, 7-12 Mar. 1993
(Contract DE-AC05-84OR-21400)
(DE93-015462; CONF-930318-10) Avail: CASI HC A03/MF A01 (US Sales Only)

An initial microgravimetric evaluation of the intrinsic reaction parameters for air reactions with H-451 graphite at 375 to 850 C at atmospheric pressure and for water contents from 0 to 2 vol% water vapor is reported. Photographic results show heterogeneous nature of the graphite and consequential variation of reaction rate as the samples are etched and

roughened in the corrosion processes. The reaction rate increases approximately two fold to a near-constant value and subsequently approaches zero as the remnant skeletal matrix is consumed. There appears to be no significant rate effect (neither catalytic nor impedimental) due to the presence of water vapor in the concentrations used. DOE

N94-16462# Cornell Univ., Ithaca, NY. Dept. of Chemistry.
STUDIES OF COMBUSTION REACTIONS AT THE STATE-RESOLVED DIFFERENTIAL CROSS SECTION LEVEL
P. L. Houston 12 Apr. 1993 5 p
(Contract DE-FG02-88ER-13934)
(DE93-017605; DOE/ER-13934/T1) Avail: CASI HC A01/MF A01

This program explores a new technique for obtaining differential cross sections with product state resolution. The three-dimensional velocity distribution of state-selected reaction products is determined by ionizing the appropriate product, waiting for a delay while it recoils along the trajectory imparted by the reaction, and finally projecting the spatial distribution of ions onto a two dimensional screen using a pulsed electric field. Knowing the arrival time allows the ion position to be converted to a velocity, and the density of velocity projections can be inverted mathematically to provide three-dimensional velocity distribution for the selected product. Apparatus has been constructed and tested using photodissociations. The proposed research will both develop the new technique and employ it to investigate methyl radical, formyl radical, and hydrogen atom reactions which are important in combustion processes. We intend specifically to characterize the reactions of CH3 with H2 and H2CO; of HCO with O2; and of H with CH4, CO2 and O2. DOE

N94-16532 Department of the Navy, Washington, DC.
ELECTRORHEOLOGICAL FLUID CHEMICAL PROCESSING Patent
Ronald P. Reitz, inventor (to Navy) 2 Mar. 1993 6 p Filed 23 Nov. 1990
(AD-D015785; US-Patent-5,190,624; US-Patent-Appl-SN-617317; US-Patent-Class-204-59R) Avail: US Patent and Trademark Office

The present invention comprises electrorheological fluids and processes. Applying an electric field to an electrorheological fluid composition electrically controls chemical reactions therein. The chemical reactions may comprise those wherein the acidity of the composition is changed. Other chemical reactions may comprise those wherein the phase of the composition is changed. DTIC

N94-16539 Department of the Navy, Washington, DC.
METHOD AND APPARATUS FOR PERFORMING SCANNING TUNNELING OPTICAL ABSORPTION SPECTROSCOPY Patent
Orest J. Glembocki, inventor (to Navy) and Eric S. Snow, inventor (to Navy) 30 Mar. 1993 7 p Filed 20 Dec. 1991
(AD-D015796; US-Patent-5,198,667; US-Patent-Appl-SN-811378; US-Patent-Class-250-306) Avail: US Patent and Trademark Office

An apparatus for performing scanning tunneling optical absorption spectroscopy includes a scanning tunneling microscope tip positioned at a tunneling distance over a surface portion of a sample to be analyzed, biasing apparatus for producing in electric potential between said scanning tunneling microscope tip and said surface portion sufficient to cause a tunneling current to flow between said scanning tunneling microscope tip and said surface portion, illumination apparatus for illuminating said surface portion with modulated monochromatic light, and a detector for detecting an AC component of the tunneling current resulting from the modulated monochromatic light. DTIC

N94-16553# Naval Research Lab., Washington, DC.
WATER ADSORPTION ON DIAMOND (110) STUDIED BY MULTIPLE INTERNAL REFLECTION INFRARED SPECTROSCOPY
M. McGonigal, J. N. Russell, Jr., P. E. Pehrsson, H. Maguire, and J. E. Butler 14 Jun. 1993 20 p
(AD-A266415; NRL/MR/6174-93-7351) Avail: CASI HC A03/MF A01

The adsorption of water on a natural, type 2a diamond (110) surface is studied by multiple internal reflection infrared spectroscopy (MIRIRS). Similar results are observed for the hydrogen-free, and hydrogen-terminated diamond (110) surfaces. Exposure of water at 100 K reveals the presence of physisorbed molecular water on the surface, with no evidence of dissociation. Upon heating to approximately 160 K, the water is desorbed from the surface without any evidence of chemisorption or decomposition. Exposure of the surface to water at elevated temperatures (373 and 773 K) also failed to produce any evidence in the infrared spectra of chemisorption or decomposition. However, the absence of water dissociative chemisorption may be the result of sp2 carbon contamination which was found on the surface at the conclusion of the experiments. DTIC

N94-16771# Boston Univ., MA. Dept. of Chemistry.
SCINTILLATION MECHANISM IN STOICHIOMETRIC CERIUM COMPOUNDS
A. J. Wojtowicz (Nicolaus Copernicus Univ., Torun, Poland.), A. Lempicki, and E. Berman 1992 5 p Presented at the Crystal 2000 International Workshop on Heavy Scintillators for Scientific and Industrial Applications, Chamonix, France, 22-26 Sep. 1992 Prepared in cooperation with ALEM Associates, Boston, MA
(Contracts DE-FG02-90ER-61033; DE-FG02-92ER-81360)
(DE93-015499; CONF-9209253-5) Avail: CASI HC A01/MF A01

These materials constitute a new class of scintillator media, with high speed and high light output. This is illustrated using CeF3, and CeP5O14. While speed, being limited by a radiative lifetime of an allowed d-f transition on the Ce(+3) ion, cannot be improved (without loss of the light output), the light output in both cases falls significantly below the estimated theoretical limit. To explain this we propose a mechanism of scintillation process, in which transfer of excitation energy from the lattice to the d-f electronic structure of Ce(+3) ions is absent and the light output of the scintillator is limited to the excitation energy directly intercepted by Ce ions. The efficiency depends, therefore, on the competition for holes between Ce(+3) ions and anions, determining the share of the total energy deposited by a high energy particle, which can be transformed into scintillation photons. The mechanism requires that the Ce ion has a stable 4+ charge state. Ionization of Ce(+3) is followed by capturing of an electron and creation of the Ce bound exciton. In the next step the energy of the bound exciton is transferred to the d-f structure of the Ce ion and, in the final step, a scintillation photon is emitted. The relatively high light output characteristic of these materials is due to the high concentration of Ce ions. The reasons for the lack of efficient energy transfer from the lattice may reside in large relaxation energies of lattice excitations. We use this model to discuss potential improvements in the light output of CeF3. DOE

N94-16772# Washington Univ., Seattle. Dept. of Physics.
CONVERGENCE OF THE MULTIPLE SCATTERING EXPANSION IN XAFS AND XANES
J. J. Rehr 1992 5 p Presented at the International Workshop on Surface X Ray Absorption Fine Structure (XAFS), Jaipur, India, Aug. 1992
(Contract DE-FG06-90ER-45415)
(DE93-011001; DOE/ER-45415/8; CONF-9208221-1) Avail: CASI HC A01/MF A01

The convergence of the multiple-scattering expansion of XAFS and XANES by explicit path-bypath calculations is discussed. The approach is based on the fast scattering matrix formalism of Rehr and Albers, together with an automated path finder and filters that exclude negligible paths. High-order scattering terms are found to be essential, especially at low energies. Several factors including the magnitude of curved wave scattering amplitudes, inelastic losses and multiple-scattering Debye-Waller factors control convergence of the expansion. The convergence is illustrated explicitly for the case of diatomic molecules. DOE

N94-16787# Wisconsin Univ., Madison. Dept. of Chemistry.
METHODS OF TUNNELING SPECTROSCOPY WITH THE STM Interim Report, 1 Jun. 1992 - 31 May 1993
R. J. Hamers 25 Jun. 1993 31 p
(Contract N00014-91-J-1629)
(AD-A266507; TR-14) Avail: CASI HC A03/MF A01

The theory and application of scanning tunneling spectroscopy techniques is reviewed. Methods of acquisition and analysis are treated in detail, with examples from the scientific literature. DTIC

N94-16821# California Univ., Berkeley. Lawrence Berkeley Lab.
ON-LINE GAS CHROMATOGRAPHIC STUDIES OF RUTHERFORDIUM (ELEMENT 104), HAHNIUM (ELEMENT 105), AND HOMOLOGS Ph.D. Thesis
B. Kadkhodayan May 1993 164 p

(Contract DE-AC03-76SF-00098)
(DE93-013890; LBL-33961) Avail: CASI HC A08/MF A02

Gas-phase isothermal chromatography is a method by which volatile compounds of different chemical elements can be separated according to their volatilities. The technique, coupled with theoretical modeling of the processes occurring in the chromatography column, provides accurate determination of thermodynamic properties (e.g., adsorption enthalpies) for compounds of elements, such as the transactinides, which can only be produced on an atom-at-a-time basis. In addition, the chemical selectivity of the isothermal chromatography technique provides the decontamination from interfering activities necessary for the determination of the nuclear decay properties of isotopes of the transactinide elements. Volatility measurements were performed on chloride species of Rf and its group 4 homologs, Zr and Hf, as well as Ha and its group 5 homologs, Nb and Ta. Adsorption enthalpies were calculated for all species using a Monte Carlo code simulation based on a microscopic model for gas thermochromatography in open columns with laminar flow of the carrier gas. Preliminary results are presented for Zr- and Nb-bromides. DOE

N94-16870# Brookhaven National Lab., Upton, NY.
BINDING OF CARBON DIOXIDE TO METAL MACROCYCLES: TOWARD A MECHANISTIC UNDERSTANDING OF ELECTROCHEMICAL AND PHOTOCHEMICAL CARBON DIOXIDE REDUCTION
E. Fujita 1993 10 p Presented at the International Conference on Carbon Dioxide Utilization, Bari (Italy), 26-30 Sep. 1993
(Contract DE-AC02-76CH-00016)
(DE93-016244; BNL-49082; CONF-9309182-1) Avail: CASI HC A02/MF A01

Efforts were made to find effective catalysts for photochemical and electrochemical reduction of CO2. We are studying the factors controlling excited-state lifetimes, electron-transfer rates to mediators/catalysts, properties of reduced mediators, binding of small molecules to reduced mediators, and reactivity of the mediators to yield the desired products. This document describes some of the results of binding on CO2 to metal macrocycles. The electrocatalytic activity of cobalt macrocycle complexes in reduction of CO2 in CO2-saturated water at the Hg electrode is being studied. We are ready to study the mechanism and kinetics of the photochemical CO2 reduction in order to design more efficient photo-energy conversion systems. DOE

N94-16876# Edgerton, Germeshausen and Grier, Inc., Goleta, CA.
ELEMENTAL IMPURITY ANALYSIS OF MERCURIC IODIDE BY ICP/MS
E. S. Cross, E. Mroz (Los Alamos National Lab., NM.), and J. A. Olivares (Los Alamos National Lab., NM.) 1993 7 p Presented at the 41st American Society of Mass Spectrometry Conference on Mass Spectrometry and Allied Topics, San Francisco, CA, 30 May - 4 Jun. 1993
(Contract DE-AC08-88NV-10617)
(DE93-015531; EGG-10617-2197; CONF-9305222-1) Avail: CASI HC A02/MF A01

A method has been developed to analyze mercuric iodide (HgI2) for elemental contamination using Inductively Coupled Plasma/Mass Spectroscopy (ICP/MS). This paper will discuss the ICP/MS method, the effectiveness of purification schemes for removing impurities from HgI2, as well as preliminary correlations between HgI2 detector performance and elemental contamination levels. DOE

N94-16891# Mississippi State Univ., Mississippi State. Diagnostic Instrumentation and Analysis Lab.
GAS ANALYSIS SYSTEM
R. A. Green 1992 64 p
(Contract DE-AC02-80ET-15601)
(DE93-014617; DOE/ET-15601/T56) Avail: CASI HC A04/MF A01

A Gas Analysis System (GAS) has been configured at the Diagnostic Instrumentation and Analysis Laboratory (DIAL) to analyze the gaseous combustion products from nearly any combustion source. GAS is a mobile system of commercially available gas analyzers capable of analyzing a sample for O2, SO2, CO, CO2, NO(x), and combustibles (as %CH4). A Gas Chromatograph is also available as a separate instrument for gas analysis. The analyzers determine the specie concentrations and send a signal to a computer used for data logging. The computer converts the electrical signal into a concentration, stores the data on a disk, displays the results on the computer display, and can also provide a printout of the results. GAS has also had several sampling systems designed for various environments. A sampling system, capable of collecting and storing samples for later analysis, has also been designed. GAS has been used to determine gas compositions at Mississippi State University and the Component Development and Integration facility in Butte, Montana, and at industrial facilities. Computer programs are included. DOE

N94-16896# Massachusetts Inst. of Tech., Cambridge. Dept. of Chemical Engineering.
DIRECT CATALYTIC DECOMPOSITION OF NITRIC OXIDE
M. Flytzani-Stephanopoulos, A. F. Sarofim, and Yanping Zhang 1993 20 p
(Contract DE-FG22-91PC-91293)
(DE93-016689; DOE/PC-91293/T2) Avail: CASI HC A03/MF A01

This project investigates a suitable catalyst system for direct NO decomposition in post-combustion gas streams. The process does not use a reductant, such as the ammonia used in Selective Catalytic Reduction (SCR) of NO(x) to nitrogen. Therefore, it is a greatly simplified process basically involving passing the flue gas through a catalytic converter. Catalysts are prepared by incorporating metal cations into zeolite supports according to ion exchange procedures widely used in preparation of metal/zeolite catalysts. The catalysts of primary interest include copper, palladium, silver, and nickel exchanged ZSM-5 catalysts. Particular emphasis is given in this work on promoted Cu-exchanged zeolites, especially the catalyst system Mg/Cu-ZSM-5 and a few others, which are promising for NO conversion to nitrogen at typical flue gas O2 and NO levels and over the temperature range of 723-873 K. Effects of zeolite modification, copper exchange level and catalyst preparation conditions on the catalyst activity are studied in a packed-bed microreactor. Temperature-programmed desorption (TPD) and reduction (TPR) experiments will be carried out in a thermogravimetric analyzer and a single-particle electrodynamic balance (EDB). Kinetic studies of NO and O2 interaction with catalysts over a wide temperature range as well as catalyst structural investigations are planned. DOE

N94-16897# AMAX Research and Development Center, Golden, CO.
DEVELOPMENT OF VANADIUM-PHOSPHATE CATALYSTS FOR METHANOL PRODUCTION BY SELECTIVE OXIDATION OF METHANE
R. L. McCormick and M. C. Jha 11 May 1993 18 p
(Contract DE-AC22-92PC-92110)
(DE93-016850; DOE/PC-92110/T2) Avail: CASI HC A03/MF A01

During the second quarter, we initiated Task 2 (Process and Catalyst Variable Study). This task involves an investigation of methods for vanadium phosphate (VPO) catalyst synthesis and activation as well as detailed testing of the catalysts produced for activity and selectivity in methane selective oxidation. As we initiated work on Task 2, three problem areas were identified: preparation of catalysts with P:V ratio greater than 1; activation of the precursor to produce the B-phase described in the patent literature; and achieving high (greater than 95 percent) carbon balances in the bench-scale test unit. Each of these problems has been addressed and overcome during this quarter. Several catalysts with P:V ratios ranging from 0.95 to 1.1 have been prepared. Activation procedures are continuing to be investigated. We have found several procedures which yield catalysts having the desired X-ray diffraction pattern. The reactor system was modified and analytical procedures improved so that in a 7-day run using V2O5 as the catalyst, carbon balances ranged from 95 to 105 percent. DOE

N94-16904# Lawrence Livermore National Lab., CA.
OBSERVATION OF NONSEQUENTIAL IONIZATION OF HELIUM AND ITS IMPACT ON INTENSITY MONITORING
D. N. Fittinghoff (California Univ., Davis.), P. R. Bolton, B. Chang, and K. C. Kulander 19 Mar. 1993 9 p Presented at the OE/LASE 1993 International Society for Optical Engineering (SPIE) Conference, Los Angeles, 16-23 Jan. 1993
(Contract W-7405-eng-48)
(DE93-017174; UCRL-JC-113277; CONF-930159-45) Avail: CASI HC A02/MF A01

The authors have measured the ion yields for helium and neon ionized by 120 femtosecond, 614 nanometer laser pulses with intensities up to 10(exp 16) watts per square centimeter. They have found that the He 2 and Ne 2 data exhibit features incompatible with standard nonresonant sequential ionization. These features reduce the usefulness of optical field

ionization for monitoring laser intensity. For the experiment, they expect dynamic resonances to have little effect on the ionization, and they attribute the features to nonsequential ionization based on the simultaneous saturation of the features and the singly ionized charge states. DOE

N94-16912# Purdue Univ., West Lafayette, IN. Dept. of Chemistry.
PRECONVERSION CATALYTIC DEOXYGENATION OF PHENOLIC FUNCTIONAL GROUPS
C. P. Kubiak 1992 19 p
(Contract DE-FG22-89PC-89770)
(DE93-017034; DOE/PC-89770/T14) Avail: CASI HC A03/MF A01

Several new catalysts for phenol deoxygenation by CO were developed in our laboratories during the grant period. The deoxygenation of phenols by CO represents a novel approach to the upgrading of coal liquids. The deoxygenation of phenols by CO is thermodynamically more favorable and potentially less expensive than current phenol hydrodeoxygenation (HDO) methods. The reaction was not known to be kinetically feasible until our recent discovery of appropriate catalysts. The catalyst precursor (Ir(triphos)((eta)(sup 4-))C8H12)(C1) was found to catalytically deoxygenate phenol and p-cresol. Reactions were conducted with varying amounts of Ar-OH (Ar = C6H5, p-Me-C6H4), NaO-Ar, and catalyst precursor. In some reactions, triethyl amine was substituted for NaO-Ar to deprotonate the Ar-OH. All reactions took place at 55 C so that Ar-OH was the solvent. One atmosphere of CO was introduced into each reactor. Periodically, gasses were sampled by gas chromatography (GC) to monitor the disappearance of CO and the appearance of CO2. After the amount of CO2 had reached a plateau, organic products were distilled from the reaction mixture and analyzed by high pressure liquid chromatography (HPLC). Significant quantities of arene (benzene or toluene) were obtained. These results are general. Initial use of phenol results in only benzene. Initial use of p-cresol results in only toluene. Control reactions eliminate the catalyst precursor as the source of CO2 or arene. No evidence is obtained for diarylcarbonate formation. HPLC and GC data consistently demonstrated that toluene and CO2 were the only products obtained from the deoxygenation of p-cresol by CO. These results were extended to a series of variously substituted phenolic and naptholic substrates related to those found in coal liquids. DOE

N94-16930# AeroChem Research Labs., Inc., Princeton, NJ.
MODELING STUDY TO EVALUATE THE IONIC MECHANISM OF SOOT FORMATION IN FLAMES Annual Report, 15 Dec. 1991 - 14 Dec. 1992
H. F. Calcote, R. J. Gill, and D. G. Keil Feb. 1993 37 p
(Contract F49620-91-C-0021)
(AD-A266242; TP-518) Avail: CASI HC A03/MF A01

A study is underway to evaluate the proposed ionic mechanism of soot formation by developing a computer model and comparing it with experimental results and with equivalent models based on neutral species. During the present report period both the thermodynamic and reaction kinetic data base for ion-molecule reactions have been updated and expanded. The CHEMKIN-2 flame code, revised last report period, to handle ions is now operating routinely and has bee used to calculate ion profiles for the standard acetylene/oxygen flame. The results are generally in good agreement with experiment, except for the benzotropylium ion, for which the calculated value is about three orders of magnitude less than the experimental value. Poor thermodynamics are suspected. A comparison of data in the literature on the effect of equivalence ratio on acetylene and soot yield with values calculated by thermodynamic equilibrium for a number of fuels show that in general measured acetylene and soot concentrations are far in excess of equilibrium, especially below the threshold soot index. The standard acetylene/oxygen flame seems to be an exception. The results continue to support an ionization mechanism of soot formation. DTIC

N94-16931# California Univ., San Diego, La Jolla.
AMIDE AND TETRAZENE COMPLEXES OF TRANSITION AND MAIN GROUP ELEMENTS AS PRECURSORS FOR THE LOW TEMPERATURE SYNTHESIS OF ELEMENTAL NITRIDES Final Report, 1 Sep. 1989 - 30 Oct. 1992
William C. Trogler May 1993 3 p
(Grant AF-AFOSR-0408-89)
(AD-A266246; AFOSR-93-0425TR) Avail: CASI HC A01/MF A01

Tetrazene complexes and nitrene compounds derived therefrom were prepared. Attempts to use these compounds as precursors to metal nitride species failed. Metal acetylide complexes were prepared and examined by x-ray crystallography. Electrochemical procedures to deposit aluminum nitride films were explored using nonaqueous solvents. The reaction of several organometallics with azide ion was studied. The disproportionation reactions between 17-electron chromium triad radicals and various nucleophiles were characterized by infrared spectroscopy. The formation of reversible adducts from the reaction between trivalent phosphorus donor ligands and unsaturated organic carbonyl compounds was observed. DTIC

N94-16952# Lawrence Livermore National Lab., CA.
ACTIVATION AND DEACTIVATION OF HIGH CONCENTRATION ARSENIC WITH SOME EVIDENCE OF PRECIPITATION
P. M. Rousseau (Stanford Univ., CA.), P. B. Griffin (Stanford Univ., CA.), J. D. Plummer (Stanford Univ., CA.), and P. G. Carey 29 Dec. 1992 9 p Presented at the 183rd Electrochemical Society Meeting, Honolulu, HI, 16-21 May 1993
(Contract W-7405-eng-48)
(DE93-016437; UCRL-JC-112521; CONF-930571-21) Avail: CASI HC A02/MF A01

Using box-shaped profiles created by laser melt annealing, the authors investigate the kinetics of arsenic activation and deactivation. They find deactivation shows no history effects which can be consistent either with clustering or precipitation for the cases considered. For activation, they notice it occurs on very short time scales, followed by a slower deactivation process. This is suggestive evidence that at least some precipitation occurs. DOE

N94-16962# Notre Dame Univ., IN. Dept. of Chemical Engineering.
TRANSIENT STUDIES OF LOW TEMPERATURE CATALYSTS FOR METHANE CONVERSION
E. E. Wolf 1993 6 p
(Contract DE-FG22-92PC-92529)
(DE93-017710; DOE/PC-92529/T1) Avail: CASI HC A02/MF A01

This report summarizes studies conducted during the past quarter on the partial oxidation of methane on the following catalysts: vanadium phosphate, unsupported and supported on silica, and on the silica (SiO2) support. It was found that the unsupported vanadium phosphate catalyst exhibits some selectivity towards formaldehyde at relatively low methane conversions (up to 5% conversion). The selectivity decreases even further on the silica supported VPO catalyst without a significant increase in conversion. In the case of silica, the reaction temperature decreases, and the formaldehyde selectivity is higher than in the case of the VPO catalyst. DOE

N94-17006# Northwestern Univ., Evanston, IL. Dept. of Chemistry.
SOLVATIONAL BARRIERS TO INTERFACIAL ELECTRON TRANSFER: MINIMIZATION BY WAY OF VALENCE DELOCALIZATION Technical Report, Jun. - Oct. 1993
Joseph T. Hupp and Xiao L. Zhang 27 Jul. 1993 11 p
(Contract N00014-91-J-1035)
(AD-A267371) Avail: CASI HC A03/MF A01

Standard rate constants (k(sub s)) for interfacial electron transfer (ET) have been obtained for several redox couples featuring very small internal activation barriers. To render these ordinarily fast rates measurable, we have employed low defect density, highly ordered pyrolytic graphite (HOPG) as an electrode material. At the HOPG/aqueous solution interface, we observe - for the first time - the systematic (exponential) increase of k(sub s) with inverse reactant size, predicted by Marcus for electrochemical reactions whose barriers are primarily defined by solvent reorganizational effects. We also observe that rates can be significantly accelerated by delocalizing electrons over multiple metal-centered trapping sites. The degree of rate acceleration is quantitatively consistent with the extent of solvent barrier lowering expected if electronic delocalization effectively increases the radius of the ET reaction site. DTIC

N94-17008 United Technologies Research Center, East Hartford, CT.
MECHANISTIC MODELS OF SOOT FORMATION Annual Report, 1 Jun. 1992 - 31 May 1993
Meredith B. Colket, III, Robert J. Hall, and Mitch D. Smooke 14 Jul. 1993 74 p Limited Reproducibility: More than 20% of this document

may be affected by microfiche quality
(Contract F49620-91-C-0056)
(AD-A267806; UTRC93-28; AFOSR-93-0592TR) Avail: CASI HC A04

The overall objectives of this work are to (1) refine and update an existing soot formation model and (2) incorporate this soot model into a code describing a laminar, opposed jet diffusion flame. To help advance the understanding of chemical limitations of PAH formation in the soot model, phenylacetylene has been pyrolyzed in a single-pulse shock tube. The formation of PAH's from aromatic-aromatic reactions have been observed and evidence has been obtained for isomerization (equilibration) among polyaromatic species. Thermodynamics of high molecular weight PAH's have been calculated. Benzene production and radiation phenomena have been modeled and where possible these calculations have been compared to experimental results. A sectional aerosol model has been added to the diffusion flame code as well as related subroutines on soot formation, growth, and oxidation and the debugging of the code is nearly complete. Comparisons of the sectional model and a global soot formation model have been made for premixed flames. DTIC

N94-17039*# Alabama Univ., Huntsville. Surface Science Labs.
ELECTRON SPECTROSCOPY ANALYSIS Final Technical Report, 13 Apr. 1990 - 12 Apr. 1992
John C. Gregory 1992 10 p
(NASA Order H-01099-D)
(NASA-CR-193591; NAS 1.26:193591; UAH-5-32465) Avail: CASI HC A02/MF A01

The Surface Science Laboratories at the University of Alabama in Huntsville (UAH) are equipped with x-ray photoelectron spectroscopy (XPS or ESCA) and Auger electron spectroscopy (AES) facilities. These techniques provide information from the uppermost atomic layers of a sample, and are thus truly surface sensitive. XPS provides both elemental and chemical state information without restriction on the type of material that can be analyzed. The sample is placed into an ultra high vacuum (UHV) chamber and irradiated with x-rays which cause the ejection of photoelectrons from the sample surface. Since x-rays do not normally cause charging problems or beam damage, XPS is applicable to a wide range of samples including metals, polymers, catalysts, and fibers. AES uses a beam of high energy electrons as a surface probe. Following electronic rearrangements within excited atoms by this probe, Auger electrons characteristic of each element present are emitted from the sample. The main advantage of electron induced AES is that the electron beam can be focused down to a small diameter and localized analysis can be carried out. On the rastering of this beam synchronously with a video display using established scanning electron microscopy techniques, physical images and chemical distribution maps of the surface can be produced. Thus very small features, such as electronic circuit elements or corrosion pits in metals, can be investigated. Facilities are available on both XPS and AES instruments for depth-profiling of materials, using a beam of argon ions to sputter away consecutive layers of material to reveal sub-surface (and even semi-bulk) analyses.
Author

N94-17050# Polish Academy of Sciences, Warsaw. Inst. Podstawowych Problemow Techniki.
AN ANALYSIS OF WAYS OF DETERMINING THE MATERIAL CONSTANTS FOR VISCOELASTIC MATERIALS [ANALIZA SPOSOBOW WYZNACZANIA STALYCH MATERIALOWYCH DLA MATERIALOW LEPKOSPREZYSTYCH]
Lech Dietrich and Karol Turski 1991 79 p In POLISH
(IFTR-28/91) Avail: CASI HC A05/MF A01

A complete solution of a fundamental equation under different initial conditions is derived for an elastoviscous material described by Burger's model. The possibilities for establishing the moduli of the materials for different sample loading schemes are defined. The experimental research results obtained for different loading methods and deformation rates for samples fabricated from an asphalt mixture are compared. It is established that the slip, cyclic deformation and loading at a constant deformation rate make it possible to determine the elasticity and viscosity moduli for different deformation rates while the results obtained from different loading methods make possible a uniform representation of the dependence of the moduli on the deformation rate. Transl. by FLS

N94-17125*# Princeton Univ., NJ. Dept. of Mechanical and Aerospace Engineering.
STUDIES OF PREMIXED LAMINAR AND TURBULENT FLAMES AT MICROGRAVITY Final Report, 15 Mar. 1991 - 31 Aug. 1993
Paul D. Ronney 31 Aug. 1993 11 p
(Grant NAG3-1242)
(NASA-CR-194656; NAS 1.26:194656) Avail: CASI HC A03/MF A01

A two and one-half year experimental and theoretical research program on the properties of laminar and turbulent premixed gas flames at microgravity was conducted. Progress during this program is identified and avenues for future studies are discussed. Author

N94-17203 Army Research Lab., Aberdeen Proving Ground, MD.
SENSITIVE DETECTION OF GAS-PHASE NITRO-CONTAINING ENERGETIC MATERIALS EMPLOYING 226-nm RADIATION Final Report, Feb. - Sep. 1992
Rosario C. Sausa, George W. Lemire, and Josef B. Simeonsson Jul. 1993 30 p Limited Reproducibility: More than 20% of this document may be affected by microfiche quality
(AD-A267633; ARL-TR-157) Avail: CASI HC A03

The development of a novel technique for sensing trace vapors of -NO2 containing compounds is reported. This technique is based on the use of one laser operating at 226 nm to both photofragment the target molecule and detect the characteristic NO fragment, formed from a rapid predissociation of NO2 by resonance-enhanced multiphoton ionization (REMPI) and/or laser-induced fluorescence (LIF) via its A2 sum (+)(-X2Pi)(0,0) band origin. The analytical utility of this technique is demonstrated on a number of compounds, including dimethylnitramine, nitromethane, nitrobenzene, TNT, and RDX, employing molecular beam sampling with time-of-flight mass spectrometric analysis of the jet cooled analyte seeded in an atmosphere of buffer gas. With the present system, limits of detection of 8 and 24 parts-per-billion (ppb) are obtained for RDX and TNT, respectively, using approx. 100 microjoules pulse of laser energy. The limits of detection of the other compounds studied are also presented and discussed. DTIC

N94-17207# Aerospace Corp., El Segundo, CA. Engineering and Technology Group.
LONG DURATION EXPOSURE FACILITY EXPERIMENT m0003 DEINTEGRATION OBSERVATION DATABASE
S. R. Gyetvay, J. M. Coggi, and M. J. Meshishnek 17 Feb. 1993 200 p
(Contract F04701-88-C-0089)
(AD-A267579; TR-92(2935)-9; SMC-TR-93-38) Avail: CASI HC A09/MF A03

The four trays of the M0003 materials experiment on LDEF contained over 1600 samples from 20 subexperiments. The complete sample complement represented a broad range of materials including thin film optical coatings, paints, polymer sheets and tape, adhesives, and composites. The materials are intended for use in various spacecraft applications including thermal control, structures, optics, and solar power. Since some subexperiments included duplicate samples exposed on the leading and trailing edge trays for 9-week, 19-week, 40-week, and 69-month durations, comparisons provided a valuable time history of degradation. During the deintegration of the subexperiments from the M0003 trays, each sample was examined using bright field, dark field, and Nomarski light microscopy techniques. Over 3,000 color macrographs and photomicrographs were made of the condition of the M0003 trays and the individual samples. Records of the condition of the samples, photographic records, and all available references of publications on postflight analyses on each sample were collected in a computer database (4th Dimension(TM) for the Macintosh computer). Upon written request, the database records and photographs for specific samples may be obtained from The Aerospace Corporation Archives. Copies of the electronic database are available on floppy disk by request, as well. Directions for requesting the records, photographs, and database copies are given in this report. DTIC

N94-17210# Consultec Scientific, Inc., Knoxville, TN.
ELECTRORHEOLOGICAL (ER) FLUIDS: A RESEARCH NEEDS ASSESSMENT
Irvin M. Krieger and Edward A. Collins May 1993 359 p

(Contract DE-AC04-91ER-30172)
(AD-A267588) Avail: CASI HC A16/MF A03

In 1947, Willis Winslow was awarded a U.S. patent on 'Methods and Means for Translating Electrical Impulse Into Mechanical Forces'. Winslow's patent makes use of an electrorheological (ER) fluid, i.e., one which is transformed from a liquid into a viscoelastic solid upon application of a strong electric field. Based on this gelation effect, a whole new technology has been proposed. This technology provides novel and efficient ways to control fluid flow and power transmission and to reduce energy loss and damage due to vibration and oscillation. A large number and variety of ER devices have been invented; they are described in publications and patents, and many exist as prototype and demonstration devices. ER devices such as shock absorbers, valves, transmissions, and fluid couplings are more energy-efficient than hydraulic, mechanical, or electromechanical devices which serve the same function. The power needed to operate an ER device is usually very low compared to the power controlled by the device, and its response can be almost instantaneous. DTIC

N94-17218# Dow Corning Corp., Carrollton, KY.
METHYL CHLORIDE VIA OXYHYDROCHLORINATION OF METHANE
B. Naasz Mar. 1993 7 p
(Contract DE-AC22-91PC-91030)
(DE93-017548; DOE/PC-91030/T4) Avail: CASI HC A02/MF A01

Work to develop a highly selective methyl chloride synthesis catalyst continued, but no stable catalyst with greater than 80% selectivity at 20% methane exists yet. An effort was made on finalizing the preengineering scope definition of the Process Demonstration Unit. Natural gas purification, reactor, reactor effluent and MeCl purification, and anhydrous HCl recovery are discussed. DOE

N94-17302 China Nuclear Information Centre, Beijing.
STRESS CORROSION CRACKING OF 316 SS AND INCOLOY-800 IN HIGH TEMPERATURE AQUEOUS CONTAINING SULFATE AND CHLORIDE
Weiguo Zhang, Fangliang Lin, Fengqin Gao, Hongyi Zhou, and Xiaoning Cao (Academia Sinica, Guiyang, China.) Mar. 1992 10 p Limited Reproducibility: More than 20% of this document may be affected by microfiche quality
(DE93-623325; CNIC-00598; IAE-0102) Avail: Issuing Activity (Department of Energy (DOE)) (US Sales Only)

The stress corrosion cracking (SCC) susceptibility of 316 stainless steel (SS) which was welded for primary pipe and Incoloy-800 (shot peening) for steam generator (SG) tube have been investigated by a slow strain rate test (SSRT) at a strain rate of 4.2 x 10(exp -6)/s. Tests were conducted at 315 C for 316 SS and 270 C for In-800 in the oxygenated simulated resin intrusion environment (acidic sulfate). Tests of the effect of combination of SO4(2-) and Cl(-) on SCC of Incoloy-800 were also carried out. The results indicate that Incoloy-800 is unsusceptible to SCC either in the environment with SO4(2-) (from a few ppm to 1000 ppm, pH approximately 3 to 4) or in the environment of combination of SO4(2-) (1000 ppm) and Cl(-) (from 2 to 1000 ppm). The 316 NG SS is susceptible to transgranular stress corrosion cracking (TGSCC) in the resin intrusion environment with SO4(2-) in high temperature water. DOE

N94-17381# California Inst. of Tech., Pasadena. Graduate Aeronautical Labs.
LIFTED TURBULENT JET FLAMES Ph.D. Thesis
Jay A. Hammer 14 Apr. 1993 156 p
(Contract N00014-89-J-1991)
(AD-A267911) Avail: CASI HC A08/MF A02

Experiments were conducted on lifted, turbulent jet diffusion flames. A linear photodiode array was used to measure the temporal history of the liftoff height, h. Measurements of the mean liftoff height, bar-h, under a wide range of flow conditions, including several fuels, nozzle diameters, and exit velocities U(sub s), showed an approximately linear relationship between bar-h and U(sub s), with a slight dependence on Reynolds number. A strain-rate model was developed for liftoff, based on far-field scaling of turbulent jets; it provides an explanation for the linear dependence of bar-h on U(sub s). When the nozzle fluid was diluted with varying amounts of air it was found that the slope of the bar-h vs. U(sub s), line increases faster than predicted by the far-field scaling. The discrepancy is attributed to near-field effects. The amplitudes of the fluctuations in bar-h were found to be of the order of the local large scale of the jet but the time scales were found to be much larger than the local large-scale time of the turbulence tau(sub delta). By using fuels of different chemical times to vary tau(sub delta), the measured correlation time tau(sub 1/2) normalized by tau(sub delta) was found to collapse with Richardson number xi(sub h). DTIC

N94-17416 North Carolina Univ., Chapel Hill. Dept. of Chemistry.
SYNTHESIS AND CHARACTERIZATION OF NEW LOW-DIMENSIONAL METAL COMPLEX CONDUCTORS Final Report
William E. Hatfield 15 Aug. 1993 8 p Limited Reproducibility: More than 20% of this document may be affected by microfiche quality
(Contract N00014-92-J-1637)
(AD-A268251) Avail: Issuing Activity (Defense Technical Information Center (DTIC))

This final report contains a recapitulation of accomplishments and conclusions. A listing of all technical reports and journal articles emanating from the grant is included along with the names of all personnel who participated in the research. DTIC

N94-17520 Air Force Inst. of Tech., Wright-Patterson AFB, OH.
LASER PHOTOIONIZATION TIME-OF-FLIGHT MASS SPECTROMETRY OF NITRATED POLYCYCLIC AROMATIC HYDROCARBONS AND NITRATED HETEROCYCLIC COMPOUNDS M.S. Thesis
Rae A. Noyes 1993 280 p Limited Reproducibility: More than 20% of this document may be affected by microfiche quality
(AD-A268126; AFIT/CI/CIA-93-070) Avail: Issuing Activity (Defense Technical Information Center (DTIC))

The partial contents of this document are as follows: Laser Desorption-Laser Photoionization Time-of-Flight Mass Spectrometry (TOFMS); Basic Principles of TOFMS; Factors Affecting Flight Time; Source of Broadening; Laser Desorption; Theory of Multiphoton Ionization: Application to Mass Spectrometry; Quantum Theory of MPI; Time-Dependent Perturbation Theory; Time-Dependent Coefficients; Probability of a Two-Photon Process; and Attributes of R2PI. DTIC

N94-17532# Pennsylvania State Univ., University Park.
SURFACE REACTIVITY OF COMBUSTION GENERATED SOOT PARTICLES Annual Technical Report, 1 Jun. 1992 - 30 May 1993
Robert J. Santoro 1 Jul. 1993 38 p
(Contract F49620-92-J-0314)
(AD-A268017; AFOSR-93-0601TR) Avail: CASI HC A03/MF A01

During the first year of this AASERT program, efforts have focused on the development of a sampling probe to extract soot particles from a laminar diffusion flame. Soot samples collected with this system are to be used to study the surface reactivity of the soot particles as a function of position in the flame. A suitable probe system has been developed and tested. Comparisons with laser-based measurements of percent conversion of fuel to soot show reasonable agreement. Additional studies have also been conducted to examine the applicability of laser-induced incandescence (LII) as a soot diagnostic. Results have demonstrated that the L2 technique compares very well with previous measurements in a well-studied ethene/air laminar diffusion flame. Measurements of soot volume fraction, particle diameter and number density have been demonstrated. DTIC

N94-17594# Deutsche Forschungsanstalt fuer Luft- und Raumfahrt, Cologne (Germany). Abt. Solarchemie.
INVESTIGATIONS INTO THE RECOVERY OF WASTE SULFURIC ACID WITH CONCENTRATED SOLAR RADIATION Thesis - Tech. Hochschule, Aachen [UNTERSUCHUNGEN ZUR AUFBEREITUNG VON ABFALLSCHWEFELSAEUREN MIT KONZENTRIERTER SOLARER STRAHLUNG]
Oliver Weinmann 23 Mar. 1993 84 p In GERMAN
(Contract BMFT-0328823A)
(DLR-FB-93-11; ETN-93-94878) Avail: CASI HC A05/MF A01

For the recovery of waste sulfuric acid solarized processes are developed. The necessary process heat for the concentration and, if required, dissociation of the acid was supplied by concentrated solar radiation. An energy loss analysis of each facility components was carried out with a calculation of entropy flows, in order to show that highest losses appear in receivers. A simulation program was developed for the calculation of distillation column for the high concentration of sulfuric acid, considering

the real material behavior. In a test facility the positive effect of the concentrated solar radiation (represented by a solar simulator) on the decomposition of organic impurities of a waste sulfuric acid was demonstrated, compared to pure thermal oxidation. ESA

N94-17649# Sandia National Labs., Albuquerque, NM.
CHARACTERIZATION OF Ni ON Si WAFERS: COMPARISON OF SURFACE ANALYSIS TECHNIQUES
W. F. Calaway (Argonne National Lab., IL.), S. R. Coon (Argonne National Lab., IL.), M. J. Pellin (Argonne National Lab., IL.), D. M. Gruen (Argonne National Lab., IL.), M. Gordon (SEMATECH, Austin, TX.), A. C. Diebold (SEMATECH, Austin, TX.), P. Maillot (SEMATECH, Austin, TX.), J. C. Banks, and J. A. Knapp Jun. 1993 28 p Presented at the 15th Symposium on Applied Surface Analysis, Cleveland, OH, 9-11 Jun. 1993
(Contracts W-31-109-eng-38; DE-AC04-76DP-00789)
(DE93-016501; SAND-93-0651C; CONF-930686-1) Avail: CASI HC A03/MF A01

This paper reports on a collaborative effort to review the capabilities of several approaches to trace surface analysis. As a test case, Ni contamination of Si wafers in the dose range 10(sup 14) to 10(sup 10)/cm(sup 2) has been chosen. Emphasis of this paper is the capabilities of SARISA (surface analysis by resonant ionization of sputtered atoms), as an example of laser postionization secondary neutral mass spectrometry (SNMS), for detection of contaminants in the near-surface region. Results on analyses of the same standard samples by other techniques will also be presented. These techniques include total reflection x-ray fluorescence (TXRF) and heavy ion backscattering spectrometry (HIBS). Results of this comparison show that there are several techniques that can accurately determine metal contaminations on Si wafers in this concentration range and that the method of choice depends on other considerations such as speed or accuracy of analysis. DOE

N94-17660# Sandia National Labs., Livermore, CA.
CONTINUUM SOLVENT MODELS FOR COMPUTATIONAL CHEMISTRY
M. Colvin and C. Melius Jun. 1993 32 p
(Contract DE-AC04-76DR-00789)
(DE93-016329; SAND-93-8239) Avail: CASI HC A03/MF A01

This report describes an alternative to MD (molecular dynamics) and the empirical methods based on treating the solvent as a polarizable continuous medium (PCM). This model excludes many important properties of water such as explicit hydrogen bonding and size effects, but includes other properties of water that would otherwise only be accessible from computationally intensive MD. This report describes work supported by an LDRD grant, 'Computer-Designed Biomolecular Engineering,' to implement a polarizable continuum model of aqueous solvation for use with ab initio self-consistent field calculations. This implementation, based on methods developed by several research groups, uses accurate quantum chemical wavefunctions optimized with respect to the induced solvent charges. It is used to calculate several chemical properties tightly coupled to solvent interactions: proton transfer in water, the pKa's of alkyl amines, the energetics of aqueous phase glycine, and the protonation state of phosphoramide mustard. DOE

N94-16188*# Minnesota Univ., Minneapolis. Dept. of Geology and Geophysics.
RHEOLOGY OF WATER AND AMMONIA-WATER ICES Abstract Only
D. L. Goldsby, D. L. Kohlstedt, and W. B. Durham (Lawrence Livermore National Lab., CA.) *In* Lunar and Planetary Inst., Twenty-Fourth Lunar and Planetary Science Conference. Part 2: G-M 1993 p 543-544 (For primary document see N94-16173 03-91)
Avail: CASI HC A01/MF A06

N94-16243*# Rice Univ., Houston, TX. Dept. of Geology and Geophysics and of Chemistry.
GEOCHEMISTRY AND COSMOCHEMISTRY OF FULLERENES 3: REACTION OF C60 AND C70 WITH OZONE Abstract Only
D. Heymann and L. P. F. Chibante *In* Lunar and Planetary Inst., Twenty-Fourth Lunar and Planetary Science Conference. Part 2: G-M 1993 p 653-654 (For primary document see N94-16173 03-91)
Avail: CASI HC A01/MF A06

N94-16247*# Lafayette Coll., Easton, PA. Dept. of Physics.
PHASE EQUILIBRIA OF THE MAGNESIUM SULFATE-WATER SYSTEM TO 4 KBARS Abstract Only
D. L. Hogenboom, J. S. Kargel (Arizona Univ., Tucson.), J. P. Ganasan, and L. Lee *In* Lunar and Planetary Inst., Twenty-Fourth Lunar and Planetary Science Conference. Part 2: G-M 1993 p 661-662 (For primary document see N94-16173 03-91)
Avail: CASI HC A01/MF A06

N94-16256*# Open Univ., Milton (England). Dept. of Earth Sciences.
REMOVAL OF CARBONACEOUS CONTAMINANTS FROM SILICA AEROGEL Abstract Only
Hui-Ping Huang, I. Gilmour, C. T. Pillinger, and M. E. Zolensky (National Aeronautics and Space Administration. Lyndon B. Johnson Space Center, Houston, TX.) *In* Lunar and Planetary Inst., Twenty-Fourth Lunar and Planetary Science Conference. Part 2: G-M 1993 p 679-680 (For primary document see N94-16173 03-91)
Avail: CASI HC A01/MF A06

N94-16259*# Chicago Univ., IL. Dept. of Geophysical Sciences.
POTASSIUM ISOTOPE COSMOCHEMISTRY, VOLATILE DEPLETION AND THE ORIGIN OF THE EARTH Abstract Only
M. Humayun and R. N. Clayton *In* Lunar and Planetary Inst., Twenty-Fourth Lunar and Planetary Science Conference. Part 2: G-M 1993 p 685-686 (For primary document see N94-16173 03-91)
Avail: CASI HC A01/MF A06

N94-16264*# Academy of Sciences (USSR), Moscow. Inst. of Geochemistry, Analysis, and Chemistry.
FIRST INVESTIGATION OF NOBLE GASES IN THE DENGLI H3,8 CHONDRITE Abstract Only
M. A. Ivanova, S. S. Assonov, and Yu. A. Shukolyukov *In* Lunar and Planetary Inst., Twenty-Fourth Lunar and Planetary Science Conference. Part 2: G-M 1993 p 695-696 (For primary document see N94-16173 03-91)
Avail: CASI HC A01/MF A06

N94-16266*# Academy of Sciences (USSR), Moscow. Inst. of Geochemistry, Analysis and Chemistry.
INDUCED THERMOLUMINESCENCE STUDY OF EXPERIMENTALLY SHOCK-LOADED OLIGOCLASE Abstract Only
A. I. Ivliev, L. L. Kashkarov, and D. D. Badjukov *In* Lunar and Planetary Inst., Twenty-Fourth Lunar and Planetary Science Conference. Part 2: G-M 1993 p 699-700 (For primary document see N94-16173 03-91)
Avail: CASI HC A01/MF A06

N94-16267*# Academy of Sciences (USSR), Moscow. Inst. of Geochemistry, Analysis and Chemistry.
SHOCK-THERMAL HISTORY OF KAPOETA HOWARDITE MATTER ON DATA OF THERMOLUMINESCENCE ANALYSIS OF INDIVIDUAL MINERAL GRAINS Abstract Only
A. I. Ivliev, L. L. Kashkarov, and Yu. Yu. Korotkova (Moscow State Univ., Russia.) *In* Lunar and Planetary Inst., Twenty-Fourth Lunar and Planetary Science Conference. Part 2: G-M 1993 p 701-702 (For primary document see N94-16173 03-91)
Avail: CASI HC A01/MF A06

N94-16283*# National Aeronautics and Space Administration. Lyndon B. Johnson Space Center, Houston, TX.
PARTITIONING OF Nb, Mo, Ba, Ce, Pb, Th AND U BETWEEN IMMISCIBLE CARBONATE AND SILICATE LIQUIDS: EVALUATING THE EFFECTS OF P2O5,F, AND CARBONATE COMPOSITION Abstract Only
J. H. Jones and D. Walker (Lamont-Doherty Geological Observatory, Palisades, NY.) *In* Lunar and Planetary Inst., Twenty-Fourth Lunar and Planetary Science Conference. Part 2: G-M 1993 p 733-734 (For primary document see N94-16173 03-91)
Avail: CASI HC A01/MF A06

N94-16313*# California Inst. of Tech., Pasadena. Div. of Geology and Planetary Sciences.
AN EXPERIMENTAL STUDY OF TRACE ELEMENT PARTITIONING BETWEEN PEROVSKITE, HIBONITE AND MELT: EQUILIBRIUM VALUES Abstract Only
A. K. Kennedy, G. E. Lofgren (National Aeronautics and Space Administration. Lyndon B. Johnson Space Center, Houston, TX.), and G. J. Wasserburg *In* Lunar and Planetary Inst., Twenty-Fourth Lunar and Planetary Science Conference. Part 2: G-M 1993 p 793-794 (For primary document see N94-16173 03-91)
Avail: CASI HC A01/MF A06

N94-16314*# California Univ., San Diego, La Jolla. Dept. of Chemistry.
NITROGEN ISOTOPIC SIGNATURES IN AGGLUTINATES FROM BRECCIA 79035 Abstract Only
John F. Kerridge, Yoosook Kim, Jin S. Kim, and Kurt Marti *In* Lunar and Planetary Inst., Twenty-Fourth Lunar and Planetary Science Conference. Part 2: G-M 1993 p 795-796 (For primary document see N94-16173 03-91)
Avail: CASI HC A01/MF A06

N94-16340*# Michigan Univ., Ann Arbor. Radiation Lab.
FAR-INFRARED SPECTRA OF CO2 CLATHRATE HYDRATE FROSTS Abstract Only
J. C. Landry and A. W. England *In* Lunar and Planetary Inst., Twenty-Fourth Lunar and Planetary Science Conference. Part 2: G-M 1993 p 847-848 (For primary document see N94-16173 03-91)
(Grant NAGw-1334)
Avail: CASI HC A01/MF A06

N94-16353*# Chicago Univ., IL.
A SEARCH FOR NOBLE-GAS EVIDENCE FOR PRESOLAR OXIDE GRAINS Abstract Only
Roy S. Lewis and B. Srinivasan *In* Lunar and Planetary Inst., Twenty-Fourth Lunar and Planetary Science Conference. Part 2: G-M 1993 p 873-874 (For primary document see N94-16173 03-91)
Avail: CASI HC A01/MF A06

N94-16372*# Hawaii Univ., Honolulu. Planetary Geosciences.
FIRST RESULTS FROM A LABORATORY FACILITY FOR MEASUREMENT OF EMISSION SPECTRA UNDER SIMULATED PLANETARY CONDITIONS Abstract Only
Paul G. Lucey, Natalie Domergue-Schmidt, Bradley G. Henderson (Colorado Univ., Boulder.), and Bruce Jakosky (Colorado Univ., Boulder.) *In* Lunar and Planetary Inst., Twenty-Fourth Lunar and Planetary Science Conference. Part 2: G-M 1993 p 911-912 (For primary document see N94-16173 03-91)
Avail: CASI HC A01/MF A06

N94-16383*# Paris Univ. (France).
CO2 PRODUCTION BY IMPACT IN CARBONATES? AN ATEM AND STABLE ISOTOPE (C,O) STUDY Abstract Only
I. Martinez, P. Agrinier, F. Guyot, Ph. Ildefonse, M. Javoy, U. Schaerer, U. Hornemann (Muenster Univ., Germany.), and A. Deutsch (Muenster Univ., Germany.) *In* Lunar and Planetary Inst., Twenty-Fourth Lunar and Planetary Science Conference. Part 2: G-M 1993 p 933-934 (For primary document see N94-16173 03-91)
Avail: CASI HC A01/MF A06

N94-16401*# Geological Survey, Denver, CO.
LIMITED SUBSOLIDUS DIFFUSION IN TYPE B1 CAI: EVIDENCE FROM TI DISTRIBUTION IN SPINEL Abstract Only
G. P. Meeker, J. E. Quick, and Julie M. Paque (National Aeronautics and Space Administration. Ames Research Center, Moffett Field, CA.) *In* Lunar and Planetary Inst., Twenty-Fourth Lunar and Planetary Science Conference. Part 2: G-M 1993 p 969-970 (For primary document see N94-16173 03-91)
Avail: CASI HC A01/MF A06

N94-16432*# Eidgenoessische Technische Hochschule, Zurich (Switzerland).
SOLAR NOBLE GASES REVEALED BY CLOSED SYSTEM STEPPED ETCHING OF A METAL SEPARATE FROM FAYETTEVILLE Abstract Only
Ch. Murer, H. Baur, P. Signer, and R. Wieler *In* Lunar and Planetary Inst., Twenty-Fourth Lunar and Planetary Science Conference. Part 2: G-M 1993 p 1031-1032 (For primary document see N94-16173 03-91)
Avail: CASI HC A01/MF A06

26 METALLIC MATERIALS

Includes physical, chemical, and mechanical properties of metals, e.g., corrosion; and metallurgy.

N94-14930# Institut National des Sciences Appliquees de Lyon, Villeurbanne (France). Groupe d'Etudes de Metallurgie Physique et Physique des Materiaux.
CHARACTERIZATION OF THE CYCLIC PLASTICITY OF POLYCRYSTALLINE ALUMINUM IN THE 90-300K DOMAIN: USE OF THE ULTRASONIC WAVE COUPLING TECHNIQUE - LOW FREQUENCY RESTRAINT Ph.D. Thesis [CARACTERISATION DE LA PLASTICITE CYCLIQUE DE L'ALUMINIUM POLYCRISTALLIN DANS LE DOMAINE 90-300K: UTILISATION DE LA TECHNIQUE DE COUPLAGE ONDE ULTRASONORE-CONTRAINTE BASSE FREQUENCE]
Franck Charvieux 1992 262 p In FRENCH
(ISAL-92-0083; ETN-93-94358) Avail: CASI HC A12/MF A03

The role of microstructure in the cyclic deformation of aluminum and the interactions between the microstructure and the dislocations which take part in the deformation are studied. The state of the art of centered face cubic metals during cyclic plastic deformation is assessed and ultrasonic methods of investigation are recalled. Models which describe the attenuation and the speed of propagation of an ultrasonic wave and show the use of the ultrasonic wave coupling technique-low frequency restraint on the characterization of the mobility of short and medium length dislocations are addressed. The methodology used to study the cyclic plasticity at different temperatures and the results obtained are presented. The results are discussed. ESA

N94-14961# Florida Univ., Gainesville. Dept. of Materials Science and Engineering.
PROCESSING AND PROTECTION OF HIGH TEMPERATURE STRUCTURAL MATERIALS Final Report, Mar. 1991 - Mar. 1993
Ellis D. Verink, Jr. Mar. 1993 90 p
(Contract N00014-88-J-1100)
(AD-A267292) Avail: CASI HC A05/MF A01

Our objective was to develop a greatly improved understanding of the thermodynamic basis for processing and performance enhancement of Nb and Ta based alloys in order to provide better, scientifically-based support for current engineering efforts aimed at development of high temperature structural aerospace applications. A number of significant accomplishments have been made by the cooperating teams of researchers involved in this program. At the University of Florida, DeHoff and Brady have completed final modification of a computer program for calculating thermochemical diagrams of the type calculated by Dr. Pourbaix for high temperature oxidation. The development of such a program was one of the major milestones of the project. The program is ready for distribution upon request. DTIC

N94-15104# Army Research Lab., Watertown, MA.
ARMY P/M RESEARCH AND DEVELOPMENT OVERVIEW Final Report
Robert J. Dowding, Martin G. Wells, and Andrew Crowson May 1993 23 p
(AD-A266921; ARL-TR-140) Avail: CASI HC A03/MF A01

The Army uses of powder metallurgy (P/M) extend from the conventional press and sinter to the more exotic processes of liquid phase sintering of tungsten heavy alloys (WHA) and powder injection molding (PIM). Many of the more advanced high performance applications require extensive research and development (R and D) prior to fielding of the application. Examples are the intense research into WHA in the last ten years. This research has led to great understanding of these heavy alloys and application into

some kinetic energy systems. The Navy has taken great advantage of WHA by employing them in the phalanx close-in weapon system (CIWS). The Army intends that research will lead to an alloy or composite of tungsten that, when used as a long rod penetrator, will perform as well as, or better than, current depleted uranium (DU) penetrators. This will allow possible replacement of the controversial DU. Powder injection molding of WHA is an area receiving attention because of the potential for producing small and medium caliber projectiles. The drawbacks at this time include the need to develop an alloy that does not require post sinter cold working to develop the strength required for these demanding applications. Other possible problems include producing slender long rod projectiles with desired product straightness. In addition to the work on tungsten alloys, a discussion is underway of other powder metallurgy R and D and is under active investigation within the Army. These topics include aluminum and titanium alloys, intermetallics, and ultrahigh strength steels for structural and propulsion applications, as well as nonequilibrium P/M produced structures. DTIC

N94-15149# Office National d'Etudes et de Recherches Aerospatiales, Paris (France).

REACTIONS OF CHEMILUMINESCENCE INDUCED BY SINGLET OXYGEN WITH METALS Ph.D. Thesis - Paris-Sud Univ. [REACTIONS DE CHIMILUMINESCENCE INDUITES PAR L'OXYGENE SINGULET SUR LES SURFACES METALLIQUES]

Jean Lamarre 1992 143 p In FRENCH

(ONERA-NT-1992-13; ETN-93-94413) Avail: CASI HC A07/MF A02

The mechanisms of the chemiluminescence induced by the reaction of singlet oxygen and chlorine with heated metals was studied. This emission was proposed as a possible candidate for a visible chemical laser. The visible and infrared emission from the flame obtained with copper are found to be identical to that obtained from CuCl2 excited by collision with singlet delta oxygen. The comparison between the spectroscopic data obtained from visible and infrared emissions of the singlet oxygen/Cl2/Cu flame and those obtained from gaseous CuCl2 by laser induced fluorescence and by absorption allow to assign the chemiluminescence to CuCl2. The spectroscopic study of the flame obtained with high purity metals confirm that CuCl2 is really the emitter with copper and other metals, the minute traces of copper being involved in the reaction scheme. The experimental failures to obtain a visible laser effect using a high power chemical singlet oxygen generator suggests that the singlet oxygen/chlorine/copper medium cannot be used to produce a chemical visible laser. The results of the spectroscopic study of CuCl2 vapor confirm that this molecule is unlikely to be involved in a visible chemically pumped laser. ESA

N94-15708*# National Aeronautics and Space Administration. Langley Research Center, Hampton, VA.

PREDICTION OF STABLE TEARING OF 2024-T3 ALUMINUM ALLOY USING THE CRACK-TIP OPENING ANGLE APPROACH

J. G. Bakuckas, Jr. and J. C. Newman, Jr. Sep. 1993 24 p

(RTOP 538-02-10-01)

(NASA-TM-109023; NAS 1.15:109023) Avail: CASI HC A03/MF A01

In this study, the crack-tip opening angle (CTOA) approach was incorporated into a damage growth finite element program, MADGIC (Micromechanics Analysis and Damage Growth in Composites), and was used to predict stable tearing in a middle-crack tension 2024-T3 aluminum alloy specimen. The MADGIC code is a displacement based finite element program implemented with an incremental elastic-plastic algorithm used to model elastic-plastic behavior and a nodal splitting and nodal force relaxation algorithm used to generate crack surfaces. Predictions of the applied stress as a function of crack extension and applied stress as a function of load-line displacement were in good agreement with experiments and with similar predictions made using an existing finite element program, ZIP2D. In addition, path integrals, namely, the J-integral and T*-integral, were also evaluated and compared with the CTOA approach. There appears to be a weak relationship between the CTOA and the T*-integral evaluated on a specific integration path during crack extension beyond maximum applied stress. This study further verifies that the CTOA can be used as an effective elastic-plastic fracture mechanics parameter to predict crack growth. Author

N94-15830# Oak Ridge National Lab., TN.

ENVIRONMENTAL EMBRITTLEMENT IN ORDERED INTERMETALLIC ALLOYS

C. T. Liu and N. S. Stoloff 1992 34 p Presented at the Minerals, Metals, and Materials Society/American Society for Metals Materials Week 1992, Chicago, IL, 2-5 Nov. 1992

(Contract DE-AC05-84OR-21400)

(DE93-015307; CONF-9211117-9) Avail: CASI HC A03/MF A01

Ordered intermetallics based on aluminides and silicides possess many promising properties for elevated-temperature applications; however, poor fracture resistance and limited fabricability restrict their use as engineering material. Recent studies have shown that environmental embrittlement is a major cause of low ductility and brittle fracture in many ordered intermetallic alloys. There are two types of environmental embrittlement observed in intermetallic alloys. One is hydrogen-induced embrittlement occurring at ambient temperatures in air. The other is oxygen-induced embrittlement in oxidizing atmospheres at elevated temperatures. In most cases, the embrittlements are due to a dynamic effect involving generation and penetration of embrittling agents (i.e., hydrogen or oxygen) during testing. Diffusion of embrittling agents plays a dominant role in fracture of these intermetallic alloys. This chapter summarizes recent progress in understanding and reducing environmental embrittlement in these alloys. DOE

N94-15832*# National Aeronautics and Space Administration. Marshall Space Flight Center, Huntsville, AL.

THE CORROSION PROTECTION OF METALS BY ION VAPOR DEPOSITED ALUMINUM

M. D. Danford Oct. 1993 25 p Sponsored by NASA. Washington

(NASA-TM-108425; NAS 1.15:108425) Avail: CASI HC A03/MF A01

A study of the corrosion protection of substrate metals by ion vapor deposited aluminum (IVD Al) coats has been carried out. Corrosion protection by both anodized and unanodized IVD Al coats has been investigated. Base metals included in the study were 2219-T87 Al, 7075-T6 Al, Titanium-6 Al-4 Vanadium (Ti-6Al-4V), 4130 steel, D6AC steel, and 4340 steel. Results reveal that the anodized IVD Al coats provide excellent corrosion protection, but good protection is also achieved by IVD Al coats that have not been anodized. Author

N94-15862# Oak Ridge National Lab., TN.

RECENT ADVANCES IN ORDERED INTERMETALLICS

C. T. Liu 1992 17 p Presented at the High-Temperature Ordered Intermetallic Alloys V, Boston, MA, 30 Nov. - 3 Dec. 1992

(Contract DE-AC05-84OR-21400)

(DE93-015308; CONF-9211205-2) Avail: CASI HC A03/MF A01

This paper briefly summarizes recent advances in intermetallic research and development. Ordered intermetallics based on aluminides and silicides possess attractive properties for structural applications at elevated temperatures in hostile environments; however, brittle fracture and poor fracture resistance limit their use as engineering materials in many cases. In recent years, considerable efforts have been devoted to the study of the brittle fracture behavior of intermetallic alloys; as a result, both intrinsic and extrinsic factors governing brittle fracture have been identified. Recent advances in first-principles calculations and atomistic simulations further help us in understanding atomic bonding, dislocation configuration, and alloying effects in intermetallics. The basic understanding has led to the development of nickel, iron, and titanium aluminide alloys with improved mechanical and metallurgical properties for structural use. Industrial interest in ductile intermetallic alloys is high, and several examples of industrial involvement are mentioned. DOE

N94-15885# Los Alamos National Lab., NM.

TERNARY ALLOYING EFFECTS IN POLYCRYSTALLINE (BETA)-NiAl

J. D. Cotton, R. D. Noebe (National Aeronautics and Space Administration. Lewis Research Center, Cleveland, OH.), and M. J. Kaufman (Florida Univ., Gainesville.) 1993 16 p Presented at the International Symposium on Structural Intermetallics, Champion, PA, 26-30 Sep. 1993

(Contract W-7405-eng-36)

(DE93-012675; LA-UR-93-1395; CONF-930997-1) Avail: CASI HC A03/MF A01

The purpose of this paper is to summarize alloying research to date in polycrystalline NiAl and its impact on microstructure and ambient temperature

properties. It is divided into the following sections: phase equilibria, solid solution effects and precipitation effects. Alloys that contain a high volume fraction of second phase (e.g. pseudobinary eutectic compositions) are not considered. Rather, the effects of dilute to moderate ternary alloying additions on the structure and properties of (beta)-NiAl are reviewed. It is already well established that stoichiometry is paramount in controlling mechanical properties of the binary compound. Since the addition of a third element is equally important, ternary phase equilibria are reviewed first. Solid solution strengthening is probably the least well understood particularly with respect to the nature of point defects and their contribution to strength. Characterization of these defects and their role in mechanical properties may well hold the key to future development of NiAl-based materials. With regard to second phases, there is limited evidence that the classical precipitation hardening mechanisms for metals are also applicable to NiAl. DOE

N94-15921# Brookhaven National Lab., Upton, NY.
APPLICATION OF IN SITU SCANNING X RAY FLUORESCENCE TO STUDY THE CONCENTRATION OF METAL IONS IN SIMULATED PITS
H. S. Isaacs, A. J. Davenport, Cho Jeong-Hwan (Yonsei Univ., Seoul, Republic of Korea.), M. L. Rivers (Chicago Univ., IL), and S. R. Sutton (Chicago Univ., IL.) 1993 8 p Presented at the 12th International Corrosion Congress, Houston, TX, 19-24 Sep. 1993
(Contract DE-AC02-76CH-00016)
(DE93-014054; BNL-48706; CONF-9309150-3) Avail: CASI HC A02/MF A01

X-ray energy-dispersive spectroscopy has been used to study the compositions of metal ions in solutions developed during localized corrosion. An electrochemical cell was designed to simulate a corrosion pit, maintaining one-dimensional diffusion and fulfilling the requirements for x-ray fluorescence measurements. The working electrode consisted of a dissolving thin foil of Type 304 stainless steel sealed between Mylar sheets through which the x-ray beam passed. Concentration gradients within the artificial pit were quantitatively determined. DOE

N94-15922# Brookhaven National Lab., Upton, NY.
POTENTIAL TRANSIENTS, TRANSMISSION AND ELECTROCHEMICAL CORROSION DETECTION
H. S. Isaacs and Jeong-Hwan Cho (Yonsei Univ., Seoul, Republic of Korea.) 1993 7 p Presented at the 12th International Corrosion Congress, Houston, TX, 19-24 Sep. 1993
(Contract DE-AC02-76CH-00016)
(DE93-014055; BNL-48707; CONF-9309150-4) Avail: CASI HC A02/MF A01

The transmission of potential along a passive metal/electrolyte interface is important in open circuit corrosion monitoring when the containment system rather than an insulated metal specimen is monitored. Potential variations have been considered for transitory and sustained corrosion processes. The observed signals are modified and delayed by the passive surface. Using a transmission line as the equivalent circuit of a pipe and incorporating the impedance characteristics of the passive-metal/solution interface enabled a quantitative analysis of the effectiveness of corrosion monitoring methods to be carried out. DOE

N94-15948*# National Aeronautics and Space Administration. Langley Research Center, Hampton, VA.
MEASUREMENT AND ANALYSIS OF CRITICAL CTOA FOR AN ALUMINUM ALLOY SHEET
D. S. Dawicke (Analytical Services and Materials, Inc., Hampton, VA.), M. A. Sutton (South Carolina Univ., Columbia.), J. C. Newman, Jr., and C. A. Bigelow Sep. 1993 33 p
(RTOP 538-02-10-01)
(NASA-TM-109024; NAS 1.15:109024) Avail: CASI HC A03/MF A01

The stable tearing behavior of thin sheets of 2024-T3 aluminum alloy was investigated for middle crack tension, M(T), and compact tension, C(T), specimens. The surface crack-tip opening angle (CTOA), applied loads, crack extension, and local displacements were measured. A critical CTOA fracture criterion was incorporated into a two-dimensional, elastic plastic finite element code and used to simulate the experimental fracture behavior. The CTOA measurements and observations of the fracture surfaces have shown that large values for surface CTOA were observed for small crack extensions (less than the sheet thickness); substantial tunneling of the crack was associated with small crack extensions; crack tunneling in the M(T) specimen was less than that observed in the C(T) configuration; for larger crack extensions, the measured CTOA values were determined to be approximately 6 degrees for both the M(T) and C(T) configuration; and for larger crack extensions, crack tunneling remained constant. The two-dimensional finite element predictions of fracture behavior assumed a constant critical CTOA value of 6 degrees and accounted for local crack tip constraint with a plane strain core of elements ahead of the crack tip. The plane strain core extended 5 mm above the crack plane. The simulations were within +/- 4 percent of the maximum applied load for the C(T) tests within 2 percent for the M(T) tests. Author (revised)

N94-15992*# National Aeronautics and Space Administration. Lewis Research Center, Cleveland, OH.
A SULFUR SEGREGATION STUDY OF PWA 1480, NiCrAl, AND NiAl ALLOYS
D. T. Jayne (Case Western Reserve Univ., Cleveland, OH.) and J. L. Smialek Mar. 1993 15 p Presented at the Second International Conference on Microscopy of Oxidation, Cambridge, England, 31 Mar. 1993; sponsored by the Inst. of Materials
(RTOP 505-63-5A)
(NASA-TM-106289; E-8001; NAS 1.15:106289) Avail: CASI HC A03/MF A01

Some nickel based superalloys show reduced oxidation resistance from the lack of an adherent oxide layer during high temperature cyclic oxidation. The segregation of sulfur to the oxide-metal interface is believed to effect oxide adhesion, since low sulfur alloys exhibit enhanced adhesion. X ray Photoelectron Spectroscopy (XPS) was combined with an in situ sample heater to measure sulfur segregation in NiCrAl, PWA 1480, and NiAl alloys. The polished samples with a 1.5 to 2.5 nm (native) oxide were heated from 650 to 1100 C with hold times up to 6 hr. The sulfur concentration was plotted as a function of temperature versus time at temperature. One NiCrAl sulfur study was performed on the same casting used by Browning to establish a base line between previous Auger Electron Spectroscopy (AES) results and the XPS results of this study. Sulfur surface segregation was similar for PWA 1480 and NiCrAl and reached a maximum of 30 at% at 800 to 850 C. Above 900 C the sulfur surface concentration decreased to about 3 at% at 1100 C. These results are contrasted to the minimal segregation observed for low sulfur hydrogen annealed materials which exhibit improved scale adhesion. Author (revised)

N94-15998# Pennsylvania State Univ., University Park. Center for Advanced Materials.
VACANCY CONDENSATION AS THE PRECURSOR TO PASSIVITY BREAKDOWN
D. D. Macdonald 1993 12 p Presented at the Fall Committee Week of the National Association of Corrosion Engineers, Houston, TX, 26 Sep. - 1 Oct. 1993
(Contract DE-FG02-91ER-45461)
(DE93-012925; DOE/ER-45461/10; CONF-930998-1) Avail: CASI HC A03/MF A01

This paper outlines the events that are envisaged to occur, according to the Point Defect Model (PDM), during 'chemically-induced' breakdown of the barrier layer on passivated metals and alloys in aqueous environments. The essential hypothesis of the model is that the local generation of cation vacancies at the barrier layer/environment interface, due to the autocatalytic adsorption of a damaging species such as chloride ion into the oxygen vacancy structure, leads to an enhanced flux of cation vacancies across the film. If the vacancies that arrive at the metal/film interface cannot be annihilated by cation ejection from the metal, the vacancies will condense leading to the local decohesion of the barrier layer from the metal. A combination of film dissolution at the barrier layer/environment interface and residual stresses in the oxide film leads to the physical rupture of the film, marking a passivity breakdown event. The PDM accounts for a variety of empirically-established relationships for the nucleation of pits, including the fact that the breakdown voltage (V(sub c)) and induction time (t(sub ind)) are distributed quantities; that V(sub c) = V(sub c)(sup o) - blog (a(sub Cl(-))), where b is greater than 2.303RT/F; and that log (t(sub ind))(alpha) 1/(Delta)V, where (Delta)V = V (applied voltage) - V(sub c). Also, the model has been extended to account for alloying effects and, indeed, new alloys are now being designed on the basis of rules that have been derived from the PDM. DOE

N94-16015# Oak Ridge National Lab., TN.
DYNAMICAL ISING MODEL SIMULATIONS OF NUCLEATION AND GROWTH IN COPPER-COBALT ALLOYS
A. Cerezo (Oxford Univ., England.), J. M. Hyde (Oxford Univ., England.), R. P. Setna (Oxford Univ., England.), G. D. W. Smith (Oxford Univ., England.), and M. K. Miller 1992 7 p Presented at the 16th Material Research Society International Symposium on the Scientific Basis for Nuclear Waste Management Fall Meeting, Boston, MA, 30 Nov. - 5 Dec. 1992
(Contract DE-AC05-84OR-21400)
(DE93-015336; CONF-921101-132) Avail: CASI HC A02/MF A01

A simple dynamical Ising model on a fixed lattice with a single bond energy parameter has been used to simulate the kinetics of diffusion during solid-state phase transformations in binary metallic alloys. Results of these simulations are compared with direct real-space measurements of the atomic distributions of elements in alloys, obtained with the position-sensitive atom probe. Despite the simplicity of the model, there is good quantitative agreement between the development of microstructure in the simulation and the nucleation and growth of cobalt-rich precipitates in copper-cobalt alloys. DOE

N94-16068# Oak Ridge National Lab., TN.
THE EFFECT OF LONG-TERM AGING ON THE IMPACT PROPERTIES OF MODIFIED 9Cr-1Mo STEEL
D. J. Alexander, P. J. Maziasz, and C. R. Brinkman 1992 7 p Presented at the Fall Meeting of the Metallurgical Society and American Institute of Metallurgical and Petroleum Engineers, Chicago, IL, 1-5 Nov. 1992
(Contract DE-AC05-84OR-21400)
(DE93-015453; CONF-921109-6) Avail: CASI HC A02/MF A01

The Charpy impact and room-temperature tensile properties of two heats of modified 9Cr-1Mo steel have been examined after aging at temperatures from 482 to 704 C for times up to 75,000 h. In general, aging at lower temperatures (482, 538, or 593 C) resulted in little change in the room-temperature tensile properties, but rapid increases in the transition temperature, with the greatest increase for an aging time of 25,000 h. The upper-shelf energy level decreased, reaching a minimum at 25,000 h, followed by recovery at 50,000-h aging. At higher aging temperatures (649 and 704 C) there was little change in the transition temperatures, but significant softening at room temperature, and large increases in the upper-shelf energy. DOE

N94-16103# Oak Ridge National Lab., TN.
THE EFFECT OF AGING AT 343 C ON THE MECHANICAL PROPERTIES AND MICROSTRUCTURE OF TYPE 308 STAINLESS STEEL WELDMENTS
D. J. Alexander, K. B. Alexander, M. K. Miller, and R. K. Nanstad 1992 8 p Presented at the Fall Meeting of the Metallurgical Society and American Institute of Metallurgical and Petroleum Engineers, Chicago, IL, 1-5 Nov. 1992
(Contract DE-AC05-84OR-21400)
(DE93-015454; CONF-921109-7) Avail: CASI HC A02/MF A01

The effect of long-term aging at intermediate temperatures on the mechanical properties of stainless steel welds was studied. Three type 308 multipass shielded metal-arc welds with ferrite levels of 4, 8, and 12% were aged up to 20,000 h at 343 C. Tensile tests showed little effect of aging on either the yield or ultimate tensile strengths, but the impact toughness was significantly degraded. The extent of the degradation increased with increasing ferrite content and increasing aging time. Examination of the microstructure with transmission electron microscopy and atom probe field-ion microscopy revealed that the ferrite phase had undergone spinodal decomposition as a result of aging. In addition, G-phase particles were observed at dislocations, and finer G-phase particles were homogeneously distributed throughout the ferrite phase. The changes in the mechanical properties and the fractography are discussed in light of the observed changes in the microstructure. DOE

N94-16106# Oak Ridge National Lab., TN.
THE INFLUENCE OF THERMAL AGING ON THE MICROSTRUCTURE AND FATIGUE PROPERTIES OF MODIFIED 9Cr-1Mo STEEL
B. G. Gieseke, C. R. Brinkman, and P. J. Maziasz 1992 10 p Presented at the Microstructure and Mechanical Properties of Aging Materials, Detroit, MI, 2-5 Nov. 1992
(Contract DE-AC05-84OR-21400)
(DE93-015489; CONF-9211110-2) Avail: CASI HC A02/MF A01

Results of elevated-temperature low cycle fatigue and creep-fatigue tests are reported for one heat of modified 9Cr-1Mo steel in the normalized and tempered condition, after pre-aging 50,000 h at 538 and 593 C, and after pre-aging for 75,000 h at 538 C. These data show that pre-aging reduces the low cycle fatigue and creep-fatigue lives in comparison to unaged material. The magnitude of these reductions are discussed along with the impact of pre-aging on the creep-fatigue damage diagrams. The effect of environment on creep-fatigue life of unaged modified 9Cr-1Mo steels is also addressed. Transmission electron microscopy explains changes in mechanical properties due to thermal aging. In the unaged alloy, TEM shows that dynamic recovery/recrystallization is occurring after significant strain-induced dislocation hardening around a stationary and stable array of as-tempered carbides during creep-fatigue. In contrast creep-fatigue testing of the pre-aged alloy produced a much coarser cellular subgrain structure and dislocation recovery without recrystallization. Aging causes as-tempered carbide dissolution and/or reprecipitation together with additional precipitation of Laves (Fe2Mo) phase, which removes some of the precipitate-strengthening effects, and depletes solid-solution hardening effects on the dislocation networks and subgrain boundary structures. DOE

N94-16163# Oak Ridge National Lab., TN.
EFFECTS OF ALLOYING AND TEMPERATURE ON THE HIGH-TEMPERATURE OXIDATION OF Cr-Cr2Nb
P. F. Tortorelli, J. H. DeVan, and L. J. Carson (Lincoln Univ., PA.) 1993 10 p Presented at the 7th Annual Conference on Fossil Energy Materials, Oak Ridge, TN, 11-13 May 1993
(Contract DE-AC05-84OR-21400)
(DE93-015800; CONF-9305135-4) Avail: CASI HC A02/MF A01

Effects of alloying additions and temperature on isothermal and cyclic oxidation resistance of Cr-Cr2Nb alloys were examined for air exposures. An isothermal exposure temperature of 1100C led to rapid reaction of binary Cr-12 at.% Nb as manifested a high oxidation rate and nonprotective behavior. Generally parabolic kinetics, complicated by some isothermal scale cracking, were observed at 900-1000C. Scale damage was exacerbated by thermal cycling. The addition of 8 at.% Al to Cr-12 at.% Nb did not effect cyclic oxidation resistance, but there was some evidence that scale adherence on Cr-6 at.% Nb-8 at.% Al was better than that for binary Cr-6 at.% Nb. Alloying additions of Al (up to 18 at.%) or Re (2 at.%) did not improve the isothermal oxidation resistance of Cr-12 at.% Nb. However, the tendency for scale damage during both isothermal and thermal cycling exposures suggests that alloying additions that specifically improve scale plasticity or modify growth stresses could be effective for Cr-Nb alloys. DOE

N94-16165# Oak Ridge National Lab., TN.
DEVELOPMENT AND COMMERCIALIZATION STATUS OF Fe3Al-BASED INTERMETALLIC ALLOYS
V. K. Sikka, S. Viswanathan, and C. G. McKamey 1993 9 p Presented at the International Symposium on Structural Intermetallics, Champion, PA, 26-30 Sep. 1993
(Contract DE-AC05-84OR-21400)
(DE93-015802; CONF-930997-3) Avail: CASI HC A02/MF A01

The Fe3Al-based intermetallic alloys offer unique benefits of excellent oxidation and sulfidation resistance, limited by poor room-temperature (RT) ductility and low high-temperature strength. Recent understanding of environmental effects on RT ductility of these alloys has led to progress toward taking commercial advantage of Fe3Al-based materials. Cause of low ductility appears to be related to hydrogen formed from reaction with moisture. The environmental effect has been reduced in these intermetallic alloys by two methods. The first deals with producing a more hydrogen-resistant microstructure through thermomechanical processing, and the second dealt with compositional modification. The alloys showing reduced environmental effect have been melted and processed by many different methods. Laboratory and commercial heats have been characterized. Tests have been conducted in both air and controlled environments to quantify environmental effects on these properties. These materials were also tested for aqueous corrosion and resistance to stress corrosion cracking. Oxidation and sulfidation data were generated and effects of minor alloying elements

on cyclic oxidation resistance were also investigated. Several applications have been identified for the newly developed iron aluminides. Commercialization status of these alloys is described. DOE

N94-16166# Oak Ridge National Lab., TN.
ENVIRONMENTAL EFFECTS ON IRON ALUMINIDES
J. H. DeVan and P. F. Tortorelli 1993 12 p Presented at the 7th Annual Conference on Fossil Energy Materials, Oak Ridge, TN, 11-13 May 1993
(Contract DE-AC05-84OR-21400)
(DE93-015820; CONF-9305135-5) Avail: CASI HC A03/MF A01

Corrosion properties of reference Fe3Al (28 at. % Al)-based compositions containing 2 and 5 at. % Cr were compared in a mixed gas composed of H2S-H2-H2O-Ar and in dehumidified air. The parabolic rate constant at 800C was a factor of 200 higher for the 5% Cr composition. Similar exposure of an alloy containing 16% Al and 5% Cr resulted in significantly higher weight gains than the Fe3Al-5% Cr composition. However all the alloys were significantly more resistant to the mixed gas than iron-based alloys with higher chromium and lower aluminum contents. The oxidation rates of the 2 and 5% Cr alloys were comparable in dry air at 800C and were a factor of two lower than the rate of the 2% Cr alloy in the mixed gas. An alloy of Fe with 16% Al, 5% Cr, and 0.1% Zr showed improved cyclic oxidation resistance in air at 900 and 1000C relative to binary alloys of 16 and 20% Al. The extent of oxidation of these 16% Al alloys was comparable to Zr-containing Fe3Al aluminides (28% Al) that develop adherent scales. DOE

N94-16168# Oak Ridge National Lab., TN.
THE EFFECT OF IRRADIATION ON THE MECHANICAL PROPERTIES OF 6061-T651 ALUMINUM
D. J. Alexander 1992 18 p Presented at the 16th Annual Symposium of American Society of Testing and Materials on Effects of Radiation on Materials, Denver, CO, 21-25 Jun. 1992
(Contract DE-AC05-84OR-21400)
(DE93-015825; CONF-920673-19) Avail: CASI HC A03/MF A01

Critical components of the Advanced Neutron Source (ANS) reactor, to be built at Oak Ridge National Laboratory (ORNL), will be fabricated from 6061-T651 aluminum alloy. This alloy has been selected for its favorable neutronic, thermal, and mechanical properties. The effect of irradiation on the tensile properties and fracture toughness has been studied to allow the lifetime of these components to be estimated. Irradiations were carried out in the High Flux Isotope Reactor at ORNL at a temperature of approximately 95 C to a fluence of approximately 10(exp 26) m(exp -2) (thermal). Testing was conducted from room temperature to 150 C. The yield and ultimate tensile strengths were increased by irradiation, and the total elongation decreased, but the fracture toughness at 26 and 95 C was not degraded by irradiation and decreased only slightly at 150 C. DOE

N94-16453# Oak Ridge National Lab., TN.
ION IMPLANTATION EFFECTS ON SURFACE-MECHANICAL PROPERTIES OF METALS AND POLYMERS
G. R. Rao Apr. 1993 207 p
(Contract DE-AC05-84OR-21400)
(DE93-014661; ORNL/M-2711) Avail: CASI HC A10/MF A03

Fatigue of 8 complex alloys based on Fe-13Cr-15Ni-2Mo-2Mn-0.2Ti-0.8Si-0.06C, and single-crystal Fe-15Cr-15Ni, implanted with 400-keV B(sup +) and 550-keV N(sup +) (total dose 2.3 x (10 exp 16) ions/sq cm) was examined. 600 C creep was also examined. The dual implantation increased hardness but decreased fatigue life of the 8 complex alloys. An optimum strengthening level and a shift to grain boundary cracking were determined. The single crystals also showed reduced fatigue life after implantation. High temperature creep of E1 and B1 alloys were improved by the dual implantation. Four polymers (PE, polypropylene, polystyrene, polyethersulfone) were implanted with 200keV B(sup +) to 3 different doses. PS was also implanted with both B(sup +) and Ar(sup +). Near-surface hardness and tribological properties were measured. The hardness increased with dose and energy; wear also improved, with an optimum dose. DOE

N94-16463# Los Alamos National Lab., NM.
METASTABLE PHASES IN MECHANICALLY ALLOYED ALUMINUM GERMANIUM POWDERS
P. J. Yvon and R. B. Schwarz 1993 21 p Presented at the 2nd Structural Applications of Mechanical Alloying Conference, Vancouver, Ontario, 20-22 Sep. 1993
(Contract W-7405-eng-36)
(DE93-008727; LA-UR-93-669; CONF-9309104-1) Avail: CASI HC A03/MF A01

Aluminum and germanium form a simple eutectic system with no stable intermetallic phase, and limited mutual solubility. We report the formation of a metastable rhombohedral gamma(sub 1) phase by mechanically alloying aluminum and germanium powders. This phase, which appears for compositions between 20 and 50 at.% germanium, has also been observed in rapidly quenched alloys, but there is disagreement as to its composition. By measuring the heat of crystallization as a function of composition, we determined the composition of the gamma(sub 1) phase to be Al70Ge30. We also produced Al70Ge30 by arc melting the pure elements, followed by splat-quenching at a cooling rate in the range of 10(exp 8) K/s. This method produced two metastable phases, one of which was found to be the gamma(sub 1) phase obtained by mechanical alloying. The other was a monoclinic phase reported earlier in the literature as gamma(sub 2). DOE

N94-16486 Department of the Navy, Washington, DC.
FORMATION OF PITTING RESISTANT ANODIZED FILMS ON ALUMINUM Patent
John S. Ahearn, Jr., inventor (to Navy), Guy D. Davis, inventor (to Navy), and William C. Moshier, inventor (to Navy) 27 Apr. 1993 4 p Filed 20 Nov. 1990
(AD-D015812; US-Patent-5,205,922; US-Patent-Appl-SN-618190; US-Patent-Class-205-332) Avail: US Patent and Trademark Office

A method and apparatus for retarding the pitting of aluminum by coating the aluminum with a film which includes molybdenum oxide is explained. The aluminum material is preexposed to a molybdate solution before anodizing in a sodium tartrate solution. DTIC

N94-16562# Florida Univ., Gainesville. Dept. of Civil Engineering.
INVESTIGATION OF THE INFLUENCE OF APPLIED POTENTIAL ON EROSION-CORROSION OF COPPER IN ALKALINE CHLORIDE SOLUTIONS Final Report, 1 Dec. 1986 - 31 Mar. 1993
Mark E. Orazem May 1993 139 p
(Contract N00014-89-J-1619)
(AD-A266448) Avail: CASI HC A07/MF A02

A novel electrochemical cell incorporating a scanning ellipsometer was designed and used to investigate the hypothesis that the critical shear observed for the erosion-corrosion of copper was associated with a shear-induced removal of protective film. While high-shear flow was shown to increase the rate of corrosion of copper in aerated and de-aerated saline solutions, ellipsometry indicated that shear induced removal of protective films did not take place, even for shear stresses ten times the reported critical shear for erosion-corrosion of copper. Subsequent work showed that a differential mass transfer mechanism could generate localized corrosion, but the visual appearance of the surface did not resemble classical products of erosion-corrosion. Separate potentiodynamic and impedance experiments were conducted to identify the electrochemical behavior, and new techniques were developed to interpret impedance spectra. Papers resulting from this work are attached. DTIC

N94-16662# Pacific Northwest Lab., Richland, WA.
EVOLUTION OF MICROSTRUCTURE IN FACE CENTERED CUBIC METALS DURING IRRADIATION: A REVIEW
F. A. Garner Jun. 1993 45 p Presented at the 3rd Conference on the Evolution of Microstructure in Metals during Irradiation, Chalk River (Canada), 29 Sep. - 2 Oct. 1992
(Contract DE-AC06-76RL-01830)
(DE93-015682; PNL-SA-21234; CONF-920970-8) Avail: CASI HC A03/MF A01

When fcc metals and alloys are irradiated at elevated temperatures, they tend to evolve toward saturation microstructures that are independent of the starting state of the metal and the early details of irradiation history. This leads to property changes and rates of dimensional change that also

eventually become independent of the starting state. The evolution of microstructure in complex alloys, especially during the transient regime, is usually determined by the complex interaction of many microstructural and microchemical processes. The more complex the alloy, the more difficult it is to identify and define the separate influence of each participating mechanism. The use of irradiation studies conducted on simple metals or model alloys assists in understanding the behavior of alloys of engineering relevance. A review of such studies shows that a number of prevailing perceptions of radiation-induced microstructural evolution are not universally correct. DOE

N94-16764# Lawrence Livermore National Lab., CA.
THE EFFECT OF OXYGEN, GRAIN SIZE, AND STRAIN RATE ON THE MECHANICAL BEHAVIOR OF FORGED P/M TANTALUM
Christopher A. Michaluk (Cabot Corp., Boston, MA.), George T. Gray, III (Los Alamos National Lab., NM.), and Tapan Chatterjee (Picatinny Arsenal, Dover, NJ.) 1993 10 p Presented at the Powder Metallurgy in Aerospace, Defense, and Demanding Applications, San Diego, CA, 8-11 Feb. 1993
(Contract W-7405-eng-36)
(DE93-011251; LA-UR-93-712; CONF-9302111-1) Avail: CASI HC A02/MF A01 (US Sales Only)

The effect of oxygen, grain size, and strain rate on the quasistatic and dynamic mechanical properties of extruded, forged, and annealed P/M tantalum containing two different levels of oxygen is addressed. The high oxygen (250-400 ppM) P/M materials were characterized as having higher flow stress and greater work hardening than wrought high purity tantalum. Work hardening and relative strain rate sensitivity exponents of the P/M materials were found to be relatively independent of oxygen level and grain size and slightly dependent on strain rate. This behavior may be due to the existence of fine dispersion of tantalum oxide particles. The state of oxygen in the P/M forgings was investigated by TEM analysis. DOE

N94-16780 General Electric Co., Cincinnati, OH. Aircraft Engines.
WEAR RESISTANT TITANIUM MATERIAL DEVELOPMENT Final Report, 1 Oct. 1991 - 30 Sep. 1992
D. G. Konitzer, N. O. Maurer, and K. P. Taylor Mar. 1993 39 p Limited Reproducibility: More than 20% of this document may be affected by microfiche quality
(Contract DAAL04-91-C-0036)
(AD-A266474; ARL-CR-51) Avail: Issuing Activity (Defense Technical Information Center (DTIC))

A method for producing a dispersion of a hard phase in a titanium alloy is being studied. The purpose of the hard phase, titanium carbide in this work, is to improve the wear and erosion resistance of the titanium matrix. The hard phase was developed in a wide range of volume fractions by nonconsumable arc melting. DTIC

N94-16781# United Technologies Research Center, East Hartford, CT.
VANADIUM CORROSION STUDIES Final Report, 1 Feb. 1989 - 30 Jun. 1993
Norman Bornstein, Hilton Roth, and Roscoe Pike 30 Jun. 1993 30 p
(Contract N00014-89-C-0053)
(AD-A266489; UTRC-R93-918120-2) Avail: CASI HC A03/MF A01

Vanadium present in certain crude and residual fuel oils is converted within the burner of the gas turbine engine to the refractory dioxide, which in flight is fully oxidized to the pentoxide. Yttrium oxide, stable in the presence of the oxides of sulfur, is identified and verified as a corrosion inhibitor. A chelation process to produce a hydrolytic stable fuel soluble yttrium additive is described. DTIC

N94-16873# Oak Ridge National Lab., TN.
BULK AND DEFECT PROPERTIES OF ORDERED INTERMETALLICS: A FIRST-PRINCIPLES TOTAL-ENERGY INVESTIGATION
C. L. Fu, Y. Y. Ye, and M. H. Yoo 1992 12 p Presented at the 16th Material Research Society International Symposium on the Scientific Basis for Nuclear Waste Management Fall Meeting, Boston, MA, 30 Nov. - 5 Dec. 1992
(Contract DE-AC05-84OR-21400)
(DE93-015492; CONF-921101-124) Avail: CASI HC A03/MF A01

First-principles quantum mechanical calculations based on local-density-functional theory have been used to investigate the fundamental factors that govern the deformation and fracture behavior of ordered intermetallic alloys. Unlike in Ni3Al, the calculated elastic constants and shear fault energies indicate that anomalous yield strength behavior is not likely to occur in Ni3Si. From the calculated Griffith strength and a phenomenological theory relating fracture toughness to ideal cleavage strength, Ni3Si is predicted to be ductile with respect to cleavage fracture. For TiAl, we find the absence of structural vacancies due to the strong Ti-Al bonding and similar atomic radii for Ti and Al. For NiAl, the defect structure is found to be dominated by two types of defects--monovacancies on the Ni sites and substitutional antisite defects on the Al sites. For FeAl, on the other hand, we find a more complex defect structure, which is closely related to the importance of electronic structure effect in FeAl. More importantly, we predict the strong tendency for vacancy clustering in FeAl due to the large binding energy found for divacancies. Effects of thermomechanical history on microhardness are discussed in terms of the calculated results. DOE

N94-16883*# National Aeronautics and Space Administration. Lewis Research Center, Cleveland, OH.
EFFECTS OF PROCESSING AND PROLONGED HIGH TEMPERATURE EXPOSURE ON THE MICROSTRUCTURE OF Nb-1Zr-C SHEET
Mehmet Uz (Lafayette Coll., Easton, PA.) and R. H. Titran Oct. 1993 12 p Prepared for the MRS 1993 Fall Meeting, Boston, MA, 29 Nov. - 3 Dec. 1993
(Contract DE-AI03-86SF-16310; RTOP 583-02-21)
(NASA-TM-106370; DOE/NASA/16310-20; E-8176; NAS 1.15:106370)
Avail: CASI HC A03/MF A01

High temperature stability of the microstructure of Nb-1Zr sheet containing 0.1 and 0.06 wt. percent C was studied as affected by processing and prolonged 1350 K exposure with and without applied stress. Sheets were fabricated by cold rolling bars that were single-, double-, or triple-extruded at 1900 K. Creep samples were double-annealed (1 h at 1755 K + 2 h at 1475 K) prior to testing at 1350 K and 10,000 - 34,500 h. The microstructures of the as-cast, extruded, rolled, DA, and crept samples were characterized using various metallographic and analytical methods. The precipitates were rather coarse Nb2C initially, but transformed to finer (less than or equal to 1 micron) carbides of (Zr, Nb)C with each subsequent high temperature process. The grain size, and the relative amount and morphology of (Zr, Nb)C were found to be affected by the number of extrusions and to some extent by C-content. However, the microstructures of all the crept samples were similar with (Zr, Nb)C distributed throughout the matrix indicating that prolonged exposure to 1350 K gave rise to complete transformation of Nb2C to (Zr, Nb)C regardless of the processing history. These and other observations are presented with the emphasis on the correlation between processing, microstructure, and creep properties. Author

N94-16890# Oak Ridge National Lab., TN.
CREEP DUCTILITY OF IRON AT VERY LOW STRAIN RATES: THE EFFECTS OF SULFUR
E. P. George, V. Sklenicka (Ceskoslovenska Akademie Ved, Brno.), and D. P. Pope (Pennsylvania Univ., Philadelphia.) 1992 6 p Presented at the Minerals, Metals, and Materials Society/American Society for Metals (TMS/ASM) Materials Week 1992, Chicago, IL, 2-5 Nov. 1992
(Contract DE-AC05-84OR-21400)
(DE93-015490; CONF-9211117-8) Avail: CASI HC A02/MF A01

Creep ductility of iron containing sulfur (200, 20 and 1 wt ppm) was measured as a function of stress and temperature in constant-stress creep tests at 673, 773, 873, and 973 K in H(sub 2). Failure times ranged from one minute to one year. Creep strengths of the 20 and 1 ppm S material were similar, but the 200 ppm S material was stronger than the other two, especially at very low strain rates. Also, at a given strain rate, a ductility minimum is seen at 873 K, the depth of which increases with sulfur content and is the result of increased intergranular failure. The strain rate (or reciprocal of failure time) at which the failure mode changes from transgranular to intergranular fracture decreases with decreasing sulfur content. Intergranular creep cavities were found to nucleate on sulfides in the high-sulfur material, and on unidentified small particles -- presumably oxides -- in the other two. It is concluded that creep cavities nucleate easily on FeS particles but that nucleation on oxide particles is more difficult, especially when the interfacial sulfur content is low. However, it is

not possible to totally prevent cavity nucleation even after reducing the sulfur level to 1 ppm. DOE

N94-16964# Auburn Univ., AL.
HIGH TEMPERATURE MATERIALS TECHNOLOGY RESEARCH FOR ADVANCED THERMIONIC SYSTEMS
R. H. Zee and M. F. Rose 1993 15 p
(Contract DE-FG03-93SF-19645)
(DE93-018302; DOE/SF-19645/T1) Avail: CASI HC A03/MF A01

Effort was concentrated on modeling the deformation process in refractory alloy single crystals and the stress distribution in metal-ceramic-metal long trilayer insulators. Resolved shear stress distributions are given for a bcc Mo single crystal tube with a (110) growth direction. Effect of 1.8% Nb additions on creep of Mo single crystals was studied, simulating the cylindrical configuration of the TFE emitter. In the area of advanced sheath trilayer insulators, radiation-induced stresses in long cylinder and effect of collector material (Nb vs Mo) were studied. DOE

N94-16972# Massachusetts Inst. of Tech., Cambridge. Dept. of Materials Science and Engineering.
SLIP, TWINNING AND TRANSFORMATION IN LAVES PHASES
S. M. Allen and J. D. Livingston 26 Jan. 1993 12 p
(Contract DE-FG02-90ER-45426)
(DE93-018164; DOE/ER-45426/2) Avail: CASI HC A03/MF A01

Research was concentrated on two-phase Ti-TiCr2 alloys, two-phase Fe-ZrFe2 alloys, and two-phase ternary Ni-Cu-Mg alloys containing MgNi2 and MgCu2 phases. Work demonstrated that a variety of room-temperature deformation processes are possible in Laves phases. A strain-induced phase transformation from C36 yields C15 structures is one mechanism for plastic deformation in ZrFe2. The C15 structure in TiCr2 deforms by slip and twinning. The microstructure after indentation of specimens containing C36 phases ZrFe2 and MgNi2 indicates that a variety of slip systems operate in this form. DOE

N94-16984# Naval Postgraduate School, Monterey, CA.
MEAN STRAIN EFFECTS ON THE STRAIN LIFE FATIGUE CURVE M.S. Thesis
Byron L. Smith 25 Mar. 1993 51 p
(AD-A267211) Avail: CASI HC A04/MF A01

Aluminum 7075-T6 was tested using a Fatigue Material Test System. After creating the monotonic and cyclic stress-strain curves to verify material properties, strain life test data were replicated twenty times each to obtain the statistical description of standard strain life curve for zero mean strain. The mean strain was then varied to create a total of four statistically described curves. Accounting for the statistical distribution, various characteristics were plotted in order to better understand the effects of mean strain. For example, strain range was plotted against the mean strain for given lives and results were compared to equations in use today that account for mean stress. DTIC

N94-17041# Washington Univ., Seattle. Dept. of Mechanical Engineering.
J-INTEGRAL AND HRR FIELD ASSOCIATED WITH STABLE CRACK GROWTH IN THIN ALUMINUM SEN SPECIMEN
G. B. May, F. X. Wang, and A. S. Kobayashi Jul. 1993 28 p
(Contract N00014-89-J-1276)
(AD-A267879; UWA/DME/TR-93/72) Avail: CASI HC A03/MF A01

Moire interferometry with line densities of 1200 and 40 lines per mm was used to determine the two orthogonal displacements surrounding a stationary and a stably extending crack, respectively in two thin 2024-T3 aluminum alloy, single-edge notched specimens. The displacement fields were used to compute the J-integrals for various contours during crack tip blunting and subsequent crack extension. As expected, the near-and far-field J-integral value prior to stable crack growth coincided with the LEFM strain energy release rate, G, and validated the experimental procedure. The far field J values increased with increasing stable crack grow-Lh but the crack tip J values within the nonlinear region remained constant. The HRR displacement field, which was computed from the experimentally determined far field J, agreed with the measured displacement field prior to stable crack growth and progressively deviated from the measured values with stable crack extension. DTIC

N94-17063# Polish Academy of Sciences, Warsaw. Inst. Podstawowych Problemow Techniki.
STUDIES OF CHANGES IN THE ENERGY STORED IN METALS AS A RESULT OF SUBJECTING THEM TO A SURFACE TYPE TECHNOLOGICAL PROCESS [BADANIA ZMIAN ENERGII ZMAGAZYNOWANEJ W METALACH W WYNIKU PODDAWANIA ICH POWIERZCHNIOWYM ZABIEGOM TECHNOLOGICZNYM]
Stefan P. Gadaj 1991 99 p In POLISH
(IFTR-25/1991) Avail: CASI HC A05/MF A02

The possibility for estimating the effect of the original state of a material on energy accumulation under plastic deformation of metal is determined based on an analysis of the literature as well as theoretical and experimental studies. It is determined that research of this type has not yet proceeded beyond the initial phase. Research on the effect of an inhomogeneous initial state attributable to surface treatments on energy accumulation during distension of Austenite steel, carbon steel, and commercial grade pure titanium is analyzed. It is noted that surface treatments modify the course of this process only in the very initial distension domain. A mathematical description of the energy accumulation process and its dependence on energy conveyed to the metal under plastic deformation is proposed. Also given is a criterion for quantitative estimation of the effect of surface treatments on energy accumulation in the metal. Transl. by FLS

N94-17079*# Alabama Univ., Tuscaloosa. College of Engineering.
PARTICLE ENGULFMENT AND PUSHING BY SOLIDIFYING INTERFACES (PEPSI) Final Report
Doru Michael Stefanescu, Peter A. Curreri (National Aeronautics and Space Administration. Marshall Space Flight Center, Huntsville, AL.), F. Juretsko, H. Pang, and R. Phalnikar 16 Aug. 1993 44 p
(Contract NAS8-39715)
(NASA-CR-193856; NAS 1.26:193856) Avail: CASI HC A03/MF A01

The preliminary definition phase included the following actions: producing a science requiring document (draft), producing a science requirements document (preliminary), updating the flight program proposal, project review at NASA Marshall Space Flight Center, and research work as defined in the statement of work. The first three items of this plan have been delivered by the University of Alabama to NASA according to schedule. A project review meeting was held at MSFC on June 29, 1993. Consequently, this part of the report will address the results of the research work performed in the Solidification Laboratory at the University of Alabama during the first six months of the project. Author (revised)

N94-17093# Polish Academy of Sciences, Warsaw. Inst. Podstawowych Problemow Techniki.
ANALYSIS OF THE STRENGTHENING OF ALUMINUM ALLOY UNDERGOING PLASTIC DEFORMATION UNDER CONDITIONS OF A COMPOUND STATE OF STRESS [ANALIZA WZMOCNIENIA STOPU ALUMINIUM ODKSZTALCONEGO PLASTYCZNIE W WARUNJKACH ZLOZONEGO STANU NAPREZENIA]
Ryszard Szczeboit 1991 94 p In POLISH
(IFTR-21/1991) Avail: CASI HC A05/MF A01

An experimental study relating to an analysis of conservation of a flow surface in a plane stressed state for material under additional reinforcement achieved by applying a load that imparts plasticity is discussed. Studies are carried out for different prestresses of the plasticity surface imposed on the side of such loading and on the opposite side of the load. Experiments were conducted to determine the contours of the complete plasticity surfaces that provided a basis for more comprehensive and extensive analysis of the conservation of such surfaces under extended preliminary strain of the test material. These results made it possible to determine the quantitative effect of material reinforcement on the change in surface dimensions and their position in the stress space and likewise served to test the theoretical principles underlying the reinforcement procedure. Transl. by FLS

N94-17100 Air Force Inst. of Tech., Wright-Patterson AFB, OH.
THE SPECIFIC HEAT OF TITANIUM DISILICIDE M.S. Thesis
William K. Sylla May 1993 73 p Limited Reproducibility: More than 20% of this document may be affected by microfiche quality
(AD-A267543; AFIT/CI/CIA-93-094) Avail: Issuing Activity (Defense Technical Information Center (DTIC))

Titanium disilicide is a promising candidate for use in the circuitry of the next generation of micro-electronics. The fabrication techniques used

by the electronics industry require accurate thermodynamic data. We have therefore undertaken the measurement of the specific heat of TiSi2. The titanium disilicide alloy has been produced and characterized. The lattice parameters of TiSi2 have been found to be as follows: a = 8.2607 +/- 0.0004 A, b = 4.7967 +/- 0.0003 A, and c = 8.545 +/- 0.002 A by x-ray diffractometry. The specific heat of titanium disilicide has been measured from 100 K to 500 K by means of differential scanning calorimetry. These data show good agreement with accepted specific heat theory following the general shape of a Debye curve and approaching a Dulong-Petit value. From these data a Debye temperature of 510 +/- 80 K has been graphically approximated. The methodology of specific heat measurements using differential scanning calorimetry has been reviewed. DTIC

N94-17106# Army Armament Research, Development and Engineering Center, Watervliet, NY. Benet Lab.

TRANSIENT PHENOMENA FOLLOWING PRECIPITATION AND RE-SOLUTION ANNEALS IN A NiTi ALLOY Final Report

L. V. Meisel and P. J. Cote May 1993 22 p

(AD-A267557; ARCCB-TR-93021) Avail: CASI HC A03/MF A01

Transient phenomena following anneals in a near stoichiometric NiTi alloy are investigated by means of differential scanning calorimetry (DSC). Precipitation anneals (350 C) raise the temperature range of the martensite and R-transformation. Subsequent cycling through the transformation range (-40 to 100 C) produces small changes in the martensite DSC peaks and no observable change in the R-peak. Subsequent re-solution anneals (600 C) produce dramatic effects: Ms rises approximately 20 C above its value preceding the precipitation anneal and the martensite DSC peak is very sharp and symmetric, while the R-transformation peak is not observable. During ensuing cycling, the martensite peak returns to its original form and position after about 300 cycles, and the R-peak appears after 4 cycles and is essentially invariant to cycling. The transient data are consistent with a dislocation model. DTIC

N94-17109# Maryland Univ., College Park. Inst. for Physical Science and Technology.

QUANTITATIVE ASSESSMENT OF THE ACCURACY OF CONSTITUTIVE LAWS FOR PLASTICITY WITH AN EMPHASIS ON CYCLIC DEFORMATION Final Report

I. Babuska, K. Jerina, Y. Li, and P. Smith Apr. 1993 99 p

(Contract N00014-87-K-0429)

(AD-A267562; BN-1146) Avail: CASI HC A05/MF A02

The paper addresses the plastic behavior of the aluminum alloys 5086 and 5454 in the H-32 temper under cyclic load. It reports the experimental results and analyzes them with the aim to design constitutive laws which could be used in the computational analysis. The reliability of the constitutive laws is analyzed. DTIC

N94-17121# Polish Academy of Sciences, Warsaw. Inst. Podstawowych Problemow Techniki.

INFLUENCE OF GRAIN SIZE ON THE ENERGY STORING ABILITY DURING UNIAXIAL STRETCHING OF AUSTENITE STEEL [WPLYW WIELKOSCI ZIARN NA ZDOLNOSC MAGAZYNOWANIA ENERGII PODCZAS JEDNOOSIOWEGO ROZCIAGANIA STALI AUSTENITYCZNEJ]

Wiera Oliferuk, Wieslaw Swiatnicki (Technical Univ. of Warsaw, Poland.), and Maciej W. Grabski (Technical Univ. of Warsaw, Poland.) 1992 33 p In POLISH

(IFTR-22/1992) Avail: CASI HC A03/MF A01

Energy accumulation in uniaxial distension along a group of austenite steel specimens with a low carbon concentration and different grain dimensions (80 micrometers, 8 micrometers) is investigated. The dislocation structure of coarse and fine grained steel with different selected deformation estimates is surveyed. An analysis of changes in its structure made possible an interpretation of the energy accumulation process bearing in mind the dislocation of the phenomenon as well as the estimate of the roll of grain and the boundaries of this process. The derived results were also analyzed from the viewpoint of the minimum free energy principle. Transl. by FLS

N94-17223# California Univ., Berkeley. Dept. of Materials Science and Mineral Engineering.

MICROMECHANISMS OF MONOTONIC AND CYCLIC SUBCRITICAL CRACK GROWTH IN ADVANCED HIGH MELTING POINT LOW-DUCTILITY INTERMETALLICS Final Report, 1 Apr. 1990 - 31 Mar. 1993

K. T. VenkateswaraRao, L. Murugesh, and R. O. Ritchie May 1993 120 p

(Grant AF-AFOSR-0167-90)

(AD-A267764; UCB/R/93/A1091) Avail: CASI HC A06/MF A02

The next generation of high-performance engines will require stiffer materials operating at higher stress levels and capable of with-standing significantly higher temperatures up to 1650 C and above. Prime candidates for such applications include ordered intermetallics, ceramics, and composites based on metal, intermetallic, and ceramic or carbon matrices. However, these materials are currently of limited use due to their low ductility and toughness properties; moreover, an understanding of their fatigue resistance is still essentially lacking. Accordingly, the present research was aimed at examining one class of these materials, namely ductile-phase toughened intermetallic alloys, with respect to the critical factors influencing crack-propagation resistance under monotonic and cyclic loading. The model systems studied included TiNb- and Nb-reinforced gamma-TiAl, Nb-reinforced Nb3Al, and Nb-reinforced MoSi2. DTIC

N94-17234# Pacific Northwest Lab., Richland, WA.

LOW-TEMPERATURE SINTERING AND PHASE CHANGES IN CHROMITE INTERCONNECT MATERIALS

L. A. Chick, T. R. Armstrong, D. E. McCready, G. W. Coffey, G. D. Maupin, and J. L. Bates May 1993 12 p Presented at the 3rd International Symposium on Solid Oxide Fuel Cells, Honolulu, HI, 16-21 May 1993

(Contract DE-AC06-76RL-01830)

(DE93-015676; PNL-SA-21622; CONF-9305100-1) Avail: CASI HC A03/MF A01

Sintering shrinkage curves and phase changes were compared for calcium-substituted lanthanum chromates with either slight Asite enrichment or depletion. Of the former type, La(0.7)Ca(0.31)CrO3 that was synthesized by the glycine-nitrate method sintered to high density in air at 1250 C, exhibiting two rapid-shrinkage events. Weight loss measurements corroborated XRD data showing that, prior to densification, over half the Ca resided in non-perovskite phases including CaCrO4. In the La(0.7)Ca(0.31)CrO3, densification was closely associated with re-dissolution of the Ca into the perovskite. DOE

N94-17251# Stanford Linear Accelerator Center, CA.

ANISOTROPIC PHASE SEPARATION IN AMORPHOUS Fe-Ge ALLOYS

M. J. Regan and A. Bienenstock Apr. 1993 7 p Presented at the Spring Meeting of the Materials Research Society, San Francisco, CA, 12-16 Apr. 1993

(Contract DE-AC03-76SF-00515)

(DE93-015255; SU-SLAC-PUB-6139; SLAC/SSRL-0010; CONF-930405-17) Avail: CASI HC A02/MF A01

Magnetron sputtered amorphous Fe(x)Ge(100-x) films have been examined with anomalous small-angle x-ray scattering (ASAXS) in an attempt to characterize composition fluctuations which have been previously reported in this system. Films grown under various deposition conditions have been studied, with the scattering vector both in and oblique to the plane of the films, to search for anisotropy. By manipulating the deposited power flux and rates of growth, films which have the same composition can be grown to different states of phase separation. The total correlation functions have been calculated from the oblique scattering experiments. The anisotropy can be successfully modeled as a close-packing of oriented prolate ellipsoidal particles, with the elongated axis along the direction of film growth. A method for using these measurements to determine the compositions of the phase-separating species has been developed and utilized. The results indicate phase separation into a-Ge and a-FeGe2 for the a-Fe(x)Ge(100-x) (x less than 33) alloy. DOE

N94-17282# Wichita State Univ., KS. National Inst. for Aviation Research.

CHARACTERIZATION OF METALLIC MULTILAYERS USING X RAY DIFFRACTION ANALYSIS

Saad Mohamed Harb Alyan and Jharna Chaudhuri 1993 87 p
(NIAR-93-13) Avail: CASI HC A05/MF A01

Kinematic x-ray diffraction analysis models are employed to study metallic multilayer films, to gain insight into the quality of these films, and to characterize their composition and interplanar spacing wave profiles. Both gold/nickel superlattice and titanium/nickel superlattice modulated films are included in this investigation. All kinematic models employed provide an excellent means to evaluate the multilayering techniques and the quality of the modulated films. Results indicate the high structural and chemical orders of the multilayered superlattices studied. Coherent interfaces, however, are found to be dependent on the thickness of each material layer within one repeat period of the superlattice film. Author

N94-17418 Naval Air Warfare Center, Warminster, PA. Air Vehicle and Crew Systems Technology Dept.

AIRCRAFT CARRIER EXPOSURE TESTS OF CAST MAGNESIUM ALLOYS Final Report

Joseph Kozol and Edwin Tankins 1 Mar. 1993 18 p Limited Reproducibility: More than 20% of this document may be affected by microfiche quality
(AD-A268260; NAWCADWAR-93015-60) Avail: CASI HC A03

This report describes the results of an ongoing effort to determine the behavior of aircraft materials and finishes in the naval environment of aircraft carrier flight decks. Coated cast magnesium alloys were exposed to the carrier environment for a relatively short time and experienced significant corrosion effects compared to aluminum control specimens. DTIC

N94-17464 Naval Surface Warfare Center, Bethesda, MD. Survivability Structures and Materials Directorate.

THE EFFECT OF ELECTRIC DISCHARGE MACHINED NOTCHES ON THE FRACTURE TOUGHNESS OF SEVERAL STRUCTURAL ALLOYS Final Report

J. A. Joyce and R. E. Link Apr. 1993 84 p Limited Reproducibility: More than 20% of this document may be affected by microfiche quality
(AD-A268605; CRDKNSWC-SSM-61-93-01; NUREG-CR-5981) Avail: CASI HC A05

Recent computational studies of the stress and strain fields at the tip of very sharp notches have shown that the stress and strain fields are very weakly dependent on the initial geometry of the notch once the notch has been blunted to a radius that is 6 to 10 times the initial root radius. It follows that if the fracture toughness of a material is sufficiently high so that fracture initiation does not occur in a specimen until the crack-tip opening displacement (CTOD) reaches a value from 6 to 10 times the size of the initial notch tip diameter, then the fracture toughness will be independent of whether a fatigue crack or a machined notch served as the initial crack. In this experimental program, the fracture toughness (Jlc and J resistance (J-R) curve, and CTOD) for several structural alloys was measured using specimens with conventional fatigue cracks and with EDM machined notches. The results of this program have shown, in fact, that most structural materials do not achieve initiation CTOD values on the order of 6 to 10 times the radius of even the smallest EDM notch tip presently achievable. DTIC

N94-17652*# National Aeronautics and Space Administration. Lewis Research Center, Cleveland, OH.

TENSILE AND STRESS-RUPTURE BEHAVIOR OF HAFNIUM CARBIDE DISPERSED MOLYBDENUM AND TUNGSTEN BASE ALLOY WIRES Final Report

Hee Mann Yun (Cleveland State Univ., OH.) and Robert H. Titran Dec. 1993 12 p Proposed for presentation at the Materials Research Society Fall Meeting, Boston, MA, 1-5 Dec. 1993
(Contract DE-AI03-86SF-16310; RTOP 590-13-11)
(NASA-TM-106350; E-8128; NAS 1.15:106350; DOE/NASA/16310-18)
Avail: CASI HC A03/MF A01

The tensile strain rate sensitivity and the stress-rupture strength of Mo-base and W-base alloy wires, 380 microns in diameter, were determined over the temperature range from 1200 K to 1600 K. Three molybdenum alloy wires; Mo + 1.1w/o hafnium carbide (MoHfC), Mo + 25w/o W + 1.1w/o hafnium carbide (MoHfC+25W) and Mo + 45w/o W + 1.1w/o hafnium carbide (MoHfC+45W), and a W + 0.4w/o hafnium carbide (WHfC) tungsten alloy wire were evaluated. The tensile strength of all wires studied was found to have a positive strain rate sensitivity. The strain rate dependency increased with increasing temperature and is associated with grain broadening of the initial fibrous structures. The hafnium carbide dispersed W-base and Mo-base alloys have superior tensile and stress-rupture properties than those without HfC. On a density compensated basis the MoHfC wires exhibit superior tensile and stress-rupture strengths to the WHfC wires up to approximately 1400 K. Addition of tungsten in the Mo-alloy wires was found to increase the long-term stress rupture strength at temperatures above 1400 K. Theoretical calculations indicate that the strength and ductility advantage of the HfC dispersed alloy wires is due to the resistance to recrystallization imparted by the dispersoid. Author

N94-16137# Martin Marietta Corp., New Orleans, LA. Manned Space Systems.

ALUMINUM-LITHIUM TECHNOLOGY

E. Powers and P. Hartley *In* Huntsville Association of Technical Societies, TABES 1993: 9th Annual Technical and Business Exhibition and Symposium 1993 4 p (For primary document see N94-16129 03-38)
(TABES Paper 93-601) Avail: CASI HC A01/MF A03

N94-16273*# Karlova Univ., Prague (Czechoslovakia). Faculty of Sciences.

TRANSITION METALS IN SUPERHEAT MELTS Abstract Only

Petr Jakes and Michael-Patrick Wolfbauer (Bemidji State Univ., MN.) *In* Lunar and Planetary Inst., Twenty-Fourth Lunar and Planetary Science Conference. Part 2: G-M 1993 p 713-714 (For primary document see N94-16173 03-91)
Avail: CASI HC A01/MF A06

N94-16287*# National Aeronautics and Space Administration. Lyndon B. Johnson Space Center, Houston, TX.

EXPERIMENTAL PARTITIONING OF Zr, Ti, AND Nb BETWEEN SILICATE LIQUID AND A COMPLEX NOBLE METAL ALLOY AND THE PARTITIONING OF Ti BETWEEN PEROVSKITE AND PLATINUM METAL Abstract Only

Stephen R. Jurewicz and John H. Jones *In* Lunar and Planetary Inst., Twenty-Fourth Lunar and Planetary Science Conference. Part 2: G-M 1993 p 741-742 (For primary document see N94-16173 03-91)
Avail: CASI HC A01/MF A06

27 NONMETALLIC MATERIALS

Includes physical, chemical, and mechanical properties of plastics, elastomers, lubricants, polymers, textiles, adhesives, and ceramic materials.

For composite materials see *24 Composite Materials*.

N94-14914# Minnesota Univ., Minneapolis. Dept. of Chemical Engineering and Materials Science.

PREPARATION OF HOMOGENEOUS ALUMINOSILICATE GELS BY SOL/GEL TECHNIQUES

M. Reese, J. Sanchez, and A. V. McCormick 12 Jul. 1993 9 p
(Contract N00014-91-J-1893)
(AD-A266823; TR-10-ONR) Avail: CASI HC A02/MF A01

The factors affecting the production of homogeneous aluminosilicate gels from alkoxide precursors were investigated. Aluminosilicate gels were made in acidic conditions with a prepolymerization of the silicate precursors followed by the addition of the alumina precursor. Confirming earlier studies, it was found that the gel homogeneity is increased when the rate of gelation decreases. The reduction of the water content and/or the aluminum precursor, and more surprisingly the increase of the acid concentratioh contributed to the gel time increase and thus the improvement of gel homogeneity. DTIC

N94-14921# Minnesota Univ., Minneapolis. Dept. of Chemical Engineering and Materials Science.

MULTINUCLEAR NMR STUDY OF ALUMINOSILICATE SOL-GEL SYNTHESIS REASONS FOR THE HOMOGENEOUS GELATION USING THE PREHYDROLYSIS METHOD

G. A. Pozarnsky and A. V. McCormick 12 Jun. 1993 40 p
(Contract N00014-91-J-1893)
(AD-A266877; TR-1) Avail: CASI HC A03/MF A01

Aluminosilicate gels have been utilized in numerous optical, dielectric, and catalytic applications. These applications require a high degree of molecular homogeneity, but reproducible means of achieving this remain unobtainable for many compositions. In this work, reaction occurring in one of the most successful sol/gel processes are examined by means of both liquid and solid C-13, Si-29, 17, and Al NMR. The synthesis process studied was the method, optimized by Krol, of prehydrolyzing tetraethyl orthosilicate, TEOS,in ethanol, and subsequently adding aluminum sec-butoxide, and then further water. After prehydrolysis and addition of aluminum sec-butoxide, an aluminosilicate precursor is formed in which the aluminum is tetrahedrally coordinated to four silicate ligands. After adding further water, gelation is accompanied by the expansion of the tetrahedral aluminum to octahedral coordination; this apparently occurs by nucleophilic attack of silanol groups on the aluminum in the aluminosilicate precursor. At sufficiently low water to silicon molar ratios, where transparent gels and longer gel times result, this coordination expansion is preceded by condensation of the silicate ligands to form Si-O-Si. Author (revised)

N94-14948# Army Research Development and Standardization Group (United Kingdom), FPO New York, NY.
PREPARATION AND INVESTIGATION OF IMPROVED LOW VOLTAGE ELECTRON EXCITABLE PHOSPHORS Annual Technical Report, May 1992 - May 1993
S. S. Chadha, D. W. Smith, and A. Vecht May 1993 53 p
(Contract DAJA45-92-C-0007)
(AD-A266852; R/D-6812-EE-01) Avail: CASI HC A04/MF A01

Recent advances in the area of field emitting arrays point to the possibility of fabricating low voltage variants of the CRT. However, these advances also highlight the lack of suitable low voltage excitable phosphors. The aim of this contract is to remedy this situation and to provide suitable phosphors emitting RBG. The problem is being tackled by making either intrinsically or extrinsically conducting phosphors, the latter by the addition of suitably conducting fine particle powders. In addition, the evaluation of phosphors was possible by acquiring a low voltage demountable CRT system. Thus, far, the results from our experiments have been promising. A bright, pure green emitting phosphors (ZnGa2O4:Mn) and a red emitting phosphor (CaTiO2:Pr) were made. In-house prepared bluish-green emitting ZnO:Zn was shown to be as bright as the commercial ZnO:Zn phosphor. Photoluminescent thin film variants of both ZnO:Zn and ZnGa2O4:Mn were made using aerosol spray pyrolysis techniques. Therefore, we now have three low voltage phosphors instead of only on available at the start of this contract. Our aims are to optimize these phosphors further and to attempt other lattices. Small sealed devices will be made to simulate condition in real FED devices and phosphors will be supplied to any US FED manufacturer. DTIC

N94-15133# Air Force Inst. of Tech., Wright-Patterson AFB, OH. Foreign Aerospace Science and Technology Center.
A STUDY OF RELAXATION TRANSITIONS IN THE POLYMERS UNDER THE INFLUENCE OF MAGNETIC FIELDS
B. Yu. Trifel and N. A. Abdullayev 15 Apr. 1993 8 p Transl. into ENGLISH from Azerbaydzhanskiy Khimicheskiy Zhurnal (USSR), no. 2, 1972 p 105-107
(AD-A263878; FASTC-ID(RS)T-0234-93) Avail: CASI HC A02/MF A01

As was mentioned in a previous work, the influence of a magnetostatic field on polymer materials results in a short-term, but considerable, increase in the dielectric power factor (tg delta). This results from the fact that during the relaxation of the polymer molecules, near the vitrification temperature (Tg) and under the influence of the magnetic field, more ordered structural formations are created. In order to determine the effect of the magnetic field on the physical structure of polymers, it was necessary to verify that during the measurement of tg delta in the magnetic field ferromagnetic impurities have no effect. The literature contains no information concerning the determination of ferromagnetic impurities (magnetic susceptibility) of polyvinyl chlorides. Analogous measurements were conducted only with inorganic simple compounds. The purpose of this work is to explain the presence of ferro- and paramagnetic impurities in the composition of previously investigated polyvinyl chloride samples. Author

N94-15179# Minnesota Univ., Minneapolis. Dept. of Chemical Engineering and Materials Science.
SELF-DIFFUSION COEFFICIENTS OF SOL-GEL INTERMEDIATES
L. Ng and A. V. McCormick 12 Jul. 1993 28 p
(Contract N00014-91-J-1893)
(AD-A266957; TR-2) Avail: CASI HC A03/MF A01

Over the past few decades, the sol-gel technique has shown great potential for producing ceramic materials of designed composition and properties. A typical sol-gel process involves the hydrolysis and polymerization of one or more metal alkoxides in an alcohol solution in a batch reactor to form a homogeneous gel, which is then further treated to provide the type of ceramic desired (aerogel, glass, crystal, coating, etc.). Several authors have suggested that diffusion effects may influence the development of the gel microstructure. To investigate if diffusion effects are important, we begin by determining what governs the diffusivity of the precursors using the pulsed-gradient-spin-echo nuclear magnetic resonance (NMR) technique. This report focuses on the early stages of the batch reaction. The system chosen is the acid catalyzed hydrolysis and condensation of tetraethyl orthosilicate (TEOS) in ethanol. Our results from H-1 PGSE NMR and Si-29 NMR show that the diffusivities of the silicate precursors are not just a function of the molecular weight. Hydrogen bonding between the polar functional groups and the solvent also decreases the mobility of the reactants. Moreover, since hydrolysis increases and polymerization reduces the concentration of these polar groups, the mobility of the reactive oligomers changes in a complex manner. Combining our results from PGSE NMR and gas chromatography, we estimate the extent of hydrogen bonding effect on the mobility of various oligomers, providing a model to predict diffusivity trends throughout the batch reaction. DTIC

N94-15313* National Aeronautics and Space Administration, Washington, DC.
RESTORING MISS LIBERTY (Videotape)
Apr. 1985 Videotape: 4 min. 25 sec. playing time, in color, with sound
(NASA-TM-109605; NONP-VT-93-190403) Avail: CASI VHS A01/BETA A22

This videotape shows how a NASA inorganic coating for metal was used on the Statue of Liberty during it recent refurbishment. CASI

N94-15490# Minnesota Univ., Minneapolis. Dept. of Chemical Engineering and Materials Science.
INTRAMOLECULAR VERSUS INTERMOLECULAR CONDENSATION RATES IN THE ACIDIC POLYMERIZATION OF OCTAETHOXYTRISILOXANE
J. Sanchez and A. V. McCormick 12 Jul. 1993 17 p
(Contract N00014-91-J-1893)
(AD-A266982; TR-5) Avail: CASI HC A03/MF A01

Octaethoxy trisiloxane, (EtO)3Si- O-Si(OEt)2- O-Si(OEt)3, was synthesized and then polymerized in water/alcohol-solution in the presence of an acid catalyst. The reaction was monitored with Si-29 NMR. The rate constants of linear and cyclic condensation were estimated by curve-fitting and were compared. No evidence of depolymerization was found, indicating that condensation is irreversible in our conditions. In addition, it was found that the formation of trimeric cyclic species by ring closure is fast and competes effectively with chain extension condensation. These observations are consistent with previous suggestions, but in addition they provide a quantitative measure of selectivity that is much needed. Quantitative kinetic models for silicon alkoxide sol-gel processes need to account for cyclization at very early stages of the polymerization. DTIC

N94-15631# Minnesota Univ., Minneapolis. Dept. of Chemical Engineering and Materials Science.
NMR AND THEORETICAL INVESTIGATION OF CATION BINDING WITH SOL-GEL SILICATES
J. Sanchez and A. V. McCormick 12 Jul. 1993 7 p
(Contract N00014-91-J-1893)
(AD-A266999; TR-3) Avail: CASI HC A02/MF A01

Previous reports suggest that the choice of base catalyst affects both the kinetics and structural evolution of SiO2 gelation from tetraethoxysilane (TEOS). Furthermore, these effects have been attributed to the interaction of the alkaline cations with charged silicate fragments. In this study, NMR analysis of alkali-metal nuclei and of Si-29 directly shows that during the condensation of silicon alkoxides in basic alcohol solutions, cations form

ion-pair complexes with negatively charged silicate groups. It is determined that the ion pair is formed most favorably with potassium. In seeking a predictive model of complex stability, we found it most successful to use a bond orbital electronegativity equalization model developed by Bergman and Hinze. DTIC

N94-15656*# Virginia Polytechnic Inst. and State Univ., Blacksburg. Dept. of Engineering Science and Mechanics.

VERIFICATION OF A TWO-DIMENSIONAL INFILTRATION MODEL FOR THE RESIN TRANSFER MOLDING PROCESS Interim Report, Aug. 1990 - Aug. 1993

Vincent H. Hammond, Alfred C. Loos, H. Benson Dexter (National Aeronautics and Space Administration. Langley Research Center, Hampton, VA.), and Gregory H. Hasko (Lockheed Engineering and Sciences Co., Hampton, VA.) Aug. 1993 100 p

(Grant NAG1-343)

(NASA-CR-194597; NAS 1.26:194597; VPI-E-93-09; CCMS-93-15) Avail: CASI HC A05/MF A02

A two-dimensional finite element model for the infiltration of a dry textile preform by an injected resin was verified. The model, which is based on the finite element/control volume technique, determines the total infiltration time and the pressure increase at the mold inlet associated with the RTM process. Important input data for the model are the compaction and permeability behavior of the preform along with the kinetic and rheological behavior of the resin. The compaction behavior for several textile preforms was determined by experimental methods. A power law regression model was used to relate fiber volume fraction to the applied compaction pressure. Results showed a large increase in fiber volume fraction with the initial application of pressure. However, as the maximum fiber volume fraction was approached, the amount of compaction pressure required to decrease the porosity of the preform rapidly increased. Similarly, a power law regression model was used to relate permeability to the fiber volume fraction of the preform. Two methods were used to measure the permeability of the textile preform. The first, known as the steady state method, measures the permeability of a saturated preform under constant flow rate conditions. The second, denoted the advancing front method, determines the permeability of a dry preform to an infiltrating fluid. Water, corn oil, and an epoxy resin, Epon 815, were used to determine the effect of fluid type and viscosity on the steady state permeability behavior of the preform. Permeability values measured with the different fluids showed that fluid viscosity had no influence on the permeability behavior of 162 E-glass and TTI IM7/8HS preforms. Permeabilities measured from steady state and advancing front experiments for the warp direction of 162 E-glass fabric were similar. This behavior was noticed for tests conducted with corn oil and Epon 815. Comparable behavior was observed for the warp direction of the TTI IM7/8HS preform and corn oil. Mold filling and flow visualization experiments were performed to verify the analytical computer model. Frequency dependent electromagnetic sensors were used to monitor the resin flow front as a function of time. For the flow visualization tests, a video camera and high resolution tape recorder were used to record the experimental flow fronts. Comparisons between experimental and model predicted flow fronts agreed well for all tests. For the mold filling tests conducted at constant flow rate injection, the model was able to accurately predict the pressure increase at the mold inlet during the infiltration process. A kinetics model developed to predict the degree of cure as a function of time for the injected resin accurately calculated the increase in the degree of cure during the subsequent cure cycle. Author (revised)

N94-15675# Massachusetts Univ., Lowell. Dept. of Chemistry.

DESIGN, SYNTHESIS AND CHARACTERIZATION OF NOVEL NONLINEAR OPTICAL POLYMERS

Sukant Tripathy 31 May 1993 19 p

(Contract N00014-90-J-1148)

(AD-A267035) Avail: CASI HC A03/MF A01

The principal focus of the project is to develop new materials chemistry based on molecular level design and solid state chemistry. The goals have been to develop electroactive polymers with novel electronic, optical, and nonlinear optical properties. Second and third order nonlinear optical materials have been developed based on conjugated macromolecules and asymmetric anharmonic molecular electronic dipolar oscillators. In this multidisciplinary research effort, starting from first principles, polymeric systems have been developed with stable large nonlinear optical coefficients, ultrathin electroactive redox monolayers, molecular superlattices, etc. Sol-gel chemistry, photochemical crosslinking, and photopolymerization have been employed as engineering tools in materials fabrication and to elicit new phenomenon. DTIC

N94-15683# Minnesota Univ., Minneapolis. Dept. of Chemical Engineering and Materials Science.

THERMOCHEMISTRY OF SILICATE SPECIATION IN AQUEOUS SODIUM SILICATE SOLUTIONS: IONIZATION AND POLYMERIZATION OF SMALL SILICATE ION

J. Yang and A. V. McCormick 12 Jul. 1993 42 p

(Contract N00014-91-J-1893)

(AD-A266825; TR-8-ONR) Avail: CASI HC A03/MF A01

The thermochemistry of simple silicate oligomers in aqueous sodium silicate solutions is rationalized by a model that qualitatively predicts equilibria among monomer, dimer, and trimer silicate structures. Unlike previous models, it incorporates the influence of both silicate bonding and ion-solvent interactions on the stability of the anions. Although semiempirical molecular orbital calculations indicate that silicate bonds become less stable as charge increases, ion-solvent interactions tend to stabilize highly charged and compact silicate oligomers. Furthermore, polymerization is favored by the formation of highly stable water molecules and by a decrease of charge repulsion within the silicate structures. Although MNDO calculations indicate that the linear structures are more stable than the cyclic structures, ion-solvent interactions tend to stabilize the cyclic structures. Polymerization of compact silicate oligomers is also favored by producing more water molecules. Implications are summarized for larger silicate species. DTIC

N94-15688# Massachusetts Univ., Lowell.

ORGANIC POLYMERIC ELECTRO-OPTIC MATERIALS: SYNTHESIS, PROCESSING, AND DEVICE APPLICATIONS Final Report, Sep. 1988 - Dec. 1991

Jayant Kumar and Sukant Tripathy Apr. 1993 35 p

(Contract F19628-88-K-0048)

(AD-A267133; RL-TR-93-36) Avail: CASI HC A03/MF A01

A number of polymeric second and third order nonlinear optical materials were designed and synthesized. The materials were characterized for their thermal properties and processed into thin films by the Langmuir-Blodgett technique or spin coating methods which then were evaluated by second harmonic generation and electric field induced phase changes by interferometry. A stable second order nonlinear coefficient was obtained in crosslinked systems. Waveguiding with low loss was achieved in spin coated nonlinear optical polymer films, and frequency doubling experiments in waveguide configuration were performed. DTIC

N94-15700*# Worcester Polytechnic Inst., MA. Mechanical Engineering.

ENGINEERING DESIGN OF SUB-MICRON TOPOGRAPHIES FOR SIMULTANEOUSLY ADHERENT AND REFLECTIVE METAL-POLYMER INTERFACES

Christopher A. Brown 29 Oct. 1993 56 p

(Grant NAG1-1476)

(NASA-CR-194573; NAS 1.26:194573) Avail: CASI HC A04/MF A01

The approach of the project is to base the design of multi-function, reflective topographies on the theory that topographically dependent phenomena react with surfaces and interfaces at certain scales. The first phase of the project emphasizes the development of methods for understanding the sizes of topographic features which influence reflectivity. Subsequent phases, if necessary, will address the scales of interaction for adhesion and manufacturing processes. A simulation of the interaction of electromagnetic radiation, or light, with a reflective surface is performed using specialized software. Reflectivity of the surface as a function of scale is evaluated and the results from the simulation are compared with reflectivity measurements made on multi-function, reflective surfaces. Derived from text

N94-15729# North Carolina Univ., Chapel Hill.

PHOTOCHEMISTRY IN THIN POLYMERIC FILMS Final Report, 15 Mar. 1990 - 14 Mar. 1993

Thomas J. Meyer and Richard W. Linton May 1993 7 p

(Contract DAAL03-90-G-0062)

(AD-A266716; ARO-27664.7-CH-SM) Avail: CASI HC A02/MF A01

A goal of the research funded by this grant was to exploit the known

photochemical and photophysical properties of (d-pi6) transition metal complexes for the preparation and utilization of novel microstructures in electroactive polymeric films. Thin polymeric films containing polypyridyl complexes of Fe(II), Ru(II), Os(II), and Zn(II) have been prepared on a variety of conducting substrates by well established electropolymerization techniques. A majority of the research involved films prepared by the reductive polymerization of vinyl substituted pyridyl ligands, such as 4-vinyl-4'methyl-2, 2'-bipyridine and 4-vinylpyridine. DTIC

N94-15773 California Univ., San Diego, La Jolla. Dept. of the Aerospace and Mechanical Engineering Sciences.

PRODUCTION AND EVALUATION OF DENSE CERAMIC COMPOUNDS BY COMBUSTION SYNTHESIS AND DYNAMIC COMPACTION Final Report, 1 Oct. 1988 - 31 Aug. 1992

M. A. Meyers, J. C. LaSalvia, and D. Hoke 15 Apr. 1993 6 p Limited Reproducibility: More than 20% of this document may be affected by microfiche quality

(Contracts DAAL03-88-K-0194; DAAL03-90-G-0204)

(AD-A266742; ARO-28368.1-MS) Avail: CASI HC A02

The objectives of this research program were to apply combustion synthesis and dynamic forging in order to produce fully dense ceramics. The program was successfully carried out but was unfortunately terminated. TiC and TiB2 ceramics, TiC-Ni cermets, and Al2O3-TiB2 an TiB2-SiC ceramic-ceramic composites were successfully produced and characterized. The research effort yielded eleven technical publications, of which seven were (or will be) published in archival journals and four in conference proceedings. The work has been presented at eight technical meetings and has been very well received by the community. Three students were supported by this research program. Three M.S. degrees were awarded and two Ph.D. theses are in progress, with projected completion in Aug. 1992 and Jan. 1993. DTIC

N94-15828# Oak Ridge National Lab., TN.

OPTICAL AND INFRARED SPECTRA OF THERMALLY ANNEALED Pb IMPLANTED SiO2 GLASSES

D. O. Henderson (Fisk Univ., Nashville, TN.), S. H. Morgan (Fisk Univ., Nashville, TN.), R. Mu (Fisk Univ., Nashville, TN.), R. H. Magruder, III (Belmont Coll., Nashville, TN.), T. S. Anderson (Belmont Coll., Nashville, TN.), J. E. Wittig (Vanderbilt Univ., Nashville, TN.), and R. A. Zuhr 1992 9 p Presented at the 37th Annual Society of Photo-Optical Instrumentation Engineers International Symposium on Optical and Optoelectronic Applied Science and Engineering, San Diego, CA, 19-24 Jul. 1992

(Contract DE-AC05-84OR-21400)

(DE93-015304; CONF-920792-61) Avail: CASI HC A02/MF A01

Infrared reflectance between 4000 and 100 cm(exp -1) and optical spectra between 1.8 and 6.2 eV of high purity silica implanted with nominal doses of 1, 3, and 6 x 10(exp 16) Pb ions/sq cm were recorded before and after annealing at 400, 600, and 800 C for 1 hour. Curve resolution analysis of the Si-O stretching region resulted in six peaks which were characterized by their lineshape parameters. The oscillator strength of the ion induced defect peak at 1035 cm(exp -1) was found to depend on ion dose. The defect band at 1035 cm(exp -1) decreased to an intensity comparable to that of the unimplanted glass after thermal annealing for 1 hour at 800 C. Far infrared spectra indicated the formation of lead silicate particles after annealing. DOE

N94-15843# Minnesota Univ., Minneapolis. Dept. of Chemical Engineering and Materials Science.

EFFECTS OF AGING TIME ON V205 SOL-GEL COATINGS

G. A. Pozarnsky, L. Wright, and A. V. McCormick 12 Jul. 1993 18 p

(Contract N00014-91-J-1893)

(AD-A266824; TR-6-ONR) Avail: CASI HC A03/MF A01

Vanadium pentoxide (V2O5) sols were used in conductive coatings and related applications. From cryo-Transmission Electron Microscopy (TEM) and Nuclear Magnetic Resonance (NMR) spectroscopic studies of the gelation, there are several intermediate structures and reactions in this process, but no information is yet available on the effects of aging on the dependent properties of viscosity, conductance, and film morphology in the coating process. The changes in these properties were observed over a 30 day period by means of rheological measurements and microscopic observation of the dried coatings obtained. The study found that the sol viscosity and ability to wet substrates is related to the initial decomposition of the precursors in solution and the start of the polymerization process. Distinct differences were observed in coating morphology as later aggregation and agglomeration processes occurred. DTIC

N94-15859# Army Research Lab., Watertown, MA.

ASSESSMENT OF CHROMATE AND NON-CHROMATE CONVERSION COATINGS FOR Al ALLOYS USING ELECTROCHEMICAL IMPEDANCE SPECTROSCOPY Final Report

F. Chang, M. Levy, and R. Huie Jun. 1993 23 p

(AD-A267205; ARL-TR-142) Avail: CASI HC A03/MF A01

A study was conducted to evaluate whether a non-chromate conversion coating (Sanchem) for Al alloys (Al 2024 and 7075) could be a suitable replacement for the currently used chromate conversion coating (Alodine) without compromising corrosion resistance. Electrochemical impedance spectroscopy (EIS) and salt spray testing were employed to compare the corrosion behavior of coatings consisting of the following: (1) pretreatment only (Sanchem or Alodine); (2) pretreatment (Sanchem or Alodine) plus primer (epoxy polyamide or waterborne epoxy); and (3) pretreatment (Sanchem or Alodine) plus epoxy polyamide primer plus polyurethane topcoat. Results indicated that the experimental impedance values provided a reliable estimate of the film integrity and corrosion protective capability, that the Sanchem conversion coating generally compared favorably with the Alodine coating, and that higher impedance values attributed to the application of topcoat of both alloys which were treated with either Sanchem or Alodine and epoxy polyamide are characteristic of low conductivity, good barrier type coatings. However, additional tests are required before the Sanchem can be recommended as a reliable alternative to the Alodine coating. DTIC

N94-15879*# National Aeronautics and Space Administration. Langley Research Center, Hampton, VA.

COMPOUNDS CONTAINING META-BIPHENYLENEDIOXY MOIETIES AND POLYMERS THEREFROM Patent Application

Terry L. St.Clair, inventor (to NASA) and John Richard Pratt, inventor (to NASA) (Lockheed Engineering and Sciences Co., Hampton, VA.) 13 May 1993 16 p

(NASA-Case-LAR-14517-1; NAS 1.71:LAR-14517-1;

US-Patent-Appl-SN-062861) Avail: CASI HC A03/MF A01

Two monomers containing meta-biphenylenedioxy moieties were prepared. One monomer, a diamine, is used to prepare polyimide, polyamide, and epoxy polymers. The other monomer, a dianhydride, was used to prepare polyimide polymers. These polymers are used to make films, coatings, and selective membranes. NASA

N94-15880*# National Aeronautics and Space Administration. Langley Research Center, Hampton, VA.

STRUCTURES FROM LOW DIELECTRIC POLYIMIDES Patent Application

Anne K. St.Clair, inventor (to NASA), Terry L. St.Clair, inventor (to NASA), and William P. Winfree, inventor (to NASA) 28 Sep. 1992 31 p

(NASA-Case-LAR-14988-1; NAS 1.71:LAR-14988-1;

US-Patent-Appl-SN-954108) Avail: CASI HC A03/MF A01

A structure which is effective as an electrical insulator or as a transmitter-receiver of electromagnetic energy is prepared by providing a suitable substrate and covering the substrate with an adhering layer of a low dielectric, high temperature, linear aromatic polyimide. This polyimide is prepared by selecting aromatic diamine and aromatic dianhydride reactants to meet at least two of the following three conditions: a reactant must have minimal permanent or inducible electrical dipolar characteristics as a result of the presence of pendant or bridging groups therein, a reactant must impart a high degree of free volume to the polymer caused by inefficient chain packing therein in the solid state as a result of the presence of pendant or bridging groups therein, and a reactant must have fluorine atoms chemically attached thereto; and chemically combining equimolar quantities of the aromatic diamine and aromatic dianhydride reactants in a solvent to form a high molecular weight polyamic acid solution, and converting the high molecular weight polyamic acid to the corresponding low dielectric, high temperature linear aromatic polyimide. NASA

N94-15920# Los Alamos National Lab., NM.

SYNTHESIS OF CERAMIC OXIDE POWDERS IN A MICROWAVE PLASMA DEVICE

D. Vollath and K. E. Sickafus 1993 11 p Presented at the 3rd European Ceramic Society Conference, Madrid, Spain, 13-17 Sep. 1993
(Contract W-7405-eng-36)
(DE93-012741; LA-UR-93-1518; CONF-930927-1) Avail: CASI HC A03/MF A01

Synthesizing oxide ceramic powders by application of a microwave plasma is of great advantage. The microwave plasma can be used two ways: to act as a source of heat for the pyrolysis of solutions and to excite gas phase reactions to obtain nanosized powders. Both applications are superior to standard methods. A microwave cavity well suited for these experiments and its operating characteristics are described. Using a microwave plasma as a source of heat for pyrolytic decomposition of nitrates in aqueous solutions leads to a fine grained product with particle sizes from 100 to 1000 nm. Crystallite sizes in those particles are in most cases less than 10 nm. This is demonstrated with zirconia-based ceramics, such as ZrO2 -- 3m% Y2O3 -- 20m% Al2O3. Depending on conditions during pyrolysis, it is possible to obtain a product in which alumina is either dissolved in zirconia or the onset of the phase separation is observed. Energy efficiency for this process is better than 80%. If the reactants are gaseous e.g., ZrCl4, it is possible to produce powders with mean crystallite sizes of about 4 nm. In the case of zirconia these particles are nanocrystalline with a cubic structure. This structure is not in equilibrium under the experimental conditions. DOE

N94-15924# Lawrence Livermore National Lab., CA.
THE EFFECT OF PROCESS PARAMETERS ON THE SURFACE FINISH OF PLASMA POLYMERS
S. A. Letts, R. C. Cook, P. Welch, R. McEachern, and E. Fearon Dec. 1992 11 p Presented at the American Chemical Society National Meeting, Denver, CO, 28 Mar. - 2 Apr. 1993
(Contract W-7405-eng-48)
(DE93-014112; UCRL-JC-112379; CONF-930304-22) Avail: CASI HC A03/MF A01

The surface finish of plasma polymers deposited in an inductively coupled discharge were measured as a function of gas flow rates. Surface finish was measured both optically and by AFM. The process parameters of the plasma polymerization were found to effect the surface finish. The gases used were trans-2-butene and hydrogen for hydrocarbon polymers. For bromocarbon polymers we added ethylbromide. The smoothest hydrocarbon polymer coatings had an RMS surface finish better than 1 nm. Bumps 200 nm high spaced approximately 1 micron apart grew on the surface of bromocarbon coatings when they were exposed to air. The composition of the bumps was found to be NH4Br by XRD and XPS analysis. We believe that nitrogen (from a small leak or desorption) dissociates in the discharge and reacts with hydrogen to form ammonia. The ammonia then reacts with HBr, a dissociation product of ethylbromide, to form NH4Br which is dispersed throughout the deposited layer. Humidity facilitates the transport of the NH4Br to the surface where it crystallizes. Bump growth was prevented by either dry storage or overcoating with 3 micron of hydrocarbon plasma polymer. Alternatively, the bumps could be washed from the surface with water. DOE

N94-15930*# National Aeronautics and Space Administration. Pasadena Office, CA.
CYANORESIN, CYANORESIN/CELLULOSE TRIACETATE BLENDS FOR THIN FILM, DIELECTRIC CAPACITORS Patent Application
Shiao-Ping Yen, inventor (to NASA) (Jet Propulsion Lab., California Inst. of Tech., Pasadena.) and T. Richard Jow, inventor (to NASA) (Jet Propulsion Lab., California Inst. of Tech., Pasadena.) 28 May 1993 17 p
(Contract NAS7-918)
(NASA-Case-NPO-18913-1-CU; NAS 1.71:NPO-18913-1-CU; US-Patent-Appl-SN-073015) Avail: CASI HC A03/MF A01

Non-brittle dielectric films are formed by blending a cyanoresin such as cyanoethyl, hydroxyethyl cellulose (CRE) with a compatible, more crystalline resin such as cellulose triacetate. The electrical breakdown strength of the blend is increased by orienting the films by uniaxial or biaxial stretching. Blends of high molecular weight CRE with high molecular weight cyanoethyl cellulose (CRC) provide films with high dielectric constants. NASA

N94-15960*# National Aeronautics and Space Administration. Pasadena Office, CA.
SELECTIVE FORMATION OF POROUS SILICON Patent Application
Jones Fathauer, inventor (to NASA) (Jet Propulsion Lab., California Inst. of Tech., Pasadena.) 7 Jun. 1993 16 p
(Contract NAS7-918)
(NASA-Case-NPO-18735-1-CU; NAS 1.71:NPO-18735-1-CU; US-Patent-Appl-SN-073019) Avail: CASI HC A03/MF A01

A pattern of porous silicon is produced in the surface of a silicon substrate by forming a pattern of crystal defects in said surface, preferably by applying an ion milling beam through openings in a photoresist layer to the surface, and then exposing said surface to a stain etchant, such as HF:HNO3:H20. The defected crystal will preferentially etch to form a pattern of porous silicon. When the amorphous content of the porous silicon exceeds 70 percent, the porous silicon pattern emits visible light at room temperature. NASA

N94-15996# California Univ., Berkeley. Lawrence Berkeley Lab.
SWELLING EQUILIBRIA FOR TEMPERATURE-SENSITIVE AMPHOLYTIC HYDROGELS
J. P. Baker, D. R. Stephens, H. W. Blanch, and J. M. Prausnitz Sep. 1992 27 p
(Contract DE-AC03-76SF-00098)
(DE93-015264; LBL-32956) Avail: CASI HC A03/MF A01

Temperature-sensitive N-isopropylacrylamide (NIPA)-based ampholytic hydrogels were synthesized by copolymerizing NIPA with the cationic monomer methacrylamidopropyl trimethylammonium chloride (MAPTAC) and the anionic monomer sodium styrene sulfonate (SSS). The total nominal charge density of the hydrogels was held constant at 8 mol % (dry basis), while the molar ratio of anionic to cationic moieties within the hydrogels was varied. Swelling equilibria were measured in water at 6 C, and in aqueous sodium chloride solutions ranging in concentration from 10(exp -5) to 5 M and temperature ranging from 6 to 56 C. Consistent with expectations, the swelling behavior of the hydrogels was found to be controlled by temperature at low salt concentrations; as the sodium chloride concentration increased, temperature control of hydrogel swelling decreased. Slight antipolyelectrolyte behavior was observed for the hydrogel prepared with equal molar amounts of MAPTAC and SSS. DOE

N94-16016# Oak Ridge National Lab., TN.
RHEOLOGY AND MICROSTRUCTURE OF CONCENTRATED ZIRCONIA-ALUMINA SUSPENSIONS FOR GELCASTING COMPOSITES
A. Bleier and O. O. Omatete 1992 8 p Presented at the 16th Material Research Society International Symposium on the Scientific Basis for Nuclear Waste Management Fall Meeting, Boston, MA, 30 Nov. - 5 Dec. 1992
(Contract DE-AC05-84OR-21400)
(DE93-015339; CONF-921101-133) Avail: CASI HC A02/MF A01

The relations among colloidal stability, suspension rheology, and solids loading are elucidated for zirconia-alumina mixtures containing 20 vol percent ZrO2, based on solids. The lower colloidal stability of ZrO2 limits the rheological properties of this system. If the zeta potential of ZrO2 is less than 49 mV, high degrees of pseudoplasticity, high yield stress, high viscosity, and long relaxation times characterize the binary suspensions. These effects occur, despite the fact that ZrO2 is the minor ceramic constituent. If the zeta potential of ZrO2 is maintained above 49 mV, suspensions with high solids loading (55 vol%) can be prepared which behave as Newtonian fluids over the 0-to-200 s(exp -1) shear rate range and as an elastic solid at higher rates. As the solids loading of a highly stable binary suspension is increased, the rheological properties change. They evolve from those of a near Newtonian-like fluid with nearly independent particles (40 vol%) to those of a pseudoplastic fluid with a weakly interacting particle network (50 vol%) to those of an elastic-like solid composed of crowded, strongly repulsive particles (55 vol%). Low-shear conditions for suspension-transport and mold-filling operations that ensure a homogeneous arrangement of ZrO2 and Al2O3 particles in a gelcast ceramic seem promising. DOE

N94-16018# Oak Ridge National Lab., TN.
THE INFLUENCE OF MICROSTRUCTURE ON THE MECHANICAL BEHAVIOR OF SILICON NITRIDE CERAMICS
P. F. Becher, H. T. Lin, S. L. Hwang, M. J. Hoffmann (Max-Planck-Inst. fuer Metallforschung, Stuttgart, Germany.), and I.-Wei Chen (Michigan Univ., Ann Arbor.) 1992 12 p Presented at the 16th Material Research Society International Symposium on the Scientific Basis for Nuclear Waste

Management Fall Meeting, Boston, MA, 30 Nov. - 5 Dec. 1992
(Contract DE-AC05-84OR-21400)
(DE93-015363; CONF-921101-131) Avail: CASI HC A03/MF A01

Elongated Si nitride grains produced during densification in a liquid phase can increase the fracture toughness, but this depends on the activation of intergranular rather than transgranular fracture. Bridging in the crack wake by elongated grains and pullout of some of these grains suggest that the crack wake mechanisms that contribute to toughening of whisker-reinforced ceramics can also operate in Si nitrides containing elongated grains. With diameters of the larger elongated grains approaching 9 microns, strengths greater than 800 MPa have been achieved along with Weibull moduli, but clustering of these larger elongated grains must be avoided. Fatigue of these toughened Si nitrides is influenced by silicate grain boundary phases. Design of toughened Si nitrides must consider effects of silicate phase composition and content on fatigue and creep. DOE

N94-16067# Oak Ridge National Lab., TN.
MULTIAXIAL DEFORMATION AND LIFE PREDICTION MODEL AND EXPERIMENTAL DATA FOR ADVANCED SILICON NITRIDE CERAMICS
J. L. Ding (Washington State Univ., Pullman.), K. C. Liu, and C. R. Brinkman 1993 48 p Presented at the 17th Annual Conference on Composites and Advanced Ceramics, Cocoa Beach, FL, 11-15 Jan. 1993
(Contract DE-AC05-84OR-21400)
(DE93-015450; CONF-930164-11) Avail: CASI HC A03/MF A01

This paper summarizes recent experimental results on creep and creep rupture behavior of a commercial grade of Si3N4 ceramic in the temperature range of 1150 to 1300 C obtained at ORNL and introduces a tentative multiaxial deformation and life prediction model for ceramic materials under general thermomechanical loadings. Issues related to the possible standardization of the data analysis methodology and possible future research needs for high temperature structural ceramics in the area of development of data base and life prediction methodology are also discussed. DOE

N94-16472# Brunel Univ., Uxbridge (England).
STRUCTURAL STUDIES OF SOL-GEL GLASSES Final Report, 15 Jul. 1989 - 14 Jul. 1992
Carole C. Perry 14 Jul. 1992 7 p
(Grant AF-AFOSR-0489-89)
(AD-A266277; AFOSR-93-0424TR) Avail: CASI HC A02/MF A01

Near and mid infrared spectroscopy and FT-Raman spectroscopy have been used to study silica/titania monoliths produced by the sol-gel route which have been subjected to selected heat treatments. Increasing thermal treatment temperature leads to a general strengthening of the gel-glass matrix although the incorporation of low levels (3% by weight) of titanium into tetrahedral sites only led to more disordered glasses than for silica alone. Evidence has been obtained for the formation of Si-O-Ti bonds principally during the later stages of densification at temperatures between 615 and 1000 C. The addition of titanium also leads to a reduction in surface 'free' silanol levels together with an increase in hydrogen bonded silanol levels and increasing amounts of water associated with the glass. The implication is that the incorporation of titanium onto the surface of the gel matrix leads to tighter binding of water molecules to silanol groups. DTIC

N94-16475# Colorado State Univ., Fort Collins. Dept. of Chemistry.
MODIFICATION OF FLUOROPOLYMER SURFACES WITH ELECTRONICALLY CONDUCTIVE POLYMERS Interim Report
Leon S. VanDyke, Charles J. Brumlik, Wenbin Liang, Junting Lei, and Charles R. Martin Jun. 1993 30 p
(Contract N00014-82-K-0612)
(AD-A266294; TR-86) Avail: CASI HC A03/MF A01

We describe methods for coating fluoropolymer surfaces with thin films of electronically conductive polymers. Modification of the fluoropolymer surface prior to coating with a conductive polymer is necessary to achieve good adhesion between the fluoropolymer membrane and the conductive polymer coating. We describe four different procedures for modifying the fluoropolymer surface so as to promote strong adhesion. These procedures are based on a wet chemical treatment of fluoropolymer or on exposure of fluoropolymer surface to a hydrogen plasma, an ultraviolet laser, or an electron beam. Finally, we show that it is possible to write patterns with the conductive polymer onto the fluoropolymer surface. DTIC

N94-16494*# Alabama Univ., Huntsville. Physics Dept.
VUV THIN FILMS, CHAPTER 7
Muamer Zukic and Douglas G. Torr [1993] 121 p
(Grant NAGw-2898)
(NASA-CR-194634; NAS 1.26:194634) Avail: CASI HC A06/MF A02

The application of thin film technology to the vacuum ultraviolet (VUV) wavelength region from 120 nm to 230 nm has not been fully exploited in the past because of absorption effects which complicate the accurate determination of the optical functions of dielectric materials. The problem therefore reduces to that of determining the real and imaginary parts of a complex optical function, namely the frequency dependent refractive index n and extinction coefficient k. We discuss techniques for the inverse retrieval of n and k for dielectric materials at VUV wavelengths from measurements of their reflectance and transmittance. Suitable substrate and film materials are identified for application in the VUV. Such applications include coatings for the fabrication of narrow and broadband filters and beamsplitters. The availability of such devices open the VUV regime to high resolution photometry, interferometry and polarimetry both for space based and laboratory applications. This chapter deals with the optics of absorbing multilayers, the determination of the optical functions for several useful materials, and the design of VUV multilayer stacks as applied to the design of narrow and broadband reflection and transmission filters and beamsplitters. Experimental techniques are discussed briefly, and several examples of the optical functions derived for selected materials are presented. Author (revised)

N94-16541*# Old Dominion Univ., Norfolk, VA. Dept. of Electrical and Computer Engineering.
PROPERTIES OF THIN FILMS FOR HIGH TEMPERATURE FLOW SENSORS Final Report, period ending 20 Aug. 1990
Sacharia Albin Jan. 1991 15 p
(Contract NAS1-18584; RTOP 505-61-01-05)
(NASA-CR-191526; NAS 1.26:191526) Avail: CASI HC A03/MF A01

Requirements of material parameters of high temperature flow sensors are identified. Refractory metal silicides offer high temperature sensitivity and high frequency response and are stable up to 1000 C. Intrinsic semiconductors of high band gap are also considered as sensor elements. SiC and diamond are identified. Combined with substrates of low thermal and electrical conductivity, such as quartz or Al2O3, these materials meet several requirements of high sensitivity and frequency response. Film deposition and patterning techniques suitable for these materials are identified. Author (revised)

N94-16543*# National Aeronautics and Space Administration. Lewis Research Center, Cleveland, OH.
PHYSICAL AND CHEMICAL PROPERTIES OF SOME NEW PERFLUOROPOLYALKYLETHER LUBRICANTS PREPARED BY DIRECT FLUORINATION
W. R. Jones, Jr., T. R. Bierschenk (Exfluor Research Corp., Austin, TX.), T. J. Juhlke (Exfluor Research Corp., Austin, TX.), H. Kawa (Exfluor Research Corp., Austin, TX.), and R. J. Lagow (Exfluor Research Corp., Austin, TX.) May 1993 23 p Presented at the STLE Annual Meeting, Calgary, Alberta, 17-21 May 1993; sponsored by Society of Tribologists and Lubrication Engineers
(RTOP 505-63-5A)
(NASA-TM-106299; E-8038; NAS 1.15:106299) Avail: CASI HC A03/MF A01

A series of perfluoropolyalkylether (PFPAE) fluids was synthesized by direct fluorination. Viscosity-temperature properties, oxidation stabilities, oxidation-corrosion properties, bulk modulus, lubricity, surface tension and density were measured. It was shown that as the carbon to oxygen ratio in the polymer repeating unit decreases, the viscometric properties improve, the fluids may become poorer boundary lubricants, the bulk modulus increases, the surface tension increases and the fluid density increases. The presence of difluoromethylene oxide units in the polymer does not significantly lower the oxidation and oxidation-corrosion stabilities as long as the difluoromethylene oxide units are separated by other units. Author

N94-16658# Argonne National Lab., IL.
DETECTION OF SUBSURFACE DEFECTS IN MACHINED SILICON NITRIDE CERAMICS BY OPTICAL SCATTERING METHODS
W. A. Ellingson, D. M. Ayaz, M. P. Brada, and W. OConnell 1993 31 p Presented at the International Conference on Machining of Advanced Materials, Gaithersburg, MD, 20-22 Jul. 1993
(Contract W-31-109-eng-38)
(DE93-015554; ANL/MCT/CP-79253; CONF-930793-1) Avail: CASI HC A03/MF A01

Si3N4 materials, from two manufacturers in the form of texture test bars, were studied by optical Fourier scattering methods. Subsurface defects were synthesized by either ultrasonically drilling or by grinding slots parallel to the surface. Because of unique optical transmission properties of ceramics subsurface defects, such as those likely to be caused by machining may be detected. S-polarized He-Ne laser light (lambda = 0.6328 microns) was used as the light source. Specular reflections were detected by an optical Fourier method which incorporated cross-polarization. Analysis of scattered laser light was accomplished using a CCD-array camera, an 8-bit A/D converter, and a PC with locally written software. Results show that subsurface defects can be detected and that for the surface finishes studied, changes in signal-to-noise (S/N) are observable. DOE

N94-16723# TRW, Inc., Redondo Beach, CA.
SPUTTERED FERROELECTRIC THIN FILMS OF KTN FOR ELECTRO-OPTIC DEVICES Final Report, 1 Aug. 1991 - 31 May 1993
Sanat Sashital May 1993 6 p
(Contract DAAL03-91-C-0048)
(AD-A266573; ARO-28979.2-PH) Avail: CASI HC A02/MF A01

Major accomplishments of this program are the demonstrations summarized as follows: (1) Large grain (0.5 to 0.8 micrometer), high preferred orientation (100) films of Pt on SiO2/Si substrates by use of high deposition temperatures (600-650 C) with a trace of reactive O2 gas in the rf-PM sputtering gas. The Pt film, besides functioning as metallization for bottom electrodes for capacitors, promotes epitaxial like growth within its large grains and high crystal quality of the overlying KTN film. (2) Epitaxial growth of KTN films on GaAs (100) and 'r' plane' (1012) Sapphire substrates with film normal along (100) polar direction. (3) First time observation of Ferroelectric Curie-Weiss behavior of KTN films by rf-PM sputtering on GaAs and Pt/SiO2/Si substrates with peak dielectric constants of nearly 2250 (at 1 KHz); Sharp Curie transition temperatures (-9 to +3 C) with bulk single crystal like characteristics. (4) High optical transmittivity of KTN films on Sapphire with nearly 99.5% of theoretical transmittivity. (5) High quadratic EO effect in paraelectric phase of KTN films on GaAs and Si substrates. Observed EO response is nearly 70% larger than for substrates. Observed EO effect is nearly 70% larger than for the same effect in PLZT thin films in ferroelectric phase. DTIC

N94-16727# State Univ. of New York, Albany. Research Foundation.
DETECTION AND DOSIMETRY OF CHEMICAL CONTAMINANTS IN POLYMERIC MATERIALS Final Report, 15 Sep. 1988 - 31 Mar. 1993
H. L. Frisch, W. M. Gibson, P. J. Toscano, and J. T. Welch 15 Jun. 1993 6 p
(Contract DAAL03-88-K-0198)
(AD-A266605; ARO-26072.25-CH-A) Avail: CASI HC A02/MF A01

New methods for the measurement of diffusion coefficients have been developed which enable the investigator to determine the local environment of a penetrant. The methods are general and facilitate discrimination between adsorbed and absorbed material. The diffusion coefficients of low molecular weight penetrants containing P-31 and F-19 can be readily measured in both glassy and rubbery polymers using solid state NMR probes that include cross-polarization, high powered H-1 decoupling and magic angle spinning. These measurements on fluorinated penetrants in both rubbery and glassy polymers have been confirmed by resonant nuclear reaction analysis using an alpha detection method of the product of F-19(p, ag)O-16 reaction at the strong 872 keV resonance. The resonant nuclear reaction techniques developed have the added feature that it is possible to investigate slowly - diffusing molecules whose study would be intractable by conventional methods. DTIC

N94-16767# Materials Modification, Inc., Fairfax, VA.
SOLID LUBRICANTS FOR SPACE STRUCTURES, PHASE 2 Final Report, 29 Jun. 1990 - 28 Jun. 1993
T. S. Sudarshan 14 Jun. 1993 97 p
(Contract DASG60-90-C-0114)
(AD-A266653) Avail: CASI HC A05/MF A02

In this Phase 2 effort, copper-lead alloys of three different compositions (90/10, 75/25, and 50/50 copper-lead) were processed by swirl die continuous casting in the form of ingots and further processed into powders using the gas atomization method. The powders were compacted using shock compaction and hot isostatic pressing. Friction and wear studies revealed that the 75/25 alloys had the best friction and wear rates under a range of sliding speeds and contact loads. Bearing cages, brushes, bushings and gears were produced from the different compositions and processing conditions. The components were tested in specially designed test rigs by the National Council for Tribology, U.K. The 90/10 hot isostatically pressed bearing cages outperformed the currently used lead-bronze cages and produced mini-noise for one (1) million revolutions. In the case of brushes, all the compositions and processing conditions outperformed all the materials that had been tested previously at NCT. Moderate to little improvements were observed in gears and bushings. DTIC

N94-16796# Duke Univ., Durham, NC. Dept. of Physics.
SPECTROSCOPIC INVESTIGATIONS OF NONAMBIENT SYSTEMS WITH MILLIMETER AND SUBMILLIMETER PROBES Final Report, 1 Oct. 1989 - 31 Dec. 1991
Frank C. DeLucia 20 Mar. 1993 20 p
(Contract DAAL03-89-K-0181)
(AD-A266537; ARO-27431.3-PH) Avail: CASI HC A03/MF A01

The project, 'Spectroscopic Investigations of nonambient systems with Millimeter and Submillimeter Probes,' addressed a broad range of scientific topics and technological developments important to this spectral region. For the purposes of this discussion, we have divided the report on research results into three parts: (1) Energy transfer in polyatomic molecules; (2) Molecular collisional processes at very low temperature (less than 5K); and (3) Development and uses of millimeter and submillimeter technology. Also included is a list of personnel who worked on these projects. DTIC

N94-16813# Oak Ridge National Lab., TN.
DEVELOPMENT OF A CONSTITUTIVE MODEL FOR CREEP AND LIFE PREDICTION OF ADVANCED SILICON NITRIDE CERAMICS
J. L. Ding (Washington State Univ., Pullman.), K. C. Liu, and C. R. Brinkman 1992 11 p Presented at the Annual Automotive Development Technology Contractors' Coordination Meeting, Dearborn, MI, 2-5 Nov. 1992
(Contract DE-AC05-84OR-21400)
(DE93-015894; CONF-9211101-11) Avail: CASI HC A03/MF A01

A constitutive model capable of describing deformation and predicting rupture life was developed for high temperature ceramic materials under general thermal mechanical loading conditions. The model was developed based on the deformation and fracture behavior observed from a systematic experimental study on an advanced silicon nitride (Si3N4) ceramic material. Validity of the model was evaluated with reference to creep and creep rupture data obtained under constant and stepwise-varied loading conditions, including the effects of annealing on creep and creep rupture behavior. DOE

N94-16843# Oak Ridge National Lab., TN.
THE CERAMIC TECHNOLOGY PROJECT: TEN YEARS OF PROGRESS
D. R. Johnson and R. B. Schulz (Department of Energy, Washington, DC.) 1993 10 p Presented at the International Gas Turbine Institute (IGTI) Meeting, Cincinnati, OH, 24 May 1993
(Contract DE-AC05-84OR-21400)
(DE93-015991; CONF-9305226-1) Avail: CASI HC A02/MF A01

The Ceramic Technology Project was initiated in 1983 for the purpose of developing highly reliable structural ceramics for applications in advanced heat engines, such as the automotive gas turbines and advanced heavy duty diesel engines. The reliability problem was determined to be a result of uncontrolled populations of processing flaws in the brittle, flaw-sensitive materials, along with microstructural features, such as grain boundary phases, that contribute to time dependent strength reduction in service at high temperatures. The approach taken to develop high reliability ceramics included the development of tougher materials with greater tolerance to microstructural flaws, the development of advanced processing technology to minimize the size and number of flaws, and the development of mechanical

testing methodology and the characterization of time dependent mechanical behavior, leading to a life prediction methodology for structural ceramics. DOE

N94-16877# Oak Ridge National Lab., TN.
PROCESSING OF COMPLEX SINTERED REACTION BONDED SILICON NITRIDE PARTS BY MICROWAVE HEATING
J. O. Kiggans, T. N. Tiegs, H. D. Kimrey, and C. E. Holcombe (Oak Ridge Y-12 Plant, TN.) 1993 9 p Presented at the 95th Annual Meeting of the American Ceramic Society, Cincinnati, OH, 18-22 Apr. 1993
(Contract DE-AC05-84OR-21400)
(DE93-015811; CONF-930438-26) Avail: CASI HC A02/MF A01

Several studies have been conducted over the last several years assessing the use of microwave heating for processing reaction-bonded silicon nitride (RBSN) and sintered reaction-bonded silicon nitride (SRBSN). Although SRBSN test specimens up to 500g have been processed by using microwave heating, samples have been limited to simple shapes such as tiles. In this study, microwave packaging techniques were developed to process complex SRBSN parts and multiple samples within a single cycle. Physical and mechanical properties of test samples were measured. Comparison studies were performed using conventional furnace processing to establish baseline values and expected statistical variation. DOE

N94-16889# Oak Ridge National Lab., TN.
CHEMICAL VAPOR DEPOSITION OF Ta2O5 CORROSION RESISTANT COATINGS
D. W. Graham and D. P. Stinton 1992 13 p Presented at the 1992 Coatings for Advanced Heat Engines Workshop, Monterey, CA, 2 Aug. 1992
(Contract DE-AC05-84OR-21400)
(DE93-015488; CONF-9208207-2) Avail: CASI HC A03/MF A01

Silicon carbide and silicon nitride heat engine components are susceptible to hot corrosion by molten Na2SO4 which forms from impurities present in fuel and the environment. Chemically vapor deposited Ta2O5 coatings are being developed as a means to protect components from reaction with these salts and preserve their structural properties. Investigations to optimize the structure of the coating have revealed that the deposition conditions dramatically affect the coating morphology. Coatings deposited at high temperatures are typically columnar in structure; high concentrations of the reactant gases produce oxide powders on the substrate surface. Ta2O5 deposited at low temperatures consists of grains that are finer and have significantly less porosity than that formed at high temperatures. Samples of coatings which have been produced by CVD have successfully completed preliminary testing for resistance to corrosion by Na2SO4. DOE

N94-16916 Department of the Navy, Washington, DC.
INTERPENETRATING POLYMER NETWORK ACOUSTIC DAMPING MATERIAL Patent
Usman A. Sorathia, inventor (to Navy), William L. Yeager, inventor (to Navy), and Timothy L. Dapp, inventor (to Navy) 6 Jul. 1993 5 p Filed 28 Aug. 1991
(AD-D015889; US-Patent-5,225,498; US-Patent-Appl-SN-750992) Avail: US Patent and Trademark Office

Improved acoustic damping materials comprise interpenetrating polymer networks having a soft polymer component and a hard polymer component. The soft polymer component, constituting from 50 to 90, preferably 70, percent by weight of the material, is made by polymerizing an aromatic diisocyanate with a polyalkylene ether glycol, and the hard polymer component is a vinyl ester polymer made by polymerization of a vinyl ester resin such as the acrylate or methacrylate ester of the diglycidyl ether of a polyphenol. Optionally, the vinyl ester resin may be brominated, whereby increased fire retardance is conferred upon the interpenetrating polymer network. The mixture is cured at room temperature. DTIC

N94-16920 Department of the Navy, Washington, DC.
MAIN CHAIN CHROMOPHORIC POLYMERS WITH SECOND ORDER NONLINEAR OPTICAL PROPERTIES Patent
John Fischer, inventor (to Navy), Ronald Henry, inventor (to Navy), James Hoover, inventor (to Navy), Geoffrey Lindsay, inventor (to Navy), and John Stenger-Smith, inventor (to Navy) 18 May 1993 8 p Filed 25 Mar. 1991
(AD-D015893; US-Patent-5,212,269; US-Patent-Appl-SN-680717) Avail: US Patent and Trademark Office

Processible chromophoric polymers are presented that have nonlinear optical properties and wherein the chromophore is present in and is a part of the polymer backbone, including substantially all of the monomer or repeat units, with the dipole moments pointing in the same direction (head-to-tail) along the polymer backbone. Such polymers include phenylene, phenylene vinylene, stilbenylene, phenyl piperdine, and coumarin polymers. DTIC

N94-16924# Polish Academy of Sciences, Warsaw. Inst. Podstawowych problemow Techniki.
SUPERCONDUCTING CERAMICS: SELECTED PROPERTIES AND METHODS OF PRODUCTION [NADPRZEWODNIKI CERAMICZNE WYBRANE WLASNOSCI I METODY WYTWARZANIA]
Jerzy Ranachowski, Zdzislaw Librant, and Jerzy Raabe (Technical Univ. of Warsaw, Poland.) 1991 34 p In POLISH
(IFTR-23/1991) Avail: CASI HC A03/MF A01

The topic 'Analysis of Acoustic Features of Selected High-Temperature Ceramic Superconductors' was discussed under Program 02.03 between 1986 and 1990. Within the framework of this Program it has become necessary to fabricate corresponding samples for ultrasonic volume wave, resonant and surface wave analyses. It has become necessary to fabricate samples of different sizes using different technologies. Structural studies of the fabricated specimens were an important task; such studies encompassed measurements of the elasticity moduli, the average grain distribution, porosity measurements as well as the contents of different crystallization phases. Primary attention has been devoted to aging of the samples and losses of superconductivity. This issue is of special significance for samples with a deposited superconductivity thin layer. Transl. by FLS

N94-16928# Colorado State Univ., Fort Collins. Dept. of Chemistry.
A SIMPLE CHEMICAL PROCEDURE FOR EXTENDING THE CONDUCTIVE STATE OF POLYPYRROLE TO MORE NEGATIVE POTENTIALS Interim Report
Leon S. VanDyke, Susumu Kuwabata, and Charles R. Martin Jun. 1993 35 p
(Contract N00014-82-K-0612)
(AD-A266235; TR-85) Avail: CASI HC A03/MF A01

The electronically conductive polymer polypyrrole is an electronic conductor at potentials positive of ca. -0.4 V vs. the saturated calomel electrode (SCE) and an electronic insulator at potentials negative of this value. As a result of this potential-dependent conductor/insulator transition, a polypyrrole film can be used as an electrode for redox couples with E(o)'s positive of ca. -0.4 V vs. SCE but cannot be used as an electrode for couples with E(o)'s negative of this value. We have discovered a simple chemical procedure that extends the conductive state of polypyrrole to ca. -1.1 V vs. SCE. This procedure entails treating the polypyrrole film with aqueous sodium hydroxide. We demonstrate this extension of the conductive state to more negative potentials in this paper. We also propose, and test, a chemical model that explains the extension of the conductive state. DTIC

N94-16946# Colorado State Univ., Fort Collins. Dept. of Chemical Engineering.
MATERIALS PROCESSING AND MANUFACTURING TECHNOLOGIES FOR DIAMOND SUBSTRATE MULTICHIP MODULES (DSMCM)
David S. Dandy 1 Jul. 1993 6 p
(Contract N00014-93-1-2002)
(AD-A267316) Avail: CASI HC A02/MF A01

A detailed surface kinetics mechanism has been developed for the deposition of CH3, C2H2, and C onto a reconstructed (100) diamond surface. The mechanism accounts for the growth of alternating dimer-trough rows. The thermophysical properties of all structures present in the mechanism have been computed using the molecular mechanics program MM3(92). A diamond growth mechanism on the unreconstructed (100) surface has been used in a stagnation flow model to examine the effect of hydrocarbon injector location and inlet temperature on gas-phase species distributions and diamond growth rate in a DC arcjet reactor system typical of that in use at the Norton Company. It is predicted that there is an optimal injector location, dictated by operating conditions, that results in

maximum concentrations of reactive growth species CH(x) and consequently, in maximum diamond growth rate. DTIC

N94-16947# University of Southern Mississippi, Hattiesburg. Dept. of Polymer Science.
PHOTODEGRADATION OF POLYIMIDES. V1: EFFECT OF DONOR-ACCEPTOR GROUPS ON THE PHOTOOXIDATIVE STABILITY OF POLYIMIDES AND MODEL COMPOUNDS Technical Report No. 19
C. E. Hoyle, D. Creed, P. Subramanian, R. Nagarajan, and C. Pandey 13 Jul. 1993 36 p
(Contract N00014-91-J-1028)
(AD-A267319) Avail: CASI HC A03/MF A01

The photophysics of polyimides and several N-arylphthalimide model compounds has been investigated as part of an effort to understand the factors that control the oxidative photodegradation of these materials. Substituents that increase the donor-acceptor (D-A) character of both polymers and models cause an enhancement of the red-shifted electronic absorption and a shift to lower energy of the broad, weak fluorescence of these materials. Increasing solvent polarity causes a similar effect on the absorption and fluorescence spectra of the model compounds. Fluorescence quantum yields decrease with increasing D-A character in the series of model compounds and with increasing solvent polarity for a given compound. The triplet states of both polymers and models have been characterized in solution by laser flash photolysis, and intersystem crossing quantum yields have been determined. The triplet yields also decrease with increasing D-A character of the chromophore and with increasing solvent polarity. A comparison of fluorescence and phosphorescence spectra reveals a very small singlet-triplet energy gap. It seems likely that the lowering, by increased D-A character, of the yields of the triplet states that are intermediates in the photooxidative degradation, enhances the photostability of aromatic based polymides. DTIC

N94-16948# University of Southern Mississippi, Hattiesburg. Dept. of Polymer Science.
THE PHOTOCHEMISTRY OF POLY(METHYLPHENYLPHOSPHAZENE) Technical Report No. 20
C. E. Hoyle, D. Creed, P. Subramanian, I. B. Rufus, and P. Chatterton 13 Jul. 1993 26 p
(Contract N00014-89-J-1028)
(AD-A267320) Avail: CASI HC A03/MF A01

The photochemical reactions of poly(methylphenyl-phosphazene) (PMPP), a disubstituted poly(phosphazene), have been studied. UV-Irradiation results in chain scission in air-saturated dichloromethane solution, whereas in the absence of molecular oxygen, a bimolecular process, leading to extensive crosslinking and gel formation, predominates. The degradation of PMPP is not inhibited by quenchers of the triplet state. The reactions of PMPP most likely originate from the singlet state. Biphenyl has been identified as a major photoproduct from PMPP both in the presence and absence of molecular oxygen. DTIC

N94-16949# University of Southern Mississippi, Hattiesburg. Dept. of Polymer Science.
THE PHOTOPHYSICS OF POLY(METHYLPHENYLPHOSPHAZENE) Annual Report, 1 May 1992 - 30 Apr. 1993
C. E. Hoyle, D. Creed, P. Subramanian, I. B. Rufus, and P. Chatterton 13 Jul. 1993 27 p
(Contract N00014-91-J-1028)
(AD-A267321) Avail: CASI HC A03/MF A01

The photophysical properties of poly(alkylarylphosphazenes), particularly poly(methylphenylphosphazene). PMPP, with a methyl and a phenyl group on the phosphazene phosphorous atom, have been investigated using absorption and emission spectroscopy, as well as laser flash photolysis. The fluorescence spectrum of PMPP shows a red-shifted emission (decay time greater than 1 nanosecond) with a maximum at 430 nm when excited at 270 nm in solvents of varying polarity. The absence of a strong solvent effect on the position and the structure of the fluorescence spectrum suggests that the emission is not due to a charge-transfer state, but originates from a significant geometry shift in the excited state. The triplet state of PMPP was identified by laser flash photolysis. The phosphorescence spectrum of PMPP indicates a triplet energy of 79 kcal/mol. DTIC

N94-16959# Lehigh Univ., Bethlehem, PA. Energy Research Center.
ROBOTIC WELD OVERLAY COATINGS FOR EROSION CONTROL
B. F. Levin, J. N. Dupont, and A. R. Marder 18 Apr. 1993 7 p
(Contract DE-FG22-92PC-92542)
(DE93-016938; DOE/PC-92542/T2) Avail: CASI HC A02/MF A01

Twelve weld overlay hardfacing alloys have been selected for preliminary erosion testing based on a literature review. These alloys have been separated into three major groups: cobalt containing alloys, nickel-base alloys, and iron base alloys. These alloys are being applied to carbon steel substrates and will undergo preliminary erosion testing to identify candidate weld overlay alloys for erosion control in CFB boilers. The candidate alloys selected from the preliminary erosion tests will then undergo more detailed evaluations in future research. DOE

N94-16963# California Inst. of Tech., Pasadena. Dept. of Chemistry.
SYNTHETIC AND MECHANISTIC INVESTIGATION OF OLEFIN POLYMERIZATION CATALYZED BY EARLY TRANSITION METAL COMPOUNDS
J. E. Bercaw 1993 13 p
(Contract DE-FG03-85ER-13431)
(DE93-018301; DOE/ER-13431/T1) Avail: CASI HC A03/MF A01

During the second year we continued to prepare and characterize organoyttrium and organoscandium compounds for use as catalysts for polymerizing simple olefins and diolefins. Simple, one-component systems are being pursued, suitable for chain initiation, propagation, and termination studies. This document is divided into the following: dicarbollide derivatives of scandium as potential catalysts; design, synthesis, and characterization of the first isospecific (alpha) olefin polymerization catalysts; polymerization of (alpha) olefins and 1,5-hexadiene using organoscandium catalysts; and attempted preparations of diastereomeric Nb and Ta olefin/hydride and olefin/alkyl derivatives. DOE

N94-16973# California Univ., Irvine. Dept. of Civil Engineering.
INVESTIGATION OF THE EFFECTS OF POLYELECTROLYTE COATINGS ON COLLOID TRANSPORT IN POROUS MEDIA
T. M. Olson 1993 8 p
(Contract DE-FG03-89ER-60849)
(DE93-018300; DOE/ER-60849/T1) Avail: CASI HC A02/MF A01

The goal is to study the repulsive interaction forces between humic-coated colloids and negatively charged porous media surfaces. Filtration experiments were carried out on hematite coated with humic acid or NOM, in porous media or packed bed (silica bed). Effects of Ca(2+) are being studied. Results so far indicate that many humic coating properties (molecular size, acidity, polarity, and surface conformation) have an important effect on colloid attachment rates but very little effect on colloid electrophoretic mobility; steric repulsive forces are proposed to account for these observations. Some humic coatings are more effective in enhancing colloid transport in quartz beds than in enhancing colloid stability. Other effects are discussed. DOE

N94-16978# Ohio State Univ., Columbus.
ELECTRICAL CONDUCTIVITY OF ION IMPLANTED LADDER AND SEMI-LADDER POLYMERS Final Report, 1 Nov. 1991 - 31 Dec. 1992
Arthur J. Epstein 2 Jul. 1993 58 p
(Contract F49620-92-C-0002)
(AD-A267432; AFOSR-93-0567TR) Avail: CASI HC A04/MF A01

Aromatic heterocyclic ordered rigid rod, ladder and semi-ladder polymers (including BBL, PBO, PBT, and BBB) combine exceptional high temperature stability with excellent mechanical properties as well as environmental stability. We have continued our systematic study of the electronic, photonic, and environmental properties of the pristine polymer. We have discovered the presence of a significant photoconductivity in PBO and characterized its photoluminescence. Extending our photoinduced absorption spectroscopy studies to the millisecond regime we have found the presence of two weak photoinduced optical absorptions. The difference in behavior as compared to other conjugated polymers likely reflects the increased order in the pristine rigid rod and ladder polymers. We have extended our temperature dependent charge transport (dc conductivity, microwave frequency conductivity and dielectric constant, thermoelectric power, magnetoconductivity, and electron spin resonance) studies of the ion implanted polymers as a function of implantation dosage. A nonmetal-to-metal transition is found as a function of increasing dosage

(occurring at 4 x 10(exp 16) ions/sq cm). For implanted samples of metallic behavior, a unique transition to a nonmetallic behavior has been discovered at 30 K. The origin of this transition is attributed to the opening up of a Coulomb gap. DTIC

N94-16980# Illinois Univ., Urbana. Dept. of Materials Science and Engineering.

TRANSFORMATION TOUGHENING OF COMPOSITE CERAMICS Final Report, 1 Mar. 1989 - 30 Sep. 1992

Waltraud M. Kriven 31 Dec. 1992 267 p

(Grant AF-AFOSR-0300-89)

(AD-A267304; UILU-ENG-93-5100; AFOSR-93-0482TR) Avail: CASI HC A12/MF A03

A systematic investigation into some possible transformation toughening alternatives to zirconia (ZrO2) has been conducted. Three systems have been focussed upon: dicalcium silicate (Ca2S104), dysprosia (DY203), and nickel sulfide (NiS). Composites of Ca2SiO4 in calcium zirconate (CaZrO3) or magnesia (MgO) or fine grained, single phase pure, and Ba-doped Ca2SiO4 were fabricated, microstructurally characterized, and mechanically evaluated. Although surface grinding was able to stress-induce the transformation in Ca2SiO4, a crack tip propagating in the bulk was not. A comprehensive crystallographic study of the transformation mechanisms implied that compressive shear, rather than tensile stresses were required. The mechanism could not controllably be nucleated by a propagating crack. Spontaneous thermal transformation of Ca2SiO4 was too powerful for a confining matrix and tended to cause dusting. The kinetics and mechanism of the transformation in single phase DY2O3 were studied and revealed that it only operated above 600 C. No transformation toughening in HIPPED SiC-DY2O3 composites could be detected at room temperature. Microstructural studies of industrial NiS in glass composites found a correlation between transformed NiS and deleterious fracture. DTIC

N94-16994# University of Southern Mississippi, Hattiesburg. Dept. of Polymer Science.

PHOTODEGRADATION OF MDI BASED POLYURETHANE/UREA ELASTOMERS Technical Report No. 17

C. E. Hoyle, H. Shah, K. Moussa, P. Berry, and I. B. Rufus 13 Jul. 1993 51 p

(Contract N00014-91-J-1028)

(AD-A267308) Avail: CASI HC A04/MF A01

A series of polyurethane urea and polyurea elastomers based on MDI, a chain extender such as ethylene glycol or ethylene diamine, and polyethylene glycol oligomers or amine end capped modified polyethylene glycol oligomers were synthesized and characterized. Photodegradation of these polymers was monitored by UV and IR spectroscopy. A review of two systems, a polyurethane urea and a polyurea, is described in depth. Formation of the photo-Fries product is observed in both the systems, although the pure polyurea exhibits a greater magnitude of change in the ultraviolet absorption spectrum. DTIC

N94-16999# University of Southern Mississippi, Hattiesburg. Dept. of Polymer Science.

RESPONSIVE COPOLYMERS FOR ENHANCED PETROLEUM RECOVERY

C. McCormick and R. Hester 1993 8 p

(Contract DE-AC22-92BC-14882)

(DE93-018030; DOE/BC-14882/3) Avail: CASI HC A02/MF A01

The overall goal of this research is the development of advanced water-soluble copolymers for use in enhanced oil recovery which rely on reversible microheterogeneous associations for mobility control and reservoir conformance. Technical progress for the quarter is summarized for the following tasks: advanced copolymer syntheses; characterization of molecular structure of copolymers; and polymer solution rheology. DOE

N94-17120# Polish Academy of Sciences, Warsaw. Inst. Podstawowych Problemow Techniki.

AN INVESTIGATION OF THE HYDROLYTIC RESISTANCE OF SODIUM-CALCIUM PLATE GLASS WITH A LAYER OF SILICA DEPOSITED ON ITS SURFACE [BADANIE ODPORNOSCI HYDROLITYCZNEJ SZKLA PLASKIEGO SODOWO-WAPNIOWEGO Z WARSTWA KRZEMIONKOWA NANIESIONA NA JEGO POWIERZCHNIE]

Malgorzata Wolna, Joanna Szwedowska-Kotlinska, and Waclaw Tuszynski 1991 22 p In POLISH

(IFTR-34/1991) Avail: CASI HC A03/MF A01

A discussion of the possibility for enhancing the resistance of a hydrolytic surface with a deposited silicon layer is discussed. The silicon layer was deposited on plane surfaces of soda glass by submersion in diluted soda-silicon aqueous solutions. The hydrolytic resistance was analyzed in accordance with the Standard DIN 52 296 (Hydrolytic resistance of the surface of glass and glass ceramic plates at 98 C. Method of test and classification for the hydrolytic resistance of the surface of glass and soda glass plates.) Since the quantity of recovered N22O from the surface of the soda-glass reaches 120 micrometers - 2. Immediately following additional treatment of the glass surface in boiling water, this quantity dropped to 30 micrograms/dm2. The silicon layer established on the surface of the plane soda glass increases the hydrolytic resistance of the glass and also induces a hydrolytic phase change from hp3 to hp2. Transl. by FLS

N94-17122*# Northwestern Univ., Evanston, IL. BIRL Industrial Research Lab.

APPLICATION OF HARD COATINGS TO SUBSTRATES AT LOW TEMPERATURES Final Report

William D. Sproul 15 Jun. 1993 57 p

(Contract NAS8-37686)

(NASA-CR-193867; NAS 1.26:193867) Avail: CASI HC A04/MF A01

BIRL, the industrial research laboratory of Northwestern University, has conducted unique and innovative research, under sponsorship from the NASA Marshall Space Flight Center (MSFC), in the application of hard, wear resistant coatings to bearing steels using the high-rate reactive sputtering (HRRS) process that was pioneered by Dr. William Sproul, the principal investigator on this program. Prior to this program, Dr. Sproul had demonstrated that it is possible to apply hard coatings such as titanium nitride (TiN) to alloy steels at low temperatures via the HRRS process without changing the metallurgical properties of the steel. The NASA MSFC program at BIRL had the specific objectives to: apply TiN to 440C stainless steel without changing the metallurgical properties of the steel; prepare rolling contact fatigue (RCF) test samples coated with binary hard coatings of TiN, zirconium nitride (ZrN), hafnium nitride (HfN), chromium nitride (CrN), and molybdenum nitride (MoN), and metal coatings of copper (Cu) and gold (Au); and develop new alloyed hard coatings of titanium aluminum nitride (Ti(0.5)Al(0.5)N), titanium zirconium nitride (Ti(0.5)Zr(0.5)N), and titanium aluminum vanadium nitride. Derived from text

N94-17198# Army Construction Engineering Research Lab., Champaign, IL.

APPLICATION OF THERMAL SPRAY AND CERAMIC COATINGS AND REINFORCED EPOXY FOR CAVITATION DAMAGE REPAIR OF HYDROELECTRIC TURBINES AND PUMPS Final Report

Richard Ruzga, Paul Willis, and Ashok Kumar Mar. 1993 52 p

(AD-A267624; CERL-TR-FM-93/01) Avail: CASI HC A04/MF A01

The U.S. Army Corps of Engineers is one of the largest single producers of hydroelectric power in the United States. The Corps' ability to generate power can be reduced by cavitation in hydroelectric turbines. Cavitation is the damage that results from high velocity liquid flow and pressure changes. Cavitation can be repaired by traditional methods, such as welding or application of epoxy, or by the newer non-fusion methods, such as thermal spray and the use of reinforced epoxies. This research shows that the performance of reinforced epoxies is sensitive to surface preparation and method of application. Repair by these compounds lasts from 6 months to 1 year, but the downtime for repair is very short. New thermal-sprayed metallized coating systems have been tested in the laboratory and show potential for application in cavitation repair. New ceramic coatings have improved cavitation resistance, but their application is limited by current thermal spray technology, which is improving. DTIC

N94-17204 SFA, Inc., Landover, MD.

INVESTIGATION OF THE OPTICAL, ELECTRONIC, AND STRUCTURAL PROPERTIES OF FIBER OPTIC GLASSES Final Report, 19 Dec. 1989 - 28 Feb. 1993

J. A. Frietas, Jr. Jun. 1993 175 p Limited Reproducibility: More than 20% of this document may be affected by microfiche quality

(Contract N00014-90-C-2020)

(AD-A267645; SFA-93/002) Avail: CASI HC A08

Under contract N00014-90-C-2020, SFA provided research support to the Naval Research Laboratory Electronic Materials Branch by conducting investigations on novel materials. These investigations ranged from using various techniques to characterize the optical, electronic, and structural properties of this semiconductor films to setting up a micro-Raman and microphotoluminescence laboratory to study microcrystalline films. The materials studied include heavy metal fluoride glasses, chalcogenide glasses, silicon carbide, diamond (chemical vapor deposition films, high-pressure, high-temperature synthetic and natural), and aluminum nitrides. These materials were investigated by such optical techniques as Raman scattering (RS), photoluminescence (PL), photoluminescence excitation, absorption, reflectivity, electron spin resonance (ESR), photo-induced ESR, optically detected magnetic response (ODMR), and Hall measurement. DTIC

N94-17227# Materials Systems, Inc., Concord, MA.
FABRICATION OF PIEZOELECTRIC CERAMIC/POLYMER COMPOSITES BY INJECTION MOLDING Final Report
15 Apr. 1993 47 p
(Contract N00014-92-C-0010)
(AD-A267302) Avail: CASI HC A03/MF A01

Piezoelectric ceramic/polymer composites have many applications in advanced Navy transducers and commercial ultrasonic imaging. Unfortunately, their application has been limited by the lack of a manufacturing-viable technology capable of meeting both the low cost and high volume production requirements. The principal manufacturing difficulty lies in the handling of millions of fine PZT fibers during their assembly into a typical composite transducer installation. In this program, Materials Systems Inc. (MSI) has demonstrated that ceramic injection molding is capable of meeting the stringent transducer cost and assembly needs of piezoelectric ceramic/polymer composites for Navy applications. The injection molding approach overcomes the difficulty of assembling oriented ceramic fibers into composite transducers by net-shape performing ceramic fiber arrays. Aside from this advantage, the process makes feasible the construction of composite transducers having more complex ceramic element geometries than those previously envisioned, leading to greater design flexibility for improved acoustic impedance matching, lateral mode cancellation and superior actuator performance. DTIC

N94-17238# Los Alamos National Lab., NM.
DYNAMIC TESTING AND CHARACTERIZATION OF PRE-FRACTURED CERAMIC
A. K. Zurek and D. A. Hunter 1993 5 p Presented at the 14th International Conference on High Pressure Science and Technology and 1993 Technical Meeting of the Topical Group on Shock Compression of Condensed Matter, Colorado Spring, CO, 28 Jun. - 3 Jul. 1993
(Contract W-7405-eng-48)
(DE93-016457; LA-UR-93-2334; CONF-9306167-6) Avail: CASI HC A01/MF A01

Nearly all of the mechanical behavior studies of armor ceramics, to date, have involved the characterization and testing of pristine ceramic material. However, ballistic impact causes a strong shock front to propagate rapidly through the ceramic before much penetration can occur. A strong shock wave can result in localized compressive failure and fragmentation of the ceramic before its amplitude is annuated below the compressive strength of the ceramic. Goals of this effort were to create shock-fractured ceramic using test assemblies which maintain the intergranular coupling and high density of the ceramic, characterize the extent and homogeneity of the fragmentation and dilatation of the ceramic, and test the compressive dynamic behavior of the shock-fractured ceramic under conditions of confining pressure. This effort will provide data to support models of the penetration resistance of fractured ceramics including degraded moduli, failure strength-strain, and post-failure characterization of the erosive properties of comminuted ceramic and penetrator materials. DOE

N94-17242# General Atomic Co., San Diego, CA.
CERAMIC FIBER COATINGS DEVELOPMENT AND DEMONSTRATION Final Technical Report, 1 Jul. 1989 - 31 May 1993
H. Streckert, D. Hazlebeck, F. Montgomery, K. Norton, and I. Schneir 28 May 1993 206 p
(Contract F49620-89-C-0078)
(AD-A267286; GA-C21284; AFOSR-93-0499TR) Avail: CASI HC A10/MF A03

The objective of this program was to develop fiber coating techniques by gas phase and liquid phase processes for interface control in ceramic matrix and metal matrix composites. Thermochemical evaluations of fiber/coating/matrix systems were performed theoretically and experimentally. Liquid phase processes were developed mainly for oxide coatings. Gas phase processes were developed for carbide, nitride, and boride coatings. Coatings were produced on continuous fiber tows and woven fabric. A small scale continuous fabric coater was designed and constructed. Coated fiber tows were infiltrated with silicon nitride matrix by chemical vapor deposition in order to study fiber matrix interactions. Composite coupons were made from Nicalon cloth and infiltrated with silicon nitride. Samples coated with high temperature BN showed flexural strengths up to 350 MPa. DTIC

N94-17253# Oak Ridge National Lab., TN.
EVALUATION OF INTERFACIAL PROPERTIES OF FIBER-REINFORCED CERAMIC COMPOSITES USING FIBER PUSH-IN TESTS
C. H. Hsueh 1993 12 p Presented at the 95th Annual Meeting of the American Ceramic Society, Cincinnati, OH, 18-22 Apr. 1993
(Contract DE-AC05-84OR-21400)
(DE93-015427; CONF-930438-25) Avail: CASI HC A03/MF A01

Evaluation of the interfacial properties of fiber-reinforced ceramic composites using fiber push-in tests is addressed. The stress-displacement relation of the embedded fiber subjected to an axial loading-unloading cycle is analyzed. The interfacial bonding, Coulomb friction at the debonded interface, Poisson's effect on the loaded fiber, and residual stresses are included in the analysis, and closed-form analytical solutions are obtained. Based on the analytical solutions, a methodology is established to extract the interfacial properties from the experimental stress-displacement curves. Roles of interfacial bonding, Poisson's effect, and residual axial stresses on residual fiber displacement after complete unloading are also addressed in the present study. DOE

N94-17273 Utah State Univ., Logan. Dept. of Chemistry and Biochemistry.
SYNTHESIS, CHARACTERIZATION, AND POLYMERIZATION OF NEW FERROCENE-FLUORENE COMPLEXES. A NOVEL HIGH-MOLECULAR WEIGHT CONJUGATED POLYMER WITH PENDANT FERROCENE GROUPS
Michael E. Wright and Brooks B. Cochran 1992 30 p Limited Reproducibility: More than 20% of this document may be affected by microfiche quality
(AD-A267717) Avail: Issuing Activity (Defense Technical Information Center (DTIC))

Ferrocenecarboxaldehyde was successfully condensed with fluorene derivatives to afford a series of new complexes, (eta5-C5H5) Fe(eta5-C5H4CH = (9-fluorenyl)) where fluorenyl = 1A, 2-bromo: 2a, 2,7-dibromo; 3, 2-nitro. The ferrocene-fluorenyl derivatives Ia and 2a were converted to the monocarboxaldehyde, tributylstannyl, bis(carboxaldehyde), and bis(tributylstannyl) complexes (Ib, Ic, 2b, and 2c, respectively). Complexes Ib and 2b were characterized by single-crystal x-ray molecular structures. The fluorenyl ring systems were tilted out of the eta5-C5H4 plane by 39 deg. Treatment of Ic and 2c with I2 afforded the mono- and bis(iodo)fluorenyl complexes Id and 2d, respectively. The reactivity of complexes 2a-d was explored. The alkynylation (alkyne, L2PdCl2, CuI, PPh3) of 2a was an extremely poor reaction giving little or no cross-coupling. Complex 2b did not undergo the Knoevenagel polycondensation with bis(cyanoacetate) comonomers. Treatment of 2c with acid chlorides under Stille cross-coupling conditions afforded ketone product and iodobenzene showed no cross-coupling. Complex 2d did copolymerize very cleanly with 2,5(diethynyl)-1,4-(decoxy)benzene using palladium catalysis to afford a soluble, high-molecular weight conjugated polymer, 4. A model compound, 5, was prepared from cross-coupling Id with 2, 5-(diethynyl)-1, 4-(decoxy)benzene. DTIC

N94-17297*# Cincinnati Univ., OH. Dept. of Chemistry.
SYNTHESIS OF NOVEL ELECTRICALLY CONDUCTING POLYMERS: POTENTIAL CONDUCTING LANGMUIR-BLODGETT FILMS AND CONDUCTING POLYMERS ON DEFINED SURFACES Final Report
Hans Zimmer 17 Nov. 1993 51 p
(Grant NAG3-995)
(NASA-CR-194651; NAS 1.26:194651) Avail: CASI HC A04/MF A01

Based on previous results involving thiophene derived electrically conducting polymers in which it was shown that thiophene, 3-substituted thiophenes, furans, and certain oligomers of these compounds showed electrical conductivity after polymerization. The conductivity was in the order of up to 500 S/cm. In addition, these polymers showed conductivity without being doped and most of all they were practically inert toward ambient conditions. They even could be used in aqueous media. With these findings as a guide, a number of 3-long-chain-substituted thiophenes and 1-substituted-3-long-chain substituted pyrrols were synthesized as monomers for potential polymeric electrically conducting Langmuir-Blodgett films.
Author (revised)

N94-17408# Geo-Centers, Inc., Newton, MA.
SYNTHESIS AND EVALUATION OF POLYMERIC MATERIALS Annual Report No. 2
E. Greenwald, J. Nagode, H. Hu, L. Levenberry, and R. Newbegin Jul. 1993 195 p
(Contract N00014-90-C-2269)
(AD-A267809; GC-TR-93-2303) Avail: CASI HC A09/MF A03

GEO-CENTERS, INC. has been supporting the research efforts at the Naval Research Laboratory including novel fluoropolymers, conductive polymers, epoxies, and modified nylons. Major efforts were conducted in radiographic analysis development and use in evaluation of Sonar Rubber Domes (SRD) and Sonar Dome Rubber Windows (SDRW). This report is a summary of accomplishments for Year Two of the contract period of performance. DTIC

N94-17413# Northwestern Univ., Evanston, IL. Dept. of Materials Science and Engineering.
DIAMOND GROWTH ON CARBIDE SURFACES USING A SELECTIVE ETCHING TECHNIQUE
K. J. Grannen and R. P. Chang Jul. 1993 30 p
(Contract N00014-89-J-1848)
(AD-A267989; TR-14) Avail: CASI HC A03/MF A01

Microwave plasma-enhanced chemical vapor deposition of diamond films on silicon carbide and tungsten carbide (with 6% cobalt) surfaces using fluorocarbon gases has been demonstrated. No diamond powder pre-treatment is necessary to grow these films with a (100) texture. The diamond films are characterized by scanning electron microscopy and Raman spectroscopy. The proposed nucleation and growth mechanism involves concurrent etching of the non-carbon component by atomic fluorine and deposition of diamond. Hydrogen is necessary in the growth process to limit the rapid etching of the substrate by fluorine atoms. DTIC

N94-17430# Naval Surface Warfare Center, Bethesda, MD. Survivability Structures and Materials Directorate.
HIGH TEMPERATURE DEFORMATION BEHAVIOR OF YBa2Cu3O(6+x) SUPERCONDUCTING CERAMIC MATERIALS
A. S. Rao, L. F. Aprigliano, and O. P. Arora 15 May 1993 38 p
(AD-A268164; CDNSWC/SSM-61-93/18) Avail: CASI HC A03/MF A01

Superplastic deformation is being explored as a means to turn the new ceramic superconducting YBa2Cu3O(6+x) into useful Naval hardware. The deformation experiments that were conducted on fine YBa2Cu3O(6+x) powders suggest that the maximum deformation that can be achieved without the degradation of superconductivity is about 62% at 850 C. The addition of silver improves the maximum deformation, and the addition of alumina has a devastating effect on the deformation mode. DTIC

N94-17434 Rome Univ. (Italy). Instituto Di Chimica.
CHARACTERIZATION OF THE LITHIUM/PAN-BASED POLYMER ELECTROLYTES INTERFACE Final Report, 1 Jan. - 31 Dec. 1992
Bruno Scrosati Mar. 1993 25 p Limited Reproducibility: More than 20% of this document may be affected by microfiche quality
(AD-A268401; WL-TR-93-2068) Avail: CASI HC A03

Polymers having transport almost exclusively of the ionic type, often named polymer electrolytes or, in a broader way, polymer ionics, have attracted large scientific and technological interest. Research on this new class of electroactive polymers has been very active and substantial progress has been achieved in recent years. Of particular interest are the new generation polymer electrolytes formed by the immobilization into a polymer matrix of common solutions of lithium salts in liquid, organic solvents. This new class of gel electrolytes offers very high ambient and subambient conductivities. In this project, we have carried out a preliminary investigation of the electrochemical properties of a typical example, namely of the membrane electrolyte obtained by gelification into a polyacrylonitrile (PAN) matrix of solutions of lithium salts (e.g., LiCl04) in aprotic solvents (e.g., an ethylene carbonate-propylene carbonate mixture). The choice was motivated by the fact that membranes of this type appear to be closest to reach a practical exploitation. DTIC

N94-17466 Pennsylvania State Univ., University Park. Dept. of Materials Science and Engineering.
INTERFACE CHEMISTRY IN CERAMIC MATRIX COMPOSITES Final Report
Carlo G. Pantano, Karl Spear, Greg Bibbo, Jim Walck, and Anant Singh Mar. 1993 29 p Limited Reproducibility: More than 20% of this document may be affected by microfiche quality
(Contract N00014-90-J-1392)
(AD-A268629) Avail: CASI HC A03

There are many possible effects of interface reactions in fiber or whisker reinforced glass or glass ceramic matrix composites. In most cases, interface reactions must be minimized because they can lead to degradation of fiber or whisker strength, destruction of interphase coatings, and modification of the interface adhesion. Nevertheless, there are systems where interface reactions are beneficial. The best example of this is in the NiCALON reinforced glass-ceramic composites where carbon interphases are generated during processing; this carbon interphase facilitates fiber pullout and thereby, is responsible for the outstanding room-temperature toughness of these materials. There have also been suggestions, although less well documented, that interface reactions can create carbide, nitride and mullite interphases that passivate the interface to subsequent oxidation. DTIC

N94-17490# North Carolina State Univ., Raleigh.
LOW TEMPERATURE DEPOSITION AND CHARACTERIZATION OF n- AND p-TYPE SILICON CARBIDE THIN FILMS AND ASSOCIATED OHMIC AND SCHOTTKY CONTACTS Semiannual Report, 1 Jan. - 30 Jun. 1993
Robert F. Davis Jun. 1993 37 p
(Contract N00014-92-J-1500)
(AD-A267966) Avail: CASI HC A03/MF A01

Monocrystalline films of SiC were grown on alpha (6H)-SiC(0001) wafers using disilane (Si2H6) and ethylene (C2H4) by gas-source MBE at 1050 deg C. The nucleation and growth of cubic beta-SiC(111) on the surface terraces of the hexagonal 6H-SiC rather than on the step surfaces and the resultant formation of double positioning boundaries is discussed. The reconfiguration of the growth system leading to enhanced control over polytype deposition is also described. Thin film contacts of Ti, Pt, Hf, and Co were deposited in UHV onto unheated, n-type vicinal alpha(6H)-SiC(0001) films by electron beam evaporation. All as-deposited contacts were rectifying with low ideality factors (n less than 1.1), low leakage currents and Schottky barrier heights between 0.85 eV and 1.15 eV. The lowest leakage currents were less than 5x10(exp -8) A/CM2 at -10V. Titanium and Pt remained relatively stable after annealing at 700-750 deg C; whereas, Co became ohmic after annealing for two minutes at 1000 deg C. UV photoemission studies on both SiC/metal interfaces and the surface of AlN(0001) deposited on SiC have been initiated. A major emphasis is on surface cleanliness prior to metal deposition. A spectral feature observed in the AlN is attributed to the initial indication of negative electron affinity in this material. Chemical interdiffusion between alpha (6H)-SiC wafers and epitaxially deposited 2H-AlN films are under investigation within the temperature range of 1500 deg C to 1700 deg C. DTIC

N94-17494# Uniax Corp., Santa Barbara, CA.
SOLUBLE PRECURSOR ROUTE TO POLYANILINES Final Report, 1 Sep. 1991 - 29 Feb. 1992
Floyd L. Klavetter Jan. 1993 9 p
(Contract F49620-91-C-0092)
(AD-A268015; AFOSR-93-0572TR) Avail: CASI HC A02/MF A01

To achieve the fundamental goal of producing a processible form of the conducting polymer polyaniline (PANI), the phase 1 program concentrated on development of the synthesis of a precursor polymer via the solution co-polymerization of bis(annellated) benzoquinone with p-phenylenediamine. The resulting polymer, expected to be soluble in common organic solvents, would be converted to PANI by thermal elimination of the pendant

cyclopentadiene groups following processing. Attempts to carry out the proposed polymerization reaction using conventional methods for ketone-amine condensation were not successful, and resulted in the conclusion that bis(annellated) benzoquinone is too 'crowded' a ketone for the polycondensation chemistry. DTIC

N94-17547# Technical Research Centre of Finland, Espoo. Fuel and Process Technology Lab.

HEATING OF LUBRICANT WITH AN ELECTRIC RESISTANCE HEATER [VOITELUOELJYN LAEMMITTAEMINEN SAEHKOEVASTUKSELLA]

Matti Kytoe Apr. 1992 34 p In FINNISH Sponsored by Technology Development Center, Finland, and Finnish Industry Original contains color illustrations

(VTT-TIED-1359; ISBN-9-51-384172-3; ETN-93-94477) Copyright Avail: CASI HC A03/MF A01

Heating of lubricant with electric resistance can result in oil cracking, and consequently, in changes in lubricant properties and in lubricant fouling. In the worst case an explosible gas mixture is formed from the cracking products in the lubricant tank or in the object of lubrication. In the experiment, three transmission oils with high pressure additives and one circulation lubricant were heated with an electric resistance heater. The aim was to determine the limits of problem free heating and to study changes in the lubricant during cracking. The lubricant is cracked and the heated coked in continuous heating of dozens of hours duration as soon as the temperature rises to 70 to 100 C. Circulation lubricant stands long term heating at a surface effect of less than 2 W/sq cm when the temperature of the lubricant is lower than 85 C. The corresponding temperature limit for the gear oil is about 60 C. The difference is due to additives; a significant part of the foul on the surface of the resistance is due to lubricant additives. The experiment indicated that short term heating does not result in oxidation of the lubricant or in the fouling of the heating resistance. In two hour tests the maximum temperature of the lubricant was 80 C and the maximum hydrocarbon content of tank air 200 ppm. In long term tests no coking appeared with less than 300 ppm hydrocarbon contents. Heating of lubricant even at temperatures below the pour point does not cause problems. The temperature peaks at the start of heating are short term, and no heater coking or lubricant cracking appears. Formation of an explosive mixture from the cracking products is possible only if the heater is coked very strongly, when the surface temperature under the foul rises even as high as to 300 C. Strong coking can be observed only as an increase in the hydrocarbon content of the tank air or as a rise in the surface temperature of the resistance heater, while the temperature of the lubricant remains stable. ESA

N94-17559*# National Aeronautics and Space Administration. Langley Research Center, Hampton, VA.

LOW DIELECTRIC POLYIMIDES Patent Application

Anne K. St.Clair, inventor (to NASA), Terry L. St.Clair, inventor (to NASA), and William P. Winfree, inventor (to NASA) 14 Jun. 1993 17 p

(NASA-Case-LAR-14987-2; NAS 1.71:LAR-14987-2; US-Patent-Appl-SN-077166) Avail: CASI HC A03/MF A01

A series of polyimides based on the dianhydride of 1,4-bis (3,4-dicarboxyphenoxy) benzene (HQDEA) or on 2,2-bis(4(3-aminophenoxy phenyl)hexafluoropropane (3-BDAF) are evolved from high molecular weight polyamic acid solutions yielding flexible free-standing films and coatings in the fully imidized form which have a dielectric constant in the range of 2.5 to 3.1 at 10 GHz. NASA

N94-17611 Bhabha Atomic Research Centre, Bombay (India).

A NEW METHOD OF DESIGNING MULTILAYER OPTICAL THIN FILM COATINGS

K. V. S. R. Apparao (Bhabha Atomic Research Centre, Bombay, India.) 1992 22 p Limited Reproducibility: More than 20% of this document may be affected by microfiche quality

(DE93-624683; BARC-1992/E/031) Avail: CASI HC A03 (US Sales Only)

A new method of designing multilayer optical thin film coatings is developed using a new optimization technique. Results obtained demonstrate that the method of damped least squares with indirect reflection derivatives give better and efficient designs compared to other known optimization methods. Many constraints and boundary conditions compatible to the available experimental facilities are incorporated in the method which enables it to give practically realizable designs. The method is successfully applied to design and develop indigenously various types of multilayer optical thin film coatings for different high power laser applications. DOE

N94-17633# Joint Inst. for Nuclear Research, Dubna (USSR). Lab. of Neutron Physics.

OXYGEN DIFFUSION IN YBa2Cu3O(6+DELTA) CERAMICS ON HEATING

A. M. Balagurov, N. V. Vuong, Ch. A. Kuan, L. K. Kui, and F. K. Chieu 1991 12 p

(DE93-629161; JINR-R-17-91-340) Avail: CASI HC A03/MF A01 (US Sales Only)

The oxygen diffusion in YBa2Cu3O(6 + delta)-ceramics by heating the samples from room temperature to 350 C with constant rate v= 0.5, 1, 2, and 3 C/min was investigated. It has been shown that the oxygen uptake in the initial sample YBa2Cu3O6 can be described by the one-dimensional diffusion model. The diffusion coefficient in the tetra-phase at T less than or equal to 500 C is confirmed to be D(sq cm/sec)= (0.84/3.4)(10)(exp -4)(exp -0.6 eV/KT). DOE

N94-17634# Joint Inst. for Nuclear Research, Dubna (USSR). Lab. of Neutron Physics.

INFLUENCE OF THE GRANULAR SURFACE ON THE OXYGEN UPTAKE IN YBa2Cu3O(6+DELTA) CERAMICS

N. V. Vuong, V. Kh. Tuong, L. K. Kui, and F. K. Chieu 1991 12 p

(DE93-629162; JINR-R-17-91-342) Avail: CASI HC A03/MF A01 (US Sales Only)

A method of 'hot grinding' for inducing quick oxygen uptake in YBa2Cu3O(x) is proposed. The oxygen content in the initial sample YBa2Cu3O(6.1), after grinding at 350 C in air for 15 min, was increased to 6.88, and a limit value of x = 6.97 was obtained in this way for 300 min. DOE

N94-17676# Brookhaven National Lab., Upton, NY.

GROWTH OF DIELECTRIC THIN FILMS BY IRRADIATION OF CONDENSED MOLECULAR PRECURSORS WITH SYNCHROTRON RADIATION

D. R. Strongin (State Univ. of New York, Stony Brook.), J. F. Moore (State Univ. of New York, Stony Brook.), M. W. Ruckman, and M. Strongin 1992 6 p Presented at the 16th Material Research Society International Symposium on the Scientific Basis for Nuclear Waste Management Fall Meeting, Boston, MA, 30 Nov. - 5 Dec. 1992

(Contract DE-AC02-76CH-00016)

(DE93-016161; BNL-48420; CONF-921101-135) Avail: CASI HC A02/MF A01

Spectroscopic evidence is presented that shows that boron nitride and aluminum oxide can be synthesized by exposing a condensed layer of molecular precursors to synchrotron radiation. In the Al2O3 circumstance a condensed layer of trimethylaluminum (TMA) and water at 78 K on a silver substrate produces pure layers of aluminum oxide. Using the same condensed layer technique, boron nitride is produced by exposing a solid matrix of diborane and ammonia to synchrotron radiation. Near edge x-ray absorption fine structure and core level photoelectron spectroscopies are used to characterize the Al2O3 and BN layers, which were typically 30 A thick. During the formation of aluminum oxide, the carbon component in the alkylaluminum precursor is completely removed during irradiation as a volatile methane product which was detected by mass spectrometry. In the absence of synchrotron radiation, the molecular precursors in both the aluminum oxide and boron nitride systems show evidence of some interactions within the solid, but upon warming to near room temperature (260 K) the layers desorb from the substrate. DOE

N94-14982*# Arizona Univ., Tucson.

MAGNETO-OPTIC SUPERLATTICE THIN FILMS: FABRICATION, STRUCTURAL AND MAGNETIC CHARACTERIZATION

C. M. Falco, B. N. Engel, R. A. VanLeeuwen, and J. Yu *In its* Research Studies on Advanced Optical Module/Head Designs for Optical Disk Recording Devices p3-5 (SEE N94-14981 03-82) 15 Mar. 1993 (For primary document see N94-14981 03-82)

Avail: CASI HC A01/MF A02

N94-16002# Krupp (Fried.) G.m.b.H., Essen (Germany).
VACUUM PLASMA SPRAYING
Friederike Deuerler, Juergen Peterseim, Juergen Willbrand, and Wolfgang Schlump *In its* Krupp Technical Reports No. 2, English Edition, October 1992 Oct. 1992 p 69-74 (For primary document see N94-16000 03-31)
Copyright Avail: CASI HC A02/MF A01

N94-16241*# Brown Univ., Providence, RI. Dept. of Geological Sciences.
THE ILMENITE LIQUIDUS AND DEPTHS OF SEGREGATION FOR HIGH-TI PICRITE GLASSES Abstract Only
P. C. Hess *In* Lunar and Planetary Inst., Twenty-Fourth Lunar and Planetary Science Conference. Part 2: G-M 1993 p 649-650 (For primary document see N94-16173 03-91)
Avail: CASI HC A01/MF A06

28 PROPELLANTS AND FUELS

Includes rocket propellants, igniters, and oxidizers; their storage and handling procedures; and aircraft fuels.

For related information see also *07 Aircraft Propulsion and Power, 20 Spacecraft Propulsion and Power,* and *44 Energy Production and Conversion.*

N94-16807# Oak Ridge National Lab., TN.
AN ADVANCED BIOPROCESSING CONCEPT FOR THE CONVERSION OF WASTEPAPER TO ETHANOL
C. D. Scott, B. H. Davison, T. C. Scott, J. Woodward, C. Dees, and D. S. Rothrock 1993 18 p Presented at the 15th Symposium on Biotechnology for Fuels, Chemicals and Materials, Colorado Springs, CO, 10-14 May 1993
(Contract DE-AC05-84OR-21400)
(DE93-015209; CONF-930552-2) Avail: CASI HC A03/MF A01

Wastepaper is a plentiful and low-cost lignocellulosic feed material that may represent the most direct way to penetrate the market with an advanced bioprocessing system. Innovative bioprocessing concepts integrated into such a system for the production of ethanol should be economically viable. Several of the proposed processing advances for such a system have only been studied on a laboratory scale, so a more thorough process development and scale-up effort will be required. DOE

N94-16898# Lehigh Univ., Bethlehem, PA.
HIGH OCTANE ETHERS FROM SYNTHESIS GAS-DERIVED ALCOHOLS
K. Klier, R. G. Herman, M. A. Johansson, and O. C. Feeley Apr. 1993 26 p
(Contract DE-AC22-90PC-90044)
(DE93-016861; DOE/PC-90044/9-Rev-1) Avail: CASI HC A03/MF A01

The objective of the proposed research is to synthesize high octane ethers, primarily methyl isobutyl ether (MIBE) and methyl tertiary butyl ether (MTBE), directly from H2/CO/CO2 coal-derived synthesis gas via alcohol mixtures that are rich in methanol and 2-methyl l-propanol (isobutanol). The overall scheme involves gasification of coal, purification and shifting of the synthesis gas, higher alcohol synthesis, and direct synthesis of ethers. The testing of strongly acidic catalysts for the conversion of a mixture of methanol and isobutanol to ethers and hydrocarbons was continued. Under standardized test conditions the catalysts tested this quarter were: phosphotungstic acid supported on zirconia (PW12/ZrO2), 'niobic acid' (Nb2O5 (center dot)xH2O), and an iron and manganese doped sulfate modified zirconia (Fe/Mn/ ZrO2/ SO4(sup 2-)). The overall activity of these catalysts followed the order of Fe/Mn/ ZrO2/ SO4(sup 2-) greater than PW12/ZrO2 greater than Nb2O5 (center dot)xH2O with the Fe/Mn/ ZrO2/ SO4(sup 2-) catalyst approaching ZrO2/SO4(sup 2-) in both activity and selectivity for isobutene production. The effect of the presence of water on the reaction of methanol and isobutanol over ZrO2/ SO4(sup 2-) was determined to be insignificant under the reaction conditions investigated. DOE

N94-16934 Department of the Navy, Washington, DC.
DENSIFYING AND STABILIZING INGREDIENT Patent
Craig E. Johnson, inventor (to Navy) and Paul F. Dendor, inventor (to Navy) 9 Mar. 1993 4 p Filed 6 Nov. 74
(AD-D015751; US-Patent-5,192,379; US-Patent-Appl-SN-521977) Avail: US Patent and Trademark Office

This invention relates to explosives and more particularly to that branch of explosives known as propellants, wherein the propellants are those stabilized and densified with at least one lead fluoride. In the explosive field there are four general subdivisions - (1) primary explosives, (2) secondary explosives, (3) pyrotechnics, and (4) propellants. The primary explosives are generally very sensitive and serve to initiate other less sensitive explosives. A secondary explosive has high brisance and shattering power but little propelling power. Most secondary explosives are usually less sensitive than primary explosives and require a primary explosives to initiate them. DTIC

N94-16996# Pennsylvania State Univ., University Park.
ADVANCED THERMALLY STABLE JET FUELS
H. H. Schobert, S. Eser, C. Song, P. G. Hatcher, P. M. Walsh, M. M. Coleman, J. Bortiatynski, C. Burgess, R. Dutta, and K. Gergova et al Feb. 1993 131 p
(Contract DE-FG22-92PC-92104)
(DE93-017711; DOE/PC-92104/T1) Avail: CASI HC A07/MF A02

The Penn State program in advanced thermally stable coal-based jet fuels has five borad objectives: (1) development of mechanisms of degradation and solids formation; (2) quantitative measurement of growth of sub-micrometer and miocrometer-sized particles suspended in fuels during thermal stressing; (3) characterization of carbonaceous deposits by various instrumental and microscopic methods; (4) elucidation of the role of additives in retarding the formation of carbonaceous solids; and (5) assessment of the potential of production of high yields of cycloalkanes by direct liquefaction of coal. Pyrolysis of four isomers of butylbenzene was investigated in static microautoclave reactors at 450 C under 0.69 MPa of UHP N2. The rates of disappearance of substrates were found to depend upon the bonding energy of C(alpha)-C(beta) bond in the side chain in the initial period of pyrolysis reactions. Possible catalytic effects of metal surfaces on thermal degradation and deposit formation at temperatures greater than 400 C have been studied. Carbon deposition depends on the composition of the metal surfaces, and also depends on the chemical compositions of the reactants. Thermal stressing of JP-8 was conducted in the presence of alumina, carbonaceous deposits recovered from earlier stressing experiments, activated carbon, carbon black, and graphite. The addition of different solid carbons during thermal stressing leads to different reaction mechanisms. C-13 NMR spectroscopy, along with C-13-labeling techniques, have been used to examine the thermal stability of a jet fuel sample mixed with 5% benzyl alcohol. Several heterometallic complexes consisting of two transition metals and sulfur in a single molecule were synthesized and tested as precursors of bimetallic dispersed catalysts for liquefaction of a Montana subbituminous and Pittsburgh No. 8 bituminous coals. DOE

N94-17073 Pennsylvania Univ., Philadelphia. Dept. of Chemistry.
SYNTHESIS OF POTENTIAL HIGH-ENERGY FUELS Final Report, 1 Jun. 1992 - 31 May 1993
William P. Dailey 13 Jul. 1993 4 p Limited Reproducibility: More than 20% of this document may be affected by microfiche quality
(Contract F49620-92-J-0273)
(AD-A267508; AFOSR-93-0566TR) Avail: Issuing Activity (Defense Technical Information Center (DTIC))

The synthesis of multigram quantities of 1,3,3- trimethyl cyclopropene was accomplished using a modified literature procedure. The stability of this material towards different conditions was studied. Oxygen reacts with the neat material to quickly form a thick polymeric gum which eventually solidifies to a white solid. In the presence of Lewis acids such as untreated glass or metals such as stainless steel or copper, neat cyclopropene will form a 2+2 dimeric product in high yield. Hydrocarbon solutions (e.g. RP-1) of the cyclopropene are much more stable to these mild Lewis acid conditions but will also produce the dimeric product. A multigram sample of the cyclopropene was sent for testing in the microthruster at Phillips Laboratory. A convenient large scale synthesis of 3-chloro- 2-chloro methyl propene was developed starting with pentaerythritol. This compound serves as the starting material for a two step synthesis of 1.1.1 propellane. DTIC

N94-17248# Air Force Inst. of Tech., Wright-Patterson AFB, OH.
ULTRASONIC WAVE PROPAGATION MODEL FOR NONDESTRUCTIVE EVALUATION OF SOLID ROCKER MOTOR PROPELLANT Ph.D. Thesis
Rosario Nici 1993 270 p
(AD-A267653; AFIT/CI/CIA-93-17D) Avail: CASI HC A12/MF A03

The detection of voids in SRM propellant is critical to the safety of Launch Vehicles. Currently this is done with the use of x-rays as an NDE technique. It is hoped to supplant this technique with the use of ultrasonic NDE methods for reasons of reduced cost, increased mobility of the NDE set-up, automated accept/reject criteria, to name a few. To be feasible the ultrasonic NDE methods must be to differentiate between a through-transmission signal from an SRM propellant segment with a void, and a signal from a segment without a void. The ability of ultrasonic NDE to penetrate one meter of propellant has already been demonstrated with sufficient signal-to-noise ratio. The crux of the ultrasonic NDE method will be in using the information present in the received signal to detect, locate, and size voids. DTIC

N94-17538# Army Research Lab., Aberdeen Proving Ground, MD.
LASER IGNITION OF SOLID PROPELLANTS: 1. IGNITION DELAYS Final Report, Jan. 1990 - Dec. 1991
Arthur Cohen and Richard A. Beyer Jul. 1993 36 p
(DA Proj. 1L1-62618-AH-80)
(AD-A268454; ARL-TR-162) Avail: CASI HC A03/MF A01

Ignition experiments on nitrate-ester and nitramine propellants have been conducted in a closed bomb. The ignition source was a variable cw C02 laser. Ambient conditions were room temperature and atmospheric pressure. Air, argon, and nitrogen gases were used. Times to detect and changes in emission rate which are attributed to onset of flamespreading have been compared with ignition delay calculations using a condensed phase radiant ignition model. Reasonable values for thermochemical properties and experimental determined values for chemical kinetic parameters and optical properties were used for the calculations. The flux dependence of the initial emission delays were in reasonable agreement with model predictions for nitrate-esters but not for nitramines. Gas phase (composition) effects on initial emission were observed with XM39, an RDX nitramine, but not with nitramines. Flamespreading delays showed gas composition effects with all propellants. These results suggest that (for all propellants) the effects of gas phase reactions on flamespreading and (for nitramines) on initiation need to be included (explicitly) in radiant ignition models for predicting pressurization in gun chambers. DTIC

N94-16146*# National Aeronautics and Space Administration. Marshall Space Flight Center, Huntsville, AL.
LIQUID OXYGEN (LO2) PROPELLANT CONDITIONING CONCEPT TESTING
Gretchen L. E. Perry, Michael S. Orth (General Dynamics Corp., Huntsville, AL.), and Gopal K. Mehta (General Dynamics Corp., Huntsville, AL.) *In* Huntsville Association of Technical Societies, TABES 1993: 9th Annual Technical and Business Exhibition and Symposium 1993 6 p (For primary document see N94-16129 03-38)
(TABES Paper 93-621) Avail: CASI HC A02/MF A03

N94-16624*# Edgerton, Germeshausen and Grier, Inc., Cocoa Beach, FL.
SPACE SHUTTLE SOLID ROCKET MOTOR EXPOSURE MONITORING
S. W. Brown *In* BioTechnology, Inc., Proceedings of the 1992 Annual Meeting NASA Occupational Health Program Jul. 1993 p 175-182 (For primary document see N94-16609 03-52)
Avail: CASI HC A02/MF A03

29 MATERIALS PROCESSING

Includes space-based development of products and processes for commercial applications.

For biological materials see *55 Space Biology.*

N94-15006*# Alabama Univ., Huntsville.
VISUALIZATION OF SOLIDIFICATION FRONT PHENOMENA Final Report
Gary L. Workman and Guy A. Smith 12 Aug. 1993 20 p Original contains color illustrations
(Contract NAS8-38609)
(NASA-CR-193838; NAS 1.26:193838) Avail: CASI HC A03/MF A01; 2 functional color pages

Directional solidification experiments have been utilized throughout the Materials Processing in Space Program to provide an experimental platform which minimizes variables in solidification experiments. Because of the wide-spread use of this experimental technique in space-based research, it has become apparent that a better understanding of all the phenomena occurring during solidification can be better understood if direct visualization of the solidification interface were possible. Author (revised)

N94-15280* National Aeronautics and Space Administration. Lyndon B. Johnson Space Center, Houston, TX.
STS-26 SSIP BRIEFING (Videotape)
Jan. 1988 Videotape: 6 min. 30 sec. playing time, in color, with sound
(NASA-TM-109556; NONP-VT-93-190354) Avail: CASI VHS A01/BETA A22

Lloyd Bruce, student experimenter, explains his Titanium Grain Formation Experiment. Dr. Charles Scaife demonstrates Richard Cavoli's Crystal Membrane Experiment. CASI

N94-15395* National Aeronautics and Space Administration. Lyndon B. Johnson Space Center, Houston, TX.
STS-26 PROTEIN GROWTH (PCG) EXPERIMENT (Videotape)
Jun. 1989 Videotape: 2 min. playing time, in color, with sound
(NASA-TM-109533; NONP-VT-93-190330) Avail: CASI VHS A01/BETA A22

Astronauts Nelson and Lounge are shown working on the Protein Crystal Growth experiment aboard the Space Shuttle. CASI

N94-15654*# Dayton Univ., OH. Mechanical and Aerospace Engineering.
EVAPORATION FROM A MENISCUS WITHIN A CAPILLARY TUBE IN MICROGRAVITY Yearly Report, 1 Dec. 1992 - 30 Nov. 1993
K. P. Hallinan 3 Nov. 1993 31 p
(Grant NAG3-1391)
(NASA-CR-194593; NAS 1.26:194593) Avail: CASI HC A03/MF A01

The following represents a summary of progress made on the project 'Evaporation from a Capillary Meniscus in Microgravity' being conducted at the University of Dayton during the period 1 Dec. 1992 to 30 Nov. 1993. The efforts during this first year of the grant focused upon the following specific tasks: (1) application of a 3-D scattering particle image velocimetry technique to thin film velocity field measurement; (2) modeling the thermo-fluid behavior of the evaporating meniscus in 0-g within large diameter capillaries; (3) conceptualization of the space flight test cell (loop) configuration; (4) construction of prototypes of the test loop configuration; (5) conduct of experiments in 0-g in the 2.2 second drop tower at NASA-LeRC to study evaporation from a capillary meniscus within a square cuvette; and (6) investigation of the effect of vibrations on the stability of the meniscus. An overview of the work completed within these six task areas is presented. Author (revised)

N94-15723*# National Aeronautics and Space Administration. Marshall Space Flight Center, Huntsville, AL.
PRIORITIZATION METHODOLOGY FOR CHEMICAL REPLACEMENT
W. Cruit, S. Schutzenhofer, B. Goldberg, and K. Everhart Oct. 1993 66 p Sponsored by NASA, Washington
(NASA-TP-3421; M-732; NAS 1.60:3421) Avail: CASI HC A04/MF A01

This project serves to define an appropriate methodology for effective prioritization of efforts required to develop replacement technologies mandated by imposed and forecast legislation. The methodology used is a semiquantitative approach derived from quality function deployment techniques (QFD Matrix). This methodology aims to weigh the full environmental, cost, safety, reliability, and programmatic implications of replacement technology development to allow appropriate identification of viable candidates and programmatic alternatives. The results are being implemented as a guideline for consideration for current NASA propulsion systems. Author

N94-16071 National Research Council of Canada, Ottawa (Ontario).
PROCEEDINGS OF THE SECOND WORKSHOP ON MICROGRAVITY EXPERIMENTATION [COMPTE RENDU DU DEUXIEME ATELIER SUR LES EXPERIENCES EN MICROGRAVITE]
1990 210 p In ENGLISH and FRENCH Workshop held in Ottawa, Ontario, 8-9 May 1990; sponsored by Canadian Space Agency
(DSS-NR15-43-1990; NRC-31485; ISBN-0-660-55771-1; CTN-93-60782)
Avail: Issuing Activity (National Research Council, Publication Sales and Distribution, Montreal Road, Ottawa, Ontario, K1A OR6 Canada)

A conference on microgravity experimentation witnessed the presentation of papers on microgravity experiments in national space programs, laser-liquid interactions, gravity effects on human physiology and performance, conditions encountered in parabolic flight, sounding rockets, microgravity test beds and experimental facilities, materials processing, behavior of liquids and gas/liquid mixtures, crystal growth, data transmission systems, radiation measurements, and experiment design. Separate abstracts have been prepared for 31 papers from this conference. For individual titles, see N94-16072 through N94-16102.

N94-16072 National Research Council of Canada, Ottawa (Ontario).
SCIENTIFIC USE OF SPACE STATION FREEDOM
Richard W. Tyson and Shelley L. Pumphrey *In its* Proceedings of the Second Workshop on Microgravity Experimentation 1990 8 p (For primary document see N94-16071 03-29)
Avail: Issuing Activity (National Research Council, Publication Sales and Distribution, Montreal Road, Ottawa, Ontario, K1A OR6 Canada)

The NASA Office of Space Science and Applications (OSSA) has developed a strategic plan providing for an integrated program that includes extending OSSA's research infrastructure beyond existing ground-based, suborbital, Shuttle, and Spacelab facilities. OSSA intends to move to develop facilities that will take advantage of the unique resources to be provided by Space Station Freedom. The Station will provide the opportunity for in-depth space research in a microgravity environment. The pressurized volume of the Station will house microgravity science and applications (MSA) and life science experiments, conducted almost entirely within experiment racks that line the pressurized modules. MSA and life sciences facilities and research goals within the space station program are outlined. Other divisions of NASA will utilize the Station's attached payload capability to carry out research in the fields of astrophysics, earth science, solar and planetary physics, space plasma physics, and communications and information systems. Future evolution of Station research facilities and utilization concerns are discussed. Author (CISTI)

N94-16073 European Space Agency, Paris (France).
THE ESA TELESCIENCE PROGRAM
G. Naja *In* National Research Council Canada, Proceedings of the Second Workshop on Microgravity Experimentation 1990 7 p (For primary document see N94-16071 03-29)
Avail: Issuing Activity (National Research Council, Publication Sales and Distribution, Montreal Road, Ottawa, Ontario, K1A OR6 Canada)

In the Columbus space station Attached Laboratory, there will be 40 experiment racks but less than two crew members available to tend them, meaning that experiment operations cannot be permanently performed by the crew. The Columbus Free Flyer will be a completely automated laboratory, serviced periodically by astronauts. To facilitate the running of experiments in the Columbus facilities, the telescience concept will be used extensively. Telescience provides ground-based users with interactive and transparent access to their on-orbit experiments. Data such as telemetry and video are received by the user, who then can react by sending telecommands to activate mechanisms or robotic systems to operate the experiment. To validate the telescience concept, to promote it, and to train telescience users, a testbed has been developed and installed. The testbed has integrated five pilot experiments operated through a user workstation. The testbed has also been used in an operational simulation of long-duration space missions. A flight test of a telescience experiment investigating Marangoni convection was performed in Nov. 1989 onboard a sounding rocket with complete success. Author (CISTI)

N94-16074 National Space Development Agency, Tokyo (Japan).
THE JAPANESE SPACE STATION UTILIZATION PLAN
S. Yoda *In* National Research Council Canada, Proceedings of the Second Workshop on Microgravity Experimentation 1990 7 p (For primary document see N94-16071 03-29)
Avail: Issuing Activity (National Research Council, Publication Sales and Distribution, Montreal Road, Ottawa, Ontario, K1A OR6 Canada)

Japan will participate in space station research by means of the Japanese Experiment Module (JEM). Utilization conditions for JEM are being investigated through preliminary surveys and a number of initiatives have been undertaken to prepare for JEM utilization. A design reference mission has been studied which includes those themes expected to receive favorable effects from a microgravity environment. Some key experimental technologies common to various research themes are being developed using reduced gravity experiments in the MU-300 jet aircraft and in a sounding rocket program. Some Japanese programs using Spacelab are also under development. Systematic research themes selected as candidate groups from a design reference mission include production of semiconductors and high purity materials, studying of natural convection and crystal growth, and measuring diffusion coefficients in a liquid phase. Author (CISTI)

N94-16075 National Research Council of Canada, Ottawa (Ontario).
CANADIAN MICROGRAVITY EXPERIMENTS FLOWN IN 1989-1990
Ron Wilkinson and Glen S. Campbell *In its* Proceedings of the Second Workshop on Microgravity Experimentation 1990 7 p (For primary document see N94-16071 03-29)
Avail: Issuing Activity (National Research Council, Publication Sales and Distribution, Montreal Road, Ottawa, Ontario, K1A OR6 Canada)

Canadian microgravity experiments flown from Apr. 1989 to Mar. 1990 included one on the Biocosmos satellite, launched for 14 days in Sep. 1989. This experiment studied the development of osteoblast progenitor cells obtained from rats flown in space. The majority of microgravity work was done on two sets of flights using NASA's KC-135 reduced gravity aircraft. Canadian experiments on the KC-135 are reviewed in the areas of data acquisition, life science, materials science, biotechnology, dynamics, and education. Topics of specific experiments included the following: eye movements, blood volume distribution, arm movements, grain refining in alloys, liquid/liquid phase separation, production of microspheres and metal foams, laser drilling and welding, bubble coalescence, protein crystallization, gyroscope drift, and production of educational video modules.
Author (CISTI)

N94-16076* National Aeronautics and Space Administration. Lewis Research Center, Cleveland, OH.
NEW FINDINGS AND INSTRUMENTATION FROM THE NASA LEWIS MICROGRAVITY FACILITY
Howard D. Ross and Paul S. Greenberg *In* National Research Council Canada, Proceedings of the Second Workshop on Microgravity Experimentation 1990 5 p (For primary document see N94-16071 03-29)
Avail: Issuing Activity (National Research Council, Publication Sales and Distribution, Montreal Road, Ottawa, Ontario, K1A OR6 Canada)

The study of fundamental combustion and fluid physics phenomena in microgravity enables a new range of experiments to be performed since buoyancy-type flows are nearly eliminated, normally obscured forces and flows may be isolated, gravitational settling or sedimentation is nearly eliminated, and larger time or length scales in experiments become permissible. Some new phenomena found through ground-based microgravity research at NASA facilities is reviewed along with the instrumentation and drop tower facilities used in the research. Experiments are described in the areas of premixed gas combustion, droplet combustion, particle cloud combustion, liquid reorientation, and two-phase flow patterns. Future plans for instrumentation development are also outlined. Author (CISTI)

N94-16077 York Univ., Toronto (Ontario). Laser Processing Lab.
LASER-LIQUID INTERACTIONS UNDER REDUCED GRAVITY CONDITIONS
R. E. Mueller and W. W. Duley *In* National Research Council Canada, Proceedings of the Second Workshop on Microgravity Experimentation 1990 5 p (For primary document see N94-16071 03-29)
Avail: Issuing Activity (National Research Council, Publication Sales and Distribution, Montreal Road, Ottawa, Ontario, K1A OR6 Canada)

An experiment was performed under microgravity conditions in a KC-135 flight to study the heat transfer and resultant mass flows in a two-phase system subjected to laser radiation. A special cell was constructed to hold liquid water and to keep the water surface at the focus of the laser beam,

an aluminum insert was used. A hole in the insert was large enough to provide a free water surface but small enough so that the surface tension would restrain the water against small upward accelerations. The results show the differences in behavior of bubbles generated by the laser beam under the reduced gravity and high gravity conditions encountered during the flight. Under normal gravity, a trapped bubble may form below the conically shaped hole formed by the laser beam in the water. Under high gravity, the bubble appears smaller and sits deeper in the cell and has a much shorter lifetime. Under reduced gravity, the bubble is unconstrained by pressure and buoyant forces and was observed to grow to 2.5 times the diameter of a bubble in normal gravity. The penetration depth of the laser drill cone does not appear to be greatly affected by the presence or absence of gravity. Author (CISTI)

N94-16078* National Aeronautics and Space Administration. Lewis Research Center, Cleveland, OH.

THE VIBRO-ACOUSTIC MAPPING OF LOW GRAVITY TRAJECTORIES ON A LEARJET AIRCRAFT

C. M. Grodsinsky and T. J. Sutliff *In* National Research Council Canada, Proceedings of the Second Workshop on Microgravity Experimentation 1990 8 p (For primary document see N94-16071 03-29)

Avail: Issuing Activity (National Research Council, Publication Sales and Distribution, Montreal Road, Ottawa, Ontario, K1A OR6 Canada)

The NASA LeRC Learjet aircraft is used to fly parabolic trajectories for carrying out in-flight microgravity experiments. To derive full benefit from data obtained in such experiments, it is not only required to understand the low- to moderate-frequency accelerations present but also necessary to characterize the broadband aircraft vibro-acoustic environment. A vibro-acoustic measurement program was conducted during a series of low-gravity trajectories flown on the Learjet. The fuselage and an experiment rack were instrumented with 13 channels of accelerometers and three channels of pressure transducers. The locations of these sensors were determined in order to build a time history of the dynamics involved in the flight of such a parabolic trajectory and thus determine the typical rigid-body and vibro-acoustic loading a payload would experience. The instrumentation, data acquisition sequence, and experimental results showing residual accelerations and high-frequency dynamics are presented. As suspected, the measurements revealed that the aircraft environment cannot simply be described in terms of the static level low-gravity g-vector obtained, but that it also must account for both rigid-body and high-frequency vibro-acoustic dynamics. Author (CISTI)

N94-16079 Swedish Space Corp., Solna.

MAXUS: THE NEW SOUNDING ROCKET PROGRAM FOR LONG DURATION MICROGRAVITY FLIGHT

Lennart Bjorn *In* National Research Council Canada, Proceedings of the Second Workshop on Microgravity Experimentation 1990 6 p (For primary document see N94-16071 03-29)

Avail: Issuing Activity (National Research Council, Publication Sales and Distribution, Montreal Road, Ottawa, Ontario, K1A OR6 Canada)

MAXUS provides easily accessible, cost-effective suborbital microgravity flight opportunities of longer duration than the seven minutes typical of existing sounding rockets. The program is jointly conducted by the Swedish and German space organizations and uses a newly developed guided sounding rocket to launch microgravity payloads of 680 kg to an altitude of 875 km, giving 14.5 minutes of exoatmospheric microgravity conditions. The payload accommodates some 420 kg of scientific experiments and is based on a modular design that allows flexibility in the configuration of each individual payload and makes testing easy and reliable. The first MAXUS launch is scheduled for the spring of 1991 and will be followed by at least one launch per year from the ESRANGE launch site in northern Sweden. A well-proven land recovery system provides rapid and reliable retrieval of samples. The telemetry and telecommand system of MAXUS provides for extensive use of telescience, enabling experimenters to have hands-on control and observation of microgravity experiments.

Author (CISTI)

N94-16080 MPB Technologies, Inc., Pointe Claire (Quebec).

DEVELOPMENT OF THE LASER-BASED R/D TEST-BED SYSTEM (LTS)

M. Olivier, S. Simard, L. Audet, A. Laferriere, and W. Jamroz *In* National Research Council Canada, Proceedings of the Second Workshop on Microgravity Experimentation 1990 6 p (For primary document see N94-16071 03-29)

Avail: Issuing Activity (National Research Council, Publication Sales and Distribution, Montreal Road, Ottawa, Ontario, K1A OR6 Canada)

The laser-based research and development testbed system (LTS), supported by Canadian Space Agency programs, is a modular multi-user research system based on commercially available components for use on the variable gravity environment provided by the NASA KC-135 aircraft. The LTS consists of seven basic units: the supporting structure, the integrated laser unit, the beam delivery unit, power supply, control and data acquisition unit, material processing unit, and the optical diagnostic unit. The units are described along with some planned experiments that will make use of LTS capabilities. The LTS is designed so that several types of laser systems can be used: CO2, He-Ne, argon, and excimer lasers.Some of the subjects to be studied using the LTS include the following: laser melting or quenching of metals and welding of thin metal sheets in near-zero gravity; laser interactions with water; laser welding of plastics and glasses; vacuum materials processing; laser chemical vapor processing; and mass spectroscopy analysis. Author (CISTI)

N94-16081 National Optics Inst., Ste-Foy (Quebec).

OPTICAL SYSTEMS FOR THE VISUALIZATION OF FLUID AND SOLID TRANSPARENT MEDIA UNDER MICROGRAVITY CONDITIONS c35

E. Harvey and P. Langlois *In* National Research Council Canada, Proceedings of the Second Workshop on Microgravity Experimentation 1990 8 p (For primary document see N94-16071 03-29)

Avail: Issuing Activity (National Research Council, Publication Sales and Distribution, Montreal Road, Ottawa, Ontario, K1A OR6 Canada)

Canada's National Optics Institute carried out, on behalf of the Canadian Space Agency, a study on the diagnosis of fluids under reduced gravity using new optical technologies. The Institute is conducting research on the adaptation of optical fluid diagnostic techniques to the visualization of laser processing of plastic in microgravity. Continuation of this project should lead to a KC-135 flight involving the optical diagnostic system. A short overview is presented of the optical techniques for fluid analysis including new techniques introduced within the last decade. Arguments are stated which lead to the choice of real-time holographic interferometry and Moire deflectometry as the most suitable techniques with respect to microgravity experiment requirements. Preliminary results are also presented from ground experiments with gas, liquid, and acrylic media. The results indicate that the two selected techniques allow visualization of temperature fields, hot spots, and convection currents with a very high sensitivity. A better understanding of the underlying phenomena can thus be acquired.

Author (CISTI)

N94-16082 Bristol Aerospace Ltd., Winnipeg (Manitoba). Space Systems Group.

QUESTS: A MICROGRAVITY RESEARCH FACILITY FOR MATERIALS SCIENCE EXPERIMENTS

G. Tyc, D. Gates, R. W. Smith (Queens Univ., Kingston, Ontario.), S. Goodman (Queens Univ., Kingston, Ontario.), and K. N. Tandon (Manitoba Univ., Winnipeg.) *In* National Research Council Canada, Proceedings of the Second Workshop on Microgravity Experimentation 1990 8 p (For primary document see N94-16071 03-29)

Avail: Issuing Activity (National Research Council, Publication Sales and Distribution, Montreal Road, Ottawa, Ontario, K1A OR6 Canada)

The QUESTS (Queen's University Experiment on the Space Transportation System) payload has a modular design to increase payload application flexibility and its controller software is also flexible in order to accommodate a large variety of materials science experiments. The QUESTS payload has evolved through several phases of study to the current configuration, which consists of three gradient-freeze furnaces conducting unidirectional freezing experiments and twelve isothermal furnaces conducting liquid diffusion experiments. The payload consists of the following major subsystems: experiment hardware, payload control and data acquisition electronics, power supply, and ground support equipment. The payload is 9.5 m in diameter, 0.68 m high, and has a mass of 90 kg. QUESTS is designed for use on space shuttle flights, but could also be used on KC-135 aircraft flights and, with minor modifications, on a sounding rocket.

Author (CISTI)

N94-16083 BM Hi-Tech, Inc., Collingwood (Ontario).
PAYLOADS FOR THE PROCESSING OF HIGH TEMPERATURE MATERIALS
S. E. Prasad, M. Verghese, A. Roorda, K. Slaughter, I. Murley, P. Stern, and P. Lave *In* National Research Council Canada, Proceedings of the Second Workshop on Microgravity Experimentation 1990 7 p (For primary document see N94-16071 03-29)
Avail: Issuing Activity (National Research Council, Publication Sales and Distribution, Montreal Road, Ottawa, Ontario, K1A OR6 Canada)

Payloads designed for microgravity processing of high temperature materials are described. The payload for use in the KC-135 aircraft includes a power supply, electronic controller, kiln, sample storage magazine, and cooling unit. The magazine can store up to eight samples and is operated by simple push-pull levers. The payload was designed to fulfill criteria including operator and aircraft safety, ease of operation, and reliability. The payload for use in the T-33F aircraft is designed to be fully automatic and can be preprogrammed to suit a broad range of experimental processes. Extremely rapid temperature cycling is possible and a closed-loop system ensures that the specimens are contained at all times, reducing the fire hazard. The payload apparatus consists of a furnace system, power supply and relay switches, and programmable logic control system. The payload for use on the Black Brant sounding rocket consists of a furnace, battery box, and card cage holding the control circuitry. The apparatus was designed to process glasses but could be modified to accommodate other materials. For ground experiments, an aerodynamic levitation unit has been developed which permits containerless processing of samples up to 6 mm in diameter. During experiments, a solid sphere sample is levitated and melted using a high intensity lamp and parabolic mirrors. Author (CISTI)

N94-16084 Canadian Space Agency, Ottawa (Ontario).
THE CANADIAN SPACE STATION USER DEVELOPMENT PROGRAM. WHERE DO WE GO FROM HERE? **c18**
Parvez Kumar *In* National Research Council Canada, Proceedings of the Second Workshop on Microgravity Experimentation 1990 3 p (For primary document see N94-16071 03-29)
Avail: Issuing Activity (National Research Council, Publication Sales and Distribution, Montreal Road, Ottawa, Ontario, K1A OR6 Canada)

The Canadian Space Station User Development Program (UDP), formally approved in March 1986, is gradually approaching maturity. As a result of limited funding, it is also approaching saturation. The remaining UDP budget is $60 million and there are no funds to build space-qualified hardware. Successful microgravity experiments in aircraft have shown that 20 seconds of microgravity are adequate for doing useful science in most cases. Spinoffs have already occurred through applications of patents for processes discovered during microgravity related work. A number of unsuccessful attempts have been made to establish drop-tube test facilities in Canada, and efforts are being made within UDP to acquire first-hand knowledge of such facilities through cooperative programs with other countries. A microgravity rocket was scheduled for a fall 1991 launch but enough experiments may not be found. The CANEX 2 flight on the space shuttle is already fully subscribed, and Canadian scientists are slowly beginning to get aboard the shuttle as co-investigators. It has been decided to book one locker on the October 1993 SPACEHAB flight. Over the long term, the high costs of participating in the space station are of concern. It is recommended that the UDP continue with its microgravity work but only use the space station on an as-required basis. Author (CISTI)

N94-16085 Garneau (Marc) Collegiate Inst., Don Mills (Ontario).
CONTAINED LIQUIDS IN MICROGRAVITY, PART 2
In National Research Council Canada, Proceedings of the Second Workshop on Microgravity Experimentation 1990 7 p (For primary document see N94-16071 03-29)
Avail: Issuing Activity (National Research Council, Publication Sales and Distribution, Montreal Road, Ottawa, Ontario, K1A OR6 Canada)

An experiment was designed to study the effects of microgravity on the behavior of contained liquids varying in viscosity, surface tension, miscibility, molecular size and shape, intermolecular forces, and molecular mass. The experimental apparatus consisted of cylindrical cavities of varying diameter cut into plexiglass, enclosed with glass plates. Additional variations included triangular and square shapes, and different cell linings. The behavior of the liquids was recorded by video camera. The liquids chosen included lubricating oils, methyl alcohol, glycerol, ethylene glycol, saline and sucrose solutions, sodium oleate, mineral oil/water, ethyl alcohol, water, and oleic acid. Experiments were conducted during microgravity flights of the KC-135 aircraft, and results of experiments using ethylene glycol and methyl alcohol mixtures with air are reported. It is suggested that observed encapsulation of air in ethylene glycol was artificially induced by the flight conditions and that true encapsulation resulting from capillary action under microgravity was only exhibited by methyl alcohol. Author (CISTI)

N94-16086 Laval Univ. (Quebec).
STUDY OF FRACTAL AGGREGATES [ETUDE DES AGREGATS FRACTALS]
C. Rioux, L. Potvin, and R. J. Slobodrian *In* National Research Council Canada, Proceedings of the Second Workshop on Microgravity Experimentation 1990 4 p In FRENCH (For primary document see N94-16071 03-29)
Avail: Issuing Activity (National Research Council, Publication Sales and Distribution, Montreal Road, Ottawa, Ontario, K1A OR6 Canada)

The properties of fractals are defined and the method of calculating fractal dimension is introduced, along with illustrative examples. Applications of knowledge about fractals are discussed and results of experiments in forming fractals are presented. Such applications include the description of particle behavior in air, the compression of information for satellite transmission, and the formation of crystals under gravitational forces. In the experiments, fractal structures were formed by depositing a fine powder suspension in water and by a chemical reaction between silver nitrate and copper. For producing fractal structures in microgravity, a literature review reveals one method which is readily applicable to use in space. The method consists of heating a filament previously coated with metal and evaporating this metal in the form of droplets, which then aggregate in the presence of a helium cooling gas. Author (CISTI)

N94-16087 Toronto Univ. (Ontario). Dept. of Chemical Engineering and Applied Chemistry.
INVESTIGATION OF TWO-PHASE FLOW AND BOILING HEAT TRANSFER DURING QUENCHING OF A TUBE UNDER MICROGRAVITY
M. Kawaji, C. J. Westbye, and B. N. Antar (Tennessee Univ. Space Inst., Tullahoma.) *In* National Research Council Canada, Proceedings of the Second Workshop on Microgravity Experimentation 1990 4 p (For primary document see N94-16071 03-29)
Avail: Issuing Activity (National Research Council, Publication Sales and Distribution, Montreal Road, Ottawa, Ontario, K1A OR6 Canada)

There are many important processes that occur under microgravity which would involve gas-liquid two-phase flow and boiling condensation heat transfer phenomena. For example, in refilling of space vehicles with liquid hydrogen or oxygen under microgravity, a transient quenching process is expected involving two-phase flow and convective boiling heat transfer due to the low boiling points of the fluids and high initial wall temperatures of the refuelling lines and receiving tanks. To elucidate the behavior of two-phase flow patterns under quenching conditions, a series of quenching experiments will be performed during microgravity flights of the KC-135. The experimental apparatus consists of a compact test loop incorporating a quartz tube test section which is heated externally. The tube contains a low boiling point refrigerant at near atmospheric pressure. When microgravity conditions are reached, a pump will inject the liquid into the tube, and the flow and heat transfer phenomena will be recorded. Results are presented from pre-flight tests conducted to obtain reference data at 1 gravity.
Author (CISTI)

N94-16088 ORTECH International, Mississauga (Ontario).
USE OF MICROGRAVITY IN THE SYNTHESIS OF CERAMICS USING SOL GEL TECHNIQUES
L. M. Luckevich, V. R. Trimble, and B. G. Sellars *In* National Research Council Canada, Proceedings of the Second Workshop on Microgravity Experimentation 1990 6 p (For primary document see N94-16071 03-29)
Avail: Issuing Activity (National Research Council, Publication Sales and Distribution, Montreal Road, Ottawa, Ontario, K1A OR6 Canada)

Using sol-gel processing techniques, it is possible to prepare sub-micron ceramic oxide powders with a narrow particle size distribution. This permits sintering to high density at lower temperatures, and allows fabrication of ceramic bodies with improved microstructures and distributions of phases. The use of microgravity to produce uniform ceramic spheres of greater

than 1 mm diameter was investigated in order to understand the kinetics of formation for terrestrial process applications and to assess application of the technology to space processing of ceramic powders and products. The sol-gel method used in the investigation was the polymerized alkoxide process, in which metal alkoxides are partially hydrolyzed or decomposed, then recombined by polymerization to form a metal-oxygen bond. Using this process in microgravity, spherical droplets are formed and there is no gravity-induced movement of the polymerizing particle. If the period of microgravity is long enough, complete reaction to the center of the particle is possible. In microgravity experiments aboard the KC-135 aircraft, several techniques for sphere production were developed, including a sphere growth and pulse-off method, a jet formation method, and an oscillating jet method. Author (CISTI)

N94-16089 British Columbia Univ., Vancouver. Dept. of Mechanical Engineering.

GAS BUBBLE GENERATION AND TRANSPORT IN MICROGRAVITY

Z. Abdullah and M. Salcudean *In* National Research Council Canada, Proceedings of the Second Workshop on Microgravity Experimentation 1990 7 p (For primary document see N94-16071 03-29)

Avail: Issuing Activity (National Research Council, Publication Sales and Distribution, Montreal Road, Ottawa, Ontario, K1A OR6 Canada)

An investigation is being conducted to develop a technique to inject and transport gas bubbles in liquid metals and then to quench the metal to form a porous solid. The objective is to vary the porosity as a function of the spatial location in a predictable and controllable manner, such that the more highly stressed parts of the solidified product would have a low void fraction and lower stressed regions would have a higher void fraction. Such a technique would only be feasible in microgravity, and in order to determine the influence of the various parameters involved in such a process, the generation and transport of gas bubbles in microgravity was studied aboard flights of the KC-135 and T-33 aircraft. The test cell consisted of an 8-cm square plexiglass enclosure containing a water-glycerine electrolyte. A well controlled flow field was established in the electrolyte using a magnetohydrodynamic pump. Gas bubbles were injected into the electrolyte using a vibrating gas injector. The gas bubble formation and movement was recorded on video. Several distinct trends were observed and simple models are presented to explain the trends. The models explain bubble detachment, breakup, and spacing. Model predictions are strongly supported by experimental observations. Author (CISTI)

N94-16090 National Research Council of Canada, Ottawa (Ontario).

KC-135 ACCELERATION MONITORING AND DATA ACQUISITION SYSTEM **c05**

Bjarni V. Tryggvason and Patrick J. Sullivan *In its* Proceedings of the Second Workshop on Microgravity Experimentation 1990 3 p (For primary document see N94-16071 03-29)

Avail: Issuing Activity (National Research Council, Publication Sales and Distribution, Montreal Road, Ottawa, Ontario, K1A OR6 Canada)

The KC-135 data acquisition system is a comprehensive data collection system designed and built for the purpose of microgravity research aboard the NASA KC-135 aircraft. The system consists of the necessary hardware for basic signal processing and an interactive software package which provides for custom specification of data collection requirements. The primary use of this system will be to monitor, record, and provide signals to other researchers of aircraft accelerations along three axes, and interior pressure, temperature, and humidity. Several data channels will also be available to record data from experiments aboard the aircraft. The components of this system are described, including the power supply, computer system, signal conditioning unit, software, and accelerometers. The system has been successfully flight-tested. Author (CISTI)

N94-16091 Simon Fraser Univ., Burnaby (British Columbia). School of Engineering Science.

INFRA LINK: A DATA TRANSMISSION SYSTEM FOR MICROGRAVITY RESEARCH **c32**

Bill Stewart, Mike Hollingshead, Jennifer Stinn, Dennis Michaelson, and Bjarni Tryggvason *In* National Research Council Canada, Proceedings of the Second Workshop on Microgravity Experimentation 1990 5 p (For primary document see N94-16071 03-29)

Avail: Issuing Activity (National Research Council, Publication Sales and Distribution, Montreal Road, Ottawa, Ontario, K1A OR6 Canada)

In microgravity experiments conducted during parabolic flight in aircraft, the experimental equipment may be freely floated in the aircraft cabin in order to improve the g-levels for the experiment. If it is necessary to transmit and/or receive data from the apparatus, a data link which does not defeat the free floating nature of the experiment is needed. In addition, in experiments where physiological data are collected from human subjects in near-weightless conditions, it is convenient to have a data link that does not require a complex and awkward umbilical cord connecting the subject to the data recording system. To this end, a data transmission system has been developed which uses infrared light as the data transmission medium. The system, called InfraLink, was designed to be able to operate and store data for at least two hours, to be compact, to be a standalone system not requiring any operator intervention during the flight, and to have a multichannel capability. The system was tested on the ground and during KC-135 flights to evaluate the range and quality of the infrared link. Results are presented showing data dropout and error rates. The results demonstrate the feasibility of the InfraLink as a data collection system for KC-135 flight experiments. Author (CISTI)

N94-16092 Thomson and Nielsen Electronics, Ottawa (Ontario).

REAL TIME RADIATION MEASUREMENTS IN SPACE **c93**

I. Thomson and G. Mackay *In* National Research Council Canada, Proceedings of the Second Workshop on Microgravity Experimentation 1990 3 p (For primary document see N94-16071 03-29)

Avail: Issuing Activity (National Research Council, Publication Sales and Distribution, Montreal Road, Ottawa, Ontario, K1A OR6 Canada)

Radiation composed of energetic electrons, protons, photons, and galactic cosmic rays will be experienced by all space missions and may have effects on radiation sensitive electronic components and biological specimens. Radiation issues of interest to microgravity and biological experiments are discussed and the design of a new direct reading electronic radiation monitoring system is described. The proposed system consists of a radiation sensitive metal oxide semiconductor field effect transistor (MOSFET) specially designed to respond to ionizing radiation. On exposure to radiation, a permanent charge is stored in the MOSFET's insulating oxide, altering the device's electrical characteristics in a manner directly proportional to the dose exposed. A simple circuit reads the MOSFET's cumulative dose, making it possible to obtain real-time measurements and store the data or transfer the data to an earth station. Tests have shown that the MOSFET dosimeter shows a linear response up to at least 30,000 centiGray at a resolution of 0.1 centiGray. The MOSFET dosimetry system will be installed on the European Space Agency's ARTEP satellite scheduled for launch in November 1991. Author (CISTI)

N94-16093 York Univ. (Ontario). Human Performance Lab.

CHARACTERISTICS OF AIMED ARM MOVEMENTS IN HUMANS UNDER LOW GRAVITY **c54**

O. Bock, K. Arnold, I. Howard, and K. Money *In* National Research Council Canada, Proceedings of the Second Workshop on Microgravity Experimentation 1990 3 p (For primary document see N94-16071 03-29)

Avail: Issuing Activity (National Research Council, Publication Sales and Distribution, Montreal Road, Ottawa, Ontario, K1A OR6 Canada)

A study was conducted to investigate the accuracy of arm pointing movements in human subjects without visual feedback on the pointing arm during low-gravity episodes of KC-135 flights, in order to gather new information on errors of visual localization and of movement execution in space. The experimental setup involved pointing at the face of a digitizing pad mounted on the back of a computer screen that provided the pointing target and faced the human subject. The time between target appearance and movement onset (reaction time), movement duration, movement velocity, and absolute pointing errors were recorded. A clear tendency was found to point too high or low in the first movement of each low-gravity episode, and to reduce these pointing errors during subsequent movements. No changes in movement kinematics between low-gravity and normal gravity were observed. Author (CISTI)

N94-16094 British Columbia Univ., Vancouver.

STATISTICAL TECHNIQUES FOR STUDY DESIGN OF MICROGRAVITY LIFE SCIENCES EXPERIMENTS **c51**

F. A. Gagnon, L. E. Susak, P. C. Wing, F. Glick, and I. K. Y. Tsang *In* National Research Council Canada, Proceedings of the Second Workshop

on Microgravity Experimentation 1990 3 p . (For primary document see N94-16071 03-29)
Avail: Issuing Activity (National Research Council, Publication Sales and Distribution, Montreal Road, Ottawa, Ontario, K1A OR6 Canada)

Small N techniques are known by such names as single system, interrupted time series, intrasubjects replication designs, single subject, or idiographic research. These techniques are ideal for application to the microgravity life sciences field, where large N studies are not feasible because they would be extremely costly and take years to conduct. Small N study techniques are the only viable method for obtaining the optimum scientific value from studies performed on the limited number of subjects in the limited time available in microgravity. The small N techniques are dependent on establishing a basic level of the dependent variable for each subject, then introducing the independent variable to determine whether there is a change in the dependent variable. Steps to be used in performing small N studies in practice are outlined. Author (CISTI)

N94-16095 Ryerson Polytechnical Inst., Toronto (Ontario).
TRANSCRANIAL DOPPLER ULTRASOUND STUDIES OF CEREBRAL BLOOD-FLOW IN MICROGRAVITY **c52**
M. S. Kassam, R. L. Bondar (Canadian Space Agency, Ottawa, Ontario.), K. W. Johnston (Toronto Univ., Ontario.), R. S. C. Cobbold (Toronto Univ., Ontario.), P. J. Vaitkus (Toronto Univ., Ontario.), F. Stein (Maple Lake Non-Invasive Vascular Lab., Farmington, NM.), and P. Dunphy *In* National Research Council Canada, Proceedings of the Second Workshop on Microgravity Experimentation 1990 8 p (For primary document see N94-16071 03-29)
Avail: Issuing Activity (National Research Council, Publication Sales and Distribution, Montreal Road, Ottawa, Ontario, K1A OR6 Canada)

Transcranial doppler ultrasound (TCD) was used to measure blood flow velocities in the middle cerebral artery of volunteers subjected to 15-20 seconds of acute microgravity in the NASA KC-135 aircraft. In addition, simultaneous recordings of acceleration in the z direction and of other systemic vascular parameters were obtained. In-flight experimental procedures and the development of a system for recording and processing a large volume of data are described. Problems in performing the experiments and in analyzing the data are noted. Results of processing seven subjects indicate a change in the quantitative indices during the flight. Of particular interest are the changes in received power of the Doppler signal and the mean flow velocity waveforms in the microgravity regions. Indices related to the mean flow of the artery appear to exhibit changes in each phase of the flight parabola that are consistent from subject to subject.
Author (CISTI)

N94-16096 Institute for Space and Terrestrial Science, York (Ontario).
HUMAN OCULAR TORSION DURING PARABOLIC FLIGHT: AN INVESTIGATION USING ELECTROMAGNETIC SCLERAL SEARCH COIL **c52**
B. Cheung, K. Money (Defence and Civil Inst. of Environmental Medicine, Downsview, Ontario.), I. Howard, N. Kirienko, W. Johnson (Saint Michael's Hospital, Toronto, Ontario.), L. Lackner (Brandeis Univ., Waltham, MA.), and Paul A. Dizio (Brandeis Univ., Waltham, MA.) *In* National Research Council Canada, Proceedings of the Second Workshop on Microgravity Experimentation 1990 8 p (For primary document see N94-16071 03-29)
Avail: Issuing Activity (National Research Council, Publication Sales and Distribution, Montreal Road, Ottawa, Ontario, K1A OR6 Canada)

Ocular counterrolling is a reflex rotation of the eyes about the visual axis opposite to the lateral inclination of the head. Attempts were made to measure the static and dynamic components of ocular counterrolling during the hypogravity and hypergravity phases of parabolic flight, using the electromagnetic scleral search-coil technique. The results provide evidence that torsional eye displacements occurred in response to the imposition of altered gravitoinertial forces. The torsional position of the eyes is not constant, when the subject's head position, both during upright or tilt, is maintained. In some subjects, the torsional displacement in microgravity is accompanied by a fine torsional nystagmus. Also, the direction and magnitude of the torsion differ substantially from one individual to another. There was a significant difference in torsional magnitude between the microgravity and hypergravity period in all head positions. Under 1-g condition, static counterroll compensated for about 16% of head roll while the dynamic counterpart was much larger, up to 36%. The gain of dynamic counterroll was also higher during the hypergravity phases than the microgravity phases. Author (CISTI)

N94-16097 Bubble Technology Industries, Inc., Chalk River (Ontario).
PRELIMINARY RESULTS FROM BUBBLE DETECTOR MEASUREMENTS ABOARD BIOCOSMOS-2044
H. Ing, K. Tremblay, A. Mortimer (Canadian Space Agency, Ottawa, Ontario.), E. E. Kovalev (Institute of Biomedical Problems, Moscow, USSR.), V. E. Dunkin (Institute of Biomedical Problems, Moscow, USSR.), and N. A. Nephedov (Institute of Biomedical Problems, Moscow, USSR.) *In* National Research Council Canada, Proceedings of the Second Workshop on Microgravity Experimentation 1990 4 p (For primary document see N94-16071 03-29)
Avail: Issuing Activity (National Research Council, Publication Sales and Distribution, Montreal Road, Ottawa, Ontario, K1A OR6 Canada)

The Bubble Detector Spectrometer (BDS) was developed primarily for the measurement of degraded fission neutrons. The Canadian Space Agency obtained a modified BDS to be used for measurement of the neutron spectrum in space. The energy responses of the five types of space BDS were measured using monoenergetic neutrons, and the measured response functions are presented. Two sets of BDS detectors were delivered, along with six pairs of bubble detectors, for placement in the Biocosmos-2044 satellite. After return of the satellite, the bubble detectors were retrieved and sent for data retrieval and processing. Spectral data from the Biocosmos bubble detectors are presented and discussed. Preliminary results show a large number of neutrons above 10 MeV, and another component spanning 0.1 to 10 MeV which bears some resemblance to an evaporation spectrum. The neutron spectrum was similar at the three locations in the satellite where the bubble detectors were located. At the location close to the small hatch, the neutron dose was comparable to that at the location of the BDS, or 82 millirems. At the other location of the dosimeter package, the dose was only 37 millirems. Author (CISTI)

N94-16098 Simon Fraser Univ., Burnaby (British Columbia). School of Kinesiology.
HEART RATE RESPONSE TO PARABOLIC FLIGHT MANOEUVRES **c52**
Daryl Leiski, Igor Makjavic, and B. V. Tryggvason *In* National Research Council Canada, Proceedings of the Second Workshop on Microgravity Experimentation 1990 9 p (For primary document see N94-16071 03-29)
Avail: Issuing Activity (National Research Council, Publication Sales and Distribution, Montreal Road, Ottawa, Ontario, K1A OR6 Canada)

Some of the physiological data on heart rate response to parabolic flight maneuvers are analyzed. Data were gathered from two subjects on flights of the KC-135 aircraft over a two year period. The electrocardiogram data retrieval system and statistical analysis methods used are described. Results are presented and discussed for heart rate versus time and versus acceleration. Heart rate versus time showed no conclusive trends. The heart rate versus acceleration levels illustrated the results that were expected based on previous studies using tilt tables to alter the hydrostatic column. The heart rate changes are directly linked to the changing hydrostatic column and the resulting fluid shifts. Coupled with this bioreceptor response is the exercise reflex, a response to the static muscular contraction of the abdominal and leg muscles maintaining body posture through the high-g portions of the parabolas. Comparison of responses between the two subjects provides insight into interindividual differences in responses to the stress of parabolic flight. Author (CISTI)

N94-16099 National Research Council of Canada, Ottawa (Ontario). Advanced Materials Engineering Centre.
FINITE ELEMENT ANALYTICAL TECHNIQUES FOR CERAMIC PRODUCTION IN MICROGRAVITY: A HYPOELASTIC MODEL
F. Taheri and J. G. Murphy *In its* Proceedings of the Second Workshop on Microgravity Experimentation 1990 7 p (For primary document see N94-16071 03-29)
Avail: Issuing Activity (National Research Council, Publication Sales and Distribution, Montreal Road, Ottawa, Ontario, K1A OR6 Canada)

Slipcasting is useful for fabricating complex structural shapes from materials such as aluminum oxide. There are many mechanisms that can generate shrinkage cracks in slipcast ceramic components, including the

residual stresses caused during the drying and firing stages of fabrication. The ceramic firing cycles necessary for sintering often produce high thermal gradients and can cause differential densification rates, resulting in formation of residual stress patterns. The methodology used in evaluating the effects of microgravity on slipcast ceramics are discussed, with the aim of increasing understanding of microstructural effects in microgravity. The analysis used the finite element method in conjunction with a hypoelastic material constitutive model. The qualitative results obtained from a preliminary run of the finite element model using the ABAQUS software package illustrate that this numerical methodology can be used to emulate the sintering mechanism and estimate the residual stresses caused by the firing process. Author (CISTI)

N94-16100 Laval Univ. (Quebec).
PRECISE MEASUREMENT AND UTILIZATION OF ACCELERATION DATA **c19**
L. Potvin, C. Rioux, and R. J. Slobodrian *In* National Research Council Canada, Proceedings of the Second Workshop on Microgravity Experimentation 1990 5 p (For primary document see N94-16071 03-29)
Avail: Issuing Activity (National Research Council, Publication Sales and Distribution, Montreal Road, Ottawa, Ontario, K1A OR6 Canada)

The causes of the main perturbations of the reduced gravity environment in a spacecraft in low earth orbit are examined. These include the variations in the earth's gravitational field, imbalances between gravitational and inertial forces, effects of the residual atmosphere, effects of solar radiation and micrometeorites, and man-made effects such as use of thrusters and movements of spacecraft personnel. To understand results of experiments carried out in this microgravity environment, an accurate record of these perturbations is needed. Specifications for a sensor of microgravity perturbations are outlined and the design of some existing accelerometers is assessed for their possible application in such a sensor. A new concept for a compact, high sensitivity accelerometer is proposed in which a small iron rod in equilibrium inside a solenoid is used. Suggestions are made for the organization and presentation of acceleration data from the proposed accelerometer system. Author (CISTI)

N94-16101 Saskatchewan Univ., Saskatoon. Dept. of Mechanical Engineering.
THE DESIGN AND ANALYSIS OF A MODULAR MICROGRAVITY TEST PLATFORM FOR USE ABOARD THE NASA KC-135 AIRCRAFT **c18**
Alain Durand, Roger Hertz, Darren Mitchell, and Kamiel S. Rezkallah *In* National Research Council Canada, Proceedings of the Second Workshop on Microgravity Experimentation 1990 7 p (For primary document see N94-16071 03-29)
Avail: Issuing Activity (National Research Council, Publication Sales and Distribution, Montreal Road, Ottawa, Ontario, K1A OR6 Canada)

A microgravity platform to be used for housing experiments aboard the NASA KC-135 aircraft was designed using a modular construction approach. Two identical modules were designed to be used in three basic configurations: side by side, vertically stacked, or separately mounted. The levels within each module were adjustable and removable, providing yet another means by which the platform could be altered to suit the experiment being conducted. The frame was designed according to the strict strength and safety specifications set out by NASA. Additional design objectives stipulated that the frame be versatile, light weight, and accessible to the experiment operator. The ANSYS finite element stress analysis package was used to simulate the frame structure and its various components. Internal moments and forces were obtained from the finite element model and were later compared to the results from material performance tests. The results indicated that the platform could withstand the gravity levels experienced on the aircraft, including crash loads, with sufficient factors of safety. Author (CISTI)

N94-16102 Ottawa Univ. (Ontario). Dept. of Chemistry.
SOLUTION BEHAVIOUR IN MICROGRAVITY: CONSIDERATIONS FOR PROTEIN CRYSTAL GROWTH
Christin T. Choma *In* National Research Council Canada, Proceedings of the Second Workshop on Microgravity Experimentation 1990 5 p (For primary document see N94-16071 03-29)
Avail: Issuing Activity (National Research Council, Publication Sales and Distribution, Montreal Road, Ottawa, Ontario, K1A OR6 Canada)

X ray crystallography can provide high resolution atomic structures of biological macromolecules such as proteins, but the technique requires uniform, large crystals of the biochemical. There is evidence that microgravity is more conducive than 1-g to the growth of protein crystals suitable for x ray analysis. Injector materials were identified which are suitable for producing the large, stable protein drops required for crystal growth. Experiments were conducted on flights of both T-33 and KC-135 aircraft involving injectors in various configurations. Protein and precipitant solutions were brought to mix together in three ways and the results were recorded on video. The results indicate that protein and precipitant solutions must be actively mixed prior to being extruded into a pendant crystallization droplet in microgravity. In the absence of density driven convection, diffusion alone is insufficient to bring about mixing. Author (CISTI)

N94-15159# Technische Univ., Munich (Germany). Sektion Physik.
BENARD CONVECTION OF MAGNETIC COLLOIDS UNDER MICROGRAVITY
S. Odenbach *In* ESA, Sounding Rocket Experiments in Fluid Science and Materials Sciences: TEXUS 25 to 27 and MASER 4, Volume 3 Feb. 1993 p 16-23 (For primary document see N94-15157 03-25)
Copyright Avail: CASI HC A02/MF A02; ESA, EPD, ESTEC, Noordwijk, Netherlands, HC

N94-15160# Technische Univ., Munich (Germany). Lab. fuer Angewandte Thermodynamik und Technologie unter Mikrogravitation.
POOL BOILING: SINGLE BUBBLE EXPERIMENT
B. Vogel and J. Straub *In* ESA, Sounding Rocket Experiments in Fluid Science and Materials Sciences: TEXUS 25 to 27 and MASER 4, Volume 3 Feb. 1993 p 24-34 Sponsored by BMFT (For primary document see N94-15157 03-25)
Copyright Avail: CASI HC A03/MF A02; ESA, EPD, ESTEC, Noordwijk, Netherlands, HC

N94-15162# Chalmers Univ. of Technology, Goeteborg (Sweden). Dept. of Physical Chemistry.
ORIENTATION OF DNA DURING FREE-SOLUTION ELECTROPHORESIS
Mats Jonsson, Ulf Jacobsson, Bengt Norden, and Tore Eriksson *In* ESA, Sounding Rocket Experiments in Fluid Science and Materials Sciences: TEXUS 25 to 27 and MASER 4, Volume 3 Feb. 1993 p 42-52 Sponsored by Swedish Board for Space Activities (For primary document see N94-15157 03-25)
Copyright Avail: CASI HC A03/MF A02; ESA, EPD, ESTEC, Noordwijk, Netherlands, HC

N94-15164# Commissariat a l'Energie Atomique, Gif-sur-Yvette (France). Service de Physique de l'Etat Condense.
DENSITY AND TEMPERATURE RELAXATION NEAR THE CRITICAL POINT OF CARBON DIOXIDE UNDER REDUCED GRAVITY
D. Beysens, Y. Garrabos (Centre National de la Recherche Scientifique, Villetaneuse, France.), P. Guenoun, B. Khalil, and B. LeNeindre (Centre National de la Recherche Scientifique, Villetaneuse, France.) *In* ESA, Sounding Rocket Experiments in Fluid Science and Materials Sciences: TEXUS 25 to 27 and MASER 4, Volume 3 Feb. 1993 p 64-78 Sponsored in part by CNES (For primary document see N94-15157 03-25)
Copyright Avail: CASI HC A03/MF A02; ESA, EPD, ESTEC, Noordwijk, Netherlands, HC

N94-15165# Deutsche Forschungsanstalt fuer Luft- und Raumfahrt, Cologne (Germany). Inst. fuer Raumsimulation.
TEMPERATURE PROPAGATION IN NEAR-CRITICAL FLUIDS PRIOR TO AND DURING SEPARATION
H. Klein, G. Schmitz, and D. Woermann (Cologne Univ., Germany.) *In* ESA, Sounding Rocket Experiments in Fluid Science and Materials Sciences: TEXUS 25 to 27 and MASER 4, Volume 3 Feb. 1993 p 80-83 Repr. from Physical Review A, v. 43, no. 8, 1991 Sponsored in part by Deutsche Agentur fuer Raumfahrtangelegenheiten G.m.b.H. (For primary document see N94-15157 03-25)
Copyright Avail: CASI HC A01/MF A02; ESA, EPD, ESTEC, Noordwijk, Netherlands, HC

N94-15167# Electrotechnical Lab., Tsukuba (Japan).
UNIDIRECTIONAL SOLIDIFICATION OF LIQUID-CRYSTAL MATERIAL
A. Iwasaki, S. Hosokawa, I. Kudo, M. Tanimoto, H. Sakurai (Ishikawajima-Harima Heavy Industries Co. Ltd., Tokyo, Japan.), Y. Arai (Ishikawajima-Harima Heavy Industries Co. Ltd., Tokyo, Japan.), T. Watanabe (Ishikawajima-Harima Heavy Industries Co. Ltd., Tokyo, Japan.), S. Kawai (Ishikawajima-Harima Heavy Industries Co. Ltd., Tokyo, Japan.), M. Ishikawa (Mitsubishi Research Inst., Inc., Tokyo, Japan.), and S. Kamei (Mitsubishi Research Inst., Inc., Tokyo, Japan.) *In* ESA, Sounding Rocket Experiments in Fluid Science and Materials Sciences: TEXUS 25 to 27 and MASER 4, Volume 3 Feb. 1993 p 92-99 Sponsored by Mechanical Social Systems Foundation and Society of Japanese Aerospace Co., Inc. Original contains color illustrations (For primary document see N94-15157 03-25)
Copyright Avail: CASI HC A02/MF A02; ESA, EPD, ESTEC, Noordwijk, Netherlands, HC

N94-15168# Hitachi Ltd., Tokyo (Japan). Research Lab.
PARTIAL MELTING EXPERIMENT OF Y-Ba-Cu OXIDE
Akira Yoshinari, Akira Okayama, H. Kodama, and N. Hamano *In* ESA, Sounding Rocket Experiments in Fluid Science and Materials Sciences: TEXUS 25 to 27 and MASER 4, Volume 3 Feb. 1993 p 100-109 (For primary document see N94-15157 03-25)
Copyright Avail: CASI HC A02/MF A02; ESA, EPD, ESTEC, Noordwijk, Netherlands, HC

N94-15169# Maschinenfabrik Augsburg-Nuernberg A.G., Munich (Germany). Centre de Geophysique Interne.
REMELTING OF Fe-C-Si-ALLOY IN A CERAMIC MOLD SKIN
W. Amende, P. Harmathy, and G. Vael *In* ESA, Sounding Rocket Experiments in Fluid Science and Materials Sciences: TEXUS 25 to 27 and MASER 4, Volume 3 Feb. 1993 p 110-119 Sponsored by BMFT (For primary document see N94-15157 03-25)
Copyright Avail: CASI HC A02/MF A02; ESA, EPD, ESTEC, Noordwijk, Netherlands, HC

N94-15170# Hamburg Univ. (Germany).
SEPARATION BEHAVIOUR OF MONOTECTIC ALLOYS
H. Ahlborn and K. Loehberg (Technische Univ., Berlin, Germany.) *In* ESA, Sounding Rocket Experiments in Fluid Science and Materials Sciences: TEXUS 25 to 27 and MASER 4, Volume 3 Feb. 1993 p 120-124 (For primary document see N94-15157 03-25)
Copyright Avail: CASI HC A01/MF A02; ESA, EPD, ESTEC, Noordwijk, Netherlands, HC

N94-15171# Royal Inst. of Tech., Stockholm (Sweden). Dept. of Casting Metals.
LIQUID PHASE SINTERING OF TUNGSTEN COMPOSITES UNDER MICROGRAVITY. EFFECT OF MATRIX COMPOSITION
L. B. Ekbom and A. Eliasson *In* ESA, Sounding Rocket Experiments in Fluid Science and Materials Sciences: TEXUS 25 to 27 and MASER 4, Volume 3 Feb. 1993 p 126-134 Sponsored in part by Swedish Board for Space Activities (For primary document see N94-15157 03-25)
Copyright Avail: CASI HC A02/MF A02; ESA, EPD, ESTEC, Noordwijk, Netherlands, HC

N94-16133# Alabama Univ., Huntsville.
MATERIALS PROCESSING IN SPACE: ISSUES FOR THE THIRD DECADE
Robert J. Naumann *In* Huntsville Association of Technical Societies, TABES 1993: 9th Annual Technical and Business Exhibition and Symposium 1993 17 p (For primary document see N94-16129 03-38)
(TABES Paper 93-260) Avail: CASI HC A03/MF A03

31 ENGINEERING (GENERAL)

Includes vacuum technology; control engineering; display engineering; cryogenics; and fire prevention.

N94-15177# Army Engineer Waterways Experiment Station, Vicksburg, MS. Geotechnical Lab.
USER'S GUIDE: HOT-MIX RECYCLING OF ASPHALT CONCRETE PAVEMENTS Final Report
James E. Shoenberger May 1993 44 p
(AD-A266939; WES/MP/GL-93-5; FEAP-UG-92/12) Avail: CASI HC A03/MF A01

This guide provides the technical information required to implement the application of hot-mix recycling of asphalt concrete pavements. Included are details on application, benefits/advantages, limitations/disadvantages, and costs associated with this technology. Information is provided on three demonstration sites at Fort Gillem, Georgia; Fort Leavenworth, Kansas; and Fort Benjamin Harrison, Indiana. Also provided is information concerning funding, procurement, maintenance, and performance monitoring. A fact sheet on recycling, contract specification example, and references are provided in the appendices. DTIC

N94-15519* National Aeronautics and Space Administration, Washington, DC.
BUILDING A LUNAR BASE (Videotape)
Jun. 1986 Videotape: 4 min. 8 sec. playing time, in color, with sound
(NASA-TM-109674; NONP-VT-93-190472) Avail: CASI VHS A01/BETA A22

This video looks at the testing of lunar materials as a possible building material for lunar bases. CASI

N94-15676# Army Cold Regions Research and Engineering Lab., Hanover, NH.
MATHEMATICAL MODEL OF FROST HEAVE AND THAW SETTLEMENT IN PAVEMENTS
Gary L. Guymon, Richard L. Berg, and Theodore V. Hromadka Apr. 1993 135 p
(AD-A267037; CREEL-93-2) Avail: CASI HC A07/MF A02

Since 1975 the U.S. Army Corps of Engineers, the Federal Highway Administration and the Federal Aviation Administration have been working cooperatively to develop a mathematical model to estimate frost heave and thaw weakening under various environmental conditions and for various pavement designs. A model has been developed. It is a one-dimensional representation of vertical heat and moisture flux. It is based on a numerical solution technique termed the nodal domain integration method, and it estimates frost heave and frost penetration reasonably well for a variety of situations. The model is now ready for additional field evaluation and implementation in appropriate cases. The main objectives of this report are: (1) to describe the model, FROST, including modeling uncertainties and errors; (2) to summarize recent comparisons between measured and computed values for frost heave and frost penetration; and (3) to describe parameters necessary for input into the model. DTIC

N94-15881*# National Aeronautics and Space Administration. Langley Research Center, Hampton, VA.
NONAQUEOUS SLIP CASTING OF HIGH TEMPERATURE CERAMIC SUPERCONDUCTORS USING AN INVESTMENT CASTING TECHNIQUE Patent Application
Matthew W. Hooker, inventor (to NASA) (Clemson Univ., SC.), Theodore D. Taylor, inventor (to NASA) (Clemson Univ., SC.), Stephanie A. Wise, inventor (to NASA), John D. Buckley, inventor (to NASA), Peter Vasquez, inventor (to NASA), Gregory M. Buck, inventor (to NASA), and Lana P. Hicks, inventor (to NASA) 16 Aug. 1993 9 p
(NASA-Case-LAR-14918-1; NAS 1.71:LAR-14918-1;
US-Patent-Appl-SN-096498) Avail: CASI HC A02/MF A01

A process for slip casting ceramic articles that does not employ parting agents and affords the casting of complete, detailed, precision articles that do not possess parting lines is presented. This process is especially useful for high temperature superconductors and water-sensitive ceramics. A wax pattern for a shell mold is provided, and an aqueous mixture of a calcium sulfate-bonded investment material is applied as a coating to the wax pattern. The coated wax pattern is then dried, followed

by curing to vaporize the wax pattern and leave a shell mold of the calcium sulfate-bonded investment material. The shell mold is cooled to room temperature, and a ceramic slip, created by dispersing a ceramic powder in an organic liquid, is poured therein. After a ceramic shell of desired thickness or a solid article has set up in the shell mold, excess ceramic slip is poured out. The shell mold is misted with water and peeled away from the ceramic article, after which the ceramic is fired to provide a complete, detailed, precision, high temperature superconductive ceramic article without parting lines. The casting technique may take place in the presence of a magnetic field to orient the ceramic powders during the casting process. NASA

N94-16000# Krupp (Fried.) G.m.b.H., Essen (Germany).
KRUPP TECHNICAL REPORTS NO. 2, ENGLISH EDITION, OCTOBER 1992 [TECHNISCHE MITTEILUNGEN KRUPP NO. 2, ENGLISH EDITION, OCTOBER 1992]
Oct. 1992 44 p In GERMAN
(ETN-93-94631) Copyright Avail: CASI HC A03/MF A01

The focal activities of the research and development establishment and its alignment in the innovation strategy are described. The use of vacuum plasma spraying as a method of coating materials to protect them against wear is discussed. An expert system developed for solving welding engineering problems is described. New possibilities offered by worldwide data transmission networks, which are being used for the remote diagnosis of mechanized parking systems, are discussed. RELMA (Remote Laser Microanalysis), which makes online quality control in the rubber industry, is introduced. In RELMA, a focused laser beam raster scans rubber slabs and reveals the material's element concentrations in fractions of a second. For individual titles, see N94-16001 through N94-16005.

N94-16001# Krupp (Fried.) G.m.b.H., Essen (Germany).
RESEARCH AND DEVELOPMENT: ENGINE OF INNOVATION AT KRUPP **c81**
Diethard Bergers *In its* Krupp Technical Reports No. 2, English Edition, October 1992 Oct. 1992 p 63-68 (For primary document see N94-16000 03-31)
Copyright Avail: CASI HC A02/MF A01

The focal activities of the research establishment and its alignment in the innovation strategy of the Krupp Group are described. Research and development plays a key role in the constant process of product and production renewal. Technological and market influences must interact in the innovation process in such a way that market needs, with ever shorter product life cycles, can be met. Factors leading to innovative success are discussed. These include: a comprehensive organizational concept to ensure smooth translation of Research and Development (R and D) work into products and processes; the continual reassessment of technical and economic risks; and the interplay of strategic planning control, marketing and technology. The organization of the centralized R and D, as undertaken at Krupp, which represents a powerful strategic element in the development and exploitation of technological synergies is discussed. The specialist capability at Krupp is said to embrace the following key technology categories: information technology and automation; mechanical engineering and process technology; and materials and components. ESA

N94-16002# Krupp (Fried.) G.m.b.H., Essen (Germany).
VACUUM PLASMA SPRAYING **c27**
Friederike Deuerler, Juergen Peterseim, Juergen Willbrand, and Wolfgang Schlump *In its* Krupp Technical Reports No. 2, English Edition, October 1992 Oct. 1992 p 69-74 (For primary document see N94-16000 03-31)
Copyright Avail: CASI HC A02/MF A01

The use of Vacuum Plasma Spraying (VPS) as a method of coating materials to protect them against wear is discussed. Vacuum plasma spraying offers a range of interesting applications which have yet to be fully exploited. Apart from conventional applications, such as wear and corrosion protection in the form of high density coatings with good bonding properties, vacuum plasma spraying can also be used to manufacture complex components with graded structures. The plasma jet can also be used for materal synthesis, for example, for producing pure diamond coatings from gaseous carbon carriers. ESA

N94-16003# Krupp (Fried.) G.m.b.H., Essen (Germany).
EXPERT SYSTEM FOR WELDING ENGINEERING **c37**
Bernd Fehsenfeld, Robert Relinghaus, and Friedhelm Troesken *In its* Krupp Technical Reports No. 2, English Edition, October 1992 Oct. 1992 p 75-84 (For primary document see N94-16000 03-31)
Copyright Avail: CASI HC A02/MF A01

The expert system developed for solving welding engineering problems, which frees welding engineers from routine tasks and enables them to concentrate on more specialized problems, is described. The objectives, development, structure, function, deployment, maintenance and benefits of this expert system are addressed. ESA

N94-16004# Krupp (Fried.) G.m.b.H., Essen (Germany).
REMOTE DIAGNOSIS AS USED FOR MECHANIZED PARKING SYSTEMS **c37**
Heinz Humberg, Hans Friedrich Maeder, and Frank Will *In its* Krupp Technical Reports No. 2, English Edition, October 1992 Oct. 1992 p 85-96 (For primary document see N94-16000 03-31)
Copyright Avail: CASI HC A03/MF A01

The new possibilities offered by worldwide data transmission networks, which are being used for the remote diagnosis of mechanized parking systems are discussed. This has led to a reduction in service costs for systems installed in Asia and elsewhere. The principles of the mechanized multistorey car park and their control concept are described. The parking facilities are fully geared up for remote diagnosis, the key functions of which are: data collection, data storage, data transmission, and data evaluation. The reports transmitted from the parking facility are analyzed using an evaluation system. The objectives are to detect impending component failures and to quickly identify the causes of irregularities which have occurred. The evaluation system can be easily adapted for other applications. ESA

N94-16005# Krupp (Fried.) G.m.b.H., Essen (Germany).
RELMA: ON-LINE QUALITY CONTROL IN THE RUBBER MIXING ROOM USING LASER ANALYSIS **c38**
Walter Haeder and Claus-Juergen Lorenzen *In its* Krupp Technical Reports No. 2, English Edition, October 1992 Oct. 1992 p 97-102 (For primary document see N94-16000 03-31)
Copyright Avail: CASI HC A02/MF A01

RELMA (Remote Laser Microanalysis), which makes online quality control in the rubber industry possible for the first time, is introduced. A focused laser beam raster scans rubber slabs and reveals the material's element concentrations in fractions of a second. The laser analysis method is described, and the optimal quality control requirements (on-line testing, composition testing, homogeneity testing and automatic measurement) are considered. The status of mixing room quality control and the determination of the homogeneity of rubber slabs are discussed. ESA

N94-16981# Industrial Technology Inst., Ann Arbor, MI.
INTEGRATION TOOLKIT AND METHODS (ITKM) MANUFACTURING METHODS AND PROTOTYPE TOOLKIT. A COMBINED MODELING METHOD USING IDEFO, IDEF1x AND XSpec Final Report, Jun. 1991 - Jun. 1992
Jul. 1992 52 p
(Contract F33615-91-C-5725)
(AD-A266176; ITI-CR-92-57A; WL-TR-93-8019) Avail: CASI HC A04/MF A01

This report develops the major theoretical concepts for the integration of three diverse engineering modeling languages: IDEFO, IDEFIx, and XSpec. IDEFO is a high level modeling tool based on functional decompositions, IDEFIx is a detailed data modeling tool, and XSpec is a simulation tool based on object-oriented decompositions. The approach used to integrate the tools is to develop a meta-model of the three modeling languages. These meta-models are examined, and a single combined meta-model is developed. All three systems use the same combined meta-model. This ensures that any changes to the system made in one language is reflected in the other languages automatically. A short description of each of the languages is given. These are not intended to be exhaustive, they are provided so that the reader is familiar with the terminology used in each of the methods and to get a feel of the types of models each language produces. The meta-models of IDEFO and XSpec are given. The approach

used to develop the combined meta-model is given. Finally, a complete description of the meta-model is presented. DTIC

N94-17068# Polish Academy of Sciences, Warsaw. Inst. Podstawowych Problemow Techniki.

A MEASUREMENT STATION FOR STUDY OF EARTH MOVING TOOLS AND GROUND CUTTING PROCESSES [STANOWISKO POMIAROWE BADANIA NARZEDZI DO ROBOT ZIEMNYCH I PROCESOW SKRAWANIA GRUNTU]

Wieslw Trampczynski, Leszek Pionecki, Julian Cendrowicz, and Dionizy Szyba 1991 65 p In POLISH

(IFTR-10/1991) Avail: CASI HC A04/MF A01

The construction and operation of a measurement station to study processes of cutting soils is discussed. It is comprised of three independent sections: simulation studies mainly of motion kinetics environment during the cutting process; studies on a semitechnical scale of both the forces acting on the tools and the kinematics of the process; and studies of the kinematics and dynamics of fittings of a hydraulic excavator with particular attention to tool/environment interaction. In the last two sections, a hydraulic drive was used with complete computer control in a closed system. The computer system also permitted collecting and processing experimental data. Transl. by FLS

N94-17482 Phillips Lab., Kirtland AFB, NM.

PROCEEDINGS OF THE 7TH INTERNATIONAL CRYOCOOLER CONFERENCE, PART 1 Final Report

Apr. 1993 320 p Conference held in Sante Fe, NM, 17-19 Nov. 1992 Limited Reproducibility: More than 20% of this document may be affected by microfiche quality

(AF Proj. 1105)

(AD-A268448; AD-E201515; PL-CP-93-1001-Pt-1) Avail: Issuing Activity (Defense Technical Information Center (DTIC))

Partial contents include: SDIO and Air Force Cryocooler Technology Developments at USAF Phillips Laboratory; JPL Cryocooler Development and Test Program Overview; Development and Demonstration of a Diaphragm Stirling 65 K Standard Spacecraft Cryocooler; Stirling Space Cooler; Thermal, Vibration, and Reliability Test Results for a Balanced 80 K Cryocooler; Spacecraft Cooler Characterization; Performance of a Long Life Reverse Brayton Cryocooler; SDI Cryocooler Producibility Program; Miniature Pulse Tube Cooler; Flow Patterns Intrinsic to the Pulse Tube Refrigerator; Experimental Investigation of the Regenerative Magnetic Refrigerator Operating Between 4.2 K and 1.8 K; A 4 K Gifford-McMahon Refrigerator for Radio Astronomy; A Stirling Cycle Cryocooler for 4 K Applications; Regenerator Performance and Refrigeration Mechanism for 4 K GM Refrigerator Using Rare Earth Compound Regenerator Materials; Superfluid Stirling Refrigerator with a Counterflow Regenerator; Graded and Nongraded Regenerator Performance; Evolution of the 10 K Periodic Sorption Refrigerator Concept; Development of a Periodic 10 K Sorption Cryocooler; Assessment of a Hydrogen Joule-Thomson Expander and Vanadium Hydride Sorption Beds for 20 K Cryocoolers; Design of a Metal Hydride Sorption Cryocooler System; Linear Compressor for JT Cryocooler; JT Cryostat with Liquid-Solid Cryogen Reservoir; Design of A Metal Hydride Sorption Cryocooler System; Linear Compressor for JT Cooler; Phase Equilibria in Cryogenic Mixtures. DTIC

N94-17484 Phillips Lab., Kirtland AFB, NM.

PROCEEDINGS OF THE 7TH INTERNATIONAL CRYOCOOLER CONFERENCE, PART 2 Final Report

Apr. 1993 306 p Conference held in Sante Fe, NM, 17-19 Nov. 1992 Limited Reproducibility: More than 20% of this document may be affected by microfiche quality

(AF Proj. 1105)

(AD-A268449; AD-E201517; PL-CP-93-1001-Pt-2) Avail: Issuing Activity (Defense Technical Information Center (DTIC))

Partial contents include: SDIO and Air Force Cryocooler Technology Developments at USAF Phillips Laboratory; JPL Cryocooler Development and Test Program Overview; Development and Demonstration of a Diaphragm Stirling 65 K Standard Spacecraft Cryocooler; Stirling Space Cooler; Thermal, Vibration, and Reliability Test Results for a Balanced 80 K Cryocooler; Spacecraft Cooler Characterization; Performance of a Long Life Reverse Brayton Cryocooler; SDI Cryocooler Producibility Program; Miniature Pulse Tube Cooler; Flow Patterns Intrinsic to the Pulse Tube Refrigerator; Experimental Investigation of the Regenerative Magnetic Refrigerator Operating Between 4.2 K and 1.8 K; A 4 K Gifford-McMahon Refrigerator for Radio Astronomy; A Stirling Cycle Cryocooler for 4 K Applications; Regenerator Performance and Refrigeration Mechanism for 4 K GM Refrigerator Using Rare Earth Compound Regenerator Materials; Superfluid Stirling Refrigerator with a Counterflow Regenerator; Graded and Nongraded Regenerator Performance; Evolution of the 10 K Periodic Sorption Refrigerator Concept; Development of a Periodic 10 K Sorption Cryocooler; Assessment of a Hydrogen Joule-Thomson Expander and Vanadium Hydride Sorption Beds for 20 K Cryocoolers; Design of a Metal Hydride Sorption Cryocooler System; Linear Compressor for JT Cryocooler; JT Cryostat with Liquid-Solid Cryogen Reservoir; Design of A Metal Hydride Sorption Cryocooler System; Linear Compressor for JT Cooler; Phase Equilibria in Cryogenic Mixtures. DTIC

N94-17485 Phillips Lab., Kirtland AFB, NM.

PROCEEDINGS OF THE 7TH INTERNATIONAL CRYOCOOLER CONFERENCE, PART 3 Final Report

Apr. 1993 342 p Conference held in Sante Fe, NM, 17-19 Nov. 1992 Limited Reproducibility: More than 20% of this document may be affected by microfiche quality

(AF Proj. 1105)

(AD-A268450; AD-E201518; PL-CP-93-1001-Pt-3) Avail: Issuing Activity (Defense Technical Information Center (DTIC))

Partial contents include: SDIO and Air Force Cryocooler Technology Developments at USAF Phillips Laboratory; JPL Cryocooler Development and Test Program Overview; Development and Demonstration of a Diaphragm Stirling 65 K Standard Spacecraft Cryocooler; Stirling Space Cooler; Thermal, Vibration, and Reliability Test Results for a Balanced 80 K Cryocooler; Spacecraft Cooler Characterization; Performance of a Long Life Reverse Brayton Cryocooler; SDI Cryocooler Producibility Program; Miniature Pulse Tube Cooler; Flow Patterns Intrinsic to the Pulse Tube Refrigerator; Experimental Investigation of the Regenerative Magnetic Refrigerator Operating Between 4.2 K and 1.8 K; A 4 K Gifford-McMahon Refrigerator for Radio Astronomy; A Stirling Cycle Cryocooler for 4 K Applications; Regenerator Performance and Refrigeration Mechanism for 4 K GM Refrigerator Using Rare Earth Compound Regenerator Materials; Superfluid Stirling Refrigerator with a Counterflow Regenerator; Graded and Nongraded Regenerator Performance; Evolution of the 10 K Periodic Sorption Refrigerator Concept; Development of a Periodic 10 K Sorption Cryocooler; Assessment of a Hydrogen Joule-Thomson Expander and Vanadium Hydride Sorption Beds for 20 K Cryocoolers; Design of a Metal Hydride Sorption Cryocooler System; Linear Compressor for JT Cryocooler; JT Cryostat with Liquid-Solid Cryogen Reservoir; Design of A Metal Hydride Sorption Cryocooler System; Linear Compressor for JT Cooler; Phase Equilibria in Cryogenic Mixtures. DTIC

N94-17544# Technical Research Centre of Finland, Espoo. Production Engineering Lab.

DRY STRIPPING AS A SURFACE TREATMENT METHOD [MUOVIRAEPUHALLUS PINNANKAESITTELYMENETELMAENAE]

Ilkka Nieminen Mar. 1992 72 p In FINNISH Sponsored by Finnish Industry, and Technical Research Centre of Finland, Espoo

(VTT-TIED-1348; ISBN-9-51-384161-8; ETN-94474) Copyright Avail: CASI HC A04/MF A01

High environmental and safety standards as well as use of new paint and substrate materials have created the need for developing stripping methods to substitute chemical and mechanical methods and on the other hand for expanding the applicability of blasting as a surface treatment. Plastic Media Blasting (PMB) (alternatively Dry Stripping System (DSS)) is an emerging technology first used in aircraft maintenance for paint stripping. Traditionally this task is performed by brushing and grinding or by using chemical solvents. With plastic media it is possible to remove thick paints with high adhesion without damaging the substrate and even layer by layer. If suitable type of plastic media, blasting pressure low enough, media concentration high enough and on the other right blasting time, blasting distance and blasting angle are chosen, the effectiveness of PMB can be varied to a large extent. In regard to the hardness of media plastic particles are situated between some organic materials and shots used in sand blasting. Therefore composite materials can be treated without damaging the substrate or thin metal plates without causing any deformations. The principle of plastic media blasting equipment is similar to traditional blasting

equipment. Nevertheless the properties of plastic media are different to harder particles used in shot peening resulting in higher demands for filtration, ventilation and recycling systems. In addition the facilities have to contain proper recovery equipment, because plastic media can be reused, even 20 times. In recycling systems plastic media is cleaned, too large and too small particles are removed, hard and magnetic particles are removed from reusable media and dust is separated from media. In addition to paint stripping PMB can successfully be used for cleaning of surfaces from contamination and to some extent for polishing, grinding and roughening. Paint stripping has been the main application so far, but there may be many other possibilities to apply the method in the future. However the PMB is not the only new technology for stripping problems. Some interesting investigations were performed for using frozen carbon dioxide, soda or high pressure water jet for paint stripping. ESA

32 COMMUNICATIONS AND RADAR

Includes radar; land and global communications; communications theory; and optical communications.

For related information see also *04 Aircraft Communications and Navigation* and *17 Space Communications, Spacecraft Communications, Command and Tracking.* For search and rescue see *03 Air Transportation and Safety,* and *16 Space Transportation.*

N94-14912# Picotronix, Inc., Ann Arbor, MI.
A NOVEL SOLID-STATE OPTICAL TEMPORAL ANALYZER WITH PICOSECOND RESOLUTION AND PICOWATT SENSITIVITY Final Report, 1 Jul. 1992 - 1 Apr. 1993
Steven Williamson 30 Apr. 1993 29 p
(Contract DAAL03-92-C-0035)
(AD-A266804; ARO-30499.1-EL-SBI) Avail: CASI HC A03/MF A01

The goal of this Phase I SBIR program was to demonstrate the feasibility and characterize a novel picosecond optical temporal analyzer based on a new 1-ps resolution photodetector. The detector/analyzer system integrates the photodetector on the same chip with a similar laser activated sampling gate. The sensor is called a Sampling Optical Temporal Analyzer, or SOTA. We have fabricated and tested this device to determine its ultimate speed, sensitivity, and dynamic range. The SOTA's system response was found to be 1.4 ps with a sensitivity of 100 pW. This is the world's fastest, most compact, ultrasensitive, picosecond optical waveform analyzer. It is completely solid-state and has a measured dynamic range of 80 dB. The potential of this technology for dual-use applications is extensive, reaching into the medical, scientific, optical communications, and automotive industries. The speed, sensitivity, and dynamic range of the SOTA, coupled with its ability to be mass produced using conventional microfabrication, offers us a unique opportunity to develop a new and greatly advanced high speed optoelectronic sensor technology. DTIC

N94-14955# Columbia Univ., New York, NY. Dept. of Electrical Engineering.
MULTICHIP MODULE HIGH SPEED TESTING Quarterly Report, 1 Apr. - 30 Jun. 1993
Robert J. Davis and David H. Auston 30 Jun. 1993 3 p
(Contract N00014-91-J-4045)
(AD-A266968) Avail: CASI HC A01/MF A01

Progress in the testing of multichip module electronic circuit packages for the period April 1, 1993 - June 30, 1993 is described below, in the areas of the testing of multichip modules using electrooptic polymers, the testing of high-speed transmission line structures, and the microfabrication of fiber optic test probes. DTIC

N94-14974 Naval Postgraduate School, Monterey, CA.
ANTENNA GAIN LOSS AND PATTERN DEGRADATION DUE TO TRANSMISSION THROUGH DIELECTRIC RADOMES M.S. Thesis
Karl A. Klopp Mar. 1993 122 p Limited Reproducibility: More than 20% of this document may be affected by microfiche quality
(AD-A267242) Avail: CASI HC A06

A computer model for axially symmetric dielectric radomes in the near field of a circular aperture has been developed. This model, based on a method of moments solution for bodies of revolution, is used to determine the electric field pattern of a linearly polarized circular aperture radiation through a dielectric radome. The program is written in FORTRAN and can accommodate rotationally symmetric radome shapes. Arbitrary illumination distributions for the aperture can be specified, and phased scanning of the aperture in both azimuth and elevation is allowed. Computational run time has been reduced by taking advantage of mode symmetry, A separate program has been developed to compute gain, and together these programs are used to determine the pattern degradation and gain loss due to the presence of a radome in the near field. DTIC

N94-14998# Rome Lab., Hanscom AFB, MA.
PROCEEDINGS OF THE 1992 ANTENNA APPLICATIONS SYMPOSIUM, VOLUME 2
Paul Mayes Jun. 1993 316 p Symposium held in Hanscom AFB, MA, 23-25 Sep. 1992
(AD-A266916; RL-TR-93-119-Vol-2) Avail: CASI HC A14/MF A03

The Proceedings of the 1992 Antenna Applications Symposium is a collection of state-of-the-art papers relating to phased array antennas, multibeam antennas, satellite antennas, microstrip antennas, reflector antennas, HF, VHF, UHF and various other antennas. DTIC

N94-15020 National Physical Lab., Teddington (England). Div. of Electrical Science.
AN OPTICALLY MODULATED SCATTERER FOR MICROWAVE ANTENNA METROLOGY
Graham Hygate May 1993 135 p
(NPL-DES-126; ETN-93-94553) Copyright Avail: Issuing Activity
(National Physical Lab., Teddington, Middlesex TW11 OLW, England)

An optically modulated dipole scatterer was developed to be used monostatically to measure microwave frequency electric field distributions. The same probe may be used over an entire waveguide band (for example, 8.5 to 12.0 GHz) and a single detection apparatus was constructed to cover the frequency range 2 to 18 GHz. The technique is particularly well suited to measuring the electric field close to conductors, where conventional techniques fail. Near field antenna measurements require exactly this capability, and the technique was used successfully to obtain the far field radiation patterns of a horn antenna by near field measurement and transformation. The chief advantages of the optically modulated scatterer over conventional methods of near field scanning are minimal perturbation of the field by the probe and the lack of any systematic phase error due to flexing of cables during the near field scan. ESA

N94-15140*# National Aeronautics and Space Administration. Langley Research Center, Hampton, VA.
WINDSHEAR RADAR CALIBRATION, 1992 FLIGHTS: TRANSMITTER POWER AND RECEIVER GAIN STABILITY
Anne I. Mackenzie Aug. 1993 10 p
(RTOP 505-64-12-02)
(NASA-TM-108997; NAS 1.15:108997) Avail: CASI HC A02/MF A01

During the 1992 NASA airborne Doppler windshear radar flights, radar calibrations were performed prior to each flight in order to determine transmitter power, receiver gain, and receiver noise power. The calibration results show that the average transmitter power in radar mode 6 was 186 watts, with a standard deviation of 7 watts. The average high power amplifier gain was 9.62 dB. At the wide IF bandwidth setting, the receiver gain was 123.1 dB, while at the narrow IF bandwidth setting, the gain was 121.8 dB. The receiver system noise as seen at the receiver input was -107.0 dBmw using the wide IF bandwidth and -107.9 dBmw using the narrow IF bandwidth. In radar mode 7, the receiver gain was the same as in mode 6. However, the receiver noise in mode 7 was about 2.5 dB less using the wide IF bandwidth and 2.0 dB less using the narrow IF bandwidth. The R/T unit flown in 1992 had also been flown the previous year when it produced comparable results. This technical memorandum was written as a follow-up to NASA TM-107589 (June 1992), which describes similar radar calibrations performed during the 1991 windshear radar flight experiments. Author

N94-15155# Deutsche Forschungsanstalt fuer Luft- und Raumfahrt, Oberpfaffenhofen (Germany). Abt. Hochfrequenztechnik.
DIFFRACTION OF MICROWAVES AT RECTANGULAR FACADES OF BUILDINGS WITH AND WITHOUT GROUND REFLECTIONS (FRESNEL-KIRCHHOFF-APPROXIMATION) [BEUGUNG VON MIKROWELLEN AN RECHTECKIGEN GEBAEUDEFRONTEN MIT UND OHNE BERUECKSICHTIGUNG VON BODENREFLEXIONEN (FRESNEL-KIRCHHOFF-NAEHERUNG)]
Michael Kleintz 14 Nov. 1992 99 p In GERMAN Original contains color illustrations
(DLR-FB-92-35; ETN-93-94620) Avail: CASI HC A05/MF A02

Multipath propagation of an airport secondary radar is analyzed by means of a theoretical model for reflection and diffraction. A lossy dielectric rectangular plate placed perpendicular to the flat ground was chosen for modeling a reflecting building facade. Diffraction diagram was calculated with the Fresnel-Kirchhoff approximation. The geometry factor of the reflection plane was calculated with a second order Taylor development around the virtual mirror reflection point, so that two Fresnel integrals with simple coefficients were obtained. The following possible ground reflections were discussed: reflection of the electromagnetic wave on the ground only, single reflection at the building face, and double reflection at ground and building facade. Interference of direct and ground reflected fields, reflection and diffraction from an isolated rectangular plate (azimuth and elevation diagrams) and influence of reflections from a flat surrounding ground were calculated. ESA

N94-15292* National Aeronautics and Space Administration. Goddard Space Flight Center, Greenbelt, MD.
COBE VIDEO NEWS (Videotape)
Oct. 1989 Videotape: 3 min. 46 sec. playing time, in color, with sound
(NASA-TM-109598; NONP-VT-93-190396) Avail: CASI VHS A01/BETA A22

This videotape was produced for hand-out to both local and national broadcast media as a prelude to the launch of the Cosmic Background Explorer. The tape consists of short clips with multi-channel sound to facilitate news media editing. CASI

N94-15439# Mitre Corp., McLean, VA.
THE NEXT GENERATION WEATHER RADAR (NEXRAD)/AIR ROUTE SURVEILLANCE RADAR (ARSR) OPERATIONAL COMPARISON Final Report
Brian Dunbar and Jeff Mittelman Jul. 1993 99 p Original contains color illustrations
(Contract DTFA01-93-C-00001)
(Rept-93W0000145; DOT/FAA/SE-93/4) Avail: CASI HC A05/MF A02

The National Weather Service (NWS), Federal Aviation Administration (FAA), and Department of Defense are in the process of fielding the Next Generation Weather Radars (NEXRAD). These doppler weather radars, also known as Weather Surveillance Radar (WSR)-88D, will be replacing the WSR-57 and WSR-74 weather radars in use today. The NEXRAD data will be used by the FAA's Advanced Automation System (AAS) in place of the Air Route Surveillance Radar (ARSR) weather data currently being used by air traffic controllers. Because the NEXRAD's scanning strategy is more time consuming than the ARSR's, there have been some concerns expressed within the FAA about using 'untimely' NEXRAD data in an Air Traffic Control (ATC) environment. In response to these concerns, the FAA's Center for Advanced Aviation System Development (CAASD) at MITRE conducted a study, under the sponsorship of the FAA's National Airspace System (NAS) System Engineering Service (ASE), to assess the relative ability of NEXRAD's and ARSR's to detect and present significant weather in order to determine the operational impact of using NEXRAD data in lieu of ARSR data. The NEXRAD/ARSR operational comparison study is documented. Author (revised)

N94-15527# Mitre Corp., Bedford, MA.
JOHNSON-GIERHART PROGRAM PREDICTIONS OF EXCESS PROPAGATION LOSS FOR SUPER-HIGH FREQUENCY AIR-TO-GROUND PATHS. VOLUME 2: APPENDICES Final Report
Melvin M. Weiner and John C. Herther Jun. 1993 223 p
(Contract F19628-89-C-0001)
(AD-A267021; MTR-92B0000027V2; ESC-TR-93-161-Vol-2) Avail: CASI HC A10/MF A03

The Johnson-Gierhart tropospheric propagation program of the Institute for Telecommunications Sciences is used to obtain predictions of excess propagation loss over that of free space for super-high frequency (SHF) air-to-ground paths within or on the radio horizon. The principal loss (gain) mechanisms considered are atmospheric absorption and refraction, surface multipath interference, smooth spherical Earth diffraction, and single knife-edge diffraction caused by terrain roughness and/or a site-specified obstacle. The program uses a semi-empirical database to statistically weigh the losses from these mechanisms. The excess propagation loss increases with increasing range and can exceed 3 decibels at distances as close as halfway to the radio horizon. DTIC

N94-15540# Naval Research Lab., Washington, DC.
COMPARISON OF RADARC HIGH-FREQUENCY RADAR PERFORMANCE PREDICTION MODEL AND ROTHR AMCHITKA DATA
Benjamin T. Root and James M. Headrick 16 Jul. 1993 62 p
(AD-A267077; NRL/MR/5320-93-7181) Avail: CASI HC A04/MF A01

Data collected with AN/TPS-71 radar has been used to validate the RADARC model. For the first ten days of Jan., Apr., and Jul., noon and midnight, the vertical ionograms, oblique backscatter soundings, radar ground backscatter amplitudes, and noise levels have been compared with Model predictions. The differences between the Model and median ionospheric soundings are small enough to have negligible effect on predictions. The coverage predicted for oblique backscatter soundings agrees well with observed median data except for sporadic E effects which were under-estimated. Medians of observed ground backscatter agree fairly well with predictions. The actual noise that controlled radar performance was the most significant deviation from the model. All nighttime and January day noise was higher than that predicted; and this was due to 'multiplicative' noise. DTIC

N94-15541# Rome Lab., Hanscom AFB, MA.
ADAPTIVE BEAMFORMING WITH IMPERFECT ARRAYS: PATTERN EFFECTS AND THEIR PARTIAL CORRECTION Report, Sep. 1991 - May 1992
Lars E. Pettersson Dec. 1992 106 p
(AD-A267079; RL-TR-92-341) Avail: CASI HC A06/MF A02

The effects of various types of imperfections on the radiation pattern of adaptive antenna arrays, using the Applebaum and Frost algorithms, are investigated. The imperfections considered are nonuniform noise figures in the channels, gain and phase shift error, IQ imbalance, DC offset, finite number of samples when forming the covariance matrix, quantization of the signals, and the weights and saturation of the signals. In particular the effects on the resulting sidelobe level, null depth, and gain are studied, and simulated results and analytical expressions for the expected pattern parameters are given. The effects of some methods to partly correct for the imperfections are also investigated. A method to obtain low sidelobe pattern when using the Frost algorithm is also discussed. DTIC

N94-15544# Naval Command, Control and Ocean Surveillance Center, San Diego, CA.
BROADBAND CONVENTIONAL BEAMFORMING INCORPORATING ADAPTIVE EQUALIZATION Final Report, Jan. - Sep. 1992
Richard C. North Sep. 1992 45 p
(AD-A267090; NRAD-TR-1575) Avail: CASI HC A03/MF A01

This report discusses methods which attempt to coherently recombine the spatially and temporally different multipaths with the direct path to enhance array gain. These methods are based on utilizing a broadband conventional beamformer incorporating adaptive equalization to recombine multipath information. Preliminary results are compared with two well-known narrow-band, purely spatial processing techniques: the Bartlett beamformer; and the minimum variance distortionless response beamformer. While preliminary results are promising, several important research issues are outlined which remain to be addressed. DTIC

N94-15644# European Space Agency, Paris (France).
ECS: NINTH YEAR IN ORBIT
D. W. Baston, P. Button, B. Demelenne, K. R. Derbyshire, P. J. Leggett, H. Meier, W. E. Neumann, E. Tilmans, R. Viddeleer, and Norman Longdon, ed. Jan. 1993 30 p Original contains color illustrations
(ESA-BR-91; ISBN-92-9092-143-9; ETN-93-94408) Copyright Avail: CASI HC A03/MF A01

Experience gained with the European Communications System (ECS) satellites during the ninth year of service in orbit from the beginning of Jul. 1991 to the end of Jun. 1992 is summarized. Appraisals are made of how various individual satellite systems have performed taking into account: thermal control; telemetry, tracking and command; attitude and orbit control and reaction control; and power. Significant events during the reporting period are identified. The accumulated total of channel years of the ECS system at the end of Jun. 1992 was close to 215, considerably in excess of the original Eutelsat requirement upon ESA to provide a minimum of 180 channel years. In the reporting period, the ECS system accumulated a total of 256,447 channel hours, or 29 channel years. Only seven of the total of 22 Spurious Switch Offs (SSO's) interrupted traffic. The total outage time due the SSO's was 29.1 channel minutes. ESA

N94-15649# Mitre Corp., Bedford, MA.
JOHNSON-GIERHART PROGRAM PREDICTIONS OF EXCESS PROPAGATION LOSS FOR SUPER-HIGH FREQUENCY AIR-TO-GROUND PATHS. VOLUME 1: THEORY AND NUMERICAL RESULTS Final Report
M. M. Weiner and J. C. Herther Jun. 1993 141 p
(Contract F19628-89-C-0001)
(AD-A267105; MTR-92B0000027V1; ESC-TR-93-161-Vol-1) Avail: CASI HC A07/MF A02

The Johnson-Gierhart tropospheric propagation program of the Institute for Telecommunications Sciences is used to obtain predictions of excess propagation loss over that of free space for super-high frequency (SHF) air-to-ground paths within or on the radio horizon. The principal loss (gain) mechanisms considered are atmospheric absorption and refraction, surface multipath interference, smooth spherical Earth diffraction, and single knife-edge diffraction caused by terrain roughness and/or a site-specified obstacle. The program uses a semi-empirical database to statistically weigh the losses from these mechanisms. The excess propagation loss increases with increasing range and can exceed 3 decibels-at distances as close as halfway to the radio horizon. DTIC

N94-15667# Dayton Univ., OH. Aerospace Medical Engineering Div.
SYSTEM ARCHITECTURE OF OPTICALLY CONTROLLED PHASED ARRAY RADAR Final Report, Aug. 1991 - Aug. 1992
K. Y. Lau May 1993 50 p
(Contract F30602-91-C-0057)
(AD-A267056; RL-TR-93-56) Avail: CASI HC A03/MF A01

The purpose of this effort is a study and analysis of architectural issues in Optically Controlled Phased Array Radar Systems. The effort is based upon progress in high speed, high efficiency, and low noise electro-optic devices and optical interconnection techniques. The aim is to provide real time delay control signals for scanning of the radar beam over wide ranges of frequencies and to simplify the hardware and power consumption at the antenna site. DTIC

N94-15668# Logicon R and D Associates, Los Angeles, CA.
DETERMINATION OF THE ELECTROMAGNETIC FIELDS RADIATED FROM THE ARES EMP SIMULATOR Technical Report, 1 Sep. 1991 - 31 Dec. 1992
Fred M. Tesche and Charles T. Mo 1 Jul. 1993 67 p
(Contract DNA001-88-C-0046)
(AD-A267069; RDA-TR-2-2240-1704-0001; DNA-TR-92-153) Avail: CASI HC A04/MF A01

This report describes a calculational model for evaluating the electromagnetic (EM) fields produced by the ARES simulator outside its normal working volume. The model employs transmission line theory to determine the simulator current distribution. Once this is determined, the radiated fields are computed approximately using the Norton surface-wave formalism. The transient electric and magnetic fields on the ground are calculated using a fast Fourier transform (FFI) and are compared with experimental magnetic field data. Accuracies on the order of 30% in the peak fields are noted in much of the data. The fields in the air above the earth also have been calculated, and the relative importance of the Norton surface wave in the overall solution has been clarified. This model and its resulting PC code provide a useful tool for further studies of the impact of radiated EM fields on distant electrical systems. The results presented here are directly applicable in defining and evaluating the EM environments produced by ARES, or by similar bounded wave simulators, and in assessing and limiting the possible biological effects of pulsed radiation. DTIC

N94-15690# California Univ., Davis. Dept. of Electrical and Computer Engineering.
EXPLOITATION OF CYCLOSTATIONARITY FOR SIGNAL-PARAMETER ESTIMATION AND SYSTEM IDENTIFICATION Semiannual Report, 1 Jan. - 30 Jun. 1993
William A. Gardner 30 Jun. 1993 3 p
(Contract N00014-92-J-1218)
(AD-A267137) Avail: CASI HC A01/MF A01

There are three particularly notable accomplishments during the present reporting period. The first is the development of a substantial generalization of our SCORE algorithm for blind adaptive spatial filtering to the Programmable Canonical Correlation Analyzer (PCCA) which can exploit any of a number of signal properties to distinguish between signals of interest (to be beamformed on) and signals not of interest (to be nulled out). The second is a new algorithm for blind adaptive channel equalization for PAM and digital QAM signals and for either single or multiple channels. The third notable achievement is the completion of the edited volume 'Cyclostationarity in Communications and Signal Processing.' DTIC

N94-15691# Boston Univ., MA.
SEGMENT-BASED ACOUSTIC MODELS FOR CONTINUOUS SPEECH RECOGNITION Progress Report, Apr. - Jun. 1993
Mari Ostendorf and J. R. Rohlicek 8 Jul. 1993 15 p
(Contract N00014-92-J-1778)
(AD-A267138) Avail: CASI HC A03/MF A01

This research aims to develop new and more accurate stochastic models for speaker-independent continuous speech recognition, by extending previous work in segment-based modeling and by introducing a new hierarchical approach to representing intra-utterance statistical dependencies. These techniques, which are more costly than traditional approaches because of the large search space associated with higher order models, are made feasible through rescoring a set of HMM-generated N-best sentence hypotheses. We expect these different modeling techniques to result in improved recognition performance over that achieved by current systems, which handle only frame-based observations and assume that these observations are independent given an underlying state sequence. In the fourth quarter of the project, we have completed the following: (1) ported our recognition system to the Wall Street Journal task, a standard task in the ARPA community; (2) developed an initial dependency-tree model of intra-utterance observation correlation; and (3) implemented baseline language model estimation software. Our initial results on the Wall Street Journal task are quite good and represent significantly improved performance over most HMM systems reporting on the Nov. 1992 5k vocabulary test set. DTIC

N94-15693# Naval Undersea Warfare Center, New London, CT.
OPERATION OF DIGITAL SYSTEMS IN SEVERE ELECTROMAGNETIC ENVIRONMENTS Final Report
K. R. Kowalczyk 11 Jun. 1993 40 p
(AD-A267176; NUWC-NL-TD-10345) Avail: CASI HC A03/MF A01

New digital communication between units is desired in the modernization of a system. Two units of an existing system are linked by circuitry that supplies direct current power, and the connecting wires have been selected for conversion to digital use. This wiring is located within a large bank of alternating current power cables and runs parallel to these cables for several hundred feet. The direct current system realizes no interference from this physical configuration; however, the power wiring radiates electromagnetic fields sufficient to couple noise voltage into a digital system. This project quantifies the effects of high levels of low frequency electromagnetic fields on standard digital communications wiring so that a sufficiently immune circuit configuration can be selected for any applications. A model of the expected electromagnetic environment is presented, and wiretermination voltage measurements are made under varying field and impedance conditions. Standard digital communication design is then examined for compatibility with this environment. DTIC

N94-15698 McMaster Univ., Hamilton (Ontario).
ADAPTIVE INTERFERENCE CANCELLER Patent
S. Haykin, inventor (to Micromedia Ltd.) and A. Ukrainec, inventor (to

Micromedia Ltd.) 24 Nov. 1992 22 p
(CA-Patent-1-310-709; Int-Patent-Class-H03H-17/04; CTN-93-60778)
Copyright Avail: Micromedia Ltd., Technical Information Centre, 165 Hotel de Ville, Place du Portage, Phase 2, Hull, Quebec J8X 3X2, Canada HC

An adaptive signal canceller is provided in which an adaptive filter effectively tracks any varying gain in the like-polar and cross-polar radar signals and compensates in response to the gain, such that in the event of a disturbance in the orthogonal signal channel, such a disturbance will appear in the output even if it does not exceed the like-polar signal in amplitude. Thus, the system of the invention enhances differences between polarizations and reduces effects common to both polarizations. This has a direct application to the enhancement and detection of a target which reflects incident signals from one polarization to another. The adaptive interference canceller includes the following: an adaptive filter with self-adjusting impulse response for filtering the second orthogonal polarized signal and in response generating an adaptive weighted version of the second signal; and circuitry for subtracting the adaptive weighted second signal from the first polarized signal and in response generating an output signal corresponding to the first polarized signal with the interference component cancelled from it. The resulting output has a high target to clutter ratio and therefore an increased probability of detection. The adaptive filter operates on baseband log video signals of the like-polar and cross-polar channels. Author (CISTI)

N94-15714# Norwegian Defence Research Establishment, Kjeller.
HIGHER ORDER STATISTICS IN SIGNAL PROCESSING [BRUK AV HOEYERE ORDENS STATISTIKK I SIGNALBEHANDLING]
Trond Jenserud 10 Nov. 1992 14 p In NORWEGIAN
(FFI-92/2008; ETN-93-94450) Avail: CASI HC A03/MF A01

A new class of signal processing tools was recently developed to the point of practical application. Known as higher order statistics, these tools are beginning to find applicability in many diverse fields; for example sonar, radar biomedicine, seismic data processing, image reconstruction, harmonic retrieval, time delay estimation, adaptive filtering, array processing, and blind equalization. Higher order statistics are useful in problems where either nonGaussianity, nonminimum phase, colored noise, or nonlinearities are important and must be accounted for. An overview of higher order statistics is presented. Some applications where these methods may be of potential value are mentioned. ESA

N94-15748 Columbia Univ., New York, NY.
CONGESTION CONTROL OF HIGH-SPEED NETWORKS Semiannual Report
30 Jun. 1993 5 p Limited Reproducibility: More than 20% of this document may be affected by microfiche quality
(Contract N00014-90-J-1289)
(AD-A267013) Avail: CASI HC A01

We report on four areas of activity in the past six months. These areas include the following: (1) work on the control of integrated video and image traffic, both at the access to a network and within a high-speed network; (2) more general/game theoretic models for flow control in networks; (3) work on fault management for high-speed heterogeneous networks to improve survivability; and (4) work on all-optical (lightwave) networks of the future, designed to take advantage of the enormous bandwidth capability available at optical frequencies. DTIC

N94-15767*# National Aeronautics and Space Administration. Langley Research Center, Hampton, VA.
RESONANT FREQUENCIES OF IRREGULARLY SHAPED MICROSTRIP ANTENNAS USING METHOD OF MOMENTS
Manohar D. Deshpande (Vigyan Research Associates, Inc., Hampton, VA.), David G. Shively, and C. R. Cockrell Washignton Oct. 1993 40 p Sponsored in part by Army Communications Electronic Command, Fort Monmouth, NJ
(RTOP 505-64-70-01)
(NASA-TP-3386; CECOM-TR-93-E-1; L-17160; NAS 1.60:3386) Avail: CASI HC A03/MF A01

This paper describes an application of the method of moments to determine resonant frequencies of irregularly shaped microstrip patches embedded in a grounded dielectric slab. For analysis, the microstrip patch is assumed to be excited by a linearly polarized plane wave that is normal to the patch. The surface-current density that is induced on the patch because of the incident field is expressed in terms of subdomain functions by dividing the patch into identical rectangular subdomains. The amplitudes of the subdomain functions, as a function of frequency, are determined using the electric-field integral equation (EFIE) approach in conjunction with the method of moments. The resonant frequencies of the patch are then obtained by selecting the frequency at which the amplitude of the surface-current density is real. The resonant frequencies of the equilateral triangular and other nonrectangular patches are computed using the present technique, and these frequencies are compared with measurements and other independent calculations. Author

N94-15786# Yale Univ., New Haven, CT. Dept. of Electrical Engineering.
DEVELOPMENT AND ANALYSIS OF ARMA PARAMETER ESTIMATION SCHEMES IN THE PRESENCE OF NOISE Final Report, 1 Feb. 1990 - 31 Jan. 1993
Arye Nehorai Jun. 1993 10 p
(Grant AF-AFOSR-0164-90)
(AD-A267184; AFOSR-93-0514TR) Avail: CASI HC A02/MF A01

This research includes the development and analysis of signal processing estimation algorithms. The main areas of application are sensor array processing for source localization, adaptive signal processing, system identification, and estimation. In the sensor array processing area, we developed algorithms for source localization with decentralized array processing, sensor localization, passive range and bearing estimation, and source localization in multipath and short data applications. We introduced statistical tools that were used to provide compact expressions of the asymptotic variances of source localization algorithms and to obtain, for the first time, concrete analytical performance comparisons. Performance bounds of the Cramer-Rao type were found and used to analyze statistical efficiency. We introduced the use of electromagnetic and acoustic vector sensors for passive source localization and for active target localization and identification. We derived performance bounds and investigated the potential advantages of methods using vector sensors. Simple algorithms for estimating source direction with a vector sensor were proposed along with their statistical performance analysis. In the adaptive signal processing and system identification area we developed algorithms for root factorization and nonlinear filtering. We analyzed the tracking properties of our previously introduced adaptive notch filter for nonstationary signals. DTIC

N94-15886*# Jet Propulsion Lab., California Inst. of Tech., Pasadena.
PROCEEDINGS OF THE THIRD SPACEBORNE IMAGING RADAR SYMPOSIUM
28 May 1993 445 p Symposium held in Pasadena, CA, 18-21 Jan. 1993
(Contract NAS7-918)
(NASA-CR-194104; JPL-Publ-93-16; NAS 1.26:194104) Avail: CASI HC A19/MF A04

This publication contains summaries of the papers presented at the Third Spaceborne Imaging Radar Symposium held at the Jet Propulsion Laboratory (JPL), California Institute of Technology, in Pasadena, California, on 18-21 Jan. 1993. The purpose of the symposium was to present an overview of recent developments in the different scientific and technological fields related to spaceborne imaging radars and to present future international plans. This symposium is the third in a series of 'Spaceborne Imaging Radar' symposia held at JPL. The first symposium was held in Jan. 1983 and the second in 1986. For individual titles, see N94-15887 through N94-15919.

N94-15887*# Jet Propulsion Lab., California Inst. of Tech., Pasadena.
MAGELLAN: PRINCIPAL VENUS SCIENCE FINDINGS **c91**
R. Stephen Saunders *In its* Proceedings of the Third Spaceborne Imaging Radar Symposium 28 May 1993 p 5-7 (For primary document see N94-15886 03-32)
Avail: CASI HC A01/MF A04

This is a brief summary of the science findings of the Magellan mission, principally based on data from the radar system. Future plans for Magellan include acquisition of high resolution gravity data from a nearly circular orbit and atmospheric drag and occultation experiments. The Magellan science results represent the combined effort of more than 100 Magellan investigators and their students and colleagues. More extensive discussions

can be found in the August and October, 1992 issues of the Journal of Geophysical Research, Planets. The Magellan mission's scientific objectives were to provide a global characterization of landforms and tectonic features; to distinguish and understand impact processes; to define and explain erosion, deposition, and chemical processes; and to model the interior density distribution. All but the last objective, which requires new global gravity data, have been accomplished, or we have acquired the data that are required to accomplish them. Author (revised)

N94-15888*# European Space Research Lab., Noordwijk (Netherlands).
ERS-1: 18 MONTHS IN ORBIT **c43**
Jacques Louet *In* JPL, Proceedings of the Third Spaceborne Imaging Radar Symposium 28 May 1993 p 9-51 (For primary document see N94-15886 03-32)
Avail: CASI HC A03/MF A04

Viewgraphs of the ERS-1 mission outline initial objectives, the orbit configuration, the instrumentation, the international cooperation, and the objectives still to be achieved. Graphs of specified performances include orbit control, inclination correction, solar array power, satellite stability, AMI performance verification, SAR radiometric stability, and RA performance stability. Also displayed are the number of planned (for November 92 through February of 93) and acquired SAR frames of the mission for each of the various sites throughout Europe and the world. A map locating these chosen sites is also included. CASI

N94-15889*# Nauchno-Proizvodstvennoe Obedinenie Radio, Moscow (USSR).
ALMAZ **c18**
V. Viter *In* JPL, Proceedings of the Third Spaceborne Imaging Radar Symposium 28 May 1993 p 53-58 (For primary document see N94-15886 03-32)
Avail: CASI HC A02/MF A04

The basic data of the automatic space station ALMAZ-1B is overviewed, including the orbit parameters and maximum power. The principal technical characteristics of its remote sensing equipment is listed for the synthetic aperture and side-looking radar, optoelectronic equipment for stereo-photography, high-resolution electronic scanner, middle-resolution optomechanical scanner, spectroradiometer for ocean satellite monitoring, and information transmission and reception. The main objectives and uses of the ALMAZ-1B information are cartography, land monitoring, geology, ecological monitoring, oceanology, pilotage, fishery, and information supply during an emergency such as controlling situation in natural disasters. CASI

N94-15890*# Jet Propulsion Lab., California Inst. of Tech., Pasadena.
SPACEBORNE IMAGING RADAR-C INSTRUMENT
Bryan L. Huneycutt *In its* Proceedings of the Third Spaceborne Imaging Radar Symposium 28 May 1993 p 61-65 (For primary document see N94-15886 03-32)
Avail: CASI HC A01/MF A04

The Spaceborne Imaging Radar-C is the next radar in the series of spaceborne radar experiments, which began with Seasat and continued with SIR-A and SIR-B. The SIR-C instrument has been designed to obtain simultaneous multifrequency and simultaneous multipolarization radar images from a low earth orbit. It is a multiparameter imaging radar that will be flown during at least two different seasons. The instrument operates in the squint alignment mode, the extended aperture mode, the scansar mode, and the interferometry mode. The instrument uses engineering techniques such as beam nulling for echo tracking, pulse repetition frequency hopping for Doppler centroid tracking, generating the frequency step chirp for radar parameter flexibility, block floating-point quantizing for data rate compression, and elevation beamwidth broadening for increasing the swath illumination. Author

N94-15891*# Deutsche Forschungs- und Versuchsanstalt fuer Luft- und Raumfahrt, Oberpfaffenhofen (Germany). Inst. fuer Hochfrequenztechnik.
X-SAR: THE X-BAND SYNTHETIC APERTURE RADAR ON BOARD THE SPACE SHUTTLE
Marian U. Werner *In* JPL, Proceedings of the Third Spaceborne Imaging Radar Symposium 28 May 1993 p 67-73 (For primary document see N94-15886 03-32)
Avail: CASI HC A02/MF A04

The X-band synthetic aperture radar (X-SAR) is the German/Italian contribution to the NASA/JPL Shuttle Radar Lab missions as part of the preparation for the Earth Observation System (EOS) program. The Shuttle Radar Lab is a combination of several radars: an L-band (1.2 GHz) and a C-band (5.3 GHz) multipolarization SAR known as SIR-C (Shuttle Imaging Radar); and an X-band (9.6 GHz) vertically polarized SAR which will be operated synchronously over the same target areas to deliver calibrated multifrequency and multipolarization SAR data at multiple incidence angles from space. A joint German/Italian project office at DARA (German Space Agency) is responsible for the management of the X-SAR project. The space hardware has been developed and manufactured under industrial contract by Dornier and Alenia Spazio. Besides supporting all the technical and scientific tasks, DLR, in cooperation with ASI (Agencia Spaziale Italiano) is responsible for mission operation, calibration, and high precision SAR processing. In addition, DLR developed an airborne X-band SAR to support the experimenters with campaigns to prepare for the missions. The main advantage of adding a shorter wavelength (3 cm) radar to the SIR-C radars is the X-band radar's weaker penetration into vegetation and soil and its high sensitivity to surface roughness and associated phenomena. The performance of each of the three radars is comparable with respect to radiometric and geometric resolution. Author (revised)

N94-15892*# European Space Research Lab., Noordwijk (Netherlands).
ENVISAT ASAR **c18**
Jacques Louet *In* JPL, Proceedings of the Third Spaceborne Imaging Radar Symposium 28 May 1993 p 75-97 (For primary document see N94-15886 03-32)
Avail: CASI HC A03/MF A04

This document is a series of viewgraphs on the Envisat advanced synthetic aperture radar (ASAR). Viewgraphs cover mission objectives, modes of operation, instrument parameters, a comparison with the European Remote Sensing Satellite (ERS-1) active microwave instrument (AMI), instrument design, transmit/receive module and antenna tile specifications, data rates, swath coverage, and ASAR program schedule. CASI

N94-15893*# Canadian Space Agency, Ottawa (Ontario).
RADARSAT PROGRAM **c18**
J. McNally and S. Parashar *In* JPL, Proceedings of the Third Spaceborne Imaging Radar Symposium 28 May 1993 p 99-117 (For primary document see N94-15886 03-32)
Avail: CASI HC A03/MF A04

Work on the RADARSAT system is progressing towards the currently scheduled launch date of early 1995. The spacecraft bus and the Synthetic Aperture Radar (SAR) payload are at various stages of development. Requirements for the ground segment have been mostly established. The design of the ground elements such as the mission control facility and the SAR data processor is underway. The SAR applications development work is continuing and the chosen distributor, RADARSAT International Inc. (RSI) is making preparations to market RADARSAT data internationally. A plan for the follow-on to RADARSAT 1 is being finalized to ensure continuity of SAR data under the Radarsat program. Author (revised)

N94-15894*# Ministry of Posts and Telecommunications, Tokyo (Japan). Communications Research Lab.
TRMM RADAR
Kenichi Okamoto *In* JPL, Proceedings of the Third Spaceborne Imaging Radar Symposium 28 May 1993 p 119-125 (For primary document see N94-15886 03-32)
Avail: CASI HC A02/MF A04

The results of a conceptual design study and the performance of key components of the Bread Board Model (BBM) of the Tropical Rainfall Measuring Mission (TRMM) radar are presented. The radar, which operates at 13.8 GHz and is designed to meet TRMM mission objectives, has a minimum measurable rain rate of 0.5 mm/h with a range resolution of 250 m, a horizontal resolution of about 4 km, and a swath width of 220 km. A 128-element active phased array system is adopted to achieve contiguous scanning within the swath. The basic characteristics of BBM were confirmed by experiments. The development of EM started with the cooperation of NASDA and CRL. Author (revised)

N94-15895*# National Aeronautics and Space Administration. Goddard Space Flight Center, Greenbelt, MD.
RECENT SCIENTIFIC ADVANCES IN THE USE OF RADAR IN SCIENTIFIC HYDROLOGY **c43**
Edwin T. Engman *In* JPL, Proceedings of the Third Spaceborne Imaging Radar Symposium 28 May 1993 p 129-134 (For primary document see N94-15886 03-32)
Avail: CASI HC A02/MF A04

The data needs in scientific hydrology involve measurements of system states and fluxes. The microwave region is particularly well suited for measuring the system states of soil moisture and snow and the major flux into the earth as rainfall. This paper discusses the unique data needs of hydrology and presents some recent examples from AIRSAR experiments.
Author (revised)

N94-15896*# Oregon State Univ., Corvallis. Coll. of Forestry.
DRIVING TERRESTRIAL ECOSYSTEM MODELS FROM SPACE **c45**
R. H. Waring *In* JPL, Proceedings of the Third Spaceborne Imaging Radar Symposium 28 May 1993 p 135-142 (For primary document see N94-15886 03-32)
Avail: CASI HC A02/MF A04

Regional air pollution, land-use conversion, and projected climate change all affect ecosystem processes at large scales. Changes in vegetation cover and growth dynamics can impact the functioning of ecosystems, carbon fluxes, and climate. As a result, there is a need to assess and monitor vegetation structure and function comprehensively at regional to global scales. To provide a test of our present understanding of how ecosystems operate at large scales we can compare model predictions of CO2, O2, and methane exchange with the atmosphere against regional measurements of interannual variation in the atmospheric concentration of these gases. Recent advances in remote sensing of the Earth's surface are beginning to provide methods for estimating important ecosystem variables at large scales. Ecologists attempting to generalize across landscapes have made extensive use of models and remote sensing technology. The success of such ventures is dependent on merging insights and expertise from two distinct fields. Ecologists must provide the understanding of how well models emulate important biological variables and their interactions; experts in remote sensing must provide the biophysical interpretation of complex optical reflectance and radar backscatter data.
Author (revised)

N94-15897*# Centre d'Etude Spatiale des Rayonnements, Toulouse (France).
RECENT ADVANCES IN RADAR REMOTE SENSING OF FOREST **c43**
Thuy LeToan *In* JPL, Proceedings of the Third Spaceborne Imaging Radar Symposium 28 May 1993 p 143-150 (For primary document see N94-15886 03-32)
Avail: CASI HC A02/MF A04

On a global scale, forests represent most of the terrestrial standing biomass (80 to 90 percent). Thus, natural and anthropogenic change in forest covers can have major impacts not only on local ecosystems but also on global hydrologic, climatic, and biogeochemical cycles that involve exchange of energy, water, carbon, and other elements between the earth and atmosphere. Quantitative information on the state and dynamics of forest ecosystems and their interactions with the global cycles appear necessary to understand how the earth works as a natural system. The information required includes the lateral and vertical distribution of forest cover, the estimates of standing biomass (woody and foliar volume), the phenological and environmental variations and disturbances (clearcutting, fires, flood), and the longer term variations following deforestation (regeneration, successional stages). To this end, seasonal, annual, and decadal information is necessary in order to separate the long term effects in the global ecosystem from short term seasonal and interannual variations. Optical remote sensing has been used until now to study the forest cover at local, regional, and global scales. Radar remote sensing, which provides recent SAR data from space on a regular basis, represents an unique means of consistently monitoring different time scales, at all latitudes and in any atmospheric conditions. Also, SAR data have shown the potential to detect several forest parameters that cannot be inferred from optical data. The differences--and complementarity--lie in the penetration capabilities of SAR data and their sensitivity to dielectric and geometric properties of the canopy volume, whereas optical data are sensitive to the chemical composition of the external foliar layer of the vegetation canopy.
Author (revised)

N94-15898*# Michigan Univ., Ann Arbor.
RADAR RESPONSE OF VEGETATION: AN OVERVIEW **c43**
Fawwaz T. Ulaby and M. Craig Dobson *In* JPL, Proceedings of the Third Spaceborne Imaging Radar Symposium 28 May 1993 p 151-183 (For primary document see N94-15886 03-32)
Avail: CASI HC A03/MF A04

This document contains a number of viewgraphs on surface and vegetation backscattering. A classification of vegetation based on general scattering properties is presented. Radar scattering mechanisms are discussed, and backscattering and reflection coefficients for soil back scattering models are given. Radar response to vegetation is presented, with the objectives to discriminate and classify vegetation; to estimate biomass, leaf area index (LAI), and soil moisture; and to monitor changes, including deforestation and growth. Both theory and observation (laboratory, field, air SAR, and European Remote Sensing Satellite (ERS-1) observations) are used to present backscatter coefficients and other data for various vegetation types. ERS-1 results include class statistics, comparison with theory, and biomass response and seasonal variation (LAI) for deciduous and coniferous forests.
CASI

N94-15899*# Jet Propulsion Lab., California Inst. of Tech., Pasadena.
IMAGING RADAR STUDIES OF POLAR ICE **c43**
Frank Carsey *In its* Proceedings of the Third Spaceborne Imaging Radar Symposium 28 May 1993 p 185-193 (For primary document see N94-15886 03-32)
Avail: CASI HC A02/MF A04

A vugraph format presentation is given. The following topics are discussed: scientific overview, radar data opportunities, sea ice investigations, and ice sheet investigations. The Sea Ice Scientific Objectives are as follows: (1) to estimate globally the surface brine generation, heat flux, and fresh water advection (as ice); (2) to monitor phasing of seasonal melt and freeze events and accurately estimate melt and growth rates; and (3) to develop improved treatment of momentum transfer and ice mechanics in coupled air-sea-ice models.
Author (revised)

N94-15900*# Jet Propulsion Lab., California Inst. of Tech., Pasadena.
GEOLOGIC REMOTE SENSING WITH RADAR **c43**
Thomas G. Farr *In its* Proceedings of the Third Spaceborne Imaging Radar Symposium 28 May 1993 p 195-203 (For primary document see N94-15886 03-32)
Avail: CASI HC A02/MF A04

Viewgraphs on geologic remote sensing with radar are presented. Ongoing studies concentrate on: weathering processes, volcanic processes, land degradation, tectonic processes, and surface and subsurface mapping.
CASI

N94-15901*# Jet Propulsion Lab., California Inst. of Tech., Pasadena.
APPLICATION OF CLOUDE'S TARGET DECOMPOSITION THEOREM TO POLARIMETRIC IMAGING RADAR DATA **c43**
Jakob J. vanZyl *In its* Proceedings of the Third Spaceborne Imaging Radar Symposium 28 May 1993 p 207-216 (For primary document see N94-15886 03-32)
Avail: CASI HC A02/MF A04

In this paper we applied Cloude's decomposition to imaging radar polarimetry. We show in detail how the decomposition results can guide the interpretation of scattering from vegetated areas. For multifrequency polarimetric radar measurements of a clear-cut area, the decomposition leads us to conclude that the vegetation is probably thin compared to even the C-band radar wavelength of 6 cm. For a frosted area, we notice an increased amount of even number of reflection scattering at P-band and L-band, probably the result of penetration through the coniferous canopy resulting in trunk-ground double reflection scattering. However, the scattering for the forested area is still dominated by scattering from randomly oriented cylinders. It is found that these cylinders are thicker than in the case of clear-cut areas, leading us to conclude that scattering from the branches probably dominates in this case.
Author (revised)

N94-15902*# Deutsche Forschungs- und Versuchsanstalt fuer Luft- und Raumfahrt, Oberpfaffenhofen (Germany). Inst. fuer Hochfrequenztechnik.
MULTIFREQUENCY OBSERVATIONS **c43**
R. Glitz, F. Heel, H. Kietzmann, H. Oettl, and C. Schmullius *In* JPL, Proceedings of the Third Spaceborne Imaging Radar Symposium 28 May 1993 p 217-227 (For primary document see N94-15886 03-32)
Avail: CASI HC A03/MF A04

Analyses of synthetic aperture radar (SAR) image data were performed at DLR to classify various kinds of vegetation and different terrain types. The data were collected both with the DLR experimental synthetic aperture radar (E-SAR) in X-band, C-band, and L-band and with the NASA/JPL DC-8 SAR in C-band, L-band, and P-band. E-SAR is a single frequency and single polarization system (both parameters can be selected) but several flights were used to collect multifrequency/multipolarization data which were geometrically matched after processing. Classification of different crop types was based on comparison of the backscatter coefficients of calibrated SAR data in different frequency bands and polarizations. The DC-8 STAR collects polarimetric data in different bands simultaneously. Data acquired with the NASA/JPL DC-8 STAR are qualified for scientific investigations by reducing the cross-talk and channel imbalance to a tolerable extent. The data are absolutely calibrated by using reference targets with known backscattering cross-sections. The signatures and polarimetric features of terrain types, such as grassland, concrete, sea, forest (coniferous; deciduous) and urban areas, are extracted and discussed with respect to frequency and incidence angle dependence. A multifrequency polarimetric feature vector was applied for classification. The results of this new approach for separating and classifying different object classes are presented.
Author (revised)

N94-15903*# National Aeronautics and Space Administration, Washington, DC.
SIR-C/X-SAR FREE FLYER CONCEPT **c18**
R. Monson *In* JPL, Proceedings of the Third Spaceborne Imaging Radar Symposium 28 May 1993 p 233-249 (For primary document see N94-15886 03-32)
Avail: CASI HC A03/MF A04

Viewgraphs on Spaceborne Imaging Radar (SAR) - C/X- Synthetic Aperture Radar (SAR) Free Flyer concept are presented. An overview, science objectives, science rationale, geophysical parameters from SAR, programmatic goals, concept description, and a candidate mission description are included.
CASI

N94-15904*# Jet Propulsion Lab., California Inst. of Tech., Pasadena.
EOS SAR: A NEW APPROACH
JoBea Way *In its* Proceedings of the Third Spaceborne Imaging Radar Symposium 28 May 1993 p 251-262 (For primary document see N94-15886 03-32)
Avail: CASI HC A03/MF A04

Viewgraphs on Earth Observing System (EOS) Synthetic Aperture Radar (SAR) are presented. The goal of the EOS is to develop the modeling and observational capabilities to predict and/or monitor atmospheric, terrestrial, and oceanic processes that are either causing global change or resulting from global change. The EOS SAR goal is to provide important geophysical products to the EOS data set to improve our understanding of the state and functioning of the Earth system. The EOS SAR strategy is to define the instrument requirements based on required input to geophysical algorithms, to provide the processing capability and algorithms to generate such products on the required spatial (global) and temporal (3-5 days) scales, and to provide the spaceborne instrumentation with international partnerships.
CASI

N94-15905*# Naples Univ. (Italy).
TOPSAT: GLOBAL SPACE TOPOGRAPHIC MISSION **c43**
Sergio Vetrella *In* JPL, Proceedings of the Third Spaceborne Imaging Radar Symposium 28 May 1993 p 263-290 (For primary document see N94-15886 03-32)
Avail: CASI HC A03/MF A04

Viewgraphs on TOPSAT Global Space Topographic Mission are presented. Topics covered include: polar region applications; terrestrial ecosystem applications; stereo electro-optical sensors; space-based stereoscopic missions; optical stereo approach; radar interferometry; along track interferometry; TOPSAT-VISTA system approach; ISARA system approach; topographic mapping laser altimeter; and role of multi-beam laser altimeter.
CASI

N94-15906*# National Aeronautics and Space Administration, Washington, DC.
SOME THOUGHTS ON FUTURE RAIN MAPPING MISSIONS (TRMM FOLLOW-ON) **c47**
John S. Theon *In* JPL, Proceedings of the Third Spaceborne Imaging Radar Symposium 28 May 1993 p 291-296 (For primary document see N94-15886 03-32)
Avail: CASI HC A02/MF A04

The release of latent heat of condensation is the largest internal energy source of the atmosphere. Latent heating is most significant during the precipitation process. Our knowledge of the distribution of precipitation is poor. It is only well observed within limited areas of the globe. Over the oceans, for example, it is known only to within a factor of two. Thus, there are strong scientific requirements for observations of precipitation from instruments on board a satellite. The Tropical Rainfall Measuring Mission (TRMM) will be the first satellite to measure rainfall with adequate accuracy and provide information about the vertical distribution of precipitation, not only in tropics and subtropics, but to plus or minus 35 degrees of latitude. There is a need for the continuity of rain observations for climate modeling purposes and to expand observations to cover more of the globe than simply plus or minus 35 degrees latitude.
Author

N94-15907*# European Space Research Lab., Noordwijk (Netherlands).
CALIBRATION: PRACTICAL EXPERIENCE WITH ERS-1
Jacques Louet *In* JPL, Proceedings of the Third Spaceborne Imaging Radar Symposium 28 May 1993 p 299-336 (For primary document see N94-15886 03-32)
Avail: CASI HC A03/MF A04

Viewgraphs and discussion of calibration:practical experience with ERS-1 are presented. Topics covered include: radiometric calibration, geometric calibration, phase calibration, and polarimetric calibration. Basic synthetic aperture radar (SAR) measurement parameters are radar backscattering, target position, target speed, and polarization. SAR calibration facilitates quantitative measurements needed to derive geophysical parameters of the area under observation from basic SAR measurements (e.g. soil moisture, biomass, ocean wave energy, ocean currents, ice type, and ice flow).
CASI

N94-15908*# Vexcel Corp., Boulder, CO.
SYNTHETIC APERTURE RADAR SIGNAL PROCESSING: TRENDS AND TECHNOLOGIES
John C. Curlander *In* JPL, Proceedings of the Third Spaceborne Imaging Radar Symposium 28 May 1993 p 337-357 (For primary document see N94-15886 03-32)
Avail: CASI HC A03/MF A04

An overview of synthetic aperture radar (SAR) technology is presented in vugraph form. The following topics are covered: an SAR ground data system; SAR signal processing algorithms; SAR correlator architectures; and current and future trends.
CASI

N94-15909*# Deutsche Forschungs- und Versuchsanstalt fuer Luft- und Raumfahrt, Oberpfaffenhofen (Germany). Remote Sensing Data Center.
RECENT ADVANCES AND PLANS IN PROCESSING AND GEOCODING OF SAR DATA AT THE DFD **c43**
W. Noack *In* JPL, Proceedings of the Third Spaceborne Imaging Radar Symposium 28 May 1993 p 359-363 (For primary document see N94-15886 03-32)
Avail: CASI HC A01/MF A04

Because of the needs of future projects like ENVISAT and the experiences made with the current operational ERS-1 facilities, a radical change in the synthetic aperture radar (SAR) processing scenarios can be predicted for the next years. At the German PAF several new developments were initialized which are driven mainly either by user needs or by system and operational constraints ('lessons learned'). At the end there will be a major simplification and uniformation of all used computer systems. Especially the following changes are likely to be implemented at the German PAF: transcription before archiving, processing of all standard products with high throughput directly at the receiving stations, processing of special

'high-valued' products at the PAF, usage of a single type of processor hardware, implementation of a large and fast on-line data archive, and improved and unified fast data network between the processing and archiving facilities. A short description of the current operational SAR facilities as well as the future implementations are given. Author (revised)

N94-15910*# Jet Propulsion Lab., California Inst. of Tech., Pasadena.
DATA DISTRIBUTION **c82**
J. E. Hilland *In its* Proceedings of the Third Spaceborne Imaging Radar Symposium 28 May 1993 p 365-380 (For primary document see N94-15886 03-32)
Avail: CASI HC A03/MF A04

A discussion of data distribution is presented in vugraph form. The following topics are discussed: data distribution from the perspective of Earth observations and the end user; problems associated with synthetic aperture radar (SAR) data distribution; and future data distribution techniques. CASI

N94-15911*# General Electric Co., Moorestown, NJ. Astro Space Div.
SAR SENSOR ELECTRONICS: T/R MODULES **c53**
MohD A. Hasan and Albert E. Preyss *In* JPL, Proceedings of the Third Spaceborne Imaging Radar Symposium 28 May 1993 p 381-402 (For primary document see N94-15886 03-32)
Avail: CASI HC A03/MF A04

A discussion concerning the architecture of transmit/receive (T/R) modules in synthetic aperture radar (SAR) systems is presented. Module requirements are discussed in the context of the following: requirements traceability; antenna configuration; and typical module specifications/requirements. Finally, module technology development in the L-, C-, and X-bands is discussed. CASI

N94-15912*# Ball Communication Systems Div., Broomfield, CO.
ADVANCED ANTENNAS FOR SAR SPACECRAFT
William B. Gail *In* JPL, Proceedings of the Third Spaceborne Imaging Radar Symposium 28 May 1993 p 403-407 (For primary document see N94-15886 03-32)
Avail: CASI HC A01/MF A04

Single and multi-frequency antenna concepts were developed to evaluate the feasibility of building large aperture polarimetric synthetic aperture radar (SAR) systems to be launched in low cost vehicles such as the Delta 2. The antennas are 18.9 m long by 2.6 m wide (L-band) and achieve single polarization imaging to an incidence angle of 55 degrees and dual/quad imaging to 42 degrees. When combined with strawman spacecraft designs, both concepts meet the mass and volume constraints imposed by a Delta 2 launch. Author (revised)

N94-15913*# Alenia Spazio S.p.A., Rome (Italy).
HIGH RESOLUTION SAR APPLICATIONS AND INSTRUMENT DESIGN
C. Dionisio and A. Torre *In* JPL, Proceedings of the Third Spaceborne Imaging Radar Symposium 28 May 1993 p 409-411 (For primary document see N94-15886 03-32)
Avail: CASI HC A01/MF A04

The Synthetic Aperture Radar (SAR) has viewed, in the last two years, a huge increment of interest from many preset and potential users. The good spatial resolution associated to the all weather capability lead to considering SAR not only a scientific instrument but a tool for verifying and controlling the daily human relationships with the Earth Environment. New missions were identified for SAR as spatial resolution became lower than three meters: disasters, pollution, ships traffic, volcanic eruptions, earthquake effect are only a few of the possible objects which can be effectively detected, controlled and monitored by SAR mounted on satellites. High resolution radar design constraints and dimensioning are discussed. Author (revised)

N94-15914*# Jet Propulsion Lab., California Inst. of Tech., Pasadena.
A SUMMARY OF MICROWAVE REMOTE SENSING INVESTIGATIONS PLANNED FOR BOREAS **c43**
Kyle C. McDonald *In its* Proceedings of the Third Spaceborne Imaging Radar Symposium 28 May 1993 p 415-416 Sponsored in part by Energy, Mines and Resources Canada (For primary document see N94-15886 03-32)
Avail: CASI HC A01/MF A04

The Boreal Ecosystem - Atmosphere Study (BOREAS) is a multidisciplinary field and remote sensing study that will be implemented jointly by the United States and Canada. The goal of BOREAS is to obtain an improved understanding of the interactions between the boreal forest biome and the atmosphere in order to clarify their roles in global change. Specific objectives are to improve the understanding of the processes that govern the exchanges of water, energy, heat, carbon, and trace gases between boreal ecosystems and the atmosphere, and to develop and validate remote sensing algorithms for transferring the understanding of these processes from local to regional scales. Two principal field sites, both within Canada, were selected. The northern site is located near Thompson, Manitoba, and the southern site encompasses Prince Albert National Park in Saskatchewan. The growing season in the northern site tends to be limited by growing-degree days while the southern site is limited by soil moisture and fire frequency. Most of the field work will occur at these two sites during 1993 and 1994 as part of six field campaigns. The first of these campaigns is scheduled for August 1993 and will involve instrument installation and an operational shakedown. Three large scale Intensive Field Campaigns (IFC's) are scheduled for 1994, along with two smaller scale Focused Field Campaigns (FFC's). The first 1994 campaign will be an FFC designed to capture the biome under completely frozen conditions during the winter. The second FFC and the first IFC are scheduled to capture the spring thaw period. Another IFC will take place in the summer during a period of maximum water stress. Finally, the third FFC will be scheduled to capture the collapse into senescence during the fall. Author (revised)

N94-15915*# Academia Sinica, Beijing (China). Inst. of Remote Sensing Applications.
SPACEBORNE RADAR FOR GEOSCIENTIFIC APPLICATIONS IN NORTH CHINA
Hua-Dong Guo, Guo-Xiang Wu (State Science and Technology Commission, Beijing, China.), and Zhen-Song Wang *In* JPL, Proceedings of the Third Spaceborne Imaging Radar Symposium 28 May 1993 p 417-419 (For primary document see N94-15886 03-32)
Avail: CASI HC A01/MF A04

The Shuttle Imaging Radar-A and -B (SIR-A and SIR-B) carried on the Space Shuttle Columbia in Nov. 1981 and the Challenger in Oct. 1984 acquired images of test sites of North China. The Russian ALMAZ SAR also acquired imagery of part of this test site in Sep. 1992. In Nov. 1990, the airborne SAR developed by the Chinese Academy of Sciences (CAS/SAR) covered this area for the purpose of Chinese spaceborne radar development. By studying and analyzing these SAR data, positive results in geoscientific applications were achieved. Author

N94-15916*# Academia Sinica, Beijing (China). Inst. of Electronics.
PRIMARY STUDIES OF CHINESE SPACEBORNE SAR
Zhen-Song Wang, Guo-Xiang Wu (State Science and Technology Commission, Beijing, China.), Hua-Dong Guo, Zhong-Quan Wei (Academia Sinica, Shanghai, China.), and Min-Hui Zhu *In* JPL, Proceedings of the Third Spaceborne Imaging Radar Symposium 28 May 1993 p 421-423 (For primary document see N94-15886 03-32)
Avail: CASI HC A01/MF A04

The primary studies on spaceborne synthetic aperture radar (SAR) in China are discussed. The SAR will be launched aboard a Chinese satellite and operated at L-band with HH polarization. The purpose of the mission in consideration is dedicated to resources and environment uses, especially to natural disaster monitoring. The ground resolution is designed as 25 m x 25 m for detailed mode and 100 m x 100 m for wide scan-SAR mode. The off-nadir angle can be varied from 20 to 40 deg. The key system concepts are introduced. Author (revised)

N94-15917*# Vexcel Corp., Boulder, CO.
INTERNATIONAL COLLABORATION IN SAR GROUND DATA SYSTEMS
John C. Curlander *In* JPL, Proceedings of the Third Spaceborne Imaging Radar Symposium 28 May 1993 p 425-430 (For primary document see N94-15886 03-32)
Avail: CASI HC A02/MF A04

A set of considerations that are pertinent to future international cooperation in the area of synthetic aperture radar (SAR) ground data systems are presented. The considerations are as follows: (1) success of future spaceborne SAR missions will require multi-agency and/or

multi-national collaboration; (2) ground processing is typically performed by each agency for their user base; (3) international standards are required to achieve a uniform data product independent of the processing center; (4) to reduce the aggregate cost of the ground data systems, collaboration is required in design and development; (5) effective utilization of the data by an international user community; (6) commercialization of data products; and (7) security of data systems. CASI

N94-15918*# Jet Propulsion Lab., California Inst. of Tech., Pasadena.
GLOBAL ENERGY AND WATER CYCLE EXPERIMENT (GEWEX) AND THE CONTINENTAL-SCALE INTERNATIONAL PROJECT (GCIP) **c45**
Deborah Vane *In its* Proceedings of the Third Spaceborne Imaging Radar Symposium 28 May 1993 p 431-439 (For primary document see N94-15886 03-32)
Avail: CASI HC A02/MF A04

A discussion of the objectives of the Global Energy and Water Cycle Experiment (GEWEX) and the Continental-scale International Project (GCIP) is presented in vugraph form. The objectives of GEWEX are as follows: determine the hydrological cycle by global measurements; model the global hydrological cycle; improve observations and data assimilation; and predict response to environmental change. The objectives of GCIP are as follows: determine the time/space variability of the hydrological cycle over a continental-scale region; develop macro-scale hydrologic models that are coupled to atmospheric models; develop information retrieval schemes; and support regional climate change impact assessment. CASI

N94-15919*# Jet Propulsion Lab., California Inst. of Tech., Pasadena.
AIRSAR SOUTH AMERICAN DEPLOYMENT: OPERATION PLAN, VERSION 3.0 **c66**
M. Kobrick *In its* Proceedings of the Third Spaceborne Imaging Radar Symposium 28 May 1993 p 441-465 (For primary document see N94-15886 03-32)
Avail: CASI HC A03/MF A04

The United States National Aeronautics and Space Administration (NASA) and the Brazilian Commission for Space Activities (COBAE) are undertaking a joint experiment involving NASA's DC-8 research aircraft and the Airborne Synthetic Aperture Radar (AIRSAR) system during late May and June 1993. The research areas motivating these activities are: (1) fundamental research in the role of soils, vegetation, and hydrology in the global carbon cycle; and (2) in cooperation with South American scientists, airborne remote sensing research for the upcoming NASA Spaceborne Imaging Radar (SIR)-C/X-SAR flights on the Space Shuttle. A flight schedule and plans for the deployment that were developed are included. Maps of the site locations and schematic indications of flight routes and dates, plots showing swath locations derived from the flight requests and generated by flight planning software, and, most importantly, a calendar showing which sites will be imaged each day are included. Author (revised)

N94-15959# Canadian Satellite Communications, Inc., Mississauga (Ontario).
[ACTIVITIES OF CANADIAN SATELLITE COMMUNICATIONS, INC.] Annual Report, 1992
1992 30 p Original contains color illustrations
(CTN-93-60864) Avail: CASI HC A03/MF A01

Canadian Satellite Communications (Cancom) has as its core business the provision of television and radio signals to cable systems in Canada, with the objective of making affordable broadcast signals available to remote and/or small communities. Cancom also provides direct-to-home services to backyard receiving dishes, as well as satellite digital data business communications services, satellite business television, and satellite network services. Its business communication services range from satellite links for big-city businesses with small branch operations located far from major centers, to a mobile messaging and tracking system for the trucking industry. Revenues in 1992 totalled $48,212,000 and net income was just over $7 million. Cancom bought 10 percent interest in Leosat Corp. of Washington, DC, who are seeking approval to operate a position locator network from low-orbit satellites. Cancom has also become a partner in SovCan Star Satellite Communications Inc., which will build an international satellite system in partnership with Russia. The first satellite in this east-west business network will be placed in a Russian orbital slot over the Atlantic by 1996, and a second satellite will follow for the Pacific region. This annual report of Cancom's activities for 1992 includes financial statements and a six year financial review. CISTI

N94-15986 Communications Research Centre, Ottawa (Ontario).
DUAL POLARIZATION MICROSTRIP ARRAY ANTENNA Patent
Adrian W. Alden, inventor (to Micromedia Ltd.) and Tom T. Ohno, inventor (to Micromedia Ltd.) 22 Sep. 1992 23 p
(CA-Patent-1-307-842; Int-Patent-Class-H01R-21/26; Int-Patent-Class-H01R-13/08; CTN-93-60779) Copyright Avail: Issuing Activity (Micromedia Ltd., Technical Information Centre, 165 Hotel de Ville, Place du Portage, Phase 2, Hull, Quebec J8X 3X2, Canada HC)

A dual polarized microstrip array antenna is provided for power reception or transmission of electromagnetic waves. The antenna has a plurality of symmetrically arranged identical antenna units. Each unit comprises a patch antenna element of given length and a plurality of identical feedlines, each of which is symmetrically attached to the patch antenna element and has identical microstrip filters, a terminal for an antenna feed, and identical microstrip matching stubs for shorting the transmission line waves at the fundamental and second harmonic. The array antenna further comprises a dielectric layer of a predetermined thickness on one side of which the plurality of the identical antenna units are arranged symmetrically in an array by direct current connecting appropriate feedlines of adjacent antenna units and a common ground plane provided on the other side of the dielectric layer. The antenna of the invention removes difficulties associated with other types of microstrip antennas and increases the overall dual polarization power conversion efficiency by a specific choice of rectenna format and dimensions. Author (CISTI)

N94-16022*# Clemson Univ., SC. Dept. of Electrical and Computer Engineering.
WINDSHEAR DETECTION RADAR SIGNAL PROCESSING STUDIES Final Technical Report No. 18, 16 Nov. 1988 - 31 Oct. 1993
Ernest G. Baxa, Jr. 1 Nov. 1993 19 p
(Grant NAG1-928)
(NASA-CR-194615; NAS 1.26:194615; TR-110193-3570F) Avail: CASI HC A03/MF A01

This final report briefly summarizes research work at Clemson in the Radar Systems Laboratory under the NASA Langley Research Grant NAG-1-928 in support of the Antenna and Microwave Branch, Guidance and Control Division, program to develop airborne sensor technology for the detection of low altitude windshear. A bibliography of all publications generated by Clemson personnel is included. An appendix provides abstracts of all publications. Author (revised)

N94-16035*# Jet Propulsion Lab., California Inst. of Tech., Pasadena.
PROCEEDINGS OF THE FIFTEENTH NASA PROPAGATION EXPERIMENTERS MEETING (NAPEX 15) AND THE ADVANCED COMMUNICATIONS TECHNOLOGY SATELLITE (ACTS) PROPAGATION STUDIES MINIWORKSHOP
Faramaz Davarian, ed. 1 Jul. 1991 275 p Miniworkshop held in London, Ontario, 28-29 Jun. 1991
(Contract NAS7-918)
(NASA-CR-194539; JPL-Publ-91-31; NAS 1.26:194539) Avail: CASI HC A12/MF A03

The NASA Propagation Experimenters Meeting (NAPEX), supported by the NASA Propagation Program, is convened annually to discuss studies made on radio wave propagation by investigators from domestic and international organizations. The meeting was organized into three technical sessions. The first session was dedicated to Olympus and ACTS studies and experiments, the second session was focused on the propagation studies and measurements, and the third session covered computer-based propagation model development. In total, sixteen technical papers and some informal contributions were presented. Following NAPEX 15, the Advanced Communications Technology Satellite (ACTS) miniworkshop was held on 29 Jun. 1991, to review ACTS propagation activities, with emphasis on ACTS hardware development and experiment planning. Five papers were presented. For individual titles, see N94-16036 through N94-16051.

N94-16036*# European Space Research Organization, Noordwikj (Netherlands).
A REVIEW OF OPEX ACTIVITIES AND MEASUREMENT RESULTS
B. Arbesser-Rastburg *In* JPL, Proceedings of the Fifteenth NASA

Propagation Experimenters Meeting (NAPEX 15) and the Advanced Communications Technology Satellite (ACTS) Propagation Studies Miniworkshop 1 Jul. 1991 p 12-19 (For primary document see N94-16035 03-32)
Avail: CASI HC A02/MF A03

A summary is given of the measurements carried out in the framework of OPEX (OLYMPUS Propagation Experimenters Group). In particular, the progress since mid-1990 is presented. In this period two OPEX meetings were held, OPEX 14 (Oct. 1990) and OPEX 15 (Apr. 1991). The First OPEX Workshop was held at ESTEC on 23-24 April 1991.
Author (revised)

N94-16037*# Virginia Polytechnic Inst. and State Univ., Blacksburg. Dept. of Electrical Engineering.
OLYMPUS PROPAGATION MEASUREMENT RESULTS AT VIRGINIA TECH
Warren Stutzman *In* JPL, Proceedings of the Fifteenth NASA Propagation Experimenters Meeting (NAPEX 15) and the Advanced Communications Technology Satellite (ACTS) Propagation Studies Miniworkshop 1 Jul. 1991 p 20-27 (For primary document see N94-16035 03-32)
Avail: CASI HC A02/MF A03

Virginia Tech is performing a comprehensive set of propagation measurements using the OLYMPUS satellite beacons at 12.5, 20, and 30 GHz. A second 20 GHz diversity terminal is portable and is moved to various spacings up to 50 m away from the fixed 20 GHz terminal. Total power radiometers are also included in each terminal. Radiometer data are used both to set the absolute level of the beacon data and to predict path attenuation. This paper presents initial results from the experiment set.
Author (revised)

N94-16038*# Virginia Polytechnic Inst. and State Univ., Blacksburg. Dept. of Electrical Engineering.
DATA ACQUISITION, PREPROCESSING AND ANALYSIS FOR THE VIRGINIA TECH OLYMPUS EXPERIMENT
P. Will Remaklus *In* JPL, Proceedings of the Fifteenth NASA Propagation Experimenters Meeting (NAPEX 15) and the Advanced Communications Technology Satellite (ACTS) Propagation Studies Miniworkshop 1 Jul. 1991 p 28-35 (For primary document see N94-16035 03-32)
Avail: CASI HC A02/MF A03

Virginia Tech is conducting a slant path propagation experiment using the 12, 20, and 30 GHz OLYMPUS beacons. Beacon signal measurements are made using separate terminals for each frequency. In addition, short baseline diversity measurements are collected through a mobile 20 GHz terminal. Data collection is performed with a custom data acquisition and control system. Raw data are preprocessed to remove equipment biases and discontinuities prior to analysis. Preprocessed data are then statistically analyzed to investigate parameters such as frequency scaling, fade slope and duration, and scintillation intensity.
Author (revised)

N94-16039*# Jet Propulsion Lab., California Inst. of Tech., Pasadena.
THE ACTS PROPAGATION PROGRAM
Dayamoy Chakraborty and Faramaz Davarian *In its* Proceedings of the Fifteenth NASA Propagation Experimenters Meeting (NAPEX 15) and the Advanced Communications Technology Satellite (ACTS) Propagation Studies Miniworkshop 1 Jul. 1991 p 50-54 (For primary document see N94-16035 03-32)
Avail: CASI HC A01/MF A03

The purpose of the Advanced Communications Technology Satellite (ACTS) is to demonstrate the feasibility of the Ka-band (20 and 30 GHz) spectrum for satellite communications, as well as to help maintain U.S. leadership in satellite communications. ACTS incorporates such innovative schemes as time division multiple access (TDMA), microwave and baseband switching, onboard regeneration, and adaptive application of coding during rain-fade conditions. The success or failure of the ACTS experiment will depend on how accurately the rain-fade statistics and fade dynamics can be predicted in order to derive an appropriate algorithm that will combat weather vagaries, specifically for links with small terminals, such as very small aperture terminals (VSAT's) where the power margin is a premium. This article describes the planning process and hardware development program that will comply with the recommendations of the ACTS propagation study groups.
Author (revised)

N94-16040*# Alaska Univ., Fairbanks. Dept. of Electrical Engineering.
PROPAGATION MEASUREMENTS IN ALASKA USING ACTS BEACONS
Charles E. Mayer *In* JPL, Proceedings of the Fifteenth NASA Propagation Experimenters Meeting (NAPEX 15) and the Advanced Communications Technology Satellite (ACTS) Propagation Studies Miniworkshop 1 Jul. 1991 p 55-60 (For primary document see N94-16035 03-32)
Avail: CASI HC A02/MF A03

The placement of an ACTS propagation terminal in Alaska has several distinct advantages. First is the inclusion of a new and important climatic zone to the global propagation model. Second is the low elevation look angle from Alaska to ACTS. These two unique opportunities also present problems unique to the location, such as extreme temperatures and lower power levels. These problems are examined and compensatory solutions are presented.
Author

N94-16041*# Johns Hopkins Univ., Laurel, MD. Applied Physics Lab.
PLANNED LMSS PROPAGATION EXPERIMENT USING ACTS: PRELIMINARY ANTENNA POINTING RESULTS DURING MOBILE OPERATIONS
John R. Rowland, Julius Goldhirsh, Wolfhard J. Vogel (Texas Univ., Austin.), and Geoffrey W. Torrence (Texas Univ., Austin.) *In* JPL, Proceedings of the Fifteenth NASA Propagation Experimenters Meeting (NAPEX 15) and the Advanced Communications Technology Satellite (ACTS) Propagation Studies Miniworkshop 1 Jul. 1991 p 61-72 (For primary document see N94-16035 03-32)
(Contracts JPL-956520; N00039-89-C-0001)
Avail: CASI HC A03/MF A03

An overview and a status description of the planned LMSS mobile K band experiment with ACTS is presented. As a precursor to the ACTS mobile measurements at 20.185 GHz, measurements at 19.77 GHz employing the Olympus satellite were originally planned. However, because of the demise of Olympus in June of 1991, the efforts described here are focused towards the ACTS measurements. In particular, we describe the design and testing results of a gyro controlled mobile-antenna pointing system. Preliminary pointing measurements during mobile operations indicate that the present system is suitable for measurements employing a 15 cm aperture (beamwidth at approximately 7 deg) receiving antenna operating with ACTS in the high gain transponder mode. This should enable measurements with pattern losses smaller than plus or minus 1 dB over more than 95 percent of the driving distance. Measurements with the present mount system employing a 60 cm aperture (beamwidth at approximately 1.7 deg) results in pattern losses smaller than plus or minus 3 dB for 70 percent of the driving distance. Acceptable propagation measurements may still be made with this system by employing developed software to flag out bad data points due to extreme pointing errors. The receiver system including associated computer control software has been designed and assembled. Plans are underway to integrate the antenna mount with the receiver on the University of Texas mobile receiving van and repeat the pointing tests on highways employing a recently designed radome system.
Author (revised)

N94-16042*# Jet Propulsion Lab., California Inst. of Tech., Pasadena.
PROPAGATION-RELATED AMT DESIGN ASPECTS AND SUPPORTING EXPERIMENTS
Khaled Dessouky and Polly Estabrook *In its* Proceedings of the Fifteenth NASA Propagation Experimenters Meeting (NAPEX 15) and the Advanced Communications Technology Satellite (ACTS) Propagation Studies Miniworkshop 1 Jul. 1991 p 73-80 (For primary document see N94-16035 03-32)
Avail: CASI HC A02/MF A03

The ACTS Mobile Terminal (AMT) is presently being developed with the goal of significantly extending commercial satellite applications and their user base. A thorough knowledge of the Ka-band channel characteristics is essential to the proper design of a commercially viable system that efficiently utilizes the valuable resources. To date, only limited tests have been performed to characterize the Ka-band channel, and they have focused on the needs of fixed terminals. As part of the value of the AMT as a Ka-band test bed is its function as a vehicle through which tests specifically applicable to the mobile satellite communications can be performed. The exact propagation environment with the proper set of elevation angles, vehicle antenna gains and patterns, roadside shadowing, rain, and Doppler is encountered. The ability to measure all of the above, as well as correlate

their effects with observed communication system performance, creates an invaluable opportunity to understand in depth Ka-band's potential in supporting mobile and personal communications. This paper discusses the propagation information required for system design, the setup with ACTS that will enable obtaining this information, and finally the types of experiments to be performed and data to be gathered by the AMT to meet this objective. Author (revised)

N94-16043*# Ministry of Posts and Telecommunications, Ibaraki (Japan). Communications Research Lab.

PROPAGATION RESEARCH IN JAPAN

Hiromitsu Wakana *In* JPL, Proceedings of the Fifteenth NASA Propagation Experimenters Meeting (NAPEX 15) and the Advanced Communications Technology Satellite (ACTS) Propagation Studies Miniworkshop 1 Jul. 1991 p 88-94 (For primary document see N94-16035 03-32)

Avail: CASI HC A02/MF A03

L-band propagation measurements for land-mobile, maritime, and aeronautical satellite communications have been carried out by using the Japanese Engineering Test Satellite-Five (ETS-5) which was launched in Aug. 1987. This paper presents propagation characteristics for each of the mobile satellite communication channels. Author (revised)

N94-16044*# Colorado Univ., Boulder. Dept. of Electrical and Computer Engineering.

A COMPARISON OF CLOUD ATTENUATION MODELS USING MEASURED CLOUD DATA

Gerald C. Gerace, Ernest K. Smith, and Edgeworth R. Westwater (National Oceanic and Atmospheric Administration, Boulder, CO.) *In* JPL, Proceedings of the Fifteenth NASA Propagation Experimenters Meeting (NAPEX 15) and the Advanced Communications Technology Satellite (ACTS) Propagation Studies Miniworkshop 1 Jul. 1991 p 95-106 (For primary document see N94-16035 03-32)

Avail: CASI HC A03/MF A03

Simultaneous measurements of surface atmospheric parameters and cloud liquid water are used to test and compare the accuracy of three different cloud models. Author

N94-16045*# National Oceanic and Atmospheric Administration, Boulder, CO. Wave Propagation Lab.

BRIGHTNESS TEMPERATURE AND ATTENUATION STATISTICS AT 20.6 AND 31.65 GHz

Edgeworth R. Westwater and M. J. Falls *In* JPL, Proceedings of the Fifteenth NASA Propagation Experimenters Meeting (NAPEX 15) and the Advanced Communications Technology Satellite (ACTS) Propagation Studies Miniworkshop 1 Jul. 1991 p 107-115 (For primary document see N94-16035 03-32)

Avail: CASI HC A02/MF A03

Attenuation and brightness temperature statistics at 20.6 and 31.65 GHz are analyzed for a year's worth of data. The data were collected in 1988 at Denver and Platteville, Colorado. The locations are separated by 49 km. Single-station statistics are derived for the entire year. Quality control procedures are discussed and examples of their application are given. Author (revised)

N94-16046*# National Oceanic and Atmospheric Administration, Boulder, CO. Wave Propagation Lab.

COMPARISON OF OLYMPUS BEACON AND RADIOMETRIC ATTENUATION MEASUREMENTS AT BLACKSBURG, VIRGINIA

J. B. Snider, M. D. Jacobson, R. H. Beeler, and D. A. Hazen *In* JPL, Proceedings of the Fifteenth NASA Propagation Experimenters Meeting (NAPEX 15) and the Advanced Communications Technology Satellite (ACTS) Propagation Studies Miniworkshop 1 Jul. 1991 p 116-122 (For primary document see N94-16035 03-32)

Avail: CASI HC A02/MF A03

Measurements of attenuation of the 20 and 30 GHz beacons onboard the OLYMPUS satellite are compared to simultaneous observations of atmospheric attenuation by a multichannel microwave radiometer along the same path. Departures from high correlation between the two measurements are believed to be related to differences in antenna beamwidths. Mean equivalent zenith attenuations derived from the slant path data are compared to zenith observations made at previous locations. Author (revised)

N94-16047*# Texas Univ., Austin. Electrical Engineering Research Lab.

SATELLITE SOUND BROADCAST PROPAGATION MEASUREMENTS

Wolfhard J. Vogel and Geoffrey W. Torrence *In* JPL, Proceedings of the Fifteenth NASA Propagation Experimenters Meeting (NAPEX 15) and the Advanced Communications Technology Satellite (ACTS) Progagation Studies Miniworkshop 1 Jul. 1991 p 123-131 (For primary document see N94-16035 03-32)

Avail: CASI HC A02/MF A03

Power transmitted from atop a 17.9 m tower in simulation of a satellite signal, emitted by a tone generator sweeping from 700 to 1800 MHz, was received using a 90 deg beamwidth linearly scanning antenna at many locations inside six buildings of solid brick, corrugated sheet-metal, wood-frame, mobile home, and concrete wall construction. The signal levels are found to have much structure in the spatial and frequency domain but were relatively stable in time. Typically, people moving nearby produced less than 0.5 dB variations, whereas a person blocking the transmission path produces 6 to 10 dB fades. Losses, which at an average position in a room increased from 6 to 12 dB over 750 to 1750 MHz, could be mitigated to 2 to 6 dB by moving the antenna typically less than 30 cm. Severe losses (17.5 dB, mitigated to 12.5 dB) were observed in a concrete wall building, which also exhibited the longest multipath delays (greater than 100 ns). Losses inside a mobile home were even larger (greater than 20 dB) and independent of antenna orientation. The losses showed a clear frequency dependence. Author (revised)

N94-16048*# Johns Hopkins Univ., Laurel, MD. Applied Physics Lab.

AN OVERVIEW OF THE TEXT PROPAGATION EFFECTS FOR LAND-MOBILE-SATELLITE SYSTEMS: EXPERIMENTAL AND MODELING RESULTS

Julius Goldhirsh and Wolfhard J. Vogel (Texas Univ., Austin.) *In* JPL, Proceedings of the Fifteenth NASA Propagation Experimenters Meeting (NAPEX 15) and the Advanced Communications Technology Satellite (ACTS) Propagation Studies Miniworkshop 1 Jul. 1991 p 132-139 (For primary document see N94-16035 03-32)

(Contracts JPL-956520; N00039-89-C-0001)

Avail: CASI HC A02/MF A03

We present an overview of the contents of the text having the above title and which is now in the form of a preliminary document titled, 'Propagation Handbook for Land-Mobile-Satellite Systems-Preliminary.' At this writing the text is undergoing peer review, and the final revised manuscript will be published in the near future as a NASA document. The text was inspired by a series of Land-Mobile-Satellite System (LMSS) experiments by the authors and other investigators at UHF and L-Band. The rationale for its writing is to place in a single document an overview of the previous propagation related salient experimental and modeling results pertaining to LMSS scenarios. It is apparent that LMSS propagation at UHF and L-Band can be seriously degraded because of attenuation (e.g., greater than 10 dB) caused by roadside tree shadowing. The extent of attenuation is shown to depend on such factors at the elevation angle to the satellite, the bearing of the line-of-signt path to the satellite relative to the line of roadside trees, the side of the road in which the vehicle is driven, the season, and the frequency. Multipath effects during line-of-sight communications are shown to cause less serious fading (e.g., smaller than 3 dB for 90 percent of the driving distance). Author (revised)

N94-16049*# Jet Propulsion Lab., California Inst. of Tech., Pasadena.

DATABASE FOR PROPAGATION MODELS

Anil V. Kantak *In its* Proceedings of the Fifteenth NASA Propagation Experimenters Meeting (NAPEX 15) and the Advanced Communications Technology Satellite (ACTS) Propagation Studies Miniworkshop 1 Jul. 1991 p 147-158 (For primary document see N94-16035 03-32)

Avail: CASI HC A03/MF A03

A propagation researcher or a systems engineer who intends to use the results of a propagation experiment is generally faced with various database tasks such as the selection of the computer software, the hardware, and the writing of the programs to pass the data through the models of interest. This task is repeated every time a new experiment is conducted or the same experiment is carried out at a different location generating different data. Thus the users of this data have to spend a considerable portion of their time learning how to implement the computer hardware and the software towards the desired end. This situation may be facilitated considerably if an easily accessible propagation database is created that

has all the accepted (standardized) propagation phenomena models approved by the propagation research community. Also, the handling of data will become easier for the user. Such a database construction can only stimulate the growth of the propagation research it if is available to all the researchers, so that the results of the experiment conducted by one researcher can be examined independently by another, without different hardware and software being used. The database may be made flexible so that the researchers need not be confined only to the contents of the database. Another way in which the database may help the researchers is by the fact that they will not have to document the software and hardware tools used in their research since the propagation research community will know the database already. The following sections show a possible database construction, as well as properties of the database for the propagation research. Author (revised)

N94-16050*# Colorado Univ., Boulder.
A CCIR-BASED PREDICTION MODEL FOR EARTH-SPACE PROPAGATION
Zengjun Zhang and Ernest K. Smith *In* JPL, Proceedings of the Fifteenth NASA Propagation Experimenters Meeting (NAPEX 15) and the Advanced Communications Technology Satellite (ACTS) Propagation Studies Miniworkshop 1 Jul. 1991 p 159-172 (For primary document see N94-16035 03-32)
Avail: CASI HC A03/MF A03

At present there is no single 'best way' to predict propagation impairments to an Earth-Space path. However, there is an internationally accepted way, namely that given in the most recent version of CCIR Report 564 of Study Group 5. This paper treats a computer code conforming as far as possible to Report 564. It was prepared for an IBM PS/2 using a 386 chip and for Macintosh SE or Mach II. It is designed to be easy to write and read, easy to modify, fast, have strong graphic capability, contain adequate functions, have dialog capability and windows capability. Computer languages considered included the following: (1) Turbo BASIC, (2) Turbo PASCAL, (3) FORTRAN, (4) SMALL TALK, (5) C++, (6) MS SPREADSHEET, (7) MS Excel-Macro, (8) SIMSCRIPT II.5, and (9) WINGZ. Author (revised)

N94-16051*# Michigan Technological Univ., Houghton. Dept. of Electrical Engineering.
A STUDY OF LAND MOBILE SATELLITE SERVICE MULTIPATH EFFECTS USING SATLAB SOFTWARE
Richard L. Campbell *In* JPL, Proceedings of the Fifteenth NASA Propagation Experimenters Meeting (NAPEX 15) and the Advanced Communications Technology Satellite (ACTS) Propagation Studies Miniworkshop 1 Jul. 1991 p 176-185 (For primary document see N94-16035 03-32)
Avail: CASI HC A02/MF A03

A software package is proposed that uses the known properties of signals received in multipath environments along with the mathematical relationships between signal characteristics to explore the effects of antenna pattern, vehicle velocity, shadowing of the direct wave, distributions of scatters around the moving vehicle and levels of scattered signals on the received complex envelope, fade rates and fade duration, Doppler spectrum, signal arrival angle spectrum, and spatial correlation. The data base may be either actual measured received signals entered as ASCII flat files or data synthesized using a built in model. An example illustrates the effect of using different antennas to receive signals in the same environment. Author (revised)

N94-16169# Lawrence Livermore National Lab., CA.
PASSIVE TRACKING OF A TARGET USING AN ARRAY OF SENSORS
M. Buhl May 1993 52 p
(Contract W-7405-eng-48)
(DE93-015870; UCRL-ID-114251) Avail: CASI HC A04/MF A01 (US Sales Only)

The problem of passively tracking a moving signal source has importance in a variety of applications such as radar, sonar, seismology, and radio astronomy. In an attempt to aid in the understanding of such problems, a passive tracking algorithm has been developed using PV-Wave, version 3.10. The objective of this document is to present this algorithm, thereby allowing others to further investigate such problems. DOE

N94-16467# Naval Command, Control and Ocean Surveillance Center, San Diego, CA.
A RAY TRACE MODEL FOR PROPAGATION LOSS Final Report
C. P. Hattan Feb. 1993 66 p
(AD-A266314; NCCOSC/RDT/E-TR-1576) Avail: CASI HC A04/MF A01

This study was conducted to determine the feasibility of replacing the optical-region propagation model currently assessing the effect of lower atmosphere refraction on electromagnetic (EM) system performance within the Engineer's Refractive Effects Prediction System (EREPS) with a complete ray trace model. The ray trace model uses a full ray trace solution to describe the propagation environment. It is implemented in a Microsoft QuickBASIC program intended for IBM-compatible personal computers. The ray trace model can determine propagation loss under certain conditions, but it resolves ray paths with increasing difficulty when the EM system frequency rises, and it produces large divergence factors. Since attempts to eliminate fluctuations in the ray trace divergence factors have failed, the study's results argue that the ray trace model is not suitable for EREPS. DTIC

N94-16477# Cornell Univ., Ithaca, NY. Dept. of Computer Science.
CONSISTENT FAILURE REPORTING IN RELIABLE COMMUNICATION SYSTEMS Special Technical Report
Kenneth P. Birman and Bradford B. Glade May 1993 20 p
(Contract N00014-92-J-1866)
(AD-A266298; CU-CSD-TR-93-1349) Avail: CASI HC A03/MF A01

The difficulty of developing reliable distributed software is an impediment to applying distributed computing technology in many settings. This paper reviews some common platforms for distributed software development and argues that inconsistent failure reporting in communication mechanisms represents a significant obstacle to reliability. DTIC

N94-16506*# Notre Dame Univ., IN. Dept. of Electrical Engineering.
LOW-COMPLEXITY, HIGH-PERFORMANCE BANDWIDTH EFFICIENT CODING AND CODED MODULATION TECHNIQUES FOR SATELLITE AND SPACE COMMUNICATIONS Semiannual Status Report
Daniel J. Costello, Jr. Nov. 1993 51 p
(Grant NAG5-557)
(NASA-CR-194623; NAS 1.26:194623) Avail: CASI HC A04/MF A01

The semi-annual progress report for NASA grant NAG5-557 is presented. The report contains three papers concerning bandwidth efficient coding and coded modulation techniques for satellite and space communications. For individual titles, see N94-16507 through N94-16509.

N94-16507*# Notre Dame Univ., IN. Dept. of Electrical Engineering.
BANDWIDTH EFFICIENT CODING: THEORETICAL LIMITS AND REAL ACHIEVEMENTS. ERROR CONTROL TECHNIQUES FOR SATELLITE AND SPACE COMMUNICATIONS Interim Report
Daniel J. Costello, Jr., Servanne Courturier, Yannick Levy, Diane G. Mills, Lance C. Perez, and Fu-Quan Wang *In its* Low-Complexity, High-Performance Bandwidth Efficient Coding and Coded Modulation Techniques for Satellite and Space Communications Nov. 1993 17 p
(For primary document see N94-16506 03-32)
(Grant NAG5-557)
Avail: CASI HC A03/MF A01

In his seminal 1948 paper 'The Mathematical Theory of Communication,' Claude E. Shannon derived the 'channel coding theorem' which has an explicit upper bound, called the channel capacity, on the rate at which 'information' could be transmitted reliably on a given communication channel. Shannon's result was an existence theorem and did not give specific codes to achieve the bound. Some skeptics have claimed that the dramatic performance improvements predicted by Shannon are not achievable in practice. The advances made in the area of coded modulation in the past decade have made communications engineers optimistic about the possibility of achieving or at least coming close to channel capacity. Here we consider the possibility in the light of current research results. Author (revised)

N94-16508*# Notre Dame Univ., IN. Dept. of Electrical Engineering.
A SIMULATION STUDY OF THE PERFORMANCE OF THE NASA (2,1,6) CONVOLUTIONAL CODE ON RFI/BURST CHANNELS
Lance C. Perez and Daniel J. Costello, Jr. *In its* Low-Complexity, High-Performance Bandwidth Efficient Coding and Coded Modulation

Techniques for Satellite and Space Communications Nov. 1993 13 p (For primary document see N94-16506 03-32)
(Grants NAG5-557; NGT-70109)
Avail: CASI HC A03/MF A01

In an earlier report, the LINKABIT Corporation studied the performance of the (2,1,6) convolutional code on the radio frequency interference (RFI)/burst channel using analytical methods. Using an R(sub 0) analysis, the report concluded that channel interleaving was essential to achieving reliable performance. In this report, Monte Carlo simulation techniques are used to study the performance of the convolutional code on the RFI/burst channel in more depth. The basic system model under consideration is shown. The convolutional code is the NASA standard code with generators g(exp 1) = 1+D(exp 2)+D(exp 3)+D(exp 5)+D(exp 6) and g(exp 2) = 1+D+D(exp 2)+D(exp 3)+D(exp 6) and d(sub free) = 10. The channel interleaver is of the convolutional or periodic type. The binary output of the channel interleaver is transmitted across the channel using binary phase shift keying (BPSK) modulation. The transmitted symbols are corrupted by an RFI/burst channel consisting of a combination of additive white Gaussian noise (AWGN) and RFI pulses. At the receiver, a soft-decision Viterbi decoder with no quantization and variable truncation length is used to decode the deinterleaved sequence. Author (revised)

N94-16509*# Notre Dame Univ., IN. Dept. of Electrical Engineering.
SEARCH FOR OPTIMAL DISTANCE SPECTRUM CONVOLUTIONAL CODES
Matthew C. Connor, Lance C. Perez, and Daniel J. Costello, Jr. *In its* Low-Complexity, High-Performance Bandwidth Efficient Coding and Coded Modulation Techniques for Satellite and Space Communications Nov. 1993 20 p Presented at the Fourth Annual Argonne Symposium for Undergraduates in Science, Engineering, and Mathematics, Argonne, IL, 6 Nov. 1993 (For primary document see N94-16506 03-32)
(Grants NAG5-557; NSF NCR-89-03429)
Avail: CASI HC A03/MF A01

In order to communicate reliably and to reduce the required transmitter power, NASA uses coded communication systems on most of their deep space satellites and probes (e.g. Pioneer, Voyager, Galileo, and the TDRSS network). These communication systems use binary convolutional codes. Better codes make the system more reliable and require less transmitter power. However, there are no good construction techniques for convolutional codes. Thus, to find good convolutional codes requires an exhaustive search over the ensemble of all possible codes. In this paper, an efficient convolutional code search algorithm was implemented on an IBM RS6000 Model 580. The combination of algorithm efficiency and computational power enabled us to find, for the first time, the optimal rate 1/2, memory 14, convolutional code. Author

N94-16535 Department of the Navy, Washington, DC.
METHOD AND APPARATUS FOR FORMING AN AGILE PLASMA MIRROR EFFECTIVE AS A MICROWAVE REFLECTOR Patent
Wallace M. Manheimer, inventor (to Navy), Anthony E. Robson, inventor (to Navy), and Robert A. Meger, inventor (to Navy) 26 Jan. 1993 15 p Filed 7 Apr. 1992
(AD-D015788; US-Patent-5,182,496; US-Patent-Appl-SN-867862; US-Patent-Class-315-111) Avail: US Patent and Trademark Office

This invention is a method and apparatus for forming plasma sheets of preselected planar curvature, which can be used as mirrors for X-band microwaves and above. A plasma is created using a shaped cathode. Confining magnetic fields maintains the plasma in the shape of the cathode. Additional magnetic fields can provide additional curvature to the plasma sheet. DTIC

N94-16557# Georgia Inst. of Tech., Atlanta. School of Electrical Engineering.
SIGNAL PROCESSING IN IMPULSIVE ELECTROMAGNETIC INTERFERENCE Progress Report
Serena M. Zabin 30 Jun. 1993 7 p
(Contract N00014-91-J-1334)
(AD-A266425) Avail: CASI HC A02/MF A01

Statistical signal processing functions such as signal detection, estimation, and identification play a key role in the development of effective communications, radar, and sonar systems. For example, advanced statistical methods are emerging as being particularly important in digital communications systems operating in channels corrupted by interference from such phenomena as multiple-access noise, intentional jamming, and impulsive noise sources. Conventional demodulation methods, such as coherent matched filtering, often suffer serious performance degradation when subject to interference of these types; however, this degradation can frequently be eliminated through the use of more sophisticated signal processing techniques. During this reporting period, the focus of our work has been on the problem of obtaining optimum and efficient identification and detection procedures for impulsive channels. Of particular interest is the Middleton Class A noise model, which is a widely-accepted statistical-physical model for impulsive interference superimposed on a Gaussian background. The model has two basic parameters that can be adjusted to fit a wide variety of impulsive noise phenomena occurring in practice. DTIC

N94-16649*# University of South Florida, Tampa. Dept. of Physics.
EFFICIENT COMPUTATIONAL METHODS TO STUDY NEW AND INNOVATIVE SIGNAL DETECTION TECHNIQUES IN SETI Final Technical Report, 1 Nov. 1988 - 30 Sep. 1991
Stanley R. Deans 30 Sep. 1991 6 p
(Contract NCC2-580)
(NASA-CR-193602; NAS 1.26:193602) Avail: CASI HC A02/MF A01

The purpose of the research reported here is to provide a rapid computational method for computing various statistical parameters associated with overlapped Hann spectra. These results are important for the Targeted Search part of the Search for ExtraTerrestrial Intelligence (SETI) Microwave Observing Project. Author (revised)

N94-16652# Polish Academy of Sciences, Warsaw. Inst. Podstawowych Problemow Techniki.
A PRIORI INEQUALITIES FOR AN IDEAL-INCOMPRESSIBLE LIQUID IN AN ELECTROMAGNETIC FIELD [NIEROWNOSCI APRIORYCZNE DLA CIECZY NIESCISLIWEJ-IDEALNEJ W POLU ELEKTROMAGNETYCZNYM]
Tadeusz Winkler-Drews 1992 16 p In POLISH
(IFTR-9/1992) Avail: CASI HC A03/MF A01

The phenomenon of variable electromagnetic field effects on an ideal non-dense fluid which is described as a homogeneous medium -- a liquid dielectric with 'E' and 'M' constants in a closed 'omega' domain in 3-D space is examined. An a priori estimate was derived for the system describing this phenomenon. Transl. by FLS

N94-16653# Polish Academy of Sciences, Warsaw. Inst. Podstawowych Problemow Techniki.
ANALYSIS OF AN ELECTROMAGNETIC FIELD IN THE VICINITY OF A CAUSTIC BY ASYMPTOTIC METHODS [ANALIZA POLA ELEKTROMAGNETYCZNEGO WOTOCZENIU KAUSTYKI METODAMI ASYMPTOTYCZNYMI]
Wlodzimierz Laprus 1991 22 p In POLISH
(IFTR-12/1991) Avail: CASI HC A03/MF A01

A number of methods leading to an asymptotic field expansion based on classical geometric optics, a constant field representation, heuristic theory of Fresnel zones and simple wave theory are analyzed. Corresponding asymptotic equations are given and the effect of the caustic surface on the asymptotic expansion is examined. A simple wave structure is given and the fundamental properties of simple waves for Maxwell's equations are defined. Transl. by FLS

N94-16655*# National Aeronautics and Space Administration. Langley Research Center, Hampton, VA.
ANALYSIS OF ELECTROMAGNETIC SCATTERING FROM IRREGULARLY SHAPED, THIN, METALLIC FLAT PLATES
Manohar D. Deshpande (Vigyan Research Associates, Inc., Hampton, VA.), C. R. Cockrell, Fred B. Beck, Erik Vedeler, and Melissa B. Koch Oct. 1993 49 p
(RTOP 505-64-70-01)
(NASA-TP-3361; L-17218; NAS 1.60:3361) Avail: CASI HC A03/MF A01

This report describes an application of the method of moments to calculate the electromagnetic scattering from irregularly shaped, thin, metallic flat plates in free space. In the present technique, an irregularly shaped plate is enclosed by a rectangle on which the surface-current density is

then expressed in terms of subdomain functions by dividing the rectangle into subsections. A shape function is introduced to ensure zero current outside the patch. The surface-current density is determined using the electric field integral equation (EFIE) approach in conjunction with the method of moments, and from a knowledge of the surface-current density, the electromagnetic scattering from a plate is calculated. Using this technique, the electromagnetic scattering from a hexagonal plate; an equilateral triangular plate; an equilateral triangular plate with a concentric, equilateral triangular hole and an inverted, equilateral triangular hole; and a diamond-shaped plate is computed and compared with the numerical results obtained by using the Electromagnetic Surface Patch (ESP) code developed by Ohio State University. The numerical results compare favorably with the measurements performed on these shapes in the Langley Experimental Test Range facility. Author (revised)

N94-16728# Wisconsin Univ., Madison.
REDUCING DATA DIMENSION TO LOWER SIGNAL PROCESSING COMPUTATIONAL REQUIREMENTS AND MAXIMIZE PERFORMANCE Final Report, 1 Sep. 1989 - 31 Mar. 1993
Barry D. VanVeen 11 May 1993 5 p
(Contract DAAL03-89-K-0141)
(AD-A266606; ARO-26460.22-EL) Avail: CASI HC A01/MF A01

The problem studied concerns reducing the dimension of data by mapping it through rectangular matrix transformations before application of signal processing algorithms. Our work addressed applications of this principle in adaptive beamforming, spectral estimation, and detection problems. While dimension reduction often leads to dramatic reductions in the computational burden of the signal processing algorithm, it can also introduce significant asymptotic performance losses if the transformation is not chosen properly. We choose dimension reducing transformations to optimize performance criteria associated with the problem of interest. Our results indicate that dramatic reductions in dimension can be achieved with relatively small asymptotic performance losses using these design procedures. Performance analyses demonstrate that dimension reduction is most profitably used in applications where relatively short data records are available or fast response time is required. In these cases dimension reduction actually improves performance. DTIC

N94-16777 Mississippi State Univ., Mississippi State.
USING MARKOV CHAINS TO MODEL THE ERROR BEHAVIOR OF DATA COMMUNICATIONS CHANNELS Final Report, Mar. 1992 - Jan. 1993
Wayne D. Smith, Karen D. Burns, and Jane N. Moorhead May 1993 59 p Limited Reproducibility: More than 20% of this document may be affected by microfiche quality
(Contract F30602-92-C-0023)
(AD-A266468; RL-TR-93-87) Avail: Issuing Activity (Defense Technical Information Center (DTIC))

A description of the work performed for a project to model data communications error patterns using Markov Models is presented. It details a method for arriving at a final Markov model starting from a collection of channel error statistics, presents a rough Markov Model for a Meteor Burst Channel, and lastly presents a theoretical model for a channel that presents a non-specific, 'N-Bits in error over M-Percent' channel error pattern. DTIC

N94-16788 Naval Air Warfare Center, China Lake, CA. Weapons Div.
ENHANCED DOWN-RANGE PROFILES OF COMPLEX TARGETS USING WIDEBAND RADAR ECHO RETURNS Interim Report, Oct. - Dec. 1992
Brett Borden May 1993 18 p Limited Reproducibility: More than 20% of this document may be affected by microfiche quality
(DA Proj. BR0-5202)
(AD-A266508; NAWC-WPNS-TP-8124) Avail: Issuing Activity (Defense Technical Information Center (DTIC))

Small radar detection and tracking systems--in particular, radar guided missile systems--are of great utility because of their all-weather performance and their long range capabilities. A major drawback with these systems results from the relatively simple data that they collect and the difficulty in using these data for target classification and identification purposes. We propose a technique which employs the statistics of the tracking data used by many missile seekers and which creates a cross-range target structure map that can be expressed as a function of the target's down-range extent. These data consist of ordinary azimuth elevation phase monopulse measurements collected from a small set of (unknown) aspects presented by the target as it maneuvers. The method requires a minimal computational burden and holds the potential to be used for automatic (machine-based) target classification in realistic (time and data limited) environments. DTIC

N94-16789 Naval Air Warfare Center, China Lake, CA. Weapons Div.
WHAT IS THE RADAR TRACKING GLINT PROBLEM AND CAN IT BE SOLVED? Interim Report, Oct. - Dec. 1992
Brett Borden May 1993 16 p Limited Reproducibility: More than 20% of this document may be affected by microfiche quality
(DA Proj. BR0-5202)
(AD-A266509; NAWC-WPNS-TP-8125) Avail: Issuing Activity (Defense Technical Information Center (DTIC))

We present an elementary tutorial on the glint problem in radar tracking. Our approach uses a very simple model; yet, because of several original observations, it allows us to make some very general observations about glint. In addition, we briefly survey the collected standard mitigating approaches and comment on their relative merits and shortcomings. DTIC

N94-16794# Rice Univ., Houston, TX. Dept. of Electrical and Computer Engineering.
ANALYSIS OF TEMPORAL SYMMETRY IN NON-GAUSSIAN RANDOM FIELDS Final Report
Don H. Johnson 22 Jun. 1993 25 p
(Contract N00014-89-J-3152)
(AD-A266496) Avail: CASI HC A03/MF A01

The goal of the proposed work was to determine if the temporal asymmetry of signals could be exploited by signal processing algorithms. We specifically intended to specify the kinds of dependence structures having physical basis (rather than those chosen for the modeler's convenience) and to develop detection or estimation algorithms sensitive to these structures that yielded signal processing gains. DTIC

N94-16797# Air Force Inst. of Tech., Wright-Patterson AFB, OH. School of Engineering.
MANUFACTURING TOLERANCE REQUIREMENTS FOR FREQUENCY SELECTIVE SURFACES M.S. Thesis
Edwin V. Chavez Jun. 1993 232 p
(AD-A266541; AFIT/GE/ENG/93J-01) Avail: CASI HC A11/MF A03

This thesis investigated the change of radome transmission behavior of Frequency Selective Surfaces (FSS), with errors introduced in the slots' geometric parameters. Three FSS's were analyzed. The first is a single thin conducting plane with an array of 35 columns of thin linear slots in free space. The second is composed of two, thin conducting planes with an array of 35 columns of thin linear slots per each FSS in free space. The third consists of two thin conducting planes with an array of 21 columns of thin linear slots per each FSS, embedded in dielectric layers. After designing the ideal FSS with the code known as PMM, Gaussian errors are introduced, on lengths, widths, locations of the slot columns and z locations of reference slots in each column, and using a 'finite by infinite' array code (SFI) the value of the peak transmitted power and the radiation pattern are obtained several times for different generated Gaussian errors. All the results are tabulated and presented in a statistical and graphical way with the purpose of defining tolerance requirements. DTIC

N94-16867*# Michigan Technological Univ., Houghton. Dept. of Computer Science.
APPLICATIONS AND DEVELOPMENT OF COMMUNICATION MODELS FOR THE TOUCHSTONE GAMMA AND DELTA PROTOTYPES Final Report, 1 Jan. 1992 - 30 Jun. 1993
Steven R. Seidel 16 Aug. 1993 4 p
(Grant NAG2-757)
(NASA-CR-193617; NAS 1.26:193617) Avail: CASI HC A01/MF A01

The goal of this project was to develop models of the interconnection networks of the Intel iPSC/860 and DELTA multicomputers to guide the design of efficient algorithms for interprocessor communication in problems that commonly occur in CFD codes and other applications. Interprocessor communication costs of codes for message-passing architectures such as the iPSC/860 and DELTA significantly affect the level of performance that can be obtained from those machines. This project addressed several

specific problems in the achievement of efficient communication on the Intel iPSC/860 hypercube and DELTA mesh. In particular, an efficient global processor synchronization algorithm was developed for the iPSC/860 and numerous broadcast algorithms were designed for the DELTA.
Author (revised)

N94-16911# Cornell Univ., Ithaca, NY. Dept. of Computer Science.
UNDERSTANDING PARTITIONS AND THE NO PARTITION ASSUMPTION
Aleta Ricciardi, Andre Schiper, and Kenneth Birman Jun. 1993 12 p
(Contract N00014-92-J-1866)
(AD-A266296; TR-93-1355) Avail: CASI HC A03/MF A01

The paper discusses partitions is asynchronous message-passing systems. In such systems slow processes and slow links can lead to virtual partitions that are indistinguishable from real ones. This raises the following question: what is a partition in an asynchronous system? To overcome the impossibility of detecting crashed processes in an asynchronous system, our system model incorporates a failure suspector to detect (possibly erroneously) process failures. Based on failure suspicions we give a definition of partitions that accounts for real partitions as well as virtual ones. We show that under certain assumptions about the process behavior, any incorrect failure suspicion inevitably partitions the system. We then show how to interpret the absence of partition assumption.
DTIC

N94-16917 Department of the Navy, Washington, DC.
MOVING TARGET INDICATOR USING HIGHER ORDER STATISTICS Patent
Robert D. Pierce, inventor (to Navy) 27 Jul. 1993 16 p Filed 30 Sep. 1992
(AD-D015890; US-Patent-5,231,403; US-Patent-Appl-SN-953622) Avail: US Patent and Trademark Office

While the computation of high resolution radar images based on higher order statistics is position insensitive, velocity estimation may be based on the ratios of values of a trispectral slice and a cross-trispectral slice computed as quadruple products of complex valued signals developed by coherent radar. Signal-to-noise ratio is improved by either averaging over a plurality of bursts during computation of both the trispectral slice and the cross-trispectral slice or averaging of values of ratios of trispectral slice and cross-trispectral slice values at particular frequencies or wavenumbers, or both.
DTIC

N94-16918 Department of the Navy, Washington, DC.
HIGH RESOLUTION RADAR PROFILING USING HIGHER-ORDER STATISTICS Patent
Robert D. Pierce, inventor (to Navy) 13 Jul. 1993 14 p Filed 26 Jun. 1992
(AD-D015891; US-Patent-5,227,801; US-Patent-Appl-SN-904927) Avail: US Patent and Trademark Office

A coherent radar is used for achieving high resolution radar imaging of a moving object in sea clutter and noise. A stored replica of the transmitted waveform is combined with the returned signal in a synchronous detector to produce in-phase and quadrature (I and Q or complex) samples. High resolution is achieved by transmitting a series of pulses, each at a different frequency, and then processing these complex samples to produce a synthetic down-range profile. To enhance the radar target or object from system noise and sea clutter, the complex I and Q (in-phase and quadrature component) samples from the radar are coherently averaged in a special two-dimensional slice of the trispectrum (e.g. quadruple product or fourth-order moment). This formulation of the fourth moment retains all important target information and suppresses Gaussian noise. Once averaged, a new set of I and Q samples are reconstructed that produce the same trispectral slice as this average. These reconstructed samples are then transformed using conventional Fourier transform methods to produce the average, or enhanced, down-range profile.
DTIC

N94-16921 Department of the Navy, Washington, DC.
ACOUSTO-OPTICAL CLASSIFIER Patent
Werner G. Hueber, inventor (to Navy) and James L. Jernigan, inventor (to Navy) 6 Oct. 1992 4 p Filed 13 Dec. 1976
(AD-D015894; US-Patent-5,153,597; US-Patent-Appl-SN-752713; US-Patent-Class-342-192) Avail: US Patent and Trademark Office

An acousto-optical classifier for classifying wide bandwidth signals such as high resolution radar returns of ships or very short pulse length signals of radar emitters is presented. This is accomplished by generating the Fourier transform power spectrum with an acousto-optic cell oriented in the Bragg configuration and a low power coherent light source such as a laser. The power spectrum is detected to provide inputs to a digital classifier.
DTIC

N94-16945# Naval Postgraduate School, Monterey, CA.
TARGET DETECTION BY WAY OF KALMAN FILTERING M.S. Thesis
Gary A. Sipe Mar. 1993 83 p
(AD-A267314) Avail: CASI HC A05/MF A01

A simple, time domain method is used to analyze moderate to high PRF radar signals. The quantities of interest are the signal's PRF, SNR, and time of arrival. The time of arrival problem is important because it can be used, with multiple sensors, to determine the position of the emitting target. An algorithm is described which will produce these values using Kalman filtering. Individual pulses in a pulsed type radar are measured against a threshold using a two sample detection scheme to provide some glitch rejection. Results of individual time domain measurements of the signal parameter are smoothed with a Kalman filter. Integrating the pulse train envelope during the radar dwell time provides the energy centroid for a scan cycle. This centroid, time differenced with multiple sensors, provides observables for an Extended Kalman Filter for emitter localization. The work here simulates all data. Tests of the algorithms developed were conducted on real, classified data in addition to the work presented here.
DTIC

N94-16965# Federal Aviation Administration, Atlantic City, NJ.
SATELLITE COMMUNICATIONS INSTALLATION PLAN
Howard Meeks May 1993 21 p
(AD-A266303; DOT/FAA/CT-TN93/1) Avail: CASI HC A03/MF A01

The installation plan describes the correct installation procedures for installing low rate Satellite Communications (SATCOM) equipment in a Federal Aviation Administration (FAA) Boeing 727 aircraft. The equipment includes an antenna, satellite communication avionics, a data collection computer, and a tape recorder.
DTIC

N94-16979# Naval Postgraduate School, Monterey, CA.
FOUR FREQUENCY-SHIFT KEYING (4-FSK) SPREAD SPECTRUM MODULATOR AND DEMODULATOR M.S. Thesis
Terrence J. Murray Mar. 1993 101 p
(AD-A267433) Avail: CASI HC A06/MF A02

This thesis explores the potential use of a four frequency-shift keying (4-FSK), spread spectrum modulator and demodulator (MODEM) in a low orbit satellite. In this first approach, a short maximal length sequence of 127 chips would be used to spread the four frequencies. After successful implementation, the design could be extended to longer codes which would provide for greater processing gain. This MODEM was not preselected for use in satellite communications based on the merits of 4-FSK, but was assigned as one of four possible digital communication designs. A MODEM would be selected for use in the Petite Amateur Navy Satellite after a thorough design review.
DTIC

N94-17000# National Academy of Sciences - National Research Council, Washington, DC.
COMPUTER SCIENCE AND TELECOMMUNICATIONS BOARD ACTIVITIES
M. S. Blumenthal 23 Feb. 1993 6 p
(Contract DE-FG05-87ER-25029)
(DE93-018141; DOE/ER-25029/4) Avail: CASI HC A02/MF A01

The board considers technical and policy issues pertaining to computer science, telecommunications, and associated technologies. Functions of the board include the following: providing a base of expertise for these fields in NRC, monitoring and promoting health of these fields, initiating studies of these fields as critical resources and sources of national economic strength, responding to requests for advice, and fostering interaction among the technologies and the other pure and applied science and technology. This document describes its major accomplishments, current programs, other sponsored activities, cooperative ventures, and plans and prospects.
DOE

N94-17011# Electronic Systems Div., Hanscom AFB, MA.
GROUND WAVE EMERGENCY NETWORK FINAL OPERATIONAL CAPABILITY: ENVIRONMENTAL ASSESSMENT FOR CENTRAL WYOMING RELAY NODE, SITE NUMBER RN 8C928WY
19 Feb. 1993 108 p
(AD-A267842) Avail: CASI HC A06/MF A02

The Ground Wave Emergency Network (GWEN), which is a radio communication system designed to relay emergency messages between strategic military areas in the continental United States, is discussed.
DTIC

N94-17019# Loral Western Development Labs., San Jose, CA.
NONLINEAR METHODS FOR COMMUNICATIONS Final Report, 1 Sep. 1990 - 31 Aug. 1992
31 Aug. 1992 186 p
(Contract F49620-90-C-0065)
(AD-A267376; AFOSR-93-0484TR) Avail: CASI HC A09/MF A02

An innovative communication system has been developed. This system has the potential for improved secure communication for covert operations. By modulating data on the chaotic signal used to synchronize two nonlinear systems, they have created a Low Probability of Intercept (LPI) communications system. The researchers derived the equations which govern the system, made models of the system, and performed numerical simulations to test these models. The theoretical and numerical studies of this system have been validated by experiment. A recent design improvement has led to a system that synchronizes at 0 db Signal-to-Noise. This development holds the promise of a Low Probability of Detection (LPD) system.
DTIC

N94-17025# Naval Postgraduate School, Monterey, CA.
DESIGN OF BROADBAND WIRE ANTENNAS FOR FREQUENCY HOPPING APPLICATIONS M.S. Thesis
Keem B. Thiem Mar. 1993 143 p
(AD-A267405) Avail: CASI HC A07/MF A02

For a variety of mechanical and electrical reasons, the U.S. Army prefers to use a wire antenna for its mobile applications in the HF and VHF bands. However, due to the rapid fluctuation of impedance with frequency, a simple wire antenna is not suitable. This research will look into the aspects of electronic switching of the antenna length and electronic switching of the accompanying tuning network for frequency hopping applications. Two separate schemes will be studied. The first one involves a chosen wire antenna loaded with PIN diodes. The diodes will be selectively switched ON or OFF at different frequencies to control the input impedance of the antenna. In the second scheme, a monopole antenna of fixed length will be considered and data on its input impedance over many sub-bands within 30 to 90 MHz will be generated. Tuning networks composed of resistors, inductors, and capacitors will be designed over each sub-band. The various networks will then be connected via PIN diodes and selectively switched to provide matching over a much wider band.
DTIC

N94-17026 Naval Postgraduate School, Monterey, CA.
AN APPROXIMATION FOR COMPUTING REDUCTION IN BANDWIDTH REQUIREMENTS USING INTELLIGENT MULTIPLEXERS M.S. Thesis
Lesley J. Henson Mar. 1993 85 p Limited Reproducibility: More than 20% of this document may be affected by microfiche quality
(AD-A267434) Avail: CASI HC A05

This paper stochastically models a single-node telecommunications system both with and without the use of intelligent multiplexing. Intelligent multiplexers take advantage of the idle periods or silences that occur during the course of speech transmissions to merge (or multiplex) packetized talkspurts from more than one source onto a single channel. This allows for a more efficient use of available bandwidth, thereby reducing the amount of bandwidth required to carry a particular traffic load. Digitizing speech into packets of equal size also allows for compression, further reducing bandwidth needs. By comparing the models for systems both with and without multiplexing, we are able to determine the reduction in bandwidth which may be expected for a particular grade of service (measured by blocking probabilities). A bivariate continuous time Markov chain model for a multiplexer is presented. An approximation is introduced to calculate limiting blocking probabilities much more quickly and for larger systems than is possible by solving a set of linear equations for the bivariate model. The accuracy of the approximation is explored through comparison with the bivariate model; the approximation provides a somewhat conservative estimate of blocking, but is close enough to be used as a tool for the range of relevant values. The approximation is then used to compare blocking probabilities for three different levels of speech activity. Results are shown in tabular form.
DTIC

N94-17031# Air Force Inst. of Tech., Wright-Patterson AFB, OH.
RADOME DEPOLARIZATION EFFECTS ON MONOPULSE RECEIVER TRACKING PERFORMANCE Ph.D. Thesis
Michael A. Temple Jun. 1993 199 p
(AD-A267446; AFIT/DS/ENG/93-03) Avail: CASI HC A09/MF A03

Boresight Error (BSE), defined as the angular deviation between the true position and the apparent position of a target as indicated by radar, is an important figure of merit for a tracking radar. A significant contributor to system BSE is the protective radome. This research effort employed a GO technique to investigate the effects of a radome on BSE, expanding previous ray-trace receiving techniques to include the following: (1) a uniquely defined/developed mathematical description for each surface within arbitrary multi-layer tapered radomes; (2) an 'ideal' taper function concept for obtaining optimum BSE prediction performance; (3) a generalized technique for calculating specular reflection points within the radome; and (4) the total retractive effects along ray propagation paths. Computer model results were compared with limiting case data (BSE = 0 deg), published experimental data, and production system acceptance test data. For all limiting cases, 'system' modeling error was less than .06 mRad. 'Excellent' (BSE within +/- 1 mRad) results were obtained using a hemispheric radome with a displaced aperture gimbal point; predicted BSE values were within +/-1 mRad of published experimental data. Likewise, BSE predictions for the production system were within +/-0.5 mRad of measured data over a 30 deg scan range. Ray refractive effects on BSE prediction were characterized using the validated model.
DTIC

N94-17033# Kaman Sciences Corp., Utica, NY.
SIGNAL DETECTION IN CORRELATED GAUSSIAN AND NON-GAUSSIAN RADAR CLUTTER Final Technical Report, Aug. 1990 - Dec. 1991
M. Rangaswamy, P. Chakravarthi, D. Weiner, L. Cai, and H. Wang May 1993 278 p
(Contract F30602-89-C-0082)
(AD-A267453; RL-TR-93-79) Avail: CASI HC A13/MF A03

The subject of this report is the detection of weak targets in a strong clutter environment. Two situations arise depending on whether or not the weak targets can be separated from the clutter. For both cases new receivers are derived which provide significant improvement in performance over other recently proposed techniques. This work includes development of an adaptive joint-domain space-time processor, effective non-gaussian weak signal detectors based on spherically invariant random processes, and a new method for approximating the underlying probability density function of random data which works extremely well with only 100 samples.
DTIC

N94-17035# Naval Postgraduate School, Monterey, CA.
EVALUATION OF SITE EFFECTS ON A HIGH FREQUENCY DIRECTION FINDING SINGLE SITE LOCATION SYSTEM M.S. Thesis
Gerasimos D. Milatos Mar. 1993 128 p
(AD-A267465) Avail: CASI HC A07/MF A02

An important resource for Signal Intelligence activity in High Frequency Direction Finding (HFDF) is the use of Single Site Location (SSL) systems. Present research and development is aimed at developing tactical, mobile, easy to deploy SSL systems for locating hostile HF transmitters. These systems can detect, determine azimuth and elevation angles of incoming signals, and using ionospheric height information can calculate emitter location. The success or failure of SSL systems is dependent on many different factors, some of which are associated with site effects. System operation over different ground parameters can affect the accuracy of locating emitters. In this thesis, the performance of an 'X' shaped interferometer HF SSL system is examined using the Numerical Electromagnetics Code (NEC). Performance in the presence of two different types of lossy ground conditions are investigated.
DTIC

N94-17048# Polish Academy of Sciences, Warsaw. Inst. Podstawowych Problemow Techniki.
AN ASYMPTOTIC EXPANSION OF AN ELECTROMAGNETIC FIELD IN THE VELOCITY OF A CAUSTIC IN THE FORM OF SIMPLE WAVES [ASYMPTOTYCZNE ROZWINIECIE POLA ELEKTROMAGNETYCZNEGO W OTOCZENIU KAUSTYKE W POSTACI FAL PROSTYCH]
Wlodzimierz Laprus 1991 12 p In POLISH
(IFTR-14/1991) Avail: CASI HC A03/MF A01

Solutions of a simple wave are found for Maxwell's equations. Based on these solutions the method employed to construct an asymptotic solution in the vicinity of the caustic which has either cylindrical or cosine symmetry is demonstrated. The effect of the waveform of a simple wave on the field magnitude at the caustic is defined. NTIS

N94-17057# Polish Academy of Sciences, Warsaw. Inst. Podstawowych Problemow Techniki.
THE EXACT SOLUTION OF THE PROBLEM OF DIFFRACTION OF AN ELECTROMAGNETIC PLANE WAVE BY A CONDUCTIVE HALF-PLANE SITUATED AT AN INTERFACE [ROZWIAZANIE SCISLE ZAGADNIENIA DYFRAKCJI ELEKTROMAGNETYCZNEJ FALI PLASKIEJ NA PRZEWODZACEJ POLPLASZCZYZNIE UMIESZCZONEJ NA GRANICY OSRODKOW]
Adam Ciarkowski 1991 23 p In POLISH
(IFTR-3/91) Avail: CASI HC A03/MF A01

An exact solution of a two-dimensional problem of electromagnetic E and H wave diffraction by an ideally conducting semi-plane at the interface between two different dielectric media is found based on the Jones method. NTIS

N94-17064# Polish Academy of Sciences, Warsaw. Inst. Podstawowych Problemow Techniki.
THE INFLUENCE OF THE LEVEL FORMANTS ON THE PERCEPTION OF SYNTHETIC VOWEL SOUNDS [WPLYW POZIOMU FORMANTOW NA PERCEPCJE SYNTETYCZNYCH DZWIEKOW SAMOZGLOSKOWYCH]
Henryk Kubzdela and Mariuz Owsianny 1991 39 p In POLISH
(IFTR-41/1991) Avail: CASI HC A03/MF A01

A computer model of a generator of periodic complex sounds simulating consonants was developed. The system makes possible independent regulation of the level of each of the formants and instant generation of the sound. A trapezoid approximates the curve of the spectrum within the range of the formant. In using this model, each person in a group of six listeners experimentally selected synthesis parameters for six sounds that to him seemed optimal approximations of Polish consonants. From these, another six sounds were selected that were identified by a majority of the six persons and several additional listeners as being best qualified to serve as prototypes of Polish consonants. These prototypes were then used to randomly create sounds with various combinations at the level of the second and third formant and these were presented to seven listeners for identification. The results of the identifications are presented in table form in three variants and are described from the point of view of the requirements of automatic recognition of consonants in continuous speech. Transl. by FLS

N94-17110# Naval Command, Control and Ocean Surveillance Center, San Diego, CA.
MEASUREMENTS OF THE RADAR CROSS SECTION AND INVERSE SYNTHETIC APERTURE RADAR (ISAR) IMAGES OF A PIPER NAVAJO AT 9.5 GHz AND 49 GHz Final Report, FY1991 - FY1993
R. Dinger, G. Kinzel, W. Lam, and S. Jones Jan. 1993 48 p
(AD-A267570; NRAD-TR-1569) Avail: CASI HC A03/MF A01

Studies were conducted of the enhanced radar cross section (RCS) and improved inverse synthetic aperture radar (ISAR) image quality that may result at millimeter-wave (mmw) frequencies. To study the potential for mmw radar in these areas, a program was initiated in FY-90 to design and fabricate a 49.0- to 49.5-GHz stepped-frequency radar. After conducting simultaneous measurements of the RCS of an airborne Piper Navajo twin-engine aircraft at 9.0 and 49.0 GHz, the RCS at 49.0 GHz was always found to be higher than at 9.0 GHz by an amount that depended on the target aspect angle. The largest increase was 19 dB and was measured at nose-on incidence; at other angles of incidence, the increase ranged from 3 to 10 dB. The increase averaged over a 360-degree aspect-angle change was 7.2 dB. The 49.0-GHz radar has demonstrated a capability to gather well-calibrated millimeter-wave RCS data of flying targets. In addition, the successful ISAR images obtainable with short aperture time suggest that 49.0-GHz radar may have a role to play in noncooperative target identification (NCTI). DTIC

N94-17196# Air Force Inst. of Tech., Wright-Patterson AFB, OH. School of Engineering.
PHASED ARRAY ANTENNA ANALYSIS USING HYBRID FINITE ELEMENT METHODS Ph.D. Thesis
Daniel T. McGrath Jun. 1993 147 p
(AD-A267620; AFIT/DS/ENG/93-4) Avail: CASI HC A07/MF A02

This research in computational electromagnetics developed a new method for predicting the near-field mutual coupling effects in phased array antennas, using the finite element method (FEM) in combination with integral equations. Accurate feed modeling is accomplished by enforcing continuity between the FEM solution and an arbitrary number of wave guide models across a ground plane aperture. A periodic integral equation is imposed above the antenna's physical structure in order to enforce the radiation condition and to confine the analysis to an array unit cell. The electric field is expanded in terms of vector finite elements, and Galerkin's method is used to write the problem as a matrix equation. A general-purpose computer code was developed and validated by comparing its results to published data for several array types. Its versatility was demonstrated with predictions of the scanning properties of arrays of printed dipoles and printed flared notches. DTIC

N94-17199# General Accounting Office, Washington, DC. National Security and International Affairs Div.
MILITARY SATELLITE COMMUNICATIONS: OPPORTUNITY TO SAVE BILLIONS OF DOLLARS. REPORT TO THE CHAIRMAN, LEGISLATION, AND NATIONAL SECURITY SUBCOMMITTEE, COMMITTEE ON GOVERNMENT OPERATIONS, HOUSE OF REPRESENTATIVES
Jul. 1993 18 p
(AD-A267627; GAO/NSIAD-93-216) Avail: CASI HC A03/MF A01

During the past several years, the Congress has been critical of DOD's management of satellite communications-a primary concern being high costs. In August 1989, the House Appropriations Committee expressed concern that DOD's satellite communications architecture was in a state of disarray. It directed DOD to provide a comprehensive plan, defining all satellite communications requirements and potential solutions to meet the requirements within realistic resource levels. In October 1990, during deliberations on the fiscal year 1991 defense appropriations bill, the conference committee expressed dissatisfaction with the plan that DOD had provided in March 1990. The committee was concerned about the lack of a comprehensive architecture and directed DOD to submit a clear and affordable plan with the fiscal year 1992 defense budget request. DTIC

N94-17200# Electronic Systems Div., Hanscom AFB, MA.
GROUND WAVE EMERGENCY NETWORK FINAL OPERATIONAL CAPABILITY: ENVIRONMENTAL ASSESSMENT FOR CENTRAL NEVADA RELAY NODE, SITE NUMBER RN 8W917NV
5 Mar. 1993 96 p
(AD-A267630) Avail: CASI HC A05/MF A01

The Ground Wave Emergency Network (GWEN) is a radio communication system designed to relay emergency messages between strategic military areas in the continental United States. DTIC

N94-17205# Electronic Systems Div., Hanscom AFB, MA.
GROUND WAVE EMERGENCY NETWORK FINAL OPERATIONAL CAPABILITY: ENVIRONMENTAL ASSESSMENT FOR SOUTHERN NEVADA RELAY NODE SITE NUMBER RN 8W918NV
5 Mar. 1993 200 p
(AD-A267647) Avail: CASI HC A09/MF A03

The Ground Wave Emergency Network (GWEN) is a radio communication system designed to relay emergency messages between strategic military areas in the continental United States. The system is immune to the effects of high-altitude electromagnetic pulse (HEMP) energy surges caused by nuclear bursts in the ionosphere that would disrupt conventional communications equipment such as telephones and shortwave radios. A failure of such equipment would prevent timely communications among top

military and civilian leaders and strategic Air Force locations and prevent U.S. assessment and retaliation during an attack. GWEN is an essential part of a defense modernization program to upgrade and improve our nation's communications system, thereby strengthening deterrence. The GWEN system consists of a network of relay nodes, receive-only stations, and input/output stations. Each relay node, such as the one proposed in southern Nevada consists of a guyed radio tower facility similar to those used by commercial AM broadcast transmitters. DTIC

N94-17206# Kaman Sciences Corp., Utica, NY.
INTELLIGENT USE OF CFAR ALGORITHMS Interim Report, Jan. - Sep. 1992
P. Antonik, B. Bowles, G. Capraro, L. Hennington, and A. Koscielny May 1993 145 p
(Contract F30602-91-C-0017)
(AD-A267755; RL-TR-93-75) Avail: CASI HC A07/MF A02

The objective of this program is to demonstrate CFAR detection improvement by applying artificial intelligence techniques. The basic concept is one in which a system that dynamically selects the most appropriate CFAR algorithms based upon the characteristics of the interference, out-perform a single, fixed CFAR algorithm. This report describes one prototype Expert System CFAR Processor, its current status, implementation details and capabilities. Also discussed are CFAR algorithm testing and evaluation, and rulebase development. DTIC

N94-17211# Electronic Systems Div., Hanscom AFB, MA.
GROUND WAVE EMERGENCY NETWORK FINAL OPERATIONAL CAPABILITY: ENVIRONMENTAL ASSESSMENT FOR CENTRAL UTAH RELAY NODE, SITE NUMBER RN 8C920UT
16 Apr. 1993 94 p
(AD-A267628) Avail: CASI HC A05/MF A01

The ground wave emergency network (GWEN) is a radio communication system designed to relay emergency messages between strategic military areas in the continental United States. DTIC

N94-17212# Electronic Systems Div., Hanscom AFB, MA.
GROUND WAVE EMERGENCY NETWORK FINAL OPERATIONAL CAPABILITY: ENVIRONMENTAL ASSESSMENT FOR NORTHWESTERN NEBRASKA RELAY NODE, SITE NUMBER RN 8C930NE
19 Feb. 1993 95 p
(AD-A267629) Avail: CASI HC A05/MF A01

The Ground Wave Emergency Network (GWEN) is a radio communication system designed to relay emergency messages between strategic military areas in the continental United States. The system is immune to the effects of high-altitude electromagnetic pulse (HEMP) energy surges caused by nuclear bursts in the ionosphere that would disrupt conventional communications equipment such as telephones and shortwave radios. A failure of such equipment would prevent timely communications among top military and civilian leaders and strategic Air Force locations and prevent U.S. assessment and retaliation during an attack. GWEN is an essential part of a defense modernization program to upgrade and improve our nation's communications system, thereby strengthening deterrence. The GWEN system consists of a network of relay nodes, receive-only stations, and input/output stations. Each relay node, such as the one proposed in northwestern Nebraska, consists of a guyed radio tower facility similar to those used by commercial AM broadcast transmitters. DTIC

N94-17228# Rome Lab., Griffiss AFB, NY.
TRUE TIME DELAY OPTICALLY CONTROLLED DUAL BAND TRANSMITTER Report, Feb. - Dec. 1992
Serey Thai May 1993 43 p
(AD-A267663; RL-TR-93-84) Avail: CASI HC A03/MF A01

The main principal of this microwave multiband phased array antenna is the use of optically controlled photonic delay line for beam forming and steering. This system is suitable for spaceborne and airborne phased array applications. It also has a potential to perform frequency hopping of transmitting signals since it is a dual band transmitter (L and X-band) and the dual band system is controlled by one set of frequency independent delay lines. The L-band (1 to 2.6 GHz) array and the X-band (8 to 12 HGz) array, each has the same physical length. Each is split into four subarrays and use a common time delay generator for each subarray on both bands. True time delay with wideband radiating elements permits large transmit and receive frequency excursions without beam wander (beam squint) as the frequency is changed, and also permits the use of wideband waveforms. The advantage also extends to both communications and surveillance applications where the beam wanders off target could occur without the use of the optically controlled true time delay beam forming and steering. DTIC

N94-17249# Electronic Systems Div., Hanscom AFB, MA.
GROUND WAVE EMERGENCY NETWORK ENVIRONMENTAL ASSESSMENT FOR NORTHWESTERN COLORADO RELAY NODE SITE NUMBER RN 8C924CO Final Report
19 Feb. 1993 200 p
(AD-A267654) Avail: CASI HC A09/MF A03

The Ground Wave Emergency Network (GWEN) is a radio communication system designed to relay emergency messages between strategic military areas in the continental United States. The system is immune to the effects of high-altitude electromagnetic pulse (HEMP) energy surges caused by nuclear bursts in the ionosphere that would disrupt conventional communications equipment such as telephones and shortwave radios. A failure of such equipment would prevent timely communications among top military and civilian leaders and strategic Air Force locations and prevent U.S. assessment and retaliation during an attack. GWEN is an essential part of a defense modernization program to upgrade and improve our nation's communications system, thereby strengthening deterrence. The GWEN system consists of a network of relay nodes, receive-only stations, and input/output stations. Each relay node, such as the one proposed in southern Nevada consists of a guyed radio tower facility similar to those used by commercial AM broadcast transmitters. DTIC

N94-17268# Sparta, Inc., Lexington, MA.
BACKSCAT LIDAR SIMULATION VERSION 3.0: TECHNICAL DOCUMENTATION AND USERS GUIDE
John R. Hummel, David R. Longtin, Nanette L. DePiero, and Robert J. Grasso 3 Dec. 1992 128 p
(Contract F19628-91-C-0093)
(AD-A267296; LTR92-017; PL-TR-92-2328; AD-E201501) Avail: CASI HC A07/MF A02

The Geophysics Directorate of Phillips Laboratory is developing a number of lidar systems for use in probing the atmosphere. These systems include backscatter lidars to study atmospheric aerosols, Doppler lidar systems to measure wind fields, and Raman lidars to study the distributions of different molecular species. To aid in the design and use of such lidar systems, SPARTA has developed a lidar simulation program, BACKSCAT. Originally developed to include only the backscattered return from aerosols, the simulation package has evolved to include Raman scattering processes. BACKSCAT Version 3.0 includes two significant improvements. The first is the inclusion of user-defined aerosol layers and the second is the consideration of Raman scattering processes. In BACKSCAT Version 3.0, a user-defined aerosol layer is defined by a number density profile, a size distribution shape, and an index of refraction. Aerosol attenuation properties are computed using an efficient Mie scattering program that is coupled to the BACKSCAT simulation system. Users can select from a library of aerosol indices of refraction for common aerosols or they can input specific values. DTIC

N94-17304# Electronic Systems Div., Hanscom AFB, MA.
GROUND WAVE EMERGENCY NETWORK. FINAL OPERATIONAL CAPABILITY. ENVIRONMENTAL ASSESSMENT FOR SOUTHEASTERN IDAHO RELAY NODE, SITE NO. RN8W927ID
19 Feb. 1993 98 p
(AD-A267796) Avail: CASI HC A05/MF A02

The Ground Wave Emergency Network (GWEN) is a radio communication system designed to relay emergency messages between strategic military areas in the continental United States. DTIC

N94-17307# Prins Maurits Lab. TNO, Rijswijk (Netherlands).
A 27 CHANNELS, 1 MHz FIBRE-OPTIC MEASURING SYSTEM [EEN 27-KANNALS, 1 MHZ OPTISCH MEETSYSTEEM]
M. A. Kaanders Mar. 1993 109 p In DUTCH
(AD-A266943; PML-1992-114; TDCK-92-2752) Avail: CASI HC A06/MF A02

The Kapitza facility is a pulse forming network consisting of an energy

source, semiconductor opening switch, pulse transformer and a load. To characterize the Kapitza facility, there is a need for a measurement system where the sensors are completely separated electrically from the Data Acquisition System. A measurement system based upon fiber-optic data transmission was finally chosen. This fiber-optic system, with a bandwidth of 1 MHz, uses FM transmission techniques; the data input is used to frequency modulate the optical carrier that is coupled to the fiber, and subsequently demodulated at the receiver to recover the analog signal. In this report the operation of the optical measurement system, the components that have been used and the calibration of the transmitter/receiver units are some of the subjects that are discussed. In the appendix, schematics, print layouts, lists with the used components, wave forms of the input output signals and specifications are given. DTIC

N94-17309 Surveillance Research Lab., Salisbury (Australia).
NOTES ON THE USE OF DEMPSTER-SHAFER AND FUZZY REASONING TO FUSE IDENTITY ATTRIBUTE DATA
D. J. Kewley Aug. 1992 22 p Limited Reproducibility: More than 20% of this document may be affected by microfiche quality
(AD-A267426; SRL-0094-TM; DODA-AR-007-012) Avail: CASI HC A03

Dempster-Shafer evidential reasoning (D-S) has been applied to fusion of identity attribute data by Filippidis and Schapel. Their example involved deciding, from a given list, which radar emitter was producing the frequency and pulse rate measured by an ESM receiver. The D-S method was used to reach conclusions under uncertainty. Here an alternative approach using fuzzy reasoning is compared to their results. It is seen that the same conclusions are reached with a considerable reduction in computation. The ability to consider new data after a conclusion is reached is seen to be an additional reason for favoring the use of fuzzy reasoning for data fusion of this type. A discussion on the relationship between the approaches is provided. DTIC

N94-17322*# National Aeronautics and Space Administration. Goddard Space Flight Center, Greenbelt, MD.
MICRO PULSE LASER RADAR Patent Application
James Spinhirne, inventor (to NASA) 13 Aug. 1992 35 p
(NASA-Case-GSC-13493-1; NAS 1.71:GSC-13493-1;
US-Patent-Appl-SN-929216) Avail: CASI HC A03/MF A01

An eye safe, compact, solid state lidar for profiling atmospheric cloud and aerosol scattering is disclosed. The transmitter of the micro pulse lidar is a diode pumped micro-J pulse energy, high repetition rate Nd:YLF laser. Eye safety is obtained through beam expansion. The receiver employs a photon counting solid state Geiger mode avalanche photodiode detector. Data acquisition is by a single card multichannel scaler. Daytime background induced quantum noise is controlled by a narrow receiver field-of-view and a narrow bandwidth temperature controlled interference filter. Dynamic range of the signal is limited to optical geometric signal compression. Signal simulations and initial atmospheric measurements indicate that micropulse lider systems are capable of detecting and profiling all significant cloud and aerosol scattering through the troposphere and into the stratosphere. The intended applications are scientific studies and environmental monitoring which require full time, unattended measurements of the cloud and aerosol height structure. NASA

N94-17364# New Mexico Inst. of Mining and Technology, Socorro. Geophysical Research Center.
REMOTE SENSING OF PRECIPITATION AND ELECTRIFICATION WITH A DUAL-POLARIZATION, COHERENT, WIDEBAND RADAR SYSTEM Final Report, 15 Jul. 1989 - 14 Jul. 1993
Paul Krehbiel and Grant Gray 10 Jul. 1993 31 p
(Grant AF-AFOSR-0450-89)
(AD-A267479; AFOSR-93-0564TR) Avail: CASI HC A03/MF A01

Electrical alignment of precipitation particles was detected in an electrified storm using the co- and cross-polar channels of the radar. The radar receiver chain was upgraded and modern signal processing and display equipment added. The system was taken to Kennedy Space Center for final checkout and data-gathering independently and in conjunction with the CaPE program. Using the cross-polar correlation magnitude and phase displays as a guide, it was possible to accurately predict the outset of electrification and attendant lightning discharges, and to determine when a storm would no longer produce lightning. Several publications documenting the effect are included. A patent on the cross-polar correlation technique is being sought. DTIC

N94-17373# Naval Research Lab., Washington, DC.
AN ELECTROMAGNETIC INTERFERENCE STUDY OF POTENTIAL TRANSMITTER SITES FOR THE HF ACTIVE AURORAL RESEARCH PROGRAM (HAARP) Interim Report
Joseph A. Goldstein, Edward J. Kennedy, Adrian S. Eley, and Michael A. Rupar 19 Jul. 1993 41 p
(AD-A267743; NRL/MR/5554-93-7375) Avail: CASI HC A03/MF A01

This report presents the results of Electromagnetic Interference (EMI) measurements conducted by the Naval Research Laboratory in June of 1991. This study examined a number of potential sites for the location of the proposed High Frequency Active Auroral Research Program (HAARP) transmitter facility. The proposed HAARP facility will consist of a large planar array of antennas excited by phased high power transmitters operating in the lower portion of the HF band (2.8 to 8 MHz). Several candidate locations were identified for study in the vicinity of Fairbanks, Alaska. The magnitude of EMI in the population centers and on other commercial and public facilities in the vicinity of Fairbanks from the high power transmitter is a major factor in the site selection process for HAARP. The EMI investigations were conducted in two phases. For Phase I of the study, EMI measurements were conducted at two receiver locations using an airborne transmitter at thirteen potential HAARP sites. The results from the Phase 1 measurements were examined and the two most promising candidate transmitter locations were selected for more comprehensive measurements during Phase 2. For Phase 2, comprehensive EMI measurements were made for each of the two candidate transmitter sites. Field strengths were measured at a variety of receiver locations that are representative of the impact area for the EMI from HAARP. The results for both the Phase 1 and Phase 2 measurements are presented in this report. DTIC

N94-17376# Electronic Systems Div., Hanscom AFB, MA.
GROUND WAVE EMERGENCY NETWORK FINAL OPERATIONAL CAPABILITY. ENVIRONMENTAL ASSESSMENT FOR SOUTHERN ARKANSAS RELAY NODE SITE NO. RN 8C912AR
19 Feb. 1993 200 p
(AD-A268001) Avail: CASI HC A09/MF A03

The Ground Wave Emergency Network (GWEN) is a radio communication system designed to relay emergency messages between strategic military areas in the continental United States. The system is immune to the effects of high-attitude electromagnetic pulse (HEMP) energy surges caused by nuclear bursts in the ionosphere that would disrupt conventional communications equipment such as telephones and shortwave radios. A failure of such equipment would prevent timely communications among top military and civilian leaders and strategic Air Force locations and prevent U.S. assessment and retaliation during an attack. GWEN is an essential part of a defense modernization program to upgrade and improve our nation's communications system, thereby strengthening deterrence. DTIC

N94-17406# Electronic Systems Div., Hanscom AFB, MA.
ENVIRONMENTAL ASSESSMENT FOR NORTHWESTERN INDIANA RELAY NODE SITE NO. RN 8C902IN Final Report
5 Mar. 1993 98 p
(AD-A267849) Avail: CASI HC A05/MF A02

The Ground Wave Emergency Network (GWEN) is a radio communication system designed to relay emergency messages between strategic military areas in the continental United States. DTIC

N94-17407 Royal Netherlands Meteorological Inst., De Bilt.
AUTOMATIC SUPPRESSION OF ANOMALOUS PROPAGATION CLUTTER FOR NONCOHERENT WEATHER RADARS
H. R. A. Wessels and J. H. Beekhuis 1992 17 p
(KNMI-WR-92-06; ISBN-90-369-2028-0; ETN-93-94538) Copyright Avail: Royal Netherlands Meteorological Institute, P.O. Box 201, 3730 AE De Bilt, Wilhelminalaan 10, Netherlands

Pulse to pulse radar echo fluctuations were used to distinguish rain from anomalous propagation clutter. For one deg sectors at a fixed range 14 echo samples from successive pulses are tested for clutter. This test has a clutter detection rate of only 45 percent, but in each 1 deg/km polar radar pixel 8 range bins can be tested. The 8 tests are shown to be

nearly independent and their combined result allows 85 percent of the clutter pixels to be detected. The pattern of suspect pixels in the completed radar picture is analyzed on a scale of about 10 km. The total result is an average removal efficiency of about 98 percent. Only echoes of very light precipitation are erroneously suppressed by this processing: at most 5 percent of light rain pixels or 15 percent of light snow pixels are removed. For online application this method requires a fast preprocessor operating in combination with the radar's digital signal integrator. ESA

N94-17431# Rome Lab., Griffiss AFB, NY.
PROCEEDINGS OF THE 1992 ANTENNA APPLICATIONS SYMPOSIUM, VOLUME 1
Paul Mayes Jun. 1993 344 p Symposium held in Griffis AFB, NY, 23-25 Sep. 1992
(AF Proj. 4600)
(AD-A268167; RL-TR-93-119-Vol-1) Avail: CASI HC A15/MF A03

The Proceedings of the 1992 Antenna Applications Symposium is a collection of state-of-the-art papers relating to phased array antennas, multibeam antennas, satellite antennas, microstrip antennas, reflector antennas, HF, VHF, UHF, and various other antennas. DTIC

N94-17463 Pennsylvania State Univ., University Park. Applied Research Lab.
HIGH ORDER NONLINEAR ESTIMATION WITH SIGNAL PROCESSING APPLICATIONS
T. W. Hilands Aug. 1993 252 p Limited Reproducibility: More than 20% of this document may be affected by microfiche quality
(AD-A268407; PSU/ARL/TR-93-08) Avail: Issuing Activity (Defense Technical Information Center (DTIC))

Two high order vector filters (HOF's) are developed for estimation in non-Gaussian noise. These filters are constructed using nonlinear functions of the innovations process. They are completely general in that the initial state covariance, the measurement noise covariance, and the process noise covariance can all have non-Gaussian distributions. The first filter is designed for systems with asymmetric probability densities. The second is designed for systems with symmetric probability densities. Experimental evaluation for estimation in non-Gaussian noise, formed from Gaussian sum distributions, shows that these filters perform much better than the standard Kalman filter, and close to the optimal Bayesian estimator. The problem of high resolution parameter estimation of superimposed sinusoids is addressed using nonlinear filtering techniques. Six separate nonlinear filters are evaluated for the estimation of the parameters of sinusoids in white and colored Gaussian noise. Experimental evaluation demonstrates that the nonlinear filters perform close to the Cramer-Rao bound for reasonable values of the initial estimation error. The recursive technique developed here is well suited for time-varying systems and for measurements with short data lengths. DTIC

N94-17496 Naval Command, Control and Ocean Surveillance Center, San Diego, CA.
APPLICATION OF THE FINITE-DIFFERENCE TIME-DOMAIN METHOD TO SCATTERING AND RADIATION PROBLEMS INVOLVING WIRES AND PLATES Final Report
B. Beker Dec. 1992 34 p Limited Reproducibility: More than 20% of this document may be affected by microfiche quality
(AD-A268396; NCCOSD/RDT/E-TD-2516) Avail: CASI HC A03

Numerical modeling of electromagnetic (EM) interaction is normally performed by using either differential or integral equation methods. Both techniques can be implemented to solve problems in frequency or time domain. The method of moments (MOM) approach to solving integral equations has matured to the point where it can be used to solve complex problems. In the past, MOM has only been applied to scattering and radiation problems involving perfectly conducting or isotropic penetrable, lossy or lossless objects. However, many materials, (e.g., composites that are used on the Navy's surface ships in practical applications) exhibit anisotropic properties. To account for these new effects, several integral equation formulations for scattering and radiation by anisotropic objects have been developed recently. The differential equation approach to EM interaction studies has seen the emergence of the finite-difference time-domain (FD-TD) method as the method of choice in many of today's scattering and radiation applications. This approach has been applied to study transient as well as steady-state scattering from many complex structures, radiation from wire antennas, and coupling into wires through narrow apertures in conducting cavities. It is important to determine whether or not, and how effectively, the FD-TD can be used to solve EM interaction problems of interest to the Navy, such as investigating potential EM interference in shipboard communication systems. Consequently, this report partly addresses this issue by dealing exclusively with FD-TD modeling of time-domain EM scattering and radiation. DTIC

N94-17498 Rice Univ., Houston, TX. Dept. of Psychology.
VISUAL DISPLAY PRINCIPLES FOR C3I SYSTEM TASKS Final Report, Sep. 1985 - Jun. 1988
William C. Howell, David M. Lane, Lila F. Laux, Loy A. Anderson, and Kritina L. Holden Jun. 1993 49 p Limited Reproducibility: More than 20% of this document may be affected by microfiche quality
(Contract MDA903-85-C-0347)
(AD-A267969; ARI-RN-93-19) Avail: Issuing Activity (Defense Technical Information Center (DTIC))

Modern C3I systems are best described as semi-automated data management and decision systems over which human operators exercise supervisory control. The effectiveness of such systems is heavily dependent on the design for human-computer interaction (HCI), an important aspect of which is the visual display interface. Current Department of Defense policy mandates consideration of such human factors issues at an early stage in the design process. Comprehensive guidelines are available for display design applications after the general system parameters have been specified. Some recommendations are general, others are specific. This report offers a set of design principles at an intermediate (conceptual) level of abstraction as a complement to existing guidelines. The purpose is to synthesize current knowledge of human cognition into a form that will be applicable to the earliest stages of display design ('cognitive' functions being the most salient and critical of those remaining for the operator in advanced C3I systems). The principles are derived from a review of the literatures on human cognition, HCI, and display design, some original research, and liberal interpretation by the authors. They are organized according to operations performed on specific categories of information in possible C3I task configurations. DTIC

N94-17519# Cornell Univ., Ithaca, NY. School of Electrical Engineering.
FEMTOSECOND CARRIER PROCESSES IN COMPOUND SEMICONDUCTORS AND REAL TIME SIGNAL PROCESSING Final Report, 1 May 1990 - 30 Apr. 1993
J. P. Krusius 1 Jul. 1993 26 p
(Contract F49620-90-C-0039)
(AD-A268122; AFOSR-0574TR) Avail: CASI HC A03/MF A01

This report is the final report on research conducted under the auspices of the Joint Services Electronics Program at Cornell University. The research is grouped under two themes: (1) femtosecond carrier processes in compound semiconductors; and (2) real time signal processing. Results on OMVPE materials growth, femtosecond laser probing of hot carriers, and ensemble Monte Carlo simulations are reported on under the first theme. Accomplishments on VLSI algorithms, fault tolerance architectures, and architectures with multiple functional units for signal processing are given under the second theme. DTIC

N94-17523# Army Test and Evaluation Command, Aberdeen Proving Ground, MD.
RADAR TRANSMITTER PROCEDURES Final Test Operations Procedure
31 Mar. 1993 76 p Supersedes TOP-6-2-517 dated 31 Dec. 1980 and TOP-5-2-530 dated 5 Dec. 1967
(AD-A268274; ITOP-6-2-530; ITOP-6-2-517) Avail: CASI HC A05/MF A01

This ITOP outlines the test methods used in evaluating the performance and characteristics of general types of radar transmitters to include single or variable frequency transmitters. The test methods serve as a guide in determining the overall efficiency of such equipment as a function of their design and their recorded performance. This ITOP is limited to methods for measuring the performance of the radar transmitter under test as a major component. Some performance aspects of the transmitter can be tested only when configured as part of a total radar system. DTIC

N94-17545 National Physical Lab., Teddington (England). Electrical Science Div.

HOW TO DEDUCE THE FAR FIELD OF AN ANTENNA FROM PLANAR NEAR-FIELD MEASUREMENTS

Graham Hygate Oct. 1992 42 p

(NPL-DES-123; ETN-93-94959) Copyright Avail: National Physical Laboratory, Teddington, Middlesex, TW11 0LW, United Kingdom

The mathematical basis for transforming measurements of a vector near field over a plane to the corresponding far field is outlined. The theory is the basis for computer programs used in the radio frequency and microwave antenna group to deduce the far field of an antenna from planar near field measurements. The Matlab program for generating the real space function and the discrete Fourier transform is given. ESA

N94-17549 National Physical Lab., Teddington (England). Materials Metrology Div.

OPTIMISATION AND SPECIFICATION OF AUGER ELECTRON SPECTROMETERS FOR SIGNAL-TO-NOISE RATIO PERFORMANCE

M. P. Seah and C. P. Hunt Apr. 1993 15 p Sponsored by Dept. of Trade and Industry, London, England

(NPL-DMM(A)-101; ETN-93-94885) Copyright Avail: Issuing Activity (National Physical Laboratory, Teddington, Middlesex, TW11 0LW, United Kingdom)

Data for the intensities of the peak and background of the Cu L(sub 3) M(sub 4,5) M(sub 4,5) Auger electron peak measured using 5 and 10 keV electron beams as a function of the angle of incidence, alpha, the angle of emission, and the spectrometer resolution, R, is presented. This data allows the performance of an instrument for sensitivity or signal to noise ratio at one condition to be related to any other condition in the ranges alpha greater than 0 and less than 7 degrees and R greater than 0.1 and less than 0.9. The performance of a cylindrical mirror analyzer with a coaxial electron gun is calculated and the behavior evaluated to show how the most sensitive operating regime differs from that of the hemispherical analyzer with an input lens. Data to relate the signal to noise ratio performances of these two forms of instruments when recorded under separate conditions is provided. ESA

N94-17565 Naval Command, Control and Ocean Surveillance Center, San Diego, CA. RDT and E Div.

ATMOSPHERIC PROPAGATION ANALYSIS PROGRAM Final Report

D. B. Law, R. Tong, T. M. Hintz, L. Terpening, and G. D. Edwards Jan. 1993 300 p Limited Reproducibility: More than 20% of this document may be affected by microfiche quality

(DA Proj. SO2-53)

(AD-A268231; NCCOSC/RDT/E-TR-1577) Avail: Issuing Activity (Defense Technical Information Center (DTIC))

The Electro-Optics Branch (Code 754) of the Naval Command, Control and Ocean Surveillance Center (NCCOSC) RDT&E Division has been assigned by NAVSEA under the Photonics Mast Program to conduct experiments to compare the performance of 3- to 5-micron and 8- to 14-micron FLIR systems in typical submarine periscope imaging environments. This report evaluates the performance of each FLIR system based on atmospheric transmittance measurements in both bands and minimum resolvable temperature (MRT) tests in two extreme weather environments (low and high precipitable water content). DTIC

N94-17582# Air Force Inst. of Tech., Wright-Patterson AFB, OH.

THE ANALYSIS OF LOW-PROFILE, BROADBAND, MONOPOLE, VEHICLE ANTENNAS AND MATCHING NETWORK SYNTHESIS M.S. Thesis

Steven D. Eiken 1993 86 p

(AD-A268340; AFIT/CI/CIA-93-051) Avail: CASI HC A05/MF A01

The characteristics of low-profile, broadband, monopole vehicle antenna designs are obtained and evaluated. This thesis describes the techniques for analysis of these antennas both numerically and experimentally. The results of these investigations are contrasted to develop an optimum design. In addition, the automated synthesis of broadband impedance matching networks was accomplished using the Real Frequency Method as well as a modification of this method. DTIC

N94-17661*# Loyola Coll., Baltimore, MD. International Technology Research Inst.

SATELLITE COMMUNICATIONS SYSTEMS AND TECHNOLOGY. EXECUTIVE SUMMARY

Burton I. Edelson (George Washington Univ., Washington, DC.), Joseph N. Pelton (Colorado Univ., Boulder.), Charles W. Bostian (Virginia Polytechnic Inst., Blacksburg.), William T. Brandon (Mitre Corp., Bedford, MA.), Vincent W. S. Chan (Massachusetts Inst. of Tech., Cambridge.), E. Paul Hager (George Mason Univ., Fairfax, VA.), Neil R. Helm (George Washington Univ., Washington, DC.), Raymond D. Jennings (Commerce Dept., Washington, DC.), Robert Kwan (Jet Propulsion Lab., California Inst. of Tech., Pasadena.), and Christoph E. Mahle (Communications Satellite Corp., Washington, DC.) et al Jul. 1993 11 p Sponsored in part by NASA, Washington and NSF

(NASA-TM-109346; NAS 1.15:109346) Avail: CASI HC A03/MF A01

The National Aeronautics and Space Administration (NASA) and the National Science Foundation (NSF) commissioned a panel of U.S. experts to study the international status of satellite communications systems and technology. The study covers emerging systems concepts, applications, services, and the attendant technologies. The panel members travelled to Europe, Japan, and Russia to gather information first-hand; they visited 17 sites in Europe, 20 sites in Japan, and four in Russia. These included major manufacturers, government organizations, service providers, and associated R&D facilities. The panel's report was reviewed by the sites visited, by the panel, and by representatives of U.S. industry. The report details the information collected and compares it to U.S. activities.

Author (revised)

N94-15222# Royal Ordnance PLC, Aylesbury (England).

MICROWAVE PROPERTIES AND SYSTEMS OVERVIEW

Ronald Lawrence *In* AGARD, Rocket Motor Plume Technology Jun. 1993 35 p (For primary document see N94-15217 03-20)

Copyright Avail: CASI HC A03/MF A03

N94-15223# Deutsche Aerospace A.G., Munich (Germany). Dynamics Systems.

PLUME RADIATION

R. Dirscherl *In* AGARD, Rocket Motor Plume Technology Jun. 1993 47 p (For primary document see N94-15217 03-20)

Copyright Avail: CASI HC A03/MF A03

N94-15566*# Academia Sinica, Shanghai (China). Lab. of Laser Technology.

SIMULTANEOUS COMPRESSION OF THE PASSIVELY MODE-LOCKED PULSEWIDTH AND PULSE TRAIN

Xiang-Chun Yang, Xiao-Lei Zhu, Zhao-Qing Wu, Zhan-Ao Sun, Fu-Min Yang (Shanghai Observatory, China.), De-Tong Tan (Shanghai Observatory, China.), Wan-Zhen Chen (Shanghai Observatory, China.), Wen-Hu Lu (Shanghai Observatory, China.), and Chi-Kun Xiao (Shanghai Observatory, China.) *In* NASA. Goddard Space Flight Center, Eighth International Workshop on Laser Ranging Instrumentation Jun. 1993 4 p (For primary document see N94-15552 03-19)

Avail: CASI HC A01/MF A06

N94-15580*# National Aeronautics and Space Administration. Goddard Space Flight Center, Greenbelt, MD.

OPTIMUM WAVELENGTHS FOR TWO COLOR RANGING

John J. Degnan *In its* Eighth International Workshop on Laser Ranging Instrumentation Jun. 1993 14 p (For primary document see N94-15552 03-19)

Avail: CASI HC A03/MF A06

N94-15582*# Institut fuer Angewandte Geodaesie, Koetzing (Germany). Forschungseinrichtung Satellitengeodaesie Fundamentalstation Wettzell.

MEASURING ATMOSPHERIC DISPERSION WITH WLRS IN MULTIPLE WAVELENGTH MODE

Ulrich Schreiber, K. H. Haufe (Institut fuer Angewandte Geodaesie, Koetzing, Germany.), and Reiner Dassing (Institut fuer Angewandte Geodaesie, Koetzing, Germany.) *In* NASA. Goddard Space Flight Center, Eighth International Workshop on Laser Ranging Instrumentation Jun. 1993 8 p (For primary document see N94-15552 03-19)

Avail: CASI HC A02/MF A06

N94-15583*# National Aeronautics and Space Administration. Goddard Space Flight Center, Greenbelt, MD.
MILLIMETER ACCURACY SATELLITES FOR TWO COLOR RANGING
John J. Degnan *In its* Eighth International Workshop on Laser Ranging Instrumentation Jun. 1993 16 p (For primary document see N94-15552 03-19)
Avail: CASI HC A03/MF A06

N94-15594*# Czech Technical Univ., Prague.
COMPUTER NETWORKING AT SLR STATIONS
Antonin Novotny *In* NASA. Goddard Space Flight Center, Eighth International Workshop on Laser Ranging Instrumentation Jun. 1993 10 p (For primary document see N94-15552 03-19)
Avail: CASI HC A02/MF A06

N94-15614*# National Aeronautics and Space Administration. Goddard Space Flight Center, Greenbelt, MD.
AIRBORNE 2 COLOR RANGING EXPERIMENT
Pamela S. Millar, James B. Abshire, Jan F. McGarry, Thomas W. Zagwodzki, and Linda K. Pacini *In its* Eighth International Workshop on Laser Ranging Instrumentation Jun. 1993 16 p (For primary document see N94-15552 03-19)
Avail: CASI HC A03/MF A06

N94-16091 Simon Fraser Univ., Burnaby (British Columbia). School of Engineering Science.
INFRA LINK: A DATA TRANSMISSION SYSTEM FOR MICROGRAVITY RESEARCH
Bill Stewart, Mike Hollingshead, Jennifer Stinn, Dennis Michaelson, and Bjarni Tryggvason *In* National Research Council Canada, Proceedings of the Second Workshop on Microgravity Experimentation 1990 5 p (For primary document see N94-16071 03-29)
Avail: Issuing Activity (National Research Council, Publication Sales and Distribution, Montreal Road, Ottawa, Ontario, K1A OR6 Canada)

N94-16197*# Brown Univ., Providence, RI.
ROVER MOUNTED GROUND PENETRATING RADAR AS A TOOL FOR INVESTIGATING THE NEAR-SURFACE OF MARS AND BEYONG Abstract Only
J. A. Grant and P. H. Schultz *In* Lunar and Planetary Inst., Twenty-Fourth Lunar and Planetary Science Conference. Part 2: G-M 1993 p 561-562 (For primary document see N94-16173 03-91)
Avail: CASI HC A01/MF A06

N94-17136 Centre National d'Etudes Spatiales, Toulouse (France).
RADIOCOMMUNICATION PROBLEMS OF A POSITION REPORTING AND BIDIRECTIONAL MESSAGERY SYSTEM USING VHF/UHF WITH LOW-EARTH ORBIT SATELLITES [ASPECTS RADIOCOMMUNICATIONS DANS UN SYSTEME DE LOCALISATION ET MESSAGERIE BIDIRECTIONNELLE EN VHF/UHF PAR SATELLITES EN ORBITE BASSE]
G. Lesthievent and M. Margery *In its* Small Satellites Systems and Services Jan. 1993 p 85-99 In FRENCH (For primary document see N94-17131 03-18)
Copyright Avail: Issuing Activity (CEPADUES-Editions, 111 rue Nicolas-Vaquelin, 31100 Toulouse, France)

N94-17160 Ministry of Posts and Telecommunications, Tokyo (Japan).
A STUDY ON AN EXPERIMENTAL COMMUNICATION SYSTEM USING MICROSATELLITES
R. Suzuki, Y. Hashimoto, R. Miura, M. Tanaka, T. Obuchi (Nippon Electric Co. Ltd., Tokyo, Japan.), K. Miyazaki (Nippon Electric Co. Ltd., Tokyo, Japan.), O. Nakagawa (Nippon Electric Co. Ltd., Tokyo, Japan.), M. Matsui (Nippon Electric Co. Ltd., Tokyo, Japan.), and N. Muranaka (Nippon Electric Co. Ltd., Tokyo, Japan.) *In* CNES, Small Satellites Systems and Services Jan. 1993 p 385-391 (For primary document see N94-17131 03-18)
Copyright Avail: Issuing Activity (CEPADUES-Editions, 111 rue Nicolas-Vaquelin, 31100 Toulouse, France)

N94-17161 Italspazio, Rome (Italy).
LEOCOM-SPES: LOW COST MESSAGE COMMUNICATIONS
G. Barresi, L. Caporicci, R. DelRicco, S. DiGirolamo, B. Pavesi, and G. Rondinelli *In* CNES, Small Satellites Systems and Services Jan. 1993 p 393-404 (For primary document see N94-17131 03-18)
Copyright Avail: Issuing Activity (CEPADUES-Editions, 111 rue Nicolas-Vaquelin, 31100 Toulouse, France)

N94-17162 Centre National d'Etudes Spatiales, Toulouse (France).
TAOS (S80): A (LEO-MSS) SYSTEM FOR POSITION REPORTING AND TELEMANAGEMENT SERVICES [TAOS (S80): UN SYSTEME LEO-MSS POUR DES SERVICES DE LOCALISATION ET DE TELEGESTION]
A. Gautier and P. Dumont *In its* Small Satellites Systems and Services Jan. 1993 p 405-415 In FRENCH (For primary document see N94-17131 03-18)
Copyright Avail: Issuing Activity (CEPADUES-Editions, 111 rue Nicolas-Vaquelin, 31100 Toulouse, France)

N94-17163 Orbital Sciences Corp., Fairfax, VA.
THE ORBCOMM SYSTEM
Martin Deckett *In* CNES, Small Satellites Systems and Services Jan. 1993 p 417-426 (For primary document see N94-17131 03-18)
Copyright Avail: Issuing Activity (CEPADUES-Editions, 111 rue Nicolas-Vaquelin, 31100 Toulouse, France)

N94-17164 European Space Agency. European Space Research and Technology Center, ESTEC, Noordwijk (Netherlands). Radiofrequency Systems Div.
MAGSS-14: MEDIUM ALTITUDE GLOBAL MOBILE SATELLITE SYSTEM WITH ENHANCED REGIONAL COVERAGE
J. Benedicto, J. Fortuny, and P. Rastrilla *In* CNES, Small Satellites Systems and Services Jan. 1993 p 427-436 (For primary document see N94-17131 03-18)
Copyright Avail: Issuing Activity (CEPADUES-Editions, 111 rue Nicolas-Vaquelin, 31100 Toulouse, France)

N94-17165 Italspazio, Rome (Italy).
FEASIBILITY STUDY OF A PERSONAL COMMUNICATIONS SYSTEM IRIDIUM-LIKE
L. Caporicci, R. DelRicco, S. DiGirolamo, C. Soddu, and G. Rondinelli *In* CNES, Small Satellites Systems and Services Jan. 1993 p 437-449 (For primary document see N94-17131 03-18)
Copyright Avail: Issuing Activity (CEPADUES-Editions, 111 rue Nicolas-Vaquelin, 31100 Toulouse, France)

N94-17168 Starsys Research Corp., Boulder, CO.
STARSYS: A VIEW AFTER WARC-92
Ashok Kaveeshwar and Raul Rodriguez *In* CNES, Small Satellites Systems and Services Jan. 1993 p 465-472 (For primary document see N94-17131 03-18)
Copyright Avail: Issuing Activity (CEPADUES-Editions, 111 rue Nicolas-Vaquelin, 31100 Toulouse, France)

33 ELECTRONICS AND ELECTRICAL ENGINEERING

Includes test equipment and maintainability; components, e.g., tunnel diodes and transistors; microminiaturization; and integrated circuitry.

For related information see also *60 Computer Operations and Hardware* and *76 Solid-State Physics.*

N94-14936# California Univ., Los Angeles.
VLSI FOR HIGH-SPEED DIGITAL SIGNAL PROCESSING Quarterly Report, 1 Apr. - 30 Jun. 1993
Alan N. Willson, Jr. 30 Jun. 1993 5 p
(Contract N00014-91-J-1852)
(AD-A267709) Avail: CASI HC A01/MF A01

During the past quarter, we have begun testing our single-processor IC's which we received from MOSIS. The chip provides for 11-bit input and output data with 16-bit internal data and 12-bit coefficients (stored in on-chip memory). The chip also has an 8-bit microprocessor bus interface for loading programs and coefficients. The IC contains 25,000 transistors

and occupies an area of 14.8 sq. mm (3.7 mm by 4.0 mm including pads) in 1.2-micron CMOS technology. A block diagram of the chip is shown. Initial testing shows that the chip is fully functional. We are in the process of testing the performance and power dissipation of the chip and characterizing the input and output timing. From simulations we expect the chip to operate at 50 MHz. DTIC

N94-15448# Technische Univ., Berlin (Germany). Fachbereich Elektrotechnik.

CIRCUITS AND CONTROL PROCESSES FOR COMBINING DIRECT CONVERTERS AND INVERTER MOTORS Ph.D. Thesis [SCHALTUNGEN UND STEUERVERFAHREN FUER DIE KOMBINATION VON DIREKTUMRICHTER UND STROMRICHTERMOTOR]

Michael Mehne 1992 131 p In GERMAN
(ETN-93-94399) Avail: CASI HC A07/MF A02

A method for inferior and superior engine speed range definition of a synchronous machine is proposed and conditions for operation interchange of direct converters and inverter motors are demonstrated. Several configurations of direct/inverse converters used as inverter motors with multiple intermediate devices were compared by simulation. It is established that the machine frequency must be chosen in the interval 5 to 12.5 Hz. The spectrum of network currents in direct operation was calculated from the simulated time curves and is found to be similar to this one of a comparable direct inverter. A higher network connection voltage is shown to be necessary for high numbers of revolution and the direct/inverse converter is found to have a lower power factor in direct operating for equal number of revolutions. It is concluded that direct/inverse converters are a powerful alternative to the well known starting processes of invertor motors and they make superfluous a system separation between direct converter and inverter motor for high power drive in any engine speed range. ESA

N94-15494# Virginia Univ., Charlottesville. School of Engineering and Applied Science.

INTEGRATED FUNDAMENTAL RESEARCH ON CURRENT COLLECTION Final Report, Feb. 1989 - Sep. 1992

Doris Kuhlmann-Wilsdorf and Leo Tran Jun. 1993 53 p
(Contract DAAA21-89-C-0027)
(AD-A266987; UVA/525234/MSE93/101; ARFSD-CR-93004) Avail: CASI HC A04/MF A01

The aim of our research was to add to the basic understanding in the area of current collection with particular emphasis on topics likely to benefit practical objectives. Under sponsorship of this contract, 23 papers were published in the international literature. Additionally, 13 invited lectures and 11 contributed lectures on various aspects of this research were delivered at universities, research laboratories, and international conferences by the principal investigator and co-workers. The development of a novel metal fiber material for sliding electrical contacts was continued with much success. This is expected to become very useful for making metal fiber brushed for homopolar motors/generators, as well as for EML armatures. Included in this report are title pages (and abstracts) for the 23 published papers. Author (revised)

N94-15547*# New Mexico Univ., Albuquerque.

NASA SPACE ENGINEERING RESEARCH CENTER FOR VLSI SYSTEM DESIGN Proposal and Annual Review

Jul. 1993 83 p
(Grant NAGw-3293)
(NASA-CR-194587; NAS 1.26:194587) Avail: CASI HC A05/MF A01

This annual report outlines the activities of the past year at the NASA SERC on VLSI Design. Highlights for this year include the following: a significant breakthrough was achieved in utilizing commercial IC foundries for producing flight electronics; the first two flight qualified chips were designed, fabricated, and tested and are now being delivered into NASA flight systems; and a new technology transfer mechanism has been established to transfer VLSI advances into NASA and commercial systems. Author (revised)

N94-15635# Varian Associates, Palo Alto, CA. Research Center.

HIGH TEMPERATURE SUPERCONDUCTIVITY Quarterly Report, period ending 31 Dec. 1992

James N. Eckstein 1 Jun. 1993 3 p
(Contract N00014-88-C-0760)
(AD-A267006) Avail: CASI HC A01/MF A01

The overall goals of this program are to develop the technology of MBE (Molecular Beam Epitaxy) growth of HTSC (High Temperature Superconductor) material, to optimize the performance of HTSC films with high transition temperatures and critical current densities, and to explore the development of electronic devices based on such material. DTIC

N94-15636# Morgan State Univ., Baltimore, MD.

A STUDY OF HIGH FIELD TRANSPORT IN WIDE BAND GAP ELECTRONIC MATERIALS USING A PICOSECOND TRANSIENT CHARGE TECHNIQUE Semiannual Report, 30 Nov. - 2 Jul. 1993

Craig J. Scott 2 Jul. 1993 9 p
(Contract N00014-93-1-0128)
(AD-A267098) Avail: CASI HC A02/MF A01

We propose a study of electron and hole traps and carrier drift velocity for high electric field strengths using the transient charge technique (TCT) with a picosecond electron beam probe. The uniqueness in the proposed approach lies in the use of a photocathode SEM to generate picosecond electron pulses with high lateral resolution to generate electron hole pairs. Ultrafast electron beam pulses allow narrow drift regions to be characterized and allow high field measurements to be performed without thermal heating. DTIC

N94-15640*# Prairie Observatory, Urbana, IL. College of Engineering and Architecture.

FAULT HANDLING SCHEMES IN ELECTRONIC SYSTEMS WITH SPECIFIC APPLICATION TO RADIATION TOLERANCE AND VLSI DESIGN Final Report, 3 Jan. 1989 - Oct. 1993

John Okyere Attia Oct. 1993 106 p
(Grant NAG9-337)
(NASA-CR-194559; NAS 1.26:194559) Avail: CASI HC A06/MF A02

Naturally occurring space radiation particles can produce transient and permanent changes in the electrical properties of electronic devices and systems. In this work, the transient radiation effects on DRAM and CMOS SRAM were considered. In addition, the effect of total ionizing dose radiation of the switching times of CMOS logic gates were investigated. Effects of transient radiation on the column and cell of MOS dynamic memory cell was simulated using SPICE. It was found that the critical charge of the bitline was higher than that of the cell. In addition, the critical charge of the combined cell-bitline was found to be dependent on the gate voltage of the access transistor. In addition, the effect of total ionizing dose radiation on the switching times of CMOS logic gate was obtained. The results of this work indicate that, the rise time of CMOS logic gates increases, while the fall time decreases with an increase in total ionizing dose radiation. Also, by increasing the size of the P-channel transistor with respect to that of the N-channel transistor, the propagation delay of CMOS logic gate can be made to decrease with, or be independent of an increase in total ionizing dose radiation. Furthermore, a method was developed for replacing polysilicon feedback resistance of SRAMs with a switched capacitor network. A switched capacitor SRAM was implemented using MOS Technology. The critical change of the switched capacitor SRAM has a very large critical charge. The results of this work indicate that switched capacitor SRAM is a viable alternative to SRAM with polysilicon feedback resistance. Author

N94-15665# Deseret Test Center, Fort Douglas, UT. Chemical Div.

RELIABILITY CHARACTERIZATION OF DIGITAL MICROCIRCUITS: INVESTIGATION OF AN IN-PROCESS OXIDE RELIABILITY SCREENING METHOD Final Report, Jan. 1991 - Nov. 1992

Chung P. Wu Apr. 1993 118 p
(Contract F30602-90-C-0063)
(AD-A267053; RL-TR-93-41) Avail: CASI HC A06/MF A02

This report covers the work performed, using a sacrificial-metal-pattern technique, to demonstrate a 100% in-process screen for oxide defects in high-density CMOS microcircuits, and to evaluate the effectiveness and side effects of the added processing steps on yield and reliability. Using large-area polysilicon capacitors and 101-stage metal-1 delay-lines in GEM WAT keys as test vehicles, experiments with split lot reliability screening and life test, first with 240 A and again with 150 A gate oxide, have demonstrated practically complete elimination of the defective populations

for test capacitors and about 50% reduction in circuit functionality failures for delay-line circuits. This is accomplished with little or no penalty in metal-polysilicon contact resistance, or in delay-line circuit yield. The technique is found to be promising and should be further investigated with more complex circuits with double-level metals. DTIC

N94-15669# Pennsylvania State Univ., University Park. Materials Research Lab.
NANOCOMPOSITES FOR ELECTRONIC APPLICATIONS, VOLUME 1 Final Report, 1 Jan. 1990 - 31 Dec. 1991
L. E. Cross 14 Jun. 1993 173 p
(Contract N00014-90-J-1558)
(AD-A267070) Avail: CASI HC A08/MF A02

Work on this program and studies associated with the ONR program on 'Piezoelectric and Electrostrictive Materials for Transducer Applications' has lead to a significantly improved understanding of the fundamental mechanisms in Relaxor Ferroelectrics. For the perovskite Lead Magnesium Niobate which is the prototype for many other relaxor perovskites, the self limiting nonstoichiometric ordering of Mg/Nb ions is shown to be the symmetry breaking key to the onset of micropolar regions at the Burns temperature well above the dielectric maximum. The simple paraelectric behavior at high temperature is shown to be modified by cooperation on cooling, leading to a Vogel/Fulcher type condensation into a glass like state at low temperature DTIC

N94-15672# Pennsylvania State Univ., University Park. Materials Research Lab.
NANOCOMPOSITES FOR ELECTRONIC APPLICATIONS, VOLUME 3 Final Report, 1 Jan. 1990 - 31 Dec. 1991
L. E. Cross 14 Jun. 1993 173 p
(Contract N00014-90-J-1558)
(AD-A267073) Avail: CASI HC A08/MF A02

Work on this program and studies associated with the ONR program on 'Piezoelectric and Electrostrictive materials for Transducer Applications' has lead to a significantly improved understanding of the fundamental mechanisms in Relaxor Ferroelectrics. For the perovskite Lead Magnesium Niobate which is the prototype for many other relaxor perovskites, the self limiting nonstoichiometric ordering of Mg/Nb ions is shown to be the symmetry breaking key to the onset of micropolar regions at the Burns temperature well above the dielectric maximum. The simple paraelectric behavior at high temperature is shown to be modified by cooperation on cooling, leading to a Vogel/Fulcher type condensation into a glass like state at low temperature DTIC

N94-15673# Pennsylvania State Univ., University Park. Materials Research Lab.
NANOCOMPOSITES FOR ELECTRONIC APPLICATIONS, VOLUME 2 Final Report, 1 Jan. 1990 - 31 Dec. 1991
L. E. Cross 14 Jun. 1993 173 p
(Contract N00014-90-J-1558)
(AD-A267074) Avail: CASI HC A08/MF A02

Work on this program and studies associated with the ONR program on 'Piezoelectric and Electrostrictive materials for Transducer Applications' has lead to a significantly improved understanding of the fundamental mechanisms in Relaxor Ferroelectrics. For the perovskite Lead Magnesium Niobate which is the prototype for many other relaxor perovskites, the self limiting nonstoichiometric ordering of Mg/Nb ions is shown to be the symmetry breaking key to the onset of micropolar regions at the Burns temperature well above the dielectric maximum. The simple paraelectric behavior at high temperature is shown to be modified by cooperation on cooling, leading to a Vogel/Fulcher type condensation into a glass like state at low temperature DTIC

N94-15706*# National Aeronautics and Space Administration. Lewis Research Center, Cleveland, OH.
A METHOD OF DETECTING AND LOCATING ELECTRICAL CURRENT IMBALANCES Patent Application
Richard L. Patterson, inventor (to NASA) 21 Jan. 1993 16 p
(NASA-Case-LEW-15407-1; NAS 1.71:LEW-15407-1;
US-Patent-Appl-SN-006413) Avail: CASI HC A03/MF A01

A method of detecting and locating current imbalances such as ground faults in multiwire systems using the Faraday effect is described. As an example, for 2-wire or 3-wire (1 ground wire) electrical systems, light is transmitted along an optical path which is exposed to magnetic fields produced by currents flowing in the hot and neutral wires. The rotations produced by these two magnetic fields cancel each other, therefore light on the optical path does not read the effect of either. However, when a ground fault occurs, the optical path is exposed to a net Faraday effect rotation due to the current imbalance thereby exposing the ground fault. NASA

N94-15726# Rockwell International Corp., Thousand Oaks, CA.
MOLTEN SALT ELECTRODEPOSITION OF HIGH TEMPERATURE SUPERCONDUCTORS Final Report, 7 Sep. 1990 - 30 Nov. 1992
D. M. Tench, M. W. Kendig, and S. Jeanjaquet Jun. 1993 52 p
(Contract N00014-90-C-0225)
(AD-A266620; SC71033.FR) Avail: CASI HC A04/MF A01

The overall objective of this project was to develop a process for direct electrodeposition of Y-Ba-Cu superconducting oxides from a molten salt at relatively low temperatures (300-550 deg C). An important finding was that cathodic deposition of metallic oxides, rather than free metals, generally occurs from nitrate melts, apparently via reduction of metal nitrato complexes. Oxide deposition was confirmed for Cu as CuO, Y as Y2O3, and Co as Co304, and apparently also occurs for Ba. Deposition of mixed Ba-Y-Cu oxides was demonstrated on both Cu and Pt substrates. Data were compiled that provide a good basis for designing schemes for deposition of various mixed oxides from nitrate melts. A sequential anodic injection method was conceived for depositing ultrathin mixed oxide layers, which can be viewed as an analog of molecular beam epitaxy. Results obtained with this approach were encouraging but were inconclusive because of contamination with Gd from the Y injection anode. Based on the results of this program and literature studies, cathodic metal oxide deposition from nitrate melts is a general phenomenon that could ultimately prove to be a practical means of preparing a variety of single and mixed anhydrous metal oxide films. It is recommended that future work focus initially on deposition of perovskite materials, which are of considerable practical interest and involve only two metallic components so that the required deposition schemes are inherently simpler. DTIC

N94-15765*# National Aeronautics and Space Administration. Ames Research Center, Moffett Field, CA.
CRYOGENIC MEASUREMENTS OF AEROJET GaAs n-JFETs
John H. Goebel and Theodore T. Weber Sep. 1993 62 p
(RTOP 590-31-11)
(NASA-TM-103972; A-92177; NAS 1.15:103972) Avail: CASI HC A04/MF A01

The spectral noise characteristics of Aerojet gallium arsenide (GaAs) junction field effect transistors (JFET's) have been investigated down to liquid-helium temperatures. Noise characterization was performed with the field effect transistor (FET) in the floating-gate mode, in the grounded-gate mode to determine the lowest noise readings possible, and with an extrinsic silicon photodetector at various detector bias voltages to determine optimum operating conditions. The measurements indicate that the Aerojet GaAs JFET is a quiet and stable device at liquid helium temperatures. Hence, it can be considered a readout line driver or infrared detector preamplifier as well as a host of other cryogenic applications. Its noise performance is superior to silicon (Si) metal oxide semiconductor field effect transistor (MOSFET's) operating at liquid helium temperatures, and is equal to the best Si n channel junction field effect transistor (n-JFET's) operating at 300 K. Author

N94-15825# Princeton Univ., NJ. Dept. of Civil Engineering and Operations Research.
STRESS SENSITIVITY OF DIELECTRIC RESONATORS Final Report, 19 Mar. 1990 - 18 Mar. 1993
Peter C. Lee 14 Jun. 1993 5 p
(Contract DAAL03-90-G-0079)
(AD-A266767; ARO-26909.6-MA) Avail: CASI HC A01/MF A01

The objective of research is to investigate the sensitivity of the frequency-shifts of the guided EM waves in dielectric resonators when they are subjected to external forces, shocks, or vibrations. Forces applied to a resonator produce stresses which, through the nonlinear piezooptical effect, changes the permittivity constant into an inhomogeneous, second-order permittivity tensor, depending upon the spatial distribution of

stresses. This changing in material property, in turn, affects the velocities and couplings of EM waves inside the resonator and hence causes the shifts of resonances. Closed form solutions of the 3-D Maxwell's equations for finite resonators are very few and they are known only for solid sphere and torus of homogeneous isotropic dielectrics. In order to study the problems of stress effect on the vibrations in dielectric plate resonators, circular or rectangular, in a systematic way, the research is conducted according to the following sequence. A system of 2-D equations for guided waves is deduced from the 3-D Maxwell's equations. Closed form solutions are obtained from these 2-D equations for circular disks embedded in free space. Then the stress sensitivity of guided waves in circular isotropic disks and in infinite anisotropic plates are studied. DTIC

N94-15874*# National Aeronautics and Space Administration. Goddard Space Flight Center, Greenbelt, MD.

FORBACK DC-TO-DC CONVERTER Patent Application

Alan T. Lukemire, inventor (to NASA) 24 Mar. 1993 33 p

(NASA-Case-GSC-13404-1; NAS 1.71:GSC-13404-1;

US-Patent-Appl-SN-038746) Avail: CASI HC A03/MF A01

A pulse-width modulated DC-to-DC power converter including a first inductor, i.e. a transformer or an equivalent fixed inductor equal to the inductance of the secondary winding of the transformer, coupled across a source of DC input voltage via a transistor switch which is rendered alternately conductive (ON) and nonconductive (OFF) in accordance with a signal from a feedback control circuit is described. A first capacitor capacitively couples one side of the first inductor to a second inductor which is connected to a second capacitor which is coupled to the other side of the first inductor. A circuit load shunts the second capacitor. A semiconductor diode is additionally coupled from a common circuit connection between the first capacitor and the second inductor to the other side of the first inductor. A current sense transformer generating a current feedback signal for the switch control circuit is directly coupled in series with the other side of the first inductor so that the first capacitor, the second inductor and the current sense transformer are connected in series through the first inductor. The inductance values of the first and second inductors, moreover, are made identical. Such a converter topology results in a simultaneous voltsecond balance in the first inductance and ampere-second balance in the current sense transformer. NASA

N94-15952*# National Aeronautics and Space Administration. Pasadena Office, CA.

CELLULOSE TRIACETATE, THIN FILM DIELECTRIC CAPACITOR Patent Application

Shiao-Ping S. Yen, inventor (to NASA) (Jet Propulsion Lab., California Inst. of Tech., Pasadena.) and T. Richard Jow, inventor (to NASA) (Jet Propulsion Lab., California Inst. of Tech., Pasadena.) 28 May 1993 13 p

(Contract NAS7-918)

(NASA-Case-NPO-18935-1-CU; NAS 1.71:NPO-18935-1-CU;

US-Patent-Appl-SN-071416) Avail: CASI HC A03/MF A01

Very thin films of cellulose triacetate are cast from a solution containing a small amount of high boiling temperature, non-solvent which evaporates last and lifts the film from the casting surface. Stretched, oriented, crystallized films have high electrical breakdown properties. Metallized films less than about 2 microns in thickness form self-healing electrodes for high energy density, pulsed power capacitors. Thicker films can be utilized as a dielectric for a capacitor. NASA

N94-15954# California Univ., Los Angeles. Dept. of Chemistry and Biochemistry.

FULLERENE SUPERCONDUCTORS Final Report, 15 May 1992 - 14 Mar. 1993

Richard B. Kaner 17 Jun. 1993 2 p

(Contract DAAL03-92-G-0188)

(AD-A266749; ARO-29708.7-CH) Avail: CASI HC A01/MF A01

The electrical, magnetic and optical properties of the fullerene superconductors K3C60 and Rb3C60 have been investigated. The room temperature microwave resistivity at 60 GHz of pressed powder samples of K3C60 is approximately 5m (ohms) cm. The resistivity drops by almost one order of magnitude on cooling to 20K, indicative of metallic behavior, before the samples superconduct at T (sub) c = 19.3K. Optical reflectivity spectra are consistent with metallic materials. An extrapolation of the frequency dependence of conductivity leads to d.c. conductivities of 1.3 x 10 (exp 3) (ohm)-I and 1.2 x 10 (exp 3) (ohm)-I for K3C60 and Rb3C60, respectively. The gap values A of 24 /cm for K3C60 and 30 /cm for Rb3C60 are consistent with weak-coupling and a BCS singlet ground state. Upper critical fields of 26-30 Tesla for K3C60 and 38-55 Tesla for Rb3C60 have been measured. The lower values are from static magnetic experiments, while the upper values used pulsed magnets. DTIC

N94-15971# Midwest Research Inst., Golden, CO. National Renewable Energy Lab.

CIRCLE DIAGRAM APPROACH FOR SELF EXCITED INDUCTION GENERATORS

E. Muljadi, P. W. Carlin, and R. M. Osgood May 1993 6 p

(Contract DE-AC02-83CH-10093)

(DE93-010031; NREL/TP-441-5611) Avail: CASI HC A02/MF A01

When an induction generator is connected to a utility line supply, the voltage and frequency at the terminal output are the same as the voltage and frequency of the utility line supply to which the generator is connected. The reactive power needed by the induction generator is supplied by the utility and the real power is returned to the utility. With a fixed frequency dictated by the utility, the induction machine starts generating above the synchronous speed. The range of speed is also limited by the slip. At a very high slip, the copper losses increases as the current increases. On the other hand, in an isolated operation, the induction generator operates in self-excitation mode. It determines its own voltage and frequency. These two quantities depend on the size of the AC capacitor, the induction machine parameters, the electrical load, and the speed of the generator. The operating speed of the induction generator is extended without generating excessive loss. This paper presents an analytical study by utilizing a circle diagram to illustrate the operation of the induction generator in isolated operation. The steady-state calculations are presented to support the analysis. Possible applications for the system in variable-speed generation are currently under investigation. The output can be directly connected to equipment that is non-sensitive to the frequency (a heater, battery charger, etc.) or can be connected to a converter to get a fixed-frequency AC output. DOE

N94-15988*# National Aeronautics and Space Administration. Langley Research Center, Hampton, VA.

A DEVICE FOR TESTING CABLES Patent Application

Arthur Ray Hayhurst, inventor (to NASA) 7 Jun. 1993 12 p

(NASA-Case-LAR-14093-1; NAS 1.71:LAR-14093-1;

US-Patent-Appl-SN-073845) Avail: CASI HC A03/MF A01

A device for testing current paths is attachable to a conductor. The device automatically checks the current paths of the conductor for continuity of a center conductor, continuity of a shield, and a short circuit between the shield and the center conductor. The device includes a pair of connectors and a circuit to provide for testing of the conductive paths of a cable to be tested with the circuit paths of the circuit. The circuit paths in the circuit include indicators to simultaneously indicate the results of the testing. NASA

N94-16061# California Univ., Berkeley. Lawrence Berkeley Lab.

IN SITU RAMAN SPECTROSCOPY OF LITHIUM ELECTRODE SURFACE IN AMBIENT TEMPERATURE LITHIUM SECONDARY BATTERY

Hiroyasu Tachikawa Sep. 1992 18 p

(Contract DE-AC03-76SF-00098)

(DE93-015238; LBL-33046) Avail: CASI HC A03/MF A01

Raman spectroscopy was used to characterize surface layers on lithium electrodes in different solvents such as propylene carbonate (PC), dimethyl carbonate (DMC), diethyl carbonate (DEC), and polyethylene glycol 400 dimethyl ether (PEG400DME). Both DMC and DEC were used singly, and also mixed with either methyl acetate (MA) or methyl formate (MF). The Raman spectra showed that passive films formed on the Li surface in different solvents may have different chemical structures, which changed during the charging and discharging processes. Raman spectroscopy was also applied to characterize zinc electrode surfaces in alkaline solutions. The results suggested that ZnO and Zn(OH)(2) formed on the Zn electrode when a passive potential was applied. A solid film of fullerene C60, which could be used as a cathode in Li rechargeable batteries, was examined in the PEG400DME solution by both electrochemical and Raman spectroscopy. Cyclic voltammograms (CV's) showed five redox peaks which suggested

the formation of C60(-), C60(2-), C60(3-), C60(4-), and C60(5-). Raman spectra obtained from a thin C60 film indicated that the thin fulleride film dissolved in the PEG400DME/LiClO4 solution at negative potentials. DOE

N94-16443# Argonne National Lab., IL.
CONTROLS OF MAGLEV SUSPENSION SYSTEMS
Y. Cai, S. Zhu, S. S. Chen, and D. M. Rote 1993 43 p Presented at the Pressure Vessels and Piping Conference, Denver, CO, 25-29 Jul. 1993
(Contract W-31-109-eng-38)
(DE93-015540; ANL/MCT/CP-78162; CONF-930702-41) Avail: CASI HC A03/MF A01

Alternative control designs of maglev vehicle suspension systems were investigated. Active and semi-active control law designs are introduced into primary and secondary suspensions of maglev vehicles. A one-dimensional vehicle with two degrees of freedom, to simulate the German Transrapid Maglev System, is used for suspension control designs. The transient and frequency responses of suspension systems and PSD's of vehicle accelerations are calculated to evaluate different control designs. The results show that active and semi-active control designs indeed improve the response of vehicle and provide an acceptable ride comfort for maglev systems. DOE

N94-16459# Department of Energy, Washington, DC. Assistant Secretary for Energy Efficiency and Renewable Energy.
UTILITY EMISSIONS ASSOCIATED WITH ELECTRIC AND HYBRID VEHICLE (EHV) CHARGING
Apr. 1993 128 p
(DE93-013734; DOE/CE-0395) Avail: CASI HC A07/MF A02

This project is a joint effort between the U.S. Department of Energy (DOE) and the Electric Power Research Institute (EPRI) to conduct a comprehensive, in-depth assessment of the emission impacts of electric and hybrid vehicles (EHV's). The study determines local and regional emission impacts under a variety of scenarios, covering both conservative and optimistic assumptions about vehicle efficiency, power plant efficiency, and other factors. In all scenarios, EHV use significantly reduces urban emissions of CO, VOC, and TSP. Changes in NO(x) and CO2 emissions are very sensitive to average or marginal power plant emissions and vehicle efficiency assumptions. NOx and CO2 emissions changes vary dramatically by region. Certain combinations of EHV and CV scenarios and regions result in significant reductions, while other combinations result in significant increases. Careful use of these results is advised. In all scenarios, SO2 increases with EHV use although the amount is small--less than 1% of total utility emissions even with the deployment of 12 million EHVS. But because of emission cap provisions of the Clean Air Act Amendments of 1990, national SO2 totals will not be allowed to increase. Thus, utilities will have to apply more stringent measures to combat increased SO2 emissions due to the increased use of electric vehicles. DOE

N94-16488 Department of the Navy, Washington, DC.
TRANSLATING WEDGE HEAT SINK Patent
Mark W. Sewell, inventor (to Navy) 8 Jun. 1993 6 p Filed 18 May 1992 Supersedes AD-D015357
(AD-D015814; US-Patent-5,218,517; US-Patent-Appl-SN-884976; US-Patent-Class-361-288) Avail: US Patent and Trademark Office

A device for dissipating heat from cased electronics where optimum heat transfer is required, and where easy removability is desired is described. The device finds utility in sonobuoys, buoys, missiles and mines, as well as cabling electronics such as transoceanic communications equipment. The device contains a translating wedge which is drawn into a forced fit between the heat generating module and a conducting wedge which contacts the electronics case, resulting in a high efficiency conducting thermal path from the electronics to the equipment case. The device is particularly efficate in circular cased electronics. DTIC

N94-16505*# Wilson Greatbatch Ltd., Clarence, NY. Electrochemical Research Div.
LITHIUM D-CELL STUDY Final Report
P. Size and Esther S. Takeuchi 31 Mar. 1993 443 p
(Contract NAS9-18395)
(NASA-CR-192705; NAS 1.26:192705) Avail: CASI HC A19/MF A04

The purpose of this contract is to evaluate parametrically the effects of various factors including the electrolyte type, electrolyte concentration, depolarizer type, and cell configuration on lithium cell electrical performance and safety. This effort shall allow for the selection and optimization of cell design for future NASA applications while maintaining close ties with WGL's continuous improvements in manufacturing processes and lithium cell design. Taguchi experimental design techniques are employed in this task, and allow for a maximum amount of information to be obtained while requiring significantly less cells than if a full factorial design were employed. Acceptance testing for this task is modeled after the NASA Document EP5-83-025, Revision C, for cell weights, OCV's and load voltages. The performance attributes that are studied in this effort are fresh capacity and start-up characteristics evaluated at two rates and two temperatures, shelf-life characteristics including start-up and capacity retention, and iterative microcalorimetry measurements. Abuse testing includes forced over discharge at two rates with and without diode protection, temperature tolerance testing, and shorting tests at three rates with the measurement of heat generated during shorting conditions. Author

N94-16549 Department of the Navy, Washington, DC.
HYDRAULIC PUMP WITH INTEGRAL ELECTRIC MOTOR Patent
William E. Schneider, inventor (to Navy) 2 Mar. 1993 8 p Filed 23 Mar. 1992
(AD-D015782; US-Patent-5,190,447; US-Patent-Appl-SN-855827; US-Patent-Class-417-356) Avail: US Patent and Trademark Office

This is a pumping mechanism featuring integration of a fixed displacement radial piston pump within an electric drive motor and cooperative operation of a radially inwardly facing piston-actuating cam with a pair of opposing axially inwardly facing spool-valve actuating cams. The piston-actuating cam is effectively the inner surface of the rotating motor rotor, the pistons extending radially from a fixed central body. Consequent benefits of the integrated configuration are greater quietness, compactness, efficiency and corrosion resistance. The external motor unit provides protection, there is a damping effect, and there are fewer parts which are subject to damage or malfunction. Further reductions in noise and leakage are gained by synchronized operation, in terms of fluid pumping, of the spool-valve actuating cams and the piston-actuating cam. The piston elements can be distributed so as to foster balanced loadings, and the pump flow rate can be controlled by varying the motor's rotational speed, thus advantageously combining the hydraulic pressure balance which is characteristic of a fixed-displacement pump with the variable delivery of a variable-displacement pump. DTIC

N94-16556# Phillips Lab., Kirtland AFB, NM.
MEASUREMENTS OF THE OPERATION OF THE SINUS-6/BWO SYSTEM Final Report, 1 Sep. - 1 Dec. 1992
Kyle J. Hendricks and Thomas A. Spencer May 1993 22 p
(AD-A266423; AD-E201487; PL-TR-93-1003) Avail: CASI HC A03/MF A01

A series of measurements were completed on the SINUS-6/BWO system presently located at the UNM EECE Dept. These measurements were necessary to establish that the rf and pulse power performances meet the contract specification. Measurements included antenna pattern plots, pulse power diagnostics, and calculations to establish what the microwave system should radiate. The SINUS-6 pulse power device produces V(sub p) approximately 600 kV, I approximately 5 kA, and tau approximately 10 ns at 200 pulses per second. The BWO parameters are P approximately 500 MW, tau approximately 10 ns, and lambda approximately 3 cm (f approximately 10 GHz). The slow wave structure is inserted into a segmented solenoid which produces a magnetic field of B(sub z) approximately 30 kG with axial uniformity over 120 mm at a radius of 20 mm. DTIC

N94-16661# Westinghouse Electric Corp., Baltimore, MD.
SONOS TECHNOLOGY FOR COMMERCIAL AND MILITARY NONVOLATILE MEMORY APPLICATIONS
D. Adams, P. Farrell, M. Jacunski, D. Williams, J. Jakubczak (Sandia National Labs., Albuquerque, NM.), M. Knoll (Sandia National Labs., Albuquerque, NM.), and J. Murray (Sandia National Labs., Albuquerque, NM.) 1993 4 p Presented at the Nonvolatile Memory Technology Review Conference, Baltimore, MD, 22 Jun. 1993
(Contract DE-AC04-76DP-00789)
(DE93-015647; SAND-93-1300C; CONF-9306181-1) Avail: CASI HC A01/MF A01

Silicon Oxide Nitride Oxide Semiconductor (SONOS) technology is well

suited for military and commercial nonvolatile memory applications. Excellent long term memory retention, radiation hardness, and endurance has been demonstrated with this technology. This paper summarizes our data in these areas for SONOS technology. DOE

N94-16765# Pacific Northwest Lab., Richland, WA.
FABRICATION OF ADVANCED DESIGN (GROOVED) CERMET ANODES
C. F. Windisch, Jr. and F. R. Huettig (Ceramic Magnetics, Inc., Fairfield, NJ.) May 1993 54 p
(Contract DE-AC06-76RL-01830)
(DE93-014590; PNL-8622) Avail: CASI HC A04/MF A01

Attempts were made to fabricate full-size anodes with advanced, or grooved, design using isostatic pressing, slip casting injection molding. Of the three approaches, isostatic pressing produced an anode with dimensions nearest to the target specifications, without serious macroscopic flaws. This approach is considered the most promising for making advanced anodes for aluminum smelting. However, significant work still remains to optimize the physical properties and microstructure of the anode, both of which were significantly different from that of previous anodes. Injection molding and slip casting yielded anode materials with serious deficiencies, including cracks and holes. Injection molding gave cermet material with the best intrinsic microstructure, i.e., the microstructure of the material between macroscopic flaws was very similar to that of anodes previously made at PNL. The reason for the similarity may have to do with amount of residual binder in the material prior to sintering. DOE

N94-16914 Department of the Navy, Washington, DC.
PROCESS OF SHAPING AN ELECTRORHEOLOGICAL SOLID Patent
Ronald P. Reitz, inventor (to Navy) 25 May 1993 13 p Filed 21 Mar. 1991
(AD-D015885; US-Patent-5,213,713; US-Patent-Appl-SN-672986; US-Patent-Class-252-500) Avail: US Patent and Trademark Office

Electrorheological solids are compositions which undergo phase change from solid phase to fluid or gel phase when activated by electric field. Objects comprising electrorheological solid compositions can be electrically repaired by electrically inducing solid to fluid phase change. Furthermore, while in fluid phase. the object shape can be altered to render a new object. DTIC

N94-16935# Lehigh Univ., Bethlehem, PA.
LARGE SIGNAL CHARACTERIZATION AND MODELING OF HETEROJUNCTION BIPOLAR TRANSISTORS Final Report, 1 Jun. 1990 - 31 May 1993
D. S. Whitefield, C. J. Wei, and J. C. Hwang 31 May 1993 29 p
(Grant AF-AFOSR-0302-90)
(AD-A266184; AFOSR-93-0438TR) Avail: CASI HC A03/MF A01

The high power operation of the heterojunction bipolar transistor (HBT) has been analyzed by experimentally determining the junction temperature and separating temperature effects from other high power effects. In addition, an HBT large signal model has been developed that is valid for the linear, saturation, and cutoff regions, with low frequency temperature effects included. This model has been implemented in a commercial harmonic balance simulator, LIBRA from EEsof, making it particularly suitable for the design and simulation of HBT microwave power integrated circuits. In addition, an analysis of the most temperature-sensitive microwave elements for the HBT has been performed using measured s-parameter data at five elevated temperatures from 23 C to 226 C. The element values were compared to a physical model showing excellent agreement in magnitude and direction of change with temperature and bias. The transistor cutoff frequencies were also measured and calculated, showing a monotonic decrease with temperature of approximately 50% over the 200 C range. DTIC

N94-16976# Naval Postgraduate School, Monterey, CA.
STRAY INSENSITIVE SWITCHED CAPACITOR COMPOSITE OPERATIONAL AMPLIFIERS M.S. Thesis
Eldon W. Bingham Mar. 1993 177 p
(AD-A267412) Avail: CASI HC A09/MF A02

In this research, analog active circuits are designed combining the properties of switched capacitors and composite operational amplifiers. This combined design improves upon the single operational amplifier's finite dc gain, smaller bandwidth, lower slew rate, finite input impedance, and less than ideal output performance. The switched capacitor is implemented using both the toggle switch capacitor and the modified open circuit floating resistor techniques. The composite operational amplifier is implemented using the C2OA-1 and C2OA-2 designs from the CNOA-1 possibilities. These four designs are evaluated in a finite-gain circuit and their results are compared with the results obtained from the continuous circuits of the same design. DTIC

N94-17023# Nebraska Univ., Lincoln. Dept. of Electrical Engineering.
SURFACE FLASHOVER OF SEMICONDUCTORS: A FUNDAMENTAL STUDY Final Report, 15 Jan. 1989 - 14 Jan. 1993
P. F. Williams and W. C. Nunnally 16 Jun. 1993 40 p
(Grant AF-AFOSR-0253-89)
(AD-A267382; AFOSR-93-0481TR) Avail: CASI HC A03/MF A01

This report presents research results and activities carried out during the period 15 Jan. 1989 through 14 Jan. 1993 sponsored by AFOSR Grant No. AFOSR-89-0253. Work was carried out at the University of Nebraska (UNL) and at the University of Texas at Arlington (UTA). The work at each of these locations is discussed in detail in separate sections of this report. Important conclusions are as follows: (1) the phenomenon commonly referred to as surface flashover in silicon results from a sequence of events occurring primarily inside the silicon, rather than in the ambient surrounding it; (2) current filamentation plays an important role in the breakdown process; (3) contacts to the silicon influence the breakdown process; (4) the condition of the sample surface strongly influences breakdown; (5) flashover can be inhibited through the action of weak visible or near infra-red illumination; (6) current before the initiation of flashover is strongly space-charge limited; and (7) double injection effects are clearly present in p+-i-n+ structures, and will limit the applicability of such structures as photoconductive switches. DTIC

N94-17040 North Carolina State Univ., Raleigh. Dept. of Materials Science and Engineering.
NITRIDE SEMICONDUCTORS FOR ULTRAVIOLET DETECTION Semiannual Report, 1 Jan. - 30 Jun. 1992
Robert F. Davis Jun. 1993 47 p Limited Reproducibility: More than 20% of this document may be affected by microfiche quality
(Contract N00014-92-J-1720)
(AD-A267877) Avail: CASI HC A03

GaN and AlN have been deposited on sapphire and SiC using gas-source MBE and extensively investigated via high resolution TEM. Below the critical thickness, AlN only contains threading dislocations emanating from the misfit dislocations; above this thickness, defects parallel to the growth surface greatly increase. The defect density of AlN grown on SiC at 1100 C is much lower than that contained in material deposited at 700 C. Deposition of GaN on sapphire or SiC results in a larger number of threading dislocations caused by the large misfit as well as a high concentration of dislocations parallel to the growth surface. Both types of defects are decreased in density if the GaN is deposited on AlN. Monocrystalline GaN thin films have also been deposited via layer-by-layer deposition on SiC(0001) substrates from triethylgallium and ammonia. Source concentrations of Ga and exposure times strongly affect the growth process. The near surface region of monocrystalline BP has been converted to BN via exposure to atomic N produced from N2 in an ECR source, as proven by XPS measurements. Current-voltage measurements show an increase in resistance by a factor of 40 after the conversion. Development of (1) ohmic and rectifying contacts, (2) facilities for reactive ion etching, and (3) a photo- and cathodoluminescence system are also underway. DTIC

N94-17062*# National Aeronautics and Space Administration. Goddard Space Flight Center, Greenbelt, MD.
THE 1987 GODDARD SPACE FLIGHT CENTER BATTERY WORKSHOP
George Morrow, ed. and Thomas Y. Yi, ed. 1993 570 p Workshop held in Greenbelt, MD, 4-5 Nov. 1987
(NASA-CP-3236; NAS 1.55:3236) Avail: CASI HC A24/MF A04

This document contains the proceedings of the 20th annual Battery Workshop held at Goddard Space Flight Center, Greenbelt, Maryland on November 4-5, 1987. The workshop attendees included manufacturers, users, and government representatives interested in the latest developments in battery technology as they relate to high reliability operations and aerospace use. The subjects covered included lithium cell technology and

safety improvements, nickel-cadmium electrode technology along with associated modifications, flight experience and life testing of nickel-cadmium cells, and nickel-hydrogen applications and technology. Author

N94-17071# Polish Academy of Sciences, Warsaw. Inst. Podstawowych Problemow Techniki.

AN ELECTROACOUSTIC TRANSDUCER FOR PURPOSES OF PHOTOACOUSTIC SPECTROSCOPY [PRZETWORNIK ELEKTROAKUSTYCZNY DO CELOW SPEKTROSKOPII FOTOAKUSTYCZNEJ]

Henryk Makowski, Wladyslaw Opydo, Jerzy Ranachowski, and Jadwiga Rzeszotarska 1992 12 p In POLISH

(IFTR-7/1992) Avail: CASI HC A03/MF A01

Requirements that must be satisfied by a broadband converter that converts acoustic signals into electric signals in a photoacoustic spectroscope chamber are given. An electroacoustic transducer that satisfies these requirements was developed and fabricated based on the commercially manufactured MS 52 microphone at the TONSIL Joint Stock Company in Wrzesien. Compared to the MS 52 microphone, the fabricated transducer prototypes have ten times greater efficiency (45 mV/Pa), a superior transmission range of 10-1000 Hz for a nonuniformity of 1 dB and 10-50,000 Hz for a nonuniformity of 2 dB. Tests on the application of the electroacoustic transducer prototypes in photoacoustic spectroscopy confirmed their suitability. Transl. by FLS

N94-17104# Air Force Inst. of Tech., Wright-Patterson AFB, OH.

A MODIFIED TWO-FLUID MODEL OF CONDUCTIVITY FOR SUPERCONDUCTING SURFACE RESISTANCE CALCULATION M.S. Thesis

Derek S. Linden May 1993 135 p

(AD-A267549; AFIT/CI/CIA-93-077) Avail: CASI HC A07/MF A02

The traditional two-fluid model of superconducting conductivity was modified to make it accurate, while remaining fast, for designing and simulating microwave devices. The modification reflects the BCS coherence effects in the conductivity of a superconductor and is incorporated through the ratio of normal to superconducting electrons. This modified ratio is a simple analytical expression which depends on frequency, temperature, and material parameters. This modified two-fluid model allows accurate and rapid calculation of the microwave surface impedance of a superconductor in the clean and dirty limits and in the weak- and strong-coupled regimes. The model compares well with surface resistance data for Nb and provides insight into Nb3Sn and YBa2Cu3O(7-delta). Numerical calculations with the modified two-fluid model are an order of magnitude faster than the quasi-classical program by Zimmermann and two to five orders of magnitude faster than Halbritter's BCS program for surface resistance. DTIC

N94-17113*# National Aeronautics and Space Administration. Lewis Research Center, Cleveland, OH.

LATTICE-MISMATCHED In(0.40)Al(0.60)As WINDOW LAYERS FOR INDIUM PHOSPHIDE SOLAR CELLS

Raj K. Jain (National Academy of Sciences - National Research Council, Washington, DC.), Geoffrey A. Landis (Sverdrup Technology, Inc., Brook Park, OH.), David M. Wilt, and Dennis J. Flood Nov. 1993 11 p Presented at the 23rd Photovoltaic Specialists Conference, Louisville, KY, 10-14 May 1993; sponsored by IEEE

(Contract NAS3-25266; RTOP 506-41-11)

(NASA-TM-106255; E-7879; NAS 1.15:106255) Avail: CASI HC A03/MF A01

The efficiency of indium phosphide (InP) solar cells is limited by its high surface recombination velocity (approximately 10(exp 7) cm/s). This might be reduced by a wide-bandgap window layer. The performance of InP solar cells with wide-bandgap (1.8 eV) lattice-mismatched In(0.40)Al(0.60)As as a window layer was calculated. Because the required window layer thickness is less than the critical layer thickness, growth of strained (pseudomorphic) layers without interfacial misfit dislocations should be possible. Calculations using the PC-ID numerical code showed that the efficiencies of baseline and optimized p(+)n (p-on-n) cells are increased to more than 22 and 24 percent, (air mass zero (AMO), 25 C), respectively for a lattice-mismatched In(0.40)Al(0.60)As window layer of 10-nm thickness. Currently, most cell development work has been focused on n(+)p (n-on-p) structures although comparatively little improvement has been found for n(+)p cells. Author (revised)

N94-17226# Argonne National Lab., IL. Materials and Components Technology Div.

ENGINEERING DESIGN OF A HIGH-TEMPERATURE SUPERCONDUCTOR CURRENT LEAD

R. C. Niemann, Y. S. Cha, J. R. Hull, M. A. Daugherty (Superconductivity, Inc., Madison, WI.), and W. E. Buckles (Superconductivity, Inc., Madison, WI.) 1993 5 p Presented at the 5th Annual International Industrial Symposium on the Super Collider and Exhibition, San Francisco, CA, 6-8 May 1993

(Contract W-31-109-eng-38)

(DE93-015156; ANL/MCT/CP-77641; CONF-930537-53) Avail: CASI HC A01/MF A01

As part of the US Department of Energy's Superconductivity Pilot Center Program, Argonne National Laboratory and Superconductivity, Inc., are developing high-temperature superconductor (HTS) current leads suitable for application to superconducting magnetic energy storage systems. The principal objective of the development program is to design, construct, and evaluate the performance of HTS current leads suitable for near-term applications. Supporting objectives are to (1) develop performance criteria; (2) develop a detailed design; (3) analyze performance; (4) gain manufacturing experience in the areas of materials and components procurement, fabrication and assembly, quality assurance, and cost; (5) measure performance of critical components and the overall assembly; (6) identify design uncertainties and develop a program for their study; and (7) develop application-acceptance criteria. DOE

N94-17316 Academy of Sciences of the Ukraine, Kiev. Inst. Yadernykh Issledovanij.

INVESTIGATION OF THE ENERGY DISTRIBUTION OF IONS, STRIKING THE CATHODE IN AN ABNORMAL GLOW DISCHARGE

A. A. Gurin, K. L. Kruglikov, A. Yu. Pankin, and V. M. Slobodyan 1992 14 p Limited Reproducibility: More than 20% of this document may be affected by microfiche quality

(DE93-623987; KIYaI-92-17) Avail: CASI HC A03 (US Sales Only)

The energy spectrum of ions at the cathode in an abnormal glow discharge has been investigated for gases H2, D2, He, and Ar at discharge current densities j(sub a) approximately greater than 10mA/sq cm and gas pressures p approximately greater than 1 Torr. It is shown that ion energy distribution is spread up to cathode fall voltages V(sub c); most of the particles in the ion stream have energies not higher than (0,1-0,3)(sub 2)V(sub c). It is found that with rising of the value j/p(sup 2) the low energy portion of the spectrum is transferred from the gradually decaying curve to one having low-energy peak. It is supposed that this phenomenon is due to peculiarities of space distribution of electron ionization intensity in dark cathode space. DOE

N94-17318# Los Alamos National Lab., NM.

PLASMA FLOW SWITCH AND FOIL IMPLOSION EXPERIMENTS ON PEGASUS 2

J. C. Cochrane, R. R. Bartsch, J. R. Benage, P. R. Forman, R. F. Gribble, J. S. Ladish, H. Oona, J. V. Parker, D. W. Scudder, and J. S. Shlachter et al 1993 4 p Presented at the 9th IEEE Pulsed Power Conference, Albuquerque, NM, 21-23 Jun. 1993

(Contract W-7405-eng-36)

(DE93-016464; LA-UR-93-2304; CONF-930616-7) Avail: CASI HC A01/MF A01

Pegasus II is the upgraded version of Pegasus, a pulsed power machine used in the Los Alamos AGEX (Above Ground Experiments) program. A goal of the program is to produce an intense (greater than 100 TW) source of soft x-rays from the thermalization of the kinetic energy of a 1 to 10 MJ plasma implosion. The radiation pulse should have a maximum duration of several 10's of nanoseconds and will be used in the study of fusion conditions and material properties. The radiating plasma source will be generated by the thermalization of the kinetic energy of an imploding cylindrical, thin, metallic foil. This paper addresses experiments done on a capacitor bank to develop a switch (plasma flow switch) to switch the bank current into the load at peak current. This allows efficient coupling of bank energy into foil kinetic energy. DOE

N94-17323*# National Aeronautics and Space Administration. Pasadena Office, CA.

LEAK DETECTION UTILIZING ANALOG BINAURAL (VLSI) TECHNIQUES Patent Application

Frank T. Hartley, inventor (to NASA) (Jet Propulsion Lab., California Inst. of Tech., Pasadena.) 18 Aug. 1993 23 p

(Contract NAS7-918)

(NASA-Case-NPO-18399-1-CU; NAS 1.71:NPO-18399-1-CU; US-Patent-Appl-SN-111317) Avail: CASI HC A03/MF A01

A detection method and system utilizing silicon models of the traveling wave structure of the human cochlea to spatially and temporally locate a specific sound source in the presence of high noise pandemonium is presented. The detection system combines two-dimensional stereausis representations, which are output by at least three VLSI binaural hearing chips, to generate a three-dimensional stereausis representation including both binaural and spectral information which is then used to locate the sound source. NASA

N94-17324*# National Aeronautics and Space Administration. Pasadena Office, CA.

OPTICALLY-SWITCHED SUBMILLIMETER-WAVE OSCILLATOR AND RADIATOR Patent Application

Michael G. Spencer, inventor (to NASA) (Jet Propulsion Lab., California Inst. of Tech., Pasadena.) and Joseph Maserjian, inventor (to NASA) (Jet Propulsion Lab., California Inst. of Tech., Pasadena.) 23 Sep. 1993 29 p

(Contract NAS7-918)

(NASA-Case-NPO-18547-1-CU; NAS 1.71:NPO-18547-1-CU; US-Patent-Appl-SN-125966) Avail: CASI HC A03/MF A01

A submillimeter wave-generating integrated circuit includes an array of N photoconductive switches biased across a common voltage source and an optical path difference from a common optical pulse of repetition rate f sub 0 providing a different optical delay to each of the switches. In one embodiment, each incoming pulse is applied to successive ones of the N switches with successive delays. The N switches are spaced apart with a suitable switch-to-switch spacing so as to generate at the output load or antenna radiation of a submillimeter wave frequency f on the order of Nf sub 0. Preferably, the optical pulse has a repetition rate of at least 10 GHz and N is of the order of 100, so that the circuit generates radiation of frequency of the order of or greater than 1 Terahertz. NASA

N94-17325*# National Aeronautics and Space Administration. Pasadena Office, CA.

THIN COMPOSITE SOLID ELECTROLYTE FILM FOR LITHIUM BATTERIES Patent Application

Emmanuel Peled, inventor (to NASA) (Jet Propulsion Lab., California Inst. of Tech., Pasadena.), Ganesan Nagasubramanian, inventor (to NASA) (Jet Propulsion Lab., California Inst. of Tech., Pasadena.), Gerald Halpert, inventor (to NASA) (Jet Propulsion Lab., California Inst. of Tech., Pasadena.), and Alan I. Attia, inventor (to NASA) (Jet Propulsion Lab., California Inst. of Tech., Pasadena.) 20 Aug. 1993 18 p

(Contract NAS7-918)

(NASA-Case-NPO-18694-1-CU; NAS 1.71:NPO-18694-1-CU; US-Patent-Appl-SN-112483) Avail: CASI HC A03/MF A01

A composite solid electrolyte film for a lithium battery comprising a dispersion of small reinforcing particles such as alumina in a binder rein such as polyethylene oxide is presented. The particles are coated with a compatible lithium salt such as lithium iodide and the alumina particles preferably have a size below 0.5 microns. NASA

N94-17375# Arizona Univ., Tucson. Optical Sciences Center

HIGH-SPEED NONLINEAR SWITCHING MECHANISMS AND DEVICES FOR MULTI-GIGABIT DATA PROCESSING Final Report, Feb. 1992 - Feb. 1993

N. Peyghambarian, S. Johns, M. Krol, R. Boncek, and J. Stacy May 1993 14 p

(Contract F30602-92-C-0020)

(AD-A267753; RL-TR-93-92) Avail: CASI HC A03/MF A01

A high contract, low intensity GaAlInAs/AlInAs multiple quantum well asymmetric Fabry-Perot reflection modulator for operation at 1.3 microns has been demonstrated. The reflection modulator takes advantage of the large absorptive and refractive nonlinearities associated with saturating the heavy-hole exciton resonance. We achieve an on/off contrast ratio in excess of 1000:1 (30 dB) and an insertion loss of 2.2 dB at a pump intensity of 30 kW/cm(exp 2), corresponding to a carrier density of 4.5 x 10(exp 17) cm(exp -3). The modulator was demonstrated to have a large operating bandwidth achieving an on/off contrast ratio of greater than 100:1 over a 5 nm optical band. The operating speed of the modulator was measured and found to approach 1 GHz. DTIC

N94-17410# Optical Society of America, Washington, DC.

OSA PROCEEDINGS ON ULTRAFAST ELECTRONICS AND OPTOELECTRONICS, VOLUME 14

Jagdeep Shah, ed. and Umesh Mishra, ed. 27 Jan. 1993 264 p Meeting held in San Francisco, CA, 25-27 Jan. 1993 Sponsored by AFOSR

(AD-A267972; AFOSR-93-0639TR-Vol-14) Avail: CASI HC A12/MF A03

This volume is comprised of papers that were presented at the Fifth Topical Meeting on Ultrafast Electronics and Optoelectronic, held in San Francisco, January 23-25, 1993. The purpose of this topical meeting, since its inception in 1985, has been to foster greater interaction between researchers in the electronics and optoelectronics communities who share a common interest in the physics and technology of ultrafast electronics and optoelectronic devices, their multigigahertz applications, and ultrafast measurement techniques. The number of abstracts submitted to this meeting was considerably larger than for the previous meetings, indicating the appeal of this interdisciplinary approach and the grow in importance of this field. The topics are ultrafast optoelectronic devices, high speed electronic devices, terahertz transients, physics of semiconductors, novel sources and techniques, (sub)millimeter wave devices, photoconductive and electro-optic sampling, and superconductors. Derived from text

N94-17423 Raytheon Co., Lexington, MA. Research Div.

RF VACUUM MICROELECTRONICS Final Report, 1 Oct. 1991 - 31 Mar. 1993

Alan Palevsky 8 Aug. 1993 57 p Limited Reproducibility: More than 20% of this document may be affected by microfiche quality

(Contracts MDA971-91-C-0032; F33615-87-C-1507)

(AD-A268399; RAY/RD/S-4921) Avail: Issuing Activity (Defense Technical Information Center (DTIC))

The result of the 18 month research and development project on high frequency Field Emission Array (FEA) cathodes is presented. Details of the process development and test procedures are discussed. The results relative to the program goals are presented. Finally, suggestions for future work in the 12 month option portion of the project are presented. DTIC

N94-17428# Massachusetts Inst. of Tech., Cambridge. Center for Materials Science and Engineering.

BASIC OPTICAL STUDIES OF HIGH T(c) OXIDE SUPERCONDUCTORS Final Report, 15 Jan. 1990 - 14 Jan. 1993

M. S. Dresselhaus and G. Dresselhaus 15 Jun. 1993 9 p

(Grant AF-AFOSR-0123-90)

(AD-A268148; AFOSR-93-0584TR) Avail: CASI HC A02/MF A01

During the 1992-93 year of the research program on Basic Optical Studies of High T(sub c) Oxide Superconductors, the effort was focused on a number of projects. The collaborative study of the microwave properties of superconductors with researchers at Rome Labs and the MIT Lincoln Laboratory continued and significant results were obtained on the microwave behavior in the non-linear high rf power regime for YBa2Cu3O(7-x) and this work will be a major part of the Ph.D. thesis of Paul Nguyen. During this year we continued study of the effect of halogen doping on the restoration of superconductivity to YBCO samples previously deoxygenated and hence rendered non-superconducting. Extensive progress was also made on our new effort in studying superconductivity and the associated phonon spectra and electron-phonon interaction in the alkali metal doped C60 materials. We review in this report the progress that was made on each of these projects, referring to the publications that were prepared on each of the topics under investigation. DTIC

N94-17505 Politecnico di Milano (Italy). Dipt. di Elettronica e Informazione.

FSM TEST: A FUNCTIONAL TEST GENERATION SYSTEM FOR SEQUENTIAL CIRCUITS

Franco Fummi Mar. 1993 32 p
(Rept-93-017; ETN-93-94569) Avail: Issuing Activity (Politecnico di Milano, Piazza Leonardo da Vinci 32, 20133 Milan, Italy)

An approach to test pattern generation for Finite State Machines (FSM's) and the relationships with their gate level implementation is presented. The algorithm is based on a functional fault model. A restricted set of transitions of the FSM is analyzed and particular state distinguishing sequences (EUIO's) are adopted to observe their final state. Overlapping and concatenation of test sequences is performed in order to reduce test length. Test length obtained is in most cases shorter than previously published functional approaches and the CPU (Central Processing Unit) time requirements are very low in comparison with the gate level ATPG's. Some polynomial complexity preserving techniques are introduced in order to improve the final fault coverage. A number of experiments on MCNC benchmarks have shown the effectiveness of the test algorithm both at the functional level and at the gate level, where the coverage of single stuck-at faults in most cases achieves 100. ESA

N94-17526 SRI International Corp., Menlo Park, CA.
FIELD-EMITTER ARRAYS FOR RF VACUUM MICROELECTRONICS Quarterly Report No. 7, 1 Apr. - 31 Jun. 1993
C. A. Spindt, A. Rosengreen, and P. R. Schwoebel 9 Aug. 1993 16 p Limited Reproducibility: More than 20% of this document may be affected by microfiche quality
(Contract MDA972-91-C-0029; ARPA Order 8162; SRI Proj. 2743)
(AD-A268397) Avail: Issuing Activity (Defense Technical Information Center (DTIC))

SRI International has completed the seventh quarter of a program to develop field-emitter arrays for vacuum microelectronics. We have met the first-phase program goals of 5 mA total emission, with a current density of 5 A/sq cm for at least 2 hours and demonstrated modulation of the emission current at a frequency of 1 GHz. A series of controlled tests with photoresist/developer/stripper combinations continued, and sulfur hexafluoride was identified as the source of a contamination problem in the low-capacitance cathode fabrication technology. The active area of the low-capacitance cathode was shielded from the base electrode to eliminate excessive gate interception of the emitter. The effects of processing on cathode performance were studied through experiments with hydrogen plasma treatment. Four cathodes were set up in a high-frequency chamber in an effort to gain data on the effectiveness of shielding the electrode. DTIC

N94-17546# Technical Research Centre of Finland, Espoo. Semiconductor Lab.
SMART POWER: NEW POWER INTEGRATED CIRCUIT TECHNOLOGIES AND THEIR APPLICATIONS [SMART POWER: UUDET TEHOMIKROPIIRITEKNOLOGIAT JA NIIDEN SOVELLUKSET]
Pekka Kuivalainen, Helena Pohjonen, Timo Yli-Pietilae, and Jaakko Lenkkeri May 1992 112 p In FINNISH Sponsored by Technical Research Centre of Finland, Espoo
(VTT-TIED-1358; ISBN-9-51-384171-5; ETN-93-94476) Copyright Avail: CASI HC A06/MF A02

Power Integrated Circuits (PIC) is one of the most rapidly growing branches of the semiconductor technology. The PIC markets has been forecast to grow from 660 million dollars in 1990 to 1658 million dollars in 1994. It has even been forecast that at the end of the 1990's the PIC markets would correspond to the value of the whole semiconductor production in 1990. Automotive electronics will play the leading role in the development of the standard PIC's. Integrated motor drivers (36 V/4 A), smart integrated switches (60 V/30 A), solenoid drivers, integrated switch-mode power supplies and regulators are the latest standard devices of the PIC manufactures. ASIC (Application Specific Integrated Circuits) PIC solutions are needed for the same reasons as other ASIC devices: there are no proper standard devices, a company has a lot of application knowhow, which should be kept inside the company, the size of the product must be reduced, and assembly costs are wished to be reduced by decreasing the number of discrete devices. During the next few years the most probable ASIC PIC applications in Finland will be integrated solenoid and motor drivers, an integrated electronic lamp ballast circuit and various sensor interface circuits. Application of the PIC technologies to machines and actuators will strongly be increased all over the world. This means that various PIC's, either standard PIC's or full custom ASIC circuits, will appear in many products which compete with the corresponding Finnish products. Therefore the development of the PIC technologies must be followed carefully in order to immediately be able to apply the latest development in the smart power technologies and their design methods. ESA

N94-17560 Cornell Univ., Ithaca, NY. Lab. of Atomic and Solid State Physics.
IN-SITU ELECTRON AND OPTICAL SPECTROSCOPIES OF TRANSLATIONAL AND VIBRATIONAL ACTIVATED BOND BREAKING AND FORMATION ON SEMICONDUCTORS Annual Report, 1 Jun. 1992 - 31 May 1993
Wilson Ho 26 Jul. 1993 7 p Limited Reproducibility: More than 20% of this document may be affected by microfiche quality
(Contract F49620-92-J-0309)
(AD-A268192; AFOSR-93-0595TR) Avail: Issuing Activity (Defense Technical Information Center (DTIC))

This experimental research program seeks a basic understanding of the growth and processing of materials on semiconductor surfaces. Interactions of molecules with surfaces are investigated by varying the translational and vibrational energies of the impinging molecules from a molecular beam and probing the resulting species on the surface by in-situ time resolved electron energy loss spectroscopy, second harmonic generation, and two-photon photoemission. The reactions of H2, CO, CO2, CH(x)F(4-x) (where x = 0-4), and CH3Cl on Si(100)2x1 were studied in order to understand the chemistry of group 4 elements: C, Si, and Ge. These studies will be extended to Ge2H6 and Si(111)7x7. The nature of bond breaking and formation of Ge and C on Si to form Ge/Si, SiC, and diamond will be investigated. DTIC

N94-17570# Imperial Coll. of Science and Technology, London (England).
PROCEEDINGS OF THE 6TH INTERNATIONAL CONFERENCE ON NARROW GAP SEMICONDUCTORS
R. A. Stradling and J. B. Mullin 23 Jul. 1992 469 p Conference held in Southampton, United Kingdom, 19-23 Jul. 1992
(Contract DAJA45-92-M-0334)
(AD-A268097; R/D-6971-EE-02) Avail: CASI HC A20/MF A04

This proceedings includes papers in the following areas: novel growth and structures; dilute magnetic semiconductors; II-VI electronics, optics, and growth; III-V devices; magnetism and magneto-optics; dots and novel confinement; linear and nonlinear optics; and material properties of IV-VI semiconductors. CASI

N94-17608# SRI International Corp., Menlo Park, CA.
FIELD EMITTER ARRAYS FOR RF VACUUM MICROELECTRONICS Quarterly Technical Report No. 6, 1 Jan. - 31 Mar. 1993
C. A. Spindt, A. Rosengreen, and P. R. Schwoebel 4 Aug. 1993 8 p
(Contract MDA972-91-C-0029; ARPA Order 8162)
(AD-A268595; SRI-2743) Avail: CASI HC A02/MF A01

SRI International has completed the sixth quarter of a program to develop field-emitter arrays for vacuum microelectronics. We have met the first-phase program goals of 5 mA total emission, with a current density of 5 A/sq cm for at least 2 hours and demonstrated modulation of the emission current at a frequency of 1 GHz. A series of controlled tests was initiated with photoresist/developer/stripper combinations to identify the source of a contamination problem in the low-capacitance cathode fabrication technology. A sequence of procedures was specified for cathode emission tests using previously developed test chambers. High-frequency testing with a triode setup at 1-GHz modulation rates was begun. DTIC

N94-17648# Sandia National Labs., Albuquerque, NM.
ELECTRICAL PROPERTIES OF SOL-GEL PZT THIN FILMS FOR DECOUPLING CAPACITOR APPLICATIONS
R. W. Schwartz, D. Dimos, S. J. Lockwood, and V. M. Torres 1992 6 p Presented at the Spring Meeting of the Materials Research Society, San Francisco, CA, 12-16 Apr. 1993
(Contract DE-AC04-76DP-00789)
(DE93-016491; SAND-92-2907C; CONF-930405-28) Avail: CASI HC A02/MF A01

The successful development of PZT thin films for decoupling capacitor devices places stringent requirements on the dielectric and leakage

properties of the films. The authors have characterized these properties for PZT thin films with compositions near the morphotropic phase boundary prepared by a sol-gel process. Capacitors were fabricated from films with thicknesses varying from 0.4 to 1.2 (mu)m. For zero applied bias, the dielectric constants of these films were in the range of 800 to 1200. The room temperature dielectric constant was observed to decrease by approximately 25% with the application of a 5 V bias. They have also characterized the interrelationships between temperature, applied bias, and dielectric constant. The capacitors exhibited asymmetry in their leakage and breakdown characteristics with bias sign, as well as non-linear I-V behavior. Breakdown fields for undoped PZT 53/47 films were typically in the range of 750 kV/cm. They have also studied the effects of La and Nb donor doping on the leakage behavior of PZT 50/50 thin films. Doping with 2 to 5 mol % of either La or Nb resulted in a reduction in film leakage current by a factor of 10(sup 3). Leakage currents of the highly doped materials were approximately 2 (times) 10(sup (minus)9) A/cm(sup 2) under an applied field of approximately 65 kV/cm at a temperature of 125 C. DOE

N94-17671# Sandia National Labs., Albuquerque, NM.
FIELD INVESTIGATION OF THE RELATIONSHIP BETWEEN BATTERY SIZE AND PV SYSTEM PERFORMANCE
J. Stevens, J. Kratochvil, and S. Harrington (Ktech Corp., Albuquerque, NM.) 1993 7 p Presented at the 23rd Institute of Electrical and Electronics Engineers (IEEE) Photovoltaic Specialits Conference, Louisville, KY, 10-14 May 1993
(Contract DE-AC04-76DP-00789)
(DE93-016503; SAND-93-1255C; CONF-930540-10) Avail: CASI HC A02/MF A01

Four photovoltaic-powered lighting systems were installed in a National Forest Service campground in June of 1991. These systems have identical arrays, loads and charge controllers. The only difference was in the rated capacity of the battery bank for each system. The battery banks all use the same basic battery as a building block with the four systems utilizing either one battery, two batteries, three batteries or four batteries. The purpose of the experiment is to examine the effect of the various battery sizes on the ability of the system to charge the battery, energy available to the load, and battery lifetime. Results show an important trend in system performance concerning the impact of charge controllers on the relation between array size and battery size which results in an inability to achieve the days of battery storage originally designed for. DOE

N94-15624*# Bendix Field Engineering Corp., Seabrook, MD.
PERFORMANCE COMPARISON OF HIGH SPEED MICROCHANNEL PLATE PHOTOMULTIPLIER TUBES
Thomas Varghese, Michael Selden, and Thomas Oldham *In* NASA. Goddard Space Flight Center, Eighth International Workshop on Laser Ranging Instrumentation Jun. 1993 9 p (For primary document see N94-15552 03-19)
Avail: CASI HC A02/MF A06

34 FLUID MECHANICS AND HEAT TRANSFER

Includes boundary layers; hydrodynamics; fluidics; mass transfer; and ablation cooling.

For related information see also *02 Aerodynamics* and *77 Thermodynamics and Statistical Physics.*

N94-15005*# Institute for Computer Applications in Science and Engineering, Hampton, VA.
ON THE RECEPTIVITY PROBLEM FOR 0(1) WAVELENGTH GOERTLER VORTICES Final Report
Andrew P. Bassom (Exeter Univ., England.) and Philip Hall (Manchester Univ., England.) Aug. 1993 25 p Submitted for publication
(Contract NAS1-19480; RTOP 505-90-52-01)
(NASA-CR-191519; NAS 1.26:191519; ICASE-93-58) Avail: CASI HC A03/MF A01

In this paper, we make an investigation of the receptivity of boundary layer flows to Gortler vortex modes. A study by Denier, Hall, and Seddougui (1991) of the generation of vortices by wall roughness elements concluded that such elements are extremely poor as mechanisms to stimulate short wavelength modes, but that analysis was in error. We re-examine this problem and demonstrate how the form of the wall roughness is crucial in determining the vortex stability characteristics downstream of the roughness. In particular, we investigate the cases of both isolated and distributed forcing functions and show that, in general, a distributed function is much more important in generating vortices than are either isolated roughness or freestream disturbances. Author (revised)

N94-15109*# Imperial Coll. of Science and Technology, London (England). Dept. of Mechanical Engineering.
COAXIAL AIRBLAST ATOMIZERS Final Report, 3 Apr. 1991 - 3 Apr. 1993
Y. Hardalupas and J. H. Whitelaw May 1993 203 p Prepared in cooperation with Scientific Research Associates, Inc., Glastonbury, CT
(Contract NAS8-38872)
(NASA-CR-193845; NAS 1.26:193845; SRA-R93-9083-F) Avail: CASI HC A10/MF A03

An experimental investigation was performed to quantify the characteristics of the sprays of coaxial injectors with particular emphasis on those aspects relevant to the performance of rocket engines. Measurements for coaxial air blast atomizers were obtained using air to represent the gaseous stream and water to represent the liquid stream. A wide range of flow conditions were examined for sprays with and without swirl for gaseous streams. The parameters varied include Weber number, gas flow rate, liquid flow rate, swirl, and nozzle geometry. Measurements were made with a phase Doppler velocimeter. Major conclusions of the study focused upon droplet size as a function of Weber number, effect of gas flow rate on atomization and spray spread, effect of nozzle geometry on atomization and spread, effect of swirl on atomization, spread, jet recirculation and breakup, and secondary atomization. Author (revised)

N94-15119# Advisory Group for Aerospace Research and Development, Neuilly-Sur-Seine (France). Propulsion and Energetics Panel.
ADVANCED METHODS FOR CASCADE TESTING [METHODES AVANCEES POUR LES ESSAIS DES GRILLES D'AUBES]
Charles Hirsch, ed. (Vrije Univ., Brussels, Belgium.) Aug. 1993 196 p
(AGARD-AG-328; ISBN-92-835-0717-7) Copyright Avail: CASI HC A09/MF A03

Considerable advances have been achieved over the last decennia in the field of cascade testing, but they were generally not reported in sufficient detail. As an example, details of transonic/supersonic cascade testing procedures were scarcely documented in literature. Many other aspects evolved considerably, originally from the progress of experimental techniques as well as from the interaction with computer data. New methodologies based on advanced instrumentation gained sufficient validation. Consequently, the Propulsion and Energetics Panel decided to initiate an AGARDograph on this subject in 1988. Since then, several authors prepared chapters for the AGARDograph, coordinated by the editor. The following chapters are included: Modeling Turbomachinery Flow Conditions, Linear Cascades, Annular Cascades, Aspects of Hot Cascades, Transient Cascade Testing, Unsteady Flow in Cascades, and 3-D Laser Anemometry in Annular Cascades. Author (revised)

N94-15151# Princeton Univ., NJ.
[LARGE-EDDY SIMULATIONS (LES) OF FLOWS AND TURBULENCE DISTRIBUTION] Final Report, 15 Jan. 1990 - 30 Sep. 1992
Steven A. Orszag 5 Mar. 1993 14 p
(Grant AF-AFOSR-0124-90)
(AD-A267182; AFOSR-93-0472TR) Avail: CASI HC A03/MF A01

This report summarizes results published with support of this grant on renormalization group methods for large-eddy simulations (LES) of fluid flows, studies of the fundamental dynamics of compressible turbulence, development of methods to study strongly interacting vortices, methods to study intermittent probability distributions in turbulence, and studies of dynamical issues involved in intermittent turbulence. Publications from 31 papers and 2 book chapters are summarized. The results demonstrate the utility of LES techniques, the differences between incompressible and compressible turbulence, and advanced models for small-scale structure that lead a series of surprising results, including a two-fluid model for small-scales in high Reynolds number turbulence. DTIC

N94-15183*# Institute for Computer Applications in Science and Engineering, Hampton, VA.

TOLLMIEN-SCHLICHTING/VORTEX INTERACTIONS IN COMPRESSIBLE BOUNDARY LAYER FLOWS Final Report

Nicholas D. Blackaby (Manchester Univ., England.) Aug. 1993 36 p Submitted for publication

(Contract NAS1-19480; RTOP 505-90-52-01)

(NASA-CR-191515; NAS 1.26:191515; ICASE-93-55) Avail: CASI HC A03/MF A01

The weakly nonlinear interaction of oblique Tollmien-Schlichting waves and longitudinal vortices in compressible, high Reynolds number, boundary-layer flow over a flat plate is considered for all ranges of the Mach number. The interaction equations comprise of equations for the vortex which is indirectly forced by the waves via a boundary condition, whereas a vortex term appears in the amplitude equation for the wave pressure. The downstream solution properties of interaction equations are found to depend on the sign of an interaction coefficient. Compressibility is found to have a significant effect on the interaction properties; principally through its impact on the waves and their governing mechanism, the triple-deck structure. It is found that, in general, the flow quantities will grow slowly with increasing downstream co-ordinate; i.e. in general, solutions do not terminate in abrupt, finite-distance 'break-ups'. Author

N94-15196# Advisory Group for Aerospace Research and Development, Neuilly-Sur-Seine (France). Fluid Dynamics Panel.

SPECIAL COURSE ON SHOCK-WAVE/BOUNDARY-LAYER INTERACTIONS IN SUPERSONIC AND HYPERSONIC FLOWS [INTERACTIONS ENTRE ONDES DE CHOC ET COUCHES LIMITES DANS LES ECOULEMENTS SUPERSONIQUES ET HYPERSONIQUES]

Aug. 1993 298 p Course held in Rhode-Saint-Genese, Belgium, 24-28 May 1993; sponsored by VKI Original contains color illustrations

(AGARD-R-792; ISBN-92-835-0718-5) Copyright Avail: CASI HC A13/MF A03

Notes for the AGARD Fluid Dynamics Panel (FDP) Special Course on 'Shock-Wave/Boundary-Layer Interactions in Supersonic and Hypersonic Flows' are presented. The objective was to report on results from recent research programs providing a consolidated review of these activities and a sound basis for developing more reliable methodologies for future vehicle design. The course also provided a focused review of recent progress for swept interactions in both laminar and turbulent flows, including discussions: flowfield structure; scaling and similarity laws; effect of shock strength on flow feature; effect of shock generator geometry for a given shock strength; techniques for investigating swept interactions, particularly optical techniques; and contributions of numerical simulations to the understanding of swept interactions. The effects of turbulence and turbulence modeling on the flowfields are provided. For individual titles, see N94-15197 through N94-15203.

N94-15197*# Pennsylvania State Univ., University Park. Gas Dynamics Lab.

SWEPT SHOCK/BOUNDARY-LAYER INTERACTIONS: SCALING LAWS, FLOWFIELD STRUCTURE, AND EXPERIMENTAL METHODS

Gary S. Settles *In* AGARD, Special Course on Shock-Wave/Boundary-Layer Interactions in Supersonic and Hypersonic Flows Aug. 1993 40 p Sponsored by NASA. Ames Research Center and AFOSR (For primary document see N94-15196 03-34)

Copyright Avail: CASI HC A03/MF A03

A general review is given of several decades of research on the scaling laws and flowfield structures of swept shock wave/turbulent boundary layer interactions. Attention is further restricted to the experimental study and physical understanding of the steady-state aspects of these flows. The interaction produced by a sharp, upright fin mounted on a flat plate is taken as an archetype. An overall framework of quasiconical symmetry describing such interactions is first developed. Boundary-layer separation, the interaction footprint, Mach number scaling, and Reynolds number scaling are then considered, followed by a discussion of the quasiconical similarity of interactions produced by geometrically-dissimilar shock generators. The detailed structure of these interaction flowfields is next reviewed, and is illustrated by both qualitative visualizations and quantitative flow images in the quasiconical framework. Finally, the experimental techniques used to investigate such flows are reviewed, with emphasis on modern non-intrusive optical flow diagnostics. Author

N94-15198# Von Karman Inst. for Fluid Dynamics, Rhode-Saint-Genese (Belgium). Aerospace Dept.

SWEPT SHOCK WAVE/LAMINAR BOUNDARY LAYER INTERACTIONS, EXPERIMENTAL, AND NUMERICAL RESULTS

G. Degrez *In* AGARD, Special Course on Shock-Wave/Boundary-Layer Interactions in Supersonic and Hypersonic Flows Aug. 1993 19 p (For primary document see N94-15196 03-34)

(Contract Aero-0027-C)

Copyright Avail: CASI HC A03/MF A03

Experimental and numerical investigations of swept shock wave/laminar boundary layer interactions are reviewed. Experimental investigations show that the flowfield is characterized by an extensive primary separation of the boundary layer upstream of the inviscid shock wave, which then rolls up into a very elongated vortex. This is often accompanied by secondary and sometimes higher order separations. Similar to turbulent interactions, the flowfield is essentially conical as far as the surface flow data are concerned (surface pressures, heat transfer, and skin friction patterns). Also, the free-interaction concept introduced for turbulent interactions is shown to apply to laminar interactions as well. Recent LDV flowfield data for a supersonic interaction are presented. They nicely confirm the vortical structure of the interaction deduced from the surface data as well as the important thickening of the viscous layer due to separation. They also show that the vertical dimension of the interaction does not obey a conical similarity rule but rather follows the classical boundary layer scaling. Numerical investigations confirm these experimental findings. None of these was however carried out with sufficient grid resolution so as to demonstrate grid convergence and code validity, in particular concerning the location of separation lines. Author (revised)

N94-15199# Rutgers - The State Univ., Piscataway, NJ. Dept. of Mechanical and Aerospace Engineering.

NUMERICAL SIMULATION OF 3-D SHOCK WAVE TURBULENT BOUNDARY LAYER INTERACTIONS

Doyle D. Knight *In* AGARD, Special Course on Shock-Wave/Boundary-Layer Interactions in Supersonic and Hypersonic Flows Aug. 1993 32 p (For primary document see N94-15196 03-34)

(Contract F49620-93-1-0005)

Copyright Avail: CASI HC A03/MF A03

The capability for numerical simulation of 3-D shock wave turbulent boundary layer interactions is assessed. Specific configurations examined include the sharp fin, blunt fin, cylinder/flare, swept compression corner and crossing shock. Future needs in improved computational methods, collaborative experimental/computational efforts and incorporation of knowledge of flowfield structure into more effective designs are discussed. Author (revised)

N94-15200*# Texas Univ., Austin. Center for Aeromechanics Research.

UNSTEADY PHENOMENA IN SHOCK WAVE/BOUNDARY LAYER INTERACTION

D. S. Dolling *In* AGARD, Special Course on Shock-Wave/Boundary-Layer Interactions in Supersonic and Hypersonic Flows Aug. 1993 46 p Sponsored by NASA. Lewis Research Center; NASA. Langley Research Center; ARO; and AFOSR (For primary document see N94-15196 03-34)

Copyright Avail: CASI HC A03/MF A03

A brief review is given of the unsteadiness of shock wave/turbulent boundary layer interaction. The focus is on interactions generated by swept and unswept compression ramps, by flares, steps and incident shock waves, by cylinders and blunt fins, and by glancing shock waves. The effects of Mach number, Reynolds number, and separated flow scale are discussed as are the physical causes of the unsteadiness. The implications that the unsteadiness has for interpreting time-average surface and flowfield data, and for comparisons of such experimental data with computation, is also briefly discussed. Finally, some suggestions for future work are given. It is clear that there are large gaps in the data base and that many aspects of such phenomena are poorly understood. Much work remains to be done. Author

N94-15201# Office National d'Etudes et de Recherches Aerospatiales, Paris (France). Aerodynamics Dept.

CONTRIBUTION OF LASER DOPPLER VELOCIMETRY TO THE PHYSICAL DESCRIPTION OF SHOCK WAVE/TURBULENT BOUNDARY LAYER INTERACTIONS WITH INCIDENCE ON TURBULENCE MODELLING

J. M. Delery *In* AGARD, Special Course on Shock-Wave/Boundary-Layer Interactions in Supersonic and Hypersonic Flows Aug. 1993 34 p Sponsored by Ministry of Defence Original contains color illustrations (For primary document see N94-15196 03-34)

Copyright Avail: CASI HC A03/MF A03

With the advent of Laser Doppler Velocimetry (LDV) in the 1970's, it became possible to investigate high speed complex flows containing shock waves, separated regions, and strong turbulent fluctuations. This powerful tool has allowed an unprecedented physical description of the flow fields resulting from shock wave/boundary layer interaction, both in two- and three-dimensional flows. It is remarkable that the development of LDV accompanied the progress in CFD, thus permitting an in depth validation of the theoretical models. The Lecture focusses on the use of LDV to investigate typical transonic and supersonic interactions occurring, firstly in nominally 2D configurations, then in a 3D channel flow. The data thus obtained are used to validate a detailed description of the flow field and to validate several equilibrium and non-equilibrium turbulence models. In 2D flows, the calculations were executed by using an economical boundary layer type approach, for the 3D case the models were implemented in a Navier-Stokes code. Author (revised)

N94-15202# Institut National des Sciences Appliquees, Routen (France). Lab. de Mecanique des Fluides Numerique.

TURBULENCE MODELLING FOR SHOCK WAVE/BOUNDARY LAYER INTERACTIONS SPECIFIC ISSUES AND EXAMPLES OF APPLICATIONS

D. Vandromme *In* AGARD, Special Course on Shock-Wave/Boundary-Layer Interactions in Supersonic and Hypersonic Flows Aug. 1993 68 p (For primary document see N94-15196 03-34)

Copyright Avail: CASI HC A04/MF A03

Since the pioneering theory of Boussinesq and the first application indicated by Prandtl, turbulence modeling has been continuously improved in order to allow effective prediction of turbulent flows. Since these early contributions, various methodologies were worked out to account properly for 'complex' effects on turbulence. Among others, these 'complex' effects are caused by curvature, body forces (gravitation or magnetic fields), unsteadiness, and variable density. In fact, in real flows situations, it is often difficult to separate these effects, and the prediction of a flow configuration of industrial interest must always combine the simultaneous treatment of several effects. Depending on the application domain, some effects can be considered as dominant which allows neglect of others completely. As an example, geophysical flows in oceans are dominated by stratification and rotation, while compressibility or solid boundary effects can be neglected. In contrast, flows around an aircraft fuselage in real flight conditions are strongly influenced by compressibility and wall effects and not at all by gravitation or rotation. Because of the requirements imposed by a wide variety of industrial and aeronautical problems, one of the biggest challenges, during the last few years in the field of turbulence modeling was the correct accountability of the variable density effects. Variable density can have different origins, which can result for instance from: (1) the mixture of gases with different density; (2) a temperature gradient within an homogeneous fluid; (3) compressibility in high speed flows; or (4) reactive flows (for instance flames, chemical or gasdynamic laser flows). Unfortunately, until now, only a small fraction of the modeling effort has been devoted to these flows. Author

N94-15203# European Space Agency. European Space Research and Technology Center, ESTEC, Noordwijk (Netherlands). Aerothermodynamics Section.

HYPERSONIC SHOCK WAVE BOUNDARY LAYER INTERACTIONS OVER SIMPLIFIED DEFLECTED CONTROL SURFACE CONFIGURATIONS

G. Simeonides *In* AGARD, Special Course on Shock-Wave/Boundary-Layer Interactions in Supersonic and Hypersonic Flows Aug. 1993 47 p Sponsored in part by Dassault Aviation Original contains color illustrations (For primary document see N94-15196 03-34)

Copyright Avail: CASI HC A03/MF A03

The problem of hypersonic shock wave boundary layer interactions over simplified geometric configurations that simulate the vicinity of deflected control surfaces on lifting reentry vehicles is addressed. The discussion evolves primarily around surface pressure and heat transfer data over flat plate/two-dimensional and swept compression ramp configurations, and the axisymmetric hyperboloid/flare configuration, emphasizing the prediction of peak heating in regions of interaction, the promotion of laminar-turbulent transition, and the performance and validation of CFD codes. Following a brief overview of the fundamental physical phenomena associated with shock wave boundary layer interactions, as these have been identified and summarized in the extensive literature available on the subject, the paper is split into three main parts. The first part concentrates on the analysis of global pressure and heat transfer distributions and their comparison with simple boundary layer theory, emphasizing peak heating at the downstream end of the interaction region. The second part addresses the formation of streamwise striations in reattaching flow regions, and the associated spanwise heat transfer variations which may exceed plus or minus 50 percent of the mean local heating level. Last but not least, the performance and limitations of state-of-the-art Navier-Stokes computations in computing hypersonic separated flows are illustrated by means of a series of computational fluid dynamics (CFD) code validation test cases assembled in recent years. Author (revised)

N94-15246* National Aeronautics and Space Administration. Ames Research Center, Moffett Field, CA.

THE 1989 COMPUTATIONAL FLUID DYNAMICS HIGHLIGHTS (Videotape)

1989 Videotape: 24 min. playing time, in color, with sound (NASA-TM-109635; NONP-VT-93-190433) Avail: CASI VHS A01/BETA A22

This document presents highlights of 1989's CFD graphics, which show shuttle flight problems, F-18 flows, artificial heart, and rotorstrator with more complex blades. CASI

N94-15252* National Aeronautics and Space Administration, Washington, DC.

RIBLETS: NEW SPEED TECHNOLOGY (Videotape)

Mar. 1987 Videotape: 3 min. 40 sec. playing time, in color, with sound (NASA-TM-109641; NONP-VT-93-190439) Avail: CASI VHS A01/BETA A22

This document discusses a new drag reduction technology called riblets, which may have helped win yachting's America's Cup. CASI

N94-15291*# National Aeronautics and Space Administration. Langley Research Center, Hampton, VA.

DSMC SIMULATIONS OF MACH 20 NITROGEN FLOWS ABOUT A 70 DEGREE BLUNTED CONE AND ITS WAKE

James N. Moss, Virendra K. Dogra (Vigyan Research Associates, Inc., Hampton, VA.), and Richard G. Wilmoth Aug. 1993 157 p (RTOP 506-40-91-03)

(NASA-TM-107762; NAS 1.15:107762) Avail: CASI HC A08/MF A02

Numerical results obtained with the direct simulation Monte Carlo (DSMC) method are presented for Mach 20 nitrogen flow about a 70-deg blunted cone. The flow conditions simulated are those that can be obtained in existing low-density hypersonic wind tunnels. Three sets of flow conditions are simulated with freestream Knudsen numbers ranging from 0.03 to 0.001. The focus is to characterize the wake flow under rarefied conditions. This is accomplished by calculating the influence of rarefaction on wake structure along with the impact that an afterbody has on flow features. This data report presents extensive information concerning flowfield features and surface quantities. Author

N94-15427*# State Univ. of New York, Buffalo. Dept. of Mechanical and Aerospace Engineering.

LARGE EDDY SIMULATION AND DIRECT NUMERICAL SIMULATION OF HIGH SPEED TURBULENT REACTING FLOWS Semiannual Report, 1 Feb. - 31 Oct. 1993

V. Adumitroaie, S. H. Frankel (Purdue Univ., West Lafayette, IN.), C. K. Madnia, and P. Givi 1993 232 p

(Contract NAG1-1122; N00014-90-J-1403; NSF CTS-92-53488)

(NASA-CR-193131; NAS 1.26:193131) Avail: CASI HC A11/MF A03

The objective of this research is to make use of Large Eddy Simulation

(LES) and Direct Numerical Simulation (DNS) for the computational analyses of high speed reacting flows. Our efforts in the first phase of this research conducted within the past three years have been directed in several issues pertaining to intricate physics of turbulent reacting flows. In our previous 5 semi-annual reports submitted to NASA LaRC, as well as several technical papers in archival journals, the results of our investigations have been fully described. In this progress report which is different in format as compared to our previous documents, we focus only on the issue of LES. The reason for doing so is that LES is the primary issue of interest to our Technical Monitor and that our other findings were needed to support the activities conducted under this prime issue. The outcomes of our related investigations, nevertheless, are included in the appendices accompanying this report. The relevance of the materials in these appendices are, therefore, discussed only briefly within the body of the report. Here, results are presented of a priori and a posterior analyses for validity assessments of assumed Probability Density Function (PDF) methods as potential subgrid scale (SGS) closures for LES of turbulent reacting flows. Simple non-premixed reacting systems involving an isothermal reaction of the type A + B yields Products under both chemical equilibrium and non-equilibrium conditions are considered. A priori analyses are conducted of a homogeneous box flow, and a spatially developing planar mixing layer to investigate the performance of the Pearson Family of PDF's as SGS models. A posteriori analyses are conducted of the mixing layer using a hybrid one-equation Smagorinsky/PDF SGS closure. The Smagorinsky closure augmented by the solution of the subgrid turbulent kinetic energy (TKE) equation is employed to account for hydrodynamic fluctuations, and the PDF is employed for modeling the effects of scalar fluctuations. The implementation of the model requires the knowledge of the local values of the first two SGS moments. These are provided by additional modeled transport equations. In both a priori and a posteriori analyses, the predicted results are appraised by comparison with subgrid averaged results generated by DNS. Based on these results, the paths to be followed in future investigations are identified. Author

N94-15431* National Aeronautics and Space Administration. Ames Research Center, Moffett Field, CA.

THE 1988 COMPUTATIONAL FLUID DYNAMICS HIGHLIGHTS (Videotape)

1988 Videotape: 15 min. playing time, in color, with sound

(NASA-TM-109645; NONP-VT-93-190443) Avail: CASI VHS A01/BETA A22

This video highlights the 1988 CFD graphics which show zero gravity phenomena, boundary layers, aeroelasticity, rotor blades, stators, jet ground effects, the F-18, flow about the shuttle, hypersonic flow, and flow in an artificial heart. CASI

N94-15475*# National Aeronautics and Space Administration. Lewis Research Center, Cleveland, OH.

PROTEUS TWO-DIMENSIONAL NAVIER-STOKES COMPUTER CODE, VERSION 2.0. VOLUME 2: USER'S GUIDE

Charles E. Towne, John R. Schwab, and Trong T. Bui Oct. 1993 134 p

(RTOP 505-62-52)

(NASA-TM-106338-Vol-2; E-8107; NAS 1.15:106338-Vol-2) Avail: CASI HC A07/MF A02

A computer code called Proteus 2D was developed to solve the two-dimensional planar or axisymmetric, Reynolds-averaged, unsteady compressible Navier-Stokes equations in strong conservation law form. The objective in this effort was to develop a code for aerospace propulsion applications that is easy to use and easy to modify. Code readability, modularity, and documentation were emphasized. The governing equations are solved in generalized nonorthogonal body-fitted coordinates, by marching in time using a fully-coupled ADI solution procedure. The boundary conditions are treated implicitly. All terms, including the diffusion terms, are linearized using second-order Taylor series expansions. Turbulence is modeled using either an algebraic or two-equation eddy viscosity model. The thin-layer or Euler equations may also be solved. The energy equation may be eliminated by the assumption of constant total enthalpy. Explicit and implicit artificial viscosity may be used. Several time step options are available for convergence acceleration. The documentation is divided into three volumes. This is the User's Guide, and describes the program's features, the input and output, the procedure for setting up initial conditions, the computer resource requirements, the diagnostic messages that may be generated, the job control language used to run the program, and several test cases. Author (revised)

N94-15478*# Institute for Computer Applications in Science and Engineering, Hampton, VA.

ON THE INTERACTION BETWEEN THE SHOCK WAVE ATTACHED TO A WEDGE AND FREESTREAM DISTURBANCES Final Report

Peter W. Duck (Manchester Univ., England.), D. Glenn Lasseigne (Old Dominion Univ., Norfolk, VA.), and M. Y. Hussaini Washington Aug. 1993 48 p Submitted for publication

(Contracts NAS1-19480; NAS1-18605; RTOP 505-90-52-01)

(NASA-CR-191528; NAS 1.26:191528; ICASE-93-61) Avail: CASI HC A03/MF A01

A study of the interaction of small amplitude, unsteady, freestream disturbances with a shock wave induced by a wedge in supersonic flow is presented. These disturbances may be acoustic waves, vorticity waves, or entropy waves (or indeed a combination of all three). Their interactions then generate behind the shock disturbances of all three classes, an aspect that is investigated in some detail, our motivation being to investigate possible mechanisms for boundary-layer receptivity, caused through the amplification and modification of freestream turbulence through the shock-body coupling. Also, the possibility of enhanced mixing owing to additional vorticity produced by the shock-body coupling is investigated. Author (revised)

N94-15479*# Institute for Computer Applications in Science and Engineering, Hampton, VA.

BOUNDARY LAYER FLOW OF AIR OVER WATER ON A FLAT PLATE Final Report

John Nelson (Air Force Systems Command, Wright-Patterson AFB, OH.), Amy E. Alving (Minnesota Univ., Minneapolis.), and Daniel D. Joseph (Minnesota Univ., Minneapolis.) Washington Aug. 1993 16 p Submitted for publication Sponsored in part by NSF, DOE, Dept. of the Army, Dept. of the Air Force, and Minnesota Univ.

(Contract NAS1-19480; RTOP 505-90-52-01)

(NASA-CR-191517; NAS 1.26:191517; ICASE-93-57) Avail: CASI HC A03/MF A01

A non-similar boundary layer theory for air blowing over a water layer on a flat plate is formulated and studied as a two-fluid problem in which the position of the interface is unknown. The problem is considered at large Reynolds number (based on x), away from the leading edge. A simple non-similar analytic solution of the problem is derived for which the interface height is proportional to x(sub 1/4) and the water and air flow satisfy the Blasius boundary layer equations, with a linear profile in the water and a Blasius profile in the air. Numerical studies of the initial value problem suggests that this asymptotic, non-similar air-water boundary layer solution is a global attractor for all initial conditions. Author (revised)

N94-15485*# National Aeronautics and Space Administration. Lewis Research Center, Cleveland, OH.

PROTEUS TWO-DIMENSIONAL NAVIER-STOKES COMPUTER CODE, VERSION 2.0. VOLUME 1: ANALYSIS DESCRIPTION

Charles E. Towne, John R. Schwab, and Trong T. Bui Oct. 1993 75 p

(RTOP 505-62-52)

(NASA-TM-106336-Vol-1; E-8105; NAS 1.15:106336-Vol-1) Avail: CASI HC A04/MF A01

A computer code called Proteus 2D was developed to solve the two-dimensional planar or axisymmetric, Reynolds-averaged, unsteady compressible Navier-Stokes equations in strong conservation law form. The objective in this effort was to develop a code for aerospace propulsion applications that is easy to use and easy to modify. Code readability, modularity, and documentation were emphasized. The governing equations are solved in generalized nonorthogonal body-fitted coordinates, by marching in time using a fully-coupled ADI solution procedure. The boundary conditions are treated implicitly. All terms, including the diffusion terms, are linearized using second-order Taylor series expansions. Turbulence is modeled using either an algebraic or two-equation eddy viscosity model. The thin-layer or Euler equations may also be solved. The energy equation may be eliminated by the assumption of constant total enthalpy. Explicit and implicit artificial viscosity may be used. Several time step options are available for convergence acceleration. The documentation is divided into three volumes.

This is the Analysis Description, and presents the equations and solution procedure. The governing equations, the turbulence model, the linearization of the equations and boundary conditions, the time and space differencing formulas, the ADI solution procedure, and the artificial viscosity models are described in detail. Author (revised)

N94-15488*# National Aeronautics and Space Administration. Lewis Research Center, Cleveland, OH.

PROTEUS THREE-DIMENSIONAL NAVIER-STOKES COMPUTER CODE, VERSION 1.0. VOLUME 2: USER'S GUIDE

Charles E. Towne, John R. Schwab, and Trong T. Bui Oct. 1993 99 p (RTOP 505-62-52)

(NASA-TM-106340-Vol-2; E-8109; NAS 1.15:106340-Vol-2) Avail: CASI HC A05/MF A02

A computer code called Proteus 3D was developed to solve the three-dimensional, Reynolds-averaged, unsteady compressible Navier-Stokes equations in strong conservation law form. The objective in this effort was to develop a code for aerospace propulsion applications that is easy to use and easy to modify. Code readability, modularity, and documentation were emphasized. The governing equations are solved in generalized nonorthogonal body-fitted coordinates, by marching in time using a fully-coupled ADI solution procedure. The boundary conditions are treated implicitly. All terms, including the diffusion terms, are linearized using second-order Taylor series expansions. Turbulence is modeled using either an algebraic or two-equation eddy viscosity model. The thin-layer or Euler equations may also be solved. The energy equation may be eliminated by the assumption of constant total enthalpy. Explicit and implicit artificial viscosity may be used. Several time step options are available for convergence acceleration. The documentation is divided into three volumes. This User's Guide describes the program's features, the input and output, the procedure for setting up initial conditions, the computer resource requirements, the diagnostic messages that may be generated, the job control language used to run the program, and several test cases. Author (revised)

N94-15526# Naval Research Lab., Washington, DC.

SURFACE AND INTERNAL SIGNATURES OF ORGANIZED VORTEX MOTIONS IN STRATIFIED FLUID

Y. T. Fung and S. W. Chang 15 Jul. 1993 50 p

(AD-A267015; NRL/MR/7225-93-7346) Avail: CASI HC A03/MF A01

Internal vortex patterns and the corresponding free surface signatures generated by a submerged sphere moving in a stratified fluid are numerically simulated by a three-dimensional time-dependent computer model. The flow is assumed to be incompressible and hydrostatic, and the Boussinesq approximation is applied. The turbulent mixing is modeled using the Smagorinsky formula for horizontal fluxes and a Richardson number closure for vertical fluxes. The numerical techniques include a second-order finite difference scheme with a staggered and stretched grid system. To efficiently handle the slow baroclinic and the fast barotropic modes in the flow, a split-explicit method is used to separately integrate the two modes in time. This method allows us to economically simulate the time history of the slowly evolving vortices. Preliminary results for the velocity field, the flow pattern, the density distribution, and the induced surface signature are presented. They consistently reveal the existence of coherent structures in the stratified flow field. A mechanism based on the interaction of the wake vorticity and the buoyancy induced oscillation is proposed for the generation and growth of the horizontal vortices in stratified fluids. This mechanism explains why the horizontal vortices appear long after the initial disturbances generated by a submerged moving body have dissipated, and why these vortices exist only in stratified fluids but not in homogenous media. In a forthcoming paper, we will examine how the density distribution, the depth of the moving object, and the depth of the channel floor affect the organized vortex structures and the corresponding surface signatures. DTIC

N94-15551*# Nevada Univ., Reno. Engineering Research and Development Center.

NUMERICAL INVESTIGATIONS IN THREE-DIMENSIONAL INTERNAL FLOWS Semiannual Status Report, 1 Jul. - 31 Dec. 1993

William C. Rose 1993 26 p

(Contract NCC2-507)

(NASA-CR-194594; NAS 1.26:194594) Avail: CASI HC A03/MF A01

In the present reporting period, the 3D version of the OVERFLOW code was used to solve the flow within the internal portion of the supersonic inlet. The internal portion of this inlet is bounded by an inflow plane containing the leading edge of the sidewalls, the sidewalls, the ramp and cowl surfaces and an outflow plane just downstream of the minimum geometric area of the inlet. Boundary layer bleed was used in the two-dimensional calculations discussed in the previous progress report and that same bleed was applied in the present study. For reference, this bleed corresponds to locations designated as R2 and R3 in the Mach 5 inlet model test. Using the GRIDGEN code, a three dimensional grid was generated that accounted for the viscous effects expected to occur on the sidewall, as well as those known to occur on the ramp and cowl surfaces. The internal flow grid size was 141 streamwise by 101 cross stream by 71 in the lateral direction between sidewalls. Since the flow entering the inlet was not symmetrical, the inlet was solved from sidewall to sidewall (without using a symmetry plane). In addition to the short sidewalls proposed in the Langley geometry database, a set of shorter sidewalls was also investigated in the present study and was shown to have beneficial effects with respect to the flow distortion exiting the supersonic inlet. In addition to these calculations, additional 3D solutions using the OVERFLOW code were obtained for the flow downstream of the throat of the supersonic inlet, including a terminal shock wave system produced by a backpressured subsonic diffuser. Author

N94-15632# Naval Surface Warfare Center, Dahlgren, VA.

INCORPORATION OF BOUNDARY LAYER HEATING PREDICTIVE METHODOLOGY INTO NSWCDD AEROPREDICTION CODE

Roy M. McInville and Frank G. Moore Feb. 1993 67 p

(AD-A267000; NSWCDD/TR-93/29) Avail: CASI HC A04/MF A01

Methods have been incorporated into the Naval Surface Warfare Center, Dahlgren Division aeroprediction code to permit the computation of heat transfer rates and recovery temperatures as part of the high Mach number solution. A mass balance technique has been included to determine the correct boundary layer edge entropy to use along the surface of blunt bodies. Refinements were also made to the pressure prediction routines to remove discontinuities and improve overall results. Comparisons of results from the new methods with those from more advanced engineering codes, with other techniques of similar technical level of detail, and with experimental data show good agreement. These new capabilities make possible the rapid computation of three-dimensional heat transfer information for a wide range of geometric configurations and flight conditions. DTIC

N94-15645# Loughborough Univ. of Technology (England). Dept. of Transport Technology.

AN EXPERIMENTAL STUDY OF ASTOVL RELATED JET FLOWS TO PRODUCE CFD CODE VALIDATION DATA. PHASE 3: RESULTS OF EXPERIMENTS Final Report

P. Behrouzi and J. J. McGuirk Oct. 1992 60 p

(TT-9203; ISBN-0-904947-38-6; ETN-93-94492) Copyright Avail: CASI HC A04/MF A01

A study aimed at the provision of experimental data for mean velocities and associated turbulence quantities in flow fields related to the ground effect phase of Advanced Short Takeoff and Vertical Landing (ASTOVL) aircraft operation is reported. These data are intended to serve as a benchmark validation data set for RANS based Computational Fluid Dynamics (CFD) codes which might in the future be used in design studies of ASTOVL aircraft. To aid the specification of boundary conditions in related CFD calculations, and to allow the isolation of several physical phenomena believed to be important in ground effect flows (in particular fountain formation), three idealized jet flow configurations were selected for study: (1) lateral pair (twin jets with line of centers perpendicular to crossflow direction) to study effect of velocity ratio (jet velocity/crossflow velocity), jet impingement height, jet splay angle, and jet spacing; (2) longitudinal pair (twin jets with line of centers aligned with crossflow direction) to study effect of velocity ratio and jet imbalance; (3) and three poster (a combination of lateral and longitudinal pair) to study effect of rear jets splay angle and jet imbalance. Low speed incompressible flows were concentrated upon. The use of laser Doppler velocimetry was selected as the measurement technique to be used, and optical access and seeding problems could be alleviated considerably by the use of a water flow rather than an air flow. Accordingly a small scale water tunnel was selected as the test facility to be used to gather the data. ESA

N94-15737# Naval Postgraduate School, Monterey, CA.
THEORETICAL STUDY OF LAMINAR FILM CONDENSATION ON HORIZONTAL ELLIPITICAL TUBES UNDER CONDITIONS OF FREE AND FORCED CONVECTION M.S. Thesis
Vance H. Adams Mar. 1993 124 p
(AD-A267161) Avail: CASI HC A06/MF A02

Analytical studies have been made of laminar film condensation on a horizontal elliptical cylinder in a pure saturated vapor under conditions of free and forced convection. Estimation of interfacial shear stress was made in two ways: the first involving an asymptotic value of the shear stress under conditions of infinite condensation rate and the second based on simultaneously solving the two-phase vapor boundary layer and condensate equations. The latter approach enables the determination of the vapor boundary layer separation point. For the assumption of asymptotic shear stress, effects of surface tension and pressure gradient in the condensate film have been included. At the extremes of eccentricity, corresponding to a circular tube and a vertical plate, the results are compared with theoretical and experimental work of others. Improvement in the condensation heat transfer coefficient was found for elliptical tubes under both free and forced convection conditions when compared to circular tubes of the same surface area. In the latter case, this improvement was due mainly to the reduced drag of the elliptical tube providing a higher vapor velocity for the same pressure drop as that across a circular tube. DTIC

N94-15751*# National Aeronautics and Space Administration. Lewis Research Center, Cleveland, OH.
PARAMETRIC RESONANT TRIAD INTERACTIONS IN A FREE SHEAR LAYER
R. Mallier (McGill Univ., Montreal, Quebec.) and S. A. Maslowe Oct. 1993 23 p
(RTOP 505-90-5K)
(NASA-TM-106365; ICOMP-93-35; E-8166; NAS 1.15:106365) Avail: CASI HC A03/MF A01

We investigate the weakly nonlinear evolution of a triad of nearly-neutral modes superimposed on a mixing layer with velocity profile u bar equals Um + tanh y. The perturbation consists of a plane wave and a pair of oblique waves each inclined at approximately 60 degrees to the mean flow direction. Because the evolution occurs on a relatively fast time scale, the critical layer dynamics dominate the process and the amplitude evolution of the oblique waves is governed by an integro-differential equation. The long-time solution of this equation predicts very rapid (exponential of an exponential) amplification and we discuss the pertinence of this result to vortex pairing phenomena in mixing layers. Author (revised)

N94-15755 Prins Maurits Lab. TNO, Rijswijk (Netherlands).
EXPERIMENTAL INVESTIGATIONS INTO THE DEFLAGRATION TO DETONATION TRANSITION AT TNO/PML Final Report [HET EXPERIMENTELE ONDERZOEK NAAR DE DEFLAGRATIE NAAR DETONATIE OVERGANG OP PML/TNO]
H. J. Verbeek, R. Oostdam, and E. G. deJong Jan. 1993 31 p In DUTCH Limited Reproducibility: More than 20% of this document may be affected by microfiche quality
(AD-A266753; PML-1992-77; TDCK-92-2743) Avail: CASI HC A03

This report presents an overview of the experimental research that has been performed at TNO-PML from 1988 to 1991 on the subject of the transition from a deflagration to a detonation (DDT) in solid explosives. A full description is given of the set-up used for the experiments, of the development in time of the set-up, and of the rationale for the applied changes. Among the experimental results that are presented, the influence on the DDT process is shown of variations in parameters such as the tube geometry, the explosive density, the particle size, and the igniter strength. The results obtained at a relatively low wall thickness of the test-tube are particularly notable. DTIC

N94-15768*# Institute for Computer Applications in Science and Engineering, Hampton, VA.
NUMERICAL SIMULATION OF THREE-DIMENSIONAL SELF-GRAVITATING FLOW
John V. Shebalin Aug. 1993 14 p Submitted for publication
(RTOP 505-90-52-01)
(NASA-TM-109021; ICASE-93-60; NAS 1.15:109021) Avail: CASI HC A03/MF A01

The three-dimensional flow of a self-gravitating fluid is numerically simulated using a Fourier pseudospectral method with a logarithmic variable formulation. Two cases with zero total angular momentum are studied in detail, a 323 simulation (Run B). Other than the grid size, the primary difference between the two cases are that Run A modeled atomic hydrogen and had considerably more compressible motion initially than Run B, which modeled molecular hydrogen. The numerical results indicate that gravitational collapse can proceed in a variety of ways. In the Run A, collapse led to an elongated tube-like structure, while in the Run B, collapse led to a flatter, disklike structure. Author (revised)

N94-15770# Clarkson Univ., Potsdam, NY.
MECHANISM OF INTERMITTENT ATOMIZATION Final Report
S. P. Lin Jun. 1993 94 p
(Contract DAAL03-89-K-0179)
(AD-A266625; ARO-26797.10-EG) Avail: CASI HC A05/MF A01

A theory is developed for the purpose of enhancing the efficiency of internal combustion engines, and to reduce the air pollution caused by inefficient combustion. The theoretical results show that the droplet formation from the leading edge of the liquid fuel jet is caused by the Taylor-Lamb instability during the deceleration phase of the intermittent spray. The mechanism of droplet formation from the rest of the liquid-gas interface is caused by the interfacial stress fluctuation. The deceleration of the liquid jet tends to reduce the droplet diameter at the same pressure. However, finer sprays can be produced with a more sudden reduction in the nozzle inlet pressure after its peak during the injection period. An increase in the compressibility of the liquid jet is shown to promote the generation of smaller droplets, although at a slower rate. The compressibility of the ambient gas, as well as the surface tension, tends to promote absolute instability. The precise physical meaning remains unclear. The absolute instability can be reduced to convective instability by reducing the surface tension and/or increasing the compressibility of the jet fluid. The convective instability is responsible for the formation of sprays. DTIC

N94-15795*# Old Dominion Univ., Norfolk, VA. Dept. of Mechanical Engineering.
INVESTIGATION OF RADIATIVE INTERACTION IN LAMINAR FLOWS USING MONTE CARLO SIMULATION
Jiwen Liu and S. N. Tiwari Jun. 1993 33 p
(Grant NAG1-363)
(NASA-CR-194604; NAS 1.26:194604; ODU/ICAM-93-101) Avail: CASI HC A03/MF A01

The Monte Carlo method (MCM) is employed to study the radiative interactions in fully developed laminar flow between two parallel plates. Taking advantage of the characteristics of easy mathematical treatment of the MCM, a general numerical procedure is developed for nongray radiative interaction. The nongray model is based on the statistical narrow band model with an exponential-tailed inverse intensity distribution. To validate the Monte Carlo simulation for nongray radiation problems, the results of radiative dissipation from the MCM are compared with two available solutions for a given temperature profile between two plates. After this validation, the MCM is employed to solve the present physical problem and results for the bulk temperature are compared with available solutions. In general, good agreement is noted and reasons for some discrepancies in certain ranges of parameters are explained. Author

N94-15834*# Institute for Computer Applications in Science and Engineering, Hampton, VA.
INVISCID INSTABILITY OF STREAMWISE CORNER FLOW
S. Balachandar (Illinois Univ., Urbana.) and M. R. Malik (High Technology Corp., Hampton, VA.) Washington Aug. 1993 25 p Submitted for publication
(Contracts NAS1-19480; NAS1-19299)
(NASA-CR-191514; ICASE-93-54; NAS 1.26:191514) Avail: CASI HC A03/MF A01

Linear stability of the incompressible flow along a stream wise corner is studied by solving the two-dimensional eigenvalue problem governed by partial differential equations. It is found that this fully three-dimensional flow is subject to inviscid instability due to the inflectional nature of the stream wise velocity profile. The higher growth rates for the inviscid instability mode, which is symmetric about the corner bisector, as compared to the viscous Tollmien-Schlichting instability operative away from the corner is

consistent with the experimental findings that the corner flow transitions to turbulence earlier than the two-dimensional Blasius flow away from the corner. Author

N94-15858# Aerospace Medical Research Labs., Brooks AFB, TX.
USAF PHYSIOLOGICAL STUDIES OF PERSONAL MICROCLIMATE COOLING: A REVIEW Final Report, Sep. 1980 - Dec. 1992
Stefan H. Constable May 1993 69 p
(AD-A267203; AL-TR-1993-0030) Avail: CASI HC A04/MF A01

The U.S. Air Force has accomplished a number of research studies which evaluated the efficacy of selected personal cooling approaches for alleviating heat stress in personnel wearing certain protective clothing. Most of this work involved laboratory, as opposed to field, studies and incorporated human subjects performing work in either warm or hot environments. Both air and liquid microclimate cooling systems were evaluated. The general findings include the following: (1) personal microclimate cooling systems (both air and liquid) were shown to remove significant quantities of body heat; (2) in general, commercially available systems were inferior to in-house prototype units; (3) backpack (ambulatory) systems usage would likely have a limited user audience for a number of reasons; (4) some near-term, partial solutions to the problem may be at hand for selected deployments; and (5) microclimate cooling technologies on the horizon will likely not provide an optimum solution for most ground crew applications. The USAF Armstrong Laboratory has limited plans for further research in this area. DTIC

N94-15860# McDonnell-Douglas Aerospace Information Services Co., Saint Louis, MO.
RECEPTIVITY OF BOUNDARY LAYERS TO CONVECTED GUSTS Final Report, 1 Apr. 1990 - 31 Mar. 1993
D. E. Parekh 31 Mar. 1993 43 p
(Contract F49620-90-C-0031)
(AD-A267206; AFOSR-93-0458TR) Avail: CASI HC A03/MF A01

The primary objective of this study is to determine experimentally the receptivity of a laminar boundary layer to convected gusts. Receptivity is the process by which external disturbances transfer energy to instabilities in the boundary layer. The term convected gust refers to a transient or periodic vortical disturbance convected by the freestream. The experimental approach consisted of hot-wire studies of the boundary layer response to vortical disturbances produced by an array of oscillating ribbons. The boundary layer is remarkably insensitive to large-scale vortical perturbations. No significant Tollmien-Schlichting waves were observed. The vortical disturbances are rapidly damped in the boundary layer and cause only weak oscillations that are primarily of the same frequency and wavelength as the external disturbance. DTIC

N94-15865*# National Aeronautics and Space Administration. Lewis Research Center, Cleveland, OH.
PROTEUS THREE-DIMENSIONAL NAVIER-STOKES COMPUTER CODE, VERSION 1.0. VOLUME 3: PROGRAMMER'S REFERENCE
Charles E. Towne, John R. Schwab, and Trong T. Bui Oct. 1993 282 p
(RTOP 505-62-52)
(NASA-TM-106341; E-8110; NAS 1.15:106341) Avail: CASI HC A13/MF A03

A computer code called Proteus 3D was developed to solve the three-dimensional, Reynolds-averaged, unsteady compressible Navier-Stokes equations in strong conservation law form. The objective in this effort was to develop a code for aerospace propulsion applications that is easy to use and easy to modify. Code readability, modularity, and documentation were emphasized. The governing equations are solved in generalized nonorthogonal body fitted coordinates, by marching in time using a fully-coupled ADI solution procedure. The boundary conditions are treated implicitly. All terms, including the diffusion terms, are linearized using second-order Taylor series expansions. Turbulence is modeled using either an algebraic or two-equation eddy viscosity model. The thin-layer or Euler equations may also be solved. The energy equation may be eliminated by the assumption of constant total enthalpy. Explicit and implicit artificial viscosity may be used. Several time step options are available for convergence acceleration. The documentation is divided into three volumes. The Programmer's Reference contains detailed information useful when modifying the program. The program structure, the Fortran variables stored in common blocks, and the details of each subprogram are described. Author (revised)

N94-15867*# National Aeronautics and Space Administration. Lewis Research Center, Cleveland, OH.
PROTEUS TWO-DIMENSIONAL NAVIER-STOKES COMPUTER CODE, VERSION 2.0. VOLUME 3: PROGRAMMER'S REFERENCE
Charles E. Towne, John R. Schwab, and Trong T. Bui Oct. 1993 266 p
(RTOP 505-62-52)
(NASA-TM-106339; E-8108; NAS 1.15:106339) Avail: CASI HC A12/MF A03

A computer code called Proteus 2D was developed to solve the two-dimensional planar or axisymmetric, Reynolds-averaged, unsteady compressible Navier-Stokes equations in strong conservation law form. The objective in this effort was to develop a code for aerospace propulsion applications that is easy to use and easy to modify. Code readability, modularity, and documentation were emphasized. The governing equations are solved in generalized nonorthogonal body-fitted coordinates, by marching in time using a fully-coupled ADI solution procedure. The boundary conditions are treated implicitly. All terms, including the diffusion terms, are linearized using second-order Taylor series expansions. Turbulence is modeled using either an algebraic or two-equation eddy viscosity model. The thin-layer or Euler equations may also be solved. The energy equation may be eliminated by the assumption of constant total enthalpy. Explicit and implicit artificial viscosity may be used. Several time step options are available for convergence acceleration. The documentation is divided into three volumes. The Programmer's Reference contains detailed information useful when modifying the program. The program structure, the Fortran variables stored in common blocks, and the details of each subprogram are described. Author (revised)

N94-15953# DCW Industries, La Canada, CA.
TURBULENCE AND TRANSITION MODELING FOR HIGH-SPEED FLOWS Final Report, 15 Sep. 1989 - 14 Mar. 1993
David C. Wilcox 15 Apr. 1993 16 p
(Contract DAAL03-92-G-0188)
(AD-A266748; ARO-26863.8-EG-S) Avail: CASI HC A03/MF A01

This report summarizes research conducted during the past three and a half years aimed at developing and testing a turbulence/transition model applicable to high-speed turbulent flows. The first two years of the project focused on fully turbulent flows, while emphasis shifted to boundary-layer development in the transition region during the final year and a half. This report includes a brief summary of research accomplished during the first three years and cites publications that describe research results in greater detail. The main body of this report summarizes research conducted during the final six months of the period of performance. The primary results of the last six months of the project are elimination of the k-omega model's sensitivity to the freestream value of omega and development of a method for triggering transition at a specified location, independent of the freestream turbulence level. DTIC

N94-15962*# National Aeronautics and Space Administration. Lyndon B. Johnson Space Center, Houston, TX.
GEOMETRICAL VAPOR BLOCKER FOR PARALLEL CONDENSATION TUBES REQUIRING COOLING Patent Application
Eugene Ungar, inventor (to NASA), John Cornwell, inventor (to NASA), and William Harwell, inventor (to NASA) 3 Sep. 1993 20 p
(NASA-Case-MSC-22090-1; NAS 1.71:MSC-22090-1;
US-Patent-Appl-SN-115832) Avail: CASI HC A03/MF A01

An apparatus and method is disclosed for regulating flow of working fluid through parallel condensation tubes requiring subcooling. The apparatus provides an elongated restriction element extending into the outlet of the respective condensation tubes to the approximate point of onset of subcooling. The elongated restriction element is braced externally to the condensation tube with a support that is used for positioning and maintaining the elongated restriction element in the correct position. The elongated restriction element has a pentagonal cross-section and is slightly undersized with respect to the working fluid passageways through the condensation tubes. The restriction member significantly restricts flow of partially vaporized

working fluid but does not significantly affect the flow of fully liquid working fluid. NASA

N94-15964*# Institute for Computer Applications in Science and Engineering, Hampton, VA.
BROKEN SYMMETRY IN IDEAL MAGNETOHYDRODYNAMIC TURBULENCE
John V. Shebalin Washington Aug. 1993 17 p Submitted for publication
(RTOP 505-90-52-01)
(NASA-TM-109017; ICASE-93-49; NAS 1.15:109017) Avail: CASI HC A03/MF A01

A numerical study of the long-time evolution of a number of cases of inviscid, isotropic, incompressible, three-dimensional fluid, and magneto-fluid turbulence has been completed. The results confirm that ideal magnetohydrodynamic turbulence is non-ergodic if there is no external magnetic field present. This is due essentially to a canonical symmetry being broken in an arbitrary dynamical representation. The broken symmetry manifests itself as a coherent structure, i.e., a non-zero time-averaged part of the turbulent magnetic field. The coherent structure is observed, in one case, to contain about eighteen percent of the total energy. Author (revised)

N94-15980# Westinghouse Savannah River Co., Aiken, SC.
GAM-HEAT: A COMPUTER CODE TO COMPUTE HEAT TRANSFER IN COMPLEX ENCLOSURES
R. E. Cooper and J. R. Taylor Dec. 1992 100 p
(Contract DE-AC09-89SR-18035)
(DE93-014724; WSRC-TR-91-372-Rev-2) Avail: CASI HC A05/MF A02

This report discusses the GAM-HEAT code which was developed for heat transfer analyses associated with postulated Double Ended Guillotine Break Loss Of Coolant Accidents (DEGB LOCA) resulting in a drained reactor vessel. In these analyses the gamma radiation resulting from fission product decay constitutes the primary source of energy as a function of time. This energy is deposited into the various reactor components and is re-radiated as thermal energy. The code accounts for all radiant heat exchanges within and leaving the reactor enclosure. The SRS reactors constitute complex radiant exchange enclosures since there are many assemblies of various types within the primary enclosure and most of the assemblies themselves constitute enclosures. GAM-HEAT accounts for this complexity by processing externally generated view factors and connectivity matrices as discussed below, and also accounts for convective, conductive, and advective heat exchanges. The code is structured such that it is applicable for many situations involving heat exchange between surfaces within a radiatively passive medium. DOE

N94-15991*# Pratt and Whitney Aircraft, East Hartford, CT.
EFFECTS OF ROTATION ON COOLANT PASSAGE HEAT TRANSFER. VOLUME 2: COOLANT PASSAGES WITH TRIPS NORMAL AND SKEWED TO THE FLOW Final Report
B. V. Johnson, J. H. Wagner, and G. D. Steuber Washington Oct. 1993 123 p
(Contract NAS3-23691; RTOP 505-62-61)
(NASA-CR-4396-Vol-2; E-6470-1; NAS 1.26:4396-Vol-2) Avail: CASI HC A06/MF A02

An experimental program was conducted to investigate heat transfer and pressure loss characteristics of rotating multipass passages, for configurations and dimensions typical of modern turbine blades. This experimental program is one part of the NASA Hot Section Technology (HOST) Initiative, which has as its overall objective the development and verification of improved analysis methods that will form the basis for a design system that will produce turbine components with improved durability. The objective of this program was the generation of a data base of heat transfer and pressure loss data required to develop heat transfer correlations and to assess computational fluid dynamic techniques for rotating coolant passages. The experimental work was broken down into two phases. Phase 1 consists of experiments conducted in a smooth wall large scale heat transfer model. A detailed discussion of these results was presented in volume 1 of a NASA Report. In Phase 2 the large scale model was modified to investigate the effects of skewed and normal passage turbulators. The results of Phase 2 along with comparison to Phase 1 is the subject of this Volume 2 NASA Report. Author (revised)

N94-16110# Scripps Institution of Oceanography, La Jolla, CA. Center for Coastal Studies.
VENTILATED OSCILLATORY BOUNDARY LAYERS
Daniel C. Conley and Douglas L. Inman Feb. 1993 80 p
(Contract N00014-89-J-1060)
(AD-A266226) Avail: CASI HC A05/MF A01

A combination of field and laboratory experiments are made in order to expand our knowledge of naturally occurring oscillatory boundary layers. Chapter 1 describes field observations of the development of wave driven boundary layers at the fluid sediment interface. Under the crest of the wave, this development can be idealized as an identifiable sequence of three parts. The latter parts of this development are never observed to occur under the trough of the wave despite similarities in wave orbital velocity and acceleration. It is proposed that wave induced boundary ventilation, the oscillatory flow through the surface of a permeable bed, may be responsible for this apparent developmental asymmetry. In chapter 2, a laboratory study is presented of ventilated oscillatory boundary layers. These are boundary layers arising from a flow which oscillates parallel to a permeable bed which is subject to oscillating percolation of the same frequency as the bed parallel flow. Measurements of boundary layer velocities, bed stress and turbulent flow properties are presented. It is observed that suction (flow into the bed) enhances the near bed velocities and bed stress while injection (flow out of the bed) leads to a reduction in these quantities. As the ventilated oscillatory boundary layer experiences both these phenomena in one full cycle, the result is a net stress and a net boundary layer velocity in an otherwise symmetric flow. While production of turbulence attributable to injection is enhanced, the finite time required for this to occur leads to greater vertically averaged turbulence in the suction half cycle. Turbulence generated in the suction half cycle is maintained in a compact layer much closer to the bed. These effects appear to hold for Re ranging from 10(exp 5) to 10(exp 6) and for oscillations other than sinusoidal. DTIC

N94-16444# Argonne National Lab., IL.
IMPLEMENTATION OF AN ANISOTROPIC TURBULENCE MODEL IN THE COMMIX-1C/ATM COMPUTER CODE
M. Bottoni and F. C. Chang 1993 19 p Presented at the Pressure Vessels and Piping Conference, Denver, CO, 25-29 Jul. 1993
(Contract W-31-109-eng-38)
(DE93-015541; ANL/MCT/CP-78185; CONF-930702-38) Avail: CASI HC A03/MF A01

The computer code COMMIX-1C/ATM, which describes single-phase, three-dimensional transient thermofluid dynamic problems, provided the framework for the extension of the standard kappa-epsilon turbulence model to a six-equation model with additional transport equations for the turbulence heat fluxes and the variance of temperature fluctuations. The new model which allows simulation of anisotropic turbulence in stratified shear flows is referred to as the Anisotropic Turbulence Model (ATM). The ATM has been verified with numerical computations of stable and unstable stratified shear flow between parallel plates. DOE

N94-16470# University of Southern California, Los Angeles. Dept. of Aerospace Engineering.
SEARCH FOR CHAOS IN FREE SHEAR FLOWS Final Technical Report, 1 May 1990 - 30 Sep. 1992
Ho Chih-Ming, Patrick Huerre, and Larry G. Redekopp 1 Sep. 1992 7 p
(Grant AF-AFOSR-0299-90)
(AD-A266245; AFOSR-93-0453TR) Avail: CASI HC A02/MF A01

Theoretical studies on the temporal and spatial structure in blunt-body wakes have revealed the necessary conditions under which global, self-sustained oscillations appear and have provided firm criteria for specifying the frequency of these oscillations. The theory has also been employed to describe the preferred mode in jets. The two-dimensional structure of these modes provides a firm basis for describing the spatial structure of the vortex pattern observed in wakes. In addition, a theoretical description of the appearance of the spatial chaos in wake-shear layers, and its representation in terms of a one-dimensional map, has been provided. An experimental facility and necessary instrumentation have been assembled and experiments are in progress on spatial chaos in wake-shear layers. Experimental results have revealed a parameter domain where a temporal

vacillation occurs between the Karman mode and the shear layer mode. Interesting results with possible application to thrust-vectoring of base flows have also been identified. DTIC

N94-16491*# California Univ., Los Angeles. Dept. of Mechanical, Aerospace and Nuclear Engineering.
FLUID FLOW AND HEAT CONVECTION STUDIES FOR ACTIVELY COOLED AIRFRAMES Report, Apr. - Nov. 1993
A. F. Mills 1993 14 p
(Contract NCC2-374)
(NASA-CR-194624; NAS 1.26:194624) Avail: CASI HC A03/MF A01

This report details progress made on the jet impingement - liquid crystal - digital imaging experiment. With the design phase complete, the experiment is currently in the construction phase. In order to reach this phase two design related issues were resolved. The first issue was to determine NASP leading edge active cooling design parameters. Meetings were arranged with personnel at SAIC International, Torrance, CA in order to obtain recent publications that characterized expected leading edge heat fluxes as well as other details of NASP operating conditions. The information in these publications was used to estimate minimum and maximum jet Reynolds numbers needed to accomplish the required leading edge cooling, and to determine the parameters of the experiment. The details of this analysis are shown in Appendix A. One of the concerns for the NASP design is that of thermal stress due to large surface temperature gradients. Using a series of circular jets to cool the leading edge will cause a non-uniform temperature distribution and potentially large thermal stresses. Therefore it was decided to explore the feasibility of using a slot jet to cool the leading edge. The literature contains many investigations into circular jet heat transfer but few investigations of slot jet heat transfer. The first experiments will be done on circular jets impinging on a flat plate and results compared to previously published data to establish the accuracy of the method. Subsequent experiments will be slot jets impinging on full scale models of the NASP leading edge. Table 1 shows the range of parameters to be explored. Next a preliminary design of the experiment was done. Previous papers which used a similar experimental technique were studied and elements of those experiments adapted to the jet impingement study. Trade-off studies were conducted to determine which design was the least expensive, easy to construct, and easy to use. Once the final design was settled, vendors were contacted to verify that equipment could be obtained to meet our specifications. Much of the equipment required to complete the construction of the experiment has been ordered or received. The material status list is shown in Appendix B. Author

N94-16527*# National Aeronautics and Space Administration. Lewis Research Center, Cleveland, OH.
PROTEUS THREE-DIMENSIONAL NAVIER-STOKES COMPUTER CODE, VERSION 1.0. VOLUME 1: ANALYSIS DESCRIPTION
Charles E. Towne, John R. Schwab, and Trong T. Bui Oct. 1993 65 p
(RTOP 505-62-52)
(NASA-TM-106337; E-8106; NAS 1.15:106337) Avail: CASI HC A04/MF A01

A computer code called Proteus 3D has been developed to solve the three dimensional, Reynolds averaged, unsteady compressible Navier-Stokes equations in strong conservation law form. The objective in this effort has been to develop a code for aerospace propulsion applications that is easy to use and easy to modify. Code readability, modularity, and documentation have been emphasized. The governing equations are solved in generalized non-orthogonal body-fitted coordinates by marching in time using a fully-coupled ADI solution procedure. The boundary conditions are treated implicitly. All terms, including the diffusion terms, are linearized using second-order Taylor series expansions. Turbulence is modeled using either an algebraic or two-equation eddy viscosity model. The thin-layer or Euler equations may also be solved. The energy equation may be eliminated by the assumption of constant total enthalpy. Explicit and implicit artificial viscosity may be used. Several time step options are available for convergence acceleration. The documentation is divided into three volumes. This is the Analysis Description, and presents the equations and solution procedure. It describes in detail the governing equations, the turbulence model, the linearization of the equations and boundary conditions, the time and space differencing formulas, the ADI solution procedure, and the artificial viscosity models. Author

N94-16542*# Old Dominion Univ., Norfolk, VA. School of Engineering.
AN ANALYSIS OF THE RADIATION FIELD BENEATH A BANK OF TUBULAR QUARTZ LAMPS
Robert L. Ash Jun. 1972 34 p
(Contract NAS1-9434; RTOP 505-63-50-10)
(NASA-CR-191551; TR-72-T3; NAS 1.26:191551) Avail: CASI HC A03/MF A01

Equations governing the incident heat flux distribution beneath a lamp-reflector system were developed. Analysis of a particular radiant heating facility showed good agreement between theory and experiment when a lamp power loss correction was used. In addition, the theory was employed to estimate thermal disruption in the radiation field caused by a protruding probe. Author

N94-16555# California Univ., Los Angeles. Dept. of Civil Engineering.
EXPERIMENTAL STUDY OF NONASSOCIATED FLOW AND INSTABILITY OF FRICTIONAL MATERIALS Final Report, Dec. 1990 - Mar. 1993
Poul V. Lade and Jerry A. Yamamuro May 1993 120 p
(Grant AF-AFOSR-0117-91)
(AD-A266421) Avail: CASI HC A06/MF A02

Experimental investigations and analyses have been performed to study the behavior of granular materials with respect to their nonassociated flow and instability under certain loading conditions. All experiments have been performed in triaxial compression and extension at high as well as at low confining pressures. Major topics that were studied include: strain localization in triaxial extension tests; drained and undrained stress-strain and strength behavior from low to high pressures in triaxial extension and compression; instability of granular materials at high pressures in triaxial compression and extension; the determination of Skempton's pore pressure parameter B at high pressures; strain rate effects of granular materials at high pressures in drained and undrained conditions; examination of the effective stress principle at high pressures; particle breakage at high pressures; behavior of sand in one-dimensional compression tests at very high pressures; determination of values of K(sub o), the coefficient of earth pressure at rest, at high pressures; evaluation of the elastic modulus and Poisson's ratio at high pressure levels; correlations of high pressure soil behavior with stress-dilatancy, critical state, and input energy; static instability and liquefaction of loose fine sandy slopes; stability of granular materials in post peak softening regime; instability of dilating sand; and creep effects on static and cyclic instability of granular soils. DTIC

N94-16763# Viscoustech, Allison Park, PA.
STABILITY OF FLOWS IN FLUIDIZED BEDS
Apr. 1993 76 p
(Contract DE-AC21-89MC-26302)
(DE93-000245; DOE/MC-26302/3269) Avail: CASI HC A05/MF A01

We study the linearized stability of the state of uniform fluidization, within the context of the theory of mixtures. The mixture is assumed to be made up of a classical linearly viscous fluid mixed with solid particles. In marked departure from most of the previous studies, we model the solid as a granular material and assume a constitutive relation that stems from classical motions in continuum mechanics. The linearized stability analysis of the state of uniform fluidization, in general, leads to an eighth order equation for the characteristic whose root implies instability, when positive. We find that the characteristic equation can be factored and one of the factors is precisely the equation that governs the stability when we use a simplified analysis akin to that of the earlier study of Anderson and Jackson. DOE

N94-16808# Oak Ridge National Lab., TN.
CYCLE PERFORMANCE TESTING OF NONAZEOTROPIC MIXTURES OF HFC-142A/HCFC-124 AND HFC-32/HCFC-124 WITH ENHANCED SURFACE HEAT EXCHANGERS
E. A. Vineyard, J. C. Conklin, and A. J. Brown 1993 20 p Presented at the 1993 American Society of Heating, Refrigerating and Air-Conditioning Engineers (ASHRAE) Summer Meeting, Denver, CO, 26-30 Jan. 1993
(Contract DE-AC05-84OR-21400)
(DE93-015215; CONF-930675-4) Avail: CASI HC A03/MF A01

In an effort to improve the efficiency of residential heat pumps using alternative refrigerants, two nonazeotropic refrigerant mixtures (NARM's) were tested over a range of heat exchanger capacities to determine their

cooling mode performance at US Department of Energy (DOE) heat pump rating conditions of 82 F (27.8 C). The two mixtures, 30% HFC-32/70% HCFC-124 and 75% HFC-143a/25% HCFC-124, were selected on the basis of a previous study that screened refrigerant pairs using such factors as boiling point, stability, ozone depletion potential (ODP), and coefficient of performance (COP) to determine suitable candidates for residential heat pump performance. Three refrigerant-side heat transfer enhancements were tested to determine improvements to overall system performance. Comparisons were made on the basis of the COP as a function of capacity. The results for one of the heat exchanger combinations, a segmented evaporator and finned condenser, were quite promising. Improvements in COP, relative to that for HCFC-22, were from 9 to 17% for the 30% HFC-32/70% HCFC-124 mixture and from 5 to 9% for the 75% HFC-143a/25% HCFC-124 NARM. Another combination, a smooth tube evaporator with a perforated foil insert and finned condenser, had similar gains at low capacities but experienced decreased performance at the higher capacities. The final combination, a smooth tube evaporator with a perforated foil insert and smooth tube condenser with a bent tab insert resulted in poor performance. DOE

N94-16842*# Colorado Univ., Boulder. Dept. of Aerospace Engineering Sciences.

NUMERICAL STUDY OF COMPRESSIBLE BOUNDARY-LEVEL TRANSITION BETWEEN TWO CONCENTRIC CYLINDERS Final Report, 15 Apr. 1990 - 31 Oct. 1993

Chuen-Yen Chow 31 Oct. 1993 2 p

(Contract NCC3-168)

(NASA-CR-194622; NAS 1.26:194622) Avail: CASI HC A01/MF A01

The period of support of this Cooperative Agreement was from April 15, 1990 to October 31, 1992, with a no-cost extension to October 31, 1993 to complete some unfinished tasks. Within this period, research associate Dr. Kai-Hsiung Kao has made tremendous contributions to this project and has produced an impressive amount of publications. At the early stage of the research, he spent some time on the extension of his doctoral thesis in a subject closely related to the present project. His major research effort was devoted to the investigation of stability of a viscous flow between two differentially rotating cylinders, with an emphasis on the effects of compressibility and heat transfer. Actually, the research topics were not restricted to those described by the title of this Agreement, as reflected in some of the more recent publications. Derived from text

N94-16879*# National Aeronautics and Space Administration. Lewis Research Center, Cleveland, OH.

COMPUTATION OF CONFINED COFLOW JETS WITH THREE TURBULENCE MODELS

J. Zhu and T. H. Shih Jul. 1993 13 p Presented at the 24th AIAA Fluid Dynamics Conference, Orlando, FL, 6-9 Jul. 1993; sponsored by AIAA

(Contract NCC2-233; RTOP 505-90-5K)

(NASA-TM-106378; ICOMP-93-40; CMOTT-93-14; AIAA Paper 93-3120; E-8191; NAS 1.15:106378) Avail: CASI HC A03/MF A01

A numerical study of confined jets in a cylindrical duct is carried out to examine the performance of two recently proposed turbulence models: an RNG-based K-epsilon model and a realizable Reynolds stress algebraic equation model. The former is of the same form as the standard K-epsilon model but has different model coefficients. The latter uses an explicit quadratic stress-strain relationship to model the turbulent stresses and is capable of ensuring the positivity of each turbulent normal stress. The flow considered involves recirculation with unfixed separation and reattachment points and severe adverse pressure gradients, thereby providing a valuable test of the predictive capability of the models for complex flows. Calculations are performed with a finite-volume procedure. Numerical credibility of the solutions is ensured by using second-order accurate differencing schemes and sufficiently fine grids. Calculations with the standard K-epsilon model are also made for comparison. Detailed comparisons with experiments show that the realizable Reynolds stress algebraic equation model consistently works better than does the standard K-epsilon model in capturing the essential flow features, while the RNG-based K-epsilon model does not seem to give improvements over the standard K-epsilon model under the flow conditions considered. Author

N94-16894# Lawrence Livermore National Lab., CA.

ADAPTIVE CARTESIAN GRID METHODS FOR REPRESENTING GEOMETRY IN INVISCID COMPRESSIBLE FLOW

R. B. Pember, J. B. Bell, W. Y. Crutchfield, M. L. Welcome, and P. Colella (California Univ., Berkeley.) 1993 11 p Presented at the 11th International Computational Fluid Dynamics Conference, 28th Thermophysics Conference and 23rd Fluid Dynamics, Plasma Dynamics and Laser Conference, Orlando, FL, 5-7 Jul. 1993

(Contracts W-7405-eng-48; DE-FG03-92ER-25140)

(DE93-016430; UCRL-JC-113851; CONF-930714-1) Avail: CASI HC A03/MF A01

In this paper, we describe a Cartesian grid algorithm for modeling time-dependent compressible flow in complex geometry. In this approach, the problem geometry is treated as an interface embedded in a regular Cartesian mesh. The discretization near the embedded boundary is based on a volume-of-fluid approach with a redistribution procedure to avoid time-step restrictions arising from small cells where the boundary intersects the mesh. The algorithm is coupled to an unsplit, second-order Godunov algorithm and is fully conservative maintaining conservation at the boundary. The Godunov/Cartesian grid integration scheme is coupled to a local adaptive mesh refinement algorithm that selectively refines regions of the computational grid to achieve a desired level of accuracy. Examples showing the results of the combined Cartesian grid/local refinement algorithm for both two- and three-dimensional flows are presented. DOE

N94-16903# Lawrence Livermore National Lab., CA.

THREE DIMENSIONAL HYDRODYNAMIC CALCULATIONS WITH ADAPTIVE MESH REFINEMENT OF THE EVOLUTION OF RAYLEIGH TAYLOR AND RICHTMYER MESHKOV INSTABILITIES IN CONVERGING GEOMETRY: MULTI-MODE PERTURBATIONS

R. I. Klein, J. Bell, R. Pember, and T. Kelleher Apr. 1993 16 p Presented at the 4th International Workshop on the Physics of Compressible Turbulent Mixing, Cambridge, (United Kingdom), 29 Mar. - 1 Apr. 1993

(Contract W-7405-eng-48)

(DE93-017155; UCRL-JC-114505; CONF-9303126-4) Avail: CASI HC A03/MF A01

The authors present results for high resolution hydrodynamic calculations of the growth and development of instabilities in shock driven imploding spherical geometries in both 2D and 3D. They solve the Eulerian equations of hydrodynamics with a high order Godunov approach using local adaptive mesh refinement to study the temporal and spatial development of the turbulent mixing layer resulting from both Richtmyer-Meshkov and Rayleigh-Taylor instabilities. The use of a high resolution Eulerian discretization with adaptive mesh refinement permits them to study the detailed three-dimensional growth of multi-mode perturbations far into the non-linear regime for converging geometries. They discuss convergence properties of the simulations by calculating global properties of the flow. They discuss the time evolution of the turbulent mixing layer and compare its development to a simple theory for a turbulent mix model in spherical geometry based on Plesset's equation. Their 3D calculations show that the constant found in the planar incompressible experiments of Read and Young's may not be universal for converging compressible flow. They show the 3D time trace of transitional onset to a mixing state using the temporal evolution of volume rendered imaging. Their preliminary results suggest that the turbulent mixing layer loses memory of its initial perturbations for classical Richtmyer-Meshkov and Rayleigh-Taylor instabilities in spherically imploding shells. They discuss the time evolution of mixed volume fraction and the role of vorticity in converging 3D flows in enhancing the growth of a turbulent mixing layer. DOE

N94-16908# Stanford Univ., CA. Dept. of Mechanical Engineering.

THREE-DIMENSIONAL TURBULENT BOUNDARY LAYER Final Report, 25 Jan. 1991 - 24 Jul. 1992

Parviz Moin 6 Jan. 1993 120 p

(Grant AF-AFOSR-0174-91)

(AD-A266261; SU-TR-57; AFOSR-93-0459TR) Avail: CASI HC A06/MF A02

The near wall mechanics of 3D turbulent boundary layers were studied using direct numerical simulation. A fully developed turbulent channel flow was suddenly subjected to a transverse pressure gradient. An explanation for the reduction in the Reynolds stresses, observed in experiments, was provided in terms of the dynamics of near-wall streamwise vortices in

turbulent boundary layers. It was shown that the effect of three-dimensionality is to change the trajectory of fluid particles in the vicinity of these vortices, and how this change leads to reductions of turbulence stresses. The proposed mechanisms are consistent with numerous statistical data and correlations which are presented. DTIC

N94-16927# Colorado Univ., Boulder.
NONLINEAR PROBLEMS IN FLUID DYNAMICS AND INVERSE SCATTERING Annual Report, 1 Jan. 1992 - 31 May 1993
Mark J. Ablowitz, Gregory Beylkin, and Duane P. Sather 31 May 1993 16 p
(Contract N00014-91-J-4037)
(AD-A266234; Rept-153-4645) Avail: CASI HC A03/MF A01

The inverse scattering of a class of differential-difference equations and multidimensional operators has been constructed. Solutions of nonlinear wave equations arising in fluid dynamics and plasma physics were found and analyzed. Novel and fast computational algorithms were developed and in relevant nonlinear problems wavelet bases with controlled localization properties in the time-frequency domain have proven to be an effective tool. Landau type amplitude equations governing the small gap Taylor problem have been obtained and analyzed. Detailed project summaries and research activities are given in the attached document. A list of published papers, preprints, and invited lectures are included. DTIC

N94-16929# Princeton Univ., NJ. Gas Dynamics Lab.
THE STRUCTURE OF TURBULENT BOUNDARY LAYERS AND SHOCK WAVE BOUNDARY LAYER INTERACTIONS Final Report, 15 Jun. 1989 - 14 Oct. 1992
Alexander J. Smits 13 Apr. 1993 23 p
(Grant AF-AFOSR-0420-89)
(AD-A266240; AFOSR-93-0451TR) Avail: CASI HC A03/MF A01

This report is the Final Technical Report for AFOSR Grant 89-0420, monitored by Dr James McMichael, for the period June 15, 1989 to October 14, 1992. Under this program, research was performed (1) to describe the structure of the large-scale motions in supersonic turbulent boundary layers, (2) to study the interaction of that turbulence with shock waves and strategies for controlling the interaction, (3) to differentiate between Mach and Reynolds number effects on turbulence structure in wall-bounded flows, and (4) to develop and implement new non-intrusive diagnostic techniques. The research is aimed at providing physical insight, and scaling information, for the development of turbulence models appropriate for supersonic shear layers. The primary experimental means used in these investigations were the Rayleigh scattering technique to study the instantaneous density field, the RELIEF line tagging method to study the instantaneous velocity field, and a dual hot-wire technique to obtain simultaneous velocity and density signals. DTIC

N94-16950# Yale Univ., New Haven, CT. Dept. of Mechanical Engineering.
STUDIES IN TURBULENCE AND TURBULENCE CONTROL Final Technical Report, 1 Jan. 1990 - 31 Dec. 1992
K. R. Sreenivasan 6 Jun. 1993 79 p
(Grant AF-AFOSR-0139-91)
(AD-A266318; AFOSR-93-0449TR) Avail: CASI HC A05/MF A01

A summary of the research performed under this grant is provided. It consists of work that bears on reacting flow research as well as basic turbulence studies. In the former category, the research involves differential diffusion, photobleaching, conditional scalar dissipation, helium jets, and the thickness-distribution of OH regions in diffusion flames. In the former category, the summary is limited to Kolmogorov's refined hypothesis, self-affine traces of turbulent signals, synthetic turbulence, wavelet decomposition of turbulence, and the intermittency exponent in the turbulence dissipation. Only briefly mentioned are other aspects such as the scaling of structure functions, the scaling of circulation, and the effect of filtering on Kolmogorov's 4/5 relation. DTIC

N94-16958# Pittsburgh Univ., PA. Dept. of Mechanical Engineering.
STABILITY ANALYSIS FOR THE FLOW OF GRANULAR MATERIALS DOWN AN INCLINED PLANE USING KINETIC MODEL
K. R. Rajagopal 1993 10 p
(Contract DE-AC22-91PC-90180)
(DE93-016852; DOE/PC-90180/T7) Avail: CASI HC A02/MF A01

In the previous report the linearized stability equations for the flow of granular materials down an inclined plane, modeled by the kinetic constitutive theory of Richman & Marciniec were derived. Here, we use the approximate solution of Richman & Marciniec as the base solution for the linearized stability analysis. The governing equations obtained are solved numerically to obtain the marginal stability curves which are presented in this report. DOE

N94-16966# Massachusetts Inst. of Tech., Cambridge. Dept. of Aeronautics and Astronautics.
ADAPTIVE NAVIER-STOKES CALCULATIONS FOR VORTICAL FLOW Final Report, 1 Jun. 1989 - 31 Oct. 1992
Earll M. Murman 12 Mar. 1993 15 p
(Grant AF-AFOSR-0395-89)
(AD-A266236; AFOSR-93-0439TR) Avail: CASI HC A03/MF A01

Brief summaries are given of research performed in the following areas: (1) adaptive Euler equation solvers; (2) adaptation parameters for vortical flow; (3) vortex breakdown calculations; (4) calculations for the F-117A; (5) normal force hysteresis; (6) visualization of vortical flows on unstructured grids; and (7) modeling of vortex breakdown. The reference list gives reports with detailed results. DTIC

N94-16985# Naval Postgraduate School, Monterey, CA.
NATURAL CONVECTION ABOVE A HORIZONTAL HEAT SOURCE M.S. Thesis
Adrian J. Jansen Mar. 1993 73 p
(AD-A267212) Avail: CASI HC A04/MF A01

An investigation of natural convection heat transfer from a flush mounted heater on a larger horizontal substrate in water has been conducted. The focus of the present investigation was on the buoyant flow above the heat source. Temperature measurements in the buoyant plume were made at various locations and heights, for a number of input powers using a traversing thermocouple probe. Simple signal processing was performed on the temperature measurements to attempt to investigate the reported meandering motions in the plume and the transition from laminar to turbulent buoyant flow. These measurements are interpreted based on flow visualizations. DTIC

N94-17003# University of Southern California, Los Angeles. Center for Applied Mathematical Sciences.
MODELING, ESTIMATION AND CONTROL OF DISTRIBUTED PARAMETER SYSTEMS Final Report, 1 Jan. 1990 - 31 Mar. 1993
H. T. Banks 3 Jun. 1993 24 p
(Grant AF-AFOSR-0091-90)
(AD-A267325; AFOSR-93-0476TR) Avail: CASI HC A03/MF A01

Research on theoretical ideas (well-posedness, feedback control, stability of inverse problems, form of damping in structures) and associated computational methods was performed. Topics include fluid/structure interaction and flow control with applications to Navier-Stokes steady flow, Burgers equation, advection diffusion, porous media flow, and acoustics/noise suppression; inverse problems for detection of semiconductor defects, electrical impedance tomography, damping, and 'smart' material actuators in composite structures; and linear, nonlinear and homogenization models for beams, plates, shells, and PZT actuators and sensors. DTIC

N94-17056*# National Aeronautics and Space Administration. Lewis Research Center, Cleveland, OH.
HIGHER-ORDER ACCURATE OSHER SCHEMES WITH APPLICATION TO COMPRESSIBLE BOUNDARY LAYER STABILITY
J. J. W. VanDerVegt Jul. 1993 16 p Presented at the AIAA 24th Fluid Dynamics Conference, Orlando, FL, 6-9 Jul. 1993; sponsored by AIAA See also A93-48231
(Contract NCC3-233; RTOP 505-90-5K)
(NASA-TM-106355; ICOMP-93-33; E-8139; CMOTT-93-12; AIAA Paper 93-3051; NAS 1.15:106355) Copyright Avail: CASI HC A03/MF A01

Two fourth order accurate Osher schemes are presented which maintain higher order accuracy on nonuniform grids. They use either a conservative finite difference or finite volume discretization. Both methods are successfully used for direct numerical simulations of flat plate boundary layer instability at different Mach numbers. Results of growth rates of Tollmien-Schlichting

waves compare well with direct simulations of incompressible flow and for compressible flow with results obtained by solving the parabolic stability equations. Author

N94-17061*# National Aeronautics and Space Administration. Langley Research Center, Hampton, VA.
AN UPWIND MULTIGRID METHOD FOR SOLVING VISCOUS FLOWS ON UNSTRUCTURED TRIANGULAR MESHES M.S. Thesis
Daryl Lawrence Bonhaus (George Washington Univ., Hampton, VA.) 13 Aug. 1993 58 p
(NASA-TM-109343; NAS 1.15:109343) Avail: CASI HC A04/MF A01

A multigrid algorithm is combined with an upwind scheme for solving the two dimensional Reynolds averaged Navier-Stokes equations on triangular meshes resulting in an efficient, accurate code for solving complex flows around multiple bodies. The relaxation scheme uses a backward-Euler time difference and relaxes the resulting linear system using a red-black procedure. Roe's flux-splitting scheme is used to discretize convective and pressure terms, while a central difference is used for the diffusive terms. The multigrid scheme is demonstrated for several flows around single and multi-element airfoils, including inviscid, laminar, and turbulent flows. The results show an appreciable speed up of the scheme for inviscid and laminar flows, and dramatic increases in efficiency for turbulent cases, especially those on increasingly refined grids. Author

N94-17095*# Texas A&M Univ., College Station. Dept. of Aerospace Engineering.
NONEQUILIBRIUM RADIATION AND CHEMISTRY MODELS FOR AEROCAPTURE VEHICLE FLOWFIELDS Semiannual Progress Report, Jan. - Jun. 1993
Leland A. Carlson Sep. 1993 39 p
(Grant NAG1-1003)
(NASA-CR-194645; NAS 1.26:194645; TAMRF-6382-93-02) Avail: CASI HC A03/MF A01

The period from Jan. 1993 thru Aug. 1993 is covered. The primary tasks during this period were the development of a single and multi-vibrational temperature preferential vibration-dissociation coupling model, the development of a normal shock nonequilibrium radiation-gasdynamic coupling model based upon the blunt body model, and the comparison of results obtained with these models with experimental data. In addition, an extensive series of computations were conducted using the blunt body model to develop a set of reference results covering a wide range of vehicle sizes, altitudes, and entry velocities. Author (revised)

N94-17112*# National Aeronautics and Space Administration. Lewis Research Center, Cleveland, OH.
THERMALLY-SUSTAINED STRUCTURE IN CONVECTIVELY UNSTABLE SYSTEMS
Robert J. Deissler Nov. 1993 17 p
(Contract NCC3-233; RTOP 505-90-5K)
(NASA-TM-106375; ICOMP-93-39; E-8185; NAS 1.15:106375) Avail: CASI HC A03/MF A01

The complex Ginzburg-Landau equation with a thermal noise term is studied under conditions when the system is convectively unstable. Under these conditions, the noise is selectively and spatially amplified giving rise to a noise-sustained structure. Analytical results, applicable to a wide range of physical systems, are derived for the variance, and the coefficients and thermal noise term are determined for Taylor-Couette flow with an axial through-flow. Comparison is made to recent experiments. Author

N94-17127*# Old Dominion Univ., Norfolk, VA. Dept. of Mechanical Engineering.
INVESTIGATION OF HIGH-SPEED FREE SHEAR FLOWS USING IMPROVED PRESSURE-STRAIN CORRELATED REYNOLDS STRESS TURBULENCE MODEL Supplemental Progress Report for period ending Aug. 1991
S. N. Tiwari and B. Lakshmanan Nov. 1993 29 p
(Grant NAG1-423)
(NASA-CR-194661; NAS 1.26:194661) Avail: CASI HC A03/MF A01

A high-speed shear layer is studied using compressibility corrected Reynolds stress turbulence model which employs newly developed model for pressure-strain correlation. MacCormack explicit prediction-corrector method is used for solving the governing equations and the turbulence transport equations. The stiffness arising due to source terms in the turbulence equations is handled by a semi-implicit numerical technique. Results obtained using the new model show a sharper reduction in growth rate with increasing convective Mach number. Some improvements were also noted in the prediction of the normalized streamwise stress and Reynolds shear stress. The computed results are in good agreement with the experimental data. Author

N94-17128*# National Aeronautics and Space Administration. Lewis Research Center, Cleveland, OH.
ON SOLVING THE COMPRESSIBLE NAVIER-STOKES EQUATIONS FOR UNSTEADY FLOWS AT VERY LOW MACH NUMBERS
R. H. Pletcher and K.-H. Chen (Ohio Aerospace Inst., Brook Park.) Jul. 1993 13 p Presented at the 24th Fluid Dynamics Conference, orlando, FL, 6-9 Jul. 1993; sponsored by AIAA See also A93-45061
(RTOP 505-90-5K)
(NASA-TM-106380; ICOMP-93-42; AIAA Paper 93-3368; E-8193; NAS 1.15:106380) Avail: CASI HC A03/MF A01

The properties of a preconditioned, coupled, strongly implicit finite difference scheme for solving the compressible Navier-Stokes equations in primitive variables are investigated for two unsteady flows at low speeds, namely the impulsively started driven cavity and the startup of pipe flow. For the shear-driven cavity flow, the computational effort was observed to be nearly independent of Mach number, especially at the low end of the range considered. This Mach number independence was also observed for steady pipe flow calculations; however, rather different conclusions were drawn for the unsteady calculations. In the pressure-driven pipe startup problem, the compressibility of the fluid began to significantly influence the physics of the flow development at quite low Mach numbers. The present scheme was observed to produce the expected characteristics of completely incompressible flow when the Mach number was set at very low values. Good agreement with incompressible results available in the literature was observed. Author

N94-17129*# Georgia Inst. of Tech., Atlanta. School of Aerospace Engineering.
DEVELOPMENT OF ITERATIVE TECHNIQUES FOR THE SOLUTION OF UNSTEADY COMPRESSIBLE VISCOUS FLOWS Final Report
Lakshmi Sankar and Duane Hixon Nov. 1993 14 p
(Grant NAG1-1217)
(NASA-CR-194657; NAS 1.26:194657) Avail: CASI HC A03/MF A01

The work done under this project was documented in detail as the Ph. D. dissertation of Dr. Duane Hixon. The objectives of the research project were evaluation of the generalized minimum residual method (GMRES) as a tool for accelerating 2-D and 3-D unsteady flows and evaluation of the suitability of the GMRES algorithm for unsteady flows, computed on parallel computer architectures. Author (revised)

N94-17130*# Florida Inst. of Tech., Melbourne. Dept. of Mechanical and Aerospace Engineering.
STRUCTURE OF TURBULENCE IN THREE-DIMENSIONAL BOUNDARY LAYERS Final Technical Report
Chelakara S. Subramanian 1993 23 p
(Grant NAG1-1541)
(NASA-CR-194655; NAS 1.26:194655) Avail: CASI HC A03/MF A01

This report provides an overview of the three dimensional turbulent boundary layer concepts and of the currently available experimental information for their turbulence modeling. It is found that more reliable turbulence data, especially of the Reynolds stress transport terms, is needed to improve the existing modeling capabilities. An experiment is proposed to study the three dimensional boundary layer formed by a 'sink flow' in a fully developed two dimensional turbulent boundary layer. Also, the mean and turbulence field measurement procedure using a three component laser Doppler velocimeter is described. Author

N94-17215*# Old Dominion Univ., Norfolk, VA. Dept. of Mechanical Engineering.
STUDIES ON NONEQUILIBRIUM PHENOMENA IN SUPERSONIC CHEMICALLY REACTING FLOWS Progress Report for period ending 31 Aug. 1993
S. N. Tiwari and Rajnish Chandrasekhar Nov. 1993 139 p

(Grant NAG1-423)
(NASA-CR-194662; NAS 1.26:194662) Avail: CASI HC A07/MF A02

This study deals with a systematic investigation of nonequilibrium processes in supersonic combustion. The two-dimensional, elliptic Navier-Stokes equations are used to investigate supersonic flows with nonequilibrium chemistry and thermodynamics, coupled with radiation, for hydrogen-air systems. The explicit, unsplit MacCormack finite-difference scheme is used to advance the governing equations in time, until convergence is achieved. For a basic understanding of the flow physics, premixed flows undergoing finite rate chemical reactions are investigated. Results obtained for specific conditions indicate that the radiative interactions vary substantially, depending on reactions involving HO2 and NO species, and that this can have a noticeable influence on the flowfield. The second part of this study deals with premixed reacting flows under thermal nonequilibrium conditions. Here, the critical problem is coupling of the vibrational relaxation process with the radiative heat transfer. The specific problem considered is a premixed expanding flow in a supersonic nozzle. Results indicate the presence of nonequilibrium conditions in the expansion region of the nozzle. This results in reduction of the radiative interactions in the flowfield. Next, the present study focuses on investigation of non-premixed flows under chemical nonequilibrium conditions. In this case, the main problem is the coupled turbulence-chemistry interaction. The resulting formulation is validated by comparison with experimental data on reacting supersonic coflowing jets. Results indicate that the effect of heat release is to lower the turbulent shear stress and the mean density. The last part of this study proposes a new theoretical formulation for the coupled turbulence-radiation interactions. Results obtained for the coflowing jets experiment indicate that the effect of turbulence is to enhance the radiative interactions. Derived from text

N94-17250# Fluid Jet Associates, Spring Valley, OH.
TWO-DIMENSIONAL, HIGH FLOW, PRECISELY CONTROLLED MONODISPERSE DROP SOURCE Final Report, 8 Nov. 1989 - 8 Mar. 1993
John L. Dressler 15 Mar. 1993 62 p
(Contract F33615-89-C-2973)
(AD-A267660; WL-TR-93-2049) Avail: CASI HC A04/MF A01

A versatile acoustically-driven fluid atomizer was designed and operated that creates precise monodisperse sprays by Rayleigh breakup or polydisperse sprays by the acoustic driving of amplitude dependent instabilities. The atomizer forms a cylindrical, conical, or flat (sheet) liquid jet by means of a photofabricated nozzle. The spray pattern and spray volume are altered by changing the nozzle. A piezoelectric driver, constructed to efficiently couple energy to the liquid, modulates the fluid velocity. When operated at low power, the drop generator can produce arrays of monodisperse drops as small as 15 microns in diameter. Operating the piezoelectric driver at high power produces perturbations with sufficient energy to break the liquid jets into drops, with a net increase in surface energy. The resulting drop sizes are influenced by the frequency and amplitude of the driving signal and nozzle size. The spatial distribution of the spray is controlled by the spacing and geometry of the holes in the nozzle plate, the amplitude of the acoustic signal, and the swirl in the fluid manifold. This device is more robust than the typical acoustic drop generator because small drops can be made from large holes, reducing the plugging problem. No air flow is used. DTIC

N94-17258*# National Aeronautics and Space Administration. Lewis Research Center, Cleveland, OH.
MULTIGRID TIME-ACCURATE INTEGRATION OF NAVIER-STOKES EQUATIONS
Andrea Arnone (Florence Univ., Italy.), Meng-Sing Liou, and Louis A. Povinelli Nov. 1993 11 p
(Contract NCC3-233; RTOP 505-90-5K)
(NASA-TM-106373; ICOMP-93-37; E-8183; NAS 1.15:106373) Avail: CASI HC A03/MF A01

Efficient acceleration techniques typical of explicit steady-state solvers are extended to time-accurate calculations. Stability restrictions are greatly reduced by means of a fully implicit time discretization. A four-stage Runge-Kutta scheme with local time stepping, residual smoothing, and multigridding is used instead of traditional time-expensive factorizations. Some applications to natural and forced unsteady viscous flows show the capability of the procedure. Author

N94-17276# Pennsylvania State Univ., University Park. Applied Research Lab.
TRANSITION INDUCED BY FIXED AND FREELY CONVECTING SPHERICAL PARTICLES IN LAMINAR BOUNDARY LAYERS Final Report
H. L. Petrie, P. J. Morris, A. R. Bajwa, and D. C. Vincent Aug. 1993 108 p
(Contract N00014-91-J-1646)
(AD-A267757; TR-93-07) Avail: CASI HC A06/MF A02

An experimental and analytical study of aspects of transition induced by disturbances from spherical particles in laminar boundary layers is discussed. The generation of turbulent wedges by fixed spherical particles in a laminar boundary layer on or near the surface of a flat plate is considered experimentally using flow visualization with fluorescent dye and laser Doppler velocimetry. Turbulent spots generated by freely convecting spherical particles that are released in the freestream to fall into a flat plate laminar boundary layer and impact the plate are also discussed. A combination of dye flow visualization and a video based particle tracking technique was used to study the convecting particle problem. Although the Reynolds number at the critical condition for turbulent wedge generation by fixed particles and turbulent spot generation by convecting particles are similar, transition in these two situations appears to be fundamentally different. The development of a turbulent wedge near the critical condition is a relatively gradual process. In contrast, turbulent spots form relatively quickly after the convecting particles enter the boundary layer and impact the plate. Turbulent wedge formation downstream of a fixed particle results from the destabilization of the near wall flow by the vortical structures shed into particle wake. This shedding process is dominated by periodically shed loop shaped hairpin vortices. Observation of subharmonic oscillations at 1/2 and 1/4 of this shedding frequency suggest that a chaotic route to turbulence by a series of period doubling bifurcations is possible. DTIC

N94-17286# Stanford Univ., CA. Thermosciences Div.
ACTIVE TURBULENCE CONTROL IN WALL BOUNDED FLOWS USING DIRECT NUMERICAL SIMULATION Final Technical Report, 1 Jul. 1989 - 30 Sep. 1992
Parviz Moin 6 Nov. 1992 292 p
(Grant AF-AFOSR-0411-89)
(AD-A267261; AFOSR-93-0467TR) Avail: CASI HC A13/MF A03

The objective of the study is to explore concepts for control of turbulent boundary layers leading to skin-friction reduction using the direct numerical simulation technique. This report is divided into three parts where different control methods are investigated: an active control by sensing and perturbing structures near the wall, a feedback control procedure guided by control theory, and a passive control by longitudinal riblets. Part 1: significant drag reduction is achieved when the surface boundary condition is modified to suppress the dynamically significant coherent structures present in the wall region. Part 2: mathematical methods of control theory are applied to the problem of control of fluid flow. Part 3: direct numerical simulation is performed to analyze turbulent flow over longitudinal riblets, and to reduce the mechanism of drag reduction by riblets. DTIC

N94-17298*# Princeton Univ., NJ. Dept. of Chemical Engineering.
THE ROLES OF FLUID MOTION AND OTHER TRANSPORT PHENOMENA IN THE MORPHOLOGY OF MATERIALS Final Report, Sep. 1988 - Dec. 1992
D. A. Saville Nov. 1993 311 p
(Grant NAG8-749)
(NASA-CR-194665; NAS 1.26:194665) Avail: CASI HC A14/MF A03

Two crystallization problems were studied: the growth of protein crystals, in particular the influence of colloidal forces and convection, and the influence of interface resistance on the growth of dendritic crystals. The protein study involved both experimental and theoretical work; the work of dendrites was entirely theoretical. In the study of protein crystallization, experiments were carried out where crystals were grown in the presence and absence of natural convection. No evidence was found that convection retards crystal growth. The theoretical study focused on the influence of colloidal forces (electrostatic and London-van der Waals) on the interaction between a protein molecule and a flat crystal surface. It was shown that the interaction is extremely sensitive to colloidal forces and that electrostatic interactions play a strong role in deciding whether or not a molecule will find a favorable site for adsorption. In the study of dendritic growth, the role of

an interfacial resistance on the selection processes was examined. Using a computational scheme, it was found that the selected velocity is strongly dependent on the magnitude of the interfacial resistance to heat transfer. This is a possible explanation for discrepancies between the theoretical and experimental results on succinonitrile. Author (revised)

N94-17363# University of Southern California, Los Angeles. Dept. of Aerospace Engineering.

A NUMERICAL INVESTIGATION OF ENERGY TRANSFER AND SUBGRID-SCALE EDDY-VISCOSITY IN HOMOGENEOUS, ISOTROPIC, AND SHEAR TURBULENCE Final Report, 15 May 1990 - 31 Aug. 1992

J. A. Domaradzki 20 Sep. 1992 78 p

(Grant AF-AFOSR-0300-90)

(AD-A267265; AFOSR-93-0479TR) Avail: CASI HC A05/MF A01

Using results of direct numerical stimulation we have analyzed nonlinear energy transfer between scales of motion in isotropic and homogeneous shear turbulence in both spectral and physical space representation. In all cases we find that the transfer is local, occurring between similar scales, but is always moderated by scales from the energy containing range (local transfer through nonlocal triad interaction). Such local energy exchanges dominate also subgrid-scale energy transfer which was found to be composed as a forward and an inverse transfer components, both being significant in dynamics of large scales. The spatial structure of the subgrid-scale transfer was compared with the structure of a number of physical quantities which are considered important in the dynamics of large scales giving usually poor correlations. Moderate correlations were observed only for the large scale energy and the Smagorinsky's transfer. Finally, a new theory of spectral energy dynamics was developed. The theory provides a plausible physical mechanism of the observed transfer process and predicts the energy spectrum in the inertial and the dissipation range in agreement with experiments and simulations. DTIC

N94-17384# Maryland Univ., College Park. Inst. for Physical Science and Technology.

ON THE a-POSTERIORI ESTIMATION OF THE MODELLING ERROR FOR THE HEAT CONDUCTION IN A PLATE AND ITS USE FOR ADAPTIVE HIERARCHIC MODELLING Final Report

I. Babuska, I. Lee, and C. Schwab Apr. 1993 30 p

(Contract N00014-90-J-1030)

(AD-A267965; BN-1145) Avail: CASI HC A03/MF A01

The paper addresses the a-posteriori error estimates of modelling heat convection problems in a plate. It derives estimators which are essentially local (of the size of the thickness of the plate). The estimator is guaranteed to be an upper bound. The lower bound of the error is also given. The asymptotic exactness of the estimator with respect to the thickness of the plate and with respect to the order of the model is proven. The adaptive procedure based on this a-posteriori error estimator is proposed. Numerical examples are given. DTIC

N94-17385*# National Aeronautics and Space Administration. Lewis Research Center, Cleveland, OH.

TIME DEPENDENT TURBULENCE MODELING AND ANALYTICAL THEORIES OF TURBULENCE

R. Rubinstein Nov. 1993 29 p

(Contract NCC3-233; RTOP 505-90-5K)

(NASA-TM-106379; ICOMP-93-41; CMOTT-93-15; E-8192; NAS 1.15:106379) Avail: CASI HC A03/MF A01

By simplifying the direct interaction approximation (DIA) for turbulent shear flow, time dependent formulas are derived for the Reynolds stresses which can be included in two equation models. The Green's function is treated phenomenologically, however, following Smith and Yakhot, we insist on the short and long time limits required by DIA. For small strain rates, perturbative evaluation of the correlation function yields a time dependent theory which includes normal stress effects in simple shear flows. From this standpoint, the phenomenological Launder-Reece-Rodi model is obtained by replacing the Green's function by its long time limit. Eddy damping corrections to short time behavior initiate too quickly in this model; in contrast, the present theory exhibits strong suppression of eddy damping at short times. A time dependent theory for large strain rates is proposed in which large scales are governed by rapid distortion theory while small scales are governed by Kolmogorov inertial range dynamics. At short times and large strain rates, the theory closely matches rapid distortion theory, but at long times it relaxes to an eddy damping model. Author

N94-17387*# Institute for Computer Applications in Science and Engineering, Hampton, VA.

CONVECTION EFFECTS ON RADIAL SEGREGATION AND CRYSTAL MELT INTERFACE IN VERTICAL BRIDGMAN GROWTH Final Report

S. Tanveer (Ohio State Univ., Columbus.) Sep. 1993 58 p Submitted for publication

(Contracts NAS1-18605; NAS1-19480; NAG3-1415; NSF DMS-91-07608; RTOP 505-90-52-01)

(NASA-CR-191541; NAS 1.26:191541; ICASE-93-72) Avail: CASI HC A04/MF A01

We analytically study the influence of convection caused by horizontal heat transfer through the sides of a vertical Bridgman apparatus. We consider the case when the heat transfer across the side walls is small so that the resulting interfacial deformation and fluid velocities are also small. This allows us to linearize the Navier-Stokes equations and express the interfacial conditions about a planar interface through a Taylor expansion. Using a no tangential stress conditions on the side walls, asymptotic expressions for both the interfacial slope, and radial segregation at the crystal-melt interface are obtained in closed form in the limit of large thermal Rayleigh number. It is suggested that these can be reduced by appropriately controlling a specific heat transfer property at the edge of the insulation zone in the solid side. Author

N94-17414# Northwestern Univ., Evanston, IL. Dept. of Engineering Science and Applied Mathematics.

THE STABILITY AND DYNAMICS OF ELASTIC STRUCTURES AND FLUID FLOWS Final Technical Report, 1 Mar. 1990 - 28 Feb. 1993

Edward Reiss 30 Jun. 1993 18 p

(Grant AF-AFOSR-0139-90)

(AD-A267990; AFOSR-93-0563TR) Avail: CASI HC A03/MF A01

Under this grant the researchers have investigated: (1) Laser instabilities, (2) Singular bifurcation to relaxation oscillations, (3) Slow passage through bifurcation points, (4) Propagation failure in discrete reaction-diffusion equations, (5) Large coherent fluid structures in boundary layers, (6) Primary and secondary flutter in flexible channel flows, (7) Energy leakage and reflection in slowly varying wave-guides, (8) Pulse dynamics in nonlinear optical fibers and switches and (9) Numerical modeling of optical pulse propagation. DTIC

N94-17440# Polish Academy of Sciences, Warsaw. Inst. Podstawowych Problemow Techniki.

OPTIMIZATION OF TWO-STAGE HOT WATER EXCHANGE POINTS [OPTYMALIZACJA WYMIENNIKOWYCH DWUSTOPNIOWYCH WEZLOW CIEPLEJ WODY]

Mariusz Adamski 1991 21 p In POLISH

Avail: CASI HC A03/MF A01

This paper presents a method of optimizing the components in hot water heat exchangers. A mathematical model is developed for both the operation of serial-parallel as well as serial-serial heat exchangers. Primary attention is devoted to the operation of the components in the maximum water consumption range. Optimization of the components makes it possible to establish the mean hot water temperature guaranteeing minimum surface area of the heat exchangers. Transl. by FLS

N94-17448*# National Aeronautics and Space Administration. Lewis Research Center, Cleveland, OH.

BOUNDARY CONDITIONS AND THE SIMULATION OF LOW MACH NUMBER FLOWS

Thomas Hagstrom and Jens Lorenz (New Mexico Univ., Albuquerque.) Nov. 1993 15 p

(Contracts NCC3-233; DE-FG03-92ER-25128; NSF DMS-91-08072; NSF DMS-91-07612)

(NASA-TM-106374; ICOMP-93-38; E-8184; NAS 1.15:106374) Avail: CASI HC A03/MF A01

The problem of accurately computing low Mach number flows, with the specific intent of studying the interaction of sound waves with incompressible flow structures, such as concentrations of vorticity is considered. This is a multiple time (and/or space) scales problem, leading to various difficulties in the design of numerical methods. Concentration is on one of these

difficulties - the development of boundary conditions at artificial boundaries which allow sound waves and vortices to radiate to the far field. Nonlinear model equations are derived based on assumptions about the scaling of the variables. Then these are linearized about a uniform flow and exact boundary conditions are systematically derived using transform methods. Finally, useful approximations to the exact conditions which are valid for small Mach number and small viscosity are computed. Author (revised)

N94-17450*# Institute for Computer Applications in Science and Engineering, Hampton, VA.
ON THE STABILITY OF A TIME DEPENDENT BOUNDARY LAYER Final Report
S. R. Otto Sep. 1993 37 p Submitted for publication
(Contract NAS1-19480; RTOP 505-90-52-01)
(NASA-CR-191542; NAS 1.26:191542; ICASE-93-73) Avail: CASI HC A03/MF A01

The aim of this article is to determine the stability characteristics of a Rayleigh layer, which is known to occur when the fluid above a flat plate has a velocity imparted to it (parallel to the plate). This situation is intrinsically unsteady, however, as a first approximation we consider the instantaneous stability of the flow. The Orr-Sommerfeld equation is found to govern fixed downstream wavelength linear perturbations to the basic flow profile. By the solution of this equation, we can determine the Reynolds numbers at which the flow is neutrally stable; this quasisteady approach is only formally applicable for infinite Reynolds numbers. We shall consider the large Reynolds number limit of the original problem and use a three deck mentality to determine the form of the modes. The results of the two calculations are compared, and the linear large Reynolds number analysis is extended to consider the effect of weak nonlinearity in order to determine whether the system is subcritical or supercritical. Author

N94-17476*# National Aeronautics and Space Administration. Langley Research Center, Hampton, VA.
SINGLE BLOCK THREE-DIMENSIONAL VOLUME GRIDS ABOUT COMPLEX AERODYNAMIC VEHICLES
Stephen J. Alter (Lockheed Engineering and Sciences Co., Hampton, VA.) and K. James Weilmuenster Nov. 1993 50 p
(RTOP 506-40-91-02)
(NASA-TM-108986; NAS 1.15:108986) Avail: CASI HC A03/MF A01

This paper presents an alternate approach for the generation of volumetric grids for supersonic and hypersonic flows about complex configurations. The method uses parametric two dimensional block face grid definition within the framework of GRIDGEN2D. The incorporation of face decomposition reduces complex surfaces to simple shapes. These simple shapes are combined to obtain the final face definition. The advantages of this method include the reduction of overall grid generation time through the use of vectorized computer code, the elimination of the need to generate matching block faces, and the implementation of simplified boundary conditions. A simple axisymmetric grid is used to illustrate this method. In addition, volume grids for two complex configurations, the Langley Lifting Body (HL-20) and the Space Shuttle Orbiter, are shown. Author

N94-17486*# National Aeronautics and Space Administration. Lewis Research Center, Cleveland, OH.
GROUND TESTING FOR THE NO-VENT FILL OF CRYOGENIC TANKS: RESULTS OF TESTS FOR A 71 CUBIC FOOT TANK
David J. Chato Jun. 1993 15 p Presented at the 29th Joint Propulsion Conference and Exhibit, Monterey, CA, 28-30 Jun. 1993; sponsored by AIAA, SAE, ASME, and ASEE See also A93-49815
(RTOP 506-42-73)
(NASA-TM-106293; E-8030; NAS 1.15:106293; AIAA Paper 93-1967)
Avail: CASI HC A03/MF A01

NASA Lewis Research has been investigating the no-vent fill method, since it is a promising approach to transfer liquid while handling the problems of low-g venting. This paper reports the results of a test series for filling a 71 cu ft tank with liquid hydrogen without venting. 22 tests were conducted, 10 with a bottom orifice as the inlet and 12 with a spray bar. Parameters investigated included inlet saturation pressures of approximately 5, 15, and 25 psia, transfer pressures of 20, 30, and 45 psia, and various starting wall temperatures. Of the tests, only the one run at the highest wall temperature (238 R) failed to fill the tank. Test results are compared to a thermodynamic equilibrium model. Overall model-data agreement was good except for the tendency of the model to overshoot during the initial wall cool down of the higher starting wall temperature fills. Author

N94-17511# Rensselaer Polytechnic Inst., Troy, NY. Center for Multiphase Research.
MEASUREMENT OF THE VELOCITY FIELD AND VOID FRACTION IN A PLANAR PLUNGING JET
F. Bonetto and R. T. Lahey, Jr. 1993 25 p
(Contract N00014-91-J-1271)
(AD-A268183) Avail: CASI HC A03/MF A01

This paper presents experimental data for a planar plunging liquid jet. Local data including the void fraction and the mean and turbulent bubble and liquid velocities were obtained using an impedance probe and a Laser Doppler Anemometer (LDA)-Fiber Optics Laser Doppler Anemometer (FPDA) system. A dual element conductivity probe was also used to measure the spatial distribution of the local void fraction. The turbulence of the plunging jet was parametrically controlled using a specially designed nozzle. DTIC

N94-17531# Institut National de Recherche d'Informatique et d'Automatique, Valbonne (France). Programme 6: Calcul Scientifique, Modelisation et Logiciels Numeriques.
COMPRESSIBLE FLOW SOLVERS USING UNSTRUCTURED GRIDS
Alain Dervieux and Jean-Antoine Desideri Jun. 1992 116 p
(INRIA-RR-1732; ETN-93-94434) Avail: CASI HC A06/MF A02

A detailed review of works related to the MUSCL FEM (Finite Element Method) upwind method for unstructured meshes is presented. Because the discrete geometry (triangulation, tetrahedrization) will likely be irregular, it is chosen to derive the approximation from both recent techniques in upwind TVD finite volume and FE in order to get an accurate, robust, and parameter free discrete model. As a result of this strategy the codes may be very time consuming, and focus is given to the important issue of efficiency. Some recent developments in mesh adaption techniques are also addressed. ESA

N94-17534# Institut National de Recherche d'Informatique et d'Automatique, Valbonne (France). Programme 6: Calcul Scientifique, Modelisation et Logiciels Numeriques.
A DOMAIN-PARTITION METHOD FOR THE ADVECTION-DIFFUSION EQUATION Thesis [UNE METHODE DE PARTITION DE DOMAINE POUR L'EQUATION D'ADVECTION-DIFFUSION]
Pierre Aubert, Marie-Claude Ciccoli, and Jean-Antoine Desideri Aug. 1992 47 p In FRENCH
(INRIA-RR-1740; ETN-93-94436) Avail: CASI HC A03/MF A01

A report corresponding to a manuscript for the degree of DEA is presented. The objective of the study was to formalize a domain partition method for a linear advection diffusion model problem, to demonstrate the properties of the basic algorithms, and thus prepare future tests of novel algorithms in a simplified context. From a technical standpoint, domain decomposition methods in general (using partition or overlapping) for the solution of partial differential equations are currently regaining interest because they are naturally adapted to parallel computing. The computational domain is decomposed in subdomains over which subproblems of reduced size are solved simultaneously and coupled iteratively to enforce matching conditions at the interfaces. A theoretical presentation of a domain partition method for the advection diffusion equation in one and two space dimensions, and numerical results, are presented. ESA

N94-17557*# National Aeronautics and Space Administration. Lewis Research Center, Cleveland, OH.
MULTIGRID DIRECT NUMERICAL SIMULATION OF THE WHOLE PROCESS OF FLOW TRANSITION IN 3-D BOUNDARY LAYERS
Chaoqun Liu and Zhining Liu (Colorado Univ., Denver.) Nov. 1993 40 p
(Contracts NAS1-10312; NCC3-233; RTOP 505-90-5K)
(NASA-TM-106369; ICOMP-93-36; E-8175; NAS 1.15:106369; CMOTT-93-13) Avail: CASI HC A03/MF A01

A new technology was developed in this study which provides a successful numerical simulation of the whole process of flow transition in 3-D boundary layers, including linear growth, secondary instability, breakdown, and transition at relatively low CPU cost. Most other spatial numerical simulations require high CPU cost and blow up at the stage of

flow breakdown. A fourth-order finite difference scheme on stretched and staggered grids, a fully implicit time marching technique, a semi-coarsening multigrid based on the so-called approximate line-box relaxation, and a buffer domain for the outflow boundary conditions were all used for high-order accuracy, good stability, and fast convergence. A new fine-coarse-fine grid mapping technique was developed to keep the code running after the laminar flow breaks down. The computational results are in good agreement with linear stability theory, secondary instability theory, and some experiments. The cost for a typical case with 162 x 34 x 34 grid is around 2 CRAY-YMP CPU hours for 10 T-S periods. Author

N94-17615# National Aerospace Lab., Emmeloord (Netherlands). Space Div.

GRAVITY DEPENDENT CONDENSATION PRESSURE DROP AND HEAT TRANSFER IN AMMONIA TWO-PHASE HEAT TRANSPORT SYSTEMS

A. A. M. Delil 1 Apr. 1992 11 p Presented at 1992 National Heat Transfer Conference AIAA Session on Phase Change Heat Transfer, San Diego, CA, 9-12 Aug. 1992 See also A92-56140

(NLR-TP-92121-U; AIAA Paper 92-4057; ETN-93-94787) Avail: CASI HC A03/MF A01

Results of calculations on condensing flow in a straight condenser duct, which investigated the impact of (reduced) gravity on the duct length required to achieve complete condensation, are reported. Condensers are critical components in two phase heat transport systems envisaged for future large spacecraft. In order to properly design such condensers, experimental data obtained from ground testing and reduced gravity aircraft and rocket flight testing, plus results of thermal modeling and scaling calculations are used. The result of such activities, frequently reported in the literature, is that condensation lengths required in low gravity environment exceed the corresponding lengths on Earth (in horizontal ducts) by at least one order of magnitude, while the accompanying pressure drops are almost the same. As the flow patterns are different in both situations, it was considered to be a better approach to theoretically (and later also experimentally) investigate the impact of gravity on condensation pressure drops and heat transfer for an identical flow pattern, namely annual-wavy-mist observed for vapor qualities ranging from 1 down to values below 0.1 (hence, almost the entire condensation length), both for low gravity conditions and for vertical downflow in a gravity field. The results of this approach are discussed for condensers using ammonia as the working fluid. ESA

N94-17627 National Aerospace Lab., Amsterdam (Netherlands). Fluid Dynamics/Informatics Div.

STUDY INTO THE LIMITS OF AN EULER EQUATION METHOD APPLIED TO LEADING-EDGE VORTEX FLOW

J. I. vandenBerg, H. W. M. Hoeijmakers, and H. A. Sytsma 9 Sep. 1991 12 p Presented at 9th GAMM Conference on Numerical Methods in Fluid Mechanics, Lausanne, Switzerland, 25-27 Sep. 1991 Limited Reproducibility: More than 20% of this document may be affected by microfiche quality

(Contract NIVR-07701N)

(NLR-TP-91350-U; ETN-93-94781) Avail: CASI HC A03

A steady fow Euler method is applied to the subsonic leading edge vortex flow about a 65 deg sharp-edged cropped delta wing at high incidence. Above a critical value of the incidence the numerical procedure fails to fully converge, the solution at successive iterations exhibiting a behavior similar to the one observed during vortex breakdown. The occurrence of this 'solution breakdown' indicates the limits of the domain of applicability of the steady flow Euler method for the case of subsonic leading edge vortex flow. Analysis of the solution at incidences just below the critical value reveals that a bubble type of flow feature develops within the vortex core. ESA

N94-16145*# National Aeronautics and Space Administration. Marshall Space Flight Center, Huntsville, AL.

LIQUID HYDROGEN AND LIQUID OXYGEN FEEDLINE PASSIVE RECIRCULATION ANALYSIS

Kimberly Ann Holt, Nicole L. Cleary, Andrew J. Nichols, and Gretchen L. E. Perry *In* Huntsville Association of Technical Societies, TABES 1993: 9th Annual Technical and Business Exhibition and Symposium 1993 5 p (For primary document see N94-16129 03-38)

(TABES Paper 93-620) Avail: CASI HC A01/MF A03

35 INSTRUMENTATION AND PHOTOGRAPHY

Includes remote sensors; measuring instruments and gages; detectors; cameras and photographic supplies; and holography.

For aerial photography see *43 Earth Resources and Remote Sensing*. For related information see also *06 Aircraft Instrumentation*, and *19 Spacecraft Instrumentation*.

N94-15018 National Physical Lab., Teddington (England). Div. of Radiation Science and Acoustics.

MEASUREMENT OF THE SPECIFIC HEAT CAPACITY OF THE ELECTRON-BEAM GRAPHITE CALORIMETER

A. J. Williams, D. T. Burns, and M. R. McEwen Mar. 1993 22 p (NPL-RSA(EXT)-40; ETN-93-94551) Copyright Avail: Issuing Activity (National Physical Lab., Teddington, Middlesex TW11 OLW, England)

The design and construction of apparatus to measure the specific heat capacity of solid materials in the temperature range 18 to 32 C are described. The apparatus is designed to minimize heat losses from the sample in order to measure the specific heat to an accuracy of better than +/- 0.2 at the 95% confidence level. The results of a set of measurements in the graphite core of the electron beam primary standard radiation calorimeter are presented, along with a measurement of the effect of a large accumulated radiation dose in the specific heat of graphite. ESA

N94-15247* National Aeronautics and Space Administration, Washington, DC.

SPACE STATION FREEDOM (Videotape)

Jul. 1990 Videotape: 3 min. 30 sec. playing time, in color, with sound (NASA-TM-109636; NONP-VT-93-190434) Avail: CASI VHS A01/BETA A22

This video presents great model photography along with astronaut activity as practiced in mockup. CASI

N94-15304* National Aeronautics and Space Administration. Lyndon B. Johnson Space Center, Houston, TX.

STS-30 CREW PHOTO IN BUILDING 4 (Videotape)

Apr. 1989 Videotape: 7 min. 20 sec. playing time, in color, with sound (NASA-TM-109573; NONP-VT-93-190371) Avail: CASI VHS A01/BETA A22

This video shows the Space Shuttle crew learning how to use the photography equipment they will have on board the Space Shuttle. CASI

N94-15316* National Aeronautics and Space Administration. Lyndon B. Johnson Space Center, Houston, TX.

STS-32 IMAX CAMERA TRAINING (Videotape)

Nov. 1989 Videotape: 10 min. 30 sec. playing time, in color, with sound (NASA-TM-109567; NONP-VT-93-190365) Avail: CASI VHS A01/BETA A22

The crew is shown learning how to load the IMAX camera and use it. This training takes place on the middeck of the CCT. CASI

N94-15374* National Aeronautics and Space Administration. Lyndon B. Johnson Space Center, Houston, TX.

STS-29 IMAX CAMERA AUDIO CLASS FFT (Videotape)

Mar. 1989 Videotape: 15 min. 30 sec. playing time, in color, with sound (NASA-TM-109543; NONP-VT-93-190340) Avail: CASI VHS A01/BETA A22

The astronauts are shown how to work the audio portion of the IMAX camera system. CASI

N94-15380* National Aeronautics and Space Administration. Lyndon B. Johnson Space Center, Houston, TX.

STS-29 CREW IMAX CAMERA TRAINING (Videotape)

Jan. 1989 Videotape: 16 min. playing time, in color, with sound (NASA-TM-109546; NONP-VT-93-190343) Avail: CASI VHS A01/BETA A22

The crew is shown learning to use the IMAX camera system. CASI

N94-15397* National Aeronautics and Space Administration. Lyndon B. Johnson Space Center, Houston, TX.

STS-34 ARRIFLEX AND IMAX CAMERA TRAINING (Videotape)

Aug. 1989 Videotape: 19 min. 17 sec. playing time, in color, with sound (NASA-TM-109467; NONP-VT-93-190264) Avail: CASI VHS A01/BETA A22

The STS-34 crew is shown being taught how to use the 16-mm Arriflex camera. CASI

N94-15405* National Aeronautics and Space Administration. Lyndon B. Johnson Space Center, Houston, TX.

STS-27 CREW PHOTO TRAINING AND HABITATION PROCEDURES (Videotape)

Nov. 1988 Videotape: 15 min. playing time, in color, with sound (NASA-TM-109553; NONP-VT-93-190351) Avail: CASI VHS A01/BETA A22

The crew is shown studying photography equipment they will carry into orbit, and how to take the best shots possible. CASI

N94-15445*# National Aeronautics and Space Administration. Lewis Research Center, Cleveland, OH.

DEVELOPMENT OF THE SEEDING SYSTEM USED FOR LASER VELOCIMETER SURVEYS OF THE NASA LOW-SPEED CENTRIFUGAL COMPRESSOR FLOW FIELD

Charles A. Wasserbauer (Sverdrup Technology, Inc., Brook Park, OH.) and Michael D. Hathaway (Army Research Lab., Cleveland, OH.) Oct. 1993 14 p

(RTOP 505-62-52)

(NASA-TM-4485; E-7810; NAS 1.15:4485) Avail: CASI HC A03/MF A01

An atomizer-based system for distributing high-volume rates of seed material was developed to support laser velocimeter investigations of the NASA Low-Speed Centrifugal Compressor flow field. The seeding system and the major concerns that were addressed during its development are described. Of primary importance were that the seed material be dispersed as single particles and that the liquid carrier used be completely evaporated before entering the compressor. Author (revised)

N94-15463* National Aeronautics and Space Administration. Lyndon B. Johnson Space Center, Houston, TX.

STS-35 PAYLOAD SPECIALISTS DURRANCE AND PARISE: 70mm PHOTO TRAINING AND CABIN FAMILIARIZATION (Videotape)

Apr. 1990 Videotape: 14 min. playing time, in color, with sound (NASA-TM-109499; NONP-VT-93-190296) Avail: CASI VHS A01/BETA A22

This video shows astronauts Durrance and Parise being trained with photography equipment. CASI

N94-15472* National Aeronautics and Space Administration. Lyndon B. Johnson Space Center, Houston, TX.

JOHNSON SPACE CENTER AND DOWNTOWN HOUSTON, TEXAS AERIALS (Videotape)

Aug. 1988 Videotape: 7 min. 5 sec. playing time, in color, with sound (NASA-TM-109522; NONP-VT-93-190319) Avail: CASI VHS A01/BETA A22

This videotape shows various aerial shots of the NASA JSC. Views of downtown Houston, TX, are also provided. CASI

N94-15697 National Defence Headquarters, Ottawa (Ontario).

MONOPIECE STRAIN GAUGE STING MOUNTED WIND TUNNEL BALANCE Patent

Gilles Faucher, inventor (to Micromedia Ltd.), Marc-Andre Paradis, inventor (to Micromedia Ltd.), and Bertrand Girard, inventor (to Micromedia Ltd.) 22 Dec. 1992 25 p Limited Reproducibility: More than 20% of this document may be affected by microfiche quality

(CA-Patent-1-311-626; Int-Patent-Class-G01M-9/00; CTN-93-60777)

Copyright Avail: Micromedia Ltd., Technical Information Centre, 165 Hotel de Ville, Place du Portage, Phase 2, Hull, Quebec J8X 3X2, Canada HC

A balance is disclosed for an apparatus for measuring the various aerodynamic coefficients of flight vehicles by testing scale models of these vehicles in a wind tunnel. The balance of the invention measures the following parameters: axial, normal, and side force; and pitching, yawing, and rolling moments. The balance is based on a monopiece center core where sensing components have a roll or primary frame as well as being reference supports to strain gauges. The dual function of the primary frame means that forces and moments, when applied to the balance, will generate interferences in several other components. Because of the center core configuration, it is possible to calibrate, calculate, and deduct with a very high precision the interferences of each component over the other. Except for the axial force sensing components, all forces and moments are sensed by two groups of crossed webs, one cross web at each end of the center core. The axial force sensing components are made of two tensioning rings, one at each end of the center core. The configuration of the balance is of the rigid-frame type, in order to make use of semiconductor strain gauges which are very precise. The resulting balance is more precise than any known balance of its size and can resist starting and stopping overloads which occur at the beginning and end of a test. Author (CISTI)

N94-15754*# National Aeronautics and Space Administration. Hugh L. Dryden Flight Research Facility, Edwards, CA.

SIMULTANEOUS MEASUREMENT OF TEMPERATURE AND STRAIN USING FOUR CONNECTING WIRES

Allen R. Parker, Jr. Nov. 1993 10 p Presented at SEM Fall Conference and Exhibit on Structural Testing Technology at High Temperature-II, Ojai, CA, 8 Nov. 1993

(RTOP 505-70-63)

(NASA-TM-104271; H-1945; NAS 1.15:104271) Avail: CASI HC A02/MF A01

This paper describes a new signal-conditioning technique for measuring strain and temperature which uses fewer connecting wires than conventional techniques. Simultaneous measurement of temperature and strain has been achieved by using thermocouple wire to connect strain gages to signal conditioning. This signal conditioning uses a new method for demultiplexing sampled analog signals and the Anderson current loop circuit. Theory is presented along with data to confirm that strain gage resistance change is sensed without appreciable error because of thermoelectric effects. Furthermore, temperature is sensed without appreciable error because of voltage drops caused by strain gage excitation current flowing through the gage resistance. Author (revised)

N94-15792* National Aeronautics and Space Administration. Lyndon B. Johnson Space Center, Houston, TX.

STS-31 CREW LINOF, ARRIFLEX, AND IMAX CAMERA TRAINING (Videotape)

Mar. 1990 Videotape: 29 min. playing time, in color, with sound (NASA-TM-109485; NONP-VT-93-190282) Avail: CASI VHS A01/BETA A22

The crew is shown on the roof of Bldg. 1 at the NASA Johnson Space Center learning about the Linof camera system. The crew is shown taking pictures with the Linof camera from the roof. CASI

N94-15797*# Lunar and Planetary Inst., Houston, TX.

WORKSHOP ON ADVANCED TECHNOLOGIES FOR PLANETARY INSTRUMENTS

J. Appleby, ed. 30 Apr. 1993 54 p Workshop held in Fairfax, VA, 28-30 Apr. 1993

(Contract NASw-4574)

(NASA-CR-194585; LPI-TR-93-02-Pt-2; NAS 1.26:194585) Avail: CASI HC A04/MF A01

NASA's robotic solar system exploration program requires a new generation of science instruments. Design concepts are now judged against stringent mass, power, and size constraints--yet future instruments must be highly capable, reliable, and, in some applications, they must operate for many years. The most important single constraint, however, is cost: new instruments must be developed in a tightly controlled design-to-cost environment. Technical innovation is the key to success and will enable the sophisticated measurements needed for future scientific exploration. As a fundamental benefit, the incorporation of breakthrough technologies in planetary flight hardware will contribute to U.S. industrial competitiveness and will strengthen the U.S. technology base. The Workshop on Advanced Technologies for Planetary Instruments was conceived to address these challenges, to provide an open forum in which the NASA and DoD space communities could become better acquainted at the working level, and to assess future collaborative efforts. Over 300 space scientists and engineers participated in the two-and-a-half-day meeting held April 28-30, 1993, in Fairfax, Virginia. It was jointly sponsored by NASA's Solar System Exploration

Division (SSED), within the Office of Space Science (OSS); NASA's Office of Advanced Concepts and Technology (OACT); DoD's Strategic Defense Initiative Organization (SDIO), now called the Ballistic Missile Defense Organization (BMDO); and the Lunar and Planetary Institute (LPI). The meeting included invited oral and contributed poster presentations, working group sessions in four sub-disciplines, and a wrap-up panel discussion. On the first day, the planetary science community described instrumentation needed for missions that may go into development during the next 5 to 10 years. Most of the second day was set aside for the DoD community to inform their counterparts in planetary science about their interests and capabilities, and to describe the BMDO technology base, flight programs, and future directions. The working group sessions and the panel discussion synthesized technical and programmatic issues from all the presentations, with a specific goal of assessing the applicability of BMDO technologies to science instrumentation for planetary exploration. Author (revised)

N94-15826 Wright Lab., Eglin AFB, FL. Armament Directorate.
AN ELECTRONIC IMAGING SYSTEM FOR THE AEROBALLISTIC RESEARCH FACILITY Final Report
G. L. Winchenbach, D. B. Snyder, M. A. Valentino, H. C. Macke, and W. J. Rowe Jul. 1993 11 p Limited Reproducibility: More than 20% of this document may be affected by microfiche quality
(AD-A267157; WL-TP-93-002) Avail: CASI HC A03

Until the present date, free-flight spark ranges used conventional film technology for recording the position-attitude histories of the projectiles as they traversed the instrumented ranges. The purpose is to describe the plans for converting the existing film based camera system in the Aeroballistic Research Facility to an electronic imaging system based on modern charge coupled device (CCD) technology. The primary concern associated with this conversion was always maintaining the facility's accuracy in measuring the projectile's position and attitude at each of the shadowgraph stations. This accuracy is directly related to the resolution of the CCD, i.e., number of pixels. Some other concerns were minimizing the facility down-time while the new imaging system is installed and maintaining a means of analyzing previous film exposures captured during the past 15 years of operation. The solution to these concerns is the development of a film reader system which also uses a CCD type camera to digitize the existing film. DTIC

N94-15872*# National Aeronautics and Space Administration. Goddard Space Flight Center, Greenbelt, MD.
CAPACIFLECTOR CAMERA Patent Application
John M. Vranish, inventor (to NASA) 12 Jul. 1993 39 p
(NASA-Case-GSC-13564-1; NAS 1.71:GSC-13564-1;
US-Patent-Appl-SN-090230) Avail: CASI HC A03/MF A01

A capacitive type proximity sensor having improved range and sensitivity between a surface and an intruding object in the vicinity of the surface having a voltage source, a number of outer electrical conductors on the surface with each forming one electrode of a number of sensor capacitors, the other electrode for each sensor capacitor being the object is described. The outer conductors are made from thin sheets of conductive material covered with insulation. An intermediate electrical conductor is located between the outer conductors and the surface and is of a size larger than the outer conductors to act as a shield for reducing the parasitic capacitance between the outer conductors and the surface. The intermediate conductor is also made from a thin sheet of conductive material covered with insulation. The outer conductors and the intermediate conductor are attached to the surface with no gap between the insulation on the conductors and no gap between the surface and the insulation on intermediate conductor, the outer conductors and the intermediate conductor conjoining with each other and with the surface, with the surface acting as a ground plane. A current-measuring voltage follower circuit is connected to the voltage source for coupling in phase and amplitude the instantaneous voltage at the voltage source to the outer electrical conductors and the intermediate electrical conductor. This circuit is responsive to the change in capacitance of the sensor capacitors and generates a number of output signals. NASA

N94-15875*# National Aeronautics and Space Administration. Pasadena Office, CA.
SUPERCONDUCTIVE MATERIAL AND MAGNETIC FIELD FOR DAMPING AND LEVITATION SUPPORT AND DAMPING OF CRYOGENIC INSTRUMENTS Patent Application
Benjamin P. Dolgin, inventor (to NASA) (Jet Propulsion Lab., California Inst. of Tech., Pasadena.) 15 Jun. 1993 14 p
(Contract NAS7-918)
(NASA-Case-NPO-18458-1-CU; NAS 1.71:NPO-18458-1-CU;
US-Patent-Appl-SN-077470) Avail: CASI HC A03/MF A01

A superconductive load bearing support without a mechanical contact and vibration damping for cryogenic instruments in space is presented. The levitation support and vibration damping is accomplished by the use of superconducting magnets and the 'Meissner' effect. The assembly allows for transfer of vibration energy away from the cryogenic instrument which then can be damped by the use of either an electronic circuit or conventional vibration damping mean. NASA

N94-15877*# National Aeronautics and Space Administration. Langley Research Center, Hampton, VA.
IMPROVEMENTS TO PULSED PHASE LOCKED LOOP STRAIN MONITOR Patent Application
Mark E. Froggatt, inventor (to NASA) 12 Aug. 1993 58 p
(NASA-Case-LAR-14887-1; NAS 1.71:LAR-14887-1;
US-Patent-Appl-SN-105161) Avail: CASI HC A04/MF A01

A pulse phase locked loop system according to the present invention is described. A frequency generator such as a voltage controlled oscillator (VCO) generates an output signal and a reference signal having a frequency equal to that of the output signal. A transmitting gate gates the output frequency signal and this gated signal drives a transmitting transducer which transmits an acoustic wave through a material. A sample/hold samples a signal indicative of the transmitted wave which is received by a receiving transducer. Divide-by-n counters control these gating and sampling functions in response to the reference signal of the frequency generator. Specifically, the output signal is gated at a rate of F/h, wherein F is the frequency of the output signal and h is an integer; and the received signal is sampled at a delay of F/n wherein n is an integer. NASA

N94-15884*# National Aeronautics and Space Administration. Langley Research Center, Hampton, VA.
REMOTE TIRE PRESSURE SENSING TECHNIQUE Patent Application
Howard H. Robinson, inventor (to NASA), Timothy A. McGinnis, inventor (to NASA) (Wyle Labs., Inc., Hampton, VA.), and Robert H. Daugherty, inventor (to NASA) 23 Aug. 1993 9 p
(NASA-Case-LAR-14160-1; NAS 1.71:LAR-14160-1;
US-Patent-Appl-SN-111321) Avail: CASI HC A02/MF A01

A remote tire pressure sensing technique is provided which uses vibration frequency to determine tire pressure. A vibration frequency measuring device is attached to the external surface of a tire which is then struck with an object, causing the tire to vibrate. The frequency measuring device measures the vibrations and converts the vibrations into corresponding electrical impulses. The electrical impulses are then fed into the frequency analyzing system which uses the electrical impulses to determine the relative peaks of the vibration frequencies as detected by the frequency measuring device. The measured vibration frequency peaks are then compared to predetermined data describing the location of vibration frequency peaks for a given pressure, thereby determining the air pressure of the tire. NASA

N94-15928*# National Aeronautics and Space Administration. Lewis Research Center, Cleveland, OH.
DUAL ACTIVE SURFACE, MINIATURE, PLUG-TYPE HEAT FLUX GAUGE Patent Application
Curt H. Liebert, inventor (to NASA) and John Koch, Jr., inventor (to NASA) 16 Apr. 1993 15 p
(NASA-Case-LEW-15643-1; NAS 1.71:LEW-15643-1;
US-Patent-Appl-SN-047120) Avail: CASI HC A03/MF A01

A plug-type heat flux gauge can simultaneously measure heat flux on two opposite surfaces of thick or very thin convection or impingement cooled metal walls. The gauge is capable of continuously measuring transient and steady heat flux under transient and steady state gauge temperature operating conditions. The length of the gauge extends through the entire

thickness of the material. A non-linear temperature gradient through the gauge can be measured by attaching 3-5 thermocouples along the length of the gauge. NASA

N94-15961*# National Aeronautics and Space Administration. Lewis Research Center, Cleveland, OH.
NEURAL-NETWORK-DIRECTED ALIGNMENT OF OPTICAL SYSTEMS USING THE LASER-BEAM SPATIAL FILTER AS AN EXAMPLE
Arthur J. Decker, Michael J. Krasowski, and Kenneth E. Weiland Aug. 1993 33 p Sponsored by NASA. Washington
(RTOP 590-21-11)
(NASA-TP-3372; E-7524; NAS 1.60:3372) Avail: CASI HC A03/MF A01

This report describes an effort at NASA Lewis Research Center to use artificial neural networks to automate the alignment and control of optical measurement systems. Specifically, it addresses the use of commercially available neural network software and hardware to direct alignments of the common laser-beam-smoothing spatial filter. The report presents a general approach for designing alignment records and combining these into training sets to teach optical alignment functions to neural networks and discusses the use of these training sets to train several types of neural networks. Neural network configurations used include the adaptive resonance network, the back-propagation-trained network, and the counter-propagation network. This work shows that neural networks can be used to produce robust sequencers. These sequencers can learn by example to execute the step-by-step procedures of optical alignment and also can learn adaptively to correct for environmentally induced misalignment. The long-range objective is to use neural networks to automate the alignment and operation of optical measurement systems in remote, harsh, or dangerous aerospace environments. This work also shows that when neural networks are trained by a human operator, training sets should be recorded, training should be executed, and testing should be done in a manner that does not depend on intellectual judgments of the human operator. Author

N94-15987*# National Aeronautics and Space Administration. Pasadena Office, CA.
ABERRATION CORRECTION OF UNSTABLE RESONATORS Patent Application
Paul D. Maker, inventor (to NASA) (Jet Propulsion Lab., California Inst. of Tech., Pasadena.) and Richard E. Muller, inventor (to NASA) (Jet Propulsion Lab., California Inst. of Tech., Pasadena.) 27 May 1993 35 p
(Contract NAS7-918)
(NASA-Case-NPO-18791-1-CU; NAS 1.71:NPO-18791-1-CU; US-Patent-Appl-SN-071131) Avail: CASI HC A03/MF A01

A method for producing a phase hologram using e-beam lithography provides n-ary levels of phase and amplitude by first producing an amplitude hologram on a transparent substrate by e-beam exposure of a resist over a film of metal by exposing n is less than or equal to m x m spots of an array of spots for each pixel, where the spots are randomly selected in proportion to the amplitude assigned to each pixel, and then after developing and etching the metal film producing a phase hologram by e-beam lithography using a low contrast resist, such as PMMA, and n-ary levels of low doses less than approximately 200 micro-C/sq cm and preferably in the range of 20-200 micro-C/sq cm and aggressive development using pure acetone for an empirically determined time (about 6 sec.) controlled to within 1/10 sec. to produce partial development of each pixel in proportion to the n-ary level of dose assigned to it. NASA

N94-15990*# National Aeronautics and Space Administration. Langley Research Center, Hampton, VA.
EFFECTS OF WINDOW SIZE AND SHAPE ON ACCURACY OF SUBPIXEL CENTROID ESTIMATION OF TARGET IMAGES
Sharon S. Welch Washington Oct. 1993 37 p
(RTOP-590-14-11-02)
(NASA-TP-3331; L-17113; NAS 1.60:3331) Avail: CASI HC A03/MF A01

A new algorithm is presented for increasing the accuracy of subpixel centroid estimation of (nearly) point target images in cases where the signal-to-noise ratio is low and the signal amplitude and shape vary from frame to frame. In the algorithm, the centroid is calculated over a data window that is matched in width to the image distribution. Fourier analysis is used to explain the dependency of the centroid estimate on the size of the data window, and simulation and experimental results are presented which demonstrate the effects of window size for two different noise models. The effects of window shape were also investigated for uniform and Gaussian-shaped windows. The new algorithm was developed to improve the dynamic range of a close-range photogrammetric tracking system that provides feedback for control of a large gap magnetic suspension system (LGMSS). Author (revised)

N94-16452# Sandia National Labs., Albuquerque, NM.
DETERMINATION OF EQUIVALENT CIRCUIT FOR PVDF SHOCK-PRESSURE GAUGES
J. D. Kotulski, M. U. Anderson, B. C. Brock, J. Gomez, R. A. Graham, and C. N. Vittitoe 1993 4 p Presented at the 14th International Conference on High Pressure Science and Technology and 1993 Technical Meeting of the Topical Group on Shock Compression of Condensed Matter, Colorado Springs, CO, 28 Jun. - 3 Jul. 1993
(Contract DE-AC04-76DP-00789)
(DE93-016492; SAND-93-0370C; CONF-9306167-8) Avail: CASI HC A01/MF A01

Broadband impedance measurements of a polyvinylidene fluoride (PVDF) shock-pressure gauge are used to build an equivalent circuit for the gauge. The essential components are a gauge capacitance and a low-loss transmission line. Component features are consistent with the physical characteristics. With knowledge of this circuit, troublesome oscillations can be anticipated and prevented. DOE

N94-16521*# Analex Corp., Brook Park, OH.
TEMPERATURE AND PRESSURE EFFECTS ON CAPACITANCE PROBE CRYOGENIC LIQUID LEVEL MEASUREMENT ACCURACY Final Report
Lawrence G. Edwards and Mark Haberbusch (Ohio Aerospace Inst., Brook Park.) Sep. 1993 32 p Presented at the 39th International Instrumentation Symposium, Albuquerque, NM, 3-6 May 1993
(Contract NAS3-25776; RTOP 506-42-00)
(NASA-CR-190763; E-8122; NAS 1.26:190763) Avail: CASI HC A03/MF A01

The inaccuracies of liquid nitrogen and liquid hydrogen level measurements by use of a coaxial capacitance probe were investigated as a function of fluid temperatures and pressures. Significant liquid level measurement errors were found to occur due to the changes in the fluids dielectric constants which develop over the operating temperature and pressure ranges of the cryogenic storage tanks. The level measurement inaccuracies can be reduced by using fluid dielectric correction factors based on measured fluid temperatures and pressures. The errors in the corrected liquid level measurements were estimated based on the reported calibration errors of the temperature and pressure measurement systems. Experimental liquid nitrogen (LN2) and liquid hydrogen (LH2) level measurements were obtained using the calibrated capacitance probe equations and also by the dielectric constant correction factor method. The liquid levels obtained by the capacitance probe for the two methods were compared with the liquid level estimated from the fluid temperature profiles. Results show that the dielectric constant corrected liquid levels agreed within 0.5 percent of the temperature profile estimated liquid level. The uncorrected dielectric constant capacitance liquid level measurements deviated from the temperature profile level by more than 5 percent. This paper identifies the magnitude of liquid level measurement error that can occur for LN2 and LH2 fluids due to temperature and pressure effects on the dielectric constants over the tank storage conditions from 5 to 40 psia. A method of reducing the level measurement errors by using dielectric constant correction factors based on fluid temperature and pressure measurements is derived. The improved accuracy by use of the correction factors is experimentally verified by comparing liquid levels derived from fluid temperature profiles. Author

N94-16536 Department of the Navy, Washington, DC.
MECHANICAL AND SURFACE FORCE NANOPROBE Patent
Nancy A. Burnham, inventor (to Navy) and Richard J. Colton, inventor (to Navy) 16 Mar. 1993 6 p Filed 11 Jul. 1990
(AD-D015792; US-Patent-5,193,383; US-Patent-Appl-SN-560391; US-Patent-Class-73-105) Avail: US Patent and Trademark Office

This invention is a method and apparatus to use an Atomic Force Microscope to take measurements of surface forces, indentation, adhesion and mechanical properties such as hardness and elasticity. The force between a probe mounted cantilever and a sample is measured as a

function cantilever deflection measured by a electron tunneling microscope. The sample and the tip of the tunneling microscope are each mounted on piezoelectric manipulators which provide for position control. Position of the sample and probe are measured from the voltages applied to the piezoelectric manipulators. Penetration is determined by the relative motion between the probe and sample. Presently, this invention has a force resolution of 1 nm and a depth resolution of 0.02 nm. DTIC

N94-16960# Lawrence Livermore National Lab., CA.
MULTI-FRAME X RAY IMAGING WITH A LARGE AREA 40ps CAMERA
P. M. Bell, J. D. Kilkenny, O. L. Landen, R. L. Hanks, J. D. Wiedwald, and D. K. Bradley (Rochester Univ., NY.) Nov. 1992 7 p Presented at the 37th Annual SPIE International Symposium on Optical and Optoelectronic Applied Science and Engineering, San Diego, CA, 19-24 Jul. 1992
(Contract W-7405-eng-48)
(DE93-017179; UCRL-JC-111213; CONF-920792-65) Avail: CASI HC A02/MF A01

The authors have developed a large area short pulse framing camera that is capable of sixteen frames and shutter times of 40ps per frame. This is accomplished with a high fidelity electrical circuit and a L/D = 20 microchannel plate, driven by a short pulse (80ps) high amplitude electrical driver. They show results of this work they have done to support this type of shutter time and the difficulties associated with large area high speed shuttering. DOE

N94-17002# Army Research Inst. of Environmental Medicine, Natick, MA.
AUTOMATED STRAIN GAUGE PLETHYSMOGRAPH
Tammy J. Doherty, Lou A. Stephenson, Margaret A. Kolka, Gary N. Sexton, and Richard R. Gonzalez May 1993 38 p
(AD-A267323; USARIEM-T13-93) Avail: CASI HC A03/MF A01

This report describes a microcomputer controlled system which measures limb blood flow by strain gauge plethysmography. Hardware components include a suitable microcomputer, compatible data acquisition unit, Hokanson EC-4 plethysmograph, pneumatic cuff inflation system, and a relay/switching unit for remote calibration of the plethysmograph unit and inflation of the pneumatic cuffs. The software developed for use with this system enables automatic electronic calibration of the plethysmograph prior to each measure of limb blood flow, collection and storage of limb volume records at user-specified time intervals, interpretation of limb volume records, and calculation of rates of limb blood flow. DTIC

N94-17197# Wright Lab., Wright-Patterson AFB, OH.
DISPLAY OF DYNAMIC, VOLUME GRAPHIC IMAGES BY HOLOGRAPHIC VOXEL PROJECTION: INITIAL INVESTIGATION Interim Report, Aug. 1989 - Jun. 1991
Shawn L. Kelly and Charles T. Robinson 29 Apr. 1993 51 p
(AD-A267622; WL-TR-93-1059) Avail: CASI HC A04/MF A01

This document presents in-house research on a holographic projector. This device operates by optically guiding the light from each pixel on an internal two dimensional display to a unique focus in a three dimensional volume. Properly addressing the 2-D pixel array via conventional computer graphics equipment will, therefore, generate transparent 3-D images which appear to float in space in front of the observer. A detailed mathematical model was created and used to design the holographic projector and simulate it's operation. Proof-of-concept experiments were conducted to test the capability of holographic materials to provide the performance predicted by the model. The results of this initial investigation support the continuation of research and development of the holographic projector as a special display for applications such as threat warning or directional indication. DTIC

N94-17401# Air Force Inst. of Tech., Wright-Patterson AFB, OH. Foreign Aerospace Science and Technology Center.
FREQUENCY RESOLUTION OF AN ACOUSTO-OPTICAL SPECTROMETER
Jing-Sheng Wang and Jian-Jun Shen 3 Aug. 1993 16 p Transl. into ENGLISH from Shengxue Xuebao (China), v. 15, no. 4, Jul. 1990 p 299-303
(AD-A267822; FASTC-ID(RS)T-0219-93) Avail: CASI HC A03/MF A01

This paper discusses the frequency resolution of an acousto-optical spectrometer (AOS) system as affected by the acousto-optical deflector and the coherent light beam truncation ratio and examines the response of the photodiode array reception system as affected by the AOS frequency resolution. The broadening of the resolution line pattern caused by the response of a photodiode pixel was computed. From this discussion, the authors proposed selection principles for AOS design parameters, including the light beam truncation ratio, focal length of the Fourier lens, and the number of photodiode array elements. These principles include the overall consideration of resolution, frequency bandwidth, and side lobes of the instrument profile in order to enable the AOS to be designed on a quantitative basis that is suitable to specific observational requirements. To verify these theoretical calculations, the frequency resolution was experimentally measured. DTIC

N94-17402# Air Force Inst. of Tech., Wright-Patterson AFB, OH. Foreign Aerospace Science and Technology Center.
STUDY OF HIGH SPEED INTERFERENCE PHOTOGRAPHY WITH TWO-DIMENSIONAL ACOUSTO-OPTICAL LATTICE DEFLECTION
Anzhi He, Da-Peng Yan, and Xiao-Wu Ni 20 Jul. 1993 15 p Transl. into ENGLISH from Guangxue Xuebao (China), v. 11, no. 4, Apr. 1991 p 364-368
(AD-A267823; FASTC-ID(RS)T-0221-93) Avail: CASI HC A03/MF A01

This paper presents the principle and method of high speed interference photography by using the technique of two dimensional acousto-optical lattice deflection. The light beam carrying the interferogram is deflected into a lattice of 10x10 light spots in a time series; the interferogram is recorded on a photographic negative. The cw laser is the light source; the exposure time can be adjusted between 10(exp -5) to approximately 3(10)(exp -6) s; the framing frequency was about 10(exp 5) frames/s. This method was used to record interferograms of transient-state temperature fields in an experimental study of the principle. DTIC

N94-17446*# National Aeronautics and Space Administration. Lewis Research Center, Cleveland, OH.
CRYOGENIC SPRAY VAPORIZATION IN HIGH-VELOCITY HELIUM, ARGON AND NITROGEN GASFLOWS
Robert D. Ingebo Oct. 1993 13 p Proposed for presentation at the AIAA 32nd Aerospace Sciences Meeting and Exhibit, Reno, NV, 10-13 Jan. 1994; sponsored by AIAA
(RTOP 505-62-52)
(NASA-TM-106363; E-8161; NAS 1.15:106363; AIAA Paper 94-0687)
Avail: CASI HC A03/MF A01

Effects of gas properties on cryogenic liquid-jet atomization in high-velocity helium, nitrogen, and argon gas flows were investigated. Volume median diameter, D(sub v.5e), data were obtained with a scattered-light scanning instrument. By calculating the change in spray drop size, -Delta D(sub v.5)(exp 2), due to droplet vaporization, it was possible to calculate D(sub v.5C). D(sub v.5C) is the unvaporized characteristic drop size formed at the fuel-nozzle orifice. This drop size was normalized with respect to liquid-jet diameter, D(sub O). It was then correlated with several dimensionless groups to give an expression for the volume median diameter of cryogenic LN2 sprays. This expression correlates drop size D(sub v.5c) with aerodynamic and liquid-surface forces so that it can be readily determined in the design of multiphase-flow propellant injectors for rocket combustors. Author (revised)

N94-17619 Nationaal Inst. voor Kernfysica en Hoge Energiefysica, Amsterdam (Netherlands).
MONTE CARLO SIMULATION OF THE MICROSTRIP GAS COUNTER
J. Schmitz 1993 8 p Presented at International Conference on Monte Carlo Simulation in High Energy and Nuclear Physics Submitted for publication Limited Reproducibility: More than 20% of this document may be affected by microfiche quality
(NIKHEF-H/93-07; ETN-93-94828) Avail: CASI HC A02

A Monte Carlo simulation to describe the microstrip gas counter is written. The simulation describes ionization, diffusion and gas amplification. Tuning of the Monte Carlo simulation on data from test beam measurements is discussed. The simulation reproduces the performance of the detector as measured in a beam test for perpendicularly incident particles. The large number of free parameters in the simulation leaves place for further optimization using dedicated measurements. It was found that the position resolution in current prototypes is dominated by the sampling error introduced

because the anode distance is larger than the radius of the electron cloud. This can be overcome by geometrical changes, leading to a resolution predicted to be of the order of 20 microns. ESA

N94-17647# Sandia National Labs., Albuquerque, NM.
RESIST PERFORMANCE IN SOFT X RAY PROJECTION LITHOGRAPHY
G. D. Kubiak (Sandia National Labs., Livermore, CA.), D. A. Tichenor (Sandia National Labs., Livermore, CA.), W. W. Chow, W. C. Sweatt, and M. D. Himel (Bell Telephone Labs., Inc., Holmdel, NJ.) 1993 12 p Presented at the SPIE Meeting on Microlithography, San Jose, CA, 28 Feb. - 5 Mar. 1993
(Contract DE-AC04-76DP-00789)
(DE93-016490; SAND-93-8541C; CONF-9302130-1) Avail: CASI HC A03/MF A01

An important issue for resists used in soft x-ray projection lithography (SXPL) is high absorption. Absorption coefficients of both organic and inorganic formulations range from 2-6 (mu)m(sup (minus)1), requiring the use of very thin (50-100 nm) layers to avoid excessive absorption and resulting pattern sidewall degradation. Such thin films are typically used as the imaging layer in a bi- or tri-level processing scheme to achieve the required pattern depth. In this work, we report experimental and theoretical studies of imaging performance in the resists PMMA and SAL 601 at an SXPL exposure wavelength of 13.9 nm. Absorption coefficients (alpha) have been measured for, and SXPL images recorded in both of these resists. A Mo/Si multilayer-coated Schwarzschild objective having known aberrations and illuminated by a laser plasma soft x-ray source has been used to produce images. Calculated aberrated aerial images are used in conjunction with the measured values of (alpha) to model the expected resist profiles and these are compared to experiment. Imaging performance as a function of resist absorption and estimates of resist exposure latitude are also discussed. DOE

N94-17655*# Southwest Sciences, Inc., Santa Fe, NM.
NONINTRUSIVE FAST RESPONSE OXYGEN MONITORING SYSTEM FOR HIGH TEMPERATURE FLOWS Final Report
Daniel B. Oh and Alan C. Stanton Oct. 1993 61 p
(Contract NAS1-19097; SBIR-02.11-1322; RTOP 324-02-01)
(NASA-CR-4553; NAS 1.26:4553) Avail: CASI HC A04/MF A01

A new technique has been developed for nonintrusive in situ measurement of oxygen concentration, gas temperature, and flow velocity of the test media in hypersonic wind tunnels. It is based on absorption of near-infrared radiation from inexpensive GaAlAs laser diodes used in optoelectronics industry. It is designed for simultaneous measurements along multiple lines of sight accessed by fiber optics. Molecular oxygen concentration is measured from the magnitude of absorption signals; rotational gas temperature is measured from the intensity ratio of two oxygen absorption lines; and the flow velocity is measured from the Doppler shift of the absorption line positions. This report describes the results of an extensive series of tests of the prototype instrument in laboratory flames emphasizing assessment of the instruments capabilities for quantitative measurement of O2 concentration (mole fraction) and gas temperature.
Author (revised)

N94-14992*# Arizona Univ., Tucson. Dept. of Electrical and Computer Engineering.
DETERMINATION OF AVERAGE REFRACTIVE INDEX OF SPIN COATED DCG FILMS FOR HOE FABRICATION
T. J. Kim, Eugene W. Campbell, and Raymond K. Kostuk *In its* Research Studies on Advanced Optical Module/Head Designs for Optical Disk Recording Devices 15 Mar. 1993 p 135-144 (For primary document see N94-14981 03-82)
Avail: CASI HC A02/MF A02

N94-15027*# National Aeronautics and Space Administration. Goddard Space Flight Center, Greenbelt, MD.
X RAY MICROCALORIMETERS: PRINCIPLES AND PERFORMANCE
S. H. Moseley, M. Juda (Wisconsin Univ., Madison.), R. L. Kelley, D. McCammon (Wisconsin Univ., Madison.), C. K. Stahle (National Academy of Sciences - National Research Council, Greenbelt, MD.), A. E. Szymkowiak, and J. Zhang (Wisconsin Univ., Madison.) *In* ESA, Proceedings of an ESA Symposium on Photon Detectors for Space Instrumentation Dec. 1992 p 13-19 (For primary document see N94-15025 03-19)
Copyright Avail: CASI HC A02/MF A04

N94-15028# European Space Agency. European Space Research and Technology Center, ESTEC, Noordwijk (Netherlands). Astrophysics Div.
A NEW APPROACH TO OPTICAL PHOTON DETECTION
M. A. C. Perryman, C. L. Foden, and A. Peacock *In its* Proceedings of an ESA Symposium on Photon Detectors for Space Instrumentation Dec. 1992 p 21-26 (For primary document see N94-15025 03-19)
Copyright Avail: CASI HC A02/MF A04

N94-15030# Danish Space Research Inst., Lyngby.
THE IMAGING MICROSTRIP PROPORTIONAL COUNTER: FEATURES OF A PRACTICAL DESIGN
C. Budtz-Jorgensen, A. Bahnsen, M. MohlMadsen, and H. W. Schnopper *In* ESA, Proceedings of an ESA Symposium on Photon Detectors for Space Instrumentation Dec. 1992 p 33-38 (For primary document see N94-15025 03-19)
Copyright Avail: CASI HC A02/MF A04

N94-15037*# California Univ., Berkeley. Experimental Astrophysics Group.
MICROCHANNEL PLATE IMAGING DETECTORS FOR THE ULTRAVIOLET
O. H. W. Siegmund, M. A. Gummin, J. Stock, and D. Marsh *In* ESA, Proceedings of an ESA Symposium on Photon Detectors for Space Instrumentation Dec. 1992 p 89-96 (For primary document see N94-15025 03-19)
(Grants NAGw-1290; NAGw-2640; NAGw-1879; NAGw-2032)
Copyright Avail: CASI HC A02/MF A04

N94-15040*# California Univ., Berkeley. Space Sciences Lab.
PROSPECTS FOR HIGH PRESSURE IMAGING GAS SCINTILLATION DRIFT CHAMBERS
T. K. Edberg, A. Parsons, B. Sadoulet, S. Weiss, J. Wilkerson, and G. Smith (California Univ., Berkeley. Lawrence Berkeley Lab.) *In* ESA, Proceedings of an ESA Symposium on Photon Detectors for Space Instrumentation Dec. 1992 p 107-110 (For primary document see N94-15025 03-19)
(Grants NAGw-2115; NGT-50462)
Copyright Avail: CASI HC A01/MF A04

N94-15049# Academy of Sciences (USSR), Moscow. Inst. of Radioengineering and Electronics.
NONSTATIONARY BEHAVIOUR OF LOW BACKGROUND PHOTON DETECTORS
B. I. Fouks *In* ESA, Proceedings of an ESA Symposium on Photon Detectors for Space Instrumentation Dec. 1992 p 167-174 (For primary document see N94-15025 03-19)
Copyright Avail: CASI HC A02/MF A04

N94-15056# Max-Planck-Inst. fuer Radioastronomie, Bonn (Germany).
SUBMM/FIR BOLOMETERS
E. Kreysa *In* ESA, Proceedings of an ESA Symposium on Photon Detectors for Space Instrumentation Dec. 1992 p 207-210 (For primary document see N94-15025 03-19)
Copyright Avail: CASI HC A01/MF A04

N94-15096# Dunsink Observatory, Dublin (Ireland). School of Cosmic Physics.
THE RUTHERFORD APPLETON LABORATORY PHOTON COUNTING DETECTOR
I. G. vanBreda, M. K. Carter (Rutherford Appleton Lab., Chilton, England.), B. E. Patchett (Rutherford Appleton Lab., Chilton, England.), and P. D. Read (Rutherford Appleton Lab., Chilton, England.) *In* ESA, Proceedings of an ESA Symposium on Photon Detectors for Space Instrumentation Dec. 1992 p 393-396 (For primary document see N94-15025 03-19)
Copyright Avail: CASI HC A01/MF A04

N94-15573*# Bendix Field Engineering Corp., Seabrook, MD.
STREAK CAMERA BASED SLR RECEIVER FOR TWO COLOR ATMOSPHERIC MEASUREMENTS

Thomas K. Varghese, Christopher Clarke, Thomas Oldham, and Michael Selden *In* NASA. Goddard Space Flight Center, Eighth International Workshop on Laser Ranging Instrumentation Jun. 1993 11 p (For primary document see N94-15552 03-19)
Avail: CASI HC A03/MF A06

N94-15581*# National Aeronautics and Space Administration. Goddard Space Flight Center, Greenbelt, MD.
TWO COLOR SATELLITE LASER RANGING UPGRADES AT GODDARD'S 1.2m TELESCOPE FACILITY
Thomas W. Zagwodzki, Jan F. McGarry, John J. Degnan, and Thomas K. Varghese (Bendix Field Engineering Corp., Seabrook, MD.) *In its* Eighth International Workshop on Laser Ranging Instrumentation Jun. 1993 13 p (For primary document see N94-15552 03-19)
Avail: CASI HC A03/MF A06

N94-15598*# McDonald Observatory, Austin, TX.
A COMPUTER-CONTROLLED x-y OFFSET GUIDING STAGE FOR THE MLRS
Peter J. Shelus, A. L. Whipple, J. R. Wiant, Randall L. Ricklefs, and Frank M. Melsheimer (DFM Engineering, Inc., Longmont, CA.) *In* NASA. Goddard Space Flight Center, Eighth International Workshop on Laser Ranging Instrumentation Jun. 1993 5 p (For primary document see N94-15552 03-19)
Avail: CASI HC A01/MF A06

N94-15618*# National Aeronautics and Space Administration. Goddard Space Flight Center, Greenbelt, MD.
BENCH CHECKOUT EQUIPMENT FOR SPACEBORNE LASER ALTIMETER SYSTEMS
James C. Smith, Gregory C. Elman (Ressler Associates, Inc., Laurel, MD.), Kent D. Christian (Bendix Field Engineering Corp., Columbia, MD.), John F. Cavanaugh, Luis Ramos-Izquierdo, and Dan E. Hopf (Science Systems and Applications, Inc., Lanham, MD.) *In its* Eighth International Workshop on Laser Ranging Instrumentation Jun. 1993 22 p (For primary document see N94-15552 03-19)
Avail: CASI HC A03/MF A06

N94-15802# Belgian Royal Observatory, Brussels. Centre de Geophysique Interne.
A NEW FEEDBACK SYSTEM FOR INSTRUMENTS EQUIPPED WITH A CAPACITIVE TRANSDUCER
M. VanRuymbeke *In its* Papers Presented at the Eleventh International Symposium on Earth Tides 1991 p 51-60 (For primary document see N94-15800 03-46)
Copyright Avail: CASI HC A02/MF A02

N94-15803# Belgian Royal Observatory, Brussels. Centre de Geophysique Interne.
LONG BASELINE WATERTUBES
M. VanRuymbeke, J. Kaeaeriaeinen (Geodetic Inst., Helsinki, Finland.), S. Hennaux, L. VanWallegem, and N. dOreye *In its* Papers Presented at the Eleventh International Symposium on Earth Tides 1991 p 61-70 (For primary document see N94-15800 03-46)
Copyright Avail: CASI HC A02/MF A02

N94-15804# Belgian Royal Observatory, Brussels. Centre de Geophysique Interne.
TEMPERATURE MEASUREMENTS
M. VanRuymbeke, H. Westerhaus (Kiel Univ., Germany.), and J. Fernandez (Universidad Complutense, Madrid, Spain.) *In its* Papers Presented at the Eleventh International Symposium on Earth Tides 1991 p 73-83 (For primary document see N94-15800 03-46)
Copyright Avail: CASI HC A03/MF A02

N94-15805# Belgian Royal Observatory, Brussels. Centre de Geophysique Interne.
CALIBRATION PLATFORMS FOR GRAVIMETERS
M. VanRuymbeke *In its* Papers Presented at the Eleventh International Symposium on Earth Tides 1991 p 95-100 (For primary document see N94-15800 03-46)
Copyright Avail: CASI HC A02/MF A02

N94-15806# State Seismological Bureau of China, Wuhan. Inst. of Seismology.
COOPERATIVE PROJECTS IN GEODYNAMICAL INSTRUMENTATION BETWEEN THE STATE SEISMOLOGICAL BUREAU (CHINA) AND THE ROYAL OBSERVATORY OF BELGIUM
Wei-Lin Cai, M. VanRuymbeke (Belgian Royal Observatory, Brussels.), Shi-Lin Tang, B. Ducarme (Belgian Royal Observatory, Brussels.), Wei-Min Du, and J. A. Flick (Laboratoire Suoterrain de Geodynamique, Luxembourg.) *In* Belgian Royal Observatory, Papers Presented at the Eleventh International Symposium on Earth Tides 1991 p 119-130 (For primary document see N94-15800 03-46)
Copyright Avail: CASI HC A03/MF A02

N94-16081 National Optics Inst., Ste-Foy (Quebec).
OPTICAL SYSTEMS FOR THE VISUALIZATION OF FLUID AND SOLID TRANSPARENT MEDIA UNDER MICROGRAVITY CONDITIONS
E. Harvey and P. Langlois *In* National Research Council Canada, Proceedings of the Second Workshop on Microgravity Experimentation 1990 8 p (For primary document see N94-16071 03-29)
Avail: Issuing Activity (National Research Council, Publication Sales and Distribution, Montreal Road, Ottawa, Ontario, K1A OR6 Canada)

N94-16426*# Los Alamos National Lab., NM.
GAMMA RAY SPECTROMETER FOR LUNAR SCOUT 2 Abstract Only
C. E. Moss, W. W. Burt (TRW Space Technology Labs., Los Angeles, CA.), B. C. Edwards, R. A. Martin, George H. Nakano (Nakano, George H., Los Altos, CA.), and R. C. Reedy *In* Lunar and Planetary Inst., Twenty-Fourth Lunar and Planetary Science Conference. Part 2: G-M 1993 p 1019-1020 (For primary document see N94-16173 03-91)
Avail: CASI HC A01/MF A06

N94-16667*# Jet Propulsion Lab., California Inst. of Tech., Pasadena.
IN-FLIGHT CALIBRATION OF THE SPECTRAL AND RADIOMETRIC CHARACTERISTICS OF AVIRIS IN 1991
Robert O. Green, James E. Conel, Carol J. Bruegge, Jack S. Margolis, Veronique Carrere, Gregg Vane, and Gordon Hoover *In its* Summaries of the Third Annual JPL Airborne Geoscience Workshop. Volume 1: AVIRIS Workshop 1 Jun. 1992 p 1-4 (For primary document see N94-16666 03-42)
Avail: CASI HC A01/MF A02

N94-16696*# Jet Propulsion Lab., California Inst. of Tech., Pasadena.
JPL ACTIVITIES ON DEVELOPMENT OF ACOUSTO-OPTIC TUNABLE FILTER IMAGING SPECTROMETER
Li-Jen Cheng, Tien-Hsin Chao, and George Reyes *In its* Summaries of the Third Annual JPL Airborne Geoscience Workshop. Volume 1: AVIRIS Workshop 1 Jun. 1992 p 88-90 (For primary document see N94-16666 03-42)
Avail: CASI HC A01/MF A02

N94-17348*# Jet Propulsion Lab., California Inst. of Tech., Pasadena.
PHASE HOLOGRAMS IN PMMA WITH PROXIMITY EFFECT CORRECTION
Paul D. Maker and R. E. Muller *In* NASA. Marshall Space Flight Center, Conference on Binary Optics: An Opportunity for Technical Exchange Aug. 1993 p 207-221 Sponsored in part by Strategic Defense Initiative Organization (For primary document see N94-17331 03-74)
Avail: CASI HC A03/MF A04

36 LASERS AND MASERS

Includes parametric amplifiers.
For related information see also *76 Solid-State Physics.*

N94-15145# University of Western Ontario, London. Dept. of Physics.
MERGED BEAM STUDIES OF LASER STIMULATED RADIATIVE RECOMBINATION Annual Report, Jun. 1992 - May 1993
J. B. Mitchell 30 Jun. 1993 25 p
(Contract F49620-92-J-0251)
(AD-A267186; AFOSR-93-0549TR) Avail: CASI HC A03/MF A01
New measurements of the stimulated recombinations of electrons and

protons to form hydrogen atoms in states n = 11, 12, and 13 are presented. Measurements have also been made for the stimulated recombination of electrons and He(+) to form n = 15 and n = 16 states. These cross sections show structure due to singlet and triplet capture. The effects of laser radiation on the dissociative recombination of molecular ions H3(+) have been examined, and the results are reported. DTIC

N94-15477*# Colorado Univ., Boulder. Cooperative Inst. for Research in the Environmental Sciences.

HETERODYNE EFFICIENCY FOR A COHERENT LASER RADAR WITH DIFFUSE OR AEROSOL TARGETS

R. G. Frehlich 26 Oct. 1993 23 p Sponsored in part by NSF
(Grant NAG8-253)
(NASA-CR-194563; NAS 1.26:194563) Avail: CASI HC A03/MF A01

The performance of a Coherent Laser Radar is determined by the statistics of the coherent Doppler signal. The heterodyne efficiency is an excellent indication of performance because it is an absolute measure of beam alignment and is independent of the transmitter power, the target backscatter coefficient, the atmospheric attenuation, and the detector quantum efficiency and gain. The theoretical calculation of heterodyne efficiency for an optimal monostatic lidar with a circular aperture and Gaussian transmit laser is presented including beam misalignment in the far-field and near-field regimes. The statistical behavior of estimates of the heterodyne efficiency using a calibration hard target are considered. For space based applications, a biased estimate of heterodyne efficiency is proposed that removes the variability due to the random surface return but retains the sensitivity to misalignment. Physical insight is provided by simulation of the fields on the detector surface. The required detector calibration is also discussed. Author

N94-15530*# Stanford Univ., CA. Center for Materials Research.

GROWTH OF NEW MATERIALS FOR SOLID STATE LASER APPLICATIONS. THE GROWTH OF ZnGeP2 BY THE VERTICAL BRIDGMAN METHOD Final Technical Report, 1 Sep. 1986 - 31 Mar. 1991

R. S. Feigelson 28 Oct. 1993 30 p
(Grant NAG1-698)
(NASA-CR-194571; NAS 1.26:194571; CMR-93-3; SPO-3952) Avail: CASI HC A03/MF A01

This is the final technical report on the cooperative NASA program 'Growth of New Materials for Solid State Laser Applications,' covering the period from 9-1-86 through 3-31-91. The first two and one half years of the program, from 9-1-86 through 3-31-89, was devoted to the development of new eye-safe laser sources. Single crystal fibers of rare earth doped and co-doped YAG were grown by the laser-heated pedestal growth method, characterized for their structural properties and supplied to NASA/Langley for spectroscopic evaluation. From 4-1-89 though 3-31-91, research focused on the growth of zinc germanium phosphide for nonlinear optical applications in the IR. The vertical Bridgman growth process was evaluated as a means to achieve better control over the short wavelength optical absorption in this material that adversely affects 2 micron-pumped optical parametric oscillators. Author

N94-15628# Naval Research Lab., Washington, DC.

X RAY LASER PROGRAM Final Report, 1 Oct. 1991 - 30 Sep. 1992

John P. Apruzese 1 Jul. 1993 86 p
(AD-A267075; NRL/MR/6721-93-7312) Avail: CASI HC A05/MF A01

This report details the progress achieved by the Radiation Hydrodynamics Branch in X-Ray Laser experiments and modeling during FY-92. Some of the experimental work discussed was carried out at Sandia National Laboratories in collaboration with NRL. It is divided into an executive summary and sections whose authors are separately identified. The individual sections describe progress in the following areas: photopumped x-ray laser research; calculations of x-ray inversions, intensities, and pulsewidths in plasmas created by ultraintense subpicosecond lasers; and effects of non-Maxwellian electron distributions on x-ray gain. DTIC

N94-15686# Naval Research Lab., Washington, DC.

THOMSON BACKSCATTERED X RAYS FROM AN INTENSE LASER BEAM Interim Report

Cha-Mei Tang, B. Hafizi (Icarus Research, Bethesda, MD.), and Sally K. Ride (California Univ., San Diego, La Jolla.) 26 Jul. 1993 19 p
(AD-A267125) Avail: CASI HC A03/MF A01

We have formulated and obtained analytical expressions for Thomson backscattered x-ray radiation for an electron beam incident on a linearly polarized electromagnetic undulator at a small angle. The analytical expressions are valid for fundamental and harmonics with arbitrarily large laser intensities. The intensity distribution pattern is evaluated numerically. DTIC

N94-15852 Illinois Univ., Urbana. Coll. of Engineering.

LASER-SHOCK DAMAGE OF IRON-BASED MATERIALS Final Report, 1990 - 1993

Jinn P. Chu, Grzegorz Banas, Frederick V. Lawrence, James M. Rigsbee, and Hani E. Elsayed-Ali 30 May 1993 156 p Limited Reproducibility: More than 20% of this document may be affected by microfiche quality
(Grant AF-AFOSR-0185-90)
(AD-A267196; AFOSR-93-0456TR) Avail: CASI HC A08

The effects of laser shock processing on the microstructure and mechanical properties of the manganese (1 percent C and 14 percent Mn) steels have been low carbon (0.04 wt. percent C) and Hadfield studied. Laser shock processing was performed with a 1.054 micrometers wavelength Nd-phosphate laser operating in a pulse mode (600 ps pulse length and up to 200 J energy) with power densities above 10 to the 11th power W/cm2. Shock waves were generated by volume expansion of the plasma formed when the material was laser irradiated. Maximum shock wave intensities were obtained using an energy-absorbing black paint coating without a plasma-confining overlay. Maximum modification of compressive residual stresses were achieved when laser shock processing induced deformation occurred without melting. Mechanical properties were improved through modifying the microstructure by laser shock processing. High density arrays of dislocations (greater than 10 to the 11th power/cm2) were generated in low carbon steel by high strain-rate deformation of laser shock processing, resulting in surface hardness increases of 30 to 80 percent. In austenitic Hadfield steel, laser shock processing caused extensive formation of Epsilon-hcp martensite (35 vol. percent), producing increases of 50 to 130 percent in surface hardness. The laser shock processing strengthening effect in Hadfield steel was attributed to the combined effects of the partial dislocation/stacking fault arrays and the grain refinement due to presence of the Epsilon-hcp martensite. DTIC

N94-15853 Spire Corp., Bedford, MA.

ION DOPED QUANTUM WELL LASERS Final Report, 15 Aug. 1992 - 14 Feb. 1993

Anton C. Greenwald Apr. 1993 13 p Limited Reproducibility: More than 20% of this document may be affected by microfiche quality
(Contract F49620-92-C-0060)
(AD-A267198; AFOSR-93-0497TR) Avail: CASI HC A03

Synthesis of erbium-doped light-emitting structures will make it possible to fabricate electrically excited ionic lasers whose output frequency is independent of temperature. The emission wavelength is determined by the ionic properties of the dopant rather than by the band structure of the semiconductor. Optical pumping efficiency would be high, as would the electrical pumping efficiency of the semiconductor. Spire's approach to fabrication of the required structure is metalorganic chemical vapor deposition (MOCVD). In this research project, Spire synthesized and tested different metalorganic chemical sources for erbium. An amide compound, trimethyldisilylamino erbium, was found superior to the cyclopentadienyls as it reduced carbon contamination in the final film, without adding nitrogen or silicon contaminants. DTIC

N94-15932*# National Aeronautics and Space Administration. Pasadena Office, CA.

LASER WITH OPTICALLY DRIVEN Q-SWITCH Patent Application

Hamid Hemmati, inventor (to NASA) (Jet Propulsion Lab., California Inst. of Tech., Pasadena.) 15 Jul. 1993 12 p
(Contract NAS7-918)
(NASA-Case-NPO-18470-1-CU; NAS 1.71:NPO-18470-1-CU;
US-Patent-Appl-SN-094332) Avail: CASI HC A03/MF A01

An optically driven interactive Q-switch, i.e., a Q-switch that responds to a short pulse of light, for example, from external light-emitting diodes (LEDs) or diode lasers, is provided for producing an output laser pulse from electronic energy stored in a laser medium. Q-switching is thus achieved

on demand by electrically pulsing the light source to produce a pulse of light directed onto a Q-switch medium in the laser cavity. Electronic control of the light pulse from the external source will thus provide not only efficient Q-switching frequency but also independent control of output laser pulse width with a fast rise time for each output laser pulse. NASA

N94-15942*# National Aeronautics and Space Administration. Langley Research Center, Hampton, VA.

REDUCTION OF PARASITIC LASING Patent Application

Mark E. Storm, inventor (to NASA) (STX Corp., Hampton, VA.) 11 Aug. 1993 24 p

(NASA-Case-LAR-14645-1-SB; NAS 1.71:LAR-14645-1-SB; US-Patent-Appl-SN-105528) Avail: CASI HC A03/MF A01

A technique was developed which carefully retro-reflects precisely controlled amounts of light back into a laser system thereby intentionally forcing the laser system components to oscillate in a new resonator called the parasitic oscillator. The parasitic oscillator uses the laser system to provide the gain and an external mirror is used to provide the output coupling of the new resonator. Any change of gain or loss inside the new resonator will directly change the lasing threshold of the parasitic oscillator. This change in threshold can be experimentally measured as a change in the absolute value of reflectivity, provided by the external mirror, necessary to achieve lasing in the parasitic oscillator. Discrepancies between experimental data and a parasitic oscillator model are direct evidence of optical misalignment or component performance problems. Any changes in the optical system can instantly be measured as a change in threshold for the parasitic oscillator. This technique also enables aligning the system for maximum parasitic suppression with the system fully operational. NASA

N94-16054# Lawrence Livermore National Lab., CA.

FULL-WAVE SIMULATION OF THE THUMBTACK LASER

R. J. Hawkins, N. K. Madsen, J. S. Kallman, M. D. Feit, C. C. Shang, B. W. Shore, and J. F. DeFord Nov. 1992 5 p Presented at the Optical Society of America Integrated Photonics Research Topical Meeting, Palm Springs, CA, 22-25 Mar. 1993

(Contract W-7405-eng-48)

(DE93-015110; UCRL-JC-112217; CONF-930332-1) Avail: CASI HC A01/MF A01

The whispering-gallery mode microdisk--or thumbtack--laser is a novel, strongly confining, microstructure with 'potential for the integrability and low-power operation required for large-scale photonic integration.' It is a thin dielectric (n approximately 3.5) cylinder--or disk--on top of a rhomboid post. Analysis of the optical modes of this structure have, to date, consisted of scaling arguments drawn from the theory of whispering-gallery spheres. While this analysis has proved useful in understanding the basic aspects of the operation of this laser, it is limited. The authors have undertaken a complete electromagnetic analysis of the thumbtack laser using 2-D, 2.5-D, and 3-D Finite-Difference Time-Domain (FDTD) codes which range in complexity from 2-D studies of the mode structure of the disk to a geometrically complete 3-D analysis of the radiation emitted from the laser. The goal of this project is to predict changes in the optical behavior that accompany structural changes in and about the laser described elsewhere in these proceedings and to guide optimized device design. DOE

N94-16114# Los Alamos National Lab., NM.

THE COOLING OF CONFINED IONS DRIVEN BY LASER BEAMS

L. G. Reyna and J. R. Sobehart 1993 13 p Presented at the New Synthesis Workshop for the Fluctuations and Order, Los Alamos, NM, 9-12 Sep. 1993

(Contract W-7405-eng-36)

(DE93-016612; LA-UR-93-2155; CONF-9309185-1) Avail: CASI HC A03/MF A01

We analyzed the dynamics of confined ions driven by a quantized radiation field. The ions can absorb photons from an incident laser beam and relax back to the ground state by either induced emissions or spontaneous emissions. Here we assume that the absorption of photons is immediately followed by spontaneous emissions, resulting in single-level ions perturbed by the exchange of momentum with the radiation field. The probability distribution of the ions is calculated using singular expansions in the low noise asymptotic limit. The present calculations reproduce the quantum results in the limit of heavy particles in static traps, and the classical results of ions in radio-frequency confining wells. DOE

N94-16124# Michigan Univ., Ann Arbor. Dept. of Physics.

SPATIAL AND FREQUENCY DIVERSITY IN LIDAR SYSTEMS Final Technical Report

John F. Ward 15 Jun. 1993 6 p

(Contract N00014-89-J-3213)

(AD-A266192) Avail: CASI HC A02/MF A01

The research is concerned with the signal to noise ratio of LIDAR signals. LIDAR is a remote sensing technique using light to gather information on molecular concentrations, wind velocities, and temperatures in the atmosphere on a temporally and spatially resolved basis. Our interest is in the statistical optics of the detection process rather than the data that might be collected in the ambient atmosphere, and our experiments, therefore, are carried out in the laboratory. The laboratory experiments are concerned with the fluctuations in LIDAR measurements. LIDAR signals typically arise from the backscatter of laser radiation from aerosols, and the return signal at the detector plane is spatially distributed in a speckle pattern. The contrast ratio in the pattern is unity, hence, an estimate of the average intensity from the intensity measured over a single speckle-area yields a signal-to-noise ratio of unity. DTIC

N94-16450# Lawrence Livermore National Lab., CA.

DESIGN OF A FORMALDEHYDE PHOTODISSOCIATION PROCESS FOR CARBON AND OXYGEN ISOTOPE SEPARATION

R. C. Stern and K. F. Scheibner 20 Jan. 1993 10 p Presented at the OE/LASE 1993 International Society for Optical Engineering Conference, Los Angeles, CA, 16-23 Jan. 1993

(Contract W-7405-eng-48)

(DE93-016435; UCRL-JC-110875; CONF-930159-40) Avail: CASI HC A02/MF A01

The current shortage of O-18 has revived interest in using one step UV photodissociation of formaldehyde to enrich C-13, O-17, and O-18. The frequency doubled output of the copper laser pumped dye laser system currently in operation at LLNL can be used to drive this dissociation. The authors use a simple kinetics model and their experience with atomic vapor laser isotope separation (AVLIS) process design to examine the relative merits of different designs for a formaldehyde photodissociation process. Given values for the molecular photoabsorption cross section, partition function, spectroscopic selectivity, collisional exchange and quenching cross sections (all as parameters), they perform a partial optimization in the space of illuminated area, formaldehyde pressure in each stage, and formaldehyde residence time in each stage. They examine the effect of cascade design (heads and tails staging) on molecule and photon utilization for each of the three isotope separation missions and look in one case at the system's response to different ratios of laser to formaldehyde costs. Finally, they examine the relative cost of enrichment as a function of isotope and product assay. Emphasis is as much on the process design methodology, which is general, as on the specific application to formaldehyde. DOE

N94-16474 Naval Command, Control and Ocean Surveillance Center, San Diego, CA. RDT and E Div.

POROUS SILICON FOR PUMPING SOLID-STATE LASERS Technical Report, Jun. - Sep. 1992

S. D. Russell, W. B. Dubbelday, and R. L. Shimabukuro Mar. 1993 18 p Limited Reproducibility: More than 20% of this document may be affected by microfiche quality

(AD-A266293; NCCOSC/RDT/E-TD-2461) Avail: Issuing Activity (Defense Technical Information Center (DTIC))

Preliminary experiments were performed to investigate the feasibility of using silicon-based sources to pump solid-state lasers. Photoluminescent porous silicon and porous silicon-on-sapphire (SOS) have been fabricated using chemical, electrochemical, and photochemical techniques. An electrochemically fabricated porous silicon sample exhibited 5% quantum efficiency when pumped with 5 mW of 457.9 nm argon ion laser light with a peak emission wavelength of 720 nm. This is consistent with other reports that efficiencies between 1 and 10% have been observed. This room temperature performance exceeds the early development of light emission from 3-5 semiconductors and suggests that continued research and development of the emission mechanism and optimization of the fabrication process can produce, at the very least, functionally equivalent results in a less expensive material which is amenable to large-scale integration. Author (DTIC)

N94-16522*# National Aeronautics and Space Administration. Lewis Research Center, Cleveland, OH.
COMPARISONS OF SELECTED LASER BEAM POWER MISSIONS TO CONVENTIONALLY POWERED MISSIONS
John M. Bozek, Steven R. Oleson (Sverdrup Technology, Inc., Brook Park, OH.), Geoffrey A. Landis (Sverdrup Technology, Inc., Brook Park, OH.), and Mark W. Stavnes (Sverdrup Technology, Inc., Brook Park, OH.) Feb. 1993 23 p Presented at the First Annual Wireless Power Transmission Conference, San Antonio, TX, 23-25 Feb. 1993; sponsored by the Center for Space Power
(Contract NAS3-25266; RTOP 593-32-41)
(NASA-TM-106110; E-7760; NAS 1.15:106110) Avail: CASI HC A03/MF A01

Earth-based laser sites beaming laser power to space assets have shown benefits over competing power system concepts for specific missions. Missions analyzed in this report that show benefits of laser beam power are low Earth orbit (LEO) to geosynchronous Earth orbit (GEO) transfer, LEO to low lunar orbit (LLO) cargo missions, and lunar-base power. Both laser- and solar-powered orbit-transfer vehicles (OTV's) make a 'tug' concept viable, which substantially reduces cumulative initial mass to LEO in comparison to chemical propulsion concepts. Lunar cargo missions utilizing laser electric propulsion from Earth-orbit to LLO show substantial mass saving to LEO over chemical propulsion systems. Lunar-base power system options were compared on a landed-mass basis. Photovoltaics with regenerative fuel cells, reactor-based systems, and laser-based systems were sized to meet a generic lunar-base power profile. A laser-based system begins to show landed mass benefits over reactor-based systems when proposed production facilities on the Moon require power levels greater than approximately 300 kWe. Benefit/cost ratios of laser power systems for an OTV, both to GEO and LLO, and for a lunar base were calculated to be greater than 1. Author (revised)

N94-16533 Department of the Navy, Washington, DC.
LASING DYE SENSOR FOR CHEMICAL VAPORS Patent
Terence W. Barrett, inventor (to Navy) and John F. Giuliani, inventor (to Navy) 9 Feb. 1993 7 p Filed 6 Dec. 1991
(AD-D015786; US-Patent-5,185,131; US-Patent-Appl-SN-802926; US-Patent-Class-422-91) Avail: US Patent and Trademark Office

In an external lasing dye sensor system, a stream of lasing dye free-flows across an open area inside a chamber. An air sample comprising chemical vapor contaminants is pumped or drawn into the chamber. A laser beam is introduced into the chamber intersecting the lasing dye. A chemical reaction between the contaminants and the lasing dye result in a change in the emission spectra of the lasing dye. The change in emission spectra is detected and thus provides an improved apparatus for detecting low concentrations of chemical vapors in an air sample. DTIC

N94-16540 Department of the Navy, Washington, DC.
DIGITAL LASER RANGE FINDER EMULATOR Patent
Vaughn P. McDowell, inventor (to Navy), Orgal T. Holland, inventor (to Navy), and Christina G. Wilkerson, inventor (to Navy) 25 May 1993 6 p Filed 6 Aug. 1992
(AD-D015811; US-Patent-5,214,483; US-Patent-Appl-SN-925217; US-Patent-Class-356-5) Avail: US Patent and Trademark Office

A digital laser range finder emulator receives N-bits of range-to-target data in a parallel format and generates N-bits of serial data representative of the range-to-target data and an external synchronization pulse whose presence is indicative of valid serial data. First and second clock pulses are generated such that the second clock pulse is delayed with respect to the first clock pulse. Control logic, responsive to the first clock pulse, generates validity logic while control logic, responsive to the second clock pulse, generates transmit logic. The parallel format range-to-target data is converted into the serial data in response to the first clock pulse. The serial data is then output in response to the transmit logic. A gate, responsive to the second clock pulse and the validity logic, generates the synchronization pulse when the second clock pulse and validity logic occupy a common logic state. DTIC

N94-16546# North Texas Research and Development Inst., Denton.
[CONTROLLING CHAOTIC BEHAVIOR IN CO2 AND OTHER LASERS] Progress Report No. 3, 16 May - 15 Jun. 1993
25 Jun. 1993 21 p
(Contract N00014-93-C-0051)
(AD-A266431) Avail: CASI HC A03/MF A01

Additional substantial experimental progress has been made, in the third month of the project, in setting up equipment and testing for producing chaotic behavior with a CO2 laser. The project goal is to synchronize and control chaos in CO2 and other lasers, and thereby increase the power in ensembles of coupled laser sources. Numerous investigations into the chaos regime have been made, a second CO2 laser has been brought on stream, and work is progressing in the fourth month toward coupling the two lasers and control of the first laser. It is also intended to submit at least two papers to the Second Experimental Chaos Conference which is supported by the Office of Naval Research. Abstracts to those two papers are attached. Last month's report discussed the experimental investigation of nonlinear dynamics of CO2 lasers which involved a new technique of inducing chaos. In this new technique, an acoustically modulated feedback of the laser light was used and led to chaotic dynamics at a very low modulation frequency of 375 Hz. Since then, new results have been obtained by an Electro-Optical Modulation (EOM) technique. In the new setup, the electro-optical modulator is placed in an external cavity outside the laser. DTIC

N94-16663# Oak Ridge National Lab., TN.
PULSED LASER DEPOSITION OF METASTABLE Ca(1-x)Sr(x)CuO2 THIN FILMS
D. P. Norton, B. C. Chakoumakos, J. D. Budai, and D. H. Lowndes 1993 7 p Presented at the 2nd International Conference on Laser Ablation: Mechanisms and Applications, Knoxville, TN, 19-22 Apr. 1993
(Contract DE-AC05-84OR-21400)
(DE93-015804; CONF-9304144-6) Avail: CASI HC A02/MF A01

One of the more interesting copper oxide materials is the tetragonal phase of Ca(1-x)Sr(x)CuO2, as it can be viewed as the parent structure of all of the high (Tc) superconducting cuprates. Although simple in structure, this copper oxide is metastable, requiring high pressures and temperatures for bulk synthesis. However, recent efforts have shown that formation of this phase can be achieved as an epitaxial thin film at low oxygen pressures (1-200 mTorr) and temperatures (450-700C) by pulsed laser deposition. We will discuss the growth of Ca(1-x)Sr(x)CuO2 by pulsed laser deposition, and the effects of various growth conditions on the transport and structural properties of these films. In particular, we will show that conductivity in this material can be significantly improved at the Sr-rich end of the solid solution. In addition, we discuss the effect of alkaline-earth (Sr, Ca) vacancies on transport properties of these thin films. DOE

N94-16664# Oak Ridge National Lab., TN.
ABLATION, SURFACE ACTIVATION, AND ELECTROLESS METALLIZATION OF INSULATING MATERIALS BY PULSED EXCIMER LASER IRRADIATION
D. H. Lowndes, M. J. Godbole, G. E. Jellison, Jr., and A. J. Pedraza 1993 9 p Presented at the 2nd International Conference on Laser Ablation: Mechanisms and Applications, Knoxville, TN, 19-22 Apr. 1993
(Contract DE-AC05-84OR-21400)
(DE93-015808; CONF-9304144-5) Avail: CASI HC A02/MF A01

Pulsed-laser irradiation of wide bandgap ceramic substrates, using photons with sub-bandgap energies, activates the ceramic surface for subsequent electroless copper deposition. The copper deposit is confined within the irradiated region when the substrate is subsequently immersed in an electroless copper bath. However, a high laser fluence (typically several j/sq cm) and repeated laser shots are needed to obtain uniform copper coverage by this direct-irradiation process. In contrast, by first applying an evaporated SiO(x) thin film (with x approximately = 1), laser ablation at quite low energy density (approximately = 0.5 J/sq cm) results in re-deposition on the ceramic substrate of material that is catalytic for subsequent electroless copper deposition. Experiments indicate that the re-deposited material is on silicon, on which copper nucleates. Using an SiO(x) film on a laser-transparent substrate, quite fine (approximately 12 microns) copper lines can be formed at the boundary of the region that is laser-etched in SiO(x). Using SiO(x) with an absorbing (polycrystalline) ceramic substrate, more-or-less uniform activation and subsequent copper deposition are obtained. In the later case, interactions with the ceramic substrate also may be important for uniform deposition. DOE

N94-16719*# Texas Univ., Austin. Center for Space Research.
LASER RANGING DATA ANALYSIS Final Report, 1987 - 1992 and Annual Report, 1991-1992
1992 4 p
(Grant NAG5-1021)
(NASA-CR-193547; NAS 1.26:193547) Avail: CASI HC A01/MF A01

Center for Space Research efforts have focused on the near real-time analysis of Lageos laser ranging data and on the production of predictive ephemerides. The data are analyzed in terms of range bias, time bias, and internal precision, and estimates for the Earth orientation parameters X(sub p), Y(sub p) and UT1 are obtained. The results of these analyses are reported in a variety of formats. In addition several additional stations began sending not only quick-look observations but also normal points created on-site with new software. These normal points are transmitted in a new standard format different from either current quick-look or MERIT-II full-rate formats. Thus new preprocessing software was written and successfully tested on these data. Inspection of the Bendix produced Lageos full-rate normal points continued, with detailed analyses and filtering of all 1991 A and B release normal points for Lageos through the beginning of 1992. A summary of the combined full-rate and quick-look normal point data set created for 1991 is provided. New long-term ephemerides for Lageos satellite, as well as for Etalon-1 and Etalon-2 (the so-called high satellites used for laser ranging) were produced and distributed to the network stations in cooperation with the Crustal Dynamics Project and Eurolas. These predictions are used by essentially every laser ranging site obtaining regular returns from any of these three satellites.
Derived from text

N94-16871# Lawrence Livermore National Lab., CA.
LASER WELD REPAIR OF TANTALUM SHEET
J. J. Oldani and C. N. Westrich Dec. 1992 9 p Presented at the 1992 International Conference on Lasers, Houston, TX, 7-11 Dec. 1992
(Contract W-7405-eng-48)
(DE93-016417; UCRL-JC-110669; CONF-921256-4) Avail: CASI HC A02/MF A01

Tantalum sheets which are used in radiographic film cassettes for high explosives studies, were repaired using Nd:YAG laser welding. The tantalum sheets can receive various levels of indentations and/or scratches which can leave radiographic indications during use in subsequent studies. Laser welding using a Raytheon 400 watt Nd:YAG laser and a 0.010 inch diameter tantalum filler wire with argon cover gas was used to fill in these false indications. A successful weld repair is required to give no radiographic indications--neither high nor low density readings. DOE

N94-16998# Utah Univ., Salt Lake City.
PULSED LASER KINETIC STUDIES OF LIQUIDS UNDER HIGH PRESSURE
E. M. Eyring 21 Jun. 1993 13 p
(Contract DE-FG02-84ER-13227)
(DE93-017826; DOE/ER-13227/7) Avail: CASI HC A03/MF A01

Experiments have been developed for measuring the rates of chemical reactions liquids and in supercritical CO2. A pulsed (Q-switch) Nd:YAG laser at 355 nm was the pump beam for laser flash photolysis studies of molybdenum and tungsten hexacarbonyls undergoing ligand displacement reactions by bidentate chelating agents such as 2,2'-bipyridine in toluene. Experiments were carried out at 0.1 to 150 MPa. In the case of molybdenum complexes, the reaction mechanism for thermal ring closure is found from activation volumes to change from associative interchange to dissociative interchange as substituents on the 2,2'-bipyridine ligands become bulkier. In a similar study of more rigid, substituted phenanthroline bidentate ligands it was found that substituent bulkiness had little effect on the thermal ring closure mechanism. Similar high pressure flash photolysis experiments with tungsten hexacarbonyl have also been completed. The concentration dependence of the fluorescence and nonradiative decay quantum yields for cresyl violet in several solvents has been reported as well as stability constants for the complexation of lithium ion by four different crown ethers dissolved in a room temperature molten salt. DOE

N94-17001# Michigan Univ., Ann Arbor. Dept. of Nuclear Engineering.
ADVANCED TRANSPORT SYSTEMS FOR ELECTRON BEAMS IN HIGH BRIGHTNESS ACCELERATORS AND FELs Annual Report, 1 May 1992 - 30 Apr. 1993
R. M. Gilgenbach, Y. Y. Lau, T. Kammash, and M. L. Brake 19 Jul. 1993 68 p
(Contract N00014-91-J-1941)
(AD-A267322) Avail: CASI HC A04/MF A01

Research on the beam breakup (BBU) instability has been performed on the following tasks during the past year: cold-test and circuit-model analysis to evaluate coupled cavity BBU experimental results, demonstration of scaling of BBU growth in a new 19 cavity system that doubles the propagation distance to about two meters, novel theoretical analysis of BBU growth in a high current annular electron beam, and theoretical studies of BBU control by gas focusing. DTIC

N94-17065# Polish Academy of Sciences, Warsaw. Inst. Podstawowych Problemow Techniki.
PROPOSAL OF A SIMPLE MATHEMATICAL MODEL FOR THE ACTION OF A LASER ON A METAL PLATE [PROPOZYCJA PROSTEGO MODELU MATEMATYCZNEGO ODDZIALYWANIA WIAZKI LASEROWEJ NA PLYTKE METALOWA]
Zbigniew Turek 1991 31 p In POLISH
(IFTR-36/1991) Avail: CASI HC A03/MF A01

By employing a number of simplifications, the effect of a laser beam packet on a metallic plate is simulated. The distension of a heat-pretreated static sample is simulated for the simplified model. It is demonstrated that on a qualitative level, the proposed model accurately describes the processes occurring in a sample fabricated from 1H18N9T steel during exposure to the laser beam packet. Transl. by FLS

N94-17193# Pacific Applied Research, Rancho Palos Verdes, CA.
PULSED HYDROGEN FLUORIDE OVERTONE CHEMICAL LASER STUDIES Final Report, 1 Nov. 1990 - 31 Jan. 1992
W. R. Warren, Jr. and Leo E. Schneider 1 Feb. 1993 80 p
(Contract F49620-90-C-0008)
(AD-A267597; PAR-TM-93-103; AFOSR-93-103TR) Avail: CASI HC A05/MF A01

An experimental study of HF chemical lasers operating on overtone transitions, OT's, in a photolytically initiated, pulsed laser facility was conducted. The primary objective was to obtain comparisons of the specific energy performance of pulsed HF, chain reaction driven, chemical laser resonators when operating only on fundamental transitions, delta V = 1, and only on first overtone transitions, delta V = 2. The initial efforts were the buildup of the experimental test facility with which excellent performance as an FT HF laser was demonstrated. However, attempts to produce OT lasing using lambda-variable reflectivity mirror coatings (to promote and suppress, simultaneously, the OT and FT mechanisms) were only marginally successful, even though major facility modifications were made to reduce cavity losses, suppress FT superradiance (ASE), suppress parasitic modes, and increase pulse duration. Finally, CW OT lasing was demonstrated using the OT optical components in a combustion driven, blowdown test facility. A specific energy level, sigma = 266 w/gm/sec, was inferred from the measurements. DTIC

N94-17195# Air Force Inst. of Tech., Wright-Patterson AFB, OH.
BIBLIOGRAPHY OF SHORT WAVELENGTH CHEMICAL LASER RESEARCH Technical Report
Glen P. Perram May 1993 64 p
(AD-A267619; AFIT/EN/TR/93-03) Avail: CASI HC A04/MF A01

High power short wavelength chemical laser (SWCL) systems offer great advantages for strategic and tactical military applications, including both weapons and imaging missions. The promise of very high brightness, high mass efficiency, and wavelength agility has justified a modest basic research program for more than a decade. Significant progress towards the demonstration of a visible chemical laser has been made during the past few years. Highly efficient methods of chemically producing metastable electronic states at concentrations exceeding 3 x 10(exp 16) molecules/cu cm have been developed. Energy transfer from these metastables to suitable lasant species has been used to demonstrate gain in the visible. Chemically generated gain of 0.029 %/cm on the (A-X) electronic transition in bismuth fluoride has been demonstrated using pulsed thermolysis of fluorine azide and trimethyl bismuth mixtures. Recently, a table-top shock facility has been used to achieve unsaturated lasing in the same system. During the past ten years, over 400 articles and reports have resulted from this

research program. This bibliography summarizes this Department of Defense sponsored research on short wavelength chemical lasers since 1980. DTIC

N94-17230# PLEX Corp., Brookline, MA.
SODIUM-MERCURY EXCIMER LASER, PHASE 1 Final Report, Jun. - Dec. 1992
Malcolm W. McGeoch Dec. 1992 42 p
(Contract DASG60-92-C-0140)
(AD-A267726; PLEX-003) Avail: CASI HC A03/MF A01

This Phase 1 work addresses the technology required to test the sodium-mercury excimer laser concept. Calculations of the optimum laser excitation conditions show that a gain of 2.8% /cm should be achievable in the 1.2 micron region for a specific discharge power input of 20kW/cu cm. At the lower power input of 2kW/cu cm the projected gain is 1.5%/cu cm. The calculations consider the electron energy distribution function and collisional dissociation of NaHg(A) state molecules. Ultraviolet pre-ionization was shown to be a viable route to the attainment of high power discharges in this system. An experimental test of 600 deg C cell technology was performed, in which windows, lead-throughs and a close-out valve were cycled repeatedly to that temperature. DTIC

N94-17285*# National Aeronautics and Space Administration. Langley Research Center, Hampton, VA.
HAZARD CALCULATIONS OF DIFFUSE REFLECTED LASER RADIATION FOR THE SELENE PROGRAM
Gilda A. Miner and Phillip D. Babb (Bionetics Corp., Hampton, VA.) Washington Oct. 1993 8 p
(RTOP 506-41-41-01)
(NASA-TM-4520; L-17008; NAS 1.15:4520) Avail: CASI HC A02/MF A01

The hazards from diffuse laser light reflections off water clouds, ice clouds, and fog and from possible specular reflections off ice clouds were assessed with the American National Standards (ANSI Z136.1-1986) for the free-electron-laser parameters under consideration for the Segmented Efficient Laser Emission for Non-Nuclear Electricity (SELENE) Program. Diffuse laser reflection hazards exist for water cloud surfaces less than 722 m in altitude and ice cloud surfaces less than 850 m in altitude. Specular reflections from ice crystals in cirrus clouds are not probable; however, any specular reflection is a hazard to ground observers. The hazard to the laser operators and any ground observers during heavy fog conditions is of such significant magnitude that the laser should not be operated in fog. Author

N94-17378# Naval Research Lab., Washington, DC.
SOFT X RAY EMISSION FROM ALEXANDRITE LASER-MATTER-INTERACTION
P. G. Burkhalter, D. J. Harter (Allied-Signal Corp., Morristown, NJ.), E. F. Gabl (MXR, Inc., Dexter, MI.), P. Bado (MXR, Inc., Dexter, MI.), and D. A. Newman (SFA, Inc., Landover, MD.) 15 Jul. 1993 29 p
(AD-A267905) Avail: CASI HC A03/MF A01

X-ray spectroscopy was used to quantify the plasma generated by a focused, Alexandrite laser as a potential alternative source in proximity lithography. An x-ray emission efficiency of 2 - 11% was determined by analysis of spectral data (10 - 14 A) from transition-metal targets. DTIC

N94-17394# Air Force Inst. of Tech., Wright-Patterson AFB, OH. Foreign Aerospace Science and Technology Center.
EXTRACAVITY FREQUENCY DOUBLING STUDY OF A PULSED PHOTODISSOCIATION IODINE LASER
Yi-Zhu Sun, Yu-Qi Jin, and Tie-Ji Gui 20 Jul. 1993 9 p Transl. into ENGLISH from Chinese Journal. of Applied Laser Technology (China), v. 10, no. 4 p 149-150
(AD-A267893; FASTC-ID(RS)T-0121-93) Avail: CASI HC A02/MF A01

An extracavity lithium metaniobate (LiNbO3) crystal and the angle-phase matching technique were used for the extracavity frequency doubling investigation of a pulsed photodissociation iodine laser. A frequency doubled laser beam of 0.657 micron wavelength and maximum energy conversion efficiency of 9.6% were obtained. DTIC

N94-17400# Air Force Inst. of Tech., Wright-Patterson AFB, OH. Foreign Aerospace Science and Technology Center.
EXPERIMENTAL STUDIES ON A GAS DYNAMIC LASER WITH NARROW THROAT AND HIGH AREA-RATIO GRID NOZZLES
20 Jul. 1993 14 p Transl. into ENGLISH from unidentified Chinese language document p 496-499
(AD-A267818; FASTC-ID(RS)T-0868-91) Avail: CASI HC A03/MF A01

This paper describes a combustion-driven CO2 gas dynamic laser (GDL) with a throat height of 0.3mm and a grid nozzle with an area-ratio of 30 and presents some experimental results. The behavior of the flow and the location of shock waves in the optical cavity were observed. The variation in small-signal gain G(sub 0) with CO2 or H2O contents were measured and compared with the experimental data from a similar set-up with a nozzle throat height of 0.8mm and an area-ratio of 17. Some of the advantages are obvious for the narrower throat height and higher area-ratio GDL: the G(sub 0) can be increased by a factor of 50%; and the H2O contents may be increased from 1% to 5%. DTIC

N94-17415 Air Force Systems Command, Wright-Patterson AFB, OH. Foreign Aerospace Science and Technology Center.
THREE SHORT ARTICLES FROM JAPANESE LASER JOURNAL
23 Jul. 1993 17 p Transl. into ENGLISH from Jiguang Zashi (China), v. 8, no. 3, 1981 p 47-49 Limited Reproducibility: More than 20% of this document may be affected by microfiche quality
(AD-A268249; FASTC-ID(RS)T-0729-92) Avail: Issuing Activity (Defense Technical Information Center (DTIC))

A branch-selected oscillation of a pulsed TEA CO2 laser with three NaCl prisms placed in the cavity as dispersive elements is reported. Sixty laser lines have been obtained. Also, an electron-beam pre-ionized, electrically excited gasdynamic CO laser was developed. Preliminary experimental research on its performance has been made. Finally, the discharging behavior of flute-type hollow cathode in limited discharge is investigated. He-Ne laser output at 6328 A is obtained at limited discharge; it is about 10 times higher than that in ordinary hollow discharge. Author

N94-17567# Tennessee Univ., Knoxville. Dept. of Physics.
BASIC STUDIES OF THE LIQUID STATE OF MATTER: ELECTRICAL PROPERTIES AND LASER INTERACTIONS Final Report
L. G. Christophorou and H. Faidas Jul. 1993 156 p
(Contracts N00014-89-J-1990; N00014-92-3-1606)
(AD-A268311) Avail: CASI HC A08/MF A02

This research involves basic studies of the electrical properties of the liquid state of matter. Given the intrinsic difficulties associated with physical studies of liquids (liquids lack the order of the crystal and the large inter-particle distances of the gas) we set out to develop new experimental techniques for and new approaches to the study of the electrical properties of liquids. The stated goals of this research were: (1) To establish a fundamental understanding of key basic processes and phenomena which determine the electrical properties of fluids; and (2) To use the new knowledge provided by the basic studies to benefit technological applications, especially in the areas of electrical breakdown of liquids, radiation detectors, pulsed power switches, and laser interactions in liquids. To meet these two goals, we emphasized studies in the following areas: (1) Electron production via ionization and injection in nonpolar liquids and dense gases; (2) Electron and ion transport in pure liquids and liquid mixtures; (3) Electron attachment and photodetachment in liquids; (4) Electron energetics in and mechanisms of the above processes; (5) Electrical breakdown and partial discharge in pure liquids and mixtures at high electric fields; (6) Technical aspects of liquids for advanced radiation detectors and pulsed power switches; and (7) Further development of liquid-filled flashlamp-operated pulsed power switch. DTIC

N94-17630 Bhabha Atomic Research Centre, Bombay (India).
DESIGN, DEVELOPMENT AND CHARACTERIZATION STUDIES OF A LARGE APERTURE HIGH POWER Nd: GLASS ROD AMPLIFIER STAGE
N. Gopi, R. C. Bapna, C. G. Murali, B. S. Narayan, and L. J. Dhareshwar (Bhabha Atomic Research Centre, Bombay, India.) 1992 53 p Limited Reproducibility: More than 20% of this document may be affected by microfiche quality
(DE93-624944; BARC-1992/E/029) Avail: CASI HC A04 (US Sales Only)

Laser-plasma interaction studies and experiments related to laser driven

shocks as well as laser induced inertially confined thermonuclear fusion have resulted in an ever increasing demand for high brightness lasers capable of producing nanosecond pulse with energy of hundreds of kilo joules. High power Nd-glass laser chains with a master oscillator followed by a number of amplifier stages made up of rods, disks, slabs etc. are in operation in many leading laboratories in the world. This report describes the design, development and characterisation studies of a large aperture Nd:glass laser amplifier which is to be incorporated on line with the existing 40 J, 5 ns high power laser chain built for laser-plasma interaction and laser driven shock wave studies in the Laser and Plasma Technology Division. The development work described in this report discusses the design based on optimum material selection, optimisation of various sub components, ease of maintenance and smooth operation. The necessary operational electronics has also been described. The characterization studies mainly include measurement of spatial gain uniformity, thermally induced depolarization effects, and thermal relaxation studies. DOE

N94-17677# Pacific Northwest Lab., Richland, WA.
ENVIRONMENTAL USE OF A LASER RANGE FINDER AND THE ADVANCED VISUALIZATION SYSTEM
E. N. Thornton, S. Bohn, C. P. Baker, D. R. Jones, and L. A. Strope May 1993 7 p Presented at the AVS 1993 Users Group Meeting, Orlando, FL, 24-26 May 1993
(Contract DE-AC06-76RL-01830)
(DE93-016163; PNL-SA-22213; CONF-9305168-5) Avail: CASI HC A02/MF A01

The United States Department of Energy (DOE) is facing a large task in characterizing and remediating the contents of hazardous waste inside storage tanks. The characterization process of these tanks is a key step to the remediation process. Due to the hazardous materials inside the waste tanks, all of the work must be done remotely utilizing robotic systems. The Laser Range Finder (LRF) is a single point sensor used to remotely collect range and intensity data. The LRF sensor data is used to reconstruct the tank surface environment based on multiple LRF scans. This reconstructed surface definition can be used by a robotic controller to perform obstacle avoidance with items in the tank. The Pacific Northwest Laboratory (PNL) has used Advanced Visualization System (AVS) to prototype the filtering, transformation, and reconstructing process. AVS software modules have been written to address LRF filtering on both the range and intensity images. A coordinate transformation module was constructed to convert the raw LRF data into a Cartesian coordinate reference frame. The results of filtering and transforms are integrated into a master map of the tank using an octree database. Master octrees are traversed and made into AVS geometry to visualize the tank interior. The graphical display of the tank interior can be used for robotic path planning and monitoring waste removal progress. DOE

N94-14994*# Arizona Univ., Tucson.
FIGURES OF MERIT FOR LASER BEAM QUALITY
T. D. Milster and E. P. Walker *In its* Research Studies on Advanced Optical Module/Head Designs for Optical Disk Recording Devices 15 Mar. 1993 p 153-159 (For primary document see N94-14981 03-82)
Avail: CASI HC A02/MF A02

N94-15092# Fraunhofer Inst. fuer Physikalische Messtechnik, Freiburg (Germany).
INFRARED DETECTOR ANNEALING AND CALIBRATION WITH IR-LASER DIODES
U. Schiessl, M. Tacke, and D. Lemke (Max-Planck-Inst. fuer Astronomie, Heidelberg, Germany.) *In* ESA, Proceedings of an ESA Symposium on Photon Detectors for Space Instrumentation Dec. 1992 p 373-377 (For primary document see N94-15025 03-19)
(Grant BMFT-511/DARA-01-RS-89376)
Copyright Avail: CASI HC A01/MF A04

N94-15553*# National Aeronautics and Space Administration. Goddard Space Flight Center, Greenbelt, MD.
LASER TRACKING FOR VERTICAL CONTROL
Peter Dunn (Hughes STX, Inc., Lanham, MD.), Mark Torrence (Hughes STX, Inc., Lanham, MD.), Erricos Pavlis (Maryland Univ., College Park.), Ron Kolenkiewicz, and David Smith *In its* Eighth International Workshop on Laser Ranging Instrumentation Jun. 1993 18 p (For primary document see N94-15552 03-19)
Avail: CASI HC A03/MF A06

N94-15554*# Deutsches Geodaetisches Forschungsinst., Munich (Germany).
LASER RANGING NETWORK PERFORMANCE AND ROUTINE ORBIT DETERMINATION AT D-PAF
Franz-Heinrich Massmann, C. Reigber, H. Li, Rolf Koenig, J. C. Raimondo, C. Rajasenan, and M. Vei *In* NASA. Goddard Space Flight Center, Eighth International Workshop on Laser Ranging Instrumentation Jun. 1993 15 p Prepared in cooperation with Deutsche Geodaetische Kommission, Munich, Germany (For primary document see N94-15552 03-19)
Avail: CASI HC A03/MF A06

N94-15555*# Ministry of Posts and Telecommunications, Tokyo (Japan). Communications Research Lab.
LASER RANGING APPLICATION TO TIME TRANSFER USING GEODETIC SATELLITE AND TO OTHER JAPANESE SPACE PROGRAMS
Hiroo Kunimori, Fujinobu Takahashi, Toshikazu Itabe, and Atsushi Yamamoto (Maritime Safety Agency, Tokyo, Japan.) *In* NASA. Goddard Space Flight Center, Eighth International Workshop on Laser Ranging Instrumentation Jun. 1993 9 p (For primary document see N94-15552 03-19)
Avail: CASI HC A02/MF A06

N94-15556*# Texas Univ., Austin. Center for Space Research.
APPLICATIONS OF SLR
Bob E. Schutz *In* NASA. Goddard Space Flight Center, Eighth International Workshop on Laser Ranging Instrumentation Jun. 1993 4 p (For primary document see N94-15552 03-19)
Avail: CASI HC A01/MF A06

N94-15557*# Royal Greenwich Observatory, Cambridge (England).
SATELLITE SIGNATURES IN SLR OBSERVATIONS
G. M. Appleby *In* NASA. Goddard Space Flight Center, Eighth International Workshop on Laser Ranging Instrumentation Jun. 1993 14 p (For primary document see N94-15552 03-19)
Avail: CASI HC A03/MF A06

N94-15563*# National Aeronautics and Space Administration. Goddard Space Flight Center, Greenbelt, MD.
Nd:YLF LASER FOR AIRBORNE/SPACEBORNE LASER RANGING
Joseph L. Dallas and Mark D. Selker *In its* Eighth International Workshop on Laser Ranging Instrumentation Jun. 1993 6 p (For primary document see N94-15552 03-19)
Avail: CASI HC A02/MF A06

N94-15564*# Czech Technical Univ., Prague. Faculty of Nuclear Science and Physical Engineering.
ALTERNATIVE WAVELENGTHS FOR LASER RANGING
Karel Hamal *In* NASA. Goddard Space Flight Center, Eighth International Workshop on Laser Ranging Instrumentation Jun. 1993 2 p (For primary document see N94-15552 03-19)
Avail: CASI HC A01/MF A06

N94-15565*# Czech Technical Univ., Prague. Faculty of Nuclear Science and Physical Engineering.
NEW METHODS OF GENERATION OF ULTRASHORT LASER PULSES FOR RANGING
Helena Jelinkova, Karel Hamal, V. Kubecek, and Ivan Prochazka *In* NASA. Goddard Space Flight Center, Eighth International Workshop on Laser Ranging Instrumentation Jun. 1993 6 p (For primary document see N94-15552 03-19)
Avail: CASI HC A02/MF A06

N94-15567*# Czech Technical Univ., Prague. Faculty of Nuclear Science and Physical Engineering.
AN IMPROVED LIGHT SOURCE FOR LASER RANGING
Karel Hamal and Martin Richardson (University of Central Florida,

Orlando.) *In* NASA. Goddard Space Flight Center, Eighth International Workshop on Laser Ranging Instrumentation Jun. 1993 2 p (For primary document see N94-15552 03-19)
Avail: CASI HC A01/MF A06

N94-15569*# Politecnico di Milano (Italy). Dipt. di Elettronica e Informazione.
PERFORMANCE OPTIMIZATION OF DETECTOR ELECTRONICS FOR MILLIMETER LASER RANGING
Sergio Cova, A. Lacaita, and Giancarlo Ripamonti (Milan Univ., Italy.) *In* NASA. Goddard Space Flight Center, Eighth International Workshop on Laser Ranging Instrumentation Jun. 1993 18 p Sponsored in part by Italian Space Agency; CNR; and Italian Ministry of University and Research (For primary document see N94-15552 03-19)
Avail: CASI HC A03/MF A06

N94-15570*# Politecnico di Milano (Italy). Dipt. di Elettronica e Informazione.
TRACKING CAPABILITIES OF SPADS FOR LASER RANGING
F. Zappa, Giancarlo Ripamonti (Milan Univ., Italy.), A. Lacaita, Sergio Cova, and C. Samori *In* NASA. Goddard Space Flight Center, Eighth International Workshop on Laser Ranging Instrumentation Jun. 1993 6 p Sponsored in part by Italian Space Agency; CNR; and Italian Ministry of University and Research (For primary document see N94-15552 03-19)
Avail: CASI HC A02/MF A06

N94-15571*# Politecnico di Milano (Italy). Dipt. di Elettronica e Informazione.
HOW TO SQUEEZE HIGH QUANTUM EFFICIENCY AND HIGH TIME RESOLUTION OUT OF A SPAD
A. Lacaita, F. Zappa, Sergio Cova, Giancarlo Ripamonti (Milan Univ., Italy.), and A. Spinelli *In* NASA. Goddard Space Flight Center, Eighth International Workshop on Laser Ranging Instrumentation Jun. 1993 6 p Sponsored in part by Italian Space Agency; CNR; and Italian Ministry of University and Research (For primary document see N94-15552 03-19)
Avail: CASI HC A02/MF A06

N94-15574*# Czech Technical Univ., Prague. Faculty of Nuclear Science and Physical Engineering.
THE FIRST SATELLITE LASER ECHOES RECORDED ON THE STREAK CAMERA
Karel Hamal, Ivan Prochazka, Georg Kirchner (Technische Univ., Graz, Austria.), and F. Koidl (Technische Univ., Graz, Austria.) *In* NASA. Goddard Space Flight Center, Eighth International Workshop on Laser Ranging Instrumentation Jun. 1993 7 p (For primary document see N94-15552 03-19)
Avail: CASI HC A02/MF A06

N94-15575*# Institut fuer Angewandte Geodaesie, Koetzing (Germany). Fundamentalstation Wettzell der Forschungsgruppe Satellitengeodaesie.
EXPERIENCE AND RESULTS OF THE 1991 MTLRS-1 USSR CAMPAIGN
Peter Sperber and H. Hauck (Institut fuer Angewandte Geodaesie, Frankfurt am Main, Germany.) *In* NASA. Goddard Space Flight Center, Eighth International Workshop on Laser Ranging Instrumentation Jun. 1993 8 p (For primary document see N94-15552 03-19)
Avail: CASI HC A02/MF A06

N94-15576*# Main Astronomical Observatory, Kiev (Ukraine).
ETALON-1,-2 CENTER OF MASS CORRECTION AND ARRAY REFLECTIVITY
N. T. Mironov, A. I. Emetz, A. N. Zaharov (United Space Device Corp., Moscow, Russia.), and V. E. Tchebotarev (United Space Device Corp., Moscow, Russia.) *In* NASA. Goddard Space Flight Center, Eighth International Workshop on Laser Ranging Instrumentation Jun. 1993 24 p (For primary document see N94-15552 03-19)
Avail: CASI HC A03/MF A06

N94-15577*# National Aeronautics and Space Administration. Goddard Space Flight Center, Greenbelt, MD.
TEST RESULTS FROM LAGEOS-2 OPTICAL CHARACTERIZATION USING PULSED LASERS
Thomas K. Varghese (Bendix Field Engineering Corp., Seabrook, MD.), Michael Selden (Bendix Field Engineering Corp., Seabrook, MD.), Thomas Oldham (Bendix Field Engineering Corp., Seabrook, MD.), Christopher Clarke (Bendix Field Engineering Corp., Seabrook, MD.), and Thomas Zagwodzki *In its* Eighth International Workshop on Laser Ranging Instrumentation Jun. 1993 14 p (For primary document see N94-15552 03-19)
Avail: CASI HC A03/MF A06

N94-15579*# Bendix Field Engineering Corp., Seabrook, MD.
HISTORICAL MOBLAS SYSTEM CHARACTERIZATION
Van S. Husson *In* NASA. Goddard Space Flight Center, Eighth International Workshop on Laser Ranging Instrumentation Jun. 1993 23 p (For primary document see N94-15552 03-19)
Avail: CASI HC A03/MF A06

N94-15584*# Czech Technical Univ., Prague. Faculty of Nuclear Science and Physical Engineering.
TWO WAVELENGTH SATELLITE LASER RANGING USING SPAD
Ivan Prochazka, Karel Hamal, Helena Jelinkova, Georg Kirchner (Technische Univ., Graz, Austria.), and F. Koidl (Technische Univ., Graz, Austria.) *In* NASA. Goddard Space Flight Center, Eighth International Workshop on Laser Ranging Instrumentation Jun. 1993 4 p (For primary document see N94-15552 03-19)
Avail: CASI HC A01/MF A06

N94-15586*# National Aeronautics and Space Administration. Goddard Space Flight Center, Greenbelt, MD.
STATE-OF-THE-ART SATELLITE LASER RANGE MODELING FOR GEODETIC AND OCEANOGRAPHIC APPLICATIONS
Steve M. Klosko (Hughes STX, Inc., Lanham, MD.) and David E. Smith *In its* Eighth International Workshop on Laser Ranging Instrumentation Jun. 1993 14 p (For primary document see N94-15552 03-19)
Avail: CASI HC A03/MF A06

N94-15590*# Geodetic Inst., Helsinki (Finland).
COMPENSATION FOR THE DISTORTION IN SATELLITE LASER RANGE PREDICTIONS DUE TO VARYING PULSE TRAVEL TIMES
Matti Paunonen *In* NASA. Goddard Space Flight Center, Eighth International Workshop on Laser Ranging Instrumentation Jun. 1993 4 p (For primary document see N94-15552 03-19)
Avail: CASI HC A01/MF A06

N94-15593*# McDonald Observatory, Austin, TX.
POISSON FILTERING OF LASER RANGING DATA
Randall L. Ricklefs and Peter J. Shelus *In* NASA. Goddard Space Flight Center, Eighth International Workshop on Laser Ranging Instrumentation Jun. 1993 7 p (For primary document see N94-15552 03-19)
Avail: CASI HC A02/MF A06

N94-15599*# McDonald Observatory, Austin, TX.
LUNAR LASER RANGING DATA PROCESSING IN A UNIX/X WINDOWS ENVIRONMENT
Randall L. Ricklefs and Judit G. Ries *In* NASA. Goddard Space Flight Center, Eighth International Workshop on Laser Ranging Instrumentation Jun. 1993 8 p (For primary document see N94-15552 03-19)
Avail: CASI HC A02/MF A06

N94-15603*# Technische Univ., Graz (Austria). Inst. for Space Research.
SUB-cm RANGING AND OTHER IMPROVEMENTS IN GRAZ
Georg Kirchner and Franz Koidl *In* NASA. Goddard Space Flight Center, Eighth International Workshop on Laser Ranging Instrumentation Jun. 1993 6 p (For primary document see N94-15552 03-19)
Avail: CASI HC A02/MF A06

N94-15607*# Naval Research Lab., Washington, DC. Optical Systems Section.
GROUND BASED LASER RANGING FOR SATELLITE LOCATION
G. C. Gilbreath and Harold D. Newby (Phillips Labs., Malabar, FL.) *In* NASA. Goddard Space Flight Center, Eighth International Workshop on Laser Ranging Instrumentation Jun. 1993 6 p (For primary document see N94-15552 03-19)
Avail: CASI HC A02/MF A06

N94-15615*# Aerospatiale, Cannes (France). Optical Dept.
GLRS-R 2-COLOUR RETROREFLECTOR TARGET DESIGN AND PREDICTED PERFORMANCE
Glenn Lund *In* NASA. Goddard Space Flight Center, Eighth International Workshop on Laser Ranging Instrumentation Jun. 1993 16 p (For primary document see N94-15552 03-19)
Avail: CASI HC A03/MF A06

N94-15616*# National Oceanic and Atmospheric Administration, Boulder, CO. Wave Propagation Lab.
EFFECTS OF TURBULENCE ON THE GEODYNAMIC LASER RANGING SYSTEM
James H. Churnside *In* NASA. Goddard Space Flight Center, Eighth International Workshop on Laser Ranging Instrumentation Jun. 1993 16 p (For primary document see N94-15552 03-19)
Avail: CASI HC A03/MF A06

N94-15617*# National Aeronautics and Space Administration. Goddard Space Flight Center, Greenbelt, MD.
DEVELOPMENT OF THE MARS OBSERVER LASER ALTIMETER (MOLA)
Bertrand L. Johnson, Jr et al *In its* Eighth International Workshop on Laser Ranging Instrumentation Jun. 1993 3 p (For primary document see N94-15552 03-19)
Avail: CASI HC A01/MF A06

N94-15619*# Czech Technical Univ., Prague. Faculty of Nuclear Science and Physical Engineering.
MARS LASER ALTIMETER BASED ON A SINGLE PHOTON RANGING TECHNIQUE
Ivan Prochazka, Karel Hamal, B. Sopko, and S. Pershin (Academy of Sciences, USSR, Moscow.) *In* NASA. Goddard Space Flight Center, Eighth International Workshop on Laser Ranging Instrumentation Jun. 1993 4 p (For primary document see N94-15552 03-19)
Avail: CASI HC A01/MF A06

N94-15620*# National Aeronautics and Space Administration. Goddard Space Flight Center, Greenbelt, MD.
MULTI-BEAM LASER ALTIMETER
Jack L. Bufton, David J. Harding, and Luis Ramos-Izquierdo *In its* Eighth International Workshop on Laser Ranging Instrumentation Jun. 1993 9 p (For primary document see N94-15552 03-19)
Avail: CASI HC A02/MF A06

N94-17349*# Rochester Univ., NY. Inst. of Optics.
CURVED GRATING FABRICATION TECHNIQUES FOR CONCENTRIC-CIRCLE GRATING, SURFACE-EMITTING SEMICONDUCTOR LASERS
Rebecca H. Jordan, Oliver King, Gary W. Wicks, Dennis G. Hall, Erik H. Anderson (International Business Machines Corp., Yorktown Heights, NY.), and Michael J. Rooks (Cornell Univ., Ithaca, NY.) *In* NASA. Marshall Space Flight Center, Conference on Binary Optics: An Opportunity for Technical Exchange Aug. 1993 p 223-235 Sponsored by ARO; New York Center for Advanced Optical Technology; and IBM (For primary document see N94-17331 03-74)
(Contract DE-AC03-76SF-00098; NSF ECS-91-12973; NSF ECS-86-19049)
Avail: CASI HC A03/MF A04

N94-17357*# Rockwell International Science Center, Thousand Oaks, CA.
LASER BEAM STEERING DEVICE
M. E. Motamedi, A. P. Andrews, and W. J. Gunning *In* NASA. Marshall Space Flight Center, Conference on Binary Optics: An Opportunity for Technical Exchange Aug. 1993 p 345-358 (For primary document see N94-17331 03-74)
Avail: CASI HC A03/MF A04

37 MECHANICAL ENGINEERING

Includes auxiliary systems (nonpower); machine elements and processes; and mechanical equipment.

N94-14920# Army Cold Regions Research and Engineering Lab., Hanover, NH.
BIBLIOGRAPHY ON SNOW AND ICE FRICTION
Samuel C. Colbeck May 1993 22 p
(DA Proj. 4A7-62784-AT-42)
(AD-A266868; CRREL-SR-93-6) Avail: CASI HC A03/MF A01

This is a bibliography compiled for use by anyone interested in friction on snow or ice surfaces. The items are separated into snow and ice categories because the physical processes and the problems on these two surfaces are somewhat different. There is some repetition between the lists because some references are appropriate for both subjects. The references were selected because they were of direct interest to the subject of friction and not just because knowledge of friction was important in the study. That is, the references selected provide information about friction and do not just use such information. DTIC

N94-14970# Carnegie-Mellon Univ., Pittsburgh, PA. Robotics Inst.
REAL-TIME IMPLEMENTATION OF NEURAL NETWORK LEARNING CONTROL OF A FLEXIBLE SPACE MANIPULATOR
R. T. Newton and Yangsheng Xu Aug. 1992 29 p
(AD-A266962; CMU-RI-TR-92-11) Avail: CASI HC A03/MF A01

This paper discusses a neural network approach to on-line control learning and real-time implementation for a flexible space robot manipulator. We at first overview the system development of the Self-Mobile Space Manipulator (SM2) and discuss the motivations of our research. Then, we propose a neural network to learn control by updating feedforward dynamics based on feedback control input. We address in great detail the implementation issues associated with on-line training strategies and present a simple stochastic training scheme. A new recurrent neural network architecture is proposed, and the performance is greatly improved in comparison to the standard neural network. By using the proposed learning scheme, manipulator trajectory error is reduced by 85 percent. At last, we discussed the implementation of the proposed scheme in teleoperated control. The approach possesses a high degree of generality and adaptability in various applications and will be a valuable method in learning control for robots working in unconstructed environments. DTIC

N94-15263* National Aeronautics and Space Administration. Goddard Space Flight Center, Greenbelt, MD.
ROBOTICS FOR SPACE STATION TAPE 2 (Videotape)
Sep. 1989 Videotape: 16 min. 18 sec. playing time, in color, with sound
(NASA-TM-109578; NONP-VT-93-190376) Avail: CASI VHS A01/BETA A22

This video shows robotics for the Space Station. CASI

N94-15268* National Aeronautics and Space Administration. Goddard Space Flight Center, Greenbelt, MD.
ROBOTICS IN SPACE (Videotape)
Nov. 1988 Videotape: 7 min. 30 sec. playing time, in color, with sound
(NASA-TM-109584; NONP-VT-93-190382) Avail: CASI VHS A01/BETA A22

Produced for the AIAA symposium, this fast paced video shows robotics and telerobotics in the exploration of space. CASI

N94-15272* National Aeronautics and Space Administration. Goddard Space Flight Center, Greenbelt, MD.
ROBOTICS FOR SPACE STATION, TAPE 1 (Videotape)
Aug. 1989 Videotape: 30 min. playing time, in color, with sound
(NASA-TM-109588; NONP-VT-93-190386) Avail: CASI VHS A01/BETA A22

Shot on location at the Goddard Robotics Laboratory, this video uses state of the art Wavefront animation to take the viewer on a tour of the robotics that may, someday, be a part of Space Station Freedom. CASI

N94-15284* National Aeronautics and Space Administration, Washington, DC.
FUTURE OF ROBOTICS (Videotape)

Apr. 1989 Videotape: 2 min. 3 sec. playing time, in color, with sound (NASA-TM-109592; NONP-VT-93-190390) Avail: CASI VHS A01/BETA A22

This videotape describes robotic research such as the EVA retriever and virtual reality. CASI

N94-15347* National Aeronautics and Space Administration, Washington, DC.

UNISTICK VEHICLE CONTROLLER (Videotape)

Oct. 1986 Videotape: 4 min. 6 sec. playing time, in color, with sound (NASA-TM-109618; NONP-VT-93-190416) Avail: CASI VHS A01/BETA A22

A single stick control system, like the lunar rover, is presented as a control to enable disadvantaged individuals to drive with only one hand. CASI

N94-15456* National Aeronautics and Space Administration. Lyndon B. Johnson Space Center, Houston, TX.

EVA RETRIEVER DEMONSTRATION (Videotape)

Apr. 1988 Videotape: 10 min. 30 sec. playing time, in color, with sound (NASA-TM-109510; NONP-VT-93-190307) Avail: CASI VHS A01/BETA A22

The EVA retriever is demonstrated in the Manipulator Development Facility (MDF). The retriever moves on the air bearing table 'searching' for its target, in this case tools 'dropped' by astronauts on orbit. CASI

N94-15459* National Aeronautics and Space Administration. Lyndon B. Johnson Space Center, Houston, TX.

STS-41 VCS TRAINING WITH MISSION SPECIALIST BRUCE MELNICK AND BILL SHEPARD (Videotape)

Sep. 1990 Videotape: 12 min. playing time, in color, with sound (NASA-TM-109513; NONP-VT-93-190310) Avail: CASI VHS A01/BETA A22

Astronaut Bill Shepard is shown using the Voice Command System (VCS) in the Manipulative Development Facility (MDF) under the eye of project engineers and crew trainers. The video shows VCS in action moving cameras around the MDF payload bay mockup. CASI

N94-15707*# National Aeronautics and Space Administration. Lyndon B. Johnson Space Center, Houston, TX.

CONNECTOR SYSTEMS FOR STRUCTURES Patent Application

Christian Lupo, inventor (to NASA), Erik Evenson, inventor (to NASA), and Clarence Wesselski, inventor (to NASA) (Lockheed Engineering and Sciences Co., Houston, TX.) 25 May 1993 19 p

(NASA-Case-MSC-21998-1; NAS 1.71:MSC-21998-1; US-Patent-Appl-SN-066271) Avail: CASI HC A03/MF A01

A releasable coupling device for connecting two members to one another where a collet type fastener has normally retracted latching fingers insertable into a latching recess and a longitudinally movable expander for activating the fastener is described. The longitudinal movement is retained with a paraffin actuated system which can reset. The longitudinal movement of the expander in one direction is through a one way threaded ratchet system which provides an automatic locking action and the expander is movable in either direction by an independently operated threaded action. NASA

N94-15738# Naval Postgraduate School, Monterey, CA.

DETERMINATION OF GTA WELDING EFFICIENCIES M.S. Thesis

Candonino P. Franche Mar. 1993 24 p

(AD-A267163) Avail: CASI HC A03/MF A01

A method is developed for estimating welding efficiencies for moving arc GTAW processes. Under quasi-conditions, the net heat transfer rate from the weld pool to the work piece is estimated from a 3-D numerical heat transfer conduction model. The dimensions of the weld pool used in the computational model are obtained experimentally using a laser vision system and by metallurgical examination. The welding efficiency is then calculated by dividing the net heat transfer rate by the total power input during the experiments. Efficiencies are measured for a range of power inputs and torch speeds and then compared with those available in the literature. DTIC

N94-15817*# National Aeronautics and Space Administration. Lewis Research Center, Cleveland, OH.

EXPLOSIVE BOILING AT VERY LOW HEAT FLUXES: A MICROGRAVITY PHENOMENON

M. M. Hasan, C. S. Lin (Analex Corp., Brook Park, OH.), R. H. Knoll, and M. D. Bentz (Boeing Defense and Space Group, Seattle, WA.) Nov. 1993 9 p Prepared for presentation at the ASME Winter Annual Meeting, New Orleans, LA, 28 Nov. - 3 Dec. 1993; sponsored by ASME (RTOP 506-42-73)

(NASA-TM-106325; E-8078; NAS 1.15:106325) Avail: CASI HC A02/MF A01

The paper presents experimental observations of explosive boiling from a large (relative to bubble sizes) flat heating surface at very low heat fluxes in microgravity. The explosive boiling is characterized as either a rapid growth of vapor mass over the entire heating surface due to the flashing of superheated liquid or a violent boiling spread following the appearance of single bubbles on the heating surface. Pool boiling data with saturated Freon 113 was obtained in the microgravity environment of the space shuttle. The unique features of the experimental results are the sustainability of high liquid superheat for long periods and the occurrence of explosive boiling at low heat fluxes (0.2 to 1.2 kW/sq m). For a heat flux of 1.0 kW/sq m a wall superheat of 17.9 degrees C was attained in ten minutes of heating. This was followed by an explosive boiling accompanied with a pressure spike and a violent bulk liquid motion. However, at this heat flux the vapor blanketing the heating surface could not be sustained. Stable nucleate boiling continued following the explosive boiling. Author (revised)

N94-15871*# National Aeronautics and Space Administration. Goddard Space Flight Center, Greenbelt, MD.

SPLINE SCREW PAYLOAD FASTENING SYSTEM Patent Application

John M. Vranish, inventor (to NASA) 21 Sep. 1992 45 p

(NASA-Case-GSC-13454-1; NAS 1.71:GSC-13454-1; US-Patent-Appl-SN-947612) Avail: CASI HC A03/MF A01

A system for coupling an orbital replacement unit (ORU) to a space station structure via the actions of a robot and/or astronaut is described. This system provides mechanical and electrical connections both between the ORU and the space station structure and between the ORU and the ORU and the robot/astronaut hand tool. Alignment and timing features ensure safe, sure handling and precision coupling. This includes a first female type spline connector selectively located on the space station structure, a male type spline connector positioned on the orbital replacement unit so as to mate with and connect to the first female type spline connector, and a second female type spline connector located on the orbital replacement unit. A compliant drive rod interconnects the second female type spline connector and the male type spline connector. A robotic special end effector is used for mating with and driving the second female type spline connector. Also included are alignment tabs exteriorally located on the orbital replacement unit for berthing with the space station structure. The first and second female type spline connectors each include a threaded bolt member having a captured nut member located thereon which can translate up and down the bolt but are constrained from rotation thereabout, the nut member having a mounting surface with at least one first type electrical connector located on the mounting surface for translating with the nut member. At least one complementary second type electrical connector on the orbital replacement unit mates with at least one first type electrical connector on the mounting surface of the nut member. When the driver on the robotic end effector mates with the second female type spline connector and rotates, the male type spline connector and the first female type spline connector lock together, the driver and the second female type spline connector lock together, and the nut members translate up the threaded bolt members carrying the first type electrical connector up to the complementary second type connector for interconnection therewith. NASA

N94-15873*# National Aeronautics and Space Administration. Goddard Space Flight Center, Greenbelt, MD.

AN IMPROVED PATCH FOR RADIATIVE COOLERS Patent Application

Vincent T. Bly, inventor (to NASA) 25 Jan. 1993 15 p

(NASA-Case-GSC-13503-1; NAS 1.71:GSC-13503-1; US-Patent-Appl-SN-008427) Avail: CASI HC A03/MF A01

A unique structure for constructing the emissive patch of a spaceborne

radiative cooler is shown. The structure has very high emissivity for all angles up to a designed-in maximum angle and near zero emissivity for greater angles. The structure also allows the use of high emissivity, nonconducting paints while fully complying with the NASA Electrostatic Discharge Susceptibility requirements for spacecraft. To accomplish these tasks, two previous disadvantages of prior art methods are addressed; eliminating background thermal radiation sources and problems concerning the high emissivity paints used in association with the black body radiator. A reflector consisting of an array of parabolic concentrators is separated from a black body element by an electrically conductive spacer. The concentrators serve to limit the field of view while the conductive spacer eliminates the need to use a conductive paint on the emissive element.
NASA

N94-15882*# National Aeronautics and Space Administration. Marshall Space Flight Center, Huntsville, AL.
WELDING NOZZLE POSITION MANIPULATOR Patent Application
Jeffrey L. Gilbert, inventor (to NASA) (Rockwell International Corp., Canoga Park, CA.) and David A. Gutow, inventor (to NASA) (Rockwell International Corp., Canoga Park, CA.) 31 Aug. 1993 16 p
(NASA-Case-MFS-29837-1; NAS 1.71:MFS-29837-1;
US-Patent-Appl-SN-114043) Avail: CASI HC A03/MF A01

The present invention is directed to a welding nozzle position manipulator. The manipulator consists of an angle support to which the remaining components of the device are attached either directly or indirectly. A pair of pivotal connections attach a weld nozzle holding link to the angle support and provide a two axis freedom of movement of the holding link with respect to the support angle. The manipulator is actuated by a pair of adjusting screws angularly mounted to the angle support. These screws contact a pair of tapered friction surfaces formed on the upper portion of the welding nozzle holding link. A spring positioned between the upper portions of the support angle and the holding link provides a constant bias engagement between the friction surfaces of the holding link and the adjustment screws, so as to firmly hold the link in position and to eliminate any free play in the adjustment mechanism. The angular relationships between the adjustment screws, the angle support and the tapered friction surfaces of the weld nozzle holding link provide a geometric arrangement which permits precision adjustment of the holding link with respect to the angle support and also provides a solid holding link mount which is resistant to movement from outside forces.
NASA

N94-15925*# National Aeronautics and Space Administration. Lyndon B. Johnson Space Center, Houston, TX.
ATTACHMENT DEVICE Patent Application
Ronald J. Zaguli, inventor (to NASA) 14 Apr. 1993 26 p
(NASA-Case-MSC-21885-1; NAS 1.71:MSC-21885-1;
US-Patent-Appl-SN-048041) Avail: CASI HC A03/MF A01

An apparatus is disclosed for capturing and holding a rod, bar or similar member; the apparatus having in one aspect a body member with a recess 5 therein and a hook extending from the body member, the hook and recess defining a capture envelope for receiving and confining the rod, etc. In one aspect such an apparatus is disclosed in which the hook is movable with respect to the body member to vary the 10 size of the capture envelope, both to initially facilitate emplacement of the apparatus about the rod, etc., and then to provide for tightening of the apparatus about the rod, etc., if desired.
NASA

N94-15949*# National Aeronautics and Space Administration. Marshall Space Flight Center, Huntsville, AL.
PLASMA ARC WELDING WELD IMAGING Patent Application
Daniel J. Rybicki, inventor (to NASA) (Martin Marietta Space Systems, Inc., Huntsville, AL.) and William F. McGee, inventor (to NASA) (Martin Marietta Space Systems, Inc., Huntsville, AL.) 29 Jul. 1993 12 p
(NASA-Case-MFS-28797-1; NAS 1.71:MFS-28797-1;
US-Patent-Appl-SN-098918) Avail: CASI HC A03/MF A01

A welding torch for plasma arc welding apparatus has a transparent shield cup disposed about the constricting nozzle, the cup including a small outwardly extending polished lip. A guide tube extends externally of the torch and has a free end adjacent to the lip. First and second optical fiber bundle assemblies are supported within the guide tube. Light from a strobe light is transmitted along one of the assemblies to the free end and through the lip onto the weld site. A lens is positioned in the guide tube adjacent to the second assembly and focuses images of the weld site onto the end of the fiber bundle of the second assembly and these images are transmitted along the second assembly to a video camera so that the weld site may be viewed continuously for monitoring the welding process.
NASA

N94-15966*# National Aeronautics and Space Administration. Lyndon B. Johnson Space Center, Houston, TX.
MECHANICAL ENERGY ABSORBER Patent Application
Clarence J. Wesselski, inventor (to NASA) (Lockheed Engineering and Sciences Co., Houston, TX.) 29 Jul. 1993 19 p
(NASA-Case-MSC-22111-1; NAS 1.71:MSC-22111-1;
US-Patent-Appl-SN-098911) Avail: CASI HC A03/MF A01

An energy absorbing system for controlling the force where a moving object engages a stationary stop and where the system utilized telescopic tubular members, energy absorbing diaphragm elements, force regulating disc springs, and a return spring to return the telescoping member to its start position after stroking is presented. The energy absorbing system has frusto-conical diaphragm elements frictionally engaging the shaft and are opposed by a force regulating set of disc springs. In principle, this force feedback mechanism serves to keep the stroking load at a reasonable level even if the friction coefficient increases greatly. This force feedback device also serves to desensitize the singular and combined effects of manufacturing tolerances, sliding surface wear, temperature changes, dynamic effects, and lubricity.
NASA

N94-16531 Department of the Navy, Washington, DC.
ELECTRO-RHEOLOGICAL DISK PUMP Patent
Vincent M. Iorio, inventor (to Navy) and Luke W. Loy, inventor (to Navy) 16 Feb. 1993 8 p Filed 23 Dec. 1991
(AD-D015783; US-Patent-5,186,604; US-Patent-Appl-SN-812477;
US-Patent-Class-415-90) Avail: US Patent and Trademark Office

The invention is directed to a device for pumping electro-rheological fluids comprising a casing that defines an inner rotor chamber having a central inlet opening and a peripheral discharge opening. Rotatably disposed within said chamber is a rotor for imparting energy to the pumped electro-rheological fluid comprising of a plurality of non-conducting coaxial substantially parallel spaced disks. On one face of each disk are embedded one or more electrodes and on the opposing face of each disk are attached one or more conductive surfaces. By selectively applying an electric charge to the embedded electrodes, an electric field is produced between the electrodes and the conducting surfaces of adjacent disks. As a result, the viscosity of the electro-rheological fluid exposed to the applied electric field is increased thereby producing electro-rheological fluid vanes between adjacent disks. When the rotor is placed in rotation and a voltage is applied to the embedded electrodes, the electro-rheological fluid that is not exposed to the applied electric field, it is accelerated from the center of the rotor towards the outer periphery by the combined action of the electro-rheological fluid vanes and the friction force acting between the fluid and the rotating disks.
DTIC

N94-16548 Department of the Navy, Washington, DC.
TILT MECHANISM Patent
Kenneth W. Stark, inventor (to Navy) 5 Jan. 1993 9 p Filed 3 Apr. 1991
(AD-D015780; US-Patent-5,177,644; US-Patent-Appl-SN-679904;
US-Patent-Class-359-896) Avail: US Patent and Trademark Office

A tilt mechanism includes a rigid base member, a first tilt plate pivotally mounted on the base member, and a second tilt plate pivotally mounted on the first tilt plate. The first and second tilt plates are pivoted via actuating mechanisms which include stepper motors, harmonic drives, and precision nuts which translate the rotational output of the harmonic drives to pivotal motion of the tilt plates. All of the movable components of the mechanism are mounted to one another via flexural pivots which allow at least limited rotation in one direction but which prevent movement in all other directions.
DTIC

N94-16806# Argonne National Lab., IL. Materials and Components Technology Div.
DYNAMICS, STABILITY, AND CONTROL OF MAGLEV SYSTEMS
Y. Cai, S. S. Chen, D. M. Rote, and H. T. Coffey 1993 7 p Presented at the 12th International Conference on Magnetically Levitated Systems

and Linear Drives, Argonne, IL, 19-21 May 1993
(Contract W-31-109-eng-38)
(DE93-015163; ANL/MCT/CP-79590; CONF-930550-5) Avail: CASI HC A02/MF A01

The dynamic response of maglev systems is important in several respects: Safety and ride quality, guideway design, and system costs. The dynamic response of vehicles is the key element in the determination of ride quality, and vehicle stability is one of the important elements relative to safety. To design a proper guideway that provides acceptable ride quality in the stable region, the vehicle dynamics must be understood. The trade-off between guideway smoothness and the levitation and control systems must be considered if maglev systems are to be economically feasible. This paper is a summary of our previous work on dynamics, stability, and control of maglev systems. First of all, the importance of dynamics of vehicle/guideway of maglev systems is discussed. Emphasis is placed on the modeling vehicle/guideway interactions of maglev systems with a multicar, or multiload vehicle traversing on a single or double-span flexible guideway. Coupled effects of vehicle/guideway interactions in wide range of vehicle speeds with various vehicle and guideway parameters for maglev systems are investigated. Secondly, the alternative control designs of maglev vehicle suspension systems are investigated in this study to achieve safe, stable operation and acceptable ride comfort requires some form of vehicle motion control. Active and semi-active control law designs are introduced into primary and secondary suspensions of maglev vehicles. Finally, this paper discusses the stability of maglev systems based on experimental data, scoping calculations, and simple mathematical models. Divergence and flutter are obtained for coupled vibration of a three-degree-of-freedom maglev vehicle on a guideway consisting of double L-shaped aluminum segments. The theory and analysis developed in this study provides basic stability characteristics and identifies future research needs for maglev systems. DOE

N94-16915 Department of the Navy, Washington, DC.
HIGH PRESSURE PUMP FOR ELECTRO-RHEOLOGICAL FLUIDS Patent
Mark E. Shiffler, inventor (to Navy) and Luke W. Loy, inventor (to Navy) 20 Jul. 1993 4 p Filed 30 Sep. 1992
(AD-D015888; US-Patent-5,226,837; US-Patent-Appl-SN-953338; US-Patent-Class-417-48) Avail: US Patent and Trademark Office

A high-pressure pump for electrorheological fluids in which the pump components operate with relatively large clearances and rely on the electrorheological fluid effect for sealing. Preferably, the electrorheological effect is induced in the fluid only in the region where a seal between relatively merging pump parts is required to generate a fluid pressure increase. DTIC

N94-16944# Naval Postgraduate School, Monterey, CA.
THREE AXIS FORCE OVERRIDE RATE CONTROL OF A PUMA 560 MANIPULATOR M.S. Thesis
Larry P. Ondrey Mar. 1993 126 p
(AD-A267313) Avail: CASI HC A07/MF A02

This paper discusses the implementation of unilateral force override of rate control of a PUMA 560 robot manipulator in three degrees of freedom. A control system is developed utilizing the necessary sensors, hardware, and software interface to enable one to operate the manipulator in rate control with unilateral force control override. A review of the theory behind such a controller is conducted and stability issues addressed. A comparison of experimental results with the theoretical results is conducted and a simple program is developed to simulate the manipulator's response. These simulation results are compared to the experimental data. DTIC

N94-16969# Argonne National Lab., IL.
ELECTRODYNAMIC FORCES OF THE CROSS-CONNECTED FIGURE-EIGHT NULL-FLUX COIL SUSPENSION SYSTEM
J. L. He, D. M. Rote, and H. T. Coffey 1993 8 p Presented at the 12th International Conference on Magnetically Levitated Systems and Linear Drives, Argonne, IL, 19-21 May 1993
(Contract W-31-109-eng-38)
(DE93-015139; ANL/ES/CP-79716; CONF-930550-2) Avail: CASI HC A02/MF A01

This paper analyzes the cross-connected figure-eight null-flux coil suspension system for maglev vehicles on the basis of dynamic circuit theory. The equivalent circuits and general magnetic force expressions for the system are developed. Simple analytical formulas for the magnetic force partitions on the basis of harmonic approximation are presented, and numerical results are also included. DOE

N94-17088*# Jackson State Univ., MS. Dept. of Technology.
END-EFFECTOR: JOINT CONJUGATES FOR ROBOTIC ASSEMBLY OF LARGE TRUSS STRUCTURES IN SPACE: EXTENDED CONCEPTS Final Progress Report, 1 Mar. 1992 - 1 Jun. 1993
W. V. Brewer, E. P. Rasis, and H. R. Shih 1 Jun. 1993 30 p
(Grant NAG1-1125)
(NASA-CR-193576; NAS 1.26:193576) Avail: CASI HC A03/MF A01

Results from NASA/HBCU Grant No. NAG-1-1125 are summarized. Designs developed for model fabrication, exploratory concepts drafted, interface of computer with robot and end-effector, and capability enhancement are discussed. Derived from text

N94-17433 McDonnell-Douglas Aerospace, Long Beach, CA. Transport Aircraft Div.
HIGH TEMPERATURE HYDRAULIC SEALS Final Report, Oct. 1987 - Nov. 1992
K. R. Williams May 1993 154 p Limited Reproducibility: More than 20% of this document may be affected by microfiche quality
(Contract F33615-87-C-2710)
(AD-A268257; MDC-92K0395; WL-TR-93-2036) Avail: Issuing Activity (Defense Technical Information Center (DTIC))

This program investigated and evaluated high temperature hydraulic sealing technology, including seals, fluids, and actuator materials. Test limits for fluid pressure and temperature were 8000 psi and 700 F respectively. The original plan to investigate CTFE fluid at 350 F as well as other fluids at higher temperatures was reduced in scope to include only the higher temperature investigation. Seals were obtained from 11 manufacturers. Design requirements including materials, dimensions, clearances, and tolerances were established and test modules were constructed from the detail designs which were produced. Nine piston seals and one rod seal were tested at temperatures ranging from -65 to +600 F and pressures to 6000 psi. Fluid performance under these conditions was evaluated. Details of this activity and results of the effort are summarized in this report. DTIC

N94-17462 Arnold Engineering Development Center, Arnold AFS, TN.
A MECHANICAL SYSTEM DAMPING MEASUREMENT TECHNIQUE USING A ONE-DEGREE-OF-FREEDOM (1DOF) CYLINDRICAL GAS BEARING Final Report, 13 Feb. - 30 Sep. 1992
C. L. Ratliff and E. J. Marquart Aug. 1993 51 p Limited Reproducibility: More than 20% of this document may be affected by microfiche quality
(AD-A268402; AEDC-TR-93-10) Avail: Issuing Activity (Defense Technical Information Center (DTIC))

An experimental investigation was conducted in the Airflow Calibration Laboratory (ACL) to separate the total rolling moment of rigid and nonrigid mechanical systems into viscous damping and coulomb rolling-moment components. The test technique consisted of measuring roll rate decay of these rigid and nonrigid mechanical systems on a one-degree-of-freedom (1 DOF) cylindrical gas bearing. To better understand the 1 DOF bearing tare damping, a significant amount of information was collected about the operational characteristics of the 1DOF cylindrical gas bearing at certain test conditions. The 1DOF bearing characteristics and test technique are described in this report. The application of the test technique developed for this investigation could be beneficial for determining damping properties of other mechanical systems such as turbomachinery, space structures, gas/ball bearings, and high-damping-capacity materials. The primary measurement uncertainties for the present investigation were determined as follows: +/- 0.01 deg/sec for roll rate obtained with a one-spot tachometer ring, +/- 0.001 in.-lbf for viscous damping moment, or, in terms of energy dissipation, +/- 1 mW. The coulomb rolling-moment uncertainty could not be established because of its variable nature. DTIC

N94-17533# Ohio State Univ., Columbus. Dept. of Mechanical Engineering.
ATOMIC-SCALE FRICTION MEASUREMENTS USING FRICTION FORCE MICROSCOPY. PART 1: GENERAL PRINCIPLES AND NEW MEASUREMENT TECHNIQUES

Ju-Ai Ruan and Bharat Bhushan 11 Feb. 1993 49 p
(Contract N00014-93-1-0067)
(AD-A268391) Avail: CASI HC A03/MF A01

Friction force measurements using modified atomic force microscopy, called here Friction Force Microscopy (FFM), are becoming increasingly important in the understanding of fundamental mechanisms of friction, wear, and lubrication, and to study interfacial phenomenon in micro- and nanostructures used in magnetic storage systems and micro-electromechanical systems (MEMS). A review of existing designs of FFM's and methods of friction force measurements is presented. In terms of friction force measurements, there are important issues related to the basic operation and calibration of these instruments which have not been fully studied. A new method of measuring friction force using a commercial FFM and a calibration procedure for conversion of measured data to normal and friction forces are presented. Atomic-scale friction data of selected materials are presented and discussed in light of macro-friction measurements. DTIC

N94-17566# Ohio State Univ., Columbus. Research Foundation.
CONTINUING RESEARCH ON FRICTION AND WEAR OF MATERIALS Fiscal Year Report, 1 Oct. 1991 - 30 Sep. 1992
D. A. Rigney 30 Jul. 1993 15 p
(Contract N00014-92-J-1608)
(AD-A268291) Avail: CASI HC A03/MF A01

This project was designed to provide new information on the effects of ion implantation on surface (adhesion) and subsurface (deformation) effects during unlubricated sliding of metals. The base materials are copper and iron, and the implanted species are also copper and iron. Thus, in some samples there should only be structural changes caused by implantation (e.g., Fe into Fe, Cu into Cu), while in others there will be composition changes as well (e.g., Cu into Fe, Fe into Cu). Copper and iron were chosen because of the considerable amount of literature available for comparison of results from testing of these metals. Also, their hardness values and deformation behavior are different, the OSU group has experience with both metals, and the phenomenon of selective transfer, extensively studied in the former USSR, usually involves both Cu and Fe. DTIC

N94-17583*# National Aeronautics and Space Administration. Lewis Research Center, Cleveland, OH.
MECHANICAL SYSTEMS TECHNOLOGY BRANCH RESEARCH SUMMARY, 1985 - 1992
Timothy L. Krantz, ed. Sep. 1993 85 p
(DA Proj. 1L1-62211-A-47-A; RTOP 505-62-10)
(NASA-TM-106329; E-6886; NAS 1.15:106329; ARL-TR-237) Avail: CASI HC A05/MF A01

A collection of significant accomplishments from the research of the Mechanical Systems Technology Branch at the NASA Lewis Research Center completed during the years 1985-1992 is included. The publication highlights and accomplishments made in bearing and gearing technology through in-house research, university grants, and industry contracted projects. The publication also includes a complete listing of branch publications for these years. Author (revised)

N94-17675# Oak Ridge National Lab., TN.
SOME SINGLE-PISTON CLOSED-CYCLE MACHINES AND PETER TAILER'S THERMAL LAG ENGINE
C. D. West 1993 8 p Presented at the 28th Intersociety Energy Conversion Engineering Conference, Atlanta, GA, 8-13 Aug. 1993
(Contract DE-AC05-84OR-21400)
(DE93-015983; CONF-930804-8) Avail: CASI HC A02/MF A01

Peter Tailer has devised, built, and operated a beautifully simple engine with a closed working gas cycle, external heating, and only a single piston. The aim of this paper is to cast some light on the possible modes of operation for his machine. The methods developed to analyze certain aspects of Stirling cycle engines, and especially the thermodynamic losses incurred in systems that are neither perfectly isothermal nor perfectly adiabatic, can be applied to Tailer's system. The results identify two idealized cycles fr such machines; relate those cycles to a single piston, ported cylinder machine proposed earlier; and offer a possible explanation for the success of the thermal lag engine. DOE

N94-16003# Krupp (Fried.) G.m.b.H., Essen (Germany).
EXPERT SYSTEM FOR WELDING ENGINEERING
Bernd Fehsenfeld, Robert Relinghaus, and Friedhelm Troesken *In its* Krupp Technical Reports No. 2, English Edition, October 1992 Oct. 1992 p 75-84 (For primary document see N94-16000 03-31)
Copyright Avail: CASI HC A02/MF A01

N94-16004# Krupp (Fried.) G.m.b.H., Essen (Germany).
REMOTE DIAGNOSIS AS USED FOR MECHANIZED PARKING SYSTEMS
Heinz Humberg, Hans Friedrich Maeder, and Frank Will *In its* Krupp Technical Reports No. 2, English Edition, October 1992 Oct. 1992 p 85-96 (For primary document see N94-16000 03-31)
Copyright Avail: CASI HC A03/MF A01

N94-16138*# National Aeronautics and Space Administration. Marshall Space Flight Center, Huntsville, AL.
THE MARSHALL AUTOMATED WELD SYSTEM (MAWS)
Carolyn K. Russell, Kirby G. Lawless, and A. C. Nunes *In* Huntsville Association of Technical Societies, TABES 1993: 9th Annual Technical and Business Exhibition and Symposium 1993 6 p (For primary document see N94-16129 03-38)
(TABES Paper 93-602) Avail: CASI HC A02/MF A03

N94-16139*# National Aeronautics and Space Administration. Marshall Space Flight Center, Huntsville, AL.
PLASMA ARC WELDING REPAIR OF SPACE FLIGHT HARDWARE
David S. Hoffman *In* Huntsville Association of Technical Societies, TABES 1993: 9th Annual Technical and Business Exhibition and Symposium 1993 5 p (For primary document see N94-16129 03-38)
(TABES Paper 93-603) Avail: CASI HC A01/MF A03

N94-16140# Applied Research, Inc., Huntsville, AL.
ADAPTIVE WELD CONTROL FOR HIGH-INTEGRITY WELDING APPLICATIONS
Bradley W. Powell *In* Huntsville Association of Technical Societies, TABES 1993: 9th Annual Technical and Business Exhibition and Symposium 1993 6 p (For primary document see N94-16129 03-38)
(TABES Paper 93-604) Avail: CASI HC A02/MF A03

38 QUALITY ASSURANCE AND RELIABILITY

Includes product sampling procedures and techniques; and quality control.

N94-15013 National Physical Lab., Teddington (England). Div. of Information Technology and Computing.
GEOMETRIC TOLERANCE ASSESSMENT
A. B. Forbes Oct. 1992 26 p Sponsored by Dept. of Trade and Industry, London, England
(NPL-DITC-210/92; ETN-93-94545) Copyright Avail: Issuing Activity (National Physical Lab., Teddington, Middlesex TW11 OLW, England)

Mathematical techniques underlying computer aided inspection methods used for checking whether a manufactured part is within tolerance are addressed. Tolerance assessment is a key step in maintaining and improving quality in manufactured products. Means by which a class of design and tolerance specifications can be formulated in terms of parametrized curves and surfaces and parameter and form constraints are described. The tolerance assessment problem can then be addressed by optimization techniques. It is shown how many important tolerance assessment problems can be formulated as simple matching problems for which efficient solution algorithms can be developed. ESA

N94-15320* National Aeronautics and Space Administration. Marshall Space Flight Center, Huntsville, AL.
IG NUTS AND BOLTS (Videotape)
Jul. 1988 Videotape: 13 min. playing time, in color, with sound
(NASA-TM-109652; NONP-VT-93-190450) Avail: CASI VHS A01/BETA A22

This videotape supports and explains the importance of Quality and Assurance Testing. CASI

N94-15870*# National Aeronautics and Space Administration. Langley Research Center, Hampton, VA.
SYNCHRONOUS SAMPLING PHASE AND AMPLITUDE DETECTION METHOD AND APPARATUS Patent Application
Mark E. Froggatt, inventor (to NASA) 19 Aug. 1993 26 p
(NASA-Case-LAR-14725-1; NAS 1.71:LAR-14725-1;
US-Patent-Appl-SN-110255) Avail: CASI HC A03/MF A01

A synchronous sampling phase and amplitude detection method and apparatus is described. An oscillator generates a signal at a particular frequency and then a frequency dividing circuit divides this signal frequency by a factor of four. This divided signal is transmitted via a transducer through a material and received by the same or another transducer. The received signal is then digitized. The received signal is next sampled at four times its frequency based on a reference signal from the oscillator and then characterized as a phasor. The phase and amplitude of the received signal are then calculated via trigonometric relationship of at least two samples separated by 90 degrees. The remaining samples are employed to reduce the noise equivalent bandwidth. NASA

N94-16055# Sandia National Labs., Albuquerque, NM.
CREATING AND MAINTAINING A VISIONARY QUALITY PROGRAM
K. W. Shirley and A. C. Spencer 1993 6 p Presented at the 2nd International Symposium on Productive and Quality Improvement with a Focus on Government, Washington, DC, 8-10 Sep. 1993
(Contract DE-AC04-76DP-00789)
(DE93-015122; SAND-93-0480C; CONF-9309168-1) Avail: CASI HC A02/MF A01

Developing a business plan that focuses on quality is not enough. It is necessary to use quality principles to affect change and improve your organization's performance. Current management practices at Sandia National Laboratory are presented. DOE

N94-16129# Huntsville Association of Technical Societies, AL.
TABES 1993: 9TH ANNUAL TECHNICAL AND BUSINESS EXHIBITION AND SYMPOSIUM
1993 259 p Symposium held in Huntsville, AL, 11-12 May 1993
Avail: CASI HC A12/MF A03

Papers under the following symposium headings are presented: space, manufacturing, defense, and environment. The papers covered the following topics: total quality management; aerospace industry; aerospace engineering; NASA space programs; engineering management; rocket engines; missiles; defense program; military technology; environmental management; pollution control; air pollution; ozone depletion; spacecraft propulsion; welding; space processing; space commercialization; etc. For individual titles, see N94-16130 through N94-16157.

N94-16130*# National Aeronautics and Space Administration. Marshall Space Flight Center, Huntsville, AL.
IMPACT OF TQM CONCEPTS ON INSPECTION OF AEROSPACE SYSTEMS
Robert W. Neuschaefer *In* Huntsville Association of Technical Societies, TABES 1993: 9th Annual Technical and Business Exhibition and Symposium 1993 4 p (For primary document see N94-16129 03-38)
(TABES Paper 93-350) Avail: CASI HC A01/MF A03

A review of TQM concepts on aerospace systems is presented in a set of viewgraphs. Author

N94-16131*# National Aeronautics and Space Administration, Washington, DC.
APPROACHING THE NEW REALITY
Al V. Diaz *In* Huntsville Association of Technical Societies, TABES 1993: 9th Annual Technical and Business Exhibition and Symposium 1993 7 p (For primary document see N94-16129 03-38)
(TABES Paper 93-230) Avail: CASI HC A02/MF A03

I'm very pleased to be here and to have this opportunity to discuss with you what I view as the current challenges in space science. Today, NASA finds itself at a major crossroads. We are in the process of moving from one era in our existence into another. As we continue to launch important science missions, we are simultaneously changing the way we do business, in a very fundamental way. We are again focusing on more frequent access to space through smaller, less costly missions. We are again focusing on NASA's role as a source of technological advancement within the U.S. economy. And we are returning to the leaner, more flexible approach to managing our projects. In short, NASA has embarked on a new journey, and a challenging journey it will be. Author

N94-16132*# National Aeronautics and Space Administration, Washington, DC.
COMMERCIAL SPACE OPPORTUNITIES ADVANCED CONCEPTS AND TECHNOLOGY OVERVIEW **c85**
Gregory M. Reck *In* Huntsville Association of Technical Societies, TABES 1993: 9th Annual Technical and Business Exhibition and Symposium 1993 7 p (For primary document see N94-16129 03-38)
(TABES Paper 93-240) Avail: CASI HC A02/MF A03

A status report on current and future commercial space opportunities is presented. Author

N94-16133# Alabama Univ., Huntsville.
MATERIALS PROCESSING IN SPACE: ISSUES FOR THE THIRD DECADE **c29**
Robert J. Naumann *In* Huntsville Association of Technical Societies, TABES 1993: 9th Annual Technical and Business Exhibition and Symposium 1993 17 p (For primary document see N94-16129 03-38)
(TABES Paper 93-260) Avail: CASI HC A03/MF A03

The present materials processing in microgravity program is reviewed and some critical issues are identified. Several suggestions are offered that would accelerate this program and strengthen its role in national competitiveness. Author

N94-16134# Boeing Co., Huntsville, AL.
GOVERNMENT/CONTRACTOR DEVELOPMENT TEAMS **c81**
James P. Noblitt *In* Huntsville Association of Technical Societies, TABES 1993: 9th Annual Technical and Business Exhibition and Symposium 1993 5 p (For primary document see N94-16129 03-38)
(TABES Paper 93-460) Avail: CASI HC A01/MF A03

As previous speakers have said, profound changes are occurring in the world and the aerospace marketplace. It seems that everyone in the industry is struggling to adapt to the new environment and to survive. To meet this challenge, new ways of doing business are being adopted. Methods that enable products to be produced better, faster, and cheaper. One of the most powerful techniques is what we call Product Development Teams (PDT's). What others may call Design-Build Teams or Concurrent Engineering. At Boeing, we have found these team approaches to be a highly effective way of increasing quality while simultaneously reducing flow time and cost. We have also found that they have a very positive effect on employee morale. Because of our successes, we are making them the standard way of operating on every program we conduct. Today, I'd like to provide a short overview of how we're using teams at Boeing with special attention to subcontractor and customer involvement. I start by reviewing why change is needed. Author (revised)

N94-16135# Xerox Corp., Webster, NY.
TOTAL QUALITY ENVIRONMENTAL MANAGEMENT LEADERSHIP THROUGH QUALITY
James C. MacKenzie *In* Huntsville Association of Technical Societies, TABES 1993: 9th Annual Technical and Business Exhibition and Symposium 1993 6 p (For primary document see N94-16129 03-38)
(TABES Paper 93-540) Avail: CASI HC A02/MF A03

The following viewgraphs are an overview of Xerox's Leadership through quality programs presented as a logical process to be applied to environmental management. Author

N94-16136# Ecolink, Inc., Atlanta, GA.
ENVIRONMENTAL MANAGEMENT LESSONS TO BE LEARNED FROM THE UPCOMING CFC PHASE OUT OR HOW TO INSURE THAT WE SURVIVE THE NEXT ENVIRONMENTALLY MANDATED PROCESS CHANGE **c45**
Bill Green *In* Huntsville Association of Technical Societies, TABES 1993: 9th Annual Technical and Business Exhibition and Symposium 1993 6 p (For primary document see N94-16129 03-38)
(TABES Paper 93-570) Avail: CASI HC A02/MF A03

Up until a few short months ago, the phase out of ozone-layer-depleting, chlorinated solvents seemed like an event in our far distant future. Then, this past November, at the Copenhagen meeting of the Montreal Protocol

Working Group, the final phase out date for CFC-113 and 1,1,1 trichloroethane was accelerated to 1995. Then DuPont, one of the world's largest producers of CFC-113, announced that they would cease production in 1994. All of a sudden, this issue became a short-term crisis to react to, rather than a long term opportunity for continuous improvement. Now we are trying to react. If we pay attention to the obstacles we encounter along the way, perhaps we can learn from this crisis -- learn how to set ourselves up to avoid this type of environmental crisis management, when the next legislative shoe drops (as it certainly will). For those of us committed to careers in environmental management or corporate industrial management, this knowledge will be invaluable in the years ahead. Author (revised)

N94-16137# Martin Marietta Corp., New Orleans, LA. Manned Space Systems.

ALUMINUM-LITHIUM TECHNOLOGY c26

E. Powers and P. Hartley *In* Huntsville Association of Technical Societies, TABES 1993: 9th Annual Technical and Business Exhibition and Symposium 1993 4 p (For primary document see N94-16129 03-38)

(TABES Paper 93-601) Avail: CASI HC A01/MF A03

Advances in ingot casting technology have enabled aluminum manufacturers to produce commercial quantities of high quality aluminum-lithium material. While still being in the specialty metal price range (greater than $10/lb), the increased strength and modulus, along with decreased density, of aluminum-lithium alloys offer attractive performance and weight savings benefits. Martin Marietta has been involved in the development of aluminum-lithium alloys for use on cryogenic launch vehicles from laboratory to production quantities. Since the inception of the Weldalite family of alloys at the Martin Marietta Laboratories, Martin Marietta has focused developmental activities on the Weldalite alloys. Now, after seven years, Weldalite alloys are available in production quantities. As the marketplace becomes more weight/performance driven, the demand for light weight alternatives to conventional metals is increasing. This paper examines the technological advances made during the Weldalite development that have enabled the alloy to become an attractive alternative to conventional aluminum alloys. Author (revised)

N94-16138*# National Aeronautics and Space Administration. Marshall Space Flight Center, Huntsville, AL.

THE MARSHALL AUTOMATED WELD SYSTEM (MAWS) c37

Carolyn K. Russell, Kirby G. Lawless, and A. C. Nunes *In* Huntsville Association of Technical Societies, TABES 1993: 9th Annual Technical and Business Exhibition and Symposium 1993 6 p (For primary document see N94-16129 03-38)

(TABES Paper 93-602) Avail: CASI HC A02/MF A03

A fully automated welding system, which can operate totally independent of human intervention, is currently unavailable in the welding industry. Development of the Marshall Automated Weld System (MAWS) has been undertaken to fill this void. The system will enable application of statistical process control practices to assure weld quality prior to post weld nondestructive testing. The Variable Polarity Plasma Arc (VPPA) welding process has been baselined for MAWS because it has eliminated process related defects in the welding of the Space Shuttle External Tank. The few remaining weld defects occurring on the tank can be associated with human error. The system integrates multiple sensors (providing real time information on weld bead geometry, weld joint location, wirefeed entry, and inert gas quality) with a weld model (describing weld geometry in relation to critical parameters) and computer controlled VPPA weld equipment. This system is designed to provide real-time, closed-loop control of the weld as it is being made. Author

N94-16139*# National Aeronautics and Space Administration. Marshall Space Flight Center, Huntsville, AL.

PLASMA ARC WELDING REPAIR OF SPACE FLIGHT HARDWARE c37

David S. Hoffman *In* Huntsville Association of Technical Societies, TABES 1993: 9th Annual Technical and Business Exhibition and Symposium 1993 5 p (For primary document see N94-16129 03-38)

(TABES Paper 93-603) Avail: CASI HC A01/MF A03

Repair and refurbishment of flight and test hardware can extend the useful life of very expensive components. A technique to weld repair the main combustion chamber of space shuttle main engines has been developed. The technique uses the plasma arc welding process and active cooling to seal cracks and pinholes in the hot-gas wall of the main combustion chamber liner. The liner hot-gas wall is made of NARloyZ, a copper alloy previously thought to be unweldable using conventional arc welding processes. The process must provide extensive heat input to melt the high conductivity NARloyZ while protecting the delicate structure of the surrounding material. The higher energy density of the plasma arc process provides the necessary heat input while active water cooling protects the surrounding structure. The welding process is precisely controlled using a computerized robotic welding system. Author

N94-16140# Applied Research, Inc., Huntsville, AL.

ADAPTIVE WELD CONTROL FOR HIGH-INTEGRITY WELDING APPLICATIONS c37

Bradley W. Powell *In* Huntsville Association of Technical Societies, TABES 1993: 9th Annual Technical and Business Exhibition and Symposium 1993 6 p (For primary document see N94-16129 03-38)

(TABES Paper 93-604) Avail: CASI HC A02/MF A03

Adaptive, closed-loop weld control is necessary to maintain high-integrity, zero-defect welds. Conventional weld control techniques using weld parameter feedback control loops are sufficient to maintain set points, but fall short when confronted with unexpected variations in part/tooling temperature and mechanical structure, weldment material, arc skew angle, or calibration in weld parameter feedback measurement. Modern technology allows closed-loop control utilizing input from real-time weld monitoring sensors and inspection devices. Weld puddle parameters, bead profile parameters, and weld seam position are fed back into the weld control loop which adapts for the weld condition variations and drives them back to a desired state, thereby preventing weld defects or perturbations. Parameters such as arc position relative to the weld seam, puddle symmetry, arc length, weld width, and bead shape can be extracted from sensor imagery and used in closed-loop active weld control. All weld bead and puddle measurements are available for real-time display and statistical process control analysis, after which the data is archived to permanent storage or later retrieval and analysis. Author

N94-16141*# National Aeronautics and Space Administration. Marshall Space Flight Center, Huntsville, AL.

THERMAL SPRAY FORMING OF REFRACTORY SAMPLE AMPOULE CARTRIDGES FOR SINGLE CRYSTAL GROWTH SPACE FURNACES c76

Frank Zimmerman, Richard Poorman, Richard Holmes, Timothy McKechnie (Rockwell International Corp., Canoga Park, CA.), Phil Krotz (Rockwell International Corp., Canoga Park, CA.), and Yoon Liaw (Rockwell International Corp., Canoga Park, CA.) *In* Huntsville Association of Technical Societies, TABES 1993: 9th Annual Technical and Business Exhibition and Symposium 1993 5 p (For primary document see N94-16129 03-38)

(TABES Paper 93-605) Avail: CASI HC A01/MF A03

A thermal spray process is being used to build up refractory metals and ceramics into a containment cartridge for high temperature, single crystal semiconductor growth experiments. This process uses high energy plasma inside a low pressure (100-200 torr) inert environment to apply layers of material onto a removable mandrel. A variety of materials are being characterized and evaluated against a demanding set of requirements, including high service temperature (1700 C), oxidation resistance, and resistance to liquid metal attack. Techniques to spray form refractory metals (tungsten, molybdenum, niobium, tantalum) and ceramics (alumina, boron nitride) are being developed in the Plasma Spray Cell at Marshall Space Flight Center. These plasma spray formed materials have been evaluated for mechanical properties, density, microstructure, and resistance to liquid metal attack. Forming techniques and the resultant mechanical and metallurgical properties are presented. Author

N94-16142*# National Aeronautics and Space Administration. Marshall Space Flight Center, Huntsville, AL.

MATERIALS, PROCESSES, AND ENVIRONMENTAL ENGINEERING NETWORK c82

Margo M. White *In* Huntsville Association of Technical Societies, TABES 1993: 9th Annual Technical and Business Exhibition and Symposium 1993 5 p (For primary document see N94-16129 03-38)

(TABES Paper 93-610) Avail: CASI HC A01/MF A03

The Materials, Processes, and Environmental Engineering Network (MPEEN) was developed as a central holding facility for materials testing

information generated by the Materials and Processes Laboratory. It contains information from other NASA centers and outside agencies, and also includes the NASA Environmental Information System (NEIS) and Failure Analysis Information System (FAIS) data. Environmental replacement materials information is a newly developed focus of MPEEN. This database is the NASA Environmental Information System, NEIS, which is accessible through MPEEN. Environmental concerns are addressed regarding materials identified by the NASA Operational Environment Team, NOET, to be hazardous to the environment. An environmental replacement technology database is contained within NEIS. Environmental concerns about materials are identified by NOET, and control or replacement strategies are formed. This database also contains the usage and performance characteristics of these hazardous materials. In addition to addressing environmental concerns, MPEEN contains one of the largest materials databases in the world. Over 600 users access this network on a daily basis. There is information available on failure analysis, metals and nonmetals testing, materials properties, standard and commercial parts, foreign alloy cross-reference, Long Duration Exposure Facility (LDEF) data, and Materials and Processes Selection List data.

Author (revised)

N94-16143*# National Aeronautics and Space Administration. Marshall Space Flight Center, Huntsville, AL.

NASA OPERATIONAL ENVIRONMENT TEAM (NOET): NASA'S KEY TO ENVIRONMENTAL TECHNOLOGY **c45**

Beth Cook *In* Huntsville Association of Technical Societies, TABES 1993: 9th Annual Technical and Business Exhibition and Symposium 1993 4 p (For primary document see N94-16129 03-38)

(TABES Paper 93-611) Avail: CASI HC A01/MF A03

NASA has stepped forward to face the environmental challenge to eliminate the use of Ozone-Layer Depleting Substances (OLDS) and to reduce our Hazardous Air Pollutants (HAP) by 50 percent in 1995. These requirements have been issued by the Clean Air Act, the Montreal Protocol, and various other legislative acts. A proactive group, the NASA Operational Environment Team or NOET, received its charter in April 1992 and was tasked with providing a network through which replacement activities and development experiences can be shared. This is a NASA-wide team which supports the research and development community by sharing information both in person and via a computerized network, assisting in specification and standard revisions, developing cleaner propulsion systems, and exploring environmentally-compliant alternatives to current processes. Author

N94-16144*# National Aeronautics and Space Administration. Marshall Space Flight Center, Huntsville, AL.

EMERGING TECHNOLOGIES FOR THE CHANGING GLOBAL MARKET **c23**

Wendy Cruit, Scott Schutzenhofer, Ben Goldberg, and Kurt Everhart (Sverdrup Technology, Inc., Huntsville, AL.) *In* Huntsville Association of Technical Societies, TABES 1993: 9th Annual Technical and Business Exhibition and Symposium 1993 11 p (For primary document see N94-16129 03-38)

(TABES Paper 93-612) Avail: CASI HC A03/MF A03

This project served to define an appropriate methodology for effective prioritization of technology efforts required to develop replacement technologies mandated by imposed and forecast legislation. The methodology used is a semi-quantative approach derived from quality function deployment techniques (QFD Matrix). This methodology aims to weight the full environmental, cost, safety, reliability, and programmatic implications of replacement technology development to allow appropriate identification of viable candidates and programmatic alternatives. The results will be implemented as a guideline for consideration for current NASA propulsion systems. Author

N94-16145*# National Aeronautics and Space Administration. Marshall Space Flight Center, Huntsville, AL.

LIQUID HYDROGEN AND LIQUID OXYGEN FEEDLINE PASSIVE RECIRCULATION ANALYSIS **c34**

Kimberly Ann Holt, Nicole L. Cleary, Andrew J. Nichols, and Gretchen L. E. Perry *In* Huntsville Association of Technical Societies, TABES 1993: 9th Annual Technical and Business Exhibition and Symposium 1993 5 p (For primary document see N94-16129 03-38)

(TABES Paper 93-620) Avail: CASI HC A01/MF A03

The primary goal of the National Launch System (NLS) program was to design an operationally efficient, highly reliable vehicle with minimal recurring launch costs. To achieve this goal, trade studies of key main propulsion subsystems were performed to specify vehicle design requirements. These requirements include the use of passive recirculation to thermally condition the liquid hydrogen (LH2) and liquid oxygen (LO2) propellant feed systems and Space Transportation Main Engine (STME) fuel pumps. Rockwell International (RI) proposed a joint independent research and development (JIRAD) program with Marshall Space Flight Center (MSFC) to study the LH2 feed system passive recirculation concept. The testing was started in July 1992 and completed in November 1992. Vertical and sloped feedline designs were used. An engine simulator was attached at the bottom of the feedline. This simulator had strip heaters that were set to equal the corresponding heat input from different engines. A computer program is currently being used to analyze the passive recirculation concept in the LH2 vertical feedline tests. Four tests, where the heater setting is the independent variable, were chosen. While the JIRAD with RI was underway, General Dynamics Space Systems (GDSS) proposed a JIRAD with MSFC to explore passive recirculation in the LO2 feed system. Liquid nitrogen (LN2) is being used instead of LO2 for safety and economic concerns. To date, three sets of calibration tests have been completed on the sloped LN2 test article. The environmental heat was calculated from the calibration tests in which the strip heaters were turned off. During the LH2 testing, the environmental heat was assumed to be constant. Therefore, the total heat was equal to the environmental heat flux plus the heater input. However, the first two sets of LN2 calibration tests have shown that the environmental heat flux varies with heater input. A Systems Improved Numerical Differencing Analyzer and Fluid Integrator (SINDA/FLUINT) model is currently being built to determine if this variation in environmental heat is due to a change in the wall temperature. During the third set of calibration tests, a faulty reference junction was found. Based on this anomaly with the reference junction, the heat flux calculations from the first two calibration sets are now considered questionable.

Author (revised)

N94-16146*# National Aeronautics and Space Administration. Marshall Space Flight Center, Huntsville, AL.

LIQUID OXYGEN (LO2) PROPELLANT CONDITIONING CONCEPT TESTING **c28**

Gretchen L. E. Perry, Michael S. Orth (General Dynamics Corp., Huntsville, AL.), and Gopal K. Mehta (General Dynamics Corp., Huntsville, AL.) *In* Huntsville Association of Technical Societies, TABES 1993: 9th Annual Technical and Business Exhibition and Symposium 1993 6 p (For primary document see N94-16129 03-38)

(TABES Paper 93-621) Avail: CASI HC A02/MF A03

Marshall Space Flight Center (MSFC) and industry contractors have undertaken activities to develop a simplified liquid oxygen (LO2) propellant conditioning concept for future expendable launch vehicles. The objective of these activities is to reduce operations costs and timelines and to improve safety of these vehicles. The approach followed has been to identify novel concepts through system level studies and demonstrate the feasibility of these concepts through small-scale and full-scale testing. Testing will also provide data for design guidelines and validation of analytical models. Four different concepts are being investigated: no-bleed, low-bleed, use of a recirculation line, and helium (He) bubbling. This investigation is being done under a Joint Institutional Research and Development (JIRAD) program currently in effect between MSFC and General Dynamics Space Systems (GDSS). A full-scale test article, which is a facsimile of a propellant feed duct with an attached section to simulate heat input from a LO2 turbopump, will be tested at the Cold Flow Facility at MSFC's West Test Area. Liquid nitrogen (LN2), which has similar properties to LO2, will be used in place of LO2 for safety and budget reasons. Work to date includes design and fabrication of the test article, design of the test facility and initial fabrication, development of a test matrix and test procedures, initial predictions of test output, and heat leak calibration and heat exchanger tests on the test article. The tests for all propellant conditioning concepts will be conducted in the summer of 1993, with the final report completed by October, 1993. Author (revised)

N94-16147# Paramax Systems Corp., Huntsville, AL.

APPLYING PAPERLESS TECHNOLOGY TO ACHIEVE EXCELLENCE IN MANUFACTURING OPERATIONS **c81**

Michael Denson and Craig Lykins *In* Huntsville Association of Technical

Societies, TABES 1993: 9th Annual Technical and Business Exhibition and Symposium 1993 6 p (For primary document see N94-16129 03-38)
(TABES Paper 93-630) Avail: CASI HC A02/MF A03

For manufacturing operations to be competitive in a global market they must integrate new technologies carefully. In the 1980's leading manufacturers spent millions of dollars implementing Paperless Manufacturing Systems. Today, low cost/high performance personal computers, very user friendly software applications, and reliable local area networks make Paperless Manufacturing Systems affordable for the smallest of operations. Widespread use of paperless manufacturing technology will be a driving force in helping U.S. manufacturers compete in the 1990's. Author

N94-16148# General Dynamics Corp., Huntsville, AL. Space Systems Div.
THE CLOSING WINDOW OF OPPORTUNITY: ADDRESSING THE US SPACE LAUNCH VEHICLE CRISIS **c15**
Todd Mosher *In* Huntsville Association of Technical Societies, TABES 1993: 9th Annual Technical and Business Exhibition and Symposium 1993 9 p (For primary document see N94-16129 03-38)
(TABES Paper 93-640) Avail: CASI HC A02/MF A03

The United States must decide if it wishes to continue as a leader or assume a lesser role in yet another high technology market. This market is for commercial space launch services and the window of opportunity to remain competitive is quickly eroding. It is clear that the current US space fleet can not meet the schedule demands, operability characteristics or reduced cost requirements to compete with the foreign competition and to meet future launch needs. Almost every recent blue ribbon panel or study has recommended a new launch vehicle development. Yet the US government has failed to embark on a new launch system program. This lack of action is already threatening to put the United States even further behind unless a new program is initiated immediately. The latest incarnation of this idea, the 'Spaceliftер', is a concept that must be embraced and accelerated if the United States is to meet the market challenge. Waiting for 'leap frog' solutions will not allow the commercial industry to survive until its arrival. To ensure that this new space launch system meets its goals and requirements new approaches must be used. These include rapid prototyping of hardware, operational demonstrations to prove the hardware's characteristics and a new industry/government relationship that ensures the maximum efficiency in this austere environment. The United States must take action to remain competitive in the space launch system business or accept a relegated market position. Author

N94-16149# Martin Marietta Corp., New Orleans, LA. Manned Space Systems.
SPACE PROPULSION SYNERGY GROUP ETO TECHNOLOGY ASSESSMENTS **c20**
James Bray *In* Huntsville Association of Technical Societies, TABES 1993: 9th Annual Technical and Business Exhibition and Symposium 1993 9 p (For primary document see N94-16129 03-38)
(TABES Paper 93-641) Avail: CASI HC A02/MF A03

There exists within the aerospace community a widely recognized need to improve future space launch systems. While these needs have been expressed by many national committees, potential solutions have not achieved consensus nor have they endured. Facing the challenge to remain competitive with limited national resources, the U.S. must improve its strategic planning efforts. A nationally accepted strategic plan for space would enable a focused research & development program. The Space Propulsion Synergy Group (SPSG), chartered to support long range strategic planning, has achieved several breakthroughs. First, using a broad industry/government team, the SPSG evaluated and achieved consensus on the vehicles, propulsion systems, and propulsion technologies that have the best long term potential for achieving desired system attributes. The breakthrough that enabled broad consensus was developing criteria that are measurable a-priori. Second, realizing that systems having the best long term payoffs can loose support when constraints are tight, the SPSG invented a dual prioritization approach that balances long term strategic thrusts with current programmatic constraints. This breakthrough enables individual program managers to make decisions based on both individual project needs and long term strategic needs. Results indicate that a SSTO using an integrated modular engine has the best long term potential for a 20 Klb class vehicle and that health monitoring and control technologies rank among the highest dual priority liquid rocket technologies. Author

N94-16150*# McDonnell-Douglas Corp., Huntsville, AL. Spacelab Design Engineering.
THE SPACELAB IPS STAR SIMULATOR **c14**
Francis C. Wessling, III *In* Huntsville Association of Technical Societies, TABES 1993: 9th Annual Technical and Business Exhibition and Symposium 1993 4 p (For primary document see N94-16129 03-38)
(Contract NAS8-39400)
(TABES Paper 93-650) Avail: CASI HC A01/MF A03

The cost of doing business in space is very high. If errors occur while in orbit the costs grow and desired scientific data may be corrupted or even lost. The Spacelab Instrument Pointing System (IPS) Star Simulator is a unique test bed that allows star trackers to interface with simulated stars in a laboratory before going into orbit. This hardware-in-the loop testing of equipment on earth increases the probability of success while in space. The IPS Star Simulator provides three fields of view 2.55 x 2.55 degrees each for input into star trackers. The fields of view are produced on three separate monitors. Each monitor has 4096 x 4096 addressable points and can display 50 stars (pixels) maximum at a given time. The pixel refresh rate is 1000 Hz. The spectral output is approximately 550 nm. The available relative visual magnitude range is 2 to 8 visual magnitudes. The star size is less than 100 arc seconds. The minimum star movement is less than 5 arc seconds and the relative position accuracy is approximately 40 arc seconds. The purpose of this paper is to describe the LPS Star Simulator design and to provide an operational scenario so others may gain from the approach and possible use of the system. Author

N94-16151*# National Aeronautics and Space Administration. Marshall Space Flight Center, Huntsville, AL.
COST-EFFECTIVE TEST METHODS FOR SHUTTLE PAYLOADS **c16**
Michael L. Tinker *In* Huntsville Association of Technical Societies, TABES 1993: 9th Annual Technical and Business Exhibition and Symposium 1993 6 p (For primary document see N94-16129 03-38)
(TABES Paper 93-651) Avail: CASI HC A02/MF A03

Techniques are discussed for deriving constrained vibration mode shapes for space shuttle payloads using unconstrained or free-boundary dynamic properties. Application of the residual flexibility method requires measurement of a set of free boundary modes plus the residual flexibility of the payload-to-orbiter interfaces. The mass-additive approach involves the measurement of unconstrained modes and frequencies of a payload with large masses attached to the interfaces. In either case, the orbiter interfaces of the test-verified payload model are analytically constrained to provide the mode shapes for the shuttle-constrained configuration. Use of these methods or a hybrid combination of them for structures to which they are applicable allows the difficulty and expense associated with development and verification of fixed-base test fixtures to be avoided. Author

N94-16152# McDonnell-Douglas Corp., Huntsville, AL. Manned Space System.
GROUND INTEGRATED ET-DERIVED SPACE PLATFORMS FOR ONORBIT APPLICATIONS **c18**
A. R. Pagano, Jr. and E. M. Enright *In* Huntsville Association of Technical Societies, TABES 1993: 9th Annual Technical and Business Exhibition and Symposium 1993 11 p (For primary document see N94-16129 03-38)
(TABES Paper 93-652) Avail: CASI HC A03/MF A03

This paper discusses a departure from the standard approach for deployment and outfitting of a Space Shuttle External Tank (ET) for on-orbit applications. Since the beginning of the development of the ET for the Space Transportation System (STS) project, a multitude of concepts have been proposed for using the ET as a space platform. The design studies are based on three major assumptions: free delivery of the ET to Low Earth Orbit (LEO), availability of the shuttle for outfitting, and extensive use of Extravehicular Activity (EVA) and telerobotics to accomplish the outfitting. However, the design studies have all encountered the following three obstacles: limited availability and timeliness of STS flights, the high cost of EVA, and reduced funding in telerobotic development. The development and use of the ETs for complex space platforms becomes even more imperative with today's space programs facing funding reduction

and/or implementation delays, cancellation, and the possible elimination or reduction in the number of STS flights in favor of various cargo vehicles and the Personnel Launch System (PLS). With these considerations and the assembly problems that influenced all the design studies, a different approach must be found to enable a more near-term realization of using the ET for on-orbit applications. That approach is not to be found in any innovative deployment and outfitting scenarios but in a return to the lessons learned from the Skylab project. An orbiting space lab/platform would be constructed from various modified ET components. The lab could vary in size depending upon how many LH2 tank barrel sections are used. The basic ET structure and tooling would be utilized to assemble a platform based on the customer's requirements. In addition, the equipment and systems for a space lab would be outfitted and tested on the ground before the platform is launched. This method follows the installation and testing procedures currently being used in the commercial satellite industry. The completed space lab/platform would be mated to a launch vehicle and delivered to orbit. Upon insertion into orbit, the lab's solar arrays, radiators, and antennas would be deployed and become fully operational. Without specifying any one particular mission, this paper examines how the modular ET-derived space platforms can offer a number of different configurations for individual users such as commercial enterprises, Government sponsored scientific research, and DoD. Author

N94-16153*# National Aeronautics and Space Administration. Marshall Space Flight Center, Huntsville, AL.

MODELING AND SIMULATION: A KEY TO FUTURE DEFENSE TECHNOLOGY **c61**

Anthony B. Muccio *In* Huntsville Association of Technical Societies, TABES 1993: 9th Annual Technical and Business Exhibition and Symposium 1993 5 p (For primary document see N94-16129 03-38)

(TABES Paper 93-654) Avail: CASI HC A01/MF A03

The purpose of this paper is to express the rationale for continued technological and scientific development of the modeling and simulation process for the defense industry. The defense industry, along with a variety of other industries, is currently being forced into making sacrifices in response to the current economic hardships. These sacrifices, which may not compromise the safety of our nation, nor jeopardize our current standing as the world peace officer, must be concentrated in areas which will withstand the needs of the changing world. Therefore, the need for cost effective alternatives of defense issues must be examined. This paper provides support that the modeling and simulation process is an economically feasible process which will ensure our nation's safety as well as provide and keep up with the future technological developments and demands required by the defense industry. The outline of this paper is as follows: introduction, which defines and describes the modeling and simulation process; discussion, which details the purpose and benefits of modeling and simulation and provides specific examples of how the process has been successful; and conclusion, which summarizes the specifics of modeling and simulation of defense issues and lends the support for its continued use in the defense arena. Author

N94-16154# Alabama Univ., Huntsville. Dept. of Civil and Environmental Engineering.

AN ANALYSIS OF THE DYNAMIC RESPONSE OF THE SPACE STATION FREEDOM DUE TO A MODULE PERFORATION BY AN ORBITAL DEBRIS PARTICLE IMPACT **c18**

William P. Schonberg and John P. Celestian *In* Huntsville Association of Technical Societies, TABES 1993: 9th Annual Technical and Business Exhibition and Symposium 1993 6 p (For primary document see N94-16129 03-38)

(TABES Paper 93-653) Avail: CASI HC A02/MF A03

The perforation of a habitable module that is part of an extended lifetime space structure in earth orbit by a orbital debris particle will result in a thrust normal to the module surface. The thrust is due to the air exhausting through the hole in the module wall created by the hypervelocity debris particle impact. This paper addresses the global dynamic response of the Space Station Freedom following such a module perforation. By varying the size of the hole through which the module air is allowed to escape, an in-depth study of the dynamic response of the Space Station Freedom to a perforating orbital debris particle impact is performed. Author

N94-16155# Army Missile Research, Development and Engineering Lab., Redstone Arsenal, AL. Weapons Sciences Directorate.

REAL-TIME ADAPTIVE NEURAL NETWORK DATA PROCESSING **c63**

S. D. Pethel, C. M. Bowden, and C. C. Sung (Alabama Univ., Huntsville.) *In* Huntsville Association of Technical Societies, TABES 1993: 9th Annual Technical and Business Exhibition and Symposium 1993 7 p (For primary document see N94-16129 03-38)

(TABES Paper 93-660) Avail: CASI HC A02/MF A03

We introduce a new training algorithm, based on a generalized matrix inverse procedure, for obtaining high-accuracy solutions of multilayer, forward-feed, neural networks for the modeling of low-dimensional chaotic systems. Our new training algorithm produces high accuracy solutions in seconds--far faster than conventional methods based on steepest descents. Application of our method is made to chaotic time series data generated from standard models to demonstrate global characterization of chaotic attractors and data window extension of stationary time series. Author

N94-16156# Dynetics, Inc., Huntsville, AL. Electro-Optics Dept.

WIDEBAND ACOUSTO-OPTIC CORRELATOR FOR AN ESM RECEIVER UPGRADE **c74**

C. Anderson, A. Dorsett, S. Tepper, M. Zari, A. Filipov (Army Research Lab., Adelphi, MD.), E. Adler (Army Research Lab., Adelphi, MD.), and J. Pellegrino (Army Research Lab., Adelphi, MD.) *In* Huntsville Association of Technical Societies, TABES 1993: 9th Annual Technical and Business Exhibition and Symposium 1993 6 p (For primary document see N94-16129 03-38)

(TABES Paper 93-661) Avail: CASI HC A02/MF A03

An acousto-optic (AO) correlator is being constructed that offers a small, lightweight solution to detecting and analyzing wide-bandwidth, spread-spectrum signals. The processor is being inserted into an existing electronic support measure (ESM) test-bed under the Defense Advanced Research Projects Agency (DARPA) Transition of Optical Processors into Systems (TOPS) program. The correlator has a processing bandwidth of 500 MHz and will be used to detect direct-sequence, phase-modulated signals, frequency-hopped signals, chirps, and impulses. A description of the processor is provided along with experimental results obtained from an interim developmental breadboard. Subsequent digital processing, which includes nonlinear detection and Fourier transformation, is used to determine center frequencies, bandwidths, and band shape. Theoretical descriptions of the post-processing are provided. Author (revised)

N94-16157# Army Missile Command, Redstone Arsenal, AL.

WIND TUNNEL INVESTIGATION WITH AN OPERATIONAL TURBOJET ENGINE **c07**

Lamar M. Auman *In* Huntsville Association of Technical Societies, TABES 1993: 9th Annual Technical and Business Exhibition and Symposium 1993 6 p (For primary document see N94-16129 03-38)

(TABES Paper 93-662) Avail: CASI HC A02/MF A03

A wind tunnel test of a turbojet powered missile with the engine installed and operating was conducted in Calspan's Transonic Wind Tunnel in Buffalo, New York from 20 May to 3 June 1991. The primary model configuration consisted of a bifurcated inlet and exhaust which was sting mounted. Instrumentation consisted of a six-component main balance, four fin balances, 39 thermocouples, 10 heat flow gages and several base pressure ports. The purpose of this test was to investigate stability and control, installed engine performance at flight conditions, and plume interactions or aft heating problems. The investigation obtained data at Mach numbers from 0.05 to 0.80, with the majority of the data collected at Mach 0.33, 0.50 and 0.60. Angle of attack was swept from -16 deg to +16 deg, with engine throttle setting, fin deflection angle and Mach number held constant. Missile stability data indicates that the operational mid-body turbojet engine has no adverse effect on missile stability or control authority. Aftbody thermal data indicates that the worst case occurs during a low Mach number (static) high engine throttle setting condition.

Author (revised)

N94-16518*# General Electric Co., Cincinnati, OH. Aircraft Engines.

THERMAL STRESS EFFECTS IN INTERMETALLIC MATRIX COMPOSITES Final Report

P. K. Wright, M. D. Sensmeier, D. S. Kupperman (Argonne National Lab., IL.), and H. N. G. Wadley (Virginia Univ., Charlottesville.) Sep. 1993 166 p

(Contract NAS3-25790; RTOP 510-01-50)
(NASA-CR-191191; E-8127; NAS 1.26:191191) Avail: CASI HC A08/MF A02

Intermetallic matrix composites develop residual stresses from the large thermal expansion mismatch (delta-alpha) between the fibers and matrix. This work was undertaken to: establish improved techniques to measure these thermal stresses in IMC's; determine residual stresses in a variety of IMC systems by experiments and modeling; and, determine the effect of residual stresses on selected mechanical properties of an IMC. X ray diffraction (XRD), neutron diffraction (ND), synchrotron XRD (SXRD), and ultrasonics (US) techniques for measuring thermal stresses in IMC were examined and ND was selected as the most promising technique. ND was demonstrated on a variety of IMC systems encompassing Ti- and Ni-base matrices, SiC, W, and Al2O3 fibers, and different fiber fractions (Vf). Experimental results on these systems agreed with predictions of a concentric cylinder model. In SiC/Ti-base systems, little yielding was found and stresses were controlled primarily by delta-alpha and Vf. In Ni-base matrix systems, yield strength of the matrix and Vf controlled stress levels. The longitudinal residual stresses in SCS-6/Ti-24Al-llNb composite were modified by thermomechanical processing. Increasing residual stress decreased ultimate tensile strength in agreement with model predictions. Fiber pushout strength showed an unexpected inverse correlation with residual stress. In-plane shear yield strength showed no dependence on residual stress. Higher levels of residual tension led to higher fatigue crack growth rates, as suggested by matrix mean stress effects.

Author (revised)

N94-17044 Air Force Inst. of Tech., Wright-Patterson AFB, OH.
A FUZZY METHOD FOR PRELIMINARY DESIGN RANDOM ACCESS MEMORY FAILURE RATE PREDICTION M.S. Thesis
Keith R. Weyenberg 1992 85 p Limited Reproducibility: More than 20% of this document may be affected by microfiche quality
(AD-A267948; AFIT/CI/CIA-93-014) Avail: Issuing Activity (Defense Technical Information Center (DTIC))

Preliminary design failure rate predictions tend to be rough approximations due to a lack of sufficient information about components, materials, requirements, etc. Often, experienced engineers can give a qualitative assessment of the possible failure rate of a given design, but have a difficult time quantifying that assessment without the aid of historical data, mathematical equations, or computers. It would be much easier if the experienced engineers judgement or verbal, qualitative evaluations could be converted to quantitative estimates? Fuzzy-set theory provides a method to convert qualitative or subjective evaluations into quantitative ones. This work looks at how fuzzy-set theory can be used to convert qualitative evaluations of factors affecting failure rates into quantitative estimates of failure rates. By using fuzzy estimates of the environment and design effects on failure rate, data is generated by the fuzzy failure rate prediction method.

DTIC

N94-17082*# Houston Univ., TX.
SIMULATION REDUCTION USING THE TAGUCHI METHOD
Farrokh Mistree, Ume Lautenschlager, Stein Owe Erikstad, and Janet K. Allen Oct. 1993 159 p
(Grant NAG9-616)
(NASA-CR-4542; S-734; NAS 1.26:4542) Avail: CASI HC A08/MF A02

A large amount of engineering effort is consumed in conducting experiments to obtain information needed for making design decisions. Efficiency in generating such information is the key to meeting market windows, keeping development and manufacturing costs low, and having high-quality products. The principal focus of this project is to develop and implement applications of Taguchi's quality engineering techniques. In particular, we show how these techniques are applied to reduce the number of experiments for trajectory simulation of the LifeSat space vehicle. Orthogonal arrays are used to study many parameters simultaneously with a minimum of time and resources. Taguchi's signal to noise ratio is being employed to measure quality. A compromise Decision Support Problem and Robust Design are applied to demonstrate how quality is designed into a product in the early stages of designing.

Author

N94-17194# Harris Corp., Melbourne, FL. Government Aerospace Systems Div.
RELIABILITY ANALYSIS OF SURFACE MOUNT TECHNOLOGY (SMT) Final Report, Feb. 1989 - Apr. 1991
Chris A. Myers, Kalyan K. Chakrabarti, Donald H. Merlino, Edward G. Palmer, and Edward F. Pello Mar. 1993 292 p
(Contract F30602-89-C-0057)
(AD-A267598; RL-TR-93-6) Avail: CASI HC A13/MF A03

This report indoctrinates the reader with the understanding of what is involved and necessary in designing and assessing the reliability of surface mount products. Deterministic methods were used to identify the primary design and environmental drivers and statistical methods were used to generate a SMT reliability assessment model. Due to the unavailability of field failure data, finite element analyses (FEA) and environmental test data were used to quantify the model parameters. Information obtained during the model development, internal Harris documents, and military and commercial standards were used to generate design, manufacturing, and quality guidelines. Finally, reliability testing and its correlation to actual life expectancy is addressed to decide the appropriateness of the existing MIL-STD testing requirements and whether these documents need to be modified to correlate to actual life conditions more accurately.

DTIC

N94-17514 Florida Atlantic Univ., Boca Raton. Center for Applied Stochastics Research.
ON PREDICTING THE PERSON-IN-WATER DRIFT FOR SEARCH AND RESCUE Final Report, 15 Nov. 1990 - 31 Mar. 1993
Tsung-Chow Su 1993 83 p Limited Reproducibility: More than 20% of this document may be affected by microfiche quality
(Contract N00014-91-J-1420)
(AD-A268083) Avail: Issuing Activity (Defense Technical Information Center (DTIC))

Search and rescue of people in distress on the high seas requires the capability to accurately predict the position of the survivors. The current approaches on drift prediction are based on an empirical correlation between wind speed and person motion from limited field data. Currently, there is no drift data available for a person wearing a survival suit. Consequently, there is not sufficient data for accurate prediction and this complicates the search and rescue operation. A study is being undertaken at Florida Atlantic University in which the essential effects of environmental forces and person-in-water characteristics will be calculated. The study is intended to provide a theoretical framework for a better understanding of the dynamics of drift and will thus lead to a reliable model of drift prediction and improved efficiency in search and rescue mission. The study consists of the following components: the development of a mathematical model for the drift prediction problem, laboratory studies of drift forces, and field experiments to calibrate the mathematical models and to verify the model prediction.

DTIC

N94-17515 Boeing Defense and Space Group, Seattle, WA.
X RAY COMPUTED TOMOGRAPHY FOR FAILURE ANALYSIS INVESTIGATIONS Interim Report, Sep. 1991 - Apr. 1993
Richard H. Bossi and William Shepherd May 1993 40 p Limited Reproducibility: More than 20% of this document may be affected by poor print and microfiche quality
(Contract F33615-88-C-5404)
(AD-A268086; WL-TR-93-4047) Avail: Issuing Activity (Defense Technical Information Center (DTIC))

Failure analysis is an important engineering evaluation in any product development cycle; it is essential to product reliability and evolution. The volumetric feature detection and three-dimensional positioning capability of X-ray computed tomography are valuable and cost saving assets to a failure analysis laboratory. Savings are realized in reduced risk, determination of proper direction for irreversible failure analysis activities, and schedule improvement. Failure analysis laboratories of sufficient size can justify the cost saving benefits of using CT for equipment procurement. Case studies of failure analyses have been demonstrated to the Air Force and industry showing the ability of CT to significantly benefit such studies. In some cases, CT can directly resolve the problem, and in other cases, CT provides key supplemental information for guiding further investigations and reducing the risk of incorrect or incomplete analysis. Examples have included mechanical and electrical system assembly, system internal measurements and fitups, and material damage evaluation. CT also can be applied to

systems to observe the internal positions as a function of test conditions. High resolution (greater than 4 lp/mm) CT with combined radioscopy (real-time radiography) capability is advocated for failure analysis facilities. DTIC

N94-17542# Technical Research Centre of Finland, Espoo. Forest Products Lab.
AUTOMATED IMAGE ANALYSIS METHOD FOR THE DETECTION OF CRACKS ON WOOD SURFACE [PINNAN HALKEILUN AUTOMAATTINEN ANALYYSIMENETELMAE]
Timo Lappalainen Jan. 1992 97 p In FINNISH Sponsored by Technology Development Center, Finland, and Technical Research Centre of Finland, Espoo
(VTT-JULK-755; ISBN-9-51-384102-2; ETN-93-94467) Copyright Avail: CASI HC A05/MF A02

An automated image analysis method was developed for the inspection of cracks on wood surfaces and on paint films. The system is capable of both detecting and analyzing the cracks. The automatic method is capable of classifying the average size of the cracks and the quantity of cracking on the scale 0 to 5 (ISO (International Standards Organization) 4628 standard) with an accuracy of +/- 1 compared to visual classification. The inspection algorithms are based on morphological preprocessing and statistical crack recognition. For optimal thresholding, an experimental system was developed. The image acquisition part of the system is based on a monochrome CCD (Charge Coupled Device) matrix camera. The image processing hardware consists of commercial modules. Information about the length, width, area, circumference, and center of mass and moment of each crack is obtained, as well as the sum of the areas of the cracks in proportion to the whole image area and the density number of the cracks based on ISO 4628 standard. The distribution of the widths and lengths of the cracks are also automatically printed on a laser printer. In the first stage, the equipment was used for determinations of the condition of surface treated boards subjected to weather tests. The performance of the system is promising. All cracks on a white paint film are detected reliably. Analysis of dark paint films is difficult because the reflectance properties of small cracks does not differ from the surrounding paint film. The system provides new possibilities to investigate the development of cracks on wood surfaces, for example, during the drying process. It takes about 3 minutes to analyze one image. The approximation of the analysis time is about 15 seconds, when using a special morphological processor and a computer. ESA

N94-17596# Boeing Defense and Space Group, Seattle, WA.
X RAY COMPUTED TOMOGRAPHY FOR CASTING DEMONSTRATION
Interim Report, Sep. 1991 - May 1993
Gary E. Georgeson, Richard H. Bossi, and Raymond D. Rempt 1 May 1993 73 p
(Contract F33615-88-C-5404)
(AD-A268084; WL-TR-93-4048) Avail: CASI HC A04/MF A01

Computed tomography (CT) has been applied to cast products demonstrating benefits to product development, dimensional measurements, and critical region evaluation. The CTAD program has produced data in a number of reports demonstrating the quantitative measurement capability of CT and its advantages for castings. CT is a measurement tool which can enable greater use of casting by assuring quality in complex structural applications. CT allows an engineering evaluation of castings for a number of criteria such as internal defects, porosity content, three-dimensional location of features, and internal and external dimensions. As casting complexity and part value increases, the application of CT increases in cost effectiveness relative to other technologies. For critical regions of a casting, CT can be superior to radiography for detail sensitivity and relatively inexpensive. Educational material is needed to aid engineers in understanding the applicability and benefits of CT to their problems. Example stories have been used by the CTAD program to demonstrate the areas of CT application and cost benefits. Readers of the case study stories are able to extrapolate from the examples to their problems and evaluate the benefits that CT may provide them. DTIC

N94-16005# Krupp (Fried.) G.m.b.H., Essen (Germany).
RELMA: ON-LINE QUALITY CONTROL IN THE RUBBER MIXING ROOM USING LASER ANALYSIS
Walter Haeder and Claus-Juergen Lorenzen *In its* Krupp Technical Reports No. 2, English Edition, October 1992 Oct. 1992 p 97-102
(For primary document see N94-16000 03-31)
Copyright Avail: CASI HC A02/MF A01

N94-16626*# Edgerton, Germeshausen and Grier, Inc., Cocoa Beach, FL.
IDENTIFYING AND RESPONDING TO CUSTOMER NEEDS AT THE KENNEDY SPACE CENTER
E. B. Ferguson *In* BioTechnology, Inc., Proceedings of the 1992 Annual Meeting NASA Occupational Health Program Jul. 1993 p 189-194
(For primary document see N94-16609 03-52)
Avail: CASI HC A02/MF A03

N94-17188 Bureau Veritas, Courbevoie (France).
SMALL SATELLITE PRODUCT ASSURANCE [L'ASSURANCE PRODUIT DES PETITS SATELLITES]
J. DeMontlivault and Jacques Cadelec (Calireal, Palaiseau, France.) *In* CNES, Small Satellites Systems and Services Jan. 1993 p 685-694
In FRENCH (For primary document see N94-17131 03-18)
Copyright Avail: Issuing Activity (CEPADUES-Editions, 111 rue Nicolas-Vaquelin, 31100 Toulouse, France)

39 STRUCTURAL MECHANICS

Includes structural element design and weight analysis; fatigue; and thermal stress.

For applications see *05 Aircraft Design, Testing and Performance* and *18 Spacecraft Design, Testing and Performance.*

N94-14945# Aerospace Corp., El Segundo, CA. Technology Operations.
XPS ANALYSIS OF Al/EPDM BONDLINES FROM IUS SRM-1 POLAR BOSSES Final Report
Carol S. Hemminger and Nicholas Marquez 10 Mar. 1993 25 p
(Contract F04701-88-C-0089)
(AD-A266851; TR-93(3464)-1; SMC-TR-93-28) Avail: CASI HC A03/MF A01

A temperature-stress rupture method using partial immersion in liquid nitrogen was developed for the aluminum/EPDM rubber insulation bondline of the IUS SRM-1 polar bosses in order to investigate a corrosion problem. Subsequent XPS analysis of the ruptured bondline followed changes in the locus of failure as corrosion progressed. Samples from the forward polar bosses had a predominantly noncorroded appearance on the ruptured surfaces. The locus of failure was predominantly through the primer layer, which is distinguished by a high concentration of chlorinated hydrocarbon. The aft polar boss segments analyzed were characterized by the presence of corrosion over the entire mid-section of the ruptured aluminum to insulation bondline. The predominant corrosion product detected was aluminum oxide/hydroxide. The corroded bondline sections had significantly higher concentrations of aluminum oxide/hydroxide than the noncorroded areas, and lower concentrations of primer material. The temperature-stress rupture appeared to progress most readily through areas of thickened aluminum oxide/hydroxide infiltrated into the primer layer. In general there was a very good correlation between the calculated Cl:Al atomic % ratio, and the visual characterization of the extent of corrosion. The Cl:Al ratio, which represents the primer to corrosion product ratio at the locus of failure, varied from 0.4 to 47. With only a few exceptions, surfaces with a predominantly noncorroded appearance had Cl:Al ratios greater than 2, and surfaces with a heavily corroded appearance had Cl:Al ratios less than 1. DTIC

N94-15004*# Eloret Corp., Sunnyvale, CA.
SIMULATION STUDIES FOR SURFACES AND MATERIALS STRENGTH
Semiannual Progress Report, 1 Nov. 1992 - 30 Apr. 1993
Timur Halicioglu 30 Apr. 1993 47 p
(Contract NCC2-297)
(NASA-CR-193387; NAS 1.26:193387) Avail: CASI HC A03/MF A01

Optimum energies and structures were estimated for single step ledges formed on the diamond (111) surface. Binding energies of carbon atoms adsorbed on a (2x1) reconstructed Si(100) surface were calculated as a function of sub-monolayer coverages. Calculations were conducted to

analyze the strain dependence of the binding energy of a carbon adatom deposited on a (2x1) dimerized Si(100) surface. Details and results of these studies are given as appendices. Derived from text

N94-15015 National Physical Lab., Teddington (England). Div. of Materials Metrology.
SYSTEMATIC STUDY OF EFFECTS OF LOAD MISALIGNMENT IN UNIAXIAL LOW CYCLE FATIGUE TESTING AT HIGH TEMPERATURES
Fathy A. Kandil and Brian F. Dyson Jul. 1991 32 p
(NPL-DMM(A)-27; ETN-93-94548) Copyright Avail: Issuing Activity
(National Physical Lab., Teddington, Middlesex TW11 OLW, England)

The influence of load misalignment in data scatter observed in uniaxial Low Cycle Fatigue (LCF) testing at high temperatures was modeled by considering the mechanisms of bending in rigid grip systems; the types of extensometer used to control the strain amplitude; and the micromechanisms of fatigue crack 'initiation'. By assuming that the scatter in fatigue lifetimes due to material inhomogeneities is negligible, it was possible not only to predict accurately the good repeatability of Nimonic 101 data found within each laboratory taking part in a worldwide LCF round robin exercise, but also to predict the very poor reproducibility between the laboratories. ESA

N94-15016 National Physical Lab., Teddington (England). Div. of Materials Metrology.
A MODEL FOR NON-LINEAR CREEP AND PHYSICAL AGEING IN PVC
G. D. Dean, P. E. Tomlins, and B. E. Read Mar. 1993 29 p Sponsored by Dept. of Trade and Industry, London, England
(NPL-DMM(A)-91; ETN-93-94549) Copyright Avail: Issuing Activity
(National Physical Lab., Teddington, Middlesex TW11 OLW, England)

An expression for the creep compliance function is derived for an amorphous polymer Polyvinyl Chloride (PVC) in terms of parameters which depend upon the applied stress and the age of the polymer. Relationships for the stress and age dependence of these parameters are investigated with the aim of establishing procedures whereby creep compliances can be derived by calculation over wide ranges of time, stress and age. Expressions for describing the increase of t(sub 0) (the mean retardation time for the creep mechanism) with creep time (apparent reactivation of physical aging) subsequent to the short term response are explored. Calculated creep compliances are compared with experimental data obtained in tension and compression. Differences in creep behavior under tensile and compressive stresses are traced to different magnitudes of two of the parameters in the model. The scope for using the model to calculate creep compliances from an analysis of a limited quantity of experimental creep data is discussed. ESA

N94-15017 National Physical Lab., Teddington (England). Div. of Materials Metrology.
MODELLING OF CREEP DATA FOR PLASTICS
B. E. Read, G. D. Dean, and P. E. Tomlins Mar. 1993 12 p
(NPL-DMM(A)-92; ETN-93-94550) Copyright Avail: Issuing Activity
(National Physical Lab., Teddington, Middlesex TW11 OLW, England)

Analytical functions capable of describing the creep behavior of plastics over wide time ranges, accounting for the effects of physical aging, stress level and temperature, are summarized. The availability of such functions and associated parameters should provide an improved basis for the prediction of creep properties and facilitate the handling of data in computerized databases. ESA

N94-15021 National Physical Lab., Teddington (England). Div. of Materials Metrology.
FRACTURE TOUGHNESS TESTS FOR PARTICULATE MMC UK COSI (IACFA) TASK GROUP. MEETING REPORT, OCTOBER 1992
B. Roebuck and J. D. Lord Apr. 1993 25 p Meeting held in Harwell, England, 15 Oct. 1992 Original contains color illustrations
(NPL-DMM(A)-81; ETN-93-94554) Copyright Avail: Issuing Activity
(National Physical Lab., Teddington, Middlesex TW11 OLW, England)

Issues related to fracture toughness tests for particulate reinforced Metal Matrix Composites (MMC) debated at the second meeting of a UK COSI (United Kingdom Committee On Structural Integrity, formerly IACFA) task group, including contacts with BSI (British Standards Institute), residual stress measurements, plane strain toughness tests, Charpy impact tests, short bar chevron notch testing and crack length measurement methods are discussed. It was agreed that the main item on the agenda for the next meeting would be to reach an agreement on a recommended test method for toughness testing of particulate MMC. ESA

N94-15150# Naval Undersea Warfare Center, Newport, RI.
FORCED HARMONIC VIBRATION OF THE GENERALLY ORTHOTROPIC CYLINDRICAL SHELL WITH INNER AND OUTER FLUID LOADING
Mark S. Peloquin 25 Nov. 1992 142 p
(AD-A266985; NUWC-NPT-TR-10199) Avail: CASI HC A07/MF A02

This report describes a modeled system comprised of an infinite shell with both inner and outer fluids subject to forced harmonic vibration in the longitudinal (x) and circumferential (0) directions. Two excitations are applied to the outer shell surface: normal pressure, Po, and longitudinal shear stress, Px. The equations of motion are derived, from first principles, for an elastic shell, including a full treatment of bending and rotatory inertia. The fluids are treated as linearly elastic, inviscid media and are subject to the wave equation in three dimensions. The stress-strain relationship for the shell is formulated to enable the treatment of isotropic, specially orthotropic, and generally orthotropic composite materials undergoing plane stress. DTIC

N94-15154*# Technische Univ., Delft (Netherlands). Faculty of Aerospace Engineering.
COMPARISON OF LEVEL-1 AND LEVEL-2 BUCKLING AND POSTBUCKLING SOLUTIONS
J. Arbocz Nov. 1992 226 p
(Grant NAGW-2736)
(NASA-CR-194611; NAS 1.26:194611; LR-700; ISBN-90-6275-839-8; ETN-93-94418) Copyright Avail: CASI HC A11/MF A03

The accuracy of the solutions obtained with the Level-1 computational modules of DISDECO (Delft Interactive Shell Design Code) are investigated by comparing them with solutions obtained with ANILISA, a Level-2 computational module. Whereas the Level-1 solutions are based on the use of trigonometric functions to represent the out-of-plane displacement W and involve Galerkin type approximations to reduce the governing partial differential equations to simple algebraic expressions, the Level-2 solutions employ a truncated Fourier expansion in the circumferential direction and solve the resulting ordinary differential equations forming a nonlinear eigenvalue problem by a Stodola like technique. This involves the numerical integration of the set of ordinary differential equations, which in turn makes it possible to satisfy the specified boundary conditions exactly. It is shown that in many applications the Level-1 predictions concerning the critical buckling load of the perfect structure and its imperfection sensitivity are quite accurate and reliable. For those cases where this is not true, it is shown how the pre and postprocessing facilities of DISDECO can be used efficiently to arrive at a reliable prediction. This involves always the use of the Level-2 computational module ANILISA with its rigorous prebuckling solution and its feature which makes it possible to satisfy the specified boundary conditions exactly. ESA

N94-15524# Naval Research Lab., Washington, DC.
PROGRESS IN THE MODELING OF THE SHOCK RESPONSE AND MITIGATION OF THICK COMPOSITE SHELLS Memorandum Report
C. T. Dyka and P. W. Randles 22 Jul. 1993 58 p
(AD-A267009; NRL/MR/6386-93-7369) Avail: CASI HC A04/MF A01

This report is a continuation of our efforts to develop a methodology for predicting the response of thick composite materials subjected to multi-dimensional shock loadings. A focus of this work was the initiation and evolution of damage in 1D, 2D, and 3D composite structures. In addition, dispersion/viscoelastic models were investigated for 1D structures and implemented. One dimensional damage predictions are made for composite plates subjected to underwater shock. The 1D and 2D continuum damage models are both applied to the impact of a plexiglass flyer and graphite/peek plate, and the results compare very well to experimental data. A new 3D continuum damage theory is developed for thick laminated composite plates. The 3D theory is in part an extension of the 2D transversely isotropic damage theory. However, three dimensional considerations as well as the inefficiencies of modeling individual plies in a thick composite require a slightly different approach. A 3D formulation is developed which applies the damage directly to the stresses, rather than the compliances as in the 2D and 1D theories. DTIC

N94-15534*# National Aeronautics and Space Administration. Marshall Space Flight Center, Huntsville, AL.

AN ASSESSMENT OF FINITE-ELEMENT MODELING TECHNIQUES FOR THICK-SOLID/THIN-SHELL JOINTS ANALYSIS

J. B. Min and S. G. Androlake Oct. 1993 30 p Sponsored by NASA, Washington

(NASA-TM-108426; NAS 1.15:108426) Avail: CASI HC A03/MF A01

The subject of finite-element modeling has long been of critical importance to the practicing designer/analyst who is often faced with obtaining an accurate and cost-effective structural analysis of a particular design. Typically, these two goals are in conflict. The purpose is to discuss the topic of finite-element modeling for solid/shell connections (joints) which are significant for the practicing modeler. Several approaches are currently in use, but frequently various assumptions restrict their use. Such techniques currently used in practical applications were tested, especially to see which technique is the most ideally suited for the computer aided design (CAD) environment. Some basic thoughts regarding each technique are also discussed. As a consequence, some suggestions based on the results are given to lead reliable results in geometrically complex joints where the deformation and stress behavior are complicated. Author (revised)

N94-15642# Technische Univ., Berlin (Germany). Inst. fuer Mechanik.

SYSTEMATOLOGY FOR ELASTIC-PLASTIC MATERIAL EQUATIONS BY LARGE DEFORMATIONS ON THE BASIS OF THE COSSERAT-CONTINUUM MODEL Ph.D. Thesis [EINE SYSTEMATIK FUER ELASTISCHE-PLASTISCHE STOFFGLEICHUNGEN BEI GROSSEN VERFORMUNGEN AUF DER BASIS DES COSSERAT-KONTINUUMSMODELLS]

Rainer Sievert 1992 300 p In GERMAN

(Schriftenr-Physikal-Ing-Bd-23; ISBN-3-79-831517-5; ETN-93-94400) Avail: CASI HC A13/MF A03

The classical continuum model is enlarged by the introduction of a rotation as an additional continuum degree of freedom (Cosserat model). The balances of momentum and internal spin were axiomatically derived from the energy conservation law by the principle of equipresence which was applied to the powerfree part of the stress. A theory for the development of elastic/plastic constitutive equations on the basis of the dissipation/inequality with a couple stress tensor as additional strength is presented. A general decomposition of deformation in an elastic and plastic part was used. The strain tensors obey a certain decomposition, if and only if the elastic constitutive laws for the stress tensors possess the same form as in the pure hyperelastic case. Also objective incremental stress strain relations were calculated by differentiating the finite elastic constitutive laws for the stress. Materials with plastic spin, like single crystals, were treated in the framework of Cosserat's continuum theory; the Eulerian plastic spin tensor turns out to be dissipative. Classical elastic-plastic materials with a multiplicative decomposition of strain were considered. A Eulerian (true) relative stress tensor was used for the description. The technical important cases of isochoric yielding and of small elastic strains at large plastic deformations were investigated. ESA

N94-15709*# National Aeronautics and Space Administration. Lewis Research Center, Cleveland, OH.

PRELIMINARY ANALYSIS AND DESIGN OPTIMIZATION OF THE SHORT SPACER TRUSS OF SPACE STATION FREEDOM

A. S. Gendy (Akron Univ., OH.), S. N. Patnaik (Ohio Aerospace Inst., Brook Park.), D. A. Hopkins, and L. Berke Aug. 1993 20 p Sponsored by NASA, Washington Original contains color illustrations

(RTOP 474-46-10)

(NASA-TM-4470; E-7653; NAS 1.15:4470) Avail: CASI HC A03/MF A01; 7 functional color pages

The analysis, dynamic simulation, and design optimization of the short spacer truss of the Space Station Freedom are presented in this report. The short spacer truss will be positioned between the integrated equipment assembly (IEA) and another truss, called the long spacer truss, in the Space Station Freedom. During its launch in the Space Shuttle, the truss will be subjected to considerable in-span distributed inertia loads due to shuttle accelerations. The short spacer truss, therefore, has been modeled as a space frame to account for flexural response. Several parameters have been assumed, since the design specifications are in the process of development; hence the results presented should be considered preliminary. However, the automated analysis and design capabilities that have been developed can readily be used to generate an optimum design of the short spacer truss once the actual specifications have been determined. This report includes static and dynamic analyses of the short spacer truss, which have been obtained with the linear elastic code LE-HOST (in these analyses, LE-HOST data files have been automated to facilitate their future use for different design specifications of the short spacer truss); the dynamic animation of the short spacer truss, which has been carried out by using the results of the dynamic analysis and a post-processing feature of the modeling code PATRAN; and the optimum-weight design of the spacer truss, which was obtained under prescribed stress, displacement, and frequency constraints by using the design code COMETBOARDS. Examination of the analysis and design results revealed that the design could be improved if the configuration of the short spacer truss were modified to a certain extent. A modified configuration, which may simplify fabrication, has been suggested. The performance of this configuration has been evaluated and was found to be satisfactory under both static and dynamic conditions. Author (revised)

N94-15710*# National Aeronautics and Space Administration. Marshall Space Flight Center, Huntsville, AL.

A SIMPLISTIC LOOK AT LIMIT STRESSES FROM RANDOM LOADING

H. M. Lee Oct. 1993 22 p

(NASA-TM-108427; NAS 1.15:108427) Avail: CASI HC A03/MF A01

Utilizing a continuous beam model, this report compares the potential stresses imposed on the beam from a random environment with those resulting from a typical static load analysis or test simulation. The Miles' equation used to develop peak response accelerations is shown to become a force equation in the hands of strength assessment personnel. This may prove to be unrealistic since hardware dynamic stresses are related to deflection rather than load. Correlation of the stress state for any static analysis or test with the actual dynamic response stress is strictly dependent upon how well the static deflections simulate the predominant dynamic mode shape. The report proposes that the general shape of this predominant mode, along with the peak response accelerations of major masses be used in strength assessments. From these data, a tailored enforced displacement loading may prove to be more effective in reproducing random induced stresses on flight hardware. Author

N94-15716*# Alabama Univ., Huntsville.

USE OF PHOTOSTRESS AND STRAIN GAGES TO ANALYZE BEHAVIOR OF WELDMENTS AND USE OF PHOTOSTRESS AND STRAIN GAGES TO ANALYZE BEHAVIOR OF AN AFT SKIRT TEST SPECIMEN Semiannual Report, 26 Dec. 1992 - 26 Jul. 1993

S. C. Gambrell (Alabama Univ., Tuscaloosa.) and Gerald R. Karr 27 Oct. 1993 15 p Original contains color illustrations

(Grant NAG8-293)

(NASA-CR-194575; NAS 1.26:194575) Avail: CASI HC A03/MF A01; 4 functional color pages

Previous work using Photostress on TIG welded, heat treated specimens of 2219-T87 parent material and 2319 weld material indicated that behavior of the joint can be highly irregular and non-uniform. Welded joints 1.40 inches thick exhibited a totally non-uniform behavior through the weld thickness with the 'wide' side of the weld being much more ductile than the 'narrow' side. It is believed that this difference in behavior through the weld is, in part, caused by procedures used when laying the weld bead. Joints similar to weldments in references 1 and 2 are an integral part of the aft skirt of the SRB of the shuttle. Since the ultimate safety factor for the lower portion of the weld is below the minimum required safety factor, a photostress analysis of this lower portion will be conducted in the vicinity of the weld. A test program using photostress will be conducted in accordance with the project planning document entitled 'Photostress Evaluation Requirements for AFT Skirt Test Article No. 4'.

Derived from text

N94-15963# Aeronautical Research Labs., Melbourne (Australia).

THE INFLUENCE OF SECONDARY BENDING ON FATIGUE LIFE IMPROVEMENT IN BOLTED JOINTS

R. L. Evans Aug. 1993 38 p

(ARL-RR-14; AR-008-384) Avail: CASI HC A03/MF A01

Secondary bending often occurs in structural joints, and to assess its influence on the fatigue life enhancement technique of hole cold-expansion, an experimental program has been undertaken. The results indicate that

the effect of cold working is substantially reduced in specimens with secondary bending. For any marked extension in fatigue life, additional treatments, for example, the combination of cold expansion and interference fit, are required. Author (revised)

N94-15983# Lawrence Livermore National Lab., CA.
SLIDESURFACES WITH ADAPTIVE NEW DEFINITIONS (SAND) FOR TRANSIENT ANALYSIS
R. G. Whirley and B. E. Engelmann 2 Jun. 1992 19 p Presented at the Winter Annual Meeting of the ASME, Anaheim, CA, 8-13 Nov. 1992
(Contract W-7405-eng-48)
(DE93-014909; UCRL-JC-108924; CONF-921110-50) Avail: CASI HC A03/MF A01

This paper describes some recent developments in adaptive contact algorithms for the transient analysis of penetration and material failure. A failure criterion is defined for volumes of potentially failing material on each side of a contact surface. As material within an element fails, the element is removed from the calculation, and the contact surface is adaptively redefined to include the newly exposed outer material boundary. This contact algorithm admits arbitrary combinations of shell and solid elements to facilitate the representation of composite or honeycomb structures. The algorithms and their application are illustrated with several large-scale simulations using the explicit transient analysis code DYNA3D. DOE

N94-15997# Argonne National Lab., Idaho Falls, ID. Materials and Components Technology Div.
WEIBULL ANALYSIS APPLIED TO THE PULL ADHESION TEST AND FRACTURE OF A METAL-CERAMIC INTERFACE
R. A. Erck, F. A. Nichols, and D. L. Schult (Illinois Univ., Urbana.) Nov. 1992 21 p Presented at the Annual Conference and Exhibition of the Society of Tribologists and Lubrication Engineers, Calgary, Canada, 17-20 Apr. 1993
(Contract W-31-109-eng-38)
(DE93-012913; ANL/MCT/CP-77789; CONF-9304133-1) Avail: CASI HC A03/MF A01

Various adhesion tests have been developed to measure the mechanical bonding of thin coatings deposited on substrates. In the pull test, pins that have been bonded to the coating under test are pulled with increasing force normal to the coating until the coating is pulled from the substrate. For many systems, large scatter in the data is often observed due to uncontrolled defects in the interface and the brittle nature of the pull test. In this study, the applicability of Weibull statistics to the analysis of adhesion of Ag films to vacuum sputter-cleaned zirconia was examined. Data were obtained for smooth and rough substrates for various levels of adhesion. A good fit of the data to the Weibull distribution was observed. The Weibull modulus was found to depend on the roughness of the substrate, but was insensitive to the adhesion strength. DOE

N94-16104# Oak Ridge National Lab., TN.
DESIGN OF A CRUCIFORM BEND SPECIMEN FOR DETERMINATION OF OUT-OF-PLANE BIAXIAL TENSILE STRESS EFFECTS ON FRACTURE TOUGHNESS FOR SHALLOW CRACKS
B. R. Bass, J. W. Bryson, W. J. Mcafee, W. E. Pennell, and T. J. Theiss 1993 12 p Presented at the 12th Biennial Conference for the International Association for Structural Mechanics in Reactor Technology (SMIRT 12), Stuttgart, Germany, 16-26 Aug. 1993
(Contract DE-AC05-84OR-21400)
(DE93-015455; CONF-930803-13) Avail: CASI HC A03/MF A01

Pressurized-thermal-shock loading in a reactor pressure vessel produces significant positive out-of-plane stresses along the crack front for both circumferential and axial cracks. Experimental evidence, while very limited, seems to indicate that a reduction in toughness is associated with out-of-plane biaxial loading when compared with toughness values obtained under uniaxial conditions. A testing program is described that seeks to determine the effects of out-of-plane biaxial tensile loading on fracture toughness of RPV steels. A cruciform bend specimen that meets specified criteria for the testing program is analyzed using three-dimensional elastic-plastic finite-element techniques. These analysis results provide the basis for proposed test conditions that are judged likely to produce a biaxial loading effect in the cruciform bend specimen. DOE

N94-16123# Rice Univ., Houston, TX. Dept. of Mechanical Engineering.
A NOVEL APPROACH FOR STRUCTURAL MECHANICS PROBLEMS WITH STOCHASTICITY Final Report, 15 Oct 1990 - 14 Jan. 1993
Pol D. Spanos and L. B. Ryon 18 Apr. 1993 58 p
(Grant AF-AFOSR-0004-91)
(AD-A266189; AFOSR-93-0430TR) Avail: CASI HC A04/MF A01

Considerable advances were made in several structural mechanics problems with stochasticity. First, a new method was developed for the solution of problems involving material variability. The Karhunen-Loeve expansion was used for this purpose. Further, a problem involving a plate with a curved boundary was solved. Also methods unifying the theory of stochastic and deterministic finite elements were developed. In parallel, a method for more efficient Monte-Carlo simulation was developed. Finally, some work in the area-of stochastic finite difference was done. DTIC

N94-16519*# National Aeronautics and Space Administration. Marshall Space Flight Center, Huntsville, AL.
ON THE DESIGN OF STRUCTURAL COMPONENTS USING MATERIALS WITH TIME-DEPENDENT PROPERTIES
Pedro I. Rodriguez Oct. 1993 55 p
(NASA-TM-108428; NAS 1.15:108428) Avail: CASI HC A04/MF A01

The application of the elastic-viscoelastic correspondence principle is presented as a design tool for structural design engineers for composite material applications. The classical problem of cantilever beams is used as the illustration problem. Both closed-form and approximate numerical solutions are presented for several different problems. The application of the collocation method is presented as a viable and simple design tool to determine the time-dependent behavior and response of viscoelastic composite beams under load. Author

N94-16587# California Inst. of Tech., Pasadena. Graduate Aeronautical Labs.
HIGHLY TRANSIENT ELASTODYNAMIC CRACK GROWTH IN A BIMATERIAL INTERFACE: HIGHER ORDER ASYMPTOTIC ANALYSIS AND OPTICAL EXPERIMENTS
Cheng Liu, John Lambros, and Ares J. Rosakis 20 Dec. 1992 98 p
(AD-A266465; SM-92-37) Avail: CASI HC A05/MF A02

A higher order asymptotic analysis of the transient deformation field surrounding the tip of a crack running dynamically along a bimaterial interface is presented. An asymptotic methodology is used to reduce the problem to one of the Riemann-Hilbert type. Its solution furnishes displacement potentials which are used to explicitly evaluate the near-tip transient stress field. Crack-tip fields corresponding to crack speeds up to the lower of the two shear wave speeds are investigated. An experimental study of dynamic crack growth in PMMA/steel interfaces using the optical method of CGS and high speed photography, is also described. Transonic terminal speeds (up to 1.4c(sub s)(PMMA) and initial accelerations (approximately 10(exp 8) m/sec(exp 2)) are reported and discussed. Transient effects are found to be severe and more important than in homogeneous dynamic fracture. For subsonic crack growth, these experiments are used to demonstrate the necessity of employing a fully transient expression in the analysis of optical data to accurately predict the complex dynamic stress intensity factor history. DTIC

N94-16651# Polish Academy of Sciences, Warsaw. Inst. Podstawowych Problemow Techniki.
ELASTOOPTICAL BRITTLE MATERIALS IN EXPERIMENTAL STUDIES OF THE STATE OF STRESS AND DEFORMATION [KRUCHE MATERIALY ELASTOOPTYCZNE W BADANIACH DOSWIADCZALNYCH STANU NAPREZENIA I ODKSZTALCENIA]
Malgorzata Wolna and Leopold Kruszka 1991 21 p In POLISH
(IFTR-22/1991) Avail: CASI HC A03/MF A01

This study contains a survey of brittle elasto-optic materials employed to simulate material failure processes. Brittle elasto-optic materials developed from an epoxy resin developed at the IPPT Institute of the Polish Academy of Sciences (IPPT AN) are presented against this background.
Transl. by FLS

N94-16815*# Hawaii Univ., Honolulu. Inst. for Astronomy.
PARTICIPATION IN THE NORTH ECLIPTIC POLE SKY SURVEY Final Technical Report, 15 Sep. 1990 - 14 Sep. 1992

J. Patrick Henry 14 Sep. 1992 2 p
(Grant NAG5-1446)
(NASA-CR-191933; NAS 1.26:191933) Avail: CASI HC A01/MF A01

This grant supported research into the nature of the faintest x-ray sources found in the ROSAT All Sky Survey, with particular emphasis on distant clusters of galaxies. The project was broadened to include sources found in the ROSAT deep pointing at the North Ecliptic Pole. Progress on the research is briefly summarized. Derived from text

N94-16881*# National Aeronautics and Space Administration. Lewis Research Center, Cleveland, OH.

FINITE ELEMENT ANALYSIS OF STRUCTURAL ENGINEERING PROBLEMS USING A VISCOPLASTIC MODEL INCORPORATING TWO BACK STRESSES

Vinod K. Arya (Toledo Univ., OH.) and Gary R. Halford Oct. 1993 26 p
(RTOP 505-63-5B)
(NASA-TM-106046; E-7922; NAS 1.15:106046) Avail: CASI HC A03/MF A01

The feasibility of a viscoplastic model incorporating two back stresses and a drag strength is investigated for performing nonlinear finite element analyses of structural engineering problems. To demonstrate suitability for nonlinear structural analyses, the model is implemented into a finite element program and analyses for several uniaxial and multiaxial problems are performed. Good agreement is shown between the results obtained using the finite element implementation and those obtained experimentally. The advantages of using advanced viscoplastic models for performing nonlinear finite element analyses of structural components are indicated. Author (revised)

N94-16923# Polish Academy of Sciences, Warsaw. Inst. Postawowych Problemow Techniki.

STATIC ANALYSIS OF BEAMS ON AN ELASTIC BASE AS STATED BY GENERALIZED FUNCTIONS [ANALIZA STATYCZNA BELEK NA SPREZYSTYM PODLOZU W UJECIU FUNKCJI UOGOLNIONYNCH]

Katarzyna Cabanska (Wyzsza Szkola Pedagogiczna, Cracow, Poland.) 1991 19 p In POLISH
(IFTR-27/1991) Avail: CASI HC A03/MF A01

This paper presents an integrated method for analytic solution of static problems for beams under Winkler stress taking into account distribution theory. A differential equation describing beam bending with zero boundary conditions on the force is solved. A general algorithm for solving the problem is derived for arbitrary loading examples. The effectiveness of the algorithm is demonstrated by a specific example and calculation results are plotted in graphs. Transl. by FLS

N94-16943# Naval Postgraduate School, Monterey, CA.

FATIGUE LIFE PROGRAM USING STRAIN-LIFE METHODS M.S. Thesis

Michael V. Skelly 25 Mar. 1993 91 p
(AD-A267310) Avail: CASI HC A05/MF A01

A user friendly program was developed to calculate fatigue life using Strain-Life equations, given either a stress history or a strain history. Additionally, the material parameters and associated stress concentration factors can be varied. Since certain material constants, such as cyclic strength coefficient (K') and cyclic strain hardening exponent (n') vary during a material's fatigue life, the program is capable of either keeping them constant or varying them as a function of elapsed cycles. The program was then utilized to examine the effects of varying K' and n' on the calculated fatigue life of aluminum 7075-T6 under a typical flight load history. DTIC

N94-17043 Air Force Inst. of Tech., Wright-Patterson AFB, OH.

INTERFACIAL SHEAR BEHAVIOR AND ITS INFLUENCE ON FIBER DAMAGE IN SAPPHIRE-REINFORCED GAMMA TITANIUM ALUMINIDE COMPOSITES Ph.D. Thesis

Jay M. Galbraith May 1993 200 p Limited Reproducibility: More than 20% of this document may be affected by microfiche quality
(AD-A267943; AFIT/CI/CIA-93-001D) Avail: Issuing Activity (Defense Technical Information Center (DTIC))

The interfacial shear behavior and its influence on fiber damage in sapphire-reinforced TiAl composites was investigated using a combination of microscopic characterization, indentation crack growth results, fiber pushout testing, fiber displacement measurements, and computational analyses. Two inter-related phenomena were studied: (1) residual stresses and resulting damage within fibers intersecting a free surface and (2) fiber/matrix interfacial strength behavior. In the first aspect of this study, experimental observations, finite element analysis, as well as analytical computations were all used to analyze the evolution of fiber damage that was observed in fibers intersecting a free surface in sapphire-reinforced Ti-48Al-4 composites. Experimental observations indicate that, under certain conditions, surface cracks introduced during specimen preparation will propagate along the fiber axis due to thermally-induced residual stresses. Finite element computations predict that significant thermally-induced residual tensile stresses exist in sapphire fibers embedded within TiAl-based matrices when they intersect and are oriented normal to a free surface. Indentation crack growth behavior within the sapphire fibers provided experimental validation of the predicted stress state. Finally, the application of an exact elastic analysis indicates that tensile stresses also exist within fibers oriented parallel to and near a free surface. DTIC

N94-17047# Polish Academy of Sciences, Warsaw. Inst. Podstawowych Problemow Techniki.

SURFACE WAVES IN AN INHOMOGENEOUS, ISOTROPIC, ELASTIC HALF-SPACE [FALE POWIERZCHNIOWE W NIEJEDORODNEJ IZOTROPOWEJ POLPRZESTRZENI SPEZYSTEJ]

Tadeusz Klecha 1991 126 p In POLISH
(IFTR-18/1991) Avail: CASI HC A07/MF A02

This study presents proof of the existence of surface waves in homogeneous media for deriving stress equations and likewise demonstrates that a propagating wave and its velocity are analytic functions of the wave number. NTIS

N94-17052# Polish Academy of Sciences, Warsaw. Inst. Podstawowych Problemow Techniki.

INFLUENCE OF THE LOADING RATE ON THE ENDURANCE AND DEFORMABILITY OF CEMENT MATRIX COMPOSITES [WPLYW PREDKOSCI OBCIAZENIA NA WYTRZYMALOSC I ODKSZTALCALNOSC KOMPOZYTOW Z MATRYCA CEMENTOWA]

Michal A. Glinicki 1992 242 p In POLISH
(IFTR-1/1992) Avail: CASI HC A11/MF A03

Results are presented of the author's experiments on the strength and deformation of composites with a cement matrix at various loading rates ranging from 10(exp -3) to 10(exp +3) MPa/s. The studies involved composites with a Portland cement base. The goal was to find the qualitative and quantitative effect of the loading rate sigma on the behavior of composites subjected to axial tension. Specifically, the studies were done to determine the sensitivity differences of composites to loading rate when these materials were used for outside construction. The effect of changes in the deformation parameters and failure with varying sigma was understood to represent sensitivity. Structural attributes of composites with a cement matrix are described in Section 2; Section 1 reviews the current state of knowledge on deformation and cracking of these composites under static and dynamic tensile loads. The experimental method in the study is described in Section 4. The structure of selected model composites revealed in a clinical way analyzed traits such as: porosity, granulation of the aggregate and content and orientation of fiber reinforcement. Apparent density, density, and porosity were identified in each of the five types of composites. Studies of direct tensile loading were carried out at rates of 0.002, 1.0, 50 and 850 MPa/s. A digital image analyzer was used for quantitative analysis of sample sections. Results are presented in Section 5; in Section 6, results are analyzed and compared to results obtained by other investigators. The results justify the theory on the significant effect of structural parameters of composites on changes in strength and resistance to damage due to changes in a under tensile loading. Increase in the rate of loading causes a definite increase in resistance to tensile motion f(sub t) as well as to deformation of the limit epsilon(sub u) of the composites. In composites with fiber reinforcement, an increase in sigma also causes an increase in failure energy. Composite porosity is the most significant structural property of these materials that affects the sensitivity to loading rate with respect to f(sub t). This sensitivity loading rate increases with increasing composite porosity. As a model (Section 7), a proposal is made that the effect of composite porosity on their sensitivity to the loading rate be interpreted with respect to f(sub t). It is demonstrated that a good agreement with experimental results can be obtained by accepting the principle that precritial cracks decrease in size increasing loading rate and that there is an increase

in loccal dispersion of material quality due to porosity. Conclusions and postulates pertaining to the direction of subsequent studies are presented in the conclusion. Transl. by FLS

N94-17058# Polish Academy of Sciences, Warsaw. Inst. Podstawowych Problemow Techniki.

THE DETERMINATION OF THE YOUNG MODULI OF A MATERIAL AFTER EXPOSURE TO LASER LIGHT AND DELINEATION OF THE ZONE OF LASER ALTERATIONS [WYZNACZANIE MODULOW YOUNG'A MATERIALU PO NASWIETLANIU LASEROWYM I OKRESLENIE STREFY ZMIAN LASEROWYCH]

Zbigniew Turek 1991 18 p In POLISH

(IFTR-37/1991) Avail: CASI HC A03/MF A01

Existing macroscopic relations derived from the literature for two-component media under serial and parallel conditions are defined in a new manner utilizing the Clapeyron theorem of deformation. The Young's moduli for material following laser treatments are defined on the basis of such relations. A different method of calculating the Young's moduli is presented for a certain laser treatment range. This paper also presents an analytic method of determining the laser treatment zone. NTIS

N94-17069# Polish Academy of Sciences, Warsaw. Inst. Podstawowych Problemow Techniki.

VARIATIONAL PRINCIPLES OF HEAT EXCHANGE AND THEIR APPLICATIONS IN CONSTRUCTION PHYSICS, PART 2 [ZASADY WARIACYJNE WYMIANY CIEPLA I ICH ZASTOSOWANIA W FIZYCE BUDOWLI, CZESC 2]

Jan Wozniak 1991 17 p In POLISH

(IFTR-19/1991) Avail: CASI HC A03/MF A01

A Lagrangian model of thermal conduction by finite element analysis, taking into account problems of control, is developed in this work. This model was used to compute the effectiveness of heat sources in maintaining a constant temperature in a room when outside temperature varies over time. Transl. by FLS

N94-17086# Polish Academy of Sciences, Warsaw. Inst. Podstawowych Problemow Techniki.

STATIC AND DYNAMIC INVESTIGATIONS OF BRITTLE ELASTO-OPTICAL MATERIAL [STATYCZNE I DYNAMICZNE BADANIA KRUCHEGO MATERIALU ELASTOOPTYCZNEGO]

Leopold Kruszka, Wojciech K. Nowacki, and Malgorzata Wolna 1992 48 p In POLISH

(IFTR-3/1992) Avail: CASI HC A03/MF A01

Results from experimental static and dynamic research on a fragile transparent material in uniaxial compression tests are presented. A multifactorial experimental method utilizing ultrasound measurement, acoustic emission, elastooptics as well as photographic recording of the changes occurring in the specimens are employed in the static tests used. This method made it possible to recover comprehensive information relating to the damage and failure mechanics of this material. Static and dynamic characteristics of the material as well as the torque resistance and the cracking and breakdown mechanisms taking into account the shape (flexibility) of the specimen were compared. Transl. by FLS

N94-17091# Polish Academy of Sciences, Warsaw. Inst. Podstawowych Problemow Techniki.

ELASTIC WAVES IN DISCRETELY CONTINUOUS MECHANICAL SYSTEMS [FALE SPREZYSTE W DYSKRETNO-CIAGLYCH UKLADACH MECHANICZNYCH]

Amalia Pielorz 1992 172 p In POLISH

(IFTR-21/1992) Avail: CASI HC A08/MF A02

Focus is on research on dynamic displacement and deformation of selected linear and non-linear discrete-continuous mechanical systems utilizing linear elasticity waves. The first portion of the study presents results from two and three dimensional wave problems of circular rolls and the possibility for their application to discrete-continuous mechanical systems under both longitudinal and transverse torsional strain. The second section of the study presents a method of finding displacement at deformation in discrete-continuous mechanical systems consisting of rotationally- or longitudinally-strained elastic elements of variable and fixed cross section connected by rigid bodies. This method is based on the use of one-dimensional elasticity waves. The method makes it possible to utilize an integrated calculation apparatus for analyzing temporary motion and steady state motion. This method is illustrated based on a linear drive system containing multiple masses for the case of longitudinally-colliding linear bar subsystems and for the case of a drive system with multiple masses with a local non-linearity. Wave solutions of equations of motion and corresponding numerical methods were used to determine the displacement. Analytic results are also given for particular linear cases of discrete-continuous mechanical systems. The proposed wave method is compared to the rigid finite element method and the separation of variables method. Transl. by FLS

N94-17105# Army Armament Research, Development and Engineering Center, Watervliet, NY. Benet Lab.

MEASUREMENT AND THEORY OF THE DEPENDENCE OF HARDNESS ON RESIDUAL STRESS Final Report

A. Abbate, J. Frankel, and W. Scholz May 1993 33 p

(AD-A267553; ARCCB-TR-93022) Avail: CASI HC A03/MF A01

The Rockwell C hardness (Rc) was measured as a function of position on the three steel rings cut from tubes with different amounts of autofrettage. These rings had different residual stress profiles through the wall that were measured using an ultrasonic technique. An experimental correlation between residual stress and Rc was obtained. In order to model the effects of residual stress on the measured hardness, the Tresca (linear) and the von Mises-Hencky (power) yield criteria were utilized within a model given by Shaw, Hoshi, and Henry that depicts the stress state within a spherical indenter. The von Mises-Hencky method was more successful in matching the data. DTIC

N94-17259*# National Aeronautics and Space Administration. Langley Research Center, Hampton, VA.

DEVELOPMENT AND COMPARISON OF ADVANCED REDUCED-BASIS METHODS FOR THE TRANSIENT STRUCTURAL ANALYSIS OF UNCONSTRAINED STRUCTURES

David M. McGowan, Susan W. Bostic, and Charles J. Camarda Nov. 1993 30 p

(RTOP 537-06-21-09)

(NASA-TM-109015; NAS 1.15:109015) Avail: CASI HC A03/MF A01

The development of two advanced reduced-basis methods, the force derivative method and the Lanczos method, and two widely used modal methods, the mode displacement method and the mode acceleration method, for transient structural analysis of unconstrained structures is presented. Two example structural problems are studied: an undamped, unconstrained beam subject to a uniformly distributed load which varies as a sinusoidal function of time and an undamped high-speed civil transport aircraft subject to a normal wing tip load which varies as a sinusoidal function of time. These example problems are used to verify the methods and to compare the relative effectiveness of each of the four reduced-basis methods for performing transient structural analyses on unconstrained structures. The methods are verified with a solution obtained by integrating directly the full system of equations of motion, and they are compared using the number of basis vectors required to obtain a desired level of accuracy and the associated computational times as comparison criteria. Author (revised)

N94-17269 Dayton Univ., OH. Research Inst.

ELASTIC-PLASTIC FINITE-DIFFERENCE ANALYSIS OF UNIDIRECTIONAL COMPOSITES SUBJECTED TO THERMOMECHANICAL CYCLIC LOADING Final Report, 1 Jan. - 1 Dec. 1992

Demirkan Coker and Noel E. Ashbaugh Dec. 1992 99 p Limited Reproducibility: More than 20% of this document may be affected by microfiche quality

(Contract F33615-91-C-5606)

(AD-A267666; WL-TR-93-4043) Avail: Issuing Activity (Defense Technical Information Center (DTIC))

An analytical tool was developed to model a unidirectional composite subjected to thermomechanical cyclic loading and processing conditions. The finite difference method was incorporated into a PC compatible computer code, FIDEP (Finite-Difference Code for Elastic-Plastic Analysis of Composites). FIDEP provides an efficient numerical procedure for analyzing a variety of problems involving thermal and mechanical cycling. The procedure allows the modeling of the constituent materials as elastic-plastic with temperature dependent properties. The concentric cylinder

approximation allows the computations to capture the three-dimensional aspects of the stress state in a real composite. Results for a thermal cool-down in an SCS-6/Ti-24Al-11Nb unidirectional composite compare well with those obtained using the finite element method. Several problems were solved for thermomechanical loading conditions and demonstrate the three-dimensional nature of the stress fields in the matrix material. DTIC

N94-17445*# Washington Univ., Saint Louis, MO. Center for Computational Mechanics.

SOLUTION OF ELASTIC-PLASTIC STRESS ANALYSIS PROBLEMS BY THE p-VERSION OF THE FINITE ELEMENT METHOD

Barna A. Szabo, Ricardo L. Actis, and Stefan M. Holzer Nov. 1993 28 p

(Grant NAG9-622)

(NASA-CR-194267; NAS 1.26:194267; WU/CCM-93/3) Avail: CASI HC A03/MF A01

The solution of small strain elastic-plastic stress analysis problems by the p-version of the finite element method is discussed. The formulation is based on the deformation theory of plasticity and the displacement method. Practical realization of controlling discretization errors for elastic-plastic problems is the main focus. Numerical examples which include comparisons between the deformation and incremental theories of plasticity under tight control of discretization errors are presented. Author

N94-17451*# National Aeronautics and Space Administration. Langley Research Center, Hampton, VA.

SPACE STATION/ORBITER BERTHING DYNAMICS DURING AN ASSEMBLY FLIGHT

Paul A. Cooper, Alan E. Stockwell (Lockheed Engineering and Sciences Co., Hampton, VA.), and Shih-Chin Wu (Lockheed Engineering and Sciences Co., Hampton, VA.) Dec. 1993 22 p Presented at the MSC World Users' Conference, Arlington, VA, 24-28 May 1993

(RTOP 585-03-11-02)

(NASA-TM-109049; NAS 1.15:109049) Avail: CASI HC A03/MF A01

A large-angle, multi-body, dynamic modeling capability was developed to help validate numerical simulations of the dynamic motion and control forces which occur while berthing Space Station Freedom to the Shuttle Orbiter during early assembly flights. The paper describes the dynamics and control of the station, the attached Shuttle Remote Manipulator System, and the Orbiter during a maneuver from a gravity-gradient attitude to a torque equilibrium attitude using the station reaction control jets. The influence of the elastic behavior of the station and of the remote manipulator system on the attitude control of the station/Orbiter system during the maneuver is investigated. The flexibility of the station and the arm had only a minor influence on the attitude control of the system during the maneuver. Author

N94-17479*# National Aeronautics and Space Administration. Langley Research Center, Hampton, VA.

STRUCTURAL MECHANICS DIVISION RESEARCH AND TECHNOLOGY ACCOMPLISHMENTS FOR CY 1992 AND PLANS FOR CY 1993

John B. Malone Nov. 1993 118 p

(RTOP 505-63-50-07)

(NASA-TM-107752; NAS 1.15:107752) Avail: CASI HC A06/MF A02

The purpose of this report is to present the Structural Mechanics Division's research accomplishments for C.Y. 1992 and plans for C.Y. 1993. The technical mission and goals of the division and its constituent research branches are described. The work under each branch is described in terms of highlights of accomplishments during the past year and plans for the current year as they relate to branch long range goals. This information is useful in program coordination with other government organizations, universities, and industry in areas of mutual interest. Author

N94-17481*# National Aeronautics and Space Administration. Lewis Research Center, Cleveland, OH.

FLUTTER ANALYSIS USING TRANSVERSALITY THEORY

D. Afolabi Nov. 1993 24 p

(Contract NCC3-233; RTOP 505-90-5K)

(NASA-TM-106382; ICOMP-93-43; E-8200; NAS 1.15:106382) Avail: CASI HC A03/MF A01

A new method of calculating flutter boundaries of undamped aeronautical structures is presented. The method is an application of the weak transversality theorem used in catastrophe theory. In the first instance, the flutter problem is cast in matrix form using a frequency domain method, leading to an eigenvalue matrix. The characteristic polynomial resulting from this matrix usually has a smooth dependence on the system's parameters. As these parameters change with operating conditions, certain critical values are reached at which flutter sets in. Our approach is to use the transversality theorem in locating such flutter boundaries using this criterion: at a flutter boundary, the characteristic polynomial does not intersect the axis of the abscissa transversally. Formulas for computing the flutter boundaries and flutter frequencies of structures with two degrees of freedom are presented, and extension to multi-degree of freedom systems is indicated. The formulas have obvious applications in, for instance, problems of panel flutter at supersonic Mach numbers. Author

N94-17507# Texas Univ., Austin. Dept. of Aerospace Engineering and Engineering Mechanics.

DAMAGE EVOLUTION IN FILLED ELASTOMERS Final Report, Oct. 1990 - Mar. 1993

K. Ha, S. Park, and R. A. Schapery 17 Jun. 1993 32 p

(Contract N00014-91-J-1738)

(AD-A268067) Avail: CASI HC A03/MF A01

This report summarizes theoretical and experimental research on distributed damage growth and its effect on stress-strain behavior and on the strain distribution around macrocracks in particle-filled rubber. Two Appendices provide details on the constitutive model, experimental determination of deformation and damage in specimens under axial straining and confining pressure, and experimental measurement of strain fields in biaxially-stressed specimens with cracks. DTIC

N94-17600 National Aerospace Lab., Amsterdam (Netherlands). Structures and Materials Div.

THE PHOTONICAL, PURE GRID METHOD

Pieter J. Sevenhuijsen 9 Dec. 1992 29 p Submitted for publication Limited Reproducibility: More than 20% of this document may be affected by microfiche quality

(NLR-TP-91478-U; ETN-93-94785) Avail: CASI HC A03

An introduction to the pure grid method for deformation measurements in experimental mechanics is presented. The pure grid method involves that the grid images are processed separately and subsequently the results of these separate processings are substrated from each other in order to obtain a quantified deformation indication. Nowadays, the recording and processing of the grid images can be performed photonically by means of digital image measurement systems. The basic data processing relations and set ups of four different applicabilities are discussed. Strains can be measured with errors smaller than 200 microstrain and displacements with errors smaller than 1/50,000 of the diameter of the object as visible in the grid image. These figures can be improved substantially by future application of high resolving power Charge Coupled Device (CCD) cameras. Two examples are shown. An extensive bibliography for further explorations is also presented. ESA

N94-17664# Los Alamos National Lab., NM.

SHEAR WAVE MEASUREMENTS IN SHOCK-INDUCED, HIGH-PRESSURE PHASES

J. B. Aidun 1993 5 p Presented at the 14th International Conference on High Pressure Science and Technology and 1993 Technical Meeting of the Topical Group on Shock Compression of Condensed Matter, Colorado Springs, CO, 28 Jun. - 3 Jul. 1993

(Contract W-7405-eng-36)

(DE93-016461; LA-UR-93-2319; CONF-9306167-9) Avail: CASI HC A01/MF A01

Structural phase transformations under shock loading are of considerable interest for understanding the response of solids under nonhydrostatic stresses and at high strain-rates. Examining shock-induced transformations from continuum level measurements is fundamentally constrained by the inability to directly identify microscopic processes, and also by the limited number of material properties that can be directly measured. The latter limitation can be reduced by measuring both shear and compression waves using Lagrangian gauges in combined, compression and shear loading. The shear wave serves as an important, real-time probe of the shocked state and unloading response. Using results from a recent study of CaCO3, the unique information obtained from the shear wave speed and the detailed

structure of the shear wave are shown to be useful for distinguishing the effects of phase transformations from yielding, as well as in characterizing the high-pressure phases and the yielding process under shock loading.
DOE

N94-16253*# National Aeronautics and Space Administration. Lyndon B. Johnson Space Center, Houston, TX.
IMPACT PENETRATION EXPERIMENTS IN TEFLON TARGETS OF VARIABLE THICKNESS Abstract Only
F. Hoerz, M. J. Cintala, R. P. Bernhard (Lockheed Engineering and Sciences Co., Houston, TX.), and T. H. See (Lockheed Engineering and Sciences Co., Houston, TX.) *In* Lunar and Planetary Inst., Twenty-Fourth Lunar and Planetary Science Conference. Part 2: G-M 1993 p 673-674 (For primary document see N94-16173 03-91)
Avail: CASI HC A01/MF A06

N94-16254*# Boeing Co., Seattle, WA. Shock Physics Group.
SIMULATION OF COLLISIONAL FRAGMENTATION WITH EXPLOSIVES Abstract Only
Kevin Housen *In* Lunar and Planetary Inst., Twenty-Fourth Lunar and Planetary Science Conference. Part 2: G-M 1993 p 675-676 (For primary document see N94-16173 03-91)
Avail: CASI HC A01/MF A06

42 GEOSCIENCES (GENERAL)

N94-16595*# Jet Propulsion Lab., California Inst. of Tech., Pasadena.
SUMMARIES OF THE THIRD ANNUAL JPL AIRBORNE GEOSCIENCE WORKSHOP. VOLUME 2: TIMS WORKSHOP
Vincent J. Realmuto, ed. 1 Jun. 1992 69 p Workshop held in Pasadena, CA, 1-5 Jun. 1992
(NASA-CR-194541; JPL-Publ-92-14-Vol-2; NAS 1.26:194541) Avail: CASI HC A04/MF A01

This publication contains the preliminary agenda and summaries for the Third Annual JPL Airborne Geoscience Workshop, held at the Jet Propulsion Laboratory, Pasadena, California, on 1-5 June 1992. This main workshop is divided into three smaller workshops as follows: (1) the Airborne Visible/Infrared Imaging Spectrometer (AVIRIS) workshop, on June 1 and 2; the summaries for this workshop appear in Volume 1; (2) the Thermal Infrared Multispectral Scanner (TIMS) workshop, on June 3; the summaries for this workshop appear in Volume 2; and (3) the Airborne Synthetic Aperture Radar (AIRSAR) workshop, on June 4 and 5; the summaries for this workshop appear in Volume 3. For individual titles, see N94-16596 through N94-16608.

N94-16596*# National Aeronautics and Space Administration. John C. Stennis Space Center, Bay Saint Louis, MS.
TIMS PERFORMANCE EVALUATION SUMMARY **c43**
Bruce Spiering, G. Meeks, J. Anderson, S. Jaggi, and S. Kuo *In* JPL, Summaries of the Third Annual JPL Airborne Geoscience Workshop. Volume 2: TIMS Workshop 1 Jun. 1992 p 1-3 (For primary document see N94-16595 03-42)
Avail: CASI HC A01/MF A01

The purpose of this effort was to investigate the Thermal Infrared Multispectral Scanner (TIMS) operation under various conditions to determine what effect, if any, there is on the TIMS performance. This effort was undertaken because of reports from investigators that the TIMS is not performing as expected when flown on the ARC C-130. This effort was initiated with a meeting at Stennis Space Center (SSC) with representatives from SSC, Jet Propulsion Laboratory (JPL), and ARC. Author (revised)

N94-16597*# Lockheed Engineering and Sciences Co., Bay Saint Louis, MS.
A QUANTITATIVE ANALYSIS OF TIMS DATA OBTAINED ON THE LEARJET 23 AT VARIOUS ALTITUDES **c43**
S. Jaggi *In* JPL, Summaries of the Third Annual JPL Airborne Geoscience Workshop. Volume 2: TIMS Workshop 1 Jun. 1992 p 4-6 (For primary document see N94-16595 03-42)
Avail: CASI HC A01/MF A01

A series of Thermal Infrared Multispectral Scanner (TIMS) data acquisition flights were conducted on the NASA Learjet 23 at different altitudes over a test site. The objective was to monitor the performance of the TIMS (its estimation of the brightness temperatures of the ground scene) with increasing altitude. The results do not show any significant correlation between the brightness temperatures and the altitude. The analysis indicates that the estimation of the temperatures is a function of the accuracy of the atmospheric correction used for each altitude.
Author (revised)

N94-16598*# Lockheed Engineering and Sciences Co., Bay Saint Louis, MS.
ANALYSIS OF TIMS PERFORMANCE SUBJECTED TO SIMULATED WIND BLAST **c43**
S. Jaggi and S. Kuo *In* JPL, Summaries of the Third Annual JPL Airborne Geoscience Workshop. Volume 2: TIMS Workshop 1 Jun. 1992 p 7-9 (For primary document see N94-16595 03-42)
Avail: CASI HC A01/MF A01

The results of the performance of the Thermal Infrared Multispectral Scanner (TIMS) when it is subjected to various wind conditions in the laboratory are described. Various wind conditions were simulated using a 24 inch fan or combinations of air jet streams blowing toward either or both of the blackbody surfaces. The fan was used to simulate a large volume of air flow at moderate speeds (up to 30 mph). The small diameter air jets were used to probe TIMS system response in reaction to localized wind perturbations. The maximum nozzle speed of the air jet was 60 mph. A range of wind directions and speeds were set up in the laboratory during the test. The majority of the wind tests were conducted under ambient conditions with the room temperature fluctuating no more than 2 C. The temperature of the high speed air jet was determined to be within 1 C of the room temperature. TIMS response was recorded on analog tape. Additional thermistor readouts of the blackbody temperatures and thermocouple readout of the ambient temperature were recorded manually to be compared with the housekeeping data recorded on the tape. Additional tests were conducted under conditions of elevated and cooled room temperatures. The room temperature was varied between 19.5 to 25.5 C in these tests. The calibration parameters needed for quantitative analysis of TIMS data were first plotted on a scanline-by-scanline basis. These parameters are the low and high blackbody temperature readings as recorded by the TIMS and their corresponding digitized count values. Using these values, the system transfer equations were calculated. This equation allows us to compute the flux for any video count by computing the slope and intercept of the straight line that relates the flux to the digital count. The actual video of the target (the lab floor in this case) was then compared with a simulated target. This simulated target was assumed to be a blackbody at emissivity of .95 degrees and the temperature was assumed to be at ambient temperature as recorded by the TIMS for each scanline. Using the slope and the intercept the flux corresponding to this target was converted into digital counts. The counts were observed to have a strong correlation with the actual video as recorded by the TIMS. The attached graphs describe the performance of the TIMS when compressed air is blown at each one of the blackbodies at different speeds. The effect of blowing a fan and changing the room temperature is also being analyzed. Results indicate that the TIMS system responds to variation in wind speed in real time and maintains the capability to produce accurate temperatures on a scan line basis.
Author

N94-16599*# Jet Propulsion Lab., California Inst. of Tech., Pasadena.
SENSITIVITY OF BLACKBODY REFERENCE PANELS TO WIND BLAST **c43**
Gordon Hoover *In its* Summaries of the Third Annual JPL Airborne Geoscience Workshop. Volume 2: TIMS Workshop 1 Jun. 1992 p 10-12 (For primary document see N94-16595 03-42)
Avail: CASI HC A01/MF A01

As part of the effort at Stennis and JPL to discover the root causes of Thermal Infrared Multispectral Scanner's (TIMS') temperature calibration errors, a series of experiments were performed to measure the sensitivity of a heated plate to cooling by wind blast. A powerful blower which was capable of generating a jet of wind in excess of 200 miles per hour was set up. In the jet, an electrically heated copper plate, one quarter of an inch thick and six inches square, was mounted. The electrical heaters were capable of delivering a total power of 800 watts. The power to the

heaters was feedback controlled with reference to a thermistor mounted on the back of the copper plate. The plate was mounted about 2.5 feet from the blower nozzle, at about 45 deg to the direction of the jet. The jet was wide enough to wash the whole surface and its temperature at the plate was about 28 C. Author (revised)

N94-16600*# JAPEX Geoscience Inst., Tokyo (Japan).
COMPARISON OF PRELIMINARY RESULTS FROM AIRBORNE ASTER SIMULATOR (AAS) WITH TIMS DATA **c43**
Yoshiaki Kannari, Franklin Mills, Hiroshi Watanabe, Teruya Ezaka, Tatsuhiko Narita, and Sheng-Huei Chang (Geophysical and Environmental Research, Inc., New York, NY.) *In* JPL, Summaries of the Third Annual JPL Airborne Geoscience Workshop. Volume 2: TIMS Workshop 1 Jun. 1992 p 13-15 Sponsored in part by Japan Resources Observation System Organization (For primary document see N94-16595 03-42)
Avail: CASI HC A01/MF A01

The Japanese Advanced Spaceborne Thermal Emission and Reflection radiometer (ASTER), being developed for a NASA EOS-A satellite, will have 3 VNIR, 6 SWIR, and 5 TIR (8-12 micron) bands. An Airborne ASTER Simulator (AAS) was developed for Japan Resources Observation System Organization (JAROS) by the Geophysical Environmental Research Group (GER) Corp. to research surface temperature and emission features in the MWIR/TIR, to simulate ASTER's TIR bands, and to study further possibility of MWIR/TIR bands. ASTER Simulator has 1 VNIR, 3 MWIR (3-5 microns), and 20 (currently 24) TIR bands. Data was collected over 3 sites - Cuprite, Nevada; Long Valley/Mono Lake, California; and Death Valley, California - with simultaneous ground truth measurements. Preliminary data collected by AAS for Cuprite, Nevada is presented and AAS data is compared with Thermal Infrared Multispectral Scanner (TIMS) data. Author (revised)

N94-16601*# Tokyo Univ. (Japan). Dept. of Mineral Development Engineering.
APPLICATION OF SPLIT WINDOW TECHNIQUE TO TIMS DATA **c43**
Tsuneo Matsunaga, Shuichi Rokugawa, and Yoshinori Ishii *In* JPL, Summaries of the Third Annual JPL Airborne Geoscience Workshop. Volume 2: TIMS Workshop 1 Jun. 1992 p 16-18 (For primary document see N94-16595 03-42)
Avail: CASI HC A01/MF A01

Absorptions by the atmosphere in thermal infrared region are mainly due to water vapor, carbon dioxide, and ozone. As the content of water vapor in the atmosphere greatly changes according to weather conditions, it is important to know its amount between the sensor and the ground for atmospheric corrections of thermal Infrared Multispectral Scanner (TIMS) data (i.e. radiosonde). On the other hand, various atmospheric correction techniques were already developed for sea surface temperature estimations from satellites. Among such techniques, Split Window technique, now widely used for AVHRR (Advanced Very High Resolution Radiometer), uses no radiosonde or any kind of supplementary data but a difference between observed brightness temperatures in two channels for estimating atmospheric effects. Applications of Split Window technique to TIMS data are discussed because availability of atmospheric profile data is not clear when ASTER operates. After these theoretical discussions, the technique is experimentally applied to TIMS data at three ground targets and results are compared with atmospherically corrected data using LOWTRAN 7 with radiosonde data. Author (revised)

N94-16602*# Purdue Univ., West Lafayette, IN. Dept. of Earth and Atmospheric Sciences.
ATMOSPHERIC CORRECTIONS FOR TIMS ESTIMATED EMITTANCE **c48**
T. A. Warner and D. W. Levandowski *In* JPL, Summaries of the Third Annual JPL Airborne Geoscience Workshop. Volume 2: TIMS Workshop 1 Jun. 1992 p 19-21 (For primary document see N94-16595 03-42)
(Contract DI-BM-G1114118)
Avail: CASI HC A01/MF A01

The estimated temperature of the average of 500 lines of Thermal Infrared Multispectral Scanner (TIMS) data of the Pacific Ocean, from flight line 94, collected on 30 Sep. 1988, at 1931 GMT is shown. With no atmospheric corrections, estimated temperature decreases away from nadir (the center of the scan line). A LOWTRAN modeled correction, using local radiosonde data and instrument scan angle information, results in reversed limb darkening effects for most bands, and does not adequately correct all bands to the same temperature. The atmosphere tends to re-radiate energy at the wavelengths at which it most absorbs, and thus the overall difference between corrected and uncorrected temperatures is approximately 40 C, despite the average LOWTRAN calculated transmittance of only 60 percent between 8.1 and 11.6 microns. An alternative approach to atmospheric correction is a black body normalization. This is done by calculating a normalization factor for each pixel position and wavelength, which when applied results in a single calculated temperature, as would be expected for a gray body with near uniform emittance. The black body adjustment is based on the atmospheric conditions over the sea. The ground elevation profile along the remaining 3520 scan lines (approximately 10 km) of flight line 94, up the slopes of Kilauea, determined from aircraft pressure and laser altimeter data is shown. This flight line includes a large amount of vegetation that is clearly discernible on the radiance image, being much cooler than the surrounding rocks. For each of the 3520 scan lines, pixels were classified as vegetation or 'other'. A moving average of 51 lines was applied to the composite vegetation emittance for each scan line, to reduce noise. Assuming vegetation to be like water, and to act as gray body with an emittance of 0.986 across the spectrum, it is shown that that the LOWTRAN induced artifacts are severe, and other than for the 0.9.9 micron channel, not significantly different from applying no corrections at all. As expected, with increasing elevation atmospheric effects are slightly reduced, because moisture tends to be concentrated in the lowermost part of the atmosphere. The black body adjustment is highly robust, and even at elevations nearly 600 meters above the sea, remains an alternative procedure for use in calculating emittance. Author (revised)

N94-16603*# National Aeronautics and Space Administration. John C. Stennis Space Center, Bay Saint Louis, MS.
AN ALGORITHM FOR THE ESTIMATION OF BOUNDS ON THE EMISSIVITY AND TEMPERATURES FROM THERMAL MULTISPECTRAL AIRBORNE REMOTELY SENSED DATA **c43**
S. Jaggi (Lockheed Engineering and Sciences Co., Bay Saint Louis, MS.), D. Quattrochi, and R. Baskin (Geological Survey, Salt Lake City, UT.) *In* JPL, Summaries of the Third Annual JPL Airborne Geoscience Workshop. Volume 2: TIMS Workshop 1 Jun. 1992 p 22-24 (For primary document see N94-16595 03-42)
Avail: CASI HC A01/MF A01

The effective flux incident upon the detectors of a thermal sensor, after it has been corrected for atmospheric effects, is a function of a non-linear combination of the emissivity of the target for that channel and the temperature of the target. The sensor system cannot separate the contribution from the emissivity and the temperature that constitute the flux value. A method that estimates the bounds on these temperatures and emissivities from thermal data is described. This method is then tested with remotely sensed data obtained from NASA's Thermal Infrared Multispectral Scanner (TIMS) - a 6 channel thermal sensor. Since this is an under-determined set of equations i.e. there are 7 unknowns (6 emissivities and 1 temperature) and 6 equations (corresponding to the 6 channel fluxes), there exist theoretically an infinite combination of values of emissivities and temperature that can satisfy these equations. Using some realistic bounds on the emissivities, bounds on the temperature are calculated. These bounds on the temperature are refined to estimate a tighter bound on the emissivity of the source. An error analysis is also carried out to quantitatively determine the extent of uncertainty introduced in the estimate of these parameters. This method is useful only when a realistic set of bounds can be obtained for the emissivities of the data. In the case of water the lower and upper bounds were set at 0.97 and 1.00 respectively. Five flights were flown in succession at altitudes of 2 km (low), 6 km (mid), 12 km (high), and then back again at 6 km and 2 km. The area selected with the Ross Barnett reservoir near Jackson, Mississippi. The mission was flown during the predawn hours of 1 Feb. 1992. Radiosonde data was collected for that duration to profile the characteristics of the atmosphere. Ground truth temperatures using thermometers and radiometers were also obtained over an area of the reservoir. The results of two independent runs of the radiometer data averaged 7.03 plus or minus .70 for the first run and 7.31 plus or minus .88 for the second run. The results of the algorithm yield a temperature of 7.68 for the low altitude data to 8.73 for the high altitude data. Author (revised)

N94-16604*# National Aeronautics and Space Administration. John C. Stennis Space Center, Bay Saint Louis, MS.

MULTI-RESOLUTION PROCESSING FOR FRACTAL ANALYSIS OF AIRBORNE REMOTELY SENSED DATA **c43**

S. Jaggi (Lockheed Engineering and Sciences Co., Bay Saint Louis, MS.), D. Quattrochi, and N. Lam (Louisiana State Univ., Baton Rouge.) *In* JPL, Summaries of the Third Annual JPL Airborne Geoscience Workshop. Volume 2: TIMS Workshop 1 Jun. 1992 p 25-27 (For primary document see N94-16595 03-42)

Avail: CASI HC A01/MF A01

Fractal geometry is increasingly becoming a useful tool for modeling natural phenomenon. As an alternative to Euclidean concepts, fractals allow for a more accurate representation of the nature of complexity in natural boundaries and surfaces. Since they are characterized by self-similarity, an ideal fractal surface is scale-independent; i.e. at different scales a fractal surface looks the same. This is not exactly true for natural surfaces. When viewed at different spatial resolutions parts of natural surfaces look alike in a statistical manner and only for a limited range of scales. Images acquired by NASA's Thermal Infrared Multispectral Scanner are used to compute the fractal dimension as a function of spatial resolution. Three methods are used to determine the fractal dimension - Schelberg's line-divider method, the variogram method, and the triangular prism method. A description of these methods and the results of applying these methods to a remotely-sensed image is also presented. Five flights were flown in succession at altitudes of 2 km (low), 6 km (mid), 12 km (high), and then back again at 6 km and 2 km. The area selected was the Ross Barnett reservoir near Jackson, Mississippi. The mission was flown during the predawn hours of 1 Feb. 1992. Radiosonde data was collected for that duration to profile the characteristics of the atmosphere. This corresponds to 3 different pixel sizes - 5m, 15m, and 30m. After, simulating different spatial sampling intervals within the same image for each of the 3 image sets, the results are cross-correlated to compare the extent of detail and complexity that is obtained when data is taken at lower spatial intervals.

Author (revised)

N94-16605*# Geological Survey, Reston, VA.

PRELIMINARY ANALYSIS OF THERMAL-INFRARED MULTISPECTRAL SCANNER DATA OF THE IRON HILL, COLORADO CARBONATITE-ALKALIC ROCK COMPLEX **c43**

Lawrence C. Rowan, Kenneth Watson (Geological Survey, Denver, CO.), and Susanne H. Miller (Geological Survey, Denver, CO.) *In* JPL, Summaries of the Third Annual JPL Airborne Geoscience Workshop. Volume 2: TIMS Workshop 1 Jun. 1992 p 28-30 (For primary document see N94-16595 03-42)

Avail: CASI HC A01/MF A01

The Iron Hill carbonatite-alkalic igneous rock complex is in the Powderhorn mining district, approximately 40 km south-southwest of Gunnison, Colorado. The complex, which occupies about 30 sq km, was emplaced in metasedimentay and metavolcanic rocks during the later Precambrian or early Cambrian. The main rock types in the complex, from oldest to youngest, are fenite, pyroxenite, uncompahgrite, ijolite, nepheline syenite, and dolomitic carbonatite. The carbonatite is limonitic and forms an elliptially shaped 4 sq km stock. Calcitic and dolomitic carbonatite dikes are also numerous throughout the complex and in the pre-existing rocks. Pyroxenite is the most widespread rock type within the complex, but pyroxene is extensively altered to biotite, phlogopite, and vermiculite. Fenite, which formed through Na, K-metasomatism of the country rocks, typically contains more feldspar and less quartz than the equivalent unaltered country rocks. The other alkalic rock types are less widespread and less well exposed. Parts of the complex are covered by Oligocene ash-flow tuff and alluvial, colluvial, and glacial deposits. Sagebrush and grass cover is moderately dense to very dense at low to intermediate elevations; coniferous tree cover is dense at high elevations and on some north-facing slopes at lower elevations. A new algorithm was used to compute spectral emissivity ratios, independent of any emissivity assumptions. This algorithm has the advantage that any of the possible emissivity ratios can be computed and, thus, a large variety of composite ratio images can be constructed, which permits examination of various geologic hypotheses based on the spectral properties of the surface materials. Author (revised)

N94-16606*# Hawaii Univ., Honolulu. Inst. of Planetary Geosciences.

THE USE OF TIMS FOR MAPPING DIFFERENT PAHOEHOE SURFACES: MAUNA IKI, KILAUEA **c43**

Scott K. Rowland *In* JPL, Summaries of the Third Annual JPL Airborne Geoscience Workshop. Volume 2: TIMS Workshop 1 Jun. 1992 p 31-33 (For primary document see N94-16595 03-42)

Avail: CASI HC A01/MF A01

S-type and p-type pahoehoe record different mechanisms and vigors of activity within an active flow field. There is some controversy about what these mechanisms are exactly, and this study was undertaken with the idea that an accurate map of the two surfaces within a pahoehoe flow field could be helpful in solving the problem. Thermal Infrared Multispectral Scanner (TIMS) allows discrimination between s-type and p-type pahoehoe, and this ability was used to map the two surface types on the Mauna Iki satellite shield (southwest rift zone, Kilauea Volcano). TIMS was previously used to discriminate a'a from pahoehoe as well as to determine relative age relationships of different flows. Although inter-flow variation was minor in the data published by these authors, a second goal presented is to understand such variations to better constrain intra-flow differences used for age dating. Author (revised)

N94-16607*# Arizona State Univ., Tempe. Dept. of Geology.

EJECTA PATTERNS OF METEOR CRATER, ARIZONA DERIVED FROM THE LINEAR UN-MIXING OF TIMS DATA AND LABORATORY THERMAL EMISSION SPECTRA **c43**

Michael S. Ramsey and Philip R. Christensen *In* JPL, Summaries of the Third Annual JPL Airborne Geoscience Workshop. Volume 2: TIMS Workshop 1 Jun. 1992 p 34-36 (For primary document see N94-16595 03-42)

Avail: CASI HC A01/MF A01

Accurate interpretation of thermal infrared data depends upon the understanding and removal of complicating effects. These effects may include physical mixing of various mineralogies and particle sizes, atmospheric absorption and emission, surficial coatings, geometry effects, and differential surface temperatures. The focus is the examination of the linear spectral mixing of individual mineral or endmember spectra. Linear addition of spectra, for particles larger than the wavelength, allows for a straight-forward method of deconvolving the observed spectra, predicting a volume percent of each endmember. The 'forward analysis' of linear mixing (comparing the spectra of physical mixtures to numerical mixtures) has received much attention. The reverse approach of un-mixing thermal emission spectra was examined with remotely sensed data, but no laboratory verification exists. Understanding of the effects of spectral mixing on high resolution laboratory spectra allows for the extrapolation to lower resolution, and often more complicated, remotely gathered data. Thermal Infrared Multispectral Scanner (TIMS) data for Meteor Crater, Arizona were acquired in Sep. 1987. The spectral un-mixing of these data gives a unique test of the laboratory results. Meteor Crater (1.2 km in diameter and 180 m deep) is located in north-central Arizona, west of Canyon Diablo. The arid environment, paucity of vegetation, and low relief make the region ideal for remote data acquisition. Within the horizontal sedimentary sequence that forms the upper Colorado Plateau, the oldest unit sampled by the impact crater was the Permian Coconino Sandstone. A thin bed of the Toroweap Formation, also of Permian age, conformably overlays the Coconino. Above the Toroweap lies the Permian Kiabab Limestone which, in turn, is covered by a thin veneer of the Moenkopi Formation. The Moenkopi is Triassic in age and has two distinct sub-units in the vicinity of the crater. The lower Wupatki member is a fine-grained sandstone, while the upper Moqui member is a fissile siltstone. Ejecta from these units are preserved as inverted stratigraphy up to 2 crater radii from the rim. The mineralogical contrast between the units, relative lack of post-emplacement erosion and ejecta mixing provide a unique site to apply the un-mixing model. Selection of the aforementioned units as endmembers reveals distinct patterns in the ejecta of the crater. Author (revised)

N94-16608*# Jet Propulsion Lab., California Inst. of Tech., Pasadena.

THE USE OF TIMS DATA TO ESTIMATE THE SO2 CONCENTRATIONS OF VOLCANIC PLUMES: A CASE STUDY AT MOUNT ETNA, SICILY **c46**

Vincent J. Realmuto *In its* Summaries of the Third Annual JPL Airborne Geoscience Workshop. Volume 2: TIMS Workshop 1 Jun. 1992

p 37-39 (For primary document see N94-16595 03-42)
Avail: CASI HC A01/MF A01

Thermal Infrared Multispectral Scanner (TIMS) data were acquired over Mount Etna, Sicily, on 29 July 1986. The volcanic activity at that time was characterized by the steady effusion of gas from the Bocca Nuova (BN), Chasm, and Southeast craters. The Northeast crater, quiet at the time of the TIMS overflight, was the site of Strombolian eruptive activity between 31 July and 24 Sep. 1986. In aerial photographs of the Etna summit region acquired during the TIMS overflight, the SO2-rich plume is visible due to the scattering of sunlight by the entrained aerosols. In the TIMS imagery, the plume is revealed by the strong absorption of SO2 between 8 and 9 microns. This absorption feature falls within the first three channels of TIMS, with the strongest absorption falling within Channel 2. Following decorrelation processing, the plume is visible in color-composites of TIMS channels 2, 3, and 5. To estimate the concentration of SO2 within the plume, the LOWTRAN 7 radiative transfer code was used to model the radiance spectra measured by TIMS. Author (revised)

N94-16666*# Jet Propulsion Lab., California Inst. of Tech., Pasadena.
SUMMARIES OF THE THIRD ANNUAL JPL AIRBORNE GEOSCIENCE WORKSHOP. VOLUME 1: AVIRIS WORKSHOP
Robert O. Green, ed. 1 Jun. 1992 184 p Workshop held in Pasadena, CA, 1-5 Jun. 1992
(NASA-CR-194540; JPL-Publ-92-14-Vol-1; NAS 1.26:194540) Avail: CASI HC A09/MF A02

This publication contains the preliminary agenda and summaries for the Third Annual JPL Airborne Geoscience Workshop, held at the Jet Propulsion Laboratory, Pasadena, California, on 1-5 June 1992. This main workshop is divided into three smaller workshops as follows: (1) the Airborne Visible/Infrared Imaging Spectrometer (AVIRIS) workshop, on June 1 and 2; (2) the Thermal Infrared Multispectral Scanner (TIMS) workshop, on June 3; and (3) the Airborne Synthetic Aperture Radar (AIRSAR) workshop, on June 4 and 5. The summaries are contained in Volumes 1, 2, and 3, respectively. For individual titles, see N94-16667 through N94-16714.

N94-16667*# Jet Propulsion Lab., California Inst. of Tech., Pasadena.
IN-FLIGHT CALIBRATION OF THE SPECTRAL AND RADIOMETRIC CHARACTERISTICS OF AVIRIS IN 1991 **c35**
Robert O. Green, James E. Conel, Carol J. Bruegge, Jack S. Margolis, Veronique Carrere, Gregg Vane, and Gordon Hoover *In its* Summaries of the Third Annual JPL Airborne Geoscience Workshop. Volume 1: AVIRIS Workshop 1 Jun. 1992 p 1-4 (For primary document see N94-16666 03-42)
Avail: CASI HC A01/MF A02

On 7 Mar. 1991, an in-flight calibration experiment was held at the Ivanpah Playa in southeastern California for the Airborne Visible/Infrared Imaging Spectrometer (AVIRIS) imaging spectrometer. Five AVIRIS overflights were acquired of a calibration target designated on the Ivanpah Playa surface. At the time of the overflights, the reflectance of the calibration target was measured with a field spectrometer. In addition, the atmospheric optical depths and water vapor abundance were measured from a radiometer station adjacent to the calibration target. These in-situ measurements were used to constrain the MODTRAN radiative transfer code to model the upwelling spectral radiance incident to the sensor aperture during the overflights. Analyses of this modeled radiance in conjunction with the laboratory-calibrated radiance were used to determine the spectral and radiometric calibration of AVIRIS while in flight. Author (revised)

N94-16668*# California Univ., Davis. Dept. of Land, Air and Water Resources.
USING AVIRIS IMAGES TO MEASURE TEMPORAL TRENDS IN ABUNDANCE OF PHOTOSYNTHETIC AND NONPHOTOSYNTHETIC CANOPY COMPONENTS **c43**
Susan L. Ustin, Milton O. Smith (Washington Univ., Seattle.), Dar Roberts (Washington Univ., Seattle.), John A. Gamon (California State Univ., Los Angeles.), and Christopher B. Field (Carnegie Institution of Washington, Stanford, CA.) *In* JPL, Summaries of the Third Annual JPL Airborne Geoscience Workshop. Volume 1: AVIRIS Workshop 1 Jun. 1992 p 5-7 (For primary document see N94-16666 03-42)
Avail: CASI HC A01/MF A02

The Jasper Ridge Biological Preserve, Stanford, California is a good example of hardwood rangeland ecosystems in California. Structurally, it is composed of a mosaic of serpentine grasslands, oak savannah, coastal chaparral, and mixed evergreen woodland, representing a broad cross-section of physiognomic classes. The Mediterranean climate produces an extended seasonal drought lasting throughout most of the growing season and has significant impact on the expression of divergent phenological patterns related to contrasting ecological strategies of these taxa. The region is well understood biologically due to the rich history of ecological research at the site. Thus, community characteristics, physiological characteristics, phenology, and temporal dynamics are reasonably well understood for many of the dominant species. Because of its proximity to NASA Ames Research Center, it has been subject to a large number of aircraft data acquisitions over many years. A more complete examination of this database would provide an opportunity to test current remote sensing hypotheses for measurement and detection of ecological attributes, particularly those involving canopy chemistry and physiology. Better definition of ecological rules might permit development of remotely sensed surrogate variables for biological properties that cannot be directly measured or measured with sufficient accuracy. Author

N94-16669*# Colorado Univ., Boulder. Center for the Study of Earth from Space.
UNMIXING AVIRIS DATA TO PROVIDE A METHOD FOR VEGETATION FRACTION SUBTRACTION **c43**
J. A. Zamudio *In* JPL, Summaries of the Third Annual JPL Airborne Geoscience Workshop. Volume 1: AVIRIS Workshop 1 Jun. 1992 p 8-10 (For primary document see N94-16666 03-42)
Avail: CASI HC A01/MF A02

Five flight lines of Airborne Visible/Infrared Imaging Spectrometer (AVIRIS) data were acquired over the Dolly Varden Mountains in northeastern Nevada on 2 June 1989. Signal-to-noise ratio values are given. The empirical line method was used to convert AVIRIS radiance values to reflectance. This method involves calculating gain and offset values for each band. These values are based upon a comparison of the imaging spectrometer data and field reflectance measurements, both taken over the same ground targets. The targets used were a dark andesite flow and a bright playa. Author (revised)

N94-16670*# Geological Survey, Denver, CO.
MAPPING THE MINERALOGY AND LITHOLOGY OF CANYONLANDS, UTAH WITH IMAGING SPECTROMETER DATA AND THE MULTIPLE SPECTRAL FEATURE MAPPING ALGORITHM **c43**
Roger N. Clark, Gregg A. Swayze, and Andrea Gallagher *In* JPL, Summaries of the Third Annual JPL Airborne Geoscience Workshop. Volume 1: AVIRIS Workshop 1 Jun. 1992 p 11-13 (For primary document see N94-16666 03-42)
Avail: CASI HC A01/MF A02

The sedimentary sections exposed in the Canyonlands and Arches National Parks region of Utah (generally referred to as 'Canyonlands') consist of sandstones, shales, limestones, and conglomerates. Reflectance spectra of weathered surfaces of rocks from these areas show two components: (1) variations in spectrally detectable mineralogy, and (2) variations in the relative ratios of the absorption bands between minerals. Both types of information can be used together to map each major lithology and the Clark spectral features mapping algorithm is applied to do the job. Author (revised)

N94-16671*# South Dakota School of Mines and Technology, Rapid City. Inst. of Atmospheric Sciences.
SPATIAL RESOLUTION AND CLOUD OPTICAL THICKNESS RETRIEVALS **c47**
Rand E. Feind, Sundar A. Christopher, and Ronald M. Welch *In* JPL, Summaries of the Third Annual JPL Airborne Geoscience Workshop. Volume 1: AVIRIS Workshop 1 Jun. 1992 p 14-16 (For primary document see N94-16666 03-42)
(Contracts NAS5-30958; NAS5-30768; NAS5-31718)
Avail: CASI HC A01/MF A02

The impact of sensor spatial resolution and accurate cloud pixel identification on cloud property retrievals was investigated. Twelve fair weather cumulus (FWC) scenes of high spectral and spatial resolution Airborne Visible and Infrared Imaging Spectrometer (AVIRIS) data are analyzed. A variation of the 3-band ratio technique of Gao and Goetz is used to discriminate clouds from the background, and then a discrete

ordinate radiative transfer model is used to obtain optical thickness of cloudy regions for each scene. To study the effect of spatial resolution upon retrieved optical thickness, the 20 m AVIRIS data was spatially degraded to spatial resolutions ranging from 40 to 960 m. Cloud area, scene average optical thickness, and distribution of retrieved optical thickness are determined at each spatial resolution. Finally, a comparison between the 3-band ratio technique and monospectral reflectance thresholding, using 20 m spatial resolution data, is presented. Author (revised)

N94-16672*# California State Univ., Los Angeles.
EVALUATION OF SPATIAL PRODUCTIVITY PATTERNS IN AN ANNUAL GRASSLAND DURING AN AVIRIS OVERFLIGHT **c43**
John A. Gamon, Christopher B. Field (Carnegie Institution of Washington, Stanford, CA.), and Susan L. Ustin (California Univ., Davis.) *In* JPL, Summaries of the Third Annual JPL Airborne Geoscience Workshop. Volume 1: AVIRIS Workshop 1 Jun. 1992 p 17-19 Sponsored in part by A. W. Mellon Foundation (For primary document see N94-16666 03-42)
(CIW-Publ-1134) Avail: CASI HC A01/MF A02

In May 1991, coincident with an Airborne Visible/Infrared Imaging Spectrometer (AVIRIS) overflight, a ground-based study covering 9 hectares of an annual grassland was completed. There were two goals of this ground study: (1) obtain ecologically and physiologically meaningful data for relating AVIRIS images to canopy structure, biochemistry, and physiology; and (2) evaluate the suitability of the 20-m AVIRIS pixel size for depicting detailed spatial patterns of productivity. Author (revised)

N94-16673*# Naval Research Lab., Bay Saint Louis, MS.
HYPERSPECTRAL MODELING FOR EXTRACTING AEROSOLS FROM AIRCRAFT/SATELLITE DATA **c43**
G. Daniel Hickman and Michael J. Duggin (State Univ. of New York, Syracuse.) *In* JPL, Summaries of the Third Annual JPL Airborne Geoscience Workshop. Volume 1: AVIRIS Workshop 1 Jun. 1992 p 20-22 (For primary document see N94-16666 03-42)
Avail: CASI HC A01/MF A02

Sensitivity studies using the Airborne Visible/Infrared Imaging Spectrometer (AVIRIS) bands are currently under investigation. The objective of this research is to develop improved algorithms for the determination of aerosol type (e.g., presently described by S(sub 12). Preliminary computer calculations were made using LOWTRAN 7, which is the most advanced atmospheric code of the Air Force Geophysics Laboratory. LOWTRAN 7 permits the calculation of atmospheric transmission and absorption caused by aerosols and molecules along a non-homogeneous path for a variety of aerosol models. The calculations used the Navy Aerosol Model (NAM), which was constructed for the marine environment using a three component size distribution model. Calculations of the total transmittance (L(sub T)), the path radiance (L(sub P)), and the reflected radiance (L(sub r)) were made as a function of wavelength (lambda) from 0.4 to 2.4 microns for each of the 224 10 nm wide AVIRIS bands. These calculations were made for various types of atmospheres for the troposphere (0-2 km).
Author (revised)

N94-16674*# Colorado Univ., Boulder. Center for the Study of Earth from Space.
THE SPECTRAL IMAGE PROCESSING SYSTEM (SIPS): SOFTWARE FOR INTEGRATED ANALYSIS OF AVIRIS DATA **c43**
F. A. Kruse, A. B. Lefkoff, J. W. Boardman, K. B. Heidebrecht, A. T. Shapiro, P. J. Barloon, and A. F. H. Goetz *In* JPL, Summaries of the Third Annual JPL Airborne Geoscience Workshop. Volume 1: AVIRIS Workshop 1 Jun. 1992 p 23-25 (For primary document see N94-16666 03-42)
(Contract NAS5-30552; NAGw-1601)
Avail: CASI HC A01/MF A02

The Spectral Image Processing System (SIPS) is a software package developed by the Center for the Study of Earth from Space (CSES) at the University of Colorado, Boulder, in response to a perceived need to provide integrated tools for analysis of imaging spectrometer data both spectrally and spatially. SIPS was specifically designed to deal with data from the Airborne Visible/Infrared Imaging Spectrometer (AVIRIS) and the High Resolution Imaging Spectrometer (HIRIS), but was tested with other datasets including the Geophysical and Environmental Research Imaging Spectrometer (GERIS), GEOSCAN images, and Landsat TM. SIPS was developed using the 'Interactive Data Language' (IDL). It takes advantage of high speed disk access and fast processors running under the UNIX operating system to provide rapid analysis of entire imaging spectrometer datasets. SIPS allows analysis of single or multiple imaging spectrometer data segments at full spatial and spectral resolution. It also allows visualization and interactive analysis of image cubes derived from quantitative analysis procedures such as absorption band characterization and spectral unmixing. SIPS consists of three modules: SIPS Utilities, SIPS—View, and SIPS Analysis. SIPS version 1.1 is described below. Author (revised)

N94-16675*# Brown Univ., Providence, RI. Dept. of Geological Sciences.
FIRST RESULTS FROM ANALYSIS OF COORDINATED AVIRIS, TIMS, AND ISM (FRENCH) DATA FOR THE RONDA (SPAIN) AND BENI BOUSERA (MOROCCO) PERIDOTITES **c43**
J. F. Mustard, S. Hurtrez (Paris-Sud Univ., Orsay, France.), P. Pinet (Centre National d'Etudes Spatiales, Toulouse, France.), and C. Sotin (Paris-Sud Univ., Orsay, France.) *In* JPL, Summaries of the Third Annual JPL Airborne Geoscience Workshop. Volume 1: AVIRIS Workshop 1 Jun. 1992 p 26-28 (For primary document see N94-16666 03-42)
Avail: CASI HC A01/MF A02

Ultramafic rocks are relatively rare at the Earth's surface but constitute the vast majority of the Earth by volume. Exposures of ultramafic bodies are therefore crucial for deducing many important processes that occur in the Earth's mantle. An important science question regarding the spatial distribution, abundance, and composition of mafic minerals in ultramafic bodies that can be examined with advanced sensor data is the melting process. When a lherzolite melts, clinopyroxene (cpx) melts first and therefore variations in the modal amount of cpx remaining in the mantle are a reflection of the amount of fractional melting that has occurred. Fe goes preferentially into the melt during melting but a 20 percent batch melting (i.e. closed system) acquires less Fe relative to 20 percent fractional melting (i.e. open system). Since the strength and wavelength of diagnostic absorptions is a strong function of Fe content, it is possible to make maps of the variation in Fe:Mg ratios which can be related to the general melting process. Accurate ground-truth information about local mineralogy provides internal calibration and consistency checks. Investigations using imaging spectrometer are very complementary to field studies because advanced sensor data can provide a synoptic view of modal mineralogy and chemical composition whereas field studies focus on detailed characterization of local areas. Two excellent exposures of ultramafic lithologies are being investigated with visible to mid-infrared imaging spectrometer data: the Ronda peridotite near Ronda, Spain and the Beni Bousera ophiolitic fragment in northern Morocco. Although separated by the Alboran Sea, these bodies are thought to be related and represent fertile sub-continental mantle. The Ronda peridotite is predominantly spinel lherzolite but grades into harzburgite and shows considerable variation in major and trace element compositions. Mafic layering and dykes (i.e. olivine gabbro) are also observed. This indicates some sections of the peridotite have experienced greater degrees of partial melting. The Beni Bousera peridotite also contains mafic layers and dykes and grades into harzburgite representing similar fundamental shifts in the bulk chemistry of this ultramafic body probably related to an episode of partial melting. The specific mode of emplacement of these bodies is controversial and important for understanding the tectonic evolution of this region. Our investigations are not necessarily designed to help resolve this controversy. Rather, these exposures provide excellent and unusual examples of fertile mantle which have undergone variable degrees of partial melting. Author (revised)

N94-16676*# Geological Survey, Reston, VA.
AVIRIS STUDY OF DEATH VALLEY EVAPORITE DEPOSITS USING LEAST-SQUARES BAND-FITTING METHODS **c43**
J. K. Crowley and R. N. Clark (Geological Survey, Denver, CO.) *In* JPL, Summaries of the Third Annual JPL Airborne Geoscience Workshop. Volume 1: AVIRIS Workshop 1 Jun. 1992 p 29-31 (For primary document see N94-16666 03-42)
Avail: CASI HC A01/MF A02

Minerals found in playa evaporite deposits reflect the chemically diverse origins of ground waters in arid regions. Recently, it was discovered that many playa minerals exhibit diagnostic visible and near-infrared (0.4-2.5 micron) absorption bands that provide a remote sensing basis for observing important compositional details of desert ground water systems. The study of such systems is relevant to understanding solute acquisition, transport,

and fractionation processes that are active in the subsurface. Observations of playa evaporites may also be useful for monitoring the hydrologic response of desert basins to changing climatic conditions on regional and global scales. Ongoing work using Airborne Visible/Infrared Imaging Spectrometer (AVIRIS) data to map evaporite minerals in the Death Valley salt pan is described. The AVIRIS data point to differences in inflow water chemistry in different parts of the Death Valley playa system and have led to the discovery of at least two new North American mineral occurrences. Seven segments of AVIRIS data were acquired over Death Valley on 31 July 1990, and were calibrated to reflectance by using the spectrum of a uniform area of alluvium near the salt pan. The calibrated data were subsequently analyzed by using least-squares spectral band-fitting methods, first described by Clark and others. In the band-fitting procedure, AVIRIS spectra are fit compared over selected wavelength intervals to a series of library reference spectra. Output images showing the degree of fit, band depth, and fit times the band depth are generated for each reference spectrum. The reference spectra used in the study included laboratory data for 35 pure evaporite spectra extracted from the AVIRIS image cube. Additional details of the band-fitting technique are provided by Clark and others elsewhere in this volume. Author (revised)

N94-16677*# Washington Univ., Seattle. Dept. of Geological Sciences.
A FIELD MEASURE OF THE SHADE FRACTION **c43**
Alan R. Gillespie, Milton O. Smith, and Donald E. Sabol *In* JPL, Summaries of the Third Annual JPL Airborne Geoscience Workshop. Volume 1: AVIRIS Workshop 1 Jun. 1992 p 32-34 (For primary document see N94-16666 03-42)
Avail: CASI HC A01/MF A02

'Shade' has a technical definition peculiar to linear spectral mixture analysis of imaging spectrometer data: it is the reduction in radiance from a surface due to lighting conditions and geometry, and includes topographic shading described by photometric functions as well as shadowing at all scales. 'Shade' is an important constituent of nearly all remotely sensed images, and is one endmember resolved in spectral mixture analysis, where it is represented as a fraction of the measured radiance and a characteristic spectrum. This spectrum is typically the null vector, provided the data have been corrected for atmospheric and instrument effects: i.e., 'shade' is the radiance from an ideal black surface. In topographic shading, irradiance is reduced - typically in proportion to cos(i), where i (incidence angle) is the angle between the sun and the local surface normal vectors. Therefore, the radiance is lowered by a multiplicative factor. Shadowing occurs when i is greater than 90 deg, or when sunlight is blocked by adjacent high terrain; the only irradiance is down-welling skylight and bounce light from adjacent terrain. In spectral mixture analysis, 'shade' is regarded as an additive term. In this regard, it is an accurate description of the proportion of a scene that consists of ideal shadows ('checkerboard mixing'); however, 'shade' represents the multiplicative cos(i) factor as well, as here it should be interpreted as the proportion of shadow that would darken the scene an equivalent amount. In either case, the 'shade' fraction is lessened by adjacency effects, because the scene has a non-zero reflectivity instead of the ideal black surface generally assumed. Author (revised)

N94-16678*# Colorado Univ., Boulder. Center for the Study of Earth from Space.
A LINEAR SPECTRAL MATCHING TECHNIQUE FOR RETRIEVING EQUIVALENT WATER THICKNESS AND BIOCHEMICAL CONSTITUENTS OF GREEN VEGETATION **c43**
Bo-Cai Gao and Alexander F. H. Goetz *In* JPL, Summaries of the Third Annual JPL Airborne Geoscience Workshop. Volume 1: AVIRIS Workshop 1 Jun. 1992 p 35-37 (For primary document see N94-16666 03-42)
(Contract NAS5-30552)
Avail: CASI HC A01/MF A02

Over the last decade, technological advances in airborne imaging spectrometers, having spectral resolution comparable with laboratory spectrometers, have made it possible to estimate biochemical constituents of vegetation canopies. Wessman estimated lignin concentration from data acquired with NASA's Airborne Imaging Spectrometer (AIS) over Blackhawk Island in Wisconsin. A stepwise linear regression technique was used to determine the single spectral channel or channels in the AIS data that best correlated with measured lignin contents using chemical methods. The regression technique does not take advantage of the spectral shape of the lignin reflectance feature as a diagnostic tool nor the increased discrimination among other leaf components with overlapping spectral features. A nonlinear least squares spectral matching technique was recently reported for deriving both the equivalent water thicknesses of surface vegetation and the amounts of water vapor in the atmosphere from contiguous spectra measured with the Airborne Visible/Infrared Imaging Spectrometer (AVIRIS). The same technique was applied to a laboratory reflectance spectrum of fresh, green leaves. The result demonstrates that the fresh leaf spectrum in the 1.0-2.5 microns region consists of spectral components of dry leaves and the spectral component of liquid water. A linear least squares spectral matching technique for retrieving equivalent water thickness and biochemical components of green vegetation is described. Author

N94-16679*# Washington Univ., Seattle. Dept. of Geological Sciences.
MAPPING THE SPECTRAL VARIABILITY IN PHOTOSYNTHETIC AND NON-PHOTOSYNTHETIC VEGETATION, SOILS, AND SHADE USING AVIRIS **c43**
Dar A. Roberts, Milton O. Smith, Donald E. Sabol, John B. Adams, and Susan L. Ustin (California Univ., Davis.) *In* JPL, Summaries of the Third Annual JPL Airborne Geoscience Workshop. Volume 1: AVIRIS Workshop 1 Jun. 1992 p 38-40 (For primary document see N94-16666 03-42)
Avail: CASI HC A01/MF A02

The primary objective of this research was to map as many spectrally distinct types of green vegetation (GV), non-photosynthetic vegetation (NPV), shade, and soil (endmembers) in an Airborne Visible/Infrared Imaging Spectrometer (AVIRIS) scene as is warranted by the spectral variability of the data. Once determined, a secondary objective was to interpret these endmembers and their abundances spatially and spectrally in an ecological context. Author (revised)

N94-16680*# Jet Propulsion Lab., California Inst. of Tech., Pasadena.
VOLCANIC THERMAL FEATURES OBSERVED BY AVIRIS **c46**
Clive Oppenheimer (Open Univ., Milton, England.), David Pieri, Veronique Carrere, Michael Abrams (Open Univ., Milton, England.), David Rothery (Open Univ., Milton, England.), and Peter Francis (Open Univ., Milton, England.) *In its* Summaries of the Third Annual JPL Airborne Geoscience Workshop. Volume 1: AVIRIS Workshop 1 Jun. 1992 p 41-43 Sponsored by Natural Environmental Research Council (For primary document see N94-16666 03-42)
Avail: CASI HC A01/MF A02

In July 1991, Airborne Visible/Infrared Imaging Spectrometer (AVIRIS) was flown over Mount Etna and Stromboli, Italy. Lava-filled vents were then present within summit craters of both volcanoes. Since surfaces at magmatic temperatures radiate strongly over the wavelength ranges of the AVIRIS C- and D-spectrometers, it was hoped that the data collected would reveal clear thermal signatures, even of sub-pixel sized features, as have been observed in the 1.65 and 2.22 microns bands of Landsat Thematic Mapper images. This would provide an opportunity to explore the potential of imaging spectrometers for deriving temperature distributions of hot volcanic surfaces. Such research has implications for volcano monitoring in the EOS era, and also for any future AVIRIS deployments above active lava flows, lakes, and domes, where understanding of their behavior may be advanced by detailed thermal observations.
Author (revised)

N94-16681*# Centre d'Etude Spatiale des Rayonnements, Toulouse (France).
RETRIEVAL OF BIOPHYSICAL PARAMETERS WITH AVIRIS AND ISM: THE LANDES FOREST, SOUTH WEST FRANCE **c43**
F. Zagolski, J. P. Gastellu-Etchegorry, E. Mougin, G. Giordano, G. Marty, T. LeToan, and A. Beaudoin *In* JPL, Summaries of the Third Annual JPL Airborne Geoscience Workshop. Volume 1: AVIRIS Workshop 1 Jun. 1992 p 44-46 (For primary document see N94-16666 03-42)
Avail: CASI HC A01/MF A02

The first steps of an experiment for investigating the capability of airborne spectrometer data for retrieval of biophysical parameters of vegetation, especially water conditions are presented. Airborne Visible/Infrared Imaging Spectrometer (AVIRIS) and ISM data were acquired in the frame of the 1991 NASA/JPL and CNES campaigns on the Landes, South west France, a large and flat forest area with mainly maritime pines. In-situ measurements were completed at that time; i.e. reflectance spectra, atmospheric profiles, sampling for further laboratory analyses of elements

concentrations (lignin, water, cellulose, nitrogen,...). All information was integrated in an already existing data base (age, LAI, DBH, understory cover,...). A methodology was designed for (1) obtaining geometrically and atmospherically corrected reflectance data, (2) registering all available information, and (3) analyzing these multi-source informations. Our objective is to conduct comparative studies with simulation reflectance models, and to improve these models, especially in the MIR. Author (revised)

N94-16682*# Geological Survey, Denver, CO.
GROUND-TRUTHING AVIRIS MINERAL MAPPING AT CUPRITE, NEVADA **c43**
Gregg Swayze, Roger N. Clark, Fred Kruse (Colorado Univ., Boulder.), Steve Sutley, and Andrea Gallagher *In* JPL, Summaries of the Third Annual JPL Airborne Geoscience Workshop. Volume 1: AVIRIS Workshop 1 Jun. 1992 p 47-49 (For primary document see N94-16666 03-42)
Avail: CASI HC A01/MF A02

Mineral abundance maps of 18 minerals were made of the Cuprite Mining District using 1990 AVIRIS data and the Multiple Spectral Feature Mapping Algorithm (MSFMA) as discussed in Clark et al. This technique uses least-squares fitting between a scaled laboratory reference spectrum and ground calibrated AVIRIS data for each pixel. Multiple spectral features can be fitted for each mineral and an unlimited number of minerals can be mapped simultaneously. Quality of fit and depth from continuum numbers for each mineral are calculated for each pixel and the results displayed as a multicolor image. Author (revised)

N94-16683*# University Coll. of Swansea (Wales). Dept. of Geography.
EXPLORING THE REMOTE SENSING OF FOLIAR BIOCHEMICAL CONCENTRATIONS WITH AVIRIS DATA **c43**
Geoffrey M. Smith and Paul J. Curran *In* JPL, Summaries of the Third Annual JPL Airborne Geoscience Workshop. Volume 1: AVIRIS Workshop 1 Jun. 1992 p 50-52 (For primary document see N94-16666 03-42)
Avail: CASI HC A01/MF A02

Airborne Visible/Infrared Imaging Spectrometer (AVIRIS) data shows promise for the estimation of foliar biochemical concentrations at the scale of the canopy. There are, however, several problems associated with the use of AVIRIS data in this way and these are detailed in recent Plant Biochemical Workshop Report. The research reported was concentrated upon three of these problems: field sampling of forest canopies, wet laboratory assay of foliar chemicals, and the visualization of AVIRIS data. Author (revised)

N94-16684*# California Univ., Santa Barbara. Dept. of Biological Sciences.
SEASONAL AND SPATIAL VARIATIONS IN PHYTOPLANKTONIC CHLOROPHYLL IN EUTROPHIC MONO LAKE, CALIFORNIA, MEASURED WITH THE AIRBORNE VISIBLE AND INFRARED IMAGING SPECTROMETER (AVIRIS) **c43**
John M. Melack and Mary Gastil *In* JPL, Summaries of the Third Annual JPL Airborne Geoscience Workshop. Volume 1: AVIRIS Workshop 1 Jun. 1992 p 53-55 (For primary document see N94-16666 03-42)
Avail: CASI HC A01/MF A02

The principal problem with application of airborne imaging spectrometers to lakes is the weak upwelling signal, especially when narrow spectral bands with high spatial resolution are sought. Furthermore, atmospheric path radiance dominates the signal received from dark targets such as lakes. Once atmospheric effects have been removed from the radiance received at the sensor, semi-empirical relationships can be developed to extract information about phytoplankton pigment concentrations for different underwater optical conditions. In lakes where concentrations of dissolved organics and suspended detritus may not co-vary with phytoplankton pigments, the many spectral channels of an imaging spectrometer such as AVIRIS are likely to be required to distinguish the various aquasols. The objectives of our study are to: (1) estimate the chlorophyll content of a lake with hundred-fold seasonal ranges in chlorophyll concentration using atmospherically corrected upwelling radiances derived from AVIRIS imagery, and (2) to examine spatial patterns in chlorophyll after reduction of the coherent noise in the imagery by filtering techniques. Author (revised)

N94-16685*# University of South Florida, Saint Petersburg. Dept. of Marine Science.
AVIRIS CALIBRATION AND APPLICATION IN COASTAL OCEANIC ENVIRONMENTS **c48**
Kendall L. Carder *In* JPL, Summaries of the Third Annual JPL Airborne Geoscience Workshop. Volume 1: AVIRIS Workshop 1 Jun. 1992 p 58-59 (For primary document see N94-16666 03-42)
Avail: CASI HC A01/MF A02

The Airborne Visible-Infrared Imaging Spectrometer (AVIRIS) is a test-bed for future spacecraft sensors such as the High-Resolution Imaging Spectrometer and the Moderate-Resolution Imaging Spectrometers planned for the Earth Observing System. To use this sensor for ocean applications, S/N was increased by spatial averaging of images. Post-flight recalibration was accomplished using in situ the water-leaving radiance measured at flight time, modeling radiance transmission to the aircraft, and adding modeled atmospheric radiance to that value. The preflight calibration curve was then adjusted until aircraft and modeled total radiance values matched. Water-leaving radiance values from the recalibrated AVIRIS imagery were consistent with in situ data supporting the validity of the approach. Imagery of the absorption coefficient at 415 nm and backscattering coefficient at 671 nm were used to depict the dissolved and particulate constituents of an ebb-tidal esturance plume on the East coast of Florida. Author (revised)

N94-16686*# Geological Survey, Denver, CO.
MAPPING VEGETATION TYPES WITH THE MULTIPLE SPECTRAL FEATURE MAPPING ALGORITHM IN BOTH EMISSION AND ABSORPTION **c43**
Roger N. Clark, Gregg A. Swayze, Christopher Koch, and Cathy Ager *In* JPL, Summaries of the Third Annual JPL Airborne Geoscience Workshop. Volume 1: AVIRIS Workshop 1 Jun. 1992 p 60-62 (For primary document see N94-16666 03-42)
Avail: CASI HC A01/MF A02

Vegetation covers a large portion of the Earth's land surface. Remotely sensing quantitative information from vegetation has proven difficult because in a broad sense, all vegetation is similar from a chemical viewpoint, and most healthy plants are green. Plant species are generally characterized by the leaf and flower or fruit morphology, not by remote sensing spectral signatures. But to the human eye, many plants show varying shades of green, so there is direct evidence for spectral differences between plant types. Quantifying these changes in a predictable manner has not been easy. The Clark spectral features mapping algorithm was applied to mapping spectral features in vegetation species. Author (revised)

N94-16687*# Jet Propulsion Lab., California Inst. of Tech., Pasadena.
MULTIPLE DATASET WATER-QUALITY ANALYSES IN THE VICINITY OF AN OCEAN WASTEWATER PLUME **c45**
Michael Hamilton, Curtiss O. Davis, W. Joseph Rhea, and Jeannette vandenBosch *In its* Summaries of the Third Annual JPL Airborne Geoscience Workshop. Volume 1: AVIRIS Workshop 1 Jun. 1992 p 63-65 (For primary document see N94-16666 03-42)
Avail: CASI HC A01/MF A02

The White's Point ocean outfall is the method of disposal for approximately 374 million gallons of treated wastewater per day from Los Angeles County. The photosynthetic characteristics and particle distributions have well-defined properties that can be exploited to yield information on transport of the plume, mixing dynamics, and resuspension of bottom sediments during periods of bottom current velocity in excess of ca. 0.1 m/s. This plume of particles serves as a conservative tracer, which was studied using a number of sampling platforms and strategies, including underway sawtooth, or 'tow-yo' sampling, moored arrays of instruments, stationary profiling, and now for the first time with remotely-sensed multispectral color imagery. Research in this area previously focused on examination of the plume as it relates to the local current field and transport of particles, and on the resuspension of bottom sediments during periods of increased currents. In addition, Wu et al elucidated techniques for separating the particle signal into photosynthetic and nonphotosynthetic components, based on the beam attenuation to chlorophyll fluorescence ratio. High-frequency time series measurements of the current field and bio-optical characteristics at a site close to the waste diffusers were also collected. These are being analyzed for the spectral characteristics of the longer-timescale variability, in order to predict particle transport through

simple meteorological measurements. With the advent of high spectral and spatial resolution imaging spectrometers such as AVIRIS, it is now possible to construct causal relationships between particle distributions and signature of the upwelled radiance from the surface. The availability of a constant and well-characterized source of material lends itself well to models which predict upwelled radiance from the surface. The availability of a constant and well-characterized source of material lends itself well to models which predict upwelled light as a function of particle distributions, photosynthetic pigments, colored dissolved organic material, and detrital and degradation products of photosynthesis. In addition, the spatial coverage provided by the tow-yo sampling device, combined with the profile measurements of the light field, should facilitate the best inverse modeling attempts possible thus far. Author (revised)

N94-16688*# Deutsche Forschungsanstalt fuer Luft- und Raumfahrt, Oberpfaffenhofen (Germany). Inst. for Microwave Technologies.

MAC EUROPE 1991: EVALUATION OF AVIRIS, GER IMAGING SPECTROMETRY DATA FOR THE LAND APPLICATION TESTSITE OBERPFAFFENHOFEN **c43**

F. Lehmann, R. Richter, H. Rothfuss, K. Werner, P. Hausknecht, A. Mueller, and P. Strobl *In* JPL, Summaries of the Third Annual JPL Airborne Geoscience Workshop. Volume 1: AVIRIS Workshop 1 Jun. 1992 p 66-68 (For primary document see N94-16666 03-42)

Avail: CASI HC A01/MF A02

During the MAC Europe 91 Campaign, the area of Oberpfaffenhofen including the land application testsite Oberpfaffenhofen was flown by the AVIRIS imaging spectrometer, the GER 2 imaging spectrometer (63 band scanner), and two SAR systems (NASA/JPL AIRSAR and DLR E-SAR). In parallel to the overflights ground spectrometry (ASD, IRIS M IV) and atmospheric measurements were carried out in order to provide data for optical sensor calibration. Ground spectrometry measurements were carried out in the runway area of the DLR research center Oberpfaffenhofen. This area was used as well during the GER 2 European flight campaign EISAC 89 as a calibration target. The land application testsite Oberpfaffenhofen is located 3 km north of the DLR research center. During the MAC Europe 91 Campaign a ground survey was carried out for documentation in the ground information data base (vegetation type, vegetation geometry, soil type, and soil mixture). Crop stands analyzed were corn, barley and rape. The DLR runway area and the land application testsite Oberpfaffenhofen were flown with the AVIRIS on 29 July and with the GER 2 on 12 and 23 July and 3 Sep. AVIRIS and GER 2 scenes were processed and atmospherically corrected for optical data analysis of optical and radar data. For the AVIRIS and the GER 2 scenes, signal-to-noise ratios (SNR) estimates were calculated. An example of the reflectance of 6 calibration targets inside a GER 2 scene of Oberpfaffenhofen is given. SNR values for the GER 2 for a medium albedo target are given. The integrated analysis for the optical and radar data was carried out in cooperation with the DLR Institute for Microwave Technologies. Author (revised)

N94-16689*# Washington Univ., Seattle. Dept. of Geological Sciences.

USING ENDMEMBERS IN AVIRIS IMAGES TO ESTIMATE CHANGES IN VEGETATIVE BIOMASS **c43**

Milton O. Smith, John B. Adams, Susan L. Ustin (California Univ., Davis.), and Dar A. Roberts *In* JPL, Summaries of the Third Annual JPL Airborne Geoscience Workshop. Volume 1: AVIRIS Workshop 1 Jun. 1992 p 69-71 (For primary document see N94-16666 03-42)

Avail: CASI HC A01/MF A02

Field techniques for estimating vegetative biomass are labor intensive, and rarely are used to monitor changes in biomass over time. Remote-sensing offers an attractive alternative to field measurements; however, because there is no simple correspondence between encoded radiance in multispectral images and biomass, it is not possible to measure vegetative biomass directly from AVIRIS images. Ways to estimate vegetative biomass by identifying community types and then applying biomass scalars derived from field measurements are investigated. Field measurements of community-scale vegetative biomass can be made, at least for local areas, but it is not always possible to identify vegetation communities unambiguously using remote measurements and conventional image-processing techniques. Furthermore, even when communities are well characterized in a single image, it typically is difficult to assess the extent and nature of changes in a time series of images, owing to uncertainties introduced by variations in illumination geometry, atmospheric attenuation, and instrumental responses. Our objective is to develop an improved method based on spectral mixture analysis to characterize and identify vegetative communities, that can be applied to multi-temporal AVIRIS and other types of images. In previous studies, multi-temporal data sets (AVIRIS and TM) of Owens Valley, CA were analyzed and vegetation communities were defined in terms of fractions of reference (laboratory and field) endmember spectra. An advantage of converting an image to fractions of reference endmembers is that, although fractions in a given pixel may vary from image to image in a time series, the endmembers themselves typically are constant, thus providing a consistent frame of reference. Author (revised)

N94-16690*# Naval Research Lab., Bay Saint Louis, MS.

ATMOSPHERIC CORRECTION OF AVIRIS DATA IN OCEAN WATERS **c48**

Gregory Terrie and Robert Arnone *In* JPL, Summaries of the Third Annual JPL Airborne Geoscience Workshop. Volume 1: AVIRIS Workshop 1 Jun. 1992 p 72-74 (For primary document see N94-16666 03-42)

Avail: CASI HC A01/MF A02

Hyperspectral data offers unique capabilities for characterizing the ocean environment. The spectral characterization of the composition of ocean waters can be organized into biological and terrigenous components. Biological photosynthetic pigments in ocean waters have unique spectral ocean color signatures which can be associated with different biological species. Additionally, suspended sediment has different scattering coefficients which result in ocean color signatures. Measuring the spatial distributions of these components in the maritime environments provides important tools for understanding and monitoring the ocean environment. These tools have significant applications in pollution, carbon cycle, current and water mass detection, location of fronts and eddies, sewage discharge and fate etc. Ocean color was used from satellite for describing the spatial variability of chlorophyll, water clarity (K(sub 490)), suspended sediment concentration, currents etc. Additionally, with improved atmospheric correction methods, ocean color results produced global products of spectral water leaving radiance (L(sub W)). Ocean color results clearly indicated strong applications for characterizing the spatial and temporal variability of bio-optical oceanography. These studies were largely the results of advanced atmospheric correction techniques applied to multispectral imagery. The atmosphere contributes approximately 80 percent - 90 percent of the satellite received radiance in the blue-green portion of the spectrum. In deep ocean waters, maximum transmission of visible radiance is achieved at 490nm. Conversely, nearly all of the light is absorbed by the water at wavelengths greater than about 650nm and thus appears black. These spectral ocean properties are exploited by algorithms developed for the atmospheric correction used in satellite ocean color processing. The objective was to apply atmospheric correction techniques that were used for procesing satellite Coastal Zone Color Scanner (CZCS) data to AVIRIS data. Quantitative measures of L(sub W) from AVIRIS are compared with ship ground truth data and input into bio-optical models. Author (revised)

N94-16691*# National Aeronautics and Space Administration. Langley Research Center, Hampton, VA.

THE 1991 AVIRIS/POLDER EXPERIMENT IN CAMARGUE, FRANCE **c43**

F. Baret (Institut National de la Recherche Agronomique, Montfavet, France.), C. Leprieur (Office National d'Etudes et de Recherches Aerospatiales, Toulouse, France.), S. Jacquemoud (Institut National de la Recherche Agronomique, Montfavet, France.), V. Carrere (Jet Propulsion Lab., California Inst. of Tech., Pasadena.), X. F. Gu (Institut National de la Recherche Agronomique, Montfavet, France.), M. Steven (Nottingham Univ., England.), V. Vanderbilt, J. F. Hanocq (Institut National de la Recherche Agronomique, Montfavet, France.), Susan L. Ustin (California Univ., Davis.), and G. Rondeaux et al *In* JPL, Summaries of the Third Annual JPL Airborne Geoscience Workshop. Volume 1: AVIRIS Workshop 1 Jun. 1992 p 75-77 Sponsored in part by PNTS (For primary document see N94-16666 03-42)

Avail: CASI HC A01/MF A02

Airborne campaigns during the eighties provided high spectral resolution data, collected with imaging instruments such as AIS, AVIRIS, FLI, CAESI, and ISM, in order to investigate the relationship with canopy biophysical characteristics. The statistical approaches used to analyze these data do not allow investigation of the causality and the applicability of the observed correlations. Further, statistical studies demonstrated the high degree of

redundancy of the spectral information amongst many others. And for retrieving vegetation biophysical characteristics, few results demonstrate the real information gain attributable to the high spectral resolution capability as compared to the use of a few wide wavelength bands. With several new imaging spectrophotometers scheduled for launch during the next 10 years (MERIS, MODIS, HIRIS), progress in the description and understanding of the mechanisms that drive the spectral variation of canopy reflectance is required. Most of these new sensor systems will also have the capability to observe the target under differing view directions. The problem of the combination and the use of the synergy between both the spectral and the directional sources of canopy reflectance variations has to be addressed. Apart from the atmospheric effects, the spectral variation of the light reflected by canopies originates from the leaves, the soil or the other vegetation elements such as branches and fruits. At leaf level, both diffuse reflectance and transmittance may be simulated by simple models, although no accurate information exists on the absorption features of the biochemicals (except water) in the 900-2500nm wavelength range. Many models mimic the directional variability of canopy reflectance at a given wavelength. Combining a leaf spectral model with a canopy directional model provides a powerful tool to analyze this problem. Some of us have initiated such a study, but our approach and theory remain to be tested using canopy data with their complexity, associated experimental error, and atmospheric effects. The main objective of the 1990 POLDER/AVIRIS experiment in Camargue was to provide a consistent data set over various canopies in order to test the applicability of the theory. The experiment, part of the 1991 MAC Europe experiment, involved simultaneous data collection using two sensors: AVIRIS and POLDER which measures the bidirectional and polarization properties of the targets at 670 and 880nm wavebands. Author (revised)

N94-16692*# Jet Propulsion Lab., California Inst. of Tech., Pasadena.
AVIRIS GROUND DATA PROCESSING SYSTEM **c43**
Earl G. Hansen, Steve Larson, H. Ian Novack, and Robert Bennett *In its* Summaries of the Third Annual JPL Airborne Geoscience Workshop. Volume 1: AVIRIS Workshop 1 Jun. 1992 p 80-82 (For primary document see N94-16666 03-42)
Avail: CASI HC A01/MF A02

During the last year and a half, Feb. 1991 to Jun. 1992, a major upgrade of the Airborne Visible/Infrared Imaging Spectrometers (AVIRIS) ground data processing system took place. Both the hardware and software components were changed significantly to improve the processing capacity and performance and to structure a data facility capable of handling the projected work load into the near future. A summary report of these changes and some projections for the future are provided. The objectives of the AVIRIS data facility are to decommutate and archive AVIRIS data and to provide raw or radiometrically calibrated data products to the science investigator. These primary objectives have not changed from the initial concepts. The upgrade effort has greatly improved the processing system. These objectives can now be accomplished in a more timely fashion at a reasonable cost and there is sufficient capacity to manage the current processing load and provide for future growth. The method of implementation added the flexibility to provide better service to the investigator and allow for future changes. Author (revised)

N94-16693*# Jet Propulsion Lab., California Inst. of Tech., Pasadena.
SIMULATION OF ASTER DATA USING AVIRIS IMAGES **c43**
Michael Abrams *In its* Summaries of the Third Annual JPL Airborne Geoscience Workshop. Volume 1: AVIRIS Workshop 1 Jun. 1992 p 83-84 (For primary document see N94-16666 03-42)
Avail: CASI HC A01/MF A02

The Advanced Thermal Emission and Reflectance Radiometer (ASTER) is a joint Japanese/US imaging instrument scheduled to fly on the first Earth Observing System (EOS) platform in 1998. The complement of scanners includes a visible, three channel module with forward-looking stereo capability, a six channel short wavelength infrared module, and a five channel thermal module. As part of the definition phase for the instrument design, AVIRIS data was used to simulate the short wave infrared (SWIR) bands to investigate the effects of widening two of the bands to increase the signal-to-noise ratio (SNR) versus loss of spectral separability due to uncertainty in the post-launch band positions. Author (revised)

N94-16694*# Institut fuer Allgemeine und Angewandte Geophysik, Munich (Germany).
USE OF AVIRIS DATA TO THE DEFINITION OF OPTIMISED SPECIFICATIONS FOR LAND APPLICATIONS WITH FUTURE SPACEBORNE IMAGING SPECTROMETERS Abstract Only **c43**
J. Bodechtel *In* JPL, Summaries of the Third Annual JPL Airborne Geoscience Workshop. Volume 1: AVIRIS Workshop 1 Jun. 1992 p 85 (For primary document see N94-16666 03-42)
Avail: CASI HC A01/MF A02

Recent experience with airborne imaging spectrometers demonstrated the advantages of narrow band sensors over broad band scanners for characterizing the nature, extent, and physical status of typical land surfaces. Information on key spectral features associated with various land surfaces can be obtained from the data of such instruments, which can be used to simulate spaceborne imaging spectrometer data and to assess their information content if comprehensive underpinning is provided by ground data. The collection of such information was an issue of airborne imaging spectrometer campaigns like the NASA MAC-Europe 1991. Airborne and ground data obtained from different test sites in Europe are utilized for a comparative analysis of the spectral signatures of various land surfaces (vegetation, bare soils and rocks, and mixed soil/rock-vegetation) as seen from different imaging spectrometers like Airborne Visible/Infrared Imaging Spectrometer (AVIRIS), GERIS 63 band scanner, and CASI. The following items are discussed: (1) the significance of different spectral regions within the wavelength interval between 0.4 m and 2.5 m for the differentiation of different land units; (2) recommendations on the optimum band selection and band-widths to be used for the application of future satellite-based imaging spectrometers for land applications; (3) the boundaries for the detection of plant features in mixed-soil plant spectra and the influence of different soil properties on the mixture of the spectra; (4) recommendations on the optimum spatial resolution and recording dates for the discrimination of spectral features of various surface types; and (5) evaluation of different data compressing techniques for the optimum extraction of spectral information from imaging spectrometry data. Author (revised)

N94-16695*# Desert Research Inst., Reno, NV. Biological Sciences Center.
PRIMARY STUDIES OF TRACE QUANTITIES OF GREEN VEGETATION IN MONO LAKE AREA USING 1990 AVIRIS DATA **c43**
Zhi-Kang Chen, Chris D. Elvidge, and David P. Groeneveld (Inyo County Water Dept., Bishop, CA.) *In* JPL, Summaries of the Third Annual JPL Airborne Geoscience Workshop. Volume 1: AVIRIS Workshop 1 Jun. 1992 p 86-87 (For primary document see N94-16666 03-42)
Avail: CASI HC A01/MF A02

Our primary results in Jasper Ridge Biological Preserve indicate that high spectral resolution Airborne Visible/Infrared Imaging Spectrometer (AVIRIS) data may provide a substantial advantage in vegetation, based on the chlorophyll red edge feature from 700-780 nm. The chlorophyll red edge was detected for green vegetation cover as low as 4.8 percent. The objective of our studies in Mono Lake area is to continue the experiments performed in Jasper Ridge and to examine the persistence of red edge feature of trace quantities of green vegetation for different plant communities with non-uniform soil backgrounds. Author (revised)

N94-16696*# Jet Propulsion Lab., California Inst. of Tech., Pasadena.
JPL ACTIVITIES ON DEVELOPMENT OF ACOUSTO-OPTIC TUNABLE FILTER IMAGING SPECTROMETER **c35**
Li-Jen Cheng, Tien-Hsin Chao, and George Reyes *In its* Summaries of the Third Annual JPL Airborne Geoscience Workshop. Volume 1: AVIRIS Workshop 1 Jun. 1992 p 88-90 (For primary document see N94-16666 03-42)
Avail: CASI HC A01/MF A02

Recent activities of JPL in the development of a new type of imaging spectrometers for earth observation and planetary exploration are reported. This instrument uses the acousto-optic tunable filter (AOTF) as high resolution and fast programmable bandpass filter. AOTF operates in the principle of acousto-optic interaction in an anisotropic medium. This filter can be tuned in sequential, random, and multiwavelength access modes, providing observational flexibility. The diffraction process in the filter generates two diffracted monochromatic beams with polarization orthogonal to each other, creating a unique capability to measure both polarimetric and spectral properties of the incoming light simultaneously with a single

instrument. The device gives wide wavelength operations with reasonably large throughput. In addition, it is in a compact solid-state structure without moving parts, providing system reliability. These attractive features give promising opportunities to develop a new generation of airborne/spaceborne and ground, real-time, imaging spectrometer systems for remote sensing applications. Author (revised)

N94-16697*# Analytical Technology Applications Corp., Moffett Field, CA.

MEASURING DRY PLANT RESIDUES IN GRASSLANDS: A CASE STUDY USING AVIRIS **c43**

Michael Fitzgerald and Susan L. Ustin (California Univ., Davis.) *In* JPL, Summaries of the Third Annual JPL Airborne Geoscience Workshop. Volume 1: AVIRIS Workshop 1 Jun. 1992 p 91-93 (For primary document see N94-16666 03-42)

Avail: CASI HC A01/MF A02

Grasslands, savannah, and hardwood rangelands are critical ecosystems and sensitive to disturbance. Approximately 20 percent of the Earth's surface are grasslands and represent 3 million ha. in California alone. Developing a methodology for estimating disturbance and the effects of cumulative impacts on grasslands and rangelands is needed to effectively monitor these ecosystems. Estimating the dry biomass residue remaining on rangelands at the end of the growing season provides a basis for evaluating the effectiveness of land management practices. The residual biomass is indicative of the grazing pressure and provides a measure of the system capacity for nutrient cycling since it represents the maximum organic matter available for decomposition, and finally, provides a measure of the erosion potential for the ecosystem. Remote sensing presents a possible method for measuring dry residue. However, current satellites have had limited application due to the coarse spatial scales (relative to the patch dynamics) and insensitivity of the spectral coverage to resolve dry plant material. Several hypotheses for measuring the biochemical constituents of dry plant material, particularly cellulose and lignin, using high spectral resolution sensors were proposed. The use of Airborne Visible/Infrared Imaging Spectrometers (AVIRIS) to measure dry plant residues over an oak savannah on the eastern slopes of the Coast Range in central California was investigated and it was asked what spatial and spectral resolutions are needed to quantitatively measure dry plant biomass in this ecosystem. Author (revised)

N94-16698*# California State Univ., Los Angeles. Dept. of Biology.

TRACKING PHOTOSYNTHETIC EFFICIENCY WITH NARROW-BAND SPECTRORADIOMETRY **c43**

John A. Gamon and Christopher B. Field (Carnegie Institution of Washington, Stanford, CA.) *In* JPL, Summaries of the Third Annual JPL Airborne Geoscience Workshop. Volume 1: AVIRIS Workshop 1 Jun. 1992 p 95-97 Sponsored in part by A. W. Mellon Foundation (For primary document see N94-16666 03-42)

(CIW-Publ-1133) Avail: CASI HC A01/MF A02

Narrow-waveband spectroradiometry presents the possibility of detecting subtle signals closely related to the current physiological state of vegetation. One such signal related to the epoxidation state of the xanthophyll cycle pigments, violaxanthin, antheraxanthin, and zeaxanthin is discussed. Recent advances in plant ecophysiology demonstrated a close relationship between these pigments and the regulatory state of photosystem 2 in photosynthesis. Our recent field studies of sunflower (Helianthus annuus) and oak (Quercus agrifolia) demonstrated that a 'xanthophyll signal' can be isolated from the diurnal reflectance spectra of intact canopies. Furthermore, the xanthophyll signal can be used to derive a 'physiological reflectance index' (PRI) that closely correlates with the actual photosynthetic efficiency (defined as the photosynthetic rate divided by the incident PAR) in closed canopies. If these signals were detectable in Airborne Visible/Infrared Imaging Spectrometers (AVIRIS) images, they could lead to improved remote estimates of photosynthetic fluxes. Author (revised)

N94-16699*# Colorado Univ., Boulder. Center for the Study of Earth from Space.

SEPARATION OF CIRRUS CLOUD FROM CLEAR SURFACE FROM AVIRIS DATA USING THE 1.38 MICRON WATER VAPOR BAND **c47**

Bo-Cai Gao and Alexander F. H. Goetz *In* JPL, Summaries of the Third Annual JPL Airborne Geoscience Workshop. Volume 1: AVIRIS Workshop 1 Jun. 1992 p 98-100 (For primary document see N94-16666 03-42)

(Contract NAS5-30552)

Avail: CASI HC A01/MF A02

Cirrus clouds play an important role in climate systems because of their large area coverage, persistence, and radiative effects. Thin cirrus clouds are difficult to detect in visible images and infrared images in the 10-12 micron atmospheric window region, particularly over land, because these clouds are partially transparent. Ackerman recently developed a method for detecting cirrus clouds using three narrow channels centered near 8, 11, and 12 microns, respectively, based on the analysis of IR emission spectra measured with a high spectral resolution interferometer. Barton also described a method for estimating cirrus cloud height and amount from measurements with two narrow channel radiometers of the Selective Chopper Radiometer on Nimbus 5. Both channels are located within the strong 2.7 micron water vapor band absorption region. One of the channels includes additional carbon dioxide absorption. A differential absorption technique with sets of empirical coefficients was used in the estimation of cirrus cloud heights and amounts. A technique using narrow channels in the strong 1.38 micron water vapor band absorption region for detecting cirrus clouds from spectral imaging data acquired by the Airborne Visible/Infrared Imaging Spectrometer (AVIRIS) on 5 Dec. 1991 during the FIRE (The First International Satellite Cloud Climatology Project (ISCCP) Regional Experiment) Phase 2 Field Experiment is described. Author (revised)

N94-16700*# Colorado Univ., Boulder. Center for the Study of Earth from Space.

SOFTWARE FOR THE DERIVATION OF SCALED SURFACE REFLECTANCES FROM AVIRIS DATA **c61**

Bo-Cai Gao, Kathleen Heidebrecht, and Alexander F. H. Goetz *In* JPL, Summaries of the Third Annual JPL Airborne Geoscience Workshop. Volume 1: AVIRIS Workshop 1 Jun. 1992 p 101-103 (For primary document see N94-16666 03-42)

(Contract NAS5-30552)

Avail: CASI HC A01/MF A02

An operational software program is now available for deriving 'scaled surface reflectances' from spectral data collected by the Airborne Visible/Infrared Imaging Spectrometer (AVIRIS). The program simulates both the atmospheric scattering and absorption effects. Brief descriptions of the algorithm, inputs, outputs, the limitations of the software, and procedures for obtaining the software are given. Author (revised)

N94-16701*# Department of Natural Resources, Salt Lake City, UT. Div. of Oil, Gas, and Mining.

INTEGRATING REMOTE SENSING TECHNIQUES AT CUPRITE, NEVADA: AVIRIS, THEMATIC MAPPER, AND FIELD SPECTROSCOPY **c43**

Bradley Hill, Greg Nash (Utah Univ., Salt Lake City.), Merrill Ridd (Utah Univ., Salt Lake City.), Phoebe L. Hauff (Spectral Research, Lafayette, CO.), and Phil Ebel (Earth Search Sciences, Inc., Salt Lake City, UT.) *In* JPL, Summaries of the Third Annual JPL Airborne Geoscience Workshop. Volume 1: AVIRIS Workshop 1 Jun. 1992 p 104-107 (For primary document see N94-16666 03-42)

Avail: CASI HC A01/MF A02

The Cuprite mining district in southwestern Nevada has become a test site for remote sensing studies with numerous airborne scanners and ground sensor data sets collected over the past fifteen years. Structurally, the Cuprite region can be divided into two areas with slightly different alteration and mineralogy. These zones lie on either side of a postulated low-angle structural discontinuity that strikes nearly parallel to US Route 95. Hydrothermal alternation at Cuprite was classified into three major zones: silicified, opalized, and argillized. These alteration types form a bulls-eye pattern east of the highway and are more linear on the west side of the highway making a striking contrast from the air and the imagery. Cuprite is therefore an ideal location for remote sensing research as it exhibits easily identified hydrothermal zoning, is relatively devoid of vegetation, and contains a distinctive spectrally diagnostic mineral suite including the ammonium feldspar buddingtonite, several types of alunite, different jarosites, illite, kaolinite, smectite, dickite, and opal. This present study brings a new dimension to these previous remote sensing and ground data sets compiled for Cuprite. The development of a higher resolution field spectrometer now provides the capability to combine extensive in-situ mineralogical data with

a new geologic field survey and detailed Airborne Visible/Infrared Imaging Spectrometers (AVIRIS) images. The various data collection methods and the refinement of the integrated techniques are discussed.

Author (revised)

N94-16702*# National Aeronautics and Space Administration. Ames Research Center, Moffett Field, CA.

OREGON TRANSECT: COMPARISON OF LEAF-LEVEL REFLECTANCE WITH CANOPY-LEVEL AND MODELLED REFLECTANCE **c43**

Lee F. Johnson (TGS Technology, Inc., Moffett Field, CA.), Frederic Baret (Institut National de la Recherche Agronomique, Avignon, France.), and David L. Peterson *In* JPL, Summaries of the Third Annual JPL Airborne Geoscience Workshop. Volume 1: AVIRIS Workshop 1 Jun. 1992 p 113-115 (For primary document see N94-16666 03-42)

Avail: CASI HC A01/MF A02

The Oregon Transect Ecosystem Research (OTTER) project involves the collection of a variety of remotely-sensed and in situ measurements for characterization of forest biophysical and biochemical parameters. The project includes nine study plots located along an environmental gradient in west-central Oregon, extending from the Pacific coast inland approximately 300km. These plots represent a broad range in ecosystem structure and function. Within the OTTER project, the sensitivity of the Airborne Visible/Infrared Imaging Spectrometer (AVIRIS) signal to absorption by foliar biochemicals is being examined. AVIRIS data were acquired over all plots in conjunction with the four OTTER Multi-sensor Aircraft Campaigns spanning the growing season. Foilage samples were gathered during each campaign for biochemical determination (at Ames Research Center), to estimate stand-level constituency at each plot. Directional-hemispheric leaf reflectance throughout the 400-2400nm region was measured in the laboratory as an aid to interpreting concurrent AVIRIS data. Obtaining leaf spectra in this manner reduces or eliminates the confounding influences of atmosphere, canopy architecture, and reflectance by woody components, understory, and exposed soils which are present in airborne observations. These laboratory spectra were compared to simulated spectra derived by inverting the PROSPECT leaf-level canopy reflectance derived from AVIRIS data by use of the LOWTRAN-7 atmospheric radiative-transfer model.

Author (revised)

N94-16703*# Geological Survey, Reston, VA.

AVIRIS AS A TOOL FOR CARBONATITE EXPLORATION: COMPARISON OF SPAM AND MBANDMAP DATA ANALYSIS METHODS **c43**

Marguerite J. Kingston and James K. Crowley *In* JPL, Summaries of the Third Annual JPL Airborne Geoscience Workshop. Volume 1: AVIRIS Workshop 1 Jun. 1992 p 116-118 (For primary document see N94-16666 03-42)

Avail: CASI HC A01/MF A02

Data acquired with the Airborne Visible/Infrared Imaging Spectrometer (AVIRIS) of the Mountain Pass, San Bernadino County, California, area were analyzed to evaluate the use of narrow-band imaging data for carbonatite exploration. Carbonatites are igneous carbonate-rich rocks that are economically important in part because they are the major source for rare-earth minerals. Because the 224 AVIRIS spectral channels have a nominal spectral resolution of 10 nm, narrow absorption features such as those displayed by the rare-earth elements neodymium (Nd) and samarium (Sm) may be detected. The Mountain Pass region encompasses a well-exposed sequence of sedimentary, metamorphic, and igneous rocks, including an alkalic carbonatite intrusion. The carbonatite was emplaced in Precambrian granitic rocks that are fault bounded by a thick suite of Paleozoic, sedimentary rock, predominantly dolomite. The carbonatite stock, the major source of light rare-earth elements (REE) in the United States, affords the opportunity to test AVIRIS capabilities for detecting REE absorption features. Nd-bearing minerals display narrow, sharp and distinctive spectral features at 580, 740, 800, and 870 nm. Minerals bearing Sm display similarly sharp features near 1090, 1250, 1410, and 1550 nm. The more common REE, lanthanum and cerium, do not display absorption features in the visible/near-infrared region in their natural oxidation states.

Author (revised)

N94-16704*# Colorado Univ., Boulder. Center for the Study of Earth from Space.

EXPERT SYSTEM-BASED MINERAL MAPPING USING AVIRIS **c43**

Fred A. Kruse, A. B. Lefkoff, and J. B. Dietz *In* JPL, Summaries of the Third Annual JPL Airborne Geoscience Workshop. Volume 1: AVIRIS Workshop 1 Jun. 1992 p 119-121 Sponsored in part by Geological Survey (For primary document see N94-16666 03-42)

(Grants NAGw-1601; NAGw-1143)

Avail: CASI HC A01/MF A02

Integrated analysis of imaging spectrometer data and field spectral measurements were used in conjunction with conventional geologic field mapping to characterize bedrock and surficial geology at the northern end of Death Valley, California and Nevada. A knowledge-based expert system was used to automatically produce image maps from Airborne Visible/Infrared Imaging Spectrometer (AVIRIS) data showing the principal surface mineralogy. The imaging spectrometer data show the spatial distribution of spectrally distinct minerals occurring both as primary rock-forming minerals and as alteration and weathering products. Field spectral measurements were used to verify the mineral maps and field mapping was used to extend the remote sensing results. Geographically referenced image-maps produced from these data form new base maps from which to develop improved understanding of the processes of deposition and erosion affecting the present land surface. The 'northern Grapevine Mountains' (NGM) study area was reported on in numerous papers. This area is an unnamed northwestward extension of the range. Most of the research here has concentrated on mapping of Jurassic-age plutons and associated hydrothermal alteration, however, the nature and scope of these studies is much broader, pertaining to the geologic history and development of the entire Death Valley region. AVIRIS data for the NGM site were obtained during May 1989. Additional AVIRIS data were acquired during September 1989 as part of the Geologic Remote Sensing Field Experiment (GRSFE). The area covered by these data overlaps slightly with the May 1989 data. Three and one-half AVIRIS scenes total were analyzed. Author (revised)

N94-16705*# Jet Propulsion Lab., California Inst. of Tech., Pasadena.

AVIRIS DATA AND NEURAL NETWORKS APPLIED TO AN URBAN ECOSYSTEM **c63**

Merrill K. Ridd (Utah Univ., Salt Lake City.), Niles D. Ritter, Nevin A. Bryant, and Robert O. Green *In its* Summaries of the Third Annual JPL Airborne Geoscience Workshop. Volume 1: AVIRIS Workshop 1 Jun. 1992 p 129-131 (For primary document see N94-16666 03-42)

Avail: CASI HC A01/MF A02

Urbanization is expanding on every continent. Although urban/industrial areas occupy a small percentage of the total landscape of the earth, their influence extends far beyond their borders, affecting terrestrial, aquatic, and atmospheric systems globally. Yet little has been done to characterize urban ecosystems of their linkages to other systems horizontally or vertically. With remote sensing we now have the tools to characterize, monitor, and model urban landscapes world-wide. However, the remote sensing performed on cities so far has concentrated on land-use patterns as distinct from land-cover or composition. The popular Anderson system is entirely land-use oriented in urban areas. This paper begins with the premise that characterizing the biophysical composition of urban environments is fundamental to understanding urban/industrial ecosystems, and, in turn, supports the modeling of other systems interfacing with urban systems. Further, it is contended that remote sensing is a tool poised to provide the biophysical composition data to characterize urban landscapes.

Author (revised)

N94-16706*# Washington Univ., Seattle. Dept. of Geological Sciences.

TEMPORAL VARIATION IN SPECTRAL DETECTION THRESHOLDS OF SUBSTRATE AND VEGETATION IN AVIRIS IMAGES **c43**

Donald E. Sabol, Jr., Dar A. Roberts, Milton O. Smith, and John B. Adams *In* JPL, Summaries of the Third Annual JPL Airborne Geoscience Workshop. Volume 1: AVIRIS Workshop 1 Jun. 1992 p 132-134 (For primary document see N94-16666 03-42)

Avail: CASI HC A01/MF A02

The ability to map changes over large surface areas over time is one of the advantages in using remote sensing as a monitoring tool. Temporal changes in the surface may be gradual, making them difficult to detect in the short-term, and because they commonly occur at the subpixel scale, they may be difficult to detect in the long-term as well. Also, subtle changes may be real or merely an artifact of image noise. It is, therefore, necessary to understand the factors that limit the detection of surface materials in evaluating temporal data. The spectral detectability of vegetation and soil

in the 1990 July and October Airborne Visible/Infrared Imaging Spectrometer (AVIRIS) data of Jasper Ridge, CA was evaluated and compared.
Author (revised)

N94-16707*# INTERA Technologies Ltd., Ottawa (Ontario).
DISCUSSION OF BAND SELECTION AND METHODOLOGIES FOR THE ESTIMATION OF PRECIPITABLE WATER VAPOUR FROM AVIRIS DATA **c43**
Dena Schanzer and Karl Staenz (Canada Centre for Remote Sensing, Ottawa, Ontario.) *In* JPL, Summaries of the Third Annual JPL Airborne Geoscience Workshop. Volume 1: AVIRIS Workshop 1 Jun. 1992 p 135-137 (For primary document see N94-16666 03-42)
Avail: CASI HC A01/MF A02

An Airborne Visible/Infrared Imaging Spectrometer (AVIRIS) data set acquired over Canal Flats, B.C., on 14 Aug. 1990, was used for the purpose of developing methodologies for surface reflectance retrieval using the 5S atmospheric code. A scene of Rogers Dry Lake, California (23 Jul. 1990), acquired within three weeks of the Canal Flats scene, was used as a potential reference for radiometric calibration purposes and for comparison with other studies using primarily LOWTRAN7. Previous attempts at surface reflectance retrieval indicated that reflectance values in the gaseous absorption bands had the poorest accuracy. Modifications to 5S to use 1 nm step size, in order to make fuller use of the 20 cm(sup -1) resolution of the gaseous absorption data, resulted in some improvement in the accuracy of the retrieved surface reflectance. Estimates of precipitable water vapor using non-linear least squares regression and simple ratioing techniques such as the CIBR (Continuum Interpolated Band Ratio) technique or the narrow/wide technique, which relate ratios of combinations of bands to precipitable water vapor through calibration curves, were found to vary widely. The estimates depended on the bands used for the estimation; none provided entirely satisfactory surface reflectance curves.
Author (revised)

N94-16708*# Science Applications International Corp., Falls Church, VA.
ABUNDANCE RECOVERY ERROR ANALYSIS USING SIMULATED AVIRIS DATA **c43**
William W. Stoner, Joseph C. Harsanyi, William H. Farrand, and Jennifer A. Wong *In* JPL, Summaries of the Third Annual JPL Airborne Geoscience Workshop. Volume 1: AVIRIS Workshop 1 Jun. 1992 p 138-140 (For primary document see N94-16666 03-42)
Avail: CASI HC A01/MF A02

Measurement noise and imperfect atmospheric correction translate directly into errors in the determination of the surficial abundance of materials from imaging spectrometer data. The effects of errors on abundance recovery were investigated previously using Monte Carlo simulation methods by Sabol et. al. The drawback of the Monte Carlo approach is that thousands of trials are needed to develop good statistics on the probable error in abundance recovery. This computational burden invariably limits the number of scenarios of interest that can practically be investigated. A more efficient approach is based on covariance analysis. The covariance analysis approach expresses errors in abundance as a function of noise in the spectral measurements and provides a closed form result eliminating the need for multiple trials. Monte Carlo simulation and covariance analysis are used to predict confidence limits for abundance recovery for a scenario which is modeled as being derived from Airborne Visible/Infrared Imaging Spectrometer (AVIRIS).
Author (revised)

N94-16709*# California Univ., Davis. Dept. of Land, Air, and Water Resources.
MULTITEMPORAL DIURNAL AVIRIS IMAGES OF A FORESTED ECOSYSTEM **c43**
Susan L. Ustin, Milton O. Smith (Washington Univ., Seattle.), and John B. Adams (Washington Univ., Seattle.) *In* JPL, Summaries of the Third Annual JPL Airborne Geoscience Workshop. Volume 1: AVIRIS Workshop 1 Jun. 1992 p 141-143 (For primary document see N94-16666 03-42)
Avail: CASI HC A01/MF A02

Both physiological and ecosystem structural information may be derived from diurnal images. Structural information may be inferred from changes in canopy shadows between images and from changes in spectral composition due to changes in proportions of subpixel mixing resulting from the differences in sun/view angles. Physiological processes having diurnal scales also may be measurable if a stable basis for spectral comparison can be established. Six diurnal images of an area east of Mt. Shasta, CA were acquired on 22 Sep. 1989. This unique diurnal data set provided an opportunity to test the consistency of endmember fractions and residuals. It was expected that shade endmember abundances would show the greatest change as lighting geometry changed and less change in the normalized fractional proportion of other endmembers. Diurnal changes in spectral features related to physiological characteristics may be identifiable as changes in wavelength specific residuals.
Author (revised)

N94-16710*# Arizona State Univ., Tempe. Dept. of Geology.
A COMPARISON OF LOWTRAN-7 CORRECTED AIRBORNE VISIBLE/INFRARED IMAGING SPECTROMETER (AVIRIS) DATA WITH GROUND SPECTRAL MEASUREMENTS **c43**
Peng-Yang Xu and Ronald Greeley *In* JPL, Summaries of the Third Annual JPL Airborne Geoscience Workshop. Volume 1: AVIRIS Workshop 1 Jun. 1992 p 144-146 (For primary document see N94-16666 03-42)
Avail: CASI HC A01/MF A02

Atmospheric correction of imaging spectroscopy data is required for quantitative analysis. Different models were proposed for atmospheric correction of these data. LOWTRAN-7 is a low-resolution model and computer code for predicting atmospheric transmittance and background radiance from 0 to 50,00 cm(sup -1) which was developed by the Air Force Geophysics Laboratory. The Airborne Visible/Infrared Imaging Spectrometer (AVIRIS) data used are radiometrically calibrated and include the 28 Sep. 1989 Providence Fan flight line segment 07, California. It includes a dark gravel surface defined as a calibration site by the Geologic Remote Sensing Field Experiment (GRSFE). Several ground measurements of portable spectrometer DAEDALUS AA440 Spectrafax were taken during the GRSFE, July 1989 field campaign. Comparisons of the LOWTRAN-7 corrected AVIRIS data with the ground spectrometer measuremont were made.
Author (revised)

N94-16711*# Colorado Univ., Boulder. Center for the Study of Earth from Space.
DISCRIMINATION AMONG SEMI-ARID LANDSCAPE ENDMEMBERS USING THE SPECTRAL ANGLE MAPPER (SAM) ALGORITHM **c43**
Roberta H. Yuhas, Alexander F. H. Goetz, and Joe W. Boardman (Commonwealth Scientific and Industrial Research Organization, North Ryde, Australia.) *In* JPL, Summaries of the Third Annual JPL Airborne Geoscience Workshop. Volume 1: AVIRIS Workshop 1 Jun. 1992 p 147-149 (For primary document see N94-16666 03-42)
(Grant NAGw-270)
Avail: CASI HC A01/MF A02

Airborne Visible/Infrared Imaging Spectrometer (AVIRIS) data were acquired during three consecutive seasons of the year (26 Sep. 1989, 22 Mar. 1990, and 7 Aug. 1990) over an area of the High Plains east of Greeley, Colorado. This region contains extensive eolian deposits in the form of stabilized dune complexes (small scale parabolic dunes superimposed on large scale longitudinal and parabolic dunes). Due to the dunes' large scale (2-10 km) and low relief (1-5 m), the scaling relationships that contribute to the evolution of this landscape are nearly impossible to understand without the use of remote sensing. Additionally, climate models indicate that the High Plains could be one of the first areas to experience changes in climate caused by either global warming or cooling. During the past 10,000 years there were at least three periods of extensive sand activity, followed by periods of landscape stability, as shown in the stratigraphic record of this area. Therefore, if the past is an indication of the future, the monitoring of this landscape and its sensitive ecosystem is important for early detection of regional and global climate change.
Author (revised)

N94-16712*# Jet Propulsion Lab., California Inst. of Tech., Pasadena.
EMPIRICAL RELATIONSHIPS AMONG ATMOSPHERIC VARIABLES FROM RAWINSONDE AND FIELD DATA AS SURROGATES FOR AVIRIS MEASUREMENTS: ESTIMATION OF REGIONAL LAND SURFACE EVAPOTRANSPIRATION **c43**
James E. Conel, Gordon Hoover, Anne Nolin, Ron Alley, and Jack Margolis *In its* Summaries of the Third Annual JPL Airborne Geoscience Workshop. Volume 1: AVIRIS Workshop 1 Jun. 1992 p 150-151 (For primary document see N94-16666 03-42)
Avail: CASI HC A01/MF A02

Empirical relationships between variables are ways of securing estimates

of quantities difficult to measure by remote sensing methods. The use of empirical functions was explored between: (1) atmospheric column moisture abundance W (gm H2O/cm(sup 2) and surface absolute water vapor density rho(q-bar) (gm H2O/cm(sup 3), with rho density of moist air (gm/cm(sup 3), q-bar specific humidity (gm H2O/gm moist air), and (2) column abundance and surface moisture flux E (gm H2O/(cm(sup 2)sec)) to infer regional evapotranspiration from Airborne Visible/Infrared Imaging Spectrometers (AVIRIS) water vapor mapping data. AVIRIS provides, via analysis of atmospheric water absorption features, estimates of column moisture abundance at very high mapping rate (at approximately 100 km(sup 2)/40 sec) over large areas at 20 m ground resolution. Author (revised)

N94-16713*# Australian Defence Force Academy, Canberra. Dept. of Electrical Engineering.

LOSSLESS COMPRESSION OF AVIRIS DATA: COMPARISON OF METHODS AND INSTRUMENT CONSTRAINTS **c43**

R. E. Roger, J. F. Arnold, M. C. Cavenor, and J. A. Richards *In* JPL, Summaries of the Third Annual JPL Airborne Geoscience Workshop. Volume 1: AVIRIS Workshop 1 Jun. 1992 p 154-156 (For primary document see N94-16666 03-42)

Avail: CASI HC A01/MF A02

A family of lossless compression methods, allowing exact image reconstruction, are evaluated for compressing Airborne Visible/Infrared Imaging Spectrometers (AVIRIS) image data. The methods are used on Differential Pulse Code Modulation (DPCM). The compressed data have an entropy of order 6 bits/pixel. A theoretical model indicates that significantly better lossless compression is unlikely to be achieved because of limits caused by the noise in the AVIRIS channels. AVIRIS data differ from data produced by other visible/near-infrared sensors, such as LANDSAT-TM or SPOT, in several ways. Firstly, the data are recorded at a greater resolution (12 bits, though packed into 16-bit words). Secondly, the spectral channels are relatively narrow and provide continuous coverage of the spectrum so that the data in adjacent channels are generally highly correlated. Thirdly, the noise characteristics of the AVIRIS are defined by the channels' Noise Equivalent Radiances (NER's), and these NER's show that, at some wavelengths, the least significant 5 or 6 bits of data are essentially noise. Author (revised)

N94-16714*# Desert Research Inst., Reno, NV. Atmospheric Sciences Center.

SIMULATION OF AVHRR-K BAND RATIOS WITH AVIRIS **c43**

Melanie A. Wetzel and Ronald M. Welch (South Dakota School of Mines and Technology, Rapid City.) *In* JPL, Summaries of the Third Annual JPL Airborne Geoscience Workshop. Volume 1: AVIRIS Workshop 1 Jun. 1992 p 157-159 (For primary document see N94-16666 03-42)

Avail: CASI HC A01/MF A02

The Advanced Very High Resolution Radiometer (AVHRR)-K polar-orbiting imager scheduled for launch by the mid-1990's will include two new near-infrared narrowband detectors, Band 3A, 1.58- 1.64 microns, and a modified (narrower) Band 2, 0.84-0.87 microns. The Airborne Visible/Infrared Imaging Spectrometer (AVIRIS) is an ideal testbed for these bands. The results of a comparison between AVIRIS band ratio values and AVHRR-K radiances simulated from AVIRIS are summarized. Author (revised)

N94-16731*# Jet Propulsion Lab., California Inst. of Tech., Pasadena.

SUMMARIES OF THE THIRD ANNUAL JPL AIRBORNE GEOSCIENCE WORKSHOP. VOLUME 3: AIRSAR WORKSHOP

Jakob vanZyl, ed. 1 Jun. 1992 120 p Workshop held in Pasadena, CA, 1-5 Jun. 1992

(NASA-CR-194542; JPL-Publ-92-14-Vol-3; NAS 1.26:194542) Avail: CASI HC A06/MF A02

This publication contains the preliminary agenda and summaries for the Third Annual JPL Airborne Geoscience Workshop, held at the Jet Propulsion Laboratory, Pasadena, California, on 1-5 June 1992. This main workshop is divided into three smaller workshops as follows: (1) the Airborne Visible/Infrared Imaging Spectrometer (AVIRIS) workshop, on June 1 and 2; the summaries for this workshop appear in Volume 1; (2) the Thermal Infrared Multispectral Scanner (TIMS) workshop, on June 3; the summaries for this workshop appear in Volume 2; and (3) the Airborne Synthetic Aperture Radar (AIRSAR) workshop, on June 4 and 5; the summaries for this workshop appear in Volume 3. For individual titles, see N94-16732 through N94-16762.

N94-16732*# National Aeronautics and Space Administration. Goddard Space Flight Center, Greenbelt, MD.

A SNOW WETNESS RETRIEVAL ALGORITHM FOR SAR **c43**

Jian-Cheng Shi (California Univ., Santa Barbara.) and Jeff Dozier *In* JPL, Summaries of the Third Annual JPL Airborne Geoscience Workshop. Volume 3: AIRSAR Workshop 1 Jun. 1992 p 1-3 (For primary document see N94-16731 03-42)

Avail: CASI HC A01/MF A02

The objectives of this study are: (1) to evaluate the backscattering signals response to snow wetness; and (2) to develop an algorithm for snow wetness measurement using C-band polarimetric synthetic aperture radar (SAR). In hydrological investigations, modeling and forecasting of snowmelt runoff requires information about snowpack properties and their spatial variability. In particular, timely measurement of snow parameters is needed for operational hydrology. The liquid water content of snowpack is one of the important parameters. Active microwave sensors are highly sensitive to liquid water in the snowpack because of the large dielectric contrast between ice and water in the microwave spectrum. They are not affected by weather and have a spatial resolution compatible with the topographic variation in alpine regions. However, a quantitative algorithm for retrieval snow wetness has not yet been developed. Author (revised)

N94-16733*# Deutsche Forschungsanstalt fuer Luft- und Raumfahrt, Oberpfaffenhofen (Germany). Inst. of Radio-Frequency Technology.

COMPARISON OF JPL-AIRSAR AND DLR E-SAR IMAGES FROM THE MAC EUROPE 1991 CAMPAIGN OVER TESTSITE OBERPFAFFENHOFEN: FREQUENCY AND POLARIZATION DEPENDENT BACKSCATTER VARIATIONS FROM AGRICULTURAL FIELDS **c43**

C. Schmullius and J. Nithack *In* JPL, Summaries of the Third Annual JPL Airborne Geoscience Workshop. Volume 3: AIRSAR Workshop 1 Jun. 1992 p 4-6 (For primary document see N94-16731 03-42)

Avail: CASI HC A01/MF A02

On July 12, the MAC Europe '91 (Multi-Sensor Airborne Campaign) took place over test site Oberpfaffenhofen. The DLR Institute of Radio-Frequency Technology participated with its C-VV, X-VV, and X-HH Experimental Synthetic Aperture Radar (E-SAR). The high resolution E-SAR images with a pixel size between 1 and 2 m and the polarimetric AIRSAR images were analyzed. Using both sensors in combination is a unique opportunity to evaluate SAR images in a frequency range from P- to X-band and to investigate polarimetric information. Author (revised)

N94-16734*# Jet Propulsion Lab., California Inst. of Tech., Pasadena.

MONITORING ENVIRONMENTAL STATE OF ALASKAN FORESTS WITH AIRSAR **c43**

Kyle C. McDonald, JoBea Way, Eric Rignot, Cindy Williams (Alaska Univ., Fairbanks.), Les Viereck (Alaska Univ., Fairbanks.), and Phylis Adams (Alaska Univ., Fairbanks.) *In its* Summaries of the Third Annual JPL Airborne Geoscience Workshop. Volume 3: AIRSAR Workshop 1 Jun. 1992 p 7-8 (For primary document see N94-16731 03-42)

Avail: CASI HC A01/MF A02

During March 1988 and May 1991, the JPL airborne synthetic aperture radar, AIRSAR, collected sets of multi-temporal imagery of the Bonanza Creek Experimental Forest near Fairbanks, Alaska. These data sets consist of series of multi-polarized images collected at P-, L-, and C-bands each over a period of a few days. The AIRSAR campaigns were complemented with extensive ground measurements that included observations of both static canopy characteristics such as forest architecture as well as properties that vary on short term time scales such as canopy dielectric conditions. Observations exist for several stands of deciduous and coniferous species including white spruce (Picea glauca), black spruce (Picea mariana), and balsam poplar (Populus balsamifera). Although the duration of each campaign was fairly short, significant changes in environmental conditions caused notable variations in the physiological state of the canopies. During the 1988 campaign, environmental conditions ranged from unseasonably warm to more normal subfreezing temperatures. This permitted AIRSAR observations of frozen and thawed canopy states. During May 1991, ice jams that occurred along the river caused many stands to flood while the subsequent clearing of the river then allowed the waters to recede, leaving a snow covered ground surface. This allowed observations of several stands during both flooded and nonflooded conditions. Furthermore, the local weather varied from clear sunny days to heavy overcast days with some

occurrence of rain. Measurements of leaf water potential indicated that this caused significant variations in canopy water status, allowing SAR observations of water stressed and unstressed trees. Mean backscatter from several stands is examined for the various canopy physiological states. The changes in canopy backscatter that occur as a function of environmental and physiological state are analyzed. Preliminary results of a backscatter signature modeling analysis are presented. The implications of using SAR to monitor canopy phenological state are addressed. Author (revised)

N94-16735*# California Univ., Santa Barbara. Dept. of Geography.
COMPARISON OF MODELED BACKSCATTER WITH SAR DATA AT P-BAND **c43**
Yong Wang, Frank W. Davis, and John M. Melack *In* JPL, Summaries of the Third Annual JPL Airborne Geoscience Workshop. Volume 3: AIRSAR Workshop 1 Jun. 1992 p 9-11 (For primary document see N94-16731 03-42)
Avail: CASI HC A01/MF A02

In recent years several analytical models were developed to predict microwave scattering by trees and forest canopies. These models contribute to the understanding of radar backscatter over forested regions to the extent that they capture the basic interactions between microwave radiation and tree canopies, understories, and ground layers as functions of incidence angle, wavelength, and polarization. The Santa Barbara microwave model backscatter model for woodland (i.e. with discontinuous tree canopies) combines a single-tree backscatter model and a gap probability model. Comparison of model predictions with synthetic aperture radar (SAR) data and L-band (lambda = 0.235 m) is promising, but much work is still needed to test the validity of model predictions at other wavelengths. The validity of the model predictions at P-band (lambda = 0.68 m) for woodland stands at our Mt. Shasta test site was tested. Author (revised)

N94-16736*# California Univ., Santa Barbara. Dept. of Geography.
SAR BACKSCATTER FROM CONIFEROUS FOREST GAPS **c43**
John L. Day and Frank W. Davis *In* JPL, Summaries of the Third Annual JPL Airborne Geoscience Workshop. Volume 3: AIRSAR Workshop 1 Jun. 1992 p 12-14 (For primary document see N94-16731 03-42)
(Contracts JPL-958468; CS-86-90)
Avail: CASI HC A01/MF A02

A study is in progress comparing Airborne Synthetic Aperture Radar (AIRSAR) backscatter from coniferous forest plots containing gaps to backscatter from adjacent gap-free plots. Issues discussed are how do gaps in the range of 400 to 1600 sq m (approximately 4-14 pixels at intermediate incidence angles) affect forest backscatter statistics and what incidence angles, wavelengths, and polarizations are most sensitive to forest gaps. In order to visualize the slant-range imaging of forest and gaps, a simple conceptual model is used. This strictly qualitative model has led us to hypothesize that forest radar returns at short wavelengths (eg., C-band) and large incidence angles (e.g., 50 deg) should be most affected by the presence of gaps, whereas returns at long wavelengths and small angles should be least affected. Preliminary analysis of 1989 AIRSAR data from forest near Mt. Shasta supports the hypothesis. Current forest backscatter models such as MIMICS and Santa Barbara Discontinuous Canopy Backscatter Model have in several cases correctly predicted backscatter from forest stands based on inputs of measured or estimated forest parameters. These models do not, however, predict within-stand SAR scene texture, or 'intrinsic scene variability' as Ulaby et al. has referred to it. For instance, the Santa Barbara model, which may be the most spatially coupled of the existing models, is not truly spatial. Tree locations within a simulated pixel are distributed according to a Poisson process, as they are in many natural forests, but tree size is unrelated to location, which is not the case in nature. Furthermore, since pixels of a simulated stand are generated independently in the Santa Barbara model, spatial processes larger than one pixel are not modeled. Using a different approach, Oliver modeled scene texture based on an hypothetical forest geometry. His simulated scenes do not agree well with SAR data, perhaps due to the simple geometric model used. Insofar as texture is the expression of biological forest processes, such as succession and disease, and physical ones, such as fire and wind-throw, it contains useful information about the forest, and has value in image interpretation and classification. Forest gaps are undoubtedly important contributors to scene variance. By studying the localized effects of gaps on forest backscatter, guided by our qualitative model, we hope to understand more clearly the manner in which spatial heterogeneities in forests produce variations in backscatter, which collectively give rise to scene texture. Author (revised)

N94-16737*# Centre d'Etude Spatiale des Rayonnements, Toulouse (France).
RETRIEVAL OF PINE FOREST BIOMASS USING JPL AIRSAR DATA **c43**
A. Beaudoin, T. LeToan, F. Zagolski, C. C. Hsu (Massachusetts Inst. of Tech., Cambridge.), H. C. Han (Massachusetts Inst. of Tech., Cambridge.), and J. A. Kong (Massachusetts Inst. of Tech., Cambridge.) *In* JPL, Summaries of the Third Annual JPL Airborne Geoscience Workshop. Volume 3: AIRSAR Workshop 1 Jun. 1992 p 15-17 (For primary document see N94-16731 03-42)
Avail: CASI HC A01/MF A02

The analysis of Jet Propulsion Laboratory (JPL) Airborne Synthetic Aperture Radar (AIRSAR) data over the Landes forest in South-West France revealed strong correlation between L- and especially P-band sigma degrees and the pine forest biomass. To explain the physical link of radar backscatter to biomass, a polarimetric backscattering model was developed and validated. Then the model was used in a simulation study to predict sigma degree sensitivity to undesired canopy and environmental parameters. Main results concerning the data analysis, modeling, and simulation at P-band are reported. Author (revised)

N94-16738*# Geo Eco Arc Research, La Canada, CA.
CHARACTERIZATION OF WETLAND, FOREST, AND AGRICULTURAL ECOSYSTEMS IN BELIZE WITH AIRBORNE RADAR (AIRSAR) **c43**
Kevin O. Pope, Jose Maria Rey-Benayas, and Jack F. Paris (California State Univ., Fresno.) *In* JPL, Summaries of the Third Annual JPL Airborne Geoscience Workshop. Volume 3: AIRSAR Workshop 1 Jun. 1992 p 18-20 (For primary document see N94-16731 03-42)
Avail: CASI HC A01/MF A02

The Shuttle Imaging Radar-C/X-SAR (Synthetic Aperture Radar) Experiment includes the study of wetland dynamics in the seasonal tropics. In preparation for these wetland studies, airborne P, L, and C band radar (AIRSAR) data of Belize, Guatemala, and Mexico acquired by NASA and JPL in March 1990 were analyzed. The first phase of our study focuses on AIRSAR data from the Gallon Jug test site in northwestern Belize, for which ground data were also collected during the three days prior to the overflight. One of the main objectives of the Gallon Jug study is to develop a method for characterizing wetland vegetation types and their flooding status with multifrequency polarimetric radar data. Author (revised)

N94-16739*# California Univ., Santa Barbara. Dept. of Geography.
STRATEGIES FOR DETECTION OF FLOODPLAIN INUNDATION WITH MULTI-FREQUENCY POLARIMETRIC SAR **c43**
Laura L. Hess and John M. Melack *In* JPL, Summaries of the Third Annual JPL Airborne Geoscience Workshop. Volume 3: AIRSAR Workshop 1 Jun. 1992 p 21-23 (For primary document see N94-16731 03-42)
(Contract JPL-958469)
Avail: CASI HC A01/MF A02

Mapping of floodplain inundation patterns is a key element in developing hydrological and biogeochemical models for large tropical river basins such as the Amazon. Knowledge of the time sequence of inundation is necessary to determine both water routing and biogenic gas fluxes. Synthetic Aperture Radar (SAR) is uniquely suited for this application because of its ability to penetrate cloud cover and, in many cases, to detect flooding beneath a forest or herbaceous canopy. A procedure for discriminating flooded forest, flooded herbaceous vegetation, and open water from other cover types for a coastal wetland site on the lower Altamaha floodplain, Georgia, emphasizing robust classifiers that are not site-specific is currently being developed. Author (revised)

N94-16740*# Commission of the European Communities, Ispra (Italy). Inst. for Remote Sensing Applications.
SUPERVISED FULLY POLARIMETRIC CLASSIFICATION OF THE BLACK FOREST TEST SITE: FROM MAESTROI TO MAC EUROPE **c43**
G. DeGrandi, C. Lavalle, H. DeGroof, and A. Sieber *In* JPL, Summaries of the Third Annual JPL Airborne Geoscience Workshop. Volume 3: AIRSAR Workshop 1 Jun. 1992 p 24-26 (For primary document see N94-16731

03-42)
Avail: CASI HC A01/MF A02

A study on the performance of a supervised fully polarimetric maximum likelihood classifier for synthetic aperture radar (SAR) data when applied to a specific classification context: forest classification based on age classes and in the presence of a sloping terrain is presented. For the experimental part, the polarimetric AIRSAR data at P, L, and C-band, acquired over the German Black Forest near Freiburg in the frame of the 1989 MAESTRO-1 campaign and the 1991 MAC Europe campaign was used, MAESTRO-1 with an ESA/JRC sponsored campaign, and MAC Europe (Multi-sensor Aircraft Campaign); in both cases the multi-frequency polarimetric JPL Airborne Synthetic Aperture Radar (AIRSAR) radar was flown over a number of European test sites. The study is structured as follows. At first, the general characteristics of the classifier and the dependencies from some parameters, like frequency bands, feature vector, calibration, using test areas lying on a flat terrain are investigated. Once it is determined the optimal conditions for the classifier performance, we then move on to the study of the slope effect. The bulk of this work is performed using the Maestrol data set. Next the classifier performance with the MAC Europe data is considered. The study is divided into two stages: first some of the tests done on the Maestro data are repeated, to highlight the improvements due to the new processing scheme that delivers 16 look data. Second we experiment with multi images classification with two goals: to assess the possibility of using a training set measured from one image to classify areas in different images; and to classify areas on critical slopes using different viewing angles. The main points of the study are listed and some of the results obtained so far are highlighted. Author (revised)

N94-16741*# National Aeronautics and Space Administration. Goddard Space Flight Center, Greenbelt, MD.
RELATING MULTIFREQUENCY RADAR BACKSCATTERING TO FOREST BIOMASS: MODELING AND AIRSAR MEASUREMENT **c43**
Guo-Qing Sun (Ressler Associates, Inc., Laurel, MD.) and K. Jon Ranson *In* JPL, Summaries of the Third Annual JPL Airborne Geoscience Workshop. Volume 3: AIRSAR Workshop 1 Jun. 1992 p 27-29 (For primary document see N94-16731 03-42)
Avail: CASI HC A01/MF A02

During the last several years, significant efforts in microwave remote sensing were devoted to relating forest parameters to radar backscattering coefficients. These and other studies showed that in most cases, the longer wavelength (i.e. P band) and cross-polarization (HV) backscattering had higher sensitivity and better correlation to forest biomass. This research examines this relationship in a northern forest area through both backscatter modeling and synthetic aperture radar (SAR) data analysis. The field measurements were used to estimate stand biomass from forest weight tables. The backscatter model described by Sun et al. was modified to simulate the backscattering coefficients with respect to stand biomass. The average number of trees per square meter or radar resolution cell, and the average tree height or diameter breast height (dbh) in the forest stand are the driving parameters of the model. The rest of the soil surface, orientation, and size distributions of leaves and branches, remain unchanged in the simulations. Author (revised)

N94-16742*# University of Southern Mississippi, Bay Saint Louis. Center for Marine Science.
SAR OBSERVATIONS IN THE GULF OF MEXICO **c43**
David Sheres *In* JPL, Summaries of the Third Annual JPL Airborne Geoscience Workshop. Volume 3: AIRSAR Workshop 1 Jun. 1992 p 30-31 (For primary document see N94-16731 03-42)
Avail: CASI HC A01/MF A02

The Gulf of Mexico (GOM) exhibits a wealth of energetic ocean features; they include the Loop Current with velocities of about 2 m/s and strong shear fronts, mesoscale eddies, double vortices, internal waves, and the outflow of the 'Mighty Mississippi' river. These energetic features can have a strong impact on the economies of the states surrounding the Gulf. Large fisheries, oil and gas production as well as pollution transport are relevant issues. These circulation features in the Gulf are invisible to conventional IR and visible satellite imagery during the Summer months due to cloud cover and uniform surface temperatures. Synthetic Aperture Radar (SAR) imagery of the Gulf does penetrate the cloud cover and shows a rich assembly of features there year-round. Below are preliminary results from GOM SAR imagery taken by SEASAT in 1978 and by the AIRSAR program in 1991. Author (revised)

N94-16743*# Naval Research Lab., Washington, DC. Center for Advanced Space Sensing.
INVESTIGATION OF AIRSAR SIGNATURES OF THE GULF STREAM **c43**
G. R. Valenzuela, J. S. Lee, D. L. Schuler, G. O. Marmorino, F. Askari, K. Hoppel, J. A. C. Kaiser, and W. C. Keller *In* JPL, Summaries of the Third Annual JPL Airborne Geoscience Workshop. Volume 3: AIRSAR Workshop 1 Jun. 1992 p 32-34 (For primary document see N94-16731 03-42)
Avail: CASI HC A01/MF A02

Extensive Airborne Synthetic Aperture Radar (AIRSAR) measurements were made on 20 July 1990 during the NRL Gulf Stream (GS) experiment which addressed a number of scientific questions relating to SAR imaging of the ocean surface in the presence of variable currents and the background thermohaline circulation. The nature of the electromagnetic (e.m.) backscatter from the North edge of the GS using polarimetric signatures and amplitude imagery from the AIRSAR data is addressed. Author (revised)

N94-16744*# Delft Hydraulics Lab., Emmeloord (Netherlands).
MAPPING OF SEA BOTTOM TOPOGRAPHY **c48**
C. J. Calkoen, G. J. Wensink, and G. H. F. M. Hesselmans *In* JPL, Summaries of the Third Annual JPL Airborne Geoscience Workshop. Volume 3: AIRSAR Workshop 1 Jun. 1992 p 35-37 (For primary document see N94-16731 03-42)
Avail: CASI HC A01/MF A02

Under suitable conditions the bottom topography of shallow seas is visible in remote sensing radar imagery. Two experiments were performed to establish which remote sensing technique or combination yields optimal imaging of bottom topography and which hydro-meteorological conditions are favorable. A further goal is to gain experience with these techniques. Two experiments were performed over an area in the North Sea near the measuring platform Meetpost Noordwijk (MPN). The bottom topography in the test area is dominated by sand waves. The crests of the sand waves are perpendicular to the coast line and the dominating (tidal-)current direction. A 4x4 sq km wide section of the test area was studied in more detail. The first experiment was undertaken on 16 Aug. 1989. During the experiment the following remote sensing instruments were used: Landsat-Thematic Mapper, and NASA/JPL Airborne Imaging Radar (AIR). The hydro-meteorological conditions; current, wind, wave, and air and water temperature were monitored by MPN, a ship of Rijkswaterstaat (the OCTANS), and a pitch-and-roll WAVEC-buoy. The second experiment took place on 12 July 1992. During this experiment data were collected with the NASA/JPL polarimetric synthetic aperture radar (SAR), and a five-band helicopter-borne scatterometer. Again the hydro-meteorological conditions were monitored at MPN and the OCTANS. Furthermore, interferometric radar data were collected. Author (revised)

N94-16745*# Organisatie voor Toegepast Natuurwetenschappelijk Onderzoek, Delft (Netherlands). Physics and Electronics Lab.
SEA BOTTOM TOPOGRAPHY IMAGING WITH SAR **c48**
M. W. A. vanderKooij, G. J. Wensink (Delft Hydraulics Lab., Emmeloord, Netherlands.), and J. Vogelzang (Rijkswaterstaat, Delft, Netherlands.) *In* JPL, Summaries of the Third Annual JPL Airborne Geoscience Workshop. Volume 3: AIRSAR Workshop 1 Jun. 1992 p 38-39 (For primary document see N94-16731 03-42)
Avail: CASI HC A01/MF A02

It is well known that under favorable meteorological and hydrodynamical conditions the bottom topography of shallow seas can be mapped with airborne or spaceborne imaging radar. This phenomenon was observed for the first time in 1969 by de Loor and co-workers in Q-band Side Looking Airborne Radar (SLAR) imagery of sandwaves in the North Sea. It is now generally accepted that the imaging mechanism consists of three steps: (1) interaction between (tidal) current and bottom topography causes spatial modulations in the surface current velocity; (2) modulations in the surface current velocity give rise to variations in the spectrum of wind-generated waves, as described by the action balance equation; and (3) variations in the wave spectrum show up as intensity modulations in radar imagery. In order to predict radar backscatter modulations caused by sandwaves, an imaging model, covering the three steps, was developed by the Dutch Sea

Bottom Topography Group. This model and some model results will be shown. On 16 Aug. 1989 an experiment was performed with the polarimetric P-, L-, and C-band synthetic aperture radar (SAR) of NASA/JPL. One scene was recorded in SAR mode. On 12 Jul. 1991 another three scenes were recorded, of which one was in the ATI-mode (Along-Track Interferometer). These experiments took place in the test area of the Sea Bottom Topography Group, 30 km off the Dutch coast, where the bottom topography is dominated by sand waves. In-situ data were gathered by a ship in the test area and on 'Measuring Platform Noordwijk', 20 km from the center of the test area. The radar images made during the experiment were compared with digitized maps of the bottom. Furthermore, the profiles of radar backscatter modulation were compared with the results of the model. During the workshop some preliminary results of the ATI measurements will be shown. Author (revised)

N94-16746*# Cornell Univ., Ithaca, NY. Dept. of Geological Sciences.
PRELIMINARY RESULTS OF POLARIZATION SIGNATURES FOR GLACIAL MORAINES IN THE MONO BASIN, EASTERN SIERRA NEVADA **c46**
Richard R. Forster, Andrew N. Fox, and Bryan Isacks *In* JPL, Summaries of the Third Annual JPL Airborne Geoscience Workshop. Volume 3: AIRSAR Workshop 1 Jun. 1992 p 40-42 (For primary document see N94-16731 03-42)
Avail: CASI HC A01/MF A02

The valleys of the Mono Basin contain several sets of lateral and terminal moraines representing multiple stages of glaciation. The semi-arid climate with slow weathering rates preserved sequences of nested younger moraines within older ones. There is a well established relative chronology and recently exposure dating provided a new set of numerical dates. The moraines span the late Wisconsin (11-25 ka) to the Illinoian (130-190 ka) glaciations. The Mono Basin area was used as a 'calibration site' to establish remote dating techniques for eventual transfer to the more inaccessible but geomorphically and climatically similar moraines of the South American Andes Mountains. Planned polarimetric synthetic aperture radar (SAR) imagery acquired by JPL AIRSAR (South American Campaign) and SIR-C (Andes super-site) are analyzed to establish chronologies of previously undated moraine sequences in a study of Pleistocene climatic change in the Southern Hemisphere. The dry climate and sparse vegetation is also favorable for correlation of ground surface roughness with radar polarization signature. The slow weathering processes acting over thousands of years reduce the size, frequency, and angularity of surface boulders while increasing soil development on the moraines. Field observations based on this hypothesis result in relative ages consistent with those inferred from nested position within the valley. Younger moraines, therefore, will appear rougher than the older smoother moraines at scales measurable at AIRSAR wavelengths. Previously documented effects of ground surface roughness on polarization signatures suggest that analysis of moraine polarization signatures can be useful for relative dating. The technique may be extended to predict numerical ages. The data set reported were acquired on 8 Sep. 1989 with the JPL Airborne SAR (AIRSAR) collecting polarimetric imagery at C- (5.6 cm), L- (24 cm), and P-band (68 cm) with a flight-line parallel to the strike of the mountains. Phase calibration was performed on the analyzed scene by setting the co-phase of a smooth lake to zero as described. Absolute amplitude calibration was not possible because corner reflectors were not deployed. Author (revised)

N94-16747*# Arizona State Univ., Tempe. Dept. of Geology.
DETECTING SURFACE ROUGHNESS EFFECTS ON THE ATMOSPHERIC BOUNDARY LAYER VIA AIRSAR DATA: A FIELD EXPERIMENT IN DEATH VALLEY, CALIFORNIA **c46**
Dan G. Blumberg and Ronald Greeley *In* JPL, Summaries of the Third Annual JPL Airborne Geoscience Workshop. Volume 3: AIRSAR Workshop 1 Jun. 1992 p 43-45 (For primary document see N94-16731 03-42)
Avail: CASI HC A01/MF A02

The part of the troposphere influenced by the surface of the earth is termed the atmospheric boundary layer. Flow within this layer is influenced by the roughness of the surface; rougher surfaces induce more turbulence than smoother surfaces and, hence, higher atmospheric transfer rates across the surface. Roughness elements also shield erodible particles, thus decreasing the transport of windblown particles. Therefore, the aerodynamic roughness length (z(sub 0)) is an important parameter in aeolian and atmospheric boundary layer processes as it describes the aerodynamic properties of the underlying surface. z(sub 0) is assumed to be independent of wind velocity or height, and dependent only on the surface topography. It is determined using in situ measurements of the wind speed distribution as a function of height. For dry, unvegetated soils the intensity of the radar backscatter (sigma(sup 0)) is affected primarily by surface roughness at a scale comparable with the radar wavelength. Thus, both wind and radar respond to surface roughness variations on a scale of a few meters or less. Greeley showed the existence of a correlation between z(sub 0) and sigma(sup 0). This correlation was based on measurements over lava flows, alluvial fans, and playas in the southwest deserts of the United States. It is shown that the two parameters behave similarly also when there are small changes over a relatively homogeneous surface.
Author (revised)

N94-16748*# Colorado Univ., Boulder. Center for the Study of Earth from Space.
EXTRACTION OF QUANTITATIVE SURFACE CHARACTERISTICS FROM AIRSAR DATA FOR DEATH VALLEY, CALIFORNIA **c43**
K. S. Kierein-Young and F. A. Kruse *In* JPL, Summaries of the Third Annual JPL Airborne Geoscience Workshop. Volume 3: AIRSAR Workshop 1 Jun. 1992 p 46-48 (For primary document see N94-16731 03-42)
(Contract JPL-958456; NGT-50728)
Avail: CASI HC A01/MF A02

Polarimetric Airborne Synthetic Aperture Radar (AIRSAR) data were collected for the Geologic Remote Sensing Field Experiment (GRSFE) over Death Valley, California, USA, in Sep. 1989. AIRSAR is a four-look, quad-polarization, three frequency instrument. It collects measurements at C-band (5.66 cm), L-band (23.98 cm), and P-band (68.13 cm), and has a GIFOV of 10 meters and a swath width of 12 kilometers. Because the radar measures at three wavelengths, different scales of surface roughness are measured. Also, dielectric constants can be calculated from the data. The AIRSAR data were calibrated using in-scene trihedral corner reflectors to remove cross-talk; and to calibrate the phase, amplitude, and co-channel gain imbalance. The calibration allows for the extraction of accurate values of rms surface roughness, dielectric constants, sigma(sub 0) backscatter, and polarization information. The radar data sets allow quantitative characterization of small scale surface structure of geologic units, providing information about the physical and chemical processes that control the surface morphology. Combining the quantitative information extracted from the radar data with other remotely sensed data sets allows discrimination, identification and mapping of geologic units that may be difficult to discern using conventional techniques. Author (revised)

N94-16749*# Jet Propulsion Lab., California Inst. of Tech., Pasadena.
THE TOPSAR INTERFEROMETRIC RADAR TOPOGRAPHIC MAPPING INSTRUMENT **c43**
Howard A. Zebker, Soren N. Madsen, Jan Martin, Giovanni Alberti (Comitato Nazionale per l'Energia Nucleare, Naples, Italy.), Sergio Vetrella (Comitato Nazionale per l'Energia Nucleare, Naples, Italy.), and Alessandro Cucci (Alenia Spazio S.p.A., Rome, Italy.) *In its* Summaries of the Third Annual JPL Airborne Geoscience Workshop. Volume 3: AIRSAR Workshop 1 Jun. 1992 p 49-52 (For primary document see N94-16731 03-42)
Avail: CASI HC A01/MF A02

The NASA DC-8 AIRSAR instrument was augmented with a pair of C-band antennas displaced across track to form an interferometer sensitive to topographic variations of the Earth's surface. The antennas were developed by the Italian consortium Co.Ri.S.T.A., under contract to the Italian Space Agency (ASI), while the AIRSAR instrument and modifications to it supporting TOPSAR were sponsored by NASA. A new data processor was developed at JPL for producing the topographic maps, and a second processor was developed at Co.Ri.S.T.A. All the results presented below were processed at JPL. During the 1991 DC-8 flight campaign, data were acquired over several sites in the United States and Europe, and topographic maps were produced from several of these flight lines. Analysis of the results indicate that statistical errors are in the 2-3 m range for flat terrain and in the 4-5 m range for mountainous areas. Author (revised)

N94-16750*# Comitato Nazionale per l'Energia Nucleare, Naples (Italy).
EVALUATION OF THE TOPSAR PERFORMANCE BY USING PASSIVE AND ACTIVE CALIBRATORS **c43**
G. Alberti, A. Moccia (Naples Univ., Italy.), S. Ponte (Naples Univ., Italy.), and S. Vetrella *In* JPL, Summaries of the Third Annual JPL Airborne

Geoscience Workshop. Volume 3: AIRSAR Workshop 1 Jun. 1992 p 53-55 Sponsored by Italian Space Agency (For primary document see N94-16731 03-42)
Avail: CASI HC A01/MF A02

The preliminary analysis of the C-band cross-track interferometric data (XTI) acquired during the MAC Europe 1991 campaign over the Matera test site, in Southern Italy is presented. Twenty three passive calibrators (Corner Reflector, CR) and 3 active calibrators (Active Radar Calibrator, ARC) were deployed over an area characterized by homogeneous background. Contemporaneously to the flight, a ground truth data collection campaign was carried out. The research activity was focused on the development of motion compensation algorithms, in order to improve the height measurement accuracy of the TOPSAR system. Author (revised)

N94-16751*# Jet Propulsion Lab., California Inst. of Tech., Pasadena.
FITTING A THREE-COMPONENT SCATTERING MODEL TO POLARIMETRIC SAR DATA **c43**
A. Freeman and S. Durden *In its* Summaries of the Third Annual JPL Airborne Geoscience Workshop. Volume 3: AIRSAR Workshop 1 Jun. 1992 p 56-58 (For primary document see N94-16731 03-42)
Avail: CASI HC A01/MF A02

A new technique for fitting a three-component scattering mechanism model to the polarimetric synthetic aperture radar (SAR) data itself, without utilizing any ground truth measurements, is presented. The three scattering mechanism components included in the model are volume scatter from randomly oriented dipoles, first-order Bragg surface scatter and a dihedral scattering mechanism for two surfaces with different dielectric constants. The model fit yields an estimate of the contribution to the total backscatter of each of the three components. The backscatter contributions can also be compared to give the relative percentage weight of each. The model fit has an equal number of input parameters (the polarimetric radar backscatter measurements) and output parameters (the backscatter parameters describing them). The model can be applied to entire images or to small areas within an image to give a first-order estimate of the relevant scattering mechanisms. The model was applied to many C-, L- and P-band Airborne SAR (AIRSAR) images of different types of terrain. Results were presented at the workshop. Author (revised)

N94-16752*# Jet Propulsion Lab., California Inst. of Tech., Pasadena.
APPLICATION OF SYMMETRY PROPERTIES TO POLARIMETRIC REMOTE SENSING WITH JPL AIRSAR DATA **c43**
S. V. Nghiem, Simon H. Yueh, R. Kwok, and F. K. Li *In its* Summaries of the Third Annual JPL Airborne Geoscience Workshop. Volume 3: AIRSAR Workshop 1 Jun. 1992 p 59-61 (For primary document see N94-16731 03-42)
Avail: CASI HC A01/MF A02

Based on symmetry properties, polarimetric remote sensing of geophysical media is studied. From the viewpoint of symmetry groups, media with reflection, rotation, azimuthal, and centrical symmetries are considered. The symmetries impose relations among polarimetric scattering coefficients, which are valid to all scattering mechanisms in the symmetrical configurations. Various orientation distributions of non-spherical scatterers can be identified from the scattering coefficients by a comparison with the symmetry calculations. Experimental observations are then analyzed for many geophysical scenes acquired with the Jet Propulsion Laboratory (JPL) airborne polarimetric SAR at microwave frequencies over sea ice and vegetation. Polarimetric characteristics of different ice types are compared with symmetry behaviors. The polarimetric response of a tropical rain forest reveals characteristics close to the centrical symmetry properties, which can be used as a distributed target to relatively calibrate polarimetric radars without any deployment of manmade calibration targets. Author (revised)

N94-16753*# Jet Propulsion Lab., California Inst. of Tech., Pasadena.
EXTERNAL CALIBRATION OF POLARIMETRIC RADAR IMAGES USING DISTRIBUTED TARGETS **c43**
Simon H. Yueh, S. V. Nghiem, and R. Kwok *In its* Summaries of the Third Annual JPL Airborne Geoscience Workshop. Volume 3: AIRSAR Workshop 1 Jun. 1992 p 62-64 (For primary document see N94-16731 03-42)
Avail: CASI HC A01/MF A02

A new technique is presented for calibrating polarimetric synthetic aperture radar (SAR) images using only the responses from natural distributed targets. The model for polarimetric radars is assumed to be X = cRST where X is the measured scattering matrix corresponding to the target scattering matrix S distorted by the system matrices T and R (in general T does not equal R(sup t)). To allow for the polarimetric calibration using only distributed targets and corner reflectors, van Zyl assumed a reciprocal polarimetric radar model with T = R(sup t); when applied for JPL SAR data, a heuristic symmetrization procedure is used by POLCAL to compensate the phase difference between the measured HV and VH responses and then take the average of both. This heuristic approach causes some non-removable cross-polarization responses for corner reflectors, which can be avoided by a rigorous symmetrization method based on reciprocity. After the radar is made reciprocal, a new algorithm based on the responses from distributed targets with reflection symmetry is developed to estimate the cross-talk parameters. The new algorithm never experiences problems in convergence and is also found to converge faster than the existing routines implemented for POLCAL. When the new technique is implemented for the JPL polarimetric data, symmetrization and cross-talk removal are performed on a line-by-line (azimuth) basis. After the cross-talks are removed from the entire image, phase and amplitude calibrations are carried out by selecting distributed targets either with azimuthal symmetry along the looking direction or with some well-known volume and surface scattering mechanisms to estimate the relative phases and amplitude responses of the horizontal and vertical channels.
Author (revised)

N94-16754*# National Aeronautics and Space Administration. Goddard Space Flight Center, Greenbelt, MD.
PROCESSING OF POLARIMETRIC SAR DATA FOR SOIL MOISTURE ESTIMATION OVER MAHANTANGO WATERSHED AREA **c43**
K. S. Rao, W. L. Teng, and J. R. Wang *In* JPL, Summaries of the Third Annual JPL Airborne Geoscience Workshop. Volume 3: AIRSAR Workshop 1 Jun. 1992 p 65-68 (For primary document see N94-16731 03-42)
Avail: CASI HC A01/MF A02

Microwave remote sensing technique has a high potential for measuring soil moisture due to the large contrast in dielectric constant of dry and wet soils. Recent work by Pults et al. demonstrated the use of X/C-band data for quantitative surface soil moisture extraction from Airborne Synthetic Aperture Radar (SAR) system. Similar technique was adopted using polarimetric SAR data acquired with the JPL-AIRSAR system over the Mahantango watershed area in central Pennsylvania during July 1990. The data sets reported include C-, L-, and P-bands of 10, 13, 15, and 17 July 1990. Author (revised)

N94-16755*# National Aeronautics and Space Administration. Goddard Space Flight Center, Greenbelt, MD.
EVALUATION OF POLARIMETRIC SAR PARAMETERS FOR SOIL MOISTURE RETRIEVAL **c43**
Jian-Cheng Shi (California Univ., Santa Barbara.), Jakob J. vanZyl (Jet Propulsion Lab., California Inst. of Tech., Pasadena.), and Edwin T. Engman *In* JPL, Summaries of the Third Annual JPL Airborne Geoscience Workshop. Volume 3: AIRSAR Workshop 1 Jun. 1992 p 69-71 (For primary document see N94-16731 03-42)
Avail: CASI HC A01/MF A02

Results of ongoing efforts to develop an algorithm for soil moisture retrieval from Synthetic Aperture Radar (SAR) imagery are reported. Estimates of soil moisture are of great importance in numerous environmental studies, including hydrology, meteorology, and agriculture. Previous studies using extensive scatterometer measurements have established the optimum parameters for moisture retrieval as C-band HH radar operating at incidence angles between 10 to 15 deg. However, these parameters were not tested or verified with imaging radar systems. The results from different investigators showed considerable variability in the relationship between soil moisture and radar backscattering. This variability suggests that those algorithms are site-specific. Furthermore, the small incidence angle requirement limits the spatial application, especially for airborne radar systems.
Author (revised)

N94-16756*# California State Univ., Fresno. GeoInformation Processing Systems.
INTERACTION TYPES AND THEIR LIKE-POLARIZATION PHASE-ANGLE DIFFERENCE SIGNATURES **c43**
Jack F. Paris *In* JPL, Summaries of the Third Annual JPL Airborne

Geoscience Workshop. Volume 3: AIRSAR Workshop 1 Jun. 1992 p 72-74 (For primary document see N94-16731 03-42)
Avail: CASI HC A01/MF A02

The JPL Airborne Synthetic Aperture Radar (AIRSAR) measures the full polarimetric properties of scene objects. AIRSAR data contain a complete set of magnitudes (for all linearly-polarized combinations (viz., VV, HH, and CS (cross Polarization))) and phase-angle differences (for all pairs of linearly-polarized components) for each image pixel. Radar images users have been greatly interested in the like-polarization (LK) phase-angle difference parameter, delta phi(sub LK). Usually, it is associated with the type of interaction between microwaves and scene-object scattering-elements. One value of delta phi(sub LK) is said to be produced by a dominant single scattering (or reflection) event, and another value is said to be the result of a dominant double-scattering (or double reflection) event. these are often called 'single bounce' and 'double bounce' interaction signatures, respectively. There appears to be a significant amount of confusion about how the interaction processes produce the characteristic values of delta phi(sub LK) and about what value of delta phi(sub LK) should be associated with each specific type. This issue is addressed.
Author (revised)

N94-16757*# Jet Propulsion Lab., California Inst. of Tech., Pasadena.
APPLICATION OF MODIFIED VICAR/IBIS GIS TO ANALYSIS OF JULY 1991 FLEVOLAND AIRSAR DATA **c43**
L. Norikane, B. Broek (Organisatie voor Toegepast Natuurwetenschappelijk Onderzoek, Delft, Netherlands.), and A. Freeman *In its* Summaries of the Third Annual JPL Airborne Geoscience Workshop. Volume 3: AIRSAR Workshop 1 Jun. 1992 p 75-77 (For primary document see N94-16731 03-42)
Avail: CASI HC A01/MF A02

Three overflights of the Flevoland calibration/agricultural site were made by the JPL Airborne Synthetic Aperture Radar (AIRSAR) on 3, 12, and 28 July 1991 as part of MAC-Europe '92. A polygon map was generated at TNO-FEL which overlayed the slant range projected July 3 data set. Each polygon was identified by a sequence of points and a crop label. The polygon map was composed of 452 uniquely identified polygons and 15 different crop types. Analysis of the data was done using our modified Video Image Communication and Retrieval/Image Based Information System Geographic Information System (VICAR/IBIS GIS). This GIS is an extension of the VICAR/IBIS GIS first developed by Bryant in the 1970's which is itself an extension of the VICAR image processing system also developed at JPL.
Author (revised)

N94-16758*# Colorado Univ., Boulder. Center for the Study of Earth from Space.
RADAR ANALYSIS AND VISUALIZATION ENVIRONMENT (RAVEN): SOFTWARE FOR POLARIMETRIC RADAR ANALYSIS **c43**
K. S. Kierein-Young, A. B. Lefkoff, and F. A. Kruse *In* JPL, Summaries of the Third Annual JPL Airborne Geoscience Workshop. Volume 3: AIRSAR Workshop 1 Jun. 1992 p 78-80 (For primary document see N94-16731 03-42)
(Contract JPL-958456; NGT-50728)
Avail: CASI HC A01/MF A02

Imaging radar data provides information about the geometric and dielectric properties of the Earth's surface. The Jet Propulsion Laboratory (JPL) polarimetric Airborne Synthetic Aperture Radar (AIRSAR) is currently obtaining imaging radar data for use in geologic, vegetation, snow and ice, and ocean studies. In the near future, the Shuttle Imaging Radar C (SIR-C/X-SAR) and the Earth Observing System Synthetic Aperture Radar (EOS SAR) will also collect polarimetric radar data. A need exists for a user-friendly, interactive software package for analysis of these polarimetric radar data sets. Previous software packages, such as JPL's Multiview, while providing some analysis capabilities for these data, did not allow interactive viewing and were tied to specific image display hardware with operating system dependencies. A prototype software system, the 'Radar Analysis and Visualization Environment' (RAVEN) under development at the Center for the Study of Earth from Space (CSES) at the University of Colorado, is designed to deal with data from the JPL AIRSAR instrument and other proposed polarimetric radar instruments. RAVEN is being developed using the Interactive Data Language (IDL). It takes advantage of high speed disk access and fast processors running under the UNIX operating system in an X-windows environment to allow for rapid, interactive visualization of AIRSAR data in both image and graphical ways. It provides a user-friendly interface through the use of menus, sliders, buttons, and display windows.
Author (revised)

N94-16759*# Jet Propulsion Lab., California Inst. of Tech., Pasadena.
MEASURING OCEAN COHERENCE TIME WITH DUAL-BASELINE INTERFEROMETRY **c48**
Richard E. Carande *In its* Summaries of the Third Annual JPL Airborne Geoscience Workshop. Volume 3: AIRSAR Workshop 1 Jun. 1992 p 81-83 Sponsored in part by DOD (For primary document see N94-16731 03-42)
Avail: CASI HC A01/MF A02

Using the Jet Propulsion Laboratory (JPL) Airborne Synthetic Aperture Radar (AIRSAR) interferometer, measurements of the ocean coherence time at L and C band can be made at high spatial resolution. Fundamental to this measurement is the ability to image the ocean interferometrically at two different time-lags, or baselines. By modifying the operating procedure of the existing two antenna interferometer, a technique was developed make these measurements. L band coherence times are measured and presented.
Author (revised)

N94-16760*# INTERA Technologies Ltd., Nepean (Ontario).
SOIL CONSERVATION APPLICATIONS WITH C-BAND SAR **c48**
B. Brisco, R. J. Brown (Canada Centre for Remote Sensing, Ottawa, Ontario.), J. Naunheimer, and D. Bedard *In* JPL, Summaries of the Third Annual JPL Airborne Geoscience Workshop. Volume 3: AIRSAR Workshop 1 Jun. 1992 p 86-88 (For primary document see N94-16731 03-42)
Avail: CASI HC A01/MF A02

Soil conservation programs are becoming more important as the growing human population exerts greater pressure on this non-renewable resource. Indeed, soil degradation affects approximately 10 percent of Canada's agricultural land with an estimated loss of 6,000 hectares of topsoil annually from Ontario farmland alone. Soil loss not only affects agricultural productivity but also decreases water quality and can lead to siltation problems. Thus, there is a growing demand for soil conservation programs and a need to develop an effective monitoring system. Topography and soil type information can easily be handled within a geographic information system (GIS). Information about vegetative cover type and surface roughness, which both experience considerable temporal change, can be obtained from remote sensing techniques. For further development of the technology to produce an operational soil conservation monitoring system, an experiment was conducted in Oxford County, Ontario which investigated the separability of fall surface cover type using C-band Synthetic Aperture Radar (SAR) data.
Author (revised)

N94-16761*# Sheffield Univ. (England). Dept. of Applied and Computational Mathematics.
COMPARISON OF EDGES DETECTED AT DIFFERENT POLARISATIONS IN MAESTRO DATA **c48**
Ronald G. Caves, Peter J. Harley, and Shaun Quegan *In* JPL, Summaries of the Third Annual JPL Airborne Geoscience Workshop. Volume 3: AIRSAR Workshop 1 Jun. 1992 p 89-91 (For primary document see N94-16731 03-42)
Avail: CASI HC A01/MF A02

Edge detection would appear to be a crucial tool for analyzing multi-polarized, multi-frequency, and multi-temporal Synthetic Aperture Radar (SAR) images. Edge structure provides a simple means for comparing different polarizations and frequencies, and for detecting changes over time. Due to the fact that edges and segments (homogeneous regions) are dual concepts, edge detection has an important role to play in identifying segments within which mean backscatter measurements for use in image classification can be made. As part of a general investigation into edge detection in SAR imagery, an initial investigation was carried out into the detectability and nature of edges in multi-polarized and multi-frequency SAR images. The contrast ratio (CR) operator was used to detect edges. This operator was previously shown to perform well at detecting edges in single-polarized and single-frequency SAR images.
Author (revised)

N94-16762*# Jet Propulsion Lab., California Inst. of Tech., Pasadena.
LITHOLOGICAL AND TEXTURAL CONTROLS ON RADAR AND DIURNAL THERMAL SIGNATURES OF WEATHERED VOLCANIC DEPOSITS, LUNAR CRATER REGION, NEVADA **c48**

Jeffrey J. Plaut and Benoit Rivard (York Univ., Ontario.) *In its* Summaries of the Third Annual JPL Airborne Geoscience Workshop. Volume 3: AIRSAR Workshop 1 Jun. 1992 p 92-95 (For primary document see N94-16731 03-42)
Avail: CASI HC A01/MF A02

Radar backscatter intensity as measured by calibrated synthetic aperture radar (SAR) systems is primarily controlled by three factors: local incidence angle, wavelength-scale roughness, and dielectric permittivity of surface materials. Radar observations may be of limited use for geological investigations of surface composition, unless the relationships between lithology and the above characteristics can be adequately understood. In arid terrains, such as the Southwest U.S., weathering signatures (e.g. soil development, fracturing, debris grain size and shape, and hill slope characteristics) are controlled to some extent by lithologic characteristics of the parent bedrock. These textural features of outcrops and their associated debris will affect radar backscatter to varying degrees, and the multiple-wavelength capability of the JPL Airborne SAR (AIRSAR) system allows sampling of textures at three distinct scales. Diurnal temperature excursions of geologic surfaces are controlled primarily by the thermal inertia of surface materials, which is a measure of the resistance of a material to a change in temperature. Other influences include albedo, surface slopes affecting insolation, local meteorological conditions and surface emissivity at the relevant thermal wavelengths. To first order, thermal inertia variations on arid terrain surfaces result from grain size distribution and porosity differences, at scales ranging from micrometers to tens of meters. Diurnal thermal emission observations, such as those made by the JPL Thermal Infrared Multispectral Scanner (TIMS) airborne instrument, are thus influenced by geometric surface characteristics at scales comparable to those controlling radar backscatter. A preliminary report on a project involving a combination of field, laboratory and remote sensing observations of weathered felsic-to basaltic volcanic rock units exposed in the southern part of the Lunar Crater Volcanic Field, in the Pancake Range of central Nevada is presented. Focus is on the relationship of radar backscatter cross sections at multiple wavelengths, apparent diurnal temperature excursions identified in multi-temporal TIMS images, surface geometries related to weathering style, and parent bedrock lithology. Author (revised)

N94-17444*# National Aeronautics and Space Administration, Washington, DC.
EARTH SYSTEM DYNAMICS: THE INTERRELATION OF ATMOSPHERIC, OCEAN AND SOLID EARTH DYNAMICS Annual Technical Report, 16 Oct. 1992 - 31 Dec. 1993
Byron D. Tapley (Texas Univ., Austin.) and Ghassem Asrar 1993 18 p
(Grant NAGw-2615)
(NASA-CR-193487; NAS 1.26:193487) Avail: CASI HC A03/MF A01

The research work performed during the time period 16 Oct. 1992 through 31 Dec. 1993 is summarized. The overall research activity, including a list of the major findings of the EOS IDS research to date, is described, the publications and presentations are listed, and a budget request for the subsequent year is attached. Specifically, the report covers: EOS panel activities; major findings of research; team member contributions; new research directions; EOS restructuring effect; changes in requirements; plans for using existing data; collaborations with other EOS and non-EOS investigations; EOS instrument team interaction; instrument development verification and validation; interaction with EOSDIS and DAAC's; team coordination; overall management; summary of response to site review questions and comments; science computing facility; and additional new research activities. Author (revised)

43 EARTH RESOURCES AND REMOTE SENSING

Includes remote sensing of earth resources by aircraft and spacecraft; photogrammetry; and aerial photography.

For instrumentation see *35 Instrumentation and Photography.*

N94-15156 Deutsche Geodaetische Kommission, Munich (Germany).
ANALYSIS OF THE ACCURACY OF STRAPDOWN INERTIAL SURVEYING SYSTEMS Ph.D. Thesis - Stuttgart Univ. [GENAUIGKEITSANALYSE INERTIALER VERMESSUNGSSYSTEME MIT FAHRZEUGFESTEN SENSOREN]
Dietrich Schroeder 1992 146 p In GERMAN
(Ser-C-391; ISBN-3-7696-9437-6; ETN-93-94618) Copyright Avail: Issuing Activity (Fachinformationszentrum Karlsruhe, 7514 Eggenstein-Leopoldshafen 2, Germany)

Different quantities effecting the accuracy of geodetic positioning by means of an inertial strapdown system are analyzed. The inertial sensors are the starting point of the theoretical analysis. Detailed models of a pendulous accelerometer, a rate integrating gyro and a ring laser gyro were introduced and discussed as examples of the method of the mathematical modeling. The transformations between the reference frames, which have be realized for the implementation of the model equation of inertial positioning, were discussed with regard to today's state of the art sensor technology. To obtain an overview of the behavior of the solutions of the differential equations simplified as a result of the above mentioned discussion, the stability of the linearized equations was analyzed, using analytical and numerical methods. Nevertheless, in the case at hand of a time variable system, only restricted statements based on the linearized equations are possible. Hence in the extensive simulations carried out the nonlinear model equations were used. The effect of different sensor parameters on position and orientation was simulated for trajectories of different dynamics. For adapting the course and the dynamics of the trajectories, observed data were used. The results obtained using a simple compensation algorithm are presented. A detailed representation of the nonlinear and linear system equations for different parametrizations of both the translation and the rotation was proposed. ESA

N94-15181*# Michigan Technological Univ., Houghton. Geological Engineering, Geology and Geophysics.
GROUND TRUTH SPECTROMETRY AND IMAGERY OF ERUPTION CLOUDS TO MAXIMIZE UTILITY OF SATELLITE IMAGERY Progress Report
William I. Rose 1993 41 p
(Grant NAG5-1838)
(NASA-CR-194358; NAS 1.26:194358) Avail: CASI HC A03/MF A01

Field experiments with thermal imaging infrared radiometers were performed and a laboratory system was designed for controlled study of simulated ash clouds. Using AVHRR (Advanced Very High Resolution Radiometer) thermal infrared bands 4 and 5, a radiative transfer method was developed to retrieve particle sizes, optical depth and particle mass involcanic clouds. A model was developed for measuring the same parameters using TIMS (Thermal Infrared Multispectral Scanner), MODIS (Moderate Resolution Imaging Spectrometer), and ASTER (Advanced Spaceborne Thermal Emission and Reflection Radiometer). Related publications are attached. Derived from text

N94-15245* National Aeronautics and Space Administration, Washington, DC.
VIEWS FROM SPACE (Videotape)
Feb. 1990 Videotape: 3 min. 25 sec. playing time, in color, with sound
(NASA-TM-109634; NONP-VT-93-190432) Avail: CASI VHS A01/BETA A22

This document shows how views from the shuttle provide valuable information as to the condition of earth. CASI

N94-15297* National Aeronautics and Space Administration, Washington, DC.
COMBATING MALARIA (Videotape)
Nov. 1989 Videotape: 3 min. 25 sec. playing time, in color, with sound
(NASA-TM-109609; NONP-VT-93-190407) Avail: CASI VHS A01/BETA A22

This videotape shows the use of remote sensing to better target mosquito larvae for more effective control. CASI

N94-15310* National Aeronautics and Space Administration, Washington, DC.
FINDING FISH FROM ABOVE (Videotape)
Jan. 1991 Videotape: 2 min. 54 sec. playing time, in color, with sound
(NASA-TM-109602; NONP-VT-93-190400) Avail: CASI VHS A01/BETA A22

This videotape shows how the use of satellites can help locate fish. The demonstration is intended for the fishing industry. CASI

N94-15334* National Aeronautics and Space Administration. Lyndon B. Johnson Space Center, Houston, TX.
STS-26 SHUTTLE EARTH VIEWS, APRIL 1990, PART 1 (Videotape)
Jan. 1990 Videotape: 1 hr. playing time, in color, with sound
(NASA-TM-109564; NONP-VT-93-190362) Avail: CASI VHS A01/BETA A22

This video features Earth views compiled from a variety of footage shot during shuttle missions. Included are parts of North America, Africa, Europe, the Orient, and the Middle East. CASI

N94-15335* National Aeronautics and Space Administration. Lyndon B. Johnson Space Center, Houston, TX.
STS-26 SHUTTLE EARTH VIEWS, APRIL 1990, PART 2 (Videotape)
Jan. 1990 Videotape: 30 min. playing time, in color, with sound
(NASA-TM-109565; NONP-VT-93-190363) Avail: CASI VHS A01/BETA A22

This video features Earth views from a variety of footage shot during Shuttle Missions. Included are parts of North America, Africa, Europe, the Orient, and the Middle East. CASI

N94-15409* National Aeronautics and Space Administration, Washington, DC.
TESTING THE WATERS FROM SPACE (Videotape)
Dec. 1986 Videotape: 2 min. 48 sec. playing time, in color, with sound
(NASA-TM-109623; NONP-VT-93-190421) Avail: CASI VHS A01/BETA A22

It is explained how an infrared radiometer can accurately measure ocean surface temperature. CASI

N94-15428* National Aeronautics and Space Administration, Washington, DC.
IMPROVED MAPPING SYSTEM (Videotape)
Jan. 1991 Videotape: 3 min. 19 sec. playing time, in color, with sound
(NASA-TM-109643; NONP-VT-93-190441) Avail: CASI VHS A01/BETA A22

This video explains the system of mapping terrain made more accurate with NASA technology. CASI

N94-15531*# JJM Systems, Inc., Ivyland, PA.
AN EXPERT SYSTEM SHELL FOR INFERRING VEGETATION CHARACTERISTICS: ATMOSPHERIC TECHNIQUES (TASK G) Final Report, Apr. - Oct. 1993
P. Ann Harrison and Patrick R. Harrison Oct. 1993 39 p
(Contract NAS5-30127; RTOP 462-61-14)
(NASA-CR-194570; NAS 1.26:194570; C931031-U-2R06) Avail: CASI HC A03/MF A01

The NASA VEGetation Workbench (VEG) is a knowledge based system that infers vegetation characteristics from reflectance data. The VEG Subgoals have been reorganized into categories. A new subgoal category 'Atmospheric Techniques' containing two new subgoals has been implemented. The subgoal Atmospheric Passes allows the scientist to take reflectance data measured at ground level and predict what the reflectance values would be if the data were measured at a different atmospheric height. The subgoal Atmospheric Corrections allows atmospheric corrections to be made to data collected from an aircraft or by a satellite to determine what the equivalent reflectance values would be if the data were measured at ground level. The report describes the implementation and testing of the basic framework and interface for the Atmospheric Techniques Subgoals. Author

N94-15646*# AI Signal Research, Inc., Huntsville, AL.
DEVELOP ADVANCED NONLINEAR SIGNAL ANALYSIS TOPOGRAPHICAL MAPPING SYSTEM Monthly Technical Progress Report, Oct. 1993
Jen-Yi Jong 31 Oct. 1993 11 p
(Contract NAS8-39393)
(NASA-CR-194577; NAS 1.26:194577; TR-4002-93-10) Avail: CASI HC A03/MF A01

The SSME has been undergoing extensive flight certification and developmental testing, which involves some 250 health monitoring measurements. Under the severe temperature pressure, and dynamic environments sustained during operation, numerous major component failures have occurred, resulting in extensive engine hardware damage and scheduling losses. To enhance SSME safety and reliability, detailed analysis and evaluation of the measurements signal are mandatory to assess its dynamic characteristics and operational condition. Efficient and reliable signal detection techniques will reduce catastrophic system failure risks and expedite the evaluation of both flight and ground test data, and thereby reduce launch turn-around time. The basic objective of this contract are threefold: (1) Develop and validate a hierarchy of innovative signal analysis techniques for nonlinear and nonstationary time-frequency analysis. Performance evaluation will be carried out through detailed analysis of extensive SSME static firing and flight data. These techniques will be incorporated into a fully automated system. (2) Develop an advanced nonlinear signal analysis topographical mapping system (ATMS) to generate a Compressed SSME TOPO Data Base (CSTDB). This ATMS system will convert tremendous amounts of complex vibration signals from the entire SSME test history into a bank of succinct image-like patterns while retaining all respective phase information. A high compression ratio can be achieved to allow the minimal storage requirement, while providing fast signature retrieval, pattern comparison, and identification capabilities. (3) Integrate the nonlinear correlation techniques into the CSTDB data base with compatible TOPO input data format. Such integrated ATMS system will provide the large test archives necessary for a quick signature comparison. This study will provide timely assessment of SSME component operational status, identify probable causes of malfunction, and indicate feasible engineering solutions. The final result of this program will yield an ATMS system of nonlinear and nonstationary spectral analysis software package integrated with the Compressed SSME TOPO Data Base (CSTDB) on the same platform. This system will allow NASA engineers to retrieve any unique defect signatures and trends associated with different failure modes and anomalous phenomena over the entire SSME test history across turbo pump families. Derived from text

N94-15842# Brown Univ., Providence, RI.
A MULTILEVEL-MULTIRESOLUTION METHOD FOR IMAGE PROCESSING. A BAYESIAN FRAMEWORK FOR RECONSTRUCTING AND REPRESENTING SHAPES Final Report, 15 Jan. 1990 - 14 Jan. 1993
Basilis Gidas 15 Apr. 1993 10 p
(Contract DAAL03-90-G-0033)
(AD-A266772; ARO-26811.7-MA-SDI) Avail: CASI HC A02/MF A01

During the period of the grant, 15 Jan. 1990 to 14 Jan. 1993, the following were developed: (1) a coherent multiresolution framework for image analysis tasks, in particular, for estimating 3-D shapes from a single video or SAR image; the algorithm was applied to constructing topographic maps of Venus' terrain, and to segmentation/classification of textures; (2) efficient procedures for estimating the parameters of Markov Random Fields (MRF's) from noisy and degraded data; (3) a fixed-length noiseless source coding for MRF's using large deviations; and (4) a multi-grid type algorithm for maximum-likelihood estimation in tomography. In addition, a new non-parametric approach to speech recognition was begun. DTIC

N94-16026*# Princeton Univ., NJ. Dept. of Civil Engineering and Operations Research.
RESEARCH INTO THE INFLUENCE OF SPATIAL VARIABILITY AND SCALE ON THE PARAMETERIZATION OF HYDROLOGICAL PROCESSES Final Technical Report
Eric F. Wood 1993 240 p
(Grant NAGw-1392)
(NASA-CR-194610; NAS 1.26:194610) Avail: CASI HC A11/MF A03

The objectives of the research were as follows: (1) Extend the Representative Elementary Area (RE) concept, first proposed and developed in Wood et al, (1988), to the water balance fluxes of the interstorm period (redistribution, evapotranspiration and baseflow) necessary for the analysis of long-term water balance processes. (2) Derive spatially averaged water balance model equations for spatially variable soil, topography and vegetation, over A RANGE OF CLIMATES. This is a necessary step in our goal to derive consistent hydrologic results up to GCM grid scales necessary for global climate modeling. (3) Apply the above macroscale water balance equations with remotely sensed data and begin to explore the feasibility of parameterizing the water balance constitutive equations at GCM grid scale. For individual titles, see N94-16027 through N94-16034.

N94-16027*# Princeton Univ., NJ. Dept. of Civil Engineering and Operations Research.

ON HYDROLOGIC SIMILARITY: A DIMENSIONLESS FLOOD FREQUENCY MODEL USING A GENERALIZED GEOMORPHOLOGIC UNIT HYDROGRAPH AND PARTIAL AREA RUNOFF GENERATION

Murugesu Sivapalan, Eric F. Wood, and Keith J. Beven (Lancaster Univ., England.) *In its* Research into the Influence of Spatial Variability and Scale on the Parameterization of Hydrological Processes 1993 16 p Repr. from Water Resources Research, v. 26, no. 1, Jan. 1990 p 43-58 (For primary document see N94-16026 03-43)

(Grants NAG5-491; USGS-14-08-0001-G1138)

(Paper-89WR01579) Avail: CASI HC A03/MF A03

One of the shortcomings of the original theory of the geomorphologic unit hydrograph (GUH) is that it assumes that runoff is generated uniformly from the entire catchment area. It is now recognized that in many catchments much of the runoff during storm events is produced on partial areas which usually form on narrow bands along the stream network. A storm response model that includes runoff generation on partial areas by both Hortonian and Dunne mechanisms was recently developed by the authors. In this paper a methodology for integrating this partial area runoff generation model with the GUH-based runoff routing model is presented; this leads to a generalized GUH. The generalized GUH and the storm response model are then used to estimate physically based flood frequency distributions. In most previous work the initial moisture state of the catchment had been assumed to be constant for all the storms. In this paper we relax this assumption and allow the initial moisture conditions to vary between storms. The resulting flood frequency distributions are cast in a scaled dimensionless framework where issues such as catchment scale and similarity can be conveniently addressed. A number of experiments are performed to study the sensitivity of the flood frequency response to some of the 'similarity' parameters identified in this formulation. The results indicate that one of the most important components of the derived flood frequency model relates to the specification of processes within the runoff generation model; specifically the inclusion of both saturation excess and Horton infiltration excess runoff production mechanisms. The dominance of these mechanisms over different return periods of the flood frequency distribution can significantly affect the distributional shape and confidence limits about the distribution. Comparisons with observed flood distributions seem to indicate that such mixed runoff production mechanisms influence flood distribution shape. The sensitivity analysis also indicated that the incorporation of basin and rainfall storm scale also greatly influences the distributional shape of the flood frequency curve. Author

N94-16028*# Princeton Univ., NJ.

SIMILARITY AND SCALE IN CATCHMENT STORM RESPONSE

Eric F. Wood, Murugesu Sivapalan (University of Western Australia, Nedlands.), and Keith Beven (Lancaster Univ., England.) *In its* Research into the Influence of Spatial Variability and Scale on the Parameterization of Hydrological Processes 1993 18 p Repr. from Reviews of Geophysics, v. 28, no. 1, Feb. 1990 p 1-18 (For primary document see N94-16026 03-43)

(Grants NAG5-491; USGS-14-08-0001-G1138; NERC-GR3/6264)

(Paper-89RG01615) Avail: CASI HC A03/MF A03

Until recently, very little progress had been made in understanding the relationship between small-scale variability of topography, soil, and rainfalls and the storm response seen at the catchment scale. The work reviewed here represents the first attempt at a systematic theoretical framework for such understanding in the context of surface runoff generation by different processes. The parameterization of hydrological processes over a range of scales is examined, and the concept of the 'representative elementary area' (REA) is introduced. The REA is a fundamental scale for catchment modeling at which continuum assumptions can be applied for the spatially variable controls and parameters, and spatial patterns no longer have to be considered explicitly. The investigation of scale leads into the concept of hydrologic similarity in which the effects of the environmental controls on runoff generation and flood frequency response be investigated independently of catchment scale. The paper reviews the authors' initial results and hopefully will motivate others to also investigate the issues of hydrologic scale and similarity. Author

N94-16029*# Princeton Univ., NJ. Dept. of Civil Engineering and Operations Research.

EVAPOTRANSPIRATION AND RUNOFF FROM LARGE LAND AREAS: LAND SURFACE HYDROLOGY FOR ATMOSPHERIC GENERAL CIRCULATION MODELS

J. S. Famiglietti and Eric F. Wood *In its* Research into the Influence of Spatial Variability and Scale on the Parameterization of Hydrological Processes 1993 28 p Repr. from Surveys in Geophysics, v. 12, 1991 p 179-204 (For primary document see N94-16026 03-43)

(Grants NGT-60153; USGS-14-08-0001-G1753)

Avail: CASI HC A03/MF A03

A land surface hydrology parameterization for use in atmospheric GCM's is presented. The parameterization incorporates subgrid scale variability in topography, soils, soil moisture and precipitation. The framework of the model is the statistical distribution of a topography-soils index, which controls the local water balance fluxes, and is therefore taken to represent the large land area. Spatially variable water balance fluxes are integrated with respect to the topography-soils index to yield our large topography-soils distribution, and interval responses are weighted by the probability of occurrence of the interval. Grid square averaged land surface fluxes result. The model functions independently as a macroscale water balance model. Runoff ratio and evapotranspiration efficiency parameterizations are derived and are shown to depend on the spatial variability of the above mentioned properties and processes, as well as the dynamics of land surface-atmosphere interactions. Author

N94-16030*# Princeton Univ., NJ.

HETEROGENEITY AND SCALING LAND-ATMOSPHERIC WATER AND ENERGY FLUXES IN CLIMATE SYSTEMS c47

Eric F. Wood *In its* Research into the Influence of Spatial Variability and Scale on the Parameterization of Hydrological Processes 1993 50 p Presented at the IHP/IAHS George Kovacs Colloquium on Space and Time Variability and Interdependencies in Various Hydrological Processes, Paris, France, 3-4 Jul. 1992 (For primary document see N94-16026 03-43)

(Grants NAG5-899)

Avail: CASI HC A03/MF A03

The effects of small-scale heterogeneity in land surface characteristics on the large-scale fluxes of water and energy in land-atmosphere system has become a central focus of many of the climatology research experiments. The acquisition of high resolution land surface data through remote sensing and intensive land-climatology field experiments (like HAPEX and FIFE) has provided data to investigate the interactions between microscale land-atmosphere interactions and macroscale models. One essential research question is how to account for the small scale heterogeneities and whether 'effective' parameters can be used in the macroscale models. To address this question of scaling, three modeling experiments were performed and are reviewed in the paper. The first is concerned with the aggregation of parameters and inputs for a terrestrial water and energy balance model. The second experiment analyzed the scaling behavior of hydrologic responses during rain events and between rain events. The third experiment compared the hydrologic responses from distributed models with a lumped model that uses spatially constant inputs and parameters. The results show that the patterns of small scale variations can be represented statistically if the scale is larger than a representative elementary area scale, which appears to be about 2 - 3 times the correlation length of the process. For natural catchments this appears to be about 1 - 2 sq km. The results concerning distributed versus lumped representations are more complicated. For conditions when the processes are nonlinear, then lumping results in biases; otherwise a one-dimensional model based on 'equivalent' parameters provides quite good results. Further research is needed to fully understand these conditions. Author (revised)

N94-16031*# Ghent Univ. (Belgium). Lab. of Hydrology and Water Management.

EVALUATION OF A DISTRIBUTED CATCHMENT SCALE WATER BALANCE MODEL

Peter A. Troch, Marco Mancini (Politecnico di Milano, Italy.), Claudio Paniconi (Padua Univ., Italy.), and Eric F. Wood (Princeton Univ., NJ.) *In* Princeton Univ., Research into the Influence of Spatial Variability and Scale on the Parameterization of Hydrological Processes 1993 13 p Repr. from Water Resources Research, v. 29, no. 6, Jun. 1993 p 1805-1817 (For

primary document see N94-16026 03-43)
(Contract NAG5-1628; DAAL03-91-G-0165; USDA-58-3K47-0-039; NRC-91-02615-PF42)
(Paper-93WR00398) Avail: CASI HC A03/MF A03

The validity of some of the simplifying assumptions in a conceptual water balance model is investigated by comparing simulation results from the conceptual model with simulation results from a three-dimensional physically based numerical model and with field observations. We examine, in particular, assumptions and simplifications related to water table dynamics, vertical soil moisture and pressure head distributions, and subsurface flow contributions to stream discharge. The conceptual model relies on a topographic index to predict saturation excess runoff and on Philip's infiltration equation to predict infiltration excess runoff. The numerical model solves the three-dimensional Richards equation describing flow in variably saturated porous media, and handles seepage face boundaries, infiltration excess and saturation excess runoff production, and soil driven and atmosphere driven surface fluxes. The study catchments (a 7.2 sq km catchment and a 0.64 sq km subcatchment) are located in the North Appalachian ridge and valley region of eastern Pennsylvania. Hydrologic data collected during the MACHYDRO 90 field experiment are used to calibrate the models and to evaluate simulation results. It is found that water table dynamics as predicted by the conceptual model are close to the observations in a shallow water well and therefore, that a linear relationship between a topographic index and the local water table depth is found to be a reasonable assumption for catchment scale modeling. However, the hydraulic equilibrium assumption is not valid for the upper 100 cm layer of the unsaturated zone and a conceptual model that incorporates a root zone is suggested. Furthermore, theoretical subsurface flow characteristics from the conceptual model are found to be different from field observations, numerical simulation results, and theoretical baseflow recession characteristics based on Boussinesq's groundwater equation.
Author

N94-16032*# Princeton Univ., NJ. Dept. of Civil Engineering and Operations Research.
A DETAILED MODEL FOR SIMULATION OF CATCHMENT SCALE SUBSURFACE HYDROLOGIC PROCESSES
Claudio Paniconi and Eric F. Wood *In its* Research into the Influence of Spatial Variability and Scale on the Parameterization of Hydrological Processes 1993 20 p Repr. from Water Resources Research, v. 29, no. 6, Jun. 1993 p 1601-1620 Sponsored in part by the Pittsburgh Supercomputing Center (For primary document see N94-16026 03-43)
(Grants NAG5-899; NAG5-1249)
(Paper-92WR02333) Avail: CASI HC A03/MF A03

A catchment scale numerical model is developed based on the three-dimensional transient Richards equation describing fluid flow in variably saturated porous media. The model is designed to take advantage of digital elevation data bases and of information extracted from these data bases by topographic analysis. The practical application of the model is demonstrated in simulations of a small subcatchment of the Konza Prairie reserve near Manhattan, Kansas. In a preliminary investigation of computational issues related to model resolution, we obtain satisfactory numerical results using large aspect ratios, suggesting that horizontal grid dimensions may not be unreasonably constrained by the typically much smaller vertical length scale of a catchment and by vertical discretization requirements. Additional tests are needed to examine the effects of numerical constraints and parameter heterogeneity in determining acceptable grid aspect ratios. In other simulations we attempt to match the observed streamflow response of the catchment, and we point out the small contribution of the streamflow component to the overall water balance of the catchment.
Author

N94-16033*# Princeton Univ., NJ. Dept. of Civil Engineering and Operations Research.
EFFECTS OF SPATIAL VARIABILITY AND SCALE ON AREAL -AVERAGE EVAPOTRANSPIRATION
J. S. Famiglietti and Eric F. Wood *In its* Research into the Influence of Spatial Variability and Scale on the Parameterization of Hydrological Processes 1993 38 p Submitted for publication (For primary document see N94-16026 03-43)
(Grants NGT-60153)
Avail: CASI HC A03/MF A03

This paper explores the effect of spatial variability and scale on areally-averaged evapotranspiration. A spatially-distributed water and energy balance model is employed to determine the effect of explicit patterns of model parameters and atmospheric forcing on modeled areally-averaged evapotranspiration over a range of increasing spatial scales. The analysis is performed from the local scale to the catchment scale. The study area is King's Creek catchment, an 11.7 sq km watershed located on the native tallgrass prairie of Kansas. The dominant controls on the scaling behavior of catchment-average evapotranspiration are investigated by simulation, as is the existence of a threshold scale for evapotranspiration modeling, with implications for explicit versus statistical representation of important process controls. It appears that some of our findings are fairly general, and will therefore provide a framework for understanding the scaling behavior of areally-averaged evapotranspiration at the catchment and larger scales.
Author

N94-16034*# Princeton Univ., NJ.
SCALING, SOIL MOISTURE AND EVAPOTRANSPIRATION IN RUNOFF MODELS
Eric F. Wood *In its* Research into the Influence of Spatial Variability and Scale on the Parameterization of Hydrological Processes 1993 30 p (For primary document see N94-16026 03-43)
(Grants NAG5-899)
Avail: CASI HC A03/MF A03

The effects of small-scale heterogeneity in land surface characteristics on the large-scale fluxes of water and energy in the land-atmosphere system has become a central focus of many of the climatology research experiments. The acquisition of high resolution land surface data through remote sensing and intensive land-climatology field experiments (like HAPEX and FIFE) has provided data to investigate the interactions between microscale land-atmosphere interactions and macroscale models. One essential research question is how to account for the small scale heterogeneities and whether 'effective' parameters can be used in the macroscale models. To address this question of scaling, the probability distribution for evaporation is derived which illustrates the conditions for which scaling should work. A correction algorithm that may appropriate for the land parameterization of a GCM is derived using a 2nd order linearization scheme. The performance of the algorithm is evaluated.
Author

N94-16831*# Purdue Univ., West Lafayette, IN.
EARTH OBSERVATIONAL RESEARCH USING MULTISTAGE EOS-LIKE DATA Semiannual Research Progress Summary, 1 Apr. - 30 Sep. 1993
C. J. Johannsen and D. A. Landgrebe 30 Sep. 1993 20 p
(Grant NAGw-925)
(NASA-CR-194626; NAS 1.26:194626) Avail: CASI HC A03/MF A01

This grant is funded as a part of a program in which both research and educational impact are intended. Research work under this grant is directed at the understanding and use of future hyperspectral data such as that from imaging spectrometers. Specifically, the objectives of the work are (1) to prepare suitable means for analyzing data from sensors which have large numbers of spectral bands, (2) to advance the fundamental understanding of the manner in which soils and vegetative materials reflect high spectral resolution optical wavelength radiation, and (3) to maximize the impact of the results on the educational community. Over the life of the grant, the work has thus involved basic Earth science research and information system technique understanding and development in a mutually supportive way, however, more recently it has become necessary to focus the work primarily on areas (1) and (3). During the last year, the level of effort on this grant has been reduced to half its previous value. We have also been advised that this grant will end with the current year, thus this will be the penultimate semiannual progress summary. Derived from text

N94-17421 Army Topographic Engineering Center, Fort Belvoir, VA.
AN AUTOMATED APPROACH FOR CLASSIFYING GENERIC TERRAIN FEATURES USING DIGITAL ELEVATION DATA
Linda H. Graff 27 May 1993 24 p Limited Reproducibility: More than 20% of this document may be affected by microfiche quality
(AD-A268385; TEC-R-197) Avail: CASI HC A03

The application of experimental SW to interface digital elevation data with knowledge representation and IP tools to automatically classify landforms is presented. I will discuss classification theory, the terrain

classification system I used in this work, the data and sites used to develop the classification method, the method itself, overall results, method limitations, and recommendations and finally conclusions. DTIC

N94-17467 Hawaii Univ., Manoa.
FABRICATION OF A NAVMAP, A DEEP-SEA MAPPING SYSTEM Final Report
Alexander Shor 1993 7 p Limited Reproducibility: More than 20% of this document may be affected by microfiche quality
(Contract N00014-90-J-4009)
(AD-A268630) Avail: CASI HC A04

This report is to develop and build a deep-sea mapping sonar system, which was to be operated on delivery by the Naval Oceanographic Office (Code OW). Intended as the first increment of a multi-part grant, it was decided in 1991 by the ONR Contracts and Grants Office that the second and subsequent funding increments were to be carried out on a contract rather than grant basis, and thus, the present grant was allowed to expire in 1991 and a contract was initiated to complete the project. The description here is of the successful completion of development efforts under the grant component of the effort; the contract effort continues as of this date (6/93), with the principal deliverables completed, tested and delivered to NAVOCEANO for operation, but some portions of the work (and the contract period) and some expansion work remain unfinished. DTIC

N94-17610# Army Research Lab., White Sands Missle Range, NM.
A SURFACE ENERGY BUDGET MODEL MODIFYING HEAT FLOW BY FOLIAGE EFFECTS Final Report
David H. Tofsted Jul. 1993 88 p
(AD-A268598; ARL-TR-60) Avail: CASI HC A05/MF A01

Propagation of energy (either acoustic or electromagnetic energy) through the region of the atmosphere close to the earth's surface depends on estimates of the vertical structure of wind, pressure, temperature, humidity, and refractive index near the earth's surface. To help predict these vertical structures, the TGRAD model has been developed. The model is based on flux-profile methods, requiring simple meteorological inputs as functions of time. The model's original purpose was to predict the vertical temperature gradient profile, hence the name TGRAD. The TGRAD model has been compared against a predecessor model (the Deardorff model) and has proven to characterize the near-surface atmosphere much better under foliated conditions. It characterizes the daytime atmosphere well under all conditions studied. It characterizes the nocturnal atmosphere well until the critical Richardson number is reached. For stronger nocturnal inversions an approach is discussed that may be capable of treating these conditions. The principal improvement provided by this model is the development of sensible and latent heat flux equations that more accurately account for a surface layer partially covered by foliage. DTIC

N94-17616# Beleidscommissie Remote Sensing, Delft (Netherlands).
SURFACE ENERGY BALANCE MODELING AT MESOSCALE: THE CONTRIBUTION OF THE FUTURE EARTH OBSERVING SYSTEM
M. Menenti (Winand Staring Centre, Wageningen, Netherlands.) Dec. 1992 18 p
(BCRS-91-04; ISBN-9-05-411054-6; ETN-93-94819) Avail: CASI HC A03/MF A01

The process leading to the formulation of international research programs, aimed at using Earth Observation Systems (EOS) to understand the processes which govern global climate, is described. This research is related to the international scientific community, national funding agencies, intergovernmental cooperation, and private industry. The plan to develop a full EOS space measurement system based on NASA, ESA and Japanese platform(s) is discussed. The role of this EOS in the U.S. global climate research program is considered. The appropriate balance between ground based and space based research activities is stressed. A Netherlands perspective concerning research on land surface processes and future EOS is given. Future developments of general circulation models and of land surface models are discussed. ESA

N94-17665*# National Aeronautics and Space Administration. Langley Research Center, Hampton, VA.
A CONCEPTUAL DESIGN STUDY FOR A TWO-DIMENSIONAL, ELECTRONICALLY SCANNED THINNED ARRAY RADIOMETER
Philip Mutton (Lockheed Engineering and Sciences Co., Hampton, VA.), Christopher C. Chromik (Lockheed Engineering and Sciences Co., Hampton, VA.), Iain Dixon (Lockheed Engineering and Sciences Co., Hampton, VA.), Richard B. Statham (Lockheed Engineering and Sciences Co., Hampton, VA.), Frederic H. Stillwagen (Lockheed Engineering and Sciences Co., Hampton, VA.), Alfred E. VonTheumer (Lockheed Engineering and Sciences Co., Hampton, VA.), Washito A. Sasamoto, and Paul A. Garn (Science and Technology Corp., Hampton, VA.) Nov. 1993 104 p
(RTOP 419-09-01)
(NASA-TM-109051; NAS 1.15:109051) Avail: CASI HC A06/MF A02

A conceptual design for the Two-Dimensional, Electronically Steered Thinned Array Radiometer (ESTAR) is described. This instrument is a synthetic aperture microwave radiometer that operates in the L-band frequency range for the measurement of soil moisture and ocean salinity. Two auxiliary instruments, an 8-12 micron, scanning infrared radiometer and a 0.4-1.0 micron, charge coupled device (CCD) video camera, are included to provided data for sea surface temperature measurements and spatial registration of targets respectively. The science requirements were defined by Goddard Space Flight Center. Instrument and the spacecraft configurations are described for missions using the Pegasus and Taurus launch vehicles. The analyses and design trades described include: estimations of size, mass and power, instrument viewing coverage, mechanical design trades, structural and thermal analyses, data and communications performance assessments, and cost estimation.
Author (revised)

N94-15888*# European Space Research Lab., Noordwijk (Netherlands).
ERS-1: 18 MONTHS IN ORBIT
Jacques Louet *In* JPL, Proceedings of the Third Spaceborne Imaging Radar Symposium 28 May 1993 p 9-51 (For primary document see N94-15886 03-32)
Avail: CASI HC A03/MF A04

N94-15895*# National Aeronautics and Space Administration. Goddard Space Flight Center, Greenbelt, MD.
RECENT SCIENTIFIC ADVANCES IN THE USE OF RADAR IN SCIENTIFIC HYDROLOGY
Edwin T. Engman *In* JPL, Proceedings of the Third Spaceborne Imaging Radar Symposium 28 May 1993 p 129-134 (For primary document see N94-15886 03-32)
Avail: CASI HC A02/MF A04

N94-15897*# Centre d'Etude Spatiale des Rayonnements, Toulouse (France).
RECENT ADVANCES IN RADAR REMOTE SENSING OF FOREST
Thuy LeToan *In* JPL, Proceedings of the Third Spaceborne Imaging Radar Symposium 28 May 1993 p 143-150 (For primary document see N94-15886 03-32)
Avail: CASI HC A02/MF A04

N94-15898*# Michigan Univ., Ann Arbor.
RADAR RESPONSE OF VEGETATION: AN OVERVIEW
Fawwaz T. Ulaby and M. Craig Dobson *In* JPL, Proceedings of the Third Spaceborne Imaging Radar Symposium 28 May 1993 p 151-183 (For primary document see N94-15886 03-32)
Avail: CASI HC A03/MF A04

N94-15899*# Jet Propulsion Lab., California Inst. of Tech., Pasadena.
IMAGING RADAR STUDIES OF POLAR ICE
Frank Carsey *In its* Proceedings of the Third Spaceborne Imaging Radar Symposium 28 May 1993 p 185-193 (For primary document see N94-15886 03-32)
Avail: CASI HC A02/MF A04

N94-15900*# Jet Propulsion Lab., California Inst. of Tech., Pasadena.
GEOLOGIC REMOTE SENSING WITH RADAR
Thomas G. Farr *In its* Proceedings of the Third Spaceborne Imaging Radar Symposium 28 May 1993 p 195-203 (For primary document see N94-15886 03-32)
Avail: CASI HC A02/MF A04

N94-15901*# Jet Propulsion Lab., California Inst. of Tech., Pasadena.
APPLICATION OF CLOUDE'S TARGET DECOMPOSITION THEOREM TO POLARIMETRIC IMAGING RADAR DATA
Jakob J. vanZyl *In its* Proceedings of the Third Spaceborne Imaging Radar Symposium 28 May 1993 p 207-216 (For primary document see N94-15886 03-32)
Avail: CASI HC A02/MF A04

N94-15902*# Deutsche Forschungs- und Versuchsanstalt fuer Luft- und Raumfahrt, Oberpfaffenhofen (Germany). Inst. fuer Hochfrequenztechnik.
MULTIFREQUENCY OBSERVATIONS
R. Glitz, F. Heel, H. Kietzmann, H. Oettl, and C. Schmullius *In* JPL, Proceedings of the Third Spaceborne Imaging Radar Symposium 28 May 1993 p 217-227 (For primary document see N94-15886 03-32)
Avail: CASI HC A03/MF A04

N94-15905*# Naples Univ. (Italy).
TOPSAT: GLOBAL SPACE TOPOGRAPHIC MISSION
Sergio Vetrella *In* JPL, Proceedings of the Third Spaceborne Imaging Radar Symposium 28 May 1993 p 263-290 (For primary document see N94-15886 03-32)
Avail: CASI HC A03/MF A04

N94-15909*# Deutsche Forschungs- und Versuchsanstalt fuer Luft- und Raumfahrt, Oberpfaffenhofen (Germany). Remote Sensing Data Center.
RECENT ADVANCES AND PLANS IN PROCESSING AND GEOCODING OF SAR DATA AT THE DFD
W. Noack *In* JPL, Proceedings of the Third Spaceborne Imaging Radar Symposium 28 May 1993 p 359-363 (For primary document see N94-15886 03-32)
Avail: CASI HC A01/MF A04

N94-15914*# Jet Propulsion Lab., California Inst. of Tech., Pasadena.
A SUMMARY OF MICROWAVE REMOTE SENSING INVESTIGATIONS PLANNED FOR BOREAS
Kyle C. McDonald *In its* Proceedings of the Third Spaceborne Imaging Radar Symposium 28 May 1993 p 415-416 Sponsored in part by Energy, Mines and Resources Canada (For primary document see N94-15886 03-32)
Avail: CASI HC A01/MF A04

N94-16318*# Geological Survey, Flagstaff, AZ.
SEPARATION OF TOPOGRAPHIC AND INTRINSIC BACKSCATTER VARIATIONS IN BISCOPIC RADAR IMAGES: A MAGIC AIRBRUSH Abstract Only
R. L. Kirk *In* Lunar and Planetary Inst., Twenty-Fourth Lunar and Planetary Science Conference. Part 2: G-M 1993 p 803-804 (For primary document see N94-16173 03-91)
Avail: CASI HC A01/MF A06

N94-16370*# Hawaii Univ., Honolulu. Planetary Geosciences.
THE CLEMENTINE INSTRUMENT COMPLEMENT Abstract Only
Paul G. Lucey *In* Lunar and Planetary Inst., Twenty-Fourth Lunar and Planetary Science Conference. Part 2: G-M 1993 p 907-908 (For primary document see N94-16173 03-91)
Avail: CASI HC A01/MF A06

N94-16407*# Saint Lawrence Univ., Canton, NY.
DO IT YOURSELF REMOTE SENSING: GENERATING AN INEXPENSIVE, HIGH TECH, REAL SCIENCE LAKE MAPPING PROJECT FOR THE CLASSROOM Abstract Only
Stephen M. Metzger *In* Lunar and Planetary Inst., Twenty-Fourth Lunar and Planetary Science Conference. Part 2: G-M 1993 p 981-982 (For primary document see N94-16173 03-91)
Avail: CASI HC A01/MF A06

N94-16437*# Brown Univ., Providence, RI. Dept. of Geological Sciences.
FROM MINERALS TO ROCKS: TOWARD MODELING LITHOLOGIES WITH REMOTE SENSING Abstract Only
John F. Mustard, Jessica M. Sunshine, Carle M. Pieters, Andrew Hoppin, and Stephan F. Pratt *In* Lunar and Planetary Inst., Twenty-Fourth Lunar and Planetary Science Conference. Part 2: G-M 1993 p 1041-1042 (For primary document see N94-16173 03-91)
Avail: CASI HC A01/MF A06

N94-16596*# National Aeronautics and Space Administration. John C. Stennis Space Center, Bay Saint Louis, MS.
TIMS PERFORMANCE EVALUATION SUMMARY
Bruce Spiering, G. Meeks, J. Anderson, S. Jaggi, and S. Kuo *In* JPL, Summaries of the Third Annual JPL Airborne Geoscience Workshop. Volume 2: TIMS Workshop 1 Jun. 1992 p 1-3 (For primary document see N94-16595 03-42)
Avail: CASI HC A01/MF A01

N94-16597*# Lockheed Engineering and Sciences Co., Bay Saint Louis, MS.
A QUANTITATIVE ANALYSIS OF TIMS DATA OBTAINED ON THE LEARJET 23 AT VARIOUS ALTITUDES
S. Jaggi *In* JPL, Summaries of the Third Annual JPL Airborne Geoscience Workshop. Volume 2: TIMS Workshop 1 Jun. 1992 p 4-6 (For primary document see N94-16595 03-42)
Avail: CASI HC A01/MF A01

N94-16598*# Lockheed Engineering and Sciences Co., Bay Saint Louis, MS.
ANALYSIS OF TIMS PERFORMANCE SUBJECTED TO SIMULATED WIND BLAST
S. Jaggi and S. Kuo *In* JPL, Summaries of the Third Annual JPL Airborne Geoscience Workshop. Volume 2: TIMS Workshop 1 Jun. 1992 p 7-9 (For primary document see N94-16595 03-42)
Avail: CASI HC A01/MF A01

N94-16599*# Jet Propulsion Lab., California Inst. of Tech., Pasadena.
SENSITIVITY OF BLACKBODY REFERENCE PANELS TO WIND BLAST
Gordon Hoover *In its* Summaries of the Third Annual JPL Airborne Geoscience Workshop. Volume 2: TIMS Workshop 1 Jun. 1992 p 10-12 (For primary document see N94-16595 03-42)
Avail: CASI HC A01/MF A01

N94-16600*# JAPEX Geoscience Inst., Tokyo (Japan).
COMPARISON OF PRELIMINARY RESULTS FROM AIRBORNE ASTER SIMULATOR (AAS) WITH TIMS DATA
Yoshiaki Kannari, Franklin Mills, Hiroshi Watanabe, Teruya Ezaka, Tatsuhiko Narita, and Sheng-Huei Chang (Geophysical and Environmental Research, Inc., New York, NY.) *In* JPL, Summaries of the Third Annual JPL Airborne Geoscience Workshop. Volume 2: TIMS Workshop 1 Jun. 1992 p 13-15 Sponsored in part by Japan Resources Observation System Organization (For primary document see N94-16595 03-42)
Avail: CASI HC A01/MF A01

N94-16601*# Tokyo Univ. (Japan). Dept. of Mineral Development Engineering.
APPLICATION OF SPLIT WINDOW TECHNIQUE TO TIMS DATA
Tsuneo Matsunaga, Shuichi Rokugawa, and Yoshinori Ishii *In* JPL, Summaries of the Third Annual JPL Airborne Geoscience Workshop. Volume 2: TIMS Workshop 1 Jun. 1992 p 16-18 (For primary document see N94-16595 03-42)
Avail: CASI HC A01/MF A01

N94-16603*# National Aeronautics and Space Administration. John C. Stennis Space Center, Bay Saint Louis, MS.
AN ALGORITHM FOR THE ESTIMATION OF BOUNDS ON THE EMISSIVITY AND TEMPERATURES FROM THERMAL MULTISPECTRAL AIRBORNE REMOTELY SENSED DATA
S. Jaggi (Lockheed Engineering and Sciences Co., Bay Saint Louis, MS.), D. Quattrochi, and R. Baskin (Geological Survey, Salt Lake City, UT.) *In* JPL, Summaries of the Third Annual JPL Airborne Geoscience Workshop. Volume 2: TIMS Workshop 1 Jun. 1992 p 22-24 (For primary document see N94-16595 03-42)
Avail: CASI HC A01/MF A01

N94-16604*# National Aeronautics and Space Administration. John C. Stennis Space Center, Bay Saint Louis, MS.
MULTI-RESOLUTION PROCESSING FOR FRACTAL ANALYSIS OF AIRBORNE REMOTELY SENSED DATA
S. Jaggi (Lockheed Engineering and Sciences Co., Bay Saint Louis, MS.), D. Quattrochi, and N. Lam (Louisiana State Univ., Baton Rouge.) *In* JPL, Summaries of the Third Annual JPL Airborne Geoscience Workshop. Volume 2: TIMS Workshop 1 Jun. 1992 p 25-27 (For primary document see N94-16595 03-42)
Avail: CASI HC A01/MF A01

N94-16605*# Geological Survey, Reston, VA.
PRELIMINARY ANALYSIS OF THERMAL-INFRARED MULTISPECTRAL SCANNER DATA OF THE IRON HILL, COLORADO CARBONATITE-ALKALIC ROCK COMPLEX
Lawrence C. Rowan, Kenneth Watson (Geological Survey, Denver, CO.), and Susanne H. Miller (Geological Survey, Denver, CO.) *In* JPL, Summaries of the Third Annual JPL Airborne Geoscience Workshop. Volume 2: TIMS Workshop 1 Jun. 1992 p 28-30 (For primary document see N94-16595 03-42)
Avail: CASI HC A01/MF A01

N94-16606*# Hawaii Univ., Honolulu. Inst. of Planetary Geosciences.
THE USE OF TIMS FOR MAPPING DIFFERENT PAHOEHOE SURFACES: MAUNA IKI, KILAUEA
Scott K. Rowland *In* JPL, Summaries of the Third Annual JPL Airborne Geoscience Workshop. Volume 2: TIMS Workshop 1 Jun. 1992 p 31-33 (For primary document see N94-16595 03-42)
Avail: CASI HC A01/MF A01

N94-16607*# Arizona State Univ., Tempe. Dept. of Geology.
EJECTA PATTERNS OF METEOR CRATER, ARIZONA DERIVED FROM THE LINEAR UN-MIXING OF TIMS DATA AND LABORATORY THERMAL EMISSION SPECTRA
Michael S. Ramsey and Philip R. Christensen *In* JPL, Summaries of the Third Annual JPL Airborne Geoscience Workshop. Volume 2: TIMS Workshop 1 Jun. 1992 p 34-36 (For primary document see N94-16595 03-42)
Avail: CASI HC A01/MF A01

N94-16668*# California Univ., Davis. Dept. of Land, Air and Water Resources.
USING AVIRIS IMAGES TO MEASURE TEMPORAL TRENDS IN ABUNDANCE OF PHOTOSYNTHETIC AND NONPHOTOSYNTHETIC CANOPY COMPONENTS
Susan L. Ustin, Milton O. Smith (Washington Univ., Seattle.), Dar Roberts (Washington Univ., Seattle.), John A. Gamon (California State Univ., Los Angeles.), and Christopher B. Field (Carnegie Institution of Washington, Stanford, CA.) *In* JPL, Summaries of the Third Annual JPL Airborne Geoscience Workshop. Volume 1: AVIRIS Workshop 1 Jun. 1992 p 5-7 (For primary document see N94-16666 03-42)
Avail: CASI HC A01/MF A02

N94-16669*# Colorado Univ., Boulder. Center for the Study of Earth from Space.
UNMIXING AVIRIS DATA TO PROVIDE A METHOD FOR VEGETATION FRACTION SUBTRACTION
J. A. Zamudio *In* JPL, Summaries of the Third Annual JPL Airborne Geoscience Workshop. Volume 1: AVIRIS Workshop 1 Jun. 1992 p 8-10 (For primary document see N94-16666 03-42)
Avail: CASI HC A01/MF A02

N94-16670*# Geological Survey, Denver, CO.
MAPPING THE MINERALOGY AND LITHOLOGY OF CANYONLANDS, UTAH WITH IMAGING SPECTROMETER DATA AND THE MULTIPLE SPECTRAL FEATURE MAPPING ALGORITHM
Roger N. Clark, Gregg A. Swayze, and Andrea Gallagher *In* JPL, Summaries of the Third Annual JPL Airborne Geoscience Workshop. Volume 1: AVIRIS Workshop 1 Jun. 1992 p 11-13 (For primary document see N94-16666 03-42)
Avail: CASI HC A01/MF A02

N94-16672*# California State Univ., Los Angeles.
EVALUATION OF SPATIAL PRODUCTIVITY PATTERNS IN AN ANNUAL GRASSLAND DURING AN AVIRIS OVERFLIGHT
John A. Gamon, Christopher B. Field (Carnegie Institution of Washington, Stanford, CA.), and Susan L. Ustin (California Univ., Davis.) *In* JPL, Summaries of the Third Annual JPL Airborne Geoscience Workshop. Volume 1: AVIRIS Workshop 1 Jun. 1992 p 17-19 Sponsored in part by A. W. Mellon Foundation (For primary document see N94-16666 03-42)
(CIW-Publ-1134) Avail: CASI HC A01/MF A02

N94-16673*# Naval Research Lab., Bay Saint Louis, MS.
HYPERSPECTRAL MODELING FOR EXTRACTING AEROSOLS FROM AIRCRAFT/SATELLITE DATA
G. Daniel Hickman and Michael J. Duggin (State Univ. of New York, Syracuse.) *In* JPL, Summaries of the Third Annual JPL Airborne Geoscience Workshop. Volume 1: AVIRIS Workshop 1 Jun. 1992 p 20-22 (For primary document see N94-16666 03-42)
Avail: CASI HC A01/MF A02

N94-16674*# Colorado Univ., Boulder. Center for the Study of Earth from Space.
THE SPECTRAL IMAGE PROCESSING SYSTEM (SIPS): SOFTWARE FOR INTEGRATED ANALYSIS OF AVIRIS DATA
F. A. Kruse, A. B. Lefkoff, J. W. Boardman, K. B. Heidebrecht, A. T. Shapiro, P. J. Barloon, and A. F. H. Goetz *In* JPL, Summaries of the Third Annual JPL Airborne Geoscience Workshop. Volume 1: AVIRIS Workshop 1 Jun. 1992 p 23-25 (For primary document see N94-16666 03-42)
(Contract NAS5-30552; NAGw-1601)
Avail: CASI HC A01/MF A02

N94-16675*# Brown Univ., Providence, RI. Dept. of Geological Sciences.
FIRST RESULTS FROM ANALYSIS OF COORDINATED AVIRIS, TIMS, AND ISM (FRENCH) DATA FOR THE RONDA (SPAIN) AND BENI BOUSERA (MOROCCO) PERIDOTITES
J. F. Mustard, S. Hurtrez (Paris-Sud Univ., Orsay, France.), P. Pinet (Centre National d'Etudes Spatiales, Toulouse, France.), and C. Sotin (Paris-Sud Univ., Orsay, France.) *In* JPL, Summaries of the Third Annual JPL Airborne Geoscience Workshop. Volume 1: AVIRIS Workshop 1 Jun. 1992 p 26-28 (For primary document see N94-16666 03-42)
Avail: CASI HC A01/MF A02

N94-16676*# Geological Survey, Reston, VA.
AVIRIS STUDY OF DEATH VALLEY EVAPORITE DEPOSITS USING LEAST-SQUARES BAND-FITTING METHODS
J. K. Crowley and R. N. Clark (Geological Survey, Denver, CO.) *In* JPL, Summaries of the Third Annual JPL Airborne Geoscience Workshop. Volume 1: AVIRIS Workshop 1 Jun. 1992 p 29-31 (For primary document see N94-16666 03-42)
Avail: CASI HC A01/MF A02

N94-16677*# Washington Univ., Seattle. Dept. of Geological Sciences.
A FIELD MEASURE OF THE SHADE FRACTION
Alan R. Gillespie, Milton O. Smith, and Donald E. Sabol *In* JPL, Summaries of the Third Annual JPL Airborne Geoscience Workshop. Volume 1: AVIRIS Workshop 1 Jun. 1992 p 32-34 (For primary document see N94-16666 03-42)
Avail: CASI HC A01/MF A02

N94-16678*# Colorado Univ., Boulder. Center for the Study of Earth from Space.
A LINEAR SPECTRAL MATCHING TECHNIQUE FOR RETRIEVING EQUIVALENT WATER THICKNESS AND BIOCHEMICAL CONSTITUENTS OF GREEN VEGETATION
Bo-Cai Gao and Alexander F. H. Goetz *In* JPL, Summaries of the Third Annual JPL Airborne Geoscience Workshop. Volume 1: AVIRIS Workshop 1 Jun. 1992 p 35-37 (For primary document see N94-16666 03-42)
(Contract NAS5-30552)
Avail: CASI HC A01/MF A02

N94-16679*# Washington Univ., Seattle. Dept. of Geological Sciences.
MAPPING THE SPECTRAL VARIABILITY IN PHOTOSYNTHETIC AND NON-PHOTOSYNTHETIC VEGETATION, SOILS, AND SHADE USING AVIRIS
Dar A. Roberts, Milton O. Smith, Donald E. Sabol, John B. Adams, and Susan L. Ustin (California Univ., Davis.) *In* JPL, Summaries of the Third Annual JPL Airborne Geoscience Workshop. Volume 1: AVIRIS Workshop 1 Jun. 1992 p 38-40 (For primary document see N94-16666 03-42)
Avail: CASI HC A01/MF A02

N94-16681*# Centre d'Etude Spatiale des Rayonnements, Toulouse (France).
RETRIEVAL OF BIOPHYSICAL PARAMETERS WITH AVIRIS AND ISM: THE LANDES FOREST, SOUTH WEST FRANCE
F. Zagolski, J. P. Gastellu-Etchegorry, E. Mougin, G. Giordano, G. Marty, T. LeToan, and A. Beaudoin *In* JPL, Summaries of the Third Annual JPL Airborne Geoscience Workshop. Volume 1: AVIRIS Workshop 1 Jun. 1992 p 44-46 (For primary document see N94-16666 03-42)
Avail: CASI HC A01/MF A02

N94-16682*# Geological Survey, Denver, CO.
GROUND-TRUTHING AVIRIS MINERAL MAPPING AT CUPRITE, NEVADA
Gregg Swayze, Roger N. Clark, Fred Kruse (Colorado Univ., Boulder.), Steve Sutley, and Andrea Gallagher *In* JPL, Summaries of the Third Annual JPL Airborne Geoscience Workshop. Volume 1: AVIRIS Workshop 1 Jun. 1992 p 47-49 (For primary document see N94-16666 03-42)
Avail: CASI HC A01/MF A02

N94-16683*# University Coll. of Swansea (Wales). Dept. of Geography.
EXPLORING THE REMOTE SENSING OF FOLIAR BIOCHEMICAL CONCENTRATIONS WITH AVIRIS DATA
Geoffrey M. Smith and Paul J. Curran *In* JPL, Summaries of the Third Annual JPL Airborne Geoscience Workshop. Volume 1: AVIRIS Workshop 1 Jun. 1992 p 50-52 (For primary document see N94-16666 03-42)
Avail: CASI HC A01/MF A02

N94-16684*# California Univ., Santa Barbara. Dept. of Biological Sciences.
SEASONAL AND SPATIAL VARIATIONS IN PHYTOPLANKTONIC CHLOROPHYLL IN EUTROPHIC MONO LAKE, CALIFORNIA, MEASURED WITH THE AIRBORNE VISIBLE AND INFRARED IMAGING SPECTROMETER (AVIRIS)
John M. Melack and Mary Gastil *In* JPL, Summaries of the Third Annual JPL Airborne Geoscience Workshop. Volume 1: AVIRIS Workshop 1 Jun. 1992 p 53-55 (For primary document see N94-16666 03-42)
Avail: CASI HC A01/MF A02

N94-16686*# Geological Survey, Denver, CO.
MAPPING VEGETATION TYPES WITH THE MULTIPLE SPECTRAL FEATURE MAPPING ALGORITHM IN BOTH EMISSION AND ABSORPTION
Roger N. Clark, Gregg A. Swayze, Christopher Koch, and Cathy Ager *In* JPL, Summaries of the Third Annual JPL Airborne Geoscience Workshop. Volume 1: AVIRIS Workshop 1 Jun. 1992 p 60-62 (For primary document see N94-16666 03-42)
Avail: CASI HC A01/MF A02

N94-16688*# Deutsche Forschungsanstalt fuer Luft- und Raumfahrt, Oberpfaffenhofen (Germany). Inst. for Microwave Technologies.
MAC EUROPE 1991: EVALUATION OF AVIRIS, GER IMAGING SPECTROMETRY DATA FOR THE LAND APPLICATION TESTSITE OBERPFAFFENHOFEN
F. Lehmann, R. Richter, H. Rothfuss, K. Werner, P. Hausknecht, A. Mueller, and P. Strobl *In* JPL, Summaries of the Third Annual JPL Airborne Geoscience Workshop. Volume 1: AVIRIS Workshop 1 Jun. 1992 p 66-68 (For primary document see N94-16666 03-42)
Avail: CASI HC A01/MF A02

N94-16689*# Washington Univ., Seattle. Dept. of Geological Sciences.
USING ENDMEMBERS IN AVIRIS IMAGES TO ESTIMATE CHANGES IN VEGETATIVE BIOMASS
Milton O. Smith, John B. Adams, Susan L. Ustin (California Univ., Davis.), and Dar A. Roberts *In* JPL, Summaries of the Third Annual JPL Airborne Geoscience Workshop. Volume 1: AVIRIS Workshop 1 Jun. 1992 p 69-71 (For primary document see N94-16666 03-42)
Avail: CASI HC A01/MF A02

N94-16691*# National Aeronautics and Space Administration. Langley Research Center, Hampton, VA.
THE 1991 AVIRIS/POLDER EXPERIMENT IN CAMARGUE, FRANCE
F. Baret (Institut National de la Recherche Agronomique, Montfavet, France.), C. Leprieur (Office National d'Etudes et de Recherches Aerospatiales, Toulouse, France.), S. Jacquemoud (Institut National de la Recherche Agronomique, Montfavet, France.), V. Carrere (Jet Propulsion Lab., California Inst. of Tech., Pasadena.), X. F. Gu (Institut National de la Recherche Agronomique, Montfavet, France.), M. Steven (Nottingham Univ., England.), V. Vanderbilt, J. F. Hanocq (Institut National de la Recherche Agronomique, Montfavet, France.), Susan L. Ustin (California Univ., Davis.), and G. Rondeaux et al *In* JPL, Summaries of the Third Annual JPL Airborne Geoscience Workshop. Volume 1: AVIRIS Workshop 1 Jun. 1992 p 75-77 Sponsored in part by PNTS (For primary document see N94-16666 03-42)
Avail: CASI HC A01/MF A02

N94-16692*# Jet Propulsion Lab., California Inst. of Tech., Pasadena.
AVIRIS GROUND DATA PROCESSING SYSTEM
Earl G. Hansen, Steve Larson, H. Ian Novack, and Robert Bennett *In its* Summaries of the Third Annual JPL Airborne Geoscience Workshop. Volume 1: AVIRIS Workshop 1 Jun. 1992 p 80-82 (For primary document see N94-16666 03-42)
Avail: CASI HC A01/MF A02

N94-16693*# Jet Propulsion Lab., California Inst. of Tech., Pasadena.
SIMULATION OF ASTER DATA USING AVIRIS IMAGES
Michael Abrams *In its* Summaries of the Third Annual JPL Airborne Geoscience Workshop. Volume 1: AVIRIS Workshop 1 Jun. 1992 p 83-84 (For primary document see N94-16666 03-42)
Avail: CASI HC A01/MF A02

N94-16694*# Institut fuer Allgemeine und Angewandte Geophysik, Munich (Germany).
USE OF AVIRIS DATA TO THE DEFINITION OF OPTIMISED SPECIFICATIONS FOR LAND APPLICATIONS WITH FUTURE SPACEBORNE IMAGING SPECTROMETERS Abstract Only
J. Bodechtel *In* JPL, Summaries of the Third Annual JPL Airborne Geoscience Workshop. Volume 1: AVIRIS Workshop 1 Jun. 1992 p 85 (For primary document see N94-16666 03-42)
Avail: CASI HC A01/MF A02

N94-16695*# Desert Research Inst., Reno, NV. Biological Sciences Center.
PRIMARY STUDIES OF TRACE QUANTITIES OF GREEN VEGETATION IN MONO LAKE AREA USING 1990 AVIRIS DATA
Zhi-Kang Chen, Chris D. Elvidge, and David P. Groeneveld (Inyo County Water Dept., Bishop, CA.) *In* JPL, Summaries of the Third Annual JPL Airborne Geoscience Workshop. Volume 1: AVIRIS Workshop 1 Jun. 1992 p 86-87 (For primary document see N94-16666 03-42)
Avail: CASI HC A01/MF A02

N94-16697*# Analytical Technology Applications Corp., Moffett Field, CA.
MEASURING DRY PLANT RESIDUES IN GRASSLANDS: A CASE STUDY USING AVIRIS
Michael Fitzgerald and Susan L. Ustin (California Univ., Davis.) *In* JPL, Summaries of the Third Annual JPL Airborne Geoscience Workshop. Volume 1: AVIRIS Workshop 1 Jun. 1992 p 91-93 (For primary document see N94-16666 03-42)
Avail: CASI HC A01/MF A02

N94-16698*# California State Univ., Los Angeles. Dept. of Biology.
TRACKING PHOTOSYNTHETIC EFFICIENCY WITH NARROW-BAND SPECTRORADIOMETRY
John A. Gamon and Christopher B. Field (Carnegie Institution of Washington,

Stanford, CA.) *In* JPL, Summaries of the Third Annual JPL Airborne Geoscience Workshop. Volume 1: AVIRIS Workshop 1 Jun. 1992 p 95-97 Sponsored in part by A. W. Mellon Foundation (For primary document see N94-16666 03-42)
(CIW-Publ-1133) Avail: CASI HC A01/MF A02

N94-16701*# Department of Natural Resources, Salt Lake City, UT. Div. of Oil, Gas, and Mining.
INTEGRATING REMOTE SENSING TECHNIQUES AT CUPRITE, NEVADA: AVIRIS, THEMATIC MAPPER, AND FIELD SPECTROSCOPY
Bradley Hill, Greg Nash (Utah Univ., Salt Lake City.), Merrill Ridd (Utah Univ., Salt Lake City.), Phoebe L. Hauff (Spectral Research, Lafayette, CO.), and Phil Ebel (Earth Search Sciences, Inc., Salt Lake City, UT.) *In* JPL, Summaries of the Third Annual JPL Airborne Geoscience Workshop. Volume 1: AVIRIS Workshop 1 Jun. 1992 p 104-107 (For primary document see N94-16666 03-42)
Avail: CASI HC A01/MF A02

N94-16702*# National Aeronautics and Space Administration. Ames Research Center, Moffett Field, CA.
OREGON TRANSECT: COMPARISON OF LEAF-LEVEL REFLECTANCE WITH CANOPY-LEVEL AND MODELLED REFLECTANCE
Lee F. Johnson (TGS Technology, Inc., Moffett Field, CA.), Frederic Baret (Institut National de la Recherche Agronomique, Avignon, France.), and David L. Peterson *In* JPL, Summaries of the Third Annual JPL Airborne Geoscience Workshop. Volume 1: AVIRIS Workshop 1 Jun. 1992 p 113-115 (For primary document see N94-16666 03-42)
Avail: CASI HC A01/MF A02

N94-16703*# Geological Survey, Reston, VA.
AVIRIS AS A TOOL FOR CARBONATITE EXPLORATION: COMPARISON OF SPAM AND MBANDMAP DATA ANALYSIS METHODS
Marguerite J. Kingston and James K. Crowley *In* JPL, Summaries of the Third Annual JPL Airborne Geoscience Workshop. Volume 1: AVIRIS Workshop 1 Jun. 1992 p 116-118 (For primary document see N94-16666 03-42)
Avail: CASI HC A01/MF A02

N94-16704*# Colorado Univ., Boulder. Center for the Study of Earth from Space.
EXPERT SYSTEM-BASED MINERAL MAPPING USING AVIRIS
Fred A. Kruse, A. B. Lefkoff, and J. B. Dietz *In* JPL, Summaries of the Third Annual JPL Airborne Geoscience Workshop. Volume 1: AVIRIS Workshop 1 Jun. 1992 p 119-121 Sponsored in part by Geological Survey (For primary document see N94-16666 03-42)
(Grants NAGw-1601; NAGw-1143)
Avail: CASI HC A01/MF A02

N94-16706*# Washington Univ., Seattle. Dept. of Geological Sciences.
TEMPORAL VARIATION IN SPECTRAL DETECTION THRESHOLDS OF SUBSTRATE AND VEGETATION IN AVIRIS IMAGES
Donald E. Sabol, Jr., Dar A. Roberts, Milton O. Smith, and John B. Adams *In* JPL, Summaries of the Third Annual JPL Airborne Geoscience Workshop. Volume 1: AVIRIS Workshop 1 Jun. 1992 p 132-134 (For primary document see N94-16666 03-42)
Avail: CASI HC A01/MF A02

N94-16707*# INTERA Technologies Ltd., Ottawa (Ontario).
DISCUSSION OF BAND SELECTION AND METHODOLOGIES FOR THE ESTIMATION OF PRECIPITABLE WATER VAPOUR FROM AVIRIS DATA
Dena Schanzer and Karl Staenz (Canada Centre for Remote Sensing, Ottawa, Ontario.) *In* JPL, Summaries of the Third Annual JPL Airborne Geoscience Workshop. Volume 1: AVIRIS Workshop 1 Jun. 1992 p 135-137 (For primary document see N94-16666 03-42)
Avail: CASI HC A01/MF A02

N94-16708*# Science Applications International Corp., Falls Church, VA.
ABUNDANCE RECOVERY ERROR ANALYSIS USING SIMULATED AVIRIS DATA
William W. Stoner, Joseph C. Harsanyi, William H. Farrand, and Jennifer A. Wong *In* JPL, Summaries of the Third Annual JPL Airborne Geoscience Workshop. Volume 1: AVIRIS Workshop 1 Jun. 1992 p 138-140 (For primary document see N94-16666 03-42)
Avail: CASI HC A01/MF A02

N94-16709*# California Univ., Davis. Dept. of Land, Air, and Water Resources.
MULTITEMPORAL DIURNAL AVIRIS IMAGES OF A FORESTED ECOSYSTEM
Susan L. Ustin, Milton O. Smith (Washington Univ., Seattle.), and John B. Adams (Washington Univ., Seattle.) *In* JPL, Summaries of the Third Annual JPL Airborne Geoscience Workshop. Volume 1: AVIRIS Workshop 1 Jun. 1992 p 141-143 (For primary document see N94-16666 03-42)
Avail: CASI HC A01/MF A02

N94-16710*# Arizona State Univ., Tempe. Dept. of Geology.
A COMPARISON OF LOWTRAN-7 CORRECTED AIRBORNE VISIBLE/INFRARED IMAGING SPECTROMETER (AVIRIS) DATA WITH GROUND SPECTRAL MEASUREMENTS
Peng-Yang Xu and Ronald Greeley *In* JPL, Summaries of the Third Annual JPL Airborne Geoscience Workshop. Volume 1: AVIRIS Workshop 1 Jun. 1992 p 144-146 (For primary document see N94-16666 03-42)
Avail: CASI HC A01/MF A02

N94-16711*# Colorado Univ., Boulder. Center for the Study of Earth from Space.
DISCRIMINATION AMONG SEMI-ARID LANDSCAPE ENDMEMBERS USING THE SPECTRAL ANGLE MAPPER (SAM) ALGORITHM
Roberta H. Yuhas, Alexander F. H. Goetz, and Joe W. Boardman (Commonwealth Scientific and Industrial Research Organization, North Ryde, Australia.) *In* JPL, Summaries of the Third Annual JPL Airborne Geoscience Workshop. Volume 1: AVIRIS Workshop 1 Jun. 1992 p 147-149 (For primary document see N94-16666 03-42)
(Grant NAGw-270)
Avail: CASI HC A01/MF A02

N94-16712*# Jet Propulsion Lab., California Inst. of Tech., Pasadena.
EMPIRICAL RELATIONSHIPS AMONG ATMOSPHERIC VARIABLES FROM RAWINSONDE AND FIELD DATA AS SURROGATES FOR AVIRIS MEASUREMENTS: ESTIMATION OF REGIONAL LAND SURFACE EVAPOTRANSPIRATION
James E. Conel, Gordon Hoover, Anne Nolin, Ron Alley, and Jack Margolis *In its* Summaries of the Third Annual JPL Airborne Geoscience Workshop. Volume 1: AVIRIS Workshop 1 Jun. 1992 p 150-151 (For primary document see N94-16666 03-42)
Avail: CASI HC A01/MF A02

N94-16713*# Australian Defence Force Academy, Canberra. Dept. of Electrical Engineering.
LOSSLESS COMPRESSION OF AVIRIS DATA: COMPARISON OF METHODS AND INSTRUMENT CONSTRAINTS
R. E. Roger, J. F. Arnold, M. C. Cavenor, and J. A. Richards *In* JPL, Summaries of the Third Annual JPL Airborne Geoscience Workshop. Volume 1: AVIRIS Workshop 1 Jun. 1992 p 154-156 (For primary document see N94-16666 03-42)
Avail: CASI HC A01/MF A02

N94-16714*# Desert Research Inst., Reno, NV. Atmospheric Sciences Center.
SIMULATION OF AVHRR-K BAND RATIOS WITH AVIRIS
Melanie A. Wetzel and Ronald M. Welch (South Dakota School of Mines and Technology, Rapid City.) *In* JPL, Summaries of the Third Annual JPL Airborne Geoscience Workshop. Volume 1: AVIRIS Workshop 1 Jun. 1992 p 157-159 (For primary document see N94-16666 03-42)
Avail: CASI HC A01/MF A02

N94-16732*# National Aeronautics and Space Administration. Goddard Space Flight Center, Greenbelt, MD.
A SNOW WETNESS RETRIEVAL ALGORITHM FOR SAR
Jian-Cheng Shi (California Univ., Santa Barbara.) and Jeff Dozier *In* JPL, Summaries of the Third Annual JPL Airborne Geoscience Workshop.

Volume 3: AIRSAR Workshop 1 Jun. 1992 p 1-3 (For primary document see N94-16731 03-42)
Avail: CASI HC A01/MF A02

N94-16733*# Deutsche Forschungsanstalt fuer Luft- und Raumfahrt, Oberpfaffenhofen (Germany). Inst. of Radio-Frequency Technology.
COMPARISON OF JPL-AIRSAR AND DLR E-SAR IMAGES FROM THE MAC EUROPE 1991 CAMPAIGN OVER TESTSITE OBERPFAFFENHOFEN: FREQUENCY AND POLARIZATION DEPENDENT BACKSCATTER VARIATIONS FROM AGRICULTURAL FIELDS
C. Schmullius and J. Nithack *In* JPL, Summaries of the Third Annual JPL Airborne Geoscience Workshop. Volume 3: AIRSAR Workshop 1 Jun. 1992 p 4-6 (For primary document see N94-16731 03-42)
Avail: CASI HC A01/MF A02

N94-16734*# Jet Propulsion Lab., California Inst. of Tech., Pasadena.
MONITORING ENVIRONMENTAL STATE OF ALASKAN FORESTS WITH AIRSAR
Kyle C. McDonald, JoBea Way, Eric Rignot, Cindy Williams (Alaska Univ., Fairbanks.), Les Viereck (Alaska Univ., Fairbanks.), and Phylis Adams (Alaska Univ., Fairbanks.) *In its* Summaries of the Third Annual JPL Airborne Geoscience Workshop. Volume 3: AIRSAR Workshop 1 Jun. 1992 p 7-8 (For primary document see N94-16731 03-42)
Avail: CASI HC A01/MF A02

N94-16735*# California Univ., Santa Barbara. Dept. of Geography.
COMPARISON OF MODELED BACKSCATTER WITH SAR DATA AT P-BAND
Yong Wang, Frank W. Davis, and John M. Melack *In* JPL, Summaries of the Third Annual JPL Airborne Geoscience Workshop. Volume 3: AIRSAR Workshop 1 Jun. 1992 p 9-11 (For primary document see N94-16731 03-42)
Avail: CASI HC A01/MF A02

N94-16736*# California Univ., Santa Barbara. Dept. of Geography.
SAR BACKSCATTER FROM CONIFEROUS FOREST GAPS
John L. Day and Frank W. Davis *In* JPL, Summaries of the Third Annual JPL Airborne Geoscience Workshop. Volume 3: AIRSAR Workshop 1 Jun. 1992 p 12-14 (For primary document see N94-16731 03-42)
(Contracts JPL-958468; CS-86-90)
Avail: CASI HC A01/MF A02

N94-16737*# Centre d'Etude Spatiale des Rayonnements, Toulouse (France).
RETRIEVAL OF PINE FOREST BIOMASS USING JPL AIRSAR DATA
A. Beaudoin, T. LeToan, F. Zagolski, C. C. Hsu (Massachusetts Inst. of Tech., Cambridge.), H. C. Han (Massachusetts Inst. of Tech., Cambridge.), and J. A. Kong (Massachusetts Inst. of Tech., Cambridge.) *In* JPL, Summaries of the Third Annual JPL Airborne Geoscience Workshop. Volume 3: AIRSAR Workshop 1 Jun. 1992 p 15-17 (For primary document see N94-16731 03-42)
Avail: CASI HC A01/MF A02

N94-16738*# Geo Eco Arc Research, La Canada, CA.
CHARACTERIZATION OF WETLAND, FOREST, AND AGRICULTURAL ECOSYSTEMS IN BELIZE WITH AIRBORNE RADAR (AIRSAR)
Kevin O. Pope, Jose Maria Rey-Benayas, and Jack F. Paris (California State Univ., Fresno.) *In* JPL, Summaries of the Third Annual JPL Airborne Geoscience Workshop. Volume 3: AIRSAR Workshop 1 Jun. 1992 p 18-20 (For primary document see N94-16731 03-42)
Avail: CASI HC A01/MF A02

N94-16739*# California Univ., Santa Barbara. Dept. of Geography.
STRATEGIES FOR DETECTION OF FLOODPLAIN INUNDATION WITH MULTI-FREQUENCY POLARIMETRIC SAR
Laura L. Hess and John M. Melack *In* JPL, Summaries of the Third Annual JPL Airborne Geoscience Workshop. Volume 3: AIRSAR Workshop 1 Jun. 1992 p 21-23 (For primary document see N94-16731 03-42)
(Contract JPL-958469)
Avail: CASI HC A01/MF A02

N94-16740*# Commission of the European Communities, Ispra (Italy). Inst. for Remote Sensing Applications.
SUPERVISED FULLY POLARIMETRIC CLASSIFICATION OF THE BLACK FOREST TEST SITE: FROM MAESTROI TO MAC EUROPE
G. DeGrandi, C. Lavalle, H. DeGroof, and A. Sieber *In* JPL, Summaries of the Third Annual JPL Airborne Geoscience Workshop. Volume 3: AIRSAR Workshop 1 Jun. 1992 p 24-26 (For primary document see N94-16731 03-42)
Avail: CASI HC A01/MF A02

N94-16741*# National Aeronautics and Space Administration. Goddard Space Flight Center, Greenbelt, MD.
RELATING MULTIFREQUENCY RADAR BACKSCATTERING TO FOREST BIOMASS: MODELING AND AIRSAR MEASUREMENT
Guo-Qing Sun (Ressler Associates, Inc., Laurel, MD.) and K. Jon Ranson *In* JPL, Summaries of the Third Annual JPL Airborne Geoscience Workshop. Volume 3: AIRSAR Workshop 1 Jun. 1992 p 27-29 (For primary document see N94-16731 03-42)
Avail: CASI HC A01/MF A02

N94-16742*# University of Southern Mississippi, Bay Saint Louis. Center for Marine Science.
SAR OBSERVATIONS IN THE GULF OF MEXICO
David Sheres *In* JPL, Summaries of the Third Annual JPL Airborne Geoscience Workshop. Volume 3: AIRSAR Workshop 1 Jun. 1992 p 30-31 (For primary document see N94-16731 03-42)
Avail: CASI HC A01/MF A02

N94-16743*# Naval Research Lab., Washington, DC. Center for Advanced Space Sensing.
INVESTIGATION OF AIRSAR SIGNATURES OF THE GULF STREAM
G. R. Valenzuela, J. S. Lee, D. L. Schuler, G. O. Marmorino, F. Askari, K. Hoppel, J. A. C. Kaiser, and W. C. Keller *In* JPL, Summaries of the Third Annual JPL Airborne Geoscience Workshop. Volume 3: AIRSAR Workshop 1 Jun. 1992 p 32-34 (For primary document see N94-16731 03-42)
Avail: CASI HC A01/MF A02

N94-16748*# Colorado Univ., Boulder. Center for the Study of Earth from Space.
EXTRACTION OF QUANTITATIVE SURFACE CHARACTERISTICS FROM AIRSAR DATA FOR DEATH VALLEY, CALIFORNIA
K. S. Kierein-Young and F. A. Kruse *In* JPL, Summaries of the Third Annual JPL Airborne Geoscience Workshop. Volume 3: AIRSAR Workshop 1 Jun. 1992 p 46-48 (For primary document see N94-16731 03-42)
(Contract JPL-958456; NGT-50728)
Avail: CASI HC A01/MF A02

N94-16749*# Jet Propulsion Lab., California Inst. of Tech., Pasadena.
THE TOPSAR INTERFEROMETRIC RADAR TOPOGRAPHIC MAPPING INSTRUMENT
Howard A. Zebker, Soren N. Madsen, Jan Martin, Giovanni Alberti (Comitato Nazionale per l'Energia Nucleare, Naples, Italy.), Sergio Vetrella (Comitato Nazionale per l'Energia Nucleare, Naples, Italy.), and Alessandro Cucci (Alenia Spazio S.p.A., Rome, Italy.) *In its* Summaries of the Third Annual JPL Airborne Geoscience Workshop. Volume 3: AIRSAR Workshop 1 Jun. 1992 p 49-52 (For primary document see N94-16731 03-42)
Avail: CASI HC A01/MF A02

N94-16750*# Comitato Nazionale per l'Energia Nucleare, Naples (Italy).
EVALUATION OF THE TOPSAR PERFORMANCE BY USING PASSIVE AND ACTIVE CALIBRATORS
G. Alberti, A. Moccia (Naples Univ., Italy.), S. Ponte (Naples Univ., Italy.), and S. Vetrella *In* JPL, Summaries of the Third Annual JPL Airborne Geoscience Workshop. Volume 3: AIRSAR Workshop 1 Jun. 1992 p 53-55 Sponsored by Italian Space Agency (For primary document see N94-16731 03-42)
Avail: CASI HC A01/MF A02

N94-16751*# Jet Propulsion Lab., California Inst. of Tech., Pasadena.
FITTING A THREE-COMPONENT SCATTERING MODEL TO POLARIMETRIC SAR DATA

A. Freeman and S. Durden *In its* Summaries of the Third Annual JPL Airborne Geoscience Workshop. Volume 3: AIRSAR Workshop 1 Jun. 1992 p 56-58 (For primary document see N94-16731 03-42)
Avail: CASI HC A01/MF A02

N94-16752*# Jet Propulsion Lab., California Inst. of Tech., Pasadena.
APPLICATION OF SYMMETRY PROPERTIES TO POLARIMETRIC REMOTE SENSING WITH JPL AIRSAR DATA
S. V. Nghiem, Simon H. Yueh, R. Kwok, and F. K. Li *In its* Summaries of the Third Annual JPL Airborne Geoscience Workshop. Volume 3: AIRSAR Workshop 1 Jun. 1992 p 59-61 (For primary document see N94-16731 03-42)
Avail: CASI HC A01/MF A02

N94-16753*# Jet Propulsion Lab., California Inst. of Tech., Pasadena.
EXTERNAL CALIBRATION OF POLARIMETRIC RADAR IMAGES USING DISTRIBUTED TARGETS
Simon H. Yueh, S. V. Nghiem, and R. Kwok *In its* Summaries of the Third Annual JPL Airborne Geoscience Workshop. Volume 3: AIRSAR Workshop 1 Jun. 1992 p 62-64 (For primary document see N94-16731 03-42)
Avail: CASI HC A01/MF A02

N94-16754*# National Aeronautics and Space Administration. Goddard Space Flight Center, Greenbelt, MD.
PROCESSING OF POLARIMETRIC SAR DATA FOR SOIL MOISTURE ESTIMATION OVER MAHANTANGO WATERSHED AREA
K. S. Rao, W. L. Teng, and J. R. Wang *In* JPL, Summaries of the Third Annual JPL Airborne Geoscience Workshop. Volume 3: AIRSAR Workshop 1 Jun. 1992 p 65-68 (For primary document see N94-16731 03-42)
Avail: CASI HC A01/MF A02

N94-16755*# National Aeronautics and Space Administration. Goddard Space Flight Center, Greenbelt, MD.
EVALUATION OF POLARIMETRIC SAR PARAMETERS FOR SOIL MOISTURE RETRIEVAL
Jian-Cheng Shi (California Univ., Santa Barbara.), Jakob J. vanZyl (Jet Propulsion Lab., California Inst. of Tech., Pasadena.), and Edwin T. Engman *In* JPL, Summaries of the Third Annual JPL Airborne Geoscience Workshop. Volume 3: AIRSAR Workshop 1 Jun. 1992 p 69-71 (For primary document see N94-16731 03-42)
Avail: CASI HC A01/MF A02

N94-16756*# California State Univ., Fresno. GeoInformation Processing Systems.
INTERACTION TYPES AND THEIR LIKE-POLARIZATION PHASE-ANGLE DIFFERENCE SIGNATURES
Jack F. Paris *In* JPL, Summaries of the Third Annual JPL Airborne Geoscience Workshop. Volume 3: AIRSAR Workshop 1 Jun. 1992 p 72-74 (For primary document see N94-16731 03-42)
Avail: CASI HC A01/MF A02

N94-16757*# Jet Propulsion Lab., California Inst. of Tech., Pasadena.
APPLICATION OF MODIFIED VICAR/IBIS GIS TO ANALYSIS OF JULY 1991 FLEVOLAND AIRSAR DATA
L. Norikane, B. Broek (Organisatie voor Toegepast Natuurwetenschappelijk Onderzoek, Delft, Netherlands.), and A. Freeman *In its* Summaries of the Third Annual JPL Airborne Geoscience Workshop. Volume 3: AIRSAR Workshop 1 Jun. 1992 p 75-77 (For primary document see N94-16731 03-42)
Avail: CASI HC A01/MF A02

N94-16758*# Colorado Univ., Boulder. Center for the Study of Earth from Space.
RADAR ANALYSIS AND VISUALIZATION ENVIRONMENT (RAVEN): SOFTWARE FOR POLARIMETRIC RADAR ANALYSIS
K. S. Kierein-Young, A. B. Lefkoff, and F. A. Kruse *In* JPL, Summaries of the Third Annual JPL Airborne Geoscience Workshop. Volume 3: AIRSAR Workshop 1 Jun. 1992 p 78-80 (For primary document see N94-16731 03-42)
(Contract JPL-958456; NGT-50728)
Avail: CASI HC A01/MF A02

N94-17150 MATRA Marconi Space, Toulouse (France).
EARTH OBSERVATION FROM SMALL SATELLITES [OBSERVATION DE LA TERRE A PARTIR DE MINISATELLITE]
C. Vialet *In* CNES, Small Satellites Systems and Services Jan. 1993 p 259-277 (For primary document see N94-17131 03-18)
Copyright Avail: Issuing Activity (CEPADUES-Editions, 111 rue Nicolas-Vaquelin, 31100 Toulouse, France)

N94-17151 Lockheed Aircraft Corp., Palo Alto, CA.
SMALL IMAGING SATELLITE FOR EARTH OBSERVING SYSTEM ADJUNCT
Steven Kilston, Vera Kilston, and Thomas F. Utsch (Air Force Space Div., Los Angeles, CA.) *In* CNES, Small Satellites Systems and Services Jan. 1993 p 279-290 (For primary document see N94-17131 03-18)
Copyright Avail: Issuing Activity (CEPADUES-Editions, 111 rue Nicolas-Vaquelin, 31100 Toulouse, France)

44 ENERGY PRODUCTION AND CONVERSION

Includes specific energy conversion systems, e.g., fuel cells; global sources of energy; geophysical conversion; and windpower.

For related information see also *07 Aircraft Propulsion and Power*, *20 Spacecraft Propulsion and Power*, and *28 Propellants and Fuels*.

N94-15984# Sandia National Labs., Albuquerque, NM.
PROGRESS IN THE CONCENTRATOR INITIATIVE PROGRAM
A. B. Maish 1992 7 p Presented at the 23rd IEEE Photovoltaic Specialists Conference, Louisville, KY, 10-14 May 1993
(Contract DE-AC04-76DP-00789)
(DE93-015006; SAND-92-2831C; CONF-930540-8) Avail: CASI HC A02/MF A01

Progress made by the eight participating cell and collector manufacturers since the beginning of the U.S. Department of Energy's multiyear photovoltaic Concentrator Initiative program is reviewed. Point and line-focus cell manufacturers achieved peak efficiencies between 19% and 25% with designs that could be manufactured commercially. Collector manufacturers delivered prototype hardware of point and line-focus collectors representing commercially producible technology. DOE

N94-15993# Sandia National Labs., Albuquerque, NM.
REVISITING THE BCS, A MEASUREMENT SYSTEM FOR CHARACTERIZING THE OPTICS OF SOLAR COLLECTORS
J. W. Strachan 1992 12 p Presented at the 39th International Instrumentation Symposium, Albuquerque, NM, 2-6 May 1993
(Contract DE-AC04-76DP-00789)
(DE93-015030; SAND-92-2789C; CONF-930561-6) Avail: CASI HC A03/MF A01

The Beam Characterization System is being employed at the Sandia's National Solar Thermal Test Facility to characterize the optical performance of heliostats, point-focus solar collectors, and their optical sub-elements as part of the on-going task to develop solar thermal technologies. With this measurement system, images of concentrated solar flux are acquired using digital imaging and processed to obtain such measures of the collector's optical performance as beam power, flux distribution, and beam diameter. Key system elements are a diffusely reflective target for imaging collector beams, meteorological instrumentation including a flux gauge to measure flux at one point in the beam, and a calibration technique to establish a pixel-intensity to flux-density conversion factor for the image. The system is employed in a variety of collector tests such as beam quality, tracking error, and wind effects. The paper describes the Beam Characterization System and its components and presents, for illustration, sample test results. An analysis of the Beam Characterization System's sources of measurement error is presented. Lastly, measurement techniques that employ the BCS to align heliostats and to measure or estimate collector surface slope errors are described. DOE

N94-15994# Sandia National Labs., Albuquerque, NM.
RECENT ADVANCES IN OUTDOOR PERFORMANCE EVALUATION OF PV SYSTEMS
M. A. Quintana, D. L. King, J. E. Cannon, J. R. Woodworth, W. E. Boyson,

N. P. Adams, and D. E. Ellibee 1992 6 p Presented at the 23rd IEEE Photovoltaic Specialists Conference, Louisville, KY, 10-14 May 1993
(Contract DE-AC04-76DP-00789)
(DE93-015031; SAND-92-2829C; CONF-930540-2) Avail: CASI HC A02/MF A01

Sandia's Photovoltaic Technology Laboratory (PTEL) routinely performs outdoor tests of a variety of one-sun and concentrator PV modules. The authors' experience is that while outdoor testing has its own set of problems, it can produce results that are more directly applicable to 'field' conditions than testing in solar simulators. They have recently improved both the hardware and software at the PTEL to improve their accuracy and to deal with the special set of problems encountered in outdoor testing. Improvements in hardware include a computer-controlled solar tracker that allows us to test arrays up to 21 sq m in size, infrared imaging of modules, and electronic loads that allow us to test components with outputs up to 1,800 watts. Improvements in software include real-time monitoring of data collection; a relational data base that has improved the reliability of test setups, operations, and analyses; and a standardized reporting process that relates module performance to a number of environmental parameters. DOE

N94-16112# Oak Ridge National Lab., TN.
PROPOSED GUIDELINES FOR REPORTING PERFORMANCE OF A SOLAR DISH/STIRLING ELECTRIC GENERATION SYSTEM
W. B. Stine (California State Polytechnic Univ., Pomona.) and M. A. Powell 1992 8 p Presented at the 28th Intersociety Energy Conversion Engineering Conference, Atlanta, GA, 8-13 Aug. 1993
(Contract DE-AC04-76DP-00789)
(DE93-016493; SAND-92-2870C; CONF-930804-9) Avail: CASI HC A02/MF A01

Experimental performance data from dish/Stirling system testing can be analyzed to generate a system performance model. An approach to developing an experimentally based performance model of a dish/Stirling system is given. Two methods for analyzing the experimental data are described. To provide information that will permit comparison of dish/Stirling systems, it is necessary to define many of the details involved in calculating system performance data such as the net system output and system solar-to-electric efficiency. This paper describes a set of guidelines for these calculations, based on past experience, especially with the Vanguard dish/Stirling system. Also presented are a set of rating conditions at which a maximum value for system efficiency can be calculated. Comparison between systems of their rated peak solar-to-electric efficiency is made possible when these rating conditions are in common use by manufacturers and testing agencies. DOE

N94-16160# Pacific Northwest Lab., Richland, WA.
CHEMICAL INTERACTIONS BETWEEN INTERCONNECT AND ELECTRODE MATERIALS DURING SINTERING IN SOLID OXIDE FUEL CELLS
T. R. Armstrong, L. A. Chick, and J. L. Bates May 1993 10 p Presented at the 3rd International Symposium on Solid Oxide Fuel Cells, Honolulu, HI, 16-21 May 1993
(Contract DE-AC06-76RL-01830)
(DE93-015696; PNL-SA-21621; CONF-9305100-2) Avail: CASI HC A02/MF A01

Chemical interactions and interdiffusion between the interconnect, (LaCa)CrO3 and (YCa)CrO3 and the anode, Ni(center dot)ZrO2, and cathode, (LaSr)MnO3 and (YCa)MnO3, were evaluated from 1300 to 1500C. Reaction of (LaCa)CrO3 and Ni(center dot)ZrO2 cermet resulted in the formation of NiCr2O4 spinel, while reaction of (YCa)CrO3 and Ni(center dot)ZrO2 resulted in the formation of both NiCr2O4 and CaZrO3, at all temperatures. Interactions between the chromites and manganites resulted in the formation of a solid solution. Dense reaction layers were observed near the interface of Ni(center dot)ZrO2/(LaCa)CrO3 and Ni(center dot)ZrO2/(YCa)CrO3 samples. These dense regions were enriched in calcium and chromium, resulting from liquid migration from the chromite to the anode. Nearly ideal interfaces were observed between (LaSr)MnO3 and (LaCa)CrO3. Interactions between (YCa)CrO3 and (YCa)MnO3 resulted in the formation of a CaCrO4 rich layer along the interface. DOE

N94-16567 Hawaii Natural Energy Inst., Honolulu.
HYDRIDE-CONTAINING MOLTEN SALTS AND THEIR TECHNOLOGY IMPLICATIONS Interim Report
Bor Y. Liaw Mar. 1993 15 p Limited Reproducibility: More than 20% of this document may be affected by microfiche quality
(Contract N00014-92-J-1673)
(AD-A266458; TR-01-ONR) Avail: CASI HC A03

Hydride-conducting molten salts such as LiH in eutectic LiCl-KCl are attractive electrolyte systems for intermediate-temperature applications. The chemically reducing characteristics of these hydride melts provide a unique method to clean metal surfaces. The high conductivity of these hydride melts makes them the best electrolytes for hydrogen-based energy applications at intermediate temperatures. We will review some earlier work on hydride-conducting molten salts and their potential applications in energy technology. We will also describe some recent work on these hydride-containing molten salts for energy conversion and storage applications, including hydrogen sensing and hydrogen storage, electrochemical characterizations, and thermodynamic and kinetic investigations of metal-hydrogen reactions. More recently, lithium deuteride containing eutectic LiCl-KCl melts have been used for excess heat production by the process of electrolysis to charge deuterium into metal matrix such as Pd and Ti. From these studies we illustrate the prospects of this hydride molten salt technology and its implications for the use in intermediate-temperature electro-chemical energy conversion configurations. It will also reveal some interesting electrochemical aspects involved in the processes. DTIC

N94-16715# Department of Energy, Morgantown, WV. Energy Technology Center.
STATUS OF MOLTEN CARBONATE FUEL CELL TECHNOLOGY DEVELOPMENT
E. L. Parsons, Jr., M. C. Williams, and T. J. George 1993 12 p Presented at the 3rd International Symposium on Carbonate Fuel Cell Technology, Honolulu, HI, 16-21 May 1993
(DE93-015666; DOE/METC-C/93/7082; CONF-9305101-2) Avail: CASI HC A03/MF A01

The MCFC technology has been identified by the DOE as a promising product for commercialization. Development of the MCFC technology supports the National Energy Strategy. Review of the status of the MCFC technology indicates that the MCFC technology developers are making rapid and significant progress. Manufacturing facility development and extensive testing is occurring. Improvements in performance (power density), lower costs, improved packaging, and scale up to full height are planned. MCFC developers need to continue to be responsive to end-users in potential markets. It will be market demands for the correct product definition which will ultimately determine the character of MCFC power plants. There is a need for continued MCFC product improvement and multiple product development tests. DOE

N94-16766# Northern Light Research and Development, Seattle, WA.
BIOMASS ENERGY: STATE OF THE TECHNOLOGY PRESENT OBSTACLES AND FUTURE POTENTIAL
Larry Dobson 23 Jun. 1993 113 p
(Contract DE-FG01-89CE-15425)
(DE93-016295; DOE/CE-15425/T11) Avail: CASI HC A06/MF A02

The prevailing image of wood and waste burning as dirty and environmentally harmful is no longer valid. The use of biomass combustion for energy can solve many of our nation's problems. Wood and other biomass residues that are now causing expensive disposal problems can be burned as cleanly and efficiently as natural gas, and at a fraction of the cost. New breakthroughs in integrated waste-to-energy systems, from fuel handling, combustion technology and control systems to heat transfer and power generation, have dramatically improved system costs, efficiencies, cleanliness of emissions, maintenance-free operation, and end-use applications. Increasing costs for fossil fuels and for waste disposal strict environmental regulations and changing political priorities have changed the economics and rules of the energy game. This report describes the new rules, new playing field and key players, in the hopes that those who make our nation's energy policy and those who play in the energy field will take biomass seriously and promote its use. DOE

N94-16824# Midwest Research Inst., Golden, CO. National Renewable Energy Lab.

MONOLITHIC, TWO-TERMINAL InP/Ga(0.47)In(0.53)As TANDEM SOLAR CELLS

M. W. Wanlass, J. S. Ward, K. A. Emery, and T. J. Coutts 1993 5 p Presented at the 5th International Conference on InP and Related Materials, Paris, France, 18-22 Apr. 1993

(Contract DE-AC02-83CH-10093)

(DE93-014037; CONF-9304151-1) Avail: CASI HC A01/MF A01

Monolithic InP/Ga(0.7)In(0.53)As tandem solar cells have been studied extensively in our laboratory over the last 4 years. Using the three-terminal approach, the tandem cell performance progressed rapidly, and improvements in the epitaxial growth and device processing procedures eventually led to a terrestrial concentrator tandem cell efficiency of 31.8%. Recently, our research has been directed towards the development of two-terminal (i.e., series-connected) monolithic InP/Ga(0.47)In(0.53)As tandem cells. Two-terminal tandem cells are desirable because they can be substituted directly for single-junction solar cells in photovoltaic module circuits that are being manufactured presently. Furthermore, in principle, two-terminal tandems should take less time to grow and process than three-terminal tandems, which would lead to reduced cell manufacturing costs. The data obtained from our previous study of three-terminal InP/Ga(0.47)In(0.53)As tandem cells have shown that the potential performance of two-terminal InP/Ga(0.47)In(0.53)As is quite high. Two fundamental problems must be addressed to realize high-performance, two-terminal cells. First, an ohmic electrical interconnect between the top and bottom subcells must be integrated into the monolithic structure to connect the subcells in series. The optical and joule losses in the interconnect should be negligible compared to the tandem cell output. Second, because the subcells are connected in series, techniques for matching the subcell photocurrents and maximizing the tandem cell photocurrent, under relevant solar spectra, are necessary to achieve the highest tandem cell efficiency. In this paper, we describe preliminary progress towards solving these problems and outline directions for future work.

DOE

N94-16954# Sandia National Labs., Albuquerque, NM.

HIGH HEAT FLUX ENGINEERING IN SOLAR ENERGY APPLICATIONS

C. P. Cameron 1993 12 p Presented at the Annual Meeting of the Society of Photo-Optical Instrumentation Engineers (SPIE), San Diego, CA, 11-16 Jul. 1993

(Contract DE-AC04-76DP-00789)

(DE93-016500; SAND-93-0229C; CONF-930722-4) Avail: CASI HC A03/MF A01

Solar thermal energy systems can produce heat fluxes in excess of 10,000 kW/sq m. This paper provides an introduction to the solar concentrators that produce high heat flux, the receivers that convert the flux into usable thermal energy, and the instrumentation systems used to measure flux in the solar environment. References are incorporated to direct the reader to detailed technical information. DOE

N94-17070# Polish Academy of Sciences, Warsaw. Inst. Podstawowych Problemow Techniki.

NUMERICAL MODELLING OF AN ACTIVE DIRECT NONPOTABLE HOT WATER HEATING SYSTEM MAKING USE OF THE ENERGY OF SOLAR RADIATION [NUMERYCZNE MODELOWANIE AKTYWNEGO BEZPOSREDNIEGO SYSTEMU PODGRZEWU CIEPLEJ WODY UZYTKOWEJ Z WYKORZYSTANIEM ENERGII PROMIENIOWANIA SLONECZNEGO]

Ryszard Wnuk 1991 37 p In POLISH

(IFTR-38/1991) Avail: CASI HC A03/MF A01

This paper presents the principles, descriptions and results from a program numerically simulating the operation of a direct hot water heating system utilizing solar energy. Discussions of the water heating systems and a simulated unit are given. The study primarily focuses on the solar energy accumulation reservoir for which a comprehensive reservoir model is given together with experimental testing results obtained on site. Also provided are the meteorological data utilized; data relating to the water delivery model and calculated parameters of the unit and its efficiency factor (the efficiency 'H'). Applied estimates derived from a numerical analysis of the simulated unit together with associated results are provided.

Transl. by FLS

N94-17092# Polish Academy of Sciences, Warsaw. Inst. Podstawowych Problemow Techniki.

ASSESSMENT OF TRENDS IN THE DEVELOPMENT OF RESIDENTIAL BUILDINGS FROM THE STANDPOINT OF THE FUEL AND ENERGY REQUIREMENTS [OCENA KIERUNKOW ROZWOJU BUDOWNICTWA MIESZKANIOWEGO Z PUNKTU WIDZENIA ZAPOTRZEBOWANIA NA PALIWA I ENERGIE]

Stanislaw Chyrczakowski 1991 49 p In POLISH

(IFTR-6/1991) Avail: CASI HC A03/MF A01

An assessment of the developmental trends in domestic housing construction from the viewpoint of energy and fuel consumption requirements was presented. The introduction provides an analysis of the developmental trends in domestic housing construction based on data reported in the literature on this topic. Primary attention is focused on technological issues and trends in construction that have a direct effect on fuel and energy use. The problem of calculating energy use in construction of residential housing units is presented. It is demonstrated that there exists significant differences between different technologies for housing construction. Monolithic technology utilizes the greatest energy (buildings for housing a large number of families), while the least energy is used by brick structures employing prefabricated elements (single family homes). Aspects of energy use for domestic housing heating applications as a function of their architectural design, height, shape, etc. are discussed. It is demonstrated that the decisive factor in energy use is not principally the building construction techniques (in the sense of the classification based on the support structure) but rather is the so-called exterior sealing methods that may or may not be related to the construction technique for the building overall. The height and shape of the building also play an important role. Supplementary aspects relating to the development of construction that the author believes are timely developments in the development of domestic housing construction in Poland were presented on the basis of the model calculations.

Transl. by FLS

N94-17217# Sandia National Labs., Albuquerque, NM.

A TEN YEAR REVIEW OF PERFORMANCE OF PHOTOVOLTAIC SYSTEMS

A. L. Rosenthal (Southwest Technology Development Inst., Las Cruces, NM.), S. J. Durand (Southwest Technology Development Inst., Las Cruces, NM.), and M. G. Thomas 1993 3 p Presented at the 23rd IEEE Photovoltaic Specialists Conference, Louisville, KY, 10-14 May 1993

(Contract DE-AC04-76DP-00789)

(DE93-015649; SAND-93-1252C; CONF-930540-9) Avail: CASI HC A01/MF A01

This paper presents data compiled by the Photovoltaic Design Assistance Center at Sandia National Laboratories from more than eighty field tests performed on over thirty-five photovoltaic systems in the United States during the last ten years. The recorded performance histories, failure rates, and degradation of post-Block 4 modules and balance-of-system (BOS) components are described in detail.

DOE

N94-17382# Air Force Inst. of Tech., Wright-Patterson AFB, OH.

ENERGY FROM THE SUN: EVOLUTION OF FEDERAL SUPPORT FOR SOLAR ENERGY M.S. Thesis

Paul C. Clark 29 May 1993 84 p

(AD-A267944; AFIT/CI/CIA-93-030) Avail: CASI HC A05/MF A01

Early civilizations workshipped the sun and relied upon it as a source of energy. Later, with the discovery of oil and coal, man looked to a new deity, fossil fuel, and the sun's importance as an energy source began to wane. Events in the last twenty years, however, indicate the sun is more important than ever as a future source of renewable energy. But, the development and commercial application of solar energy technologies will never occur without the commitment of the American people and their elected representatives in Congress.

DTIC

N94-17668# Midwest Research Inst., Golden, CO. National Renewable Energy Lab.

DOE/NREL ADVANCED WIND TURBINE DEVELOPMENT PROGRAM

C. P. Butterfield, B. Smith, A. Laxson, B. Thresher, and P. Goldman (Department of Energy, Washington, DC.) May 1993 7 p Presented at the ECWEC 1993 European Community Wind Energy Conference and Exhibition, Travemuende, Germany, 8-12 Mar. 1993

(Contract DE-AC02-83CH-10093)
(DE93-010028; NREL/TP-422-5415; CONF-930315-1) Avail: CASI HC A02/MF A01

The development of technologically advanced, high-efficiency wind turbines continues to be a high-priority activity of the US wind industry. The National Renewable Energy Laboratory (formerly the Solar Energy Research Institute), sponsored by the US Department of Energy (DOE), has initiated the Advanced Wind Turbine Program to assist the wind industry in the development of a new class of advanced wind turbines. The initial phase of the program focused on developing conceptual designs for near-term and advanced turbines. The goal of the second phase of this program is to use the experience gained over the last decade of turbine design and operation combined with the latest existing design tools to develop a turbine that will produce energy at $0.05 per kilowatt-hour (kWh) in a 5.8-m/s (13-mph) wind site. Three contracts have been awarded, and two more are under negotiation in the second phase. The third phase of the program will use new innovations and state-of-the-art wind turbine design technology to produce a turbine that will generate energy at $0.04/kWh in a 5.6-m/s wind site. Details of the third phase will be announced in early 1993. DOE

N94-15172# Deutsche Forschungsanstalt fuer Luft- und Raumfahrt, Stuttgart (Germany). Inst. fuer Technische Thermodynamik.
HEAT STORAGE MODULE
H. J. Staehle and F. Lindner *In* ESA, Sounding Rocket Experiments in Fluid Science and Materials Sciences: TEXUS 25 to 27 and MASER 4, Volume 3 Feb. 1993 p 136-141 (For primary document see N94-15157 03-25)
Copyright Avail: CASI HC A02/MF A02; ESA, EPD, ESTEC, Noordwijk, Netherlands, HC

N94-17174 Fabrica Italiana Apparecchiature Radioelettriche S.p.A., Milan.
ARSENE GaAs SOLAR ARRAY
L. Brambilla, A. Caon, R. Contini, G. DAccolti, E. Rossi, G. Verzeni, B. Boliani (Centro Informazioni Studi Esperienze, Milan, Italy.), C. Flores (Centro Informazioni Studi Esperienze, Milan, Italy.), F. Paletta (Centro Informazioni Studi Esperienze, Milan, Italy.), and D. Passoni (Centro Informazioni Studi Esperienze, Milan, Italy.) et al *In* CNES, Small Satellites Systems and Services Jan. 1993 p 537-546 (For primary document see N94-17131 03-18)
Copyright Avail: Issuing Activity (CEPADUES-Editions, 111 rue Nicolas-Vaquelin, 31100 Toulouse, France)

45 ENVIRONMENT POLLUTION

Includes atmospheric, noise, thermal, and water pollution.

N94-15136# IT Corp., Knoxville, TN.
HyperVentilate: DECISION-SUPPORT SOFTWARE FOR SOIL VAPOR EXTRACTION TECHNOLOGY APPLICATION
C. A. Kruger and J. G. Morse Feb. 1993 172 p Sponsored by EPA, Cincinnati, OH Prepared in cooperation with Midwest Research Inst., Falls Church, VA
(Contract EPA-68-C2-0108)
(PB93-134880; EPA/600/R-93/028; AEPA/SW/DK-A93/033A) Avail: CASI HC A08/MF A02

Soil vapor extraction (SVE) is a proven, in situ corrective action technology that can remove volatile organic compounds (VOC) and selected residual petroleum hydrocarbons from unsaturated soils. To assist regulators, investigators, and UST owners in evaluating whether SVE is an appropriate cleanup technology for use at UST sites, decision-support software entitled HyperVentilate has been developed. HyperVentilate is an interactive, software guidance system for evaluating the feasibility of using SVE at a specific site based on site and contaminant characteristics. HyperVentilate is designed to do the following: (1) identify the level of site data required to evaluate SVE systems; (2) evaluate soil permeability test results; (3) approximate the minimum number of extraction wells likely to be needed; and (4) provide a rough approximation of the system's desired and maximum removal rates. The document provides guidance in evaluating the use of the IBM-compatible version of HyperVentilate that requires a computer equipped with (minimally) a 80386 processor, 4 MB RAM, DOS 3.1, Microsoft Windows 3.x, and Spinnaker PLUS 2.5. An overview of SVE principles and procedures is presented along with the basic model principles and a sensitivity analysis of HyperVentilate. A sample application of the software is also presented using data from an actual UST site. NTIS

N94-15185 National Inst. of Water and Atmospheric Research, Lower Hutt (New Zealand).
PROJECTIONS OF FUTURE CO2
I. G. Enting (Commonwealth Scientific and Industrial Research Organization, Mordialoc, Australia.), K. R. Lassey, and R. A. Houghton (Woods Hole Research Center, MA.) 1993 45 p
(NIWA/Atmos/R/93-001; ISBN-0-643-05252-6) Copyright Avail: Issuing Activity

A box-diffusion model is used to calculate the projected atmospheric CO2 concentrations resulting from the various emission scenarios proposed in the 1992 IPCC supplementary report. The terrestrial biota are treated in terms of a release from land-use change and an uptake from enhanced growth so that (1) the contemporary budget balances, and (2) the treatment of the biota in the past is consistent with the approach used in the projections. We refine the modeling by making use of C-14 data to recalibrate the model and translate the calibration uncertainty into estimates of the uncertainties on the projections. We analyze the projections under a range of assumptions that reflect the uncertainties in the current atmospheric carbon budget. We find that the range of uncertainty implies an uncertainty of about +/- 15 percent in the predicted change in CO2 concentrations between 1990 and 2100. Author (revised)

N94-15238* National Aeronautics and Space Administration, Washington, DC.
MARS LOOK-ALIKE (Videotape)
Oct. 1987 Videotape: 4 min. 7 sec. playing time, in color, with sound
(NASA-TM-109667; NONP-VT-93-190465) Avail: CASI VHS A01/BETA A22

This video presentation describes a research trek to western Antarctica to study it's ecosystem as a first step in the future exploration of Mars. CASI

N94-15289* National Aeronautics and Space Administration, Washington, DC.
SAVING YELLOWSTONE (Videotape)
Nov. 1988 Videotape: 3 min. 46 sec. playing time, in color, with sound
(NASA-TM-109596; NONP-VT-93-190394) Avail: CASI VHS A01/BETA A22

This videotape explains how NASA participated in controlling the devastating forest fires that consumed parts of Yellowstone National Park. CASI

N94-15290* National Aeronautics and Space Administration. Goddard Space Flight Center, Greenbelt, MD.
TOMS COMPUTER GRAPHICS (Videotape)
Nov. 1988 Videotape: 3 min. 46 sec. playing, in color, with sound
(NASA-TM-109597; NONP-VT-93-190395) Avail: CASI VHS A01/BETA A22

This videotape explains how NASA participated in controlling the devastating forest fires that consumed parts of Yellowstone National Park. CASI

N94-15329* National Aeronautics and Space Administration. Goddard Space Flight Center, Greenbelt, MD.
ATLAS OF TOMS OZONE, 1978-1988 (Videotape)
Feb. 1989 Videotape: 41 min. playing time, in color, with sound
(NASA-TM-109456; NONP-VT-93-190253) Avail: CASI VHS A01/BETA A22

This video contains very graphic images of the seasonal accumulation and depletion of the world's ozone layer, as depicted by the Total Ozone Mapping Satellite (TOMS). CASI

N94-15350* National Aeronautics and Space Administration, Washington, DC.
WHAT'S KILLING THE TREES? (Videotape)
Oct. 1987 Videotape: 3 min. 7 sec. playing time, in color, with sound

(NASA-TM-109621; NONP-VT-93-190419) Avail: CASI VHS A01/BETA A22

The possible causes for forest decline are discussed, including acid rain on Camel's Hump Mountain, Vermont. CASI

N94-15364* National Aeronautics and Space Administration, Washington, DC.

GLOBAL GREENHOUSE EXPEDITION (Videotape)

Oct. 1990 Videotape: 3 min. 18 sec. playing time, in color, with sound (NASA-TM-109613; NONP-VT-93-190411) Avail: CASI VHS A01/BETA A22

This video covers an airborne study of greenhouse gases in the atmosphere. CASI

N94-15365* National Aeronautics and Space Administration, Washington, DC.

ARCTIC OZONE (Videotape)

Apr. 1989 Videotape: 4 min. 35 sec. playing time, in color, with sound (NASA-TM-109614; NONP-VT-93-190412) Avail: CASI VHS A01/BETA A22

Recent research on ozone done in the Arctic region is detailed and an update on information is gained from the previous Antarctic research. CASI

N94-15408* National Aeronautics and Space Administration, Washington, DC.

LOUISIANA DELTA STUDY (Videotape)

Feb. 1990 Videotape: 3 min. 15 sec. playing time, in color, with sound (NASA-TM-109622; NONP-VT-93-190420) Avail: CASI VHS A01/BETA A22

The project studies the causes of land erosion and sediment transport in order to protect the Delta's resources. CASI

N94-15425* National Aeronautics and Space Administration, Washington, DC.

FOREST FIRE STUDY (Videotape)

Mar. 1987 Videotape: 3 min. 49 sec. playing time, in color, with sound (NASA-TM-109615; NONP-VT-93-190413) Avail: CASI VHS A01/BETA A22

The impact of natural fires on our environment is examined, especially regarding greenhouse gases. CASI

N94-15781*# National Aeronautics and Space Administration, Washington, DC.

DIRECTORY OF RESEARCH PROJECTS: PLANETARY MATERIALS AND GEOCHEMISTRY Annual Report, 1 Oct. 1992 - 30 Sep. 1993

Tamara Dickinson, ed. Oct. 1993 114 p

(NASA-TM-4484; NAS 1.15:4484) Avail: CASI HC A06/MF A02

Abstracts of FY 93 research in the Planetary Materials and Geochemistry Program are included. The annual program report is also included. Author (revised)

N94-15790# University of Western Washington, Bellingham. Inst. of Environmental Toxicology and Chemistry.

DEVELOPMENT OF PATTERN RECOGNITION TECHNIQUES FOR THE EVALUATION OF TOXICANT IMPACTS TO MULTISPECIES SYSTEMS Annual Technical Report, 1 Jun. 1992 - 31 May 1993

Wayne G. Landis and Robin A. Matthews 18 Jun. 1993 255 p

(Grant AF-AFOSR-0291-91)

(AD-A267197; AFOSR-93-0460TR) Avail: CASI HC A12/MF A03

A common assumption in environmental toxicology is that after the initial impact, ecosystems recover to resemble the control state. This assumption may be based more on our inability to observe an ecosystem with sufficient resolution to detect differences than reality. Recent findings of complex and perhaps chaotic dynamics in two relatively simple types of microcosms demonstrate that complex dynamics and nonequilibrium systems are the rule rather than the exception. In the Standardized Aquatic Microcosm and the Mixed Flask Culture (MFC) microcosms, multivariate analysis and clustering methods derived from artificial intelligence research was able to differentiate oscillations that separate the treatments from the reference group, followed by what would normally appear as recovery, followed by another separation into treatment groups as distinct from the reference treatment. The explanation may be that the oscillations are the result of the intrinsic chaotic behavior of population interactions, of which the alteration of detrital quality is but one of many. In fact, preliminary data indicate that material derived from the jet fuel may be released back into the water column due to the decay of organic material. The initial impact of the toxicant re-set the dosed communities into different regions of the n-dimensional space where recovery may be an illusion due to the incidental overlap of the oscillation trajectories occurring along a few axes. DTIC

N94-15940# Brookhaven National Lab., Upton, NY.

AN ASSESSMENT OF ACID FOG

F. W. Lipfert 1992 11 p Presented at the International Symposium on Measurement of Toxic and Related Air Pollutants, Durham, NC, 4-8 May 1992

(Contract DE-AC02-76CH-00016)

(DE93-009347; BNL-48499; CONF-920556-1) Avail: CASI HC A03/MF A01

Airborne particles have long been associated with adverse effects on public health beginning with the notorious air pollution disasters of several decades ago. Although H2SO4 was identified early on as a potential causal factor during these episodes (in part because of fog), concern for potential health effects of particle acidity per se has intensified only recently. Most of the recent aerometric research in the U.S. on acid fog has focused on the ability of clouds and fog to deliver acidity to vegetation and ecosystems. Strong acids are characterized chemically by their pH or H(+) concentration. For fog, concentrations are referred to the droplet liquid content; for other (i.e., 'clear air') aerosols, concentrations are referred to the volume of air sampled. A useful measure of the relationship between aerosol and fog is obtained by comparing their mass concentrations on the basis of the same volume of air, by multiplying fogwater concentrations by liquid water content (LWC). This paper reviews fog measurement capability, physical properties and chemistry, and presents a simple urban airshed model which is used to simulate the evolution of fog and aerosol concentrations under urban stagnation conditions. DOE

N94-15999# Brookhaven National Lab., Upton, NY.

NEW YORK MARKAL: AN EVALUATION OF CARBON DIOXIDE EMISSION CONTROL STRATEGIES IN NEW YORK STATE

L. D. Hamilton 1992 11 p Presented at the International CHALLENGE Symposium, Laxenburg, Austria, 30-31 Jan. 1992

(Contract DE-AC02-76CH-00016)

(DE93-013149; BNL-48755; CONF-9201150-1) Avail: CASI HC A03/MF A01

A MARKAL model was developed for the State of New York. It represents the State's energy system as a set of typical technologies for generating, converting, and using energy as it evolves over a 45-year period. NYMARKAL was applied here in demonstration analyses to explore strategies to reduce CO2 emissions. NYMARKAL was installed at the State Energy Office and in the Offices of the New York Power Pool. Example scenarios showed that it is more difficult and more expensive to reduce carbon emissions in New York State than in the United States as a whole. Were a common carbon tax instituted, it would have less effect in New York and most carbon emissions reduction would take place elsewhere in the country where it is more cost-effective. Alternatively, were all states required to reduce CO2 emission an equal percentage (say by 20%), the cost per unit emissions reduction to New York would be much greater than in the rest of the country. DOE

N94-16006# Pacific Northwest Lab., Richland, WA.

STATEMENT ON GLOBAL CLIMATE CHANGE BEFORE THE SUBCOMMITTEE ON ENERGY AND POWER, UNITED STATES HOUSE OF REPRESENTATIVES

J. A. Edmonds Apr. 1993 9 p

(Contract DE-AC06-76RL-01830)

(DE93-013163; PNL-SA-22080) Avail: CASI HC A02/MF A01

Greenhouse gases are gases which are effectively transparent to incoming sunlight but absorb infrared radiation escaping to space and thereby warm the surface of the Earth. Human activities result in the release of greenhouse and related gases in such quantities that they are changing the composition of the atmosphere. Greenhouse and related gases which human activities release include carbon dioxide (CO2), methane

(CH4), carbon monoxide (CO), nitrous oxide (N2O), nitrogen oxides (NO(x)), chlorofluorocarbons (CFCs) and sulphur dioxide (SO2). The emission and effects of these gases are detailed in this report. DOE

N94-16445# Pacific Northwest Lab., Richland, WA.
GLOBAL CHANGE RESEARCH: SCIENCE AND POLICY
S. Rayner May 1993 20 p Presented at the Global Change Research: Science and Policy Meeting, Washington, DC, 17 May 1993
(Contract DE-AC06-76RL-01830)
(DE93-015675; PNL-SA-22390; CONF-9305219-1) Avail: CASI HC A03/MF A01

This report characterizes certain aspects of the Global Change Research Program of the U.S. Government, and its relevance to the short and medium term needs of policy makers in the public and private sectors. It addresses some of the difficulties inherent in the science and policy interface on the issues of global change. Finally, this report offers some proposals for improving the science for policy process in the context of global environmental change. DOE

N94-16449# Lawrence Livermore National Lab., CA.
APPLICATION OF NON-THERMAL PLASMAS TO POLLUTION CONTROL
B. M. Penetrante, G. E. Vogtlin, J. N. Bardsley, P. A. Vitello, and P. H. Wallman Jun. 1993 11 p Presented at the 2nd International Plasma Symposium on World Progress in Plasma Applications, Palo Alto, CA, 9-11 Feb. 1993
(Contract W-7405-eng-48)
(DE93-016432; UCRL-JC-112689-Rev-1; CONF-930256-1-Rev-1) Avail: CASI HC A03/MF A01

Non-thermal plasma techniques can be used to destroy many types of hazardous molecules. They are particularly efficient when the toxic materials are present in very small concentrations. This paper discusses three particular applications of non-thermal plasmas: decomposition of hydrogen sulfide (H2S), removal of trichloro ethylene (TCE), and removal of nitrogen oxides (NO(x)). Emphasis is placed on the energy cost for implementing the decomposition or removal of these pollutants. Some of the factors affecting the energy cost are discussed. The authors discuss in detail their work at LLNL on pulsed plasma processing for the treatment of NO(x) in diesel engine exhaust. The results suggest that their plasma reactor can remove up to 70% of NO with relatively high initial concentrations (up to 500 ppM) at a power consumption cost of 2.5% for an engine with an output of 14 kW and an exhaust gas flow rate of 1,200 liters per minute. DOE

N94-16589# Army Research Lab., White Sands Missle Range, NM.
COMPLEX TERRAIN WIND MODEL EVALUATION Final Report
Martin E. Lee Jun. 1993 169 p
(AD-A266467; ARL-TR-54) Avail: CASI HC A08/MF A02

The Winds on Critical Steamline Surfaces (WOCSS) complex terrain wind flow model is designed to simulate lateral, mechanical forcing effects on air flows along elevated, solid boundaries. These effects exert significant influence on observed flow field properties, such as transport and diffusion. The degree to which WOCSS model outputs are more reliable than a basic mass consistency model (that does not address lateral forcing dynamics in complex terrain) is discussed in terms of statistical and spatial results, and conclusions regarding this comparison are presented. Results indicate that the WOCSS model does not predict directional changes resulting from lateral forcing, which is a serious limiting factor in its potential application. The WOCSS model was also found to have an oversimplified mass consistency algorithm, averaging speed-up effects over the entire lateral free-flow surface, which restricts prediction of localized lateral speed-up effects in the vicinity of mechanical flow obstacles. Finally, the WOCSS model tends to over-predict the quantity of flow restricted space under both stable and unstable conditions in the transition from moderate to rugged complex terrain when wind speeds are generally less than or equal to 4.0 m/s. However, despite the observed WOCSS model limitations, the WOCSS model did demonstrate the potential to selectivity predict reasonable and significant dynamic lateral forcing spaces over a variety of terrain and stability conditions. DTIC

N94-16802# Lawrence Livermore National Lab., CA.
THE USE OF GENERAL CIRCULATION MODELS IN DETECTING CLIMATE CHANGE INDUCED BY GREENHOUSE GASES
B. D. Santer, U. Cubasch (Deutsches Klimarechenzentrum G.m.b.H., Hamburg, Germany.), U. Mikolajewicz (Max-Planck-Inst. fuer Meteorologie, Hamburg, Germany.), and G. Hegerl (Max-Planck-Inst. fuer Meteorologie, Hamburg, Germany.) Mar. 1993 32 p
(Contract W-7405-eng-48)
(DE93-014369; UCRL-ID-113627; PCMDI-10) Avail: CASI HC A03/MF A01

This article reviews some problems associated with the use of coupled atmosphere-ocean General Circulation Models (GCM's) in studies which attempt to detect a greenhouse-gas-induced signal in observed climate records. We show that model uncertainties affect both our predictions of how climate might change in response to greenhouse-gas (GHG) changes and our estimates of the decadal- to century-time scale natural variability properties of the climate system. Knowledge of the latter are essential in order to make meaningful statements about when and even whether we could expect to detect a greenhouse-gas signal. We show that GHG signal uncertainties are associated with errors in simulating the current climate in uncoupled and coupled climate models, the possible omission of relevant feedbacks, the non-uniqueness of the signal (due to the twin problems of the model's internally-generated natural variability and its sensitivity to initial conditions), uncertainties regarding the future GHG forcing and atmospheric GHG concentrations, and the so-called 'cold start' error. Results from recent time-dependent greenhouse warming experiments are used to illustrate some of these points. We then discuss how energy-balance models, stochastic-forced ocean GCM's, and fully-coupled atmosphere-ocean GCM's have been used to derive estimates of decadal- to century-time scale natural variability, and consider some of the uncertainties associated with these estimates. This review illustrates that it will be necessary to reduce both model signal and model natural variability uncertainties in order to detect a climate change signal and attribute this convincingly to changes in CO2 and other greenhouse gases. DOE

N94-16825# Lawrence Livermore National Lab., CA.
EMISSIONS OF VOLATILE ORGANIC COMPOUNDS FROM STATIONARY COMBUSTION SOURCES: NUMERICAL MODELING CAPABILITIES
J. G. Seebold (Chevron Research Co., Richmond, CA.), R. J. Kee (Sandia National Labs., Albuquerque, NM.), A. J. Lutz (Sandia National Labs., Albuquerque, NM.), W. J. Pitz, and C. K. Westbrook Sep. 1992 10 p Presented at the 1992 American Flame Research Committee Fall International Symposium, Cambridge, MA, 19-21 Oct. 1992
(Contracts W-7405-eng-48; DE-AC04-76DP-00789)
(DE93-014123; UCRL-JC-111829; CONF-9210359-1) Avail: CASI HC A02/MF A01

A collaborative research program was initiated to study the emissions of a wide variety of chemical species from stationary combustion systems. These product species have been included in the Clean Air Act legislation and their emissions must be rigidly controlled, but there is a need for much better understanding of the physical and chemical mechanisms that produce and consume them. We are using numerical modeling to study the chemical reactions and fluid mechanical factors that occur in industrial processes: we are examining systems including premixed and diffusion flames, stirred reactors and plug flow reactors in these modeling studies to establish the major factors leading to emissions of these chemicals. In addition, we are applying advanced laser diagnostic techniques to validate the model predictions and to study the possibilities of developing sophisticated sensors to detect emissions of undesirable species in real time. This paper will discuss the organization of this collaborative effort and its results to date. DOE

N94-17289# California Univ., Berkeley. Lawrence Berkeley Lab.
INCORPORATING GLOBAL WARMING RISKS IN POWER SECTOR PLANNING. VOLUME 1: A CASE STUDY OF THE NEW ENGLAND REGION
F. Krause, J. Busch, and J. Koomey Nov. 1992 127 p
(Contract DE-AC03-76SF-00098)
(DE93-015241; LBL-30797-Vol-1) Avail: CASI HC A07/MF A02

Growing international concern over the threat of global climate change has led to proposals to buy insurance against this threat by reducing

emissions of carbon (short for carbon dioxide) and other greenhouse gases below current levels. Concern over these and other, non-climatic environmental effects of electricity generation has led a number of states to adopt or explore new mechanisms for incorporating environmental externalities in utility resource planning. For example, the New York and Massachusetts utility commissions have adopted monetized surcharges (or adders) to induce emission reductions of federally regulated air pollutants (notably, SO(sub 2), NO(sub x), and particulates) beyond federally mandated levels. These regulations also include preliminary estimates of the cost of reducing carbon emissions, for which no federal regulations exist at this time. Within New England, regulators and utilities have also held several workshops and meetings to discuss alternative methods of incorporating externalities as well as the feasibility of regional approaches. This study examines the potential for reduced carbon emissions in the New England power sector as well as the cost and rate impacts of two policy approaches: environmental externality surcharges and a target- based approach. We analyze the following questions: Does New England have sufficient low-carbon resources to achieve significant reductions (10% to 20% below current levels) in fossil carbon emissions in its utility sector? What reductions could be achieved at a maximum? What is the expected cost of carbon reductions as a function of the reduction goal? How would carbon reduction strategies affect electricity rates? How effective are environmental externality cost surcharges as an instrument in bringing about carbon reductions? To what extent could the minimization of total electricity costs alone result in carbon reductions relative to conventional resource plans?. DOE

N94-17426# Oak Ridge National Lab., TN.
A GEOGRAPHIC INFORMATION SYSTEM APPROACH TO MODELING NUTRIENT AND SEDIMENT TRANSPORT
Daniel A. Levine (Automated Sciences Group, Inc., Oak Ridge, TN.), Carolyn T. Hunsaker, John J. Beauchamp, and Sidey P. Timmins (Analysas Corp., Oak Ridge, TN.) Feb. 1993 177 p
(Contract DE-AC05-84OR-21400)
(DE93-013747; ORNL-6736) Avail: CASI HC A09/MF A02

The objective of this study was to develop a water quality model to quantify nonpoint-source (NPS) pollution that uses a geographic information system (GIS) to link statistical modeling of nutrient and sediment delivery with the spatial arrangement of the parameters that drive the model. The model predicts annual nutrient and sediment loading and was developed, calibrated, and tested on 12 watersheds within the Lake Ray Roberts drainage basin in north Texas. Three physiographic regions are represented by these watersheds, and model success, as measured by the accuracy of load estimates, was compared within and across these regions. DOE

N94-17625# National Defence Research Establishment, Umea (Sweden). NBC Defence Dept.
TRACE ANALYSIS OF CHEMICAL WARFARE AGENTS IN AIR: SAMPLING IN POROUS POLYMERS FOLLOWED WITH THERMAL DESORPTION ANALYSIS [SPAARANALYS AV KEMISTA STRIDSMEDEL I LUFT: PROVTAGNING PAA POROESA POLYMERER MED EFTERFOELJANDE TERMISK DESORPTION]
Hans-Aake Lakso Nov. 1992 38 p In SWEDISH
(FOA-C-40302-4.6; ETN-93-94630) Avail: CASI HC A03/MF A01

Three adsorbents were evaluated for their capacity on sampling chemical warfare agents in air. The materials were Carbotrap, Chromosorb 102 and Tenax TA. After the sampling was completed the adsorbents were analyzed with thermal desorption. This means that the adsorbent is heated and at the same time flushed with gas, which leads to complete desorption on everything on the adsorbents surface. For the analysis of the adsorbents, a thermal desorption injector (Chrompack) in connection with a gas chromatogaph (Hewlett-Packard) was used. The gas chromatograph was equipped with flame ionization and nitrogen phosphorous detectors. It was shown that Tenax TA was the most suitable adsorbent for sampling and thermal desorption of organic phosphorous compounds. ESA

N94-15896*# Oregon State Univ., Corvallis. Coll. of Forestry.
DRIVING TERRESTRIAL ECOSYSTEM MODELS FROM SPACE
R. H. Waring *In* JPL, Proceedings of the Third Spaceborne Imaging Radar Symposium 28 May 1993 p 135-142 (For primary document see N94-15886 03-32)
Avail: CASI HC A02/MF A04

N94-15918*# Jet Propulsion Lab., California Inst. of Tech., Pasadena.
GLOBAL ENERGY AND WATER CYCLE EXPERIMENT (GEWEX) AND THE CONTINENTAL-SCALE INTERNATIONAL PROJECT (GCIP)
Deborah Vane *In its* Proceedings of the Third Spaceborne Imaging Radar Symposium 28 May 1993 p 431-439 (For primary document see N94-15886 03-32)
Avail: CASI HC A02/MF A04

N94-16136# Ecolink, Inc., Atlanta, GA.
ENVIRONMENTAL MANAGEMENT LESSONS TO BE LEARNED FROM THE UPCOMING CFC PHASE OUT OR HOW TO INSURE THAT WE SURVIVE THE NEXT ENVIRONMENTALLY MANDATED PROCESS CHANGE
Bill Green *In* Huntsville Association of Technical Societies, TABES 1993: 9th Annual Technical and Business Exhibition and Symposium 1993 6 p (For primary document see N94-16129 03-38)
(TABES Paper 93-570) Avail: CASI HC A02/MF A03

N94-16143*# National Aeronautics and Space Administration. Marshall Space Flight Center, Huntsville, AL.
NASA OPERATIONAL ENVIRONMENT TEAM (NOET): NASA'S KEY TO ENVIRONMENTAL TECHNOLOGY
Beth Cook *In* Huntsville Association of Technical Societies, TABES 1993: 9th Annual Technical and Business Exhibition and Symposium 1993 4 p (For primary document see N94-16129 03-38)
(TABES Paper 93-611) Avail: CASI HC A01/MF A03

N94-16687*# Jet Propulsion Lab., California Inst. of Tech., Pasadena.
MULTIPLE DATASET WATER-QUALITY ANALYSES IN THE VICINITY OF AN OCEAN WASTEWATER PLUME
Michael Hamilton, Curtiss O. Davis, W. Joseph Rhea, and Jeannette vandenBosch *In its* Summaries of the Third Annual JPL Airborne Geoscience Workshop. Volume 1: AVIRIS Workshop 1 Jun. 1992 p 63-65 (For primary document see N94-16666 03-42)
Avail: CASI HC A01/MF A02

46 GEOPHYSICS

Includes aeronomy; upper and lower atmosphere studies; ionospheric and magnetospheric physics; and geomagnetism.
For space radiation see *93 Space Radiation.*

N94-14960# Weston Observatory, MA.
BROADBAND TELESEISMIC ARRAY RECORDING IN THE ADIRONDACK MOUNTAINS, NEW YORK STATE Final Report, 1 May 1992 - 30 Apr. 1993
S. Mangino, J. Ebel, and K. Priestley 30 Apr. 1993 29 p
(Contract F19628-91-K-0009)
(AD-A267290; PL-TR-93-2108; AD-E201548) Avail: CASI HC A03/MF A01

This is a data report on the Adirondack Teleseismic (ATA) experiment, conducted during June to November, 1992. In this experiment, five portable seismic stations were run in the Adirondack Mountains of upstate New York in order to record teleseismic body waveform in a tight array configuration. Seventy-eight regional and teleseismic earthquakes were detected by the array during its operation. The purpose of this experiment is to acquire a data set where array processing techniques can be used to enhance the signals used in a teleseismic receiver structure analysis. DTIC

N94-15003*# Iowa Univ., Iowa City. Dept. of Physics and Astronomy.
GLOBAL AURORAL IMAGING: DYNAMICS OF EXPLORER MISS ION Semiannual Status Report, 1 Jan. - 30 Jun. 1993
L. A. Frank Sep. 1993 3 p
(Grant NAG5-483)
(NASA-CR-194284; NAS 1.26:194284) Avail: CASI HC A01/MF A01

An automated contour analysis of auroral images from the DESAI database is being developed. The goal is to be able to feed DESAI images to the software and let it automatically determine the inner and outer boundaries of the auroral oval of a given set of DESAI images. With these contours established, the software will determine the enclosed polar

cap area and (model based) integrated magnetic flux through that area. Through the use of this automated system, it will be possible to analyze a large fraction of the DESAI database and correlate it with various other solar-terrestrial space plasma physics parameters and indices.
Derived from text

N94-15132 Reading Univ. (England).
MESOSCALE MODELING OF THE ATMOSPHERE Interim Report No. 9
R. P. Pearce 31 Mar. 1993 28 p Limited Reproducibility: More than 20% of this document may be affected by microfiche quality
(Contract DAJA45-90-C-0009)
(AD-A263236) Avail: CASI HC A03

The Naval Research Laboratory (NRL) is presently developing a non-hydrostatic mesoscale model which is suitable for forecasting meso-Beta and gamma scale phenomena over complex terrain. The model will be delivered to the Army in 1997. However, until the non-hydrostatic model becomes operational, HOTMAC (Higher Order Turbulence Model for Atmospheric Circulation) will be used as an operational model in the U.S. Army's IMETS (Integrated METeorological System) to make a short-range (up to 24 hours) forecast of battlescale atmospheric phenomena. The U.S. Army is mainly concerned with meteorological conditions spatially within the area of 500 km x 500 km x 10 km or less and temporally within the period of 24 hours or less. The Army Research Laboratory's (ARL) prototype IMETS is currently receiving the forecast and analysis fields of meteorological variables produced from the U.S. Air Force Global Spectral Model (GSM) through the Automated Weather Distribution System (AWDS). In the near future, the Relocatable Window Model (RWM) output is expected to become available. The RWM is the Air Force's regional meso-alpha model similar to the Navy Operational Regional Atmospheric Prediction System (NORAPS). The U.S. Army is planning to use the output of GSM (or RWM) to initialize and assimilate into HOTMAC. HOTMAC has been used extensively at the ARL (formerly Atmospheric Sciences Laboratory), and simulate the evolution of locally forced circulations due to surface heating and cooling over meso-Beta and gamma scale areas. HOTMAC is numerically stable and easy to use and thus, suitable for operational use. Author

N94-15153 Deutsche Geodaetische Kommission, Munich (Germany).
NEW TECHNIQUES FOR THE COMBINATION OF HETEROGENOUS DATA WHEN DETERMINING THE EARTH'S GRAVITY FIELD Ph.D. Thesis - Stuttgart Univ. [NEUE VERFAHREN ZUR KOMBINATION HETEROGENER DATEN BEI DER BESTIMMUNG DES ERDSCHWEREFELDES]
Burkhard Middel 1992 124 p In GERMAN
(Ser-C-395; ISBN-3-7696-9441-4; ETN-93-94619) Copyright Avail: Issuing Activity (Fachinformationszentrum Karlsruhe, 7514 Eggenstein-Leopoldshafen 2, Germany)

A concept for the solution of data combination is developed in which the idea of robust collocation, based on a random effects model, is generalized. With the multi-hom BLUP (Best homogeneously Linear Unbiased Prediction) and mixed BLUP predictors, two approaches are presented where the influence of possible systematic errors in the data set, being interpreted as stochastic prior information, can be reduced. In order to estimate the different combination solutions a statistical test strategy was developed, which involved identity and compatibility tests. These techniques were numerically tested by means of an expansion of the Earth's gravitational potential in spherical harmonics based on terrestrial gravity data and satellite orbit information. Due to the robustification very homogenous combination solutions could be obtained using the predictors; they turn out to be superior when compared with the traditional approaches. ESA

N94-15282* National Aeronautics and Space Administration. Goddard Space Flight Center, Greenbelt, MD.
SOUTHERN AND NORTHERN HEMISPHERE TOTAL OZONE AS SEEN BY TOMS (Videotape)
Mar. 1989 Videotape: 24 min. playing time, in color, with sound
(NASA-TM-109591; NONP-VT-93-190389) Avail: CASI VHS A01/BETA A22

This videotape contains raw footage of this planet's upper atmosphere for use in the preparation of environmental and Earth monitoring presentation. CASI

N94-15363* National Aeronautics and Space Administration, Washington, DC.
GLOBAL CLIMATE STUDY (Videotape)
Jul. 1989 Videotape: 3 min. 18 sec. playing time, in color, with sound
(NASA-TM-109612; NONP-VT-93-190410) Avail: CASI VHS A01/BETA A22

The Global Surface Radiation Budget Experiment, which determines if current climate models are accurate, is explained. CASI

N94-15433*# Aerospace Corp., El Segundo, CA. Engineering and Technology Group.
FORMATION OF THE STABLE AURORAL ARC THAT INTENSIFIES AT SUBSTORM ONSET
L. R. Lyons and J. C. Samson (Alberta Univ., Edmonton.) 15 Oct. 1993 9 p See also A93-16192
(Grants NAG5-1541; NSF ATM-90-17637)
(NASA-CR-193637; NAS 1.26:193637; ATR-92(7248)-2) Copyright Avail: CASI HC A02/MF A01

In a companion paper, we present observational evidence that the stable, growth-phase auroral arc that intensifies at substorm expansion phase onset often forms on magnetic field lines that map to within approximately 1 to 2 R(sub e) of synchronous. The equatorial plasma pressure is 1 to 10 nPa in this region, which can give a cross-tail current greater than 0.1 A/m. In this paper, we propose that the arc is formed by a perpendicular magnetospheric-current divergence that results from a strong dawn-to-dusk directed pressure gradient in the vicinity of magnetic midnight. We estimate that the current divergence is sufficiently strong that a is greater than 1 kV field-aligned potential drop is required to maintain ionospheric-current continuity. We suggest that the azimuthal pressure gradient results from proton drifts in the vicinity of synchronous orbit that are directed nearly parallel to the cross-tail electric field. Author

N94-15539# Naval Research Lab., Washington, DC.
ATMOSPHERIC TRANSMITTANCE BETWEEN 1.0 AND 2.0 MICROMETERS Interim Report, 1991 - 1993
G. L. Trusty and J. A. Welch 30 Jun. 1993 133 p
(AD-A267076; NRL/MR/5632-93-7336) Avail: CASI HC A07/MF A02

Calculated high resolution extinction plots at sea level are presented for the spectral region between 1 and 2 micrometers using a mid-latitude summer atmospheric model. DTIC

N94-15639*# Michigan Univ., Ann Arbor. Dept. of Atmospheric, Oceanic and Space Sciences.
[INVESTIGATE WAVE-MEAN FLOW INTERACTION AND TRANSPORT IN THE EXTRATROPICAL WINTER STRATOSPHERE] Final Report
Anne K. Smith 20 Oct. 1993 3 p
(Grant NAGw-1744)
(NASA-CR-194555; NAS 1.26:194555) Avail: CASI HC A01/MF A01

The grant supported studies using several models along with observations in order to investigate some questions of wave-mean flow interaction and transport in the extratropical winter stratosphere. A quasi-geostrophic wave model was used to investigate the possibility that resonant growth of planetary wave 2 may have played a role in the sudden stratospheric warming of February 1979. The results of the time-dependent integration support the interpretation of resonance during February, 1979. Because of the possibility that the model treatment of critical line interactions exerted a controlling influence on the atmospheric dynamics, a more accurate model was needed for wave-mean flow interaction studies. A new model was adapted from the 3-dimensional primitive equation model developed by K. Rose and G. Brasseur. In its present form the model is global, rather than hemispheric; it contains an infrared cooling algorithm and a parameterized solar heating; it has parameterized gravity wave drag; and the chemistry has been entirely revised. Derived from text

N94-15800# Belgian Royal Observatory, Brussels.
PAPERS PRESENTED AT THE ELEVENTH INTERNATIONAL SYMPOSIUM ON EARTH TIDES
J. Kakkuri, ed. 1991 187 p Repr. from Proceedings of 11th Symposium on Earth Tides (Stuttgart, Germany, Schweizerbart'sche Verlagsbuchhandlung), 1991 Symposium held in Helsinki, Finland, 31 Jul.

- 5 Aug. 1989
(Communications-Ser-B-158; Ser-Geophys-177; ETN-93-94625) Copyright Avail: CASI HC A09/MF A02

The following papers are presented: report of the International Center for Earth Tides for 1985-1989; a feedback system for instruments equipped with a capacitive transducer; long baseline watertubes; temperature measurements; calibration platforms for gravimeters; cooperative projects in geodynamical instrumentation between the State Seismological Bureau (China) and the Royal Observatory of Belgium; tidal parameters at Brussels fundamental station; nontidal gravity changes observed with a superconducting gravimeter; Earth tidal results obtained with gravimeters; clinometers and strainmeters in Belgium and Luxembourg; results of tidal gravity observations with a conical pendulum; knowledge of ocean tides from tide gauge and gravity loading measurements; water-levels fluctuation in a borehole; study of the observed tidal residue vectors B versus oceanic tidal load vectors L; and tidal gravity anomalies and tectonics. For individual titles, see N94-15801 through N94-15815.

N94-15801# Belgian Royal Observatory, Brussels. Ist. di Chimica Fisica Applicata dei Materiali.

REPORT OF THE INTERNATIONAL CENTER FOR EARTH TIDES FOR THE PERIOD 1985-1989

P. Melchior *In its* Papers Presented at the Eleventh International Symposium on Earth Tides 1991 p 9-22 (For primary document see N94-15800 03-46)

Copyright Avail: CASI HC A03/MF A02

Tables of tidal tilts recorded by the International Center for Earth Tides (IECT) are presented. The evaluation of the data collected from 309 (245 in 1985) worldwide stations involved the comparison of the new extended tidal potentials. Great attention was given to the calibration problem of the gravimeters. IECT has continued to extend the transworld tidal gravity profiles by establishing temporary stations with geodynamics and LaCoste Romberg (zero method) gravimeters in South America and Africa. The results of the I/h ratio derived from 11 years of measurements with an Ozawa horizontal extensometer installed in the azimuth 37.8 deg south-east at Walferdange (Luxembourg) and for the vertical strain parameter obtained from 9 years registration with a 3.4 m vertical extensometer at Walferdange are given. A comparison of the results of the superconducting gravimeter with the mean of three modified (Bonatz) Azania gravimeters installed in the Walferdange mine is offered. In all these results, the hydrodynamical effects of the Earth's liquid core are clearly visible. The method of analysis is the least squares method with Venedikov filters.
ESA

N94-15802# Belgian Royal Observatory, Brussels. Centre de Geophysique Interne.

A NEW FEEDBACK SYSTEM FOR INSTRUMENTS EQUIPPED WITH A CAPACITIVE TRANSDUCER **c35**

M. VanRuymbeke *In its* Papers Presented at the Eleventh International Symposium on Earth Tides 1991 p 51-60 (For primary document see N94-15800 03-46)

Copyright Avail: CASI HC A02/MF A02

The feedback system under test on a LaCoste Romberg gravimeter is directly connected to the transducer without (LCR) CPI card. The bridge capacitors are measured by the phase shift of a square wave signal applied to the two capacitors. The voltage inducing the electrostatic force is applied to the short capacitor which corresponds to the largest gap. After a while the situation is reversed. By averaging the excitation signals, a figure proportional to the mean restoring force is obtained. For voltages as large as 60 v, the gravimeter remains stable without a feedback range of about 100 milligal.
ESA

N94-15803# Belgian Royal Observatory, Brussels. Centre de Geophysique Interne.

LONG BASELINE WATERTUBES **c35**

M. VanRuymbeke, J. Kaeaeriaeinen (Geodetic Inst., Helsinki, Finland.), S. Hennaux, L. VanWallegem, and N. dOreye *In its* Papers Presented at the Eleventh International Symposium on Earth Tides 1991 p 61-70 (For primary document see N94-15800 03-46)

Copyright Avail: CASI HC A02/MF A02

A comparison of the long baseline watertubes installed at the underground laboratory in Walferdange (Luxembourg) is presented and an instrument using a capacitive or inductive transducer placed directly in the tube connecting the two pots is described. Experiments using electrostatic and magnetic forces for feedback system are described.
ESA

N94-15804# Belgian Royal Observatory, Brussels. Centre de Geophysique Interne.

TEMPERATURE MEASUREMENTS **c35**

M. VanRuymbeke, H. Westerhaus (Kiel Univ., Germany.), and J. Fernandez (Universidad Complutense, Madrid, Spain.) *In its* Papers Presented at the Eleventh International Symposium on Earth Tides 1991 p 73-83 (For primary document see N94-15800 03-46)

Copyright Avail: CASI HC A03/MF A02

An electronic interface adapted to solid state thermistors, placed in a probe for boreholes, is described. Four applications are detailed: temperature profiles in a borehole at the Royal Observatory of Belgium (ROB); continuous records of water temperature in boreholes in Turkey which confirm that a thermal wave is induced by Earth tides; high precision temperature profiles along an underground gallery in the Corona volcano (Lanzarote island); continuous records of rock temperature in the same site to check the thermal influence in the tidal instruments installed nearby. In conclusion, thermometers developed at the ROB give a precision of 5 mK for differential measurements in different sites. Placed in permanent position, a long term precision of 1 mK seems possible. For detection of thermal waves induced at a well defined period (for example Earth tides), a 10 microK precision is clearly obtained. A noise level of 1 microK or better seems to be achieved. The noise decreases during one week after the set pump of thermistors. The grounding of the supply, a moisture protection and a close contact between the thermistor and the environment are the key points for the best performances.
ESA

N94-15805# Belgian Royal Observatory, Brussels. Centre de Geophysique Interne.

CALIBRATION PLATFORMS FOR GRAVIMETERS **c35**

M. VanRuymbeke *In its* Papers Presented at the Eleventh International Symposium on Earth Tides 1991 p 95-100 (For primary document see N94-15800 03-46)

Copyright Avail: CASI HC A02/MF A02

Several methods investigated in order to calibrate gravimeters by the inertial acceleration produced by a vertical motion are described. The VRR 8601 calibrating platform is especially designed to calibrate La Coste and Romberg gravimeters. For heavier gravimeters such as tidal La Coste or superconducting instruments, two other principles are possible to lift up sinusoidally the platform: a mercury crapaudine or the rotation on an inclined plane.
ESA

N94-15806# State Seismological Bureau of China, Wuhan. Inst. of Seismology.

COOPERATIVE PROJECTS IN GEODYNAMICAL INSTRUMENTATION BETWEEN THE STATE SEISMOLOGICAL BUREAU (CHINA) AND THE ROYAL OBSERVATORY OF BELGIUM **c35**

Wei-Lin Cai, M. VanRuymbeke (Belgian Royal Observatory, Brussels.), Shi-Lin Tang, B. Ducarme (Belgian Royal Observatory, Brussels.), Wei-Min Du, and J. A. Flick (Laboratoire Suoterrain de Geodynamique, Luxembourg.) *In* Belgian Royal Observatory, Papers Presented at the Eleventh International Symposium on Earth Tides 1991 p 119-130 (For primary document see N94-15800 03-46)

Copyright Avail: CASI HC A03/MF A02

Since 1981, the State Seismological Bureau of China (BES) and the Royal Observatory of Belgium (ORB) have cooperated for instrumentation in the ORBES project. The results of the horizontal strainmeter ORBES 81 installed at Huangshi (China) station confirm the quality of the mechanical design and of the VLR electronics. New prototypes of vertical strainmeters (ORBES 84) with two kinds of transducers (capacitive and inductive) are installed at Huangshi and Walferdange (Luxembourg) stations. The drift rate is low and the calibration system has been improved. The inductive and capacitive sensors give quite similar results in amplitude and phase. A new barometer ORBES 83 is now recording at Brussels (Belgium) near the superconducting gravimeter and is compared with a standard barometer. A Chinese FSQ watertube is installed in Walferdange. The analysis results are in very good agreement with the VM pendulums and the error level is very low.
ESA

N94-15807# Belgian Royal Observatory, Brussels. Centre de Geophysique Interne.

ON TIDAL PARAMETERS AT BRUSSELS FUNDAMENTAL STATION

c48

B. Ducarme and M. VanRuymbeke *In its* Papers Presented at the Eleventh International Symposium on Earth Tides 1991 p 157-166 (For primary document see N94-15800 03-46)

Copyright Avail: CASI HC A02/MF A02

The accepted values of the tidal factor delta at Brussels (Belgium) disagree by about 1 percent with the most recent model based on the Wahr-Dehant model for the body tides and in the Schwiderski maps for the tidal loading computation. Several attempts previously made to redetermine more precisely these parameters are described, and the results obtained with a zero method LaCoste and Romberg gravimeter calibrated by means of an oscillating platform are given. This experiment confirms that a 1 percent decrease of the accepted value of delta(O(sub 1)) at Brussels seems to be required. This is also confirmed by an independently calibrated Askania gravimeter installed at the Dourbes station. ESA

N94-15808# Institut Royal Meteorologique de Belgique, Brussels. Dept. Inwendige Geophysica.

NONTIDAL GRAVITY CHANGES OBSERVED WITH A SUPERCONDUCTING GRAVIMETER

F. DeMayer and B. Ducarme (Belgian Royal Observatory, Brussels.) *In* Belgian Royal Observatory, Papers Presented at the Eleventh International Symposium on Earth Tides 1991 p 167-184 (For primary document see N94-15800 03-46)

Copyright Avail: CASI HC A03/MF A02

Recordings made by a superconducting gravimeter GWR at the Royal Observatory of Belgium (Brussels) are reported. Its long term trend is difficult to model due to instrumental perturbations. When a reliable drift model is built, periodical gravity changes show up at the annual and Chandlerian (430 days) periods. Unfortunately the length of the observation (four and a half years) does not yet allow a complete separation of the two contributions and a correct evaluation of the amplitude factor delta associated with the Chandler term. The amplitude of the anomalous annual term reaches 3 microgal. It is however possible to suppress the annual contribution by introducing a phase shift to the polar motion effect. With this model an amplitude factor delta close to unity but a phase lag of 44 days is obtained, which is unrealistic. In any case a complete model for the gravity variations leaves final residues with a standard deviation of 1.7 microgral bit these residues do not yet exhibit a white noise structure which implies the necessity of including other perturbing factors. ESA

N94-15809# Belgian Royal Observatory, Brussels.

EARTH TIDES RESULTS OBTAINED WITH GRAVIMETERS, CLINOMETERS, AND STRAINMETERS IN BELGIUM AND IN GRAND DUCHY OF LUXEMBOURG

P. Melchior, J. A. Flick (Laboratoire Suoterrain de Geodynamique, Luxembourg.), B. Ducarme, M. VanRuymbeke, F. DeMayer (Institut Royal Meteorologique de Belgique, Brussels.), and J. Rasson (Institut Royal Meteorologique de Belgique, Dourbes.) *In its* Papers Presented at the Eleventh International Symposium on Earth Tides 1991 p 197-210 (For primary document see N94-15800 03-46)

Copyright Avail: CASI HC A03/MF A02

Very long series of tidal registrations in the horizontal and vertical components and in the horizontal and vertical strain have been obtained in Belgium and in the Grand Duchy of Luxembourg since 1961. In 1988, the Sclaigneaux station was closed, not only because of practical difficulties of maintenance but also because the 27 years series obtained looked sufficiently informative. Sclaigneaux was the station where the resonance effect in diurnal waves K(sub 1) and P(sub 1) was for the first time experimentally demonstrated. Results on tilt, strain and gravity are tabulated. ESA

N94-15810# Institut Royal Meteorologique de Belgique, Dourbes. Centre de Physique du Globe.

RESULTS OF TIDAL GRAVITY OBSERVATIONS WITH A CONICAL PENDULUM

J. Rasson *In* Belgian Royal Observatory, Papers Presented at the Eleventh International Symposium on Earth Tides 1991 p 211-215 (For primary document see N94-15800 03-46)

Copyright Avail: CASI HC A01/MF A02

Several years of observations of the gravity tide were recorded with the conical pendulum in the feedback mode. This means that the instrument is calibrated by design and that the calibration factor is traceable to a frequency standard. The noise level is in the range of tens of microgals, and the delta factors are estimated at the percent level. The results are presented and discussed. Various suggestions are given for improving the instrument so that full use can be made of its calibration accuracy. ESA

N94-15811# Belgian Royal Observatory, Brussels.

WHAT WE CAN LEARN ABOUT OCEAN TIDES FROM TIDE GAUGE AND GRAVITY LOADING MEASUREMENTS?

O. Francis and P. Mazzega (Centre National d'Etudes Spatiales, Toulouse, France.) *In its* Papers Presented at the Eleventh International Symposium on Earth Tides 1991 p 287-298 (For primary document see N94-15800 03-46)

Copyright Avail: CASI HC A03/MF A02

The harmonic constants from tide gauge stations and from gravity loading measurements of the ICET (International Center for Earth Tides) data bank are separately inverted to produce M2 cotidal maps on a global scale. The optimal interpolation of these data, based on the total inverse theory in L2 norm, makes use of a set of a priori stationary and isotropic covariance functions deduced from a global hydrodynamical model and from its corresponding gravity loading map. The preliminary results presented with formal error estimates are surprisingly good, in particular the M2 maps obtained from the numerous tide gauge data. These results are discussed and further lines of work are drawn. ESA

N94-15812# Belgian Royal Observatory, Brussels. Centre de Geophysique Interne.

WATER-LEVELS FLUCTUATIONS IN A BOREHOLE AT THE ROYAL OBSERVATORY OF BELGIUM: EFFECTS ON LOCAL GRAVITY, EARTH TIDAL, AND BAROMETRIC RESPONSES

M. Delcourt-Honorez *In its* Papers Presented at the Eleventh International Symposium on Earth Tides 1991 p 389-411 (For primary document see N94-15800 03-46)

Copyright Avail: CASI HC A03/MF A02

A borehole was drilled at the Royal Observatory of Belgium in Brussels, next to the superconducting gravimeter. Three aquifers belong to the 'multiple aquifer-aquitard system'. Continuously since Jun. 1984, various kinds of water levels variations are registered: long term and short term variations and, in the intermediate and deep wells, periodic tidal oscillations. Moreover, the water table and the pressure heads respond to the atmospheric pressure variations. The water levels variations perturbing effects in the superconducting gravimeter registrations are estimated and the hydraulic problem and the consolidation problem are studied. The classical Bouguer's formula in theories is enlarged, taking into account the nature of the layers, the expansions or compressions of each layer, the global land surface displacement and the various hydrostatic occurrences of phases on porous media. The Bouguer's theory is also extended to the case of a finite thickness layer, by a numerical integration. The water levels variations in the intermediate and deep aquifers (at long term, at short term, and the barometric and tidal responses) are only inducing negligible perturbing effects on the superconducting gravimeter registrations but the effect of the water table drift is at the limit of the actual precision of the gravimeter registrations. On the other hand, the barometric and tidal responses of the well-aquifer systems are used to estimate the in situ parameters of both the aquifers and the aquifer system (porosity, specific storage, vertical compressibility, and permeability). The estimated values are in good agreement with those deduced by using hydrogeological, soil, and rock mechanics considerations. The research presented can be applied to any hydrogeological configuration with any complexity. ESA

N94-15813# Belgian Royal Observatory, Brussels.

A STUDY OF THE OBSERVED TIDAL RESIDUE VECTORS B VERSUS OCEANIC TIDAL LOAD VECTORS L

P. Melchior and B. Ducarme *In its* Papers Presented at the Eleventh International Symposium on Earth Tides 1991 p 431-444 (For primary document see N94-15800 03-46)

Copyright Avail: CASI HC A03/MF A02

The Earth Tides Data Bank holds the results of more than three

hundred tidal gravity stations. Fifty percent of them are directly connected to the ICET (International Center for Earth Tides) network and outside of Europe it is ninety percent of them. The correlation between the tidal loading vector L computed from Schwiderski maps and the tidal residual vector B deduced from these observations by computing the linear regression of the in phase and the out of phase components is studied. If the coastal stations (D less than or equal to 5 km) are discarded, the slopes of the regression lines are equal to unity except for the sine components in Europe where the observed effect is 5% larger than the computed one. A phase lag of the body tides is observed: the independent term is not significantly different from zero for the cosine components while, for the sine components, and for any combination of stations, it takes negative values comprised between -0.200 and -0.300 which corresponds to a phase lag of -0.4 deg. This value is in agreement with the evaluation by Schwiderski of the effect of the pressure of the oceanic tides on the tidally deformed bottom of the ocean. ESA

N94-15814# Belgian Royal Observatory, Brussels.
TIDAL GRAVITY ANOMALIES AND TECTONICS
P. Melchior and B Ducarme *In its* Papers Presented at the Eleventh International Symposium on Earth Tides 1991 p 445-454 (For primary document see N94-15800 03-46)
Copyright Avail: CASI HC A02/MF A02

A statistical study of the two components of tidal residues X(Khi, khi) shows a larger scattering for the in phase component X cos Khi corresponding to regional effects. Further investigations demonstrate a clear correlation between X cos Khi and the regional heat flow for the waves O(sub 1) and M(sub 2). The existence of a linear dependence is established: an increase of 0.4 to 0.5% of the body tides amplitude corresponds to an increase of 10 mW/sq m. ESA

N94-15815# Belgian Royal Observatory, Brussels.
REPORT OF THE WORKING GROUP ON THEORETICAL TIDAL MODEL
V. Dehant (Belgian National Foundation for Scientific Research, Brussels.), B. Ducarme, G. Jentzsch, J. Kaeaeriaeinen, G. Y. Li, S. M. Molodensky, S. Okubo, J. M. Wahr, Qin-Wen Xi, and J. Zschau *In its* Papers Presented at the Eleventh International Symposium on Earth Tides 1991 p 533-548 (For primary document see N94-15800 03-46)
Copyright Avail: CASI HC A03/MF A02

Three tasks are analyzed: to agree upon one definition of the tidal parameters to be proposed for a recommendation; to agree upon one tidal model to account for as many physical phenomena as possible according to the advance of the technology used for the observation; and to agree on a tidal potential development. Tidal parameters are defined as Earth's transfer functions, and include the tidal gravimetric factor, Love number, tilt, and strain. The main results of the discussions are summarized and problems to be investigated are pointed out. ESA

N94-16021*# California Univ., Los Angeles.
TECTONIC DEFORMATION IN SOUTHERN CALIFORNIA Final Technical Report
David D. Jackson 1 Nov. 1993 4 p
(Grant NAG5-447)
(NASA-CR-194621; NAS 1.26:194621) Avail: CASI HC A01/MF A01

Our objectives were to use modern geodetic data, especially those derived from space techniques like Very Long Baseline Interferometry (VLBI), Satellite Laser Ranging (SLR), and the Global Positioning System (GPS) to infer crustal deformation in southern California and relate it to plate tectonics and earthquake hazard. To do this, we needed to collect some original data, write computer programs to determine positions of survey markers from geodetic observables, interpret time dependent positions in terms of velocity and earthquake caused episodic displacements, and construct a model to explain these velocities and displacements in terms of fault slip and plate movements. Author (revised)

N94-16125# Royal Norwegian Council for Scientific and Industrial Research, Kjeller.
NORSAR BASIC SEISMOLOGICAL RESEARCH Final Report, 1 Oct. 1991 - 30 Sep. 1992
Svein Mykkeltveit 29 Nov. 1992 54 p
(Contract F49620-89-C-0038)
(AD-A266193; PL-TR-93-2085) Avail: CASI HC A04/MF A01

This report contains 4 separate contributions, as well as abstracts of the investigations submitted as quarterly technical reports during FY-92. A systematic analysis of teleseismic P-wave travel time and amplitude variations across the NORSAR array reveals the following: (1) SP time and amplitude anomalies are related; (2) SP and LP time variations are only partially related; and (3) LP amplitude variations are very small. It is generally appreciated that later arrivals contain important information about the seismic source and about the earth's structure. The arrival times of later phases reported to the ISC have been used for tomographic studies of the earth's deep interior by several workers. The phases of PcP and PKKP were analyzed as the detections of these phases were sufficiently numerous product meaningful statistics. The results of the investigations are given. Synthetic seismograms may provide a better understanding of wave propagation in complex media. A novel scheme for computing 2D synthetics based on numerical solutions of the elastic wave equation using finite-difference techniques has been presented in a previous contribution. Recently this scheme has been generalized to models with free surface tomography, and the usefulness of synthetic seismogram analysis to elucidate wave propagation in the crust and mantle lithosphere is demonstrated. The status of development of the Northern Europe Regional Array Network is summarized. DTIC

N94-16469# Orion International Technologies, Albuquerque, NM.
CHARACTERIZATION OF UV EMISSIONS RESULTING FROM ELECTRONIC ENERGY TRANSFER IN ATMOSPHERIC MOLECULES Final Report, 23 Oct. 1989 - 1992
Joseph M. Thomas and Anthony V. Dentamaro 28 Apr. 1993 63 p
(Contract F19628-90-C-0030)
(AD-A266244; PL-TR-93-2042) Avail: CASI HC A04/MF A01

Electronically excited metastable diatomics are energy rich and are known to play an important role in the chemistry of normal and perturbed atmospheres. The dynamics of these species includes both chemical reactivity and collisional energy transfer. The dynamics are investigated. DTIC

N94-16551# Technology International Corp., Bedford, MA.
OPTICAL MEASUREMENTS OF NASA/USAF CRRES HIGH ALTITUDE ROCKET BORNE CHEMICAL RELEASE EXPERIMENTS IN CONJUNCTION WITH THE USAF AIRBORNE IONOSPHERIC OBSERVATORY AIRCRAFT Final Report, 9 Jan. 1991 - 30 Sep. 1992
W. P. Boquist and B. G. Ledley Oct. 1992 32 p
(Contract F19628-91-C-0010)
(AD-A266404; AD-E201480; PL-TR-92-2326) Avail: CASI HC A03/MF A01

In order to provide post experiment optical imagery data for correlation of airborne measurements of satellite signal modification from intervening chemical vapor clouds released in the upper atmosphere, Technology International Corporation provided and operated as part of the NASA/USAF PL/CRRES research program a ground optics station on Grand Turk Island in the Caribbean during June-July 1992. Optical data was acquired on the AA-1 event (approximately 95%) and the AA-7 event (approximately 60%). The third release (AA-2 event) occurred when the Grand Turk optics site was fully obscured by clouds for the duration of the normal period of visibility. All three rocket borne experiments were launched at morning twilight. DTIC

N94-16840# American Museum of Natural History, New York, NY.
THE ROLE OF CARBON AND TEMPERATURE IN DETERMINING ELECTRICAL CONDUCTIVITY OF BASINS, CRUST AND MANTLE
E. Mathez 1992 2 p
(Contract DE-FG02-92ER-14265)
(DE93-015936; DOE/ER-14265/1) Avail: CASI HC A01/MF A01

The initial phase concentrated on improving electron microprobe techniques for carbon mapping of polished sections. Experiments were carried out on the utility of Au/Pd, Cr, and Ag coats; results shows that Cr and Ag gave good results. Observations were made on maps of carbon distribution in rocks; low magnification base maps consisting of a mosaic of BSE images were produced on the SEM, and traverses were plotted. The metamorphic rocks adjacent to the Denali fault were chosen for study. DOE

N94-17214*# Michigan Univ., Ann Arbor.
THE FEASIBILITY OF TROPOSPHERIC AND TOTAL OZONE DETERMINATION USING A FABRY-PEROT INTERFEROMETER AS A SATELLITE-BASED NADIR-VIEWING ATMOSPHERIC SENSOR Ph.D. Thesis
Allen Maurice Larar 1993 194 p Sponsored by NASA Original contains color illustrations
(NASA-TM-109342; NAS 1.15:109342) Avail: CASI HC A09/MF A03; 3 functional color pages

Monitoring of the global distribution of tropospheric ozone (O3) is desirable for enhanced scientific understanding as well as to potentially lessen the ill-health impacts associated with exposure to elevated concentrations in the lower atmosphere. Such a capability can be achieved using a satellite-based device making high spectral resolution measurements with high signal-to-noise ratios; this would enable observation in the pressure-broadened wings of strong O3 lines while minimizing the impact of undesirable signal contributions associated with, for example, the terrestrial surface, interfering species, and clouds. The Fabry-Perot Interferometer (FPI) provides high spectral resolution and high throughput capabilities that are essential for this measurement task. Through proper selection of channel spectral regions, the FPI optimized for tropospheric O3 measurements can simultaneously observe a stratospheric component and thus the total O3 column abundance. Decreasing stratospheric O3 concentrations may lead to an increase in biologically harmful solar ultraviolet radiation reaching the earth's surface, which is detrimental to health. In this research, a conceptual instrument design to achieve the desired measurement has been formulated. This involves a double-etalon fixed-gap series configuration FPI along with an ultra-narrow bandpass filter to achieve single-order operation with an overall spectral resolution of approximately .068 cm(exp -1). A spectral region of about 1 cm(exp -1) wide centered at 1054.73 cm(exp -1) within the strong 9.6 micron ozone infrared band is sampled with 24 spectral channels. Other design characteristics include operation from a nadir-viewing satellite configuration utilizing a 9 inch (diameter) telescope and achieving horizontal spatial resolution with a 50 km nadir footprint. A retrieval technique has been implemented and is demonstrated for a tropical atmosphere possessing enhanced tropospheric ozone amounts. An error analysis assessing the impact on retrieved O3 amounts of the most significant uncertainties associated with this particular measurement has been performed for several different types of atmospheres. Results show the proposed instrumentation to enable a good measurement of absolute ozone amounts and an even better determination of relative changes, with a range of accuracy to within 7.55 to 20.6 percent for integrated tropospheric amounts (and 1.99 to 4.02 percent for total O3 column abundance) and a corresponding range in precision to within 7.73 to 10.4 percent (and 3.30 to 3.95 percent for total O3 column abundance), for the atmospheric conditions considered. Author

N94-17252# California Univ., Berkeley. Lawrence Berkeley Lab.
A SEARCH FOR EVIDENCE OF NONLINEAR ELASTICITY IN THE EARTH
T. M. Daley, J. E. Peterson, Jr., and T. V. McEvilly Dec. 1992 61 p
(Contract DE-AC03-76SF-00098)
(DE93-015279; LBL-33313) Avail: CASI HC A04/MF A01

Attempts to observe nonlinear elasticity in seismic wave propagation have been made in recent years. The sought-after nonlinear effects include harmonic distortion of a monofrequency wave and nonlinear superposition of two waves of differing frequencies. Most recent work has focused on laboratory measurements in rock samples, and there has been no definitive publication of nonlinear wave propagation in situ in rocks of the earth. Because LBL research has involved crustal seismic experiments over a wide range of scales, there exists an excellent data base from which we can draw appropriate experimental data. In mid-1991, we proceeded to use in-house data in a search for effects of nonlinear elasticity. The data sets selected include seismic reflection profiles from the Tehachapi Mountains area of California and seismic wave monitoring data from the Parkfield earthquake prediction experiment. In addition, we conducted one field experiment explicitly for detection of nonlinear wave propagation in conjunction with a previously planned Vertical Seismic Profile (VSP) at the Dept. of Energy's Nevada Test Site (NTS), and we analyzed a special data set acquired recently by Los Alamos National Lab (LANL) in West Texas in an attempt to verify nonlinear wave propagation during a seismic reflection profile. These data sets used Vibroseis energy sources which allowed analysis of time-separated frequency-domain data. DOE

N94-17493 Air Force Inst. of Tech., Wright-Patterson AFB, OH.
OPTIMIZATION OF SATELLITE COVERAGE IN OBSERVING CAUSE AND EFFECT CHANGES IN THE IONOSPHERE, MAGNETOSPHERE, AND SOLAR WIND M.S. Thesis
Martin J. Loveless Jun. 1993 103 p Limited Reproducibility: More than 20% of this document may be affected by microfiche quality
(AD-A267956; AFIT/CI/CIA-93-118) Avail: Issuing Activity (Defense Technical Information Center (DTIC))

Disturbances in the ionosphere sometimes cause adverse effects to communications systems, power grids, etc. on the earth. Currently, very little, if any, lead time is given to warn of an impending problem. If a forecast could be made of ionospheric occurrences, some lead time may be given to appropriate agencies and equipment may be saved. Most changes that occur in the ionosphere are a result of interaction of energy, currents, etc. between the magnetosphere and/or solar wind. Before a forecast can be made, however, improvement of ionospheric models currently in use need to be made. The models currently depict features in various regions of the ionosphere but not always where these features are actually observed. So an improvement to the model is needed to create an accurate baseline condition, or in other words an accurate depiction of the current ionosphere. Models could be improved by inputting real-time data from the ionosphere into the model. This data would come from satellites and/or ground-based stations. DTIC

N94-17499 Pacific-Sierra Research Corp., Los Angeles, CA.
EFFECT OF POWERFUL OBLIQUE HF WAVES ON IONOSPHERIC D-LAYER ABSORPTION Technical Report
R. M. Bloom 13 Apr. 1993 18 p Limited Reproducibility: More than 20% of this document may be affected by microfiche quality
(Contract F19628-90-C-0100)
(AD-A268443; PL-TR-93-2098) Avail: Issuing Activity (Defense Technical Information Center (DTIC))

A simple model of D-layer ionospheric heating in the presence of strong, high frequency (HF) radio waves is used to predict the anomalous, nonlinear wave absorption due to collisional and recombination effects induced by the indirect signal. It is found that little anomalous absorption occurs until effective radiated power (ERP) approaches 100 dBW; further increases in power of several dB beyond this 100 dBW threshold are frustrated by a comparable increase in self-induced, one-way absorption. This trend of increasing absorption with increasing transmitter ERP has considerable implications for design of communication or radar systems that use ultra-powerful, high-gain HF transmitters. DTIC

N94-17512 Air Force Inst. of Tech., Wright-Patterson AFB, OH.
A CORRELATIVE COMPARISON OF GEOMAGNETIC STORMS AND AURORAL SUBSTORMS USING GEOMAGNETIC INDECES M.S. Thesis
William B. Cade, III Jun. 1993 118 p Limited Reproducibility: More than 20% of this document may be affected by microfiche quality
(AD-A268081; AFIT/CI/CIA-93-116) Avail: Issuing Activity (Defense Technical Information Center (DTIC))

The partial contents of this document include the following: (1) geomagnetic storm and substorm processes; (2) magnetospheric structure; (3) substorm processes; (4) data description; (5) geomagnetic indices; and (6) data period and data sets. DTIC

N94-17527*# Alaska Univ., Fairbanks. Geophysical Inst.
[MICRO- AND MESO-SCALE SIMULATIONS OF MAGNETOSPHERIC PROCESSES RELATED TO THE AURORA AND SUBSTORM MORPHOLOGY] Final Technical Report, Jun. 1989 - Nov. 1991
Daniel W. Swift 1991 4 p
(Grant NAGw-1787)
(NASA-CR-193437; NAS 1.26:193437) Avail: CASI HC A01/MF A01

The primary methodology during the grant period has been the use of micro or meso-scale simulations to address specific questions concerning magnetospheric processes related to the aurora and substorm morphology. This approach, while useful in providing some answers, has its limitations. Many of the problems relating to the magnetosphere are inherently global and kinetic. Effort during the last year of the grant period has increasingly

focused on development of a global-scale hybrid code to model the entire, coupled magnetosheath - magnetosphere - ionosphere system. In particular, numerical procedures for curvilinear coordinate generation and exactly conservative differencing schemes for hybrid codes in curvilinear coordinates have been developed. The new computer algorithms and the massively parallel computer architectures now make this global code a feasible proposition. Support provided by this project has played an important role in laying the groundwork for the eventual development or a global-scale code to model and forecast magnetospheric weather. Derived from text

N94-17631 International Centre for Theoretical Physics, Trieste (Italy).
A PHYSICAL MODEL FOR ONE-DIMENSION AND TIME-DEPENDENT IONOSPHERE. PART 2: RESULTS AND DISCUSSIONS
Shunrong Zhang and S. M. Radicella Mar. 1993 16 p Limited Reproducibility: More than 20% of this document may be affected by microfiche quality
(DE93-627959; IC-93/46-Pt-2) Avail: CASI HC A03 (US Sales Only)

Results of a one-dimension time-dependent ionospheric theoretical model when experimental critical frequency of the F(sub 2) region are used as input data are given. Evidences of the validity of the mentioned model are shown; and it is indicated that the bottom side F region described by IRI90 empirical model for Wuchang (30.5 deg N, 11.4 deg E) are well reproduced by the theoretical model for different seasons and low solar activity, meanwhile, it is shown that IRI gives values of the electron concentration in the topside larger than the model. Also, the effect of the dynamics and the photo-ionization on the variation of the height of the peak is discussed. DOE

N94-16203*# Museum of Natural History, London (England). Dept. of Mineralogy.
PETROGRAPHY, MINERALOGY, AND Mg ISOTOPE COMPOSITION OF VICTA: A VIGARANO CaAl4O7-BEARING TYPE A INCLUSION Abstract Only
R. C. Greenwood, A. Morse (Open Univ., Milton, England.), and J. V. P. Long (Cambridge Univ., England.) *In* Lunar and Planetary Inst., Twenty-Fourth Lunar and Planetary Science Conference. Part 2: G-M 1993 p 573-574 (For primary document see N94-16173 03-91)
Avail: CASI HC A01/MF A06

N94-16211*# Academy of Sciences of the Ukraine, Kiev. Inst. of Geological Sciences.
THE ACRAMAN IMPACT STRUCTURE: ESTIMATION OF THE DIAMETER BY THE EJECTA LAYER THICKNESS Abstract Only
E. P. Gurov *In* Lunar and Planetary Inst., Twenty-Fourth Lunar and Planetary Science Conference. Part 2: G-M 1993 p 589-590 (For primary document see N94-16173 03-91)
Avail: CASI HC A01/MF A06

N94-16214*# Washington Univ., Saint Louis, MO. Dept. of Earth and Planetary Sciences.
ASSIMILATION OF SOLIDS DURING ASCENT OF MAGMAS FROM THE BARTOY FIELD OF THE BAIKAL REGION, SIBERIA Abstract Only
Johnson R. Haas, Larry A. Haskin, James Luhr (Smithsonian Institution, Washington, DC.), and Sergei Rasskazov (Academy of Sciences, USSR, Irkutsk.) *In* Lunar and Planetary Inst., Twenty-Fourth Lunar and Planetary Science Conference. Part 2: G-M 1993 p 595-596 (For primary document see N94-16173 03-91)
Avail: CASI HC A01/MF A06

N94-16222*# Planetary Science Inst., Tucson, AZ.
CONFIRMATION OF SATURATION EQUILIBRIUM CONDITIONS IN CRATER POPULATIONS Abstract Only
William K. Hartmann and Robert W. Gaskell (Jet Propulsion Lab., California Inst. of Tech., Pasadena.) *In* Lunar and Planetary Inst., Twenty-Fourth Lunar and Planetary Science Conference. Part 2: G-M 1993 p 611-612 (For primary document see N94-16173 03-91)
Avail: CASI HC A01/MF A06

N94-16237*# Lancaster Univ. (England). Environmental Sciences Div.
BUBBLE COALESCENCE IN MAGMAS Abstract Only
Richard A. Herd and Harry Pinkerton *In* Lunar and Planetary Inst., Twenty-Fourth Lunar and Planetary Science Conference. Part 2: G-M 1993 p 641-642 (For primary document see N94-16173 03-91)
Avail: CASI HC A01/MF A06

N94-16250*# Max-Planck-Inst. fuer Chemie, Mainz (Germany).
SIDEROPHILE ELEMENTS IN THE UPPER MANTLE OF THE EARTH: NEW CLUES FROM METAL-SILICATE PARTITION COEFFICIENTS Abstract Only
A. Holzheid, A. Borisov, and H. Palme *In* Lunar and Planetary Inst., Twenty-Fourth Lunar and Planetary Science Conference. Part 2: G-M 1993 p 667-668 (For primary document see N94-16173 03-91)
Avail: CASI HC A01/MF A06

N94-16269*# Geological Survey, Denver, CO. Federal Center.
A DISCONTINUOUS MELT SHEET IN THE MANSON IMPACT STRUCTURE Abstract Only
G. A. Izett, R. L. Reynolds, J. G. Rosenbaum, and J. M. Nishi *In* Lunar and Planetary Inst., Twenty-Fourth Lunar and Planetary Science Conference. Part 2: G-M 1993 p 705-706 (For primary document see N94-16173 03-91)
Avail: CASI HC A01/MF A06

N94-16271*# Harvard Univ., Cambridge, MA. Dept. of Earth and Planetary Sciences.
CONSTRAINTS ON THE DIFFERENTIATION OF THE EARTH FROM THE COUPLED Sm-146,147-Nd-142,143 SYSTEMATICS Abstract Only
S. B. Jacobsen and C. L. Harper, Jr. *In* Lunar and Planetary Inst., Twenty-Fourth Lunar and Planetary Science Conference. Part 2: G-M 1993 p 709-710 (For primary document see N94-16173 03-91)
Avail: CASI HC A01/MF A06

N94-16282*# Lancaster Univ. (England). Inst. of Environmental and Biological Sciences.
THE COOLING RATES OF PAHOEHOE FLOWS: THE IMPORTANCE OF LAVA POROSITY Abstract Only
Alun C. Jones *In* Lunar and Planetary Inst., Twenty-Fourth Lunar and Planetary Science Conference. Part 2: G-M 1993 p 731-732 (For primary document see N94-16173 03-91)
Avail: CASI HC A01/MF A06

N94-16285*# Lockheed Engineering and Sciences Co., Houston, TX.
ANGRITE LEW87051: ARE THE OLIVINES PHENO'S OR XENO'S? A CONTINUING STORY Abstract Only
A. J. G. Jurewicz and G. A. McKay (National Aeronautics and Space Administration. Lyndon B. Johnson Space Center, Houston, TX.) *In* Lunar and Planetary Inst., Twenty-Fourth Lunar and Planetary Science Conference. Part 2: G-M 1993 p 737-738 (For primary document see N94-16173 03-91)
Avail: CASI HC A01/MF A06

N94-16307*# Kansas Univ., Lawrence.
HIGH-RESOLUTION SEISMIC REFLECTION SURVEY AT THE MANSON CRATER, IOWA Abstract Only
D. A. Keiswetter, R. Black, D. W. Steeples, and R. R. Anderson (Geological Survey, Iowa City, IA.) *In* Lunar and Planetary Inst., Twenty-Fourth Lunar and Planetary Science Conference. Part 2: G-M 1993 p 781-782 (For primary document see N94-16173 03-91)
Avail: CASI HC A01/MF A06

N94-16316*# Lancaster Univ. (England). Environmental Science Div.
LAVA CRUSTS AND FLOW DYNAMICS Abstract Only
C. R. J. Kilburn *In* Lunar and Planetary Inst., Twenty-Fourth Lunar and Planetary Science Conference. Part 2: G-M 1993 p 799 (For primary document see N94-16173 03-91)
Avail: CASI HC A01/MF A06

N94-16322*# Wien Univ. (Austria). Inst. of Geochemistry.
MANSON IMPACT STRUCTURE, IOWA: FIRST GEOCHEMICAL RESULTS FOR DRILL CORE M-1
Christian Koeberl, Raymond R. Anderson (Geological Survey, Iowa City, IA.), Jack B. Hartung (Geological Survey, Iowa City, IA.), and Wolf Uwe Reimold (Witwatersrand Univ., Johannesburg, South Africa.) *In* Lunar

and Planetary Inst., Twenty-Fourth Lunar and Planetary Science Conference. Part 2: G-M 1993 p 811-812 (For primary document see N94-16173 03-91)
(FWF Proj. P6794-GEO)
Avail: CASI HC A01/MF A06

N94-16334*# Geological Survey, Reston, VA.
PRELIMINARY Ar-40/Ar-39 AGE SPECTRUM AND LASER PROBE DATING OF THE M1 CORE OF THE MANSON IMPACT STRUCTURE, IOWA: A K-T BOUNDARY CRATER CANDIDATE Abstract Only
M. J. Kunk, L. W. Snee (Geological Survey, Denver, CO.), B. M. French (National Aeronautics and Space Administration, Washington, DC.), S. S. Harlan (Geological Survey, Denver, CO.), and J. J. McGee *In* Lunar and Planetary Inst., Twenty-Fourth Lunar and Planetary Science Conference. Part 2: G-M 1993 p 835-836 (For primary document see N91-16173 03-91)
Avail: CASI HC A01/MF A06

N94-16336*# Tsukuba Univ. (Japan). Inst. of Geoscience.
WATER IN EARTH'S MANTLE: HYDROGEN ANALYSIS OF MANTLE OLIVINE, PYROXENES AND GARNET USING THE SIMS Abstract Only
Masanori Kurosawa, Hisayoshi Yurimoto, and Shigeho Sueno *In* Lunar and Planetary Inst., Twenty-Fourth Lunar and Planetary Science Conference. Part 2: G-M 1993 p 839-840 (For primary document see N94-16173 03-91)
Avail: CASI HC A01/MF A06

N94-16349*# California Univ., Los Angeles. Dept. of Earth and Space Sciences.
ON THE RELATIONSHIP BETWEEN TECTONIC PLATES AND THERMAL MANTLE PLUME MORPHOLOGY Abstract Only
A. Lenardic and W. M. Kaula *In* Lunar and Planetary Inst., Twenty-Fourth Lunar and Planetary Science Conference. Part 2: G-M 1993 p 865-866 (For primary document see N94-16173 03-91)
Avail: CASI HC A01/MF A06

N94-16358*# Oregon State Univ., Corvallis. Depts. of Chemistry and Geosciences.
EARTH'S PARTIAL PRESSURE OF CO2 OVER THE PAST 120 Ma; EVIDENCE FROM Ce ANOMALIES IN THE DEEP (GREATER THAN 600 m) PACIFIC OCEAN, 1 Abstract Only
Y.-G Liu and R. A. Schmitt *In* Lunar and Planetary Inst., Twenty-Fourth Lunar and Planetary Science Conference. Part 2: G-M 1993 p 883-884 (For primary document see N94-16173 03-91)
Avail: CASI HC A01/MF A06

N94-16360*# Oregon State Univ., Corvallis. Depts. of Chemistry and Geosciences.
EARTH'S PARTIAL PRESSURE OF CO2 OVER THE PAST 100-500 Ma; EVIDENCE FROM Ce ANOMALIES IN MOSTLY SHALLOW SEAS (LESS THAN 200 m) AS RECORDED IN CARBONATE SEDIMENTS, 2 Abstract Only
Y.-G. Liu, J. W. Reinhardt (Erlangen-Nuremberg Univ., Germany.), and R. A. Schmitt *In* Lunar and Planetary Inst., Twenty-Fourth Lunar and Planetary Science Conference. Part 2: G-M 1993 p 887-888 (For primary document see N94-16173 03-91)
Avail: CASI HC A01/MF A06

N94-16365*# Lamont-Doherty Geological Observatory, Palisades, NY.
THE MONZONORITE-ANORTHOSITE CONNECTION: THE PETROGENESIS OF TERRESTRIAL KREEP Abstract Only
J. Longhi and J. Vander Auwera (Liege Univ., Belgium.) *In* Lunar and Planetary Inst., Twenty-Fourth Lunar and Planetary Science Conference. Part 2: G-M 1993 p 897-898 (For primary document see N94-16173 03-91)
Avail: CASI HC A01/MF A06

N94-16396*# Massachusetts Inst. of Tech., Cambridge. Dept. of Earth, Atmospheric, and Planetary Sciences.
ASPECTS OF MODELLING THE TECTONICS OF LARGE VOLCANOES ON THE TERRESTRIAL PLANETS Abstract Only
Patrick J. McGovern and Sean C. Solomon (Carnegie Institution of Washington, DC.) *In* Lunar and Planetary Inst., Twenty-Fourth Lunar and Planetary Science Conference. Part 2: G-M 1993 p 959-960 (For primary document see N94-16173 03-91)
Avail: CASI HC A01/MF A06

N94-16416*# Tokyo Univ. (Japan). Mineralogical Inst.
THE THICKNESS OF EUCRITIC CRUST IN THE HED PARENT BODY Abstract Only
M. Miyamoto and H. Takeda *In* Lunar and Planetary Inst., Twenty-Fourth Lunar and Planetary Science Conference. Part 2: G-M 1993 p 999-1000 (For primary document see N94-16173 03-91)
Avail: CASI HC A01/MF A06

N94-16424*# National Aeronautics and Space Administration. Lyndon B. Johnson Space Center, Houston, TX.
TERRESTRIAL IMPACT MELTS AS ANALOGUES FOR THE HEMATIZATION OF MARTIAN SURFACE MATERIALS Abstract Only
R. V. Morris, H. V. Lauer, Jr. (Lockheed Engineering and Sciences Co., Houston, TX.), and D. C. Golden *In* Lunar and Planetary Inst., Twenty-Fourth Lunar and Planetary Science Conference. Part 2: G-M 1993 p 1015-1016 (For primary document see N94-16173 03-91)
Avail: CASI HC A01/MF A06

N94-16608*# Jet Propulsion Lab., California Inst. of Tech., Pasadena.
THE USE OF TIMS DATA TO ESTIMATE THE SO2 CONCENTRATIONS OF VOLCANIC PLUMES: A CASE STUDY AT MOUNT ETNA, SICILY
Vincent J. Realmuto *In its* Summaries of the Third Annual JPL Airborne Geoscience Workshop. Volume 2: TIMS Workshop 1 Jun. 1992 p 37-39 (For primary document see N94-16595 03-42)
Avail: CASI HC A01/MF A01

N94-16680*# Jet Propulsion Lab., California Inst. of Tech., Pasadena.
VOLCANIC THERMAL FEATURES OBSERVED BY AVIRIS
Clive Oppenheimer (Open Univ., Milton, England.), David Pieri, Veronique Carrere, Michael Abrams (Open Univ., Milton, England.), David Rothery (Open Univ., Milton, England.), and Peter Francis (Open Univ., Milton, England.) *In its* Summaries of the Third Annual JPL Airborne Geoscience Workshop. Volume 1: AVIRIS Workshop 1 Jun. 1992 p 41-43 Sponsored by Natural Environmental Research Council (For primary document see N94-16666 03-42)
Avail: CASI HC A01/MF A02

N94-16746*# Cornell Univ., Ithaca, NY. Dept. of Geological Sciences.
PRELIMINARY RESULTS OF POLARIZATION SIGNATURES FOR GLACIAL MORAINES IN THE MONO BASIN, EASTERN SIERRA NEVADA
Richard R. Forster, Andrew N. Fox, and Bryan Isacks *In* JPL, Summaries of the Third Annual JPL Airborne Geoscience Workshop. Volume 3: AIRSAR Workshop 1 Jun. 1992 p 40-42 (For primary document see N94-16731 03-42)
Avail: CASI HC A01/MF A02

N94-16747*# Arizona State Univ., Tempe. Dept. of Geology.
DETECTING SURFACE ROUGHNESS EFFECTS ON THE ATMOSPHERIC BOUNDARY LAYER VIA AIRSAR DATA: A FIELD EXPERIMENT IN DEATH VALLEY, CALIFORNIA
Dan G. Blumberg and Ronald Greeley *In* JPL, Summaries of the Third Annual JPL Airborne Geoscience Workshop. Volume 3: AIRSAR Workshop 1 Jun. 1992 p 43-45 (For primary document see N94-16731 03-42)
Avail: CASI HC A01/MF A02

N94-16762*# Jet Propulsion Lab., California Inst. of Tech., Pasadena.
LITHOLOGICAL AND TEXTURAL CONTROLS ON RADAR AND DIURNAL THERMAL SIGNATURES OF WEATHERED VOLCANIC DEPOSITS, LUNAR CRATER REGION, NEVADA
Jeffrey J. Plaut and Benoit Rivard (York Univ., Ontario.) *In its* Summaries of the Third Annual JPL Airborne Geoscience Workshop. Volume 3: AIRSAR Workshop 1 Jun. 1992 p 92-95 (For primary document see N94-16731 03-42)
Avail: CASI HC A01/MF A02

47 METEOROLOGY AND CLIMATOLOGY

Includes weather forecasting and modification.

N94-14938# Risoe National Lab., Roskilde (Denmark).
THE MADONA EXPERIMENTS (METEOROLOGY AND DIFFUSION OVER NON-UNIFORM AREAS): HIGH-RESOLUTION IN-PLUME CONCENTRATION FLUCTUATIONS MEASUREMENTS USING LIDAR REMOTE SENSING TECHNIQUE Interim Data and Analysis Report
Torben Mikkelsen, Hans E. Joergensen, Soeren Thykier-Nielsen, Soern W. Lund, and Josep M. Santabarbara 16 Apr. 1993 73 p
(Contract DAJA45-92-M-0344)
(AD-A267711; R/D-6858-EN-09) Avail: CASI HC A04/MF A01

The scientific objective for our participation in MADONA was to investigate fundamental questions regarding the statistical properties of the instantaneous concentration fluctuations in smoke plumes and puffs. The joint-venture Porton Down experiments, with international participation and support, facilitated this objective. Modeling objectives included investigation and experimental evaluation of flow and diffusion modelling based on our LINCOM/RIMPUFF real-time codes. DTIC

N94-14958# Atmospheric and Environmental Research, Inc., Cambridge, MA.
SENSITIVITY TESTING OF A SINGLE-DOPPLER TEMPERATURE RETRIEVAL AND FORECAST SYSTEM
Thomas M. Hamill and Thomas Nehrkorn 1 Feb. 1993 94 p
(Contract F19628-91-C-0011)
(AD-A267278; PL-TR-93-2071; SR-4) Avail: CASI HC A05/MF A01

Results are presented from the second year of a three-year contract to explore the feasibility of local thunderstorm forecasting based on the assimilation of single-Doppler radar data. The method used can assimilate Doppler radial winds, derive a tangential component, infer temperature distributions from the wind, and assimilate the resultant information. The underlying analysis and assimilation methodology is explained in detail. This is then followed with a set of sensitivity experiments using simulated Doppler radar data generated from a numerical model forecast. A simple 2-D experiment is first presented which confirms the benefit of temperature assimilation to complement wind data assimilation. Second, a set of 3-D model experiments is presented to test the sensitivity of the model to observational data type and error characteristics. The results suggest that forecast accuracy is relatively insensitive to the observational error, though this result is in part due to the inherent smoothing built into the objective analysis and the assumption of no biases in the wind observations. DTIC

N94-15137# Air Force Inst. of Tech., Wright-Patterson AFB, OH.
DETERMINATION OF MOMENTUM FLUX USING A BIVANE AND CUP ANEMOMETER M.S. Thesis
Thomas L. Schiano Dec. 1992 219 p
(AD-A265414; AFIT/CI/CIA-92-119) Avail: CASI HC A10/MF A03

The ability of a bivane and cup anemometer system to provide data that can be used to determine momentum flux is examined for conditions in the near-surface boundary layer. Use of a bivane for such a purpose was first proposed by Chimonas, who suggested a method for obtaining an approximation of the flux magnitude from time-mean values of angular deflection and horizontal wind speed. Both the approximation proposed by Chimonas and an accepted statistical method (covariance of wind components, u'w') are examined. A three-axis sonic anemometer was used to obtain the reference values of u'w'. The evaluated system consisted of a three-cup anemometer for determination of the horizontal wind vector, and a dual annulus bivane, used to determine the elevation (vertical) angle of the wind vector. In three field tests under various degrees of stability, the instruments were suspended from an instrumented tower on a boom oriented relative to the prevailing horizontal wind flow. Output voltages from the instrumentation were collected and subsequently converted to the desired components through the use of empirically-derived transfer functions. Examination of data reveals high degrees of correlation between the patterns and magnitudes of the components derived from the bivane/three-cup anemometer system as compared to those measured with the sonic anemometer. Computations of momentum flux yielded comparable values between the two systems. Based on these results, conclusions are presented concerning the validity of the different methods of estimating momentum flux. Author

N94-15142# Massachusetts Univ., Lowell.
SHORT TERM WEATHER FORECASTING IN REAL TIME IN A BASE WEATHER STATION SETTING
Frank P. Colby, Jr. and Keith L. Seitter Oct. 1992 21 p
(Contract F19628-91-K-0040)
(AD-A266872; AD-E201472; TR-92-2341; SR-1) Avail: CASI HC A03/MF A01

Starting with computer code for a research model developed by Seitter and Colby (1992), initial steps were taken to make the model a real-time forecasting tool. Several procedures are required to initialize and run the model from real data. The code to automate this process has been written and tested. In addition, an error condition in the interactive nesting region related to terrain has been corrected. DTIC

N94-15226* National Aeronautics and Space Administration. Marshall Space Flight Center, Huntsville, AL.
MESOSCALE LIGHTNING (Videotape)
Apr. 1989 Videotape: 2 min. 16 sec. playing time, in color, with sound
(NASA-TM-109655; NONP-VT-93-190453) Avail: CASI VHS A01/BETA A22

This video tape addresses ongoing lightning research and how data is valuable to upcoming projects. CASI

N94-15302 Deutscher Wetterdienst, Offenbach am Main (Germany).
DETERMINATION OF SUNSHINE DURATION FROM RADIATION INTENSITY PYRANOMETRIC MEASUREMENTS OF GLOBAL AND SKY RADIATION [ERMITTLUNG DER SONNENSCHEINDAUER AUS PYRANOMETRISCH GEMESSENEN BESTRAHLUNGSSTAERKEN DER GLOBAL- UND HIMMELSSTRAHLUNG]
Dietrich Sonntag and Klaus Behrens 1992 69 p In GERMAN
(Ber-181; ISBN-3-88-148273-3; ETN-93-94617) Copyright Avail: Issuing Activity (Deutscher Wetterdienst, Zentralamt, Frankfurter Str. 135, D-6050 Offenbach am Main, Germany)

On the basis of the definition of the meteorological parameter 'sunshine duration', the application in practice of sunshine duration values is discussed. Measuring methods and instruments are described taking into consideration both calorimetric and photometric instruments. Several calorimetric measuring methods are described. The first method provides the utilization of a Sun tracked pyroheliometer: there is sunshine as soon as the direct solar irradiance exceeds 120 W/sq m. In the case of the second method, the direct solar irradiance on a horizontal surface resulting from a global and sky irradiance measured with pyranometers was determined and divided by the sine of the altitude of the Sun. The value obtained was compared with the threshold of 120 W/sq m. As the calculation of the sine of the altitude of the Sun is rather difficult, two approximation procedures are given as methods 3 and 4 utilizing the forest solar irradiance in a horizontal surface determined by pyranometric measurements as described under method 2. ESA

N94-15326* National Aeronautics and Space Administration, Washington, DC.
WIND SHEAR AND HEAVY RAIN (Videotape)
Jul. 1989 Videotape: 2 min. 56 sec. playing time, in color, with sound
(NASA-TM-109453; NONP-VT-93-190250) Avail: CASI VHS A01/BETA A22

This document looks at research on countering the effects of wind shear and heavy rain situations on flight stability. CASI

N94-15430* National Aeronautics and Space Administration. Ames Research Center, Moffett Field, CA.
VENUS LIGHTNING (Videotape)
Jul. 1990 Videotape: 3 min. playing time, in color, with sound
(NASA-TM-109644; NONP-VT-93-190442) Avail: CASI VHS A01/BETA A22

This document presents scenes of earth lightning with dramatic sound, views of Venus clouds rotating, and diagrams of Venusian weather. CASI

N94-15480*# National Aeronautics and Space Administration. Langley Research Center, Hampton, VA.
ATLAS-2 AND UARS CORRELATIVE MEASUREMENT OPPORTUNITIES DURING SPACE SHUTTLE MISSION ON APRIL 8-17, 1993
Edwin F. Harrison, Fred M. Denn (Lockheed Engineering and Sciences

Co., Hampton, VA.), and Gary G. Gibson (Lockheed Engineering and Sciences Co., Hampton, VA.) Oct. 1993 69 p
(RTOP 618-22-31-03)
(NASA-TM-109020; NAS 1.15:109020) Avail: CASI HC A04/MF A01

The second ATmospheric Laboratory for Applications and Science (ATLAS-2) mission was flown aboard the Space Shuttle Discovery from 8-17 Apr. 1993. The nighttime launch at 0529 Greenwich Mean Time provided maximum solar occultation sunrise coverage of the northern latitudes by the Atmospheric Trace Molecule Spectroscopy instrument. The ATLAS-2 Earth-viewing instruments provided a large number of measurements which were nearly coincident with observations from experiments on the Upper Atmosphere Research Satellite (UARS). Based on instrument operating schedules during the ATLAS-2 mission, simulations were performed to determine when and where correlative measurements between ATLAS and UARS instruments occurred. Results of these orbital and instrument simulations provide valuable information for the ATLAS and UARS scientists to compare measurements between various instruments on the two satellites. Author

N94-15757 Air Force Environmental Technical Applications Center, Scott AFB, IL.
TAFVER 2 USERS MANUAL
Christopher A. Donahue May 1993 29 p Limited Reproducibility: More than 20% of this document may be affected by microfiche quality
(AD-A266850; USAFETAC/TN-93/003; AWS-TN-93/003) Avail: Issuing Activity (Defense Technical Information Center (DTIC))

TAFVER 2 is an automated quality control program designed to provide headquarters staff (at HQ USAF/XOW, HQ Air Weather Service, and the Major Command Directorates of Weather) a tool they can use to measure the quality of weather support provided by the Air Force weather community. The TAFVER 2 program, run by the USAF Environmental Technical Applications Center (USAFETAC) at Scott AFB, verifies all Terminal Aerodrome Forecasts (TAF's) issued by Air Force weather forecasters providing there are corresponding observations against which to verify them. TAFVER 2 accommodates customer-tailored output by incorporating command-unique category thresholds. This technical note tells users how the TAFVER 2 program verifies weather forecasts and explains the output statistics. Appendices provide major command verification categories and USAFETAC's weather station information databases. DTIC

N94-15851 Army Engineer Waterways Experiment Station, Vicksburg, MS. Environmental Lab.
ENVIRONMENTAL CHARACTERIZATION FOR TARGET ACQUISITION. REPORT 1: SITE DESCRIPTIONS AND MEASUREMENTS
Tommy Berry, Salvador Rivera, Jr., and Bruce Sabol Jun. 1993 198 p Limited Reproducibility: More than 20% of this document may be affected by microfiche quality
(AD-A267192; WES/TR/EL-93-9-Rept-1) Avail: CASI HC A09

Automatic/Aided Target Recognition (ATR) systems are being developed for current and next generation attack and reconnaissance helicopters. Part of the development cycle consists of testing and evaluation of these systems at field test facilities within the United States. Preliminary tests of ATR systems have demonstrated a high sensitivity to terrain and environmental conditions. Testers and analysts must therefore have an understanding of the relationship between system performance and terrain/environmental conditions to plan tests and interpret data. To develop an understanding of this relationship, the Environmental Characterization for Target Acquisition (ECTA) Program was initiated. As part of this program, visible and thermal infrared imagery, meteorological data, and terrain characterization data were systematically collected from six different United States testing sites for different times of year and times of day. This report (Report 1) describes field and laboratory procedures used to obtain this data. Analysis of these data is described in Report 2. DTIC

N94-16465# National Weather Service, Fort Worth, TX.
RADAR DIAGNOSTIC PARAMETERS AS INDICATORS OF SEVERE WEATHER IN CENTRAL FLORIDA
C. H. Paxton and J. M. Shepherd Jun. 1993 19 p See also PB92-101823 Prepared in cooperation with Florida State Univ., Tallahassee, FL.
(PB93-183507; NOAA-TM-NWS-SR-149) Avail: CASI HC A03/MF A01

Diagnostic techniques based on WSR-88D radar observations and sounding data are needed to assess severe storm potential in Florida's semi-tropical thunderstorm environment. To begin this effort, nearly 100 severe weather events involving hail 3/4 in (1.9 cm) or greater in diameter, thunderstorm wind gusts 50 kt (26 m/s) or greater, or tornadoes were examined, along with RADAP II reflectivity and VIL (Vertically Integrated Liquid) observations. RADAP II algorithms are similar to those which will be employed with the WSR-88D's. Several other parameters, including (1) cell density (VIL divided by echo top), (2) cell momentum (VIL (mass per unit area) multiplied by storm velocity produces a quantity proportional to momentum and will be referred to as momentum for the study), and (3) echo top growth rates were calculated for comparison with severe storm reports. In addition, a formula for hail detection was derived to represent processes responsible for different types of severe weather. Tornadoes are classified by the method of formation as stretched vortex, gust induced or dynamic. Severe wind gusts are classified primarily by the time of year in which they occur. Results from the study could be integrated into WSR-88D severe weather algorithms designed more specifically for the Florida environment. NTIS

N94-16493*# Washington Univ., Seattle. Coll. of Arts and Sciences.
MIDDLE ATMOSPHERIC ELECTRIC FIELDS OVER THUNDERSTORMS Final Report, 1 May 1982 - 30 Jun. 1992
Robert H. Holzworth 30 Jun. 1992 18 p
(Grant NAG5-604)
(NASA-CR-194619; NAS 1.26:194619) Avail: CASI HC A03/MF A01

This grant has supported a variety of investigations all having to do with the external electrodynamics of thunderstorms. The grant was a continuation of work begun while the PI was at the Aerospace Corporation (under NASA Grant NAS6-3109) and the general line of investigation continues today under NASA Grants NAG5-685 and NAG6-111. This report will briefly identify the subject areas of the research and associated results. The period actually covered by the grant NAG5-604 included the following analysis and flights: (1) analysis of five successful balloon flights in 1980 and 1981 (under the predecessor NASA grant) in the stratosphere over thunderstorms; (2) development and flight of the Hy-wire tethered balloon system for direct measurement of the atmospheric potential to 250 kV (this involved multiple tethered balloon flight periods from 1981 through 1986 from several locations including Wallops Island, VA, Poker Flat and Ft. Greely, AK and Holloman AFB, NM.); (3) balloon flights in the stratosphere over thunderstorms to measure vector electric fields and associated parameters in 1986 (2 flights), 1987 (4 flights), and 1988 (2 flights); and (4) rocket-borne optical lightning flash detectors on two rocket flights (1987 and 1988) (the same detector design that was used for the balloon flights listed under #3). In summary this grant supported 8 stratospheric zero-pressure balloon flights, tethered aerostat flights every year between 1982-1985, instruments on 2 rockets, and analysis of data from 6 stratospheric flights in 1980/81. Author (revised)

N94-16568 Naval Research Lab., Monterey, CA.
THE MULTIVARIATE OPTIMUM INTERPOLATION ANALYSIS OF METEOROLOGICAL DATA AT THE FLEET NUMERICAL OCEANOGRAPHY CENTER Final Report
James S. Goerss and Patricia A. Phoebus Apr. 1993 61 p Limited Reproducibility: More than 20% of this document may be affected by microfiche quality
(AD-A266459; NRL/FR/7531-92-9413; NOARL-31) Avail: CASI HC A04

The operational global database at the Fleet Numerical Oceanography Center (FNOC) is the most complete in the world. In addition to conventional radiosonde and surface data, it includes satellite-derived temperature soundings and satellite-derived wind information, along with synthetic observations in the vicinity of extratropical and tropical storms. To take full advantage of this database for improved meteorological analyses and forecasts, significant upgrades were made to the Navy Operational Global Atmospheric Prediction System (NOGAPS) at FNOC in January of 1988. These improvements included the implementation of a global spectral forecast model, a normal-mode initialization, improved data quality control, and a multivariate optimum interpolation (MVOI) analysis scheme. Since that time, the MVOI has become the centerpiece of all the Navy's meteorological data assimilation systems, providing global, regional, and local analysis capability both ashore and afloat. In a data assimilation system like NOGAPS, the 6-hour model forecast valid at the analysis time is used as the background for the analysis. The analysis, in turn, combines

information from the background with the quality-controlled observations to provide updated fields that are used to initialize the forecast model. The MVOI analysis utilizes data from all available platforms to produce analyzed fields that possess minimum error in a statistical sense, while taking into account the error properties of the model forecast used for the background fields and the error properties of the observational data used to update the background. DTIC

N94-16717*# Wisconsin Univ., Madison.
INVESTIGATION OF CLOUD PROPERTIES AND ATMOSPHERIC STABILITY WITH MODIS Semiannual Report, Jan. - Jun. 1993
Paul Menzel 1993 9 p Original contains color illustrations
(Contract NAS5-31367)
(NASA-CR-193475; NAS 1.26:193475) Avail: CASI HC A02/MF A01; 1 functional color page

The work accomplished with the MAS (MODIS Airborne Simulator) during the TOGA-COARE (Tropical Ocean Global Atmosphere - Coupled Ocean Atmosphere Response Experiment) from January through June 1993 included cloud investigations with longwave CO2 channels (out to 13.9 microns) that reconfigured spectral channels. The comparison data was used with HIRS (high resolution Infrared Radiation Sounder) data from FIRE (First ISSCP Regional Experiment), CEPEX, and SCAR (Smoke Clouds, Aerosol and Radiation) data for the development of a two layer cloud CO2 slicing algorithm and the development of multi-spectral cloud detection algorithms (specifically tri-spectral) for cloud identification. Regarding the latter, a clustering analysis was added to improve cloud identification within the scatter diagram of tri-spectral (8, 11, and 12 microns) brightness temperatures. Via the regressions of the 8 - 11 and the 11 - 12 micron brightness temperature differences versus precipitable water, the problem of clear sky identification in the scatter diagram was further addressed. Comparison of the tri-spectral technique and visible channel reflectance ratioing indicate the tri-spectral infrared method distinguishes cloud phase more consistently in mixed cloud scenes rather than single phase cloud scenes where visible ratioing performs best. CASI

N94-17029# Naval Postgraduate School, Monterey, CA.
ENSEMBLE FORECASTING TECHNIQUES IN MEDIUM-RANGE FORECASTING M.S. Thesis
Steven W. Warren Mar. 1993 126 p
(AD-A267443) Avail: CASI HC A07/MF A02

A continuing trend in numerical weather prediction (NWP) is the desire for reduced model forecast error. Developments in NWP such as advanced computing power and improved model physics and analysis methods have been successful in lowering error but are potentially limited. The regression method of ensemble forecasting is used to further reduce mean forecast error when compared to individual model forecast performances. A statistical regression scheme is utilized to achieve an optimum combination fitting of the National Meteorological Center, the European Centre for Medium-Range Weather Forecasts, and the U.S. Navy Fleet Numerical Oceanography Center forecast models. The performance of the regression model is evaluated for 72-h and 108-h prediction cycles through statistical and subjective comparisons with the individual models and an equally weighted ensemble model at the surface and at 500 hPa. The regression model is shown to produce gains through the reduction of systematic error present in the individual model forecasts. DTIC

N94-17054 Air Force Inst. of Tech., Wright-Patterson AFB, OH.
MESOSCALE FRONTOGENESIS: AN ANALYSIS OF TWO COLD FRONT CASE STUDIES M.S. Thesis
William J. Spendley, Jr. 1993 120 p Limited Reproducibility: More than 20% of this document may be affected by microfiche quality
(AD-A267950; AFIT/CI/CIA-93-037) Avail: Issuing Activity (Defense Technical Information Center (DTIC))

A comparative analysis of mesoscale-Beta frontogenesis is presented for two case studies of cold fronts that originated west of the Appalachians and moved across North Carolina during the Genesis of Atlantic Lows Experiment (GALE). The evolution of the fronts is depicted with a detailed three-dimensional analysis. The two cold fronts are compared to the classic model of fronts established by the Norwegian school. Diagnostic computations of divergence, vorticity, dynamical forces, and frontogenesis were performed. The individual contributions of shear, confluence, and diabatic terms were determined to assess their relative importance in frontogenetical forcing. The diabatic process of differential cloud shading and its thermal impact at the surface contributed significantly to the development of a zone of strong temperature gradient ahead of both wind shift lines. A more extensive cloud free area contributed to more widespread diabatic forcing in case 1 as compared to case 2. Meteograms, satellite imagery, and diagnostic computations of divergence, vorticity, and frontogenesis confirm that only the extreme eastern portion of both wind shift lines over the coastal plain and adjacent waters of North Carolina remained active and well-defined. The confluence term dominated frontogenetical forcing over this region. It is hypothesized that the pre-existing baroclinic zone over the cold Atlantic shelf waters had a pronounced influence on the regeneration of the frontal boundaries along extreme eastern North Carolina. Results of other relevant studies confirm this possibility. The dynamical force balance and parcel trajectories were computed at selected times. DTIC

N94-17102# Air Force Inst. of Tech., Wright-Patterson AFB, OH.
THE STANDARDIZED PRECIPITATION INDEX AND ITS USE IN THE WESTERN CONTIGUOUS UNITED STATES M.S. Thesis
Keith Forman 3 May 1993 124 p
(AD-A267547; AFIT/CI/CIA-93-097) Avail: CASI HC A06/MF A02

Droughts have been a concern to all sectors of the economy since the beginning of mankind. The importance of understanding, monitoring, and forecasting these dry events is of paramount concern to the world considering the population increases seen over the last few decades. There is a finite supply of water available to the world in the relatively inexpensive forms needed for drinking and to support food productions. DTIC

N94-17244# Phillips Lab., Hanscom AFB, MA.
PHILLIPS LABORATORY GLOBAL SPECTRAL NUMERICAL WEATHER PREDICTION MODEL Final Report, Oct. 1988 - Sep. 1991
Donald C. Norquist, Chien-Hsiung Yang, Sam Chang, and Douglas C. Hahn 11 Sep. 1992 166 p
(AD-A267293; AD-E201500; PL-TR-92-2225; ERP-1108) Avail: CASI HC A08/MF A02

This report documents the ten-year (1981-91) development of the Phillips Laboratory Global Spectral Model (PL GSM). Beginning with the National Meteorological Center Model of 1980, the hydrodynamics of the model were recoded and new physical parameterizations were developed for radiation, planetary boundary layer, cumulus convection, and gravity wave drag effects on the large-scale forecast fields. A sequence of tests and parameterization refinements were carried out to arrive ultimately at the current version of the PL GSM, termed PL-91. The report describes its performance with respect to that of the operational AFGWC GSM in a series of six January and June forecasts. The PL-91 version appears to produce better forecasts of virtually all parameters, producing small systematic errors and slower error growth. The model is envisioned to serve as a research tool to develop techniques for global cloud forecasting. DTIC

N94-17245 Pennsylvania State Univ., University Park.
THE USE OF THE AIR FORCE ACADEMY HIGH WIND ALERT SYSTEM IN FORECASTING MODERATE INTENSITY WIND EVENTS FOR MILITARY BASES IN THE COLORADO SPRINGS AREA M.S. Thesis
Douglas S. Clark Aug. 1993 45 p Limited Reproducibility: More than 20% of this document may be affected by microfiche quality
(AD-A267648) Avail: CASI HC A03

A study of the problem of forecasting moderate intensity wind events in the Colorado Springs area, which are operationally significant to the military bases there, was conducted over a three year period. This study centered on the use of the United States Air Force Academy High Wind Alert System, a network of automatic observing stations in the foothills of the Air Force Academy. The usefulness of the High Wind Alert System as an aid to forecasting the onset of moderate intensity events at the other bases was investigated. The results of a statistical analysis of data taken from the High Wind Alert System on a number of days during which the synoptic conditions indicated the possibility of a moderate intensity wind event are presented, with emphasis on the correlation between the output from the High Wind Alert System and the time of onset of moderate intensity winds at the concerned bases. The results of this analysis, along with the possible empirical forecasting rules they suggest, are explained. DTIC

N94-17247# Air Force Inst. of Tech., Wright-Patterson AFB, OH.
OROGRAPHIC MICROBURSTS IN A SEVERE WINTER WINDSTORM M.S. Thesis
Zena A. Tucker 1993 49 p
(AD-A267651; AFIT/CI/CIA-93-019) Avail: CASI HC A03/MF A01

Orographic microbursts in a remarkable winter wind storm caused severe damage to the San Juan Islands and coastal regions of Washington State on 28 Dec. 1990. The microbursts, associated with trapped lee mountain waves, produced winds in excess of 50 m/s on Guemes Island. The damage patterns of the tree fall and debris reveal small scale swaths and pockets of high winds similar to those patterns caused by convective downbursts. Analysis of large scale features reveal that an underlying cause of the strong winds was a strong pressure gradient behind an arctic front. The strong pressure gradient was due to cold air damming on the eastern slopes of the Canadian Coast and Cascade Mountains. Gap wind acceleration was noted over Puget Sound by the sharp boundary between the high speed jet of dry air emanating from the Fraser River Valley, a gap between the Coast and Cascade Mountains, and the ambient lower speed marine winds. DTIC

N94-17267# Atmospheric and Environmental Research, Inc., Cambridge, MA.
NOWCASTING METHODS FOR SATELLITE IMAGERY
Thomas Nehrkorn, Thomas C. Hamill, and Lawrence W. Knowlton 27 May 1993 122 p
(Contract F19628-92-C-0014)
(AD-A267294; PL-TR-93-2021; SR-1) Avail: CASI HC A06/MF A02

This report documents the development and testing of nowcasting methods for satellite imagery. Techniques for identifying, tracking, and forecasting features of interest through contours of brightness temperature in geostationary IR imagery were evaluated in a study covering over 200 features from all four seasons. Results indicate that because contours frequently split, merge, or dissipate, contour based techniques are successful in only a minority of cases. The most skillful contour extrapolation technique is movable persistence, which simply extrapolates the position of the contour based on the past movement of its centroid position. Its verification scores are significantly better than persistence for forecasts from 1/2 to 3 hours in advance. As an alternative to the contour-based schemes, a cross-correlation technique for predicting short-term changes in pixel grayshade values (brightness temperatures) was developed and tested. Pixel-based verification of the cross-correlation forecasts show an improvement over persistence out to 2 1/2 hours (the longest time period studied for this technique). Contour forecasts derived from cross-correlation are significantly more skillful than those of the best contour extrapolation technique (movable persistence) out to 1 hour and no worse out to 2 1/2 hours. DTIC

N94-17283*# National Aeronautics and Space Administration. Langley Research Center, Hampton, VA.
WINDSHEAR DATABASE FOR FORWARD-LOOKING SYSTEMS CERTIFICATION
G. F. Switzer (Research Triangle Inst., Research Triangle Park, NC.), F. H. Proctor, D. A. Hinton, and J. V. Aanstoos (Research Triangle Inst., Research Triangle Park, NC.) Nov. 1993 128 p
(RTOP 505-64-12-01)
(NASA-TM-109012; NAS 1.15:109012) Avail: CASI HC A07/MF A02

This document contains a description of a comprehensive database that is to be used for certification testing of airborne forward-look windshear detection systems. The database was developed by NASA Langley Research Center, at the request of the Federal Aviation Administration (FAA), to support the industry initiative to certify and produce forward-look windshear detection equipment. The database contains high resolution, three dimensional fields for meteorological variables that may be sensed by forward-looking systems. The database is made up of seven case studies which have been generated by the Terminal Area Simulation System, a state-of-the-art numerical system for the realistic modeling of windshear phenomena. The selected cases represent a wide spectrum of windshear events. General descriptions and figures from each of the case studies are included, as well as equations for F-factor, radar-reflectivity factor, and rainfall rate. The document also describes scenarios and paths through the data sets, jointly developed by NASA and the FAA, to meet FAA certification testing objectives. Instructions for reading and verifying the data from tape are included. Author

N94-17303# Air Force Inst. of Tech., Wright-Patterson AFB, OH.
VALIDATION AND ANALYSIS OF MICROWAVE-DERIVED RAINFALL OVER THE TROPICS M.S. Thesis
Robert P. Fleishauer 1993 89 p
(AD-A267785; AFIT/CI/CIA-93-020) Avail: CASI HC A05/MF A01

A recently developed single channel microwave rain rate retrieval algorithm exists to measure global precipitation over the data-sparse tropical oceans. The objective of this study is to retrieve and validate rainfall using this algorithm, followed by an analysis of the derived rainfall fields. Retrieval consists of applying the algorithm technique to the extraction of four years worth of achieved data from the Electrically Scanning Microwave Radiometer (ESMR) instrument flown aboard the NIMBUS 5 satellite. The Pacific Atoll Raingage Data Set is chosen as a ground truth measure to validate the ESMR-Derived rainfall data against, comparing slope, intercept and correlation between 5 deg x 5 deg area average. Despite limitations imposed by the comparison of point measurements to area-averaged rainfall, results show a 0.80 correlation. Monthly and quarterly climatological mean rainfall estimates are produced, with a consequent analysis of prominent signals, especially in the Intertropical Convergence Zone (ITCZ), South Pacific Convergence Zone (SPCZ) and the Indian monsoon. Latent heat flux is computed, using the ESMR-derived rainfall, and plotted to show qualitatively where seasonal latent thermodynamic energy sources and sinks exist in the atmosphere. A comparison of the summer and winter quarterly composites of the above products with previously compiled climatologies and Outgoing Longwave Radiation (OLR) showed only minor discrepancies in location and intensity, which are discussed in some detail. DTIC

N94-17459 Air Force Inst. of Tech., Wright-Patterson AFB, OH.
A COMPARISON OF CEILING AND VISIBILITY OBSERVATION FOR NWS MANNED OBSERVATION SITES AND ASOS SITES M.S. Thesis
Jon C. Cornick May 1993 80 p Limited Reproducibility: More than 20% of this document may be affected by microfiche quality
(AD-A268356; AFIT/CI/CIA-93-022) Avail: CASI HC A05

The National Weather Service modernization program involves, among other things, a shift from manned weather observation to automated, unmanned instrument sensing. The Automated Surface Observing System (ASOS) is the device that will replace the conventional manned weather observation in use today. ASOS observations of ceiling and visibility were compared to the standard manual observations at 16 sites having at least four months of overlap data. The 16 sites were located in the central plains states of Colorado, Nebraska, Missouri, Kansas, Oklahoma, and Texas. The period of study was confined to the precommissioning period of the sites when both conventional data and ASOS data were available. The study spans from mid September of 1991 to late July 1992, with the greatest amount of data collected between February and June 1992. The overall results show that ASOS ceiling reports were within 1000 ft of conventional ceiling reports 92.7% of the time. Similarly, ASOS derived visibility was within one reportable category of conventionally derived visibility 93.7% of the time. These percentages were determined from a data base composed of approximately 64,000 observations. DTIC

N94-17465 Naval Postgraduate School, Monterey, CA.
ARCTIC CYCLONES AND MARGINAL ICE ZONE (MIZ) VARIABILITY M.S. Thesis
John Rutherford Mar. 1993 87 p Limited Reproducibility: More than 20% of this document may be affected by microfiche quality
(AD-A268610) Avail: CASI HC A05

The Seasonal Ice Zone Experiment (SIZEX), conducted in January 1992, was designed as the European Space Agency's ERS-1 synthetic-aperture radar (SAR) validation experiment. The satellite was placed in a three day exact repeat orbit, with ascending and descending passes which crossed the Greenland Sea marginal ice zone. In conjunction with SAR imagery collected by the Nansen Environmental and Remote Sensing Center, the research vessel Hakon Mosby recorded meteorological data on station near the ice edge. The marginal ice zone was subjected to atmospheric and oceanographic forcing during the 7-16 January period which resulted in significant changes in ice edge morphology. As intense low pressure systems propagated across the Greenland Sea, strong easterly and northerly winds dominated oceanographic forcing and created a compact

ice edge which correlated with the 50% ice concentration isopleth from the SSM/I passive microwave sensor. Conversely, during periods of weak atmospheric forcing, the ice edge became diffuse and the ice edge morphology was determined by a variety of oceanic circulations. In this instance the actual ice edge position was well correlated with a 30% concentration isopleth. DTIC

N94-17492# Air Force Inst. of Tech., Wright-Patterson AFB, OH.
OPPOSING MESOSCALE FLOWS IN A BROKEN MIDLATITUDE SQUALL LINE M.S. Thesis
Barbara D. Miner 1993 126 p
(AD-A268011; AFIT/CI/CIA-93-012) Avail: CASI HC A07/MF A02

During the period 14-15 June 1985 a broken line of convection with one primary gap (echo-free) region developed along a cold front passing through the Oklahoma-Kansas Preliminary Regional Experiment for STORM-Central (OK PRESTORM) domain. Radar and satellite data are presented to provide an overview of the life cycle of the line. Observations from the OK PRESTORM mesonetwork and upper air soundings are used to document the occurrence of the gap and an associated surface mesolow. The convective line initially developed as two mesoscale convective systems (MCS's), one in northeast Kansas, the other in the Texas panhandle, along a weak cold front. As the two MCS's matured, convection developed between the two similar to the broken-line squall line formation described by Bluestein and Jain (1985). Despite strong low-level convergence and strong moisture convergence, an echo-free region remained between the two MCS's throughout the life cycle of the line. DTIC

N94-17522# Air Force Inst. of Tech., Wright-Patterson AFB, OH.
PROPAGATION CHARACTERISTICS OF MESOSCALE CONVECTIVE SYSTEMS M.S. Thesis
Charles H. Pappas 1993 99 p
(AD-A268130; AFIT/CI/CIA-93-021) Avail: CASI HC A05/MF A02

Case studies were undertaken of mesoscale convective systems (MCS) on an individual storm basis to examine factors influencing MCS propagation characteristics. This was done by examining numerous specific storms during a portion of the warm seasons (June-September) of 1990 through 1992. Three cases were presented in detail to illustrate the types of propagation typically exhibited by mesoscale convective systems. This research attempts to analyze why MCS's exhibit a particular type of propagation and if that propagation can be accurately predicted by forecasters on an operation basis. Parameters such as moisture convergence, surface boundaries (fronts, dry lines, etc), Convective Available Potential Energy (CAPE), equivalent potential temperature, vertical wind shear, and others were used in the diagnosis of a particular region where a storm grew and propagated toward. DTIC

N94-17525*# Simpson Weather Associates, Inc., Charlottesville, VA.
EOS LASER ATMOSPHERE WIND SOUNDER (LAWS) INVESTIGATION Final Report, 24 Jan. - 14 Dec. 1990
George D. Emmitt 11 Mar. 1991 40 p
(Contract NAS5-30751)
(NASA-CR-193445; NAS 1.26:193445) Avail: CASI HC A03/MF A01

The related activities of the contract are outlined for the first year. These include: (1) attend team member meetings; (2) support EOS Project with science related activities; (3) prepare and Execution Phase plan; and (4) support LAWS and EOSDIS related work. Attached to the report is an appendix, 'LAWS Algorithm Development and Evaluation Laboratory (LADEL)'. Also attached is a copy of a proposal to the NASA EOS for 'LAWS Sampling Strategies and Wind Computation Algorithms -- Storm-Top Divergence Studies. Volume I: Investigation and Technical Plan, Data Plan, Computer Facilities Plan, Management Plan.' CASI

N94-17552# Air Force Inst. of Tech., Wright-Patterson AFB, OH.
FURTHER DEVELOPMENT AND TESTING OF A SECOND-ORDER BULK BOUNDARY LAYER MODEL M.S. Thesis
Richard D. Krasner 3 May 1993 134 p
(AD-A268071; AFIT/CI/CIA-93-018) Avail: CASI HC A07/MF A02

A one-layer bulk boundary layer model is developed. The model predicts the mixed layer values of the potential temperature, mixing ratio, and u- and v-momentum. The model also predicts the depth of the boundary layer and the vertically integrated turbulence kinetic energy (TKE). The TKE is determined using a second-order closure that relates the rate of dissipation to the TKE. The fractional area covered by rising motion sigma and the entrainment rate (E) are diagnostically determined. The model is used to study the clear convective boundary layer (CBL) using data from the Wangara, Australia boundary layer experiment. The Wangara data is also used as an observation base to validate model results. A further study is accomplished by simulating the planetary boundary layer (PBL) over an ocean surface. This study is designed to find the steady-state solutions of the prognostic variable. DTIC

N94-17571# Air Force Inst. of Tech., Wright-Patterson AFB, OH.
FORECASTING THE DUCTING OF ELECTROMAGNETIC WAVES ON THE MESOSCALE M.S. Thesis
Scott P. Simcox Aug. 1993 85 p
(AD-A268101; AFIT/CI/CIA-93-122) Avail: CASI HC A05/MF A01

Ducting of electromagnetic waves in the lower troposphere can have a significant impact on radar coverage. However, despite the importance of identifying ducting conditions, operational forecasts of these conditions are still based on a primitive, single-station approach. Single-Station ducting analyses are available operationally through the Navy's Integrated Refractive Effects Prediction System (IREPS) software. This software can provide a satisfactory point analysis of ducting conditions, but significant spatial and temporal variations of ducting in the atmosphere can also seriously limit the utility of the output. By combining IREPS with mesoscale model output, however, there is the opportunity for significant improvement in the predictability of ducting conditions. Subsidence inversions are a primary cause of atmospheric ducting. These inversions are common during the summer season over the west coast of the United States, particularly west-central California. Fortunately, they can be effectively modeled because they are generally very strong and quite persistent. In this thesis, a study of the predictability of inversion-generated ducting conditions over west-central California is conducted by combining output from the Penn State/NCAR non-hydrostatic mesoscale modeling system (MM5) with the IREPS ducting analysis software. DTIC

N94-17572# Air Force Inst. of Tech., Wright-Patterson AFB, OH.
THREE DIMENSIONAL VISUALIZATION OF GOES CLOUD DATA USING OCTRESS M.S. Thesis
Bruce H. VanAartsen Jun. 1993 86 p
(AD-A268102; AFIT/CI/CIA-93-119) Avail: CASI HC A05/MF A01

Geostationary Operational Environmental Satellite (GOES) imagery is commonly displayed in a two-dimensional format. This is adequate to portray areas as being simply cloudy or clear, but often more information is desired. A three-dimensional display could be helpful in analyzing the information, and could improve understanding of the atmospheric conditions. Many three-dimensional visualization packages model just the smoothed object surfaces. While this may be aesthetically pleasing, it does not effectively represent volumetric data, and the smoothed surfaces may compromise data integrity. This thesis presents octree encoding as a structure that can effectively represent volumetric data with the added benefits of data compression and acceleration of volume rendering. The fundamentals of octree encoding are introduced, along with strengths and weaknesses, and which data sets are better suited to octree compression. To demonstrate the capabilities of octree encoding of cloud data, GOES imagery was gathered over Central America for the month of December 1990, and a program called VOXEL (VOlumetric piXEL) was utilized for octree encoding and three-dimensional visualization. VOXEL displays are shown to illustrate the greater visual impact of three-dimensional vs. two-dimensional data. VOXEL is also used to demonstrate how two-dimensional cloud climatologies are overlaid to create a three-dimensional array, which can then be rotated, sliced, or thresholded as desired. DTIC

N94-17573# Air Force Inst. of Tech., Wright-Patterson AFB, OH.
AN ANALYSIS OF SIMULATED AND ACTUAL DMSP SSM/T-2 BRIGHTNESS TEMPERATURES M.S. Thesis
Frank A. Leute, IV May 1993 213 p
(AD-A268103; AFIT/CI/CIA-93-016) Avail: CASI HC A10/MF A03

Defense Meteorological Satellite Program (DMSP) Special Sensor Microwave/T-2 (SSM/T-2 or T-2) global brightness temperature maps are related to some of the known observed general circulation features of the atmosphere and surface characteristics of Earth. The brightness temperatures from two regions with different large scale circulations are compared and contrasted. The concept of the invariance of the weighting

functions with respect to water vapor overburden is tested. It is demonstrated that the levels where the 183 + or - 1 and 3 GHz brightness temperatures match the thermodynamic temperature are levels of approximately equal overburden. Water vapor overburden (integrated water vapor above a given level) was retrieved and mapped on a constant pressure surface from T-2 brightness temperatures and atmospheric temperature-pressure data. A simple physical retrieval scheme based on the approximately equal overburden, irrespective of the moisture profile, for the 183 + or - 1 GHz frequency was developed and demonstrated. This simple retrieval could be used to initialize more sophisticated retrievals. DTIC

N94-17593 Stockholm Univ. (Sweden). Dept. of Meteorology.
A TWO-LAYER QUASI-GEOTROPHIC SPHERICAL MODEL: FORMULATION AND CLIMATOLOGY
Shuting Yang 22 Apr. 1993 39 p Prepared in cooperation with International Meteorologicl Inst., Stockholm, Sweden Limited Reproducibility: More than 20% of this document may be affected by microfiche quality
(DM-63; ETN-93-94629) Avail: CASI HC A03

A two layer, quasi-geostrophic spherical model is developed for the purpose of studying weather regimes. The model can successfully reproduce a realistic zonal mean structure and a large scale energy spectrum. The geographical distribution of the model climatology and the time variability is reasonable. The location relation of the maximum low frequency variability and the maximum baroclinic activity also resembles observations, although the baroclinic activity is underestimated by the model. Weather regime events can be identified in the simulated circulations in terms of localized persistent anomalies. The transitions to the regime events are not as persistent as in the atmosphere. These features of the model suggest that the model can be used for understanding the internal dynamical processes of weather regime phenomena in the atmosphere. ESA

N94-17595# Air Force Inst. of Tech., Wright-Patterson AFB, OH.
AN EMPIRICAL STUDY OF TROPICAL CLOUD CLUSTERS USING SPECIAL SENSOR MICROWAVE IMAGER DATA M.S. Thesis
Mark P. Weadon Aug. 1993 100 p
(AD-A268072; AFIT/CI/CIA-93-120) Avail: CASI HC A05/MF A02

Fifteen cases of Tropical Cloud Clusters (TCC's) in the western Pacific were analyzed using infrared satellite imagery and microwave satellite data from the Special Sensor Microwave Imager (SSM/I). Microwave data yielded atmospheric parameters of integrated water vapor, liquid water path, ice water path, and surface rainrate. Analyzed fields of SSM/I-derived parameters were then compared with each other and with infrared blackbody cloud top temperatures of TCC's in various stages of development. It was found that TCC's form preferentially in regions of elevated integrated water vapor. It is hypothesized that this extremely humid pre-storm environment signals large scale ascent, contributing to favorable conditions for tropical convection. Areas of surface precipitation retrieved from SSM/I were found, in general, to correlate to infrared cloud top temperatures of less than -65 C, though the coldest cloud tops did not necessarily coincide with the heaviest rain. It was found that the microwave signature of a TCC changes over the course of its life cycle, from a balance of liquid water emission and ice scattering in the intensifying and mature phases, to a predominance of liquid water emission over ice scattering in the dissipating phase. DTIC

N94-17607# Texas A&M Univ., College Station.
THE CENTRAL AMERICAN COLD SURGE: AN OBSERVATIONAL ANALYSIS OF THE DEEP SOUTHWARD PENETRATION OF NORTH AMERICAN COLD FRONTS M.S. Thesis
Philip J. Reding Dec. 1992 191 p
(AD-A268592) Avail: CASI HC A09/MF A02

The occurrence and structure of the Central American Cold Surge (CACS) is quantified using surface and upper air observations, GOES satellite imagery and satellite estimates of total precipitable water (TPW) and rain rate. A quantitative CACS definition, similar to established East Asian Cold Surge definitions, is developed and used to construct an eleven winter season climatology of CACS frequency and relative strength. Central America experiences between 11 and 21 CACS events each winter season, with a winter season average of 16 events. GOES imagery is analyzed to quantify the duration and southward penetration of CACS events. Each cold surge typically affects Central America for 3 to 6 days, but may persist for up to 13 days. The mean CACS southward penetration ranges from 12 deg N to 14 deg N, while the maximum southward penetration is approximately 7 deg N. Over 76% of CACS events penetrate south of 15 deg N and over 26% penetrate south of 10 deg N. CACS onset characteristics are described from Belize City, Belize surface observations. A wind shift to the north, a sharp rise in sea level pressure, and an increase in low-level cloud cover are the best cold surge indicators. CACS events contribute from 70% to 90% of the winter season precipitation across Central America. Temporal cross sections of upper air data are constructed to quantify the vertical structural characteristics of the pre- and post-CACS atmosphere. The most common feature is an increase in the depth of the moist layer after frontal passage. TPW and rain rate are estimated from satellite microwave observations. DTIC

N94-17673# Argonne National Lab., IL.
BOUNDARY LAYER STRUCTURE OVER AREAS OF HETEROGENEOUS HEAT FLUXES
J. C. Doran (Pacific Northwest Lab., Richland, WA.), F. J. Barnes (Los Alamos National Lab., NM.), R. L. Coulter, and T. L. Crawford (National Oceanic and Atmospheric Administration, Oak Ridge, TN.) 1993 6 p Presented at the 73rd American Meteorological Society (AMS) Annual Meeting, Anaheim, CA, 17-22 Jan. 1993
(Contracts W-31-109-eng-38; W-7405-eng-36; DE-AC06-76RL-01830)
(DE93-010657; ANL/ER/CP-79191; CONF-930133-11) Avail: CASI HC A02/MF A01

In general circulation models (GCM's), some properties of a grid element are necessarily considered homogeneous. That is, for each grid volume there is associated a particular combination of boundary layer depth, vertical profiles of wind and temperature, surface fluxes of sensible and latent heat, etc. In reality, all of these quantities may exhibit significant spatial variations within the grid area, and the larger the area the greater the likely variations. In balancing the benefits of higher resolution against increased computational time and expense, it is useful to consider what the consequences of such subgrid-scale variability may be. Moreover, in interpreting the results of a simulation, one must be able to define an appropriate average value over a grid. There are two aspects of this latter problem: (1) in observations, how does one take a set of discrete or volume-averaged measurements and relate these to properties of the entire domain?, and (2) in computations, how can subgrid-scale features be accounted for in the model parameterizations? To address these and related issues, two field campaigns were carried out near Boardman, Oregon, in June 1991 and 1992. These campaigns were designed to measure the surface fluxes of latent and sensible heat over adjacent areas with strongly contrasting surface types and to measure the response of the boundary layer to those fluxes. This paper discusses some initial findings from those campaigns. DOE

N94-15906*# National Aeronautics and Space Administration, Washington, DC.
SOME THOUGHTS ON FUTURE RAIN MAPPING MISSIONS (TRMM FOLLOW-ON)
John S. Theon *In* JPL, Proceedings of the Third Spaceborne Imaging Radar Symposium 28 May 1993 p 291-296 (For primary document see N94-15886 03-32)
Avail: CASI HC A02/MF A04

N94-16030*# Princeton Univ., NJ.
HETEROGENEITY AND SCALING LAND-ATMOSPHERIC WATER AND ENERGY FLUXES IN CLIMATE SYSTEMS
Eric F. Wood *In its* Research into the Influence of Spatial Variability and Scale on the Parameterization of Hydrological Processes 1993 50 p Presented at the IHP/IAHS George Kovacs Colloquium on Space and Time Variability and Interdependencies in Various Hydrological Processes, Paris, France, 3-4 Jul. 1992 (For primary document see N94-16026 03-43)
(Grants NAG5-899)
Avail: CASI HC A03/MF A03

N94-16671*# South Dakota School of Mines and Technology, Rapid City. Inst. of Atmospheric Sciences.
SPATIAL RESOLUTION AND CLOUD OPTICAL THICKNESS RETRIEVALS
Rand E. Feind, Sundar A. Christopher, and Ronald M. Welch *In* JPL, Summaries of the Third Annual JPL Airborne Geoscience Workshop. Volume

1: AVIRIS Workshop 1 Jun. 1992 p 14-16 (For primary document see N94-16666 03-42)
(Contracts NAS5-30958; NAS5-30768; NAS5-31718)
Avail: CASI HC A01/MF A02

N94-16699*# Colorado Univ., Boulder. Center for the Study of Earth from Space.
SEPARATION OF CIRRUS CLOUD FROM CLEAR SURFACE FROM AVIRIS DATA USING THE 1.38 MICRON WATER VAPOR BAND
Bo-Cai Gao and Alexander F. H. Goetz *In* JPL, Summaries of the Third Annual JPL Airborne Geoscience Workshop. Volume 1: AVIRIS Workshop 1 Jun. 1992 p 98-100 (For primary document see N94-16666 03-42)
(Contract NAS5-30552)
Avail: CASI HC A01/MF A02

48 OCEANOGRAPHY

Includes biological, dynamic, and physical oceanography; and marine resources.

For related information see also *43 Earth Resources and Remote Sensing.*

N94-14947# Scripps Institution of Oceanography, La Jolla, CA. Inst. of Geophysics and Planet Ary Physics.
LFASE REPORT: CRUSTAL STUDY Final Report, 1 Oct. 1988 - 31 Mar. 1991
Liliya V. Posiolova and John A. Orcutt 12 Jul. 1993 37 p
(Contract N00014-89-C-0064)
(AD-A266893) Avail: CASI HC A03/MF A01

The data set described was collected on 150-154 Ma oceanic crust during the DARPA/Navy Low Frequency Acoustic Seismic Experiment (LFASE). This is some of the oldest lithosphere remaining in the modern oceans. The experiment used an array of airguns as a source and ocean bottom seismographs (OBS) and a borehole array as receivers. Our final model of the seismic structure of oceanic crust at the LFASE site was obtained using travel times along with general characteristics of amplitudes and waveforms of the crustal P-wave arrivals. The results of the LFASE seismic data interpretation are discussed and our results are compared to those of Purdy for 140 Ma lithosphere. DTIC

N94-15134# Quadrant Engineering, Inc., Amherst, MA.
FINE SCALE MEASUREMENTS OF MICROWAVE BACKSCATTER FROM THE OCEAN SURFACE
James B. Mead 13 May 1993 40 p
(Contract N00014-91-C-0138)
(AD-A264516) Avail: CASI HC A03/MF A01

This report summarizes work performed under an ONR contract entitled 'Fine Scale Measurements of Microwave Backscatter from the Ocean Surface'. During this Phase 2 SBIR project we built a new-concept Focused Phased Array Imaging Radar (FOPAIR) system capable of producing very fine scale (approximately 1m x 1m) radar cross-section and radial velocity images of the ocean surface. Phase 2 work began in July of 1991 and within 20 months we had completed preliminary tests of the entire FOPAIR system from a roof top site in Amherst, MA. On 5 May 1993 we brought the FOPAIR system to North Truro, MA, where we demonstrated the system's ability to image ocean surface waves at ranges up to 500 m. Following submission of this report, Quadrant will deliver FOPAIR to the University of Massachusetts Microwave Remote Sensing Laboratory. FOPAIR will be used initially to study scattering from breaking waves and will participate in the upcoming Marine Boundary Layer Accelerated Research Initiative (MBL-ARI). Author

N94-15139# Oregon State Univ., Corvallis.
ARCTIC INTERNAL WAVES (CEAREX) Final Report
Murray Levine and Clayton Paulson 1993 1 p
(Contract N00014-90-J-1036)
(AD-A265822) Avail: CASI HC A01/MF A01

We successfully deployed a horizontal and vertical array of instruments beneath the Arctic pack ice during the Coordinated Eastern Arctic Experiment (CEAREX). The measurements were made near 83 deg N and 5 to 11 deg E at the 'C' Camp during Mar.-Apr. 1989. A variety of sensors were deployed: 7 current meters, 11 temperature sensors, 9 conductivity sensors, 5 temperature-conductivity recorders, and 1 acoustic Doppler profiler. The measurements were made between the surface and 250 m depth; horizontal separations ranged from 75 to 500 m. The drifting ice camp permitted us to observe the upper ocean internal wave in a variety of different background conditions including: quiescent deep water, strong diurnal oscillations, and an eddy. Spectra and coherences of the velocity and temperature time series show that the internal wave field varies significantly with the background. In the quiescent period over deep water internal wave energy was the lowest observed during CEAREX--about one-half of the mid-ocean value given by the Garrett-Munk model (GM). As the camp drifted over the slope of the Yemak Plateau, strong diurnal oscillations were observed. The energy in the high-frequency internal wave field also increased--to about three times the GM level. Near the end of the experiment the camp drifted over an eddy; internal wave energy dropped. Author

N94-15186# Instituto de Pesquisas Espaciais, Sao Jose dos Campos (Brazil).
IAI TOPIC: EL NINO. SOUTHERN OSCILLATION AND INTERANNUAL CLIMATE VARIABILITY
Antonio Divino Moura and Vernon Edgard Kousky 1992 21 p Presented at the Scientific Experts Meeting of the Inter-American Inst. for Global Change Research, Washington, DC, 5-6 Mar. 1992
(INPE-5410-PRE/1757) Avail: CASI HC A03/MF A01

Observational, modeling and theoretical work by scientists all over the world, especially during the last decade, has lead to an understanding that the abnormal warming of the Pacific Ocean is intimately related to a consistent pattern of climate anomalies throughout the tropics and many parts of the globe. The climatic disasters of 1982-83 are an extreme example of an irregular but recurring pattern known as the warm episode phase of the El Nino-Southern Oscillation (ENSO) cycle. ENSO is an irregular cycle, with extremes of variable amplitude recurring at intervals of 3 to 7 years. The impact of ENSO warm episodes is such that warmer than normal winters are expected in northwestern United States and southeastern Canada, due to a jet stream split, that brings warmer tropical air to the region, while flooding are likely to occur in the Gulf Coast States. Increased frequency of forest fires has been associated with the cold phases of ENSO due to low precipitation in many areas. Global Circulation Models which are incapable of properly simulating interannual time scale ocean variability in the tropical Pacific are being argued as not being well suited for longer (decadal to centennial) time scale simulation of climate change. These scientific facts added to the tremendous economic value of the climate information on these time scales for socio-economic planning, make this topic a natural choice to be included among those of relevance in the scientific agenda of the Inter-American Institute (IAI) for Global Change Research. Derived from text

N94-15281* National Aeronautics and Space Administration. Goddard Space Flight Center, Greenbelt, MD.
COASTAL ZONE COLOR SCANNER: NIMBUS 7 (Videotape)
May 1989 Videotape: 15 min. 10 sec. playing time, in color, no sound
(NASA-TM-109590; NONP-VT-93-190388) Avail: CASI VHS A01/BETA A22

This videotape is a soundless presentation showing the global ocean color for scientific purposes. The tape makes excellent B-roll for use in editing. CASI

N94-15349* National Aeronautics and Space Administration, Washington, DC.
OCEAN WAVE STUDY (Videotape)
May 1991 Videotape: 3 min. 15 sec. playing time, in color, with sound
(NASA-TM-109620; NONP-VT-93-190418) Avail: CASI VHS A01/BETA A22

An international study of waves in the Atlantic Ocean is explained. The study is to determine the effect of the waves on the transfer of energy between sea and air. CASI

N94-15529*# National Aeronautics and Space Administration. Goddard Space Flight Center, Greenbelt, MD.
SeaWIFS TECHNICAL REPORT SERIES. VOLUME 12, SeaWIFS TECHNICAL REPORT SERIES CUMULATIVE INDEX: VOLUMES 1-11
Elaine R. Firestone, ed. (General Sciences Corp., Laurel, MD.) and Stanford

B. Hooker, ed. Washington Aug. 1993 30 p
(NASA-TM-104566-Vol-12; Rept-93B00034; NAS 1.15:104566-Vol-12)
Avail: CASI HC A03/MF A01

The Sea-viewing Wide Field-of-view Sensor (SeaWiFS) is the follow-on ocean color instrument to the Coastal Zone Color Scanner (CZCS), which ceased operations in 1986, after an 8-year mission. SeaWiFS is expected to be launched in 1994, on the SeaStar satellite, being built by Orbital Sciences Corporation (OSC). The SeaWiFS Project at the National Aeronautics and Space Administration's (NASA) Goddard Space Flight Center (GSFC) has undertaken the responsibility of documenting all aspects of this mission, which is critical to the ocean color and marine science communities. This documentation, entitled the SeaWiFS Technical Report Series, is in the form of NASA Technical Memorandum Number 104566. All reports published are volumes within the series. This particular volume serves as a reference, or guidebook, to the previous 11 volumes and consists of 6 sections including: an errata, an addendum (a summary of the SeaWiFS Working Group Bio-optical Algorithm and Protocols Subgroups Workshops), an index to keywords and phrases, a list of all references cited, and lists of acronyms and symbols used. It is the editors' intention to publish a cumulative index of this type after every five volumes in the series. This will cover the topics published in all previous editions of the indices, that is, each new index will include all of the information contained in the preceding indices. Author

N94-15680*# Columbia Univ., New York, NY.
EXPLORING THE SOUTHERN OCEAN RESPONSE TO CLIMATE CHANGE Final Report
Douglas G. Martinson, David Rind (National Aeronautics and Space Administration. Goddard Inst. for Space Studies, New York, NY.), and Claire Parkinson (National Aeronautics and Space Administration. Goddard Space Flight Center, Greenbelt, MD.) 1993 3 p
(Grant NAGw-1844)
(NASA-CR-194601; NAS 1.26:194601) Avail: CASI HC A01/MF A01

The purpose of this project was to couple a regional (Southern Ocean) ocean/sea ice model to the existing Goddard Institute for Space Science (GISS) atmospheric general circulation model (GCM). This modification recognizes: the relative isolation of the Southern Ocean; the need to account, prognostically, for the significant air/sea/ice interaction through all involved components; and the advantage of translating the atmospheric lower boundary (typically the rapidly changing ocean surface) to a level that is consistent with the physical response times governing the system evolution (that is, to the base of the fast responding ocean surface layer). The deeper ocean beneath this layer varies on time scales several orders of magnitude slower than the atmosphere and surface ocean, and therefore the boundary between the upper and deep ocean represents a more reasonable fixed boundary condition. Author (revised)

N94-15701*# Colorado Univ., Boulder. Center for Astrodynamics Research.
SEA ICE MOTIONS IN THE CENTRAL ARCTIC ICE CENTRAL ARCTIC PACK ICE AS INFERRED FROM AVHRR IMAGERY Annual Progress Report
William Emery, James Maslanik, and Charles Fowler Oct. 1993 10 p
(Grant NAGw-2948)
(NASA-CR-194572; NAS 1.26:194572) Avail: CASI HC A02/MF A01

Synoptic observations of ice motion in the Arctic Basin are currently limited to those acquired by drifting buoys and, more recently, radar data from ERS-1. Buoys are not uniformly distributed throughout the Arctic, and SAR coverage is limited regionally and temporally due to the data volume, swath width, processing requirements, and power needs of the SAR. Additional ice-motion observations that can map ice responses simultaneously over large portions of the Arctic on daily to weekly time intervals are thus needed to augment the SAR and buoy data and to provide an intermediate-scale measure of ice drift suitable for climatological analyses and ice modeling. Merging the remotely-sensed ice motions with SAR, AVHRR, OLS, and SSM/I imagery permits studies of ice processes over a range of space and time scales. A medium-resolution passive microwave sensor might be ideal for this purpose, but no such satellite will be available in the near future. Combinations of existing data types are thus likely to be our best bet for generating motion fields with a coverage and resolution best suited to climate studies. Principal objectives of this project are to: (1) demonstrate whether sufficient ice features and ice motion existed within the consolidated ice pack to permit motion tracking using AVHRR imagery; (2) determine the limits imposed on AVHRR mapping by cloud cover; and (3) test the applicability of AVHRR-derived motions in studies of ice-atmosphere interactions. Derived from text

N94-15771# Mississippi State Univ., Mississippi State. Center for Air Sea Technology.
ON THE APPLICATION AND EVALUATION OF THE RELOCATABLE DIECAST OCEAN CIRCULATION MODEL IN COASTAL AND SEMI-ENCLOSED SEAS
David E. Dietrich, Dong-Shan Ko, and Lanny A. Yeske 1 Jul. 1993 71 p
(Contract N00014-92-J-4109)
(AD-A266626; CAST-TR-93-1) Avail: CASI HC A04/MF A01

To improve coastal and semi-enclosed seas modeling, a new DieCAST Ocean Model has been developed. In application to the Gulf of Mexico (GOM), this model gives remarkably similar results to that obtained from the Sandia Ocean Model System (SOMS) and at a computational speed much faster than SOMS or other ocean models presently available. The results are supported by many GOM observations including GEOSAT rms sea-surface-height anomaly data; mean thermocline and empirical orthogonal functions; the evolution of vortex pairs in the western GOM; major loop current eddy shedding period; shed eddy size, phase speed, dispersion rate and vorticity; and detailed loop current and shed eddy structure. Finally, a major advantage of DieCAST is its capability to be easily relocated to any geographical region of the globe. Preliminary applications in several regions such as the Mediterranean, South China Sea, Great Lakes, and Labrador Current are described. Author (revised)

N94-15844 Rhode Island Univ., Narragansett. Graduate School of Oceanography.
RAY TRACING ON TOPOGRAPHIC ROSSBY WAVES Summary Report
Christopher Meinen, Erik Fields, Robert Pickart, and D. R. Watts May 1993 47 p Limited Reproducibility: More than 20% of this document may be affected by microfiche quality
(Contracts N00014-92-J-4013; N00014-90-J-1568; NSF OCE-87-17144)
(AD-A267014; GSO-TR-93-1) Avail: CASI HC A03

Topographic Rossby Waves (TRW's) were identified with the largest variability in deep current meter records along the continental slope in the Mid-Atlantic Bight (MAB). Ray tracing theory is applied to TRW's using the real bottom topography of the MAB and the observed stratification. The depression relation for TRW's is derived and various wavenumber limits are discussed. A computational method for tracing the waves is presented including the necessity of smoothing the bathymetry. In the examples shown, TRW's with periods of 24-48 days generally propagate southwestward, changing their wavelengths from 400 to 100 kilometers in response to the change in bottom slope. TRW paths are shown that connect from the SYNOP Central Array near 68 deg W to the SYNOP Inlet Array near Cape Hatteras. DTIC

N94-16009# Westinghouse Savannah River Co., Aiken, SC.
COMPOSITE REFRACTION-REFLECTION STACK SECTIONS: TRACING FAULTS IN THE ATLANTIC COASTAL PLAIN SEDIMENTS
D. E. Stephenson, C. Coruh (Virginia Polytechnic Inst. and State Univ., Blacksburg.), and J. K. Costain (Virginia Polytechnic Inst. and State Univ., Blacksburg.) 1993 4 p Presented at the Annual Meeting of the Society of Exploration Geophysicists, Washington, DC, 26-30 Sep. 1993
(Contract DE-AC09-89SR-18035)
(DE93-013581; WSRC-MS-93-179; CONF-930901-4) Avail: CASI HC A01/MF A01

Seismic data from the Atlantic Coastal Plain are reprocessed and composite refraction-reflection stack sections are produced to investigate basement faults that penetrate upward into Atlantic Coastal Plain sediments in South Carolina. Reprocessing recovered reflections from within the deep crust to the Moho as well as from within thin veneer (300) of the Atlantic Coastal Plain sediments. One of the major objectives of this paper is to discuss the use of shallow refracted arrivals to construct a composite refraction-reflection stack that allows better imaging of the subsurface at shallow depths. DOE

N94-16517# Coastal Engineering Research Center, Vicksburg, MS.
OBSERVATIONS AND MODELLING OF WINDS AND WAVES DURING THE SURFACE WAVE DYNAMICS EXPERIMENT. REPORT 1: INTENSIVE OBSERVATION PERIOD IOP-1, 20-31 OCTOBER 1990
Michael J. Caruso, Hans C. Graber, Robert E. Jensen, and Mark A. Donelan Apr. 1993 200 p
(Contracts N00014-90-J-1464; N00014-92-J-1546; N00014-88-J-1028)
(AD-A266384; CERC-93-6) Avail: CASI HC A09/MF A03

This report describes the compilation of observed and modelled wind and wave parameters during the first intensive observation period (IOP-1) from October 20-31, 1990, of the Surface Wave Dynamics Experiment. The measurements include wind speeds and directions, wave heights and periods, air and sea temperatures, and atmospheric pressures from three directional wave buoys, four meteorological buoys, and several routinely operated buoys from the National Data Buoy Center (NDBC). In addition, a summary of directional wave spectra is presented for this period. The model data include examples of wind fields from six numerical weather prediction models and the corresponding wave height maps as derived from the 3G-WAM ocean wave model. Estimated surface current velocities and directions from the Harvard quasi geostrophic model are also presented for this time period. DTIC

N94-16561# Quest Integrated, Inc., Kent, WA.
FIELD OBSERVATIONS OF INFRAGRAVITY, SEA AND SWELL DIRECTIONAL SPECTRA
Joan Oltman-Shay 1992 22 p
(Contract N00014-91-C-0004)
(AD-A266439) Avail: CASI HC A03/MF A01

Infragravity, sea, and swell wavenumber-frequency (k-f) spectra from an alongshore-aligned array of bottom-mounted pressure sensors in 8 m depth (800 m offshore) are analyzed for their insight into edge wave generation mechanisms. Eight months of nearly continuous data are analyzed. Earlier analysis of infragravity k-f spectra from this site identified the presence of trapped edge waves, distinct from leaky waves at this offshore location. Here, edge wave variance is separated from other infragravity motions (leaky and bound waves) by their k-f location in the spectra. It is observed that on average edge waves account for approximately 50% of the total infragravity variance at this offshore location, and occasionally dominate with approximately 80% of the variance. Significant wave heights greater than 20 cm are observed. Correlation analysis of up- and downcoast progressive edge wave variance with sea and swell directional distributions suggest that swell waves propagating from the same directional quadrant as the edge wave are the dominant generation source; sea waves had significantly lower correlations. An order of magnitude difference in up- and downcoast progressive edge wave variance is occasionally observed and is shown to be expected from the theory of resonant excitation of edge waves through nonlinear difference interaction of swell waves incident to the beach at oblique angles to the normal. The correlation between swell and edge waves from the same directional quadrant is approximately linear and accounts for more than 90% of the up- and down coast edge wave variance over the 8 months. DTIC

N94-16588# Naval Oceanographic Office, Bay Saint Louis, MS.
OPTICAL PROPERTIES OF THE RED SEA
Christine M. Kirby, Michelle M. Parmeter, Robert A. Arnone, and R. A. Oriol May 1993 46 p
(AD-A266466; NOO-TN-03-93) Avail: CASI HC A03/MF A01

Optical properties of the Red Sea are characterized using the Coastal Zone Color Scanner (CZCS) for the period of Jan. 1979 to Dec. 1980. The ocean color imagery gathered by the CZCS is used to determine the diffuse attenuation coefficient, K, at 490 nm. The distribution of K(490) is shown to change spatially and temporally during the 2-year period. The Red Sea circulation is influenced by the monsoons which have significant effect on the surface optical properties. Optical properties of five different regions within the Red Sea are identified and statistics determined. The southern Red Sea exhibits a higher variability than the northern Red Sea. The K(490) optical properties were low during the summer months of June and July but showed a significant increase in November as a result of the onset of the Northeast monsoon. A strong interannual difference in K(490) between 1979 and 1980 is shown for the five Red Sea regions. DTIC

N94-17241# Naval Research Lab., Bay Saint Louis, MS.
DEVELOPING AUTOMATED ANALYSIS METHODS FOR SEA ICE IMAGERY: A STATUS REPORT WITH RECOMMENDATIONS Final Report
Florence M. Fetterer May 1993 43 p
(AD-A267284; NRL/FR/7240-93-9422) Avail: CASI HC A03/MF A01

The 1990's will see a rapid increase in the amount of satellite data available for the analysis and forecasting of sea ice conditions. Planning is underway to bring altimetry from the Geosat Follow-on satellite and synthetic aperture radar (SAR) imagery from the European Space Agency's Earth Remote Sensing Satellite (ERS-1), Canada's Radarsat, and Japan's Earth Resources Satellite (JERS-1) to the Navy/National Oceanic and Atmospheric Administration (NOAA) Joint Ice Center (JIC). In addition, JIC will continue to rely on visible and infrared imagery from the Advanced Very High Resolution Radiometer (AVHRR) sensor on the NOAA series of polar-orbiting satellites and passive microwave data from the Special Sensor Microwave Imager (SSM/1) onboard the Defense Meteorological Satellite Program (DMSP) satellites. JIC has relied on manual analysis of AVHRR imagery in the past. The introduction of data from new sources will require automated methods for quickly and accurately analyzing data without necessitating additional personnel. This report surveys automated analysis methods which are being explored in the sea ice research community. Recommendations are made concerning automated analysis methods which are likely candidates for development under the Remote Sensing Applications Branch's 6.2 program, followed by transition to operational use at JIC. The long-term goal of 6.2 ice work is an automated system for near-real-time analysis and forecasting of ice conditions that uses all data available at JIC. Four milestones emerge as instrumental in meeting this goal, given the present status of automated analysis research, resources, and JIC requirements. DTIC

N94-17383# Woods Hole Oceanographic Inst., MA.
ABSTRACTS OF MANUSCRIPTS SUBMITTED IN 1992 FOR PUBLICATION Abstracts Only
Alora Paul, ed. Apr. 1993 189 p
(AD-A267963; WHOI-93-11) Avail: CASI HC A09/MF A02

This volume contains the abstracts of manuscripts submitted for publication during calendar year 1992 by the staff and students of the Woods Hole Oceanographic Institution. We identify the journal of those manuscripts which are in press or have been published. The volume is intended to be informative, but not a bibliography. The abstracts are listed by title in the Table of Contents and are grouped into one of our five departments, the Marine Policy Center, the Coastal Research Center, or the student category. An author index is presented in the back to facilitate locating specific papers. DTIC

N94-17391# Woods Hole Oceanographic Inst., MA.
REAL TIME SYSTEM FOR PRACTICAL ACOUSTIC MONITORING OF GLOBAL OCEAN TEMPERATURE Quarterly Progress Report No. 1
15 Jul. 1993 54 p
(Contract MDA972-93-1-0004)
(AD-A267868) Avail: CASI HC A04/MF A01

Work completed includes the algorithms which calculate the loss for geometric and diffracted rays. An algorithm was written which does not generate extraneous eigenrays. Work on the calculation of acoustic travel times using ocean models is also on schedule. Multi-year runs of the wind driven equatorial Pacific model have been completed, allowing for the extraction of the Kelvin wave signal. Remote-forced NE Pacific (NEP) model runs have been completed for 1961-1991. Two main features appear in these calculations: (1) when realistic bottom topography is included, cyclonic eddies form on the American coast, and slowly propagate westward; and (2) Kelvin waves from El Nino events produce Rossby waves with amplitude much larger than in non-El Nino years and therefore should significantly effect acoustic travel times. Algorithms for calculating the travel time from acoustic source to receiver have been developed for great circle paths. All elements of the SSAR development are well underway. The array design (spacing and number of hydrophones) is complete, as is the optimum depth determination. DTIC

N94-17439* National Aeronautics and Space Administration, Washington, DC.
ARCTIC AND ANTARCTIC SEA ICE, 1978-1987: SATELLITE PASSIVE-MICROWAVE OBSERVATIONS AND ANALYSIS
Per Gloersen (National Aeronautics and Space Administration. Goddard Space Flight Center, Greenbelt, MD.), William J. Campbell (Geological Survey, Tacoma, WA.), Donald J. Cavalieri (National Aeronautics and Space Administration. Goddard Space Flight Center, Greenbelt, MD.), Josefino C. Comiso (National Aeronautics and Space Administration. Goddard Space Flight Center, Greenbelt, MD.), Claire L. Parkinson (National Aeronautics and Space Administration. Goddard Space Flight Center, Greenbelt, MD.), and H. Jay Zwally (National Aeronautics and Space Administration. Goddard Space Flight Center, Greenbelt, MD.) 1992 306 p Limited Reproducibility: More than 20% of this document may be affected by color photographs
Original contains color illustrations
(NASA-SP-511; NAS 1.21:511; LC-93-22329) Avail: CASI HC A14; 152 functional pages

This book contains a description and analysis of the spatial and temporal variations in the Arctic and Antarctic sea ice covers from October 26, 1978 through August 20, 1987. It is based on data collected by the Scanning Multichannel Microwave Radiometer (SMMR) onboard the NASA Nimbus 7 satellite. The 8.8-year period, together with the 4 years of the Nimbus 5 Electrically Scanning Microwave Radiometer (ESMR) observations presented in two earlier volumes, comprises a sea ice record spanning almost 15 years. Author

N94-17489# Institute of Oceanographic Sciences, Wormley (England).
CHEMICAL TRACER STUDIES AT IOSDL. 3: THE MEASUREMENT OF SILICATE, NITRATE AND PHOSPHATE IN SEAWATER
D. Smythe-Wright, R. Paylor, and S. E. Holley 1992 73 p
(IOS-302-1992; ETN-93-94565) Avail: CASI HC A04/MF A01; Inst. of Oceanographic Sciences, Deacon Library, Wormley, Godalming, Surrey GU8 5UB, England, HC

The measurement of nutrient species for chemical tracer studies at the Institute of Oceanographic Sciences Deacon Laboratory (IOSDL) is addressed. Analytical techniques for the measurement of silicate, nitrate and phosphate were developed using an autoanalyzer system. The analyses are based on the formation of colored complexes; the intensity of the color being directly proportional to the concentration of the nutrient in the sea water sample. The color is measured at specific wavelengths using photometric techniques. Details of the design and full analytical methods are given. ESA

N94-17497 Coastal Engineering Research Center, Vicksburg, MS.
PRELIMINARY ESTIMATES OF FREQUENCY-DIRECTION SPECTRA DERIVED FROM THE SAMSON PRESSURE GAGE ARRAY, NOVEMBER 1990 TO MAY 1991 Final Report
Charles E. Long and Joan M. Oltman-Shay (Quest Integrated, Inc., Kent, WA.) May 1993 94 p Limited Reproducibility: More than 20% of this document may be affected by microfiche quality
(AD-A267960; CERC-MP-93-3) Avail: Issuing Activity (Defense Technical Information Center (DTIC))

In the course of the SAMSON (Sources of Ambient Micro-Seismic Noise) experiment conducted by researchers from Scripps Institution of Oceanography at the Coastal Engineering Research Center (CERC) Field Research Facility (FRF) near Duck, NC, a two-dimensional array of 24 bottom-mounted pressure sensors was deployed near the 13-m depth contour to detect unattenuated pressure signals arising from interactions of directionally opposed wave trains. The geometry of the array was ideal for wind wave directional spectral estimation in the 0.04- to 0.24-Hz frequency band. The formal SAMSON experiment took place in October and early November 1990, but data collection continued until June 1991. Data from this post-experiment period were made available to CERC and were subsequently processed with a 360-deg Iterative Maximum Likelihood Estimation algorithm to determine the general character of the local wave field, including specifically any indications of significant seaward-propagating wind wave energy. This report contains descriptions of the SAMSON array and the type of data collected, and an estimate of error for reported reflection coefficients. It contains displays, both graphic and tabular, of relevant wind wave parameters deduced from the analysis. DTIC

N94-17503# Air Force Inst. of Tech., Wright-Patterson AFB, OH.
AN INVESTIGATION OF THE GROUND-BASED HIGH-RESOLUTION INTERFEROMETER SOUNDER (GB-HIS) IN A COSTAL MARINE ENVIRONMENT M.S. Thesis
Steven A. Rugg Dec. 1992 99 p
(AD-A268052; AFIT/CI/CIA-93-054) Avail: CASI HC A05/MF A02

Vertical temperature and moisture profiles from the Ground-Based High-Resolution Interferometer Sounder (GB-HIS) are studied for the coastal marine atmosphere. In May of 1991 and 1992, the GB-HIS instrument was operated on the Research Vessel Point Sur during a cruise off the central California coast. The ability of the GB-HIS retrieval algorithm to produce accurate temperature and moisture profiles is evaluated using Root Mean Square (RMS) difference, Bias, and Explained Variance statistics. In addition, objective analysis is performed on timesections of temperature and moisture. Temperature retrievals, on average, attained significant skill throughout the low troposphere. Moisture retrievals attained moderate skill in the lower and upper boundary layer, but no skill in the mid-boundary layer due to non-depiction of small scale moisture features. Results showed a maximum RMS temperature difference of less than 3 C and RMS dewpoint difference of less than 12 C in the low troposphere (up to 700 mb) over both cruises. Preliminary analysis of the updated retrieval algorithm is performed and further improvements are discussed. DTIC

N94-17509# Naval Research Lab., Bay Saint Louis, MS. Stennis Space Center.
REPORT DETAILING MODIFICATIONS TO THE 1/8 DEGREE GLOBAL BATHYMETRY Final Report
Wesley J. Youtsey May 1993 129 p
(AD-A268178; NRL/MR/7323-93-7023) Avail: CASI HC A07/MF A02

This report describes the modifications made to the 1/8 deg global topography used in the Navy Layered Ocean Model. The regions, which were modified, are listed, and figures are provided to show the Earth Topography 5-minute (ETOP05) global topography, the 1/8 deg global topography prior to modification, and both the smoothed and unsmoothed versions of the 1/8 deg global topography after modification. DTIC

N94-17516# Institute of Oceanographic Sciences, Wormley (England). Deacon Lab.
THE IOSDL SeaSoar HYDRAULIC UNIT Laboratory Test Report
T. J. P. Gwilliam, D. Grohmann, and R. F. Wallace 1992 37 p
(IOS-300-1992; ETN-93-94563) Avail: CASI HC A03/MF A01

A series of static and dynamic laboratory measurements taken on five IOSDL (Institute of Oceanographic Sciences Deacon Laboratory) SeaSoar hydraulic units is reported. Their operation, the test equipment and the test methods used are described. Analysis of the test results provide power efficiency and loss information for each unit. An estimate of the input on output torque requirements at peak load conditions is also included. ESA

N94-17518# Institute of Oceanographic Sciences, Wormley (England). Deacon Lab.
LIST OF THE SCIENTIFIC AND PERSONAL PAPERS OF SIR GEORGE DEACON, FRS
M. B. Deacon (Southampton Univ., England.) 1992 82 p
(IOS-301-1992; ETN-93-94564) Avail: CASI HC A05/MF A01

A list of the scientific and personal papers of Sir George Deacon which fall into two main categories, oceanographic research and scientific administration, is presented. On the scientific side are data, notes and drafts for publication from his days with the Discovery Committee onwards, together with correspondence on scientific and related topics, such as attendance at meetings, etc. Administrative papers from the period when he headed Group W and the National Institute of Oceanography include files of official correspondence, relating to work in progress and to his membership of national and international committees. The importance of the collection, taken as a whole, therefore lies as much and possibly more in its documentation of the growth of an institution and the contribution of its staff to the science of oceanography at a time when both were rapidly developing, as in its reflection of the career of an individual. ESA

N94-17555# Woods Hole Oceanographic Inst., MA.
MERIDIONAL CIRCULATION IN THE TROPICAL NORTH ATLANTIC Technical Report

Marjorie A. Friedrichs Jan. 1993 92 p
(Grants NSF OCE-91-01636; NSF OCE-87-16314)
(AD-A268222; WHOI-93-06) Avail: CASI HC A05/MF A01

A transatlantic CTD/ADCP section nominally located at 11 deg N was carried out in March 1989. In this paper relative geostrophic velocities are computed from these data via the thermal wind balance, with reference level choices based primarily on water mass distributions. A brief overview of the meridional circulation of the upper waters resulting from these analysis techniques is presented. Schematic circulation patterns of the NADW and AABW are also presented. In both the western and eastern basins these waters are characterized by cyclonic recirculation gyres. A particularly notable result of the deep western basin analysis is the negligible net flow of middle NADW. Although the horizontal circulation patterns described in this study agree well with results from many previous studies, the meridional overturning cell and net heat flux are considerably lower, while the net freshwater flux is slightly higher than previous estimates. These discrepancies may be attributed to: differences in methodologies, the increased resolution of this section, and temporal (including decadal, synoptic, and most importantly, seasonal) variability. DTIC

N94-17598# National Academy of Sciences - National Research Council, Washington, DC.
STATISTICS AND PHYSICAL OCEANOGRAPHY
1993 70 p Sponsored by ONR
(AD-A268565) Avail: CASI HC A04/MF A01

Research in oceanography has historically been pursued to better understand the oceans as, for example, avenues to exploration, routes for commerce, theaters for military operations, and components in the weather system. Today this research is also done in conjunction with studies on major issues such as global climate environmental change, and bio-diversity, among many others. Statistical techniques have always been important in the analysis of oceanographic data. With the recent introduction of oceanographic observational mechanisms that yield much larger quantities of data than ever before statistical considerations have gained even more prominence in oceanographic research contexts. Yet disciplinary distinctions have limited interactions across discipline boundaries in many national and global research areas; traditional statistics and oceanography are not exceptions. To stimulate progress in important research questions now arising at this interface, more cross-disciplinary efforts between statistics and oceanography are needed. This report is thus presented to help encourage successful collaborations between statistics and oceanography that are focused on potentially fruitful cross-disciplinary research areas. DTIC

N94-15807# Belgian Royal Observatory, Brussels. Centre de Geophysique Interne.
ON TIDAL PARAMETERS AT BRUSSELS FUNDAMENTAL STATION
B. Ducarme and M. VanRuymbeke *In its* Papers Presented at the Eleventh International Symposium on Earth Tides 1991 p 157-166
(For primary document see N94-15800 03-46)
Copyright Avail: CASI HC A02/MF A02

N94-16602*# Purdue Univ., West Lafayette, IN. Dept. of Earth and Atmospheric Sciences.
ATMOSPHERIC CORRECTIONS FOR TIMS ESTIMATED EMITTANCE
T. A. Warner and D. W. Levandowski *In* JPL, Summaries of the Third Annual JPL Airborne Geoscience Workshop. Volume 2: TIMS Workshop 1 Jun. 1992 p 19-21 (For primary document see N94-16595 03-42)
(Contract DI-BM-G1114118)
Avail: CASI HC A01/MF A01

N94-16685*# University of South Florida, Saint Petersburg. Dept. of Marine Science.
AVIRIS CALIBRATION AND APPLICATION IN COASTAL OCEANIC ENVIRONMENTS
Kendall L. Carder *In* JPL, Summaries of the Third Annual JPL Airborne Geoscience Workshop. Volume 1: AVIRIS Workshop 1 Jun. 1992 p 56-59 (For primary document see N94-16666 03-42)
Avail: CASI HC A01/MF A02

N94-16690*# Naval Research Lab., Bay Saint Louis, MS.
ATMOSPHERIC CORRECTION OF AVIRIS DATA IN OCEAN WATERS
Gregory Terrie and Robert Arnone *In* JPL, Summaries of the Third Annual JPL Airborne Geoscience Workshop. Volume 1: AVIRIS Workshop 1 Jun. 1992 p 72-74 (For primary document see N94-16666 03-42)
Avail: CASI HC A01/MF A02

N94-16744*# Delft Hydraulics Lab., Emmeloord (Netherlands).
MAPPING OF SEA BOTTOM TOPOGRAPHY
C. J. Calkoen, G. J. Wensink, and G. H. F. M. Hesselmans *In* JPL, Summaries of the Third Annual JPL Airborne Geoscience Workshop. Volume 3: AIRSAR Workshop 1 Jun. 1992 p 35-37 (For primary document see N94-16731 03-42)
Avail: CASI HC A01/MF A02

N94-16745*# Organisatie voor Toegepast Natuurwetenschappelijk Onderzoek, Delft (Netherlands). Physics and Electronics Lab.
SEA BOTTOM TOPOGRAPHY IMAGING WITH SAR
M. W. A. vanderKooij, G. J. Wensink (Delft Hydraulics Lab., Emmeloord, Netherlands.), and J. Vogelzang (Rijkswaterstaat, Delft, Netherlands.) *In* JPL, Summaries of the Third Annual JPL Airborne Geoscience Workshop. Volume 3: AIRSAR Workshop 1 Jun. 1992 p 38-39 (For primary document see N94-16731 03-42)
Avail: CASI HC A01/MF A02

N94-16759*# Jet Propulsion Lab., California Inst. of Tech., Pasadena.
MEASURING OCEAN COHERENCE TIME WITH DUAL-BASELINE INTERFEROMETRY
Richard E. Carande *In its* Summaries of the Third Annual JPL Airborne Geoscience Workshop. Volume 3: AIRSAR Workshop 1 Jun. 1992 p 81-83 Sponsored in part by DOD (For primary document see N94-16731 03-42)
Avail: CASI HC A01/MF A02

N94-16760*# INTERA Technologies Ltd., Nepean (Ontario).
SOIL CONSERVATION APPLICATIONS WITH C-BAND SAR
B. Brisco, R. J. Brown (Canada Centre for Remote Sensing, Ottawa, Ontario.), J. Naunheimer, and D. Bedard *In* JPL, Summaries of the Third Annual JPL Airborne Geoscience Workshop. Volume 3: AIRSAR Workshop 1 Jun. 1992 p 86-88 (For primary document see N94-16731 03-42)
Avail: CASI HC A01/MF A02

N94-16761*# Sheffield Univ. (England). Dept. of Applied and Computational Mathematics.
COMPARISON OF EDGES DETECTED AT DIFFERENT POLARISATIONS IN MAESTRO DATA
Ronald G. Caves, Peter J. Harley, and Shaun Quegan *In* JPL, Summaries of the Third Annual JPL Airborne Geoscience Workshop. Volume 3: AIRSAR Workshop 1 Jun. 1992 p 89-91 (For primary document see N94-16731 03-42)
Avail: CASI HC A01/MF A02

51 LIFE SCIENCES (GENERAL)

N94-14918# Naval Medical Research Inst., Bethesda, MD.
NEUROPEPTIDE-Y (NPY) INCREASES TOTAL BLOOD FLOW IN THE TAIL, AND REDUCES CUTANEOUS MICROVASCULAR BLOOD FLOW IN THE TAIL AND FOOT OF THE RAT Technical Report, 1990 - 1991
M. E. Heath and J. R. Thomas 10 Feb. 1993 22 p
(DA Proj. MR0-4120)
(AD-A266839; NMRI-93-34) Avail: CASI HC A03/MF A01

The purpose of this study was to describe the in vivo effects of neuropeptide-Y (NPY) on total blood flow (BF(sub T)) and on microvascular skin blood flow (BF(sub sk)) in appendages of a whole animal model. This study is important to understanding the medical relevance of NPY in cardiovascular physiology. The tail and foot of the rat were used as the model. BF(sub sk) and skin temperature (T(sub sk)) were measured on the foot pad and mid-way along the tail with a laser Doppler flowmeter and a 40-gauge thermocouple. BF(sub T) was measured mid-way along the tail (distal to the laser Doppler flowmeter) via venous occlusion plethysmography. NPY (16, 32, 64, and 128 microgram/kg), norepinephrine

(NE) (25, 50, 100, and 400 microgram/kg), or saline alone was administered i.v. in 300 microliter volume. NE caused marked reductions in blood flow at all three sites. The duration of the contraction was correlated with the dose. NPY caused immediate marked decreases in BF(sub sk) and significant increases in tail BF(sub T), tail blood volume, and tail T(sub sk). The magnitude and duration of the changes in BF were correlated to dose. These results indicte that some vessels in the tail are dilating in response to NPY. The most likely site of this vasodilation is the arteriovenous anastoma (AVA), which are shunts between arterioles and veins. When AVA's are open, the blood volume in the tissue increases, and the BF through the tissue increases because of the decrease in resistance, and capillary BF(sub sk) often decreases as blood follows the path of least resistance. T(sub sk) also increases when AVA's are opened. DTIC

N94-15138 Materials Research Society, Pittsburg, PA.
MATERIALS RESEARCH SOCIETY SYMPOSIUM PROCEEDINGS, VOLUME 292: BIOMOLECULAR MATERIALS
Christopher Viney, ed. (Washington Univ., Seattle.), Steven T. Case, ed. (Mississippi Univ., Jackson.), and J. H. Waite, ed. (Delaware Univ., Lewes.) 3 Dec. 1992 300 p Symposium held in Boston, MA, 1-3 Dec. 1992 Limited Reproducibility: More than 20% of this document may be affected by microfiche quality
(Contract N00014-93-1-0120)
(AD-A265776) Avail: CASI HC A13

Biological materials are naturally occurring substances produced and utilized internally or externally by living organisms. In contrast, biomolecular materials are partial, complete, or modified replicas of biological materials whose synthesis and utilization may be unrelated to their original biological source. Whether the objective is to replicate the properties of a biological material, or to produce derivatives with novel properties, the ultimate goal is to attain biomolecular materials that have industrial, medical, or agricultural applications. This symposium, held at the 1992 Fall Meeting of the Materials Research Society, brought together an interdisciplinary group of scientists (zoologists, molecular biologists, biochemists, inorganic and organic chemists, materials scientists, and mathematicians) that are directly or indirectly involved in some aspect of biomolecular materials research. The diversity of biological (Nature's) materials was amply demonstrated: cockroach elastin, mussel adhesives, trematode and avian eggshells, spider and midge silks, abalone shell, rhinoceros horn, algal pigments, a bacterial hemolytic protein, and nut shells. Descriptions of these biological systems ranged from the relatively unknown to detailed information regarding the structure, composition, processing, and physical properties of the biological material. In several instances, particularly for protein-based polymers, biomolecular materials have been obtained by cellular synthesis through biotechnology. Bacterial cells have been engineered to synthesize discrete portions of insect silk and mussle adhesive proteins, multifunctional proteins with a unique combination of multiple binding sites, and recombinant proteins with specific combinations of functional groups that lead to ordered assembly into supramolecular complexes. DTIC

N94-15235* National Aeronautics and Space Administration, Washington, DC.
PLANT RESEARCH (Videotape)
Apr. 1985 Videotape: 3 min. 14 sec. playing time, in color, with sound
(NASA-TM-109664; NONP-VT-93-190462) Avail: CASI VHS A01/BETA A22

This video presentation addresses Stennis research on the use of plants for the purification of water and air for living in space and on Earth. CASI

N94-15378* National Aeronautics and Space Administration. Lyndon B. Johnson Space Center, Houston, TX.
STS-29 CREW WITH STUDENT EXPERIMENT (Videotape)
Feb. 1989 Videotape: 15 min. playing time, in color, with sound
(NASA-TM-109545; NONP-VT-93-190342) Avail: CASI VHS A01/BETA A22

John Vellinger, student experimenter, and Mark Deuser, Kentucky Fried Chicken Sponsor, are shown explaining the Chicken Embryo experiment to the crew. CASI

N94-15548*# National Aeronautics and Space Administration. Ames Research Center, Moffett Field, CA.
FAULT MANAGEMENT FOR DATA SYSTEMS
Mark A. Boyd, David L. Iverson, and F. Ann Patterson-Hine Sep. 1993 23 p Sponsored by NASA, Washington
(RTOP 476-14-03)
(NASA-TM-103953; A-92147; NAS 1.15:103953) Avail: CASI HC A03/MF A01

Issues related to automating the process of fault management (fault diagnosis and response) for data management systems are considered. Substantial benefits are to be gained by successful automation of this process, particularly for large, complex systems. The use of graph-based models to develop a computer assisted fault management system is advocated. The general problem is described and the motivation behind choosing graph-based models over other approaches for developing fault diagnosis computer programs is outlined. Some existing work in the area of graph-based fault diagnosis is reviewed, and a new fault management method which was developed from existing methods is offered. Our method is applied to an automatic telescope system intended as a prototype for future lunar telescope programs. Finally, an application of our method to general data management systems is described. Author (revised)

N94-15633# Delaware Univ., Newark. Coll. of Marine Studies.
CHARACTERIZATION OF SPATIAL AND TEMPORAL VARIABILITY OF PHYTOPLANKTON BLOOMS IN COASTAL WATERS Final Report
V. Klemas 1 Mar. 1993 11 p
(Contract N00014-91-J-1737)
(AD-A267102) Avail: CASI HC A03/MF A01

The tide-related parameters of the Delaware Bay are derived from space shuttle time-series photographs. The water areas in the bay are measured from interpretation maps of the photographs with a CALCOMP 9100 digitizer and ERDAS Image Processing System. The corresponding tidal levels are calculated using the exposure time annotated on the photographs. From these data, an approximate function relating the water area to the tidal level at a reference point is determined. Based on the function, the water areas of the Delaware Bay at mean high water (MHW) and mean low water (MLW), below 0 m, and for the tidal zone are inferred. With MHW and MLW areas and the mean tidal range, we calculate the tidal influx of the Delaware Bay, which is 2.76(10)(exp 9) cu m. Furthermore, the velocity of flood tide at the bay mouth is determined using the tidal flux and an integral of the velocity distribution function at the cross section between Cape Henlopen and Cape May. The result is 132 cm/s, which compares well with the data on tidal current charts. DTIC

N94-15643# Laboratoire d'Automatique et d'Analyse des Systemes, Toulouse (France). Equipe Conduite Automatique de Procedes Biotechnologiques.
CONTRIBUTION TO THE ELABORATION OF SOME ADAPTIVE CONTROL ALGORITHMS FOR FERMENTATION PROCESSES MONITORING Ph.D. Thesis - Toulouse Univ. [CONTRIBUTION A L'ELABORATION D'ALGORITHMES DE COMMANDE ADAPTATIVE POUR LA CONDUITE DE PROCEDES FERMENTAIRES]
Gilles Roux 1992 201 p In FRENCH
(LAAS-92513; ETN-93-94405) Avail: CASI HC A10/MF A03

Several problems arising from the continuous fermentation process monitoring are studied. Nonlinear systems control as well as flexible and robust adaptive control techniques are discussed. They are of crucial interest for an efficiency monitoring of the biotechnological processes. These techniques are based on the implementation of parameter estimation procedures for the modeling and real time tracking of certain physical values characterizing the process operation. They also appeal to filtering techniques for the estimation of non-measured relevant quantities which determine the process evolution. These processes are clearly nonstationary processes and ask for the development of adaptive linear or nonlinear control methods. They allow the representation of the model nonlinearities and the parameter variations to be taken into consideration. Algorithms using the inherent nonlinear structure of the fermentation process models were developed, using a single variable, then a multivariate case was studied. The control laws were theoretically studied then validated on an experimental plant. ESA

N94-15662# Naval Command, Control and Ocean Surveillance Center, San Diego, CA.
LOOKING AT FOKKER-PLANCK DYNAMICS WITH A NOISY INSTRUMENT
Gabor Schmera, Adi Bulsara, David Pierson, Frank Moss, and Enrico DiCera May 1993 3 p
(AD-A267049) Avail: CASI HC A01/MF A01

We consider the class of experiments which can be characterized by a Fokker-Planck dynamics corresponding to the overdamped motion of a state point in a suitable stochastic potential. We assume that the general form of the potential is known (or can be guessed with reasonable accuracy), but that its parameters are to be determined experimentally by measurements made with a noisy instrument. This possible method for determining the potential parameters, which exploits the system's own internal stochastic motion in order to rapidly explore its available parameter space, is substantially more efficient than traditional methods involving time averages of single point measurements, and yet does not appear to have been previously considered. The method could be important, when, for example, the experiment must be completed in a limited time owing either to the expense of the experimental materials or to the temporary stationarity of the preparation, situations which are commonly encountered in experimental biochemistry and biology. DTIC

N94-15967*# National Aeronautics and Space Administration. Lyndon B. Johnson Space Center, Houston, TX.
QUANTITATIVE METHOD OF MEASURING CANCER CELL UROKINASE AND METASTATIC POTENTIAL Patent Application
Dennis R. Morrison, inventor (to NASA) 27 Jul. 1993 27 p
(NASA-Case-MSC-21715-1; NAS 1.71:MSC-21715-1;
US-Patent-Appl-SN-097186) Avail: CASI HC A03/MF A01

The metastatic potential of tumors can be evaluated by the quantitative detection of urokinase and DNA. The cell sample selected for examination is analyzed for the presence of high levels of urokinase and abnormal DNA using analytical flow cytometry and digital image analysis. Other factors such as membrane associated urokinase, increased DNA synthesis rates and certain receptors can be used in the method for detection of potentially invasive tumors. NASA

N94-15969*# National Aeronautics and Space Administration. Lyndon B. Johnson Space Center, Houston, TX.
CULTURED NORMAL MAMMALIAN TISSUE AND PROCESS Patent Application
Thomas J. Goodwin, inventor (to NASA) (Krug Life Sciences, Inc., Houston, TX.), Tacey L. Prewett, inventor (to NASA), David A. Wolf, inventor (to NASA), and Glenn F. Spaulding, inventor (to NASA) 25 May 1993 40 p
(NASA-Case-MSC-21984-1; NAS 1.71:MSC-21984-1;
US-Patent-Appl-SN-066292) Avail: CASI HC A03/MF A01

Normal mammalian tissue and the culturing process has been developed for the three groups of organ, structural and blood tissue. The cells are grown in vitro under microgravity culture conditions and form three dimensional cell aggregates with normal cell function. The microgravity culture conditions may be microgravity or simulated microgravity created in a horizontal rotating wall culture vessel. NASA

N94-16441# Du Pont de Nemours (E. I.) and Co., Wilmington, DE.
BIOORGANIC MODELS FOR PROTEIN ION CHANNELS Progress Report, 30 Jun. 1991 - 1 Jun. 1992
William F. DeGrado 1 Jun. 1992 7 p
(Contract N00014-90-C-0083)
(AD-A266365) Avail: CASI HC A02/MF A01

Biophysical characterization of ion channel peptides is discussed. We are using single-channel voltage clamp methods to study the model ion channel peptide, Ac-(LSSLLSL)3-CONH2 in an attempt to determine how selective it is for the conductance of cations versus anions. Both ends of the peptide are masked with neutral blocking groups allowing us to eliminate effects that are due to formal charges. Because the peptides can reorient upon a voltage change, we must use voltage pulses or fast ramps (approximately 100 msec) to measure full current-voltage relations on single open channels; the longer lifetime of the acetylated peptide facilitates this measurement. The open channel 1-5 relation rectifies in symmetrical 1 M KC1, with larger currents at the holding potential than at the opposite potential. According to our gating model, the larger currents flow from C-terminus to N-terminus. DTIC

N94-16514 Wisconsin Univ., Madison.
ISOLATION OF THERMOSTABLE ENZYME MUTANTS BY CLONING AND SELECTION IN THERMOPHILIC BACTERIA Final Technical Report, 1 Jul. 1989 - 31 Dec. 1992
Hans H. Liao 22 Jun. 1993 4 p Limited Reproducibility: More than 20% of this document may be affected by microfiche quality
(Contract N00014-89-J-3134)
(AD-A266378) Avail: Issuing Activity (Defense Technical Information Center (DTIC))

The objective of this project was to isolate thermostable variants of enzymes and to understand the molecular basis for their increased stability. Such variants may be isolated by introducing the gene encoding the enzyme into a thermophile and selecting for enzymatic activity at the high growth temperatures of these organisms. Thermostable mutants of kanamycin nucleotidyl transferase (KNTase) were obtained in this way and found to be also more resistant to chemical denaturants, to protease, and to inclusion body formation during their overexpression in Escherichia coli. The tools for obtaining mutants at up to 80 C by cloning in Thermus thermophilus, including a plasmid that transforms and expresses heterologous genes in this thermophile, were constructed, and more thermostable mutants of KNTase were isolated. Crystals of a thermostable KNTase were obtained and the structure was solved to 2.7A; comparison with the wildtype structure will allow correlation of the known genetic change with the structural basis for enhanced stability. Work was also begun on isolating thermostable mutants of another enzyme, chloramphenicol acetyltransferase. DTIC

N94-16545# Letterman Army Inst. of Research, San Francisco, CA.
HEAT SHOCK PROTEIN INDUCTION IN HUMAN CELLS BY CO2 LASER IRRADIATION Final Report
Ronald E. Ferrando, Steven T. Schuschereba, Phillip D. Bowman, Julie A. Quong, and Janet M. Yang 14 Jun. 1993 54 p
(AD-A266430; LAIR-486) Avail: CASI HC A04/MF A01

This study investigated the effect of millisecond exposures from a carbon dioxide (CO2) laser on the production of heat shock proteins in human fibroblast cell cultures. Heat shock or stress proteins (hsp) are induced to high levels by heat shock, transition series and heavy metals, amino acid analogs, certain chemicals, and ultraviolet radiation. These proteins are highly conserved throughout nature and their regulation and cellular functions are just beginning to be understood. The production of hsps was monitored by S-35-methionine incorporation into newly synthesized heat shock protein and by immunocytochemistry. It was shown that CO2 laser irradiation could induce the production of hsps. The time course of hsp synthesis and localization within cells was also determined. The hsp synthesis produced by the CO2 laser was compared to the effects of sodium arsenite and heat. The results of this study indicate that hsp 70 is the major heat shock protein induced by CO2 laser radiation and that this response is most likely due to the thermal effects of the laser. DTIC

N94-16893# Argonne National Lab., IL.
TRANSRAPID TR-07 MAGLEV-SPECTRUM MAGNETIC FIELD EFFECTS ON DAILY PINEAL INDOLEAMINE METABOLIC RHYTHMS IN RODENTS
K. R. Groh 1993 6 p Presented at the 12th International Conference on Magnetically Levitated Systems and Linear Drives, Argonne, IL, 19-21 May 1993
(Contract W-31-109-eng-38)
(DE93-015143; ANL/BIM/CP-79650; CONF-930550-1) Avail: CASI HC A02/MF A01

This study examined the effects on pineal function of magnetic field (MF) exposures (ac and dc components) similar to those produced by the TransRapid TR-07 and other electromagnetic maglev systems (EMS). Rats were entrained to a light-dark cycle and then exposed to a continuous, or to an inverted, intermittent (on = 45 s, off = 15 s, induced current = 267 G/s) simulated multifrequency ac and dc magnetic field (MF) at 1 or 7 times the TR-07 maglev vehicle MF intensity for 2 hr. Other groups of rats were exposed to only the ac or the dc-component of the maglev MF. For comparison, one group was exposed to an inverted, intermittent 60-Hz MF. Each group was compared to an unexposed group of rats for changes

in pineal melatonin and serotonin-N-acetyltransferase (NAT). MF exposures at an intensity equivalent to that produced by the TR-07 vehicle had no effect on melatonin or NAT compared with sham-exposed animals under any of the conditions examined. However, 7X TR-07-level continuous 2-h MF exposures significantly depressed pineal NAT by 45%. Pineal melatonin was also depressed 33-43% by a continuous 7X TR-07 MF exposure and 28% by an intermittent 60-Hz 850-mG MF, but the results were not statistically significant. This study demonstrates that intermittent, combined ac and dc MF's similar to those produced by the TR-07 EMS maglev vehicle alter the normal circadian rhythm of pineal indoleamine metabolism. The pineal regulatory enzyme NAT was more sensitive to MF exposure than melatonin and may be a more desirable measure of the biological effects of MF exposure. DOE

N94-16989# Illinois Univ., Urbana.
BIOFILM STRUCTURE AND DIVERSITY Final Technical Report
David A. Stahl 1993 5 p
(Contract N00014-92-J-1710)
(AD-A267254) Avail: CASI HC A01/MF A01

The objective of this project is to develop molecular measures of the identity, activity, and spatial distribution of microbial populations making up natural (multispecies) biofilms. A further goal of this project is to use biofilm bioreactors to characterize the relationship between biochemical transformations and community structure, focusing on the terminal steps of anaerobic mineralization and emphasizing competitive and cooperative interactions among sulfate-reducing and methanogenic biofilm populations. Long term objectives include the identification and characterization of obligate symbioses among attached microbial populations and the refinement of mathematical models to predict the behavior of biofilm communities. DTIC

N94-17090*# Wright State Univ., Dayton, OH.
EVALUATION OF PUTATIVE NEUROCHEMICAL INTERMEDIARIES IN SPACE/MOTION SICKNESS Final Report, 1 Jan. 1966 - 31 Dec. 1991
James B. Lucot and George H. Crampton 31 Dec. 1991 23 p
(Contract NCC2-229)
(NASA-CR-193607; NAS 1.26:193607) Avail: CASI HC A03/MF A01

The topics covered include the following: the emetic stimuli used on the cats in the study; analysis of the constituents of the cerebral spinal fluid (CSF) during motion sickness; evaluation of serotonin-1A agonists; other 5-HT receptors; and additional studies and activities. Derived from text

N94-17224# Society of Toxicology, Washington, DC.
[FACTORS DETERMINING THE RELEASE OF NITRIC OXIDE] Thesis Final Report, 1 Dec. 1991 - 30 Nov. 1992
Joan Walsh Cassedy 30 Nov. 1992 7 p
(Grant AF-AFOSR-0187-89)
(AD-A266232; AFOSR-93-0448TR) Avail: CASI HC A02/MF A01

Cortical collecting duct cells were cultured on permeable membranes and used to assess cellular transport properties for calcium/cadmium. Functional viability of the cells in culture were affirmed by their ability to absorb sodium and chloride, secrete protons and potassium, and respond appropriately to the hormones vassopressin and aldosterone. Calcium absorption by these cells was affected neither by sodium blockers or hormone inducers of cyclic AMP nor, surprisingly, by various calcium channel blockers. However, when the pH of the culture medium on the apical side of the cells was controlled artificially by buffer, calcium absorption was found to be affected. Decreasing the pH inhibited calcium uptake by cells, indicating that calcium and H+ transport were linked, possibly by a mechanism involving a H+/Ca++ exchanger. Cadmium had no apparent effect on calcium absorption until cadmium concentrations reached levels at which nonspecific, cytotoxic effects were observed. In another separate project, initial research efforts were undertaken to use electron paramagnetic resonance (EPR) to explain the mechanism by which endothelial/smooth muscle cells release the putative endothelium-derived relaxing factor (EDRF), nitric oxide (NO), from vasodilator drugs. DTIC

N94-17232# Georgia Inst. of Tech., Atlanta. Bioengineering Center.
BIOEFFECTS OF RADIOFREQUENCY RADIATION ON CELL GROWTH AND DIFFERENTATION. VOLUME 1: ENGINEERING CONSIDERATIONS Final Report, Jan. 1988 - Oct. 1991
David L. Banks, Wesley W. Shelton, and James C. Toler Jun. 1993 42 p
(Contract F33615-83-K-0600)
(AD-A267754; AL-TR-1992-0106-Vol-1) Avail: CASI HC A03/MF A01

This report details the engineering considerations of a program designed to investigate the effects of chronic low-level radiofrequency radiation (RFR) exposure on cell growth and differentiation. The protocol required the exposure (1 mW/cm2 20 hours daily, average, 7 days per week) of 200 female, mammary-tumor-prone mice (strain C3H/HeJ) to 435-MHz pulsed-wave (1.0 us pulse width, 1.0 kHz pulse rate) RFR for a duration of 21 months. In addition, a sham-exposure group consisting of 200 female, C3H/HeJ mice was housed under identical conditions, but not exposed to the 435-MHz pulsed-wave radiation. The program's engineering considerations involved developing and providing the facility and equipment used to expose the mammary-tumor-prone mice and the development of a procedure for reliable identification of the mice. Also described are the design of the antenna and transmitter system, animal caging, cage washing procedures, and the data collection system. DTIC

N94-17257*# National Aeronautics and Space Administration, Washington, DC.
THE 1990-1991 NASA SPACE BIOLOGY ACCOMPLISHMENTS
Thora W. Halstead, ed. (George Washington Univ., Washington, DC.) Oct. 1993 259 p
(NASA-TM-4501; NAS 1.15:4501) Avail: CASI HC A12/MF A03

This report consists of individual technical summaries of research projects of NASA's Space Biology Program, for research conducted during the period May 1990 through May 1991. This program includes both plant and animal research, and is dedicated to understanding the role of gravity and other environmental factors on biological systems and to using the microgravity of the space environment as a tool to advance fundamental scientific knowledge in the biological sciences to improve the quality of life on Earth and contribute to NASA's goal of manned exploration of space. The summaries for each project include a description of the research, a list of the accomplishments, an explanation of the significance of the accomplishments, and a list of publications. Author

N94-17275# Delaware Univ., Lewes. Coll. of Marine Studies.
REGULATION OF ATTACHED BACTERIAL GROWTH BY ADSORBED PROTEINS Final Report, 1 May 1990 - 30 Jun. 1993
David L. Kirchman 28 Jul. 1993 4 p
(Contract N00014-90-J-1973)
(AD-A267756) Avail: CASI HC A01/MF A01

The general objective of this project was to examine one component of the primary biofilm, protein, which has been hypothesized to be a major component of both dissolved and adsorbed organic pools in seawater. In previous work we found that surface energy was important in determining adsorption of protein to surfaces in seawater and degradation rates by bacteria and bacterial growth. In the last phase of this work, we examined the chemical nature of actual protein in seawater using HPLC techniques which we developed, standard chemical assays, and bioassays. We showed that protein in seawater is not the same chemically as cellular protein. Bacteria appear to treat nearly all seawater protein as if it were glycolated and degrade it at much lower rates than unmodified, fresh protein. Other experiments showed that cellular protein introduced into seawater is quickly modified by abiotic reactions and becomes less easily hydrolyzed by bacterial proteases within hours. The abiotic reactions appear to include adsorption to small colloids. These results begin to explain the growth dynamics of microorganisms on surfaces and the origin of refractory organic matter which is highly abundant in seawater. DTIC

N94-17279*# New York Univ., New York. Dept. of Applied Science.
THE DYNAMICS OF HYDROPONIC CROPS FOR SIMULATION STUDIES OF THE CELSS INITIAL REFERENCE CONFIGURATIONS Final Report, 1 Apr. 1989 - 31 Aug. 1993
Tyler Volk 31 Aug. 1993 45 p
(Contract NCC2-608)
(NASA-CR-194654; NAS 1.26:194654) Avail: CASI HC A03/MF A01

During the past several years, the NASA Program in Controlled Ecological Life Support Systems (CELSS) has continued apace with crop research and logistic, technological, and scientific strides. These include the CELSS Test Facility planned for the space station and its prototype Engineering

Development Unit, soon to be active at Ames Research Center (as well as the advanced crop growth research chamber at Ames); the large environmental growth chambers and the planned human test bed facility at Johnson Space Center; the NSCORT at Purdue with new candidate crops and diverse research into the CELSS components; the gas exchange data for soy, potatoes, and wheat from Kennedy Space Center (KSC); and the high-precision gas exchange data for wheat from Utah State University (USU). All these developments, taken together, speak to the need for crop modeling as a means to connect the findings of the crop physiologists with the engineers designing the system. A need also exists for crop modeling to analyze and predict the gas exchange data from the various locations to maximize the scientific yield from the experiments. One fruitful approach employs what has been called the 'energy cascade'. Useful as a basis for CELSS crop growth experimental design, the energy cascade as a generic modeling approach for CELSS crops is a featured accomplishment in this report. The energy cascade is a major tool for linking CELSS crop experiments to the system design. The energy cascade presented here can help collaborations between modelers and crop experimenters to develop the most fruitful experiments for pushing the limits of crop productivity. Furthermore, crop models using the energy cascade provide a natural means to compare, feature for feature, the crop growth components between different CELSS experiments, for example, at Utah State University and Kennedy Space Center. Author (revised)

N94-16094 British Columbia Univ., Vancouver.
STATISTICAL TECHNIQUES FOR STUDY DESIGN OF MICROGRAVITY LIFE SCIENCES EXPERIMENTS
F. A. Gagnon, L. E. Susak, P. C. Wing, F. Glick, and I. K. Y. Tsang *In* National Research Council Canada, Proceedings of the Second Workshop on Microgravity Experimentation 1990 3 p (For primary document see N94-16071 03-29)
Avail: Issuing Activity (National Research Council, Publication Sales and Distribution, Montreal Road, Ottawa, Ontario, K1A OR6 Canada)

52 AEROSPACE MEDICINE

Includes physiological factors; biological effects of radiation; and effects of weightlessness on man and animals.

N94-14916# Naval Medical Research Inst., Bethesda, MD.
AN APPARATUS FOR MEASURING THE BIOLOGICAL OXIDATION OF HYDROGEN GAS UNDER HYPERBARIC CONDITIONS
S. R. Kayar, G. S. Goehring, W. E. Long, Jr., and A. L. Harabin Jun. 1993 35 p
(DA Proj. MR0-4101)
(AD-A266834; NMRI-93-38) Avail: CASI HC A03/MF A01

An apparatus was designed, constructed, and operated to permit us to expose mammalian tissues to high pressures and concentrations of hydrogen (H2), using the radioisotope tritium (T2) as a label. As part of a study of H2 as a breathing gas for deep diving, it was necessary to determine if mammalian tissues have a latent capacity to metabolize H2 that is only evident under hyperbaric conditions. The apparatus was designed to store up to 1 Curie T2 between experiments, mix T2 and H2 with air in the experimental chamber without producing an explosive mixture, and reclaim the T2 at the end of the experiment for safe disposal. The T2 was purchased in glass ampules. Storage of T2 was accomplished by placing the T2 ampule in a steel pressure chamber and breaking the ampule to release the T2 under complete containment. The potential problems from explosivity were solved by diluting the T2 and H2 with helium. Reclamation of the T2 was accomplished by passing a controlled stream of the T2 and H2 along with a controlled stream of air through a combustion trap. DTIC

N94-14917# Letterman Army Inst. of Research, San Francisco, CA. Military Trauma Research Div.
A MATHEMATICAL MODEL FOR THE STUDY OF HEMORRHAGIC SHOCK AND FLUID RESUSCITATION: THE SYSTEMIC AND PULMONARY VASCULATURE Final Report No. 479
Tammy J. Doherty Jun. 1993 24 p
(AD-A266835) Avail: CASI HC A03/MF A01

In systemic and pulmonary circuit models, the number and configuration of vascular compartments may affect predictions of vascular volume and blood flow. Various models of the pulmonary and systemic vascular circuits are considered to identify models appropriate for studies of hemorrhage and fluid resuscitation. It was found that at least one pulmonary vascular compartment, made up of one resistance and one capacitance element, was required to describe the response of pulmonary blood volume to changes in pulmonary inflow rate (i.e., right heart output). Incorporation of additional pulmonary vascular segments did not altar predictions of pulmonary volume or flow rate. Therefore, one lumped pulmonary vascular compartment appears to be sufficient. It may be necessary to incorporate multiple pulmonary vascular segments, however, for studies of pulmonary transcapillary exchange or cardiovascular control. The initial model for the systemic circuit included a separate capillary compartment for studies of transcapillary exchange as well as variable resistance and compliance elements for studies of cardiovascular control. Model identification for the systemic circulation focused on the most appropriate number of parallel vascular pathways for predicting the response of systemic outflow (i.e., venous return) to changes in systemic inflow (i.e., left heart output). At least two separate parallel pathways were required to predict systemic outflow rate because of differences in the distribution time constant between skeletal muscle and other vascular beds. DTIC

N94-14923# FORSS, Inc., Naperville, IL.
VALIDATION OF RESPIRATORY INDUCTIVE PLETHYSMOGRAPHY FOR MEASURING EXERCISE TIDAL VOLUMES Final Report, Nov. 1991 - Jun. 1992
David M. Caretti, Paul V. Pullen, Leslie A. Premo, and Wade D. Kuhlmann May 1993 25 p
(AD-A266883; ERDEC-TR-078) Avail: CASI HC A03/MF A01

This study validated the accuracy of tidal volume (V(sub T)) measurements obtained with a respiratory inductive plethysmograph (RIP) to determine its reliability for measuring ventilation during studies of exercise and respirator wear. Values from the RIP were compared with simultaneous flowmeter volumes in 8 healthy subjects at 5 incremental work rates (60, 90, 120, 150, and 180 W) of cycling and treadmill exercise. During cycling, average RIP and flowmeter values did not differ significantly at work rates below 180 W for 5 of the 8 subjects. Average RIP and flowmeter V(sub T) were similar at work rates below 150 W for 5 of the 6 subjects who completed the treadmill iteration. The variability in these results may be attributed to several factors including RIP calibration errors and slippage of the RIP elastic bands containing the inductive coils. Correlations of breath-by-breath flowmeter and RIP V(sub T) were significant for each subject during cycling and treadmill exercise. These findings suggest that the RIP can provide reliable, noninvasive measurements of ventilation during exercise with and without respirator wear. Author (revised)

N94-14943 Naval Health Research Center, San Diego, CA.
SLEEP MANAGEMENT USER'S GUIDE FOR SPECIAL OPERATIONS PERSONNEL Final Report
Paul Naitoh and Tamsin Kelly Jul. 1992 47 p Limited Reproducibility: More than 20% of this document may be affected by microfiche quality
(AD-A267746; NHRC-92-28) Avail: CASI HC A03

The objective of sleep logistics is to ensure that fighting men and women at all levels obtain sufficient sleep to maintain combat effectiveness. Special warfare missions frequently involve night work and arduous operational schedules. This User's Guide explains selected sleep management techniques for use during military operations, with particular emphasis on special operations mission. The guide will assist field commanders in using sleep logistics to prevent compromise of mission accomplishment due to sleep deprivation. In addition, it provides techniques for assessing severity of sleep debt and compensating for its ill effects. DTIC

N94-14952# Army Aeromedical Research Lab., Fort Rucker, AL.
MONOGRAPH OF THE AVIATION EPIDEMIOLOGY DATA REGISTER FOR FY 1991 Final Report
Robert H. Schrimsher and S. G. Shannon Jan. 1993 117 p
(DA Proj. 3M1-62787-A-879)
(AD-A266896; USAARL-93-12) Avail: CASI HC A06/MF A02

The purpose of this monograph was to provide descriptive statistics within the Aviation Epidemiology Data Register (AEDR) of selected variables from an aviator's annual class 2 or class 2A Flying Duty Medical Examination (FDME) that was performed in 1991. Only aviators from a major Army

component were considered, active duty, reserve, or National Guard. Descriptive data are presented in tables, which normally are defined by component, age group, and gender. Due to the small number of female aviators, some of the age-group cells are sparsely populated, especially within the reserve component. The data were organized into three areas: laboratory/clinical, vision, and hearing. Within the laboratory/clinical area, age was correlated with increases in mean values and percentages of population with values over a threshold for systolic and diastolic blood pressure, pulse, and cholesterol. Within the vision area, the likelihood of corrective lens use increased with age. For males, visual acuity decreased for both distant and near vision. DTIC

N94-15180# East Carolina Univ., Greenville, NC. School of Medicine.
EVALUATION OF DRIED STORAGE OF PLATELETS FOR TRANSFUSION: PHYSIOLOGIC INTEGRITY AND HEMOSTATIC FUNCTIONALITY Triannual Report No. 1, 1 Feb. - 3 May 1993
Arthur P. Bode 28 Jun. 1993 5 p
(Contract N00014-92-J-1244)
(AD-A266958) Avail: CASI HC A01/MF A01

In the last report period, we received a statement of rejection of claims from the U.S. Patent Office on our filing of May 1992 for use of lyophilized platelets in continuation-in-part (CIP) response which included aspects of applications of lyophilized platelets in wound healing. The CIP added much new data to strengthen the prior claims and listed others related to activity of platelet-derived growth factor (PDGF) expressed by freeze-dried platelets as an adjunct application in surface dressings. DTIC

N94-15250* National Aeronautics and Space Administration, Washington, DC.
COOL SUIT (Videotape)
Feb. 1988 Videotape: 3 min. 5 sec. playing time, in color, with sound (NASA-TM-109639; NONP-VT-93-190437) Avail: CASI VHS A01/BETA A22

This video explains how a boy born with no sweat glands now lives a relatively normal life. CASI

N94-15253* National Aeronautics and Space Administration, Washington, DC.
NEW INSULIN PUMP (Videotape)
Feb. 1988 Videotape: 3 min. 30 sec. playing time, in color, with sound (NASA-TM-109642; NONP-VT-93-190440) Avail: CASI VHS A01/BETA A22

This video details the Programmable Implant Medicine Monitoring System. CASI

N94-15271* National Aeronautics and Space Administration. Goddard Space Flight Center, Greenbelt, MD.
GSFC FUN RUN (Videotape)
Oct. 1988 Videotape: 10 min. playing time, in color, with sound (NASA-TM-109587; NONP-VT-93-190385) Avail: CASI VHS A01/BETA A22

This video shows Goddard's commitment to it's employees physical well-being by highlighting the Spring 1988 Goddard Fun Run. CASI

N94-15309* National Aeronautics and Space Administration, Washington, DC.
SPACE ADAPTATION (Videotape)
May 1991 Videotape: 3 min. 15 sec. playing time, in color, with sound (NASA-TM-109601; NONP-VT-93-190399) Avail: CASI VHS A01/BETA A22

This videotape discusses space adaptation syndrome and a training simulator that may help astronauts adjust to microgravity before space flight. CASI

N94-15312* National Aeronautics and Space Administration, Washington, DC.
LASER ARTERY REPAIR (Videotape)
Apr. 1985 Videotape: 3 min. 51 sec. playing time, in color, with sound (NASA-TM-109604; NONP-VT-93-190402) Avail: CASI VHS A01/BETA A22

This videotape demonstrates the capabilities of the excimer laser and the angioscope for treating heart disease. CASI

N94-15368* National Aeronautics and Space Administration. Lyndon B. Johnson Space Center, Houston, TX.
LIVING WELL IN SPACE: MONITORING ENVIRONMENT (Videotape)
Jul. 1989 Videotape: 9 min. 45 sec. playing time, in color, with sound (NASA-TM-109537; NONP-VT-93-190334) Avail: CASI VHS A01/BETA A22

This video describes the Environmental Health Systems (EHS). Progress in experiments concerning water quality, toxicology, microbiology, and radiation are addressed. CASI

N94-15369* National Aeronautics and Space Administration. Lyndon B. Johnson Space Center, Houston, TX.
LIVING WELL IN SPACE: ENSURING CREW CAPABILITY (Videotape)
Jul. 1989 Videotape: 7 min. 45 sec. playing time, in color, with sound (NASA-TM-109538; NONP-VT-93-190335) Avail: CASI VHS A01/BETA A22

This video describes the Exercise Countermeasure Facility (ECF). The ECF provides a comprehensive exercise program to allow astronauts to remain physically fit during extended stays in space. Featured are the Exercise Development Laboratory, the Exercise Physiology Laboratory, the Anthromorphic and Biomechanical Laboratory, and the Artificial Intelligence Laboratory. CASI

N94-15370* National Aeronautics and Space Administration. Lyndon B. Johnson Space Center, Houston, TX.
LIVING WELL IN SPACE: CLINICAL CARE CHALLENGE (Videotape)
Jul. 1989 Videotape: 9 min. 15 sec. playing time, in color, with sound (NASA-TM-109539; NONP-VT-93-190336) Avail: CASI VHS A01/BETA A22

This video describes the Health Maintenance Facility (HMF). The HMF provides inflight medical care including prevention, diagnosis, and care during transport if the patient must be evacuated. A comparison to medical services found in a large hospital is used to describe the HMP's subsystems. CASI

N94-15381* National Aeronautics and Space Administration. Lyndon B. Johnson Space Center, Houston, TX.
STS-32 CREW TRAINING FOR LOWER BODY NEGATIVE PRESSURE UNIT AND AFE (Videotape)
Nov. 1989 Videotape: 13 min. playing time, in color, with sound (NASA-TM-109475; NONP-VT-93-190272) Avail: CASI VHS A01/BETA A22

Astronauts Dunbar, Ivins, and Low are shown preparing for the checkouts of the Lower Body Negative Pressure (LBNP) and American Flight Echocardiograph (AFE) tests. Dunbar gets into the LBNP suit, while technicians look on. Experiments on Dunbar are conducted while other crew members and technicians record data. CASI

N94-15457* National Aeronautics and Space Administration. Lyndon B. Johnson Space Center, Houston, TX.
ANSWERING THE SPACE MEDICINE CHALLENGE (Videotape)
Aug. 1988 Videotape: 15 min. playing time, in color, with sound (NASA-TM-109511; NONP-VT-93-190308) Avail: CASI VHS A01/BETA A22

The development of the Space Station Health Maintenance Facility (HMF) is featured. The HMF will provide necessary inflight medical care, including prevention, diagnosis, treatment, and care during transport if the patient must be evacuated from Space Station. CASI

N94-15537*# National Aeronautics and Space Administration. Ames Research Center, Moffett Field, CA.
AUTOGENIC-FEEDBACK TRAINING (AFT) AS A PREVENTIVE METHOD FOR SPACE MOTION SICKNESS: BACKGROUND AND EXPERIMENTAL DESIGN
Patricia S. Cowings and William B. Toscano (California Univ., Los Angeles.) Aug. 1993 16 p Sponsored by NASA, Washington
(RTOP 199-70-12-14)
(NASA-TM-108780; A-93095; NAS 1.15:108780) Avail: CASI HC A03/MF A01

Finding an effective treatment for the motion sickness-like symptoms that occur in space has become a high priority for NASA. The background research is reviewed and the experimental design of a formal life sciences

shuttle flight experiment designed to prevent space motion sickness in shuttle crew members is presented. This experiment utilizes a behavioral medicine approach to solving this problem. This method, Autogenic-Feedback Training (AFT), involves training subjects to voluntarily control several of their own physiological responses to environmental stressors. AFT has been used reliably to increase tolerance to motion sickness during ground-based tests in over 200 men and women under a variety of conditions that induce motion sickness, and preliminary evidence from space suggests that AFT may be an effective treatment for space motion sickness as well. Proposed changes to this experiment for future manifests are included. Author (revised)

N94-15634# Massachusetts Inst. of Tech., Lexington. Lincoln Lab.
EXPERIMENTAL EVALUATION OF AN ADAPTIVE FOCUSING ALGORITHM FOR A MICROWAVE PLANAR PHASED-ARRAY HYPERTHERMIA SYSTEM AT UCSF
Alan J. Fenn, Chris J. Diederich, and Paul R. Stauffer 17 May 1993 52 p
(Contract F19628-90-C-0002)
(AD-A267004; TR-977; ESC-TR-92-203) Avail: CASI HC A04/MF A01

An adaptive focusing microwave planar phased-array hyperthermia system for improved heating of superficial tumors is experimentally investigated. A commercial microwave hyperthermia planar phased-array antenna system at the University of California at San Francisco (UCSF) Radiation Oncology Department has been modified to implement a gradient-search adaptive focusing algorithm. Adaptive focusing measurements in a muscle-equivalent liquid phantom with a 915-MHz microwave planar phased-array hyperthermia system comprising 16 independent amplitude/phase-controlled waveguide antenna elements (Microtherm-1000, Labthermics Technologies, Inc.) are reported. An electric-(E-)-field feedback probe detector, fabricated at UCSF, measures the E-field generated by the hyperthermia phased array. A method of steepest-ascent gradient-search feedback algorithm, implemented in software, controls the hyperthermia array phase shifters and focuses the transmitted radiation beam. In 10 to 15 iterations, the measured phantom data indicate rapid convergence of the adaptive focusing algorithm and significant increase of the focal region field strength due to the adaptive focusing. Two-dimensional E-field radiation pattern measurements were collected by scanning the E-field dipole probe antenna inside the muscle-equivalent liquid phantom. The measured, adaptively phase-focused radiation pattern data indicate a maximum useful heating depth of about 3 cm in a muscle-equivalent sugar/saline phantom having dielectric losses of 3 dB/cm. DTIC

N94-15658*# National Aeronautics and Space Administration. John F. Kennedy Space Center, Cocoa Beach, FL.
TOXIC SUBSTANCES REGISTRY SYSTEM: INDEX OF MATERIAL SAFETY DATA SHEETS
Oct. 1993 915 p
(NASA-TM-109332; NAS 1.15:109332; GP-23-1) Avail: CASI HC A99/MF A10

The Material Safety Data Sheets (MSDS's) listed in this index reflect product inventories and associated MSDS's which were submitted to the Toxic Substances Registry database maintained by the Base Operations Contractor at the Kennedy Space Center. The purpose of this index is to provide KSC government, contractor, and tenant organizations a means to access information on the hazards associated with these chemicals. The Toxic Substance Registry Service (TSRS) was established to manage information dealing with the storage and use of toxic and otherwise hazardous materials at KSC. As a part of this service, the BOC Environmental Health Services maintains a central repository of MSDS's which were provided to TSRS. The data on the TSRS are obtained from NASA, contractor, and tenant organizations who use or store hazardous materials at KSC. It is the responsibility of these organizations to conduct inventories, obtain MSDS's, distribute Hazard Communication information to their employees, and otherwise implement compliance with appropriate Federal, State, and NASA Hazard Communication and Worker Right-to-Know regulations and policies. Author (revised)

N94-15660# Columbia Univ., New York, NY.
DIFFUSIBLE DRIVING AND COUPLING SIGNALS OF THE BIOLOGICAL CLOCK Annual Report, 1 Apr. 1992 - 31 Mar. 1993
Rae Silver and Joseph LeSauter 18 May 1993 12 p
(Contract F49620-92-J-0195)
(AD-A267046; AFOSR-93-0548TR) Avail: CASI HC A03/MF A01

It is well established that the mammalian suprachiasmatic nucleus (SCN) is a biological pacemaker which entrains the activity of organisms to their environment and controls circadian rhythmicity. However, neither the nature of these coupling signal(s) from the SCN, nor their target(s) in the brain are well understood. Fiber efferents from the SCN reach nearby hypothalamic regions, suggesting a coupling role for neural efferent pathways. The SCN produces diffusible signals that reach nearby hypothalamic sites and the cerebrospinal fluid, suggesting a role for a diffusible efferent pathway. We consider the possibility of redundant coupling signals of the SCN and review evidence suggesting that diffusible elements may-be sufficient to sustain locomotor rhythmicity in adult animals and to restore locomotor rhythmicity in lesioned hamsters bearing SCN grafts. We also provide data for the occurrence of signals that synchronize oscillators irrespective of initial phase. The distinct role of neural and diffusible SCN coupling signals and the role of SCN-driven systems (pineal melatonin rhythms, body temperature) remains to be explored. DTIC

N94-15663# Army Research Inst. of Environmental Medicine, Natick, MA.
ANNUAL HISTORICAL REPORT, CALENDAR YEAR 1992
Apr. 1993 152 p
(AD-A267050) Avail: CASI HC A08/MF A02

This report contains information concerning the mission, organization, key staff, overall funding and significant research accomplishments of the US Army Research Institute of Environmental Medicine, a subordinate element of the US Army Medical Research and Development Command, for calendar year 1992. Also included are listings of published reports, abstracts, presentations, and key briefings for each Research Division of the Institute and significant accomplishments and appointments of the professional staff. DTIC

N94-15711*# National Aeronautics and Space Administration. Ames Research Center, Moffett Field, CA.
RELIABILITY OF AUTONOMIC RESPONSES AND MALAISE ACROSS MULTIPLE MOTION SICKNESS STIMULATION TESTS
Cynthia S. Stout, William B. Toscano (California Univ., Los Angeles.), and Patricia S. Cowings Sep. 1993 10 p Sponsored by NASA, Washington
(RTOP 199-70-12-14)
(NASA-TM-108787; A-93118; NAS 1.15:108787) Avail: CASI HC A02/MF A01

There is general agreement that a high degree of variability exists between subjects in their autonomic nervous system responses to motion sickness stimulation. Additionally, a paucity of data exists that examines the variability within an individual across repeated motion sickness tests. Investigators have also examined the relationship of autonomic responses to motion sickness development. These investigations have used analyses at discrete points in time to describe this relationship. This approach fails to address the time course of autonomic responses and malaise development throughout the motion sickness test. Our objectives were to examine the reliability of autonomic responses and malaise using the final minute of the motion sickness test across five testing occasions, to examine the reliability of the change in autonomic responses and the change in malaise across five testing occasions, and to examine the relationship between changes in autonomic responses and changes in malaise level across the entire motion sickness test. Our results indicate that, based on the final minute of testing, the autonomic responses of heart rate, blood volume pulse, and respiration rate are moderately stable across multiple tests. Changes in heart rate, blood volume pulse, respiration rate, and malaise throughout the test duration were less stable across the tests. We attribute this instability to variations in individual susceptibility and the error associated with estimating a measure of autonomic gain. Author

N94-15736# Alabama Univ., Birmingham. School of Medicine.
CUMULATIVE EFFECT OF REPEATED BRIEF CEREBRAL ISCHEMIA Final Report, 1 Jun. 1992 - 31 May 1993
Hoby Hetherington 31 May 1993 34 p
(Contract F49620-92-J-0362)
(AD-A267155; AFOSR-93-0459TR) Avail: CASI HC A03/MF A01

The purpose of this grant is to investigate the metabolic and physiological factors determining the extent of ischemic damage in a model of brief repetitive ischemia. The model is intended to simulate the effects of Gz induced blackout experienced by fighter pilots undergoing high gravitational stress maneuvers. To achieve this goal a rat model was developed whereby ischemia could be induced remotely (under computer regulation) by inflation of occlusive cuff about the common carotid artery of the rat. Metabolic parameters were determined by performing in vivo NMR measurements throughout the repetitive ischemic insult. The non-destructive nature of the NMR measurement permits complete time courses to be monitored in each animal thereby minimizing animal variability. NMR measurements of metabolite content are then used in conjunction with histologic evaluations of neuronal death to assess which metabolic factors have the strongest influence on ischemic damage. During the past year we have completed our studies: (1) investigating the correlations between EEG, phosphocreatine (PCr), adenosine triphosphate (ATP), inorganic phosphate (P), pH and lactate as a function of increasing ischemic severity in our model of brief repetitive ischemia and (2) characterizing substrate utilization and lactate clearance curves using the same model. These experiments have been performed in the rat brain using the repetitive ischemia model with in vivo NMR to measure metabolite content. DTIC

N94-15740# Letterman Army Inst. of Research, San Francisco, CA.
A REVIEW OF THE EFFICACY OF 7.5 PERCENT NaCl/6 PERCENT DEXTRAN-70 (HSD) IN EXPERIMENTAL ANIMALS AND HUMANS
M. A. Dubick and C. E. Wade Jan. 1993 31 p
(AD-A266633; LAIR-IR-481) Avail: CASI HC A03/MF A01

Recent years have seen a renewed interest in the use of hypertonic-hyperoncotic solutions as plasma volume expanders for the treatment of hemorrhagic hypotension. In particular, a number of studies in experimental animals have addressed the efficacy and safety of small volume infusions of 7.5% NaCl/6% Dextran-70 (HSD). Employing models of fixed volume or fixed pressure hemorrhage, HSD has improved survival, and reversed many of the hemodynamic, hormonal, and metabolic abnormalities associated with hemorrhagic shock. In the few human field trials completed to date, HSD has been shown to be potentially beneficial in hypotensive trauma patients who require surgery or have concomitant head injury. Extensive toxicological evaluations and lack of reports of adverse effects in the human trials indicate that, at the proposed therapeutic dose of 4 ml/kg, HSD should present little risk. DTIC

N94-15741# Letterman Army Inst. of Research, San Francisco, CA.
THE RELATIONSHIP OF METALLOTHIONEIN INDUCTION TO THE HEAT SHOCK RESPONSE
J. M. Yang, P. D. Bowman, M. A. Deaton, S. T. Schuschereba, and B. E. Stuck Apr. 1993 46 p
(AD-A266634; LAIR-IR-480) Avail: CASI HC A03/MF A01

Heat shock proteins (hsp's) and Metallothioneins (MT's) are sets of proteins specifically synthesized by cells in response to sublethal injury such as heat, heavy metals, or radiation. This dissertation investigated the relationship of metallothionein induction to the heat shock response. Sodium arsenite, which induces both hsp's and MT's was used to establish a model system for investigation. Electrophoresis conditions that allowed simultaneous identification and quantitation of hsp's and MT's were then developed. Identification of MT's was achieved by (S-35) cysteine and methionine labeling and (Cd-109)-binding. The results of this study indicate that MT's undergo increased synthesis following both heat shock and sodium arsenite treatment. The level of increase of MT's after heat shock was about one-tenth of the increase after sodium arsenite treatment. These results suggest that MT's are heat shock and stress proteins. DTIC

N94-15759 Naval Air Station, Pensacola, FL. Computer and Telecommunications Station.
DEVELOPMENT OF THE OMPAT NEUROPSYCHOLOGICAL/PSYCHOMOTOR PERFORMANCE EVALUATION AND OMPAT DATA AND TIMING SUPPORT PROGRAMS Annual Report, 1 Oct. 1991 - 1 Oct. 1992
Kathryn P. Winter and Dennis L. Reeves 15 Oct. 1992 11 p Limited Reproducibility: More than 20% of this document may be affected by microfiche quality
(Contract MIPR-91MM1504; DA Proj. 302-63002-D-995)
(AD-A266954) Avail: CASI HC A03

The objectives of this project were as follows: (1) to create a millisecond accuracy software timer module that could be incorporated into OMPAT and other testing programs; (2) to construct a set of automated, i.e., 'computerized' OMPAT Level 1 neuropsychological and psychomotor tests with documentation that provide a standardized, clinically relevant, and rapid method for assessment of nervous system integrity; and (3) to construct a version of UTCPAB that incorporates the software timer. DTIC

N94-15845 Dayton Univ. Research Inst., OH.
FLIGHT SIMULATOR-INDUCED SICKNESS AND VISUAL DISPLAYS EVALUATION Final Report, Oct. 1989 - Jan. 1992
Harold D. Warner May 1993 102 p Limited Reproducibility: More than 20% of this document may be affected by microfiche quality
(Contract F33615-90-C-0005)
(AD-A267019; AL/HR-TR-1993-0056) Avail: CASI HC A06

The objectives of this investigation were to compare the incidence and severity of simulator sickness associated with the use of two flight simulator visual systems and to evaluate the performance characteristics of the visual displays. The visual systems were the Display for Advanced Research and Training (DART) and the Limited Field-of-View Dome (LFOVD). Two groups of pilots served as subjects. One group consisted of active duty U.S. Air Force instructor pilots. The second group was comprised of pilots who were no longer flying military aircraft. The pilots performed a series of single-ship and formation flights, and an F-16 simulated fighter aircraft was used in conjunction with both visual systems. It was observed that both visual systems induced simulator sickness symptoms, and some of the pilots were forced to prematurely terminate the flights due to severe discomfort. For the pilots who were able to complete the flights, there was a significant increase in self reports of discomfort over time, an increase in simulator sickness symptomatology, and a decline in postural equilibrium. However, there were no differences in the incidence of simulator sickness between the two visual systems or pilot groups. The pilots recovered from the adverse effects of the simulation within 30 min following the flights. The means and medians of the pilots' ratings of the visual display characteristics indicated that the only problems encountered with the two visual systems were the resolution of the peripheral field and the vertical excursion limits of the high-resolution inset for the LFOVD. DTIC

N94-16113# Massachusetts General Hospital, Boston. Labs. of Photomedicine.
CENTER OF EXCELLENCE IN LASER MEDICINE
J. A. Parrish 29 Apr. 1993 6 p
(Contract DE-FG02-91ER-61228)
(DE93-016541; DOE/ER-61228/T1) Avail: CASI HC A02/MF A01

Achievements during the last 12 months of funding to initiate a Center of Excellence in biomedical laser development include the following: seven specific research projects within the Center's three broad interest areas; and program development to establish the MGH Laser Center and its activities. Progress is reported in three areas of interest: new medical laser systems development; optical diagnostics; and photo sensitization. Feasibility studies and prototype development were emphasized, to enhance establishing a substantial Center through future support. Specific projects are outlined. In addition, the interdepartmental MGH Laser Center's activities and accomplishments are reported. DOE

N94-16478* National Aeronautics and Space Administration, Washington, DC.
AEROSPACE MEDICINE AND BIOLOGY: A CONTINUING BIBLIOGRAPHY WITH INDEXES (SUPPLEMENT 378)
Aug. 1993 72 p
(NASA-SP-7011(378); NAS 1.21:7011(378)) Avail: CASI HC A04

This bibliography lists 185 reports, articles and other documents introduced into the NASA Scientific and Technical Information System during Aug. 1993. Subject coverage includes: aerospace medicine and physiology, life support systems and man/system technology, protective clothing, exobiology and extraterrestrial life, planetary biology, and flight crew behavior and performance. Author

N94-16479* National Aeronautics and Space Administration, Washington, DC.
AEROSPACE MEDICINE AND BIOLOGY: A CONTINUING

BIBLIOGRAPHY WITH INDEXES (SUPPLEMENT 380)
Oct. 1993 72 p
(NASA-SP-7011(380); NAS 1.21:7011(380)) Avail: CASI HC A04

This bibliography lists 192 reports, articles and other documents introduced into the NASA Scientific and Technical Information System during Oct. 1993. Subject coverage includes: aerospace medicine and physiology, life support systems and man/system technology, protective clothing, exobiology and extraterrestrial life, planetary biology, and flight crew behavior and performance. Author

N94-16515# Armed Forces Radiobiology Research Inst., Bethesda, MD.
AFRRI REPORTS, FIRST QUARTER 1993
May 1993 81 p
(DA Proj. NWE-DQAX)
(AD-A266380; AFRRI-SR93-1; AFRRI-SR93-2) Avail: CASI HC A05/MF A01

Contents include the following Armed Forces Radiobiology Research Institute reports: .effects of WR-1065 and WR-151326 on survival and neoplastic transformation in C3H/10T1/2 cells exposed to TRIGA or JANUS fission neutrons; behavioral differences of irradiated persons associated with the Kyshtym, Chelyabinsk, and Chernobyl nuclear accidents; involvement of superoxide dismutase and glutathione peroxidase in attenuation of radiation induced hyperthermia; implication of nitric oxide synthase in radiation induced decrease in hippocampal noradrenaline release in rats; energy deposition in a spherical cavity of arbitrary size and composition; inhibition of c-kit ligand/steel factor by antibodies reduces survival of lethally irradiated mice; effects of combined administration of interleukin-6 and granulocyte colony stimulating factor on recovery from radiation induced hemopoietic aplasia; synergistic roles of interleukin-6, interleukin-1, and tumor necrosis factor in the adreno corticotropin response to bacterial lipo polysaccharide in vivo; electron paramagnetic resonance detection of nitric oxide-dependent spin adducts in mouse jejunum; radiolysis of dinucleoside monophosphates by high-energy electrons and fission neutrons; effects of sublethal doses of ionizing radiation; and differences in unwinding of supercoiled DNA induced by the two enantiomers of anti benzo(a)pyrene diol epoxide. DTIC

N94-16544# Letterman Army Inst. of Research, San Francisco, CA.
A MATHEMATICAL MODEL FOR THE STUDY OF HEMORRHAGIC SHOCK AND FLUID RESUSCITATION: TRANSCAPILLARY EXCHANGE Final Report, 1989 - 1993
Tammy J. Doherty Mar. 1993 37 p
(AD-A266427; LAIR-477) Avail: CASI HC A03/MF A01

Mathematical models used to predict plasma volume responses to hemorrhage and fluid resuscitation must consider both fluid and solute exchange across the capillary wall. In this paper, we review four models of transcapillary exchange that might be incorporated into a compartmental model for plasma volume prediction. The simplest of the four transcapillary flux models assumes a discrete capillary wall structure, ideal solutions, and capillary wall homogeneity. The remaining models become progressively more complex by successive elimination of these three assumptions. To assess their effects on whole-body plasma volume predictions, the four models of transcapillary exchange were incorporated into a simple two-compartment (blood and interstitial space) model. Next, plasma volume predictions were generated for the following simulation conditions: instantaneous 25% loss of blood volume, instantaneous 50% increase in plasma NaCl concentration, instantaneous 50% increase in plasma albumin concentration, and instantaneous 25% loss of blood volume with a 50% increase in plasma NaCl concentration. Plasma volume predictions, generated by the four models, were indistinguishable over these simulation conditions. From these results, we conclude that the simplest of the transcapillary flux models may be used for predicting plasma volume responses to hemorrhage and resuscitative fluid administration. DTIC

N94-16558# Letterman Army Inst. of Research, San Francisco, CA.
A MATHEMATICAL MODEL FOR THE STUDY OF HEMORRHAGIC SHOCK AND FLUID RESUSCITATION: EXCHANGE OF FLUID AND SOLUTES BETWEEN VASCULAR, INTERSTITIAL, AND TISSUE CELL COMPARTMENTS Final Report, 1989 - 1993
Tammy J. Doherty Jun. 1993 26 p
(AD-A266426; LAIR-478) Avail: CASI HC A03/MF A01

The transfer of fluid from extravascular compartments into the vasculature is an important recovery mechanism for hemorrhage. This paper describes a three-compartment model (i.e., vascular, interstitial, and tissue cell) that predicts intra-extravascular fluid exchange following hemorrhage and fluid resuscitation. This three-compartment model assumes that capillary pressure is a linear function of blood volume, that interstitial pressure is a nonlinear function of extravascular volume, and that lymph flow is a function of interstitial pressure. Starting with this simple three-compartment model, the effects of model assumptions on plasma volume predictions were assessed. By varying model assumptions and comparing plasma volume predictions, we determined that separate tissue cell and interstitial compartments were required for predicting the plasma volume response to infusions of resuscitative solutions containing small, permeable solutes (e.g., NaCl). We also determined that the interstitial space could be described by a constant hydrostatic pressure, that considerations of interstitial exclusion volumes were not required, and that lymph flow could be considered constant. Plasma volume predictions generated by the three-compartment model were also compared to observed plasma volumes for validation. DTIC

N94-16564# Letterman Army Inst. of Research, San Francisco, CA. Div. of Blood Research.
EVALUATION OF HEMOGLOBIN-OXYGEN EQUILIBRIUM BINDING BY RAPID-SCANNING SPECTROPHOTOMETRY AND SINGULAR-VALUE DECOMPOSITION
Kim D. Vandegriff and Richard I. Shrager 8 Mar. 1993 21 p
(AD-A266453) Avail: CASI HC A03/MF A01

A review of a new method to measure oxygen equilibrium binding to hemoglobin solutions by rapid-scanning spectrophotometry is presented. State-of-the-art technologies are reviewed and compared. The new method is based on rapid-scanning spectrophotometry that is used to resolve directly unique optical transitions during continuous hemoglobin oxygenation. Mathematical techniques for matrix multicomponent analysis and singular value decomposition (SVD) are described, and spectral artifacts that are resolved by these sensitive techniques are discussed. DTIC

N94-16565# Letterman Army Inst. of Research, San Francisco, CA.
INCREASED VASCULAR RESISTANCE WITH HEMOGLOBIN-BASED OXYGEN CARRIERS
J. R. Hess, V. W. MacDonald, C. S. Gomez, and V. Copper 1993 13 p
(AD-A266454) Avail: CASI HC A03/MF A01

The purpose of this project was as follows: to compare the effects of resuscitation with hemoglobin-based oxygen-carriers and conventional crystalloid and colloid resuscitation fluids on hemodynamics, oxygen transport, and oxygen consumption in an animal model of the field medical use of these fluids in the treatment of hemorrhagic shock. Twenty-eight immature swine were tested in accordance with the following protocol: they were surgically prepared; allowed to recover five days; water deprived for 48 hours; hemorrhaged of 25 ml/kg over one hour; resuscitated promptly with (1) Ringer's lactate, 75 ml/kg, (2) 7% albumin in Ringer's acetate, 25 ml/kg, (3) 9% unmodified hemoglobin in Ringer's acetate, 25 ml/kg, or (4) 9% alpha alpha-crosslinked hemoglobin in Ringer's acetate, 25 ml/kg; observed with three hours of hemodynamic and oxygen transport measurements; and, finally, blood which had been removed previously was returned. DTIC

N94-16566# Letterman Army Inst. of Research, San Francisco, CA. Div. of Blood Research.
HEMOGLOBIN
Kim D. Vandegriff 8 Mar. 1993 11 p
(AD-A266455) Avail: CASI HC A03/MF A01

This is a review of hemoglobin structure and function. The role of hemoglobin as the red blood cell oxygen-transport protein is outlined. The structure is defined in terms of amino acid sequence, x-ray crystallographic structure, and subunit interaction. The function is described for reversible oxygen binding, carbon dioxide, and protein mechanism. DTIC

N94-16609*# BioTechnology, Inc., Falls Church, VA.
PROCEEDINGS OF THE 1992 ANNUAL MEETING NASA OCCUPATIONAL HEALTH PROGRAM
Jul. 1993 312 p Meeting held in San Jose, CA, 30 Nov. - 4 Dec. 1992
(Contract NASw-4176)
(NASA-CR-193462; NAS 1.26:193462) Avail: CASI HC A14/MF A03

The purpose of this meeting was to exchange information across NASA facilities that is critical to agency-wide improvement in the efforts to maintain and enhance employee health. The topics covered include the following: occupational medicine, environmental health, physical fitness, and health education. For individual titles, see N94-16610 through N94-16645.

N94-16610*# Department of Energy, Washington, DC.
NEW HEALTH AND SAFETY INITIATIVES AT THE DEPARTMENT OF ENERGY (DOE)
Paul L. Ziemer *In* BioTechnology, Inc., Proceedings of the 1992 Annual Meeting NASA Occupational Health Program Jul. 1993 p 9-26 (For primary document see N94-16609 03-52)
Avail: CASI HC A03/MF A03

This document touches on some of the more important lessons learned and the more noteworthy initiatives DOE has put into motion in the last three years to protect the health and safety of our contractor employees. What we have learned in the process should come as no surprise to those of you who have been working in the field: (1) that management commitment to safety and health is critical to a successful program; (2) that meaningful employee participation in all aspects of the program enhances its effectiveness at every level; and (3) that the dedication and expertise of medical and occupational safety and health professionals are needed if the challenging problems presented by the complex and technologically advanced environment at DOE facilities are to be overcome. I believe that we have made a good beginning in the long and arduous task of building an Occupational Safety and Health Program that will serve as a model for others, and I can assure you that we intend to continue our efforts to protect every worker within the complex from occupational injury and disease. Derived from text

N94-16611*# Medical Associates, Inc., Charlotte, NC.
AMERICANS WITH DISABILITIES ACT CONSIDERATIONS FOR THE PRACTICE OF OCCUPATIONAL MEDICINE
Steven St.Clair and Theodore Shults (Shults and Associates, Chapel Hill, NC.) *In* BioTechnology, Inc., Proceedings of the 1992 Annual Meeting NASA Occupational Health Program Jul. 1993 p 27-43 (For primary document see N94-16609 03-52)
Avail: CASI HC A03/MF A03

The Americans with Disabilities Act (ADA), although developed in the context of civil rights legislation, is likely to have notable impact on the practice of occupational medicine. The ADA contains provisions limiting the use of preplacement examinations to determinations of the capability to perform the essential functions of the job and of direct threat to the health and safety of the job applicant and others. The Title 1 employment provisions of the ADA established definitions and requirements similar to those found in section 504 of the Rehabilitation Act of 1973, as amended; leading cases that have been litigated under the Rehabilitation Act, as amended, are described. The limitations of available scientific and medical information related to determinations of job capability and direct threat and ramifications of the ADA on the practice of occupational medicine are discussed. Author

N94-16612*# Georgia Inst. of Tech., Atlanta.
ERGONOMICS IN THE OFFICE ENVIRONMENT **c54**
Theodore K. Courtney *In* BioTechnology, Inc., Proceedings of the 1992 Annual Meeting NASA Occupational Health Program Jul. 1993 p 45-60 (For primary document see N94-16609 03-52)
Avail: CASI HC A03/MF A03

Perhaps the four most popular 'ergonomic' office culprits are: (1) the computer or visual display terminal (VDT); (2) the office chair; (3) the workstation; and (4) other automated equipment such as the facsimile machine, photocopier, etc. Among the ergonomics issues in the office environment are visual fatigue, musculoskeletal disorders, and radiation/electromagnetic (VLF,ELF) field exposure from VDT's. We address each of these in turn and then review some regulatory considerations regarding such stressors in the office and general industrial environment. Author

N94-16613*# Monsanto Co., Luling, LA.
EMERGENCY PREPAREDNESS AND PLANNING
Kenneth Bouvier *In* BioTechnology, Inc., Proceedings of the 1992 Annual Meeting NASA Occupational Health Program Jul. 1993 p 61-68 (For primary document see N94-16609 03-52)
Avail: CASI HC A02/MF A03

Monsanto's emergency response plan in dealing with hazardous materials at their facilities is presented. Topics discussed include the following: CPR training; emergency medial training; incident reports; contractor injuries; hazardous materials transport; evacuation; and other industrial safety concerns. CASI

N94-16614*# Coalition to Prevent Lead Poisoning, San Francisco, CA.
LEAD POISONING: AN OVERVIEW
Neil Gendel *In* BioTechnology, Inc., Proceedings of the 1992 Annual Meeting NASA Occupational Health Program Jul. 1993 p 69-78 (For primary document see N94-16609 03-52)
Avail: CASI HC A02/MF A03

A problem that should be of great concern to all of us is the lead poisoning of children. First, I would like to present a short overview concerning the reasons everyone should care about lead poisoning, then discuss the history of lead poisoning, what is happening today across the country, and the future. Author

N94-16615*# Edgerton, Germeshausen and Grier, Inc., Cocoa Beach, FL.
MEDICAL SURVEILLANCE AND BIOLOGICAL MONITORING OF LEAD EXPOSED EMPLOYEES
E. B. Ferguson *In* BioTechnology, Inc., Proceedings of the 1992 Annual Meeting NASA Occupational Health Program Jul. 1993 p 79-85 (For primary document see N94-16609 03-52)
Avail: CASI HC A02/MF A03

Employee health protection is an employer responsibility. The multi-faceted aspects of employee protection from the potentially harmful effects of inorganic lead sometimes stress the relationships of several employer units. These include supervision and management, safety, operations and maintenance, engineering, environmental health, environmental management, and occupational medicine. The administrative aspects of program development are discussed. The purpose is to emphasize the opportunity for cooperation by all of the employee health components in developing an optimum surveillance and protection program. Author (revised)

N94-16616*# Center for Occupational Programs for Employees, Inc., Washington, DC.
ONGOING RECOVERY BASIC INFORMATION TOOL (ORBIT)
Donald Oberg *In* BioTechnology, Inc., Proceedings of the 1992 Annual Meeting NASA Occupational Health Program Jul. 1993 p 87-89 (For primary document see N94-16609 03-52)
Avail: CASI HC A01/MF A03

The Federal Drug Free Work Place Program (DFWP) has now matured to the point of being able to return employees to sensitive testing designated positions (TDP) after completion of treatment of their addiction. The known tendency of addicted individuals to suffer multiple relapses prior to their final recovery has resulted in several positive urine tests (relapses) occurring among those Federal employees who have already completed treatment and who have been returned to TDP's. The very real potential for further relapses occurring after additional employees return to TDP's will be a critical factor in the ultimate success of the DFWP and in the public's impression of the program's effectiveness. In response to this concern, NASA has begun development of its Ongoing Recovery Basic Information Tool (ORBIT) instrument. The aim of the NASA ORBIT is to provide Employee Assistance Program (EAP) professionals with an advanced clinical tool which will be helpful in supporting recovery from substance abuse and which will allow more accurate determinations of when clients may be successfully returned to sensitive positions. Author (revised)

N94-16617*# Office of Personnel Management, Washington, DC.
PROGRAMS AND RESOURCES FOR CONTROL OF JOB STRESS IN THE FEDERAL WORKPLACE **c53**
Wendell Joice *In* BioTechnology, Inc., Proceedings of the 1992 Annual Meeting NASA Occupational Health Program Jul. 1993 p 91-98 (For primary document see N94-16609 03-52)
Avail: CASI HC A02/MF A03

A couple of weeks ago, the American Psychological Association and

the National Institute of Occupational Safety and Health held a conference in Washington, D.C. entitled 'Stress in the 90's'. At this conference the Office of Personnel Management (OPM) conducted a session on 'Programs and Resources for the Control of Job Stress in the Federal Workplace'. I am going to present an overview of that three-hour session and some related information from the conference. My discussion covers stress terminology and models, selected programs and resources, evaluation research, some concerns about our progress, and plans to expand our efforts at OPM. Author (revised)

N94-16618*# Harvard School of Public Health, Boston, MA.
EDUCATION AND TRAINING OF PROFESSIONAL INDUSTRIAL HYGIENISTS FOR 2020 **c80**
R. J. Sherwood *In* BioTechnology, Inc., Proceedings of the 1992 Annual Meeting NASA Occupational Health Program Jul. 1993 p 99-120 (For primary document see N94-16609 03-52)
Avail: CASI HC A03/MF A03

Four questions are addressed: (1) Are we giving sufficient attention to the professional education of industrial hygienists?; (2) Are we achieving an adequate measure of control of hazards at the workplace?; (3) What is our record of success in this field?; and (4) Do we have clear objectives, both as a profession and as individuals? I discuss some aspects of these but will not attempt to provide answers, hoping thereby to stimulate discussion and to conceal the fact that I do not know the answers myself. I will, however, follow this discussion with a review of the overall need for training in industrial hygiene, and will conclude with some comments about needed changes in the education of future professional industrial hygienists. Author (revised)

N94-16619*# National Aeronautics and Space Administration. Lyndon B. Johnson Space Center, Houston, TX.
PHYSICAL FITNESS AND THE HEALTHY PEOPLE 2000 GOALS
Larry T. Wier *In* BioTechnology, Inc., Proceedings of the 1992 Annual Meeting NASA Occupational Health Program Jul. 1993 p 121-142 (For primary document see N94-16609 03-52)
Avail: CASI HC A03/MF A03

Healthy People 2000 is a statement of national objectives with the overall goal of improving American health. Various aspects of endeavor are discussed. Derived from text

N94-16620*# National Aeronautics and Space Administration. Ames Research Center, Moffett Field, CA.
SEARCH FOR EXTRATERRESTRIAL INTELLIGENCE (SETI) **c55**
John Billingham *In* BioTechnology, Inc., Proceedings of the 1992 Annual Meeting NASA Occupational Health Program Jul. 1993 p 143-151 (For primary document see N94-16609 03-52)
Avail: CASI HC A02/MF A03

Various aspects of project SETI are discussed. Some of the topics discussed include spectrum analyzers, signal processing, sky surveys, radiotelescopes, high resolution microwave survey, Deep Space Network, and signal detection. CASI

N94-16621*# National Health Services, Inc., New York, NY.
THE GODDARD SPACE FLIGHT CENTER ERGONOMICS PROGRAM **c54**
Eileen Batson and Theodore Unite *In* BioTechnology, Inc., Proceedings of the 1992 Annual Meeting NASA Occupational Health Program Jul. 1993 p 153-158 (For primary document see N94-16609 03-52)
Avail: CASI HC A02/MF A03

Since the Kennedy Space Center (KSC) Cardiovascular Screening Program started in 1984, we have made many changes to accommodate the growing number of participants. As a result of these changes, screening of KSC employees has become more efficient and productive. Various aspects of the program are covered. Derived from text

N94-16622*# Edgerton, Germeshausen and Grier, Inc., Cocoa Beach, FL.
EFFICIENT MANAGEMENT OF CARDIOVASCULAR RISK SCREENING PROGRAMS
Carol Roth *In* BioTechnology, Inc., Proceedings of the 1992 Annual Meeting NASA Occupational Health Program Jul. 1993 p 159-165 (For primary document see N94-16609 03-52)
Avail: CASI HC A02/MF A03

The Environmental Health Unit, located on-site at the Goddard Space Flight Center (GSFC), is responsible for the implementation of the Center's Employee Environmental and Occupational Health Program. The Health Unit, Health Physics (HP), and Industrial Hygiene (IH) staffs collaborate to provide quality service to the employees at GSFC. The Health Unit staff identifies, evaluates, and ensures the control of occupational hazards on the Center. In the past, components of the Industrial Hygiene Program have included the Industrial Hygiene Health Hazard Identification Program (IHHIP), the Hearing Conservation Program (HCP), the Hazard Communication Program, and the bi-annual fume hood survey. More recently, the Environmental Health Unit has expanded its services by adding the Ergonomics Program. Various aspects of the Ergonomics Program are discussed. Derived from text

N94-16623*# Kelsey Seybold Clinic, P.A., Houston, TX.
INDUSTRIAL HYGIENE LABORATORY ACCREDITATION: THE JSC EXPERIENCE
Dawn E. Fadner *In* BioTechnology, Inc., Proceedings of the 1992 Annual Meeting NASA Occupational Health Program Jul. 1993 p 167-174 (For primary document see N94-16609 03-52)
Avail: CASI HC A02/MF A03

The American Industrial Hygiene Association (AIHA) is a society of professionals dedicated to the health and safety of workers and community. With more than 10,000 members, the AIHA is the largest international association serving occupational and environmental health professionals practicing industrial hygiene in private industry, academia, government, labor, and independent organizations. In 1973, AIHA developed a National Industrial Hygiene Laboratory Accreditation Program. The purposes of this program are shown. Derived from text

N94-16624*# Edgerton, Germeshausen and Grier, Inc., Cocoa Beach, FL.
SPACE SHUTTLE SOLID ROCKET MOTOR EXPOSURE MONITORING **c28**
S. W. Brown *In* BioTechnology, Inc., Proceedings of the 1992 Annual Meeting NASA Occupational Health Program Jul. 1993 p 175-182 (For primary document see N94-16609 03-52)
Avail: CASI HC A02/MF A03

During the processing of the Space Shuttle Solid Rocket Booster (SRB), segments at the Kennedy Space Center, an odor was detected around the solid propellant. An Industrial Hygiene survey was conducted to determine the chemical identity of the SRB offgassing constituents. Air samples were collected inside a forward SRB segment and analyzed to determine chemical composition. Specific chemical analysis for suspected offgassing constituents of the propellant indicated ammonia to be present. A gas chromatograph mass spectroscopy (GC/MS) analysis of the air samples detected numerous high molecular weight hydrocarbons. Author

N94-16625*# Edgerton, Germeshausen and Grier, Inc., Cocoa Beach, FL.
ILLNESS/INJURY PATTERN COMPLEX 40 (TITAN)
Sharon Blasdell *In* BioTechnology, Inc., Proceedings of the 1992 Annual Meeting NASA Occupational Health Program Jul. 1993 p 183-188 (For primary document see N94-16609 03-52)
Avail: CASI HC A02/MF A03

On July 31, 1991, EG&G Medical began providing medical support at the Titan Area Clinic (TAC). The hours of operation are 0700-2300, Monday through Friday, with Emergency Medical Services (EMS) provided 24-hours a day, seven days a week. The TAC consists of a 10 x 10 ft section of a trailer that also houses Bechtel Safety. Supplies consisted of an examining table, an eye wash chair, first aid equipment, over-the-counter medications, spine boards, a portable rescuscitator, etc. All of the nurses are Advanced Cardiac Life Support (ACLS) certified. Although the Titan Area Clinic is strictly a first-aid station with no ACLS facilities on-site, it is staffed with an Occupational Health Nurse with ACLS certification. If ACLS or additional help is needed, the nurse activates EMS by dialing 911. The nurse responds to any medical problems or emergencies on the complex, but activates EMS prior to leaving the TAC. A Bechtel Safety Representative accompanies the nurse to the site and assists as needed. Other aspects of the complex and its functions are presented. Derived from text

N94-16626*# Edgerton, Germeshausen and Grier, Inc., Cocoa Beach, FL.

IDENTIFYING AND RESPONDING TO CUSTOMER NEEDS AT THE KENNEDY SPACE CENTER c38

E. B. Ferguson *In* BioTechnology, Inc., Proceedings of the 1992 Annual Meeting NASA Occupational Health Program Jul. 1993 p 189-194 (For primary document see N94-16609 03-52)

Avail: CASI HC A02/MF A03

The Patient Questionnaire Program at the Kennedy Space Center (KSC) has been in place for several years. It has helped to identify customer perceptions and needs. The questionnaire is presented and the survey results are discussed with respect to total quality management.

Derived from text

N94-16627*# National Aeronautics and Space Administration. Lewis Research Center, Cleveland, OH.

TUBERCULOSIS: A CASE FOR INCREASED SCREENING

Stephen A. Weirich *In* BioTechnology, Inc., Proceedings of the 1992 Annual Meeting NASA Occupational Health Program Jul. 1993 p 199-210 (For primary document see N94-16609 03-52)

Avail: CASI HC A03/MF A03

The topics discussed include the following: background; epidemiological shifts; pathophysiology of turberculosis; screening for turberculosis; and recommendations.

Derived from text

N94-16628*# National Aeronautics and Space Administration. Lewis Research Center, Cleveland, OH.

SUMMARY OF FOLLOW-UP RESULTS FROM POTENTIAL TUBERCULOSIS EXPOSURES

Stephen A. Weirich *In* BioTechnology, Inc., Proceedings of the 1992 Annual Meeting NASA Occupational Health Program Jul. 1993 p 211-212 (For primary document see N94-16609 03-52)

Avail: CASI HC A01/MF A03

There were two isolated episodes of LeRC workers who were diagnosed with pulmonary tuberculosis (TB) during the fall of 1990. The specifics surrounding each case were very different, and it is clear that the two episodes were completely unrelated. The fact that the final diagnoses of pulmonary tuberculosis came within three weeks of each other was purely coincidental. The Occupational Medicine Service (OMS) conducted separate informational sessions and offered free PPD skin testing to all employees, both NASA and contractors, who felt that they were at risk of having been exposed to tuberculosis from either individual. The procedures and results of these are briefly discussed.

Derived from text

N94-16629*# National Aeronautics and Space Administration. Lewis Research Center, Cleveland, OH.

LEGIONELLA: AN OVERVIEW

Stephen A. Weirich *In* BioTechnology, Inc., Proceedings of the 1992 Annual Meeting NASA Occupational Health Program Jul. 1993 p 213-219 (For primary document see N94-16609 03-52)

Avail: CASI HC A02/MF A03

The topics discussed include the following: history; bacteriology, ecology, and transmission; epidemiology; clinical manifestations; Pontiac Fever; diagnosis; treatment; and prevention.

Derived from text

N94-16630*# National Aeronautics and Space Administration. Lewis Research Center, Cleveland, OH.

SCREENING FOR PROSTATE CANCER

Stephen A. Weirich *In* BioTechnology, Inc., Proceedings of the 1992 Annual Meeting NASA Occupational Health Program Jul. 1993 p 221-223 (For primary document see N94-16609 03-52)

Avail: CASI HC A01/MF A03

Despite recent advances in both the survival and cure rates for many forms of cancer, unfortunately the same has not been true for prostate cancer. In fact, the age-adjusted death rate from prostate cancer has not significantly improved since 1949, and prostate cancer remains the most common cancer in American men, causing the second highest cancer mortality rate. Topics discussed include the following: serum testosterone levels; diagnosis; mortality statistics; prostate-sppecific antigen (PSA) tests; and the Occupational Medicine Services policy at LeRC.

Derived from text

N94-16631*# National Aeronautics and Space Administration, Washington, DC.

PHYSICAL FITNESS AND HEALTH EDUCATION PROGRAM AT NASA HEADQUARTERS

Cathy Angotti *In* BioTechnology, Inc., Proceedings of the 1992 Annual Meeting NASA Occupational Health Program Jul. 1993 p 233-235 (For primary document see N94-16609 03-52)

Avail: CASI HC A01/MF A03

The topics discussed include the following: policy procedures to enter the NASA Headquarters Physical Fitness and Health Program; eligibility; TDY eligibility; health promotions offered; and general facility management.

Derived from text

N94-16632*# National Aeronautics and Space Administration. Ames Research Center, Moffett Field, CA.

AMES FITNESS PROGRAM

Randy Pratt *In* BioTechnology, Inc., Proceedings of the 1992 Annual Meeting NASA Occupational Health Program Jul. 1993 p 237 (For primary document see N94-16609 03-52)

Avail: CASI HC A01/MF A03

The Ames Fitness Program services 5,000 civil servants and contractors working at Ames Research Center. A 3,000 square foot fitness center, equipped with cardiovascular machines, weight training machines, and free weight equipment is on site. Thirty exercise classes are held each week at the Center. A weight loss program is offered, including individual exercise prescriptions, fitness testing, and organized monthly runs. The Fitness Center is staffed by one full-time program coordinator and 15 hours per week of part-time help. Membership is available to all employees at Ames at no charge, and there are no fees for participation in any of the program activities. Prior to using the Center, employees must obtain a physical examination and complete a membership package. Funding for the Ames Fitness Program was in jeopardy in December 1992; however, the employees circulated a petition in support of the program and collected more than 1500 signatures in only three days. Funding has been approved through October 1993.

Author (revised)

N94-16633*# National Aeronautics and Space Administration. Lyndon B. Johnson Space Center, Houston, TX.

JOHNSON SPACE CENTER HEALTH RELATED FITNESS PROGRAM

Larry T. Wier *In* BioTechnology, Inc., Proceedings of the 1992 Annual Meeting NASA Occupational Health Program Jul. 1993 p 239-243 (For primary document see N94-16609 03-52)

Avail: CASI HC A01/MF A03

The topics covered include the following: educational component; activity ratings; lecture topics; program evaluation; Nutrition Intervention Program; and research.

CASI

N94-16634*# Bionetics Corp., Cocoa Beach, FL.

KENNEDY SPACE CENTER EXERCISE PROGRAM

Cristy Hoffman *In* BioTechnology, Inc., Proceedings of the 1992 Annual Meeting NASA Occupational Health Program Jul. 1993 p 245-248 (For primary document see N94-16609 03-52)

Avail: CASI HC A01/MF A03

The Kennedy Space Center (KSC) Fitness Program began in Feb. 1993. The program is managed by the Biomedical Operations and Research Office and operated by the Bionetics Corporation. The facilities and programs are offered to civil servants, all contractors, temporary duty assignment (TDY) participants, and retirees. All users must first have a medical clearance. A computer-generated check-in system is used to monitor participant usage. Various aspects of the program are discussed.

Derived from text

N94-16635*# National Aeronautics and Space Administration. Langley Research Center, Hampton, VA.

THE LANGLEY FITNESS CENTER

In BioTechnology, Inc., Proceedings of the 1992 Annual Meeting NASA Occupational Health Program Jul. 1993 p 249-253 (For primary document see N94-16609 03-52)

Avail: CASI HC A01/MF A03

NASA Langley recognizes the importance of healthy employees by committing itself to offering a complete fitness program. The scope of the program focuses on promoting overall health and wellness in an effort to reduce the risks of illness and disease and to increase productivity. This is

accomplished through a comprehensive Health and Fitness Program offered to all NASA employees. Various aspects of the program are discussed.
Derived from text

N94-16636*# National Aeronautics and Space Administration. Marshall Space Flight Center, Huntsville, AL.
PHYSICAL EXERCISE PROGRAM
In BioTechnology, Inc., Proceedings of the 1992 Annual Meeting NASA Occupational Health Program Jul. 1993 p 255-257 (For primary document see N94-16609 03-52)
Avail: CASI HC A01/MF A03
The topics discussed include the following: the Marshall Space Flight Center Physical Education Program and the physical fitness and health breakout session. CASI

N94-16637*# National Aeronautics and Space Administration. Lewis Research Center, Cleveland, OH.
ARSENIC SURVEILLANCE PROGRAM
In BioTechnology, Inc., Proceedings of the 1992 Annual Meeting NASA Occupational Health Program Jul. 1993 p 261-266 (For primary document see N94-16609 03-52)
Avail: CASI HC A02/MF A03
Background information about arsenic is presented including forms, common sources, and clinical symptoms of arsenic exposure. The purpose of the Arsenic Surveillance Program and LeRC is outlined, and the specifics of the Medical Surveillance Program for Arsenic Exposure at LeRC are discussed. CASI

N94-16638*# National Aeronautics and Space Administration. Lewis Research Center, Cleveland, OH.
ASBESTOS SURVEILLANCE PROGRAM
In BioTechnology, Inc., Proceedings of the 1992 Annual Meeting NASA Occupational Health Program Jul. 1993 p 267-271 (For primary document see N94-16609 03-52)
Avail: CASI HC A01/MF A03
Background on asbestos is presented including the different types and the important medical distinctions between those different types. The four diseases associated with asbestos exposure are discussed: mesothelioma, lung cancer, asbestosis, and benign pleural disorders. The purpose of the LeRC Asbestos Surveillance Program is outlined, and the specifics of the Medical Surveillance Program for Asbestos Monitoring at LeRC are discussed. Derived from text

N94-16639*# National Aeronautics and Space Administration. Lewis Research Center, Cleveland, OH.
HEARING CONSERVATION MEDICAL PROGRAM
In BioTechnology, Inc., Proceedings of the 1992 Annual Meeting NASA Occupational Health Program Jul. 1993 p 273-279 (For primary document see N94-16609 03-52)
Avail: CASI HC A02/MF A03
Background on hearing impairment is presented including causes and criteria for safe noise levels. The purpose of the Hearing Conservation Program at LeRC is outlined, and the specifics of the Medical Surveillance Program for Hearing Impairment at LeRC are discussed. CASI

N94-16640*# National Aeronautics and Space Administration. Lewis Research Center, Cleveland, OH.
LEAD SURVEILLANCE PROGRAM
In BioTechnology, Inc., Proceedings of the 1992 Annual Meeting NASA Occupational Health Program Jul. 1993 p 281-289 (For primary document see N94-16609 03-52)
Avail: CASI HC A02/MF A03
Background on lead exposure is presented including forms of lead, sources, hematologic effects, neurologic effects, endocrine effects, renal effects, and reproductive and developmental effects. The purpose of the Lead Surveillance Program at LeRC is outlined, and the specifics of the Medical Surveillance Program for Lead Exposure at LeRC are discussed. CASI

N94-16641*# National Aeronautics and Space Administration. Lewis Research Center, Cleveland, OH.
MERCURY SURVEILLANCE PROGRAM
In BioTechnology, Inc., Proceedings of the 1992 Annual Meeting NASA Occupational Health Program Jul. 1993 p 291-295 (For primary document see N94-16609 03-52)
Avail: CASI HC A01/MF A03
Background on mercury exposure is presented including forms, sources, permissible exposure limits, and physiological effects. The purpose of the Mercury Surveillance Program at LeRC is outlined, and the specifics of the Medical Surveillance Program for Mercury Exposure at LeRC are discussed. CASI

N94-16642*# National Aeronautics and Space Administration. Lewis Research Center, Cleveland, OH.
RESPIRATORY PROTECTION PROGRAM MEDICAL CLEARANCE FOR RESPIRATOR USE
In BioTechnology, Inc., Proceedings of the 1992 Annual Meeting NASA Occupational Health Program Jul. 1993 p 297-303 (For primary document see N94-16609 03-52)
Avail: CASI HC A02/MF A03
Background on occupational exposure to various inhalents is discussed including on-site hazard control measures, procedures, physiological effects, and interpretation of results for the medical clearance of employee for use of personal respiratory protection devices. The purpose of the Respiratory Protection Program at LeRC is outlined, and the specifics of the Medical Surveillance Program for Respiratory Protection at LeRC are discussed. CASI

N94-16643*# National Aeronautics and Space Administration. Lewis Research Center, Cleveland, OH.
GENERAL MEDICAL SURVEILLANCE PROGRAM
In BioTechnology, Inc., Proceedings of the 1992 Annual Meeting NASA Occupational Health Program Jul. 1993 p 305-308 (For primary document see N94-16609 03-52)
Avail: CASI HC A01/MF A03
Background on the General Medical Surveillance Program at LeRC is presented. The purpose of the General Medical Surveillance Program at LeRC is outlined, and the specifics of the program are discussed. CASI

N94-16644*# Edgerton, Germeshausen and Grier, Inc., Cocoa Beach, FL.
BLOODBORNE PATHOGENS PROGRAM
Sharon Blasdell *In* BioTechnology, Inc., Proceedings of the 1992 Annual Meeting NASA Occupational Health Program Jul. 1993 p 309-311 (For primary document see N94-16609 03-52)
Avail: CASI HC A01/MF A03
The final rule on the Occupational Exposure to Bloodborne Pathogens was published in the Federal Register on Dec. 6, 1991. This Standard, 29 CFR Part 1910.130, is expected to prevent 8,900 hepatitis B infections and nearly 200 deaths a year in healthcare workers in the U.S. The Occupational Medicine and Environmental Health Services at KSC has been planning to implement this standard for several years. Various aspects of this standard and its Bloodborne Pathogens Program at KSC are discussed. Derived from text

N94-16645*# Hummer Associates, Washington, DC.
OSHA BLOODBORNE PATHOGENS STANDARDS EXPOSURE CONTROL PLAN
Caro Elise Luhrs and Rita Teitelbaum *In* BioTechnology, Inc., Proceedings of the 1992 Annual Meeting NASA Occupational Health Program Jul. 1993 p 313-327 Revised (For primary document see N94-16609 03-52)
Avail: CASI HC A03/MF A03
The Hummer Associates Exposure Control Plan is designed to reduce significant occupational exposure to bloodborne pathogens and infectious materials for Hummer Associates health care personnel. Under universal precautions, all patients and all body fluids are considered potentially infectious for bloodborne pathogens. Medical personnel need not be at increased risk if universal precautions are correctly understood and followed. This program covers all employees who could reasonably anticipate contact with blood or other potentially infectious materials during the performance of their job responsibilities. Although HIV and hepatitis B are mentioned most often, this program applies to all bloodborne diseases. The two main components needed to implement this program are universal precautions

and engineering/work practice controls. This program covers all employees who may have occupational exposure to blood or other potentially infectious materials. Other aspects of this program are discussed. Derived from text

N94-16779 Letterman Army Inst. of Research, San Francisco, CA.
WOUND HEALING AFTER LASER INJURY TO SKIN: THE EFFECT OF OCCLUSION AND VITAMIN E Final Report
Gad A. Simon, Peter Schmid, William G. Reifenrath, Theodore VanRavenswaay, and Bruce E. Stuck May 1993 36 p Limited Reproducibility: More than 20% of this document may be affected by microfiche quality
(AD-A266473) Avail: Issuing Activity (Defense Technical Information Center (DTIC))

The skin of the Yorkshire pig was irradiated with various doses of argon and copper vapor laser and evaluated for effects on healing time of pretreatment with topical or intramuscular vitamin E or the Op-Site wound dressing. Incident irradiance for both lasers was between 3.5 and 4.5 watts/cm(sup 2) for a 10-14 mm beam diameter with a near uniform intensity profile. Minimal erythemic dose for the copper vapor laser was 35 +/- 2 J/cm(sup 2) (10 second exposure) and 22.4 +/- 0.1 J/cm(sup 2) (6 second exposure) for the argon laser. Three dose levels were administered: a low dose causing light erythema, an intermediate dose, and a high dose causing dermal stasis. Exposure to argon and copper vapor lasers generally caused wounds with similar healing times. Healing time was significantly decreased for wounds caused by intermediate exposure of the copper vapor laser and either pretreated with vitamin E or treated with the wound dressing. Healing times for corresponding argon laser exposure were significantly decreased with pretreatment of intramuscular vitamin E only or after treatment with the wound dressing. These findings may be valuable in selecting treatment for accidental laser skin injuries in man. DTIC

N94-16783# Letterman Army Inst. of Research, San Francisco, CA.
THE NATURE OF DYNAMIC ARTERIOLAR VASOREACTIVITY: A MINI-REVIEW AND A CLASSIFICATION SCHEME Final Report
K. E. Arfors, M. Intaglietta, S. P. Bruttig, P. Borgstrom, and J. A. Schmidt 8 Jun. 1993 28 p
(AD-A266499; LAIR-IR-482) Avail: CASI HC A03/MF A01

Changes in microvascular caliber are frequently observed both during normal, resting physiological conditions, as well as during physiologic stresses such as hemorrhage and fluid volume resuscitation. Many of the dynamic changes have been described with the singular term vasomotion. However, many types of frequently observed vasomotive behavior are a typical of either microvascular inactivity or vasomotion. This review describes a simple classification scheme for four types of arteriolar behavior observed routinely in our laboratory in the microvasculature of skeletal muscle of the anesthetized rabbit. These patterns include inactivity (static diameter of the open vessel which does not dynamically affect flow), vasoactivity (random, non-rhythmic changes in vessel diameter, which effect step-wise or non-rhythmic increases or decreases in flow), vasomotion (regular, rhythmic, repetitive constriction and dilation of arterioles with either a fast or slow period), and vessel closure (closure occludes flow entirely, and may divert flow to other adjoining microvascular beds). Although these patterns may not represent a functional continuum, each pattern of behavior is distinct in its effect on blood flow. Therefore, our study proposes a simple classification scheme, which will aid in understanding the dynamic response of the microvasculature to moderate or severe physiologic stress as well as the local, dynamic regulation of microcirculatory flow during pathophysiologic states. DTIC

N94-16784 Letterman Army Inst. of Research, San Francisco, CA.
RELEASE OF IRON FROM HEMOGLOBIN
S. S. Panter 17 Feb. 1993 26 p Limited Reproducibility: More than 20% of this document may be affected by microfiche quality
(AD-A266503) Avail: Issuing Activity (Defense Technical Information Center (DTIC))

The measurement of free iron in hemoglobin solutions as well as the measurement of total hemoglobin-bound iron are important validation assays for large-scale production of hemoglobin-based oxygen carriers. In addition, the detection of iron released from hemoglobin by oxidation or reduction reactions provides information about the stability of iron in heme. These stability measurements may be important in the characterization of structurally modified hemoglobins and can be conducted using spectrophotometric assays based on ferrozine, a chelator of ferrous iron. Techniques for the measurement of free iron in hemoglobin solutions, total hemoglobin-bound iron, and iron released from hemoglobin are described in detail. DTIC

N94-16785 Letterman Army Inst. of Research, San Francisco, CA. Div. of Blood Research.
ENCAPSULATION OF HEMOGLOBIN IN NON-PHOSPHOLIPID VESICLES
K. D. Vandegriff, D. F. Wallach, and R. M. Winslow 1993 6 p Limited Reproducibility: More than 20% of this document may be affected by microfiche quality
(AD-A266505) Avail: Issuing Activity (Defense Technical Information Center (DTIC))

The efficiency of encapsulating hemoglobin in non-phospholipid liposomes by rapidly mixing hemoglobin with lipids heated above their solid-liquid phase transition temperature was examined. Human hemoglobin was mixed at 55-60 C with a lipid solution containing polyoxyethylene-2 cetyl ether and cholesterol (molar ratio, 3:1) at 60-65 C. Repeated mixing was carried out through a high-shear orifice, followed by rapid cooling and additional mixing. Lipid vesicles were heterogeneous in size, with diameters from approximately 300 nm to 10 micrometers. The non-encapsulated aqueous phase was removed by centrifugation, and total hemoglobin was determined spectrophotometrically. Encapsulation efficiency was calculated as the percentage of hemoglobin associated with the liposome phase (i.e., encapsulated) as a function of hemoglobin concentration and the aqueous:lipid hydration ratio. Hemoglobin concentrations were varied from 1 to 10 mM (in heme). Aqueous:lipid ratios of 8:1 and 4:1 were tested. Percent encapsulation varied from 13-30%, with the greatest efficiency, i.e., 30%, at a 4:1 hydration ratio of hemoglobin:lipid at 5.6 mM hemoglobin. DTIC

N94-16786 Letterman Army Inst. of Research, San Francisco, CA. Div. of Blood Research.
NEUROTOXICITY OF HEMOGLOBIN IN CORTICAL CELL CULTURE Final Report
Raymond F. Regan and S. S. Panter 23 Sep. 1992 37 p Limited Reproducibility: More than 20% of this document may be affected by microfiche quality
(AD-A266506) Avail: Issuing Activity (Defense Technical Information Center (DTIC))

Hemoglobin (Hb) has been demonstrated to be neurotoxic when injected into the cerebral cortex, in vivo. However, associated systemic factors such as ischemia and epileptogenesis have limited investigations of Hb toxicity in the intact central nervous system (CNS). In this study, the neurotoxicity of human Hb was assessed in mixed neuronal and glial neocortical cell cultures derived from fetal mice. Exposure of cultures to Hb for 24-28 hours produced widespread and concentration-dependent neuronal death (EC50 1-2.5 uM), without injuring glia. Brief exposures (1-2 hours) were not toxic. Neuronal death was completely blocked by the 21-aminosteroid U74500A, the antioxidant Trolox, and the ferric iron chelator deferoxamine. The results of these experiments suggest that, in this system, chromatographically pure Hb is a potent neurotoxin, and that Hb neurotoxicity may contribute to secondary injury processes after trauma and intracranial hemorrhage. DTIC

N94-16812# California Univ., Berkeley. Lawrence Berkeley Lab.
QUANTIFYING LIFETIME EXPOSURE TO ULTRAVIOLET RADIATION IN THE EPIDEMIOLOGY OF CUTANEOUS MALIGNANT MELANOMA: A PILOT STUDY
C. S. Lea (California Univ., Berkeley.), S. Selvin (California Univ., Berkeley.), and P. A. Buffler (California Univ., Berkeley.) Oct. 1992 21 p
(Contract DE-AC03-76SF-00098)
(DE93-015274; LBL-32745) Avail: CASI HC A03/MF A01

This pilot study uses a unique method to calculate cumulative lifetime exposure to ultraviolet radiation-b (UVB) to determine if this refined method would indicate differences in lifetime cumulative UVB exposure between age and sex matched controls. Forty-four age and sex matched cases and controls demonstrated no significant difference in mean cumulative lifetime UVB exposure based on the duration and location of residence. This pilot study suggests that further analysis of the dataset should be conducted to

determine if the cumulative lifetime exposure hypothesis is of primary importance regarding the association between UVB exposure and development of cutaneous malignant melanoma. DOE

N94-16970# Argonne National Lab., IL.
THE ROLE OF CONSTITUTIVE AND INDUCIBLE PROCESSES IN THE RESPONSE OF HUMAN SQUAMOUS CELL CARCINOMA CELL LINES TO IONIZING RADIATION
J. L. Schwartz 1993 13 p Presented at the Molecular, Genetics and Cellular Basis of Radiosensitivity at Low Doses Workshop, Vancouver, British Columbia, 9-13 May 1993
(Contract W-31-109-eng-38)
(DE93-015150; ANL/BIM/CP-79672; CONF-9305202-2) Avail: CASI HC A03/MF A01

The inherent radiation sensitivity of the cells within a tumor is thought to contribute to the success or failure of radiation therapy. In vitro studies have shown that radiation sensitivity differences in squamous cell carcinoma cell lines reflect alterations in DNA repair. These alterations result from constitutive changes in chromosome organization, not radiation-inducible processes. While inducible responses may play some role in the radiation response of tumor cells, there is no evidence for their involvement in inherent tumor cell radiosensitivity differences or in the success or failure of radiotherapy for squamous cell carcinomas. DOE

N94-17085*# National Aeronautics and Space Administration. Langley Research Center, Hampton, VA.
METHOD AND APPARATUS TO CHARACTERIZE ULTRASONICALLY REFLECTIVE CONTRAST AGENTS Patent Application
Robert A. Pretlow, III, inventor (to NASA) (Lockheed Engineering and Sciences Co., Hampton, VA.) 15 Nov. 1993 27 p
(NASA-Case-LAR-14969-1; NAS 1.71:LAR-14969-1;
US-Patent-Appl-SN-153930) Avail: CASI HC A03/MF A01

A method and apparatus for characterizing the time and frequency response of an ultrasonically reflective contrast agent is disclosed. An ultrasonically reflective contrast agent is injected, under constant pressure, into a fluid flowing through a pump flow circuit. The fluid and the ultrasonically reflective contrast agent are uniformly mixed in a mixing chamber, and the uniform mixture is passed through a contrast agent chamber. The contrast agent chamber is acoustically and axially interposed between an ultrasonic transducer chamber and an acoustic isolation chamber. A pulse of ultrasonic energy is transmitted into the contrast agent chamber from the ultrasonic transducer chamber. An echo waveform is received from the ultrasonically reflective contrast agent, and it is analyzed to determine the time and frequency response of the ultrasonically reflective contrast agent. NASA

N94-17374 Naval Health Research Center, San Diego, CA.
CARPAL TUNNEL SYNDROME AND OTHER CUMULATIVE TRAUMA DISORDERS OF THE ARM AND HAND AND OCCUPATION IN US NAVY ENLISTED PERSONNEL Final Report, 1 Oct. 1991 - 30 Sep. 1992
F. C. Garland, C. F. Garland, E. J. Doyle, Jr., L. Balazs, and R. Levine 15 Feb. 1993 21 p Limited Reproducibility: More than 20% of this document may be affected by microfiche quality
(AD-A267747; NHRC-93-7) Avail: CASI HC A03

The majority of reported occupational illnesses in the United States are cumulative trauma disorders of the arm and hand due to repeated motion, vibration, or pressure; among these is carpal tunnel syndrome (CTS). The objectives of this study were to describe demographic factors associated with high rates of CTS and other nerve entrapment disorders and to identify high-risk Navy occupations. Computerized records of first hospitalizations of all Navy enlisted personnel for CTS and other nerve entrapment disorders (ICD-9-CM codes 354.0-354.9) were identified during 1980 to 1988. Age-, sex-, and race-specific incidence rates and age-standardized incidence rates were calculated. There were 493 first hospitalizations for CTS in 4,095,708 person-years in men and 90 in 365,668 person-years in women. Rates of CTS rose with age in both sexes. Rates in white women were about triple those in white men, but rates in black women were not significantly different from black men. In men, occupations with significantly high standardized incidence ratios (SIRs) for CTS included aviation support equipment technician, engineman, hull maintenance technician, boatswain's mate, and machinist's mate. In women they included boatswain's mate, engineman, hospital corpsman, ocean systems technician, and personnelman. Sex and race differences do not account for the occupations at highest risk. DTIC

N94-17424 Air Force Systems Command, Brooks AFB, TX. Operations and Support Directorate.
AUTOMATED DATA COLLECTION SYSTEM FOR THE TCM3 TRANSCUTANEOUS pO2/pCO2 MONITORING SYSTEM Final Report, Jan. - Jun. 1993
Roxanne Constabe Aug. 1993 18 p Limited Reproducibility: More than 20% of this document may be affected by microfiche quality
(AD-A268400; AL/DO-TP-1993-0025) Avail: CASI HC A03

The Hyperbaric Medicine Division of the Armstrong Laboratory (AL/AOHP) routinely uses the TCM3 Transcutaneous system for monitoring of patients and during research protocols. The monitor is used to measure the amount of oxygen/carbon dioxide at the skin surface. Up to 3 monitors may be utilized, and all data must be written down by hand at some interval. This method requires an individual to be watching the monitors at all times. If any further data analysis is to be performed, then the data must be entered into a computer by hand, or the manipulations are performed on paper. The purpose of this technical paper is to describe a data acquisition system designed to automate the collection and analysis of information processed by the TCM3 transcutaneous monitor. The hardware portion of the system is designed around a Macintosh 2 computer, and the software was written using LabVIEW 2. DTIC

N94-17456 Texas A&M Univ., College Station. Research Foundation.
MICROMECHANICS MODELING AND ANALYSIS OF HAVERSIAN COMPACT BONE TISSUES AS A FIBER REINFORCED COMPOSITE MATERIAL Annual Report, 1 Apr. 1992 - 31 Mar. 1993
Harry A. Hogan and Raymond J. DeFrese 30 Jun. 1993 35 p Limited Reproducibility: More than 20% of this document may be affected by microfiche quality
(Contract F49620-92-J-0208)
(AD-A268250; AFOSR-93-0598TR) Avail: Issuing Activity (Defense Technical Information Center (DTIC))

This research is part of the recent AFOSR initiative in biomimetics, which has the broad overall goal of seeking to elucidate and understand the salient characteristics of naturally occurring biological composite materials with an aim toward mimicking these features in devising improved man-made composite materials. The biological composite of interest in this effort is bone tissue, or more specifically Haversian compact bone tissue. The main objective of the project is to develop a deterministic understanding of the relationships between microstructural details and macroscopic mechanical behavior. The unique fiber/matrix interphase material, which is distinctive of this type of bone tissue, is of particular interest because of the recognized significance of interfaces in developing new higher performance composites. The methodology combines composite micromechanics modeling techniques to analytically model structure/property relationships with companion experimental testing of tissue samples to evaluate and validate the modeling. DTIC

N94-17478 Texas A&M Univ., College Station. Dept. of Biology.
MELATONIN, THE PINEAL GLAND, AND CIRCADIAN RHYTHMS Annual Report, 1 Jun. 1992 - 31 May 1993
Vincent M. Cassone, Wade S. Warren, David S. Brooks, and Jun Lu 31 May 1993 83 p Limited Reproducibility: More than 20% of this document may be affected by microfiche quality
(Contract F49620-92-J-0238)
(AD-A268200; AFOSR-93-0602TR) Avail: CASI HC A05/MF A01

Amniote circadian organization derives from the interactions of the circadian oscillator and photoreceptors located in the hypothalamic suprachiasmatic nuclei (SCN), the pineal gland, and the eyes. In mammals, circadian organization is dominated by the SCN, which serve as master pacemakers in the control of a wide array of behavioral and physiological rhythms (including locomotion, sleep-wake, thermoregulation, cardiovascular function, and many endocrine processes). Among the rhythms under SCN control in mammals are the circadian synthesis and secretion of the pineal hormone melatonin, which relies on a multisynaptic pathway via the sympathetic nervous system to maintain and entrain rhythmicity in this hormone. Several studies have indicated that pineal melatonin feeds back on SCN rhythmicity to modulate circadian patterns of activity and other

processes. However, the nature and system-level significance of this feedback are unknown. Recently published work indicates that although pinealectomy does not affect rat circadian rhythms in light-dark cycles or constant darkness, wheel-running activity rhythms are severely disrupted in constant light. These data suggest that either pineal feedback regulates the light sensitivity of the SCN, and/or it affects coupling among circadian oscillators within the SCN or between the SCN and its output. DTIC

N94-17554 Krug Life Sciences, Inc., San Antonio, TX.
METABOLIC MONITORING OF HYPOBARIC SUBJECTS Final Report, 16 Mar. 1990 - 16 Mar. 1991
Janet F. Wiegman, Sean A. McLean, Robert W. Olson, and Andrew A. Pilmanis Apr. 1993 37 p Limited Reproducibility: More than 20% of this document may be affected by microfiche quality
(Contract F33615-89-C-0603)
(AD-A268221; AL-TR-1991-0057) Avail: CASI HC A03/MF A01

The objective of Task Order No. 0013, amendment to USAF Contract No. F33615-89-C0603, was to quantify the metabolic activity of subjects during isometric and isotonic exercise to develop procedures for individualized exercise performance during simulated high altitude exposures. To satisfy the stated objective, KRUG Life Sciences performed the following tasks: designed and instrumented a stack-weight machine suitable for isometric or isotonic exercise performed with the arm or legs; provided and operated an advanced metabolic measurement system capable of breath-by-breath analysis of low-level oxygen consumption data; provided for administration of criterion tests for maximal oxygen consumption (VO2 max) and maximal voluntary contraction; developed procedures for equating and individualizing the isometric and isotonic work by means of oxygen consumption (% of VO2 max); and provided procedures for training subjects on the individual exercise programs. DTIC

N94-17556# Naval Medical Research Inst., Bethesda, MD.
HUMAN CENTRAL NERVOUS SYSTEM OXYGEN TOXICITY DATA FROM 1945 TO 1986 Technical Report, 1986 - 1992
Andrea L. Harabin Jan. 1993 142 p
(AD-A268225; NMRI-93-03) Avail: CASI HC A07/MF A02

This report contains a summary of all known results from controlled human exposures to hyperbaric O2. The data were collected for analysis and development of predictive models relating the risk of developing a symptom of central nervous system O2 toxicity as a function of time, depth, and condition of exposure. Data were obtained from publications and technical reports and verified by original records and log books. A total of 2,170 exposures, at depths ranging from 12 feet of sea water (fsw) to 100 fsw for up to 240 min, are included. The data consist of exposure time, depth, fraction of inspired O2, temperature, whether or not subjects exercised, whether they were immersed in water or exposed in a dry chamber, and outcome of the exposure, i.e., whether a symptom developed or the exposure was completed safely. Studies conducted under the following conditions were found: dry, no exercise; dry, exercise; immersed, no exercise; and immersed, exercise. The final category was divided into old (before 1972) and new. DTIC

N94-17562# Naval Medical Research Inst., Bethesda, MD.
METHODS TO OBTAIN BLOOD SAMPLES PERIODICALLY DURING EXERCISE RESEARCH STUDIES WHILE SUBJECTS ARE IMMERSED IN WATER OR OTHERWISE INACCESSIBLE Technical Report, 1990 - 1992
J. W. Thorp, J. R. Roberts, and T. J. Doubt Jan. 1993 14 p
(AD-A268227; NMRI-93-02) Avail: CASI HC A03/MF A01

We describe a method to obtain periodic blood samples during exercise studies by use of an indwelling intravenous catheter. A step-by-step process for establishing the intravenous line and obtaining samples is also described. Steps we have found especially useful to facilitate the process and to avoid complications are presented in more detail. A list of supplies required for the process is included. With these methods, we have been able to obtain samples from subjects performing heavy exercise on cycle ergometers and from other subjects who were immersed for up to three hours in water at 18 deg C and working on an underwater ergometer. Hemorrhage, infection, or other complications did not occur. The only failure has been occasional inability to obtain a blood sample because blood flow was inadequate. DTIC

N94-17621# Utah Univ., Salt Lake City. Dept. of Electrical Engineering.
CURRENTS INDUCED IN THE HUMAN BODY FOR EXPOSURE TO ULTRAWIDEBAND ELECTROMAGNETIC PULSES Final Report, Aug. - Nov. 1992
Om P. Gandhi and Cynthia M. Furse May 1993 32 p
(Contract F33615-91-C-0600)
(AD-A268570; AL-TR-1992-0156) Avail: CASI HC A03/MF A01

We have used the recently developed frequency-dependent finite-difference time-domain ((FD)(sup 2)TD) method to calculate internal electric fields and induced current densities in a 1.31-cm resolution anatomically based model of the human body for exposure to an ultrawideband vertically polarized electromagnetic pulse (EMP). The Fourier spectrum of the pulse revealed that it had energy content to about 1500 MHz with the bulk of the energy being in the frequency band 400-800 MHz. The complex permittivities epsilon*(w) for the various tissues are known to vary a great deal over the wide bandwidth of the incident pulse. In the ((FD)(sup 2)TD) formulation, these frequency-dependent epsilon*(w) have been described by the best-fit two-relaxation Debye equations with different constants epsilon(sub infinity), epsilon(sub s1), and epsilon(sub s2) for the sixteen tissues (fat, muscle, blood, etc.) that are used in defining the anatomically based model. From the values of the induced electric displacement vector D, we have calculated the time variations of the vertical currents that pass through each of the sections of the model that is assumed to be either isolated or shoe-wearing, standing above a perfectly conducting ground plane. Peak vertical currents with magnitudes on the order of 1-4 mA per V/m of incident electric fields are calculated with the highest values calculated for the sections through the bladder and slightly above it. DTIC

N94-16095 Ryerson Polytechnical Inst., Toronto (Ontario).
TRANSCRANIAL DOPPLER ULTRASOUND STUDIES OF CEREBRAL BLOOD-FLOW IN MICROGRAVITY
M. S. Kassam, R. L. Bondar (Canadian Space Agency, Ottawa, Ontario.), K. W. Johnston (Toronto Univ., Ontario.), R. S. C. Cobbold (Toronto Univ., Ontario.), P. J. Vaitkus (Toronto Univ., Ontario.), F. Stein (Maple Lake Non-Invasive Vascular Lab., Farmington, NM.), and P. Dunphy *In* National Research Council Canada, Proceedings of the Second Workshop on Microgravity Experimentation 1990 8 p (For primary document see N94-16071 03-29)
Avail: Issuing Activity (National Research Council, Publication Sales and Distribution, Montreal Road, Ottawa, Ontario, K1A OR6 Canada)

N94-16096 Institute for Space and Terrestrial Science, York (Ontario).
HUMAN OCULAR TORSION DURING PARABOLIC FLIGHT: AN INVESTIGATION USING ELECTROMAGNETIC SCLERAL SEARCH COIL
B. Cheung, K. Money (Defence and Civil Inst. of Environmental Medicine, Downsview, Ontario.), I. Howard, N. Kirienko, W. Johnson (Saint Michael's Hospital, Toronto, Ontario.), L. Lackner (Brandeis Univ., Waltham, MA.), and Paul A. Dizio (Brandeis Univ., Waltham, MA.) *In* National Research Council Canada, Proceedings of the Second Workshop on Microgravity Experimentation 1990 8 p (For primary document see N94-16071 03-29)
Avail: Issuing Activity (National Research Council, Publication Sales and Distribution, Montreal Road, Ottawa, Ontario, K1A OR6 Canada)

N94-16098 Simon Fraser Univ., Burnaby (British Columbia). School of Kinesiology.
HEART RATE RESPONSE TO PARABOLIC FLIGHT MANOEUVRES
Daryl Leiski, Igor Makjavic, and B. V. Tryggvason *In* National Research Council Canada, Proceedings of the Second Workshop on Microgravity Experimentation 1990 9 p (For primary document see N94-16071 03-29)
Avail: Issuing Activity (National Research Council, Publication Sales and Distribution, Montreal Road, Ottawa, Ontario, K1A OR6 Canada)

53 BEHAVIORAL SCIENCES

Includes psychological factors; individual and group behavior; crew training and evaluation; and psychiatric research.

N94-15108# Dayton Univ., OH. Research Inst.
AN INFORMATION PROCESSING CLASSIFICATION OF BEYOND-VISUAL-RANGE AIR INTERCEPTS Final Technical Report, Jan. - Dec. 1991
Michael R. Houck, Leslie A. Whitaker, and Robert R. Kendall May 1993 53 p
(Contract F33615-90-C-0005)
(AD-A266927; AL/HR-TR-1993-0061) Avail: CASI HC A04/MF A01

This research produced a descriptive classification of the task behaviors and cognitive processing associated with performing a beyond-visual-range (BVR) air combat mission. An F-15C defensive counter air mission scenario was analyzed to identify the critical tactical decisions required of the pilot, the information that must be processed in order to make these decisions, and the overt behaviors associated with pilots' information processing. The goal of this classification scheme was to determine observable behaviors that can be used as overt indicators of cognitive information processing. For future research purposes, the classification will provide a framework for identifying observable task behaviors that may be worthy candidates for developing and testing measures of performance. Such measures are essential for assessing the effectiveness of simulator-based training programs for enhancing the cognitive skills necessary for BVR employment. DTIC

N94-15148# Illinois Univ., Champaign.
THE 12TH ANNUAL CARMEL CONFERENCE, DISTINCTIVENESS AND MEMORY: COGNITIVE PSYCHOPHYSIOLOGICAL AND PHYSIOLOGICAL CONSIDERATIONS Final Report, 10 Jan. 1992
Emanuel Donchin 10 Jun. 1993 12 p Conference held in Carmel Highland, CA, 5-10 Jan. 1992
(Contract F49620-92-J-0102)
(AD-A267181; AFOSR-93-0525TR) Avail: CASI HC A03/MF A01

A workshop concerned with the integration of data obtained by a number of recently developed imaging methods with data obtained by more traditional means was conducted in Carmel Highlands, California, January 5-10, 1992. The thirty-four attendees focused, as a context for considering the challenge of integration, on the degree to which converging information makes it possible to develop models accounting for the effects of distinctiveness on recall, with particular emphasis on models of hippocampal function. Special consideration was given to the relationship between scalp recordings of ERP's and the neuroanatomical information that can be obtained on related processes by MRI, PET, numerical estimation procedures, and the study of focal lesions. The conference paid particular attention to the need to develop a common vocabulary and novel research paradigms if we are to gain the full benefits of current technological innovations. DTIC

N94-15237* National Aeronautics and Space Administration, Washington, DC.
TEACHER IN SPACE (Videotape)
Dec. 1985 Videotape: 4 min. 50 sec. playing time, in color, with sound
(NASA-TM-109666; NONP-VT-93-190464) Avail: CASI VHS A01/BETA A22

This video presentation covers the Teacher in Space program from the competition and selection process to the training of Christa McAuliffe and Barbara Morgan. CASI

N94-15499* National Aeronautics and Space Administration. Lewis Research Center, Cleveland, OH.
ASTRONAUTS NUMBER 1 (Videotape)
Sep. 1988 Videotape: 28 min. 51 sec. playing time, in color, with sound
(NASA-TM-109428; NONP-VT-93-190225) Avail: CASI VHS A01/BETA A22

The story of the selection and training of the seven Mercury astronauts is presented. A re-release of US Project Mercury. CASI

N94-15659# Army Aeromedical Research Lab., Fort Rucker, AL.
ACTIVITY/REST PATTERNS OF INSTRUCTOR AND RATES STUDENT PILOTS DURING RAPID TRANSITIONS FROM DAYTIME TO NIGHTTIME DUTY HOURS AT THE EASTERN ARMY AVIATION TRAINING SITE
Carlos A. Comperatore, James A. Chiaramonte, Jacquelyn Y. Pearson, Lewis W. Stone, and Gerald L. Hess Feb. 1993 62 p
(DA Proj. 3M1-62787-A-879)
(AD-A267038; USAARL-93-16) Avail: CASI HC A04/MF A01

Rapid shifts in work schedules demand that pilots and aircrew quickly adapt to new sleep schedules. Transitions to nighttime duty hours lacking planned work/rest schedules can result in the delay of physiological and cognitive adaptation, fatigue, and performance degradation (shift lag). The objective of this study was to determine the effects of a night shift coping strategy in the adaptation of helicopter pilots (UH-1) to nighttime (2100 to 0100) flying schedules. Daily activity/rest rhythms of instructor and rated student pilots (IP's/RSP's) were monitored 24 h perday for a total of 21 to 28 days using individual wrist activity monitors. RSP's ($n = 6$) lived in dormitories with complete blocking of daylight (below 10 lux) and reduced environmental noise until 1000. Meals and academic activities were scheduled to all RSP's the opportunity to sleep until 1000 after night flights. IP's lived in private homes and were expected to meet administrative, academic, and flight instruction demands. Throughout the NVG course, RSP's elected to retire between 0040 and 0200, to rise at approximately 0900, and to delay morning daylight exposure between 0900 1000. This schedule of activities resulted in an average of 7 h of bedrest under both daytime and nighttime duty schedules. In contrast, IP's exhibited variable rise times, usually occurring between 0700 and 0830 during both daytime and nighttime duty schedules. After night flights, IP's exhibited a delay of bedtime (2 h) but failed to consistently delay rise times. DTIC

N94-15694# Harvard Univ., Cambridge, MA.
COOPERATIVITY AND 3-D REPRESENTATION Annual Technical Report, 1 Feb. 1992 - 31 Jan. 1993
Patrick Cavanagh 28 Feb. 1993 7 p
(Grant AF-AFOSR-0169-91)
(AD-A267180; AFOSR-93-0547TR) Avail: CASI HC A02/MF A01

Recent evidence indicates that the early stages in visual processing may be broken into several parallel streams that are specialized for the analysis of different visual attributes. A contour localization task showed that all attributes can contribute equally to border localization no particular attribute dominated position decisions. A series of experiments on transparency perception showed that transparency is analyzed rapidly (within 60 msec) and influences early levels of visual processing. We have also investigated the early stages that lead from the initial 2D representation to object recognition. Visual priming studies have been completed which suggest that object recognition begins, not with the construction of a 3-D model, but with a crude match of 2-D views to internal prototypes. The prototype that has the best match then guides the construction of an internal 3-D model. An analysis of drawing techniques has led to ideas about memory codes for the depth structure of an image and to simplified mechanisms for understanding shadows and shading and to renewed interest in 'isophot' models of shading. Visual search studies have shown that some scene features may be rapidly suppressed. For example, shadows appear to be identified early and discounted in order to allow object contours to be processed. Finally, long-term practice in visual search tasks leads to learning of both object-centered and retinotopic properties of the stimuli. DTIC

N94-15742# Carnegie-Mellon Univ., Pittsburgh, PA. School of Computer Science.
COMPLEXITY ANALYSIS OF REAL-TIME REINFORCEMENT LEARNING APPLIED TO FINDING SHORTEST PATHS IN DETERMINISTIC DOMAINS
Sven Koenig and Reid G. Simmons Dec. 1992 102 p
(AD-A266636; CMU-CS-93-106) Avail: CASI HC A06/MF A02

This report analyzes the complexity of on-line reinforcement learning algorithms, namely asynchronous real-time versions of Q-learning and value-iteration, applied to the problems of reaching any goal state from the given start state and finding shortest paths from all states to a goal state. Previous work had concluded that, in many cases, initially uninformed (i.e. tabula rasa) reinforcement learning was exponential for such problems,

THE PAPER AND INK USED IN THE ORIGINAL PUBLICATION MAY AFFECT THE QUALITY OF THE MICROFORM EDITION.

or that it was tractable (i.e. of polynomial time-complexity) only if the learning algorithm was augmented. We prove that, to the contrary, the algorithms are tractable with only a simple change in the task representation (penalizing the agent for action executions) or initialization (initializing high). We provide tight bounds on their worst-case complexity, and show how the complexity is even smaller if the state space has certain special properties. We compare these reinforcement learning algorithms to other uninformed on-line search methods and to informed off-line search methods and investigate how initial knowledge of the topology of the state space can decrease their complexity. We also present two novel algorithms, the bi-directional Q-learning algorithms and the bi-directional value-iteration algorithm, for finding shortest paths from all states to a goal state and show that they are no more complex than their counterparts for reaching a goal state from a given start state. The worst-case analysis of the reinforcement learning algorithms is complemented by an empirical study of their average-case complexity in three domains. DTIC

N94-15762 Vanderbilt Univ., Nashville, TN.
COMPLEX INFORMATION COORDINATION PERFORMANCE: DIFFERENTIAL CHANGES IN WORKING MEMORY CONTRIBUTIONS FOLLOWING TRAINING Final Report
David J. Law, Kevin A. Morrin, and James W. Pellegrino 30 Jun. 1993 70 p Limited Reproducibility: More than 20% of this document may be affected by microfiche quality
(Contract N00014-91-J-1709; NR Proj. S11-42-CS)
(AD-A267007) Avail: CASI HC A04

Yee, Hunt, and Pellegrino introduced the concept of information coordination tasks--tasks that require the concurrent performance of two or more component tasks and the subsequent coordination of component information. In the present experiment different procedures, componential and contextual, were used to train separate groups (N = 35, N = 33) in a coordination task that involved dynamic spatial and verbal components. Within and between group analyses indicated that post-training performance improved and the improvement was equivalent across treatments. However, individual differences analyses indicated the treatments promoted different ability-performance profiles, which were related to differential dependencies on working memory resources. The differential dependence on working memory appears related to the functional consistency of information in the different treatments. Further analyses indicated that both treatments fostered the coordination of the dynamic spatial information within the relative arrival time task--a dynamic spatial coordination task. Sensitivity to relative velocity, working memory capacity, verbal processing ability, and gender mediated whether individuals became coordinators of dynamic spatial information. The broad implications of this study include the importance of combining mean and individual differences analyses in studies of human cognition. DTIC

N94-15938# Haifa Univ. (Israel).
SCUBA-DIVING, ANXIETY AND TASK PERFORMANCE
Baruch Nevo and Moshe Zeidner [1984] 18 p
Avail; CASI HC A03/MF A01

This study was primarily designed to examine the effect of scuba-diving on anxiety and cognitive performance in divers. In addition, this study experimentally tested the validity of the state-trait anxiety distinction. The sample was composed of 7 female and 6 male university students. Using a repeated measures design counterbalanced for testing conditions, subjects were administered a series of cognitive and anxiety measures both on land and when scuba-diving underwater. Whereas Trait-Anxiety scores were not significantly elevated by diving, State-Anxiety scores and heartbeat were significantly higher when diving underwater compared to surface conditions. Time estimation was significantly impacted by diving conditions, with subjects providing shorter time estimates for underwater conditions relative to control conditions. However, diving had no significant impact upon either the quantity or quality of simple math calculations. Overall, there is a tendency for diving conditions to impact upon some cognitive measures but not others. Since only state scores, but not trait scores, were affected by the experimental conditions, this study provides additional support for the construct validity of the State-Trait Anxiety Inventory in differentiating between anxiety as a state and trait. Author

N94-16456# Johns Hopkins Univ., Baltimore, MD. Dept. of Psychology.
NEURAL MECHANISMS OF ATTENTION Final Technical Report, 15 Dec. 1990 - 14 Nov 1992
David S. Olton, Kevin Pang, and Howard Egeth 21 May 1993 125 p
(Grant AF-AFOSR-0110-91)
(AD-A266315; AFOSR-93-0454TR) Avail: CASI HC A06/MF A02

This project was successful in examining the neural mechanisms involved in attention. An important outcome is the conclusion that modification of neural transmission by attentional processes takes place in many different places in the nervous system and at many different levels of information processing. Animal models of attentional processes are being developed that allow more extensive analysis of the neuroplastic changes involved in attention. The field of attention is now able to proceed in an integrated fashion similar to the way that memory has been pursued. DTIC

N94-16819# Sandia National Labs., Albuquerque, NM.
A COMPUTER-BASED TRAINING SYSTEM COMBINING VIRTUAL REALITY AND MULTIMEDIA
S. A. Stansfield 28 Apr. 1993 8 p Presented at the 1993 Conference on Intelligent, Computer-Aided Training and Virtual Environments, Houston, TX, 5-7 May 1993
(Contract DE-AC04-76DP-00789)
(DE93-013768; SAND-93-0967C; CONF-9305194-1) Avail: CASI HC A02/MF A01

Training new users of complex machines is often an expensive and time-consuming process. This is particularly true for special purpose systems, such as those frequently encountered in DOE applications. This paper presents a computer-based training system intended as a partial solution to this problem. The system extends the basic virtual reality (VR) training paradigm by adding a multimedia component which may be accessed during interaction with the virtual environment: The 3D model used to create the virtual reality is also used as the primary navigation tool through the associated multimedia. This method exploits the natural mapping between a virtual world and the real world that it represents to provide a more intuitive way for the student to interact with all forms of information about the system. DOE

N94-16925# Rochester Univ., NY. Center for Visual Science.
REFERENCE FRAMES IN VISION Annual Report, 15 Feb. 1992 - 14 Feb. 1993
Mary M. Hayhoe 26 May 1993 5 p
(Grant AF-AFOSR-0332-91)
(AD-A266174; AFOSR-93-0422TR) Avail: CASI HC A01/MF A01

This research examines the consequences of observer motion for visual functioning. Two major visual issues are addressed. The first issue is how a grossly time-varying retinal input (due to eye, head, and body motion) results in the perception of a continuous and directionally stable world. The second issue concerns the relatedness of the visual information that is retained from previous viewing. An examination of 'deictic primitives' (e.g., fixation points) and their importance for accurate internal representations is being investigated by covarying the temporal access to the sensory input during the problem solving process. Preliminary observations reveal some notable features of the-eye and head coordination: (1) Head movement frequently leads the gaze change, and (2) The fraction of gaze shift due to head movement varied from 20% for short, vertical movements, to nearly 100% for large horizontal movements. It was in general dependent on the sub-task, and was larger for horizontal than vertical gaze changes. In addition, it was shown that the gaze moved first to the model area, then is refined down to the workspace, while the head simply moves to the model area. DTIC

N94-16942# Southeastern Center for Electrical Engineering Education, Inc., Saint Cloud, FL.
STATES OF AWARENESS 1: SUBLIMINAL PERCEPTION RELATIONSHIP TO SITUATIONAL AWARENESS Final Report, 30 Nov. 1988 - 31 May 1991
Grant E. Secrist and Bryce O. Hartman May 1993 67 p
(AF Proj. 7755)
(AD-A267249; AL-TR-1992-0085) Avail: CASI HC A04/MF A01

On the face of it, subliminal perception violates common sense. How can a stimulus for which you have no knowledge make any difference? In its simplest terms, the answer is as follows. When you have a known

stimulus at a known intensity, which is at or below the level of conscious awareness, and behavior on a concurrent or subsequent task is modified, then you have a subliminal perception. This report reviews and integrates the literature on subliminal perception. We review the history (early research was weak) and theoretical roots. Then we examine in detail the five prominent methodologies: signal detection; dual channel; masking; lexical decision; and neurophysiologic--the latter very briefly. The main part of the review addresses two major areas: Subthreshold information acquisition; and subconscious information processing. Current criticisms are examined. Operational relevance is discussed. The significance of subliminal perception for operational applications is that it provides a methodological basis for one kind of training to enhance situational awareness. DTIC

N94-17020# Rochester Univ., NY. Center for Visual Science.
LOCALIZING VISUAL FUNCTION IN THE BRAIN Final Report, 1 Jun. 1992 - 31 Jan. 1993
William H. Merigan 13 Aug. 1992 16 p
(Contract F49620-92-J-0369)
(AD-A267381; AFOSR-93-0527TR) Avail: CASI HC A03/MF A01

The subject of 'Localizing Visual Function in the Brain' was discussed at a three-day meeting in Rochester. The meeting consisted of presentations by 15 prominent scientists of topics including the following: the anatomy of modular connections in the primate visual system; computational advantages of modular organization; imaging of the function of visual cortex; and physiological and behavioral evidence of modular processing. Each group of presentations was followed by a wide ranging discussion of the theme of the session. An audience of about 200 researchers and students included visual and computational scientists, neurologists, and radiologists, as well as a diverse group of investigators (largely physicists and engineers) interested in brain imaging. Many participants felt that it was an unusually productive meeting because of the broad range of related issues covered and the, at times intense, discussions that filled the meeting. DTIC

N94-17022# Brown Univ., Providence, RI. Inst. for Brain and Neural Systems.
THEORETICAL AND EXPERIMENTAL RESEARCH INTO BIOLOGICAL MECHANISMS UNDERLYING LEARNING AND MEMORY
30 Jun. 1993 34 p
(Contract N00014-91-J-1316)
(AD-A267441) Avail: CASI HC A03/MF A01

This is written to provide a semi-annual progress report for the contract N00014-91-J-1316 entitled 'Theoretical and Experimental Research into Biological Mechanisms Underlying Learning and Memory.' The major goal of our research is to elucidate the biological mechanisms that underlie learning and memory: to find principles of organization that can account both for experimental data on the cellular level and, when applied to large numbers of neurons that receive sensory and/or interneuronal information, for various higher level system properties. Among our detailed objectives are the following: to clarify the dependence of learning on synaptic modification; to elucidate the principles that govern synapse formation or modification; and to use principles of organization that can account for observations on a cellular level to construct neural-like systems that can learn, associate, and reproduce such higher level cognitive acts as abstraction and computation. DTIC

N94-17265# California Univ., San Diego, La Jolla.
NEURAL BASIS OF MOTION PERCEPTION Final Report, 1 Jun. 1990 - 31 May 1992
V. S. Ramachandran 18 Feb. 1993 6 p
(Grant AF-AFOSR-0414-89)
(AD-A267267; AFOSR-93-0464TR) Avail: CASI HC A02/MF A01

Our research has been concerned with visual surface representation and the manner in which visual image segmentation influences certain early visual processes such as stereopsis, motion correspondence, structure from motion, shape from shading, and the aperture problem. A number of new visual effects in our laboratory (e.g., motion capture, stereoscopic capture, etc.) have given us novel insights into the mechanisms underlying human motion perception and stereopsis. DTIC

N94-17296*# Georgia Inst. of Tech., Atlanta. School of Industrial and Systems Engineering.
ACQUISITION AND PRODUCTION OF SKILLED BEHAVIOR IN DYNAMIC DECISION-MAKING TASKS Final Report
Alex Kirlik 12 Nov. 1993 30 p
(Grant NAG2-656)
(NASA-CR-194658; NAS 1.26:194658) Avail: CASI HC A03/MF A01

Summaries of the four projects completed during the performance of this research are included. The four projects described are: Perceptual Augmentation Aiding for Situation Assessment, Perceptual Augmentation Aiding for Dynamic Decision-Making and Control, Action Advisory Aiding for Dynamic Decision-Making and Control, and Display Design to Support Time-Constrained Route Optimization. Papers based on each of these projects are currently in preparation. The theoretical framework upon which the first three projects are based, Ecological Task Analysis, was also developed during the performance of this research, and is described in a previous report. A project concerned with modeling strategies in human control of a dynamic system was also completed during the performance of this research. Author (revised)

N94-17397 Harvard Univ., Cambridge, MA. Div. of Applied Sciences.
THE EFFECTS OF LUMINANCE BOUNDARIES ON COLOR PERCEPTION Final Report, 15 Mar. 1989 - 14 Jan. 1993
Richard E. Kronauer, Charles F. Stromeyer, III, and Alex Chaparro 20 Jul. 1993 39 p Limited Reproducibility: More than 20% of this document may be affected by microfiche quality
(Grant AF-AFOSR-0304-89)
(AD-A268398) Avail: Issuing Activity (Defense Technical Information Center (DTIC))

The luminance and red-green chromatic detection mechanisms respond to, respectively, the sum and difference of the long-wave (L) and middle-wave (M) cone contrast signals. The most-detectable stimulus is not a small patch of luminance drifting grating, as suggested by others, but rather a small, foveal red-green chromatic flash. Even at the smallest test size examined, 2.3 ft. diameter, the red-green mechanism is more sensitive than the luminance mechanism, which has profound implication for visual physiology. When a suprathreshold luminance flash (a pedestal) occurs coincidentally with a red-green chromatic flash, detection of color is facilitated approximately 2-fold, regardless of spot size, as shown by forced-choice results, and this constant facilitation contrasts with the much larger facilitation reported earlier for small flashes. The lack of chromatic masking by suprathreshold luminance pedestals supports the view of separable luminance and red-green detectors. DTIC

N94-17453# California Univ., Irvine. Center for the Neurobiology of Learning and Memory.
SYNAPTIC PLASTICITY AND MEMORY FORMATION Annual Technical Report, 1 Jun. 1992 - 31 May 1993
Gary Lynch 30 Jun. 1993 5 p
(Contract F49620-92-J-0307)
(AD-A267988; AFOSR-93-0565TR) Avail: CASI HC A01/MF A01

The physiological effect known as long-term potentiation (LTP) is widely suspected of being the substrate of several forms of memory encoded by synapses in the forebrain of humans and other mammals. Work in the past year established that translational suppression with antisense oligonucleotides of one of the subunits of the AMPA (glutamate) transmitter receptor blocks the capacity of synapses to exhibit LTP. This confirms the hypothesis that the AMPA receptor is the agent of LTP expression. Changes in the waveform of the synaptic responses were found to occur in conjunction with LTP and were suggestive of a shift in the kinetic properties of the AMPA receptor channel. Computer simulations of the receptor led to the discovery that all known phenomenology of LTP expression can be reproduced by simply increasing the rates at which the receptor channel opens and closes. In parallel studies, a drug which acts on the AMPA receptor channel was shown to facilitate the induction of LTP. This led to a drug development program to find potent compounds of this kind which cross the blood-brain barrier and enhance the AMPA receptor and LTP in behaving rats. This effort was successful and one of the new drugs was then tested extensively in large numbers of rats across three learning tasks; as predicted, this compound produced substantial improvements in the encoding of short and long-term memories. DTIC

N94-17468# Wisconsin Univ., Madison. Dept. of Psychology.
PROCESSES INVOLVED IN THE INTEGRATION OF PICTURES AND DISCOURSE Annual Report, 1 Jun. 1992 - 31 May 1993
Arthur Glenberg 7 Jul. 1993 2 p
(Contract F49620-92-J-0310)
(AD-A268150; AFOSR-93-0615TR) Avail: CASI HC A01/MF A01

During the period 7/92 to 6/93 Peter Kruley conducted experiments studying the comprehension of illustrated texts; he took a leading role in designing the experiments, writing and debugging computer programs used in the collection of data, collecting actual subject data, and analyzing the data. In two experiments conducted from June to Nov. 1992, subjects read scientific texts, either with or without illustrations, while simultaneously performing tasks that stressed working memory. The goal of the experiments was to investigate the contribution of spatial and non-spatial working memory to the comprehension of texts; the results showed that performance of a concurrent spatial task was impaired when subjects read illustrated texts, whereas performance of a non-spatial task was not so impaired. Thus evidence was found for on-line use of the visuo-spatial sketchpad during comprehension of illustrated texts. DTIC

N94-17510# Krug Life Sciences, Inc., San Antonio, TX.
A VIRTUAL ACOUSTIC ORIENTATION INSTRUMENT Final Report, Nov. 1991 - 1992
Don C. Teas Jan. 1993 44 p
(Contract F33615-89-C-0603)
(AD-A268181; AL-TR-1992-0157) Avail: CASI HC A03/MF A01

Virtual instrumentation developed to create acoustic stimuli for use as orientation signals and the rationale for selecting these target signals is described. A commercially available computer-assisted software engineered programming system, LabVIEW, was used to develop the acoustic signals and the manner of their presentation. Two different acoustic signals are presented. One sound seems to change pitch without limit, and the other is a narrow band-pass noise. The pitch, loudness, and lateral position of the signals are controlled by different functions. Listeners can control the variations in pitch and lateralization and also the rate at which these features change. Programs to generate the signals with sinusoids or with noise bands are described. LabVIEW representations of the programs are included with text descriptions. DTIC

N94-17513 Retina Foundation, Boston, MA. Eye Research Inst.
PERCEPTION OF LIGHTNESS AND BRIGHTNESS IN COMPLEX PATTERNS Final Report, 1 May 1991 - 30 Apr. 1993
Lawrence E. Arend, Jr. 30 Jun. 1993 24 p Limited Reproducibility: More than 20% of this document may be affected by microfiche quality
(Grant AF-AFOSR-0377-89)
(AD-A268435; AFOSR-93-0617TR) Avail: CASI HC A03

Perception of surface color plays an important part in many everyday visual tasks. Psychophysical and neurophysiological data on early visual processes suggest a number of potential sensory limitations on the accuracy of surface-color perception. A new paradigm has been used to clarify the relationships between early visual processes and perception of achromatic surface colors (shades of gray). Psychophysical measurements of perceived surface color were made using achromatic stimulus patterns that were complex enough to support unambiguous perception of surfaces and lights. Lightness (apparent reflectance), brightness (apparent luminance) and local brightness contrasts were all measured using the same stimulus patterns. According to a number of models, lightness is closely related to local brightness contrast, but the data indicated that the relationship is more complicated than previously supposed. The brightness contrast data are well described by Stiles' threshold-vs-radiance curve, which is widely thought to be a characteristic of retinal adaptation processes. Both brightness and lightness are slightly higher on dark gray backgrounds than on white backgrounds. This perceptual error appears to be independent of illumination level. DTIC

N94-17535# Walter Reed Army Inst. of Research, Washington, DC.
THE BEHAVIORAL TOXICOLOGY OF HIGH-PEAK, LOW AVERAGE POWER, PULSED MICROWAVE IRRADIATION Interim Report, 20 Oct. 1989 - 31 Dec. 1992
T. G. Raslear, Y. Akyel, F. Bates, S.-T. Lu, and E. C. Elson 25 Jan. 1993 95 p
(AD-A268392) Avail: CASI HC A05/MF A01

The TEMPO microwave bioeffects exposure platform at the Department of Microwave Research, Walter Reed Army Institute of Research, produces an 80 ns, 3 GHz microwave pulse with a peak power of 700 MW. The energy transmitted is approximately 16 J, so that at a pulse repetition rate of 0.125 Hz, the duty factor is 10(exp -8) and the average power is 2 W. The time-averaged SAR for TEMPO exposures at full power is 0.072 W/kg, a value well-below suggested exposure limits. Five behavioral tasks were used to determine if exposure affected subsequent task performance: temporal bisection, Y-maze, treadmill running, food motivation (behavioral economics), and Persolt swim test. Reliable effects were found with the temporal bisection, Y-maze, treadmill, and behavioral economics tasks. The pattern of results suggests at least two effects of high-power pulsed microwaves: memory impairment and decreased physical endurance. It was suggested that research be expanded in this area, and that tasks which are specifically sensitive to memory function and physical endurance receive especial attention. DTIC

N94-17576# Intelligent Reasoning Systems, Inc., Las Cruces, NM.
A HIGH-SPEED OBJECT RECOGNITION CHIP BASED ON A BIOLOGICALLY-REALISTIC HYBRID TEMPORAL PROCESSING Progress Report No. 2
4 Aug. 1993 78 p
(Contract N00014-93-C-0118)
(AD-A268270) Avail: CASI HC A05/MF A01

This report traces the progress made by Intelligent Reasoning System, Inc. (IRSI) on contract N00014-93-C-0118, from June 1, 1993 to July 31, 1993. The technical objective of this Phase 1 effort is to evaluate the feasibility of a binocular object recognition system for the Integrated Active VISION System (INAVISIONS) currently under development at IRSI. The INAVISIONS is based on a custom Very Large Scale Integration (VLSI) Hybrid Temporal Processing Element (HTPE) developed by IRSI (patent pending). Active vision implies that the image collection and processing operations form a single, integrated, adaptive system in which high-level processes, such as object recognition can augment lower level processes through feedback connections and can itself be controlled by higher levels. For example, the object recognition process can instruct the oscillating saccadic perception system to enhance the image resolution by a particular amount to assist in the object recognition process. Higher level perception systems can guide the object recognition processes by using expectations of what objects might be present in the image. Therefore, the INAVISIONS behaves a single image collection and processing system with coupled low- and high-level capabilities. DTIC

N94-15911*# General Electric Co., Moorestown, NJ. Astro Space Div.
SAR SENSOR ELECTRONICS: T/R MODULES
MohD A. Hasan and Albert E. Preyss *In* JPL, Proceedings of the Third Spaceborne Imaging Radar Symposium 28 May 1993 p 381-402 (For primary document see N94-15886 03-32)
Avail: CASI HC A03/MF A04

N94-16617*# Office of Personnel Management, Washington, DC.
PROGRAMS AND RESOURCES FOR CONTROL OF JOB STRESS IN THE FEDERAL WORKPLACE
Wendell Joice *In* BioTechnology, Inc., Proceedings of the 1992 Annual Meeting NASA Occupational Health Program Jul. 1993 p 91-98 (For primary document see N94-16609 03-52)
Avail: CASI HC A02/MF A03

54 MAN/SYSTEM TECHNOLOGY AND LIFE SUPPORT

Includes human engineering; biotechnology; and space suits and protective clothing.

For related information see also *16 Space Transportation.*

N94-15194* National Aeronautics and Space Administration. Lyndon B. Johnson Space Center, Houston, TX.
STS-35 CREW TRAINING: EMU WALK THROUGH AND EVA PREP AND POST (Videotape)

Apr. 1990 Videotape: 12 min. 30 sec. playing time, in color, with sound (NASA-TM-109488; NONP-VT-93-190285) Avail: CASI VHS A01/BETA A22

This video tape shows astronauts Hoffman, Gardner, and Lounge donning the Extravehicular Mobility Unit (EMU) and performing checks on the system. CASI

N94-15195* National Aeronautics and Space Administration. Lyndon B. Johnson Space Center, Houston, TX.

STS-35 CREW TRAINING: BAILOUT IN CCT, FIREFIGHTING, TAGS CLASS AND BAILOUT IN WFTF (Videotape)

Apr. 1990 Videotape: 30 min. playing time, in color, with sound (NASA-TM-109489; NONP-VT-93-190286) Avail: CASI VHS A01/BETA A22

Several aspects of crew training are shown including bailout exercises from the CCT and in the Weightless Environment Training Facility. CASI

N94-15224* National Aeronautics and Space Administration. Lyndon B. Johnson Space Center, Houston, TX.

BROWN, MARK (Videotape)

Jul. 1989 Videotape: 8 min. 20 sec. playing time, in color, with sound (NASA-TM-109505; NONP-VT-93-190302) Avail: CASI VHS A01/BETA A22

Mark Brown is shown during ASCAN training programs including parachute and classroom instruction. CASI

N94-15285* National Aeronautics and Space Administration, Washington, DC.

SUPPORTING LIFE IN SPACE (Videotape)

Apr. 1989 Videotape: 3 min. 45 sec. playing time, in color, with sound (NASA-TM-109593; NONP-VT-93-190391) Avail: CASI VHS A01/BETA A22

This videotape examines NASA research regarding the growing of plants for food during long-duration space travel. The primary focus is on the Controlled Ecological Life Support System (CELLS). CASI

N94-15286* National Aeronautics and Space Administration, Washington, DC.

ANCIENT SKILLS: MODERN USE (Videotape)

Nov. 1988 Videotape: 2 min. 42 sec. playing time, in color, with sound (NASA-TM-109594; NONP-VT-93-190392) Avail: CASI VHS A01/BETA A22

This videotape shows how Navajo Indians are involved in making the spacesuits of the future. CASI

N94-15303* National Aeronautics and Space Administration. Lyndon B. Johnson Space Center, Houston, TX.

STS-30 EVA PREP IN CCT: GRABE, LEE, AND THAGARD (Videotape)

Apr. 1989 Videotape: 5 min. playing time, in color, with sound (NASA-TM-109572; NONP-VT-93-190370) Avail: CASI VHS A01/BETA A22

Astronauts Grabe, Thagard, and Lee practice donning extravehicular activity (EVA) suits while in the CCT. CASI

N94-15305* National Aeronautics and Space Administration. Lyndon B. Johnson Space Center, Houston, TX.

STS-29 PRE-LAUNCH AND POST-LANDING EGRESS (Videotape)

Mar. 1989 Videotape: 18 min. 10 sec. playing time, in color, with sound (NASA-TM-109574; NONP-VT-93-190372) Avail: CASI VHS A01/BETA A22

This video shows crew emergency egress training. It includes practice after being hoisted to the ceiling and descending a rope. CASI

N94-15330* National Aeronautics and Space Administration. Lyndon B. Johnson Space Center, Houston, TX.

STS-37 CETA EVALUATION WITH ROSS (Videotape)

Jul. 1990 Videotape: 5 min. 25 sec. playing time, in color, with sound (NASA-TM-109495; NONP-VT-93-190292) Avail: CASI VHS A01/BETA A22

This video shows Astronaut Ross donning an EVA suit and performing various tasks on the Crew and Equipment Translation Aide (CETA) equipment. CASI

N94-15359* National Aeronautics and Space Administration. Lyndon B. Johnson Space Center, Houston, TX.

STS-34 FINAL BENCH REVIEW (Videotape)

Oct. 1989 Videotape: 14 min. playing time, in color, with sound (NASA-TM-109464; NONP-VT-93-190261) Avail: CASI VHS A01/BETA A22

The Space Shuttle crew is shown looking through equipment they will carry into orbit, including clothing, personal effects, and camera. CASI

N94-15360* National Aeronautics and Space Administration. Lyndon B. Johnson Space Center, Houston, TX.

STS-34 CREW BAILOUT EXERCISE IN CCT (Videotape)

Aug. 1989 Videotape: 10 min. 40 sec. playing time, in color, with sound (NASA-TM-109465; NONP-VT-93-190262) Avail: CASI VHS A01/BETA A22

This video shows crews practicing bailout procedures in the CCT. CASI

N94-15361* National Aeronautics and Space Administration. Lyndon B. Johnson Space Center, Houston, TX.

STS-34 CHANG-DIAZ AND E. BAKER DURING GALILEO CONTINGENCY TRAINING IN WFTF (Videotape)

Sep. 1989 Videotape: 16 min. 15 sec. playing time, in color, with sound (NASA-TM-109466; NONP-VT-93-190263) Avail: CASI VHS A01/BETA A22

Chang-Diaz and Baker are shown donning suits for submersion in the Weightless Environment Training Facility (WETF). Once in the water, they work on the Galileo mockup. CASI

N94-15362* National Aeronautics and Space Administration, Washington, DC.

FIREFIGHTERS BREATHING SYSTEM (Videotape)

Apr. 1989 Videotape: 2 min. 50 sec. playing time, in color, with sound (NASA-TM-109611; NONP-VT-93-190409) Avail: CASI VHS A01/BETA A22

The improvement of protective gear for fire fighters is presented, including the breathing system. CASI

N94-15371* National Aeronautics and Space Administration. Lyndon B. Johnson Space Center, Houston, TX.

INTERNATIONAL FOOD RESEARCH PROJECT (Videotape)

Oct. 1989 Videotape: 5 min. 30 sec. playing time, in color, with sound (NASA-TM-109540; NONP-VT-93-190337) Avail: CASI VHS A01/BETA A22

Dr. Selina Ahmed, an associate professor of Human Nutrition, explains the purpose of the international Food Research Project to food tasters. CASI

N94-15375* National Aeronautics and Space Administration. Lyndon B. Johnson Space Center, Houston, TX.

STS-29 EVA PREP IN FFT (Videotape)

Jan. 1989 Videotape: 11 min. playing time, in color, with sound (NASA-TM-109544; NONP-VT-93-190341) Avail: CASI VHS A01/BETA A22

Astronauts Blaha, Springer, and Bagian are shown donning suits in the FFT. Blaha runs through checklists while the other two suit up in the airlock. CASI

N94-15377* National Aeronautics and Space Administration. Lyndon B. Johnson Space Center, Houston, TX.

STS-32 LDEF EVA TRAINING IN WETF WITH LOW AND DUNBAR (Videotape)

Nov. 1989 Videotape: 14 min. playing time, in color, with sound (NASA-TM-109473; NONP-VT-93-190270) Avail: CASI VHS A01/BETA A22

Astronauts Low and Dunbar are shown entering the Weightless Environment Training Facility to perform tasks they might be called on to do if extravehicular activity were required during their mission to retrieve the Long Duration Exposure Facility. CASI

N94-15382* National Aeronautics and Space Administration. Lyndon B. Johnson Space Center, Houston, TX.
STS-29 CREW FOOD TASTING IN BUILDING 45 (Videotape)
Jan. 1989 Videotape: 3 min. 28 sec. playing time, in color, with sound (NASA-TM-109547; NONP-VT-93-190345) Avail: CASI VHS A01/BETA A22

The crew is shown tasting food that will be served on the Space Shuttle. CASI

N94-15383* National Aeronautics and Space Administration. Lyndon B. Johnson Space Center, Houston, TX.
STS-32 BAILOUT TRAINING IN WETF (Videotape)
Dec. 1989 Videotape: 13 min. playing time, in color, with sound (NASA-TM-109476; NONP-VT-93-190273) Avail: CASI VHS A01/BETA A22

The crew is shown practicing water survival techniques in the Weightless Environment Training Facility in case of a bailout during the launch or landing. CASI

N94-15385* National Aeronautics and Space Administration. Lyndon B. Johnson Space Center, Houston, TX.
STS-29 CREW BAILOUT IN WETF (Videotape)
Feb. 1989 Videotape: 7 min. 30 sec. playing time, in color, with sound (NASA-TM-109548; NONP-VT-93-190346) Avail: CASI VHS A01/BETA A22

The crew is donning life vests and being dropped into the WETF. Once in the water, the crew is trained on water survival techniques. CASI

N94-15387* National Aeronautics and Space Administration. Lyndon B. Johnson Space Center, Houston, TX.
STS-28 ADAMSON AND BROWN EMU WALK THROUGH (Videotape)
Jul. 1989 Videotape: 10 min. playing time, in color, with sound (NASA-TM-109549; NONP-VT-93-190347) Avail: CASI VHS A01/BETA A22

Astronauts Adamson and Brown are shown working on EMU suit, donning EVA gear, and entering vacuum chamber. CASI

N94-15388* National Aeronautics and Space Administration. Lyndon B. Johnson Space Center, Houston, TX.
STS-33 EMERGENCY EGRESS TRAINING (Videotape)
Nov. 1989 Videotape: 15 min. playing time, in color, with sound (NASA-TM-109525; NONP-VT-93-190322) Avail: CASI VHS A01/BETA A22

The STS-33 crew is shown donning flight survival gear, then entering the CCT for bailout exercises. After completion of the exercises in the CCT, the bailout procedures are practiced in the FFT. CASI

N94-15390* National Aeronautics and Space Administration. Lyndon B. Johnson Space Center, Houston, TX.
1990 ASCAN LAND SURVIVAL TRAINING (Videotape)
Feb. 1991 Videotape: 32 min. playing time, in color, with sound (NASA-TM-109527; NONP-VT-93-190324) Avail: CASI VHS A01/BETA A22

This video tape shows astronaut candidates training at Fairchild AFB with signal flares, setting up tents, making fires, fishing, and signaling a helicopter with mirrors and radios. CASI

N94-15391* National Aeronautics and Space Administration. Lyndon B. Johnson Space Center, Houston, TX.
1990 ASCAN GROUND EGRESS/PARASAIL (Videotape)
Feb. 1991 Videotape: 32 min. playing time, in color, with sound (NASA-TM-109528; NONP-VT-93-190325) Avail: CASI VHS A01/BETA A22

This video tape shows astronaut candidates practicing ground egress and parachute landing procedures. CASI

N94-15392* National Aeronautics and Space Administration. Lyndon B. Johnson Space Center, Houston, TX.
CREW ESCAPE CERTIFICATION TEST (Videotape)
Aug. 1988 Videotape: 2 min. 50 sec. playing time, in color, with sound (NASA-TM-109530; NONP-VT-93-190327) Avail: CASI VHS A01/BETA A22

This video tape shows the Shuttle hatch jettison test at Rockwell facilities. The video also shows a Shuttle escape pole deployment test from a NASA aircraft, and an emergency egress test performed by a volunteer Navy parachutist using the pole and a parachute escape system. CASI

N94-15401* National Aeronautics and Space Administration. Lyndon B. Johnson Space Center, Houston, TX.
STS-27 EMU AND RMS CONTINGENCY TRAINING (Videotape)
Dec. 1988 Videotape: 23 min. playing time, in color, with sound (NASA-TM-109550; NONP-VT-93-190348) Avail: CASI VHS A01/BETA A22

This video shows astronauts donning their EMU suits and Astronauts Shepard and Ross training in the WETF on the RMS, which will not come down. CASI

N94-15402* National Aeronautics and Space Administration. Lyndon B. Johnson Space Center, Houston, TX.
STS-33 CARTER AND THORTON DURING WETF ACTIVITIES (Videotape)
Nov. 1989 Videotape: 8 min. 54 sec. playing time, in color, with sound (NASA-TM-109471; NONP-VT-93-190268) Avail: CASI VHS A01/BETA A22

Astronauts Carter and Thorton are shown suiting up for work in the WETF (Weightless Environment Training Facility). (The payload mockup shown is not related to the STS-33 mission. It is a mockup of the Upper Atmosphere Research Satellite (UARS), which is scheduled to fly in the early 1990's.) CASI

N94-15404* National Aeronautics and Space Administration. Lyndon B. Johnson Space Center, Houston, TX.
STS-27 CREW POST-INSERTION DEORBIT-PREP IN CCT (Videotape)
Nov. 1988 Videotape: 14 min. playing time, in color, with sound (NASA-TM-109552; NONP-VT-93-190350) Avail: CASI VHS A01/BETA A22

The crew is shown donning harness backpacks and suits for post-insertion activities in the CCT. Once on the CCT middeck, astronauts take off suits and practice stowing seats. CASI

N94-15406* National Aeronautics and Space Administration. Lyndon B. Johnson Space Center, Houston, TX.
STS-27 CREW FIRE TRAINING AND GLOVE MOLDING (Videotape)
Nov. 1988 Videotape: 14 min. 30 sec. playing time, in color, with sound (NASA-TM-109554; NONP-VT-93-190352) Avail: CASI VHS A01/BETA A22

The crew is shown during fire training exercises and space suit glove molding. CASI

N94-15435* National Aeronautics and Space Administration, Washington, DC.
FOOD FOR SPACE (Videotape)
Jan. 1985 Videotape: 3 min. 20 sec. playing time, in color, with sound (NASA-TM-109668; NONP-VT-93-190466) Avail: CASI VHS A01/BETA A22

This video explores the food preparation and selection over the years of space flight. CASI

N94-15441* National Aeronautics and Space Administration. Lyndon B. Johnson Space Center, Houston, TX.
STS-31 HUBBLE SPACE TELESCOPE CONTINGENCY TRAINING IN WETF WITH MCCANDLESS AND SULLIVAN (Videotape)
Feb. 1989 Videotape: 13 min. playing time, in color, with sound (NASA-TM-109480; NONP-VT-93-190277) Avail: CASI VHS A01/BETA A22

Astronauts McCandless adn Sullivan are shown suiting up for training with a telescope mockup in the Weightless Environment Training Facility (WETF). CASI

N94-15453* National Aeronautics and Space Administration. Lyndon B. Johnson Space Center, Houston, TX.
STS-38 CREW TRAINING: HABITATION EQUIPMENT PROCEDURES, BAILOUT IN CCT, 70mm PHOTO CLASS, EVA PREP AND POST, AND FIREFIGHTING (Videotape)

Jul. 1990 Videotape: 20 min. playing time, in color, with sound (NASA-TM-109494; NONP-VT-93-190291) Avail: CASI VHS A01/BETA A22

Several aspects of crew training are shown, including habitation equipment procedures and bailout procedures (both in CCT), 70mm photo class, EVA prep and post, and firefighting. Author (revised)

N94-15454* National Aeronautics and Space Administration. Lyndon B. Johnson Space Center, Houston, TX.

ADAMSON, JIM (Videotape)

Jul. 1989 Videotape: 11 min. 34 sec. playing time, in color, with sound (NASA-TM-109507; NONP-VT-93-190304) Avail: CASI VHS A01/BETA A22

Jim Adamson is shown during ASCAN training programs including T-38 training, parachute and liferaft training, and classroom instruction. CASI

N94-15460* National Aeronautics and Space Administration. Lyndon B. Johnson Space Center, Houston, TX.

STS-37 ASTRONAUTS ROSS AND APT DURING CETA HARDWARE CHECKOUT (Videotape)

Mar. 1990 Videotape: 7 min. 15 sec. playing time, in color, with sound (NASA-TM-109496; NONP-VT-93-190293) Avail: CASI VHS A01/BETA A22

Astronauts Ross and Apt are shown checking out Crew and Equipment Translation Aide (CETA) equipment. CASI

N94-15462* National Aeronautics and Space Administration. Lyndon B. Johnson Space Center, Houston, TX.

STS-36 CREW EVA PREP AND POST-TRAINING, BAILOUT EXERCISES, FINAL BENCH REVIEW (Videotape)

Feb. 1990 Videotape: 14 min. 30 sec. playing time, in color, with sound (NASA-TM-109498; NONP-VT-93-190295) Avail: CASI VHS A01/BETA A22

The crew is shown in the CCT airlock checking out EVA equipment and practicing bailout exercises. They are also shown looking over equipment they will carry into space including medical equipment, clothing, and cameras. CASI

N94-15470* National Aeronautics and Space Administration. Lyndon B. Johnson Space Center, Houston, TX.

STS-26 CREW CLOTHING, GLOVE MOLDING, AND PERSONAL HYGIENE (Videotape)

Jul. 1988 Videotape: 19 min. 41 sec. playing time, in color, with sound (NASA-TM-109520; NONP-VT-93-190317) Avail: CASI VHS A01/BETA A22

This videotape shows the crew during various phases of flight clothing fit checks, space suit glove molding, and selection of personal hygiene articles for use onboard the Shuttle. CASI

N94-15507* National Aeronautics and Space Administration, Washington, DC.

SPACE SUIT DESIGN (Videotape)

Jun. 1987 Videotape: 3 min. 48 sec. playing time, in color, with sound (NASA-TM-109670; NONP-VT-93-190468) Avail: CASI VHS A01/BETA A22

This video shows how space suits evolved to those being designed for the Space Station Freedom. CASI

N94-15514* National Aeronautics and Space Administration. Lyndon B. Johnson Space Center, Houston, TX.

MARK 111 SUIT TEST EVALUATION IN WETF WITH JERRY ROSS (Videotape)

Oct. 1989 Videotape: 7 min. 50 sec. playing time, in color, with sound (NASA-TM-109504; NONP-VT-93-190301) Avail: CASI VHS A01/BETA A22

Astronaut Jerry Ross tests the new Mark 111 spacesuit in the WETF. The Mark 111 could be used as the main spacesuit on the Space Station Freedom. CASI

N94-15717*# National Aeronautics and Space Administration. Lyndon B. Johnson Space Center, Houston, TX.

INVESTIGATION OF THE EFFECTS OF EXTRAVEHICULAR ACTIVITY (EVA) GLOVES ON PERFORMANCE

Ram R. Bishu (Nebraska Univ., Lincoln.) and Glenn Klute Oct. 1993 49 p

(NASA-TP-3401; S-732; NAS 1.60:3401) Avail: CASI HC A03/MF A01

The objective was to assess the effects of extravehicular activity (EVA) gloves at different pressures on human hand capabilities. A factorial experiment was performed in which three types of EVA gloves were tested at five pressure differentials. The independent variables tested in this experiment were gender, glove type, pressure differential, and glove make. Six subjects participated in an experiment where a number of dexterity measures, namely time to tie a rope, and the time to assemble a nut and bolt were recorded. Tactility was measured through a two point discrimination test. The results indicate that with EVA gloves strength is reduced by nearly 50 percent, there is a considerable reduction in dexterity, performance decrements increase with increasing pressure differential, and some interesting gender glove interactions were observed, some of which may have been due to the extent (or lack of) fit of the glove to the hand. The implications for the designer are discussed. Author (revised)

N94-15820# Dayton Univ., OH. Research Inst.

COMPARATIVE NIGHT VISION GOGGLE VISUAL ACUITY MEASUREMENTS PERFORMED IN THE A-10 AIRCRAFT IN AN OPERATIONAL SETTING Final Report, Apr. - Sep. 1992

Carita A. Devilbiss and Joseph C. Antonio Apr. 1993 29 p

(Contract F33615-90-C-0005)

(AD-A266721; AL/HR-TR-1993-0066) Avail: CASI HC A03/MF A01

The Night Vision Programs Office of the Aircrew Training Research Division, Armstrong Laboratory, responded to a request from the 422nd Operational Test Squadron at Nellis AFB to conduct the ground testing portion of their A-10 Night Vision Goggle (NVG) special project. Evaluations were conducted comparing the performance of four different NVG's under both laboratory and representative operational conditions. The performance of the F4949 'Super ANVIS' was superior to that of the other NVG's tested. Additionally, a comparative study was conducted evaluating the impact of two different windscreens on NVG image quality. The new windscreen allowed the transmission of more energy usable to the NVG's, thus enhancing image quality over that possible with the old windscreen. DTIC

N94-15883*# National Aeronautics and Space Administration. Lyndon B. Johnson Space Center, Houston, TX.

INFLATABLE RESCUE DEVICE Patent Application

Scott A. Swan, inventor (to NASA) 4 May 1993 21 p

(NASA-Case-MSC-22244-1; NAS 1.71:MSC-22244-1;

US-Patent-Appl-SN-066274) Avail: CASI HC A03/MF A01

This invention discloses, in one aspect, a personal rescue device for use in outer space which has an inflatable flexible tube with a shaper apparatus herein. Gas under pressure flows through the shaper apparatus and into the flexible tube. The flexible tube is mounted to the shaper so that as it inflates it expands and deploys lengthwise away from the shaper. In one embodiment a housing contains the shaper and the flexible tube and the housing is designed to facilitate movement of the expanding tube from the housing so the expanding tube does not bunch up in the housing. NASA

N94-16108# Memphis State Univ., TN. Dept. of Psychology.

QUESTIONING MECHANISMS DURING TUTORING, CONVERSATION, AND HUMAN-COMPUTER INTERACTION Final Report, 15 Jun. 1992 - 14 Jun. 1993

Arthur C. Graesser Jun. 1993 51 p

(Contract N00014-92-J-1826)

(AD-A266199; ONR-TR-93-1) Avail: CASI HC A04/MF A01

One-to-one tutoring is more effective than alternative training methods, yet there have been few attempts to examine the process of naturalistic tutoring. This project explored dialogue patterns in two corpora: graduate students tutoring undergraduates in research methods; and high school students tutoring 7th graders in algebra. We analyzed pedagogical strategies, feedback mechanisms, question asking, question answering, and pragmatic assumptions during the tutoring process. One pervasive dialogue pattern

was a five-step frame: (1) tutor asks question, (2) student answers question, (3) tutor gives short feedback on answer quality, (4) tutor and student collaboratively improve on answer quality, and (5) tutor assesses the student's understanding of the answer. Tutor questions were primarily motivated by curriculum scripts and the process of coaching students through exemplar problems--rarely by attempts to diagnose and remediate the student's idiosyncratic knowledge deficits. Dialogue patterns were simulated by two computational models: a recurrent connectionist network, and a recursive transition network. These models capture the systematicity in the sequential ordering of speech act categories. That is, to what extent does a model accurately predict the category of speech act N+1, given speech acts 1 through N? DTIC

N94-16793 Analysis and Technology, Inc., New London, CT.
EVALUATION OF NIGHT VISION GOGGLES (NVG) FOR MARITIME SEARCH AND RESCUE (HH-3/HH-60) COMPARISON REPORT Final Report, Mar. 1989 - Jan. 1993
R. Q. Robe and J. V. Plourde Jan. 1993 97 p Limited Reproducibility: More than 20% of this document may be affected by microfiche quality
(Contract DTCG39-89-C-E10G56)
(AD-A266493; USCG-D-09-93) Avail: Issuing Activity (Defense Technical Information Center (DTIC))

Eight experiments, including seven involving helicopters, have been conducted by the U.S. Coast Guard Research and Development (R and D) Center to evaluate night vision goggles (NVG's) for their effectiveness in detecting small targets at night. Three types of NVG's have been evaluated. The AN/AVS-6 Aviator's Night Vision Imaging System (ANVIS) was evaluated onboard U.S. Coast Guard HH-3F, CH-3E, and HH-60J helicopters and HU-25C and RG-8A fixed-wing aircraft. The AN/PVS-5C and AN/PVS-7A NVG's were evaluated onboard U.S. and Canadian Coast Guard Search and Rescue Units (SRU's) in the 200-foot size range and onboard U.S. Coast Guard 41-foot utility boats (UTB's). A total of 3029 target detection opportunities were generated during searches from helicopters for all the target types employed during the eight experiments. These data were first analyzed to determine whether a statistically significant difference existed in the detection performance of the HH-3/CH-3 and HH-60 helicopters. The data were then analyzed to determine which of 25 search parameters of interest exerted a statistically significant influence on target detection probability. Lateral range curves and sweep width estimates are presented for SRU/target type combinations that contained sufficient data to support this detailed analysis. Human factors data are presented and discussed. DTIC

N94-16983# Krug Life Sciences, Inc., San Antonio, TX.
REGULATED EMERGENCY OXYGEN SYSTEM Final Report, Jan. 1990 - Jan. 1991
Nancy J. Balkus, Edward W. Hade, and John H. Ohlhausen Jun. 1993 31 p
(Contract F33615-89-C-0603)
(AD-A266228; AL-TP-1992-0041) Avail: CASI HC A03/MF A01

This paper describes the accomplishments of the Regulated Emergency, Oxygen System (REOS) task. A true emergency secondary oxygen system is nonexistent in current aircraft. The current system is inadequate in regulating pressure, is ineffective at altitudes below 10,000 ft, and provides no option except to activate the emergency oxygen bottle if a malfunction of the primary regulator occurs. The REOS concept alleviates these inadequacies by providing an option to select a secondary regulated oxygen source, rather than the emergency bottle, if there is a malfunction of the primary regulator. Also of significance is that altitude protection has been incorporated into the REOS. The contents of this paper provide greater details as to the background, development, and testing of the REOS. DTIC

N94-17077# Anacapa Sciences, Inc., Fort Rucker, AL.
PRELIMINARY VALIDATION OF THE TASK ANALYSIS/WORKLOAD METHODOLOGY Interim Report, Jul. 1990 - Dec. 1991
David B. Hamilton and Kenneth D. Cross Jun. 1993 147 p
(AD-A267514; AS1690-353-92; ARI-93-18) Avail: CASI HC A07/MF A02

Over the past 8 years, the U.S. Army Research Institute for the Behavioral and Social Sciences (ARI) has sponsored the development of the Task Analysis/Workload (TAWL) methodology. The methodology is used to develop computer-based models that predict the operator workload of Army weapon systems. The TAWL methodology has been used to predict operator workload in existing and modified versions of the AH-64, UH-60, and CH-47 aircraft. This preliminary research was designed to assess the validity of the methodology. Seven experimental task conditions, analogous to rotorcraft operation and designed to vary in workload, were used in the research. Two TAWL workload prediction models of the conditions were independently developed by two analysts. Twenty AH-64A aviators performed repeated trials in each of the task conditions. Measures of the aviators' task performance, subjective workload, and physiological workload were obtained as TAWL model validity criteria. Although there were some differences between the models developed by the two analysts, the predictions generated by the models were highly correlated. In addition, the correlations between the average TAWL predictions for both models and the criterion measures were significant and high (between .89 and .99). The results support the validity of the TAWL methodology. DTIC

N94-17452*# National Aeronautics and Space Administration. Langley Research Center, Hampton, VA.
STRATEGY FOR THE REDUCTION OF TOTAL INTEGRATED FLUID LOGISTICS TO THE SPACE STATION FREEDOM
Marston J. Gould and David T. Shannon, Jr. Nov. 1993 66 p
(RTOP 476-14-06)
(NASA-TM-107744; NAS 1.15:107744) Avail: CASI HC A04/MF A01

The use of an integrated environmental control and life support system (ECLSS) and secondary propulsion system (SRS) on the Space Station Freedom (SSF) has many potential advantages. Through the metabolism of food, the crew on-board the station will produce carbon dioxide as a waste gas and an excess of water in the form of urine and condensate. The processing of these waste fluids by the ECLSS could produce quantities of oxygen that would eliminate the need for cryogenic oxygen resupply and hydrogen, carbon dioxide, and/or methane that could be used with the addition of a resistojet system to provide a constant low thrust for station. This additional thrust would represent significant savings in required hydrazine resupply. Author

N94-17460 Science Applications International Corp., McLean, VA.
PREDICTING RADIATION INDUCED PERFORMANCE DECREMENTS OF AH-1 HELICOPTER CREWS. VOLUME 1: PREDICTED VEERSUS ACTUAL PERFORMANCE OF AH-1 CREWS INDUCED WITH SYMPTOMS SIMULATING RADIATION SICKNESS Technical Report, 25 Sep. 1986 - 30 Nov. 1991
Vaughn W. Inman, William A. Perez, Joseph I. Peters, Robert R. Sanchez, and Robert W. Young 1 Jul. 1993 213 p Limited Reproducibility: More than 20% of this document may be affected by microfiche quality
(Contract DNA001-86-C-0308)
(AD-A268376; DNA-TR-92-54-Vol-1) Avail: Issuing Activity (Defense Technical Information Center (DTIC))

The purpose of this study was to assess the utility of the Performance Decrement Questionnaire (PDO) technique for prediction of radiation induced performance decrements in Army personnel. Twenty AH-1 pilots participated in an experiment in which they (1) predicted the effects of various symptom complexes on their performance, (2) went through a 36-hour protocol to induce symptoms similar to those that are followed by intermediate doses of radiation exposure, and (3) performed a simulated AH-1 mission before and after symptom induction. The participants' performance time predictions were compared to actual performance times. The comparisons between predicted and actual performance were conducted with correlational and modeling (MicroSAINT) techniques. The modeling analysis suggested greater concordance between predicted and actual performance than did the correlational analysis. DTIC

N94-17475 Air Force Inst. of Tech., Wright-Patterson AFB, OH.
COMPUTER-HUMAN INTERFACE ISSUES: THEORY AND APPLICATION M.S. Thesis
Michael Joseph 11 May 1993 71 p Limited Reproducibility: More than 20% of this document may be affected by microfiche quality
(AD-A268013; AFIT/CI/CIA-93-117) Avail: Issuing Activity (Defense Technical Information Center (DTIC))

This paper addresses the process by which an organization implements a human-machine interface and what factors need to be considered to insure that the interface meets the needs of its human users. This latter

goal is composed of objectives such as acceptance of the interface by the computer users, providing an acceptable means of assisting the human in accomplishing his/her computer assisted task, and related interface characteristics which help support these other two objectives. DTIC

N94-17563 Krug International, San Antonio, TX.
AIRCREW/GROUNDCREW LIFE SUPPORT SYSTEMS RESEARCH. VOLUME 1: CLIN 0001 RESEARCH REQUIREMENTS Final Report, May 1989 - Nov. 1992
Robert W. Krutz, Jr. and James T. Webb Jul. 1993 50 p Limited Reproducibility: More than 20% of this document may be affected by microfiche quality
(Contract F33615-89-C-0603)
(AD-A268229; AL-TR-1993-0012-Vol-1) Avail: Issuing Activity (Defense Technical Information Center (DTIC))

USAF Contract F33615-89-C-0603 (SOW Section 3.2; CLIN 0001) with KRUG Life Sciences, Incorporated, San Antonio Division, supported the Armstrong Laboratory by providing for research in the following areas: human research subjects; experimental life support equipment development laboratory; anti-G suit research, development, test, and evaluation (RDT&E); research databases; sub-atmospheric research; molecular sieve technology; centrifuge testing of life support equipment; centrifuge support; cockpit integration and crew performance; and spatial disorientation research. This final report provides summaries of objectives and accomplishments including citations and abstracts for the publications documenting the work. AL-TR-1993- 0012-VOL-2 is the final report for the CLIN 0002 portion of this contract. DTIC

N94-17564 Krug Life Sciences, Inc., San Antonio, TX.
AIRCREW/GROUNDCREW LIFE SUPPORT SYSTEMS RESEARCH. VOLUME 2: CLIN 0002 TASK ORDER REQUIREMENTS Final Report, May 1989 - Nov. 1992
James T. Webb and Robert W. Krutz, Jr. Jul. 1993 45 p Limited Reproducibility: More than 20% of this document may be affected by microfiche quality
(Contract F33615-89-C-0603)
(AD-A268230; AL-TR-1993-0012-Vol-2) Avail: Issuing Activity (Defense Technical Information Center (DTIC))

USAF Contract F33615-89-C-0603 (SOW Section 3.3; CLIN 0002) with KRUG Life Sciences, Incorporated, San Antonio Division, supported the Armstrong Laboratory by providing for research in the form of professional and technical personnel, resources, and, when required, facilities necessary to accomplish task orders for research, development, test, and evaluation (RDT&E) to include, but not be limited to, the following topics: chemical defense, experimental aeromedical and casualty care equipment laboratory support, biochemical laboratory support, test studies and evaluations, system integration/equipment modification, equipment design package, independent engineering tests, equipment fabrication, design and development, computer programs, specialized and unique R&D laboratory facilities, and altitude research. This final report provides summaries of objectives and accomplishments including citations and abstracts for the publications documenting the work. AL-TR-19930012-VOL-I is the final report for the CLIN 0001 portion of this contract. DTIC

N94-17653*# National Aeronautics and Space Administration. Lyndon B. Johnson Space Center, Houston, TX.
FORCE-ENDURANCE CAPABILITIES OF EXTRAVEHICULAR ACTIVITY (EVA) GLOVES AT DIFFERENT PRESSURE LEVELS
Ram R. Bishu (Nebraska Wesleyan Univ., Lincoln.) and Glenn K. Klute 1 Dec. 1993 13 p
(NASA-TP-3420; S-746; NAS 1.60:3420) Avail: CASI HC A03/MF A01

The human hand is a very useful multipurpose tool in all environments. However, performance capabilities are compromised considerably when gloves are donned. This is especially true to extravehicular activity (EVA) gloves. The primary intent was to answer the question of how long a person can perform tasks requiring certain levels of exertion. The objective was to develop grip force-endurance relations. Six subjects participated in a factorial experiment involving three hand conditions, three pressure differentials, and four levels of force exertion. The results indicate that, while the force that could be exerted depended on the glove, pressure differential, and the level of exertion, the endurance time at any exertion level depended just on the level of exertion expressed as a percentage of maximum exertion possible at that condition. The impact of these findings for practitioners as well as theoreticians is discussed. Author

N94-16093 York Univ. (Ontario). Human Performance Lab.
CHARACTERISTICS OF AIMED ARM MOVEMENTS IN HUMANS UNDER LOW GRAVITY
O. Bock, K. Arnold, I. Howard, and K. Money *In* National Research Council Canada, Proceedings of the Second Workshop on Microgravity Experimentation 1990 3 p (For primary document see N94-16071 03-29)
Avail: Issuing Activity (National Research Council, Publication Sales and Distribution, Montreal Road, Ottawa, Ontario, K1A OR6 Canada)

N94-16612*# Georgia Inst. of Tech., Atlanta.
ERGONOMICS IN THE OFFICE ENVIRONMENT
Theodore K. Courtney *In* BioTechnology, Inc., Proceedings of the 1992 Annual Meeting NASA Occupational Health Program Jul. 1993 p 45-60 (For primary document see N94-16609 03-52)
Avail: CASI HC A03/MF A03

N94-16621*# National Health Services, Inc., New York, NY.
THE GODDARD SPACE FLIGHT CENTER ERGONOMICS PROGRAM
Eileen Batson and Theodore Unite *In* BioTechnology, Inc., Proceedings of the 1992 Annual Meeting NASA Occupational Health Program Jul. 1993 p 153-158 (For primary document see N94-16609 03-52)
Avail: CASI HC A02/MF A03

55 SPACE BIOLOGY

Includes exobiology; planetary biology; and extraterrestrial life.

N94-17017*# National Aeronautics and Space Administration, Washington, DC.
PUBLICATIONS OF THE EXOBIOLOGY PROGRAM FOR 1991: A SPECIAL BIBLIOGRAPHY
Oct. 1993 64 p
(NASA-TM-4483; NAS 1.15:4483) Avail: CASI HC A04/MF A01

This document contains a list of 1991 publications resulting from research pursued under the auspices of NASA's Exobiology Program.
Author (revised)

N94-17636*# National Aeronautics and Space Administration. Ames Research Center, Moffett Field, CA.
ONTOGENESIS OF MAMMALS IN MICROGRAVITY
O. G. Gazenko, ed. (Academy of Sciences, USSR, Moscow.) Apr. 1993 167 p
(RTOP 106-10-04)
(NASA-TM-103978; A-92192; NAS 1.15:103978) Avail: CASI HC A08/MF A02

This report is an English translation of a Russian report prepared by a group of authors from the USSR, Bulgaria, Hungary, the GDR, Poland, Czechoslovakia, France, and the USA. It presents results of the first microgravity experiment on mammalian embryology performed during the flight of the biosatellite Cosmos-1514 and in ground-based simulation studies. An overview is provided of the data available about the role of gravity in animal growth and development, and future studies into this problem are discussed. A new introduction has been provided for the English version.
Author (revised)

N94-16620*# National Aeronautics and Space Administration. Ames Research Center, Moffett Field, CA.
SEARCH FOR EXTRATERRESTRIAL INTELLIGENCE (SETI)
John Billingham *In* BioTechnology, Inc., Proceedings of the 1992 Annual Meeting NASA Occupational Health Program Jul. 1993 p 143-151 (For primary document see N94-16609 03-52)
Avail: CASI HC A02/MF A03

59 MATHEMATICAL AND COMPUTER SCIENCES (GENERAL)

N94-17623# Office of Naval Research, Arlington, VA.
MATHEMATICAL SCIENCES DIVISION 1992 PROGRAMS Summary Report, 1 Oct. 1991 - 30 Sep. 1992
Neil L. Gerr 1 Oct. 1992 124 p
(AD-A268586; OCNR-111192-12) Avail: CASI HC A06/MF A02

This report documents research performed under the sponsorship of the ONR Mathematical Sciences Division during fiscal year 1992. DTIC

60 COMPUTER OPERATIONS AND HARDWARE

Includes hardware for computer graphics, firmware, and data processing.

For components see *33 Electronics and Electrical Engineering.*

N94-15174# Illinois Univ., Urbana-Champaign. Coordinated Science Lab.
RELAXING CONSISTENCY IN RECOVERABLE DISTRIBUTED SHARED MEMORY
Bob Janssens and W. K. Fuchs 1993 9 p
(Contract N00014-91-J-1283)
(AD-A266931) Avail: CASI HC A02/MF A01

Relaxed memory consistency models tolerate increased memory access latency in both hardware and software distributed shared memory systems. In recoverable systems, relaxing consistency has the added benefit of reducing the number of checkpoints needed to avoid rollback propagation. New checkpointing algorithms that take advantage of relaxed consistency to reduce the performance overhead of checkpointing are introduced. A scheme based on lazy relaxed consistency, that reduces both checkpointing overhead and the overhead of avoiding error propagation in systems with error latency is also introduced. Multiprocessor address traces are used to evaluate the relaxed consistency approach to checkpointing with distributed shared memory. DTIC

N94-15228* National Aeronautics and Space Administration. Marshall Space Flight Center, Huntsville, AL.
NASA SPACELINK COMPUTER (Videotape)
May 1989 Videotape: 2 min. 13 sec. playing time, in color, with sound
(NASA-TM-109657; NONP-VT-93-190455) Avail: CASI VHS A01/BETA A22

This video tape introduces Spacelink, a computer resource that educators and students can access. The purpose of Spacelink is to stimulate interest in math and science. CASI

N94-15455* National Aeronautics and Space Administration. Lyndon B. Johnson Space Center, Houston, TX.
FREEDOM SYSTEM TEXT AND GRAPHICS SYSTEMS (TAGS) (Videotape)
Apr. 1989 Videotape: 1 min. 50 sec. playing time, in color, with sound
(NASA-TM-109509; NONP-VT-93-190306) Avail: CASI VHS A01/BETA A22

The Text and Graphics Systems (TAGS) is a high-resolution facsimile system that scans test or graphics material and converts the analog SCAN data into serial digital data. This video shows the TAGS in operation. CASI

N94-15744# Carnegie-Mellon Univ., Pittsburgh, PA. School of Computer Science.
FAST INTERRUPT PRIORITY MANAGEMENT IN OPERATING SYSTEM KERNELS
Daniel Stodolsky, J. B. Chen, and Brian N. Bershad May 1993 8 p
(Contract MDA972-90-C-0035; ARPA Order 7330)
(AD-A266638; CMU-CS-93-152) Avail: CASI HC A02/MF A01

This paper describes a new technique, optimistic interrupt protection, that efficiently schedules and handles processor interrupts. While modern processor architectures have led to substantial overall performance improvements, operating systems have received significantly less benefit than application codes. One processor function that has not scaled well with processor speed is interrupt management. Operating systems use interrupts to control scheduling and input/output and use interrupt masking to guarantee integrity of system resources shared across interrupt levels. This approach was efficient in many previous processor architectures (e.g, VAX) where the cost changing interrupt levels was small--generally less than ten instructions 4,5. In modern architectures, however, interrupt masking may be up to an order of magnitude more expensive, contributing to poorer performance of system code. DTIC

N94-15763 University of Southwestern Louisiana, Lafayette.
THE DESIGN OF SELF-CHECKING REDUCED INSTRUCTION SET COMPUTERS Final Report
T. R. Rao 31 Mar. 1993 32 p Limited Reproducibility: More than 20% of this document may be affected by microfiche quality
(Contract N00014-91-J-1067)
(AD-A267012) Avail: CASI HC A03

The overall goal of this project is the design of self-checking computers and fault-tolerant memory systems with low overhead and high reliability. During the research, we focused our research on the determination of more efficient approach for realization of self-checking systems and developing new approach for fault-tolerant memory systems. The research conducted in this project is summarized under five different topics given below. Fifteen papers have been published by the PI under the contract and were listed in Section 6. Abstracts of these papers are included at the end of this report. DTIC

N94-16716*# Georgia Inst. of Tech., Atlanta. Center for Human-Machine Systems Research.
COGNITIVE ENGINEERING MODELS IN SPACE SYSTEMS Final Report
Christine M. Mitchell Aug. 1993 52 p
(Grant NAG9-422)
(NASA-CR-193473; NAS 1.26:193473) Avail: CASI HC A04/MF A01

NASA space systems, including mission operations on the ground and in space, are complex, dynamic, predominantly automated systems in which the human operator is a supervisory controller. Models of cognitive functions in complex systems are needed to describe human performance and form the theoretical basis of operator workstation design, including displays, controls, and decision aids. Currently, there several candidate modeling methodologies. They include the Rasmussen abstraction/aggregation hierarchy and decision ladder, the goal-means network, the problem behavior graph, and the operator function model. The research conducted under the sponsorship of this grant focuses on the extension of the theoretical structure of the operator function model and its application to NASA Johnson mission operations and space station applications. The initial portion of this research consists of two parts. The first is a series of technical exchanges between NASA Johnson and Georgia Tech researchers. The purpose is to identify candidate applications for the current operator function model; prospects include mission operations and the Data Management System Testbed. The second portion will address extensions of the operator function model to tailor it to the specific needs of Johnson applications. At this point, we have accomplished two things. During a series of conversations with JSC researchers, we have defined the technical goal of the research supported by this grant to be the structural definition of the operator function model and its computer implementation, OFMspert. Both the OFM and OFMspert have matured to the point that they require infrastructure to facilitate use by researchers not involved in the evolution of the tools. The second accomplishment this year was the identification of the Payload Deployment and Retrieval System (PDRS) as a candidate system for the case study. In conjunction with government and contractor personnel in the Human-Computer Interaction Lab, the PDRS was identified as the most accessible system for the demonstration. Pursuant to this a PDRS simulation was obtained from the HCIL and an initial knowledge engineering effort was conducted to understand the operator's tasks in the PDRS application. The preliminary results of the knowledge engineering effort and an initial formulation of an operator function model (OFM) are contained in the appendices. Derived from text

N94-17005# Massachusetts Univ., Amherst. Dept. of Electrical and Computer Engineering.
FAULT-TOLERANT ARCHITECTURES FOR MULTIPROCESSOR AND VLSI-BASED SYSTEMS Final Report, 30 Sep. 1991 - 29 Sep. 1992

Dhiraj K. Pradhan 29 Sep. 1992 36 p
(Grant AF-AFOSR-0403-91)
(AD-A267370; AFOSR-93-0561TR) Avail: CASI HC A03/MF A01

The research investigated under this grant includes: a virtual checkpointing scheme for recovery; schemes for implementing reliable memory; roll-forward recovery schemes for duplex systems; REACT, a tool for reliable architecture characterization and its application to reliability evaluation of triple modular redundant (TMR) systems; a new approach for low-cost system level diagnosis; and the reliability safety trade-off in modular redundant systems. DTIC

N94-17015 Air Force Inst. of Tech., Wright-Patterson AFB, OH. Foreign Aerospace Science and Technology Center.
OPTICAL COMPUTING
Hiroyoshi Yajima 3 Aug. 1993 15 p Transl. into ENGLISH from Technical Survey (Japan), v. 74, no. 12, 1991 p 1284-1287 Limited Reproducibility: More than 20% of this document may be affected by microfiche quality
(AD-A267881; FASTC-ID(RS)T-0890-92) Avail: Issuing Activity (Defense Technical Information Center (DTIC))

The advantage of optical computing is its parallelism. In the case of photography, every part of an object is focused by a camera lens onto a film to construct an image of the object. This image forming process constitutes the basis of optical parallel processing and optical computing is a technology that transforms the concept of optical processing into various information processing techniques. Various research has been conducted in the field of optical information processing to develop retrievable optical memories using the lens as the means to perform Fourier transformations or the holograms, but none of the methods has been put into practical use. They utilize the devices in classical optics such as the lenses to perform basically different functions from electronic devices. DTIC

N94-17030# Naval Postgraduate School, Monterey, CA.
EFFICIENT SCHEDULING OF REAL-TIME COMPUTE-INTENSIVE PERIODIC GRAPHS ON LARGE GRAIN DATA FLOW MULTIPROCESSOR M.S. Thesis
Cem Akin Mar. 1993 171 p
(AD-A267444) Avail: CASI HC A08/MF A02

Architectures of computer systems based on Data Flow (DF) concepts attracted great attention as an alternative to conventional sequential architectures (Von Neumann). DF architectures are capable of efficiently exploiting a massive amount of parallelism inherent in many types of computation. They are programmed using directed graphs whose vertices are function modules and whose edges denote data dependencies between function modules. An important subclass of DF is Large Grain Data Flow (LGDF) which is efficiently used in computation intensive applications, such as signal processing. Presently, most leadoffs incorporate a nondeterministic run-time technique to allocate system resources to support the execution (One such technique could be First Come First Served). Despite of the usual simplistic nature of scheduling techniques, which results in a low run-time overhead, the system throughput and predictability could rapidly degrade under high system load. To provide uniform output and improve the resource usage even under a high load, a compile-time technique called Revolving Cylinder (RC) was introduced. In this thesis, we present a LGDF simulator and a Graph restructurer that restructures the given graph according to the RC technique. We then perform a comparative experimental study of the different implementation of RC and the FCFS scheduling techniques. Our results demonstrate that there is a high potential for the RC technique, if a satisfactory node mapping technique is developed. DTIC

N94-17115# Carnegie-Mellon Univ., Pittsburgh, PA. Dept. of Computer Science.
EXPERIENCE WITH DISCONNECTED OPERATION IN A MOBILE COMPUTING ENVIRONMENT
M. Satyanarayanan, James J. Kistler, Lily B. Mummert, Maria R. Ebling, and Puneet Kumar Jun. 1993 20 p
(Contract F33615-90-C-1465; ARPA Order 7597)
(AD-A267524; CMU-CS-93-168) Avail: CASI HC A03/MF A01

In this paper we present qualitative and quantitative data on file access in a mobile computing environment. This information is based on actual usage experience with the Coda File System over a period of about two years. Our experience confirms the viability and effectiveness of disconnected operation. It also exposes certain deficiencies of the current implementation of Coda, and identifies new functionality that would enhance its usefulness for mobile computing. The paper concludes with a description of what we are doing to address these issues DTIC

N94-17380# California Inst. of Tech., Pasadena. Dept. of Electrical Engineering.
3-D OPTICAL MEMORY DISK Annual Technical Report, 1 Jul. 1992 - 30 Jun. 1993
Demetri Psaltis 23 Jul. 1993 23 p
(Contract F49620-92-J-0400)
(AD-A267908; AFOSR-93-0594TR) Avail: CASI HC A03/MF A01

In this report we describe optical disks that store data holographically in three dimensions using either angle multiplexing or wavelength multiplexing. Data is stored and retrieved in parallel blocks or pages. Each page consists of approximately one million bits. The storage capacity of such disks is derived as a function of disk thickness, pixel size, page size, and scanning parameters. The optimum storage density is approximately 120 bits/sq micron. DTIC

N94-15595*# National Aeronautics and Space Administration. Goddard Space Flight Center, Greenbelt, MD.
UPGRADING NASA/DOSE LASER RANGING SYSTEM CONTROL COMPUTERS
Randall L. Ricklefs (McDonald Observatory, Austin, TX.), Jack Cheek (Hughes STX, Inc., Lanham, MD.), Paul J. Seery (Bendix Field Engineering Corp., Seabrook, MD.), Kenneth S. Emenheiser (Bendix Field Engineering Corp., Seabrook, MD.), William P. Hanrahan, III (Bendix Field Engineering Corp., Seabrook, MD.), and Jan F. McGarry *In its* Eighth International Workshop on Laser Ranging Instrumentation Jun. 1993 6 p (For primary document see N94-15552 03-19)
Avail: CASI HC A02/MF A06

N94-15596*# Bendix Field Engineering Corp., Seabrook, MD.
HP UPGRADE OPERATIONAL STREAMLINING
David R. Edge, Kenneth S. Emenheiser, William P. Hanrahan, III, D. McCollums, Paul J. Seery, and Randall L. Ricklefs (McDonald Observatory, Austin, TX.) *In* NASA. Goddard Space Flight Center, Eighth International Workshop on Laser Ranging Instrumentation Jun. 1993 8 p (For primary document see N94-15552 03-19)
Avail: CASI HC A02/MF A06

61 COMPUTER PROGRAMMING AND SOFTWARE

Includes computer programs, routines, alogorithms, and specific applications, e.g., CAD/CAM.

N94-14915# Carnegie-Mellon Univ., Pittsburgh, PA. School of Computer Science.
CONCURRENT GARBAGE COLLECTION OF PERSISTENT HEAPS
Scott Nettles, James OToole (Massachusetts Inst. of Tech., Cambridge.), and David Gifford Apr. 1993 25 p
(Contracts F33615-90-C-1465; F19628-91-C-0168)
(AD-A266831; CMU-CS-93-137; MIT-LCS-TR-569) Avail: CASI HC A03/MF A01

The first concurrent compacting garbage collector for a persistent heap is described. Client threads read and write the heap in primary memory, and can independently commit or abort their write operations. When write operations are committed they are preserved in stable storage and thus survive system failures. Clients can freely access the heap during a garbage collection because a replica of the heap is created by the stable replica collector. A log is maintained to capture client write operations. This log is used to support both the transaction system and the replication-based garbage collection algorithm. Experimental data from our implementation was obtained from a transactional version of the SML/NJ compiler and modified versions of the TPC-B and 001 database benchmarks. The pause time latency results show that the prototype implementation

provides significantly better latencies than stop-and-copy collection. For small transactions, throughput is limited by the logging bandwidth of the underlying log manager. The results provide strong evidence that the replication copying algorithm imposes less overhead on transaction commit operations than other algorithms. DTIC

N94-14924# Army Materiel Systems Analysis Activity, Aberdeen Proving Ground, MD.

ARMY SOFTWARE TEST AND EVALUATION PANEL (STEP) SOFTWARE METRICS INITIATIVES REPORT

Henry P. Betz and Patrick J. ONeill Apr. 1993 98 p

(AD-A266889) Avail: CASI HC A05/MF A02

This report documents the efforts and portrays the findings and recommendations of the Army Software Test and Evaluation Panel (STEP) Subgroup on measures. The final recommendations include the mandatory use of a minimum, common set of software metrics in order to better measure and manage software development from the test and evaluation perspective. This set of measures should be used to help determine whether the system under consideration has demonstrated the necessary functionality, maturity, and readiness to proceed to the next stage of development or testing. This set of metrics is a minimum set; other metrics of specific interest to a certain agency or point of view can and should be collected if desired. Of course, there are many characteristics of the software that need to be evaluated for quality and conformance but do not lend themselves to measurement. These quality factors remain important to any evaluation of software. Metrics are simply one element of a set of tools that should be used in a software evaluation. DTIC

N94-14944 National Physical Lab., Teddington (England). Information Technology and Computing Div.

VDM SPECIFICATION OF THE MD4 MESSAGE DIGEST ALGORITHM

A. Harry Aug. 1992 50 p Sponsored by Dept. of Trade and Industry, London, England

(NPL-DITC-204/92; ETN-93-94539) Copyright Avail: Issuing Activity (National Physical Laboratory, Teddington, Middlesex TW11 0LW, United Kingdom)

The use of a formal description language in the specification of an algorithm related to secure transmission of messages is illustrated. The example presented is the MD4 (Message Digest) algorithm, written in the formal notation VDM (Vienna Development Method). It is shown by example how expression in a formal language can expose possible ambiguities in natural language. It highlights the suitability of formal methods for describing security standards in a clear, concise way allowing easy implementation in any of the many different programming styles. ESA

N94-14967# Carnegie-Mellon Univ., Pittsburgh, PA. Software Engineering Inst.

LECTURE NOTES ON ENGINEERING MEASUREMENT FOR SOFTWARE ENGINEERS Final Report

Gary Ford Apr. 1993 95 p

(Contract F19628-90-C-0003)

(AD-A266959; CMY/SEI-93-EM-9) Avail: CASI HC A05/MF A01

Measurement is a fundamental skill for engineers. To facilitate teaching software engineering measurement, materials are provided to support three lectures: introduction to engineering measurement, measurement theory, and software engineering measures. These materials include lecture notes suitable for class handouts and additional information for instructors-educational objectives, pedagogical considerations, suggestions for class projects, an annotated bibliography, and transparency masters for use in the delivery of the lectures. DTIC

N94-14978# Institut National de Recherche d'Informatique et d'Automatique, Valbonne (France). Programme 2: Calcul Symbolique, Programmation et Genie Logiciel.

A CENTAUR TUTORIAL

Ian Jacobs (Institut National de Recherche d'Informatique et d'Automatique, Le Chesnay, France.) and Laurence Rideau-Gallot 16 Jul. 1992 108 p

(INRIA-RT-140; ETN-93-94427) Avail: CASI HC A06/MF A02

The CENTAUR system is presented through a tutorial describing the creation of an environment for a small language of mathematical expressions called EXP. With CENTAUR, the user may interactively generate programming language environments, including structured editors, debuggers, interpreters, and other tools. In this tutorial, all phases of language specification are covered: the design of the abstract and concrete syntax of EXP in METAL and SDF, the pretty printing rules in PPML, and the semantics of an EXP intepreter in TYPOL. The tools generated by CENTAUR based on these specifications are enhanced by a user interface built with CENTAUR graphic primitives. ESA

N94-14979# Institut National de Recherche d'Informatique et d'Automatique, Valbonne (France). Programme 2: Calcul Symbolique, Programmation et Genie Logiciel.

THE CAML NUMBERS REFERENCE MANUAL

Valerie Menissier-Morain Jul. 1992 147 p Sponsored by Institut National de Recherche en Informatique et en Automatique

(Contract MRT-89553)

(INRIA-RT-141; ETN-93-94428) Avail: CASI HC A07/MF A02

The reference manual for the arithmetic of the functional language CAML V3.1 is presented. It is available by anonymous ftp from ftp.inria.fr as a compressed PostScript file lang/cam1/ V3.1/docarith.tar.z. This arithmetic includes floating point numbers, arbitrary large integers and rationals, and a complete set of primitives. Its implementation relies on the efficient BigNum package. ESA

N94-15008 National Physical Lab., Teddington (England). Div. of Information Technology and Computing.

THE USE OF FORMAL METHODS IN DATA SECURITY STANDARDS

Andrew Harry Aug. 1992 13 p Sponsored by Dept. of Trade and Industry, London, England

(NPL-DITC-205/92; ETN-93-94540) Copyright Avail: Issuing Activity (National Physical Lab., Teddington, Middlesex TW11 OLW, England)

The advantages of using formal languages over normal natural language in the description of standards is explained. A number of examples of natural descriptions of security related algorithms are given, showing how these can be ambiguous and misconstrued. The advantages of formal methods in the areas of proof analysis and refinement are also discussed. ESA

N94-15010 National Physical Lab., Teddington (England). Div. of Information Technology and Computing.

RAISE SPECIFICATION OF THE MD4 MESSAGE DIGEST ALGORITHM

Andrew Harry Sep. 1992 53 p Sponsored by Dept. of Trade and Industry, London, England

(NPL-DITC-206/92; ETN-93-94541) Copyright Avail: Issuing Activity (National Physical Lab., Teddington, Middlesex TW11 OLW, England)

The use of a formal description language in the specification of an algorithm related to secure transmission of messages is illustrated. The example presented is the MD4 (Message Digest) algorithm, written in the formal notation RAISE (Rigorous Approach to Industrial Software Engineering). It is shown by example how expression in a formal language can expose possible ambiguities in natural language. It highlights the suitability of formal methods for describing security standards in a clear, concise way allowing easy implemetnation in any of the many different programming styles. ESA

N94-15011 National Physical Lab., Teddington (England). Div. of Information Technology and Computing.

THE VALUE OF REFERENCE IMPLEMENTATIONS AND PROTOTYPING IN A FORMAL DESIGN AND TESTING METHODOLOGY

Andrew Harry Oct. 1992 18 p Sponsored by Dept. of Trade and Industry, London, England

(NPL-DITC-208/92; ETN-93-94543) Copyright Avail: Issuing Activity (National Physical Lab., Teddington, Middlesex TW11 OLW, England)

The application of prototypes and reference implementations to a formal methodology for the writing and testing of formal specifications is reported. Exploratory prototyping is seen as being of value in the conversion of natural language standards into formally specified ones. However, the value of this may diminish as formal methods become established and algorithms are written directly from a formal notation. The use of reference implementations in the testing of security standards may become of increasing value. Greater tool support is also required, particularly in the area of verified compilers if the use of reference implementations for testing is to form part of a certifiable evaluation process. Ways of testing for security weaknesses also have to be defined. ESA

N94-15012 National Physical Lab., Teddington (England). Div. of Information Technology and Computing.

THE APPLICATION OF PROGRAMMING LANGUAGES TO THE PRODUCTION OF REFERENCE IMPLEMENTATIONS

Andrew Harry Oct. 1992 20 p Sponsored by Dept. of Trade and Industry, London, England

(NPL-DITC-209/92; ETN-93-94544) Copyright Avail: Issuing Activity (National Physical Lab., Teddington, Middlesex TW11 OLW, England)

The suitability of imperative, functional and logic based implementation languages for the production of reference implementations from formally defined specifications is examined. Reference implementations are prototype implementations of a formally defined specification which rigorously conforms to the formal definition, the resultant system being used for testing purposes. It is concluded that functional languages are the most suitable. Their use for both constructive and behavioral specification is discussed. ESA

N94-15014 National Physical Lab., Teddington (England). Data Security Group.

STANDARDS AND CONFORMANCE TESTING IN DATA SECURITY: RESULTS OF INITIAL PROGRAMME OF INVESTIGATION

Mar. 1993 47 p Sponsored by Dept. of Trade and Industry, London, England

(NPL-DITC-218/92; ETN-93-94547) Copyright Avail: Issuing Activity (National Physical Lab., Teddington, Middlesex TW11 OLW, England)

Results of a program of research concerned with the testing of implementations of data security standards are presented. These standards range from simple mechanisms for message authentication to those that form part of a large open system. The types of standard, how they can be improved by the use of formal specification languages, and how the corresponding implementations may be tested, are explored. An analysis of areas where further action is needed is given in the conclusion. ESA

N94-15022 National Physical Lab., Teddington (England). Div. of Information Technology and Computing.

TESTABILITY OF DATA SECURITY STANDARDS

Roger Manning, Bronia Szczygiel, and Andrew Harry Feb. 1993 27 p Sponsored by Dept. of Trade and Industry, London, England

(NPL-DITC-217/93; ETN-93-94605) Copyright Avail: Issuing Activity (National Physical Lab., Teddington, Middlesex TW11 OLW, England)

The requirements of security evaluation are examined. Areas that must be addressed in defining and testing implementations of standards, including such problems as inadequate specification of security, programming language and compiler insecurities, and difficulties in testing embedded systems are investigated. For each of these issues solutions and/or areas of research likely to address these problems are suggested. ESA

N94-15110# Scranton Univ., PA.

EVALUATION OF ALSYS 037 ADA COMPILER Final Report, Jun. - Aug. 1992

Richard M. Plishka and Agustin Ifarraguerri May 1993 16 p

(Contract DAAL03-91-C-0034)

(AD-A266972; ERDEC-CR-040) Avail: CASI HC A03/MF A01

Several standard benchmarks were implemented in order to study the real-time performance of the Alsys.037 Ada Compiler for the Inmos T800 Transputer. A limited comparison to the Transputer's native language, Occam, was possible. The key aspects that were investigated were the computational speed, using the Whetstone benchmark, the clock resolution, delay resolution, procedure call overhead and general performance. These were measured using the Performance Issues Working Group (PWIG) test suite. The Whetstone benchmark was implemented on the T800 in both Ada and Occam, making this measurement the most informative. DTIC

N94-15114*# North Carolina State Univ., Raleigh. Dept. of Computer Science.

SOFTWARE RELIABILITY THROUGH FAULT-AVOIDANCE AND FAULT-TOLERANCE Progress Report, 1 Mar. 1992 - 1 Sep. 1993

Mladen A. Vouk and David F. McAllister 1993 61 p

(Grant NAG1-983)

(NASA-CR-194353; NAS 1.26:194353) Avail: CASI HC A04/MF A01

Strategies and tools for the testing, risk assessment and risk control of dependable software-based systems were developed. Part of this project consists of studies to enable the transfer of technology to industry, for example the risk management techniques for safety-concious systems. Theoretical investigations of Boolean and Relational Operator (BRO) testing strategy were conducted for condition-based testing. The Basic Graph Generation and Analysis tool (BGG) was extended to fully incorporate several variants of the BRO metric. Single- and multi-phase risk, coverage and time-based models are being developed to provide additional theoretical and empirical basis for estimation of the reliability and availability of large, highly dependable software. A model for software process and risk management was developed. The use of cause-effect graphing for software specification and validation was investigated. Lastly, advanced software fault-tolerance models were studied to provide alternatives and improvements in situations where simple software fault-tolerance strategies break down. CASI

N94-15175# University of Southern California, Marina del Rey. Information Sciences Inst.

SIMS: SINGLE INTERFACE TO MULTIPLE SYSTEMS Final Report, 1 Sep. 1987 - 31 Aug. 1992

Yigal Arens 31 Aug. 1992 24 p

(Contract MDA903-87-C-0641; DARPA Order 6096)

(AD-A266934) Avail: CASI HC A03/MF A01

The Services and Information Management for Decision Systems (SIMS) project integrates several computer services into a single, seamless system, as seen from the user's perspective. This relieves the user of the need to be familiar with all the services available from the system, enabling the user to make requests as though he or she were dealing with a single entity. SIMS analyzes the user request, plans the necessary sequence of calls on the services and executes them. Until now, the only approach to the problem of software integration has been to build custom systems that support an integrated view of the underlying servers. Such systems are expensive, are suitable only for the application for which they were crafted, are not very flexible with respect to functionality, and are difficult to modify. In contrast, SIMS would allow maintainers to assimilate servers into the system through a much less painful process of building a declarative model of the servers, and allowing the SIMS planner to perform the actual integration task. DTIC

N94-15189*# Research Inst. for Advanced Computer Science, Moffett Field, CA.

A BROWSING TOOL FOR THE INTERNET LOGICAL LIBRARY OF THE HPCC SOFTWARE EXCHANGE

Ross Biro Sep. 1993 22 p

(Contract NAS2-13721)

(NASA-CR-194545; NAS 1.26:194545; RIACS-TR-93.09) Avail: CASI HC A03/MF A01

As the quantity of information available on the Internet grows, locating a particular piece of information becomes more difficult. One possible solution is for a database of pointers to all available information to be maintained at a central site. Subject classifications for all the information could also be maintained in order to make searching possible. This paper describes one possible method of searching such an index. In particular a prototype browsing tool has been created using TCL/TK to demonstrate several possible features: rapidly scanning at any rank of the index, narrowing the index to any scope, regular-expression searching, and creation of a list of pointers answering to any set of index terms. The prototype browser is an easy-to-use independent X application designed for use in the Catalog of Repositories of the HPCC (High Performance Computing and Communications) Software Exchange. Author (revised)

N94-15212# Carnegie-Mellon Univ., Pittsburgh, PA. Robotics Inst.

FINDING STABLE ORIENTATIONS OF ASSEMBLIES WITH LINEAR PROGRAMMING

David Baraff, Raju Mattikalli, Bruno Repetto, and Pradeep Khosla Jun. 1993 21 p

(AD-A266990; CMU/RI-TR-93-13) Avail: CASI HC A03/MF A01

In the paper by Mattikalli et al.(5), the stability of an assemblage of frictionless contacting bodies with uniform gravity was considered. The problem of finding a stable orientation for such an assembly was formulated as a constrained maximun problem. A solution to the maximun problem yielded an orientation of the assembly that was stable under gravity; however, if no such orientation existed, then the solution to the maximun problem yielded the most stable orientation possible for the assembly. The maximun

problem was solved using a numerical iteration procedure that solved a linear program for each step of the iteration. In this paper, we show that the stability problem can be considered a variant of standard zero-sum matrix games. A solution to the maximun problem can be found by solving a single linear program. DTIC

N94-15214# Carnegie-Mellon Univ., Pittsburgh, PA. Software Engineering Inst.

SAFETY-CRITICAL SOFTWARE: STATUS REPORT AND ANNOTATED BIBLIOGRAPHY Final Report

Patrick R. Place and Kyo C. Kang Jun. 1993 84 p

(Contract F19628-90-C-0003)

(AD-A266993; CMU/SEI-93-TR-05; ESC-TR-93-182) Avail: CASI HC A05/MF A01

Many systems are deemed safety-critical and these systems are increasingly dependent on software. Much has been written in the literature with respect to system and software safety. This report summarizes some of that literature and outlines the development of safety-critical software. Techniques for hazard identification and analysis are discussed. Further, techniques for the development of safety-critical software are mentioned. A partly annotated bibliography of literature concludes the report. DTIC

N94-15215# Carnegie-Mellon Univ., Pittsburgh, PA. Software Engineering Inst.

CONCEPTS ON MEASURING THE BENEFITS OF SOFTWARE PROCESS IMPROVEMENTS Final Report

James A. Rozum Jun. 1993 52 p

(Contract F19628-90-C-0003)

(AD-A266994; CMU/SEI-93-TR-09; ESC-TR-93-186) Avail: CASI HC A04/MF A01

The software community initially became aware of process improvement from the works of Deming, Juran, and Crosby. The current awareness and activity regarding software process improvement was sparked by the Software Engineering Institute (SEI) with the release of its original software process maturity model. Following the advice of the SEI, many software organizations initiated software process improvement efforts to improve the quality of their products by improving the processes that produce those products. The question that many managers are continually asking today, though, is: How much has my organization benefited from the changes we have made? Unfortunately, many organizations did not include a method of measuring those benefits in their improvement activities. This report describes some concepts that organizations can tailor and build upon to develop a method for determining the benefits they have received from their software process improvement activities. DTIC

N94-15216# Carnegie-Mellon Univ., Pittsburgh, PA. Software Engineering Inst.

SOFTWARE ARCHITECTURE FOR SHARED INFORMATION SYSTEMS Final Report

Mary Shaw Mar. 1993 50 p

(Contract F19628-90-C-0003)

(AD-A266995; CMU/SEI-93-TR-3; ESC-TR-93-180) Avail: CASI HC A03/MF A01

Software system design takes place at many levels. Different kinds of design elements, notations, and analyses distinguish these levels. At the software architecture level, designers combine subsystems into complete systems. This paper studies some of the common patterns of idioms, that guide these configurations. Results from software architecture offer some insight into the problems of systems integration-the task of connecting individual, isolated, pre-existing software systems to provide coherent, distributed solutions to large problems. As computing has become more sophisticated, so too have the software structures used in the integration task. This paper reviews historical examples of shared information systems in three different applications whose requirements share some common features about collecting, manipulating, and preserving large bodies of complex information. These applications have similar architectural histories in which a succession of designs responds to new technologies and new requirements for flexible, highly dynamic responses. DTIC

N94-15443*# Computational Logic, Inc., Austin, TX.

A FORMAL LANGUAGE FOR THE SPECIFICATION AND VERIFICATION OF SYNCHRONOUS AND ASYNCHRONOUS CIRCUITS Final Report

David M. Russinoff Sep. 1993 89 p

(Contract NAS1-18878; RTOP 505-64-10-13)

(NASA-CR-191509; NAS 1.26:191509) Avail: CASI HC A05/MF A01

A formal hardware description language for the intended application of verifiable asynchronous communication is described. The language is developed within the logical framework of the Nqthm system of Boyer and Moore and is based on the event-driven behavioral model of VHDL, including the basic VHDL signal propagation mechanisms, the notion of simulation deltas, and the VHDL simulation cycle. A core subset of the language corresponds closely with a subset of VHDL and is adequate for the realistic gate-level modeling of both combinational and sequential circuits. Various extensions to this subset provide means for convenient expression of behavioral circuit specifications. Author (revised)

N94-15483*# Institute for Computer Applications in Science and Engineering, Hampton, VA.

PARALLEL SPATIAL DIRECT NUMERICAL SIMULATIONS ON THE INTEL IPSC/860 HYPERCUBE Final Report

Ronald D. Joslin (National Aeronautics and Space Administration. Langley Research Center, Hampton, VA.) and Mohammad Zubair (Old Dominion Univ., Norfolk, VA.) Aug. 1993 46 p Submitted for publication

(Contract NAS1-19480; RTOP 505-90-52-01)

(NASA-CR-191513; NAS 1.26:191513; ICASE-93-53) Avail: CASI HC A03/MF A01

The implementation and performance of a parallel spatial direct numerical simulation (PSDNS) approach on the Intel iPSC/860 hypercube is documented. The direct numerical simulation approach is used to compute spatially evolving disturbances associated with the laminar-to-turbulent transition in boundary-layer flows. The feasibility of using the PSDNS on the hypercube to perform transition studies is examined. The results indicate that the direct numerical simulation approach can effectively be parallelized on a distributed-memory parallel machine. By increasing the number of processors nearly ideal linear speedups are achieved with nonoptimized routines; slower than linear speedups are achieved with optimized (machine dependent library) routines. This slower than linear speedup results because the Fast Fourier Transform (FFT) routine dominates the computational cost and because the routine indicates less than ideal speedups. However with the machine-dependent routines the total computational cost decreases by a factor of 4 to 5 compared with standard FORTRAN routines. The computational cost increases linearly with spanwise wall-normal and streamwise grid refinements. The hypercube with 32 processors was estimated to require approximately twice the amount of Cray supercomputer single processor time to complete a comparable simulation; however it is estimated that a subgrid-scale model which reduces the required number of grid points and becomes a large-eddy simulation (PSLES) would reduce the computational cost and memory requirements by a factor of 10 over the PSDNS. This PSLES implementation would enable transition simulations on the hypercube at a reasonable computational cost. Author (revised)

N94-15486*# National Aeronautics and Space Administration. Langley Research Center, Hampton, VA.

OPEN ENVIRONMENTS TO SUPPORT SYSTEMS ENGINEERING TOOL INTEGRATION: A STUDY USING THE PORTABLE COMMON TOOL ENVIRONMENT (PCTE)

Dave E. Eckhardt, Jr., Michael J. Jipping (Hope College, Holland, MI.), Chris J. Wild (Old Dominion Univ., Norfolk, VA.), Steven J. Zeil (Old Dominion Univ., Norfolk, VA.), and Cathy C. Roberts Sep. 1993 17 p

(RTOP 505-64-50-05)

(NASA-TM-4489; L-17202; NAS 1.15:4489) Avail: CASI HC A03/MF A01

A study of computer engineering tool integration using the Portable Common Tool Environment (PCTE) Public Interface Standard is presented. Over a 10-week time frame, three existing software products were encapsulated to work in the Emeraude environment, an implementation of the PCTE version 1.5 standard. The software products used were a computer-aided software engineering (CASE) design tool, a software reuse tool, and a computer architecture design and analysis tool. The tool set was then demonstrated to work in a coordinated design process in the Emeraude environment. The project and the features of PCTE used are described, experience with the use of Emeraude environment over the project time frame is summarized, and several related areas for future research are summarized. Author (revised)

N94-15489*# Institute for Computer Applications in Science and Engineering, Hampton, VA.
MULTIPHASE COMPLETE EXCHANGE: A THEORETICAL ANALYSIS Final Report
Shahid H. Bokhari (University of Engineering and Technology, Lahore, Pakistan.) Aug. 1993 28 p
(Contracts NAS1-19480; NAS1-18605; RTOP 505-90-52-01)
(NASA-CR-191531; NAS 1.26:191531; ICASE-93-64) Avail: CASI HC A03/MF A01

Complete Exchange requires each of N processors to send a unique message to each of the remaining N-1 processors. For a circuit switched hypercube with N = 2(sub d) processors, the Direct and Standard algorithms for Complete Exchange are optimal for very large and very small message sizes, respectively. For intermediate sizes, a hybrid Multiphase algorithm is better. This carries out Direct exchanges on a set of subcubes whose dimensions are a partition of the integer d. The best such algorithm for a given message size m could hitherto only be found by enumerating all partitions of d. The Multiphase algorithm is analyzed assuming a high performance communication network. It is proved that only algorithms corresponding to equipartitions of d (partitions in which the maximum and minimum elements differ by at most 1) can possibly be optimal. The run times of these algorithms plotted against m form a hull of optimality. It is proved that, although there is an exponential number of partitions, (1) the number of faces on this hull is Theta(square root of d), (2) the hull can be found in theta(square root of d) time, and (3) once it has been found, the optimal algorithm for any given m can be found in Theta(log d) time. These results provide a very fast technique for minimizing communication overhead in many important applications, such as matrix transpose, Fast Fourier transform, and ADI. Author (revised)

N94-15525# Boeing Computer Services Co., Seattle, WA.
RAMCAD DESIGN METHODOLOGY Interim Technical Report, Apr. 1988 - Dec. 1992
Charles T. Kitzmiller, Matthew C. Tracy, II, and Michael W. Anderson May 1993 122 p
(Contract F33615-87-C-0001)
(AD-A267010; AL/HR-TP-1993-0017) Avail: CASI HC A06/MF A02

The goal of the Reliability, Availability, and Maintainability in Computer Aided Design (RAMCAD) research effort is to define environment that fully supports reliability, maintainability, and supportability issues through the use of computer aided design/computer aided engineering workstations. As part of this effort, the current design methodology was analyzed and a new variation of the methodology was proposed. The proposed methodology as well as the computer support requirements, measures of effectiveness, and design techniques that are required to implement the methodology are described. DTIC

N94-15538*# National Aeronautics and Space Administration. Ames Research Center, Moffett Field, CA.
REACTIVE SYSTEM VERIFICATION CASE STUDY: FAULT-TOLERANT TRANSPUTER COMMUNICATION
D. Francis Crane and Philip J. Hamory Sep. 1993 12 p Sponsored by NASA, Washington
(RTOP 505-64-52)
(NASA-TM-108784; A-93103; NAS 1.15:108784) Avail: CASI HC A03/MF A01

A reactive program is one which engages in an ongoing interaction with its environment. A system which is controlled by an embedded reactive program is called a reactive system. Examples of reactive systems are aircraft flight management systems, bank automatic teller machine (ATM) networks, airline reservation systems, and computer operating systems. Reactive systems are often naturally modeled (for logical design purposes) as a composition of autonomous processes which progress concurrently and which communicate to share information and/or to coordinate activities. Formal (i.e., mathematical) frameworks for system verification are tools used to increase the users' confidence that a system design satisfies its specification. A framework for reactive system verification includes formal languages for system modeling and for behavior specification and decision procedures and/or proof-systems for verifying that the system model satisfies the system specifications. Using the Ostroff framework for reactive system verification, an approach to achieving fault-tolerant communication between transputers was shown to be effective. The key components of the design, the decoupler processes, may be viewed as discrete-event-controllers introduced to constrain system behavior such that system specifications are satisfied. The Ostroff framework was also effective. The expressiveness of the modeling language permitted construction of a faithful model of the transputer network. The relevant specifications were readily expressed in the specification language. The set of decision procedures provided was adequate to verify the specifications of interest. The need for improved support for system behavior visualization is emphasized. Author (revised)

N94-15627# California Univ., San Diego, La Jolla.
DATABASE SYSTEM STUDIES IN FINE GRAIN OPTOELECTRONIC COMPUTING Quarterly Technical Report
Sadik C. Esener 14 May 1993 9 p
(Contract N00014-93-I-0414)
(AD-A267026) Avail: CASI HC A02/MF A01

This document describes investigations which were carried out by a select team of researchers centered at UCSD together with researchers from other institutions and industry: UCSB and UCLA (focused on smart pixels integration); the packaging alliance at Cornell and UCLA (for array interfaces and system packaging); and our industrial partners including Hughes (for 3-D electronics and optical storage interfacing), Honeywell and Rockwell (for packaging), and AT&T (for diffractive optics). DTIC

N94-15629# Carnegie-Mellon Univ., Pittsburgh, PA. Software Engineering Inst.
AN ANALYSIS OF SEI SOFTWARE PROCESS ASSESSMENT RESULTS: 1987-1991 Final Report
David H. Kitson and Stephen Masters Jul. 1992 37 p
(Contract F19628-90-C-0003)
(AD-A266996; CMU/SEI-92-TR-24; ESC-TR-92-24) Avail: CASI HC A03/MF A01

This report focuses on the results of SEI (Software Engineering Institute) software process assessments conducted over a four year period beginning in 1987. It characterizes the software processes used by software managers and practitioners at the assessed sites and classifies issues identified during the assessments. The basis for the characterization and classification is a software process maturity model developed by the SEI. This report contributes to the existing body of knowledge on the state of practice of software engineering in the U.S. by characterizing the sites from a software process maturity perspective and profiling site software process weaknesses. The data analyzed is drawn from SEI software process assessments of 59 government and industry software sites. This work is an analysis of existing assessment data rather than a designed study. The participating sites were not randomly selected; accordingly, they do not necessarily constitute a statistically valid sampling of the U.S. software industry. DTIC

N94-15630# Carnegie-Mellon Univ., Pittsburgh, PA. Software Engineering Inst.
PROCESS-CENTERED DEVELOPMENT ENVIRONMENTS: AN EXPLORATION OF ISSUES Final Report
Alan M. Christie Jun. 1993 74 p
(Contract F19628-90-C-0003)
(AD-A266997; CMU/SEI-93-TR-04; ESC-TR-93-181) Avail: CASI HC A04/MF A01

Software development environments are beginning to move from research communities to commercial applications. As this occurs, the need to address process issues related to such environments is becoming increasingly apparent. Thus there is a growing awareness of the need for process-centered development environments (PCDEs). This report addresses process definition and enactment issues which pertain to the specification and design of a PCDE. The first part of the report explores some of the required characteristics of an enactable graphical language and the relationship between process definition and enactment. This process language naturally led to the ability to perform process verification, i.e., a verification that the actual process path taken throughout a project conforms to the defined process. The issue of process verification is thus also explored. The success of PCDEs rests heavily on end-user acceptance. Because of this, the report concludes with a review of user-oriented process and social issues relevant to the successful adoption of PCDEs. DTIC

N94-15638# Carnegie-Mellon Univ., Pittsburgh, PA. Software Engineering Inst.
DEPENDABLE SOFTWARE TECHNOLOGY EXCHANGE Final Report
Charles B. Weinstock and Fred B. Scheneider Jun. 1993 34 p
(Contract F19628-90-C-0003)
(AD-A267103; CMU/SEI-93-SR-04) Avail: CASI HC A03/MF A01

On 18 and 19 Mar. 1993, the Dependable Real-Time Software Project hosted a Dependable Software Technology Exchange. The exchange, sponsored by the Air Force Space and Missile Systems Center and the Office of Naval Research, brought together researchers and system developers, providing an opportunity for the researchers to learn the needs of the developers and for the developers to learn about techniques being investigated by the researchers. This report summarizes what transpired at the meeting. DTIC

N94-15650# Aeronautical Research Labs., Melbourne (Australia).
A SOFTWARE INTERFACE FOR THE ARL WIND TUNNEL DATA ACQUISITION SYSTEM
B. D. Fairlie and S. S. Sam Mar. 1993 55 p
(AD-A267114; ARL-TR-14; DODA-AR-007-135) Avail: CASI HC A04/MF A01

A software interface for the data acquisition system has been developed on a MicroVAX II computer for the transonic and low speed wind tunnels at ARL. The software is responsible for handling instrumentation control and data transfer requests between the data acquisition software and the parallel data bus via a DRV11 parallel I/O interface adapter. Access to the DRV11 registers is effected by direct mapping of the Q22-Bus I/O page to program variables, giving fast and efficient transfer of data to and from the parallel data bus. Up to five processes may access the parallel data bus at one time via this software interface thus allowing great flexibility in the development of data acquisition software. This report details the necessary programming steps which must be included in data acquisition software to access the parallel data bus via the software interface. DTIC

N94-15653# Carnegie-Mellon Univ., Pittsburgh, PA. Software Engineering Inst.
REENGINEERING: AN ENGINEERING PROBLEM Special Report
Peter H. Feiler Jul. 1993 42 p
(Contract F19628-90-C-0003)
(AD-A267117; CMU/SEI-93-SR-5) Avail: CASI HC A03/MF A01

This paper discusses a plan that addresses how the Software Engineering Institute (SEI) may assist the Department of Defense (DoD) in reengineering its large software-intensive systems. This plan is based on a view of reengineering as an engineering problem to improve the cost-effective evolution of large software-intensive systems. This view of reengineering, which takes the whole software engineering process into account, fosters a growth path by leveraging promising emerging software engineering technologies. Reengineering also builds on the industry's improvement in its ability to manage the software engineering process, an accomplishment of SEI work in the Capability Maturity Model (CMM) and its key process areas. DTIC

N94-15670# Naval Air Warfare Center, Warminster, PA. Systems and Software Technology Dept.
MULTIOBJECTIVE FUNCTIONS OPTIMIZATION FOR TASK ALLOCATION MAPPING TO MULTICOMPUTER NODES Final Report
Jesse Williams 7 Aug. 1992 14 p
(NR Proj. RS3-4-P-11)
(AD-A267071; NAWCADWAR-92103-70) Avail: CASI HC A03/MF A01

The Naval Air Warfare Center-Aircraft Division Warminster, Software and Computer Technology Division, is developing software to allocate tasks to multicomputer nodes such that multiple objectives are optimized. The eventual goal of this project is to allow the decision maker to have design optimization capabilities available to her/him when designing complex system. Two key aspects of the allocation problem are discussed: (1) the techniques used to treat multiple objectives simultaneously; and (2) the techniques used to perform the search for the optimal set of model parameters. The report discusses current research reported in the literature and makes several suggestions for continuing the current effort. The current technique being used for treating multiple objectives simultaneously is to use a weighted sum of each of the individual objective functions as the objective function for the search. It is suggested that a vector of objective functions approach be implemented and experimentally compared to the weighted sum approach. Two algorithms are being used in the software: the genetic algorithm and the simulated annealing algorithm. DTIC

N94-15674# ORA Corp., Ithaca, NY.
INTEGRATED TRUSTED SYSTEMS DEVELOPMENT ENVIRONMENT Final Report
Tanya Korelsky and David Rosenthal May 1993 72 p
(Contract F30602-91-C-0058)
(AD-A267029; RL-TR-93-49) Avail: CASI HC A04/MF A01

This document is the Final Report of the Integrated Trusted Systems Development Environment (ITSDE) project. The ITSDE project was a feasibility study that addressed the software development process for trusted systems. The goals of this effort were as follows: (1) to elaborate the Integrated Development Process (IDP) for trusted systems outlined in 'Developing Trusted Systems Using DoD-STD-2167A' and to elaborate the corresponding documentation suite; and (2) to investigate how formal specification and verification tools developed at ORA for Rome Laboratory fit into the elaborated IDP for trusted systems of high assurance. The IDP attempts to integrate activities by the DOD-STD2167A and the 'Trusted Computer System Evaluation Criteria' (TCSEC) into a unified approach for the development of trusted systems. We chose to investigate the elaboration of the IDP by developing requirements, design, and formal specification of a particular example. This approach allowed us to illustrate the findings and recommendations produced by the study. As our example for the study we chose to add a trusted mail service, which we call the Trusted Mail Handler, to the THETA (Trusted Heterogeneous Architecture) distributed operating system. THETA adds trusted distributed operating system functionality on top of commercial-off-the-shelf (COTS) trusted operating systems. DTIC

N94-15687# Naval Postgraduate School, Monterey, CA.
SOFTWARE RELIABILITY MANAGEMENT THROUGH METRICS M.S. Thesis
Douglas R. Burton Mar. 1993 70 p
(AD-A267129) Avail: CASI HC A04/MF A01

As systems become increasingly software dependent, their reliability will accordingly depend more so on the reliability of their resident software. Just as techniques and processes were developed and improved to ensure hardware reliability, so must techniques evolve to ensure software reliability. Two questions are addressed by this thesis. First, how do we measure software reliability throughout a project's lifecycle? Second, is there a tool which will provide effective insight into the test-now-or-later problem? The solution to our first question is a U.S. Army software procurement methodology which is briefly outlined as the overall framework for software procurement in this thesis. A software fault analysis tool is developed and programmed. Some results from this algorithm are provided and their potential resource saving impact explored. Program managers of software-intensive projects would be well advised to use the Army's methodology and this fault analysis tool to potentially save critically short procurement resources. DTIC

N94-15702# Admiralty Research Establishment, Gosport (England).
THE FREE DECAY OF COUPLED HEAVE AND PITCH MOTIONS OF A MODEL FRIGATE
P. Crossland, P. A. Wilson (Southampton Univ., England.), and J. C. Bradburn (Imperial Coll. of Science and Technology, London, England.) Oct. 1992 27 p
(DRA/TM(AWMH)92340; BR315173; ETN-93-94503) Copyright Avail: CASI HC A03/MF A01

A comparison of the heave and pitch motion decay time histories together with the analytical decay time histories synthesized using the hydrodynamic coefficients predicted by the PAT-91 ship motion computer program is provided. The PAT-91 ship program was found to overpredict damping especially at resonant frequencies, resulting in there being no significant peak in the transfer function of pitch at resonance. The results of a series of experiments that measured the decay time histories of a model frigate free to move in the vertical plane, in an attempt to identify where the problems might be occurring, are presented. Judgements are made concerning the components in the heave and pitch motions using the terms in the full two dimensional strip theory heave and pitch motion equations to explain the trends shown. The investigation showed that the

sectional damping coefficient appears to be over predicted. This results in a relatively poor prediction of heave decay curves at low speed and overestimates the damping in the pitch decay curves. It appears that the discrepancies seen in the heave and pitch transfer functions could be due to the wave excitation being predicted incorrectly. ESA

N94-15703*# National Aeronautics and Space Administration. Goddard Space Flight Center, Greenbelt, MD.
LINEAR ENCODING DEVICE Patent Application
Douglas B. Leviton, inventor (to NASA) 29 Mar. 1993 22 p
(NASA-Case-GSC-13562-1; NAS 1.71:GSC-13562-1;
US-Patent-Appl-SN-037876) Avail: CASI HC A03/MF A01

A Linear Motion Encoding device for measuring the linear motion of a moving object is disclosed in which a light source is mounted on the moving object and a position sensitive detector such as an array photodetector is mounted on a nearby stationary object. The light source emits a light beam directed towards the array photodetector such that a light spot is created on the array. An analog-to-digital converter, connected to the array photodetector is used for reading the position of the spot on the array photodetector. A microprocessor and memory is connected to the analog-to-digital converter to hold and manipulate data provided by the analog-to-digital converter on the position of the spot and to compute the linear displacement of the moving object based upon the data from the analog-to-digital converter. NASA

N94-15721*# National Aeronautics and Space Administration. Marshall Space Flight Center, Huntsville, AL.
REPORT ON COMPUTING AND NETWORKING IN THE SPACE SCIENCE LABORATORY BY THE SSL COMPUTER COMMITTEE
D. L. Gallagher, ed. Sep. 1993 18 p Sponsored by NASA, Washington
(NASA-TM-108422; NAS 1.15:108422) Avail: CASI HC A03/MF A01

The Space Science Laboratory (SSL) at Marshall Space Flight Center is a multiprogram facility. Scientific research is conducted in four discipline areas: earth science and applications, solar-terrestrial physics, astrophysics, and microgravity science and applications. Representatives from each of these discipline areas participate in a Laboratory computer requirements committee, which developed this document. The purpose is to establish and discuss Laboratory objectives for computing and networking in support of science. The purpose is also to lay the foundation for a collective, multiprogram approach to providing these services. Special recognition is given to the importance of the national and international efforts of our research communities toward the development of interoperable, network-based computer applications. Author (revised)

N94-15725# Carnegie-Mellon Univ., Pittsburgh, PA. Dept. of Computer Science.
ACM SIGPLAN WORKSHOP ON ML AND ITS APPLICATIONS
Peter Lee Jun. 1992 209 p Workshop held in San Francisco, CA, 20-21 Jun. 1992
(AD-A266617; CMU-CS-93-105) Avail: CASI HC A10/MF A03

The Workshop on ML and its Applications was held June 20-21, 1992 in San Francisco, CA, in conjunction with the ACM SIGPLAN '92 Conferences and Workshops. The ML programming language has been an important tool and framework for research in language design and implementation. As the language and its implementations have matured, the range of applications has increased greatly. New applications, combined with new ideas in design and implementation, have stimulated a large number of significant activities in research and software development. This workshop, like the previous workshops in Princeton, Edinburgh, and Pittsburgh, provided a forum for theses activities, with a special emphasis on applications of the language. A total of 21 abstracts were selected for presentation and discussion at the workshop: 12 were chosen for conference-style presentations and 9 for presentation in a poster session. DTIC

N94-15728# Carnegie-Mellon Univ., Pittsburgh, PA. Dept. of Computer Science.
ARCHITECTURES FOR SOFTWARE SYSTEMS: A CURRICULUM DEVELOPMENT PROPOSAL IN UNDERGRADUATE SOFTWARE ENGINEERING Final Technical Report, 1 Jan. - 31 Dec. 1992
David Garlan and Mary Shaw May 1993 23 p
(Contract MDA972-92-J-1002)
(AD-A266703) Avail: CASI HC A03/MF A01

This curriculum development project had as its primary goal the development of a course that augments existing undergraduate software curricula by teaching concepts, techniques, and examples at the architectural level of software design. Specifically, Architectures for Software Systems would: (1) teach students how to understand and evaluate designs of existing software systems from an architectural perspective; (2) provide students with the intellectual building blocks for designing new systems in principled ways using well-understood architectural paradigms; (3) show students how formal notations and models can be used to characterize and reason about a system design; and (4) familiarize students with concrete examples of actual system architectures that can serve as models for new designs. DTIC

N94-15743# Carnegie-Mellon Univ., Pittsburgh, PA. School of Computer Science.
USING INTERACTIVE SKETCH INTERPRETATION TO DESIGN SOLID OBJECTS Ph.D. Thesis
David Pugh 4 Apr. 1993 101 p
(AD-A266637; CMU-CS-93-147) Avail: CASI HC A06/MF A02

Before the introduction of Computer Aided Design and solid modeling systems, designers had developed a set of methods for designing solid objects by sketching their ideas using pencil and paper and refining these ideas into workable designs. These methods are different from those used for designing objects with a conventional solid modeler. Not only does this dichotomy waste a vast reserve of talent and experience (people typically start sketching from the moment they first pick up a crayon), but it also has a more fundamental problem: designers can use their intuition more effectively when sketching than they can when using a solid modeler. This dissertation introduces interactive sketch interpretation as a new user interface paradigm for solid modeling systems. Interactive sketch interpretation makes it possible to use the computer as a sketchpad for designing three-dimension objects. The premise behind interactive sketch interpretation is to let the designer change an object's design by modifying a computer generated the line drawing of the object. Sketch interpretation maps the designer's changes onto a boundary representation model of the object. The designer can continue the design process by then changing the line drawing of the modified object. This design cycle is highly interactive and, as a result, incorrect interpretations can be easily corrected by the designer. Viking is a solid modeling system whose user interface is based on interactive sketch interpretation. With Viking, the designer can modify his or her design by either changing the line drawing or placing geometric constraints on the object. Sketch interpretation changes Viking's model of the object so that it is consistent with the modified line drawing and the geometric constraints placed by the user. DTIC

N94-15772 New Jersey Inst. of Tech., Newark.
THE BOOTSTRAPPED ALGORITHM: FAST ALGORITHM FOR BLIND SIGNAL SEPARATION Final Report, Mar. 1991 - Jun. 1992
Yeheskel Bar-Ness, A. Dinc, and H. Messer-Yaron Apr. 1993 249 p
Limited Reproducibility: More than 20% of this document may be affected by microfiche quality
(Contract F30602-88-D-0025)
(AD-A266671; RL-TR-93-24) Avail: CASI HC A11

An adaptive algorithm termed 'Bootstrapped Algorithm' is proposed and analyzed, and its performance is evaluated in this report. Using this algorithm as an interference canceller results in structures which are unique in that they are composed of multi-cancellers; each uses the outputs of other cancellers as references (desired signals) or in other forms to further improve performance. As a result of such unique structures, the bootstrapped algorithm is shown to perform as a 'Signal Separator' rather than as an interference canceller. Clearly, because it does not require a reference signal in the form of decision feedback or training sequence, it is sometimes justifiably referred to by the term 'Blind Separator.' DTIC

N94-15776 Prins Maurits Lab. TNO, Rijswijk (Netherlands).
USER MANUAL AND PROGRAM DESCRIPTION OF THE DATA ACQUISITION SYSTEM OF PML-PULSE PHYSICS Final Report [GEBRUIKERSHANDLEIDING EN PROGRAMMATUURBESCHRIJVING VAN HET DATA ACQUISITIE SYSTEEM VAN HET LABORATORIUM VOOR PULSFYSICA]

G. H. Olthof Jan. 1993 31 p In DUTCH Limited Reproducibility: More than 20% of this document may be affected by microfiche quality
(AD-A266752; PML-1992-72; TDCK-92-2416) Avail: CASI HC A03

This report describes the hardware and software of the Data Acquisition System (DAS) used at the TNO-PML Pulse Physics Laboratory for their experimental research. The first part deals with the hardware specifications. The DAS set-up for performing measurements is described in the second part of this report. This part can be used as a user's manual of the DAS. For documentation purposes a detailed description of the software is added at the end of the report. DTIC

N94-15784*# National Aeronautics and Space Administration. Ames Research Center, Moffett Field, CA.
USER'S MANUAL FOR THE HYPGEN HYPERBOLIC GRID GENERATOR AND THE HGUI GRAPHICAL USER INTERFACE
William M. Chan (MCAT Inst., San Jose, CA.), Ing-Tsau Chiu (Overset Methods, Inc., Vacaville, CA.), and Pieter G. Buning Oct. 1993 44 p
(RTOP 505-59-00)
(NASA-TM-108791; A-93133; NAS 1.15:108791) Avail: CASI HC A03/MF A01

The HYPGEN program is used to generate a 3-D volume grid over a user-supplied single-block surface grid. This is accomplished by solving the 3-D hyperbolic grid generation equations consisting of two orthogonality relations and one cell volume constraint. In this user manual, the required input files and parameters and output files are described. Guidelines on how to select the input parameters are given. Illustrated examples are provided showing a variety of topologies and geometries that can be treated. HYPGEN can be used in stand-alone mode as a batch program or it can be called from within a graphical user interface HGUI that runs on Silicon Graphics workstations. This user manual provides a description of the menus, buttons, sliders, and typein fields in HGUI for users to enter the parameters needed to run HYPGEN. Instructions are given on how to configure the interface to allow HYPGEN to run either locally or on a faster remote machine through the use of shell scripts on UNIX operating systems. The volume grid generated is copied back to the local machine for visualization using a built-in hook to PLOT3D. Author

N94-15840# Army Natick Research and Development Command, MA. Engineering Center.
EFFICACY OF FLOCCULATING AND OTHER EMERGENCY WATER PURIFICATION TABLETS Final Report, Oct. 1989 - Sep. 1991
Edmund M. Powers May 1993 39 p
(AD-A266695) Avail: CASI HC A03/MF A01

Chlor-Floc (CF) emergency water purification tablets were tested in the following areas: bactericidal, viricidal, and cysticical efficacy; removal of turbidity and chemical agents in water at temperatures ranging from 5 to 25 C; and storage stability at 5, 25, and 40 deg C. The minimal required reduction was achieved for bacteria, Rotavirus, and Giardia, but CF did not achieve the required reduction of Poliovirus at any of the temperatures or time periods investigated. Clarification of water was effective in turbid waters, but filtration through a cloth is necessary to prevent flocculated sediment from entering the canteen. Removal of chemical agents from water was a function of the solubility of the chemical agent, the rate of hydrolysis, and the composition of the water. The free residual chlorine in CF tablets remained stable at 5 and 25 C for 27 months, but declined rapidly after three months at 40 C and three days at 60 C. To be acceptable to the Military, the tablets must be approved and registered by the EPA and must be stable during normal storage for three years. Commercial Item Descriptions have been written for CF tablets and for a kit containing tablets, filters, and a water treatment bag. Both may be procured through the Defense General Supply Center, Richmond, VA. DTIC

N94-15841# Carnegie-Mellon Univ., Pittsburgh, PA. School of Computer Science.
A SCIENTIFIC BASIS FOR COMPUTATIONAL SCIENCE
Raul E. Valdes-Perez May 1993 19 p
(AD-A266697; CMU-CS-93-162) Avail: CASI HC A03/MF A01

Computational science is a productive intellectual activity. It produces highly useful computer programs that require much creativity and ingenuity to develop. Moreover, computation is a powerful theoretical tool for natural scientists. However, can computational science have a scientific foundation, quite apart from its roles as a juxtaposition of disciplines and as another theoretical tool for scientists? That is, can computational science develop concepts that enable a broad systematic understanding of inference and discovery in science? This paper makes a case for an affirmative answer that relies on the concept of generic scientific task. We will argue that theoretical understanding is to be attained by identifying and automating such tasks. To develop the idea, we configure samples of previous work in computational science (broadly construed), lay a road map to guide further research, and suggest experimental tools to generate research problems and to re-deploy proven techniques. DTIC

N94-15943*# National Aeronautics and Space Administration. Goddard Space Flight Center, Greenbelt, MD.
ROTARY ENCODING DEVICE Patent Application
Douglas B. Leviton, inventor (to NASA) 25 Feb. 1993 26 p
(NASA-Case-GSC-13556-1; NAS 1.71:GSC-13556-1;
US-Patent-Appl-SN-022219) Avail: CASI HC A03/MF A01

A device for position encoding of a rotating shaft in which a polygonal mirror having a number of facets is mounted to the shaft and a light beam is directed towards the facets is presented. The facets of the polygonal mirror reflect the light beam such that a light spot is created on a linear array detector. An analog-to-digital converter is connected to the linear array detector for reading the position of the spot on the linear array detector. A microprocessor with memory is connected to the analog-to-digital converter to hold and manipulate the data provided by the analog-to-digital converter on the position of the spot and to compute the position of the shaft based upon the data from the analog-to-digital converter. NASA

N94-15956*# Research Inst. for Advanced Computer Science, Moffett Field, CA.
THE ALIGNMENT-DISTRIBUTION GRAPH
Siddhartha Chatterjee, John R. Gilbert, and Robert Schreiber Aug. 1993 17 p Presented at the 6th Annual Languages and Compilers for Parallelism Workshop, Portland, OR, 12-14 Aug. 1993
(Contract NAS2-13721)
(NASA-CR-194609; RIACS-TR-93.06; NAS 1.26:194609) Avail: CASI HC A03/MF A01

Implementing a data-parallel language such as Fortran 90 on a distributed-memory parallel computer requires distributing aggregate data objects (such as arrays) among the memory modules attached to the processors. The mapping of objects to the machine determines the amount of residual communication needed to bring operands of parallel operations into alignment with each other. We present a program representation called the alignment-distribution graph that makes these communication requirements explicit. We describe the details of the representation, show how to model communication cost in this framework, and outline several algorithms for determining object mappings that approximately minimize residual communication. Author

N94-15965*# Institute for Computer Applications in Science and Engineering, Hampton, VA.
CLOUDING TRACING: VISUALIZATION OF THE MIXING OF FLUID ELEMENTS IN CONVECTION-DIFFUSION SYSTEMS Final Report
Kwan-Liu Ma and Philip J. Smith (Utah Univ., Salt Lake City.) Washington Aug. 1993 17 p Submitted for publication Original contains color illustrations
(Contract NAS1-19480; RTOP 505-90-52-01)
(NASA-CR-191529; NAS 1.26:191529; ICASE-93-62) Avail: CASI HC A03/MF A01; 1 functional color page

This paper describes a highly interactive method for computer visualization of the basic physical process of dispersion and mixing of fluid elements in convection-diffusion systems. It is based on transforming the vector field from a traditionally Eulerian reference frame into a Lagrangian reference frame. Fluid elements are traced through the vector field for the mean path as well as the statistical dispersion of the fluid elements about the mean position by using added scalar information about the root mean square value of the vector field and its Lagrangian time scale. In this way, clouds of fluid elements are traced and are not just mean paths. We have used this method to visualize the simulation of an industrial incinerator to help identify mechanisms for poor mixing. Author (revised)

N94-15985# Sandia National Labs., Albuquerque, NM.
C++ AS A LANGUAGE FOR OBJECT-ORIENTED NUMERICS

K. G. Budge, J. S. Peery, A. C. Robinson, and M. K. Wong 1993 13 p Presented at the European C++ Users Group Meeting, Munich, Germany, 7-9 Jul. 1993
(Contract DE-AC04-76DP-00789)
(DE93-015027; SAND-93-1353C; CONF-930791-1) Avail: CASI HC A03/MF A01

C++ is commonly described as an object-oriented programming language because of its strong support for classes with multiple inheritance and polymorphism. However, for a growing community of numerical programmers, an equally important feature of C++ is its support of operator overloading on abstract data types. The authors choose to call the resulting style of programming object-oriented numerics. They believe that much of object-oriented numerics is orthogonal to conventional object-oriented programming. As a case study, they discuss two strong shock physics codes written in C++ that they're currently developing. These codes use both polymorphic classes (typical of traditional object-oriented programming) and abstract data types with overloaded operators (typical of object-oriented numerics). They believe that C++ translators can generate efficient code for many numerical objects. However, for the important case of smart arrays (which are used to represent matrices and the fields found in partial differential equations) fundamental difficulties remain. The authors discuss the two most important of these, namely, the aliasing ambiguity and the proliferation of temporaries, and they present some possible solutions. DOE

N94-15989*# Institute for Computer Applications in Science and Engineering, Hampton, VA.
DISTRIBUTED COMPUTING FEASIBILITY IN A NON-DEDICATED HOMOGENEOUS DISTRIBUTED SYSTEM
Scott T. Leutenegger and Xian-He Sun Washington Sep. 1993 25 p Submitted for publication
(Contract NAS1-19480; RTOP 505-90-52-01)
(NASA-CR-191532; NAS 1.26:191532; ICASE-93-65) Avail: CASI HC A03/MF A01

The low cost and availability of clusters of workstations have lead researchers to re-explore distributed computing using independent workstations. This approach may provide better cost/performance than tightly coupled multiprocessors. In practice, this approach often utilizes wasted cycles to run parallel jobs. The feasibility of such a non-dedicated parallel processing environment assuming workstation processes have preemptive priority over parallel tasks is addressed. An analytical model is developed to predict parallel job response times. Our model provides insight into how significantly workstation owner interference degrades parallel program performance. A new term task ratio, which relates the parallel task demand to the mean service demand of nonparallel workstation processes, is introduced. It was proposed that task ratio is a useful metric for determining how large the demand of a parallel applications must be in order to make efficient use of a non-dedicated distributed system.
Author (revised)

N94-16119# Lawrence Livermore National Lab., CA.
A TASK ADAPTIVE PARALLEL GRAPHICS RENDERER
S. Whitman 21 Dec. 1992 19 p Presented at the Siggraph 1993 Conference, Anaheim, CA, 2-6 Aug. 1993
(Contract W-7405-eng-48)
(DE93-017123; UCRL-JC-112572; CONF-930881-3) Avail: CASI HC A03/MF A01

This paper presents a graphics renderer which incorporates new partitioning methodologies of memory and work for efficient execution on a parallel computer. The Task Adaptive domain decomposition scheme is an image space method involving dynamic partitioning of rectangular pixel area tasks. The author shows that this method requires little overhead, allows coherence within a parallel context, handles worst case scenarios effectively, and executes efficiently with little processor synchronization necessary. Previous research in the area of memory and work decompositions for graphics rendering has been primarily limited to simulation studies and little practical experience. The algorithm presented here has been implemented on a scalable distributed memory multiprocessor and tested on a variety of input scenes. The author presents a theoretical and practical analysis in order to contrast its predicted and actual success. The implementation analysis indicates that load imbalance is the major cause of performance degradation at the higher processor counts. Even so, on a variety of test scenes, an average rendering speedup of 79 was achieved utilizing 96 processors on the BBN TC2000 multiprocessor with a processor efficiency range of 66% to 94%. DOE

N94-16120# Stanford Univ., CA. Systems Optimization Lab.
A SEQUENTIAL QUADRATIC PROGRAMMING ALGORITHM USING AN INCOMPLETE SOLUTION OF THE SUBPROBLEM
W. Murray and F. J. Prieto May 1993 54 p
(Contract DE-FG03-92ER-25117)
(DE93-017439; SU-SOL-93-3; AD-A267216) Avail: CASI HC A04/MF A01

We analyze sequential quadratic programming (SQP) methods to solve nonlinear constrained optimization problems that are more flexible in their definition than standard SQP methods. The type of flexibility introduced is motivated by the necessity to deviate from the standard approach when solving large problems. Specifically we no longer require a minimizer of the QP subproblem to be determined or particular Lagrange multiplier estimates to be used. Our main focus is on an SQP algorithm that uses a particular augmented Lagrangian merit function. New results are derived for this algorithm under weaker conditions than previously assumed; in particular, it is not assumed that the iterates lie on a compact set. DOE

N94-16554*# Stanford Univ., CA. Dept. of Computer Science.
MODELS FOR REACTIVITY
Zohar Manna and Amir Pnueli 7 Jan. 1993 75 p
(Grants NAG2-703; AF-AFOSR-0057-90)
(AD-A266419; STAN-CS-92-1461) Avail: CASI HC A04/MF A01

A hierarchy of models that capture realistic aspects of reactive, realtime, and hybrid systems is introduced. On the most abstract level, the qualitative (non-quantitative) model of reactive systems captures the temporal precedence aspect of time. A more refined model is that of real-time systems, which represents the metric aspect of time. The third and most detailed model is that of hybrid systems, which allows the incorporation of continuous components into a reactive system. For each of the three levels, we present a computational model, a requirement specification language based on extensions of temporal logic, system description languages based on state charts and a textual programming language, proof rules for proving validity of properties, and examples of such proofs.
DTIC

N94-16560# Air Force Inst. of Tech., Wright-Patterson AFB, OH. School of Engineering.
A DECISION CRITERIA TO SELECT AN ASSOCIATIVE-MEMORY ORGANIZATION THAT MINIMIZES THE EXECUTION TIME OF A MIX OF ASSOCIATIVE-SEARCH OPERATIONS Ph.D. Thesis
David W. Banton Jun. 1993 205 p
(AD-A266438; AFIT/DS/ENG/93-02) Avail: CASI HC A10/MF A03

The dissertation develops a decision criteria to select an associative-memory organization that minimizes the execution time of a mix of associative-search operations and a decision criteria to estimate the layout dimensions of each organization for a specified memory size. The dissertation reclassifies Feng's associative-search operations into three hardware-influenced categories: bit-position independent (BPI), record-content independent (RCI); bit-position dependent (BPD), RCI; and BPD, record-content dependent (RCD). It develops a relationship between the categories and three associative-memory organizations: the CAM, the bit-serial word-parallel associative memory (BSWPAM), and the extreme-search associative memory (ESAM). A version of the CAM, three versions of the BSWPAM, and a version of the ESAM organizations were designed and simulated to show that for most memory sizes, BPI, RCI operations require less time when executed on a CAM, BPD, RCI operations require less time when executed on a BSWPAM organization, and for many memory sizes, BPD, RCD operations require less time when executed on an ESAM. The dissertation calculates the layout dimensions of each memory. The results indicate the CAM is the most area efficient followed by the single, and two BSWPAM, the ESAM, and the four BSWPAM.
DTIC

N94-16575# Rochester Univ., NY. Computer Science and Philosophy Dept.
COMBINATORIAL SEMANTICS

Henry E. Kyburg, Jr. Dec. 1992 24 p Replaces TR-408
(Grant NSF IRI-90-02659)
(TR-444) Avail: CASI HC A03/MF A01

In ordinary first order logic, a valid inference in a language L is one in which the conclusion is true in every model of the language in which the premises are true. To accommodate inductive/uncertain/probabilistic/non-monotonic inference, we weaken that demand to the demand that the conclusion be true in a large proportion of the models in which the premises are true. More generally, we say that an inference is (p,q) valid if it is true in a proportion lying between p and q of those models in which the premises are true. If we include a statistical variable binding operator 'percent' in our language, there are many quite general things we can say about uncertain validity. Author (revised)

N94-16579# Rochester Univ., NY. Dept. of Computer Science.
REDUCTIONS TO SETS OF LOW INFORMATION CONTENT
V. Arvind (Indian Inst. of Tech., New Delhi.), Y. Han, L. Hemachandra, J. Koebler (Ulm Univ., Germany.), A. Lozano (Universidad Politecnica de Catalunya, Spain.), M. Mundhenk (Ulm Univ., Germany.), M. Ogiwara (University of Electro-Communications, Tokyo, Japan.), U. Schoening (Ulm Univ., Germany.), R. Silvestri (La Sapienza Univ., Rome, Italy.), and T. Thierauf (Ulm Univ., Germany.) Apr. 1992 57 p
(Grants NSF CCR-89-57604; NSF CCR-90-02292)
(TR-417) Avail: CASI HC A04/MF A01

This paper is concerned with three basic questions about sparse sets: With respect to what types of reductions might NP have hard or complete sparse sets?; If a set A reduces to a sparse set, does it follow that A is reducible to some sparse set that is 'simple' relative to A?; With respect to what types of reductions might NP have hard or complete sets of low instance complexity, and, relatedly, what is the structure of the class of sets with low instance complexity?; With respect to the first and third questions, intuitively one would expect that even with respect to flexible reductions NP is unlikely to have complete sets whose information content is low. With respect to the second question, one might intuitively feel that the structure imposed on a set by the fact that it reduces to a sparse set makes it plausible that we can indeed find a simple sparse set that can masquerade as the original sparse set. These two intuitions are in many ways certified by the current literature, and by the results of this paper. Derived from text

N94-16585# Carnegie-Mellon Univ., Pittsburgh, PA. School of Computer Science.
USING MULTIPLE ADAPTIVELY-WEIGHTED STRATEGIES FOR THE RESOLUTION OF DEMONSTRATIVES Ph.D. Thesis
Ralf D. Brown 10 May 1993 188 p
(AD-A266463; CMU-CS-93-148) Avail: CASI HC A09/MF A02

The resolution of demonstratives is an interesting topic which nonetheless has received relatively little attention. As with pronominal anaphora, there is currently no comprehensive theory of demonstrative references, although there are numerous partial or microtheories. This dissertation describes a multistrategy approach to resolving demonstrative pronouns and noun phrases, using constraint, preference, and recovery strategies implementing various microtheories and heuristics. The multistrategy approach, which has proven itself for resolving pronominal anaphora, allows easy integration of new microtheories. This provides incremental improvements in performance, permitting a decreasing reliance on user intervention as the system is able to resolve a larger percentage of demonstratives. A major weakness of the multistrategy approach, the necessity to carefully choose the weights of the strategy is overcome by automatically optimizing the weights as demonstratives are resolved. Such an adaptively-weighted multistrategy approach has been implemented in the modular and extensible MASTER-D system which is expected to be applicable to other linguistic phenomena in addition to the resolution of demonstratives. DTIC

N94-16591# European Space Agency. European Space Research and Technology Center, ESTEC, Noordwijk (Netherlands).
THE ESA TELE-INVOICING SYSTEM (ETIS)
Charles Pridgeon, Stephen Kahn, and Norman Longdon, ed. Feb. 1993 14 p Original contains color illustrations
(ESA-INT-6) Copyright Avail: CASI HC A03/MF A01

ETIS was introduced in 1987 with the aim of linking industry to ESA for the transmission of invoices electronically. After trials with one of ESA's Prime Contractors, Dornier GmbH, the system was considered proven and was introduced on a wider scale. A brochure on ETIS (ESA BR-53) was subsequently distributed throughout European space-related industry. This system was known as ETIS Mk. 1. At a seminar held on 26 and 27 April 1990 in Florence, Italy, ESA proposed a new procedure to industry that found general favor with the major space companies represented. Various aspects of the ETIS are discussed. Derived from text

N94-16594*# Northwestern Univ., Evanston, IL. Dept. of Mechanical Engineering.
GENERAL MONTE CARLO RELIABILITY SIMULATION CODE INCLUDING COMMON MODE FAILURES AND HARP FAULT/ERROR-HANDLING
M. E. Platt, E. E. Lewis, and F. Boehm Jan. 1991 101 p
(Grant NAG1-1031; RTOP 505-66-21)
(NASA-CR-187587; NAS 1.26:187587) Avail: CASI HC A06/MF A02

A Monte Carlo Fortran computer program was developed that uses two variance reduction techniques for computing system reliability applicable to solving very large highly reliable fault-tolerant systems. The program is consistent with the hybrid automated reliability predictor (HARP) code which employs behavioral decomposition and complex fault-error handling models. This new capability is called MC-HARP which efficiently solves reliability models with non-constant failures rates (Weibull). Common mode failure modeling is also a specialty. Author

N94-16656*# Sterling Software, Inc., Palo Alto, CA.
SOFTWARE ENGINEERING GUIDEBOOK
John Connell and Greg Wenneson Sep. 1993 67 p
(Contract NAS2-13210)
(NASA-CR-177625; A-93135; NAS 1.26:177625) Avail: CASI HC A04/MF A01

The Software Engineering Guidebook describes SEPG (Software Engineering Process Group) supported processes and techniques for engineering quality software in NASA environments. Three process models are supported: structured, object-oriented, and evolutionary rapid-prototyping. The guidebook covers software life-cycles, engineering, assurance, and configuration management. The guidebook is written for managers and engineers who manage, develop, enhance, and/or maintain software under the Computer Software Services Contract. Author

N94-16659# Argonne National Lab., IL.
DISCOVERING SEQUENCE SIMILARITY BY THE ALGORITHMIC SIGNIFICANCE METHOD
A. Milosavljevic Feb. 1993 11 p Presented at the 1st International Conference in Intelligent Systems for Molecular Biology, Washington, DC, 7-9 Jul. 1993
(Contracts W-31-109-eng-38; DE-FG03-91ER-61152)
(DE93-015556; ANL/BIM/CP-78918; CONF-930745-2) Avail: CASI HC A03/MF A01

The minimal-length encoding approach is applied to define concept of sequence similarity. A sequence is defined to be similar to another sequence or to a set of keywords if it can be encoded in a small number of bits by taking advantage of common subwords. Minimal-length encoding of a sequence is computed in linear time, using a data compression algorithm that is based on a dynamic programming strategy and the directed acyclic word graph data structure. No assumptions about common word ('k-tuple') length are made in advance, and common words of any length are considered. The newly proposed algorithmic significance method provides an exact upper bound on the probability that sequence similarity has occurred by chance, thus eliminating the need for any arbitrary choice of similarity thresholds. Preliminary experiments indicate that a small number of keywords can positively identify a DNA sequence, which is extremely relevant in the context of partial sequencing by hybridization. DOE

N94-16721# Interface Foundation of North America, Inc., Fairfax Station, VA.
COMPUTING SCIENCE AND STATISTICS. VOLUME 24: GRAPHICS AND VISUALIZATION Final Report, 1 Mar. 1992 - 28 Feb. 1993
H. J. Newton 20 Mar. 1993 642 p
(Contract DAAL03-92-G-0035)

(AD-A266571; ARO-29748.1-MA-CF-Vol-24) Avail: CASI HC A99/MF A06

The 24th Symposium on the Interface: Computing Science and Statistics was held March 18-21, 1992 in College Station, Texas. The theme was Graphics and Visualization. Sixty invited papers were presented to more than 300 attendees. James Blinn gave the Keynote Address while Edward Tufte gave the Plenary Address. There were 38 technical sessions, including a poster session. There was also a short course, Visualization. This report presents papers based on the presentations. Also included is a list of attendees. DTIC

N94-16768# Universal Analytics, Inc., Torrance, CA.
ASTROS ENHANCEMENTS. VOLUME 1: ASTRO USER'S MANUAL Interim Report, 15 Jan. 1987 - 30 Oct. 1992
D. J. Neill and D. L. Herendeen Mar. 1993 439 p
(Contract F33615-87-C-3216)
(AD-A266818; WL-TR-93-3025-Vol-1) Avail: CASI HC A19/MF A04

ASTROS (Automated STRuctural Optimization System) is a computer program for the multidisciplinary design and analysis of aerospace structures. ASTROS combines mathematical optimization algorithms with traditional structural analysis disciplines such as static forces, normal modes, static aeroelasticity, and dynamic aeroelasticity (flutter), all in a finite element context, to perform automated preliminary design of an aircraft structure. This report is a complete user's manual that documents the many features of ASTROS through version 10 of the software package. It also provides information on system architecture and other topics of interest. This report is Volume 1 of a set; Volume 2 (WL-TR-93-3038) is the programmer's manual. DTIC

N94-16769 Universal Analytics, Inc., Torrance, CA.
ASTROS ENHANCEMENTS. VOLUME 2: ASTRO PROGRAMMER'S MANUAL Interim Report, 15 Jan. 1987 - 30 Oct. 1992
D. J. Neill, D. L. Herendeen, and R. L. Hoesly Mar. 1993 711 p Limited Reproducibility: More than 20% of this document may be affected by microfiche quality
(Contract F33615-87-C-3216)
(AD-A266819; WL-TR-93-3025-Vol-2) Avail: CASI HC A99

ASTROS (Automated STRuctural Optimization System) is a computer program for the multidisciplinary design and analysis of aerospace structures. ASTROS combines mathematical optimization algorithms with traditional structural analysis disciplines such as static forces, normal modes, static aeroelasticity, and dynamic aeroelasticity (flutter), all in a finite element context, to perform automated preliminary design of an aircraft structure. This report is a complete user's manual that documents the many features of ASTROS through version 10 of the software package. It also provides information on system architecture and other topics of interest. This report is Volume 2 of a set; Volume 1 (WL-TR-93-3025) is the user's manual. DTIC

N94-16790 Carnegie-Mellon Univ., Pittsburgh, PA. Dept. of Computer Science.
MONADS AND COMONADS IN INTENSIONAL SEMANTICS
Stephen Brookes and Kathryn VanStone Apr. 1993 43 p Limited Reproducibility: More than 20% of this document may be affected by microfiche quality
(Grant NSF CCR-90-06064)
(AD-A266522; CMU-CS-93-140) Avail: Issuing Activity (Defense Technical Information Center (DTIC))

Kleisli categories over monads have been used in denotational semantics to describe functional languages using various notions of computations as values. Kleisli categories over comonads have also been used to describe intensional semantics rather than extensional. This paper explores the possibilities of combining monads and comonads to obtain an intensional semantics using computations as values. We give three alternative ways to combine the two and explore which apply to known monads and comonads of interest. We will also look at various intensional semantics for an example programming language that uses monads for computations and compare them to the original extensional semantics. DTIC

N94-16892# Brookhaven National Lab., Upton, NY.
EIGENFUNCTIONS OF THE TRANSFER MATRIX IN THE PRESENCE OF LINEAR COUPLING
G. Parzen 1993 4 p Presented at the International Particle Accelerator Conference, Washington, DC, 17-20 May 1993
(Contract DE-AC02-76CH-00016)
(DE93-015020; BNL-48268; CONF-930511-161) Avail: CASI HC A01/MF A01

This paper presents an approach to computing the change in the linear orbit parameters, due to a perturbing field that couples the x and y motions, by computing to change in the eigenfunctions of the transfer matrix and then using the relationship between the eigenfunctions and the orbit parameters. This can be compared with the approach that computes the change in the transfer matrix and uses the relationship between the elements of the transfer matrix and the orbit parameters. For the case of coupled motion, the eigenfunction approach appears to be easier to apply than the transfer matrix approach, partly because the relationship between the transfer matrix and the linear orbit parameters is considerably more complicated in this case. Results are found for the change in the four eigenfunctions of the transfer matrix in the presence of linear coupling and for the relationship between the eigenfunctions and the orbit parameters. DOE

N94-16902# Pacific Northwest Lab., Richland, WA.
COMPUTING AND INFORMATION SCIENCES
T. H. Dunning, Jr. and J. R. Lewis Jun. 1993 4 p
(Contract DE-AC06-76RL-01830)
(DE93-017149; PNL-SA-22693) Avail: CASI HC A01/MF A01

Computing is an integral part of the research being conducted by scientists in the Molecular Sciences Research Center at Pacific Northwest Laboratory. The advanced computing infrastructure for the Computing and Information Sciences (C&IS) program of the Environmental and Molecular Sciences Laboratory will provide a state-of-the-art facility where scientific research can be performed to support US Department of Energy missions in environmental restoration and waste management, energy and environmental quality, and science and technology. The C&IS program is composed of five research and applied development facilities: High Performance Computing, Data Management and Archiving, Graphics and Visualization, Distributed Computing, Network Infrastructure, and Computer Instrumentation and Electronics. This report briefly describes the programs of these five facilities. DOE

N94-16910# Science Applications International Corp., San Diego, CA.
THE IMS SOFTWARE INTEGRATION PLATFORM Special Technical Report, 27 Nov. 1991 - 21 Mar. 1993
J. W. Given, W. K. Fox, J. Wang, and T. C. Bache 12 Apr. 1993 81 p
(Contract MDA972-92-C-0026)
(AD-A266285; SAIC-93/1069) Avail: CASI HC A05/MF A01

The Software Integration Platform (SIP) supports automated and interactive distributed processing for the Intelligent Monitoring System (IMS). The SIP addresses the practical problem of integrating existing software and data archives into a processing system distributed on a network of UNIX workstations. It consists of software components that are widely applicable to other scientific data-processing operations. The SIP is divided into two subsystems. The Data Management System (DMS) manages shared data stored in archives distributed over a wide-area network. The Distributed Applications Control System (DACS) handles inter-process communication (IPC) and process control for user applications distributed over a local-area network. The data archives managed by the DMS consists of commercial relational database management systems (RDBMS) supplemented by UNIX file systems. User applications access data stored in the archives through the Data Management System Interface (DMSI). The DMSI allows global access to data independent of a specific physical archive. Because IMS requires the capabilities provided by commercial RDBMS products, the DMSI includes extensive support for these products. The CommAgent provides message routing and queueing. DTIC

N94-16941# Rochester Inst. of Tech., NY.
CONFLICT RESOLUTION (CORE) FOR SOFTWARE QUALITY FACTORS Final Report, May 1990 - Sep. 1992
Jeffrey A. Lasky and Kevin H. Donaghy May 1993 40 p
(Contract F30602-88-D-0026)
(AD-A267248; RL-TR-93-80) Avail: CASI HC A03/MF A01

The software quality problem can be formulated as maximizing the quality goals within the constraints of cost, schedule, and technical feasibility. This is a difficult problem which belongs to a class known as multiobjective

or multiattribute optimization problems. These problems are characterized by the presence of multiple, conflicting goals accompanied by a large candidate solution space. The goals conflict because they are somehow interrelated. In software development, there are several quality characteristics, or software quality factors, that inherently conflict. For example, efficiency and maintainability conflict and the objective is to improve code understandability, since efficiency frequently required reliance on exceptional code. The same is true for expandability and reliability (increased risk to acquire more functionality), safety and availability (fail-soft/failsafe requirements reduce the set of available system capabilities). This effort developed a prototype tool which provides computer support for the Rome Laboratory Software Quality Methodology. Conflict Resolution (CORE) determines whether quality factor goals are achievable. If not, CORE then adjusts factor goals until an achievable solution is identified. In a session, there may be several candidate solutions. DTIC

N94-16974# Naval Postgraduate School, Monterey, CA.
DEVELOPMENT OF DYNAMIC, CONTEX-DRIVEN HELP SYSTEMS M.S. Thesis
Nancy J. McClellan Mar. 1993 128 p
(AD-A267409) Avail: CASI HC A07/MF A02

This thesis develops a methodology to identify and employ elements of the user's context in the help system architecture, thereby improving the response provided by the online help system. Typical online help system structures are static, providing a pre-programmed response to a specific assistance request and are not effected by the dynamics of the user or the task being attempted. A dynamic, context driven help system has been developed that uses user- and system-based components of the working environment to influence the system access and presentation strategies. The provided response is tailored specifically to the user, based on the user's level of experience and help system command history; and specifically to the situation, based on the task being attempted. The resulting online system provides a more flexible interface that can serve the needs of all types of users and can evolve as the user's skill with the application grows. The dynamic, context-driven help system methodology is explained through design and implementation of a prototype help system for an interactive software environment. TAE+ Help is a help component designed to assist users of the Transportable Application Environment Plus (TAE+). It is initiated separately from TAE+ but runs concurrently in the XWindows environment. When the user requests assistance, TAE+ Help initiates a dialogue with the user, collecting situational environmental information and employs these dynamics in the help system access process. DTIC

N94-16982# Cornell Univ., Ithaca, NY. Dept. of Computer Science.
A SECURITY ARCHITECTURE FOR FAULT-TOLERANT SYSTEMS Special Report
Michael Reiter, Kenneth Birman, and Robbert VanRenesse Jun. 1993 32 p
(Contract N00014-92-J-1866)
(AD-A266178; TR-93-1354) Avail: CASI HC A03/MF A01

Process groups are a common abstraction for fault-tolerant computing in distributed systems. We present a security architecture that extends the process group into a security abstraction. Integral parts of this architecture are services that securely and fault-tolerantly support cryptographic key distribution using novel techniques. We detail the design and implementation of these services and the secure process group abstraction they support. We also give performance figures for some common group operations. DTIC

N94-17009# Carnegie-Mellon Univ., Pittsburgh, PA. Dept. of Computer Science.
SEQUENTIAL FUNCTIONS ON INDEXED DOMAINS AND FULL ABSTRACTION FOR A SUB-LANGUAGE OF PCF
Stephen Brookes and Shai Geva Apr. 1993 16 p Submitted for publication
(Grant NSF CCR-90-06064)
(AD-A267838; CMU-CS-93-163) Avail: CASI HC A03/MF A01

We present a general semantic framework of sequential functions on domains equipped with a parameterized notion of incremental sequential computation. Under the simplifying assumption that computation other function spaces proceeds by successive application to constants, we construct a sequential semantic model for a non-trivial sub-language of PCF with a corresponding syntactic restriction - that variables of function type may only be applied to closed terms. We show that the model is fully abstract for the sub-language, with respect to the usual notion of program behavior. DTIC

N94-17014 Wright Lab., Wright-Patterson AFB, OH.
DETAILED EXAMPLE OF USING ACEC RELEASE 3.0 WITH THE DEC VAX Ada COMPILER Final Report, 13 - 24 Jul. 1992
Steven A. Davidson Dec. 1992 46 p Limited Reproducibility: More than 20% of this document may be affected by microfiche quality
(AD-A267880; WL-TR-93-1046) Avail: Issuing Activity (Defense Technical Information Center (DTIC))

This report provides explicit, step-by-step instructions on how to execute the Ada Compiler Evaluation Capability (ACEC) software tool on a Digital Equipment Corp. VAX computer. It provides the reader a worked example of execution for using this tool more effectively. It covers version 3.0 release of the ACEC. DTIC

N94-17027# Naval Postgraduate School, Monterey, CA.
APPLICABILITY OF COMPUTER SPREADSHEET SIMULATION FOR SOLVING RESOURCE ALLOCATION PROBLEMS M.S. Thesis
Dixon K. Hicks Mar. 1993 140 p
(AD-A267436) Avail: CASI HC A07/MF A02

This thesis investigates the possibility of employing computer spreadsheets as a sophisticated tool to resolve resource allocation dilemmas through simulation techniques. Microsoft's Excel 4.0 is used to analyze three separate and unique resource allocation problems: (1) an inventory distribution system involving different distribution points to illustrate the magnification of uncertainty as the distribution system is lengthened; (2) a queuing utilization problem faced by an emergency room of a hospital; and (3) a scenario that looks at the uncertainty in a financial budgeting situation as reflected in the Navy's CHAMPUS budget. A spreadsheet macro using simulation techniques is created for each scenario to illustrate that computer spreadsheets are fully capable of analyzing resource allocation enigmas through simulation methodology. DTIC

N94-17032# McDonnell-Douglas Corp., Saint Louis, MO.
MISSILE DATCOM USER'S MANUAL Final Report, 1 Aug. 1992 - 31 Mar. 1993
K. A. Burns, K. J. Deters, S. L. Stoy, S. R. Vukelich, and W. B. Blake (Wright Lab., Wright-Patterson AFB, OH.) Jun. 1993 239 p
(Contract F33615-89-D-2198)
(AD-A267447; WL-TR-93-3043) Avail: CASI HC A11/MF A03

In missile preliminary design it is necessary to quickly and economically estimate the aerodynamics of a wide variety of missile configuration designs. Since the ultimate shape and aerodynamic performance are so dependent upon the subsystems utilized, such as payload size, propulsion system selection, and launch mechanism, the designer must be capable of predicting a wide variety of configurations accurately. The fundamental purpose of Missile Datcom is to provide an aerodynamic design tool which has the predictive accuracy suitable for preliminary design and the capability for the user to easily substitute methods to fit specific applications. DTIC

N94-17060*# National Aeronautics and Space Administration. Langley Research Center, Hampton, VA.
INTEL NX TO PVM 3.2 MESSAGE PASSING CONVERSION LIBRARY
Trey Arthur (Computer Sciences Corp., Hampton, VA.) and Michael L. Nelson Oct. 1993 14 p
(RTOP 505-90-53-02)
(NASA-TM-109038; NAS 1.15:109038) Avail: CASI HC A03/MF A01

NASA Langley Research Center has developed a library that allows Intel NX message passing codes to be executed under the more popular and widely supported Parallel Virtual Machine (PVM) message passing library. PVM was developed at Oak Ridge National Labs and has become the defacto standard for message passing. This library will allow the many programs that were developed on the Intel iPSC/860 or Intel Paragon in a Single Program Multiple Data (SPMD) design to be ported to the numerous architectures that PVM (version 3.2) supports. Also, the library adds global operations capability to PVM. A familiarity with Intel NX and PVM message passing is assumed. Author

N94-17075# Air Force Inst. of Tech., Wright-Patterson AFB, OH.
EFFECTS OF INSPECTION ERROR ON OPTIMAL INSPECTION POLICIES AND SOFTWARE FAULT DETECTION MODELS Ph.D. Thesis
Donna C. Herge Aug. 1993 112 p
(AD-A267511; AFIT/CI/CIA-93-014D) Avail: CASI HC A06/MF A02

Inspection policies are essential for many types of systems for which the status (functioning or failed) can be determined only by actual inspection. Two types of inspection error may occur. A functioning system may be incorrectly assessed as having failed or a failed system may be incorrectly assessed as functioning. These errors are designated as Types I and II respectively, and their impact on optimal inspection policies and software fault detection models is analyzed. For a periodic inspection model with Type I error, an optimal replacement age is obtained, then monotonicity and asymptotic properties of the long-run expected cost per unit of time are presented. Type I error is incorporated into a cumulative damage model. When the failure density is reverse rule of order 2, an algorithm to compute an optimal inspection sequence is derived, and it is proven that optimal intervals are increasing. Extending the optimal inspection sequence model of Barlow, Hunter, and Proschan to include Type II inspection error, it is proven that optimal intervals are nonincreasing for a PF(sub 2) density, and an algorithm to compute optimal intervals is derived. Additionally, monoticity and majorization results are obtained for an optimal inspection sequence with Type II error. The impact of fault-detection error on a software release time model is shown. The effect of fault diversity on the Jelinski-Moranda model and how this relates to imperfect fault detection is demonstrated. DTIC

N94-17078 University of Southern California, Marina del Rey. Information Sciences Inst.
A PROPOSED RESEARCH PROGRAM IN STRATEGIC COMPUTING Final Report
Yigal Arens 31 Aug. 1992 24 p *Limited Reproducibility:* More than 20% of this document may be affected by microfiche quality
(Contract MDA903-87-C-0641)
(AD-A267516) Avail: CASI HC A03

The Services and Information Management for Decision Systems (SIMS) project integrates several computer services into a single, seamless system, as seen from the user's perspective. This relieves the user of the need to be familiar with all the services available from the system, enabling the user to make requests as though he or she were dealing with a single entity. SIMS analyzes the user request, plans the necessary sequence of calls on the services, and executes them. Until now, the only approach to the problem of software integration has been to build custom systems that support an integrated view of the underlying servers. Such systems are expensive, are suitable only for the application for which they were crafted, are not very flexible with respect to functionality, and are difficult to modify. In contrast, SIMS would allow maintainers to assimilate servers into the system through a much less painful process of building a declarative model of the servers and allowing the SIMS planner to perform the actual integration task. DTIC

N94-17107# Carnegie-Mellon Univ., Pittsburgh, PA. Dept. of Computer Science.
VISUAL PARALLEL PROGRAMMING WITH DETERMINACY: A LANGUAGE SPECIFICATION, AN ANALYSIS TECHNIQUE, AND A PROGRAMMING TOOL
Adam Beguelin and Gary Nutt 7 Jun. 1993 36 p
(Grant NSF CCR-88-02283)
(AD-A267560; CMU-CS-93-166) Avail: CASI HC A03/MF A01

Phred is a visual parallel programming language in which programs can be statically analyzed for deterministic behavior. This paper presents the Phred language, techniques for analyzing the language, and a programming environment which supports Phred programming. There are many methods for specifying synchronization and data sharing in parallel programs. The Phred programmer uses graph constructs for describing parallelism, synchronization, and data sharing. These graphs are formally described in this paper as a graph grammar. The use of graphs in Phred provides an intuitive and visual representation for parallel computations. The inadvertent specification of nondeterministic computations is a common error in parallel programming. Phred addresses the issue of determinacy by visually indicating regions of a program where nondeterminacy may exist. This analysis and its integration into a programming environment is presented here. The Phred programming environment supports the specification, analysis, and execution of Phred programs. The distribution of the programming environment itself over several workstations is also described. DTIC

N94-17118# Carnegie-Mellon Univ., Pittsburgh, PA. Dept. of Computer Science.
CAUSALITY-PRESERVING TIMESTAMPS IN DISTRIBUTED PROGRAMS
Adam Beguelin and Erik Seligman Jun. 1993 13 p
(Contract MDA972-90-C-0035; ARPA Order 7330)
(AD-A267534; CMU-CS-93-167) Avail: CASI HC A03/MF A01

A tachyon is an improperly ordered event in a distributed program. Tachyons are most often manifested as messages which are received before they are sent, violating the principle of causality. Although tachyons are not possible in real life, they may appear to occur in distributed parallel program traces due to coarse clock granularity or poor clock synchronization. In this paper, we establish that tachyons do in fact occur commonly in distributed programs on our Ethernet at Carnegie Mellon University, and we discuss some ways of eliminating them from program traces while preserving at least some knowledge of the length of time intervals in our programs. Our methods are based on Lamport-style clock corrections; when a process receives a message stamped with a later sending time, it sets its own clock ahead to a time at least as great as the sending timestamp. We have implemented this both in real time and in a more comprehensive post-processor for Xab. DTIC

N94-17220# RTware, Inc., Durham, NC.
MODULE INTERCONNECTION FRAMEWORKS FOR A REAL-TIME SPREADSHEET
Richard Clarke 30 May 1993 12 p
(AD-A267317) Avail: CASI HC A03/MF A01

The first month of this work has been very fruitful, yielding a detailed understanding of how module interconnection frameworks (MIF) can be used to implement specific features of a real-time distributed spreadsheet. A number of ideas will be presented in this report. These ideas envision a system which combines the advantages of high-level system design with the very rapid implementation/prototyping capabilities already demonstrated in numerous applications by the ControlCalc system. In particular, an MIF system solves a number of problems of distributed programming and of integrating service provided by the spreadsheet into a large scale modular system implemented in non-spreadsheet languages. The focus of the investigation so far has been Polylith, a software bus system developed at the University of Maryland. DTIC

N94-17231# RTware, Inc., Durham, NC.
MODULE INTERCONNECTION FRAMEWORKS FOR A REAL-TIME SPREADSHEET Progress Report
Richard Clark 29 Jul. 1993 12 p
(AD-A267752) Avail: CASI HC A03/MF A01

RTware is working on a proposal for an SBIR Phase 2 software research and development project for distributed control systems (DCS) using Module Interconnect Frameworks (MIF). SBIR Phase 1 work includes research into the feasibility, design and benefits of such a system, resulting in a detailed Phase 2 proposal. The proposed software package will be based on RTware's Control-Calc real-time spreadsheet control system and the Polylith MIF system from the University of Maryland. Work in the initial stage of Phase 1 has identified the main outlines of the package, and described key benefits to the Department of Defense (see the May 30th Progress Report). Work in the latest time period involved developing a detailed description of the proposed system and trying test implementations with the Polylith package. That description breaks the system down into two major components: The first component (DCS-I) is a distributed services capability for accessing remote procedures and data both into and out of the Control-Calc spreadsheet. The second component (DCS-II) will allow the largely transparent distribution of compiled Control-Calc code segment across remote, and heterogeneous, platforms. DTIC

N94-17299# Wichita State Univ., KS. National Inst. for Aviation Research.
COMPUTER MODELING AND ANIMATION OF MECHANICAL SYSTEMS
Li Wen and Behnam Bahr 1993 88 p
(NIAR-93-3) Avail: CASI HC A05/MF A01

A new methodology for mechanism modeling and animation using 2-D or 3-D computer graphics techniques is presented. Simulation systems based on this method enable mechanical designers, educators and management to evaluate the motion performance of mechanisms in effective, flexible and inexpensive ways. This method is particularly well suited for use in small manufacturing companies and educational institutes because of the small required expense. The emphasis is given to the system structure, the design procedures, and a wide variety of its applications.
Author (revised)

N94-17326*# National Aeronautics and Space Administration. Pasadena Office, CA.
METHOD AND APPARATUS FOR SPUR-REDUCED DIGITAL SINUSOID SYNTHESIS Patent Application
George A. Zimmerman, inventor (to NASA) (Jet Propulsion Lab., California Inst. of Tech., Pasadena.) and Michael J. Flanagan, inventor (to NASA) (Jet Propulsion Lab., California Inst. of Tech., Pasadena.) 20 Oct. 1993 56 p
(Contract NAS7-918)
(NASA-Case-NPO-18789-1-CU; NAS 1.71:NPO-18789-1-CU; US-Patent-Appl-SN-141295) Avail: CASI HC A04/MF A01

A technique for reducing the spurious signal content in digital sinusoid synthesis is presented. Spur reduction is accomplished through dithering both amplitude and phase values prior to word-length reduction. The analytical approach developed for analog quantization is used to produce new bounds on spur performance in these dithered systems. Amplitude dithering allows output word-length reduction without introducing additional spurs. Effects of periodic dither similar to that produced by a pseudo-noise (PN) generator are analyzed. This phase dithering method provides a spur reduction of 6(M + 1) dB per phase bit when the dither consists of M uniform variates. While the spur reduction is at the expense of an increase in system noise, the noise power can be made white, making the power spectral density small. This technique permits the use of a smaller number of phase bits addressing sinusoid look-up tables, resulting in an exponential decrease in system complexity. Amplitude dithering allows the use of less complicated multipliers and narrower data paths in purely digital applications, as well as the use of coarse-resolution, highly-linear digital-to-analog converters (DACs) to obtain spur performance limited by the DAC linearity rather than its resolution.
NASA

N94-17366# Air Force Inst. of Tech., Wright-Patterson AFB, OH.
AN EXAMINATION OF TWO Ada LANGUAGE OBJECT-ORIENTED DATABASES Technical Report
Karl S. Mathias and Mark A. Roth Jul. 1993 12 p
(AD-A267486; AFIT/EN/TR-93-6) Avail: CASI HC A03/MF A01

Many object-oriented databases marketed today target themselves to either C++ or Lisp as a host language. This presents problems to Department of Defense contractors who need to utilize Ada for development. This paper examines two Ada object-oriented databases: Classic-Ada with Persistence and Science Applications International Corporation's OODBMS developed for the US Air Force's Dental Data System.
DTIC

N94-17370# Yale Univ., New Haven, CT. Dept. of Computer Science.
FAST ALGORITHMS FOR POLYNOMIAL INTERPOLATION, INTEGRATION AND DIFFERENTIATION Research Report
A. Dutt, M. Gu, and V. Rokhlin Jul. 1993 39 p
(Contract N00014-89-J-1527; NSF MDS-90-12751)
(AD-A267505; YALEU/DCS/RR-977) Avail: CASI HC A03/MF A01

For functions tabulated at Chebyshev nodes on an interval, spectral interpolation, integration and differentiation can be performed stably and efficiently via the fast Fourier transform. In this paper, a group of algorithms is presented for the efficient evaluation of Lagrange polynomial interpolants at multiple points on the line, and for the rapid spectral integration and differentiation of functions tabulated at nodes other than Chebyshev.
DTIC

N94-17371 Air Force Inst. of Tech., Wright-Patterson AFB, OH. School of Engineering.
AN OBJECT-ORIENTED DYNAMIC SOFTWARE PROCESS MODEL M.S. Thesis
Bradley J. Smith Jan. 1993 112 p Limited Reproducibility: More than 20% of this document may be affected by microfiche quality
(AD-A267726; AFIT/CI/CIA-93-092) Avail: CASI HC A06

This thesis describes a new method for modeling complex dynamic processes using object-oriented techniques. These techniques are applied to develop a sophisticated model of the software development process. This object-oriented approach has many advantages over non-object-oriented System Dynamics models. Non-homogeneous resource allocation can be explicitly modeled. This allows resource allocation strategies and management decisions to be modeled and assessed in a realistic manner. Since software development tasks and resources are modeled as objects, they can be flexibly created and manipulated to capture the dynamics of a particular project. Furthermore, the principles of object-oriented inheritance lets the modeler or analyst easily extend the model to include new resources and tasks. The thesis addresses major considerations in modeling the software development process, as well as the detailed development of an object-oriented software process model in C++. A comparison is done between this dynamic model and the empirical predictions of the popular COCOMO software estimation system. This new object-oriented approach is not limited to software process modeling and could be applied to a wide variety, of scientific, business, and social simulations.
DTIC

N94-17390# Rutgers - The State Univ., New Brunswick, NJ. Dept. of Computer Science.
COMPUTER-AIDED DESIGN PACKAGE FOR DESIGNERS OF DIGITAL OPTICAL COMPUTERS Report, 1 May 1990 - 30 Apr. 1993
Miles Murdocca, David Berger, Apostolos Gerasoulis, Vipul Gupta, and Saul Levy Jul. 1993 42 p
(Contract N00014-90-J-4018)
(AD-A267866) Avail: CASI HC A03/MF A01

The primary goals of the effort are to create methods for designing digital optical computers and to investigate aspects of optical interconnection that influence the design process. The emphasis is on the Bell Labs style of architecture, in which arrays of optical logic gates are interconnected in free space with regular patterns at the gate-level. Other approaches are also explored that make use of hybrid technology (smart pixels), irregular interconnects, and reconfigurable interconnects.
DTIC

N94-17395# Carnegie-Mellon Univ., Pittsburgh, PA. Software Engineering Inst.
SOFTWARE CAPABILITY EVALUATION (SCE) VERSION 1.5 METHOD DESCRIPTION. SOFTWARE CAPABILITY EVALUATION PROJECT
Jul. 1993 182 p Sponsored by AFSC
(AD-A267895; CMU/SEI-93-TR-17; ESC-TR-93-194) Avail: CASI HC A09/MF A02

This report describes Version 1.5 of the Software Capability Evaluation (SCE) method, as taught at the Software Engineering Institute (SEI) from Jan. 1992 to June 1993. This version of the SCE method is based on the process maturity framework defined in Characterizing the Software Process: Maturity Framework (CMU/SEI-87-TR-11, ADA197671), which predates Version 1.0 of the Capability Maturity Model (CMM) described in Capability Maturity Model for Software (CMU/SEI-91-TR 24, ADA240603). The document includes a background overview of the SCE method and its evolution, a detailed description of the activities performed during an SCE, and a discussion of the characteristics of the method and their implications for the use of the method. This built description provides a baseline for future evolution of the SCE method.
DTIC

N94-17396# Carnegie-Mellon Univ., Pittsburgh, PA. Software Engineering Inst.
ESTABLISHING A SOFTWARE MEASUREMENT PROCESS
Donald R. McAndrews Jul. 1993 54 p Sponsored by AFSC
(AD-A267896; CMU/SEI-93-TR-16; ESC-TR-93-193) Avail: CASI HC A04/MF A01

This report presents guidelines for establiishing a measurement process as part of an organization's overall software process. Methods are suggested that can be used to design a repeatable measurement process that is focused on goal setting, data analysis, and decision making rather than on just data collection and numbers. Examples are included to illustrate these methods in the context of some common software process management issues involving basic measures of size, effort, and schedule. This report also suggests some steps for starting a measurement program. These

steps focus on identifying an organizational strategy for improvement and designing a process for measurement to support this strategy. DTIC

N94-17398# Columbia Univ., New York, NY. Dept. of Computer Science.
PROCESS EVOLUTION FOR THE MARVEL ENVIRONMENT
Gail E. Kaiser, Israel Z. Ben-Shaul, George T. Heineman, John K. Hinsdale, and Wilfredo Marrero 8 Nov. 1992 32 p
(Grants NSF CCR-91-06368; NSF CCR-88-58029)
(AD-A267813; CUCS-047-92) Avail: CASI HC A03/MF A01

We present a schema and process evolution tool, called the Evolver, for the MARVEL process-centered environment. The Evolver analyzes the differences between the new and installed process models of an existing environment and detects each case where the notion of consistency defined by the process model has been strengthened or weakened. The Evolver then automatically updates the environment's object-base to guarantee that the objects are consistent according to the new specifications. The Evolver can be applied while the installed process is in progress, temporarily halting normal operation while it updates the object-base, after which development continues using the new process. We have had several months of experience using the Evolver to make repeated changes in the process that supports our own further development of MARVEL and include in this paper one small but practical example of a recent change made to a real MARVEL process. DTIC

N94-17399# Columbia Univ., New York, NY. Dept. of Computer Science.
TESTING STRING SUPERPRIMITIVITY IN PARALLEL
Dany Breslauer 1992 6 p
(AD-A267814; CUCS-053-92) Avail: CASI HC A02/MF A01

A string w covers another string z if every symbol of z is within some occurrence of w in z. A string is called superprimitive if it is covered only by itself and quasiperiodic if it is covered by some shorter string. This paper presents an O(log(log n)) time n(log n)/log(log n)-processor CRCW-PRAM algorithm that tests if a string is superprimitive. The algorithm is the fastest possible with this number of processors over a general alphabet. DTIC

N94-17404# Columbia Univ., New York, NY. Graduate School of Arts and Sciences.
CONCURRENCY CONTROL IN RULE-BASED SOFTWARE DEVELOPMENT ENVIRONMENTS Ph.D. Thesis
Naser S. Barghouti 1992 286 p
(AD-A267829; TR/CUCS-001-92) Avail: CASI HC A13/MF A03

This dissertation investigates the concurrency control problem in software development environments (SDE's). The problem arises when multiple developers perform activities that concurrently access the project's components, stored as database objects. The interleaved execution of the developers' activities leads to interference if they access overlapping sets of objects concurrently. An SDE can ensure that activities never interfere by modeling their execution in terms of atomic transactions and allowing only serializable schedules. This prevents cooperation, which requires some degree of interference between the activities of multiple developers. To allow cooperation, an SDE must be provided with semantic information about development activities. In rule-based SDE's, the necessary information is readily available in the set of rules that defines the process model of a project. The rules are loaded into the SDE, which provides process-specific assistance through a rule chaining engine. A single user command might lead the chaining engine to initiate a rule chain. The concurrency control problem in rule-based SDE's manifests itself in terms of interference between concurrent rule chains. We present a mechanism that extracts semantic information from the process model to solve the concurrency control problem without obstructing cooperation. DTIC

N94-17411# Army Inst. for Research in Management Information and Computer Sciences, Atlanta, GA.
ACE: LESSONS LEARNED, VOLUME 1
Gerald McCoyd and Adrienne Raglin 30 Sep. 1992 59 p
(AD-A267979; ASQB-GC-92-023-Vol-1) Avail: CASI HC A04/MF A01

This report describes AIRMICS involvement with the development of three prototypes using AT and T's Application Connectivity Engineering (ACE) Tool. The prototyping tool, ETIP, and the communications and file transfer tool, ESCORT, were used. This report includes the lessons learned during this project. The principle lesson learned was that success in using ACE demands an environment that provides the programmers with a wide array of tools to simplify and coordinate their work. In this report summaries of the experiences we had with ACE are included, as well as, presenting the tools that we developed and those which were supplied to us by other organizations, most notable Information Foundation. This report is intended primarily for programmers who are familiar with ACE. DTIC

N94-17429 Carnegie-Mellon Univ., Pittsburgh, PA. Software Engineering Inst.
AN INTRODUCTION TO STRUCTURAL MODELS Final Report, Jun. 1986 - Aug. 1992
Joe Batman, Larry Howard, and Bill Schelker Aug. 1992 30 p Limited Reproducibility: More than 20% of this document may be affected by microfiche quality
(Contract F19628-90-C-0003)
(AD-A268151; ASC-TR-93-5008) Avail: Issuing Activity (Defense Technical Information Center (DTIC))

This paper introduces structural models for flight simulators to technical managers. It gives the rationale for using structural models, defines structural models, and discusses practices associated with their use. The paper provides an example of a structural model based on the model used on a number of recent simulator acquisitions. The paper also discusses what ASC/YT expects in proposals for the use of structural models in the development of training simulators. DTIC

N94-17447*# National Aeronautics and Space Administration. Langley Research Center, Hampton, VA.
TUTORIAL: ADVANCED FAULT TREE APPLICATIONS USING HARP
Joanne Bechta Dugan (Duke Univ., Durham, NC.), Salvatore J. Bavuso, and Mark A. Boyd (Duke Univ., Durham, NC.) Nov. 1993 30 p
(RTOP 505-66-21)
(NASA-TM-102747; NAS 1.15:102747) Avail: CASI HC A03/MF A01

Reliability analysis of fault tolerant computer systems for critical applications is complicated by several factors. These modeling difficulties are discussed and dynamic fault tree modeling techniques for handling them are described and demonstrated. Several advanced fault tolerant computer systems are described, and fault tree models for their analysis are presented. HARP (Hybrid Automated Reliability Predictor) is a software package developed at Duke University and NASA Langley Research Center that is capable of solving the fault tree models presented.
Author (revised)

N94-17491# Mitre Corp., Bedford, MA.
INCREMENTAL REDERIVATION OF SOFTWARE ARTIFACTS: FY 1992 Final Report, Oct. 1991 - Sep. 1992
Melissa Chase, Howard Reubenstein, and Alexander Yeh May 1993 19 p
(Contract F19628-89-C-0001)
(AD-A267968; RL-TR-93-60) Avail: CASI HC A03/MF A01

Design relay presents a possible enabling technology to the Knowledge-Based Software Assistant specification maintenance and implementation derivation approach to software development. More generally, design replay can also be applied to derivations between a variety of different software description abstraction levels. Radical changes to a software artifact cannot generally be addressed by designed replay as they require new design input. Evolutionary changes are more amenable to design replay and often involve incremental changes to derived artifacts. This report outlines an approach to rederivation that exploits the incrementality of evolutionary maintenance changes, describes the state at which the implementation of this approach is at, and what remains to be done to test this approach. DTIC

N94-17500 Army Inst. for Research in Management Information and Computer Sciences, Atlanta, GA.
INTEGRATION OF SEVERAL COMPUTER SYSTEMS WITHIN A HETEROGENEOUS ENVIRONMENT Final Report
William O. Putnam and Ian E. Smith Sep. 1992 29 p Limited Reproducibility: More than 20% of this document may be affected by microfiche quality
(AD-A267978; ASQB-GM-92-024) Avail: CASI HC A03

This project prepared the AIRMICS testbed for an evaluation of the Information Architecture Reference Model (IARM). Plans are to perform the evaluation by integrating a set of independently developed applications into a heterogeneous environment. Tbe project also modified and enhanced the IARM to incorporate it into the Army's Information Systems Architecture Circa 1997 plan (ISA97). DTIC

N94-17501 Politecnico di Milano (Italy). Dipt. di Elettronica e Informazione.

AUTOMATIC GENERATION OF PRODUCTION RULES FOR INTEGRITY MAINTENANCE

Stefano Ceri, Piero Fraternali, Stefano Paraboschi, and Letizia Tanca 29 Apr. 1993 47 p Sponsored by Commission of the European Communities and CNR

(Rept-92-054; ETN-93-94566) Avail: Issuing Activity (Politecnico di Milano, Piazza Leonardo da Vinci 32, 20133 Milan, Italy)

An approach to integrity maintenance, consisting of automatically generating production rules for integrity enforcement is presented. Constraints are expressed as particular formulas of Domain Relational Calculus; they are automatically translated into a set of compensating actions, encoded as production rules of an active database system. Prodution rules may be redundant (they enforce the same constraint in different ways) and conflicting (because repairing one constraint may cause the violation of another constraint). Thus, it is necessary to develop techniques for analyzing the properties of the set of active rules and for ensuring that any computation of production rules after any faulty transaction terminates and produces a consistent database state. Among these guidelines, a specific architecture for constraint definition and their enforcement is described. The components of the architecture include a Rule Generator, for producing all possible compensating actions, and a Rule Analyzer and Selector, for producing a collection of production rules such that their execution after a faulty transaction always terminates in a consistent state (possibly by rolling back the transaction); moreover, the needs of applications are modeled, so that integrity enforcing rules reach the final state that better represents the original intentions of the transaction's supplier. Experimental results of a prototype implementation of the proposed architecture are also described. ESA

N94-17504 Politecnico di Milano (Italy). Dipt. di Elettronica e Informazione.

ORPHEUS: A SYNTHESIS FRAMEWORK FOR REGULAR ARCHITECTURES

Franco Fummi Mar. 1993 29 p

(Rept-93-016; ETN-93-94568) Avail: Issuing Activity (Politecnico di Milano, Piazza Leonardo da Vinci 32, 20133 Milan, Italy)

A global methodology to extract from the behavioral description of a circuit all information concerning the regularity of the computation is presented; such regular parts of the entire circuit are easily implemented into systolic arrays. Some criteria to evaluate the optimal combination of scheduling and allocation of user's constraints are also presented. All such algorithms are implemented in Orpheus, a synthesis framework that guides the user to analyze different implementations and choose the optimal. The results achieved using Orpheus were checked on some benchmarks and the complete synthesis of a IIR (Infinite Impulse Response) filter is presented. The main innovative contributions may be summarized as follows: the analysis starts from a behavioral description of a circuit that is written using a general purpose language; the circuit description is translated into an internal representation (DFG/CFG (Data Flow Graph/Control FG)) suitable to analyze the main characteristics of different architectures, with focus on systolic arrays based architectures; an innovative methodology to extract the regular parts of the computation and to obtain a description useful to apply the Kung's synthesis strategy is presented; a set of criteria to choose the optimal combination of scheduling and allocation of a systolic array is explained with all parameters that can be constrained by the user to guide the synthesis. ESA

N94-17528# Institut National de Recherche d'Informatique et d'Automatique, Valbonne (France). Programme 4: Robotique, Image et Vision.

TOWARDS DYNAMIC RANDOMIZED ALGORITHMS IN COMPUTATIONAL GEOMETRY Ph.D. Thesis - Paris-Sud Univ., 10 Dec. 1991

Monique Teillaud Jul. 1992 180 p Sponsored by EEC

(INRIA-RR-1727; ETN-93-94432) Avail: CASI HC A09/MF A02

Computational geometry aims to design and analyze algorithms for solving geometric problems. Randomization allows the use of complicated data structures to be avoided, and was proved to be very efficient, from both points of view of theoretical complexity and practical results. Particular interest is shown in designing dynamic algorithms: in practice, the data of a problem are often acquired progressively. It is obviously not reasonable to compute the whole result again each time a new data is inserted, (semi)dynamic schemes are thus necessary. A very general data structure, the Influence Graph, is introduced, that allows the construction of various geometric structures: Voronoi diagrams, arrangements of line segments, etc. Both theoretical complexity and practical efficiency of the algorithms are studied. ESA

N94-17530 Army Research Lab., Aberdeen Proving Ground, MD.

TDNOVA INTERACTIVE GRAPHICS Interim Report, Jan. 1990 - Dec. 1992

Ronald D. Anderson Jul. 1993 34 p Limited Reproducibility: More than 20% of this document may be affected by poor print and microfiche quality

(DA Proj. 1L1-61102-AH-43)

(AD-A268000; ARL-TR-165) Avail: Issuing Activity (Defense Technical Information Center (DTIC))

As computational resources have expanded, the computer codes have kept pace with increased complexity and have grown in sheer volume of output-so much that the millions of numbers are difficult to comprehend without a visualizing tool. A graphical analysis program has been developed to view the huge amount of data produced by the two-dimensional (2-D) NOVA interior ballistics code (TDNOVA). By using color plots and drawings, the TDNOVA Graphical Analysis Program (TGAP) can display 2-D and 3-D information in four separate, independent windows. Besides the standard interior ballistic (IB) data, such as pressure, temperature, and gas velocity, the TGAP program can also show deformation of the computational grid, movement of propellant increments, and composite gas velocity vectors (radial and axial directions). Three-dimensional drawings of computed IB physical quantities can be rotated, shifted, and sized to produce the desired view for the scientist. Any of the four windows may be chosen for enlargement to full-screen size to make color screen copies or viewgraphs. The windows may show four different types of data from a single TDNOVA calculation, or may be used to display data from up to four completely independent computations. DTIC

N94-17541# Naval Postgraduate School, Monterey, CA.

A PROTOCOL VALIDATOR FOR THE SCM AND CFSM MODELS M.S. Thesis

Zeki B. Bulbul Jun. 1993 141 p

(AD-A268523) Avail: CASI HC A07/MF A02

This thesis introduces and describes a software tool called Mushroom which automates the analysis of network protocols specified by the Systems of Communicating Machines (SCM) and the Communicating Finite State Machines (CFSM) models. SCM is a formal model for the specification, verification, and testing of communication protocols. This model was originally developed to improve the CFSM model which is a simpler and earlier Formal Description Technique (FDT). The program is developed as two separate programs in the Ada programming language. The first program automates either the system state analysis (Smart Mushroom), or the full global analysis (Big Mushroom) for a protocol specified by the SCM model. The second program called Simple Mushroom, automates the global reachability analysis for the CFSM model. Mushroom greatly facilitates the use of these models for protocol design and analysis. The run time and memory efficiency of a previous program was improved to allow the analysis of larger and more complex protocols. The program was also extended to accept up to eight machines (processes) in the protocol specification. The user interface of the program has also been improved. Mushroom has been used to verify some well known protocols specified by the SCM and CFSM models such as the token bus protocol, Go Back N and Lap-B data link control protocol. DTIC

N94-17588 Carnegie-Mellon Univ., Pittsburgh, PA. Software Engineering Inst.

A SOFTWARE PROCESS FRAMEWORK FOR THE SEI CAPABILITY MATURITY MODEL: REPEATABLE LEVEL Final Report

Timothy G. Olson, L. P. Gates, J. L. Mullaney, J. W. Over, and N. R. Reizer Jun. 1993 305 p Limited Reproducibility: More than 20% of this document may be affected by microfiche quality

(Contract F19628-90-C-0003)

(AD-A268059) Avail: Issuing Activity (Defense Technical Information Center (DTIC))

This document describes a Software Process Framework (SPF) based on the Software Engineering Institute's (SEI) Capability Maturity Model (CMM) for the Repeatable Level (Level 2). The purpose of the SPF is to provide guidance for designing, analyzing, and reviewing software processes (consisting of standards, processes, procedures, training, and tools) so that they are consistent with the CMM. As a thesaurus is a companion book to a dictionary (both are useful for different purposes) the SPF is a companion guide to the CMM for defining software processes. For each key process area in the CMM, the SPF defines roles, entry and exit criteria, inputs and outputs, activities, reviews and audits, measurements, etc. This information can also be used to help build process models and process guides that are consistent with the CMM. The primary audiences of the SPF are software engineering process groups (SEPG's), process engineers, process action teams, and software quality assurance groups. Secondary audiences include anyone interested in software process improvement, or anyone using the CMM. DTIC

N94-17590# Boeing Defense and Space Group, Seattle, WA.

X RAY COMPUTED TOMOGRAPHY FOR GEOMETRY ACQUISITION Interim Report, May 1991 - Feb. 1992

Alan R. Crews, Richard H. Bossi, and Gary E. Georgeson 1 Mar. 1993 22 p

(Contract F33615-88-C-5404)

(AD-A268085; WL-TR-93-4036) Avail: CASI HC A03/MF A01

X-ray computed tomography (CT) provides quantitative measures of component feature dimensions and density as related to the linear X-ray attenuation of the material under study. The data are available in digital format to be input not only to NDE workstations but also design workstations. By converting the CT data to computer aided design/engineering (CAD/E) workstations, the designer/engineer can access the as-built component geometry. Productivity gains are realized in generating computer drawings for as-built components. In the case of components that do not have adequate drawing documentation, particularly ergonomically, aesthetically or aerodynamically shaped parts, the CT data provide a highly cost effective approach for generating digital format documentation. Multiple slice CT data may be used to completely define the object, or CT data at selected orientations may be used to define specific features. Once data are transferred to a workstation, the designer can manipulate the data to create a part drawing. The process of obtaining digital definition of an existing component is referred to as geometry acquisition. DTIC

N94-17620# Army Construction Engineering Research Lab., Champaign, IL.

RESEARCH IN PRESISTENT SIMULATION: DEVELOPMENT OF THE PERSISTENT ModSim OBJECT-ORIENTED PROGRAMMING LANGUAGE Interim Report

Charles Herring, Biju Kalathil, and Joseph Teo Jul. 1993 52 p

(DA Proj. 4A1-62784-AT-41)

(AD-A268568; CERL-IR-FF-93/07) Avail: CASI HC A04/MF A01

A general trend in object-oriented programming language development is the addition of features for consistent storage of objects. This capability is implemented through persistent programming languages and object-oriented databases. The U.S. Army Construction Engineering Research Laboratories has developed Persistent ModSim, an enhanced version of the ModSim programming language previously developed to provide a general-purpose, object-oriented, process-based simulation language with support for programming large-scale simulations. This report describes the pilot and prototype experiments leading to the development of a robust version of Persistent ModSim. Details of the database class libraries, transient and persistent object allocation, transactions, and compilation management are given. Example programs are provided to show how Persistent Modsim's facilities are used. Directions for future research in this area are outlined. DTIC

N94-17626 National Aerospace Lab., Amsterdam (Netherlands). Informatics Div.

THE DEVELOPMENT OF FLEXIBLE SOFTWARE FOR THE ITALIAN/DUTCH SATELLITE SAX: ADVANTAGES AND DISADVANTAGES OF THE USE OF CASE TOOLS

G. J. Dekker and G. J. Hameetman 29 Jul. 1991 13 p Presented at AIAA Computing on Aerospace 8 Conference, Baltimore, MD, 21-24 Oct. 1991 Limited Reproducibility: More than 20% of this document may be affected by microfiche quality

(Contract FSS-SAX-90/005-NL/TS)

(NLR-TP-91288-U; ETN-93-94780) Avail: CASI HC A03

The application software is described in relation with the overall SAX (Italian acronym for X-ray Astronomy Satellite) Attitude and Orbit Control Subsystem (AOCS). The ACOS onboard application software is being developed using a suite of CASE (Computer Aided Systems Engineering) tools, the CASE software configuration management package, processor emulation hardware and software, and a number of special test and simulation tools. The CASE tools that were used during the development, the advantages and disadvantages of the use of these tools, the measures taken to meet the more or less conflicting requirements of reliability and flexibility, and the lessons learned during development are described. On board software was also developed for other satellites but this was done without the help of commercial CASE tools. Both approaches, with and without CASE tools, are compared. The current status of the software is that it is being coded and module tested. ESA

N94-15562*# Bendix Field Engineering Corp., Seabrook, MD.

SATCOP MISSION PLANNING SOFTWARE PACKAGE

Steve Bucey *In* NASA. Goddard Space Flight Center, Eighth International Workshop on Laser Ranging Instrumentation Jun. 1993 13 p (For primary document see N94-15552 03-19)

Avail: CASI HC A03/MF A06

N94-16153*# National Aeronautics and Space Administration. Marshall Space Flight Center, Huntsville, AL.

MODELING AND SIMULATION: A KEY TO FUTURE DEFENSE TECHNOLOGY

Anthony B. Muccio *In* Huntsville Association of Technical Societies, TABES 1993: 9th Annual Technical and Business Exhibition and Symposium 1993 5 p (For primary document see N94-16129 03-38)

(TABES Paper 93-654) Avail: CASI HC A01/MF A03

N94-16700*# Colorado Univ., Boulder. Center for the Study of Earth from Space.

SOFTWARE FOR THE DERIVATION OF SCALED SURFACE REFLECTANCES FROM AVIRIS DATA

Bo-Cai Gao, Kathleen Heidebrecht, and Alexander F. H. Goetz *In* JPL, Summaries of the Third Annual JPL Airborne Geoscience Workshop. Volume 1: AVIRIS Workshop 1 Jun. 1992 p 101-103 (For primary document see N94-16666 03-42)

(Contract NAS5-30552)

Avail: CASI HC A01/MF A02

62 COMPUTER SYSTEMS

Includes computer networks and special application computer systems.

N94-14927# Sandia National Labs., Albuquerque, NM.

PARTICLE SIMULATIONS ON MASSIVELY PARALLEL MACHINES

S. Plimpton 1993 4 p Presented at the Conference on High Speed Computing, Salisham, OR, Apr. 1993

(Contract DE-AC04-76DP-00789)

(DE93-015644; SAND-93-0507C; CONF-9304159-1) Avail: CASI HC A01/MF A01

A wide variety of physical phenomena can be modeled with particles. Such simulations pose interesting challenges for parallel machines since the computations are often difficult to load-balance and can require irregular

communication. We discuss the size of problems that can be simulated today, obstacles to higher performance, and areas where algorithmic improvements are needed. The relevant issues are illustrated with two prototypical simulations: a Monte Carlo model of low-density fluid flow and molecular dynamics. DOE

N94-14980# Institut National de Recherche d'Informatique et d'Automatique, Valbonne (France). Programme 1: Architectures Paralleles, Bases de Donnees, Reseaux et Systemes Distribues.

APPLICABILITY OF THE SESSION AND THE PRESENTATION LAYERS FOR THE SUPPORT OF HIGH SPEED APPLICATIONS

Walid Dabbous, Christian Huitema, Leon VidallerSiso (Universidad Politecnica de Madrid, Spain.), Joaquin Seoane (Universidad Politecnica de Madrid, Spain.), and Julio Berrocal (Universidad Politecnica de Madrid, Spain.) Nov. 1992 61 p

(INRIA-RT-144; ETN-93-94429) Avail: CASI HC A04/MF A01

A detailed assessment of the session and presentation services and protocols is given in order to study their suitability to support high speed applications. Focus is thus on the performance aspects of these standard protocols. The evaluation is focused on the following topics: the assessment of the session layer, the suitability of some Interface Description languages, data transparency and transfer syntaxes, and the presentation protocol. A special interest is given to the description and evaluation of a light weight transfer syntax called FTLWS (Flat Tree Light Weight Syntax) proposed as an alternative to the ASN.1 Basic Encoding Rules. ESA

N94-15113*# Research Inst. for Advanced Computer Science, Moffett Field, CA.

MOBILE AND REPLICATED ALIGNMENT OF ARRAYS IN DATA-PARALLEL PROGRAMS

Siddhartha Chatterjee, John R. Gilbert (Xerox Palo Alto Research Center, CA.), and Robert Schreiber Sep. 1993 12 p Proposed for presentation at the 1993 Proceedings of Supercomputing, Portland, OR, 15-19 Nov. 1993

(Contracts NAS2-13721; NCC2-387)

(NASA-CR-194294; NAS 1.26:194294; RIACS-TR-93-08) Copyright Avail: CASI HC A03/MF A01

When a data-parallel language like FORTRAN 90 is compiled for a distributed-memory machine, aggregate data objects (such as arrays) are distributed across the processor memories. The mapping determines the amount of residual communication needed to bring operands of parallel operations into alignment with each other. A common approach is to break the mapping into two stages: first, an alignment that maps all the objects to an abstract template, and then a distribution that maps the template to the processors. We solve two facets of the problem of finding alignments that reduce residual communication: we determine alignments that vary in loops, and objects that should have replicated alignments. We show that loop-dependent mobile alignment is sometimes necessary for optimum performance, and we provide algorithms with which a compiler can determine good mobile alignments for objects within do loops. We also identify situations in which replicated alignment is either required by the program itself (via spread operations) or can be used to improve performance. We propose an algorithm based on network flow that determines which objects to replicate so as to minimize the total amount of broadcast communication in replication. This work on mobile and replicated alignment extends our earlier work on determining static alignment. Author

N94-15173# Illinois Univ., Urbana-Champaign. Coordinated Science Lab.

THE APPLICATION OF COMPILER-ASSISTED MULTIPLE INSTRUCTION RETRY TO VLIW ARCHITECTURES

Shyh-Kwei Chen, W. K. Fuchs, and Wen-Mei W. Hwu 1993 19 p

(Contract N00014-91-J-1128)

(AD-A266930) Avail: CASI HC A03/MF A01

Very Long Instruction Word (VLIW) architectures enhance performance by exploiting fine instruction level parallelism. The development of two compiler assisted multiple instruction word retry schemes for VLIW architectures are described. The first scheme utilizes the compiler techniques previously developed for processors with single functional units. Compiler generated hazard-free code with different degrees of rollback capability for uni-processors is compacted by a modified VLIW trace scheduling algorithm. Nops are then inserted in the scheduled code words to resolve data hazards for VLIW architectures. Performance is compared under three parameters: N, the rollback distance for uni-processors; P, the number of functional units; and n, the rollback distance for VLIW architectures. The second scheme employs a hardware read buffer to resolve frequently occurring data hazards, and utilizes the compiler to resolve the remaining hazards. Performance results are shown for six benchmark programs. DTIC

N94-15492# Massachusetts Inst. of Tech., Lexington.

OVERVIEW OF ENHANCED DATA STREAM ARRAY PROCESSOR (EDSAP)

A. G. Rocco, P. D. Linton, and J. K. Noonan 6 May 1993 54 p

(Contract F19628-90-C-0002)

(AD-A266986; TR-974; TR-92-159) Avail: CASI HC A04/MF A01

The Enhanced Data Stream Array Processor (EDSAP) is a scalable version of the DSAP processing architecture that will allow massively parallel processing. Lincoln Laboratory previously designed two generations of DSAP processors; these programmable signal/data processors provide very high throughput in small, lightweight packages that require low power use. The EDSAP design builds upon the DSAP architecture in a way that provides for processing in the gigaop (billion operations per second) to teraop (trillion operations per second) range. This capability is being accomplished primarily by a significant redesign of high-speed I/O and interprocessor communication. Other architectural improvements, as well as rapid technological advances, contribute to the improved processor. This report provides an overview of the architecture of the EDSAP. The first EDSAP board is expected to be available in late 1993. DTIC

N94-15536*# National Aeronautics and Space Administration. Langley Research Center, Hampton, VA.

AN ELEMENTARY TUTORIAL ON FORMAL SPECIFICATION AND VERIFICATION USING PVS

Ricky W. Butler Sep. 1993 71 p Sponsored by NASA, Washington

(RTOP 505-64-10-13)

(NASA-TM-108991; NAS 1.15:108991) Avail: CASI HC A04/MF A01

A tutorial on the development of a formal specification and its verification using the Prototype Verification System (PVS) is presented. The tutorial presents the formal specification and verification techniques by way of specific example - an airline reservation system. The airline reservation system is modeled as a simple state machine with two basic operations. These operations are shown to preserve a state invariant using the theorem proving capabilities of PVS. The technique of validating a specification via 'putative theorem proving' is also discussed and illustrated in detail. This paper is intended for the novice and assumes only some of the basic concepts of logic. A complete description of user inputs and the PVS output is provided and thus it can be effectively used while one is sitting at a computer terminal. Author (revised)

N94-15671# Naval Command, Control and Ocean Surveillance Center, San Diego, CA. Research, Development, Test and Evaluation Div.

DECOMPOSITION OF LARGE SPARSE SYMMETRIC SYSTEMS FOR PARALLEL COMPUTATION. PART 2: PARALLELIZATION TOOL ROADMAP

A. K. Kevorkian Mar. 1993 22 p

(Proj. ZW6-2)

(AD-A267072; NCCOSC/RDT/E-TR-1601-Pt-2) Avail: CASI HC A03/MF A01

In this report we give a complete computer implementation of an automated algorithmic tool for exploiting the parallelism hidden in the sparsity structure of large symmetric matrices with regular and irregular structures. With this parallelization tool, large sparse symmetric systems of equations are automatically decomposed into independently solvable smaller tasks that can be executed in parallel on different processors of a parallel architecture computer. DTIC

N94-15745# Carnegie-Mellon Univ., Pittsburgh, PA. School of Computer Science.

PROCESSOR CAPACITY RESERVES FOR MULTIMEDIA OPERATING SYSTEMS

Clifford W. Mercer, Stefan Savage, and Hideyuki Tokuda May 1993 17 p

(Contract N00014-91-J-4061)
(AD-A266639; CMU-CS-93-157) Avail: CASI HC A03/MF A01

Multimedia applications have timing requirements that cannot generally be satisfied using time-sharing scheduling algorithms and system structures. To effectively support these types of programs, operating systems must support processor capacity reservation. A capacity reservation and enforcement mechanism isolates programs from the timing and execution characteristics of other programs in the same way that a memory protection system isolates programs from memory access by other programs. In this paper, we characterize the timing requirements and processor capacity reservation requirements for multimedia applications, we describe a scheduling framework to support reservation and admission control, and we introduce a novel reserve abstraction, specifically designed for the microkernel architecture, for controlling processor usage. DTIC

N94-15750# Naval Command, Control and Ocean Surveillance Center, San Diego, CA. Research, Development, Test and Evaluation Div.
DECOMPOSITION OF LARGE SPARSE SYMMETRIC SYSTEMS FOR PARALLEL COMPUTATION. PART 1: THEORETICAL FOUNDATIONS Final Report
A. K. Kevorkian Mar. 1993 62 p
(AD-A267144; NRAD-TR-1572-Pt-1) Avail: CASI HC A04/MF A01

Given a sparse symmetric matrix M, we develop a linear-time algorithm to construct in the undirected graph G = (V, E) of M a vertex partition Π* = (V1, V2, ..., Vr, S*) satisfying the following three properties. First, for any two distinct elements Vi and Vj of the partition, no vertex in Vi is adjacent to a vertex in Vj. Second, every element Vi of the partition induces a clique in G. Third, if A is a full principal submatrix of M such that the symbolic factorization of A does not produce fill-in, then the set of vertices in G corresponding to the rows of A is a subset of an element Vi of the partition. By the first two properties of the vertex partition Π*, the solution of a sparse symmetric problem is reduced to the solution of smaller dense symmetric subproblems. In the case where M is a positive definite matrix, the first property allows us to factorize r dense symmetric blocks in parallel as well as solve in parallel r triangular systems with multiple right-hand sides. The third property is a means for computing an ordering that produces acceptably small fill-in. DTIC

N94-15796*# Research Inst. for Advanced Computer Science, Moffett Field, CA.
GENERATING LOCAL ADDRESSES AND COMMUNICATION SETS FOR DATA-PARALLEL PROGRAMS
Siddhartha Chatterjee, John R. Gilbert, Fred J. E. Long, Robert Schreiber, and Shang-Hua Teng Apr. 1993 11 p Presented at the Fourth ACM SIGPLAN Symposium on Principles and Practice of Parallel Programming, San Diego, CA, May 1993 See also A93-51951
(Contract NCC2-387)
(NASA-CR-194605; RIACS-TR-93.03; NAS 1.26:194605) Avail: CASI HC A03/MF A01

Generating local addresses and communication sets is an important issue in distributed-memory implementations of data-parallel languages such as High Performance Fortran. We show that for an array A affinely aligned to a template that is distributed across p processors with a cyclic(k) distribution, and a computation involving the regular section A, the local memory access sequence for any processor is characterized by a finite state machine of at most k states. We present fast algorithms for computing the essential information about these state machines, and extend the framework to handle multidimensional arrays. We also show how to generate communication sets using the state machine approach. Performance results show that this solution requires very little runtime overhead and acceptable preprocessing time. Author

N94-15849 Colorado Univ., Boulder. Dept. of Computer Science.
PARALLEL PROCESSING AND SCIENTIFIC APPLICATIONS Final Report, 1 Jul. 1989 - 30 Nov. 1992
Charbel Farhat and Oliver A. McBryan 30 Nov. 1992 24 p Limited Reproducibility: More than 20% of this document may be affected by microfiche quality
(Grant AF-AFOSR-0422-89)
(AD-A267179; AFOSR-93-0470TR) Avail: CASI HC A03

Even though today supercomputers are routinely used by large industrial corporations, parallel processors are thought of as exotic machines. Currently, only a fraction of the engineering community is engaged in applying the concurrent computation technology. Incorporation of these new machines in the mainstream of large scale computations is more challenging than that of supercomputers, and will have a greater impact on computational engineering power. Moving engineering applications to concurrent processors faces significant obstacles that will have to be resolved as such machines are becoming available on a commercial scale. These obstacles center on: (1) methods, (2) algorithms, and (3) software. The present proposal addresses all of these issues. 3ore specifically, the objectives of this research are: (1) to investigate, (2) implement, and (3) evaluate tools for concurrent processing of very large structural engineering problems. DTIC

N94-16172# Superconducting Super Collider Lab., Dallas, TX.
THE 3D-FLOW PROCESSOR FOR A PROGRAMMABLE LEVEL-1 TRIGGER (FEASIBILITY STUDY)
D. Crosetto Oct. 1992 11 p
(Contract DE-AC35-89ER-40486)
(DE93-016045; SSCL-601) Avail: CASI HC A03/MF A01

A feasibility study has been made to use the 3D-Flow processor in a pipelined programmable parallel processing architecture to identify particles such as electrons, jets, muons, etc., in high-energy physics experiments. DOE

N94-16577# Rochester Univ., NY. Dept. of Computer Science.
A TRACE-BASED COMPARISON OF SHARED MEMORY MULTIPROCESSOR ARCHITECTURES
William J. Bolosky and Michael L. Scott Jul. 1992 29 p
(Grant NSF CDA-88-22724)
(TR-432) Avail: CASI HC A03/MF A01

There are three major classes of MIMD multiprocessors: cache-coherent machines, NUMA (non-uniform memory reference) machines without cache coherence, and distributed memory multicomputers. All three classes can be used to run shared-memory applications, though the third requires software support in order to do so, and the second requires software support in order to do so well. We use trace-driven simulation to compare the performance of these classes, in an attempt to determine the effact of various architectural features and parameters on overall program performance. For those systems whose hardware or software supports both coherent caching (migration, replication) and remote reference, we use optimal off-line analysis to make the correct decision in all cases. This technique allows us to evaluate architectural alternatives without worrying that the results may be biased by a poor data placement policy. We find that the size of the unit of coherence (page or cache line) is the dominant factor in performance; that NUMA systems can have performance comparable to that of cache coherent machines; and that even relatively expensive, software-implemented remote reference is beneficial in distributed shared memory machines. Author (revised)

N94-16578# Rochester Univ., NY. Dept. of Computer Science.
SHARED-MEMORY MULTIPROCESSOR TRENDS AND THE IMPLICATIONS FOR PARALLEL PROGRAM PERFORMANCE
Evangelos P. Markatos and Thomas J. LeBlanc May 1992 30 p
(Grants NSF CDA-88-22724; NSF CCR-90-05633)
(TR-420) Avail: CASI HC A03/MF A01

The last decade has produced enormous improvements in processor speeds without a corresponding improvement in bus or interconnection network speeds. As a result, the relative costs of communication and computation in shared-memory multiprocessors have changed dramatically. An important consequence of this trend is that many parallel applications, which depend on a delicate balance between the cost of communication and computation, do not execute efficiently on today's shared-memory multiprocessors. We quantify the effect of this trend in multiprocessor architecture on parallel program performance. Our experiments on bus-based, cache-coherent machines like the Sequent Symmetry, and large-scale distributed-memory machines like the BBN Butterfly, demonstrate that applications scale much better on previous-generation machines than on current machines. In addition, we show that some scalable machines support fine-grain, shared-memory programs better than some bus-based, cache-coherent machines, without significantly greater programming effort. From our experiments we conclude that communication has become a dominant source of inefficiency in shared-memory multiprocessors, with

serious consequences for system software involved in scheduling and decomposition decisions. In particular, we argue that shared-memory programming models that could be implemented efficiently on the machines of yesterday do not readily port to state-of-the-art machines, and that current software trends in support of fine-grain parallel programming are at odds with hardware trends. Author (revised)

N94-16724# Carnegie-Mellon Univ., Pittsburgh, PA. School of Computer Science.

EFFICIENT COMPILATION OF ARRAY STATEMENTS FOR PRIVATE MEMORY MULTICOMPUTERS

James M. Stichnoth Feb. 1993 54 p

(Contract MDA972-90-C-0035; ARPA Order 7330)

(AD-A266595; CMU-CS-93-109) Avail: CASI HC A04/MF A01

One of the core constructs of High Performance Fortran (HPF) is the array-slice assignment statement combined with the rich choice of data distribution options available to the programmer. On a private memory multicomputer, the HPF compiler writer faces the difficult task of automatically generating the necessary communication for assignment statements involving arrays with arbitrary block-cyclic data distributions. In this paper we present a framework for representing array slices and block-cyclic distributions, and we derive efficient algorithms for sending and receiving the necessary data for array-slice assignment statements. The algorithms include a memory-efficient method of managing the layout of the distributed arrays in each processor's local memory. We also provide a means of converting the user's TEMPLATE, ALIGN, and DISTRIBUTE statements into a convenient array ownership descriptor. In addition, we present several optimizations for common distributions and easily-recognized communication patterns. The work presented makes minimal assumptions regarding the processor architecture, the communication architecture, or the underlying language being compiled. DTIC

N94-16774# Department of Energy, Washington, DC. Office of Energy Research.

REQUIREMENTS FOR SUPERCOMPUTING IN ENERGY RESEARCH: THE TRANSITION TO MASSIVELY PARALLEL COMPUTING

Feb. 1993 73 p

(DE93-012376; DOE/ER-0587) Avail: CASI HC A04/MF A01

This report discusses: The emergence of a practical path to TeraFlop computing and beyond; requirements of energy research programs at DOE; implementation--supercomputer production computing environment on massively parallel computers; and implementation--user transition to massively parallel computing. DOE

N94-16791# Stanford Univ., CA.

ASYNCHRONOUS DESIGN FOR PARALLEL PROCESSING ARCHITECTURES Final Report

Teresa H.-Y. Meng Jun. 1993 5 p

(Contract N00014-89-J-3036)

(AD-A266523) Avail: CASI HC A01/MF A01

As the integration of VLSI systems becomes larger and denser, implementing a high-performance parallel architecture using a global clock is becoming more inefficient and difficult to design, primarily due to concerns related to clock skew and data synchronization. To solve this problem, a large system may be broken up into asynchronously communicating processors. Each processor can be either asynchronous or synchronous and therefore execute at a rate best suited for individual tasks. Using such asynchronous communication provides a modular design environment in which processors can be individually optimized to yield prominent performance improvement. However the advantages of asynchronous design do not come without a cost, due to two-way communication and design restrictions necessary to avoid hazards and races. In addition, adopting an asynchronous design style requires new methods for synthesis and verification. This research work addressed these methods to simplify the design methodology for asynchronous processors and improve their performance. To provide similar easy-to-use synthesis tools for the design of asynchronous systems, as are available and widely used in the design of synchronous systems, we have developed CAD tools that allow automated design of synchronous, asynchronous, and mixed synchronous/asynchronous circuits. Our work can be summarized in three major topics: automated gate-level synthesis of asynchronous circuits, a uniform approach to both synchronous and asynchronous circuit synthesis, and efficient verification. DTIC

N94-16878*# National Aeronautics and Space Administration. Langley Research Center, Hampton, VA.

A COMPARISON OF QUEUEING, CLUSTER AND DISTRIBUTED COMPUTING SYSTEMS

Joseph A. Kaplan and Michael L. Nelson Oct. 1993 49 p

(RTOP 505-90-53-02)

(NASA-TM-109025; NAS 1.15:109025) Avail: CASI HC A03/MF A01

Using workstation clusters for distributed computing has become popular with the proliferation of inexpensive, powerful workstations. Workstation clusters offer both a cost effective alternative to batch processing and an easy entry into parallel computing. However, a number of workstations on a network does not constitute a cluster. Cluster management software is necessary to harness the collective computing power. A variety of cluster management and queuing systems are compared: Distributed Queueing Systems (DQS), Condor, Load Leveler, Load Balancer, Load Sharing Facility (LSF - formerly Utopia), Distributed Job Manager (DJM), Computing in Distributed Networked Environments (CODINE), and NQS/Exec. The systems differ in their design philosophy and implementation. Based on published reports on the different systems and conversations with the system's developers and vendors, a comparison of the systems are made on the integral issues of clustered computing. Author (revised)

N94-16993# General Accounting Office, Washington, DC. Information Management and Technology Div.

EMBEDDED COMPUTER SYSTEMS: STATUS OF C-17 SOFTWARE

18 Mar. 1993 6 p

(AD-A267307; GAO/T-IMTEC-93-2) Avail: CASI HC A02/MF A01

The C-17 will be the most computerized, software-intensive, transport aircraft ever built. Embedded computers are essential for the C-17 to accomplish its mission; the aircraft depends on these computers to control basic avionics functions such as flight control, communication, and instrument displays. The C-17 relies on 19 different types of embedded computers incorporating over 80 microprocessors and about 1.3 million lines of code. This statement provides information on the current status of embedded computer and software development for the C-17. In summary, we have observed a pattern of the Air Force continuing to permit its prime contractor, McDonnell Douglas Corporation, to defer software development to future aircraft. Originally, the first aircraft (T-1), delivered in September 1991, was supposed to include all the software. But, McDonnell was unable to develop and deliver the software on time. Rather than slowing aircraft production until the software could be completed, McDonnell deferred software development, initially to the P-2 aircraft, then to the P-5 aircraft, and now to the P-6 and future aircraft. Each software development deferral further delays the Air Force's ability to fully test the software and demonstrate that the C-17 can meet all of its requirements. DTIC

N94-17034# Naval Postgraduate School, Monterey, CA.

NETWORKED WORKSTATIONS AND PARALLEL PROCESSING UTILIZING FUNCTIONAL LANGUAGES M.S. Thesis

Stanley L. Fox, II Mar. 1993 124 p

(AD-A267464) Avail: CASI HC A06/MF A02

Alternative computer architectures are necessary to replace the traditional 'von Neumann' computer organization in order to obtain large increases in performance. The traditional 'von Neumann' architecture uses a timer based (e.g., the program counter), sequentially programmed, single processor approach to problem solving. Today's new hardware technology allows for the utilization of multiple processors. By programming and operating these processors in parallel, this alternative architecture will provide for greater computing speed, improved system reliability, enhanced software manageability, and a more cost-effective approach than our present computing practices. DTIC

N94-17209# Air Force Systems Command, Wright-Patterson AFB, OH. CALS Test Network.

CALS TEST NETWORK HANDBOOK

Mar. 1993 77 p

(AD-A267587) Avail: CASI HC A05/MF A01

This Computer-aided Acquisition and Logistic Support (CALS) Test Network (CTN) Handbook will have periodic updates. These will occur as

the technology of CALS standards and testing grows and matures. CALS Standards and Specifications require three levels of testing. The testing includes the following: (1) Standards Validation Testing; (2) Conformance Testing; and (3) User Application Testing. The management of CALS Standards Validation Testing and user Application Testing has been assigned to the CALS Test Network. Conformance Testing wil be assigned to other agencies. The purpose of this handbook is twofold. First, it provides an introduction to the CTN and identifies the managers and testing analysts. Second, it lists CTN reference material such as testing platforms used by CTN, testing tools, CTN reference test packet descriptions, and how to receive some of these materials. The writing style and format of the document is concise. DTIC

N94-17239*# Cornell Univ., Ithaca, NY. Dept. of Computer Science.
LIGHT-WEIGHT PROCESS GROUPS IN THE ISIS SYSTEM
Bradford B. Glade, Robert C. Cooper, Kenneth P. Birman, and Robbert vanRenesse 1993 22 p
(Contract NAG2-593; N00014-92-J-1866)
(NASA-CR-194544; NAS 1.26:194544; AD-A267270) Avail: CASI HC A03/MF A01

ISIS is a toolkit for building applications consisting of cooperating processes in a distributed system. Group management and group communication are two basic building blocks provided by ISIS. This approach has proven successful, and ISIS' large user community is putting substantial demands on these mechanisms. To accommodate these demands a complete redesign of the system, called HORUS, is being done to build a simpler and faster system that scales well. Of particular concern is the support and management of hundreds of thousands or more process groups. This paper describes a component of HORUS known as light-weight process groups that addresses this scaling issue. DTIC

N94-17328*# National Aeronautics and Space Administration. Pasadena Office, CA.
NON-BLOCKING CROSSBAR PERMUTATION ENGINE WITH CONSTANT ROUTING LATENCY Patent Application
Steve P. Monacos, inventor (to NASA) (Jet Propulsion Lab., California Inst. of Tech., Pasadena.) 18 Aug. 1993 60 p
(Contract NAS7-918)
(NASA-Case-NPO-18864-1-CU; NAS 1.71:NPO-18864-1-CU; US-Patent-Appl-SN-111318) Avail: CASI HC A04/MF A01

The invention is embodied in an N x N crossbar for routing packets from a set of N input ports to a set of N output ports, each packet having a header identifying one of the output ports as its destination, including a plurality of individual links which carry individual packets. Each link has a link input end and a link output end, a plurality of switches. Each of the switches has at least top and bottom switch inputs connected to a corresponding pair of the link output ends and top and bottom switch outputs connected to a corresponding pair of link input ends, whereby each switch is connected to four different links. Each of the switches has an exchange state which routes packets from the top and bottom switch inputs to the bottom and top switch outputs, respectively, and a bypass state which routes packets from the top and bottom switch inputs to the top and bottom switch outputs, respectively. A plurality of individual controller devices governing respective switches for sensing from a header of a packet at each switch input for the identity of the destination output port of the packet and selecting one of the exchange and bypass states in accordance with the identity of the destination output port and with the location of the corresponding switch relative to the destination output port. NASA

N94-17330*# National Aeronautics and Space Administration. Pasadena Office, CA.
A SCALABLE WRAP-AROUND SHUFFLE EXCHANGE NETWORK WITH DEFLECTION ROUTING Patent Application
Steve P. Monacos, inventor (to NASA) (Jet Propulsion Lab., California Inst. of Tech., Pasadena.) 18 Aug. 1993 36 p
(Contract NAS7-918)
(NASA-Case-NPO-18983-1-CU; NAS 1.71:NPO-18983-1-CU; US-Patent-Appl-SN-112497) Avail: CASI HC A03/MF A01

The invention in one embodiment is a communication network including plural non-blocking crossbar nodes, first apparatus for connecting the nodes in a first layer of connecting links, and second apparatus for connecting the nodes in a second layer of connecting links independent of the first layer, whereby each layer is connected to the other layer at each one of the nodes. Preferably, each one of the layers of connecting links corresponds to one recirculating network topology that closes in on itself. NASA

N94-17367 Air Force Inst. of Tech., Wright-Patterson AFB, OH.
ESTIMATING TASK EXECUTION DELAY IN A REAL-TIME SYSTEM VIA STATIC SOURCE CODE ANALYSIS M.S. Thesis
Steve B. Treadwell Jun. 1993 125 p Limited Reproducibility: More than 20% of this document may be affected by microfiche quality
(AD-A267496; AFIT/CI/CIA-93-072) Avail: Issuing Activity (Defense Technical Information Center (DTIC))

In a hard-real-time system, it is critical that application tasks complete their iterative execution cycles within their allotted time frames. For a highly configurable parallel processing system, there exists an overwhelming set of hardware and software configurations, and it is useful to know a priori if a particular configuration satisfies hard-real-time constraints. This thesis presents an automated timing analysis tool which attempts to accurately characterize the timing behavior of the C3 Fault-Tolerant Parallel Processor (FTPP) developed at the Charles Stark Draper Laboratory. For each application task hosted by the FTPP, this automated tool performs a static source code analysis in an effort to estimate a lower bound on worst case execution delay. Then, using the specified mapping between software tasks and hardware processing sites, the analysis tool integrates the results of the individual task analyses in an effort to account for delays due to operating system overhead. The final portion of the analysis involves a prediction of possible performance failures based upon the given system configuration and the timing deadlines imposed by the FTPP's rate group scheduling paradigm. It is intended that the results of this timing analysis will help the user to develop a system configuration that optimizes throughput while minimizing the risk, of performance failures. DTIC

N94-17409# Columbia Univ., New York, NY. Dept. of Computer Science.
ISOCHRONETS: A HIGH-SPEED NETWORK SWITCHING ARCHITECTURE
Yechiam Yemini and Danilo Florissi 1992 8 p
(Grant NSF NCR-91-01627)
(AD-A267811; CUCS-050-92) Avail: CASI HC A02/MF A01

This paper overviews a novel switching architecture for high-speed networks: Isochronets. Isochronets time-divide network bandwidth among routing trees. Traffic moves down a routing tree to the root during its time band. Network functions such as routing and flow control are entirely governed by band timers and require no processing of frame headers bits. Frame motions need not be delayed for switch processing allowing Isochronets to scale over a large spectrum of transmission speeds and support all-optical implementations. The network functions as a media-access layer that can support multiple framing protocols simultaneously, handled by higher layers at the periphery. Internetworking is reduced to a simple media-layer bridging. Isochronets provide flexible quality of service control and multicasting through allocation of bands to routing trees. They can be tuned to span a spectrum of performance behaviors outperforming both circuit or packet switching. DTIC

N94-17449*# National Aeronautics and Space Administration. Langley Research Center, Hampton, VA.
VERIFICATION OF FAULT-TOLERANT CLOCK SYNCHRONIZATION SYSTEMS M.S. Thesis - College of William and Mary, 1992
Paul S. Miner Nov. 1993 143 p
(RTOP 505-64-50-03)
(NASA-TP-3349; L-17209; NAS 1.60:3349) Avail: CASI HC A07/MF A02

A critical function in a fault-tolerant computer architecture is the synchronization of the redundant computing elements. The synchronization algorithm must include safeguards to ensure that failed components do not corrupt the behavior of good clocks. Reasoning about fault-tolerant clock synchronization is difficult because of the possibility of subtle interactions involving failed components. Therefore, mechanical proof systems are used to ensure that the verification of the synchronization system is correct. In 1987, Schneider presented a general proof of correctness for several fault-tolerant clock synchronization algorithms.

Subsequently, Shankar verified Schneider's proof by using the mechanical proof system EHDM. This proof ensures that any system satisfying its underlying assumptions will provide Byzantine fault-tolerant clock synchronization. The utility of Shankar's mechanization of Schneider's theory for the verification of clock synchronization systems is explored. Some limitations of Shankar's mechanically verified theory were encountered. With minor modifications to the theory, a mechanically checked proof is provided that removes these limitations. The revised theory also allows for proven recovery from transient faults. Use of the revised theory is illustrated with the verification of an abstract design of a clock synchronization system.
Author (revised)

N94-17537# Institut National de Recherche d'Informatique et d'Automatique, Valbonne (France). Programme 1: Architectures Paralleles, Bases de Donnees, Reseaux et Systemes Distribues.
STOCHASTIC SCHEDULING IN A MULTICLASS G/G/1 QUEUE
Philippe Nain and Don Towsley (Massachusetts Univ., Amherst.) Sep. 1992 14 p
(Grants NSF ASC-88-02764; NSF NCR-91-16183)
(INRIA-RR-1746; ETN-93-94437) Avail: CASI HC A03/MF A01

The problem of scheduling customers in a multiclass G/G/1 queue so as to minimize a weighted sum of the workloads of the different classes is addressed. The nonidling, preemptive, fixed priority policy that schedules customers belonging to the class having the maximum weight is established as minimizing the cost function pathwise at any point in time. This result is based on the application of elementary forward induction arguments and is shown to hold for a very general class of policies. A proof for the optimality of the mu-c rule in the multiclass G/M/1 queue is then obtained as an easy corollary of the first result.
ESA

N94-17539# Institut National de Recherche d'Informatique et d'Automatique, Valbonne (France). Programme 4: Robotique, Image et Vision.
CONSTRUCTION OF d-DIMENSIONAL HYPEROCTREES ON A HYPERCUBE MULTIPROCESSOR
Frank Dehne (Ottawa Univ., Ontario.), Andreas Fabri, Mostafa Nassar (Acadia Univ., Wolfville, Nova Scotia.), Andrew Rau-Chaplin (Ottawa Univ., Ontario.), and Rada Valiveti (Ottawa Univ., Ontario.) Sep. 1992 13 p Sponsored in part by Natural Sciences and Engineering Research Council of Canada, and EEC
(INRIA-RR-1752; ETN-93-94438) Avail: CASI HC A03/MF A01

A parallel algorithm for the construction of the hyperoctree representing a d dimensional object from a set of n(d-1) dimensional hyperoctrees, representing adjacent crossections of this object, is presented. On a p-processor SIMD hypercube the time complexity of the algorithm is O((m/p)log(p)log(n)), where m is the maximum of input and output size.
ESA

N94-17550# Stanford Univ., CA. Dept. of Computer Science.
ACCURATE ANALYSIS OF ARRAY REFERENCES M.S. Thesis
Dror E. Maydan 22 Sep. 1992 144 p
(Contract N00039-91-C-0138)
(AD-A268069; STAN-CS-92-1449; CSL-TR-92-547) Avail: CASI HC A07/MF A02

This thesis addresses the problem of data dependence analysis, the base step in detecting loop level parallelism in scientific programs. Traditional data dependence analysis research has concentrated on the simpler problem of affine memory disambiguation. Many algorithms have been developed that conservatively approximate even this simpler problem. Using a series of algorithms, each one guaranteed to be exact for a certain class of input, we are able to devise a new method that in practice solves exactly and efficiently the affine memory disambiguation problem. Because our system is exact, we can devise an experiment to test the effectiveness of affine memory disambiguation at approximating the full dependence problem. We discover that the lack of dataflow information on array elements is the key limitation of affine memory disambiguators. We develop a new representation and algorithm to efficiently calculate these data-flow dependences. Finally, we address the problem of interprocedural data dependence analysis. By using an array summary representation that is guaranteed to be exact when applicable, we can combine summaries with inlining to exactly and efficiently analyze affine array references across procedure boundaries. Taken together, our algorithms generate the more accurate information that will be needed to exploit parallelism in the future.
DTIC

N94-17551# Air Force Inst. of Tech., Wright-Patterson AFB, OH.
SYSTEM PERFORMANCE MODELING AND ANALYSIS OF A FAULT-TOLERANT, REAL TIME PARALLEL PROCESSOR M.S. Thesis
Robert J. Clasen 27 May 1993 142 p
(AD-A268070; AFIT/CI/CIA-93-112) Avail: CASI HC A07/MF A02

The use of fault-tolerant, real-time systems for the control of life-critical processes is becoming increasingly common, with examples including flight and nuclear reactor control systems. In such systems, the overhead associated with managing redundancy, communication, and task scheduling is critical due to real-time constraints imposed by the application; missed time deadlines can be viewed as system failures, with results as consequential as hardware failures. The Fault-Tolerant Parallel Processor (FTPP) was developed by Draper Laboratory as a fault-tolerant, real-time computing platform. This thesis analyzes the FTPP prototype operating system overhead through the use of empirical performance measurement and two performance models based on these measurements. One model is developed to predict the operating system overhead under various configurations and workloads; accurate prediction of overhead provides confidence that real-time constraints can be satisfied. Because the system communication overhead may vary depending upon the amount of contention by Processing Elements for service by the Network Element, a second model is developed to account for performance delays that may result from this contention. When such performance analysis and modeling are an integral part of a concurrent build-analyze-improve methodology, performance bottlenecks can be cost effectively removed at an early stage in development.
DTIC

N94-17622# Naval Research Lab., Washington, DC.
AN INTERNETWORK AUTHENTICATION ARCHITECTURE
Randall J. Atkinson 5 Aug. 1993 15 p
(AD-A268579; NRL/FR/5544-93-9561) Avail: CASI HC A03/MF A01

Current internetworks do not have effective host-to-host authentication mechanisms. The lack of these mechanisms contributes substantially to currently widespread network security problems. Public key authentication is a good approach to providing optional authentication in internetworks. An internetwork authentication architecture using public key authentication technology is proposed as a possible mechanism to substantially improve the security of large internetworks. Limitations of the proposed authentication architecture are also described.
DTIC

N94-17646# Los Alamos National Lab., NM.
BENCHMARKING MASSIVELY PARALLEL ARCHITECTURES
O. Lubeck, J. Moore, M. Simmons, and H. Wasserman 1993 7 p Presented at the Workshop on Benchmark and Performance Evaluation in High Performance Computing, Tokyo, Japan, 23 Jul. 1993
(Contract W-7405-eng-36)
(DE93-016486; LA-UR-93-2373; CONF-9307100-1) Avail: CASI HC A02/MF A01

The purpose of this paper is to summarize some initial experiences related to measuring the performance of massively parallel processors (MPP's) at Los Alamos National Laboratory (LANL). Actually, the range of MPP architectures the authors have used is rather limited, being confined mostly to the Thinking Machines Corporation (TMC) Connection Machine CM-2 and CM-5. Some very preliminary work has been carried out on the Kendall Square KSR-1, and efforts related to other machines, such as the Intel Paragon and the soon-to-be-released CRAY T3D are planned. This paper will concentrate more on methodology rather than discuss specific architectural strengths and weaknesses; the latter is expected to be the subject of future reports. MPP benchmarking is a field in critical need of structure and definition. As the authors have stated previously, such machines have enormous potential, and there is certainly a dire need for orders of magnitude computational power over current supercomputers. However, performance reports for MPP's must emphasize actual sustainable performance from real applications in a careful, responsible manner. Such has not always been the case. A recent paper has described in some detail, the problem of potentially misleading performance reporting in the parallel scientific computing field. Thus, in this paper, the authors briefly offer a few general ideas on MPP performance analysis.
DOE

63 CYBERNETICS

Includes feedback and control theory, artificial intelligence, robotics and expert systems.

For related information see also 54 Man/System Technology and Life Support.

N94-14910# Carnegie-Mellon Univ., Pittsburgh, PA. School of Computer Science.
YARF: AN OPEN-ENDED FRAMEWORK FOR ROBOT ROAD FOLLOWING Ph.D. Thesis
Karl Kluge 24 Feb. 1993 98 p
(AD-A266788; CMU-CS-93-104) Avail: CASI HC A05/MF A02

This thesis describes YARF (Yet Another Road Follower), a vision-based system for autonomous road following. Video data from a camera mounted *on a robot vehicle is fed into a computer, which analyzes the image data* to locate the position of the vehicle relative to the road. The computer then issues command to actuators attached to the throttle, brakes, and steering in order to drive the vehicle along the road. YARF has been extensively tested using a combination of open- and closed-loop runs on testbed vehicles, simulation, and data from videotapes. YARF provides a set of perception capabilities to locate the position of the vehicle relative to the road, to detect changes in the lane structure of the road, to navigate through intersections given a model of the intersection geometry, and to extract the lane structure of the road without a prior model. The central theme of YARF is that using richer models improves road following performance. Models of geometric structure, of road appearance, and of segmentation performance all simplify processing and contribute to improve reliability. YARF uses road models in several ways: Model drive segmentation; Exploitation of model coherence to avoid the influence of contaminating data; and Data driven recognition of model changes. While YARF assumes that the models of road structure used are generated off line, the thesis presents an algorithm designed to automatically extract much of the needed model information. The algorithm uses a weak domain model to filter a noisy image segmentation, extracting both feature geometry and type.
DTIC

N94-14937# Stanford Univ., CA. Dept. of Mechanical Engineering.
TACTILE SENSING AND CONTROL IN HUMANS AND ROBOTIC/TELEOPERATED SYSTEMS Progress Report
Mark R. Cutkosky, Gregory T. Kovacs, Robert D. Howe, Roger Brockett, and Roland Johansson Jul. 1993 7 p
(Contract N00014-90-J-1887)
(AD-A267710) Avail: CASI HC A02/MF A01

Over the last several years, a number of sophisticated robot hands have been developed for laboratory use. However, while such hands approximate the mechanical complexity of human hands, their application in manipulation tasks remains in a primitive stage. Unlike human hands, they rely on minutely programmed task descriptions that are time-consuming to generate and susceptible to unanticipated changes in the task or the immediate environment. This is largely because they cannot use tactile information to detect and respond to changes in an event-driven fashion as humans do. Similarly, teleoperated manipulation systems are slow and difficult to use because the operator does not receive appropriate tactile feedback from the manipulator.
DTIC

N94-14950# Carnegie-Mellon Univ., Pittsburgh, PA. Robotics Inst.
FUZZY CONTROL AND FUZZY KINEMATIC MAPPING FOR A REDUNDANT SPACE ROBOT
Alois Schacherbauer and Yangsheng Xu Aug. 1992 72 p
(AD-A266866; CMU-RI-TR-92-12) Avail: CASI HC A04/MF A01

Parts of the research in the Self Mobile Space Manipulator (SM2) project at Carnegie Mellon University are documented. Fuzzy Logic Friction Compensation schemes that improve motion performance of SM2 were developed. Both static and dynamic errors are reduced. Also, Fuzzy Inverse Kinematic Mapping is proposed to resolve the redundancy problem in SM2. The proposed scheme works identically for redundant and non-redundant robots, does not require any constraints to be imposed on the robot configuration, and provides a closed-form solution. This scheme in simulation is investigated and then implemented for real-time teleoperation of SM2.
DTIC

N94-14953# Carnegie-Mellon Univ., Pittsburgh, PA. Robotics Inst.
VIDEO APPLICATIONS DEVELOPMENT PLATFORM
Robert Thibadeau, Robert Berger, David Touretzky, and Don Lindsay Mar. 1993 23 p
(Contract MDA972-92-J-1010; DARPA Order 6873)
(AD-A266966; CMU-RI-TR-93-04) Avail: CASI HC A03/MF A01

The objective of the video applications development platform research is to develop the technical basis for intelligent frame buffers useful in high definition displays. This project has three components: physical *implementation of the Intelligent Frame Buffer (IFB) which includes multiple* cooperating CPU's on a single display, software operating system support *which forms the basis for display sharing and display cooperation, and* applications-level software support which forms the basis for programming the intelligent frame buffer in such applications as intelligent sensor fusion. The focus of the work is on display sharing by multiple processors and intelligent autonomous display manipulation. The IFB project operates in a *domain that minimizes the need for explicit user input as opposed to* domains which involve pure user manipulation, e.g. 'smart controls,' such *as 'fly by wire' systems which have no need for display, or 'user monitoring.'* This report describes the results of the first year of a multi-year project, *namely: architectural design and hardware prototype of regular resolution* IFB; survey of work in real time operating systems for imagery and MACH, resulting in an architectural design of real-time MACH kernel for imagery; prototype regular resolution workstation integrating realtime MACH kernel, IFB, and Advanced Video Display Systems (AVDS) applications building *environments; and designs, prototypes, and systems architecture design* for high resolution IFB, MACH kernel, and applications building environment *with networking.*
Author (revised)

N94-14954# Carnegie-Mellon Univ., Pittsburgh, PA. Robotics Inst.
FUZZY INVERSE KINEMATIC MAPPING: RULE GENERATION, EFFICIENCY, AND IMPLEMENTATION
Yangsheng Xu and Michael C. Nechyba Jan. 1993 34 p
(AD-A266967; CMU-RI-TR-93-02) Avail: CASI HC A03/MF A01

Inverse kinematics is computationally expensive and can result in significant control delays in real time. For a redundant robot, additional computations are required for the inverse kinematic solution through optimization schemes. Based on the fact that humans do not compute exact inverse kinematics, but can do precise positioning from heuristics, we developed an inverse kinematic mapping through fuzzy logic. The implementation of the proposed scheme has demonstrated that it is feasible for both redundant and nonredundant cases, and that it is very computationally efficient. The result provides sufficient precision, and transient tracking error can be controlled based on a fuzzy adaptive scheme proposed in this paper. This paper discusses the automatic generation of the Fuzzy Inverse Kinematic Mapping (FIKM) from specification of the Denavit-Hartenberg (DH) parameters, the efficiency of the scheme in comparison to conventional approaches, and the implementation results for both redundant and nonredundant robots.
Author (revised)

N94-14968# Carnegie-Mellon Univ., Pittsburgh, PA. Robotics Inst.
SEGMENTING TEXTURED 3D SURFACES USING THE SPACE/FREQUENCY REPRESENTATION
John Krumm and Steven A. Shafer Apr. 1993 32 p
(AD-A266960; CMU-RI-TR-93-14) Avail: CASI HC A03/MF A01

Segmenting 3D textured surfaces is critical for general image understanding. Unfortunately, current efforts at automatically understanding image texture are based on assumptions that make this goal impossible. Texture segmentation research assumes that the textures are flat and viewed from the front, while shape-from-texture work assumes that the textures have already been segmented. This deadlock means that none of these algorithms can be successfully applied to images of 3D textured surfaces. We have developed an algorithm that can segment an image containing nonfrontally viewed, planar, periodic textures. We use the spectrogram to compute local surface normals from many different regions of the image. This algorithm does not require unreliable image feature detection. Based on these surface normals, we compute a 'frontalized' version of the local power spectrum which shows what the region's power spectrum would look like if viewed from the front. If neighboring regions have similar frontalized power spectra, they are merged. To our knowledge, this is the first program that can segment 3D textured surfaces by explicitly accounting for shape effects.
DTIC

N94-15502# Carnegie-Mellon Univ., Pittsburgh, PA. Robotics Inst.
HIDDEN MARKOV MODEL APPROACH TO SKILL LEARNING AND ITS APPLICATION TO TELEROBOTICS
Jie Yang, Yangsheng Xu, and C. S. Chen Jan. 1993 32 p
(AD-A266989; CMU/RI-TR-93-01) Avail: CASI HC A03/MF A01

In this paper, we discuss the problem of how human skill can be represented as a parametric model using a hidden Markov model (HMM), and how a HMM-based skill model can be used to learn human skill. HMM is feasible to characterize two stochastic processes--measurable action and immeasurable mental states--which are involved in the skill learning. We formulated the learning problem as a multi-dimensional HMM and developed a programming system which serves as a skill learning testbed for a variety of applications. Based on 'the most likely performance' criterion, we can select the best action sequence from all previously measured action data by modeling the skill as HMM. This selection process can be updated in real-time by feeding new action data and modifying HMM parameters. We address the implementation of the proposed method in a teleoperation-controlled space robot. An operator specifies the control command by a hand controller for the task of exchanging Orbit Replaceable Unit, and the robot learns the operation skill by selecting the sequence which represents the most likely performance of the operator. The skill is learned in Cartesian space, joint space, and velocity domain. The experimental results demonstrate the feasibility of the proposed method in learning human skill and teleoperation control. The learning is significant in eliminating sluggish motion and correcting the motion command which the operator mistakenly generates. DTIC

N94-15515* National Aeronautics and Space Administration. Lyndon B. Johnson Space Center, Houston, TX.
PROGRAMMABLE REMAPPER PROJECT (Videotape)
Jul. 1990 Videotape: 23 min. 50 sec. playing time, in color, with sound
(NASA-TM-109508; NONP-VT-93-190305) Avail: CASI VHS A01/BETA A22

This video shows how the Remapper Project helps with many problems including vision problems. It shows the Remapper in action as it tracks several objects around the moon. The video is narrated by Dr. Richard Juday, Robotic Vision, Manager at the Johnson Space Center. CASI

N94-15695# Institut National de Recherche d'Informatique et d'Automatique, Valbonne (France). Programme 1: Architectures Paralleles, Bases de Donnees, Reseaux et Systemes Distribues.
STOCHASTIC SCHEDULING IN IN-FOREST NETWORKS
Zhen Liu and Don Towsley (Massachusetts Univ., Amherst.) Jul. 1992 36 p
(Grant NSF ASC-88-02764)
(INRIA-RR-1719; ETN-93-94430) Avail: CASI HC A03/MF A01

The extremal properties of several scheduling policies in a queueing network consisting of multiserver queues where the topology is that of an in-forest are studied. Associated with each customer is a due date. It is assumed that service times at the different queues form mutually independent sequences of independent and identically distributed random variables independent of the arrival times and due dates. Furthermore, the network is assumed to consist of a mixture of nodes, some of which only permit non-preemptive service policies whereas the others permit preemptive resume policies. In the case of nonpreemptive queues, service times may be generally distributed provided there is only one server; otherwise the service times are required to be increased in likelihood ratio. In the case of preemptive queues, service times are restricted to be exponentially distributed random variables. Using stochastic majorization and a partial order on permutations, it is established that, the class of work conserving service policies, the Smallest Due Date (SDD) and Largest Due Date (LDD) policies minimize and maximize, respectively, the vector of the customer latenesses of the first 'n' customers in the sense of the Schur-convex order. From this, it is concluded that the First Come First Serve (FCFS) and Last Come First Serve (LCFS) policies minimize and maximize, respectively, the vector of the response times of the first n customers in the sense of the Schur-convex order. If due dates are only known stochastically, then it is established that the stochastic SDD and the stochastic LDD policies minimize and maximize the vector of latenesses according to a weaker ordering. It is shown that the FCFS and LCFS policies minimize and maximize, respectively, the vector of customer end-to-end delays in the sense of the strong stochastic order. When idling policies are under consideration, the FCFS policy is shown to be optimal for various performance metrics in the case that all queues permit preemptive resume policies and all service times are exponentially distributed. Extensions of these results to the stationary regime are also given. ESA

N94-15704*# National Aeronautics and Space Administration. Goddard Space Flight Center, Greenbelt, MD.
STEERING CAPACIFLECTOR SENSOR Patent Application
Del T. Jenstrom, inventor (to NASA) and Robert L. McConnell, inventor (to NASA) (West Virginia Univ., Morgantown.) 23 Nov. 1992 15 p
(NASA-Case-GSC-13489-1; NAS 1.71:GSC-13489-1;
US-Patent-Appl-SN-979987) Avail: CASI HC A03/MF A01

A capacitive type proximity sensor having substantial range and sensitivity between a machine and an intruding object in the immediate vicinity of the machine and having a steerable sensing field has an outer electrical conductor on the machine forming one electrode of a sensor capacitor, the other electrode is the object. The outer conductor is a thin sheet of conductive material with a pair (or more) of intermediate electrical conductors located between the outer conductor and the machine. The pair of intermediate electrical conductors are in close proximity to each other and together form a surface having a size substantially larger than the outer conductor to act as a shield for reducing the parasitic capacitance between the outer conductor and the machine and to steer the sensor field. The pair of intermediate conductors are thin sheets of conductive material substantially wider than the first conductor. The outer and pair of intermediate conductors are attached to a surface on the machine in electrical isolation and with no gaps between the conductors and no gap between the surface and the pair of intermediate conductors. The outer and pair of intermediate conductors are also in conformance with each other and the surface of the machine, and the surface of the machine acts as a ground plane. Variable gain voltage follower circuits are used for coupling, in phase, the instantaneous voltage at the outer electrical conductor to the pair of intermediate electrical conductors and a signal generator is coupled to the outer conductor and is responsive to the capacitance of the sensor capacitor for generating a control signal to the machine. NASA

N94-15746# Massachusetts Inst. of Tech., Lexington.
PIXEL-LEVEL FUSION USING INTEREST IMAGES
Richard L. Delanoy, Jacques G. Verly, and Dan E. Dudgeon 26 Apr. 1993 22 p
(Contract F19628-90-C-0002)
(AD-A266640; TR-979; ESC-TR-92-206) Avail: CASI HC A03/MF A01

A simple general-purpose means of representing image sensory data at the pixel level is presented in the context of target detection. One or more interest operators (i.e., feature detectors) are applied to one or more sensory images. The output of each operator is an interest image in which high pixel values are assigned to locations where features are found that are indicative of the object (or target) being sought. Any relevant sensory data that are transformed into interest images can then be fused in a pixel-wise manner by means as simple as computing averages, maxima or minima. The approach has been implemented in the detection module of an automatic target recognition system built at Lincoln Laboratory. DTIC

N94-15756 Carnegie-Mellon Univ., Pittsburgh, PA. Robotics Inst.
IMPENDING MOTION DIRECTION OF CONTACTING RIGID BODIES
David Baraff and Raju Mattikali Jun. 1993 19 p Limited Reproducibility: More than 20% of this document may be affected by poor print and microfiche quality
(AD-A266814; CMU-RI-TR-93-15) Avail: Issuing Activity (Defense Technical Information Center (DTIC))

Three different formulations are presented for expressing the initial motion direction of a system of contacting frictionless rigid bodies under gravity. The bodies are assumed to have no initial velocity. The first formulation expresses the accelerations of the bodies in terms of the contact forces between the bodies. The contact forces are themselves expressed as the solution to a quadratic programming problem. The second formulation expresses the accelerations of the bodies according to Gauss' principle of least constraint. This principle is well-known to apply to systems with holonomic motion constraints (such as joints or hinges); in this paper, we show that the principle extends to the nonholonomic constraints that arise due to contact between bodies. The third formulation is conceptually the simplest; it says simply that the initial acceleration of the system is in

the direction that most quickly decreases the gravitational potential energy of the system without violating the contact constraints between the bodies. DTIC

N94-15775 Stanford Univ., CA. Operations Research House.
LOGARITHMIC ASYMPTOTICS FOR STEADY-STATE TAIL PROBABILITIES IN A SINGLE-SERVER QUEUE
Peter W. Glynn and Ward Whitt Jan. 1993 40 p Limited Reproducibility: More than 20% of this document may be affected by microfiche quality
(Contract DAAL03-91-G-0101)
(AD-A266746; ARO-28809.13-MA-SDI) Avail: CASI HC A03

We consider the standard single-server queue with unlimited waiting space and the first-out service discipline. We find conditions for the steady-state waiting-time distribution to have small-tail asymptotics of a certain form. We require only stationarity of the basic sequence of service times minus interarrival times and a Gaertner-Ellis condition for the cumulant generating function of the associated partial sums. DTIC

N94-15778# Michigan Univ., Ann Arbor. Dept. of Electrical Engineering and Computer Science.
THE DESIGN AND ANALYSIS OF ROBUST FEEDBACK SYSTEMS Final Report, 1 Nov. 1989 - 31 Oct. 1992
Pramod P. Khargonekar 31 Oct. 1992 14 p
(Grant AF-AFOSR-0053-90)
(AD-A267152; AFOSR-93-0475TR) Avail: CASI HC A03/MF A01

In this report, we give a brief summary of the work done by the principal investigator and his students on the design and analysis of robust feedback systems. Under this contract, we have conducted research on a number of problems in robust control and identification theory. In particular, we have obtained significant new results on H2, H-infinity, and H2/H-infinity control theory, robust digital control in the framework of sampled-data systems, identification in H-infinity, etc. In this report, we will present a brief summary of the main results obtained under the AFOSR contract. Author (revised)

N94-15855 Naval Postgraduate School, Monterey, CA.
AN EXPERIMENTAL COMPARISON OF CLOS AND C(++) IMPLEMENTATIONS OF AN OBJECT-ORIENTED GRAPHICAL SIMULATION OF WALKING ROBOT KINEMATICS M.S. Thesis
Sandra L. Davidson 25 Mar. 1993 146 p Limited Reproducibility: More than 20% of this document may be affected by microfiche quality
(AD-A267168) Avail: CASI HC A07

The ability to conduct research in the robotic field in new areas can be accomplished safely and efficiently using computer graphic simulation. Object-oriented languages provide a powerful and flexible capability in defining rigid body manipulators that can be adapted in the use and design of many types of systems. The very nature of object-oriented programming permits modification and improvement of the code with ease. The major capabilities of object-oriented programming in conjunction with kinematic equations that simulate a six-legged walking robot are examined. A comparison is conducted between programs using CLOS (LISP) and C++ to graphically simulate the Aquarobot - an existing underwater walking robot. It is found that both languages are effective, but CLOS programming is easier while C++ code executes more than twice as fast as compiled CLOS. DTIC

N94-15946*# National Aeronautics and Space Administration. Goddard Space Flight Center, Greenbelt, MD.
DOUBLE-DRIVEN SHIELD CAPACITIVE TYPE PROXIMITY SENSOR Patent Application
John M. Vranish, inventor (to NASA) 25 Jan. 1993 24 p
(NASA-Case-GSC-13541-1; NAS 1.71:GSC-13541-1;
US-Patent-Appl-SN-008426) Avail: CASI HC A03/MF A01

A capacity type proximity sensor comprised of a capacitance type sensor, a capacitance type reference, and two independent and mutually opposing driven shields respectively adjacent to the sensor and reference and which are coupled in an electrical bridge circuit configuration and driven by a single frequency crystal controlled oscillator is presented. The bridge circuit additionally includes a pair of fixed electrical impedance elements which form adjacent arms of the bridge and which comprise either a pair of precision resistances or capacitors. Detection of bridge unbalance provides an indication of the mutual proximity between an object and the sensor. Drift compensation is also utilized to improve performance and thus increase sensor range and sensitivity. NASA

N94-15958*# National Aeronautics and Space Administration. Pasadena Office, CA.
UNIPOLAR TERMINAL-ATTRACTOR BASED NEURAL ASSOCIATIVE MEMORY WITH ADAPTIVE THRESHOLD Patent Application
Hua-Kuang Liu, inventor (to NASA) (Jet Propulsion Lab., California Inst. of Tech., Pasadena.), Jacob Barhen, inventor (to NASA) (Jet Propulsion Lab., California Inst. of Tech., Pasadena.), Nabil H. Farhat, inventor (to NASA) (Jet Propulsion Lab., California Inst. of Tech., Pasadena.), and Chwan-Hwa Wu, inventor (to NASA) 7 Jun. 1993 66 p
(Contract NAS7-918)
(NASA-Case-NPO-18790-1-CU; NAS 1.71:NPO-18790-1-CU;
US-Patent-Appl-SN-073018) Avail: CASI HC A04/MF A01

A unipolar terminal-attractor based neural associative memory (TABAM) system with adaptive threshold for perfect convergence is presented. By adaptively setting the threshold values for the dynamic iteration for the unipolar binary neuron states with terminal-attractors for the purpose of reducing the spurious states in a Hopfield neural network for associative memory and using the inner product approach, perfect convergence and correct retrieval is achieved. Simulation is completed with a small number of stored states (M) and a small number of neurons (N) but a large M/N ratio. An experiment with optical exclusive-OR logic operation using LCTV SLMs shows the feasibility of optoelectronic implementation of the models. A complete inner-product TABAM is implemented using a PC for calculation of adaptive threshold values to achieve a unipolar TABAM (UIT) in the case where there is no crosstalk, and a crosstalk model (CRIT) in the case where crosstalk corrupts the desired state. NASA

N94-16559# Mitre Corp., Bedford, MA.
PROCEEDINGS OF THE ASSOCIATION FOR COMPUTING MACHINERY SPECIAL INTEREST GROUP FOR Ada ARTIFICIAL INTELLIGENCE WORKING GROUP
Janet F. Johns Jun. 1993 122 p Workshop held in Bedford, MA, 22-27 Jun. 1992
(AD-A266422; M93B0000072) Avail: CASI HC A06/MF A02

On 24-27 June 1992, the Association for Computing Machinery (ACM) Special Interest Group for Ada (SIGAda) Artificial Intelligence Working Group held a workshop to discuss Ada real-time and Artificial Intelligence (AI) issues. Workshop discussions covered blackboard architectures, experiences and lessons learned, real-time development approaches and issues, and Ada 9X issues for AI systems. These proceedings included papers by workshop participants describing their large-scale AI with Ada systems. A summary of the related workshop experiences and lessons learned discussions in the areas of requirements analysis, design methodologies, development techniques, test and validation, and maintainability are included. DTIC

N94-16580# Rochester Univ., NY. Dept. of Computer Science.
CONTEXTUALLY DEPENDENT CONTROL STRATEGIES FOR MANIPULATION
Polly K. Pook and Dana H. Ballard Apr. 1992 27 p
(Grants NSF IRI-89-03582; NSF IRI-90-10692)
(TR-416) Avail: CASI HC A03/MF A01

Traditional analytic robotics defines grasping by knowing the task geometry and the forces acting on the manipulator precisely. This method is particularly important for non-compliant manipulators with few degrees of freedom, such as a parallel jaw gripper, that overconstrain the solution space. In contrast, the advent of anthropomorphic, high degree-of-freedom grippers allows us to use closed-loop strategies that depend heavily on the task context but do not require precise positioning knowledge. To demonstrate, a robotic hand flips a plastic egg, using the finger joint tendon tensions as the the sole control signal. The manipulator is a compliant, sixteen degree-of-freedom, Utah/MIT hand mounted on a Puma 760 arm. The completion of each subtask, such as picking up the spatula, finding the pan, and sliding the spatula under the egg, is detected by sensing when the tensions of the hand tendons pass a threshold. Beyond this use of tendon tensions and the approximate starting position of the spatula and pan, no model of the task is constructed. The routine is found to be robust to different spatulas and to changes in the location and

orientation of the spatula, egg, and table, with some exceptions. The egg-flipping example relies on interpreting fluctuating tension values within a known temporal sequence of actions. For instance, knowing when the manipulator is trying to touch the pan with the spatula provides the context to interpret changes in tendon tensions. Given the success of this task, we go on to propose a method for analyzing the temporal sensory output for tasks that have not been previously segmented. This method suggests a means for automatically generating robust force control programs to perform previously teleoperated manipulation tasks. Author (revised)

N94-16581# Rochester Univ., NY. Dept. of Computer Science.
VISUALLY GUIDED TOUCHING AND MANUAL TRACKING
Peter A. Sandon Mar. 1992 35 p
(Grant NSF IRI-90-108999)
(TR-412) Avail: CASI HC A03/MF A01

Animate vision depends on an ability to choose a region of the visual environment for task-specific processing. This processing may involve extraction of image features for object classification or identification, or it may involve extraction of viewpoint parameters, such as position, scale and orientation, for guiding movement. It is the role of selective attention to choose the region to be processed in a task-dependent way. This paper describes a real-time implementation of a vision-robotics system that uses the location information provided by the attention mechanism to guide eye movements and arm movements in touching and manual tracking behaviors. Author (revised)

N94-16725# Carnegie-Mellon Univ., Pittsburgh, PA. School of Computer Science.
TEMPORAL SEGMENTATION OF TASKS FROM HUMAN HAND MOTION Report, 1989 - 1993
Sing B. Kang and Katsushi Ikeuchi Apr. 1993 47 p
(Contract F33615-90-C-1465; ARPA Order 7597)
(AD-A266596; CMU-CS-93-150) Avail: CASI HC A03/MF A01

This report describes work on the temporal segmentation of grasping task sequences based on human hand motion. The segmentation process results in the identification of motion breakpoints separating the different constituent phases of the grasping task. A grasping task is composed of three basic phases: pregrasp phase, static grasp phase, and manipulation phase. The pregrasp phase is the initial stage of the grasping task prior to the establishment of a stable grasp (static grasp phase) involved in the task. The manipulation phase refers to the purposeful hand-object interaction performed to achieve a goal in the task. In the pregrasp phase, the trajectory of the hand and the movement of the fingers follow an established pattern. Specifically, it comprises two parallel and simultaneous components: the hand transportation, and the hand preshape. We show that by analyzing the fingertip polygon area (which is an indication of the hand preshape) and the speed of hand movement (which is an indication of the hand transportation), we can divide a task into meaningful action segments such as approach object (which corresponds to the pregrasp phase), grasp object, manipulate object, place object, and depart (a special case of the pregrasp phase which signals the termination of the task). We introduce a measure called the volume sweep rate, which is the product of the fingertip polygon area and the hand speed. The profile of this measure is also used in the determination of the task breakpoints. DTIC

N94-16770# Andersen (Arthur) and Co., Chicago, IL. Center for Strategic Technology Research.
KBSA CONCEPT DEMO Final Report, Sep. 1989 - Sep. 1992
Michael DeBellis, Kanth Miriyala, Sudin Bhat, William C. Sasso, and Owen Rambow Apr. 1993 147 p
(Contract F30602-89-C-0160)
(AD-A267054; RL-TR-93-38) Avail: CASI HC A07/MF A02

The Knowledge-Based Software Assistant (KBSA) Concept Demonstration System project had three main goals: (1) to integrate KBSA technology concepts developed up to the time of the effort into a single life cycle processing system and also to provide additional insight to guide the direction of later KBSA contractual efforts (in particular, to provide insights into the requirements for an integrated high-to-medium-level interface suite, and high-to-medium-level process mediation and coordination); (2) to gain leverage from current industry research in, or related to, KBSA technology areas; and (3) to provide a vehicle for technology transfer to complement the efforts of the KBSA technology Transfer Consortium. This report describes the work accomplished under the project and presents its suggestions for future work in the area. DTIC

N94-16888# Oak Ridge National Lab., TN.
A MODULAR CONTROL ARCHITECTURE FOR REAL-TIME SYNCHRONOUS AND ASYNCHRONOUS SYSTEMS
P. L. Butler and J. P. Jones 1993 12 p Presented at the Society of Photo-Optical Instrumentation Engineers (SPIE) OE/Aerospace Science and Sensing Meeting, Orlando, FL, 11-16 Apr. 1993
(Contract DE-AC05-84OR-21400)
(DE93-015439; CONF-930445-15) Avail: CASI HC A03/MF A01

This paper describes a control architecture for real-time control of complex robotic systems. The Modular Integrated Control Architecture (MICA), which is actually two complementary control systems, recognizes and exploits the differences between asynchronous and synchronous control. The asynchronous control system simulates shared memory on a heterogeneous network. For control information, a portable event-scheme is used. This scheme provides consistent interprocess coordination among multiple tasks on a number of distributed systems. The machines in the network can vary with respect to their native operating systems and the internal representation of numbers they use. The synchronous control system is needed for tight real-time control of complex electromechanical systems such as robot manipulators, and the system uses multiple processors at a specified rate. Both the synchronous and asynchronous portions of MICA have been developed to be extremely modular. MICA presents a simple programming model to code developers and also considers the needs of system integrators and maintainers. MICA has been used successfully in a complex robotics project involving a mobile 7-degree-of-freedom manipulator in a heterogeneous network with a body of software totaling over 100,000 lines of code. MICA has also been used in another robotics system, controlling a commercial long-reach manipulator. DOE

N94-16938# Naval Research Lab., Washington, DC.
INFORMATION TECHNOLOGY DIVISION TECHNICAL PAPER ABSTRACTS
Cathy J. Wiley (JAYCOR, Vienna, VA.) 11 Jun. 1993 76 p
(AD-A266227; NRL/MR/5510-93-7350) Avail: CASI HC A05/MF A01

The accomplishments of projects at the six branches of the Information Technology Division are documented. The six branches are: Navy Center for Applied Research in Artificial Intelligence (NCARAI) including machine learning, intelligent decision aids, natural language, sensor-based systems, and neural networks; Communication Systems; Human-Computer Interaction; Center for Computer High Assurance Systems; Transmission Technology; and Advanced Information Technology. Points of contact are indicated for acquiring additional technical information about the projects, and an order form is provided for obtaining copies of the publications abstracted. DTIC

N94-16986# Naval Postgraduate School, Monterey, CA.
AN OBJECT-ORIENTED PROGRAM SPECIFICATION FOR A MOBILE ROBOT MOTION CONTROL LANGUAGE M.S. Thesis
Carl J. Grim 25 Mar. 1993 119 p
(AD-A267213) Avail: CASI HC A06/MF A02

The Yamabico Research Group at the Naval Postgraduate School is actively pursuing improvements in design and implementation of applications for it's family of autonomous mobile robots. This paper describes a new high level language for controlling the Yamabico-11, surnamed OOPS-MML (Object-Oriented Program Specification for a Mobile robot Motion control Language). Conceptual goals included a user friendly, high level interface coupled with a very abstract, efficient and compartmentalized architecture to employ a path planning and tracking application developed at NPS. The result is a robust and flexible robot control system that is intended to be implemented and employed onboard the Yamabico-11. DTIC

N94-17201 Carnegie-Mellon Univ., Pittsburgh, PA. Dept. of Computer Science.
INTEGRATING REACTIVE AND DELIBERATIVE PLANNING FOR AGENTS
Jim Blythe and W. S. Reilly May 1993 28 p Limited Reproducibility: More than 20% of this document may be affected by microfiche quality
(Contract F33615-90-C-1465; ARPA Order 7597)

(AD-A267631; CMU-CS-93-155) Avail: Issuing Activity (Defense Technical Information Center (DTIC))

Autonomous agents that respond intelligently in dynamic, complex environments need to be both reactive and deliberative. Reactive systems have traditionally fared better than deliberative planners in such environments, but are often hard to code and inflexible. To fill in some of these gaps, we propose a hybrid system that exploits the strengths of both reactive and deliberative systems. We demonstrate how out system controls a simulated household robot and compare our system to a purely reactive one in this domain. We also look at a number of relevant issues in anytime planning. DTIC

N94-17202 Teleos Research, Palo Alto, CA.
ARPA UNMANNED GROUND VEHICLE STEREO VISION PROGRAM AT TELEOS RESEARCH Annual Report, Dec. 1991 - 1992
H. K. Nishihara Apr. 1993 36 p Limited Reproducibility: More than 20% of this document may be affected by microfiche quality
(Contract DACA76-92-C-0005)
(AD-A267632; TEC-0034) Avail: Issuing Activity (Defense Technical Information Center (DTIC))

This report reviews the work done during 1992 at Teleos Research in support of ARPA's UGV program. It first gives a broad overview of Teleos' approach to studying visual perception. In particular, the concept of minimal-meaningful-measurement tools is developed as a natural methodology for allowing a higher level application process to easily influence and exploit basic measurement modalities. The sign correlation algorithm under development at Teleos is then described in this context and the current performance benchmarks of our accelerator technology are presented. Several important results in stereo theory were obtained this year including: the development of techniques for automatically setting stereo matcher operating parameters, an analysis identifying the principal parameters affecting the magnitude of the disparity gradient effects, and a technique for improving area correlator performance in the presence of large stereo disparity gradients. Contributions were also made to the development and implementation of methods for evaluating stereo matching algorithms. UGV application specific studies were carried out in the areas of narrow-field-of-view stereo; wide field-of-view, high-resolution stereo mosaic building; stereo landmark navigation; 3-D tracking of moving objects; evaluation of hardware accelerators; and development of a low-cost mobile test facility. DTIC

N94-17287 Oak Ridge National Lab., TN.
IMAGE ACCURACY AND REPRESENTATIONAL ENHANCEMENT THROUGH LOW-LEVEL, MULTI-SENSOR INTEGRATION TECHNIQUES
J. E. Baker May 1993 43 p Limited Reproducibility: More than 20% of this document may be affected by microfiche quality
(Contract DE-AC05-84OR-21400)
(DE93-014888; ORNL/TM-12218) Avail: CASI HC A03

Multi-Sensor Integration (MSI) is the combining of data and information from more than one source in order to generate a more reliable and consistent representation of the environment. The need for MSI derives largely from basic ambiguities inherent in our current sensor imaging technologies. These ambiguities exist as long as the mapping from reality to image is not 1-to-1. That is, if different 'realities' lead to identical images, a single image cannot reveal the particular reality which was the truth. MSI techniques can be divided into three categories based on the relative information content of the original images with that of the desired representation: (1) 'detail enhancement,' wherein the relative information content of the original images is less rich than the desired representation; (2) 'data enhancement,' wherein the MSI techniques are concerned with improving the accuracy of the data rather than either increasing or decreasing the level of detail; and (3) 'conceptual enhancement,' wherein the image contains more detail than is desired, making it difficult to easily recognize objects of interest. In conceptual enhancement one must group pixels corresponding to the same conceptual object and thereby reduce the level of extraneous detail. This research focuses on data and conceptual enhancement algorithms. To be useful in many real-world applications, e.g., autonomous or teleoperated robotics, real-time feedback is critical. But, many MSI/image processing algorithms require significant processing time. This is especially true of feature extraction, object isolation, and object recognition algorithms due to their typical reliance on global or large neighborhood information. This research attempts to exploit the speed currently available in state-of-the-art digitizers and highly parallel processing systems by developing MSI algorithms based on pixel rather than global-level features. DOE

N94-17369# Air Force Inst. of Tech., Wright-Patterson AFB, OH.
DISCRETE SLIDING MODE CONTROL FOR NONLINEAR SAMPLED DATA SYSTEMS Ph.D. Thesis
Jean M. Fernand 1993 190 p
(AD-A267500; AFIT/CI/CIA-93-008D) Avail: CASI HC A09/MF A02

Nonlinear control theory has been successfully applied to continuous, nonlinear, autonomous plant models. Implementation of these continuous control laws, using digital computers, has relied upon high sample frequencies to approximate the performance of continuous control. This thesis extends the design of continuous sliding mode control to discrete and to sampled data systems. Continuous, nonlinear, autonomous, second order dynamic plant models are discretized using an approximation to a Taylor series expansion. The discretization process accounts for the Zero Order Hold circuit, used to convert the discrete control output of the digital computer, into a piecewise continuous control input to the plant. A Discrete Sliding Mode Control is developed using Feedback Linearization to account for plant model nonlinearities, and Lyapunov Stability analysis to guarantee convergence to the sliding manifold. A five step design process systematizes the design technique. The design technique was applied to two unstable nonlinear second order plant models. Stability was confirmed by simulation studies. Comparison with the Continuous Sliding Mode Control implemented digitally, at a sample rate five times the plant model fundamental frequency, showed that the Discrete Sliding Mode Control retained asymptotic stability while the Continuous Sliding Mode Control did not. DTIC

N94-17392# Naval Civil Engineering Lab., Port Hueneme, CA.
OPTIMAL TUNING OF HEAVY EQUIPMENT MOTION CONTROLLERS Final Report
William V. Miller and William N. Varnava Feb. 1993 102 p
(AD-A267873; NCEL-TR-940) Avail: CASI HC A06/MF A02

The objective of this work is the demonstration of feasibility of computerized optimal tuning of electronic motion controllers for mobile heavy equipment end-effectors. A backhoe yaw mode position control system was selected as the application for the purpose of proof of concept. The control algorithm selected for use in the servocontroller is Pseudo-Derivative Feedback (PDF). A computer model and an operational laboratory model of a translational electrohydraulic position control system dynamically analogous to the structural, mechanical, and hydraulic components of the selected backhoe position control system were constructed. These models were exercised in simulation of the backhoe system equipped with an electronic servocontroller incorporating the PDF algorithm. The computer model was first validated in its baseline configuration by way of comparison with baseline laboratory model test results. 'Baseline' refers to the complete system, but with proportional position feedback control in place of the PDF algorithm. An interesting aspect of this project is the two degree-of-freedom system constituted by the relatively compliant boom coupling the hydraulic actuator with a fully loaded bucket. This is of particular interest since the bucket does not lend itself to position instrumentation, thereby precluding load position feedback. Data supporting the successful demonstration of computerized automation of optimal tuning is presented. DTIC

N94-17506# California Inst. of Tech., Pasadena. Dept. of Electrical Engineering.
ROBUST CONTROL OF UNCERTAIN NONLINEAR SYSTEMS Final Report
1992 5 p
(AD-A268056) Avail: CASI HC A01/MF A01

Several new results were obtained extending standard analysis techniques to Linear Fractional Transformations (LFT) using Structured Singular Value, Micron, and Linear Matrix Inequalities (LMI) in solving LFT problems. LFT's and LMI's play a very important role in postmodern control theory by providing a framework that unifies many concepts and generalizes transfer functions and their state-space realizations to include uncertainty. Doyle, Zhou, and Packard reviews known results on robust stability and performance and establishes a common and unified framework for the companion papers, which consider generalizations and extensions of

balanced realizations and model reduction, stabilization, optimal control, mixed real/complex micron, model validation, and LMI computation. DTIC

N94-17517 Air Force Inst. of Tech., Wright-Patterson AFB, OH.
RELIABILITY AND MAINTAINABILITY OF MODULAR ROBOT SYSTEMS: A ROADMAP FOR DESIGN Ph.D. Thesis
Dean L. Schneider Aug. 1993 441 p Limited Reproducibility: More than 20% of this document may be affected by microfiche quality
(AD-A268104; AFIT/CI/CIA-93-004D) Avail: Issuing Activity (Defense Technical Information Center (DTIC))

As robotic technology is considered for use in extreme environments, such as on-orbit and planetary exploration missions, the availability of the robotic systems become of paramount concern. Availability has two components: Reliability and Maintainability (R and M). Modular robotic systems address the maintainability portion of availability by minimizing repair time and allowing for the optimal reconfiguration of the robotic system for different tasks. The remaining portion of availability is the reliability of the modular robotic system. This dissertation presents a review of robotic system reliability technology and develops a technology roadmap outlining future directions for research and technology application that will improve the reliability of modular robotic systems. Also developed and tested is a design index based upon a modular robotic system's hardware and software reliability and the precision of the system. DTIC

N94-16155# Army Missile Research, Development and Engineering Lab., Redstone Arsenal, AL. Weapons Sciences Directorate.
REAL-TIME ADAPTIVE NEURAL NETWORK DATA PROCESSING
S. D. Pethel, C. M. Bowden, and C. C. Sung (Alabama Univ., Huntsville.) *In* Huntsville Association of Technical Societies, TABES 1993: 9th Annual Technical and Business Exhibition and Symposium 1993 7 p (For primary document see N94-16129 03-38)
(TABES Paper 93-660) Avail: CASI HC A02/MF A03

N94-16705*# Jet Propulsion Lab., California Inst. of Tech., Pasadena.
AVIRIS DATA AND NEURAL NETWORKS APPLIED TO AN URBAN ECOSYSTEM
Merrill K. Ridd (Utah Univ., Salt Lake City.), Niles D. Ritter, Nevin A. Bryant, and Robert O. Green *In its* Summaries of the Third Annual JPL Airborne Geoscience Workshop. Volume 1: AVIRIS Workshop 1 Jun. 1992 p 129-131 (For primary document see N94-16666 03-42)
Avail: CASI HC A01/MF A02

64 NUMERICAL ANALYSIS

Includes iteration, difference equations, and numerical approximation.

N94-14928# Fermi National Accelerator Lab., Batavia, IL.
AUTOMATIC DIFFERENTIATION OF LIMIT FUNCTIONS
L. Michelotti May 1993 5 p Presented at the International Particle Accelerator Conference, Washington, DC, 17-20 May 1993
(Contract DE-AC02-76CH-03000)
(DE93-016376; FNAL/C-93/135; CONF-930511-209) Avail: CASI HC A01/MF A01

Automatic differentiation can be used to evaluate the derivatives of and set up Taylor series for implicitly defined functions and maps. The author provides several examples of how this works, within the context of the MXYZPTLK class library, and discusses its extension to inverse functions. The techniques of automatic differentiation and differential algebra are rapidly becoming a standard part of accelerator physicists' arsenals. DOE

N94-14933 Joint Inst. for Nuclear Research, Dubna (USSR). Lab. of Computing Techniques and Automation.
ITERATION SCHEME FOR THE MULTIPARAMETER NONLINEAR BOUNDARY VALUE PROBLEM WITH THE ADDITIONAL CONDITIONS AND ITS APPLICATION TO SOME FIELD MODELS
I. V. Amirkhanov, I. V. Puzynin, and T. A. Strizh 1992 14 p Limited Reproducibility: More than 20% of this document may be affected by microfiche quality
(DE93-626638; JINR-E-11-92-236) Avail: CASI HC A03 (US Sales Only)

The iterative scheme based on the combination of continuous analog of the Newton's method and continuation method was developed for the solving a boundary value problem together with an additional condition. The accuracy was investigated numerically. The suggested method was applied for the numerical investigation of the equations of the solvated electron problem, of some bielectron problem, and one QCD problem with an increasing potential. DOE

N94-14939 Maryland Univ., College Park. Inst. for Physical Science and Technology.
A POSTERIORI ERROR ESTIMATION FOR HIERARCHIC MODELS OF ELLIPTIC BOUNDARY VALUE PROBLEMS ON THIN DOMAINS Final Report
Ivo Babuska and C. Schwab May 1993 45 p Limited Reproducibility: More than 20% of this document may be affected by microfiche quality
(Contract N00014-90-J-1030)
(AD-A267714) Avail: Issuing Activity (Defense Technical Information Center (DTIC))

The boundary value problem of heat conduction in a three dimensional, laminated plate is approximated by a hierarchy of two dimensional models. Computable a-posteriori indicators and estimators of the modeling error in various norms are derived and their local spectral and asymptotic exactness is proved. Sharp estimates for their effectivity indices are also obtained. DTIC

N94-15112*# Research Inst. for Advanced Computer Science, Moffett Field, CA.
THE ALIGNMENT-DISTRIBUTION GRAPH
Siddhartha Chatterjee, John R. Gilbert (Xerox Palo Alto Research Center, CA.), and Robert Schreiber Aug. 1993 17 p Proceeding of the Sixth Annual Languages and Compilers for Parallelism Workshop held in Portland, OR, 12-14 Aug. 1993
(Contract NAS2-13721)
(NASA-CR-194292; NAS 1.26:194292; RIACS-TR-93-06) Copyright Avail: CASI HC A03/MF A01

Implementing a data-parallel language such as Fortran 90 on a distributed-memory parallel computer requires distributing aggregate data objects (such as arrays) among the memory modules attached to the processors. The mapping of objects to the machine determines the amount of residual communication needed to bring operands of parallel operations into alignment with each other. We present a program representation called the alignment distribution graph that makes these communication requirements explicit. We describe the details of the representation, show how to model communication cost in this framework, and outline several algorithms for determining object mappings that approximately minimize residual communication. Author

N94-15724*# Institute for Computer Applications in Science and Engineering, Hampton, VA.
A PARALLEL ADAPTIVE MESH REFINEMENT ALGORITHM
James J. Quirk and Ulf R. Hanebutte Washington Aug. 1993 31 p Submitted for publication
(Contract NAS1-19480; RTOP 505-90-52-01)
(NASA-CR-191530; NAS 1.26:191530; ICASE-93-63) Avail: CASI HC A03/MF A01

Over recent years, Adaptive Mesh Refinement (AMR) algorithms which dynamically match the local resolution of the computational grid to the numerical solution being sought have emerged as powerful tools for solving problems that contain disparate length and time scales. In particular, several workers have demonstrated the effectiveness of employing an adaptive, block-structured hierarchical grid system for simulations of complex shock wave phenomena. Unfortunately, from the parallel algorithm developer's viewpoint, this class of scheme is quite involved; these schemes cannot be distilled down to a small kernel upon which various parallelizing strategies may be tested. However, because of their block-structured nature such schemes are inherently parallel, so all is not lost. In this paper we describe the method by which Quirk's AMR algorithm has been parallelized. This method is built upon just a few simple message passing routines and so it may be implemented across a broad class of MIMD machines. Moreover, the method of parallelization is such that the original serial code is left virtually intact, and so we are left with just a single product to support. The importance of this fact should not be underestimated given the size and complexity of the original algorithm. Author

N94-15779# Illinois Univ., Urbana. Dept. of Computer Science.
MONOTONE APPROXIMATE QUERY PROCESSING Final Report, 1 Apr. 1990 - 30 Sep. 1992
Jane Liu 30 Sep. 1992 19 p
(Grant AF-AFOSR-0193-90)
(AD-A267153; AFOSR-93-0478TR) Avail: CASI HC A03/MF A01

This project was concerned with means to provide approximate answers to queries. The researchers developed a monotone query processing scheme. This scheme allows a data base system to provide for each a series of intermediate answers that are approximations of the exact answer. The approximate answers improve monotonically in accuracy as more data are retrieved and processed to answer the query. If for any reason query processing must be terminated prematurely before the exact answer is produced, the latest intermediate answer, that is, the best approximate answer produced so far, is made available to the application. For many time-critical applications, a timely approximate answer that is sufficiently good is better than no answer at all or the late exact answer. DTIC

N94-15785 Lowell Univ., MA. Research Foundation.
VOLUME INTEGRAL EQUATIONS APPLIED TO CIRCULAR AND SQUARE CYLINDERS Final Report
Rose W. Wang Dec. 1992 100 p Limited Reproducibility: More than 20% of this document may be affected by poor print
(Contract F30602-91-D-0001)
(AD-A266635; RL-TR-92-300) Avail: Issuing Activity (Defense Technical Information Center (DTIC))

Three numerical integration methods are developed and used for evaluating the highly singular dyadic Green's function in the volume integral equations for scattering from dielectric cylinders. Numerical results indicate that for small permittivities or relatively small dielectric cylinders, the methods are quite efficient and give comparable accuracy. However, when both the relative permittivity and the size of the cylinder are increased, we experienced problems similar to those encountered by a number of previous researchers, namely, the results converge slowly for the TE polarization. DTIC

N94-15799*# National Aeronautics and Space Administration. Lewis Research Center, Cleveland, OH.
MODAL ELEMENT METHOD FOR POTENTIAL FLOW IN NON-UNIFORM DUCTS: COMBINING CLOSED FORM ANALYSIS WITH CFD
Kenneth J. Baumeister and Joseph F. Baumeister Jan. 1994 18 p Prepared for presentation at the 32nd Aerospace Sciences Meeting and Exhibit, Reno, NV, 10-13 Jan. 1994; sponsored by AIAA
(RTOP 505-62-52)
(NASA-TM-106347; AIAA Paper 93-0813; E-8118; NAS 1.15:106347)
Avail: CASI HC A03/MF A01

An analytical procedure is presented, called the modal element method, that combines numerical grid based algorithms with eigenfunction expansions developed by separation of variables. A modal element method is presented for solving potential flow in a channel with two-dimensional cylindrical like obstacles. The infinite computational region is divided into three subdomains; the bounded finite element domain, which is characterized by the cylindrical obstacle and the surrounding unbounded uniform channel entrance and exit domains. The velocity potential is represented approximately in the grid based domain by a finite element solution and is represented analytically by an eigenfunction expansion in the uniform semi-infinite entrance and exit domains. The calculated flow fields are in excellent agreement with exact analytical solutions. By eliminating the grid surrounding the obstacle, the modal element method reduces the numerical grid size, employs a more precise far field boundary condition, as well as giving theoretical insight to the interaction of the obstacle with the mean flow. Although the analysis focuses on a specific geometry, the formulation is general and can be applied to a variety of problems as seen by a comparison to companion theories in aeroacoustics and electromagnetics. Author

N94-15818*# National Aeronautics and Space Administration. Lewis Research Center, Cleveland, OH.
ON THE STABILITY ANALYSIS OF APPROXIMATE FACTORIZATION METHODS FOR 3D EULER AND NAVIER-STOKES EQUATIONS
A. O. Demuren (Old Dominion Univ., Norfolk, VA.) and S. O. Ibraheem (Old Dominion Univ., Norfolk, VA.) Oct. 1993 39 p
(Contract NCC3-233; RTOP 505-90-5K)
(NASA-TM-106314; ICOMP-93-29; E-8054; NAS 1.15:106314) Avail: CASI HC A03/MF A01

The convergence characteristics of various approximate factorizations for the 3D Euler and Navier-Stokes equations are examined using the von-Neumann stability analysis method. Three upwind-difference based factorizations and several central-difference based factorizations are considered for the Euler equations. In the upwind factorizations both the flux-vector splitting methods of Steger and Warming and van Leer are considered. Analysis of the Navier-Stokes equations is performed only on the Beam and Warming central-difference scheme. The range of CFL numbers over which each factorization is stable is presented for one-, two-, and three-dimensional flow. Also presented for each factorization is the CFL number at which the maximum eigenvalue is minimized, for all Fourier components, as well as for the high frequency range only. The latter is useful for predicting the effectiveness of multigrid procedures with these schemes as smoothers. Further, local mode analysis is performed to test the suitability of using a uniform flow field in the stability analysis. Some inconsistencies in the results from previous analyses are resolved. Author

N94-15833*# Institute for Computer Applications in Science and Engineering, Hampton, VA.
ADAPTIVE WAVELET COLLOCATION METHODS FOR INITIAL VALUE BOUNDARY PROBLEMS OF NONLINEAR PDE'S Final Report
Wei Cai and Jian-Zhong Wang Jul. 1993 53 p Submitted for publication
(Contract NAS1-19480; NSF ASC-91-13895; RTOP 505-90-52-01)
(NASA-CR-191507; NAS 1.26:191507; ICASE-93-48) Avail: CASI HC A04/MF A01

We have designed a cubic spline wavelet decomposition for the Sobolev space H(sup 2)(sub 0)(I) where I is a bounded interval. Based on a special 'point-wise orthogonality' of the wavelet basis functions, a fast Discrete Wavelet Transform (DWT) is constructed. This DWT transform will map discrete samples of a function to its wavelet expansion coefficients in O(N log N) operations. Using this transform, we propose a collocation method for the initial value boundary problem of nonlinear PDE's. Then, we test the efficiency of the DWT transform and apply the collocation method to solve linear and nonlinear PDE's. Author

N94-15979# Los Alamos National Lab., NM.
EFFICIENCY EFFECTS OF VARIATION IN CONTROLLED EXPERIMENTAL VARIABLES
J. R. Wendelberger 1993 19 p Presented at the American Statistical Association Conference, San Francisco, CA, 11 Aug. 1993
(Contract W-7405-eng-36)
(DE93-014345; LA-UR-93-1981; CONF-9308107-1) Avail: CASI HC A03/MF A01

When a designed experiment is conducted, the exact levels of controlled experimental variables specified by the design may not be attainable. Two different types of situations can occur in which the actual settings of the design variables deviate from the target design settings. In one case, the actual settings obtained are unknown. In the other case, the actual settings are known; however, desirable design properties such as orthogonality may have been lost. This paper examines the impact of known and unknown errors in experimental variables for designed experiments in which the response is assumed to be approximately linear in the region of interest. For comparison, the well known situation where the target values of the experimental variables can actually be obtained will also be considered. DOE

N94-16127# Vanderbilt Univ., Nashville, TN. Dept. of Mathematics.
HOMOGENEOUSLY TRACEABLE RESULTS IN CLAW-FREE GRAPHS
Lisa R. Markus Jun. 1993 26 p
(Contract N00014-91-J-1142)
(AD-A266196) Avail: CASI HC A03/MF A01

A graph is homogeneously traceable if for each v in V(C) there is a Hamilton path starting at v. In this paper we find a sufficient condition for a claw-free graph to be homogeneously traceable in terms of a neighborhood union condition. DTIC

N94-16167# Oak Ridge National Lab., TN.
GENERAL ORDER CHARACTERISTIC METHODS FOR SOLVING NEUTRON TRANSPORT PROBLEMS
Y. Y. Azmy 1992 27 p Presented at the International Symposium on Transport Theory, Moscow, Russia, 23-31 May 1992
(Contract DE-AC05-84OR-21400)
(DE93-015824; CONF-9205173-1-Vugraphs) Avail: CASI HC A03/MF A01

The neutron transport equation in Cartesian geometry possesses straight line characteristics along which the streaming operator can be written as a full differential in terms of the characteristic length. This idea was used by Lathrop to develop the step characteristic method, which he showed to be positive definite but less accurate than conventional Diamond-Difference schemes. Several authors since then have developed new methods utilizing the characteristic curves (including non-Cartesian geometry). A Linear Characteristic Method, based on a more consistent linear representation of the incoming-surface and within-cell angular flux, has been developed and tested in two-dimensional geometry producing highly accurate and computationally efficient results. A similar linear method, with several modifications, was developed for three-dimensional Cartesian geometry, and implemented in ORNL's production code TORT. In this paper is presented a fully consistent, two-dimensional Cartesian geometry, general order characteristic method, in the same spirit as the previously developed, general order nodal method. Preliminary tests and numerical error analysis of the new method for orders up to five are also presented. DOE

N94-16582# Rochester Univ., NY. Dept. of Computer Science.
SET-BASED BAYESIANISM
Henry E. Kyburg, Jr. and Michael Pittarelli Mar. 1992 42 p Sponsored in part by NSF, Army Signals Warfare Center and State Univ. of New York (TR-407) Avail: CASI HC A03/MF A01

Problems for strict and convex Bayesianism are discussed. A set-based Bayesianism generalizing convex Bayesianism and intervalism is proposed. This approach abandons not only the strict Bayesian requirement of a unique real-valued probability function in any decision-making context but also the requirement of convexity for a set-based representation of uncertainty. Levi's E-admissibility decision criterion is retained and is shown to be applicable in the non-convex case. Author (revised)

N94-16778# Argonne National Lab., IL.
OPERATOR OVERLOADING AS AN ENABLING TECHNOLOGY FOR AUTOMATIC DIFFERENTIATION
G. F. Corliss (Marquette Univ., Milwaukee, WI.) and A. Griewank 1993 12 p Presented at the Object-Oriented Numerics Conference, Sunriver, OR, 25-27 Apr. 1993
(Contract W-31-109-eng-38)
(DE93-012899; ANL/MCS/CP-79481; CONF-9304114-5) Avail: CASI HC A03/MF A01

We present an example of the science that is enabled by object-oriented programming techniques. Scientific computation often needs derivatives for solving nonlinear systems such as those arising in many PDE algorithms, optimization, parameter identification, stiff ordinary differential equations, or sensitivity analysis. Automatic differentiation computes derivatives accurately and efficiently by applying the chain rule to each arithmetic operation or elementary function. Operator overloading enables the techniques of either the forward or the reverse mode of automatic differentiation to be applied to real-world scientific problems. We illustrate automatic differentiation with an example drawn from a model of unsaturated flow in a porous medium. The problem arises from planning for the long-term storage of radioactive waste. DOE

N94-16882*# National Aeronautics and Space Administration. Lewis Research Center, Cleveland, OH.
ACCURATE UPWIND METHODS FOR THE EULER EQUATIONS
Hung T. Huynh Nov. 1993 76 p
(RTOP 505-62-52)
(NASA-TM-106388; E-8210; NAS 1.15:106388) Avail: CASI HC A05/MF A01

A new class of piecewise linear methods for the numerical solution of the one-dimensional Euler equations of gas dynamics is presented. These methods are uniformly second-order accurate, and can be considered as extensions of Godunov's scheme. With an appropriate definition of monotonicity preservation for the case of linear convection, it can be shown that they preserve monotonicity. Similar to Van Leer's MUSCL scheme, they consist of two key steps: a reconstruction step followed by an upwind step. For the reconstruction step, a monotonicity constraint that preserves uniform second-order accuracy is introduced. Computational efficiency is enhanced by devising a criterion that detects the 'smooth' part of the data where the constraint is redundant. The concept and coding of the constraint are simplified by the use of the median function. A slope steepening technique, which has no effect at smooth regions and can resolve a contact discontinuity in four cells, is described. As for the upwind step, existing and new methods are applied in a manner slightly different from those in the literature. These methods are derived by approximating the Euler equations via linearization and diagonalization. At a 'smooth' interface, Harten, Lax, and Van Leer's one intermediate state model is employed. A modification for this model that can resolve contact discontinuities is presented. Near a discontinuity, either this modified model or a more accurate one, namely, Roe's flux-difference splitting. is used. The current presentation of Roe's method, via the conceptually simple flux-vector splitting, not only establishes a connection between the two splittings, but also leads to an admissibility correction with no conditional statement, and an efficient approximation to Osher's approximate Riemann solver. These reconstruction and upwind steps result in schemes that are uniformly second-order accurate and economical at smooth regions, and yield high resolution at discontinuities. Author

N94-16940# South Carolina Univ., Columbia. Dept. of Mathematics and Statistics.
APPLICATIONS OF THE PHI-TRANSFORM Final Report, 1 Oct. 1989 - Mar. 1993
Ronald DeVore and B. Jawerth Mar. 1993 9 p
(Grant AF-AFOSR-0455-89)
(AD-A266247; AFOSR-93-0442TR) Avail: CASI HC A02/MF A01

Research on this project has centered on the Phi-transform and wavelets and their application to various problems in image/signal processing, differential equations, and computer aided design. While the Phi-transform and wavelets have been developed in a quite general setting, several applications, most notably in image processing and numerical methods for differential equations, have pointed to several deficiencies in the traditional wavelet constructions. This has led researchers to consider alternate constructions of wavelets and related questions. Partial Differential Equations Concentration has been on two of the most prominent problems in partial differential equations: nonlinear equations such as conservation laws which arise in the study of wave propagation; and elliptic problems on nonsmooth domains which arise in scattering theory and many aspects of computer aided design. Researchers have investigated algorithms for image and surface compression based on wavelet decompositions. The algorithms developed have been shown by researchers to be optimal methods for compression in the sense of width or optimal recovery. They have continued their development of the second generation of the CAD system SLIP. They now have a prototype running which allows them to reconstruct a 3D CAD description from photographic images of a manufactured part. They continue their collaboration with various industries, government laboratories, and university centers. DTIC

N94-17045# Polish Academy of Sciences, Warsaw. Inst. Podstawowych Problemow Techniki.
INVARIANCE OF SLIP MOVEMENTS WITH RESPECT TO THE CONTROL MATRIX [INWARIANTNOSC RUCHOW POSLIZGOWYCH WZGLEDEM MACIERZY STERIOWANIA]
Stefan Kotowski 1991 19 p In POLISH
(IFTR-43/1991) Avail: CASI HC A03/MF A01

This study proves the claim that smooth solutions of systems of differential equations with discontinuous functions and a linear control describing mechanical systems are independent of the parameters of the matrix executing control. NTIS

N94-17076# Air Force Inst. of Tech., Wright-Patterson AFB, OH.
ENERGY POTENTIAL ANALYSIS OF ZERO VELOCITY CURVES IN THE RESTRICTED THREE-BODY PROBLEM M.S. Thesis
Christopher M. Tuason May 1993 63 p
(AD-A267512; AFIT/CI/CIA-93-096) Avail: CASI HC A04/MF A01

The restricted problem of three bodies is a more tractable case than

the general three-body problem. Two primary celestial bodies are restricted to a circular orbit while a third body of negligible mass orbits in the plane of motion established by the primaries. Among many other practical applications, these restrictions form a rough approximation to the Earth, Moon, and spacecraft problem. This study analyzes the restricted problem by superposition of the energy potential wells that arise from the gravitational and inertial forces of the primaries in their circular motion. Three dimensional computer graphics are used to illustrate the surfaces that are created by the potential of the primaries. Zero velocity curves, also known as Hill's curves, describe the boundary between regions of possible motion and forbidden regions for the third body. These curves are the principle qualitative aspect of the restricted problem. A curve of zero velocity is found by taking a cross-section of the potential surface at a specific energy level corresponding to the Jacobian constant of the third body. The topology of a zero velocity curve may change depending on the energy of the third body. The Lagrange equilibrium points are clearly shown to be located at the critical energy levels where the topology of the zero velocity curves change. The superposition analysis in a three dimensional representation clearly reveals the component forces involved in the restricted problem and provide a visual model for understanding the stability of motion near the equilibrium points. DTIC

N94-17314 Joint Inst. for Nuclear Research, Dubna (USSR). Lab. of Theoretical Physics.
MULTIPOLAR-LIKE FORM OF NONABELIAN GAUGE THEORIES
M. I. Shirokov 1992 14 p Limited Reproducibility: More than 20% of this document may be affected by microfiche quality
(DE93-626690; JINR-E-2-92-269) Avail: CASI HC A03 (US Sales Only)

A notion of the multipolar form of QED is exemplified by using its version valid for neutral systems such as two unlike charges. A new potential-like term P(sub perpendicular) arises in the multipolar Hamiltonian. It is shown to be a confining potential in a regularized variant of the multipolar form. This attracts interest to the discussion of multipolar-like form of nonabelian theories. The form is constructed for the case of nonquantized quarks interacting with gluons. A confining potential is shown to arise which is similar to P(sub perpendicular). But its relevance to the quark confinement problem requires further investigations. DOE

N94-17393# Naval Undersea Warfare Center, Newport, RI.
CLOSED FORM CHARACTERISTIC FUNCTION FOR GENERAL COMPLEX SECOND-ORDER FORM IN CORRELATED COMPLEX GAUSSIAN RANDOM VARIABLES Progress Report
Albert H. Nuttall 12 Jul. 1993 64 p
(AD-A267883; NUWC-NPT-TR-10403) Avail: CASI HC A04/MF A01

The properties of the left and right eigenvectors of generalized characteristic value problems with non-Hermitian complex matrices are reviewed, and diagonal expansions of various matrix combinations and inverses are derived. The interrelationships of the solutions of two related non-Hermitian characteristic value problems are determined and found to be simply related to the earlier eigenvectors and their properties. These results are then applied to the evaluation of the characteristic function of a general complex second-order form in correlated Gaussian random variables. The end result is a compact closed form result involving a finite product and a finite sum, along with one square root and exponential. This expression allows for rapid evaluation of the characteristic function for numerous values of its complex argument. DTIC

N94-17420 Yale Univ., New Haven, CT. Dept. of Computer Science.
FAST FOURIER TRANSFORMS FOR NONEQUISPACED DATA 2 Research Report
A. Dutt and V. Rokhlin Aug. 1993 30 p Limited Reproducibility: More than 20% of this document may be affected by microfiche quality
(Contract N00014-89-J-1527)
(AD-A268383; YALEU/DCS/RR-980) Avail: CASI HC A03

A group of algorithms is presented generalizing the Fast Fourier Transform to the case of noninteger frequencies and non equispaced nodes on the interval (-Pi, Pi). The schemes of this paper are based on a combination of the classical Fast Fourier Transform with a version of the Fast Multipole Method, and generalize both the forward and backward FFT's. DTIC

N94-17521 Air Force Inst. of Tech., Wright-Patterson AFB, OH.
NUMERICAL SOLUTION OF A SECOND ORDER BOUNDARY PROBLEM FOR TWO DIMENSIONS USING GALERKIN APPROXIMATIONS M.S. Thesis
Craig L. Arnold Apr. 1993 148 p Limited Reproducibility: More than 20% of this document may be affected by microfiche quality
(AD-A268126; AFIT/CI/CIA-93-058) Avail: CASI HC A07

This report outlines the development and use of the program LAPLACE. LAPLACE is capable of solving a second order two dimensional boundary value problem, employing graphics to assist in mesh generation and solution presentation. Galerkin approximation methods, along with the development of a finite element mesh, permit the program to calculate nodal results over the domain of the problem. The use of these nodal solutions with additional subroutines allows for the computation of equipotential lines and lines perpendicular to the equipotential lines. The current format of this program solves Laplace's Equation. Nodal solutions to Laplace's Equation are calculated over the domain of the problem and used as the basis for the generation of equipotential lines and their perpendiculars. Equipotential lines are interpreted as contours and their perpendiculars represent flow lines for the solution to Laplace's Equation. These lines are used in combination to develop a flow net over the domain of the problem and this flow net is graphically displayed. This program was written with the capability of solving several types of second order two dimensional boundary value problems. The calculation of solutions to other second order two dimensional boundary value problems is accomplished by entering the appropriate functional coefficients of the differential equation into one subroutine. DTIC

N94-17613 International Centre for Theoretical Physics, Trieste (Italy).
ON A CLASS OF SINGULAR QUASILINEAR ELLIPTIC EQUATIONS WITH GENERAL STRUCTURE AND DISTRIBUTION DATA
Le Dung May 1993 26 p Limited Reproducibility: More than 20% of this document may be affected by microfiche quality
(DE93-628585; IC-93/108) Avail: CASI HC A03 (US Sales Only)

We present a C(sup 1,(alpha)) regularity theory for a large class of singular quasilinear elliptic equations having general structure and involving distribution data in some Campanato-Morrey spaces M(sub (lambda))(sup -1,p'). An optimal equivalent relation between the regularity of weak solutions and the growth of data will be proved. The Holder continuity of solutions near the boundary is also given. Our results extend and complete those of Rakotoson and Ziemer. DOE

N94-17640 International Centre for Theoretical Physics, Trieste (Italy).
GLOBAL SOLUTIONS TO A SYSTEM OF STRONGLY COUPLED REACTION-DIFFUSION EQUATIONS
Mokhtar Kirane and Said Kouachi (Ecole Normale Superieure, Abidjan, Ivory Coast.) Apr. 1993 14 p Limited Reproducibility: More than 20% of this document may be affected by microfiche quality
(DE93-628587; IC-93/72) Avail: CASI HC A03 (US Sales Only)

The paper discusses the existence of globally bounded-in-time classical solutions for a system of strongly coupled reaction-diffusion equations under homogenous boundary conditions. DOE

N94-17642 International Centre for Theoretical Physics, Trieste (Italy).
ASYMPTOTIC BEHAVIOR OF FIRMLY NON EXPANSIVE SEQUENCES
B. D. Rouhani Apr. 1993 12 p Limited Reproducibility: More than 20% of this document may be affected by microfiche quality
(DE93-628589; IC-93/82) Avail: CASI HC A03 (US Sales Only)

We introduce the notion of firmly non expansive sequences in a Banach space and present several results concerning their asymptotic behaviour extending previous results and giving an affirmative answer to an open question raised by S. Reich and I. Shafir. Applications to averaged mappings are also given. DOE

N94-17667 International Centre for Theoretical Physics, Trieste (Italy).
STEEPEST DESCENT APPROXIMATIONS FOR ACCRETIVE OPERATOR EQUATIONS
C. E. Chidume Mar. 1993 20 p Limited Reproducibility: More than 20% of this document may be affected by microfiche quality
(DE93-628586; IC-93/43) Avail: CASI HC A03 (US Sales Only)

A necessary and sufficient condition is established for the strong

convergence of the steepest descent approximation to a solution of equations involving quasi-accretive operators defined on a uniformly smooth Banach space. DOE

N94-15592*# Royal Greenwich Observatory, Cambridge (England).
FORMATION OF ON-SITE NORMAL POINTS
G. M. Appleby and Andrew T. Sinclair *In* NASA. Goddard Space Flight Center, Eighth International Workshop on Laser Ranging Instrumentation Jun. 1993 7 p (For primary document see N94-15552 03-19)
Avail: CASI HC A02/MF A06

65 STATISTICS AND PROBABILITY

Includes data sampling and smoothing; Monte Carlo method; and stochastic processes.

N94-15002# Stanford Univ., CA. Dept. of Statistics.
THE DISTRIBUTION OF A SUM OF BINOMIAL RANDOM VARIABLES
Ken Butler and Michael Stephens 28 Apr. 1993 15 p
(Contract N00014-92-J-1264)
(AD-A266969) Avail: CASI HC A03/MF A01

In this paper we examine the distribution of a sum S of binomial random variables, each with different success probabilities. The distribution arises in reliability analysis and in survival analysis. An algorithm is given to calculate the exact distribution of S, and several approximations are examined. An approximation based on a method of Kolmogorov, and another based on fitting a distribution from the Pearson family, can be recommended. DTIC

N94-15298# Norwegian Defence Research Establishment, Kjeller.
A NEW METHOD FOR GENERATING BAYES CLASSIFIERS ASSUMING MIXTURES OF GAUSSIAN DENSITIES
Hans Christian Palm 22 Dec. 1992 33 p
(FFI-91/4029; ETN-93-94449) Avail: CASI HC A03/MF A01

A method for generating a Bayes classifier assuming linear mixtures of Gaussian probability densities is presented. The aim was to create reliable and computationally efficient classifiers for real time applications. The concept consists of first designing a Bayes classifier assuming Gaussian densities. If the error rate is unacceptable, the number of Gaussian components in one of the classes is increased by one, new classifier parameters are estimated and the error rate is computed. This process of classifier generation and evaluation continues until a set of criteria is fulfilled. The classifier is compared with other relevant classifiers such as Bayes classifier with Gaussian assumptions, Bayes classifier assuming a linear mixture of two Gaussian densities, various piecewise linear classifiers and the nearest neighbor rule. Both synthetic and real data sets were used. Tests indicate that the algorithm produces fast and reliable classifiers with equal or better performance than the 'real time' classifiers used in the comparison. ESA

N94-15535*# National Aeronautics and Space Administration. Marshall Space Flight Center, Huntsville, AL.
STATISTICAL COMPUTATION OF TOLERANCE LIMITS
J. T. Wheeler Oct. 1993 45 p Sponsored by NASA, Washington
(NASA-TM-108424; NAS 1.15:108424) Avail: CASI HC A03/MF A01

Based on a new theory, two computer codes were developed specifically to calculate the exact statistical tolerance limits for normal distributions within unknown means and variances for the one-sided and two-sided cases for the tolerance factor, k. The quantity k is defined equivalently in terms of the noncentral t-distribution by the probability equation. Two of the four mathematical methods employ the theory developed for the numerical simulation. Several algorithms for numerically integrating and iteratively root-solving the working equations are written to augment the program simulation. The program codes generate some tables of k's associated with the varying values of the proportion and sample size for each given probability to show accuracy obtained for small sample sizes. Author (revised)

N94-15641*# Illinois Univ., Urbana-Champaign.
STATISTICAL ANALYSIS OF TRIGONOMETRIC PARALLAXES Final Technical Report, 1 Jan. 1992 - 30 Sep. 1993
Stefano Casertano, Kavan U. Ratnatunga (Johns Hopkins Univ., Baltimore, MD.), and Mario G. Lattanzi (Space Telescope Science Inst., Baltimore, MD.) 1993 4 p
(Grant NAGw-2945)
(NASA-CR-194558; NAS 1.26:194558) Avail: CASI HC A01/MF A01

The present project was initiated with two specific medium-term goals: first, to develop a novel approach, based on global modeling and maximum likelihood, to the study of databases of stellar data, with specific attention to the results to be obtained by the Hipparcos mission; and second, to apply and test the methodology developed to existing ground-based data. The long-term goal was of course to integrate the methodology and the ground-based data into a global study of the results of the Hipparcos mission, which were expected to be made available in 1995 or 1996. The closing of the project is due to the recent change of home institution of the PI, who has moved from the University of Illinois to Johns Hopkins University. As a consequence of this move, the three scientists involved in this project will be in close proximity, thereby hopefully improving their ability to collaborate and increasing the productivity of the project. Continued funding for the project has been requested from Johns Hopkins University. This report describes briefly the results obtained so far both on the technical aspect of software development and on the scientific side of applications to existing ground-based data. Significant progress has been made on both counts, with several papers published in (or submitted to) refereed journals and in conference proceedings. Because it is hoped that the project can be successfully continued with NASA support, the report of the progress in each area includes also an assessment of how the current results fit in the expected continuation of the project. Our results to date include: code development (essentially completed); a detailed study of the kinematics and dynamics of stars escaping from the Hyades cluster, relevant to the question of membership in the Hyades; a study of the kinematics and luminosity calibration of nearby dwarfs; an assessment of the quality of the photometry included in the Hipparcos Input Catalog; and two studies of properties of nearby clusters, including a moving-cluster determination of the distance to Praesepe. The bibliography includes three papers submitted to refereed journals, two of which have already been published, and four contributions to conference proceedings. Finally, the work so far has also provided a very good introduction to stellar dynamics and astrometry for an undergraduate student, with educational benefits that had not been foreseen in the original proposal. Derived from text

N94-15733# Harvard Univ., Cambridge, MA. Dept. of Statistics.
BOUNDS ON INCONSISTENT INFERENCES FOR SEQUENCES OF TRIALS WITH VARYING PROBABILITIES
Herman Chernoff and Ying-Nian Wu 21 Jun. 1993 20 p Sponsored by ONR
(AD-A267146; ONR-C-13) Avail: CASI HC A03/MF A01

Consider independent pairs of Bernoulli trials on two unknown sequences of probabilities p(1) = (p(sub i)(1) : 1 less than or equal to i less than or equal to n) and p(2) = (p(sub i)(2) : less than or equal to i less than or equal to n). The data are the numbers of pairs which consist of (0,0), (0,1), (1,0), and (1,1) and can be summarized in a two-way table with entries n(sub 00), n(sub 01), n(sub 10) and n(sub 11) adding up to n. The two problems of estimating the mean and variance of the number of discordant pairs n(sub 01) + n(sub 10) when H(sub 0) : p(l) = p(2) is true, and of testing H(sub 0) using the number of discordant pairs as a test statistic are considered. Two novel issues arise. While relevant parameters can not be estimated consistently from the available data, useful bounds on these can be derived. While the test is poor for alternatives typically considered in the literature, it may be effective for detecting the presence of unknown explanatory factors which discriminate between supposedly matched pairs. DTIC

N94-15777# Purdue Univ., West Lafayette, IN. Research Foundation.
EFFICIENT ALGORITHMIC TECHNIQUES FOR COMBINATORIAL PROBLEMS Final Report, 1 Jan. 1990 - 31 Dec. 1992
M. J. Atallah, A. Apostolico, and W. Szpankowski 31 Dec. 1992 13 p
(Grant AF-AFOSR-0107-90)
(AD-A267151; AFOSR-93-0474TR) Avail: CASI HC A03/MF A01

Important algorithms for parallel computational geometry and for string recognition have been developed. These algorithms have been developed for application in a parallel and stochastic setting. DTIC

N94-16657# North Carolina Central Univ., Durham.
NONPARAMETRIC STATISTICS: WEIGHTED RANKINGS ANALYSIS Final Report, 15 May 1966 - 14 Sep. 1989
Ibrahim A. Salama 20 Apr. 1993 17 p
(Contract DAAL03-86-G-0084)
(AD-A266607; ARO-23369.6-MA) Avail: CASI HC A03/MF A01

We examine the credibility hypothesis associated with the method of Weighted Rankings Analysis. We consider a multivariate test for homogeneity based on all nearest neighbors. We extend exact tables for Spearman's footrule by using a Markov chain structure over the permutation group of 1,...,n. We prove the asymptotic permutational normality of certain weighted measures of correlation. DTIC

N94-16726# Stanford Univ., CA. Dept. of Statistics.
MOMENTS IN STATISTICS: APPROXIMATIONS TO DENSITIES AND GOODNESS-OF-FIT
Michael A. Stephens 11 May 1993 20 p
(AD-A266600; TR-469) Avail: CASI HC A03/MF A01

In this article the author discusses ways in which moments are used (1) to approximate distributions, and (2) to test fit to a given distribution. DTIC

N94-16937# Illinois Univ., Urbana. Dept. of Aeronautical and Astronautical Engineering.
NONLINEAR ANALYSIS OF MECHANICAL SYSTEMS UNDER COMBINED HARMONIC AND STOCHASTIC EXCITATION Annual Report, 15 Nov. 1991 - 14 Nov. 1992
N. S. Namachchivaya 27 May 1993 73 p
(Grant AF-AFOSR-0041-91)
(AD-A266217; AFOSR-93-0444TR) Avail: CASI HC A04/MF A01

In the AFOSR grant, the complex interaction between noise, stability and nonlinear dynamics inherent in mechanical systems was examined and a consistent method for analyzing stochastic nonlinear systems was developed. The specific objective of the current work, is to examine, both theoretically and experimentally, the nonlinear response of gyroscopic systems under stochastic and harmonic excitation. This study will include the following: examination of the combined effects of mass imbalance, asymmetry, and realistic boundary conditions on the nonlinear response of rotating systems; development of a general nonlinear control technique designed to suppress unwanted vibrations and chaotic motions in gyroscopic systems; and experimental verification of the theories developed. DTIC

N94-17236# Superconducting Super Collider Lab., Dallas, TX.
STATISTICS OF THE HALF-INTEGER STOPBAND
S. Dutt, F. Chautard, R. Gerig, and S. Kauffmann May 1993 5 p
Presented at the International Particle Accelerator Conference, Washington, DC, 17-20 May 1993
(Contract DE-AC35-89ER-40486)
(DE93-016101; SSCL-Preprint-442; CONF-930511-185) Avail: CASI HC A01/MF A01

We consider the statistical nature of the stopband set up in the vicinity of a half-integer tune when a linear lattice is subjected to quadrupole errors distributed according to Gaussians. The probability density function of the stopband, treated as a complex number, is found to be a correlated bivariate Gaussian in the real and imaginary parts. The mean magnitude of the stopband is calculated in terms of the complete elliptic integral of the first kind, and the conditional probability density of its magnitude is obtained in closed form. A number of limiting conditions are studied. Finally, we estimate the requirements on a correction system for neutralizing the stopband with a given probability of success. DOE

N94-17372# Naval Undersea Warfare Center, New London, CT. New London Detachment.
EXPANSIONS OF CUMULATIVE DISTRIBUTION FUNCTIONS DIRECTLY FROM CHARACTERISTIC FUNCTIONS Technical Progress Report
Albert H. Nuttall 8 Jun. 1993 69 p
(AD-A267727; NUWC-NPT-TR-10371) Avail: CASI HC A04/MF A01

Expansions of probability density functions and their corresponding cumulative distribution functions, directly from given characteristic functions, have been achieved in a series form, with four parameters which are under the control of the user, thereby enabling realization of more rapidly convergent terms. Typical examples of characteristic functions encountered in detection of multiple matched filter outputs are presented, along with an application to a noisy channel with partially correlated fading. The series presented here enable immediate evaluation of performance of a related normalizer once the expansion coefficients have been determined. An extension to allow for additive Gaussian noise is realized through a set of simple but efficient recursions. DTIC

N94-17495 Naval Research Lab., Washington, DC.
ENERGY DEPOSITION FLUCTUATIONS INDUCED BY IONS IN MICROVOLUMES AND NANOVOLUMES: AN ANALYTIC APPROACH. 1: THEORY Final Report
Michael A. Xapsos, Edward A. Burke, and Geoffrey P. Summers (Maryland Univ., Baltimore.) 22 Jul. 1993 66 p Limited Reproducibility: More than 20% of this document may be affected by microfiche quality
(AD-A267959; NRL/MR/6615-93-6948) Avail: Issuing Activity (Defense Technical Information Center (DTIC))

A new analytic method is developed for calculating fluctuations in energy deposition induced by ions in sites having dimensions as small as one nanometer. The method considers two contributions to the fluctuation phenomena. The first is due to direct ion interactions with the site. The second is due to secondary electrons that strike the site but which are produced by ion interactions in the surrounding medium. Particular attention is given to the way the two contributions are combined to describe the complete stochastic process. This analytic combination of the two contributions has not previously been developed in the context of microdosimetry where Monte Carlo simulations are often used to describe the combined processes. The new analytic approach is much more versatile than Monte Carlo methods and can easily be applied to different incident radiations, target materials and target geometries. In addition to its versatility and convenience, the physical factors which contribute to the fluctuations in energy deposition are brought clearly into focus. DTIC

N94-17585 Air Force Inst. of Tech., Wright-Patterson AFB, OH.
STATE SPACE PARTITIONING METHODS FOR SOLVING A CLASS OF STOCHASTIC NETWORK PROBLEMS Ph.D. Thesis
Jay A. Jacobson May 1993 134 p Limited Reproducibility: More than 20% of this document may be affected by poor print and microfiche quality
(AD-A267494; AFIT/CI/CIA-93-006D) Avail: Issuing Activity (Defense Technical Information Center (DTIC))

This study focuses on state space partitioning techniques for computing measures related to the operation of stochastic systems. These methods iteratively decompose the system state space until the measure of interest has been determined. The information available in each iteration yields lower and upper bounds on this measure, and can be used to design efficient Monte Carlo estimation routines. We present here new theoretical results identifying strategies for significantly enhancing the performance of these algorithms. Using these results, we describe a generalized algorithm that can easily be tailored to address a variety of problems. We net use this algorithm to analyze two important models in the area of stochastic network optimization. The first concerns the probabilistic behavior of minimum spanning trees in graphs with discrete random arc weights. Specifically, we compute the probability distribution of the weight of a minimum spanning tree and the probability that a given arc is on a minimum spanning tree. Both of these problems are shown to be P-hard. The second model considers minimum cost flows in networks with discrete random arc costs and capacities. DTIC

N94-15561*# Geodetic Inst., Helsinki (Finland).
ADAPTIVE MEDIAN FILTERING FOR PREPROCESSING OF TIME SERIES MEASUREMENTS
Matti Paunonen *In* NASA. Goddard Space Flight Center, Eighth International Workshop on Laser Ranging Instrumentation Jun. 1993 7 p (For primary document see N94-15552 03-19)
Avail: CASI HC A02/MF A06

66 SYSTEMS ANALYSIS

Includes mathematical modeling; network analysis; and operations research.

N94-15823# Stanford Univ., CA. Operations Research House.
FAST SIMULATION OF STEADY-STATE AVAILABILITY IN NON-MARKOVIAN HIGHLY DEPENDABLE SYSTEMS
Peter W. Glynn, Victor F. Nicola, Perwez Shahabuddin, and Philip Heidelberger Dec. 1992 22 p
(Contract DAAL03-91-G-0101)
(AD-A266747; ARO-26863.8-EG-S) Avail: CASI HC A03/MF A01

This paper considers efficient simulation techniques for estimating steady-state quantities in models of highly dependable computing systems with general component failure and repair time distributions. Earlier approaches in this application setting for steady-state estimation rely on the regenerative method of simulation which can be used when the failure time distributions are exponentially distributed. However, when the failure times are generally distributed the regenerative structure is lost and a new approach must be taken. The approach we take is to exploit a ratio representation for steady-state quantities in terms of cycles that are no longer independent and identically distributed. A splitting technique is used in which importance sampling is used to speed up the simulation of rare system failure events during a cycle, and standard simulation is used to estimate the expected cycle length. Experimental results show that the method is effective in practice. DTIC

N94-16109# Army War Coll., Carlisle Barracks, PA.
THE STRATEGIC ENVIRONMENTAL RESEARCH AND DEVELOPMENT PROGRAM: A NEW PARADIGM FOR SPACE, THE ENVIRONMENT, AND NATIONAL SECURITY Individual Study Project
Thomas C. Suermann 17 Mar. 1993 44 p
(AD-A266222) Avail: CASI HC A03/MF A01

Future U.S. national security objectives will encompass a broader range of technological systems and applications than they have in the past. Dual-use technologies will be vitally important to maintaining U.S. leadership in the world community, in space-based security, and in global environmental security and stewardship. The Strategic Environmental Research and Development Program (SERDP), as well as NASA's emerging, Mission-To-Planet-Earth Program, individually and collectively offer national ways of leveraging technology. They will provide mutually reinforcing endeavors which will enhance our national security. This study focuses on the benefits of using space technology applications within these programs to enhance military and environmental security. It is an attempt to define part of the peace dividend which is emerging from the end of the Cold War, and it offers some recommendations for improving dual-technology synergism in augmenting national military security and environmental stewardship. DTIC

N94-16665# Naval War Coll., Newport, RI. Dept. of Operations.
NOT READY FOR THE FIRST SPACE WAR. WHAT ABOUT THE SECOND? Final Report
Steven J. Bruger 17 May 1993 34 p
(AD-A266557) Avail: CASI HC A03/MF A01

For the first time in history, space systems were employed during the Persian Gulf War at not only the strategic level of war, but also at the operational and tactical levels as well. Spaceborne assets had a dramatic effect on the ability of the operational level commander to successfully plan and prosecute a comprehensive warfighting campaign. This paper outlines the mission capabilities of U.S. Space Command, and its components, and examines how space assets contributed to concrete, coherent military action at the operational level of war in support of the ultimate national political goals and objectives. The impact of space forces during Operations Desert Shield/Desert Storm, specifically force enhancement assets, is examined and six implications for the future are offered. DTIC

N94-17219# Air Force Academy, CO.
HYPERVELOCITY ORBITAL INTERCEPT GUIDANCE USING CERTAINTY CONTROL
Salvatore Alfano and Charles E. Fosha, Jr. Jun. 1993 8 p Repr. from Journal of Guidance, Control, and Dynamics, v. 14, no. 3, May-Jun. 1991 p 574-580 See also A91-39411
(AF Proj. 9993)
(AD-A267297; PL-TR-93-1020; AD-E201508) Avail: CASI HC A02/MF A01

Terminal guidance of a hypervelocity exoatmospheric orbital interceptor with free end time is examined. A new approach called certainty control is developed where control energy expenditure is reduced by constraining the expected final state to a function of projected estimate error. Conceptually, the constraint produces a shrinking sphere about the predicted impact point with the radius being a function of estimated error. If the predicted miss is inside or touching the sphere, thrusting is not necessary. The interceptor is modeled as a satellite with lateral thrusting capability using two-body orbital dynamics. The target is modeled as an intercontinental ballistic missile (ICBM) in its final boost phase prior to burnout. Filtering is accomplished using an eight-state extended Kalman filter with line-of-sight and range updates. The estimated relative trajectory and variances are propagated numerically to predicted impact time and then approximated by splines which eliminate the need to propagate new data repeatedly when present conditions are varied. A search is then made for a new impact time and point that will minimize present interceptor velocity changes and final miss distance. This control strategy, which is applied to two intercept problems, substantially reduces fuel consumption. DTIC

N94-17469*# National Aeronautics and Space Administration. Marshall Space Flight Center, Huntsville, AL.
STUDY OF THE NATIONAL SCIENCE FOUNDATION'S SOUTH POLE STATION AS AN ANALOGOUS DATA BASE FOR THE LOGISTICAL SUPPORT OF A MOON LABORATORY Final Report
H. H. Hickam, Jr. Oct. 1993 47 p
(RTOP 307-52-00)
(NASA-TM-108429; NAS 1.15:108429) Avail: CASI HC A03/MF A01

The day will come when the United States will want to return to the Earth's Moon. When that occurs, NASA may look to the Apollo program for technical and inspirational guidance. The Apollo program, however, was designed to be an end to itself--the landing of a man on the Moon and his return safely within the decade of the 1960's. When that was accomplished, the program folded because it was not self-sustaining. The next time we return to the Moon, we should base our planning on a program that is designed to be a sustained effort for an indefinite period. It is the thrust of this report that the South Pole Station of the National Science Foundation can be used to develop analogs for the construction, funding, and logistical support of a lunar base. Other analogs include transportation and national efforts versus international cooperation. A recommended lunar base using the South Pole Station as inspiration is provided, as well as details concerning economical construction of the base over a 22-year period. Author

N94-15919*# Jet Propulsion Lab., California Inst. of Tech., Pasadena.
AIRSAR SOUTH AMERICAN DEPLOYMENT: OPERATION PLAN, VERSION 3.0
M. Kobrick *In its* Proceedings of the Third Spaceborne Imaging Radar Symposium 28 May 1993 p 441-465 (For primary document see N94-15886 03-32)
Avail: CASI HC A03/MF A04

67 THEORETICAL MATHEMATICS

Includes topology and number theory.

N94-16820# Texas Univ., Austin.
LINEAR STABILITY OF STATIONARY SOLUTIONS OF THE VLASOV-POISSON SYSTEM IN THREE DIMENSIONS
J. Batt (Ludwig-Maximilians-Univ., Munich, Germany.), G. Rein (Ludwig-Maximilians-Univ., Munich, Germany.), and P. J. Morrison Mar. 1993 26 p
(Contract DE-FG05-80ET-53088)
(DE93-013873; DOE/ET-53088/597; IFSR-597) Avail: CASI HC A03/MF A01

Rigorous results on the stability of stationary solutions of the Vlasov-Poisson system are obtained in both the plasma physics and stellar

dynamics contexts. It is proven that stationary solutions in the plasma physics (stellar dynamics) case are linearly stable if they are decreasing (increasing) functions of the local, i.e. particle, energy. The main tool in the analysis is the free energy of the system, a conserved quantity. In addition, an appropriate global existence result is proven for the linearized Vlasov-Poisson system and the existence of stationary solutions that satisfy the above stability condition is established. DOE

N94-17641 International Centre for Theoretical Physics, Trieste (Italy).
DISTRIBUTIVELY GENERATED MATRIX NEAR RINGS
S. J. Abbasi Apr. 1993 5 p Limited Reproducibility: More than 20% of this document may be affected by poor print
(DE93-628588; IC-93/79) Avail: Issuing Activity (Department of Energy (DOE)) (US Sales Only)

It is known that if R is a near ring with identity then (I,+) is abelian if (I(sup +),+) is abelian and (I,+) is abelian if (I*,+) is abelian. This paper extends these results. We show that if R is a distributively generated near ring with identity then (I,+) is included in Z(R), the center of R, if and only if (I(sup +),+) is included in Z(M(sub n)(R)), the center of matrix near ring M(sub n)(R). Furthermore (I,+) is included in Z(R) if and only if (I*,+) is included in Z(M(sub n)(R)). DOE

N94-17643 International Centre for Theoretical Physics, Trieste (Italy).
QUANTUM HEISENBERG GROUPS AND SKLYANIN ALGEBRAS
Nicolas Andruskiewitsch (Max-Planck-Inst. fuer Mathematik, Bonn, Germany.), Jorge Devoto, and Alejandro Tiraboschi May 1993 15 p Limited Reproducibility: More than 20% of this document may be affected by microfiche quality
(DE93-628590; IC-93/93) Avail: CASI HC A03 (US Sales Only)

We define new quantizations of the Heisenberg group by introducing new quantizations in the universal enveloping algebra of its Lie algebra. Matrix coefficients of the Stone-von Neumann representation are preserved by these new multiplications on the algebra of functions on the Heisenberg group. Some of the new quantizations provide also a new multiplication in the algebra of theta functions; we obtain in this way Sklyanin algebras. DOE

N94-17644 International Centre for Theoretical Physics, Trieste (Italy).
FIXED POINT ITERATIONS FOR STRICTLY HEMI-CONTRACTIVE MAPS IN UNIFORMLY SMOOTH BANACH SPACES
C. E. Chidume and M. O. Osilike May 1993 15 p Limited Reproducibility: More than 20% of this document may be affected by microfiche quality
(DE93-628591; IC-93/96) Avail: CASI HC A03 (US Sales Only)

It is proved that the Mann iteration process converges strongly to the fixed point of a strictly hemi-contractive map in real uniformly smooth Banach spaces. The class of strictly hemi-contractive maps includes all strictly pseudo-contractive maps with nonempty fixed point sets. A related result deals with the Ishikawa iteration scheme when the mapping is Lipschitzian and strictly hemi-contractive. Our theorems generalize important known results. DOE

70 PHYSICS (GENERAL)

For precision time and time interval (PTTI) see *35 Instrumentation and Photography;* for geophysics, astrophysics or solar physics see *46 Geophysics, 90 Astrophysics,* or *92 Solar Physics.*

N94-15233* National Aeronautics and Space Administration. Marshall Space Flight Center, Huntsville, AL.
AUTOMATED DIRECTIONAL SOLIDIFICATION FURNACE (Videotape)
Aug. 1989 Videotape: 1 min. 42 sec. playing time, in color, with sound
(NASA-TM-109662; NONP-VT-93-190460) Avail: CASI VHS A01/BETA A22

This video presentation addresses space research supporting the development of longer lasting, lighter weight, and more powerful magnets. CASI

N94-15758 California Univ., Berkeley. Dept. of Electrical Engineering and Computer Science.
[TECHNOLOGY TRANSFERS AND RELIABLE OXIDES] Annual Progress Report, 1 Aug. 1992 - 1 Jul. 1993
Chen-Ming Hu 1 Jul. 1993 68 p Limited Reproducibility: More than 20% of this document may be affected by microfiche quality
(Contract N00014-92-J-1757)
(AD-A266948) Avail: CASI HC A04

The aims of this research grant have not been modified. The aims are to do the following: to extend the reliability models for oxide wearout and hot-electron-induced degradation from DC stress to AC stress by arbitrary waveforms as encountered in circuits; to develop a circuit reliability simulator that incorporates the best known reliability models for oxide and hot electrons effects; and to develop improved device and reliable oxides. We have set a new world record in silicon transistor speed--13.5ps at room temperature and at 1.5 volt. This was a result of our research into the design and fabrication of advanced silicon-on-insulator MOS transistors. The goal is to understand the reliability limits of transistor scaling. DTIC

N94-15978# Brookhaven National Lab., Upton, NY.
MAGNETIC EFFECTS IN ANOMALOUS DISPERSION
M. Blume 1992 19 p Presented at the International Conference on Anomalous Scattering, Hamburg, Germany, 17-21 Aug. 1992
(Contract DE-AC02-76CH-00016)
(DE93-014291; BNL-48895; CONF-9208186-2) Avail: CASI HC A03/MF A01

Spectacular enhancements of magnetic x-ray scattering have been predicted and observed experimentally. These effects are the result of resonant phenomena closely related to anomalous dispersion, and they are strongest at near-edge resonances. The theory of these resonances will be developed with particular attention to the symmetry properties of the scatterer. While the phenomena to be discussed concern magnetic properties, the transitions are electric dipole or electric quadrupole in character and represent a subset of the usual anomalous dispersion phenomena. The polarization dependence of the scattering is also considered, and the polarization dependence for magnetic effects is related to that for charge scattering and to Templeton type anisotropic polarization phenomena. It has been found that the strongest effects occur in rare-earths and in actinides for M shell edges. In addition to the scattering properties the theory is applicable to 'forward scattering' properties such as the Faraday effect and circular dichroism. DOE

N94-17288# California Univ., Berkeley. Lawrence Berkeley Lab.
THE INVERSE PROBLEM TO THE EVALUATION OF MAGNETIC FIELDS
S. Caspi, M. Helm, L. J. Laslett, and V. Brady Dec. 1992 26 p
(Contract DE-AC03-76SF-00098)
(DE93-015239; LBL-33316; SC-MAG-412) Avail: CASI HC A03/MF A01

In the design of superconducting magnet elements, such as may be required to guide and focus ions in a particle accelerator, one frequently premises some particular current distribution and then proceeds to compute the consequent magnetic field through use of the laws of Biot and Savart or of Ampere. When working in this manner one of course may need to revise frequently the postulated current distribution before arriving at a resulting magnetic field of acceptable field quality. It therefore is of interest to consider an alternative ('inverse') procedure in which one specifies a desired character for the field required in the region interior to the winding and undertakes them to evaluate the current distribution on the specified winding surface that would provide this desired field. We may note that in undertaking such an inverse procedure we would wish, on practical grounds, to avoid the use of any 'double-layer' distributions of current on the winding surface or interface but would not demand that no fields be generated in the exterior region, so that in this respect the goal would differ in detail from that discussed by other authors, in analogy to the distribution sought in electrostatics by the so-caged Green's equivalent stratum. DOE

N94-17317 China Nuclear Information Centre, Beijing.
A REVIEW OF SOME DYNAMICS MODELS IN SIX-DIMENSIONAL PHASE SPACE AND THEIR SUITABLE CONDITIONS OF MOTION EQUATION
Qingxi Cao and Guan Xialing (Academia Sinica, Beijing, China.) Sep. 1991 12 p Limited Reproducibility: More than 20% of this document may be affected by microfiche quality
(DE93-623741; CNIC-00537; IAE-0094) Avail: Issuing Activity (Department of Energy (DOE)) (US Sales Only)

Based on the analysis of motion features for a pulse beam, as the

dynamics models of motion system in a six-dimensional phase space, target measuring model and instantaneous distribution model are described. The strict dynamics motion equations of particle beams have been derived both in Cartesian coordinate system and in curvilinear coordinate system for two kinds of models mentioned above. The force components in three directions have been given for two models and two coordinate systems. The model of Karl L. Brown's theory and his dynamics motion equations were also analyzed. The features of two theory models and their suitable conditions were discussed. It is confirmed that the 'target measuring model' is a better one to describe a pulse beam. That is because the time t and t' = dt/d(zeta) are selected as the longitudinal coordinate of six dimensional coordinate system. The status described by this model is not instantaneous but a status with time distribution in a fixed position, eg. in a target. With this model, the time features of a pulse beam can be given directly. But when the space charge has to be considered, the instantaneous distribution model will be better than the target measuring model. DOE

N94-17581# Wisconsin Univ., Madison. Center for Mathematical Sciences.

[A BASIC PRINCIPLES DESCRIPTION OF LIQUID VAPOR PHASE TRANSITIONS] Progress Report

15 Jul. 1993 4 p

(Contract N00014-93-1-0015)

(AD-A268331) Avail: CASI HC A01/MF A01

The research effort of Slemrod has been directed to developing a discrete velocity kinetic theory model for liquid-vapor phase transitions. The aim of the research is to develop a 'basic principles' description of liquid-vapor phase transitions (such as those occurring in an internal combustion engine) which is not a priori biased by ad hoc equations of state (constitutive relations). The modelling is almost completely finished, numerical simulations are being run, and a first draft of the results is being written. The model is of the following form: We consider a gas of clusters in three dimensional space made up monomers, dimers, trimers, etc. which can move with seven fixed momenta: the six unit vectors + or - i, + or - j, + or - k plus the 0 vector. The clusters can collide elastically and inelastically. The elastic collisions conserve mass, momentum, and energy. The inelastic collisions occur when clusters coagulate or fragment and conserve mass and momentum. In an inelastic collisions kinetic energy is lost. DTIC

N94-17605# Georgia Inst. of Tech., Atlanta.

LOW DIELECTRIC CONSTANT INSULATORS AND GOLD METALLIZATION FOR GHz MULTI-CHIP MODULES, PART 2 Annual Performance Report

Paul Kohl, Sue A. Bidstrup, and David Hertling Jul. 1993 60 p

(Contract N00014-91-J-4008)

(AD-A268590) Avail: CASI HC A04/MF A01

The goal of this program is to investigate new dielectrics, metals, and processes for the fabrication of multi-chip modules which hold the promise of exceptional electrical performance in the GHz region in addition to high yield and high reliability. The low dielectric constant insulators are being evaluated through the fabrication of in-situ test structures using noble metals. In the course of doing this evaluation, a simple process for gold or silver MCM's has been investigated. A processing scheme using noble metals (gold and silver) as the interconnection metallization in the module has been developed and is being characterized. The noble metal process has fewer process steps than the equivalent copper process and is potentially lower cost, particularly when high reliability is important. It has been observed that silver has an advantage in that it maintains its bulk conductivity during high temperature processing and has low residual stress. DTIC

N94-17658# Brookhaven National Lab., Upton, NY.

COMPARISON OF COMPUTER PREDICTIONS AND MAGNETIC FIELD MEASUREMENTS FOR AN IRON SPECTROMETER MAGNET

G. T. Danby, J. W. Jackson, W. Meng, and C. Spataro 1993 3 p Presented at the International Particle Accelerator Conference, Washington, DC, 17-20 May 1993

(Contract DE-AC02-76CH-00016)

(DE93-016164; BNL-48306; CONF-930511-196) Avail: CASI HC A01/MF A01

Three dimensional computer calculations using the Program TOSCA have been made for a complex-shaped iron magnet. Precision field measurements were made on this magnet in preparation for its installation in a new Low Energy Separated Beam for the post-Booster high proton intensity AGS at Brookhaven National Laboratory. Point-by-point direct comparisons for field values are described encompassing the entire useful acceptance. The predictability of high order multipoles is described, including the region of the magnet ends. Computer predicted focal properties are compared with results of experimental data analysis. The method of measurement and analysis, as well as comments on the computer calculations are described. Conclusions are drawn on the accuracy of calculations with respect to higher order moments and the impact on future beam optical design and execution of three dimensional computer codes. DOE

71 ACOUSTICS

Includes sound generation, transmission and attenuation.
For noise pollution see *45 Environmental Pollution.*

N94-15019 National Physical Lab., Teddington (England). Div. of Radiation Science and Acoustics.

FREE-FIELD SENSITIVITY CALIBRATION OF LABORATORY STANDARD MICROPHONES BY THE RECIPROCITY TECHNIQUE: MEASUREMENTS FOR THE 1991 EEC INTERCOMPARISON

D. R. Jarvis and R. G. Barham May 1993 34 p

(NPL-RSA(EXT)-0043; ETN-93-94552) Copyright Avail: Issuing Activity (National Physical Lab., Teddington, Middlesex TW11 OLW, England)

The free field sensitivity levels of eight laboratory standard microphones were measured, as part of an intercomparison exercise, with an uncertainty of better than 0.1 dB. The pressure sensitivity of each of the microphones was also measured in order to determine the difference between the free field and pressure sensitivity levels of the microphones. This was also determined with an uncertainty of about 0.1 dB. ESA

N94-15115*# National Aeronautics and Space Administration. Lewis Research Center, Cleveland, OH.

CRUISE NOISE MEASUREMENTS OF A SCALE MODEL ADVANCED DUCTED PROPULSOR

James H. Dittmar, Christopher E. Hughes, Lawrence A. Bock (Pratt and Whitney Aircraft, East Hartford, CT.), and David G. Hall (Sverdrup Technology, Inc., Brook Park, OH.) Oct. 1993 12 p Proposed for presentation at the 15th AIAA Aeroacoustics Conference, Long Beach, CA, 25-27 Oct. 1993; sponsored by AIAA

(RTOP 535-03-10)

(NASA-TM-105808; E-8042; NAS 1.15:105808; AIAA Paper 93-4400) Avail: CASI HC A03/MF A01

A scale model Advanced Ducted Propulsor (ADP) was tested in NASA Lewis Research Center's 8- by 6-Foot Wind Tunnel to obtain acoustic data at cruise conditions. The model, designed and manufactured by Pratt & Whitney Division of United Technologies, was tested with three inlet lengths. The model has 16 rotor blades and 22 stator vanes, which results in a cut-on condition with respect to rotor-stator interaction noise. Comparisons of the noise directivity of the ADP with that of a previously tested high-speed, unducted propeller showed that the ADP peak blade passing tone was about 30 dB below that of the propeller, and therefore, should not present a cabin or enroute noise problem. The maximum blade passing tone first increased with increasing helical tip Mach number, peaked, and then decreased at a higher Mach number. The ADP tests with the shortest inlet showed more noise in the inlet arc than did tests with either of the other two inlet lengths. Author

N94-15487*# Lockheed Engineering and Sciences Co., Hampton, VA.

ON THE USE OF THE NONCENTRAL CHI-SQUARE DENSITY FUNCTION FOR THE DISTRIBUTION OF HELICOPTER SPECTRAL ESTIMATES

Donald P. Garber Oct. 1993 41 p

(Contract NAS1-19000; RTOP 505-63-70-02)

(NASA-CR-191546; NAS 1.26:191546) Avail: CASI HC A03/MF A01

A probability density function for the variability of ensemble averaged spectral estimates from helicopter acoustic signals in Gaussian background noise was evaluated. Numerical methods for calculating the density function

and for determining confidence limits were explored. Density functions were predicted for both synthesized and experimental data and compared with observed spectral estimate variability. Author

N94-15506 National Aerospace Lab., Amsterdam (Netherlands). Aerodynamics Div.
TECHNICAL EVALUATION REPORT ON THE AGARD-PEP SPECIALISTS MEETING ON COMBAT AIRCRAFT NOISE
W. B. deWolf 14 Nov. 1991 8 p Meeting held in Bonn, Germany, 23-25 Oct. 1991 Limited Reproducibility: More than 20% of this document may be affected by poor print and microfiche quality
(NLR-TP-91445-U; ETN-93-94342) Avail: Issuing Activity (European Space Agency (ESA))

A technical evaluation of the AGARD-PEP specialists' meeting on combat aircraft noise at Bonn (Germany), Oct. 1991 which concentrated on the noise from combat aircraft in low altitude high speed training missions, is presented. Considerable improvement on the understanding and prediction of various noise components was reported. One of the main conclusions was that the overall effectiveness of reduction of engine based noise critically depends on the airframe noise level at high flight speeds, and more work is required in this area to clarify the situation. ESA

N94-15549*# National Aeronautics and Space Administration. Ames Research Center, Moffett Field, CA.
CALL SIGN INTELLIGIBILITY IMPROVEMENT USING A SPATIAL AUDITORY DISPLAY
Durand R. Begault Apr. 1993 11 p Sponsored by NASA, Washington
(RTOP 505-67-01)
(NASA-TM-104014; A-93067; NAS 1.15:104014) Avail: CASI HC A03/MF A01

A spatial auditory display was used to convolve speech stimuli, consisting of 130 different call signs used in the communications protocol of NASA's John F. Kennedy Space Center, to different virtual auditory positions. An adaptive staircase method was used to determine intelligibility levels of the signal against diotic speech babble, with spatial positions at 30 deg azimuth increments. Non-individualized, minimum-phase approximations of head-related transfer functions were used. The results showed a maximal intelligibility improvement of about 6 dB when the signal was spatialized to 60 deg or 90 deg azimuth positions. Author (revised)

N94-15732# Texas Univ., Austin. Applied Research Lab.
NONLINEAR ACOUSTICS: PERIODIC WAVEGUIDE, SCATTERING OF SOUND BY SOUND, THREE-LAYER FLUID, FINITE AMPLITUDE SOUND IN A MEDIUM HAVING A DISTRIBUTION OF RELAXATION PROCESSES, AND PRODUCTION OF AN ISOLATED NEGATIVE PULSE IN WATER Annual Summary Report No. 4, 1 Oct. 1991 - 30 Sep. 1992
David T. Blackstock 3 Jun. 1993 59 p
(Contract N00014-89-J-1109)
(AD-A267145; ARL-TR-93-11) Avail: CASI HC A04/MF A01

Research on nonlinear acoustics has been carried out during the 12-month period ending 30 September 1992. Progress is reported on the following projects: (1) propagation in a periodic waveguide; (2) scattering of sound by sound; (3) finite-amplitude waves in a three-layer fluid; (4) finite-amplitude waves in a medium having a distribution of relaxation processes; and, (5) propagation of an isolated negative-pressure pulse in water. DTIC

N94-16448# Lawrence Livermore National Lab., CA.
ACOUSTO-OPTICAL CONFIRMATION OF THE LOCALIZED WAVE PHENOMENA
D. K. Lewis Sep. 1992 7 p Presented at the 5th Spring School on Acousto-Optics and Applications, Gdansk, Poland, 25-29 May 1992
(Contract W-7405-eng-48)
(DE93-016425; UCRL-JC-111951; CONF-9205354-1) Avail: CASI HC A02/MF A01

An acousto-optical measurement method is described which was used to conduct proof of principle experiments for a novel acoustic pulse system. The pulse theory, the localized wave pulse, is discussed and the system explained and described. The results of the experiments confirm the localized wave theory. DOE

N94-16497*# National Aeronautics and Space Administration. Lewis Research Center, Cleveland, OH.
MODAL RING METHOD FOR THE SCATTERING OF SOUND
Kenneth J. Baumeister and Kevin L. Kreider (Akron Univ., OH.) Nov. 1993 10 p Presented at the ASME Winter Annual Meeting, New Orleans, LA, 28 Nov. - 3 Dec. 1993; sponsored by ASME
(RTOP 505-62-52)
(NASA-TM-106342; E-8111; NAS 1.15:106342) Avail: CASI HC A02/MF A01

The modal element method for acoustic scattering can be simplified when the scattering body is rigid. In this simplified method, called the modal ring method, the scattering body is represented by a ring of triangular finite elements forming the outer surface. The acoustic pressure is calculated at the element nodes. The pressure in the infinite computational region surrounding the body is represented analytically by an eigenfunction expansion. The two solution forms are coupled by the continuity of pressure and velocity on the body surface. The modal ring method effectively reduces the two-dimensional scattering problem to a one-dimensional problem capable of handling very high frequency scattering. In contrast to the boundary element method or the method of moments, which perform a similar reduction in problem dimension, the model line method has the added advantage of having a highly banded solution matrix requiring considerably less computer storage. The method shows excellent agreement with analytic results for scattering from rigid circular cylinders over a wide frequency range (1 is equal to or less than ka is less than or equal to 100) in the near and far fields. Author

N94-16650# Polish Academy of Sciences, Warsaw. Inst. Podstawowych Problemow Techniki.
STUDIES OF AURAL ACOUSTIC EMMISSIONS WITH THE USE OF AN ORIGINAL APPARATUS AND INVESTIGATIVE METHODOLOGY [BADANIA USZNYCH EMISJI AKUSTYCZNYCH Z ZASTOSOWANIEM ORYGINALNEJ APARATURY I METODYKI BADAWCZEJ]
Wanda Bochenek (Medical Academy, Warsaw, Poland.), Zbigniew Ranachowski, Jan Kiciak, and Andrzej Kukwa (Medical Academy, Warsaw, Poland.) 1992 21 p In POLISH
(IFTR-20/1992) Avail: CASI HC A03/MF A01

The physiological bases for phenomena of aural acoustic emissions are presented; a study of these is essential to analysis of the operation of the aural cochlea. The authors also describe an apparatus they constructed and an original research method and present the results of studies with a group of 20 probationers. The results lead to the conclusion that the method proposed by the authors for distinguishing nonlinear aural emissions may be an effective tool in clinical studies of the cochlea. Transl. by FLS

N94-16919 Department of the Navy, Washington, DC.
DIGITAL REVERBERATION TIME MEASUREMENT SYSTEM Patent
Blair M. Kipple, inventor (to Navy), Douglas A. Noll, inventor (to Navy), and Andrew H. Chiang, inventor (to Navy) 13 Jul. 1993 15 p Filed 28 Feb. 1991
(AD-D015892; US-Patent-5,227,982; US-Patent-Appl-SN-661932; US-Patent-Class-364-508) Avail: US Patent and Trademark Office

An apparatus and method, having both structural and acoustical applicability, for measuring damping of a solid or fluid resonant physical system in terms of reverberation or decay time, featuring a digital computer based measurement system in which plural numbers of resonances are grouped into single analysis bands are presented. The resonant response is converted into an electronic signal, which is then pre-amplified, filtered, post-amplified, digitized and finally processed so as to determine the reverberation time in the resonant physical system. DTIC

N94-16939# California Univ., Irvine. Center for Neurobiology of Learning and Memory.
CORTICAL ADAPTIVE FILTERING IN BIOACOUSTIC SIGNAL CLASSIFICATION Progress Report, 1 Nov. 1992 - 30 Apr. 1993
Norman M. Weinberger 30 Apr. 1993 13 p
(Contract N00014-91-J-1193)
(AD-A266229) Avail: CASI HC A03/MF A01

Frequency receptive fields (RF) in the auditory cortex are systematically altered as a result of a brief training experience. Responses to training signals (conditioned stimulus, CS) are increased whereas responses to other frequency, including the pretraining best frequency (BF) are decreased.

These changes can be sufficiently large so that the frequency of the CS becomes the new BF. Frequency RFs describe the frequency filtering characteristics of auditory system neurons. Systematic changes of these RF may then be seen to indicate adaptive filtering; i.e., adaptive filtering may be said to have occurred when training with a selected acoustic signal results in plasticity of the receptive field that is highly specific to that signal. The goal of this project is to determine the underlying processes of adaptive filtering both neurophysiologically and computationally. Of particular, we are applying findings from olfactory (paleo) cortex and training rules derived from the hippocampus (archicortex) to the architecture of the thalamo-neocortical auditory system to determine computational implications for bioacoustic signal classification. An initial stage of this project has been to determine fundamental characteristics of adaptive filtering which are essential for computational analysis. These findings provide a basis for experiments to test predictions which have been generated by the computational work. DTIC

N94-16955# Los Alamos National Lab., NM.

THE SHOCK HUGONIOT OF 316 SS AND SOUND VELOCITY MEASUREMENTS

R. S. Hixson, R. G. McQueen, and J. N. Fritz 1993 8 p Presented at the 14th International Conference on High Pressure Science and Technology and Technical Meeting of the Topical Group on Shock Compression of Condensed Matter, Colorado Springs, CO, 28 Jun. - 3 Jul. 1993

(Contract W-7405-eng-36)

(DE93-016525; LA-UR-93-2386; CONF-9306167-12) Avail: CASI HC A02/MF A01

Type 316 stainless steel has been characterized for its high-pressure, shock-wave response. Measurements have been made of shock-wave and particle velocity and of sound velocity. Our preliminary results for shock and particle velocity have been combined with previously unpublished results, and an overall fit was made. Sound velocity results show a discontinuity that is attributed to shock-induced melting. DOE

N94-16991# Pennsylvania State Univ., University Park. Dept. of Mechanical Engineering.

ACOUSTIC WAVES IN COMPLICATED GEOMETRIES AND THEIR INTERACTIONS WITH LIQUID-PROPELLANT DROPLET COMBUSTION Final Report, 14 Mar. 1991 - 14 May 1993

Vigor Yang, M. W. Yoon, and J. M. Wicker 14 May 1993 145 p

(Grant AF-AFOSR-0171-91)

(AD-A267260; AFOSR-93-0463TR) Avail: CASI HC A07/MF A02

A linear and nonlinear acoustic wave analysis has been developed for baffled combustion chambers. Results suggest three important effects of baffles on transverse modes of combustion instability. First, transverse waves can be longitudinalized inside baffle compartments. This may decouple combustion response from oscillatory motions if the processes near the injector face are sensitive to transverse variations in pressure. Second, severe restriction of the transverse component of acoustic velocity fluctuations is observed in baffle compartments. This may be key in stabilizing systems with velocity-sensitive combustion. Third, the frequency of oscillation is decreased with the addition of baffles, in agreement with experiments. One potentially destabilizing effect of baffles is the observed pressure concentration at the injector face. Pressure sensitive processes in this region may enhance instability. Limit cycles were observed for both two- and three-dimensional baffled chambers. Their most remarkable characteristic is high frequency modulation of the limit cycle amplitude. DTIC

N94-17051# Polish Academy of Sciences, Warsaw. Inst. Podstawowych Problemow Techniki.

DISCRETE MODELS OF THE BOLTZMANN EQUATION: STRUCTURE OF THE COLLISION OPERATOR OF SOUND PROPAGATION [DYSKRETNE MODELE ROWNANIA BOLTZMANNA: STRUKTURA OPERATORA ZDERZENIOWEGO PROPAGACJA DZWIEKU]

Kazimierz Piechor 1992 68 p In POLISH

(IFTR-2/1992) Avail: CASI HC A04/MF A01

Given the extensive range of literature relating to discrete kinetic theory, the discussion of results obtained by other authors was minimized, and primary attention was on such studies as the relation between results obtained in the discrete kinetic theory and corresponding results obtained within the framework of the so-called true kinetic theory based on Boltzmann's complete equation. In the first section, the discrete collision operator is analyzed. The primary conclusion is the statement that in the class of bilinear operators that copy Rn x Rp onto Rp, only operators (1.6), the so-called classical discrete collision operators, are characterized by collision in variants that vanish only for the Maxwellian and solutions of system (1.5) satisfy Statement H. The approximation is axiomatic and the conclusion is constructive. The proposed structure was used to construct discrete models of mixtures of noble gases and gases with binary chemical reactions. Let us consider existing models as such cases. The uniform balance principle largely does not hold for the case of gases in chemical reactions, i.e. forward and reverse reactions do not have equal probabilities. Only in the case of so-called chemical equilibrium can we assume that this principle will hold. Our models require that this principle holds since a classical form of the Maxwellian is used for discrete theory. It is the author's belief that discrete kinetic models can be extended to permit a polymolecular reaction with a different quantity of molecules following the reaction compared to the quantity of molecules prior to the reaction and an exception or even a weakening of the universal balance principle requires a different form of the Maxwellian rather than the classical form and, consequently, a new form of collision operator. Research on nonclassical collision operators continues, while the first incomplete model is the model proposed by the author. Necesary and sufficient results are presented to assure that this discrete model is not trivial, i.e. so system 1.5 and 1.6 does not decompose into multiple independent subsystems.

Transl. by FLS

N94-17087# Polish Academy of Sciences, Warsaw. Inst. Podstawowych Problemow Techniki.

AN AUTOMATED SYSTEM FOR ULTRASOUND MEASUREMENTS OF LIQUIDS BY THE RESONANCE (EGGERS) METHOD [ZAUTOMATYZOWANY UKLAD DO POMIAROW ULTRADZWIEKOWYCH O CIECZACH METODA REZONACYJNA]

Andrzej Balcerzak, Zbigniew Bazior, and Zdzislaw Kozlowski 1992 15 p In POLISH

(IFTR-17/1992) Avail: CASI HC A03/MF A01

The principles of measuring the damping and velocity of ultrasonic waves in fluids by the Eggers resonant method are discussed and likewise an automated system for such measurements operating in the 0.5-10 MHz range is described. The general operating principles of the system illustrated by test studies utilizing a fluid sample are given. Results obtained for resonators in which transducers with different surfaces were employed were compared. Transl. by FLS

N94-17119 Army Construction Engineering Research Lab., Champaign, IL.

SOUND EXPOSURE LEVEL PREDICTION FOR IMPULSE SOUND SOURCES ABOVE VARIABLE TERRAIN Final Report

Hong C. Zhuang, Leslie J. Benson, and Michael J. White May 1993 57 p Limited Reproducibility: More than 20% of this document may be affected by microfiche quality

(DA Proj. 4A1-62720-A-896)

(AD-A267535; CERL-TR-EC-93/02) Avail: Issuing Activity (Defense Technical Information Center (DTIC))

The influence of the ground surface makes it difficult to calculate the propagation of impulse noise from Army type blasts such as that produced by heavy-weapons fire on training ranges. This study developed the computer program gtdcom, which extends the Geometrical Theory of Diffraction (GTD) propagation model to include realistic, three-dimensional terrain, broadband sounds (blast waves), and frequency weighting factors. This report describes the theoretical basis used to broaden the GTD model, and briefly outlines the use of GTDCOM. The new program was interfaced with the Geographic Resources Analysis Support System (GRASS) to calculate sound exposure levels (SEL's) from blast sources using map elevation contour data. A user specifies the source position of the blast, a charge size, and an expected frequency weighting factor; the program calculates the SEL for each terrain cell, displays the results on the screen, and prepares a contour map for printer output. DTIC

N94-17278*# Georgia Inst. of Tech., Atlanta.

STRATEGIC PLANNING FOR AIRCRAFT NOISE ROUTE IMPACT ANALYSIS: A THREE DIMENSIONAL APPROACH Final Report, 12 Jul. 1991 - 15 Jan. 1993

C. R. Bragdon, M. J. Rowan, and K. K. Ahuja Sep. 1993 259 p
(Contract NAS1-19061; RTOP 537-03-21-03)
(NASA-CR-191484; A8612-009/1; NAS 1.26:191484) Avail: CASI HC A12/MF A03

The strategic routing of aircraft through navigable and controlled airspace to minimize adverse noise impact over sensitive areas is critical in the proper management and planning of the U.S. based airport system. A major objective of this phase of research is to identify, inventory, characterize, and analyze the various environmental, land planning, and regulatory data bases, along with potential three dimensional software and hardware systems that can be potentially applied for an impact assessment of any existing or planned air route. There are eight data bases that have to be assembled and developed in order to develop three dimensional aircraft route impact methodology. These data bases which cover geographical information systems, sound metrics, land use, airspace operational control measures, federal regulations and advisories, census data, and environmental attributes have been examined and aggregated. A three dimensional format is necessary for planning, analyzing space and possible noise impact, and formulating potential resolutions. The need to develop this three dimensional approach is essential due to the finite capacity of airspace for managing and planning a route system, including airport facilities. It appears that these data bases can be integrated effectively into a strategic aircraft noise routing system which should be developed as soon as possible, as part of a proactive plan applied to our FAA controlled navigable airspace for the United States. Author (revised)

N94-17599# Federal Aviation Administration, Cambridge, MA. National Transportation Systems Center.
NOISE MEASUREMENT FLIGHT TEST OF FIVE LIGHT HELICOPTERS Final Report, Jul. 1991 - May 1993
Edward J. Rickley, Kenneth E. Jones, Amanda S. Keller, and Gregg G. Fleming Jul. 1993 400 p
(AD-A268566; DOTVNTSC-FAA-93-5; DOT/FAA/EE-93-01) Avail: CASI HC A17/MF A04

The U.S. Department of Transportation, Federal Aviation Administration, (U.S.DOT/FAA), along with the U.S.DOT, Research and Special Programs Administration, Volpe National Transportation Systems Center (RSPA/Volpe Center) conducted a helicopter noise measurement flight test in Champaign, Illinois, during the period 22-26 July 1991. The primary objective of the study was to obtain the field data necessary to examine the feasibility of a simplified helicopter-noise-certification procedure (screening test). Acoustic data were measured by and stored on a hand-held sound-level meter (on-line processing) and recorded on digital tape for later off-line processing. A comparison of the measured on-line acoustic data with the acoustic data processed off-line provided the foundation necessary to evaluate the feasibility of the proposed screening test. In addition to acoustic measurements, meteorological data and helicopter tracking and performance data were also obtained. DTIC

N94-17650*# National Aeronautics and Space Administration. Langley Research Center, Hampton, VA.
NONLINEAR RANDOM RESPONSE PREDICTION USING MSC/NASTRAN
J. H. Robinson, C. K. Chiang (Old Dominion Univ., Hampton, VA.), and S. A. Rizzi Oct. 1993 62 p
(RTOP 505-63-50-10)
(NASA-TM-109029; NAS 1.15:109029) Avail: CASI HC A04/MF A01

An equivalent linearization technique was incorporated into MSC/NASTRAN to predict the nonlinear random response of structures by means of Direct Matrix Abstract Programming (DMAP) modifications and inclusion of the nonlinear differential stiffness module inside the iteration loop. An iterative process was used to determine the rms displacements. Numerical results obtained for validation on simple plates and beams are in good agreement with existing solutions in both the linear and linearized regions. The versatility of the implementation will enable the analyst to determine the nonlinear random responses for complex structures under combined loads. The thermo-acoustic response of a hexagonal thermal protection system panel is used to highlight some of the features of the program. Author

N94-15161# Technische Hochschule, Aachen (Germany). Zentrum fuer Physikalische Chemie unter Mikrogravitation.
ULTRASOUND ABSORPTION IN MOLTEN SALTS
E. P. Rejek, J. Richter, L. Schoester, and M. Vogt *In* ESA, Sounding Rocket Experiments in Fluid Science and Materials Sciences: TEXUS 25 to 27 and MASER 4, Volume 3 Feb. 1993 p 36-41 (For primary document see N94-15157 03-25)
Copyright Avail: CASI HC A02/MF A02; ESA, EPD, ESTEC, Noordwijk, Netherlands, HC

72 ATOMIC AND MOLECULAR PHYSICS

Includes atomic structure, electron properties, and molecular spectra.

N94-14931 Academy of Sciences of the Ukraine, Kharkov. Fiziko-Tekhnicheskij Inst.
CHANNEL OF THE SYSTEM FOR PULSE CHARGED PARTICLE BEAM DIAGNOSTICS
Yu. V. Vladimirov, V. M. Denyak, N. V. Perun, and V. P. Sergienko 1992 6 p Limited Reproducibility: More than 20% of this document may be affected by microfiche quality
(DE93-623867; KFTI-92-3) Avail: Issuing Activity (Department of Energy (DOE)) (US Sales Only)

A channel of the system for pulse charged particle beam diagnostics is described. It measures: beam current in pulse I(sub p) greater than or = 1 mA at T=1...10 microsecond duration and pulse frequency f=50...300 Hz with relative errors less than or = 0.1%; deviation from the beam 'equilibrium center' with resolving in X,Y coordinates in a circle of 40...0.05 mm radius; form of the beam pulse envelope by stroboscope method with 20 ns discreteness. DOE

N94-14932 Academy of Sciences of the Ukraine, Kiev. Inst. Yadernykh Issledovanij.
MULTIPLE PROCESS SIMULATIONS FOR CORRECTION FACTOR CALCULATIONS IN EXPERIMENTS WITH NEUTRONS. LUSMK PROGRAM
L. L. Litvinskij 1992 20 p Limited Reproducibility: More than 20% of this document may be affected by microfiche quality
(DE93-623957; KIYal-92-19) Avail: CASI HC A03 (US Sales Only)

The method of multiple process correction factor calculations for neutron experiments in unresolved and overlapping resonance energy regions is described. The weight method of random simulation has been used for the calculations. The LUSMK FORTRAN program is published destined for correction factor calculations in neutron scattering, neutron capture experiments. The control examples of the simulation are presented. DOE

N94-14934 Joint Inst. for Nuclear Research, Dubna (USSR). Lab. of Computing Techniques and Automation.
ON THE NATURE OF MIRROR PARTICLES
G. G. Takhtamyshev 1992 12 p Limited Reproducibility: More than 20% of this document may be affected by microfiche quality
(DE93-626670; JINR-D-2-92-44) Avail: CASI HC A03 (US Sales Only)

Consequences of the experiments demonstrating non-conservation of spatial and combined (CP) parity are considered. A hypothesis is proposed according to which the results of the experiments do not contradict the mirror symmetry of our World. According to the hypothesis the fundamental particles (quarks and leptons) consist of moving constituents which do not possess charges of any of the three known interactions. Strong, weak, and electromagnetic interactions arise as a result of internal motion of the constituents; on reversal of the direction of this motion, a particle transforms into its antiparticle, whereas spatial inversion transforms usual particles into mirror ones (and vice versa). Consequences of the hypothesis for neutral kaons system are also considered, and some experiments aimed at searching for mirror particles are suggested. DOE

N94-14949# New York Univ., New York. Dept. of Physics.
THEORETICAL STUDIES RELATING TO THE INTERACTION OF RADIATION WITH MATTER Annual Report, 1 Jan. 1992 - 31 May 1993
P. R. Berman 1 Jun. 1993 6 p

(Contract N00014-91-J-1146)
(AD-A266894) Avail: CASI HC A02/MF A01

During the past year, progress was made in the areas of: (1) coherent transients using counterpropagating fields; (2) new resonances in cold-atom spectroscopy; (3) laser cooling in one dimension using linearly polarized fields; and, (4) theory of four-wave mixing. DTIC

N94-15135# Tokyo Univ. (Japan).
STUDY OF THE RARE DECAYS K(SUB L)(SUP 0) YIELDS (MU)e, K(SUB L)(SUP 0) YIELDS ee, AND K(SUB L)(SUP 0) YIELDS (MU)(MU) AT KEK
Takeshi K. Komatsubara Jun. 1992 5 p
(DE93-753247; INS-934) Avail: CASI HC A01/MF A01

An experimental study of the rare decays K(sub L)(sup 0) yields (mu)e, K(sub L)(sup 0) yields ee, and K(sub L)(sup 0) yields (mu)(mu) was performed at the KEK 12-GeV Proton Synchrotron. No event was observed in the fiducial region for the decay K(sub L)(sup 0) yields (mu)e. There was one event in the fiducial region for the decay K(sub L)(sup 0) yields ee, which was indistinguishable from the background. Normalizing to the decay K(sub L)(sup 0) yields (pi)(+)(pi)(-), the upper limits on the branching ratios at 90 percent confidence level were B(K(sub L)(sup 0) yields (mu)e) less than 9.4 x 10(exp -11) and B(K(sub L)(sup 0) yields ee) less than 1.6 x 10(exp -10). We observed 179 k(sub L)(sup 0) yields (mu)(mu) events in the fiducial region, and the branching ratio B(K(sub L)(sup 0) yields (mu)(mu)) = (7.9 (+/-) 0.6(stat) (+/-) 0.3(syst)) x 10(exp -9) was obtained. DOE

N94-15283 Tel-Aviv Univ. (Israel).
THE QUANTUM MASS SHIFT OF THE SOLITON IN SKYRME MODEL Ph.D. Thesis
Hillel Livne Sep. 1991 92 p In HEBREW
(ITN-93-85219) Copyright Avail: Issuing Activity (Tel-Aviv Univ., Exact Sciences Library, Ramat Aviv 69978, Israel)

Quantum chromodynamics (QCD) is a fundamental field theory describing the strong forces in nature. At present, it is unknown how to calculate the spectrum of the hadrons from QCD in the low energy limit. One of the ways to overcome this difficulty is to use effective models with the same global symmetries as QCD. The Skyrme model represents a class of such models. The Skyrme model is an effective QCD model at the limit of small momenta and large number of colors. Quantities such as the spectrum of the lightest baryons or the isoscalar mean square radius and the magnetic moment of the baryon, were calculated by quantization of rotational zero modes (ZM). In addition, the meson-baryon scattering cross-sections and S-matrix elements were calculated by quantization of the non-ZM up to the second order in the Lagrangian. The contribution of the quantum mass shift from some of the non-ZM to the soliton, was also calculated. It was found that it cannot be neglected when compared with the mass calculated from ZM only. Values calculated via the Skyrme model deviate from experimental values by about 30% and it is, therefore, interesting to ask whether these values could be improved by including the quantum mass contribution from all the non-ZM in the calculations. The quantum mass shift which arises from all non-ZM to the soliton mass in the Skyrme model were calculated. The mass shift does not depend on the baryonic spin, so that it is the same for the nucleon and for the delta.
Author (ISA)

N94-15288 Tel-Aviv Univ. (Israel). School of Physics and Astronomy.
EFFECTS OF SPIN-ORBIT COUPLING ON DISORDERED MESOSCOPIC SYSTEMS M.S. Thesis
Yuval Oreg Sep. 1991 86 p In HEBREW
(ITN-93-85220) Copyright Avail: Issuing Activity (Tel-Aviv Univ., Exact Sciences Library, Ramat Aviv 69978, Israel)

The effect of spin-orbit interaction on one- and two-dimensional mesoscopic disordered systems is studied in general and in terms of the tight-binding model in particular. It is shown that spin-orbit coupling can be formulated in the non-relativistic limit as a vector potential. By averaging over arbitrarily strong spin-orbit coupling, it is shown that the transmission of a one-dimensional ring, subject to a magnetic flux, contains only the second harmonic of the flux and a constant term (zeroth harmonic). The transverse ('Hall') conductance of a one-dimensional disordered ring is studied as well and it is shown that in the presence of spin-orbit coupling it may change its sign for some values of the flux threading the ring. The analysis of two-dimensional systems, with a well-defined plaquette size, shows that the zeroth and the second harmonics of the flux per plaquette are dominant in the transmission and in the transverse ('Hall') resistance of the sample. For the calculation of transport properties, a closed expression for the scattering matrix of a sample connected to a few wires is derived. The scattering matrix is expressed as a function of (1) the Green's function of the isolated system and (2) the coupling between the system and the wires. Chapters 1, 3 and 5 are devoted to reviews and to rederivation of previous results which provided the motivation for this study and are essential for the thesis. In chapter 2, an intuitive physical approach to the problem of spin-orbit coupling is presented. In chapters 4, 6, and 7, the new results and methods are derived rigorously (analytically and numerically). The last chapter is devoted to summary, specluations and possible continuations of the work. Author (ISA)

N94-15689# New York Univ., New York. Dept. of Physics.
THEORETICAL STUDIES RELATING TO THE INTERACTION OF RADIATION WITH MATTER Final Report, 1 Jan. 1991 - 30 Jun. 1993
P. R. Berman 30 Jun. 1993 8 p
(Contract N00014-91-J-1146)
(AD-A267134) Avail: CASI HC A02/MF A01

The final report for Grant No. N00014-91-J7-1146 is divided into seven subject areas as follows: (1) coherent transients using broadband optical pulses; (2) four-wave mixing in magnetically degenerate systems; (3) interpretation of laser cooling mechanisms; (4) laser cooling in one and two dimensions; (5) nonlinear spectroscopy of cold atoms; (6) transient spectroscopy using counterpropagating pulses; and (7) theory of four-wave mixing. A detailed description of the work carried out under this Grant can be found in the articles listed at the end of this report as well as in Annual Reports GAR1 and GAR2 associated with this Grant. In this Final Report, the research areas are summarized briefly, with references to the appropriate articles. DTIC

N94-15715*# Christopher Newport Coll., Newport News, VA.
SHIELDING FROM SPACE RADIATIONS Annual Technical Report, 1 Dec. 1992 - 1 Jun. 1993
C. Ken Chang, Forooz F. Badavi, and Ram K. Tripathi 1993 91 p
(Contract NAS1-1286)
(NASA-CR-194578; NAS 1.26:194578) Avail: CASI HC A05/MF A01

This Progress Report covering the period of December 1, 1992 to June 1, 1993 presents the development of an analytical solution to the heavy ion transport equation in terms of Green's function formalism. The mathematical development results are recasted into a highly efficient computer code for space applications. The efficiency of this algorithm is accomplished by a nonperturbative technique of extending the Green's function over the solution domain. The code may also be applied to accelerator boundary conditions to allow code validation in laboratory experiments. Results from the isotopic version of the code with 59 isotopes present for a single layer target material, for the case of an iron beam projectile at 600 MeV/nucleon in water is presented. A listing of the single layer isotopic version of the code is included. Author

N94-15727# Florida Univ., Gainesville.
MANY-BODY QUANTUM MECHANICAL STUDIES OF MOLECULAR CLUSTERS Final Report
Rodney J. Bartlett 1 Jun. 1992 21 p
(Contracts N00014-88-J-1046; N00014-91-J-1282)
(AD-A266624) Avail: CASI HC A03/MF A01

The following final report summarizes four years of research for ONR on the topic of 'Many-Body Quantum Mechanical Studies of Molecular Clusters.' There are two primary aspects of this effort, a methodological part focusing on new first principle (i.e. ab initio) multi-reference coupled-cluster methods for obtaining improved solutions to the Schroedinger equation for the structure and spectra of molecular clusters; and applications of these new, coupled-cluster (CC) and many-body perturbation theory (MBPT) methods to several fascinating problems with emphasis on the structure and spectra of carbon clusters and borane (BH3) containing clusters. The substantial accomplishments of this effort are summarized. DTIC

N94-15752*# Old Dominion Univ., Norfolk, VA. Dept. of Mechanical Engineering.
STUDY OF MULTI-DIMENSIONAL RADIATIVE ENERGY TRANSFER IN MOLECULAR GASES
Jiwen Liu and S. N. Tiwari Oct. 1993 71 p
(Grant NAG1-363)
(NASA-CR-194613; NAS 1.26:194613; ODU/ICAM-93-102) Avail: CASI HC A04/MF A01

The Monte Carlo method (MCM) is applied to analyze radiative heat transfer in nongray gases. The nongray model employed is based on the statistical arrow band model with an exponential-tailed inverse intensity distribution. Consideration of spectral correlation results in some distinguishing features of the Monte Carlo formulations. Validation of the Monte Carlo formulations has been conducted by comparing results of this method with other solutions. Extension of a one-dimensional problem to a multi-dimensional problem requires some special treatments in the Monte Carlo analysis. Use of different assumptions results in different sets of Monte Carlo formulations. The nongray narrow band formulations provide the most accurate results. Author (revised)

N94-15774 Georgia State Univ., Atlanta.
INVESTIGATION OF THE INTERACTIONS OF RADIATION WITH MATTER Final Report, 1 Mar. 1990 - 28 Feb. 1993
Steven T. Manson 31 May 1993 9 p Limited Reproducibility: More than 20% of this document may be affected by microfiche quality
(Contract DAAL03-89-K-0098)
(AD-A266743; ARO-26709.13-PH) Avail: CASI HC A02

Theoretical studies of the interaction of charged particles and electromagnetic radiation with matter have been performed. Particular emphasis has been given to ionizing radiation and the details of energy deposition by the radiation. New phenomena have been discovered in the area of ionization in ion-atom and atom-atom collisions. Models of electron impact ionization of atoms and molecules have been extended to the relativistic range. In addition, relativistic effects in the photoionization of very heavy atoms and ions have been delineated in detail for the first time. Finally, a number of investigations of various aspects of photoionization of excited atoms have been carried out which have given new insight into the process, both for outer and inner shell ionization. Of particular interest is the discovery that inner shell photoionization of excited atoms is primarily a many-body process. DTIC

N94-15863# Oak Ridge K-25 Site, TN.
MULTIPHOTON IONIZATION STUDIES OF WF6 AND UF6
D. A. Harkins, D. P. Armstrong, R. N. Compton (Oak Ridge National Lab., TN.), and Dajun Ding (Oak Ridge National Lab., TN.) 1993 18 p Presented at the 6th International Conference on Multiphoton Processes, Quebec City, Ontario, 25-30 Jun. 1993
(Contracts DE-AC05-84OT-21400; DE-AC05-76OR-00001)
(DE93-016232; K/ETO-127; CONF-9306125-2) Avail: CASI HC A03/MF A01

Multiphoton ionization of UF6 and WF6 has been studied from low (approximately 10(exp 5) W/sq cm) to high (approximately 10(exp 16) W/sq cm) power density. The role of 'collective states' in MPI is considered. DOE

N94-15974# Los Alamos National Lab., NM.
ON THE 17-keV NEUTRINO
A. Hime Apr. 1993 17 p Presented at the 5th International Workshop on Neutrino Telescopes, Venice, Italy, 2-4 Mar. 1993
(Contract W-7405-eng-36)
(DE93-012638; LA-UR-93-1348; CONF-9303160-1) Avail: CASI HC A03/MF A01

A brief review on the status of the 17-keV neutrino is presented. Several different experiments found spectral distortions which were consistently interpreted as evidence for a heavy neutrino admixture in beta decay. Recent experiments, however, rule out the existence of a 17-keV neutrino as well as escape criticisms of earlier null results. Moreover, the majority of positive results have been reinterpreted in terms of instrumental effects, despite the need for a different explanation in each case. Anomalies persist in the low energy region of the tritium spectrum which deserve further investigation. DOE

N94-15995# California Univ., Berkeley. Lawrence Berkeley Lab.
MOLECULAR BEAM STUDIES OF REACTION DYNAMICS
Yuan T. Lee Mar. 1993 7 p Presented at the 15th Combustion Research Contractors' Meeting, Lake Harmony, PA, 2-4 Jun. 1993
(Contract DE-AC03-76SF-00098)
(DE93-015035; LBL-33919-ABS; CONF-9306172-1) Avail: CASI HC A02/MF A01

The major goal of this research is to elucidate simple elementary reactions and to unravel mechanism of complex/photochemical reactions. Molecular beams are used to study reactions between molecules or to monitor photodissociation events in a collision-free environment. Recent activities centered on reactions involving oxygen atoms with unsaturated hydrocarbons, endothermic substitution reactions, dependence of reactivity of excited atoms on alignment of excited orbitals, photochemical reactions of polyatomic molecules, energy transfer, free radicals in combustion processes, infrared absorption spectra of carbonium ions and hydrated hydronium ions, and bond-selective photodissociation. Author (revised)

N94-16013# California Univ., Berkeley. Lawrence Berkeley Lab.
RELATIVISTIC MEAN-FIELD CALCULATIONS OF LAMBDA AND SIGMA HYPERNUCLEI
N. K. Glendenning, D. VonEiff, M. Haft, H. Lenske, and M. K. Weigel 24 Oct. 1992 19 p
(Contract DE-AC03-76SF-00098)
(DE93-015269; LBL-33031) Avail: CASI HC A03/MF A01

Single-particle spectra of lambda and sigma hypernuclei are calculated within a relativistic mean-field theory. The hyperon couplings used are compatible with the lambda binding in saturated nuclear matter, neutron-star masses, and experimental data on lambda levels in hypernuclei. Special attention is devoted to the spin-orbit potential for the hyperons and the influence of the rho-meson field (isospin dependent interaction). DOE

N94-16020# Brookhaven National Lab., Upton, NY.
CONFINEMENT AND STABILITY OF A CRYSTAL BEAM
A. G. Ruggiero 1993 4 p Presented at the International Particle Accelerator Conference, Washington, DC, 17-20 May 1993
(Contract DE-AC02-76CH-00016)
(DE93-015400; BNL-48373; CONF-930511-152) Avail: CASI HC A01/MF A01

The following is an analysis of the confinement and stability issues of a Crystal Beam. A method is described to determine the equilibrium configuration of a beam of highly charged particles. It is required that the beam has a uniform distribution in the direction of motion, which is stable and does not need therefore confinement with external means. It is shown that this can be obtained only for a relatively longitudinally compact beam. Confinement in the plane transverse to the direction of motion is obtained with external means, which also provide stability. It is important that particles are distributed so that the resulting space charge forces are linear with respect to the particle transverse coordinates. DOE

N94-16053# California Univ., Berkeley. Lawrence Berkeley Lab.
ELECTROWEAK PHYSICS FROM D0
N. A. Roe May 1993 11 p Presented at the 1993 Recontres De Physique De La Vallee D'Aoste, LaThuile, Italy, 8-13 Mar. 1993
(Contract DE-AC03-76SF-00098)
(DE93-015041; LBL-34077; CONF-9303172-1) Avail: CASI HC A03/MF A01

The D0 detector was recently commissioned at the Tevatron p(bar-p) collider and is presently taking data. Preliminary results from D0 are presented on properties of the W and Z electroweak gauge bosons using final states containing electrons and muons. DOE

N94-16059# California Univ., Berkeley. Lawrence Berkeley Lab.
STATUS OF (ALPHA)(SUB s) MEASUREMENTS
I. Hinchliffe May 1993 10 p Presented at the 28th Recontres De Moriond Conference on Electroweak Interaction and Unified Theories, Les Arcs, France, 13-20 Mar. 1993
(Contract DE-AC03-76SF-00098)
(DE93-015179; LBL-33952; CONF-9303171-2) Avail: CASI HC A02/MF A01

I review the current determinations of alpha(sub s). Attention is given to the theoretical uncertainties inherent in most determinations. All current

determinations are consistent with an average of alpha(sub s)(M(sub Z)) = 0.119 +/- 0.005. Prospects for reduction of the errors in the future are discussed. DOE

N94-16064# Oak Ridge National Lab., TN.
NEGATIVE ION FORMATION IN SMALL CARBON CLUSTERS
H. S. Carman, Jr. and R. N. Compton 1993 7 p Presented at the 2nd International Conference on Laser Ablation, Knoxville, TN, 19-22 Apr. 1993
(Contract DE-AC05-84OR-21400)
(DE93-015436; CONF-9304144-3) Avail: CASI HC A02/MF A01

Laser ablation of graphite into a rare gas supersonic jet has been used to generate C(sub m) clusters (both neutral and ionic) in the size range m less than or equal to 30. Negative ions produced by three different mechanisms have been studied: ion formation during the ablation process, low energy electron attachment (Rydberg electron transfer) to neutral clusters, and charge transfer from ground state rubidium atoms to neutral clusters. The C(sub m)(sup (minus)) distributions observed for the three cases are distinctly different, providing insights into the structures, stabilities, and electron attachment dynamics of small carbon clusters. DOE

N94-16111# Emory Univ., Atlanta, GA. Dept. of Chemistry.
THE INTERACTION OF HCN(DCN) WITH Si(111)-7X7 STUDIED WITH HREELS, UPS, AND XPS Technical Report
Y. Bu, L. Ma, and M. C. Lin 1993 24 p
(Contract N00014-89-J-1235)
(AD-A266237; TR-19) Avail: CASI HC A03/MF A01

The interaction of HCN (DCN) with Si(111)-7x7 was studied with high resolution electron energy loss spectroscopy (HREELS), ultra-violet photo-electron spectroscopy (UPS), and X-ray photoelectron spectroscopy (XPS). HCN (DCN) formed dimers and/or polymers on the surface at 100 K with higher dosages (D greater than 4 L). Above 200 K, CN radicals in an end-on adsorption geometry were identified as the major species which survived up to 600 K on the surface. This observation was different from that with HCN (DCN) on Si(100)-2x1, where the relative concentration of the HCNH species was higher. The observed difference in the behavior of HCN (DCN) on Si(111)-7x7 and Si(100)-2x1 could be ascribed to the different topologies of the two surfaces. DTIC

N94-16115# Los Alamos National Lab., NM.
PAST, PRESENT AND FUTURE ((PI),(ETA)) EXPERIMENTS
J. C. Peng 1993 7 p Presented at the Future Directions in Particle and Nuclear Physics at Multi-GeV Hadron Beam Facilities, Upton, NY, 4-6 Mar. 1993
(Contract W-7405-eng-36)
(DE93-016631; LA-UR-93-2021; CONF-930389-21) Avail: CASI HC A02/MF A01

Following a discussion of some physics issues in eta experiments, the current status of the (pi,eta) experiments is reviewed. Future prospects for eta experiments are also presented. DOE

N94-16117# Chicago Univ., IL.
EXPERIMENTAL STUDY OF WEAK INTERACTIONS BY PRECISION MEASUREMENT BY RARE KAON DECAY
R. Winston Apr. 1993 3 p
(Contract DE-FG02-90ER-40560)
(DE93-016864; DOE/ER-40560/4B) Avail: CASI HC A01/MF A01

Brief status reports are given on searches for direct CP and CPT violation. Additionally, a search for further evidence of CP violation through rare kaon decays such as K(sub L) yields pi(sup 0)e(+)e(-) is presented. DOE

N94-16121# Columbia Univ., New York, NY.
SINGLE-COLLISION STUDIES OF ENERGY TRANSFER AND CHEMICAL REACTION
J. J. Valentini 1993 3 p
(Contract DE-FG02-91ER-14225)
(DE93-017603; DOE/ER-14225/2) Avail: CASI HC A01/MF A01

The dynamics of the H + RH yields H2 + R (RH = CH4, C2H6, C3H8, and CHCl3) abstraction reactions were studied. We reported absolute partial and total cross sections for the H2 product as a function of rotational and vibrational state. DOE

N94-16161# Brookhaven National Lab., Upton, NY.
PHENIX CONCEPTUAL DESIGN REPORT
29 Jan. 1993 480 p
(Contract DE-AC02-76CH-00016)
(DE93-015759; BNL-48922) Avail: CASI HC A21/MF A04

The PHENIX Conceptual Design Report (CDR) describes the detector design of the PHENIX experiment for Day-1 operation at the Relativistic Heavy Ion Collider (RHIC). The CDR presents the physics capabilities, technical details, cost estimate, construction schedule, funding profile, management structure, and possible upgrade paths of the PHENIX experiment. The primary goals of the PHENIX experiment are to detect the quark-gluon plasma (QGP) and to measure its properties. Many of the potential signatures for the QGP are measured as a function of a well-defined common variable to see if any or all of these signatures show a simultaneous anomaly due to the formation of the QGP. In addition, basic quantum chromodynamics phenomena, collision dynamics, and thermodynamic features of the initial states of the collision are studied. To achieve these goals, the PHENIX experiment measures lepton pairs (dielectrons and dimuons) to study various properties of vector mesons, such as the mass, the width, and the degree of yield suppression due to the formation of the QGP. The effect of thermal radiation on the continuum is studied in different regions of rapidity and mass. The e(mu) coincidence is measured to study charm production, and aids in understanding the shape of the continuum dilepton spectrum. Photons are measured to study direct emission of single photons and to study (pi)(sup 0) and (eta) production. Charged hadrons are identified to study the spectrum shape, production of antinuclei, the (phi) meson (via K(sup +)K(sup -) decay), jets, and two-boson correlations. The measurements are made down to small cross sections to allow the study of high p(sub T) spectra, and J/(psi) and (upsilon) production. The PHENIX collaboration consists of over 300 scientists, engineers, and graduate students from 43 institutions in 10 countries. This large international collaboration is supported by U.S. resources and significant foreign resources. DOE

N94-16466# Northwestern Univ., Evanston, IL. Dept. of Chemistry.
STRUCTURAL EFFECTS IN ELECTRON TRANSFER REACTIONS: COMPARATIVE INTERFACIAL ELECTROCHEMICAL KINETICS FOR CIS- VERSUS TRANS-DIOXORHENIUM (V) (BI)PYRIDINE OXIDATION Technical Report, Jul. 1992 - Jul. 1993
Xiao L. Zhang, Joseph T. Hupp, and Gerald D. Danzer 29 May 1993 26 p
(Contract N00014-91-J-1035)
(AD-A266307; TR-14) Avail: CASI HC A03/MF A01

We have been exploring the proton-coupled reductions of various dioxorhenium (5) species because of the more general insights they provide into the kinetics and thermodynamics of multielectron transfer processes. The rhenium (5) complexes are also amenable, however, to proton-decoupled one-electron oxidation--both optically (via metal-to-ligand charge-transfer excitation) and electrochemically. Our prior studies of electron transfer (ET) thermodynamics revealed a strong dependence of the Re (6/5) formal potential on ligand substituent characteristics (most notably, substituent electron donating or withdrawing characteristics). The studies also showed--independent of ligand substituent identity--a strong dependence of E(sub f) on isomeric form cis versus trans coordination geometry. In all cases the cis form was more easily oxidized than the corresponding trans, generally by about 600mV. DTIC

N94-16586# SRI International Corp., Menlo Park, CA.
DISSOCIATION RATES OF DIATOMIC MOLECULES Final Report, 15 Sep. 1985 - 15 May 1992
Philip C. Cosby and Hanspeter Helm Dec. 1992 233 p
(Contract F33615-85-C-2560)
(AD-A266464; SRI-PYU-1147/MP-92-280; WL-TR-93-2004) Avail: CASI HC A11/MF A03

Absolute cross sections were measured for the electron-impact dissociation of simple molecules using a novel fast beam technique with multicoincident detection of the dissociation fragments. Translational energy released in the dissociation and product mass ratios were explicitly measured, allowing a detailed understanding of the dissociation mechanisms. The technique was applied to the molecules of nitrogen, oxygen, carbon monoxide, carbon dioxide, nitrogen dioxide, chlorine, and other molecules.

A detailed description of the measurement technique is presented together with the measured data. DTIC

N94-16722# Princeton Univ., NJ. Dept. of Chemistry.
A MOLECULAR DYNAMICS SIMULATOR FOR OPTIMAL CONTROL OF MOLECULAR MOTION Final Report, 1 Oct. 1991 - 31 Mar. 1993
Herschel Rabitz 18 Jun. 1993 19 p
(Contract DAAL03-91-G-0012)
(AD-A266572; ARO-28555.1-CH) Avail: CASI HC A03/MF A01

This report presents results of a Molecular Dynamics Simulator (MDS) used to explore optimal control of molecular motion. A realistic model of an interatomic potential is created by a configuration of magnets. This simulated potential approximately models both the short and long range portions of true molecular potentials. Atoms within a polyatomic molecule are simulated using carts which float on an airtrack, and a mechanical driver simulates the action of a controlling laser. In analogy with a molecular system, the potential is determined by analysis of a series of dynamics experiments. Knowledge of the potential, combined with optimal control theory, enables the design of the driver motion necessary to achieve controlled dissociation. Successful control requires overcoming a variety of difficulties analogous to those expected to be faced in the control of true molecular systems. The MDS provides insight into factors affecting the molecular control by demonstrating a real-time simulation of laser-controlled molecular dynamics. DTIC

N94-16801# Los Alamos National Lab., NM.
NEUTRINO MASS AND MIXING: SUMMARY OF THE NEUTRINO SESSIONS
T. J. Bowles 1993 25 p Presented at the 13th Moriond Workshop on Perspectives in Neutrinos, Atomic Physics, and Gravitation, Villars-sur-Ollon, Switzerland, 30 Jan. - 6 Feb. 1993
(Contract W-7405-eng-36)
(DE93-014342; LA-UR-93-2006; CONF-930187-3) Avail: CASI HC A03/MF A01

A great deal of experimental and theoretical effort is underway to use neutrinos as a probe for Physics Beyond the Standard Model. Most of these efforts center on the questions of the possible existence of non zero neutrino mass and mixing. Sessions at the Moriond conferences have dealt with these questions at most of the meetings during the last several years and this year was no exception. Presentations covering most of the current and planned research in this field were presented and discussed. Although there is, at present, no definitive evidence for a non zero neutrino mass and mixing, several unresolved problems (in particular solar neutrinos) do seem to be indicating the likely existence of new neutrino properties. It is likely that before the end of this decade, efforts now being initiated will be able to determine whether or not the hints we are now seeing are really due to new physics. DOE

N94-16809# Stanford Linear Accelerator Center, CA.
FUNDAMENTAL-MODE RF DESIGN IN e(+)e(-) STORAGE RING FACTORIES
P. B. Wilson Mar. 1993 10 p Presented at the Joint US/CERN School on Particle Accelerators Frontiers of Particle Beams: Factories with e(+)e(-) Rings, Benalmadena, Spain, 28 Oct. - 5 Nov. 1992
(Contract DE-AC03-76SF-00515)
(DE93-015249; SU-SLAC-PUB-6062; CONF-9210313-3) Avail: CASI HC A02/MF A01

The difficulties arising in the design of the RF system for a factory-type storage ring lie mainly in two areas. First, a gap in the circulating beam current is required for ion clearing. Because of the high beam loading current, this gap produces a strong transient variation in the RF cavity voltage, which can in turn lead to a significant shift in the synchronous phases between bunches on either side of the gap. This phase shift would produce an unacceptable shift in the collision point, unless compensated by a corresponding shift in the bunch phases in the other ring. In order to work out the details of this compensation, the transient beams loading effects produced by the gap must be calculated quite carefully. A major goal of this chapter is to provide the insight and the basic analytic tools necessary for this analysis. The second major problem for the fundamental mode RF design is also a consequence of the high average current needed for a storage ring particle factory: longitudinal multibunch beam instabilities at sideband frequencies within the passband of the accelerating mode. These instabilities can be damped by an appropriate feedback system, as discussed elsewhere in these proceedings. However, as background for this problem, we need to understand the phase and amplitude variations produced in the cavity voltage when the bunches undergo small-amplitude synchrotron oscillations. In the final section, the cavity voltage variation induced by such oscillations is calculated and applied to compute the Robinson damping time. The emphasis throughout this paper will be to provide a thorough understanding of beam loading effects. DOE

N94-16811# Stanford Linear Accelerator Center, CA.
APPLICATION OF CYLINDRICAL DISTRIBUTION FUNCTIONS TO ANISOTROPIC SCATTERING FROM AMORPHOUS FILMS
M. J. Regan and A. Bienenstock Apr. 1993 5 p Presented at the 9th International Conference on Small-angle Scattering, Saclay, France, 27-30 Apr. 1993
(Contract DE-AC03-76SF-00515)
(DE93-015256; SU-SLAC-PUB-6140; SLAC/SSRL-0011; CONF-9304155-1)
Avail: CASI HC A01/MF A01

The cylindrical pair correlation function has been utilized as a structural tool in the study of anisotropic phase separation in magnetron-sputtered amorphous Fe(x)Ge(100-x) films. Anomalous small-angle x-ray scattering (ASAXS) measurements have been performed with the scattering vector both in and oblique to the plane of the films, to search for anisotropy. The cylindrical correlation function has been calculated from these measurements, and indicates that there exist well-defined regions of electron density that are elongated (7 A by 12 A) in the direction of film growth. In addition, for a composition of x = 6, these regions are well-correlated on a length scale of 27 A for those correlation vectors oriented in the plane of the film surface, whereas the correlations are far weaker and longer in length for those vectors aligned in the direction of growth. These results are in agreement with a previous qualitative model of packed, prolate ellipsoids oriented in the direction of growth. DOE

N94-16817# Lawrence Livermore National Lab., CA.
ATOMIC PROCESSES IN HYDROGEN AND DEUTERIUM NEGATIVE ION DISCHARGES
J. R. Hiskes Nov. 1992 14 p Presented at the Production and Neutralization of Negative Ions and Beams, Upton, NY, 9-13 Nov. 1992
(Contract W-7405-eng-48)
(DE93-013432; UCRL-JC-112220; CONF-921145-7) Avail: CASI HC A03/MF A01

A knowledge of the atomic processes active in a hydrogen negative ion discharge and their respective rates is an essential component of the interpretation, modeling, and enhancement of negative ion systems. The generation of the cross sections and rate processes appropriate to this problem has been a principal activity at several laboratories. In this paper is discussed those collision processes that are of major importance for the destruction of the vibrationally excited molecules generated in the discharge, processes that are essential to the valuation of the optimization procedure that is discussed in this paper. DOE

N94-16818# Texas Univ., Austin. Dept. of Physics.
FEMTOSECOND GROWTH DYNAMICS OF AN UNDERDENSE IONIZATION FRONT MEASURED BY SPECTRAL BLUESHIFTING
W. M. Wood, C. W. Siders, and M. C. Downer 1993 53 p
(Contract DE-FG05-92ER-40739)
(DE93-013582; DOE/ER-40739/T1) Avail: CASI HC A04/MF A01

A comprehensive report of time-resolved spectral blue shifts of 100-femtosecond laser pulses caused by ionization of atmospheric density N(sub 2) and noble gases subjected to high (10(sup 14) W/cm(sup 2) - 10(sup 16) W/cm(sup 2)) light intensities is presented. Included are data for two experiments: (1) self-shifting of the ionizing laser pulses for varying peak intensities, pressures (1-5 atm.), and gas species; and (2) time-resolved blueshifts of a weak copropagating probe pulse for the same range of ionization conditions. The self-shift data reveal a universal, reproducible pattern in the shape of the blueshifted spectra: as laser intensity, gas pressure, or atomic number increase, the self-blueshifted spectra develop from a near replica of the incident pulse spectrum into a complex structure consisting of two spectral peaks. The time-resolved data reveal different temporal dependence for each of these two features. A quantitative model for a simplified cylindrical focal geometry is presented which explains the

presence of the two spectral features in terms of two distinct ionization mechanisms: collisionless tunneling ionization, which dominates early in the ionizing pulse profile, and electron impact ionization, which dominates during the intense maximum of the ionizing pulse. Transient resonant enhancements may also contribute to ionization near the peak of the pulse. DOE

N94-16826# Brookhaven National Lab., Upton, NY.
EVOLUTION OF HADRON BEAMS UNDER INTRABEAM SCATTERING
Jie Wei 1993 4 p Presented at the International Particle Accelerator Conference, Washington, DC, 17-20 May 1993
(Contract DE-AC02-76CH-00016)
(DE93-014330; BNL-48384; CONF-930511-71) Avail: CASI HC A01/MF A01

Based on assumptions applicable to many circular accelerators, we simplify into analytical form the growth rates of a hadron beam under Coulomb intrabeam scattering (IBS). Because of the dispersion that correlates the horizontal closed orbit to the momentum, the scaling behavior of the growth rates are drastically different at energies low and high compared with the transition energy. At high energies the rates are approximately independent of the energy. Asymptotically, the horizontal and longitudinal beam amplitudes are linearly related by the average dispersion. At low energies, the beam evolves such that the velocity distribution in the rest frame becomes isotropic in all the directions. DOE

N94-16828# Brookhaven National Lab., Upton, NY.
THE STABILITY OF IONS IN A STORAGE RING IN THE PRESENCE OF SMALL GAP INSERTION DEVICES
E. Bozoki 1993 4 p Presented at the International Particle Accelerator Conference, Washington, DC, 17-20 May 1993
(Contract DE-AC02-76CH-00016)
(DE93-015387; BNL-48965; CONF-930511-153) Avail: CASI HC A01/MF A01

With more and more insertion devices in storage rings, where the vacuum chamber size can be suddenly different, ionization pockets may develop, thus ions may be trapped leading to beam blow up, beam instabilities or even beam loss. One has to take a closer took at the stability conditions of the ions in these longitudinal equidistant bunches: are the ions above or below the Ac critical mass? For a bunch tram followed by a gap: is the ion of mass A stable or unstable for a given current at a given azimuthal location in the ring? Are the ions longitudinally mobile and able to get to an unstable region? If the ions proved to be stable in that region and if their longitudinal energy is less then the depth of the potential well, then they have to be statically cleared at that location. We are going to investigate the question of ion stability in the NSLS X-ray ring with a .32 m long variable gap (4-18 mm) undulator and a .95 m long 27 mm gap undulator in it. We will concentrate our attention to CO ions (A=28) since they are the most bothersome in the ring. We will show the effect of gap in the bunch train, the effect of nonlinearity in the beam kicks and the effect of restricted longitudinal mobility of ions. The methods used and the calculations performed are general enough to be applied to any other storage ring or accelerator, thus representing general interest. DOE

N94-16838# Oak Ridge National Lab., TN.
NEUTRON AND X RAY SCATTERING STUDIES OF (FeF2)(SUB m)(CoF2)(SUB n) MULTILAYERS
D. Lederman (California Univ., San Diego, La Jolla.), D. P. Belanger (California Univ., Santa Cruz.), J. Wang (California Univ., Santa Cruz.), and S. J. Han (California Univ., Santa Cruz.) 1993 7 p Presented at the Spring Meeting of the Materials Research Society, San Francisco, CA, 12-16 Apr. 1993
(Contracts DE-AC05-84OR-21400; DE-FG03-87ER-45324)
(DE93-015809; CONF-930405-24) Avail: CASI HC A02/MF A01

We have performed elastic neutron scattering measurements of the staggered magnetization in (FeF2)(sub m)(CoF2)(sub n) superlattices. Thermal expansion measurements, which are proportional to the magnetic contribution to the specific heat, were also carried out using high resolution x-ray diffraction. One of the two measured samples has thicknesses of m = n = 4.5 and the other m = 26 and n = 28 monolayers, as determined from high angle x-ray theta - 2(theta) scans. In the m = n = 4.5 sample, only one transition is observed at T(sub N) = 62.9 K. Analysis of the neutron data, including the rounding effects, indicates an effective beta approximately equal to 0.42. This does not compare well with the 3D Ising exponent beta = 0.325. The X-ray data also shows the existence of only one specific heat anomaly at T = 62.8 K. For the m = 26, n = 28 sample, dips in the staggered magnetization, and peaks in the thermal expansion were observed at T approximately equal to 40 K and 74 K. The higher temperature anomaly, associated primarily with the FeF2 layers, is sharper than the lower one, which is presumably rounded by the staggered ordering field imposed by the long range order in the FeF2 regions on the CoF2 regions. DOE

N94-16885# Brookhaven National Lab., Upton, NY.
SIX DIMENSIONAL TRACKING SIMULATOR FOR H(-) INJECTION IN AGS BOOSTER
S. Y. Lee and S. Tepikian 27 Apr. 1993 6 p
(Contract DE-AC02-76CH-00016)
(DE93-015396; BNL-48950; AGS/AD-93-7) Avail: CASI HC A02/MF A01

The effect of Coulomb multipole scattering on the beam emittance is studied with the 6 dimensional injection program ARCHSIM by A. Thiessen. Since the energy loss due to Bhabha scattering is small, the six dimensional simulation can be approximated into transverse 4 dimensional and longitudinal 2 dimensional tracking. The emittance growth agrees well with the multiple scattering theory. The beam loss occurs mainly in the adiabatic capture process in the longitudinal phase space. DOE

N94-16886# Brookhaven National Lab., Upton, NY.
EMITTANCE AND BEAM SIZE DISTORTION DUE TO LINEAR COUPLING
G. Parzen 1993 4 p Presented at the International Particle Accelerator Conference, Washington, DC, 17-20 May 1993
(Contract DE-AC02-76CH-00016)
(DE93-015402; BNL-48269; CONF-930511-154) Avail: CASI HC A01/MF A01

At injection, the presence of linear coupling may result in an increased beam emittance and in increased beam dimensions. Results for the emittance in the presence of linear coupling will be found. These results for the emittance distortion show that the harmonics of the skew quadrupole field close to (nu)(sub x) + (nu)(sub y) are the important harmonics. Results will be found for the important driving terms for the emittance distortion. It will be shown that if these driving terms are corrected, then the total emittance is unchanged, (var epsilon)(sub x) + (var epsilon)(sub y) = (var epsilon)(sub 1) + (var epsilon)(sub 2). Also, the increase in the beam dimensions will be limited to a factor which is less than 1.414. If the correction is good enough, one can achieve (var epsilon)(sub 1) = (var epsilon)(sub x), (var epsilon)(sub 2) = (var epsilon) where (var epsilon)(sub 1), (var epsilon)(sub 2) are the emittances in the presence of coupling, and the beam dimensions are unchanged. Global correction of the emittance and beam size distortion appears possible. DOE

N94-16899# Chicago Univ., IL.
A HIGH SENSITIVITY SEARCH FOR CP VIOLATING RARE K(SUB L) DECAYS AND PRECISION MEASUREMENT OF THE DIRECT CP VIOLATION PARAMETER (EPSILON)(PRIME)/(EPSILON) VIA THE FOUR K (YIELDS) 2(PI) DECAY MODES
Yau W. Wah May 1993 8 p
(Contract DE-FG02-90ER-40560)
(DE93-016866; DOE/ER-40560/4J) Avail: CASI HC A02/MF A01

Fermilab experiments E731, E773, E799, and E832 are a series of experiments to investigate the physics of CP violation, CPT violation, and rare decays of the neutral kaon system. E731 finished data taking in 1988; during the past year the full data set analysis was completed and yielded ((epsilon)(sup prime) / (epsilon)) (sub (2 x pi)) = (7.4 plus or minus 5.2 (stat) plus or minus 2.9 (syst)) x10(sup -4). The value favors a high top quark mass value within the Standard Model. E773 tests CPT violation by determining (Delta-phi)(sub (2 x pi)) with an accuracy of about 0.5(sup 0). Data were taken during the last Fermilab Fixed Target run period between September and November 1991. It is anticipated the data analysis will be finished within a year. E799, with the primary goal of observing direct Cp violation via searching for the rare decay K(sub L) yields (pi)(sup 0) l(sup +) l(sup -) (where l = e, mu, nu) took test data between November 1991 and January 1992 (Phase 1). Some preliminary

results are shown here. E799 (Phase II) and E832 (a follow up experiment of E731) are scheduled to take data after the current Fermilab collider run with a new facility and detector. DOE

N94-16951# Los Alamos National Lab., NM.
NEUTRAL-CURRENT DETECTION IN THE SUDBURY NEUTRINO OBSERVATORY
T. J. Bowles, P. J. Doe, M. M. Fowler, A. Hime, R. G. H. Robertson, P. M. Thornewell, J. B. Wilhelmy, J. F. Wilkerson, and J. M. Wouters 1993 9 p Presented at the 13th Moriond Workshop on Perspectives in Neutrinos, Atomic Physics, and Gravitation, Villars-sur-Ollon, Switzerland, 30 Jan. - 6 Feb. 1993
(Contract W-7405-eng-36)
(DE93-014481; LA-UR-93-1855; CONF-930187-4) Avail: CASI HC A02/MF A01

The Sudbury Neutrino Observatory (SNO) will have the capability of detecting all active species of neutrinos with energies greater than 2.2 MeV by the neutral-current disintegration of deuterium. The comparison of this rate with the rate of inverse beta decay of the deuteron will yield a nearly model-independent answer to the question of whether electron neutrinos from the sun oscillate into mu or tau neutrinos. The signal of a neutral-current interaction is the liberation of a free neutron in the heavy-water detector, and we discuss a technique employing He-3 proportional counters for registering these neutrons, particularly from the standpoint of the ultra-low backgrounds needed. DOE

N94-16957# Creighton Univ., Omaha, NE.
HEAVY ION PHYSICS RESEARCH AT CREIGHTON UNIVERSITY
M. Cherney 1992 8 p
(Contract DE-FG02-91ER-40652)
(DE93-016809; DOE/ER-40652/2) Avail: CASI HC A02/MF A01

This research continues the baseline efforts in the investigation of the behavior of hadronic matter under extreme conditions. The project is concerned with the search for indications of a phase transition from hadronic to quark matter in the STAR, NA44, and NA36 experiments. It is believed that the conditions necessary for the formation of this quark-gluon plasma include large energy densities over extended volumes. These large energy densities may be produced in heavy ion interactions. The technique of boson interferometry may prove to be an effective tool in verifying the existence of a quark-gluon plasma. The measurement of enhanced strangeness production may also provide an indication of plasma formation. This project contributes to the development of a slow control system and time projection chamber tracking for the STAR experiment, upgrades for the NA44 experiment at CERN through studies of a spot focusing Cherenkov-detector, and the remaining analysis of data collected with the NA36 experiment at CERN. DOE

N94-16968# Fermi National Accelerator Lab., Batavia, IL.
ELECTROWEAK RESULTS FROM D0
M. Demarteau May 1993 9 p Presented at the 28th Conference on Quantum Chromodynamics and High Energy Hadronic Interactions, Les Arcs, France, 20-27 Mar. 1993
(Contract DE-AC02-76CH-03000)
(DE93-014926; FNAL/C-93/127; CONF-930363-2) Avail: CASI HC A02/MF A01

Preliminary results from D0 are presented on properties of the W(+/-) and Z(sup 0) electroweak gauge bosons using final states containing electrons and muons. In particular, preliminary measurements of the W(+/-) and Z(sup 0) production cross sections with decay into final states containing electrons are shown and a status report on the determination of M(sub w)/M(sub z) is given. DOE

N94-16971# Texas Univ., Austin. Dept. of Chemistry.
VECTORIAL ELECTRON TRANSFER IN SPATIALLY ORDERED ARRAYS
M. A. Fox Feb. 1993 5 p
(Contract DE-FG05-85ER-13387)
(DE93-018150; DOE/ER-13387/T1) Avail: CASI HC A01/MF A01

Progress was made on synthesis of new materials for directional electron transfer (block copolymers and helical oligopeptides), preparation and characterization of anisotropic composites bearing organics and inorganics, electrocatalysis (redox-activated catalysts), and surface modifications of metals and semiconductors. DOE

N94-17310 Joint Inst. for Nuclear Research, Dubna (USSR). Lab. of Theoretical Physics.
MESONS AT FINITE TEMPERATURE IN THE NJL MODEL WITH GLUON CONDENSATE
D. Ebert, Yu. L. Kalinovskij, and M. K. Volkov 1992 10 p Limited Reproducibility: More than 20% of this document may be affected by microfiche quality
(DE93-626697; JINR-E-2-92-268) Avail: CASI HC A02 (US Sales Only)

The QCD-motivated NJL-model with gluon condensate is studied at finite temperature and baryon number density. We investigate the behavior of the constituent quark mass, quark condensate, meson masses, F(sub (pi)), coupling constants g(sub (pi)qq-bar), g(sub (sigma)qq-bar) and Z as function of temperature T. It is shown that the gluon condensate plays a stabilizing role for behavior of different physical quantities when temperature changes. DOE

N94-17312# Joint Inst. for Nuclear Research, Dubna (USSR). Lab. of Nuclear Problems.
PRODUCTION OF D-MESONS IN pp-COLLISIONS AND QUARK-GLUON STRING MODEL
G. I. Lykasov and M. N. Sergeenko 1992 12 p
(DE93-626721; JINR-E-2-92-51) Avail: CASI HC A03/MF A01 (US Sales Only)

The calculation results of the inclusive spectra of D-mesons produced in pp-collisions as the functions of the Feynman variable x and transverse momentum P-I are presented in the frame of the Quark-gluon string model. The satisfactory description of the experimental data in the frame of QGSM indicated domination of the peripheral mechanism of the D-meson production at high energies. DOE

N94-17329*# National Aeronautics and Space Administration. Pasadena Office, CA.
ELECTRON REVERSAL IONIZER FOR DETECTION OF TRACE SPECIES USING A SPHERICAL CATHODE Patent Application
Said Boumsellek, inventor (to NASA) (Jet Propulsion Lab., California Inst. of Tech., Pasadena.) and Ara Chutjian, inventor (to NASA) (Jet Propulsion Lab., California Inst. of Tech., Pasadena.) 15 Sep. 1993 27 p
(Contract NAS7-918)
(NASA-Case-NPO-18870-1-CU; NAS 1.71:NPO-18870-1-CU; US-Patent-Appl-SN-127653) Avail: CASI HC A03/MF A01

A reversal electron, high-current ionizer capable of focusing a beam of electrons to a reversal region employs an indirectly heated cathode having a concave emitting surface of width of W less than 2r, where r is the radius of curvature and preferably a ratio of width to radius approximately equal to one for optimum high current for a given cathode width. NASA

N94-17365# Air Force Inst. of Tech., Wright-Patterson AFB, OH.
LINEAR CHARACTERISTIC SPATIAL QUADRATURE FOR DISCRETE ORDINATES NEUTRAL PARTICLE TRANSPORT ON ARBITRARY TRIANGLES Ph.D. Thesis
Dennis J. Miller Jun. 1993 135 p
(AD-A267485; AFIT/DS/ENP/93-02) Avail: CASI HC A07/MF A02

A new discrete ordinates spatial quadrature for arbitrary triangular cells is derived and compared to its rectangular cell linear characteristic counterpart. The triangular mesh is more flexible, allowing curved surfaces and off-axis angles to be approximated with many fewer spatial cells. The triangle method is consistently more accurate on example problems tested here. Arbitrary orientation and size of the triangles allow non-patterned meshes to be developed which appears to ameliorate numerical diffusion. The triangle linear characteristic quadrature converges at nearly the same rate as rectangular Linear characteristic on Lathrop's problem. Mesh sensitivity measurements show large variations in triangle vertex locations produce less than 1.0 percent variation in results. Test cases included a rectangular region with diagonal vacuum duct, and cylindrical source region with rotated rings of annular segmented reflectors. The triangle linear characteristic quadrature is more cost effective on these problems achieving a relative error of less than 1.0 percent with a factor of three to over a hundred fewer spatial cells, with less than three times the computational

cost per cell. This spatial cell savings should increase the practical problem domain for which discrete ordinates is usable. DTIC

N94-17436 Denver Univ., CO. Dept. of Physics.
ATOMIC BEAM STUDIES RELEVANT TO THE SPACE ENVIRONMENT Final Report, 1 Dec. 1989 - 31 Mar. 1993
Robert C. Amme 31 Mar. 1993 22 p Limited Reproducibility: More than 20% of this document may be affected by microfiche quality
(Grant AF-AFOSR-0119-90)
(AD-A268628; AFOSR-93-0621TR) Avail: CASI HC A03

This final report describes the development, testing, and utilization of an atomic oxygen beam apparatus, capable of energies ranging from approximately 4 eV to over 500 eV. The technique employed is that of creating a beam of negative oxygen ions, typically from electron impact on N2O, then focusing and deceleration with subsequent electron photodetachment employing an argon-ion laser cavity with boosted power. Up to 30% of the ion beam may be photodetached at maximum laser powers, producing approximately 50 na of equivalent neutral flux. Angular divergence and energy spread are both well controlled and the total beam intensity is known to about 3 to 5%. Higher beam fluxes may be attained, but at the cost of filament and laser window lifetimes. Several measurements are described employing the beam apparatus in conjunction with a high stability quartz crystal mass monitor. Capabilities of the system have been demonstrated for studies of erosion, secondary charged particle production, and related work. DTIC

N94-17536# United Technologies Research Center, East Hartford, CT.
CATHODE SHEATH CHARGE TRANSFER EFFECTS Final Report, 10 Jun. 1987 - 28 Mar. 1993
H. H. Michels and R. H. Hobbs Mar. 1993 126 p
(Contract F33615-87-C-2718)
(AD-A268393; UTRC-927703-1; WL-TR-93-2071) Avail: CASI HC A07/MF A02

The United Technologies Research Center, under Contract No. F33615-87-C-2718, has carried out a theoretical research investigation of ion-molecule reactions that take place in the sheath region of low pressure discharges in silane gas mixtures. Of particular interest were the dissociative charge transfer mechanism(s) and energy dependent reaction rates of electrons, H(+), H(-), H(3+) and several noble gas ions (He+, Ne+, Ar+) in collisions with silane (SiH4). Such reactions are an important component in the modeling of plasma-processing discharges for producing device-quality silicon films and a detailed understanding of their kinetics is required. Similar ion-molecule reactions with methane and other lower member alkanes have proven to be of importance in the analysis of hydrocarbon combustion. The results of this theoretical investigation furnish fundamental data and provide a better understanding of the role of ion collision-induced molecular decomposition. The initial program for the research effort under this contract was formulated into three phases. Phase 1 consisted of a critical examination of available theoretical methods, including R-matrix methods, that are applicable to the prediction of the rates of dissociative charge transfer in ion-molecule collisions. These studies resulted in the development of an improved R-matrix code which incorporated analysis of reaction products. DTIC

N94-17578# Maryland Univ., College Park. Lab. for Plasma Research.
STUDY OF BRIGHTNESS AND CURRENT LIMITATIONS IN INTENSE CHARGED PARTICLE BEAMS Progress Report, 1 Jul. 1992 - 30 Jun. 1993
M. Reiser and S. Guharay 30 Jun. 1993 87 p
(Contract N00014-90-J-1913)
(AD-A268283) Avail: CASI HC A05/MF A01

Over the past several years of ONR support for our research program we have mainly studied the various schemes for intense, high-brightness H(-) beam transport and focusing in the context of its application in space defense. Detailed theoretical studies revealed that the conventional gas focusing system is not suitable as a low-energy beam transport (LEBT) system and also that there are too many unknown parameters to model accurately the behavior of partially charge-neutralized particle beams. We concluded that the electrostatic quadrupole lens system will be a good choice. We have developed a large number of simulation codes and also accessed into the existing codes in the accelerator community (e.g., PARMILA, SNOW-2D, PARMTEQ, etc.) to strengthen our analysis. During the 1992-93 contract period we focused our attention to the experimental activities on H(-) beam characterization and on the installation of a LEBT system for beam transport experiments. We have simultaneously improved our code by incorporating many practical features that we encountered during the analysis of experimental data. We have studied H(-) beams from two types of ion sources: a volume ionization type and a magnetron type source. One of the major problems in this work is to transform a highly diverging beam from the source into a highly converging one so that the output beam from the LEBT can be matched into the acceptance ellipse of an RFQ. Furthermore, the emittance budget is quite restricted. DTIC

N94-17601 Nationaal Inst. voor Kernfysica en Hoge Energiefysica, Amsterdam (Netherlands).
EXISTENCE OF A NEW INSTANTON IN CONSTRAINED YANG-MILLS-HIGGS THEORY
F. R. Klinkhamer Mar. 1993 42 p Sponsored by Royal Netherlands Academy of Arts and Sciences Limited Reproducibility: More than 20% of this document may be affected by microfiche quality
(NIKHEF-H/93-02; ETN-93-94824) Avail: CASI HC A03

The goal of the study is to discover possible new four dimensional euclidean solutions (instantons) in fundamental supersymmetry SU(2) Yang-Mills-Higgs theory, with a constraint added to prevent collapse of the scale. It is shown that there exists one particular new constrained instanton (I star) with vanishing Pontryagin index. This is based on a topological argument that involves the construction of a noncontractible loop of four dimensional configurations with a certain upperbound on the action, which were established numerically. I star is expected to be the lowest action nontrivial solution in the vacuum sector of the theory. There also exists a related static, but unstable, solution, the new sphaleron. Possible applications of I star to the electroweak interactions include the asymptotics of perturbation theory and the high energy behavior of the total cross section. ESA

N94-17612 Joint Inst. for Nuclear Research, Dubna (USSR). Lab. of Theoretical Physics.
QUANTUM PHASE FLUCTUATIONS IN THE JAYNES-CUMMINGS MODEL: EFFECTS OF CAVITY DAMPING
Trung Dung Ho and A. S. Shumovskij 1992 19 p Limited Reproducibility: More than 20% of this document may be affected by microfiche quality
(DE93-627984; JINR-E-17-92-201) Avail: CASI HC A03 (US Sales Only)

Phase properties of a coherent field interacting with a two-level atom in a cavity with very high but finite Q are studied. It is shown that due to the cavity damping the field phase is randomized more quickly than in the ideal-losslesscavity case. The Hermitian phase distribution and the phase distributions associated with the Q function and the Wigner function are compared. The similarities between them have a clear interpretation in terms of the area-of-overlap in phase space. DOE

N94-17617 Nationaal Inst. voor Kernfysica en Hoge Energiefysica, Amsterdam (Netherlands).
THE THREE-LOOP QCD BETA-FUNCTION AND ANOMALOUS DIMENSIONS
S. A. Larin and J. A. M. Vermaseren 1992 6 p Limited Reproducibility: More than 20% of this document may be affected by microfiche quality
(NIKHEF-H/92-17; ETN-93-94822) Avail: CASI HC A02

The analytic calculation of the three loop Quantum Chromodynamics (QCD) beta function and anomalous dimensions within the minimal subtraction scheme in an arbitrary covariant gage is presented. The result for the beta function coincides with the previous calculation. Throughout the calculations, dimensional regularization and the minimal subtraction scheme are used. The unrenormalized three loop one particle irreducible quark-quark-gluon vertex and inverted quark and gluon propagators are computed. ESA

N94-17662# Fermi National Accelerator Lab., Batavia, IL.
SEARCH FOR THE TOP QUARK FROM (e(MU)) AND (e,e) EVENTS IN THE D0 DETECTOR IN p(BAR-p) COLLISIONS AT THE SQUARE ROOT OF s = 1.8 TeV
R. Raja 3 Jun. 1993 20 p Presented at the 1993 Recontres De Physique De La Vallee D'Aoste, LaThuile, Italy, 8-13 Mar. 1993

(Contract DE-AC02-76CH-03000)
(DE93-016350; FNAL/C-93/143-E; CONF-9303172-2) Avail: CASI HC A03/MF A01

We present results from searches for top quark production in p(bar p) collisions at the Tevatron collider based on an integrated luminosity of 7.5 pb(sup -1) obtained during the 1992-1993 run. The present results are confined to decay modes where both the top and anti-top quarks in the event decay semi-leptonically to the ee and e(mu) channels. A lower limit of 103 (99) GeV/c(exp 2) is obtained at 95% confidence level for the top quark mass from the absence of events consistent with standard model top quark decays with background subtraction (no background subtraction). We do, however, observe one event in the e(mu) channel which cannot be explained by the known backgrounds. While we make no claim that this event is due to top quark decay, it is not inconsistent with a top quark mass in the range 130-170 GeV/c exp 2. DOE

N94-17674# Wisconsin Univ., Madison. Plasma Physics Research.
GRANULAR FLUCTUATIONS IN PLASMA TURBULENCE AND THEIR ROLE IN TRANSPORT
P. W. Terry Apr. 1993 17 p Presented at the Interdisciplinary Workshop on Statistical Description of Transport in Astro- and Nuclear Physics, Les Houches, France, 2-11 Feb. 1993
(Contract DE-FG02-89ER-53291)
(DE93-013465; DOE/ER-53291/217; CONF-9302117-1) Avail: CASI HC A03/MF A01

Three general types of granular or discrete fluctuations in plasma turbulence are reviewed, with emphasis placed on their unique role in fluctuation-induced transport. These fluctuations are clumps, holes, and vortices, and represent structures that are not part of the normal mode response, the basis of conventional descriptions of plasma turbulence and transport. These fluctuations interact with the normal mode response to produce profound modifications of transport. The self-consistent linking of fields and particle distributions through quasineutrality and Ampere's law is shown to be crucial in calculating these modifications. In particular, it is pointed out that collisionless electron motion along perturbed magnetic fields produces almost no transport of field aligned current across equilibrium surfaces. It is also shown that clumps are granular structures which are turbulently mixed, whereas holes and vortices avoid mixing and relaxation through strong self-binding effects. The distinction between structures that are mixed and those that are persistent is probed in an analysis of the interaction of an intense vortex and ambient turbulent fluctuations. It is shown that, above a critical amplitude, the shearing of eddies due to the differential rotation of the vortex suppresses the fluctuations that mix its vorticity, allowing it to achieve a lifetime greatly in excess of the turbulent interaction time scale. DOE

N94-16194*# California Univ., San Diego, La Jolla. Dept. of Chemistry.
A CALIBRATION OF THE PRODUCTION RATE RATIO P-21/P-26 BY LOW ENERGY SECONDRY NEUTRONS: IDENTIFICATION OF Ne SPALLATION COMPONENTS AT THE 10(EXP 6) ATOMS/g LEVEL IN TERRESTRIAL SAMPLES Abstract Only
Th. Graf, S. Niedermann (Bern Univ., Switzerland.), and K. Marti *In* Lunar and Planetary Inst., Twenty-Fourth Lunar and Planetary Science Conference. Part 2: G-M 1993 p 555-556 (For primary document see N94-16173 03-91)
Avail: CASI HC A01/MF A06

73 NUCLEAR AND HIGH-ENERGY PHYSICS

Includes elementary and nuclear particles; and reactor theory. For space radiation see *93 Space Radiation.*

N94-16116# Chicago Univ., IL.
THEORETICAL HIGH ENERGY PHYSICS RESEARCH AT THE UNIVERSITY OF CHICAGO
J. L. Rosner, E. J. Martinec, and R. G. Sachs Apr. 1993 31 p
(Contract DE-FG02-90ER-40560)
(DE93-016863; DOE/ER-40560/4A) Avail: CASI HC A03/MF A01

Brief narrative descriptions of work performed are given on numerous topics including the following: CP violation, Cabibbo--Kobayashi--Maskawa matrix, and B physics; radiative corrections and electroweak observables; heavy quark symmetry; heavy meson spectroscopy; composite models of quarks and leptons; supersymmetric quantum mechanics, inverse scattering, and the vertex operator; cosmological constraints on lepton-number violation in SO(10) models; black hole evaporation; the light cone in string theory; surfaces in the 3D Ising model; and conformal field theories. DOE

N94-16170# Columbia Univ., New York, NY.
THEORETICAL HIGH ENERGY PHYSICS
T. D. Lee 1993 25 p
(Contract DE-FG02-92ER-40699)
(DE93-015884; DOE/ER-40699/2) Avail: CASI HC A03/MF A01

Brief reports are given on the work of several professors. The following areas are included: quantum chromodynamics calculations using numerical lattice gauge theory and a high-speed parallel computer; the 'spin wave' description of bosonic particles moving on a lattice with same-site exclusion; a high-temperature expansion to 13th order for the O(4)-symmetric (phi)(sup 4) model on a four-dimensional F(sub 4) lattice; spin waves and lattice bosons; superconductivity of C60; meson-meson interferometry in heavy-ion collisions; baryon number violation in the Standard Model in high-energy collisions; hard thermal loops in QCD; electromagnetic interactions of anyons; the relation between Bose-Einstein and BCS condensations; Euclidean wormholes with topology S(sup 1) x S(sup 2) x R; vacuum decay and symmetry breaking by radiative corrections; inflationary solutions to the cosmological horizon and flatness problems; and magnetically charged black holes. DOE

N94-16660# Texas Univ., Austin. Inst. for Fusion Studies.
THE (DELTA)F ALGORITHM FOR BEAM DYNAMICS
J. Koga and T. Tajima May 1993 51 p
(Contract DE-FG05-80ET-53088)
(DE93-015632; DOE/ET-53088-601; IFSR-601) Avail: CASI HC A04/MF A01

An algorithm is developed to study particle dynamics of beams including collective interaction with high accuracy and low noise. Particle dynamics with collective interactions is treated through particle simulation, where the main or average distribution f(sub 0) and the deviation away from it (delta)f are separately followed. The main distribution f(sub 0) is handled by an analytic equilibrium solution and the perturbation away from it (delta)f is followed by the method of characteristics. We call this the (delta)f algorithm. We specifically model a synchrotron collider which includes the collision section where collective effects of collisions are simulated by this (delta)f algorithm and the rest of the collider where single particle dynamics are treated by simple harmonic transport. The most important target of this simulation is to understand and predict the long-time behavior of the beam luminosity and lifetime. The (delta)f method allows the study of the effect of small perturbations over long timescales on beam lifetime by eliminating the numerical noise problem inherent in Particle-in-Cell techniques. In the (delta)f code using the reference parameters of the SSC (Superconducting Super Collider), beam blow-up near resonances and oscillations in the tune shift, (delta)(nu), far from resonances are observed. In studying long timescale particle diffusion in the phase space of the beams away from resonances, the (delta)f code performance is compared with a tracking code which does not incorporate collective interaction. DOE

N94-16829# Brookhaven National Lab., Upton, NY.
THE pp ELASTIC SCATTERING EXPERIMENT AT RHIC AND POLARIZATION STUDIES IN THE COULOMB NUCLEAR INTERFERENCE REGION
W. Guryn and N. Akchurin (Iowa Univ., Iowa City.) 1993 6 p Presented at the Future Directions in Particle and Nuclear Physics At Multi-GeV Hadron Beam Facilities, Upton, NY, 4-6 Mar. 1993
(Contract DE-AC02-76CH-00016)
(DE93-015391; BNL-48932; CONF-930389-18) Avail: CASI HC A02/MF A01

We have examined the feasibility of measuring proton proton (pp) elastic scattering at small four momentum transfer t. The application of the measurement as a polarimeter in the Coulomb Nuclear Interference (CNI) region for polarized pp collisions is discussed. In addition, other fundamental polarization phenomena can be explored by making use of the same setup. The configuration of the lattice of the Relativistic Heavy Ion Collider (RHIC) which allows the measurement of scattering in CNI region is

presented. The t range of the experiment is 0.0005 less than t less than 0.2(GeV/c)(sup 2). DOE

N94-16900# State Univ. of New York, Albany. Research Foundation.
CALORIMETER BASED DETECTORS FOR HIGH ENERGY HADRON COLLIDERS
23 Jun. 1993 43 p
(Contract DE-FG02-92ER-40697)
(DE93-017055; DOE/ER-40697/2) Avail: CASI HC A03/MF A01

The work was directed in two complementary directions: the D0 experiment at Fermilab, and the GEM detector for the SSC. Efforts have been towards the data taking and analysis with the newly commissioned D0 detector at Fermilab in the (bar-p)p Collider run that started in May 1992 and ended on 1 Jun. 1993. We were involved running and calibration of the calorimeter and tracking chambers, the second level trigger development, and various parts of the data analysis, as well as studies for the D0 upgrade planned in the second half of this decade. Another major accomplishment was the 'delivery' of the Technical Design Report for the GEM SSC detector. Efforts to the overall detector and magnet design, design of the facilities, installation studies, muon system coordination, muon chamber design and tests, muon system simulation studies, and physics simulation studies are described individually in this document. DOE

N94-17018*# National Aeronautics and Space Administration. Langley Research Center, Hampton, VA.
ENERGY-LOSS CROSS SECTIONS FOR INCLUSIVE CHARGE-EXCHANGE REACTIONS AT INTERMEDIATE ENERGIES
Francis A. Cucinotta, Lawrence W. Townsend, and Rajendra R. Dubey (Old Dominion Univ., Norfolk, VA.) Nov. 1993 22 p
(RTOP 199-45-16-11)
(NASA-TM-4522; L-17277; NAS 1.15:4522) Avail: CASI HC A03/MF A01

Charge-exchange reactions for scattering to the continuum are considered in a high-energy multiple scattering model. Calculations for (p,n) and (He-3,H-3) reactions are made and compared with experimental results for C-12, O-16, and Al-27 targets. Coherent effects are shown to lead to an important role for inelastic multiple scattering terms when light projectiles are considered. Author

N94-17313 Joint Inst. for Nuclear Research, Dubna (USSR). Lab. of Theoretical Physics.
QUARK-LOOP EFFECTS IN HIGH ENERGY SPIN-FLIP PROCESSES
S. V. Goloskokov 1992 15 p Limited Reproducibility: More than 20% of this document may be affected by microfiche quality
(DE93-626692; JINR-E-2-92-103) Avail: Issuing Activity (Department of Energy (DOE)) (US Sales Only)

On the basis of QCD long-distance model, the qq-sea contribution to the spin effects is analyzed in the s approaches infinity, t-fixed limit, and it is shown that such effects lead to the spin-flip amplitude growing as s. The magnitude of spin-flip and spin-nonflip amplitudes is estimated within some models for quark and gluon propagators. The relative role of spin effects, the wave function, and the elementary quark subprocess is discussed too. It is shown that the quark-sea effects in the scattering amplitude can reach 30-40% of the contribution of the simple two-gluon exchange at small momenta transfer. DOE

N94-17672# Lawrence Livermore National Lab., CA.
EMITTANCE GROWTH IN DISPLACED, SPACE-CHARGE-DOMINATED BEAMS WITH ENERGY SPREAD
J. J. Barnard, J. Miller, and I. Haber (Naval Research Lab., Washington, DC.) 11 May 1993 3 p Presented at the International Particle Accelerator Conference, Washington, DC, 17-20 May 1993
(Contract W-7405-eng-48)
(DE93-016514; UCRL-JC-112340; CONF-930511-212) Avail: CASI HC A01/MF A01

Conversion of transverse energy associated with the coherent motion of displaced beams into thermal energy, and thus emittance growth, has been predicted theoretically by a number of authors. Here, they authors show, using 2-D particle-in-cell simulations, that emittance growth is inhibited for tune depressed beams, if the energy spread of the beam is not too large. Further, using a uniform density model to calculate the space charge field of the beam, they numerically determine the criteria for emittance growth as a function of tune depression, energy spread, and beam displacement over a wide range of parameters. A theoretical interpretation of the results is presented. This study is applicable to an inertial fusion reactor driven by a heavy ion accelerator. DOE

74 OPTICS

Includes light phenomena; and optical devices.
For lasers see *36 Lasers and Masers.*

N94-14940 BDM International, Inc., McLean, VA.
OPTICAL RESIDUE PROCESSING MODULE Final Report, Jul. 1991 - Dec. 1992
Michael W. Haney, James J. Levy, Ravindra A. Athale, and Gary W. Euliss May 1993 36 p Limited Reproducibility: More than 20% of this document may be affected by microfiche quality
(Contract F30602-91-C-0052)
(AD-A267721; RL-TR-93-58) Avail: Issuing Activity (Defense Technical Information Center (DTIC))

An experimental program was conducted which demonstrated the Source Modulator Outer Product (SMOP) concept for high speed, high efficiency residue number system (RNS) computation. The optical architecture includes the outer product portion and a mapping portion to implement a Lookup Table (LUT). A Fourier transform based approach proved better suited to this architecture than did an image-based approach. Also, while the mapping was experimentally performed with optical fibers, a free-space approach based on an array of holographic optical elements is also contemplated. The end product of this research effort included experimental demonstration and a preliminary design of a high performance optical RNS processor based on the SMOP approach. DTIC

N94-14957# California Inst. of Tech., Pasadena. Dept. of Electrical Engineering.
VELOCITY MATCHED MILLIMETERWAVE ELECTRO-OPTIC MODULATOR Final Technical Report, Aug. 1990 - Sep. 1991
William B. Bridges and Finbar T. Sheehy May 1993 49 p
(Contract F30602-88-D-0026)
(AD-A267264; RL-TR-93-57) Avail: CASI HC A03/MF A01

This effort has resulted in the fabrication and demonstration of an optical phase modulator at RF frequencies as high as 64 GHz while using a visible light source. This technique, which is extendable to higher RF frequencies and to longer optical wavelengths, uses a series of high dielectric materials, set at an angle, between the RF signal source to match the resultant velocity of the RF wave with the optical signal in the photonic waveguide. The coupling of the RF wave to the optical signal in the modulator is enhanced by plating resonant antenna structures onto the modulator substrate and electronically interfacing them with the modulator electrodes. This technique can also be applied to interferometric type modulators. DTIC

N94-15144# Carnegie-Mellon Univ., Pittsburgh, PA. Robotics Inst.
INFRARED REMOTE ACTIVITY TRANSCEIVER UNIVERSAL MODEL
William Sands, Robert Thibadeau, and Drew Anderson Apr. 1993 28 p
(Contract MDA972-92-J-1010; ARPA Order 6873)
(AD-A266965; CMU-RI-TR-93-12) Avail: CASI HC A03/MF A01

The IR-RAT was developed as the result of a need to remotely control computers. It is a microcontroller based infrared remote control interface. This document describes its design and operation so that it might be used or altered for use in the future. DTIC

N94-15447# Technische Univ., Berlin (Germany). Fachbereich fuer Elektrotechnik.
OPTICAL COUPLING ELEMENTS FOR COHERENT OPTICAL MULTIPORT RECEIVERS Ph.D. Thesis [OPTISCHE KOPPELEMENTE FUER DEN KOHAERENT OPTISCHEN MEHRTOREMPFAENGER]
Ralf Langenhorst 1992 177 p In GERMAN
(ETN-93-94398) Avail: CASI HC A09/MF A02

Three by three (3 by 3) and four by four (4 by 4) port coupling elements and receivers for heterodyne multiport systems are realized. Commercial (3 by 3) fiber coupling elements were used to achieve a usual (3 by 3) port receiver and a (3 by 3) port receiver in pushpull switching,

whose concept was theoretically and experimentally analyzed. It is established that intensity oscillations of laser sources are suppressed by pushpull switching. The influence of thermal noise of opto-electronic input levels is shown to be weaker than in usual (3 by 3) port and (4 by 4) port receivers. Thermal noise effect in pushpull switching is similar to this one in heterodyne receivers. An integrated optical coupling element in LiNbO3 was made with bridge circuit from four waveguide coupling elements and two phase converters, which are electro-optically tunable so that a continuous regulation of intermediate frequency phase can be compensated by temperature variations of the element. To obtain fiber-to-fiber losses lower than a dB, a compact crystal optical coupling element was developed with reference to polarization properties of optical waves. This element supplied the eight necessary intermediate frequency output signals. A direct experimental comparison of bandwidth efficiency of multiport and heterodyne receivers shows a factor two in optical area and a factor three in electrical frequency area. ESA

N94-15647*# Christopher Newport Coll., Newport News, VA. Dept. of Physics and Computer Science.
OPTICAL FIBER SPECTROSCOPY: A STUDY OF THE LUMINESCENT PROPERTIES OF THE EUROPIUM ION FOR THERMAL SENSORS Annual Technical Report
A. Martin Buoncristiani 1992 12 p
(Grant NAG1-1443)
(NASA-CR-194576; NAS 1.26:194576) Avail: CASI HC A03/MF A01

Recently, there has been interest in developing a distributed temperature sensor integrated into an optical fiber. Such a system would allow embedding of the optical fiber within or on a structural material to provide for continuous monitoring of the material's temperature. Work has already begun on the development of a temperature sensor using the temperature dependent emission spectra from the lanthanide rare earths doped into crystalline hosts. The lifetime, the linewidth and the integrated intensity of this emission are each sensitive to changes in the temperature and can provide a basis for thermometry. One concept for incorporating this phenomena into an optical fiber based sensor involves bonding the optically active material to the cladding of an optical fiber and allowing the luminescent light to couple into the the fiber by the evanescent wave. Experimental work developing this concept has already been reported. Measurements of the linewidth of Eu3+:Y2O3, diffused into a fiber, made by Albin clearly show a strong and regular dependence on temperature over the range of 300 to 1000 K. We report here on a study of the temperature dependence of the lineshape of the emission at 611 nm using the data in references. We focus attention on understanding the general behavior of the Eu3+:Y2O3 system. Building upon understanding of this system we will be able to establish the physical criterial for a good optical fiber based temperature sensor and then to examine available data on other lanthanide rare earths and transition metal ions to determine the best luminescent system for temperature sensing in an optical fiber. Derived from text

N94-15664# Dynetics, Inc., Huntsville, AL.
ALTERNATIVE OPTICAL ARCHITECTURES FOR MULTICHANNEL ADAPTIVE OPTICAL PROCESSING Final Report, Jan. - Oct. 1992
R. J. Berinato, M. C. Zari, and M. C. Budge, Jr. Apr. 1993 150 p
(Contract F30602-92-C-0026)
(AD-A267052; RL-TR-93-34) Avail: CASI HC A07/MF A02

This final report describes the continued design and hardware implementation of an acousto-optic (AO) multichannel adaptive optical processor (MADOP) for application to the cancellation of multipath jamming interference in advanced surveillance radars. The work described in this report was performed for the Photonics Center at Rome Laboratory and represents the second year of Dynetics support on this project. The objective of this effort was the continued fabrication and performance characterization of a multichannel adaptive system that can perform cancellation of multiple wideband (10 MHz) interference sources in the presence of multipath. Specific activities included the following: (1) the simulation of convergence performance of the MADOP algorithms against a variety of multipath conditions; (2) the reconfiguration of the multichannel AO time-integrating correlator for improved stability; (3) the refinement of the AO tapped delay line to achieve better frequency response; (4) the development of the radio frequency interface between the two AO subsystems; and (5) the design and development of a single-loop electronic canceller for improved phase stability after the AO tapped delay line system. DTIC

N94-15705*# National Aeronautics and Space Administration. Goddard Space Flight Center, Greenbelt, MD.
ROTARY ENCODING DEVICE Patent Application
Douglas B. Leviton, inventor (to NASA) 3 Nov. 1992 32 p
(NASA-Case-GSC-13543-1; NAS 1.71:GSC-13543-1;
US-Patent-Appl-SN-971035) Avail: CASI HC A03/MF A01

A device for position encoding of a rotating shaft in which a polygonal mirror having a number of facets is mounted to the shaft and a monochromatic light beam is directed towards the facets. The facets of the polygonal mirror each have a low line density diffraction grating to diffract the monochromatic light beam into a number of diffracted light beams such that a number of light spots are created on a linear array detector. An analog-to-digital converter is connected to the linear array detector for reading the position of the spots on the linear array detector means. A microprocessor with memory is connected to the analog-to-digital converter to hold and manipulate the data provided by the analog-to-digital converter on the position of the spots and to compute the position of the shaft based upon the data from the analog-to-digital converter. NASA

N94-15735# Arizona Univ., Tucson. Optical Sciences Center.
LABORATORY FOR X RAY OPTICS Final Report, 1 Jan. 1990 - 28 Feb. 1993
Charles M. Falco 29 Apr. 1993 9 p
(Grant AF-AFOSR-0140-90)
(AD-A267149; AFOSR-93-0480TR) Avail: CASI HC A02/MF A01

During this period we concentrated our effort in two areas: (1) growth of epitaxial single-crystal beryllium films; and (2) multilayers and interfaces of material pairs incorporating 'new' materials for multilayer x-ray optics. To date we have succeeded in growing epitaxial single-crystal films of beryllium on alpha-Al2O3 (sapphire), silicon, and germanium using molecular beam epitaxy (MBE). This is a major development since beryllium is an excellent spacer for the difficult but desirable water window wavelengths (24 A less than lambda less than 44 A). To our knowledge, this is the first time beryllium has been grown epitaxially on any substrate. Our best quality beryllium films were grown on silicon. The ability to grow a single crystal layer of beryllium is a promising first step toward a beryllium-based single-crystal mirror. In the area of new material pairs. we began by using theoretical reflectivity calculations to assemble a list of promising new material pairs. We then prioritized this list by using what was already known about the materials, such as phase diagrams and diffusion studies. These materials pairs then were studied by sputtering and/or MBE. DTIC

N94-15739# Naval Postgraduate School, Monterey, CA.
THE THREE-DIMENSIONAL RAY TRAJECTORIES OF THE WKB OPTICAL FIBER MODES M.S. Thesis
Athanasios Nassopoulos Mar. 1993 102 p
(AD-A267167) Avail: CASI HC A06/MF A02

A model that produces three-dimensional ray trajectories in an optical fiber is derived through the use of a simple correspondence rule. The analysis and simulations presented will be in terms of dimensionless parameters. The curves prepared are presented for allowed radial and azimuthal mode numbers and are presented in terms of dimensions which are normalized by the core radius. The model presented will be shown to be in agreement with the standard Eikonal ray theory and will serve as a link between the ray trajectories and the mode numbers of the WKB waveguide solutions of an optical fiber. DTIC

N94-15791# Dayton Univ. Research Inst., OH.
SPATIAL FILTERS FOR OPTICAL CORRELATION Final Technical Report, May 1991 - May 1992
David L. Flannery May 1993 17 p
(Contract F30602-88-D-0028)
(AD-A267199; RL-TR-93-65) Avail: CASI HC A03/MF A01

A set of images comprising an azimuthal training set of M-48 tank images was used as the basis of simulation studies to assess the performance of improved metric sort ternary phase-amplitude filters using gray scale inputs. Results compared favorably with those obtained with other filter formulations. Binary versions of these images were used as the basis for a study of image binarization effects on optical correlation performance. The study indicated excellent correlation performance with binarized inputs and references. A set of T-72 tank images, including an azimuthal training set and input scenes with clutter, was the basis for a

simulation study comparing correlation performance of smart TPAF's with gray scale and binary input scenes. The correlation results with binary images were at least equal in quality to those using gray scale inputs. 128 x 128 correlation filters were generated on a zero-filled 256 x 256-pixel array. These filters were correlated with 128 x 128-pixel input scenes (imbedded in a zero-filled 256 x 256 array for digital simulations). Methods for implementing these filters in a correlator with 128 x 128-pixel SLM's at both input and filter planes were investigated by both simulation and experimentation. The two methods provided acceptable results. DTIC

N94-15845 Surveillance Research Lab., Salisbury (Australia).
SENSOR MODELLING FOR THE CYCLOPS FOCAL PLANE DETECTOR ARRAY BASED TECHNOLOGY DEMONSTRATOR
G. V. Poropat Dec. 1992 29 p Limited Reproducibility: More than 20% of this document may be affected by microfiche quality
(AD-A267172; SRL-0112-RN; DODA-AR-008-151) Avail: Issuing Activity (Defense Technical Information Center (DTIC))

The Surveillance Research Laboratory of the DSTO has developed a technology demonstrator utilizing an infrared focal plane detector array to assess the feasibility of using large scale infrared detector arrays for ADF applications. The imaging sensor which has been developed requires no scanning mechanism and uses an array of mercury cadmium telluride detectors sensitive to radiation in the 8 um to 12 um spectral region to produce an image. The sensor was tested in a series of airborne trails and the results obtained from these trials will be used to evaluate the performance of focal plane detector array based systems. A mathematical model of the sensor has been used to evaluate the performance of the sensor. The mathematical model has been developed to meet the requirements imposed by analysis of the performance of this sensor. The model is based on the description of the operation of the elements of the detector array as photon counters. A description of the model used for the analysis of the data obtained using the sensor is presented here. DTIC

N94-15848 California Univ., Los Angeles. Dept. of Electrical Engineering.
OPTOELECTRONICS BASED ON SiGe/Si HETEROSTRUCTURES
Annual Report, 15 Oct. 1991 - 14 Oct. 1992
Kang L. Wang 14 Jan. 1993 18 p Limited Reproducibility: More than 20% of this document may be affected by microfiche quality
(Grant AF-AFOSR-0313-91)
(AD-A267176; AFOSR-93-0545TR) Avail: CASI HC A03

The overall objective of the research is to explore SiGe/Si heterostructures for optoelectronic applications. In addition to exploration of new devices, alternative growth techniques for achieving layer thickness to monolayer scale and doping control are also investigated. We have discovered a new transition at normal incidence for p-type quantum well structures, in addition to previously observed intersubband transition. One of the advantages of this intervalence band transition is the detection of infrared at normal incidence. The application of these transitions for the fabrication of tunable normal incidence infrared detectors have also demonstrated. We have also demonstrated normal incidence intersubband transition in the conduction band of SiGe/Si quantum wells grown on (110) Si substrate due to the nonvanishing off-diagonal elements of the effective mass tensor. In the area of transport properties, we have studied the in-plane mobility of coupled delta-doped quantum wells as a function of spacing between the wells. An enhancement of hole mobility above that of the Si was found due to the penetration of wavefunctions into the spacer where the impurity scattering is minimal. In the area of the growth control of SiGe epitaxial layers, we have modified a MBE system for handling the gaseous species for gas beam epitaxy study. DTIC

N94-15854# California Univ., Berkeley. Lawrence Berkeley Lab.
CLOSED ORBIT DISTORTION AND THE BEAM-BEAM INTERACTION
M. Furman, Y. H. Chin, J. Eden, W. Kozanecki (Commissariat a l'Energie Atomique, Saclay, France.), and J Tennyson 1 Jun. 1992 48 p
(Contract DE-AC03-76SF-00098)
(DE93-015284; LBL-32435-Draft; ESG-193; SLAC-ABC-49) Avail: CASI HC A03/MF A01

We study the applicability of beam-beam deflection techniques as a tuning tool for the SLAC/LBL/LLNL B factory, PEP-II. Assuming that the closed orbits of the two beams are separated vertically at the interaction point by a local orbit bump that is nominally closed, we calculate the residual beam orbit distortions due to the beam-beam interaction. Difference orbit measurements, performed at points conveniently distant from the IP, provide distinct coordinator frequency-space signatures that can be used to maintain the beams in collision and perform detailed optical diagnostics at the IP. A proposal to test this method experimentally at the TRISTAN ring is briefly discussed. DOE

N94-15868*# Alabama Univ., Huntsville. Physics Dept.
FILTERS FOR THE INTERNATIONAL SOLAR TERRESTRIAL PHYSICS (ISTP) MISSION FAR ULTRAVIOLET IMAGER
Muamer Zukic, Douglas G. Torr, Jongmin Kim, James F. Spann, and Marsha R. Torr 1993 29 p
(Contract NAGw-2898; NAS8-38145)
(NASA-CR-194633; NAS 1.26:194633) Avail: CASI HC A03/MF A01

The far ultraviolet (FUV) imager for the International Solar Terrestrial Physics (ISTP) mission is designed to image four features of the aurora: O I lines at 130.4 nm and 135.6 nm and the N2 Lyman-Birge-Hopfield (LBH) bands between 140 nm - 160 nm (LBH long) and 160 nm - 180 nm (LBH long). In this paper we report the design and fabrication of narrow-band and broadband filters for the ISTP FUV imager. Narrow-band filters designed and fabricated for the O I lines have a bandwidth of less than 5 nm and a peak transmittance of 23.9 percent and 38.3 percent at 130.4 nm and 135.6 nm, respectively. Broadband filters designed and fabricated for LBH bands have the transmittance close to 60 percent. Blocking of out-of-band wavelengths for all filters is better than 5x10(exp -3) percent with the transmittance at 121.6 nm of less than 10(exp -6) percent. Author

N94-15869*# Alabama Univ., Huntsville. Physics Dept.
MULTILAYER THIN FILM DESIGN FOR FAR ULTRAVIOLET POLARIZERS USING AN INDUCED TRANSMISSION AND ABSORPTION TECHNIQUE
Jongmin Kim, Muamer Zukic, and Douglas G. Torr 1993 14 p
(Contract NAGw-2898; NAS8-38145)
(NASA-CR-194631; NAS 1.26:194631) Avail: CASI HC A03/MF A01

An explanation of induced transmission for spectral regions excluding the far ultraviolet (FUV) is given to better understand how induced transmission and absorption can be used to design effective polarizers in the FUV spectral region. We achieve high s-polarization reflectance and a high degree of polarization (P equals (Rs-Rp)/(Rs+Rp)) by means of a MgF2/Al/MgF2 three layer structure on an opaque thick film of Al as the substrate. For example, our polarizer designed for the Lyman-alpha line (lambda equals 121.6 nm) has 87.95 percent reflectance for the s-polarization case and 0.43 percent for the p-polarization case, with a degree of polarization of 99.03 percent. If a double reflection polarizer is made with this design, it will have a degree of polarization of 99.99 percent and s-polarization throughput of 77.35 percent. Author (revised)

N94-15933*# National Aeronautics and Space Administration. Pasadena Office, CA.
DISPLAY SYSTEM EMPLOYING ACOUSTO-OPTIC TUNABLE FILTER
Patent Application
James L. Lambert, inventor (to NASA) (Jet Propulsion Lab., California Inst. of Tech., Pasadena.) 7 Jun. 1993 22 p
(Contract NAS7-918)
(NASA-Case-NPO-18736-1-CU; NAS 1.71:NPO-18736-1-CU; US-Patent-Appl-SN-073235) Avail: CASI HC A03/MF A01

An acousto-optic tunable filter (AOTF) is employed to generate a display by driving the AOTF with a RF electrical signal comprising modulated red, green, and blue video scan line signals and scanning the AOTF with a linearly polarized, pulsed light beam, resulting in encoding of color video columns (scan lines) of an input video image into vertical columns of the AOTF output beam. The AOTF is illuminated periodically as each acoustically-encoded scan line fills the cell aperture of the AOTF. A polarizing beam splitter removes the unused first order beam component of the AOTF output and, if desired, overlays a real world scene on the output plane. Resolutions as high as 30,000 lines are possible, providing holographic display capability. NASA

N94-15975# Lawrence Livermore National Lab., CA.
POLISHED SUBSTRATE SURFACE AND CLEANING STUDY FOR COATED OPTIC QUALITY

A. Tesar, W. Eickelberg, K. Koons (Optical Coating Lab., Inc., Santa Rosa, CA.), and K. Davis (Optical Coating Lab., Inc., Santa Rosa, CA.) Nov. 1992 5 p Presented at the OPTCON 1992 Optical Fabrication and Testing Workshop, Boston, MA, 17 Nov. 1992
(Contract W-7405-eng-48)
(DE93-014116; UCRL-JC-111397; CONF-9211104-9) Avail: CASI HC A01/MF A01

The optical substrate-coating interface is established by the following: (1) the original polished condition of the substrate; (2) the substrate cleaning process; and (3) the environment of the coating process. The substrate-coating interface has the following characteristics: affects the coating adhesion properties; is where most coating defects and scatter sites are thought to initiate; and, in some instances, may control the structure of the coating as it is deposited. Often features appear on an optic after coating which could not be observed after cleaning and prior to coating. Because of the wide variety of possible substrate materials, surface problems, and contaminants, the cleaning processes are constantly evolving. Our study has clearly shown that the coating appearance is dependent not only on the cleaning method, but on the initial character of the substrate surface. DOE

N94-16007# Maryland Univ. Baltimore County, Catonsville. Dept. of Electrical Engineering.
PULSE PROPAGATION IN INHOMOGENEOUS OPTICAL WAVEGUIDES
C. R. Menyuk 28 Apr. 1993 6 p
(Contract DE-FG05-89ER-14090)
(DE93-013378; DOE/ER-14090/4) Avail: CASI HC A02/MF A01

This report discusses pulse propagation in inhomogeneous optical waveguides and fibers. DOE

N94-16023*# Alabama Univ., Huntsville. Physics Dept.
DESIGN AND FABRICATION OF A REFLECTION FAR ULTRAVIOLET POLARIZER AND RETARDER
Jongmin Kim, Muamer Zukic, Michele M. Wilson, and Douglas G. Torr 1993 19 p
(Contract NAGw-2898; NAS8-38145)
(NASA-CR-194630; NAS 1.26:194630) Avail: CASI HC A03/MF A01

New methods have been developed for the design of a far ultraviolet multilayer reflection polarizer and retarder. A MgF2/Al/MgF2 three-layer structure deposited on a thick opaque Al film (substrate) is used for the design of polarizers and retarders. The induced transmission and absorption method is used for the design of a polarizer and layer-by-layer electric field calculation method is used for the design of a quarterwave retarder. In order to fabricate these designs in a conventional high vacuum chamber, we have to minimize the oxidation of the Al layers and somehow characterize the oxidized layer. X-ray photoelectron spectroscopy is used to investigate the amount and profile of oxidation. Depth profiling results and a seven layer oxidation model are presented. Author (revised)

N94-16024*# Alabama Univ., Huntsville. Physics Dept.
TRANSPARENT CONDUCTIVE COATINGS IN THE FAR ULTRAVIOLET
Jongmin Kim, Muamer Zukic, Jung Ho Park, Michele M. Wilson, Charles E. Keffer, and Douglas G. Torr 1993 8 p
(Contract NAGw-2898; NAS8-38145)
(NASA-CR-194632; NAS 1.26:194632) Avail: CASI HC A02/MF A01

In certain cases a space-borne optical instrument with a dielectric window requires a transparent conductive coating deposited on the window to remove the electrostatic charge collected due to the bombardment of ionized particles. Semiconductor and metal films are studied for use as transparent conductive coatings for the front window of far ultraviolet camera. Cr is found to be the best coating material. The theoretical search for the semiconductor and metal coating materials and experimental results for ITO and Cr films are reported. Author (revised)

N94-16126# Air Force Systems Command, Wright-Patterson AFB, OH. Foreign Aerospace Science and Technology Center.
HIGH-PERFORMANCE NONLINEAR OPTICAL MATERIAL DEVELOPED IN JAPAN
Sheng Li 25 May 1993 6 p Transl. into ENGLISH from unidentified Chinese language document, cols 2-4 p 3
(AD-A266194; FASTC-IR(RS)T-0959-92) Avail: CASI HC A02/MF A01

The world's best performing nonlinear optical material was recently developed by the Asahi Corporation. The nonlinear three-dimensionality of this new material is 1000 times higher than any known material. This new material is made by spreading fine particles of cuprous chloride (with semiconductor properties) onto a special glass. The fine cuprous chloride particles are only 5 to 10 nanometers in diameter. After the cuprous chloride particles are melted onto the special glass, they are subjected to heat treatment before cooling, thus producing uniform fine particles. DTIC

N94-16128# International Business Machines Corp., Yorktown Heights, NY. Research Div.
OETC OPTICAL BACKPLANE BUS TESTBED. IBM TASKS: RECEIVER OEIC AND LINK SIMULATION TOOLS AND ANALYSIS Milestone Report
John Crow, Richard Bates, Young Kwark, Dennis Rogers, and Dan Kuchta 20 May 1993 17 p
(Contract MDA972-92-C-0075)
(AD-A266198) Avail: CASI HC A03/MF A01

This report describes the following: the strategy adopted for developing a bus simulation tool; the parameters chosen for the component models which are used in the tool; the experimental determination of the parameters for one of the key devices in the link, the VSEL; and the experimental and simulation analysis used to predict the first pass link behavior. The major accomplishments are as follows: (1) that a set of specifications were developed; and (2) that a design for the VSEL source for the transmitter was established based on device and link characterization at IBM. Operational parameters for the transmitter simulation model were developed. With these accomplishments, first pass components for the link can, and are, being designed and fabricated. DTIC

N94-16454# Northwestern Univ., Evanston, IL.
RATIONAL DESIGN, CONSTRUCTION, AND PROCESSING OF HIGH-PERFORMANCE NONLINEAR OPTICAL MATERIALS Final Report, 1 Dec. 1990 - 30 Nov. 1992
T. J. Marks, G. K. Wong, and M. A. Ratner 14 May 1993 16 p
(Grant AF-AFOSR-0071-90)
(AD-A266185; AFOSR-93-0440TR) Avail: CASI HC A03/MF A01

This project consists of a collaborative synthetic, processing, physical characterization, and theoretical program aimed at the rational design, construction, evaluation, and fundamental understanding of new types of maximum-performance molecule/polymer-based materials exhibiting high second-order (CHI(2)) optical nonlinearities. Areas of emphasis include poled chromophore-functionalized glassy polymers, poled chromophore-embedded crosslinkable matrices, chromophoric self-assembled superlattices, the theoretical design and analysis of novel chromophores and chromophore environments, theoretical studies of poling dynamics, studies of optical damage phenomena, and fabrication of new types of NLO waveguides. Each research component of this highly interactive effort builds upon work already in progress as well as upon strong on-going collaborations in laser optics and quantum theory. DTIC

N94-16489 Department of the Navy, Washington, DC.
FABRICATION AND PHASE TUNING OF AN OPTICAL WAVEGUIDE DEVICE Patent
William K. Burns, inventor (to Navy), Catherine H. Bulmer, inventor (to Navy), and Arthur S. Greenblatt, inventor (to Navy) 16 Mar. 1993 7 p Filed 27 Sep. 1991 Supersedes AD-D015179
(AD-D015815; US-Patent-5,195,163; US-Patent-Appl-SN-766939; US-Patent-Class-385-132) Avail: US Patent and Trademark Office

The manufacture of an optical waveguide device utilizing a fast, accurate method for tuning of the output phase angle of such devices to a desired operating point is described. Tuning is accomplished by adjusting the accumulated phase along a waveguide arm of the device by removing optical waveguide material using laser ablation. Due to the change in waveguide geometry in the ablated region, the optical phase velocity is changed and thus the optical path length is affected in that section of waveguide, thereby resulting in a change in output phase angle. DTIC

N94-16547 Department of the Navy, Washington, DC.
INFRARED SPOT TRACKER Patent
Albert H. Marshall, inventor (to Navy), Edward J. Purvis, inventor (to Navy), Robert T. McCormack, inventor (to Navy), and Ronald S. Wolff, inventor

(to Navy) 1 Jun. 1993 168 p Filed 5 Nov. 1991
(AD-D015778; US-Patent-5,215,465; US-Patent-Appl-SN-788073; US-Patent-Class-434-22) Avail: US Patent and Trademark Office

The apparatus is an interactive, scenario based simulator for training a weapons team in close encounter combat. Employed is a large screen projection system, a plurality of trainee positions, and means to remove aggressor images when neutralized by the team, to provide an apparent threat to the trainees from the simulated aggressors, and to track each trainees performance throughout the training scenario. DTIC

N94-16550# Keo Consultants, Brookline, MA.
OPTICAL IONOSPHERIC INSTRUMENTATION AND RESEARCH Final Report, 3 Nov. 1989 - 3 Nov. 1992
Robert H. Eather and Peter A. Ning 18 Dec. 1992 52 p
(Contract F19628-89-C-0187)
(AD-A266403; PL-TR-92-2342) Avail: CASI HC A04/MF A01

Keo Consultants participated in the research of the Ionospheric Applications Branch at Phillips Laboratory by implementing improvements in research optical instrumentation (photometers and imagers). This research involved numerous field trips to study aurora, airglow, ionospheric scintillations, barium releases, and heater experiments. Keo customized instrument control software for each application, and developed software to display the resultant images and compare with other data sets. DTIC

N94-16563# University of Northern Illinois, De Kalb. Dept. of Chemistry.
NEW ORGANIC MATERIALS FOR NONLINEAR OPTICS APPLICATIONS Final Report, 1 Nov. 1989 - 31 Oct. 1992
Charles W. Spangler 29 Jan. 1993 45 p
(Grant AF-AFOSR-0060-90)
(AD-A266451; AFOSR-93-0195TR) Avail: CASI HC A03/MF A01

The formation of polaron-like radical cations and bipolaron-like dictations in oligomer series related to polyacetylene, polyP-PHENYLENE (PPV), poly2,5-THIENYLENE VINYLENE (PTV), POL, and PTL were studied in solution and composite films. Chi(3) measurements were carried out in collaboration with Professors Larry Dalton and Robert Hellwarth (USC). Conclusive evidence was obtained that demonstrates bipolaronic-enhancement of X(3). DTIC

N94-16718*# Case Western Reserve Univ., Cleveland, OH. Dept. of Chemical Engineering.
MAXIMUM LIKELIHOOD TECHNIQUES APPLIED TO QUASI-ELASTIC LIGHT SCATTERING Final Report
Robert V. Edwards 24 Aug. 1992 3 p
(Contract NCC3-115)
(NASA-CR-193550; NAS 1.26:193550) Avail: CASI HC A01/MF A01

There is a necessity of having an automatic procedure for reliable estimation of the quality of the measurement of particle size from QELS (Quasi-Elastic Light Scattering). Getting the measurement itself, before any error estimates can be made, is a problem because it is obtained by a very indirect measurement of a signal derived from the motion of particles in the system and requires the solution of an inverse problem. The eigenvalue structure of the transform that generates the signal is such that an arbitrarily small amount of noise can obliterate parts of any practical inversion spectrum. This project uses the Maximum Likelihood Estimation (MLE) as a framework to generate a theory and a functioning set of software to oversee the measurement process and extract the particle size information, while at the same time providing error estimates for those measurements. The theory involved verifying a correct form of the covariance matrix for the noise on the measurement and then estimating particle size parameters using a modified histogram approach. Derived from text

N94-16926# Aerospace Medical Research Labs., Wright-Patterson AFB, OH.
OPTICAL DISPLAYS: A TUTORIAL ON IMAGES AND IMAGE FORMATION Final Report, Oct. 1990 - Oct. 1992
Herschel C. Self Oct. 1992 115 p
(AD-A266230; AL-TR-1992-0178) Avail: CASI HC A06/MF A02

The tutorial presents basic image and optical display concepts. To aid in understanding the concepts, discussion, figures, and tables, derivations in detail of optical equations are presented. Examples and alternative derivations clarify the concepts. High school algebra and trigonometry are adequate for following the derivations. Extensive use is made of the basic Gauss lens equation relating object distance and lens focal length to image distance. Topics include real and virtual images, image size and distance, proper viewing distance, exit pupil diameter and location, varying optical distance with a magnifier, focal length, objectives and eyepieces, relays, microscopes and telescopes, optical system complexity, etc. Compound optical systems with an objective and an eyepiece, and systems that also include a relay lens, are examined. Optical and mechanical considerations for helmet-mounted displays (HMDs), and the compromises and trade-offs required in designing such systems are presented in considerable detail. DTIC

N94-16936# Photometrics, Inc., Woburn, MA.
OPTICAL PROPERTIES OF WATER RELEASED IN LOW EARTH ORBIT
James A. Gardner, II, David L. Rall, Christian A. Trowbridge, Irving L. Kofsky, and Rodney A. Viereck 21 Jun. 1993 13 p
(Contract F19628-91-C-0061)
(AD-A266197; PL-TR-93-2134) Avail: CASI HC A03/MF A01

Analysis of intensified video photographs of a twilight venting of excess water from the space shuttle showed that the approx. 1 mm diameter stream cavitationally fragments within about 1 m, forming two discrete-particle components and vapor. The images from nearby cameras are dominated by irregular, polydisperse water/ice droplets with sizes comparable with the venting orifice and outward velocity indistinguishable from that of the initially coherent liquid. In contrast the 2 1/2 km-long quasiconical trail imaged from a distant ground station consists of accompanying submicron ice spherules that were produced by partial recondensation of the overexpanded vacuum-evaporated water gas, which are sublimating at rates that we calculated from the measured falloff of axial sunlight-scatter radiance and the energy balance of progressively roughening ice at 329 km altitude; at low latitudes they cool to 180 K in less than 1 s, and their radii transition to the Rayleigh-scattering range in approx. 1 min. The very much larger fragmentation particles come to a slightly higher equilibrium temperature within approx. 2 min, and persist for a few earth orbits. These three components of the vented water (and other high vapor pressure liquids) radiate and scatter earthshine and solar photons, and the orbital-velocity molecules are also excited by collisions with the residual atmospheric gas, overlaying wide-angle contaminating foregrounds on remote optical sensing from onboard. DTIC

N94-16953# Los Alamos National Lab., NM.
FUNDAMENTAL THEORY OF LIGHT FOR APPLICATIONS: NOTES FOR FIVE INFORMAL LECTURES
P. W. Milonni 18 Jun. 1993 34 p Presented at the International School and Workshop in Photonics and 4th Latin American Encounter on Optics, Lasers, and Their Applications, Oaxtepec (Mexico), 21 Jun. - 2 Jul. 1993
(Contract W-7405-eng-36)
(DE93-016463; LA-UR-93-2307; CONF-9306186-1) Avail: CASI HC A03/MF A01

These notes give an overview of some aspects of the quantum theory of light and its interaction with matter. A description is given of basic emission and absorption processes, as well as the theory of photodetection and optical coherence. Basic research in this area is increasingly relevant to areas of technological importance including microlaser devices and the noise characteristics of semiconductor lasers. DOE

N94-16975# Naval Postgraduate School, Monterey, CA.
A FORMAL PROTOCOL TEST PROCEDURE FOR THE SURVIVABLE ADAPTABLE FIBER OPTIC EMBEDDED NETWORK (SAFENET) M.S. Thesis
Wayne High Mar. 1993 118 p
(AD-A267410) Avail: CASI HC A06/MF A02

This thesis focuses upon a new method for verifying the correct operation of a complex, high speed fiber optic communication network. These networks are of growing importance to the military because of their increased connectivity, survivability, and reconfigurability. With the introduction and increased dependence on sophisticated software and protocols, it is essential that their operation be correct. Because of the speed and complexity of fiber optic networks being designed today, they are becoming increasingly difficult to test. Previously, testing was accomplished by application of conformance test methods which had little connection with an implementation's specification. The major goal of

conformance testing is to ensure that the implementation of a profile is consistent with its specification. Formal specification is needed to ensure that the implementation performs its intended operations while exhibiting desirable behaviors. The new conformance test method presented is based upon the System of Communicating Machine model which uses a formal protocol specification to generate a test sequence. The major contribution of this thesis is the application of the System of Communicating Machine model to formal profile specifications of the Survivable Adaptable Fiber Optic Embedded Network (SAFENET) standard which results in the derivation of test sequences for a SAFENET profile. The results applying this new method to SAFENET's OSI and Lightweight profiles are presented. DTIC

N94-17012# Aerospace Corp., El Segundo, CA. Technology Operations.
SPECKLES STATISTICS AND DECORRELATION EFFECTS IN COMPLEX ABCD OPTICAL SYSTEMS
H. T. Yura, S. G. Hanson, and T. P. Grum 15 Dec. 1992 36 p
(Contract F04701-88-C-0089)
(AD-A267843; TR-92(2409)-3; SMC-TR-93-35) Avail: CASI HC A03/MF A01

The mean, variance, and correlation function of the intensity pattern resulting from an incoherent source that has propagated through a complex ABCD optical system is derived. The number of speckle correlation cells (or modes) within an effective measurement area is presented and discussed. Optical field decorrelation effects regarding secondary fringe formation in phase shifting speckle interferometry is discussed. In particular, the correlation coefficient resulting from load-induced object tilt, in-plane translations, and displacements parallel to the optic axis as a function of the number of modes propagating through the optical system is described and discussed. DTIC

N94-17024# Massachusetts Inst. of Tech., Cambridge. Dept. of Chemistry.
THEORETICAL STUDIES OF NONLINEAR OPTICAL PROPERTIES OF CONJUGATED POLYMERS Final Report, 1 Jan. - 31 Dec. 1992
Robert J. Silbey 21 May 1993 9 p
(Grant AF-AFOSR-0077-90)
(AD-A267390; AFOSR-93-0560TR) Avail: CASI HC A02/MF A01

The study of the nonlinear optical properties of polymeric systems is a challenging and exciting field of research ranging from device engineering, optical measurements, chemical synthesis to design and theoretical issues. At the present time, most of the basic science needed for the synthesis of molecules and the design of devices utilizing second order optical susceptibilities is in hand, although certain issues remain to be resolved. On the other hand, many important questions regarding the design and use of third order optical susceptibilities are still unanswered. The earliest ideas of the importance of low dimensionality optical band gaps suggests the use of conjugated molecules. At present, there is considerable effort, both experimentally and theoretically, in optimizing the value of gamma for polymers or oligomers with conjugated segments, because such conjugated polymers (like polyacetylene, polythiophenes, and the poly-diacetylenes) have very large gamma. These polymers have also been under intense scrutiny because of their large conductivities when doped. Although we are beginning to understand the theoretical reasons for the various unusual properties of the materials, we do not understand the factors that limit the ultimate value of gamma. For example, what are the important structures and interactions in the molecule the prevent gamma from being as large as possible while still having a small absorption coefficient, and how can we design molecules with these constraints in mind. DTIC

N94-17028# Naval Postgraduate School, Monterey, CA.
PERFORMANCE OF CODED COHERENT FSK LIGHTWAVE SYSTEM WITH NONCOHERENT DETECTION
Thomas E. Neely Mar. 1993 76 p
(AD-A267442) Avail: CASI HC A05/MF A01

The original coherent lightwave systems were expected to offer significant performance gains relative to standard direct detection systems. This expectation has not been realized due to the effects of laser phase noise. The laser phase noise process results in the integration of a random variable that transitions over the integration period from a Gaussian distribution to a uniform distribution. The use of convolutional coding effectively replaces a single bit time, with its mostly noncoherently integrating latter portion, by several more coherently integrating bits. This primary bit-time effect comes in addition to the normal coding effect of efficiently trading bandwidth for error performance. The improvement in performance brought about from coding may enable coherent systems to live up to previous expectations. The contributions of this thesis include the visualization of the phase noise process, the efficient computation of the laser phase noise power factor probability density function, and the computation of performance curves for uncoded and coded systems. Additional sections on coherent lightwave systems and coding provide tutorial information. A potential military application is discussed, along with practical implementation issues. DTIC

N94-17049# Polish Academy of Sciences, Warsaw. Inst. Podstawowych Problemow Techniki.
REGULAR AND IRREGULAR REFLECTION OF A WAVE FROM A SLANTING FLAT WALL [REGULARNE I NIEREGULARNE ODBICIE FALI UDERZENIOWEJ OD SKOSNIE USTAWIONEJ PLASKIEJ SCIANKI]
Zbigniew A. Walenta 1991 37 p In POLISH
(IFTR-13/1991) Avail: CASI HC A03/MF A01

This survey contains a discussion of theoretical and experimental studies that the author considers to be the most important research for understanding quasi-stationary reflection of a plane wave by a prism. Primary attention is focused on recently published experimental studies carried out with strong gas rarification relating to phenomena adjacent to the edge of the reflecting prism. Attention is also focused on significant qualitative differences between wave reflection under stationary and quasi-stationary conditions that cause such phenomena to be treated as equivalent, solely for the case of strong waves. NTIS

N94-17254# Air Force Inst. of Tech., Wright-Patterson AFB, OH. Foreign Aerospace Science and Technology Center.
TWO-DIMENSIONAL ACOUSTO-OPTICAL INTERACTION THEORY AND EXPERIMENTAL ANALYSIS
Zhan-Xiang Ren, Xiaoyi Dong, Jian-Zhong Zhang, Qui-Qin Sheng, and Qida Zhao 6 Aug. 1993 12 p Transl. into ENGLISH from Guangxue Xuebao (China), v. 10, no. 11, Nov. 1990 p 1047-1051
(AD-A267761; FASTC-ID(RS)T-0220-93) Avail: CASI HC A03/MF A01

In the paper, the universal coupling wave equation of two-dimensional acousto-optical interaction is theoretically derived. The solution of Raman-Nath diffraction under normal acousto-optical (A-O) interaction is derived. The theoretical results are compared with the experimental results of a two-dimensional A-O device consisting of two one-dimensional Raman-Nath type A-O modulators. The two results are in agreement. DTIC

N94-17264# California Inst. of Tech., Pasadena. Graduate Aeronautical Labs.
TRANSMISSION OF LIGHT THROUGH A TURBULENT MIXING LAYER Final Report, 30 Sep. 1989 - 30 Jun. 1992
Anatol Roshko and John Wissler 14 Aug. 1992 5 p
(Grant AF-AFOSR-0552-89)
(AD-A267266; AFOSR-93-0468TR) Avail: CASI HC A01/MF A01

Light transmission through incompressible gaseous turbulent mixing layers was investigated with the objective of understanding the effects of large-scale coherent structures and mixing transition on the optical quality of the mixing layer. Experiments were done in a vertically flowing mixing layer which is enclosed inside a pressure tank and fed by two banks of high-pressure gas bottles. The study considered both the unequal density (high-speed He and low-speed N2) and equal density (high-speed N2 and low-speed He-Ar) cases; the mixing of dissimilar gases is the source of the optical aberrations. Large-scale Reynolds numbers ranged between 3500 and 80000 over pressures from 2 to 6 bar. Light transmission characteristics were first studied qualitatively using a network of thin sheets of short-exposure (approximately 1 microsec) white light which were aberrated by the mixing layer and then imaged directly onto photographic film. Light transmission characteristics were then studied quantitatively using a lateral effect detector to dynamically track a thin He-Ne laser beam as it wandered under the influence of the passing coherent structures. The study found that the spanwise coherent structures generate systematic deflections of the light beam in the streamwise direction; the greatest deflections occur near the trailing edges of the structures at a formation called the cusp, where the high-speed fluid and low-speed fluid are entrained

into the vortex core. The streamwise coherent structures, which form later in the mixing layer's development than the spanwise structures, generate substantial beam deflections in the spanwise direction which are closely associated with the streamwise streaks in plan-view shadowgraphs. DTIC

N94-17321*# National Aeronautics and Space Administration. Goddard Space Flight Center, Greenbelt, MD.
CONICALLY SCANNED HOLOGRAPHIC LIDAR TELESCOPE Patent Application
Geary Schwemmer, inventor (to NASA) 10 Mar. 1992 21 p
(NASA-Case-GSC-13462-1; NAS 1.71:GSC-13462-1;
US-Patent-Appl-SN-848885) Avail: CASI HC A03/MF A01

An optical scanning device utilizing a source of optical energy such as laser light backscattered from the earth's atmosphere or transmitted outward as in a lidar, a rotating holographic optical element having an axis of rotation perpendicular to the plane of its substrate, and having a stationary focus which may or may not be located on its axis of rotation, with the holographic optical element diffracting the source of optical energy at an angle to its rotation axis enabling a conical scanning area and a motor for supporting and rotating the rotating holographic optical element. NASA

N94-17331*# National Aeronautics and Space Administration. Marshall Space Flight Center, Huntsville, AL.
CONFERENCE ON BINARY OPTICS: AN OPPORTUNITY FOR TECHNICAL EXCHANGE
Helen J. Cole, ed. and William C. Pittman, ed. (Army Missile Command, Redstone Arsenal, AL.) Washington Aug. 1993 426 p Conference held in Huntsville, AL, 23-25 Feb. 1993 Sponsored by NASA, Washington; ARO; Army Missile Research and Development Command; Army Strategic Defense Command; Army Night Vision Lab.; and Army Test Measurement and Diagnostic Equipment Activity
(NASA-CP-3227; M-728; NAS 1.55:3227) Avail: CASI HC A19/MF A04

The papers herein were presented at the Conference on Binary Optics held in Huntsville, AL, February 23-25, 1993. The papers were presented according to subject as follows: modeling and design, fabrication, and applications. Invited papers and tutorial viewgraphs presented on these subjects are included. For individual titles, see N94-17332 through N94-17362.

N94-17332*# Army Research Office, Research Triangle Park, NC.
MANUFACTURING THE KEY TO BINARY OPTICS
Bob D. Guenther *In* NASA. Marshall Space Flight Center, Conference on Binary Optics: An Opportunity for Technical Exchange Aug. 1993 p 1-17 (For primary document see N94-17331 03-74)
Avail: CASI HC A03/MF A04

The topics are presented in viewgraph form, and the topics covered include the following: gratings, grating characteristics, grating manufacture, zone plate, zone plate characteristics, zone plate manufacture, holography, holographic aberration correction, wavefront generated holograms, computer generated holograms, fabrication, fabrication capabilities, replication, processing errors, and quality control. CASI

N94-17333*# Massachusetts Inst. of Tech., Lexington. Lincoln Lab.
BINARY OPTICS: TRENDS AND LIMITATIONS
Michael W. Farn and Wilfrid B. Veldkamp *In* NASA. Marshall Space Flight Center, Conference on Binary Optics: An Opportunity for Technical Exchange Aug. 1993 p 19-29 (For primary document see N94-17331 03-74)
Avail: CASI HC A03/MF A04

We describe the current state of binary optics, addressing both the technology and the industry (i.e., marketplace). With respect to the technology, the two dominant aspects are optical design methods and fabrication capabilities, with the optical design problem being limited by human innovation in the search for new applications and the fabrication issue being limited by the availability of resources required to improve fabrication capabilities. With respect to the industry, the current marketplace does not favor binary optics as a separate product line and so we expect that companies whose primary purpose is the production of binary optics will not represent the bulk of binary optics production. Rather, binary optics' more natural role is as an enabling technology - a technology which will directly result in a competitive advantage in a company's other business areas - and so we expect that the majority of binary optics will be produced for internal use. Author

N94-17334*# Rochester Univ., NY. Inst. of Optics.
DIFFRACTIVE OPTICS: DESIGN, FABRICATION, AND APPLICATIONS
G. Michael Morris *In* NASA. Marshall Space Flight Center, Conference on Binary Optics: An opportunity for Technical Exchange Aug. 1993 p 31-60 Prepared in cooperation with Rochester Photonics Corp., NY (For primary document see N94-17331 03-74)
Avail: CASI HC A03/MF A04

The topics are presented in viewgraph form and include the following: features, applications, surface relief diffractive optics, optical data storage, waveguide lenses, diffractive lense imaging, phase grating synthesis, sub-wavelength structured surfaces, etc. CASI

N94-17335*# Georgia Inst. of Tech., Atlanta. School of Electrical Engineering.
REVIEW OF RIGOROUS COUPLED-WAVE ANALYSIS AND OF HOMOGENEOUS EFFECTIVE MEDIUM APPROXIMATIONS FOR HIGH SPATIAL-FREQUENCY SURFACE-RELIEF GRATINGS
Elias N. Glytsis, David L. Brundrett, and Thomas K. Gaylord *In* NASA. Marshall Space Flight Center, Conference on Binary Optics: An Opportunity for Technical Exchange Aug. 1993 p 61-76 (For primary document see N94-17331 03-74)
Avail: CASI HC A03/MF A04

A review of the rigorous coupled-wave analysis as applied to the diffraction of electro-magnetic waves by gratings is presented. The analysis is valid for any polarization, angle of incidence, and conical diffraction. Cascaded and/or multiplexed gratings as well as material anisotropy can be incorporated under the same formalism. Small period rectangular groove gratings can also be modeled using approximately equivalent uniaxial homogeneous layers (effective media). The ordinary and extraordinary refractive indices of these layers depend on the gratings filling factor, the refractive indices of the substrate and superstrate, and the ratio of the freespace wavelength to grating period. Comparisons of the homogeneous effective medium approximations with the rigorous coupled-wave analysis are presented. Antireflection designs (single-layer or multilayer) using the effective medium models are presented and compared. These ultra-short period antireflection gratings can also be used to produce soft x-rays. Comparisons of the rigorous coupled-wave analysis with experimental results on soft x-ray generation by gratings are also included. Author

N94-17336*# Teledyne Brown Engineering, Huntsville, AL. Sensor Systems Dept.
SCALAR LIMITATIONS OF DIFFRACTIVE OPTICAL ELEMENTS
Eric G. Johnson, Diane Hochmuth, M. G. Moharam (University of Central Florida, Orlando.), and Drew Pommet (University of Central Florida, Orlando.) *In* NASA. Marshall Space Flight Center, Conference on Binary Optics: An Opportunity for Technical Exchange Aug. 1993 p 77-86 (For primary document see N94-17331 03-74)
Avail: CASI HC A02/MF A04

In this paper, scalar limitations of diffractive optic components are investigated using coupled wave analyses. Results are presented for linear phase gratings and fanout devices. In addition, a parametric curve is given which correlates feature size with scalar performance. Author

N94-17337*# Rochester Univ., NY. Inst. of Optics.
SUBWAVELENGTH STRUCTURED SURFACES AND THEIR APPLICATIONS
Daniel H. Raguin and G. Michael Morris *In* NASA. Marshall Space Flight Center, Conference on Binary Optics: An Opportunity for Technical Exchange Aug. 1993 p 87-97 (For primary document see N94-17331 03-74)
Avail: CASI HC A03/MF A04

The term subwavelength structured (SWS) surface describes any surface that contains a subwavelength-period grating or gratings. The grating may be of any type provided the period is sufficiently fine so that, unlike conventional gratings, no diffraction orders propagate other than the zeroth orders. Because of the fine periods involved, the fabrication of such surfaces for applications in the visible and infrared portions of the spectral regime have only recently been considered. With refinements in holographic procedures and the push of the semiconductor industry for submicron

lithography, production of SWS surfaces is becoming increasingly viable. The topics covered include the following: analytic approaches to analyze SWS surfaces, 1D periodic stratification and effective medium theory, design of waveplates using form birefringence, and 2D binary antireflection structured surfaces. Derived from text

N94-17338*# Army Research Lab., Adelphi, MD.
DIFFRACTIVE OPTICAL ELEMENTS FOR GENERATING ARBITRARY LINE FOCI
Joseph N. Mait, Dennis W. Prather, Joseph vanderGracht, and Tristan J. Tayag *In* NASA. Marshall Space Flight Center, Conference on Binary Optics: An Opportunity for Technical Exchange Aug. 1993 p 99-105 (For primary document see N94-17331 03-74)
Avail: CASI HC A02/MF A04

The key optical component in the architecture of the linearly variable magnification telescope presented here is a conical lens. This architecture has application to Doppler radar processing and to wavelet processing. Unfortunately, the unique surface profile of a conical lens does not allow traditional grinding techniques to be used for fabrication; therefore, its fabrication is considered custom. In addition to the requirement of custom fabrication, a refractive conical lens introduces phase aberrations that are intrinsic to its conic shape. Further, due to the large prismatic component of the lens, the variable magnification telescope architecture is off-axis. To overcome the fabrication and application difficulties of a refractive lens, we consider the construction of a hybrid diffractive-refractive lens. Derived from text

N94-17339*# Teledyne Brown Engineering, Huntsville, AL.
FINITE DIFFERENCE TIME DOMAIN ANALYSIS OF CHIRPED DIELECTRIC GRATINGS
Diane H. Hochmuth and Eric G. Johnson *In* NASA. Marshall Space Flight Center, Conference on Binary Optics: An Opportunity for Technical Exchange Aug. 1993 p 107-110 (For primary document see N94-17331 03-74)
Avail: CASI HC A01/MF A04

The finite difference time domain (FDTD) method for solving Maxwell's time-dependent curl equations is accurate, computationally efficient, and straight-forward to implement. Since both time and space derivatives are employed, the propagation of an electromagnetic wave can be treated as an initial-value problem. Second-order central-difference approximations are applied to the space and time derivatives of the electric and magnetic fields providing a discretization of the fields in a volume of space, for a period of time. The solution to this system of equations is stepped through time, thus, simulating the propagation of the incident wave. If the simulation is continued until a steady-state is reached, an appropriate far-field transformation can be applied to the time-domain scattered fields to obtain reflected and transmitted powers. From this information diffraction efficiencies can also be determined. In analyzing the chirped structure, a mesh is applied only to the area immediately around the grating. The size of the mesh is then proportional to the electric size of the grating. Doing this, however, imposes an artificial boundary around the area of interest. An absorbing boundary condition must be applied along the artificial boundary so that the outgoing waves are absorbed as if the boundary were absent. Many such boundary conditions have been developed that give near-perfect absorption. In this analysis, the Mur absorbing boundary conditions are employed. Several grating structures were analyzed using the FDTD method. Derived from text

N94-17340*# Teledyne Brown Engineering, Huntsville, AL.
ASYMMETRIC THREE-BEAM BINARY OPTIC GRATING
Alan D. Kathman, Eric G. Johnson, and Miles L. Scott *In* NASA. Marshall Space Flight Center, Conference on Binary Optics: An Opportunity for Technical Exchange Aug. 1993 p 111-115 (For primary document see N94-17331 03-74)
Avail: CASI HC A01/MF A04

Binary and diffractive optical components are finding many applications in optical systems and integrated optical devices. A recent application required the development of a two-dimensional diffraction grating to perform an asymmetric, three-beam fanout. In this paper, techniques are presented for the design of arbitrary fanout grating devices. Modeling and optimization processes are demonstrated for the three-beam grating. The counter-intuitive results of the initial design are discussed, and experimental data verifying performance are presented. Author

N94-17341*# Naval Air Warfare Center, China Lake, CA. Weapons Div.
SCATTERING FROM BINARY OPTICS
Douglas W. Ricks *In* NASA. Marshall Space Flight Center, Conference on Binary Optics: An Opportunity for Technical Exchange Aug. 1993 p 117-134 (For primary document see N94-17331 03-74)
Avail: CASI HC A03/MF A04

There are a number of sources of scattering in binary optics: etch depth errors, line edge errors, quantization errors, roughness, and the binary approximation to the ideal surface. These sources of scattering can be systematic (deterministic) or random. In this paper, scattering formulas for both systematic and random errors are derived using Fourier optics. These formulas can be used to explain the results of scattering measurements and computer simulations. Author

N94-17342*# Minnesota Univ., Minneapolis. School of Mathematics.
MATHMATICAL MODELING FOR DIFFRACTIVE OPTICS
David Dobson and J. Allen Cox (Honeywell, Inc., Bloomington, MN.) *In* NASA. Marshall Space Flight Center, Conference on Binary Optics: An Opportunity for Technical Exchange Aug. 1993 p 135-151 (For primary document see N94-17331 03-74)
Avail: CASI HC A03/MF A04

We consider a 'diffractive optic' to be a biperiodic surface separating two half-spaces, each having constant constitutive parameters; within a unit cell of the periodic surface and across the transition zone between the two half-spaces, the constitutive parameters can be a continuous, complex-valued function. Mathematical models for diffractive optics have been developed, and implemented as numerical codes, both for the 'direct' problem and for the 'inverse' problem. In problems of the 'direct' class, the diffractive optic is specified, and the full set of Maxwell's equations is cast in a variational form and solved numerically by a finite element approach. This approach is well-posed in the sense that existence and uniqueness of the solution can be proved and specific convergence conditions can be derived. An example of a metallic grating at a Wood anomaly is presented as a case where other approaches are known to have convergence problems. In problems of the 'inverse' class, some information about the diffracted field (e.g., the far-field intensity) is given, and the problem is to find the periodic structure in some optimal sense. Two approaches are described: phase reconstruction in the far-field approximation; and relaxed optimal design based on the Helmholtz equation. Practical examples are discussed for each approach to the inverse problem, including array generators in the far-field case and antireflective structures for the relaxed optimal design. Author

N94-17343*# Massachusetts Inst. of Tech., Lexington. Lincoln Lab.
FABRICATING BINARY OPTICS: AN OVERVIEW OF BINARY OPTICS PROCESS TECHNOLOGY
Margaret B. Stern *In* NASA. Marshall Space Flight Center, Conference on Binary Optics: An Opportunity for Technical Exchange Aug. 1993 p 153-166 Sponsored by DARPA (For primary document see N94-17331 03-74)
Avail: CASI HC A03/MF A04

A review of binary optics processing technology is presented. Pattern replication techniques have been optimized to generate high-quality efficient microoptics in visible and infrared materials. High resolution optical photolithography and precision alignment is used to fabricate maximally efficient fused silica diffractive microlenses at lambda = 633 nm. The degradation in optical efficiency of four-phase-level fused silica microlenses resulting from an intentional 0.35 micron translational error has been systematically measured as a function of lens speed (F/2 - F/60). Novel processes necessary for high sag refractive IR microoptics arrays, including deep anisotropic Si-etching, planarization of deep topography and multilayer resist techniques, are described. Initial results are presented for monolithic integration of photonic and microoptic systems. Author

N94-17344*# Hughes Danbury Optical Systems, Inc., CT.
BINARY OPTICS AT HUGHES DANBURY OPTICAL SYSTEMS
James Logue and Michael Power *In* NASA. Marshall Space Flight Center, Conference on Binary Optics: An Opportunity for Technical

Exchange Aug. 1993 p 167-177 (For primary document see N94-17331 03-74)
Avail: CASI HC A03/MF A04

An overview of binary optics development at Hughes Danbury Optical Systems is presented. Design software used for mask design is presented. A brief discussion of fabrication follows. Two examples of actual projects are used to highlight the discussion: (1) a large aspheric lens; and (2) a set of grating and lenslet arrays. Author

N94-17345*# Environmental Research Inst. of Michigan, Ann Arbor.
FABRICATION TECHNIQUES FOR VERY FAST DIFFRACTIVE LENSES
Anthony M. Tai and Joseph C. Marron *In* NASA. Marshall Space Flight Center, Conference on Binary Optics: An Opportunity for Technical Exchange Aug. 1993 p 179-185 (For primary document see N94-17331 03-74)
Avail: CASI HC A02/MF A04

Aspheric lenses with arbitrary phase functions can be fabricated on thin light weight substrates via the binary optics fabrication technique. However, it is difficult and costly to fabricate a fast lens (f/number less than 1) for use as the shorter wavelengths. The pitch of the masks and the alignment accuracy must be very fine. For a large lens, the space-bandwidth product of the element can also become impractically large. In this paper, two alternate approaches for the fabrication of fast aspheric diffractive lenses are described. The first approach fabricates the diffractive lens interferometrically, utilizing a spherical wavefront to provide the optical power of the lens and a computer generated hologram to create the aspheric components. The second approach fabricates the aspheric diffractive lens in the form if a higher order kinoform which trades groove profile fidelity for coarser feature size. The design and implementation issues for these two fabrication techniques are discussed. Author

N94-17346*# Hughes Danbury Optical Systems, Inc., CT.
LASER FIGURING FOR THE GENERATION OF ANALOG MICRO-OPTICS AND KINEFORM SURFACES
Edward J. Gratrix *In* NASA. Marshall Space Flight Center, Conference on Binary Optics: An Opportunity for Technical Exchange Aug. 1993 p 187-193 Sponsored in part by Strategic Defense Initiative Organization (For primary document see N94-17331 03-74)
Avail: CASI HC A02/MF A04

To date, there have been many techniques used to generate micro-optic structures in glass or other materials. Using methods common to the lithographic industry, the manufacturing technique known as 'binary optics,' has demonstrated the use of diffractive optics in a variety of micro-optic applications. It is well established that diffractive structures have limited capability when applied in a design more suited for a refractive element. For applications that demand fast, highly efficient, broadband designs, we have developed a technique which uses laser figuring to generate the refractive micro-optical surface. This paper describes the technique used to fabricate refractive micro-optics. Recent results of micro-optics in CdZnTe focal planes are shown. Author

N94-17347*# California Univ., San Diego, La Jolla. Dept. of Electrical and Computer Engineering.
DIFFRACTIVE OPTICS FABRICATED BY DIRECT WRITE METHODS WITH AN ELECTRON BEAM
Bernard Kress, David Zaleta, Walter Daschner, Kris Urquhart, Robert Stein, and Sing H. Lee *In* NASA. Marshall Space Flight Center, Conference on Binary Optics: An Opportunity for Technical Exchange Aug. 1993 p 195-205 (For primary document see N94-17331 03-74)
Avail: CASI HC A03/MF A04

State-of-the-art diffractive optics are fabricated using e-beam lithography and dry etching techniques to achieve multilevel phase elements with very high diffraction efficiencies. One of the major challenges encountered in fabricating diffractive optics is the small feature size (e.g. for diffractive lenses with small f-number). It is not only the e-beam system which dictates the feature size limitations, but also the alignment systems (mask aligner) and the materials (e-beam and photo resists). In order to allow diffractive optics to be used in new optoelectronic systems, it is necessary not only to fabricate elements with small feature sizes but also to do so in an economical fashion. Since price of a multilevel diffractive optical element is closely related to the e-beam writing time and the number of etching steps, we need to decrease the writing time and etching steps without affecting the quality of the element. To do this one has to utilize the full potentials of the e-beam writing system. In this paper, we will present three diffractive optics fabrication techniques which will reduce the number of process steps, the writing time, and the overall fabrication time for multilevel phase diffractive optics. Author

N94-17348*# Jet Propulsion Lab., California Inst. of Tech., Pasadena.
PHASE HOLOGRAMS IN PMMA WITH PROXIMITY EFFECT CORRECTION **c35**
Paul D. Maker and R. E. Muller *In* NASA. Marshall Space Flight Center, Conference on Binary Optics: An Opportunity for Technical Exchange Aug. 1993 p 207-221 Sponsored in part by Strategic Defense Initiative Organization (For primary document see N94-17331 03-74)
Avail: CASI HC A03/MF A04

Complex computer generated phase holograms (CGPH's) have been fabricated in PMMA by partial e-beam exposure and subsequent partial development. The CGPH was encoded as a sequence of phase delay pixels and written by the JEOL JBX-5D2 E-beam lithography system, a different dose being assigned to each value of phase delay. Following carefully controlled partial development, the pattern appeared rendered in relief in the PMMA, which then acts as the phase-delay medium. The exposure dose was in the range 20-200 micro-C/sq cm, and very aggressive development in pure acetone led to low contrast. This enabled etch depth control to better than plus or minus lambda(sub vis)/60. That result was obtained by exposing isolated 50 micron square patches and measuring resist removal over the central area where the proximity effect dose was uniform and related only to the local exposure. For complex CGPH's with pixel size of the order of the e-beam proximity effect radius, the patterns must be corrected for the extra exposure caused by electrons scattered back up out of the substrate. This has been accomplished by deconvolving the two-dimensional dose deposition function with the desired dose pattern. The deposition function, which plays much the same role as an instrument response function, was carefully measured under the exact conditions used to expose the samples. The devices fabricated were designed with 16 equal phase steps per retardation cycle, were up to 1 cm square, and consisted of up to 100 million 0.3-2.0 micron square pixels. Data files were up to 500 MB long and exposure times ranged to tens of hours. A Fresnel phase lens was fabricated that hed diffraction limited optical performance with better than 85 percent efficiency. Author

N94-17349*# Rochester Univ., NY. Inst. of Optics.
CURVED GRATING FABRICATION TECHNIQUES FOR CONCENTRIC-CIRCLE GRATING, SURFACE-EMITTING SEMICONDUCTOR LASERS **c36**
Rebecca H. Jordan, Oliver King, Gary W. Wicks, Dennis G. Hall, Erik H. Anderson (International Business Machines Corp., Yorktown Heights, NY.), and Michael J. Rooks (Cornell Univ., Ithaca, NY.) *In* NASA. Marshall Space Flight Center, Conference on Binary Optics: An Opportunity for Technical Exchange Aug. 1993 p 223-235 Sponsored by ARO; New York Center for Advanced Optical Technology; and IBM (For primary document see N94-17331 03-74)
(Contract DE-AC03-76SF-00098; NSF ECS-91-12973; NSF ECS-86-19049)
Avail: CASI HC A03/MF A04

We describe the fabrication and operational characteristics of a novel, surface-emitting semiconductor laser that makes use of a concentric-circle grating to both define its resonant cavity and to provide surface emission. A properly fabricated circular grating causes the laser to operate in radially inward- and outward-going circular waves in the waveguide, thus, introducing the circular symmetry needed for the laser to emit a beam with a circular cross-section. The basic circular-grating-resonator concept can be implemented in any materials system; an AlGaAs/GaAs graded-index, separate confinement heterostructure (GRINSCH), single-quantum-well (SQW) semiconductor laser, grown by molecular beam epitaxy (MBE), was used for the experiments discussed here. Each concentric-circle grating was fabricated on the surface of the AlGaAs/GaAs semiconductor laser. The circular pattern was first defined by electron-beam (e-beam) lithography in a layer of polymethylmethacrylate (PMMA) and subsequently etched into the semiconductor surface using chemically-assisted (chlorine) ion-beam etching (CAIBE). We consider issues that affect the fabrication and quality of the gratings. These issues include grating design requirements, data representation of the grating pattern, and e-beam scan method. We provide examples of how these techniques can be implemented and their impact

on the resulting laser performance. A comparison is made of the results obtained using two fundamentally different electron-beam writing systems. Circular gratings with period lambda = 0.25 microns and overall diameters ranging from 80 microns to 500 microns were fabricated. We also report our successful demonstration of an optically pumped, concentric-circle grating, semiconductor laser that emits a beam with a far-field divergence angle that is less than one degree. The emission spectrum is quite narrow (less than 0.1 nm) and is centered at wavelength lambda = 0.8175 microns. Author

N94-17350*# Lockheed Missiles and Space Co., Palo Alto, CA. Research Lab.

MICRO-OPTICS TECHNOLOGY AND SENSOR SYSTEMS APPLICATIONS

George Gal, B. Herman, W. Anderson, R. Whitney, and H. Morrow *In* NASA. Marshall Space Flight Center, Conference on Binary Optics: An Opportunity for Technical Exchange Aug. 1993 p 237-254 Sponsored in part by Army Strategic Defense Command (For primary document see N94-17331 03-74)

Avail: CASI HC A03/MF A04

The current generation of electro-optical sensors utilizing refractive and reflective optical elements require sophisticated, complex, and expensive designs. Advanced-technology-based electro-optical sensors of minimum size and weight require miniaturization of optical, electrical, and mechanical devices with an increasing trend toward integration of various components. Micro-optics technology has the potential in a number of areas to simplify optical design with improved performance. This includes internally cooled apertures, hybrid optical design, microlenses, dispersive multicolor microlenses, active dither, electronically controlled optical beam steer, and microscopic integration of micro-optics, detectors, and signal processing layers. This paper describes our approach to the development of micro-optics technology with our main emphasis for sensors applications. Author

N94-17351*# Lockheed Missiles and Space Co., Palo Alto, CA. Research Lab.

FABRICATION OF MICRO-OPTICAL DEVICES

W. W. Anderson, J. Marley, George Gal, and Don Purdy (Philips Components Ltd., Southampton, England.) *In* NASA. Marshall Space Flight Center, Conference on Binary Optics: An Opportunity for Technical Exchange Aug. 1993 p 255-269 (For primary document see N94-17331 03-74)

Avail: CASI HC A03/MF A04

We have fabricated a variety of micro-optic components including Fresnel and non-Frensel lenses, off-axis and dispersive lenses with binary stepped contours, and analog contours. Process details for all lens designs fabricated are given including multistep photolithography for binary fabrication and grayscale mask photolithography for analog fabrication. Reactive ion etching and ion beam milling are described for the binary fabrication process, while ion beam milling was used for the analog fabrication process. Examples of micro-optic components fabricated in both Si and CdTe substrates are given. Author

N94-17352*# Army Research Lab., Adelphi, MD.

DIFFRACTIVE OPTICS IN ADVERSE ENVIRONMENTS

Gregory P. Behrmann *In* NASA. Marshall Space Flight Center, Conference on Binary Optics: An Opportunity for Technical Exchange Aug. 1993 p 271-281 (For primary document see N94-17331 03-74)

Avail: CASI HC A03/MF A04

An investigation at the Army Research Laboratory is in progress to characterize DOE performance in mil-spec environments. One of the most significant environmental influences is temperature. An analysis of a diffractive lens is presented in which optical performance is described as a function of temperature. In particular, we review the thermal dependence of focal length and diffraction efficiency. It is shown that the change in these parameters is independent of lens shape and relates only to material properties. Thermalized hybrid refractive/diffractive designs are discussed. Author

N94-17353*# Foster-Miller Associates, Inc., Waltham, MA.

LOW COST PATHS TO BINARY OPTICS

Arthur Nelson and Lawrence Domash *In* NASA. Marshall Space Flight Center, Conference on Binary Optics: An Opportunity for Technical Exchange Aug. 1993 p 283-302 Sponsored by NSWC and Center for Night Vision and Electro-Optics (For primary document see N94-17331 03-74)

Avail: CASI HC A03/MF A04

Application of binary optics has been limited to a few major laboratories because of the limited availability of fabrication facilities such as e-beam machines and the lack of standardized design software. Foster-Miller has attempted to identify low cost approaches to medium-resolution binary optics using readily available computer and fabrication tools, primarily for the use of students and experimenters in optical computing. An early version of our system, MacBEEP, made use of an optimized laser film recorder from the commercial typesetting industry with 10 micron resolution. This report is an update on our current efforts to design and build a second generation MacBEEP, which aims at 1 micron resolution and multiple phase levels. Trails included a low cost scanning electron microscope in microlithography mode, and alternative laser inscribers or photomask generators. Our current software approach is based on Mathematica and PostScript compatibility. Author

N94-17354*# Hughes Aircraft Co., El Segundo, CA. Electro-Optical Systems.

THERMAL WEAPON SIGHT (TWS) AN/PAS-13 DIFFRACTIVE OPTICS DESIGNED FOR PRODUCIBILITY

J. Steven Anderson, Chungte W. Chen, and Robert A. Spande (Army Night Vision Lab., Fort Belvoir, VA.) *In* NASA. Marshall Space Flight Center, Conference on Binary Optics: An Opportunity for Technical Exchange Aug. 1993 p 303-324 (For primary document see N94-17331 03-74)

(Contract DAAB07-91-C-K254)

Avail: CASI HC A03/MF A04

The Thermal Weapon Sight (TWS) program is a manportable 3-5 micrometer forward-looking-infrared (FLIR) rifle sight. The manportable nature requires that the optics modules be lightweight, low cost and compact while maximizing performance. These objectives were met with diffractive optics. TWS promises to be the first FLIR sensor to incorporate kinoform surfaces in full scale production. Author

N94-17355*# Lockheed Missiles and Space Co., Palo Alto, CA. Research Lab.

MEASUREMENTS OF MICROLENS PERFORMANCE

D. Shough, B. Herman, and George Gal *In* NASA. Marshall Space Flight Center, Conference on Binary Optics: An Opportunity for Technical Exchange Aug. 1993 p 325-339 (For primary document see N94-17331 03-74)

Avail: CASI HC A03/MF A04

We present results of laboratory evaluations of several microlens types that have been designed and fabricated at the Lockheed Research and Development Division. The microlenses include wideband and dispersive types, in isolation and in arrays, and fabricated with binary or grayscale methods. Different lens pixel geometries are considered, including square, hexagonal, and skewed microlenses. We describe our micro-optics laboratory testbed which has been designed for the evaluation of individual lenslets or 2D arrays at selected spectral wavelengths. Measurement capabilities include focal length, point-spread functions, wavefront quality, and modulation transfer functions. Our present effort focuses on the results of point spread function measurements and their comparison with design predictions. Author

N94-17356*# Digital Optics Corp., Charlotte, NC.

APPLICATIONS OF ADVANCED DIFFRACTIVE OPTICAL ELEMENTS

W. Hudson Welch, James E. Morris, and Michael R. Feldman *In* NASA. Marshall Space Flight Center, Conference on Binary Optics: An Opportunity for Technical Exchange Aug. 1993 p 341-343 Prepared in cooperation with North Carolina Univ., Charlotte (For primary document see N94-17331 03-74)

Avail: CASI HC A01/MF A04

Digital Optics Corporation is a UNC-Charlotte spin-off company, established to transfer technology developed at UNC-Charlotte for the design and manufacture Computer Generated Holograms (CGH's) and to market products based on CGH technology. DOC acquired core technologies from UNC-Charlotte including: (1) a CGH encoding process that can provide holograms with extremely high diffraction efficiency; (2) a low cost, high precision CGH manufacturing process; and (3) extensive holographic and

refractive element design capabilities for design and evaluation of complex optical systems. These technologies have been used to design and/or manufacture optical components for a variety of applications including: (1) generation of Spot arrays; (2) fiber optic coupling elements; (3) optical interconnects between VLSI chips within and between multichip modules; and (4) imaging systems for head-mounted displays (HMD's). Author

N94-17357*# Rockwell International Science Center, Thousand Oaks, CA.

LASER BEAM STEERING DEVICE **c36**

M. E. Motamedi, A. P. Andrews, and W. J. Gunning *In* NASA. Marshall Space Flight Center, Conference on Binary Optics: An Opportunity for Technical Exchange Aug. 1993 p 345-358 (For primary document see N94-17331 03-74)

Avail: CASI HC A03/MF A04

Agile beam steering is a critical requirement for airborne and space based LIDAR and optical communication systems. Design and test results are presented for a compact beam steering device with low inertia which functions by dithering two complementary (positive and negative) binary optic microlens arrays relative to each other in directions orthogonal to the direction of light propagation. The miniaturized system has been demonstrated at scan frequencies as high as 300 Hz, generating a 13 x 13 spot array with a total field of view of 2.4 degrees. The design is readily extendable to a 9.5 degree field of view and a 52 x 52 scan pattern. The system is compact - less than 2 in. on a side. Further size reductions are anticipated. Author

N94-17358*# Du Pont de Nemours (E. I.) and Co., Wilmington, DE. Imaging Systems.

SURPHEX (TM): NEW DRY PHOTOPOLYMERS FOR REPLICATION OF SURFACE RELIEF DIFFRACTIVE OPTICS

Felix P. Shvartsman *In* NASA. Marshall Space Flight Center, Conference on Binary Optics: An Opportunity for Technical Exchange Aug. 1993 p 359-368 Submitted for publication (For primary document see N94-17331 03-74)

Avail: CASI HC A02/MF A04

High efficiency, deep groove, surface relief Diffractive Optical Elements (DOE) with various optical functions can be recorded in a photoresist using conventional interferometric holographic and computer generated photolithographic recording techniques. While photoresist recording media are satisfactory for recording individual surface relief DOE, a reliable and precise method is needed to replicate these diffractive microstructures to maintain the high aspect ratio in each replicated DOE. The term 'high aspect ratio' means that the depth of a groove is substantially greater, i.e. 2, 3, or more times greater, than the width of the groove. A new family of dry photopolymers SURPHEX was developed recently at Du Pont to replicate such highly efficient, deep groove DOE's. SURPHEX photopolymers are being utilized in Du Pont's proprietary Dry Photopolymer Embossing (DPE) technology to replicate with very high degree of precision almost any type of surface relief DOE. Surfaces relief microstructures with width/depth aspect ratio of 1:20 (0.1 micron/2.0 micron) were faithfully replicated by DPE technology. Several types of plastic and glass/quartz optical substrates can be used for economical replication of DOE. Author

N94-17359*# OFC Corp., Keene, NH. Diamond Turning Div.

PREDESIGN OF DIAMOND TURNED REFRACTIVE/DIFFRACTIVE ELEMENTS FOR IR OBJECTIVES

Max J. Riedl *In* NASA. Marshall Space Flight Center, Conference on Binary Optics: An Opportunity for Technical Exchange Aug. 1993 p 369-385 (For primary document see N94-17331 03-74)

Avail: CASI HC A03/MF A04

Diffractive lenses have arrived. Literally hundreds of papers have been published and technology impact reports have been written about the exciting addition of a new tool for the lens designer. Sophisticated computer programs have been developed to aid in the optimization of these diffractive phase profiles for a wide variety of applications. Now, several fabrication methods are being pursued to produce these diffractive elements economically. The best known process is the etching of a multi-level relief grating, known as binary optics. This process uses sets of computer generated lithographic masks. Another, more recently developed method is Dry Photopolymer Embossing (DPE). This replication process uses master holograms. And now, diamond turning is being applied for the machining of these elements. Diamond turning is especially well suited for infrared optics. As any process has advantages and limitations, so has diamond turning. These advantages and limitations are discussed and general guidelines are presented to aid the designer and systems engineer in the project predesign stage. Author

N94-17360*# Arizona Univ., Tucson. Dept. of Electrical and Computer Engineering.

OPTICAL SYSTEM STORAGE DESIGN WITH DIFFRACTIVE OPTICAL ELEMENTS

Raymond K. Kostuk and Charles W. Haggans (Minnesota Mining and Mfg. Co., Vadnais.) *In* NASA. Marshall Space Flight Center, Conference on Binary Optics: An Opportunity for Technical Exchange Aug. 1993 p 387-394 (For primary document see N94-17331 03-74)

Avail: CASI HC A02/MF A04

Optical data storage systems are gaining widespread acceptance due to their high areal density and the ability to remove the high capacity hard disk from the system. In magneto-optical read-write systems, a small rotation of the polarization state in the return signal from the MO media is the signal which must be sensed. A typical arrangement used for detecting these signals and correcting for errors in tracking and focusing on the disk is illustrated. The components required to achieve these functions are listed. The assembly and alignment of this complex system has a direct impact on cost, and also affects the size, weight, and corresponding data access rates. As a result, integrating these optical components and improving packaging techniques is an active area of research and development. Most designs of binary optic elements have been concerned with optimizing grating efficiency. However, rigorous coupled wave models for vector field diffraction from grating surfaces can be extended to determine the phase and polarization state of the diffracted field, and the design of polarization components. A typical grating geometry and the phase and polarization angles associated with the incident and diffracted fields are shown. In our current stage of work, we are examining system configurations which cascade several polarization functions on a single substrate. In this design, the beam returning from the MO disk illuminates a cascaded grating element which first couples light into the substrate, then introduces a quarter wave retardation, then a polarization rotation, and finally separates s- and p-polarized fields through a polarization beam splitter. The input coupler and polarization beam splitter are formed in volume gratings, and the two intermediate elements are zero-order elements. Derived from text

N94-17361*# Lockheed Missiles and Space Co., Palo Alto, CA. Research Lab.

THEORY OF DISPERSIVE MICROLENSES

B. Herman and George Gal *In* NASA. Marshall Space Flight Center, Conference on Binary Optics: An Opportunity for Technical Exchange Aug. 1993 p 395-408 (For primary document see N94-17331 03-74)

Avail: CASI HC A03/MF A04

A dispersive microlens is a miniature optical element which simultaneously focuses and disperses light. Arrays of dispersive mircolenses have potential applications in multicolor focal planes. They have a 100 percent optical fill factor and can focus light down to detectors of diffraction spot size, freeing up areas on the focal plane for on-chip analog signal processing. Use of dispersive microlenses allows inband color separation within a pixel and perfect scene registration. A dual-color separation has the potential for temperature discrimination. We discuss the design of dispersive microlenses and present sample results for efficient designs. Author

N94-17362*# Massachusetts Inst. of Tech., Lexington. Lincoln Lab.

COLOR SEPARATION GRATINGS

Michael W. Farn and Robert E. Knowlden *In* NASA. Marshall Space Flight Center, Conference on Binary Optics: An Opportunity for Technical Exchange Aug. 1993 p 409-421 (For primary document see N94-17331 03-74)

Avail: CASI HC A03/MF A04

In this paper, we describe the theory, fabrication and test of a binary optics 'echelon'. The echelon is a grating structure which separates electromagnetic radiation of different wavelengths, but it does so according to diffraction order rather than by dispersion within one diffraction order, as is the case with conventional gratings. A prototype echelon, designed for the visible spectrum, is fabricated using the binary optics process.

Tests of the prototype show good agreement with theoretical predictions.
Author

N94-17427 Texas Univ. at Dallas, Richardson. Center for Applied Optics.
SPECTRAL INVERSE SCATTERING THEORY FOR DIELECTRIC MEDIA: APPLICATION TO OPTICAL DEVICES Yearly Report, 1992 - 1993
Lakshman S. Tamil 23 Aug. 1993 148 p Limited Reproducibility: More than 20% of this document may be affected by microfiche quality
(Contract N00014-92-J-1030)
(AD-A268635; UTD/CAO/26) Avail: CASI HC A07/MF A02

The report contains discussions on (1) synthesis and analysis of guided wave optical interconnects; (2) synthesis and analysis of optical waveguides with prescribed TM modes; (3) development and testing of direct scattering solver to analyze optical waveguides; (4) development of inverse scattering theory for the design of planar optical waveguides with same propagation constants for different frequencies; (5) analysis of coupling in multilayered waveguides using inverse scattering techniques; and (6) soliton-soliton interaction in nonlinear optical waveguides and bistability in nonlinear periodic media.
DTIC

N94-17443*# California Inst. of Tech., Pasadena. Infrared Processing and Analysis Center.
[A TYPICAL POINTED OBSERVATION IN IRAS DESIGNED TO FIT INTO A 15 MINUTE WINDOW] Final Report, 1 Aug. 1992 - 31 Jul. 1993
G. Neugebauer and D. Gregorich 18 Nov. 1993 3 p
(Grant NAG5-1710)
(NASA-CR-194653; NAS 1.26:194653) Avail: CASI HC A01/MF A01

A typical pointed observation in the Infrared Astronomical Satellite (IRAS) was designed to fit into a 15 minute window. Observing constraints, however, did not always permit targets from the scientific program to be observed on exactly 15 minute centers and a few months into the mission it was realized that the automatic scheduling program left times when no observations were being made. In order to use this potentially wasted observing time, a mode of pointed observations, the 'filler' mode, with shorter observation duration was initiated. Locations were picked on an arbitrary grid, spaced relatively uniformly in ecliptic coordinates, and the telescope was pointed to one of these sites whenever a gap potentially occurred. One of us (GXN) was the coordinator of this effort (the FL sub-group). There are a total of 22 FL fields, 13 of which have more than 50 component observations. These 13 fields cover about 30 square degrees. It was proposed to concentrate on one filler field, FL29, a field with 53 coverages which thus had among the deepest coverage of those observed in this mode. This field was also observed extensively at various non-infrared wavelengths by a variety of techniques. Because the IRAS observations of FL29 were made at the limits of the survey sensitivity and at different twist angles it was necessary to make significant technical advances in the methods used in the processing and analyzing the data. In particular, if normal IRAS coaddition procedures were used, the noise resulting from coaddition of the multiple frames did not decrease in the manner expected once significantly different twist angles were included in the coaddition. The technical effort needed to reduce the observations of FL29 was completed and now the noise behavior is understood and well behaved. The reduction of the field FL29 observations is done.
Author (revised)

N94-17455 Alabama A & M Univ., Normal.
OPTICAL STUDIES OF GLASSES EMBEDDED WITH INORGANIC IONS AND ORGANIC DYES Final Report, 15 Feb. 1990 - 31 May 1993
B. R. Reddy 22 Jul. 1993 105 p Limited Reproducibility: More than 20% of this document may be affected by microfiche quality
(Grant AF-AFOSR-0160-90)
(AD-A268146; AFOSR-93-0579TR) Avail: Issuing Activity (Defense Technical Information Center (DTIC))

We performed optical studies of organic dye doped glasses and rare earth ion doped glasses. We doped several organic dyes in boric acid, sucrose, and polycarbonate hosts and detected phase conjugate signals from all these samples. Sucrose samples are hygroscopic and hence are useful for characterizing dyes only. Boric acid samples were damaged even at moderate laser powers. On the other hand polycarbonate samples could withstand high input powers and hence will be useful in device applications. Styryl 7 doped boric acid sample exhibited several interesting nonlinear optical phenomena and was also found to be useful for long-term/permanent information storage due to photochemical effects undergone by the excited molecules. PC signals in Pyridine 1 dye doped samples exhibited oscillations (period-hour) which was found to be due to thermal effects/large Stokes shift in the emission. DCM and RI 10 doped boric acid samples are found to be chemically stable even after three years. We measured third order susceptibilities of DCF, DCM, RIIO, AY, and R6G doped samples. We experimentally demonstrated that excited state absorption alters the transmission/saturation characteristics of the dyes in condensed media. These results have been published in three journal papers.
DTIC

N94-14986*# Arizona Univ., Tucson.
DYNAMIC TESTBED LABORATORY AND MICRO-OPTICS
T. Milster, K. Erwin, F. Froehlich, J. Kann, W. Li, W. Schlichting, R. Shetty, E. Walker, and M. Wang *In its* Research Studies on Advanced Optical Module/Head Designs for Optical Disk Recording Devices 15 Mar. 1993 p 19-23 (For primary document see N94-14981 03-82)
Avail: CASI HC A01/MF A02

N94-14993*# Arizona Univ., Tucson.
EFFECTS OF A SHADING BAND IN THE DATA PATH OF AN OPTICAL DRIVE
T. D. Milster, M. S. Wang, and Weiquan Li (Shanghai Inst. of Metallurgy, China.) *In its* Research Studies on Advanced Optical Module/Head Designs for Optical Disk Recording Devices 15 Mar. 1993 p 147-149 (For primary document see N94-14981 03-82)
Avail: CASI HC A01/MF A02

N94-14995*# Arizona Univ., Tucson.
A NEAR-FIELD SCANNING OPTICAL MICROSCOPE FOR ANALYSIS OF MAGNETO-OPTIC MEDIA
Fred F. Froehlich and Tom D. Milster *In its* Research Studies on Advanced Optical Module/Head Designs for Optical Disk Recording Devices 15 Mar. 1993 p 163-165 (For primary document see N94-14981 03-82)
Avail: CASI HC A01/MF A02

N94-14996*# Arizona Univ., Tucson.
A COMPLETE STUDY OF DIFFERENTIAL WAX-WANE FOCUS SERVO TECHNIQUE
Mark S. Wang and Tom D. Milster *In its* Research Studies on Advanced Optical Module/Head Designs for Optical Disk Recording Devices 15 Mar. 1993 p 169-171 (For primary document see N94-14981 03-82)
Avail: CASI HC A01/MF A02

N94-15044# National Optical Astronomy Lab. Tucson, AZ.
LARGE SCIENTIFIC 2-D ARRAYS FOR THE 1-5 MICRON REGION
A. M. Fowler *In* ESA, Proceedings of an ESA Symposium on Photon Detectors for Space Instrumentation Dec. 1992 p 129-135 Sponsored by NSF (For primary document see N94-15025 03-19)
Copyright Avail: CASI HC A02/MF A04

N94-15045# Max-Planck-Inst. fuer Astronomie, Heidelberg (Germany).
PHOTOCONDUCTORS AND ARRAYS FOR THE FAR-INFRARED
J. Wolf *In* ESA, Proceedings of an ESA Symposium on Photon Detectors for Space Instrumentation Dec. 1992 p 137-146 Sponsored in part by Deutsche Agentur fuer Raumfahrtangelegenheite G.m.b.H. (For primary document see N94-15025 03-19)
Copyright Avail: CASI HC A02/MF A04

N94-15058# European Space Agency. European Space Research and Technology Center, ESTEC, Noordwijk (Netherlands). Space Science Dept.
DEVELOPMENTS IN EXTREME ULTRAVIOLET AND X RAY INSTRUMENTATION
A. Peacock and J. A. M. Bleeker (Space Research Organization Netherlands, Utrecht.) *In its* Proceedings of an ESA Symposium on Photon Detectors for Space Instrumentation Dec. 1992 p 217-218 (For primary document see N94-15025 03-19)
Copyright Avail: CASI HC A01/MF A04

N94-15072*# National Aeronautics and Space Administration. Goddard Space Flight Center, Greenbelt, MD.
X-RAY SPECTROSCOPY WITH SILICON PIN AND AVALANCHE PHOTO DIODES
U. D. Desai *In* ESA, Proceedings of an ESA Symposium on Photon Detectors for Space Instrumentation Dec. 1992 p 285-287 (For primary document see N94-15025 03-19)
Copyright Avail: CASI HC A01/MF A04

N94-16156# Dynetics, Inc., Huntsville, AL. Electro-Optics Dept.
WIDEBAND ACOUSTO-OPTIC CORRELATOR FOR AN ESM RECEIVER UPGRADE
C. Anderson, A. Dorsett, S. Tepper, M. Zari, A. Filipov (Army Research Lab., Adelphi, MD.), E. Adler (Army Research Lab., Adelphi, MD.), and J. Pellegrino (Army Research Lab., Adelphi, MD.) *In* Huntsville Association of Technical Societies, TABES 1993: 9th Annual Technical and Business Exhibition and Symposium 1993 6 p (For primary document see N94-16129 03-38)
(TABES Paper 93-661) Avail: CASI HC A02/MF A03

75 PLASMA PHYSICS

Includes magnetohydrodynamics and plasma fusion.

For ionospheric plasmas see *46 Geophysics*. For space plasmas see *90 Astrophysics*.

N94-14966 Max-Planck-Inst. fuer Plasmaphysik, Munich (Germany).
DESCRIPTION OF COOLING WATER CALORIMETRY AND WALL THERMOMETRY DIAGNOSTIC AT TOKAMAK ASDEX-UPGRADE [BESCHREIBUNG DER KUEHLWASSERKALORIMETRIE UND DER WANDTHERMOMETRIEDIGNOSTIK AM TOKAMAK ASDEX-UPGRADE]
Th. Richter and H. Vernickel Aug. 1992 36 p In GERMAN
(IPP-5/46; ETN-93-94611) Copyright Avail: Issuing Activity (Fachinformationszentrum Karslruhe, 7511 Eggenstein-Leopoldshafen 2, Germany)

Hardware and software of the cooling water calorimetry and the wall thermometry diagnostics at the tokamak ASDEX-Upgrade are described. These diagnostics were used to analyze the energy deposition on the first wall elements in ASDEX-Upgrade. The cooling water calorimetry system consists of 130 platinum resistor thermometers Pt-100 and 27 annular flow meters located in the cooling water system of the tokamak downstream and upstream near the individual cooling units. In addition to the cooling water calorimetry system in some sections of the torus a wall thermometry diagnostic was installed to reach a higher poloidal resolution of the energy deposition measurements. The electrical measuring signals from the sensors were amplified, converted into digital signals, multiplexed with a frequency of 500 Hz, and sent over a fiber optics system into the control room. There a transputer system consisting of five T800 transputers receives the signals and stores a complete set of data about every three seconds during the 10 minute pause between the shots. These raw data were sent into the data analysis system of the experiment and the deposited energy for each cooling unit was calculated. First experimental results of the cooling water calorimetry show toroidal and poloidal asymmetries in the energy deposition in the ASDEX-Upgrade walls. ESA

N94-15204# Technical Research Centre of Finland, Espoo. Nuclear Engineering Lab.
STUDIES ON THE PARAMETRIC DECAY OF WAVES IN FUSION PLASMAS Ph.D. Thesis - Helsinki Univ. of Technology
Timo Pattikangas 1992 165 p Sponsored by Jenny and Antti Wihuri Foundation and Finnish Cultural Foundation
(VTT-Pubs-110; ISBN-951-38-4228-2; ETN-93-94484) Copyright Avail: CASI HC A08/MF A02

Parametric instabiliies of large amplitude electromagnetic waves are investigated in fusion applications. In Double Stimulated Brillouin Scattering (DSBS), both the incoming and the reflected pump wave scatter from a common ion sound wave. The stationary states and the dynamics of DSBS are investigated by using a simple envelope model. The ion sound wave that is excited in DSBS is shown to have soliton like properties. The Stimulated Raman Scattering (SRS) of free electron laser radiation can be applied to current drive in tokamaks. The feasibility of the Raman current drive in tokamaks is investigated theoretically. The energy transfer to the fast electrons from the electrostatic wave is studied with relativistic Vlaslov-Maxwell simulations. The parametric decay of a wave to half harmonics is investigated. It is shown that the growth rate of the decay vanishes in the limit of a long wavelength even for general decay modes. For individual titles, see N94-15205 through N94-15211.

N94-15205# Helsinki Univ. of Technology, Espoo (Finland). Dept. of Technical Physics.
DOUBLE STIMULATED BRILLOUIN SCATTERING
T. J. H. Pattikangas and R. R. E. Salomaa *In* Technical Research Centre of Finland, Studies on the Parametric Decay of Waves in Fusion Plasmas 1992 10 p Repr. from Physica Scripta, v. 40, 1989 p 99-108 Presented at 2nd Nordic Symposium on Nonlinear Phenomena in Plastics and Related Topics, Riso, Denmark, 8-12 Aug. 1992 (For primary document see N94-15204 03-75)
Copyright Avail: CASI HC A02/MF A02

To explain discrepancies between experiments and standard theories of stimulated Brillouin scattering, a parametric process called Double Stimulated Brillouin Scattering (DSBS) was developed. In DSBS the incident pump wave is reflected from the critical surface and the two waves scatter from a common ion wave. Some of the properties of DSBS are reviewed. Complete formulary for calculating the stationary eigensolutions of the fields and the eigenvalues of the reflection coefficients and oscillation frequencies is presented. The approach allows inhomogeneous plasma density and temperature. Temperature gradient effects are studied. Numerical solutions including the temporal variation of the ion wave show that the fields start to pulsate above a critical intensity. The backscattering and specular reflections in DSBS develop into regular pulse trains. ESA

N94-15206# Helsinki Univ. of Technology, Espoo (Finland). Dept. of Technical Physics.
DYNAMICS OF DOUPLE STIMULATED BRILLOUIN SCATTERING
T. J. H. Pattikangas and R. R. E. Salomaa *In* Technical Research Centre of Finland, Studies on the Parametric Decay of Waves in Fusion Plasmas 1992 17 p Repr. from Laser and Particle Beams, v. 8, 1990 p 209-225 (For primary document see N94-15204 03-75)
Copyright Avail: CASI HC A03/MF A02

The pump wave reflected from the overdense plasma may play an important role in the dynamics of stimulated Brillouin scattering. The particular case of Double Stimulated Brillouin Scattering (DSBS) is studied. In DSBS the incident pump wave and the reflected pump wave scatter from a common ion acoustic wave. Some steady state properties of DSBS are reviewed. The analysis of DSBS dynamics is based on a series of 'numerical experiments'. At small pump intensities the system asymptotically approaches a true steady state. When the intensity is increased the solution turns into a regular pulse train with intensity dependent period. Connections between the pulses and soliton like solutions of a damped sine Gordon equation are discussed. ESA

N94-15207# Helsinki Univ. of Technology, Espoo (Finland). Dept. of Technical Physics.
SOLITON-LIKE STRUCTURES IN DOUBLE STIMULATED BRILLOUIN SCATTERING
T. J. H. Pattikangas and R. R. E. Salomaa *In* Technical Research Centre of Finland, Studies on the Parametric Decay of Waves in Fusion Plasmas 1992 5 p Repr. from Europhysics Conference Abstracts (Frankfurt am Main, Germany, European Physical Society), v. 13B, pt. 4, 1989 p 1345-1348 Presented at 16th European Conference on Controlled Fusion and Plasma Physics, Venice, Italy, 13-17 Mar. 1989 (For primary document see N94-15204 03-75)
Copyright Avail: CASI HC A01/MF A02

Some results of numerical and analytical investigations in soliton like behavior occurring in Double Stimulated Brillouin Scattering (DSBS) are reviewed. The soliton-like properties of the ion acoustic wave in DSBS are investigated. It is shown that the ion wave area obeys a damped sine Gordon equation. During propagation the total area of the ion acoustic pulse is approximately (+/-) pi/2 and the shape of the pulse resembles a hyperbolic secant. The pulse height equals its inverse width and its length increases with increasing pump intensity. In the 'numerical experiments' any sign of chaotic behavior of the scattering, and any evidence of transitions between the fundamental and the higher order modes were observed. The

boundaries seem to play an important role in the dynamics of the system. The pulsation of the ion wave is due to the boundaries and the continuous feeding of pump energy into the system. ESA

N94-15208# Technical Research Centre of Finland, Espoo. Nuclear Engineering Lab.

HIGH FREQUENCY RAMAN CURRENT DRIVE

S. J. Karttunen, T. J. H. Pattikangas (Helsinki Univ. of Technology, Espoo, Finland.), R. R. E. Salomaa (Helsinki Univ. of Technology, Espoo, Finland.), and S. K. Sipila (Helsinki Univ. of Technology, Espoo, Finland.) *In its* Studies on the Parametric Decay of Waves in Fusion Plasmas 1992 19 p Repr. from Nuclear Fusion, v. 31, no. 6, 1991 p 1079-1097 Sponsored in part by Ministry of Trade and Industry (For primary document see N94-15204 03-75)

Copyright Avail: CASI HC A03/MF A02

Current drive in reactor grade tokamak plasmas with a pulsed, high power Free Electron Laser (FEL) is investigated. The stimulated Raman process generates fast, longitudinal electron plasma waves which accelerate electrons to relativistic energies. The fast electrons with parallel velocities much greater than perpendicular velocities are not trapped toroidally and the resulting current decays slowly. A systematic study on different combinations of Raman forward and backward scattering and FEL polarization is presented. The optimal FEL frequencies fall within the range 2.2 to 4 omega sub p and 3.8 to 7 omega sub p. In a reactor grade plasma the best current drive efficiency is obtained by using the stimulated Raman forward process and a left circularly polarized FEL beam. The FEL driven current can be localized to the plasma center and amplified by the bootstrap effect to further enhance the overall efficiency. Raman current drive in high temperature reactor plasma is quite different from small scale experiments with the electron temperature approximately equal to 1 keV, where the Raman backward process dominates and the current drive efficiency remain rather low. ESA

N94-15209# Technical Research Centre of Finland, Espoo. Nuclear Engineering Lab.

CURRENT DRIVE WITH FREE ELECTRON LASERS IN HIGH AND LOW TEMPERATURE TOKAMAKS

T. J. H. Pattikangas, S. J. Karttunen, and R. R. E. Salomaa (Helsinki Univ. of Technology, Espoo, Finland.) *In its* Studies on the Parametric Decay of Waves in Fusion Plasmas 1992 9 p Repr. from Societa Italiana di Fisica, 1992 p 503-510 Presented at High Power Microwave Generation and Applications Course and Workshop, Varenna, Italy, 9-17 Sep. 1991 Sponsored by Finnish Cultural Foundation (For primary document see N94-15204 03-75)

Copyright Avail: CASI HC A02/MF A02

The requirements for the Free Electron Laser (FEL) performance in Stimulated Raman Scattering (SRS) current drive tokamaks are investigated. High power FEL's are promising power sources for current drive in tokamak plasmas. The high intensities of FEL's make it possible to excite fast electrostatic waves in nonlinear wave-wave interactions, such as SRS and beat wave process. At high and at low temperatures, better efficiencies are obtained with left circularly polarized beams than with right circularly polarized beams. The performance requirements for FEL's are less stringent in the left circularly polarized case than in the right circularly polarized case. In MTX size tokamaks, the needed average and peak power, pulse energy and repetition rate are not much higher than those of the present day FEL's. The FEL's that are needed in reactor size tokamaks are still beyond the present state of the art. FEL's with higher peak powers and pulse energies have to be developed in order to drive a current of 15 MA in a tokamak reactor. ESA

N94-15210# Nancy Univ. (France).

SIMULATIONS OF WAVE-PARTICLE INTERACTIONS IN STIMULATED RAMAN FORWARD SCATTERING IN A MAGNETIZED PLASMA

P. Bertrand, A. Ghizzo, S. J. Karttunen (Technical Research Centre of Finland, Espoo.), T. J. H. Pattikangas (Technical Research Centre of Finland, Espoo.), R. R. E. Salomaa (Helsinki Univ. of Technology, Espoo, Finland.), and M. Shoucri (Hydro-Quebec Inst. for Research, Varennes.) *In* Technical Research Centre of Finland, Studies on the Parametric Decay of Waves in Fusion Plasmas 1992 47 p Submitted for publication Sponsored by Finnish Cultural Foundation and Ministry of Trade and Industry (For primary document see N94-15204 03-75)

(TKK-F-A704; ISBN-951-22-1091-6) Copyright Avail: CASI HC A03/MF A02

Stimulated Raman forward scattering in a high temperature, magnetized plasma is investigated with relativistic Vlasov-Maxwell simulations and with envelope and test particle calculations. The parameters correspond to Raman current drive by free electron lasers in reactor trade tokamak plasmas. The phase velocity of the Raman excited plasma wave is large. The electron plasma wave grows to a large amplitude and accelerates electrons to high energies. Simultaneous pump depletion weakens the driving ponderomotive force. Spatially the wave-particle interaction takes place in a distance of a few wavelengths of the plasma wave. The electron energies can largely exceed the kinetic energy at the phase velocity of the electron plasma wave. Short wavelength amplitude modulations of the plasma wave appears at high amplitudes. Efficient generation of the nonresonant anti-Stokes wave and of the second Stokes wave are also observed. Analytical growth rates and envelope calculation explain the early evolution of the Raman process. Later on nonlinear wave-particle interactions and relativistic effects start to dominate and the system is not satisfactorily described by simple envelope equations. ESA

N94-15211# Technical Research Centre of Finland, Espoo. Nuclear Engineering Lab.

ON THE DECAY OF A DIPOLE PUMP WAVE TO HALF-HARMONICS

J. A. Heikkinen, T. J. H. Pattikangas (Helsinki Univ. of Technology, Espoo, Finland.), and G. Devillers (Joint European Torus Project, Abingdon, England.) *In its* Studies on the Parametric Decay of Waves in Fusion Plasmas 1992 6 p Repr. from Journal of Plasma Physics, v. 46, pt. 2, 1991 p 231-236 (For primary document see N94-15204 03-75)

Copyright Avail: CASI HC A02/MF A02

Starting from a three wave interaction coefficient for a homogeneous Vlasov plasma, it is shown that the parametric decay to half harmonics has zero growth rate if the wavenumber of the pump wave vanishes. This result is valid for electromagnetic decay waves to any order in ion or electron Larmor radius. An earlier proof of this fact for electrostatic decay modes is thus extended to a general case. As an application, the decay of a fast magnetosonic wave to two slow waves was studied in the cold plasma approximation. Simple analytical expressions for the coupling coefficient were found for a finite wavenumber of the pump wave as well as with a finite difference between the decay wave frequencies. ESA

N94-15661# Tennessee Univ., Knoxville.

MICROWAVE INTERACTION WITH PLASMAS Final Report, 1 May 1992 - 30 Apr. 1993

Igor Alexeff and Mark Radar 30 Apr. 1993 21 p

(Contract F49620-92-J-0266)

(AD-A267048; AFOSR-93-0526TR) Avail: CASI HC A03/MF A01

The object of this work is to create dense plasmas for research and development that are accessable--not confined in vacuum systems. The corona method of production by high D.C. and A.C. voltages is simple and convenient. Much work was done in this field in the 1900-1940 time frame, but the field seems to be neglected now. Multiple points were used on positive and negative electrodes at voltages of 6000 to 1200 volts D.C. The current appears to comprise equal negative and positive ion species, as an metal plate blocking the current flow reduced the current exactly to 1/2 of its initial value. An electrostatic voltmeter (zero current drain) was used to obtain the potential profiles. DTIC

N94-15981# Lawrence Livermore National Lab., CA.

ITER-HARD TOROIDAL FIELD COIL STRUCTURAL ANALYSIS

S. J. Wineman 15 Oct. 1992 17 p

(Contract W-7405-eng-48)

(DE93-014834; UCRL-ID-111954) Avail: CASI HC A03/MF A01

The High Aspect Ratio Design (HARD) for the International Thermonuclear Experimental Reactor (ITER) has Toroidal Field (TF) coils that are farther out from the center of the Toroidal ring and more elongated than the previous design (CDA). These coils should see higher forces than in CDA and were designed accordingly. The objective of this work, conducted at LLNL and the MIT Plasma Fusion Center, was to determine whether stress levels in the ITER-HARD design are acceptable. A global finite element model, representing one of the coils, was modeled at MIT to obtain stresses and displacements both during operation of the TF coils

alone and during the End of Burn phase with TF and PF (Poloidal Field) coils operating. At LLNL, a detailed model of the TF coil straight leg near the equator was used to obtain stresses and displacements during TF operation only. Further detailed analysis of the winding pack of this model was done to estimate stress concentrations in the conduit and insulation. DOE

N94-16019# Brookhaven National Lab., Upton, NY.
NUCLEAR FUSION OF PROTONS WITH IONS OF BORON
A. G. Ruggiero 1993 5 p Presented at the International Symposium on Heavy Ion Fusion, Frascati, Italy, 25-28 May 1993
(Contract DE-AC02-76CH-00016)
(DE93-015399; BNL-48642; CONF-9305136-1) Avail: CASI HC A01/MF A01

This paper describes a method of extracting energy from the fusion events occurring between the collision of a beam of protons with a beam of ions of Boron 11. The two beams are circulating in separated and intersecting storage rings where they collide head-on in a common long-straight section. Requirements on the beam parameters in the collider are presented. Limitations due to space-charge forces are discussed; it is found necessary to provide beam-charge neutralization with electrons. The paper discusses also the effects of Coulomb scattering between particles of the same beam and in the opposing beams. Methods are proposed for the controlling of the electromagnetic interaction. DOE

N94-16162# Oak Ridge National Lab., TN. Fusion Energy Div.
ACTIVE PROBING OF PLASMA EDGE TURBULENCE AND FEEDBACK STUDIES ON THE TEXAS EXPERIMENTAL TOKAMAK (TEXT)
T. Uckan, B. Richards (Texas Univ., Austin.), Roger D. Bengtson (Texas Univ., Austin.), B. A. Carreras, D. B. Crockett (Texas Univ., Austin.), K. W. Gentle (Texas Univ., Austin.), G. X. Li (Texas Univ., Austin.), P. D. Hurwitz (Texas Univ., Austin.), W. L. Rowan (Texas Univ., Austin.), and H. Y. W. Tsui (Texas Univ., Austin.) et al 1993 4 p Presented at the 20th European Conference on Controlled Fusion and Plasma Physics, Lisbon, Portugal, 26-30 Jul. 1993
(Contracts DE-AC05-84OR-21400; DE-FG05-88ER-53267)
(DE93-015799; CONF-930720-11) Avail: CASI HC A01/MF A01

The edge fluctuations play a critical role in the overall tokamak confinement. Experiments on TEXT show that electrostatic fluctuations in the edge plasma are the dominant mechanism for energy and particle transport. The basic mechanisms responsible for the edge turbulence are the subject of ongoing research in fusion devices. To understand the driving forces responsible for edge fluctuations, a novel experiment is underway on TEXT to actively modify the turbulence at the plasma edge by launching waves using electrostatic probes in the shadow of the limiter. This technique permits active probing of the spectral properties of the edge turbulence. This new approach to the study of edge fluctuations can provide more insight into the basic dynamics of the turbulence and may, in turn, enable detailed comparison with the theory. These experiments, which rely on the use of oscillating electric fields at the plasma edge, complement edge fluctuation control studies that are presently limited to the use of applied dc biasing to influence the edge electric field profile. These experiments have been extended to control of the edge plasma fluctuation level, using feedback to explore its effects on the edge turbulence characteristics as well as on confinement. DOE

N94-16446# Columbia Univ., New York, NY.
HIGH BETA AND CONFINEMENT STUDIES OF TFTR
G. A. Navratil, A. Bhattacharjee, R. Iacono, M. E. Mauel, S. A. Sabbagh (Columbia Univ., New York, NY.), and J. Kesner (Massachusetts Inst. of Tech., Cambridge.) 1993 49 p
(Contract DE-FG02-89ER-53297)
(DE93-016204; DOE/ER-53297/5) Avail: CASI HC A03/MF A01

The projects discussed in this report are as follows: enhanced high poloidal beta operation in TFTR with deuterium pellet injection; approaching high Q by utilizing high (beta)(sub p) operation in TFTR; advanced tokamak regime experiment; and second regime studies at large major radius high (beta)(sub p) plasmas. Analysis of the data taken during these experiments as well as continuing analysis of earlier data led to a number of important results described in publications in the past year including two invited presentations at the 1992 American Physical Society Division of Plasma Physics Meeting in Seattle, an oral presentation at the 1992 IAEA Meeting in Wuertzburg, Germany, and a Physical Review Letter. These results included the following: extending the high 11/2 regime to 1.2 MA current and neutron production rates to more than 3 x 10(exp 16)/sec; the first experiments with 4 sec neutral beam injection on TFRR; the creation of the first beam and bootstrap current sustained plasmas on TFTR for more than a current relaxation time scale; the first observation of ideal NM ballooning modes in a large tokamak; and production of plasmas with the inner 3/4 of the plasma in or with stable access to the second stability regime. The principal results of these papers and supporting theory work are summarized. DOE

N94-16451# Los Alamos National Lab., NM.
A MICROSECOND-PULSEWIDTH, INTENSE, LIGHT-ION BEAM ACCELERATOR
D. J. Rej, R. R. Bartsch, H. A. Davis, J. B. Greenly, and W. J. Waganaar 1993 5 p Presented at the 9th IEEE Pulsed Power Conference, Albuquerque, NM, 21-23 Jun. 1993
(Contract W-7405-eng-48)
(DE93-016455; LA-UR-93-2354; CONF-930616-5) Avail: CASI HC A01/MF A01

A relatively long-pulsewidth (0.1-1 microsecond) intense ion beam accelerator has been built for materials processing applications. An applied-B(sub r), magnetically-insulated extraction ion diode with dielectric flashover ion source is installed directly onto the output of a 1.2-MV, 300-kJ Marx generator. Initial operation of the accelerator at 0.4 MV indicates satisfactory performance without the need for additional pulse-shaping. DOE

N94-16776# Los Alamos National Lab., NM.
DIRECT DRIVE FOIL IMPLOSION EXPERIMENTS ON PEGASUS 2
J. C. Cochrane, R. R. Bartsch, J. F. Benage, P. R. Forman, R. F. Gribble, M. Y. P. Hockaday, R. G. Hockaday, J. S. Ladish, H. Oona, and J. V. Parker et al 1993 8 p Presented at the 3rd International Conference on Dense Z-Pinches, London, England, 19-23 Apr. 1993
(Contract W-7405-eng-36)
(DE93-012666; LA-UR-93-1448; CONF-9304126-4) Avail: CASI HC A02/MF A01

Pegasus 2 is the upgraded version of Pegasus, a pulsed power machine used in the Los Alamos Above Ground Experiments (AGEX) program. The goal of the program is to produce an intense (greater than 100 TW) source of soft x-rays from the thermalization of the KE of a 1 to 10 MJ collapsing plasma source. The radiation pulse should have a maximum duration of several tens of nanoseconds and will be used in the study of fusion conditions and material properties. This paper addresses z-pinch experiments done on a capacitor bank where the radiating plasma source is formed by an imploding annular aluminum foil driven by the J X B forces generated by the current flowing through the foil. DOE

N94-16803# General Atomic Co., San Diego, CA.
INDUCTIVE EFFECTS DURING SECOND HARMONIC CURRENT DRIVE EXPERIMENTS ON T-10
C. B. Forest, R. W. Harvey, J. Lohr, T. C. Luce, Y. R. Linliu, Y. Esipchuk (Gosudarstvennyi Komitet po Ispolzovaniyu Atomnoi Energii, Moscow, USSR.), G. Notkin (Gosudarstvennyi Komitet po Ispolzovaniyu Atomnoi Energii, Moscow, USSR.), and K. Razumova (Gosudarstvennyi Komitet po Ispolzovaniyu Atomnoi Energii, Moscow, USSR.) Apr. 1993 4 p Presented at the 10th Topical Conference on Radio Frequency Power in Plasmas, Boston, MA, 1-3 Apr. 1993
(Contract DE-AC03-89ER-51114)
(DE93-014411; GA-A-21293; CONF-9304112-15) Avail: CASI HC A01/MF A01

Current drive during second harmonic, electron cyclotron heating experiments performed on the T-10 tokamak have been simulated with the ONETWO transport code to determine the effects of induction on the time evolution of the loop voltage and current density profile. Ray tracing shows the well focused RF power can generate centrally peaked current densities which exceed the Ohmic current densities by a factor of five, causing very peaked plasma current profiles which will be unable to sawteeth. A Kadomtsev model of the sawtooth shows that a limit cycle is quickly reached which maintains a broad current profile and requires generation of a negative dc component of the loop voltage localized near the magnetic

axis. This negative electric field effectively drive efficiency. A broader profile of driven current, as in the fundamental current drive experiment on T-10, would not suffer this effect. DOE

N94-16816# General Atomic Co., San Diego, CA.
RECENT RESULTS FROM THE 60 GHz INSIDE LAUNCH ECH SYSTEM ON THE D3-D TOKAMAK
T. C. Luce, C. C. Petty, R. Prater, R. W. Harvey, Y. R. Lin-Liu, J. Lohr, K. Matsuda, C. P. Moeller, and R. A. James (Lawrence Livermore National Lab., CA.) Nov. 1992 31 p Presented at the EC 8th Joint Workshop on Electron Cyclotron Emission and Electron Cyclotron Heating, Gut Ising, Germany, 19-21 Oct. 1992
(Contracts DE-AC03-89ER-51114; W-7405-eng-48)
(DE93-013027; GA-A-21134; CONF-9210300-3) Avail: CASI HC A03/MF A01

Electron cyclotron heating (ECH) is a useful tool in global transport and local confinement studies. Operational experience with the inside launch ECH system on DIII-D shows that reliable operations are possible with power densities up to 0.7 GW/m(sup 2) in vacuum waveguide. Global confinement is roughly predicted by the Rebut-Lallia or ITER-89P scaling law, but direct analysis indicates a nearly linear scaling with toroidal field not found in these scaling laws. Local transport studies with off-axis heating clearly show inward transport in the electron fluid. This implies that diffusive and critical gradient models cannot completely describe plasma transport. DOE

N94-16822# Texas Univ., Austin. Inst. for Fusion Studies.
STRUCTURE AND DAMPING OF TOROIDAL DRIFT WAVES (AND THEIR IMPLICATIONS FOR ANOMALOUS TRANSPORT)
J. B. Taylor, J. Connor (United Kingdom Atomic Energy Authority, Abingdon, England.), and H. R. Wilson (United Kingdom Atomic Energy Authority, Abingdon, England.) May 1993 14 p
(Contract DE-FG05-80ET-53088)
(DE93-014005; DOE/ET-53088/605; IFSR-605) Avail: CASI HC A03/MF A01

The conventional theory of high-n toroidal drift waves, based on the ballooning representation, indicates that shear-damping is generally reduced in a torus compared to its plane-slab value. It therefore describes the most unstable class of toroidal drift waves. However, modes of this type occur only if the diamagnetic frequency omega*(r) has a maximum in r, and they affect only a small fraction, Omicron(1/n(sup 1/2)), of the plasma radius around this maximum. Consequently they may produce little anomalous transport. In the present work we show that, within the ballooning description, there is another class of toroidal drift waves with very different properties to the conventional ones. The new modes have greater shear-damping (closer to that in a plane-slab) than the conventional ones and so have a higher instability threshold. However, they occur for any plasma profile and at all radii, and they have larger radial extent. Consequently they may produce much greater anomalous transport than the possibly benign conventional modes. This suggests a picture of anomalous transport in which the plasma profile is determined by marginal stability, but marginal to the new class of modes not to the conventional ones. This might explain why marginally stable profiles calculated for drift waves with plane-slab damping sometimes agree well with the profiles in toroidal experiments. It is also consistent with the fact that experimental profiles may exceed conventional toroidal instability thresholds. The new modes may also be related to the long radial structures which appear in some plasma simulations and in experiments. DOE

N94-16823# General Atomic Co., San Diego, CA.
SIMULATION OF ENHANCED TOKAMAK PERFORMANCE ON D3-D USING FAST WAVE CURRENT DRIVE
J. S. deGrassie, Y. R. Lin-Liu, R. I. Pinsker, V. S. Chan, R. Prater, H. St.John, F. W. Baity (Oak Ridge National Lab., TN.), R. H. Goulding (Oak Ridge National Lab., TN.), D. J. Hoffman (Oak Ridge National Lab., TN.), and C. C. Petty May 1993 4 p Presented at the 20th European Conference on Controlled Fusion and Plasma Physics, Lisbon, Portugal, 26-30 Jul. 1993
(Contracts DE-AC03-89ER-51114; DE-AC05-84OR-21400)
(DE93-014009; GA-A-21312; CONF-930720-2) Avail: CASI HC A01/MF A01

The fast magnetosonic wave is now recognized to be a leading candidate for noninductive current drive for the tokamak reactor due to the ability of the wave to penetrate to the hot dense core region. Fast wave current drive (FWCD) experiments on D3-D have realized up to 120 kA of RF current drive, with up to 40% of the plasma current driven noninductively. The success of these experiments at 60 MHz with a 2 MW transmitter source capability has led to a major upgrade of the FWCD system. Two additional transmitters, 30 to 120 MHz, with a 2 MW source capability each, will be added together with two new four-strap antennas in early 1994. Another major thrust of the D3-D program is to develop advanced tokamak modes of operation, simultaneously demonstrating improvements in confinement and stability in quasi-steady-state operation. In some of the initial advanced tokamak experiments on D3-D with neutral beam heated (NBI) discharges it has been demonstrated that energy confinement time can be improved by rapidly elongating the plasma to force the current density profile to be more centrally peaked. However, this high-l(sub i) phase of the discharge with the commensurate improvement in confinement is transient as the current density profile relaxes. By applying FWCD to the core of such a (kappa)-ramped discharge it may be possible to sustain the high internal inductance and elevated confinement. Using computational tools validated on the initial DM-D FWCD experiments we find that such a high-l(sub i) advanced tokamak discharge should be capable of sustainment at the 1 MA level with the upgraded capability of the FWCD system. DOE

N94-16869# Oak Ridge National Lab., TN.
NONLINEAR GYROFLUID MODELS OF SHEAR ALFVEN INSTABILITIES IN IGNITED AND BEAM HEATED TOROIDAL PLASMAS
D. A. Spong, C. L. Hedrick, and B. A. Carreras 1993 20 p Presented at the International Atomic Energy Agency (IAEA) Technical Committee Meeting, Trieste (Italy), 10-14 May 1993
(Contract DE-AC05-84OR-21400)
(DE93-016235; CONF-9305231-1) Avail: CASI HC A03/MF A01

Shear Alfven instabilities driven by energetic beams and alpha populations are investigated using a reduced MHD-gyrofluid model with Landau closure. The moment equations for the fast ions are truncated in a way which incorporates the wave particle resonances that are required to destabilize the shear Alfven mode. These are coupled to an Ohm's law and vorticity equations which have been generalized to include ion FLR, electron and ion Landau damping. This model has been applied to experimentally observed regimes in a number of tokamak and stellarator devices. Both linearized growth rates and the nonlinear evolution are obtained. The saturated nonlinear regimes indicate mode number and frequency spectra which are generally consistent with experiment. A detailed examination of one typical nonlinear state has allowed identification of the dominant saturation mechanisms. This indicates that generation of $n = 0$, $m = 0$ sheared poloidal velocity flows and quasi linear modification of the q(r) profile can be important factors in reaching saturation. DOE

N94-16901# Rensselaer Polytechnic Inst., Troy, NY. Dept. of Nuclear Engineering and Engineering Physics.
ARIES TOKAMAK REACTOR STUDY
D. Steiner Jul. 1993 10 p
(Contract DE-FG02-85ER-52118)
(DE93-017059; DOE/ER-52118/8) Avail: CASI HC A02/MF A01

This report examines the feasibility of a standard poloidal diverter design for ARIES-2/4 with the determination of the peak thermal loading on and the plasma temperature facing a poloidal double null diverter. The ARIES-2/4 reactors produce 2,141 MW of fusion power of which 1712 MW is contained in the neutron channel. Of the remaining 429 MW of charged particle power, 47 MW is radiated from the core by bremsstrahlung and synchrotron modes to the vessel walls. The remaining 382 MW of charged particle or transport power crosses the core/edge interface. The fact that the bulk of the power is contained in the neutron channel makes the application of a poloidal divertor possible. The ARIES-2/4 diverter constraints for peak heat load and peak particle temperature are set by current technology and materials knowledge. Divertor geometry constraints are imposed by the plasma equilibrium and the 2/4 vacuum vessel. The diverter heat load and plasma temperatures are determined from edge particle and energy balances. These balances are important characteristics of the plasma edge because the transport power from the plasma core must pass through the edge and be deposited on tokamak components.

The Braams' B2 code is a multifluid ion and electron energy and momentum transport code for the plasma edge and is adopted for the design of the ARIES-2/4 diverter. DOE

N94-16987# Naval Postgraduate School, Monterey, CA.
INVESTIGATION OF ONSET OF PLASMA FORMATION AT ANODE OF FAST-PULSED HIGH-VOLTAGE VACUUM DIODE M.S. Thesis
Gregory Willis Mar. 1993 62 p
(AD-A267214) Avail: CASI HC A04/MF A01

The mechanism by which plasma forms in a fast pulsed high vacuum diode has been greatly studied. For the most part, efforts have been concentrated on plasma formation at the cathode. Recently, investigators improved the popular explosive emission model, taking into account the ion current density and surface heating through ion bombardment. This model provides total current densities of the order necessary for exploding whiskers on the cathode surface, and explains the cathode spot phenomena. The general belief is that a fast pulsed high voltage diode event is dominated by cathodic processes, and little research into plasma formation at the anode has been conducted. This study presents experimental results which support the above model applied to both the cathode and anode regions of the diode. It is shown here that plasma formation does indeed take place in the anode region, and that the formation occurs nearly simultaneously with plasma formation at the cathode. Also, photographic evidence of postbreakdown cratering on the anode surface, similar to the cathode spot phenomena, is presented. DTIC

N94-16995# National Academy of Sciences - National Research Council, Washington, DC.
PLASMA SCIENCE COMMITTEE (PLSC) AND THE PANEL ON OPPORTUNITIES IN PLASMA SCIENCE AND TECHNOLOGY (OPST)
1993 5 p
(Contract DE-FG05-88ER-53279)
(DE93-018142; DOE/ER-53279/3) Avail: CASI HC A01/MF A01

The Plasma Science Committee (PLSC) of the National Research Council (NRC) is charged with monitoring the health of the field of plasma science in the United States, and it identifies and examines both broad and specific issues affecting the field. Regular meetings, teleconferences, briefings from agencies and the scientific community, the formation of study panels to prepare reports, and special symposia are among the mechanisms used by the PLSC to meet its charge. During July 1992, the PLSC sponsored a workshop on nonneutral plasmas in traps. Although no written report on the workshop results was prepared for public distribution, a summary of highlights was provided to the OPST Subpanel on Nonneutral Plasmas. The PLSC also continued its follow-up briefings and discussions on the results of the results of the report 'Plasma Processing of Materials: Scientific and Technological Opportunities'. As a result of these activities, the Committee is now working with the NRC Committee on Atomic, Molecular, and Optical Sciences (CAMOS) to organize a symposium on database needs in plasma processing of materials. DOE

N94-17066# Polish Academy of Sciences, Warsaw. Inst. Podstawowych Problemow Techniki.
SPECTROSCOPIC AND COMPUTER MODELING INVESTIGATIONS OF A LASER-SUSTAINED PLASMA [BADANIA SPEKTROSKOPOWE I MODELOWANIE NUMERYCZNE PLAZMY PODTRZYMYWANEJ LASEREM]
Zygmunt Szymanski 1991 74 p In POLISH
(IFTR-30/1991) Avail: CASI HC A04/MF A01

Results from a spectral analysis of a laser-generated plasma are presented. The studies were carried out in argon at a pressure of 10 atm under both steady-state conditions and during the decay and new accumulation of plasma. The local thermodynamic equilibrium conditions are stipulated together with problems associated with determining plasma parameters based on measurements of constant radiation intensity and spectral line measurements. A quasi-two-dimensional cylindrical model is employed to describe the theoretical laser-generated plasma; this model provides a good description of laser-generated plasma under natural convection conditions and likewise by modification under forced convection conditions. The effect of the laser packet geometry and the inlet rate of the working gas on laser radiation absorption by the plasma at atmospheric pressure was also analyzed. Transl. by FLS

N94-17067# Polish Academy of Sciences, Warsaw. Inst. Podstawowych Problemow Techniki.
APPLICATION OF GROUP THEORY TO INTEGRAL-DIFFERENCE EQUATIONS OF PLASMA PHYSICS [ZASTOSOWANIE TEORII GRUP DO ROWNAN ROZNICZKOWO-CALKOWYCH FIZYKI PLAZMY]
Jacek Zawistowski 1992 52 p In POLISH
(IFTR-23/1992) Avail: CASI HC A04/MF A01

The Ovsyannikov method of determining the symmetry groups of differential equations was generalized to the case of integrodifferential equations. The new method is designed for the Vlasov-Maxwell equations describing plasma in zero magnetic field. In the case of single-component plasma, Taranov's result obtained indirectly was reproduced. A new result with respect to the indirect method was derived for a multi-component plasma: a complete symmetry group was defined. Transl. by FLS

N94-17237 Lawrence Livermore National Lab., CA.
A STATE-OF-THE-ART PLASMA POLYMERIZATION COATER FOR ICF TARGETS
G. Devine, S. Letts, R. Cook, and R. Brusasco Dec. 1992 6 p Presented at the 205th American Chemical Society National Meeting, Denver, CO, 28 Mar. - 2 Apr. 1993 Limited Reproducibility: More than 20% of this document may be affected by microfiche quality
(Contract W-7405-eng-48)
(DE93-016452; UCRL-JC-112360; CONF-930304-29) Avail: CASI HC A02/MF A01

Increasingly stringent demands on the characteristics of plasma polymer coatings for use in Inertial Confinement Fusion (ICF) experiments have created a need for a plasma polymerization coating system with the capability of producing a wide variety of different types of coatings as well as one that can be used to do fundamental investigations of the process conditions leading to desirable films. We report on the construction and use of just such a coating instrument. We have recognized the usefulness of computer assisted process monitoring and control, currently being developed by the semiconductor industry, in designing our own, state-of-the-art plasma polymerization device. Our system is fully computer interfaced to provide the user with the capability of collecting system parameter data over the length of the deposition experiment. The system is also designed to allow for any degree of computer control of the deposition process in the future. DOE

N94-17311 Ceskoslovenska Akademie Ved, Prague. Ustav. Fyziky Plazmatu.
STATIC CHARACTERISTICS OF A CONDUCTION AND RADIATION DOMINATED ELECTRIC ARC IN NITROGEN
J. Jenista Jul. 1992 37 p Limited Reproducibility: More than 20% of this document may be affected by microfiche quality
(DE93-627106; IPPCZ-323) Avail: CASI HC A03 (US Sales Only)

The time-dependent energy and circuit equations are solved numerically to obtain temperature profiles, current-voltage characteristics and electric field strength vs. axis temperature diagrams in the asymptotic region of a wall-stabilized electric arc operated in nitrogen. The numerical calculations demonstrate the splitting of the rising branch of the stationary solutions in the current-voltage characteristic. This phenomenon was earlier found experimentally for air. The computations were made for various channel radii and for various series resistances. The steady-state characteristics and convergence to the single branch of solutions is explained on the basis of the linearized Lyapunov stability theory (LLST). Comparison with available results of other authors shows that the analytical solution based on simple polynomial approximation to thermodynamic and transport functions differs significantly from numerical computations. DOE

N94-17575# Princeton Univ., NJ. Dept. of Mechanical and Aerospace Engineering.
PLASMA INSTABILITIES AND TRANSPORT IN THE MPD THRUSTER Final Technical Report, 1 Feb. 1991 - 1993
Edgar Y. Choueiri, Arnold J. Kelly, and Robert G. Jahn Jun. 1993 53 p
(Grant AF-AFOSR-0162-91)
(AD-A268268; AFOSR-93-0569TR) Avail: CASI HC A04/MF A01

This study deals with the development and testing of anomalous (turbulent) transport coefficient models that include the effects of plasma turbulence and that can be used in plasma fluid codes for more realistic numerical simulations. The anomalous transport models were derived using

a kinetic description of microinstabilities in the MPD thruster plasma. Nonlinear plasma theory was used under the valid approximation of weak turbulence and the resulting transport models were studied in detail. A strong dependence of anomalous transport on the electron Hall parameter was found. The models were then reduced to a set of compact polynomials ideally suited for inclusion in fluid codes. The usefulness and importance of these models were demonstrated by including them in an advanced plasma fluid code and carrying numerical simulations of realistic MPD thruster flows. The results show the impact of turbulence on various aspects of dissipation in the thruster as well as on the overall propulsive efficiency. Fluid codes that include these models are more accurate engineering tools for the design and study of high efficiency plasma thrusters. DTIC

N94-17635# Ceskoslovenska Akademie Ved, Prague. Ustav Fyziky Plazmatu.

DYNAMIC BEHAVIOR OF AN ELECTRIC ARC GAS DISCHARGE

J. Jenista Aug. 1992 30 p

(DE93-630197; IPPCZ-324) Avail: CASI HC A03/MF A01 (US Sales Only)

The time-dependent energy and circuit equations are solved numerically to obtain temperature profiles, current-voltage characteristics, and electric field strength vs. axial temperature diagrams in the asymptotic region of a wall-stabilized electric arc operated in nitrogen. Dynamic current-voltage characteristics and transient phenomena of steady state formation during the spark ignition phase are studied. The arc time-constant for free decay is computed and compared with approximate analytical results. It is found that for fixed initial conditions, the arc response to the variable applied voltage is several times longer than the arc time-constant for free decay. DOE

N94-17645# Los Alamos National Lab., NM.

OPTIMAL PULSE MODULATOR DESIGN CRITERIA FOR PLASMA SOURCE ION IMPLANTERS

W. Reass 1993 5 p Presented at the 9th IEEE Pulsed Power Conference, Albuquerque, NM, 21-23 Jun. 1993

(Contract W-7405-eng-36)

(DE93-016465; LA-UR-93-2303; CONF-930616-6) Avail: CASI HC A01/MF A01

This paper describes what are believed to be the required characteristics of a high-voltage modulator for efficient and optimal ion deposition from the 'Plasma Source Ion Implantation' (PSII) process. The PSII process is a method to chemically or physically alter and enhance surface properties of objects by placing them in a weakly ionized plasma and pulsing the object with a high negative voltage. The attracted ions implant themselves and form chemical bonds or are interstitially mixed with the base material. Present industrial uses of implanted objects tends to be for limited-production, high-value-added items. Traditional implanting hardware uses the typical low-current (ma) semiconductor 'raster scan' implanters. The targets must also be manipulated to maintain a surface normal to the ion beam. The PSII method can provide 'bulk' equipment processing on a large industrial scale. For the first generation equipment, currents are scaled from milliamps to hundreds of amps, voltages to -175kV, at kilohertz rep-rates, and high plasma ion densities. DOE

N94-17663# Lawrence Livermore National Lab., CA.

THE EFFECTS OF RADIATION TRANSPORT ON LINE RATIOS USED AS TEMPERATURE AND DENSITY DIAGNOSTIC

S. H. Langer and C. J. Keane Jul. 1992 23 p Presented at the 22nd Anomalous Absorption Conference, Lake Placid, NY, 12-17 Jul. 1992

(Contract W-7405-eng-48)

(DE93-016424; UCRL-JC-110695; CONF-9207204-1) Avail: CASI HC A03/MF A01

The ability to diagnose the conditions of the fuel in an Inertial Confinement Fusion (ICF) capsule is a fundamental requirement for progress in ICF. Current ICF experiments are concentrating on high convergence capsules, and the capsules will be larger on the more powerful lasers that are currently under development. Both of these developments make it harder to diagnose fuel conditions because of the larger column density in the target. This has led to increased interest in the use of line ratios as temperature and density diagnostics. For a line ratio to be a good temperature diagnostic, the ratio must be relatively insensitive to density and vary strongly with temperature. Given the atomic rates, it is relatively easy to find candidate line ratios in the coronal limit where all lines are optically thin. In this paper, the authors consider the effects of optical depth on line ratios. They show that, even if both of the lines used in the ratio are optically thin, the line ratio can depend on optical depth effects if one of the levels involved in the line ratio is pumped by an optically thick line. They present results from several different radiation transport models and attempt to draw conclusions about whether it is possible to calculate the effects of optical depth accurately enough that line ratios can still be used as diagnostics. They also consider the effects of uncertainties in atomic rates on predicted line ratios. DOE

N94-17670# Lawrence Livermore National Lab., CA.

3D AND r,z PARTICLE SIMULATIONS OF HEAVY ION FUSION BEAMS

A. Friedman, D. P. Grote, D. A. Callahan, A. B. Langdon, and I. Haber (Naval Research Lab., Washington, DC.) 21 Aug. 1992 5 p Presented at the 16th International LINAC Conference, Ottawa, Ontario, 23-28 Aug. 1992

(Contracts W-7405-eng-48; DE-AC03-76SF-00098)

(DE93-013417; UCRL-JC-110201; CONF-9208109-84) Avail: CASI HC A01/MF A01

The space-charge-dominated beams in a heavy ion beam driven inertial fusion (HIF) accelerator must be focused onto small (few mm) spots at the fusion target, and so preservation of a small emittance is crucial. The nonlinear beam self-fields can lead to emittance growth; thus, a self-consistent field description is necessary. We have developed a multi-dimensional time-dependent discrete particle simulation code, WARP, and are using it to study the behavior of HIF beams. The code's 3d package combines features of an accelerator code and a particle-in-cell (PIC) plasma simulation. Novel techniques allow it to follow beams through many accelerator elements over long distances and around bends. We have used the code to understand the emittance growth observed in the MBE4 experiment at Lawrence Berkeley Laboratory (LBL) under conditions of aggressive drift-compression. We are currently applying it to LBL's planned ILSE experiments, and (most recently) to an ESQ injector option being evaluated for ILSE. The code's r, z package is being used to study the axial confinement afforded by the shaped ends of the accelerating pulses, and to study longitudinal instability induced by induction module impedance. DOE

N94-17149 Max-Planck-Inst. fuer Extraterrestrische Physik, Garching (Germany).

ROLE AND DEVELOPMENT OF SMALL SATELLITE MISSIONS IN SPACE PLASMA PHYSICS

A. Valenzuela *In* CNES, Small Satellites Systems and Services Jan. 1993 p 229-254 (For primary document see N94-17131 03-18)

Copyright Avail: Issuing Activity (CEPADUES-Editions, 111 rue Nicolas-Vaquelin, 31100 Toulouse, France)

76 SOLID-STATE PHYSICS

Includes superconductivity.

For related information, see also *33 Electronics and Electrical Engineering* and *36 Lasers and Masers.*

N94-14913# Trieste Univ. (Italy). Inst. Di Fisica.

ELECTRONIC AND ATOMIC STRUCTURE OF SEMICONDUCTORS AND OF HIGH-TEMPERATURE SUPERCONDUCTORS Final Report

E. Tosatti and R. Car Feb. 1993 28 p

(Contract DAJA45-89-C-0025)

(AD-A266805) Avail: CASI HC A03/MF A01

In this final technical report we summarize the activity carried out within the present research project, conducted over a three year period, under the sponsorship of the European Research Office of the U.S. Army. The work done covers different areas, namely: (1) Microscopic simulations of solid, amorphous and liquid semiconductors and semimetals, of their defects, vacancies, and surfaces, and of hydrogen diffusion, using Car-Parrinello and related methods; (2) Theory of the electronic and vibrational properties of semiconductors, semiconductor alloys, interfaces, microstructures, and of GaAs - based semiconductor superlattices; (3) Quantum simulations and theory of highly correlated electron systems particularly as models for

high-T (sub c). superconducting materials; The body of the report will briefly outline the work done in each area, and highlight the main achievements which have been made possible by the project. DTIC

N94-14922# Northwestern Univ., Evanston, IL. Dept. of Electrical Engineering and Computer Science.
CHARACTERIZATION OF InTlSb GROWN BY LOW PRESSURE METALORGANIC CHEMICAL VAPOR DEPOSITION ON GaAs SUBSTRATE
Y. H. Choi, P. T. Staveteig, E. Bigan, and M. Razeghi 1993 11 p
(AD-A266878) Avail: CASI HC A03/MF A01

Optical properties of InTlSb, a new long wavelength infrared material, are investigated. InTlSb/InSb epilayers grown by low-pressure metalorganic chemical vapor deposition on semi-insulating Ga-As substrates were characterized using Auger electron spectroscopy and Fourier transform infrared spectroscopy. Auger electron spectra confirm the presence of Thallium. Transmission measurements at 77 K indicate an absorption shift from 5.5 micrometers for InSb up to 8 micrometers for InTlSb, which is confirmed by photoconductivity measurements. Author (revised)

N94-14925# Oak Ridge Inst. for Science and Education, TN.
ION MIXING OF THIN ZrO2 FILMS ON SAPPHIRE
N. D. Evans, D. L. Joslin (Tennessee Univ., Knoxville.), and C. J. McHargue (Tennessee Univ., Knoxville.) 1993 3 p Presented at the 27th Microbeam Analysis Society Meeting, Los Angeles, CA, 11-16 Jul. 1993
(Contracts DE-AC05-84OR-21400; DE-AC05-76OR-00033)
(DE93-015214; CONF-930783-2) Avail: CASI HC A01/MF A01

Ion beam induced mixing, a process useful in various applications such as adhesion enhancement, involving, metal films on either metal or either metal or oxide substrates has been studied for several years. For this study, analytical electron microscopy (AEM) has been used to investigate ion mixing in an oxide-oxide system: ZrO2 thin film on alpha-Al2O3. DOE

N94-15107# Space Exploration Association, Cedarville, OH.
DIAMOND p-n JUNCTION COLD CATHODE Final Report, 30 Nov. 1992 - 25 Jun. 1993
Elliot B. Kennel, Vladimir Z. Zaibyshev, Rafail Y. Kucherov, C. Robert Svensson, Paul R. Davis (Linfield Research Inst., McMinnville, OR.), and William A. Mackie (Linfield Research Inst., McMinnville, OR.) 29 Jun. 1993 46 p
(Contract DAAH01-93-C-R031)
(AD-A266926) Avail: CASI HC A03/MF A01

This effort successfully demonstrated that intercalated graphite fibers are outstanding cathode materials. Such fibers are stable in air at ambient temperature and offer current densities of over 100 Amps/sq cm at 10 volts bias voltage (at 700 K). Ambient temperature cathodes also offer high current capability at somewhat higher bias voltage. Cesiated graphite and diamond both exhibit these characteristics, but graphite intercalation compounds are stable in air whereas the diamond/cesium system is not. The graphite cathodes do not require a cesium reservoir in order to function. DTIC

N94-15295# Office National d'Etudes et de Recherches Aerospatiales, Paris (France).
ELECTRON-MICROSCOPY STUDY OF ANTIPHASE BOUNDARIES IN Cu3Pd AND Fe3Al ALLOYS NEAR THE ORDER-DISORDER TRANSITION Ph.D. Thesis - Paris 6 Univ., 15 Dec. 1992 [ETUDE PAR MICROSCOPIE ELECTRONIQUE DES PAROIS D'ANTIPHASE DANS LES ALLIAGES CU3PD ET FE3AL A L'APPROCHE DE LA TRANSITION ORDRE-DESORDRE]
Christian Ricolleau 1993 202 p In FRENCH
(ONERA-NT-1993-1; ETN-93-94414) Avail: CASI HC A10/MF A03

Order-disorder transitions on a fixed lattice are generally characterized by a loss of symmetry. When the ordered structures are cubic, there is only a loss of translational symmetry which implies the formation, during the ordering process, of translational variants bounded by domain wall so called Antiphase Boundaries (APB). In the particular case of the L1(sub 2) yields Disorder FCC (A1) first order phase transition, the Cu-17%Pd alloy which exhibits a two phase field over 1C was investigated. At low temperature, the APB are perfectly thin. When the temperature increases, a boundary extends over a few atomic planes which become partially disordered. At transition T(sub C), the width of the domain walls becomes macroscopic (divergence) compared to the domain size. This is the wetting phenomenon. In order to characterize the nature of the divergence of the domain wall width, strictly controlled heat treatments were performed in the (T(sub C) - 10 C, T(sub C)) range, the smallest temperature steps being 0.2C. The determination of the quantitative law and the measurements were achieved using carefully constant experimental conditions. The results showed that the APB width diverges logarithmically as -Log(T(sub C) - T) in the wetting regime, as expected theoretically. A thermodynamic model which allows a detailed analysis of the cross over regime occurring between the wetting and the two phase regime was developed. In order to compare a first and a second order phase transition, an in situ heating experiment in the FeAl(27%) alloy was performed. ESA

N94-15476*# Alabama Univ., Huntsville. Center for Microgravity and Materials Research.
CONVECTIVE FLOW EFFECTS ON PROTEIN CRYSTAL GROWTH Semiannual Progress Report No. 1, 1 Feb. - 31 Jul. 1993
Franz Rosenberger and Lisa A. Monaco 1993 29 p
(Grant NAG8-950)
(NASA-CR-194560; NAS 1.26:194560) Avail: CASI HC A03/MF A01

The experimental setup for the in-situ high resolution optical monitoring of protein crystal growth/dissolution morphologies was substantially improved. By augmenting the observation system with a temperature-controlled enclosure, laser illumination for the interferometric microscope, and software for pixel by pixel light intensity recording, a height resolution of about two unit cells for lysozyme can now be obtained. The repartitioning of Na(+) and Cl(-) ions between lysozyme solutions and crystals was studied. Quite unexpectedly, it was found that the longer crystals were in contact with their solution, the lower was their ion content. The development of a model for diffusive-convective transport and resulting distribution of the growth rate on facets was completed. Results obtained for a realistic growth cell geometry show interesting differences between 'growth runs' at 1g and 0g. The kinematic viscosity of lysozyme solutions of various supersaturations and salt concentrations was monitored over time. In contrast to the preliminary finding of other authors, no changes in viscosity were found over four days. The experimental setup for light scattering investigations of aggregation and nucleation in protein solutions was completed, and a computer program for the evaluation of multi-angle light scattering data was acquired. Author (revised)

N94-15747# North Carolina State Univ., Raleigh.
DIAMOND EPITAXY AND DIAMONDLIKE COATINGS Final Report, 1 Sep. 1989 - 28 Feb. 1993
J. Narayan 10 Jun. 1993 22 p
(Contract DAAL03-89-K-0118)
(AD-A266657; ARO-26601.2-MS) Avail: CASI HC A03/MF A01

Significant progress has been made in synthesis and processing and characterization and modelling of defects in diamond and diamondlike films. Specific areas of research include the following: (1) enhancement of nucleation and adhesion of diamond films on nondiamond substrates; (2) laser patterning of diamond films on nondiamond substrates; (3) novel methods of formation of diamond films on nondiamond substrates; (4) characterization of diamond films--defects and grain boundaries; and (5) laser processing and characterization of diamondlike films. DTIC

N94-15764# Howard Univ., Washington, DC. Dept. of Chemistry.
LASER ASSISTED CVD GROWTH OF AlN AND GaN Final Report, Aug. 1989 - Feb. 1993
Joshua B. Halpern and Joan M. Frye 20 Jun. 1993 39 p
(Contract F49620-89-C-0108)
(AD-A267150; AFOSR-93-0498TR) Avail: CASI HC A03/MF A01

This is the final report of a project for investigating laser (assisted) methods of growing nitrile thin films. We have grown thin films of AlN and SiN by laser ablation from powders. We have also developed an efficient method for laser assisted chemical vapor deposition (CVD) of aluminum, or aluminum containing films from trimethylalaminum. Author (revised)

N94-15822# Minnesota Univ., Minneapolis. Dept. of Computer Science.
SEARCH FOR FAR INFRARED RADIATION FROM OPTICALLY PUMPED DEFECT MODES Final Report, 1 Mar. 1990 - 28 Feb. 1993
A. J. Sievers 5 May 1993 34 p

(Contract DAAL03-90-G-0040)
(AD-A266744; ARO-26996.8-PH) Avail: CASI HC A03/MF A01

Five different experimental studies are described. Hole burning in chalcogenide glasses: the quantitative form of the hole relaxation depends solely on the average coordination number of the glass independent of chemical composition. PIRSH burning of Tb(3+) in alkaline earth fluoride crystals: these PIRSHs in 'glassy' crystals display the characteristic properties of spectral holes burned in true glasses. NO2(-) ions in alkali halides: four different kinds of vibrational hole burning have been carried out, namely, the hole and antihole in the same absorption line, the antihole removed in frequency from the inhomogeneously broadened line, multiple antiholes, and the burning at one vibrational mode frequency while monitoring the persistent changes produced in the other internal (IR) or external (FIR) modes with a high resolution FT interferometer. Calculations and simulations of vibrational solitons in crystals: the stationary localized mode results for perfect anharmonic crystals are reminiscent of the defect induced local modes studied in the harmonic approximation. KI:Ag(+) vibrational dynamics, first evidence for vibrational solitons: the silver ion in KI is the most thermally unstable lattice-defect combination known. It may result from localized anharmonic modes being released into the lattice.

Author (revised)

N94-15827# Oak Ridge National Lab., TN.
STRUCTURAL INVESTIGATION OF ELECTROCHEMICALLY ETCHED SILICON

B. J. Heuser (Missouri Univ., Columbia.), S. Spooner, and C. J. Glinka (National Inst. of Standards and Technology, Gaithersburg, MD.) 1992 4 p Presented at the Materials Research Society Symposium, Boston, MA, 2-6 Dec. 1992
(Contract DE-AC05-84OR-21400)
(DE93-015300; CONF-921206-13) Avail: CASI HC A01/MF A01

Small-angle neutron scattering (SANS) measurements of four electrochemically etched, porous (PS) samples have been performed over a wide wavevector transfer (Q) range. The intermediate to high Q results can be modeled with a non-particulate, random phase model. Correlation length scales on the order of 1 to 2 nm thought to characterize the PS skeleton have been deduced from the SANS data. The microstructural anisotropy was studied by tilting two of the samples with respect to the neutron beam. These samples exhibited an asymmetric scattering pattern at intermediate Q (0.1 less than or equal to Q less than or equal to 0.6 nm(exp -1)) in this condition. Photoluminescence spectra from all four samples have been recorded as well. A correlation appears to exist between the SANS and photoluminescence measurements. An x-ray diffraction measurement of one sample demonstrates that the PS layer retains the silicon lattice structure. Significant peak broadening is observed and is interpreted as a quasi-particle size effect. The PS particle size calculated from the x-ray diffraction measurement is equal to the correlation length obtained in the SANS measurement. DOE

N94-15829# Oak Ridge National Lab., TN.
EXPERIMENTAL INVESTIGATIONS OF SUPERCONDUCTIVITY IN QUASI-TWO-DIMENSIONAL EPITAXIAL COPPER OXIDE SUPERLATTICES AND TRILAYERS

D. H. Lowndes and D. P. Norton 1993 28 p Presented at the Annual Meeting of The Metallurgical Society, Denver, CO, 21-25 Feb. 1993
(Contract DE-AC05-84OR-21400)
(DE93-015306; CONF-930202-10) Avail: CASI HC A03/MF A01

Epitaxial trilayer and superlattice structures grown by pulsed laser ablation have been used to study the superconducting-to-normal transition of ultrathin (one and two c-axis unit cells) YBa2Cu3O(7 - x) layers. The normalized flux-flow resistances for several epitaxial structures containing two-cell-thick YBa2Cu3O(7 - x) films collapse onto the 'universal' curve of the Ginzburg-Landau Coulomb Gas (GLCG) model. Analysis of normalized resistance data for a series of superlattices containing one-cell-thick YBa2Cu3O(7 - x) layers also is consistent with the behavior expected for quasi-two-dimensional layers in a highly anisotropic, layered three-dimensional superconductor. Current-voltage measurements for one of the trilayer structures also are consistent with the normalized resistance data, and with the GLCG model. Scanning tunneling microscopy, transmission electron microscopy, and electrical transport studies show that growth-related steps in ultrathin YBa2Cu3O(7 - x) layers affect electrical continuity over macroscopic distances, acting as weak links. However , the perturbation of the superconducting order parameter can be minimized by utilizing hole-doped buffer and cap layers, on both sides of the YBa2Cu3O(7 - x) layer, in trilayers and superlattices. These results demonstrate the usefulness of epitaxial trilayer and superlattice structures as tools for systematic, fundamental studies of high-temperature superconductivity. DOE

N94-15923# Brookhaven National Lab., Upton, NY.
PASSIVE OXIDE FILMS ON WELL-DEFINED NICKEL SURFACES: AN EXAMINATION OF FILM GROWTH ON Ni(100) WITH EX SITU SCANNING TUNNELING MICROSCOPY

C. M. Vitus and A. J. Davenport 1993 5 p Presented at the 12th International Corrosion Congress, Houston, TX, 19-24 Sep. 1993
(Contract DE-AC02-76CH-00016)
(DE93-014056; BNL-48655; CONF-9309150-2) Avail: CASI HC A01/MF A01

The surface morphology and atomic structure of air-formed and passive oxide films on a Ni(100) single crystal is presented. The passive oxide film was formed in a 0.15N Na2SO4 solution (pH = 2.8) anodized at 0.0 V vs. Hg/Hg2SO4 reference. DOE

N94-15955# Wisconsin Univ., Madison. Dept. of Physics.
A HIGH FLUX RADICAL BEAM DIAMOND GROWTH Final Report, 30 Apr. 1990 - 29 Apr. 1993

J. E. Lawler and L. W. Anderson 10 Jun. 1993 5 p
(Contract DAAL03-90-G-0115)
(AD-A266754; ARO-27646.9-PH) Avail: CASI HC A01/MF A01

Research on chemical vapor deposition (CVD) of diamond films is summarized. The development of a technique for High Sensitivity Absorption Spectroscopy at deep ultraviolet wavelengths in CVD systems is reported. Diagnostic experiments on the diamond CVD environment are described.

DTIC

N94-15972# Los Alamos National Lab., NM.
THE FRACTIONAL QUANTUM HALL EFFECT AND THE ROTATION GROUP

J. N. Ginocchio and W. C. Haxton (Washington Univ., Seattle.) 1992 12 p Presented at the 6th Symmetries in Science, Bregenz, Austria, 2-7 Aug. 1992
(Contracts DE-FG06-90ER-40561; DE-FG06-88ER-40427)
(DE93-010348; DOE/ER-40561/084; CONF-9208164-3) Avail: CASI HC A03/MF A01

The fractional quantum Hall effect is thought to be the result of correlations between electrons induced by their mutual interactions. This paper explores the consequences of these correlations numerically and analytically. The problem is mapped onto the surface of a sphere, so that the number of states in the first Landau level is finite. The following three sections review this geometry, give the matrix elements of the Coulomb interaction, and compare exact wave functions with the Laughlin/Haldane ground state ansatz for fractional fillings 1/m, m an odd integer. While this ansatz accounts for many of the J = 0 ground states found in numerical diagonalizations, it does not explain all such states. To make progress on this problem, a complete characterization of the most general four-particle J = 0 wave function is given, including an algebraic enumeration of the number of such states. This construction provides one example of a 2/3-filled state, the particle-hole conjugate of the 3-particle Laughlin/Haldane m = 3 state. This result suggests a generalization that may give the particle-hole conjugates of all Laughlin/Haldane states of arbitrary N: the construction depends on an equivalence of single-particle spinors of rank N/2 and ones formed by coupling the elementary spinors of N different particles. This result is further generalized to produce a wave function ansatz that may account for other fractional fillings of physical interest. DOE

N94-15973# EG and G Energy Measurements, Inc., Goleta, CA.
OPTICAL PROPERTIES AND SURFACE MORPHOLOGY STUDIES OF PALLADIUM CONTACTS ON MERCURIC IODIDE SINGLE CRYSTALS

M. A. George (Fisk Univ., Nashville, TN.), M. Azoulay (Fisk Univ., Nashville, TN.), A. Burger (Fisk Univ., Nashville, TN.), Y. Biao (Fisk Univ., Nashville, TN.), E. Silberman (Fisk Univ., Nashville, TN.), and D. Nason 1993 16 p Presented at the International Conference on Metallurgical Coatings and Thin Films, San Diego, CA, 19-23 Apr. 1993
(Contract DE-AC08-88NV-10617)

(DE93-012510; EGG-10617-2168; CONF-930419-2) Avail: CASI HC A03/MF A01

Palladium is chemically suitable for electric contacts on mercuric iodide detectors for photon and nuclear radiation detection, so the understanding of palladium contacts is important for fundamental and practical scientific purposes. A study has been conducted on the surface morphology of evaporated contacts using atomic force microscopy (AFM) and optical transmission and reflection. Evaporated palladium coatings are typically nonuniform and may deposit selectively on mercuric iodide surface defects. Reflection measurements show that coating thickness and surface treatment affect intensity, position, and shape of a reflected peak characteristic of the mercuric iodide structure. Results indicate that the band gap energy in the surface of the mercuric iodide is lowered by palladium contacts. DOE

N94-15976# Lawrence Livermore National Lab., CA.
ELECTRONIC STRUCTURE AND ENTHALPY OF HYDROGEN AND HELIUM MIXTURES

M. Ross, J. E. Klepeis, K. J. Schafer, and T. W. Barbee, III Nov. 1992 3 p Presented at the International Conference on the Physics of Strongly Coupled Plasmas, Rochester, NY, 17-21 Aug. 1992

(Contract W-7405-eng-48)
(DE93-014128; UCRL-JC-112346; CONF-9208135-7) Avail: CASI HC A01/MF A01

The first local density approximation (LDA) calculations of the electronic structure, equation of state, and enthalpy of mixing were carried out for a number of different compositions of hydrogen and helium in bcc and fcc lattices. These are fully quantum mechanical, self-consistent calculations utilizing state-of-the-art methods of electron band theory, which make no assumptions regarding pressure ionization. The major approximation in the LDA method is that the exchange and correlation energy is given by a free electron functional in terms of the local electron density. The majority of previous mixture calculations start with the assumption that both hydrogen and helium are pressure-ionized so that the electronic structure is approximately that of free or weakly screened electrons in the presence of positive ions. Stevenson used a hard-sphere mixture model for the ions with an ion-ion pseudopotential to account for electron screening and predicted that a mixture containing 7% helium by number, the composition believed to be present in Jupiter and Saturn, would phase separate at a temperature of about 7000 K at 8 Mbar. Subsequent calculations carried out for the fully ionized mixture and for a mixture of screened ions (linear response theory) have all arrived at predictions similar to those of Stevenson. MacFarlane and Hubbard performed Thomas-Fermi-Dirac calculations for mixing enthalpies of hydrogen and helium in bcc and fcc lattices and predicted that phase separation would not occur at any temperature. DOE

N94-15982# Argonne National Lab., Idaho Falls, ID.
ROLES OF OXYGEN DEFECTS IN COPPER-OXIDE SUPERCONDUCTORS

J. D. Jorgensen, P. G. Radaelli, H. Shaked, J. L. Wagner, B. A. Hunter, J. F. Mitchell, R. L. Litterman, and D. G. Hinks Apr. 1993 6 p Presented at the International Workshop on Superconductivity, Hokkaido, Japan, 28 Jun. - 1 Jul. 1993

(Contract W-31-109-eng-38)
(DE93-014875; ANL/MSD/CP-79578; CONF-930682-1) Avail: CASI HC A02/MF A01

Oxygen vacancy and interstitial defects can have a profound effect on the superconducting compounds. Recent work on compounds such as La2CuO(4+x) provided new insight into the role of interstitial oxygen defects as a doping mechanism. Studies of (La,Sr,Ca)(3)Cu2O(6+x) with various metal compositions and metal-site ordering show that interstitial oxygen defects that form between the CuO2 layers in this structure systematically lower (Tc) and eventually destroy superconductivity. However, oxygen vacancies in the CuO2 planes have surprisingly little effect at concentrations below 3%. The infinite-layer compounds, ACuO2 where A = La, Sr, Ca, Nd, etc., in solid-solution combinations, offer a very similar environment for the formation of interstitial oxygen defects between the CuO2 planes. However, neutron diffraction experiments on Sr(0.9)La(0.1)CuO2 (T(sub c) = 42 K) have not found any interstitial oxygen. DOE

N94-16012# Sandia National Labs., Albuquerque, NM.
THE GROWTH OF InAs(1-x)Sb(x)/InAs STRAINED-LAYER SUPERLATTICES BY METAL-ORGANIC CHEMICAL VAPOR DEPOSITION

R. M. Biefeld, K. C. Baucom, and S. R. Kurtz 1993 14 p Presented at the 9th American Conference on Crystal Growth, Characterization and Applications, Baltimore, MD, 1-6 Aug. 1993

(Contract DE-AC04-76DP-00789)
(DE93-015028; SAND-93-0300C; CONF-930851-1) Avail: CASI HC A03/MF A01

InAs(1-x)Sb(x)/InAs strained-layer superlattice (SLS) semiconductors and thick epitaxial layers of InAs(1-x)Sb(x) were grown under a variety of conditions by metal-organic chemical vapor deposition on InAs substrates. The 3/5 ratio was varied from 0.026 to 1.0 over a temperature range of 475-525C, at pressures of 200 to 660 torr and growth rates of 0.75 to 3.0 micron/hour. The composition of the ternary can be predicted from the input gas molar flow rates using a thermodynamic model. At lower temperatures, the thermodynamic model must be modified to take account of the incomplete decomposition of arsine and trimethyl antimony. These layers were characterized by optical microscopy, SIMS, and x-ray diffraction. The optical properties of these SLS's were determined by infrared photoluminescence and absorption measurements. The PL peak energies of the alloys and the SLS's are consistently lower than the previously reported values for the bandgap of InAs(1-x)Sb(x) alloys. DOE

N94-16058# Argonne National Lab., IL.
INTERFACIAL STRUCTURE OF LATTICE MISMATCHED BCC(110)/BCC(110) TRANSITION METAL SUPERLATTICES

E. E. Fullerton, C. H. Sowers, S. D. Bader, S. Mini, A. S. Bommannavar (City Univ. of New York, Brooklyn.), and S. N. Ehrlich (Purdue Univ., West Lafayette, IN.) Mar. 1993 7 p Presented at the Spring Meeting of the Materials Research Society, San Francisco, CA, 12-16 Apr. 1993

(Contract W-31-109-eng-38)
(DE93-015162; ANL/XFD/CP-79634; CONF-930405-18) Avail: CASI HC A02/MF A01

We present structural characterizations of a series of sputtered Fe/Nb and V/Nb superlattices by high-angle x-ray diffraction. Diffraction scans were performed with the scattering vector at various angles (chi) with respect to the layers. Chi = 0 deg diffraction spectra (normal to the layers) were fitted to a general structural model to determine the (110) lattice strains, interfacial disorder and interdiffusion. Chi greater than 0 deg spectra probe the lattice strain of the individual layers and the in-plane interfacial coherence. Both systems form incoherent interfaces above a critical modulation wavelength (lambda(sub C)). At lambda(sub C), the Fe/Nb system undergoes a crystalline-to-amorphous transition while the V/Nb forms in-plane coherent interfaces. DOE

N94-16062# Stanford Linear Accelerator Center, CA.
PHOTOEMISSION STUDY OF DIAMOND (100) SURFACE

J. Wu, R. Cao, X. Yang, P. Pianetta, and I. Lindau Mar. 1993 7 p Presented at the 39th National Symposium of the American Vacuum Society, Chicago, IL, 9-13 Nov. 1992

(Contract DE-AC03-76SF-00515)
(DE93-015251; SU-SLAC-PUB-6078; SLAC/SSRL-0015; CONF-921129-10) Avail: CASI HC A02/MF A01

The electronic structure of the diamond C(100)-(2 x 1)/(2 x 2) has been investigated by means of angle-resolved photoelectron spectroscopy for the first time. A surface-related shift has been observed in the C 1s core level spectrum. The surface-state band dispersion was measured along the symmetry axis Gamma-J' in the surface Brillouin zone. For k(sub (parallel)) = 0, there is a very pronounced surface state 1.5 eV below Fermi level E(sub F), and it disperses downwards with increasing k(sub (parallel)). Near the boundary of the surface Brillouin zone J', we find two states with binding energies of 1.9 and 2.4 eV with respect to E(sub F). DOE

N94-16063# Oak Ridge National Lab., TN.
A REEXAMINATION OF GRAIN BOUNDARY FRACTURE IN NI3AL: ENVIRONMENTAL AND ALLOYING EFFECTS

E. P. George, C. T. Liu, and D. P. Pope (Pennsylvania Univ., Philadelphia.) 1993 9 p Presented at the International Symposium on Structural

Intermetallics, Champion, PA, 26-30 Sep. 1993
(Contract DE-AC05-84OR-21400)
(DE93-015431; CONF-930997-2) Avail: CASI HC A02/MF A01

The intrinsic room-temperature ductility (approximately 23 percent) of polycrystalline Ni3Al is considerably higher than previously thought. Environmental embrittlement, caused by moisture in ordinary ambient air, reduces significantly the maximum attainable ductility in air. Microcracks (introduced during processing) can also reduce the maximum attainable ductility in air. A consequence of these extrinsic factors is that polycrystalline Ni3Al is usually found to be quite brittle in air, and very careful experimental procedures are required if its (higher) intrinsic ductility is to be measured. The addition of B essentially suppresses environmental embrittlement in Ni3Al, thereby improving ductility. The substitutional elements Zr and Hf also improve ductility, but Ti (which is from the same group in the periodic table) does not. The mechanism by which Zr and Hf improve ductility is not known, but they appear to both alleviate environmental embrittlement and enhance grain-boundary cohesion. DOE

N94-16066# Oak Ridge National Lab., TN.
THIN NI SILICIDE FORMATION BY LOW TEMPERATURE-INDUCED METAL ATOM REACTION WITH ION IMPLANTED AMORPHOUS SILICON

Y. N. Erokhin (North Carolina State Univ., Raleigh.), S. Pramanick (North Carolina Univ., Chapel Hill.), F. Hong (North Carolina State Univ., Raleigh.), G. A. Rozgonyi (North Carolina State Univ., Raleigh.), B. K. Patnaik (North Carolina Univ., Chapel Hill.), and C. W. White 1992 5 p Presented at the 16th Material Research Society International Symposium on the Scientific Basis for Nuclear Waste Management Fall Meeting, Boston, MA, 30 Nov. - 5 Dec. 1992
(Contract DE-AC05-84OR-21400)
(DE93-015449; CONF-921101-126) Avail: CASI HC A01/MF A01

We have extended our recent work on buried silicide formation by Ni diffusion into a buried amorphous silicon layer to the case where silicide formation is at lower temperatures on silicon substrates which have been preamorphized. The reaction of metal atoms from a 12 nm Ni film evaporated on top of a 65 nm thick surface amorphous layer formed by 35 keV Si(+) ion implantation has been investigated at temperature less than or equal to 400 C. Rutherford Backscattering Spectrometry (RBS) with channeling, cross-sectional transmission electron microscopy (XTEM), x-ray diffraction and four-point probe measurements were used to determine structure, interfacial morphology, composition, and resistivity of the silicide films. It has been found that an increased rate of silicidation occurs for amorphous silicon with respect to crystalline areas permitting a selective control of the silicon area to be contacted during silicide growth. Vacuum furnace annealing at 360 C for 8 hours followed by an additional step at 400 C for one hour produces a continuous NiSi2 layer with a resistivity 44 (mu)(Omega) cm. DOE

N94-16159# Pacific Northwest Lab., Richland, WA.
THE ROLE OF INTERFACIAL CHEMISTRY IN SURFACE NUCLEATION AND GROWTH OF CALCIUM OXALATE

L. Song, A. A. Campbell, and B. C. Bunker 1993 6 p Presented at the Spring Meeting of the Materials Research Society, San Francisco, CA, 12-16 Apr. 1993
(Contracts DE-AC06-76RL-01830; DE-FG06-89ER-75522)
(DE93-015689; PNL-SA-22038; CONF-930405-20) Avail: CASI HC A02/MF A01

The surface adsorption of Ca(2+) and oxalate anions Ox(2-) on SiO2, TiO2 and Al2O3 oxide colloids were by electrosonic amplitude measurements. Kinetics studies of CaO(x) formation on the model oxide surfaces were carried out using constant composition method. Results suggested Ca(2+) and Ox(2-) adsorption was promoted on the oxide surfaces with opposite charges, and the specific adsorption of the divalent ions also resulted in surface charge reversal. For heterogeneous nucleation of CaO(x) on the three model oxide surfaces, induction times ranged from 270 to 360 minutes compared with 1200 minutes estimated for homogeneous nucleation and 700 minutes for spontaneous or nucleation at pH 6.5 and S = 3.3. Lower nucleation barriers, 27 mJ/sq m for SiO2, 26 mJ/sq m for TiO2, were observed by studying the dependence of nucleation induction times as the function of solution supersaturation. DOE

N94-16164# Oak Ridge National Lab., TN.
CRYSTALLIZATION OF GRAIN BOUNDARY PHASES IN SILICON NITRIDE WITH LOW ADDITIVE CONTENTS BY MICROWAVE ANNEALING

T. N. Tiegs, K. L. Ploetz, J. O. Kiggans, and R. L. Yeckley 1993 11 p Presented at the 95th Annual Meeting of the American Ceramic Society, Cincinnati, OH, 18-22 Apr. 1993
(Contract DE-AC05-84OR-21400)
(DE93-015801; CONF-930438-24) Avail: CASI HC A03/MF A01

Microwave annealing of dense Si3N4-4% Y2O3 materials showed improvements over conventional heating. Increases in fracture toughness were observed for annealing between 1200-1650C. The high temperature strength was related to the residual (alpha)-Si3N4 content which is indicative of a finer average grain size in the specimens. The high temperature dynamic fatigue showed increased stress to failure for specimens microwave annealed between 1400-1550C for periods greater than 5 h. Silicon nitrides with different sintering additives would require different conditions for optimum crystallization. While there were some observed property improvements, they were not so dramatic to justify abandoning conventional over microwave heating. The Si3N4-4% Y2O3 materials used in the study were developed for elevated temperature use and already possesses excellent to good high temperature strength, fatigue resistance and creep properties. This is due to the very refractory nature of the grain boundary phases and the small quantity of secondary phase present. However, microwave annealing of these materials may be necessary in applications where the maximum in fracture toughness and fatigue resistance are required and thus justifies its use. DOE

N94-16171# Oak Ridge National Lab., TN.
CHEMICAL AND DISPLACEMENT ATOMIC PAIR CORRELATIONS IN CRYSTALLINE SOLID SOLUTIONS RECOVERED BY ANOMALOUS X RAY SCATTERING IN Fe-Ni ALLOYS

G. E. Ice, C. J. Sparks, and L. B. Shaffer 1992 30 p Presented at the Anomalous Scattering International Conference, Malente, Germany, 17-21 Aug. 1992
(Contract DE-AC05-84OR-21400)
(DE93-015906; CONF-9208184-2) Avail: CASI HC A03/MF A01

Short-range pair correlations of atoms in crystalline solid solutions consist of both chemical and displacement correlations. Measurement of these pair correlations is fundamental to understanding the properties of solid solutions. We discuss anomalous scattering techniques which have provided an important advance in our ability to recover these pair correlations and to model the local atomic arrangements in crystalline solid solutions of Fe-Ni alloys. DOE

N94-16442# EG and G Energy Measurements, Inc., Goleta, CA.
GROWTH OF SINGLE CRYSTALS OF MERCURIC IODIDE ON THE GROUND AND IN SPACE

L. vandenBerg 1993 10 p Presented at the Spring Meeting of the Materials Research Society, San Francisco, CA, 12-16 Apr. 1993
(Contract DE-AC08-88NV-10617)
(DE93-015523; EGG-10617-2186; CONF-930405-21) Avail: CASI HC A02/MF A01

A short review is given of the methods by which mercuric iodide is prepared and purified to obtain material suitable for the growth of single crystals. The method used in our laboratory to grow single crystals up to 1,000 grams in weight from the vapor is discussed. Effects of gravity on the growth process are described. A crystal growth system suitable for operation in the reduced gravity environment of space was designed and crystal growth experiments were performed during the flights of Spacelab 3 (April 1985) and the International Microgravity Laboratory (January 1992). Structural quality and electronic properties of ground-based and space-grown crystals are compared. DOE

N94-16447# Brookhaven National Lab., Upton, NY.
LOCAL ENVIRONMENT ABOUT O ATOMS IN Pr-Y-Ba-Cu-O FILMS STUDIED BY O K-EDGE XAFS

A. Krol, Y. L. Soo, S. Huang, Z. H. Ming, L. W. Song, Y. H. Kao, and G. C. Smith (Brookhaven National Lab., Upton, NY.) Sep. 1992 8 p Presented at the 6th Annual New York State Inst. on Superconductivity Conference on Superconductivity and Applications, Buffalo, NY, 15-17 Sep. 1992

(Contracts DE-AC02-76CH-00016; DE-FG02-87ER-45283)
(DE93-016218; BNL-48361; CONF-920944-7) Avail: CASI HC A02/MF A01

The local environment about oxygen atoms in Pr(x)Y(1-x)Ba2Cu3O7 films obtained by laser ablation has been investigated by means of the x-ray absorption fine structure (XAFS) spectroscopy at the O K-edge. It has been found that the Pr atoms do not substitute for the Cu atoms nor do they form interstitial defects in the CuO2 planes and that the presence of Pr dopant does not disturb the local environment of oxygen.
Author (revised)

N94-16460# Oak Ridge National Lab., TN.
FAST-ICCD PHOTOGRAPHY AND GATED PHOTON COUNTING MEASUREMENTS OF BLACKBODY EMISSION FROM PARTICULATES GENERATED IN THE KrF-LASER ABLATION OF BN AND YBC
D. B. Geohegan Nov. 1992 7 p Presented at the 16th Material Research Society International Symposium on the Scientific Basis for Nuclear Waste Management Fall Meeting, Boston, MA, 30 Nov. - 5 Dec. 1992
(Contract DE-AC05-84OR-21400)
(DE93-015491; CONF-921101-123) Avail: CASI HC A02/MF A01

Fast intensified CCD photography and gated photon counting following KrF-laser irradiation of YBCO and BN targets reveals the first observations of very weak emission from slow-moving ejecta up to 2 cm from the target and times extending to approximately 1.5 ms. Time-of-flight velocities inferred from the emission measurements indicate velocities (v approximately (0.45-1.2) x 10(exp 4) cm s(exp -1) comparable to those measured for the large particles which often accompany the pulsed laser deposition process. Gated photon counting is employed to obtain temporally resolved spectra of this weak emission. The spectral shape is characteristic of blackbody emission, which shifts to longer wavelengths as the particles cool during flight in vacuum. Estimates of the temperature of the particles are made based on the emissivity of a perfect blackbody and range from 2200 K to 3200 K for both BN and YBCO when irradiated at Phi(sub 248) = 3.5 J cm(exp -2) and 1.5 J cm(exp -2), respectively. The temperature decrease of the particles in vacuum is compared to a radiative cooling model which gives estimates of the initial surface temperature and radii of the particles.
DOE

N94-16476# Pittsburgh Univ., PA. Surface Science Center.
THERMAL DISORDER IN ADSORBED Cl ON Si(100)
C. C. Cheng, Q. Gao, Z. Dohnalek, W. J. Choyky, and J. T. Yates, Jr. 21 May 1993 24 p
(Contract N00014-82-K-0280)
(AD-A266295; TR-56) Avail: CASI HC A03/MF A01

Thermal broadening of Cl(+) ESDIAD patterns, related to the vibrational motion of the adsorbate, has been investigated by subtraction of patterns measured at different temperatures. In the case of Cl on Si(100), the observed difference pattern between 130 K and 305 K indicates that azimuthally isotropic motion of Cl occurs about the most probable Si-Cl bond direction. Equal distributions from the in-plane and out-of-plane bending motions are observed, correlating with the approx 200/cm frequencies associated with these motions.
DTIC

N94-16487 Department of the Navy, Washington, DC.
APPARATUS FOR AND A METHOD OF GROWING THIN FILMS OF ELEMENTAL SEMICONDUCTORS Patent
Max N. Yoder, inventor (to Navy) 6 Jul. 1993 16 p Filed 22 Jun. 1990
(AD-D015813; US-Patent-5,225,366; US-Patent-Appl-SN-541990;
US-Patent-Class-437-108) Avail: US Patent and Trademark Office

An apparatus for and a method of growing thin films of the elemental semiconductors (group IVB), i.e., silicon, germanium, tin, lead. and, especially diamond, using modified atomic layer epitaxial (ALE) growth techniques are disclosed. In addition, stoichiometric and nonstoichiometric compounds of the group IVB elements are also grown by a variation of the method according to the present invention. The ALE growth of diamond thin films is carried-out, inter alia, by exposing a plurality of diamond or like substrates alternately to a halocarbon reactant gas, e.g., carbon tetrafluoride (CF4), and a hydrocarbon reactant gas, e.g., methane (CH4), at substrate temperatures between 300 and 650 C. A stepping motor device portion of the apparatus is controlled by a programmable controller portion such that the surfaces of the plurality of substrates are given exposures of at least 10(exp 15) molecules/sq cm of each of the reactant gases. The chemical reaction time to complete the growth of an individual atom layer is approximately 25 x 10(exp -6) second.
DTIC

N94-16538 Department of the Navy, Washington, DC.
METHOD FOR DOPING GaAs WITH HIGH VAPOR PRESSURE ELEMENTS Patent
Bijan Tadayon, inventor (to Navy) and Saied Tadayon, inventor (to Navy) 2 Feb. 1993 7 p Filed 3 May 1991
(AD-D015794; US-Patent-5,183,779; US-Patent-Appl-SN-695018;
US-Patent-Class-437-165) Avail: US Patent and Trademark Office

A method is disclosed for the incorporation of relatively high vapor pressure elements into good quality GaAs at extremely low T(sub s) using the migration enhanced epitaxy technique. Zinc was doped in GaAs material grown at a low T, of 120 C. Zinc may thus be used as a p-type dopant replacing more toxic Be. Similarly, other high vapor pressure elements can be incorporated much more efficiently into the material grown at low T(sub s).
DTIC

N94-16646*# Alabama Univ., Huntsville. Center for Microgravity and Materials Research.
RESEARCH SUPPORT FOR CADMIUM TELLURIDE CRYSTAL GROWTH Semiannual Report No. 6, 11 Feb. 1992 - 10 Aug. 1993
Franz Rosenberger and Michael Banish 1993 3 p
(Grant NAG8-842)
(NASA-CR-193557; NAS 1.26:193557) Avail: CASI HC A01/MF A01

Work performed during the period 11 Feb. 1992 to 10 Aug. 1993 on research support for cadmium telluride crystal growth is reported. Work on chemical impurity characterization and mass spectroscopy is described.
CASI

N94-16720# City Coll. of the City Univ. of New York, NY.
ULTRAFAST PROCESSES IN TUNNELING MICROSTRUCTURE DEVICES Final Report, 15 Sep. 1989 - 14 Dec. 1992
R. R. Alfano and Kai Shum 21 Jun. 1993 5 p
(Contract DAAL03-89-G-0110)
(AD-A266570; ARO-27154-8-PH-SAH) Avail: CASI HC A01/MF A01

A systematic investigation of ultrafast electron tunneling processes in semiconductor microstructures in presence of inter-valley (X-gamma) scattering, infrared radiation, phonons, and Coulomb interaction has been undertaken. Various important time constants involved in high speed electronic and photonic device operation were obtained such as the lifetime of a quasi-bound state, the time needed for an electron to tunnel into a well through a barrier, and the escape time for an electron to tunnel out from a well through a barrier. Our investigation under the period supported by the grant has resulted in ten journal publications.
DTIC

N94-16775# Brookhaven National Lab., Upton, NY.
POWDER DIFFRACTION STUDIES USING ANOMALOUS DISPERSION
D. E. Cox and A. P. Wilkinson (California Univ., Santa Barbara.) 1993 25 p Presented at the International Conference on Anomalous Scattering, Malente, Germany, 15-19 Aug. 1993
(Contract DE-AC02-76CH-00016)
(DE93-012531; BNL-48626; CONF-930899-1) Avail: CASI HC A03/MF A01

With the increasing availability and accessibility of high resolution powder diffractometers at many synchrotron radiation sources throughout the world, there is rapidly-growing interest in the exploitation of anomalous dispersion techniques for structural studies of polycrystalline materials. In conjunction with the Rietveld profile method for structure refinement, such studies are especially useful for the determination of the site distributions of two or more atoms which are near neighbors in the periodic table, or atoms which are distributed among partially occupied sites. Additionally, it is possible to (1) determine the mean-square displacements associated with different kinds of atoms distributed over a single set of sites, (2) distinguish between different oxidation states and coordination geometries of a particular atom in a compound, and (3) to determine f' for a wide range of atomic species as a function of energy in the vicinity of an absorption edge. Experimental methods for making anomalous dispersion measurements are described in some detail, including data collection strategies, data analysis and correlation problems, possible systematic errors, and the accuracy of the results. Recent work in the field is reviewed, including cation site-distribution studies

(e.g. doped high (Tc) superconductors, ternary alloys, FeCo2(PO4)3, FeNi2BO5), oxidation-state contrast (e.g. YBa2Cu3O(6+x), Eu3O4, GaCl2, Fe2PO5), and the effect of coordination geometry (e.g. Y3Ga5O12). DOE

N94-16782 Northwestern Univ., Evanston, IL. Dept. of Chemistry.
HIGH-VALENT OXO, METHOXORHENIUM COMPLEXES: MODELS FOR INTERMEDIATES AND TRANSITION STATES IN PROTON-COUPLED MULTI-ELECTRON TRANSFER REACTIONS Technical Report, Jun. 1992 - Jun. 1993
M. S. Ram, Lisa M. Skeens-Jones, Christopher S. Johnson, Xiao L. Zhang, and Joseph T. Hupp 30 May 1993 59 p Limited Reproducibility: More than 20% of this document may be affected by microfiche quality
(Contract N00014-91-J-1035)
(AD-A266492; TR-15) Avail: Issuing Activity (Defense Technical Information Center (DTIC))

Dioxorhenium(V) tetrapyridyl species are currently under active investigation as model systems for interfacial two-electron, two-proton transfer reaction sequences. We now find that the corresponding oxo,methoxo complexes can be prepared from dioxo species and methyl trifluoromethanesulfonate. The new complexes behave nearly identically to the analogous oxo,hydroxo complexes - with one important exception: CH3(+), unlike H(+), does not dissociate from the oxo ligand. As a direct consequence, the usually elusive rhenium oxidation state, IV, is stabilized with respect to redox disproportionation and is observable for several complexes at high pH. The ability to detect this state, in turn leads to: (1) direct access to the formal reduction potentials for the isolated 1e(-) redox couples comprising the overall two electron transfer (key information for understanding multi-ET kinetics); (2) elucidation of the profound structural and energetic consequences of the initial protonation (methylation) step in the dioxorhenium(V) reduction kinetics; (3) estimates for pK(sub s) of (O)(HO)Re(sup IV)L4(3+) (exceptionally negative); and (4) estimates for the first pK(sub s) of (HO)2Re(III)L4(+) (extremely large and positive). The combination of (1) and (2), in principle, provides sufficient information to characterize completely the energetic accessiblity of key intermediate species lying just before or just after the transition state for the two-electron, two-proton reduction of dioxorhenium(V) at electrochemical interfaces.
Author (DTIC)

N94-16800# Texas Univ., Austin. Electronics Research Center.
JSEP FELLOWSHIP Final Report, May 1991 - Dec. 1992
Alvin M. Goodman and Edward J. Powers 28 Jun. 1993 5 p
(Contract N00014-91-J-1636)
(AD-A266568) Avail: CASI HC A01/MF A01

In this dissertation, the precision of molecular-beam epitaxy (MBE) is taken advantage of in order to grow semiconductor reflectors, microcavities, and quantum wells for studies of vertical-cavity surface-emitting lasers (VCSEL's) and the coupling between reflectors and the spatially localized dipoles of semiconductor quantum wells. The design of the structures and the choice of epitaxial growth parameters used for the structures are discussed in detail. Experimental techniques and results are discussed which relate to studies that advance the optoelectronics technology and our understanding of fundamental physics. MBE is used to grow epitaxial structures in which a QW is precisely placed either in close proximity to a DBR, or near the surface of the epitaxial layer, so that a highly reflective mirror can be placed in close proximity to the QW. DTIC

N94-16805# Argonne National Lab., IL.
TRITIUM DIFFUSION AND DESORPTION IN SINGLE CRYSTAL LIAIO2
J. P. Kopasz, C. A. Seils, and C. E. Johnson 1992 11 p Presented at the International Workshop on Ceramic Breeder Blanket Interactions, Tokyo, Japan, 26-29 Oct. 1992
(Contract W-31-109-eng-38)
(DE93-015140; ANL/CMT/CP-79667; CONF-9210255-2) Avail: CASI HC A03/MF A01

In an attempt to determine the diffusivity of tritium in lithium aluminate, we have performed isothermal annealing tests on single crystal samples (approximately 1.5 mm dia.). Large single crystals were used to minimize the contributions from desorption. Diffusion kinetics become more dominant as the crystal radius increases due to the decreasing surface area to volume ratio. However, the release may still be in the mixed diffusion-desorption regime which would make obtaining the rate constants from the time dependence of the tritium release difficult. Therefore, we have decided to section the samples and determine the diffusivity from the tritium concentration profile within the sample. In addition, in an attempt to understand the effects of impurities on the tritium transport, we have studied the tritium profiles in pure and Mg doped (0.3%) LiAlO2. DOE

N94-16814# Oak Ridge National Lab., TN.
MICROSTRUCTURE OF Zr3Al AFTER 2 MeV PROTON BOMBARDMENT
F. C. Chen (University of Southern California, Los Angeles.), A. J. Ardell (University of Southern California, Los Angeles.), D. F. Pedraza, and R. A. Buhl 1992 6 p Presented at the 16th Material Research Society International Symposium on the Scientific Basis for Nuclear Waste Management Fall Meeting, Boston, MA, 30 Nov. - 5 Dec. 1992
(Contract DE-AC05-84OR-21400)
(DE93-015331; CONF-921101-127) Avail: CASI HC A02/MF A01

The ordered intermetallic Ll2 alloy Zr3Al was irradiated with 2 MeV protons at -124 C to fluences up to 2(10)(exp 15) H(+)/sq mm and at 250 C to fluences 1(10)(exp 15) H(+)/sq mm. Defects with spherically symmetric strain fields were produced at both irradiation temperatures. They are of interstitial character at -124 C and vacancy character at 250 C. Disordering is induced at -124 C, whereas irradiating at 250 C initially lowers, then slightly raises, the degree of long-range order above its unirradiated value. Additional defects that appear as black spots were imaged using superlattice reflections in dark field. For the low-temperature irradiations they were seen at all doses, but were present at only the lowest dose for the high-temperature irradiations. They are probably disordered zones, although some of the zones may be amorphous at the higher doses in the low-temperature irradiations. DOE

N94-16827# Brookhaven National Lab., Upton, NY.
CRYSTALLINE BEAM GROUND STATE
Jie Wei, Xiao-Ping Li (California Univ., Berkeley. Lawrence Berkeley Lab.), and A. M. Sessler (California Univ., Berkeley. Lawrence Berkeley Lab.) 1993 4 p Presented at the International Particle Accelerator Conference, Washington, DC, 17-20 May 1993
(Contracts DE-AC02-76CH-00016; DE-AC03-76SF-00098)
(DE93-014331; BNL-48385; CONF-930511-63) Avail: CASI HC A01/MF A01

In order to employ Molecular Dynamics method, commonly used in condensed matter physics, we have derived the equations of motion for a beam of charged particles in the rotating rest frame of the reference particle. We include in the formalism that the particles are confined by the guiding and focusing magnetic fields, and that they are confined in a conducting vacuum pipe while interacting with each other via a Coulomb force. Numerical simulation has been performed to obtain the equilibrium structure. The effects of the shearing force, centrifugal force, and azimuthal variation of the focusing strength are investigated. It is found that a constant gradient storage ring can not give a crystalline beam, but that an alternating-gradient (AG) structure can. In such a machine the ground state is, except for one-dimensional (1-D) crystals, time-dependent. The ground state is a zero entropy state, despite the time-dependent, periodic variation of the focusing force. The nature of the ground state, similar to that found by Rahman and Schiffer, depends upon the density and the relative focusing strengths in the transverse directions. At low density, the crystal is 1-D. As the density increases, it transforms into various kinds of 2-D and 3-D crystals. If the energy of the beam is higher than the transition energy of the machine, the crystalline structure can not be formed for lack of radial focusing. DOE

N94-16839# Oak Ridge National Lab., TN.
DENSITY OF STATES AND TUNNELING CHARACTERISTICS OF LAYERED SUPERCONDUCTORS
S. H. Liu and R. A. Klemm (Argonne National Lab., Idaho Falls, ID.) Apr. 1993 3 p Presented at the Conference of the International Union of Pure and Applied Physics on Low Temperature Physics (LT 20), Eugene, OR, 1-11 Aug. 1993
(Contracts DE-AC05-84OR-21400; W-31-109-eng-38)
(DE93-015898; CONF-930801-5) Avail: CASI HC A01/MF A01

We have studied the structure of the density of states (DOS) curves and tunneling characteristics of layered superconductors with two distinct layers in a unit cell. In general, the peaks of the DOS curves do not correspond to energy gaps of each layer, but depend on the gaps and the interlayer hopping strengths in a complex manner. This makes the

interpretation of tunneling data of layered superconductors much less straightforward than isotropic superconductors. Our simulated tunneling characteristics bear certain resemblance to experimental results. DOE

N94-16841# Oak Ridge National Lab., TN.
INSIGHTS INTO SEMICONDUCTING MATERIALS AND GROWTH PHENOMENA THROUGH Z-CONTRAST STEM
S. J. Pennycook, D. E. Jesson, M. F. Chisholm, and N. D. Browning Apr. 1993 5 p Presented at the 20th Annual Meeting of the Microscopical Society of Canada, Toronto (Canada), 2-5 Jun. 1993
(Contract DE-AC05-84OR-21400)
(DE93-015964; CONF-9306183-1) Avail: CASI HC A01/MF A01

The high-angle annular detector proposed by Howie is used to form an atomic resolution Z-contrast image in a high-resolution scanning transmission electron microscope. For incoherent scattering, the coherent probe is effectively channeled along each individual atomic column, forming a basis for atomic resolution incoherent imaging and atomic resolution microanalysis. Incoherent imaging is combined with strong compositional sensitivity. Since a model structure is not needed to interpret the images to first order, unexpected interfacial phenomena are immediately apparent, such as the compositional ordering at a CoSi2/Si(100) interface made by high-dose Co implantation and annealing. Growth and relaxation of strained Si(x)Ge(1-x) layers are studied. Combining atomic resolution imaging and analysis on a single microscope is a powerful method for studying interfaces without any prior knowledge or model structures. DOE

N94-16844# Brookhaven National Lab., Upton, NY.
DIFFUSE SCATTERING AND IMAGE CONTRAST OF TWEED IN SUPERCONDUCTING OXIDES: A SIMULATION AND INTERPRETATION
Yimei Zhu and Zhi-Xiong Cai 1993 23 p Presented at the John M. Crowley Symposium on Ultramicroscopy, Scottsdale, AZ, 5-8 Jan. 1993
(Contract DE-AC02-76CH-00016)
(DE93-016131; BNL-48498; CONF-9301114-1) Avail: CASI HC A03/MF A01

Monte Carlo simulations were performed with a lattice gas model which represents the interactions between oxygen atoms in YBa2 (Cu(1-x)M(x))(sub 3) O(7+delta) (M=Fe, Co, or Al, 0.03 less than x less than 0.1) system. The amplitudes of concentration waves/displacement waves obtained from these simulations were then used to calculate the intensity of the diffuse scattering of tweed seen in the electron diffraction pattern. The characteristic features of the tweed image were produced by calculation, using a model based on the contrast originating from structures with displacive modulation, stacking on the top of each other. Both calculations agree well with the TEM observations and provide a useful basis for a better insight into the origin of the tweed structure. DOE

N94-16868# Oak Ridge National Lab., TN.
STRUCTURAL PHASE TRANSITION AND SUPERCONDUCTIVITY IN La(2-x)Ba(x)CuO4
S. Katano (Japan Atomic Energy Research Inst., Tokai.), S. Funahashi (Japan Atomic Energy Research Inst., Tokai.), J. A. Fernandez-Baca, N. Mori (Tokyo Univ., Japan.), C. Murayama (Tokyo Univ., Japan.), and Y. Ueda (Tokyo Univ., Japan.) 1993 7 p Presented at the International Symposium on Advanced Nuclear Energy Research: Neutrons As Microscopic Probes, Mito Ibaraki (Japan), 10-12 Mar. 1993
(Contract DE-AC05-84OR-21400)
(DE93-015812; CONF-9303190-1) Avail: CASI HC A02/MF A01

High-resolution neutron powder diffraction experiments and ac magnetic susceptibility measurements have been performed on La(2-x)Ba(x)CuO(4) (where x = 0.125) at ambient pressure and under high pressures. Crystal parameters including bond lengths and angle are refined by profile analysis at ambient pressure. Results suggest that the changes in the Cu-O bonds accompanied with the structural phase transition may be related to the suppression of the superconductivity. Effects of pressure on the structural transition is fairly large. The LTT phase is greatly suppressed and disappears at 0.7 GPa. The superconducting transition temperature (Tc) remains almost constant up to 0.5 GPa; however, above this pressure it increases at the rate of about 10 K/GPa. These results clearly indicate a strong correlation between the crystal structure and the superconductivity in this system. DOE

N94-16887# Brookhaven National Lab., Upton, NY.
SUPPRESSION OF CHARGE SCATTERING IN MOESSBAUER EXPERIMENTS USING SYNCHROTRON RADIATION
U. Bergmann, D. P. Siddons, and J. B. Hastings 1992 17 p Presented at the International Conference on Anomalous Scattering (ICAS), Hamburg, Germany, 17-21 Aug. 1992
(Contract DE-AC02-76CH-00016)
(DE93-015406; BNL-48963; CONF-9208186-4) Avail: CASI HC A03/MF A01

The extremely small ratio of linewidth to energy combined with the character of recoil free absorption and reemission makes the low lying nuclear resonances a unique spectroscopic tool. Further, considering the simplicity of performing Moessbauer experiments, they have become very useful in a wide range of disciplines. (sup 57)Fe has remained the most widely used isotope despite its low natural abundance (2%) because iron is ubiquitous in nature and shows a strong effect. The energy width of this resonance corresponds to a lifetime of 140 nsec of the excited state. Therefore in principle time differential spectroscopy is possible. Using the time differential measurement one is no longer restricted to a nuclear source, in fact a short pulse excitation is favored in such experiments. The concept of using a pulsed source and time gating to isolate the resonant scattering was already suggested in 1962. In 1974 it was noted that synchrotron radiation (SR) was ideally suited to this task. Although the time gating technique is conceptually simple the bandwidth of SR poses significant technical difficulties. In this paper we will discuss the extraction of the nuclear signal from the overwhelming background, which is the central problem in SR-based Moessbauer experiments. We will only, consider the (sup 57)Fe-isotope, although other isotopes might be of interest in a SR-based experiment. Although SR sources have the disadvantages of creating this high background and being limited in beam-time and location, new and unique opportunities make them very attractive even with these difficulties. For this reason research and development groups at every major SR facility worldwide are increasingly working on Moessbauer experiments, stimulated by the first successful observation of nuclear Bragg scattering (NBS) using SR in 1984. DOE

N94-16932# APA Optics, Inc., Blaine, MN.
ATOMIC LAYER EPITAXY OF BORON NITRIDE Final Report, 1 Jun. - 31 Dec. 1992
M. A. Khan 3 Jun. 1993 16 p
(Contract F49620-92-C-0037)
(AD-A266260; AFOSR-93-0388TR) Avail: CASI HC A03/MF A01

This document summarizes the work performed under the phase 1 project aimed at developing the wide bandgap nitrides for high temperature electronics and optoelectronics applications. The focus was on the study of atomic layer epitaxy of BN, AlN, and GaN. We present a summary of the program accomplishments. This is followed by a description of the technical effort including the data obtained. Finally, we outline a potential phase 2 program. DTIC

N94-16961# Cornell Univ., Ithaca, NY.
UHV-STEM STUDIES ON NUCLEATION AND GROWTH OF THIN METAL SILICIDE FILMS ON SILICON
J. Silcox and E. J. Kirkland 1992 21 p
(Contract DE-FG02-87ER-45322)
(DE93-017604; DOE/ER-45322/6) Avail: CASI HC A03/MF A01

Work centers on the multiple imaging and spectroscopy operating modes of an ultra-high vacuum scanning transmission electron microscope. Three research topics were as follows: single atom structures on Si, grain boundaries in Ni3Al, and the simulations to interpret the observations. DOE

N94-16992# Boston Univ., MA. Dept. of Electrical Computer and Systems Engineering.
GROWTH AND DOPING OF Al(x)Ga(1-x)N FILMS BY ELECTRON CYCLOTRON RESONANCE ASSISTED MOLECULAR BEAM EPITAXY Annual Report, May 1992 - 30 Apr. 1993
Theodore D. Moustakas 30 May 1993 104 p
(Contract N00014-92-J-1436)
(AD-A267305) Avail: CASI HC A06/MF A02

During this funding period, the work focused on the heteroepitaxial growth, doping, and characterization of GaN by the ECR-MBE method.

Nitrogen-ECR plasmas were investigated by Optical Emission Spectroscopy. Work was also initiated in the growth of AlN. In the area of GaN growth on (0001) sapphire, we identified ECR-plasma conditions to grow the material in the layer-by-layer growth mode to a layer-by-layer growth followed by an island growth mode. Such films were grown in semi-insulating form (p approximately equal to 10(exp 12) omega-cm) and doped p- and n-type with Mg and Si at the level of 10(exp 19) cm(exp -3) RIE of GaN using CCl2F2 and CF3Br/Ar as well as Ohmic contacts to n-GaN were developed. Defects in the films were characterized by photoluminescence and EPR studies. Initial studies of AlN growth indicate that the material can grow in the single crystal form at temperatures comparable to that of GaN. DTIC

N94-17037 Southampton Univ. (England). Dept. of Chemistry.
AN ALTERNATIVE APPROACH TO THE GROWTH OF SINGLE CRYSTAL GALLIUM NITRIDE Final Report, 1 Sep. 1990 - 31 Jan. 1993
Neville Jonathan 30 Jun. 1993 15 p Limited Reproducibility: More than 20% of this document may be affected by microfiche quality
(Grant AF-AFOSR-0337-90)
(AD-A267876; AFGAN-2; EOARD-TR-93-08) Avail: Issuing Activity (Defense Technical Information Center (DTIC))

This project has been primarily concerned with investigating a new approach to the synthesis of epitaxial layers of high purity gallium nitride. The new approach involves the use of hydrazoic acid, HN3, a previously untried precursor as the source of active nitrogen. A new, all-stainless steel apparatus which is UHV compatible, has been constructed. It has been designed to allow growth studies to be made by the chemical beam epitaxy (CBE) technique or by low pressure metal organic vapour phase deposition (LPMOCVD) at pressures up to ca. 1 mbar. During the grant period, the apparatus has been constructed, tested, and modified. Experiments have been carried out which show that gallium nitride and aluminium nitride can be made from the reaction of hydrazoic acid with trimethyl gallium and trimethyl aluminium respectively, at a hot substrate surface. In-situ RHEED patterns and ex-situ Auger spectra and x-ray diffraction data have been obtained. Systematic studies aimed at producing high quality single crystal films have been made. The results are promising and uniform, golden yellow films of gallium nitride can now be produced. RHEED data show that the films are composed of highly orientated crystals. The x-ray results support this, with crystal sizes being at least 1000 A with the crystals strongly orientated along the c-axis. DTIC

N94-17042 California Univ., San Diego, La Jolla. Dept. of Electrical and Computer Engineering.
PHOTO-ASSISTED EPITAXIAL GROWTH FOR III-V SEMICONDUCTORS Interim Report, 1 Sep. 1990 - 31 Oct. 1992
C. W. Tu Feb. 1993 58 p Limited Reproducibility: More than 20% of this document may be affected by microfiche quality
(Contract F33615-90-C-5946)
(AD-A267889; UCSD-CWT-93-R1; WL-TR-93-4029) Avail: Issuing Activity (Defense Technical Information Center (DTIC))

Photo-assisted metalorganic molecular beam epitaxy (MOMBE), with an argon ion laser, has been used to grow GaAs. The substrate temperature was calibrated by an infrared laser interferometric technique with an accuracy of + or - 3 C. The MOMBE growth of GaAs, InAs, and InGaAs was first studied, by monitoring intensity oscillations of reflection high-energy electron diffraction (RHEED). The actual arsenic incorporation rate was deduced from As-induced RHEED oscillations, and a unity V/III incorporation ratio could be obtained. In growing InGaAs, indium segregation suppresses the InGaAs growth rate. In laser-assisted MOMBE, the enhancement of arsenic desorption with laser irradiation and its effects were observed. The decomposition of triethylgallium and desorption of arsenic compete with each other, resulting in a saturation in the enhanced growth rate in the arsenic-controlled growth regime. The initial growth behavior was also studied by inspecting the details of the RHEED behavior and arsenic surface coverage. DTIC

N94-17046# Polish Academy of Sciences, Warsaw. Inst. Podstawowych Problemow Techniki.
THE INFLUENCE OF AN ELECTRIC FIELD ON THE KINETICS OF NUCLEATION [WPLYW POLA ELEKTRYCZNEGO NA KINETYKE NUKLEACJI]
Leszek Jarecki 1991 62 p In POLISH
(IFTR-2/91) Avail: CASI HC A04/MF A01

This paper examines in detail a crystallization model in an electric field that has been proposed previously for systems in oriented fields. The model takes into account the angular configuration of the crystal nuclei and the effect of rotational diffusion of the nuclei on nucleation kinetics. The orientation state of the amorphous phase in an electrostatic field, where the particles manifest uniaxial symmetry under polarization and are subject to a constant dipole moment are analyzed. An expression is given for the free formation energy of the polar and non-polar aggregates of the crystallized stated depending on the angle within the field assuming uniaxial symmetry of the polarization tensor of the crystal grid. A solution of a continuity equation expanded in terms of the magnitude and orientation of the aggregates is given; this solution takes into account the growth and rotational diffusion of the aggregates where the motive force behind such processes consists of the free growth energy and the free energy of the aggregates in the field. The solution takes a form that accounts for the kinetic parameter representing the ratio of the continuous rotation diffusion of the nucleus and the reaction constant of the aggregate with a single element. An expression is derived for the angular distribution of the nucleation rate in the form of an expansion in an established parameter; an expression for independent diffusion is derived together with expressions corresponding to rotational diffusion and nucleation in a system disrupted by diffusion. Certain values of the angular distributions of the nucleation rate and diffusion corrections as a function of field intensity and temperature for polar and non-polar phases of polyfluorovinylide are discussed. NTIS

N94-17108# North Carolina State Univ., Raleigh. Dept. of Materials Science and Engineering.
PSEUDOMORPHIC SEMICONDUCTING HETEROSTRUCTURES FROM COMBINATIONS OF AlN, GaN AND SELECTED SiC POLYTYPES: THEORETICAL ADVANCEMENT AND ITS COORDINATION WITH EXPERIMENTAL STUDIES OF NUCLEATION, GROWTH, CHARACTERIZATION AND DEVICE DEPLOYMENT Semiannual Report, 1 Jan. - 30 Jun. 1993
Robert F. Davis, K. S. Ailey, R. S. Kern, R. Patterson, and S. Tanaka Jun. 1993 33 p
(Contract N00014-90-J-1427)
(AD-A267561) Avail: CASI HC A03/MF A01

Solid solutions and pseudomorphic heterostructures of AlN and SiC have been grown on vicinal alpha (6H)-SiC substrates via plasma-assisted, gas-source molecular beam epitaxy at 1050 C. Reflection high energy electron diffraction, high resolution TEM, and Auger depth profiling show the films to be monocrystalline and to possess the desired chemical compositions. The solid solutions have the wurtzite structure. The multilayers have the following phases: alpha (6H)-SiC substrate, 2H-AlN, and 3C-SiC. Chemical interdiffusion between alpha (6H)-SiC wafers and epitaxially deposited 2H-AlN films are under investigation within the temperature range of 1500 C to 1700 C. Scanning Auger spectroscopy and XTEM is being used to determine the diffusion profiles and the occurrence of new phases. The Auger data and electron energy loss measurements are in disagreement. Additional diffusion and segregation research is under way to resolve this conflict. Superlattices of GaN/AlN on sapphire and SiC have been extensively investigated via HRTEM. Below the critical thickness, AlN only contains threading dislocations emanating from the misfit dislocations; above this thickness, defects parallel to the growth surface greatly increase. Deposition of GaN on sapphire or SiC results in a larger number of threading dislocations caused by the large misfit as well as a high concentration of dislocations parallel to the growth surface. Both types of defects are decreased in density if the GaN is deposited on AlN. DTIC

N94-17116# North Carolina State Univ., Raleigh.
ATOMIC LAYER EPITAXY GROUP IV MATERIALS: SURFACE PROCESSES, THIN FILMS, DEVICES AND THEIR CHARACTERIZATION Semiannual Report, 1 Jan. - 30 Jun. 1993
Robert F. Davis, Salah Bedair, Nadia El-Masry, and Jeffrey T. Glass Jun. 1993 43 p
(Contract N00014-91-J-1416)
(AD-A267527) Avail: CASI HC A03/MF A01

The maximum temperature at which self-terminating monolayers of Si can be formed on Si(100) from Si2H6 has been determined to be 570 deg C. As such, the chemical reactivity of C2H4 has been determined to be insufficient at this temperature, and acetylene has been selected as the successor C precursor due to its superior reactivity and chemisorption

properties. A cryogenic purifier for removing acetone has been commissioned. Trenched Si(100) wafers are also being made to assess the ALE process for sidewall deposition uniformity and future bipolar devices. Nonstoichiometric, Si-rich SiC has been produced with an associated decrease in the band gap. An AES/XPS UHV analytical system and associated ALE deposition system has been commissioned and integrated into a much larger surface science system. These dual systems will allow a thorough study and characterization of both the initial nucleation of SiC and the overall ALE growth process of SiC. Tetramethylsilane and hexamethyldisilane have been deposited onto Si substrates in a hot filament CVD chamber to investigate their ability to promote ALE of diamond under DC biasing and a variety of system parameters. An electron gun and heating stage has been added to the growth chamber to enable AES and substrate heating. Good quality diamond films have been nucleated on deposited interlayers of both precursor compounds. The films have been examined by SEM and Raman spectroscopy. Good quality epitaxial films of CeO2 have been grown on Si(111) using laser ablation. Atomically clean substrates and slow growth rates were determined necessary for epitaxy. DTIC

N94-17216# Epion Corp., Bedford, MA.
SINGLE CRYSTAL DIAMOND THIN FILMS Technical Progress Report, 28 Jul. 1992 - 27 Apr. 1993
Allen Kirkpatrick May 1993 13 p
(Contract N00014-92-C-0172; DA Proj. S40-030)
(AD-A266457) Avail: CASI HC A03/MF A01

One possibility for accomplishing growth of single crystal diamond film on a nondiamond substrate is based upon ion implantation of carbon atoms into crystalline copper. In spite of widespread interest in the concept, heteroepitaxial diamond growth by this approach has never been confirmed. The objective of this program is to develop specialized ion implantation capabilities for C(+) into Cu processing under conditions for which heteroepitaxial formation of diamond on copper may be feasible. A 200 keV medium current ion implantation system has been modified to allow implantations to be performed into substrates at temperatures up to 1000 C, to incorporate background atomic hydrogen in the vicinity of the substrate surface during implantation, and to facilitate in-situ CVD diamond growth processing. Apparatus development has been completed, and process investigations have been initiated. DTIC

N94-17243# George Mason Univ., Fairfax, VA.
DLTS AND DYNAMIC TRANSCONDUCTANCE ANALYSIS OF DEEP-SUBMICRON FULLY-DEPLETED SOI MOSFET'S Quarterly Technical Report, 1 Apr. - 30 Jun. 1993
Dimitris E. Ioannou 30 Jun. 1993 9 p
(Contract N00014-91-J-1441)
(AD-A267291) Avail: CASI HC A02/MF A01

Progress this period was accomplished in two areas: hot electron degradation studies of partially- and fully-depleted transistors; and measurement and analysis of relaxation parameters (generation lifetime) in fully-depleted enhancement and accumulation mode transistors. A summary of the results is given in the attached abstracts: Successive Charging/Discharging of Gate Oxides in SOI MOSFET's by Sequential Hot Electron Stressing of Front/Back Channel and Generation Lifetime Measurements in Fully Depleted Enhancement and Accumulation Mode SOI MOSFET's submitted for presentation in the forthcoming 1993 IEEE SOI Conference; and Sequential Stressing of Front/Back Gate Oxides in SOI MOSFET's for Device Characterization and Applications submitted for presentation in the forthcoming 1993 IEEE IEDM. A presentation was given at INFOS' 93 (8th biennial conference on Insulating Films on Semiconductors) on the topic of Mechanisms of Hot-Carrier Induced Degradation of SOI (SIMOX) MOSFET's. A full length paper on the mechanisms of our hot carrier degradation studies is under preparation for IEEE Transactions on Electron Devices. DTIC

N94-17270# Naval Surface Warfare Center, Dahlgren, VA.
INVESTIGATION OF THE ORIGIN OF HOT SPOTS IN DEFORMED CRYSTALS: AMMONIUM PERCHLORATE STUDIES Final Report, Jan. 1986 - Sep. 1990
W. L. Elban, H. W. Sandusky, B. C. Beard, and B. C. Glancy 19 Jul. 1993 40 p
(AD-A267692; NSWCDD/TR-92/206) Avail: CASI HC A03/MF A01

A number of single crystals of ammonium perchlorate (AP) were shock loaded near the reaction threshold to investigate the effects of concentrated lattice defects (dislocations) and differing crystal orientations on chemical reactivity. Large, optical quality crystals of pure AP were immersed in mineral oil and shocked through either the (001) or 210 surfaces by a detonator. Prior to shock loading, some crystals had localized regions of increased lattice defects and strain created by placing diamond pyramid (Vickers) hardness impressions into their exterior cleavage surfaces. High-speed photographs showed preferential cracking and luminosity near some of the hardness impressions. The photographs also revealed the occurrence of the same slip deformation identified previously from hardness testing. The shocked crystals were recovered, sometimes intact, for microstructural characterization and chemical analyses. Crystal orientation relative to the shock propagation direction changed the dynamic response and threshold for decomposition of the crystal, indicating the influence of material microstructure. Along these freshly cleaved surfaces, the XPS results showed enhanced lattice disruption and perchlorate decomposition as a result of the hardness impressions. The greatest decomposition was not immediately adjacent to the impressions, but near the tips of cracks and along slip planes emanating from the impressions several millimeters, or more, into the crystal. DTIC

N94-17272 Florida Univ., Gainesville. Dept. of Electrical Engineering.
DEVELOPMENT OF ULTRA-LOW NOISE, HIGH PERFORMANCE 3-V QUANTUM WELL INFRARED PHOTODECTORS (QWIP'S) FOR FOCAL PLANE ARRAY STARING IMAGE SENSOR SYSTEMS Quarterly Progress Report No. 8, 1 May - 31 Jul. 1993
Sheng S. Li 1 Aug. 1993 64 p Limited Reproducibility: More than 20% of this document may be affected by microfiche quality
(Contract N00014-91-J-1976)
(AD-A267715) Avail: Issuing Activity (Defense Technical Information Center (DTIC))

During this reporting period we have continued to make excellent progress towards the program goals. We have made a major breakthrough in the development of a new normal incidence p-type strained layer InGaAs/InAlAs QWIP grown on InP by MBE, which achieved both the lowest dark current and highest detectivity ever reported for a QWIP operating at 8.1 um and 77 K. The device dark current at 77 K is one to two orders of magnitude smaller than its 300 K background photocurrent, which shows that this p-type strained layer QWIP is under BLIP operation at 77 K. Other tasks performed during this period include: (1) measured and compared the device dark current with 300 K background limited photocurrent (BLIP) for several QWIP's fabricated from GaAs/AlGaAs, InGaAs/InAlAs, and AlAs/AlGaAs material systems, (2) designed a broad band 2-D square mesh grating coupler for the dual-mode operation GaAs QWIP to enhance the coupling quantum efficiency and responsivity of this QWIP in the 3-5 and 8-12 um bands, (3) using a 2-D square mesh grating coupler to achieve maximum responsivity for an InGaAs SBTM QWIP, and (4) performed noise characterization on four different types of III-V QWIP's and identified their noise sources. Detailed results and accomplishments are discussed in this report. DTIC

N94-17301# Los Alamos National Lab., NM.
THEORETICAL STUDIES OF THE CRYSTAL STRUCTURE OF RARE EARTHS AND ACTINIDES AT ZERO TEMPERATURE
J. M. Wills and O. Eriksson (Uppsala Univ., Sweden.) 1993 9 p Presented at the 14th International Conference on High Pressure Science and Technology and the 1993 Meeting of the Topical Group on Shock Compression of Condensed Matter, Colorado Springs, CO, 28 Jun - 3 Jul. 1993
(Contract W-7405-eng-36)
(DE93-016488; LA-UR-93-2368; CONF-9306167-7) Avail: CASI HC A02/MF A01

Accurate total energy electronic structure calculations have recently been carried out over a range of volumes for selected rare-earth and actinide elements in crystal structures experimentally observed in these elements. Correct zero temperature crystal structures are obtained, and calculated equilibrium properties are in reasonable agreement with experiment. Results of these calculations indicate that the interactions underlying crystal structure stability are similar in itinerant f-electron metals and transition metals. The stable crystal structure at a particular volume is determined by a balance between one-electron bandwidths and band fillings

and the electrostatic energy of the crystal lattice. Broad bands favor high-symmetry, close-packed structures while narrow bands favor low-symmetry, open structures; allowing for expansion as well as contraction, both transition and actinide elements can be stabilized in both low- and high-symmetry crystal structures. DOE

N94-17319# Pacific Northwest Lab., Richland, WA.
THEORETICAL CRYSTALLOGRAPHY WITH THE ADVANCED VISUALIZATION SYSTEM
C. R. Younkin, E. N. Thornton, J. B. Nicholas, D. R. Jones, and A. C. Hess May 1993 4 p Presented at the Advanced Visualization System (AVS) 1993 Users Group Meeting, Orlando, FL, 24-26 May 1993
(Contract DE-AC06-76RL-01830)
(DE93-015692; PNL-SA-22209; CONF-9305168-4) Avail: CASI HC A01/MF A01

Space is an Application Visualization System (AVS) graphics module designed for crystallographic and molecular research. The program can handle molecules, two-dimensional periodic systems, and three-dimensional periodic systems. All are referred to in the paper as models. Using several methods, the user can select atoms, groups of atoms, or entire molecules. Selections can be moved, copied, deleted, and merged. An important feature of Space is the crystallography component. The program allows the user to generate the unit cell from the asymmetric unit, manipulate the unit cell, and replicate it in three dimensions. Space includes the Buerger reduction algorithm which determines the asymmetric unit and the space group of highest symmetry of an input unit cell. Space also allows the user to display planes in the lattice based on Miller indices and to cleave the crystal to expose the surface. The user can display important precalculated volumetric data in Space, such as electron densities and electrostatic surfaces. With a variety of methods, Space can compute the electrostatic potential of any chemical system based on input point charges. DOE

N94-17327*# National Aeronautics and Space Administration. Pasadena Office, CA.
BURIED POROUS SILICON-GERMANIUM LAYERS IN MONOCRYSTALLINE SILICON LATTICES AND METHOD OF PRODUCING Patent Application
Robert W. Fathauer, inventor (to NASA) (Jet Propulsion Lab., California Inst. of Tech., Pasadena.) and Thomas George, inventor (to NASA) (Jet Propulsion Lab., California Inst. of Tech., Pasadena.) 11 Aug. 1993 23 p
(Contract NAS7-918)
(NASA-Case-NPO-18836-1-CU; NAS 1.71:NPO-18836-1-CU; US-Patent-Appl-SN-105728) Avail: CASI HC A03/MF A01

Lattices of alternating layers of monocrystalline silicon and porous silicon-germanium have been produced. These single crystal lattices have been fabricated by epitaxial growth of Si and Si-Ge layers followed by patterning into mesa structures. The mesa structures are stain etched resulting in porosification of the Si-Ge layers with a minor amount of porosification of the monocrystalline Si layers. Thicker Si-Ge layers produced in a similar manner emitted visible light at room temperature. NASA

N94-17377 North Carolina State Univ., Raleigh.
INTERFACE PROPERTIES OF WIDE BANDGAP SEMICONDUCTOR STRUCTURES Semiannual Report, 1 Jan. - 30 Jun. 1993
Robert F. Davis and R. J. Nemanich Jun. 1993 122 p Limited Reproducibility: More than 20% of this document may be affected by microfiche quality
(Contract N00014-92-J-1477)
(AD-A268269) Avail: CASI HC A06

Theoretical studies have involved calculations of the electronic states of hydrogenated surfaces and the properties of defect and impurities in GaN. Infrared studies on diamond films have indicated SiC at the interface and the lack of C-H bonding in the films. To investigate SiC growth, two chambers have been integrated into the surface science facility. Studies of the interdiffusion of SiC-AlN have indicated new results concerning SiC-AlN phase diagrams. The use of ALE for SiC deposited on patterned substrates has been initiated. Low temperature (LT) GaP and InGaP films produced by gas source MBE proved the first demonstration of high resistivity, semi-insulating properties. Using an ALE reactor, layer-by-layer growth of GaN has been demonstrated. The CVD deposition of AlN nitride has been demonstrated on various substrates. A combined photo/cathodo-luminescence system is being assembled. The effects of hydrogen and oxygen on the Schottky barrier of Ni/diamond has been studied, and negative electron affinity effects are observed. The Schottky barrier properties of various metals on clean n-type 6H-SiC have been measured. Approaches have been developed for contacts on GaN and AlN. A reactive ion etching system has been configured for patterning of GaN and AlN films. DTIC

N94-17389# Stanford Univ., CA. Center for Integrated Systems.
LOW VOLTAGE ELECTRON BEAM LITHOGRAPHY
May 1993 5 p Sponsored by NRL
(AD-A267865) Avail: CASI HC A01/MF A01

The contract has three parts covering aspects of high precision electron beam lithography: (1) comprehensive computer modeling of the electron beam tool; (2) experimental determination of the properties of sources, columns, and targets; and (3) the use of silicon single crystals as straightness and orthogonality standards using orientation dependent etching techniques. DTIC

N94-17417 Superior Vacuum Technology, Eden Prairie, NM.
PRECISE FLUX CONTROL FOR LATTICE MATCHED SUPERLATTICE MATERIALS Final Report, 1 May - 30 Nov. 1992
Peter P. Chow Feb. 1993 19 p Limited Reproducibility: More than 20% of this document may be affected by microfiche quality
(Contract F33615-92-C-5937)
(AD-A268254; WL-TR-93-4072) Avail: Issuing Activity (Defense Technical Information Center (DTIC))

Flux transients in molecular beam epitaxy (MBE) sources has been investigated. A detailed study of the relevant factors has been carried out. For the first time Ga transient was measured in the presence of As in a realistic growth environment. Growth rate variation due to transients can be accurately monitored by RHEED analysis. We demonstrated that transients could be minimized or even eliminated by source temperature ramping and mass spectrometer feedback control. DTIC

N94-17422 Colorado Univ., Boulder.
LASER PROBING OF THE KINETICS AND DYNAMICS OF 3-5 SEMICONDUCTOR GROWTH Final Report, Feb. 1990 - 30 Jun. 1993
Stephen R. Leone 30 Jun. 1993 15 p Limited Reproducibility: More than 20% of this document may be affected by microfiche quality
(Grant AF-AFOSR-0166-90)
(AD-A268388; AFOSR-93-0583TR) Avail: CASI HC A03

Work is carried out on the dynamics of Ga, In, and As scattering, sticking, and desorption from silicon single crystals using laser induced fluorescence and laser ionization probing of the Ga and In atoms and As atoms, dimers, and tetramers in the gas phase. Desorption kinetics are used to probe the InAs and GaAs heterostructures on silicon and the islanding behavior that occurs for the mixed systems. It is observed that islands form readily when In and Ga are grown on a prelayer of As on Si(100). State-resolved detection of As2 species is demonstrated by laser-induced fluorescence probing for the first time. Laser single photon ionization detection of III-V semiconductor species is also demonstrated with high sensitivity and species specific detection. These results are relevant to the epitaxial growth of GaAs and InAs on silicon. DTIC

N94-17437 International Centre for Theoretical Physics, Trieste (Italy).
LATTICE RELAXATION THEORY OF LOCALIZED EXCITATIONS IN QUASI-ONE-DIMENSIONAL SYSTEMS
Chui-Lin Wang (China Center for Advanced Science and Technology, Beijing.), Zhao-Bin Su, and Yu Lu Apr. 1993 20 p Limited Reproducibility: More than 20% of this document may be affected by microfiche quality
(DE93-624947; IC-93/71) Avail: CASI HC A03 (US Sales Only)

The lattice relaxation theory developed earlier by Su and Yu for solitons and polarons in conducting polymers is applied to systems with both electron-phonon and electron-electron interactions, described by a single band Peierls-Hubbard model. The localized excitations in the competing bond-order-wave (BOW), charge-density-wave (CDW) and spin-density-wave (SDW) systems show interesting new features in their dynamics. In particular, a non-monotonic dependence of the relaxation rate on the coupling strength is predicted from the theory. The possible connection of this effect with photo-luminescence experiments is discussed. Similar phenomena may occur in other quasi-one-dimensional systems as well. DOE

N94-17454 Stanford Univ., CA. Dept. of Materials Science and Engineering.
MECHANICAL PROPERTIES AND CRYSTAL GROWTH STUDIES OF SEMICONDUCTOR ALLOYS Final Report, 18 Sep. 1989 - 17 Sep. 1992
David A. Stevenson Jun. 1993 28 p Limited Reproducibility: More than 20% of this document may be affected by microfiche quality
(Grant AF-AFOSR-0537-89)
(AD-A268144; AFOSR-93-0585TR) Avail: Issuing Activity (Defense Technical Information Center (DTIC))

Compound semiconductors are attractive materials for optoelectronic devices since they present a broad selection of band gaps. The mechanical properties of these materials is of interest for both practical and theoretical reasons; however, there is a paucity of experimental information on this topic. The objective of this research program was to develop methods for providing reliable experimental information on the mechanical properties of compound semiconductors and their alloys. The main activity has been the measurement of the hardness of these materials. We have used two basic hardness measurements: conventional microhardness measurements, such as the Vickers hardness test; and the Nanoindentor hardness. For the former measurements, bulk crystals or thick films were needed. A significant part of the program was devoted to preparing relevant samples for these measurements. We used conventional methods of crystal growth for producing bulk crystals, and we developed novel methods of vapor phase epitaxial growth to prepare thick films of variable composition. The Nanoindentor was used for measuring the hardness and the modulus of thin films, and bulk samples were measured by Vickers or with the Nanoindentor. We investigated a wide variety of semiconductor systems for measurement, but we selected a few systems that had well established device applications for particular emphasis in our studies. DTIC

N94-17477# Wayne State Univ., Detroit, MI. Dept. of Physics.
INVESTIGATIONS OF YBaCuO MATERIALS WITH NEAR-ROOM-TEMPERATURE RESISTIVITY TRANSITIONS Annual Report, 15 Jun. 1993 - 14 Jun. 1993
Lowell E. Wenger and J. T. Chen 14 Jul. 1993 6 p
(Grant AF-AFOSR-0319-91)
(AD-A268016; AFOSR-93-0587TR) Avail: CASI HC A02/MF A01

This annual technical report describes the continual superconductivity research on the materials and structural phases responsible for the above 200-K superconducting transitions, their synthesis conditions, and the study of the physical properties associated with these transitions. Superconducting resistive transition and magnetic flux trapping phenomena have been observed in mixed-phase ceramic samples of YBaCuO e.g. Y5Ba6Cu11O(x) and on the surfaces of YBa2Cu3O7 single crystals in the temperature range 230 K to 270 K. Near room-temperature oxidation studies show that the properties can change, including a large resistance decrease over a 3-month period. This behavior is consistent with the formation of a different oxide phase on the surface of the grains. Structural analyses by x-ray diffraction and high-resolution transmission electron microscopy indicate these samples have surfaces with large amounts of defect structures as well. Correspondingly these surface phases/structures may be responsible for the above 200-K transitions. DTIC

N94-17480 Army Lab. Command, Fort Monmouth, NJ. Electronics Technology and Devices Lab.
QUARTZ CRYSTAL RESONATORS AND OSCILLATORS FOR FREQUENCY CONTROL AND TIMING APPLICATIONS: A TUTORIAL, REVISION 6.1
John R. Vig May 1993 272 p Limited Reproducibility: More than 20% of this document may be affected by microfiche quality
(DA Proj. 1L1-72605-AH-94)
(AD-A268205; SLCET-TR-88-1-Rev-6.1) Avail: Issuing Activity (Defense Technical Information Center (DTIC))

The following subjects are covered: applications of frequency standards; types of oscillators (quartz and atomic); quartz resonator properties; quartz growing, sweeping, and material characteristics; Q and its significance; resonator and oscillator stability, including aging, short-term instability, frequency vs. temperature characteristics, oscillator circuit caused instabilities, frequency vs. drive level effects, acceleration effects, the effect of shock, and radiation effects; emerging technologies; atomic frequency standards; comparison of the major oscillator types; oscillator specifications and selection guidelines; time and timekeeping; clock errors; relativistic time; time transfer; time and frequency subsystem; and other applications of quartz resonators. The goal of this document is to assist in presenting to the nonspecialist the most frequently encountered concepts in frequency control and timing. The document originated as a set of hard copies of presentation visual graphs (i.e., vugraphs). DTIC

N94-17553 North Carolina State Univ., Raleigh.
GROWTH, CHARACTERIZATION AND DEVICE DEVELOPMENT IN MONOCRYSTALLINE DIAMOND FILMS Quarterly Report, 31 Mar. - 30 Jun. 1993
Robert F. Davis, J. T. Glass, R. J. Nemanich, P. K. Baumann, and T. P. Humphreys Jun. 1993 27 p Limited Reproducibility: More than 20% of this document may be affected by microfiche quality
(Contract N00014-93-I-0437)
(AD-A268206) Avail: Issuing Activity (Defense Technical Information Center (DTIC))

A series of computer-based statistical experimental designs have been conducted to determine the optimum conditions for negative bias-enhanced nucleation of diamond. The concentration of CH4 and the effects of pressure and bias voltage on the time for complete coverage of the substrate, film uniformity, and nucleation density were the experimental parameters and desired results investigated. Time to complete film formation, uniformity, and nucleation density were all improved with the use of both a negative bias voltage and high CH4 concentrations. Diamond has also been formed on diamond seeds placed on nickel substrates via microwave plasma CVD. The long range nucleation density was low and the formation of clusters of diamond more common. Polycrystalline Si-Ge films have been grown by e(-) beam deposition on naturally occurring p-type semiconducting diamond C(001) substrates. Room temperature and 300 C I-V data show the formation of a low-barrier rectifying contacts which exhibit ohmic behavior. Annealing at 850 C under UHV conditions resulted in apparent degradation in the I-V characteristics. DTIC

N94-17561 Stanford Univ., CA. Lab. of Physics.
ADVANCED THIN-FILM DEPOSITION AND PHYSICAL PROPERTIES OF HIGH-TEMPERATURE AND OTHER NOVEL SUPERCONDUCTING MATERIALS Annual Report, 15 Oct. 1991 - 31 Oct. 1992
M. R. Beasley, T. H. Geballe, and A. Kapitulnik 3 Jun. 1993 9 p Limited Reproducibility: More than 20% of this document may be affected by microfiche quality
(Contract F49620-92-C-0004)
(AD-A268199; AFOSR-93-0593TR) Avail: CASI HC A02

Progress under AFOSR Contract F49620-92-C-0004 for the period 15 Oct. 1991 to 31 Oct. 1992 is reported. Important results include studies of the grain boundaries in a-axis oriented high-Tc superconducting 123 YBCO thin films, the study of the vortex properties of high-Tc single crystals of the superconductor 2212 BSCCO, and the artificially structured Mo-Ge/Ge quasi-two-dimensional superconductors. The latter provide an outstanding model system for the study of vortices in highly anisotropic superconductors, such at the high-Tc cuprates, without all the attendant difficult materials problems. Progress in the synthesis and study of the so-called infinite layer cuprate SrCuO4 and the normally conducting oxide SrRuO3 of interest as a barrier materials in high-Tc SNS devices are also reported. Finally, we report the development of advanced approaches to rate control of the cation fluxes in the reactive coevaporation of the high-Tc superconductors. DTIC

N94-17577# Microtronics Associates, Pittsburgh, PA.
RARE EARTH DOPED III-V SEMICONDUCTORS FOR OPTOELECTRONICS Final Report, 1 Jul. - 31 Dec. 1992
Victoria T. Coon 1 Mar. 1993 21 p
(Contract F49620-92-C-0038)
(AD-A268279; AFOSR-93-0573TR) Avail: CASI HC A03/MF A01

The overall goal of this Phase 1 project was to focus on developing procedures for the fabrication and evaluation of epitaxial layers of GaAs which are doped with rare earth (RE) ions of Erbium. The essential elements of the originally proposed approach have been demonstrated through the efforts on this Phase 1 project. Erbium was successfully incorporated in epitaxially grown Gallium Arsenide (GaAs) and Aluminum-Gallium Arsenide (AlGaAs) by using the Metal Organic Chemical Vapor Deposition (MOCVD) method and using Tris(n-butylcyclopentadienyl)erbium Er(C4H9C5H4)3 as Er source material. Concentrations of Erbium as high as 10(exp 19)/cm(exp

-3) were detected by Secondary Ion Mass Spectroscopy (SIMS). A substantial, though unknown, amount of the Erbium was incorporated in the form of trivalent ions; this was evident by the observation of the characteristic Er(3+) light emission from photoluminescence spectra of our samples. DTIC

N94-17579# Minnesota Univ., Minneapolis. Dept. of Physics.
EPITAXIAL IRON FILMS Annual Report, 1 Mar. 1992 - 1993
E. D. Dahlbert 15 Jun. 1993 9 p
(Contract F49620-92-J-0185)
(AD-A268286; AFOSR-93-0596TR) Avail: CASI HC A02/MF A01

This research involved studies of the magnetic properties of multilayered magnetic films and high quality thin films. Both ultra high vacuum sputtering and molecular beam epitaxy techniques were utilized to prepare the films. Both electrical transport and magneto-optic effects were used to measure the magnetic properties of the films. The primary focus during this year was to develop high quality trilayers consisting of a magnetic layer, nonmagnetic layer, and a magnetic layer. These structures are being developed to determine the scattering origin of the giant magnetoresistance phenomena. In addition, other investigations included the determination of the temperature dependence of the magnetic anisotropy energies of epitaxial iron films, the magnetization dynamics of thin films, and the general transport properties of multilayers. The transport effort utilized multilayers of magnetic and nonmagnetic metals to study the interfacial scattering. The combination of a magnetic and nonmagnetic metal in this work facilitates the origin of the scattering by use of the anisotropic magnetoresistance. DTIC

N94-17606# California Univ., San Diego, La Jolla. Dept. of Physics.
MECHANICAL PROPERTIES OF INTERFACES AND SUPERLATTICES Final Report
Ivan K. Schuller 1993 13 p
(Contract N00014-91-J-1177)
(AD-A268591) Avail: CASI HC A03/MF A01

This proposal was dedicated to the study of mechanical properties of interfaces and superlattices. These properties were correlated with growth techniques and extensive structural characterization. The principal goal of this proposal was to ascertain whether structural or electronic effects control the mechanical properties of interfaces and superlattices. Molecular Beam Epitaxy (MBE) and Sputtering were used to prepare single interfaces and multilayers. In-situ structural characterization was accomplished mainly using High Energy Electron Diffraction (HEED). Post preparation Micro-cleavage Transmission Electron Microscopy (MTEM), together with temperature dependent x-ray diffraction was performed to characterize the structure of the sample. The main successes during the last funding period of this proposal includes the simultaneous study of a variety of elastic constants of Cu/Nb, Fe/Cr, and W/Ni superlattices together with detailed structural studies, the measurement of the elastic constants of GaAs/AlAs superlattices and the development of a vibrating drum method for measurements of the biaxial modulus of thin films. DTIC

N94-17659# Los Alamos National Lab., NM.
KINETICS OF SILICA-PHASE TRANSITIONS
C. J. Duffy Jul. 1993 23 p
(Contract W-7405-eng-36)
(DE93-016231; LA-12564-MS) Avail: CASI HC A03/MF A01

In addition to the stable silica polymorph quartz, several metastable silica phases are present in Yucca Mountain. The conversion of these phases to quartz is accompanied by volume reduction and a decrease in the aqueous silica activity, which may destabilize clinoptilolite and mordenite. The primary reaction sequence for the silica phases is from opal or glass to disordered opal-CT, followed by ordering of the opal-CT and finally by the crystallization of quartz. The ordering of opal-CT takes place in the solid state, whereas the conversion of opal-CT takes place through dissolution-reprecipitation involving the aqueous phase. It is proposed that the rate of conversion of opal-CT to quartz is controlled by diffusion of defects out of a disordered surface layer formed on the crystallizing quartz. The reaction rates are observed to be dependent on temperature, pressure, degree of supersaturation, and pH. Rate equations selected from the literature appear to be consistent with observations at Yucca Mountain. DOE

N94-15031# Space Research Organization Netherlands, Utrecht. Space Research Lab.
SUPERCONDUCTIVE X RAY PHOTON DETECTORS
P. A. J. deKorte *In* ESA, Proceedings of an ESA Symposium on Photon Detectors for Space Instrumentation Dec. 1992 p 41-50 Sponsored by Netherlands Technology Foundation (For primary document see N94-15025 03-19)
Copyright Avail: CASI HC A02/MF A04

N94-15032# Paris VI Univ. (France).
METASTABLE SUPERCONDUCTORS AS PHOTON DETECTORS
T. Girard, V. Jeudy, D. Limagne, V. Pagesy, A. Pagesy, and G. Waysand *In* ESA, Proceedings of an ESA Symposium on Photon Detectors for Space Instrumentation Dec. 1992 p 51-55 Prepared in cooperation with Paris VII Univ., Fra nce (For primary document see N94-15025 03-19)
Copyright Avail: CASI HC A01/MF A04

N94-15034# Max-Planck-Inst. fuer Extraterrestrische Physik, Garching (Germany).
THE XMM pn-CCD DETECTOR SYSTEM: FIRST RESULTS
H. Braeuninger, R. Danner, N. Findeis (KETEK G.m.b.H., Haimhausen, Germany.), D. Hauff, P. Holl (KETEK G.m.b.H., Haimhausen, Germany.), J. Kemmer (KETEK G.m.b.H., Haimhausen, Germany.), E. Kendziorra (Tuebingen Univ., Germany.), J. Kraemer (Tuebingen Univ., Germany.), P. Lechner, and G. Lutz et al *In* ESA, Proceedings of an ESA Symposium on Photon Detectors for Space Instrumentation Dec. 1992 p 69-73 (For primary document see N94-15025 03-19)
(Contract BMFT-50-OX-90020/XMM-EPIC)
Copyright Avail: CASI HC A01/MF A04

N94-15035# Space Research Organization Netherlands, Utrecht. Space Research Lab.
THE DEVELOPMENT OF BACK-ILLUMINATED CCD'S FOR XMM
P. W. A. M. Verhoeve, F. A. Jansen (Space Research Organization Netherlands, Leiden.), P. A. J. deKorte, A. J. F. denBoggende, A. C. Brinkman, H. J. M. Aarts (Space Research Organization Netherlands, Leiden.), D. Burt (GEC Hirst Research Centre, Wembley, England.), and P. Pool (English Electric Valve Co. Ltd., Chelmsford, England.) *In* ESA, Proceedings of an ESA Symposium on Photon Detectors for Space Instrumentation Dec. 1992 p 75-80 (For primary document see N94-15025 03-19)
Copyright Avail: CASI HC A02/MF A04

N94-15036# Interuniversity Micro-Electronics Center, Leuven (Belgium).
THINNED, BACKSIDE ILLUMINATED, AREA CCD IMAGER FOR ELECTRON DETECTION
I. Debusschere, I. Born, C. Claeys, K. DeBackker, A. Verbist, J. Adema (Delft Electronic Products, Roden, Netherlands.), and L. Bosch (Delft Electronic Products, Roden, Netherlands.) *In* ESA, Proceedings of an ESA Symposium on Photon Detectors for Space Instrumentation Dec. 1992 p 81-85 (For primary document see N94-15025 03-19)
(Contract HV-CCD-N88/20/21/22)
Copyright Avail: CASI HC A01/MF A04

N94-15041*# Ball Aerospace Systems Div., Boulder, CO.
CCDS AND PHOTON COUNTING DEVICES: APPLICATIONS IN SPACE AND FROM THE GROUND
W. A. Delamere, M. M. Blouke (Tektronix, Inc., Beaverton, OR.), J. S. Flores, and W. W. Frame *In* ESA, Proceedings of an ESA Symposium on Photon Detectors for Space Instrumentation Dec. 1992 p 111-113 Sponsored by NASA. Langley Research Center and Tektronix, Inc. (For primary document see N94-15025 03-19)
Copyright Avail: CASI HC A01/MF A04

N94-15050# Universidad Politecnica de Barcelona (Spain).
SCHOTTKY BARRIER FOCAL PLANE ARRAYS FOR SWIR AND MWIR
E. Roca, J. Vermeiren (Interuniversity Micro-Electronics Center, Leuven, Belgium.), W. Platz (Messerschmitt-Boelkow-Blohm G.m.b.H., Munich, Germany.), G. Marangoni (Elettronica S.R.L., Rome, Italy.), and M. Fabbricotti (European Space Agency. European Space Research and Technology Center, ESTEC, Noordwijk, Netherlands.) *In* ESA, Proceedings of an

ESA Symposium on Photon Detectors for Space Instrumentation Dec. 1992 p 175-179 (For primary document see N94-15025 03-19)
(Contract ESA-6044/84/NL/PB)
Copyright Avail: CASI HC A01/MF A04

N94-15051# Philips Components Ltd., Southampton (England).
ADVANCED HIGH PERFORMANCE CdHgTe MULTIPLEXED ARRAYS
I. M. Baker, D. E. Charlton, C. Arthurs, and G. Crimes *In* ESA, Proceedings of an ESA Symposium on Photon Detectors for Space Instrumentation Dec. 1992 p 181-185 Sponsored by Ministry of Defence (For primary document see N94-15025 03-19)
Copyright Avail: CASI HC A01/MF A04

N94-15053# Academy of Sciences (USSR), Saint Petersburg. National Research Inst.
LEAD CHALCOGENIDES BASED IR PHOTOSENSITIVE ARRAY DETECTORS WITH COORDINATE ADDRESSING
G. A. Agranov, S. K. Novoselov, R. M. Stepanov, A. Z. Doon, A. V. Pashkevich, A. I. Ivanov, I. K. Nemchuk, V. K. Nesterov, and V. E. Skoriukin *In* ESA, Proceedings of an ESA Symposium on Photon Detectors for Space Instrumentation Dec. 1992 p 191-195 (For primary document see N94-15025 03-19)
Copyright Avail: CASI HC A01/MF A04

N94-15054# Space Research Organization Netherlands, Groningen.
SUBMILLIMETERWAVE SIS MIXER DEVELOPMENTS
H. vandeStadt, T. deGraauw, C. E. Honingh, R. A. Panhuyzen, H. H. A. Schaeffer, E. Armandillo (European Space Agency. European Space Research and Technology Center, ESTEC, Noordwijk, Netherlands.), M. M. T. M. Dierichs (Groningen Rijksuniv., Netherlands.), T. M. Klapwijk (Groningen Rijksuniv., Netherlands.), G. deLange (Groningen Rijksuniv., Netherlands.), and A. Skalare (Chalmers Univ. of Technology, Goeteborg, Sweden.) *In* ESA, Proceedings of an ESA Symposium on Photon Detectors for Space Instrumentation Dec. 1992 p 197-200 Sponsored in part by Science Research Council (For primary document see N94-15025 03-19)
(Contract ESA-7898/88/NL/PB(SC))
Copyright Avail: CASI HC A01/MF A04

N94-15068# Consiglio Nazionale delle Ricerche, Naples (Italy). Ist. di Cibernetica.
Nb-BASED SJTJ FOR NUCLEAR DETECTION: PRELIMINARY RESULTS WITH ALPHA RADIATION
R. Cristiano, E. Esposito, L. Frunzio, S. Pagano, A. Barone (Naples Univ., Italy.), G. Peluso (Naples Univ., Italy.), G. Pepe (Naples Univ., Italy.), H. Akoh (Tsukuba Univ., Ibaraki, Japan.), H. Nakagawa (Tsukuba Univ., Ibaraki, Japan.), and S. Takada (Tsukuba Univ., Ibaraki, Japan.) *In* ESA, Proceedings of an ESA Symposium on Photon Detectors for Space Instrumentation Dec. 1992 p 265-268 Sponsored by CNR and ETL (For primary document see N94-15025 03-19)
Copyright Avail: CASI HC A01/MF A04

N94-15071# Interuniversity Micro-Electronics Center, Leuven (Belgium).
RADIATION HARDENING OF A CCD TECHNOLOGY THROUGH PROCESS AND DESIGN MODIFICATIONS
I. Debusschere, A. Simone, A. Alaerts, and C. Claeys *In* ESA, Proceedings of an ESA Symposium on Photon Detectors for Space Instrumentation Dec. 1992 p 281-284 (For primary document see N94-15025 03-19)
(Contract ESTEC-8615/90/NL/PM(SC))
Copyright Avail: CASI HC A01/MF A04

N94-15073# Battelle Inst., Frankfurt am Main (Germany).
EXTRINSIC PHOTOCONDUCTOR DETECTORS FOR THE WAVELENGTH RANGE 2 MICRONS TO 240 MICRONS
D. Engemann, R. Faymonville, R. Felten, O. Frenzl, M. Overhamm, M. Griffin (London Univ., England.), P. Ade (London Univ., England.), S. Church (London Univ., England.), and A. Murray (London Univ., England.) *In* ESA, Proceedings of an ESA Symposium on Photon Detectors for Space Instrumentation Dec. 1992 p 289-292 Sponsored by DLR and ESTEC (For primary document see N94-15025 03-19)
Copyright Avail: CASI HC A01/MF A04

N94-15075# National Physical Lab., Teddington (England). Quantum Metrology Div.
IMPROVED OPTICAL RADIATION DETECTORS AND THEIR CALIBRATION: 200 nm - 30 MICRONS
Nigel Fox *In* ESA, Proceedings of an ESA Symposium on Photon Detectors for Space Instrumentation Dec. 1992 p 299-301 (For primary document see N94-15025 03-19)
Copyright Avail: CASI HC A01/MF A04

N94-15077# London Univ. (England). Dept. of Physics.
IONISING RADIATION-INDUCED EFFECTS IN DOPED GERMANIUM FIR PHOTOCONDUCTORS
M. C. Price, M. J. Griffin, S. E. Church, A. G. Murray, and P. A. R. Ade *In* ESA, Proceedings of an ESA Symposium on Photon Detectors for Space Instrumentation Dec. 1992 p 309-312 (For primary document see N94-15025 03-19)
Copyright Avail: CASI HC A01/MF A04

N94-15078# Institut de Radio Astronomie Millimetrique, Grenoble (France).
PREPARATION AND PROPERTIES OF Nb/Al SIS AND SIN JUNCTIONS FOR MILLIMETER AND SUBMILLIMETER RADIOASTRONOMICAL RECEIVERS
K. H. Gundlach, T. Lehnert, D. Billon-Pierron, M. Voss, and P. Pasturel *In* ESA, Proceedings of an ESA Symposium on Photon Detectors for Space Instrumentation Dec. 1992 p 313-316 (For primary document see N94-15025 03-19)
Copyright Avail: CASI HC A01/MF A04

N94-15080# Leicester Univ. (England). X Ray Astronomy Group.
CCD'S ON HIGH RESISTIVITY BULK SILICON FOR X RAY SPECTROSCOPY ON XMM
A. D. Holland, M. J. L. Turner, A. A. Wells, and D. J. Burt (GEC Hirst Research Centre, Wembley, England.) *In* ESA, Proceedings of an ESA Symposium on Photon Detectors for Space Instrumentation Dec. 1992 p 321-324 Sponsored by Science Research Council (For primary document see N94-15025 03-19)
Copyright Avail: CASI HC A01/MF A04

N94-15083# Tuebingen Univ. (Germany). Physikalisches Inst.
SUBSTRATE EFFECTS IN SUPERCONDUCTING TUNNEL JUNCTION DETECTORS
S. Lemke, F. Hebrank, R. Gross, R. P. Huebener, T. Weimann (Physikalisch-Technische Bundesanstalt, Brunswick, Germany.), R. Poepel (Physikalisch-Technische Bundesanstalt, Brunswick, Germany.), J. Niemeyer (Physikalisch-Technische Bundesanstalt, Brunswick, Germany.), U. Schnakenberg (Fraunhofer-Inst. fuer Mikrostrukturtechnik, Berlin, Germany.), and W. Benecke (Bremen Univ., Germany.) *In* ESA, Proceedings of an ESA Symposium on Photon Detectors for Space Instrumentation Dec. 1992 p 335-338 Sponsored by DFG (For primary document see N94-15025 03-19)
Copyright Avail: CASI HC A01/MF A04

N94-15089*# Northwestern Univ., Evanston, IL. Dept. of Physics and Astronomy.
A MULTILAYERED APPROACH TO SUPERCONDUCTING TUNNEL JUNCTION X RAY DETECTORS
E. D. Rippert, S. N. Song, J. B. Ketterson, S. R. Maglic, S. Lomatch, C. Thomas, M. A. Cheida, and M. P. Ulmer *In* ESA, Proceedings of an ESA Symposium on Photon Detectors for Space Instrumentation Dec. 1992 p 361-363 (For primary document see N94-15025 03-19)
(Grants NAGw-2859; NSF DMR-88-09864)
Copyright Avail: CASI HC A01/MF A04

N94-15095# Center for Industrial Research, Oslo (Norway).
SILICON RADIATION SENSOR SYSTEMS FOR GAMMA AND X RAY DETECTION AT SI
Svein Tunheim, Einar Nygaard, Arne Kjensmo, Lars Evensen, Fin Serck-Hanssen, and Per Ohlckers *In* ESA, Proceedings of an ESA Symposium on Photon Detectors for Space Instrumentation Dec. 1992 p 389-391 (For primary document see N94-15025 03-19)
Copyright Avail: CASI HC A01/MF A04

N94-15098# Interuniversity Micro-Electronics Center, Leuven (Belgium).
A LINEAR MONOLITHIC 4-6 ON SILICON IR DETECTOR ARRAY
J. VanDamme, J. Vermeiren, H. Zogg (Eidgenoessische Technische Hochschule, Zurich, Switzerland.), J. Masek (Eidgenoessische Technische Hochschule, Zurich, Switzerland.), and M. Fabbricotti (European Space Agency. European Space Research and Technology Center, ESTEC, Noordwijk, Netherlands.) *In* ESA, Proceedings of an ESA Symposium on Photon Detectors for Space Instrumentation Dec. 1992 p 401-404 Sponsored by Gruppe fuer Ruestungsdienste and Swiss NSF (For primary document see N94-15025 03-19)
(Contract ESA-7085/87/NL/PB)
Copyright Avail: CASI HC A01/MF A04

N94-15100# Interuniversity Micro-Electronics Center, Leuven (Belgium).
A MONOLITHIC PbTeCCD FOCAL PLANE ARRAY FOR MWIR IMAGING
J. VanDamme, J. Vermeiren, G. Marangoni (Elettronica S.R.L., Rome, Italy.), M. DAntoni (Elettronica S.R.L., Rome, Italy.), W. Platz (Messerschmitt-Boelkow-Blohm G.m.b.H., Munich, Germany.), and M. Fabbricotti (European Space Agency. European Space Research and Technology Center, ESTEC, Noordwijk, Netherlands.) *In* ESA, Proceedings of an ESA Symposium on Photon Detectors for Space Instrumentation Dec. 1992 p 409-412 (For primary document see N94-15025 03-19)
(Contract ESA-6044/84/NL/PB)
Copyright Avail: CASI HC A01/MF A04

N94-15101# Cambridge Univ. (England). Dept. of Materials Science and Metallurgy.
QUASIPARTICLE TRAPPING IN DISTRIBUTED SUPERCONDUCTING THREE-TERMINAL TUNNEL JUNCTION DEVICES
P. A. Warburton and M. G. Blamire *In* ESA, Proceedings of an ESA Symposium on Photon Detectors for Space Instrumentation Dec. 1992 p 413-416 Sponsored in part Science Research Council; Royal Society; and NRL (For primary document see N94-15025 03-19)
Copyright Avail: CASI HC A01/MF A04

N94-15103# Imperial Coll. of Science and Technology, London (England).
THE EPITAXIAL Si X RAY BOLOMETER AN ALTERNATIVE TO ION IMPLANTED DEVICES
C. C. Zammit, T. J. Sumner, I. D. Hepburn (London Univ., England.), P. A. R. Ade (London Univ., England.), P. Hutchin (Southampton Univ., England.), and G. Ensell (Southampton Univ., England.) *In* ESA, Proceedings of an ESA Symposium on Photon Detectors for Space Instrumentation Dec. 1992 p 423-425 (For primary document see N94-15025 03-19)
Copyright Avail: CASI HC A01/MF A04

N94-15572*# Czech Technical Univ., Prague. Faculty of Nuclear Science and Physical Engineering.
THE SOLID STATE DETECTOR TECHNOLOGY FOR PICOSECOND LASER RANGING
Ivan Prochazka *In* NASA. Goddard Space Flight Center, Eighth International Workshop on Laser Ranging Instrumentation Jun. 1993 5 p (For primary document see N94-15552 03-19)
Avail: CASI HC A01/MF A06

N94-16141*# National Aeronautics and Space Administration. Marshall Space Flight Center, Huntsville, AL.
THERMAL SPRAY FORMING OF REFRACTORY SAMPLE AMPOULE CARTRIDGES FOR SINGLE CRYSTAL GROWTH SPACE FURNACES
Frank Zimmerman, Richard Poorman, Richard Holmes, Timothy McKechnie (Rockwell International Corp., Canoga Park, CA.), Phil Krotz (Rockwell International Corp., Canoga Park, CA.), and Yoon Liaw (Rockwell International Corp., Canoga Park, CA.) *In* Huntsville Association of Technical Societies, TABES 1993: 9th Annual Technical and Business Exhibition and Symposium 1993 5 p (For primary document see N94-16129 03-38)
(TABES Paper 93-605) Avail: CASI HC A01/MF A03

N94-16255*# Arizona State Univ., Tempe. Dept. of Geology and Chemistry.
OLIVINES IN THE KABA CARBONACEOUS CHONDRITE AND CONSTRAINTS ON THEIR FORMATION Abstract Only
X. Hua and P. R. Buseck *In* Lunar and Planetary Inst., Twenty-Fourth Lunar and Planetary Science Conference. Part 2: G-M 1993 p 677-678 (For primary document see N94-16173 03-91)
Avail: CASI HC A01/MF A06

N94-16331*# California Inst. of Tech., Pasadena. Div. of Geological and Planetary Sciences.
EVAPORATION KINETICS OF Mg2SiO4 CRYSTALS AND MELTS FROM MOLECULAR DYNAMICS SIMULATIONS Abstract Only
J. D. Kubicki and E. M. Stolper *In* Lunar and Planetary Inst., Twenty-Fourth Lunar and Planetary Science Conference. Part 2: G-M 1993 p 829-830 (For primary document see N94-16173 03-91)
Avail: CASI HC A01/MF A06

N94-16341*# Muenster Univ. (Germany).
ORIENTATION OF PLANAR DEFORMATION FEATURES (PDFs) IN QUARTZ Abstract Only
F. Langenhorst and A. Deutsch *In* Lunar and Planetary Inst., Twenty-Fourth Lunar and Planetary Science Conference. Part 2: G-M 1993 p 849-850 (For primary document see N94-16173 03-91)
Avail: CASI HC A01/MF A06

N94-16420*# National Aeronautics and Space Administration. Goddard Space Flight Center, Greenbelt, MD.
CATALYTIC CRYSTALLIZATION OF ICES BY SMALL SILICATE SMOKES AT TEMPERATURES LESS THAN 20K Abstract Only
M. Moore, R. Ferrante, R. Hudson, T. Tanabe, and J. Nuth *In* Lunar and Planetary Inst., Twenty-Fourth Lunar and Planetary Science Conference. Part 2: G-M 1993 p 1007-1008 (For primary document see N94-16173 03-91)
Avail: CASI HC A01/MF A06

77 THERMODYNAMICS AND STATISTICAL PHYSICS

Includes quantum mechanics; theoretical physics; and Bose and Fermi statistics.

For related information see also *25 Inorganic and Physical Chemistry* and *34 Fluid Mechanics and Heat Transfer.*

N94-14935 Joint Inst. for Nuclear Research, Dubna (USSR). Lab. of Theoretical Physics.
SUPERSYMMETRY OF GAUGE EQUATIONS AND GEOMETRIC NONADIABATIC PHASES
A. A. Suzko 1992 11 p Limited Reproducibility: More than 20% of this document may be affected by microfiche quality
(DE93-626671; JINR-E-4-92-282) Avail: Issuing Activity (Department of Energy (DOE)) (US Sales Only)

It is shown that nondiagonal elements of the connection operator A generate the nonadiabatic geometric phase in addition to Aharonov-Anandan one. The extra geometric phases are produced by A-singularities arising due to crossing of potential curves and in certain case of supersymmetry. The supersymmetric extension for the system of gauge equations is discussed. DOE

N94-14977# Naval Postgraduate School, Monterey, CA.
BREAKDOWN OF ADIABATIC INVARIANCE M.S. Thesis
Charolette V. Leigh Mar. 1993 84 p
(AD-A267246) Avail: CASI HC A05/MF A01

Adiabatic invariance, in which certain quantities of a system remain unchanged as a parameter of the system is infinitely slowly altered, plays a fundamental role in many areas of physics. For any harmonic oscillator, the adiabatic invariant is the energy divided by the frequency. When the alterations are slow but occur over a finite time, there is predicted to be an exponential suppression of the change in adiabatic invariant; that is, if epsilon is a dimensionless positive number that tends to zero in the limit of infinitely slow alterations, then the change in adiabatic invariant is proportional to exp(-1/epsilon). We report numerical simulations of three oscillators whose parameters are varied at rates ranging from very slow to very fast compared to the oscillation frequency. The models are single-degree-of-freedom oscillators that are based on simple physical

systems. The exponential suppression is not observed, which indicates that its observation may be extremely difficult or impossible. Furthermore, the change in adiabatic invariant is found tc depend upon the initial phase even in the limit of infinitely slow changes. In the case of abrupt alterations, the numerical simulations verify some theoretical calculations, but reveal that other theoretical calculations are incorrect. DTIC

N94-16810# Oak Ridge National Lab., TN.
NUMERICAL STUDIES OF THE PHOTOLUMINESCENCE SPECTRUM OF QUANTUM HALL SYSTEMS
X. M. Chen (Tennessee Univ., Knoxville.) and J. J. Quinn (Tennessee Univ., Knoxville.) Apr. 1993 6 p Presented at the Electronic Properties of Two-Dimensional Systems Conference, Newport, RI, 31 May - 4 Jun. 1993
(Contract DE-AC05-84OR-21400)
(DE93-015822; CONF-9305225-1) Avail: CASI HC A02/MF A01

The eigenfunctions and eigenvalues of a system consisting of a finite number of electrons on a two dimensional plane together with a few holes on a neighboring plane are obtained by numerical diagonalization within the subspace of the lowest Landau level. The energy spectrum and ground state energy per particle are studied as a function of the Landau level degeneracy and the interlayer separation. By evaluating the square of the matrix element of the luminescence operator between the initial state with N(sub e) electrons and one hole and various final states with N(sub e) - 1 electrons and no hole, and multiplying by a delta function which conserves energy, the luminescence intensity I(omega) is obtained. DOE

N94-16956# Los Alamos National Lab., NM.
STOCHASTIC CHAOS: AN ANALOG OF QUANTUM CHAOS
M. M. Millonas 1993 5 p Presented at the 12th International Conference on Noise in Physical Systems and 1/f Fluctuations, Saint Louis, MO, 16-20 Aug. 1993
(Contract W-7405-eng-36)
(DE93-016619; LA-UR-93-2133; CONF-930866-2) Avail: CASI HC A01/MF A01

Some intriguing connections between the properties of nonlinear, noise driven systems and the nonlinear dynamics of a particular set of Hamilton's equation are discussed. A large class of Fokker-Planck equations, like the Schroedinger equation, can exhibit a transition in their spectral statistics as a coupling parameter is varied. This transition is connected to the transition to non-integrability in the Hamilton's equations. DOE

N94-16997# Georgia Inst. of Tech., Atlanta. School of Chemical Engineering.
SUPERCRITICAL THERMODYNAMICS OF SULFUR AND NITROGEN SPECIES
C. A. Eckert 1993 11 p
(Contract DE-FG22-91PC-91287)
(DE93-017727; DOE/PC-91287/8) Avail: CASI HC A03/MF A01

Significant opportunity exists for the application of supercritical fluid (SCF) technology to coal processing, both for pretreatment of high sulfur coals, as well as liquefaction and treatment of coal liquids. Supercritical fluids are attractive solvents for a variety of coal processing applications because of their unusual solvating and mass transfer properties. Solubility studies have been carried out for a number of model coal and coal-liquid compounds, primarily in pure supercritical fluids. We are extending this database of model coal compound equilibria using modern techniques that have the advantage of being much more rapid than traditional techniques. Cosolvent effects on solubility are being investigated over a variety of solvent properties. In addition, specific molecular interactions are being investigated through spectroscopic techniques. The resulting data are being used to develop a chemical-physical equation of state (EOS) model of SCF solution with meaningful parameters. The equation of state will be used to predict solubility behavior, which will permit the design and tailoring of SCF cosolvent systems for specific coal processing applications. DOE

N94-17315 Joint Inst. for Nuclear Research, Dubna (USSR). Lab. of Theoretical Physics.
CLUSTERIZATION OF QUANTUM STATES IN THE HARTMANN MODEL
I. V. Lutsenko, A. D. Magakyan, A. N. Sisakyan, and V. M. Ter-Antonyan 1992 6 p Limited Reproducibility: More than 20% of this document may be affected by microfiche quality
(DE93-626624; JINR-R-2-92-48) Avail: CASI HC A02 (US Sales Only)

The effect of clusterization of quantum states in the Hartmann is predicted and explained. DOE

N94-17540# Naval Postgraduate School, Monterey, CA.
NUMERICALLY SOLVING A TRANSIENT HEAT CONDUCTION PROBLEM WITH CONVECTION AND RADIATION M.S. Thesis
David J. Albert Jun. 1993 98 p
(AD-A268521) Avail: CASI HC A05/MF A02

The transient surface temperature distribution is determined for the flat plate and sphere subjected to cooling by combined convection and radiation. In the study, the initial boundary value problem is reduced to a singular nonlinear Volterra integral equation of the second kind using the integral transform method. Several numerical techniques are introduced in an attempt to find an approximate solution of the problem: The method of successive approximations, the Runge-Kutta method, and the finite difference method. The integral equation is solved numerically by the Runge-Kutta method of orders 1, 3, and 5. In addition, the finite difference method is implemented to solve the initial boundary value problem, and the solutions are compared with those generated by the Runge-Kutta method. All the numerical results are presented graphically. Limitations and difficulties involved in these schemes are discussed. At the end, a numerical algorithm for solving the problem is proposed. DTIC

N94-17602 Nationaal Inst. voor Kernfysica en Hoge Energiefysica, Amsterdam (Netherlands).
THE UNIVERSALITY OF THE SHIFT OF THE CHERN-SIMONS PARAMETER FOR A GENERAL CLASS OF BRS INVARIANT REGULARIZATIONS
G. Giavarini (Paris VII Univ., France.), C. P. Martin (Universidad Autonoma de Madrid, Cantoblanco, Spain.), and F. RuizRuiz 1993 8 p Sponsored in part by Stichting voor Fundamenteel Onderzoek der Materie, Netherlands, and Comisionn de Investigacion Cientifica y Tecnica, Spain Limited Reproducibility: More than 20% of this document may be affected by microfiche quality
(Contract SC-900376)
(NIKHEF-H/93-03; FTUAM-93/03; LPTHE-93/06; ETN-93-94825) Avail: CASI HC A02

A biparametric family of BRS invariant regularization methods of SU(N) Chern-Simons theory (the parameters defining the family taking arbitrary values in the two dimensional real space) is presented and it is shown that the shift k (tends to) k + sign(k)N of the Chern-Simons parameter k occurs for arbitrary values of the family defining parameters. This supports irrefutably the conjecture that the shift of k is universal for BRS invariant regulators. ESA

N94-17618# Nationaal Inst. voor Kernfysica en Hoge Energiefysica, Amsterdam (Netherlands).
THE RENORMALIZATION OF THE AXIAL ANOMALY IN DIMENSIONAL REGULARIZATION
S. A. Larin 1992 12 p
(NIKHEF-H/92-18; ETN-93-94823) Avail: CASI HC A03/MF A01

The prescription for the gamma(sub five) matrix within dimensional regularization in multiloop calculations is elaborated. The three loop anomalous dimension of the singlet axial current is calculated. Thoughout the calculations minimal subtraction scheme or its standard variation are used to perform renormalizations. The dimension of space time is defined in the standard way as D 4 - 2 epsilon. All calculations were performed within massless perturbative quantum chromodynamics. ESA

N94-17624*# National Aeronautics and Space Administration. Lewis Research Center, Cleveland, OH.
COEFFICIENTS FOR CALCULATING THERMODYNAMIC AND TRANSPORT PROPERTIES OF INDIVIDUAL SPECIES
Bonnie J. McBride, Sanford Gordon (Gordon, Sanford, Cleveland, OH.), and Martin A. Reno (Heidelberg Coll., Tiffin, OH.) Oct. 1993 92 p
(RTOP 505-62-52)
(NASA-TM-4513; E-7981; NAS 1.15:4513) Avail: CASI HC A05/MF A01

Libraries of thermodynamic data and transport properties are given for individual species in the form of least-squares coefficients. Values of C(sup

0)(sub p)(T), H(sup 0)(T), and S(sup 0)(T) are available for 1130 solid, liquid, and gaseous species. Viscosity and thermal conductivity data are given for 155 gases. The original C(sup 0)(sub p)(T) values were fit to a fourth-order polynomial with integration constants for H(sup 0)(T) and S(sup 0)(T). For each species the integration constant for H(sup 0)(T) includes the heat of formation. Transport properties have a different functional form. The temperature range for most of the data is 300 to 5000 K, although some of the newer thermodynamic data have a range of 200 to 6000 K. Because the species are mainly possible products of reaction, the data are useful for chemical equilibrium and kinetics computer codes. Much of the data has been distributed for several years with the NASA Lewis equilibrium program CET89. The thermodynamic properties of the reference elements were updated along with about 175 species that involve the elements carbon, hydrogen, oxygen, and nitrogen. These sets of data will be distributed with the NASA Lewis personal computer program for calculating chemical equilibria, CETPC. Author (revised)

N94-17632# International Centre for Theoretical Physics, Trieste (Italy).
DERIVATION OF THE VERLINDE FORMULA FROM CHERN-SIMONS THEORY AND THE G/G MODEL
M. Blau and G. Thompson May 1993 49 p
(DE93-628620; IC-93/83) Avail: CASI HC A03/MF A01 (US Sales Only)

We give a derivation of the Verlinde formula for the G(sub k) WZW model from Chern-Simons theory, without taking recourse to CFT, by calculating explicitly the partition function Z(sub (Sigma x S(sup 1))) of Sigma x S(sup 1) with an arbitrary number of labelled punctures. By a suitable gauge choice, Z(sub (Sigma x S(sup 1))) is reduced to the partition function of an Abelian topological field theory on Sigma (a deformation of non-Abelian BF and Yang-Mills theory) whose evaluation is straightforward. This relates the Verlinde formula to the Ray-Singer torsion of Sigma x S(sup 1). We derive the G(sub k)/G(sub k) model from Chern-Simons theory, proving their equivalence and give an alternative derivation of the Verlinde formula by calculating the G(sub k)/G(sub k) path integral via a functional version of the Weyl integral formula. From this point of view the Verlinde formula arises from the corresponding Jacobian, the Weyl determinant. Also, a novel derivation of the shift k(yields)k+h is given, based on the index of the twisted Dolbeault complex. DOE

80 SOCIAL SCIENCES (GENERAL)

Includes educational matters.

N94-15230* National Aeronautics and Space Administration. Marshall Space Flight Center, Huntsville, AL.
SHARP (Videotape)
Jan. 1989 Videotape: 7 min. 20 sec. playing time, in color, with sound (NASA-TM-109659; NONP-VT-93-190457) Avail: CASI VHS A01/BETA A22

This video tape describes the benefits of NASA's Summer High School Apprenticeship Research Program to participating students. CASI

N94-15232* National Aeronautics and Space Administration. Marshall Space Flight Center, Huntsville, AL.
SPACE CLASSROOM (Videotape)
Nov. 1990 Videotape: 2 min. 21 sec. playing time, in color, with sound (NASA-TM-109661; NONP-VT-93-190459) Avail: CASI VHS A01/BETA A22

This video presentation provides information on the first classroom taught from space to encourage student interest in astronomy and space exploration. CASI

N94-15248* National Aeronautics and Space Administration, Washington, DC.
ENHANCING SIGHT (Videotape)
Feb. 1990 Videotape: 3 min. 54 sec. playing time, in color, with sound (NASA-TM-109637; NONP-VT-93-190435) Avail: CASI VHS A01/BETA A22

This video describes a new reading program for people with limited sight. CASI

N94-15340* National Aeronautics and Space Administration, Washington, DC.
STUDENT RESEARCHERS (Videotape)
Jul. 1990 Videotape: 3 min. 28 sec. playing time, in color, with sound (NASA-TM-109441; NONP-VT-93-190238) Avail: CASI VHS A01/BETA A22

The videotape shows students and their NASA-related research at LeRC. CASI

N94-15372* National Aeronautics and Space Administration. Lyndon B. Johnson Space Center, Houston, TX.
SHORT WALK TO EVERYWHERE (Videotape)
Jul. 1988 Videotape: 17 min. 43 sec. playing time, in color, with sound (NASA-TM-109541; NONP-VT-93-190338) Avail: CASI VHS A01/BETA A22

This video details the activities of the Space, Earth, Ocean Center (SEOC), an environmental residential camp held in the summer for elementary school children. Students are shown participating in hands on activities designed to encourage environmental awareness and interests in the environmental sciences. CASI

N94-15418* National Aeronautics and Space Administration. Lewis Research Center, Cleveland, OH.
CORE/TRC (Videotape)
Feb. 1990 Videotape: 7 min. playing time, in color, with sound (NASA-TM-109434; NONP-VT-93-190231) Avail: CASI VHS A01/BETA A22

This video looks at the Central Operations for Educators in Ohio, and the LeRC Teacher Resource Center. CASI

N94-15420* National Aeronautics and Space Administration. Lewis Research Center, Cleveland, OH.
SPACEWORK 16 (Videotape)
Jan. 1988 Videotape: 28 min. playing time, in color, with sound (NASA-TM-109436; NONP-VT-93-190233) Avail: CASI VHS A01/BETA A22

This video consists of the Simulated Space Shuttle Program for schools and also has clips on wind tunnel research and on JPL's 'Miranda the Movie'. CASI

N94-15504* National Aeronautics and Space Administration. Lewis Research Center, Cleveland, OH.
CHALLENGER CENTER (Videotape)
Nov. 1989 Videotape: 8 min. 18 sec. playing time, in color, with sound (NASA-TM-109432; NONP-VT-93-190229) Avail: CASI VHS A01/BETA A22

This video explains the objectives of the Challenger Center for Space Education and how it got started. CASI

N94-15505* National Aeronautics and Space Administration. Lewis Research Center, Cleveland, OH.
CHALLENGER CENTER: ORIENTATION (Videotape)
Jul. 1989 Videotape: 7 min. 40 sec. playing time, in color, with sound (NASA-TM-109433; NONP-VT-93-190230) Avail: CASI VHS A01/BETA A22

This is a video orientation to the Challenger Center for Space Science Education in Prince Georges County, Maryland. CASI

N94-15719*# Massachusetts Univ., Amherst. Dept. of Computer Science.
REPRESENTATION IN INCREMENTAL LEARNING
1993 4 p
(Contract NCC2-658)
(NASA-CR-194595; NAS 1.26:194595) Avail: CASI HC A01/MF A01

Work focused on two areas in machine learning: representation for inductive learning and how to apply concept learning techniques to learning state preferences, which can represent search control knowledge for problem solving. Specifically, in the first area the issues of the effect of representation on learning, on how learning formalisms are biased, and how concept learning can benefit from the use of a hybrid formalism are addressed. In the second area, the issues of developing an agent to learn search control knowledge from the relative values of states, of the source of that qualitative

information, and of the ability to use both quantitative and qualitative information in order to develop an effective problem-solving policy are examined. Author (revised)

N94-17261# Wichita State Univ., KS. National Inst. for Aviation Research.
MAXIMIZING PARTICIPATION OF WOMEN IN COLLEGIATE AVIATION EDUCATION Ph.D. Thesis
Jacqueline R. Luedtke Jul. 1993 112 p
(NIAR-93-14) Avail: CASI HC A06/MF A02

The purpose of this study is to collect and analyze information which can be used to examine the reasons for the seemingly low number of women in the United States' collegiate aviation educational system. With ever-increasing global competition, it is vital to assist all qualified persons in the aviation field to succeed in their chosen area of this profession. Only by utilizing all trained persons, men and women, will the United States remain competitive in aviation. With women comprising such a large percentage of the work force, it is only logical to employ the best and brightest of both genders to accomplish this goal. Data will be collected directly from program directors and/or aviation faculty at each participating member institution in the UAA with a four-year degree program in aviation. These directors and faculty members can offer insight into whether or not women are, in fact, under-represented in higher aviation education, and, if so, what they believe can be done to rectify this situation. They will be able to evaluate the status of aviation education and what the future needs might be. This research endeavor will attempt to determine what progress has been made in recent years to increase the percentage of women in collegiate aviation education. Both factual data and perceptions from the respondents will be acquired. By analyzing the history of women aviation educators, this study hopes to offer means of maximizing participation of women in collegiate aviation education. Recommendations for improvements which will allow the integration of women more readily into this field will be sought. The information gathered through this study will allow persons in higher aviation education at all colleges and universities and at the University Aviation Association to better understand the role women should be playing in this field. Such information will also be useful to the aviation industry at large as women become a larger force in this area of study and expertise. Author

N94-17441* National Aeronautics and Space Administration, Washington, DC.
THE IMPACT OF INDUSTRY/UNIVERSITY CONSORTIA PROGRAMS ON SPACE EDUCATION
John R. Page (New South Wales Univ., Kensington, Australia.) and Barbara A. Stone 1993 7 p Presented at the 44th Congress of the IAF Symposium on Space and Education, Graz, Austria, 16-22 Oct. 1993
(NASA-TM-109340; NAS 1.15:109340; IAF-93-P.2.365) Copyright Avail: Issuing Activity

Australia and the United States have each established industry/university consortia programs to facilitate and promote the development of their space industry. The universities also benefit from being involved in the discipline associated with real commercial space projects and access to current industrial practice. Generically, the consortia are composed of universities and companies seeking to identify and exploit potentially commercially-significant technologies. Australia has two programs: Space Industry Development Centers (spacebased technologies) and Cooperative Research Centers (not limited to space research but including Centers with a space interest). In the United States, the Centers for the Commercial Development of Space Program was established in 1985 to stimulate interest and expand private sector investment in commercial space activities. This paper examines these programs from the standpoint of their impact on space education in their respective counties. Author

N94-15130# Haarlem Univ. (Netherlands).
DEVELOPMENTS IN THE HIGHER TECHNICAL AEROSPACE EDUCATION [ONTWIKKELINGEN IN HET VLIEGTUIGBOUWKUNDIG HOGER TECHNISCH ONDERWIJS]
P. J. L. M. vanderZanden *In* NAL, Symposium on the Future of Aeronautics in the Netherlands 1991 12 p In DUTCH (For primary document see N94-15120 03-01)
Avail: CASI HC A03/MF A02

N94-15131# Technische Univ., Delft (Netherlands). Faculteit der Luchtvaart- en Ruimtevaarttechniek.
EXPECTATIONS FOR THE FUTURE OF THE FACULTY OF AERONAUTICS AND ASTRONAUTICS OF THE TECHNICAL UNIVERSITY OF DELFT [TOEKOMSTVERWACHTINGEN FACULTEIT DER LUCHTVAART- EN RUIMTEVAARTTECHNIEK TU-DELFT]
T. deJong *In* NAL, Symposium on the Future of Aeronautics in the Netherlands 1991 9 p In DUTCH (For primary document see N94-15120 03-01)
Avail: CASI HC A02/MF A02

N94-16346*# Arizona Univ., Tucson. Lunar and Planetary Lab.
TEACHING PLANETARY SCIENCES TO ELEMENTARY SCHOOL TEACHERS: PROGRAMS THAT WORK Abstract Only
Larry A. Lebofsky and Nancy R. Lebofsky *In* Lunar and Planetary Inst., Twenty-Fourth Lunar and Planetary Science Conference. Part 2: G-M 1993 p 859 (For primary document see N94-16173 03-91)
Avail: CASI HC A01/MF A06

N94-16356*# National Aeronautics and Space Administration. Lyndon B. Johnson Space Center, Houston, TX.
SPACESHIP EARTH: A PARTNERSHIP IN CURRICULUM WRITING Abstract Only
Marilyn M. Lindstrom *In* Lunar and Planetary Inst., Twenty-Fourth Lunar and Planetary Science Conference. Part 2: G-M 1993 p 879 (For primary document see N94-16173 03-91)
Avail: CASI HC A01/MF A06

N94-16618*# Harvard School of Public Health, Boston, MA.
EDUCATION AND TRAINING OF PROFESSIONAL INDUSTRIAL HYGIENISTS FOR 2020
R. J. Sherwood *In* BioTechnology, Inc., Proceedings of the 1992 Annual Meeting NASA Occupational Health Program Jul. 1993 p 99-120 (For primary document see N94-16609 03-52)
Avail: CASI HC A03/MF A03

81 ADMINISTRATION AND MANAGEMENT

Includes management planning and research.

N94-15213# Carnegie-Mellon Univ., Pittsburgh, PA. Robotics Inst.
HSTS: INTEGRATING PLANNING AND SCHEDULING
Nicola Muscettola Mar. 1993 40 p
(Contract F30602-91-F-0016)
(AD-A266991; CMU/RI-TR-93-05) Avail: CASI HC A03/MF A01

In the traditional approach to managing complex systems, planning and scheduling are two very distinct phases. However, in a wide variety of applications this strict separation is not possible or beneficial. During scheduling it is often necessary to make planning decisions (plan the setup of a machine); moreover planning decisions can benefit from scheduling information (choose a process plan depending on resource loads). HSTS (Heuristic Scheduling Testbed System) is a representation and problem solving framework that provides an integrated view of planning and scheduling. HSTS emphasizes the decomposition of a domain into state variables evolving over continuous time. This allows the description and manipulation of resources far more complex than it is possible in classical scheduling. The inclusion of time and resource capacity into the description of causal justifications allows a fine-grain integration of planning and scheduling and a better adaptation to problem and domain structure. HSTS puts special emphasis on leaving as much temporal flexibility as possible during the planning/scheduling process to generate better plan/schedules with less computation effort. Within the HSTS framework we have implemented several planning/scheduling systems. In the paper we describe an integrated planner and scheduler for short term scheduling of the Hubble Space Telescope. This system has demonstrated the ability to deal effectively with all of the important constraints of the domain. Experimental results show that executable schedules for Hubble can be built in a time compatible with operational needs. The paper also describes a methodology for job-shop scheduling problems. The methodology exploits the temporal flexibility provided by HSTS. DTIC

N94-15234* National Aeronautics and Space Administration. Marshall Space Flight Center, Huntsville, AL.
RETURN TO FLIGHT 1 (Videotape)
Sep. 1987 Videotape: 17 min. 21 sec. playing time, in color, with sound (NASA-TM-109663; NONP-VT-93-190461) Avail: CASI VHS A01/BETA A22

This video tape presents a dynamic overview of the hard work and tireless efforts of NASA employees and contractors. CASI

N94-15293* National Aeronautics and Space Administration. Goddard Space Flight Center, Greenbelt, MD.
PET TEAM (Videotape)
Mar. 1989 Videotape: 15 min. playing time, in color, with sound (NASA-TM-109599; NONP-VT-93-190397) Avail: CASI VHS A01/BETA A22

This videotape shows the Productivity Enhancement Team's (PET) presentation to management regarding ways to make the workforce more responsive to overall corporate goals. CASI

N94-15319* National Aeronautics and Space Administration. Marshall Space Flight Center, Huntsville, AL.
RETURN TO FLIGHT 3, THE JOURNEY CONTINUES (Videotape)
Feb. 1989 Videotape: 15 min. 17 sec. playing time, in color, with sound (NASA-TM-109651; NONP-VT-93-190449) Avail: CASI VHS A01/BETA A22

This videotape presents a dynamic overview of the hard work and tireless efforts of NASA employees and contractors. CASI

N94-15367* National Aeronautics and Space Administration. Lyndon B. Johnson Space Center, Houston, TX.
COHEN PROGRAM MANAGEMENT BRIEFING (Videotape)
Dec. 1989 Videotape: 55 min. playing time, in color, with sound (NASA-TM-109536; NONP-VT-93-190333) Avail: CASI VHS A01/BETA A22

Dr. Aaron Cohen, Director of NASA Johnson Space Center, discusses management issues as they have appeared in the manned space flight programs. CASI

N94-15545*# National Aeronautics and Space Administration. John F. Kennedy Space Center, Cocoa Beach, FL.
SPACE STATION FACILITY GOVERNMENT ESTIMATING
Joseph A. Brown 1993 26 p Presented at the Florida Chapter, Orlando, FL, 8 Oct. 1993
(NASA-TM-109324; NAS 1.15:109324) Avail: CASI HC A03/MF A01

This new, unique Cost Engineering Report introduces the 800-page, C-100 government estimate for the Space Station Processing Facility (SSPF) and Volume IV Aerospace Construction Price Book. At the January 23, 1991, bid opening for the SSPF, the government cost estimate was right on target. Metric, Inc., Prime Contractor, low bid was 1.2 percent below the government estimate. This project contains many different and complex systems. Volume IV is a summary of the cost associated with construction, activation and Ground Support Equipment (GSE) design, estimating, fabrication, installation, testing, termination, and verification of this project. Included are 13 reasons the government estimate was so accurate; abstract of bids, for 8 bidders and government estimate with additive alternates, special labor and materials, budget comparison and system summaries; and comments on the energy credit from local electrical utility. This report adds another project to our continuing study of 'How Does the Low Bidder Get Low and Make Money?' which was started in 1967, and first published in the 1973 AACE Transaction with 18 ways the low bidders get low. The accuracy of this estimate proves the benefits of our Kennedy Space Center (KSC) teamwork efforts and KSC Cost Engineer Tools which are contributing toward our goals of the Space Station. Author (revised)

N94-15546*# National Aeronautics and Space Administration. Lyndon B. Johnson Space Center, Houston, TX.
ESTIMATING AND BIDDING FOR THE SPACE STATION PROCESSING FACILITY
Joseph A. Brown 1993 29 p Presented at the AACE International 37th Annual Meeting, Dearborn, MI, 11-14 Jul. 1993
(NASA-TM-109323; NAS 1.15:109323) Avail: CASI HC A03/MF A01

This new, unique Cost Engineering Report introduces the 800-page, C-100 government estimate for the Space Station Processing Facility (SSPF) and Volume IV Aerospace Construction Price Book. At the January 23, 1991, bid opening for the SSPF, the government cost estimate was right on target. Metric, Inc., Prime Contractor, low bid was 1.2 percent below the government estimate. This project contains many different and complex systems. Volume IV is a summary of the cost associated with construction, activation and Ground Support Equipment (GSE) design, estimating, fabrication, installation, testing, termination, and verification of this project. Included are 13 reasons the government estimate was so accurate; abstract of bids, for 8 bidders and government estimate with additive alternates, special labor and materials, budget comparison and system summaries; and comments on the energy credit from local electrical utility. This report adds another project to our continuing study of 'How Does the Low Bidder Get Low and Make Money?' which was started in 1967, and first published in the 1973 AACE Transaction with 10 more ways the low bidder got low. The accuracy of this estimate proves the benefits of our Kennedy Space Center (KSC) teamwork efforts and KSC Cost Engineer Tools which are contributing toward our goals of the Space Station. Author (revised)

N94-15682# Defense Personnel Security Research Centre, Monterey, CA.
THE IMPACT OF REPORT OF INVESTIGATION WRITING STYLE ON THE ASSESSMENT TIMES, IMPRESSIONS, PERCEPTIONS AND PREFERENCES OF ADJUDICATORS Technical Report
James E. Suchan (Naval Postgraduate School, Monterey, CA.) and Mark LaViolette Jan. 1993 95 p
(AD-A265748; PERS-TR-93-003) Avail: CASI HC A05/MF A01

This report examines the effect of style of written communication on processing of information and readers' perceptions of the writer. Forty senior adjudicators from four sites reviewed two cases containing significant derogatory information. The reports of investigation (ROI's) were written in two styles: high- and low-impact. High-impact reports were designed to facilitate information processing through structural and stylistic features such as lists, bullets, active verbs and subject-verb-object sentence construction. The results show that adjudicators prefer a high-impact ROI for its presentation of information, ease of reading, remembering and applying adjudication criteria, and limited amount of re-reading. With the high-impact ROI adjudicators also formed a more favorable impression of the quality of investigation and the competence of field agents. There was no evidence of a shorter reading time for high-impact ROI's. DTIC

N94-15782*# National Aeronautics and Space Administration, Washington, DC.
NASA TREND ANALYSIS PROCEDURES
Oct. 1993 71 p
(NASA-RP-1290; NAS 1.61:1290) Avail: CASI HC A04/MF A01

This publication is primarily intended for use by NASA personnel engaged in managing or implementing trend analysis programs. 'Trend analysis' refers to the observation of current activity in the context of the past in order to infer the expected level of future activity. NASA trend analysis was divided into 5 categories: problem, performance, supportability, programmatic, and reliability. Problem trend analysis uncovers multiple occurrences of historical hardware or software problems or failures in order to focus future corrective action. Performance trend analysis observes changing levels of real-time or historical flight vehicle performance parameters such as temperatures, pressures, and flow rates as compared to specification or 'safe' limits. Supportability trend analysis assesses the adequacy of the spaceflight logistics system; example indicators are repair-turn-around time and parts stockage levels. Programmatic trend analysis uses quantitative indicators to evaluate the 'health' of NASA programs of all types. Finally, reliability trend analysis attempts to evaluate the growth of system reliability based on a decreasing rate of occurrence of hardware problems over time. Procedures for conducting all five types of trend analysis are provided in this publication, prepared through the joint efforts of the NASA Trend Analysis Working Group. Author (revised)

N94-15931*# National Aeronautics and Space Administration, Washington, DC.
PERMANENT CHANGE OF STATION: THE NASA EMPLOYEE'S GUIDE TO AN EASIER MOVE
Apr. 1993 68 p
(NHB-9760.1A; NAS 1.18:9760.1A) Avail: CASI HC A04/MF A01

This guide is for the NASA employee preparing to make a permanent change of station. Whether a transferee or a new appointee, this guide contains information that will help a Government-authorized move go more smoothly from start to finish. The guide outlines the allowances and expense reimbursements one is entitled to under Federal Travel Regulations (FTR). It provides samples of forms one may need to fill out to start the transfer rolling and to claim reimbursements. However, it is important to note that this guide is not a copy of the FTR. Information in the FTR and the NASA Travel Regulations, FMM 9760, is far more detailed and is always updated and correct. Derived from text

N94-15934*# National Aeronautics and Space Administration, Washington, DC.

FACILITIES MAINTENANCE HANDBOOK

Dec. 1991 283 p

(NHB-8831.2; NAS 1.18:8831.2) Avail: CASI HC A13/MF A03

This handbook is a guide for facilities maintenance managers. Its objective is to set minimum facilities maintenance standards. It also provides recommendations on how to meet the standards to ensure that NASA maintains its facilities in a manner that protects and preserves its investment in the facilities in a cost-effective manner while safely and efficiently performing its mission. This handbook implements NMI 8831.1, which states NASA facilities maintenance policy and assigns organizational responsibilities for the management of facilities maintenance activities on all properties under NASA jurisdiction. It is a reference for facilities maintenance managers, not a step-by-step procedural manual. Because of the differences in NASA Field Installation organizations, this handbook does not assume or recommend a typical facilities maintenance organization. Instead, it uses a systems approach to describe the functions that should be included in any facilities maintenance management system, regardless of its organizational structure. For documents referenced in the handbook, the most recent version of the documents is applicable. This handbook is divided into three parts: Part 1 specifies common definitions and facilities maintenance requirements and amplifies the policy requirements contained in NMI 8831. 1; Part 2 provides guidance on how to meet the requirements of Part 1, containing recommendations only; Part 3 contains general facilities maintenance information. One objective of this handbook is to fix commonality of facilities maintenance definitions among the Centers. This will permit the application of uniform measures of facilities conditions, of the relationship between current replacement value and maintenance resources required, and of the backlog of deferred facilities maintenance. The utilization of facilities maintenance system functions will allow the Centers to quantitatively define maintenance objectives in common terms, prepare work plans, and develop management information in order to statistically identify and analyze variances from those plans. It will also add credibility to the NASA facilities maintenance budgeting process. The key to a successful maintenance program is the understanding and support of the senior Center managers. Derived from text

N94-15937*# National Aeronautics and Space Administration, Washington, DC.

NASA SECURITY HANDBOOK

Feb. 1993 361 p

(NHB-1620.3C; NAS 1.18:1620.3C) Avail: CASI HC A16/MF A03

This 'NASA Security Handbook' provides basic information regarding the assignment of individual security responsibilities within NASA. It sets forth minimum standards, procedures, specifications, and guidelines for the protection of classified information, material, facilities, and property in the possesion of NASA. It expands upon and further specifies NASA security policy spelled out in NMI 1600.2. This Handbook implements the provisions of Executive Order 12356, 'National Security Information,' dated April 2, 1982, 'Information Security Oversight Office Directive No. 1 Concerning National Security Information,' dated June 25, 1982, Executive Order 10450, 'Security Requirements for Government Employees' dated April 27, 1953, and the Federal Personnel Manual, Chapters 731, 732, and 736.

Derived from text

N94-15939*# National Aeronautics and Space Administration, Washington, DC.

INDUSTRIAL LABOR RELATIONS MANUAL

Nov. 1992 50 p

(NHB-5200.1B; NAS 1.18:5200.1B) Avail: CASI HC A03/MF A01

The NASA Industrial Labor Relations Manual provides internal guidelines and procedures to assist NASA Field Installations in dealing with contractor labor management disputes, Service Contract Act variance hearings, and to provide access of Labor Union Representatives to NASA for the purpose of maintaining schedules and goals in connection with vital NASA programs. This manual will be revised by page changes as revisions become necessary. Initial distribution of this manual has been made to NASA Headquarters and Field Installations. Derived from text

N94-15944*# National Aeronautics and Space Administration, Washington, DC.

THE NASA COMPETITIVE PLACEMENT PLAN FOR POSITIONS GS-15 AND BELOW (INCLUDING TRADES AND LABOR POSITIONS)

1 Feb. 1993 19 p

(NHB-3335.1C; NAS 1.18:3335.1C) Avail: CASI HC A03/MF A01

This plan provides the framework for selection based on merit from among the best qualified candidates available. Selections will be made without regard to political, religious, or labor organization affiliation or nonaffiliation, marital status, race, color, sex, national origin, nondisqualifying disability, or age. This plan does not guarantee promotion but rather ensures that all qualified available candidates receive fair and equitable consideration for positions filled under these competitive procedures. Announcing a vacancy under this plan is only one method of locating applicants for a position and can be used in conjunction with other methods. Subject to applicable law and regulation, selection of an individual to fill a position is the decision of management, as is the decision as to the method(s) to be used in identifying candidates. This plan is applicable to all NASA Installations. It covers all positions in the competitive service at (and below) the GS/GM-15 level (including all trades and labor positions), except positions in the Office of the Inspector General. The requirements herein are not intended to, nor should they be construed to limit in any way, the independent personnel authority of the Inspector General under the Inspector General Act, as Amended. Derived from text

N94-15945*# National Aeronautics and Space Administration, Washington, DC.

THE SENIOR EXECUTIVE SERVICE

Dec. 1992 42 p

(NHB-3100.6; NAS 1.18:3100.6) Avail: CASI HC A03/MF A01

A major innovation of the Civil Service Reform Act of 1978 was the creation of a Senior Executive Service (SES). The purpose of the SES is both simple and bold: to attract executives of the highest quality into Federal service and to retain them by providing outstanding opportunities for career growth and reward. The SES is intended to: provide greater authority in managing executive resources; attract and retain highly competent executives, and assign them where they will effectively accomplish their missions and best use their talents; provide for systematic development of executives; hold executives accountable for individual and organizational performance; reward outstanding performers and remove poor performers; and provide for an executive merit system free of inappropriate personnel practices and arbitrary actions. This Handbook summarizes the key features of the SES at NASA. It is intended as a special welcome to new appointees and also as a general reference document. It contains an overview of SES management at NASA, including the Executive Resources Board and the Performance Review Board, which are mandated by law to carry out key SES functions. In addition, assistance is provided by a Senior Executive Committee in certain reviews and decisions and by Executive Position Managers in day-to-day administration and oversight. Derived from text

N94-15957*# National Aeronautics and Space Administration, Washington, DC.

EQUIPMENT MANAGEMENT USER'S HANDBOOK FOR PROPERTY CUSTODIANS

Mar. 1993 86 p

(NHB-4200.2A; NAS 1.18:4200.2A) Avail: CASI HC A05/MF A01

The NASA Equipment Management User's Handbook for Property Custodians is issued as an instructional guide for personnel designated as property custodians and technical personnel involved in the acquisition, management, and use of NASA-owned equipment. This handbook provides general information and basic operational procedures for processing equipment transactions through the agency-wide NASA Equipment Management System (NEMS). Each NASA installation must prepare

supplementary instructions for local requirements beyond the scope of NASA-wide policies and procedures contained herein, or as specified for local implementation in NHB 4200.1, 'NASA Equipment Management Manual.' NHB 4200.1 sets forth policy, uniform performance standards, and procedural guidance to NASA personnel for the acquisition, management, and use of NASA-owned equipment. This handbook is a controlled document, issued in loose-leaf form and revised by page changes. Additional copies for internal use may be obtained through normal distribution. Author (revised)

N94-16473 Army Engineer Studies Center, Fort Belvoir, VA.
DESIGN QUALITY TASK FORCE SURVEY COMMENTS Final Report, Feb. - Apr. 1992
Larry Lang May 1993 64 p Limited Reproducibility: More than 20% of this document may be affected by microfiche quality
(AD-A266283; CETEC-ES-P-93-7) Avail: CASI HC A04

In November 1991, the U.S. Army Corps of Engineers (USACE) commissioned a Design Quality Task Force (DQTF). Its objective was to identify problems with, and recommend improvements in the quality of, design products in the Corps' Engineering Divisions. As part of this overall effort, the Engineer Strategic Studies Center (ESSC) performed a comprehensive district-level survey in Feb. 1992 to assess the importance of issues and the Corps' perception of where it is performing today on these issues. The questionnaire collected data by program (Civil Works and Military Construction), by function (Planning, Construction, Program and Project Management (PPM), Operations, and Engineering), and by position (Division Chief, Branch/Section Chief, or Journeyman). Approximately one-third of the 1231 people who returned questionnaires wrote in optional comments. This report contains verbatim comments from the questionnaire forms. The report has a section for each function, and comments for each function are sorted by position. These comments provide grass roots insight into Design Quality in USACE. DTIC

N94-16593# European Space Agency. European Space Research and Technology Center, ESTEC, Noordwijk (Netherlands).
THE EARLY ACTIVITIES OF THE COPERS AND THE DRAFTING OF THE ESRO CONVENTION (1961/62)
John Krige Jan. 1993 47 p
(ESA-HSR-4) Avail: CASI HC A03/MF A01

The aim of this report is to describe the main activities of these two groups, particularly in so far as they bore on the drafting of the convention of the new European Space Research Organization (ESRO). This convention was laid before an intergovernmental conference in Paris on 14 and 15 June 1962. By restricting our time span and our subject matter in this way we do not, of course, deal with all matters handled by the working groups in this period, and not by the LAFWG in particular (staff policy and internal structure, privileges and immunities, etc.). We do, however, throw into relief the most significant issues which were 'settled' in the run up to the signature of the convention, so exploring in depth the history of some key clauses in that important legal document. Derived from text

N94-16729*# National Aeronautics and Space Administration, Washington, DC.
MISSION MANAGEMENT AIRCRAFT OPERATIONS MANUAL
Mar. 1992 75 p
(NHB-7900.3; NAS 1.18:7900.3) Avail: CASI HC A04/MF A01

This manual prescribes the NASA mission management aircraft program and provides policies and criteria for the safe and economical operation, maintenance, and inspection of NASA mission management aircraft. The operation of NASA mission management aircraft is based on the concept that safety has the highest priority. Operations involving unwarranted risks will not be tolerated. NASA mission management aircraft will be designated by the Associate Administrator for Management Systems and Facilities. NASA mission management aircraft are public aircraft as defined by the Federal Aviation Act of 1958. Maintenance standards, as a minimum, will meet those required for retention of Federal Aviation Administration (FAA) airworthiness certification. Federal Aviation Regulation Part 91, Subparts A and B, will apply except when requirements of this manual are more restrictive. Derived from text

N94-16730*# National Aeronautics and Space Administration, Washington, DC.
AIRCRAFT OPERATIONS MANAGEMENT MANUAL
Mar. 1992 80 p
(NHB-7900.3(V1); NAS 1.18:7900.3(V1)) Avail: CASI HC A05/MF A01

The NASA aircraft operations program is a multifaceted, highly diverse entity that directly supports the agency mission in aeronautical research and development, space science and applications, space flight, astronaut readiness training, and related activities through research and development, program support, and mission management aircraft operations flights. Users of the program are interagency, inter-government, international, and the business community. This manual provides guidelines to establish policy for the management of NASA aircraft resources, aircraft operations, and related matters. This policy is an integral part of and must be followed when establishing field installation policy and procedures covering the management of NASA aircraft operations. Each operating location will develop appropriate local procedures that conform with the requirements of this handbook. This manual should be used in conjunction with other governing instructions, handbooks, and manuals. Author

N94-16799*# National Aeronautics and Space Administration, Washington, DC.
EQUIPMENT MANAGEMENT MANUAL
1 Apr. 1992 222 p
(NHB-4200.1D; NAS 1.18:4200.1D) Avail: CASI HC A10/MF A03

The NASA Equipment Management Manual (NHB 4200.1) is issued pursuant to Section 203(c)(1) of the National Aeronautics and Space Act of 1958, as amended (42 USC 2473), and sets forth policy, uniform performance standards, and procedural guidance to NASA personnel for the acquisition, management, and use of NASA-owned equipment. This revision is effective upon receipt. This is a controlled manual, issued in loose-leaf form, and revised through page changes. Additional copies for internal use may be obtained through normal distribution. Author

N94-16830*# National Aeronautics and Space Administration, Washington, DC.
MATERIALS INVENTORY MANAGEMENT MANUAL
Mar. 1992 88 p
(NHB-4100.1C; NAS 1.18:4100.1C) Avail: CASI HC A05/MF A01

This NASA Materials Inventory Management Manual (NHB 4100.1) is issued pursuant to Section 203(c)(1) of the National Aeronautics and Space Act of 1958 (42 USC 2473). It sets forth policy, performance standards, and procedures governing the acquisition, management and use of materials. This Manual is effective upon receipt. Derived from text

N94-16907*# National Aeronautics and Space Administration, Washington, DC.
RESEARCH GRANT HANDBOOK
1 Dec. 1993 52 p
(NHB-5800.1C; NAS 1.18:5800.1C) Avail: CASI HC A04/MF A01

This handbook prescribes policies and procedures relating to the award and administration of NASA research grants and cooperative agreements with educational institutions and other nonprofit organizations. The handbook is divided into six subparts: (1) general; (2) definitions; (3) the process; (4) provisions and special conditions; (5) administration; and (6) reports. The appendix includes a listing of exhibits. Author (revised)

N94-16001# Krupp (Fried.) G.m.b.H., Essen (Germany).
RESEARCH AND DEVELOPMENT: ENGINE OF INNOVATION AT KRUPP
Diethard Bergers *In its* Krupp Technical Reports No. 2, English Edition, October 1992 Oct. 1992 p 63-68 (For primary document see N94-16000 03-31)
Copyright Avail: CASI HC A02/MF A01

N94-16134# Boeing Co., Huntsville, AL.
GOVERNMENT/CONTRACTOR DEVELOPMENT TEAMS
James P. Noblitt *In* Huntsville Association of Technical Societies, TABES 1993: 9th Annual Technical and Business Exhibition and Symposium 1993 5 p (For primary document see N94-16129 03-38)
(TABES Paper 93-460) Avail: CASI HC A01/MF A03

N94-16147# Paramax Systems Corp., Huntsville, AL.
APPLYING PAPERLESS TECHNOLOGY TO ACHIEVE EXCELLENCE IN MANUFACTURING OPERATIONS
Michael Denson and Craig Lykins *In* Huntsville Association of Technical Societies, TABES 1993: 9th Annual Technical and Business Exhibition and Symposium 1993 6 p (For primary document see N94-16129 03-38)
(TABES Paper 93-630) Avail: CASI HC A02/MF A03

82 DOCUMENTATION AND INFORMATION SCIENCE

Includes information management; information storage and retrieval technology; technical writing; graphic arts; and micrography.

For computer documentation see *61 Computer Programming and Software*.

N94-14981*# Arizona Univ., Tucson. Optical Sciences Center.
RESEARCH STUDIES ON ADVANCED OPTICAL MODULE/HEAD DESIGNS FOR OPTICAL DISK RECORDING DEVICES
James J. Burke and Bernard D. Seery 15 Mar. 1993 168 p
(Grant NAG5-1346)
(NASA-CR-194390; NAS 1.26:194390) Avail: CASI HC A08/MF A02

The Annual Report of the Optical Data Storage Center of the University of Arizona is presented. Summary reports on continuing projects are presented. Research areas include: magneto-optic media, optical heads, and signal processing. For individual titles, see N94-14982 through N94-14997.

N94-14982*# Arizona Univ., Tucson.
MAGNETO-OPTIC SUPERLATTICE THIN FILMS: FABRICATION, STRUCTURAL AND MAGNETIC CHARACTERIZATION **c27**
C. M. Falco, B. N. Engel, R. A. VanLeeuwen, and J. Yu *In its* Research Studies on Advanced Optical Module/Head Designs for Optical Disk Recording Devices p3-5 (SEE N94-14981 03-82) 15 Mar. 1993 (For primary document see N94-14981 03-82)
Avail: CASI HC A01/MF A02

During this quarter studies were extended to determine the electronic contribution to the perpendicular interface anisotropy in Co-based multilayers. Using in situ Kerr effect measurements, the influences of different transition metals (TM = Ag, Au, Cu, and Pd) on the magnetic properties of single-crystal Co films grown on Pd (111) and Au (111) surfaces are investigated. Last quarter the discovery of a large peak in the perpendicular anisotropy when approximately one monolayer of Cu or Ag is deposited on the Co surface was reported. We now have added a computer-controlled stepper-motor drive to our MBE sample transfer mechanism. The motor allows us to move the sample at a constant velocity from behind a shutter during deposition. The film, therefore, is deposited as a wedge with a linear variation of thickness across the substrate. In this way, a continuous range of coverage on a single sample is studied. The stepper motor also provides the necessary control for precisely positioning the sample in the laser beam for Kerr effect measurements at the different coverages.
Author (revised)

N94-14983*# Arizona Univ., Tucson.
CHARACTERIZATION FACILITY FOR MAGNETO-OPTIC MEDIA AND SYSTEMS
M. Mansuripur, H. Fu, S. Gadetsky, S. Sugaya, T. H. Wu, J. Zambuto, R. Gerber, T. Goodman, and J. K. Erwin *In its* Research Studies on Advanced Optical Module/Head Designs for Optical Disk Recording Devices 15 Mar. 1993 p 7-9 (For primary document see N94-14981 03-82)
Avail: CASI HC A01/MF A02

Objectives of this research are: (1) to measure the hysteresis loop, Kerr rotation angle, anisotropy energy profile, Hall voltage, and magnetoresistance of thin-film magneto-optic media using our loop-tracer; (2) measure the wavelength-dependence of the Kerr rotation angle, Theta(sub k), and ellipticity, epsilon(sub k), for thin-film media using our magneto-optic Kerr spectrometer (MOKS); (3) measure the dielectric tensor of thin-film and multilayer samples using our variable-angle magneto-optic ellipsometer (VAMOE); (4) measure the hysteresis loop, coercivity, remanent magnetization, saturation magnetization, and anisotropy energy constant for thin film magnetic media using vibrating sample magnetometry; (5) observe small magnetic domains and investigate their interaction with defects using magnetic force microscopy; (6) perform static read/write/erase experiments on thin-film magneto-optic media using our static test station; (7) integrate the existing models of magnetization, magneto-optic effects, coercivity, and anisotropy in an interactive and user-friendly environment, and analyze the characterization data obtained in the various experiments, using this modeling package; (8) measure focusing- and tracking-error signals on a static testbed, determine the 'feedthrough' for various focusing schemes, investigate the effects of polarization and birefringence, and compare the results with diffraction-based calculations; and (9) measure the birefringence of optical disk substrates using two variable angle ellipsometers.
Author (revised)

N94-14984*# Arizona Univ., Tucson.
MeV ION-BEAM ANALYSIS OF OPTICAL DATA STORAGE FILMS
J. A. Leavitt, L. C. McIntyre, Jr., and Z. Lin *In its* Research Studies on Advanced Optical Module/Head Designs for Optical Disk Recording Devices 15 Mar. 1993 p 11-13 (For primary document see N94-14981 03-82)
Avail: CASI HC A01/MF A02

Our objectives are threefold: (1) to accurately characterize optical data storage films by MeV ion-beam analysis (IBA) for ODSC collaborators; (2) to develop new and/or improved analysis techniques; and (3) to expand the capabilities of the IBA facility itself. Using H-1(+), He-4(+), and N-15(++) ion beams in the 1.5 MeV to 10 MeV energy range from a 5.5 MV Van de Graaff accelerator, film thickness (in atoms/sq cm), stoichiometry, impurity concentration profiles, and crystalline structure were determined by Rutherford backscattering (RBS), high-energy backscattering, channeling, nuclear reaction analysis (NRA) and proton induced X-ray emission (PIXE). Most of these techniques are discussed in detail in the ODSC Annual Report (February 17, 1987), p. 74. The PIXE technique is briefly discussed in the ODSC Annual Report (March 15, 1991), p. 23.
Author (revised)

N94-14985*# Arizona Univ., Tucson.
APPLICATION OF HOLOGRAPHIC OPTICAL ELEMENTS TO MAGNETO-OPTIC READ/WRITE HEADS
R. K. Kostuk, E. Campbell, and T. Kim *In its* Research Studies on Advanced Optical Module/Head Designs for Optical Disk Recording Devices 15 Mar. 1993 p 15-18 (For primary document see N94-14981 03-82)
Avail: CASI HC A01/MF A02

Objectives of this research are to determine the theoretical and practical performance limits of holographic optical elements (HOE's) formed in different recording materials, and to evaluate the application of these components to magneto-optic read/write heads.
Author (revised)

N94-14986*# Arizona Univ., Tucson.
DYNAMIC TESTBED LABORATORY AND MICRO-OPTICS **c74**
T. Milster, K. Erwin, F. Froehlich, J. Kann, W. Li, W. Schlichting, R. Shetty, E. Walker, and M. Wang *In its* Research Studies on Advanced Optical Module/Head Designs for Optical Disk Recording Devices 15 Mar. 1993 p 19-23 (For primary document see N94-14981 03-82)
Avail: CASI HC A01/MF A02

Objectives of this research are as follows: to understand the three classes of superresolution and their behavior in optical data storage systems; to investigate new and improved components and techniques in the optical system for data detection and servo control; to apply micro-optic components to the optical system to reduce size and weight; to investigate techniques, such as near-field optical probes, for recording data densities beyond that possible with superresolution; and to understand and find solutions for problems associated with dynamic testing, especially those that arise when evaluating blue-sensitive media.
Author (revised)

N94-14987*# Arizona Univ., Tucson.
GRATINGS AND WAVEGUIDES
K. A. Bates, J. K. Erwin, L. Li, J. J. Burke, and N. Ramanujam *In its* Research Studies on Advanced Optical Module/Head Designs for Optical Disk Recording Devices 15 Mar. 1993 p 25-26 (For primary document

see N94-14981 03-82)
Avail: CASI HC A01/MF A02

Our immediate objective is to understand the limitations of guided-wave and grating coupler devices in their application to optical data storage. Our long-range goal is to develop and validate design codes for integrated optic devices. The principal research activity was in the development of numerical models for the design of a blue wavelength integrated optical source for data storage applications. Author (revised)

N94-14988*# Arizona Univ., Tucson.
COMPACT DISK ERROR MEASUREMENTS
D. Howe, K. Harriman, and B. Tehranchi *In its* Research Studies on Advanced Optical Module/Head Designs for Optical Disk Recording Devices 15 Mar. 1993 p 27-31 (For primary document see N94-14981 03-82)
Avail: CASI HC A01/MF A02

The objectives of this project are as follows: provide hardware and software that will perform simple, real-time, high resolution (single-byte) measurement of the error burst and good data gap statistics seen by a photoCD player read channel when recorded CD write-once discs of variable quality (i.e., condition) are being read; extend the above system to enable measurement of the hard decision (i.e., 1-bit error flags) and soft decision (i.e., 2-bit error flags) decoding information that is produced/used by the Cross Interleaved - Reed - Solomon - Code (CIRC) block decoder employed in the photoCD player read channel; construct a model that uses data obtained via the systems described above to produce meaningful estimates of output error rates (due to both uncorrected ECC words and misdecoded ECC words) when a CD disc having specific (measured) error statistics is read (completion date to be determined); and check the hypothesis that current adaptive CIRC block decoders are optimized for pressed (DAD/ROM) CD discs. If warranted, do a conceptual design of an adaptive CIRC decoder that is optimized for write-once CD discs. Author (revised)

N94-14989*# Arizona Univ., Tucson.
MEASUREMENT OF BIREFRINGENCE FOR OPTICAL RECORDING DISK SUBSTRATES
Hong Fu, S. Sugaya (Nippon Electric Co. Ltd., Japan.), J. K. Erwin, T. Goodman, Z. Yan, W. J. Tang, and M. Mansuripur *In its* Research Studies on Advanced Optical Module/Head Designs for Optical Disk Recording Devices 15 Mar. 1993 p 37-75 (For primary document see N94-14981 03-82)
Avail: CASI HC A03/MF A02

The birefringence of bare and coated substrates for magneto-optical recording is experimentally investigated using ellipsometry at the wavelengths of 632.8 nm and 780 nm. The rotation and ellipticity of the polarization state of the reflected or transmitted light is measured for different incident angles and different orientations of the incident linear polarization. The measured data is then fitted by a computer program which solves the Maxwell equations for the plane-wave propagation in a multilayer structure and minimizes the error between the measured and calculated data by adjusting the unknown parameters of the multilayer. This approach enables us to determine orientations of the three principal axes in the substrate and the corresponding refractive indices. A special feature of our ellipsometers is that a glass hemisphere is placed in contact with the substrate, which eliminates the refraction of the incident light and enables a maximum propagation angle of 70 degrees (with respect to the normal) in the substrate. This increases the sensitivity of the measurement. Certain anomalies were observed, which we believe are associated with the presence of grooves on these substrates. Author (revised)

N94-14990*# Arizona Univ., Tucson.
RING LENS FOCUSING AND PUSH-PULL TRACKING SCHEME FOR OPTICAL DISK SYSTEMS
R. Gerber, J. Zambuto, J. K. Erwin, and M. Mansuripur *In its* Research Studies on Advanced Optical Module/Head Designs for Optical Disk Recording Devices 15 Mar. 1993 p 79-105 (For primary document see N94-14981 03-82)
Avail: CASI HC A03/MF A02

An experimental comparison of the ring lens and the astigmatic techniques of generating focus-error-signal (FES) in optical disk systems reveals that the ring lens generates a FES over two times steeper than that produced by the astigmat. Partly due to this large slope and, in part, because of its diffraction-limited behavior, the ring lens scheme exhibits superior performance characteristics. In particular the undesirable signal known as 'feedthrough' (induced on the FES by track-crossings during the seek operation) is lower by a factor of six compared to that observed with the astigmatic method. The ring lens is easy to align and has reasonable tolerance for positioning errors. Author (revised)

N94-14991*# Arizona Univ., Tucson.
MAGNETIC AND MAGNETO-OPTICAL PROPERTIES AND DOMAIN STRUCTURE OF Co/Pd MULTILAYERS
S. Gadetsky, Teho Wu, T. Suzuki (International Business Machines Corp., San Jose, CA.), and M. Mansuripur *In its* Research Studies on Advanced Optical Module/Head Designs for Optical Disk Recording Devices 15 Mar. 1993 p 109-132 (For primary document see N94-14981 03-82)
Avail: CASI HC A03/MF A02

The domain structure of Co/Pd(1.6/6.3 A)xN multilayers and its relation to the bulk magnetic properties of the samples were studied. The Co/Pd multilayers were deposited by rf and dc magnetron sputtering onto different substrates. It was found that magnetic and magnetooptical properties and domain structure of the multilayers were affected by total film thickness and substrate condition. Magnetization, coercivity, and anisotropy of the films decreased significantly as the film thickness dropped below 100 A. However, Kerr rotation angle had a maximum at the same thickness. The width of the domain structure increased with the decrease of the film thickness attaining the single domain state at N = 10. The initial curves in Co/Pd multilayers were found to depend on demagnetization process. The samples demagnetized by inplane field showed the largest difference between initial curves and the corresponding parts of the loops. Different domain structures were observed in the samples demagnetized by perpendicular and in-plane magnetic fields. Author (revised)

N94-14992*# Arizona Univ., Tucson. Dept. of Electrical and Computer Engineering.
DETERMINATION OF AVERAGE REFRACTIVE INDEX OF SPIN COATED DCG FILMS FOR HOE FABRICATION **c35**
T. J. Kim, Eugene W. Campbell, and Raymond K. Kostuk *In its* Research Studies on Advanced Optical Module/Head Designs for Optical Disk Recording Devices 15 Mar. 1993 p 135-144 (For primary document see N94-14981 03-82)
Avail: CASI HC A02/MF A02

The refractive index of holographic emulsions is an important parameter needed for designing holographic optical elements (HOE's). Theoretical calculations of the accuracy required for the refractive index and thickness of emulsions needed to meet predetermined Bragg angle conditions are presented. A modified interferometric method is used to find average refractive index of the unexposed and the developed dichromated gelatin holographic films. Slanted transmission HOE's are designed considering the index and thickness variations, and used to verify the index measurement results. The Brewster angle method is used to measure surface index of the unexposed and the developed films. The differences between average index and surface index are discussed. Theoretical calculation of the effects of index variation on diffraction efficiency, and experimental results for index modulation variation caused by process changes are also presented. Author (revised)

N94-14993*# Arizona Univ., Tucson.
EFFECTS OF A SHADING BAND IN THE DATA PATH OF AN OPTICAL DRIVE **c74**
T. D. Milster, M. S. Wang, and Weiquan Li (Shanghai Inst. of Metallurgy, China.) *In its* Research Studies on Advanced Optical Module/Head Designs for Optical Disk Recording Devices 15 Mar. 1993 p 147-149 (For primary document see N94-14981 03-82)
Avail: CASI HC A01/MF A02

A shading band can alter the system transfer function. In our theory and experiment, both contrast improvement and enhanced carrier-to-noise ratio are investigated. Author

N94-14994*# Arizona Univ., Tucson.
FIGURES OF MERIT FOR LASER BEAM QUALITY **c36**
T. D. Milster and E. P. Walker *In its* Research Studies on Advanced Optical Module/Head Designs for Optical Disk Recording Devices 15

Mar. 1993 p 153-159 (For primary document see N94-14981 03-82)
Avail: CASI HC A02/MF A02

It was shown how full-width at half maximum (FWHM), full-width at 1/e(sup 2) (FW1/e(sup 2)), Strehl ratio, and encircled energy figures of merit vary with different types of aberration and measurement methods. The array sampling method and the slit-scan method are examined in detail. Our irradiance in the exit pupil of the optical system is a simple gaussian. It was found that in general the slit-scan method and the array method do not yield the same result. The width measurements for the central lobe of the diffraction pattern are very insensitive to aberration.
Author (revised)

N94-14995*# Arizona Univ., Tucson.
A NEAR-FIELD SCANNING OPTICAL MICROSCOPE FOR ANALYSIS OF MAGNETO-OPTIC MEDIA **c74**
Fred F. Froehlich and Tom D. Milster *In its* Research Studies on Advanced Optical Module/Head Designs for Optical Disk Recording Devices 15 Mar. 1993 p 163-165 (For primary document see N94-14981 03-82)
Avail: CASI HC A01/MF A02

The design of a near-field scanning optical microscope (NSOM) is described. Applications to the study of magneto-optic media and domain detection are discussed.
Author

N94-14996*# Arizona Univ., Tucson.
A COMPLETE STUDY OF DIFFERENTIAL WAX-WANE FOCUS SERVO TECHNIQUE **c74**
Mark S. Wang and Tom D. Milster *In its* Research Studies on Advanced Optical Module/Head Designs for Optical Disk Recording Devices 15 Mar. 1993 p 169-171 (For primary document see N94-14981 03-82)
Avail: CASI HC A01/MF A02

A thorough study of differential wax-wane focus servo technique including effects of aberration and cancellation of crosstalk is presented.
Author (revised)

N94-14997*# Arizona Univ., Tucson.
DETERMINING THE LOCATIONS OF THE VARIOUS CIRC RECORDING FORMAT INFORMATION BLOCKS (USER DATA BLOCKS, C2 AND C1 WORDS AND EFM FRAMES) ON A RECORDED COMPACT DISC
Dennis G. Howe *In its* Research Studies on Advanced Optical Module/Head Designs for Optical Disk Recording Devices 15 Mar. 1993 p 175-186 (For primary document see N94-14981 03-82)
Avail: CASI HC A03/MF A02

Just prior to its being EFM modulated (i.e., converted to eight-to-fourteen channel data by the EFM encoder) and written to a Compact Disc (CD), information that passes through the CIRC Block Encoder is grouped into 33-byte blocks referred to as EFM frames. Twenty four of the bytes that make up a given EFM frame are user data that was input into the CIRC encoder at various (different) times, 4 of the bytes of this same EFM frame were created by the C2 ECC encoder (each at a different time), and another 4 were created by the C1 ECC encoder (again, each at a different time). The one remaining byte of the given EFM frame, which is known as the EFM frame C&D (for Control & Display) byte, carries information that identifies which portion of the current disc program track the given EFM frame belongs to and also specifies the location of the given EFM frame on the disc (in terms of a time stamp that has a resolution of 1/75th second, or 98 EFM frames). (Note: since the program track and time information is stored as a 98-byte word, a logical group consisting of 98 consecutive EFM frames must be read, and their respective C&D bytes must be catenated and decoded, before the program track identification and time position information that pertains to the entire block of 98 EFM frames can be obtained.) The C&D byte is put at the start (0th byte) of an EFM frame in real time; its placement completes the construction of the EFM frame - it is assigned just before the EFM frame enters the EFM encoder. Four distinct blocks of data are referred to: 24-byte User Input Data Blocks; 28-byte C2 words; 32-byte C1 words; and 33-byte EFM frames.
Author (revised)

N94-15009*# NASA Center for AeroSpace Information, Baltimore-Washington International Airport, MD.
NASA'S ONLINE MACHINE AIDED INDEXING SYSTEM Final Report
June P. Silvester (RMS Associates, Linthicum Heights, MD.), Michael T. Genuardi (RMS Associates, Linthicum Heights, MD.), and Paul H. Klingbiel (RMS Associates, Linthicum Heights, MD.) Sep. 1993 60 p
(Contract NASw-4584)
(NASA-CR-4518; NAS 1.26:4518) Avail: CASI HC A04/MF A01

This report describes the NASA Lexical Dictionary, a machine aided indexing system used online at the National Aeronautics and Space Administration's Center for Aerospace Information (CASI). This system is comprised of a text processor that is based on the computational, non-syntactic analysis of input text, and an extensive 'knowledge base' that serves to recognize and translate text-extracted concepts. The structure and function of the various NLD system components are described in detail. Methods used for the development of the knowledge base are discussed. Particular attention is given to a statistically-based text analysis program that provides the knowledge base developer with a list of concept-specific phrases extracted from large textual corpora. Production and quality benefits resulting from the integration of machine aided indexing at CASI are discussed along with a number of secondary applications of NLD-derived systems including on-line spell checking and machine aided lexicography.
Author

N94-15116*# National Aeronautics and Space Administration. Goddard Space Flight Center, Greenbelt, MD.
THE THIRD ANNUAL NASA SCIENCE INTERNET USER WORKING GROUP CONFERENCE
Brian S. Lev, ed. (Hughes STX, Inc., Lanham, MD.) and J. Patrick Gary, ed. Washington May 1993 464 p Conference held in Greenbelt, MD, 30 Mar. - 3 Apr. 1992
(RTOP 656-63-00)
(NASA-CP-3170; Rept-93B00048; NAS 1.55:3170) Avail: CASI HC A20/MF A04

The NASA Science Internet (NSI) User Support Office (USO) sponsored the Third Annual NSI User Working Group (NSIUWG) Conference March 30 through April 3, 1992, in Greenbelt, MD. Approximately 130 NSI users attended to learn more about the NSI, hear from projects which use NSI, and receive updates about new networking technologies and services. This report contains material relevant to the conference; copies of the agenda, meeting summaries, presentations, and descriptions of exhibitors. Plenary sessions featured a variety of speakers, including NSI project management, scientists, and NSI user project managers whose projects and applications effectively use NSI, and notable citizens of the larger Internet community. The conference also included exhibits of advanced networking applications; tutorials on internetworking, computer security, and networking technologies; and user subgroup meetings on the future direction of the conference, networking, and user services and applications.
Author

N94-15152# Defense Information Systems Agency, Arlington, VA. Center for Information Management.
DEPARTMENT OF DEFENSE TECHNICAL ARCHITECTURE FRAMEWORK FOR INFORMATION MANAGEMENT. VOLUME 1: OVERVIEW, VERSION 2.0
John Keane 22 Jun. 1993 58 p Supersedes AD-A261911; N93-26531
(AD-A267193; AD-A261911) Avail: CASI HC A04/MF A01

This volume provides an overview of the Technical Architecture Framework for Information Management (TAFIM) project. It describes a conceptual approach to using the TAFIM. It also relates information technology (IT) and information management (IM) guidance published in the Department of Defense (DoD) directives, instructions, and manuals to the TAFIM guidance.
DTIC

N94-15176# General Accounting Office, Washington, DC. National Security and International Affairs Div.
CLASSIFIED INFORMATION: VOLUME COULD BE REDUCED BY CHANGING RETENTION POLICY
May 1993 44 p
(AD-A266938; GAO/NSIAD-93-127) Avail: CASI HC A03/MF A01

The U.S. government maintains a large but unquantifiable volume of classified documents, some dating to before World War II. The Chairmen, House Committees on Government Operations and on Foreign Affairs, expressed concerns about whether this is warranted and asked GAO to review the classification of national security information. Accordingly, GAO examined the reasons for the retention of large volumes of documents as

classified for long periods of time. GAO also reviewed documents for classification errors, reports on government-wide classification and declassification activity and adherence to policies and procedures, and various executive orders that have governed national security information. DTIC

N94-15178# Army Training and Doctrine Command, Fort Monroe, VA.
A TRALINET GUIDE TO THE INTERNET Final Report
Leroy Bell and Ed Burgess Jun. 1993 32 p
(AD-A266946) Avail: CASI HC A03/MF A01

This workbook was put together for the benefit of TRALINET librarians. It addresses some specific problems that TRADOC libraries will face in accessing Internet resources. Some assumptions: Most TRALINET librarians will go through Profs. Most use an IBM 4381 running the VM operating system. About half of all TRALINET libraries dial into Profs using a modem and communications software. In some cases, this workbook will talk about commands and practices which are in use at Fort Monroe. Readers should be aware that those practices are not universal. The reader is advised to speak with the local system administrators. Anyone wishing to actually do work on the Internet is advised to bring along an extra helping of patience. Partly because of the hosts that TRADOC uses, and partly because the reality of the software you will be interacting with is far removed from the promotional literature, Internet surfers often get stuck. The Internet is new, evolving, constantly changing, designed by computer systems people rather than information retrieval people. Things don't always go as well as one would hope. DTIC

N94-15231* National Aeronautics and Space Administration. Marshall Space Flight Center, Huntsville, AL.
UNIVERSITY JOINT VENTURE: JOVE (Videotape)
Mar. 1989 Videotape: 2 min. 12 sec. playing time, in color, with sound
(NASA-TM-109660; NONP-VT-93-190458) Avail: CASI VHS A01/BETA A22

This video presentation explains how NASA shares its several trillion bits of raw science and engineering data with universities who help NASA analyze and distribute that data. CASI

N94-15251* National Aeronautics and Space Administration, Washington, DC.
MONITORING HISTORY (Videotape)
Jun. 1987 Videotape: 3 min. 25 sec. playing time, in color, with sound
(NASA-TM-109640; NONP-VT-93-190438) Avail: CASI VHS A01/BETA A22

Deep space technology is applied to help monitor the aging process of the treasured documents in the National Archives. CASI

N94-15300* National Aeronautics and Space Administration. Lyndon B. Johnson Space Center, Houston, TX.
TEXT AND GRAPHICS SYSTEMS (Videotape)
Mar. 1989 Videotape: 1 min. 55 sec. playing time, in color, with sound
(NASA-TM-109570; NONP-VT-93-190368) Avail: CASI VHS A01/BETA A22

This video shows Text and Graphics Systems (TAGS) in action and describes how the system will be used on Space Shuttle missions. CASI

N94-15414*# National Aeronautics and Space Administration, Washington, DC.
NASA DIRECTIVES MASTER LIST AND INDEX
31 Mar. 1993 95 p
(NHB-1410.13L) Avail: CASI HC A05/MF A01

This Handbook sets forth in two parts the following information for the guidance of users of the NASA Management Directives System. Part A is a master list of management directives in force as of March 31, 1993. Chapter 1 contains introductory informative material on how to use this Handbook. Chapter 2 is a complete master list of Agencywide management directives, describing each directive by type, number, effective date, expiration date, title, and organization code of the office responsible for the directive. Chapter 3 includes a consolidated numerical list of all delegations of authority and a breakdown of such delegation by the office or installation to which special authority is assigned. Chapter 4 sets forth a consolidated list of all NASA Handbooks (NHB's) and important footnotes covering the control and ordering of such documents. Chapter 5 is a consolidated list of NASA management directives applicable to the Jet Propulsion Laboratory. Chapter 6 is a consolidated list of NASA management directives published in the Code of Federal Regulations. Complementary manuals to the NASA Management Directives System are described in Chapter 7. Part B is the index to NASA management directives in force as of March 31, 1993. This part contains an in-depth alphabetical index to all NASA management directives other than Handbooks. NHB's 1610.6, 'NASA Personnel Security Handbook,' 1620.3, 'NASA Physical Security Handbook,' 1640.4, 'NASA Information Security Program,' 1900.1, 'Standards of Conduct for NASA Employees,' 5103.6, 'Source Evaluation Board Handbook,' and 7400.1, 'Budget Administration Manual,' are indexed in-depth. All other NHB's are indexed by titles only. Derived from text

N94-15437# Advisory Group for Aerospace Research and Development, Neuilly-Sur-Seine (France). Technical Information Panel.
ELECTRONIC MESSAGING FOR THE 1990'S Report No. 309 [LES MESSAGERIES ELECTRONIQUES DES ANNEES 90]
Jean Mourain May 1993 44 p In ENGLISH and FRENCH
(AD-A267143; AGARD-AR-309; ISBN-92-835-2117-X) Copyright Avail: CASI HC A03/MF A01

Electronic messaging systems, including their general principles, potential uses for transmitting information between people and between applications, problems of compatibility and possible solutions, messaging and data formats, and system architecture are discussed as well as the advantages and disadvantages of these systems in relation to competitors such as telefax, and the risks inherent in introducing them and ways of overcoming these risks. This publication is concluded with recommendations for AGARD (NATO's Advisory Group for Aerospace Research and Development). This publication was sponsored by the Technical Information Panel of AGARD. The volume contains the original French text and a translation into English. Author

N94-15520* National Aeronautics and Space Administration, Washington, DC.
MEDICAL IMAGING (Videotape)
Jun. 1986 Videotape: 3 min. 40 sec. playing time, in color, with sound
(NASA-TM-109675; NONP-VT-93-190473) Avail: CASI VHS A01/BETA A22

This video shows how satellite data processing techniques (multispectral scanning) can improve disease detection and treatment. CASI

N94-15523* National Aeronautics and Space Administration. John C. Stennis Space Center, Bay Saint Louis, MS.
COAST ENCOUNTERS: A SPACE AGE ADVENTURE IN SCIENCE LITERACY (Videotape)
Apr. 1989 Videotape: 6 min. 20 sec. playing time, in color, with sound
(NASA-TM-109334; NONP-VT-93-190475) Avail: CASI VHS A01/BETA A22

This video recaps the NASA Community Involvement Program for education held on the Mississippi Gulf Coast, April 1989. CASI

N94-15652# Electronics Research Lab., Salisbury (Australia).
THE DISTRIBUTED DATABASE DYNAMIC RECONFIGURATION PROJECT Interim Report
Damian ODea Jan. 1993 34 p
(AD-A267116; ERL-0663-RN; DODA-AR-007-015) Avail: CASI HC A03/MF A01

This paper discusses the work which took place in the first phase of the development of the Distributed Database Dynamic Reconfiguration (D3R) project. The concepts of object-oriented programming and multitasking are introduced and explained. Each stage of the project is detailed, and where relevant, concepts from the Distributed Database Management Evaluation Software (DBMES) system are introduced and explained. The paper concludes with recommendations for future developments to both systems as they approach completion. Author (revised)

N94-15788# Defense Information Systems Agency, Arlington, VA. Center for Information Management.
DEPARTMENT OF DEFENSE TECHNICAL ARCHITECTURE FRAMEWORK FOR INFORMATION MANAGEMENT. VOLUME 2: TECHNICAL REFERENCE MODEL AND STANDARDS PROFILE,

VERSION 2.0
John Keane 22 Jun. 1993 110 p
(AD-A267194) Avail: CASI HC A06/MF A02

This document discusses the services and standards needed to support DoD's Distributed Computing requirements. In addition, requirements for internationalization services resulting from harmonization of the Technical Reference Model with NATO reference model development efforts are addressed. DTIC

N94-15789# Defense Information Systems Agency, Arlington, VA. Center for Information Management.
DEPARTMENT OF DEFENSE TECHNICAL ARCHITECTURE FRAMEWORK FOR INFORMATION MANAGEMENT. VOLUME 3: ARCHITECTURE CONCEPTS AND DESIGN GUIDANCE, VERSION 2.0
John Keane 22 Jun. 1993 97 p
(AD-A267195) Avail: CASI HC A05/MF A02

For purposes of the Technical Architecture Framework for Information Management (TAFIM), an information system may be characterized as composed of the following components: data; mission-specific applications; and a technical infrastructure consisting of support applications, computing platforms, and communications networks. This document presents the technical architecture concepts and the design guidance for information systems in the Department of Defense (DoD). As part of the TAFIM, this volume provides guidance for the evolution of the Department's technical infrastructure in support of specific mission requirements. The data and mission-specific software architectures are critical elements in information system development. Guidance on their development and use will be provided in separate documents outside of the TAFIM. DTIC

N94-15838*# National Aeronautics and Space Administration. Langley Research Center, Hampton, VA.
NASA/DOD AEROSPACE KNOWLEDGE DIFFUSION RESEARCH PROJECT. PAPER 32: A NEW ERA IN INTERNATIONAL TECHNICAL COMMUNICATION: AMERICAN-RUSSIAN COLLABORATION
Madelyn Flammia (University of Central Florida, Orlando.), Rebecca O. Barclay (Rensselaer Polytechnic Inst., Troy, NY.), Thomas E. Pinelli, Michael L. Keene (Tennessee Univ., Knoxville.), Robert H. Burger (Illinois Univ., Urbana.), and John M. Kennedy (Indiana Univ., Bloomington.) 1993 6 p Presented at the International Professional Communication Conference, Philadelphia, PA, 5-8 Oct. 1993
(NASA-TM-109336; NAS 1.15:109336) Avail: CASI HC A02/MF A01

Until the recent dissolution of the Soviet Union, the Communist Party exerted a strict control of access to and dissemination of scientific and technical information (STI). This article presents models of the Soviet-style information society and the Western-style information society and discusses the effects of centralized governmental control of information on Russian technical communication practices. The effects of political control on technical communication are then used to interpret the results of a survey of Russian and U.S. aerospace engineers and scientists concerning the time devoted to technical communication, their collaborative writing practices and their attitudes toward collaboration, the kinds of technical documents they produce and use, their views regarding the appropriate content for an undergraduate technical communication course, and their use of computer technology. Finally, the implications of these findings for future collaboration between Russian and U.S. engineers and scientists are examined. Author

N94-15839*# National Aeronautics and Space Administration. Langley Research Center, Hampton, VA.
NASA/DOD AEROSPACE KNOWLEDGE DIFFUSION RESEARCH PROJECT. PAPER 34: TECHNICAL COMMUNICATIONS PRACTICES AND THE USE OF INFORMATION TECHNOLOGIES AS REPORTED BY DUTCH AND US AEROSPACE ENGINEERS
Rebecca O. Barclay (Rensselaer Polytechnic Inst., Troy, NY.), Thomas E. Pinelli, Axel S. T. Tan (National Aerospace Lab., Amsterdam, Netherlands.), and John M. Kennedy (Indiana Univ., Bloomington.) 1993 7 p Presented at the International Professional Communication Conference, Philadelphia, PA, 5-8 Oct. 1993
(NASA-TM-109337; NAS 1.15:109337) Avail: CASI HC A02/MF A01

As part of Phase 4 of the NASA/DOD Aerospace Knowledge Diffusion Research Project, two studies were conducted that investigated the technical communications practices of Dutch and U.S. aerospace engineers and scientists. A self-administered questionnaire was distributed to aerospace engineers and scientists at the National Aerospace Laboratory (The Netherlands), and NASA ARC (U.S.), and NASA LaRC (U.S.). This paper presents responses of the Dutch and U.S. participants to selected questions concerning four of the seven project objectives: determining the importance of technical communications to aerospace engineering professionals, investigating the production of technical communications, examining the use and importance of computer and information technology, and exploring the use of electronic networks. Author (revised)

N94-15850 Air Force Office of Scientific Research, Bolling AFB, Washington, DC.
AFOSR TECHNICAL REPORT SUMMARIES, JANUARY - MARCH 1993
Mar. 1993 313 p Limited Reproducibility: More than 20% of this document may be affected by microfiche quality
(AD-A267187) Avail: CASI HC A14

The AFOSR technical report summaries are published quarterly of each calendar year. They consist of a brief summary of each AFOSR technical report received in the technical information division and submitted to the Defense Technical Information Center for that quarter. DTIC

N94-15936*# National Aeronautics and Space Administration, Washington, DC.
INDEX OF NASA PREFIXED FORMS
Jan. 1992 34 p
(NHB-1420.21; NAS 1.18:1420.21) Avail: CASI HC A03/MF A01

This Handbook sets forth information for the guidance of all users of the NASA Forms Management Program System. It is issued in accordance with the Federal Information Resources Management Regulation (FIRMR), Subpart 201-9.1. This Handbook sets forth an alpha-functional index of NASA-prefixed forms by title, identifying number, and unit of issue. The automated processing two-letter code (NF) has been substituted for the spelling out of the NASA form-prefix preceding the form number. To indicate a description in lieu of a distinct title, the entire reference under the Form Title/Description column has been enclosed in parentheses. A list of current forms, shown by number and page, is included for cross-reference and to preclude the ordering of those forms which have been deleted from the system. This Handbook will be updated, as appropriate. NHB 1420.2H dated July 1986, is cancelled. Derived from text

N94-15941*# National Aeronautics and Space Administration, Washington, DC.
NASA INFORMATION RESOURCES MANAGEMENT HANDBOOK
Apr. 1992 218 p
(NHB-2410.1E; NAS 1.18:2410.1E) Avail: CASI HC A10/MF A03

This National Aeronautics and Space Administration (NASA) Handbook (NHB) implements recent changes to Federal laws and regulations involving the acquisition, management, and use of Federal Information Processing (FIP) resources. This document defines NASA's Information Resources Management (IRM) practices and procedures and is applicable to all NASA personnel. The dynamic nature of the IRM environment requires that the controlling management practices and procedures for an Agency at the leading edge of technology, such as NASA, must be periodically updated to reflect the changes in this environment. This revision has been undertaken to accommodate changes in the technology and the impact of new laws and regulations dealing with IRM. The contents of this document will be subject to a complete review annually to determine its continued applicability to the acquisition, management, and use of FIP resources by NASA. Updates to this document will be accomplished by page changes. This revision cancels NHB 2410.1D, dated April 1985. Derived from text

N94-16010# Department of Energy, Washington, DC. Office of Information Resources Management.
INFORMATION TECHNOLOGY RESOURCES ASSESSMENT
Apr. 1993 70 p
(DE93-013899; DOE/AD-0044) Avail: CASI HC A04/MF A01

The Information Technology Resources Assessment (ITRA) is being published as a companion document to the Department of Energy (DOE) FY 1994-FY 1998 Information Resources Management Long-Range Plan. This document represents a collaborative effort between the Office of Information Resources Management and the Office of Energy Research that was undertaken to achieve, in part, the Technology Strategic Objective of IRM Vision 21. An integral part of this objective, technology forecasting

provides an understanding of the information technology horizon and presents a perspective and focus on technologies of particular interest to DOE program activities. Specifically, this document provides site planners with an overview of the status and use of new information technology for their planning consideration. DOE

N94-16458# Naval Air Station, Pensacola, FL. Computer and Telecommunications.
PERFORMANCE INFORMATION MANAGEMENT SYSTEM (PIMS) COMMUNICATION Annual Report, 1 Oct. 1991-1992
Kathryn P. Winter 15 Oct. 1992 8 p
(Contract MIPR-9MM2501)
(AD-A267040) Avail: CASI HC A02/MF A01

The objective of this project is to modify and enhance the capabilities of the Mailnet telephonic bulletin board system and create 'hooks' for accessing a performance database remotely. DTIC

N94-16490 Department of the Navy, Washington, DC.
METHOD FOR RESTRUCTURING A DATABASE USING A RELATIONAL DATABASE SCHEME DERIVED BY SELECTING SUBSCHEME JOINS TO AVOID CYCLES Patent
Allen D. Parks, inventor (to Navy) 22 Jun. 1993 6 p Filed 9 Jul. 1990 Supersedes AD-D014755
(AD-D015816; US-Patent-5,222,233; US-Patent-Appl-SN-551104; US-Patent-Class-395-600) Avail: US Patent and Trademark Office

A method for relational database scheme design with the aid of a digital computer for a database having attributes A(sub i), i = 1 to n and relational schemes R(sub j), j = 1 to m is described. Each relational scheme Rj is a non-empty subset of the attributes Ai. The method detects any scheme that is non-acyclic in a simple manner that is easily adapted to a digital computer environment. The resulting relational database scheme design is thereby prevented from being non-acyclic. DTIC

N94-16499*# Research Inst. for Computing and Information Systems, Houston, TX.
NASA ELECTRONIC LIBRARY SYSTEM (NELS): THE SYSTEM IMPACT OF SECURITY
Terry L. McGregor (I-NET, Inc., Bethesda, MD.) Jul. 1993 19 p
(Contract NCC9-16; RICIS Proj. RB-08)
(NASA-CR-194614; NAS 1.26:194614) Avail: CASI HC A03/MF A01

This paper discusses security issues as they relate to the NASA Electronic Library System which is currently in use as the repository system for AdaNET System Version 3 (ASV3) being operated by MountainNET, Inc. NELS was originally designed to provide for public, development, and secure collections and objects. The secure feature for collections and objects was deferred in the initial system for implementation at a later date. The NELS system is now 9 months old and many lessons have been learned about the use and maintenance of library systems. MountainNET has 9 months of experience in operating the system and gathering feedback from the ASV3 user community. The user community has expressed an interest in seeing security features implemented in the current system. The time has come to take another look at the whole issue of security for the NELS system. Two requirements involving security have been put forth by MountainNET for the ASV3 system. The first is to incorporate at the collection level a security scheme to allow restricted access to collections. This should be invisible to end users and be controlled by librarians. The second is to allow inclusion of applications which can be executed only by a controlled group of users; for example, an application which can be executed by librarians only. The requirements provide a broad framework in which to work. These requirements raise more questions than answers. To explore the impact of these requirements a top down approach will be used. Author (revised)

N94-16570# Carnegie-Mellon Univ., Pittsburgh, PA. School of Computer Science.
DISCONNECTED OPERATION IN A DISTRIBUTED FILE SYSTEM Ph.D. Thesis
James J. Kistler May 1993 268 p
(Contract F33615-90-C-1465; ARPA Order 7597)
(AD-A266461; CMU-CS-93-156) Avail: CASI HC A12/MF A03

Disconnected operation refers to the ability of a distributed system client to operate despite server inaccessibility by emulating services locally. The capability to operate disconnected is already valuable in many systems, and its importance is growing with two major trends: the increasing scale of distributed systems, and the proliferation of powerful mobile computers. The former makes clients vulnerable to more frequent and less controllable system failures, and the latter introduces an important class of clients which are disconnected frequently and for long durations--often as a matter of choice. This dissertation shows that it is practical to support disconnected operation for a fundamental system service: general purpose file management. It describes the architecture, implementation, and evaluation of disconnected file service in the Coda file system. The architecture is centered on the idea that the disconnected service agent should be one and the same with the client cache manager. The Coda cache manager prepares for disconnection by pre-fetching and hoarding copies of critical files; while disconnected it logs all update activity and otherwise emulates server behavior; upon reconnection it reintegrates by sending its log to the server for replay. This design achieves the goal of high data availability--users can access many of their files while disconnected, but it does not sacrifice the other positive properties of contemporary distributed file systems: scalability, performance, security, and transparency. DTIC

N94-16576# Rochester Univ., NY. Computer Science Dept.
EXPLOITING WORLD STRUCTURE TO EFFICIENTLY SEARCH FOR OBJECTS
Lambert E. Wixson Nov. 1992 56 p
(Grant NSF IRI-89-03582)
(TR-434) Avail: CASI HC A04/MF A01

This paper studies the task of using a mobile camera platform to search a region of space for a target object. Our goal is to maximize the efficiency of such searches. The problem is analyzed using a simple mathematical description of the factors that affect search efficiency. This analysis suggests that one way to improve efficiency is to take advantage of the spatial relationships in which the target object commonly participates. Searches that do so, which we call indirect searches, are modeled as two-stage processes that first find an intermediate object that commonly participates in a spatial relationship for the target object, and then look for the target in the restricted region specified by this relationship. A mathematical model of search efficiency is then used to analyze the efficiency of indirect search over a wide range of situations that vary the spatial structure of the domain as well as recognition performance. The model predicts that, for searches that involve rotating a camera about a fixed location, indirect searches improve efficiency by factors of 2 to 8. An implemented robot search system substantiates these predictions. Finally, we highlight some areas in need of further research if these efficiencies are to be achieved. Author (revised)

N94-16874# Oak Ridge National Lab., TN.
PROCESSING OF RESONANCE PARAMETER COVARIANCE FILES
B. L. Broadhead 1992 16 p Presented at the Nuclear Energy Agency Science Committee (NEANSC) Specialists Meeting on Evaluation and Processing of Covariance Data, Oak Ridge, TN, 7-9 Oct. 1992
(Contract DE-AC05-84OR-21400)
(DE93-015506; CONF-9210173-5) Avail: CASI HC A03/MF A01

The prudent use of resonance parameter covariance information requires the availability of a means of error propagation from the resonance parameters to the cross sections. This work presents an approach to obtaining these so-called resonance parameter sensitivities. The resonance parameter sensitivity methodology developed herein generally provides accurate results when compared to direct recalculations using existing and wellknown cross-section processing codes. However, it has been shown in several cases that self-shielded cross sections can be very nonlinear functions of the basic parameters. For this reason, caution must be used in any study which assumes that a linear relationship exists between a given self-shielded group cross section and its corresponding basic data parameters. The study also has pointed out the need for more approximate techniques which will allow the required sensitivity information to be obtained in a more cost-effective manner. This paper is a synopsis of major work that was completed nearly ten years ago. However, due to the lack of additional development in the field, it remains essentially the current state-of-the-art. DOE

N94-16875# Martin Marietta Energy Systems, Inc., Oak Ridge, TN.
MANAGING INFORMATION AS A CORPORATE ASSET: KEY STRATEGIES FOR INFORMATION PROFESSIONALS TO REMAIN COMPETITIVE
B. G. Ashdown 1993 29 p Presented at the Special Libraries Association Annual Conference, Cincinnati, OH, Jun. 1993
(Contract DE-AC05-84OR-21400)
(DE93-015515; CONF-9306177-1) Avail: CASI HC A03/MF A01

This report discusses the concepts and efforts involved in competitively managing an information organization that supports the 20,000 staff members of Martin Marietta Energy Systems, Inc., a government-contracted organization run for the Department of Energy (DOE) by Martin Marietta Corporation. A range of library and records management services to three different plant locations and several off-site locations in Oak Ridge, Tennessee is provided. Library and records management consulting to the plants in Paducah, Kentucky and Portsmouth, Ohio are also provided. A dozen libraries, six records centers, 15 document management centers, a centralized policy management group, and other groups provide customized information analysis and database development services. Subjects supporting business include multidisciplinary basic and applied scientific research and development, manufacturing process support, environmental restoration and waste management, and legislative and management information. These endeavors are supported through 176 regular staff and about 25 subcontracted staff members, who reside in eight major site locations in the Oak Ridge vicinity. DOE

N94-16967# Oak Ridge National Lab., TN.
PUBLICATIONS OF THE OAK RIDGE NATIONAL LABORATORY FOSSIL ENERGY PROGRAM, 1 OCTOBER 1991 - 31 MARCH 1993
P. T. Carlson, comp. Jun. 1993 53 p
(Contract DE-AC05-84OR-21400)
(DE93-014643; ORNL-6755) Avail: CASI HC A04/MF A01

The Oak Ridge National Laboratory (ORNL) Fossil Energy Program, organized in FY-74 as the Coal Technology Program, involves research and development activities for the Department of Energy (DOE) Assistant Secretary for Fossil Energy that cover a wide range of fossil energy technologies. The principal focus of the Laboratory's fossil energy activities relates to coal, with current emphasis on the following: materials research and development; environmental, health, and safety research; and the bioprocessing of coal to produce liquid or gaseous fuels. This bibliography covers the period of 1 Oct. 1991 through 31 Mar. 1993. DOE

N94-16977# Naval Postgraduate School, Monterey, CA.
DESIGN AND IMPLEMENTATION OF AN OBJECT-ORIENTED INTERFACE FOR THE MULTI-MODEL/MULTI-LINGUAL DATABASE SYSTEM M.S. Thesis
John W. Moore and Turgay Karlidere Mar. 1993 196 p
(AD-A267413) Avail: CASI HC A09/MF A03

Database designs in today's information-intensive environment, challenge the database-system user to adhere to strict and somewhat archaic means, i.e., traditional data models and their data languages, of expressing their database applications. In light of these requirements, the user must purchase the new database system that supports the latest data model and its data language. We design and implement a comprehensive data-model-and-data-language interface which is a simple and yet effective alternative to the costly and cumbersome standard method of purchasing or developing a new database system. Our solution is two-fold. First, we use the concept of a data-model-and-data-language interface to an existing database system. This not only eliminates the costs associated with building a separate, stand-alone database system to support each new data model and its language, but also allows for resource consolidation and data duplication elimination. Second, using the data-model-and-data-language interface concept, we design and implement an object-oriented-data-model-and-data-language interface for the multimodel/multilingual database system. DTIC

N94-17007 Defense Logistics Services Center, Battle Creek, MI.
DEFENSE LOGISTICS INFORMATION SYSTEM (DLIS) PROCEDURES MANUAL. PRODUCTS AND SERVICES END-USER MANUAL
Jul. 1992 170 p Limited Reproducibility: More than 20% of this document may be affected by microfiche quality
(AD-A267766; DOD-4100.39-M) Avail: CASI HC A08

The contents are as follows: Certified Contractor Access List (CCAL); Commercial and Government Entity (CAGE), Handbook; Depot Maintenance; Descriptive Publication Requirements Guide; DLA Federal Supply Catalog for Civil Agencies (CAC); DoD Ammunition Code Publication, H3; DoD Consolidated Ammunition Catalog; DoD Interchangeability and Substitutability; DoD Medical Catalog; DRMS Demil Reference File; Federal Aviation Administration (FAA) Catalog; Federal Item Logistics Data Record (FILDR); Federal Item Name Directory (FIND); Federal Logistics Data on Compact Disk (FED LOG). DTIC

N94-17036# Cornell Univ., Ithaca, NY. Inst. for the Study of the Continents.
A GEOLOGICAL AND GEOPHYSICAL INFORMATION SYSTEM FOR EURASIA Semiannual Technical Report No. 3, 30 Oct. 1992 - 30 Apr. 1993
Eric J. Fielding, Muawia Barazangi, and Bryan L. Isacks 29 Jun. 1993 16 p
(Contract F29601-91-K-DB08)
(AD-A267841) Avail: CASI HC A03/MF A01

Topography and heterogeneous crustal structure have major effects on the propagation of regional seismic phases. We are collecting topographical, geological, and geophysical datasets for Eurasia into an information system that can be accessed via Internet connections. Now available are digital topography, satellite imagery, and data on sedimentary basins and crustal structure thicknesses. We are expanding the scope of our information system to include data on the Middle East and North Africa. Under the auspices of several other ongoing projects at Cornell, we have collected a very large literature collection, satellite imagery and some detailed datasets, especially in Syria and Morocco. New datasets for Eurasia include maps of depth to Moho beneath Europe and Scandinavia. We have created regularly spaced grids of the crustal thickness values from these maps that can be used to create profiles of crustal structure. These profiles can be compared by an analyst or an automatic program with the crustal seismic phases received along the propagation path to better understand and predict the path effects on phase amplitudes, a key to estimating magnitudes and yields, and for understanding variations in travel-time delays for phases such as Pn which are important for improving regional event locations. The gridded data could also be used to model propagation of crustal phases in three dimensions. In the near future, we will be making new databases from the Middle East and North Africa available via the Internet. We encourage ARPA and Air Force researchers to contact us about gaining access to our databases. DTIC

N94-17038*# Colorado Univ., Boulder. Center for Astro-Physics and Space Astronomy.
CRITICALLY EVALUATED/DISTRIBUTED DATABASE OF IRAS LRS SPECTRA Final Report, 15 Aug. 1990 - 14 Aug. 1993
R. E. Stencel 1993 10 p
(Grant NAG5-1214)
(NASA-CR-193611; NAS 1.26:193611) Avail: CASI HC A02/MF A01

Accomplishments under this grant effort include: successful scientific utilization of the IRAS Low Resolution Spectrometer (LRS) database of over 150,000 scans of 7-23 micron spectra for over 50,000 celestial sources; publication in refereed journal of an additional 486 critically evaluated spectra of sources brighter than 20 Jy, completing the LRS ATLAS (Olnon and Raimond 1986 A&A) uniformly to that level, and production of an additional 1,830 critically evaluated spectra of sources brighter than 10 Jy; creation and maintenance of on-line, remotely accessible LRS spectra of over 7500 sources; cooperation with Astrophysics Data System personnel for transitioning this LRS database to the ADS access system after funding for this project expires; and publication of research highlights, which include a systematic variation of the shapes of LRS silicate features among stars of differing IRAS broad-band colors, maser characteristics and light curve asymmetries, all correlated with the chemical and physical development and processing of solid phase materials, and preliminary evidence for silicate profile variations in individual stars as a function of visual light curve phase. Author

N94-17101 Defense Technical Information Center, Alexandria, VA.
DEFENSE RDT&E ONLINE SYSTEM (DROLS) HANDBOOK Final Report
Barbara Lesser, Christian M. Cupp, Richard J. Wayman, Keith L. Thompson, and Holly J. Wilson Jul. 1993 250 p Supersedes DLAM 4185.4,

dated Sep. 1990 Limited Reproducibility: More than 20% of this document may be affected by microfiche quality
(AD-A267546; DTIC/TR/93-20; DLAM 4185.4) Avail: CASI HC A11

This training handbook provides basic instruction in the use of the Defense RDT and E Online System (DROLS), an automated system providing access to major research and development (R and D) data collections. The Technical Report Database (TR) and Current File Technical Report Database (CF) both address completed R and D work efforts, whereas the Work Unit Database (WU) addresses work in progress. The IR and D Database, representing planned work efforts by Department of Defense (DoD) contractors wholly funded by the DoD. It is intended to be used in conjunction with the DROLS Workbook AD-A259033. DTIC

N94-17114# Naval Postgraduate School, Monterey, CA.
DESIGN AND IMPLEMENTATION OF AN INTERFACE EDITOR FOR THE AMADEUS MULTI-RELATIONAL DATABASE FRONT-END SYSTEM M.S. Thesis
James P. Hargrove 25 Mar. 1993 286 p
(AD-A267403) Avail: CASI HC A13/MF A03

This thesis extends the Graphical User Interface of a prototype multi-relational database front-end system, called Amadeus. System enhancements are realized through the application of Object-Oriented Programming (OOP) and Human-Computer Interface (HCI) design principles. Knowledge gained from each topic has been incorporated into the design and implementation of a Form-based interface for database data entry and display. The focus of this thesis is divided between two issues: the development of a set of tools for creating and using Form objects; and the design of the Form object itself. Form creation is accomplished using an application program called the Interface Editor module. The Interface Editor is one of six modules which, together, comprise the Amadeus system. Form manipulation occurs in a second application which implements basic program methods for controlling Data entry and display processes. Design and implementation of this thesis was accomplished using the Prograph programming language and development environment, which provided a basic set of system classes essential to the implementation of the Form object and Graphical User Interfaces. DTIC

N94-17229# Defense Logistics Services Center, Battle Creek, MI.
DEFENSE LOGISTICS INFORMATION SYSTEM (DLIS). PROCEDURES MANUAL: LOGISTICS ON-LINE ACCESS (LOLA) PROCEDURES MANUAL
Jul. 1992 122 p
(AD-A267685; DOD-4100.39-M) Avail: CASI HC A06/MF A02

This section provides a non-technical presentation of information on the overall system. Detailed technical information, i.e., how to use the Logistics On-Line Access (LOLA) Procedures Application, is presented in other sections of this manual. The LOLA Procedures Application is a component of an automated customer service system provided by the Defense Logistics Services Center (DLSC). LOLA Procedures was designed, developed, and implemented as part of an overall modernization effort at DLSC which was undertaken to address End-User considerations. These considerations include reliability transparency where possible, seamless integration, quick response, single user interface, inter-operability, connectivity, availability, and growth. The LOLA Procedures Application accomplishes these tasks by providing timely responsiveness for customers, increasing reliability and performance, increasing responsiveness to change, and reducing dependence on hardcopy. The Defense Logistics Information System (DLIS) is a centralized, large-scale, fully-integrated, mainframe system. As a part of this System, LOLA Procedures provides the on-line software designed to permit easy access to volumes of information stored in DLSC's databases. LOLA Procedures provides the End-User with user-friendly, help-responsive, interactive screens from which data is requested and then displayed. DTIC

N94-17291*# National Aeronautics and Space Administration. Langley Research Center, Hampton, VA.
NASA/DOD AEROSPACE KNOWLEDGE DIFFUSION RESEARCH PROJECT. REPORT 15: TECHNICAL UNCERTAINTY AND PROJECT COMPLEXITY AS CORRELATES OF INFORMATION USE BY US INDUSTRY-AFFILIATED AEROSPACE ENGINEERS AND SCIENTISTS: RESULTS OF AN EXPLORATORY INVESTIGATION
Thomas E. Pinelli, Nanci A. Glassman (Continental Research, Norfolk, VA.), Linda O. Affelder (Continental Research, Norfolk, VA.), Laura M. Hecht (Indiana Univ., Bloomington.), John M. Kennedy (Indiana Univ., Bloomington.), and Rebecca O. Barclay (Rensselaer Polytechnic Inst., Troy, NY.) Washington Sep. 1993 71 p
(RTOP 505-90-00)
(NASA-TM-107693; NAS 1.15:107693; Rept-15) Avail: CASI HC A04/MF A01

An exploratory study was conducted that investigated the influence of technical uncertainty and project complexity on information use by U.S. industry-affiliated aerospace engineers and scientists. The study utilized survey research in the form of a self-administered mail questionnaire. U.S. aerospace engineers and scientists on the Society of Automotive Engineers (SAE) mailing list served as the study population. The adjusted response rate was 67 percent. The survey instrument is appendix C to this report. Statistically significant relationships were found to exist between technical uncertainty, project complexity, and information use. Statistically significant relationships were found to exist between technical uncertainty, project complexity, and the use of federally funded aerospace R&D. The results of this investigation are relevant to researchers investigating information-seeking behavior of aerospace engineers. They are also relevant to R&D managers and policy planners concerned with transferring the results of federally funded aerospace R&D to the U.S. aerospace industry. Author

N94-17300*# National Aeronautics and Space Administration. Langley Research Center, Hampton, VA.
NASA/DOD AEROSPACE KNOWLEDGE DIFFUSION RESEARCH PROJECT. REPORT 15: TECHNICAL UNCERTAINTY AND PROJECT COMPLEXITY AS CORRELATES OF INFORMATION USE BY US INDUSTRY-AFFILIATED AEROSPACE ENGINEERS AND SCIENTISTS: RESULTS OF AN EXPLORATORY INVESTIGATION
Thomas E. Pinelli, Nanci A. Glassman (Continental Research, Norfolk, VA.), Linda O. Affelder (Continental Research, Norfolk, VA.), Laura M. Hecht (Indiana Univ., Bloomington.), John M. Kennedy (Indiana Univ., Bloomington.), and Rebecca O. Barclay (Rensselaer Polytechnic Inst., Troy, NY.) Sep. 1993 71 p
(RTOP 505-90-00)
(NASA-TM-107693; NAS 1.15:107693) Avail: CASI HC A04/MF A01

The NASA/DOD Aerospace Knowledge Diffusion Research Project attempts to understand, among other things, the information environment in which U.S. aerospace engineers and scientists work and the factors that influence their use of scientific and technical information (STI). Such an understanding could do the following: (1) lead to the development of practical theory; (2) contribute to the design and development of aerospace information systems; and (3) have practical implications for transferring the results of federally funded aerospace research and development (R&D) to the U.S. aerospace community. In this report, the results of an exploratory study that investigated the influence of two variables--technical uncertainty and project complexity--on the use of information and information sources in completing or solving a project, task, or problem are reported. Several authors have explored relationships among uncertainty, complexity, and information use (Tushman and Nadler; Gifford, Bobbitt, and Slocum; and Randolph). Tushman and Nadler, for example, reported that the more complex the R&D task, the greater the use of STI. Randolph found that the greater the uncertainty associated with the task, the greater the use of STI. These findings, plus the work of Bodensteiner; Holland, Stead, and Leibrock; Atkin; and Kuhlthau, led us to investigate the extent to which the perceived technical uncertainty and complexity of a project, task, or problem affected the use of information and information sources by U.S. aerospace engineers and scientists. The work of Paisley, Wilson, Roberts, Dervin, and Taylor regarding 'information use environments' influenced the conceptual framework, underlying assumptions, and direction of this study. Finally, information on the aerospace information environment and on the information seeking behavior of U.S. aerospace engineers and scientists is included to help establish a context for the study. The study's methodology is described in detail. The variables and their measurement are explained. The study's hypotheses, the data used to test the hypothesis, and a discussion of the results are presented. Author (revised)

N94-17419 Ohio State Univ., Columbus. Dept. of Computer and Information Science.
DESIGN AND DIAGNOSIS PROBLEM SOLVING WITH MULTIFUNCTIONAL TECHNICAL KNOWLEDGE BASES Final Report, 1 Sep. 1989 - 31 Oct. 1992
B. Chandrasekaran and John Josephson 29 Sep. 1992 226 p Limited Reproducibility: More than 20% of this document may be affected by microfiche quality
(Contract F49620-89-C-0110; DARPA Order 6919)
(AD-A268375; AFOSR-93-0575TR) Avail: Issuing Activity (Defense Technical Information Center (DTIC))

The research goal for the project reported here has been to develop enabling technology for building large knowledge bases designed to support automated and semi-automated problem solving for scientific and engineering domains. The work on analyzing problem-solving tasks, much of it preceding the project reported here, has led to the view that there are distinct, analyzable Generic Tasks (GT's) that occur naturally in problem-solving activity. The Functional Representation Language (FR), was originally introduced by Sembugamoorthy and Chandrasekaran as a device representation from which diagnosis specific knowledge could be derived by a process of knowledge compilation. It was subsequently applied to support other tasks besides diagnosis (most notably forms of qualitative simulation), and used to represent a wide variety of device types. DTIC

N94-17502 Politecnico di Milano (Italy). Dipt. di Elettronica e Informazione.
AUTOMATIC TRANSLATION OF DATABASE INTEGRITY CONSTRAINTS INTO COMPENSATING PRODUCTION RULES
Piero Fraternali 1992 27 p
(Rept-92-055; ETN-93-94567) Avail: Issuing Activity (Politecnico di Milano, Piazza Leonardo da Vinci 32, 20133 Milan, Italy)

In conventional database systems, consistency is preserved either by forbidding operations that violate integrity constraints or by rolling back transactions that produce inconsistent database states. A third way to integrity maintenance is that of post processing faulty transactions, by introducing system generated compensating actions that lead to a database state which is consistent and as close as possible to that intended by the user. Active databases provide the appropriate technology to implement this paradigm. A framework in which constraints are expressed in a logical language and automatically translated into a set of database rules is introduced. Automatic derivation not only of the triggering conditions of rules but also of the compensating actions is stressed, so that the user is presented with the complete set of actions available to repair constraints violations. This approach ensures that if the execution of the rules triggered by a faulty transaction eventually comes to an end, the final state reached is correct with respect to all the declared constraints. Compile time analysis of termination is then discussed and the features of the run time needed to cope with conflicts among rules enforcing different constraints or the same constraint in several ways are presented. ESA

N94-17529# Institut National de Recherche d'Informatique et d'Automatique, Valbonne (France). Programme 2: Calcul Symbolique, Programmation et Genie Logiciel.
LANGUAGE-BASED DOCUMENT PROCESSING
Dennis S. Arnon (Xerox Corp., Palo Alto, CA.), Isabelle Attali, and Paul Franchi-Zannettacci (Nice Univ., France.) Jul. 1992 21 p
(INRIA-RR-1731; ETN-93-94433) Avail: CASI HC A03/MF A01

An application of programming environments generation to structured documents manipulation is proposed. Centaur is used as a formal tool to model and implement logical and physical structure, logical editing and layout processing, document analysis, re-use and conversion for a sample class of documents: scientific articles including equations and figures. To make connections with real document systems, two particular external forms are given to the logical structure: Tioga source and LATEX source. From the specifications of the logical and physical structures of the Article document class on one hand, and, on the other hand, the specification of the layout processing (viewed as its semantics according to the Tioga or the LATEX layout model) and other semantic tools, the Centaur system automatically generates structured environments for Tioga and LATEX documents and conversions between them. ESA

N94-15560*# Royal Greenwich Observatory, Cambridge (England).
SLR DATA SCREENING; LOCATION OF PEAK OF DATA DISTRIBUTION
Andrew T. Sinclair *In* NASA. Goddard Space Flight Center, Eighth International Workshop on Laser Ranging Instrumentation Jun. 1993 10 p (For primary document see N94-15552 03-19)
Avail: CASI HC A02/MF A06

N94-15587*# National Aeronautics and Space Administration. Goddard Space Flight Center, Greenbelt, MD.
GEOMETRIC ANALYSIS OF SATELLITE LASER RANGING DATA
Brion Conklin (Bendix Field Engineering Corp., Seabrook, MD.), Steven Bucey (Bendix Field Engineering Corp., Seabrook, MD.), Van S. Husson (Bendix Field Engineering Corp., Seabrook, MD.), Winfield M. Decker (Bendix Field Engineering Corp., Seabrook, MD.), and John J. Degnan *In its* Eighth International Workshop on Laser Ranging Instrumentation Jun. 1993 8 p (For primary document see N94-15552 03-19)
Avail: CASI HC A02/MF A06

N94-15597*# Shanghai Observatory (China).
APPLICATION OF THE ROBUST ESTIMATE IN SLR DATA PREPROCESSING
De-Tong Tan, Zhong-Ping Zhang, Hua-Guan Xu, and Peiz-Hang Jia (Academia Sinica, Shanghai, China.) *In* NASA. Goddard Space Flight Center, Eighth International Workshop on Laser Ranging Instrumentation Jun. 1993 9 p (For primary document see N94-15552 03-19)
Avail: CASI HC A02/MF A06

N94-15910*# Jet Propulsion Lab., California Inst. of Tech., Pasadena.
DATA DISTRIBUTION
J. E. Hilland *In its* Proceedings of the Third Spaceborne Imaging Radar Symposium 28 May 1993 p 365-380 (For primary document see N94-15886 03-32)
Avail: CASI HC A03/MF A04

N94-16142*# National Aeronautics and Space Administration. Marshall Space Flight Center, Huntsville, AL.
MATERIALS, PROCESSES, AND ENVIRONMENTAL ENGINEERING NETWORK
Margo M. White *In* Huntsville Association of Technical Societies, TABES 1993: 9th Annual Technical and Business Exhibition and Symposium 1993 5 p (For primary document see N94-16129 03-38)
(TABES Paper 93-610) Avail: CASI HC A01/MF A03

N94-16209*# Washington Univ., Saint Louis, MO. Dept. of Earth and Planetary Sciences.
THE PLANETARY DATA SYSTEM EDUCATIONAL CD-ROM Abstract Only
E. A. Guinness, R. E. Arvidson, M. Martin (Jet Propulsion Lab., California Inst. of Tech., Pasadena.), and S. Dueck (Jet Propulsion Lab., California Inst. of Tech., Pasadena.) *In* Lunar and Planetary Inst., Twenty-Fourth Lunar and Planetary Science Conference. Part 2: G-M 1993 p 585-586 (For primary document see N94-16173 03-91)
Avail: CASI HC A01/MF A06

N94-17177 INISEL, Torrejon de Ardoz (Spain).
DATA HANDLING STRATEGY FOR THE SPANISH SMALL SATELLITE PROGRAM (MINISAT)
X. Lobao and L. Pina *In* CNES, Small Satellites Systems and Services Jan. 1993 p 567-575 (For primary document see N94-17131 03-18)
Copyright Avail: Issuing Activity (CEPADUES-Editions, 111 rue Nicolas-Vaquelin, 31100 Toulouse, France)

N94-17178 Centre National d'Etudes Spatiales, Toulouse (France).
THE STRV ON BOARD DATA HANDLING (OBDH) SYSTEM: AN INTRODUCTION
H. G. Andrews *In its* Small Satellites Systems and Services Jan. 1993 p 577-578 (For primary document see N94-17131 03-18)
Copyright Avail: Issuing Activity (CEPADUES-Editions, 111 rue Nicolas-Vaquelin, 31100 Toulouse, France)

83 ECONOMICS AND COST ANALYSIS

Includes cost effectiveness studies.

N94-16988# Institute for Defense Analyses, Alexandria, VA.
A HANDBOOK OF COST RISK ANALYSIS METHODS Final Report, Oct. 1991 - Apr. 1993
Philip M. Lurie, Matthew S. Goldberg, and Mitchell S. Robinson Apr. 1993 50 p
(AD-A267253; IDA-P-2734; IDA/HQ-92-41686; AD-E501670) Avail: CASI HC A03/MF A01

When estimating costs, interval estimates are more informative than simple point estimates. Interval estimates are sometimes available using analytical methods. These methods may be either exact (for example, a sum of random variables) or approximate (for example, based on Taylor series). When analytical methods are not available, simulation may be used instead. This paper illustrates the application of both analytical and simulation methods to the three main types of cost analysis: cost-estimating relationships, work breakdown structures, and stochastic network models. In addition, the paper contains descriptions of some commercially-available software products that can be used to perform simulations for the types of cost-risk analysis described. DTIC

N94-17190 Smith System Engineering Ltd., Guildford (England).
COST DRIVERS: WHY DO CONVENTIONAL SATELLITES COST SO MUCH?
Chris Elliott *In* CNES, Small Satellites Systems and Services Jan. 1993 p 703-708 (For primary document see N94-17131 03-18)
Copyright Avail: Issuing Activity (CEPADUES-Editions, 111 rue Nicolas-Vaquelin, 31100 Toulouse, France)

N94-17191 Euroconsult, Paris (France).
KEY TRENDS OF THE SMALL SATELLITE MARKET
Stephane Chenard *In* CNES, Small Satellites Systems and Services Jan. 1993 p 709-722 (For primary document see N94-17131 03-18)
Copyright Avail: Issuing Activity (CEPADUES-Editions, 111 rue Nicolas-Vaquelin, 31100 Toulouse, France)

84 LAW, POLITICAL SCIENCE AND SPACE POLICY

Includes NASA appropriation hearings; aviation law; space law and policy; international law; international cooperation; and patent policy.

N94-17290* National Aeronautics and Space Administration, Washington, DC.
SPACE COMMERCE IN A GLOBAL ECONOMY: COMPARISON OF US AND AUSTRALIAN APPROACHES
Barbara A. Stone and John R. Page (New South Wales Univ., Kensington, Australia.) 1993 17 p Presented at the 44th Congress of the International Astronautical Federation, Graz, Austria, 16-22 Oct. 1993
(NASA-TM-109341; NAS 1.15:109341; IAA.1.2-93-651) Copyright Avail: Issuing Activity

The United States and Australia are among the 20 or more nations of the world having industries currently engaging in some form of space commerce. As a matter of national policy, the United States has encouraged private investment and involvement in space activities since 1984, when the Congress declared it in the best interest of the Nation that NASA '...seek and encourage to the maximum extent possible, the fullest commercial use of space.' Australia's space policy, announced in 1986, has the objective of encouraging greater involvement by industry in space research and development, and the development of commercial space activities. This paper discusses the underlying policies, current status, and prospects for the future of commercial space business activities in the two countries. Author (revised)

85 URBAN TECHNOLOGY AND TRANSPORTATION

Includes applications of space technology to urban problems; technology transfer; technology assessment; and surface and mass transportation.

For related information see also *03 Air Transportation and Safety, 16 Space Transportation,* and *44 Energy Production and Conversion.*

N94-15249* National Aeronautics and Space Administration, Washington, DC.
FROM SPACE TO EARTH (Videotape)
Jun. 1987 Videotape: 3 min. 30 sec. playing time, in color, with sound
(NASA-TM-109638; NONP-VT-93-190436) Avail: CASI VHS A01/BETA A22

This video presents a few NASA spinoffs, including Statue of Liberty paint, Unistick, an ocular screening device, and running shoes. CASI

N94-15337* National Aeronautics and Space Administration. Lewis Research Center, Cleveland, OH.
NASA IMAGES 7 (Videotape)
Mar. 1988 Videotape: 27 min. 49 sec. playing time, in color, with sound
(NASA-TM-109438; NONP-VT-93-190235) Avail: CASI VHS A01/BETA A22

This videotape shows how space derived technology is being used to benefit people on Earth. CASI

N94-15339* National Aeronautics and Space Administration. Lewis Research Center, Cleveland, OH.
NASA IMAGES 16 (Videotape)
May 1988 Videotape: 28 min. 25 sec. playing time, in color, with sound
(NASA-TM-109440; NONP-VT-93-190237) Avail: CASI VHS A01/BETA A22

The videotape describes NASA technology that is in everyday use. CASI

N94-17293*# Tennessee Univ. Space Inst., Tullahoma.
TECHNOLOGY TRANSFER. DETERMINING INDUSTRY NEEDS: A GUIDE FOR COMMUNITIES
31 Mar. 1993 28 p Sponsored by NASA. Marshall Space Flight Center
(NASA-CR-194676; NAS 1.26:194676) Avail: CASI HC A01/MF A01

This Guide was developed in accordance with the Memorandum of Understanding between the NASA George C. Marshall Space Flight Center and the following States: Alabama, Georgia, Louisiana, Mississippi, Tennessee, West Virginia. The economic welfare of individual communities is currently a matter of considerable interest. Concern for the position of US industry in the competitive world marketplace is a matter of growing concern as well. This 'guide' describes a process whereby communities may seize the opportunity to improve their own economic destiny. The method described involves linking the technology needs of existing industries to the technologies which are available from Federal Laboratories. Community technology transfer is an 'action possibility' which allows individual citizen groups to do something tangible to improve the economic climate of the places where they live and work. The George C. Marshall Space Flight Center in Huntsville, Alabama is pledged to promote and encourage such efforts, and stands ready to help communities both large and small in that regard. Derived from text

N94-17294*# National Aeronautics and Space Administration. Marshall Space Flight Center, Huntsville, AL.
TECHNOLOGY IN ACTION Annual Report
1992 88 p
(NASA-TM-109345; NAS 1.15:109345) Avail: CASI HC A05/MF A01

In keeping with the NASA Administrator's announcement that technology transfer will become a fundamental mission of NASA, the Marshall Space Flight Center (MSFC) has initiated new programs to reach the heartland of U.S. industry. The Center has continued to expand its already well-established outreach program aimed at helping American business, industry, and academia at the grassroots level. The goal is to ensure that America regains and maintains its proper place of leadership among the world's technologically developed nations. MSFC's national goal is to

enhance America's competitiveness in the world marketplace, fortify the value of the dollar, and ensure technological breakthroughs by American laboratories benefit taxpayers and industries. The Technology Utilization (TU) Office at MSFC believes a number of measures are possible to slow, then halt, and ultimately reverse the erosion of American technological leadership. MSFC's TU Office is reaching out to American industry on an increasingly broadening scope, facilitating the transfer of NASA derived technologies to American businesses, industries, educational institutions, and individuals. There are many valid approaches to achieving this goal. Some, such as the National Technology Initiative, begin at the top and work down through America's top corporate structure. Others, such as the technology transfer program that MSFC has implemented, begin at the one-on-one, grassroots level -- working with small and medium-sized firms that form the bulk of American industry. What can be done by one NASA center is, admittedly, limited. But by extrapolating this one-on-one approach to the more than 700 Federal laboratories, a great deal can be accomplished. This report contains an examination of outreach and in reach programs, problem statements programs, applications projects, new technology reporting, new technology administration, and the need for increased resources to further facilitate technology transfer. Derived from text

N94-16132*# National Aeronautics and Space Administration, Washington, DC.
COMMERCIAL SPACE OPPORTUNITIES ADVANCED CONCEPTS AND TECHNOLOGY OVERVIEW
Gregory M. Reck *In* Huntsville Association of Technical Societies, TABES 1993: 9th Annual Technical and Business Exhibition and Symposium 1993 7 p (For primary document see N94-16129 03-38)
(TABES Paper 93-240) Avail: CASI HC A02/MF A03

88 SPACE SCIENCES (GENERAL)

No abstracts in this category.

89 ASTRONOMY

Includes radio, gamma-ray, and infrared astronomy, and astrometry.

N94-14929# Lawrence Livermore National Lab., CA.
DESIGN OF PULSE STRETCHING CELL FOR A SODIUM GUIDE STAR OPTICAL SYSTEM
H. W. Friedman, J. A. Horton, T. J. Kuklo, and N. J. Wong 10 Nov. 1992 4 p Presented at the OPTCON 1992 Optical Fabrication and Testing Workshop, Boston, MA, 17 Nov. 1992
(Contract W-7405-eng-48)
(DE93-016436; UCRL-JC-110714; CONF-9211104-10) Avail: CASI HC A01/MF A01

A pulse stretcher has been designed for the LLNL sodium guide star experiment to lower the laser flux and avoid saturation effects. The optical design, mechanical layout, and wavefront error analysis are presented. DOE

N94-15311* National Aeronautics and Space Administration, Washington, DC.
LUNAR RANGING (Videotape)
Aug. 1985 Videotape: 4 min. 38 sec. playing time, in color, with sound
(NASA-TM-109603; NONP-VT-93-190401) Avail: CASI VHS A01/BETA A22

This videotape describes the work at the Lure observatory (Hawaii) in the area of Lunar rangefinding. This work uses laser technology to range the moon with an accuracy of one inch. CASI

N94-15422* National Aeronautics and Space Administration. Goddard Space Flight Center, Greenbelt, MD.
NASA'S HUBBLE SPACE TELESCOPE: THE CHALLENGE AND COMPLEXITY OF OPERATIONS (Videotape)
Jun. 1989 Videotape: 16 min. 5 sec. playing time, in color, with sound
(NASA-TM-109577; NONP-VT-93-190375) Avail: CASI VHS A01/BETA A22

This video presentation touches on the truly fast complexity of the first of NASA's great observatories, the Hubble Space Telescope. CASI

N94-15481*# National Aeronautics and Space Administration. Goddard Space Flight Center, Greenbelt, MD.
TOTAL SOLAR ECLIPSE OF 3 NOVEMBER 1994
Fred Espenak and Jay Anderson (Prairie Weather Centre, Winnipeg, Manitoba.) Oct. 1993 69 p
(RTOP 693-00-00)
(NASA-RP-1318; Rept-93B00120; NAS 1.61:1318) Avail: CASI HC A04/MF A01

A total eclipse of the Sun will be visible from the southern half of the Western Hemisphere on 3 November 1994. The path of the Moon's shadow passes through Peru, Chile, Bolivia, Paraguay, and Brazil. Detailed predictions for this event are presented and include tables of geographic coordinates of the path of totality, local circumstances for hundreds of cities, maps of the path of total and partial eclipse, weather prospects, and the lunar limb profile. Author

N94-15679*# Pennsylvania State Univ., University Park.
THE THEORY OF QSO ABSORPTION LINE SYSTEMS AND THEIR RELATIONSHIP TO THE GALAXIES Annual Status Report
Jane Charlton 1 Nov. 1993 3 p
(Grant NAGw-3571)
(NASA-CR-194596; NAS 1.26:194596) Avail: CASI HC A01/MF A01

The fundamental goal of this effort is to paint a picture of what the Ly-alpha forest clouds are and how they are distributed in space. Progress during the first phase of this program involved development of the 'Cheshire Cat Model' of Ly-alpha clouds in which systems over a large range of column densities are produced by disks with somewhat smaller column densities than those of normal galaxies. A prediction of the slab model of Ly-alpha clouds was confirmed by a new observational result, and the comparison of models to the new data allowed an estimate of the pressure of the intergalactic medium. This result should be forthcoming in pre-print form within the next month. The various results will now be described in more detail. Derived from text

N94-16492*# Colorado Univ., Boulder.
ROSAT-IUE OBSERVATIONS OF SYMBIOTIC STARS. THE X RAY MORPHOLOGY OF HIGH LATITUDE ASSOCIATIONS Final Report
Robert E. Stencel 31 Oct. 1993 2 p
(Grant NAG5-1798)
(NASA-CR-194616; NAS 1.26:194616) Avail: CASI HC A01/MF A01

The purposes of this grant included: to provide for continuing investigations of the x-ray properties of a class of interacting binaries known as symbiotic stars through analysis of their detection statistics in the ROSAT All-Sky Survey and simultaneous IUE observations; and to obtain and analyze ROSAT images of selected high latitude OB star associations, in order to permit multi-wavelength dissection of their contents and energetics. The first study is expected to result in enhanced information on mass transfer and accretion in such systems, and provide a more quantitative basis for interpretation of the spectra of these and similar stellar and extragalactic systems. This particular effort represents NASA support for an approved collaboration between the PI and the ROSAT Team at MPE Garching. In the second study, we seek to correlate the strength with which the diffuse clouds have been shocked and the recent star formation triggered, namely, the O and B stars of the Association, as well as nearby T Tauri stars. The large scale X-ray emission in deep ROSAT PSPC images will be compared with the optical, infrared, and radio topology of nearby supernova remnants, molecular clouds, and the distribution of massive stars in the regions. This should enable us to test whether the star formation triggering shocks originate from in the galactic plane (nearby supernovae) or from the collision of infalling matter with the disk material (galactic fountain dynamics). Author

N94-16833*# Northwestern Univ., Chicago, IL.
COMPLEX QSO ABSORBERS: HIGH-REDSHIFT CLUSTERS OF GALAXIES? Final Technical Report
David M. Meyer 9 Nov. 1993 2 p
(Grant NAG5-1779)
(NASA-CR-194617; NAS 1.26:194617) Avail: CASI HC A01/MF A01

Using the PSPC instrument on the ROSAT satellite, we have obtained deep exposures of the fields centered on the QSO's 1556+335, 1037-271, and 0854+191 in an effort to search for extended X-ray emission corresponding to complex QSO absorption-line systems (QALS's) that could be indicative of clusters of galaxies at high redshift. The QSO 1556+335 is known to have a pair of complicated C IV absorption systems at z equals 1.610 (Delta v = 988 km/s) and z equals 1.650 (Delta v = 1677 km/s) near the z equals 1.641 QSO redshift. It has been suggested that the absorption may be due to two rich clusters, one containing the QSO itself. The QSO 0854+191 (z(sub em) = 1.89) has 6 strong C IV absorption systems in 2 close groups at z equals 1.2954, 1.2973,1.3019 and z equals 1.3522, 1.3543, 1.3558. Assuming q(sub O) equals 0.5 and H(sub O) equals 50 km/s Mpc(exp -l), the redshift range of this absorption-line cluster corresponds to a radial distance of 44 Mpc. Interestingly, there is a nearby (approximately 30') QSO (0856+189) with a projected separation of 16 Mpc whose redshift (z = 1.29) is similar to that of the absorbing material toward 0854+191. In the case of 1037-271 (Z(sub em) = 2.18), common QALSs have been observed at z equals I.90, 1.96, 2.02, 2.08, and 2.14 (a radial range of 66 Mpc) in its spectrum and that of its neighbor Tol 1038-272 (Z(sub em) = 2.32) whose 18' separation corresponds to a linear distance of 9 Mpc at z approximately equals 2. The length scales implied by the absorbers toward 0854+191 and 1037-271 are interesting in that they suggest structures more akin to superclusters than clusters. Derived from text

N94-16872# Lawrence Livermore National Lab., CA.
TIP-TILT COMPENSATION: RESOLUTION LIMITS FOR GROUND-BASED TELESCOPES USING LASER GUIDE STAR ADAPTIVE OPTICS
S. S. Olivier, C. E. Max, D. T. Gavel, and J. M. Brase Oct. 1992 52 p Presented at the Laser Guide Star Adaptive Optics Workshop, Albuquerque, NM, 10-12 Mar. 1992
(Contract W-7405-eng-48)
(DE93-016426; UCRL-JC-109219-Rev-2; CONF-9203139-5-Rev-2) Avail: CASI HC A04/MF A01

The angular resolution of long-exposure images from ground-based telescopes equipped with laser guide star adaptive optics systems is fundamentally limited by the the accuracy with which the tip-tilt aberrations introduced by the atmosphere can be corrected. Assuming that a natural star is used as the tilt reference, the residual error due to tilt anisoplanatism can significantly degrade the long-exposure resolution even if the tilt reference star is separated from the object being imaged by a small angle. Given the observed distribution of stars in the sky, the need to find a tilt reference star quite close to the object restricts the fraction of the sky over which long-exposure images with diffraction limited resolution can be obtained. In this paper, the authors present a comprehensive performance analysis of tip-tilt compensation systems that use a natural star as a tilt reference, taking into account properties of the atmosphere and of the Galactic stellar populations and optimizing over the system operating parameters to determine the fundamental limits to the long-exposure resolution. Their results show that for a ten meter telescope on Mauna Kea, if the image of the tilt reference star is uncorrected, about half the sky can be imaged in the V band with long-exposure resolution less than 60 milli-arc-seconds (mas), while if the image of the tilt reference star is fully corrected, about half the sky can be imaged in the V band with long-exposure resolution less than 16 mas. Furthermore, V band images long-exposure resolution of less than 16 mas may be obtained with a ten meter telescope on Mauna Kea for unresolved objects brighter than magnitude 22 that are fully corrected by a laser guide star adaptive optics system. This level of resolution represents about 70% of the diffraction limit of a ten meter telescope in the V band and is more than a factor of 45 better than the median seeing in the V band on Mauna Kea. DOE

N94-17225# Air Force Operational Test and Evaluation Center, Scott AFB, IL. Detachment 1.
SOLAR ELECTRO-OPTICAL NETWORK (SEON) UPGRADE/REPLACEMENT PROGRAM. PHASE 1: QUALIFICATION OPERATIONAL TEST AND EVALUATION PLAN Test Report
Stephen D. Fitts and Herman E. Loftin Jun. 1993 84 p
(AD-A266364; AFOTEC-DET1/TP-92-007) Avail: CASI HC A05/MF A01

Detachment 1, Air Force Operational Test and Evaluation Center will conduct a Qualification Operational Test and Evaluation (QOT&E) on the SEON Upgrade/Replacement Program during the fourth quarter of FY 1993 and the first quarter of FY1994 at the Palehua Solar Observatory in Hawaii. The purpose of this QOT&E is to determine the operational suitability and effectiveness of the upgraded SEON so decision makers can decide what changes, if any, need to be made prior to upgrading the other sites. SEON measures solar events to predict their impact on manned space activities and satellite communication, and validates ionospheric disturbances. SEON interfaces with the Air Force Space Forecast Center and the Air Force Global Weather Central. It is comprised of five Solar Observing Optical Networks (SOONs) and four Radio Solar Telescope Networks (RSTNs) longitudinally separated to ensure the sun is constantly monitored. Each SOON is composed of a solar optical telescope (AN/FMQ-7) with automatic solar tracking. Each RSTN is composed of a solar radio telescope (AN/FRR-95) with automatic solar tracking. This equipment also measures the magnitude of solar flares and prepares the necessary solar event messages for release by the operator into the Automated Weather Network. DTIC

N94-17438*# National Aeronautics and Space Administration. Pasadena Office, CA.
WIDE ANGLE, SINGLE SCREEN, GRIDDED SQUARE-LOOP FREQUENCY SELECTIVE SURFACE FOR DIPLEXING TWO CLOSELY SEPARATED FREQUENCY BANDS Patent Application
Te-Kao Wu, inventor (to NASA) (Jet Propulsion Lab., California Inst. of Tech., Pasadena.) 15 Jul. 1993 26 p
(Contract NAS7-918)
(NASA-Case-NPO-18664-1-CU; NAS 1.71:NPO-18664-1-CU; US-Patent-Appl-SN-094331) Avail: CASI HC A03/MF A01

The design and performance of a wide angle, single screen, frequency selective surface (FSS) with gridded square-loop path elements are described for diplexing closely separated signal bands, for example, X- and Ku-band signals in an Orbiting Very Long Baseline Interferometer (OVLBI) earth station reflector antenna system, as well as other applications such as military and commercial communications via satellites. Excellent agreement is obtained between the predicted and measured results of this FSS design using the gridded square-loop patch elements sandwiched between 0.0889 cm thick tetrafluoroethylene fluorocarbon polymer (PTFE) slabs. Resonant frequency drift is reduced by 1 GHz with an incident angle from n degrees normal to 40 degrees from normal. NASA

N94-17568# Range Commanders Council, White Sands Missile Range, NM. Optical Systems Group.
TEST METHODS FOR ACCEPTANCE TESTING OF TELESCOPES
Jul. 1993 40 p
(AD-A268316; RCC-457-93) Avail: CASI HC A03/MF A01

This guide will provide government organizations who are responsible for the procurement of long focal-length optical systems (telescopes) with a general knowledge of what tests can, and generally should, be performed on these systems to ensure compliance with the required specifications. General test procedures are also included. Since test facilities and test equipment available vary considerably among organizations, it is impractical to write a 'cookbook' type of guide to be followed rigorously by all. It is also true that some procured systems may possess special features not generally found in the normal imaging telescope system such as beam splitters, special filters, and reticles. DTIC

N94-17629 Max-Planck-Inst. fuer Physik und Astrophysik, Garching (Germany). Inst. fuer Astrophysik.
A COMPARISON OF CALCULATED AND OBSERVED MONOCHROMATIC TYPE Ia SUPERNOVA LIGHT CURVES
E. Mueller and P. Hoeflich (Technische Univ., Munich, Germany.) Dec. 1992 35 p Submitted for publication

(MPA-709; ETN-93-94916) Copyright Avail: Issuing Activity (Max-Planck-Institut fuer Physik und Astrophysik, Karl-Schwarzschild-Strasse 1, 8046 Garching, Germany)

The calculated monochromatic light curves of a set of type Ia supernova models are compared with the observed monochromatic light curves of 13 type Ia Supernovae (SNIa). The set consists of 11 type Ia supernova models including deflagrations, detonations, delayed detonations, pulsating delayed detonations and tamped detonations. The theoretical light curves were calculated using our recently developed light curve model. The model incorporates a detailed equation of state with an elaborate treatment of the ionization balance, an implicit grey LTE (Local Thermodynamic Equilibrium) radiation transport scheme based on the moment equations, a total energy equation for the gas and the radiation field, expansion opacities, and a Monte Carlo gamma ray deposition scheme. To evolve the structure of the underlying explosion models homologous expansion is assumed. Based on a comparison of theoretical light curves and observational data, the distances of the patent galaxies were determined. It is shown that SNe Ia allow for a measurement of the value of the Hubble constant provided individual fits are used and if they are located at distances larger than 15 Mpc, because only then they are in the 'Hubble' flow. Taking this restriction into account a Hubble constant can be derived within a 2 sigma error. ESA

N94-15029# Consiglio Nazionale delle Ricerche, Bologna (Italy). Ist. di Tecnologie e Studio sulle Radiazioni Extraterrestri.

CdTe ARRAY DETECTORS FOR HIGH ENERGY ASTRONOMY

E. Caroli, G. Baldazzi (Bologna Univ., Italy.), G. DiCocco, A. Donati, W. Dusi, G. Malaguti (Bologna Univ., Italy.), J. B. Stephen, and M. Trifoglio *In* ESA, Proceedings of an ESA Symposium on Photon Detectors for Space Instrumentation Dec. 1992 p 27-31 (For primary document see N94-15025 03-19)

Copyright Avail: CASI HC A01/MF A04

N94-15033# GEC Hirst Research Centre, Wembley (England).

DEVELOPMENT OF X RAY CCDS

D. J. Burt *In* ESA, Proceedings of an ESA Symposium on Photon Detectors for Space Instrumentation Dec. 1992 p 57-67 Prepared in cooperation with English Electric Valve Co. Ltd., Chelmsford, England (For primary document see N94-15025 03-19)

Copyright Avail: CASI HC A03/MF A04

N94-15038# Leicester Univ. (England). X Ray Astronomy Group.

MICROCHANNEL PLATE DETECTORS FOR SPACE ASTRONOMY

G. W. Fraser *In* ESA, Proceedings of an ESA Symposium on Photon Detectors for Space Instrumentation Dec. 1992 p 97-102 (For primary document see N94-15025 03-19)

Copyright Avail: CASI HC A02/MF A04

N94-15039# University Coll., London (England). Dept. of Physics and Astronomy.

THE MIC PHOTON COUNTING DETECTOR

J. L. A. Fordham, D. A. Bone, M. K. Oldfield, J. G. Bellis, and T. J. Norton (Imperial Coll. of Science and Technology, London, England.) *In* ESA, Proceedings of an ESA Symposium on Photon Detectors for Space Instrumentation Dec. 1992 p 103-106 (For primary document see N94-15025 03-19)

(Contract ESA-8819/90/NL/US(SC))

Copyright Avail: CASI HC A01/MF A04

N94-15043# Rockwell International Science Center, Anaheim, CA.

VISIBLE LIGHT PHOTON COUNTERS FOR ASTRONOMY

M. G. Stapelbroek, M. D. Petroff, and R. Bharat *In* ESA, Proceedings of an ESA Symposium on Photon Detectors for Space Instrumentation Dec. 1992 p 125-128 (For primary document see N94-15025 03-19)

Copyright Avail: CASI HC A01/MF A04

N94-15055# Chalmers Univ. of Technology, Goeteborg (Sweden).

HOT ELECTRON MIXERS, THE POTENTIAL COMPETITION

Erik L. Kollberg, E. Gershenzon (Academy of Pedagogical Sciences of the USSR, Moscow.), G. Goltsman (Academy of Pedagogical Sciences of the USSR, Moscow.), and K. S. Yngvesson (Massachusetts Univ., Amherst.) *In* ESA, Proceedings of an ESA Symposium on Photon Detectors for Space Instrumentation Dec. 1992 p 201-206 (For primary document see N94-15025 03-19)

Copyright Avail: CASI HC A02/MF A04

N94-15057# Danish Space Research Inst., Lyngby.

OUTLOOK FOR HARD X RAY AND GAMMA RAY ASTRONOMY

Niels Lund *In* ESA, Proceedings of an ESA Symposium on Photon Detectors for Space Instrumentation Dec. 1992 p 213-216 (For primary document see N94-15025 03-19)

Copyright Avail: CASI HC A01/MF A04

N94-15061# Stanford Linear Accelerator Center, CA.

GAMMA LARGE AREA SILICON TELESCOPE: APPLYING SI STRIP DETECTOR TECHNOLOGY TO THE DETECTION OF GAMMA RAYS IN SPACE

W. B. Atwood, E. D. Bloom, G. L. Godfrey, P. L. Hertz (Naval Research Lab., Washington, DC.), Ying-Chi Lin (Stanford Univ., CA.), P. L. Nolan (Stanford Univ., CA.), A. E. Snyder (Stanford Univ., CA.), R. E. Taylor, K. S. Wood (Naval Research Lab., Washington, DC.), and P. F. Michelson (Stanford Univ., CA.) *In* ESA, Proceedings of an ESA Symposium on Photon Detectors for Space Instrumentation Dec. 1992 p 227-232 (For primary document see N94-15025 03-19)

Copyright Avail: CASI HC A02/MF A04

N94-15087# Institut National des Sciences Appliquees, Toulouse (France). Lab. de Physique des Solides.

SILICON GALLIUM DOPED PHOTOCONDUCTOR DEVELOPMENT FOR THE AROME BALLOON BORNE INSTRUMENT

C. Meny, I. Ristorcelli (Centre d'Etude Spatiale des Rayonnements, Toulouse, France.), M. Giard (Centre d'Etude Spatiale des Rayonnements, Toulouse, France.), G. Sirmain, G. Serra (Centre d'Etude Spatiale des Rayonnements, Toulouse, France.), G. Lucas (Commissariat a l'Energie Atomique, Grenoble, France.), and J. Leotin *In* ESA, Proceedings of an ESA Symposium on Photon Detectors for Space Instrumentation Dec. 1992 p 353-356 (For primary document see N94-15025 03-19)

Copyright Avail: CASI HC A01/MF A04

N94-15090# Imperial Coll. of Science and Technology, London (England). Blackett Lab.

APPLICATIONS FOR LARGE AREA SILICON DRIFT DETECTORS ON X RAY AND GAMMA RAY ASTRONOMY

G. K. Rochester, T. J. Sumner, R. J. Wheadon, G. Hall, B. Swinyard (Rutherford Appleton Lab., Chilton, England.), and P. Seller (Rutherford Appleton Lab., Chilton, England.) *In* ESA, Proceedings of an ESA Symposium on Photon Detectors for Space Instrumentation Dec. 1992 p 365-368 (For primary document see N94-15025 03-19)

Copyright Avail: CASI HC A01/MF A04

N94-15093# Swedish Inst. of Space Physics, Kiruna.

REQUIREMENTS ON CCD-DETECTORS FOR GROUND-BASED AURORAL IMAGING

A. Steen and U. Braendstroem *In* ESA, Proceedings of an ESA Symposium on Photon Detectors for Space Instrumentation Dec. 1992 p 379-382 (For primary document see N94-15025 03-19)

Copyright Avail: CASI HC A01/MF A04

N94-15099# Interuniversity Micro-Electronics Center, Leuven (Belgium).

CRYOGENIC READOUT ELECTRONICS FOR ASTRONOMICAL APPLICATIONS

B. Dierickx, J. Vermeiren, S. Cos, R. Faymonville (Battelle Inst., Frankfurt am Main, Germany.), and D. Lemke (Max-Planck-Inst. fuer Astronomie, Heidelberg, Germany.) *In* ESA, Proceedings of an ESA Symposium on Photon Detectors for Space Instrumentation Dec. 1992 p 405-408 Sponsored by Deutsche Agentur fuer Raumfahrtangelegenheiten G.m.b.H. (For primary document see N94-15025 03-19)

Copyright Avail: CASI HC A01/MF A04

N94-15625*# National Aeronautics and Space Administration. Goddard Space Flight Center, Greenbelt, MD.

STATION REPORT ON THE GODDARD SPACE FLIGHT CENTER (GSFC) 1.2 METER TELESCOPE FACILITY

Jan F. McGarry, Thomas W. Zagwodzki, Arnold Abbott, John J. Degnan,

Jack W. Cheek (Hughes STX, Inc., Lanham, MD.), Richard S. Chabot (Bendix Field Engineering Corp., Seabrook, MD.), David A. Grolemund (Bendix Field Engineering Corp., Seabrook, MD.), and Jim D. Fitzgerald (Bendix Field Engineering Corp., Seabrook, MD.) *In its* Eighth International Workshop on Laser Ranging Instrumentation Jun. 1993 8 p (For primary document see N94-15552 03-19)
Avail: CASI HC A02/MF A06

N94-16433*# Lockheed Aircraft Corp., Palo Alto, CA. Research Lab.
EFFECTS OF LEVITATED DUST ON ASTRONOMICAL OBSERVATIONS FROM THE LUNAR SURFACE Abstract Only
D. L. Murphy and R. R. Vondrak *In* Lunar and Planetary Inst., Twenty-Fourth Lunar and Planetary Science Conference. Part 2: G-M 1993 p 1033-1034 (For primary document see N94-16173 03-91)
Avail: CASI HC A01/MF A06

90 ASTROPHYSICS

Includes cosmology; celestial mechanics; space plasmas; and interstellar and interplanetary gases and dust.

For related information see also *75 Plasma Physics*.

N94-15188*# Smithsonian Astrophysical Observatory, Cambridge, MA.
MOLECULAR PROCESSES IN COMETS Annual Progress Report No. 2, 1 Nov. 1992 - 31 Oct. 1993
A. Dalgarno Aug. 1993 38 p
(Grant NAGw-1561)
(NASA-CR-194148; NAS 1.26:194148) Avail: CASI HC A03/MF A01

Classical trajectory calculations of the cross sections for vibrational and rotational energy exchange in direct and reactive collisions of hydrogen atoms and hydrogen molecules have been carried out. To test the sensitivity, three potential energy surfaces have been used. For the exchange transitions which occur at small internuclear distances, the rate coefficients for the three surfaces agree quite well. For the direct transitions, there are significant differences for the pure rotational transitions from j=0 to 2 and from j=1 to j=3 in which there is no change in vibration. For higher j the differences tend to disappear, suggesting that the rotational angular momentum can couple to the orbital angular momentum to overcome the centrifugal barrier. Complete numerically exact quantum mechanical calculations for the process in which vJ changes have been performed. Dr. M. A'Hearn has provided data on the fluorescent population of the NH rotational and fine-structure levels from which we should be able to predict accurate photodissociation lifetimes. The distribution rate of C2 is being investigated. A review of H3(+) in terrestrial and extraterrestrial environments was prepared for a volume of Advances in Atomic, Molecular and Optical Physics.
Derived from text

N94-15495* National Aeronautics and Space Administration. Ames Research Center, Moffett Field, CA.
PIONEER-VENUS PRESS CLIP (Videotape)
May 1988 Videotape: 11 min. playing time, in color, with sound
(NASA-TM-109425; NONP-VT-93-190222) Avail: CASI VHS A01/BETA A22

This video shows, with high quality animation, the formation of the Solar System: comets, Jupiter, Europa, Saturn, Titan, Mars, the Sun, and early Earth. The focus is on life elsewhere in the Solar System. The recording was prepared for a news conference.
CASI

N94-15970# *Aarhus Univ. (Denmark). Inst. of Physics and Astronomy.*
ASTRONOMY AND ASTROPHYSICS Biannual Report, 1991-1992
Helge Knudsen, ed. and Alice Grandjean, ed. 1992 23 p
Avail: CASI HC A03/MF A01

The possibility that strange quark matter (SQM), rather than Fe-56, could be the ground state of hadronic matter has attracted a lot of attention since Witten resurrected the idea in 1984. Stable or metastable SQM can play an important role in cosmology, neutron stars, cosmic ray physics, and relativistic heavy-ion collisions. The following is a brief introduction (with a bias towards Arhus-activities) to the physics and astrophysics of SQM. Further details can be found in the Proceedings of the International Workshop on Strange Quark Matter in Physics and Astrophysics, which was held at Aarhus University from May 20-24, 1991. Derived from text

N94-16052# California Univ., Berkeley. Lawrence Berkeley Lab.
FAST PULSARS, COMPACT STARS, AND THE STRANGE MATTER HYPOTHESIS
F. Weber and N. K. Glendenning 17 Mar. 1993 5 p Presented at the 2nd International Conference on Physics and Astrophysics of Quark-Gluon Plasma, Calcutta, India, 19-23 Jan. 1993
(Contract DE-AC03-76SF-00098)
(DE93-015039; LBL-33771; CONF-9301109-3) Avail: CASI HC A01/MF A01

Part one of this paper deals with the recent finding of the possible existence of a mixed phase of baryon matter and quark matter inside neutron stars. In part two, we review the theoretically determined minimum rotational periods of neutron stars, which serve to distinguish between pulsars that can be understood as rotating neutron stars and those that can not. Likely candidates for the latter are hypothetical strange stars. Their mass-radius relationship is discussed in the last part. It is pointed out that strange stars with a nuclear crust can give rise to the observed phenomena of pulsar glitches, thus passing the only astrophysical test of the strange-matter hypothesis existing to date.
DOE

N94-16118# Chicago Univ., IL.
PARTICLE PHYSICS AND COSMOLOGY, TASK C
M. S. Turner May 1993 15 p
(Contract DE-FG02-90ER-40560)
(DE93-016865; DOE/ER-40560/4C) Avail: CASI HC A03/MF A01

The research has spanned many topics at the boundary of particle physics and cosmology. The major focus has been in the general areas of inflationary cosmology, cosmological phase transitions, astrophysical constraints to particle physics theories, and dark matter/structure formation as it relates to particle physics. Some attention is given to axion physics. Narrative summaries of the research of the individual group members are given, followed by a list of publications.
DOE

N94-16524# European Space Agency. European Space Research and Technology Center, ESTEC, Noordwijk (Netherlands).
GIOTTO'S SECOND ENCOUNTER: THE MISSION TO COMET GRIGG-SKJELLERUP
B. Battrick, ed. 1993 52 p Repr. from ESA Bulletins Original contains color illustrations
(ESA-BR-93; ISBN-92-9092-151-X) Copyright Avail: CASI HC A04/MF A01

Papers on Giotto's second encounter, the mission to Comet Grigg-Skjellerup are included. Topics covered include: (1) a close encounter of the second kind - Giotto Extended Mission (GEM); (2) Giotto's reactivation and Earth swingby; (3) Giotto - the second encounter; (4) Giotto's encounter with Comet Grigg-Skjellerup: the first results; (5) the Giotto extended mission to Comet Grigg-Skjellerup: summary of preliminary results; and (6) the Giotto extended mission - high risk, high pay-off.
CASI

N94-16647*# Columbia Univ., New York, NY.
LINEAR AND NON-LINEAR STUDIES OF ALFVEN WAVES IN SPACE. STATIONARY AND DYNAMIC PROCESSES IN MAGNETOSPHERIC PLASMAS Final Technical Report, 15 Jan. 1986 - 14 Jan. 1990, 14 Jan. 1989 - 14 Mar. 1990
A. Bhattacharjee and A. Hasegawa 1990 4 p
(Grants NAGw-894; NAGw-1610)
(NASA-CR-193585; NAS 1.26:193585) Avail: CASI HC A01/MF A01

The Final Technical Report on linear and non-linear studies of Alfven waves in space is presented. Areas of research included relaxation of magnetotail plasmas with field-aligned currents; the equilibrium dayside magnetosphere; macroscale particle simulation of kinetic Alfven wave physics; ballooning stability of plasmas with sheared equilibrium flows; theory of the drift-mirror instability; collisionless tearing instability in magnetotail plasmas; and nonadiabatic behavior of the magnetic moment of a charged particle in a dipole magnetic field and the development of stochastic webs.
Author (revised)

N94-16648*# Virginia Univ., Charlottesville. Dept. of Applied Mathematics.
COLLISIONAL DYNAMICS OF PERTURBED PARTICLE DISKS IN THE SOLAR SYSTEM Final Technical Report, 1 Jul. 1986 - 31 Dec. 1989

William W. Roberts, Jr. 1989 7 p
(Grant NAGw-929)
(NASA-CR-193584; NAS 1.26:193584) Avail: CASI HC A02/MF A01

Theoretical and computational studies were carried out on galactic and planetary disks. With the goal of addressing important open questions centered on galactic structure, the cloudy interstellar medium, giant molecular clouds, and star formation in galactic disks and the collisional dynamics of perturbed particulate matter in planetary disks, focus was largely on the self-gravitational effects, dissipative effects, and collisional dynamics of cloud-particle disks. N-body, 'cloud-particle' computational algorithms were developed for the purpose of isolating the role of gaseous self gravity from the roles of other dominant physical mechanisms and dynamical processes, e.g. the collisional dynamics and dissipative processes. The efforts focused largely on galactic disks show that observational constraints provide stringent tests of the numerical simulation techniques developed. Self gravitational effects of the galactic interstellar medium's gas clouds are included by means of Fourier Transform technique. Author (revised)

N94-17059*# California Univ., Berkeley. Dept. of Astronomy.
FROM THE MOONS OF JUPITER TO THE MILKY WAY Final Report
Martin Cohen 12 Nov. 1993 12 p
(Grant NAGw-3154)
(NASA-CR-194649; NAS 1.26:194649) Avail: CASI HC A03/MF A01

In this report we will describe the successes and problems encountered in carrying out the above project. Due to funding delays, we were unable to begin the project until February, 1993. The telescopes were ordered in September, 1992. We arranged with the principals of the participating schools, Fruitvale Elementary and Allendale year-Round, to conduct the building and lecture phases of the project during the second and third weeks of February. The principals chose to employ totally different methods of selecting children to participate. Author

N94-17094*# Iowa State Univ. of Science and Technology, Ames.
THE FORMATION PROCESS OF THE He I LAMBDA 10830 LINE IN COOL GIANT STARS Final Report, 1 Jul. 1991 - 30 Jun. 1993
Donald G. Luttermoser 29 Oct. 1993 12 p Submitted for publication
(Grant NAG5-1655)
(NASA-CR-194648; NAS 1.26:194648) Avail: CASI HC A03/MF A01

The Final Report on the formation process of the He I lambda 10830 line in cool giant stars is presented. The research involves observing a sample of cool giant stars with ROSAT. These stars were selected from the list of bright stars which display He I lambda 10830 in absorption or emission and lie on the cool side of the coronal dividing line. With measured x ray fluxes or upper limits measured by the Position Sensitive Proportional Counter (PSPC), the role x rays play in the formation of this important line was investigated using the non-LTE radiative transfer code PANDORA. Hydrodynamic calculations were performed to investigate the contributions of acoustic wave heating in the formation of this line as well.
Author (revised)

N94-17591 Max-Planck-Inst. fuer Physik und Astrophysik, Garching (Germany).
VARIABILITY OF THE SEYFERT GALAXY MKN 766 IN THE ROSAT ALL SKY SURVEY
Silvano Molendi, Tommaso Maccacaro (Osservatorio Astronomico, Brera, Milan, Italy.), and Stefan Schaeidt 19 Oct. 1992 22 p Submitted for publication Sponsored by Max-Planck-Inst. fuer Physik und Astrophysik, Garching, Germany, and Italian Space Agency, Rome, Italy
(MPE-Preprint-221; ETN-93-94613) Copyright Avail: Max-Planck-Institut fuer Physik und Astrophysik, Giessenbachstrasse, 8046 Garching, Germany

Results from the Rosat All Sky Survey (RASS) observation of the Seyfert galaxy MKN 766 are presented. Using a technique developed for the analysis of point sources in the RASS it is shown that MKN 766 is highly variable. Comparison of the soft X-ray spectrum with Exosat medium energy archive data shows that the spectrum of MKN 766 is characterized by a strong soft excess. The low energy resolution of the Position Sensitive Proportional Counter (PSPC) instrument on board the Rosat spacecraft does not allow discrimination between different spectral models for the soft access. Both a power law or a thermal component yield an acceptable fit. Of the two thermal models only the first can be accepted since the best fitting parameters derived for the latter are not consistent with bremsstrahlung emission. A comparison with theoretical models for the soft excess is presented. The lack of a strong bump rules out models in which soft X-ray are produced by Comptonizing ultraviolet photons. The soft excess in the spectrum of MKN 766 can be fitted with the emission spectrum from an accretion disk. The accretion disk parameters derived from the fit, the mass, and the accretion rate are consistent with those found by comparing the two variability timescales observed in the lightcurve to two fundamental timescales operating in the disk. ESA

N94-17603 Nationaal Inst. voor Kernfysica en Hoge Energiefysica, Amsterdam (Netherlands).
SUSY IN THE SKY
G. W. Gibbons (Cambridge Univ., England.), R. H. Rietdijk (Durham Univ., England.), and J. W. vanHolten 1993 29 p Limited Reproducibility: More than 20% of this document may be affected by microfiche quality
(NIKHEF-H/93-04; DAMTP-R92/43; ETN-93-94826) Avail: CASI HC A03

Spinning particles in curved space time can have fermionic symmetries generated by the square root of bosonic constants of motion other than the Hamiltonian. A general analysis of the conditions under which such new supersymmetries appear is presented. The Poisson-Dirac algebra of the resulting set of charges, including the conditions of closure of the new algebra are discussed. An example of a new nontrivial supersymmetry is found in black hole solutions of the Kerr-Newmann type and corresponds to the Killing-Yano tensor, which plays an important role in solving the Dirac equation in these black hole metrics. ESA

N94-17604 Nationaal Inst. voor Kernfysica en Hoge Energiefysica, Amsterdam (Netherlands).
RELATIVISTIC DYNAMICS OF SPIN IN STRONG EXTERNAL FIELDS
J. W. vanHolten 1993 12 p Presented at 4th Hellenic School on Elementary Particle Physics, Corfu, Italy, Sep. 1992 Limited Reproducibility: More than 20% of this document may be affected by microfiche quality
(NIKHEF-H/93-06; ETN-93-94827) Avail: Issuing Activity (European Space Agency (ESA))

The dynamics of relativistic spinning particles in strong external electromagnetic or gravitational fields is discussed. The purpose is to present some examples of this dynamical phenomenon which satisfy the equations of motion of the type proposed by other authors for motion in an electromagnetic field, or a generalization of these equations to motion in gravitational fields. Spin-orbit is shown to affect such relativistic phenomena as time dilation and perihelion shift. Possible applications include muon decay in a magnetic field and the dynamics of neutrion stars in binary systems. ESA

N94-17628 Max-Planck-Inst. fuer Physik und Astrophysik, Garching (Germany). Inst. fuer Astrophysik.
PROPERTIES OF NUCLEI IN ASTROPHYSICAL ENVIRONMENTS: BINDING ENERGIES, WEAK-INTERACTION RATES
K. Takahashi and W. Hillebrandt Dec. 1992 15 p Submitted for publication
(MPA-706; ETN-93-94913) Copyright Avail: Issuing Activity
(Max-Planck-Institut fuer Physik und Astrophysik, Karl-Schwarzschild-Strasse 1, 8046 Garching, Germany)

Some of the problems related to the evaluation of binding energies (masses) and weak interaction rates in nuclei of astrophysical interest are discussed. Selected examples of those arising in stellar evolution and nucleosynthesis studies are considered. Judging from the progress made in developing new experiment techniques, it can be expected that some data in the quest will become available in the near future. This concerns masses and beta decay half lives of neutron rich nuclei involved in the r-process nucleosynthesis ESA

N94-17657# Los Alamos National Lab., NM.
ASTROPHYSICS WITH MILAGRO
1993 4 p Presented at the International Cosmic-Ray Conference, Calgary, Alberta, 19-20 Jul. 1993
(Contract W-7405-eng-36)
(DE93-012722; LA-UR-93-1603; CONF-930779-1) Avail: CASI HC A01/MF A01

This paper describes how data from a new type of air shower detector, MILAGRO, can shed light on a variety of interesting problems in astrophysics. MILAGRO has the capability to make observations of VHE/UHE emission from the recently discovered TeV gamma-ray source Markarian 421, an

Active Galactic Nucleus (AGN). An observation of the attenuation of this signal in the range of 1-20 TeV can be used to make the first measurement of the intergalactic infrared radiation. We also describe how MILAGRO can improve the existing limits on the density of Primordial Black Holes (PBH) by three orders of magnitude. Finally, we discuss how this instrument can be used to measure the diffuse galactic emission of gamma-rays which must come from the disk. DOE

N94-16174*# Jet Propulsion Lab., California Inst. of Tech., Pasadena.
SPECTRAL EVIDENCE OF SIZE DEPENDENT SPACE WEATHERING PROCESSES ON ASTEROID SURFACES Abstract Only
M. J. Gaffey (Rensselaer Polytechnic Inst., Troy, NY.), J. F. Bell (Hawaii Univ., Honolulu.), R. H. Brown, T. H. Burbine (Smithsonian Astrophysical Observatory, Cambridge, MA.), J. L. Piatek (Arizona State Univ., Tempe.), K. L. Reed (Rensselaer Polytechnic Inst., Troy, NY.), and D. A. Chaky (Rensselaer Polytechnic Inst., Troy, NY.) *In* Lunar and Planetary Inst., Twenty-Fourth Lunar and Planetary Science Conference. Part 2: G-M 1993 p 515-516 (For primary document see N94-16173 03-91)
(Grants NAGw-642; NSF AST-90-12180)
Avail: CASI HC A01/MF A06

N94-16175*# Arizona Univ., Tucson. Dept. of Geosciences.
THE Fe2(+)-Mg INTERDIFFUSION IN ORTHOPYROXENE: CONSTRAINTS FROM CATION ORDERING AND STRUCTURAL DATA AND IMPLICATIONS FOR COOLING RATES OF METEORITES Abstract Only
J. Ganguly and V. Tazzoli (Pavia Univ., Italy.) *In* Lunar and Planetary Inst., Twenty-Fourth Lunar and Planetary Science Conference. Part 2: G-M 1993 p 517-518 (For primary document see N94-16173 03-91)
Avail: CASI HC A01/MF A06

N94-16176*# Arizona Univ., Tucson. Dept. of Geosciences.
CATION ORDERING IN ORTHOPYROXENES AND COOLING RATES OF METEORITES: LOW TEMPERATURE COOLING RATES OF ESTHERVILLE, BONDOC AND SHAW Abstract Only
J. Ganguly, H. Yang (Washington Univ., Seattle.), and S. Ghose (Washington Univ., Seattle.) *In* Lunar and Planetary Inst., Twenty-Fourth Lunar and Planetary Science Conference. Part 2: G-M 1993 p 519-520 (For primary document see N94-16173 03-91)
Avail: CASI HC A01/MF A06

N94-16184*# Open Univ., Milton (England). Dept. of Earth Sciences.
EXTRACTION AND ISOTOPIC ANALYSIS OF MEDIUM MOLECULAR WEIGHT HYDROCARBONS FROM MURCHISON USING SUPERCRITICAL CARBON DIOXIDE Abstract Only
Iain Gilmour and Colin Pillinger *In* Lunar and Planetary Inst., Twenty-Fourth Lunar and Planetary Science Conference. Part 2: G-M 1993 p 535-536 (For primary document see N94-16173 03-91)
Avail: CASI HC A01/MF A06

N94-16186*# Delaware Univ., Newark. Dept. of Geology.
CRETACEOUS-TERTIARY BOUNDARY SPHERULES AND CENOZOIC MICROTEKTITES: SIMILARITIES AND DIFFERENCES Abstract Only
B. P. Glass, Bruce F. Bohor (Geological Survey, Denver, CO.), and William J. Betterton (Geological Survey, Denver, CO.) *In* Lunar and Planetary Inst., Twenty-Fourth Lunar and Planetary Science Conference. Part 2: G-M 1993 p 539-540 (For primary document see N94-16173 03-91)
Avail: CASI HC A01/MF A06

N94-16190*# Arizona Univ., Tucson. Lunar and Planetary Lab.
STALKING THE LREE-ENRICHED COMPONENT IN UREILITES Abstract Only
Cyrena Anne Goodrich and Guenter W. Lugmair (Scripps Institution of Oceanography, San Diego, CA.) *In* Lunar and Planetary Inst., Twenty-Fourth Lunar and Planetary Science Conference. Part 2: G-M 1993 p 547-548 (For primary document see N94-16173 03-91)
Avail: CASI HC A01/MF A06

N94-16191*# Physical Research Lab., Ahmedabad (India).
GROSNAJA ABCs: MAGNESIUM ISOTOPE COMPOSITIONS Abstract Only
J. N. Goswami, G. Srinivasan, and A. A. Ulyanov (Moscow State Univ., Russia.) *In* Lunar and Planetary Inst., Twenty-Fourth Lunar and Planetary Science Conference. Part 2: G-M 1993 p 549-550 (For primary document see N94-16173 03-91)
Avail: CASI HC A01/MF A06

N94-16192*# Museum of Natural History, London (England). Dept. of Mineralogy.
EUROMET UREILITE CONSORTIUM: A PRELIMINARY REPORT ON CARBON AND NITROGEN GEOCHEMISTRY Abstract Only
Monica M. Grady and C. T. Pillinger (Open Univ., Milton, England.) *In* Lunar and Planetary Inst., Twenty-Fourth Lunar and Planetary Science Conference. Part 2: G-M 1993 p 551-552 (For primary document see N94-16173 03-91)
Avail: CASI HC A01/MF A06

N94-16195*# Hawaii Univ., Honolulu. Planetary Geosciences.
NEW K TYPE ASTEROIDS Abstract Only
James C. Granahan, Greg Smith, and Jeffrey F. Bell *In* Lunar and Planetary Inst., Twenty-Fourth Lunar and Planetary Science Conference. Part 2: G-M 1993 p 557-558 (For primary document see N94-16173 03-91)
Avail: CASI HC A01/MF A06

N94-16202*# Arizona Univ., Phoenix. Lunar and Planetary Lab.
COLLISIONAL AND DYNAMICAL HISTORY OF GASPRA Abstract Only
R. Greenberg, M. C. Nolan, W. F. Bottke, Jr., and R. A. Kolvoord *In* Lunar and Planetary Inst., Twenty-Fourth Lunar and Planetary Science Conference. Part 2: G-M 1993 p 571-572 (For primary document see N94-16173 03-91)
Avail: CASI HC A01/MF A06

N94-16205*# Arizona State Univ., Tempe. Dept. of Geology.
HELIOCENTRIC ZONING OF THE ASTEROID BELT BY ALUMINUM-26 HEATING Abstract Only
R. E. Grimm and H. Y. McSween, Jr. (Tennessee Univ., Knoxville.) *In* Lunar and Planetary Inst., Twenty-Fourth Lunar and Planetary Science Conference. Part 2: G-M 1993 p 577-578 (For primary document see N94-16173 03-91)
Avail: CASI HC A01/MF A06

N94-16208*# Massachusetts Inst. of Tech., Cambridge. Dept. of Earth, Atmospheric and Planetary Sciences.
PETROLOGIC CONSTRAINTS ON THE SURFACE PROCESSES ON ASTEROID 4 VESTA AND ON EXCAVATION DEPTHS OF DIOGENITE FRAGMENTS Abstract Only
T. L. Grove *In* Lunar and Planetary Inst., Twenty-Fourth Lunar and Planetary Science Conference. Part 2: G-M 1993 p 583-584 (For primary document see N94-16173 03-91)
Avail: CASI HC A01/MF A06

N94-16210*# Arizona Univ., Tucson. Dept. of Geosciences.
FLUVIAL EROSION ON MARS: IMPLICATIONS FOR PALEOCLIMATIC CHANGE Abstract Only
Virginia C. Gulick and Victor R. Baker *In* Lunar and Planetary Inst., Twenty-Fourth Lunar and Planetary Science Conference. Part 2: G-M 1993 p 587-588 (For primary document see N94-16173 03-91)
Avail: CASI HC A01/MF A06

N94-16212*# Academy of Sciences of the Ukraine, Kiev. Inst. of Geological Sciences.
THE KARAKUL DEPRESSION IN PAMIRS: THE FIRST IMPACT STRUCTURE IN CENTRAL ASIA Abstract Only
E. P. Gurov, H. P. Gurova, R. B. Rakitskaya, and A. Yu. Yamnichenko *In* Lunar and Planetary Inst., Twenty-Fourth Lunar and Planetary Science Conference. Part 2: G-M 1993 p 591-592 (For primary document see N94-16173 03-91)
Avail: CASI HC A01/MF A06

N94-16213*# Hawaii Univ., Honolulu. Planetary Geosciences.
SYSTEMATIC CHEMICAL VARIATIONS IN LARGE 3AB IRON METEORITES: CLUES TO CORE CRYSTALLIZATION Abstract Only
H. Haack, E. R. D. Scott, G. S. Rubio (Universidad Nacional Autonoma de

Mexico, Mexico City.), D. F. Gutierrez (Universidad Nacional Autonoma de Mexico, Mexico City.), C. F. Lewis (Arizona State Univ., Tempe.), J. T. Wasson (California Univ., Los Angeles.), R. R. Brooks (Massey Univ., Palmerston North, New Zealand.), X. Guo (Massey Univ., Palmerston North, New Zealand.), D. E. Ryan (Dalhousie Univ., Halifax, Nova Scotia.), and J. Holzbecher (Dalhousie Univ., Halifax, Nova Scotia.) *In* Lunar and Planetary Inst., Twenty-Fourth Lunar and Planetary Science Conference. Part 2: G-M 1993 p 593-594 (For primary document see N94-16173 03-91)
(Grants NAGw-3281; NAG9-454)
Avail: CASI HC A01/MF A06

N94-16221*# Planetary Science Inst., Tucson, AZ.
THE PHYSICAL MECHANISM OF COMET OUTBURSTS: AN EXPERIMENT Abstract Only
William K. Hartmann *In* Lunar and Planetary Inst., Twenty-Fourth Lunar and Planetary Science Conference. Part 2: G-M 1993 p 609-610 (For primary document see N94-16173 03-91)
Avail: CASI HC A01/MF A06

N94-16223*# Hartung (Jack B.), Great Falls, VA.
CORVID METEOROIDS AND A GIORDANO BRUNO RAY ARE GENETICALLY RELATED Abstract Only
Jack B. Hartung *In* Lunar and Planetary Inst., Twenty-Fourth Lunar and Planetary Science Conference. Part 2: G-M 1993 p 613-614 (For primary document see N94-16173 03-91)
Avail: CASI HC A01/MF A06

N94-16224*# Tennessee Univ., Knoxville. Dept. of Geological Sciences.
PYROXENE EQUILIBRATION TEMPERATURES IN METAMORPHOSED ORDINARY CHONDRITES Abstract Only
R. P. Harvey, M. L. Bennett, and H. Y. McSween, Jr. *In* Lunar and Planetary Inst., Twenty-Fourth Lunar and Planetary Science Conference. Part 2: G-M 1993 p 615-616 (For primary document see N94-16173 03-91)
Avail: CASI HC A01/MF A06

N94-16240*# Rutgers Univ., New Brunswick, NJ. Dept. of Chemistry.
Al-26-Mg-26 AGES OF IRON METEORITES Abstract Only
G. F. Herzog, A. E. Souzis (Army Research Lab., Fort Belvoir, VA.), S. Xue, J. Klein (Pennsylvania Univ., Philadelphia.), D. Juenemann (Pennsylvania Univ., Philadelphia.), and R. Middleton (Pennsylvania Univ., Philadelphia.) *In* Lunar and Planetary Inst., Twenty-Fourth Lunar and Planetary Science Conference. Part 2: G-M 1993 p 647-648 (For primary document see N94-16173 03-91)
Avail: CASI HC A01/MF A06

N94-16245*# Geological Survey of Canada, Ottawa (Ontario).
TRACE-ELEMENT COMPOSITION OF CHICXULUB CRATER MELT ROCK, K/T TEKTITES AND YUCATAN BASEMENT Abstract Only
A. R. Hildebrand, D. C. Gregoire, M. Attrep, Jr. (Los Alamos National Lab., NM.), P. Claeys (California Univ., Davis.), C. M. Thompson (Arizona Univ., Tucson.), and W. V. Boynton (Arizona Univ., Tucson.) *In* Lunar and Planetary Inst., Twenty-Fourth Lunar and Planetary Science Conference. Part 2: G-M 1993 p 657-658 (For primary document see N94-16173 03-91)
Avail: CASI HC A01/MF A06

N94-16246*# National Aeronautics and Space Administration. Lyndon B. Johnson Space Center, Houston, TX.
COMPARISON OF REFLECTANCE SPECTRA OF C ASTEROIDS AND UNIQUE C CHONDRITES Y86720, Y82162, AND B7904 Abstract Only
T. Hiroi, C. M. Pieters (Brown Univ., Providence, RI.), and M. E. Zolensky *In* Lunar and Planetary Inst., Twenty-Fourth Lunar and Planetary Science Conference. Part 2: G-M 1993 p 659-660 (For primary document see N94-16173 03-91)
(Grant NAGw-748)
Avail: CASI HC A01/MF A06

N94-16257*# Arkansas Univ., Fayetteville. Cosmochemistry Group.
THE GROUP A3 CHONDRULES OF KRYMKA: FURTHER EVIDENCE FOR MAJOR EVAPORATIVE LOSS DURING THE FORMATION OF CHONDRULES Abstract Only
S. Huang, P. H. Benoit, and D. W. G. Sears *In* Lunar and Planetary Inst., Twenty-Fourth Lunar and Planetary Science Conference. Part 2: G-M 1993 p 681-682 (For primary document see N94-16173 03-91)
(Grant NAG9-81)
Avail: CASI HC A01/MF A06

N94-16260*# California Inst. of Tech., Pasadena. Div. of Geology and Planet Science.
DO SiC GRAINS IN ORGUEIL DIFFER FROM THOSE IN MURCHISON? Abstract Only
Gary R. Huss, Ian D. Hutcheon, and G. J. Wasserburg *In* Lunar and Planetary Inst., Twenty-Fourth Lunar and Planetary Science Conference. Part 2: G-M 1993 p 687-688 (For primary document see N94-16173 03-91)
Avail: CASI HC A01/MF A06

N94-16265*# Academy of Sciences (USSR), Moscow. Inst. of Geochemistry, Analysis and Chemistry.
SILICA-BEARING OBJECTS IN THE DENGLI H3.8 AND GORLOVKA H3-4 CHONDRITES Abstract Only
M. A. Ivanova, N. N. Kononkova, and M. I. Petaev *In* Lunar and Planetary Inst., Twenty-Fourth Lunar and Planetary Science Conference. Part 2: G-M 1993 p 697-698 (For primary document see N94-16173 03-91)
Avail: CASI HC A01/MF A06

N94-16270*# Lockheed Engineering and Sciences Co., Houston, TX.
ORBITAL EVOLUTION OF DUST FROM COMET SCHWASSMANN-WACHMANN 1: A CASE OF ONE-TO-ONE RESONANCE TRAPPING Abstract Only
A. A. Jackson and H. A. Zook (National Aeronautics and Space Administration. Lyndon B. Johnson Space Center, Houston, TX.) *In* Lunar and Planetary Inst., Twenty-Fourth Lunar and Planetary Science Conference. Part 2: G-M 1993 p 707-708 (For primary document see N94-16173 03-91)
Avail: CASI HC A01/MF A06

N94-16272*# Max-Planck-Inst. fuer Chemie, Mainz (Germany).
Os ISOTOPES IN SNC METEORITES AND THEIR IMPLICATIONS TO THE EARLY EVOLUTION OF MARS AND EARTH
E. Jagoutz, J. M. Luck (Montpellier Univ., France.), D. Ben Othman (Montpellier Univ., France.), and H. Wanke *In* Lunar and Planetary Inst., Twenty-Fourth Lunar and Planetary Science Conference. Part 2: G-M 1993 p 711-712 (For primary document see N94-16173 03-91)
Avail: CASI HC A01/MF A06

N94-16274*# Wright State Univ., Dayton, OH. Dept. of Geology.
IRON OXIDE BANDS IN THE VISIBLE AND NEAR-INFRARED REFLECTANCE SPECTRA OF PRIMITIVE ASTEROIDS Abstract Only
Kandy S. Jarvis, Faith Vilas (National Aeronautics and Space Administration. Lyndon B. Johnson Space Center, Houston, TX.), and Michael J. Gaffey (Rensselaer Polytechnic Inst., Troy, NY.) *In* Lunar and Planetary Inst., Twenty-Fourth Lunar and Planetary Science Conference. Part 2: G-M 1993 p 715-716 (For primary document see N94-16173 03-91)
(Grant NAGw-642)
Avail: CASI HC A01/MF A06

N94-16281*# Washington Univ., Saint Louis, MO. Dept. of Earth and Planetary Sciences.
AN IRIDIUM-RICH IRON MICROMETEORITE WITH SILICATE INCLUSIONS FROM THE MOON Abstract Only
Bradley L. Jolliff, Randy L. Korotev, and Larry A. Haskin *In* Lunar and Planetary Inst., Twenty-Fourth Lunar and Planetary Science Conference. Part 2: G-M 1993 p 729-730 (For primary document see N94-16173 03-91)
(Grant NAG9-56)
Avail: CASI HC A01/MF A06

N94-16284*# New Mexico Univ., Albuquerque. Dept. of Earth and Planetary Sciences.
COMPLEX ZONING BEHAVIOR IN PYROXENE IN FeO-RICH CHONDRULES IN THE SEMARKONA ORDINARY CHONDRITE Abstract Only
Rhian H. Jones and J. J. Papike *In* Lunar and Planetary Inst., Twenty-Fourth Lunar and Planetary Science Conference. Part 2: G-M 1993 p 735-736 (For primary document see N94-16173 03-91)
(Grant NAG9-497)
Avail: CASI HC A01/MF A06

N94-16286*# Lockheed Engineering and Sciences Co., Houston, TX.
PARTIAL MELTING OF ORDINARY CHONDRITES: LOST CITY (H) AND ST. SEVERIN (LL) Abstract Only
Amy J. G. Jurewicz, John H. Jones (National Aeronautics and Space Administration. Lyndon B. Johnson Space Center, Houston, TX.), Egon T. Weber (Michigan Univ., Ann Arbor.), and David W. Mittlefehldt *In* Lunar and Planetary Inst., Twenty-Fourth Lunar and Planetary Science Conference. Part 2: G-M 1993 p 739-740 (For primary document see N94-16173 03-91)
Avail: CASI HC A01/MF A06

N94-16288*# National Aeronautics and Space Administration. Lyndon B. Johnson Space Center, Houston, TX.
EXPERIMENTAL SEGREGATION OF IRON-NICKEL METAL, IRON-SULFIDE, AND OLIVINE IN A THERMAL GRADIENT: PRELIMINARY RESULTS Abstract Only
Stephen R. Jurewicz and J. H. Jones *In* Lunar and Planetary Inst., Twenty-Fourth Lunar and Planetary Science Conference. Part 2: G-M 1993 p 743-744 (For primary document see N94-16173 03-91)
Avail: CASI HC A01/MF A06

N94-16290*# California Univ., Los Angeles. Inst. of Geophysics and Planetary Physics.
THE AL RAIS METEORITE: A CR CHONDRITE OR CLOSE RELATIVE? Abstract Only
G. W. Kallemeyn *In* Lunar and Planetary Inst., Twenty-Fourth Lunar and Planetary Science Conference. Part 2: G-M 1993 p 747-748 (For primary document see N94-16173 03-91)
Avail: CASI HC A01/MF A06

N94-16291*# Tokyo Univ. (Japan). Inst. for Cosmic Ray Research.
CHEMICAL AND ISOTOPIC COMPOSITIONS IN ACID RESIDUES FROM VARIOUS METEORITES Abstract Only
N. Kano, K. Yamakoshi, H. Matsuzaki, and K. Nogami (Dokkyo Univ., Tochigi, Japan.) *In* Lunar and Planetary Inst., Twenty-Fourth Lunar and Planetary Science Conference. Part 2: G-M 1993 p 749-750 (For primary document see N94-16173 03-91)
Avail: CASI HC A01/MF A06

N94-16292*# Geological Survey, Flagstaff, AZ.
CRUSTAL STRUCTURE AND IGNEOUS PROCESSES IN A CHONDRITIC IO Abstract Only
J. S. Kargel *In* Lunar and Planetary Inst., Twenty-Fourth Lunar and Planetary Science Conference. Part 2: G-M 1993 p 751-752 (For primary document see N94-16173 03-91)
Avail: CASI HC A01/MF A06

N94-16294*# Geological Survey, Flagstaff, AZ.
THE RHEOLOGY AND COMPOSITION OF CRYOVOLCANIC FLOWS ON ICY SATELLITES Abstract Only
Jeffrey S. Kargel *In* Lunar and Planetary Inst., Twenty-Fourth Lunar and Planetary Science Conference. Part 2: G-M 1993 p 755-756 (For primary document see N94-16173 03-91)
Avail: CASI HC A01/MF A06

N94-16296*# Academy of Sciences (USSR), Moscow. Inst. of Geochemistry, Analysis and Chemistry.
DIFFERENT RADIATION AND METAMORPHIC HISTORY OF THE KAINSAZ CO 3.2 CHONDRULES Abstract Only
L. L. Kashkarov and G. V. Kalinina *In* Lunar and Planetary Inst., Twenty-Fourth Lunar and Planetary Science Conference. Part 2: G-M 1993 p 759-760 (For primary document see N94-16173 03-91)
Avail: CASI HC A01/MF A06

N94-16297*# Academy of Sciences (USSR), Moscow. Inst. of Geochemistry, Analysis and Chemistry.
COMPLEX RADIATION-THERMAL HISTORY OF KAIDUN METEORITE ON DATA OF TRACK STUDY OF SILICATE MINERALS Abstract Only
L. L. Kashkarov, N. N. Korotkova, and A. Ya. Skripnik *In* Lunar and Planetary Inst., Twenty-Fourth Lunar and Planetary Science Conference. Part 2: G-M 1993 p 761-762 (For primary document see N94-16173 03-91)
Avail: CASI HC A01/MF A06

N94-16305*# Washington Univ., Saint Louis, MO. Center for Space Sciences.
I-Xe STRUCTURE OF ILAFEGH 009 AND SHALLOWATER: EVIDENCE FOR EARLY FORMATION AND RAPID COOLING OF IMPACT-DERIVED ENSTATITE METEORITES Abstract Only
K. Kehm, R. H. Nichols, Jr., C. M. Hohenberg, T. J. McCoy (Hawaii Univ., Honolulu.), and K. Keil (Hawaii Univ., Honolulu.) *In* Lunar and Planetary Inst., Twenty-Fourth Lunar and Planetary Science Conference. Part 2: G-M 1993 p 777-778 (For primary document see N94-16173 03-91)
Avail: CASI HC A01/MF A06

N94-16306*# Hawaii Univ., Honolulu. Dept. of Geology and Geophysics.
EXPLOSIVE VOLCANISM AND THE COMPOSITIONS OF THE CORES OF DIFFERENTIATED ASTEROIDS Abstract Only
Klaus Keil and Lionel Wilson *In* Lunar and Planetary Inst., Twenty-Fourth Lunar and Planetary Science Conference. Part 2: G-M 1993 p 779-780 (For primary document see N94-16173 03-91)
Avail: CASI HC A01/MF A06

N94-16308*# National Aeronautics and Space Administration. Lyndon B. Johnson Space Center, Houston, TX.
HETEROGENEOUS PLAGIOCLASE COMPOSITIONS IN THE MARALINGA CK4 CHONDRITE Abstract Only
Lindsay P. Keller *In* Lunar and Planetary Inst., Twenty-Fourth Lunar and Planetary Science Conference. Part 2: G-M 1993 p 783-784 (For primary document see N94-16173 03-91)
Avail: CASI HC A01/MF A06

N94-16309*# National Aeronautics and Space Administration. Lyndon B. Johnson Space Center, Houston, TX.
CARBON ABUNDANCES, MAJOR ELEMENT CHEMISTRY, AND MINERALOGY OF HYDRATED INTERPLANETARY DUST PARTICLES Abstract Only
L. P. Keller, K. L. Thomas (Lockheed Engineering and Sciences Co., Houston, TX.), and D. S. McKay *In* Lunar and Planetary Inst., Twenty-Fourth Lunar and Planetary Science Conference. Part 2: G-M 1993 p 785-786 (For primary document see N94-16173 03-91)
Avail: CASI HC A01/MF A06

N94-16310*# Rensselaer Polytechnic Inst., Troy, NY. Dept. of Earth and Environmental Science.
AN INITIAL PERSPECTIVE OF S-ASTEROID SUBTYPES WITHIN ASTEROID FAMILIES Abstract Only
M. S. Kelley and M. J. Gaffey *In* Lunar and Planetary Inst., Twenty-Fourth Lunar and Planetary Science Conference. Part 2: G-M 1993 p 787-788 (For primary document see N94-16173 03-91)
(Grants NAGw-642; NSF AST-90-12180)
Avail: CASI HC A01/MF A06

N94-16317*# California Univ., San Diego, La Jolla. Dept. of Chemistry.
ISOTOPIC SIGNATURES AND DISTRIBUTION OF NITROGEN AND TRAPPED AND RADIOGENIC XENON IN THE ACAPULCO AND FRO90011 METEORITES Abstract Only
Y. Kim and K. Marti *In* Lunar and Planetary Inst., Twenty-Fourth Lunar and Planetary Science Conference. Part 2: G-M 1993 p 801-802 (For primary document see N94-16173 03-91)
Avail: CASI HC A01/MF A06

N94-16321*# Wien Univ. (Austria). Inst. of Geochemistry.
OSMIUM ISOTOPES IN IVORY COAST TEKTITES: CONFIRMATION OF A METEORITIC COMPONENT AND RHENIUM DEPLETION Abstract Only
Christian Koeberl and Steven B. Shirey (Carnegie Institution of Washington, DC.) *In* Lunar and Planetary Inst., Twenty-Fourth Lunar and Planetary Science Conference. Part 2: G-M 1993 p 809-810 (For primary document see N94-16173 03-91)
(Grant NSF EAR-92-18847; FWF Proj. P9026-GEO)
Avail: CASI HC A01/MF A06

N94-16328*# Arizona Univ., Tucson. Lunar and Planetary Lab.
CAT MOUNTAIN: A METEORITIC SAMPLE OF AN IMPACT-MELTED CHONDRITIC ASTEROID Abstract Only
David A. Kring *In* Lunar and Planetary Inst., Twenty-Fourth Lunar and Planetary Science Conference. Part 2: G-M 1993 p 823-824 (For primary document see N94-16173 03-91)
Avail: CASI HC A01/MF A06

N94-16329*# Polish Academy of Sciences, Warsaw. Inst. of Geophysics.
COMPARATIVE MAGNETIC AND THERMOANALYTICAL STUDY OF TWO ENSTATITE CHONDRITES: ADHI KOT AND ATLANTA Abstract Only
Elizabeth Krol and Bruno Lang (Warsaw Univ., Poland.) *In* Lunar and Planetary Inst., Twenty-Fourth Lunar and Planetary Science Conference. Part 2: G-M 1993 p 825-826 (For primary document see N94-16173 03-91)
Avail: CASI HC A01/MF A06

N94-16330*# California Univ., Los Angeles. Inst. of Geophysics and Planetary Physics.
CHROMITE-RICH MAFIC SILICATE CHONDRULES IN ORDINARY CHONDRITES: FORMATION BY IMPACT MELTING Abstract Only
Alexander N. Krot and Alan E. Rubin *In* Lunar and Planetary Inst., Twenty-Fourth Lunar and Planetary Science Conference. Part 2: G-M 1993 p 827-828 (For primary document see N94-16173 03-91)
Avail: CASI HC A01/MF A06

N94-16343*# Academy of Sciences (USSR), Moscow. Inst. of Geochemistry and Analytical Chemistry.
THE ASTROPHYSICAL INTERPRETATION OF ISOTOPE ANOMALIES IN GRAPHITE AND SIC GRAINS OF CHONDRITES Abstract Only
A. K. Lavrukhina *In* Lunar and Planetary Inst., Twenty-Fourth Lunar and Planetary Science Conference. Part 2: G-M 1993 p 853-854 (For primary document see N94-16173 03-91)
Avail: CASI HC A01/MF A06

N94-16344*# Academy of Sciences (USSR), Moscow. Inst. of Geochemistry and Analytical Chemistry.
ON POSSIBLE Mn-53 HETEROGENEITY IN THE EARLY SOLAR SYSTEM Abstract Only
A. K. Lavrukhina and G. K. Ustinova *In* Lunar and Planetary Inst., Twenty-Fourth Lunar and Planetary Science Conference. Part 2: G-M 1993 p 855-856 (For primary document see N94-16173 03-91)
Avail: CASI HC A01/MF A06

N94-16345*# Academy of Sciences (USSR), Moscow. Inst. of Geochemistry and Analytical Chemistry.
ON ORIGIN OF THE OLIVINE INCLUSIONS FROM THE KAINSAZ CO CARBONACEOUS CHONDRITE Abstract Only
A. K. Lavrukhina, Z. A. Lavrentjeva, A. Yu. Ljul, and K. I. Ignatenko *In* Lunar and Planetary Inst., Twenty-Fourth Lunar and Planetary Science Conference. Part 2: G-M 1993 p 857-858 (For primary document see N94-16173 03-91)
Avail: CASI HC A01/MF A06

N94-16352*# Arizona Univ., Tucson. Lunar and Planetary Lab.
POSSIBLE DUST CONTAMINATION OF THE EARLY SOLAR SYSTEM Abstract Only
E. H. Levy and T. V. Ruzmaikina *In* Lunar and Planetary Inst., Twenty-Fourth Lunar and Planetary Science Conference. Part 2: G-M 1993 p 871-872 (For primary document see N94-16173 03-91)
Avail: CASI HC A01/MF A06

N94-16355*# National Aeronautics and Space Administration. Lyndon B. Johnson Space Center, Houston, TX.
INAA OF CAIs FROM THE MARALINGA CK4 CHONDRITE: EFFECTS OF PARENT BODY THERMAL METAMORPHISM Abstract Only
D. J. Lindstrom, L. P. Keller, and R. R. Martinez (Lockheed Engineering and Sciences Co., Houston, TX.) *In* Lunar and Planetary Inst., Twenty-Fourth Lunar and Planetary Science Conference. Part 2: G-M 1993 p 877-878 (For primary document see N94-16173 03-91)
Avail: CASI HC A01/MF A06

N94-16357*# Oregon State Univ., Corvallis. Depts. of Chemistry and Geosciences.
CHONDRITIC RATIOS OF Fe/Cr/Ir IN KERGUELEN PLATEAU (HOLE 738C) K/T CARBONATE-RICH SEDIMENTS SUPPORT ASTEROID-COMETARY IMPACT AT K/T TIME Abstract Only
Y. G. Liu and R. A. Schmitt *In* Lunar and Planetary Inst., Twenty-Fourth Lunar and Planetary Science Conference. Part 2: G-M 1993 p 881-882 (For primary document see N94-16173 03-91)
Avail: CASI HC A01/MF A06

N94-16359*# Oregon State Univ., Corvallis. Depts. of Chemistry and Geosciences.
GEOCHEMICAL EVIDENCES FOR TWO CHONDRITIC-LIKE COMETARY OR ASTEROIDAL IMPACTS BEFORE AND AT THE K/T BOUNDARY Abstract Only
Y.-G. Liu and R. A. Schmitt *In* Lunar and Planetary Inst., Twenty-Fourth Lunar and Planetary Science Conference. Part 2: G-M 1993 p 885-886 (For primary document see N94-16173 03-91)
Avail: CASI HC A01/MF A06

N94-16361*# Max-Planck-Inst. fuer Chemie, Mainz (Germany).
NOBLE GASES IN TWENTY YAMATO H-CHONDRITES: COMPARISON WITH ALLAN HILLS CHONDRITES AND MODERN FALLS Abstract Only
Th. Loeken, P. Scherer, and L. Schultz *In* Lunar and Planetary Inst., Twenty-Fourth Lunar and Planetary Science Conference. Part 2: G-M 1993 p 889-890 (For primary document see N94-16173 03-91)
Avail: CASI HC A01/MF A06

N94-16363*# National Aeronautics and Space Administration. Lyndon B. Johnson Space Center, Houston, TX.
EXPERIMENTALLY REPRODUCED RELICT ENSTATITE IN PORPHYRITIC CHONDRULES OF ENSTATITE CHONDRITE COMPOSITION Abstract Only
Gary E. Lofgren, John M. DeHart, and Tammy L. Dickinson (National Aeronautics and Space Administration, Washington, DC.) *In* Lunar and Planetary Inst., Twenty-Fourth Lunar and Planetary Science Conference. Part 2: G-M 1993 p 893-894 (For primary document see N94-16173 03-91)
Avail: CASI HC A01/MF A06

N94-16367*# Washington Univ., Seattle. Dept. of Astronomy.
DENSITIES OF 5-15 MICRON INTERPLANETARY DUST PARTICLES Abstract Only
S. G. Love, D. J. Joswiak, and D. E. Brownlee *In* Lunar and Planetary Inst., Twenty-Fourth Lunar and Planetary Science Conference. Part 2: G-M 1993 p 901-902 (For primary document see N94-16173 03-91)
Avail: CASI HC A01/MF A06

N94-16377*# Academy of Sciences (USSR), Moscow. Inst. of Physics of the Earth.
POSSIBLE SOURCES OF H2 TO H2O ENRICHMENT AT EVAPORATION OF PARENT CHONDRITIC MATERIAL Abstract Only
A. B. Makalkin, V. A. Dorofeyeva, and A. V. Vityazev *In* Lunar and Planetary Inst., Twenty-Fourth Lunar and Planetary Science Conference. Part 2: G-M 1993 p 921-922 (For primary document see N94-16173 03-91)
Avail: CASI HC A01/MF A06

N94-16378*# Denison Univ., Granville, OH. Dept. of Geology and Geography.
TIDAL REGIME OF INTACT PLANETOID CAPTURE MODEL FOR THE EARTH-MOON SYSTEM: DOES IT RELATE TO THE ARCHEAN SEDIMENTARY ROCK RECORD? Abstract Only
Robert J. Malcuit and Ronald R. Winters *In* Lunar and Planetary Inst., Twenty-Fourth Lunar and Planetary Science Conference. Part 2: G-M 1993 p 923-924 (For primary document see N94-16173 03-91)
Avail: CASI HC A01/MF A06

N94-16379*# Lunar and Planetary Inst., Houston, TX.
ON THE DELIVERY OF PLANETESIMALS TO A PROTOPLANET IN THE SOLAR NEBULA Abstract Only
Renu Malhotra *In its* Twenty-Fourth Lunar and Planetary Science Conference. Part 2: G-M 1993 p 925-926 (For primary document see N94-16173 03-91)
Avail: CASI HC A01/MF A06

N94-16384*# Padua Univ. (Italy). Dept. of Physics.
DUST GRAIN RESONANT CAPTURE: A STATISTICAL STUDY Abstract Only
F. Marzari, V. Vanzani, and S. J. Weidenschilling (Planetary Science Inst., Tucson, AZ.) *In* Lunar and Planetary Inst., Twenty-Fourth Lunar and Planetary Science Conference. Part 2: G-M 1993 p 935-936 (For primary document see N94-16173 03-91)
Avail: CASI HC A01/MF A06

N94-16385*# Los Alamos National Lab., NM. Space Science and Technology Div.
EFFECTS OF BULK COMPOSITION ON PRODUCTION RATES OF COSMOGENIC NUCLIDES IN METEORITES Abstract Only
Jozef Masarik and Robert C. Reedy *In* Lunar and Planetary Inst., Twenty-Fourth Lunar and Planetary Science Conference. Part 2: G-M 1993 p 937-938 (For primary document see N94-16173 03-91)
Avail: CASI HC A01/MF A06

N94-16386*# Jet Propulsion Lab., California Inst. of Tech., Pasadena.
A DECADE'S OVERVIEW OF IO'S VOLCANIC ACTIVITY Abstract Only
D. L. Matson, G. J. Veeder, T. V. Johnson, D. L. Blaney, and J. D. Goguen *In* Lunar and Planetary Inst., Twenty-Fourth Lunar and Planetary Science Conference. Part 2: G-M 1993 p 939-940 (For primary document see N94-16173 03-91)
Avail: CASI HC A01/MF A06

N94-16388*# Tokyo Univ. (Japan). Inst. for Cosmic Ray Research.
SIZE DISTRIBUTION OF INTERPLANETARY IRON AND STONY PARTICLES RELATED WITH DEEP-SEA SPHERULES Abstract Only
H. Matsuzaki and K. Yamakoshi *In* Lunar and Planetary Inst., Twenty-Fourth Lunar and Planetary Science Conference. Part 2: G-M 1993 p 943-944 (For primary document see N94-16173 03-91)
Avail: CASI HC A01/MF A06

N94-16389*# Hawaii Univ., Honolulu. Dept. of Geology and Geophysics.
CLASSIFICATIONAL PARAMETERS FOR ACAPULCOITES AND LODRANITES: THE CASES OF FRO 90011, EET 84302 AND ALH A81187/84190 Abstract Only
T. J. McCoy, K. Keil, R. N. Clayton (Chicago Univ., IL), and T. K. Mayeda (Chicago Univ., IL.) *In* Lunar and Planetary Inst., Twenty-Fourth Lunar and Planetary Science Conference. Part 2: G-M 1993 p 945-946 (For primary document see N94-16173 03-91)
Avail: CASI HC A01/MF A06

N94-16390*# Hawaii Univ., Honolulu. Dept. of Geology and Geophysics.
THE DREGS OF CRYSTALLIZATION IN ZAGAMI Abstract Only
T. J. McCoy, K. Keil, and G. J. Taylor *In* Lunar and Planetary Inst., Twenty-Fourth Lunar and Planetary Science Conference. Part 2: G-M 1993 p 947-948 (For primary document see N94-16173 03-91)
(Grant NAG9-454)
Avail: CASI HC A01/MF A06

N94-16391*# Kent Univ., Canterbury (England). Unit for Space Sciences.
RESOLVING LDEF'S FLUX DISTRIBUTION: ORBITAL (DEBRIS?) AND NATURAL METEOROID POPULATIONS Abstract Only
J. A. M. McDonnell *In* Lunar and Planetary Inst., Twenty-Fourth Lunar and Planetary Science Conference. Part 2: G-M 1993 p 949-950 (For primary document see N94-16173 03-91)
Avail: CASI HC A01/MF A06

N94-16399*# National Aeronautics and Space Administration. Lyndon B. Johnson Space Center, Houston, TX.
THE NAKHLA PARENT MELT: REE PARTITION COEFFICIENTS AND CLUES TO MAJOR ELEMENT COMPOSITION Abstract Only
G. McKay, L. Le (Lockheed Engineering and Sciences Co., Houston, TX.), and J. Wagstaff (Lockheed Engineering and Sciences Co., Houston, TX.) *In* Lunar and Planetary Inst., Twenty-Fourth Lunar and Planetary Science Conference. Part 2: G-M 1993 p 965-966 (For primary document see N94-16173 03-91)
Avail: CASI HC A01/MF A06

N94-16400*# National Aeronautics and Space Administration. Lyndon B. Johnson Space Center, Houston, TX.
MORE ON THE COOLING HISTORY OF ANGRITE LEW 86010 Abstract Only
G. McKay, T. Ogawa (Tokyo Univ., Japan.), M. Miyamoto (Tokyo Univ., Japan.), and H. Takeda (Tokyo Univ., Japan.) *In* Lunar and Planetary Inst., Twenty-Fourth Lunar and Planetary Science Conference. Part 2: G-M 1993 p 967-968 (For primary document see N94-16173 03-91)
Avail: CASI HC A01/MF A06

N94-16409*# Purdue Univ., West Lafayette, IN. Depts. of Physics and Chemistry.
Al-26 PRODUCTION PROFILE AND MODEL COMPARISONS IN CANYON DIABLO Abstract Only
E. Michlovich, D. Elmore, S. Vogt, M. Lipschutz, J. Masarik (Los Alamos National Lab., NM.), and R. C. Reedy (Los Alamos National Lab., NM.) *In* Lunar and Planetary Inst., Twenty-Fourth Lunar and Planetary Science Conference. Part 2: G-M 1993 p 985-986 (For primary document see N94-16173 03-91)
Avail: CASI HC A01/MF A06

N94-16410*# Tokyo Univ. (Japan). Mineralogical Inst.
EXSOLVED KIRSCHSTEINITE IN ANGRITE LEW86010 OLIVINE Abstract Only
Takashi Mikouchi, Hiroshi Takeda, Hiroshi Mori, Masamichi Miyamoto, and Gordon McKay (National Aeronautics and Space Administration. Lyndon B. Johnson Space Center, Houston, TX.) *In* Lunar and Planetary Inst., Twenty-Fourth Lunar and Planetary Science Conference. Part 2: G-M 1993 p 987-988 (For primary document see N94-16173 03-91)
Avail: CASI HC A01/MF A06

N94-16412*# National Inst. of Polar Research, Tokyo (Japan). Dept. of Antarctic Meteorites.
REFRACTORY PRECURSOR COMPONENTS IN AN ALLENDE FERROMAGNESIAN CHONDRULE Abstract Only
Keiji Misawa, Takashi Fujita (Kyoto Univ., Japan.), Masao Kitamura (Kyoto Univ., Japan.), and Noboru Nakamura (Kobe Univ., Japan.) *In* Lunar and Planetary Inst., Twenty-Fourth Lunar and Planetary Science Conference. Part 2: G-M 1993 p 991-992 (For primary document see N94-16173 03-91)
Avail: CASI HC A01/MF A06

N94-16413*# Lockheed Engineering and Sciences Co., Houston, TX.
IGNEOUS FRACTIONATION AND SUBSOLIDUS EQUILIBRATION OF DIOGENITE METEORITES Abstract Only
David W. Mittlefehldt *In* Lunar and Planetary Inst., Twenty-Fourth Lunar and Planetary Science Conference. Part 2: G-M 1993 p 993-994 (For primary document see N94-16173 03-91)
Avail: CASI HC A01/MF A06

N94-16414*# Lockheed Engineering and Sciences Co., Houston, TX.
SIDEROPHILE ELEMENT FRACTIONATION IN METEOR CRATER IMPACT GLASSES AND METALLIC SPHERULES Abstract Only
David W. Mittlefehldt, T. H. See, and E. R. D. Scott (Hawaii Univ., Honolulu.) *In* Lunar and Planetary Inst., Twenty-Fourth Lunar and Planetary Science Conference. Part 2: G-M 1993 p 995-996 (For primary document see N94-16173 03-91)
Avail: CASI HC A01/MF A06

N94-16415*# Yamaguchi Univ. (Japan).
IDENTIFICATION OF NEW METEORITE, MIHONOSEKI (L), FROM BROKEN FRAGMENTS IN JAPAN Abstract Only
Y. Miura and Y. Noma *In* Lunar and Planetary Inst., Twenty-Fourth Lunar and Planetary Science Conference. Part 2: G-M 1993 p 997-998 (For primary document see N94-16173 03-91)
Avail: CASI HC A01/MF A06

N94-16417*# Padua Univ. (Italy). Dipartimento di Mineralogia and Petrologia.
ZAOYANG CHONDRITE COOLING HISTORY FROM PYROXENE Fe(2+)-Mg INTRACRYSTALLINE ORDERING AND EXOLUTIONS Abstract Only
G. M. Molin, M. Tribaudino (Turin Univ., Italy.), and E. Brizi (Perugia Univ., Italy.) *In* Lunar and Planetary Inst., Twenty-Fourth Lunar and Planetary Science Conference. Part 2: G-M 1993 p 1001 (For primary document see N94-16173 03-91)
Avail: CASI HC A01/MF A06

N94-16422*# Academy of Sciences (USSR), Moscow.
OPTICAL EFFECTS OF REGOLITH PROCESSES ON S ASTEROIDS AS SIMULATED BY LASER IMPULSE ALTERATION OF ORDINARY CHONDRITE Abstract Only
L. V. Moroz, A. V. Fisenko, L. F. Semjonova, and C. M. Pieters (Brown Univ., Providence, RI.) *In* Lunar and Planetary Inst., Twenty-Fourth Lunar and Planetary Science Conference. Part 2: G-M 1993 p 1011-1012 (For primary document see N94-16173 03-91)
Avail: CASI HC A01/MF A06

N94-16425*# Open Univ., Milton (England). Dept. of Earth Sciences.
A HYDROGEN ISOTOPE STUDY OF CO3 TYPE CARBONACEOUS CHONDRITES; COMPARISON WITH TYPE 3 ORDINARY CHONDRITES Abstract Only
A. D. Morse, J. Newton, and C. T. Pillinger *In* Lunar and Planetary Inst., Twenty-Fourth Lunar and Planetary Science Conference. Part 2: G-M 1993 p 1017-1018 (For primary document see N94-16173 03-91)
Avail: CASI HC A01/MF A06

N94-16435*# Physical Research Lab., Ahmedabad (India).
NITROGEN AND LIGHT NOBLE GASES IN PARSA ENSTATITE CHONDRITE Abstract Only
S. V. S. Murty *In* Lunar and Planetary Inst., Twenty-Fourth Lunar and Planetary Science Conference. Part 2: G-M 1993 p 1037-1038 (For primary document see N94-16173 03-91)
Avail: CASI HC A01/MF A06

N94-17147 Bremen Univ. (Germany). Center of Applied Space Technology and Microgravity.
COSMIC DUST AND SPACE DEBRIS MEASUREMENTS ON BOARD THE SMALL SATELLITES HITEN AND BREM-SAT
H. Igiseder *In* CNES, Small Satellites Systems and Services Jan. 1993 p 209-217 (For primary document see N94-17131 03-18)
Copyright Avail: Issuing Activity (CEPADUES-Editions, 111 rue Nicolas-Vaquelin, 31100 Toulouse, France)

91 LUNAR AND PLANETARY EXPLORATION

Includes planetology; and manned and unmanned flights.

For spacecraft design or space stations see *18 Spacecraft Design, Testing and Performance.*

N94-15182*# Cornell Univ., Ithaca, NY. Center for Radiophysics and Space Research.
A GLOBAL TRAVELING WAVE ON VENUS Final Report
Michael D. Smith, Peter J. Gierasch, and Paul J. Schinder 16 Sep. 1993 88 p
(Grant NAG2-680)
(NASA-CR-194356; NAS 1.26:194356) Avail: CASI HC A05/MF A01

The dominant large-scale pattern in the clouds of Venus has been described as a 'Y' or 'Psi' and tentatively identified by earlier workers as a Kelvin wave. A detailed calculation of linear wave modes in the Venus atmosphere verifies this identification. Cloud feedback by infrared heating fluctuations is a plausible excitation mechanism. Modulation of the large-scale pattern by the wave is a possible explanation for the Y. Momentum transfer by the wave could contribute to sustaining the general circulation.
Derived from text

N94-15239* Jet Propulsion Lab., California Inst. of Tech., Pasadena.
VOYAGER ENCOUNTER HIGHLIGHTS (Videotape)
28 Jun. 1989 Videotape: 30 min. 18 sec. playing time, in color, with sound
(NASA-TM-109420; NONP-VT-93-190217) Avail: CASI VHS A01/BETA A22

The following are presented: computer animation of trajectories for both Voyagers 1 and 2; view of Jupiter during one orbit of Ganymede; computer animation of Voyager 2's encounter with Jupiter and its satellites; time lapse of the planet's rotation and its satellites; stroboscopic sequence of selected frames; cloud motion; Jupiter's Great Red Spot (4/25 - 5/24, 1979) through a violet filter; and the Great Red Spot through a blue filter by Voyager 1. The dynamics of Jupiter's clouds are shown - the whole planet is shown first, then two closer looks are repeated several times. Also included are pans of stills of Jupiter's satellites and a computer simulation tour of Saturn system from POV just behind Voyager, made of 116 images of Saturn through a green filter and of 516 images taken by Voyager 1 (9/12 - 9/14, 1980). Frames are enhanced to show the motion of features in Saturn's rings. Pans of stills of Saturn's satellites are shown. There is computer animation of the planet's system, rings, and Sigma Sagittari. Images on January 14, 1986 are through an orange filter. Uranus's satellites are shown as is computer animation of an August 1989 encounter.
CASI

N94-15240* Jet Propulsion Lab., California Inst. of Tech., Pasadena.
NEPTUNE ENCOUNTER HIGHLIGHTS (Videotape)
28 Nov. 1989 Videotape: 32 min. 38 sec. playing time, in color, with sound
(NASA-TM-109421; NONP-VT-93-190218) Avail: CASI VHS A01/BETA A22

Voyager encounter data are presented in computer animation (CA) and real (R) animation. The highlights include a view of 2 full rotations of Neptune. It shows spacecraft trajectory 'diving' over Neptune and intercepting Triton's orbit, depicting radiation and occulation zones. Also shown are a renegade orbit of Triton and Voyager's encounter with Neptune's Magnetopause. A model of the spacecraft's complex maneuvers during close encounters of Neptune and Triton is presented. A view from Earth of Neptune's occulation experiment is is shown as well as a recreation of Voyager's final pass. There is detail of Voyager's Image Compensation technique which produces Voyager images. Eighteen images were produced on June 22 - 23, 1989, from 57 million miles away. A 68 day sequence which provides a stroboscopic view - colorization approximates what is seen by the human eye. Real time images recorded live from Voyager on 8/24/89 are presented. Photoclinometry produced the topography of Triton. Three images are used to create a sequence of Neptune's rings. The globe of Neptune and 2 views of the south pole are shown as well as Neptune rotating. The rotation of a scooter is frozen in images showing differential motion. There is a view of rotation of the Great Dark Spot about its own axis. Photoclinometry provides a 3-dimensional perspective

using a color mosaic of Triton images. The globe is used to indicate the orientation of Neptune's crescent. The east and west plumes on Triton are shown. CASI

N94-15294* National Aeronautics and Space Administration, Washington, DC.
LUNAR BASE CONCEPTS (Videotape)
Apr. 1985 Videotape: 3 min. 2 sec. playing time, in color, with sound
(NASA-TM-109607; NONP-VT-93-190405) Avail: CASI VHS A01/BETA A22

This videotape discusses NASA's plans for a lunar base. Additionally, the videotape features interviews with George Keyworth, James Beggs, and Harrison Schmidt. CASI

N94-15342* National Aeronautics and Space Administration, Washington, DC.
THE 1979 HIGHLIGHTS (Videotape)
Dec. 1979 Videotape: 14 min. 30 sec. playing time, in color, with sound
(NASA-TM-109443; NONP-VT-93-190240) Avail: CASI VHS A01/BETA A22

The videotape includes footage of the following: Voyagers to Jupiter, Pioneer to Saturn, High Energy Astronomy Observatory, space telescope, space shuttle, astronauts Young and Crippen, 10th anniversary of Apollo 11, Skylab reentry, Landsat, satellite freeze warning, Fire Fighting Module, SAGE, wind generators, Solar Energy Project, electric car research, XV-15, HiMAT, and crash worthiness tests. CASI

N94-15348* National Aeronautics and Space Administration, Washington, DC.
VOYAGER ENCOUNTERS URANUS (Videotape)
Jun. 1986 Videotape: 3 min. 2 sec. playing time, in color, with sound
(NASA-TM-109619; NONP-VT-93-190417) Avail: CASI VHS A01/BETA A22

Early results from Voyager's pass of Uranus and its moon, Miranda, are shown. CASI

N94-15419* National Aeronautics and Space Administration. Lewis Research Center, Cleveland, OH.
NASA REPORT TO EDUCATION, VOLUME 7 (Videotape)
Dec. 1989 Videotape: 26 min. 14 sec. playing time, in color, with sound
(NASA-TM-109435; NONP-VT-93-190232) Avail: CASI VHS A01/BETA A22

Segments of this video include the STS-34 Mission, Pegesus tests, and Voyager's Neptune. CASI

N94-15432* National Aeronautics and Space Administration. Ames Research Center, Moffett Field, CA.
GALILEO PROBE READY TO GO (Videotape)
Feb. 1989 Videotape: 4 min. playing time, in color, with sound
(NASA-TM-109648; NONP-VT-93-190446) Avail: CASI VHS A01/BETA A22

This video presents close cloud views of Jupiter, probe deployment, descent, chute opening, trajectories, and views of assembly at Hughes. CASI

N94-15491* Jet Propulsion Lab., California Inst. of Tech., Pasadena.
VOYAGER 2: NEPTUNE ENCOUNTER (Videotape)
8 Aug. 1989 Videotape: 11 min. 31 sec. playing time, in color, with sound
(NASA-TM-109423; NONP-VT-93-190220) Avail: CASI VHS A01/BETA A22

Computer graphics, actual images, and stock footage of the Voyager 2's Neptune encounter are narrated with music. CASI

N94-15511* National Aeronautics and Space Administration. Lewis Research Center, Cleveland, OH.
NASA IMAGES 12 (Videotape)
Apr. 1988 Videotape: 28 min. 7 sec. playing time, in color, with sound
(NASA-TM-109417; NONP-VT-93-190214) Avail: CASI VHS A01/BETA A22

Voyager's encounters with Jupiter, Saturn, Uranus, and pre-Neptune are reviewed. CASI

N94-15512* National Aeronautics and Space Administration. Lewis Research Center, Cleveland, OH.
NASA IMAGES 13 (Videotape)
Apr. 1988 Videotape: 28 min. 30 sec. playing time, in color, with sound
(NASA-TM-109418; NONP-VT-93-190215) Avail: CASI VHS A01/BETA A22

Clips on Voyager 2 at Uranus and Venus are presented. CASI

N94-15513* Jet Propulsion Lab., California Inst. of Tech., Pasadena.
LIFE AND THE SOLAR SYSTEM: THE CRAF AND CASSINI MISSIONS (Videotape)
21 Mar. 1993 Videotape: 9 min. playing time, in color, with sound
(NASA-TM-109422; NONP-VT-93-190219) Avail: CASI VHS A01/BETA A22

Animation and interviews describe the proposed missions to study comets and Saturn. CASI

N94-16070* National Aeronautics and Space Administration. Ames Research Center, Moffett Field, CA.
GALILEO PROBE SPACECRAFT MISSION TO JUPITER (Videotape)
Oct. 1989 Videotape: 9 min. playing time, in color, with sound
(NASA-TM-109646; NONP-VT-93-190444) Avail: CASI VHS A01/BETA A22

This video contains Galileo probe animation, mission diagrams, and testing and manufacturing footage. CASI

N94-16173*# Lunar and Planetary Inst., Houston, TX.
TWENTY-FOURTH LUNAR AND PLANETARY SCIENCE CONFERENCE. PART 2: G-M Abstracts Only
1993 609 p Conference held in Houston, TX, 15-19 Mar. 1993
(Contract NASw-4574)
(NASA-CR-193174; NAS 1.26:193174) Avail: CASI HC A99/MF A06

The topics covered include the following: meteorites, meteoritic composition, geochemistry, planetary geology, planetary composition, planetary craters, the Moon, Mars, Venus, asteroids, planetary atmospheres, meteorite craters, space exploration, lunar geology, planetary surfaces, lunar surface, lunar rocks, lunar soil, planetary atmospheres, lunar atmosphere, lunar exploration, space missions, geomorphology, lithology, petrology, petrography, planetary evolution, Earth surface, planetary surfaces, volcanology, volcanos, lava, magma, mineralogy, minerals, ejecta, impact damage, meteoritic damage, tectonics, etc. For individual titles, see N94-16174 through N94-16437.

N94-16174*# Jet Propulsion Lab., California Inst. of Tech., Pasadena.
SPECTRAL EVIDENCE OF SIZE DEPENDENT SPACE WEATHERING PROCESSES ON ASTEROID SURFACES Abstract Only **c90**
M. J. Gaffey (Rensselaer Polytechnic Inst., Troy, NY.), J. F. Bell (Hawaii Univ., Honolulu.), R. H. Brown, T. H. Burbine (Smithsonian Astrophysical Observatory, Cambridge, MA.), J. L. Piatek (Arizona State Univ., Tempe.), K. L. Reed (Rensselaer Polytechnic Inst., Troy, NY.), and D. A. Chaky (Rensselaer Polytechnic Inst., Troy, NY.) *In* Lunar and Planetary Inst., Twenty-Fourth Lunar and Planetary Science Conference. Part 2: G-M 1993 p 515-516 (For primary document see N94-16173 03-91)
(Grants NAGw-642; NSF AST-90-12180)
Avail: CASI HC A01/MF A06

Most compositional characterizations of the minor planets are derived from analysis of visible and near-infrared reflectance spectra. However, such spectra are derived from light which has only interacted with a very thin surface layer. Although regolith processes are assumed to mix all near-surface lithologic units into this layer, it has been proposed that space weathering processes can alter this surface layer to obscure the spectral signature of the bedrock lithology. It has been proposed that these spectral alteration processes are much less pronounced on asteroid surfaces than on the lunar surface, but the possibility of major spectral alteration of asteroidal optical surfaces has been invoked to reconcile S-asteroids with ordinary chondrites. The reflectance spectra of a large subset of the S-asteroid population have been analyzed in a systematic investigation of the mineralogical diversity within the S-class. In this sample, absorption band depth is a strong function of asteroid diameter. The S-asteroid band depths are relatively constant for objects larger than 100 km and increase linearly by factor of two toward smaller sizes (approximately 40 km). Although the S-asteroid surface materials includes a diverse variety

of silicate assemblages, ranging from dunites to basalts, all compositional subtypes of the S-asteroids conform to this trend. The A-, R-, and V-type asteroids which are primarily silicate assemblages (as opposed to the metal-silicate mixtures of most S-asteroids) follow a parallel but displaced trend. Some sort of textural or regolith equilibrium appears to have been attained in the optical surfaces of asteroids larger than about 100 km diameter but not on bodies below this size. The relationships between absorption band depth, spectral slope, surface albedo and body size provide an intriguing insight into the nature of the optical surfaces of the S-asteroids and space weathering on these objects. Author

N94-16175*# Arizona Univ., Tucson. Dept. of Geosciences.

THE Fe2(+)-Mg INTERDIFFUSION IN ORTHOPYROXENE: CONSTRAINTS FROM CATION ORDERING AND STRUCTURAL DATA AND IMPLICATIONS FOR COOLING RATES OF METEORITES Abstract Only **c90**

J. Ganguly and V. Tazzoli (Pavia Univ., Italy.) *In* Lunar and Planetary Inst., Twenty-Fourth Lunar and Planetary Science Conference. Part 2: G-M 1993 p 517-518 (For primary document see N94-16173 03-91)

Avail: CASI HC A01/MF A06

Orthopyroxene crystals in a number of meteorites exhibit compositional zoning of Fe and Mg, which provide important constraint on their cooling rates. However, attempts to model cooling rate of these crystals from Fe-Mg zoning profiles suffer from the lack of any measured or theoretically well constrained Fe-Mg interdiffusion data in OP(x) It has been assumed that Fe-Mg interdiffusion in OP(x) only slightly slower than that in olivine. The purpose of this paper is to (1) calculate the Fe-Mg fractionation, and (2) provide analytical formulation relating cooling rate to the length of the diffusion zone across the interface of the overgrowth of a mineral on itself with application to Mg diffusion profile across OP(x) growth on OP(x) in certain mesosiderites. Derived from text

N94-16176*# Arizona Univ., Tucson. Dept. of Geosciences.

CATION ORDERING IN ORTHOPYROXENES AND COOLING RATES OF METEORITES: LOW TEMPERATURE COOLING RATES OF ESTHERVILLE, BONDOC AND SHAW Abstract Only **c90**

J. Ganguly, H. Yang (Washington Univ., Seattle.), and S. Ghose (Washington Univ., Seattle.) *In* Lunar and Planetary Inst., Twenty-Fourth Lunar and Planetary Science Conference. Part 2: G-M 1993 p 519-520 (For primary document see N94-16173 03-91)

Avail: CASI HC A01/MF A06

The cooling rates of meteorites provide important constraints on the size of their parent bodies, and their accretionary and evolutionary histories. However, the cooling rates obtained so far from the commonly used metallographic, radiometric and fission-track methods have been sometimes quite controversial, such as in the case of the mesosiderites and the meteorite Shaw. We have undertaken a systematic study of the cooling rates of meteorites using a different approach, which involves single crystal x-ray determination of Fe(2+)-Mg ordering in orthopyroxenes (OP(x)) in meteorites, subject to bulk compositional constraints, and numerical simulation of the evolution of the ordering state as a function of cooling rate, within the framework of the thermodynamic and kinetic principles governing cation ordering. We report the results obtained for OP(x) crystals from Shaw and two mesosiderites, Estherville and Bondoc.

Derived from text

N94-16177*# National Aeronautics and Space Administration. Lyndon B. Johnson Space Center, Houston, TX.

THE SCR Ne-21 AND Ar-38 IN LUNAR ROCK 68815: THE SOLAR PROTON ENERGY SPECTRUM OVER THE PAST 2 MYR Abstract Only

D. H. Garrison, M. N. Rao, and D. D. Bogard (Los Alamos National Lab., NM.) *In* Lunar and Planetary Inst., Twenty-Fourth Lunar and Planetary Science Conference. Part 2: G-M 1993 p 521-522 (For primary document see N94-16173 03-91)

Avail: CASI HC A01/MF A06

We determined concentration profiles of Ne-21, Ne-22, and Ar-38 produced by solar protons as a function of depth in oriented lunar rock 68815. A comparison with model predictions indicate a solar proton flux J(4(pi)(r); E greater than 10 MeV) of 100-125 p/sq. cm/s and a rigidity, R sub 0, of 85-100 MV, assuming an erosion rate of 1-2 mm/Myr. These results for 68815 and similar results on 61016 define the integrated solar proton energy spectrum at the moon over the past approximately 2 Myr.

Author (revised)

N94-16178*# National Aeronautics and Space Administration. Goddard Space Flight Center, Greenbelt, MD.

MORPHOMETRIC COMPARISON OF ICELANDIC LAVA SHIELD VOLCANOES VERSUS SELECTED VENUSIAN EDIFICES Abstract Only

James B. Garvin and Richard S. Williams, Jr. (Geological Survey, Woods Hole, MA.) *In* Lunar and Planetary Inst., Twenty-Fourth Lunar and Planetary Science Conference. Part 2: G-M 1993 p 523-524 Sponsored by NASA. Washington (For primary document see N94-16173 03-91)

Avail: CASI HC A01/MF A06

Shield volcanoes are common landforms on the silicate planets of the inner Solar System, and a wide variety have recently been documented on Venus by means of Magellan observations. In this report, we emphasize our recently completed morphometric analysis of three representative Icelandic lava shields: the classic Skjaldbreidur edifice, the low-reflief Lambahraun feature, and the monogenetic Sandfellshaed shield, as the basis for comparison with representative venusian edifices (greater than 60 km in diameter). Our detailed morphometric measurements of a representative and well-studied set of Icelandic volcanoes permits us to make comparisons with our measurements of a reasonable subset of shield-like edifices on Venus on the basis of Magellan global radar altimetry. Our study has been restricted to venusian features larger than approximately 60 km in basal diameter, on the basis of the minimum intrinsic spatial resolution (8 km) of the Magellan radar altimetry data. Finally, in order to examine the implications of landform scaling from terrestrial simple and composite shields to larger venusian varieties, we have considered the morphometry of the subaerial component of Mauna Loa, a type-locality for a composite shield edifice on Earth. Author

N94-16179*# Arizona Univ., Tucson. Dept. of Planetary Sciences.

A MINERALIZED ZONE IN WESTERN CANDOR CHASMA, MARS Abstract Only

P. E. Geissler, R. B. Singer, and G. Komatsu *In* Lunar and Planetary Inst., Twenty-Fourth Lunar and Planetary Science Conference. Part 2: G-M 1993 p 525-526 (For primary document see N94-16173 03-91)

Avail: CASI HC A01/MF A06

Spectral evidence from Viking and Phobos orbiting spacecraft suggests the local development of crystalline ferric oxides in a small region within Mars' equatorial Valles Marineris canyon system. This is the same area noted for its anomalous coloration in Viking Orbiter image 583 A by McEwen. The unique hue of the region in Viking color data is due to a reduced green filter reflectance, relative to violet and red, in comparison to surrounding materials of similar albedo or average reflectance. For this reason, the region does not appear spectrally distinctive in later Survey Mission images which were acquired without the green filter. In high resolution, the spectral unit can be seen to correspond to two 20 km long depressions on the margins of Candor Mensa, a heavily eroded plateau-forming deposit on the canyon floor. Laminae are conspicuous in several places on the plateau, particularly where 15 to 20 cycles of alternating bright and dark laminae are exposed at approximately 200 meter vertical intervals. Laminae are also visible on the steep, vertically fluted cliffs to the south of this depression. Concentric laminae indicate a basis in the depression on the southeastern margin of Candor Mensa at the location of the less pronounced hue anomaly. A distinct lineation at the base of the scarp at the western end of the canyon transects mottled canyon floor deposits believed to be among the youngest in the Valles marineris. Water is implicated in the formation of the iron oxides, since the steep surfaces of layered sediments elsewhere on Candor Mensa show no evidence of unusual coloration despite the fact that these materials were deposited concurrently with the strata exposed in the depressions. This suggests that the mineralization is secondary in nature and developed locally in association with the depressions, which could have ponded surface runoff or groundwater seepage. Author

N94-16180*# Academy of Sciences (USSR), Moscow. Space Research Inst.

TRAPPING OF WATER VAPOR FROM AN ATMOSPHERE BY CONDENSED SILICATE MATTER FORMED BY HIGH-TEMPERATURE PULSE VAPORIZATION Abstract Only

M. V. Gerasimov, Yu. P. Dikov, O. I. Yakovlev, and F. Wlotzka

(Max-Planck-Inst. fuer Chemie, Mainz, Germany.) *In* Lunar and Planetary Inst., Twenty-Fourth Lunar and Planetary Science Conference. Part 2: G-M 1993 p 527-528 (For primary document see N94-16173 03-91)
Avail: CASI HC A01/MF A06

The origin of planetary atmospheres is thought to be the result of bombardment of a growing planet by massive planetesimals. According to some models, the accumulation of released water vapor and/or carbon dioxide can result in the formation of a dense and hot primordial atmosphere. Among source and sink processes of atmospheric water vapor the formation of hydroxides was considered mainly as rehydration of dehydrated minerals (foresterite and enstatite). From our point of view, the formation of hydroxides is not limited to rehydration. Condensation of small silicate particles in a spreading vapor cloud and their interaction with a wet atmosphere can also result in the origin of hydrated phases which have no genetic connections with initial water bearing minerals. We present results of two experiments of a simulated interaction of condensed silicate matter which originated during vaporization of dry clinopyroxene in a wet helium atmosphere. Author

N94-16181*# Lancaster Univ. (England).
PARGO CHASMA AND ITS RELATIONSHIP TO GLOBAL TECTONICS Abstract Only
R. C. Ghail *In* Lunar and Planetary Inst., Twenty-Fourth Lunar and Planetary Science Conference. Part 2: G-M 1993 p 529 (For primary document see N94-16173 03-91)
Avail: CASI HC A01/MF A06

Pargo Chasma was first identified on Pioneer Venus data as a 10,000 km long lineation extending from Atla Regio in the north terminating in the plains south of Phoebe Regio. More recent Magellan data have revealed this feature to be one of the longest chains of coronae so far identified on the planet. Stofan et al have identified 60 coronae and 2 related features associated with this chain; other estimates differ according to the classification scheme adopted, for example Head et al. identify only 29 coronae but 43 arachnoids in the same region. This highlights one of the major problems associated with the preliminary mapping of the Magellan data: there has been an emphasis on identifying particular features on Venus without a universally accepted scheme to classify those features. Nevertheless, Pargo Chasma is clearly identified as a major tectonic belt of global significance. Together with the Artemis-Atla-Beta tectonic zone and the Beta-Phoebe rift belt, Pargo Chasma defines a region on Venus with an unusually high concentration of tectonic and volcanic features. Thus, an understanding of the processes involved in the formation of Pargo Chasma may lend significant insight into the evolution of the region and the planet as a whole. I have produced a detailed 1 to 10 million scale map of Pargo Chasma and the surrounding area from preliminary USGS controlled mosaiced image maps of Venus constructed from Magellan data. In view of the problems highlighted above in relation the efforts already made at identifying a particular set of features I have mapped the region purely on the basis of the geomorphology visible in the magellan data without any attempt at identifying a particular set or class of features. Thus, the map produced distinguishes between areas of different brightness and texture. This has the advantage of highlighting the tectonic fabric of Pargo Chasma and clearly illustrates the close inter-relationship between individual coronae and the surrounding tectonic belts. Author

N94-16182*# Carbotek, Inc., Houston, TX.
FIRST OXYGEN FROM LUNAR BASALT Abstract Only
M. A. Gibson, C. W. Knudsen, D. J. Brueneman, H. Kanamori (Shimizu Corp., Japan.), R. O. Ness (Energy Research and Development Administration, Grand Forks, ND.), L. L. Sharp (Energy Research and Development Administration, Grand Forks, ND.), D. W. Brekke (Energy Research and Development Administration, Grand Forks, ND.), C. C. Allen (Lockheed Engineering and Sciences Co., Houston, TX.), R. V. Morris (National Aeronautics and Space Administration. Lyndon B. Johnson Space Center, Houston, TX.), and L. P. Keller (National Aeronautics and Space Administration. Lyndon B. Johnson Space Center, Houston, TX.) et al *In* Lunar and Planetary Inst., Twenty-Fourth Lunar and Planetary Science Conference. Part 2: G-M 1993 p 531-532 (For primary document see N94-16173 03-91)
Avail: CASI HC A01/MF A06

The Carbotek/Shimizu process to produce oxygen from lunar soils has been successfully demonstrated on actual lunar samples in laboratory facilities at Carbotek with Shimizu funding and support. Apollo sample 70035 containing approximately 25 percent ilmenite ($FeTiO_3$) was used in seven separate reactions with hydrogen varying temperature and pressure: $FeTiO_3 + H_2$ yields $Fe + TiO_2 + H_2O$. The experiments gave extremely encouraging results as all ilmenite was reduced in every experiment. The lunar ilmenite was found to be about twice as reactive as terrestrial ilmenite samples. Analytical techniques of the lunar and terrestrial ilmenite experiments performed by NASA Johnson Space Center include iron Mossbauer spectroscopy (FeMS), optical microscopy, SEM, TEM, and XRD. The Energy and Environmental Research Center at the University of North Dakota performed three SEM techniques (point count method, morphology determination, elemental mapping), XRD, and optical microscopy. Author

N94-16183*# Brown Univ., Providence, RI. Dept. of Geological Sciences.
THE FORMATION AND EVOLUTION OF ALPHA AND TELLUS TESSERAE ON VENUS Abstract Only
M. S. Gilmore and J. W. Head *In* Lunar and Planetary Inst., Twenty-Fourth Lunar and Planetary Science Conference. Part 2: G-M 1993 p 533-534 (For primary document see N94-16173 03-91)
Avail: CASI HC A01/MF A06

Although tesserae comprise at approximately 10 percent of the surface of Venus, the nature of their formation and evolution is not well understood. One important clue to elucidate this problem is tessera boundaries which are of two types: type 1 are generally embayed by plains; type 2 boundaries are characterized by being linear at the hundred kilometer scale and often associated with steep scarps or tectonic features. Previous study of a distinctive type 2 boundary at Alpha Regio was pursued in order to characterize and assess the implications for this style in general. A model of gravitational relaxation of the tessera block was presented to explain the specific style of type 2 feature seen at western Alpha; however, this model cannot account for the full range of interior structures of Alpha, namely widespread compressional features overprinted by extensional features and volcanism. In order to explain the features of Alpha, we have considered a three-stage model involving (1) mantle downwelling and compression of the lithosphere, (2) delamination of the thickened tessera root, and (3) gravitational relaxation and extension of the tessera plateau. We compare this to the characteristics of Tellus Regio in order to test its broader application. Derived from text

N94-16184*# Open Univ., Milton (England). Dept. of Earth Sciences.
EXTRACTION AND ISOTOPIC ANALYSIS OF MEDIUM MOLECULAR WEIGHT HYDROCARBONS FROM MURCHISON USING SUPERCRITICAL CARBON DIOXIDE Abstract Only **c90**
Iain Gilmour and Colin Pillinger *In* Lunar and Planetary Inst., Twenty-Fourth Lunar and Planetary Science Conference. Part 2: G-M 1993 p 535-536 (For primary document see N94-16173 03-91)
Avail: CASI HC A01/MF A06

The large variety of organic compounds present in carbonaceous chondrites poses particular problems in their analysis not the least of which is terrestrial contamination. Conventional analytical approaches employ simple chromatographic techniques to fractionate the extractable compounds into broad classes of similar chemical structure. However, the use of organic solvents and their subsequent removal by evaporation results in the depletion or loss of semi-volatile compounds as well as requiring considerable preparative work to assure solvent purity. Supercritical fluids have been shown to provide a powerful alternative to conventional liquid organic solvents used for analytical extractions. A sample of Murchison from the Field Museum was analyzed. Two interior fragments were used; the first (2.85 g) was crushed in an agate pestel and mortar to a grain size of ca. 50-100 micron, the second (1.80 g) was broken into chips 3-8 mm in size. Each sample was loaded into a stainless steel bomb and placed in the extraction chamber of an Isco supercritical fluid extractor maintained at 35 C. High purity (99.9995 percent) carbon dioxide was used and was pressurized using an Isco syringe pump. The samples were extracted dynamically by flowing CO_2 under pressure through the bomb and venting via a 50 micron fused filica capillary into 5 mls of hexane used as a collection solvent. The hexane was maintained at a temperature of 0.5 C. A series of extractions were done on each sample using CO_2 of increasing density. The principal components extracted in each fraction are summarized. Author

N94-16185*# California Univ., Berkeley. Center for Extreme Ultraviolet Astrophysics.

EUVE OBSERVATIONS OF THE MOON Abstract Only

G. R. Gladstone, J. S. McDonald, and W. T. Boyd *In* Lunar and Planetary Inst., Twenty-Fourth Lunar and Planetary Science Conference. Part 2: G-M 1993 p 537 (For primary document see N94-16173 03-91)

Avail: CASI HC A01/MF A06

During its all-sky survey, the Extreme Ultraviolet Explorer (EUVE) satellite observed the Moon several times at first and last quarters, and once near the Dec. 10, 1992 lunar eclipse. We present a preliminary reduction and analysis of this data, in the form of EUV images of the Moon and derived albedos. Author

N94-16186*# Delaware Univ., Newark. Dept. of Geology.

CRETACEOUS-TERTIARY BOUNDARY SPHERULES AND CENOZOIC MICROTEKTITES: SIMILARITIES AND DIFFERENCES Abstract Only **c90**

B. P. Glass, Bruce F. Bohor (Geological Survey, Denver, CO.), and William J. Betterton (Geological Survey, Denver, CO.) *In* Lunar and Planetary Inst., Twenty-Fourth Lunar and Planetary Science Conference. Part 2: G-M 1993 p 539-540 (For primary document see N94-16173 03-91)

Avail: CASI HC A01/MF A06

Bohor and Betterton pointed out that the K-T spherules can be divided into three groups. Their Type 1 spherules appear to be found in or adjacent to North America, particularly the Western Interior and in Haiti and Mexico. The Type 1 spherules occur in the lower part of the K-T boundary clay below an Ir anomaly. It is the Type 1 spherules which are most similar to microtektites. The discovery of K-T boundary spherules in Beloc, Haiti, and Mimbral, Mexico, with residual tektite-like glass cores supports the hypothesis that the Type 1 spherules are diagenetically altered microtektites. The similarities and differences of the Type 1 K-T boundary spherules to previously described Cenozoic microtektites are discussed. Author

N94-16187*# Jet Propulsion Lab., California Inst. of Tech., Pasadena.

A TEST OF THE APPLICABILITY OF INDEPENDENT SCATTERING TO HIGH ALBEDO PLANETARY REGOLITHS Abstract Only

J. D. Goguen *In* Lunar and Planetary Inst., Twenty-Fourth Lunar and Planetary Science Conference. Part 2: G-M 1993 p 541-542 (For primary document see N94-16173 03-91)

Avail: CASI HC A01/MF A06

We show that 'independent scattering' is a useful approximation for high albedo particles whose size and packing density are similar to typical particles in the lunar regolith. Laboratory measurements of the intensity and linear polarization of light scattered from a laboratory sample of glass spheres of know size and composition are compared to radiative transfer calculations of the same observable quantities. Mie scattering is integrated over the size distribution of the particles to determine the mean phase and polarization functions, or phase matrix, of the particle. Assuming that the particles scatter independently, the 'doubling method' is used to rigorously calculate multiple scattering in an optically thick layer of these anisotropically scattering particles. All of the major features 'predicted' in the calculated intensity (double peaks at small phase angles) and polarization (negative branch at small phase angles, large positive peak near 20 degrees phase, and small polarization elsewhere) are observed in the laboratory measurements, with good quantitative agreement indicated at phase angles less than 90 degrees. Even though the particles are supported by physical contact with each other in the sample, as are the particles in planetary regoliths, the independent scattering calculation yields a good approximation to both the intensity and polarization. The physical parameters input to the calculation are only the size distribution of the particles and their complex index of refraction (composition). Significant advantages of this approach are that the phase matrix is calculated from basic physical principles and both the intensity and polarization are determined simultaneously. This model may have broad applications to the interpretation of photometry, spectroscopy, and polarimetry of the icy regoliths of high albedo satellites. The intent of this effort is to perform a controlled experiment that tests the utility of the independent scattering assumption Author

N94-16188*# Minnesota Univ., Minneapolis. Dept. of Geology and Geophysics.

RHEOLOGY OF WATER AND AMMONIA-WATER ICES Abstract Only **c25**

D. L. Goldsby, D. L. Kohlstedt, and W. B. Durham (Lawrence Livermore National Lab., CA.) *In* Lunar and Planetary Inst., Twenty-Fourth Lunar and Planetary Science Conference. Part 2: G-M 1993 p 543-544 (For primary document see N94-16173 03-91)

Avail: CASI HC A01/MF A06

Creep experiments on fine-grained water and ammonia-water ices have been performed at one atmosphere and high confining pressure in order to develop constitutive relationships necessary to model tectonic processes and interpret surface features of icy moons of the outer solar system. The present series of experiments explores the effects of temperature, strain rate, grain size, and melt fraction on creep strength. In general, creep strength decreases with increasing temperature, decreasing strain rate, and increasing melt fraction. A transition from dislocation creep to diffusion creep occurs at finer grain sizes, higher temperatures, and lower strain rates. Author

N94-16189*# Jet Propulsion Lab., California Inst. of Tech., Pasadena.

IMPORTANCE OF EXPANSION AND CONTRACTION IN THE FORMATION OF TECTONIC FEATURES ON THE MOON Abstract Only

M. P. Golombek and W. B. Banerdt *In* Lunar and Planetary Inst., Twenty-Fourth Lunar and Planetary Science Conference. Part 2: G-M 1993 p 545-546 (For primary document see N94-16173 03-91)

Avail: CASI HC A01/MF A06

The lack of globally distributed tectonic features on the lunar surface has been used to argue against significant changes in the radius of the Moon since the formation of the presently observed surface, which dates to the end of heavy bombardment about 3.9 Ga. This observation has been used previously to limit the maximum stresses to approximately 100 MPa that could be supported by the lunar lithosphere without the formation of globally distributed tectonic features, which in turn limits the maximum radius changes to plus or minus 1 km for a purely elastic lithosphere. In a previous abstract, limits on the elastic expansion or contraction of the Moon were reexamined with respect to realistic failure stresses necessary to produce actual lunar tectonic features. In addition, limits on the permanent (plastic) strain that could be accommodated by non-mascon grabens and wrinkle ridges were considered with more severe constraints placed on the total reasonable expansion and contraction of the Moon since 3.9 Ga. In this abstract, considerations of the distribution and mechanisms of formation due to a planetary radius change or their accommodating much permanent plastic planetary expansion or contraction. Author

N94-16190*# Arizona Univ., Tucson. Lunar and Planetary Lab.

STALKING THE LREE-ENRICHED COMPONENT IN UREILITES Abstract Only **c90**

Cyrena Anne Goodrich and Guenter W. Lugmair (Scripps Institution of Oceanography, San Diego, CA.) *In* Lunar and Planetary Inst., Twenty-Fourth Lunar and Planetary Science Conference. Part 2: G-M 1993 p 547-548 (For primary document see N94-16173 03-91)

Avail: CASI HC A01/MF A06

Ureilites contain a LREE-enriched component whose origin and identity are unknown, but which may have been introduced into 4.55 Ga olivine + pyroxene assemblages at various times in the period 4.55 - 3.74 Ga. This component is volumetrically minor, inhomogeneously distributed, and can be removed with concentrated HNO3, which suggests that it may be contained in minor, interstitial phases not previously recognized in ureilites. There is evidence, however, that not all of this component is leachable. Whole rock samples of Kenna, Novo Urei, and ALHA77257 form a Nd-143/Nd-144-Sm-147/Nd-144 line with a slope corresponding to an age of 3.74 Ga. Although this line could be a mixing line, with one end-member being the LREE-enriched component and the other being a 4.55 Ga olivine + pyroxene assemblage, the observation that a pyroxene separate from Kenna plots on the line suggests that the LREE-enriched component at least partially equilibrated with the olivine and pyroxene and that the line is an isochron. We performed a leaching experiment on Kenna, using various acids and concentrations, in an attempt to isolate the LREE-enriched component and differentiate between possible hosts for it, and to determine whether all of it is leachable. Our results suggest that most of the LREE-enriched component is surface-sited, rather than contained in a

discrete mineral. However, some of it is not readily leachable because it equilibrated with Kenna olivine + pyroxene at 3.79 plus or minus 0.05 Ga. Author

N94-16191*# Physical Research Lab., Ahmedabad (India).
GROSNAJA ABCs: MAGNESIUM ISOTOPE COMPOSITIONS Abstract Only **c90**
J. N. Goswami, G. Srinivasan, and A. A. Ulyanov (Moscow State Univ., Russia.) *In* Lunar and Planetary Inst., Twenty-Fourth Lunar and Planetary Science Conference. Part 2: G-M 1993 p 549-550 (For primary document see N94-16173 03-91)
Avail: CASI HC A01/MF A06

Three CAI's from the Grosnaja CV3 chondrite were analyzed for their magnesium isotopic compositions by the ion microprobe. The selected CAI's represent three distinct types: GR4(compact Type A), GR7(Type B) and GR2(Type C). Petrographic studies indicate that all three Grosnaja inclusions were subjected to secondary alterations. The Type A CAI GR4 is primarily composed of melilite with spinel and pyroxene occurring as minor phases. The rim of the inclusion does not exhibit distinct layered structure and secondary alteration products (garnet, Fe-rich olivine and Na-rich plagioclase) are present in some localized areas near the rim region. The average major element compositions of different mineral phases in GR4 are given. Preliminary REE data suggest a depletion of HREE relative to LREE by about a factor of 3 without any clear indication of interelement fractionation. The CAI GR7 has textural and minerological characteristics similar to Type B inclusions. The REE data show a pattern that is similar to Group 6 with enrichment in Eu and Yb. In addition, a depletion of HREE compared to LREE is also evident in this object. Melilite composition shows a broad range of akermanite content (Ak(sub 15-55)). Detailed petrographic study is in progress. GR2 is a anorthite-rich Type C inclusion with large plagioclase laths intergrown with Ti-rich pyroxene. The average plagioclase composition is close to pure anorthite (An99). Author

N94-16192*# Museum of Natural History, London (England). Dept. of Mineralogy.
EUROMET UREILITE CONSORTIUM: A PRELIMINARY REPORT ON CARBON AND NITROGEN GEOCHEMISTRY Abstract Only **c90**
Monica M. Grady and C. T. Pillinger (Open Univ., Milton, England.) *In* Lunar and Planetary Inst., Twenty-Fourth Lunar and Planetary Science Conference. Part 2: G-M 1993 p 551-552 (For primary document see N94-16173 03-91)
Avail: CASI HC A01/MF A06

The first Euromet expedition to the Frontier Mountain in Antarctica in December 1990 recovered two ureilites, FRO 90036 (34.6g) and FRO 90054 (17.5g). Preliminary classification indicated that the specimens had very different textures and mineral chemistries, and hence were not paired. A third ureilite, Acfer 277 (41.0 g), has also recently been returned from the Sahara. Due to the small sample sizes of the meteorites, and the unusual mineralogy of FRO 90054, a consortium was established to ensure the most effective study of these samples; this abstract reports on the carbon and nitrogen stable isotope geochemistry of two of the three ureilites issued to the consortium. Author

N94-16193*# Museum of Natural History, London (England).
NITRATES IN SNCs: IMPLICATIONS FOR THE NITROGEN CYCLE ON MARS Abstract Only
Monica M. Grady, I. P. Wright (Open Univ., Milton, England.), I. A. Franchi (Open Univ., Milton, England.), and C. T. Pillinger (Open Univ., Milton, England.) *In* Lunar and Planetary Inst., Twenty-Fourth Lunar and Planetary Science Conference. Part 2: G-M 1993 p 553-554 (For primary document see N94-16173 03-91)
Avail: CASI HC A01/MF A06

Nitrogen is the second most abundant constituent of the Martian atmosphere, after CO2, present at a level of ca. 2.7 percent. Several authors have hypothesized that earlier in the planet's history, nitrogen was more abundant, but has been removed by processes such as exospheric loss from the atmosphere. However, an alternative sink for atmospheric nitrogen is the regolith; model calculations have predicted that, via the formation of NOx, HNO2 and HNO3 in the lower layers of the Martian atmosphere, the regolith might trap nitrite and nitrate anions, leading to the build-up of involatile nitrates. Integrated over 4.5 x 10(exp 9) yr, such a mechanism would contribute the equivalent of a layer of nitrates up to 0.3 cm thick distributed across the Martian surface. Features in thermal emission spectra of the surface of Mars have been interpreted tentatively as emanating from various anions (carbonates, bicarbonates, sulphates, etc.), and the presence of nitrates has also been addressed as a possibility. The identification of carbonates in SCN meteorites has allowed inferences to be drawn concerning the composition and evolution of the Martian atmosphere in terms of its carbon isotope systematics; if nitrites, nitrates, or other nitrogen-bearing salts could be isolated from SNC's, similar conclusions might be possible for an analogous nitrogen cycle. Nitrates are unstable, being readily soluble in water, and decomposed at temperatures between 50 C and 600 C, depending on composition. Any nitrates present in SNC's might be removed during ejection from the planet's surface, passage to Earth, or during the sample's terrestrial history, by weathering etc. The same might have been said for carbonates, but pockets of shock-produced glass (lithology C) from within the EET A79001 shergottite and bulk samples of other SNC contain this mineral, which did apparently survive. Nitrates occurring within the glassy melt pockets of lithology C in EET A79001 might likewise be protected. Lithology C glass was therefore selected for nitrate analysis, first by non-destructive infra red spectroscopy, and then by stepped combustion. Author

N94-16194*# California Univ., San Diego, La Jolla. Dept. of Chemistry.
A CALIBRATION OF THE PRODUCTION RATE RATIO P-21/P-26 BY LOW ENERGY SECONDRY NEUTRONS: IDENTIFICATION OF Ne SPALLATION COMPONENTS AT THE 10(EXP 6) ATOMS/g LEVEL IN TERRESTRIAL SAMPLES Abstract Only **c72**
Th. Graf, S. Niedermann (Bern Univ., Switzerland.), and K. Marti *In* Lunar and Planetary Inst., Twenty-Fourth Lunar and Planetary Science Conference. Part 2: G-M 1993 p 555-556 (For primary document see N94-16173 03-91)
Avail: CASI HC A01/MF A06

The spallation ratio (Ne-22/Ne-21)(sub c) from Si was determined as 1.243 plus or minus 0.022 in a terrestrial quartz sample. We carried out a calibration of the in-situ production rate ratio P-21/P-26 in quartz samples for which Be-10 and Al-26 production rates were previously measured. A ratio P-21/P-26 of 0.67 plus or minus 0.12 is obtained. Author

N94-16195*# Hawaii Univ., Honolulu. Planetary Geosciences.
NEW K TYPE ASTEROIDS Abstract Only **c90**
James C. Granahan, Greg Smith, and Jeffrey F. Bell *In* Lunar and Planetary Inst., Twenty-Fourth Lunar and Planetary Science Conference. Part 2: G-M 1993 p 557-558 (For primary document see N94-16173 03-91)
Avail: CASI HC A01/MF A06

Several new K type asteroids were identified during near infrared spectral observations on July 30, 1992 at NASA's infrared telescope facility (IRTF) at Mauna Kea, Hawaii. These K asteroids are 513 Centesima, 633 Zelima, 1129 Neujmina, 1416 Renauxa, 1799 Koussevitzky, and 1883 Rauma. A K asteroid is an asteroid which possesses a S type spectra in visible wavelengths and a C type spectra visible in near-infrared wavelengths. These objects are usually misclassified as S asteroids on the basis of visible spectra alone. This type was first detected by the 52 infrared color asteroid survey also conducted at the IRTF. Our observations utilized a new seven color infrared asteroid filter system which allows near-infrared data to be collected from asteroids as faint as 16th 5 magnitude. Author

N94-16196*# Brown Univ., Providence, RI.
MARTIAN CRATER DEGRADATION BY EOLIAN PROCESSES: ANALOGY WITH THE RIO CUARTO CRATER FIELD, ARGENTINA Abstract Only
J. A. Grant and P. H. Schultz *In* Lunar and Planetary Inst., Twenty-Fourth Lunar and Planetary Science Conference. Part 2: G-M 1993 p 559-560 (For primary document see N94-16173 03-91)
Avail: CASI HC A01/MF A06

Numerous degraded and rimless craters occur across broad areas of the Martian surface that are mantled by thick, unconformable deposits. These regions include Arabia, Mesogaea, Electris, Tempe, the interior and surface to the northwest of Isidis Basin, southern Ismenius Lacus, and the polar layered terrains. Occurrence of the deposits and low regional thermal inertias indicate that at least some accumulated fine-grained sediment (effective particle diameters of 0.1-0.5 mm or coarse silt to medium sand) to a thickness of 100's to 1000's of meters. Most unconformable deposits

experienced some eolian modification that may be recent in some locales. Despite the presence of these deposits, simple eolian deposition appears incapable of creating the numerous degraded and rimless craters occurring within their limits. Nevertheless, terrestrial analyses of the Rio Cuario craters formed into loessoid deposits demonstrates that eolian redistribution of fine-grained sediment in and around craters produces degraded morphologies that are analogous to some found in mantled regions on Mars.

Derived from text

N94-16197*# Brown Univ., Providence, RI.

ROVER MOUNTED GROUND PENETRATING RADAR AS A TOOL FOR INVESTIGATING THE NEAR-SURFACE OF MARS AND BEYONG

Abstract Only **c32**

J. A. Grant and P. H. Schultz *In* Lunar and Planetary Inst., Twenty-Fourth Lunar and Planetary Science Conference. Part 2: G-M 1993 p 561-562 (For primary document see N94-16173 03-91)

Avail: CASI HC A01/MF A06

In spite of the highly successful nature of recent planetary missions to the terrestrial planets and outer satellites a number of questions concerning the evolution of their surfaces remain unresolved. For example, knowledge of many characteristics of the stratigraphy and soils comprising the near-surface on Mars remains largely unknown, but is crucial in order to accurately define the history of surface processes and near-surface sedimentary record. Similar statements can be made regarding our understanding of near-surface stratigraphy and processes on other extraterrestrial planetary bodies. Ground penetrating radar (GPR) is a proven and standard instrument capable of imaging the subsurface at high resolution to 10's of meters depth in a variety of terrestrial environments. Moreover, GPR is portable and easily modified for rover deployment. Data collected with a rover mounted GPR could resolve a number of issues related to planetary surface evolution by defining shallow stratigraphic records and would provide context for interpreting results of other surface analyses (e.g. elemental or mineralogical). A discussion of existing GPR capabilities is followed first by examples of how GPR might be used to better define surface evolution on Mars and then by a brief description of possible GPR applications to the Moon and other planetary surfaces. Author

N94-16198*# Arizona State Univ., Tempe.

SAND TRANSPORT ON MARS: PRELIMINARY RESULTS FROM MODELS Abstract Only

R. Greeley, F. S. Anderson, D. Blumberg, E. Lo, P. Xu, and J. Pollack (National Aeronautics and Space Administration. Ames Research Center, Moffett Field, CA.) *In* Lunar and Planetary Inst., Twenty-Fourth Lunar and Planetary Science Conference. Part 2: G-M 1993 p 563-564 (For primary document see N94-16173 03-91)

Avail: CASI HC A01/MF A06

Most studies of active aeolian processes on Mars have focused on dust, i.e., particles approximately 1 micron in diameter that are transported in suspension by wind. The presence of sand dunes on Mars indicates that larger grains (approximately greater than 60 microns, transported primarily in saltation) are also present. Although indirect evidence suggests that some dunes may be active, definitive evidence is lacking. Nonetheless, numerous studies demonstrate that sand is substantially easier to transport by wind than dust, and it is reasonable to infer that sand transportation in saltation occurs under present Martian conditions. In order to assess potential source regions, transportation pathways, and sites of deposition for sand on Mars, an iterative sand transport algorithm was developed that is based on the Mars General Circulation Model of Pollack et al. The results of the dust transport model are then compared with observed surface features, such as dune field locations observed on images, and surficial deposits as inferred from Viking IRTM observations. Preliminary results suggest that the north polar dune fields in the vicinity of 270 degrees W, 70 degrees N originated from weathered polar layered plains centered at 280 degrees W, 85 degrees N, and that Thaumasia Fossae, southern Hellas Planitia, and the area west of Hellespontus Montes are sand depositional sites. Examples of transportation 'corridors' include a westward pathway in the latitudinal band 35 degrees N to 45 degrees N, and a pathway southward from Solis Planum to Thaumasia Fossae, among others. Author

N94-16199*# Arizona State Univ., Tempe.

GALILEO IMAGING RESULTS FROM THE SECOND EARTH-MOON FLYBY: LUNAR MARIA AND RELATED UNITS

R. Greeley, M. J. S. Belton (Kitt Peak National Observatory, Tucson, AZ.), J. W. Head (Brown Univ., Providence, RI.), A. S. McEwen (Geological Survey, Flagstaff, AZ.), C. M. Pieters (Brown Univ., Providence, RI.), G. Neukum (Deutsche Forschungsanstalt fuer Luft- und Raumfahrt, Oberpfaffenhofen, Germany.), T. L. Becker (Geological Survey, Flagstaff, AZ.), E. M. Fischer (Brown Univ., Providence, RI.), S. D. Kadel, and M. S. Robinson (Hawaii Univ., Honolulu.) et al *In* Lunar and Planetary Inst., Twenty-Fourth Lunar and Planetary Science Conference. Part 2: G-M 1993 p 565-566 (For primary document see N94-16173 03-91)

Avail: CASI HC A01/MF A06

The second flyby of the Earth-Moon System by Galileo occurred on December 7, 1992, on its trajectory toward Jupiter. The flyby took the spacecraft over the lunar north polar region from the dark farside and continued across the illuminated nearside. This provided the first opportunity to observe northern and northeastern limb regions with a modern, multispectral imaging system with high spatial resolution (up to 1.1 km/pixel). Scientific objectives included compositional assessment of previously uncharacterized mare regions, study of various light plains materials, and assessment of dark mantle deposits (DMD) and dark halo craters (DHC). Color composite images were prepared from ratios of Galileo SSI filter data (0.76/0.41 yields red; 0.76/0.99 yields green; 0.41/0.76 yields blue) and used for preliminary comparison of units. The 0.41/0.76 ratio has been empirically correlated to Ti content of mare soils (blue is relatively high, red is relatively low). The relative strengths of the ferrous one micron absorption in mafic minerals can be compared using the 0.76/0.99 ratio. In addition, relative ages of units analyzed spectrally were determined from crater statistics using Lunar Orbiter images following the techniques of Neukum et al. Mare deposits analyzed include Mare Humboldtianum, central and eastern Mare Frigoris, Mare Crisium and other deposits in the Crisium Basin, and isolated mare patches on the northeastern lunar limb. Preliminary results show a diversity of 0.41/0.76 micron signatures, implying a wide range of titanium contents. Some light plains units are similar to units found at the Apollo 16 site; others may be ancient mare materials. Dark mantle deposits (DMD) analyzed also are available. Author

N94-16200*# Arizona State Univ., Tempe.

MARS ANALOG SITE STUDY (MASS) Abstract Only

R. Greeley, R. Kuzmin (Academy of Sciences, USSR, Moscow.), F. Costard (Centre National de la Recherche Scientifique, Meudon-Bellevue, France.), F. S. Anderson (Arizona State Univ., Tempe.), M. A. Geringer (Arizona State Univ., Tempe.), R. Landheim (Arizona State Univ., Tempe.), and M. L. Wenrich (Arizona State Univ., Tempe.) *In* Lunar and Planetary Inst., Twenty-Fourth Lunar and Planetary Science Conference. Part 2: G-M 1993 p 567-568 (For primary document see N94-16173 03-91)

Avail: CASI HC A01/MF A06

Many proposed missions to Mars involve landing vehicles, including the Mars 94/96 (Russia), Mars Environmental Survey (MESUR, US), and the Marsnet (ESA) missions. Most landers involve in situ measurements of rock and soil compositions, study of local geology by imaging, and establishment of seismic and meteorological networks. The selection of landing sites on Mars is a complex process that must meet engineering constraints and scientific objectives, using available and anticipated data. The goal of the MASS project is to conduct an 'end-to-end' test of the site selection process using Earth analogs. Derived from text

N94-16201*# Arizona Univ., Tucson.

EARTH IMAGING RESULTS FROM GALILEO'S SECOND ENCOUNTER Abstract Only

R. Greenberg, M. Belton (Kitt Peak National Observatory, Tucson, AZ.), E. DeJong (Jet Propulsion Lab., California Inst. of Tech., Pasadena.), A. Ingersoll (California Inst. of Tech., Pasadena.), K. Klaasen (Jet Propulsion Lab., California Inst. of Tech., Pasadena.), P. Geissler (Arizona Univ., Tucson.), J. Moersch (Cornell Univ., Ithaca, NY.), and W. R. Thompson (Cornell Univ., Ithaca, NY.) *In* Lunar and Planetary Inst., Twenty-Fourth Lunar and Planetary Science Conference. Part 2: G-M 1993 p 569 (For primary document see N94-16173 03-91)

Avail: CASI HC A01/MF A06

The recent flyby of the Galileo spacecraft en route to Jupiter contributes a unique perspective to our view of our home planet. Imaging activities conducted during the second Earth encounter provide an important opportunity to assess new methods and approaches on familiar territory. These include unique multispectral observations, low light-level imaging

(searches for aurorae, lightning and artificial lights on the nightside) and experiments with multiple exposure times to extend the effective radiometric resolution and dynamic range of the camera system. Galileo imaging data has the potential to make important contributions to terrestrial remote sensing. This is because the particular set of filters included in the Solid State Imaging system are not presently incorporated in any currently operating Earth-orbiting sensor system. The visible/near-infrared bandpasses of the SSI filters are well suited to remote sensing of geological, glaciological, botanical, and meteorological phenomena. Data from this and the previous Earth encounter may provide an extremely valuable reference point in time for comparison with similar data expected from EOS or other systems in the future, contributing directly to our knowledge of global change. The highest resolution imaging (0.2 km/pixel) during the December, 1992 encounter occurred over the central Andes; a five filter mosaic of visible and near infrared bands displays the remarkable spectral heterogeneity of this geologically diverse region. As Galileo departed the Earth, cooperative imaging with the Near Infrared Mapping Spectrometer (NIMS) instrument targeted Antarctica, Australia, and Indonesia at 1.0 to 2.5 km/pixel resolutions in the early morning local times near the terminator. The Antarctic data are of particular interest, potentially allowing ice grain size mapping using the 889 and 968 nm filters and providing an important means of calibrating the technique for application to the Galilean satellites. As the spacecraft receded further, regional scale imaging provided data which, along with data from the previous encounter, will enable the production of global multispectral mosaics of Earth in each of the SSI filters. Author

N94-16202*# Arizona Univ., Phoenix. Lunar and Planetary Lab.
COLLISIONAL AND DYNAMICAL HISTORY OF GASPRA Abstract Only **c90**
R. Greenberg, M. C. Nolan, W. F. Bottke, Jr., and R. A. Kolvoord *In* Lunar and Planetary Inst., Twenty-Fourth Lunar and Planetary Science Conference. Part 2: G-M 1993 p 571-572 (For primary document see N94-16173 03-91)
Avail: CASI HC A01/MF A06

Interpretation of the impact record on Gaspra requires understanding of the effects of collisions on a target body of Gaspra's size and shape, recognition of impact features that may have different morphologies from craters on larger planets, and models of the geological processes that erase and modify impact features. Crater counts on the 140 sq km of Gaspra imaged at highest resolution by the Galileo spacecraft show a steep size-frequency distribution (cumulative power-law index near -3.5) from the smallest resolvable size (150 m diameter) up through the large feature (1.5 km diameter crater) of familiar crater-like morphology. In addition, there appear to be as many as eight roughly circular concavities with diameters greater than 3 km visible on the asteroid. If we restrict our crater counts to features with traditionally recognized crater morphologies, these concavities would not be included. However, if we define craters to include any concave structures that may represent local or regional damage at an impact size, then the larger features on Gaspra are candidates for consideration. Acceptance of the multi-km features as craters has been cautious for several reasons. First, scaling laws (the physically plausible algorithms for extrapolating from experimental data) indicate that Gaspra could not have sustained such large-crater-forming impacts without being disrupted; second, aside from concavity, the larger structures have no other features (e.g. rims) that can be identified with known impact craters; and third, extrapolation of the power-law size distribution for smaller craters predicts no craters larger than 3 km over the entire surface. On the other hand, recent hydrocode modeling of impacts shows that for given impact (albeit into a sphere), the crater size is much larger than given by scaling laws. Gaspra-size bodies can sustain formation of up to 8-km craters without disruption. Besides allowing larger impact craters, this result doubles the lifetime since the last catastrophic fragmentation event up to one billion years. Events that create multi-km craters also globally damage the material structure, such that regolith is produced, whether or not Gaspra 'initially' had a regolith, contrary to other models in which initial regolith is required in order to allow current regolith. Because the globally destructive shock wave precedes basin formation, crater size is closer to the large size extrapolated from gravity-scaling rather than the strength-scaling that had earlier been assumed for such small bodies. This mechanism may also help explain the existence of Stickney on Phobos. Moreover, rejection of the large concavities as craters based on unfamiliar morphology would be premature, because (aside from Stickney) we have no other data on such large impact structures on such a small, irregular body. The eight candidate concavities cover an area greater than that counted for smaller craters, because they are most apparent where small craters cannot be seen: on low resolution images and at the limb on high resolution images. We estimate that there are at least two with diameter greater than 4 km per 140 sq km, which would have to be accounted for in any model that claims these are impact craters. Author

N94-16203*# Museum of Natural History, London (England). Dept. of Mineralogy.
PETROGRAPHY, MINERALOGY, AND Mg ISOTOPE COMPOSITION OF VICTA: A VIGARANO CaAl4O7-BEARING TYPE A INCLUSION Abstract Only **c46**
R. C. Greenwood, A. Morse (Open Univ., Milton, England.), and J. V. P. Long (Cambridge Univ., England.) *In* Lunar and Planetary Inst., Twenty-Fourth Lunar and Planetary Science Conference. Part 2: G-M 1993 p 573-574 (For primary document see N94-16173 03-91)
Avail: CASI HC A01/MF A06

Thermodynamic calculations predict that Ca-dialuminate ($CaAl_4O_7$) condenses from a cooling gas of solar composition after hibonite and before melilite. Although Ca-dialuminate has now been recorded from Ca Al-rich inclusions (CAI's) in at least 9 meteorites, compared to hibonite it is a relatively rare phase. As pointed out by Michel-Levy et al., the absence of Ca-dialuminate from most hibonite-bearing inclusions poses a serious problem for the condensation model of CAI formation. Here we describe an inclusion which contains abundant CA-dialuminate partially altered to a hercynite-rich ($FeAl_2O_4$) assemblage. The evidence from VICTA indicates that compared to all other phases in type A inclusions, Ca-dialuminate is the most susceptible to secondary alteration; a feature which may explain its restricted occurrence. Unaltered Ca-dialuminate and melilite in VICTA display excess Mg-26 indicative of in situ decay of Al-26. Author

N94-16204*# Arizona State Univ., Tempe. Dept. of Geology.
EXPLOSIVE MAFIC VOLCANISM ON EARTH AND MARS Abstract Only
Tracy K. P. Gregg and Stanley N. Williams *In* Lunar and Planetary Inst., Twenty-Fourth Lunar and Planetary Science Conference. Part 2: G-M 1993 p 575-576 (For primary document see N94-16173 03-91)
Avail: CASI HC A01/MF A06

Deposits within Amazonia Planitia, Mars, have been interpreted as ignimbrite plains on the basis of their erosional characteristics. The western flank of Hecates Tholus appears to be mantled by an airfall deposit, which was produced through magma-water interactions or exsolution of magmatic volatiles. Morphologic studies, along with numerical and analytical modeling of Martian plinian columns and pyroclastic flows, suggest that shield materials of Tyrrhena and Hadriaca paterae are composed of welded pyroclastic flows. Terrestrial pyroclastic flows, ignimbrites, and airfall deposits are typically associated with silicic volcanism. Because it is unlikely that large volumes of silicic lavas have been produced on Mars, we seek terrestrial analogs of explosives, mafic volcanism. Plinian basaltic airfall deposits have been well-documented at Masaya, Nicaragua, and basaltic ignimbrite and surge deposits also have been recognized there. Ambrym and Yasour, both in Vanuatu, are mafic stratovolcanioes with large central calderas, and are composed of interbedded basaltic pyrocalstic deposits and lava flows. Zavaritzki, a mafic stratovolcano in the Kurile Islands, may have also produced pyroclastic deposits, although the exact nature of these deposits in unknown. Masaya, Ambrym and Yasour are known to be located above tensional zones. Hadriaca and Tyrrhena Paterae may also be located above zones of tension, resulting from the formation and evolution of Hellas basin, and, thus, may be directly analogous to these terrestrial mafic, explosive volcanoes. Author

N94-16205*# Arizona State Univ., Tempe. Dept. of Geology.
HELIOCENTRIC ZONING OF THE ASTEROID BELT BY ALUMINUM-26 HEATING Abstract Only **c90**
R. E. Grimm and H. Y. McSween, Jr. (Tennessee Univ., Knoxville.) *In* Lunar and Planetary Inst., Twenty-Fourth Lunar and Planetary Science Conference. Part 2: G-M 1993 p 577-578 (For primary document see N94-16173 03-91)
Avail: CASI HC A01/MF A06

Variations in petrology among meteorites attest to a strong heating event early in solar system history, but the heat source has remained

unresolved. Aluminum-26 has been considered the most likely high-energy, short-lived radionuclide (half-life 0.72 million years) since the discovery of its decay product - excess Mg-26 - in Allende CAI's. Furthermore, observation of relict Mg-26 in an achondritic clast and in feldspars within ordinary chondrites (3,4) provided strong evidence for live Al-26 in meteorite parent bodies and not just in refractory nebular condensates. The inferred amount of Al-26 is consistent with constraints on the thermal evolution of both ordinary and carbonaceous chondrite parent objects up to a few hundred kilometers in diameter. Meteorites can constrain the early thermal evolution of their parent body locations, provided that a link can be established between asteroid spectrophotometric signature and meteorite class. Asteroid compositions are heliocentrically distributed: objects thought to have experienced high metamorphic or even melting temperatures are located closer to the sun, whereas apparently unaltered or mildly heated asteroids are located farther away. Heliocentric zoning could be the result of Al-26 heating if the initial amount of the radionuclide incorporated into planetesimals was controlled by accretion time, which in turn varies with semimajor axis. Analytic expressions for planetary accretion may be integrated to given the time, tau, required for a planetesimal to grow to a specified radius: tau varies as a(sup n), where n = 1.5 to 3 depending on the assumptions about variations in the surface density of the planetesimal swarm. Numerical simulations of planetesimal accretion at fixed semimajor axis demonstrate that variations in accretion time among small planetesimals can be strongly nonlinear depending on the initial conditions and model assumptions. The general relationship with semimajor axis remains valid because it depends only on the initial orbit properties and distribution of the planesimal swarm. In order to demonstrate the basic dependence of thermal evolution on semimajor axis, we parameterized accretion time across the asteroid belt according to tau varies as a(sup n) and calculated the subsequent thermal history. Objects at a specified semimajor axis were assumed to have the same accretion time, regardless of size. We set the initial Al-26/Al-27 ratio = 6 x 10(exp -5) and treated n and tau(sub 0) at a(sub 0) = 3 AU as adjustable parameters. The thermal model included temperature-dependent properties of ice and rock (CM chondrite analog) and the thermodynamic effects of phase transitions. Author

N94-16206*# Colorado Univ., Boulder. Lab. for Atmospheric and Space Physics.

EVOLUTIONARY IMPLICATIONS OF A STEADY-STATE WATER ABUNDANCE ON VENUS Abstract Only

David H. Grinspoon *In* Lunar and Planetary Inst., Twenty-Fourth Lunar and Planetary Science Conference. Part 2: G-M 1993 p 579-580 (For primary document see N94-16173 03-91)

Avail: CASI HC A01/MF A06

In 1987, Grinspoon proposed that the data on hydrogen abundance, isotopic composition, and escape rate were consistent with the hypothesis that water on Venus might be in steady-state rather than monotonic decline since the dawn of time. This conclusion was partially based on a derived water lifetime against nonthermal escape of approximately 10(exp 8) years. Others have questioned this conclusion. De Bergh et al. found H2O lifetimes of greater than 10(exp 9) years. Donahue and Hodges derived H2O lifetimes of 0.4 - 5 x 10(exp 9) years. The most sophisticated analysis to date of near-IR radiation from Venus' nightside reveals a water mixing ratio of approximately 30 ppm. Recent re-analysis of Pioneer Venus Mass Spectrometer Data are consistent with a water abundance of 30 ppm. Hodges and Tinsley found an escape flux due to charge exchange with hot H(+) of 2.8 x 10(exp 7) cm(exp -2) s(exp -1). Gurwell and Yung estimated an escape flux of 3.5 x 10(exp 6) cm(exp -2) s(exp -1) from collisions with hot O produced by dissociative recombination of O2(+). Brace et al. estimated an escape flux of 5 x 10(exp 6) cm(exp -2) s(exp -1) from ion escape from the ionotail of Venus. The combined estimated escape flux from all of these processes is 3.7 x 10(exp 7) cm(exp -2) s(exp -1), suggesting a lifetime against escape for water of less than 10(exp 8) years. A recent estimate of H escape flux employing a different ionospheric model and using Pioneer Venus reentry data to estimate the response of the escape flux to the solar cycle finds a somewhat lower escape flux of 1.4 x 10(exp 7) cm(exp -2) s(exp -1), suggesting a water lifetime closer to 2 x 10(exp 8) years, significantly less than the age of the planet. Large uncertainties remain in these quantities, yet the data suggest that a source of water more recent than primordial sources is required and that a steady-state is likely. To obvious candidates for this source water are cometary impact and volcanic outgassing. Other aspects of this investigation are discussed. Author

N94-16207*# Brown Univ., Providence, RI. Dept. of Geological Sciences.

SPATIALLY EXTENSIVE UNIFORM STRESS FIELDS ON VENUS INFERRED FROM RADIAL DIKE SWARM GEOMETRIES: THE APHRODITE TERRA EXAMPLE Abstract Only

Eric B. Grosfils and James W. Head *In* Lunar and Planetary Inst., Twenty-Fourth Lunar and Planetary Science Conference. Part 2: G-M 1993 p 581-582 (For primary document see N94-16173 03-91)

Avail: CASI HC A01/MF A06

The high resolution and near global coverage of Magellan radar images is facilitating attempts to systematically investigate the stresses that have deformed the venusian crust. Here we continue earlier efforts to utilize approximately 170 large, radially lineated structures interpreted as dike swarms to assess the orientation of the regional maximum horizontal compressive stress (MHCS) which existed in their vicinities during emplacement. Examination of swarms near the equator reveals a link to broad scale regional structures, such as Aphrodite Terra, across distances in excess of 1000 km, suggesting the existence of first order stress fields which affect areas of more than 10(exp 6) sq km in a uniform fashion. Focusing further upon the Aphrodite Terra region, the MHCS field in the surrounding lowlands inferred from radial swarms is oriented approximately normal to the slope of the highland topography. This stress configuration appears, at a simple level, to be incompatible with that expected during either upwelling or downwelling construction of the highlands. In addition, the relatively undeformed geometry of the radial structures within the highlands implies that these dike swarm features formed more recently than their highly deformed surroundings. We conclude that the differential stresses which existed during emplacement of the dike swarms within and adjacent to the Aphrodite Terra highlands are related to the gravitational relaxation of pre-existing topography. Author

N94-16208*# Massachusetts Inst. of Tech., Cambridge. Dept. of Earth, Atmospheric and Planetary Sciences.

PETROLOGIC CONSTRAINTS ON THE SURFACE PROCESSES ON ASTEROID 4 VESTA AND ON EXCAVATION DEPTHS OF DIOGENITE FRAGMENTS Abstract Only **c90**

T. L. Grove *In* Lunar and Planetary Inst., Twenty-Fourth Lunar and Planetary Science Conference. Part 2: G-M 1993 p 583-584 (For primary document see N94-16173 03-91)

Avail: CASI HC A01/MF A06

The eucrite-howardite-diogenite meteorite groups are though to be related by magmatic processes. Asteroid 4 Vesta has been proposed as the parent body for these basaltic achondrite meteorites. The similarity of the planetesimal's surface composition to eucrite and diogenite meteorites and the large size of the asteroid (r = 250 km) make it an attractive source, but its position in the asteroid belt far from the known resonances from which meteorites originate make a relation between Vesta and eucrite-howardite-giogenite group problematic. It has been proposed that diogenites are low-Ca pyroxene-rich cumulates that crystallized from a magnesian parent (identified in howardite breccias), and this crystallization process led to evolved eucrite derivative magmas. This eucrite-diogenite genetic relationship places constraints on the physical conditions under which crystallization occurred. Elevated pressure melting experiments on magnesian eucrite parent compositions show that the minimum pressure at which pyroxene crystallization could lead to the observed compositions of main series eucrites is 500 bars, equivalent to a depth of 135 km in a 4 Vesta-sized eucrite parent body. Therefore, the observation of diogenite on the surface of 4 Vesta requires a post-crystallization process that excavates diogenite cumulate from depth. The discovery of diogenite asteroidal fragments is consistent with an impact event on 4 Vesta that penetrated the deep interior of this planetesimal. Author

N94-16209*# Washington Univ., Saint Louis, MO. Dept. of Earth and Planetary Sciences.

THE PLANETARY DATA SYSTEM EDUCATIONAL CD-ROM Abstract Only **c82**

E. A. Guinness, R. E. Arvidson, M. Martin (Jet Propulsion Lab., California Inst. of Tech., Pasadena.), and S. Dueck (Jet Propulsion Lab., California

Inst. of Tech., Pasadena.) *In* Lunar and Planetary Inst., Twenty-Fourth Lunar and Planetary Science Conference. Part 2: G-M 1993 p 585-586 (For primary document see N94-16173 03-91)
Avail: CASI HC A01/MF A06

The Planetary Data System (PDS) is producing a special educational CD-ROM that contains samples of PDS datasets and is expected to be released in 1993. The CD-ROM will provide university-level instructors with PDS-compatible materials and information that can be used to construct student problem sets using real datasets. The main purposes of the CD-ROM are to facilitate wide use of planetary data and to introduce a large community to the PDS. To meet these objectives the Educational CD-ROM will also contain software to manipulate the data, background discussions about scientific questions that can be addressed with the data, and a suite of exercises that illustrate analysis techniques. Students will also be introduced to the SPICE concept, which is a new way of maintaining geometry and instrument information. The exercises will be presented at the freshman through graduate student levels. With simplification, some of the material should also be of use at the high school level. Author

N94-16210*# Arizona Univ., Tucson. Dept. of Geosciences.
FLUVIAL EROSION ON MARS: IMPLICATIONS FOR PALEOCLIMATIC CHANGE Abstract Only **c90**
Virginia C. Gulick and Victor R. Baker *In* Lunar and Planetary Inst., Twenty-Fourth Lunar and Planetary Science Conference. Part 2: G-M 1993 p 587-588 (For primary document see N94-16173 03-91)
Avail: CASI HC A01/MF A06

Fluvial erosion on Mars has been nonuniform in both time and space. Viking orbiter images reveal a variety of different aged terrains exhibiting widely different degrees of erosion. Based on our terrestrial analog studies, rates of fluvial erosion associated with the formation of many of the valleys on Mars is probably on the order of hundreds of meters per million years, while rates of erosion associated with the formation of the outflow channels probably ranged from tens to hundreds of meters in several weeks to months. However, estimated rates of erosion of the Martian surface at the Viking Lander sites are extremely low, on the order of 1 micron/yr or less. At most this would result in a meter of material removed per million years, and it is unlikely that such an erosion rate would be able to produce the degree of geomorphic work required to form the fluvial features present elsewhere on the surface. In addition, single terrain units are not eroded uniformly by fluvial processes. Instead fluvial valleys, particularly in the cratered highlands, typically are situated in clusters surrounded by vast expanses of uneroded surfaces of the same apparent lithologic, structural, and hydrological setting. Clearly throughout its geologic history, Mars has experienced a nonuniformity in erosion rates. By estimating the amount of fluvial erosion on dissected terrains and by studying the spatial distribution of those locations which have experienced above normal erosion rates, it should be possible to place further constraints on Mars' paleoclimatic history. Author

N94-16211*# Academy of Sciences of the Ukraine, Kiev. Inst. of Geological Sciences.
THE ACRAMAN IMPACT STRUCTURE: ESTIMATION OF THE DIAMETER BY THE EJECTA LAYER THICKNESS Abstract Only **c46**
E. P. Gurov *In* Lunar and Planetary Inst., Twenty-Fourth Lunar and Planetary Science Conference. Part 2: G-M 1993 p 589-590 (For primary document see N94-16173 03-91)
Avail: CASI HC A01/MF A06

The big role of gigantic craters formation in geological history of the Earth was established by the example of the K/T boundary event. The discovery of the iridium anomaly in the sedimentary rocks of Vendian in the western part of Ukrainian shield allows to suppose its origin in connection with the great impact of that time. The only big impact structure of that age is the Acraman Crater in south-eastern part of Australia. The Acraman Crater is presented by deeply eroded structure, original diameter of which it is difficult to determine. By geological and morphological data the Acraman Crater is presented by an inner ring 30 km in diameter, an intermediate ring 90 km in diameter, and an outer ring about 150-160 km in diameter. Author

N94-16212*# Academy of Sciences of the Ukraine, Kiev. Inst. of Geological Sciences.
THE KARAKUL DEPRESSION IN PAMIRS: THE FIRST IMPACT STRUCTURE IN CENTRAL ASIA Abstract Only **c90**
E. P. Gurov, H. P. Gurova, R. B. Rakitskaya, and A. Yu. Yamnichenko *In* Lunar and Planetary Inst., Twenty-Fourth Lunar and Planetary Science Conference. Part 2: G-M 1993 p 591-592 (For primary document see N94-16173 03-91)
Avail: CASI HC A01/MF A06

The Karakul depression was picked out as the possible impact structure by the study of space images of Tadjikistan. Its striking similarity with some complex impact craters such as Dellen and Gosses Bluff is evident. Our investigations of the Karakul depression in 1987 and 1989-1991 years allowed to determine it as the impact crater with the central uplift. The target of the crater is presented by slightly metamorphosed sedimentary rocks of Paleozoic, intensively folded and intruded with granites during the Gercynian orogeny. The modern structure of north-eastern Pamirs was formed by Alpinian orogeny; the raise of the area in Neogene was about 4000-7000 m. Author

N94-16213*# Hawaii Univ., Honolulu. Planetary Geosciences.
SYSTEMATIC CHEMICAL VARIATIONS IN LARGE 3AB IRON METEORITES: CLUES TO CORE CRYSTALLIZATION Abstract Only **c90**
H. Haack, E. R. D. Scott, G. S. Rubio (Universidad Nacional Autonoma de Mexico, Mexico City.), D. F. Gutierrez (Universidad Nacional Autonoma de Mexico, Mexico City.), C. F. Lewis (Arizona State Univ., Tempe.), J. T. Wasson (California Univ., Los Angeles.), R. R. Brooks (Massey Univ., Palmerston North, New Zealand.), X. Guo (Massey Univ., Palmerston North, New Zealand.), D. E. Ryan (Dalhousie Univ., Halifax, Nova Scotia.), and J. Holzbecher (Dalhousie Univ., Halifax, Nova Scotia.) *In* Lunar and Planetary Inst., Twenty-Fourth Lunar and Planetary Science Conference. Part 2: G-M 1993 p 593-594 (For primary document see N94-16173 03-91)
(Grants NAGw-3281; NAG9-454)
Avail: CASI HC A01/MF A06

Analysis of numerous individual iron meteorites have shown that fractional crystallization of iron cores result in variations in chemical concentration of the solid core which span several orders of magnitude. The magnitude and direction of the resulting spatial gradients in the core can provide clues to the physical nature of the core crystallization process. We have analyzed suites of samples from three large 3AB irons (Cape York, 58t; Chupaderos, 24t; Morito, 10t) in order to estimate local chemical gradients. Initial results for the concentrations of Ge, Pd, Pt (Massey group), Ir, Au, As, Co, Os, and Rh (Dalhouse group), and P (Arizona group) show significant ranges among the Cape York and Chupaderos samples and marginally significant ranges among the Morito samples. Measurements of Au, Ir, Co, Ni, Cu, Ga, As, W, Re (from UCLA) and Ni and Co (Arizona group) are in progress. We find a spatial Ir gradient in Chupaderos with a magnitude similar to the one reported for Agpalilik (Cape York iron) by Esbensen et al. Author

N94-16214*# Washington Univ., Saint Louis, MO. Dept. of Earth and Planetary Sciences.
ASSIMILATION OF SOLIDS DURING ASCENT OF MAGMAS FROM THE BARTOY FIELD OF THE BAIKAL REGION, SIBERIA Abstract Only **c46**
Johnson R. Haas, Larry A. Haskin, James Luhr (Smithsonian Institution, Washington, DC.), and Sergei Rasskazov (Academy of Sciences, USSR, Irkutsk.) *In* Lunar and Planetary Inst., Twenty-Fourth Lunar and Planetary Science Conference. Part 2: G-M 1993 p 595-596 (For primary document see N94-16173 03-91)
Avail: CASI HC A01/MF A06

Most investigators ascribe mare basalt magma genesis to partial melting at depths of approximately 130 to greater than 400 km within the cumulate pile deposited from a lunar magma ocean. Mare basalts share with mid-ocean ridge basalts the characteristic of relative depletion in LREE and other incompatible trace elements that arises from melting within 'used' mantle, from which crust-forming elements have already been separated. Some mare basalt types do not show the classical, La-Nd depleted mare basalt REE distributions; however, some types are isotopically heterogeneous. These differences have been ascribed to assimilation, mainly AFC-style, of KREEPy highland material overlying the source region. Might such

assimilation occur during magma ascent through the KREEPy material? To gain information from a terrestrial setting on possible assimilation during ascent, we have studied a suite of Quaternary nepheline-hawalites and nepheline-mugearites from the Bartoy cinder cone complex of the Baikal Rift, Siberia. The Bartoy magmas originated from greater than 80 km deep, and erupted through thick Archean crust. We find evidence for assimilation of approximately 31 wt. percent xenocrysts of garnet, aluminous clinopyroxene, kaersutite, and olivine, all presumably from the basalt source region, but no appreciable assimilation of overlying crust, consistent with isotopic constraints. Magmatic superheat made available by rapid ascent and decomposition accounts adequately for the energy of assimilation; no accompanying fractional crystallization is required or evident. Author

N94-16215*# Occidental Coll., Los Angeles, CA. Dept. of Geology.

MORPHOLOGY AND MODELS FOR THE EVOLUTION OF EASTERN HECATE CHASMA, VENUS Abstract Only

Victoria E. Hamilton and Ellen R. Stofan (Jet Propulsion Lab., California Inst. of Tech., Pasadena.) *In* Lunar and Planetary Inst., Twenty-Fourth Lunar and Planetary Science Conference. Part 2: G-M 1993 p 597-598 (For primary document see N94-16173 03-91)

Avail: CASI HC A01/MF A06

Hecate Chasma is a deep trough characterized by a chain-like concentration of coronae and corona-like features trending approximately southwest-northeast between approximately 200 and 260 degrees east longitude (terminating at Beta Regio). The section of Hecate in which we have concentrated our study is centered at 15N, 249, where the trough is especially well-defined. Nearby, a smaller chain of eight coronae lies along a minor trough parallel to the general trend of the greater chain. The trough itself is unusual in this area because it has a highly asymmetric profile. Using Magellan radar and topography data, we have examined the morphology of this area in order to assess the tectonic and volcanic history of the area. After examining the most important types of features (linear, arcuate and circular) in eastern Hecate, we present two possible models of origin. A companion abstract presents an overview of the Hecate and Parga linear deformation zones. Author

N94-16216*# Jet Propulsion Lab., California Inst. of Tech., Pasadena.

A PLUTO THERMAL MODEL Abstract Only

C. J. Hansen and D. A. Paige (California Univ., Los Angeles.) *In* Lunar and Planetary Inst., Twenty-Fourth Lunar and Planetary Science Conference. Part 2: G-M 1993 p 599 (For primary document see N94-16173 03-91)

Avail: CASI HC A01/MF A06

The recent discovery of nitrogen on Pluto suggests that Pluto's volatile cycles may be similar to those on Neptune's moon Triton. Here, we report the first results of our efforts to apply a thermal model that we developed to study the seasonal nitrogen cycle on Triton to the case of Pluto. The model predicts volatile behavior as a function of time to calculate frost deposit depth, polar cap boundaries, temperature of the frost and substrate, and atmospheric pressure, assuming nitrogen frost deposits in solid-vapor equilibrium with nitrogen in the atmosphere. Author

N94-16217*# Washington Univ., Seattle.

MODELING THE REFLECTANCE OF CO2 FROST WITH NEW OPTICAL CONSTANTS: APPLICATION TO MARTIAN SOUTH POLAR CAP SPECTRA Abstract Only

Gary B. Hansen and Terry Z. Martin (Jet Propulsion Lab., California Inst. of Tech., Pasadena.) *In* Lunar and Planetary Inst., Twenty-Fourth Lunar and Planetary Science Conference. Part 2: G-M 1993 p 601-602 (For primary document see N94-16173 03-91)

Avail: CASI HC A01/MF A06

New measurements of the absorption coefficients of CO2 ice, in most of the spectral range 0.2 to 3.9 microns where absorption coefficients are below 1.5 per cm, have recently been made. Although these measurements are preliminary, they contain spectral detail not seen previously in the literature. Therefore, it is useful to combine these new data with older data from spectral regions of stronger absorption and reformulate models of the albedo or reflectance of CO2 frost. These models can then be adjusted in an attempt to match measurements of Martian polar deposits, such as the set of spectra returned by the IRS instrument on Mariner 7 (1969). The new absorption coefficients of CO2 ice were measured on several samples of 41-mm thickness at 150-155 K. A portion of the spectrum from 1.9 to 3.9 microns wavelength is shown in the form of imaginary coefficient of refraction (= linear absorption x wavelength / 4 pi). The data above 3x10(exp -5) are obtained from, except for the absorption line at 3.32 micrometers, which is extrapolated in a way that is consistent with laboratory frost measurements, but the peak level is still highly uncertain. This new imagary coefficient, combined with the real coefficient, can be immediately applied to the models for hemispherical albedo, resulting in markedly different results from those in that study. The results for an infinite optical depth layer and solar incidence of 60 degrees are plotted for a range of mean particle radii from 0.03 to 3 mm. Author

N94-16218*# Southern Methodist Univ., Dallas, TX. Dept. of Geological Sciences.

ISHTAR DEFORMED BELTS: EVIDENCE FOR DEFORMATION FROM BELOW? Abstract Only

V. L. Hansen and R. J. Phillips (Washington Univ., Saint Louis, MO.) *In* Lunar and Planetary Inst., Twenty-Fourth Lunar and Planetary Science Conference. Part 2: G-M 1993 p 603-604 (For primary document see N94-16173 03-91)

Avail: CASI HC A01/MF A06

The mountain belts of Ishtar Terra are unique on Venus. Models for their formation include mantle upwelling, mantle downwelling, and horizontal convergence. The present forms of these models are too simple to predict surface strain, topography, or gravity. More detailed models will require specific constraints as imposed by geologic relations. In order to develop specific constraints for geodynamic models, we examine the geology of Ishtar Terra as viewed in Magellan SAR imagery in an attempt to interpret regional surface strain patterns. In this paper, we present geologic and structural relations that leads us to postulate that Ishtar deformed belts result from shear forces within the mantle acting on the lithosphere, and not by horizontal forces from colliding plates. We propose that the surface strains result from differential strain and displacement of domains within the upper mantle, and that further analysis of Ishtar deformation may allow us to identify individual domains within the mantle, and to constrain displacement trajectories between domains. Author

N94-16219*# Pittsburgh Univ., PA.

WHY IS THE MOON DARK? Abstract Only

B. Hapke *In* Lunar and Planetary Inst., Twenty-Fourth Lunar and Planetary Science Conference. Part 2: G-M 1993 p 605-606 (For primary document see N94-16173 03-91)

Avail: CASI HC A01/MF A06

This paper reports the results of attempts to model the spectral properties of the lunar regolith as consisting of crystalline rocks, glass and submicroscopic metallic iron (SMFe), produced by a process involving vapor phase differentiation. The models differ in the location of the SMFe.

Author

N94-16220*# Harvard Univ., Cambridge, MA. Dept. of Earth and Planetary Sciences.

Nd-142/Nd-144 IN BULK PLANETARY RESERVOIRS, THE PROBLEM OF INCOMPLETE MIXING OF INTERSTELLAR COMPONENTS AND SIGNIFICANCE OF VERY HIGH PRECISION Nd-145/Nd-144 MEASUREMENTS Abstract Only

C. L. Harper, Jr. and S. B. Jacobsen *In* Lunar and Planetary Inst., Twenty-Fourth Lunar and Planetary Science Conference. Part 2: G-M 1993 p 607-608 (For primary document see N94-16173 03-91)

Avail: CASI HC A01/MF A06

Apart from the challange of very high precision Nd-142/Nd-144 ratio measurement, accurate applications of the coupled Sm-(146,147)-Nd-(142,143) systematics in planetary differentiation studies require very precise knowledge of the present-day (post-Sm-146 decay) Nd-142/Nd-144 ratios of bulk planetary objects (BP). The coupled systematics yield model ages for the time of formation of Sm/Nd-fractionated reservoirs by differentiation of Sm/Nd-unfractionated bulk planetary reservoirs. Estimates of (Nd-142/Nd-144)(sub BP) and (Nd-143/Nd-144)(sub BP) therefore provide the critical baseline relative to which these model ages are referenced. In the Sm-147-Nd-143 systematics, Nd-143/Nd-144 variations are mostly large; therefore, small variations in initial Nd-143/Nd-144 ratios generally can be ignored. However, in the case of Sm-146-Nd-142, the range of Nd-142/Nd-144 divergence for differentiated planetary reservoirs is much smaller. Consequently Sm-(146,147)-Nd-(142,143) model ages are

sensitive to small variations in bulk planetary Nd-142/Nd-144 (both present-day and initial). One major unanswered question is whether or not Nd shelf standards (CIT Nd beta/Ames metal, La Jolla, NASA-JSC/Ames metal) have Nd-142/Nd-144 identical to the bulk Earth or otherwise might record some degree of radiogenic evolution in an early-fractionated reservoir. Our discussions of earth Earth differentiation based on Nd-142/Nd-144 in Isua and Acasta samples have employed a working assumption: (Nd-142/Nd-144)(sub Nd beta) = (Nd-142/Nd-144)(sub Bulk Earth). This requires experimental justification and is apparently contradicted by chondrite Nd-142/Nd-144 measurements, which have been interpreted to indicate: (Nd-142/Nd-144)(sub JSC/Ames metal) = ((Nd-142/Nd-144)(sub CHUR) = 35 plus or minus 8 ppm). At present, interpretations of the early Earth and Moon hinge largely on this issue. Because Ba in bulk chondrite samples exhibit similar magnitude nuclear anomalies, attributable to incomplete mixing of interstellar components, a critical question is whether or not nuclear effects are also present in Nd-142/Nd-144, both in bulk chondrites and between planetary objects. Author

N94-16221*# Planetary Science Inst., Tucson, AZ.
THE PHYSICAL MECHANISM OF COMET OUTBURSTS: AN EXPERIMENT Abstract Only **c90**
William K. Hartmann *In* Lunar and Planetary Inst., Twenty-Fourth Lunar and Planetary Science Conference. Part 2: G-M 1993 p 609-610 (For primary document see N94-16173 03-91)
Avail: CASI HC A01/MF A06

During a series of impact experiments into regolith-like powders at the NASA Ames Research Center Vertical Gun Facility in 1976, I observed and filmed a unique anomalous event that may illuminate outburst mechanisms in comets. During one test, a new batch of basalt powder (half the mass in particles less than 800 microns in diameter) retained some air pressure while the vacuum chamber was being evacuated. As a result, the projectile impacted into gas-charged regolith. Instead of ejecting the normal, relatively negligible amount of debris, the disturbance triggered a major eruption that lasted at least 18 seconds. The experimental results have been recently re-analyzed with reference to cometary phenomena. A series of frames from this eruption experiment are shown. The ejecta velocities of 150 to 300 cm/s would have been sufficient to drive debris into the coma of a comet nucleus smaller than a few kilometers diameter. The event suggests a mechanism for comet outbursts, discussed briefly by Hartmann et al.: the pore space in a layer of regolith, possibly with weak effective tensile strength, becomes gas charged as ice slowly sublimates. Once the effective tensile strength is exceeded by the gas pressure, the surface fails locally, triggering an eruption such as photographed here. This model is consistent with the emerging view of regolith materials on comets and is closest to the recent model of Rickman et al. The earlier models generally picture a more uniform flow of debris off the comet, not outbursts. Rickman et al. allow gas pressure to build until it matches the overburden pressure, followed by 'instantaneous blow-off'. They note that as soon as the mantle is found to be unstable, we consider it to be instantaneously swept away by the gas pressure. The main new points made here are that the experiment gives a more realistic view of the blow-off process after surface failure occurs, and the present model gives a recharge mechanism that can explain recurrent outbursts on comets such as P/Schwassmann-Wachmann 1 and 2060 Chiron. In fact, the resulting jets resemble distinct jet structures in high-resolution comet comae.

Author

N94-16222*# Planetary Science Inst., Tucson, AZ.
CONFIRMATION OF SATURATION EQUILIBRIUM CONDITIONS IN CRATER POPULATIONS Abstract Only **c46**
William K. Hartmann and Robert W. Gaskell (Jet Propulsion Lab., California Inst. of Tech., Pasadena.) *In* Lunar and Planetary Inst., Twenty-Fourth Lunar and Planetary Science Conference. Part 2: G-M 1993 p 611-612 (For primary document see N94-16173 03-91)
Avail: CASI HC A01/MF A06

We have continued work on realistic numerical models of cratered surfaces, as first reported at last year's LPSC. We confirm the saturation equilibrium level with a new, independent test. One of us has developed a realistic computer simulation of a cratered surface. The model starts with a smooth surface or fractal topography, and adds primary craters according to the cumulative power law with exponent -1.83, as observed on lunar maria and Martian plains. Each crater has an ejecta blanket with the volume of the crater, feathering out to a distance of 4 crater radii. We use the model to test the levels of saturation equilibrium reached in naturally occurring systems, by increasing crater density and observing its dependence on various parameters. In particular, we have tested to see if these artificial systems reach the level found by Hartmann on heavily cratered planetary surfaces, hypothesized to be the natural saturation equilibrium level. This year's work gives the first results of a crater population that includes secondaries. Our model 'Gaskell-4' (September, 1992) includes primaries as described above, but also includes a secondary population, defined by exponent -4. We allowed the largest secondary from each primary to be 0.10 times the size of the primary. These parameters will be changed to test their effects in future models. The model gives realistic images of a cratered surface although it appears richer in secondaries than real surfaces are. The effect of running the model toward saturation gives interesting results for the diameter distribution. Our most heavily cratered surface had the input number of primary craters reach about 0.65 times the hypothesized saturation equilibrium, but the input number rises to more than 100 times that level for secondaries below 1.4 km in size. Author

N94-16223*# Hartung (Jack B.), Great Falls, VA.
CORVID METEOROIDS AND A GIORDANO BRUNO RAY ARE GENETICALLY RELATED Abstract Only **c90**
Jack B. Hartung *In* Lunar and Planetary Inst., Twenty-Fourth Lunar and Planetary Science Conference. Part 2: G-M 1993 p 613-614 (For primary document see N94-16173 03-91)
Avail: CASI HC A01/MF A06

Both Corvid meteoroids and the Giordano Bruno (GB) crater are products of recent events. On June 25, or 26, 1178, Corvid meteoroids and a portion of GB ejecta were at the same place in the Solar System and moved in the same direction (right ascension = 12 degrees and declination = +19 degrees). The ground track of this direction is the same as that of the most prominant GB ray (azimuth = 237 degrees). These 'coincidences' could not have occurred by change and, therefore, support the conclusions that the GB impact occurred on June 26, 1178, and that Corvid meteoroids are high-velocity ejecta fragments from that impact. Finally, those fragments ejected with somewhat lower velocities failed to escape from the Earth-Moon system and produced the prominant ray extending southwest from the GB crater. Between June 25 and July 2, 1937, a Corvid meteor shower was observed. The apparent lack of Corvid showers in other years suggests that Corvids are the product of a recent break-up event. The right ascension and declination, corrected for zenith attraction, of 192 degrees and -19 degrees were reported for the radiant of this shower. This corresponds to a right ascension and declination of the direction of motion of Corvid meteoroids of 12 degrees and +19 degrees. In ecliptic coordinates the celestial longitude and latitude of this direction are 18 degrees and +13 degrees. Author

N94-16224*# Tennessee Univ., Knoxville. Dept. of Geological Sciences.
PYROXENE EQUILIBRATION TEMPERATURES IN METAMORPHOSED ORDINARY CHONDRITES Abstract Only **c90**
R. P. Harvey, M. L. Bennett, and H. Y. McSween, Jr. *In* Lunar and Planetary Inst., Twenty-Fourth Lunar and Planetary Science Conference. Part 2: G-M 1993 p 615-616 (For primary document see N94-16173 03-91)
Avail: CASI HC A01/MF A06

Ordinary chondrites are divided into petrographic types based on observed mineralogical and textural properties consistent with progressive thermal metamorphism from low grade (type 3) to high (type 7). Regardless of the exact cause of the metamorphism, higher-type chondrites should retain information concerning peak temperatures reached and for what duration. Using the two-pyroxene geothermometer of Lindsley, we have calculated the equilibration temperatures for 26H, L and LL type 5 and 6 ordinary chondrites, to investigate the relative peak temperatures and equilibration-states reached by these various meteorite classes. The Lindsley thermometer relies on a detailed accounting of non-quadrilateral components in pyroxenes, whose recalculated compositions are then plotted onto an empirically-derived polythermal diagram from which temperatures can be interpolated. The reported uncertainty of this method is plus or minus 50 C; in addition, close spacing of isotherms on the graph (particularly for orthopyroxene compositions) increase this uncertainty. We have parameterized the Lindsley polythermal quadrilateral for 1 atm pressure (less than 2 bar), and interpreted recalculated coordinates directly in terms

of 25 C temperature intervals. Meteorites selected for this study include both relatively shocked and unshoked specimens; heavily weathered or visibly brecciated specimens were avoided. Temperatures were calculated from orthopyroxene (opx) and clinopyroxene (cpx) analyses within one relative percent of ideal sums and stoichiometry. Histograms summarizing the calculated temperatures for type 5 and 6 ordinary chondrites are shown. Author

N94-16225*# Hawaii Univ., Honolulu. Planetary Geosciences.
REMOTE SENSING STUDIES OF THE NORTHEASTERN PORTION OF THE LUNAR NEARSIDE Abstract Only
B. R. Hawke, D. T. Blewett, P. G. Lucey, G. J. Taylor, C. A. Peterson, J. F. Bell, M. S. Robinson, J. F. Bell, III (National Aeronautics and Space Administration. Ames Research Center, Moffett Field, CA.), C. R. Coombs (POD Associates, Inc., Albuquerque, NM.), and R. Jaumann (Deutsche Forschungsanstalt fuer Luft- und Raumfahrt, Oberpfaffenhofen, Germany.) et al *In* Lunar and Planetary Inst., Twenty-Fourth Lunar and Planetary Science Conference. Part 2: G-M 1993 p 617-618 (For primary document see N94-16173 03-91)
Avail: CASI HC A01/MF A06

During the Galileo spacecraft encounter with the Earth-Moon system in December, 1992, a variety of spectral data and imagery were obtained for the eastern limb region as well as much of the lunar nearside. In order to support this encounter, we have been collecting near-infrared spectra and other remote sensing data for that portion of the northeastern nearside (NEM region) for which the highest resolution Galileo data were obtained. Analysis of spectra obtained for highlands units in the NEN region indicates that most surface units are dominated by anorthositic norite. To date, no pure anorthosites have been identified in the region. Several dark-haloed impact craters have exposed mare material from beneath highlands-rich surface units. Hence, ancient mare volcanism occurred in at least a portion of the NEN region. Endogenic dark-haloed craters in the region are the source of localized dark mantle deposits (LDMD) of pyroclastic origin and at least two compositional groups are present. The Galileo spacecraft obtained very high-resolution remote sensing data for the northeastern part of the nearside of the Moon. In order to prepare for and support this encounter, we have collected and analyzed a variety of spectral data for the NEN region. Numerous unanswered questions exist for this region. These include: (1) the composition and stratigraphy of the local highlands crust, (2) the nature and mode of formation of regional light plains, (3) the composition of localized pyroclastic deposits, and (4) the distribution of possible cryptomare in the region. The purpose of this paper is to present the preliminary results of our analyzes of remote sensing data of remote sensing data obtained for the NEN region. Author

N94-16226*# Brown Univ., Providence, RI. Dept. of Geological Sciences.
TESSERA TERRAIN ON VENUS: IMPLICATIONS OF TESSERA FLOODING MODELS AND BOUNDARY CHARACTERISTICS FOR GLOBAL DISTRIBUTION AND MODE OF FORMATION Abstract Only
James W. Head and Mikhail Ivanov (Academy of Sciences, USSR, Moscow.) *In* Lunar and Planetary Inst., Twenty-Fourth Lunar and Planetary Science Conference. Part 2: G-M 1993 p 619-620 (For primary document see N94-16173 03-91)
Avail: CASI HC A01/MF A06

Mapping of tessera terrain using Magellan global high-resolution data has shown that it comprises about 10 percent of the surface area of Venus, is not randomly distributed, is extremely highly deformed relative to intervening plains, lies at a wide range of elevations, is embayed by and largely predates adjacent volcanic plains, is generally negatively correlated with broad lowlands and volcanic rises, may underlie a considerable percentage of the superposed volcanic plains, and has linear/tectonic margins for about 27 percent of its boundaries. In this paper, we investigate further the distribution and origin of tessera through analysis of the changing nature of tessera occurrences during sequential flooding, and assessment of the nature and distribution of Type 2 (linear/tectonic) tessera boundaries. Author

N94-16227*# Brown Univ., Providence, RI. Dept. of Geological Sciences.
MODE OF EMPLACEMENT OF LUNAR MARE VOLCANIC DEPOSITS: GRABEN FORMATION DUE TO NEAR SURFACE DEFORMATION ACCOMPANYING DIKE EMPLACEMENT AT RIMA PARRY 5 Abstract Only
J. W. Head and L. Wilson (Lancaster Univ., England.) *In* Lunar and Planetary Inst., Twenty-Fourth Lunar and Planetary Science Conference. Part 2: G-M 1993 p 621-622 (For primary document see N94-16173 03-91)
Avail: CASI HC A01/MF A06

Theoretical analyses, together with the observed style of emplacement of lunar mare volcanic deposits, strongly suggest that mare volcanic eruptions are fed by dikes from source regions at the base of the crust or deeper in the lunar mantle. Some dikes intrude into the lower crust, while others penetrate to the surface and are the sources for voluminous outpourings of lava. Still others stall near the surface generating a near-surface extensional stress field. We have investigated the hypothesis that some lunar linear rilles (graben) are the near-surface manifestations of dikes intruded to shallow depths. For a specific example (Rima Parry 5), we show that the geometry of the faults implies a mean dike width of about 150 m and depth to the dike top of about 500 m, values consistent with other theoretical and observational data on lunar dike geometry. Localized pyroclastic deposits along Rima Parry 5 are evidence for the presence of near-surface magma, and are interpreted to be the result of degassing and pyroclastic eruption subsequent to the emplacement of the dike. Author

N94-16228*# Brown Univ., Providence, RI.
LUNAR IMPACT BASINS: NEW DATA FOR THE NEARSIDE NORTHERN HIGH LATITUDES AND EASTERN LIMB FROM THE SECOND GALILEO FLYBY Abstract Only
J. W. Head, M. Belton (Kitt Peak National Observatory, Tucson, AZ.), R. Greeley (Arizona State Univ., Tempe.), C. Pieters, E. Fischer, J. Sunshine, K. Klaasen (Jet Propulsion Lab., California Inst. of Tech., Pasadena.), A. McEwen (Geological Survey, Flagstaff, AZ.), T. Becker (Geological Survey, Flagstaff, AZ.), and G. Neukum (Deutsche Forschungsanstalt fuer Luft- und Raumfahrt, Oberpfaffenhofen, Germany.) et al *In* Lunar and Planetary Inst., Twenty-Fourth Lunar and Planetary Science Conference. Part 2: G-M 1993 p 623-624 (For primary document see N94-16173 03-91)
Avail: CASI HC A01/MF A06

During the December 1992 Galileo Earth/Moon encounter the northern half of the nearside, the eastern limb, and parts of the western farside of the Moon were illuminated and in view, a geometry that was complementary to the first lunar encounter in December, 1990, which obtained images of the western limb and eastern farside. The Galileo Solid State Imaging System (SSI) obtained multispectral images for these regions during the second encounter and color ratio composite images were compiled using combinations of band ratios chosen on the basis of telescopic spectra and laboratory spectra of lunar samples. Ratios of images taken at 0.41 and 0.76 micron are sensitive to changes in the slope in the visible portion of the spectrum, and ratios of 0.99 and 0.76 micron relate to the strength of near-infrared absorptions due to iron-rich mafic minerals (0.76/0.99 ratio) such as olivine and pyroxene. Results of the analyses of the compositional diversity of the crust, maria, and Copernican craters are presented elsewhere. Primary objectives for lunar basin analysis for the second encounter include analysis of: the north polar region and the Humboldtianum basin; the characteristics of the Imbrium basin along its northern border and the symmetry of associated deposits; the origin of light plains north of Mare Frigoris and associated with several other basins; the nature and significance of pre-basin substrate; the utilization of the stereo capability to assess subtle basis structure; the identification of previously unrecognized ancient basins; basin deposits and structure for limb and farside basins; and assessment of evidence for proposed ancient basins. These data and results will be applied to addressing general problems of evaluation of the nature and origin of basin deposits, investigation of mode of ejecta emplacement and ejecta mixing, analysis of the origin of light plains deposits, analysis of basin deposit symmetry/asymmetry, investigation of basin depth of excavation and crustal stratigraphy, and assessment of models for basin formation and evolution. Here we discuss some preliminary results concerning

lunar impact basins, their deposits, and prebasin substrates, using the same approaches that we employed for the Orientale and South Pole-Aitken basins using the data from the first encounter. Author

N94-16229*# Brown Univ., Providence, RI.
LUNAR SCOUT MISSIONS: GALILEO ENCOUNTER RESULTS AND APPLICATION TO SCIENTIFIC PROBLEMS AND EXPLORATION REQUIREMENTS Abstract Only
J. W. Head, M. Belton (Kitt Peak National Observatory, Tucson, AZ.), R. Greeley (Arizona State Univ., Tempe.), C. Pieters, A. McEwen (Geological Survey, Flagstaff, AZ.), G. Neukum (Deutsche Forschungsanstalt fuer Luft- und Raumfahrt, Berlin, Germany.), and T. McCord (Hawaii Univ., Honolulu.) *In* Lunar and Planetary Inst., Twenty-Fourth Lunar and Planetary Science Conference. Part 2: G-M 1993 p 625-626 (For primary document see N94-16173 03-91)
Avail: CASI HC A01/MF A06

The Lunar Scout Missions (payload: x-ray fluorescence spectrometer, high-resolution stereocamera, neutron spectrometer, gamma-ray spectrometer, imaging spectrometer, gravity experiment) will provide a global data set for the chemistry, mineralogy, geology, topography, and gravity of the Moon. These data will in turn provide an important baseline for the further scientific exploration of the Moon by all-purpose landers and micro-rovers, and sample return missions from sites shown to be of primary interest from the global orbital data. These data would clearly provide the basis for intelligent selection of sites for the establishment of lunar base sites for long-term scientific and resource exploration and engineering studies. The two recent Galileo encounters with the Moon (December, 1990 and December, 1992) illustrate how modern technology can be applied to significant lunar problems. We emphasize the regional results of the Galileo SSI to show the promise of geologic unit definition and characterization as an example of what can be done with the global coverage to be obtained by the Lunar Scout Missions. Author

N94-16230*# Brown Univ., Providence, RI. Dept. of Geological Sciences.
LAVA FLOW-FIELD MORPHOLOGICAL CLASSIFICATION AND INTERPRETATION: EXAMPLES FROM VENUS Abstract Only
J. W. Head, K. Magee Roberts, L. Wilson (Lancaster Univ., England.), and H. Pinkerton *In* Lunar and Planetary Inst., Twenty-Fourth Lunar and Planetary Science Conference. Part 2: G-M 1993 p 627-628 (For primary document see N94-16173 03-91)
Avail: CASI HC A01/MF A06

Recent analyses suggest that thermal constraints will act to limit the maximum length of an advancing lava flow being fed at a given volume or mass effusion rate from a vent. These constraints can be characterized through the Gratz number, which has a large value at the vent and decreases down flow; under a wide range of conditions, motion apparently ceases when the Gratz number has decreased to a value close to 300. In cooling-limited flows, effusion from the vent should be steady; the flow front thickens, eventually stops due to this cooling, and the central channel does not drain. If the vent remains active, a break-out flow will form from some point on the margin of the initial flow unit. If flows on planetary surfaces can be shown to be cooling limited, eruption rates can be estimated. In this analysis, we illustrate the morphological characteristics of various flow configurations, and we describe the application of these concepts to a flow length histogram for a hypothetical flow field and then apply this to an example on Venus. Author

N94-16231*# Brown Univ., Providence, RI. Dept. of Geological Sciences.
MODES OF FORMATION OF LUNAR LIGHT PLAINS AND THE DETECTION OF CRYPTOMARIA DEPOSITS Abstract Only
James W. Head, John Mustard, Irene Antonenko, and B. Ray Hawke (Hawaii Univ., Honolulu.) *In* Lunar and Planetary Inst., Twenty-Fourth Lunar and Planetary Science Conference. Part 2: G-M 1993 p 629-630 (For primary document see N94-16173 03-91)
Avail: CASI HC A01/MF A06

The early volcanic and impact histories of the Moon are closely linked and the record preserved in surface morphology and samples is tightly convolved because of the interaction of the two processes. The deconvolution of the record is an important goal in order to assess early volcanic flux and the mode of emplacement of large crater and basin deposits. For example, lunar light plains have been variously interpreted as volcanic, impact, and volcanic covered by impact deposits. The development of criteria for the determination of the origin of light plains and the detection of cryptomaria is a key to the deconvolution of this early record. We outline the various hypotheses for the origin of and potential modes of occurrence of light plains and cryptomaria, and develop criteria for their recognition and documentation. We use the example of the Schiller-Schickard and Balmer cryptomaria to illustrate the application of these techniques to the problem of light plains interpretation and cryptomaria documentation. Author

N94-16232*# Brown Univ., Providence, RI. Dept. of Geological Sciences.
CHEMICAL DIFFERENTIATION, THERMAL EVOLUTION, AND CATASTROPHIC OVERTURN ON VENUS: PREDICTIONS AND GEOLOGIC OBSERVATIONS Abstract Only
James W. Head, E. M. Parmentier, and P. C. Hess *In* Lunar and Planetary Inst., Twenty-Fourth Lunar and Planetary Science Conference. Part 2: G-M 1993 p 631-632 (For primary document see N94-16173 03-91)
Avail: CASI HC A01/MF A06

Observations from Magellan show that: (1) the surface of Venus is generally geologically young, (2) there is no evidence for widespread recent crustal spreading or subduction, (3) the crater population permits the hypothesis that the surface is in production, and (4) relatively few impact craters appear to be embayed by volcanic deposits suggesting that the volcanic flux has drastically decreased as a function of time. These observations have led to consideration of hypotheses suggesting that the geological history of Venus may have changed dramatically as a function of time due to general thermal evolution, and/or thermal and chemical evolution of a depleted mantle layer, perhaps punctuated by catastrophic overturn of upper layers or episodic plate tectonics. We have previously examined the geological implications of some of these models, and here we review the predictions associated with two periods of Venus history. Stationary thick lithosphere and depleted mantle layer, and development of regional to global development of regional to global instabilities, and compare these predictions to the geological characteristics of Venus revealed by Magellan. Author

N94-16233*# Technische Univ., Darmstadt (Germany). Inst. fur Kernphysik.
A MOESSBAUER SPECTROMETER FOR THE MINERALOGICAL ANALYSIS OF THE MARS SURFACE: FIRST TEMPERATURE DEPENDENT TESTS OF THE DETECTOR AND DRIVE SYSTEM Abstract Only
P. Held, R. Teucher, G. Klingelhoefer, J. Foh, H. Jaeger, and E. Kankeleit *In* Lunar and Planetary Inst., Twenty-Fourth Lunar and Planetary Science Conference. Part 2: G-M 1993 p 633-634 (For primary document see N94-16173 03-91)
Avail: CASI HC A01/MF A06

Part of the scientific payload of the Mars-96 mission is a Fe-(57)Mossbauer (MB) spectrometer installed on a small rover to be placed on the surface of Mars. The instrument is under development at the University of Darmstadt. This instrument, with some modifications, is also included in the scientific payload of the proposed MARSNET mission of the European Space Agency (ESA). A similar instrument is currently under development in the US. The reason for developing a Mossbauer spectrometer for space applications is the high abundance of the element iron, especially on the surface of Mars. The elemental composition of Martian soil was determined during the Viking mission in 1976 but not it's mineralogical composition. One believes that it is composed mainly of iron-rich clay minerals, with an iron content of about 14 (plus or minus 2) wt-percent, partly magnetic. Of extremely great interest are the oxidation state of the iron, the magnetic phases and the mineral composition of the Mars surface. To these questions MB spectroscopy can provide important information, which are not available by other methods. We report on first tests of the experimental setup in the temperature range plus 20 C to -70 C, roughly corresponding to the temperature range on the surface of Mars. Also questions concerning the signal/noise ratio (S/N) are discussed. Author

N94-16234*# Cornell Univ., Ithaca, NY.
GALILEO PHOTOMETRY OF APOLLO LANDING SITES Abstract Only

P. Helfenstein, J. Veverka, James W. Head (Brown Univ., Providence, RI.), C. Pieters (Brown Univ., Providence, RI.), S. Pratt (Brown Univ., Providence, RI.), J. Mustard (Brown Univ., Providence, RI.), K. Klaasen (Jet Propulsion Lab., California Inst. of Tech., Pasadena.), G. Neukum (Deutsche Forschungsanstalt fuer Luft- und Raumfahrt, Oberpfaffenhofen, Germany.), H. Hoffmann (Deutsche Forschungsanstalt fuer Luft- und Raumfahrt, Oberpfaffenhofen, Germany.), and R. Jaumann (Deutsche Forschungsanstalt fuer Luft- und Raumfahrt, Oberpfaffenhofen, Germany.) et al *In* Lunar and Planetary Inst., Twenty-Fourth Lunar and Planetary Science Conference. Part 2: G-M 1993 p 635-636 (For primary document see N94-16173 03-91)

Avail: CASI HC A01/MF A06

As of December 1992, the Galileo spacecraft performed its second and final flyby (EM2), of the Earth-Moon system, during which it acquired Solid State Imaging (SSI) camera images of the lunar surface suitable for photometric analysis using Hapke's, photometric model. These images, together with those from the first flyby (EM1) in December 1989, provide observations of all of the Apollo landing sites over a wide range of photometric geometries and at eight broadband filter wavelengths ranging from 0.41 micron to 0.99 micron. We have completed a preliminary photometric analysis of Apollo landing sites visible in EM1 images and developed a new strategy for a more complete analysis of the combined EM1 and EM2 data sets in conjunction with telescopic observations and spectrogoniometric measurements of returned lunar samples. No existing single data set, whether from spacecraft flyby, telescopic observation, or laboratory analysis of returned samples, describes completely the light scattering behavior of a particular location on the Moon at all angles of incidence (i), emission (e), and phase angles (a). Earthbased telescopic observations of particular lunar sites provide good coverage of incidence nad phase angles, but their range in emission angle is limited to only a few degrees because of the Moon's synchronous rotation. Spacecraft flyby observations from Galileo are now available for specific lunar features at many photometric geometries unobtainable from Earth; however, this data set lacks coverage at very small phase angles (a less than 13 deg) important for distinguishing the well-known 'opposition effect'. Spectrogoniometric measurements from returned lunar samples can provide photometric coverage at almost any geometry; however, mechanical properties of prepared particulate laboratory samples, such as particle compaction and macroscopic roughness, likely differ from those on the lunar surface. In this study, we have developed methods for the simultaneous analysis of all three types of data: we combine Galileo and telescopic observations to obtain the most complete coverage with photometric geometry, and use spectrogoniometric observations of lunar soils to help distinguish the photometric effects of macroscopic roughness from those caused by particle phase function behavior (i.e., the directional scattering properties of regolith particles). Author

N94-16235*# Carleton Coll., Northfield, MN.

EMPLACEMENT OF MULTIPLE FLOW UNITS ON VERY SHALLOW SLOPES, EAST KAWELU PLANITIA FLOW FIELD, VENUS Abstract Only

Michael B. Helgerud and James R. Zimbelman (Smithsonian Institution, Washington, DC.) *In* Lunar and Planetary Inst., Twenty-Fourth Lunar and Planetary Science Conference. Part 2: G-M 1993 p 637-638 (For primary document see N94-16173 03-91)

Avail: CASI HC A01/MF A06

Lobate flows with variable radar brightness occur at several locations on Venus. Here we present preliminary mapping results for a lava flow field on the eastern side of Kawelu Planitia, centered at approximately 41 deg N, 251 deg E. Numerous individual flows of varying brightness can be traced for up to 400 km at this location. Megallan image F-MIDRP.40N251;1 contains two major flow complexes as well as a distinct minor flow field associated with a volcanic dome. The southern flow field (unit F) changes from radar dark to radar bright in a convex arc from west to east. The flow path is diverted by a ridge system (unit B) and associated N-S faulted zone (unit A) evident in the Magellan altimetry data. The 130-km-long radar-bright flow field located at 41.5 deg N and 249-250 deg E is comprised of a narrow, channeled flow (unit E) overlying an intermediate brightness flow (unit D), all of which appears to emanate from a solitary dome at 249 deg E. The southern lobe of unit E disappears under a broad leveed channel (41.3 deg N, 250.1 deg E) in unit 5, only to reappear south of the unit 5 boundary. The source of this largest flow field is not evident, but could be associated with the region of small domes west of the F-MIDRP image (centered at 41 deg N, 246 deg E). Another possible source is the fractured area south of unit C. The flow complex is clearly a conglomeration of many flow episodes, not necessarily from a single source. Author

N94-16236*# Colorado Univ., Boulder. Lab. for Atmospheric and Space Physics.

NEAR-SURFACE TEMPERATURE GRADIENTS AND THEIR EFFECTS ON THERMAL-INFRARED EMISSION SPECTRA OF PARTICULATE PLANETARY SURFACES Abstract Only

B. G. Henderson and B. M. Jakosky *In* Lunar and Planetary Inst., Twenty-Fourth Lunar and Planetary Science Conference. Part 2: G-M 1993 p 639-640 (For primary document see N94-16173 03-91)

Avail: CASI HC A01/MF A06

The infrared energy emitted from a planetary surface is generated within a finite depth determined by the material's absorption skin depth. This parameter varies significantly with wavelength in the infrared but has an average value of around 50 microns for most geologic materials. In solid rock, heat transfer is efficient enough so that this 50 micron zone of the near surface from which the radiation emanates will be more or less isothermal. In particulate materials, however, heat transfer is more complicated and occurs via a combination of mechanisms, including solid conduction within grains and across grain contacts, conduction through the interstitial gas, and thermal radiation within individual particles and across the void spaces in between grains. On planets with substantial atmospheres, the gas component dominates the heat transfer and tends to mitigate near-surface thermal gradients. However, on airless bodies, the gas component is absent and heat transfer occurs via solid conductions and radiation. If the particles are small relative to the average absorption skin depth, then the top 50-100 microns or so of the surface will be cooled by radiation to space allowing the creation of significant near-surface thermal gradients. In those regions of the spectrum where the absorption coefficient is low, the emission will come from the deeper, warmer parts of the medium, whereas in regions of high absorption, the emission will emanate from shallower, cooler parts of the medium. The resulting emission spectrum will show non-compositional features as a result of the thermal structure in the material. We have modeled the heat transfer in a particulate medium in order to determine the magnitude of near-surface thermal gradients for surfaces on airless bodies and on Mars. We use the calculated thermal structure to determine the effects it has on the infrared emission spectrum of the surface. Author (revised)

N94-16237*# Lancaster Univ. (England). Environmental Sciences Div.

BUBBLE COALESCENCE IN MAGMAS Abstract Only **c46**

Richard A. Herd and Harry Pinkerton *In* Lunar and Planetary Inst., Twenty-Fourth Lunar and Planetary Science Conference. Part 2: G-M 1993 p 641-642 (For primary document see N94-16173 03-91)

Avail: CASI HC A01/MF A06

The most important factors governing the nature of volcanic eruptions are the primary volatile contents, the ways in which volatiles exsolve, and how the resulting bubbles grow and interact. In this contribution we assess the importance of bubble coalescence. The degree of coalescence in alkali basalts has been measured using Image Analysis techniques and it is suggested to be a process of considerable importance. Binary coalescence events occur every few minutes in basaltic melts with vesicularities greater than around 35 percent. Author (revised)

N94-16238*# Jet Propulsion Lab., California Inst. of Tech., Pasadena. Geology and Planetology Section.

THERMAL INERTIA AND RADAR REFLECTIVITY OF THE MARTIAN NORTH POLAR ERG: LOW-DENSITY AGGREGATES Abstract Only

K. E. Herkenhoff *In* Lunar and Planetary Inst., Twenty-Fourth Lunar and Planetary Science Conference. Part 2: G-M 1993 p 643-644 (For primary document see N94-16173 03-91)

Avail: CASI HC A01/MF A06

The north polar layered deposits on Mars appear to be the source of the dark material that comprises the north polar erg. The physical properties and chemical composition of the erg material therefore have important implications for the origin and evolution of the Martian layered deposits. Viking bistatic radar and infrared thermal mapping (IRTM) data indicate that the bulk density of the erg material is lower than that of the average

Martian surface. These data are consistent with hypotheses involving formation of filamentary sublimation residue (FSR) particles from erosion of the layered deposits. The color and albedo of the erg and of the layered deposits, and the presence of magnetic material on Mars, suggest that the dark material is composed of low-density aggregates of magnetic dust grains, perhaps similar to FSR particles created in laboratory experiments.
Author (revised)

N94-16239*# Lunar and Planetary Inst., Houston, TX.
THE THREE AGES OF VENUS: A HYPOTHESIS BASED ON THE CRATERING RECORD Abstract Only
R. R. Herrick *In its* Twenty-Fourth Lunar and Planetary Science Conference. Part 2: G-M 1993 p 645-646 (For primary document see N94-16173 03-91)
Avail: CASI HC A01/MF A06

The elevation range of 6051.9 - 6053.9 km on Venus is deficient in craters but has a high proportion of embayed and tectonically deformed craters. On the basis of this data and previous work, I propose that Venus has experienced three distinct geologic ages: pseudo-plate tectonics until 1 - 2 Ga, volcanic flooding of low-lying areas, and currently hot spot tectonics.
Author

N94-16240*# Rutgers Univ., New Brunswick, NJ. Dept. of Chemistry.
Al-26-Mg-26 AGES OF IRON METEORITES Abstract Only c90
G. F. Herzog, A. E. Souzis (Army Research Lab., Fort Belvoir, VA.), S. Xue, J. Klein (Pennsylvania Univ., Philadelphia.), D. Juenemann (Pennsylvania Univ., Philadelphia.), and R. Middleton (Pennsylvania Univ., Philadelphia.) *In* Lunar and Planetary Inst., Twenty-Fourth Lunar and Planetary Science Conference. Part 2: G-M 1993 p 647-648 (For primary document see N94-16173 03-91)
Avail: CASI HC A01/MF A06

An exposure age for an iron meteorite can be calculated from measurements of a radioactive nuclide and a stable nuclide that are produced by similar sets of nuclear reactions, provided that the stable nuclide is present with low initial abundance. The standard methods rely on either K-40 (t(sub 1/2) = 1.26 Gy), K-39, and K-41 or on a shorter-lived radionuclide and a stable, noble gas isotope. Widely used pairs of this type include Cl-36/Ar-36 and Al-26/Ne-21. Other pairs that may serve the purpose for iron meteorites contain many stable isotopes besides those of K and the noble gases that are produced partly by cosmic rays. We consider here the calculation of exposure ages, t(sub 26), from measurements of Al-26 (t(sub 1/2) = 0.7 My) and (stable) Mg-26. Ages based on Al-26/Mg-26 ratios, like those based on Cl-36/Ar-36 ratios, are 'buffered' against changes in relative production rates due to shielding because decay of the radioactive nuclide accounts for a good part of the inventory of the stable nuclide.
Author (revised)

N94-16241*# Brown Univ., Providence, RI. Dept. of Geological Sciences.
THE ILMENITE LIQUIDUS AND DEPTHS OF SEGREGATION FOR HIGH-Ti PICRITE GLASSES Abstract Only c27
P. C. Hess *In* Lunar and Planetary Inst., Twenty-Fourth Lunar and Planetary Science Conference. Part 2: G-M 1993 p 649-650 (For primary document see N94-16173 03-91)
Avail: CASI HC A01/MF A06

Lunar picrite glasses represent primitive and perhaps near primary liquids which have suffered only minor degrees of crystallization or near crustal modification. These glasses are multisaturated with olivine and orthopyroxene at pressures from 20-25 kb. I argue below that high TiO2 mare glasses were indeed equilibrated with orthopyroxene and were segregated from the lunar mantle at mean depths of 400-500 km. The glasses are typically modelled as products of relatively low degrees of melting of an hybridized source resulting from the overturn and mixing of the gravitationally unstable cumulate pile. But the models are neither unique nor, in some cases, correct.
Author (revised)

N94-16242*# Brown Univ., Providence, RI. Dept. of Geological Sciences.
OVERTURN OF MAGMA OCEAN ILMENITE CUMULATE LAYER: IMPLICATIONS FOR LUNAR MAGMATIC EVOLUTION AND FORMATION OF A LUNAR CORE Abstract Only
P. C. Hess and E. M. Parmentier *In* Lunar and Planetary Inst., Twenty-Fourth Lunar and Planetary Science Conference. Part 2: G-M 1993 p 651-652 (For primary document see N94-16173 03-91)
Avail: CASI HC A01/MF A06

We explore a model for the chemical evolution of the lunar interior that explains the origin and evolution of lunar magmatism and possibly the existence of a lunar core. A magma ocean formed during accretion differentiates into the anorthositic crust and chemically stratified cumulate mantle. The cumulative mantle is gravitationally unstable with dense ilmenite cumulate layers overlying olivine-orthopyroxene cumulates with Fe/Mg that decreases with depth. The dense ilmenite layer sinks to the center of the moon forming the core. The remainder of the gravitationally unstable cumulate pile also overturns. Any remaining primitive lunar mantle rises to its level of neutral buoyancy in the cumulate pile. Perhaps melting of primitive lunar mantle due to this decompression results in early lunar Mg-rich magmatism. Because of its high concentration of incompatible heat producing elements, the ilmenite core heats the overlying orthopyroxene-bearing cumulates. As a conductively thickening thermal boundary layer becomes unstable, the resulting mantle plumes rise, decompress, and partially melt to generate the mare basalts. This model explains both the timing and chemical characteristics of lunar magmatism.
Author (revised)

N94-16243*# Rice Univ., Houston, TX. Dept. of Geology and Geophysics and of Chemistry.
GEOCHEMISTRY AND COSMOCHEMISTRY OF FULLERENES 3: REACTION OF C60 AND C70 WITH OZONE Abstract Only c25
D. Heymann and L. P. F. Chibante *In* Lunar and Planetary Inst., Twenty-Fourth Lunar and Planetary Science Conference. Part 2: G-M 1993 p 653-654 (For primary document see N94-16173 03-91)
Avail: CASI HC A01/MF A06

C60 and C70 dissolved in toluene were treated with O2 gas containing 2.6 volume percent ozone and with O3-free oxygen. No reaction products were detected for 0.1 mole of O2 passed through the solution, but destruction of C60 was clearly detectable for a dose of 10(exp -6) moles of O3. C70 was destroyed more slowly than C60. Among the substances remaining in solution, we identified C60O, C70O, C60O2, C60O3, and C60O4. C60 crystals exposed to O3 at room temperature became less soluble in toluene in a matter of days, but oxides were apparently not formed.
Author (revised)

N94-16244*# Deutsche Forschungsanstalt fuer Luft- und Raumfahrt, Oberpfaffenhofen (Germany). Inst. for Planetary Exploration.
EARTH-BASED AND GALILEO SSI MULTISPECTRAL OBSERVATIONS OF EASTERN MARE SERENITATIS AND THE APOLLO 17 LANDING SITE Abstract Only
H. Hiesinger, R. Jaumann, and G. Neukum *In* Lunar and Planetary Inst., Twenty-Fourth Lunar and Planetary Science Conference. Part 2: G-M 1993 p 655-656 (For primary document see N94-16173 03-91)
Avail: CASI HC A01/MF A06

Both the Apollo 17 and the Mare Serenitatis region were observed by Galileo during its fly-by in December 1992. We used earth-based multispectral data to define mare units which then can be compared with the results of the Galileo SSI data evaluation.
Author (revised)

N94-16245*# Geological Survey of Canada, Ottawa (Ontario).
TRACE-ELEMENT COMPOSITION OF CHICXULUB CRATER MELT ROCK, K/T TEKTITES AND YUCATAN BASEMENT Abstract Only c90
A. R. Hildebrand, D. C. Gregoire, M. Attrep, Jr. (Los Alamos National Lab., NM.), P. Claeys (California Univ., Davis.), C. M. Thompson (Arizona Univ., Tucson.), and W. V. Boynton (Arizona Univ., Tucson.) *In* Lunar and Planetary Inst., Twenty-Fourth Lunar and Planetary Science Conference. Part 2: G-M 1993 p 657-658 (For primary document see N94-16173 03-91)
Avail: CASI HC A01/MF A06

The Cretaceous/Tertiary (K/T) boundary Chicxulub impact is the best preserved large impact in the geologic record. The Chicxulub crater has been buried with no apparent erosion of its intracrater deposits, and its ejecta blanket is known and is well preserved at hundreds of localities globally. Although most of the molten material ejected from the crater has been largely altered, a few localities still preserve tektite glass. Availability of intra- and extracrater impact products as well as plausible matches to the targeted rocks allows the comparison of compositions of the different

classes of impact products to those of the impacted lithologies. Determination of trace-element compositions of the K/T tektites, Chicxulub melt rock, and the targeted Yucatan silicate basement and carbonate/evaporite lithologies have been made using instrumental neutron activation analysis (INAA) and inductively coupled plasma mass spectrometry (ICP-MS). Some sample splits were studied with both techniques to ensure that inter-laboratory variation was not significant or could be corrected. The concentration of a few major and minor elements was also checked against microprobe results. Radiochemical neutron activation analysis (RNAA) was used to determine Ir abundances in some samples. Author (revised)

N94-16246*# National Aeronautics and Space Administration. Lyndon B. Johnson Space Center, Houston, TX.

COMPARISON OF REFLECTANCE SPECTRA OF C ASTEROIDS AND UNIQUE C CHONDRITES Y86720, Y82162, AND B7904 Abstract Only **c90**

T. Hiroi, C. M. Pieters (Brown Univ., Providence, RI.), and M. E. Zolensky *In* Lunar and Planetary Inst., Twenty-Fourth Lunar and Planetary Science Conference. Part 2: G-M 1993 p 659-660 (For primary document see N94-16173 03-91)

(Grant NAGw-748)

Avail: CASI HC A01/MF A06

Reflectance spectra (0.3-2.6 microns) of 11 carbonaceous (C) chondrite powders (less than 100 or less than 125 microns) including 'unique' ones Y86720, Y82162, and B7904, have been measured and compared with those of 14 C asteroids. Among those C chondrites, only three 'unique' ones had close counterparts among C asteroids (Y86720 and 1 Ceres, Y82162 and 704 Interamnia, and B7904 and 31 Euphrosyne). Mixing calculations of those C chondrites by Hapke's isotropic model were also performed to improve fits of reflectance spectra of all the 14 C asteroids. If the grain-size distributions of those asteroid surfaces are similar to those C chondrite powders, the result suggests that all tested C asteroids contain a high amount of heated C chondrite material, such as Y86720, Y82162, and B7904. Author (revised)

N94-16247*# Lafayette Coll., Easton, PA. Dept. of Physics.

PHASE EQUILIBRIA OF THE MAGNESIUM SULFATE-WATER SYSTEM TO 4 KBARS Abstract Only **c25**

D. L. Hogenboom, J. S. Kargel (Arizona Univ., Tucson.), J. P. Ganasan, and L. Lee *In* Lunar and Planetary Inst., Twenty-Fourth Lunar and Planetary Science Conference. Part 2: G-M 1993 p 661-662 (For primary document see N94-16173 03-91)

Avail: CASI HC A01/MF A06

Magnesium sulfate is the most abundant salt in carbonaceous chondrites, and it may be important in the low-temperature igneous evolution and aqueous differentiation of icy satellites and large chondritic asteroids. Accordingly, we are investigating high-pressure phase equilibria in MgSO4-H2O solutions under pressures up to four kbars. An initial report was presented two years ago. This abstract summarizes our results to date including studies of solutions containing 15.3 percent, 17 percent, and 22 percent MgSO4. Briefly, these results demonstrate that increasing pressure causes the eutectic and peritectic compositions to shift to much lower concentrations of magnesium sulfate, and the existence of a new low-density phase of magnesium sulfate hydrate. Author (revised)

N94-16248*# Arizona State Univ., Tempe. Dept. of Geology.

EXPERIMENTAL CONSTRAINTS ON CO2 AND H2O IN THE MARTIAN MANTLE AND PRIMARY MAGMAS Abstract Only

John R. Holloway, Kenneth J. Domanik, and Peter A. Cocheo *In* Lunar and Planetary Inst., Twenty-Fourth Lunar and Planetary Science Conference. Part 2: G-M 1993 p 663-664 (For primary document see N94-16173 03-91)

Avail: CASI HC A01/MF A06

We present new data on the stability of hornblende in a Martian mantle composition, on CO2 solubility in iron-rich basaltic magmas, and on the solubility of H2O in an alkalic basaltic magma. These new data are combined with a summary of data from the literature to present a summary of the current state of our estimates of solubilities of H2O and CO2 in probable Martian magmas and the stability of hornblende in a slightly hydrous mantle. The new results suggest that hornblende stability is not sensitive to the Mg/(Mg+Fe) ratio (mg#) of the mantle, that is the results for terrestrial mantle compositions are similar to the more iron-rich Martian composition. Likewise, CO2 solubility in iron-rich tholeiitic basaltic magmas is similar to iron-poor terrestrial compositions. The solubility of H2O has been measured in an alkalic basaltic (basanite) composition for the first time, and it is significantly lower than predicted for models of water solubility in magmas. The lack of mg# dependence observed in hornblende stability and on CO2 solubility that in many cases terrestrial results can be applied to Martian compositions. This conclusion does not apply to other phenomena such as primary magma compositions and major mantle mineral mineralogy. Author (revised)

N94-16249*# Washington Univ., Seattle.

THE SIZE OF COMPLEX CRATERS Abstract Only

K. A. Holsapple *In* Lunar and Planetary Inst., Twenty-Fourth Lunar and Planetary Science Conference. Part 2: G-M 1993 p 665-666 (For primary document see N94-16173 03-91)

Avail: CASI HC A01/MF A06

Lunar craters larger than about 15 km and terrestrial craters larger than about 3 km in diameter presumably underwent gravity-driven, 'late-stage' collapse that modified an initial transient bowl-shaped 'simple' crater into the flat-floored complex craters observed. These same mechanisms were operative for the larger craters on other solar system bodies, at a threshold size inversely proportional to gravity. This paper presents a new look at the scaling relations for these complex craters. Author (revised)

N94-16250*# Max-Planck-Inst. fuer Chemie, Mainz (Germany).

SIDEROPHILE ELEMENTS IN THE UPPER MANTLE OF THE EARTH: NEW CLUES FROM METAL-SILICATE PARTITION COEFFICIENTS Abstract Only **c46**

A. Holzheid, A. Borisov, and H. Palme *In* Lunar and Planetary Inst., Twenty-Fourth Lunar and Planetary Science Conference. Part 2: G-M 1993 p 667-668 (For primary document see N94-16173 03-91)

Avail: CASI HC A01/MF A06

New, precise data on the solubilities of Ni, Co, and Mo in silicate melts at 1400 C and fO2 from IW to IW-2 are presented. The results suggest NiO, CoO as stable species in the melt. No evidence for metallic Ni or Co was found. Equilibrium was ensured by reversals with initially high Ni and Co in the glass. Mo appears to change oxidation state at IW-1, from MoO3 to MoO2. Metal-silicate partition coefficients calculated from these data and recent data on Pd indicate similar partition coefficients for Pd and Mo at the conditions of core formation. This unexpected result constrains models of core formation in the Earth. Author (revised)

N94-16251*# Arizona Univ., Tucson. Lunar and Planetary Lab.

GAS-GRAIN ENERGY TRANSFER IN SOLAR NEBULA SHOCK WAVES: IMPLICATIONS FOR THE ORIGIN OF CHONDRULES Abstract Only **c92**

L. L. Hood and M. Horanyi (Colorado Univ., Boulder.) *In* Lunar and Planetary Inst., Twenty-Fourth Lunar and Planetary Science Conference. Part 2: G-M 1993 p 669-670 (For primary document see N94-16173 03-91)

Avail: CASI HC A01/MF A06

Meteoritic chondrules provide evidence for the occurrence of rapid transient heating events in the protoplanetary nebula. Astronomical evidence suggests that gas dynamic shock waves are likely to be excited in protostellar accretion disks by processes such as protosolar mass ejections, nonaxisymmetric structures in an evolving disk, and impact on the nebula surface of infalling 'clumps' of circumstellar gas. Previous detailed calculations of gas-grain energy and momentum transfer have supported the possibility that such shock waves could have melted pre-existing chondrule-sized grains. The main requirement for grains to reach melting temperatures in shock waves with plausibly low Mach numbers is that grains existed in dust-rich zones (optical depth greater than 1) where radiative cooling of a given grain can be nearly balanced by radiation from surrounding grains. Localized dust-rich zones also provide a means of explaining the apparent small spatial scale of heating events. For example, the scale size of at least some optically thick dust-rich zones must have been relatively small (less than 10 kilometers) to be consistent with petrologic evidence for accretion of hot material onto cold chondrules. The implied number density of mm-sized grains for these zones would be greater than 30 m(exp -3). In this paper, we make several improvements of our earlier calculations to include radiation self-consistently in the shock jump conditions, and we include heating of grains due to radiation from the

shocked gas. In addition, we estimate the importance of momentum feedback of dust concentrations onto the shocked gas which would tend to reduce the efficiency of gas dynamic heating of grains in the center of the dust cloud. Author (revised)

N94-16252*# Jet Propulsion Lab., California Inst. of Tech., Pasadena.
MASS OF SATURN'S A RING Abstract Only
L. J. Horn and C. T. Russell (California Univ., Los Angeles.) *In* Lunar and Planetary Inst., Twenty-Fourth Lunar and Planetary Science Conference. Part 2: G-M 1993 p 671-672 (For primary document see N94-16173 03-91)
Avail: CASI HC A01/MF A06

The mass of Saturn's A ring is reestimated using the behavior of spiral density waves embedded in the ring. The Voyager photopolarimeter (PPS) observed the star delta-Scorpii as it was occulted by Saturn's rings during the Voyager 2 flyby of Saturn in 1981 producing a radial profile of the rings. We examined forty spiral density waves in the Voyager PPS data of the A ring including 10 weaker waves that have not been previously analyzed by means of an autoregressive power spectral technique called Burg. The strengths of this new method for ring studies are that weaker, less extended waves are easily detected and characterized. This method is also the first one which does not require precise knowledge of the resonance location and phase of the wave in order to calculate the surface mass density. Uncertainties of up to 3 km are present in the currently available radial scales for Saturn's rings. Author (revised)

N94-16253*# National Aeronautics and Space Administration. Lyndon B. Johnson Space Center, Houston, TX.
IMPACT PENETRATION EXPERIMENTS IN TEFLON TARGETS OF VARIABLE THICKNESS Abstract Only **c39**
F. Hoerz, M. J. Cintala, R. P. Bernhard (Lockheed Engineering and Sciences Co., Houston, TX.), and T. H. See (Lockheed Engineering and Sciences Co., Houston, TX.) *In* Lunar and Planetary Inst., Twenty-Fourth Lunar and Planetary Science Conference. Part 2: G-M 1993 p 673-674 (For primary document see N94-16173 03-91)
Avail: CASI HC A01/MF A06

Approximately 20.4 sq m of Teflon thermal blankets on the nonspinning Long Duration Exposure Facility (LDEF) were exposed to the orbital debris and micrometeoroid environment in low-Earth orbit (LEO) for approximately 5.7 years. Each blanket consisted of an outer layer (approximately 125 micron thick) of FEP Teflon that was backed by a vapor-deposited metal mirror (Inconel; less than 1 micron thick). The inner surface consisted of organic binders and Chemglaze thermal protective paint (approximately 50 micron thick) resulting in a somewhat variable, total blanket thickness of approximately 180 to 200 microns. There was at least one of these blankets, each exposing approximately 1.2 sq m of surface area, on nine of LDEF's 12 principal pointing directions, the exceptions being Rows 3, 9, and 12. As a consequence, these blankets represent a significant opportunity for micrometeoroid and debris studies, in general, and specifically they provide an opportunity to address those issues that require information about pointing direction (i.e., spatial density of impact events as a function of instrument orientation). During deintegration of the LDEF spacecraft at KSC, all penetration holes greater than or equal to 300 micron in diameter were documented and were recently synthesized in terms of spatial density as a function of LDEF viewing direction by. The present report describes ongoing cratering and penetration experiments in pure Teflon targets, which are intended to establish the relationships between crater or penetration-hole diameters and the associated projectile dimensions at laboratory velocities (i.e., 6 km/s). The ultimate objective of these efforts is to extract reliable mass-frequencies and associated fluxes of hypervelocity particles in LEO. Author (revised)

N94-16254*# Boeing Co., Seattle, WA. Shock Physics Group.
SIMULATION OF COLLISIONAL FRAGMENTATION WITH EXPLOSIVES Abstract Only **c39**
Kevin Housen *In* Lunar and Planetary Inst., Twenty-Fourth Lunar and Planetary Science Conference. Part 2: G-M 1993 p 675-676 (For primary document see N94-16173 03-91)
Avail: CASI HC A01/MF A06

For practical reasons, experimental studies of collisional fragmentation must at times rely on explosives to fragment a target body. For example, Housen et al., described experiments in which spheres were fragmented in a pressurized atmosphere. Explosives were used because impacts could not be performed in the pressure chamber. Explosives can also be used to study targets much larger than those which can be disrupted by conventional light-gas guns, thereby allowing size- and rate-effects to be investigated. The purpose of this study is to determine the charge burial depth required to simulate various aspects of collisions. Author (revised)

N94-16255*# Arizona State Univ., Tempe. Dept. of Geology and Chemistry.
OLIVINES IN THE KABA CARBONACEOUS CHONDRITE AND CONSTRAINTS ON THEIR FORMATION Abstract Only **c76**
X. Hua and P. R. Buseck *In* Lunar and Planetary Inst., Twenty-Fourth Lunar and Planetary Science Conference. Part 2: G-M 1993 p 677-678 (For primary document see N94-16173 03-91)
Avail: CASI HC A01/MF A06

Kaba is unique in containing almost pure fayalitic olivine (Fo(sub 0.1)). Its coexistence with pure forsterite up to Fo(sub 99.6) and normal (Fo(sub 92) to Fo(sub 59)) and reversely (Fo(sub 0.4) to Fo(sub 4.7)) zoned olivines suggest that the Kaba olivines are in thermodynamic disequilibrium and experienced a complicated history. The fayalite is sufficiently pure that it is unlikely that it could have been produced by fractional crystallization. A gas-solid reaction under oxidizing conditions (H2O/H2 ratio approximately 10) is probably responsible for its formation. Author (revised)

N94-16256*# Open Univ., Milton (England). Dept. of Earth Sciences.
REMOVAL OF CARBONACEOUS CONTAMINANTS FROM SILICA AEROGEL Abstract Only **c25**
Hui-Ping Huang, I. Gilmour, C. T. Pillinger, and M. E. Zolensky (National Aeronautics and Space Administration. Lyndon B. Johnson Space Center, Houston, TX.) *In* Lunar and Planetary Inst., Twenty-Fourth Lunar and Planetary Science Conference. Part 2: G-M 1993 p 679-680 (For primary document see N94-16173 03-91)
Avail: CASI HC A01/MF A06

Capture of micrometeorite material from low Earth orbit or dust grains around active comets for return to terrestrial laboratories, capable of practicing the most up to date techniques of chemical isotopic and mineralogical analysis, will greatly enhance our knowledge of primitive material in the solar system. The next generation of space launched cosmic dust collectors will undoubtedly include extremely low density target materials such as silica aerogel as the decelerating and arresting medium. This material has been found to be clean from the point of view of inorganic elements and is thus acceptable for the purpose of harvesting grains to be studied by, for example PIXE, INAA, or SXRF. However, the process used in making aerogel leaves substantial carbon and hydrogen containing residues which would negate their suitability for collection and subsequent investigation of the very important CHON particles. Attempts to precondition aerogel by solvent extraction or heating at 500 C and 750 C in air for 24 hours or under a vacuum of 2(7)(exp -7) torr at 260 C were largely ineffective except that pyrolysis did reduce volatile species. In this investigation we have examined the use of supercritical fluids for the purpose of extracting organic residues. The logic of the new approach is that beyond the supercritical point a substance has the solvating properties of a liquid but the viscosity characteristics of a gas. For example carbon dioxide becomes supercritical at a pressure of 73 atmospheres and a temperature of 31 C; in consequence it can transform to a very powerful and ultraclean solvent. It can dissolve organic matter from low molecular weight up to molecules containing 90 carbon atoms. On release of pressure the fluid reverts to a gas which can easily be pumped away and removed from the substrate being extracted. Author (revised)

N94-16257*# Arkansas Univ., Fayetteville. Cosmochemistry Group.
THE GROUP A3 CHONDRULES OF KRYMKA: FURTHER EVIDENCE FOR MAJOR EVAPORATIVE LOSS DURING THE FORMATION OF CHONDRULES Abstract Only **c90**
S. Huang, P. H. Benoit, and D. W. G. Sears *In* Lunar and Planetary Inst., Twenty-Fourth Lunar and Planetary Science Conference. Part 2: G-M 1993 p 681-682 (For primary document see N94-16173 03-91)
(Grant NAG9-81)
Avail: CASI HC A01/MF A06

Like Semarkona (type 3.0), Krymka (type 3.1) contains two distinct types of chondrule (namely groups A and B) which differ in their bulk compositions, phase compositions, and CL properties. The group A

chondrules in both meteorites show evidence for major loss of material by evaporation(i.e. elemental abundance patterns, size, redox state, olivine-pyroxene abundances). Group A and B chondrules probably formed from common or very similar precursors by the same processes acting with different intensities, group A suffering greater mass-loss by evaporation and reduction of FeO and SiO2. While Krymka chondrules share many primary mineralogical and compositional properties with Semarkona chondrules, the minimal metamorphism it has suffered has also had a significant effect on its chondrules. Author (revised)

N94-16258*# Idaho State Univ., Pocatello. Dept. of Geology.
PETROLOGIC MODELS OF 15388, A UNIQUE APOLLO 15 MARE BASALT Abstract Only
S. S. Hughes, E. J. Dasch (National Aeronautics and Space Administration, Washington, DC.), and L. E. Nyquist (National Aeronautics and Space Administration. Lyndon B. Johnson Space Center, Houston, TX.) *In* Lunar and Planetary Inst., Twenty-Fourth Lunar and Planetary Science Conference. Part 2: G-M 1993 p 683-684 (For primary document see N94-16173 03-91)
Avail: CASI HC A01/MF A06

Mare basalt 15388, a feldspathic microgabbro from the Apennine Front, is chemically and petrographically distinct from Apollo 15 picritic, olivine-normative (ON), and quartz-normative basalts. The evolved chemistry, coarse texture, lack of olivine, and occurrence of cristobalite in 15388 argue for derivation by a late-stage magmatic process that is significantly removed from parental magma. It either crystallized from a magma evolved from the more mafic Apollo 15 basalts, or it crystallized from a currently unrepresented magma. Rb-Sr and Sm-Nd isotopic systematics yield isochron ages of 3.391 plus or minus 0.036 and 3.42 plus or minus 0.07 Ga, respectively, and epsilon(sub Nd) = 8.6 plus or minus 2.4, which is relatively high for Apollo 15 mare basalts. In contrast to chemical patterns of average Apollo 15 ON basalts and Apollo 15 picritic basalt, 15388 has a strongly positive LREE slope, high Ti, shallower HREE slope and a slightly positive Eu anomaly. These features argue against 15388 evolution by simple olivine fractionation of a parental ON or picritic basalt magma, although olivine is a dominant liquidus phase in both potential parents. Author (revised)

N94-16259*# Chicago Univ., IL. Dept. of Geophysical Sciences.
POTASSIUM ISOTOPE COSMOCHEMISTRY, VOLATILE DEPLETION AND THE ORIGIN OF THE EARTH Abstract Only **c25**
M. Humayun and R. N. Clayton *In* Lunar and Planetary Inst., Twenty-Fourth Lunar and Planetary Science Conference. Part 2: G-M 1993 p 685-686 (For primary document see N94-16173 03-91)
Avail: CASI HC A01/MF A06

We report the first results obtained by our techniques for the precise and accurate determination of the isotopic composition of potassium to constrain the mechanism of volatile element depletion in the formation of the Earth, Moon, and meteorites. Our measurements of delta(K-41) for six chondrites and ten terrestrial rocks attained an average precision of the individual measurement of plus or minus 0.4 percent (2 sigma; plus or minus 0.2 percent/a.m.u. and yield a net chondrite-Earth difference unresolved at the 99 percent confidence limit, delta(K-41) = 0.32 plus or minus 0.35 percent (3 delta). This sets a firm upper limit of 1.3 plus or minus 1.4 percent Rayleigh evaporation of terrestrial potassium (using alpha = square root of 41/39), compared with an observed approximately equals 85 percent chemical depletion of K relative to C1 chondrites. Similar conclusions are reached for the SNC meteorites, Shergotty and Zagami, for 15495 (lunar mare gabbro), and for the eucrite Juvinas. Our conclusion is that direct evaporation of volatile elements from planets (e.g. from silicate vapor atmospheres following giant impact) can be ruled out, and the cause of volatile loss must be sought elsewhere, e.g. nebular processes. Our present findings do not support the conclusions of Hinton et al., the discrepancy to be resolved at a later date. We also find lunar soil 64801, delta(K-41) = +4.99 plus or minus 0.53 percent, to be distinctly heavy in accord with Garner et al. Author (revised)

N94-16260*# California Inst. of Tech., Pasadena. Div. of Geology and Planet Science.
DO SIC GRAINS IN ORGUEIL DIFFER FROM THOSE IN MURCHISON? Abstract Only **c90**
Gary R. Huss, Ian D. Hutcheon, and G. J. Wasserburg *In* Lunar and Planetary Inst., Twenty-Fourth Lunar and Planetary Science Conference. Part 2: G-M 1993 p 687-688 (For primary document see N94-16173 03-91)
Avail: CASI HC A01/MF A06

Studies of individual presolar SiC grains have shown that most are enriched in Si-29, Si-30, and C-13, and depleted in N-15, compared to solar-system abundances and that many have large excesses of Mg-26, most plausibly from in situ decay of Al-26. Stone et al., observed that Si from a family of platy SiC grains define a linear array on a 3-isotope plot that does not pass through normal solar-system Si. In contrast, Si-isotope data from over 100 3-4 micron SiC grains from Murchison from an elongate ellipse enclosing the Stone et al. linear array but also including 'normal' solar-system Si. To investigate whether this difference in Si isotopes indicates different populations of SiC in the two meteorites and to improve the characterization of Orgueil SiC, we used the PANURGE ion microprobe to measure Si, C, N, and Mg isotopes and Al and Na concentrations in a suite of 2-5 micron SiC grains from a new sample of Orgueil. Author (revised)

N94-16261*# Academy of Sciences (USSR), Moscow. Inst. for Dynamics of Geospheres.
THE DEPTHS OF THE LARGEST IMPACT CRATERS ON VENUS Abstract Only
B. A. Ivanov and P. G. Ford (Massachusetts Inst. of Tech., Cambridge.) *In* Lunar and Planetary Inst., Twenty-Fourth Lunar and Planetary Science Conference. Part 2: G-M 1993 p 689-690 (For primary document see N94-16173 03-91)
Avail: CASI HC A01/MF A06

The largest impact craters on Venus may be used as evidence of various geological processes within the Venusian crust. We are continuing to construct a data base for the further investigation of large craters on Venus (LCV). We hope to find evidence of crater relaxation that might constrain the thickness and thermal gradient of the crust, as was proposed in an earlier work. The current work concentrates on 27 impact craters with diameters (d) larger than 70 km, i.e., large enough that the footprint of the Magellan altimeter has a good chance of sampling the true crater bottom. All altimeter echoes from points located within (d/2)+70 km from the crater center have been inspected. Author (revised)

N94-16262*# Academy of Sciences (USSR), Moscow.
TESSERA TERRAIN ON VENUS: GLOBAL CHARACTERIZATION FROM MAGELLAN DATA Abstract Only
Mikhail Ivanov and James W. Head (Brown Univ., Providence, RI.) *In* Lunar and Planetary Inst., Twenty-Fourth Lunar and Planetary Science Conference. Part 2: G-M 1993 p 691-692 (For primary document see N94-16173 03-91)
Avail: CASI HC A01/MF A06

Tessera terrain is characterized by relatively high elevations and complex tectonic patterns; analysis of Venera 15/16 data showed that large (up to thousands of km across) and small (up to hundreds of km across) occurrences of tesserae are widespread and non-randomly distributed and make up about 10-15 percent of the surface of Venus north of approximately 30 deg N. In a previous analysis, we used the Magellan Cycle 1 and 2 data to map the global distribution of tesserae on the basis of the following: (1) complex deformational patterns (two or more trends); (2) relatively high radar backscatter; and (3) relatively high elevation. Here we report on the quantitative aspects of tesserae areal, size, and shape distribution and on the characteristics and distribution of tesserae boundaries. Experiments on volcanic flooding of tessera and implications for tessera presence beneath the plains and analysis of the distribution of impact craters on tesserae and the plains are reported elsewhere. Author (revised)

N94-16263*# Academy of Sciences (USSR), Moscow.
DENSITY OF IMPACT CRATERS ON TESSERA, VENUS Abstract Only
M. A. Ivanov and A. T. Basilevsky (Brown Univ., Providence, RI.) *In* Lunar and Planetary Inst., Twenty-Fourth Lunar and Planetary Science Conference. Part 2: G-M 1993 p 693-694 (For primary document see N94-16173 03-91)
Avail: CASI HC A01/MF A06

After the plains, tessera is the most abundant terrain on Venus. It occupies about 10 percent of the Venusian surface, forming the continent-like blocks and small islands above the adjacent plains. Tessera is a result of tectonic deformations of some precursor terrain. However, the nature of

that precursor, as well as the causes and mechanisms of its formations, are under debate. Any models considering tessera terrain involve estimation of tessera age, either relative or absolute. It is well known that the important information on the age of a planetary surface comes from impact crater statistics. The Magellan global overview of Venus with improved resolution provides an opportunity to gather data on impact craters in amounts large enough for statistically reliable estimations of crater density for different terrains. Our study of impact crater density on tesserae compared to the surrounding terrains has a goal to determine whether it is higher, lower, or the same and to interpret it in terms of the tessera age and processes involved. Author (revised)

N94-16264*# Academy of Sciences (USSR), Moscow. Inst. of Geochemistry, Analysis, and Chemistry.

FIRST INVESTIGATION OF NOBLE GASES IN THE DENGLI H3,8 CHONDRITE Abstract Only **c25**

M. A. Ivanova, S. S. Assonov, and Yu. A. Shukolyukov *In* Lunar and Planetary Inst., Twenty-Fourth Lunar and Planetary Science Conference. Part 2: G-M 1993 p 695-696 (For primary document see N94-16173 03-91)

Avail: CASI HC A01/MF A06

The Dengli (H3,8) meteorite, which weighs 243.5 g, is a find from the Karakum desert. It is a complex microbreccia containing unusual clasts which are more typical for regolithic breccias than for H-chondrites. Based on comparisons of Xe and Kr content and isotopic composition, the Dengli does not differ significantly from other H-chondrites. Its exposure age is 7.6 Ma. That is in agreement with common data for the exposure age (6.2 + 0.2 Ma) of 350 H-chondrites. Dengli's K/Ar age (4.01 Ga) coincides with the same ages of many other H-chondrites. Thus the Dengli is not regolithic breccia, and it probably formed during accretion of its parent body. Author (revised)

N94-16265*# Academy of Sciences (USSR), Moscow. Inst. of Geochemistry, Analysis and Chemistry.

SILICA-BEARING OBJECTS IN THE DENGLI H3.8 AND GORLOVKA H3-4 CHONDRITES Abstract Only **c90**

M. A. Ivanova, N. N. Kononkova, and M. I. Petaev *In* Lunar and Planetary Inst., Twenty-Fourth Lunar and Planetary Science Conference. Part 2: G-M 1993 p 697-698 (For primary document see N94-16173 03-91)

Avail: CASI HC A01/MF A06

Silica-bearing objects are enigmatic components of the olivine-normative ordinary chondrites. Several papers have been devoted to the study of these objects in various chondrite types. While a relatively large body of information has been collected, the origin of these objects is still controversial. Here we report new data on silica-bearing objects in the unequilibrated H-chondrites Dengli and Gorlovka. The crystallization history of these objects could be explained on the basis of the phase diagram of the Q-Ol-Pl (Al_2O_3) system, but the origin of the silica-rich liquids remains unclear. Author (revised)

N94-16266*# Academy of Sciences (USSR), Moscow. Inst. of Geochemistry, Analysis and Chemistry.

INDUCED THERMOLUMINESCENCE STUDY OF EXPERIMENTALLY SHOCK-LOADED OLIGOCLASE Abstract Only **c25**

A. I. Ivliev, L. L. Kashkarov, and D. D. Badjukov *In* Lunar and Planetary Inst., Twenty-Fourth Lunar and Planetary Science Conference. Part 2: G-M 1993 p 699-700 (For primary document see N94-16173 03-91)

Avail: CASI HC A01/MF A06

Artificially induced thermoluminescence (TL) in oligoclase samples which were shock-loaded up to 27 GPa was measured. The essential increase of the TL sensitivity in relation to the total gamma-ray irradiation dose was observed only in samples at the 27 GPa pressure. This result can be explained by the initiation of additional radiation damages in the shocked oligoclace crystal lattice. Author (revised)

N94-16267*# Academy of Sciences (USSR), Moscow. Inst. of Geochemistry, Analysis and Chemistry.

SHOCK-THERMAL HISTORY OF KAPOETA HOWARDITE MATTER ON DATA OF THERMOLUMINESCENCE ANALYSIS OF INDIVIDUAL MINERAL GRAINS Abstract Only **c25**

A. I. Ivliev, L. L. Kashkarov, and Yu. Yu. Korotkova (Moscow State Univ., Russia.) *In* Lunar and Planetary Inst., Twenty-Fourth Lunar and Planetary Science Conference. Part 2: G-M 1993 p 701-702 (For primary document see N94-16173 03-91)

Avail: CASI HC A01/MF A06

The artificially induced thermoluminescence (TL) was measured in OPx grains from Kapoeta howardite. The TL glow curves for individual OPx grains are significantly distinguished from each other both by their shape and TL sensitivity; five groups of OPx grains were characterized. The observed variety of glow curves of OPx grains could be caused by their distinct shock-thermal events at the regolith stage of meteorite parent body formation. Author (revised)

N94-16268*# Washington Univ., Saint Louis, MO. Dept. of Earth and Planetary Sciences.

A FIRST-ORDER MODEL FOR IMPACT CRATER DEGRADATION ON VENUS Abstract Only

Noam R. Izenberg, Raymond E. Arvidson, and Roger J. Phillips *In* Lunar and Planetary Inst., Twenty-Fourth Lunar and Planetary Science Conference. Part 2: G-M 1993 p 703-704 (For primary document see N94-16173 03-91)

Avail: CASI HC A01/MF A06

A first-order impact crater aging model is presented based on observations of the global crater population of Venus. The total population consists of 879 craters found over the approximately 98 percent of the planet that has been mapped by the Magellan spacecraft during the first three cycles of its mission. The model is based upon three primary aspects of venusian impact craters: (1) extended ejecta deposits (EED's); (2) crater rims and continuous ejecta deposits; and (3) crater interiors and floors. Author (revised)

N94-16269*# Geological Survey, Denver, CO. Federal Center.

A DISCONTINUOUS MELT SHEET IN THE MANSON IMPACT STRUCTURE Abstract Only **c46**

G. A. Izett, R. L. Reynolds, J. G. Rosenbaum, and J. M. Nishi *In* Lunar and Planetary Inst., Twenty-Fourth Lunar and Planetary Science Conference. Part 2: G-M 1993 p 705-706 (For primary document see N94-16173 03-91)

Avail: CASI HC A01/MF A06

Petrologic studies of the core recovered from holes drilled in the Manson, Iowa, buried impact structure may unravel the thermal history of the crater-fill debris. We made a cursory examination of about 200 m of core recovered from the M-1 bore hole. The M-1 bore hole was the first of 12 holes drilled as part of a cooperative drilling program between the U.S. Geological Survey and the Iowa Geological Survey Bureau. The M-1 core hole is about 6 km northeast of the center of the impact structure, apparently on the flank of its central peak. We developed a working hypothesis that a 30-m-thick breccia unit within a 53-m-thick unit previously termed the 'crystalline clast breccia with glassy matrix' is part of a discontinuous melt sheet in the crater-fill impact debris. The 30-m-thick breccia unit reached temperatures sufficient to partially melt some small breccia clasts and convert the fine-grained breccia matrix into a silicate melt that cooled to a greenish-black, flinty, microcrystalline rock. The results of the investigation of this unit are presented. Author (revised)

N94-16270*# Lockheed Engineering and Sciences Co., Houston, TX.

ORBITAL EVOLUTION OF DUST FROM COMET SCHWASSMANN-WACHMANN 1: A CASE OF ONE-TO-ONE RESONANCE TRAPPING Abstract Only **c90**

A. A. Jackson and H. A. Zook (National Aeronautics and Space Administration. Lyndon B. Johnson Space Center, Houston, TX.) *In* Lunar and Planetary Inst., Twenty-Fourth Lunar and Planetary Science Conference. Part 2: G-M 1993 p 707-708 (For primary document see N94-16173 03-91)

Avail: CASI HC A01/MF A06

In a recent study we have modeled the orbital evolution of dust particles released from comets and asteroids in the solar system. The source bodies were either asteroids inside Jupiter's orbit or comets from the Jupiter family of comets. However there are other dust producing parent bodies in the solar system of interest, one of these is comet P/Schwassman-Wachmann 1. Since comet Schwassman-Wachmann 1, which has an orbit outside of Jupiter's orbit, is an active dust producer

and has low eccentricity, dust particle evolution from it is of interest. We report on a particular 2 micron radius particle that captured into a 1 to 1 mean motion resonance orbit with Saturn. Author (revised)

N94-16271*# Harvard Univ., Cambridge, MA. Dept. of Earth and Planetary Sciences.
CONSTRAINTS ON THE DIFFERENTIATION OF THE EARTH FROM THE COUPLED Sm-146,147-Nd-142,143 SYSTEMATICS Abstract Only **c46**

S. B. Jacobsen and C. L. Harper, Jr. *In* Lunar and Planetary Inst., Twenty-Fourth Lunar and Planetary Science Conference. Part 2: G-M 1993 p 709-710 (For primary document see N94-16173 03-91)
Avail: CASI HC A01/MF A06

The coupled Sm-Nd systematics are a powerful (albeit analytically challenging) tool for investigating the geodynamic history of the Earth. We have previously reported evidence for a 33 ppm difference of an Isua sample relative to our terrestrial standard. Interpretation yields a formation age range for the depleted mantle (DM) source reservoir of 4.45-4.55 Ga. This is consistent with an epoch of LREE-enriched melt extraction from the mantle (proto-crust formation), soon after magma ocean freeze-up following the putative Moon forming giant impact. Author (revised)

N94-16272*# Max-Planck-Inst. fuer Chemie, Mainz (Germany).
Os ISOTOPES IN SNC METEORITES AND THEIR IMPLICATIONS TO THE EARLY EVOLUTION OF MARS AND EARTH **c90**

E. Jagoutz, J. M. Luck (Montpellier Univ., France.), D. Ben Othman (Montpellier Univ., France.), and H. Wanke *In* Lunar and Planetary Inst., Twenty-Fourth Lunar and Planetary Science Conference. Part 2: G-M 1993 p 711-712 (For primary document see N94-16173 03-91)
Avail: CASI HC A01/MF A06

A new development on the measurement of the Os isotopic composition by mass spectrometry using negative ions opened a new field of applications. The Re-Os systematic provides time information on the differentiation of the nobel metals. The nobel metals are strongly partitioned into metal and sulphide phases, but also the generation of silicate melts might fractionate the Re-Os system. Compared to the other isotopic systems which are mainly dating the fractionation of the alkalis and alkali-earth elements, the Re-Os system is expected to disclose entirely new information about the geochemistry. Especially the differentiation and early evolution of the planets such as the formation of the core will be elucidated with this method.
Author (revised)

N94-16273*# Karlova Univ., Prague (Czechoslovakia). Faculty of Sciences.
TRANSITION METALS IN SUPERHEAT MELTS Abstract Only **c26**

Petr Jakes and Michael-Patrick Wolfbauer (Bemidji State Univ., MN.) *In* Lunar and Planetary Inst., Twenty-Fourth Lunar and Planetary Science Conference. Part 2: G-M 1993 p 713-714 (For primary document see N94-16173 03-91)
Avail: CASI HC A01/MF A06

A series of experiments with silicate melts doped with transition element oxides was carried out at atmospheric pressures of inert gas at temperatures exceeding liquidus. As predicted from the shape of fO2 buffer curves in T-fO2 diagrams the reducing conditions for a particular oxide-metal pair can be achieved through the T increase if the released oxygen is continuously removed. Experimental studies suggest that transition metals such as Cr or V behave as siderophile elements at temperatures exceeding liquidus temperatures if the system is not buffered by the presence of other oxide of more siderophile element. For example the presence of FeO prevents the reduction of Cr2O3. The sequence of decreasing siderophility of transition elements at superheat conditions (Mo, Ni, Fe, Cr) matches the decreasing degree of depletion of siderophile elements in mantle rocks as compared to chondrites. Author

N94-16274*# Wright State Univ., Dayton, OH. Dept. of Geology.
IRON OXIDE BANDS IN THE VISIBLE AND NEAR-INFRARED REFLECTANCE SPECTRA OF PRIMITIVE ASTEROIDS Abstract Only **c90**

Kandy S. Jarvis, Faith Vilas (National Aeronautics and Space Administration. Lyndon B. Johnson Space Center, Houston, TX.), and Michael J. Gaffey (Rensselaer Polytechnic Inst., Troy, NY.) *In* Lunar and Planetary Inst., Twenty-Fourth Lunar and Planetary Science Conference. Part 2: G-M 1993 p 715-716 (For primary document see N94-16173 03-91)
(Grant NAGw-642)
Avail: CASI HC A01/MF A06

High resolution reflectance spectra of primitive asteroids (C, P, and D class and associated subclasses) have commonly revealed an absorption feature centered at 0.7 microns attributed to an Fe(2+)-Fe(3+) charge transfer transition in iron oxides and/or oxidized iron in phyllosilicates. A smaller feature identified at 0.43 microns has been attributed to an Fe(3+) spin-forbidden transition in iron oxides. In the spectra of the two main-belt primitive asteroids 368 Haidea (D) and 877 Walkure (F), weak absorption features which were centered near the location of 0.60-0.65 microns and 0.80-0.90 microns prompted a search for features at these wavelengths and an attempt to identify their origin(s). The CCD reflectance spectra obtained between 1982-1992 were reviewed for similar absorption features located near these wavelengths. The spectra of asteroids in which these absorption features have been identified are shown. These spectra are plotted in order of increasing heliocentric distance. No division of the asteroids by class has been attempted here (although the absence of these features in the anhydrous S-class asteroids, many of which have presumably undergone full heating and differentiation should be noted). For this study, each spectrum was treated as a continuum with discrete absorption features superimposed on it. For each object, a linear least squares fit to the data points defined a simple linear continuum. The linear continuum was then divided into each spectrum, thus removing the sloped continuum and permitting the intercomparison of residual spectral features.
Author (revised)

N94-16275*# Tennessee Univ., Knoxville. Dept. of Geological Sciences.
SEARCHING FOR neuKREEP: AN EMP STUDY OF APOLLO 11 GROUP A BASALTS Abstract Only

Eric A. Jerde and Lawrence A. Taylor *In* Lunar and Planetary Inst., Twenty-Fourth Lunar and Planetary Science Conference. Part 2: G-M 1993 p 717-718 (For primary document see N94-16173 03-91)
Avail: CASI HC A01/MF A06

The Apollo 11 and 17 landing sites are characterized by the presence of high-Ti basalts (TiO2 greater than 6 percent). The Group A basalts of Apollo 11 have elevated K compositions (greater than 2000 ppm); and are enriched in incompatible trace elements relative to the other types of high-Ti basalt found in the region. These unique basalts also are the youngest of all high-Ti basalts, with an age of 3.56 +/- 0.02 Ga. Recent modelling of the Apollo 11 Group A basalts by Jerde et al. has demonstrated that this unique variety of high-Ti basalt may have formed through fractionation of a liquid with the composition of the Apollo 11 orange glass, coupled with assimilation of evolved material (dubbed neuKREEP and having similarities to lunar quartz monzodiorite). Assimilation of this material would impart its REE signature on the liquid, resulting in the elevated REE abundances observed. Minerals such as whitlockite which contain a large portion of the REE budget can be expected to reflect the REE characteristics of the assimilant. To this end, an examination of the whitlockite present in the Apollo 11 Group A basalts was undertaken to search for evidence of the neuKREEP material assimilated.
Author (revised)

N94-16276*# Tennessee Univ., Knoxville. Dept. of Geological Sciences.
ON THE COMPOSITION OF neuKREEP: QMD CONTAMINATION AT APOLLO 11? Abstract Only

Eric A. Jerde, Gregory A. Snyder, and Lawrence A. Taylor *In* Lunar and Planetary Inst., Twenty-Fourth Lunar and Planetary Science Conference. Part 2: G-M 1993 p 719-720 (For primary document see N94-16173 03-91)
Avail: CASI HC A01/MF A06

The Group A basalts of Apollo 11 differ in many respects from other high-Ti basalts of the region. Chemically, they are the only high-K (greater than 2000 ppm K) variety of high-Ti basalt and are enriched in incompatible trace elements relative to other basalts from both the Apollo 11 and Apollo 17 sites. In addition, Group A basalts are the youngest of all high-Ti basalts, with an age of 3.56 +/- 0.02 Ga. The cluster of compositions is consistent with the Apollo 11 Group A basalts representing a single flow. Papanastassiou et al. have also indicated the uniqueness of these basalts, based particularly on relatively young Rb-Sr model ages (3.8 - 3.9 Ga). A model for the formation of the Group A basalts was presented by Jerde et al., wherein the Apollo 17 orange volcanic glass is the parent

liquid. Fractionation of this composition, coupled with the assimilation of incompatible-element-rich material, results in compositions akin to those of the Apollo 11 Group A basalt population. Orange glass of similar major-element composition is present at the Apollo 11 site as well, although complete trace element analyses are not available. New modelling results using the Apollo 11 orange glass major elements are grossly similar to those obtained using the Apollo 17 orange glass, indicating approximately 30 percent fractionation. Author (revised)

N94-16277*# Scripps Institution of Oceanography, La Jolla, CA.
ESTIMATES OF LITHOSPHERIC THICKNESS ON VENUS Abstract Only
C. L. Johnson and D. T. Sandwell *In* Lunar and Planetary Inst., Twenty-Fourth Lunar and Planetary Science Conference. Part 2: G-M 1993 p 721-722 (For primary document see N94-16173 03-91)
Avail: CASI HC A01/MF A06

Magellan altimetry data have revealed many examples of topographic flexure on Venus. Modeling of flexural features is of interest as it provides information on spatial (and for the earth, temporal) variations in lithospheric thickness. Lithospheric thickness may be determined solely from modeling topographic flexure or by combining gravity and topography data. On Venus even the highest resolution gravity is insufficient for modeling all but the very longest wavelength flexural features, so we rely heavily on altimetry data for information about lithospheric thickness. Sandwell and Schubert modeled flexure around four coronae and found lithospheric thicknesses h, in the range 35 - 70 km. Studies of several more flexural features suggests that these are typical of Aphrodite Terra and other chasmata regions on Venus. However lithospheric thicknesses associated with other regions are in the range 15-30 km. McKenzie et al. noted that part of Aphrodite Terra appeared similar in planform and morphology to the subduction zones of the East Indies on Earth. Other flexure studies using Magellan data have looked at smaller coronae (h = 5-30 km) and rifts (h = 8-20 km). It can be seen that the range of thicknesses suggested by studies to date is extremely large, and it is difficult to establish whether their mean is in agreement with that predicted by heat flow scaling arguments (h approximately 18 km). Here we present results from a global study of flexure on Venus, with particular emphasis on the variation in our results with different tectonic settings. Author (revised)

N94-16278*# Arizona Univ., Tucson. Lunar and Planetary Lab.
RADAR PROPERTIES OF SEVERAL FLUIDIZED EJECTA BLANKETS ON VENUS Abstract Only
J. R. Johnson and V. R. Baker *In* Lunar and Planetary Inst., Twenty-Fourth Lunar and Planetary Science Conference. Part 2: G-M 1993 p 723-724 (For primary document see N94-16173 03-91)
Avail: CASI HC A01/MF A06

Magellan SAR imagery, altimetry, and radiometry are being analyzed to characterize the radar properties of the fluidized ejecta blankets (FEB's) that are associated with over 40 percent of the impact craters on Venus. The FEB flows and plains units surrounding the craters Isabella (175 km), Addams (90 km), Seymore (65 km), and a crater located at 4 S, 155.5 E (70 km) are examined here using the MIT-produced ARCDR and GxDR data. Individual orbital footprints obtained from the ARCDR's have been classified according to their dominant simple geologic unit (e.g., plains, FEB flows). This permits average values of reflectivity (corrected for diffuse scattering), rms meter-scale slopes, emissivity, and SAR backscatter to be calculated for each unit. GxDR images provide a means of visualizing the spatial relations between the various data sets. Variability of radar properties within the FEB's and relative to surrounding regions may have implications concerning the genesis and possible emplacement mechanisms of fluidized ejecta. Author (revised)

N94-16279*# Washington Univ., Saint Louis, MO. Dept. of Earth and Planetary Sciences.
A MONAZITE-BEARING CLAST IN APOLLO 17 MELT BRECCIA Abstract Only
Bradley L. Jolliff *In* Lunar and Planetary Inst., Twenty-Fourth Lunar and Planetary Science Conference. Part 2: G-M 1993 p 725-726 (For primary document see N94-16173 03-91)
(Grant NAG9-56)
Avail: CASI HC A01/MF A06

A phosphate-rich clast in a pigeonite-plagioclase mineral assemblage occurs in Apollo 17 impact-melt breccia 76503,7025. The clast, measuring 0.9 x 0.4 mm in thin section, contains 3.3 percent (volume) apatite ($Ca_5P_3O_{12}(F,Cl)$), 0.8 percent whitlockite ($Ca_{16}(Mg,Fe)_2REE_2P_{14}O_{56}$), and trace monazite ((LREE)PO_4). Major minerals include 26 percent pigeonite, En53-57FS34-35W08-13, and 69 percent plagioclase, An84-92Ab7-15Oro.6-1.1. Troilite, ilmenite, and other accessory minerals constitute less than 1 percent of the assemblage and Fe-metal occurs along fractures. Also present in the melt breccia as a separate clast is a fragment of felsite. Based on the association of these clasts and their assemblages, a parent lithology of alkali-anorthositic monzogabbro is postulated. Monazite occurs in the phosphate-bearing clast as two less than 10 micron grains intergrown with whitlockite. The concentration of combined REE oxides in monazite is 63.5 percent and the chondrite-normalized REE pattern is strongly enriched in LREE, similar to lunar monazite in 10047,68 and terrestrial monazite. Thorium concentration was not measured in monazite, but based on oxide analyses of approximately 100 percent (including interpolated values for REE not measured), substantial Th concentration is not indicated, similar to monazite in 10047,68. Measured monazite/whitlockite REE ratios are La: 11, Ce: 8, Sm: 3.6, Y: 0.9, and Yb: 0.5. Compositions of monazite and coexisting whitlockite and apatite are given. Author

N94-16280*# Washington Univ., Saint Louis, MO. Dept. of Earth and Planetary Sciences.
APOLLO 17 MATERIALS VIEWED FROM 2 TO 4 mm SOIL PARTICLES: PRE-SERENITATIS HIGHLANDS COMPONENTS Abstract Only
Bradley L. Jolliff and Kaylynn M. Bishop *In* Lunar and Planetary Inst., Twenty-Fourth Lunar and Planetary Science Conference. Part 2: G-M 1993 p 727-728 (For primary document see N94-16173 03-91)
(Grant NAG9-56)
Avail: CASI HC A01/MF A06

Among the highland lithologies of 2-4 mm rock fragments in North Massif soil 76503, we have found a compositional group, low in incompatible element concentrations, that we interpret as representing the pre-Serenitatis surface. A component of these materials is an igneous-textured lithology that we believe formed in large impact melts. These are compositionally similar to, and possibly precursors of, many of the granulitic breccias that appear to be mixtures of ferroan and magnesian-suite rocks. The polymict, or old, upper-crustal breccias, along with granulitic breccias and the endogenous igneous lithologies found particularly at the North Massif stations, constitute the poorly consolidated portions of North Massif. Highland samples from the South Massif, on the other hand, are enriched in materials of the competent, impact-melt breccias formed by the Serenitatis impact. The competent melt-breccias contain clasts of most of the pre-existing surface materials, but they also contain components not found in the rocks of the poorly consolidated massif materials. Author

N94-16281*# Washington Univ., Saint Louis, MO. Dept. of Earth and Planetary Sciences.
AN IRIDIUM-RICH IRON MICROMETEORITE WITH SILICATE INCLUSIONS FROM THE MOON Abstract Only **c90**
Bradley L. Jolliff, Randy L. Korotev, and Larry A. Haskin *In* Lunar and Planetary Inst., Twenty-Fourth Lunar and Planetary Science Conference. Part 2: G-M 1993 p 729-730 (For primary document see N94-16173 03-91)
(Grant NAG9-56)
Avail: CASI HC A01/MF A06

We have found a 0.1 mg iron micrometeorite containing meteoritic silicate inclusions in an agglutinate from 2-2.5 cm deep in regolith core 60014. The metal is 93 percent iron, 6.5 percent nickel, 0.5 percent cobalt, approximately 150 ppm iridium, and less than 2 ppm gold. Although the Ir concentration is higher than that reported previously for any iron meteorite group, it lies on the extrapolation to low Ni and high Ir concentrations of several meteorite groups on Ni,Ir plots (groups 2C,D,E, and 3AB,E,F). Tiny, subrounded silicate inclusions comprise low-Ca pyroxene (En83), olivine (FO80), and albitic and potassic feldspars, as mixtures of minerals or glasses. Minor phases include oldhamite (CaS) and, tentatively, hercynite ($FeAl_2O_4$). The inclusions have pyroxene FeO/MnO of approximately 25 and olivine FeO/MnO of 40-60. In comparison with known iron meteorites, the inclusions are most similar to those in type 2E, e.g., Weekeroo Station, Colomera, and Kodaikanal. As far as we know, this is the first observation of an iron meteorite with silicate inclusions from a lunar sample. No metal

fragments with meteoritic, nonmetallic inclusions were reported in several previous, exhaustive studies of soil particles. Author (revised)

N94-16282*# Lancaster Univ. (England). Inst. of Environmental and Biological Sciences.
THE COOLING RATES OF PAHOEHOE FLOWS: THE IMPORTANCE OF LAVA POROSITY Abstract Only **c46**
Alun C. Jones *In* Lunar and Planetary Inst., Twenty-Fourth Lunar and Planetary Science Conference. Part 2: G-M 1993 p 731-732 (For primary document see N94-16173 03-91)
Avail: CASI HC A01/MF A06

Many theoretical models have been put forward to account for the cooling history of a lava flow; however, only limited detailed field data exist to validate these models. To accurately model the cooling of lava flows, data are required, not only on the heat loss mechanisms, but also on the surface skin development and the causes of differing cooling rates. This paper argues that the cause of such variations in the cooling rates are attributed, primarily, to the vesicle content and degassing history of the lava. Author (revised)

N94-16283*# National Aeronautics and Space Administration. Lyndon B. Johnson Space Center, Houston, TX.
PARTITIONING OF Nb, Mo, Ba, Ce, Pb, Th AND U BETWEEN IMMISCIBLE CARBONATE AND SILICATE LIQUIDS: EVALUATING THE EFFECTS OF P2O5,F, AND CARBONATE COMPOSITION Abstract Only **c25**
J. H. Jones and D. Walker (Lamont-Doherty Geological Observatory, Palisades, NY.) *In* Lunar and Planetary Inst., Twenty-Fourth Lunar and Planetary Science Conference. Part 2: G-M 1993 p 733-734 (For primary document see N94-16173 03-91)
Avail: CASI HC A01/MF A06

Previously we have reported carbonate liq./silicate liq. partition coefficients (D) for a standard suite of trace elements (Nb, Mo, Ba, Ce, Pb, Th, and U) and Ra and Pa as well. In brief, we have found that immiscible liquid partitioning is a strong function of temperature. As the critical temperature of the carbonate-silicate solvus is approached, all partition coefficients approach unity. Additionally, for the overwhelming majority of the partitioning elements, lnD is a linear function of 'ionic field strength,' z/r, where z is the charge of the partitioned cation and r is its ionic radius. Author (revised)

N94-16284*# New Mexico Univ., Albuquerque. Dept. of Earth and Planetary Sciences.
COMPLEX ZONING BEHAVIOR IN PYROXENE IN FeO-RICH CHONDRULES IN THE SEMARKONA ORDINARY CHONDRITE Abstract Only **c90**
Rhian H. Jones and J. J. Papike *In* Lunar and Planetary Inst., Twenty-Fourth Lunar and Planetary Science Conference. Part 2: G-M 1993 p 735-736 (For primary document see N94-16173 03-91)
(Grant NAG9-497)
Avail: CASI HC A01/MF A06

A detailed understanding of the properties of silicate minerals in chondrules is essential to the interpretation of chondrule formation conditions. This study is further work in a series of petrologic studies of chondrules in the least equilibrated LL chondrite, Semarkona (LL3.0). The objectives of this work are as follows: (1) to understand chondrule formation conditions and nebular processes; and (2) to use the data as a basis for understanding the effects of metamorphism in more equilibrated chondrites. FeO-rich pyroxene in the chondrules described shows complex zoning behavior. Low-Ca clinopyroxene, orthopyroxene, pigeonite, and augite are all observed, in various associations with one another. Coexisting olivine phenocrysts are also FeO-rich and strongly zoned. Compositional and zoning properties are similar to those observed in boninites and are interpreted as resulting from rapid cooling of individual chondrules. Author (revised)

N94-16285*# Lockheed Engineering and Sciences Co., Houston, TX.
ANGRITE LEW87051: ARE THE OLIVINES PHENO'S OR XENO'S? A CONTINUING STORY Abstract Only **c46**
A. J. G. Jurewicz and G. A. McKay (National Aeronautics and Space Administration. Lyndon B. Johnson Space Center, Houston, TX.) *In* Lunar and Planetary Inst., Twenty-Fourth Lunar and Planetary Science Conference. Part 2: G-M 1993 p 737-738 (For primary document see N94-16173 03-91)
Avail: CASI HC A01/MF A06

The achondrite LEW87051 is a porphyritic basalt consisting of large subhedral to euhedral zoned olivines in a finer-grained groundmass. The texture of this groundmass looks remarkably like a quenched melt. However, although the rock is clearly igneous, its exact origins and history are under dispute. From petrographic observations, Prinz felt that the large olivines were xenocrysts and that the zoning reflected interaction with an unrelated, CAI-enriched melt. McKay et al. was able to model the olivines as phenocrysts, whose zoning was the result of a parent melt that changed in composition as material crystallized, e.g., fractional crystallization in a closed system, and calculated a parent melt composition. Jurewicz and McKay compared the calculated parent melt composition with actual partial melts from CV and CM chondrites. They showed that the calculated melt was substantially different from equilibrium melts of these chondrites; however, the LEW87051 groundmass composition was similar to some of the low temperature partial melts, although slightly enriched in AN (or depleted in OL) components. This study presents the results of an independent petrologic look at other olivines in LEW87051 and the preliminary results of a quantitative model for the major zoning in these olivines as diffusive-exchange with an olivine-saturated, low temperature angritic melt. Author (revised)

N94-16286*# Lockheed Engineering and Sciences Co., Houston, TX.
PARTIAL MELTING OF ORDINARY CHONDRITES: LOST CITY (H) AND ST. SEVERIN (LL) Abstract Only **c90**
Amy J. G. Jurewicz, John H. Jones (National Aeronautics and Space Administration. Lyndon B. Johnson Space Center, Houston, TX.), Egon T. Weber (Michigan Univ., Ann Arbor.), and David W. Mittlefehldt *In* Lunar and Planetary Inst., Twenty-Fourth Lunar and Planetary Science Conference. Part 2: G-M 1993 p 739-740 (For primary document see N94-16173 03-91)
Avail: CASI HC A01/MF A06

Eucrites and diogenites are examples of asteroidal basalts and orthopyroxenites, respectively. As they are found intermingled in howardites, which are inferred to be regolith breccias, eucrites and diogenites are thought to be genetically related. But the details of this relationship and of their individual origins remain controversial. Work by Jurewicz et al. showed that 1170-1180 C partial melts of the (anhydrous) Murchison (CM) chondrite have major element compositions extremely similar to primitive eucrites, such as Sioux County. However, the MnO contents of these melts were about half that of Sioux County, a problem for the simple partial melting model. In addition, partial melting of Murchison could not produce diogenites, because residual pyroxenes in the Murchison experiments were too Fe- and Ca-rich and were minor phases at all but the lowest temperatures. A parent magma for diogenites needs an expanded low-calcium pyroxene field. In their partial melting study of an L6 chondrite, Kushiro and Mysen found that ordinary chondrites did have an expanded low-Ca pyroxene field over that of CV chondrites (i.e., Allende), probably because ordinary chondrites have lower Mg/Si ratios. This study expands that of both Kushiro and Mysen and Jurewicz et al. to the Lost City (H) and St. Severin (LL) chondrites at temperatures ranging from 1170 to 1325 C, at an fO2 of one log unit below the iron-wuestite buffer (IW-1). Author (revised)

N94-16287*# National Aeronautics and Space Administration. Lyndon B. Johnson Space Center, Houston, TX.
EXPERIMENTAL PARTITIONING OF Zr, Ti, AND Nb BETWEEN SILICATE LIQUID AND A COMPLEX NOBLE METAL ALLOY AND THE PARTITIONING OF Ti BETWEEN PEROVSKITE AND PLATINUM METAL Abstract Only **c26**
Stephen R. Jurewicz and John H. Jones *In* Lunar and Planetary Inst., Twenty-Fourth Lunar and Planetary Science Conference. Part 2: G-M 1993 p 741-742 (For primary document see N94-16173 03-91)
Avail: CASI HC A01/MF A06

El Goresy et al.'s observation of Nb, Zr, and Ta in refractory platinum metal nuggets (RPMN's) from Ca-Al-rich inclusions (CAI's) in the Allende meteorite led them to propose that these lithophile elements alloyed in the metallic state with noble metals in the early solar nebula. However, Grossman pointed out that the thermodynamic stability of Zr in the oxide phase is vastly greater than metallic Zr at estimated solar nebula conditions. Jones and Burnett suggested this discrepancy may be explained by the very

non-ideal behavior of some lithophile transition elements in noble metal solutions and/or intermetallic compounds. Subsequently, Fegley and Kornacki used thermodynamic data taken from the literature to predict the stability of several of these intermetallic compounds at estimated solar nebula conditions. Palme and Schmitt and Treiman et al. conducted experiments to quantify the partitioning behavior of certain lithophile elements between silicate liquid and Pt-metal. Although their results were somewhat variable, they did suggest that Zr partition coefficients were too small to explain the observed 'percent' levels in some RPMN's. Palme and Schmitt also observed large partition coefficients for Nb and Ta. No intermetallic phases were identified. Following the work of Treiman et al., Jurewicz and Jones performed experiments to examine Zr, Nb, and Ti partitioning near solar nebula conditions. Their results showed that Zr, Nb, and Ti all have an affinity for the platinum metal, with Nb and Ti having a very strong preference for the metal. The intermetallic phases (Zr,Fe)Pt3, (Nb,Fe)Pt3, and (Ti,Fe)Pt3 were identified. Curiously, although both experiments and calculations indicate that Ti should partition strongly into Pt-metal (possibly as TiPt3), no Ti has ever been observed in any RPMN's. Fegley and Kornacki also noticed this discrepancy and hypothesized that the Ti was stabilized in perovskite which is a common phase in Allende CAI's.

Author (revised)

N94-16288*# National Aeronautics and Space Administration. Lyndon B. Johnson Space Center, Houston, TX.

EXPERIMENTAL SEGREGATION OF IRON-NICKEL METAL, IRON-SULFIDE, AND OLIVINE IN A THERMAL GRADIENT: PRELIMINARY RESULTS Abstract Only **c90**

Stephen R. Jurewicz and J. H. Jones *In* Lunar and Planetary Inst., Twenty-Fourth Lunar and Planetary Science Conference. Part 2: G-M 1993 p 743-744 (For primary document see N94-16173 03-91)

Avail: CASI HC A01/MF A06

Speculation about the possible mechanisms for core formation in small asteroids raises more questions than answers. Petrologic evidence from iron meteorites, pallasites, and astronomical observations of M asteroids suggests that many small bodies were capable of core formation. Recent work by Taylor reviews the geochemical evidence and examines the possible physical/mechanical constraints on segregation processes. Taylor's evaluation suggests that extensive silicate partial melting (preferably 50 vol. percent or greater) is required before metal can segregate from the surrounding silicate and form a metal core. The arguments for large degrees of silicate partial melting are two-fold: (1) elemental trends in iron meteorites require that the metal was at is liquidus; and (2) experimental observations of metal/sulfide inclusions in partially molten silicate meteorites show that the metal/sulfide tends to form spherules in the liquid silicate due to surface tension effects. Taylor points out that for these metal spherules to sink through a silicate mush, high degrees of silicate partial melting are required to lower the silicate yield strength. Although some qualitative experimental data exists, little is actually known about the behavior of metals and liquid sulfides dispersed in silicate systems. In addition, we have been impressed with the ability of cumulative olivine to expel trapped liquid when placed in a thermal gradient. Consequently, we undertook to accomplish the following: (1) experimentally evaluate the potential for metal/sulfide/silicate segregation in a thermal gradient; and (2) obtain quantitative data of the wetting parameters of metal-sulfide melts among silicate grains.

Author (revised)

N94-16289*# Arizona State Univ., Tempe. Dept. of Geology.

THE HISTORY OF MARE VOLCANISM IN THE ORIENTALE BASIN: MARE DEPOSIT AGES, COMPOSITIONS AND MORPHOLOGIES Abstract Only

S. D. Kadel, R. Greeley, G. Neukum (Deutsche Versuchsanstalt fuer Luft- und Raumfahrt, Oberpfaffenhofen, Germany.), and R. Wagner (Deutsche Versuchsanstalt fuer Luft- und Raumfahrt, Oberpfaffenhofen, Germany.) *In* Lunar and Planetary Inst., Twenty-Fourth Lunar and Planetary Science Conference. Part 2: G-M 1993 p 745-746 (For primary document see N94-16173 03-91)

Avail: CASI HC A01/MF A06

The eruptive history of mare basalts in the Orientale Basin has been studied, using Lunar Orbiter 4 high-resolution photographs, Zond 8 photographs, and recently acquired Galileo EM-1 multispectral images. This work represents a refined set of compositional data incorporating the use of a linear mixing model for mare compositions, crater count data, and a comprehensive morphologic analysis of Orientale Basin mare deposits. Evidence for multiple eruptive episodes has been found, with compositions ranging from medium- to high-Ti basalt (less than 4 to greater than 6 wt. percent TiO2). Eruptive styles included flood, rille-forming, and shield-forming eruptions. Impact crater densities of mare units in the Orientale Basin enable determination of the ages of these deposits, using the method of Neukum et al. Earliest eruptions of mare basalt in the basin occurred at greater than or equal to 3.80 Ga and the latest eruptions occurred at about 2.3-2.5 Ga. Hence, mare volcanism occurred over a period of nearly 1.5 Ga.

Author (revised)

N94-16290*# California Univ., Los Angeles. Inst. of Geophysics and Planetary Physics.

THE AL RAIS METEORITE: A CR CHONDRITE OR CLOSE RELATIVE? Abstract Only **c90**

G. W. Kallemeyn *In* Lunar and Planetary Inst., Twenty-Fourth Lunar and Planetary Science Conference. Part 2: G-M 1993 p 747-748 (For primary document see N94-16173 03-91)

Avail: CASI HC A01/MF A06

Although the classificational group 'CR' was first put forth by McSween more than 10 years ago, it included only the Al Rais and Renazzo meteorites. It has only been the relatively recent discovery of several CR-related chondrites in Antarctica and the Sahara that has provided the necessary research material for an extensive group description and classification. Some 22 separate specimens representing at least 6 falls are now purportedly members of the CR group. In light of all this new data, an old question can once again be raised as to whether or not Al Rais should be classified in the same distinct group as Renazzo. This paper explores that question.

Author (revised)

N94-16291*# Tokyo Univ. (Japan). Inst. for Cosmic Ray Research.

CHEMICAL AND ISOTOPIC COMPOSITIONS IN ACID RESIDUES FROM VARIOUS METEORITES Abstract Only **c90**

N. Kano, K. Yamakoshi, H. Matsuzaki, and K. Nogami (Dokkyo Univ., Tochigi, Japan.) *In* Lunar and Planetary Inst., Twenty-Fourth Lunar and Planetary Science Conference. Part 2: G-M 1993 p 749-750 (For primary document see N94-16173 03-91)

Avail: CASI HC A01/MF A06

We are planning to carry out systematic isotopic investigations of Ru, Mg, etc., in primordial samples. The investigations will be pursued in the context of a study of the pre-history of the solar system. It is hoped that the study will yield direct evidence for processes of nucleosynthesis in the pre-solar stage and detection of extinct radioactive nuclides. In this paper, we present the results of chemical compositions of acid residues obtained from three types of meteorites: Canyon Diablo (IA), Allende (CV3), and Nuevo Mercuro (H5); and the preliminary results of Ru isotopic compositions.

Author (revised)

N94-16292*# Geological Survey, Flagstaff, AZ.

CRUSTAL STRUCTURE AND IGNEOUS PROCESSES IN A CHONDRITIC IO Abstract Only **c90**

J. S. Kargel *In* Lunar and Planetary Inst., Twenty-Fourth Lunar and Planetary Science Conference. Part 2: G-M 1993 p 751-752 (For primary document see N94-16173 03-91)

Avail: CASI HC A01/MF A06

Liquid sulfur can form when metal-free C1 or C2 chondrites are heated. It may be obtained either by direct melting of native sulfur in disequilibrated C1 or C2 chondrites or by incongruent melting of pyrite and other sulfides in thermodynamically equilibrated rocks of the same composition. Hence, Lewis considered C2 chondrites to be the best meteoritic analog for Io's bulk composition. Metal-bearing C3 and ordinary chondrites are too chemically reduced to yield liquid sulfur and are not thought tc represent plausible analogs of Io's bulk composition. An important aspect of Lewis' work is that CaSO4 and MgSO4 are predicted to be important in Io. Real C1 and C2 chondrites contain averages of, respectively, 11 percent and 3 percent by mass of salts (plus water of hydration). The most abundant chondritic salts are magnesium and calcium sulfates, but other important components include sulfates of sodium, potassium, and nickel and carbonates of magnesium, calcium, and iron. It is widely accepted that chondritic salts are formed by low-temperature aqueous alteration. Even if Io originally did not contain salts, it is likely that aqueous alteration would have yielded several percent sulfates and carbonates. In any event, Io

probably contains sulfates and carbonates. This report presents the results of a model of differentiation of a simplified C2 chondrite-like composition that includes 1.92 percent MgSO4, 0.56 percent CaSO4, 0.53 percent CaCO3, and 0.094 percent elemental sulfur. The temperature of the model is gradually increased; ensuing fractional melting results in these components extruding or intruding at gravitationally stable levels in Io's crust. Relevant phase equilibria were reviewed. A deficiency of high-pressure phase equilibria renders the present model qualitative. Author (revised)

N94-16293*# Geological Survey, Flagstaff, AZ.
GEOMORPHIC PROCESSES IN THE ARGYRE-DORSA ARGENTEA REGION OF MARS Abstract Only
J. S. Kargel *In* Lunar and Planetary Inst., Twenty-Fourth Lunar and Planetary Science Conference. Part 2: G-M 1993 p 753-754 (For primary document see N94-16173 03-91)
Avail: CASI HC A01/MF A06

Among many indications of possible ancient Martian galciation are sinuous eskerlike ridges in southern Argyre Planitia and the Dorsa Argentea region. But, in photogeology, other interpretations are always possible, and what appears eskerlike to one set of eyes may appear quite different to another. Interpretations of these ridges are about as numerous as observers, who collectively have suggested nine distinct hypotheses. Martian sinuous ridges have been interpreted as wrinkle ridges, lava flows, igneous dikes, clastic dikes, linear sand dunes, spits or bars, examples of inverted stream topography, or glacial crevasse fill. With Mars Observer en route to Mars, the prospects for a narrowing of the debate are bright. The esker hypothesis will gain support if Mars Observer images show that the ridges contain boulders, that the ridges are layered and contain channel structures, that the ridges are modified by thermokarst, or that the ridges occur in close, logical associations with other glacial landforms such as flutes, oriented grooves, and moraines. In the meantime, the evidence presented below bolsters the esker hypothesis, challenges certain alternative ideas, and draws a tentative geomorphic connection between the sinuous ridges of Argyre and those of Dorsa Argentea. Author (revised)

N94-16294*# Geological Survey, Flagstaff, AZ.
THE RHEOLOGY AND COMPOSITION OF CRYOVOLCANIC FLOWS ON ICY SATELLITES Abstract Only **c90**
Jeffrey S. Kargel *In* Lunar and Planetary Inst., Twenty-Fourth Lunar and Planetary Science Conference. Part 2: G-M 1993 p 755-756 (For primary document see N94-16173 03-91)
Avail: CASI HC A01/MF A06

The rheologic properties of terrestrial lavas have been related to morphologic features of their flows, such as levees, banked surfaces, multilobate structures, and compressible folds. These features also have been used to determine rheologies and constrain the compositions of extraterrestrial flows. However, with rare exceptions, such features are not resolvable in Voyager images of the satellites of outer planets. Often only flow length and edge thickness of cryovolcanic flows can be measured reasonably accurately from Voyager images. The semiempirical lava-flow model presented here is a renewed effort to extract useful information from such measurements. Author

N94-16295*# Texas Technological Univ., Lubbock. Dept. of Geosciences and Dept. of Chemistry and Biochemistry.
MARTIAN CARBON DIOXIDE: CLUES FROM ISOTOPES IN SNC METEORITES Abstract Only
H. R. Karlsson, R. N. Clayton (Chicago Univ., IL.), T. K. Mayeda (Chicago Univ., IL.), A. J. T. Jull (Arizona Univ., Tucson.), and E. K. Gibson, Jr. (National Aeronautics and Space Administration. Lyndon B. Johnson Space Center, Houston, TX.) *In* Lunar and Planetary Inst., Twenty-Fourth Lunar and Planetary Science Conference. Part 2: G-M 1993 p 757-758 (For primary document see N94-16173 03-91)
Avail: CASI HC A01/MF A06

Attempts to unravel the origin and evolution of the atmosphere and hydrosphere on Mars from isotopic data have been hampered by the impreciseness of the measurements made by the Viking Lander and by Earth-based telescopes. The SNC meteorites which are possibly pieces of the Martian surface offer a unique opportunity to obtain more precise estimates of the planet's volatile inventory and isotopic composition. Recently, we reported results on oxygen isotopes of water extracted by pyrolysis from samples of Shergotty, Zagami, Nakhla, Chassigny, Lafayette, and EETA-79001. Now we describe complementary results on the stable isotopic composition of carbon dioxide extracted simultaneously from those same samples. We will also report on C-14 abundances obtained by accelerator mass spectrometry (AMS) for some of these CO2 samples. Author (revised)

N94-16296*# Academy of Sciences (USSR), Moscow. Inst. of Geochemistry, Analysis and Chemistry.
DIFFERENT RADIATION AND METAMORPHIC HISTORY OF THE KAINSAZ CO 3.2 CHONDRULES Abstract Only **c90**
L. L. Kashkarov and G. V. Kalinina *In* Lunar and Planetary Inst., Twenty-Fourth Lunar and Planetary Science Conference. Part 2: G-M 1993 p 759-760 (For primary document see N94-16173 03-91)
Avail: CASI HC A01/MF A06

Track and thermoluminescence parameters in chondrules from the Kainsaz CO 3.2 chondrite have been studied. Obtained results elucidate their individual shock-thermal history and the early pre-accretion stage of the meteorite parent body formation. Author (revised)

N94-16297*# Academy of Sciences (USSR), Moscow. Inst. of Geochemistry, Analysis and Chemistry.
COMPLEX RADIATION-THERMAL HISTORY OF KAIDUN METEORITE ON DATA OF TRACK STUDY OF SILICATE MINERALS Abstract Only **c90**
L. L. Kashkarov, N. N. Korotkova, and A. Ya. Skripnik *In* Lunar and Planetary Inst., Twenty-Fourth Lunar and Planetary Science Conference. Part 2: G-M 1993 p 761-762 (For primary document see N94-16173 03-91)
Avail: CASI HC A01/MF A06

The results of track study of approximately 80 individual silicate mineral crystals (ol, px, plag) picked out from Kaidun meteorite are presented. A wide range of observed rho(sub VH) value distributions indicate the complex irradiation history of Kaidun minerals. In one anortite crystal having two track groups with different parameters the pre-accretion irradiation traces were observed in all probability. Author (revised)

N94-16298*# Oulu Univ. (Finland). Dept. of Astronomy.
FRACTAL GEOMETRY OF SOME MARTIAN LAVA FLOW MARGINS: ALBA PATERA Abstract Only
K. Kauhanen *In* Lunar and Planetary Inst., Twenty-Fourth Lunar and Planetary Science Conference. Part 2: G-M 1993 p 763-764 (For primary document see N94-16173 03-91)
Avail: CASI HC A01/MF A06

Fractal dimension for a few lava flow margins on the gently sloping flanks of Alba Patera were measured using the structured walk method. Fractal behavior was observed at scales ranging from 20 to 100 pixels. The upper limit of the linear part of log(margin length) vs. log(scale) profile correlated well to the margin length. The lower limit depended on resolution and flow properties. Author

N94-16299*# Oulu Univ. (Finland). Dept. of Astronomy.
TECTONICS OF NEYTERKOB CORONA ON VENUS Abstract Only
K. Kauhanen *In* Lunar and Planetary Inst., Twenty-Fourth Lunar and Planetary Science Conference. Part 2: G-M 1993 p 765-766 (For primary document see N94-16173 03-91)
Avail: CASI HC A01/MF A06

Neyterkob double corona (50 deg N 202 deg) presents an area of corona-related interfering tectonic patterns which are formed in different phases of evolution of the corona and modified by regional stresses. Analyzing the patterns can reveal something about the coronal formation. Tectonic features form distinct units on topographic depressions, slopes, and volcanic flows extending over one radius of the corona. A remarkable amount of compressional features were found near the rim and related to interaction between adjacent coronae. Radial extension was mainly observed on a peculiar NE-SW trending high crossing the corona. Concentric fractures were found to the east partly connected to the lithospheric flexure. Tectonic features indicate movements of volcanic activity and modification of the area by more regional stresses. Author (revised)

N94-16300*# California Univ., Los Angeles.
IMPLICATIONS OF CRATER DISTRIBUTIONS ON VENUS Abstract Only
W. M. Kaula *In* Lunar and Planetary Inst., Twenty-Fourth Lunar and

Planetary Science Conference. Part 2: G-M 1993 p 767-768 (For primary document see N94-16173 03-91)
Avail: CASI HC A01/MF A06

The horizontal locations of craters on Venus are consistent with randomness. However, (1) randomness does not make crater counts useless for age indications; (2) consistency does not imply necessity or optimality; and (3) horizontal location is not the only reference frame against which to test models. Re (1), the apparent smallness of resurfacing areas means that a region on the order of one percent of the planet with a typical number of craters, 5-15, will have a range of feature ages of several 100 My. Re (2), models of resurfacing somewhat similar to Earth's can be found that are also consistent and more optimal than random: i.e., resurfacing occurring in clusters, that arise and die away in lime intervals on the order of 50 My. These agree with the observation that there are more areas of high crater density, and fewer of moderate density, than optimal for random. Re (3), 799 crater elevations were tested; there are more at low elevations and fewer at high elevations than optimal for random: i.e., 54.6 percent below the median. Only one of 40 random sets of 799 was as extreme.
Author (revised)

N94-16301*# California Univ., Los Angeles.
MEGAPLUMES ON VENUS Abstract Only
W. M. Kaula *In* Lunar and Planetary Inst., Twenty-Fourth Lunar and Planetary Science Conference. Part 2: G-M 1993 p 769-770 (For primary document see N94-16173 03-91)
Avail: CASI HC A01/MF A06

The geoid and topography heights of Atla Regio and Beta Regio, both peaks and slopes, appear explicable as steady-state plumes, if non-linear viscosity eta(Tau, epsilon) is taken into account. Strongly constrained by the data are an effective plume depth of about 700 km, with a temperature anomaly thereat of about 30 degrees, leading to more than 400 degrees at the plume head. Also well constrained is the combination Q(eta)/s(sup 4)(sub 0) = (volume flow rate)(viscosity)/(plume radius): about 11 Pa/m/sec. The topographic slopes dh/ds constrain the combination Q/A, where A is the thickness of the spreading layer, since the slope varies inversely with velocity. The geoid slopes dN/ds require enhancement of the deeper flow, as expected from non-linear viscosity. The Beta data are best fit by Q = 500 m(sup 3)/sec and A equals 140 km; the Atla, by Q equals 440 m(exp 3)/sec and A equals 260 km. The dynamic contribution to the topographic slope is minor.
Author (revised)

N94-16302*# Brown Univ., Providence, RI. Dept. of Geological Sciences.
PRELIMINARY ANALYSIS OF DIONE REGIO, VENUS: THE FINAL MAGELLAN REGIONAL IMAGING GAP Abstract Only
S. T. Keddie *In* Lunar and Planetary Inst., Twenty-Fourth Lunar and Planetary Science Conference. Part 2: G-M 1993 p 771-772 (For primary document see N94-16173 03-91)
Avail: CASI HC A01/MF A06

In Sep. 1992, the Magellan spacecraft filled the final large gap in its coverage of Venus when it imaged an area west of Alpha Regio. F-BIDR's and some test MIDR's of parts of this area were available as of late December. Dione Regio was imaged by the Arecibo observatory and a preliminary investigation of Magellan images supports the interpretations made based on these earlier images: Dione Regio is a regional highland on which is superposed three large, very distinct volcanic edifices. The superior resolution and different viewing geometry of the Magellan images also clarified some uncertainties and revealed fascinating details about this region.
Author (revised)

N94-16303*# Brown Univ., Providence, RI.
THE DISTRIBUTION OF LARGE VOLCANOES ON VENUS AS A FUNCTION OF HEIGHT AND ALTITUDE Abstract Only
S. T. Keddie and J. W. Head *In* Lunar and Planetary Inst., Twenty-Fourth Lunar and Planetary Science Conference. Part 2: G-M 1993 p 773-774 (For primary document see N94-16173 03-91)
Avail: CASI HC A01/MF A06

Theory predicts that the slower cooling of lava flows on Venus should result in lava flows that are typically 20 percent longer than their terrestrial counterparts and that the development of neutral buoyancy zones (NBZ) on Venus may be strongly influenced by altitude-controlled variations in surface pressure. Observations that support these predictions would include relatively low heights for Venus volcanoes, and an increase in both the number and development of large edifices with increasing basal altitude. The results of an analysis of the height and altitude distribution of 123 large (diameter greater than 100 km) volcanoes made using Magellan image and altimetry data are presented and these results are used to begin to test the predications of the above theories.
Author (revised)

N94-16304*# Southern Methodist Univ., Dallas, TX.
STRUCTURAL MAPPING OF MAXWELL MONTES Abstract Only
Myra Keep and Vicki L. Hansen *In* Lunar and Planetary Inst., Twenty-Fourth Lunar and Planetary Science Conference. Part 2: G-M 1993 p 775-776 (For primary document see N94-16173 03-91)
Avail: CASI HC A01/MF A06

Four sets of structures were mapped in the western and southern portions of Maxwell Montes. An early north-trending set of penetrative lineaments is cut by dominant, spaced ridges and paired valleys that trend northwest. To the south the ridges and valleys splay and graben form in the valleys. The spaced ridges and graben are cut by northeast-trending graben. The northwest-trending graben formed synchronously with or slightly later than the spaced ridges. Formation of the northeast-trending graben may have overlapped with that of the northwest-trending graben, but occurred in a spatially distinct area (regions of 2 deg slope). Graben formation, with northwest-southeast extension, may be related to gravity-sliding. Individually and collectively these structures are too small to support the immense topography of Maxwell, and are interpreted as parasitic features above a larger mass that supports the mountain belt.
Author (revised)

N94-16305*# Washington Univ., Saint Louis, MO. Center for Space Sciences.
I-Xe STRUCTURE OF ILAFEGH 009 AND SHALLOWATER: EVIDENCE FOR EARLY FORMATION AND RAPID COOLING OF IMPACT-DERIVED ENSTATITE METEORITES Abstract Only **c90**
K. Kehm, R. H. Nichols, Jr., C. M. Hohenberg, T. J. McCoy (Hawaii Univ., Honolulu.), and K. Keil (Hawaii Univ., Honolulu.) *In* Lunar and Planetary Inst., Twenty-Fourth Lunar and Planetary Science Conference. Part 2: G-M 1993 p 777-778 (For primary document see N94-16173 03-91)
Avail: CASI HC A01/MF A06

Enstatite meteorites have proven to be ideal samples for past studies of the I-Xe system. This work focuses on two enstatite meteorites that were formed by impact processes. Ilafegh 009 is a clast-free impact melt rock from the EL chondrite parent body. The Shallowater aubrite likely formed when a fully molten planetesimal collided with a solid planetesimal, mixing fragments of the solid planetesimal into the enstatite mantle of the molten planetesimal. A complex three-stage cooling history resulted from this mixing and later break-up and reassembly of the parent body. The present study indicates that the I-Xe structure of these two meteorites resulted from in situ decay of live I-129 and that both experienced xenon closure of the iodine host phase at approximately the same time. I-Xe cooling rates are consistent with the cooling rates derived from mineralogic and petrologic studies of these objects. The similarities in ages suggest that the region of the nebula in which enstatite parent bodies formed must have experienced an intense early bombardment.
Author (revised)

N94-16306*# Hawaii Univ., Honolulu. Dept. of Geology and Geophysics.
EXPLOSIVE VOLCANISM AND THE COMPOSITIONS OF THE CORES OF DIFFERENTIATED ASTEROIDS Abstract Only **c90**
Klaus Keil and Lionel Wilson *In* Lunar and Planetary Inst., Twenty-Fourth Lunar and Planetary Science Conference. Part 2: G-M 1993 p 779-780 (For primary document see N94-16173 03-91)
Avail: CASI HC A01/MF A06

Eleven iron meteorite groups showing correlations between Ni and siderophile trace elements that are predictable by distribution coefficients between liquid and solid metal of fractionally crystallizing metal magmas, are interpreted to be fragments of the fractionally crystallized cores of 11 differentiated asteroids. Many of these groups crystallized from S-depleted magmas which we propose resulted from removal of the first partial melt (a Fe,Ni-FeS cotectic) by explosive pyroclastic volcanism. It is shown that these dense, negatively buoyant melts can be driven to asteroidal surfaces by the combination of an excess pressure in the melt and the presence of buoyant bubbles of gas which decrease the bulk density of the melt. It is also shown that in typical asteroidal materials, veins will form which grow

into dikes and serve as pathways for migration of melt and gas to asteroidal surfaces. Since cotectic Fe,Ni-FeS melt consists of about 85 wt. percent FeS and 15 wt. percent Fe,Ni, removal of small volumes of eutectic melts results in major loss of S but only minor loss of Fe,Ni, thus leaving sufficient Fe,Ni to form sizeable asteroidal cores. Author (revised)

N94-16307*# Kansas Univ., Lawrence.
HIGH-RESOLUTION SEISMIC REFLECTION SURVEY AT THE MANSON CRATER, IOWA Abstract Only **c46**
D. A. Keiswetter, R. Black, D. W. Steeples, and R. R. Anderson (Geological Survey, Iowa City, IA.) *In* Lunar and Planetary Inst., Twenty-Fourth Lunar and Planetary Science Conference. Part 2: G-M 1993 p 781-782 (For primary document see N94-16173 03-91)
Avail: CASI HC A01/MF A06

Approximately 17.4 km of high-resolution reflection data were acquired along an east-west radius of the Manson Impact Structure (MIS) to delineate the shallow (upper 300 m) subsurface structural configuration. The geometry of the shallow structure is poorly known due to a 30-90 m thick Pleistocene till cover. The resolution of the new seismic data is roughly 5-10 times that of existing Vibroseis data. Data quality varies rapidly along the line from exceptional to poor, due primarily to velocity variations associated with the geological complexity of the area. Preliminary results indicate subsurface structural blocks previously envisioned to be several hundreds of meters in size are actually an order of magnitude smaller and more complex. A seismogram-by-seismogram analysis is necessary to confidently identify intricate stratigraphic and structural relationships seen on preliminary CDP sections, as numerous faults, diffractions, and complicated reflection patterns create potential pitfalls. Author (revised)

N94-16308*# National Aeronautics and Space Administration. Lyndon B. Johnson Space Center, Houston, TX.
HETEROGENEOUS PLAGIOCLASE COMPOSITIONS IN THE MARALINGA CK4 CHONDRITE Abstract Only **c90**
Lindsay P. Keller *In* Lunar and Planetary Inst., Twenty-Fourth Lunar and Planetary Science Conference. Part 2: G-M 1993 p 783-784 (For primary document see N94-16173 03-91)
Avail: CASI HC A01/MF A06

One of the characteristic features of CK chondrites is the wide compositional range displayed by feldspar grains in matrix relative to the narrow range of compositions exhibited by the highly equilibrated olivines and pyroxenes. Recently, it was suggested that these heterogeneous feldspar compositions may have been strongly influenced by shock metamorphisms. It is shown that the apparent range of feldspar compositions in Maralinga probably results from annealing during parent body thermal metamorphism rather than shock. The majority of matrix feldspars in Maralinga are typically 50 microns in size and are compositionally zoned, with oligoclase cores (approximately An40) and bytownite rims (approximately An80). The contact between core and rim is sharp and abrupt and is readily observed in backscattered scanning electron microscopy (SEM) images.
Author (revised)

N94-16309*# National Aeronautics and Space Administration. Lyndon B. Johnson Space Center, Houston, TX.
CARBON ABUNDANCES, MAJOR ELEMENT CHEMISTRY, AND MINERALOGY OF HYDRATED INTERPLANETARY DUST PARTICLES Abstract Only **c90**
L. P. Keller, K. L. Thomas (Lockheed Engineering and Sciences Co., Houston, TX.), and D. S. McKay *In* Lunar and Planetary Inst., Twenty-Fourth Lunar and Planetary Science Conference. Part 2: G-M 1993 p 785-786 (For primary document see N94-16173 03-91)
Avail: CASI HC A01/MF A06

Hydrated interplanetary dust particles (IDP's) comprise a major fraction of the interplanetary dust particles collected in the stratosphere. While much is known about the mineralogy and chemistry of hydrated IDP's, little is known about the C abundance in this class of IDP's, the nature of the C-bearing phases, and how the C abundance is related to other physical properties of hydrated IDP's. Bulk compositional data (including C and O) for 11 hydrated IDP's that were subsequently examined by the transition electron microscopy (TEM) to determine their mineralogy and mineral chemistry are reported. Our analysis indicates that these hydrated IDP's are strongly enriched in C relative to the most C-rich meteorites. The average abundance of C in these hydrated IDP's is 4X CI chondrite values. The bulk compositions (including C and O) of 11 hydrated IDP's were determined by thin-window, energy-dispersive x ray (EDX) spectroscopy of the uncoated IDP's on Be substrates in the scanning electron microscopy (SEM). As a check on our C measurements, one of the IDP's (L2006H5) was embedded in glassy S, and microtome thin sections were prepared and placed onto Be substrates. Thin-film EDX analyses of multiple thin sections of L2006H5 show good agreement with the bulk value determined in the SEM. Following EDX analysis, the mineralogy and mineral chemistry of each IDP was determined by analyzing ultramicrotome thin sections in a TEM equipped with an EDX spectrometer. Author (revised)

N94-16310*# Rensselaer Polytechnic Inst., Troy, NY. Dept. of Earth and Environmental Science.
AN INITIAL PERSPECTIVE OF S-ASTEROID SUBTYPES WITHIN ASTEROID FAMILIES Abstract Only **c90**
M. S. Kelley and M. J. Gaffey *In* Lunar and Planetary Inst., Twenty-Fourth Lunar and Planetary Science Conference. Part 2: G-M 1993 p 787-788 (For primary document see N94-16173 03-91)
(Grants NAGw-642; NSF AST-90-12180)
Avail: CASI HC A01/MF A06

Many main belt asteroids cluster around certain values of semi-major axis (a), inclination (i), and eccentricity (e). Hirayama was the first to notice these concentrations which he interpreted as evidence of disruptions of larger parent bodies. He called these clusters 'asteroid families'. The term 'families' is increasingly reserved for genetic associations to distinguish them from clusters of unknown or purely dynamical origin (e.g. the Phocaea cluster). Members of a genetic asteroid family represent fragments derived from various depths within the original parent planetesimal. Thus, family members offer the potential for direct examination of the interiors of parent bodies which have undergone metamorphism and differentiation similar to that occurring in the inaccessible interiors of terrestrial planets. The differentiation similar to that occurring in the inaccessible interiors of terrestrial planets. The condition that genetic family members represent the fragments of a parent object provides a critical test of whether an association (cluster in proper element space) is a genetic family. Compositions (types and relative abundances of materials) of family members must permit the reconstruction of a compositionally plausible parent body. The compositions of proposed family members can be utilized to test the genetic reality of the family and to determine the type and degree of internal differentiation within the parent planetesimal. The interpretation of the S-class mineralogy provides a preliminary evaluation of family memberships. Detailed mineralogical and petrological analysis was done based on the reflectance spectra of 39 S-type asteroids. The result is a division of the S-asteroid class into seven subtypes based on compositional differences. These subtypes, designated S(I) to S(VII), correspond to surface silicate assemblages ranging from monomineralic olivine (dunites) through olivine-pyroxene mixtures to pure pyroxene or pyroxene-feldspar mixtures (basalts). The most general conclusion is that the S-asteroids cannot be treated as a single group of objects without greatly oversimplifying their properties. Each S-subtype needs to be treated as an independent group with a distinct evolutionary history. Author (revised)

N94-16311*# Lockheed Engineering and Sciences Co., Houston, TX.
TIDAL INTERACTION: A POSSIBLE EXPLANATION FOR GEYSERS AND OTHER FLUID PHENOMENA IN THE NEPTUNE-TRITON SYSTEM Abstract Only
W. D. Kelly and C. L. Wood *In* Lunar and Planetary Inst., Twenty-Fourth Lunar and Planetary Science Conference. Part 2: G-M 1993 p 789-790 (For primary document see N94-16173 03-91)
Avail: CASI HC A01/MF A06

Discovery of geyser-like plumes on the surface of Triton was a highlight of Voyager 2's passage through the Neptune planetary system. Remarkable as these observations were, they were not entirely without precedent. Considering the confirmed predictions for the 1979 Voyager Jovian passage, it was logical to consider other solar system bodies beside Io where tidal effects could be a significant factor in surface processes. It was our intuition that the Neptune-Triton gravitational bond acting at high inclination to the Neptune equator and the fact that Neptune was a fluid body was significant oblateness would produce tidal and mechanical forces that could be transformed into thermal energy vented on Triton's surface. Prior to the Voyager flyby, others have noted that capture and evolution of Triton's orbit from extreme eccentricity to near circular state today would have

resulted in significant tidal heating, but these analysts disregard current day forces. Our calculations indicate that the time varying forces between Neptune-Triton fall midway between those exerted in the Earth-Moon and Jupiter-Io systems, and considering the low level of other energy inputs, this source of internal energy should not be ignored when seeking an explanation for surface activity. In each planet-satellite case, residual or steady-state eccentricity causes time-varying stresses on internal satellite strata. In the case of Jupiter the residual eccentricity is due largely to Galilean satellite interactions, particularly Io-Europa, but in the case of Neptune-Triton, it is the effect of Triton's inclined orbit about an oblate primary. Author (revised)

N94-16312*# Academy of Sciences (USSR), Saint Petersburg. Mobile Vehicle Engineering Inst.

INTERNATIONAL TESTING OF A MARS ROVER PROTOTYPE Abstract Only

Alexsandr Leonovich Kemurjian, V. Linkin (Academy of Sciences, USSR, Moscow.), and L. Friedman (Planetary Society, Pasadena, CA.) *In* Lunar and Planetary Inst., Twenty-Fourth Lunar and Planetary Science Conference. Part 2: G-M 1993 p 791 (For primary document see N94-16173 03-91)

Avail: CASI HC A01/MF A06

Tests on a prototype engineering model of the Russian Mars 96 Rover were conducted by an international team in and near Death Valley in the United States in late May, 1992. These tests were part of a comprehensive design and testing program initiated by the three Russian groups responsible for the rover development. The specific objectives of the May tests were: (1) evaluate rover performance over different Mars-like terrains; (2) evaluate state-of-the-art teleoperation and autonomy development for Mars rover command, control and navigation; and (3) organize an international team to contribute expertise and capability on the rover development for the flight project. The range and performance that can be planned for the Mars mission is dependent on the degree of autonomy that will be possible to implement on the mission. Current plans are for limited autonomy, with Earth-based teleoperation for the nominal navigation system. Several types of television systems are being investigated for inclusion in the navigation system including panoramic camera, stereo, and framing cameras. The tests used each of these in teleoperation experiments. Experiments were included to consider use of such TV data in autonomy algorithms. Image processing and some aspects of closed-loop control software were also tested. A micro-rover was tested to help consider the value of such a device as a payload supplement to the main rover. The concept is for the micro-rover to serve like a mobile hand, with its own sensors including a television camera. Author (revised)

N94-16313*# California Inst. of Tech., Pasadena. Div. of Geology and Planetary Sciences.

AN EXPERIMENTAL STUDY OF TRACE ELEMENT PARTITIONING BETWEEN PEROVSKITE, HIBONITE AND MELT: EQUILIBRIUM VALUES Abstract Only **c25**

A. K. Kennedy, G. E. Lofgren (National Aeronautics and Space Administration. Lyndon B. Johnson Space Center, Houston, TX.), and G. J. Wasserburg *In* Lunar and Planetary Inst., Twenty-Fourth Lunar and Planetary Science Conference. Part 2: G-M 1993 p 793-794 (For primary document see N94-16173 03-91)

Avail: CASI HC A01/MF A06

The presence of perovskite (CATiO3) and hibonite (Ca Al12O19) within different regions of Calcium-, Aluminum-rich Inclusions (CAI) and the trace element concentrations of these minerals in each circumstance, constrain models of precursor formation, nebular condensation, the thermal history of inclusions with relict perovskite and hibonite, and the formation of the Wark-Lovering rim. At present mineral/melt partition coefficient data for hibonite are limited to a few elements in simple experimental systems, or to those derived from hibonite-glass pairs in hibonite/glass microspherules. Similarly, there is only limited data on perovskite D that are applicable to meteorite compositions. Apart from the importance of partitioning studies to meteorite research, D values also are invaluable in the development of thermodynamic models, especially when data is available for a large number of elements that have different ionic charge and radii. In addition, study of the effect of rapid cooling on partitioning is crucial to our understanding of meteorite inclusions. To expand our knowledge of mineral/melt D for perovskite and hibonite, a study was instituted where D values are obtained in both equilibrium and dynamic cooling experiments. As an initial phase of this study mineral/melt D was measured for major elements (Ca, Mg, Al, Ti, and Si), 15 rare earth elements (La-Lu) and 8 other elements (Ba, Sr, U, Th, Nb, Zr, Hf, and Ge) in perovskite and hibonite grown under equilibrium conditions, in bulk compositions that are respectively similar to Compact Type A (CTA) CAI and to a hibonite/glass microspherule. Experimental mixes were doped with REE at 20-50x chondritic (ch) abundances, Ba at 50 ppm, Sr, Hf, Nb, and Zr at 100 ppm and, U and Th at 200 ppm. Trace element abundances were measured with the PANURGE ion microprobe. Major element compositions were obtained by electron microprobe analysis. Author (revised)

N94-16314*# California Univ., San Diego, La Jolla. Dept. of Chemistry.

NITROGEN ISOTOPIC SIGNATURES IN AGGLUTINATES FROM BRECCIA 79035 Abstract Only **c25**

John F. Kerridge, Yoosook Kim, Jin S. Kim, and Kurt Marti *In* Lunar and Planetary Inst., Twenty-Fourth Lunar and Planetary Science Conference. Part 2: G-M 1993 p 795-796 (For primary document see N94-16173 03-91)

Avail: CASI HC A01/MF A06

Agglutinates in the size range 125-175 microns from regolith breccia 79035 are substantially depleted in N compared with bulk 79035. Isotopically, agglutinate N closely resembles that found previously in ilmenite separates. The minimum (delta)N-15 value found during stepwise pyrolysis of agglutinates is significantly heavier than that observed for bulk 79035. The major host phase for trapped N in 79035, and the host phase of the lightest isotopic component(s), remain unidentified. Author (revised)

N94-16315*# National Aeronautics and Space Administration. Goddard Space Flight Center, Greenbelt, MD.

AN INVERSION OF GEOID AND TOPOGRAPHY FOR MANTLE AND CRUSTAL STRUCTURE ON MARS Abstract Only

Walter Kiefer, Bruce Bills, Herb Frey, Steve Nerem, Jim Roark, and Maria Zuber *In* Lunar and Planetary Inst., Twenty-Fourth Lunar and Planetary Science Conference. Part 2: G-M 1993 p 797-798 (For primary document see N94-16173 03-91)

Avail: CASI HC A01/MF A06

Mars has the largest amplitude geoid anomalies and surface topography known on the terrestrial planets. A number of prior studies have analyzed Martian gravity anomalies and topography in terms of isostasy and flexure of the crust and lithosphere. Other studies have emphasized the role of mantle convection in producing gravity anomalies and topography in some regions of Mars. Geoid and topography observations for simultaneous estimates of density anomalies in the crust and mantle of Mars are inverted. In performing this study, a recent degree 50 spherical harmonic expansion of the Martian gravity field (GMM-l) and a corresponding resolution expansion of the USGS Mars topography model are used. However, our analysis is restricted to harmonic degrees up to L equals 25, which are better determined than the higher harmonics. This provides a half-wavelength horizontal resolution of 425 km. Author (revised)

N94-16316*# Lancaster Univ. (England). Environmental Science Div.

LAVA CRUSTS AND FLOW DYNAMICS Abstract Only **c46**

C. R. J. Kilburn *In* Lunar and Planetary Inst., Twenty-Fourth Lunar and Planetary Science Conference. Part 2: G-M 1993 p 799 (For primary document see N94-16173 03-91)

Avail: CASI HC A01/MF A06

Lava flows can be considered as hot viscous cores within thinner, solidified crusts. Interaction between crust and core determines a flow's morphological and dynamical evolution. When the lava core dominates, flow advance approaches a steady state. When crusts are the limiting factor, advance is more irregular. These two conditions can be distinguished by a timescale ratio comparing rates of core deformation and crustal formation. Aa and budding pahoehoe lavas are used as examples of core- and crustal-dominated flows, respectively. A simple model describes the transition between pahoehoe and aa flow in terms of lava discharge rate, underlying slope, and either the thickness or velocity of the flow front. The model shows that aa morphologies are characterized by higher discharge rates and frontal velocities and yields good quantitative agreement with empirical relations distinguishing pahoehoe and aa emplacement on Hawaii. Author (revised)

N94-16317*# California Univ., San Diego, La Jolla. Dept. of Chemistry.
ISOTOPIC SIGNATURES AND DISTRIBUTION OF NITROGEN AND TRAPPED AND RADIOGENIC XENON IN THE ACAPULCO AND FRO90011 METEORITES Abstract Only **c90**
Y. Kim and K. Marti *In* Lunar and Planetary Inst., Twenty-Fourth Lunar and Planetary Science Conference. Part 2: G-M 1993 p 801-802 (For primary document see N94-16173 03-91)
Avail: CASI HC A01/MF A06

Acapulco metal and silicate show distinct N isotopic signatures. Trapped heavy noble gases are carried by 'magnetic' opx and radiogenic Xe-129 excesses are observed in phosphate and in minor surficial phases on metal grains. N and Xe isotopic signatures in FRO90011 do not agree with those observed in Acapulco. The Acapulco meteorite is unique in having achondritic texture and chondritic composition. Its mineralogical study shows the record of high temperature (1100 C) recrystallization. However, this meteorite shows abundances of volatile elements close to the levels observed in carbonaceous chondrites and concentrations of heavy noble gases comparable to those observed in type 4 ordinary chondrites, not expected for a presumed highly equilibrated object. Nitrogen measurements in bulk Acapulco revealed two different isotopic signatures, in apparent conflict with evidence for a high degree of recrystallization. N and Xe were studied in separated mineral phases to search for the carriers in order to better understand the formation and thermal history of the Acapulco parent body. Author (revised)

N94-16318*# Geological Survey, Flagstaff, AZ.
SEPARATION OF TOPOGRAPHIC AND INTRINSIC BACKSCATTER VARIATIONS IN BISCOPIC RADAR IMAGES: A MAGIC AIRBRUSH Abstract Only **c43**
R. L. Kirk *In* Lunar and Planetary Inst., Twenty-Fourth Lunar and Planetary Science Conference. Part 2: G-M 1993 p 803-804 (For primary document see N94-16173 03-91)
Avail: CASI HC A01/MF A06

Shaded-relief maps portraying landforms as they would appear in the absence of variations in the intrinsic brightness of the surface are a venerable and extremely useful tool in planetary geology. Such maps have traditionally been produced by a highly labor intensive manual process. Skilled cartographer-artists develop detailed mental images of landforms by meticulous scrutiny of all available data, and are able to use an airbrush and electric eraser to draw these images on a map. This process becomes increasingly time-consuming or even impossible if - as is true for radar data in general and Magellan data in particular - the effects on image brightness of varying scattering properties greatly outweigh those of slope variations. Because of the difficulty of interpreting relief in the Magellan images, the airbrush technique is being used only to remove obvious artifacts from low-resolution, shaded-relief images computed digitally from altimetric data. A surprisingly simple digital-processing technique that can be applied to pairs of radar images to produce shaded-relief-like results at the full image resolution is described. These shaded-relief images can be used not only as base maps, but to improve the accuracy of quantitative topographic mapping by radarclinometry and stereoanalysis.
Author (revised)

N94-16319*# Geological Survey, Flagstaff, AZ.
GLOBAL MAGELLAN-IMAGE MAP OF VENUS AT FULL RESOLUTION Abstract Only
R. L. Kirk, K. B. Edwards, H. F. Morgan, L. A. Soderblom, and T. L. Stoewe *In* Lunar and Planetary Inst., Twenty-Fourth Lunar and Planetary Science Conference. Part 2: G-M 1993 p 805-806 (For primary document see N94-16173 03-91)
Avail: CASI HC A01/MF A06

During its first 243-day mapping cycle, the Magellan spacecraft succeeded in imaging 84 percent of the surface of Venus at resolutions on the order of 100 meters; subsequent cycles have increased the total coverage to over 97 percent and provided redundant coverage of much of the planet with differing viewing geometries. Unfortunately, this full-resolution global dataset is in the form of thousands of individual orbit tracks (F-BIDR's) whose length-to-width ratio of nearly 1000:1 makes them minimally useful unless mosaicked. The Magellan project produced full-resolution mosaics (F-MIDR's) only for selected regions on the planet, whereas a global set of mosaics was made only at threefold degraded resolution (C1-MIDR's). Furthermore, although the F-MIDR's, which are approximately equidimensional, are much better suited for scientific interpretation than the F-BIDR's, they are still an unwieldy dataset: over 1500 quadrangles, each showing a region only about 600 km on a side, would be required to cover the entire planet. The USGS has therefore undertaken to produce and distribute a global, full resolution set of mosaics of the Magellan image data in a format that will be efficient for both hardcopy and digital use. The initial motivation was that it would provide an efficient means of verifying the integrity of the F-BIDR's to be archived on computer-compatible tape at the USGS Flagstaff facility. However, the resulting product, known as the FMAP, should also serve as an important resource for future scientific interpretation. It will offer several advantages beyond global coverage at full resolution. The first, alluded to above, is its division of the planet's surface to minimize the number of quadrangles and maximize their area, subject to the limits on the number of pixels imposed by state-of-the-art digital recording media and hardcopy output devices. The second, the use of improved 'cosmetic' processing techniques, will greatly reduce tonal discontinuities between component F-BIDR's in the FMAP compared to the standard Magellan mosaic products. Finally, wherever possible, the FMAP will incorporate data that were unavailable (e.g., because of processing delays) when the standard MIDR products were created, as well as data that were reprocessed to improve their radiometric or geometric quality.
Author (revised)

N94-16320*# Geological Survey, Flagstaff, AZ.
THE CARTOGRAPHY OF VENUS WITH MAGELLAN DATA Abstract Only
R. L. Kirk, H. F. Morgan, and J. F. Russell *In* Lunar and Planetary Inst., Twenty-Fourth Lunar and Planetary Science Conference. Part 2: G-M 1993 p 807 (For primary document see N94-16173 03-91)
Avail: CASI HC A01/MF A06

Maps of Venus based on Magellan data are being compiled at 1:50,000,000, 1:5,000,000 and 1:1,500,000 scales. Topographic contour lines based on radar altimetry data are overprinted on the image maps, along with feature nomenclature. Map controls are based on existing knowledge of the spacecraft orbit; photogrammetric triangulation, a traditional basis for geodetic control for bodies where framing cameras were used, is not feasible with the radar images of Venus. Preliminary synthetic aperture radar (SAR) image maps have some data gaps and cosmetic inconsistencies, which will be corrected on final compilations. Eventual revision of geodetic controls and of the adopted Venusian spin-axis location will result in geometric adjustments, particularly on large-scale maps. Author

N94-16321*# Wien Univ. (Austria). Inst. of Geochemistry.
OSMIUM ISOTOPES IN IVORY COAST TEKTITES: CONFIRMATION OF A METEORITIC COMPONENT AND RHENIUM DEPLETION Abstract Only **c90**
Christian Koeberl and Steven B. Shirey (Carnegie Institution of Washington, DC.) *In* Lunar and Planetary Inst., Twenty-Fourth Lunar and Planetary Science Conference. Part 2: G-M 1993 p 809-810 (For primary document see N94-16173 03-91)
(Grant NSF EAR-92-18847; FWF Proj. P9026-GEO)
Avail: CASI HC A01/MF A06

The sensitive negative thermal ionization mass spectrometry method was used for the measurement of concentrations and isotopic ratios of osmium and rhenium in four Ivory Coast tektites. These tektites have crustal major and trace element composition, as well as large negative epsilon(sub Nd)(-20) and positive epsilon(sub Sr)(+260 to +300) which are characteristic for old continental crust. Os concentrations ranging from 0.09 to 0.30 ppb were found, clearly much higher than average crustal values, Os-187/Os-186 ratios of about 1.2-1.7, and low Re-187/Os-186 ratios. These results show unambiguously the existence of a meteoritic component (on the order of 0.06%) in the Ivory Coast tektites. Low Re abundances are the result of fractionation of Re during the impact.
Author (revised)

N94-16322*# Wien Univ. (Austria). Inst. of Geochemistry.
MANSON IMPACT STRUCTURE, IOWA: FIRST GEOCHEMICAL RESULTS FOR DRILL CORE M-1 **c46**
Christian Koeberl, Raymond R. Anderson (Geological Survey, Iowa City, IA.), Jack B. Hartung (Geological Survey, Iowa City, IA.), and Wolf Uwe Reimold (Witwatersrand Univ., Johannesburg, South Africa.) *In* Lunar and Planetary Inst., Twenty-Fourth Lunar and Planetary Science Conference.

Part 2: G-M 1993 p 811-812 (For primary document see N94-16173 03-91)
(FWF Proj. P8794-GEO)
Avail: CASI HC A01/MF A06

The Manson Impact Structure is a large complex impact crater centered ca. S km north of the town of Manson, Iowa. It is the largest intact impact structure recognized in the United States (35 km in diameter). Its Ar-40/Ar-39 age is indistinguishable from that of the Cretaceous-Tertiary (K-T) boundary. The Manson structure may be one element of the events at the K-T boundary. The crater is completely covered by Quaternary glacial sedimentary deposits that are normally underlain by Cretaceous clastic sediments and flat-lying carbonate sediments of Phanerozoic age, as well as Proterozoic red clastic, metamorphic, volcanic, and plutonic rock sequences. The study of a reflection seismic profile, provided by Amoco, was critical in interpreting the structure. In the 35 km diameter zone that marks the extension of the crater the normal rock sequence is disturbed due to the impact, and at the center of the structure granitic basement rocks are present that have been uplifted from about 4 km depth. Our studies consist of detailed petrological and geochemical characterization of all cores, with emphasis on a detailed description of all rock types found in the core samples and their relationship to target rocks. Geochemical data on samples from the Manson M-1 core are presented. Author (revised)

N94-16323*# Deutsche Forschungsanstalt fuer Luft- und Raumfahrt, Oberpfaffenhofen (Germany). Inst. for Planetary Exploration.
AGE DETERMINATIONS AND EARTH-BASED MULTISPECTRAL OBSERVATIONS OF LUNAR LIGHT PLAINS Abstract Only
U. Koehler, R. Jaumann, and G. Neukum *In* Lunar and Planetary Inst., Twenty-Fourth Lunar and Planetary Science Conference. Part 2: G-M 1993 p 813-814 (For primary document see N94-16173 03-91)
Avail: CASI HC A01/MF A06

The history of light plains still remains doubtful, but there are good arguments - mainly obtained by age determinations and supported by multispectral observations - for an endogenic (magmatic) instead of an (exclusively) impact related origin. Light plains are characterized by smooth areas with an albedo lower than the surrounding highlands (12 - 13 percent), but significantly higher than maria (5 - 6 percent). Before Apollo 16 a volcanic source has been supposed, but analysis of returned samples (highly brecciated and metamorphosed rocks) favored an impact ejecta related origin. Among the currently discussed models are formation by ejecta sedimentation from multi-ringed basins, formation by secondary and tertiary cratering action of ballistically ejected material during the formation of multi-ringed basins, in situ formation by impact melt of large events, and premare (crypto-) volcanism basalts covered by a thin ejecta cover; younger impacts penetrated the ejecta surface to create the dark haloed craters. To find arguments in favor or against these ideas the chronology of light plains is of major importance. Obviously a genetic relationship between the evolution of light plains and the basin forming impacts can be possible only if the events of emplacement features happened simultaneously. Author (revised)

N94-16324*# Arizona Univ., Tucson. Lunar and Planetary Lab.
MEANDER PROPERTIES OF VENUSIAN CHANNELS Abstract Only
G. Komatsu and V. R. Baker *In* Lunar and Planetary Inst., Twenty-Fourth Lunar and Planetary Science Conference. Part 2: G-M 1993 p 815-816 (For primary document see N94-16173 03-91)
Avail: CASI HC A01/MF A06

Venusian lava channels have meander dimensions that relate to their mode of formation. Their meander properties generally follow terrestrial river trends of wavelength (L) to width (W) ratios, suggesting an equilibrium adjustment of channel form. Slightly higher L/W for many Venusian channels in comparison to terrestrial rivers may relate to nonaqueous flow processes. The unusually low L/W values for some Venusian and lunar sinuous rilles probably indicate modification of original meander patterns by lava-erosional channel widening. Author (revised)

N94-16325*# Academy of Sciences (USSR), Moscow.
TERRESTRIAL BITUMEN ANALOGUE OF ORGUEIL ORGANIC MATERIAL DEMONSTRATES HIGH SENSITIVITY TO USUAL HF-HCl TREATMENT Abstract Only **c23**
A. V. Korochantsev and O. V. Nikolaeva *In* Lunar and Planetary Inst., Twenty-Fourth Lunar and Planetary Science Conference. Part 2: G-M 1993 p 817-818 (For primary document see N94-16173 03-91)
Avail: CASI HC A01/MF A06

The relationship between the chemical composition and the interlayer spacing (d002) of organic materials (OM's) is known for various terrestrial OM's. We improved this general trend by correlation with corresponding trend of natural solid bitumens (asphaltite-kerite-anthraxolite) up to graphite. Using the improved trend we identified bitumen analogs of carbonaceous chondrite OM's residued after HF-HCl treatment. Our laboratory experiment revealed that these analogs and, hence, structure and chemical composition of carbonaceous chondrite OM's are very sensitive to the HF-HCl treatment. So, usual extraction of OM from carbonaceous chondrites may change significantly structural and chemical composition of extracted OM.
Author (revised)

N94-16326*# Washington Univ., Saint Louis, MO. Dept. of Earth and Planetary Sciences.
COMPOSITION OF APOLLO 17 CORE 76001 Abstract Only
Randy L. Korotev and Kaylynn M. Bishop *In* Lunar and Planetary Inst., Twenty-Fourth Lunar and Planetary Science Conference. Part 2: G-M 1993 p 819-820 (For primary document see N94-16173 03-91)
(Grant NAG9-56)
Avail: CASI HC A01/MF A06

Core 76001 is a single drive tube containing a column of regolith taken at the base of the North Massif, station 6, Apollo 17. The core material is believed to have accumulated through slow downslope mass wasting from the massif. As a consequence, the core soil is mature throughout its length. Results of INAA for samples taken every half centimeter along the length of the core indicate that there is only minor systematic compositional variation with depth. Concentrations of elements primarily associated with mare basalt (Sc, Fe) and noritic impact melt breccia (Sm) decrease slightly with depth, particularly between 20 cm and the bottom of the core at 32 cm depth. This is consistent with petrographic studies that indicate a greater proportion of basalt and melt breccia in the top part of the core. However, Sm/Sc and La/Sm ratios are remarkably constant with depth, indicating no variation in the ratio of mare material to Sm-rich highlands material with depth. Other than these subtle changes, there is no compositional evidence for the two stratigraphic units (0-20 cm and 20-32 cm) defined on the basis of modal petrography, although all samples with anomalously high Ni concentrations (Fe-Ni metal nuggets) occur above 20 cm depth. Author (revised)

N94-16327*# Washington Univ., Saint Louis, MO. Dept. of Earth and Planetary Sciences.
COMPOSITION AND MATURITY OF THE 60013/14 CORE Abstract Only
Randy L. Korotev, Richard V. Morris (National Aeronautics and Space Administration. Lyndon B. Johnson Space Center, Houston, TX.), and Howard V. Lauer, Jr. (Lockheed Engineering and Sciences Co., Houston, TX.) *In* Lunar and Planetary Inst., Twenty-Fourth Lunar and Planetary Science Conference. Part 2: G-M 1993 p 821-822 (For primary document see N94-16173 03-91)
Avail: CASI HC A01/MF A06

The 60013/14 double drive tube (62 cm deep) is one of three regolith cores taken 35-40 m apart in a triangular array on the Cayley plains at station 10' (LM/ALSEP), Apollo 16. This trio, which includes double drive tube 60009/10 (59 cm deep) and deep drill core 60001-7 (220 cm), is the only such array of cores returned from the Moon. The top 45 cm of 60013/14 is mature, as is surface reference soil 60601 taken nearby. Maturity generally decreases with depth, with soil below 45 cm being submature. The zone of lowest maturity (34 is less than or equal to I(sub s)/FeO is less than 50) extends from 46 to 58 cm depth, and corresponds to the distinct region of light-colored soil observed during core processing. In the other two cores, most of the compositional variation results from mixing between fine-grained, mature soil with 10-11 micro-g/g Sc and coarse-grained ferroan anorthosite consisting of greater than 99% plagioclase with less than 0.5 micro-g/g Sc. This is most evident in 60009/10 which contains a high abundance of plagioclase at about 54 cm depth (minimum Sc: 3-4 micro-g/g); a similar zone occurs in 60001-7 at 17-22 cm (MPU-C), although it is not as rich in plagioclase (minimum Sc: 6-7 micro-g/g). Compositional variations are less in 60013/14 than in the other two cores (range: 7.9-10.0 micro-g/g Sc), but are generally consistent with

the 'plagioclase dilution' effect seen in 60009/10, i.e., most 60013/14 samples plot along the mixing line of 60009/10. However, a plagioclase component is not the cause of the lower maturity and lighter color of the unit at 46-58 cm depth in 60013/14. Many of the samples in this zone have distinctly lower Sm/Sc ratios than typical LM-area soils and plot off the mixing trend defined by 60009/10. This requires a component with moderately high Sc, but low-Sm/Sc, such as feldspathic fragmental breccia (FFB) or granulitic breccia. A component of Descartes regolith, such as occurs at North Ray Crater (NRC) and which is rich in FFB, could account for the composition of these soils (i.e., a 3:1 mixture of 60601 and NRC soil). It seems unlikely that NRC ejecta would occur half a meter deep at the LM station, thus this low-Sm/Sc component may result from an older, local crater that penetrated the Cayley surface layer and excavated underlying Descartes material, as did North Ray Crater. There is no evidence for such a unit or component in the other two cores. Soil below the light-colored unit (58-62) cm has 'typical' Sm/Sc ratios, but the lowest absolute Sc concentrations, i.e., it is compositionally equivalent to a mixture of surface soil and plagioclase such as that in ferroan anorthosite. This is the only soil that might be related to the plagioclase-rich units in the other two cores. Except for the mature soil at the top of each core and, perhaps, the plagioclase-rich layers, there is little compositional evidence for any common unit among the three cores. Soil corresponding to the mare-glass-bearing unit (MPU-B) and regolith-breccia-bearing unit (MPU-A) of 60001-7 do not occur in 60013/14 or 60009/10. Author (revised)

N94-16328*# Arizona Univ., Tucson. Lunar and Planetary Lab.

CAT MOUNTAIN: A METEORITIC SAMPLE OF AN IMPACT-MELTED CHONDRITIC ASTEROID Abstract Only **c90**

David A. Kring *In* Lunar and Planetary Inst., Twenty-Fourth Lunar and Planetary Science Conference. Part 2: G-M 1993 p 823-824 (For primary document see N94-16173 03-91)

Avail: CASI HC A01/MF A06

Although impact cratering and collisional disruption are the dominant geologic processes affecting asteroids, samples of impact melt breccias comprise less than 1 percent of ordinary chondritic material and none exist among enstatite and carbonaceous chondrite groups. Because the average collisional velocity among asteroids is sufficiently large to produce impact melts, this paucity of impact-melted material is generally believed to be a sampling bias, making it difficult to determine the evolutionary history of chondritic bodies and how impact processes may have affected the physical properties of asteroids (e.g., their structural integrity and reflectance spectra). To help address these and related issues, the first petrographic description of a new chondritic impact melt breccia sample, tentatively named Cat Mountain, is presented. Author (revised)

N94-16329*# Polish Academy of Sciences, Warsaw. Inst. of Geophysics.

COMPARATIVE MAGNETIC AND THERMOANALYTICAL STUDY OF TWO ENSTATITE CHONDRITES: ADHI KOT AND ATLANTA Abstract Only **c90**

Elizabeth Krol and Bruno Lang (Warsaw Univ., Poland.) *In* Lunar and Planetary Inst., Twenty-Fourth Lunar and Planetary Science Conference. Part 2: G-M 1993 p 825-826 (For primary document see N94-16173 03-91)

Avail: CASI HC A01/MF A06

With allowance for the discussion of classification of enstatite chondrites and their relation to aubrites, the obtained magnetic and thermoanalytical data is submitted to be considered as additive arguments. Our study covered the Adhi Kot (EH4) and Atlanta (EL6). meteorites belonging to two distinct groups of enstatite chondrites. Applying AF demagnetization the intensity of natural remanent magnetization (NRM) was measured and the mean magnetic susceptibility of the samples was determined. The differential thermal (DTA) and thermogravimetric (TG) curves were obtained for meteorites under study. For measurements of the intensity of NRM, a superconducting cryomagnetometer SQUID (2 G Enterprise, USA), while magnetic susceptibility Kappabridge KLY-2 (Czechoslovakia) were used. The abbreviated magnetic data sheets are given. The values 786 x 10(exp -4)A/mkg and 196.1 x 10(exp -4)A/mkg were obtained as NRM intensities for Atlanta and Adhi Kot respectively, while 17.4 x 10(exp -6) Slu/kg and 43.4 x 10(exp -6) Slu/kg for their susceptibilities. Both meteorites proved to be strongly magnetized. The demagnetization down to 3.2 percent of NMR was received for Atlanta at AF field intensity of 250 Oe. For Adhi Kot at this level rested 13.2 percent of NRM intensity, this sample being demagnetized without change of direction till 750 Oe field. The demagnetization curves are similar to those obtained for Abee (EL4) chondrite by Sugiura and Strangway. Against Abee the Adhi Kot exhibited a little bit steeper downfall, and in both cases dominate one component of magnetization. The DTA and TG curves were obtained with Rigaku-Denki thermoanalytical instrument. The DTA curves exhibit striking similarity in their shape and relatively close temperature values for various features. The same is valid for TG curves. The higher values for TG for Adhi Kot express its higher content of oxydable (Fe, Ni) whose oxidation in air is reached at 1000-1200 C. Author (revised)

N94-16330*# California Univ., Los Angeles. Inst. of Geophysics and Planetary Physics.

CHROMITE-RICH MAFIC SILICATE CHONDRULES IN ORDINARY CHONDRITES: FORMATION BY IMPACT MELTING Abstract Only **c90**

Alexander N. Krot and Alan E. Rubin *In* Lunar and Planetary Inst., Twenty-Fourth Lunar and Planetary Science Conference. Part 2: G-M 1993 p 827-828 (For primary document see N94-16173 03-91)

Avail: CASI HC A01/MF A06

Chromium-rich chondrules constitute less than 0.1 percent of all ordinary chondrite (OC) chondrules and comprise three groups: chromian-spinel chondrules, chromian-spinel inclusions, and chromite-rich mafic silicate (CRMS) chondrules. Chromian-spinel chondrules (typically 100-300 microns in apparent diameter) exhibit granular, porphyritic and unusual textures and occur mainly in H chondrites. Their morphologies are distinct from the irregularly shaped chromian-spinel inclusions of similar mineralogy. Chromian-spinel chondrules and inclusions consist of grains of chromian-spinel embedded in plagioclase (Pl) or mesostasis of Pl composition. Many also contain accessory ilmenite (Ilm), high-Ca pyroxene (Px), merrillite (Mer), and rare olivine (Ol); some exhibit concentric mineral and chemical zoning. CRMS chondrules (300-1100 microns in apparent diameter) are generally larger than chromian-spinel chondrules and occur in all metamorphosed OC groups. Most CRMS chondrules are nearly spherical although a few are ellipsoidal with a/b aspect ratios ranging up to 1.7. Textures include cryptocrystalline, granular, radial, barred, and porphyritic varieties; some contain apparently relict grains. The chondrules consist of chromite (Chr), Ol and Pl, along with accessory Mer, troilite (Tr), metallic Fe-Ni (Met), Px and Ilm. The mesostasis in CRMS chondrules is nearly opaque in transmitted light; thus, they can be easily recognized in the optical microscope. Based on the similarity of mineralogy and chemistry between CRMS chondrules of different textures (opaque chromite-rich mesostasis, skeletal morphology of Ol grains, similar bulk compositions) we suggest that these chondrules form a genetically related population. Author (revised)

N94-16331*# California Inst. of Tech., Pasadena. Div. of Geological and Planetary Sciences.

EVAPORATION KINETICS OF Mg_2SiO_4 CRYSTALS AND MELTS FROM MOLECULAR DYNAMICS SIMULATIONS Abstract Only **c76**

J. D. Kubicki and E. M. Stolper *In* Lunar and Planetary Inst., Twenty-Fourth Lunar and Planetary Science Conference. Part 2: G-M 1993 p 829-830 (For primary document see N94-16173 03-91)

Avail: CASI HC A01/MF A06

Computer simulations based on the molecular dynamics (MD) technique were used to study the mechanisms and kinetics of free evaporation from crystalline and molten forsterite (i.e., Mg_2SiO_4) on an atomic level. The interatomic potential employed for these simulations reproduces the energetics of bonding in forsterite and in gas-phase MgO and SiO_2 reasonably accurately. Results of the simulation include predicted evaporation rates, diffusion rates, and reaction mechanisms for Mg_2SiO_4(s or l) yields $2Mg(g) + 2O(g) + SiO_2(g)$. Author (revised)

N94-16332*# Jet Propulsion Lab., California Inst. of Tech., Pasadena.

SPECTRAL STUDY OF VENUS GLOBAL TOPOGRAPHY AND GEOID FROM MAGELLAN AND PVO DATA Abstract Only

A. B. Kucinskas, N. J. Borderies, and D. L. Turcotte (Cornell Univ., Ithaca, NY.) *In* Lunar and Planetary Inst., Twenty-Fourth Lunar and Planetary Science Conference. Part 2: G-M 1993 p 831-832 (For primary document see N94-16173 03-91)

Avail: CASI HC A01/MF A06

An analysis of newly available global harmonic models for topography

and geoid on Venus was conducted. It was found that the power spectral density for Venus topography has a power law dependence on wave-number characteristic of Brown Noise, similar to what is found for the Earth. However, the Venus topography spectrum presents a rollover at lower degree (l = 3) than is observed for the Earth spectrum and has smaller amplitudes than that of the Earth's. The Venus geoid also obeys a power law relationship, at least for small values of l, but with a smaller slope and more power (for l greater than 3) than the Earth geoid. Author (revised)

N94-16333*# Pittsburgh State Univ., KS.

VERTICAL STRUCTURE MODELS OF THE 1990 EQUATORIAL DISTURBANCE ON SATURN Abstract Only

D. M. Kuehn, Christopher Dwight Barnet (Institute for Space and Terrestrial Science, Concord, Ontario.), and R. F. Beebe (New Mexico State Univ., University Park.) *In* Lunar and Planetary Inst., Twenty-Fourth Lunar and Planetary Science Conference. Part 2: G-M 1993 p 833 (For primary document see N94-16173 03-91)

Avail: CASI HC A01/MF A06

In September 1990, an atmospheric disturbance in the form of an abnormally high albedo area developed in the equatorial region of Saturn. Events of this nature are exceedingly rare for this planet as they have been detected in the equatorial region on only two other occasions in over a century. In ongoing monitoring of the atmospheres of the outer planets, CCD imaging observations of Saturn by New Mexico State University's Tortugas Mountain Station were made before, during, and after the disturbance's formation through both broad-band filters and narrow-band visible/near-IR filters centered in methane absorption bands. Also, multispectral Hubble Space Telescope observations were made within weeks of the event and later in 1991. These observations were calibrated and scans of reflectivity at constant latitude are being modeled with a vertically inhomogeneous, multiple scattering model previously used to model Jupiter's South Equatorial Belt brightening event in 1989. In addition, the reflectivity of the disturbance as a function of the scattering angles is being obtained so as to model this feature's vertical structure in particular. A preliminary report of the modeling results will be presented. Author (revised)

N94-16334*# Geological Survey, Reston, VA.

PRELIMINARY Ar-40/Ar-39 AGE SPECTRUM AND LASER PROBE DATING OF THE M1 CORE OF THE MANSON IMPACT STRUCTURE, IOWA: A K-T BOUNDARY CRATER CANDIDATE Abstract Only c46

M. J. Kunk, L. W. Snee (Geological Survey, Denver, CO.), B. M. French (National Aeronautics and Space Administration, Washington, DC.), S. S. Harlan (Geological Survey, Denver, CO.), and J. J. McGee *In* Lunar and Planetary Inst., Twenty-Fourth Lunar and Planetary Science Conference. Part 2: G-M 1993 p 835-836 (For primary document see N94-16173 03-91)

Avail: CASI HC A01/MF A06

Preliminary Ar-40/Ar-39 age spectrum and laser probe dating results from new drill core from the 35-km-diameter Manson Impact Structure (MIS), Iowa indicates a reasonable possibility that the MIS is a Cretaceous-Tertiary (K-T) boundary impact event. Several different types of samples from a melt-matrix breccia, a unit of apparent crater fill intersected by the M1 core, were analyzed. Ar-40/Ar-39 results from these samples indicate a maximum age for the MIS of about 65.4 plus or minus 0.4(2 sigma) Ma. Petrographic analyses of the samples indicate a high probability that all the dated samples from the melt-matrix breccia contain relict grains that were not entirely melted or degassed at the time of impact, suggesting that the actual age of the MIS could be somewhat younger than our preliminary results indicate. The results are consistent with a previously published age estimate of shocked microcline from the MIS central uplift of 65.7 plus or minus 1.0 Ma. Author (revised)

N94-16335*# Tokyo Univ. (Japan). Dept. of Earth and Planetary Physics.

WAS MARTIAN MANTLE WET? A POSSIBLE CONSEQUENCE OF RAPID CORE FORMATION Abstract Only

Kiyoshi Kuramoto and Takafumi Matsui *In* Lunar and Planetary Inst., Twenty-Fourth Lunar and Planetary Science Conference. Part 2: G-M 1993 p 837-838 (For primary document see N94-16173 03-91)

Avail: CASI HC A01/MF A06

Degassing of H2O in the planetary interior possibly plays an important role in the evolution of surface environment as well as geologic activity on the terrestrial planets. Mars may be such a planet that well preserves the materials and the geologic features directly related to early evolution of H2O. H2O content in the interior of proto-Mars during accretion and also core formation were investigated. Geodetic data shows that Mars has a dense core. The existence of iron-rich core on Mars may be also supported by the depletion of siderophile elements in SNC meteorites assuming that these samples came from Mars. Isotope systematics of these meteorites indicate that the core formation occurred very early, probably concurrently with Mars formation. Considering the kinetics of metal segregation from silicate, the melting of silicate is likely to precede the core formation. Once the core formation occurs, substantial amount of gravitational energy is released and thus the planetary interior is heated. This energy may be large enough to keep the silicate material in partially molten state along with the accretional heating. Under such circumstances, the silicate melt probably migrates to the surface. Early crustal formation, therefore, is also likely to be associated with the core formation. Author (revised)

N94-16336*# Tsukuba Univ. (Japan). Inst. of Geoscience.

WATER IN EARTH'S MANTLE: HYDROGEN ANALYSIS OF MANTLE OLIVINE, PYROXENES AND GARNET USING THE SIMS Abstract Only c46

Masanori Kurosawa, Hisayoshi Yurimoto, and Shigeho Sueno *In* Lunar and Planetary Inst., Twenty-Fourth Lunar and Planetary Science Conference. Part 2: G-M 1993 p 839-840 (For primary document see N94-16173 03-91)

Avail: CASI HC A01/MF A06

Hydrogen (or water) in the Earth's interior plays a key role in the evolution and dynamics of the planet. However, the abundance and the existence form of the hydrogen have scarcely been clear in practice. Hydrogen in the mantle was incorporated in the interior during the formation of the Earth. The incorporated hydrogen was hardly possible to concentrate locally inside the Earth considering its high mobility and high reactivity. The hydrogen, preferably, could be distributed homogeneously over the mantle and the core by the subsequent physical and chemical processes. Therefore, hydrogen in the mantle could be present in the form of trace hydrogen in nominally anhydrous mantle minerals. The hydrogen and the other trace elements in mantle olivines, orthopyroxenes, clinopyroxenes, and garnets were determined using secondary ion mass spectrometry (SIMS) for elucidating (1) the exact hydrogen contents, (2) the correlation between the hydrogen and the other trace elements, (3) the dependence of the hydrogen contents on the depth, and (4) the dependence of the whole rock water contents on the depth. Author (revised)

N94-16337*# Lockheed Engineering and Sciences Co., Houston, TX.

LUNAR LIGO: A NEW CONCEPT IN GRAVITATIONAL WAVE ASTRONOMY Abstract Only

Norman LaFave and Thomas L. Wilson (National Aeronautics and Space Administration. Lyndon B. Johnson Space Center, Houston, TX.) *In* Lunar and Planetary Inst., Twenty-Fourth Lunar and Planetary Science Conference. Part 2: G-M 1993 p 841-842 (For primary document see N94-16173 03-91)

Avail: CASI HC A01/MF A06

For three decades, physicists have been in search of an elusive phenomenon predicted by Einstein's general theory of relativity; gravitational radiation. These weak vibrations of spacetime have, thus far, eluded conclusive Earth-based detection due in part to insufficient detector sensitivity and noise isolation. The detection of gravitational waves is crucial for two reasons. It would provide further evidence for the validity of Einstein's theory of relativity, the presently accepted theory of gravitation. Furthermore, the ability to identify the location of a source of a detected gravitational wave event would yield a radical new type of astronomy based on non-electromagnetic emissions. We continue our study of a lunar-based system which can provide an important complement to Earth-based analysis because it is completely independent of the geophysical sources of noise on Earth, while providing an Earth-Moon baseline for pin-pointing burst sources in the Universe. We also propose for the first time that a simplified version of the LIGO beam detector optical system, which we will call LLIGO (Lunar LIGO), could be emplaced on the Moon as part of NASA's robotic lander program now under study (Artemis). The Earth-based investigation has two major programs underway. Both involve large interferometer-type gravitational wave antennas. Author (revised)

N94-16338*# London Univ. Observatory (England).
SHEET FLOW FIELDS ON VENUS
M. G. Lancaster, J. E. Guest, and K. M. Roberts (Brown Univ., Providence, RI.) *In* Lunar and Planetary Inst., Twenty-Fourth Lunar and Planetary Science Conference. Part 2: G-M 1993 p 843-844 (For primary document see N94-16173 03-91)
Avail: CASI HC A01/MF A06

A survey of flow fields with areas greater than 50,000 sq km revealed fields with sheet-like morphology. These sheet flow fields are distinguished by their relatively uniform backscatter, lack of internal flow structure such as well defined lava streams or channels, absence of flow lobes, and irregular boundaries. Internal flow boundaries are essentially absent in these fields, and as such they cannot usually be divided into separate stratigraphic units or eruptive episodes. This is unlike other flow fields with more digitate morphologies, which are made up of discrete flow lobes, and can usually be divided into several episodes of flow emplacement. Five sheet flow fields were studied so far, and other candidates were found. A flow field associated with Lauma Dorsa is taken as an example and examined in detail. Author (revised)

N94-16339*# Arizona State Univ., Tempe. Dept. of Geology.
MARS EXOBIOLOGY LANDING SITES FOR FUTURE EXPLORATION Abstract Only
Ragnhild Landheim, Ronald Greeley, David DesMarais (National Aeronautics and Space Administration. Ames Research Center, Moffett Field, CA.), Jack D. Farmer (National Aeronautics and Space Administration. Ames Research Center, Moffett Field, CA.), and Harold Klein (Santa Clara Univ., CA.) *In* Lunar and Planetary Inst., Twenty-Fourth Lunar and Planetary Science Conference. Part 2: G-M 1993 p 845-846 (For primary document see N94-16173 03-91)
Avail: CASI HC A01/MF A06

The selection of landing sites for Exobiology is an important issue for planning for future Mars missions. Results of a recent site selection study which focused on potential landing sites described in the Mars Landing Site Catalog are presented. In addition, basic Exobiology science objectives in Mars exploration are reviewed, and the procedures used in site evaluation and prioritization are outlined. Author (revised)

N94-16340*# Michigan Univ., Ann Arbor. Radiation Lab.
FAR-INFRARED SPECTRA OF CO2 CLATHRATE HYDRATE FROSTS Abstract Only **c25**
J. C. Landry and A. W. England *In* Lunar and Planetary Inst., Twenty-Fourth Lunar and Planetary Science Conference. Part 2: G-M 1993 p 847-848 (For primary document see N94-16173 03-91)
(Grant NAGw-1334)
Avail: CASI HC A01/MF A06

As a product of our interest in remote sensing of planetary ices, frost samples of CO2 clathrate hydrate were grown by depositing water vapor on a cooled surface and pressurizing the resulting water frost with CO2 gas. At pressures above the dissociation pressure of the clathrate, the samples exhibit an absorption peak at 75 cm (sup -1). At pressures below the dissociation pressure, the peak disappears. Since the free CO2 molecule does not have rotational or vibrational absorption in this region, the absorption is attributed to a CO2 rattling mode within a clathrate cage. Author (revised)

N94-16341*# Muenster Univ. (Germany).
ORIENTATION OF PLANAR DEFORMATION FEATURES (PDFs) IN QUARTZ Abstract Only **c76**
F. Langenhorst and A. Deutsch *In* Lunar and Planetary Inst., Twenty-Fourth Lunar and Planetary Science Conference. Part 2: G-M 1993 p 849-850 (For primary document see N94-16173 03-91)
Avail: CASI HC A01/MF A06

Differently oriented single crystal quartz was shocked experimentally at pressures of 20 to 32 GPa and pre-shock temperatures up to 630 C. Based on this systematic investigation, we can demonstrate that the orientation of planar deformation features in quartz is not only dependent on shock pressure but also on pre-shock temperature and shock direction. Moreover, the orientation of Planar Deformation Features (PDF's) is strongly influenced by the set-up in recovery experiments. PDF's in quartz are defined as optically recognizable, planar microstructures diagnostically produced by shock compression. PDF's differ from all kinds of microstructures found in volcanic environment and therefore, their presence is a primary criterion for recognizing impact craters and ejecta layers such as the K/T boundary. Because experiments have shown a pressure dependence of the orientation of PDF's, this property is used extensively for shock wave barometry in natural impact sites. However, the unreflected application of experimental results neglects that parameters such as pre-shock temperature, shock direction, or the experimental arrangement may influence the spatial distribution of PDF's. In order to test this assumption, shock experiments on single crystal quartz at pre-shock temperatures of 20, 275, 540, and 630 C, and with shock directions (1010) and (0001) were performed. Most of the recovery experiments were carried out by using a reverberation technique, whereas in only one experiment a single shock was produced (impedance method). In the former case 0.5 mm thin discs of single crystal quartz were used, in the latter a 15 mm thick cylinder. The orientation of PDF's was measured by means of a conventional universal stage and the results are given. Effects of the experimentation technique can be derived showing the orientation of PDF's in quartz shocked at 27.5 GPa. In comparison to the well defined peaks at (1012) found in samples from reverberation experiments, the impedance matching technique causes PDF's with a broad distribution pattern and indistinct maxima. Our results have serious implications for shock-wave barometry in nature: the existing classification scheme which relates PDF orientation exclusively to shock pressure is no longer applicable. In consequence more experimental data is needed. Author (revised)

N94-16342*# Arizona Univ., Tucson. Dept. of Geosciences.
LUNAR PHASE FUNCTION EFFECTS ON SPECTRAL RATIOS USED FOR RESOURCE ASSESSMENT Abstract Only
S. M. Larson, J. Collins, R. B. Singer, J. R. Johnson, and D. E. Melendrez *In* Lunar and Planetary Inst., Twenty-Fourth Lunar and Planetary Science Conference. Part 2: G-M 1993 p 851-852 (For primary document see N94-16173 03-91)
Avail: CASI HC A01/MF A06

Groundbased telescopic CCD images of 36 selected locations on the moon were obtained in five 'standard' bandpasses at 12 phase angles ranging from -78 deg to +75 deg to measure phase function effects on the ratio values used to quantify the abundance of TiO2 and qualitatively indicate soil maturity. Consistent with previous studies, we find that the moon is 'bluer' at small phase angles, but that the effect on the ratio values for TiO2 abundance for the phase angles of our data is on the order of the measurement uncertainties throughout the range of abundances found in the mare. The effect is more significant as seen from orbiting spacecraft over a range of selenographic latitude. Spectral ratio images (400/560 and 400/730 nm) were used to map the abundance of TiO2 using the empirical relation found by Charlette et al from analysis of returned lunar soils. Additionally, the 950/560 and 950/730 nm image ratios were used to define the regions of mature mare soil in which the relation is valid. Although the phase function dependence on wavelength was investigated and quantified for small areas and the integrated disc, the effect specifically on TiO2 mapping was not rigorously determined. For consistency and convenience in observing the whole lunar front side, our mapping utilized images taken -15 deg less than alpha less than 15 deg when the moon was fully illuminated from earth; however, this includes the strong opposition peak. Author (revised)

N94-16343*# Academy of Sciences (USSR), Moscow. Inst. of Geochemistry and Analytical Chemistry.
THE ASTROPHYSICAL INTERPRETATION OF ISOTOPE ANOMALIES IN GRAPHITE AND SiC GRAINS OF CHONDRITES Abstract Only **c90**
A. K. Lavrukhina *In* Lunar and Planetary Inst., Twenty-Fourth Lunar and Planetary Science Conference. Part 2: G-M 1993 p 853-854 (For primary document see N94-16173 03-91)
Avail: CASI HC A01/MF A06

The C, N, and Mg isotopic compositions in graphite and SiC grains of carbonaceous chondrites can be explained by nuclear processes in massive O,B stars of second generation passed a stage of WR star with intensive stellar wind, where grain condensation had taken place. The interstellar graphite and SiC grains with anomalous isotopic compositions of C, N, Ne, and Si and other elements of nucleosynthetic origin, found in non-equilibrated chondrites, are most suitable for determination of astro-physical objects, where nucleosynthesis had taken place. Two objects were examined: (1) massive O,B stars of second generation passed a stage of WR star with

intensive stellar wind (O,B-WR model) and (2) low-mass stars (1 less than or equal to M/solar mass less than or equal to 3) during thermally pulsing asymptotic giant branch phase (TP-AGB model). Author

N94-16344*# Academy of Sciences (USSR), Moscow. Inst. of Geochemistry and Analytical Chemistry.

ON POSSIBLE Mn-53 HETEROGENEITY IN THE EARLY SOLAR SYSTEM Abstract Only **c90**

A. K. Lavrukhina and G. K. Ustinova *In* Lunar and Planetary Inst., Twenty-Fourth Lunar and Planetary Science Conference. Part 2: G-M 1993 p 855-856 (For primary document see N94-16173 03-91)

Avail: CASI HC A01/MF A06

The effects of influence of shock wave propagation on the energy spectrum of accelerated particles that lead to different production rates of radionuclides, in particular, Mn-53, on small scales in the early solar system are shown. Search for evidence for extinct Mn-53 has stimulated investigations of Cr isotope anomalies in meteorites. The linear correlation between the magnitude of the Cr-53* excesses and the Mn/Cr ratio that unambiguously proves the in situ decay of Mn-53 was detected, really, in different mineral phases of some carbonaceous and enstatite chondrites, primitive achondrites, pallasites and iron meteorites. However, the data on the Cr-53* excess rarely defines a single linear array on a Mn-53-Cr-52 evolution diagram even for meteorites of the same chemical group. A clear isochron with Mn-53/Mn-55 = 4.4 plus or minus 1.0 x 10(exp -5) (in range of approximately 2.4 to approximately 9 x 10(exp -5)) is observed for CAI of the Allende C3-chondrite while the data for the Murchison C2- and Orgueil C1-chondrites fall much lower corresponding rather to Mn-53/Mn-55 less than 2 x 10(exp -5). In the case of iron meteorites it ranges from less than 5 x 10(exp -8) to less than 5 x 10(exp -5).

Author (revised)

N94-16345*# Academy of Sciences (USSR), Moscow. Inst. of Geochemistry and Analytical Chemistry.

ON ORIGIN OF THE OLIVINE INCLUSIONS FROM THE KAINSAZ CO CARBONACEOUS CHONDRITE Abstract Only **c90**

A. K. Lavrukhina, Z. A. Lavrentjeva, A. Yu. Ljul, and K. I. Ignatenko *In* Lunar and Planetary Inst., Twenty-Fourth Lunar and Planetary Science Conference. Part 2: G-M 1993 p 857-858 (For primary document see N94-16173 03-91)

Avail: CASI HC A01/MF A06

Olivine inclusions and chondrules of Kainsaz were formed in a unique process of dust matter melting. The elemental abundances of four fractions of olivine (01) inclusions from Kainsaz were analyzed by INAA. The inclusions of fraction A (160 less than d less than 260 microns) have Fe-Ni grains, the inclusions of fractions B (100 less than d less than 160 microns), C (160 less than d less than 260 microns), and D (260 less than d less than 360 microns) do not. The average elemental enrichment factors relative to CI chondrite for each fraction and chondrules of Kainsaz is shown. The enrichment factors of siderophile Co, Ni, Ir, Au, and non-refractory Na in all fractions are less than 1. The factors of refractory Ca, Sc, La, Sm, and Yb are comparative with the corresponding values of O1 aggregates of Allende CV (average 4.76). For chondrules of Kainsaz these values are lower. Fraction A is enriched in Co, Ir, Au, and relative Ni and CI chondrites: Ir greater than Au greater than Co. The values of (Me/Ni)inc/(Me/Ni)CI are equal to 3.25 for Ir, 2.1 for Au, and 1.2 for Co. The superabundances in Ir and Au relative to Ni witness to formation of Fe-Ni grains of O1 inclusions by agglomeration of grains enriched in refractory metal with grains enriched in non-refractory metal (Au). The enrichments of fraction A in Ca, Sc, La, Sm, and Yb witness about presence of high-temperature phases in O1 inclusions. Author (revised)

N94-16346*# Arizona Univ., Tucson. Lunar and Planetary Lab.

TEACHING PLANETARY SCIENCES TO ELEMENTARY SCHOOL TEACHERS: PROGRAMS THAT WORK Abstract Only **c80**

Larry A. Lebofsky and Nancy R. Lebofsky *In* Lunar and Planetary Inst., Twenty-Fourth Lunar and Planetary Science Conference. Part 2: G-M 1993 p 859 (For primary document see N94-16173 03-91)

Avail: CASI HC A01/MF A06

Planetary sciences can be used to introduce students to the natural world which is a part of their lives. Even children in an urban environment are aware of such phenomena as day and night, shadows, and the seasons. It is a science that transcends cultures, has been prominent in the news in recent years, and can generate excitement in young minds as no other science can. Planetary sciences also provides a useful tool for understanding other sciences and mathematics, and for developing problem solving skills which are important in our technological world. However, only 15 percent of elementary school teachers feel very well qualified to teach earth/space science, while better than 80 percent feel well qualified to teach reading; many teachers avoid teaching science; very little time is actually spent teaching science in the elementary school: 19 minutes per day in K-3 and 38 minutes per day in 4-6. While very little science is taught in elementary and middle school, earth/space science is taught at the elementary level in less than half of the states. It was pointed out that science is not generally given high priority by either teachers or school districts, and is certainly not considered on a par with language arts and mathematics. Therefore, in order to teach science to our youth, we must empower our teachers, making them familiar and comfortable with existing materials. In our earlier workshops, several of our teachers taught in classrooms where the majority of the students were Hispanic (over 90 percent). However, few space sciences materials existed in Spanish. Therefore, most of our materials could not be used effectively in the classroom. To address this issue, NASA materials were translated into Spanish and a series of workshops for bilingual classroom teachers from Tucson and surrounding cities was conducted. Our space sciences workshops and our bilingual classroom workshops and how they address the needs of elementary school teachers in Arizona are addressed in detail. Author (revised)

N94-16347*# National Aeronautics and Space Administration. Goddard Space Flight Center, Greenbelt, MD.

A SIMULTANEOUS ESTIMATION OF THE MASS OF MARS AND ITS NATURAL SATELLITES, PHOBOS AND DEIMOS, FROM THE ORBITAL PERTURBATIONS ON THE MARINER 9, VIKING 1, AND VIKING 2 ORBITERS Abstract Only

F. G. Lemoine, D. E. Smith (Maryland Univ., College Park.), S. K. Fricke (RMS Technologies, Inc., Landover, MD.), and J. J. McCarthy (Hughes STX, Inc., Lanham, MD.) *In* Lunar and Planetary Inst., Twenty-Fourth Lunar and Planetary Science Conference. Part 2: G-M 1993 p 861-862 (For primary document see N94-16173 03-91)

Avail: CASI HC A01/MF A06

The natural satellites of Mars, Phobos and Deimos, caused perturbations on the orbits of the Mariner 9, and the Viking spacecraft that were used to estimate the satellite masses. The Viking spacecraft were specifically targeted to make close flybys (within a few hundred kilometers) of Phobos in February 1977 and of Deimos in October 1977. These close encounters were used to estimate the moon's gravitational constant, GM (the universal constant of gravitation multiplied by the satellite mass). However, the Viking and Mariner 9 spacecraft made numerous flybys of Phobos and Deimos at distances of a few thousand kilometers. The tracking data from these more 'distant' encounters were processed to estimate the masses of Mars, Phobos, and Deimos. Author (revised)

N94-16348*# California Univ., Los Angeles. Dept. of Earth and Space Sciences.

MODELS OF THERMAL/CHEMICAL BOUNDARY LAYER CONVECTION: POTENTIAL APPLICATION TO VENUS Abstract Only

A. Lenardic and W. M. Kaula *In* Lunar and Planetary Inst., Twenty-Fourth Lunar and Planetary Science Conference. Part 2: G-M 1993 p 863-864 (For primary document see N94-16173 03-91)

Avail: CASI HC A01/MF A06

The upper boundary layer of Venus is comprised of at least two distinct chemical components, mantle and crust. Fluid dynamical models of convection within Venus' mantle were primarily of the thermal boundary layer type. Models assessing the ability of convective mantle flows to deform the crust were undertaken, but models exploring the effects of a variable thickness crust on mantle convection were largely lacking. A Venusian crust of variable thickness could couple back into, and alter, the mantle flow patterns that helped create it, leading to deformation mechanisms not predicted by purely thermal boundary layer convection models. This possibility is explored through a finite element model of thermal/chemical boundary layer convection. Model results suggest that a crust of variable thickness can serve as a mantle flow driver by perturbing lateral temperature gradients in the upper mantle. Resulting mantle flow is driven by the combination of free convective and nonuniform crustal distribution. This combination can lead to a flow instability manifest in the occurrence of

episodic mantle lithosphere subduction initiated at the periphery of a crustal plateau. The ability of a light, near surface, chemical layer to potentially alter mantle flow patterns suggest that mantle convection and the creation and/or deformation of such a chemical layer may be highly nonseparable problems on time scales of 10(exp 8) years. Author (revised)

N94-16349*# California Univ., Los Angeles. Dept. of Earth and Space Sciences.
ON THE RELATIONSHIP BETWEEN TECTONIC PLATES AND THERMAL MANTLE PLUME MORPHOLOGY Abstract Only **c46**
A. Lenardic and W. M. Kaula *In* Lunar and Planetary Inst., Twenty-Fourth Lunar and Planetary Science Conference. Part 2: G-M 1993 p 865-866 (For primary document see N94-16173 03-91)
Avail: CASI HC A01/MF A06

Models incorporating plate-like behavior, i.e., near uniform surface velocity and deformation concentrated at plate boundaries, into a convective system, heated by a mix of internal and basal heating and allowing for temperature dependent viscosity, were constructed and compared to similar models not possessing plate-like behavior. The simplified numerical models are used to explore how plate-like behavior in a convective system can effect the lower boundary layer from which thermal plumes form. A principal conclusion is that plate-like behavior can significantly increase the temperature drop across the lower thermal boundary layer. This temperature drop affects the morphology of plumes by determining the viscosity drop across the boundary layer. Model results suggest that plumes on planets possessing plate-like behavior, e.g., the Earth, may differ in morphologic type from plumes on planets not possessing plate-like behavior, e.g., Venus and Mars. Author

N94-16350*# Geological Survey, Flagstaff, AZ.
HELLAS BASIN, MARS: FORMATION BY OBLIQUE IMPACT Abstract Only
Gregory J. Leonard and Kenneth L. Tanaka *In* Lunar and Planetary Inst., Twenty-Fourth Lunar and Planetary Science Conference. Part 2: G-M 1993 p 867-868 (For primary document see N94-16173 03-91)
Avail: CASI HC A01/MF A06

Hellas, a 2,000-km-diameter, roughly circular multiring impact basin in the southern highlands of Mars, has a pronounced southeastern lobe of rim material that extends for some 1,500 km. This lobe and a system of ridges concentric to the southern part of the basin (including part of the lobe) were interpreted to be formed by an oblique impact that was inclined in the direction of the lobe. Our preliminary geologic mapping of the Hellas region (lat -20 to -65 deg, long 250 to 320 deg) at 1:5,000,000 scale gives this hypothesis additional supporting evidence, including a symmetric distribution of basin ejecta and volcanic centers across the inferred trend of the impact. Furthermore, measurements of relief indicate that the downrange ejecta may be about twice as thick as they are elsewhere around the rim. Author (revised)

N94-16351*# Southwest Research Inst., San Antonio, TX.
MAPPING THE STABILITY REGION OF THE 3:2 NEPTUNE-PLUTO RESONANCE Abstract Only
H. F. Levison and S. A. Stern *In* Lunar and Planetary Inst., Twenty-Fourth Lunar and Planetary Science Conference. Part 2: G-M 1993 p 869-870 (For primary document see N94-16173 03-91)
Avail: CASI HC A01/MF A06

Pluto and Charon are most likely the remnants of a large number of objects that existed in the Uranus-Neptune region at early epochs of the solar system. Numerical integrations have shown that, in general, such objects were ejected from the planetary region on timescales of approximately 10(exp 7) years after Neptune and Uranus reached their current masses. It is thought that the Pluto-Charon system survived to current times without being dynamically removed in this way because it is trapped in a set of secular and mean motion resonances with Neptune. The best-known Pluto-Neptune orbit coupling is the 3:2 mean motion resonance discovered almost 30 years ago by C. Cohen and E. Hubbard. These workers showed that the resonance angle, delta is equivalent to 3(lambda(sub P)) - 2(lambda(sub N)) - omega-bar(sub P) where omega-bar(sub P) is the longitude of perihelion of the Pluto-Charon system, and lambda(sub N) and lambda(sub P) are the mean longitude of Neptune and Pluto-Charon respectively, librates about 180 deg with an amplitude, A(sub delta), of 76 deg. A numerical simulation project to map out the stability region of the 3:2 resonance is reported. The results of these simulations are important to understanding whether Pluto's long-term heliocentric stability requires only the 3:2 resonance, or whether it instead requires one or more of the other Pluto-Neptune resonances. Our study also has another important application. By investigating stability timescales as a function of orbital elements, we gain insight into the fraction of orbital phase space which the stable 3:2 resonance occupies. This fraction is directly related to the probability that the Pluto-Charon system (and possibly other small bodies) could have been captured into this resonance. Author (revised)

N94-16352*# Arizona Univ., Tucson. Lunar and Planetary Lab.
POSSIBLE DUST CONTAMINATION OF THE EARLY SOLAR SYSTEM Abstract Only **c90**
E. H. Levy and T. V. Ruzmaikina *In* Lunar and Planetary Inst., Twenty-Fourth Lunar and Planetary Science Conference. Part 2: G-M 1993 p 871-872 (For primary document see N94-16173 03-91)
Avail: CASI HC A01/MF A06

Measurements carried out over more than twenty years indicate a deficiency of neutrinos emitted from the deep interior of the Sun in conjunction with the neutrino flux expected from canonical solar models. The early measurements were sensitive only to high-energy neutrinos emitted from B-8 on a minor branch of the energy-producing nuclear reactions in the solar interior. Thus these measurements were not widely considered to be a definitive test of solar physics. However the more recent measurements, which are sensitive to lower energy neutrinos, produced primarily by the p-p reaction on the main energy-producing branch of the solar nuclear reactions, pose a far more significant mystery in physics. One possibility is that the Sun's interior opacity is lower than expected due to a paucity of elements. This paper discusses that the Sun formed from material less abundant in heavy elements than usually believed, and the subsequent contamination due to the settling of surrounding dust brought the abundance of heavy elements - in the protoplanetary nebula, and in the Sun's convective envelope - up to the currently observed value. Author (revised)

N94-16353*# Chicago Univ., IL.
A SEARCH FOR NOBLE-GAS EVIDENCE FOR PRESOLAR OXIDE GRAINS Abstract Only **c25**
Roy S. Lewis and B. Srinivasan *In* Lunar and Planetary Inst., Twenty-Fourth Lunar and Planetary Science Conference. Part 2: G-M 1993 p 873-874 (For primary document see N94-16173 03-91)
Avail: CASI HC A01/MF A06

Early results from an ongoing search for isotopically distinctive noble gases as evidence for presolar oxide grains are presented. With some qualifications, we do not see such evidence in spinel rich acid residue fractions from the Allende meteorite. We remain hopeful that less abundant mineral separates may yet be fruitful. Presolar grains, micro-diamonds, silicon carbide, and graphite, were found in primitive meteorites. While the abundances of these three refractory C rich grains are low, a few hundred ppm, a few ppm, & less than 1 ppm, respectively in primitive meteorites, they are tagged with high concentrations of isotopically anomalous noble gas components, Xe-HL, KR & Xe-s and Ne-E(H), and Ne-E(L). These tags have served as tracers and allowed the development of techniques for their purification and eventual identification. One might expect similar amounts of refractory presolar oxides to have survived, but so far only three cases exist for their identification. The first two cases are individual corundum oxide grains. Huss et al. found one such grain from an Orgueil residue with an Al-26/Al-27 ratio of 8.9 x 10(exp -5), about 18 times higher than the canonical initial solar system value. The second corundum grain, from Murchison, was found by Nittler et al. to have unusual oxygen in addition to a similar Al-26/Al-27 ratio of 8.7 x 10(exp -4). The oxygen was depleted in O-18 by 22 percent and enriched in O-17 by a factor of 2. The third case is a measurement by Zinner et al. on an aggregate of fine grained spinels from a Murray residue with an O-17 enrichment and a possible O-18 depletion similar to the second grain, but much subdued. This is consistent with a few such presolar grains diluted by a much larger population of isotopically normal corundum grains and an even larger number of normal spinel grains. Author (revised)

N94-16354*# California Inst. of Tech., Pasadena.
THE SEISMIC RESPONSE OF AN AQUIFER TO THE PROPAGATION OF AN IMPACT GENERATED SHOCK WAVE: A POSSIBLE TRIGGER OF THE MARTIAN OUTFLOW CHANNELS? Abstract Only
Ivett A. Leyva and Stephen M. Clifford (Lunar and Planetary Inst., Houston, TX.) *In* Lunar and Planetary Inst., Twenty-Fourth Lunar and Planetary Science Conference. Part 2: G-M 1993 p 875-876 (For primary document see N94-16173 03-91)
Avail: CASI HC A01/MF A06

Aquifer dilation from shock waves produced by the 8.4 magnitude Alaskan earthquake of 1964 led to water and sediment ejection from the ground up to 400 km away from the earthquake's epicenter. Groundwater disturbances were observed as far away as Perry, Florida (approximately 5500 km), where well water fluctuations with an amplitude of as much as 2.3 m were reported. The martian cratering record provides evidence that the planet has experienced numerous seismic events of a similar, and often much greater, magnitude. Given this fact, and the photogeologic evidence for abundant water in the early crust, the response of a basalt aquifer to the propagation of compressional waves (P-waves) produced by impacts in the 33-1000 km diameter size range were investigated. The resulting one-dimensional changes in effective stress and pore pressure were calculated - as a function of both distance and time - based on the following assumptions: (1) that all of the seismic energy radiated by an impact is transmitted as a single compressional wave; (2) that both the host rock and groundwater are compressible; and (3) that there is no net flow between the water-filled pores. Author (revised)

N94-16355*# National Aeronautics and Space Administration. Lyndon B. Johnson Space Center, Houston, TX.
INAA OF CAIs FROM THE MARALINGA CK4 CHONDRITE: EFFECTS OF PARENT BODY THERMAL METAMORPHISM Abstract Only c90
D. J. Lindstrom, L. P. Keller, and R. R. Martinez (Lockheed Engineering and Sciences Co., Houston, TX.) *In* Lunar and Planetary Inst., Twenty-Fourth Lunar and Planetary Science Conference. Part 2: G-M 1993 p 877-878 (For primary document see N94-16173 03-91)
Avail: CASI HC A01/MF A06

Maralinga is an anomalous CK4 carbonaceous chondrite which contains numerous Ca-, Al-rich inclusions (CAI's) unlike the other members of the CK group. These CAI's are characterized by abundant green hercynitic spinel intergrown with plagioclase and high-Ca clinopyroxene, and a total lack of melilite. Instrumental Neutron Activation Analysis (INAA) was used to further characterize the meteorite, with special focus on the CAI's. High sensitivity INAA was done on eight sample disks about 100-150 microns in diameter obtained from a normal 30 micron thin section with a diamond microcoring device. The CAI's are enriched by 60-70X bulk meteorite values in Zn, suggesting that the substantial exchange of Fe for Mg that made the spinel in the CAI's hercynitic also allowed efficient scavenging of Zn from the rest of the meteorite during parent body thermal metamorphism. Less mobile elements appear to have maintained their initial heterogeneity. Author (revised)

N94-16356*# National Aeronautics and Space Administration. Lyndon B. Johnson Space Center, Houston, TX.
SPACESHIP EARTH: A PARTNERSHIP IN CURRICULUM WRITING Abstract Only c80
Marilyn M. Lindstrom *In* Lunar and Planetary Inst., Twenty-Fourth Lunar and Planetary Science Conference. Part 2: G-M 1993 p 879 (For primary document see N94-16173 03-91)
Avail: CASI HC A01/MF A06

As the Apollo astronauts left Earth to venture onto the surface of another planetary body, they saw their home planet in a new global perspective. Unmanned NASA missions have given us a closer look at all the other planets in our solar system and emphasized the uniqueness of Earth as the only place in our solar system that can sustain life as we know it. Spaceship Earth is a new science curriculum which was developed to help students and teachers to explore the Earth, to see it in the global perspective, and to understand the relationships among life, the planet, and the sun. Astronaut photographs, especially shuttle pictures, are used as groundbased studies to help students to understand global Earth Science and integrate various aspects of physical, life, and social science. The Spaceship Earth curriculum was developed at by a team of JSC scientists working in collaboration with teachers from local school districts. This project was done under the auspices of Partner-In-Space, a local non-profit organization dedicated to improving science education and our general knowledge of space. The team met once a month for a year then assembled the curriculum during the summer. The project is now in the testing stage as the teachers try it out in their classrooms. It was supported by the Texas Education Agency and will be offered by the State of Texas as a supplemental curriculum for statewide use. Because the curriculum was developed by teachers, it is self contained and the lessons are easy to implement and give students concrete experiences. The three sub-units follow in a logical order, but may be used independently. If they are used separately, they may be tied together by the teacher returning to the basic theme of the global Earth as each unit is completed. Author (revised)

N94-16357*# Oregon State Univ., Corvallis. Depts. of Chemistry and Geosciences.
CHONDRITIC RATIOS OF Fe/Cr/Ir IN KERGUELEN PLATEAU (HOLE 738C) K/T CARBONATE-RICH SEDIMENTS SUPPORT ASTEROID-COMETARY IMPACT AT K/T TIME Abstract Only c90
Y. G. Liu and R. A. Schmitt *In* Lunar and Planetary Inst., Twenty-Fourth Lunar and Planetary Science Conference. Part 2: G-M 1993 p 881-882 (For primary document see N94-16173 03-91)
Avail: CASI HC A01/MF A06

In the study of marine carbonate sediments from Holes 577 and 577B, Shatsky Plateau (Rise), a net extraterrestrial Fe/Ir = C1 chondritic ratio at the K/T boundary was reported. Applying a similar procedure to Hole 738C (Kerguelen Plateau) data reported, Fe/Cr/Ir ratios similar to C1 or C2 chondritic ratios were obtained. Author (revised)

N94-16358*# Oregon State Univ., Corvallis. Depts. of Chemistry and Geosciences.
EARTH'S PARTIAL PRESSURE OF CO2 OVER THE PAST 120 Ma; EVIDENCE FROM Ce ANOMALIES IN THE DEEP (GREATER THAN 600 m) PACIFIC OCEAN, 1 Abstract Only c46
Y.-G Liu and R. A. Schmitt *In* Lunar and Planetary Inst., Twenty-Fourth Lunar and Planetary Science Conference. Part 2: G-M 1993 p 883-884 (For primary document see N94-16173 03-91)
Avail: CASI HC A01/MF A06

It was found that Ce serves as a chemical tracer of paleo-oceanic redox conditions. It was shown that the unoxidized and soluble Ce(3+) in modern seawater exhibits a negative anomaly relative to the other soluble REE(3+). An expression of soluble Ce(3+) in seawater that was approximately 1900X greater than the average observed in Ce in 600-5000 m Pacific seawater was derived. Since Ce(CO3)(+) and Ce(CO3)2(-) complexes greatly exceed the Ce(PO4) complexes in seawater, the formulations of using carbonate complexes were followed and it was found that the calculated Ce and observed concentrations in the deep 600-5000 m Pacific Ocean agree within the uncertainties of the thermodynamic data. As expected, the calculated Ce concentrations are a strong function of pH and found to be lesser functions of CO3(2-) activities. Author (revised)

N94-16359*# Oregon State Univ., Corvallis. Depts. of Chemistry and Geosciences.
GEOCHEMICAL EVIDENCES FOR TWO CHONDRITIC-LIKE COMETARY OR ASTEROIDAL IMPACTS BEFORE AND AT THE K/T BOUNDARY Abstract Only c90
Y.-G. Liu and R. A. Schmitt *In* Lunar and Planetary Inst., Twenty-Fourth Lunar and Planetary Science Conference. Part 2: G-M 1993 p 885-886 (For primary document see N94-16173 03-91)
Avail: CASI HC A01/MF A06

A number of geological and palaeontological evidences support multiple impacts of cometary showers within a short time (approximately 1-3 Ma) and their connection with mass extinctions. Observations include clustered crater ages, stratigraphic horizons of impact ejecta closely spaced in time, and evidence for stepwise mass extinctions spanning intervals of 1-3 Ma. For the K/T boundary, three candidates, Popigai, Manson, and Yucatan, have been proposed as impact craters. Two distinct strata at the K/T boundary in western North America have been interpreted as evidence for two sequential impacts. If multiple impacts occurred within a time span of about 1 Ma then multiple Ir enrichments should be observed. DSDP Hole 577B on the Shatsky Plateau in the northern Pacific at K/T time is the first site. Samples contain approximately greater than 97 percent CaCO3, which exhibit clear chemical signals associated with asteroidal/cometary

impact. Ir, Fe, and Cr data are presented. From the Th-normalized data, two satellite peaks below the major peak at 78 cm and 81 cm of 577B-1-4 are clearly shown. The major Ir peak (K/T boundary) is at 72 cm. Fe and Cr, from C1-like impactor ejecta fallout, also show two peaks at the same positions. For hole 738C on the southern Kerguelen Plateau, Ir values reach a peak concentration of 18 ppb in the clay layer at 96.0-96.2 cm in section 20R-5, and gradually tail off. In the sample 115 cm above the boundary, Ir concentrations have still not reached background levels. From the Ir peak downward to the lowermost sample analyzed at 102 cm, the Ir concentration is still as high as 1.7 ppb. From the Th-normalized data, we observe a small Ir/Th peak at 100-101 cm. Though this peak is within the error margin, the trend is clear. Fe and Cr exhibit the same pattern. The third case is Hole 690C on the Queen Maud Ridge. Again, the Ir/Th plot indicates the strong possibility of satellite peaks at approximately 52 cm. The main peak is at 39-40 cm. For the Stevns Klint K/T boundary layers, the stratification of trace elements appears threefold with peak concentrations in sublayers A1, A3, and B2 for different element groups, including Ir. C1 ratios for many siderophile elements found in combined layers III and IV, corresponding to layers A, B, C, and D, strongly support the impact hypothesis. Also, multiple Ir anomalies in the K/T section at Lattengebirge, Bavarian Alps are reported. Recent works on Ni-rich spinels and Ir at the K/T boundaries clearly establish cometary/asteroidal impacts at the K/T boundary. Lastly, cometary showers can explain the enhanced Ir contents over approximately a 1 Ma interval in Gubbio shales. CASI

N94-16360*# Oregon State Univ., Corvallis. Depts. of Chemistry and Geosciences.

EARTH'S PARTIAL PRESSURE OF CO2 OVER THE PAST 100-500 Ma; EVIDENCE FROM Ce ANOMALIES IN MOSTLY SHALLOW SEAS (LESS THAN 200 m) AS RECORDED IN CARBONATE SEDIMENTS, 2 Abstract Only **c45**

Y.-G. Liu, J. W. Reinhardt (Erlangen-Nuremberg Univ., Germany.), and R. A. Schmitt *In* Lunar and Planetary Inst., Twenty-Fourth Lunar and Planetary Science Conference. Part 2: G-M 1993 p 887-888 (For primary document see N94-16173 03-91)

Avail: CASI HC A01/MF A06

We reported the direct relationship of Ce anomalies recorded in 0.2-119 Ma CaCO3 sediments (Ce(sup A*)) to the Ce anomalies in the parental Pacific deep seawater (Ce(sup A)) and their relationship to atmospheric P(CO2) relative to present P(CO2). We have analyzed continental CaCO3 samples that were deposited in ancient oceans and shallow sea platforms less than 200 m over central USA, central Europe, China, and Saudi-Arabia/Oman. We have plotted Ce(sup A*) over the 75-470 Ma interval. For P(CO2) calculations, we assumed as a reference standard the less than 200 m mixed Pacific Ocean with a Ce(sup A) geometric mean of 0.22 and a range of 0.10-0.43. Because P(CO2) values obtained from reliable deep Pacific Ocean carbonates in the 67-119 Ma interval were similar to the present P(CO2) values, we have drawn a 1.0 ratio for that interval. Although there is considerable scatter among the approximately 150 Ma carbonates, the average Ce(sup A*) value suggests that P(CO2) increased during the early Cretaceous, from 1.0X at approximately 120 Ma to about 1.4X at approximately 150 Ma. At approximately 250 Ma, the average Ce(sup A*) in 13 shallow sea China carbonates agrees well with the single and more reliable approximately 250 Ma China carbonate deposited in deeper open platform. We suggest that P(CO2) ranged from 1.4-1.7X over the Jurassic and Triassic periods. At approximately 280 Ma, three China carbonates deposited in deeper open platforms and therefore considered more reliable are consistent with a European carbonate, which indicate Ce(sup A) and P(CO2) values similar to the present. The minimum at this time corresponds to the great Permo-Carboniferous glaciation. From 280 Ma to 470 Ma, the trend favors increasing Ce(sup A*) and corresponding P(CO2) values between 1.9-2.7X, with a more reliable value closer to 2.7X at 430 Ma because of the unknown higher temperature in the less than 100 m seawater over continental USA which was located just south of the equator at approximately 430 Ma. CASI

N94-16361*# Max-Planck-Inst. fuer Chemie, Mainz (Germany).

NOBLE GASES IN TWENTY YAMATO H-CHONDRITES: COMPARISON WITH ALLAN HILLS CHONDRITES AND MODERN FALLS Abstract Only **c90**

Th. Loeken, P. Scherer, and L. Schultz *In* Lunar and Planetary Inst., Twenty-Fourth Lunar and Planetary Science Conference. Part 2: G-M 1993 p 889-890 (For primary document see N94-16173 03-91)

Avail: CASI HC A01/MF A06

Concentration and isotopic composition of noble gases have been measured in 20 H-chrondrites found on the Yamato Mountains ice fields in Antarctica. The distribution of exposure ages as well as of radiogenic He-4 contents is similar to that of H-chrondrites collected at the Allan Hills site. Furthermore, a comparison of the noble gas record of Antarctic H-chrondrites and finds or falls from non-Antarctic areas gives no support to the suggestion that Antarctic H-chrondrites and modern falls derive from differing interplanetary meteorite populations. Author

N94-16362*# National Aeronautics and Space Administration. Lyndon B. Johnson Space Center, Houston, TX.

THE FIRST LUNAR OUTPOST: THE DESIGN REFERENCE MISSION AND A NEW ERA IN LUNAR SCIENCE Abstract Only **c12**

Gary E. Lofgren *In* Lunar and Planetary Inst., Twenty-Fourth Lunar and Planetary Science Conference. Part 2: G-M 1993 p 891-892 (For primary document see N94-16173 03-91)

Avail: CASI HC A01/MF A06

The content of the First Lunar Outpost (FLO) Design Reference Mission has been formulated and a 'strawman' science program has been established. The mission consists of two independent launches using heavy lift vehicles that land directly on the lunar surface. A habitat module and support systems are flown to the Moon first. After confirmation of a successful deployment of the habitat systems, the crewed lunar lander is launched and piloted to within easy walking distance (2 km) of the habitat. By eliminating the Apollo style lunar orbit rendezvous, landing sites at very high latitudes can be considered. A surface rover and the science experiments will accompany the crew. The planned stay time is 45 days, two lunar days and one night. A payload of 3.3 metric tons will support a series of geophysics, geology, astronomy, space physics, resource utilization, and life science experiments. Sample return is 150 to 200 kg. The rover is unpressurized and can carry four astronauts or two astronauts and 500 kg of payload. The rover can also operate in robotic mode with the addition of a robotics package. The science and engineering experiment strategy is built around a representative set of place holder experiments.

Author (revised)

N94-16363*# National Aeronautics and Space Administration. Lyndon B. Johnson Space Center, Houston, TX.

EXPERIMENTALLY REPRODUCED RELICT ENSTATITE IN PORPHYRITIC CHONDRULES OF ENSTATITE CHONDRITE COMPOSITION Abstract Only **c90**

Gary E. Lofgren, John M. DeHart, and Tammy L. Dickinson (National Aeronautics and Space Administration, Washington, DC.) *In* Lunar and Planetary Inst., Twenty-Fourth Lunar and Planetary Science Conference. Part 2: G-M 1993 p 893-894 (For primary document see N94-16173 03-91)

Avail: CASI HC A01/MF A06

Experiments are presented that test a model for the origin of porphyritic pyroxene (PP) chondrules in enstatite chondrites that contain phenocrysts of enstatite with blue cathodoluminescence (CL) set in a matrix of radial, dendritic enstatite with red CL. Established one-atmosphere, gas-mixing techniques were used. Relict enstatite phenocrysts with blue CL in a matrix of coarsely radial to dendritic enstatite with red CL were successfully produced. The relict crystals are preserved in runs with a melt time of 36 minutes or less at 1537 C. The relicts remain angular with smooth crystal/melt interfaces, and thus melting has occurred uniformly. Partial melting does occur along fractures produced when the blue CL enstatite was initially grown and cooled through the proto/ortho enstatite transition with the attendent volume change. There is either reaction with the melt and diffusion of Mn and Cr into the blue CL En, or there is an overgrowth of red CL En along the fractures. The bulk of the relicts remain blue. The melt enclosing the relicts crystalized to a coarsely radial to dendritic to micro porphyritic texture comprised of enstatite that has a bright red CL with decreasing melt time. The blue CL En has Mn and Cr contents at or below detection limits of the electron probe as described in earlier studies and in natural blue CL En. In the red CL En in this study, the Mn, Al2O3, and Cr are at previously observed levels and the levels change rapidly.

CASI

N94-16364*# Lamont-Doherty Geological Observatory, Palisades, NY.
LIQUIDUS EQUILIBRIA OF LUNAR ANALOGS AT HIGH PRESSURE Abstract Only
J. Longhi *In* Lunar and Planetary Inst., Twenty-Fourth Lunar and Planetary Science Conference. Part 2: G-M 1993 p 895-896 (For primary document see N94-16173 03-91)
Avail: CASI HC A01/MF A06

Melting experiments have been performed in the range of 20 to 40 kbar on partially crystallized synthetic glasses in order to test the accuracy of the polybaric fractional fusion model for picritic lunar green glasses. Results show that the model predicts the position of the olivine (ol) + orthopyroxene (opx) liquidus boundary within the uncertainty of the measurements, but that details of the calculations are subject to change because of new crystal/liquid partitioning data for olivine and pyroxene.
Author

N94-16365*# Lamont-Doherty Geological Observatory, Palisades, NY.
THE MONZONORITE-ANORTHOSITE CONNECTION: THE PETROGENESIS OF TERRESTRIAL KREEP Abstract Only **c46**
J. Longhi and J. Vander Auwera (Liege Univ., Belgium.) *In* Lunar and Planetary Inst., Twenty-Fourth Lunar and Planetary Science Conference. Part 2: G-M 1993 p 897-898 (For primary document see N94-16173 03-91)
Avail: CASI HC A01/MF A06

There is a suite of rocks typically associated with Proterozoic massif anorthosites that bear some interesting similarities to lunar KREEP. In many cases these rocks are plutonic and have traditionally been referred to as the jotunite-mangerite-+/-charnockite-+/-syenite suite. However, in the Rogaland district of southwestern Norway, where they are referred to as 'monzonorites', these rocks are also present as fine-grained dikes and as the chill margin of a layered intrusion, and thus approximate magmatic liquid compositions are readily obtained by chemical analysis. Monzonorites are typically enriched in incompatible lithophile elements such as K (alkali feldspar is present), the rare earths (REE), and P. They have intermediate to low Mg', low-Ca pyroxene, and more evolved types have low Ti/Sm ratios. Much debate has developed over attempts to explain the link between monzonorites and massif anorthosites. One feature seems clear: monzonorites and associated anorthosites have different initial isotopic ratios, so a simple relation is not possible. However, there is apparently a continuum in major elements between the monzonorites and gabbros believed to represent magmas parental to the anorthosites. This continuum suggests a link via high pressure fractionation coupled with assimilation. Although more complicated, this scenario is similar to that evoked for the early Moon: following the formation of ferroan anorthosites, continued fractional crystallization of the residual liquids at the base of the crust led to the formation of KREEP. An attempt is made here to establish a link between monzonorites and high-Al gabbros which are nearly always found as ancillary intrusions associated with anorthosites, and which may record processes in lower crustal magma chambers.
Author (revised)

N94-16366*# Jet Propulsion Lab., California Inst. of Tech., Pasadena.
MARTIAN LAVAS: THREE COMPLEMENTARY REMOTE SENSING TECHNIQUES TO DERIVE FLOW PROPERTIES Abstract Only
R. Lopes-Gautier, B. C. Bruno (Hawaii Univ., Honolulu.), G. J. Taylor (Hawaii Univ., Honolulu.), S. Rowland, and C. R. J. Kilburn (Lancaster Univ., England.) *In* Lunar and Planetary Inst., Twenty-Fourth Lunar and Planetary Science Conference. Part 2: G-M 1993 p 899-900 (For primary document see N94-16173 03-91)
Avail: CASI HC A01/MF A06

Several remote sensing techniques have been developed to determine various properties of lava flows. We are currently focusing on three such techniques to interpret Martian lava flows on Alba Patera, which are based on measurements of distal flow lobe widths which can be used to infer silica content; convolution of flow margins which can distinguish between pahoehoe and a'a types of basaltic flows; final flow field dimensions which can be combined with ground slope to derive effusion duration and average effusion rate. These methods are extremely complementary and together provide a more significant and complete understanding of extra-terrestrial lava flows. However, each of these techniques have specific and distinct data requirements.
Author

N94-16367*# Washington Univ., Seattle. Dept. of Astronomy.
DENSITIES OF 5-15 MICRON INTERPLANETARY DUST PARTICLES Abstract Only **c90**
S. G. Love, D. J. Joswiak, and D. E. Brownlee *In* Lunar and Planetary Inst., Twenty-Fourth Lunar and Planetary Science Conference. Part 2: G-M 1993 p 901-902 (For primary document see N94-16173 03-91)
Avail: CASI HC A01/MF A06

We have measured the densities of about 100 5-15 micron stratospheric IDPs. Great care was taken to minimize selection bias in the sample population. Masses were determined using an absolute x-ray analysis technique with a transmission electron microscope, and volumes were found using scanning electron microscope imagery. Unmelted chondritic particles have densities between 0.5 and 6.0 g/cc. Roughly half of the particles have densities below 2 g/cc, indicating appreciable porosity, but porosities greater than about 70 percent are rare. IDPs with densities above 3.5 g/cc usually contain large sulfide grains. We find no evidence of bimodality in the unmelted particle density distribution. Chondritic spherules (melted particles) have densities near 3.5 g/cc, consistent with previous results for deep sea spherules.
Author

N94-16368*# Massachusetts Univ., Amherst. Dept. of Physics and Astronomy.
RESOLVING TOPOGRAPHIC DETAIL ON VENUS BY MODELING COMPLEX MAGELLAN ALTIMETRY ECHOES Abstract Only
Amy J. Lovell, F. Peter Schloerb, and George E. McGill *In* Lunar and Planetary Inst., Twenty-Fourth Lunar and Planetary Science Conference. Part 2: G-M 1993 p 903-904 (For primary document see N94-16173 03-91)
Avail: CASI HC A01/MF A06

Magellan's altimeter is providing some of the finest resolution topography of Venus achieved to date. Nevertheless, efforts continue to improve the topographic resolution whenever possible. One effort to this end is stereoscopic imaging, which provides topography at scales similar to that of the synthetic aperture radar (SAR). However, this technique requires two SAR images of the same site to be obtained and limits the utility of this method. In this paper, we present another method to resolve topographic features at scales smaller than that of an altimeter footprint, which is more globally applicable than the stereoscopic approach. Each pulse which is transmitted by Magellan's altimeter scatters from the planet and echoes to the receiver, delayed based on the distance between the spacecraft and each surface element. As resolved in time, each element of an altimetry echo represents the sum of all points on the surface which are equidistant from the spacecraft. Thus, individual returns, as a function of time, create an echo profile which may be used to derive properties of the surface, such as the scattering law or, in this case, the topography within the footprint. The Magellan project has derived some of this information by fitting model templates to radar echo profiles. The templates are calculated based on Hagfor's Law, which assumes a smooth, gently undulating surface. In most regions these templates provide a reasonable fit to the observed echo profile; however, in some cases the surface departs from these simple assumptions and more complex profiles are observed. Specifically, we note that sub-footprint topographic relief apparently has a strong effect on the shape of the echo profile. To demonstrate the effects of sub-resolution relief on echo profiles, we have calculated the echo shapes from a wide range of simple topographic models. At this point, our topographic models have emphasized surfaces where only two dominant elevations are contained within a footprint, such as graben, ridges, crater rims, and central features in impact craters.
Author (revised)

N94-16369*# Geological Survey, Flagstaff, AZ.
SEDIMENTATION, VOLCANISM, AND ANCESTRAL LAKES IN THE VALLES MARINERIS: CLUES FROM TOPOGRAPHY Abstract Only
B. K. Lucchitta, N. K. Isbell, and A. Howington-Kraus *In* Lunar and Planetary Inst., Twenty-Fourth Lunar and Planetary Science Conference. Part 2: G-M 1993 p 905-906 (For primary document see N94-16173 03-91)
Avail: CASI HC A01/MF A06

Compilation of a simplified geologic/geomorphic map onto a digital terrain model of Valles Marineris has permitted quantitative evaluations of topographic parameters. The study showed that, if their interior layered deposits are lacustrine, the ancestral Valles Marineris must have consisted of isolated basins. If, on the other hand, the troughs were interconnected

as they are today, the deposits are most likely to volcanic origin, and the mesas in the peripheral troughs may be table mountains. The material eroded from the trough walls was probably not sufficient to form all of the interior layered deposits, but it may have contributed significantly to their formation.
Author

N94-16370*# Hawaii Univ., Honolulu. Planetary Geosciences.
THE CLEMENTINE INSTRUMENT COMPLEMENT Abstract Only **c43**
Paul G. Lucey *In* Lunar and Planetary Inst., Twenty-Fourth Lunar and Planetary Science Conference. Part 2: G-M 1993 p 907-908 (For primary document see N94-16173 03-91)
Avail: CASI HC A01/MF A06

The recent successes of the Galileo solid-state imaging (SSI) experiment at the Moon and Gaspra show the utility of multispectral imaging of planetary objects. 'Clementine' is the planetary community's 'code name' for the SDIO (Space Defense Initiative Organization), mission to the Moon and the asteroid Geographos. This mission is designed as a long term stressing test on sensors and space systems developed for SDIO. In the course of this test Clementine will obtain science data using a varied and powerful array of remote sensing instruments which were developed by or for Lawrence Livermore National Laboratory in Livermore, California. Clementine carries five cameras, one for navigation and four for science experiments. In addition, a laser ranger is included which will serve as a laser altimeter. The Clementine cameras cover a wider range of spatial resolutions and wavelength range than did Galileo and are almost ideally suited to mapping of mafic rock types as are present on the Moon and expected at Geographos. Calibration of the cameras will occur at the sensor calibration laboratory at LLNL. In flight calibrations, using standard stars and other standards should improve the stated accuracies. Signal-to-noise ratios (SNRs) include the following noise sources: shot noise, calibration error, digitization noise, readout noise, and frame transfer noise (where applicable). The achieved SNRs are a balance between detector saturation and acceptable image smear. The 'worst' case uses the longest possible integration times.
Author (revised)

N94-16371*# Hawaii Univ., Honolulu. Planetary Geosciences.
MIXING MODEL ANALYSIS OF TELESCOPIC LUNAR SPECTRA Abstract Only
Paul G. Lucey, Beth C. Clark, and B. Ray Hawke *In* Lunar and Planetary Inst., Twenty-Fourth Lunar and Planetary Science Conference. Part 2: G-M 1993 p 909-910 (For primary document see N94-16173 03-91)
Avail: CASI HC A01/MF A06

We have analyzed very high quality reflectance spectra of the lunar surface from the University of Hawaii lunar spectral data collection using a spectral mixing model. The spectra analyzed are those of 45 mare sites and 75 highland sites. The spectra were selected on the basis of very high signal to noise ratios based on error bars and point to point scatter, and on quality of removal of telluric water bands. The spectral mixing model used 7 components, not all of which were used in each fit. Four of the components were mineral spectra of the orthopyroxene, a clinopyroxene, an olivine and an anorthite, measured at the Brown University's RELAB. All of the minerals were 45-90 micron splits. Lunar soil contains other components which have the effect of reddening and darkening the soil as well as reducing spectral contrast. In addition, lunar soil contains spectral neutral bright material (likely very fine grained feldspar) which serves to reduce spectral contrast and brighten soils. Early attempts to fit many of the spectra pointed out the need for a component which has a very broad smooth absorption feature centered near 1.1 microns. Glass is a good candidate for this component. For the bright component we used a flat reflectance of 70 percent to represent fine grained feldspar. For the 'glass' component we used a telescopic spectrum of a pyroclastic glass present on the Aristarchus plateau which is characterized by a strong smooth band centered at 1.07 microns. In addition to exhibiting the glass band this spectrum is very red and has a low albedo. On the assumption that the dark component and the red component are agglutinates, which is reasonable but not necessarily true, we sought a dark red component. To derive its properties we modelled the spectrum of an Apollo 16 soil (16xxx) and assumed the dark red component to comprise 60 percent of the soil, appropriate to agglutinate abundance in mature soil. We adjusted the albedo and slope of a straight line representing the dark red component until the contrast and albedo of the model spectrum matched the soil spectrum. The mixing was done after conversion to a single scattering albedo.
Author

N94-16372*# Hawaii Univ., Honolulu. Planetary Geosciences.
FIRST RESULTS FROM A LABORATORY FACILITY FOR MEASUREMENT OF EMISSION SPECTRA UNDER SIMULATED PLANETARY CONDITIONS Abstract Only **c25**
Paul G. Lucey, Natalie Domergue-Schmidt, Bradley G. Henderson (Colorado Univ., Boulder.), and Bruce Jakosky (Colorado Univ., Boulder.) *In* Lunar and Planetary Inst., Twenty-Fourth Lunar and Planetary Science Conference. Part 2: G-M 1993 p 911-912 (For primary document see N94-16173 03-91)
Avail: CASI HC A01/MF A06

We have developed a laboratory spectroscopic facility for the measurement of emission spectra under simulated planetary conditions. Spectral measurements are made from 6 to 13 microns with a scanning grating monochromator equipped with a HgCdTl detector. An environment chamber in service in Hawaii for several years in which we can control the temperature from 77 K to 500 K, the pressure from 10(exp -5) torr to two atmospheres, has been equipped with a 77 K or 273 K cold shield. The shield serves to minimize light reflected off the sample and to aid in development of thermal gradients for obtaining spectra under conditions simulating the thermal environment of airless bodies. Samples are placed in small cups on a temperature controlled substrate allowing measurements of emission due to heating from below by the substrate, or from illumination from a solar simulation source.
Author

N94-16373*# Arizona Univ., Tucson.
EVOLUTION OF TRITON'S VOLATILE BUDGET Abstract Only
J. I. Lunine *In* Lunar and Planetary Inst., Twenty-Fourth Lunar and Planetary Science Conference. Part 2: G-M 1993 p 913-914 (For primary document see N94-16173 03-91)
Avail: CASI HC A01/MF A06

Triton's volatile budget provides important links to planetary formation processes in the cold outer solar nebula. However, the budget has been modified by processes subsequent to the accretion of this body. It is of interest to assess whether certain formation environments can be ruled out for Triton on the basis of its current volatile abundances, and also to quantify some of the post-accretional processes by which the abundances have been modified.
Author

N94-16374*# Science Applications International Corp., Glendora, CA.
THE EFFECT OF AN ON-ORBIT NEAR ENCOUNTER ON THE NUMBER FLUX DENSITY OF MICRON SIZED PARTICLES Abstract Only **c18**
Carl R. Maag, William G. Tanner (Baylor Univ., Waco, TX.), Tim J. Stevenson (Kent Univ., Canterbury, England.), Janet Borg (Institut d'Astrophysique, Paris, France.), Jean-Pierre Bibring (Institut d'Astrophysique, Paris, France.), W. Merle Alexander (Baylor Univ., Waco, TX.), and Andrew J. Maag (Stanford Univ., CA.) *In* Lunar and Planetary Inst., Twenty-Fourth Lunar and Planetary Science Conference. Part 2: G-M 1993 p 915 (For primary document see N94-16173 03-91)
Avail: CASI HC A01/MF A06

Many materials and techniques have been developed by the authors to sample the flux of particles in Low Earth Orbit (LEO), and through regular insitu sampling of the flux in LEO, the materials and techniques have produced data which complement the data now being amassed by the Long Duration Exposure Facility (LDEF) research activities. Recent flight experiments on STS-32, STS-44, STS-46, and STS-52 have been conducted to develop an understanding of the spatial density as a function of size (mass) for particle sizes 1x10(exp -6) cm and larger. In addition to the enumeration of particle impacts, it was also the intent of these experiments that hypervelocity particles be captured and returned intact. Measurements were performed post-flight to determine the flux density, diameters, and subsequent effects on various optical, thermal control, and structural materials. During the course of the STS-44 mission, the Space Shuttle corrected its altitude by 26 km to evade a spent upper stage. The results of this near encounter suggests that a cloud of micron sized particles exist in the vicinity of the object. Data also suggest that the flux density is nearly two (2) orders of magnitude higher than background flux. A comparison of the number flux density along with microphotographs of the captured particles will be presented for the referenced shuttle flights.
Author (revised)

N94-16375*# Orsted Inst., Copenhagen (Denmark). Physics Lab.
SUGGESTION FOR EXTENDED VIKING MAGNETIC PROPERTIES EXPERIMENT ON FUTURE MARS MISSIONS Abstract Only
M. B. Madsen, J. M. Knudsen, L. Vistisen (Niels Bohr Inst., Copenhagen, Denmark.), and R. B. Hargraves (Princeton Univ., NJ.) *In* Lunar and Planetary Inst., Twenty-Fourth Lunar and Planetary Science Conference. Part 2: G-M 1993 p 917-918 (For primary document see N94-16173 03-91)
Avail: CASI HC A01/MF A06

A remarkable result from the Viking missions was the discovery that the Martian soil is highly magnetic, in the sense that the soil is attracted by a small magnet. The soil was found to adhere almost equally well to a strong and a weak SmCo magnet in the Viking lander backhoe at both landing sites. An array of permanent magnets, with the purpose of establishing if the magnetic particles on Mars are present as discrete or as composite particles, has been constructed. Author

N94-16376*# Brown Univ., Providence, RI. Dept. of Geological Sciences.
LARGE-SCALE VOLCANISM ASSOCIATED WITH CORONAE ON VENUS Abstract Only
K. Magee Roberts and James W. Head *In* Lunar and Planetary Inst., Twenty-Fourth Lunar and Planetary Science Conference. Part 2: G-M 1993 p 919-920 (For primary document see N94-16173 03-91)
Avail: CASI HC A01/MF A06

The formation and evolution of coronae on Venus are thought to be the result of mantle upwellings against the crust and lithosphere and subsequent gravitational relaxation. A variety of other features on Venus have been linked to processes associated with mantle upwelling, including shield volcanoes on large regional rises such as Beta, Atla and Western Eistla Regiones and extensive flow fields such as Mylitta and Kaiwan Fluctus near the Lada Terra/Lavinia Planitia boundary. Of these features, coronae appear to possess the smallest amounts of associated volcanism, although volcanism associated with coronae has only been qualitatively examined. An initial survey of coronae based on recent Magellan data indicated that only 9 percent of all coronae are associated with substantial amounts of volcanism, including interior calderas or edifices greater than 50 km in diameter and extensive, exterior radial flow fields. Sixty-eight percent of all coronae were found to have lesser amounts of volcanism, including interior flooding and associated volcanic domes and small shields; the remaining coronae were considered deficient in associated volcanism. It is possible that coronae are related to mantle plumes or diapirs that are lower in volume or in partial melt than those associated with the large shields or flow fields. Regional tectonics or variations in local crustal and thermal structure may also be significant in determining the amount of volcanism produced from an upwelling. It is also possible that flow fields associated with some coronae are sheet-like in nature and may not be readily identified. If coronae are associated with volcanic flow fields, then they may be a significant contributor to plains formation on Venus, as they number over 300 and are widely distributed across the planet. As a continuation of our analysis of large-scale volcanism on Venus, we have reexamined the known population of coronae and assessed quantitatively the scale of volcanism associated with them. In particular, we have examined the percentage of coronae associated with volcanic flow fields (i.e., a collection of digitate or sheet-like lava flows extending from the corona interior or annulus); the range in scale of these flow fields; the variations in diameter, structure and stratigraphy of coronae with flow fields; and the global distribution of coronae associated with flow fields. Author (revised)

N94-16377*# Academy of Sciences (USSR), Moscow. Inst. of Physics of the Earth.
POSSIBLE SOURCES OF H2 TO H2O ENRICHMENT AT EVAPORATION OF PARENT CHONDRITIC MATERIAL Abstract Only **c90**
A. B. Makalkin, V. A. Dorofeyeva, and A. V. Vityazev *In* Lunar and Planetary Inst., Twenty-Fourth Lunar and Planetary Science Conference. Part 2: G-M 1993 p 921-922 (For primary document see N94-16173 03-91)
Avail: CASI HC A01/MF A06

One of the results obtained from thermodynamic simulation of recondensation of the source chondritic material is that at 1500-1800 K it's possible to form iron-rich olivine by reaction between enstatite, metallic iron and water vapor in the case of (H2O)/(H2) approximately equal to 0.1. This could be reached if the gas depletion in hydrogen is 200-300 times relative to solar abundance. To get this range of depletion one needs some source material more rich in hydrogen than the carbonaceous CI material which is the richest in volatiles among chondrites. In the case of recondensation at impact heating and evaporation of colliding planetesimals composed of CI material, we obtain insufficiently high value of (H2)/(H2O) ratio. In the present paper we consider some possible source materials and physical conditions necessary to reach gas composition with (H2)/(H2O) approximately 10 at high temperature. Author

N94-16378*# Denison Univ., Granville, OH. Dept. of Geology and Geography.
TIDAL REGIME OF INTACT PLANETOID CAPTURE MODEL FOR THE EARTH-MOON SYSTEM: DOES IT RELATE TO THE ARCHEAN SEDIMENTARY ROCK RECORD? Abstract Only **c90**
Robert J. Malcuit and Ronald R. Winters *In* Lunar and Planetary Inst., Twenty-Fourth Lunar and Planetary Science Conference. Part 2: G-M 1993 p 923-924 (For primary document see N94-16173 03-91)
Avail: CASI HC A01/MF A06

Regardless of one's favorite model for the origin of the Earth-Moon system (fission, coformation, tidal capture, giant-impact) the early history of lunar orbital evolution would produce significant thermal and earth and ocean tidal effects on the primitive earth. Three of the above lunar origin models (fission, coformation, giant-impact) feature a circular orbit which undergoes a progressive increase in orbital radius from the time of origin to the present time. In contrast, a tidal capture model places the moon in an elliptical orbit undergoing progressive circularization from the time of capture (for model purposes about 3.9 billion years ago) for at least a few 10(exp 8) years following the capture event. Once the orbit is circularized, the subsequent tidal history for a tidal capture scenario is similar to that for other models of lunar origin and features a progressive increase in orbital radius to the current state of the lunar orbit. This elliptical orbit phase, if it occurred, should have left a distinctive signature in the terrestrial and lunar rock records. Depositional events would be associated terrestrial shorelines characterized by abnormally high, but progressively decreasing, ocean tidal amplitudes and ranges associated with such an orbital evolution. Several rock units in the age range 3.6-2.5 billion years before present are reported to have a major tidal component. Examples are the Warrawoona, Fortescue, and Hamersley Groups of Western Australia and the Pangola and Witwatersand Supergroups of South Africa. Detailed study of the features of these tidal sequences may be helpful in deciphering the style of lunar orbital evolution during the Archean Eon. Author

N94-16379*# Lunar and Planetary Inst., Houston, TX.
ON THE DELIVERY OF PLANETESIMALS TO A PROTOPLANET IN THE SOLAR NEBULA Abstract Only **c90**
Renu Malhotra *In its* Twenty-Fourth Lunar and Planetary Science Conference. Part 2: G-M 1993 p 925-926 (For primary document see N94-16173 03-91)
Avail: CASI HC A01/MF A06

A planetesimal moving in the solar nebula experiences an aerodynamic drag which causes its orbit to circularize and shrink. However resonant perturbations from a protoplanet interior to the planetesimal's orbit can counteract both the orbital decay and the damping of the eccentricity: the planetesimal can be captured into an orbital resonance and its eccentricity pumped up to an equilibrium value. The resonance trapping phenomenon is sensitive to several factors and we elaborate on these below. Orbital resonances form (partial) barriers to the transport of planetesimals into the feeding zone of the protoplanet. Here we report on a systematic study of the idealized system of a single protoplanet of mass much larger than the masses of the planetesimals, comparing relevant analytic estimates with numerical simulations. Our principal conclusion is that in a gas-rich environment, the bulk of the solid material delivered to the feeding zone of the protoplanet is in the form of bodies of small radius. Author

N94-16380*# Malin Space Science Systems, San Diego, CA.
TECTONIC RESURFACING OF VENUS Abstract Only
Michael C. Malin, Robert E. Grimm (Arizona State Univ., Tempe.), and Robert R. Herrick (Lunar and Planetary Inst., Houston, TX.) *In* Lunar and Planetary Inst., Twenty-Fourth Lunar and Planetary Science Conference. Part 2: G-M 1993 p 927-928 (For primary document see N94-16173

03-91)
Avail: CASI HC A01/MF A06

Impact crater distributions and morphologies have traditionally played an important role in unraveling the geologic histories of terrestrial objects, and Venus has proved no exception. The key observations are: mean crater retention age about 500 Ma; apparently random spatial distribution; modest proportion (17 percent) of modified craters; and preferential association of modified craters with areas of low crater density. The simplest interpretation of these data alone is that Venus experienced global resurfacing (assumed to be largely volcanic) prior to 500 Ma, after which time resurfacing rates decreased dramatically. This scenario does not totally exclude present geological activity: some resurfacing and crater obliteration is occurring on part of the planet, but at rates much smaller than on Earth. An alternative endmember model holds that resurfacing is also spatially randomly distributed. Resurfacing of about 1 sq km/yr eliminates craters such that a typical portion of the surface has an age of 500 Ma, but actual ages range from zero to about 1000 Ma. Monte Carlo simulation indicates that the typical resurfacing 'patch' cannot exceed about 500 km in diameter without producing a crater distribution more heterogeneous than observed. Volcanic or tectonic processes within these patches must be locally intense to be able to obliterate craters completely and leave few modified. In this abstract, we describe how global geologic mapping may be used to test resurfacing hypotheses. We present preliminary evidence that the dominant mode of resurfacing on Venus is tectonism, not volcanism, and that this process must be ongoing today. Lastly, we outline a conceptual model in which to understand the relationship between global tectonics and crater distribution and preservation. Author

N94-16381*# Arizona State Univ., Tempe. Dept. of Geology.
VENUSIAN PANCAKE DOMES: INSIGHTS FROM TERRESTRIAL VOLUMINOUS SILICIC LAVAS AND THERMAL MODELING Abstract Only
Curtis R. Manley *In* Lunar and Planetary Inst., Twenty-Fourth Lunar and Planetary Science Conference. Part 2: G-M 1993 p 929-930 (For primary document see N94-16173 03-91)
Avail: CASI HC A01/MF A06

The so-called 'pancake' domes, and several other volcanoes on Venus, appear to represent large extrusions of silicic lava. Similar voluminous rhyolite lava flows, often associated with mantle plumes, are known on Earth. Venus' high ambient temperature, and insulation by the dome's brecciated carapace, both act to prolong cooling of a dome's interior, allowing for episodic lava input over an extended period of time. Field relations and aspect ratios of terrestrial voluminous rhyolite lavas imply continuous, non-episodic growth, reflecting tapping of a large volume of dry, anatectic silicic magma. Petrogenetically, the venusian domes may be analogous to chains of small domes on Earth, which represent 'leakage' of evolved material from magma bodies fractionating from much more mafic liquids. Author

N94-16382*# Academy of Sciences (USSR), Moscow. Inst. of Physics of the Earth.
GEOPHYSICAL MODELS OF WESTERN APHRODITE-NIOBE REGION: VENUS Abstract Only
K. I. Marchenkov, R. S. Saunders (Jet Propulsion Lab., California Inst. of Tech., Wrightwood.), and W. B. Banerdt (Jet Propulsion Lab., California Inst. of Tech., Wrightwood.) *In* Lunar and Planetary Inst., Twenty-Fourth Lunar and Planetary Science Conference. Part 2: G-M 1993 p 931-932 (For primary document see N94-16173 03-91)
Avail: CASI HC A01/MF A06

The new topography and gravitational field data for Venus expressed in spherical harmonics of degree and order up to 50 allow us to analyze the crust-mantle boundary relief and stress state of the Venusian lithosphere. In these models, we consider models in which convection is confined beneath a thick, buoyant lithosphere. We divide the convection regime into an upper mantle and lower mantle component. The lateral scales are smaller than on Earth. In these models, relative to Earth, convection is reflected in higher order terms of the gravitational field. On Venus geoid height and topography are highly correlated, although the topography appears to be largely compensated. We hypothesize that Venus topography for those wavelengths that correlate well with the geoid is partly compensated at the crust-mantle boundary, while for the others compensation may be distributed over the whole mantle. In turn the strong sensitivity of the stresses to parameters of the models of the external layers of Venus together with geological mapping allows us to begin investigations of the tectonics and geodynamics of the planet. For stress calculations we use a new technique of space- and time-dependent Green's response functions using Venus models with rheologically stratified lithosphere and mantle and a ductile lower crust. In the basic model of Venus the mean crust is 50-70 km thick, the density contrast across the crust-mantle boundary is in the range from 0.3 to 0.4 g/cm(exp -3). The thickness of a weak mantle zone may be from 350 to 1000 km. Strong sensitivity of calculated stress to various parameters of the layered model of Venus together with geological mapping and analysis of surface tectonic patterns allow us to investigate the tectonics and geodynamics of the planet. The results are presented in the form of maps of compression-extension and maximum shear stresses in the lithosphere and maps of crust-mantle boundary relief, which can be presented as a function of time. We have modeled the region of Western Aphrodite and the Niobe plains to get reasonable depths of compensation. Crust mantle boundary relief is calculated for Western Aphrodite-Niobe relative to a mean crustal thickness of 50 km. The calculations include the consequences of simple crust models and more complicated models with a weak, ductile lower crust, a strong upper mantle and a weak lower mantle layer. Author

N94-16383*# Paris Univ. (France).
CO2 PRODUCTION BY IMPACT IN CARBONATES? AN ATEM AND STABLE ISOTOPE (C,O) STUDY Abstract Only **c25**
I. Martinez, P. Agrinier, F. Guyot, Ph. Ildefonse, M. Javoy, U. Schaerer, U. Hornemann (Muenster Univ., Germany.), and A. Deutsch (Muenster Univ., Germany.) *In* Lunar and Planetary Inst., Twenty-Fourth Lunar and Planetary Science Conference. Part 2: G-M 1993 p 933-934 (For primary document see N94-16173 03-91)
Avail: CASI HC A01/MF A06

Carbonates may have been a common target for large impacts on the Earth and possible related CO2 outgassing would have important consequences for the composition of the atmosphere. To estimate volatile release during such impacts, isotopic ratios (C-13/C-12 and O-18/O-16) were determined on highly shocked carbonate samples in combination with SEM and analytical transmission electron microscopy (ATEM) investigations. The study was performed on both naturally and experimentally shocked rocks, i.e. 50-60 GPa shocked limestone-dolomite fragments from the Haughton impact crater (Canada), and carbonates shocked in shock recovery experiments. For the experiments, unshocked carbonates consisting of mixture of dolomite and calcite from the Haughton area were used. Naturally shocked samples were collected in the polymict breccia near the center of the Haughton crater. Author

N94-16384*# Padua Univ. (Italy). Dept. of Physics.
DUST GRAIN RESONANT CAPTURE: A STATISTICAL STUDY Abstract Only **c90**
F. Marzari, V. Vanzani, and S. J. Weidenschilling (Planetary Science Inst., Tucson, AZ.) *In* Lunar and Planetary Inst., Twenty-Fourth Lunar and Planetary Science Conference. Part 2: G-M 1993 p 935-936 (For primary document see N94-16173 03-91)
Avail: CASI HC A01/MF A06

A statistical approach, based on a large number of simultaneous numerical integrations, is adopted to study the capture in external mean motion resonances with the Earth of micron size dust grains perturbed by solar radiation and wind forces. We explore the dependence of the resonant capture phenomenon on the initial eccentricity e(sub 0) and perihelion argument w(sub 0) of the dust particle orbit. The intensity of both the resonant and dissipative (Poynting-Robertson and wind drag) perturbations strongly depends on the eccentricity of the particle while the perihelion argument determines, for low inclination, the mutual geometrical configuration of the particle's orbit with respect to the Earth's orbit. We present results for three j:j+1 commensurabilities (2:3, 4:5 and 6:7) and also for particle sizes s = 15, 30 microns. This study extends our previous work on the long term orbital evolution of single dust particles trapped into resonances with the Earth. Author

N94-16385*# Los Alamos National Lab., NM. Space Science and Technology Div.
EFFECTS OF BULK COMPOSITION ON PRODUCTION RATES OF COSMOGENIC NUCLIDES IN METEORITES Abstract Only **c90**

Jozef Masarik and Robert C. Reedy *In* Lunar and Planetary Inst., Twenty-Fourth Lunar and Planetary Science Conference. Part 2: G-M 1993 p 937-938 (For primary document see N94-16173 03-91)
Avail: CASI HC A01/MF A06

The bulk chemical composition of meteorites has been suggested as a main factor influencing the production of cosmogenic nuclides. Numerical simulations with Los Alamos Monte Carlo production and transport codes were done for Ne-21/Ne-22 ratios and Ar-38 production rates in meteorites with a wide range of compositions. The calculations show that an enhanced flux of low-energy secondary particles in metal-rich phases is the essential key for the explanation of experimentally observed differences in nuclide production processes in various meteorite classes. Author

N94-16386*# Jet Propulsion Lab., California Inst. of Tech., Pasadena.
A DECADE'S OVERVIEW OF IO'S VOLCANIC ACTIVITY Abstract Only **c90**

D. L. Matson, G. J. Veeder, T. V. Johnson, D. L. Blaney, and J. D. Goguen *In* Lunar and Planetary Inst., Twenty-Fourth Lunar and Planetary Science Conference. Part 2: G-M 1993 p 939-940 (For primary document see N94-16173 03-91)
Avail: CASI HC A01/MF A06

Over the past decade some aspects of Io's volcanic activity have changed greatly, while others have essentially remained constant. This contrast has emerged from our study of multi-wavelength, infrared, observations of Io's thermal emission. From 1983 to 1992 we observed the disk integrated flux density of Io from the NASA Infrared Telescope Facility (IRTF) on Mauna Kea, Hawaii. Our spectral coverage allows us to separate out the emission components due to volcanic thermal anomalies which are warmer than the background emission caused by solar heating. Our temporal coverage allows us to resolve individual eruptions and also to obtain the disk-integrated flux density as a function of longitude (or, equivalently, orbital phase angle). Characteristics that persisted over the decade involve Loki's location and intensity of emission, the leading hemisphere emission, and the average heat flow. The variable aspects of Io over the decade include Loki's hotter area(s) and the outbursts in the leading hemisphere. Author

N94-16387*# National Aerospace Lab., Tokyo (Japan). Control Systems Div.
A MISSION CONCEPT OF PHOBOS/DEIMOS EXPLORATION Abstract Only

K. Matsushima, J. Saito, M. Utashima (National Space Development Agency, Saitama, Japan.), and H. Koshiishi (Remote Sensing Technology Center, Tokyo, Japan.) *In* Lunar and Planetary Inst., Twenty-Fourth Lunar and Planetary Science Conference. Part 2: G-M 1993 p 941-942 (For primary document see N94-16173 03-91)
Avail: CASI HC A01/MF A06

We have been designing the concept of Phobos/Deimos mission using the Japanese H-2 rocket as a first step in asteroid exploration. In planning the mission concept, we focused on development of methods to characterize the materials of Phobos/Deimos. The development of such methods will contribute to both scientific and resource explorations of asteroids. Here we report the preliminary concept of the mission. Author

N94-16388*# Tokyo Univ. (Japan). Inst. for Cosmic Ray Research.
SIZE DISTRIBUTION OF INTERPLANETARY IRON AND STONY PARTICLES RELATED WITH DEEP-SEA SPHERULES Abstract Only **c90**

H. Matsuzaki and K. Yamakoshi *In* Lunar and Planetary Inst., Twenty-Fourth Lunar and Planetary Science Conference. Part 2: G-M 1993 p 943-944 (For primary document see N94-16173 03-91)
Avail: CASI HC A01/MF A06

To study origin and evolution of the interplanetary dust, it is very important to investigate the size distribution. Here the changes of the size distributions of meteoroid particles due to the ablative effects during atmospheric entry were investigated by numerical computer simulation. Using the results, the pre-atmospheric size distributions of the interplanetary dust particles could be estimated from that of ablated spherules taken from deep-sea sediments. We are now analyzing deep-sea spherules from some aspects and examining if we could get any information about the interplanetary dust. Author

N94-16389*# Hawaii Univ., Honolulu. Dept. of Geology and Geophysics.
CLASSIFICATIONAL PARAMETERS FOR ACAPULCOITES AND LODRANITES: THE CASES OF FRO 90011, EET 84302 AND ALH A81187/84190 Abstract Only **c90**

T. J. McCoy, K. Keil, R. N. Clayton (Chicago Univ., IL.), and T. K. Mayeda (Chicago Univ., IL.) *In* Lunar and Planetary Inst., Twenty-Fourth Lunar and Planetary Science Conference. Part 2: G-M 1993 p 945-946 (For primary document see N94-16173 03-91)
Avail: CASI HC A01/MF A06

Acapulcoites and lodranites probably sample a common parent body, which has experienced a range of partial melting. We present classificational parameters which allow acapulcoites-lodranites to be distinguished from other groups of meteorites, as well as from each other. Petrography can complement oxygen isotopic compositions in separating these meteorites from other groups of stony-irons and primitive achondrites, while petrographic properties alone distinguish acapulcoites from lodranites. Acapulcoites differ from lodranites in having smaller grain sizes, abundant Fe, Ni-FeS as micron-sized veins and plagioclase which escaped melting. We have applied these criteria to three new members of the group. FRO 90011 is a typical lodranite; EET 84302 is intermediate in many properties between acapulcoites and lodranites; and ALH A81187/84190 are paired meteorites and are first low-FeO acapulcoites. These meteorites provide a wider spectrum of samples from the acapulcoite-lodranite parent body and suggests that this body may have had a complex structure. Author

N94-16390*# Hawaii Univ., Honolulu. Dept. of Geology and Geophysics.
THE DREGS OF CRYSTALLIZATION IN ZAGAMI Abstract Only **c90**

T. J. McCoy, K. Keil, and G. J. Taylor *In* Lunar and Planetary Inst., Twenty-Fourth Lunar and Planetary Science Conference. Part 2: G-M 1993 p 947-948 (For primary document see N94-16173 03-91)
(Grant NAG9-454)
Avail: CASI HC A01/MF A06

The Zagami shergottite is a basaltic meteorite which formed when a phenocryst-bearing lava flow was emplaced at or near the surface of Mars. Recently, a cm-sized olivine-rich lithology has been identified in Zagami by Mossbauer spectroscopy. Olivine is extremely rare in shergottites, particularly in Zagami and Shergotty, where it occurs only as minute grains. We report petrologic and microprobe studies of this olivine-rich lithology. This material represents the last few percent of melt and is highly enriched in phosphates, opaques and mesostases, all of which are late-stage crystallization products. Phosphates replaced augite as a phenocryst phase when the magma became saturated in P. This late stage melt also includes a fayalite-bearing, multi-phase intergrowth which crystallized after the melt became too rich in iron to crystallize pigeonite. We can now reconstruct the entire crystallization history of the Zagami shergottite from a deep-seated magma chamber to crystallization of the final few percent of melt in a near-surface dike or thick flow. Small pockets (tens of microns) of late-stage melt pockets are ubiquitous but volumetrically minor in Zagami. We do not know the physical relationship between these areas and the cm-sized olivine-rich material described here. It is possible that these small pockets were mobile, forming larger areas. Perhaps inspection of the entire hand specimen of Zagami would clarify this relationship. Derived from text

N94-16391*# Kent Univ., Canterbury (England). Unit for Space Sciences.
RESOLVING LDEF'S FLUX DISTRIBUTION: ORBITAL (DEBRIS?) AND NATURAL METEOROID POPULATIONS Abstract Only **c90**

J. A. M. McDonnell *In* Lunar and Planetary Inst., Twenty-Fourth Lunar and Planetary Science Conference. Part 2: G-M 1993 p 949-950 (For primary document see N94-16173 03-91)
Avail: CASI HC A01/MF A06

A consistent methodology for the collation of data from both penetration and perforation experiments and from data in the Meteoroid and Debris Special Investigator Group (M-D SIG) data-base has led to the derivation of the average impact flux over LDEF's exposure history 1984-1990. Data are first presented for LDEF's N,S,E,W and Space faces ('offset' by 8 deg and 'tilted' by 1 deg respectively). A model fit is derived for ballistic limits of penetration from 1 micron to 1mm of aluminium target, corresponding to impactor masses from 10(exp -18) kg (for rho sub p = 2g/cu cm) to 10(exp -10) kg (for rho sub p = 1g/cu cm). A second order harmonic

function is fitted to the N,S,E, and W fluxes to establish the angular distribution at regular size intervals; this fit is then used to provide 'corrected' data corresponding to fluxes applicable to true N,S,E,W and Space directions for a LEO 28.5 degree inclination orbit at a mean altitude of 465 km.
Derived from text

N94-16392*# Geological Survey, Flagstaff, AZ.
CLEMENTINE: ANTICIPATED SCIENTIFIC DATASETS FROM THE MOON AND GEOGRAPHOS Abstract Only
A. S. McEwen *In* Lunar and Planetary Inst., Twenty-Fourth Lunar and Planetary Science Conference. Part 2: G-M 1993 p 951-952 (For primary document see N94-16173 03-91)
Avail: CASI HC A01/MF A06

The Clementine spacecraft mission is designed to test the performance of new lightweight and low-power detectors developed at the Lawrence Livermore National Laboratory (LLNL) for the Strategic Defense Initiative Office (SDIO). A secondary objective of the mission is to acquire useful scientific data, principally of the Moon and the near-Earth asteroid Geographos. The spacecraft will be in an elliptical polar orbit about the Moon for about 2 months beginning in February of 1994 and it will fly by Geographos on August 31. Clementine will carry seven detectors each weighing less than about 1 kg: two Star Trackers wide-angle uv/vis wide-angle Short Wavelength IR (SWIR) Long-Wavelength IR (LWIR) and LIDAR (Laser Image Detection And Ranging) narrow-angle imaging and ranging. Additional presentations about the mission detectors and related science issues are in this volume. If fully successful Clementine will return about 3 million lunar images, a dataset with nearly as many bits of data (uncompressed) as the first cycle of Magellan and more than 5000 images of Geographos. The complete and efficient analysis of such large data sets requires systematic processing efforts. Described below are concepts for two such efforts for the Clementine mission: global multispectral imaging of the Moon and videos of the Geographos flyby. Other anticipated datasets for which systematic processing might be desirable include multispectral observations of Earth; LIDAR altimetry of the Moon with high-resolution imaging along each ground track; high-resolution LIDAR color along each lunar ground track which could be used to identify potential titanium-rich deposits at scales of a few meters; and thermal IR imaging along each lunar ground track (including nighttime observations near the poles).
Derived from text

N94-16393*# Geological Survey, Flagstaff, AZ.
GLOBAL AND REGIONAL/SEASONAL COLOR MOSAICS OF MARS Abstract Only
Alfred S. McEwen and Laurence A. Soderblom *In* Lunar and Planetary Inst., Twenty-Fourth Lunar and Planetary Science Conference. Part 2: G-M 1993 p 953-954 (For primary document see N94-16173 03-91)
Avail: CASI HC A01/MF A06

Four regional mosaics of Mars acquired during different seasons, along with their composite as a single global mosaic, have been completed in two colors (red and violet) at scales of 1/16 and 1/64 degrees/pixel. These mosaics were put together from a set of 51 separate mosaics, each acquired from a single Viking orbiter spacecraft orbital revolution. Special techniques were developed and applied to suppress large variations between mosaics introcued by highly variable, optically thin, condensate hazes. The techniques utilize a combination of the spatial characteristics of the hazes (generally broad, low-frequency) along with their modulation of the reginal color ratios (strongly enhancing the violet/red ratios). Photometric-function normalization was applied following the haze removal. Most of the single-orbit mosaics consist of red and violet or red, green, and violet filters, but a few mosaics with only red-filter data were included to fill gaps in global coverage at high northern latitudes. Global coverage is approximately 99 percent complete in red-filter mosaics and approximately 95 percent and approximately 60 percent complete in corresponding violet- and green-filter mosaics, respectively. All of the mosaics are geometrically tied to the 1/256 deg per pixel Mars Digital Image Map (MDIM), which is available on Compact Disk (CD), and which will be used as the base map for Mars Observer data sets. Early in 1993, the single-orbit color mosaics will be distributed to the science community in a six-volume set of CDs. Perhaps the most scientifically interesting parts of this dataset are the overlap regions, which show significant temporal variations in surface and atmospheric features. Surface changes can be categorized as (1) changes that probably occurred during the great dust storms of 1977; (2) changes that occurred soon after 1977 storms due to removal of redistribution of recently deposited dust; (3) changes in the northern lowlands that probably occurred during the dusty southern summer of 1979 (when no great dust storm occurred); and (4) changes associated with strong slope winds in the Tharsis and Elysium regions.
Derived from text

N94-16394*# Geological Survey, Flagstaff, AZ.
LUNAR MULTISPECTRAL MOSAICS FROM GALILEO'S SECOND EARTH-MOON FLYBY Abstract Only
A. S. McEwen, T. L. Becker, M. S. Robinson (Hawaii Univ., Honolulu.), K. P. Klaasen (Jet Propulsion Lab., California Inst. of Tech., Pasadena.), C. Heffernan (Jet Propulsion Lab., California Inst. of Tech., Pasadena.), and J. M. Sunshine (Brown Univ., Providence, RI.) *In* Lunar and Planetary Inst., Twenty-Fourth Lunar and Planetary Science Conference. Part 2: G-M 1993 p 955-956 (For primary document see N94-16173 03-91)
Avail: CASI HC A01/MF A06

Galileo's Solid-State Imaging (SSI) experiment acquired about 800 images of the Moon from the second Earth-Moon flyby (EM2) in December of 1992. Ten major sequences were acquired; each consists of mosaics of the entire or nearly entire visible and illuminated surface from each viewing geometry in at least six spectral filters (effective wavelengths for the Moon of 420, 564, 660, 756, 890, and 990 nm). The geometries of LUNMOS numbers 3, 4, 5, and 6 were designed to provide stereo data at the best possible resolutions. The purpose of this abstract is to describe the sequences, calibration, processing, and mosaicking, and to present a set of color products in a poster session.
Derived from text

N94-16395*# Geological Survey, Flagstaff, AZ.
GALILEO SSI LUNAR OBSERVATIONS: COPERNICAN CRATERS AND SOILS Abstract Only
A. S. McEwen, R. Greeley (Arizona State Univ., Tempe.), James W. Head (Brown Univ., Providence, RI.), C. M. Pieters (Brown Univ., Providence, RI.), E. M. Fischer (Brown Univ., Providence, RI.), T. V. Johnson (Jet Propulsion Lab., California Inst. of Tech., Pasadena.), and G. Neukum (Deutsche Forschungs- und Versuchsanstalt fuer Luft- und Raumfahrt, Berlin, Germany.) *In* Lunar and Planetary Inst., Twenty-Fourth Lunar and Planetary Science Conference. Part 2: G-M 1993 p 957-958 (For primary document see N94-16173 03-91)
Avail: CASI HC A01/MF A06

The Galileo spacecraft completed its first Earth-Moon flyby (EMI) in December 1990 and its second flyby (EM2) in December 1992. Copernican-age craters are among the most prominent features seen in the SSI (Solid-State Imaging) multispectral images of the Moon. The interiors, rays, and continuous ejecta deposits of these youngest craters stand out as the brightest features in images of albedo and visible/1-micron color ratios (except where impact melts are abundant). Crater colors and albedos (away from impact melts) are correlated with their geologic emplacement ages as determined from counts of superposed craters; these age-color relations can be used to estimate the emplacement age (time since impact event) for many Copernican-age craters on the near and far sides of the Moon. The spectral reflectivities of lunar soils are controlled primarily by (1) soil maturity, resulting from the soil's cumulative age of exposure to the space environment; (2) steady-state horizontal and vertical mixing of fresh crystalline materials ; and (3) the mineralogy of the underlying bedrock or megaregolith. Improved understanding of items (1) and (2) above will improve our ability to interpret item (3), especially for the use of crater compositions as probes of crustal stratigraphy. We have examined the multispectral and superposed crater frequencies of large isolated craters, mostly of Eratosthenian and Copernican ages, to avoid complications due to (1) secondaries (as they affect superposed crater counts) and (2) spatially and temporally nonuniform regolith mixing from younger, large, and nearby impacts. Crater counts are available for 11 mare craters and 9 highlands craters within the region of the Moon imaged during EM1. The EM2 coverage provides multispectral data for 10 additional craters with superposed crater counts. Also, the EM2 data provide improved spatial resolution and signal-to-noise ratios over the western nearside.
Author

N94-16396*# Massachusetts Inst. of Tech., Cambridge. Dept. of Earth, Atmospheric, and Planetary Sciences.
ASPECTS OF MODELLING THE TECTONICS OF LARGE VOLCANOES ON THE TERRESTRIAL PLANETS Abstract Only **c46**
Patrick J. McGovern and Sean C. Solomon (Carnegie Institution of

Washington, DC.) *In* Lunar and Planetary Inst., Twenty-Fourth Lunar and Planetary Science Conference. Part 2: G-M 1993 p 959-960 (For primary document see N94-16173 03-91)
Avail: CASI HC A01/MF A06

Analytic solutions for the responses of planetary lithospheres to volcanic loads have been used to model faulting and infer elastic plate thicknesses. Predictions of the distribution of faulting around volcanic loads, based on the application of Anderson's criteria for faulting to the results of the models, do not agree well with observations. Such models do not give the stress state in the load itself, but only suggest a state of horizontal compressive stress there. Further, these models have considered only the effect of an instantaneously emplaced load. They do not address the time evolution of stresses, nor do they consider the effect of a load which grows. A finite element approach allows us to assign elements to the load itself, and thus permits calculation of the stress state and stress history within the edifice. The effects of episodic load growth can also be treated. When these effects are included, models give much better agreement with observations. We use the finite element code TECTON to construct axisymmetric models of volcanoes resting on an elastic lithospheric plate overlying a viscoelastic asthenosphere. We have implemented time-dependent material properties in order to simulate incremental volcano growth. The viscoelastic layer was taken to extend to a sufficient depth so that a rigid lower boundary has no significant influence on the results. The code first calculates elastic deformations and stresses and then determines the time-dependent viscous deformations and stresses. Time in the model scales as the Maxwell time tau(m) in the asthenosphere. We consider a volcano 25 km in height and 200 km in radius on an elastic lithosphere 40 km thick (parameters approximately appropriate to Ascraeus Mons). The volcano consists of three load increments applied at intervals of 1000 tau(m). Contours of maximum deviatoric stress in the fully-grown edifice at the conclusion of flexure (t = 3000 tau(m)) are shown. Derived from text

N94-16397*# National Aeronautics and Space Administration. Lyndon B. Johnson Space Center, Houston, TX.
GRAIN SURFACE FEATURES OF APOLLO 17 ORANGE AND BLACK GLASS Abstract Only
David S. McKay and Sue J. Wentworth (Lockheed Engineering and Sciences Co., Houston, TX.) *In* Lunar and Planetary Inst., Twenty-Fourth Lunar and Planetary Science Conference. Part 2: G-M 1993 p 961-962 (For primary document see N94-16173 03-91)
Avail: CASI HC A01/MF A06

Lunar soil sample 74220 and core samples 74001/2 consist mainly of orange glass droplets, droplet fragments, and their crystallized equivalents. These samples are now generally accepted to be pyroclastic ejecta from early lunar volcanic eruptions. It has been known that they contain surface coatings and material rich in volatile condensable phases including S, Zn, F, Cl, and many volatile metals. Meyer summarizes the voluminous published chemical data and calculates the volatile enrichment ratios for most of the surface condensates. In an attempt to more completely understand this enrichment of surface volatiles, we have searched for carbon and carbon-bearing phases on droplet surfaces. We have reviewed many of our existing photomicrographs and energy dispersive analysis (EDX) of grain surfaces and have reexamined some of our older SEM mounts using an improved EDXA system capable of light element detection and analysis (oxygen, nitrogen, and carbon). In addition, we have made fresh mounts using procedures which should minimize carbon contamination or extraneous carbon x-rays and have analyzed for carbon. Derived from text

N94-16398*# National Aeronautics and Space Administration. Lyndon B. Johnson Space Center, Houston, TX.
JSC-1: A NEW LUNAR REGOLITH SIMULANT Abstract Only
David S. McKay, James L. Carter (Texas Univ., Dallas.), Walter W. Boles (Texas A&M Univ., College Station.), Carlton C. Allen (Lockheed Engineering and Sciences Co., Houston, TX.), and Judith H. Allton (Lockheed Engineering and Sciences Co., Houston, TX.) *In* Lunar and Planetary Inst., Twenty-Fourth Lunar and Planetary Science Conference. Part 2: G-M 1993 p 963-964 (For primary document see N94-16173 03-91)
Avail: CASI HC A01/MF A06

Simulants of lunar rocks and soils with appropriate properties, although difficult to produce in some cases, will be essential to meeting the system requirements for lunar exploration. In order to address this need a new lunar regolith simulant, JSC-1, has been developed. JSC-1 is a glass-rich basaltic ash which approximates the bulk chemical composition and mineralogy of some lunar soils. It has been ground to produce a gain size distribution approximating that of lunar regolith samples. The simulant is available in large quantities (greater than 2000 lb; 907 kg). JSC-1 was produced specifically for large- and medium-scale engineering studies in support of future human activities on the Moon. Such studies include material handling, construction, excavation, and transportation. The simulant is also appropriate for research on dust control and spacesuit durability. JSC-1 can be used as a chemical or mineralogical analog to some lunar soils for resource studies such as oxygen or metal production, sintering, and radiation shielding. Derived from text

N94-16399*# National Aeronautics and Space Administration. Lyndon B. Johnson Space Center, Houston, TX.
THE NAKHLA PARENT MELT: REE PARTITION COEFFICIENTS AND CLUES TO MAJOR ELEMENT COMPOSITION Abstract Only **c90**
G. McKay, L. Le (Lockheed Engineering and Sciences Co., Houston, TX.), and J. Wagstaff (Lockheed Engineering and Sciences Co., Houston, TX.) *In* Lunar and Planetary Inst., Twenty-Fourth Lunar and Planetary Science Conference. Part 2: G-M 1993 p 965-966 (For primary document see N94-16173 03-91)
Avail: CASI HC A01/MF A06

Nakhla is one of the SNC meteorites, generally believed to be of Martian origin. It is a medium-grained augite-olivine cumulate with a variolitic groundmass of sodic plagioclase, alkali feldspar, and Fe-rich pyroxenes and olivine. One of the major tasks in deciphering Nakhla's petrogenesis is determining the composition of its parent melt. Gaining an understanding of the composition and petrogenesis of this parent melt may help unravel Nakhla's relationship to the other SNCs, and provide clues to Martian petrogenesis in general. Our experimental partitioning studies provide new information that helps constrain both the major and trace element composition of the Nakhla parent melt. Author

N94-16400*# National Aeronautics and Space Administration. Lyndon B. Johnson Space Center, Houston, TX.
MORE ON THE COOLING HISTORY OF ANGRITE LEW 86010 Abstract Only **c90**
G. McKay, T. Ogawa (Tokyo Univ., Japan.), M. Miyamoto (Tokyo Univ., Japan.), and H. Takeda (Tokyo Univ., Japan.) *In* Lunar and Planetary Inst., Twenty-Fourth Lunar and Planetary Science Conference. Part 2: G-M 1993 p 967-968 (For primary document see N94-16173 03-91)
Avail: CASI HC A01/MF A06

Antarctic angrite LEW 86010 has many chemical and mineralogical characteristics which suggest it is closely related to Angra dos Reis (ADOR). However, these meteorites have had very different thermal histories. Olivines and pyroxenes in ADOR are nearly homogeneous, suggesting very slow cooling or extensive subsolidus equilibration. In contrast, LEW 86010 pyroxenes are extensively zoned in both major and trace elements, while olivines are nearly homogeneous, suggesting that cooling of this sample was slow enough to homogenize olivines, but too fast to homogenize pyroxenes. In an earlier study, we used Ca diffusion gradients associated with exsolution lamellae of kirsh-steinite in LEW 86010 olivines to estimate the cooling rate of this sample. We obtained cooling rates of a few x.01 deg C/yr, corresponding to a burial depth of approximately 10(exp 2) m under solid rock (thermal diffusivity = 0.004 sq cm/s), or approximately m under regolith material (10(exp -5) sq cm/s). Unfortunately, this calculation was very sensitive to the assumed temperature of initial exsolution, which we approximated from the estimated initial olivine bulk Ca content, and also to the extrapolated values for the Ca diffusion coefficient (D sub Ca). This abstract reports new cooling rate estimates obtained using a refined approach that includes the initial temperature of exsolution as one of the fitted parameters. The purpose of our new calculations is (1) to reduce uncertainties in cooling rate due to uncertainties in bulk olivine Ca content and initial exsolution temperature, (2) to investigate the effects of using different values for D sub Ca, and (3) to determine how well constrained the cooling rate is for any particular Ca diffusion coefficient.
Derived from text

N94-16401*# Geological Survey, Denver, CO.
LIMITED SUBSOLIDUS DIFFUSION IN TYPE B1 CAI: EVIDENCE FROM TI DISTRIBUTION IN SPINEL Abstract Only **c25**
G. P. Meeker, J. E. Quick, and Julie M. Paque (National Aeronautics and

Space Administration. Ames Research Center, Moffett Field, CA.) *In* Lunar and Planetary Inst., Twenty-Fourth Lunar and Planetary Science Conference. Part 2: G-M 1993 p 969-970 (For primary document see N94-16173 03-91)
Avail: CASI HC A01/MF A06

Most models of calcium aluminum-rich inclusions (CAI) have focused on early stages of formation by equilibrium crystallization of a homogeneous liquid. Less is known about the subsolidus cooling history of CAI. Chemical and isotopic heterogeneties on a scale of tens to hundreds of micrometers (e.g. MacPherson et al. (1989) and Podosek, et al. (1991)) suggest fairly rapid cooling with a minimum of subsolidus diffusion. However, transmission electron microscopy indicates that solid state diffusion may have been an important process at a smaller scale (Barber et al. 1984). If so, chemical evidence for diffusion could provide constraints on cooling times and temperatures. With this in mind, we have begun an investigation of the Ti distribution in spinels from two type B1 CAI from Allende to determine if post-crystallization diffusion was a significant process. The type B1 CAIs, 3529Z and 5241 have been described by Podosek et al. (1991) and by El Goresy et al. (1985) and MacPherson et al. (1989). We have analyzed spinels in these inclusions using the electron microprobe. These spinels are generally euhedral, range in size from less than 10 to 15 micron and are poikilitically enclosed by millimeter-sized pyroxene, melilite, and anorthite. Analyses were obtained from both the mantles and cores of the inclusions. Compositions of pyroxene in the vicinity of individual spinel grains were obtained by analyzing at least two points on opposite sides of the spinel and averaging the compositions. The pyroxene analyses were obtained within 15 microns of the spinel-pyroxene interface. No compositional gradients were observed within single spinel crystals. Ti concentrations in spinels included within pyroxene, melilite, and anorthite are presented.

Derived from text

N94-16402*# Colorado Univ., Boulder. Lab. for Atmospheric and Space Physics.
THE EFFECTS OF ORBITAL AND CLIMATIC VARIATIONS ON MARTIAN SURFACE HEAT FLOW Abstract Only
Michael T. Mellon and Bruce M. Jakosky *In* Lunar and Planetary Inst., Twenty-Fourth Lunar and Planetary Science Conference. Part 2: G-M 1993 p 971 (For primary document see N94-16173 03-91)
Avail: CASI HC A01/MF A06

Large changes in the orbital elements of Mars on timescales of 10(exp 4) to 10(exp 6) years will cause widely varying climate, specifically surface temperatures, as a result of varying insolation. These surface temperature oscillations will produce subsurface thermal gradients which contribute to the total surface heat flux. We investigate the thermal behavior of the Martian regolith on orbital timescales and show that this climatological surface heat flux is spatially variable and contributes significantly to the total surface heat flux at many locations. We model the thermal behavior of the Martian regolith by calculating the mean annual surface temperatures for each epoch (spaced 1000 years apart to resolve orbital variations) for the past 200,000 years at a chosen location on the surface. These temperatures are used as a boundary condition for the deeper regolith and subsurface temperature oscillation are then computed. The surface climatological heat flux due to past climate changes can then be found from the temperature gradient between the surface and about 150 m depth (a fraction of the thermal skin depth on these timescales). This method provides a fairly accurate determination of the climatological heat flow component at a point; however, this method is computationally time consuming and cannot be applied to all points on the globe. To map the spatial variations in the surface heat flow we recognize that the subsurface temperature structure will be largely dominated by the most recent surface temperature oscillations. In fact, the climate component of the surface heat flow will be approximately proportional to the magnitude of the most recent surface temperature change. By calculating surface temperatures at all points globally for the present epoch and an appropriate past epoch, and combining these results with a series of more precise calculations described above, we estimate the global distribution of climatological surface heat flow.

Derived from text

N94-16403*# Colorado Univ., Boulder. Lab. for Atmospheric and Space Physics.
EQUATORIAL GROUND ICE ON MARS: STEADY-STATE STABILITY Abstract Only
Michael T. Mellon, Bruce M. Jakosky, and Susan E. Postawko (Oklahoma Univ., Norman.) *In* Lunar and Planetary Inst., Twenty-Fourth Lunar and Planetary Science Conference. Part 2: G-M 1993 p 973-974 (For primary document see N94-16173 03-91)
Avail: CASI HC A01/MF A06

Current Martian equatorial surface temperatures are too warm for water ice to exist at the surface for any appreciable length of time before subliming into the atmosphere. Subsurface temperatures are generally warmer still and, despite the presence of a diffusive barrier of porous regolith material, it has been shown by Smoluchowski, Clifford and Hillel, and Fanale et al. that buried ground ice will also sublime and be lost to the atmosphere in a relatively short time. We investigate the behavior of this subliming subsurface ice and show that it is possible for ice to maintain at a steady-state depth, where sublimation and diffusive loss to the atmosphere is balanced by resupply from beneath by diffusion and recondensation of either a deeper buried ice deposits or ground water. We examine the behavior of equatorial ground ice with a numercial time-marching molecular diffusion model. In our model we allow for diffusion of water vapor through a porous regolith, variations in diffusivity and porosity with ice content, and recondensation of sublimed water vapor. A regolith containing considerable amounts of ice can still be very porous, allowing water vapor to diffuse up from deeper within the ice layer where temperatures are warmer due to the geothermal gradient. This vapor can then recondense nearer to the surface where ice had previously sublimed and been lost to the atmosphere. As a result we find that ice deposits migrate to find a steady-state depth, which represents a balance between diffusive loss to the atmosphere through the overlying porous regolith and diffusive resupply through a porous icy regolith below. This depth depends primarily on the long-term mean surface temperature and the nature of the geothermal gradient, and is independent of the ice-free porosity and the regolith diffusivity. Only the rate of loss of ground ice depends on diffusive properties.

Derived from text

N94-16404*# Arizona Univ., Tucson. Lunar and Planetary Lab.
REMOTE VISUAL DETECTION OF IMPACTS ON THE LUNAR SURFACE Abstract Only
H. Jay Melosh, N. A. Artemjeva (Academy of Sciences, USSR, Moscow.), A. P. Golub (Academy of Sciences, USSR, Moscow.), I. V. Nemchinov (Academy of Sciences, USSR, Moscow.), V. V. Shuvalov (Academy of Sciences, USSR, Moscow.), and I. A. Trubetskaya (Academy of Sciences, USSR, Moscow.) *In* Lunar and Planetary Inst., Twenty-Fourth Lunar and Planetary Science Conference. Part 2: G-M 1993 p 975-976 (For primary document see N94-16173 03-91)
Avail: CASI HC A01/MF A06

We propose a novel method of remotely observing impacts on the airless Moon that may extend the present data base on meteoroids down to 1 m in diameter. Meteorites or comets of radius approximately 1-100 m are burnt away or dispersed in the atmospheres of the Earth and Venus. However, when such objects strike the Moon they deposit their energy in a small initial volume, forming a plasma plume whose visible and infrared radiation may be visible from the Earth. We consider impacts of model SiO2 projectiles on the surface of an SiO2 model Moon.

Derived from text

N94-16405*# National Aeronautics and Space Administration. Lyndon B. Johnson Space Center, Houston, TX.
THERMOGEOLOGIC MAPPING OF THE MOON FROM LUNAR ORBIT Abstract Only
W. W. Mendell and M. A. Wieczorek (State Univ. of New York, Buffalo.) *In* Lunar and Planetary Inst., Twenty-Fourth Lunar and Planetary Science Conference. Part 2: G-M 1993 p 977-978 (For primary document see N94-16173 03-91)
Avail: CASI HC A01/MF A06

The Infrared Scanning Radiometer (ISR) onboard the Apollo 17 Command-Service Module (CSM) mapped thermal emission of the lunar surface from orbit. Measured temperature values span the diurnal range of lunar temperatures (85 K to 400 K) and have an accuracy of approximately plus or minus 2 K. Surface spatial resolution at nadir is 2.2 km. This Apollo data is being revisited using data presentation software for the Macintosh computer, which was not available 20 years ago, even on mainframes. The new thermal images exhibit subtleties in the delineation of geophysical surface units that were unappreciated in the original survey

of the data. Looking first at nighttime thermal emission from the ground tracks over Oceanus Procellarum to Mare Orientale, we have confirmed and expanded on earlier observations of regolith differences between mare and highlands and of a scheme for relative age-dating of larger impact craters of the Copernican age. We see an impact crater near Lenz, just north of Orientale, which exhibits an extraordinarily fresh ejecta blanket. Photography of this area is extremely poor, but we can see the feature in the Galileo data. We plan to derive geophysical surface properties of the overflown region using thermal models of regolith structures.

Derived from text

N94-16406*# Arizona Univ., Tucson. Lunar and Planetary Lab.

DEUCALIONIS REGIO, MARS: EVIDENCE FOR A UNIQUE MINERALOGIC ENDMEMBER AND A CRUSTED SURFACE Abstract Only

E. Merenyi, K. S. Edgett (Arizona State Univ., Tempe.), and R. B. Singer *In* Lunar and Planetary Inst., Twenty-Fourth Lunar and Planetary Science Conference. Part 2: G-M 1993 p 979-980 (For primary document see N94-16173 03-91)

Avail: CASI HC A01/MF A06

A small equatorial region south of Sinus Meridiani, Deucalionis Regio, has been found spectrally distinct from other regions as seen in a high spectral resolution telescopic image of the meridian hemisphere of Mars. Analysis of Viking IRTM and other related data suggest that Deucalionis Regio has a crusted surface. The crust-bonding minerals may contribute to the spectral uniqueness of this region. Two independent analyses of spectral images, linear spectral mixing and supervised classification based on the spectral shapes, showed that in addition to the well-known spectral endmember regions in this image (western Arabia, south Acidalia, and Sinus Meridiani), Deucalionis Regio has spectral properties that are unique enough to make it a principle endmember unit. In those earlier works, Deucalionis Regio was referred to as 'Meridiani Border.' Analysis of thermal inertia, rock abundance, and albedo information derived from Viking images and Infrared Thermal Mapper (IRTM) data obtained 1977-80 also indicate that Deucalionis Regio has a surface of distinctly different physical properties when compared to Arabia, Sinus Meridiani, and Acidalia. Deucalionis Regio has a thermal inertia equivalent to the Martian average, a low rock abundance (less than 5 percent), and an intermediate albedo and color. Considerable effort by previous investigators has revealed a consistent model for the surface (upper few cm) properties of the endmember reigons Arabia, Sinus Meridiani, and Acidalia. Compared with these regions, we consider that Deucalionis Regio is not a region of either (1) unconsolidated, fine bright dust like Arabia, (2) considerable windblown unconsolidated sand like Sinus Meridiani, or (3) a rocky-and-sandy surface like Acidalia. Thus, we are forced to consider that either the surface of Deucalionis Regio is made of unconsolidated fine to medium sand (about 250 microns) of an unusual and previously unreported color and albedo, or that the surface is crusted, fine-grained weathered soil, and the thermal inertia is an indicator of the degree to which the surface sediments have become indurated. We favor the latter.

Derived from text

N94-16407*# Saint Lawrence Univ., Canton, NY.

DO IT YOURSELF REMOTE SENSING: GENERATING AN INEXPENSIVE, HIGH TECH, REAL SCIENCE LAKE MAPPING PROJECT FOR THE CLASSROOM Abstract Only **c43**

Stephen M. Metzger *In* Lunar and Planetary Inst., Twenty-Fourth Lunar and Planetary Science Conference. Part 2: G-M 1993 p 981-982 (For primary document see N94-16173 03-91)

Avail: CASI HC A01/MF A06

The utilization of modest equipment and software revealed bottom contours and water column conditions of a dynamic water body. Classroom discussions of field techniques and equipment capabilities followed by exercises with the data sets in cause-and-effect analysis all contributed to participatory education in the process of science. This project is presented as a case study of the value of engaging secondary and collegiate level students in planning, executing and appraising a real world investigation which they can directly relate to. A 1 km wide bay, experiencing marsh inflow, along an 8 km long lake situated 120 km north of Ottawa, Canada, on the glaciated Canadian Precambrian Shield was mapped in midsummer for submerged topography, bottom composition, temperature profile, turbudity, dissolved oxygen and biota distribution. Low level aerial photographs scanned into image processing software are permitting spatial classification of bottom variations in biology and geology. Instrumentation consisted of a portable sport fishing SONAR depth finder, an electronic lead line multiprobe with photocell, thermistor and dissolved oxygen sensors, a selective depth water sampler, portable pH meter, an underwater camera mounted on a home-made platform with a bottom-contact trigger and a disposable underwater camera for shallow survey work. Sampling transects were referenced using a Brunton hand transit triangulating several shore markers.

Derived from text

N94-16408*# National Aeronautics and Space Administration. Lyndon B. Johnson Space Center, Houston, TX.

OPPORTUNITY FOR EARLY SCIENCE RETURN BY THE ARTEMIS PROGRAM Abstract Only

Charles Meyer *In* Lunar and Planetary Inst., Twenty-Fourth Lunar and Planetary Science Conference. Part 2: G-M 1993 p 983-984 (For primary document see N94-16173 03-91)

Avail: CASI HC A01/MF A06

The purpose of the Artemis Program is to gather vital scientific and engineering data by conducting robotic exploration missions on the lunar surface both prior to and concurrent with human missions. The Artemis Program includes rapid, near-term development of a variety of small experimental and operational payloads, a low-cost capacity to deliver these payloads to any location on the lunar surface, and the analysis of the data returned. The Artemis Program will provide opportunities to improve the understanding of lunar geosciences, to demonstrate the Moon's unique capacity as an astronomical platform to study the universe, to conduct scientific and technology development experiments, and to prepare for and complement human missions.

Derived from text

N94-16409*# Purdue Univ., West Lafayette, IN. Depts. of Physics and Chemistry.

Al-26 PRODUCTION PROFILE AND MODEL COMPARISONS IN CANYON DIABLO Abstract Only **c90**

E. Michlovich, D. Elmore, S. Vogt, M. Lipschutz, J. Masarik (Los Alamos National Lab., NM.), and R. C. Reedy (Los Alamos National Lab., NM.) *In* Lunar and Planetary Inst., Twenty-Fourth Lunar and Planetary Science Conference. Part 2: G-M 1993 p 985-986 (For primary document see N94-16173 03-91)

Avail: CASI HC A01/MF A06

The large preatmospheric size of the Canyon Diablo meteorite, a radius of about 15 m, makes it especially suitable for systematic studies of cosmogenic nuclide production rates of iron objects in a 2 pi geometry. To reconstruct the exposure history of the meteoroid, Heymann et al. investigated several fragments recovered from known geographic locations around the crater for their shock features and cosmogenic nobel gases. They applied the Signer-Nier noble gas production rate model to establish the preatmospheric depth of the specimens in the meteoroid. Cosmic ray exposure ages suggested a multi-episodic irradiation, with 170 or 540 Ma being inferred for most of the samples studied while two anomalous specimens indicated a possible third exposure age at 940 Ma. Be-10 and Cl-36 have been measured in a number of these same samples by accelerator mass spectrometry (AMS), with use being made of the preatmospheric depths determined in Heymann et al. to construct production profiles. The present study extends the cosmogenic radionuclide data to Al-26 and compares the results with both the production rate model of Reedy and Arnold and production rates determined from the cross sections used by the Reedy-Arnold model (for the major nuclear reactions making Al-26) in combination with differential fluxes calculated using the Los Alamos High Energy Transport (LAHET) Code System. Model calculations for Be-10 and Cl-36 have also been obtained.

Derived from text

N94-16410*# Tokyo Univ. (Japan). Mineralogical Inst.

EXSOLVED KIRSCHSTEINITE IN ANGRITE LEW86010 OLIVINE Abstract Only **c90**

Takashi Mikouchi, Hiroshi Takeda, Hiroshi Mori, Masamichi Miyamoto, and Gordon McKay (National Aeronautics and Space Administration. Lyndon B. Johnson Space Center, Houston, TX.) *In* Lunar and Planetary Inst., Twenty-Fourth Lunar and Planetary Science Conference. Part 2: G-M 1993 p 987-988 (For primary document see N94-16173 03-91)

Avail: CASI HC A01/MF A06

Mineralogy of kirschsteinite exsolution in olivine from Antarctic meteorite LEW86010 has been studied by single crustal X-ray diffraction technique.

The LEW86010 olivine crystals have exsolution lamellae of kirschteinite about 15 microns wide. Determination of crystallographic orientation of exsolved kirschsteinite in an olivine grain has been made. Weak reflections of exsolved kirschsteinite share common crystallographic orientation with the host olivine. The cell dimensions of the exsolved phase (a - 4.87 plus or minus 0.05A, b - 11.14 plus or minus 0.10A, c - 6.36 plus or minus 0.05A) and intensities were in well accord with those of kirschsteinite previously reported. Oriented section perpendicular to the a axis shows exsolution lamellae in two directions parallel to (031) and (031). The lamellae are up to 10 microns in width and spacings between them are usually 50-100 microns. Author (revised)

N94-16411*# Arizona Univ., Tucson. Planetary Image Research Lab.
ANALYSIS OF PYROXENE ABSORPTIONS OBSERVED IN MARTIAN DARK REGIONS Abstract Only
J. S. Miller and R. B. Singer *In* Lunar and Planetary Inst., Twenty-Fourth Lunar and Planetary Science Conference. Part 2: G-M 1993 p 989-990 (For primary document see N94-16173 03-91)
Avail: CASI HC A01/MF A06

We have investigated the mineralogy of the Martian dark regions by analysis of the pyroxene Fe(2+) absorption band near 1.0 micron in a set of VIS/NIR reflectance spectral images. The data used for these analyses were selected from a larger set, extending from 0.44 to 1.02 microns, obtained during the close 1988 opposition and covering substantially all of Mars south of 40 degrees N. This data set is being used in regional mapping of spectral parameters related to surface mineralogy. Martian dark regions are of interest in reconstructing the geologic history because they contain exposures of unaltered or little-altered basaltic crustal material; mapping differences in composition among dark regions could reveal regional or temporal variation in magmatic activity or mantle source composition. Two types of dark regions are seen, with the pyroxene band present and absent; where present, the inferred composition is in the range pigeonite-augite to very high-Fe, low-Ca pyroxene, with a two-pyroxene mixture possible. Derived from text

N94-16412*# National Inst. of Polar Research, Tokyo (Japan). Dept. of Antarctic Meteorites.
REFRACTORY PRECURSOR COMPONENTS IN AN ALLENDE FERROMAGNESIAN CHONDRULE Abstract Only **c90**
Keiji Misawa, Takashi Fujita (Kyoto Univ., Japan.), Masao Kitamura (Kyoto Univ., Japan.), and Noboru Nakamura (Kobe Univ., Japan.) *In* Lunar and Planetary Inst., Twenty-Fourth Lunar and Planetary Science Conference. Part 2: G-M 1993 p 991-992 (For primary document see N94-16173 03-91)
Avail: CASI HC A01/MF A06

Chemical and petrological studies of chondrules revealed that they were formed through melting of pre-existing solid precursor materials, and that one of the refractory lithophile precursors was a high temperature condensate from the nebular gas and related to Ca, Al-rich inclusions (CAIs). Sheng et al. found relict spinel grains with isotopically fractionated Mg in plagioclase-olivine inclusions from CV chondrites and suggested that the major fractionation processes were common to CAIs and chondrules. We have determined the Mg isotopic compositon of five barred olivine chondrules and one coarse-grained rim from the Allende (CV3) meteorite. A reproducibility of instrumental isotope fractionation is plus or minus 2 per thousand per amu. The precision of the Mg-26/Mg-24 data after normalization for mass fractionation can be as good as 0.5 per thousand (2 sigma(mean)). The Mg analytical results are given and indicate that delta Mg-25/Mg-24 and sigma Mg-26 of the chondrules are normal within errors. Derived from text

N94-16413*# Lockheed Engineering and Sciences Co., Houston, TX.
IGNEOUS FRACTIONATION AND SUBSOLIDUS EQUILIBRATION OF DIOGENITE METEORITES Abstract Only **c90**
David W. Mittlefehldt *In* Lunar and Planetary Inst., Twenty-Fourth Lunar and Planetary Science Conference. Part 2: G-M 1993 p 993-994 (For primary document see N94-16173 03-91)
Avail: CASI HC A01/MF A06

Diogenites are coarse-grained orthopyroxenite breccias of remarkably uniform major element composition. Most diogenites contain homogeneous pyroxene fragments up to 5 cm across of Wo2En74Fs24 composition. Common minor constituents are chromite, olivine, trolite and metal, while silica, plagioclase, merrillite and diopside are trace phases. Diogenites are generally believed to be cumulates from the eucrite parent body, although their relationship with eucrites remains obscure. It has been suggested that some diogenites are residues after partial melting. I have performed EMPA and INAA for major, minor and trace elements on most diogenites, concentrating on coarse-grained mineral and lithic clasts in order to elucidate their igneous formation and subsequent metamorphic history. Major element compositions of diogenites are decoupled from minor and trace element compositions; the latter record an igneous fractionation sequence that is not preserved in the former. Low equilibration temperatures indicate that major element diffusion continued long after crystallization. Diffusion coefficients for trivalent and tetravalent elements in pyroxene are lower than those of divalent elements. Therefore, major element compositions of diogenites may represent means of unknown portions of a cumulate homogenized by diffusion, while minor and trace elements still yield information on their igneous history. The scale of major element equilibration is unknown, but is likely to be on the order of a few cm. Therefore, the diogenite precursors may have consisted largely of cm-sized, igneously zoned orthopyroxene grains, which were subsequently annealed during slow cooling, obliterating major element zoning but preserving minor and trace incompatible element zoning. Derived from text

N94-16414*# Lockheed Engineering and Sciences Co., Houston, TX.
SIDEROPHILE ELEMENT FRACTIONATION IN METEOR CRATER IMPACT GLASSES AND METALLIC SPHERULES Abstract Only **c90**
David W. Mittlefehldt, T. H. See, and E. R. D. Scott (Hawaii Univ., Honolulu.) *In* Lunar and Planetary Inst., Twenty-Fourth Lunar and Planetary Science Conference. Part 2: G-M 1993 p 995-996 (For primary document see N94-16173 03-91)
Avail: CASI HC A01/MF A06

Meteor Crater, Arizona provides an opportunity to study, in detail, elemental fractionation processes occurring during impacts through the study of target rocks, meteorite projectile and several types of impact products. We have performed EMPA and INAA on target rocks, two types of impact glass and metallic spherules from Meteor Crater. Using literature data for the well studied Canyon Diablo iron we can show that different siderophite element fractionations affected the impact glasses than affected the metallic spherules. The impact glasses primarily lost Au, while the metallic spherules lost Fe relative to other siderophile elements. Author (revised)

N94-16415*# Yamaguchi Univ. (Japan).
IDENTIFICATION OF NEW METEORITE, MIHONOSEKI (L), FROM BROKEN FRAGMENTS IN JAPAN Abstract Only **c90**
Y. Miura and Y. Noma *In* Lunar and Planetary Inst., Twenty-Fourth Lunar and Planetary Science Conference. Part 2: G-M 1993 p 997-998 (For primary document see N94-16173 03-91)
Avail: CASI HC A01/MF A06

New meteorite of Mihonoseki fallen in Shimane-ken was identified by fine broken pieces by using an energy-dispersive scanning electron microprobe analyzer. It shows fusion-crust (i.e. Fe-Si melt), meteoritic minerals (kamacite, taenite, troilite, amorphous plagioclase etc.) and chrondrule with clear glassy rim. Mineralogical, and petrological data of several fine grains suggest that broken fragments of Mihonoseki are L3/4 chondritic meteorite which is the first identification in a Japanese fallen meteorite. The prompt identification method of meteorite-fragments will be applied to the next lunar, Martian and asteroid explorations, as well as meteorite falls on the terrestrial surface. Derived from text

N94-16416*# Tokyo Univ. (Japan). Mineralogical Inst.
THE THICKNESS OF EUCRITIC CRUST IN THE HED PARENT BODY Abstract Only **c46**
M. Miyamoto and H. Takeda *In* Lunar and Planetary Inst., Twenty-Fourth Lunar and Planetary Science Conference. Part 2: G-M 1993 p 999-1000 (For primary document see N94-16173 03-91)
Avail: CASI HC A01/MF A06

Because cumulate eucrites are generally thought to be located at the lower part in eucritic crust on a diogenitic mantle in the HED parent body, the burial depth of cumulate eucrites gives information on the thickness of the eucritic crust. We estimated the burial depth and cooling rate of cumulate eucrites, Serra de Mage and Moore County on the basis of the width of augite lamellae and compositional gradients of Ca in pyroxenes by

numerically solving the diffusion equation. We obtained the burial depth of the eucrites of 7-8 km and cooling rate of 0.00016-0.0002 degrees C/yr.
Derived from text

N94-16417*# Padua Univ. (Italy). Dipartimento di Mineralogia and Petrologia.
ZAOYANG CHONDRITE COOLING HISTORY FROM PYROXENE Fe(2+)-Mg INTRACRYSTALLINE ORDERING AND EXOLUTIONS Abstract Only **c90**
G. M. Molin, M. Tribaudino (Turin Univ., Italy.), and E. Brizi (Perugia Univ., Italy.) *In* Lunar and Planetary Inst., Twenty-Fourth Lunar and Planetary Science Conference. Part 2: G-M 1993 p 1001 (For primary document see N94-16173 03-91)
Avail: CASI HC A01/MF A06

The Zaoyang ordinary chondrite fell as a single 14.15-kg mass in Hubey province (China) in October 1984 and was classified as a non-brecciated H5 chondrite, shock facies b. Cooling rate in pyroxenes can be calculated down to about 1000 C by using fine textures and at still lower temperatures (700 to 200 C) by intracrystalline ordering processes. The crystal chemistry of clinopyroxene and orthopyroxene from the matrix of the H5 Zaoyang chondrite has been investigated by X-ray structure refinement and detailed microprobe analysis. By comparison with terrestrial pyroxenes cell and polyhedral volumes in clino- and orthopyroxenes show a low crystallization pressure. Fe(2+) and Mg are rather disordered in M1 and M2 sites of clino- and orthopyroxenes; the closure temperatures of the exchange reaction are 600 and 512 C respectively, which is consistent with a quite fast cooling rate, estimated of the order of one degree per day. The closure temperature for the intercrystalline Ca-Mg exchange reaction for clino- and orthopyroxene showing clinopyroxene lamellae about 10 microns thick. Kinetic evaluations based on the thickness of exolved lamellae give a cooling rate of not more than a few degrees per 10(exp 4) years. The different cooling rates obtained from Fe(2+)-Mg intracrystalline partitioning and exolution lamellae suggest an initial episode of slow cooling at 900 C, followed by faster cooling at temperatures of 600-500 C at low pressure conditions. The most probable scenario of the meteorite history seems that the exolved orthopyroxene entered the parental chondrite body after exolution had taken place at high temperature. Subsequent fast cooling occurred at low temperature after the formation of the body.
Author (revised)

N94-16418*# Geological Survey, Menlo Park, CA.
RELIEF OF SOME SMALL LANDFORMS ON VENUS Abstract Only
H. J. Moore, J. J. Plaut (Jet Propulsion Lab., California Inst. of Tech., Pasadena.), and T. J. Parker (Jet Propulsion Lab., California Inst. of Tech., Pasadena.) *In* Lunar and Planetary Inst., Twenty-Fourth Lunar and Planetary Science Conference. Part 2: G-M 1993 p 1003-1004 (For primary document see N94-16173 03-91)
Avail: CASI HC A01/MF A06

Three sets of radar images have been acquired under different viewing conditions by the Magellan synthetic aperture radar: (1) left-looking with varied incidence angles (cycle 1); (2) right-looking with nearly constant incidence angles (cycle 2); and (3) left-looking with varied incidence angles, most of which were smaller than those in (1) except for those acquired on passes across Maxwell Montes with incidence angles larger than those in (1) (cycle 3). Image displacements in the radar images that are caused by the relief of landforms provide several methods of estimating this relief: (1) monoscopic measurements of foreshortening of landforms that are symmetrical in the plane of the look-direction of the radar (includes radial symmetry); (2) stereoscopic measurements of parallax in same-side image pairs (cycles 1-2 and 3); and (3) measurements of parallax in opposite-side image pairs (cycles 1-2 and/or 2-3). Success in methods 2 and 3 (especially 3) depends on identifying conjugate image points in the two images. Here, we report our preliminary results for five impact craters, seven small volcanic edifices, and two lava flows. The three methods mentioned above lead to the interesting result that Venusian impact craters have depth-diameter ratios like those on Mars rather than those on Earth, but some appear partly filled. Our results for de Lalande and Melba also suggest filling, but there may be other causes for their relatively small depth-diameter ratios. A host of small volcanic edifices have relief that can be crudely estimated using the above methods. Relief/diameter ratios for our cratered cones are about the same as those of Icelandic lava shields; some Venusian cones resemble the Martian shields of Mareotis-Tempe and Ceraunius Fossae, but the Venusian relief diameter ratios are larger. The smallest cratered dome is similar in size and profile to a Martian dome north of Uranius Patera; the smallest cratered cone resembles one in Chryse Planitia. Lava flows on Venus that are thick enough to measure are rare, but we have applied methods 1 and 3 to the huge flow of Ovda Regio and flows of an unusual volcano, Mahuea Tholus.
Author (revised)

N94-16419*# National Aeronautics and Space Administration. Ames Research Center, Moffett Field, CA.
MARS BRINE FORMATION EXPERIMENT Abstract Only
Jeffrey M. Moore, Mark A. Bullock (Colorado Univ., Boulder.), and Carol R. Stoker *In* Lunar and Planetary Inst., Twenty-Fourth Lunar and Planetary Science Conference. Part 2: G-M 1993 p 1005-1006 (For primary document see N94-16173 03-91)
Avail: CASI HC A01/MF A06

The presence of water-soluble cations and anions in the Martian regolith has been the subject of speculation for some time. Viking lander data provided evidence for salt-cemented crusts on the Martian surface. If the crusts observed at the two Viking landing sites are, in fact, cemented by salts, and these crusts are globally widespread, as IRTM-derived thermal inertia studies of the Martian surface seem to suggest, then evaporite deposits, probably at least in part derived from brines, are a major component of the Martian regolith. The composition of liquid brines in the subsurface, which not only may be major agents of physical weathering but may also presently constitute a major deep subsurface liquid reservoir, is currently unconstrained by experimental work. A knowledge of the chemical identity and rate of production of Martian brines is a critical first-order step toward understanding the nature of both these fluids and their precipitated evaporites. Laboratory experiments are being conducted to determine the identity and production rate of water-soluble ions that form in initially pure liquid water in contact with Mars-mixture gases and unaltered Mars-analog minerals.
Derived from text

N94-16420*# National Aeronautics and Space Administration. Goddard Space Flight Center, Greenbelt, MD.
CATALYTIC CRYSTALLIZATION OF ICES BY SMALL SILICATE SMOKES AT TEMPERATURES LESS THAN 20K Abstract Only **c76**
M. Moore, R. Ferrante, R. Hudson, T. Tanabe, and J. Nuth *In* Lunar and Planetary Inst., Twenty-Fourth Lunar and Planetary Science Conference. Part 2: G-M 1993 p 1007-1008 (For primary document see N94-16173 03-91)
Avail: CASI HC A01/MF A06

Samples of methanol and water ices condensed from the vapor onto aluminum substrates at low temperatures (below approximately 80 K) form amorphous ices; annealing at temperatures in excess of 140-155 K is usually required to convert such amorphous samples to crystalline ices. However, we have found that when either methanol or water vapor is deposited on to aluminum substrates that have been coated with a thin (0.1-0.5 mm) layer of amorphous silicate smoke, the ices condense in crystalline form. We believe that crystalline ice forms as the result of energy liberated at the ice/silicate interface perhaps due to weak bonding of the ice at defect sites on the grains and the very high surface to volume ratio and defect density of these smokes. Annealing of amorphous water ice mixed with more volatile components such as methane, carbon monoxide, etc., has been suggested as an efficient way to produce clatherates in the outer solar nebula and thus explain the volatile content of comets and icy satellites of the outer planets. This hypothesis may need to be re-examined if amorphous ice does not form on cold silicate grains.
Derived from text

N94-16421*# California Inst. of Tech., Pasadena. Seismological Lab.
EFFECTIVE ELASTIC THICKNESS OF THE VENUSIAN LITHOSPHERE WITH LATERAL VISCOSITY VARIATIONS IN THE MANTLE Abstract Only
Louis Moresi *In* Lunar and Planetary Inst., Twenty-Fourth Lunar and Planetary Science Conference. Part 2: G-M 1993 p 1009-1010 (For primary document see N94-16173 03-91)
Avail: CASI HC A01/MF A06

Both the Earth and Venus have a convecting mantle at the top of which is a relatively strong, mechanical boundary layer. The surface topography and gravity signals which result from the convection within the viscous mantle are modified by the elastic properties of this lithospheric

boundary layer. In particular the ability of the lithosphere to support loads and transmit stresses from below is a function of the wavelength of the load--the lithosphere is strong to loading at shorter wavelengths. As a consequence it is usual to expect that long wavelength topography cannot be supported by the mechanical strength of the lithosphere and must be compensated--isostatically or dynamically--within the uppermost mantle or the crust. The flexural rigidity of the lithosphere can therefore be determined by estimating the greatest wavelength at which uncompensated surface topography can be supported, usually by measuring the admittance as a function of wavelength. In fact this procedure for determining the elastic thickness relies upon being able to distinguish topography with underlying support from that supported by the brittle lithosphere on the basis of their each having a characteristic value of the admittance. However, in the presence of lateral viscosity variations in the mantle, it is possible for topography to be generated which is NOT compensated by density anomalies in the underlying mantle at the same wavelength. Although this effect is not likely to be important for the Earth, on Venus, where the high surface temperatures would be expected to give a weaker lithosphere, lateral viscosity variations in the mantle can give a misleadingly large apparent elastic thickness for the lithosphere. Derived from text

N94-16422*# Academy of Sciences (USSR), Moscow.
OPTICAL EFFECTS OF REGOLITH PROCESSES ON S ASTEROIDS AS SIMULATED BY LASER IMPULSE ALTERATION OF ORDINARY CHONDRITE Abstract Only **c90**

L. V. Moroz, A. V. Fisenko, L. F. Semjonova, and C. M. Pieters (Brown Univ., Providence, RI.) *In* Lunar and Planetary Inst., Twenty-Fourth Lunar and Planetary Science Conference. Part 2: G-M 1993 p 1011-1012 (For primary document see N94-16173 03-91)
Avail: CASI HC A01/MF A06

The spectral properties of some powdered chondrites and minerals altered by lsser impulse are studied in order to estimate possible optical effects of regolith processes (micrometeoritic bombardment). Gradual reduction of overall reflectance and spectral contrast, the increase of continuum slope, the increase of spectrally derived olivine/pyroxene ratio and Fs content of orthopyroxene with increasing alteration degree show that regolith processes could affect optical properties of surface material more heavily than has been previously appreciated. Ordinary chondrites (OC's) are known to account for 80 percent of observed meteorite falls, but so far no main belt parent bodies have been identified for these meteorites. S-asteroids resemble OC's spectrally, but are characterized by a steeper red continuum unlike that of OC's and their spectrally derived mineralogies are far outside OC range. Attempts were made to explain the spectral mismatch between OC's and S asteroids by some process, which alters optical properties of uppermost regolith. However, the spectral studies of shocked (black) OC's, gas-rich OC's, melted OC's and synthetic metal-rich regoliths derived from OC's demonstrate that such altered OC materials darken, but do not redden. Derived from text

N94-16423*# Academy of Sciences (USSR), Moscow. Space Research Inst.
ALTITUDE PROFILE OF AEROSOLS ON MARS FROM MEASUREMENTS OF ITS THERMAL RADIATION ON LIMB Abstract Only

V. I. Moroz, D. V. Titov, Yu. M. Gektin, M. K. Naraeva, and A. S. Selivanov *In* Lunar and Planetary Inst., Twenty-Fourth Lunar and Planetary Science Conference. Part 2: G-M 1993 p 1013-1014 (For primary document see N94-16173 03-91)
Avail: CASI HC A01/MF A06

Measurements of the thermal (range 7 - 13 micrometers) radiation of Mars with the high space resolution (approximately 2 km) were made by the TERMOSKAN experiment of the Phobos mission. Some of the results were published earlier but only the surface radiation was analyzed in detail. However some part of these measurements was made near the limb of the planet. The atmosphere gives an important input here in the planetary thermal radiation. Beyond the limb the atmosphere is the only source. The task of this work is to estimate some characteristics of the atmosphere using brightness profiles of the thermal radiation near the limb. An appropriate model of the temperature profile T(h) is necessary for such an analysis. A set of T(h) models (nominal, maximal and minimal) was defined using various sources including MARSGRAM, Viking-1 lander data, its theoretical considerations and boundary layer models. On the next step the possible input of the atmospheric gaseous emissions (wing of CO2 15 micrometer band) was estimated. It was found that even for the maximal T(h) this input is no more than a few percents of the measured radiation beyond the limb. Consequently the aerosols are responsible for almost all measured emission. The analysis of the observed profile showed that these aerosols have two components: (1) exponential with the scale height about 10 km and (2) some layered structure (two layers with maxima about 23 and 33 km consisted probably of ice). Derived from text

N94-16424*# National Aeronautics and Space Administration. Lyndon B. Johnson Space Center, Houston, TX.
TERRESTRIAL IMPACT MELTS AS ANALOGUES FOR THE HEMATIZATION OF MARTIAN SURFACE MATERIALS Abstract Only **c46**

R. V. Morris, H. V. Lauer, Jr. (Lockheed Engineering and Sciences Co., Houston, TX.), and D. C. Golden *In* Lunar and Planetary Inst., Twenty-Fourth Lunar and Planetary Science Conference. Part 2: G-M 1993 p 1015-1016 (For primary document see N94-16173 03-91)
Avail: CASI HC A01/MF A06

Visible and near-IR reflectivity and Mossbauer data were obtained on powders of hydrothermally-altered impact melt sheets from West Clearwater Lake, Manicouagan, and Ries (Polsingen) impact structures. The data support previous interpretations that Martian bright regions spectra can be interpreted by a ferric-bearing phase that has a relatively featureless absorption edge together with some well-crystalline (bulk) hematite to account for the 860 nm hematite band. The data also show that bands at wavelengths longer than 900 nm, which are characteristic of Martian dark regions, occur when both hematite and pyroxene are present. It thus follows that hematization of Mars can be attributed, at least in part, to hydrothermal alterations of impact melt sheets. Impact heating could also form bulk-Hm from nanophase ferric oxides. Author

N94-16425*# Open Univ., Milton (England). Dept. of Earth Sciences.
A HYDROGEN ISOTOPE STUDY OF CO3 TYPE CARBONACEOUS CHONDRITES; COMPARISON WITH TYPE 3 ORDINARY CHONDRITES Abstract Only **c90**

A. D. Morse, J. Newton, and C. T. Pillinger *In* Lunar and Planetary Inst., Twenty-Fourth Lunar and Planetary Science Conference. Part 2: G-M 1993 p 1017-1018 (For primary document see N94-16173 03-91)
Avail: CASI HC A01/MF A06

Meteorites of the Ornans type 3 carbonaceous chondrites exhibit a range in degree of equilibration, attributed to differing amounts of thermal metamorphism. These differences have been used to split the CO3 chondrites into petrologic sub-types from 3.0, least equilibrated, to 3.7, being most equilibrated. This is similar to the system of assigning the type 3 ordinary chondrites into petrologic sub-types 3.0 to 3.9 based upon thermoluminescence (TL) and other properties; however, the actual range of thermal metamorphism experienced by CO3 chondrites is much less than that of the type 3 ordinary chondrites. The least equilibrated ordinary chondrites show evidence of aqueous alteration and have high D/H ratios possibly due to a deuterium-rich organic carrier. The aim of this study was to determine whether the CO3 chondrites, which have experienced similar secondary conditions to the type 3 ordinary chondrites, also contain a similar deuterium-rich carrier. To date a total of 5 CO3 meteorites, out of a set of 11 for which carbon and nitrogen isotopic data are available, have been analyzed. Ornans has not been analyzed yet, because it does not appear to fit in with the metamorphic sequence exhibited by the other CO3 chondrites; it also has an extremely high delta-D value of +2150 percent, unusual for such a comparatively equilibrated meteorite (type 3.4). Initial results indicate that the more equilibrated CO3's tend to have lower delta-D values, analogous to the higher petrologic type ordinary chondrites. However this is complicated by the effects of terrestrial weathering and the small data-set. Derived from text

N94-16426*# Los Alamos National Lab., NM.
GAMMA RAY SPECTROMETER FOR LUNAR SCOUT 2 Abstract Only **c35**

C. E. Moss, W. W. Burt (TRW Space Technology Labs., Los Angeles, CA.), B. C. Edwards, R. A. Martin, George H. Nakano (Nakano, George H., Los Altos, CA.), and R. C. Reedy *In* Lunar and Planetary Inst., Twenty-Fourth Lunar and Planetary Science Conference. Part 2: G-M

1993 p 1019-1020 (For primary document see N94-16173 03-91)
Avail: CASI HC A01/MF A06

We review the current status of the Los Alamos program to develop a high-resolution gamma-ray spectrometer for the Lunar Scout-II mission, which is the second of two Space Exploration Initiative robotic precursor missions to study the Moon. This instrument will measure gamma rays in the energy range of approximately 0.1 - 10 MeV to determine the composition of the lunar surface. The instrument is a high-purity germanium crystal surrounded by an CsI anticoincidence shield and cooled by a split Stirling cycle cryocooler. It will provide the abundance of many elements over the entire lunar surface. Derived from text

N94-16427*# Hawaii Univ., Honolulu. Planetary Geosciences, Geology and Geophysics.

THE INFLUENCE OF OCEANS ON MARTIAN VOLCANISM Abstract Only

Peter Mouginis-Mark *In* Lunar and Planetary Inst., Twenty-Fourth Lunar and Planetary Science Conference. Part 2: G-M 1993 p 1021-1022 (For primary document see N94-16173 03-91)
Avail: CASI HC A01/MF A06

Geomorphological evidence for episodic oceans on Mars has recently been identified. This idea of large bodies of water on Mars is innovative and controversial compared to the more generally accepted view of a 'dry Mars', but also enables some of the more enigmatic volcanic landforms to be reinterpreted in a self-consistent model. This hypothesis can be used to develop new models for the mode of formation of several volcanic landforms in the W. Tharsis and S.E. Elysium Planitia regions of Mars. Derived from text

N94-16428*# Lamar Univ., Beaumont, TX. Earth and Space Resources Lab.

HELIUM-3 INVENTORY OF LUNAR SAMPLES: A POTENTIAL FUTURE ENERGY RESOURCE FOR MANKIND? Abstract Only

A. V. Murali and J. L. Jordan *In* Lunar and Planetary Inst., Twenty-Fourth Lunar and Planetary Science Conference. Part 2: G-M 1993 p 1023-1024 (For primary document see N94-16173 03-91)
(Contract NAS9-17900)
Avail: CASI HC A01/MF A06

Recent public concern over the safety, cost, and environmental impact of the worldwide fission reactors has focused the attention of scientists and engineers towards perfecting fusion technology because it promises a much more environmentally acceptable 'clean' energy supply. The fusion reaction D-2 + He-3 yields p(14.7 MeV) + He-4(3.6 MeV) has long been recognized as an ideal candidate for producing commercially 'safer and cleaner' fusion power. Naturally occurring He-3 is scarce on earth; however, lunar regolith is a potential ore for He-3 because the high He-3 in solar wind has been implanted in the lunar regolith for more than 4 x 10(exp 9) years, along with other volatile species. The helium abundance in lunar soils is dependent not only on the maturity of soils (I(sub S)/FeO) but also on their mineralogy. The titanium-rich (ilmenite) lunar soils are important repositories for volatiles, which may be released by heating these soils up to approximately 700 C. CASI

N94-16429*# Lunar and Planetary Inst., Houston, TX.

THE SPECTRUM OF PHOBOS FROM PHOBOS 2 OBSERVATIONS AT 0.3-2.6 MICRONS: COMPARISON TO PREVIOUS DATA AND METEORITE ANALOGS Abstract Only

Scott Murchie and Stephane Erard (Rome Univ., Italy.) *In its* Twenty-Fourth Lunar and Planetary Science Conference. Part 2: G-M 1993 p 1025-1026 (For primary document see N94-16173 03-91)
Avail: CASI HC A01/MF A06

The surface of Phobos has been proposed to consist of carbonaceous chondrite or optically darkened ordinary chondrite ('black chondrite'). Measurements of Phobos's spectrum are key evidence for testing these hypotheses. Disk-integrated measurements were obtained by the Mariner 9 UV spectrometer, Viking Lander cameras, and groundbased observations. In 1989 disk-resolved measurements of Phobos and Mars were obtained by three instruments on Phobos 2: the KRFM spectrometer, which covered the wavelength range 0.32 - 0.6 microns; the ISM imaging spectrometer, which covered the wavelength range 0.76 - 3.16 microns; and the VSK TV cameras, whose wavelength ranges overlap those of KRFM and ISM. Here we report analysis of the Phobos 2 measurements completed since earlier results were reported. We validated calibration of the Phobos measurements using observations of Mars for reference, and compared them with pre-1989 measurements. We also combined spectra from the three detectors to produce an integrated spectrum of Phobos from 0.3 - 2.6 microns. Phobos 2 results agree well with previous measurements, contrary to some reports. The general shape of the spectrum is consistent with both proposed analogues. However position and depth of the previously unobserved 1 micron absorption are more diagnostic, and indicate the composition of typical surfaces to be more consistent with black chondrite. Derived from text

N94-16430*# Lunar and Planetary Inst., Houston, TX.

BRIGHT SOIL UNITS ON MARS DETERMINED FROM ISM IMAGING SPECTROMETER DATA Abstract Only

Scott Murchie and John Mustard (Brown Univ., Providence, RI.) *In its* Twenty-Fourth Lunar and Planetary Science Conference. Part 2: G-M 1993 p 1027-1028 (For primary document see N94-16173 03-91)
Avail: CASI HC A01/MF A06

The lithology of bright Martian soil provides evidence for chemical and physical processes that have modified the planet's surface. Data from the ISM imaging spectrometer, which observed much of the equatorial region at a spatial resolution of approximately 22 km, cover the NIR wavelength range critical to ascertaining the presence and abundance of Fe-containing phases, hydroxylated silicates, and H2O in the bright soil. ISM data previously have revealed spatial variations in depth of the 3.0-microns H2O absorption suggesting differences in water content, a weak absorption at 2.2 microns indicative of metal-OH in phyllosilicate, and variations in the 1-micron Fe absorption indicative of differences in Fe mineralogy. This paper summarizes first results of a systematic investigation of spectral heterogeneity in bright soils observed by ISM. At least seven 'units' with distinctive properties were discriminated. Comparison of their spatial distributions with Viking data shows that they generally correspond with previously recognized morphologic, color, and thermal features. These correspondences and the units' spectral attributes provide evidence for lithologic differences between the soils in different geologic settings. Derived from text

N94-16431*# Lunar and Planetary Inst., Houston, TX.

VARIATIONS IN THE Fe MINERALOGY OF BRIGHT MARTIAN SOIL Abstract Only

Scott Murchie, John Mustard (Brown Univ., Providence, RI.), Stephane Erard (Rome Univ., Italy.), Paul Geissler (Arizona Univ., Tucson.), and Robert Singer (Arizona Univ., Tucson.) *In its* Twenty-Fourth Lunar and Planetary Science Conference. Part 2: G-M 1993 p 1029-1030 (For primary document see N94-16173 03-91)
Avail: CASI HC A01/MF A06

Bright regions on Mars are interpreted as 'soil' derived by chemical alteration of crustal rocks, whose main pigmentary component is ferric oxide or oxyhydroxide. The mineralogy and mineralogic variability of ferric iron are important evidence for the evolution of Martian soil: mineralogy of ferric phases is sensitive to chemical conditions in their genetic environments, and the spatial distributions of different ferric phases would record a history of both chemical environments and physical mixing. Reflectance spectroscopic studies provide several types of evidence that discriminate possible pigmentary phases, including the position of a crystal field absorption near 0.9 microns and position and strengths of absorptions in the UV-visible wavelength region. Recent telescopic spectra and laboratory measurements of Mars soil analogs suggest that spectral features of bright soil can be explained based on a single pigmentary phase, hematite (alpha-Fe2O3), occurring in both 'nanophase' and more crystalline forms. Here we report on a systematic investigation of Martian bright regions using ISM imaging spectrometer data, in which we examined spatial variations in the position and shape of the approximately 0.9 microns absorption. We found both local and regional heterogeneities that indicate differences in Fe mineralogy. These results demonstrate that bright soils do not represent a single lithology that has been homogenized by eolian mixing, and suggest that weathering of soils in different geologic settings has followed different physical and chemical pathways. Derived from text

N94-16432*# Eidgenoessische Technische Hochschule, Zurich (Switzerland).
SOLAR NOBLE GASES REVEALED BY CLOSED SYSTEM STEPPED ETCHING OF A METAL SEPARATE FROM FAYETTEVILLE Abstract Only **c25**
Ch. Murer, H. Baur, P. Signer, and R. Wieler *In* Lunar and Planetary Inst., Twenty-Fourth Lunar and Planetary Science Conference. Part 2: G-M 1993 p 1031-1032 (For primary document see N94-16173 03-91)
Avail: CASI HC A01/MF A06

Solar He, Ne, and Ar in a Fe-Ni separate from the chondrite Fayetteville are analyzed by closed system stepped oxidation. We report here data of the first 15 steps comprising 55 percent of the total solar gases. He-4/Ar-36 and Ne-20/Ar-36 are quite constant at values about 20 percent below those of present day solar wind (SWC). In this, Fe-Ni differs from lunar ilmenites where He-4/Ar-36 and Ne-20/Ar-36 in the first steps are several times below SWC. Thus, metal retains SW-noble gases even better than ilmenite, almost without element fractionation. Nevertheless, the isotopic composition of SW-He, -Ne, and -Ar in the first steps of the metal sample are identical to those found in a recently irradiated lunar ilmenite, indicating that ilmenites and chondritic metal both contain isotopically unfractionated SW noble gases. A preliminary analysis of a smaller Fayetteville metal separate shows Ne from solar energetic particles (SEP-Ne) with Ne-20/Ne-22 less than or equal to 11.5. Author

N94-16433*# Lockheed Aircraft Corp., Palo Alto, CA. Research Lab.
EFFECTS OF LEVITATED DUST ON ASTRONOMICAL OBSERVATIONS FROM THE LUNAR SURFACE Abstract Only **c89**
D. L. Murphy and R. R. Vondrak *In* Lunar and Planetary Inst., Twenty-Fourth Lunar and Planetary Science Conference. Part 2: G-M 1993 p 1033-1034 (For primary document see N94-16173 03-91)
Avail: CASI HC A01/MF A06

It is believed that a substantial population of levitated dust is present in the terminator region of the moon. Stray light scattered by this dust layer may contaminate astronomical observations made from the lunar surface using infrared, visible, and ultraviolet light. The evidence for dust levitation stems from: Surveyor vidicon images of horizon glow; anomalous brightness in photographs of the solar corona taken by Apollo astronauts while the spacecraft was just inside the moon's shadow; and observations by Apollo astronauts of streamers just prior to lunar orbital sunrise or just after lunar orbital sunset. It has been proposed that the differential charging of the lunar surface in the terminator region due to photoemission and the consequent strong local electric fields comprise the mechanism responsible for this levitation. Although quantitative data on the levitated lunar dust distribution are meager, it is possible to estimate column densities and sizes. In this paper we summarize the estimates of particulate sizes and number densities of previous authors, and construct a nominal terminator dust distribution, as a function of particulate radius and altitude above the lunar surface. Using the model we estimate the brightness of scattered sunshine for three wavelength bands. For the results in the visible wavelengths, we compare the estimated brightness with the known brightness of selected astronomical objects and discuss the implications for lunar-based astronomy. Derived from text

N94-16434*# National Aeronautics and Space Administration. Ames Research Center, Moffett Field, CA.
DUST-DYNAMIC FEEDBACKS IN THE MARTIAN ATMOSPHERE: SURFACE DUST LIFTING Abstract Only
James R. Murphy and James B. Pollack *In* Lunar and Planetary Inst., Twenty-Fourth Lunar and Planetary Science Conference. Part 2: G-M 1993 p 1035-1036 (For primary document see N94-16173 03-91)
Avail: CASI HC A01/MF A06

Numerical models have been developed to study surface dust lifting in the Martian atmosphere. The present model is comprised of interactively coupled 3-D dynamical and aerosol transport/microphysical models. The nature of possible feedbacks between surface dust lifting and the amplification/damping of near-surface wind and thermal fields and their implications for additional lifting is investigated. These studies have examined large scale Martian topography for its impact upon the ability of the atmospheric circulation to lift dust from the surface, and the particular component(s) responsible for the lifting (e.g. overturning circulation, thermal tides, baroclinic waves). Analogous experiments in which the lifted dust is radiatively inactive (passive tracer) have been conducted to act as a control against which feedbacks are defined. CASI

N94-16435*# Physical Research Lab., Ahmedabad (India).
NITROGEN AND LIGHT NOBLE GASES IN PARSA ENSTATITE CHONDRITE Abstract Only **c90**
S. V. S. Murty *In* Lunar and Planetary Inst., Twenty-Fourth Lunar and Planetary Science Conference. Part 2: G-M 1993 p 1037-1038 (For primary document see N94-16173 03-91)
Avail: CASI HC A01/MF A06

Solar gases have been recently reported in Parsa, an EH3 chondrite. In an effort to check whether solar gases are uniformly distributed throughout Parsa or they are located in specific phases, we analyzed two additional samples of bulk Parsa and one aubritic nodule for N and noble gases. Nitrogen studies are intended for the understanding of the nitrogen components distribution in E-chondrites. The N-systematics of the nodule are entirely different from the bulk samples. The higher N contents in this nodule, as well as its complex delta(sup 15)N structure, as compared to the normal aubrites, is suggestive that the nodule is not a genuine aubrite. Derived from text

N94-16436*# Brown Univ., Providence, RI. Dept. of Geological Sciences.
COMPOSITION OF WEAKLY ALTERED MARTIAN CRUST Abstract Only
J. F. Mustard, S. L. Murchie (Lunar and Planetary Inst., Houston, TX.), and S. Erard (Rome Univ., Italy.) *In* Lunar and Planetary Inst., Twenty-Fourth Lunar and Planetary Science Conference. Part 2: G-M 1993 p 1039-1040 (For primary document see N94-16173 03-91)
Avail: CASI HC A01/MF A06

The mineralogic and chemical composition of weakly altered crust remains an unresolved question for Mars. Dark regions hold clues to the composition since they are thought to comprise surface exposures of weakly altered crustal materials. Understanding the in situ composition of relatively pristine crustal rocks in greater detail is important for investigating basic volcanic processes. Also, this will provide additional constraints on the chemical pathways by which pristine rocks are altered to produce the observed ferric iron-bearing assemblages and inferred clay silicate, sulphate, and magnetic oxide phases. Reflectance spectra of dark regions obtained with the ISM instrument are being used to determine the basic mineralogy of weakly altered crust for a variety of regions on Mars. Derived from text

N94-16437*# Brown Univ., Providence, RI. Dept. of Geological Sciences.
FROM MINERALS TO ROCKS: TOWARD MODELING LITHOLOGIES WITH REMOTE SENSING Abstract Only **c43**
John F. Mustard, Jessica M. Sunshine, Carle M. Pieters, Andrew Hoppin, and Stephan F. Pratt *In* Lunar and Planetary Inst., Twenty-Fourth Lunar and Planetary Science Conference. Part 2: G-M 1993 p 1041-1042 (For primary document see N94-16173 03-91)
Avail: CASI HC A01/MF A06

High spectral resolution imaging spectroscopy will play an important role in future planetary missions. Sophisticated approaches will be needed to unravel subtle, super-imposed spectral features typically of natural systems, and to maximize the science return of these instruments. Carefully controlled laboratory investigations using homogeneous mineral separates have demonstrated that variations due to solid solution, changes in modal abundances, and the effects of particle size are well understood from a physical basis. In many cases, these variations can be modeled quantitatively using photometric models, mixing approaches, and deconvolution procedures. However, relative to the spectra of individual mineral components, reflectance spectra of rocks and natural surfaces exhibit a reduced spectral contrast. In addition, soils or regolith, which are likely to dominate any natural planetary surface, exhibit spectral properties that have some similarities to the parent materials, but due to weathering and alteration, differences remain that cannot yet be fully recreated in the laboratory or through mixture modeling. A significant challenge is therefore to integrate modeling approaches to derive both lithologic determinations and include the effects of alteration. We are currently conducting laboratory investigations in lithologic modeling to expand upon the basic results of previous analyses with our initial goal to more closely match physical state

of natural systems. The effects of alteration are to be considered separately. Derived from text

N94-16832*# Southwest Research Inst., San Antonio, TX.
CHAIRMANSHIP OF THE NEPTUNE/PLUTO OUTER PLANETS SCIENCE WORKING GROUP Annual Report
S. Alan Stern 1 Nov. 1993 7 p
(Grant NAGw-2914; SwRI Proj. 15-4945)
(NASA-CR-194625; NAS 1.26:194625) Avail: CASI HC A02/MF A01

The Outer Planets Science Working Group (OPSWG) is the NASA Solar System Exploration Division (SSED) scientific steering committee for the Outer Solar System missions. OPSWG consists of 19 members and is chaired by Dr. S. Alan Stern. This proposal summarizes the FY93 activities of OPSWG, describes a set of objectives for OPSWG in FY94, and outlines the SWG's activities for FY95. As chair of OPSWG, Dr. Stern will be responsible for: organizing priorities, setting agendas, conducting meetings of the Outer Planets SWG; reporting the results of OPSWG's work to SSED; supporting those activities relating to OPSWG work, such as briefings to the SSES, COMPLEX, and OSS; supporting the JPL/SAIC Pluto study team; and other tasks requested by SSED. As the Scientific Working Group (SWG) for Jupiter and the planets beyond, OPSWG is the SSED SWG chartered to study and develop mission plans for all missions to the giant planets, Pluto, and other distant objects in the remote outer solar system. In that role, OPSWG is responsible for: defining and prioritizing scientific objectives for missions to these bodies; defining and documenting the scientific goals and rationale behind such missions; defining and prioritizing the datasets to be obtained in these missions; defining and prioritizing measurement objectives for these missions; defining and documenting the scientific rationale for strawman instrument payloads; defining and prioritizing the scientific requirements for orbital tour and flyby encounter trajectories; defining cruise science opportunities plan; providing technical feedback to JPL and SSED on the scientific capabilities of engineering studies for these missions; providing documentation to SSED concerning the scientific goals, objectives, and rationale for the mission; interfacing with other SSED and OSS committees at the request of SSED's Director or those committee chairs; providing input to SSED concerning the structure and content of the Announcement of Opportunity for payload and scientific team selection for such missions; and providing other technical or programmatic inputs concerning outer solar system missions at the request of the Director of SSED. Derived from text

N94-16866*# Wellesley Coll., MA.
THE CHROMOSPHERE OF VV CEPHEI AND THE DISTRIBUTION OF CIRCUMSTELLAR DUST AROUND RED GIANTS AND SUPERGIANTS Final Report, 1 Aug. 1990 - 21 Jan. 1992
Wendy Hagen Bauer 31 Jan. 1992 5 p
(Grant NAG5-1213)
(NASA-CR-193594; NAS 1.26:193594) Avail: CASI HC A01/MF A01

The work on this project has followed two separate paths of inquiry. The first project was entitled 'the Chromosphere of VV Cephei.' The examination of the archival spectra revealed significant changes in the spectra. Therefore, we obtained additional observing time with IUE to monitor the system during the summer of 1991. Short-term changes continue to be seen in both the overall spectrum and individual line profiles. Work continues on this object. The second project was entitled 'the Distribution of Circumstellar Dust around Red Giants and Supergiants.' A number of cool evolved stars are surrounded by dust shells of sufficient angular size as to appear extended in the IRAS survey data. The aim of this project has been to convolve the predictions of the flux distribution from model dust shells with the IRAS beam profiles in order to reproduce the observed IRAS scans. At the time of the last status report, the cross-scan profiles of the IRAS detectors had just been added to the modeling procedure. For scans in which the star passed near the detector center, there was no significant variation in predicted scan profile for different detectors. Scans in which the detector did not pass over the bright central star had been anticipated to be particularly useful in determining the dust distribution; however, significant differences in the predicted scan profiles were seen for different detector profiles. For this reason, and due to the cross-talk effects discussed in the previous status report, further work on the scans not including a central star has been postponed in favor of further analysis of scans passing over the central star. Author (revised)

N94-16884*# Southwest Research Inst., San Antonio, TX.
MULTISPECTRAL OBSERVATIONS OF THE JOVIAN AURORA
[1992] 23 p Original contains color illustrations
(Grant NAGw-1657)
(NASA-CR-193628; NAS 1.26:193628) Avail: CASI HC A03/MF A01; 4 functional color pages

This paper presents and analyzes images of the Jovian aurora gathered by the Hubble Space Telescope Faint Object Camera (FOC) and the ROSAT Position Sensitive Proportional Counter (PSPC) to determine the function of energetic heavy ion precipitation in the inner magnetosphere and electron acceleration in the outer magnetosphere. Hubble data includes hydrogen auroral spectra and reduced images of Jupiter's north and south poles. One important result is that acceleration of electrons may be largely responsible for the discrete auroral emission features seen in the data set. ROSAT PSPC data presented includes a photon energy spectrum. A two line emission model is shown to produce the best fit to the data. The production of these emission lines occurs as a result of recombination lines that are produced from the slowing of the energetic ion beam as it enters the Jupiter upper atmosphere. It is noted that the observed energetic ion precipitation does not contain sufficient power to explain the observed ultraviolet aurora; it is therefore concluded that both electrons and ions play a role in the Jupiter auroral emissions, but that the bulk of the ultraviolet emissions comes from electron processes. Derived from text

N94-17292*# Knudsen Geophysical Branch, Monte Sereno, CA.
PIONEER VENUS DATA ANALYSIS FOR THE RETARDING POTENTIAL ANALYZER Final Technical Report, Aug. 1988 - Sep. 1993
William C. Knudsen 5 Oct. 1993 86 p
(Contract NAS2-12902; RTOP 370-24-11)
(NASA-CR-194673; NAS 1.26:194673) Avail: CASI HC A05/MF A01

This report describes the data analysis and archiving activities, analysis results, and instrument performance of the orbiter retarding potential analyzer (ORPA) flown on the Pioneer Venus Orbiter spacecraft during the period, Aug. 1, 1988 to Sept. 30, 1993. During this period, the periapsis altitude of the Orbiter spacecraft descended slowly from 1900 km altitude, at which altitude the spacecraft was outside the Venus ionosphere, to approximately 130 km altitude in Oct. 1992 at which time communication with the spacecraft ceased as a result of entry of the spacecraft into the Venus atmosphere. The quantity of ORPA data returned during this reporting period was greatly reduced over that recovered in the previous years of the mission because of the reduced power capability of the spacecraft, loss of half of the onboard data storage, and partial failure of the ORPA. Despite the reduction in available data, especially ionospheric data, important scientific discoveries resulted from this extended period of the Pioneer Venus mission. The most significant discovery was that of a strong solar cycle change in the size of the dayside ionosphere and the resulting shutoff of flow of dayside ions into the nightside hemisphere. The large, topside O+ F2 ionospheric layer observed during the first three years of the Pioneer Venus mission, a period of solar cycle maximum activity, is absent during the solar cycle minimum activity period. Author

N94-17637*# Lunar and Planetary Inst., Houston, TX. MSATT Study Group.
WORKSHOP ON EARLY MARS: HOW WARM AND HOW WET, PART 2?
S. Squyres, ed. and J. Kasting, ed. 1993 14 p Workshop held in Breckenridge, CO, 26-28 Jul. 1993
(Contract NASw-4574)
(NASA-CR-193503; NAS 1.26:193503; LPI-TR-93-03-Pt-2) Avail: CASI HC A03/MF A01

In 1992 the MSATT program conducted a workshop on modeling of the Martian climate. At that workshop it became clear that a serious problem had arisen concerning the early climate of Mars. Based on the evidence for smallscale fluvial activity, the view had been widely held that early in its history Mars had a climate that was much warmer and wetter than today's. However, most plausible recent climate models have fallen far short of the warm temperatures often inferred from the geologic evidence. Moreover, recent geophysical work has suggested that early geothermal warming may also have played a significant role in allowing fluvial activity. In order to address the issue of just how warm and how wet early Mars was, a workshop was convened in July of 1993, in Breckenridge, Colorado. The results of the workshop are reported here. Author

N94-17654*# Jet Propulsion Lab., California Inst. of Tech., Pasadena.
GUIDE TO MAGELLAN IMAGE INTERPRETATION
John P. Ford, Jeffrey J. Plaut, Catherine M. Weitz, Tom G. Farr, David A. Senske, Ellen R. Stofan, Gregory Michaels, Timothy J. Parker, and D. Fulton, ed. 1 Nov. 1993 150 p Original contains color illustrations
(NASA-CR-194340; JPL-Publ-93-24; NAS 1.26:194340) Avail: CASI HC A07/MF A02; 9 functional color pages

An overview of Magellan Mission requirements, radar system characteristics, and methods of data collection is followed by a description of the image data, mosaic formats, areal coverage, resolution, and pixel DN-to-dB conversion. The availability and sources of image data are outlined. Applications of the altimeter data to estimate relief, Fresnel reflectivity, and surface slope, and the radiometer data to derive microwave emissivity are summarized and illustrated in conjunction with corresponding SAR image data. Same-side and opposite-side stereo images provide examples of parallax differences from which to measure relief with a lateral resolution many times greater than that of the altimeter. Basic radar interactions with geologic surfaces are discussed with respect to radar-imaging geometry, surface roughness, backscatter modeling, and dielectric constant. Techniques are described for interpreting the geomorphology and surface properties of surficial features, impact craters, tectonically deformed terrain, and volcanic landforms. The morphologic characteristics that distinguish impact craters from volcanic craters are defined. Criteria for discriminating extensional and compressional origins of tectonic features are discussed. Volcanic edifices, constructs, and lava channels are readily identified from their radar outlines in images. Geologic map units are identified on the basis of surface texture, image brightness, pattern, and morphology. Superposition, cross-cutting relations, and areal distribution of the units serve to elucidate the geologic history. Author (revised)

N94-15887*# Jet Propulsion Lab., California Inst. of Tech., Pasadena.
MAGELLAN: PRINCIPAL VENUS SCIENCE FINDINGS
R. Stephen Saunders *In its* Proceedings of the Third Spaceborne Imaging Radar Symposium 28 May 1993 p 5-7 (For primary document see N94-15886 03-32)
Avail: CASI HC A01/MF A04

92 SOLAR PHYSICS

Includes solar activity, solar flares, solar radiation and sunspots. For related information see *93 Space Radiation.*

N94-15023*# Teledyne Brown Engineering, Huntsville, AL.
ULTRAVIOLET SPECTROMETER AND POLARIMETER (UVSP) CATALOG OF OBSERVATIONS. VOLUME 1: EXPERIMENTS 1-30719, FEBRUARY 1980 - APRIL 1985
William Henze, Jr. Washington NASA Jul. 1993 668 p
(Contract NAS8-35921)
(NASA-CR-4529-Vol-1; M-724-Vol-1; NAS 1.26:4529-Vol-1) Avail: CASI HC A99/MF A06

A catalog of observations (experiments) obtained by the Ultraviolet Spectrometer and Polarimeter (UVSP) on the Solar Maximum Mission (SMM) from Feb. 1980 to Nov. 1989 is presented. The information for each entry includes the time of each observation, the observed position of the Sun, the spacecraft roll angle, the slit used, and instrument parameters such as raster size, pixel spacing, wavelength, polarimeter usage, gate time, etc. The document is split into three volumes: Volume 1 contains experiments 1-30719 (February 1980-April 1985); Volume 2 contains experiments 30720-63057 (April 1985-February 1988); and Volume 3 contains experiments 63058-99771 (February 1988-November 1989). Author (revised)

N94-15024*# Teledyne Brown Engineering, Huntsville, AL.
ULTRAVIOLET SPECTROMETER AND POLARIMETER (UVSP) CATALOG OF OBSERVATIONS. VOLUME 2: EXPERIMENTS 30720-63057, APRIL 1985 - FEBRUARY 1988
William Henze, Jr. Washington NASA Jul. 1993 915 p
(Contract NAS8-35921)
(NASA-CR-4529-Vol-2; M-724-Vol-2; NAS 1.26:4529-Vol-2) Avail: CASI HC A99/MF A10

A catalog of observations (experiments) obtained by the Ultraviolet Spectrometer and Polarimeter (UVSP) on the Solar Maximum Mission (SMM) from Feb. 1980 to Nov. 1989 is presented. The information for each entry includes the time of each observation, the observed position of the Sun, the spacecraft roll angle, the slit used, and instrument parameters such as raster size, pixel spacing, wavelength, polarimeter usage, gate time, etc. The document is split into three volumes: Volume 1 contains experiments 1-30719 (February 1980-April 1985); Volume 2 contains experiments 30720-63057 (April 1985-February 1988); and Volume 3 contains experiments 63058-99771 (February 1988-November 1989). Author (revised)

N94-15287* National Aeronautics and Space Administration, Washington, DC.
UNMASKING THE SUN (Videotape)
Nov. 1988 Videotape: 3 min. 42 sec. playing time, in color, with sound
(NASA-TM-109595; NONP-VT-93-190393) Avail: CASI VHS A01/BETA A22

This videotape describes solar-related research at the Mt. Palomar Observatory. CASI

N94-15421*# Massachusetts Univ., Amherst. Dept. of Physics and Astronomy.
BOUNDARY CONDITIONS FOR THE PALEOENVIRONMENT: CHEMICAL AND PHYSICAL PROCESSES IN THE PRE-SOLAR NEBULA Semiannual Status Report No. 21, 16 Feb. - 15 Aug. 1993
William M. Irvine and F. Peter Schloerb 1993 6 p
(Grant NAGw-436)
(NASA-CR-194418; NAS 1.26:194418) Avail: CASI HC A02/MF A01

In observations with the NRAO 12m telescope at Kitt Peak, Arizona, Irvine, a new interstellar radical, CH2N, has been detected. This identification is important for the study of hydrogenation processes in the interstellar medium. In particular, although the abundance of hydrogen is some four orders of magnitude higher than that of other reactive elements in this environment, many organic molecules in quiescent clouds are very unsaturated. This is a consequence of activation barriers which cannot be overcome at the temperatures of cold clouds, even when such reactions are energetically allowed. The hydrogenation series based on the cyanide radical (HnCN) has had four members previously detected in the interstellar medium: CN (n equals O), HCN (n equals I), CH2CN (n equals 3), and CH3NH2 (n equals 5). The recent determination of the rotational spectrum of the CH2N radical through microwave spectroscopy in Japan has made possible a search for this species. In addition to its potential importance for interstellar chemistry, the CH2N radical has been proposed as a reaction intermediate for HCN production in the atmosphere of Jupiter, and as a possible species in the expanding envelopes of oxygen--rich evolved stars. We detected CH2N in the cold cloud TMC--1 where the abundance seems to be some three orders of magnitude lower than that of HCN. A tentative detection was made in the Galactic Center molecular cloud Sgr B2. To our knowledge, there are no predicted abundances of CH2N from models of interstellar chemistry. Derived from text

N94-15522* National Aeronautics and Space Administration. Ames Research Center, Moffett Field, CA.
C 141 KAO SOLAR ECLIPSE MISSION (Videotape)
Apr. 1988 Videotape: 4 min. playing time, in color, with sound
(NASA-TM-109676; NONP-VT-93-190474) Avail: CASI VHS A01/BETA A22

This video presents the C 141 Kuiper Airborne Observatory Solar Eclipse Mission. CASI

N94-15821# Total Army Personnel Agency (Provisional), Alexandria, VA.
A COMPARISON OF SOLAR WIND PARAMETERS MEASURED BY IMP 8, VOYAGER 1 AND VOYAGER 2 M.S. Thesis
Stephen J. Simmerer 7 May 1993 138 p
(AD-A266728) Avail: CASI HC A07/MF A02

This thesis analyzes measurements of four solar wind parameters (radial velocity, density, ram pressure, and flux density) as observed by three spacecraft: IMP 8 (Interplanetary Monitoring Platform 8, also called Explorer 50), Voyager 1, and Voyager 2. First, a brief discussion of the evolution of the solar wind within the solar system is presented in order to establish a basis for understanding observed trends in spacecraft data. Then following is an explanation and comparison of the data gathering instruments and collection methods of IMP 8 and the Voyager spacecraft including a discussion of the data analysis. Next, solar wind parameters are compared

over four averaging periods: 25/27 days, representing the period of one solar rotation as seen by the Voyagers/IMP 8; 50/54 days, to coincide with two solar rotations; 100 days and 200 days, approximating four and eight solar rotations, respectively. Similarities and differences between spacecraft observations are discussed. DTIC

N94-15836 Harvard Coll. Observatory, Cambridge, MA.
ABSOLUTE, EXTREME-ULTRAVIOLET SOLAR SPECTRAL IRRADIANCE MONITOR (AESSIM) Annual Report, 15 Nov. 1991 - 14 Nov. 1992
W. H. Parkinson 14 Nov. 1992 3 p Limited Reproducibility: More than 20% of this document may be affected by microfiche quality
(Grant AF-AFOSR-0063-90)
(AD-A267045; AFOSR-93-0546TR) Avail: CASI HC A01

The goal of this research program is development of a method for obtaining daily, radiometrically accurate, solar spectral irradiance data at extreme-ultraviolet (EUV) wavelengths. In-orbit radiometric instrumentation recalibration is a fundamental requirement for such measurements. It was proposed to investigate, design, and test smaller and less massive, low power, in-space version of a 'standard' EUV radiance source, which was developed for laboratory use and to assess the merits of innovative combinations of rare-gas ionization cells and thin film filters to make absolute measurements of EUV radiation over a number of wavelength bands. DTIC

N94-15968*# Aarhus Univ. (Denmark). Inst. of Physics and Astronomy.
GENERATION OF ARTIFICIAL HELIOSEISMIC TIME-SERIES
J. Schou (Stanford Univ., CA.) and T. M. Brown (National Center for Atmospheric Research, Boulder, CO.) Oct. 1993 10 p Submitted for publication
(Contract NAS5-30386; NASA Order W-17678)
(NASA-CR-194612; NAS 1.26:194612; AARHUS-ASTRO-93-12; IFA-93/40) Avail: CASI HC A02/MF A01

We present an outline of an algorithm to generate artificial helioseismic time-series, taking into account as much as possible of the knowledge we have on solar oscillations. The hope is that it will be possible to find the causes of some of the systematic errors in analysis algorithms by testing them with such artificial time-series. Author

N94-16895# Los Alamos National Lab., NM.
THE SOLAR FLARE MYTH IN SOLAR-TERRESTRIAL PHYSICS
J. T. Gosling 1993 15 p Presented at the AGU Monograph/Solar System Plasma Physics Meeting on Resolution of Processes in Space and Time, Yosemite, CA, Feb. 1993
(Contract W-7405-eng-36)
(DE93-016487; LA-UR-93-2371; CONF-9302115-4) Avail: CASI HC A03/MF A01

Early observations of associations between solar flares and large non-recurrent geomagnetic storms, large 'solar' energetic particle events, and transient shock wave disturbances in the solar wind led to a paradigm of cause and effect that gave flares a central position in the chain of events leading from solar activity to major transient disturbances in the near-earth space environment. However, research in the last two decades shows that this emphasis on flares is misplaced. In this paper the author outlines briefly the rationale for a different paradigm of cause and effect in solar-terrestrial physics that removes solar flares from their central position as the 'cause' of major disturbances in the near-earth space environment. Instead, this central role of 'cause' is played by events now known as coronal mass ejections, or CME's. DOE

N94-17004# Johns Hopkins Univ., Laurel, MD. Applied Physics Lab.
SOLAR VECTOR MAGNETIC FIELD RESEARCH Final Report, 1 Dec. 1989 - 31 Mar. 1993
David M. Rust 31 Mar. 1993 18 p
(Grant AF-AFOSR-0102-90)
(AD-A267367; AFOSR-93-0558TR) Avail: CASI HC A03/MF A01

The objective of the project was to measure the magnetic fields in solar active regions, develop methods for predicting solar flares on the basis of the measurements, and improve the instrumentation for solar magnetic field measurements. In cooperation with the staff at the Solar Branch of the USAF Phillips Laboratory, field measurements were made almost daily during the grant period. The principal result of analyses carried out so far is that so-called sheared magnetic fields are neither necessary nor sufficient for solar flaring. The crucial element seems to be emerging magnetic flux and local development of shear in the hour before flare onset. A need for greatly improved instrumentation was identified. A new vector magnetograph was designed for operation above the image-degrading layers of the atmosphere. Fourteen technical publications and presentations appeared under grant sponsorship. DTIC

N94-17089*# Alabama Univ., Huntsville.
FNAS/SOLAR FLARE ENERGETICS Final Technical Report, 15 Apr. 1991 - 14 Oct. 1992
M. E. Machado 20 Nov. 1992 3 p
(Grant NAG8-872)
(NASA-CR-193574; NAS 1.26:193574) Avail: CASI HC A01/MF A01

We have performed an extensive study of solar flare energy buildup and release, concentrating in two aspects: (1) relationship with 3D field topology and measured electric currents; and (2) flare onset characteristics as determined from combined x ray and ultraviolet observations. We extended our previous studies on the characteristic topology of flaring regions, by following the evolution of an active region over three consecutive days. From comparison with flare observations in x rays and h alpha, we found further support for the hypothesis that flares were triggered by taking place at the separators (3D generalization of and x-type neutral point). Furthermore, we found that emerging in flux at a site within the active regions where no (or little) activity was previously observed, caused the appearance of a secondary separator and thereon continuous triggering of activity at such site. Our topology arguments were then applied to a study of sympathetic activity between two regions within an active complex. Here again we found that interacting field structures along separators and separatrices, which act as pathways for recurrent flaring to spread between the regions, could be used to understand how activity spread to potentially explosive sites with the complex. We also finished our study of flare onset characteristics as determined from combined x ray and ultraviolet observations. Using a quasi-static modeling approach, we find that this phase is characterized by a relatively low level of energy release, 10 exp 26-27 erg/s, which is sufficient to produce 'gentle' evaporation, a shift in the location of the transition zone as compared to pre-flare conditions, and an increase in the temperature and density of coronal loops. All these changes have profound implications on the observed signatures of impulsive phase phenomena, which had been neglected in the past. As a follow-up of this investigation, we now plan to apply our results to the interpretation of high-sensitivity spectroscopic and hard x-ray data currently being gathered by the Yohkoh and Compton Gamma Ray Observatory satellites. Derived from text

N94-17208# Kansas Univ. Center for Research, Inc., Lawrence.
ATMOSPHERIC IONIZATION BY SOLAR PARTICLES DETECTED BY NITRATE MEASUREMENT IN ANTARCTIC SNOW Annual Technical Report, 1 Jun. 1992 - 31 May 1993
G. Dreschhoff, T. P. Armstrong, T. Cravens, and F. Vitt 30 Jun. 1993 121 p
(Contract F49620-92-J-0235)
(AD-A267583; AFOSR-93-0556TR) Avail: CASI HC A06/MF A02

Nitrates are observed in polar snow, firn, and ice in variable amounts and concentrations. Hundred-year or longer time series of nitrate observations can be obtained from ice cores. It is important to identify possible and probable sources of nitrates and mechanisms by which surface deposition and incorporation into ice occurs. Several important sources of nitrate are solar protons and auroral electrons producing ionization in the D-region. Chemical reactions energized by this ionization produce nitrates. Transport mechanisms can move nitrates from the stratosphere into the troposphere where it becomes incorporated into precipitation. From the amounts of nitrates deposited in polar snow over long times it may be possible to determine atmospheric characteristics of importance to climate and global change studies. The specific goal of this study is to evaluate carefully and completely the atmospheric nitrates produced by solar flare protons and auroral electrons and to estimate the amounts deposited in snow. DTIC

N94-17281*# Southwest Research Inst., San Antonio, TX.
MAGNETIC EFFECTS IN VENUS/SOLAR WIND INTERACTION Final Report

Richard S. Steinolfson 31 Jul. 1993 5 p
(Grant NAG2-692; SwRI Proj. 15-4170)
(NASA-CR-194666; NAS 1.26:194666) Avail: CASI HC A01/MF A01

The overall objective of this research program is to better understand the interaction of a magnetized solar wind with the Venus atmosphere through the use of numerical solutions of the time-dependent, 2-D and 3-D magnetohydrodynamic (MHD) equations. Due to the more modest CPU requirements for the 2-D simulations, they were used for studies in which useful information not dependent on the third dimension could be obtained. The 2-D simulations served several purposes in addition to providing useful physical insight. They were used to determine the numerical parameters required in the 3-D studies, such as the grid spacing required to resolve particular features, and the damping that must be included to remove high-frequency oscillations. Among the specific studies performed with support from this grant that are discussed in this report are the following: comparison with other available models for purposes of testing the code and obtaining a baseline with which to evaluate the effects of additional physical processes, effects of a finite planet conductivity, bow shock standoff distance, and formation of the magnetic barrier and slippage of the magnetic field around the planet. A brief description of the methodology is presented before discussing the results. Author (revised)

N94-17524*# Alabama Univ., Huntsville. Dept. of Physics.
KINETIC PLASMA PROCESSES OCCURRING IN THE OUTER PLASMASPHERE Final Progress Report, Nov. 1991 - Apr. 1992
Gordon R. Wilson 6 May 1992 4 p
(Grant NAG5-1555)
(NASA-CR-193452; NAS 1.26:193452) Avail: CASI HC A01/MF A01

One area of data analysis work that was begun under this contract is the fitting of the perpendicular velocity distributions of equatorially trapped ions with a Kappa function. This type of characterization of the trapped ions will be very useful for comparison with velocity distributions produced by the model. A second area of data analysis is to study data from consecutive passes when DE 1's apogee was near the magnetic equator and the spacecraft was often skimming along nearly the same L shell. In 1982 three such periods occurred in May, June, and July. For these consecutive events we have Kp histories, density measurements from a number of sources (Whistler data, DE SFR, ISEE SFR) and consecutive samples of ion pitch angle distributions along field lines. It is clear from this data how the pitch angle distributions evolve during a flux tube refilling event. Our modeling of the flow of plasma along closed field lines is following two basic tracks. The first is a study of the basic refilling process without the effect of wave-particle heating near the equator or the effect of large or abrupt field-aligned electric potential drops. This model includes the effects of Coulomb self-collisions and collisions with the O+ ions in the topside ionosphere. The second track is a study of the effects of wave produced pitch-angle scattering and perpendicular heating occurring near the magnetic equator, in connection with the development of large potential drops that result from electron heating and the development of density gradients. Derived from text

N94-16251*# Arizona Univ., Tucson. Lunar and Planetary Lab.
GAS-GRAIN ENERGY TRANSFER IN SOLAR NEBULA SHOCK WAVES: IMPLICATIONS FOR THE ORIGIN OF CHONDRULES Abstract Only
L. L. Hood and M. Horanyi (Colorado Univ., Boulder.) *In* Lunar and Planetary Inst., Twenty-Fourth Lunar and Planetary Science Conference. Part 2: G-M 1993 p 669-670 (For primary document see N94-16173 03-91)
Avail: CASI HC A01/MF A06

93 SPACE RADIATION

Includes cosmic radiation; and inner and outer earth's radiation belts.

For biological effects of radiation see *52 Aerospace Medicine*. For theory see *73 Nuclear and High-Energy Physics*.

N94-15533*# Applied Research Corp., Landover, MD.
X RAY EMISSION FROM WOLF-RAYET STARS WITH RECURRENT DUST FORMATION Final Report, 2 Nov. 1992 - 1 Nov. 1993
Gayle L. Rawley 29 Oct. 1993 7 p
(NASA Order S-93065-E)
(NASA-CR-194567; NAS 1.26:194567; R93-213) Avail: CASI HC A02/MF A01

We were granted a ROSAT observation of the Wolf-Rayet star WR 137 (equals HD 192641) to test a proposed mechanism for producing the infrared variability reported by Williams et al. (1987). These studies showed one clear infrared outburst preceded by what may be the dimming of a previous outburst. The recurrent dust formation model was put forward by Williams et al. (1990) to account for similar variability seen in WR 140, which varies in both the infrared and X-ray bands. The detected X-ray flux from WR 140 was observed to decrease from its normally high (for Wolf-Rayet stars) level as the infrared flux increased. Observation of two apparently-periodic infrared outbursts led to the hypothesis that WR 140 had an O star companion in an eccentric orbit, and that the increase in infrared flux came from a dust formation episode triggered by the compression of the O star and Wolf-Rayet star winds. The absorption of the X-rays by the increased material explained the decrease in flux at those wavelengths. If the infrared variability in WR 137 were caused by a similar interaction of the Wolf-Rayet star with a companion, we might expect that WR 137 would show corresponding X-ray variability and an X-ray luminosity somewhat higher than typical WC stars, as well as a phase-dependent non-thermal X-ray spectrum. Our goals in this study were to obtain luminosity estimates from our counting rates for comparison with previous observations of WR 137 and other WC class stars, especially WR 140; to compare the luminosity with the IR lightcurve; and to characterize the spectral shape of the X-ray emission, including the column density. Author (revised)

N94-15816*# National Aeronautics and Space Administration. Langley Research Center, Hampton, VA.
EXPOSURE FLUCTUATIONS OF ASTRONAUTS DUE TO ORIENTATION
John W. Wilson, John E. Nealy, James S. Wood (FMC Corp., Hampton, VA.), Gary Qualls (FMC Corp., Hampton, VA.), William Atwell (Rockwell International Corp., Houston, TX.), Judy L. Shinn, and Lisa C. Simonsen Washington Sep. 1993 54 p Sponsored by NASA. Washington Original contains color illustrations
(RTOP 199-45-16-11)
(NASA-TP-3364; L-17254; NAS 1.60:3364) Avail: CASI HC A04/MF A01; 5 functional color pages

The dose incurred in an anisotropic environment depends on the orientation of the astronaut's body relative to the direction of the radiation field. The fluctuations in exposure of specific organs due to astronaut orientation are found to be a factor of 2 or more in a typical space habitation module and typical space radiations. An approximation function is found that overestimates astronaut exposure in most cases studied and is recommended as a shield design guide for future space missions. Derived from text

N94-17084*# National Aeronautics and Space Administration. Langley Research Center, Hampton, VA.
APPROXIMATE GREEN'S FUNCTION METHODS FOR HZE TRANSPORT IN MULTILAYERED MATERIALS
John W. Wilson, Francis F. Badavi (Christopher Newport Coll., Newport News, VA.), Judy L. Shinn, and Robert C. Costen Oct. 1993 16 p
(RTOP 199-45-16-11)
(NASA-TM-4519; L-17302; NAS 1.15:4519) Avail: CASI HC A03/MF A01

A nonperturbative analytic solution of the high charge and energy (HZE) Green's function is used to implement a computer code for laboratory ion beam transport in multilayered materials. The code is established to operate on the Langley nuclear fragmentation model used in engineering applications. Computational procedures are established to generate linear energy transfer (LET) distributions for a specified ion beam and target for comparison with experimental measurements. The code was found to be highly efficient and compared well with the perturbation approximation. Author

N94-17233# Argonne National Lab., IL.
CONTAINED (nu) EVENTS OBSERVED IN SOUDAN 2
I. Ambats, D. S. Ayres, L. Balka, W. L. Barrett, J. Dawson, T. Fields, M. C. Goodman, N. Hill, J. H. Hoftiezer, and D. J. Jankowski et al 1993 3 p Presented at the International Cosmic-ray Conference, Calgary, Canada, 19-20 Jul. 1993

(Contract W-31-109-eng-38)
(DE93-015548; ANL-HEP-CP-93-34; CONF-930779-15) Avail: CASI HC A01/MF A01

Atmospheric nu(sub mu) and nu(sub e) are created in cosmic ray interactions in the atmosphere and can be detected in underground detectors. The Kamiokande and IMB water Cerenkov detectors have found fewer nu(sub mu) interactions (relative to nu(sub e)) than are expected. Results are usually expressed by the ratio: R is equivalent (nu(sub mu)/nu(sub mu)) measured/(nu(sub mu)/nu(sub e)) predicted with R found to be less than 1. The Soudan 2 detector is an iron calorimeter, which has different systematic effects than the water Cerenkov counters. Results from the Frejus and NUSEX calorimeters do not suggest a deficit of nu(sub mu)'s in iron implying that perhaps there is a systematic effect in Cerenkov detectors or some unexpected nuclear effect. Here we report on a preliminary analysis of 0.5 kton-year of data in Soudan 2. We are presently analyzing our second 0.5 kt-year of data, and will present new results at the meeting. DOE

N94-17255*# Christopher Newport Coll., Newport News, VA. Dept. of Biology, Chemistry and Environmental Sciences.
SHIELDING FROM SPACE RADIATIONS Annual Progress Report, 1 Dec. 1992 - 1 Jun. 1993
C. Ken Chang, Forooz F. Badavi, and Ram K. Tripathi 1 Dec. 1993 39 p
(Grant NAG1-1286)
(NASA-CR-194664; NAS 1.26:194664) Avail: CASI HC A03/MF A01

This Progress Report covering the period of 1 June 1993 to 1 Dec. 1993 presents the development of an analytical solution to the heavy ion transport equation in terms of a one-layer Green's function formalism. The mathematical developments are recasted into an efficient computer code for space applications. The efficiency of this algorithm is accomplished by a nonperturbative technique of extending the Green's function over the solution domain. The code may also be applied to accelerator boundary conditions to allow code validation in laboratory experiments. Results from the isotopic version of the code with 80 isotopes present for a single layer target material, for the case of an Iron beam projectile at 600 MeV/nucleon in water is presented. Author (revised)

N94-17666*# National Aeronautics and Space Administration. Langley Research Center, Hampton, VA.
CALCULATIONS OF COSMIC-RAY HELIUM TRANSPORT IN SHIELDING MATERIALS
Francis A. Cucinotta Nov. 1993 33 p
(RTOP 199-45-16-11)
(NASA-TP-3354; L-17225; NAS 1.60:3354) Avail: CASI HC A03/MF A01

The transport of galactic cosmic-ray helium nuclei and their secondaries through bulk shielding is considered using the straight-ahead approximation to the Boltzmann equation. A data base for nuclear interaction cross sections and secondary particle energy spectra for high-energy light-ion breakup is presented. The importance of the light ions H-2, H-3, and He-3 for cosmic-ray risk estimation is discussed, and the estimates of the fractional contribution to the neutron flux from helium interactions compared with other particle interactions are presented using a 1977 solar minimum cosmic-ray spectrum. Author (revised)

N94-16092 Thomson and Nielsen Electronics, Ottawa (Ontario).
REAL TIME RADIATION MEASUREMENTS IN SPACE
I. Thomson and G. Mackay *In* National Research Council Canada, Proceedings of the Second Workshop on Microgravity Experimentation 1990 3 p (For primary document see N94-16071 03-29)
Avail: Issuing Activity (National Research Council, Publication Sales and Distribution, Montreal Road, Ottawa, Ontario, K1A OR6 Canada)

99 GENERAL

N94-14926 Oak Ridge National Lab., TN.
ENGINEERING PHYSICS AND MATHEMATICS DIVISION PROGRESS REPORT, PERIOD ENDING 31 DECEMBER 1992
R. C. Ward May 1993 273 p Limited Reproducibility: More than 20% of this document may be affected by microfiche quality
(Contract DE-AC05-84OR-21400)
(DE93-015118; ORNL-6753) Avail: CASI HC A12

In this report, our research is described through abstracts of journal articles, technical reports, and presentations organized into sections following the five major operating units in the division: Mathematical Sciences, Intelligent Systems, Nuclear Data and Measurement Analysis, Nuclear Analysis and Shielding, and the Engineering Physics Information Centers. Each section begins with an introduction highlighting honors, awards, and significant research accomplishments in that unit during the reporting period. DOE

N94-15241* National Aeronautics and Space Administration, Washington, DC.
THE 1969 HIGHLIGHTS (Videotape)
Dec. 1969 Videotape: 14 min. 30 sec. playing time, in color, with sound (NASA-TM-109630; NONP-VT-93-190428) Avail: CASI VHS A01/BETA A22

This video includes Mariners to Mars; Orbiting Solar Observatory; Orbiting Geophysical Observatory; sounding rockets; weather satellites - Tiros and Nimbus; applications technology; advanced research; space shuttle research; V/STOL; jet noise abatement; and Apollo 9, 10, 11, and 12 missions. CASI

N94-15242* National Aeronautics and Space Administration, Washington, DC.
THE 1972 HIGHLIGHTS (Videotape)
Jan. 1973 Videotape: 14 min. 30 sec. playing time, in color, with sound (NASA-TM-109631; NONP-VT-93-190429) Avail: CASI VHS A01/BETA A22

This document includes Mariners to Mars, Pioneer to Jupiter, Orbiting Astronomical Observatory, Small Astronomy Satellite, sounding rockets, earth resources, Nimbus weather watcher, communication satellites, aeronautics, wind tunnel research, STOL, noise abatement, lifting bodies, US/Soviet cooperation, preparation for Skylab, and the Apollo 16 and 17 missions. CASI

N94-15243* National Aeronautics and Space Administration, Washington, DC.
THE 1965 HIGHLIGHTS (Videotape)
Dec. 1965 Videotape: 4 min. 40 sec. playing time, in color, with sound (NASA-TM-109632; NONP-VT-93-190430) Avail: CASI VHS A01/BETA A22

This document includes Ranger to the Moon, Mariner to Mars, Tiros weather watcher, Early Bird satellite, scientific satellites, sounding rockets, aeronautical research, preparation for the moon, and manned Gemini flights. CASI

N94-15244* National Aeronautics and Space Administration, Washington, DC.
THE 1967 HIGHLIGHTS (Videotape)
Dec. 1967 Videotape: 15 min. playing time, in color, with sound (NASA-TM-109633; NONP-VT-93-190431) Avail: CASI VHS A01/BETA A22

This document includes Surveyor, Lunar Orbiter, Apollo 4, Biosatellite, Orbiting Geophysical Observatory, Orbiting Solar Observatory, Explorers, Applications Technology satellites, operational satellites, Mariner to Venus, San Marco, sounding rockets, and aeronautical research. CASI

N94-15315* National Aeronautics and Space Administration. Lyndon B. Johnson Space Center, Houston, TX.
STS-26 THROUGH STS-34, DEPLOY ACTIVITIES (Videotape)
Dec. 1989 Videotape: 28 min. 34 sec. playing time, in color, with sound (NASA-TM-109566; NONP-VT-93-190364) Avail: CASI VHS A01/BETA A22

This video shows on orbit deployments since Shuttle flights resumed in 1988. These deployments include TDRS-C and TDRS-D, and the Magellan and Galileo spacecrafts. CASI

N94-15322* National Aeronautics and Space Administration, Washington, DC.
NACA-NASA: 75 YEARS OF FLIGHT (Videotape)
Oct. 1990 Videotape: 3 min. 11 sec. playing time, in color, with sound (NASA-TM-109449; NONP-VT-93-190246) Avail: CASI VHS A01/BETA A22

This document presents historical footage used to recollect the last 75 years of aeronautical and space-related research. CASI

N94-15343* National Aeronautics and Space Administration, Washington, DC.
THE 1966 HIGHLIGHTS (Videotape)
Dec. 1966 Videotape: 14 min. 30 sec. playing time, in color, with sound (NASA-TM-109444; NONP-VT-93-190241) Avail: CASI VHS A01/BETA A22

The videotape includes footage of the following: space and aeronautic montage, Surveyor lands on the Moon, Lunar Orbiter, weather satellites, Orbiting Geophysical Observatory, Pagoes, Pioneer, sounding rockets, solar eclipse, X-15, lifting bodies, solid rockets, nuclear powered engines, Project Gemini ends, and Apollo-Saturn. CASI

N94-15352* National Aeronautics and Space Administration, Washington, DC.
NASA: THE 25TH YEAR (Videotape)
Sep. 1983 Videotape: 50 min. playing time, in color, with sound (NASA-TM-109457; NONP-VT-93-190254) Avail: CASI VHS A01/BETA A22

This video tape chronicles NASA's research and development programs, especially regarding space travel from 1958 to 1983. CASI

N94-15366* National Aeronautics and Space Administration. Lyndon B. Johnson Space Center, Houston, TX.
APOLLO PRESENTATION FOR ASTRODOME (Videotape)
Aug. 1989 Videotape: 7 min. playing time, in color, with sound (NASA-TM-109535; NONP-VT-93-190332) Avail: CASI VHS A01/BETA A22

This video features a condensed look at Apollo milestones. It was created for presentation at the Houston Astrodome during Apollo 11's 20th Anniversity celebrations. CASI

N94-15394* National Aeronautics and Space Administration. Lyndon B. Johnson Space Center, Houston, TX.
PRESIDENT KENNEDY'S SPEECH AT RICE UNIVERSITY (Videotape)
Nov. 1988 Videotape: 34 min. playing time, in color, with sound (NASA-TM-109532; NONP-VT-93-190329) Avail: CASI VHS A01/BETA A22

This video tape presents unedited film footage of President John F. Kennedy's speech at Rice University, Houston, Texas, September 12, 1962. The speech expresses the commitment of the United States to landing an astronaut on the Moon. CASI

N94-15399* National Aeronautics and Space Administration. Lyndon B. Johnson Space Center, Houston, TX.
ASTP 15TH ANNIVERSARY CLIP-MEDIA RELEASE (Videotape)
Sep. 1990 Videotape: 42 min. playing time, in color, with sound (NASA-TM-109534; NONP-VT-93-190331) Avail: CASI VHS A01/BETA A22

This release is comprised of 5 separate clips, including the following: CL 762 Astronauts/Cosmonauts Visit to KSC and Walt Disney World; CL 739 ASTP Joint Crew Activities; CL 748 ASTP Astronauts/Cosmonauts Horlock Ranch Visit; CL 758 T-21 ASTP Training - US/USSR; and CL 743 ASTP Joint Crew Training in the Soviet Union. CASI

N94-15410* National Aeronautics and Space Administration, Washington, DC.
THE 1973 HIGHLIGHTS (Videotape)
Dec. 1973 Videotape: 14 min. 30 sec. playing time, in color, with sound (NASA-TM-109624; NONP-VT-93-190422) Avail: CASI VHS A01/BETA A22

These highlights include man in space, Pioneer to Jupiter, Mariner to Venus and Mercury, sounding rockets, comet Kohoutek, Earth resources, and aeronautics. CASI

N94-15411* National Aeronautics and Space Administration, Washington, DC.
THE 1978 HIGHLIGHTS (Videotape)
Dec. 1978 Videotape: 14 min. 30 sec. playing time, in color, with sound (NASA-TM-109625; NONP-VT-93-190423) Avail: CASI VHS A01/BETA A22

These highlights include the space shuttle, new astronauts, Pioneers to Venus, Voyagers to Jupiter and Saturn, High Energy Astronomy Observatories Space Telescope, Landsat/Seasat, space applications, wind energy research, and aeronautics. CASI

N94-15412* National Aeronautics and Space Administration, Washington, DC.
THE 1977 HIGHLIGHTS (Videotape)
Dec. 1977 Videotape: 14 min. 30 sec. playing time, in color, with sound (NASA-TM-109626; NONP-VT-93-190424) Avail: CASI VHS A01/BETA A22

These highlights include the Space Shuttle, the Voyagers, Landsat, aeronautics, Spacelab, HEAO-1, and energy research. CASI

N94-15413* National Aeronautics and Space Administration, Washington, DC.
THE 1968 HIGHLIGHTS (Videotape)
Jan. 1969 Videotape: 14 min. 30 sec. playing time, in color, with sound (NASA-TM-109627; NONP-VT-93-190425) Avail: CASI VHS A01/BETA A22

These highlights include the end of the Surveyor Program, planetary studies, Pioneers, Orbiting Geophysical Observatory, sounding rockets, radio astronomy Explorer, Orbiting Astronomical Observatory, Nimbus, lifting bodies, X-15 Program, XB-70, V/TOL, model research, jet noise reduction, flight safety, nuclear engines, Project Apollo (testing and training), and Apollo 5,6,7, and 8. CASI

N94-15415* National Aeronautics and Space Administration, Washington, DC.
THE 1970 HIGHLIGHTS (Videotape)
Dec. 1970 Videotape: 28 min. 30 sec. playing time, in color, with sound (NASA-TM-109628; NONP-VT-93-190426) Avail: CASI VHS A01/BETA A22

These highlights include the 1970 solar eclipse, Tiros, Nimbus, Intelsat, wake turbulence, the Peru earthquake, Oregon fishing grounds, Apollo 13, SI-C static firing, McDonnell/Douglas 90-day confinement test, and the moon from Galileo to 1971. CASI

N94-15417* National Aeronautics and Space Administration, Washington, DC.
THE 1971 HIGHLIGHTS (Videotape)
Dec. 1971 Videotape: 14 min. 30 sec. playing time, in color, with sound (NASA-TM-109629; NONP-VT-93-190427) Avail: CASI VHS A01/BETA A22

These highlights include Mariner orbit of Mars, Interplanetary Monitoring Platform, Orbiting Solar Observatory, small scientific satellite, sounding rockets, Stratoscope 11, earth resources, aeronautics, jet noise abatement, airport runway safety, Apollo 14 and 15, and Skylab. CASI

N94-15424* National Aeronautics and Space Administration, Washington, DC.
SIGHTS AND SOUNDS OF SPACE (Videotape)
Nov. 1989 Videotape: 3 min. 19 sec. playing time, in color, with sound (NASA-TM-109610; NONP-VT-93-190408) Avail: CASI VHS A01/BETA A22

This video details the progress of the first musician's work, based on the STS-26 mission, in the NASA Fine Arts Program. CASI

N94-15434* National Aeronautics and Space Administration. Ames Research Center, Moffett Field, CA.
UNITARY PLAN WIND TUNNEL LANDMARK DEDICATION AND REVITALIZATION (Videotape Supplement)
Sep. 1990 Videotape: 21 min. playing time, in color, with sound (NASA-TM-109649; NONP-VT-93-190447) Avail: CASI VHS A01/BETA A22

This video shows construction scenes of unitary plan wind tunnel, aerials,

and views of various models, including an MD-11 in the 11 ft, an Apollo in the 8x7, Dynasoar in the 8x7, a one inch scale shuttle in the 8x7, and an artist's concept of a 12 ft test section. CASI

N94-15508* National Aeronautics and Space Administration, Washington, DC.
THE 1982 HIGHLIGHTS (Videotape)
Dec. 1982 Videotape: 14 min. 30 sec. playing time, in color, with sound (NASA-TM-109671; NONP-VT-93-190469) Avail: CASI VHS A01/BETA A22

This video includes STS 3 & 4, Challenger completed, unmanned launches, the Hubble Space Telescope, Pioneers 8 & 9 encounter, Mars Pictures, Landsat 4, wind energy, ion-electric engines, solar powered medical system, medical image analysis, rotor systems research aircraft, XV-15, propfan research, aircraft icing studies, and Oshkosh Sirshow. CASI

N94-15509* National Aeronautics and Space Administration, Washington, DC.
THE 1980 HIGHLIGHTS (Videotape)
Dec. 1980 Videotape: 14 min. 30 sec. playing time, in color, with sound (NASA-TM-109672; NONP-VT-93-190470) Avail: CASI VHS A01/BETA A22

This video includes Voyager 1 to Saturn, Solar Maximum Mission, sounding rockets/balloons, Space Shuttle, GOES 4 weather satellite, Mount St. Helen's Research, wind energy, rotor systems research aircraft, quiet shorthaul aircraft, AD-1 Scissor Wing, and automated pilot advisory system. CASI

N94-16069* National Aeronautics and Space Administration. Lyndon B. Johnson Space Center, Houston, TX.
HISTORY OF THE MANNED SPACE FLIGHT PROGRAM (Videotape)
Aug. 1990 Videotape: 13 min. playing time, in color, with sound (NASA-TM-109529; NONP-VT-93-190326) Avail: CASI VHS A01/BETA A22

Astronaut Marsha Ivins tracks the history of America's space program, from Alan Shepard's Mercury flight to Space Shuttle flight STS-26. CASI

N94-16495*# National Aeronautics and Space Administration. Langley Research Center, Hampton, VA.
THIRD LDEF POST-RETRIEVAL SYMPOSIUM ABSTRACTS Abstracts Only
Arlene S. Levine, comp. 1993 150 p Symposium held in Williamsburg, VA, 8-12 Nov. 1993; sponsored by NASA, Washington and AIAA
(NASA-CP-10120; NAS 1.55:10120) Avail: CASI HC A07/MF A02

This volume is a compilation of abstracts submitted to the Third Long Duration Exposure Facility (LDEF) Post-Retrieval Symposium. The abstracts represent the data analysis of the 57 experiments flown on the LDEF. The experiments include materials, coatings, thermal systems, power and propulsion, science (cosmic ray, interstellar gas, heavy ions, micrometeoroid, etc.), electronics, optics, and life science. Author

N94-16500# European Space Agency. European Space Research and Technology Center, ESTEC, Noordwijk (Netherlands).
THE DEFINITION OF A SCIENTIFIC POLICY: ESRO'S SATELLITE PROGRAMME IN 1969-1973
Arturo Russo Mar. 1993 57 p
(ESA-HSR-6) Avail: CASI HC A04/MF A01

The development of the European Space Research Organization's (ESRO's) scientific satellite program in the period 1969-1973 is analyzed. These four years were the most important in the history of European cooperation in space. The paper is organized in three main parts. In the first part, the main features of the two satellite projects approved by the ESRO council in 1969, namely COS-B and GEOS, are reviewed. In the second part, the discussions within the European space science community which led to the important policy statement issued by ESRO's Launching Program Advisory Committee (LPAC) in early 1970 are analyzed. In the third part, the important 'Package Deal' agreed on by the ESRO Council in December 1971 which formally established application satellite programs is reported and the choice of ISEE-2 and Exosat, the coherent conclusion of four years of scientific discussions and feasibility studies, is discussed. Derived from text

N94-16526# European Space Agency. European Space Research and Technology Center, ESTEC, Noordwijk (Netherlands).
EUROPE IN SPACE: EDOARDO AMALDI AND THE INCEPTION OF ESRO
Michelangelo DeMaria (La Sapienza Univ., Rome, Italy.) Mar. 1993 38 p
(ESA-HSR-5) Avail: CASI HC A03/MF A01

This European Space Agency (ESA) History Study Report discusses Edoardo Amaldi and the inception of the European Space Research Organization. Topics covered include: Amaldi's dream of a Euroluna before 1965; Franco-Italian alliance and Auger's Comite des Recherches Spatiales as a model for Europe; first public discussions of Amaldi's project: the British enter the field; and Amaldi's role in the development of a national space program in Italy and his lost battle against the European Space Vehicle Launcher Development Organization (ELDO). CASI

N94-16592# European Space Agency. European Space Research and Technology Center, ESTEC, Noordwijk (Netherlands).
EUROPE INTO SPACE: THE AUGER YEARS (1959-1967)
John Krige May 1993 76 p
(ESA-HSR-8) Avail: CASI HC A05/MF A01

This is the first of a series of working papers dealing with an overview of the history of ESRO, ELDO and ESA. As such it represents a synthesis of hundreds, even thousands of pages of source material. To reduce the volume of material in this way, the historian has to make two related intellectual choices. The first concerns what to include (and what to leave out), the second the level at which an issue is to be handled. Both of these choices are difficult and negotiable, in the sense that disagreements are inevitable both between historian and those who lived this history, and between the historian and his or her professional colleagues. The topics I have chosen to concentrate on in this rich and difficult start to Europe's space effort are identified in the table of contents above. As source material I have drawn on previously published, more detailed, work by myself and my colleagues in the ESA History Team, notably results which have already appeared in this series of working papers. It has been supplemented by original documents, particularly those which arrived at the level of the ESRO Council, as well as by articles in the ESRO and the ESRO/ELDO Bulletins. References, as well as material in the notes, have been restricted to the minimum so as not to impede the narrative flow. The series of overviews, of which this is the first, has two main purposes. Firstly, it is intended to provide the general intellectual framework for the detailed two-volume history of the European Space Agency which the Team is to produce. Secondly, parts are to serve for a shorter volume to be published in 1994 to coincide with ESRO's thirtieth birthday. Derived from text

N94-16792# European Space Agency. European Space Research and Technology Center, ESTEC, Noordwijk (Netherlands).
[RESOURCES AND ACTIVITIES OF THE EUROPEAN SPACE AGENCY] Annual Report, 1992
N. Longdon and T. D. Guyenne May 1993 116 p Original contains color illustrations
Copyright Avail: CASI HC A06/MF A02

The European Space Agency (ESA) Annual Report for 1992 is presented. An explanation of major aspects of the work that affects all Member States is reported. This work includes scientific projects, scientific research, Earth observation, telecommunications, space transportation, Colombus/Space Station, microgravity, technology, operations, international cooperation, and public relations. The recent evolution of ESA contractual methods that have had to be adapted to the changing industrial pattern of Europe is explained. The agency's budget, industrial policy, and contracts are described. CASI

N94-16804# Organization for Economic Co-Operation and Development, Paris (France).
THE MEGASCIENCE FORUM Progress Report, 15 Jun. 1992 - 14 Jun. 1993
M. W. Oborne May 1993 6 p
(Contract DE-FG02-92ER-35166)
(DE93-014445; DOE/ER-35166/1) Avail: CASI HC A02/MF A01

This report gives an account of the activities of the OECD Megascience Forum following its creation in June 1992, in particular the reviews of two areas of megascience: Astronomy and deep drilling (both deep sea and

continental). It presents the main policy conclusions reached by the Megascience Forum on these areas. It also gives an indication of ongoing and future work. With regard to ongoing and future work, the Forum will review at its next meeting, in July 1993, the area of global change research, and for this purpose an expert meeting was held in late Mar. 1993 in Cambridge, Mass. (USA). Areas to be reviewed later in 1993 include oceanography, and neutron sources and synchrotron radiation sources as multipurpose facilities for the study of condensed matter, as well as for other applications such as element transmutation. The Megascience Forum will also undertake to discuss generic science and technology policy issues related to the development and management of megascience, starting with a discussion, at its next meeting, of national decision-making structure and processes. DOE

N94-17305# Office of Naval Research Liaison Office, Far East, APO San Francisco, CA.

ONRASIA SCIENTIFIC INFORMATION BULLETIN, VOLUME 18, NUMBER 2 Quarterly Report, Apr. - Jun. 1993

Jun. 1993 176 p

(AD-A267798) Avail: CASI HC A09/MF A02

This is a quarterly publication presenting articles covering recent developments in Far Eastern (particularly Japanese) scientific research. It is hoped that these reports (which do not constitute part of the scientific literature) will prove to be of value to scientists by providing items of interest well in advance of the usual scientific publications. The articles are written primarily by members of the staff of ONRASIA, with certain reports also being contributed by visiting stateside scientists. Occasionally, a regional scientist will be invited to submit an article covering his own work, considered to be of special interest. This publication is approved for official dissemination of technical and scientific information of interest to the Defense research community and the scientific community at large. DTIC

N94-17651# Massachusetts Inst. of Tech., Cambridge. Research Lab. of Electronics.

[ACTIVITIES OF THE RESEARCH LABORATORY OF ELECTRONICS] Progress Report No. 135, 1 Jan. - 31 Dec. 1992

Jonathan Allen and Daniel Kleppner Jun. 1993 399 p

(Contract DAAL03-92-C-0001)

(AD-A266730; ARO-28925.58-EL) Avail: CASI HC A17/MF A04

The activities and topics include: Solid State Physics, Electronics and Optics: Materials and Fabrication: Heterostructures for High Performance Devices, High-Frequency InAlAs/InGaAs Metal-Insulator-Doped Semiconductor Field-Effect Transistors (MIDFET's) for Telecommunications, Chemical Beam Epitaxy of Compound Semiconductors, Focused Ion Beam Microfabrication; Quantum-Effect Devices: Statistical Mechanics of Quantum Dots, Single Electron Transistors, Differential Resistance Through a Quantum Dot: Signature of Kondo Correlation, Submicron and Nanometer Structures Technology and Research; Optics and Devices: Optics and Quantum Electronics, Optical Propagation and Communication, and High-Frequency (greater than 100 GHz) Electronic Devices; Surfaces and Interfaces; Atomic, Molecular and Optical Physics; Plasma Physics; Electromagnetics; Radio Astronomy; Computer-Aided Design; Digital Signal Processing; Genetic Analysis; Speech and Sensory Communication; Auditory Physiology; and Linguistics. DTIC

N94-15126# KLM Aerocarto, Schiphol (Netherlands).

AVIATION AND THE KLM: PAST AND FUTURE [DE LUCHTVAART EN DE KLM: VERLEDEN EN TOEKOMST]

C. denHartog *In* NAL, Symposium on the Future of Aeronautics in the Netherlands 1991 7 p In DUTCH (For primary document see N94-15120 03-01)

Avail: CASI HC A02/MF A02

Typical Subject Index Listing

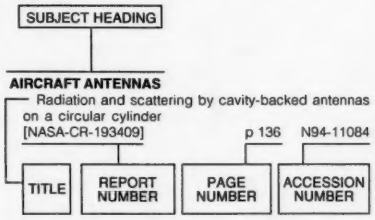

The subject heading is a key to the subject content of the document. Titles, report numbers, and accession numbers of pertinent documents are provided under each subject heading. When the title is insufficiently descriptive of the document content, a title extension is added, separated from the title by three hyphens. The report number helps to indicate the type of document cited (e.g., NASA report, NASA translation, NASA contractor report). The accession number is the number by which the document abstracts are arranged in this journal and by which the document is sold or requested. The page number helps you locate the citation in the abstract section. The titles, with title extensions if present, are arranged under each subject heading in ascending accession number order. The subject headings have been selected from the latest revision of the *NASA Thesaurus*.

A

ABEL FUNCTION
Distributively generated matrix near rings
[DE93-628588] p 1175 N94-17641

ABERRATION
Figures of merit for laser beam quality p 1043 N94-14994
A complete study of differential wax-wane focus servo technique p 1199 N94-14996
Aberration correction of unstable resonators
[NASA-CASE-NPO-18791-1-CU] p 1034 N94-15987
Tip-tilt compensation: Resolution limits for ground-based telescopes using laser guide star adaptive optics
[DE93-016426] p 1237 N94-16872

ABILITIES
Hidden Markov model approach to skill learning and its application to telerobotics
[AD-A266989] p 1164 N94-15502

ABLATION
Size distribution of interplanetary iron and stony particles related with deep-sea spherules p 1245 N94-16388
Ablation, surface activation, and electroless metallization of insulating materials by pulsed excimer laser irradiation
[DE93-015808] p 1040 N94-16664

ABSORBERS (MATERIALS)
Interpenetrating polymer network acoustic damping material
[AD-D015889] p 969 N94-16916
Factors determining the release of nitric oxide — Calcium/cadmium transport by renal cortical collectin duct cells
[AD-A266232] p 1118 N94-17224

ABSORPTANCE
VUV thin films, chapter 7
[NASA-CR-194634] p 967 N94-16494

ABSORPTION SPECTRA
The theory of QSO absorption line systems and their relationship to the galaxies
[NASA-CR-194596] p 1236 N94-15679
Spectral studies of solid propellant combustion 4: Absorption and burn rate results for M43, XM39, and M10 propellants
[AD-A267119] p 946 N94-15685
Optical and infrared spectra of thermally annealed Pb implanted SiO2 glasses
[DE93-015304] p 965 N94-15828
Spectral evidence of size dependent space weathering processes on asteroid surfaces p 1241 N94-16174
Analysis of pyroxene absorptions observed in Martian dark regions p 1292 N94-16411
Bright soil units on Mars determined from ISM imaging spectrometer data p 1295 N94-16430
From minerals to rocks: Toward modeling lithologies with remote sensing p 1086 N94-16437
Mapping the mineralogy and lithology of Canyonlands, Utah with imaging spectrometer data and the multiple spectral feature mapping algorithm p 1066 N94-16670
The Spectral Image Processing System (SIPS): Software for integrated analysis of AVIRIS data p 1067 N94-16674
AVIRIS study of Death Valley evaporite deposits using least-squares band-fitting methods p 1067 N94-16676
Separation of cirrus cloud from clear surface from AVIRIS data using the 1.38 micron water vapor band p 1072 N94-16699
AVIRIS as a tool for carbonatite exploration: Comparison of SPAM and Mbandmap data analysis methods p 1073 N94-16703
Discussion of band selection and methodologies for the estimation of precipitable water vapour from AVIRIS data p 1074 N94-16707
Convergence of the multiple scattering expansion in XAFS and XANES
[DE93-011001] p 948 N94-16772
Complex QSO absorbers: High-redshift clusters of galaxies?
[NASA-CR-194617] p 1237 N94-16833

ABSORPTION SPECTROSCOPY
A high flux radical beam diamond growth
[AD-A266754] p 1207 N94-15955
In situ studies of passive film chemistry using x ray absorption spectroscopy
[DE93-014023] p 947 N94-16011
Method and apparatus for performing scanning tunneling optical absorption spectroscopy
[AD-D015796] p 948 N94-16539
Characterization of nanoscale oxide and oxyhydroxide powders using EXAFS spectroscopy
[DE93-015683] p 940 N94-17235

ABSORPTIVITY
Characterization of InTISb grown by low pressure metalorganic chemical vapor deposition on GaAs substrate
[AD-A266878] p 1206 N94-14922
Modeling the reflectance of CO2 frost with new optical constants: Application to Martian south polar cap spectra p 1256 N94-16217
Near-surface temperature gradients and their effects on thermal-infrared emission spectra of particulate planetary surfaces p 1260 N94-16236
Theoretical studies of nonlinear optical properties of conjugated polymers
[AD-A267390] p 1193 N94-17024
Resist performance in soft x ray projection lithography
[DE93-016490] p 1036 N94-17647

ABSTRACTS
Annual historical report, calendar year 1992
[AD-A267050] p 1121 N94-15663
AFOSR technical report summaries, January - March 1993
[AD-A267187] p 1230 N94-15850
Proceedings of the Second Workshop on Microgravity Experimentation
[DSS-NR15-43-1990] p 977 N94-16071
DLTS and dynamic transconductance analysis of deep-submicron fully-depleted SOI MOSFET's
[AD-A267291] p 1214 N94-17243
Abstracts of manuscripts submitted in 1992 for publication
[AD-A267963] p 1113 N94-17383

ABUNDANCE
Evolutionary implications of a steady-state water abundance on Venus p 1254 N94-16206
Do SiC grains in Orgueil differ from those in Murchison? p 1242 N94-16260
Carbon abundances, major element chemistry, and mineralogy of hydrated interplanetary dust particles p 1243 N94-16309
Isotopic signatures and distribution of nitrogen and trapped and radiogenic xenon in the Acapulco and FRO90011 meteorites p 1243 N94-16317
A search for noble-gas evidence for presolar oxide grains p 954 N94-16353
Abundance recovery error analysis using simulated AVIRIS data p 1074 N94-16708

AC GENERATORS
Circle diagram approach for self excited induction generators
[DE93-010031] p 1010 N94-15971

ACCELERATED LIFE TESTS
Analytical and experimental investigation of the feasibility of accelerated lifetime testing of materials exposed to an atomic oxygen beam
[NASA-CR-193851] p 946 N94-15766

ACCELERATION (PHYSICS)
A simplistic look at limit stresses from random loading
[NASA-TM-108427] p 1058 N94-15710

ACCELERATION TOLERANCE
Cumulative effect of repeated brief cerebral ischemia
[AD-A267155] p 1121 N94-15736

ACCELEROMETERS
Analysis of the accuracy of strapdown inertial surveying systems
[SER-C-391] p 1081 N94-15156
A feasibility study of a microgravity enhancement system for Space Station Freedom
[NASA-CR-191550] p 886 N94-15864
KC-135 acceleration monitoring and data acquisition system p 868 N94-16090
Precise measurement and utilization of acceleration data p 923 N94-16100

ACCEPTABILITY
Environment tests for mini satellites p 896 N94-17189

ACCEPTOR MATERIALS
Photodegradation of polyimides. V1: Effect of donor-acceptor groups on the photooxidative stability of polyimides and model compounds
[AD-A267319] p 970 N94-16947

ACCIDENT INVESTIGATION
The fragmentation of the Nimbus 6 rocket body
[NASA-CR-191645] p 926 N94-16504

ACCIDENT PREVENTION
The 1971 highlights — NASA programs and research
[NASA-TM-109629] p 1302 N94-15417
OSHA bloodborne pathogens standards exposure control plan p 1127 N94-16645

ACCOUNTING
The ESA Tele-Invoicing System (ETIS)
[ESA-INT-6] p 1150 N94-16591

ACCRETION DISKS
Gas-grain energy transfer in solar nebula shock waves: Implications for the origin of chondrules p 1262 N94-16251

ACCURACY
New perspectives for high accuracy SLR with second generation geodesic satellites p 916 N94-15585
Improvement of SLR accuracy, a possible new step p 917 N94-15588
On the accuracy of ERS-1 orbit predictions p 874 N94-15589
Sub-cm ranging and other improvements in Graz p 919 N94-15603
Temperature and pressure effects on capacitance probe cryogenic liquid level measurement accuracy
[NASA-CR-190763] p 1034 N94-16521

ACETATES
Cyanoresin, cyanoresin/cellulose triacetate blends for thin film, dielectric capacitors
[NASA-CASE-NPO-18913-1-CU] p 966 N94-15930
Cellulose triacetate, thin film dielectric capacitor
[NASA-CASE-NPO-18935-1-CU] p 1010 N94-15952

ACETONE
Aberration correction of unstable resonators
[NASA-CASE-NPO-18791-1-CU] p 1034 N94-15987

ACETYLATION
Bioorganic models for protein ion channels
[AD-A266365] p 1117 N94-16441

ACETYLENE
Modeling study to evaluate the ionic mechanism of soot formation in flames
[AD-A266242] p 950 N94-16930

ACHONDRITES
Petrologic constraints on the surface processes on asteroid 4 Vesta and on excavation depths of diogenite fragments p 1241 N94-16208
Potassium isotope cosmochemistry, volatile depletion and the origin of the Earth p 953 N94-16259
Angrite LEW87051: Are the olivines pheno's or xeno's? A continuing story p 1103 N94-16285
Partial melting of ordinary chondrites: Lost City (H) and St. Severin (LL) p 1243 N94-16286
Exsolved kirschsteinite in angrite LEW86010 olivine p 1245 N94-16410
Igneous fractionation and subsolidus equilibration of diogenite meteorites p 1245 N94-16413

ACID RAIN
What's killing the trees? --- causes for forest decline
[NASA-TM-109621] p 1094 N94-15350

ACIDITY
Intramolecular versus intermolecular condensation rates in the acidic polymerization of octaethoxytrisiloxane
[AD-A266982] p 963 N94-15490

ACOUSTIC ATTENUATION
Interpenetrating polymer network acoustic damping material
[AD-D015889] p 969 N94-16916
Cortical adaptive filtering in bioacoustic signal classification
[AD-A266229] p 1177 N94-16939

ACOUSTIC EMISSION
Studies of aural acoustic emmissions with the use of an original apparatus and investigative methodology
[IFTR-20/1992] p 1177 N94-16650

ACOUSTIC EXCITATION
Sound radiation from infinite laminated composite shell with periodic rib stiffening
[DRA/TM(USGR)92326] p 933 N94-15699

ACOUSTIC FATIGUE
Vibro-acoustic analysis of an aircraft maintenance dock
[AD-A266778] p 871 N94-14908

ACOUSTIC MEASUREMENT
Vibro-acoustic analysis of an aircraft maintenance dock
[AD-A266778] p 871 N94-14908
Free-field sensitivity calibration of laboratory standard microphones by the reciprocity technique: Measurements for the 1991 EEC intercomparison
[NPL-RSA(EXT)-0043] p 1176 N94-15019
Ultrasound absorption in molten salts p 944 N94-15161
Acousto-optical confirmation of the localized wave phenomena
[DE93-016425] p 1177 N94-16448
Digital reverberation time measurement system
[AD-D015892] p 1177 N94-16919
An automated system for ultrasound measurements of liquids by the resonance (Eggers) method
[IFTR-17/1992] p 1178 N94-17087
Noise measurement flight test of five light helicopters
[AD-A268566] p 1179 N94-17599

ACOUSTIC PROPAGATION
Vibro-acoustic analysis of an aircraft maintenance dock
[AD-A266778] p 871 N94-14908
Nonlinear acoustics: Periodic waveguide, scattering of sound by sound, three-layer fluid, finite amplitude sound in a medium having a distribution of relaxation processes, and production of an isolated negative pulse in water
[AD-A267145] p 1177 N94-15732
Sound exposure level prediction for impulse sound sources above variable terrain
[AD-A267535] p 1178 N94-17119

ACOUSTIC PROPERTIES
Segment-based acoustic models for continuous speech recognition
[AD-A267138] p 988 N94-15691
Effect of wind tunnel acoustic modes on linear oscillating cascade aerodynamics
[NASA-TM-106367] p 869 N94-15866
Real time system for practical acoustic monitoring of global ocean temperature
[AD-A267868] p 1113 N94-17391
Noise measurement flight test of five light helicopters
[AD-A268566] p 1179 N94-17599

ACOUSTIC SCATTERING
Nonlinear acoustics: Periodic waveguide, scattering of sound by sound, three-layer fluid, finite amplitude sound in a medium having a distribution of relaxation processes, and production of an isolated negative pulse in water
[AD-A267145] p 1177 N94-15732
Modal ring method for the scattering of sound
[NASA-TM-106342] p 1177 N94-16497

ACOUSTIC VELOCITY
The shock Hugoniot of 316 SS and sound velocity measurements
[DE93-016525] p 1178 N94-16955
Acoustic waves in complicated geometries and their interactions with liquid-propellant droplet combustion
[AD-A267260] p 1178 N94-16991
Real time system for practical acoustic monitoring of global ocean temperature
[AD-A267868] p 1113 N94-17391

ACOUSTO-OPTICS
Alternative optical architectures for multichannel adaptive optical processing
[AD-A267052] p 1189 N94-15664
Display system employing acousto-optic tunable filter
[NASA-CASE-NPO-18736-1-CU] p 1190 N94-15933
Wideband acousto-optic correlator for an ESM receiver upgrade
[TABES PAPER 93-661] p 1054 N94-16156
Acousto-optical confirmation of the localized wave phenomena
[DE93-016425] p 1177 N94-16448
JPL activities on development of acousto-optic tunable filter imaging spectrometer p 1037 N94-16696
Acousto-optical classifier
[AD-D015894] p 1000 N94-16921
Two-dimensional acousto-optical interaction theory and experimental analysis
[AD-A267761] p 1193 N94-17254
Frequency resolution of an acousto-optical spectrometer
[AD-A267822] p 1035 N94-17401
Study of high speed interference photography with two-dimensional acousto-optical lattice deflection
[AD-A267823] p 1035 N94-17402

ACRYLATES
Interpenetrating polymer network acoustic damping material
[AD-D015889] p 969 N94-16916

ACRYLONITRILES
Characterization of the lithium/pan-based polymer electrolytes interface
[AD-A268401] p 973 N94-17434

ACTINIDE SERIES
Theoretical studies of the crystal structure of rare earths and actinides at zero temperature
[DE93-016488] p 1214 N94-17301

ACTIVATION ENERGY
Structural effects in electron transfer reactions: Comparative interfacial electrochemical kinetics for cis-versus trans-dioxorhenium (V) (bi)pyridine oxidation
[AD-A266307] p 1182 N94-16466
Solvational barriers to interfacial electron transfer: Minimization by way of valence delocalization
[AD-A267371] p 950 N94-17006

ACTIVE CONTROL
Aerodynamic/dynamic/control interaction
[AD-A266187] p 871 N94-16107
Controls of maglev suspension systems
[DE93-015540] p 1011 N94-16443
Active turbulence control in wall bounded flows using direct numerical simulation
[AD-A267261] p 1028 N94-17286

ACTIVE GALACTIC NUCLEI
Astrophysics with MILAGRO
[DE93-012722] p 1240 N94-17657

ACTS
Proceedings of the Fifteenth NASA Propagation Experimenters Meeting (NAPEX 15) and the Advanced Communications Technology Satellite (ACTS) Propagation Studies Miniworkshop
[NASA-CR-194539] p 994 N94-16035
The ACTS propagation program p 995 N94-16039
Propagation measurements in Alaska using ACTS beacons p 995 N94-16040
Planned LMSS propagation experiment using ACTS: Preliminary antenna pointing results during mobile operations p 995 N94-16041
Propagation-related AMT design aspects and supporting experiments p 995 N94-16042

ACTUATOR DISKS
Electro-rheological disk pump
[AD-D015783] p 1047 N94-16531

ACTUATORS
YARF: An open-ended framework for robot road following
[AD-A266788] p 1163 N94-14910
Advanced cooling for high power electric actuators
[AD-A266984] p 866 N94-15761
ALS engine propellant effector system
[NASA-CR-194650] p 926 N94-16590
Design of a fluid elastic actuator with application to structure control
[AD-A267649] p 897 N94-17246
Optimal tuning of heavy equipment motion controllers
[AD-A267873] p 1167 N94-17392
A comparative study of analog and digital control laws for the UMCSL truss
[AD-A267980] p 871 N94-17412

ADA (PROGRAMMING LANGUAGE)
Evaluation of ALSYS 037 Ada Compiler
[AD-A266972] p 1143 N94-15110
Proceedings of the Association for Computing Machinery Special Interest Group for Ada Artificial Intelligence Working Group
[AD-A266422] p 1165 N94-16559
An examination of two Ada language object-oriented databases
[AD-A267486] p 1154 N94-17366

ADAPTATION
The bootstrapped algorithm: Fast algorithm for blind signal separation
[AD-A266671] p 1147 N94-15772

ADAPTIVE CONTROL
Contribution to the elaboration of some adaptive control algorithms for fermentation processes monitoring
[LAAS-92513] p 1116 N94-15643
Neural-network-directed alignment of optical systems using the laser-beam spatial filter as an example
[NASA-TP-3372] p 1034 N94-15961
Adaptive weld control for high-integrity welding applications
[TABES PAPER 93-604] p 1049 N94-16140
Information technology division technical paper abstracts
[AD-A266227] p 1166 N94-16938

ADAPTIVE FILTERS
Broadband conventional beamforming incorporating adaptive equalization
[AD-A267090] p 987 N94-15544
Adaptive median filtering for preprocessing of time series measurements p 912 N94-15561
Adaptive interference canceller
[CA-PATENT-1-310-709] p 988 N94-15698
Development and analysis of ARMA parameter estimation schemes in the presence of noise
[AD-A267184] p 989 N94-15786
Cortical adaptive filtering in bioacoustic signal classification
[AD-A266229] p 1177 N94-16939

ADAPTIVE OPTICS
Neural-network-directed alignment of optical systems using the laser-beam spatial filter as an example
[NASA-TP-3372] p 1034 N94-15961
Tip-tilt compensation: Resolution limits for ground-based telescopes using laser guide star adaptive optics
[DE93-016426] p 1237 N94-16872

ADDITIVES
Growth of new materials for solid state laser applications. The growth of ZnGeP2 by the vertical Bridgman method
[NASA-CR-194571] p 1038 N94-15530
Optoelectronics based on SiGe/Si heterostructures
[AD-A267178] p 1190 N94-15848
Ion doped quantum well lasers
[AD-A267198] p 1038 N94-15853
Local environment about O atoms in Pr-Y-Ba-Cu-O films studied by O K-edge XAFS
[DE93-016218] p 1209 N94-16447
Method for doping GaAs with high vapor pressure elements
[AD-D015794] p 1210 N94-16538
Vanadium corrosion studies
[AD-A266489] p 959 N94-16781

ADDRESSING
Generating local addresses and communication sets for data-parallel programs
[NASA-CR-194605] p 1159 N94-15796

ADHESION
Ion mixing of thin ZrO2 films on sapphire
[DE93-015214] p 1206 N94-14925
The effect of plasma treatment on interfacial bond characteristics of Kevlar/epoxy laminates as measured by T-peel tests
[AD-A266920] p 930 N94-14999
Engineering design of sub-micron topographies for simultaneously adherent and reflective metal-polymer interfaces
[NASA-CR-194573] p 964 N94-15700

Weibull analysis applied to the pull adhesion test and fracture of a metal-ceramic interface
[DE93-012913] p 1059 N94-15997
Interface chemistry in ceramic matrix composites
[AD-A268629] p 973 N94-17466
Continuing research on friction and wear of materials
[AD-A268291] p 1049 N94-17566

ADHESION TESTS
Weibull analysis applied to the pull adhesion test and fracture of a metal-ceramic interface
[DE93-012913] p 1059 N94-15997

ADHESIVE BONDING
Weibull analysis applied to the pull adhesion test and fracture of a metal-ceramic interface
[DE93-012913] p 1059 N94-15997

ADHESIVES
Materials Research Society Symposium Proceedings, Volume 292: Biomolecular Materials
[AD-A265776] p 1116 N94-15138

ADIABATIC CONDITIONS
Breakdown of adiabatic invariance
[AD-A267246] p 1219 N94-14977

ADIRONDACK MOUNTAINS (NY)
Broadband teleseismic array recording in the Adirondack Mountains, New York State
[AD-A267290] p 1097 N94-14960

ADSORBENTS
Structural and dynamical aspects of electrodeposition
[AD-A266786] p 942 N94-14909
Trace analysis of chemical warfare agents in air: Sampling in porous polymers followed with thermal desorption analysis
[FOA-C-40302-4.6] p 1097 N94-17625

ADSORPTION
The thermal dissociation of NH2CHO(ND2CHO) on Si(100)-2x1
[AD-A266903] p 942 N94-14956
Theoretical prediction of the UV adsorption and fluorescence spectra of tyrosine and phenylalanine
[AD-A266970] p 943 N94-15111
The role of interfacial chemistry in surface nucleation and growth of calcium oxalate
[DE93-015689] p 1209 N94-16159
Thermal disorder in adsorbed Cl on Si(100)
[AD-A266295] p 1210 N94-16476
On-line gas chromatographic studies of Rutherfordium (element 104), hahnium (element 105), and homologs
[DE93-013890] p 948 N94-16821
Regulation of attached bacterial growth by adsorbed proteins
[AD-A267756] p 1118 N94-17275

ADVANCED LAUNCH SYSTEM (STS)
ALS engine propellant effector system
[NASA-CR-194650] p 926 N94-16590
ALS engine controller system
[NASA-CR-194647] p 926 N94-16654
ALS liquid hydrogen turbopump
[NASA-CR-194646] p 927 N94-17016

ADVANCED SOLID ROCKET MOTOR (STS)
Advanced Solid Rocket Motor
[NASA-TM-109658] p 924 N94-15229
ASRM nozzle thermal analysis
[NASA-CR-194672] p 928 N94-17277

ADVANCED VERY HIGH RESOLUTION RADIOMETER
Sea ice motions in the central arctic ice central arctic pack ice as inferred from AVHRR imagery
[NASA-CR-194572] p 1112 N94-15701
Simulation of AVHRR-K band ratios with AVIRIS
p 1075 N94-16714

ADVECTION
A domain-partition method for the advection-diffusion equation
[INRIA-RR-1740] p 1030 N94-17534

AERATION
Investigation of the influence of applied potential on erosion-corrosion of copper in alkaline chloride solutions
[AD-A266448] p 958 N94-16562

AERIAL PHOTOGRAPHY
Johnson Space Center and downtown Houston, Texas aerials
[NASA-TM-109522] p 1032 N94-15472
The use of TIMS data to estimate the SO2 concentrations of volcanic plumes: A case study at Mount Etna, Sicily p 1065 N94-16608

AERIAL RECONNAISSANCE
AIRSAR South American deployment: Operation plan, version 3.0 p 994 N94-15919

AEROBRAKING
Minimum accommodation for aerobrake assembly. Phase 2: Structural concepts for a lunar transfer vehicle aerobrake which can be assembled on orbit
[NASA-TM-107610] p 885 N94-15446

AEROCAPTURE
Nonequilibrium radiation and chemistry models for aerocapture vehicle flowfields
[NASA-CR-194645] p 1027 N94-17095

AERODYNAMIC BRAKES
Tetrahedral lander
[NASA-CASE-MSC-22082-1] p 886 N94-15951

AERODYNAMIC CHARACTERISTICS
Vertical-tail aerodynamic configuration of space shuttle orbiter
[AD-A267723] p 879 N94-14941
Aerodynamic flight control to increase payload capability of future launch vehicles
[NASA-CR-193850] p 870 N94-15532
Heat transfer and aerodynamics of a 3D design nozzle guide vane tested in the Pyestock isentropic light piston facility
[RAE-TM-AERO/PROP-19] p 856 N94-15696
Aerodynamic control of NASP-type vehicles through vortex manipulation, volume 4
[NASA-CR-177626-VOL-4] p 857 N94-15720
Experimental study of vortex and aerodynamic characteristics of stack wings with sideslip
[AD-A267722] p 860 N94-17274
Subsonic aerodynamic characteristics of the HL-20 lifting-body configuration
[NASA-TM-4515] p 861 N94-17284

AERODYNAMIC CONFIGURATIONS
Vertical-tail aerodynamic configuration of space shuttle orbiter
[AD-A267723] p 879 N94-14941
The effect of the nose shape and wing location toward the wing vortex breakdown
[AD-A267724] p 855 N94-14942
Aerodynamic control of NASP-type vehicles through Vortex manipulation. Volume 1: Static water tunnel tests
[NASA-CR-177626-VOL-1] p 855 N94-15655
Aerodynamic control of NASP-type vehicles through Vortex manipulation. Volume 2: Static wind tunnel tests
[NASA-CR-177626-VOL-2] p 856 N94-15677
Missile datcom user's manual
[AD-A267447] p 1152 N94-17032
Single block three-dimensional volume grids about complex aerodynamic vehicles
[NASA-TM-108986] p 1030 N94-17476

AERODYNAMIC DRAG
The turbulent wall jet
[AD-A267675] p 855 N94-14963
On the delivery of planetesimals to a protoplanet in the solar nebula p 1245 N94-16379
Dust grain resonant capture: A statistical study
p 1245 N94-16384
Low Earth orbit constellations: Orbit control or not
p 875 N94-17134
Equations of motion of a hinged body over a spherical earth
[AD-A268408] p 868 N94-17435

AERODYNAMIC FORCES
Aeroelastic airfoil smart spar p 868 N94-16865

AERODYNAMIC HEATING
Incorporation of boundary layer heating predictive methodology into NSWCDD aeroprediction code
[AD-A267000] p 1020 N94-15632
Aerothermoelastic analysis of a NASP demonstrator model
[NASA-TM-109007] p 867 N94-17055

AERODYNAMIC INTERFERENCE
Development of an air-to-air refueling automatic flight control system using quantitative feedback theory
[AD-A266718] p 870 N94-15730
Wall interference and boundary simulation in a transonic wind tunnel with a discretely slotted test section
[NASA-TP-3334] p 872 N94-15794
Determination of the effect of the walls of a wind-tunnel from the parameters of flow near them
[RAE-LIB-TRANS-2201] p 859 N94-16583

AERODYNAMIC LOADS
Aerodynamic/dynamic/control interaction
[AD-A266187] p 871 N94-16107
Computation of a controlled store separation from a cavity p 858 N94-16513
Fatigue life program using strain-life methods
[AD-A267310] p 1060 N94-16943
A review of Australian and New Zealand investigations on aeronautical fatigue during the period April 1991 to March 1993
[AD-A267532] p 868 N94-17117

AERODYNAMIC NOISE
Development of a quiet supersonic wind tunnel with a cryogenic adaptive nozzle
[NASA-CR-194548] p 871 N94-15117

AERODYNAMIC STABILITY
Static aeroelastic response of an aircraft with asymmetric wing planforms representative of combat damage
[AD-A266890] p 865 N94-14951
Wind shear and heavy rain --- effects on flight stability
[NASA-TM-109453] p 1105 N94-15326
Aerodynamic control of NASP-type vehicles through Vortex manipulation. Volume 1: Static water tunnel tests
[NASA-CR-177626-VOL-1] p 855 N94-15655
Wind tunnel investigation with an operational turbojet engine
[TABES PAPER 93-662] p 870 N94-16157
Aerothermoelastic analysis of a NASP demonstrator model
[NASA-TM-109007] p 867 N94-17055
Subsonic aerodynamic characteristics of the HL-20 lifting-body configuration
[NASA-TM-4515] p 861 N94-17284

AERODYNAMIC STALLING
Suppression of dynamic stall with a leading-edge slat on a VR-7 airfoil
[NASA-TP-3357] p 856 N94-15657

AERODYNAMICS
Aerodynamic flight control to increase payload capability of future launch vehicles
[NASA-CR-193850] p 870 N94-15532
An electronic imaging system for the Aeroballistic Research Facility
[AD-A267157] p 1033 N94-15826
Aeronautical engineering: A continuing bibliography with indexes (supplement 295)
[NASA-SP-7037(295)] p 854 N94-16480
Missile datcom user's manual
[AD-A267447] p 1152 N94-17032
Computational aerodynamics with icing effects
[AD-A267509] p 860 N94-17074
User's manual for the Langley Research Center 14- by 22- foot subsonic tunnel static data acquisition system
[NASA-TM-109027] p 861 N94-17639

AEROELASTICITY
Static aeroelastic response of an aircraft with asymmetric wing planforms representative of combat damage
[AD-A266890] p 865 N94-14951
Physical properties of the benchmark models program supercritical wing
[NASA-TM-4457] p 866 N94-15722
Center for Rotorcraft Education and Research progress report, 1987 - 1992
[AD-A266760] p 857 N94-15824
A rapid computational model for estimating the performance of compliant airfoils in cascades
[AD-A266275] p 857 N94-16471
ASTROS enhancements. Volume 1: ASTRO user's manual
[AD-A266818] p 1151 N94-16768
ASTROS enhancements. Volume 2: ASTRO programmer's manual
[AD-A266819] p 1151 N94-16769
Aeroelastic airfoil smart spar p 868 N94-16865
Flutter analysis using transversality theory
[NASA-TM-106382] p 1062 N94-17481

AEROGELS
Removal of carbonaceous contaminants from silica aerogel p 953 N94-16256

AERONAUTICAL ENGINEERING
Symposium on the Future of Aeronautics in the Netherlands
[ETN-93-93780] p 853 N94-15120
Fifty years of the Netherlands Association of Aeronautical Engineers p 853 N94-15121
Predicted and real development in the aviation in the period 1961-1991 p 853 N94-15122
Center for Rotorcraft Education and Research progress report, 1987 - 1992
[AD-A266760] p 857 N94-15824
Aeronautical engineering: A continuing bibliography with indexes (supplement 295)
[NASA-SP-7037(295)] p 854 N94-16480

AERONAUTICAL SATELLITES
Propagation research in Japan p 996 N94-16043

AERONAUTICS
NACA-NASA: 75 years of flight
[NASA-TM-109449] p 1302 N94-15322
Maximizing participation of women in collegiate aviation education
[NIAR-93-14] p 1222 N94-17261

AERONOMY
An assessment of acid fog
[DE93-009347] p 1095 N94-15940

AEROSOLS
Preliminary analysis of University of North Dakota aircraft data from the FIRE Cirrus IFO-2
[NASA-CR-193357] p 866 N94-15429
An assessment of acid fog
[DE93-009347] p 1095 N94-15940
Spatial and frequency diversity in lidar systems
[AD-A266192] p 1039 N94-16124
Altitude profile of aerosols on Mars from measurements of its thermal radiation on limb p 1294 N94-16423
Hyperspectral modeling for extracting aerosols from aircraft/satellite data p 1067 N94-16873

Mechanistic models of soot formation
[AD-A267806] p 950 N94-17008
BACKSCAT lidar simulation version 3.0: Technical documentation and users guide
[AD-A267296] p 1003 N94-17268

AEROSPACE ENGINEERING
Processing and protection of high temperature structural materials
[AD-A267292] p 954 N94-14961
Symposium on the Future of Aeronautics in the Netherlands
[ETN-93-93780] p 853 N94-15120
Developments in the Higher Technical Aerospace Education p 854 N94-15130
Expectations for the future of the Faculty of Aeronautics and Astronautics of the Technical University of Delft p 854 N94-15131
The 1969 highlights
[NASA-TM-109630] p 1301 N94-15241
The 1972 highlights
[NASA-TM-109631] p 1301 N94-15242
The 1965 highlights — NASA programs
[NASA-TM-109632] p 1301 N94-15243
The 1967 highlights
[NASA-TM-109633] p 1301 N94-15244
NACA-NASA: 75 years of flight
[NASA-TM-109449] p 1302 N94-15322
NASA images 7
[NASA-TM-109438] p 1235 N94-15337
NAS technical summaries: Numerical aerodynamic simulation program, March 1991 - February 1992
[NASA-TM-109335] p 854 N94-15798
NASA/DOD Aerospace Knowledge Diffusion Research Project. Paper 32: A new era in international technical communication: American-Russian collaboration
[NASA-TM-109336] p 1230 N94-15838
NASA/DOD Aerospace Knowledge Diffusion Research Project. Paper 34: Technical communications practices and the use of information technologies as reported by Dutch and US aerospace engineers
[NASA-TM-109337] p 1230 N94-15839
TABES 1993: 9th Annual Technical and Business Exhibition and Symposium p 1050 N94-16129
Impact of TQM concepts on inspection of aerospace systems
[TABES PAPER 93-350] p 1050 N94-16130
Approaching the new reality
[TABES PAPER 93-230] p 1050 N94-16131
Commercial space opportunities advanced concepts and technology overview
[TABES PAPER 93-240] p 1050 N94-16132
Commonwealth of Independent States aerospace science and technology, 1992: A bibliography with indexes
[NASA-SP-7106] p 854 N94-16481
Space Nuclear Facility test capability at the Baikal-1 and IGR sites Semipalatinsk-21, Kazakhstan
[DE93-011662] p 926 N94-16773
NASA/DOD Aerospace Knowledge Diffusion Research Project. Report 15: Technical uncertainty and project complexity as correlates of information use by US industry-affiliated aerospace engineers and scientists: Results of an exploratory investigation
[NASA-TM-107693] p 1233 N94-17291
NASA/DOD Aerospace Knowledge Diffusion Research Project. Report 15: Technical uncertainty and project complexity as correlates of information use by US industry-affiliated aerospace engineers and scientists: Results of an exploratory investigation
[NASA-TM-107693] p 1233 N94-17300

AEROSPACE ENVIRONMENTS
Autogenic-Feedback Training (AFT) as a preventive method for space motion sickness: Background and experimental design
[NASA-TM-108780] p 1120 N94-15537
Atomic beam studies relevant to the space environment
[AD-A268628] p 1186 N94-17436
Design of an experiment hardware for the ESA space facility BIOPAN
[DLR-FB-93-06] p 876 N94-17548

AEROSPACE INDUSTRY
TABES 1993: 9th Annual Technical and Business Exhibition and Symposium p 1050 N94-16129
Government/contractor development teams
[TABES PAPER 93-460] p 1050 N94-16134
Space Propulsion Synergy Group ETO technology assessments
[TABES PAPER 93-641] p 929 N94-16149
NASA/DOD Aerospace Knowledge Diffusion Research Project. Report 15: Technical uncertainty and project complexity as correlates of information use by US industry-affiliated aerospace engineers and scientists: Results of an exploratory investigation
[NASA-TM-107693] p 1233 N94-17291
NASA/DOD Aerospace Knowledge Diffusion Research Project. Report 15: Technical uncertainty and project complexity as correlates of information use by US industry-affiliated aerospace engineers and scientists: Results of an exploratory investigation
[NASA-TM-107693] p 1233 N94-17300

AEROSPACE MEDICINE
Living well in space: Ensuring crew capability
[NASA-TM-109538] p 1120 N94-15369
Living well in space: Clinical care challenge
[NASA-TM-109539] p 1120 N94-15370
Answering the space medicine challenge
[NASA-TM-109511] p 1120 N94-15457
Autogenic-Feedback Training (AFT) as a preventive method for space motion sickness: Background and experimental design
[NASA-TM-108780] p 1120 N94-15537
Reliability of autonomic responses and malaise across multiple motion sickness stimulation tests
[NASA-TM-108787] p 1121 N94-15711
Exposure fluctuations of astronauts due to orientation
[NASA-TP-3364] p 1300 N94-15816
Aerospace medicine and biology: A continuing bibliography with indexes (supplement 378)
[NASA-SP-7011(378)] p 1122 N94-16478
Aerospace medicine and biology: A continuing bibliography with indexes (supplement 380)
[NASA-SP-7011(380)] p 1122 N94-16479
Evaluation of putative neurochemical intermediaries in space/motion sickness
[NASA-CR-193607] p 1118 N94-17090
Aircrew/groundcrew life support systems research. Volume 1: CLIN 0001 research requirements
[AD-A268229] p 1139 N94-17563
Aircrew/groundcrew life support systems research. Volume 2: CLIN 0002 task order requirements
[AD-A268230] p 1139 N94-17564

AEROSPACE PLANES
Aerothermoelastic analysis of a NASP demonstrator model
[NASA-TM-109007] p 867 N94-17055

AEROSPACE SAFETY
Gearing up for 1988
[NASA-TM-109617] p 880 N94-15346
Living well in space: Clinical care challenge
[NASA-TM-109539] p 1120 N94-15370

AEROSPACE SCIENCES
Short walk to everywhere --- Space, Earth, Ocean Center
[NASA-TM-109541] p 1221 N94-15372
Challenger Center
[NASA-TM-109432] p 1221 N94-15504
Challenger Center: Orientation
[NASA-TM-109433] p 1221 N94-15505
Coast encounters: A space age adventure in science literacy
[NASA-TM-109334] p 1229 N94-15523
Report on computing and networking in the Space Science Laboratory by the SSL Computer Committee
[NASA-TM-108422] p 1147 N94-15721
Teaching planetary sciences to elementary school teachers: Programs that work p 1222 N94-16346
Spaceship Earth: A partnership in curriculum writing p 1222 N94-16356
Commonwealth of Independent States aerospace science and technology, 1992: A bibliography with indexes
[NASA-SP-7106] p 854 N94-16481
The impact of industry/university consortia programs on space education
[NASA-TM-109340] p 1222 N94-17441

AEROSPACE SYSTEMS
Impact of TQM concepts on inspection of aerospace systems
[TABES PAPER 93-350] p 1050 N94-16130
Liquid Oxygen (LO2) propellant conditioning concept testing
[TABES PAPER 93-621] p 976 N94-16146
Not ready for the first space war. What about the second?
[AD-A266557] p 1174 N94-16665
ASTROS enhancements. Volume 1: ASTRO user's manual
[AD-A266818] p 1151 N94-16768
ASTROS enhancements. Volume 2: ASTRO programmer's manual
[AD-A266819] p 1151 N94-16769
Satellite control: A comprehensive approach p 878 N94-17158
Space systems environmental interaction studies
[AD-A267280] p 897 N94-17240
Model designation of military aerospace vehicles
[AD-A267852] p 898 N94-17388

AEROSPACE TECHNOLOGY TRANSFER
From space to Earth
[NASA-TM-109638] p 1235 N94-15249
Monitoring history
[NASA-TM-109640] p 1229 N94-15251
NASA images 7
[NASA-TM-109438] p 1235 N94-15337
Improved mapping system
[NASA-TM-109643] p 1082 N94-15428
NASA/DOD Aerospace Knowledge Diffusion Research Project. Paper 32: A new era in international technical communication: American-Russian collaboration
[NASA-TM-109336] p 1230 N94-15838
NASA/DOD Aerospace Knowledge Diffusion Research Project. Paper 34: Technical communications practices and the use of information technologies as reported by Dutch and US aerospace engineers
[NASA-TM-109337] p 1230 N94-15839
Commercial space opportunities advanced concepts and technology overview
[TABES PAPER 93-240] p 1050 N94-16132

AEROSPACE VEHICLES
Results of an electrical power system fault study (CDDF)
[NASA-TP-3413] p 884 N94-15007
Model designation of military aerospace vehicles
[AD-A267852] p 898 N94-17388

AEROTHERMODYNAMICS
A rapid computational model for estimating the performance of compliant airfoils in cascades
[AD-A266275] p 857 N94-16471

AEROTHERMOELASTICITY
Aerothermoelastic analysis of a NASP demonstrator model
[NASA-TM-109007] p 867 N94-17055

AGGLOMERATION
Separation behaviour of monotectic alloys p 945 N94-15170

AGGLUTINATION
Nitrogen isotopic signatures in agglutinates from breccia 79035 p 954 N94-16314

AGGREGATES
Study of fractal aggregates p 979 N94-16086
Thermal inertia and radar reflectivity of the Martian north polar ERG: Low-density aggregates p 1260 N94-16238

AGING (MATERIALS)
A model for non-linear creep and physical ageing in PVC
[NPL-DMM(A)-91] p 1057 N94-15016
Monitoring history
[NASA-TM-109640] p 1229 N94-15251
Effects of aging time on V205 sol-gel coatings
[AD-A266824] p 965 N94-15843
The effect of aging at 343 C on the mechanical properties and microstructure of type 308 stainless steel weldments
[DE93-015454] p 957 N94-16103
The influence of thermal aging on the microstructure and fatigue properties of modified 9Cr-1Mo steel
[DE93-015489] p 957 N94-16106
Superconducting ceramics: Selected properties and methods of production
[IFTR-23/1991] p 969 N94-16924

AGING (METALLURGY)
The effect of long-term aging on the impact properties of modified 9Cr-1Mo steel
[DE93-015453] p 957 N94-16068

AGRICULTURE
Comparison of JPL-AIRSAR and DLR E-SAR images from the MAC Europe 1991 campaign over testsite Oberpfaffenhofen: Frequency and polarization dependent backscatter variations from agricultural fields p 1075 N94-16733
Characterization of wetland, forest, and agricultural ecosystems in Belize with airborne radar (AIRSAR) p 1076 N94-16738

AH-64 HELICOPTER
Basic principles of helicopter crashworthiness
[AD-A267099] p 862 N94-15637

AIR
Effects of alloying and temperature on the high-temperature oxidation of Cr-Cr2Nb
[DE93-015800] p 957 N94-16163
Lasing dye sensor for chemical vapors
[AD-D015786] p 1040 N94-16533

AIR BREATHING ENGINES
Flight testing of airbreathing hypersonic vehicles
[NASA-TM-4524] p 886 N94-15753

AIR COOLING
USAF physiological studies of personal microclimate cooling: A review
[AD-A267203] p 1022 N94-15858
Fluid flow and heat convection studies for actively cooled airframes
[NASA-CR-194624] p 1024 N94-16491
Sensitivity of blackbody reference panels to wind blast p 1063 N94-16599

AIR DEFENSE
Expectations for the future of military aviation
p 854 N94-15128
AIR FLOW
The MADONA experiments (Meteorology and Diffusion Over Non-uniform Areas): High-resolution in-plume concentration fluctuations measurements using lidar remote sensing technique
[AD-A267711] p 1105 N94-14938
Boundary layer flow of air over water on a flat plate
[NASA-CR-191517] p 1019 N94-15479
Complex terrain wind model evaluation
[AD-A266467] p 1096 N94-16589
AIR JETS
Fluid flow and heat convection studies for actively cooled airframes
[NASA-CR-194624] p 1024 N94-16491
Analysis of TIMS performance subjected to simulated wind blast p 1063 N94-16598
A comparative study of analog and digital control laws for the UMCSL truss
[AD-A267980] p 871 N94-17412
AIR LAND INTERACTIONS
Evapotranspiration and runoff from large land areas: Land surface hydrology for atmospheric general circulation models p 1083 N94-16029
Heterogeneity and scaling land-atmospheric water and energy fluxes in climate systems p 1083 N94-16030
Effects of spatial variability and scale on areal -average evapotranspiration p 1084 N94-16033
AIR LOCKS
STS-36 crew EVA prep and post-training, bailout exercises, final bench review
[NASA-TM-109498] p 1137 N94-15462
AIR PIRACY
Criminal acts against civil aviation, fiscal year 1992
[AD-A268014] p 863 N94-17586
AIR POLLUTION
An assessment of acid fog
[DE93-009347] p 1095 N94-15940
New York MARKAL: An evaluation of carbon dioxide emission control strategies in New York State
[DE93-013149] p 1095 N94-15999
TABES 1993: 9th Annual Technical and Business Exhibition and Symposium p 1050 N94-16129
NASA Operational Environment Team (NOET): NASA's key to environmental technology
[TABES PAPER 93-611] p 1052 N94-16143
Emerging technologies for the changing global market
[TABES PAPER 93-612] p 930 N94-16144
Utility emissions associated with electric and hybrid vehicle (EHV) charging
[DE93-013734] p 1011 N94-16459
Biomass energy: State of the technology present obstacles and future potential
[DE93-016295] p 1092 N94-16766
Incorporating global warming risks in power sector planning. Volume 1: A case study of the New England region
[DE93-015241] p 1096 N94-17289
AIR PURIFICATION
Plant research
[NASA-TM-109664] p 1116 N94-15235
AIR QUALITY
NASA Operational Environment Team (NOET): NASA's key to environmental technology
[TABES PAPER 93-611] p 1052 N94-16143
Utility emissions associated with electric and hybrid vehicle (EHV) charging
[DE93-013734] p 1011 N94-16459
The 11th annual report of accomplishments under the airport improvement program: Fiscal year 1992
[AD-A268328] p 865 N94-17458
AIR SAMPLING
Space Shuttle solid rocket motor exposure monitoring
p 976 N94-16624
Trace analysis of chemical warfare agents in air: Sampling in porous polymers followed with thermal desorption analysis
[FOA-C-40302-4.6] p 1097 N94-17625
AIR SEA ICE INTERACTIONS
Sea ice motions in the central arctic ice central arctic pack ice as inferred from AVHRR imagery
[NASA-CR-194572] p 1112 N94-15701
AIR TO AIR REFUELING
Development of an air-to-air refueling automatic flight control system using quantitative feedback theory
[AD-A266718] p 870 N94-15730
AIR TRAFFIC
Strategic planning for aircraft noise route impact analysis: A three dimensional approach
[NASA-CR-191484] p 1178 N94-17278
AIR TRAFFIC CONTROL
Symposium on the Future of Aeronautics in the Netherlands
[ETN-93-93780] p 853 N94-15120
Developments in the European air traffic control
p 853 N94-15124
The Next Generation Weather Radar (NEXRAD)/Air Route Surveillance Radar (ARSR) operational comparison
[REPT-93W0000145] p 987 N94-15439
ATCRBS reply environment at Memphis International Airport
[AD-A266322] p 864 N94-16439
The 11th annual report of accomplishments under the airport improvement program: Fiscal year 1992
[AD-A268328] p 865 N94-17458
AIR TRAFFIC CONTROLLERS (PERSONNEL)
Developments in the European air traffic control
p 853 N94-15124
AIR TRANSPORTATION
An analysis of tactical airlifter characteristics and their impact on theater airlift system performance
[AD-A266719] p 866 N94-15731
The airline quality report 1993
[NIAR-93-11] p 863 N94-17262
Annual review of aircraft accident data. US air carrier operations, calendar year 1990
[PB94-102787] p 863 N94-17471
AIR WATER INTERACTIONS
Fine scale measurements of microwave backscatter from the ocean surface
[AD-A264516] p 1111 N94-15134
Ocean wave study
[NASA-TM-109620] p 1111 N94-15349
Exploring the southern ocean response to climate change
[NASA-CR-194601] p 1112 N94-15680
Ventilated oscillatory boundary layers
[AD-A266226] p 1023 N94-16110
Observations and modelling of winds and waves during the Surface Wave Dynamics Experiment. Report 1: Intensive observation period IOP-1, 20-31 October 1990
[AD-A266384] p 1113 N94-16517
The use of General Circulation Models in detecting climate change induced by greenhouse gases
[DE93-014369] p 1096 N94-16802
Orographic microbursts in a severe winter windstorm
[AD-A267651] p 1108 N94-17247
Abstracts of manuscripts submitted in 1992 for publication
[AD-A267963] p 1113 N94-17383
Real time system for practical acoustic monitoring of global ocean temperature
[AD-A267868] p 1113 N94-17391
Preliminary estimates of frequency-direction spectra derived from the SAMSON pressure gage array, November 1990 to May 1991
[AD-A267960] p 1114 N94-17497
Meridional circulation in the tropical north atlantic
[AD-A268222] p 1114 N94-17555
AIRBORNE EQUIPMENT
Windshear detection radar signal processing studies
[NASA-CR-194615] p 994 N94-16022
Optical measurements of NASA/USAF CRRES high altitude rocket borne chemical release experiments in conjunction with the USAF airborne ionospheric observatory aircraft
[AD-A266404] p 1101 N94-16551
Summaries of the Third Annual JPL Airborne Geoscience Workshop. Volume 3: AIRSAR Workshop
[NASA-CR-194542] p 1075 N94-16731
Laser beam steering device p 1045 N94-17357
AIRBORNE LASERS
Nd:YLF laser for airborne/spaceborne laser ranging
p 913 N94-15563
AIRBORNE/SPACEBORNE COMPUTERS
STS-34 Space Shuttle Portable Onboard Computer (SPOC) briefing
[NASA-TM-109458] p 880 N94-15353
NASA Space Engineering Research Center for VLSI System Design
[NASA-CR-194587] p 1008 N94-15547
Satellite communications installation plan
[AD-A266303] p 1000 N94-16965
Data handling strategy for the Spanish small satellite program (MINISAT) p 895 N94-17177
The STRV On Board Data Handling (OBDH) system: An introduction p 895 N94-17178
AIRCRAFT ACCIDENT INVESTIGATION
Aircraft accident investigation at ARL: The first 50 years
[AD-A267086] p 862 N94-15542
Annual review of aircraft accident data. US air carrier operations, calendar year 1990
[PB94-102787] p 863 N94-17471
AIRCRAFT ACCIDENTS
Aircraft accident investigation at ARL: The first 50 years
[AD-A267086] p 862 N94-15542
Basic principles of helicopter crashworthiness
[AD-A267099] p 862 N94-15637
National Transportation Safety Board annual review of aircraft accident data, US general aviation, calendar year 1989
[PB93-160687] p 863 N94-16464
Annual review of aircraft accident data. US air carrier operations, calendar year 1990
[PB94-102787] p 863 N94-17471
AIRCRAFT COMMUNICATION
Johnson-Gierhart program predictions of excess propagation loss for super-high frequency air-to-ground paths. Volume 1: Theory and numerical results
[AD-A267105] p 988 N94-15649
AIRCRAFT CONFIGURATIONS
Adaptive algorithm for aircraft configuration in turbulent flow
[AD-A266188] p 867 N94-16122
Computational aerodynamics with icing effects
[AD-A267509] p 860 N94-17074
AIRCRAFT CONSTRUCTION MATERIALS
An overview of the NASA textile composites program
p 937 N94-16846
Techno-economic requirements for composite aircraft components p 940 N94-16864
Aircraft carrier exposure tests of cast magnesium alloys
[AD-A268260] p 962 N94-17418
AIRCRAFT CONTROL
Aerodynamic control of NASP-type vehicles through vortex manipulation, volume 4
[NASA-CR-177626-VOL-4] p 857 N94-15720
Development of an air-to-air refueling automatic flight control system using quantitative feedback theory
[AD-A266718] p 870 N94-15730
AIRCRAFT DESIGN
Expectations for the future of Fokker
p 854 N94-15127
Better airplane wings
[NASA-TM-109446] p 933 N94-15345
The lift-fan powered-lift aircraft concept: Lessons learned
[NASA-CR-177616] p 866 N94-15718
AIRCRAFT ENGINES
Flight-determined engine exhaust characteristics of an F404 engine in an F-18 airplane
[NASA-TM-4538] p 869 N94-15141
A review of Australian and New Zealand investigations on aeronautical fatigue during the period April 1991 to March 1993
[AD-A267532] p 868 N94-17117
Micromechanisms of monotonic and cyclic subcritical crack growth in advanced high melting point low-ductility intermetallics
[AD-A267764] p 961 N94-17223
Structured finite volume modeling of US Navy aircraft engine test cells task 2: Turboprop engine, volume 1
[AD-A267833] p 872 N94-17405
Structured finite volume modeling of US Navy aircraft engine test cells. Task 1: Turboshaft engine, volume 1
[AD-A268176] p 873 N94-17432
Structured finite volume modeling of US Navy aircraft engine test cells. Task 1: Turboshaft engine-code documentation and listings, volume 2
[AD-A268177] p 873 N94-17508
Structured finite volume modeling of US Navy aircraft engine test cells. Task 2: Turboprop engine. Volume 2: Code documentation and listings
[AD-A268386] p 873 N94-17569
AIRCRAFT EQUIPMENT
Regulated emergency oxygen system
[AD-A266228] p 1138 N94-16983
AIRCRAFT HAZARDS
Development of a proposed international standard for certification of aircraft to High Intensity Radiated Fields (HIRF)
[NASA-TM-106357] p 863 N94-16520
Windshear database for forward-looking systems certification
[NASA-TM-109012] p 1108 N94-17283
AIRCRAFT HYDRAULIC SYSTEMS
High temperature hydraulic seals
[AD-A268257] p 1048 N94-17433
AIRCRAFT ICING
The 1982 highlights
[NASA-TM-109671] p 1303 N94-15508
Computational aerodynamics with icing effects
[AD-A267509] p 860 N94-17074
AIRCRAFT LANDING
An analysis of tactical airlifter characteristics and their impact on theater airlift system performance
[AD-A266719] p 866 N94-15731
AIRCRAFT MAINTENANCE
Mission management aircraft operations manual
[NHB-7900.3] p 1225 N94-16729

Definitions of terms relating to aircraft windscreens, canopies, and transparencies
[AD-A268403] p 868 N94-17425
Overview of the FAA/DCA/NLR programs related to ageing aircraft
[NLR-TR-92119-U] p 854 N94-17614

AIRCRAFT MANEUVERS
Aerodynamic/dynamic/control interaction
[AD-A266187] p 871 N94-16107

AIRCRAFT MODELS
National Aero-Space Plane
[NASA-TM-109450] p 865 N94-15323
National Aero-Space Plane resource reel
[NASA-TM-109451] p 865 N94-15324
An introduction to structural models
[AD-A268151] p 1155 N94-17429

AIRCRAFT NOISE
On the use of the noncentral chi-square density function for the distribution of helicopter spectral estimates
[NASA-CR-191546] p 1176 N94-15487
Strategic planning for aircraft noise route impact analysis: A three dimensional approach
[NASA-CR-191484] p 1178 N94-17278
Noise measurement flight test of five light helicopters
[AD-A268566] p 1179 N94-17599

AIRCRAFT PERFORMANCE
Naval aviation: The Navy is taking actions to improve the combat capabilities of its tactical aircraft. Report to Congressional Requesters
[AD-A268002] p 868 N94-17472

AIRCRAFT PILOTS
Monograph of the aviation epidemiology data register for FY 1991
[AD-A266896] p 1119 N94-14952
US civil airmen statistics: Calendar year 1992
[AD-A267708] p 853 N94-14965
Human factor studies
[NASA-TM-109665] p 875 N94-15236

AIRCRAFT PRODUCTION
Government/contractor development teams
[TABES PAPER 93-460] p 1050 N94-16134

AIRCRAFT RELIABILITY
Aircraft operations management manual
[NHB-7900.3(V1)] p 1225 N94-16730

AIRCRAFT SAFETY
NASA images 6
[NASA-TM-109437] p 862 N94-15336
Altitude deviations: Breakdowns of an error-tolerant system
[NASA-TM-108788] p 862 N94-15550
An analysis of tactical airlifter characteristics and their impact on theater airlift system performance
[AD-A266719] p 866 N94-15731
National Transportation Safety Board annual review of aircraft accident data, US general aviation, calendar year 1989
[PB93-160687] p 863 N94-16464
Mission management aircraft operations manual
[NHB-7900.3] p 1225 N94-16729
Aircraft operations management manual
[NHB-7900.3(V1)] p 1225 N94-16730
Regulated emergency oxygen system
[AD-A266228] p 1138 N94-16983
The 11th annual report of accomplishments under the airport improvement program: Fiscal year 1992
[AD-A268328] p 865 N94-17458

AIRCRAFT STABILITY
Wind shear and heavy rain --- effects on flight stability
[NASA-TM-109453] p 1105 N94-15326
Development of an air-to-air refueling automatic flight control system using quantitative feedback theory
[AD-A266718] p 870 N94-15730

AIRCRAFT STRUCTURES
ASTROS enhancements. Volume 1: ASTRO user's manual
[AD-A266818] p 1151 N94-16768
ASTROS enhancements. Volume 2: ASTRO programmer's manual
[AD-A266819] p 1151 N94-16769
An overview of the NASA textile composites program
p 937 N94-16846
Development of test methods for textile composites
p 939 N94-16862
Techno-economic requirements for composite aircraft components p 940 N94-16864
Definitions of terms relating to aircraft windscreens, canopies, and transparencies
[AD-A268403] p 868 N94-17425
Structural mechanics division research and technology accomplishments for CY 1992 and plans for CY 1993
[NASA-TM-107752] p 1062 N94-17479

AIRCRAFT SURVIVABILITY
A review of Australian and New Zealand investigations on aeronautical fatigue during the period April 1991 to March 1993
[AD-A267532] p 868 N94-17117

AIRFIELD SURFACE MOVEMENTS
The use of the Air Force Academy high wind alert system in forecasting moderate intensity wind events for military bases in the Colorado Springs area
[AD-A267648] p 1107 N94-17245

AIRFOILS
Unsteady separated flows: Empirical model and control
[AD-A267282] p 855 N94-14959
Suppression of dynamic stall with a leading-edge slat on a VR-7 airfoil
[NASA-TP-3357] p 856 N94-15657
A rapid computational model for estimating the performance of compliant airfoils in cascades
[AD-A266275] p 857 N94-16471
Hoph bifurcation in viscous, low speed flows about an airfoil with structural coupling
[AD-A266542] p 859 N94-16798

AIRFRAMES
Technical evaluation report on the AGARD-PEP Specialists Meeting on Combat Aircraft Noise
[NLR-TP-91445-U] p 1177 N94-15506
Helicopter structures: A review of loads, fatigue design techniques, and usage monitoring
[AD-A267115] p 866 N94-15651

AIRGLOW
Altitude profile of aerosols on Mars from measurements of its thermal radiation on limb p 1294 N94-16423
Optical ionospheric instrumentation and research
[AD-A266403] p 1192 N94-16550

AIRLINE OPERATIONS
Aviation and the KLM: Past and future
p 853 N94-15126
An elementary tutorial on formal specification and verification using PVS
[NASA-TM-108991] p 1158 N94-15536
The airline quality report 1993
[NIAR-93-11] p 863 N94-17262

AIRPORT PLANNING
Symposium on the Future of Aeronautics in the Netherlands
[ETN-93-93780] p 853 N94-15120
The future of Schiphol: Growth within boundaries
p 853 N94-15123
ATCRBS reply environment at Memphis International Airport
[AD-A266322] p 864 N94-16439

AIRPORTS
The future of Schiphol: Growth within boundaries
p 853 N94-15123
The 11th annual report of accomplishments under the airport improvement program: Fiscal year 1992
[AD-A268328] p 865 N94-17458
Criminal acts against civil aviation, fiscal year 1992
[AD-A268014] p 863 N94-17586

ALASKA
An electromagnetic interference study of potential transmitter sites for the HF Active Auroral Research Program (HAARP)
[AD-A267743] p 1004 N94-17373

ALBEDO
A test of the applicability of independent scattering to high albedo planetary regoliths p 1250 N94-16187
Age determinations and Earth-based multispectral observations of lunar light plains p 1275 N94-16323
Vertical structure models of the 1990 equatorial disturbance on Saturn p 1277 N94-16333

ALBUMINS
Increased vascular resistance with hemoglobin-based oxygen carriers
[AD-A266454] p 1123 N94-16565

ALCOHOLS
Intramolecular versus intermolecular condensation rates in the acidic polymerization of octaethoxytrisiloxane
[AD-A266982] p 963 N94-15490
High octane ethers from synthesis gas-derived alcohols
[DE93-016861] p 975 N94-16898

ALEXANDRITE
Soft x ray emission from Alexandrite laser-matter-interaction
[AD-A267905] p 1042 N94-17378

ALGEBRA
Automatic differentiation of limit functions
[DE93-016376] p 1168 N94-14928

ALGORITHMS
VDM specification of the MD4 message digest algorithm
[NPL-DITC-204/92] p 1142 N94-14944
RAISE specification of the MD4 message digest algorithm
[NPL-DITC-206/92] p 1142 N94-15010
Massively parallel, adaptive, color image processing for autonomous road following
[AD-A266988] p 864 N94-15498
Contribution to the elaboration of some adaptive control algorithms for fermentation processes monitoring
[LAAS-92513] p 1116 N94-15643
Software reliability management through metrics
[AD-A267129] p 1146 N94-15687
Segment-based acoustic models for continuous speech recognition
[AD-A267138] p 988 N94-15691
A parallel adaptive mesh refinement algorithm
[NASA-CR-191530] p 1168 N94-15724
Complexity analysis of real-time reinforcement learning applied to finding shortest paths in deterministic domains
[AD-A266636] p 1131 N94-15742
Processor capacity reserves for multimedia operating systems
[AD-A266639] p 1158 N94-15745
The bootstrapped algorithm: Fast algorithm for blind signal separation
[AD-A266671] p 1147 N94-15772
Efficient algorithmic techniques for combinatorial problems
[AD-A267151] p 1172 N94-15777
Development and analysis of ARMA parameter estimation schemes in the presence of noise
[AD-A267184] p 989 N94-15786
Parallel processing and scientific applications
[AD-A267179] p 1159 N94-15849
Synthetic aperture radar signal processing: Trends and technologies p 992 N94-15908
The alignment-distribution graph
[NASA-CR-194609] p 1148 N94-15956
Generation of artificial helioseismic time-series
[NASA-CR-194612] p 1299 N94-15968
Slidesurfaces with adaptive new definitions (SAND) for transient analysis
[DE93-014909] p 1059 N94-15983
A sequential quadratic programming algorithm using an incomplete solution of the subproblem
[DE93-017439] p 1149 N94-16120
Adaptive algorithm for aircraft configuration in turbulent flow
[AD-A266188] p 867 N94-16122
Passive tracking of a target using an array of sensors
[DE93-015870] p 997 N94-16169
Search for optimal distance spectrum convolutional codes p 998 N94-16509
The (delta)f algorithm for beam dynamics
[DE93-015632] p 1187 N94-16660
Accurate upwind methods for the Euler equations
[NASA-TM-106388] p 1170 N94-16882
Adaptive Cartesian grid methods for representing geometry in inviscid compressible flow
[DE93-016430] p 1025 N94-16894
Applications of the phi-transform
[AD-A266247] p 1170 N94-16940
Target detection by way of Kalman filtering
[AD-A267314] p 1000 N94-16945
Modeling, estimation and control of distributed parameter systems
[AD-A267325] p 1026 N94-17003
Progress in computational unsteady aerodynamics
[NASA-CR-177630] p 860 N94-17081
Intelligent use of CFAR algorithms
[AD-A267755] p 1003 N94-17206
Development and comparison of advanced reduced-basis methods for the transient structural analysis of unconstrained structures
[NASA-TM-109015] p 1061 N94-17259
Validation and analysis of microwave-derived rainfall over the tropics
[AD-A267785] p 1108 N94-17303
Fast algorithms for polynomial interpolation, integration and differentiation
[AD-A267505] p 1154 N94-17370
Optimal tuning of heavy equipment motion controllers
[AD-A267873] p 1167 N94-17392
Testing string superprimitivity in parallel
[AD-A267814] p 1155 N94-17399
Fast Fourier Transforms for nonequispaced data 2
[AD-A268383] p 1171 N94-17420
Orpheus: A synthesis framework for regular architectures
[REPT-93-016] p 1156 N94-17504
FSM test: A functional test generation system for sequential circuits
[REPT-93-017] p 1014 N94-17505
Towards dynamic randomized algorithms in computational geometry
[INRIA-RR-1727] p 1156 N94-17528
How to deduce the far field of an antenna from planar near-field measurements
[NPL-DES-123] p 1006 N94-17545
State space partitioning methods for solving a class of stochastic network problems
[AD-A267494] p 1173 N94-17585

ALIGNMENT
Mobile and replicated alignment of arrays in data-parallel programs
[NASA-CR-194294] p 1158 N94-15113
Heterodyne efficiency for a coherent laser radar with diffuse or aerosol targets
[NASA-CR-194563] p 1038 N94-15477
ALIPHATIC HYDROCARBONS
Cycle performance testing of nonazeotropic mixtures of HFC-142A/HCFC-124 and HFC-32/HCFC-124 with enhanced surface heat exchangers
[DE93-015215] p 1024 N94-16808
ALKALI METALS
Basic optical studies of high T(c) oxide superconductors
[AD-A268148] p 1014 N94-17428
ALKALIES
Analysis of an electromagnetic field in the vicinity of a caustic by asymptotic methods
[IFTR-12/1991] p 998 N94-16653
An asymptotic expansion of an electromagnetic field in the velocity of a caustic in the form of simple waves
[IFTR-14/1991] p 1002 N94-17048
ALKALINE BATTERIES
Lithium D-cell study
[NASA-CR-192705] p 1011 N94-16505
ALKALINE EARTH METALS
Investigation of the influence of applied potential on erosion-corrosion of copper in alkaline chloride solutions
[AD-A266448] p 958 N94-16562
Pulsed laser deposition of metastable Ca(1-x)Sr(x)CuO2 thin films
[DE93-015804] p 1040 N94-16663
ALKANES
Advanced thermally stable jet fuels
[DE93-017711] p 975 N94-16996
ALKENES
Synthetic and mechanistic investigation of olefin polymerization catalyzed by early transition metal compounds
[DE93-018301] p 970 N94-16963
ALLENDE METEORITE
Experimental partitioning of Zr, Ti, and Nb between silicate liquid and a complex noble metal alloy and the partitioning of Ti between perovskite and platinum metal p 962 N94-16287
Chemical and isotopic compositions in acid residues from various meteorites p 1243 N94-16291
A search for noble-gas evidence for presolar oxide grains p 954 N94-16353
Refractory precursor components in an Allende ferromagnesian chondrule p 1245 N94-16412
ALLOCATIONS
Regulation of low Earth orbit satellites p 892 N94-17159
ALLOYING
Ternary alloying effects in polycrystalline (beta)-NiAl
[DE93-012675] p 955 N94-15885
Effects of alloying and temperature on the high-temperature oxidation of Cr-Cr2Nb
[DE93-015800] p 957 N94-16163
Metastable phases in mechanically alloyed aluminum germanium powders
[DE93-008727] p 958 N94-16463
ALLOYS
Visualization of solidification front phenomena
[NASA-CR-193838] p 976 N94-15006
Electron-microscopy study of antiphase boundaries in Cu3Pd and Fe3Al alloys near the order-disorder transition
[ONERA-NT-1993-1] p 1206 N94-15295
Vacancy condensation as the precursor to passivity breakdown
[DE93-012925] p 956 N94-15998
ALPHA PARTICLES
Nb-based SJTJ for nuclear detection: Preliminary results with alpha radiation p 905 N94-15068
Nonlinear gyrofluid models of shear Alfven instabilities in ignited and beam heated toroidal plasmas
[DE93-016235] p 1203 N94-16869
ALPHABETS
Testing string superprimitivity in parallel
[AD-A267814] p 1155 N94-17399
ALTERNATING CURRENT
Technology transfers and reliable oxides
[AD-A266948] p 1175 N94-15758
Method and apparatus for performing scanning tunneling optical absorption spectroscopy
[AD-D015796] p 948 N94-16539
ALTERNATING DIRECTION IMPLICIT METHODS
Development of iterative techniques for the solution of unsteady compressible viscous flows
[NASA-CR-194657] p 1027 N94-17129
ALTIMETERS
Analysis of TOPEX laser retroreflector array characteristics p 915 N94-15578
ALTIMETRY
Emplacement of multiple flow units on very shallow slopes, east Kawelu Planitia flow field, Venus p 1260 N94-16235
Clementine: Anticipated scientific datasets from the Moon and Geographos p 1288 N94-16392
Adequation of mini satellites to oceanic altimetry missions p 891 N94-17152
ALTITUDE
The distribution of large volcanoes on Venus as a function of height and altitude p 1271 N94-16303
A quantitative analysis of TIMS data obtained on the Learjet 23 at various altitudes p 1063 N94-16597
ALTITUDE SICKNESS
Metabolic monitoring of hypobaric subjects
[AD-A268221] p 1130 N94-17554
ALTITUDE SIMULATION
Metabolic monitoring of hypobaric subjects
[AD-A268221] p 1130 N94-17554
ALTITUDE TESTS
Effects of RVP, T(50), and oxygenates on hot-start and driveability performance at high and low altitude
[AD-A266382] p 869 N94-16516
ALUMINATES
Tritium diffusion and desorption in single crystal LiAlO2
[DE93-015140] p 1211 N94-16805
ALUMINIDES
Environmental embrittlement in ordered intermetallic alloys
[DE93-015307] p 955 N94-15830
Recent advances in ordered intermetallics
[DE93-015308] p 955 N94-15862
Environmental effects on iron aluminides
[DE93-015820] p 958 N94-16166
Interfacial shear behavior and its influence on fiber damage in sapphire-reinforced gamma titanium aluminide composites
[AD-A267943] p 1060 N94-17043
ALUMINUM
Characterization of the cyclic plasticity of polycrystalline aluminum in the 90-300K domain: Use of the ultrasonic wave coupling technique - low frequency restraint
[ISAL-92-0083] p 954 N94-14930
The corrosion protection of metals by ion vapor deposited aluminum
[NASA-TM-108425] p 955 N94-15832
Mean strain effects on the strain life fatigue curve
[AD-A267211] p 960 N94-16984
J-integral and HRR field associated with stable crack growth in thin aluminum SEN specimen
[AD-A267879] p 960 N94-17041
ALUMINUM ALLOYS
XPS analysis of Al/EPDM bondlines from IUS SRM-1 polar bosses
[AD-A266851] p 1056 N94-14945
Crack-tip-opening angle measurements and crack tunneling under stable tearing in thin sheet 2024-T3 aluminum alloy
[NASA-CR-191523] p 931 N94-15184
Prediction of stable tearing of 2024-T3 aluminum alloy using the crack-tip opening angle approach
[NASA-TM-109023] p 955 N94-15708
The corrosion protection of metals by ion vapor deposited aluminum
[NASA-TM-108425] p 955 N94-15832
Assessment of chromate and non-chromate conversion coatings for Al alloys using electrochemical impedance spectroscopy
[AD-A267205] p 965 N94-15859
Ternary alloying effects in polycrystalline (beta)-NiAl
[DE93-012675] p 955 N94-15885
Measurement and analysis of critical CTOA for an aluminum alloy sheet
[NASA-TM-109024] p 956 N94-15948
A reexamination of grain boundary fracture in Ni3Al: Environmental and alloying effects
[DE93-015431] p 1208 N94-16063
Environmental effects on iron aluminides
[DE93-015820] p 958 N94-16166
The effect of irradiation on the mechanical properties of 6061-T651 aluminum
[DE93-015825] p 958 N94-16168
Metastable phases in mechanically alloyed aluminum germanium powders
[DE93-008727] p 958 N94-16463
Bulk and defect properties of ordered intermetallics: A first-principles total-energy investigation
[DE93-015492] p 959 N94-16873
Fatigue life program using strain-life methods
[AD-A267310] p 1060 N94-16943
Mean strain effects on the strain life fatigue curve
[AD-A267211] p 960 N94-16984
J-integral and HRR field associated with stable crack growth in thin aluminum SEN specimen
[AD-A267879] p 960 N94-17041
Analysis of the strengthening of aluminum alloy undergoing plastic deformation under conditions of a compound state of stress
[IFTR-21/1991] p 960 N94-17093
Quantitative assessment of the accuracy of constitutive laws for plasticity with an emphasis on cyclic deformation
[AD-A267562] p 961 N94-17109
The effect of electric discharge machined notches on the fracture toughness of several structural alloys
[AD-A268605] p 962 N94-17464
ALUMINUM COATINGS
Improved composite flexible blanket insulation
[NASA-CASE-ARC-11955-1-CU] p 934 N94-15926
Formation of pitting resistant anodized films on aluminum
[AD-D015812] p 958 N94-16486
ALUMINUM COMPOUNDS
Lattice-mismatched In(0.40)Al(0.60)As window layers for indium phosphide solar cells
[NASA-TM-106255] p 1013 N94-17113
ALUMINUM FLUORIDES
An improved light source for laser ranging p 913 N94-15567
ALUMINUM GALLIUM ARSENIDE LASERS
Development of the Mars Observer Laser Altimeter (MOLA) p 921 N94-15617
ALUMINUM GALLIUM ARSENIDES
Large signal characterization and modeling of heterojunction bipolar transistors
[AD-A266184] p 1012 N94-16935
Curved grating fabrication techniques for concentric-circle grating, surface-emitting semiconductor lasers p 1045 N94-17349
Rare earth doped III-V semiconductors for optoelectronics
[AD-A268279] p 1216 N94-17577
Nonintrusive fast response oxygen monitoring system for high temperature flows
[NASA-CR-4553] p 1036 N94-17655
ALUMINUM ISOTOPES
Petrography, mineralogy, and Mg isotope composition of VICTA: A vigarano CaAl4O7-bearing type A inclusion p 1103 N94-16203
Heliocentric zoning of the asteroid belt by aluminum-26 heating p 1241 N94-16205
Al-26 production profile and model comparisons in Canyon Diablo p 1245 N94-16409
ALUMINUM NITRIDES
Laser assisted CVD growth of AlN and GaN
[AD-A267150] p 1206 N94-15764
Amide and tetrazene complexes of transition and main group elements as precursors for the low temperature synthesis of elemental nitrides
[AD-A266246] p 950 N94-16931
An alternative approach to the growth of single crystal gallium nitride
[AD-A267876] p 1213 N94-17037
ALUMINUM OXIDES
Ion mixing of thin ZrO2 films on sapphire
[DE93-015214] p 1206 N94-14925
Method of producing a silicon carbide fiber reinforced strontium aluminosilicate glass-ceramic matrix composite
[NASA-CASE-LEW-15263-2] p 934 N94-15929
Rheology and microstructure of concentrated zirconia-alumina suspensions for gelcasting composites
[DE93-015339] p 966 N94-16016
Thin composite solid electrolyte film for lithium batteries
[NASA-CASE-NPO-18694-1-CU] p 1014 N94-17325
Direct observation of fracture of CAS-glass/SiC composites and processing of toughened alumina
[AD-A268275] p 941 N94-17457
Growth of dielectric thin films by irradiation of condensed molecular precursors with synchrotron radiation
[DE93-016161] p 974 N94-17676
ALUMINUM SILICATES
Preparation of homogeneous aluminosilicate gels by sol/gel techniques
[AD-A266823] p 962 N94-14914
Multinuclear NMR study of aluminosilicate sol-gel synthesis reasons for the homogeneous gelation using the prehydrolysis method
[AD-A266877] p 962 N94-14921
ALUMINUM-LITHIUM ALLOYS
Aluminum-lithium technology
[TABES PAPER 93-601] p 962 N94-16137
AMBIENT TEMPERATURE
Diamond p-n junction cold cathode
[AD-A266926] p 1206 N94-15107
In situ Raman spectroscopy of lithium electrode surface in ambient temperature lithium secondary battery
[DE93-015238] p 1010 N94-16061
AMERICAN INDIANS
Ancient skills: Modern use
[NASA-TM-109594] p 1135 N94-15286

AMIDES
Amide and tetrazene complexes of transition and main group elements as precursors for the low temperature synthesis of elemental nitrides
[AD-A266246] p 950 N94-16931
Responsive copolymers for enhanced petroleum recovery
[DE93-018030] p 971 N94-16999
AMINO ACIDS
Study of protein-H2O interactions by multidimensional NMR spectroscopy
[AD-A266955] p 946 N94-15760
Heat shock protein induction in human cells by CO2 laser irradiation
[AD-A266430] p 1117 N94-16545
Hemoglobin
[AD-A266455] p 1123 N94-16566
AMMONIA
Rheology of water and ammonia-water ices p 953 N94-16188
Gravity dependent condensation pressure drop and heat transfer in ammonia two-phase heat transport systems
[NLR-TP-92121-U] p 1031 N94-17615
Growth of dielectric thin films by irradiation of condensed molecular precursors with synchrotron radiation
[DE93-016161] p 974 N94-17676
AMMONIUM COMPOUNDS
The effect of process parameters on the surface finish of plasma polymers
[DE93-014112] p 966 N94-15924
AMMONIUM PERCHLORATES
Investigation of the origin of hot spots in deformed crystals: Ammonium perchlorate studies
[AD-A267692] p 1214 N94-17270
AMMONIUM PHOSPHATES
Mechanical properties of magnesium ammonium phosphate cements and their zeolite composites
[DE93-015155] p 934 N94-16057
AMORPHOUS MATERIALS
Application of cylindrical distribution functions to anisotropic scattering from amorphous films
[DE93-015256] p 1183 N94-16811
Anisotropic phase separation in amorphous Fe-Ge alloys
[DE93-015255] p 961 N94-17251
AMORPHOUS SILICON
Thin Ni silicide formation by low temperature-induced metal atom reaction with ion implanted amorphous silicon
[DE93-015449] p 1209 N94-16066
AMPLIFICATION
Antenna gain loss and pattern degradation due to transmission through dielectric radomes
[AD-A267242] p 986 N94-14974
AMPLITUDES
Synchronous sampling phase and amplitude detection method and apparatus
[NASA-CASE-LAR-14725-1] p 1050 N94-15870
AMPOULES
Thermal spray forming of refractory sample ampoule cartridges for single crystal growth space furnaces
[TABES PAPER 93-605] p 1051 N94-16141
ANALOG CIRCUITS
Stray insensitive switched capacitor composite operational amplifiers
[AD-A267412] p 1012 N94-16976
ANALOG DATA
Freedom system Text and Graphics Systems (TAGS)
[NASA-TM-109509] p 1140 N94-15455
Simultaneous measurement of temperature and strain using four connecting wires
[NASA-TM-104271] p 1032 N94-15754
Evaluation of midband analog fiber optic telemetry links
[DE93-015128] p 883 N94-16056
Leak detection utilizing analog binaural (VLSI) techniques
[NASA-CASE-NPO-18399-1-CU] p 1014 N94-17323
ANALOG TO DIGITAL CONVERTERS
Two color satellite laser ranging upgrades at Goddard's 1.2m telescope facility p 915 N94-15581
Linear encoding device
[NASA-CASE-GSC-13562-1] p 1147 N94-15703
Rotary encoding device
[NASA-CASE-GSC-13543-1] p 1189 N94-15705
Rotary encoding device
[NASA-CASE-GSC-13556-1] p 1148 N94-15943
Image accuracy and representational enhancement through low-level, multi-sensor integration techniques
[DE93-014888] p 1167 N94-17287
ANALOGS
Mars Analog Site Study (MASS) p 1252 N94-16200
ANALYSIS OF VARIANCE
Simulation reduction using the Taguchi method
[NASA-CR-4542] p 1055 N94-17082
ANALYZERS
Prototype instrumentation and design studies
[AD-A266402] p 882 N94-16530
Electron reversal ionizer for detection of trace species using a spherical cathode
[NASA-CASE-NPO-18870-1-CU] p 1185 N94-17329
ANATOMY
Localizing visual function in the brain
[AD-A267381] p 1133 N94-17020
ANDES MOUNTAINS (SOUTH AMERICA)
Earth imaging results from Galileo's second encounter p 1252 N94-16201
ANGLE OF ATTACK
The effect of the nose shape and wing location toward the wing vortex breakdown
[AD-A267724] p 855 N94-14942
Wind tunnel investigation of three axisymmetric cowls of different lengths at Mach numbers from 0.60 to 0.92
[NASA-TM-4488] p 856 N94-15681
Particle simulation of hypersonic flow
[AD-A267185] p 857 N94-15787
Wind tunnel investigation with an operational turbojet engine
[TABES PAPER 93-662] p 870 N94-16157
Flow analysis for the nacelle of an advanced ducted propeller at high angle-of-attack and at cruise with boundary layer control
[NASA-TM-106371] p 858 N94-16571
An experimental study of fluctuating wall pressures in a highly swept, sharp fin-induced, Mach 5 shock wave/turbulent boundary layer interaction
[AD-A268394] p 861 N94-17461
ANGLES (GEOMETRY)
Measurements of the radar cross section and Inverse Synthetic Aperture Radar (ISAR) images of a Piper Navajo at 9.5 GHz and 49 GHz
[AD-A267570] p 1002 N94-17110
Review of rigorous coupled-wave analysis and of homogeneous effective medium approximations for high spatial-frequency surface-relief gratings p 1194 N94-17335
ANGULAR DISTRIBUTION
Past, present and future ((pi),(eta)) experiments
[DE93-016631] p 1182 N94-16115
The influence of an electric field on the kinetics of nucleation
[IFTR-2/91] p 1213 N94-17046
SYNMOD: A low-resource, low-cost means of monitoring the near-Earth space debris environment p 891 N94-17148
ANGULAR MOMENTUM
Numerical simulation of three-dimensional self-gravitating flow
[NASA-TM-109021] p 1021 N94-15768
ANGULAR RESOLUTION
Tip-tilt compensation: Resolution limits for ground-based telescopes using laser guide star adaptive optics
[DE93-016426] p 1237 N94-16872
ANGULAR VELOCITY
Determination of momentum flux using a bivane and cup anemometer
[AD-A265414] p 1105 N94-15137
ANHYDRIDES
Compounds containing meta-biphenylenedioxy moieties and polymers therefrom
[NASA-CASE-LAR-14517-1] p 965 N94-15879
Low dielectric polyimides
[NASA-CASE-LAR-14987-2] p 974 N94-17559
ANILINE
Soluble precursor route to polyanilines
[AD-A268015] p 973 N94-17494
ANIMALS
A review of the efficacy of 7.5 percent NaCl/6 percent Dextran-70 (HSD) in experimental animals and humans
[AD-A266633] p 1122 N94-15740
The 1990-1991 NASA space biology accomplishments
[NASA-TM-4501] p 1118 N94-17257
ANIONS
Thermochemistry of silicate speciation in aqueous sodium silicate solutions: Ionization and polymerization of small silicate ion
[AD-A266825] p 964 N94-15683
Swelling equilibria for temperature-sensitive ampholytic hydrogels
[DE93-015264] p 966 N94-15996
Scintillation mechanism in stoichiometric cerium compounds
[DE93-015499] p 948 N94-16771
ANISOTROPIC MEDIA
Measurement of birefringence for optical recording disk substrates p 1227 N94-14989
Dynamic behavior of fiber and particle reinforced composites
[AD-A266905] p 930 N94-15143
ANISOTROPIC PLATES
Three-dimensional analysis of anisotropic spatially reinforced structures p 939 N94-16863
ANISOTROPY
Magnetic and magneto-optical properties and domain structure of Co/Pd multilayers p 1227 N94-14991
Magnetic effects in anomalous dispersion
[DE93-014291] p 1175 N94-15978
Anisotropic damage mechanics modeling in metal matrix composites
[AD-A266328] p 934 N94-16440
Application of cylindrical distribution functions to anisotropic scattering from amorphous films
[DE93-015256] p 1183 N94-16811
Anisotropic phase separation in amorphous Fe-Ge alloys
[DE93-015255] p 961 N94-17251
Advanced thin-film deposition and physical properties of high-temperature and other novel superconducting materials
[AD-A268199] p 1216 N94-17561
ANNEALING
The thermal dissociation of NH2CHO(ND2CHO) on Si(100)-2x1
[AD-A266903] p 942 N94-14956
Infrared detector annealing and calibration with IR-laser diodes p 909 N94-15092
Optical and infrared spectra of thermally annealed Pb implanted SiO2 glasses
[DE93-015304] p 965 N94-15828
Thin Ni silicide formation by low temperature-induced metal atom reaction with ion implanted amorphous silicon
[DE93-015449] p 1209 N94-16066
Crystallization of grain boundary phases in silicon nitride with low additive contents by microwave annealing
[DE93-015801] p 1209 N94-16164
The effect of oxygen, grain size, and strain rate on the mechanical behavior of forged P/M tantalum
[DE93-011251] p 959 N94-16764
Tritium diffusion and desorption in single crystal LiAlO2
[DE93-015140] p 1211 N94-16805
Transient phenomena following precipitation and re-solution anneals in a NiTi alloy
[AD-A267557] p 961 N94-17106
ANNIHILATION REACTIONS
Status of (alpha)(sub s) measurements
[DE93-015179] p 1181 N94-16059
ANNUAL VARIATIONS
Atlas of TOMS ozone, 1978-1988
[NASA-TM-109456] p 1094 N94-15329
Validation and analysis of microwave-derived rainfall over the tropics
[AD-A267785] p 1108 N94-17303
ANNULAR FLOW
Heat transfer and aerodynamics of a 3D design nozzle guide vane tested in the Pyestock isentropic light piston facility
[RAE-TM-AERO/PROP-19] p 856 N94-15696
ANODES
Fabrication of advanced design (grooved) cermet anodes
[DE93-014590] p 1012 N94-16765
Investigation of onset of plasma formation at anode of fast-pulsed high-voltage vacuum diode
[AD-A267214] p 1204 N94-16987
ANODIC COATINGS
Formation of pitting resistant anodized films on aluminum
[AD-D015812] p 958 N94-16486
ANODIZING
The corrosion protection of metals by ion vapor deposited aluminum
[NASA-TM-108425] p 955 N94-15832
Formation of pitting resistant anodized films on aluminum
[AD-D015812] p 958 N94-16486
ANOMALIES
Cretaceous-tertiary boundary spherules and Cenozoic microtektites: Similarities and differences p 1241 N94-16186
ANORTHOSITE
Remote sensing studies of the northeastern portion of the lunar nearside p 1258 N94-16225
The monzonorite-anorthosite connection: The petrogenesis of terrestrial KREEP p 1104 N94-16365
ANTARCTIC OCEAN
Exploring the southern ocean response to climate change
[NASA-CR-194601] p 1112 N94-15680
Arctic and Antarctic sea ice, 1978-1987: Satellite passive-microwave observations and analysis
[NASA-SP-511] p 1114 N94-17439

ANTARCTIC REGIONS
Mars look-alike
[NASA-TM-109667] p 1094 N94-15238
Exploring the southern ocean response to climate change
[NASA-CR-194601] p 1112 N94-15680
Noble gases in twenty Yamato H-chondrites: Comparison with Allan Hills chondrites and modern falls p 1244 N94-16361
Atmospheric ionization by solar particles detected by nitrate measurement in antarctic snow
[AD-A267583] p 1299 N94-17208

ANTENNA ARRAYS
Velocity matched millimeterwave electro-optic modulator
[AD-A267264] p 1188 N94-14957
Adaptive beamforming with imperfect arrays: Pattern effects and their partial correction
[AD-A267079] p 987 N94-15541
Dual polarization microstrip array antenna
[CA-PATENT-1-307-842] p 994 N94-15986
Phased array antenna analysis using hybrid finite element methods
[AD-A267620] p 1002 N94-17196
Proceedings of the 1992 Antenna Applications Symposium, volume 1
[AD-A268167] p 1005 N94-17431

ANTENNA COMPONENTS
Velocity matched millimeterwave electro-optic modulator
[AD-A267264] p 1188 N94-14957

ANTENNA DESIGN
Advanced antennas for SAR spacecraft p 993 N94-15912
Dual polarization microstrip array antenna
[CA-PATENT-1-307-842] p 994 N94-15986
Manufacturing tolerance requirements for frequency selective surfaces
[AD-A266541] p 999 N94-16797
Design of broadband wire antennas for frequency hopping applications
[AD-A267405] p 1001 N94-17025
Proceedings of the 1992 Antenna Applications Symposium, volume 1
[AD-A268167] p 1005 N94-17431
The analysis of low-profile, broadband, monopole, vehicle antennas and matching network synthesis
[AD-A268340] p 1006 N94-17582

ANTENNA RADIATION PATTERNS
Antenna gain loss and pattern degradation due to transmission through dielectric radomes
[AD-A267242] p 986 N94-14974
An optically modulated scatterer for microwave antenna metrology
[NPL-DES-126] p 986 N94-15020
Adaptive beamforming with imperfect arrays: Pattern effects and their partial correction
[AD-A267079] p 987 N94-15541
Experimental evaluation of an adaptive focusing algorithm for a microwave planar phased-array hyperthermia system at UCSF
[AD-A267004] p 1121 N94-15634
Propagation-related AMT design aspects and supporting experiments p 995 N94-16042
Manufacturing tolerance requirements for frequency selective surfaces
[AD-A266541] p 999 N94-16797
Design of broadband wire antennas for frequency hopping applications
[AD-A267405] p 1001 N94-17025
How to deduce the far field of an antenna from planar near-field measurements
[NPL-DES-123] p 1006 N94-17545

ANTENNAS
Antenna gain loss and pattern degradation due to transmission through dielectric radomes
[AD-A267242] p 986 N94-14974

ANTIMISSILE DEFENSE
Hypervelocity orbital intercept guidance using certainty control
[AD-A267297] p 1174 N94-17219

ANTIMONY
BIB photodetectors based on antimony doped silicon p 902 N94-15047

ANTIMONY COMPOUNDS
Characterization of InTISb grown by low pressure metalorganic chemical vapor deposition on GaAs substrate
[AD-A266878] p 1206 N94-14922

ANTIPARTICLES
On the nature of mirror particles
[DE93-626670] p 1179 N94-14934

ANTIPROTONS
Search for the top quark from (e(mu)) and (e,e) events in the D0 detector in p(bar-p) collisions at the square root of s = 1.8 TeV
[DE93-016350] p 1186 N94-17662

ANTIREFLECTION COATINGS
Review of rigorous coupled-wave analysis and of homogeneous effective medium approximations for high spatial-frequency surface-relief gratings p 1194 N94-17335
Subwavelength structured surfaces and their applications p 1194 N94-17337
A new method of designing multilayer optical thin film coatings
[DE93-624683] p 974 N94-17611

ANXIETY
Scuba-diving, anxiety and task performance p 1132 N94-15938

APERTURES
Display system employing acousto-optic tunable filter
[NASA-CASE-NPO-18736-1-CU] p 1190 N94-15933
Design, development and characterization studies of a large aperture high power Nd: Glass rod amplifier stage
[DE93-624944] p 1042 N94-17630

APOLLO PROJECT
The 1966 highlights --- NASA research programs
[NASA-TM-109444] p 1302 N94-15343
Apollo presentation for Astrodome
[NASA-TM-109535] p 1302 N94-15366
President Kennedy's speech at Rice University
[NASA-TM-109532] p 1302 N94-15394
Galileo photometry of Apollo landing sites p 1259 N94-16234

APOLLO SOYUZ TEST PROJECT
ASTP 15th anniversary clip-media release
[NASA-TM-109534] p 1302 N94-15399

APPALACHIAN MOUNTAINS (NORTH AMERICA)
Mesoscale frontogenesis: An analysis of two cold front case studies
[AD-A267950] p 1107 N94-17054

APPLICATION SPECIFIC INTEGRATED CIRCUITS
Smart Power: New power integrated circuit technologies and their applications
[VTT-TIED-1358] p 1015 N94-17546

APPLICATIONS PROGRAMS (COMPUTERS)
HyperVentilate: Decision-support software for soil vapor extraction technology application
[PB93-134880] p 1094 N94-15136
An expert system shell for inferring vegetation characteristics: Atmospheric techniques (Task G)
[NASA-CR-194570] p 1082 N94-15531
SATCOP mission planning software package p 912 N94-15562
Preliminary analysis and design optimization of the short spacer truss of Space Station Freedom
[NASA-TM-4470] p 1058 N94-15709
A study of land mobile satellite service multipath effects using SATLAB software p 997 N94-16051
Proteus three-dimensional Navier-Stokes computer code, version 1.0. Volume 1: Analysis description
[NASA-TM-106337] p 1024 N94-16527
The Spectral Image Processing System (SIPS): Software for integrated analysis of AVIRIS data p 1067 N94-16674
Radar Analysis and Visualization Environment (RAVEN): Software for polarimetric radar analysis p 1080 N94-16758
ASTROS enhancements. Volume 1: ASTRO user's manual
[AD-A266818] p 1151 N94-16768
ASTROS enhancements. Volume 2: ASTRO programmer's manual
[AD-A266819] p 1151 N94-16769
Module interconnection frameworks for a real-time spreadsheet
[AD-A267752] p 1153 N94-17231

APPROACH
Category (CAT) 3B level 1 test plan for Global Positioning System (GPS)
[DOT/FAA/RD-93/21] p 864 N94-16835

APPROACH CONTROL
Wide-area Differential Global Positioning System (WDGPS)/Wide-area Integrity Broadcast (WIB) alternatives analysis
[DOT/FAA/SE-93/3] p 864 N94-16906
Hypervelocity orbital intercept guidance using certainty control
[AD-A267297] p 1174 N94-17219

APPROXIMATION
Monotone approximate query processing
[AD-A267153] p 1169 N94-15779
On the stability analysis of approximate factorization methods for 3D Euler and Navier-Stokes equations
[NASA-TM-106314] p 1169 N94-15818
Moments in statistics: Approximations to densities and goodness-of-fit
[AD-A266600] p 1173 N94-16726
Numerically solving a transient heat conduction problem with convection and radiation
[AD-A268521] p 1220 N94-17540
Steepest descent approximations for accretive operator equations
[DE93-628586] p 1171 N94-17667

AQUEOUS SOLUTIONS
Pressures of supercritical salt solutions p 945 N94-15166
Thermochemistry of silicate speciation in aqueous sodium silicate solutions: Ionization and polymerization of small silicate ion
[AD-A266825] p 964 N94-15683
Swelling equilibria for temperature-sensitive ampholytic hydrogels
[DE93-015264] p 966 N94-15996
Contained liquids in microgravity, part 2 p 979 N94-16085
Rheology of water and ammonia-water ices p 953 N94-16188
An investigation of the hydrolytic resistance of sodium-calcium plate glass with a layer of silica deposited on its surface
[IFTR-34/1991] p 971 N94-17120

AQUIFERS
Water-levels fluctuations in a borehole at the Royal Observatory of Belgium: Effects on local gravity, Earth tidal, and barometric responses p 1100 N94-15812
The seismic response of an aquifer to the propagation of an impact generated shock wave: A possible trigger of the Martian outflow channels? p 1281 N94-16354

ARAMID FIBER COMPOSITES
The effect of plasma treatment on interfacial bond characteristics of Kevlar/epoxy laminates as measured by T-peel tests
[AD-A266920] p 930 N94-14999
New textile composite materials development, production, application p 938 N94-16853

ARC DISCHARGES
Dynamic behavior of an electric arc gas discharge
[DE93-630197] p 1205 N94-17635

ARC WELDING
Adaptive weld control for high-integrity welding applications
[TABES PAPER 93-604] p 1049 N94-16140

ARCHITECTURE (COMPUTERS)
Video applications development platform
[AD-A266966] p 1163 N94-14953
The application of compiler-assisted multiple instruction retry to VLIW architectures
[AD-A266930] p 1158 N94-15173
Relaxing consistency in recoverable distributed shared memory
[AD-A266931] p 1140 N94-15174
Software architecture for shared information systems
[AD-A266995] p 1144 N94-15216
Overview of Enhanced Data Stream Array Processor (EDSAP)
[AD-A266986] p 1158 N94-15492
System architecture of optically controlled phased array radar
[AD-A267056] p 988 N94-15667
Integrated trusted systems development environment
[AD-A267029] p 1146 N94-15674
Architectures for software systems: A curriculum development proposal in undergraduate software engineering
[AD-A266703] p 1147 N94-15728
Department of Defense technical architecture framework for information management. Volume 2: Technical reference model and standards profile, version 2.0
[AD-A267194] p 1229 N94-15788
A decision criteria to select an associative-memory organization that minimizes the execution time of a mix of associative-search operations
[AD-A266438] p 1149 N94-16560
Disconnected operation in a distributed file system
[AD-A266461] p 1231 N94-16570
Efficient compilation of array statements for private memory multicomputers
[AD-A266595] p 1160 N94-16724
ASTROS enhancements. Volume 1: ASTRO user's manual
[AD-A266818] p 1151 N94-16768
ASTROS enhancements. Volume 2: ASTRO programmer's manual
[AD-A266819] p 1151 N94-16769
A modular control architecture for real-time synchronous and asynchronous systems
[DE93-015439] p 1166 N94-16888
Development of dynamic, contex-driven help systems
[AD-A267409] p 1152 N94-16974

A security architecture for fault-tolerant systems
[AD-A266178] p 1152 N94-16982
An object-oriented program specification for a mobile robot motion control language
[AD-A267213] p 1166 N94-16986
Fault-tolerant architectures for multiprocessor and VLSI-based systems
[AD-A267370] p 1140 N94-17005
Efficient scheduling of real-time compute-intensive periodic graphs on large grain data flow multiprocessor
[AD-A267444] p 1141 N94-17030
Networked workstations and parallel processing utilizing functional languages
[AD-A267464] p 1160 N94-17034
A proposed ground segment design for small satellites
p 878 N94-17154
Integrating reactive and deliberative planning for agents
[AD-A267631] p 1166 N94-17201
Light-weight process groups in the ISIS system
[NASA-CR-194544] p 1161 N94-17239
Computer-aided design package for designers of digital optical computers
[AD-A267866] p 1154 N94-17390
Integration of several computer systems within a heterogeneous environment
[AD-A267978] p 1155 N94-17500
Femtosecond carrier processes in compound semiconductors and real time signal processing
[AD-A268122] p 1005 N94-17519

ARCTIC OCEAN
Sea ice motions in the central arctic ice central arctic pack ice as inferred from AVHRR imagery
[NASA-CR-194572] p 1112 N94-15701
Arctic and Antarctic sea ice, 1978-1987: Satellite passive-microwave observations and analysis
[NASA-SP-511] p 1114 N94-17439

ARCTIC REGIONS
Arctic internal waves (CEAREX)
[AD-A265822] p 1111 N94-15139
Arctic ozone
[NASA-TM-109614] p 1095 N94-15365
Arctic cyclones and Marginal Ice Zone (MIZ) variability
[AD-A268610] p 1108 N94-17465

ARGENTINA
Martian crater degradation by eolian processes: Analogy with the Rio Cuarto Crater Field, Argentina
p 1251 N94-16196

ARGON
Investigation of the energy distribution of ions, striking the cathode in an abnormal glow discharge
[DE93-623987] p 1013 N94-17316
Laser ignition of solid propellants: 1. Ignition delays
[AD-A268454] p 976 N94-17538

ARGON ISOTOPES
The SCR Ne-21 and Ar-38 in lunar rock 68815: The solar proton energy spectrum over the past 2 MYR
p 1248 N94-16177
Preliminary Ar-40/Ar-39 age spectrum and laser probe dating of the M1 core of the Manson Impact Structure, Iowa: A K-T boundary crater candidate
p 1104 N94-16334
Effects of bulk composition on production rates of cosmogenic nuclides in meteorites p 1245 N94-16385
Solar noble gases revealed by closed system stepped etching of a metal separate from Fayetteville
p 954 N94-16432

ARGON LASERS
Photo-assisted epitaxial growth for III-V semiconductors
[AD-A267889] p 1213 N94-17042
Atomic beam studies relevant to the space environment
[AD-A268628] p 1186 N94-17436

ARIANE LAUNCH VEHICLE
ARIANE 5 light derivatives p 878 N94-17140

ARID LANDS
AVIRIS study of Death Valley evaporite deposits using least-squares band-fitting methods p 1067 N94-16676
Discrimination among semi-arid landscape endmembers using the Spectral Angle Mapper (SAM) algorithm
p 1074 N94-16711

ARITHMETIC
Operator overloading as an enabling technology for automatic differentiation
[DE93-012899] p 1170 N94-16778

ARKANSAS
Ground wave emergency network final operational capability. Environmental assessment for southern Arkansas relay node site no. RN 8C912AR
[AD-A268001] p 1004 N94-17376

ARMATURES
Integrated fundamental research on current collection
[AD-A266987] p 1008 N94-15494
Numerical modeling of the temperature gradients and spectra of the plasma armature on Thunderbolt
[AD-A266414] p 878 N94-16552

ARMED FORCES (UNITED STATES)
Monograph of the aviation epidemiology data register for FY 1991
[AD-A266896] p 1119 N94-14952
AFOSR technical report summaries, January - March 1993
[AD-A267187] p 1230 N94-15850

ARMOR
Dynamic testing and characterization of pre-fractured ceramic
[DE93-016457] p 972 N94-17238

ARPA COMPUTER NETWORK
A geological and geophysical information system for Eurasia
[AD-A267841] p 1232 N94-17036
ARPA unmanned ground vehicle stereo vision program at Teleos Research
[AD-A267632] p 1167 N94-17202

ARRAYS
Broadband teleseismic array recording in the Adirondack Mountains, New York State
[AD-A267290] p 1097 N94-14960
CdTe array detectors for high energy astronomy
p 899 N94-15029
Large scientific 2-D arrays for the 1-5 micron region
p 902 N94-15044
Photoconductors and arrays for the far-infrared
p 902 N94-15045
Nonstationary behaviour of low background photon detectors p 902 N94-15049
Schottky barrier focal plane arrays for SWIR and MWIR p 903 N94-15050
Advanced high performance CdHgTe multiplexed arrays p 903 N94-15051
Lead chalcogenides based IR photosensitive array detectors with coordinate addressing
p 903 N94-15053
The alignment-distribution graph
[NASA-CR-194292] p 1168 N94-15112
Mobile and replicated alignment of arrays in data-parallel programs
[NASA-CR-194294] p 1158 N94-15113
Work at Graz on satellite signatures
p 898 N94-15558
Binary optics at Hughes Danbury Optical Systems
p 1195 N94-17344
Field-emitter arrays for RF vacuum microelectronics
[AD-A268397] p 1015 N94-17526

ARSENIC
Arsenic surveillance program p 1127 N94-16637
Activation and deactivation of high concentration arsenic with some evidence of precipitation
[DE93-016437] p 950 N94-16952
Photo-assisted epitaxial growth for III-V semiconductors
[AD-A267889] p 1213 N94-17042

ARTERIES
Laser artery repair
[NASA-TM-109604] p 1120 N94-15312
The nature of dynamic arteriolar vasoreactivity: A mini-review and A classification scheme
[AD-A266499] p 1128 N94-16783

ARTIFICIAL GRAVITY
Apparatus and method for producing an artificial gravitational field
[NASA-CASE-MSC-22021-1] p 886 N94-15935

ARTIFICIAL INTELLIGENCE
YARF: An open-ended framework for robot road following
[AD-A266788] p 1163 N94-14910
A scientific basis for computational science
[AD-A266697] p 1148 N94-15841
Proceedings of the Association for Computing Machinery Special Interest Group for Ada Artificial Intelligence Working Group
[AD-A266422] p 1165 N94-16559
Combinatorial semantics
[TR-444] p 1149 N94-16575
Temporal segmentation of tasks from human hand motion
[AD-A266596] p 1166 N94-16725
KBSA concept demo
[AD-A267054] p 1166 N94-16770
Information technology division technical paper abstracts
[AD-A266227] p 1166 N94-16938
Integrating reactive and deliberative planning for agents
[AD-A267631] p 1166 N94-17201
ARPA unmanned ground vehicle stereo vision program at Teleos Research
[AD-A267632] p 1167 N94-17202
Intelligent use of CFAR algorithms
[AD-A267755] p 1003 N94-17206
Developing automated analysis methods for sea ice imagery: A status report with recommendations
[AD-A267284] p 1113 N94-17241
Notes on the use of Dempster-Shafer and fuzzy reasoning to fuse identity attribute data
[AD-A267426] p 1004 N94-17309
Incremental rederivation of software artifacts: FY 1992
[AD-A267968] p 1155 N94-17491
A high-speed object recognition chip based on a biologically-realistic hybrid temporal processing
[AD-A268270] p 1134 N94-17576

ARTIFICIAL SATELLITES
Proceedings of the 1992 Antenna Applications Symposium, volume 2
[AD-A266916] p 986 N94-14998
Satellite situation report, volume 33, no. 3
[NASA-TM-109278] p 885 N94-15712
Solar absorptance of optical surfaces contaminated with spacecraft material outgassing products
[AD-A267202] p 886 N94-15857
History of on-orbit satellite fragmentations
[NASA-CR-191644] p 887 N94-16502
L-shell binning and display of sensor data from the CRRES spacecraft
[AD-A267256] p 888 N94-16990
Implementing a 50x50 gravity field model in an orbit determination system
[AD-A267548] p 888 N94-17103
Space systems environmental interaction studies
[AD-A267280] p 897 N94-17240
Satellite situation report, volume 31, number 1
[NASA-TM-105088] p 898 N94-17584

ASBESTOS
Asbestos Surveillance Program p 1127 N94-16638

ASCENT
STS-30 suited ascent training in fixed base SMS
[NASA-TM-109581] p 875 N94-15265
Assimilation of solids during ascent of magmas from the Bartoy Field of the Baikal Region, Siberia
p 1103 N94-16214

ASCENT TRAJECTORIES
Trajectory optimization for the National Aerospace Plane
[NASA-CR-194618] p 867 N94-16498

ASIA
The Karakul depression in Pamirs: The first impact structure in Central Asia p 1241 N94-16212
A geological and geophysical information system for Eurasia
[AD-A267841] p 1232 N94-17036

ASPHALT
User's guide: Hot-mix recycling of asphalt concrete pavements
[AD-A266939] p 983 N94-15177
An analysis of ways of determining the material constants for viscoelastic materials
[IFTR-28/91] p 951 N94-17050

ASPHERICITY
Binary optics at Hughes Danbury Optical Systems
p 1195 N94-17344
Fabrication techniques for very fast diffractive lenses
p 1196 N94-17345

ASSIMILATION
Assimilation of solids during ascent of magmas from the Bartoy Field of the Baikal Region, Siberia
p 1103 N94-16214

ASSOCIATIVE PROCESSING (COMPUTERS)
Unipolar terminal-attractor based neural associative memory with adaptive threshold
[NASA-CASE-NPO-18790-1-CU] p 1165 N94-15958

ASSURANCE
Software Engineering Guidebook
[NASA-CR-177625] p 1150 N94-16656

ASTEROID BELTS
Heliocentric zoning of the asteroid belt by aluminum-26 heating p 1241 N94-16205
Petrologic constraints on the surface processes on asteroid 4 Vesta and on excavation depths of diogenite fragments p 1241 N94-16208
An initial perspective of S-asteroid subtypes within asteroid families p 1243 N94-16310

ASTEROID MISSIONS
The Clementine instrument complement
p 1086 N94-16370
Small spacecraft for planetary exploration
p 874 N94-17145

ASTEROIDS
Twenty-Fourth Lunar and Planetary Science Conference. Part 2: G-M
[NASA-CR-193174] p 1247 N94-16173
Spectral evidence of size dependent space weathering processes on asteroid surfaces p 1241 N94-16174
New K type asteroids p 1241 N94-16195

Collisional and dynamical history of Gaspra
p 1241 N94-16202
Heliocentric zoning of the asteroid belt by aluminum-26 heating
p 1241 N94-16205
Comparison of reflectance spectra of C asteroids and unique C chondrites Y86720, Y82162, and B7904
p 1242 N94-16246
Iron oxide bands in the visible and near-infrared reflectance spectra of primitive asteroids
p 1242 N94-16274
Explosive volcanism and the compositions of the cores of differentiated asteroids
p 1243 N94-16306
An initial perspective of S-asteroid subtypes within asteroid families
p 1243 N94-16310
Cat Mountain: A meteoritic sample of an impact-melted chondritic asteroid
p 1244 N94-16328
Clementine: Anticipated scientific datasets from the Moon and Geographos
p 1288 N94-16392
Optical effects of regolith processes on S asteroids as simulated by laser impulse alteration of ordinary chondrite
p 1246 N94-16422

ASTRO MISSIONS (STS)
STS-35 onboard photography quick release
[NASA-TM-109500] p 881 N94-15464
STS-35 mission highlights resource tape
[NASA-TM-109501] p 881 N94-15465

ASTRODYNAMICS
Linear stability of stationary solutions of the Vlasov-Poisson system in three dimensions
[DE93-013873] p 1174 N94-16820

ASTRONAUT LOCOMOTION
STS-37 CETA evaluation with Ross
[NASA-TM-109495] p 1135 N94-15330

ASTRONAUT MANEUVERING EQUIPMENT
STS-37 CETA evaluation with Ross
[NASA-TM-109495] p 1135 N94-15330
STS-37 astronauts Ross and Apt during CETA hardware checkout
[NASA-TM-109496] p 1137 N94-15460

ASTRONAUT TRAINING
STS-35 crew training: EMU walk through and EVA prep and post
[NASA-TM-109488] p 1134 N94-15194
STS-35 Crew training: Bailout in CCT, firefighting, TAGS class and bailout in WFTF
[NASA-TM-109489] p 1135 N94-15195
Brown, Mark --- astronaut candidate training
[NASA-TM-109505] p 1135 N94-15224
Space Station Freedom
[NASA-TM-109636] p 1031 N94-15247
STS-30 suited ascent training in fixed base SMS
[NASA-TM-109581] p 875 N94-15265
STS-26 STA training (Hauck)
[NASA-TM-109555] p 870 N94-15279
The 61-M long duration sim video highlights resource tape
[NASA-TM-109569] p 875 N94-15299
STS-30 Magellan deploy Sim in SMS and MOCR
[NASA-TM-109571] p 875 N94-15301
STS-30 EVA prep in CCT: Grabe, Lee, and Thagard
[NASA-TM-109572] p 1135 N94-15303
STS-30 crew photo in building 4
[NASA-TM-109573] p 1031 N94-15304
STS-29 pre-launch and post-landing egress
[NASA-TM-109574] p 1135 N94-15305
Space adaptation
[NASA-TM-109601] p 1120 N94-15309
STS-32 IMAX camera training
[NASA-TM-109567] p 1031 N94-15316
STS-26 IUS and latch contingency training
[NASA-TM-109561] p 875 N94-15331
STS-26 generic integrated IUS deploy simulation
[NASA-TM-109562] p 875 N94-15332
STS-26 EVA rescue training
[NASA-TM-109563] p 875 N94-15333
STS-34 McCully and Baker during IFM training
[NASA-TM-109462] p 880 N94-15357
STS-34 crew bailout exercise in CCT
[NASA-TM-109465] p 1135 N94-15360
STS-34 Chang-Diaz and E. Baker during Galileo contingency training in WFTF
[NASA-TM-109466] p 1135 N94-15361
STS-29 IMAX camera audio class FFT
[NASA-TM-109543] p 1031 N94-15374
STS-32 LDEF EVA training in WETF with Low and Dunbar
[NASA-TM-109473] p 1135 N94-15377
STS-32 LDEF approach in SES
[NASA-TM-109474] p 880 N94-15379
STS-29 crew IMAX camera training
[NASA-TM-109546] p 1031 N94-15380
STS-32 crew training for lower body negative pressure unit and AFE
[NASA-TM-109475] p 1120 N94-15381
STS-32 bailout training in WETF
[NASA-TM-109476] p 1136 N94-15383
STS-29 crew bailout in WETF
[NASA-TM-109548] p 1136 N94-15385
STS-28 Adamson and Brown EMU walk through
[NASA-TM-109549] p 1136 N94-15387
STS-33 emergency egress training
[NASA-TM-109525] p 1136 N94-15388
1990 ASCAN land survival training
[NASA-TM-109527] p 1136 N94-15390
1990 ASCAN ground egress/parasail
[NASA-TM-109528] p 1136 N94-15391
ASTP 15th anniversary clip-media release
[NASA-TM-109534] p 1302 N94-15399
STS-27 EMU and RMS contingency training
[NASA-TM-109550] p 1136 N94-15401
STS-33 Carter and Thorton during WETF activities
[NASA-TM-109471] p 1136 N94-15402
STS-27 crew photo training and habitation procedures
[NASA-TM-109553] p 1032 N94-15405
STS-27 crew fire training and glove molding
[NASA-TM-109554] p 1136 N94-15406
STS-31 Hubble space telescope contingency training in WETF with McCandless and Sullivan
[NASA-TM-109480] p 1136 N94-15441
STS-31 Hubble space telescope deploy: Training at MDF with Hawley
[NASA-TM-109481] p 876 N94-15442
STS-31 HST deploy sim in SMS and MOCR
[NASA-TM-109482] p 876 N94-15449
STS-31 crew training inflight maintenance and bailout exercises in CCT and WFTF
[NASA-TM-109483] p 876 N94-15450
STS-31 crew training: firefighting, food tasting, EVA prep and post
[NASA-TM-109484] p 876 N94-15451
STS-38 crew training: Habitation equipment procedures, bailout in CCT, 70mm photo class, EVA prep and post, and firefighting
[NASA-TM-109494] p 1136 N94-15453
STS-36 crew EVA prep and post-training, bailout exercises, final bench review
[NASA-TM-109498] p 1137 N94-15462
STS-35 payload specialists Durrance and Parise: 70mm photo training and cabin familiarization
[NASA-TM-109499] p 1032 N94-15463
Richards, Dick: Training clip
[NASA-TM-109503] p 876 N94-15467
STS-27 crew deorbit prep in SMS with Gibson, Shepard, Mullane, Ross, and G. Gardner
[NASA-TM-109518] p 882 N94-15468
STS-26 long duration simulation: Crew entering SMS
[NASA-TM-109560] p 876 N94-15474
Astronauts number 1 --- mercury project
[NASA-TM-109428] p 1131 N94-15499
STS-41 crew training bailout in CCT, 16mm camera class EVA prep, habitation equipment procedures, and food tasting
[NASA-TM-109517] p 876 N94-15517
STS-31 crew Linof, Arriflex, and IMAX camera training
[NASA-TM-109485] p 1032 N94-15792

ASTRONAUTICS
Commonwealth of Independent States aerospace science and technology, 1992: A bibliography with indexes
[NASA-SP-7106] p 854 N94-16481

ASTRONAUTS
Brown, Mark --- astronaut candidate training
[NASA-TM-109505] p 1135 N94-15224
Teacher in space
[NASA-TM-109666] p 1131 N94-15237
STS-26 IUS and latch contingency training
[NASA-TM-109561] p 875 N94-15331
Living well in space: Ensuring crew capability
[NASA-TM-109538] p 1120 N94-15369
STS-29 mission highlights resource tape
[NASA-TM-109542] p 880 N94-15373
STS-29 IMAX camera audio class FFT
[NASA-TM-109543] p 1031 N94-15374
STS-29 EVA prep in FFT
[NASA-TM-109544] p 1135 N94-15375
STS-32 LDEF EVA training in WETF with Low and Dunbar
[NASA-TM-109473] p 1135 N94-15377
STS-32 crew training for lower body negative pressure unit and AFE
[NASA-TM-109475] p 1120 N94-15381
STS-28 Adamson and Brown EMU walk through
[NASA-TM-109549] p 1136 N94-15387
ASTP 15th anniversary clip-media release
[NASA-TM-109534] p 1302 N94-15399
STS-27 EMU and RMS contingency training
[NASA-TM-109550] p 1136 N94-15401
STS-33 Carter and Thorton during WETF activities
[NASA-TM-109471] p 1136 N94-15402
STS-27 crew post-insertion deorbit-prep in CCT
[NASA-TM-109552] p 1136 N94-15404
STS-26 missions highlight resource tape
[NASA-TM-109559] p 881 N94-15407
STS-36 crew presentation clip
[NASA-TM-109497] p 881 N94-15461
STS-35 payload specialists Durrance and Parise: 70mm photo training and cabin familiarization
[NASA-TM-109499] p 1032 N94-15463
STS-35 onboard photography quick release
[NASA-TM-109500] p 881 N94-15464
STS-35 mission highlights resource tape
[NASA-TM-109501] p 881 N94-15465
Science operation in space: Lessons
[NASA-TM-109502] p 881 N94-15466
Richards, Dick: Training clip
[NASA-TM-109503] p 876 N94-15467
STS-26 long duration simulation: Crew entering SMS
[NASA-TM-109560] p 876 N94-15474
Astronauts number 3 --- Friendship 7
[NASA-TM-109430] p 874 N94-15501
Exposure fluctuations of astronauts due to orientation
[NASA-TP-3364] p 1300 N94-15816

ASTRONOMICAL CATALOGS
Critically evaluated/distributed database of IRAS LRS spectra
[NASA-CR-193611] p 1232 N94-17038

ASTRONOMICAL MODELS
The physical mechanism of comet outbursts: An experiment
p 1242 N94-16221

ASTRONOMICAL OBSERVATORIES
Matera Laser Ranging Observatory (MLRO): An overview
p 877 N94-15601
TLRS-3 system upgrades
p 877 N94-15609

ASTRONOMICAL PHOTOMETRY
Heliocentric zoning of the asteroid belt by aluminum-26 heating
p 1241 N94-16205
Galileo photometry of Apollo landing sites
p 1259 N94-16234
Earth-based and Galileo SSI multispectral observations of eastern mare serenitatis and the Apollo 17 landing site
p 1261 N94-16244

ASTRONOMICAL SPECTROSCOPY
CdTe array detectors for high energy astronomy
p 899 N94-15029
Spectral evidence of size dependent space weathering processes on asteroid surfaces
p 1241 N94-16174
New K type asteroids
p 1241 N94-16195
Heliocentric zoning of the asteroid belt by aluminum-26 heating
p 1241 N94-16205
Earth-based and Galileo SSI multispectral observations of eastern mare serenitatis and the Apollo 17 landing site
p 1261 N94-16244
The spectrum of Phobos from Phobos 2 observations at 0.3-2.6 microns: Comparison to previous data and meteorite analogs
p 1295 N94-16429

ASTRONOMY
Large scientific 2-D arrays for the 1-5 micron region
p 902 N94-15044
Astronomy and astrophysics
p 1239 N94-15970
The planetary data system educational CD-ROM
p 1234 N94-16209
From the Moons of Jupiter to the Milky Way
[NASA-CR-194649] p 1240 N94-17059

ASTROPHYSICS
NASA's Ultraviolet Astrophysics Branch: Present and future detector program
p 910 N94-15102
Astronomy and astrophysics
p 1239 N94-15970
Particle physics and cosmology, Task C
[DE93-016865] p 1239 N94-16118
The Megascience Forum
[DE93-014445] p 1303 N94-16804
ALEXIS and HETE: Two small, low cost, scientific satellite systems
p 896 N94-17185

ASYMMETRY
Structural investigation of electrochemically etched silicon
[DE93-015300] p 1207 N94-15827
Analysis of temporal symmetry in non-gaussian random fields
[AD-A266496] p 999 N94-16794
Asymmetric three-beam binary optic grating
p 1195 N94-17340
High order nonlinear estimation with signal processing applications
[AD-A268407] p 1005 N94-17463

ASYMPTOTIC METHODS
Analysis of an electromagnetic field in the vicinity of a caustic by asymptotic methods
[IFTR-12/1991] p 998 N94-16653

ASYMPTOTIC PROPERTIES
Asymptotic behavior of firmly non expansive sequences
[DE93-628589] p 1171 N94-17642

ASYMPTOTIC SERIES
Highly transient elastodynamic crack growth in a bimaterial interface: Higher order asymptotic analysis and optical experiments
[AD-A266465] p 1059 N94-16587
Convection effects on radial segregation and crystal melt interface in vertical Bridgman growth
[NASA-CR-191541] p 1029 N94-17387
ATLANTIC OCEAN
Ray tracing on topographic Rossby waves
[AD-A267014] p 1112 N94-15844
Meridional circulation in the tropical north atlantic
[AD-A268222] p 1114 N94-17555
ATMOSPHERIC & OCEANOGRAPHIC INFORM SYS
Observations and modelling of winds and waves during the Surface Wave Dynamics Experiment. Report 1: Intensive observation period IOP-1, 20-31 October 1990
[AD-A266384] p 1113 N94-16517
ATMOSPHERIC ATTENUATION
Johnson-Gierhart program predictions of excess propagation loss for super-high frequency air-to-ground paths. Volume 2: Appendices
[AD-A267021] p 987 N94-15527
Johnson-Gierhart program predictions of excess propagation loss for super-high frequency air-to-ground paths. Volume 1: Theory and numerical results
[AD-A267105] p 988 N94-15649
Olympus propagation measurement results at Virginia Tech p 995 N94-16037
Data acquisition, preprocessing and analysis for the Virginia Tech OLYMPUS experiment p 995 N94-16038
A comparison of cloud attenuation models using measured cloud data p 996 N94-16044
Brightness temperature and attenuation statistics at 20.6 and 31.65 GHz p 996 N94-16045
Comparison of OLYMPUS beacon and radiometric attenuation measurements at Blacksburg, Virginia p 996 N94-16046
A CCIR-based prediction model for Earth-Space propagation p 997 N94-16050
Application of split window technique to TIMS data p 1064 N94-16601
The use of TIMS data to estimate the SO2 concentrations of volcanic plumes: A case study at Mount Etna, Sicily p 1065 N94-16608
Hyperspectral modeling for extracting aerosols from aircraft/satellite data p 1067 N94-16673
Software for the derivation of scaled surface reflectances from AVIRIS data p 1072 N94-16700
Atmospheric propagation analysis program
[AD-A268231] p 1006 N94-17565
ATMOSPHERIC BOUNDARY LAYER
Detecting surface roughness effects on the atmospheric boundary layer via AIRSAR data: A field experiment in Death Valley, California p 1078 N94-16747
An investigation of the Ground-Based High-Resolution Interferometer Sounder (GB-HIS) in a costal marine environment
[AD-A268052] p 1114 N94-17503
ATMOSPHERIC CHEMISTRY
Electronic spectroscopy of the gas-phase OH-Kr van der Waals complex
[AD-A266891] p 942 N94-14946
Mesoscale modeling of the atmosphere
[AD-A263236] p 1098 N94-15132
Projections of future CO2
[NIWA/ATMOS/R/93-001] p 1094 N94-15185
ATLAS-2 and UARS correlative measurement opportunities during Space Shuttle mission on April 8-17, 1993
[NASA-TM-109020] p 1105 N94-15480
Characterization of UV emissions resulting from electronic energy transfer in atmospheric molecules
[AD-A266244] p 1101 N94-16469
BACKSCAT lidar simulation version 3.0: Technical documentation and users guide
[AD-A267296] p 1003 N94-17268
ATMOSPHERIC CIRCULATION
Mesoscale modeling of the atmosphere
[AD-A263236] p 1098 N94-15132
A global traveling wave on Venus
[NASA-CR-194356] p 1246 N94-15182
IAI topic: El Nino. Southern oscillation and interannual climate variability
[INPE-5410-PRE/1757] p 1111 N94-15186
Effects of spatial variability and scale on areal -average evapotranspiration p 1084 N94-16033
Sand transport on Mars: Preliminary results from models p 1252 N94-16198
Dust-dynamic feedbacks in the Martian atmosphere: Surface dust lifting p 1296 N94-16434
Mesoscale frontogenesis: An analysis of two cold front case studies
[AD-A267950] p 1107 N94-17054
Orographic microbursts in a severe winter windstorm
[AD-A267651] p 1108 N94-17247
BACKSCAT lidar simulation version 3.0: Technical documentation and users guide
[AD-A267296] p 1003 N94-17268
A correlative comparison of geomagnetic storms and auroral substorms using geomagnetic indeces
[AD-A268081] p 1102 N94-17512
Propagation characteristics of mesoscale convective systems
[AD-A268130] p 1109 N94-17522
Further development and testing of a second-order bulk boundary layer model
[AD-A268071] p 1109 N94-17552
A two-layer quasi-geotrophic spherical model: Formulation and climatology
[DM-63] p 1110 N94-17593
ATMOSPHERIC COMPOSITION
Projections of future CO2
[NIWA/ATMOS/R/93-001] p 1094 N94-15185
Global Greenhouse Expedition
[NASA-TM-109613] p 1095 N94-15364
Preliminary analysis of University of North Dakota aircraft data from the FIRE Cirrus IFO-2
[NASA-CR-193357] p 866 N94-15429
Driving terrestrial ecosystem models from space p 991 N94-15896
Trapping of water vapor from an atmosphere by condensed silicate matter formed by high-temperature pulse vaporization p 1248 N94-16180
A Pluto thermal model p 1256 N94-16216
Martian carbon dioxide: Clues from isotopes in SNC meteorites p 1270 N94-16295
Evolution of Triton's volatile budget p 1284 N94-16373
Retrieval of biophysical parameters with AVIRIS and ISM: The Landes Forest, south west France p 1068 N94-16681
Investigation of cloud properties and atmospheric stability with MODIS
[NASA-CR-193475] p 1107 N94-16717
The use of General Circulation Models in detecting climate change induced by greenhouse gases
[DE93-014369] p 1096 N94-16802
The feasibility of tropospheric and total ozone determination using a Fabry-Perot interferometer as a satellite-based nadir-viewing atmospheric sensor
[NASA-TM-109342] p 1102 N94-17214
Second flight of the Spacelab grille spectrometer during the Atlas-1 mission
[AERONAUTICA-ACTA-A-367-199] p 923 N94-17592
ATMOSPHERIC CORRECTION
An expert system shell for inferring vegetation characteristics: Atmospheric techniques (Task G)
[NASA-CR-194570] p 1082 N94-15531
New methods of generation of ultrashort laser pulses for ranging p 913 N94-15565
New perspectives for high accuracy SLR with second gpneration geodesic satellites p 916 N94-15585
Test plan for the evaluation of the initial capability of the National Satellite Test Bed: Phase 1D
[DOT/FAA/RD-93/20] p 876 N94-16025
Application of split window technique to TIMS data p 1064 N94-16601
Atmospheric corrections for TIMS estimated emittance p 1064 N94-16602
Atmospheric correction of AVIRIS data in ocean waters p 1070 N94-16690
A comparison of LOWTRAN-7 corrected Airborne Visible/Infrared Imaging Spectrometer (AVIRIS) data with ground spectral measurements p 1074 N94-16710
ATMOSPHERIC DENSITY
BRIDGE: A small scientific satellite for geodesy p 890 N94-17146
ATMOSPHERIC EFFECTS
A ray trace model for propagation loss
[AD-A266314] p 997 N94-16467
The 1991 AVIRIS/POLDER experiment in Camargue, France p 1070 N94-16691
Aircraft carrier exposure tests of cast magnesium alloys
[AD-A268260] p 962 N94-17418
Forecasting the ducting of electromagnetic waves on the mesoscale
[AD-A268101] p 1109 N94-17571
ATMOSPHERIC ELECTRICITY
Remote sensing of precipitation and electrification with a dual-polarization, coherent, wideband radar system
[AD-A267479] p 1004 N94-17364
ATMOSPHERIC ENTRY
Size distribution of interplanetary iron and stony particles related with deep-sea spherules p 1245 N94-16388
ATMOSPHERIC GENERAL CIRCULATION MODELS
Exploring the southern ocean response to climate change
[NASA-CR-194601] p 1112 N94-15680
Evapotranspiration and runoff from large land areas: Land surface hydrology for atmospheric general circulation models p 1083 N94-16029
The use of General Circulation Models in detecting climate change induced by greenhouse gases
[DE93-014369] p 1096 N94-16802
Surface energy balance modeling at mesoscale: The contribution of the future Earth observing system
[BCRS-91-04] p 1085 N94-17616
Boundary layer structure over areas of heterogeneous heat fluxes
[DE93-010657] p 1110 N94-17673
ATMOSPHERIC HEATING
Some thoughts on future rain mapping missions (TRMM follow-on) p 992 N94-15906
ATMOSPHERIC MODELS
Engineering Physics and Mathematics Division progress report, period ending 31 December 1992
[DE93-015118] p 1301 N94-14926
Sensitivity testing of a single-Doppler temperature retrieval and forecast system
[AD-A267278] p 1105 N94-14958
Mesoscale modeling of the atmosphere
[AD-A263236] p 1098 N94-15132
Short term weather forecasting in real time in a base weather station setting
[AD-A266872] p 1105 N94-15142
IAI topic: El Nino. Southern oscillation and interannual climate variability
[INPE-5410-PRE/1757] p 1111 N94-15186
Atmospheric transmittance between 1.0 and 2.0 micrometers
[AD-A267076] p 1098 N94-15539
Comparison of RADARC high-frequency radar performance prediction model and ROTHR Amchitka data
[AD-A267077] p 987 N94-15540
Two color satellite laser ranging upgrades at Goddard's 1.2m telescope facility p 915 N94-15581
Two wavelength satellite laser ranging using SPAD p 916 N94-15584
State-of-the-art satellite laser range modeling for geodetic and oceanographic applications p 916 N94-15586
Investigate wave-mean flow interaction and transport in the extratropical winter stratosphere
[NASA-CR-194555] p 1098 N94-15639
Some thoughts on future rain mapping missions (TRMM follow-on) p 992 N94-15906
Global Energy and Water Cycle Experiment (GEWEX) and the Continental-scale International Project (GCIP) p 994 N94-15918
Evolutionary implications of a steady-state water abundance on Venus p 1254 N94-16206
A Pluto thermal model p 1256 N94-16216
Vertical structure models of the 1990 equatorial disturbance on Saturn p 1277 N94-16333
Observations and modelling of winds and waves during the Surface Wave Dynamics Experiment. Report 1: Intensive observation period IOP-1, 20-31 October 1990
[AD-A266384] p 1113 N94-16517
The multivariate optimum interpolation analysis of meteorological data at the Fleet Numerical Oceanography Center
[AD-A266459] p 1106 N94-16568
Hyperspectral modeling for extracting aerosols from aircraft/satellite data p 1067 N94-16673
Oregon transect: Comparison of leaf-level reflectance with canopy-level and modelled reflectance p 1073 N94-16702
Discrimination among semi-arid landscape endmembers using the Spectral Angle Mapper (SAM) algorithm p 1074 N94-16711
Mechanistic models of soot formation
[AD-A267806] p 950 N94-17008
On-board spatial scientific experiment project on small satellites p 896 N94-17184
Phillips Laboratory global spectral numerical weather prediction model
[AD-A267293] p 1107 N94-17244
Optimization of satellite coverage in observing cause and effect changes in the ionosphere, magnetosphere, and solar wind
[AD-A267956] p 1102 N94-17493
Further development and testing of a second-order bulk boundary layer model
[AD-A268071] p 1109 N94-17552
Forecasting the ducting of electromagnetic waves on the mesoscale
[AD-A268101] p 1109 N94-17571
A two-layer quasi-geotrophic spherical model: Formulation and climatology
[DM-63] p 1110 N94-17593
Workshop on early Mars: How warm and how wet, part 2?
[NASA-CR-193503] p 1297 N94-17637

Boundary layer structure over areas of heterogeneous heat fluxes
[DE93-010657] p 1110 N94-17673

ATMOSPHERIC MOISTURE
Trapping of water vapor from an atmosphere by condensed silicate matter formed by high-temperature pulse vaporization p 1248 N94-16180
Empirical relationships among atmospheric variables from rawinsonde and field data as surrogates for AVIRIS measurements: Estimation of regional land surface evapotranspiration p 1074 N94-16712
An investigation of the Ground-Based High-Resolution Interferometer Sounder (GB-HIS) in a costal marine environment
[AD-A268052] p 1114 N94-17503
An analysis of simulated and actual DMSP SSM/T-2 brightness temperatures
[AD-A268103] p 1109 N94-17573

ATMOSPHERIC PHYSICS
Mesoscale modeling of the atmosphere
[AD-A263236] p 1098 N94-15132
Atmospheric transmittance between 1.0 and 2.0 micrometers
[AD-A267076] p 1098 N94-15539
Micro- and meso-scale simulations of magnetospheric processes related to the aurora and substorm morphology
[NASA-CR-193437] p 1102 N94-17527

ATMOSPHERIC PRESSURE
Transition metals in superheat melts
p 962 N94-16273

ATMOSPHERIC RADIATION
Statement on global climate change before the Subcommittee on Energy and Power, United States House of Representatives
[DE93-013163] p 1095 N94-16006

ATMOSPHERIC REFRACTION
Johnson-Gierhart program predictions of excess propagation loss for super-high frequency air-to-ground paths. Volume 2: Appendices
[AD-A267021] p 987 N94-15527
Two color satellite laser ranging upgrades at Goddard's 1.2m telescope facility p 915 N94-15581
Airborne 2 color ranging experiment
p 920 N94-15614
Johnson-Gierhart program predictions of excess propagation loss for super-high frequency air-to-ground paths. Volume 1: Theory and numerical results
[AD-A267105] p 988 N94-15649
Forecasting the ducting of electromagnetic waves on the mesoscale
[AD-A268101] p 1109 N94-17571

ATMOSPHERIC SCATTERING
Software for the derivation of scaled surface reflectances from AVIRIS data p 1072 N94-16700
Micro pulse laser radar
[NASA-CASE-GSC-13493-1] p 1004 N94-17322

ATMOSPHERIC SOUNDING
Streak camera based SLR receiver for two color atmospheric measurements p 914 N94-15573
Electron reversal ionizer for detection of trace species using a spherical cathode
[NASA-CASE-NPO-18870-1-CU] p 1185 N94-17329
Opposing mesoscale flows in a broken midlatitude squall line
[AD-A268011] p 1109 N94-17492
An investigation of the Ground-Based High-Resolution Interferometer Sounder (GB-HIS) in a costal marine environment
[AD-A268052] p 1114 N94-17503
EOS Laser Atmosphere Wind Sounder (LAWS) investigation
[NASA-CR-193445] p 1109 N94-17525

ATMOSPHERIC TEMPERATURE
Application of split window technique to TIMS data
p 1064 N94-16601
Atmospheric corrections for TIMS estimated emittance
p 1064 N94-16602
An investigation of the Ground-Based High-Resolution Interferometer Sounder (GB-HIS) in a costal marine environment
[AD-A268052] p 1114 N94-17503
Propagation characteristics of mesoscale convective systems
[AD-A268130] p 1109 N94-17522
Boundary layer structure over areas of heterogeneous heat fluxes
[DE93-010657] p 1110 N94-17673

ATMOSPHERIC TURBULENCE
Effects of turbulence on the geodynamic laser ranging system p 921 N94-15616
Further development and testing of a second-order bulk boundary layer model
[AD-A268071] p 1109 N94-17552

ATMOSPHERIC WINDOWS
Separation of cirrus cloud from clear surface from AVIRIS data using the 1.38 micron water vapor band
p 1072 N94-16699

ATMOSPHERICS
Earth system dynamics: The interrelation of atmospheric, ocean and solid earth dynamics
[NASA-CR-193487] p 1081 N94-17444

ATOMIC BEAMS
Atomic beam studies relevant to the space environment
[AD-A268628] p 1186 N94-17436

ATOMIC CLOCKS
Quartz crystal resonators and oscillators for frequency control and timing applications: A tutorial, revision 6.1
[AD-A268205] p 1216 N94-17480

ATOMIC COLLISIONS
Atomic processes in hydrogen and deuterium negative ion discharges
[DE93-013432] p 1183 N94-16817

ATOMIC ENERGY LEVELS
Merged beam studies of laser stimulated radiative recombination
[AD-A267186] p 1037 N94-15145
Photodegradation of polyimides. V1: Effect of donor-acceptor groups on the photooxidative stability of polyimides and model compounds
[AD-A267319] p 970 N94-16947
The photochemistry of poly(methylphenylphosphazene)
[AD-A267320] p 970 N94-16948
The photophysics of poly(methylphenylphosphazene)
[AD-A267321] p 970 N94-16949

ATOMIC EXCITATIONS
Molecular processes in comets
[NASA-CR-194148] p 1239 N94-15188

ATOMIC INTERACTIONS
Single-collision studies of energy transfer and chemical reaction
[DE93-017603] p 1182 N94-16121

ATOMIC STRUCTURE
Electronic and atomic structure of semiconductors and of high-temperature superconductors
[AD-A266805] p 1205 N94-14913
Passive oxide films on well-defined nickel surfaces: An examination of film growth on Ni(100) with ex situ scanning tunneling microscopy
[DE93-014056] p 1207 N94-15923
Electronic structure and enthalpy of hydrogen and helium mixtures
[DE93-014128] p 1208 N94-15976
Photoemission study of diamond (100) surface
[DE93-015251] p 1208 N94-16062
Water adsorption on diamond (110) studied by multiple internal reflection infrared spectroscopy
[AD-A266415] p 948 N94-16553
Scintillation mechanism in stoichiometric cerium compounds
[DE93-015499] p 948 N94-16771
Growth and doping of Al(x)Ga(1-x)N films by electron cyclotron resonance assisted molecular beam epitaxy
[AD-A267305] p 1212 N94-16992
Atomic layer epitaxy group IV materials: Surface processes, thin films, devices and their characterization
[AD-A267527] p 1213 N94-17116
Theoretical studies of the crystal structure of rare earths and actinides at zero temperature
[DE93-016488] p 1214 N94-17301

ATOMIZERS
Coaxial airblast atomizers
[NASA-CR-193845] p 1016 N94-15109
Two-dimensional, high flow, precisely controlled monodisperse drop source
[AD-A267660] p 1028 N94-17250
Cryogenic spray vaporization in high-velocity helium, argon and nitrogen gasflows
[NASA-TM-106363] p 1035 N94-17446

ATOMIZING
Cryogenic spray vaporization in high-velocity helium, argon and nitrogen gasflows
[NASA-TM-106363] p 1035 N94-17446

ATOMS
Chemical and displacement atomic pair correlations in crystalline solid solutions recovered by anomalous x ray scattering in Fe-Ni alloys
[DE93-015906] p 1209 N94-16171

ATTENUATION COEFFICIENTS
Optical properties of the Red Sea
[AD-A266466] p 1113 N94-16588

ATTITUDE (INCLINATION)
Interferometric GPS attitude: A stochastic error model, DREO report
[AD-A266411] p 864 N94-16457
Tilt mechanism
[AD-D015780] p 1047 N94-16548
Space Station/Orbiter berthing dynamics during an assembly flight
[NASA-TM-109049] p 1062 N94-17451

ATTITUDE CONTROL
Standard platforms for small satellites
p 895 N94-17181
Space Station/Orbiter berthing dynamics during an assembly flight
[NASA-TM-109049] p 1062 N94-17451

ATTITUDE STABILITY
ERS-1: 18 months in orbit p 990 N94-15888

AUDIO EQUIPMENT
STS-29 IMAX camera audio class FFT
[NASA-TM-109543] p 1031 N94-15374

AUDITORY DEFECTS
Hearing Conservation Medical Program
p 1127 N94-16639

AUDITORY PERCEPTION
A virtual acoustic orientation instrument
[AD-A268181] p 1134 N94-17510

AUDITORY SENSATION AREAS
Cortical adaptive filtering in bioacoustic signal classification
[AD-A266229] p 1177 N94-16939

AUDITORY SIGNALS
Cortical adaptive filtering in bioacoustic signal classification
[AD-A266229] p 1177 N94-16939
A virtual acoustic orientation instrument
[AD-A268181] p 1134 N94-17510
Activities of the Research Laboratory of Electronics
[AD-A266730] p 1304 N94-17651

AUGER SPECTROSCOPY
A sulfur segregation study of PWA 1480, NiCrAl, and NiAl alloys
[NASA-TM-106289] p 956 N94-15992
Electron spectroscopy analysis
[NASA-CR-193591] p 951 N94-17039
Optimisation and specification of Auger electron spectrometers for signal-to-noise ratio performance
[NPL-DMM(A)-101] p 1006 N94-17549

AURORAL ARCS
Formation of the stable auroral arc that intensifies at substorm onset
[NASA-CR-193637] p 1098 N94-15433
Micro- and meso-scale simulations of magnetospheric processes related to the aurora and substorm morphology
[NASA-CR-193437] p 1102 N94-17527

AURORAL IONIZATION
Atmospheric ionization by solar particles detected by nitrate measurement in antarctic snow
[AD-A267583] p 1299 N94-17208

AURORAL SPECTROSCOPY
Global auroral imaging: Dynamics of Explorer Miss ion
[NASA-CR-194284] p 1097 N94-15003

AURORAL ZONES
A correlative comparison of geomagnetic storms and auroral substorms using geomagnetic indeces
[AD-A268081] p 1102 N94-17512

AURORAS
Global auroral imaging: Dynamics of Explorer Miss ion
[NASA-CR-194284] p 1097 N94-15003
Development of an ultra violet auroral imager for the Freja project p 904 N94-15060
A new detector concept for energetic auroral x ray imaging p 907 N94-15081
Requirements on CCD-detectors for ground-based auroral imaging p 909 N94-15093
Optical ionospheric instrumentation and research
[AD-A266403] p 1192 N94-16550
Multispectral observations of the Jovian aurora
[NASA-CR-193628] p 1297 N94-16884
An electromagnetic interference study of potential transmitter sites for the HF Active Auroral Research Program (HAARP)
[AD-A267743] p 1004 N94-17373
A correlative comparison of geomagnetic storms and auroral substorms using geomagnetic indeces
[AD-A268081] p 1102 N94-17512

AUSTENITE
Influence of grain size on the energy storing ability during uniaxial stretching of austenite steel
[IFTR-22/1992] p 961 N94-17121

AUSTRALIA
Space commerce in a global economy: Comparison of US and Australian approaches
[NASA-TM-109341] p 1235 N94-17290

AUTOCATALYSIS
Studies of premixed laminar and turbulent flames at microgravity
[NASA-CR-194656] p 951 N94-17125

AUTOMATED PILOT ADVISORY SYSTEM
The 1980 highlights
[NASA-TM-109672] p 1303 N94-15509

AUTOMATED TRANSIT VEHICLES
YARF: An open-ended framework for robot road following
[AD-A266788] p 1163 N94-14910
AUTOMATIC CONTROL
RACCOON: A Real-Time Autonomous Car Chaser Operating Optimally at Night
[AD-A266963] p 863 N94-14971
The Marshall Automated Weld System (MAWS)
[TABES PAPER 93-602] p 1049 N94-16138
Cognitive engineering models in space systems
[NASA-CR-193473] p 1140 N94-16716
An object-oriented program specification for a mobile robot motion control language
[AD-A267213] p 1166 N94-16986
Automated image analysis method for the detection of cracks on wood surface
[VTT-JULK-755] p 1056 N94-17542
AUTOMATIC FLIGHT CONTROL
Development of an air-to-air refueling automatic flight control system using quantitative feedback theory
[AD-A266718] p 870 N94-15730
AUTOMATIC WEATHER STATIONS
A comparison of ceiling and visibility observation for NWS manned observation sites and ASOS sites
[AD-A268356] p 1108 N94-17459
AUTOMATION
Fault management for data systems
[NASA-TM-103953] p 1116 N94-15548
AUTOMOBILES
RACCOON: A Real-Time Autonomous Car Chaser Operating Optimally at Night
[AD-A266963] p 863 N94-14971
Techno-economic requirements for automotive composites p 937 N94-16847
AUTONOMIC NERVOUS SYSTEM
Reliability of autonomic responses and malaise across multiple motion sickness stimulation tests
[NASA-TM-108787] p 1121 N94-15711
AUTONOMOUS NAVIGATION
YARF: An open-ended framework for robot road following
[AD-A266788] p 1163 N94-14910
Perception for outdoor navigation
[AD-A266867] p 863 N94-14919
Panacea: An active sensor controller for the ALVINN autonomous driving system
[AD-A266964] p 864 N94-14972
Massively parallel, adaptive, color image processing for autonomous road following
[AD-A266988] p 864 N94-15498
AVALANCHE DIODES
X-ray spectroscopy with silicon pin and avalanche photo diodes p 906 N94-15072
Work at Graz on satellite signatures p 898 N94-15558
Performance optimization of detector electronics for millimeter laser ranging p 913 N94-15569
Tracking capabilities of SPADs for laser ranging p 914 N94-15570
How to squeeze high quantum efficiency and high time resolution out of a SPAD p 914 N94-15571
Measuring atmospheric dispersion with WLRS in multiple wavelength mode p 916 N94-15582
The new MTLRS-1 receiving system p 877 N94-15611
The new MTLRS transmitting system p 877 N94-15612
AVIATION METEOROLOGY
Windshear database for forward-looking systems certification
[NASA-TM-109012] p 1108 N94-17283
AVIONICS
Development of a proposed international standard for certification of aircraft to High Intensity Radiated Fields (HIRF)
[NASA-TM-106357] p 863 N94-16520
Power Reactant Storage Assembly (PRSA) (Space Shuttle). PRSA hydrogen and oxygen DVT tank refurbishment
[NASA-CR-188262] p 926 N94-16922
Satellite communications installation plan
[AD-A266303] p 1000 N94-16965
Embedded computer systems: Status of C-17 software
[AD-A267307] p 1160 N94-16993
AXIAL LOADS
Design of a cruciform bend specimen for determination of out-of-plane biaxial tensile stress effects on fracture toughness for shallow cracks
[DE93-015455] p 1059 N94-16104
The processing and mechanical properties of high temperature/high performance composites. Book 5: Processing and miscellaneous properties
[AD-A266398] p 935 N94-16529
Overview of the FAA/DCA/NLR programs related to ageing aircraft
[NLR-TR-92119-U] p 854 N94-17614
AXIAL STRAIN
Damage evolution in filled elastomers
[AD-A268067] p 1062 N94-17507
AXIAL STRESS
Evaluation of the interfacial mechanical properties in fiber-reinforced ceramic composites
[DE93-015494] p 935 N94-16461
Evaluation of interfacial properties of fiber-reinforced ceramic composites using fiber push-in tests
[DE93-015427] p 972 N94-17253
AXISYMMETRIC BODIES
Wind tunnel investigation of three axisymmetric cowls of different lengths at Mach numbers from 0.60 to 0.92
[NASA-TM-4488] p 856 N94-15681
AZIDES (ORGANIC)
Amide and tetrazene complexes of transition and main group elements as precursors for the low temperature synthesis of elemental nitrides
[AD-A266246] p 950 N94-16931

B

B-70 AIRCRAFT
The 1968 highlights — NASA programs and research
[NASA-TM-109627] p 1302 N94-15413
BACKSCATTERING
Fine scale measurements of microwave backscatter from the ocean surface
[AD-A264516] p 1111 N94-15134
Double stimulated Brillouin scattering p 1200 N94-15205
Dynamics of douple stimulated Brillouin scattering p 1200 N94-15206
New methods of generation of ultrashort laser pulses for ranging p 913 N94-15565
Thomson backscattered x rays from an intense laser beam
[AD-A267125] p 1038 N94-15686
Method and apparatus for non-destructive evaluation of composite materials with cloth surface impressions
[NASA-CASE-LAR-14535-1] p 933 N94-15878
Radar response of vegetation: An overview p 991 N94-15898
Multifrequency observations p 992 N94-15902
Spatial and frequency diversity in lidar systems
[AD-A266192] p 1039 N94-16124
Radar properties of several fluidized ejecta blankets on Venus p 1267 N94-16278
Comparison of modeled backscatter with SAR data at P-band p 1076 N94-16735
SAR backscatter from coniferous forest gaps p 1076 N94-16736
Retrieval of pine forest biomass using JPL AIRSAR data p 1076 N94-16737
Relating multifrequency radar backscattering to forest biomass: Modeling and AIRSAR measurement p 1077 N94-16741
Investigation of AIRSAR signatures of the Gulf Stream p 1077 N94-16743
Detecting surface roughness effects on the atmospheric boundary layer via AIRSAR data: A field experiment in Death Valley, California p 1078 N94-16747
Extraction of quantitative surface characteristics from AIRSAR data for Death Valley, California p 1078 N94-16748
Fitting a three-component scattering model to polarimetric SAR data p 1079 N94-16751
Evaluation of polarimetric SAR parameters for soil moisture retrieval p 1079 N94-16755
Interaction types and their like-polarization phase-angle difference signatures p 1079 N94-16756
Lithological and textural controls on radar and diurnal thermal signatures of weathered volcanic deposits, Lunar Crater region, Nevada p 1080 N94-16762
BACKSCAT lidar simulation version 3.0: Technical documentation and users guide
[AD-A267296] p 1003 N94-17268
Characterization of Ni on Si wafers: Comparison of surface analysis techniques
[DE93-016501] p 953 N94-17649
BACKWARD WAVE TUBES
Measurements of the operation of the SINUS-6/BWO system
[AD-A266423] p 1011 N94-16556
BACKWARD WAVES
Measurements of the operation of the SINUS-6/BWO system
[AD-A266423] p 1011 N94-16556
BACTERIA
Efficacy of flocculating and other emergency water purification tablets
[AD-A266695] p 1148 N94-15840
Isolation of thermostable enzyme mutants by cloning and selection in thermophilic bacteria
[AD-A266378] p 1117 N94-16514
Biofilm structure and diversity
[AD-A267254] p 1118 N94-16989
Regulation of attached bacterial growth by adsorbed proteins
[AD-A267756] p 1118 N94-17275
BACTERIOLOGY
Legionella: An overview p 1126 N94-16629
BAFFLES
Acoustic waves in complicated geometries and their interactions with liquid-propellant droplet combustion
[AD-A267260] p 1178 N94-16991
BAILOUT
STS-35 Crew training: Bailout in CCT, firefighting, TAGS class and bailout in WFTF
[NASA-TM-109489] p 1135 N94-15195
STS-34 crew bailout exercise in CCT
[NASA-TM-109465] p 1135 N94-15360
STS-32 bailout training in WETF
[NASA-TM-109476] p 1136 N94-15383
STS-29 crew bailout in WETF
[NASA-TM-109548] p 1136 N94-15385
STS-33 emergency egress training
[NASA-TM-109525] p 1136 N94-15388
STS-31 crew training inflight maintenance and bailout exercises in CCT and WFTF
[NASA-TM-109483] p 876 N94-15450
STS-38 crew training: Habitation equipment procedures, bailout in CCT, 70mm photo class, EVA prep and post, and firefighting
[NASA-TM-109494] p 1136 N94-15453
STS-41 crew training bailout in CCT, 16mm camera class EVA prep, habitation equipment procedures, and food tasting
[NASA-TM-109517] p 876 N94-15517
BALLISTICS
An electronic imaging system for the Aeroballistic Research Facility
[AD-A267157] p 1033 N94-15826
BALLOON FLIGHT
Middle atmospheric electric fields over thunderstorms
[NASA-CR-194619] p 1106 N94-16493
BALLOON SOUNDING
The 1980 highlights
[NASA-TM-109672] p 1303 N94-15509
BALLOON-BORNE INSTRUMENTS
Silicon gallium doped photoconductor development for the AROME balloon borne instrument p 908 N94-15087
Mars laser altimeter based on a single photon ranging technique p 921 N94-15619
BALLOONING MODES
High beta and confinement studies of TFTR
[DE93-016204] p 1202 N94-16446
Structure and damping of toroidal drift waves (and their implications for anomalous transport)
[DE93-014005] p 1203 N94-16822
BANACH SPACE
Asymptotic behavior of firmly non expansive sequences
[DE93-628589] p 1171 N94-17642
Fixed point iterations for strictly hemi-contractive maps in uniformly smooth Banach spaces
[DE93-628591] p 1175 N94-17644
Steepest descent approximations for accretive operator equations
[DE93-628586] p 1171 N94-17667
BAND STRUCTURE OF SOLIDS
Optoelectronics based on SiGe/Si heterostructures
[AD-A267178] p 1190 N94-15848
Theoretical studies of the crystal structure of rare earths and actinides at zero temperature
[DE93-016488] p 1214 N94-17301
BANDPASS FILTERS
Filters for the International Solar Terrestrial Physics (ISTP) mission far ultraviolet imager
[NASA-CR-194633] p 1190 N94-15868
JPL activities on development of acousto-optic tunable filter imaging spectrometer p 1037 N94-16696
BANDWIDTH
Bandwidth characteristics of multimedia data traffic on a local area network
[NASA-TM-104026] p 883 N94-15648
Low-Complexity, High-Performance Bandwidth Efficient Coding and Coded Modulation Techniques for Satellite and Space Communications
[NASA-CR-194623] p 997 N94-16506
Bandwidth efficient coding: Theoretical limits and real achievements. Error control techniques for satellite and space communications p 997 N94-16507
An approximation for computing reduction in bandwidth requirements using intelligent multiplexers
[AD-A267434] p 1001 N94-17026

Isochronets: A high-speed network switching architecture
[AD-A267811] p 1161 N94-17409
BAROCLINITY
Mesoscale frontogenesis: An analysis of two cold front case studies
[AD-A267950] p 1107 N94-17054
BAROMETERS
Cooperative projects in geodynamical instrumentation between the State Seismological Bureau (China) and the Royal Observatory of Belgium p 1037 N94-15806
BARRIER LAYERS
Vacancy condensation as the precursor to passivity breakdown
[DE93-012925] p 956 N94-15998
BARYONS
The quantum mass shift of the soliton in Skyrme model
[ITN-93-85219] p 1180 N94-15283
BASALT
First oxygen from lunar basalt p 1249 N94-16182
Assimilation of solids during ascent of magmas from the Bartoy Field of the Baikal Region, Siberia p 1103 N94-16214
The physical mechanism of comet outbursts: An experiment p 1242 N94-16221
Bubble coalescence in magmas p 1103 N94-16237
Overturn of magma ocean ilmenite cumulate layer: Implications for lunar magmatic evolution and formation of a lunar core p 1261 N94-16242
Petrologic models of 15388, a unique Apollo 15 mare basalt p 1264 N94-16258
Searching for neuKREEP: An EMP study of Apollo 11 Group A basalts p 1266 N94-16275
On the composition of neuKREEP: QMD contamination at Apollo 11? p 1266 N94-16276
Angrite LEW87051: Are the olivines pheno's or xeno's? A continuing story p 1103 N94-16285
Partial melting of ordinary chondrites: Lost City (H) and St. Severin (LL) p 1243 N94-16286
The history of mare volcanism in the Orientale Basin: Mare deposit ages, compositions and morphologies p 1269 N94-16289
JSC-1: A new lunar regolith simulant p 1289 N94-16398
BATHYMETERS
Report detailing modifications to the 1/8 degree global bathymetry
[AD-A268178] p 1114 N94-17509
BAYES THEOREM
A new method for generating Bayes classifiers assuming mixtures of Gaussian densities
[FFI-91/4029] p 1172 N94-15298
A multilevel-multiresolution method for image processing. A Bayesian framework for reconstructing and representing shapes
[AD-A266772] p 1082 N94-15842
Set-based Bayesianism
[TR-407] p 1170 N94-16582
High order nonlinear estimation with signal processing applications
[AD-A268407] p 1005 N94-17463
BAYS (STRUCTURAL UNITS)
Computation of a controlled store separation from a cavity p 858 N94-16513
BEAM CURRENTS
Channel of the system for pulse charged particle beam diagnostics
[DE93-623867] p 1179 N94-14931
High beta and confinement studies of TFTR
[DE93-016204] p 1202 N94-16446
Fundamental-mode RF design in e(+)e(-) storage ring factories
[DE93-015249] p 1183 N94-16809
A review of some dynamics models in six-dimensional phase space and their suitable conditions of motion equation
[DE93-623741] p 1175 N94-17317
BEAM INJECTION
High beta and confinement studies of TFTR
[DE93-016204] p 1202 N94-16446
Six dimensional tracking simulator for H(-) injection in AGS Booster
[DE93-015396] p 1184 N94-16885
Emittance and beam size distortion due to linear coupling
[DE93-015402] p 1184 N94-16886
BEAM INTERACTIONS
Closed orbit distortion and the beam-beam interaction
[DE93-015284] p 1190 N94-15854
BEAM SPLITTERS
Display system employing acousto-optic tunable filter
[NASA-CASE-NPO-18736-1-CU] p 1190 N94-15933
VUV thin films, chapter 7
[NASA-CR-194634] p 967 N94-16494
Optical system storage design with diffractive optical elements p 1198 N94-17360
Test methods for acceptance testing of telescopes
[AD-A268316] p 1237 N94-17568
BEAMFORMING
Adaptive beamforming with imperfect arrays: Pattern effects and their partial correction
[AD-A267079] p 987 N94-15541
Broadband conventional beamforming incorporating adaptive equalization
[AD-A267090] p 987 N94-15544
BEAMS (RADIATION)
Experimental evaluation of an adaptive focusing algorithm for a microwave planar phased-array hyperthermia system at UCSF
[AD-A267004] p 1121 N94-15634
Six dimensional tracking simulator for H(-) injection in AGS Booster
[DE93-015396] p 1184 N94-16885
Laser beam steering device p 1045 N94-17357
BEAMS (SUPPORTS)
A novel approach for structural mechanics problems with stochasticity
[AD-A266189] p 1059 N94-16123
Static analysis of beams on an elastic base as stated by generalized functions
[IFTR-27/1991] p 1060 N94-16923
BEARINGS
Solid lubricants for space structures, phase 2
[AD-A266653] p 968 N94-16767
BED REST
Activity/rest patterns of instructor and rates student pilots during rapid transitions from daytime to nighttime duty hours at the Eastern Army Aviation Training site
[AD-A267038] p 1131 N94-15659
BEDROCK
Lithological and textural controls on radar and diurnal thermal signatures of weathered volcanic deposits, Lunar Crater region, Nevada p 1080 N94-16762
BEHAVIOR
The behavioral toxicology of high-peak, low average power, pulsed microwave irradiation
[AD-A268392] p 1134 N94-17535
BELLOWS
Design of a fluid elastic actuator with application to structure control
[AD-A267649] p 897 N94-17246
BENDING
Direct observation of fracture of CAS-glass/SiC composites and processing of toughened alumina
[AD-A268275] p 941 N94-17457
BENDING FATIGUE
The influence of secondary bending on fatigue life improvement in bolted joints
[ARL-RR-14] p 1058 N94-15963
BENZENE
Mechanistic models of soot formation
[AD-A267806] p 950 N94-17008
BERNOULLI THEOREM
Bounds on inconsistent inferences for sequences of trials with varying probabilities
[AD-A267146] p 1172 N94-15733
BERYLLIUM
Laboratory for x ray optics
[AD-A267149] p 1189 N94-15735
BETA PARTICLES
On the 17-keV neutrino
[DE93-012638] p 1181 N94-15974
Neutrino mass and mixing: Summary of the neutrino sessions
[DE93-014342] p 1183 N94-16801
Neutral-current detection in the Sudbury Neutrino Observatory
[DE93-014481] p 1185 N94-16951
BIAS
Timebias corrections to predictions p 875 N94-15591
Formation of on-site normal points p 917 N94-15592
Laser ranging data analysis
[NASA-CR-193547] p 1041 N94-16719
BIBLIOGRAPHIES
Bibliography on snow and ice friction
[AD-A266868] p 1045 N94-14920
SeaWiFS technical report series. Volume 12, SeaWiFS technical report series cumulative index: Volumes 1-11
[NASA-TM-104566-VOL-12] p 1111 N94-15529
Aeronautical engineering: A continuing bibliography with indexes (supplement 295)
[NASA-SP-7037(295)] p 854 N94-16480
Commonwealth of Independent States aerospace science and technology, 1992: A bibliography with indexes
[NASA-SP-7106] p 854 N94-16481
Publications of the Exobiology Program for 1991: A special bibliography
[NASA-TM-4483] p 1139 N94-17017
Bibliography of short wavelength chemical laser research
[AD-A267619] p 1041 N94-17195
The 1990-1991 NASA space biology accomplishments
[NASA-TM-4501] p 1118 N94-17257
Abstracts of manuscripts submitted in 1992 for publication
[AD-A267963] p 1113 N94-17383
BINARY ALLOYS
Transient phenomena following precipitation and re-solution anneals in a NiTi alloy
[AD-A267557] p 961 N94-17106
BINARY CODES
Search for optimal distance spectrum convolutional codes p 998 N94-16509
BINARY DATA
Spatial filters for optical correlation
[AD-A267199] p 1189 N94-15791
Unipolar terminal-attractor based neural associative memory with adaptive threshold
[NASA-CASE-NPO-18790-1-CU] p 1165 N94-15958
BINARY MIXTURES
Rheology and microstructure of concentrated zirconia-alumina suspensions for gelcasting composites
[DE93-015339] p 966 N94-16016
BINARY PHASE SHIFT KEYING
Low-Complexity, High-Performance Bandwidth Efficient Coding and Coded Modulation Techniques for Satellite and Space Communications
[NASA-CR-194623] p 997 N94-16506
A simulation study of the performance of the NASA (2,1,6) convolutional code on RFI/burst channels p 997 N94-16508
BINARY SYSTEMS (MATERIALS)
Highly transient elastodynamic crack growth in a bimaterial interface: Higher order asymptotic analysis and optical experiments
[AD-A266465] p 1059 N94-16587
BINAURAL HEARING
Leak detection utilizing analog binaural (VLSI) techniques
[NASA-CASE-NPO-18399-1-CU] p 1014 N94-17323
BINDERS (MATERIALS)
Fabrication of advanced design (grooved) cermet anodes
[DE93-014590] p 1012 N94-16765
Thin composite solid electrolyte film for lithium batteries
[NASA-CASE-NPO-18694-1-CU] p 1014 N94-17325
BINOMIAL THEOREM
The distribution of a sum of binomial random variables
[AD-A266969] p 1172 N94-15002
BIOACOUSTICS
Cortical adaptive filtering in bioacoustic signal classification
[AD-A266229] p 1177 N94-16939
BIOASTRONAUTICS
Movement in microgravity
[NASA-TM-109526] p 881 N94-15389
Exposure fluctuations of astronauts due to orientation
[NASA-TP-3364] p 1300 N94-15816
Aircrew/groundcrew life support systems research. Volume 1: CLIN 0001 research requirements
[AD-A268229] p 1139 N94-17563
Aircrew/groundcrew life support systems research. Volume 2: CLIN 0002 task order requirements
[AD-A268230] p 1139 N94-17564
BIOCHEMISTRY
Evaluation of spatial productivity patterns in an annual grassland during an AVIRIS overflight
[CIW-PUBL-1134] p 1067 N94-16672
A linear spectral matching technique for retrieving equivalent water thickness and biochemical constituents of green vegetation p 1068 N94-16678
Exploring the remote sensing of foliar biochemical concentrations with AVIRIS data p 1069 N94-16683
Biofilm structure and diversity
[AD-A267254] p 1118 N94-16989
Aircrew/groundcrew life support systems research. Volume 2: CLIN 0002 task order requirements
[AD-A268230] p 1139 N94-17564
BIOCONVERSION
Publications of the Oak Ridge National Laboratory Fossil Energy Program, 1 October 1991 - 31 March 1993
[DE93-014643] p 1232 N94-16967
BIODYNAMICS
Living well in space: Ensuring crew capability
[NASA-TM-109538] p 1120 N94-15369
BIOGEOCHEMISTRY
Strategies for detection of floodplain inundation with multi-frequency polarimetric SAR p 1076 N94-16739

BIOLOGICAL EFFECTS
Determination of the electromagnetic fields radiated from the ARES EMP simulator
[AD-A267069] p 988 N94-15668
Aerospace medicine and biology: A continuing bibliography with indexes (supplement 378)
[NASA-SP-7011(378)] p 1122 N94-16478
Aerospace medicine and biology: A continuing bibliography with indexes (supplement 380)
[NASA-SP-7011(380)] p 1122 N94-16479
TransRapid TR-07 maglev-spectrum magnetic field effects on daily pineal indoleamine metabolic rhythms in rodents
[DE93-015143] p 1117 N94-16893
The role of constitutive and inducible processes in the response of human squamous cell carcinoma cell lines to ionizing radiation
[DE93-015150] p 1129 N94-16970
Bioeffects of radiofrequency radiation on cell growth and differentation. Volume 1: Engineering considerations
[AD-A267754] p 1118 N94-17232
The behavioral toxicology of high-peak, low average power, pulsed microwave irradiation
[AD-A268392] p 1134 N94-17535
BIOLOGICAL EVOLUTION
Publications of the Exobiology Program for 1991: A special bibliography
[NASA-TM-4483] p 1139 N94-17017
BIOMASS
Recent advances in radar remote sensing of forest p 991 N94-15897
Using endmembers in AVIRIS images to estimate changes in vegetative biomass p 1070 N94-16689
Measuring dry plant residues in grasslands: A case study using AVIRIS p 1072 N94-16697
Retrieval of pine forest biomass using JPL AIRSAR data p 1076 N94-16737
Relating multifrequency radar backscattering to forest biomass: Modeling and AIRSAR measurement p 1077 N94-16741
Biomass energy: State of the technology present obstacles and future potential
[DE93-016295] p 1092 N94-16766
BIOPHYSICS
Driving terrestrial ecosystem models from space p 991 N94-15896
Bioorganic models for protein ion channels
[AD-A266365] p 1117 N94-16441
Retrieval of biophysical parameters with AVIRIS and ISM: The Landes Forest, south west France p 1068 N94-16681
BIOPROCESSING
An advanced bioprocessing concept for the conversion of wastepaper to ethanol
[DE93-015209] p 975 N94-16807
Publications of the Oak Ridge National Laboratory Fossil Energy Program, 1 October 1991 - 31 March 1993
[DE93-014643] p 1232 N94-16967
BIOREACTORS
Biofilm structure and diversity
[AD-A267254] p 1118 N94-16989
BIOSATELLITES
Ontogenesis of mammals in microgravity
[NASA-TM-103978] p 1139 N94-17636
BIOTECHNOLOGY
Materials Research Society Symposium Proceedings, Volume 292: Biomolecular Materials
[AD-A265776] p 1116 N94-15138
Annual historical report, calendar year 1992
[AD-A267050] p 1121 N94-15663
Canadian microgravity experiments flown in 1989-1990 p 977 N94-16075
BIPOLAR TRANSISTORS
Large signal characterization and modeling of heterojunction bipolar transistors
[AD-A266184] p 1012 N94-16935
BIREFRINGENCE
Characterization facility for magneto-optic media and systems p 1226 N94-14983
Measurement of birefringence for optical recording disk substrates p 1227 N94-14989
Pulse propagation in inhomogeneous optical waveguides
[DE93-013378] p 1191 N94-16007
Subwavelength structured surfaces and their applications p 1194 N94-17337
BIT ERROR RATE
Using Markov chains to model the error behavior of data communications channels
[AD-A266468] p 999 N94-16777
BITUMENS
Terrestrial bitumen analogue of orgueil organic material demonstrates high sensitivity to usual HF-HCl treatment p 930 N94-16325
BIVARIATE ANALYSIS
Statistics of the half-integer stopband
[DE93-016101] p 1173 N94-17236
BLACK BODY RADIATION
Fast-ICCD photography and gated photon counting measurements of blackbody emission from particulates generated in the KrF-laser ablation of BN and YBC
[DE93-015491] p 1210 N94-16460
BLACK HOLES (ASTRONOMY)
SUSY in the sky
[NIKHEF-H/93-04] p 1240 N94-17603
BLACKOUT (PHYSIOLOGY)
Cumulative effect of repeated brief cerebral ischemia
[AD-A267155] p 1121 N94-15736
BLADE TIPS
Turbine blade tip film cooling measurements
[AD-A267686] p 868 N94-14964
BLANKETS
Improved composite flexible blanket insulation
[NASA-CASE-ARC-11955-1-CU] p 934 N94-15926
BLASIUS FLOW
Inviscid instability of streamwise corner flow
[NASA-CR-191514] p 1021 N94-15834
BLINDNESS
Enhancing sight
[NASA-TM-109637] p 1221 N94-15248
BLOCK COPOLYMERS
Vectorial electron transfer in spatially ordered arrays
[DE93-018150] p 1185 N94-16971
BLOCKING
Optimisation of FIR photoconductors for atmospheric spectroscopy p 902 N94-15048
BLOOD
A mathematical model for the study of hemorrhagic shock and fluid resuscitation: Transcapillary exchange
[AD-A266427] p 1123 N94-16544
Bloodborne Pathogens Program p 1127 N94-16644
OSHA bloodborne pathogens standards exposure control plan p 1127 N94-16645
Release of iron from hemoglobin
[AD-A266503] p 1128 N94-16784
Methods to obtain blood samples periodically during exercise research studies while subjects are immersed in water or otherwise inaccessible
[AD-A268227] p 1130 N94-17562
Currents induced in the human body for exposure to ultrawideband electromagnetic pulses
[AD-A268570] p 1130 N94-17621
BLOOD CIRCULATION
A mathematical model for the study of hemorrhagic shock and fluid resuscitation: The systemic and pulmonary vasculature
[AD-A266835] p 1119 N94-14917
Increased vascular resistance with hemoglobin-based oxygen carriers
[AD-A266454] p 1123 N94-16565
The nature of dynamic arteriolar vasoreactivity: A mini-review and A classification scheme
[AD-A266499] p 1128 N94-16783
BLOOD FLOW
A mathematical model for the study of hemorrhagic shock and fluid resuscitation: The systemic and pulmonary vasculature
[AD-A266835] p 1119 N94-14917
Neuropeptide-Y (NPY) increases total blood flow in the tail, and reduces cutaneous microvascular blood flow in the tail and foot of the rat
[AD-A266839] p 1115 N94-14918
Transcranial Doppler ultrasound studies of cerebral blood-flow in microgravity p 981 N94-16095
The nature of dynamic arteriolar vasoreactivity: A mini-review and A classification scheme
[AD-A266499] p 1128 N94-16783
Automated strain gauge plethysmograph
[AD-A267323] p 1035 N94-17002
BLOOD PLASMA
A review of the efficacy of 7.5 percent NaCl/6 percent Dextran-70 (HSD) in experimental animals and humans
[AD-A266633] p 1122 N94-15740
BLOOD VESSELS
The nature of dynamic arteriolar vasoreactivity: A mini-review and A classification scheme
[AD-A266499] p 1128 N94-16783
BLOOD VOLUME
A mathematical model for the study of hemorrhagic shock and fluid resuscitation: The systemic and pulmonary vasculature
[AD-A266835] p 1119 N94-14917
A review of the efficacy of 7.5 percent NaCl/6 percent Dextran-70 (HSD) in experimental animals and humans
[AD-A266633] p 1122 N94-15740
A mathematical model for the study of hemorrhagic shock and fluid resuscitation: Transcapillary exchange
[AD-A266427] p 1123 N94-16544
A mathematical model for the study of hemorrhagic shock and fluid resuscitation: Exchange of fluid and solutes between vascular, interstitial, and tissue cell compartments
[AD-A266426] p 1123 N94-16558
BLOWING
Aerodynamic control of NASP-type vehicles through Vortex manipulation. Volume 1: Static water tunnel tests
[NASA-CR-177626-VOL-1] p 855 N94-15655
Aerodynamic control of NASP-type vehicles through Vortex manipulation. Volume 2: Static wind tunnel tests
[NASA-CR-177626-VOL-2] p 856 N94-15677
Aerodynamic control of NASP-type vehicles through vortex manipulation. Volume 3: Wing rock experiments
[NASA-CR-177626] p 857 N94-15780
BLUE STREAK LAUNCH VEHICLE
The launch of ELDO
[ESA-HSR-7] p 886 N94-16501
BLUNT BODIES
DSMC simulations of Mach 20 nitrogen flows about a 70 degree blunted cone and its wake
[NASA-TM-107762] p 1018 N94-15291
Particle simulation of hypersonic flow
[AD-A267185] p 857 N94-15787
Search for chaos in free shear flows
[AD-A266245] p 1023 N94-16470
Nonequilibrium radiation and chemistry models for aerocapture vehicle flowfields
[NASA-CR-194645] p 1027 N94-17095
BODY CENTERED CUBIC LATTICES
Electronic structure and enthalpy of hydrogen and helium mixtures
[DE93-014128] p 1208 N94-15976
Interfacial structure of lattice mismatched bcc(110)/bcc(110) transition metal superlattices
[DE93-015162] p 1208 N94-16058
High temperature materials technology research for advanced thermionic systems
[DE93-018302] p 960 N94-16964
BODY FLUIDS
A mathematical model for the study of hemorrhagic shock and fluid resuscitation: Exchange of fluid and solutes between vascular, interstitial, and tissue cell compartments
[AD-A266426] p 1123 N94-16558
OSHA bloodborne pathogens standards exposure control plan p 1127 N94-16645
BODY-WING AND TAIL CONFIGURATIONS
Aerodynamic control of NASP-type vehicles through vortex manipulation. Volume 3: Wing rock experiments
[NASA-CR-177626] p 857 N94-15780
BODY-WING CONFIGURATIONS
The effect of the nose shape and wing location toward the wing vortex breakdown
[AD-A267724] p 855 N94-14942
BOEING 727 AIRCRAFT
Satellite communications installation plan
[AD-A266303] p 1000 N94-16965
BOEING 747 AIRCRAFT
Computation of the Fluid and Optical Fields About the Stratospheric Observatory for Infrared Astronomy (SOFIA) and the Coupling of Fluids, Dynamics, and Control Laws on Parallel Computers
[NASA-CR-193168] p 858 N94-16510
BOILING
Pool boiling: Single bubble experiment p 944 N94-15160
Explosive boiling at very low heat fluxes: A microgravity phenomenon
[NASA-TM-106325] p 1046 N94-15817
Cellulose triacetate, thin film dielectric capacitor
[NASA-CASE-NPO-18935-1-CU] p 1010 N94-15952
Investigation of two-phase flow and boiling heat transfer during quenching of a tube under microgravity p 979 N94-16087
Cycle performance testing of nonazeotropic mixtures of HFC-142A/HCFC-124 and HFC-32/HCFC-124 with enhanced surface heat exchangers
[DE93-015215] p 1024 N94-16808
BOLOMETERS
Future development in cryogenic techniques for space p 901 N94-15042
Hot electron mixers, the potential competition p 903 N94-15055
Submm/FIR bolometers p 904 N94-15056
Developments in extreme ultraviolet and x ray instrumentation p 904 N94-15058
In orbit adiabatic demagnetization refrigeration for bolometric and microcalorimetric detectors p 907 N94-15079
The epitaxial Si x ray bolometer an alternative to ion implanted devices p 911 N94-15103
BOLTED JOINTS
The influence of secondary bending on fatigue life improvement in bolted joints
[ARL-RR-14] p 1058 N94-15963

BOLTZMANN TRANSPORT EQUATION
Discrete models of the Boltzmann equation: Structure of the collision operator of sound propagation
[IFTR-2/1992] p 1178 N94-17051
Linear characteristic spatial quadrature for discrete ordinates neutral particle transport on arbitrary triangles
[AD-A267485] p 1185 N94-17365
Calculations of cosmic-ray helium transport in shielding materials
[NASA-TP-3354] p 1301 N94-17666
BOLTZMANN-VLASOV EQUATION
Linear stability of stationary solutions of the Vlasov-Poisson system in three dimensions
[DE93-013873] p 1174 N94-16820
BONDED JOINTS
XPS analysis of Al/EPDM bondlines from IUS SRM-1 polar bosses
[AD-A266851] p 1056 N94-14945
Physical interpretation and development of ultrasonic nondestructive evaluation techniques applied to the quantitative characterization of textile composite materials
[NASA-CR-194549] p 931 N94-15190
BONDING
Evaluation of interfacial properties of fiber-reinforced ceramic composites using fiber push-in tests
[DE93-015427] p 972 N94-17253
BONDOC METEORITE
Cation ordering in orthopyroxenes and cooling rates of meteorites: Low temperature cooling rates of Estherville, Bondoc and Shaw p 1241 N94-16176
BONES
Micromechanics modeling and analysis of Haversian compact bone tissues as a fiber reinforced composite material
[AD-A268250] p 1129 N94-17456
BOOSTER ROCKET ENGINES
CPIA/M5 liquid propellant engine manual
[AD-A268062] p 929 N94-17589
BOREHOLES
Water-levels fluctuations in a borehole at the Royal Observatory of Belgium: Effects on local gravity, Earth tidal, and barometric responses p 1100 N94-15812
BORESIGHT ERROR
Radome depolarization effects on monopulse receiver tracking performance
[AD-A267446] p 1001 N94-17031
BORESIGHTS
Radome depolarization effects on monopulse receiver tracking performance
[AD-A267446] p 1001 N94-17031
BORON ISOTOPES
Nuclear fusion of protons with ions of boron
[DE93-015399] p 1202 N94-16019
BORON NITRIDES
Atomic layer epitaxy of boron nitride
[AD-A266260] p 1212 N94-16932
Growth of dielectric thin films by irradiation of condensed molecular precursors with synchrotron radiation
[DE93-016161] p 974 N94-17676
BOSONS
Theoretical high energy physics
[DE93-015884] p 1187 N94-16170
Heavy ion physics research at Creighton University
[DE93-016809] p 1185 N94-16957
BOUNDARY CONDITIONS
Boundary conditions for the paleoenvironment: Chemical and physical processes in the pre-solar nebula
[NASA-CR-194418] p 1298 N94-15421
Shielding from space radiations
[NASA-CR-194578] p 1180 N94-15715
A novel approach for structural mechanics problems with stochasticity
[AD-A266189] p 1059 N94-16123
An analysis of ways of determining the material constants for viscoelastic materials
[IFTR-28/91] p 951 N94-17050
Structured finite volume modeling of US Navy aircraft engine test cells. Task 1: Turboshaft engine, volume 1
[AD-A268176] p 873 N94-17432
Boundary conditions and the simulation of low Mach number flows
[NASA-TM-106374] p 1029 N94-17448
Global solutions to a system of strongly coupled reaction-diffusion equations
[DE93-628587] p 1171 N94-17640
BOUNDARY LAYER CONTROL
The turbulent wall jet
[AD-A267675] p 855 N94-14963
Riblets: New speed technology
[NASA-TM-109641] p 1018 N94-15252
Flow analysis for the nacelle of an advanced ducted propeller at high angle-of-attack and at cruise with boundary layer control
[NASA-TM-106371] p 858 N94-16571
Determining the effect of endwall boundary layer suction in a large scale subsonic compressor cascade
[AD-A267208] p 859 N94-16913
Active turbulence control in wall bounded flows using direct numerical simulation
[AD-A267261] p 1028 N94-17286
BOUNDARY LAYER EQUATIONS
Boundary layer flow of air over water on a flat plate
[NASA-CR-191517] p 1019 N94-15479
BOUNDARY LAYER FLOW
On the receptivity problem for 0(1) wavelength Goertler vortices
[NASA-CR-191519] p 1016 N94-15005
Tollmien-Schlichting/vortex interactions in compressible boundary layer flows
[NASA-CR-191515] p 1017 N94-15183
Special course on Shock-Wave/Boundary-Layer Interactions in Supersonic and Hypersonic Flows
[AGARD-R-792] p 1017 N94-15196
Swept shock/boundary-layer interactions: Scaling laws, flowfield structure, and experimental methods
p 1017 N94-15197
On the interaction between the shock wave attached to a wedge and freestream disturbances
[NASA-CR-191528] p 1019 N94-15478
Boundary layer flow of air over water on a flat plate
[NASA-CR-191517] p 1019 N94-15479
Parallel spatial direct numerical simulations on the Intel iPSC/860 hypercube
[NASA-CR-191513] p 1144 N94-15483
Complex terrain wind model evaluation
[AD-A266467] p 1096 N94-16589
Three-dimensional turbulent boundary layer
[AD-A266261] p 1025 N94-16908
Studies in turbulence and turbulence control
[AD-A266318] p 1026 N94-16950
Higher-order accurate Osher schemes with application to compressible boundary layer stability
[NASA-TM-106355] p 1026 N94-17056
Structure of turbulence in three-dimensional boundary layers
[NASA-CR-194655] p 1027 N94-17130
On the stability of a time dependent boundary layer
[NASA-CR-191542] p 1030 N94-17450
BOUNDARY LAYER SEPARATION
Unsteady separated flows: Empirical model and control
[AD-A267282] p 855 N94-14959
Swept shock/boundary-layer interactions: Scaling laws, flowfield structure, and experimental methods
p 1017 N94-15197
BOUNDARY LAYER STABILITY
Numerical study of compressible boundary-level transition between two concentric cylinders
[NASA-CR-194622] p 1025 N94-16842
Higher-order accurate Osher schemes with application to compressible boundary layer stability
[NASA-TM-106355] p 1026 N94-17056
On the stability of a time dependent boundary layer
[NASA-CR-191542] p 1030 N94-17450
Multigrid direct numerical simulation of the whole process of flow transition in 3-D boundary layers
[NASA-TM-106369] p 1030 N94-17557
BOUNDARY LAYER TRANSITION
Development of a quiet supersonic wind tunnel with a cryogenic adaptive nozzle
[NASA-CR-194548] p 871 N94-15117
Parallel spatial direct numerical simulations on the Intel iPSC/860 hypercube
[NASA-CR-191513] p 1144 N94-15483
Receptivity of boundary layers to convected gusts
[AD-A267206] p 1022 N94-15860
Turbulence and transition modeling for high-speed flows
[AD-A266748] p 1022 N94-15953
Natural convection above a horizontal heat source
[AD-A267212] p 1026 N94-16985
An experimental study of fluctuating wall pressures in a highly swept, sharp fin-induced, Mach 5 shock wave/turbulent boundary layer interaction
[AD-A268394] p 861 N94-17461
Multigrid direct numerical simulation of the whole process of flow transition in 3-D boundary layers
[NASA-TM-106369] p 1030 N94-17557
BOUNDARY LAYERS
Unsteady phenomena in shock wave/boundary layer interaction p 1017 N94-15200
Hypersonic shock wave boundary layer interactions over simplified deflected control surface configurations
p 1018 N94-15203
Supersonic flow visualization of a nacelle in close proximity to a simulated wing
[NASA-CR-194675] p 860 N94-17260
The stability and dynamics of elastic structures and fluid flows
[AD-A267990] p 1029 N94-17414
On the stability of a time dependent boundary layer
[NASA-CR-191542] p 1030 N94-17450
Boundary layer structure over areas of heterogeneous heat fluxes
[DE93-010657] p 1110 N94-17673
BOUNDARY LUBRICATION
Physical and chemical properties of some new perfluoropolyalkylether lubricants prepared by direct fluorination
[NASA-TM-106299] p 967 N94-16543
BOUNDARY VALUE PROBLEMS
Iteration scheme for the multiparameter nonlinear boundary value problem with the additional conditions and its application to some field models
[DE93-626638] p 1168 N94-14933
A posteriori error estimation for hierarchic models of elliptic boundary value problems on thin domains
[AD-A267714] p 1168 N94-14939
Adaptive wavelet collocation methods for initial value boundary problems of nonlinear PDE's
[NASA-CR-191507] p 1169 N94-15833
Finite difference time domain analysis of chirped dielectric gratings p 1195 N94-17339
Numerical solution of a second order boundary problem for two dimensions using galerkin approximations
[AD-A268128] p 1171 N94-17521
Numerically solving a transient heat conduction problem with convection and radiation
[AD-A268521] p 1220 N94-17540
Global solutions to a system of strongly coupled reaction-diffusion equations
[DE93-628587] p 1171 N94-17640
BRACKETS
RSRM nozzle actuator bracket/lug fracture mechanics qualification test
[NASA-CR-193859] p 927 N94-17080
BRAIDED COMPOSITES
Design and cost drivers in 2-D braiding
p 937 N94-16849
Development of braided fiber seals for engine applications p 939 N94-16859
Development of test methods for textile composites
p 939 N94-16862
Three-dimensional analysis of anisotropic spatially reinforced structures p 939 N94-16863
Evaluation of hybrid reinforcement (fiber-reinforced-plastic rod with steel core)
[AD-A268009] p 941 N94-17473
BRAIN
Neural mechanisms of attention
[AD-A266315] p 1132 N94-16456
Localizing visual function in the brain
[AD-A267381] p 1133 N94-17020
Synaptic plasticity and memory formation
[AD-A267988] p 1133 N94-17453
BREADBOARD MODELS
Results of an electrical power system fault study (CDDF)
[NASA-TP-3413] p 884 N94-15007
TRMM radar p 990 N94-15894
Wideband acousto-optic correlator for an ESM receiver upgrade
[TABES PAPER 93-661] p 1054 N94-16156
BREATHING APPARATUS
An apparatus for measuring the biological oxidation of hydrogen gas under hyperbaric conditions
[AD-A266834] p 1119 N94-14916
Firefighters breathing system
[NASA-TM-109611] p 1135 N94-15362
BRECCIA
First investigation of noble gases in the Dengli H3,8 chondrite p 953 N94-16264
A discontinuous melt sheet in the Manson impact structure p 1103 N94-16269
A Monazite-bearing clast in Apollo 17 melt breccia
p 1267 N94-16279
Apollo 17 materials viewed from 2 to 4 mm soil particles: Pre-serenitatis highlands components
p 1267 N94-16280
Partial melting of ordinary chondrites: Lost City (H) and St. Severin (LL) p 1243 N94-16286
Nitrogen isotopic signatures in agglutinates from breccia 79035 p 954 N94-16314
BREMSSTRAHLUNG
ARIES tokamak reactor study
[DE93-017059] p 1203 N94-16901
BRIDGMAN METHOD
Growth of new materials for solid state laser applications. The growth of ZnGeP2 by the vertical Bridgman method
[NASA-CR-194571] p 1038 N94-15530
Convection effects on radial segregation and crystal melt interface in vertical Bridgman growth
[NASA-CR-191541] p 1029 N94-17387
BRIGHTNESS
Effects of levitated dust on astronomical observations from the lunar surface p 1239 N94-16433

Perception of lightness and brightness in complex patterns
[AD-A268435] p 1134 N94-17513
Study of brightness and current limitations in intense charged particle beams
[AD-A268283] p 1186 N94-17578

BRIGHTNESS DISTRIBUTION
Optical effects of regolith processes on S asteroids as simulated by laser impulse alteration of ordinary chondrite p 1246 N94-16422

BRIGHTNESS TEMPERATURE
Brightness temperature and attenuation statistics at 20.6 and 31.65 GHz p 996 N94-16045
A quantitative analysis of TIMS data obtained on the Learjet 23 at various altitudes p 1063 N94-16597
Analysis of TIMS performance subjected to simulated wind blast p 1063 N94-16598
Application of split window technique to TIMS data p 1064 N94-16601
Investigation of cloud properties and atmospheric stability with MODIS
[NASA-CR-193475] p 1107 N94-16717
Nowcasting methods for satellite imagery
[AD-A267294] p 1108 N94-17267
An analysis of simulated and actual DMSP SSM/T-2 brightness temperatures
[AD-A268103] p 1109 N94-17573
An empirical study of tropical cloud clusters using special sensor microwave imager data
[AD-A268072] p 1110 N94-17595

BRILLOUIN EFFECT
Studies on the parametric decay of waves in fusion plasmas
[VTT-PUBS-110] p 1200 N94-15204
Double stimulated Brillouin scattering p 1200 N94-15205
Dynamics of douple stimulated Brillouin scattering p 1200 N94-15206
Soliton-like structures in double stimulated Brillouin scattering p 1200 N94-15207

BRILLOUIN ZONES
Photoemission study of diamond (100) surface
[DE93-015251] p 1208 N94-16062

BRINES
Mars brine formation experiment p 1293 N94-16419

BRITTLE MATERIALS
Elastooptical brittle materials in experimental studies of the state of stress and deformation
[IFTR-22/1991] p 1059 N94-16651
Static and dynamic investigations of brittle elasto-optical material
[IFTR-3/1992] p 1061 N94-17086

BRITTLENESS
Recent advances in ordered intermetallics
[DE93-015308] p 955 N94-15862
A reexamination of grain boundary fracture in Ni3Al: Environmental and alloying effects
[DE93-015431] p 1208 N94-16063
The processing and mechanical properties of high temperature/high performance composites. Book 1: Coonstituent properties of composites
[AD-A266394] p 935 N94-16483
The processing and mechanical properties of high temperature/high performance composites. Book 2: Coonstituent properties and macroscopic performance
[AD-A266395] p 935 N94-16484
The processing and mechanical properties of high temperature/high performance composites. Book 4: Coonstitutive laws and design
[AD-A266397] p 935 N94-16528

BROADBAND
Broadband teleseismic array recording in the Adirondack Mountains, New York State
[AD-A267290] p 1097 N94-14960
Broadband conventional beamforming incorporating adaptive equalization
[AD-A267090] p 987 N94-15544
Theoretical studies relating to the interaction of radiation with matter
[AD-A267134] p 1180 N94-15689
Filters for the International Solar Terrestrial Physics (ISTP) mission far ultraviolet imager
[NASA-CR-194633] p 1190 N94-15868
Wideband acousto-optic correlator for an ESM receiver upgrade
[TABES PAPER 93-661] p 1054 N94-16156
Enhanced down-range profiles of complex targets using wideband radar echo returns
[AD-A266508] p 999 N94-16788
Design of broadband wire antennas for frequency hopping applications
[AD-A267405] p 1001 N94-17025
On-board B-ISDN fast packet switching architectures. Phase 1: Study
[NASA-CR-191143] p 883 N94-17111
The analysis of low-profile, broadband, monopole, vehicle antennas and matching network synthesis
[AD-A268340] p 1006 N94-17582

BROADCASTING
Activities of Canadian Satellite Communications, Inc.
[CTN-93-60864] p 994 N94-15959
Test plan for the evaluation of the initial capability of the National Satellite Test Bed: Phase 1D
[DOT/FAA/RD-93/20] p 876 N94-16025

BROKEN SYMMETRY
Broken symmetry in ideal magnetohydrodynamic turbulence
[NASA-TM-109017] p 1023 N94-15964

BROMIDES
The effect of process parameters on the surface finish of plasma polymers
[DE93-014112] p 966 N94-15924

BROMINATION
Interpenetrating polymer network acoustic damping material
[AD-D015889] p 969 N94-16916

BRUSHES
Solid lubricants for space structures, phase 2
[AD-A266653] p 968 N94-16767

BRUSHES (ELECTRICAL CONTACTS)
Integrated fundamental research on current collection
[AD-A266987] p 1008 N94-15494

BSCCO SUPERCONDUCTORS
Advanced thin-film deposition and physical properties of high-temperature and other novel superconducting materials
[AD-A268199] p 1216 N94-17561

BUBBLE CHAMBERS
Preliminary results from bubble detector measurements aboard Biocosmos-2044 p 981 N94-16097

BUBBLES
Pool boiling: Single bubble experiment p 944 N94-15160
Laser-liquid interactions under reduced gravity conditions p 977 N94-16077
Gas bubble generation and transport in microgravity p 980 N94-16089
Bubble coalescence in magmas p 1103 N94-16237
Measurement of the velocity field and void fraction in a planar plunging jet
[AD-A268183] p 1030 N94-17511

BUCKLING
Comparison of level-1 and level-2 buckling and postbuckling solutions
[NASA-CR-194611] p 1057 N94-15154

BUCKMINSTERFULLERENE
Geochemistry and cosmochemistry of fullerenes 3: Reaction of C60 and C70 with ozone p 953 N94-16243

BUDGETS
Resources and activities of the European Space Agency p 1303 N94-16792

BUILDINGS
Satellite sound broadcast propagation measurements p 996 N94-16047
Assessment of trends in the development of residential buildings from the standpoint of the fuel and energy requirements
[IFTR-6/1991] p 1093 N94-17092

BULK MODULUS
Physical and chemical properties of some new perfluoropolyalkylether lubricants prepared by direct fluorination
[NASA-TM-106299] p 967 N94-16543

BURGER EQUATION
Numerical solution of SUPG finite-element method for supersonic viscous flow
[AD-A267762] p 860 N94-17222

BURNING RATE
Spectral studies of solid propellant combustion 4: Absorption and burn rate results for M43, XM39, and M10 propellants
[AD-A267119] p 946 N94-15685

BUS CONDUCTORS
VLSI for high-speed digital signal processing
[AD-A267709] p 1007 N94-14936
OETC optical backplane bus testbed. IBM tasks: Receiver OEIC and link simulation tools and analysis
[AD-A266198] p 1191 N94-16128

BUSHINGS
Solid lubricants for space structures, phase 2
[AD-A266653] p 968 N94-16767

C

C (PROGRAMMING LANGUAGE)
User manual and program description of the data acquisition system of PML-pulse physics
[AD-A266752] p 1147 N94-15776

C BAND
Evaluation of the TOPSAR performance by using passive and active calibrators p 1078 N94-16750

C++ (PROGRAMMING LANGUAGE)
An experimental comparison of CLOS and C(++) implementations of an object-oriented graphical simulation of walking robot kinematics
[AD-A267168] p 1165 N94-15855
C++ as a language for object-oriented numerics
[DE93-015027] p 1148 N94-15985

C-135 AIRCRAFT
Canadian microgravity experiments flown in 1989-1990 p 977 N94-16075
Development of the Laser-based R/D Test-bed System (LTS) p 978 N94-16080
Optical systems for the visualization of fluid and solid transparent media under microgravity conditions p 978 N94-16081
KC-135 acceleration monitoring and data acquisition system p 868 N94-16090

CADMIUM TELLURIDES
CdTe array detectors for high energy astronomy p 899 N94-15029
Research support for cadmium telluride crystal growth
[NASA-CR-193557] p 1210 N94-16646
Laser figuring for the generation of analog micro-optics and kineform surfaces p 1196 N94-17346
Fabrication of micro-optical devices p 1197 N94-17351

CALCITE
CO2 production by impact in carbonates? An ATEM and stable isotope (C,O) study p 954 N94-16383

CALCIUM CARBONATES
Earth's partial pressure of CO2 over the past 100-500 Ma; evidence from Ce anomalies in mostly shallow seas (less than 200 m) as recorded in carbonate sediments, 2 p 1104 N94-16360

CALCIUM COMPOUNDS
The role of interfacial chemistry in surface nucleation and growth of calcium oxalate
[DE93-015689] p 1209 N94-16159
Transformation toughening of composite ceramics
[AD-A267304] p 971 N94-16980

CALCIUM ISOTOPES
The role of interfacial chemistry in surface nucleation and growth of calcium oxalate
[DE93-015689] p 1209 N94-16159

CALCIUM OXIDES
Low-temperature sintering and phase changes in chromite interconnect materials
[DE93-015676] p 961 N94-17234

CALIBRATING
Validation of respiratory inductive plethysmography for measuring exercise tidal volumes
[AD-A266883] p 1119 N94-14923
Free-field sensitivity calibration of laboratory standard microphones by the reciprocity technique: Measurements for the 1991 EEC intercomparison
[NPL-RSA(EXT)-0043] p 1176 N94-15019
A test facility to calibrate EUV detectors p 873 N94-15062
Characterization of detectors and calibration of the ISOPHOT experiment p 907 N94-15082
Infrared detector annealing and calibration with IR-laser diodes p 909 N94-15092
Windshear radar calibration, 1992 flights: Transmitter power and receiver gain stability
[NASA-TM-108997] p 986 N94-15140
Testing and management of flight instruments and their data
[NASA-CR-194332] p 868 N94-15187
Heterodyne efficiency for a coherent laser radar with diffuse or aerosol targets
[NASA-CR-194563] p 1038 N94-15477
The precision of today's satellite laser ranging systems p 912 N94-15559
Sub-cm ranging and other improvements in Graz p 919 N94-15603
Optical attenuation mechanism upgrades, MOBLAS, and TLRS systems p 922 N94-15622
Calibration platforms for gravimeters p 1037 N94-15805
On tidal parameters at Brussels fundamental station p 1100 N94-15807
Calibration: Practical experience with ERS-1 p 992 N94-15907
A calibration of the production rate ratio P-21/P-26 by low energy secondry neutrons: Identification of Ne spallation components at the 10(exp 6) atoms/g level in terrestrial samples p 1187 N94-16194
The Clementine instrument complement p 1086 N94-16370
In-flight calibration of the spectral and radiometric characteristics of AVIRIS in 1991 p 1037 N94-16667
AVIRIS calibration and application in coastal oceanic environments p 1069 N94-16685

MAC Europe 1991: Evaluation of AVIRIS, GER imaging spectrometry data for the land application testsite Oberpfaffenhofen p 1070 N94-16688
Application of symmetry properties to polarimetric remote sensing with JPL AIRSAR data p 1079 N94-16752
External calibration of polarimetric radar images using distributed targets p 1079 N94-16753
Photo-assisted epitaxial growth for III-V semiconductors [AD-A267889] p 1213 N94-17042
Microwave reflectometer ionization sensor [NASA-CR-191464] p 922 N94-17083

CALIFORNIA
Tectonic deformation in southern California [NASA-CR-194621] p 1101 N94-16021

CALORIMETERS
Measurement of the specific heat capacity of the electron-beam graphite calorimeter [NPL-RSA(EXT)-40] p 1031 N94-15018
X ray microcalorimeters: Principles and performance p 899 N94-15027
Calorimeter based detectors for high energy hadron colliders [DE93-017055] p 1188 N94-16900
Contained (nu) events observed in Soudan 2 [DE93-015548] p 1300 N94-17233

CAMERAS
Development of an ultra violet auroral imager for the Freja project p 904 N94-15060
A new detector concept for energetic auroral x ray imaging p 907 N94-15081
STS-32 IMAX camera training [NASA-TM-109567] p 1031 N94-15316
STS-29 IMAX camera audio class FFT [NASA-TM-109543] p 1031 N94-15374
STS-29 crew IMAX camera training [NASA-TM-109546] p 1031 N94-15380
STS-34 Arriflex and IMAX camera training [NASA-TM-109467] p 1031 N94-15397
STS-31 crew Linof, Arriflex, and IMAX camera training [NASA-TM-109485] p 1032 N94-15792
Capaciflector camera [NASA-CASE-GSC-13564-1] p 1033 N94-15872
Transparent conductive coatings in the far ultraviolet [NASA-CR-194632] p 1191 N94-16024
The Clementine instrument complement p 1086 N94-16370
Exploiting world structure to efficiently search for objects [TR-434] p 1231 N94-16576

CAMS
Hydraulic pump with integral electric motor [AD-D015782] p 1011 N94-16549

CANADA
Optical systems for the visualization of fluid and solid transparent media under microgravity conditions p 978 N94-16081

CANADIAN SPACE PROGRAM
Canadian microgravity experiments flown in 1989-1990 p 977 N94-16075
Development of the Laser-based R/D Test-bed System (LTS) p 978 N94-16080
The Canadian Space Station user development program. Where do we go from here? p 898 N94-16084

CANCELLATION
A complete study of differential wax-wane focus servo technique p 1199 N94-14996

CANCER
Experimental evaluation of an adaptive focusing algorithm for a microwave planar phased-array hyperthermia system at UCSF [AD-A267004] p 1121 N94-15634
Quantitative method of measuring cancer cell urokinase and metastatic potential [NASA-CASE-MSC-21715-1] p 1117 N94-15967
Screening for prostate cancer p 1126 N94-16630
Asbestos Surveillance Program p 1127 N94-16638
Quantifying lifetime exposure to ultraviolet radiation in the epidemiology of cutaneous malignant melanoma: A pilot study [DE93-015274] p 1128 N94-16812
The role of constitutive and inducible processes in the response of human squamous cell carcinoma cell lines to ionizing radiation [DE93-015150] p 1129 N94-16970

CANOPIES
Definitions of terms relating to aircraft windscreens, canopies, and transparencies [AD-A268403] p 868 N94-17425

CANOPIES (VEGETATION)
Using AVIRIS images to measure temporal trends in abundance of photosynthetic and nonphotosynthetic canopy components p 1066 N94-16668
Evaluation of spatial productivity patterns in an annual grassland during an AVIRIS overflight [CIW-PUBL-1134] p 1067 N94-16672
A linear spectral matching technique for retrieving equivalent water thickness and biochemical constituents of green vegetation p 1068 N94-16678
Exploring the remote sensing of foliar biochemical concentrations with AVIRIS data p 1069 N94-16683
The 1991 AVIRIS/POLDER experiment in Camargue, France p 1070 N94-16691
Monitoring environmental state of Alaskan forests with AIRSAR p 1075 N94-16734
Comparison of modeled backscatter with SAR data at P-band p 1076 N94-16735

CANTILEVER BEAMS
On the design of structural components using materials with time-dependent properties [NASA-TM-108428] p 1059 N94-16519
Mechanical and surface force nanoprobe [AD-D015792] p 1034 N94-16536

CANYONS
A mineralized zone in Western Candor Chasma, Mars p 1248 N94-16179
AI-26 production profile and model comparisons in Canyon Diablo p 1245 N94-16409

CAPACITANCE
Steering capaciflector sensor [NASA-CASE-GSC-13489-1] p 1164 N94-15704
Capaciflector camera [NASA-CASE-GSC-13564-1] p 1033 N94-15872
Double-driven shield capacitive type proximity sensor [NASA-CASE-GSC-13541-1] p 1165 N94-15946
Determination of equivalent circuit for PVDF shock-pressure gauges [DE93-016492] p 1034 N94-16452
Temperature and pressure effects on capacitance probe cryogenic liquid level measurement accuracy [NASA-CR-190763] p 1034 N94-16521

CAPACITORS
Reliability characterization of digital microcircuits: Investigation of an in-process oxide reliability screening method [AD-A267053] p 1008 N94-15665
Forback DC-to-DC converter [NASA-CASE-GSC-13404-1] p 1010 N94-15874
Cyanoresin, cyanoresin/cellulose triacetate blends for thin film, dielectric capacitors [NASA-CASE-NPO-18913-1-CU] p 966 N94-15930
Cellulose triacetate, thin film dielectric capacitor [NASA-CASE-NPO-18935-1-CU] p 1010 N94-15952
Stray insensitive switched capacitor composite operational amplifiers [AD-A267412] p 1012 N94-16976
Plasma flow switch and foil implosion experiments on Pegasus 2 [DE93-016464] p 1013 N94-17318
Electrical properties of sol-gel PZT thin films for decoupling capacitor applications [DE93-016491] p 1015 N94-17648

CAPE KENNEDY LAUNCH COMPLEX
Identifying and responding to customer needs at the Kennedy Space Center p 1056 N94-16626
Bloodborne Pathogens Program p 1127 N94-16644

CAPILLARY FLOW
Neuropeptide-Y (NPY) increases total blood flow in the tail, and reduces cutaneous microvascular blood flow in the tail and foot of the rat [AD-A266839] p 1115 N94-14918
Characterization of voids formed during liquid impregnation of nonwoven multifilament glass networks as related to composite processing p 939 N94-16858

CAPILLARY TUBES
Evaporation from a meniscus within a capillary tube in microgravity [NASA-CR-194593] p 976 N94-15654

CAPTURE EFFECT
Multiple process simulations for correction factor calculations in experiments with neutrons. LUSMK program [DE93-623957] p 1179 N94-14932

CARBIDES
Interface chemistry in ceramic matrix composites [AD-A268629] p 973 N94-17466

CARBON
Simulation studies for surfaces and materials strength [NASA-CR-193387] p 1056 N94-15004
Negative ion formation in small carbon clusters [DE93-015436] p 1182 N94-16064
Euromet Ureilite Consortium: A preliminary report on carbon and nitrogen geochemistry p 1241 N94-16192
Carbon abundances, major element chemistry, and mineralogy of hydrated interplanetary dust particles p 1243 N94-16309
Water adsorption on diamond (110) studied by multiple internal reflection infrared spectroscopy [AD-A266415] p 948 N94-16553
The role of carbon and temperature in determining electrical conductivity of basins, crust and mantle [DE93-015936] p 1101 N94-16840
Single crystal diamond thin films [AD-A266457] p 1214 N94-17216

CARBON CYCLE
AIRSAR South American deployment: Operation plan, version 3.0 p 994 N94-15919

CARBON DIOXIDE
Density and temperature relaxation near the critical point of carbon dioxide under reduced gravity p 944 N94-15164
Analysis of leading edge and trailing edge cover glass samples before and after treatment with advanced satellite contamination removal techniques [AD-A267055] p 885 N94-15666
New York MARKAL: An evaluation of carbon dioxide emission control strategies in New York State [DE93-013149] p 1095 N94-15999
Statement on global climate change before the Subcommittee on Energy and Power, United States House of Representatives [DE93-013163] p 1095 N94-16006
Extraction and isotopic analysis of medium molecular weight hydrocarbons from Murchison using supercritical carbon dioxide p 1241 N94-16184
Nitrates in SNCs: Implications for the nitrogen cycle on Mars p 1251 N94-16193
Modeling the reflectance of CO2 frost with new optical constants: Application to Martian south polar cap spectra p 1256 N94-16217
Experimental constraints on CO2 and H2O in the Martian mantle and primary magmas p 1262 N94-16248
Removal of carbonaceous contaminants from silica aerogel p 953 N94-16256
Martian carbon dioxide: Clues from isotopes in SNC meteorites p 1270 N94-16295
Far-infrared spectra of CO2 clathrate hydrate frosts p 954 N94-16340
Earth's partial pressure of CO2 over the past 120 Ma; evidence from Ce anomalies in the deep (greater than 600 m) Pacific Ocean, 1 p 1104 N94-16358
Earth's partial pressure of CO2 over the past 100-500 Ma; evidence from Ce anomalies in mostly shallow seas (less than 200 m) as recorded in carbonate sediments, 2 p 1104 N94-16360
CO2 production by impact in carbonates? An ATEM and stable isotope (C,O) study p 954 N94-16383
Investigation of cloud properties and atmospheric stability with MODIS [NASA-CR-193475] p 1107 N94-16717
Binding of carbon dioxide to metal macrocycles: Toward a mechanistic understanding of electrochemical and photochemical carbon dioxide reduction [DE93-016244] p 949 N94-16870
Incorporating global warming risks in power sector planning. Volume 1: A case study of the New England region [DE93-015241] p 1096 N94-17289
Automated data collection system for the TCM3 transcutaneous pO2/pCO2 monitoring system [AD-A268400] p 1129 N94-17424
Strategy for the reduction of total integrated fluid logistics to the Space Station Freedom [NASA-TM-107744] p 1138 N94-17452

CARBON DIOXIDE CONCENTRATION
Projections of future CO2 [NIWA/ATMOS/R/93-001] p 1094 N94-15185

CARBON DIOXIDE LASERS
Heat shock protein induction in human cells by CO2 laser irradiation [AD-A266430] p 1117 N94-16545
Controlling chaotic behavior in CO2 and other lasers [AD-A266431] p 1040 N94-16546
Experimental studies on a gas dynamic laser with narrow throat and high area-ratio grid nozzles [AD-A267818] p 1042 N94-17400
Three short articles from Japanese laser journal [AD-A268249] p 1042 N94-17415
Laser ignition of solid propellants: 1. Ignition delays [AD-A268454] p 976 N94-17538

CARBON FIBER REINFORCED PLASTICS
Polymer Infiltration Studies [NASA-CR-194494] p 932 N94-15275
Effect of Impact Damage and Open Hole on Compressive Strength of Hybrid Composite Laminates [NASA-CR-194603] p 936 N94-16836
Low and high velocity impact response of thick hybrid composites p 936 N94-16837

CARBON FIBERS
Polymer Infiltration Studies [NASA-CR-194494] p 932 N94-15275
Processing, properties and applications of composites using powder-coated epoxy towpreg technology p 933 N94-15277

Carbon-carbon grid for ion engines
[NASA-CASE-NPO-19174-1-CU] p 925 N94-15876
Continuous fabrication of SiC fiber tows by chemical vapor deposition
[AD-A266460] p 936 N94-16569
Production and application of chemical fibers with special properties for manufacturing composite materials and goods of different usage p 938 N94-16854
Fibers and materials of medical application p 938 N94-16855
Fiber strength utilization in carbon/carbon composites
[AD-A267713] p 940 N94-17271
Interface chemistry in ceramic matrix composites
[AD-A268629] p 973 N94-17466

CARBON ISOTOPES
Euromet Ureilite Consortium: A preliminary report on carbon and nitrogen geochemistry p 1241 N94-16192
CO2 production by impact in carbonates? An ATEM and stable isotope (C,O) study p 954 N94-16383

CARBON MONOXIDE
Preconversion catalytic deoxygenation of phenolic functional groups
[DE93-017034] p 950 N94-16912

CARBON MONOXIDE LASERS
Three short articles from Japanese laser journal
[AD-A268249] p 1042 N94-17415

CARBON STEELS
Robotic weld overlay coatings for erosion control
[DE93-016938] p 970 N94-16959

CARBON 13
Do SiC grains in Orgueil differ from those in Murchison? p 1242 N94-16260
Design of a formaldehyde photodissociation process for carbon and oxygen isotope separation
[DE93-016435] p 1039 N94-16450

CARBON-CARBON COMPOSITES
Carbon-carbon grid for ion engines
[NASA-CASE-NPO-19174-1-CU] p 925 N94-15876
The processing and mechanical properties of high temperature/high performance composites. Book 2: Coonstituent properties and macroscopic performance
[AD-A266395] p 935 N94-16484
Fiber strength utilization in carbon/carbon composites
[AD-A267713] p 940 N94-17271
Thermo-mechanical analysis of oxidation protected carbon-carbon composites
[AD-A268191] p 941 N94-17597

CARBONACEOUS CHONDRITES
Comparison of reflectance spectra of C asteroids and unique C chondrites Y86720, Y82162, and B7904 p 1242 N94-16246
Phase equilibria of the magnesium sulfate-water system to 4 kbars p 953 N94-16247
Olivines in the Kaba carbonaceous chondrite and constraints on their formation p 1219 N94-16255
Different radiation and metamorphic history of the Kainsaz CO 3.2 chondrules p 1243 N94-16296
Cat Mountain: A meteoritic sample of an impact-melted chondritic asteroid p 1244 N94-16328
The astrophysical interpretation of isotope anomalies in graphite and SiC grains of chondrites p 1244 N94-16343
On origin of the olivine inclusions from the Kainsaz CO carbonaceous chondrite p 1244 N94-16345
INAA of CAIs from the Maralinga CK4 chondrite: Effects of parent body thermal metamorphism p 1244 N94-16355
Possible sources of H2 to H2O enrichment at evaporation of parent chondritic material p 1244 N94-16377
A hydrogen isotope study of CO3 type carbonaceous chondrites; comparison with type 3 ordinary chondrites p 1246 N94-16425
The spectrum of Phobos from Phobos 2 observations at 0.3-2.6 microns: Comparison to previous data and meteorite analogs p 1295 N94-16429

CARBONACEOUS METEORITES
Complex radiation-thermal history of Kaidun meteorite on data of track study of silicate minerals p 1243 N94-16297

CARBONATES
Partitioning of Nb, Mo, Ba, Ce, Pb, Th and U between immiscible carbonate and silicate liquids: Evaluating the effects of P2O5,F, and carbonate composition p 953 N94-16283
Crustal structure and igneous processes in a chondritic Io p 1243 N94-16292
Earth's partial pressure of CO2 over the past 120 Ma; evidence from Ce anomalies in the deep (greater than 600 m) Pacific Ocean, 1 p 1104 N94-16358
CO2 production by impact in carbonates? An ATEM and stable isotope (C,O) study p 954 N94-16383
Status of molten carbonate fuel cell technology development
[DE93-015666] p 1092 N94-16715

CARBONIZATION
Fiber strength utilization in carbon/carbon composites
[AD-A267713] p 940 N94-17271

CARBONYL COMPOUNDS
Synthesis, reactivity, and characterization of (-hexacarbocyclic) manganese dicarbonyl complexes with sulfur and phosphorus ligands
[AD-A267592] p 930 N94-17192

CARBOXYL GROUP
Synthesis, characterization, and polymerization of new ferrocene-fluorene complexes. A novel high-molecular weight conjugated polymer with pendant ferrocene groups
[AD-A267717] p 972 N94-17273

CARDIOVASCULAR SYSTEM
A mathematical model for the study of hemorrhagic shock and fluid resuscitation: The systemic and pulmonary vasculature
[AD-A266835] p 1119 N94-14917
Neuropeptide-Y (NPY) increases total blood flow in the tail, and reduces cutaneous microvascular blood flow in the tail and foot of the rat
[AD-A266839] p 1115 N94-14918
Increased vascular resistance with hemoglobin-based oxygen carriers
[AD-A266454] p 1123 N94-16565
The Goddard Space Flight Center ergonomics program p 1125 N94-16621
Efficient management of cardiovascular risk screening programs p 1125 N94-16622
Illness/injury pattern complex 40 (Titan) p 1125 N94-16625
Melatonin, the pineal gland, and circadian rhythms
[AD-A268200] p 1129 N94-17478

CARGO SPACECRAFT
Space transfer concepts and analyses for exploration missions, phase 4
[NASA-CR-193849] p 882 N94-15831

CAROTENE
Tracking photosynthetic efficiency with narrow-band spectroradiometry
[CIW-PUBL-1133] p 1072 N94-16698

CARRIER INJECTION
Nonstationary behaviour of low background photon detectors p 902 N94-15049

CARTESIAN COORDINATES
Adaptive Cartesian grid methods for representing geometry in inviscid compressible flow
[DE93-016430] p 1025 N94-16894
A review of some dynamics models in six-dimensional phase space and their suitable conditions of motion equation
[DE93-623741] p 1175 N94-17317

CARTRIDGES
Thermal spray forming of refractory sample ampoule cartridges for single crystal growth space furnaces
[TABES PAPER 93-605] p 1051 N94-16141

CASCADE FLOW
Advanced methods for cascade testing
[AGARD-AG-328] p 1016 N94-15119
Heat transfer and aerodynamics of a 3D design nozzle guide vane tested in the Pyestock isentropic light piston facility
[RAE-TM-AERO/PROP-19] p 856 N94-15696
Effect of wind tunnel acoustic modes on linear oscillating cascade aerodynamics
[NASA-TM-106367] p 869 N94-15866
Determining the effect of endwall boundary layer suction in a large scale subsonic compressor cascade
[AD-A267208] p 859 N94-16913

CASCADE WIND TUNNELS
Effect of wind tunnel acoustic modes on linear oscillating cascade aerodynamics
[NASA-TM-106367] p 869 N94-15866

CASE HISTORIES
Lift-fan aircraft: Lessons learned-the pilot's perspective
[NASA-CR-177620] p 867 N94-15950

CASSEGRAIN OPTICS
Matera Laser Ranging Observatory (MLRO): An overview p 877 N94-15601

CASSINI MISSION
Life and the solar system: The CRAF and Cassini missions
[NASA-TM-109422] p 1247 N94-15513

CAST ALLOYS
Aircraft carrier exposure tests of cast magnesium alloys
[AD-A268260] p 962 N94-17418

CASTING
STS-27 crew fire training and glove molding
[NASA-TM-109554] p 1136 N94-15406
Method of producing a silicon carbide fiber reinforced strontium aluminosilicate glass-ceramic matrix composite
[NASA-CASE-LEW-15263-2] p 934 N94-15929
Cellulose triacetate, thin film dielectric capacitor
[NASA-CASE-NPO-18935-1-CU] p 1010 N94-15952
Aluminum-lithium technology
[TABES PAPER 93-601] p 962 N94-16137
Fabrication of advanced design (grooved) cermet anodes
[DE93-014590] p 1012 N94-16765
Solid lubricants for space structures, phase 2
[AD-A266653] p 968 N94-16767
Techniques for preparation of ingot metallurgical discontinuous composites
[AD-D015748] p 940 N94-16933
X ray computed tomography for casting demonstration
[AD-A268084] p 1056 N94-17596

CASTINGS
X ray computed tomography for casting demonstration
[AD-A268084] p 1056 N94-17596

CATALOGS (PUBLICATIONS)
Satellite situation report, volume 33, no. 3
[NASA-TM-109278] p 885 N94-15712
Defense Logistics Information System (DLIS) procedures manual. Products and services end-user manual
[AD-A267766] p 1232 N94-17007
Satellite situation report, volume 31, number 1
[NASA-TM-105088] p 898 N94-17584

CATALYSIS
Catalytic crystallization of ices by small silicate smokes at temperatures less than 20K p 1219 N94-16420
Synthetic and mechanistic investigation of olefin polymerization catalyzed by early transition metal compounds
[DE93-018301] p 970 N94-16963
Methyl chloride via oxyhydrochlorination of methane
[DE93-017548] p 952 N94-17218

CATALYSTS
Intramolecular versus intermolecular condensation rates in the acidic polymerization of octaethoxytrisiloxane
[AD-A266982] p 963 N94-15490
Direct catalytic decomposition of nitric oxide
[DE93-016689] p 949 N94-16896
Development of vanadium-phosphate catalysts for methanol production by selective oxidation of methane
[DE93-016850] p 949 N94-16897
High octane ethers from synthesis gas-derived alcohols
[DE93-016861] p 975 N94-16898
Preconversion catalytic deoxygenation of phenolic functional groups
[DE93-017034] p 950 N94-16912
Transient studies of low temperature catalysts for methane conversion
[DE93-017710] p 950 N94-16962
Synthetic and mechanistic investigation of olefin polymerization catalyzed by early transition metal compounds
[DE93-018301] p 970 N94-16963
Methyl chloride via oxyhydrochlorination of methane
[DE93-017548] p 952 N94-17218

CATALYTIC ACTIVITY
Preconversion catalytic deoxygenation of phenolic functional groups
[DE93-017034] p 950 N94-16912

CATASTROPHE THEORY
Flutter analysis using transversality theory
[NASA-TM-106382] p 1062 N94-17481

CATHETERIZATION
Methods to obtain blood samples periodically during exercise research studies while subjects are immersed in water or otherwise inaccessible
[AD-A268227] p 1130 N94-17562

CATHODE RAY TUBES
Preparation and investigation of improved low voltage electron excitable phosphors
[AD-A266852] p 963 N94-14948

CATHODES
Status of molten carbonate fuel cell technology development
[DE93-015666] p 1092 N94-16715
Investigation of the energy distribution of ions, striking the cathode in an abnormal glow discharge
[DE93-623987] p 1013 N94-17316
Electron reversal ionizer for detection of trace species using a spherical cathode
[NASA-CASE-NPO-18870-1-CU] p 1185 N94-17329
RF vacuum microelectronics
[AD-A268399] p 1014 N94-17423
Cathode sheath charge transfer effects
[AD-A268393] p 1186 N94-17536

CATHODOLUMINESCENCE
Experimentally reproduced relict enstatite in porphyritic chondrules of enstatite chondrite composition p 1244 N94-16363
Nitride semiconductors for ultraviolet detection
[AD-A267877] p 1012 N94-17040

CATIONS
NMR and theoretical investigation of cation binding with sol-gel silicates
[AD-A266999] p 963 N94-15631
Vacancy condensation as the precursor to passivity breakdown
[DE93-012925] p 956 N94-15998
The Fe2(+)-Mg interdiffusion in orthopyroxene: Constraints from cation ordering and structural data and implications for cooling rates of meteorites
p 1241 N94-16175
Cation ordering in orthopyroxenes and cooling rates of meteorites: Low temperature cooling rates of Estherville, Bondoc and Shaw p 1241 N94-16176
Direct catalytic decomposition of nitric oxide
[DE93-016689] p 949 N94-16896
CATS
Evaluation of putative neurochemical intermediaries in space/motion sickness
[NASA-CR-193607] p 1118 N94-17090
CAVITATION FLOW
Application of thermal spray and ceramic coatings and reinforced epoxy for cavitation damage repair of hydroelectric turbines and pumps
[AD-A267624] p 971 N94-17198
CAVITIES
Selected computations of transonic cavity flows
p 858 N94-16511
Unsteady fluid and optical simulation of transonic aero-windows
[AIAA PAPER 93-3017] p 858 N94-16512
Computation of a controlled store separation from a cavity p 858 N94-16513
Advanced transport systems for electron beams in high brightness accelerators and FELs
[AD-A267322] p 1041 N94-17001
Quantum phase fluctuations in the Jaynes-Cummings model: Effects of cavity damping
[DE93-627984] p 1186 N94-17612
CAVITY FLOW
Computation of the Fluid and Optical Fields About the Stratospheric Observatory for Infrared Astronomy (SOFIA) and the Coupling of Fluids, Dynamics, and Control Laws on Parallel Computers
[NASA-CR-193168] p 858 N94-16510
Selected computations of transonic cavity flows
p 858 N94-16511
Unsteady fluid and optical simulation of transonic aero-windows
[AIAA PAPER 93-3017] p 858 N94-16512
On solving the compressible Navier-Stokes equations for unsteady flows at very low Mach numbers
[NASA-TM-106380] p 1027 N94-17128
An investigation of oblique shock/boundary layer interaction control
[AD-A268106] p 861 N94-17574
CAVITY RESONATORS
Quantum phase fluctuations in the Jaynes-Cummings model: Effects of cavity damping
[DE93-627984] p 1186 N94-17612
CD-ROM
The planetary data system educational CD-ROM
p 1234 N94-16209
CEILINGS (METEOROLOGY)
A comparison of ceiling and visibility observation for NWS manned observation sites and ASOS sites
[AD-A268356] p 1108 N94-17459
CELESTIAL MECHANICS
Total solar eclipse of 3 November 1994
[NASA-RP-1318] p 1236 N94-15481
Mapping the stability region of the 3:2 Neptune-Pluto resonance p 1280 N94-16351
Energy potential analysis of zero velocity curves in the restricted three-body problem
[AD-A267512] p 1170 N94-17076
AMIGAU: A prototype tool aimed at mission analysis for satellites and satellite constellations
p 888 N94-17133
CELL DIVISION
Bioeffects of radiofrequency radiation on cell growth and differentation. Volume 1: Engineering considerations
[AD-A267754] p 1118 N94-17232
CELL MEMBRANES (BIOLOGY)
Factors determining the release of nitric oxide --- Calcium/cadmium transport by renal cortical collectin duct cells
[AD-A266232] p 1118 N94-17224
CELLS (BIOLOGY)
The role of constitutive and inducible processes in the response of human squamous cell carcinoma cell lines to ionizing radiation
[DE93-015150] p 1129 N94-16970
Factors determining the release of nitric oxide --- Calcium/cadmium transport by renal cortical collectin duct cells
[AD-A266232] p 1118 N94-17224
Bioeffects of radiofrequency radiation on cell growth and differentation. Volume 1: Engineering considerations
[AD-A267754] p 1118 N94-17232
CELLULOSE
Cyanoresin, cyanoresin/cellulose triacetate blends for thin film, dielectric capacitors
[NASA-CASE-NPO-18913-1-CU] p 966 N94-15930
Cellulose triacetate, thin film dielectric capacitor
[NASA-CASE-NPO-18935-1-CU] p 1010 N94-15952
CEMENTS
Mechanical properties of magnesium ammonium phosphate cements and their zeolite composites
[DE93-015155] p 934 N94-16057
Influence of the loading rate on the endurance and deformability of cement matrix composites
[IFTR-1/1992] p 1060 N94-17052
CENTER OF MASS
ETALON-1,-2 center of mass correction and array reflectivity p 915 N94-15576
A feasibility study of a microgravity enhancement system for Space Station Freedom
[NASA-CR-191550] p 886 N94-15864
CENTRAL AMERICA
The Central American cold surge: An observational analysis of the deep southward penetration of North American cold fronts
[AD-A268592] p 1110 N94-17607
CENTRAL NERVOUS SYSTEM
Neurotoxicity of hemoglobin in cortical cell culture
[AD-A266506] p 1128 N94-16786
Human central nervous system oxygen toxicity data from 1945 to 1986
[AD-A268225] p 1130 N94-17556
CENTRAL PROCESSING UNITS
A microprocessor controller for a towing tank drive and flow visualisation system
[AD-A267087] p 872 N94-15543
Space systems environmental interaction studies
[AD-A267280] p 897 N94-17240
CENTRIFUGAL COMPRESSORS
Development of the seeding system used for laser velocimeter surveys of the NASA Low-Speed Centrifugal Compressor flow field
[NASA-TM-4485] p 1032 N94-15445
Experimental and computational investigation of the NASA low-speed centrifugal compressor flow field
[NASA-TM-4481] p 869 N94-17386
CENTROIDS
Effects of window size and shape on accuracy of subpixel centroid estimation of target images
[NASA-TP-3331] p 1034 N94-15990
CEPHEUS CONSTELLATION
The chromosphere of VV cephei and the distribution of circumstellar dust around red giants and supergiants
[NASA-CR-193594] p 1297 N94-16866
CERAMIC COATINGS
Application of thermal spray and ceramic coatings and reinforced epoxy for cavitation damage repair of hydroelectric turbines and pumps
[AD-A267624] p 971 N94-17198
Ceramic fiber coatings development and demonstration
[AD-A267286] p 972 N94-17242
CERAMIC FIBERS
Continuous fabrication of SiC fiber tows by chemical vapor deposition
[AD-A266460] p 936 N94-16569
Fabrication of piezoelectric ceramic/polymer composites by injection molding
[AD-A267302] p 972 N94-17227
Ceramic fiber coatings development and demonstration
[AD-A267286] p 972 N94-17242
CERAMIC MATRIX COMPOSITES
High temperature advanced structural composites. Volume 2: Ceramic matrix composites, fiber processiing and properties, and interfaces
[AD-A267023] p 933 N94-15528
High temperature advanced structural composites. Volume 3: Mechanics
[AD-A267024] p 933 N94-15626
High temperature advanced structural composites. Volume 1: Executive summary and intermetallic compounds
[AD-A267022] p 933 N94-15835
Method of producing a silicon carbide fiber reinforced strontium aluminosilicate glass-ceramic matrix composite
[NASA-CASE-LEW-15263-2] p 934 N94-15929
Modeling the thermal conductivity of fiber-reinforced ceramic composites
[DE93-015340] p 934 N94-16017
Overview of chemical vapor infiltration
[DE93-015440] p 934 N94-16065
Environmental effects on elevated temperature subcritical crack growth of SiC/SiC composites
[DE93-015688] p 934 N94-16158
Evaluation of the interfacial mechanical properties in fiber-reinforced ceramic composites
[DE93-015494] p 935 N94-16461
The processing and mechanical properties of high temperature/high performance composites. Book 1: Coonstituent properties of composites
[AD-A266394] p 935 N94-16483
The processing and mechanical properties of high temperature/high performance composites. Book 2: Coonstituent properties and macroscopic performance
[AD-A266395] p 935 N94-16484
The processing and mechanical properties of high temperature/high performance composites. Book 3: Coonstituent properties and macroscopic performance
[AD-A266396] p 935 N94-16485
The processing and mechanical properties of high temperature/high performance composites. Book 4: Coonstitutive laws and design
[AD-A266397] p 935 N94-16528
Transformation toughening of composite ceramics
[AD-A267304] p 971 N94-16980
Micromechanisms of monotonic and cyclic subcritical crack growth in advanced high melting point low-ductility intermetallics
[AD-A267764] p 961 N94-17223
Ceramic fiber coatings development and demonstration
[AD-A267286] p 972 N94-17242
Evaluation of interfacial properties of fiber-reinforced ceramic composites using fiber push-in tests
[DE93-015427] p 972 N94-17253
Direct observation of fracture of CAS-glass/SiC composites and processing of toughened alumina
[AD-A268275] p 941 N94-17457
Interface chemistry in ceramic matrix composites
[AD-A268629] p 973 N94-17466
CERAMICS
Remelting of Fe-C-Si-alloy in a ceramic mold skin
p 945 N94-15169
Self-diffusion coefficients of sol-gel intermediates
[AD-A266957] p 963 N94-15179
The friction and wear of ceramic/ceramic and ceramic/metal combinations in sliding contact
[NASA-TM-106348] p 930 N94-15769
Production and evaluation of dense ceramic compounds by combustion synthesis and dynamic compaction
[AD-A266742] p 965 N94-15773
Gas separations using ceramic membranes
[DE93-000278] p 947 N94-15861
Nonaqueous slip casting of high temperature ceramic superconductors using an investment casting technique
[NASA-CASE-LAR-14918-1] p 983 N94-15881
Synthesis of ceramic oxide powders in a microwave plasma device
[DE93-012741] p 965 N94-15920
The influence of microstructure on the mechanical behavior of silicon nitride ceramics
[DE93-015363] p 966 N94-16018
Multiaxial deformation and life prediction model and experimental data for advanced silicon nitride ceramics
[DE93-015450] p 967 N94-16067
Use of microgravity in the synthesis of ceramics using sol gel techniques p 979 N94-16088
Finite element analytical techniques for ceramic production in microgravity: A hypoelastic model
p 981 N94-16099
Thermal spray forming of refractory sample ampoule cartridges for single crystal growth space furnaces
[TABES PAPER 93-605] p 1051 N94-16141
Continuous fabrication of SiC fiber tows by chemical vapor deposition
[AD-A266460] p 936 N94-16569
Detection of subsurface defects in machined silicon nitride ceramics by optical scattering methods
[DE93-015554] p 968 N94-16658
Ablation, surface activation, and electroless metallization of insulating materials by pulsed excimer laser irradiation
[DE93-015808] p 1040 N94-16664
Development of a constitutive model for creep and life prediction of advanced silicon nitride ceramics
[DE93-015894] p 968 N94-16813
The Ceramic Technology Project: Ten years of progress
[DE93-015991] p 968 N94-16843
Superconducting ceramics: Selected properties and methods of production
[IFTR-23/1991] p 969 N94-16924
High temperature materials technology research for advanced thermionic systems
[DE93-018302] p 960 N94-16964
Transformation toughening of composite ceramics
[AD-A267304] p 971 N94-16980
Fabrication of piezoelectric ceramic/polymer composites by injection molding
[AD-A267302] p 972 N94-17227

Dynamic testing and characterization of pre-fractured ceramic
[DE93-016457] p 972 N94-17238
High temperature deformation behavior of YBa2Cu3O(6+x) superconducting ceramic materials
[AD-A268164] p 973 N94-17430
Investigations of YBaCuO materials with near-room-temperature resistivity transitions
[AD-A268016] p 1216 N94-17477
Oxygen diffusion in YBa2Cu3O(6+delta) ceramics on heating
[DE93-629161] p 974 N94-17633
Influence of the granular surface on the oxygen uptake in YBa2Cu3O(6+delta) ceramics
[DE93-629162] p 974 N94-17634

CEREBRAL CORTEX
Neurotoxicity of hemoglobin in cortical cell culture
[AD-A266506] p 1128 N94-16786

CEREBROSPINAL FLUID
Diffusible driving and coupling signals of the biological clock
[AD-A267046] p 1121 N94-15660
Evaluation of putative neurochemical intermediaries in space/motion sickness
[NASA-CR-193607] p 1118 N94-17090

CEREBRUM
Cumulative effect of repeated brief cerebral ischemia
[AD-A267155] p 1121 N94-15736

CERENKOV COUNTERS
Contained (nu) events observed in Soudan 2
[DE93-015548] p 1300 N94-17233

CERENKOV RADIATION
Contained (nu) events observed in Soudan 2
[DE93-015548] p 1300 N94-17233

CERIUM COMPOUNDS
Scintillation mechanism in stoichiometric cerium compounds
[DE93-015499] p 948 N94-16771

CERMETS
Production and evaluation of dense ceramic compounds by combustion synthesis and dynamic compaction
[AD-A266742] p 965 N94-15773
Chemical interactions between interconnect and electrode materials during sintering in solid oxide fuel cells
[DE93-015696] p 1092 N94-16160
Fabrication of advanced design (grooved) cermet anodes
[DE93-014590] p 1012 N94-16765

CERTIFICATION
Development of a proposed international standard for certification of aircraft to High Intensity Radiated Fields (HIRF)
[NASA-TM-106357] p 863 N94-16520
Windshear database for forward-looking systems certification
[NASA-TM-109012] p 1108 N94-17283

CESIUM
Earth's partial pressure of CO2 over the past 120 Ma; evidence from Ce anomalies in the deep (greater than 600 m) Pacific Ocean, 1 p 1104 N94-16358
Earth's partial pressure of CO2 over the past 100-500 Ma; evidence from Ce anomalies in mostly shallow seas (less than 200 m) as recorded in carbonate sediments, 2 p 1104 N94-16360

CETYL COMPOUNDS
Encapsulation of hemoglobin in non-phospholipid vesicles
[AD-A266505] p 1128 N94-16785

CHALCOGENIDES
Lead chalcogenides based IR photosensitive array detectors with coordinate addressing p 903 N94-15053
A linear monolithic 4-6 on silicon IR detector array p 910 N94-15098

CHALLENGER (ORBITER)
The 1982 highlights
[NASA-TM-109671] p 1303 N94-15508

CHANNEL CAPACITY
Bandwidth efficient coding: Theoretical limits and real achievements. Error control techniques for satellite and space communications p 997 N94-16507

CHANNEL FLOW
Modal element method for potential flow in non-uniform ducts: Combining closed form analysis with CFD
[NASA-TM-106347] p 1169 N94-15799
Three-dimensional turbulent boundary layer
[AD-A266261] p 1025 N94-16908
The stability and dynamics of elastic structures and fluid flows
[AD-A267990] p 1029 N94-17414

CHANNEL NOISE
Lossless compression of AVIRIS data: Comparison of methods and instrument constraints p 1075 N94-16713

CHANNELS
Channel of the system for pulse charged particle beam diagnostics
[DE93-623867] p 1179 N94-14931

CHANNELS (DATA TRANSMISSION)
A software interface for the ARL wind tunnel data acquisition system
[AD-A267114] p 1146 N94-15650
A simulation study of the performance of the NASA (2,1,6) convolutional code on RFI/burst channels p 997 N94-16508
Search for optimal distance spectrum convolutional codes p 998 N94-16509
Using Markov chains to model the error behavior of data communications channels
[AD-A266468] p 999 N94-16777
Small satellite constellation system: Optimization criteria p 888 N94-17132
Strategy for a small satellite program and a proposal for a first mission p 874 N94-17143

CHAOS
Looking at Fokker-Planck dynamics with a noisy instrument
[AD-A267049] p 1117 N94-15662
Development of pattern recognition techniques for the evaluation of toxicant impacts to multispecies systems
[AD-A267197] p 1095 N94-15790
Real-time adaptive neural network data processing
[TABES PAPER 93-660] p 1054 N94-16155
Search for chaos in free shear flows
[AD-A266245] p 1023 N94-16470
Controlling chaotic behavior in CO2 and other lasers
[AD-A266431] p 1040 N94-16546
Stochastic chaos: An analog of quantum chaos
[DE93-016619] p 1220 N94-16956
Nonlinear methods for communications
[AD-A267376] p 1001 N94-17019
Extracavity frequency doubling study of a pulsed photodissociation iodine laser
[AD-A267893] p 1042 N94-17394

CHARACTER RECOGNITION
Freedom system Text and Graphics Systems (TAGS)
[NASA-TM-109509] p 1140 N94-15455

CHARACTERIZATION
Characterization facility for magneto-optic media and systems p 1226 N94-14983
Tessera terrain on Venus: Global characterization from Magellan data p 1264 N94-16262

CHARGE CARRIERS
A study of high field transport in wide band gap electronic materials using a picosecond transient charge technique
[AD-A267098] p 1008 N94-15636

CHARGE COUPLED DEVICES
Development of x ray CCDs p 900 N94-15033
The XMM pn-CCD detector system: First results p 900 N94-15034
The development of back-illuminated CCD's for XMM p 900 N94-15035
Thinned, backside illuminated, area CCD imager for electron detection p 901 N94-15036
The MIC photon counting detector p 901 N94-15039
CCDs and photon counting devices: Applications in space and from the ground p 901 N94-15041
Schottky barrier focal plane arrays for SWIR and MWIR p 903 N94-15050
A 12.5 micron infrared detector for Earth observation p 903 N94-15052
Developments in extreme ultraviolet and x ray instrumentation p 904 N94-15058
Radiation hardening of a CCD technology through process and design modifications p 906 N94-15071
CCD's on high resistivity bulk silicon for x ray spectroscopy on XMM p 907 N94-15080
Requirements on CCD-detectors for ground-based auroral imaging p 909 N94-15093
Assessment of TDI operation of a frame transfer CCD for high resolution imaging from a fast spinning spacecraft p 910 N94-15097
A conceptual design study for a two-dimensional, electronically scanned thinned array radiometer
[NASA-TM-109051] p 1085 N94-17665

CHARGE TRANSFER
Negative ion formation in small carbon clusters
[DE93-015436] p 1182 N94-16064
Iron oxide bands in the visible and near-infrared reflectance spectra of primitive asteroids p 1242 N94-16274
Structural effects in electron transfer reactions: Comparative interfacial electrochemical kinetics for cis- versus trans-dioxorhenium (V) (bi)pyridine oxidation
[AD-A266307] p 1182 N94-16466
Energy-loss cross sections for inclusive charge-exchange reactions at intermediate energies
[NASA-TM-4522] p 1188 N94-17018
Cathode sheath charge transfer effects
[AD-A268393] p 1186 N94-17536

CHARGED PARTICLES
Channel of the system for pulse charged particle beam diagnostics
[DE93-623867] p 1179 N94-14931
Investigation of the interactions of radiation with matter
[AD-A266743] p 1181 N94-15774
Confinement and stability of a Crystal Beam
[DE93-015400] p 1181 N94-16020
Inductive effects during second harmonic current drive experiments on T-10
[DE93-014411] p 1202 N94-16803
Study of brightness and current limitations in intense charged particle beams
[AD-A268283] p 1186 N94-17578

CHARM (PARTICLE PHYSICS)
Status of (alpha)(sub s) measurements
[DE93-015179] p 1181 N94-16059

CHARON
Mapping the stability region of the 3:2 Neptune-Pluto resonance p 1280 N94-16351

CHASSIGNITES
Nitrates in SNCs: Implications for the nitrogen cycle on Mars p 1251 N94-16193
Os isotopes in SNC meteorites and their implications to the early evolution of Mars and Earth p 1242 N94-16272
Martian carbon dioxide: Clues from isotopes in SNC meteorites p 1270 N94-16295

CHEBYSHEV APPROXIMATION
Fast algorithms for polynomial interpolation, integration and differentiation
[AD-A267505] p 1154 N94-17370

CHECKOUT
STS-37 astronauts Ross and Apt during CETA hardware checkout
[NASA-TM-109496] p 1137 N94-15460
Bench checkout equipment for spaceborne laser altimeter systems p 921 N94-15618
Galileo probe spacecraft mission to Jupiter
[NASA-TM-109646] p 1247 N94-16070

CHELATION
Vanadium corrosion studies
[AD-A266489] p 959 N94-16781

CHEMICAL ANALYSIS
Lasing dye sensor for chemical vapors
[AD-D015786] p 1040 N94-16533

CHEMICAL BONDS
The thermal dissociation of NH2CHO(ND2CHO) on Si(100)-2x1
[AD-A266903] p 942 N94-14956
Materials Research Society Symposium Proceedings, Volume 292: Biomolecular Materials
[AD-A265776] p 1116 N94-15138
NMR and theoretical investigation of cation binding with sol-gel silicates
[AD-A266999] p 963 N94-15631
Thermochemistry of silicate speciation in aqueous sodium silicate solutions: Ionization and polymerization of small silicate ion
[AD-A266825] p 964 N94-15683
Structural studies of sol-gel glasses
[AD-A266277] p 967 N94-16472

CHEMICAL COMPOSITION
Compounds containing meta-biphenylenedioxy moieties and polymers therefrom
[NASA-CASE-LAR-14517-1] p 965 N94-15879
An assessment of acid fog
[DE93-009347] p 1095 N94-15940
Systematic chemical variations in large 3AB iron meteorites: Clues to core crystallization p 1241 N94-16213
A Moessbauer spectrometer for the mineralogical analysis of the Mars surface: First temperature dependent tests of the detector and drive system p 1259 N94-16233
Thermal inertia and radar reflectivity of the Martian north polar ERG: Low-density aggregates p 1260 N94-16238
Chemical and isotopic compositions in acid residues from various meteorites p 1243 N94-16291
Carbon abundances, major element chemistry, and mineralogy of hydrated interplanetary dust particles p 1243 N94-16309
An initial perspective of S-asteroid subtypes within asteroid families p 1243 N94-16310
Terrestrial bitumen analogue of orgueil organic material demonstrates high sensitivity to usual HF-HCl treatment p 930 N94-16325
Composition of Apollo 17 core 76001 p 1275 N94-16326
Evolution of Triton's volatile budget p 1284 N94-16373

Effects of bulk composition on production rates of cosmogenic nuclides in meteorites p 1245 N94-16385
Composition of weakly altered Martian crust p 1296 N94-16436
Metastable phases in mechanically alloyed aluminum germanium powders
[DE93-008727] p 958 N94-16463
Method for doping GaAs with high vapor pressure elements
[AD-D015794] p 1210 N94-16538
First results from analysis of coordinated AVIRIS, TIMS, and ISM (French) data for the Ronda (Spain) and Beni Bousera (Morocco) peridotites p 1067 N94-16675
Advanced thermally stable jet fuels
[DE93-017711] p 975 N94-16996
Pseudomorphic semiconducting heterostructures from combinations of AlN, GaN and selected SiC polytypes: Theoretical advancement and its coordination with experimental studies of nucleation, growth, characterization and device deployment
[AD-A267561] p 1213 N94-17108

CHEMICAL EFFECTS
Analytical and experimental investigation of the feasibility of accelerated lifetime testing of materials exposed to an atomic oxygen beam
[NASA-CR-193851] p 946 N94-15766

CHEMICAL ELEMENTS
Elemental impurity analysis of mercuric iodide by ICP/MS
[DE93-015531] p 949 N94-16876

CHEMICAL ENGINEERING
Prioritization methodology for chemical replacement
[NASA-TP-3421] p 976 N94-15723

CHEMICAL EQUILIBRIUM
Large eddy simulation and direct numerical simulation of high speed turbulent reacting flows
[NASA-CR-193131] p 1018 N94-15427
Evaluation of hemoglobin-oxygen equilibrium binding by rapid-scanning spectrophotometry and singular-value decomposition
[AD-A266453] p 1123 N94-16564
Coefficients for calculating thermodynamic and transport properties of individual species
[NASA-TM-4513] p 1220 N94-17624

CHEMICAL EVOLUTION
Publications of the Exobiology Program for 1991: A special bibliography
[NASA-TM-4483] p 1139 N94-17017

CHEMICAL LASERS
Reactions of chemiluminescence induced by singlet oxygen with metals
[ONERA-NT-1992-13] p 955 N94-15149
Pulsed hydrogen fluoride overtone chemical laser studies
[AD-A267597] p 1041 N94-17193
Bibliography of short wavelength chemical laser research
[AD-A267619] p 1041 N94-17195

CHEMICAL PROPERTIES
Physical and chemical properties of some new perfluoropolyalkylether lubricants prepared by direct fluorination
[NASA-TM-106299] p 967 N94-16543
Continuum solvent models for computational chemistry
[DE93-016329] p 953 N94-17660

CHEMICAL PROPULSION
Emerging technologies for the changing global market
[TABES PAPER 93-612] p 930 N94-16144

CHEMICAL REACTIONS
A proposed mechanism for the pyrolysis of diborane
[DE93-014275] p 947 N94-15977
Study of fractal aggregates p 979 N94-16086
Single-collision studies of energy transfer and chemical reaction
[DE93-017603] p 1182 N94-16121
Chemical interactions between interconnect and electrode materials during sintering in solid oxide fuel cells
[DE93-015696] p 1092 N94-16160
Structural effects in electron transfer reactions: Comparative interfacial electrochemical kinetics for cis- versus trans-dioxorhenium (V) (bi)pyridine oxidation
[AD-A266307] p 1182 N94-16466
Characterization of UV emissions resulting from electronic energy transfer in atmospheric molecules
[AD-A266244] p 1101 N94-16469
Apparatus for and a method of growing thin films of elemental semiconductors
[AD-D015813] p 1210 N94-16487
Electrorheological fluid chemical processing
[AD-D015785] p 948 N94-16532
Evaluation of hemoglobin-oxygen equilibrium binding by rapid-scanning spectrophotometry and singular-value decomposition
[AD-A266453] p 1123 N94-16564
Dissociation rates of diatomic molecules
[AD-A266464] p 1182 N94-16586
Release of iron from hemoglobin
[AD-A266503] p 1128 N94-16784
Pulsed laser kinetic studies of liquids under high pressure
[DE93-017826] p 1041 N94-16998
Synthesis of potential high-energy fuels
[AD-A267508] p 975 N94-17073
Atmospheric ionization by solar particles detected by nitrate measurement in antarctic snow
[AD-A267583] p 1299 N94-17208
Studies on nonequilibrium phenomena in supersonic chemically reacting flows
[NASA-CR-194662] p 1027 N94-17215
Investigation of the origin of hot spots in deformed crystals: Ammonium perchlorate studies
[AD-A267692] p 1214 N94-17270
Interface chemistry in ceramic matrix composites
[AD-A268629] p 973 N94-17466
Soluble precursor route to polyanilines
[AD-A268015] p 973 N94-17494
Chemical reactions in turbulent mixing flows
[AD-A268287] p 861 N94-17580

CHEMICAL VAPOR INFILTRATION
NEXTEL(trademark)/SiC composites using forced chemical vapor infiltration
[DE93-013532] p 934 N94-16008
Overview of chemical vapor infiltration
[DE93-015440] p 934 N94-16065

CHEMICAL WARFARE
Trace analysis of chemical warfare agents in air: Sampling in porous polymers followed with thermal desorption analysis
[FOA-C-40302-4.6] p 1097 N94-17625

CHEMICALS
Prioritization methodology for chemical replacement
[NASA-TP-3421] p 976 N94-15723

CHEMILUMINESCENCE
Reactions of chemiluminescence induced by singlet oxygen with metals
[ONERA-NT-1992-13] p 955 N94-15149

CHEMISORPTION
Structural and dynamical aspects of electrodeposition
[AD-A266[illegible]] p 942 N94-14909
Water adsorption on diamond (110) studied by multiple internal reflection infrared spectroscopy
[AD-A266415] p 948 N94-16553
Atomic layer epitaxy group IV materials: Surface processes, thin films, devices and their characterization
[AD-A267527] p 1213 N94-17116

CHEMOTHERAPY
Evaluation of putative neurochemical intermediaries in space/motion sickness
[NASA-CR-193607] p 1118 N94-17090

CHICKENS
STS-29 crew with student experiment
[NASA-TM-109545] p 1116 N94-15378

CHILDREN
Short walk to everywhere --- Space, Earth, Ocean Center
[NASA-TM-109541] p 1221 N94-15372
Lead poisoning: An overview p 1124 N94-16614

CHIPS (ELECTRONICS)
Multichip module high speed testing
[AD-A266968] p 986 N94-14955
NASA Space Engineering Research Center for VLSI System Design
[NASA-CR-194587] p 1008 N94-15547
Reliability analysis of Surface Mount Technology (SMT)
[AD-A267598] p 1055 N94-17194
Leak detection utilizing analog binaural (VLSI) techniques
[NASA-CASE-NPO-18399-1-CU] p 1014 N94-17323
A high-speed object recognition chip based on a biologically-realistic hybrid temporal processing
[AD-A268270] p 1134 N94-17576
Low dielectric constant insulators and gold metallization for GHz multi-chip modules, part 2
[AD-A268590] p 1176 N94-17605

CHIRP SIGNALS
Spaceborne Imaging Radar-C instrument p 990 N94-15890

CHLORIDES
Thermal disorder in adsorbed Cl on Si(100)
[AD-A266295] p 1210 N94-16476
Stress corrosion cracking of 316 SS and Incoloy-800 in high temperature aqueous containing sulfate and chloride
[DE93-623325] p 952 N94-17302

CHLORINATION
Methyl chloride via oxyhydrochlorination of methane
[DE93-017548] p 952 N94-17218

CHLORINE COMPOUNDS
The photochemistry of poly(methylphenylphosphazene)
[AD-A267320] p 970 N94-16948

CHLOROCARBONS
Environmental management lessons to be learned from the upcoming CFC phase out or how to insure that we survive the next environmentally mandated process change
[TABES PAPER 93-570] p 1050 N94-16136

CHLOROFLUOROCARBONS
Environmental management lessons to be learned from the upcoming CFC phase out or how to insure that we survive the next environmentally mandated process change
[TABES PAPER 93-570] p 1050 N94-16136

CHLOROPHYLLS
Seasonal and spatial variations in phytoplanktonic chlorophyll in eutrophic Mono Lake, California, measured with the Airborne Visible and Infrared Imaging Spectrometer (AVIRIS) p 1069 N94-16684
Multiple dataset water-quality analyses in the vicinity of an ocean wastewater plume p 1069 N94-16687
Primary studies of trace quantities of green vegetation in Mono Lake area using 1990 AVIRIS data p 1071 N94-16695

CHOLESTEROL
Encapsulation of hemoglobin in non-phospholipid vesicles
[AD-A266505] p 1128 N94-16785

CHONDRITES
Grosnaja ABCs: Magnesium isotope compositions p 1241 N94-16191
Nd-142/Nd-144 in bulk planetary reservoirs, the problem of incomplete mixing of interstellar components and significance of very high precision Nd-145/Nd-144 measurements p 1256 N94-16220
Pyroxene equilibration temperatures in metamorphosed ordinary chondrites p 1242 N94-16224
Potassium isotope cosmochemistry, volatile depletion and the origin of the Earth p 953 N94-16259
First investigation of noble gases in the Dengli H3,8 chondrite p 953 N94-16264
Silica-bearing objects in the Dengli H3.8 and Gorlovka H3-4 chondrites p 1242 N94-16265
Transition metals in superheat melts p 962 N94-16273
Complex zoning behavior in pyroxene in FeO-rich chondrules in the Semarkona ordinary chondrite p 1243 N94-16284
Angrite LEW87051: Are the olivines pheno's or xeno's? A continuing story p 1103 N94-16285
Partial melting of ordinary chondrites: Lost City (H) and St. Severin (LL) p 1243 N94-16286
The Al Rais meteorite: A CR chondrite or close relative? p 1243 N94-16290
Crustal structure and igneous processes in a chondritic Io p 1243 N94-16292
Heterogeneous plagioclase compositions in the Maralinga CK4 chondrite p 1243 N94-16308
Comparative magnetic and thermoanalytical study of two enstatite chondrites: Adhi Kot and Atlanta p 1244 N94-16329
Chromite-rich mafic silicate chondrules in ordinary chondrites: Formation by impact melting p 1244 N94-16330
Chondritic ratios of Fe/Cr/Ir in Kerguelen Plateau (Hole 738C) K/T carbonate-rich sediments support asteroid-cometary impact at K/T time p 1244 N94-16357
Noble gases in twenty Yamato H-chondrites: Comparison with Allan Hills chondrites and modern falls p 1244 N94-16361
Experimentally reproduced relict enstatite in porphyritic chondrules of enstatite chondrite composition p 1244 N94-16363
Refractory precursor components in an Allende ferromagnesian chondrule p 1245 N94-16412
Identification of new meteorite, Mihonoseki (L), from broken fragments in Japan p 1246 N94-16415
Zaoyang chondrite cooling history from pyroxene Fe(2+)-Mg intracrystalline ordering and exolutions p 1246 N94-16417
Optical effects of regolith processes on S asteroids as simulated by laser impulse alteration of ordinary chondrite p 1246 N94-16422
Nitrogen and light noble gases in Parsa enstatite chondrite p 1246 N94-16435

CHONDRULE
Gas-grain energy transfer in solar nebula shock waves: Implications for the origin of chondrules p 1262 N94-16251
The group A3 chondrules of Krymka: Further evidence for major evaporative loss during the formation of chondrules p 1242 N94-16257

Complex zoning behavior in pyroxene in FeO-rich chondrules in the Semarkona ordinary chondrite
p 1243 N94-16284
Different radiation and metamorphic history of the Kainsaz CO 3.2 chondrules p 1243 N94-16296
Chromite-rich mafic silicate chondrules in ordinary chondrites: Formation by impact melting
p 1244 N94-16330
On origin of the olivine inclusions from the Kainsaz CO carbonaceous chondrite p 1244 N94-16345
Experimentally reproduced relict enstatite in porphyritic chondrules of enstatite chondrite composition
p 1244 N94-16363
Refractory precursor components in an Allende ferromagnesian chondrule p 1245 N94-16412

CHORDS (GEOMETRY)
Wind-tunnel investigation of aerodynamic efficiency of three planar elliptical wings with curvature of quarter-chord line
[NASA-TP-3359] p 859 N94-16574

CHROMATES
Assessment of chromate and non-chromate conversion coatings for Al alloys using electrochemical impedance spectroscopy
[AD-A267205] p 965 N94-15859

CHROMITES
Chemical interactions between interconnect and electrode materials during sintering in solid oxide fuel cells
[DE93-015696] p 1092 N94-16160
Low-temperature sintering and phase changes in chromite interconnect materials
[DE93-015676] p 961 N94-17234

CHROMIUM ALLOYS
In situ studies of passive film chemistry using x ray absorption spectroscopy
[DE93-014023] p 947 N94-16011
Effects of alloying and temperature on the high-temperature oxidation of Cr-Cr2Nb
[DE93-015800] p 957 N94-16163

CHROMIUM COMPOUNDS
Chromite-rich mafic silicate chondrules in ordinary chondrites: Formation by impact melting
p 1244 N94-16330

CHROMIUM OXIDES
Low-temperature sintering and phase changes in chromite interconnect materials
[DE93-015676] p 961 N94-17234

CHROMIUM STEELS
The effect of long-term aging on the impact properties of modified 9Cr-1Mo steel
[DE93-015453] p 957 N94-16068

CHROMOSPHERE
The chromosphere of VV cephei and the distribution of circumstellar dust around red giants and supergiants
[NASA-CR-193594] p 1297 N94-16866

CHRONIC CONDITIONS
Cool suit
[NASA-TM-109639] p 1120 N94-15250

CHRONOLOGY
Preliminary results of polarization signatures for glacial moraines in the Mono Basin, Eastern Sierra Nevada
p 1078 N94-16746

CIRCADIAN RHYTHMS
Diffusible driving and coupling signals of the biological clock
[AD-A267046] p 1121 N94-15660
TransRapid TR-07 maglev-spectrum magnetic field effects on daily pineal indoleamine metabolic rhythms in rodents
[DE93-015143] p 1117 N94-16893
Melatonin, the pineal gland, and circadian rhythms
[AD-A268200] p 1129 N94-17478

CIRCUIT DIAGRAMS
Circle diagram approach for self excited induction generators
[DE93-010031] p 1010 N94-15971

CIRCUIT RELIABILITY
Technology transfers and reliable oxides
[AD-A266948] p 1175 N94-15758

CIRCULAR CYLINDERS
Volume integral equations applied to circular and square cylinders
[AD-A266635] p 1169 N94-15785
Modal ring method for the scattering of sound
[NASA-TM-106342] p 1177 N94-16497

CIRRUS CLOUDS
Preliminary analysis of University of North Dakota aircraft data from the FIRE Cirrus IFO-2
[NASA-CR-193357] p 866 N94-15429
Separation of cirrus cloud from clear surface from AVIRIS data using the 1.38 micron water vapor band
p 1072 N94-16699

CIVIL AVIATION
US civil airmen statistics: Calendar year 1992
[AD-A267708] p 853 N94-14965
Symposium on the Future of Aeronautics in the Netherlands
[ETN-93-93780] p 853 N94-15120
Predicted and real development in the aviation in the period 1961-1991 p 853 N94-15122
The future of Schiphol: Growth within boundaries
p 853 N94-15123
Aviation inspection prospects p 853 N94-15125
Aviation and the KLM: Past and future
p 853 N94-15126
Expectations for the future of Fokker
p 854 N94-15127
Back to propellers
[NASA-TM-109445] p 869 N94-15344
Criminal acts against civil aviation, fiscal year 1992
[AD-A268014] p 863 N94-17586

CLASSICAL MECHANICS
Stability of flows in fluidized beds
[DE93-000245] p 1024 N94-16763

CLASSIFICATIONS
A browsing tool for the Internet Logical Library of the HPCC Software Exchange
[NASA-CR-194545] p 1143 N94-15189
A new method for generating Bayes classifiers assuming mixtures of Gaussian densities
[FFI-91/4029] p 1172 N94-15298
Multifrequency observations p 992 N94-15902
Lava flow-field morphological classification and interpretation: Examples from Venus
p 1259 N94-16230
The Al Rais meteorite: A CR chondrite or close relative? p 1243 N94-16290
The nature of dynamic arteriolar vasoreactivity: A mini-review and A classification scheme
[AD-A266499] p 1128 N94-16783

CLASSIFIERS
Acousto-optical classifier
[AD-D015894] p 1000 N94-16921

CLATHRATES
Far-infrared spectra of CO2 clathrate hydrate frosts
p 954 N94-16340

CLEAN ENERGY
Helium-3 inventory of lunar samples: A potential future energy resource for mankind? p 1295 N94-16428

CLEAN FUELS
Utility emissions associated with electric and hybrid vehicle (EHV) charging
[DE93-013734] p 1011 N94-16459

CLEANING
Polished substrate surface and cleaning study for coated optic quality
[DE93-014116] p 1190 N94-15975
Dry stripping as a surface treatment method
[VTT-TIED-1348] p 985 N94-17544

CLEARANCES
Soyuz/ACRV accommodation study
[NASA-TM-107733] p 888 N94-17072

CLEAVAGE
Bulk and defect properties of ordered intermetallics: A first-principles total-energy investigation
[DE93-015492] p 959 N94-16873

CLIMATE
IAI topic: El Nino. Southern oscillation and interannual climate variability
[INPE-5410-PRE/1757] p 1111 N94-15186
Global climate study
[NASA-TM-109612] p 1098 N94-15363
Exploring the southern ocean response to climate change
[NASA-CR-194601] p 1112 N94-15680
Research into the influence of spatial variability and scale on the parameterization of hydrological processes
[NASA-CR-194610] p 1082 N94-16026
Heterogeneity and scaling land-atmospheric water and energy fluxes in climate systems p 1083 N94-16030
Further development and testing of a second-order bulk boundary layer model
[AD-A268071] p 1109 N94-17552
Workshop on early Mars: How warm and how wet, part 2?
[NASA-CR-193503] p 1297 N94-17637
Boundary layer structure over areas of heterogeneous heat fluxes
[DE93-010657] p 1110 N94-17673

CLIMATE CHANGE
IAI topic: El Nino. Southern oscillation and interannual climate variability
[INPE-5410-PRE/1757] p 1111 N94-15186
Exploring the southern ocean response to climate change
[NASA-CR-194601] p 1112 N94-15680
Recent scientific advances in the use of radar in scientific hydrology p 991 N94-15895
Driving terrestrial ecosystem models from space
p 991 N94-15896
EOS SAR: A new approach p 992 N94-15904
A summary of microwave remote sensing investigations planned for BOREAS p 993 N94-15914
Statement on global climate change before the Subcommittee on Energy and Power, United States House of Representatives
[DE93-013163] p 1095 N94-16006
The effects of orbital and climatic variations on Martian surface heat flow p 1290 N94-16402
Global change research: Science and policy
[DE93-015675] p 1096 N94-16445
Discrimination among semi-arid landscape endmembers using the Spectral Angle Mapper (SAM) algorithm
p 1074 N94-16711
The use of General Circulation Models in detecting climate change induced by greenhouse gases
[DE93-014369] p 1096 N94-16802
Atmospheric ionization by solar particles detected by nitrate measurement in antarctic snow
[AD-A267583] p 1299 N94-17208
Incorporating global warming risks in power sector planning. Volume 1: A case study of the New England region
[DE93-015241] p 1096 N94-17289
Statistics and physical oceanography
[AD-A268565] p 1115 N94-17598
Surface energy balance modeling at mesoscale: The contribution of the future Earth observing system
[BCRS-91-04] p 1085 N94-17616

CLIMATOLOGY
Exploring the southern ocean response to climate change
[NASA-CR-194601] p 1112 N94-15680
Recent advances in radar remote sensing of forest
p 991 N94-15897
The effects of orbital and climatic variations on Martian surface heat flow p 1290 N94-16402
The use of General Circulation Models in detecting climate change induced by greenhouse gases
[DE93-014369] p 1096 N94-16802
Orographic microbursts in a severe winter windstorm
[AD-A267651] p 1108 N94-17247
Validation and analysis of microwave-derived rainfall over the tropics
[AD-A267785] p 1108 N94-17303
Further development and testing of a second-order bulk boundary layer model
[AD-A268071] p 1109 N94-17552
A two-layer quasi-geotrophic spherical model: Formulation and climatology
[DM-63] p 1110 N94-17593
Statistics and physical oceanography
[AD-A268565] p 1115 N94-17598
The Central American cold surge: An observational analysis of the deep southward penetration of North American cold fronts
[AD-A268592] p 1110 N94-17607
Workshop on early Mars: How warm and how wet, part 2?
[NASA-CR-193503] p 1297 N94-17637

CLIMBING FLIGHT
Trajectory optimization for the National Aerospace Plane
[NASA-CR-194618] p 867 N94-16498

CLINICAL MEDICINE
Living well in space: Clinical care challenge
[NASA-TM-109539] p 1120 N94-15370
Center of Excellence in Laser Medicine
[DE93-016541] p 1122 N94-16113
Tuberculosis: A case for increased screening
p 1126 N94-16627
Summary of follow-up results from potential tuberculosis exposures p 1126 N94-16628
Legionella: An overview p 1126 N94-16629

CLOCKS
Asynchronous design for parallel processing architectures
[AD-A266523] p 1160 N94-16791
Verification of fault-tolerant clock synchronization systems
[NASA-TP-3349] p 1161 N94-17449

CLOSED CYCLES
Some single-piston closed-cycle machines and Peter Tailer's thermal lag engine
[DE93-015983] p 1049 N94-17675

CLOSED ECOLOGICAL SYSTEMS
The dynamics of hydroponic crops for simulation studies of the CELSS initial reference configurations
[NASA-CR-194654] p 1118 N94-17279
Strategy for the reduction of total integrated fluid logistics to the Space Station Freedom
[NASA-TM-107744] p 1138 N94-17452

CLOUD COVER
Venus lightning
[NASA-TM-109644] p 1105 N94-15430
Simulation of AVHRR-K band ratios with AVIRIS
p 1075 N94-16714

Three dimensional visualization of GOES cloud data using OCTRESS
[AD-A268102] p 1109 N94-17572
The Central American cold surge: An observational analysis of the deep southward penetration of North American cold fronts
[AD-A268592] p 1110 N94-17607

CLOUD HEIGHT INDICATORS
An empirical study of tropical cloud clusters using special sensor microwave imager data
[AD-A268072] p 1110 N94-17595

CLOUD PHYSICS
A global traveling wave on Venus
[NASA-CR-194356] p 1246 N94-15182
Preliminary analysis of University of North Dakota aircraft data from the FIRE Cirrus IFO-2
[NASA-CR-193357] p 866 N94-15429
Investigation of cloud properties and atmospheric stability with MODIS
[NASA-CR-193475] p 1107 N94-16717

CLOUDS
Ground truth spectrometry and imagery of eruption clouds to maximize utility of satellite imagery
[NASA-CR-194358] p 1081 N94-15181
Clouding tracing: Visualization of the mixing of fluid elements in convection-diffusion systems
[NASA-CR-191529] p 1148 N94-15965

CLOUDS (METEOROLOGY)
A comparison of cloud attenuation models using measured cloud data p 996 N94-16044
Three dimensional visualization of GOES cloud data using OCTRESS
[AD-A268102] p 1109 N94-17572

CLUSTER ANALYSIS
Massively parallel, adaptive, color image processing for autonomous road following
[AD-A266988] p 864 N94-15498

CLUTTER
Designing clutter rejection filters with complex coefficients for airborne pulsed Doppler weather radar
[NASA-CR-4550] p 862 N94-15444
High resolution radar profiling using higher-order statistics
[AD-D015891] p 1000 N94-16918
Signal detection in correlated Gaussian and non-Gaussian radar clutter
[AD-A267453] p 1001 N94-17033
Automatic suppression of anomalous propagation clutter for noncoherent weather radars
[KNMI-WR-92-06] p 1004 N94-17407

CMOS
VLSI for high-speed digital signal processing
[AD-A267709] p 1007 N94-14936
The XMM pn-CCD detector system: First results
p 900 N94-15034
A linear monolithic 4-6 on silicon IR detector array
p 910 N94-15098
Fault handling schemes in electronic systems with specific application to radiation tolerance and VLSI design
[NASA-CR-194559] p 1008 N94-15640
Reliability characterization of digital microcircuits: Investigation of an in-process oxide reliability screening method
[AD-A267053] p 1008 N94-15665

COAL
Publications of the Oak Ridge National Laboratory Fossil Energy Program, 1 October 1991 - 31 March 1993
[DE93-014643] p 1232 N94-16967

COAL DERIVED GASES
High octane ethers from synthesis gas-derived alcohols
[DE93-016861] p 975 N94-16898

COAL DERIVED LIQUIDS
Preconversion catalytic deoxygenation of phenolic functional groups
[DE93-017034] p 950 N94-16912
Advanced thermally stable jet fuels
[DE93-017711] p 975 N94-16996

COAL LIQUEFACTION
Advanced thermally stable jet fuels
[DE93-017711] p 975 N94-16996
Supercritical thermodynamics of sulfur and nitrogen species
[DE93-017727] p 1220 N94-16997

COAL UTILIZATION
High octane ethers from synthesis gas-derived alcohols
[DE93-016861] p 975 N94-16898

COALESCING
Bubble coalescence in magmas p 1103 N94-16237

COASTAL CURRENTS
On the application and evaluation of the relocatable diecast ocean circulation model in coastal and semi-enclosed seas
[AD-A266626] p 1112 N94-15771

COASTAL PLAINS
Composite refraction-reflection stack sections: Tracing faults in the Atlantic coastal plain sediments
[DE93-013581] p 1112 N94-16009

COASTAL WATER
Characterization of spatial and temporal variability of phytoplankton blooms in coastal waters
[AD-A267102] p 1116 N94-15633
Preliminary estimates of frequency-direction spectra derived from the SAMSON pressure gage array, November 1990 to May 1991
[AD-A267960] p 1114 N94-17497

COASTAL ZONE COLOR SCANNER
Coastal zone color scanner: Nimbus 7
[NASA-TM-109590] p 1111 N94-15281
Optical properties of the Red Sea
[AD-A266466] p 1113 N94-16588
Atmospheric correction of AVIRIS data in ocean waters p 1070 N94-16690

COASTS
Ventilated oscillatory boundary layers
[AD-A266226] p 1023 N94-16110
Field observations of infragravity, sea and swell directional spectra
[AD-A266439] p 1113 N94-16561

COATING
A new NASA LaRC Multi-Purpose Prepregging Unit
p 932 N94-15276
Effects of aging time on V205 sol-gel coatings
[AD-A266824] p 965 N94-15843
Investigation of the effects of polyelectrolyte coatings on colloid transport in porous media
[DE93-018300] p 970 N94-16973
A state-of-the-art plasma polymerization coater for ICF targets
[DE93-016452] p 1204 N94-17237

COATINGS
The effect of process parameters on the surface finish of plasma polymers
[DE93-014112] p 966 N94-15924
Polished substrate surface and cleaning study for coated optic quality
[DE93-014116] p 1190 N94-15975
Weibull analysis applied to the pull adhesion test and fracture of a metal-ceramic interface
[DE93-012913] p 1059 N94-15997
Investigation of the effects of polyelectrolyte coatings on colloid transport in porous media
[DE93-018300] p 970 N94-16973
Thin composite solid electrolyte film for lithium batteries
[NASA-CASE-NPO-18694-1-CU] p 1014 N94-17325

COAXIAL CABLES
Determination of equivalent circuit for PVDF shock-pressure gauges
[DE93-016492] p 1034 N94-16452

COBALT
Robotic weld overlay coatings for erosion control
[DE93-016938] p 970 N94-16959

COBALT ALLOYS
Dynamical Ising model simulations of nucleation and growth in copper-cobalt alloys
[DE93-015336] p 957 N94-16015

COBALT FLUORIDES
Neutron and x ray scattering studies of (FeF2)(sub m)(CoF2)(sub n) multilayers
[DE93-015809] p 1184 N94-16838

COBALT OXIDES
Siderophile elements in the upper mantle of the Earth: New clues from metal-silicate partition coefficients
p 1103 N94-16250

COCHLEA
Studies of aural acoustic emmissions with the use of an original apparatus and investigative methodology
[IFTR-20/1992] p 1177 N94-16650

COCKPITS
Better way to fly
[NASA-TM-109447] p 866 N94-15396
Basic principles of helicopter crashworthiness
[AD-A267099] p 862 N94-15637

CODE DIVISION MULTIPLE ACCESS
The ELLIPSO (tm) system: Elliptical low orbits for mobile communications p 893 N94-17167

CODING
Rotary encoding device
[NASA-CASE-GSC-13543-1] p 1189 N94-15705
Rotary encoding device
[NASA-CASE-GSC-13556-1] p 1148 N94-15943
Bandwidth efficient coding: Theoretical limits and real achievements. Error control techniques for satellite and space communications p 997 N94-16507
Search for optimal distance spectrum convolutional codes p 998 N94-16509
Discovering sequence similarity by the algorithmic significance method
[DE93-015556] p 1150 N94-16659

COERCIVITY
Magnetic and magneto-optical properties and domain structure of Co/Pd multilayers p 1227 N94-14991

COGNITION
Altitude deviations: Breakdowns of an error-tolerant system
[NASA-TM-108788] p 862 N94-15550
Complex information coordination performance: Differential changes in working memory contributions following training
[AD-A267007] p 1132 N94-15762
Scuba-diving, anxiety and task performance
p 1132 N94-15938

COGNITIVE PSYCHOLOGY
Neural mechanisms of attention
[AD-A266315] p 1132 N94-16456
States of awareness 1: Subliminal perception relationship to situational awareness
[AD-A267249] p 1132 N94-16942
Theoretical and experimental research into biological mechanisms underlying learning and memory
[AD-A267441] p 1133 N94-17022
Processes involved in the integration of pictures and discourse
[AD-A268150] p 1134 N94-17468

COHERENT RADAR
Heterodyne efficiency for a coherent laser radar with diffuse or aerosol targets
[NASA-CR-194563] p 1038 N94-15477
High resolution radar profiling using higher-order statistics
[AD-D015891] p 1000 N94-16918
Remote sensing of precipitation and electrification with a dual-polarization, coherent, wideband radar system
[AD-A267479] p 1004 N94-17364

COHERENT RADIATION
Theoretical studies relating to the interaction of radiation with matter
[AD-A266894] p 1179 N94-14949

COLD CATHODES
Diamond p-n junction cold cathode
[AD-A266926] p 1206 N94-15107

COLD FRONTS
Mesoscale frontogenesis: An analysis of two cold front case studies
[AD-A267950] p 1107 N94-17054
Opposing mesoscale flows in a broken midlatitude squall line
[AD-A268011] p 1109 N94-17492
The Central American cold surge: An observational analysis of the deep southward penetration of North American cold fronts
[AD-A268592] p 1110 N94-17607

COLD WORKING
The influence of secondary bending on fatigue life improvement in bolted joints
[ARL-RR-14] p 1058 N94-15963
Evolution of microstructure in face centered cubic metals during irradiation: A review
[DE93-015682] p 958 N94-16662

COLLAPSE
The size of complex craters p 1262 N94-16249

COLLIMATORS
Test methods for acceptance testing of telescopes
[AD-A268316] p 1237 N94-17568

COLLISION AVOIDANCE
Path planning for robotic truss assembly
[NASA-CR-194652] p 897 N94-17280

COLLISION PARAMETERS
Closed orbit distortion and the beam-beam interaction
[DE93-015284] p 1190 N94-15854

COLLISIONAL PLASMAS
Dynamic behavior of an electric arc gas discharge
[DE93-630197] p 1205 N94-17635

COLLISIONS
Collisional and dynamical history of Gaspra
p 1241 N94-16202
Simulation of collisional fragmentation with explosives
p 1063 N94-16254
Stability analysis for the flow of granular materials down an inclined plane using kinetic model
[DE93-016852] p 1026 N94-16958
Discrete models of the Boltzmann equation: Structure of the collision operator of sound propagation
[IFTR-2/1992] p 1178 N94-17051
Cathode sheath charge transfer effects
[AD-A268393] p 1186 N94-17536

COLLOCATION
Adaptive wavelet collocation methods for initial value boundary problems of nonlinear PDE's
[NASA-CR-191507] p 1169 N94-15833

COLLOIDS
Rheology and microstructure of concentrated zirconia-alumina suspensions for gelcasting composites
[DE93-015339] p 966 N94-16016

Investigation of the effects of polyelectrolyte coatings on colloid transport in porous media
[DE93-018300] p 970 N94-16973
Regulation of attached bacterial growth by adsorbed proteins
[AD-A267756] p 1118 N94-17275

COLOR
Optimum wavelengths for two color ranging p 915 N94-15580
Two color satellite laser ranging upgrades at Goddard's 1.2m telescope facility p 915 N94-15581
Millimeter accuracy satellites for two color ranging p 916 N94-15583
Airborne 2 color ranging experiment p 920 N94-15614
Color separation gratings p 1198 N94-17362
The effects of luminance boundaries on color perception
[AD-A268398] p 1133 N94-17397
Perception of lightness and brightness in complex patterns
[AD-A268435] p 1134 N94-17513

COLOR PHOTOGRAPHY
Global and regional/seasonal color mosaics of Mars p 1288 N94-16393

COLOR TELEVISION
Display system employing acousto-optic tunable filter
[NASA-CASE-NPO-18736-1-CU] p 1190 N94-15933

COLOR VISION
Massively parallel, adaptive, color image processing for autonomous road following
[AD-A266988] p 864 N94-15498
The effects of luminance boundaries on color perception
[AD-A268398] p 1133 N94-17397

COMBAT
Sleep management user's guide for special operations personnel
[AD-A267746] p 1119 N94-14943
Infrared spot tracker
[AD-D015778] p 1191 N94-16547

COMBINATIONS (MATHEMATICS)
New techniques for the combination of heterogenous data when determining the Earth's gravity field
[SER-C-395] p 1098 N94-15153

COMBINATORIAL ANALYSIS
Efficient algorithmic techniques for combinatorial problems
[AD-A267151] p 1172 N94-15777
Combinatorial semantics
[TR-444] p 1149 N94-16575

COMBUSTION
Mechanisms of combustion limits in premixed gas flames at microgravity
[NASA-CR-194557] p 946 N94-15713

COMBUSTION CHAMBERS
Supersonic Combustion Research Laboratory. Volume 1: Design and fabrication
[AD-A267667] p 943 N94-14962
Acoustic waves in complicated geometries and their interactions with liquid-propellant droplet combustion
[AD-A267260] p 1178 N94-16991

COMBUSTION CHEMISTRY
A proposed mechanism for the pyrolysis of diborane
[DE93-014275] p 947 N94-15977
Fundamental studies of rocket combustion chemistry and combustion instability
[AD-A266248] p 925 N94-16482
Gas Analysis System
[DE93-014617] p 949 N94-16891

COMBUSTION CONTROL
Biomass energy: State of the technology present obstacles and future potential
[DE93-016295] p 1092 N94-16766

COMBUSTION EFFICIENCY
Space Shuttle main engine. NASA has not evaluated the alternate fuel turbopump costs and benefits. Report to the Administrator of the National Aeronautics and Space Administration
[GAO/NSIAD-94-54] p 926 N94-16834

COMBUSTION PHYSICS
Rotary engine performance computer program (RCEMAP and RCEMAPPC): User's guide
[NASA-CR-191192] p 869 N94-15192
Clouding tracing: Visualization of the mixing of fluid elements in convection-diffusion systems
[NASA-CR-191529] p 1148 N94-15965
New findings and instrumentation from the NASA Lewis Microgravity Facility p 977 N94-16076
Studies of combustion reactions at the state-resolved differential cross section level
[DE93-017605] p 948 N94-16462
Acoustic waves in complicated geometries and their interactions with liquid-propellant droplet combustion
[AD-A267260] p 1178 N94-16991
Lifted turbulent jet flames
[AD-A267911] p 952 N94-17381
Experimental studies on a gas dynamic laser with narrow throat and high area-ratio grid nozzles
[AD-A267818] p 1042 N94-17400

COMBUSTION PRODUCTS
Scholarly research program in fuel analysis and combustion research
[AD-A266789] p 942 N94-14911
Rocket Motor Plume Technology
[AGARD-LS-188] p 923 N94-15217
Plume primary smoke p 923 N94-15218
Secondary smoke p 924 N94-15220
Rocket motor plume flowfields: Phenomenology and simulation p 924 N94-15221
NASA Operational Environment Team (NOET): NASA's key to environmental technology
[TABES PAPER 93-611] p 1052 N94-16143
Emerging technologies for the changing global market
[TABES PAPER 93-612] p 930 N94-16144
Fundamental studies of rocket combustion chemistry and combustion instability
[AD-A266248] p 925 N94-16482
Biomass energy: State of the technology present obstacles and future potential
[DE93-016295] p 1092 N94-16766
Emissions of volatile organic compounds from stationary combustion sources: Numerical modeling capabilities
[DE93-014123] p 1096 N94-16825
Gas Analysis System
[DE93-014617] p 949 N94-16891
Modeling study to evaluate the ionic mechanism of soot formation in flames
[AD-A266242] p 950 N94-16930
Surface reactivity of combustion generated soot particles
[AD-A268017] p 952 N94-17532

COMBUSTION STABILITY
Fundamental studies of rocket combustion chemistry and combustion instability
[AD-A266248] p 925 N94-16482
Acoustic waves in complicated geometries and their interactions with liquid-propellant droplet combustion
[AD-A267260] p 1178 N94-16991

COMBUSTION SYNTHESIS
Production and evaluation of dense ceramic compounds by combustion synthesis and dynamic compaction
[AD-A266742] p 965 N94-15773

COMET NUCLEI
The physical mechanism of comet outbursts: An experiment p 1242 N94-16221

COMET RENDEZVOUS ASTEROID FLYBY MISSION
Life and the solar system: The CRAF and Cassini missions
[NASA-TM-109422] p 1247 N94-15513

COMETS
Molecular processes in comets
[NASA-CR-194148] p 1239 N94-15188
Life and the solar system: The CRAF and Cassini missions
[NASA-TM-109422] p 1247 N94-15513
The physical mechanism of comet outbursts: An experiment p 1242 N94-16221
Small satellite missions to long-period comets p 874 N94-17144

COMMAND AND CONTROL
Decomposition of large sparse symmetric systems for parallel computation. Part 1: Theoretical foundations
[AD-A267144] p 1159 N94-15750
International testing of a Mars rover prototype p 1273 N94-16312
Not ready for the first space war. What about the second?
[AD-A266557] p 1174 N94-16665
Data processing system for ARSENE ground station: A tool for small satellite control and development p 878 N94-17157
S 80/T: A micro satellite system combining high performances and limited resources p 893 N94-17166
Visual display principles for C3I system tasks
[AD-A267969] p 1005 N94-17498

COMMERCE
Approaching the new reality
[TABES PAPER 93-230] p 1050 N94-16131
Space commerce in a global economy: Comparison of US and Australian approaches
[NASA-TM-109341] p 1235 N94-17290

COMMERCIAL AIRCRAFT
Criminal acts against civil aviation, fiscal year 1992
[AD-A268014] p 863 N94-17586

COMMERCIAL ENERGY
Energy from the sun: Evolution of federal support for solar energy
[AD-A267944] p 1093 N94-17382

COMMINUTION
Dynamic testing and characterization of pre-fractured ceramic
[DE93-016457] p 972 N94-17238

COMMUNICATION EQUIPMENT
Operation of digital systems in severe electromagnetic environments
[AD-A267176] p 988 N94-15693
Satellite communications installation plan
[AD-A266303] p 1000 N94-16965
Ground wave emergency network final operational capability: Environmental assessment for central Nevada relay node, site number RN 8W917NV
[AD-A267630] p 1002 N94-17200
Ground wave emergency network final operational capability: Environmental assessment for southern Nevada relay node site number RN 8W918NV
[AD-A267647] p 1002 N94-17205
Ground wave emergency network final operational capability: Environmental assessment for northwestern Nebraska relay node, site number RN 8C930NE
[AD-A267629] p 1003 N94-17212
Ground wave emergency network environmental assessment for northwestern Colorado relay node site number RN 8C924CO
[AD-A267654] p 1003 N94-17249

COMMUNICATION NETWORKS
The Third Annual NASA Science Internet User Working Group Conference
[NASA-CP-3170] p 1228 N94-15116
Electronic messaging for the 1990's
[AD-A267143] p 1229 N94-15437
Multiphase complete exchange: A theoretical analysis
[NASA-CR-191531] p 1145 N94-15489
Overview of Enhanced Data Stream Array Processor (EDSAP)
[AD-A266986] p 1158 N94-15492
Congestion control of high-speed networks
[AD-A267013] p 989 N94-15748
Logarithmic asymptotics for steady-state tail probabilities in a single-server queue
[AD-A266746] p 1165 N94-15775
Department of Defense technical architecture framework for information management. Volume 3: Architecture concepts and design guidance, version 2.0
[AD-A267195] p 1230 N94-15789
Data distribution p 993 N94-15910
Remote diagnosis as used for mechanized parking systems p 984 N94-16004
Performance Information Management System (PIMS) communication
[AD-A267040] p 1231 N94-16458
Consistent failure reporting in reliable communication systems
[AD-A266298] p 997 N94-16477
Information technology division technical paper abstracts
[AD-A266227] p 1166 N94-16938
A formal protocol test procedure for the Survivable Adaptable Fiber Optic Embedded Network (SAFENET)
[AD-A267410] p 1192 N94-16975
Ground wave emergency network final operational capability: Environmental assessment for central Wyoming relay node, site number RN 8C928WY
[AD-A267842] p 1001 N94-17011
Low Earth orbit constellations: Orbit control or not p 875 N94-17134
Impact of launching uncertainties on the visibility of communication satellite constellations without orbit control p 889 N94-17135
A study on an experimental communication system using microsatellites p 892 N94-17160
Feasibility study of a personal communications system IRIDIUM-like p 893 N94-17165
Ground wave emergency network final operational capability: Environmental assessment for central Utah relay node, site number RN 8C920UT
[AD-A267628] p 1003 N94-17211
Ground wave emergency network. Final operational capability. Environmental assessment for southeastern Idaho relay node, site no. RN8W927ID
[AD-A267796] p 1003 N94-17304
Non-blocking crossbar permutation engine with constant routing latency
[NASA-CASE-NPO-18864-1-CU] p 1161 N94-17328
A scalable wrap-around shuffle exchange network with deflection routing
[NASA-CASE-NPO-18983-1-CU] p 1161 N94-17330
Ground wave emergency network final operational capability. Environmental assessment for southern Arkansas relay node site no. RN 8C912AR
[AD-A268001] p 1004 N94-17376
Environmental assessment for northwestern Indiana relay node site no. RN 8C902IN
[AD-A267849] p 1004 N94-17406

A protocol validator for the SCM and CFSM models
[AD-A268523] p 1156 N94-17541

COMMUNICATION SATELLITES

Activities of Canadian Satellite Communications, Inc.
[CTN-93-60864] p 994 N94-15959

Olympus propagation measurement results at Virginia Tech p 995 N94-16037

Data acquisition, preprocessing and analysis for the Virginia Tech OLYMPUS experiment p 995 N94-16038

Comparison of OLYMPUS beacon and radiometric attenuation measurements at Blacksburg, Virginia p 996 N94-16046

Satellite sound broadcast propagation measurements p 996 N94-16047

The early development of the Telecommunications Satellite Programme in ESRO (1965-1971)
[ESA-HSR-9] p 887 N94-16525

Small satellite constellation system: Optimization criteria p 888 N94-17132

Impact of launching uncertainties on the visibility of communication satellite constellations without orbit control p 889 N94-17135

Small satellite constellation deployment strategies p 878 N94-17138

Adequation of mini satellites to oceanic altimetry missions p 891 N94-17152

Satellite control: A comprehensive approach p 878 N94-17158

Regulation of low Earth orbit satellites p 892 N94-17159

Feasibility study of a personal communications system IRIDIUM-like p 893 N94-17165

STARSYS: A view after WARC-92 --- satellite position and messaging system p 893 N94-17168

UoSAT: A decade of experience pioneering microsatellites p 894 N94-17169

Arsene GaAs solar array p 894 N94-17174

The STRV On Board Data Handling (OBDH) system: An introduction p 895 N94-17178

Standard platforms for small satellites p 895 N94-17181

Big results with small space systems: What small systems are doing today p 896 N94-17187

Key trends of the small satellite market p 897 N94-17191

Military satellite communications: Opportunity to save billions of dollars. Report to the Chairman, Legislation, and National Security Subcommittee, Committee on Government Operations, House of Representatives
[AD-A267627] p 1002 N94-17199

On-board packet switch architectures for communication satellites
[NASA-TM-106328] p 883 N94-17488

Satellite communications systems and technology. Executive summary
[NASA-TM-109346] p 1006 N94-17661

COMPACTING

Verification of a two-dimensional infiltration model for the resin transfer molding process
[NASA-CR-194597] p 964 N94-15656

Production and evaluation of dense ceramic compounds by combustion synthesis and dynamic compaction
[AD-A266742] p 965 N94-15773

COMPETITION

The NASA competitive placement plan for positions GS-15 and below (including trades and labor positions)
[NHB-3335.1C] p 1224 N94-15944

COMPILERS

Concurrent garbage collection of persistent heaps
[AD-A266831] p 1141 N94-14915

Applicability of the session and the presentation layers for the support of high speed applications
[INRIA-RT-144] p 1158 N94-14980

Evaluation of ALSYS 037 Ada Compiler
[AD-A266972] p 1143 N94-15110

The application of compiler-assisted multiple instruction retry to VLIW architectures
[AD-A266930] p 1158 N94-15173

Efficient compilation of array statements for private memory multicomputers
[AD-A266595] p 1160 N94-16724

Detailed example of using ACEC release 3.0 with the DEC VAX Ada compiler
[AD-A267880] p 1152 N94-17014

COMPLEX COMPOUNDS

High-valent oxo, methoxorhenium complexes: Models for intermediates and transition states in proton-coupled multi-electron transfer reactions
[AD-A266492] p 1211 N94-16782

Synthesis, reactivity, and characterization of (-hexacarbocyclic) manganese dicarbonyl complexes with sulfur and phosphorus ligands
[AD-A267592] p 930 N94-17192

Synthesis, characterization, and polymerization of new ferrocene-fluorene complexes. A novel high-molecular weight conjugated polymer with pendant ferrocene groups
[AD-A267717] p 972 N94-17273

COMPLEX SYSTEMS

Multiobjective functions optimization for task allocation mapping to multicomputer nodes
[AD-A267071] p 1146 N94-15670

Development of pattern recognition techniques for the evaluation of toxicant impacts to multispecies systems
[AD-A267197] p 1095 N94-15790

A modular control architecture for real-time synchronous and asynchronous systems
[DE93-015439] p 1166 N94-16888

Speckles statistics and decorrelation effects in complex ABCD optical systems
[AD-A267843] p 1193 N94-17012

COMPLEX VARIABLES

Closed form characteristic function for general complex second-order form in correlated complex Gaussian random variables
[AD-A267883] p 1171 N94-17393

COMPONENT RELIABILITY

The design of self-checking reduced instruction set computers
[AD-A267012] p 1140 N94-15763

Reduction of parasitic lasing
[NASA-CASE-LAR-14645-1-SB] p 1039 N94-15942

COMPOSITE MATERIALS

Production Technology for Components from Nonmetallic Fiber Reinforced Materials
[ETN-93-94607] p 931 N94-15254

Production process p 931 N94-15257

Machine development p 932 N94-15258

Component testing and quality assurance p 932 N94-15259

Development of a computer supported instrumentation for economic planning and evaluation of production facilities for fiber reinforced composites elements p 932 N94-15260

Processing, properties and applications of composites using powder-coated epoxy towpreg technology p 933 N94-15277

Better airplane wings
[NASA-TM-109446] p 933 N94-15345

Illustrated glossary of textile terms for composites
[NASA-CR-191539] p 933 N94-15484

Method and apparatus for non-destructive evaluation of composite materials with cloth surface impressions
[NASA-CASE-LAR-14535-1] p 933 N94-15878

On the design of structural components using materials with time-dependent properties
[NASA-TM-108428] p 1059 N94-16519

An overview of the NASA textile composites program p 937 N94-16846

Techno-economic requirements for automotive composites p 937 N94-16847

Fibers and materials of medical application p 938 N94-16855

Techno-economic requirements for composite aircraft components p 940 N94-16864

Influence of the loading rate on the endurance and deformability of cement matrix composites
[IFTR-1/1992] p 1060 N94-17052

Fabrication of piezoelectric ceramic/polymer composites by injection molding
[AD-A267302] p 972 N94-17227

Thin composite solid electrolyte film for lithium batteries
[NASA-CASE-NPO-18694-1-CU] p 1014 N94-17325

COMPOSITE STRUCTURES

Dynamic behavior of fiber and particle reinforced composites
[AD-A266905] p 930 N94-15143

Better airplane wings
[NASA-TM-109446] p 933 N94-15345

Progress in the modeling of the shock response and mitigation of thick composite shells
[AD-A267009] p 1057 N94-15524

High temperature advanced structural composites. Volume 2: Ceramic matrix composites, fiber processiing and properties, and interfaces
[AD-A267023] p 933 N94-15528

High temperature advanced structural composites. Volume 3: Mechanics
[AD-A267024] p 933 N94-15626

Center for Rotorcraft Education and Research progress report, 1987 - 1992
[AD-A266760] p 857 N94-15824

High temperature advanced structural composites. Volume 1: Executive summary and intermetallic compounds
[AD-A267022] p 933 N94-15835

Improved composite flexible blanket insulation
[NASA-CASE-ARC-11955-1-CU] p 934 N94-15926

Slidesurfaces with: adaptive new definitions (SAND) for transient analysis
[DE93-014909] p 1059 N94-15983

On the design of structural components using materials with time-dependent properties
[NASA-TM-108428] p 1059 N94-16519

FIBER-TEX 1992: The Sixth Conference on Advanced Engineering Fibers and Textile Structures for Composites
[NASA-CP-3211] p 936 N94-16845

Thin composite solid electrolyte film for lithium batteries
[NASA-CASE-NPO-18694-1-CU] p 1014 N94-17325

Structural mechanics division research and technology accomplishments for CY 1992 and plans for CY 1993
[NASA-TM-107752] p 1062 N94-17479

COMPOSITE WRAPPING

Production process p 931 N94-15257

Machine development p 932 N94-15258

COMPRESSED GAS

Inflatable rescue device
[NASA-CASE-MSC-22244-1] p 1137 N94-15883

Transmission of light through a turbulent mixing layer
[AD-A267266] p 1193 N94-17264

COMPRESSIBILITY

The processing and mechanical properties of high temperature/high performance composites. Book 5: Processing and miscellaneous properties
[AD-A266398] p 935 N94-16529

COMPRESSIBILITY EFFECTS

Turbulence modelling for shock wave/boundary layer interactions specific issues and examples of applications p 1018 N94-15202

COMPRESSIBLE BOUNDARY LAYER

Tollmien-Schlichting/vortex interactions in compressible boundary layer flows
[NASA-CR-191515] p 1017 N94-15183

Higher-order accurate Osher schemes with application to compressible boundary layer stability
[NASA-TM-106355] p 1026 N94-17056

COMPRESSIBLE FLOW

Large-Eddy Simulations (LES) of flows and turbulence distribution
[AD-A267182] p 1016 N94-15151

Turbulence modelling for shock wave/boundary layer interactions specific issues and examples of applications p 1018 N94-15202

Proteus two-dimensional Navier-Stokes computer code, version 2.0. Volume 2: User's guide
[NASA-TM-106338-VOL-2] p 1019 N94-15475

Proteus two-dimensional Navier-Stokes computer code, version 2.0. Volume 1: Analysis description
[NASA-TM-106336-VOL-1] p 1019 N94-15485

Proteus three-dimensional Navier-Stokes computer code, version 1.0. Volume 2: User's guide
[NASA-TM-106340-VOL-2] p 1020 N94-15488

Proteus three-dimensional Navier-Stokes computer code, version 1.0. Volume 3: Programmer's reference
[NASA-TM-106341] p 1022 N94-15865

Proteus two-dimensional Navier-Stokes computer code, version 2.0. Volume 3: Programmer's reference
[NASA-TM-106339] p 1022 N94-15867

Proteus three-dimensional Navier-Stokes computer code, version 1.0. Volume 1: Analysis description
[NASA-TM-106337] p 1024 N94-16527

Numerical study of compressible boundary-level transition between two concentric cylinders
[NASA-CR-194622] p 1025 N94-16842

Adaptive Cartesian grid methods for representing geometry in inviscid compressible flow
[DE93-016430] p 1025 N94-16894

Three dimensional hydrodynamic calculations with adaptive mesh refinement of the evolution of Rayleigh Taylor and Richtmyer Meshkov instabilities in converging geometry: Multi-mode perturbations
[DE93-017155] p 1025 N94-16903

On solving the compressible Navier-Stokes equations for unsteady flows at very low Mach numbers
[NASA-TM-106380] p 1027 N94-17128

Development of iterative techniques for the solution of unsteady compressible viscous flows
[NASA-CR-194657] p 1027 N94-17129

Compressible flow solvers using unstructured grids
[INRIA-RR-1732] p 1030 N94-17531

COMPRESSION RATIO

Jet engine performance enhancement through use of a wave-rotor topping cycle
[NASA-TM-4486] p 870 N94-17470

COMPRESSION TESTS

Experimental study of nonassociated flow and instability of frictional materials
[AD-A266421] p 1024 N94-16555

Development of test methods for textile composites p 939 N94-16862

Static and dynamic investigations of brittle elasto-optical material
[IFTR-3/1992] p 1061 N94-17086
COMPRESSION WAVES
The seismic response of an aquifer to the propegation of an impact generated shock wave: A possible trigger of the Martian outflow channels? p 1281 N94-16354
Shear wave measurements in shock-induced, high-pressure phases
[DE93-016461] p 1062 N94-17664
COMPRESSIVE STRENGTH
Simulation studies for surfaces and materials strength
[NASA-CR-193387] p 1056 N94-15004
Mechanical properties of magnesium ammonium phosphate cements and their zeolite composites
[DE93-015155] p 934 N94-16057
Effect of Impact Damage and Open Hole on Compressive Strength of Hybrid Composite Laminates
[NASA-CR-194603] p 936 N94-16836
Dynamic testing and characterization of pre-fractured ceramic
[DE93-016457] p 972 N94-17238
COMPRESSOR BLADES
Determining the effect of endwall boundary layer suction in a large scale subsonic compressor cascade
[AD-A267208] p 859 N94-16913
COMPUTATION
A formal language for the specification and verification of synchronous and asynchronous circuits
[NASA-CR-191509] p 1144 N94-15443
Decomposition of large sparse symmetric systems for parallel computation. Part 2: Parallelization tool roadmap
[AD-A267072] p 1158 N94-15671
A scientific basis for computational science
[AD-A266697] p 1148 N94-15841
Efficient computational methods to study new and innovative signal detection techniques in SETI
[NASA-CR-193602] p 998 N94-16649
COMPUTATIONAL CHEMISTRY
Continuum solvent models for computational chemistry
[DE93-016329] p 953 N94-17660
COMPUTATIONAL FLUID DYNAMICS
Large-Eddy Simulations (LES) of flows and turbulence distribution
[AD-A267182] p 1016 N94-15151
Swept shock wave/laminar boundary layer interactions, experimental, and numerical results
p 1017 N94-15198
Numerical simulation of 3-D shock wave turbulent boundary layer interactions p 1017 N94-15199
Unsteady phenomena in shock wave/boundary layer interaction p 1017 N94-15200
Hypersonic shock wave boundary layer interactions over simplified deflected control surface configurations
p 1018 N94-15203
Rocket motor plume flowfields: Phenomenology and simulation p 924 N94-15221
The 1989 computational fluid dynamics highlights
[NASA-TM-109635] p 1018 N94-15246
The 1988 computational fluid dynamics highlights
[NASA-TM-109645] p 1019 N94-15431
Proteus two-dimensional Navier-Stokes computer code, version 2.0. Volume 2: User's guide
[NASA-TM-106338-VOL-2] p 1019 N94-15475
Proteus two-dimensional Navier-Stokes computer code, version 2.0. Volume 1: Analysis description
[NASA-TM-106336-VOL-1] p 1019 N94-15485
Proteus three-dimensional Navier-Stokes computer code, version 1.0. Volume 2: User's guide
[NASA-TM-106340-VOL-2] p 1020 N94-15488
Numerical investigations in three-dimensional internal flows
[NASA-CR-194594] p 1020 N94-15551
Particle kinetic simulation of high altitude hypervelocity flight
[NASA-CR-194599] p 856 N94-15678
On the application and evaluation of the relocatable diecast ocean circulation model in coastal and semi-enclosed seas
[AD-A266626] p 1112 N94-15771
User's manual for the HYPGEN hyperbolic grid generator and the HGUI graphical user interface
[NASA-TM-108791] p 1148 N94-15784
NAS technical summaries: Numerical aerodynamic simulation program, March 1991 - February 1992
[NASA-TM-109335] p 854 N94-15798
Modal element method for potential flow in non-uniform ducts: Combining closed form analysis with CFD
[NASA-TM-106347] p 1169 N94-15799
On the stability analysis of approximate factorization methods for 3D Euler and Navier-Stokes equations
[NASA-TM-106314] p 1169 N94-15818
Proteus three-dimensional Navier-Stokes computer code, version 1.0. Volume 3: Programmer's reference
[NASA-TM-106341] p 1022 N94-15865
Proteus two-dimensional Navier-Stokes computer code, version 2.0. Volume 3: Programmer's reference
[NASA-TM-106339] p 1022 N94-15867
Clouding tracing: Visualization of the mixing of fluid elements in convection-diffusion systems
[NASA-CR-191529] p 1148 N94-15965
Effects of rotation on coolant passage heat transfer. Volume 2: Coolant passages with trips normal and skewed to the flow
[NASA-CR-4396-VOL-2] p 1023 N94-15991
Aerodynamic/dynamic/control interaction
[AD-A266187] p 871 N94-16107
Implementation of an anisotropic turbulence model in the COMMIX-1C/ATM computer code
[DE93-015541] p 1023 N94-16444
Computation of the Fluid and Optical Fields About the Stratospheric Observatory for Infrared Astronomy (SOFIA) and the Coupling of Fluids, Dynamics, and Control Laws on Parallel Computers
[NASA-CR-193168] p 858 N94-16510
Proteus three-dimensional Navier-Stokes computer code, version 1.0. Volume 1: Analysis description
[NASA-TM-106337] p 1024 N94-16527
Flow analysis for the nacelle of an advanced ducted propeller at high angle-of-attack and at cruise with boundary layer control
[NASA-TM-106371] p 858 N94-16571
Applications and development of communication models for the touchstone GAMMA and DELTA prototypes
[NASA-CR-193617] p 999 N94-16867
Computation of confined coflow jets with three turbulence models
[NASA-TM-106378] p 1025 N94-16879
Accurate upwind methods for the Euler equations
[NASA-TM-106388] p 1170 N94-16882
Three-dimensional turbulent boundary layer
[AD-A266261] p 1025 N94-16908
An upwind multigrid method for solving viscous flows on unstructured triangular meshes
[NASA-TM-109343] p 1027 N94-17061
Computational aerodynamics with icing effects
[AD-A267509] p 860 N94-17074
Progress in computational unsteady aerodynamics
[NASA-CR-177630] p 860 N94-17081
Investigation of high-speed free shear flows using improved pressure-strain correlated Reynolds stress turbulence model
[NASA-CR-194661] p 1027 N94-17127
On solving the compressible Navier-Stokes equations for unsteady flows at very low Mach numbers
[NASA-TM-106380] p 1027 N94-17128
Development of iterative techniques for the solution of unsteady compressible viscous flows
[NASA-CR-194657] p 1027 N94-17129
Studies on nonequilibrium phenomena in supersonic chemically reacting flows
[NASA-CR-194662] p 1027 N94-17215
Multigrid time-accurate integration of Navier-Stokes equations
[NASA-TM-106373] p 1028 N94-17258
Active turbulence control in wall bounded flows using direct numerical simulation
[AD-A267261] p 1028 N94-17286
Experimental and computational investigation of the NASA low-speed centrifugal compressor flow field
[NASA-TM-4481] p 869 N94-17386
Structured finite volume modeling of US Navy aircraft engine test cells task 2: Turboprop engine, volume 1
[AD-A267833] p 872 N94-17405
Computational analysis of Variable Thrust Engine (VTE) performance
[NASA-CR-193852] p 928 N94-17442
Boundary conditions and the simulation of low Mach number flows
[NASA-TM-106374] p 1029 N94-17448
Single block three-dimensional volume grids about complex aerodynamic vehicles
[NASA-TM-108986] p 1030 N94-17476
Compressible flow solvers using unstructured grids
[INRIA-RR-1732] p 1030 N94-17531
A domain-partition method for the advection-diffusion equation
[INRIA-RR-1740] p 1030 N94-17534
Multigrid direct numerical simulation of the whole process of flow transition in 3-D boundary layers
[NASA-TM-106369] p 1030 N94-17557
Thin-layer and full Navier-Stokes calculations for turbulent supersonic flow over a cone at an angle of attack
[NASA-CR-189103] p 861 N94-17558
Structured finite volume modeling of US Navy aircraft engine test cells. Task 2: Turboprop engine. Volume 2: Code documentation and listings
[AD-A268386] p 873 N94-17569
Study into the limits of an Euler equation method applied to leading-edge vortex flow
[NLR-TP-91350-U] p 1031 N94-17627
COMPUTATIONAL GEOMETRY
Efficient algorithmic techniques for combinatorial problems
[AD-A267151] p 1172 N94-15777
Towards dynamic randomized algorithms in computational geometry
[INRIA-RR-1727] p 1156 N94-17528
Construction of d-dimensional hyperoctrees on a hypercube multiprocessor
[INRIA-RR-1752] p 1162 N94-17539
COMPUTATIONAL GRIDS
A parallel adaptive mesh refinement algorithm
[NASA-CR-191530] p 1168 N94-15724
Modal element method for potential flow in non-uniform ducts: Combining closed form analysis with CFD
[NASA-TM-106347] p 1169 N94-15799
Design of round-to-square transition section; analysis and computer code
[AD-A267173] p 872 N94-15847
A detailed model for simulation of catchment scale subsurface hydrologic processes
[PAPER-92WR02333] p 1084 N94-16032
Adaptive algorithm for aircraft configuration in turbulent flow
[AD-A266188] p 867 N94-16122
Modal ring method for the scattering of sound
[NASA-TM-106342] p 1177 N94-16497
Adaptive Cartesian grid methods for representing geometry in inviscid compressible flow
[DE93-016430] p 1025 N94-16894
Three dimensional hydrodynamic calculations with adaptive mesh refinement of the evolution of Rayleigh Taylor and Richtmyer Meshkov instabilities in converging geometry: Multi-mode perturbations
[DE93-017155] p 1025 N94-16903
An upwind multigrid method for solving viscous flows on unstructured triangular meshes
[NASA-TM-109343] p 1027 N94-17061
Linear characteristic spatial quadrature for discrete ordinates neutral particle transport on arbitrary triangles
[AD-A267485] p 1185 N94-17365
Single block three-dimensional volume grids about complex aerodynamic vehicles
[NASA-TM-108986] p 1030 N94-17476
Numerical solution of a second order boundary problem for two dimensions using galerkin approximations
[AD-A268128] p 1171 N94-17521
Compressible flow solvers using unstructured grids
[INRIA-RR-1732] p 1030 N94-17531
Multigrid direct numerical simulation of the whole process of flow transition in 3-D boundary layers
[NASA-TM-106369] p 1030 N94-17557
Thin-layer and full Navier-Stokes calculations for turbulent supersonic flow over a cone at an angle of attack
[NASA-CR-189103] p 861 N94-17558
The photonical, pure grid method
[NLR-TP-91478-U] p 1062 N94-17600
COMPUTER AIDED DESIGN
A CENTAUR tutorial
[INRIA-RT-140] p 1142 N94-14978
Gratings and waveguides p 1226 N94-14987
Geometric tolerance assessment
[NPL-DITC-210/92] p 1049 N94-15013
Open environments to support systems engineering tool integration: A study using the Portable Common Tool Environment (PCTE)
[NASA-TM-4489] p 1144 N94-15486
RAMCAD design methodology
[AD-A267010] p 1145 N94-15525
An assessment of finite-element modeling techniques for thick-solid/thin-shell joints analysis
[NASA-TM-108426] p 1058 N94-15534
The free decay of coupled heave and pitch motions of a model frigate
[DRA/TM(AWMH)92340] p 1146 N94-15702
Using interactive sketch interpretation to design solid objects
[AD-A266637] p 1147 N94-15743
Asynchronous design for parallel processing architectures
[AD-A266523] p 1160 N94-16791
Applications of the phi-transform
[AD-A266247] p 1170 N94-16940
Missile datcom user's manual
[AD-A267447] p 1152 N94-17032
Computer modeling and animation of mechanical systems
[NIAR-93-3] p 1153 N94-17299
Binary optics at Hughes Danbury Optical Systems
p 1195 N94-17344
Fabrication techniques for very fast diffractive lenses
p 1196 N94-17345

Computer-aided design package for designers of digital optical computers
[AD-A267866] p 1154 N94-17390
Structural mechanics division research and technology accomplishments for CY 1992 and plans for CY 1993
[NASA-TM-107752] p 1062 N94-17479
X ray computed tomography for geometry acquisition
[AD-A268085] p 1157 N94-17590
The development of flexible software for the Italian/Dutch satellite SAX: Advantages and disadvantages of the use of CASE tools
[NLR-TP-91288-U] p 1157 N94-17626
Activities of the Research Laboratory of Electronics
[AD-A266730] p 1304 N94-17651

COMPUTER AIDED MANUFACTURING

Applying paperless technology to achieve excellence in manufacturing operations
[TABES PAPER 93-630] p 1052 N94-16147
The processing and mechanical properties of high temperature/high performance composites. Book 5: Processing and miscellaneous properties
[AD-A266398] p 935 N94-16529
A decision criteria to select an associative-memory organization that minimizes the execution time of a mix of associative-search operations
[AD-A266438] p 1149 N94-16560

COMPUTER AIDED MAPPING

Separation of topographic and intrinsic backscatter variations in biscopic radar images: A magic airbrush
p 1086 N94-16318
Fabrication of a NAVMAP, a deep-sea mapping system
[AD-A268630] p 1085 N94-17467

COMPUTER AIDED TOMOGRAPHY

X ray computed tomography for failure analysis investigations
[AD-A268086] p 1055 N94-17515
X ray computed tomography for geometry acquisition
[AD-A268085] p 1157 N94-17590
X ray computed tomography for casting demonstration
[AD-A268084] p 1056 N94-17596

COMPUTER ANIMATION

Galileo probe spacecraft mission to Jupiter
[NASA-TM-109646] p 1247 N94-16070
Computer modeling and animation of mechanical systems
[NIAR-93-3] p 1153 N94-17299

COMPUTER ASSISTED INSTRUCTION

The application of compiler-assisted multiple instruction retry to VLIW architectures
[AD-A266930] p 1158 N94-15173
Questioning mechanisms during tutoring, conversation, and human-computer interaction
[AD-A266199] p 1137 N94-16108
The planetary data system educational CD-ROM
p 1234 N94-16209
A computer-based training system combining virtual reality and multimedia
[DE93-013768] p 1132 N94-16819
Development of dynamic, contex-driven help systems
[AD-A267409] p 1152 N94-16974
Theoretical implications and empirical findings on instructional control and part-whole-task training
[AD-A267826] p 872 N94-17403

COMPUTER DESIGN

The design of self-checking reduced instruction set computers
[AD-A267012] p 1140 N94-15763

COMPUTER GRAPHICS

TOMS computer graphics
[NASA-TM-109597] p 1094 N94-15290
Text and graphics systems
[NASA-TM-109570] p 1229 N94-15300
The 1988 computational fluid dynamics highlights
[NASA-TM-109645] p 1019 N94-15431
Freedom system Text and Graphics Systems (TAGS)
[NASA-TM-109509] p 1140 N94-15455
Using interactive sketch interpretation to design solid objects
[AD-A266637] p 1147 N94-15743
Flight instrument software for the F/A-18 research simulator
[AD-A267170] p 872 N94-15856
A CCIR-based prediction model for Earth-Space propagation p 997 N94-16050
A task adaptive parallel graphics renderer
[DE93-017123] p 1149 N94-16119
Computing science and statistics. Volume 24: Graphics and visualization
[AD-A266571] p 1150 N94-16721
Development of a prototype kinestatic platform for application to space and ground servicing tasks. Phase 1: Concept Modeling
[NASA-CR-194036] p 887 N94-16905
Display of dynamic, volume graphic images by holographic voxel projection: Initial investigation
[AD-A267622] p 1035 N94-17197
Module interconnection frameworks for a real-time spreadsheet
[AD-A267317] p 1153 N94-17220
Computer modeling and animation of mechanical systems
[NIAR-93-3] p 1153 N94-17299
Theoretical crystallography with the Advanced Visualization System
[DE93-015692] p 1215 N94-17319
TDNOVA interactive graphics
[AD-A268000] p 1156 N94-17530

COMPUTER INFORMATION SECURITY

VDM specification of the MD4 message digest algorithm
[NPL-DITC-204/92] p 1142 N94-14944
The use of formal methods in data security standards
[NPL-DITC-205/92] p 1142 N94-15008
RAISE specification of the MD4 message digest algorithm
[NPL-DITC-206/92] p 1142 N94-15010
The value of reference implementations and prototyping in a formal design and testing methodology
[NPL-DITC-208/92] p 1142 N94-15011
Standards and conformance testing in data security: Results of initial programme of investigation
[NPL-DITC-218/92] p 1143 N94-15014
Testability of data security standards
[NPL-DITC-217/93] p 1143 N94-15022
The Third Annual NASA Science Internet User Working Group Conference
[NASA-CP-3170] p 1228 N94-15116
Integrated trusted systems development environment
[AD-A267029] p 1146 N94-15674
NASA Electronic Library System (NELS): The system impact of security
[NASA-CR-194614] p 1231 N94-16499
A security architecture for fault-tolerant systems
[AD-A266178] p 1152 N94-16982
An internetwork authentication architecture
[AD-A268579] p 1162 N94-17622

COMPUTER NETWORKS

The Third Annual NASA Science Internet User Working Group Conference
[NASA-CP-3170] p 1228 N94-15116
A TRALINET guide to the Internet
[AD-A266946] p 1229 N94-15178
A browsing tool for the Internet Logical Library of the HPCC Software Exchange
[NASA-CR-194545] p 1143 N94-15189
Computer networking at SLR stations
p 917 N94-15594
Bandwidth characteristics of multimedia data traffic on a local area network
[NASA-TM-104026] p 883 N94-15648
The distributed database dynamic reconfiguration project
[AD-A267116] p 1229 N94-15652
Report on computing and networking in the Space Science Laboratory by the SSL Computer Committee
[NASA-TM-108422] p 1147 N94-15721
Congestion control of high-speed networks
[AD-A267013] p 989 N94-15748
Unipolar terminal-attractor based neural associative memory with adaptive threshold
[NASA-CASE-NPO-18790-1-CU] p 1165 N94-15958
Consistent failure reporting in reliable communication systems
[AD-A266298] p 997 N94-16477
The ESA Tele-Invoicing System (ETIS)
[ESA-INT-6] p 1150 N94-16591
A comparison of queueing, cluster and distributed computing systems
[NASA-TM-109025] p 1160 N94-16878
A modular control architecture for real-time synchronous and asynchronous systems
[DE93-015439] p 1166 N94-16888
Computing and Information Sciences
[DE93-017149] p 1151 N94-16902
The IMS software integration platform
[AD-A266285] p 1151 N94-16910
Understanding partitions and the no partition assumption
[AD-A266296] p 1000 N94-16911
Computer Science and Telecommunications Board activities
[DE93-018141] p 1000 N94-17000
Networked workstations and parallel processing utilizing functional languages
[AD-A267464] p 1160 N94-17034
Causality-preserving timestamps in distributed programs
[AD-A267534] p 1153 N94-17118
CALS test network handbook
[AD-A267587] p 1160 N94-17209
Isochronets: A high-speed network switching architecture
[AD-A267811] p 1161 N94-17409
A protocol validator for the SCM and CFSM models
[AD-A268523] p 1156 N94-17541
An internetwork authentication architecture
[AD-A268579] p 1162 N94-17622

COMPUTER PROGRAM INTEGRITY

Automatic generation of production rules for integrity maintenance
[REPT-92-054] p 1156 N94-17501
Automatic translation of database integrity constraints into compensating production rules
[REPT-92-055] p 1234 N94-17502

COMPUTER PROGRAMMING

Concurrent garbage collection of persistent heaps
[AD-A266831] p 1141 N94-14915
Lecture notes on engineering measurement for software engineers
[AD-A266959] p 1142 N94-14967
Safety-critical software: Status report and annotated bibliography
[AD-A266993] p 1144 N94-15214
Software architecture for shared information systems
[AD-A266995] p 1144 N94-15216
Open environments to support systems engineering tool integration: A study using the Portable Common Tool Environment (PCTE)
[NASA-TM-4489] p 1144 N94-15486
Process-centered development environments: An exploration of issues
[AD-A266997] p 1145 N94-15630
Multiobjective functions optimization for task allocation mapping to multicomputer nodes
[AD-A267071] p 1146 N94-15670
Integrated trusted systems development environment
[AD-A267029] p 1146 N94-15674
ACM SIGPLAN Workshop on ML and Its Applications
[AD-A266617] p 1147 N94-15725
Architectures for software systems: A curriculum development proposal in undergraduate software engineering
[AD-A266703] p 1147 N94-15728
Proteus three-dimensional Navier-Stokes computer code, version 1.0. Volume 3: Programmer's reference
[NASA-TM-106341] p 1022 N94-15865
Proteus two-dimensional Navier-Stokes computer code, version 2.0. Volume 3: Programmer's reference
[NASA-TM-106339] p 1022 N94-15867
C++ as a language for object-oriented numerics
[DE93-015027] p 1148 N94-15985
Consistent failure reporting in reliable communication systems
[AD-A266298] p 997 N94-16477
Models for reactivity
[AD-A266419] p 1149 N94-16554
Reductions to sets of low information content
[TR-417] p 1150 N94-16579
Software Engineering Guidebook
[NASA-CR-177625] p 1150 N94-16656
ASTROS enhancements. Volume 1: ASTRO user's manual
[AD-A266818] p 1151 N94-16768
ASTROS enhancements. Volume 2: ASTRO programmer's manual
[AD-A266819] p 1151 N94-16769
KBSA concept demo
[AD-A267054] p 1166 N94-16770
Operator overloading as an enabling technology for automatic differentiation
[DE93-012899] p 1170 N94-16778
Monads and comonads in intensional semantics
[AD-A266522] p 1151 N94-16790
Information technology division technical paper abstracts
[AD-A266227] p 1166 N94-16938
Development of dynamic, contex-driven help systems
[AD-A267409] p 1152 N94-16974
Design and implementation of an object-oriented interface for the multi-model/multi-lingual database system
[AD-A267413] p 1232 N94-16977
A handbook of cost risk analysis methods
[AD-A267253] p 1235 N94-16988
Sequential functions on indexed domains and full abstraction for a sub-language of PCF
[AD-A267838] p 1152 N94-17009
Detailed example of using ACEC release 3.0 with the DEC VAX Ada compiler
[AD-A267880] p 1152 N94-17014
Applicability of computer spreadsheet simulation for solving resource allocation problems
[AD-A267436] p 1152 N94-17027

Design and implementation of an interface editor for the Amadeus multi-relational database front-end system
[AD-A267403] p 1233 N94-17114
Causality-preserving timestamps in distributed programs
[AD-A267534] p 1153 N94-17118
Module interconnection frameworks for a real-time spreadsheet
[AD-A267317] p 1153 N94-17220
Module interconnection frameworks for a real-time spreadsheet
[AD-A267752] p 1153 N94-17231
Software Capability Evaluation (SCE) version 1.5 method description. Software capability evaluation project
[AD-A267895] p 1154 N94-17395
Process evolution for the MARVEL environment
[AD-A267813] p 1155 N94-17398
Concurrency control in rule-based software development environments
[AD-A267829] p 1155 N94-17404
ACE: Lessons learned, volume 1
[AD-A267979] p 1155 N94-17411
Incremental rederivation of software artifacts: FY 1992
[AD-A267968] p 1155 N94-17491
Reliability and maintainability of modular robot systems: A roadmap for design
[AD-A268104] p 1168 N94-17517
A protocol validator for the SCM and CFSM models
[AD-A268523] p 1156 N94-17541
A software process framework for the SEI capability maturity model: Repeatable level
[AD-A268059] p 1157 N94-17588

COMPUTER PROGRAMS

A CENTAUR tutorial
[INRIA-RT-140] p 1142 N94-14978
The CAML numbers reference manual
[INRIA-RT-141] p 1142 N94-14979
Global auroral imaging: Dynamics of Explorer Miss ion
[NASA-CR-194284] p 1097 N94-15003
Testability of data security standards
[NPL-DITC-217/93] p 1143 N94-15022
The alignment-distribution graph
[NASA-CR-194292] p 1168 N94-15112
Software reliability through fault-avoidance and fault-tolerance
[NASA-CR-194353] p 1143 N94-15114
Rotary engine performance computer program (RCEMAP and RCEMAPPC): User's guide
[NASA-CR-191192] p 869 N94-15192
Safety-critical software: Status report and annotated bibliography
[AD-A266993] p 1144 N94-15214
Concepts on measuring the benefits of software process improvements
[AD-A266994] p 1144 N94-15215
Software architecture for shared information systems
[AD-A266995] p 1144 N94-15216
Upgrading NASA/DOSE laser ranging system control computers p 918 N94-15595
An analysis of SEI software process assessment results: 1987-1991
[AD-A266996] p 1145 N94-15629
Statistical analysis of trigonometric parallaxes
[NASA-CR-194558] p 1172 N94-15641
Software reliability management through metrics
[AD-A267129] p 1146 N94-15687
The free decay of coupled heave and pitch motions of a model frigate
[DRA/TM(AWMH)92340] p 1146 N94-15702
Architectures for software systems: A curriculum development proposal in undergraduate software engineering
[AD-A266703] p 1147 N94-15728
An analysis of tactical airlifter characteristics and their impact on theater airlift system performance
[AD-A266719] p 866 N94-15731
Design of round-to-square transition section; analysis and computer code
[AD-A267173] p 872 N94-15847
Parallel processing and scientific applications
[AD-A267179] p 1159 N94-15849
GAM-HEAT: A computer code to compute heat transfer in complex enclosures
[DE93-014724] p 1023 N94-15980
Information Technology Resources Assessment
[DE93-013899] p 1230 N94-16010
Database for propagation models p 996 N94-16049
A CCIR-based prediction model for Earth-Space propagation p 997 N94-16050
Liquid hydrogen and liquid oxygen feedline passive recirculation analysis
[TABES PAPER 93-620] p 1031 N94-16145
Applying paperless technology to achieve excellence in manufacturing operations
[TABES PAPER 93-630] p 1052 N94-16147
Consistent failure reporting in reliable communication systems
[AD-A266298] p 997 N94-16477
Laser ranging data analysis
[NASA-CR-193547] p 1041 N94-16719
ASTROS enhancements. Volume 1: ASTRO user's manual
[AD-A266818] p 1151 N94-16768
ASTROS enhancements. Volume 2: ASTRO programmer's manual
[AD-A266819] p 1151 N94-16769
Earth observational research using multistage EOS-like data
[NASA-CR-194626] p 1084 N94-16831
The IMS software integration platform
[AD-A266285] p 1151 N94-16910
Information technology division technical paper abstracts
[AD-A266227] p 1166 N94-16938
Conflict Resolution (CORE) for software quality factors
[AD-A267248] p 1151 N94-16941
Development of dynamic, contex-driven help systems
[AD-A267409] p 1152 N94-16974
Design and implementation of an object-oriented interface for the multi-model/multi-lingual database system
[AD-A267413] p 1232 N94-16977
Integration ToolKit and Methods (ITKM) manufacturing methods and prototype toolkit. A combined modeling method using IDEFO, IDEF1x and XSpec
[AD-A266176] p 984 N94-16981
Embedded computer systems: Status of C-17 software
[AD-A267307] p 1160 N94-16993
Detailed example of using ACEC release 3.0 with the DEC VAX Ada compiler
[AD-A267880] p 1152 N94-17014
Applicability of computer spreadsheet simulation for solving resource allocation problems
[AD-A267436] p 1152 N94-17027
Design and implementation of an interface editor for the Amadeus multi-relational database front-end system
[AD-A267403] p 1233 N94-17114
Sound exposure level prediction for impulse sound sources above variable terrain
[AD-A267535] p 1178 N94-17119
A proposed ground segment design for small satellites p 878 N94-17154
OREMUS: Prototype of an orbit determination center dedicated to mini-satellite control p 878 N94-17156
Data processing system for ARSENE ground station: A tool for small satellite control and development p 878 N94-17157
Defense Logistics Information System (DLIS). Procedures manual: Logistics On-Line Access (LOLA) procedures manual
[AD-A267685] p 1233 N94-17229
Module interconnection frameworks for a real-time spreadsheet
[AD-A267752] p 1153 N94-17231
ONRASIA scientific information bulletin, volume 18, number 2
[AD-A267798] p 1304 N94-17305
Concurrency control in rule-based software development environments
[AD-A267829] p 1155 N94-17404
Incremental rederivation of software artifacts: FY 1992
[AD-A267968] p 1155 N94-17491
Micro- and meso-scale simulations of magnetospheric processes related to the aurora and substorm morphology
[NASA-CR-193437] p 1102 N94-17527
TDNOVA interactive graphics
[AD-A268000] p 1156 N94-17530
Structured finite volume modeling of US Navy aircraft engine test cells. Task 2: Turboprop engine. Volume 2: Code documentation and listings
[AD-A268386] p 873 N94-17569
Environmental use of a Laser Range Finder and the Advanced Visualization System
[DE93-016163] p 1043 N94-17677

COMPUTER STORAGE DEVICES

Concurrent garbage collection of persistent heaps
[AD-A266831] p 1141 N94-14915
Relaxing consistency in recoverable distributed shared memory
[AD-A266931] p 1140 N94-15174
The design of self-checking reduced instruction set computers
[AD-A267012] p 1140 N94-15763
SONOS technology for commercial and military nonvolatile memory applications
[DE93-015647] p 1011 N94-16661
Detailed example of using ACEC release 3.0 with the DEC VAX Ada compiler
[AD-A267880] p 1152 N94-17014
Experience with disconnected operation in a mobile computing environment
[AD-A267524] p 1141 N94-17115
Causality-preserving timestamps in distributed programs
[AD-A267534] p 1153 N94-17118
3-D optical memory disk
[AD-A267908] p 1141 N94-17380

COMPUTER SYSTEMS DESIGN

Software architecture for shared information systems
[AD-A266995] p 1144 N94-15216
Reengineering: An engineering problem
[AD-A267117] p 1146 N94-15653
Multiobjective functions optimization for task allocation mapping to multicomputer nodes
[AD-A267071] p 1146 N94-15670
Report on computing and networking in the Space Science Laboratory by the SSL Computer Committee
[NASA-TM-108422] p 1147 N94-15721
The design of self-checking reduced instruction set computers
[AD-A267012] p 1140 N94-15763
Information Technology Resources Assessment
[DE93-013899] p 1230 N94-16010
NASA Electronic Library System (NELS): The system impact of security
[NASA-CR-194614] p 1231 N94-16499
Design and implementation of an object-oriented interface for the multi-model/multi-lingual database system
[AD-A267413] p 1232 N94-16977
A security architecture for fault-tolerant systems
[AD-A266178] p 1152 N94-16982
Fault-tolerant architectures for multiprocessor and VLSI-based systems
[AD-A267370] p 1140 N94-17005
Data handling strategy for the Spanish small satellite program (MINISAT) p 895 N94-17177
Light-weight process groups in the ISIS system
[NASA-CR-194544] p 1161 N94-17239
Computer-aided design package for designers of digital optical computers
[AD-A267866] p 1154 N94-17390
Integration of several computer systems within a heterogeneous environment
[AD-A267978] p 1155 N94-17500
Orpheus: A synthesis framework for regular architectures
[REPT-93-016] p 1156 N94-17504
System performance modeling and analysis of a fault-tolerant, real time parallel processor
[AD-A268070] p 1162 N94-17551

COMPUTER SYSTEMS PERFORMANCE

Applicability of the session and the presentation layers for the support of high speed applications
[INRIA-RT-144] p 1158 N94-14980
Concepts on measuring the benefits of software process improvements
[AD-A266994] p 1144 N94-15215
Process-centered development environments: An exploration of issues
[AD-A266997] p 1145 N94-15630
Reengineering: An engineering problem
[AD-A267117] p 1146 N94-15653
NASA trend analysis procedures
[NASA-RP-1290] p 1223 N94-15782
Parallel processing and scientific applications
[AD-A267179] p 1159 N94-15849
Performance Information Management System (PIMS) communication
[AD-A267040] p 1231 N94-16458
Shared-memory multiprocessor trends and the implications for parallel program performance
[TR-420] p 1159 N94-16578
Estimating task execution delay in a real-time system via static source code analysis
[AD-A267496] p 1161 N94-17367
Benchmarking massively parallel architectures
[DE93-016486] p 1162 N94-17646

COMPUTER SYSTEMS PROGRAMS

Software architecture for shared information systems
[AD-A266995] p 1144 N94-15216
Software reliability management through metrics
[AD-A267129] p 1146 N94-15687
Orpheus: A synthesis framework for regular architectures
[REPT-93-016] p 1156 N94-17504

COMPUTER TECHNIQUES

NASA's online machine aided indexing system
[NASA-CR-4518] p 1228 N94-15009
Report on computing and networking in the Space Science Laboratory by the SSL Computer Committee
[NASA-TM-108422] p 1147 N94-15721
A scientific basis for computational science
[AD-A266697] p 1148 N94-15841

Parallel processing and scientific applications
[AD-A267179] p 1159 N94-15849
Plasma arc welding repair of space flight hardware
[TABES PAPER 93-603] p 1049 N94-16139
A computer-based training system combining virtual reality and multimedia
[DE93-013768] p 1132 N94-16819
Development of dynamic, contex-driven help systems
[AD-A267409] p 1152 N94-16974
Experience with disconnected operation in a mobile computing environment
[AD-A267524] p 1141 N94-17115
A state-of-the-art plasma polymerization coater for ICF targets
[DE93-016452] p 1204 N94-17237
Low cost paths to binary optics p 1197 N94-17353
Design and diagnosis problem solving with multifunctional technical knowledge bases
[AD-A268375] p 1234 N94-17419
System performance modeling and analysis of a fault-tolerant, real time parallel processor
[AD-A268070] p 1162 N94-17551
X ray computed tomography for geometry acquisition
[AD-A268085] p 1157 N94-17590

COMPUTER VISION
YARF: An open-ended framework for robot road following
[AD-A266788] p 1163 N94-14910
Perception for outdoor navigation
[AD-A266867] p 863 N94-14919
Segmenting textured 3D surfaces using the space/frequency representation
[AD-A266960] p 1163 N94-14968
RACCOON: A Real-Time Autonomous Car Chaser Operating Optimally at Night
[AD-A266963] p 863 N94-14971
Panacea: An active sensor controller for the ALVINN autonomous driving system
[AD-A266964] p 864 N94-14972
Massively parallel, adaptive, color image processing for autonomous road following
[AD-A266988] p 864 N94-15498
Programmable Remapper project
[NASA-TM-109508] p 1164 N94-15515
Exploiting world structure to efficiently search for objects
[TR-434] p 1231 N94-16576
Reference frames in vision
[AD-A266174] p 1132 N94-16925
ARPA unmanned ground vehicle stereo vision program at Teleos Research
[AD-A267632] p 1167 N94-17202
A high-speed object recognition chip based on a biologically-realistic hybrid temporal processing
[AD-A268270] p 1134 N94-17576

COMPUTERIZED SIMULATION
Particle simulations on massively parallel machines
[DE93-015644] p 1157 N94-14927
Multiple process simulations for correction factor calculations in experiments with neutrons. LUSMK program
[DE93-623957] p 1179 N94-14932
Rotorcraft research
[NASA-TM-109452] p 871 N94-15325
STS-26 EVA rescue training
[NASA-TM-109563] p 875 N94-15333
Large eddy simulation and direct numerical simulation of high speed turbulent reacting flows
[NASA-CR-193131] p 1018 N94-15427
The 1988 computational fluid dynamics highlights
[NASA-TM-109645] p 1019 N94-15431
Parallel spatial direct numerical simulations on the Intel iPSC/860 hypercube
[NASA-CR-191513] p 1144 N94-15483
Surface and internal signatures of organized vortex motions in stratified fluid
[AD-A267015] p 1020 N94-15526
Statistical computation of tolerance limits
[NASA-TM-108424] p 1172 N94-15535
Numerical simulation of three-dimensional self-gravitating flow
[NASA-TM-109021] p 1021 N94-15768
NAS technical summaries: Numerical aerodynamic simulation program, March 1991 - February 1992
[NASA-TM-109335] p 854 N94-15798
An experimental comparison of CLOS and C(++) implementations of an object-oriented graphical simulation of walking robot kinematics
[AD-A267168] p 1165 N94-15855
Clouding tracing: Visualization of the mixing of fluid elements in convection-diffusion systems
[NASA-CR-191529] p 1148 N94-15965
A CCIR-based prediction model for Earth-Space propagation p 997 N94-16050
Modeling and simulation: A key to future defense technology
[TABES PAPER 93-654] p 1054 N94-16153
Evaporation kinetics of Mg2SiO4 crystals and melts from molecular dynamics simulations p 1219 N94-16331
Size distribution of interplanetary iron and stony particles related with deep-sea spherules p 1245 N94-16388
A trace-based comparison of shared memory multiprocessor architectures
[TR-432] p 1159 N94-16577
General Monte Carlo reliability simulation code including common mode failures and HARP fault/error-handling
[NASA-CR-187587] p 1150 N94-16594
Linear and non-linear studies of Alfven waves in space. Stationary and dynamic processes in magnetospheric plasmas
[NASA-CR-193585] p 1239 N94-16647
Collisional dynamics of perturbed particle disks in the solar system
[NASA-CR-193584] p 1239 N94-16648
A molecular dynamics simulator for optimal control of molecular motion
[AD-A266572] p 1183 N94-16722
A computer-based training system combining virtual reality and multimedia
[DE93-013768] p 1132 N94-16819
Simulation of enhanced tokamak performance on D3-D using fast wave current drive
[DE93-014009] p 1203 N94-16823
Crystalline beam ground state
[DE93-014331] p 1211 N94-16827
Influence of fiber packing structure on permeability p 938 N94-16857
Modeling study to evaluate the ionic mechanism of soot formation in flames
[AD-A266242] p 950 N94-16930
Applicability of computer spreadsheet simulation for solving resource allocation problems
[AD-A267436] p 1152 N94-17027
The influence of the level formants on the perception of synthetic vowel sounds
[IFTR-41/1991] p 1002 N94-17064
Module interconnection frameworks for a real-time spreadsheet
[AD-A267752] p 1153 N94-17231
An introduction to structural models
[AD-A268151] p 1155 N94-17429
Space Station Freedom electrical performance model
[NASA-TM-106395] p 929 N94-17483
Research in presistent simulation: Development of the persistent ModSim object-oriented programming language
[AD-A268568] p 1157 N94-17620
3D and r,z particle simulations of heavy ion fusion beams
[DE93-013417] p 1205 N94-17670

COMPUTERS
Infrared remote activity transceiver universal model
[AD-A266965] p 1188 N94-15144
NASA Spacelink computer
[NASA-TM-109657] p 1140 N94-15228

CONCENTRATING
Investigations into the recovery of waste sulfuric acid with concentrated solar radiation
[DLR-FB-93-11] p 952 N94-17594

CONCENTRATION (COMPOSITION)
Second flight of the Spacelab grille spectrometer during the Atlas-1 mission
[AERONAUTICA-ACTA-A-367-199] p 923 N94-17592

CONCENTRATORS
An improved patch for radiative coolers
[NASA-CASE-GSC-13503-1] p 1046 N94-15873
Progress in the concentrator initiative program
[DE93-015006] p 1091 N94-15984

CONCENTRIC CYLINDERS
Numerical study of compressible boundary-level transition between two concentric cylinders
[NASA-CR-194622] p 1025 N94-16842
Elastic-plastic finite-difference analysis of unidirectional composites subjected to thermomechanical cyclic loading
[AD-A267666] p 1061 N94-17269

CONCRETE STRUCTURES
Evaluation of hybrid reinforcement (fiber-reinforced-plastic rod with steel core)
[AD-A268009] p 941 N94-17473

CONCRETES
User's guide: Hot-mix recycling of asphalt concrete pavements
[AD-A266939] p 983 N94-15177

CONCURRENT PROCESSING
Parallel processing and scientific applications
[AD-A267179] p 1159 N94-15849
Concurrency control in rule-based software development environments
[AD-A267829] p 1155 N94-17404

CONDENSATES
Mesons at finite temperature in the NJL model with gluon condensate
[DE93-626697] p 1185 N94-17310
Strategy for the reduction of total integrated fluid logistics to the Space Station Freedom
[NASA-TM-107744] p 1138 N94-17452

CONDENSED MATTER PHYSICS
The Megascience Forum
[DE93-014445] p 1303 N94-16804

CONDENSERS (LIQUEFIERS)
Theoretical study of laminar film condensation on horizontal elliptical tubes under conditions of free and forced convection
[AD-A267161] p 1021 N94-15737

CONDENSING
Gravity dependent condensation pressure drop and heat transfer in ammonia two-phase heat transport systems
[NLR-TP-92121-U] p 1031 N94-17615

CONDUCTING POLYMERS
Photochemistry in thin polymeric films
[AD-A266716] p 964 N94-15729
Synthesis of novel electrically conducting polymers: Potential conducting Langmuir-Blodgett films and conducting polymers on defined surfaces
[NASA-CR-194651] p 972 N94-17297
Characterization of the lithium/pan-based polymer electrolytes interface
[AD-A268401] p 973 N94-17434
Lattice relaxation theory of localized excitations in quasi-one-dimensional systems
[DE93-624947] p 1215 N94-17437
Soluble precursor route to polyanilines
[AD-A268015] p 973 N94-17494

CONDUCTION BANDS
Optoelectronics based on SiGe/Si heterostructures
[AD-A267178] p 1190 N94-15848

CONDUCTION ELECTRONS
Growth and doping of Al(x)Ga(1-x)N films by electron cyclotron resonance assisted molecular beam epitaxy
[AD-A267305] p 1212 N94-16992

CONDUCTIVE HEAT TRANSFER
A posteriori error estimation for hierarchic models of elliptic boundary value problems on thin domains
[AD-A267714] p 1168 N94-14939
Advanced cooling for high power electric actuators
[AD-A266984] p 866 N94-15761
On the a-posteriori estimation of the modelling error for the heat conduction in a plate and its use for adaptive hierarchic modelling
[AD-A267965] p 1029 N94-17384
Numerically solving a transient heat conduction problem with convection and radiation
[AD-A268521] p 1220 N94-17540
Heat transfer parametric system identification
[AD-A268525] p 929 N94-17543

CONDUCTIVITY
Theoretical studies of nonlinear optical properties of conjugated polymers
[AD-A267390] p 1193 N94-17024

CONDUCTORS
A device for testing cables
[NASA-CASE-LAR-14093-1] p 1010 N94-15988
A simple chemical procedure for extending the conductive state of polypyrrole to more negative potentials
[AD-A266235] p 969 N94-16928

CONES (VOLCANOES)
Assimilation of solids during ascent of magmas from the Bartoy Field of the Baikal Region, Siberia p 1103 N94-16214
Emplacement of multiple flow units on very shallow slopes, east Kawelu Planitia flow field, Venus p 1260 N94-16235
Venusian pancake domes: Insights from terrestrial voluminous silicic lavas and thermal modeling p 1286 N94-16381

CONFERENCES
The Third Annual NASA Science Internet User Working Group Conference
[NASA-CP-3170] p 1228 N94-15116
Symposium on the Future of Aeronautics in the Netherlands
[ETN-93-93780] p 853 N94-15120
Materials Research Society Symposium Proceedings, Volume 292: Biomolecular Materials
[AD-A265776] p 1116 N94-15138
Eighth International Workshop on Laser Ranging Instrumentation
[NASA-CP-3214] p 911 N94-15552
ACM SIGPLAN Workshop on ML and Its Applications
[AD-A266617] p 1147 N94-15725
Papers presented at the Eleventh International Symposium on Earth Tides
[COMMUNICATIONS-SER-B-158] p 1098 N94-15800

Proceedings of the Third Spaceborne Imaging Radar Symposium
[NASA-CR-194104] p 989 N94-15886
Proceedings of the Fifteenth NASA Propagation Experimenters Meeting (NAPEX 15) and the Advanced Communications Technology Satellite (ACTS) Propagation Studies Miniworkshop
[NASA-CR-194539] p 994 N94-16035
A review of OPEX activities and measurement results p 994 N94-16036
Proceedings of the Second Workshop on Microgravity Experimentation
[DSS-NR15-43-1990] p 977 N94-16071
TABES 1993: 9th Annual Technical and Business Exhibition and Symposium p 1050 N94-16129
Twenty-Fourth Lunar and Planetary Science Conference. Part 2: G-M
[NASA-CR-193174] p 1247 N94-16173
Controlling chaotic behavior in CO2 and other lasers
[AD-A266431] p 1040 N94-16546
Proceedings of the Association for Computing Machinery Special Interest Group for Ada Artificial Intelligence Working Group
[AD-A266422] p 1165 N94-16559
Proceedings of the 1992 Annual Meeting NASA Occupational Health Program
[NASA-CR-193462] p 1123 N94-16609
Neutrino mass and mixing: Summary of the neutrino sessions
[DE93-014342] p 1183 N94-16801
Fundamental-mode RF design in e(+)e(-) storage ring factories
[DE93-015249] p 1183 N94-16809
Plasma Science Committee (PLSC) and the Panel on Opportunities in Plasma Science and Technology (OPST)
[DE93-018142] p 1204 N94-16995
DLTS and dynamic transconductance analysis of deep-submicron fully-depleted SOI MOSFET's
[AD-A267291] p 1214 N94-17243
Conference on Binary Optics: An Opportunity for Technical Exchange
[NASA-CP-3227] p 1194 N94-17331
Proceedings of the 1992 Antenna Applications Symposium, volume 1
[AD-A268167] p 1005 N94-17431
Proceedings of the 7th International Cryocooler Conference, part 1
[AD-A268448] p 985 N94-17482
Proceedings of the 7th International Cryocooler Conference, part 2
[AD-A268449] p 985 N94-17484
Proceedings of the 7th International Cryocooler Conference, part 3
[AD-A268450] p 985 N94-17485
Proceedings of the 6th International Conference on Narrow Gap Semiconductors
[AD-A268097] p 1015 N94-17570

CONFIDENCE LIMITS
Study of the rare decays K(sub L)(sup 0) yields (mu)e, K(sub L)(sup 0) yields ee, and K(sub L)(sup 0) yields (mu)(mu) at KEK
[DE93-753247] p 1180 N94-15135
Search for the top quark from (e(mu)) and (e,e) events in the D0 detector in p(bar-p) collisions at the square root of s = 1.8 TeV
[DE93-016350] p 1186 N94-17662

CONFIGURATION MANAGEMENT
Software Engineering Guidebook
[NASA-CR-177625] p 1150 N94-16656

CONFINEMENT
Microwave interaction with plasmas
[AD-A267048] p 1201 N94-15661
Confinement and stability of a Crystal Beam
[DE93-015400] p 1181 N94-16020
The cooling of confined ions driven by laser beams
[DE93-016612] p 1039 N94-16114
High beta and confinement studies of TFTR
[DE93-016204] p 1202 N94-16446

CONGESTION
Congestion control of high-speed networks
[AD-A267013] p 989 N94-15748

CONGRESSIONAL REPORTS
Naval aviation: The Navy is taking actions to improve the combat capabilities of its tactical aircraft. Report to Congressional Requesters
[AD-A268002] p 868 N94-17472

CONICAL FLOW
Thin-layer and full Navier-Stokes calculations for turbulent supersonic flow over a cone at an angle of attack
[NASA-CR-189103] p 861 N94-17558

CONICAL SCANNING
Conically scanned holographic lidar telescope
[NASA-CASE-GSC-13462-1] p 1194 N94-17321

CONIFERS
Radar response of vegetation: An overview p 991 N94-15898
Application of Cloude's target decomposition theorem to polarimetric imaging radar data p 991 N94-15901
SAR backscatter from coniferous forest gaps p 1076 N94-16736

CONJUGATES
End-effector: Joint conjugates for robotic assembly of large truss structures in space: Extended concepts
[NASA-CR-193576] p 1048 N94-17088

CONJUGATION
Synthesis, characterization, and polymerization of new ferrocene-fluorene complexes. A novel high-molecular weight conjugated polymer with pendant ferrocene groups
[AD-A267717] p 972 N94-17273

CONNECTIVE TISSUE
Micromechanics modeling and analysis of Haversian compact bone tissues as a fiber reinforced composite material
[AD-A268250] p 1129 N94-17456

CONNECTORS
Connector systems for structures
[NASA-CASE-MSC-21998-1] p 1046 N94-15707
A device for testing cables
[NASA-CASE-LAR-14093-1] p 1010 N94-15988

CONSERVATION
Soil conservation applications with C-band SAR p 1080 N94-16760

CONSERVATION EQUATIONS
A comparison of one and two dimensional flame quenching: Heat transfer results
[DE93-015196] p 947 N94-16060

CONSISTENCY
Process evolution for the MARVEL environment
[AD-A267813] p 1155 N94-17398

CONSOLES
Ergonomics in the office environment p 1124 N94-16612

CONSOLIDATION
Processing, properties and applications of composites using powder-coated epoxy towpreg technology p 933 N94-15277

CONSONANTS (SPEECH)
The influence of the level formants on the perception of synthetic vowel sounds
[IFTR-41/1991] p 1002 N94-17064

CONSTITUTIVE EQUATIONS
Systematology for elastic-plastic material equations by large deformations on the basis of the Cosserat-continuum model
[SCHRIFTENR-PHYSIKAL-ING-BD] p 1058 N94-15642

CONSTRAINTS
Automatic generation of production rules for integrity maintenance
[REPT-92-054] p 1156 N94-17501
Automatic translation of database integrity constraints into compensating production rules
[REPT-92-055] p 1234 N94-17502

CONSTRICTIONS
The nature of dynamic arteriolar vasoreactivity: A mini-review and A classification scheme
[AD-A266499] p 1128 N94-16783

CONSTRUCTION
Unitary plan wind tunnel landmark dedication and revitalization
[NASA-TM-109649] p 1302 N94-15434
Space Station Facility government estimating
[NASA-TM-109324] p 1223 N94-15545
Estimating and bidding for the Space Station Processing Facility
[NASA-TM-109323] p 1223 N94-15546
A state-of-the-art plasma polymerization coater for ICF targets
[DE93-016452] p 1204 N94-17237
Study of the National Science Foundation's South Pole Station as an analogous data base for the logistical support of a Moon laboratory
[NASA-TM-108429] p 1174 N94-17469

CONSTRUCTION INDUSTRY
Assessment of trends in the development of residential buildings from the standpoint of the fuel and energy requirements
[IFTR-6/1991] p 1093 N94-17092

CONSTRUCTION MATERIALS
Building a lunar base
[NASA-TM-109674] p 983 N94-15519
Synthesis and evaluation of polymeric materials
[AD-A267809] p 973 N94-17408

CONSUMABLES (SPACECREW SUPPLIES)
Supporting life in space
[NASA-TM-109593] p 1135 N94-15285
STS-29 crew food tasting in building 45
[NASA-TM-109547] p 1136 N94-15382
Food for space
[NASA-TM-109668] p 1136 N94-15435
STS-31 crew training: firefighting, food tasting, EVA prep and post
[NASA-TM-109484] p 876 N94-15451

CONTACTORS
Hollow cathode heater development for the Space Station plasma contactor
[NASA-CR-191131] p 926 N94-16880

CONTAINMENT
Mechanical properties of magnesium ammonium phosphate cements and their zeolite composites
[DE93-015155] p 934 N94-16057

CONTAMINANTS
HyperVentilate: Decision-support software for soil vapor extraction technology application
[PB93-134880] p 1094 N94-15136
Solar absorptance of optical surfaces contaminated with spacecraft material outgassing products
[AD-A267202] p 886 N94-15857
Polished substrate surface and cleaning study for coated optic quality
[DE93-014116] p 1190 N94-15975
Removal of carbonaceous contaminants from silica aerogel p 953 N94-16256
Detection and dosimetry of chemical contaminants in polymeric materials
[AD-A266605] p 968 N94-16727
Emissions of volatile organic compounds from stationary combustion sources: Numerical modeling capabilities
[DE93-014123] p 1096 N94-16825

CONTAMINATION
On the composition of neuKREEP: QMD contamination at Apollo 11? p 1266 N94-16276
Possible dust contamination of the early solar system p 1244 N94-16352
Field emitter arrays for RF vacuum microelectronics
[AD-A268595] p 1015 N94-17608
Characterization of Ni on Si wafers: Comparison of surface analysis techniques
[DE93-016501] p 953 N94-17649

CONTEXT
Development of dynamic, contex-driven help systems
[AD-A267409] p 1152 N94-16974

CONTINENTAL SHELVES
Ray tracing on topographic Rossby waves
[AD-A267014] p 1112 N94-15844

CONTINUOUS WAVE LASERS
Test results from LAGEOS-2 optical characterization using pulsed lasers p 915 N94-15577
Study of high speed interference photography with two-dimensional acousto-optical lattice deflection
[AD-A267823] p 1035 N94-17402
Laser ignition of solid propellants: 1. Ignition delays
[AD-A268454] p 976 N94-17538

CONTINUOUS WAVE RADAR
Microwave reflectometer ionization sensor
[NASA-CR-191464] p 922 N94-17083

CONTINUUM MECHANICS
Stability of flows in fluidized beds
[DE93-000245] p 1024 N94-16763

CONTINUUM MODELING
Progress in the modeling of the shock response and mitigation of thick composite shells
[AD-A267009] p 1057 N94-15524
Systematology for elastic-plastic material equations by large deformations on the basis of the Cosserat-continuum model
[SCHRIFTENR-PHYSIKAL-ING-BD] p 1058 N94-15642
Continuum solvent models for computational chemistry
[DE93-016329] p 953 N94-17660

CONTOURS
Nowcasting methods for satellite imagery
[AD-A267294] p 1108 N94-17267

CONTRACT MANAGEMENT
Industrial labor relations manual
[NHB-5200.1B] p 1224 N94-15939
NASA information resources management handbook
[NHB-2410.1E] p 1230 N94-15941

CONTRACT NEGOTIATION
Industrial labor relations manual
[NHB-5200.1B] p 1224 N94-15939

CONTRACTORS
Space Station Facility government estimating
[NASA-TM-109324] p 1223 N94-15545
Estimating and bidding for the Space Station Processing Facility
[NASA-TM-109323] p 1223 N94-15546
Government/contractor development teams
[TABES PAPER 93-460] p 1050 N94-16134
New health and safety initiatives at the Department of Energy (DOE) p 1124 N94-16610
Emergency preparedness and planning p 1124 N94-16613

CONTRACTS
Space Station Facility government estimating
[NASA-TM-109324] p 1223 N94-15545
Estimating and bidding for the Space Station Processing Facility
[NASA-TM-109323] p 1223 N94-15546
CONTRAST
Perception of lightness and brightness in complex patterns
[AD-A268435] p 1134 N94-17513
CONTROL EQUIPMENT
Serpentine manipulator planning and control for NASA Space-Shuttle payload servicing
[AD-A266961] p 879 N94-14969
ALS engine propellant effector system
[NASA-CR-194650] p 926 N94-16590
CONTROL SIMULATION
Theoretical implications and empirical findings on instructional control and part-whole-task training
[AD-A267826] p 872 N94-17403
CONTROL STABILITY
Three axis force override rate control of a PUMA 560 manipulator
[AD-A267313] p 1048 N94-16944
Robust control of uncertain nonlinear systems
[AD-A268056] p 1167 N94-17506
CONTROL STICKS
Unistick vehicle controller
[NASA-TM-109618] p 1046 N94-15347
CONTROL SURFACES
Static aeroelastic response of an aircraft with asymmetric wing planforms representative of combat damage
[AD-A266890] p 865 N94-14951
Aerodynamic flight control to increase payload capability of future launch vehicles
[NASA-CR-193850] p 870 N94-15532
Aerodynamic control of NASP-type vehicles through Vortex manipulation. Volume 1: Static water tunnel tests
[NASA-CR-177626-VOL-1] p 855 N94-15655
Aerodynamic control of NASP-type vehicles through Vortex manipulation. Volume 2: Static wind tunnel tests
[NASA-CR-177626-VOL-2] p 856 N94-15677
Aerodynamic control of NASP-type vehicles through vortex manipulation, volume 4
[NASA-CR-177626-VOL-4] p 857 N94-15720
Equations of motion of a hinged body over a spherical earth
[AD-A268408] p 868 N94-17435
CONTROL SYSTEMS DESIGN
Research in robust control for hypersonic aircraft
[NASA-CR-194106] p 870 N94-15416
Transputer based control system for MTLRS
p 877 N94-15613
System architecture of optically controlled phased array radar
[AD-A267056] p 988 N94-15667
Adaptive weld control for high-integrity welding applications
[TABES PAPER 93-604] p 1049 N94-16140
Controls of maglev suspension systems
[DE93-015540] p 1011 N94-16443
ALS engine controller system
[NASA-CR-194647] p 926 N94-16654
Cognitive engineering models in space systems
[NASA-CR-193473] p 1140 N94-16716
A modular control architecture for real-time synchronous and asynchronous systems
[DE93-015439] p 1166 N94-16888
Development and analysis of startup strategies for particle bed nuclear rocket engine
[AD-A267949] p 927 N94-17053
A proposed ground segment design for small satellites
p 878 N94-17154
Ground segment definition for the Spanish small satellite program (MINISAT) p 878 N94-17155
Discrete sliding mode control for nonlinear sampled data systems
[AD-A267500] p 1167 N94-17369
CONTROL THEORY
Aerodynamic flight control to increase payload capability of future launch vehicles
[NASA-CR-193850] p 870 N94-15532
Contribution to the elaboration of some adaptive control algorithms for fermentation processes monitoring
[LAAS-92513] p 1116 N94-15643
The design and analysis of robust feedback systems
[AD-A267152] p 1165 N94-15778
Controls of maglev suspension systems
[DE93-015540] p 1011 N94-16443
Computation of the Fluid and Optical Fields About the Stratospheric Observatory for Infrared Astronomy (SOFIA) and the Coupling of Fluids, Dynamics, and Control Laws on Parallel Computers
[NASA-CR-193168] p 858 N94-16510
Cognitive engineering models in space systems
[NASA-CR-193473] p 1140 N94-16716
A molecular dynamics simulator for optimal control of molecular motion
[AD-A266572] p 1183 N94-16722
Dynamics, stability, and control of maglev systems
[DE93-015163] p 1047 N94-16806
Modeling, estimation and control of distributed parameter systems
[AD-A267325] p 1026 N94-17003
Hypervelocity orbital intercept guidance using certainty control
[AD-A267297] p 1174 N94-17219
Active turbulence control in wall bounded flows using direct numerical simulation
[AD-A267261] p 1028 N94-17286
Discrete sliding mode control for nonlinear sampled data systems
[AD-A267500] p 1167 N94-17369
A comparative study of analog and digital control laws for the UMCSL truss
[AD-A267980] p 871 N94-17412
CONTROL VALVES
ALS engine propellant effector system
[NASA-CR-194650] p 926 N94-16590
CONTROLLABILITY
Aerodynamic control of NASP-type vehicles through vortex manipulation, volume 4
[NASA-CR-177626-VOL-4] p 857 N94-15720
Fidelity assessment of a UH-60A simulation on the NASA Ames vertical motion simulator
[NASA-TM-104016] p 870 N94-15793
CONTROLLED FUSION
3D and r,z particle simulations of heavy ion fusion beams
[DE93-013417] p 1205 N94-17670
CONTROLLERS
A microprocessor controller for a towing tank drive and flow visualisation system
[AD-A267087] p 872 N94-15543
ALS engine controller system
[NASA-CR-194647] p 926 N94-16654
Three axis force override rate control of a PUMA 560 manipulator
[AD-A267313] p 1048 N94-16944
Space systems environmental interaction studies
[AD-A267280] p 897 N94-17240
Optimal tuning of heavy equipment motion controllers
[AD-A267873] p 1167 N94-17392
A comparative study of analog and digital control laws for the UMCSL truss
[AD-A267980] p 871 N94-17412
Environmental use of a Laser Range Finder and the Advanced Visualization System
[DE93-016163] p 1043 N94-17677
CONVECTION
Clouding tracing: Visualization of the mixing of fluid elements in convection-diffusion systems
[NASA-CR-191529] p 1148 N94-15965
Geophysical models of Western Aphrodite-Niobe region: Venus p 1286 N94-16382
Unsteady fluid and optical simulation of transonic aero-windows
[AIAA PAPER 93-3017] p 858 N94-16512
Convection effects on radial segregation and crystal melt interface in vertical Bridgman growth
[NASA-CR-191541] p 1029 N94-17387
Opposing mesoscale flows in a broken midlatitude squall line
[AD-A268011] p 1109 N94-17492
Propagation characteristics of mesoscale convective systems
[AD-A268130] p 1109 N94-17522
CONVECTION CURRENTS
Orographic microbursts in a severe winter windstorm
[AD-A267651] p 1108 N94-17247
A correlative comparison of geomagnetic storms and auroral substorms using geomagnetic indeces
[AD-A268081] p 1102 N94-17512
Propagation characteristics of mesoscale convective systems
[AD-A268130] p 1109 N94-17522
Further development and testing of a second-order bulk boundary layer model
[AD-A268071] p 1109 N94-17552
CONVECTION-DIFFUSION EQUATION
Convective flow effects on protein crystal growth
[NASA-CR-194560] p 1206 N94-15476
CONVECTIVE FLOW
Visualization of solidification front phenomena
[NASA-CR-193838] p 976 N94-15006
Convective flow effects on protein crystal growth
[NASA-CR-194560] p 1206 N94-15476
Clouding tracing: Visualization of the mixing of fluid elements in convection-diffusion systems
[NASA-CR-191529] p 1148 N94-15965
Models of thermal/chemical boundary layer convection: Potential application to Venus p 1279 N94-16348
CONVECTIVE HEAT TRANSFER
Dual active surface, miniature, plug-type heat flux gauge
[NASA-CASE-LEW-15643-1] p 1033 N94-15928
GAM-HEAT: A computer code to compute heat transfer in complex enclosures
[DE93-014724] p 1023 N94-15980
On the relationship between tectonic plates and thermal mantle plume morphology p 1104 N94-16349
Fluid flow and heat convection studies for actively cooled airframes
[NASA-CR-194624] p 1024 N94-16491
Natural convection above a horizontal heat source
[AD-A267212] p 1026 N94-16985
On the a-posteriori estimation of the modelling error for the heat conduction in a plate and its use for adaptive hierarchic modelling
[AD-A267965] p 1029 N94-17384
Numerically solving a transient heat conduction problem with convection and radiation
[AD-A268521] p 1220 N94-17540
Heat transfer parametric system identification
[AD-A268525] p 929 N94-17543
CONVENTIONS
The early activities of the COPERS and the drafting of the ESRO Convention (1961/62)
[ESA-HSR-4] p 1225 N94-16593
CONVERGENCE
On the stability analysis of approximate factorization methods for 3D Euler and Navier-Stokes equations
[NASA-TM-106314] p 1169 N94-15818
Unipolar terminal-attractor based neural associative memory with adaptive threshold
[NASA-CASE-NPO-18790-1-CU] p 1165 N94-15958
Convergence of the multiple scattering expansion in XAFS and XANES
[DE93-011001] p 948 N94-16772
Asymptotic behavior of firmly non expansive sequences
[DE93-628589] p 1171 N94-17642
Fixed point iterations for strictly hemi-contractive maps in uniformly smooth Banach spaces
[DE93-628591] p 1175 N94-17644
CONVERGENT-DIVERGENT NOZZLES
Design of round-to-square transition section; analysis and computer code
[AD-A267173] p 872 N94-15847
Effects of internal yaw-vectoring devices on the static performance of a pitch-vectoring nonaxisymmetric convergent-divergent nozzle
[NASA-TP-3369] p 858 N94-16572
CONVERSATION
Questioning mechanisms during tutoring, conversation, and human-computer interaction
[AD-A266199] p 1137 N94-16108
CONVOLUTION INTEGRALS
A simulation study of the performance of the NASA (2,1,6) convolutional code on RFI/burst channels
p 997 N94-16508
COOL STARS
The formation process of the He I lambda 10830 line in cool giant stars
[NASA-CR-194648] p 1240 N94-17094
COOLERS
Future development in cryogenic techniques for space
p 901 N94-15042
Infrared detectors and coolers for space instrumentation: Summary and concluding remarks p 904 N94-15059
Proceedings of the 7th International Cryocooler Conference, part 1
[AD-A268448] p 985 N94-17482
Proceedings of the 7th International Cryocooler Conference, part 2
[AD-A268449] p 985 N94-17484
Proceedings of the 7th International Cryocooler Conference, part 3
[AD-A268450] p 985 N94-17485
COOLING
Theoretical studies relating to the interaction of radiation with matter
[AD-A266894] p 1179 N94-14949
Advanced cooling for high power electric actuators
[AD-A266984] p 866 N94-15761
The cooling of confined ions driven by laser beams
[DE93-016612] p 1039 N94-16114
Cation ordering in orthopyroxenes and cooling rates of meteorites: Low temperature cooling rates of Estherville, Bondoc and Shaw p 1241 N94-16176
The cooling rates of pahoehoe flows: The importance of lava porosity p 1103 N94-16282
More on the cooling history of angrite LEW 86010
p 1245 N94-16400
Limited subsolidus diffusion in type B1 CAI: Evidence from Ti distribution in spinel p 954 N94-16401

Zaoyang chondrite cooling history from pyroxene Fe(2+)-Mg intracrystalline ordering and exolutions
p 1246 N94-16417
Techniques for preparation of ingot metallurgical discontinuous composites
[AD-D015748] p 940 N94-16933
Numerically solving a transient heat conduction problem with convection and radiation
[AD-A268521] p 1220 N94-17540

COOLING SYSTEMS
Cool suit
[NASA-TM-109639] p 1120 N94-15250
USAF physiological studies of personal microclimate cooling: A review
[AD-A267203] p 1022 N94-15858
Geometrical vapor blocker for parallel condensation tubes requiring cooling
[NASA-CASE-MSC-22090-1] p 1022 N94-15962
Effects of rotation on coolant passage heat transfer. Volume 2: Coolant passages with trips normal and skewed to the flow
[NASA-CR-4396-VOL-2] p 1023 N94-15991
Cycle performance testing of nonazeotropic mixtures of HFC-142A/HCFC-124 and HFC-32/HCFC-124 with enhanced surface heat exchangers
[DE93-015215] p 1024 N94-16808

COORDINATION
Complex information coordination performance: Differential changes in working memory contributions following training
[AD-A267007] p 1132 N94-15762

COPOLYMERIZATION
Swelling equilibria for temperature-sensitive ampholytic hydrogels
[DE93-015264] p 966 N94-15996

COPOLYMERS
Vectorial electron transfer in spatially ordered arrays
[DE93-018150] p 1185 N94-16971
Responsive copolymers for enhanced petroleum recovery
[DE93-018030] p 971 N94-16999

COPPER
Ablation, surface activation, and electroless metallization of insulating materials by pulsed excimer laser irradiation
[DE93-015808] p 1040 N94-16664
Single crystal diamond thin films
[AD-A266457] p 1214 N94-17216
Continuing research on friction and wear of materials
[AD-A268291] p 1049 N94-17566

COPPER ALLOYS
Dynamical Ising model simulations of nucleation and growth in copper-cobalt alloys
[DE93-015336] p 957 N94-16015
Aluminum-lithium technology
[TABES PAPER 93-601] p 962 N94-16137
Fabrication of advanced design (grooved) cermet anodes
[DE93-014590] p 1012 N94-16765

COPPER CHLORIDES
High-performance nonlinear optical material developed in Japan
[AD-A266194] p 1191 N94-16126
Investigation of the influence of applied potential on erosion-corrosion of copper in alkaline chloride solutions
[AD-A266448] p 958 N94-16562

COPPER OXIDES
Roles of oxygen defects in copper-oxide superconductors
[DE93-014875] p 1208 N94-15982
Pulsed laser deposition of metastable Ca(1-x)Sr(x)CuO2 thin films
[DE93-015804] p 1040 N94-16663

CORE FLOW
Lava crusts and flow dynamics p 1103 N94-16316

CORE SAMPLING
A discontinuous melt sheet in the Manson impact structure p 1103 N94-16269
Manson impact structure, Iowa: First geochemical results for drill core M-1 p 1103 N94-16322
Composition of Apollo 17 core 76001 p 1275 N94-16326
Composition and maturity of the 60013/14 core p 1275 N94-16327

CORES
Atmospheric ionization by solar particles detected by nitrate measurement in antarctic snow
[AD-A267583] p 1299 N94-17208

CORNER FLOW
Inviscid instability of streamwise corner flow
[NASA-CR-191514] p 1021 N94-15834

CORONAL LOOPS
FNAS/solar flare energetics
[NASA-CR-193574] p 1299 N94-17089

CORONAS
Microwave interaction with plasmas
[AD-A267048] p 1201 N94-15661
Morphology and models for the evolution of eastern Hecate Chasma, Venus p 1256 N94-16215
Tectonics of Neyterkob corona on Venus p 1270 N94-16299
Large-scale volcanism associated with coronae on Venus p 1285 N94-16376

CORRECTION
Timebias corrections to predictions p 875 N94-15591

CORRELATION
Chemical and displacement atomic pair correlations in crystalline solid solutions recovered by anomalous x ray scattering in Fe-Ni alloys
[DE93-015906] p 1209 N94-16171
Powder diffraction studies using anomalous dispersion
[DE93-012531] p 1210 N94-16775
To extend the thirteen-moment theory and its application to problems in rarefied hypersonic flow
[AD-A267384] p 859 N94-17021

CORRELATION COEFFICIENTS
Speckles statistics and decorrelation effects in complex ABCD optical systems
[AD-A267843] p 1193 N94-17012

CORRELATORS
Synthetic aperture radar signal processing: Trends and technologies p 992 N94-15908
Wideband acousto-optic correlator for an ESM receiver upgrade
[TABES PAPER 93-661] p 1054 N94-16156
High resolution radar profiling using higher-order statistics
[AD-D015891] p 1000 N94-16918

CORROSION
Application of in situ scanning x ray fluorescence to study the concentration of metal ions in simulated pits
[DE93-014054] p 956 N94-15921
Corrosion kinetics and mechanisms for nuclear grade graphites
[DE93-015462] p 947 N94-16105
Environmental effects on iron aluminides
[DE93-015820] p 958 N94-16166
Status of molten carbonate fuel cell technology development
[DE93-015666] p 1092 N94-16715
Aircraft carrier exposure tests of cast magnesium alloys
[AD-A268260] p 962 N94-17418

CORROSION PREVENTION
XPS analysis of Al/EPDM bondlines from IUS SRM-1 polar bosses
[AD-A266851] p 1056 N94-14945
The corrosion protection of metals by ion vapor deposited aluminum
[NASA-TM-108425] p 955 N94-15832
Assessment of chromate and non-chromate conversion coatings for Al alloys using electrochemical impedance spectroscopy
[AD-A267205] p 965 N94-15859
Formation of pitting resistant anodized films on aluminum
[AD-D015812] p 958 N94-16486
Vanadium corrosion studies
[AD-A266489] p 959 N94-16781
Evaluation of hybrid reinforcement (fiber-reinforced-plastic rod with steel core)
[AD-A268009] p 941 N94-17473

CORROSION RESISTANCE
Assessment of chromate and non-chromate conversion coatings for Al alloys using electrochemical impedance spectroscopy
[AD-A267205] p 965 N94-15859
Environmental effects on elevated temperature subcritical crack growth of SiC/SiC composites
[DE93-015688] p 934 N94-16158
Development and commercialization status of Fe3Al-based intermetallic alloys
[DE93-015802] p 957 N94-16165
Wear resistant titanium material development
[AD-A266474] p 959 N94-16780
Chemical vapor deposition of Ta2O5 corrosion resistant coatings
[DE93-015488] p 969 N94-16889
Evaluation of hybrid reinforcement (fiber-reinforced-plastic rod with steel core)
[AD-A268009] p 941 N94-17473

CORROSION TESTS
Application of in situ scanning x ray fluorescence to study the concentration of metal ions in simulated pits
[DE93-014054] p 956 N94-15921
Potential transients, transmission and electrochemical corrosion detection
[DE93-014055] p 956 N94-15922

COSMIC BACKGROUND EXPLORER SATELLITE
COBE video news
[NASA-TM-109598] p 987 N94-15292

COSMIC DUST
X ray emission from Wolf-Rayet stars with recurrent dust formation
[NASA-CR-194567] p 1300 N94-15533
Removal of carbonaceous contaminants from silica aerogel p 953 N94-16256
The astrophysical interpretation of isotope anomalies in graphite and SiC grains of chondrites p 1244 N94-16343
The chromosphere of VV cephei and the distribution of circumstellar dust around red giants and supergiants
[NASA-CR-193594] p 1297 N94-16866
Cosmic dust and space debris measurements on board the small satellites HITEN and BREM-SAT p 890 N94-17147

COSMIC RAY SHOWERS
Astrophysics with MILAGRO
[DE93-012722] p 1240 N94-17657

COSMIC RAYS
Astronomy and astrophysics p 1239 N94-15970
Al-26-Mg-26 ages of iron meteorites p 1242 N94-16240
Contained (nu) events observed in Soudan 2
[DE93-015548] p 1300 N94-17233
Astrophysics with MILAGRO
[DE93-012722] p 1240 N94-17657

COSMOCHEMISTRY
Geochemistry and cosmochemistry of fullerenes 3: Reaction of C60 and C70 with ozone p 953 N94-16243
Potassium isotope cosmochemistry, volatile depletion and the origin of the Earth p 953 N94-16259
Catalytic crystallization of ices by small silicate smokes at temperatures less than 20K p 1219 N94-16420

COSMOLOGY
Astronomy and astrophysics p 1239 N94-15970
Theoretical high energy physics research at the University of Chicago
[DE93-016863] p 1187 N94-16116
Particle physics and cosmology, Task C
[DE93-016865] p 1239 N94-16118

COSMONAUTS
ASTP 15th anniversary clip-media release
[NASA-TM-109534] p 1302 N94-15399

COSPAS
Life saving satellites
[NASA-TM-109616] p 862 N94-15426

COST ANALYSIS
Concepts on measuring the benefits of software process improvements
[AD-A266994] p 1144 N94-15215
Space Station Facility government estimating
[NASA-TM-109324] p 1223 N94-15545
Estimating and bidding for the Space Station Processing Facility
[NASA-TM-109323] p 1223 N94-15546
New York MARKAL: An evaluation of carbon dioxide emission control strategies in New York State
[DE93-013149] p 1095 N94-15999
Space Shuttle main engine. NASA has not evaluated the alternate fuel turbopump costs and benefits. Report to the Administrator of the National Aeronautics and Space Administration
[GAO/NSIAD-94-54] p 926 N94-16834
A handbook of cost risk analysis methods
[AD-A267253] p 1235 N94-16988
Cost drivers: Why do conventional satellites cost so much? p 897 N94-17190
X ray computed tomography for failure analysis investigations
[AD-A268086] p 1055 N94-17515

COST EFFECTIVENESS
Reengineering: An engineering problem
[AD-A267117] p 1146 N94-15653
Facilities maintenance handbook
[NHB-8831.2] p 1224 N94-15934
Cost-effective test methods for Shuttle payloads
[TABES PAPER 93-651] p 883 N94-16151
Modeling and simulation: A key to future defense technology
[TABES PAPER 93-654] p 1054 N94-16153

COST ESTIMATES
Space Station Facility government estimating
[NASA-TM-109324] p 1223 N94-15545
Estimating and bidding for the Space Station Processing Facility
[NASA-TM-109323] p 1223 N94-15546
A handbook of cost risk analysis methods
[AD-A267253] p 1235 N94-16988
A conceptual design study for a two-dimensional, electronically scanned thinned array radiometer
[NASA-TM-109051] p 1085 N94-17665

COST REDUCTION
Techno-economic requirements for composite aircraft components p 940 N94-16864
A mini satellite called Arsene: The way to make it at a minimum cost p 895 N94-17179
MINISAT programme p 896 N94-17182
Small satellite product assurance p 896 N94-17188
Cost drivers: Why do conventional satellites cost so much? p 897 N94-17190

COSTS
Space Station Facility government estimating
[NASA-TM-109324] p 1223 N94-15545
Estimating and bidding for the Space Station Processing Facility
[NASA-TM-109323] p 1223 N94-15546
Approaching the new reality
[TABES PAPER 93-230] p 1050 N94-16131
Design of a formaldehyde photodissociation process for carbon and oxygen isotope separation
[DE93-016435] p 1039 N94-16450
Comparisons of selected laser beam power missions to conventionally powered missions
[NASA-TM-106110] p 1040 N94-16522
Military satellite communications: Opportunity to save billions of dollars. Report to the Chairman, Legislation, and National Security Subcommittee, Committee on Government Operations, House of Representatives
[AD-A267627] p 1002 N94-17199

COUETTE FLOW
Numerical study of compressible boundary-level transition between two concentric cylinders
[NASA-CR-194622] p 1025 N94-16842
Thermally-sustained structure in convectively unstable systems
[NASA-TM-106375] p 1027 N94-17112

COULOMB COLLISIONS
Nuclear fusion of protons with ions of boron
[DE93-015399] p 1202 N94-16019
Ultrafast processes in tunneling microstructure devices
[AD-A266570] p 1210 N94-16720
Evolution of hadron beams under intrabeam scattering
[DE93-014330] p 1184 N94-16826
Six dimensional tracking simulator for H(-) injection in AGS Booster
[DE93-015396] p 1184 N94-16885

COUNTERMEASURES
Space countersurveillance: A requisite for theater defense planning
[AD-A266871] p 884 N94-15147
Living well in space: Ensuring crew capability
[NASA-TM-109538] p 1120 N94-15369

COUPLED MODES
Emittance and beam size distortion due to linear coupling
[DE93-015402] p 1184 N94-16886

COUPLERS
Gratings and waveguides p 1226 N94-14987
Optical system storage design with diffractive optical elements p 1198 N94-17360

COUPLINGS
Connector systems for structures
[NASA-CASE-MSC-21998-1] p 1046 N94-15707
Attachment device
[NASA-CASE-MSC-21885-1] p 1047 N94-15925
Electrorheological (ER) fluids: A research needs assessment
[AD-A267588] p 951 N94-17210

COVARIANCE
Abundance recovery error analysis using simulated AVIRIS data p 1074 N94-16708
Maximum likelihood techniques applied to quasi-elastic light scattering
[NASA-CR-193550] p 1192 N94-16718
Processing of resonance parameter covariance files
[DE93-015506] p 1231 N94-16874
High order nonlinear estimation with signal processing applications
[AD-A268407] p 1005 N94-17463

COWLINGS
Wind tunnel investigation of three axisymmetric cowls of different lengths at Mach numbers from 0.60 to 0.92
[NASA-TM-4488] p 856 N94-15681

CRACK GEOMETRY
Crack-tip-opening angle measurements and crack tunneling under stable tearing in thin sheet 2024-T3 aluminum alloy
[NASA-CR-191523] p 931 N94-15184
Measurement and analysis of critical CTOA for an aluminum alloy sheet
[NASA-TM-109024] p 956 N94-15948
Prediction of thermal cycling induced cracking in polymer matrix composites
[NASA-CR-194677] p 941 N94-17295

CRACK PROPAGATION
Crack-tip-opening angle measurements and crack tunneling under stable tearing in thin sheet 2024-T3 aluminum alloy
[NASA-CR-191523] p 931 N94-15184
Prediction of stable tearing of 2024-T3 aluminum alloy using the crack-tip opening angle approach
[NASA-TM-109023] p 955 N94-15708
Measurement and analysis of critical CTOA for an aluminum alloy sheet
[NASA-TM-109024] p 956 N94-15948
Design of a cruciform bend specimen for determination of out-of-plane biaxial tensile stress effects on fracture toughness for shallow cracks
[DE93-015455] p 1059 N94-16104
Environmental effects on elevated temperature subcritical crack growth of SiC/SiC composites
[DE93-015688] p 934 N94-16158
Anisotropic damage mechanics modeling in metal matrix composites
[AD-A266328] p 934 N94-16440
The processing and mechanical properties of high temperature/high performance composites. Book 3: Coonstituent properties and macroscopic performance
[AD-A266396] p 935 N94-16485
Highly transient elastodynamic crack growth in a bimaterial interface: Higher order asymptotic analysis and optical experiments
[AD-A266465] p 1059 N94-16587
Mean strain effects on the strain life fatigue curve
[AD-A267211] p 960 N94-16984
J-integral and HRR field associated with stable crack growth in thin aluminum SEN specimen
[AD-A267879] p 960 N94-17041
Interfacial shear behavior and its influence on fiber damage in sapphire-reinforced gamma titanium aluminide composites
[AD-A267943] p 1060 N94-17043
RSRM nozzle actuator bracket/lug fracture mechanics qualification test
[NASA-CR-193859] p 927 N94-17080
Micromechanisms of monotonic and cyclic subcritical crack growth in advanced high melting point low-ductility intermetallics
[AD-A267764] p 961 N94-17223
Aspects of high temperature damage in fiber reinforced titanium metal matrix composites
[AD-A267907] p 941 N94-17379
Direct observation of fracture of CAS-glass/SiC composites and processing of toughened alumina
[AD-A268275] p 941 N94-17457
Damage evolution in filled elastomers
[AD-A268067] p 1062 N94-17507
Thermo-mechanical analysis of oxidation protected carbon-carbon composites
[AD-A268191] p 941 N94-17597
Environment enhanced fatigue crack propagation in metals: Inputs to fracture mechanics life prediction models
[NASA-CR-191538] p 942 N94-17638

CRACK TIPS
Crack-tip-opening angle measurements and crack tunneling under stable tearing in thin sheet 2024-T3 aluminum alloy
[NASA-CR-191523] p 931 N94-15184
Prediction of stable tearing of 2024-T3 aluminum alloy using the crack-tip opening angle approach
[NASA-TM-109023] p 955 N94-15708
Measurement and analysis of critical CTOA for an aluminum alloy sheet
[NASA-TM-109024] p 956 N94-15948
Highly transient elastodynamic crack growth in a bimaterial interface: Higher order asymptotic analysis and optical experiments
[AD-A266465] p 1059 N94-16587
Transformation toughening of composite ceramics
[AD-A267304] p 971 N94-16980
J-integral and HRR field associated with stable crack growth in thin aluminum SEN specimen
[AD-A267879] p 960 N94-17041
The effect of electric discharge machined notches on the fracture toughness of several structural alloys
[AD-A268605] p 962 N94-17464
Environment enhanced fatigue crack propagation in metals: Inputs to fracture mechanics life prediction models
[NASA-CR-191538] p 942 N94-17638

CRACKING (CHEMICAL ENGINEERING)
Investigation of the origin of hot spots in deformed crystals: Ammonium perchlorate studies
[AD-A267692] p 1214 N94-17270
Heating of lubricant with an electric resistance heater
[VTT-TIED-1359] p 974 N94-17547

CRACKING (FRACTURING)
Creep ductility of iron at very low strain rates: The effects of sulfur
[DE93-015490] p 959 N94-16890
Static and dynamic investigations of brittle elasto-optical material
[IFTR-3/1992] p 1061 N94-17086
Prediction of thermal cycling induced cracking in polymer matrix composites
[NASA-CR-194677] p 941 N94-17295
Automated image analysis method for the detection of cracks on wood surface
[VTT-JULK-755] p 1056 N94-17542

CRACKS
Application of in situ scanning x ray fluorescence to study the concentration of metal ions in simulated pits
[DE93-014054] p 956 N94-15921
The influence of microstructure on the mechanical behavior of silicon nitride ceramics
[DE93-015363] p 966 N94-16018
Anisotropic damage mechanics modeling in metal matrix composites
[AD-A266328] p 934 N94-16440
Highly transient elastodynamic crack growth in a bimaterial interface: Higher order asymptotic analysis and optical experiments
[AD-A266465] p 1059 N94-16587
Prediction of thermal cycling induced cracking in polymer matrix composites
[NASA-CR-194677] p 941 N94-17295
Direct observation of fracture of CAS-glass/SiC composites and processing of toughened alumina
[AD-A268275] p 941 N94-17457
The effect of electric discharge machined notches on the fracture toughness of several structural alloys
[AD-A268605] p 962 N94-17464
Damage evolution in filled elastomers
[AD-A268067] p 1062 N94-17507

CRASH INJURIES
National Transportation Safety Board annual review of aircraft accident data, US general aviation, calendar year 1989
[PB93-160687] p 863 N94-16464
Design of non-sled setup to measure head injury criteria
[NIAR-92-20] p 872 N94-17263

CRASHES
Basic principles of helicopter crashworthiness
[AD-A267099] p 862 N94-15637
National Transportation Safety Board annual review of aircraft accident data, US general aviation, calendar year 1989
[PB93-160687] p 863 N94-16464
Design of non-sled setup to measure head injury criteria
[NIAR-92-20] p 872 N94-17263

CRASHWORTHINESS
Basic principles of helicopter crashworthiness
[AD-A267099] p 862 N94-15637

CRATERING
Impact penetration experiments in teflon targets of variable thickness p 1063 N94-16253
Cat Mountain: A meteoritic sample of an impact-melted chondritic asteroid p 1244 N94-16328

CREATIVITY
A scientific basis for computational science
[AD-A266697] p 1148 N94-15841

CREEP ANALYSIS
Modelling of creep data for plastics
[NPL-DMM(A)-92] p 1057 N94-15017
Multiaxial deformation and life prediction model and experimental data for advanced silicon nitride ceramics
[DE93-015450] p 967 N94-16067
On the design of structural components using materials with time-dependent properties
[NASA-TM-108428] p 1059 N94-16519
Development of a constitutive model for creep and life prediction of advanced silicon nitride ceramics
[DE93-015894] p 968 N94-16813

CREEP PROPERTIES
A model for non-linear creep and physical ageing in PVC
[NPL-DMM(A)-91] p 1057 N94-15016
Modelling of creep data for plastics
[NPL-DMM(A)-92] p 1057 N94-15017
Multiaxial deformation and life prediction model and experimental data for advanced silicon nitride ceramics
[DE93-015450] p 967 N94-16067
The influence of thermal aging on the microstructure and fatigue properties of modified 9Cr-1Mo steel
[DE93-015489] p 957 N94-16106
Rheology of water and ammonia-water ices p 953 N94-16188
Ion implantation effects on surface-mechanical properties of metals and polymers
[DE93-014661] p 958 N94-16453

The processing and mechanical properties of high temperature/high performance composites. Book 2: Coonstituent properties and macroscopic performance
[AD-A266395] p 935 N94-16484
The processing and mechanical properties of high temperature/high performance composites. Book 3: Coonstituent properties and macroscopic performance
[AD-A266396] p 935 N94-16485
Development of a constitutive model for creep and life prediction of advanced silicon nitride ceramics
[DE93-015894] p 968 N94-16813
The Ceramic Technology Project: Ten years of progress
[DE93-015991] p 968 N94-16843
Effects of processing and prolonged high temperature exposure on the microstructure of Nb-1Zr-C sheet
[NASA-TM-106370] p 959 N94-16883
Creep ductility of iron at very low strain rates: The effects of sulfur
[DE93-015490] p 959 N94-16890

CREEP RUPTURE STRENGTH
Modelling of creep data for plastics
[NPL-DMM(A)-92] p 1057 N94-15017
Multiaxial deformation and life prediction model and experimental data for advanced silicon nitride ceramics
[DE93-015450] p 967 N94-16067
Tensile and stress-rupture behavior of hafnium carbide dispersed molybdenum and tungsten base alloy wires
[NASA-TM-106350] p 962 N94-17652

CREEP STRENGTH
Rheology of water and ammonia-water ices
p 953 N94-16188
The processing and mechanical properties of high temperature/high performance composites. Book 3: Coonstituent properties and macroscopic performance
[AD-A266396] p 935 N94-16485
Creep ductility of iron at very low strain rates: The effects of sulfur
[DE93-015490] p 959 N94-16890

CRETACEOUS-TERTIARY BOUNDARY
Cretaceous-tertiary boundary spherules and Cenozoic microtektites: Similarities and differences
p 1241 N94-16186
The Acraman impact structure: Estimation of the diameter by the ejecta layer thickness
p 1103 N94-16211
Trace-element composition of Chicxulub crater melt rock, K/T tektites and Yucatan basement
p 1242 N94-16245
Manson impact structure, Iowa: First geochemical results for drill core M-1 p 1103 N94-16322
Preliminary Ar-40/Ar-39 age spectrum and laser probe dating of the M1 core of the Manson Impact Structure, Iowa: A K-T boundary crater candidate
p 1104 N94-16334
Chondritic ratios of Fe/Cr/Ir in Kerguelen Plateau (Hole 738C) K/T carbonate-rich sediments support asteroid-cometary impact at K/T time
p 1244 N94-16357
Geochemical evidences for two chondritic-like cometary or asteroidal impacts before and at the K/T boundary
p 1244 N94-16359

CREW PROCEDURES (INFLIGHT)
STS-30 Post-Flight Press Conference --- Space Shuttle Launch, Magellan/IUS deploy, Crew Activites, and Landing
[NASA-TM-109580] p 879 N94-15264
STS-30 mission tape --- Space Shuttle Launch, Crew Activities, Landing, and Air-to-Ground Transmission
[NASA-TM-109582] p 879 N94-15266
STS-29 pre-launch and post-landing egress
[NASA-TM-109574] p 1135 N94-15305
STS-29 Post-Flight Press Conference --- Shuttle Launch, TDRS-D/IUS Deployment, Crew Activites, and Shuttle Landing
[NASA-TM-109575] p 880 N94-15306
STS-29 onboard 16mm photography quick release
[NASA-TM-109576] p 880 N94-15307
STS-34 McCully and Baker during IFM training
[NASA-TM-109462] p 880 N94-15357
STS-34 Galileo integrated deploy sim
[NASA-TM-109463] p 880 N94-15358
STS-34 Chang-Diaz and E. Baker during Galileo contingency training in WFTF
[NASA-TM-109466] p 1135 N94-15361
STS-30 onboard 16mm photography quick release
[NASA-TM-109579] p 881 N94-15423
STS-31 onboard 16mm photography quick release --- Onboard Activities
[NASA-TM-109478] p 881 N94-15438
STS-31 mission highlights resource tape
[NASA-TM-109479] p 881 N94-15440
STS-31 crew training inflight maintenance and ballout exercises in CCT and WFTF
[NASA-TM-109483] p 876 N94-15450

CREW PROCEDURES (PREFLIGHT)
STS-29 pre-launch and post-landing egress
[NASA-TM-109574] p 1135 N94-15305

CREWS
Carpal tunnel syndrome and other cumulative trauma disorders of the arm and hand and occupation in US Navy enlisted personnel
[AD-A267747] p 1129 N94-17374

CRIME
Criminal acts against civil aviation, fiscal year 1992
[AD-A268014] p 863 N94-17586

CRITERIA
Slidesurfaces with adaptive new definitions (SAND) for transient analysis
[DE93-014909] p 1059 N94-15983

CRITICAL LOADING
RSRM nozzle actuator bracket/lug fracture mechanics qualification test
[NASA-CR-193859] p 927 N94-17080

CRITICAL MASS
The stability of ions in a storage ring in the presence of small gap insertion devices
[DE93-015387] p 1184 N94-16828

CRITICAL POINT
Density and temperature relaxation near the critical point of carbon dioxide under reduced gravity
p 944 N94-15164
Temperature propagation in near-critical fluids prior to and during separation p 944 N94-15165
Pressures of supercritical salt solutions
p 945 N94-15166

CRITICAL TEMPERATURE
Partitioning of Nb, Mo, Ba, Ce, Pb, Th and U between immiscible carbonate and silicate liquids: Evaluating the effects of P2O5,F, and carbonate composition
p 953 N94-16283

CROP GROWTH
The dynamics of hydroponic crops for simulation studies of the CELSS initial reference configurations
[NASA-CR-194654] p 1118 N94-17279

CROSS CORRELATION
Nowcasting methods for satellite imagery
[AD-A267294] p 1108 N94-17267

CROSS COUPLING
Synthesis, characterization, and polymerization of new ferrocene-fluorene complexes. A novel high-molecular weight conjugated polymer with pendant ferrocene groups
[AD-A267717] p 972 N94-17273

CROSS POLARIZATION
External calibration of polarimetric radar images using distributed targets p 1079 N94-16753
Comparison of edges detected at different polarisations in MAESTRO data p 1080 N94-16761
Remote sensing of precipitation and electrification with a dual-polarization, coherent, wideband radar system
[AD-A267479] p 1004 N94-17364

CROSSLINKING
Rational design, construction, and processing of high-performance nonlinear optical materials
[AD-A266185] p 1191 N94-16454
The photochemistry of poly(methylphenylphosphazene)
[AD-A267320] p 970 N94-16948

CROSSTALK
A complete study of differential wax-wane focus servo technique p 1199 N94-14996
Unipolar terminal-attractor based neural associative memory with adaptive threshold
[NASA-CASE-NPO-18790-1-CU] p 1165 N94-15958
External calibration of polarimetric radar images using distributed targets p 1079 N94-16753

CRRES (SATELLITE)
Optical measurements of NASA/USAF CRRES high altitude rocket borne chemical release experiments in conjunction with the USAF airborne ionospheric observatory aircraft
[AD-A266404] p 1101 N94-16551
L-shell binning and display of sensor data from the CRRES spacecraft
[AD-A267256] p 888 N94-16990

CRUCIFORM WINGS
The effect of the nose shape and wing location toward the wing vortex breakdown
[AD-A267724] p 855 N94-14942

CRUDE OIL
Responsive copolymers for enhanced petroleum recovery
[DE93-018030] p 971 N94-16999

CRUISING FLIGHT
Flow analysis for the nacelle of an advanced ducted propeller at high angle-of-attack and at cruise with boundary layer control
[NASA-TM-106371] p 858 N94-16571

CRUSTAL FRACTURES
Composite refraction-reflection stack sections: Tracing faults in the Atlantic coastal plain sediments
[DE93-013581] p 1112 N94-16009
Tectonic deformation in southern California
[NASA-CR-194621] p 1101 N94-16021
High-resolution seismic reflection survey at the Manson crater, Iowa p 1103 N94-16307

CRUSTS
Crustal structure and igneous processes in a chondritic Io p 1243 N94-16292
The thickness of eucritic crust in the HED parent body
p 1104 N94-16416

CRYOGENIC COOLING
Future development in cryogenic techniques for space
p 901 N94-15042
Proceedings of the 7th International Cryocooler Conference, part 1
[AD-A268448] p 985 N94-17482
Proceedings of the 7th International Cryocooler Conference, part 2
[AD-A268449] p 985 N94-17484
Proceedings of the 7th International Cryocooler Conference, part 3
[AD-A268450] p 985 N94-17485

CRYOGENIC EQUIPMENT
X ray microcalorimeters: Principles and performance
p 899 N94-15027
Cryogenic readout electronics for astronomical applications p 910 N94-15099
Superconductive material and magnetic field for damping and levitation support and damping of cryogenic instruments
[NASA-CASE-NPO-18458-1-CU] p 1033 N94-15875
Aluminum-lithium technology
[TABES PAPER 93-601] p 962 N94-16137
Proceedings of the 7th International Cryocooler Conference, part 1
[AD-A268448] p 985 N94-17482
Proceedings of the 7th International Cryocooler Conference, part 2
[AD-A268449] p 985 N94-17484
Proceedings of the 7th International Cryocooler Conference, part 3
[AD-A268450] p 985 N94-17485

CRYOGENIC FLUID STORAGE
Power Reactant Storage Assembly (PRSA) (Space Shuttle). PRSA hydrogen and oxygen DVT tank refurbishment
[NASA-CR-188262] p 926 N94-16922
Ground testing for the no-vent fill of cryogenic tanks: Results of tests for a 71 cubic foot tank
[NASA-TM-106293] p 1030 N94-17486

CRYOGENIC FLUIDS
Temperature and pressure effects on capacitance probe cryogenic liquid level measurement accuracy
[NASA-CR-190763] p 1034 N94-16521

CRYOGENIC TEMPERATURE
Cryogenic measurements of aerojet GaAs n-JFETs
[NASA-TM-103972] p 1009 N94-15765

CRYPTOGRAPHY
A security architecture for fault-tolerant systems
[AD-A266178] p 1152 N94-16982

CRYSTAL DEFECTS
Search for far infrared radiation from optically pumped defect modes
[AD-A266744] p 1206 N94-15822
Selective formation of porous silicon
[NASA-CASE-NPO-18735-1-CU] p 966 N94-15960
Roles of oxygen defects in copper-oxide superconductors
[DE93-014875] p 1208 N94-15982
Research support for cadmium telluride crystal growth
[NASA-CR-193557] p 1210 N94-16646
Microstructure of Zr3Al after 2 MeV proton bombardment
[DE93-015331] p 1211 N94-16814
Nitride semiconductors for ultraviolet detection
[AD-A267877] p 1012 N94-17040
Investigation of the origin of hot spots in deformed crystals: Ammonium perchlorate studies
[AD-A267692] p 1214 N94-17270
Kinetics of silica-phase transitions
[DE93-016231] p 1217 N94-17659

CRYSTAL DISLOCATIONS
Diffuse scattering and image contrast of tweed in superconducting oxides: A simulation and interpretation
[DE93-016131] p 1212 N94-16844

CRYSTAL GROWTH
Visualization of solidification front phenomena
[NASA-CR-193838] p 976 N94-15006
Growth of new materials for solid state laser applications. The growth of ZnGeP2 by the vertical Bridgman method
[NASA-CR-194571] p 1038 N94-15530
Laser assisted CVD growth of AlN and GaN
[AD-A267150] p 1206 N94-15764

Dynamical Ising model simulations of nucleation and growth in copper-cobalt alloys
[DE93-015336] p 957 N94-16015
Thermal spray forming of refractory sample ampoule cartridges for single crystal growth space furnaces
[TABES PAPER 93-605] p 1051 N94-16141
Evaporation kinetics of Mg2SiO4 crystals and melts from molecular dynamics simulations p 1219 N94-16331
Experimentally reproduced relict enstatite in porphyritic chondrules of enstatite chondrite composition
p 1244 N94-16363
Growth of single crystals of mercuric iodide on the ground and in space
[DE93-015523] p 1209 N94-16442
Research support for cadmium telluride crystal growth
[NASA-CR-193557] p 1210 N94-16646
Insights into semiconducting materials and growth phenomena through Z-contrast STEM
[DE93-015964] p 1212 N94-16841
Growth of dielectric thin films by irradiation of condensed molecular precursors with synchrotron radiation
[DE93-016161] p 974 N94-17676

CRYSTAL LATTICES
Simulation studies for surfaces and materials strength
[NASA-CR-193387] p 1056 N94-15004
Induced thermoluminescence study of experimentally shock-loaded oligoclase p 953 N94-16266
New organic materials for nonlinear optics applications
[AD-A266451] p 1192 N94-16563
Diffuse scattering and image contrast of tweed in superconducting oxides: A simulation and interpretation
[DE93-016131] p 1212 N94-16844
Investigation of the origin of hot spots in deformed crystals: Ammonium perchlorate studies
[AD-A267692] p 1214 N94-17270
Theoretical studies of the crystal structure of rare earths and actinides at zero temperature
[DE93-016488] p 1214 N94-17301
Theoretical crystallography with the Advanced Visualization System
[DE93-015692] p 1215 N94-17319
Buried porous silicon-germanium layers in monocrystalline silicon lattices and method of producing
[NASA-CASE-NPO-18836-1-CU] p 1215 N94-17327
Lattice relaxation theory of localized excitations in quasi-one-dimensional systems
[DE93-624947] p 1215 N94-17437

CRYSTAL OSCILLATORS
Double-driven shield capacitive type proximity sensor
[NASA-CASE-GSC-13541-1] p 1165 N94-15946
Quartz crystal resonators and oscillators for frequency control and timing applications: A tutorial, revision 6.1
[AD-A268205] p 1216 N94-17480

CRYSTAL STRUCTURE
MeV ion-beam analysis of optical data storage films
p 1226 N94-14984
STS-26 SSIP briefing --- Titanium Grain Formation Experiment and Crystal Membrane Experiment
[NASA-TM-109556] p 976 N94-15280
Cation ordering in orthopyroxenes and cooling rates of meteorites: Low temperature cooling rates of Estherville, Bondoc and Shaw p 1241 N94-16176
Zaoyang chondrite cooling history from pyroxene Fe(2+)-Mg intracrystalline ordering and exolutions
p 1246 N94-16417
Local environment about O atoms in Pr-Y-Ba-Cu-O films studied by O K-edge XAFS
[DE93-016218] p 1209 N94-16447
Hemoglobin
[AD-A266455] p 1123 N94-16566
JSEP fellowship
[AD-A266568] p 1211 N94-16800
Structural phase transition and superconductivity in La(2-x)Ba(x)CuO4
[DE93-015812] p 1212 N94-16868
Structural characterization of epitaxial layers for infrared detectors
[AD-A267875] p 940 N94-17013
Pseudomorphic semiconducting heterostructures from combinations of AlN, GaN and selected SiC polytypes: Theoretical advancement and its coordination with experimental studies of nucleation, growth, characterization and device deployment
[AD-A267561] p 1213 N94-17108
Investigation of the origin of hot spots in deformed crystals: Ammonium perchlorate studies
[AD-A267692] p 1214 N94-17270
Buried porous silicon-germanium layers in monocrystalline silicon lattices and method of producing
[NASA-CASE-NPO-18836-1-CU] p 1215 N94-17327

CRYSTAL SURFACES
Theoretical crystallography with the Advanced Visualization System
[DE93-015692] p 1215 N94-17319

CRYSTALLINITY
Chemical and displacement atomic pair correlations in crystalline solid solutions recovered by anomalous x ray scattering in Fe-Ni alloys
[DE93-015906] p 1209 N94-16171

CRYSTALLIZATION
Crystallization of grain boundary phases in silicon nitride with low additive contents by microwave annealing
[DE93-015801] p 1209 N94-16164
Systematic chemical variations in large 3AB iron meteorites: Clues to core crystallization
p 1241 N94-16213
The ilmenite liquidus and depths of segregation for high-Ti picrite glasses p 975 N94-16241
Olivines in the Kaba carbonaceous chondrite and constraints on their formation p 1219 N94-16255
Petrologic models of 15388, a unique Apollo 15 mare basalt p 1264 N94-16258
Silica-bearing objects in the Dengli H3.8 and Gorlovka H3-4 chondrites p 1242 N94-16265
Explosive volcanism and the compositions of the cores of differentiated asteroids p 1243 N94-16306
The dregs of crystallization in Zagami
p 1245 N94-16390
Catalytic crystallization of ices by small silicate smokes at temperatures less than 20K p 1219 N94-16420
Crystalline beam ground state
[DE93-014331] p 1211 N94-16827
Superconducting ceramics: Selected properties and methods of production
[IFTR-23/1991] p 969 N94-16924
The influence of an electric field on the kinetics of nucleation
[IFTR-2/91] p 1213 N94-17046
The roles of fluid motion and other transport phenomena in the morphology of materials
[NASA-CR-194665] p 1028 N94-17298

CRYSTALLOGRAPHY
Solution behaviour in microgravity: Considerations for protein crystal growth p 982 N94-16102
Exsolved kirschsteinite in angrite LEW86010 olivine
p 1245 N94-16410
Amide and tetrazene complexes of transition and main group elements as precursors for the low temperature synthesis of elemental nitrides
[AD-A266246] p 950 N94-16931
Transformation toughening of composite ceramics
[AD-A267304] p 971 N94-16980
Theoretical studies of the crystal structure of rare earths and actinides at zero temperature
[DE93-016488] p 1214 N94-17301
Theoretical crystallography with the Advanced Visualization System
[DE93-015692] p 1215 N94-17319

CRYSTALS
Search for far infrared radiation from optically pumped defect modes
[AD-A266744] p 1206 N94-15822
Confinement and stability of a Crystal Beam
[DE93-015400] p 1181 N94-16020

CULTURE TECHNIQUES
Cultured normal mammalian tissue and process
[NASA-CASE-MSC-21984-1] p 1117 N94-15969
Factors determining the release of nitric oxide --- Calcium/cadmium transport by renal cortical collectin duct cells
[AD-A266232] p 1118 N94-17224

CUMULUS CLOUDS
Spatial resolution and cloud optical thickness retrievals p 1066 N94-16671

CURING
Process for shaping articles from electrosetting compositions
[AD-D015787] p 935 N94-16534

CURRENT CONVERTERS (AC TO DC)
Circuits and control processes for combining direct converters and inverter motors
[ETN-93-94399] p 1008 N94-15448

CURRENT DENSITY
High temperature superconductivity
[AD-A267006] p 1008 N94-15635
Resonant frequencies of irregularly shaped microstrip antennas using method of moments
[NASA-TP-3386] p 989 N94-15767
Inductive effects during second harmonic current drive experiments on T-10
[DE93-014411] p 1202 N94-16803
The inverse problem to the evaluation of magnetic fields
[DE93-015239] p 1175 N94-17288
Field-emitter arrays for RF vacuum microelectronics
[AD-A268397] p 1015 N94-17526
Field emitter arrays for RF vacuum microelectronics
[AD-A268595] p 1015 N94-17608
Currents induced in the human body for exposure to ultrawideband electromagnetic pulses
[AD-A268570] p 1130 N94-17621

CURRENT DISTRIBUTION
Determination of the electromagnetic fields radiated from the ARES EMP simulator
[AD-A267069] p 988 N94-15668
The inverse problem to the evaluation of magnetic fields
[DE93-015239] p 1175 N94-17288

CURTAINS
SRB thermal curtain design support
[NASA-CR-193857] p 927 N94-17123

CURVATURE
Wind-tunnel investigation of aerodynamic efficiency of three planar elliptical wings with curvature of quarter-chord line
[NASA-TP-3359] p 859 N94-16574

CURVE FITTING
Formation of on-site normal points
p 917 N94-15592
Moments in statistics: Approximations to densities and goodness-of-fit
[AD-A266600] p 1173 N94-16726

CYCLES
Nitrates in SNCs: Implications for the nitrogen cycle on Mars p 1251 N94-16193
A Pluto thermal model p 1256 N94-16216

CYCLIC ACCELERATORS
Evolution of hadron beams under intrabeam scattering
[DE93-014330] p 1184 N94-16826

CYCLIC HYDROCARBONS
Advanced thermally stable jet fuels
[DE93-017711] p 975 N94-16996
Synthesis of potential high-energy fuels
[AD-A267508] p 975 N94-17073
Laser photoionization time-of-flight mass spectrometry of nitrated polycyclic aromatic hydrocarbons and nitrated heterocyclic compounds
[AD-A268126] p 952 N94-17520

CYCLIC LOADS
Quantitative assessment of the accuracy of constitutive laws for plasticity with an emphasis on cyclic deformation
[AD-A267562] p 961 N94-17109
Elastic-plastic finite-difference analysis of unidirectional composites subjected to thermomechanical cyclic loading
[AD-A267666] p 1061 N94-17269

CYCLONES
Arctic cyclones and Marginal Ice Zone (MIZ) variability
[AD-A268810] p 1108 N94-17465

CYCLOTRON RESONANCE
Growth and doping of Al(x)Ga(1-x)N films by electron cyclotron resonance assisted molecular beam epitaxy
[AD-A267305] p 1212 N94-16992

CYLINDRICAL BODIES
A mechanical system damping measurement technique using a one-degree-of-freedom (1DOF) cylindrical gas bearing
[AD-A268402] p 1048 N94-17462

CYLINDRICAL SHELLS
Forced harmonic vibration of the generally orthotropic cylindrical shell with inner and outer fluid loading
[AD-A266985] p 1057 N94-15150
Sound radiation from infinite laminated composite shell with periodic rib stiffening
[DRA/TM(USGR)92326] p 933 N94-15699

CYSTEINE
The relationship of metallothionein induction to the heat shock response
[AD-A266634] p 1122 N94-15741

CYTOLOGY
Cultured normal mammalian tissue and process
[NASA-CASE-MSC-21984-1] p 1117 N94-15969
Heat shock protein induction in human cells by CO2 laser irradiation
[AD-A266430] p 1117 N94-16545

CYTOMETRY
Quantitative method of measuring cancer cell urokinase and metastatic potential
[NASA-CASE-MSC-21715-1] p 1117 N94-15967

D

D REGION
Effect of powerful oblique HF waves on ionospheric D-layer absorption
[AD-A268443] p 1102 N94-17499

DAMAGE
Slidesurfaces with adaptive new definitions (SAND) for transient analysis
[DE93-014909] p 1059 N94-15983

Anisotropic damage mechanics modeling in metal matrix composites
[AD-A266328] p 934 N94-16440
Interfacial shear behavior and its influence on fiber damage in sapphire-reinforced gamma titanium aluminide composites
[AD-A267943] p 1060 N94-17043
Aspects of high temperature damage in fiber reinforced titanium metal matrix composites
[AD-A267907] p 941 N94-17379

DAMAGE ASSESSMENT

Effect of tow alignment on the mechanical performance of 3D woven textile composites p 937 N94-16851
Stochastic damage evolution in textile laminates p 939 N94-16861
Techno-economic requirements for composite aircraft components p 940 N94-16864
X ray computed tomography for failure analysis investigations
[AD-A268086] p 1055 N94-17515
Overview of the FAA/DCA/NLR programs related to ageing aircraft
[NLR-TR-92119-U] p 854 N94-17614

DAMPING

Soliton-like structures in double stimulated Brillouin scattering p 1200 N94-15207
Mechanical energy absorber
[NASA-CASE-MSC-22111-1] p 1047 N94-15966
Hydraulic pump with integral electric motor
[AD-D015782] p 1011 N94-16549
Interpenetrating polymer network acoustic damping material
[AD-D015889] p 969 N94-16916
Design of a fluid elastic actuator with application to structure control
[AD-A267649] p 897 N94-17246
Quantum phase fluctuations in the Jaynes-Cummings model: Effects of cavity damping
[DE93-627984] p 1186 N94-17612

DATA ACQUISITION

Preliminary analysis of University of North Dakota aircraft data from the FIRE Cirrus IFO-2
[NASA-CR-193357] p 866 N94-15429
A software interface for the ARL wind tunnel data acquisition system
[AD-A267114] p 1146 N94-15650
User manual and program description of the data acquisition system of PML-pulse physics
[AD-A266752] p 1147 N94-15776
NASA Lewis 9- by 15-foot low-speed wind tunnel user manual
[NASA-TM-106247] p 872 N94-15819
International collaboration in SAR ground data systems p 993 N94-15917
Index of NASA prefixed forms
[NHB-1420.21] p 1230 N94-15936
Recent advances in outdoor performance evaluation of PV systems
[DE93-015031] p 1091 N94-15994
Test plan for the evaluation of the initial capability of the National Satellite Test Bed: Phase 1D
[DOT/FAA/RD-93/20] p 876 N94-16025
Data acquisition, preprocessing and analysis for the Virginia Tech OLYMPUS experiment p 995 N94-16038
Development of the Laser-based R/D Test-bed System (LTS) p 978 N94-16080
KC-135 acceleration monitoring and data acquisition system p 868 N94-16090
Ejecta patterns of Meteor Crater, Arizona derived from the linear un-mixing of TIMS data and laboratory thermal emission spectra p 1065 N94-16607
AVIRIS ground data processing system p 1071 N94-16692
Powder diffraction studies using anomalous dispersion
[DE93-012531] p 1210 N94-16775
Automated strain gauge plethysmograph
[AD-A267323] p 1035 N94-17002
Small imaging satellite for Earth observing system adjunct p 891 N94-17151
OREMUS: Prototype of an orbit determination center dedicated to mini-satellite control p 878 N94-17156
The STRV On Board Data Handling (OBDH) system: An introduction p 895 N94-17178
A state-of-the-art plasma polymerization coater for ICF targets
[DE93-016452] p 1204 N94-17237
Automated data collection system for the TCM3 transcutaneous pO2/pCO2 monitoring system
[AD-A268400] p 1129 N94-17424
User's manual for the Langley Research Center 14- by 22- foot subsonic tunnel static data acquisition system
[NASA-TM-109027] p 861 N94-17639

DATA BASE MANAGEMENT SYSTEMS

The distributed database dynamic reconfiguration project
[AD-A267116] p 1229 N94-15652
Monotone approximate query processing
[AD-A267153] p 1169 N94-15779
Method for restructuring a database using a relational database scheme derived by selecting subscheme joins to avoid cycles
[AD-D015816] p 1231 N94-16490
Managing information as a corporate asset: Key strategies for information professionals to remain competitive
[DE93-015515] p 1232 N94-16875
Computing and Information Sciences
[DE93-017149] p 1151 N94-16902
The IMS software integration platform
[AD-A266285] p 1151 N94-16910
A proposed research program in strategic computing
[AD-A267516] p 1153 N94-17078
An examination of two Ada language object-oriented databases
[AD-A267486] p 1154 N94-17366

DATA BASES

Engineering Physics and Mathematics Division progress report, period ending 31 December 1992
[DE93-015118] p 1301 N94-14926
Database system studies in fine grain optoelectronic computing
[AD-A267026] p 1145 N94-15627
The distributed database dynamic reconfiguration project
[AD-A267116] p 1229 N94-15652
Toxic substances registry system: Index of material safety data sheets
[NASA-TM-109332] p 1121 N94-15658
TAFVER 2 users manual
[AD-A266850] p 1106 N94-15757
Monotone approximate query processing
[AD-A267153] p 1169 N94-15779
A study of the observed tidal residue vectors B versus oceanic tidal load vectors L p 1100 N94-15813
Recent advances in outdoor performance evaluation of PV systems
[DE93-015031] p 1091 N94-15994
Database for propagation models p 996 N94-16049
A study of land mobile satellite service multipath effects using SATLAB software p 997 N94-16051
Materials, processes, and environmental engineering network
[TABES PAPER 93-610] p 1051 N94-16142
Method for restructuring a database using a relational database scheme derived by selecting subscheme joins to avoid cycles
[AD-D015816] p 1231 N94-16490
The multivariate optimum interpolation analysis of meteorological data at the Fleet Numerical Oceanography Center
[AD-A266459] p 1106 N94-16568
Managing information as a corporate asset: Key strategies for information professionals to remain competitive
[DE93-015515] p 1232 N94-16875
Design and implementation of an object-oriented interface for the multi-model/multi-lingual database system
[AD-A267413] p 1232 N94-16977
Defense Logistics Information System (DLIS) procedures manual. Products and services end-user manual
[AD-A267766] p 1232 N94-17007
A geological and geophysical information system for Eurasia
[AD-A267841] p 1232 N94-17036
Critically evaluated/distributed database of IRAS LRS spectra
[NASA-CR-193611] p 1232 N94-17038
Defense RDT&E online system (DROLS) handbook
[AD-A267546] p 1232 N94-17101
Design and implementation of an interface editor for the Amadeus multi-relational database front-end system
[AD-A267403] p 1233 N94-17114
Long duration exposure facility experiment m0003 deintegration observation database
[AD-A267579] p 951 N94-17207
Strategic planning for aircraft noise route impact analysis: A three dimensional approach
[NASA-CR-191484] p 1178 N94-17278
Windshear database for forward-looking systems certification
[NASA-TM-109012] p 1108 N94-17283
An examination of two Ada language object-oriented databases
[AD-A267486] p 1154 N94-17366
Process evolution for the MARVEL environment
[AD-A267813] p 1155 N94-17398
Automatic generation of production rules for integrity maintenance
[REPT-92-054] p 1156 N94-17501
Automatic translation of database integrity constraints into compensating production rules
[REPT-92-055] p 1234 N94-17502

DATA COMPRESSION

Computer networking at SLR stations p 917 N94-15594
HP upgrade operational streamlining p 918 N94-15596
Efficient algorithmic techniques for combinatorial problems
[AD-A267151] p 1172 N94-15777
Spaceborne Imaging Radar-C instrument p 990 N94-15890
Discovering sequence similarity by the algorithmic significance method
[DE93-015556] p 1150 N94-16659
Use of AVIRIS data to the definition of optimised specifications for land applications with future spaceborne imaging spectrometers p 1071 N94-16694
Lossless compression of AVIRIS data: Comparison of methods and instrument constraints p 1075 N94-16713

DATA CORRELATION

Comparison of preliminary results from Airborne Aster Simulator (AAS) with TIMS data p 1064 N94-16600

DATA FLOW ANALYSIS

Generating local addresses and communication sets for data-parallel programs
[NASA-CR-194605] p 1159 N94-15796
The alignment-distribution graph
[NASA-CR-194609] p 1148 N94-15956
Efficient compilation of array statements for private memory multicomputers
[AD-A266595] p 1160 N94-16724
Efficient scheduling of real-time compute-intensive periodic graphs on large grain data flow multiprocessor
[AD-A267444] p 1141 N94-17030
Accurate analysis of array references
[AD-A268069] p 1162 N94-17550

DATA INTEGRATION

Pixel-level fusion using interest images
[AD-A266640] p 1164 N94-15746
Notes on the use of Dempster-Shafer and fuzzy reasoning to fuse identity attribute data
[AD-A267426] p 1004 N94-17309

DATA LINKS

Evaluation of midband analog fiber optic telemetry links
[DE93-015128] p 883 N94-16056
Infra Link: A data transmission system for microgravity research p 980 N94-16091
Performance Information Management System (PIMS) communication
[AD-A267040] p 1231 N94-16458
Category (CAT) 3B level 1 test plan for Global Positioning System (GPS)
[DOT/FAA/RD-93/21] p 864 N94-16835
A study on an experimental communication system using microsatellites p 892 N94-17160
TAOS (S80): A (LEO-MSS) system for position reporting and telemanagement services p 893 N94-17162
MAGSS-14: Medium Altitude Global Mobile Satellite System with enhanced regional coverage p 893 N94-17164
Feasibility study of a personal communications system IRIDIUM-like p 893 N94-17165
A protocol validator for the SCM and CFSM models
[AD-A268523] p 1156 N94-17541

DATA MANAGEMENT

Fast interrupt priority management in operating system kernels
[AD-A266638] p 1140 N94-15744
NASA information resources management handbook
[NHB-2410.1E] p 1230 N94-15941
Computing and Information Sciences
[DE93-017149] p 1151 N94-16902
The IMS software integration platform
[AD-A266285] p 1151 N94-16910
Design and implementation of an object-oriented interface for the multi-model/multi-lingual database system
[AD-A267413] p 1232 N94-16977
Defense Logistics Information System (DLIS) procedures manual. Products and services end-user manual
[AD-A267766] p 1232 N94-17007
Experience with disconnected operation in a mobile computing environment
[AD-A267524] p 1141 N94-17115
Accurate analysis of array references
[AD-A268069] p 1162 N94-17550

DATA PROCESSING
Channel of the system for pulse charged particle beam diagnostics
[DE93-623867] p 1179 N94-14931
Multiple process simulations for correction factor calculations in experiments with neutrons. LUSMK program
[DE93-623957] p 1179 N94-14932
Sensitivity testing of a single-Doppler temperature retrieval and forecast system
[AD-A267278] p 1105 N94-14958
Data processing system for flight spectrometer
p 908 N94-15086
An uncertainty analysis of inlet dynamic flow distortion using an analog/digital hybrid editing system
[AD-A266924] p 855 N94-15105
SLR data screening; location of peak of data distribution p 912 N94-15560
Application of the robust estimate in SLR data preprocessing p 918 N94-15597
Lunar laser ranging data processing in a Unix/X windows environment p 918 N94-15599
Workshop on advanced technologies for planetary instruments
[NASA-CR-194585] p 1032 N94-15797
Recent advances and plans in processing and geocoding of SAR data at the DFD p 992 N94-15909
International collaboration in SAR ground data systems p 993 N94-15917
Recent advances in outdoor performance evaluation of PV systems
[DE93-015031] p 1091 N94-15994
Remote diagnosis as used for mechanized parking systems p 984 N94-16004
Test plan for the evaluation of the initial capability of the National Satellite Test Bed: Phase 1D
[DOT/FAA/RD-93/20] p 876 N94-16025
Real-time adaptive neural network data processing
[TABES PAPER 93-660] p 1054 N94-16155
Neural mechanisms of attention
[AD-A266315] p 1132 N94-16456
AVIRIS ground data processing system
p 1071 N94-16692
Processing of resonance parameter covariance files
[DE93-015506] p 1231 N94-16874
The IMS software integration platform
[AD-A266285] p 1151 N94-16910
Sequential functions on indexed domains and full abstraction for a sub-language of PCF
[AD-A267838] p 1152 N94-17009
Data processing system for ARSENE ground station: A tool for small satellite control and development
p 878 N94-17157
LEOCOM-SPES: Low cost message communications
p 892 N94-17161
Data handling strategy for the Spanish small satellite program (MINISAT) p 895 N94-17177
The STRV On Board Data Handling (OBDH) system: An introduction p 895 N94-17178
TUBSAT: Low cost access to space technology
p 895 N94-17180
Automatic suppression of anomalous propagation clutter for noncoherent weather radars
[KNMI-WR-92-06] p 1004 N94-17407
Language-based document processing
[INRIA-RR-1731] p 1234 N94-17529

DATA PROCESSING EQUIPMENT
Laser ranging network performance and routine orbit determination at D-PAF p 911 N94-15554
NASA Lewis 9- by 15-foot low-speed wind tunnel user manual
[NASA-TM-106247] p 872 N94-15819
S 80/T: A micro satellite system combining high performances and limited resources
p 893 N94-17166
Detecting small debris using a ground-based photon counting detector
[DE93-012623] p 898 N94-17669

DATA PROCESSING TERMINALS
Ergonomics in the office environment
p 1124 N94-16612

DATA RECORDERS
Prototype instrumentation and design studies
[AD-A266402] p 882 N94-16530

DATA RECORDING
Research Studies on Advanced Optical Module/Head Designs for Optical Disk Recording Devices
[NASA-CR-194390] p 1226 N94-14981
Determining the locations of the various CIRC recording format information blocks (user data blocks, C2 and C1 words and EFM frames) on a recorded compact disc
p 1228 N94-14997

DATA REDUCTION
Test plan for the evaluation of the initial capability of the National Satellite Test Bed: Phase 1D
[DOT/FAA/RD-93/20] p 876 N94-16025
EUVE observations of the Moon p 1250 N94-16185
Reductions to sets of low information content
[TR-417] p 1150 N94-16579
Reducing data dimension to lower signal processing computational requirements and maximize performance
[AD-A266606] p 999 N94-16728
Developing automated analysis methods for sea ice imagery: A status report with recommendations
[AD-A267284] p 1113 N94-17241

DATA RETRIEVAL
NASA Electronic Library System (NELS): The system impact of security
[NASA-CR-194614] p 1231 N94-16499
A proposed research program in strategic computing
[AD-A267516] p 1153 N94-17078

DATA STORAGE
Concurrent garbage collection of persistent heaps
[AD-A266831] p 1141 N94-14915
Monograph of the aviation epidemiology data register for FY 1991
[AD-A266896] p 1119 N94-14952
Research Studies on Advanced Optical Module/Head Designs for Optical Disk Recording Devices
[NASA-CR-194390] p 1226 N94-14981
MeV ion-beam analysis of optical data storage films
p 1226 N94-14984
Dynamic testbed laboratory and micro-optics
p 1199 N94-14986
Gratings and waveguides p 1226 N94-14987
Compact disk error measurements
p 1227 N94-14988
Determination of average refractive index of spin coated DCG films for HOE fabrication p 1036 N94-14992
Effects of a shading band in the data path of an optical drive p 1199 N94-14993
Figures of merit for laser beam quality
p 1043 N94-14994
A near-field scanning optical microscope for analysis of magneto-optic media p 1199 N94-14995
Determining the locations of the various CIRC recording format information blocks (user data blocks, C2 and C1 words and EFM frames) on a recorded compact disc
p 1228 N94-14997
Recent advances and plans in processing and geocoding of SAR data at the DFD p 992 N94-15909
Data distribution p 993 N94-15910
AVIRIS ground data processing system
p 1071 N94-16692
Optical system storage design with diffractive optical elements p 1198 N94-17360
3-D optical memory disk
[AD-A267908] p 1141 N94-17380

DATA STRUCTURES
Generating local addresses and communication sets for data-parallel programs
[NASA-CR-194605] p 1159 N94-15796
The alignment-distribution graph
[NASA-CR-194609] p 1148 N94-15956
Discovering sequence similarity by the algorithmic significance method
[DE93-015556] p 1150 N94-16659
Research in presistent simulation: Development of the persistent ModSim object-oriented programming language
[AD-A268568] p 1157 N94-17620

DATA SYSTEMS
Fault management for data systems
[NASA-TM-103953] p 1116 N94-15548
International collaboration in SAR ground data systems p 993 N94-15917
The planetary data system educational CD-ROM
p 1234 N94-16209

DATA TRANSFER (COMPUTERS)
Electronic messaging for the 1990's
[AD-A267143] p 1229 N94-15437
A software interface for the ARL wind tunnel data acquisition system
[AD-A267114] p 1146 N94-15650
The distributed database dynamic reconfiguration project
[AD-A267116] p 1229 N94-15652
A parallel adaptive mesh refinement algorithm
[NASA-CR-191530] p 1168 N94-15724
The alignment-distribution graph
[NASA-CR-194609] p 1148 N94-15956
Information Technology Resources Assessment
[DE93-013899] p 1230 N94-16010
Efficient compilation of array statements for private memory multicomputers
[AD-A266595] p 1160 N94-16724

DATA TRANSMISSION
Electronic messaging for the 1990's
[AD-A267143] p 1229 N94-15437
Computer networking at SLR stations
p 917 N94-15594
HP upgrade operational streamlining
p 918 N94-15596
Information Technology Resources Assessment
[DE93-013899] p 1230 N94-16010
Evaluation of midband analog fiber optic telemetry links
[DE93-015128] p 883 N94-16056
Infra Link: A data transmission system for microgravity research p 980 N94-16091
Performance Information Management System (PIMS) communication
[AD-A267040] p 1231 N94-16458
Using Markov chains to model the error behavior of data communications channels
[AD-A266468] p 999 N94-16777
The ORBCOMM system p 893 N94-17163
STARSYS: A view after WARC-92 --- satellite position and messaging system p 893 N94-17168
TUBSAT: Low cost access to space technology
p 895 N94-17180
CALS test network handbook
[AD-A267587] p 1160 N94-17209
A 27 channels, 1 MHz fibre-optic measuring system
[AD-A266943] p 1003 N94-17307

DC 8 AIRCRAFT
AIRSAR South American deployment: Operation plan, version 3.0 p 994 N94-15919

DEACTIVATION
Activation and deactivation of high concentration arsenic with some evidence of precipitation
[DE93-016437] p 950 N94-16952

DEATH VALLEY (CA)
Expert system-based mineral mapping using AVIRIS
p 1073 N94-16704

DEBRIS
The physical mechanism of comet outbursts: An experiment p 1242 N94-16221
A discontinuous melt sheet in the Manson impact structure p 1103 N94-16269

DECARBONATION
CO2 production by impact in carbonates? An ATEM and stable isotope (C,O) study p 954 N94-16383

DECIDUOUS TREES
Radar response of vegetation: An overview
p 991 N94-15898

DECISION MAKING
An information processing classification of beyond-visual-range air intercepts
[AD-A266927] p 1131 N94-15108
HyperVentilate: Decision-support software for soil vapor extraction technology application
[PB93-134880] p 1094 N94-15136
The impact of report of investigation writing style on the assessment times, impressions, perceptions and preferences of adjudicators
[AD-A265748] p 1223 N94-15682
A scientific basis for computational science
[AD-A266697] p 1148 N94-15841
A decision criteria to select an associative-memory organization that minimizes the execution time of a mix of associative-search operations
[AD-A266438] p 1149 N94-16560
The Megascience Forum
[DE93-014445] p 1303 N94-16804
Simulation reduction using the Taguchi method
[NASA-CR-4542] p 1055 N94-17082
Acquisition and production of skilled behavior in dynamic decision-making tasks
[NASA-CR-194658] p 1133 N94-17296
Establishing a software measurement process
[AD-A267896] p 1154 N94-17396

DECODING
A simulation study of the performance of the NASA (2,1,6) convolutional code on RFI/burst channels
p 997 N94-16508

DECOMPOSITION
Decomposition of large sparse symmetric systems for parallel computation. Part 2: Parallelization tool roadmap
[AD-A267072] p 1158 N94-15671
Decomposition of large sparse symmetric systems for parallel computation. Part 1: Theoretical foundations
[AD-A267144] p 1159 N94-15750
Gas separations using ceramic membranes
[DE93-000278] p 947 N94-15861
Application of Cloude's target decomposition theorem to polarimetric imaging radar data p 991 N94-15901
A task adaptive parallel graphics renderer
[DE93-017123] p 1149 N94-16119
Application of non-thermal plasmas to pollution control
[DE93-016432] p 1096 N94-16449
Evaluation of hemoglobin-oxygen equilibrium binding by rapid-scanning spectrophotometry and singular-value decomposition
[AD-A266453] p 1123 N94-16564
Direct catalytic decomposition of nitric oxide
[DE93-016689] p 949 N94-16896

Studies in turbulence and turbulence control
[AD-A266318] p 1026 N94-16950
DECOMPRESSION SICKNESS
Aircrew/groundcrew life support systems research. Volume 1: CLIN 0001 research requirements
[AD-A268229] p 1139 N94-17563
DECOUPLING
Electrical properties of sol-gel PZT thin films for decoupling capacitor applications
[DE93-016491] p 1015 N94-17648
DEEP SPACE NETWORK
Search for Extraterrestrial Intelligence (SETI)
p 1125 N94-16620
DEEP WATER
Arctic internal waves (CEAREX)
[AD-A265822] p 1111 N94-15139
DEFECTS
Reliability characterization of digital microcircuits: Investigation of an in-process oxide reliability screening method
[AD-A267053] p 1008 N94-15665
Diamond epitaxy and diamondlike coatings
[AD-A266657] p 1206 N94-15747
Roles of oxygen defects in copper-oxide superconductors
[DE93-014875] p 1208 N94-15982
Microstructure of Zr3Al after 2 MeV proton bombardment
[DE93-015331] p 1211 N94-16814
Growth and doping of Al(x)Ga(1-x)N films by electron cyclotron resonance assisted molecular beam epitaxy
[AD-A267305] p 1212 N94-16992
X ray computed tomography for casting demonstration
[AD-A268084] p 1056 N94-17596
DEFENSE INDUSTRY
Modeling and simulation: A key to future defense technology
[TABES PAPER 93-654] p 1054 N94-16153
DEFENSE PROGRAM
Expectations for the future of military aviation
p 854 N94-15128
Department of Defense technical architecture framework for information management. Volume 1: Overview, version 2.0
[AD-A267193] p 1228 N94-15152
STS-36 crew presentation clip
[NASA-TM-109497] p 881 N94-15461
Reengineering: An engineering problem
[AD-A267117] p 1146 N94-15653
Department of Defense technical architecture framework for information management. Volume 2: Technical reference model and standards profile, version 2.0
[AD-A267194] p 1229 N94-15788
Department of Defense technical architecture framework for information management. Volume 3: Architecture concepts and design guidance, version 2.0
[AD-A267195] p 1230 N94-15789
The strategic environmental research and development program: A new paradigm for space, the environment, and national security
[AD-A266222] p 1174 N94-16109
TABES 1993: 9th Annual Technical and Business Exhibition and Symposium p 1050 N94-16129
The Clementine instrument complement
p 1086 N94-16370
A handbook of cost risk analysis methods
[AD-A267253] p 1235 N94-16988
Defense RDT&E online system (DROLS) handbook
[AD-A267546] p 1232 N94-17101
DEFLAGRATION
Experimental investigations into the deflagration to detonation transition at TNO/PML
[AD-A266753] p 1021 N94-15755
DEFLECTION
Study of high speed interference photography with two-dimensional acousto-optical lattice deflection
[AD-A267823] p 1035 N94-17402
DEFLECTORS
Effects of internal yaw-vectoring devices on the static performance of a pitch-vectoring nonaxisymmetric convergent-divergent nozzle
[NASA-TP-3369] p 858 N94-16572
DEFORESTATION
Recent advances in radar remote sensing of forest
p 991 N94-15897
DEFORMATION
Characterization of the cyclic plasticity of polycrystalline aluminum in the 90-300K domain: Use of the ultrasonic wave coupling technique - low frequency restraint
[ISAL-92-0083] p 954 N94-14930
Inelastic deformation of metal matrix composites
[NASA-CR-191522] p 930 N94-15106
Tectonic deformation in southern California
[NASA-CR-194621] p 1101 N94-16021
Multiaxial deformation and life prediction model and experimental data for advanced silicon nitride ceramics
[DE93-015450] p 967 N94-16067
Spatially extensive uniform stress fields on Venus inferred from radial dike swarm geometries: The Aphrodite Terra example p 1254 N94-16207
Ishtar deformed belts: Evidence for deformation from below? p 1256 N94-16218
A rapid computational model for estimating the performance of compliant airfoils in cascades
[AD-A266275] p 857 N94-16471
Highly transient elastodynamic crack growth in a bimaterial interface: Higher order asymptotic analysis and optical experiments
[AD-A266465] p 1059 N94-16587
Influence of the loading rate on the endurance and deformability of cement matrix composites
[IFTR-1/1992] p 1060 N94-17052
Elastic waves in discretely continuous mechanical systems
[IFTR-21/1992] p 1061 N94-17091
Influence of grain size on the energy storing ability during uniaxial stretching of austenite steel
[IFTR-22/1992] p 961 N94-17121
Design of a fluid elastic actuator with application to structure control
[AD-A267649] p 897 N94-17246
High temperature deformation behavior of YBa2Cu3O(6+x) superconducting ceramic materials
[AD-A268164] p 973 N94-17430
The photonical, pure grid method
[NLR-TP-91478-U] p 1062 N94-17600
DEGASSING
The cooling rates of pahoehoe flows: The importance of lava porosity p 1103 N94-16282
DEGRADATION
Non-linear effects in doped-germanium photoconductors for the ISO long wavelength spectrometer p 905 N94-15067
A first-order model for impact crater degradation on Venus p 1265 N94-16268
The processing and mechanical properties of high temperature/high performance composites. Book 2: Coonstituent properties and macroscopic performance
[AD-A266395] p 935 N94-16484
Long duration exposure facility experiment m0003 deintegration observation database
[AD-A267579] p 951 N94-17207
DEGREES OF FREEDOM
Three axis force override rate control of a PUMA 560 manipulator
[AD-A267313] p 1048 N94-16944
DEIMOS
A simultaneous estimation of the mass of Mars and its natural satellites, Phobos and Deimos, from the orbital perturbations on the Mariner 9, Viking 1, and Viking 2 orbiters p 1279 N94-16347
A mission concept of Phobos/Deimos exploration
p 1287 N94-16387
DELAMINATING
The processing and mechanical properties of high temperature/high performance composites. Book 2: Coonstituent properties and macroscopic performance
[AD-A266395] p 935 N94-16484
Research in textile composites at KU, Leuven
p 937 N94-16848
DELAWARE BAY (US)
Characterization of spatial and temporal variability of phytoplankton blooms in coastal waters
[AD-A267102] p 1116 N94-15633
DELAY LINES
Reliability characterization of digital microcircuits: Investigation of an in-process oxide reliability screening method
[AD-A267053] p 1008 N94-15665
True time delay optically controlled dual band transmitter
[AD-A267663] p 1003 N94-17228
DELTA LAUNCH VEHICLE
Delta launch vehicle: Accommodations for small satellites p 878 N94-17139
DELTA WINGS
Unsteady separated flows: Empirical model and control
[AD-A267282] p 855 N94-14959
Aerodynamic control of NASP-type vehicles through vortex manipulation. Volume 3: Wing rock experiments
[NASA-CR-177626] p 857 N94-15780
Study into the limits of an Euler equation method applied to leading-edge vortex flow
[NLR-TP-91350-U] p 1031 N94-17627
DEMAGNETIZATION
An adiabatic demagnetisation refrigerator with a mechanical pre-cooler for space applications
p 906 N94-15070
In orbit adiabatic demagnetization refrigeration for bolometric and microcalorimetric detectors
p 907 N94-15079
DEMODULATION
Signal processing in impulsive electromagnetic interference
[AD-A266425] p 998 N94-16557
Nonlinear methods for communications
[AD-A267376] p 1001 N94-17019
A 27 channels, 1 MHz fibre-optic measuring system
[AD-A266943] p 1003 N94-17307
DEMODULATORS
Four Frequency-Shift Keying (4-FSK) spread spectrum modulator and demodulator
[AD-A267433] p 1000 N94-16979
DEMULTIPLEXING
Simultaneous measurement of temperature and strain using four connecting wires
[NASA-TM-104271] p 1032 N94-15754
DENDRITIC CRYSTALS
The roles of fluid motion and other transport phenomena in the morphology of materials
[NASA-CR-194665] p 1028 N94-17298
DENSE PLASMAS
Microwave interaction with plasmas
[AD-A267048] p 1201 N94-15661
DENSIFICATION
The influence of microstructure on the mechanical behavior of silicon nitride ceramics
[DE93-015363] p 966 N94-16018
Densifying and stabilizing ingredient
[AD-D015751] p 975 N94-16934
DENSITY (MASS/VOLUME)
Influence of the loading rate on the endurance and deformability of cement matrix composites
[IFTR-1/1992] p 1060 N94-17052
DENSITY (NUMBER/VOLUME)
A comparison of solar wind parameters measured by IMP 8, Voyager 1 and Voyager 2
[AD-A266728] p 1298 N94-15821
Swelling equilibria for temperature-sensitive ampholytic hydrogels
[DE93-015264] p 966 N94-15996
DENSITY DISTRIBUTION
Densities of 5-15 micron interplanetary dust particles
p 1244 N94-16367
DEOXYGENATION
Preconversion catalytic deoxygenation of phenolic functional groups
[DE93-017034] p 950 N94-16912
DEOXYRIBONUCLEIC ACID
Orientation of DNA during free-solution electrophoresis p 944 N94-15162
Quantitative method of measuring cancer cell urokinase and metastatic potential
[NASA-CASE-MSC-21715-1] p 1117 N94-15967
Discovering sequence similarity by the algorithmic significance method
[DE93-015556] p 1150 N94-16659
DEPLETION
Do SiC grains in Orgueil differ from those in Murchison? p 1242 N94-16260
DEPLOYMENT
STS-26 Post-Flight Press Conference
[NASA-TM-109557] p 879 N94-15261
STS-26 onboard 16mm photography quick release
[NASA-TM-109558] p 879 N94-15262
STS-26 through STS-34, deploy activities
[NASA-TM-109566] p 1301 N94-15315
Return to Space Mission: The STS-26 crew report
[NASA-TM-109568] p 880 N94-15317
Galileo probe ready to go
[NASA-TM-109648] p 1247 N94-15432
STS-41 post-flight press presentation
[NASA-TM-109514] p 882 N94-15516
STS-41 onboard 16mm photography quick release
[NASA-TM-109515] p 882 N94-15518
STS-41 mission highlights resource tape
[NASA-TM-109516] p 882 N94-15521
DEPOLARIZATION
Radome depolarization effects on monopulse receiver tracking performance
[AD-A267446] p 1001 N94-17031
DEPOLYMERIZATION
Intramolecular versus intermolecular condensation rates in the acidic polymerization of octaethoxytrisiloxane
[AD-A266982] p 963 N94-15490
DEPOSITION
Study of fractal aggregates p 979 N94-16086
Sand transport on Mars: Preliminary results from models p 1252 N94-16198
Materials processing and manufacturing technologies for diamond substrate multichip modules (DSMCM)
[AD-A267316] p 969 N94-16946
Nitride semiconductors for ultraviolet detection
[AD-A267877] p 1012 N94-17040

Phase holograms in PMMA with proximity effect correction p 1037 N94-17348
Advanced thin-film deposition and physical properties of high-temperature and other novel superconducting materials
[AD-A268199] p 1216 N94-17561

DEPOSITS
Sand transport on Mars: Preliminary results from models p 1252 N94-16198
A Pluto thermal model p 1256 N94-16216
Modes of formation of lunar light plains and the detection of cryptomaria deposits p 1259 N94-16231
The history of mare volcanism in the Orientale Basin: Mare deposit ages, compositions and morphologies p 1269 N94-16289

DEPTH
Arctic internal waves (CEAREX)
[AD-A265822] p 1111 N94-15139
Near-surface temperature gradients and their effects on thermal-infrared emission spectra of particulate planetary surfaces p 1260 N94-16236

DESCENT TRAJECTORIES
Galileo probe ready to go
[NASA-TM-109648] p 1247 N94-15432

DESIGN ANALYSIS
Vertical-tail aerodynamic configuration of space shuttle orbiter
[AD-A267723] p 879 N94-14941
Supersonic Combustion Research Laboratory. Volume 1: Design and fabrication
[AD-A267667] p 943 N94-14962
Discrete CMT infrared detectors for space application, from ISSR to second generation Meteosat and MIPAS p 905 N94-15065
Development of a quiet supersonic wind tunnel with a cryogenic adaptive nozzle
[NASA-CR-194548] p 871 N94-15117
Space suit design
[NASA-TM-109670] p 1137 N94-15507
Mark 111 suit test evaluation in WETF with Jerry Ross
[NASA-TM-109504] p 1137 N94-15514
Reengineering: An engineering problem
[AD-A267117] p 1146 N94-15653
Preliminary analysis and design optimization of the short spacer truss of Space Station Freedom
[NASA-TM-4470] p 1058 N94-15709
The lift-fan powered-lift aircraft concept: Lessons learned
[NASA-CR-177616] p 866 N94-15718
Efficiency effects of variation in controlled experimental variables
[DE93-014345] p 1169 N94-15979
The Spacelab IPS Star Simulator
[TABES PAPER 93-650] p 877 N94-16150
International testing of a Mars rover prototype p 1273 N94-16312
The processing and mechanical properties of high temperature/high performance composites. Book 1: Coonstituent properties of composites
[AD-A266394] p 935 N94-16483
Development of a prototype kinestatic platform for application to space and ground servicing tasks. Phase 1: Concept Modeling
[NASA-CR-194036] p 887 N94-16905
Small satellite constellation system: Optimization criteria p 888 N94-17132
Engineering design of a high-temperature superconductor current lead
[DE93-015156] p 1013 N94-17226
Diffractive optics: Design, fabrication, and applications p 1194 N94-17334
Space Station Freedom electrical performance model
[NASA-TM-106395] p 929 N94-17483

DESIGN TO COST
Cost drivers: Why do conventional satellites cost so much? p 897 N94-17190

DESORPTION
Tritium diffusion and desorption in single crystal LiAlO2
[DE93-015140] p 1211 N94-16805
Direct catalytic decomposition of nitric oxide
[DE93-016689] p 949 N94-16896
Laser photoionization time-of-flight mass spectrometry of nitrated polycyclic aromatic hydrocarbons and nitrated heterocyclic compounds
[AD-A268126] p 952 N94-17520
Trace analysis of chemical warfare agents in air: Sampling in porous polymers followed with thermal desorption analysis
[FOA-C-40302-4.6] p 1097 N94-17625

DETECTION
Proceedings of an ESA Symposium on Photon Detectors for Space Instrumentation
[ESA-SP-356] p 899 N94-15025
A method of detecting and locating electrical current imbalances
[NASA-CASE-LEW-15407-1] p 1009 N94-15706
Sensitive detection of gas-phase nitro-containing energetic materials employing 226-nm radiation
[AD-A267633] p 951 N94-17203
Leak detection utilizing analog binaural (VLSI) techniques
[NASA-CASE-NPO-18399-1-CU] p 1014 N94-17323

DETECTORS
Requirements on CCD-detectors for ground-based auroral imaging p 909 N94-15093
Electron reversal ionizer for detection of trace species using a spherical cathode
[NASA-CASE-NPO-18870-1-CU] p 1185 N94-17329

DETONATION
Experimental investigations into the deflagration to detonation transition at TNO/PML
[AD-A266753] p 1021 N94-15755

DEUTERIDES
Hydride-containing molten salts and their technology implications
[AD-A266458] p 1092 N94-16567

DEUTERIUM
A hydrogen isotope study of CO3 type carbonaceous chondrites; comparison with type 3 ordinary chondrites p 1246 N94-16425
Atomic processes in hydrogen and deuterium negative ion discharges
[DE93-013432] p 1183 N94-16817
Investigation of the energy distribution of ions, striking the cathode in an abnormal glow discharge
[DE93-623987] p 1013 N94-17316

DEUTERONS
Neutral-current detection in the Sudbury Neutrino Observatory
[DE93-014481] p 1185 N94-16951

DIAGNOSIS
Channel of the system for pulse charged particle beam diagnostics
[DE93-623867] p 1179 N94-14931
Medical imaging
[NASA-TM-109675] p 1229 N94-15520
Measurements of the operation of the SINUS-6/BWO system
[AD-A266423] p 1011 N94-16556
Summary of follow-up results from potential tuberculosis exposures p 1126 N94-16628
Legionella: An overview p 1126 N94-16629
Screening for prostate cancer p 1126 N94-16630
Mercury Surveillance Program p 1127 N94-16641

DIALS
Flight instrument software for the F/A-18 research simulator
[AD-A267170] p 872 N94-15856

DIAMAGNETISM
Superconductive material and magnetic field for damping and levitation support and damping of cryogenic instruments
[NASA-CASE-NPO-18458-1-CU] p 1033 N94-15875

DIAMINES
Compounds containing meta-biphenylenedioxy moieties and polymers therefrom
[NASA-CASE-LAR-14517-1] p 965 N94-15879

DIAMOND FILMS
Diamond epitaxy and diamondlike coatings
[AD-A266657] p 1206 N94-15747
A high flux radical beam diamond growth
[AD-A266754] p 1207 N94-15955
Vacuum plasma spraying p 975 N94-16002
Apparatus for and a method of growing thin films of elemental semiconductors
[AD-D015813] p 1210 N94-16487
Properties of thin films for high temperature flow sensors
[NASA-CR-191526] p 967 N94-16541
Atomic layer epitaxy group IV materials: Surface processes, thin films, devices and their characterization
[AD-A267527] p 1213 N94-17116
Single crystal diamond thin films
[AD-A266457] p 1214 N94-17216
Diamond growth on carbide surfaces using a selective etching technique
[AD-A267989] p 973 N94-17413
Growth, characterization and device development in monocrystalline diamond films
[AD-A268206] p 1216 N94-17553

DIAMONDS
Simulation studies for surfaces and materials strength
[NASA-CR-193387] p 1056 N94-15004
Diamond p-n junction cold cathode
[AD-A266926] p 1206 N94-15107
Diamond epitaxy and diamondlike coatings
[AD-A266657] p 1206 N94-15747
Photoemission study of diamond (100) surface
[DE93-015251] p 1208 N94-16062
Water adsorption on diamond (110) studied by multiple internal reflection infrared spectroscopy
[AD-A266415] p 948 N94-16553
Materials processing and manufacturing technologies for diamond substrate multichip modules (DSMCM)
[AD-A267316] p 969 N94-16946
Predesign of diamond turned refractive/diffractive elements for IR objectives p 1198 N94-17359

DIATOMIC MOLECULES
Characterization of UV emissions resulting from electronic energy transfer in atmospheric molecules
[AD-A266244] p 1101 N94-16469
Dissociation rates of diatomic molecules
[AD-A266464] p 1182 N94-16586
Convergence of the multiple scattering expansion in XAFS and XANES
[DE93-011001] p 948 N94-16772

DIBORANE
A proposed mechanism for the pyrolysis of diborane
[DE93-014275] p 947 N94-15977
Growth of dielectric thin films by irradiation of condensed molecular precursors with synchrotron radiation
[DE93-016161] p 974 N94-17676

DICTIONARIES
SeaWiFS technical report series. Volume 12, SeaWiFS technical report series cumulative index: Volumes 1-11
[NASA-TM-104566-VOL-12] p 1111 N94-15529
Definitions of terms relating to aircraft windscreens, canopies, and transparencies
[AD-A268403] p 868 N94-17425

DIELECTRIC POLARIZATION
Resonant frequencies of irregularly shaped microstrip antennas using method of moments
[NASA-TP-3386] p 989 N94-15767

DIELECTRIC PROPERTIES
Far-infrared spectra of CO2 clathrate hydrate frosts p 954 N94-16340
Radar Analysis and Visualization Environment (RAVEN): Software for polarimetric radar analysis p 1080 N94-16758
High voltage conductors in spacecraft
[AD-A267268] p 897 N94-17266
Electrical properties of sol-gel PZT thin films for decoupling capacitor applications
[DE93-016491] p 1015 N94-17648

DIELECTRICS
Velocity matched millimeterwave electro-optic modulator
[AD-A267264] p 1188 N94-14957
Antenna gain loss and pattern degradation due to transmission through dielectric radomes
[AD-A267242] p 986 N94-14974
A study of relaxation transitions in the polymers under the influence of magnetic fields
[AD-A263878] p 963 N94-15133
Nanocomposites for electronic applications, volume 1
[AD-A267070] p 1009 N94-15669
Nanocomposites for electronic applications, volume 3
[AD-A267073] p 1009 N94-15672
Nanocomposites for electronic applications, volume 2
[AD-A267074] p 1009 N94-15673
Volume integral equations applied to circular and square cylinders
[AD-A266635] p 1169 N94-15785
Stress sensitivity of dielectric resonators
[AD-A266767] p 1009 N94-15825
Structures from low dielectric polyimides
[NASA-CASE-LAR-14988-1] p 965 N94-15880
Cyanoresin, cyanoresin/cellulose triacetate blends for thin film, dielectric capacitors
[NASA-CASE-NPO-18913-1-CU] p 966 N94-15930
Cellulose triacetate, thin film dielectric capacitor
[NASA-CASE-NPO-18935-1-CU] p 1010 N94-15952
Transparent conductive coatings in the far ultraviolet
[NASA-CR-194632] p 1191 N94-16024
Full-wave simulation of the thumbtack laser
[DE93-015110] p 1039 N94-16054
VUV thin films, chapter 7
[NASA-CR-194634] p 967 N94-16494
A priori inequalities for an ideal-incompressible liquid in an electromagnetic field
[IFTR-9/1992] p 998 N94-16652
The exact solution of the problem of diffraction of an electromagnetic plane wave by a conductive half-plane situated at an interface
[IFTR-3/91] p 1002 N94-17057
Finite difference time domain analysis of chirped dielectric gratings p 1195 N94-17339
Spectral inverse scattering theory for dielectric media: Application to optical devices
[AD-A268635] p 1199 N94-17427
Low dielectric polyimides
[NASA-CASE-LAR-14987-2] p 974 N94-17559
Low dielectric constant insulators and gold metallization for GHz multi-chip modules, part 2
[AD-A268590] p 1176 N94-17605

Growth of dielectric thin films by irradiation of condensed molecular precursors with synchrotron radiation
[DE93-016161] p 974 N94-17676

DIES
Solid lubricants for space structures, phase 2
[AD-A266653] p 968 N94-16767

DIFFERENTIAL CALCULUS
Automatic differentiation of limit functions
[DE93-016376] p 1168 N94-14928

DIFFERENTIAL EQUATIONS
Comparison of level-1 and level-2 buckling and postbuckling solutions
[NASA-CR-194611] p 1057 N94-15154
Operator overloading as an enabling technology for automatic differentiation
[DE93-012899] p 1170 N94-16778
Application of group theory to integral-difference equations of plasma physics
[IFTR-23/1992] p 1204 N94-17067
Global solutions to a system of strongly coupled reaction-diffusion equations
[DE93-628587] p 1171 N94-17640

DIFFERENTIAL PULSE CODE MODULATION
Lossless compression of AVIRIS data: Comparison of methods and instrument constraints
p 1075 N94-16713

DIFFRACTION
Powder diffraction studies using anomalous dispersion
[DE93-012531] p 1210 N94-16775
Conference on Binary Optics: An Opportunity for Technical Exchange
[NASA-CP-3227] p 1194 N94-17331
Diffractive optics: Design, fabrication, and applications
p 1194 N94-17334
Scalar limitations of diffractive optical elements
p 1194 N94-17336
Subwavelength structured surfaces and their applications p 1194 N94-17337
Diffractive optical elements for generating arbitrary line foci p 1195 N94-17338
Finite difference time domain analysis of chirped dielectric gratings p 1195 N94-17339
Asymmetric three-beam binary optic grating
p 1195 N94-17340
Scattering from binary optics p 1195 N94-17341
Mathmatical modeling for diffractive optics
p 1195 N94-17342
Fabricating binary optics: An overview of binary optics process technology p 1195 N94-17343
Fabrication techniques for very fast diffractive lenses
p 1196 N94-17345
Laser figuring for the generation of analog micro-optics and kineform surfaces p 1196 N94-17346
Diffractive optics fabricated by direct write methods with an electron beam p 1196 N94-17347
Phase holograms in PMMA with proximity effect correction p 1037 N94-17348
Diffractive optics in adverse environments
p 1197 N94-17352
Thermal Weapon Sight (TWS) AN/PAS-13 diffractive optics designed for producibility p 1197 N94-17354
Applications of advanced diffractive optical elements
p 1197 N94-17356
SURPHEX (tm): New dry photopolymers for replication of surface relief diffractive optics p 1198 N94-17358
Predesign of diamond turned refractive/diffractive elements for IR objectives p 1198 N94-17359
Optical system storage design with diffractive optical elements p 1198 N94-17360
Theory of dispersive microlenses
p 1198 N94-17361
Color separation gratings p 1198 N94-17362

DIFFRACTION PATTERNS
Prelaunch optical characterization of the Laser Geodynamic Satellite (LAGEOS 2)
[NASA-TP-3400] p 884 N94-15193
Diffuse scattering and image contrast of tweed in superconducting oxides: A simulation and interpretation
[DE93-016131] p 1212 N94-16844
Mathmatical modeling for diffractive optics
p 1195 N94-17342
Fabricating binary optics: An overview of binary optics process technology p 1195 N94-17343

DIFFRACTION PROPAGATION
Sound exposure level prediction for impulse sound sources above variable terrain
[AD-A267535] p 1178 N94-17119

DIFFRACTOMETERS
Powder diffraction studies using anomalous dispersion
[DE93-012531] p 1210 N94-16775

DIFFUSE RADIATION
Hazard calculations of diffuse reflected laser radiation for the SELENE program
[NASA-TM-4520] p 1042 N94-17285

DIFFUSION
The MADONA experiments (Meteorology and Diffusion Over Non-uniform Areas): High-resolution in-plume concentration fluctuations measurements using lidar remote sensing technique
[AD-A267711] p 1105 N94-14938
Self-diffusion coefficients of sol-gel intermediates
[AD-A266957] p 963 N94-15179
Diffusible driving and coupling signals of the biological clock
[AD-A267046] p 1121 N94-15660
Environmental embrittlement in ordered intermetallic alloys
[DE93-015307] p 955 N94-15830
Clouding tracing: Visualization of the mixing of fluid elements in convection-diffusion systems
[NASA-CR-191529] p 1148 N94-15965
The Fe2(+)-Mg interdiffusion in orthopyroxene: Constraints from cation ordering and structural data and implications for cooling rates of meteorites
p 1241 N94-16175
Rheology of water and ammonia-water ices
p 953 N94-16188
Tritium diffusion and desorption in single crystal LiAlO2
[DE93-015140] p 1211 N94-16805
Linear characteristic spatial quadrature for discrete ordinates neutral particle transport on arbitrary triangles
[AD-A267485] p 1185 N94-17365
A domain-partition method for the advection-diffusion equation
[INRIA-RR-1740] p 1030 N94-17534
Oxygen diffusion in YBa2Cu3O(6+delta) ceramics on heating
[DE93-629161] p 974 N94-17633
Kinetics of silica-phase transitions
[DE93-016231] p 1217 N94-17659

DIFFUSION COEFFICIENT
Detection and dosimetry of chemical contaminants in polymeric materials
[AD-A266605] p 968 N94-16727

DIFFUSION FLAMES
Studies in turbulence and turbulence control
[AD-A266318] p 1026 N94-16950
Mechanistic models of soot formation
[AD-A267806] p 950 N94-17008
Lifted turbulent jet flames
[AD-A267911] p 952 N94-17381
Surface reactivity of combustion generated soot particles
[AD-A268017] p 952 N94-17532

DIFFUSIVITY
Self-diffusion coefficients of sol-gel intermediates
[AD-A266957] p 963 N94-15179
Low temperature deposition and characterization of n- and p-type silicon carbide thin films and associated ohmic and Schottky contacts
[AD-A267966] p 973 N94-17490

DIGITAL COMPUTERS
Digital reverberation time measurement system
[AD-D015892] p 1177 N94-16919

DIGITAL DATA
Freedom system Text and Graphics Systems (TAGS)
[NASA-TM-109509] p 1140 N94-15455
Global Magellan-image map of Venus at full resolution
p 1274 N94-16319
CALS test network handbook
[AD-A267587] p 1160 N94-17209
An automated approach for classifying generic terrain features using digital elevation data
[AD-A268385] p 1084 N94-17421

DIGITAL ELECTRONICS
Orpheus: A synthesis framework for regular architectures
[REPT-93-016] p 1156 N94-17504

DIGITAL FILTERS
Designing clutter rejection filters with complex coefficients for airborne pulsed Doppler weather radar
[NASA-CR-4550] p 862 N94-15444

DIGITAL SYSTEMS
VLSI for high-speed digital signal processing
[AD-A267709] p 1007 N94-14936
Streak camera based SLR receiver for two color atmospheric measurements p 914 N94-15573
Operation of digital systems in severe electromagnetic environments
[AD-A267176] p 988 N94-15693
Digital laser range finder emulator
[AD-D015811] p 1040 N94-16540
Digital reverberation time measurement system
[AD-D015892] p 1177 N94-16919
On-board B-ISDN fast packet switching architectures. Phase 1: Study
[NASA-CR-191143] p 883 N94-17111
Method and apparatus for spur-reduced digital sinusoid synthesis
[NASA-CASE-NPO-18789-1-CU] p 1154 N94-17326
A comparative study of analog and digital control laws for the UMCSL truss
[AD-A267980] p 871 N94-17412
Fabrication of a NAVMAP, a deep-sea mapping system
[AD-A268630] p 1085 N94-17467
Activities of the Research Laboratory of Electronics
[AD-A266730] p 1304 N94-17651

DIGITAL TECHNIQUES
Spaceborne Imaging Radar-C instrument
p 990 N94-15890
Revisiting the BCS, a measurement system for characterizing the optics of solar collectors
[DE93-015030] p 1091 N94-15993
Method and apparatus for spur-reduced digital sinusoid synthesis
[NASA-CASE-NPO-18789-1-CU] p 1154 N94-17326

DIGITAL TO ANALOG CONVERTERS
Channel of the system for pulse charged particle beam diagnostics
[DE93-623867] p 1179 N94-14931
Method and apparatus for spur-reduced digital sinusoid synthesis
[NASA-CASE-NPO-18789-1-CU] p 1154 N94-17326

DIISOCYANATES
Interpenetrating polymer network acoustic damping material
[AD-D015889] p 969 N94-16916

DIMENSIONAL MEASUREMENT
X ray computed tomography for casting demonstration
[AD-A268084] p 1056 N94-17596

DIMERS
The interaction of HCN(DCN) with Si(111)-7x7 studied with HREELS, UPS, and XPS
[AD-A266237] p 1182 N94-16111

DIODES
A new detector concept for energetic auroral x ray imaging p 907 N94-15081
A microsecond-pulsewidth, intense, light-ion beam accelerator
[DE93-016455] p 1202 N94-16451
Investigation of onset of plasma formation at anode of fast-pulsed high-voltage vacuum diode
[AD-A267214] p 1204 N94-16987

DIPOLE ANTENNAS
Proceedings of the 1992 Antenna Applications Symposium, volume 2
[AD-A266916] p 986 N94-14998

DIPOLE MOMENTS
The pressure broadening of HDO by O2, N2, H2, and He between 100 K and 600 K
[AD-A267118] p 946 N94-15684

DIRAC EQUATION
SUSY in the sky
[NIKHEF-H/93-04] p 1240 N94-17603

DIRECTION FINDING
Interferometric GPS attitude: A stochastic error model, DREO report
[AD-A266411] p 864 N94-16457
Evaluation of site effects on a high frequency direction finding single site location system
[AD-A267465] p 1001 N94-17035

DIRECTIONAL CONTROL
Wind tunnel investigations of forebody strakes for yaw control on F/A-18 model at subsonic and transonic speeds
[NASA-TP-3360] p 859 N94-16573
Equations of motion of a hinged body over a spherical earth
[AD-A268408] p 868 N94-17435

DIRECTIONAL SOLIDIFICATION (CRYSTALS)
Visualization of solidification front phenomena
[NASA-CR-193838] p 976 N94-15006
Unidirectional solidification of liquid-crystal material
p 945 N94-15167
Automated directional solidification furnace
[NASA-TM-109662] p 1175 N94-15233

DIRECTORIES
Defense Logistics Information System (DLIS) procedures manual. Products and services end-user manual
[AD-A267766] p 1232 N94-17007

DIRICHLET PROBLEM
On a class of singular quasilinear elliptic equations with general structure and distribution data
[DE93-628585] p 1171 N94-17613

DISABILITIES
Americans with Disabilities Act considerations for the practice of occupational medicine p 1124 N94-16611

DISASTERS
IAI topic: El Nino. Southern oscillation and interannual climate variability
[INPE-5410-PRE/1757] p 1111 N94-15186

Primary studies of Chinese spaceborne SAR
p 993 N94-15916
Technical urban search and rescue, System To Locate Survivors (STOLS) units: Operator's manual
[AD-A266317] p 862 N94-16438

DISCONTINUITY
Stress analysis of laminated composites with preformed holes. Part 1: Single plies with embedded material discontinuities
[AD-A266524] p 936 N94-16795

DISCOVERY (ORBITER)
Small spacecraft for planetary exploration
p 874 N94-17145

DISCRETE FUNCTIONS
Adaptive wavelet collocation methods for initial value boundary problems of nonlinear PDE's
[NASA-CR-191507] p 1169 N94-15833

DISEASES
Cool suit
[NASA-TM-109639] p 1120 N94-15250
Medical imaging
[NASA-TM-109675] p 1229 N94-15520
Proceedings of the 1992 Annual Meeting NASA Occupational Health Program
[NASA-CR-193462] p 1123 N94-16609
Legionella: An overview p 1126 N94-16629
OSHA bloodborne pathogens standards exposure control plan p 1127 N94-16645

DISILICIDES
The specific heat of titanium disilicide
[AD-A267543] p 960 N94-17100

DISK GALAXIES
Collisional dynamics of perturbed particle disks in the solar system
[NASA-CR-193584] p 1239 N94-16648

DISLOCATIONS (MATERIALS)
Characterization of the cyclic plasticity of polycrystalline aluminum in the 90-300K domain: Use of the ultrasonic wave coupling technique - low frequency restraint
[ISAL-92-0083] p 954 N94-14930

DISORDERS
Cool suit
[NASA-TM-109639] p 1120 N94-15250

DISPLACEMENT
Elastic waves in discretely continuous mechanical systems
[IFTR-21/1992] p 1061 N94-17091
Nonlinear random response prediction using MSC/NASTRAN
[NASA-TM-109029] p 1179 N94-17650

DISPLACEMENT MEASUREMENT
Mechanical and surface force nanoprobe
[AD-D015792] p 1034 N94-16536

DISPLAY DEVICES
Video applications development platform
[AD-A266966] p 1163 N94-14953
Flight simulator-induced sickness and visual displays evaluation
[AD-A267019] p 1122 N94-15845
Display system employing acousto-optic tunable filter
[NASA-CASE-NPO-18736-1-CU] p 1190 N94-15933
Ergonomics in the office environment
p 1124 N94-16612
Optical displays: A tutorial on images and image formation
[AD-A266230] p 1192 N94-16926
Applications of advanced diffractive optical elements
p 1197 N94-17356
Visual display principles for C3I system tasks
[AD-A267969] p 1005 N94-17498

DISSIPATION
Translating wedge heat sink
[AD-D015814] p 1011 N94-16488

DISSOCIATION
Water adsorption on diamond (110) studied by multiple internal reflection infrared spectroscopy
[AD-A266415] p 948 N94-16553
Cathode sheath charge transfer effects
[AD-A268393] p 1186 N94-17536
Investigations into the recovery of waste sulfuric acid with concentrated solar radiation
[DLR-FB-93-11] p 952 N94-17594

DISSOLVING
In situ studies of passive film chemistry using x ray absorption spectroscopy
[DE93-014023] p 947 N94-16011

DISTORTION
Closed orbit distortion and the beam-beam interaction
[DE93-015284] p 1190 N94-15854
Emittance and beam size distortion due to linear coupling
[DE93-015402] p 1184 N94-16886

DISTRIBUTED PARAMETER SYSTEMS
Modeling, estimation and control of distributed parameter systems
[AD-A267325] p 1026 N94-17003
Module interconnection frameworks for a real-time spreadsheet
[AD-A267752] p 1153 N94-17231

DISTRIBUTED PROCESSING
The alignment-distribution graph
[NASA-CR-194292] p 1168 N94-15112
Relaxing consistency in recoverable distributed shared memory
[AD-A266931] p 1140 N94-15174
The distributed database dynamic reconfiguration project
[AD-A267116] p 1229 N94-15652
A parallel adaptive mesh refinement algorithm
[NASA-CR-191530] p 1168 N94-15724
Department of Defense technical architecture framework for information management. Volume 2: Technical reference model and standards profile, version 2.0
[AD-A267194] p 1229 N94-15788
Generating local addresses and communication sets for data-parallel programs
[NASA-CR-194605] p 1159 N94-15796
Distributed computing feasibility in a non-dedicated homogeneous distributed system
[NASA-CR-191532] p 1149 N94-15989
Consistent failure reporting in reliable communication systems
[AD-A266298] p 997 N94-16477
Disconnected operation in a distributed file system
[AD-A266461] p 1231 N94-16570
A comparison of queueing, cluster and distributed computing systems
[NASA-TM-109025] p 1160 N94-16878
The IMS software integration platform
[AD-A266285] p 1151 N94-16910
A security architecture for fault-tolerant systems
[AD-A266178] p 1152 N94-16982
Intel NX to PVM 3.2 message passing conversion library
[NASA-TM-109038] p 1152 N94-17060
Light-weight process groups in the ISIS system
[NASA-CR-194544] p 1161 N94-17239

DISTRIBUTION (PROPERTY)
Large-scale volcanism associated with coronae on Venus p 1285 N94-16376

DISTRIBUTION FUNCTIONS
The alignment-distribution graph
[NASA-CR-194292] p 1168 N94-15112
Mobile and replicated alignment of arrays in data-parallel programs
[NASA-CR-194294] p 1158 N94-15113
Application of cylindrical distribution functions to anisotropic scattering from amorphous films
[DE93-015256] p 1183 N94-16811
To extend the thirteen-moment theory and its application to problems in rarefied hypersonic flow
[AD-A267384] p 859 N94-17021

DISTRIBUTION MOMENTS
Moments in statistics: Approximations to densities and goodness-of-fit
[AD-A266600] p 1173 N94-16726

DIURNAL VARIATIONS
Arctic internal waves (CEAREX)
[AD-A265822] p 1111 N94-15139
Multitemporal diurnal AVIRIS images of a forested ecosystem p 1074 N94-16709
Field investigation of the relationship between battery size and PV system performance
[DE93-016503] p 1016 N94-17671

DIVERTERS
ARIES tokamak reactor study
[DE93-017059] p 1203 N94-16901

DIVING (UNDERWATER)
An apparatus for measuring the biological oxidation of hydrogen gas under hyperbaric conditions
[AD-A266834] p 1119 N94-14916
Scuba-diving, anxiety and task performance
p 1132 N94-15938
Human central nervous system oxygen toxicity data from 1945 to 1986
[AD-A268225] p 1130 N94-17556

DOCUMENTS
Monitoring history
[NASA-TM-109640] p 1229 N94-15251
Language-based document processing
[INRIA-RR-1731] p 1234 N94-17529

DOLOMITE (MINERAL)
CO2 production by impact in carbonates? An ATEM and stable isotope (C,O) study p 954 N94-16383

DOMAINS
Complexity analysis of real-time reinforcement learning applied to finding shortest paths in deterministic domains
[AD-A266636] p 1131 N94-15742

DONOR MATERIALS
Photodegradation of polyimides. V1: Effect of donor-acceptor groups on the photooxidative stability of polyimides and model compounds
[AD-A267319] p 970 N94-16947

DOPED CRYSTALS
BIB photodetectors based on antimony doped silicon
p 902 N94-15047
The epitaxial Si x ray bolometer an alternative to ion implanted devices p 911 N94-15103
Growth of new materials for solid state laser applications. The growth of ZnGeP2 by the vertical Bridgman method
[NASA-CR-194571] p 1038 N94-15530
Ion doped quantum well lasers
[AD-A267198] p 1038 N94-15853
Transition metals in superheat melts
p 962 N94-16273
Method for doping GaAs with high vapor pressure elements
[AD-D015794] p 1210 N94-16538
Powder diffraction studies using anomalous dispersion
[DE93-012531] p 1210 N94-16775
Tritium diffusion and desorption in single crystal LiAlO2
[DE93-015140] p 1211 N94-16805
Growth and doping of Al(x)Ga(1-x)N films by electron cyclotron resonance assisted molecular beam epitaxy
[AD-A267305] p 1212 N94-16992
Theoretical studies of nonlinear optical properties of conjugated polymers
[AD-A267390] p 1193 N94-17024
Basic optical studies of high T(c) oxide superconductors
[AD-A268148] p 1014 N94-17428
Optical studies of glasses embedded with inorganic ions and organic dyes
[AD-A268146] p 1199 N94-17455
Low temperature deposition and characterization of n- and p-type silicon carbide thin films and associated ohmic and Schottky contacts
[AD-A267966] p 973 N94-17490
Rare earth doped III-V semiconductors for optoelectronics
[AD-A268279] p 1216 N94-17577

DOPPLER RADAR
Sensitivity testing of a single-Doppler temperature retrieval and forecast system
[AD-A267278] p 1105 N94-14958
Windshear radar calibration, 1992 flights: Transmitter power and receiver gain stability
[NASA-TM-108997] p 986 N94-15140
The Next Generation Weather Radar (NEXRAD)/Air Route Surveillance Radar (ARSR) operational comparison
[REPT-93W0000145] p 987 N94-15439
Diffractive optical elements for generating arbitrary line foci p 1195 N94-17338

DOSAGE
Ion implantation effects on surface-mechanical properties of metals and polymers
[DE93-014661] p 958 N94-16453

DOSIMETERS
Real time radiation measurements in space
p 980 N94-16092
Space systems environmental interaction studies
[AD-A267280] p 897 N94-17240

DOWNRANGE
Enhanced down-range profiles of complex targets using wideband radar echo returns
[AD-A266508] p 999 N94-16788
High resolution radar profiling using higher-order statistics
[AD-D015891] p 1000 N94-16918

DOWNTIME
Fast simulation of steady-state availability in non-Markovian highly dependable systems
[AD-A266747] p 1174 N94-15823

DRAG MEASUREMENT
Suppression of dynamic stall with a leading-edge slat on a VR-7 airfoil
[NASA-TP-3357] p 856 N94-15657

DRAG REDUCTION
Riblets: New speed technology
[NASA-TM-109641] p 1018 N94-15252
Active turbulence control in wall bounded flows using direct numerical simulation
[AD-A267261] p 1028 N94-17286

DRAINAGE
On hydrologic similarity: A dimensionless flood frequency model using a generalized geomorphologic unit hydrograph and partial area runoff generation
[PAPER-89WR01579] p 1083 N94-16027
Similarity and scale in catchment storm response
[PAPER-89RG01615] p 1083 N94-16028

Evapotranspiration and runoff from large land areas: Land surface hydrology for atmospheric general circulation models p 1083 N94-16029
Evaluation of a distributed catchment scale water balance model
[PAPER-93WR00398] p 1083 N94-16031
A detailed model for simulation of catchment scale subsurface hydrologic processes
[PAPER-92WR02333] p 1084 N94-16032
Scaling, soil moisture and evapotranspiration in runoff models p 1084 N94-16034
A Geographic Information System approach to modeling nutrient and sediment transport
[DE93-013747] p 1097 N94-17426

DRAINAGE PATTERNS
Similarity and scale in catchment storm response
[PAPER-89RG01615] p 1083 N94-16028
Sedimentation, volcanism, and ancestral lakes in the Valles Marineris: Clues from topography p 1283 N94-16369

DRIFT (INSTRUMENTATION)
Nontidal gravity changes observed with a superconducting gravimeter p 1100 N94-15808

DRIFT RATE
A study of high field transport in wide band gap electronic materials using a picosecond transient charge technique
[AD-A267098] p 1008 N94-15636

DRILLING
Detection of subsurface defects in machined silicon nitride ceramics by optical scattering methods
[DE93-015554] p 968 N94-16658
The Megascience Forum
[DE93-014445] p 1303 N94-16804

DROP SIZE
Mechanism of intermittent atomization
[AD-A266625] p 1021 N94-15770
Two-dimensional, high flow, precisely controlled monodisperse drop source
[AD-A267660] p 1028 N94-17250
Cryogenic spray vaporization in high-velocity helium, argon and nitrogen gasflows
[NASA-TM-106363] p 1035 N94-17446

DROP TOWERS
New findings and instrumentation from the NASA Lewis Microgravity Facility p 977 N94-16076
Design of non-sled setup to measure head injury criteria
[NIAR-92-20] p 872 N94-17263

DROPS (LIQUIDS)
Mechanism of intermittent atomization
[AD-A266625] p 1021 N94-15770
Acoustic waves in complicated geometries and their interactions with liquid-propellant droplet combustion
[AD-A267260] p 1178 N94-16991
Two-dimensional, high flow, precisely controlled monodisperse drop source
[AD-A267660] p 1028 N94-17250

DROUGHT
The standardized precipitation index and its use in the western contiguous United States
[AD-A267547] p 1107 N94-17102

DRUGS
Ongoing Recovery Basic Information Tool (ORBIT) p 1124 N94-16616

DUCTED FANS
Cruise noise measurements of a scale model advanced ducted propulsor
[NASA-TM-105808] p 1176 N94-15115

DUCTED FLOW
Modal element method for potential flow in non-uniform ducts: Combining closed form analysis with CFD
[NASA-TM-106347] p 1169 N94-15799
Computation of confined coflow jets with three turbulence models
[NASA-TM-106378] p 1025 N94-16879

DUCTILITY
Environmental embrittlement in ordered intermetallic alloys
[DE93-015307] p 955 N94-15830
Recent advances in ordered intermetallics
[DE93-015308] p 955 N94-15862
A reexamination of grain boundary fracture in Ni3Al: Environmental and alloying effects
[DE93-015431] p 1208 N94-16063
The processing and mechanical properties of high temperature/high performance composites. Book 4: Coonstitutive laws and design
[AD-A266397] p 935 N94-16528
Bulk and defect properties of ordered intermetallics: A first-principles total-energy investigation
[DE93-015492] p 959 N94-16873
Creep ductility of iron at very low strain rates: The effects of sulfur
[DE93-015490] p 959 N94-16890
Micromechanisms of monotonic and cyclic subcritical crack growth in advanced high melting point low-ductility intermetallics
[AD-A267764] p 961 N94-17223

DUNES
Sand transport on Mars: Preliminary results from models p 1252 N94-16198
Discrimination among semi-arid landscape endmembers using the Spectral Angle Mapper (SAM) algorithm p 1074 N94-16711

DUST
Sand transport on Mars: Preliminary results from models p 1252 N94-16198
On origin of the olivine inclusions from the Kainsaz CO carbonaceous chondrite p 1244 N94-16345
Possible dust contamination of the early solar system p 1244 N94-16352
Dust-dynamic feedbacks in the Martian atmosphere: Surface dust lifting p 1296 N94-16434

DUST COLLECTORS
Removal of carbonaceous contaminants from silica aerogel p 953 N94-16256

DUST STORMS
Global and regional/seasonal color mosaics of Mars p 1288 N94-16393

DYE LASERS
Design of pulse stretching cell for a sodium guide star optical system
[DE93-016436] p 1236 N94-14929
Lasing dye sensor for chemical vapors
[AD-D015786] p 1040 N94-16533

DYES
Optical studies of glasses embedded with inorganic ions and organic dyes
[AD-A268146] p 1199 N94-17455

DYNAMIC CHARACTERISTICS
Particle simulations on massively parallel machines
[DE93-015644] p 1157 N94-14927
Dynamic behavior of fiber and particle reinforced composites
[AD-A266905] p 930 N94-15143
Develop advanced nonlinear signal analysis topographical mapping system
[NASA-CR-194577] p 1082 N94-15646
The vibro-acoustic mapping of low gravity trajectories on a Learjet aircraft p 978 N94-16078
Cost-effective test methods for Shuttle payloads
[TABES PAPER 93-651] p 883 N94-16151
Static and dynamic investigations of brittle elasto-optical material
[IFTR-3/1992] p 1061 N94-17086
Dynamic testing and characterization of pre-fractured ceramic
[DE93-016457] p 972 N94-17238
Dynamic behavior of an electric arc gas discharge
[DE93-630197] p 1205 N94-17635

DYNAMIC CONTROL
Aerodynamic flight control to increase payload capability of future launch vehicles
[NASA-CR-193850] p 870 N94-15532
A molecular dynamics simulator for optimal control of molecular motion
[AD-A266572] p 1183 N94-16722
Dynamics, stability, and control of maglev systems
[DE93-015163] p 1047 N94-16806
Space Station/Orbiter berthing dynamics during an assembly flight
[NASA-TM-109049] p 1062 N94-17451

DYNAMIC MODELS
State-of-the-art satellite laser range modeling for geodetic and oceanographic applications p 916 N94-15586
Cost-effective test methods for Shuttle payloads
[TABES PAPER 93-651] p 883 N94-16151
An object-oriented dynamic software process model
[AD-A267726] p 1154 N94-17371

DYNAMIC PRESSURE
Wall interference and boundary simulation in a transonic wind tunnel with a discretely slotted test section
[NASA-TP-3334] p 872 N94-15794
A comparison of solar wind parameters measured by IMP 8, Voyager 1 and Voyager 2
[AD-A266728] p 1298 N94-15821
Mechanical and surface force nanoprobe
[AD-D015792] p 1034 N94-16536

DYNAMIC PROGRAMMING
Discovering sequence similarity by the algorithmic significance method
[DE93-015556] p 1150 N94-16659
Towards dynamic randomized algorithms in computational geometry
[INRIA-RR-1727] p 1156 N94-17528

DYNAMIC RANGE
A novel solid-state optical temporal analyzer with picosecond resolution and picowatt sensitivity
[AD-A266804] p 986 N94-14912
Evaluation of midband analog fiber optic telemetry links
[DE93-015128] p 883 N94-16056

DYNAMIC RESPONSE
Static aeroelastic response of an aircraft with asymmetric wing planforms representative of combat damage
[AD-A266890] p 865 N94-14951
Dynamic behavior of fiber and particle reinforced composites
[AD-A266905] p 930 N94-15143
A simplistic look at limit stresses from random loading
[NASA-TM-108427] p 1058 N94-15710
Aerodynamic/dynamic/control interaction
[AD-A266187] p 871 N94-16107
An analysis of the dynamic response of the Space Station Freedom due to a module perforation by an orbital debris particle impact
[TABES PAPER 93-653] p 899 N94-16154
The nature of dynamic arteriolar vasoreactivity: A mini-review and A classification scheme
[AD-A266499] p 1128 N94-16783
Dynamics, stability, and control of maglev systems
[DE93-015163] p 1047 N94-16806
Aerothermoelastic analysis of a NASP demonstrator model
[NASA-TM-109007] p 867 N94-17055
Method and apparatus to characterize ultrasonically reflective contrast agents
[NASA-CASE-LAR-14969-1] p 1129 N94-17085
Integrating reactive and deliberative planning for agents
[AD-A267631] p 1166 N94-17201
Nonlinear random response prediction using MSC/NASTRAN
[NASA-TM-109029] p 1179 N94-17650

DYNAMIC STABILITY
Aerodynamic flight control to increase payload capability of future launch vehicles
[NASA-CR-193850] p 870 N94-15532

DYNAMIC STRUCTURAL ANALYSIS
Vibro-acoustic analysis of an aircraft maintenance dock
[AD-A266778] p 871 N94-14908
Research in robust control for hypersonic aircraft
[NASA-CR-194106] p 870 N94-15416
Preliminary analysis and design optimization of the short spacer truss of Space Station Freedom
[NASA-TM-4470] p 1058 N94-15709
A simplistic look at limit stresses from random loading
[NASA-TM-108427] p 1058 N94-15710
Physical properties of the benchmark models program supercritical wing
[NASA-TM-4457] p 866 N94-15722
In-flight investigation of a rotating cylinder-based structural excitation system for flutter testing
[NASA-TM-4512] p 867 N94-15783
Aerodynamic/dynamic/control interaction
[AD-A266187] p 871 N94-16107
Cost-effective test methods for Shuttle payloads
[TABES PAPER 93-651] p 883 N94-16151
An analysis of the dynamic response of the Space Station Freedom due to a module perforation by an orbital debris particle impact
[TABES PAPER 93-653] p 899 N94-16154
A rapid computational model for estimating the performance of compliant airfoils in cascades
[AD-A266275] p 857 N94-16471
Hoph bifurcation in viscous, low speed flows about an airfoil with structural coupling
[AD-A266542] p 859 N94-16798
Development and comparison of advanced reduced-basis methods for the transient structural analysis of unconstrained structures
[NASA-TM-109015] p 1061 N94-17259
A mechanical system damping measurement technique using a one-degree-of-freedom (1DOF) cylindrical gas bearing
[AD-A268402] p 1048 N94-17462

DYNAMIC TESTS
Dynamic testing and characterization of pre-fractured ceramic
[DE93-016457] p 972 N94-17238
Structured finite volume modeling of US Navy aircraft engine test cells. Task 1: Turboshaft engine-code documentation and listings, volume 2
[AD-A268177] p 873 N94-17508
Structured finite volume modeling of US Navy aircraft engine test cells. Task 2: Turboprop engine. Volume 2: Code documentation and listings
[AD-A268386] p 873 N94-17569

E

EARTH (PLANET)
Explosive mafic volcanism on Earth and Mars p 1253 N94-16204
Venusian pancake domes: Insights from terrestrial voluminous silicic lavas and thermal modeling p 1286 N94-16381

EARTH ATMOSPHERE
ATLAS-2 and UARS correlative measurement opportunities during Space Shuttle mission on April 8-17, 1993 [NASA-TM-109020] p 1105 N94-15480
Investigation of cloud properties and atmospheric stability with MODIS [NASA-CR-193475] p 1107 N94-16717
Boundary layer structure over areas of heterogeneous heat fluxes [DE93-010657] p 1110 N94-17673

EARTH CORE
Lava crusts and flow dynamics p 1103 N94-16316

EARTH CRUST
LFASE report: Crustal study [AD-A266893] p 1111 N94-14947
Composite refraction-reflection stack sections: Tracing faults in the Atlantic coastal plain sediments [DE93-013581] p 1112 N94-16009
NORSAR basic seismological research [AD-A266193] p 1101 N94-16125
The Acraman impact structure: Estimation of the diameter by the ejecta layer thickness p 1103 N94-16211
Assimilation of solids during ascent of magmas from the Bartoy Field of the Baikal Region, Siberia p 1103 N94-16214
Constraints on the differentiation of the Earth from the coupled Sm-146,147-Nd-142,143 systematics p 1103 N94-16271
Lava crusts and flow dynamics p 1103 N94-16316
A search for evidence of nonlinear elasticity in the earth [DE93-015279] p 1102 N94-17252

EARTH GRAVITATION
New techniques for the combination of heterogenous data when determining the Earth's gravity field [SER-C-395] p 1098 N94-15153
Papers presented at the Eleventh International Symposium on Earth Tides [COMMUNICATIONS-SER-B-158] p 1098 N94-15800
Report of the International Center for Earth Tides for the period 1985-1989 p 1099 N94-15801
Nontidal gravity changes observed with a superconducting gravimeter p 1100 N94-15808
Earth tides results obtained with gravimeters, clinometers, and strainmeters in Belgium and in Grand Duchy of Luxembourg p 1100 N94-15809
Results of tidal gravity observations with a conical pendulum p 1100 N94-15810
What we can learn about ocean tides from tide gauge and gravity loading measurements? p 1100 N94-15811
Water-levels fluctuations in a borehole at the Royal Observatory of Belgium: Effects on local gravity, Earth tidal, and barometric responses p 1100 N94-15812
A study of the observed tidal residue vectors B versus oceanic tidal load vectors L p 1100 N94-15813
Tidal gravity anomalies and tectonics p 1101 N94-15814
Report of the working group on theoretical tidal model p 1101 N94-15815
BRIDGE: A small scientific satellite for geodesy p 890 N94-17146

EARTH IONOSPHERE
Comparison of RADARC high-frequency radar performance prediction model and ROTHR Amchitka data [AD-A267077] p 987 N94-15540
Optimization of satellite coverage in observing cause and effect changes in the ionosphere, magnetosphere, and solar wind [AD-A267956] p 1102 N94-17493

EARTH MAGNETOSPHERE
The Solar Flare Myth in solar-terrestrial physics [DE93-016487] p 1299 N94-16895
Micro- and meso-scale simulations of magnetospheric processes related to the aurora and substorm morphology [NASA-CR-193437] p 1102 N94-17527

EARTH MANTLE
NORSAR basic seismological research [AD-A266193] p 1101 N94-16125
Siderophile elements in the upper mantle of the Earth: New clues from metal-silicate partition coefficients p 1103 N94-16250
Constraints on the differentiation of the Earth from the coupled Sm-146,147-Nd-142,143 systematics p 1103 N94-16271
Water in Earth's mantle: Hydrogen analysis of mantle olivine, pyroxenes and garnet using the SIMS p 1104 N94-16336
First results from analysis of coordinated AVIRIS, TIMS, and ISM (French) data for the Ronda (Spain) and Beni Bousera (Morocco) peridotites p 1067 N94-16675

EARTH MOVEMENTS
Laser tracking for vertical control p 911 N94-15553

EARTH OBSERVATIONS (FROM SPACE)
A 12.5 micron infrared detector for Earth observation p 903 N94-15052
Views from space [NASA-TM-109634] p 1081 N94-15245
STS-26 Shuttle Earth views, April 1990, part 1 [NASA-TM-109564] p 1082 N94-15334
STS-26 Shuttle Earth views, April 1990, part 2 [NASA-TM-109565] p 1082 N94-15335
Testing the waters from space --- Thermal mapping [NASA-TM-109623] p 1082 N94-15409
X-SAR: The X-band synthetic aperture radar on board the Space Shuttle p 990 N94-15891
Data distribution p 993 N94-15910
The Spectral Image Processing System (SIPS): Software for integrated analysis of AVIRIS data p 1067 N94-16674
JPL activities on development of acousto-optic tunable filter imaging spectrometer p 1037 N94-16696
Radar Analysis and Visualization Environment (RAVEN): Software for polarimetric radar analysis p 1080 N94-16758
Small Satellites Systems and Services [ISBN-2-85-428327-9] p 888 N94-17131
Earth observation from small satellites p 891 N94-17150
Small imaging satellite for Earth observing system adjunct p 891 N94-17151
SYDONI: An intensified system for night observation p 891 N94-17153
Standard platforms for small satellites p 895 N94-17181

EARTH OBSERVING SYSTEM (EOS)
Effects of turbulence on the geodynamic laser ranging system p 921 N94-15616
EOS SAR: A new approach p 992 N94-15904
Surface energy balance modeling at mesoscale: The contribution of the future Earth observing system [BCRS-91-04] p 1085 N94-17616

EARTH ORBITAL ENVIRONMENTS
Long Duration Exposure Facility experiment M0003 deintegration/findings and impacts [AD-A267140] p 885 N94-15749
Third LDEF Post-Retrieval Symposium Abstracts [NASA-CP-10120] p 1303 N94-16495
History of on-orbit satellite fragmentations [NASA-CR-191644] p 887 N94-16502
Performance of silvered Teflon thermal control blankets on spacecraft [AD-A266284] p 887 N94-16909
Optical properties of water released in low Earth orbit [AD-A266197] p 1192 N94-16936
Low Earth orbit constellations: Orbit control or not p 875 N94-17134
High voltage conductors in spacecraft [AD-A267268] p 897 N94-17266

EARTH ORBITAL RENDEZVOUS
The effect of an on-orbit near encounter on the number flux density of micron sized particles p 899 N94-16374

EARTH ORBITS
Satellite situation report, volume 33, no. 3 [NASA-TM-109278] p 885 N94-15712
Tidal regime of intact planetoid capture model for the Earth-Moon system: Does it relate to the archean sedimentary rock record? p 1245 N94-16378
History of on-orbit satellite fragmentations [NASA-CR-191644] p 887 N94-16502
Implementing a 50x50 gravity field model in an orbit determination system [AD-A267548] p 888 N94-17103
BRIDGE: A small scientific satellite for geodesy p 890 N94-17146
SYNMOD: A low-resource, low-cost means of monitoring the near-Earth space debris environment p 891 N94-17148

EARTH ORIENTATION
Laser ranging data analysis [NASA-CR-193547] p 1041 N94-16719

EARTH RADIATION BUDGET EXPERIMENT
Global climate study [NASA-TM-109612] p 1098 N94-15363

EARTH RESOURCES
The 1973 highlights --- Pioneer and Mariner space probes and other advancements [NASA-TM-109624] p 1302 N94-15410

EARTH SCIENCES
Short walk to everywhere --- Space, Earth, Ocean Center [NASA-TM-109541] p 1221 N94-15372
High-resolution seismic reflection survey at the Manson crater, Iowa p 1103 N94-16307
Spaceship Earth: A partnership in curriculum writing p 1222 N94-16356
Earth system dynamics: The interrelation of atmospheric, ocean and solid earth dynamics [NASA-CR-193487] p 1081 N94-17444

EARTH SURFACE
Primary studies of Chinese spaceborne SAR p 993 N94-15916
Use of AVIRIS data to the definition of optimised specifications for land applications with future spaceborne imaging spectrometers p 1071 N94-16694
Lithological and textural controls on radar and diurnal thermal signatures of weathered volcanic deposits, Lunar Crater region, Nevada p 1080 N94-16762
Earth observational research using multistage EOS-like data [NASA-CR-194626] p 1084 N94-16831

EARTH TIDES
Papers presented at the Eleventh International Symposium on Earth Tides [COMMUNICATIONS-SER-B-158] p 1098 N94-15800
Report of the International Center for Earth Tides for the period 1985-1989 p 1099 N94-15801
A new feedback system for instruments equipped with a capacitive transducer p 1037 N94-15802
Long baseline watertubes p 1037 N94-15803
Temperature measurements p 1037 N94-15804
On tidal parameters at Brussels fundamental station p 1100 N94-15807
Earth tides results obtained with gravimeters, clinometers, and strainmeters in Belgium and in Grand Duchy of Luxembourg p 1100 N94-15809
Results of tidal gravity observations with a conical pendulum p 1100 N94-15810
What we can learn about ocean tides from tide gauge and gravity loading measurements? p 1100 N94-15811
Water-levels fluctuations in a borehole at the Royal Observatory of Belgium: Effects on local gravity, Earth tidal, and barometric responses p 1100 N94-15812
A study of the observed tidal residue vectors B versus oceanic tidal load vectors L p 1100 N94-15813
Tidal gravity anomalies and tectonics p 1101 N94-15814
Report of the working group on theoretical tidal model p 1101 N94-15815
Tidal regime of intact planetoid capture model for the Earth-Moon system: Does it relate to the archean sedimentary rock record? p 1245 N94-16378

EARTH-MOON SYSTEM
Remote sensing studies of the northeastern portion of the lunar nearside p 1258 N94-16225
Tidal regime of intact planetoid capture model for the Earth-Moon system: Does it relate to the archean sedimentary rock record? p 1245 N94-16378

EARTHQUAKES
Broadband teleseismic array recording in the Adirondack Mountains, New York State [AD-A267290] p 1097 N94-14960
The 1970 highlights --- NASA programs and research [NASA-TM-109628] p 1302 N94-15415
Tectonic deformation in southern California [NASA-CR-194621] p 1101 N94-16021
A search for evidence of nonlinear elasticity in the earth [DE93-015279] p 1102 N94-17252

ECCENTRIC ORBITS
Tidal regime of intact planetoid capture model for the Earth-Moon system: Does it relate to the archean sedimentary rock record? p 1245 N94-16378

ECCENTRICITY
Tidal interaction: A possible explanation for geysers and other fluid phenomena in the Neptune-Triton system p 1272 N94-16311
On the delivery of planetesimals to a protoplanet in the solar nebula p 1245 N94-16379
Dust grain resonant capture: A statistical study p 1245 N94-16384

ECHOCARDIOGRAPHY
STS-32 crew training for lower body negative pressure unit and AFE [NASA-TM-109475] p 1120 N94-15381

ECOLOGY
Driving terrestrial ecosystem models from space p 991 N94-15896

ECONOMIC ANALYSIS
Techno-economic requirements for automotive composites p 937 N94-16847
ECONOMIC FACTORS
New York MARKAL: An evaluation of carbon dioxide emission control strategies in New York State
[DE93-013149] p 1095 N94-15999
Approaching the new reality
[TABES PAPER 93-230] p 1050 N94-16131
ECONOMIC IMPACT
Technology transfer. Determining industry needs: A guide for communities
[NASA-CR-194676] p 1235 N94-17293
ECONOMICS
Technology transfer. Determining industry needs: A guide for communities
[NASA-CR-194676] p 1235 N94-17293
ECOSYSTEMS
Development of pattern recognition techniques for the evaluation of toxicant impacts to multispecies systems
[AD-A267197] p 1095 N94-15790
Driving terrestrial ecosystem models from space
p 991 N94-15896
Recent advances in radar remote sensing of forest
p 991 N94-15897
TOPSAT: Global space topographic mission
p 992 N94-15905
Measuring dry plant residues in grasslands: A case study using AVIRIS p 1072 N94-16697
Oregon transect: Comparison of leaf-level reflectance with canopy-level and modelled reflectance
p 1073 N94-16702
AVIRIS data and neural networks applied to an urban ecosystem p 1073 N94-16705
Multitemporal diurnal AVIRIS images of a forested ecosystem p 1074 N94-16709
Discrimination among semi-arid landscape endmembers using the Spectral Angle Mapper (SAM) algorithm
p 1074 N94-16711
EDDY VISCOSITY
A numerical investigation of energy transfer and subgrid-scale eddy-viscosity in homogeneous, isotropic, and shear turbulence
[AD-A267265] p 1029 N94-17363
EDGE DETECTION
Massively parallel, adaptive, color image processing for autonomous road following
[AD-A266988] p 864 N94-15498
Comparison of edges detected at different polarisations in MAESTRO data p 1080 N94-16761
EDUCATION
Symposium on the Future of Aeronautics in the Netherlands
[ETN-93-93780] p 853 N94-15120
Developments in the Higher Technical Aerospace Education p 854 N94-15130
Expectations for the future of the Faculty of Aeronautics and Astronautics of the Technical University of Delft
p 854 N94-15131
NASA Spacelink computer
[NASA-TM-109657] p 1140 N94-15228
SHARP
[NASA-TM-109659] p 1221 N94-15230
Space classroom
[NASA-TM-109661] p 1221 N94-15232
Teacher in space
[NASA-TM-109666] p 1131 N94-15237
Short walk to everywhere --- Space, Earth, Ocean Center
[NASA-TM-109541] p 1221 N94-15372
STS-29 crew IMAX camera training
[NASA-TM-109546] p 1031 N94-15380
CORE/TRC
[NASA-TM-109434] p 1221 N94-15418
NASA report to education, volume 7
[NASA-TM-109435] p 1247 N94-15419
Spacework 16 --- Simulated Space Shuttle Program
[NASA-TM-109436] p 1221 N94-15420
Challenger Center
[NASA-TM-109432] p 1221 N94-15504
Challenger Center: Orientation
[NASA-TM-109433] p 1221 N94-15505
Coast encounters: A space age adventure in science literacy
[NASA-TM-109334] p 1229 N94-15523
NASA Space Engineering Research Center for VLSI System Design
[NASA-CR-194587] p 1008 N94-15547
Questioning mechanisms during tutoring, conversation, and human-computer interaction
[AD-A266199] p 1137 N94-16108
The planetary data system educational CD-ROM
p 1234 N94-16209
Teaching planetary sciences to elementary school teachers: Programs that work p 1222 N94-16346
Spaceship Earth: A partnership in curriculum writing
p 1222 N94-16356
Do it yourself remote sensing: Generating an inexpensive, high tech, real science lake mapping project for the classroom p 1086 N94-16407
Proceedings of the 1992 Annual Meeting NASA Occupational Health Program
[NASA-CR-193462] p 1123 N94-16609
Emergency preparedness and planning
p 1124 N94-16613
Education and training of professional industrial hygienists for 2020 p 1125 N94-16618
Physical fitness and health education program at NASA Headquarters p 1126 N94-16631
Ames Fitness Program p 1126 N94-16632
Johnson Space Center health related fitness program
p 1126 N94-16633
From the Moons of Jupiter to the Milky Way
[NASA-CR-194649] p 1240 N94-17059
Defense RDT&E online system (DROLS) handbook
[AD-A267546] p 1232 N94-17101
Maximizing participation of women in collegiate aviation education
[NIAR-93-14] p 1222 N94-17261
Theoretical implications and empirical findings on instructional control and part-whole-task training
[AD-A267826] p 872 N94-17403
The impact of industry/university consortia programs on space education
[NASA-TM-109340] p 1222 N94-17441
EFFECTORS
ALS engine propellant effector system
[NASA-CR-194650] p 926 N94-16590
EFFICIENCY
Wind-tunnel investigation of aerodynamic efficiency of three planar elliptical wings with curvature of quarter-chord line
[NASA-TP-3359] p 859 N94-16574
EGRESS
STS-35 Crew training: Bailout in CCT, firefighting, TAGS class and bailout in WFTF
[NASA-TM-109489] p 1135 N94-15195
STS-29 pre-launch and post-landing egress
[NASA-TM-109574] p 1135 N94-15305
STS-33 emergency egress training
[NASA-TM-109525] p 1136 N94-15388
1990 ASCAN ground egress/parasail
[NASA-TM-109528] p 1136 N94-15391
Crew escape certification test
[NASA-TM-109530] p 1136 N94-15392
EIGENVALUES
On the stability analysis of approximate factorization methods for 3D Euler and Navier-Stokes equations
[NASA-TM-106314] p 1169 N94-15818
Numerical studies of the photoluminescence spectrum of quantum Hall systems
[DE93-015822] p 1220 N94-16810
Eigenfunctions of the transfer matrix in the presence of linear coupling
[DE93-015020] p 1151 N94-16892
Closed form characteristic function for general complex second-order form in correlated complex Gaussian random variables
[AD-A267883] p 1171 N94-17393
EIGENVECTORS
Modal element method for potential flow in non-uniform ducts: Combining closed form analysis with CFD
[NASA-TM-106347] p 1169 N94-15799
The fractional quantum Hall effect and the rotation group
[DE93-010348] p 1207 N94-15972
Modal ring method for the scattering of sound
[NASA-TM-106342] p 1177 N94-16497
Numerical studies of the photoluminescence spectrum of quantum Hall systems
[DE93-015822] p 1220 N94-16810
Eigenfunctions of the transfer matrix in the presence of linear coupling
[DE93-015020] p 1151 N94-16892
Closed form characteristic function for general complex second-order form in correlated complex Gaussian random variables
[AD-A267883] p 1171 N94-17393
EJECTA
The Acraman impact structure: Estimation of the diameter by the ejecta layer thickness
p 1103 N94-16211
The physical mechanism of comet outbursts: An experiment p 1242 N94-16221
Confirmation of saturation equilibrium conditions in crater populations p 1103 N94-16222
Corvid meteoroids and a Giordano Bruno ray are genetically related p 1242 N94-16223
Lunar impact basins: New data for the nearside northern high latitudes and eastern limb from the second Galileo flyby p 1258 N94-16228
Trace-element composition of Chicxulub crater melt rock, K/T tektites and Yucatan basement
p 1242 N94-16245
A first-order model for impact crater degradation on Venus p 1265 N94-16268
Radar properties of several fluidized ejecta blankets on Venus p 1267 N94-16278
Geochemical evidences for two chondritic-like cometary or asteroidal impacts before and at the K/T boundary
p 1244 N94-16359
Galileo SSI lunar observations: Copernican craters and soils p 1288 N94-16395
Grain surface features of Apollo 17 orange and black glass p 1289 N94-16397
Ejecta patterns of Meteor Crater, Arizona derived from the linear un-mixing of TIMS data and laboratory thermal emission spectra p 1065 N94-16607
EL NINO
IAI topic: El Nino. Southern oscillation and interannual climate variability
[INPE-5410-PRE/1757] p 1111 N94-15186
ELASTIC BENDING
Static analysis of beams on an elastic base as stated by generalized functions
[IFTR-27/1991] p 1060 N94-16923
ELASTIC DAMPING
Suppression of charge scattering in Moessbauer experiments using synchrotron radiation
[DE93-015406] p 1212 N94-16887
ELASTIC DEFORMATION
An analysis of ways of determining the material constants for viscoelastic materials
[IFTR-28/91] p 951 N94-17050
ELASTIC PROPERTIES
Effective elastic thickness of the Venusian lithosphere with lateral viscosity variations in the mantle
p 1293 N94-16421
The processing and mechanical properties of high temperature/high performance composites. Book 3: Coonstituent properties and macroscopic performance
[AD-A266396] p 935 N94-16485
Elastooptical brittle materials in experimental studies of the state of stress and deformation
[IFTR-22/1991] p 1059 N94-16651
Bulk and defect properties of ordered intermetallics: A first-principles total-energy investigation
[DE93-015492] p 959 N94-16873
Superconducting ceramics: Selected properties and methods of production
[IFTR-23/1991] p 969 N94-16924
Design of a fluid elastic actuator with application to structure control
[AD-A267649] p 897 N94-17246
A search for evidence of nonlinear elasticity in the earth
[DE93-015279] p 1102 N94-17252
Solution of elastic-plastic stress analysis problems by the p-version of the finite element method
[NASA-CR-194267] p 1062 N94-17445
Mechanical properties of interfaces and superlattices
[AD-A268591] p 1217 N94-17606
ELASTIC SCATTERING
The pp elastic scattering experiment at RHIC and polarization studies in the Coulomb Nuclear Interference region
[DE93-015391] p 1187 N94-16829
ELASTIC SHELLS
Forced harmonic vibration of the generally orthotropic cylindrical shell with inner and outer fluid loading
[AD-A266985] p 1057 N94-15150
ELASTIC WAVES
NORSAR basic seismological research
[AD-A266193] p 1101 N94-16125
Elastic waves in discretely continuous mechanical systems
[IFTR-21/1992] p 1061 N94-17091
ELASTIN
Materials Research Society Symposium Proceedings, Volume 292: Biomolecular Materials
[AD-A265776] p 1116 N94-15138
ELASTODYNAMICS
Highly transient elastodynamic crack growth in a bimaterial interface: Higher order asymptotic analysis and optical experiments
[AD-A266465] p 1059 N94-16587
ELASTOMERS
Photodegradation of MDI based polyurethane/urea elastomers
[AD-A267308] p 971 N94-16994
Damage evolution in filled elastomers
[AD-A268067] p 1062 N94-17507

ELASTOPLASTICITY
Systematology for elastic-plastic material equations by large deformations on the basis of the Cosserat-continuum model
[SCHRIFTENR-PHYSIKAL-ING-BD] p 1058 N94-15642
Prediction of stable tearing of 2024-T3 aluminum alloy using the crack-tip opening angle approach
[NASA-TM-109023] p 955 N94-15708
Elastic-plastic finite-difference analysis of unidirectional composites subjected to thermomechanical cyclic loading
[AD-A267666] p 1061 N94-17269

ELDO LAUNCH VEHICLE
The launch of ELDO
[ESA-HSR-7] p 886 N94-16501

ELECTRIC ARCS
High voltage conductors in spacecraft
[AD-A267268] p 897 N94-17266
Static characteristics of a conduction and radiation dominated electric arc in nitrogen
[DE93-627106] p 1204 N94-17311
Dynamic behavior of an electric arc gas discharge
[DE93-630197] p 1205 N94-17635

ELECTRIC BATTERIES
Utility emissions associated with electric and hybrid vehicle (EHV) charging
[DE93-013734] p 1011 N94-16459
The 1987 Goddard Space Flight Center Battery Workshop
[NASA-CP-3236] p 1012 N94-17062
Thin composite solid electrolyte film for lithium batteries
[NASA-CASE-NPO-18694-1-CU] p 1014 N94-17325

ELECTRIC CHARGE
Swelling equilibria for temperature-sensitive ampholytic hydrogels
[DE93-015264] p 966 N94-15996

ELECTRIC CONDUCTORS
Steering capacitlector sensor
[NASA-CASE-GSC-13489-1] p 1164 N94-15704
Capacitlector camera
[NASA-CASE-GSC-13564-1] p 1033 N94-15872
High voltage conductors in spacecraft
[AD-A267268] p 897 N94-17266
Synthesis and characterization of new low-dimensional metal complex conductors
[AD-A268251] p 952 N94-17416

ELECTRIC CONNECTORS
Simultaneous measurement of temperature and strain using four connecting wires
[NASA-TM-104271] p 1032 N94-15754
Spline screw payload fastening system
[NASA-CASE-GSC-13454-1] p 1046 N94-15871
Engineering design of a high-temperature superconductor current lead
[DE93-015156] p 1013 N94-17226

ELECTRIC CONTACTS
Integrated fundamental research on current collection
[AD-A266987] p 1008 N94-15494
Optical properties and surface morphology studies of palladium contacts on mercuric iodide single crystals
[DE93-012510] p 1207 N94-15973
Growth, characterization and device development in monocrystalline diamond films
[AD-A268206] p 1216 N94-17553

ELECTRIC CORONA
Electrostatic fiber spreader including a corona discharge device
[AD-D015793] p 936 N94-16537

ELECTRIC CURRENT
Potential transients, transmission and electrochemical corrosion detection
[DE93-014055] p 956 N94-15922
Polar 2 model of the wake shield experiment
[AD-A266243] p 882 N94-16468
Surface flashover of semiconductors: A fundamental study
[AD-A267382] p 1012 N94-17023
FNAS/solar flare energetics
[NASA-CR-193574] p 1299 N94-17089
Development of ultra-low noise, high performance 3-V Quantum Well Infrared Photodectors (QWIP's) for focal plane array staring image sensor systems
[AD-A267715] p 1214 N94-17272
Static characteristics of a conduction and radiation dominated electric arc in nitrogen
[DE93-627106] p 1204 N94-17311

ELECTRIC DIPOLES
Magnetic effects in anomalous dispersion
[DE93-014291] p 1175 N94-15978

ELECTRIC DISCHARGES
An improved patch for radiative coolers
[NASA-CASE-GSC-13503-1] p 1046 N94-15873
Electrostatic fiber spreader including a corona discharge device
[AD-D015793] p 936 N94-16537
The effect of electric discharge machined notches on the fracture toughness of several structural alloys
[AD-A268605] p 962 N94-17464

ELECTRIC FIELD STRENGTH
Static characteristics of a conduction and radiation dominated electric arc in nitrogen
[DE93-627106] p 1204 N94-17311
Dynamic behavior of an electric arc gas discharge
[DE93-630197] p 1205 N94-17635

ELECTRIC FIELDS
Antenna gain loss and pattern degradation due to transmission through dielectric radomes
[AD-A267242] p 986 N94-14974
An optically modulated scatterer for microwave antenna metrology
[NPL-DES-126] p 986 N94-15020
Experimental evaluation of an adaptive focusing algorithm for a microwave planar phased-array hyperthermia system at UCSF
[AD-A267004] p 1121 N94-15634
Resonant frequencies of irregularly shaped microstrip antennas using method of moments
[NASA-TP-3386] p 989 N94-15767
Middle atmospheric electric fields over thunderstorms
[NASA-CR-194619] p 1106 N94-16493
Electro-rheological disk pump
[AD-D015783] p 1047 N94-16531
Electrorheological fluid chemical processing
[AD-D015785] p 948 N94-16532
Process for shaping articles from electrosetting compositions
[AD-D015787] p 935 N94-16534
TransRapid TR-07 maglev-spectrum magnetic field effects on daily pineal indoleamine metabolic rhythms in rodents
[DE93-015143] p 1117 N94-16893
Surface flashover of semiconductors: A fundamental study
[AD-A267382] p 1012 N94-17023
The influence of an electric field on the kinetics of nucleation
[IFTR-2/91] p 1213 N94-17046
Electrorheological (ER) fluids: A research needs assessment
[AD-A267588] p 951 N94-17210
Currents induced in the human body for exposure to ultrawideband electromagnetic pulses
[AD-A268570] p 1130 N94-17621

ELECTRIC GENERATORS
Application of thermal spray and ceramic coatings and reinforced epoxy for cavitation damage repair of hydroelectric turbines and pumps
[AD-A267624] p 971 N94-17198
Two-dimensional, high flow, precisely controlled monodisperse drop source
[AD-A267660] p 1028 N94-17250

ELECTRIC HYBRID VEHICLES
Utility emissions associated with electric and hybrid vehicle (EHV) charging
[DE93-013734] p 1011 N94-16459

ELECTRIC MOTORS
Hydraulic pump with integral electric motor
[AD-D015782] p 1011 N94-16549

ELECTRIC NETWORKS
Circuits and control processes for combining direct converters and inverter motors
[ETN-93-94399] p 1008 N94-15448

ELECTRIC POTENTIAL
Microwave interaction with plasmas
[AD-A267048] p 1201 N94-15661
Operation of digital systems in severe electromagnetic environments
[AD-A267176] p 988 N94-15693
Simultaneous measurement of temperature and strain using four connecting wires
[NASA-TM-104271] p 1032 N94-15754
Capacitlector camera
[NASA-CASE-GSC-13564-1] p 1033 N94-15872
Bioorganic models for protein ion channels
[AD-A266365] p 1117 N94-16441
Electro-rheological disk pump
[AD-D015783] p 1047 N94-16531
Inductive effects during second harmonic current drive experiments on T-10
[DE93-014411] p 1202 N94-16803
Fundamental-mode RF design in e(+)e(-) storage ring factories
[DE93-015249] p 1183 N94-16809
High voltage conductors in spacecraft
[AD-A267268] p 897 N94-17266
Static characteristics of a conduction and radiation dominated electric arc in nitrogen
[DE93-627106] p 1204 N94-17311
Dynamic behavior of an electric arc gas discharge
[DE93-630197] p 1205 N94-17635
Optimal pulse modulator design criteria for plasma source ion implanters
[DE93-016465] p 1205 N94-17645

ELECTRIC PROPULSION
NASA images 10
[NASA-TM-109419] p 924 N94-15351
High power steady state MPD thrusters
[AD-A267277] p 928 N94-17308

ELECTRIC PULSES
User manual and program description of the data acquisition system of PML-pulse physics
[AD-A266752] p 1147 N94-15776

ELECTRIC ROCKET ENGINES
Application of a NEPTUNE propulsion concept to a manned Mars excursion
[AD-A268053] p 929 N94-17587

ELECTRIC SWITCHES
A 27 channels, 1 MHz fibre-optic measuring system
[AD-A266943] p 1003 N94-17307

ELECTRIC WIRE
Operation of digital systems in severe electromagnetic environments
[AD-A267176] p 988 N94-15693
Simultaneous measurement of temperature and strain using four connecting wires
[NASA-TM-104271] p 1032 N94-15754

ELECTRICAL FAULTS
Results of an electrical power system fault study (CDDF)
[NASA-TP-3413] p 884 N94-15007
A method of detecting and locating electrical current imbalances
[NASA-CASE-LEW-15407-1] p 1009 N94-15706
Cellulose triacetate, thin film dielectric capacitor
[NASA-CASE-NPO-18935-1-CU] p 1010 N94-15952
Surface flashover of semiconductors: A fundamental study
[AD-A267382] p 1012 N94-17023
Electrical properties of sol-gel PZT thin films for decoupling capacitor applications
[DE93-016491] p 1015 N94-17648

ELECTRICAL IMPEDANCE
Determination of equivalent circuit for PVDF shock-pressure gauges
[DE93-016492] p 1034 N94-16452
Stray insensitive switched capacitor composite operational amplifiers
[AD-A267412] p 1012 N94-16976
A modified two-fluid model of conductivity for superconducting surface resistance calculation
[AD-A267549] p 1013 N94-17104
Optimal pulse modulator design criteria for plasma source ion implanters
[DE93-016465] p 1205 N94-17645

ELECTRICAL INSULATION
Structures from low dielectric polyimides
[NASA-CASE-LAR-14988-1] p 965 N94-15880
Low dielectric polyimides
[NASA-CASE-LAR-14987-2] p 974 N94-17559

ELECTRICAL PROPERTIES
Partial melting experiment of Y-Ba-Cu oxide p 945 N94-15168
Basic studies of the liquid state of matter: Electrical properties and laser interactions
[AD-A268311] p 1042 N94-17567

ELECTRICAL RESISTANCE
Nonstationary behaviour of low background photon detectors p 902 N94-15049
Integrated fundamental research on current collection
[AD-A266987] p 1008 N94-15494

ELECTRICAL RESISTIVITY
Integrated fundamental research on current collection
[AD-A266987] p 1008 N94-15494
Fullerene superconductors
[AD-A266749] p 1010 N94-15954
A simple chemical procedure for extending the conductive state of polypyrrole to more negative potentials
[AD-A266235] p 969 N94-16928
Electrical conductivity of ion implanted ladder and semi-ladder polymers
[AD-A267432] p 970 N94-16978
Interface properties of wide bandgap semiconductor structures
[AD-A268269] p 1215 N94-17377
Synthesis and characterization of new low-dimensional metal complex conductors
[AD-A268251] p 952 N94-17416
Investigations of YBaCuO materials with near-room-temperature resistivity transitions
[AD-A268016] p 1216 N94-17477
Dynamic behavior of an electric arc gas discharge
[DE93-630197] p 1205 N94-17635

ELECTRIFICATION
Remote sensing of precipitation and electrification with a dual-polarization, coherent, wideband radar system
[AD-A267479] p 1004 N94-17364

ELECTRO-OPTICAL PHOTOGRAPHY
An electronic imaging system for the Aeroballistic Research Facility
[AD-A267157] p 1033 N94-15826

ELECTRO-OPTICS
A novel solid-state optical temporal analyzer with picosecond resolution and picowatt sensitivity
[AD-A266804] p 986 N94-14912
Velocity matched millimeterwave electro-optic modulator
[AD-A267264] p 1188 N94-14957
Proceedings of the 1992 Antenna Applications Symposium, volume 2
[AD-A266916] p 986 N94-14998
Database system studies in fine grain optoelectronic computing
[AD-A267026] p 1145 N94-15627
System architecture of optically controlled phased array radar
[AD-A267056] p 988 N94-15667
Organic polymeric electro-optic materials: Synthesis, processing, and device applications
[AD-A267133] p 964 N94-15688
Optoelectronics based on SiGe/Si heterostructures
[AD-A267178] p 1190 N94-15848
TOPSAT: Global space topographic mission
p 992 N94-15905
Method and apparatus for performing scanning tunneling optical absorption spectroscopy
[AD-D015796] p 948 N94-16539
Atomic layer epitaxy of boron nitride
[AD-A266260] p 1212 N94-16932
Solar Electro-Optical Network (SEON) upgrade/replacement program. Phase 1: Qualification operational test and evaluation plan
[AD-A266364] p 1237 N94-17225
Laser figuring for the generation of analog micro-optics and kineform surfaces p 1196 N94-17346
Micro-optics technology and sensor systems applications p 1197 N94-17350
OSA proceedings on Ultrafast Electronics and Optoelectronics, volume 14
[AD-A267972] p 1014 N94-17410
Femtosecond carrier processes in compound semiconductors and real time signal processing
[AD-A268122] p 1005 N94-17519
Rare earth doped III-V semiconductors for optoelectronics
[AD-A268279] p 1216 N94-17577

ELECTROACOUSTIC TRANSDUCERS
An electroacoustic transducer for purposes of photoacoustic spectroscopy
[IFTR-7/1992] p 1013 N94-17071

ELECTROCATALYSTS
Binding of carbon dioxide to metal macrocycles: Toward a mechanistic understanding of electrochemical and photochemical carbon dioxide reduction
[DE93-016244] p 949 N94-16870
Vectorial electron transfer in spatially ordered arrays
[DE93-018150] p 1185 N94-16971

ELECTROCHEMICAL CELLS
Application of in situ scanning x ray fluorescence to study the concentration of metal ions in simulated pits
[DE93-014054] p 956 N94-15921
Investigation of the influence of applied potential on erosion-corrosion of copper in alkaline chloride solutions
[AD-A266448] p 958 N94-16562

ELECTROCHEMICAL CORROSION
Potential transients, transmission and electrochemical corrosion detection
[DE93-014055] p 956 N94-15922

ELECTROCHEMISTRY
Binding of carbon dioxide to metal macrocycles: Toward a mechanistic understanding of electrochemical and photochemical carbon dioxide reduction
[DE93-016244] p 949 N94-16870
Process of shaping an electrorheological solid
[AD-D015885] p 1012 N94-16914
A simple chemical procedure for extending the conductive state of polypyrrole to more negative potentials
[AD-A266235] p 969 N94-16928
Activation and deactivation of high concentration arsenic with some evidence of precipitation
[DE93-016437] p 950 N94-16952

ELECTRODE MATERIALS
Chemical interactions between interconnect and electrode materials during sintering in solid oxide fuel cells
[DE93-015696] p 1092 N94-16160

ELECTRODEPOSITION
Structural and dynamical aspects of electrodeposition
[AD-A266786] p 942 N94-14909
Molten salt electrodeposition of high temperature superconductors
[AD-A266620] p 1009 N94-15726

ELECTRODES
Structural and dynamical aspects of electrodeposition
[AD-A266786] p 942 N94-14909
Microwave interaction with plasmas
[AD-A267048] p 1201 N94-15661
Cellulose triacetate, thin film dielectric capacitor
[NASA-CASE-NPO-18935-1-CU] p 1010 N94-15952
In situ studies of passive film chemistry using x ray absorption spectroscopy
[DE93-014023] p 947 N94-16011
In situ Raman spectroscopy of lithium electrode surface in ambient temperature lithium secondary battery
[DE93-015238] p 1010 N94-16061
Electro-rheological disk pump
[AD-D015783] p 1047 N94-16531
Solvational barriers to interfacial electron transfer: Minimization by way of valence delocalization
[AD-A267371] p 950 N94-17006

ELECTRODYNAMICS
Middle atmospheric electric fields over thunderstorms
[NASA-CR-194619] p 1106 N94-16493
Electrodynamic forces of the cross-connected figure-eight null-flux coil suspension system
[DE93-015139] p 1048 N94-16969

ELECTROHYDRODYNAMICS
Electrophoresis visualisation p 944 N94-15163

ELECTROLESS DEPOSITION
Ablation, surface activation, and electroless metallization of insulating materials by pulsed excimer laser irradiation
[DE93-015808] p 1040 N94-16664

ELECTROLYTES
Hydride-containing molten salts and their technology implications
[AD-A266458] p 1092 N94-16567
Characterization of the lithium/pan-based polymer electrolytes interface
[AD-A268401] p 973 N94-17434
Environment enhanced fatigue crack propagation in metals: Inputs to fracture mechanics life prediction models
[NASA-CR-191538] p 942 N94-17638

ELECTROMAGNETIC ABSORPTION
Spectral studies of solid propellant combustion 4: Absorption and burn rate results for M43, XM39, and M10 propellants
[AD-A267119] p 946 N94-15685
Multilayer thin film design for far ultraviolet polarizers using an induced transmission and absorption technique
[NASA-CR-194631] p 1190 N94-15869
Effect of powerful oblique HF waves on ionospheric D-layer absorption
[AD-A268443] p 1102 N94-17499

ELECTROMAGNETIC COMPATIBILITY
Radar transmitter procedures
[AD-A268274] p 1005 N94-17523

ELECTROMAGNETIC COUPLING
Phased array antenna analysis using hybrid finite element methods
[AD-A267620] p 1002 N94-17196

ELECTROMAGNETIC FIELDS
Determination of the electromagnetic fields radiated from the ARES EMP simulator
[AD-A267069] p 988 N94-15668
Operation of digital systems in severe electromagnetic environments
[AD-A267176] p 988 N94-15693
Full-wave simulation of the thumbtack laser
[DE93-015110] p 1039 N94-16054
A priori inequalities for an ideal-incompressible liquid in an electromagnetic field
[IFTR-9/1992] p 998 N94-16652
Analysis of an electromagnetic field in the vicinity of a caustic by asymptotic methods
[IFTR-12/1991] p 998 N94-16653
An asymptotic expansion of an electromagnetic field in the velocity of a caustic in the form of simple waves
[IFTR-14/1991] p 1002 N94-17048
Relativistic dynamics of spin in strong external fields
[NIKHEF-H/93-06] p 1240 N94-17604

ELECTROMAGNETIC INTERACTIONS
On the nature of mirror particles
[DE93-626670] p 1179 N94-14934
Engineering design of sub-micron topographies for simultaneously adherent and reflective metal-polymer interfaces
[NASA-CR-194573] p 964 N94-15700
Confinement and stability of a Crystal Beam
[DE93-015400] p 1181 N94-16020
Electroweak physics from D0
[DE93-015041] p 1181 N94-16053
Theoretical high energy physics research at the University of Chicago
[DE93-016863] p 1187 N94-16116
Electroweak results from D0
[DE93-014926] p 1185 N94-16968
The exact solution of the problem of diffraction of an electromagnetic plane wave by a conductive half-plane situated at an interface
[IFTR-3/91] p 1002 N94-17057
Application of the finite-difference time-domain method to scattering and radiation problems involving wires and plates
[AD-A268396] p 1005 N94-17496
Basic studies of the liquid state of matter: Electrical properties and laser interactions
[AD-A268311] p 1042 N94-17567

ELECTROMAGNETIC INTERFERENCE
Signal processing in impulsive electromagnetic interference
[AD-A266425] p 998 N94-16557
An electromagnetic interference study of potential transmitter sites for the HF Active Auroral Research Program (HAARP)
[AD-A267743] p 1004 N94-17373
Forecasting the ducting of electromagnetic waves on the mesoscale
[AD-A268101] p 1109 N94-17571

ELECTROMAGNETIC NOISE
Looking at Fokker-Planck dynamics with a noisy instrument
[AD-A267049] p 1117 N94-15662
What is the radar tracking Glint problem and can it be solved?
[AD-A266509] p 999 N94-16789

ELECTROMAGNETIC PULSES
Determination of the electromagnetic fields radiated from the ARES EMP simulator
[AD-A267069] p 988 N94-15668
Theoretical studies relating to the interaction of radiation with matter
[AD-A267134] p 1180 N94-15689
Ground wave emergency network final operational capability: Environmental assessment for central Wyoming relay node, site number RN 8C928WY
[AD-A267842] p 1001 N94-17011
Ground wave emergency network final operational capability: Environmental assessment for southern Nevada relay node site number RN 8W918NV
[AD-A267647] p 1002 N94-17205
Ground wave emergency network final operational capability: Environmental assessment for northwestern Nebraska relay node, site number RN 8C930NE
[AD-A267629] p 1003 N94-17212
Ground wave emergency network environmental assessment for northwestern Colorado relay node site number RN 8C924CO
[AD-A267654] p 1003 N94-17249
Ground wave emergency network. Final operational capability. Environmental assessment for southeastern Idaho relay node, site no. RN8W927ID
[AD-A267796] p 1003 N94-17304
Ground wave emergency network final operational capability. Environmental assessment for southern Arkansas relay node site no. RN 8C912AR
[AD-A268001] p 1004 N94-17376
Environmental assessment for northwestern Indiana relay node site no. RN 8C902IN
[AD-A267849] p 1004 N94-17406
Currents induced in the human body for exposure to ultrawideband electromagnetic pulses
[AD-A268570] p 1130 N94-17621

ELECTROMAGNETIC RADIATION
Future development in cryogenic techniques for space
p 901 N94-15042
Double stimulated Brillouin scattering
p 1200 N94-15205
Plume radiation p 924 N94-15223
Engineering design of sub-micron topographies for simultaneously adherent and reflective metal-polymer interfaces
[NASA-CR-194573] p 964 N94-15700
Investigation of the interactions of radiation with matter
[AD-A266743] p 1181 N94-15774
Development of a proposed international standard for certification of aircraft to High Intensity Radiated Fields (HIRF)
[NASA-TM-106357] p 863 N94-16520
Ergonomics in the office environment
p 1124 N94-16612
Phased array antenna analysis using hybrid finite element methods
[AD-A267620] p 1002 N94-17196

Bioeffects of radiofrequency radiation on cell growth and differentation. Volume 1: Engineering considerations
[AD-A267754] p 1118 N94-17232
Color separation gratings p 1198 N94-17362

ELECTROMAGNETIC SCATTERING
Analysis of electromagnetic scattering from irregularly shaped, thin, metallic flat plates
[NASA-TP-3361] p 998 N94-16655
Ultrafast processes in tunneling microstructure devices
[AD-A266570] p 1210 N94-16720
Application of the finite-difference time-domain method to scattering and radiation problems involving wires and plates
[AD-A268396] p 1005 N94-17496

ELECTROMAGNETIC WAVE FILTERS
VUV thin films, chapter 7
[NASA-CR-194634] p 967 N94-16494

ELECTROMAGNETIC WAVE TRANSMISSION
The three-dimensional ray trajectories of the WKB optical fiber modes
[AD-A267167] p 1189 N94-15739
Stress sensitivity of dielectric resonators
[AD-A266767] p 1009 N94-15825
A ray trace model for propagation loss
[AD-A266314] p 997 N94-16467
Speckles statistics and decorrelation effects in complex ABCD optical systems
[AD-A267843] p 1193 N94-17012
Frequency resolution of an acousto-optical spectrometer
[AD-A267822] p 1035 N94-17401
Forecasting the ducting of electromagnetic waves on the mesoscale
[AD-A268101] p 1109 N94-17571

ELECTROMAGNETISM
Proceedings of the 1992 Antenna Applications Symposium, volume 2
[AD-A266916] p 986 N94-14998

ELECTROMECHANICAL DEVICES
Advanced cooling for high power electric actuators
[AD-A266984] p 866 N94-15761
ALS engine propellant effector system
[NASA-CR-194650] p 926 N94-16590
Stress analysis of laminated composites with preformed holes. Part 1: Single plies with embedded material discontinuities
[AD-A266524] p 936 N94-16795
Development of a prototype kinestatic platform for application to space and ground servicing tasks. Phase 1: Concept Modeling
[NASA-CR-194036] p 887 N94-16905
Electrorheological (ER) fluids: A research needs assessment
[AD-A267588] p 951 N94-17210

ELECTROMETERS
Space systems environmental interaction studies
[AD-A267280] p 897 N94-17240

ELECTRON ACCELERATION
Multispectral observations of the Jovian aurora
[NASA-CR-193628] p 1297 N94-16884

ELECTRON ACCELERATORS
Measurements of the operation of the SINUS-6/BWO system
[AD-A266423] p 1011 N94-16556
Advanced transport systems for electron beams in high brightness accelerators and FELs
[AD-A267322] p 1041 N94-17001

ELECTRON ATTACHMENT
Negative ion formation in small carbon clusters
[DE93-015436] p 1182 N94-16064

ELECTRON BEAMS
Measurement of the specific heat capacity of the electron-beam graphite calorimeter
[NPL-RSA(EXT)-40] p 1031 N94-15018
A study of high field transport in wide band gap electronic materials using a picosecond transient charge technique
[AD-A267098] p 1008 N94-15636
Thomson backscattered x rays from an intense laser beam
[AD-A267125] p 1038 N94-15686
Aberration correction of unstable resonators
[NASA-CASE-NPO-18791-1-CU] p 1034 N94-15987
Modification of fluoropolymer surfaces with electronically conductive polymers
[AD-A266294] p 967 N94-16475
Measurements of the operation of the SINUS-6/BWO system
[AD-A266423] p 1011 N94-16556
Advanced transport systems for electron beams in high brightness accelerators and FELs
[AD-A267322] p 1041 N94-17001
Electron reversal ionizer for detection of trace species using a spherical cathode
[NASA-CASE-NPO-18870-1-CU] p 1185 N94-17329
Diffractive optics fabricated by direct write methods with an electron beam p 1196 N94-17347
Phase holograms in PMMA with proximity effect correction p 1037 N94-17348
Curved grating fabrication techniques for concentric-circle grating, surface-emitting semiconductor lasers p 1045 N94-17349
Low cost paths to binary optics p 1197 N94-17353
Low voltage electron beam lithography
[AD-A267865] p 1215 N94-17389

ELECTRON CYCLOTRON HEATING
Inductive effects during second harmonic current drive experiments on T-10
[DE93-014411] p 1202 N94-16803
Recent results from the 60 GHz inside launch ECH system on the D3-D tokamak
[DE93-013027] p 1203 N94-16816

ELECTRON DENSITY (CONCENTRATION)
Electronic structure and enthalpy of hydrogen and helium mixtures
[DE93-014128] p 1208 N94-15976
Application of cylindrical distribution functions to anisotropic scattering from amorphous films
[DE93-015256] p 1183 N94-16811

ELECTRON DENSITY PROFILES
A physical model for one-dimension and time-dependent ionosphere. Part 2: Results and discussions
[DE93-627959] p 1103 N94-17631

ELECTRON DIFFRACTION
Diffuse scattering and image contrast of tweed in superconducting oxides: A simulation and interpretation
[DE93-016131] p 1212 N94-16844
Photo-assisted epitaxial growth for III-V semiconductors
[AD-A267889] p 1213 N94-17042
Mechanical properties of interfaces and superlattices
[AD-A268591] p 1217 N94-17606

ELECTRON DISTRIBUTION
X ray laser program
[AD-A267075] p 1038 N94-15628

ELECTRON EMISSION
Dissociation rates of diatomic molecules
[AD-A266464] p 1182 N94-16586

ELECTRON ENERGY
Characterization of InTISb grown by low pressure metalorganic chemical vapor deposition on GaAs substrate
[AD-A266878] p 1206 N94-14922
Application of Z-contrast imaging to obtain column-by-column spectroscopic analysis of materials
[DE93-015333] p 947 N94-16014
The interaction of HCN(DCN) with Si(111)-7x7 studied with HREELS, UPS, and XPS
[AD-A266237] p 1182 N94-16111
ARIES tokamak reactor study
[DE93-017059] p 1203 N94-16901
Sodium-mercury excimer laser, phase 1
[AD-A267728] p 1042 N94-17230
In-situ electron and optical spectroscopies of translational and vibrational activated bond breaking and formation on semiconductors
[AD-A268192] p 1015 N94-17560

ELECTRON IMPACT
Investigation of the interactions of radiation with matter
[AD-A266743] p 1181 N94-15774
Dissociation rates of diatomic molecules
[AD-A266464] p 1182 N94-16586
Atomic beam studies relevant to the space environment
[AD-A268628] p 1186 N94-17436

ELECTRON MICROSCOPES
Mechanical and surface force nanoprobe
[AD-D015792] p 1034 N94-16536

ELECTRON MICROSCOPY
Electron-microscopy study of antiphase boundaries in Cu3Pd and Fe3Al alloys near the order-disorder transition
[ONERA-NT-1993-1] p 1206 N94-15295

ELECTRON MOBILITY
Granular fluctuations in plasma turbulence and their role in transport
[DE93-013465] p 1187 N94-17674

ELECTRON ORBITALS
Water adsorption on diamond (110) studied by multiple internal reflection infrared spectroscopy
[AD-A266415] p 948 N94-16553

ELECTRON PARAMAGNETIC RESONANCE
Investigation of the optical, electronic, and structural properties of fiber optic glasses
[AD-A267645] p 971 N94-17204
Factors determining the release of nitric oxide --- Calcium/cadmium transport by renal cortical collectin duct cells
[AD-A266232] p 1118 N94-17224
Synthesis and characterization of new low-dimensional metal complex conductors
[AD-A268251] p 952 N94-17416

ELECTRON PHONON INTERACTIONS
Basic optical studies of high T(c) oxide superconductors
[AD-A268148] p 1014 N94-17428
Lattice relaxation theory of localized excitations in quasi-one-dimensional systems
[DE93-624947] p 1215 N94-17437

ELECTRON PLASMA
High frequency Raman current drive
p 1201 N94-15208

ELECTRON PROBES
The role of carbon and temperature in determining electrical conductivity of basins, crust and mantle
[DE93-015936] p 1101 N94-16840

ELECTRON SCATTERING
On the 17-keV neutrino
[DE93-012638] p 1181 N94-15974

ELECTRON SPECTROSCOPY
Electron spectroscopy analysis
[NASA-CR-193591] p 951 N94-17039
In-situ electron and optical spectroscopies of translational and vibrational activated bond breaking and formation on semiconductors
[AD-A268192] p 1015 N94-17560

ELECTRON STATES
Photodegradation of polyimides. V1: Effect of donor-acceptor groups on the photooxidative stability of polyimides and model compounds
[AD-A267319] p 970 N94-16947
Bibliography of short wavelength chemical laser research
[AD-A267619] p 1041 N94-17195
Sodium-mercury excimer laser, phase 1
[AD-A267728] p 1042 N94-17230
Interface properties of wide bandgap semiconductor structures
[AD-A268269] p 1215 N94-17377

ELECTRON TRANSFER
Structural effects in electron transfer reactions: Comparative interfacial electrochemical kinetics for cis- versus trans-dioxorhenium (V) (bi)pyridine oxidation
[AD-A266307] p 1182 N94-16466
Characterization of UV emissions resulting from electronic energy transfer in atmospheric molecules
[AD-A266244] p 1101 N94-16469
Scintillation mechanism in stoichiometric cerium compounds
[DE93-015499] p 948 N94-16771
High-valent oxo, methoxorhenium complexes: Models for intermediates and transition states in proton-coupled multi-electron transfer reactions
[AD-A266492] p 1211 N94-16782
Binding of carbon dioxide to metal macrocycles: Toward a mechanistic understanding of electrochemical and photochemical carbon dioxide reduction
[DE93-016244] p 949 N94-16870
Photodegradation of polyimides. V1: Effect of donor-acceptor groups on the photooxidative stability of polyimides and model compounds
[AD-A267319] p 970 N94-16947
Vectorial electron transfer in spatially ordered arrays
[DE93-018150] p 1185 N94-16971
Solvational barriers to interfacial electron transfer: Minimization by way of valence delocalization
[AD-A267371] p 950 N94-17006

ELECTRON TRANSITIONS
Optoelectronics based on SiGe/Si heterostructures
[AD-A267178] p 1190 N94-15848
Dissociation rates of diatomic molecules
[AD-A266464] p 1182 N94-16586

ELECTRON TUBES
RF vacuum microelectronics
[AD-A268399] p 1014 N94-17423

ELECTRON TUNNELING
Mechanical and surface force nanoprobe
[AD-D015792] p 1034 N94-16536
Method and apparatus for performing scanning tunneling optical absorption spectroscopy
[AD-D015796] p 948 N94-16539
Ultrafast processes in tunneling microstructure devices
[AD-A266570] p 1210 N94-16720
Density of states and tunneling characteristics of layered superconductors
[DE93-015898] p 1211 N94-16839

ELECTRONIC CONTROL
Transputer based control system for MTLRS
p 877 N94-15613
Laser with optically driven Q-switch
[NASA-CASE-NPO-18470-1-CU] p 1038 N94-15932
Mechanical properties of interfaces and superlattices
[AD-A268591] p 1217 N94-17606

ELECTRONIC EQUIPMENT
The specific heat of titanium disilicide
[AD-A267543] p 960 N94-17100

ELECTRONIC EQUIPMENT TESTS
Multichip module high speed testing
[AD-A266968] p 986 N94-14955
ELECTRONIC FILTERS
Poisson filtering of laser ranging data
p 917 N94-15593
ELECTRONIC MAIL
Electronic messaging for the 1990's
[AD-A267143] p 1229 N94-15437
Computer networking at SLR stations
p 917 N94-15594
Performance Information Management System (PIMS) communication
[AD-A267040] p 1231 N94-16458
The ESA Tele-Invoicing System (ETIS)
[ESA-INT-6] p 1150 N94-16591
ELECTRONIC MODULES
Multichip module high speed testing
[AD-A266968] p 986 N94-14955
Module interconnection frameworks for a real-time spreadsheet
[AD-A267752] p 1153 N94-17231
Low dielectric constant insulators and gold metallization for GHz multi-chip modules, part 2
[AD-A268590] p 1176 N94-17605
ELECTRONIC PACKAGING
Stress analysis of laminated composites with preformed holes. Part 1: Single plies with embedded material discontinuities
[AD-A266524] p 936 N94-16795
ELECTRONIC WARFARE
Evaluation of site effects on a high frequency direction finding single site location system
[AD-A267465] p 1001 N94-17035
ELECTRONICS
Cryogenic readout electronics for astronomical applications p 910 N94-15099
Translating wedge heat sink
[AD-D015814] p 1011 N94-16488
ELECTRONS
Iteration scheme for the multiparameter nonlinear boundary value problem with the additional conditions and its application to some field models
[DE93-626638] p 1168 N94-14933
Thinned, backside illuminated, area CCD imager for electron detection p 901 N94-15036
Electroweak physics from D0
[DE93-015041] p 1181 N94-16053
The 3D-Flow processor for a programmable level-1 trigger (feasibility study)
[DE93-016045] p 1159 N94-16172
Numerical studies of the photoluminescence spectrum of quantum Hall systems
[DE93-015822] p 1220 N94-16810
Multispectral observations of the Jovian aurora
[NASA-CR-193628] p 1297 N94-16884
Electron reversal ionizer for detection of trace species using a spherical cathode
[NASA-CASE-NPO-18870-1-CU] p 1185 N94-17329
ELECTROPHORESIS
Orientation of DNA during free-solution electrophoresis p 944 N94-15162
Electrophoresis visualisation p 944 N94-15163
Investigation of the effects of polyelectrolyte coatings on colloid transport in porous media
[DE93-018300] p 970 N94-16973
ELECTRORHEOLOGICAL FLUIDS
Electrorheological fluid chemical processing
[AD-D015785] p 948 N94-16532
Process of shaping an electrorheological solid
[AD-D015885] p 1012 N94-16914
High pressure pump for electro-rheological fluids
[AD-D015888] p 1048 N94-16915
Electrorheological (ER) fluids: A research needs assessment
[AD-A267588] p 951 N94-17210
ELECTROSTATIC BONDING
Electrostatic fiber spreader including a corona discharge device
[AD-D015793] p 936 N94-16537
ELECTROSTATIC CHARGE
An improved patch for radiative coolers
[NASA-CASE-GSC-13503-1] p 1046 N94-15873
Process for shaping articles from electrosetting compositions
[AD-D015787] p 935 N94-16534
Electrostatic fiber spreader including a corona discharge device
[AD-D015793] p 936 N94-16537
ELECTROSTATIC PROBES
Prototype instrumentation and design studies
[AD-A266402] p 882 N94-16530
Space systems environmental interaction studies
[AD-A267280] p 897 N94-17240
ELECTROSTATICS
Microwave interaction with plasmas
[AD-A267048] p 1201 N94-15661
Theoretical crystallography with the Advanced Visualization System
[DE93-015692] p 1215 N94-17319
ELECTROSTRICTION
Nanocomposites for electronic applications, volume 1
[AD-A267070] p 1009 N94-15669
Nanocomposites for electronic applications, volume 3
[AD-A267073] p 1009 N94-15672
Nanocomposites for electronic applications, volume 2
[AD-A267074] p 1009 N94-15673
ELEMENT 104
On-line gas chromatographic studies of Rutherfordium (element 104), hahnium (element 105), and homologs
[DE93-013890] p 948 N94-16821
ELEMENT 105
On-line gas chromatographic studies of Rutherfordium (element 104), hahnium (element 105), and homologs
[DE93-013890] p 948 N94-16821
ELEMENTARY EXCITATIONS
Quasiparticle trapping in distributed superconducting three-terminal tunnel junction devices
p 910 N94-15101
ELEMENTARY PARTICLE INTERACTIONS
Search for the top quark from (e(mu)) and (e,e) events in the D0 detector in p(bar-p) collisions at the square root of s = 1.8 TeV
[DE93-016350] p 1186 N94-17662
ELEMENTARY PARTICLES
Particle physics and cosmology, Task C
[DE93-016865] p 1239 N94-16118
ELEVATION ANGLE
Determination of momentum flux using a bivane and cup anemometer
[AD-A265414] p 1105 N94-15137
Propagation measurements in Alaska using ACTS beacons p 995 N94-16040
Propagation-related AMT design aspects and supporting experiments p 995 N94-16042
ELEVONS
Subsonic aerodynamic characteristics of the HL-20 lifting-body configuration
[NASA-TM-4515] p 861 N94-17284
ELLIPSES
Wind-tunnel investigation of aerodynamic efficiency of three planar elliptical wings with curvature of quarter-chord line
[NASA-TP-3359] p 859 N94-16574
ELLIPSOMETERS
Investigation of the influence of applied potential on erosion-corrosion of copper in alkaline chloride solutions
[AD-A266448] p 958 N94-16562
ELLIPSOMETRY
Investigation of the influence of applied potential on erosion-corrosion of copper in alkaline chloride solutions
[AD-A266448] p 958 N94-16562
ELLIPTIC DIFFERENTIAL EQUATIONS
On a class of singular quasilinear elliptic equations with general structure and distribution data
[DE93-628585] p 1171 N94-17613
ELLIPTIC FUNCTIONS
Statistics of the half-integer stopband
[DE93-016101] p 1173 N94-17236
ELLIPTICAL ORBITS
The ELLIPSO (tm) system: Elliptical low orbits for mobile communications p 893 N94-17167
EMBEDDED COMPUTER SYSTEMS
A formal protocol test procedure for the Survivable Adaptable Fiber Optic Embedded Network (SAFENET)
[AD-A267410] p 1192 N94-16975
Embedded computer systems: Status of C-17 software
[AD-A267307] p 1160 N94-16993
EMBOSSING
Predesign of diamond turned refractive/diffractive elements for IR objectives p 1198 N94-17359
EMBRITTLEMENT
A reexamination of grain boundary fracture in Ni3Al: Environmental and alloying effects
[DE93-015431] p 1208 N94-16063
The effect of long-term aging on the impact properties of modified 9Cr-1Mo steel
[DE93-015453] p 957 N94-16068
EMBRYOLOGY
Ontogenesis of mammals in microgravity
[NASA-TM-103978] p 1139 N94-17636
EMBRYOS
STS-29 crew with student experiment
[NASA-TM-109545] p 1116 N94-15378
EMERGENCIES
Emergency preparedness and planning
p 1124 N94-16613
Illness/injury pattern complex 40 (Titan)
p 1125 N94-16625
Regulated emergency oxygen system
[AD-A266228] p 1138 N94-16983
Ground wave emergency network final operational capability: Environmental assessment for central Wyoming relay node, site number RN 8C928WY
[AD-A267842] p 1001 N94-17011
Ground wave emergency network environmental assessment for northwestern Colorado relay node site number RN 8C924CO
[AD-A267654] p 1003 N94-17249
Ground wave emergency network final operational capability. Environmental assessment for southern Arkansas relay node site no. RN 8C912AR
[AD-A268001] p 1004 N94-17376
EMISSION
Statement on global climate change before the Subcommittee on Energy and Power, United States House of Representatives
[DE93-013163] p 1095 N94-16006
EMISSION SPECTRA
Optical fiber spectroscopy: A study of the luminescent properties of the europium ion for thermal sensors
[NASA-CR-194576] p 1189 N94-15647
Remote sensing studies of the northeastern portion of the lunar nearside p 1258 N94-16225
Near-surface temperature gradients and their effects on thermal-infrared emission spectra of particulate planetary surfaces p 1260 N94-16236
First results from a laboratory facility for measurement of emission spectra under simulated planetary conditions
p 954 N94-16372
Lasing dye sensor for chemical vapors
[AD-D015786] p 1040 N94-16533
Ejecta patterns of Meteor Crater, Arizona derived from the linear un-mixing of TIMS data and laboratory thermal emission spectra p 1065 N94-16607
Soft x ray emission from Alexandrite laser-matter-interaction
[AD-A267905] p 1042 N94-17378
EMISSIVITY
Radar properties of several fluidized ejecta blankets on Venus p 1267 N94-16278
An algorithm for the estimation of bounds on the emissivity and temperatures from thermal multispectral airborne remotely sensed data p 1064 N94-16603
Preliminary analysis of thermal-infrared multispectral scanner data of the Iron Hill, Colorado carbonatite-alkalic rock complex p 1065 N94-16605
EMITTANCE
Emittance and beam size distortion due to linear coupling
[DE93-015402] p 1184 N94-16886
Emittance growth in displaced, space-charge-dominated beams with energy spread
[DE93-016514] p 1188 N94-17672
EMITTERS
Acousto-optical classifier
[AD-D015894] p 1000 N94-16921
Evaluation of site effects on a high frequency direction finding single site location system
[AD-A267465] p 1001 N94-17035
Space systems environmental interaction studies
[AD-A267280] p 897 N94-17240
Field-emitter arrays for RF vacuum microelectronics
[AD-A268397] p 1015 N94-17526
Field emitter arrays for RF vacuum microelectronics
[AD-A268595] p 1015 N94-17608
EMPLOYEE RELATIONS
Industrial labor relations manual
[NHB-5200.1B] p 1224 N94-15939
EMPLOYMENT
The NASA competitive placement plan for positions GS-15 and below (including trades and labor positions)
[NHB-3335.1C] p 1224 N94-15944
EMULSIONS
Determination of average refractive index of spin coated DCG films for HOE fabrication p 1036 N94-14992
ENCAPSULATING
Contained liquids in microgravity, part 2
p 979 N94-16085
Encapsulation of hemoglobin in non-phospholipid vesicles
[AD-A266505] p 1128 N94-16785
END EFFECTORS
Tactile sensing and control in humans and robotic/teleoperated systems
[AD-A267710] p 1163 N94-14937
Spline screw payload fastening system
[NASA-CASE-GSC-13454-1] p 1046 N94-15871
Contextually dependent control strategies for manipulation
[TR-416] p 1165 N94-16580
End-effector: Joint conjugates for robotic assembly of large truss structures in space: Extended concepts
[NASA-CR-193576] p 1048 N94-17088

Optimal tuning of heavy equipment motion controllers
[AD-A267873] p 1167 N94-17392
ENDOCRINOLOGY
New insulin pump
[NASA-TM-109642] p 1120 N94-15253
Melatonin, the pineal gland, and circadian rhythms
[AD-A268200] p 1129 N94-17478
ENDURANCE
Force-endurance capabilities of extravehicular activity (EVA) gloves at different pressure levels
[NASA-TP-3420] p 1139 N94-17653
ENERGETIC PARTICLES
The Solar Flare Myth in solar-terrestrial physics
[DE93-016487] p 1299 N94-16895
ENERGY ABSORPTION
Investigation of the optical, electronic, and structural properties of fiber optic glasses
[AD-A267645] p 971 N94-17204
Resist performance in soft x ray projection lithography
[DE93-016490] p 1036 N94-17647
ENERGY BUDGETS
Heterogeneity and scaling land-atmospheric water and energy fluxes in climate systems p 1083 N94-16030
Effects of spatial variability and scale on areal -average evapotranspiration p 1084 N94-16033
Heat transfer parametric system identification
[AD-A268525] p 929 N94-17543
A surface energy budget model modifying heat flow by foliage effects
[AD-A268598] p 1085 N94-17610
ENERGY CONSERVATION
Systematology for elastic-plastic material equations by large deformations on the basis of the Cosserat-continuum model
[SCHRIFTENR-PHYSIKAL-ING-BD] p 1058 N94-15642
Biomass energy: State of the technology present obstacles and future potential
[DE93-016295] p 1092 N94-16766
ENERGY CONSUMPTION
Application of non-thermal plasmas to pollution control
[DE93-016432] p 1096 N94-16449
Assessment of trends in the development of residential buildings from the standpoint of the fuel and energy requirements
[IFTR-6/1991] p 1093 N94-17092
ENERGY CONVERSION
New York MARKAL: An evaluation of carbon dioxide emission control strategies in New York State
[DE93-013149] p 1095 N94-15999
Emittance growth in displaced, space-charge-dominated beams with energy spread
[DE93-016514] p 1188 N94-17672
ENERGY CONVERSION EFFICIENCY
Progress in the concentrator initiative program
[DE93-015006] p 1091 N94-15984
Numerical modelling of an active direct nonpotable hot water heating system making use of the energy of solar radiation
[IFTR-38/1991] p 1093 N94-17070
ENERGY DISSIPATION
The interaction of HCN(DCN) with Si(111)-7x7 studied with HREELS, UPS, and XPS
[AD-A266237] p 1182 N94-16111
Six dimensional tracking simulator for H(-) injection in AGS Booster
[DE93-015396] p 1184 N94-16885
Energy-loss cross sections for inclusive charge-exchange reactions at intermediate energies
[NASA-TM-4522] p 1188 N94-17018
Structure of high Reynolds number turbulent boundary layer
[AD-A267476] p 860 N94-17099
Electrorheological (ER) fluids: A research needs assessment
[AD-A267588] p 951 N94-17210
Low temperature deposition and characterization of n- and p-type silicon carbide thin films and associated ohmic and Schottky contacts
[AD-A267966] p 973 N94-17490
In-situ electron and optical spectroscopies of translational and vibrational activated bond breaking and formation on semiconductors
[AD-A268192] p 1015 N94-17560
ENERGY GAPS (SOLID STATE)
A study of high field transport in wide band gap electronic materials using a picosecond transient charge technique
[AD-A267098] p 1008 N94-15636
Ablation, surface activation, and electroless metallization of insulating materials by pulsed excimer laser irradiation
[DE93-015808] p 1040 N94-16664
Density of states and tunneling characteristics of layered superconductors
[DE93-015898] p 1211 N94-16839
Atomic layer epitaxy of boron nitride
[AD-A266260] p 1212 N94-16932
Interface properties of wide bandgap semiconductor structures
[AD-A268269] p 1215 N94-17377
ENERGY LEVELS
Investigation of the interactions of radiation with matter
[AD-A266743] p 1181 N94-15774
ENERGY REQUIREMENTS
Assessment of trends in the development of residential buildings from the standpoint of the fuel and energy requirements
[IFTR-6/1991] p 1093 N94-17092
ENERGY SPECTRA
The SCR Ne-21 and Ar-38 in lunar rock 68815: The solar proton energy spectrum over the past 2 MYR p 1248 N94-16177
On possible Mn-53 heterogeneity in the early solar system p 1244 N94-16344
Numerical studies of the photoluminescence spectrum of quantum Hall systems
[DE93-015822] p 1220 N94-16810
Investigation of the energy distribution of ions, striking the cathode in an abnormal glow discharge
[DE93-623987] p 1013 N94-17316
ENERGY STORAGE
Advanced cooling for high power electric actuators
[AD-A266984] p 866 N94-15761
Influence of grain size on the energy storing ability during uniaxial stretching of austenite steel
[IFTR-22/1992] p 961 N94-17121
ENERGY TECHNOLOGY
Space Station thermal storage/refrigeration system research and development
[NASA-CR-193841] p 879 N94-15191
The 1979 highlights
[NASA-TM-109443] p 1247 N94-15342
The 1978 highlights
[NASA-TM-109625] p 1302 N94-15411
The 1977 highlights
[NASA-TM-109626] p 1302 N94-15412
Requirements for supercomputing in energy research: The transition to massively parallel computing
[DE93-012376] p 1160 N94-16774
Publications of the Oak Ridge National Laboratory Fossil Energy Program, 1 October 1991 - 31 March 1993
[DE93-014643] p 1232 N94-16967
Energy from the sun: Evolution of federal support for solar energy
[AD-A267944] p 1093 N94-17382
DOE/NREL Advanced Wind Turbine Development Program
[DE93-010028] p 1093 N94-17668
ENERGY TRANSFER
Molecular processes in comets
[NASA-CR-194148] p 1239 N94-15188
Studies on the parametric decay of waves in fusion plasmas
[VTT-PUBS-110] p 1200 N94-15204
Ocean wave study
[NASA-TM-109620] p 1111 N94-15349
Theoretical studies relating to the interaction of radiation with matter
[AD-A267134] p 1180 N94-15689
Study of multi-dimensional radiative energy transfer in molecular gases
[NASA-CR-194613] p 1181 N94-15752
Investigation of the interactions of radiation with matter
[AD-A266743] p 1181 N94-15774
Single-collision studies of energy transfer and chemical reaction
[DE93-017603] p 1182 N94-16121
Active probing of plasma edge turbulence and feedback studies on the Texas experimental tokamak (TEXT)
[DE93-015799] p 1202 N94-16162
Gas-grain energy transfer in solar nebula shock waves: Implications for the origin of chondrules p 1262 N94-16251
Characterization of UV emissions resulting from electronic energy transfer in atmospheric molecules
[AD-A266244] p 1101 N94-16469
Spectroscopic investigations of nonambient systems with millimeter and submillimeter probes
[AD-A268537] p 968 N94-16796
Bibliography of short wavelength chemical laser research
[AD-A267619] p 1041 N94-17195
Plasma flow switch and foil implosion experiments on Pegasus 2
[DE93-016464] p 1013 N94-17318
A numerical investigation of energy transfer and subgrid-scale eddy-viscosity in homogeneous, isotropic, and shear turbulence
[AD-A267265] p 1029 N94-17363
Energy deposition fluctuations induced by ions in microvolumes and nanovolumes: An analytic approach. 1: Theory
[AD-A267959] p 1173 N94-17495
ENGINE CONTROL
ALS engine controller system
[NASA-CR-194647] p 926 N94-16654
Development and analysis of startup strategies for particle bed nuclear rocket engine
[AD-A267949] p 927 N94-17053
ENGINE DESIGN
Turbine blade tip film cooling measurements
[AD-A267686] p 868 N94-14964
SPDE/SPRE final summary report
[NASA-CR-187086] p 924 N94-15482
NASA Operational Environment Team (NOET): NASA's key to environmental technology
[TABES PAPER 93-611] p 1052 N94-16143
Emerging technologies for the changing global market
[TABES PAPER 93-612] p 930 N94-16144
Advanced transportation system studies technical area 3: Alternate propulsion subsystem concepts, volume 2
[NASA-CR-193863] p 927 N94-17096
Some single-piston closed-cycle machines and Peter Tailer's thermal lag engine
[DE93-015983] p 1049 N94-17675
ENGINE INLETS
An uncertainty analysis of inlet dynamic flow distortion using an analog/digital hybrid editing system
[AD-A266924] p 855 N94-15105
Wind tunnel investigation of three axisymmetric cowls of different lengths at Mach numbers from 0.60 to 0.92
[NASA-TM-4488] p 856 N94-15681
ENGINE NOISE
Technical evaluation report on the AGARD-PEP Specialists Meeting on Combat Aircraft Noise
[NLR-TP-91445-U] p 1177 N94-15506
ENGINE PARTS
Chemical vapor deposition of Ta2O5 corrosion resistant coatings
[DE93-015488] p 969 N94-16889
ENGINE TESTING LABORATORIES
Structured finite volume modeling of US Navy aircraft engine test cells task 2: Turboprop engine, volume 1
[AD-A267833] p 872 N94-17405
Structured finite volume modeling of US Navy aircraft engine test cells. Task 1: Turboshaft engine, volume 1
[AD-A268176] p 873 N94-17432
Structured finite volume modeling of US Navy aircraft engine test cells. Task 1: Turboshaft engine-code documentation and listings, volume 2
[AD-A268177] p 873 N94-17508
ENGINE TESTS
Effects of RVP, T(50), and oxygenates on hot-start and driveability performance at high and low altitude
[AD-A266382] p 869 N94-16516
Structured finite volume modeling of US Navy aircraft engine test cells task 2: Turboprop engine, volume 1
[AD-A267833] p 872 N94-17405
Structured finite volume modeling of US Navy aircraft engine test cells. Task 1: Turboshaft engine, volume 1
[AD-A268176] p 873 N94-17432
Structured finite volume modeling of US Navy aircraft engine test cells. Task 1: Turboshaft engine-code documentation and listings, volume 2
[AD-A268177] p 873 N94-17508
Structured finite volume modeling of US Navy aircraft engine test cells. Task 2: Turboprop engine. Volume 2: Code documentation and listings
[AD-A268386] p 873 N94-17569
ENGINEERING DRAWINGS
Using interactive sketch interpretation to design solid objects
[AD-A266637] p 1147 N94-15743
ENGINEERING MANAGEMENT
An analysis of SEI software process assessment results: 1987-1991
[AD-A266996] p 1145 N94-15629
Prioritization methodology for chemical replacement
[NASA-TP-3421] p 976 N94-15723
TABES 1993: 9th Annual Technical and Business Exhibition and Symposium p 1050 N94-16129
Impact of TQM concepts on inspection of aerospace systems
[TABES PAPER 93-350] p 1050 N94-16130
Medical surveillance and biological monitoring of lead exposed employees p 1124 N94-16615
ENGINEERS
Fifty years of the Netherlands Association of Aeronautical Engineers p 853 N94-15121
NASA/DOD Aerospace Knowledge Diffusion Research Project. Report 15: Technical uncertainty and project complexity as correlates of information use by US industry-affiliated aerospace engineers and scientists: Results of an exploratory investigation
[NASA-TM-107693] p 1233 N94-17291

ENGINES
NASA images 10
[NASA-TM-109419] p 924 N94-15351
ENRICHMENT
Possible sources of H2 to H2O enrichment at evaporation of parent chondritic material
p 1244 N94-16377
ENSTATITE
I-Xe structure of ILAFEGH 009 and shallowater: Evidence for early formation and rapid cooling of impact-derived enstatite meteorites
p 1243 N94-16305
Comparative magnetic and thermoanalytical study of two enstatite chondrites: Adhi Kot and Atlanta
p 1244 N94-16329
Experimentally reproduced relict enstatite in porphyritic chondrules of enstatite chondrite composition
p 1244 N94-16363
Nitrogen and light noble gases in Parsa enstatite chondrite p 1246 N94-16435
ENTHALPY
Electronic structure and enthalpy of hydrogen and helium mixtures
[DE93-014128] p 1208 N94-15976
On-line gas chromatographic studies of Rutherfordium (element 104), hahnium (element 105), and homologs
[DE93-013890] p 948 N94-16821
To extend the thirteen-moment theory and its application to problems in rarefied hypersonic flow
[AD-A267384] p 859 N94-17021
ENTRAPMENT
Characterization of voids formed during liquid impregnation of nonwoven multifilament glass networks as related to composite processing p 939 N94-16858
Particle Engulfment and Pushing by Solidifying Interfaces (PEPSI)
[NASA-CR-193856] p 960 N94-17079
ENTROPY
Set-based Bayesianism
[TR-407] p 1170 N94-16582
ENVIRONMENT EFFECTS
Development of Japanese Earth Resources Satellite-1 (JERS-1; FUYO-1) and it's operational results
[NASDA-SPP-930001] p 884 N94-15001
The future of Schiphol: Growth within boundaries
p 853 N94-15123
Aviation inspection prospects p 853 N94-15125
Forest fire study
[NASA-TM-109615] p 1095 N94-15425
Statement on global climate change before the Subcommittee on Energy and Power, United States House of Representatives
[DE93-013163] p 1095 N94-16006
Environmental effects on elevated temperature subcritical crack growth of SiC/SiC composites
[DE93-015688] p 934 N94-16158
Development and commercialization status of Fe3Al-based intermetallic alloys
[DE93-015802] p 957 N94-16165
Environmental effects on iron aluminides
[DE93-015820] p 958 N94-16166
Utility emissions associated with electric and hybrid vehicle (EHV) charging
[DE93-013734] p 1011 N94-16459
Ground wave emergency network final operational capability: Environmental assessment for central Nevada relay node, site number RN 8W917NV
[AD-A267630] p 1002 N94-17200
Ground wave emergency network final operational capability: Environmental assessment for southern Nevada relay node site number RN 8W918NV
[AD-A267647] p 1002 N94-17205
Ground wave emergency network final operational capability: Environmental assessment for central Utah relay node, site number RN 8C920UT
[AD-A267628] p 1003 N94-17211
Ground wave emergency network final operational capability: Environmental assessment for northwestern Nebraska relay node, site number RN 8C930NE
[AD-A267629] p 1003 N94-17212
Incorporating global warming risks in power sector planning. Volume 1: A case study of the New England region
[DE93-015241] p 1096 N94-17289
Ground wave emergency network. Final operational capability. Environmental assessment for southeastern Idaho relay node, site no. RN8W927ID
[AD-A267796] p 1003 N94-17304
Environment enhanced fatigue crack propagation in metals: Inputs to fracture mechanics life prediction models
[NASA-CR-191538] p 942 N94-17638
ENVIRONMENT MANAGEMENT
The future of Schiphol: Growth within boundaries
p 853 N94-15123
TABES 1993: 9th Annual Technical and Business Exhibition and Symposium p 1050 N94-16129
Total quality environmental management leadership through quality
[TABES PAPER 93-540] p 1050 N94-16135
Environmental management lessons to be learned from the upcoming CFC phase out or how to insure that we survive the next environmentally mandated process change
[TABES PAPER 93-570] p 1050 N94-16136
Global change research: Science and policy
[DE93-015675] p 1096 N94-16445
Medical surveillance and biological monitoring of lead exposed employees p 1124 N94-16615
Computing and Information Sciences
[DE93-017149] p 1151 N94-16902
ENVIRONMENT MODELS
Driving terrestrial ecosystem models from space
p 991 N94-15896
A Pluto thermal model p 1256 N94-16216
Modeling the reflectance of CO2 frost with new optical constants: Application to Martian south polar cap spectra p 1256 N94-16217
Tessera terrain on Venus: Implications of tessera flooding models and boundary characteristics for global distribution and mode of formation p 1258 N94-16226
ENVIRONMENT PROTECTION
The future of Schiphol: Growth within boundaries
p 853 N94-15123
Aviation inspection prospects p 853 N94-15125
Prioritization methodology for chemical replacement
[NASA-TP-3421] p 976 N94-15723
NASA Operational Environment Team (NOET): NASA's key to environmental technology
[TABES PAPER 93-611] p 1052 N94-16143
Emerging technologies for the changing global market
[TABES PAPER 93-612] p 930 N94-16144
ENVIRONMENT SIMULATORS
First results from a laboratory facility for measurement of emission spectra under simulated planetary conditions
p 954 N94-16372
ENVIRONMENTAL ENGINEERING
Materials, processes, and environmental engineering network
[TABES PAPER 93-610] p 1051 N94-16142
ENVIRONMENTAL LABORATORIES
Computing and Information Sciences
[DE93-017149] p 1151 N94-16902
ENVIRONMENTAL MONITORING
Views from space
[NASA-TM-109634] p 1081 N94-15245
Living well in space: Monitoring environment
[NASA-TM-109537] p 1120 N94-15368
Laser tracking for vertical control p 911 N94-15553
Toxic substances registry system: Index of material safety data sheets
[NASA-TM-109332] p 1121 N94-15658
Environmental characterization for target acquisition. Report 1: Site descriptions and measurements
[AD-A267192] p 1106 N94-15851
A summary of microwave remote sensing investigations planned for BOREAS p 993 N94-15914
The strategic environmental research and development program: A new paradigm for space, the environment, and national security
[AD-A266222] p 1174 N94-16109
Global change research: Science and policy
[DE93-015675] p 1096 N94-16445
Monitoring environmental state of Alaskan forests with AIRSAR p 1075 N94-16734
Soil conservation applications with C-band SAR
p 1080 N94-16760
ENVIRONMENTAL QUALITY
Computing and Information Sciences
[DE93-017149] p 1151 N94-16902
ENVIRONMENTAL SURVEYS
Tectonic deformation in southern California
[NASA-CR-194621] p 1101 N94-16021
Mars Analog Site Study (MASS) p 1252 N94-16200
ENVIRONMENTAL TESTS
Long Duration Exposure Facility experiment M0003 deintegration/findings and impacts
[AD-A267140] p 885 N94-15749
Materials, processes, and environmental engineering network
[TABES PAPER 93-610] p 1051 N94-16142
Environment tests for mini satellites
p 896 N94-17189
Reliability analysis of Surface Mount Technology (SMT)
[AD-A267598] p 1055 N94-17194
Aircraft carrier exposure tests of cast magnesium alloys
[AD-A268260] p 962 N94-17418
ENZYME ACTIVITY
An advanced bioprocessing concept for the conversion of wastepaper to ethanol
[DE93-015209] p 975 N94-16807
ENZYMES
Isolation of thermostable enzyme mutants by cloning and selection in thermophilic bacteria
[AD-A266378] p 1117 N94-16514
An advanced bioprocessing concept for the conversion of wastepaper to ethanol
[DE93-015209] p 975 N94-16807
EPHEMERIDES
Laser ranging data analysis
[NASA-CR-193547] p 1041 N94-16719
EPIDEMIOLOGY
Monograph of the aviation epidemiology data register for FY 1991
[AD-A266896] p 1119 N94-14952
Proceedings of the 1992 Annual Meeting NASA Occupational Health Program
[NASA-CR-193462] p 1123 N94-16609
Tuberculosis: A case for increased screening
p 1126 N94-16627
Legionella: An overview p 1126 N94-16629
Screening for prostate cancer p 1126 N94-16630
Quantifying lifetime exposure to ultraviolet radiation in the epidemiology of cutaneous malignant melanoma: A pilot study
[DE93-015274] p 1128 N94-16812
Global solutions to a system of strongly coupled reaction-diffusion equations
[DE93-628587] p 1171 N94-17640
EPITAXY
The epitaxial Si x ray bolometer an alternative to ion implanted devices p 911 N94-15103
Diamond epitaxy and diamondlike coatings
[AD-A266657] p 1206 N94-15747
Experimental investigations of superconductivity in quasi-two-dimensional epitaxial copper oxide superlattices and trilayers
[DE93-015306] p 1207 N94-15829
The growth of InAs(1-x)Sb(x)/InAs strained-layer superlattices by metal-organic chemical vapor deposition
[DE93-015028] p 1208 N94-16012
Apparatus for and a method of growing thin films of elemental semiconductors
[AD-D015813] p 1210 N94-16487
Method for doping GaAs with high vapor pressure elements
[AD-D015794] p 1210 N94-16538
Pulsed laser deposition of metastable Ca(1-x)Sr(x)CuO2 thin films
[DE93-015804] p 1040 N94-16663
Sputtered ferroelectric thin films of KTN for electro-optic devices
[AD-A266573] p 968 N94-16723
Atomic layer epitaxy of boron nitride
[AD-A266260] p 1212 N94-16932
Structural characterization of epitaxial layers for infrared detectors
[AD-A267875] p 940 N94-17013
An alternative approach to the growth of single crystal gallium nitride
[AD-A267876] p 1213 N94-17037
Photo-assisted epitaxial growth for III-V semiconductors
[AD-A267889] p 1213 N94-17042
Atomic layer epitaxy group IV materials: Surface processes, thin films, devices and their characterization
[AD-A267527] p 1213 N94-17116
Buried porous silicon-germanium layers in monocrystalline silicon lattices and method of producing
[NASA-CASE-NPO-18836-1-CU] p 1215 N94-17327
Growth, characterization and device development in monocrystalline diamond films
[AD-A268206] p 1216 N94-17553
Rare earth doped III-V semiconductors for optoelectronics
[AD-A268279] p 1216 N94-17577
Epitaxial iron films
[AD-A268286] p 1217 N94-17579
EPOXY MATRIX COMPOSITES
The effect of plasma treatment on interfacial bond characteristics of Kevlar/epoxy laminates as measured by T-peel tests
[AD-A266920] p 930 N94-14999
Physical interpretation and development of ultrasonic nondestructive evaluation techniques applied to the quantitative characterization of textile composite materials
[NASA-CR-194549] p 931 N94-15190
Construction, testing, and representation of resin and fiber reinforced materials p 931 N94-15255
Synthesis and evaluation of polymeric materials
[AD-A267809] p 973 N94-17408

EPOXY RESINS
Processing, properties and applications of composites using powder-coated epoxy towpreg technology
p 933 N94-15277
Elastooptical brittle materials in experimental studies of the state of stress and deformation
[IFTR-22/1991] p 1059 N94-16651
Process of shaping an electrorheological solid
[AD-D015885] p 1012 N94-16914
Application of thermal spray and ceramic coatings and reinforced epoxy for cavitation damage repair of hydroelectric turbines and pumps
[AD-A267624] p 971 N94-17198
Synthesis and evaluation of polymeric materials
[AD-A267809] p 973 N94-17408
EQUATIONS OF MOTION
Particle simulations on massively parallel machines
[DE93-015644] p 1157 N94-14927
Forced harmonic vibration of the generally orthotropic cylindrical shell with inner and outer fluid loading
[AD-A266985] p 1057 N94-15150
Trajectory optimization for the National Aerospace Plane
[NASA-CR-194618] p 867 N94-16498
Elastic waves in discretely continuous mechanical systems
[IFTR-21/1992] p 1061 N94-17091
A review of some dynamics models in six-dimensional phase space and their suitable conditions of motion equation
[DE93-623741] p 1175 N94-17317
Equations of motion of a hinged body over a spherical earth
[AD-A268408] p 868 N94-17435
Flutter analysis using transversality theory
[NASA-TM-106382] p 1062 N94-17481
EQUATIONS OF STATE
Electronic structure and enthalpy of hydrogen and helium mixtures
[DE93-014128] p 1208 N94-15976
EQUATORIAL REGIONS
Equatorial ground ice on Mars: Steady-state stability
p 1290 N94-16403
Deucalionis Regio, Mars: Evidence for a unique mineralogic endmember and a crusted surface
p 1291 N94-16406
EQUILIBRIUM METHODS
Preliminary analysis and design optimization of the short spacer truss of Space Station Freedom
[NASA-TM-4470] p 1058 N94-15709
EQUIPMENT
Equipment Management Manual
[NHB-4200.1D] p 1225 N94-16799
EQUIPMENT SPECIFICATIONS
Development of Japanese Earth Resources Satellite-1 (JERS-1; FUYO-1) and it's operational results
[NASDA-SPP-930001] p 884 N94-15001
Bench checkout equipment for spaceborne laser altimeter systems p 921 N94-15618
MINISAT programme p 896 N94-17182
EQUIPOTENTIALS
Numerical solution of a second order boundary problem for two dimensions using galerkin approximations
[AD-A268128] p 1171 N94-17521
EQUIVALENT CIRCUITS
Circle diagram approach for self excited induction generators
[DE93-010031] p 1010 N94-15971
Determination of equivalent circuit for PVDF shock-pressure gauges
[DE93-016492] p 1034 N94-16452
ERBIUM
Rare earth doped III-V semiconductors for optoelectronics
[AD-A268279] p 1216 N94-17577
ERBIUM COMPOUNDS
Ion doped quantum well lasers
[AD-A267198] p 1038 N94-15853
EROSION
Louisiana delta study
[NASA-TM-109622] p 1095 N94-15408
Fluvial erosion on Mars: Implications for paleoclimatic change p 1241 N94-16210
ASRM nozzle thermal analysis
[NASA-CR-194672] p 928 N94-17277
ERROR ANALYSIS
A posteriori error estimation for hierarchic models of elliptic boundary value problems on thin domains
[AD-A267714] p 1168 N94-14939
Compact disk error measurements
p 1227 N94-14988
An uncertainty analysis of inlet dynamic flow distortion using an analog/digital hybrid editing system
[AD-A266924] p 855 N94-15105
Fault management for data systems
[NASA-TM-103953] p 1116 N94-15548
Generation of artificial helioseismic time-series
[NASA-CR-194612] p 1299 N94-15968
Interferometric GPS attitude: A stochastic error model, DREO report
[AD-A266411] p 864 N94-16457
The multivariate optimum interpolation analysis of meteorological data at the Fleet Numerical Oceanography Center
[AD-A266459] p 1106 N94-16568
Set-based Bayesianism
[TR-407] p 1170 N94-16582
TIMS performance evaluation summary
p 1063 N94-16596
Abundance recovery error analysis using simulated AVIRIS data p 1074 N94-16708
Maximum likelihood techniques applied to quasi-elastic light scattering
[NASA-CR-193550] p 1192 N94-16718
Processing of resonance parameter covariance files
[DE93-015506] p 1231 N94-16874
On the a-posteriori estimation of the modelling error for the heat conduction in a plate and its use for adaptive hierarchic modelling
[AD-A267965] p 1029 N94-17384
ERROR CORRECTING CODES
Adaptive beamforming with imperfect arrays: Pattern effects and their partial correction
[AD-A267079] p 987 N94-15541
ERROR CORRECTING DEVICES
Ring lens focusing and push-pull tracking scheme for optical disk systems p 1227 N94-14990
ERRORS
Efficiency effects of variation in controlled experimental variables
[DE93-014345] p 1169 N94-15979
Manufacturing tolerance requirements for frequency selective surfaces
[AD-A266541] p 999 N94-16797
Ensemble forecasting techniques in medium-range forecasting
[AD-A267443] p 1107 N94-17029
Effects of inspection error on optimal inspection policies and software fault detection models
[AD-A267511] p 1153 N94-17075
Hypervelocity orbital intercept guidance using certainty control
[AD-A267297] p 1174 N94-17219
On the a-posteriori estimation of the modelling error for the heat conduction in a plate and its use for adaptive hierarchic modelling
[AD-A267965] p 1029 N94-17384
ERS-1 (ESA SATELLITE)
The laboratory performance of the short wavelength instrument for the Along Track Scanning Radiometer ATSR-2 (initial results) p 908 N94-15088
Laser ranging network performance and routine orbit determination at D-PAF p 911 N94-15554
On the accuracy of ERS-1 orbit predictions
p 874 N94-15589
ERS-1: 18 months in orbit p 990 N94-15888
Calibration: Practical experience with ERS-1
p 992 N94-15907
ERYTHROCYTES
Hemoglobin
[AD-A266455] p 1123 N94-16566
ESCAPE SYSTEMS
Crew escape certification test
[NASA-TM-109530] p 1136 N94-15392
ESTIMATES
Estimates of lithospheric thickness on Venus
p 1267 N94-16277
ESTIMATING
Space Station Facility government estimating
[NASA-TM-109324] p 1223 N94-15545
Estimating and bidding for the Space Station Processing Facility
[NASA-TM-109323] p 1223 N94-15546
Application of the robust estimate in SLR data preprocessing p 918 N94-15597
Development and analysis of ARMA parameter estimation schemes in the presence of noise
[AD-A267184] p 989 N94-15786
High order nonlinear estimation with signal processing applications
[AD-A268407] p 1005 N94-17463
ESTIMATORS
Application of the robust estimate in SLR data preprocessing p 918 N94-15597
ETA-MESONS
Past, present and future ((pi),(eta)) experiments
[DE93-016631] p 1182 N94-16115
ETCHANTS
Selective formation of porous silicon
[NASA-CASE-NPO-18735-1-CU] p 966 N94-15960
ETCHING
Selective formation of porous silicon
[NASA-CASE-NPO-18735-1-CU] p 966 N94-15960
Aberration correction of unstable resonators
[NASA-CASE-NPO-18791-1-CU] p 1034 N94-15987
Atomic layer epitaxy of boron nitride
[AD-A266260] p 1212 N94-16932
Structural characterization of epitaxial layers for infrared detectors
[AD-A267875] p 940 N94-17013
Nitride semiconductors for ultraviolet detection
[AD-A267877] p 1012 N94-17040
Scattering from binary optics p 1195 N94-17341
Diffractive optics fabricated by direct write methods with an electron beam p 1196 N94-17347
Phase holograms in PMMA with proximity effect correction p 1037 N94-17348
Curved grating fabrication techniques for concentric-circle grating, surface-emitting semiconductor lasers p 1045 N94-17349
Fabrication of micro-optical devices
p 1197 N94-17351
Predesign of diamond turned refractive/diffractive elements for IR objectives p 1198 N94-17359
Low voltage electron beam lithography
[AD-A267865] p 1215 N94-17389
Diamond growth on carbide surfaces using a selective etching technique
[AD-A267989] p 973 N94-17413
ETHERS
Encapsulation of hemoglobin in non-phospholipid vesicles
[AD-A266505] p 1128 N94-16785
High octane ethers from synthesis gas-derived alcohols
[DE93-016861] p 975 N94-16898
ETHYL ALCOHOL
An advanced bioprocessing concept for the conversion of wastepaper to ethanol
[DE93-015209] p 975 N94-16807
ETHYLENE
Application of non-thermal plasmas to pollution control
[DE93-016432] p 1096 N94-16449
ETHYLENE COMPOUNDS
Contained liquids in microgravity, part 2
p 979 N94-16085
EUCLIDEAN GEOMETRY
Multi-resolution processing for fractal analysis of airborne remotely sensed data p 1065 N94-16604
EULER EQUATIONS OF MOTION
On the stability analysis of approximate factorization methods for 3D Euler and Navier-Stokes equations
[NASA-TM-106314] p 1169 N94-15818
Flow analysis for the nacelle of an advanced ducted propeller at high angle-of-attack and at cruise with boundary layer control
[NASA-TM-106371] p 858 N94-16571
Accurate upwind methods for the Euler equations
[NASA-TM-106388] p 1170 N94-16882
Study into the limits of an Euler equation method applied to leading-edge vortex flow
[NLR-TP-91350-U] p 1031 N94-17627
EURECA (ESA)
Third LDEF Post-Retrieval Symposium Abstracts
[NASA-CP-10120] p 1303 N94-16495
Looking at science on board Eureca
[ESA-BR-80] p 874 N94-16584
EUROPE
Developments in the European air traffic control
p 853 N94-15124
A geological and geophysical information system for Eurasia
[AD-A267841] p 1232 N94-17036
EUROPEAN COMMUNICATIONS SATELLITE
ECS: Ninth year in orbit
[ESA-BR-91] p 987 N94-15644
EUROPEAN SPACE AGENCY
The definition of a scientific policy: ESRO's satellite programme in 1969-1973
[ESA-HSR-6] p 1303 N94-16500
Choosing ESRO's first scientific satellites
[ESA-HSR-3] p 887 N94-16523
The early development of the Telecommunications Satellite Programme in ESRO (1965-1971)
[ESA-HSR-9] p 887 N94-16525
Europe in space: Edoardo Amaldi and the inception of ESRO
[ESA-HSR-5] p 1303 N94-16526
The ESA Tele-Invoicing System (ETIS)
[ESA-INT-6] p 1150 N94-16591
Europe into space: The Auger years (1959-1967)
[ESA-HSR-8] p 1303 N94-16592
The early activities of the COPERS and the drafting of the ESRO Convention (1961/62)
[ESA-HSR-4] p 1225 N94-16593

Resources and activities of the European Space Agency p 1303 N94-16792
Small missions for space science p 874 N94-17142

EUROPEAN SPACE PROGRAMS
Absolute Radiometric Measurements in Space: ARMS p 908 N94-15085
The ESA telescience program p 977 N94-16073
Europe into space: The Auger years (1959-1967) [ESA-HSR-8] p 1303 N94-16592
The early activities of the COPERS and the drafting of the ESRO Convention (1961/62) [ESA-HSR-4] p 1225 N94-16593
Strategy for a small satellite program and a proposal for a first mission p 874 N94-17143

EUTECTICS
Phase equilibria of the magnesium sulfate-water system to 4 kbars p 953 N94-16247
Hydride-containing molten salts and their technology implications [AD-A266458] p 1092 N94-16567

EVALUATION
Helicopter structures: A review of loads, fatigue design techniques, and usage monitoring [AD-A267115] p 866 N94-15651
Software Capability Evaluation (SCE) version 1.5 method description. Software capability evaluation project [AD-A267895] p 1154 N94-17395

EVAPORATION
Evaporation from a meniscus within a capillary tube in microgravity [NASA-CR-194593] p 976 N94-15654
The group A3 chondrules of Krymka: Further evidence for major evaporative loss during the formation of chondrules p 1242 N94-16257
Evaporation kinetics of Mg2SiO4 crystals and melts from molecular dynamics simulations p 1219 N94-16331
Possible sources of H2 to H2O enrichment at evaporation of parent chondritic material p 1244 N94-16377

EVAPORATORS
Cycle performance testing of nonazeotropic mixtures of HFC-142A/HCFC-124 and HFC-32/HCFC-124 with enhanced surface heat exchangers [DE93-015215] p 1024 N94-16808

EVAPOTRANSPIRATION
Evapotranspiration and runoff from large land areas: Land surface hydrology for atmospheric general circulation models p 1083 N94-16029
A detailed model for simulation of catchment scale subsurface hydrologic processes [PAPER-92WR02333] p 1084 N94-16032
Effects of spatial variability and scale on areal -average evapotranspiration p 1084 N94-16033
Scaling, soil moisture and evapotranspiration in runoff models p 1084 N94-16034
Empirical relationships among atmospheric variables from rawinsonde and field data as surrogates for AVIRIS measurements: Estimation of regional land surface evapotranspiration p 1074 N94-16712

EXCAVATION
Petrologic constraints on the surface processes on asteroid 4 Vesta and on excavation depths of diogenite fragments p 1241 N94-16208
A measurement station for study of Earth moving tools and ground cutting processes [IFTR-10/1991] p 985 N94-17068

EXCIMER LASERS
Laser artery repair [NASA-TM-109604] p 1120 N94-15312
Ablation, surface activation, and electroless metallization of insulating materials by pulsed excimer laser irradiation [DE93-015808] p 1040 N94-16664
Sodium-mercury excimer laser, phase 1 [AD-A267728] p 1042 N94-17230

EXCITATION
Preparation and investigation of improved low voltage electron excitable phosphors [AD-A266852] p 963 N94-14948
Field observations of infragravity, sea and swell directional spectra [AD-A266439] p 1113 N94-16561

EXCITONS
Scintillation mechanism in stoichiometric cerium compounds [DE93-015499] p 948 N94-16771
Lattice relaxation theory of localized excitations in quasi-one-dimensional systems [DE93-624947] p 1215 N94-17437

EXERCISE PHYSIOLOGY
Validation of respiratory inductive plethysmography for measuring exercise tidal volumes [AD-A266883] p 1119 N94-14923
Living well in space: Ensuring crew capability [NASA-TM-109538] p 1120 N94-15369
Metabolic monitoring of hypobaric subjects [AD-A268221] p 1130 N94-17554
Methods to obtain blood samples periodically during exercise research studies while subjects are immersed in water or otherwise inaccessible [AD-A268227] p 1130 N94-17562

EXHAUST CLOUDS
Plume primary smoke p 923 N94-15218

EXHAUST EMISSION
Rocket Motor Plume Technology [AGARD-LS-188] p 923 N94-15217
Microwave properties and systems overview p 924 N94-15222
New York MARKAL: An evaluation of carbon dioxide emission control strategies in New York State [DE93-013149] p 1095 N94-15999
Utility emissions associated with electric and hybrid vehicle (EHV) charging [DE93-013734] p 1011 N94-16459
Emissions of volatile organic compounds from stationary combustion sources: Numerical modeling capabilities [DE93-014123] p 1096 N94-16825

EXHAUST GASES
Scholarly research program in fuel analysis and combustion research [AD-A266789] p 942 N94-14911
Flight-determined engine exhaust characteristics of an F404 engine in an F-18 airplane [NASA-TM-4538] p 869 N94-15141
Propulsion p 924 N94-15219
Secondary smoke p 924 N94-15220
Microwave properties and systems overview p 924 N94-15222
Plume radiation p 924 N94-15223
Application of non-thermal plasmas to pollution control [DE93-016432] p 1096 N94-16449
Emissions of volatile organic compounds from stationary combustion sources: Numerical modeling capabilities [DE93-014123] p 1096 N94-16825

EXHAUST NOZZLES
Flight-determined engine exhaust characteristics of an F404 engine in an F-18 airplane [NASA-TM-4538] p 869 N94-15141
Equations of motion of a hinged body over a spherical earth [AD-A268408] p 868 N94-17435

EXISTENCE THEOREMS
Bandwidth efficient coding: Theoretical limits and real achievements. Error control techniques for satellite and space communications p 997 N94-16507

EXOBIOLOGY
Living well in space: Ensuring crew capability [NASA-TM-109538] p 1120 N94-15369
STS-40 crew during spacelab Sim [NASA-TM-109493] p 876 N94-15452
Mars exobiology landing sites for future exploration p 1278 N94-16339
Aerospace medicine and biology: A continuing bibliography with indexes (supplement 378) [NASA-SP-7011(378)] p 1122 N94-16478
Aerospace medicine and biology: A continuing bibliography with indexes (supplement 380) [NASA-SP-7011(380)] p 1122 N94-16479
Publications of the Exobiology Program for 1991: A special bibliography [NASA-TM-4483] p 1139 N94-17017
The 1990-1991 NASA space biology accomplishments [NASA-TM-4501] p 1118 N94-17257
Design of an experiment hardware for the ESA space facility BIOPAN [DLR-FB-93-06] p 876 N94-17548

EXPERIMENT DESIGN
STS-29 crew with student experiment [NASA-TM-109545] p 1116 N94-15378
Science operation in space: Lessons [NASA-TM-109502] p 881 N94-15466
Autogenic-Feedback Training (AFT) as a preventive method for space motion sickness: Background and experimental design [NASA-TM-108780] p 1120 N94-15537
PHENIX Conceptual Design Report [DE93-015759] p 1182 N94-16161
Fluid flow and heat convection studies for actively cooled airframes [NASA-CR-194624] p 1024 N94-16491
Lithium D-cell study [NASA-CR-192705] p 1011 N94-16505
Principal investigators data package for Project Initiation Conference (PIC): EUVS sounding rocket no. 36.117CL. Target: Venus [NASA-CR-194663] p 923 N94-17126
Design of an experiment hardware for the ESA space facility BIOPAN [DLR-FB-93-06] p 876 N94-17548

EXPERIMENTATION
On the 17-keV neutrino [DE93-012638] p 1181 N94-15974

EXPERT SYSTEMS
Development of a computer supported instrumentation for economic planning and evaluation of production facilities for fiber reinforced composites elements p 932 N94-15260
An expert system shell for inferring vegetation characteristics: Atmospheric techniques (Task G) [NASA-CR-194570] p 1082 N94-15531
Krupp technical reports no. 2, English edition, October 1992 [ETN-93-94631] p 984 N94-16000
Expert system for welding engineering p 984 N94-16003
KBSA concept demo [AD-A267054] p 1166 N94-16770
Intelligent use of CFAR algorithms [AD-A267755] p 1003 N94-17206

EXPLOSIONS
Explosive boiling at very low heat fluxes: A microgravity phenomenon [NASA-TM-106325] p 1046 N94-15817
Laser weld repair of tantalum sheet [DE93-016417] p 1041 N94-16871

EXPLOSIVES
Experimental investigations into the deflagration to detonation transition at TNO/PML [AD-A266753] p 1021 N94-15755
Simulation of collisional fragmentation with explosives p 1063 N94-16254
Densifying and stabilizing ingredient [AD-D015751] p 975 N94-16934

EXPOSURE
Analytical and experimental investigation of the feasibility of accelerated lifetime testing of materials exposed to an atomic oxygen beam [NASA-CR-193851] p 946 N94-15766
Environmental effects on iron aluminides [DE93-015820] p 958 N94-16166
Al-26-Mg-26 ages of iron meteorites p 1242 N94-16240
Composition of weakly altered Martian crust p 1296 N94-16436
Arsenic surveillance program p 1127 N94-16637
Asbestos Surveillance Program p 1127 N94-16638
Lead Surveillance Program p 1127 N94-16640
Mercury Surveillance Program p 1127 N94-16641
Respiratory Protection Program medical clearance for respirator use p 1127 N94-16642
OSHA bloodborne pathogens standards exposure control plan p 1127 N94-16645
Quantifying lifetime exposure to ultraviolet radiation in the epidemiology of cutaneous malignant melanoma: A pilot study [DE93-015274] p 1128 N94-16812
TransRapid TR-07 maglev-spectrum magnetic field effects on daily pineal indoleamine metabolic rhythms in rodents [DE93-015143] p 1117 N94-16893
Performance of silvered Teflon thermal control blankets on spacecraft [AD-A266284] p 887 N94-16909
Aircraft carrier exposure tests of cast magnesium alloys [AD-A268260] p 962 N94-17418
Currents induced in the human body for exposure to ultrawideband electromagnetic pulses [AD-A268570] p 1130 N94-17621

EXTERNAL TANKS
Ground integrated ET-derived space platforms for onorbit applications [TABES PAPER 93-652] p 899 N94-16152

EXTINCTION
Atmospheric transmittance between 1.0 and 2.0 micrometers [AD-A267076] p 1098 N94-15539

EXTRACTION
HyperVentilate: Decision-support software for soil vapor extraction technology application [PB93-134880] p 1094 N94-15136
Extraction and isotopic analysis of medium molecular weight hydrocarbons from Murchison using supercritical carbon dioxide p 1241 N94-16184
Extraction of quantitative surface characteristics from AIRSAR data for Death Valley, California p 1078 N94-16748
Surface reactivity of combustion generated soot particles [AD-A268017] p 952 N94-17532

EXTRAPOLATION
Nowcasting methods for satellite imagery [AD-A267294] p 1108 N94-17267

EXTRATERRESTRIAL ENVIRONMENTS
Publications of the Exobiology Program for 1991: A special bibliography
[NASA-TM-4483] p 1139 N94-17017
EXTRATERRESTRIAL INTELLIGENCE
Search for Extraterrestrial Intelligence (SETI)
p 1125 N94-16620
EXTRATERRESTRIAL LIFE
Pioneer-Venus press clip --- Solar System formation and extraterrestrial life
[NASA-TM-109425] p 1239 N94-15495
Publications of the Exobiology Program for 1991: A special bibliography
[NASA-TM-4483] p 1139 N94-17017
EXTRATERRESTRIAL RADIATION
Fault handling schemes in electronic systems with specific application to radiation tolerance and VLSI design
[NASA-CR-194559] p 1008 N94-15640
Shielding from space radiations
[NASA-CR-194578] p 1180 N94-15715
Real time radiation measurements in space
p 980 N94-16092
Preliminary results from bubble detector measurements aboard Biocosmos-2044 p 981 N94-16097
Shielding from space radiations
[NASA-CR-194664] p 1301 N94-17255
EXTRAVEHICULAR ACTIVITY
STS-35 crew training: EMU walk through and EVA prep and post
[NASA-TM-109488] p 1134 N94-15194
Future of robotics
[NASA-TM-109592] p 1045 N94-15284
STS-37 CETA evaluation with Ross
[NASA-TM-109495] p 1135 N94-15330
STS-26 EVA rescue training
[NASA-TM-109563] p 875 N94-15333
STS-29 EVA prep in FFT
[NASA-TM-109544] p 1135 N94-15375
STS-32 LDEF EVA training in WETF with Low and Dunbar
[NASA-TM-109473] p 1135 N94-15377
STS-28 Adamson and Brown EMU walk through
[NASA-TM-109549] p 1136 N94-15387
STS-33 EVA prep and post with Gregory, Blaha, Carter, Thorton, and Musgrave in FFT
[NASA-TM-109469] p 881 N94-15398
STS-38 crew training: Habitation equipment procedures, bailout in CCT, 70mm photo class, EVA prep and post, and firefighting
[NASA-TM-109494] p 1136 N94-15453
EVA retriever demonstration
[NASA-TM-109510] p 1046 N94-15456
STS-37 astronauts Ross and Apt during CETA hardware checkout
[NASA-TM-109496] p 1137 N94-15460
STS-36 crew EVA prep and post-training, bailout exercises, final bench review
[NASA-TM-109498] p 1137 N94-15462
Investigation of the effects of extravehicular activity (EVA) gloves on performance
[NASA-TP-3401] p 1137 N94-15717
Ground integrated ET-derived space platforms for onorbit applications
[TABES PAPER 93-652] p 899 N94-16152
Force-endurance capabilities of extravehicular activity (EVA) gloves at different pressure levels
[NASA-TP-3420] p 1139 N94-17653
EXTRAVEHICULAR MOBILITY UNITS
STS-35 crew training: EMU walk through and EVA prep and post
[NASA-TM-109488] p 1134 N94-15194
STS-28 Adamson and Brown EMU walk through
[NASA-TM-109549] p 1136 N94-15387
STS-27 EMU and RMS contingency training
[NASA-TM-109550] p 1136 N94-15401
EXTREME ULTRAVIOLET RADIATION
Microchannel plate detectors for space astronomy
p 901 N94-15038
Developments in extreme ultraviolet and x ray instrumentation p 904 N94-15058
A test facility to calibrate EUV detectors
p 873 N94-15062
Absolute, Extreme-Ultraviolet Solar Spectral Irradiance Monitor (AESSIM)
[AD-A267045] p 1299 N94-15836
EUVE observations of the Moon p 1250 N94-16185
Principal investigators data package for Project Initiation Conference (PIC): EUVS sounding rocket no. 36.117CL. Target: Venus
[NASA-CR-194663] p 923 N94-17126
EXTREMELY HIGH FREQUENCIES
The ACTS propagation program p 995 N94-16039
EXTRUDING
The effect of oxygen, grain size, and strain rate on the mechanical behavior of forged P/M tantalum
[DE93-011251] p 959 N94-16764
EYE MOVEMENTS
Human ocular torsion during parabolic flight: An investigation using electromagnetic scleral search coil
p 981 N94-16096
Visually guided touching and manual tracking
[TR-412] p 1166 N94-16581
Reference frames in vision
[AD-A266174] p 1132 N94-16925
EYE PROTECTION
Micro pulse laser radar
[NASA-CASE-GSC-13493-1] p 1004 N94-17322
EYEPIECES
Optical displays: A tutorial on images and image formation
[AD-A266230] p 1192 N94-16926

F

F REGION
A physical model for one-dimension and time-dependent ionosphere. Part 2: Results and discussions
[DE93-627959] p 1103 N94-17631
F-16 AIRCRAFT
In-flight investigation of a rotating cylinder-based structural excitation system for flutter testing
[NASA-TM-4512] p 867 N94-15783
Flight simulator-induced sickness and visual displays evaluation
[AD-A267019] p 1122 N94-15845
Adaptive algorithm for aircraft configuration in turbulent flow
[AD-A266188] p 867 N94-16122
F-18 AIRCRAFT
Flight-determined engine exhaust characteristics of an F404 engine in an F-18 airplane
[NASA-TM-4538] p 869 N94-15141
Wind tunnel investigations of forebody strakes for yaw control on F/A-18 model at subsonic and transonic speeds
[NASA-TP-3360] p 859 N94-16573
FABRICATION
Construction, testing, and representation of resin and fiber reinforced materials p 931 N94-15255
Machine development p 932 N94-15258
Design and fabrication of a reflection far ultraviolet polarizer and retarder
[NASA-CR-194630] p 1191 N94-16023
Fabrication and phase tuning of an optical waveguide device
[AD-D015815] p 1191 N94-16489
Continuous fabrication of SiC fiber tows by chemical vapor deposition
[AD-A266460] p 936 N94-16569
Fabrication of advanced design (grooved) cermet anodes
[DE93-014590] p 1012 N94-16765
The Ceramic Technology Project: Ten years of progress
[DE93-015991] p 968 N94-16843
Conference on Binary Optics: An Opportunity for Technical Exchange
[NASA-CP-3227] p 1194 N94-17331
Binary optics: Trends and limitations
p 1194 N94-17333
Diffractive optics: Design, fabrication, and applications
p 1194 N94-17334
Fabricating binary optics: An overview of binary optics process technology p 1195 N94-17343
Binary optics at Hughes Danbury Optical Systems
p 1195 N94-17344
Fabrication techniques for very fast diffractive lenses
p 1196 N94-17345
Laser figuring for the generation of analog micro-optics and kineform surfaces p 1196 N94-17346
Diffractive optics fabricated by direct write methods with an electron beam p 1196 N94-17347
Phase holograms in PMMA with proximity effect correction p 1037 N94-17348
Curved grating fabrication techniques for concentric-circle grating, surface-emitting semiconductor lasers p 1045 N94-17349
Fabrication of micro-optical devices
p 1197 N94-17351
Low cost paths to binary optics p 1197 N94-17353
Measurements of microlens performance
p 1197 N94-17355
Predesign of diamond turned refractive/diffractive elements for IR objectives p 1198 N94-17359
Color separation gratings p 1198 N94-17362
Rare earth doped III-V semiconductors for optoelectronics
[AD-A268279] p 1216 N94-17577
FABRICS
Production process p 931 N94-15257
FIBER-TEX 1992: The Sixth Conference on Advanced Engineering Fibers and Textile Structures for Composites
[NASA-CP-3211] p 936 N94-16845
Weaving multi-layer fabrics for reinforcement of engineering components p 937 N94-16850
New textile composite materials development, production, application p 938 N94-16853
FABRY-PEROT INTERFEROMETERS
The feasibility of tropospheric and total ozone determination using a Fabry-Perot interferometer as a satellite-based nadir-viewing atmospheric sensor
[NASA-TM-109342] p 1102 N94-17214
FACE CENTERED CUBIC LATTICES
Electronic structure and enthalpy of hydrogen and helium mixtures
[DE93-014128] p 1208 N94-15976
Evolution of microstructure in face centered cubic metals during irradiation: A review
[DE93-015682] p 958 N94-16662
FACILITIES
Short walk to everywhere --- Space, Earth, Ocean Center
[NASA-TM-109541] p 1221 N94-15372
Building 46 grand opening
[NASA-TM-109524] p 875 N94-15386
CORE/TRC
[NASA-TM-109434] p 1221 N94-15418
Challenger Center
[NASA-TM-109432] p 1221 N94-15504
Challenger Center: Orientation
[NASA-TM-109433] p 1221 N94-15505
Proceedings of the 1992 Annual Meeting NASA Occupational Health Program
[NASA-CR-193462] p 1123 N94-16609
New health and safety initiatives at the Department of Energy (DOE) p 1124 N94-16610
Illness/injury pattern complex 40 (Titan)
p 1125 N94-16625
Summary of follow-up results from potential tuberculosis exposures p 1126 N94-16628
Johnson Space Center health related fitness program
p 1126 N94-16633
Kennedy Space Center exercise program
p 1126 N94-16634
The Langley Fitness Center p 1126 N94-16635
Physical Exercise Program p 1127 N94-16636
Arsenic surveillance program p 1127 N94-16637
Asbestos Surveillance Program p 1127 N94-16638
Hearing Conservation Medical Program
p 1127 N94-16639
Lead Surveillance Program p 1127 N94-16640
Respiratory Protection Program medical clearance for respirator use p 1127 N94-16642
General Medical Surveillance Program
p 1127 N94-16643
FACTORIAL DESIGN
An analysis of tactical airlifter characteristics and their impact on theater airlift system performance
[AD-A266719] p 866 N94-15731
FACTORIZATION
Decomposition of large sparse symmetric systems for parallel computation. Part 2: Parallelization tool roadmap
[AD-A267072] p 1158 N94-15671
On the stability analysis of approximate factorization methods for 3D Euler and Navier-Stokes equations
[NASA-TM-106314] p 1169 N94-15818
FAILURE
General Monte Carlo reliability simulation code including common mode failures and HARP fault/error-handling
[NASA-CR-187587] p 1150 N94-16594
A ten year review of performance of photovoltaic systems
[DE93-015649] p 1093 N94-17217
FAILURE ANALYSIS
Software reliability through fault-avoidance and fault-tolerance
[NASA-CR-194353] p 1143 N94-15114
Concepts on measuring the benefits of software process improvements
[AD-A266994] p 1144 N94-15215
Remote diagnosis as used for mechanized parking systems p 984 N94-16004
Materials, processes, and environmental engineering network
[TABES PAPER 93-610] p 1051 N94-16142
Elastooptical brittle materials in experimental studies of the state of stress and deformation
[IFTR-22/1991] p 1059 N94-16651

A fuzzy method for preliminary design random access memory failure rate prediction
[AD-A267948] p 1055 N94-17044
Static and dynamic investigations of brittle elasto-optical material
[IFTR-3/1992] p 1061 N94-17086
Dynamic testing and characterization of pre-fractured ceramic
[DE93-016457] p 972 N94-17238
X ray computed tomography for failure analysis investigations
[AD-A268086] p 1055 N94-17515

FAILURE MODES
Slidesurfaces with adaptive new definitions (SAND) for transient analysis
[DE93-014909] p 1059 N94-15983
General Monte Carlo reliability simulation code including common mode failures and HARP fault/error-handling
[NASA-CR-187587] p 1150 N94-16594
Quantification of processing artifacts in textile composites p 939 N94-16860
Reliability analysis of Surface Mount Technology (SMT)
[AD-A267598] p 1055 N94-17194

FAINT OBJECTS
A typical pointed observation in IRAS designed to fit into a 15 minute window
[NASA-CR-194653] p 1199 N94-17443

FALSE ALARMS
Intelligent use of CFAR algorithms
[AD-A267755] p 1003 N94-17206

FAR FIELDS
Mathmatical modeling for diffractive optics p 1195 N94-17342
How to deduce the far field of an antenna from planar near-field measurements
[NPL-DES-123] p 1006 N94-17545

FAR INFRARED RADIATION
Photoconductors and arrays for the far-infrared p 902 N94-15045
BIB photodetectors based on antimony doped silicon p 902 N94-15047
Optimisation of FIR photoconductors for atmospheric spectroscopy p 902 N94-15048
Submm/FIR bolometers p 904 N94-15056
Performance testing of doped-germanium photoconductors for the ISO long wavelength spectrometer p 905 N94-15066
Non-linear effects in doped-germanium photoconductors for the ISO long wavelength spectrometer p 905 N94-15067
Ionising radiation-induced effects in doped germanium FIR photoconductors p 907 N94-15077
Search for far infrared radiation from optically pumped defect modes
[AD-A266744] p 1206 N94-15822

FAR ULTRAVIOLET RADIATION
Filters for the International Solar Terrestrial Physics (ISTP) mission far ultraviolet imager
[NASA-CR-194633] p 1190 N94-15868
Multilayer thin film design for far ultraviolet polarizers using an induced transmission and absorption technique
[NASA-CR-194631] p 1190 N94-15869
Design and fabrication of a reflection far ultraviolet polarizer and retarder
[NASA-CR-194630] p 1191 N94-16023
Transparent conductive coatings in the far ultraviolet
[NASA-CR-194632] p 1191 N94-16024
VUV thin films, chapter 7
[NASA-CR-194634] p 967 N94-16494

FARADAY EFFECT
A method of detecting and locating electrical current imbalances
[NASA-CASE-LEW-15407-1] p 1009 N94-15706

FARM CROPS
MAC Europe 1991: Evaluation of AVIRIS, GER imaging spectrometry data for the land application testsite Oberpfaffenhofen p 1070 N94-16688
The dynamics of hydroponic crops for simulation studies of the CELSS initial reference configurations
[NASA-CR-194654] p 1118 N94-17279

FAST FOURIER TRANSFORMATIONS
Fast algorithms for polynomial interpolation, integration and differentiation
[AD-A267505] p 1154 N94-17370
Fast Fourier Transforms for nonequispaced data 2
[AD-A268383] p 1171 N94-17420

FASTENERS
Connector systems for structures
[NASA-CASE-MSC-21998-1] p 1046 N94-15707
Attachment device
[NASA-CASE-MSC-21885-1] p 1047 N94-15925

FATIGUE (MATERIALS)
The influence of thermal aging on the microstructure and fatigue properties of modified 9Cr-1Mo steel
[DE93-015489] p 957 N94-16106
The processing and mechanical properties of high temperature/high performance composites. Book 3: Coonstituent properties and macroscopic performance
[AD-A266396] p 935 N94-16485
Micromechanisms of monotonic and cyclic subcritical crack growth in advanced high melting point low-ductility intermetallics
[AD-A267764] p 961 N94-17223
The effect of electric discharge machined notches on the fracture toughness of several structural alloys
[AD-A268605] p 962 N94-17464
Environment enhanced fatigue crack propagation in metals: Inputs to fracture mechanics life prediction models
[NASA-CR-191538] p 942 N94-17638

FATIGUE LIFE
Helicopter structures: A review of loads, fatigue design techniques, and usage monitoring
[AD-A267115] p 866 N94-15651
The influence of secondary bending on fatigue life improvement in bolted joints
[ARL-RR-14] p 1058 N94-15963
Ion implantation effects on surface-mechanical properties of metals and polymers
[DE93-014661] p 958 N94-16453
Fatigue life program using strain-life methods
[AD-A267310] p 1060 N94-16943
Mean strain effects on the strain life fatigue curve
[AD-A267211] p 960 N94-16984
Application of hard coatings to substrates at low temperatures
[NASA-CR-193867] p 971 N94-17122
Overview of the FAA/DCA/NLR programs related to ageing aircraft
[NLR-TR-92119-U] p 854 N94-17614

FATIGUE TESTS
Systematic study of effects of load misalignment in uniaxial low cycle fatigue testing at high temperatures
[NPL-DMM(A)-27] p 1057 N94-15015
Fracture toughness tests for particulate MMC UK COSI (IACFA) task group. Meeting report, October 1992
[NPL-DMM(A)-81] p 1057 N94-15021
Crack-tip-opening angle measurements and crack tunneling under stable tearing in thin sheet 2024-T3 aluminum alloy
[NASA-CR-191523] p 931 N94-15184
Helicopter structures: A review of loads, fatigue design techniques, and usage monitoring
[AD-A267115] p 866 N94-15651
Laser-shock damage of iron-based materials
[AD-A267196] p 1038 N94-15852
Mean strain effects on the strain life fatigue curve
[AD-A267211] p 960 N94-16984
RSRM nozzle actuator bracket/lug fracture mechanics qualification test
[NASA-CR-193859] p 927 N94-17080
A review of Australian and New Zealand investigations on aeronautical fatigue during the period April 1991 to March 1993
[AD-A267532] p 868 N94-17117
Application of hard coatings to substrates at low temperatures
[NASA-CR-193867] p 971 N94-17122

FAULT DETECTION
Understanding partitions and the no partition assumption
[AD-A266296] p 1000 N94-16911
Effects of inspection error on optimal inspection policies and software fault detection models
[AD-A267511] p 1153 N94-17075

FAULT TOLERANCE
Software reliability through fault-avoidance and fault-tolerance
[NASA-CR-194353] p 1143 N94-15114
A formal language for the specification and verification of synchronous and asynchronous circuits
[NASA-CR-191509] p 1144 N94-15443
Reactive system verification case study: Fault-tolerant transputer communication
[NASA-TM-108784] p 1145 N94-15538
Altitude deviations: Breakdowns of an error-tolerant system
[NASA-TM-108788] p 862 N94-15550
The design of self-checking reduced instruction set computers
[AD-A267012] p 1140 N94-15763
General Monte Carlo reliability simulation code including common mode failures and HARP fault/error-handling
[NASA-CR-187587] p 1150 N94-16594
A security architecture for fault-tolerant systems
[AD-A266178] p 1152 N94-16982
Fault-tolerant architectures for multiprocessor and VLSI-based systems
[AD-A267370] p 1140 N94-17005
Estimating task execution delay in a real-time system via static source code analysis
[AD-A267496] p 1161 N94-17367
Tutorial: Advanced fault tree applications using HARP
[NASA-TM-102747] p 1155 N94-17447
Verification of fault-tolerant clock synchronization systems
[NASA-TP-3349] p 1161 N94-17449
NASA Lewis Meshed VSAT Workshop meeting summary
[NASA-TM-106332] p 883 N94-17487
System performance modeling and analysis of a fault-tolerant, real time parallel processor
[AD-A268070] p 1162 N94-17551

FAULT TREES
Fault management for data systems
[NASA-TM-103953] p 1116 N94-15548
Tutorial: Advanced fault tree applications using HARP
[NASA-TM-102747] p 1155 N94-17447

FAYALITE
Olivines in the Kaba carbonaceous chondrite and constraints on their formation p 1219 N94-16255

FEASIBILITY
Distributed computing feasibility in a non-dedicated homogeneous distributed system
[NASA-CR-191532] p 1149 N94-15989
Center of Excellence in Laser Medicine
[DE93-016541] p 1122 N94-16113
The 3D-Flow processor for a programmable level-1 trigger (feasibility study)
[DE93-016045] p 1159 N94-16172

FEASIBILITY ANALYSIS
A feasibility study of a microgravity enhancement system for Space Station Freedom
[NASA-CR-191550] p 886 N94-15864
Liquid Oxygen (LO2) propellant conditioning concept testing
[TABES PAPER 93-621] p 976 N94-16146
Category (CAT) 3B level 1 test plan for Global Positioning System (GPS)
[DOT/FAA/RD-93/21] p 864 N94-16835

FEDERAL BUDGETS
Space Shuttle main engine. NASA has not evaluated the alternate fuel turbopump costs and benefits. Report to the Administrator of the National Aeronautics and Space Administration
[GAO/NSIAD-94-54] p 926 N94-16834

FEED SYSTEMS
Liquid hydrogen and liquid oxygen feedline passive recirculation analysis
[TABES PAPER 93-620] p 1031 N94-16145

FEEDBACK
Questioning mechanisms during tutoring, conversation, and human-computer interaction
[AD-A266199] p 1137 N94-16108
Active probing of plasma edge turbulence and feedback studies on the Texas experimental tokamak (TEXT)
[DE93-015799] p 1202 N94-16162
Controlling chaotic behavior in CO2 and other lasers
[AD-A266431] p 1040 N94-16546

FEEDBACK CONTROL
YARF: An open-ended framework for robot road following
[AD-A266788] p 1163 N94-14910
Development of an air-to-air refueling automatic flight control system using quantitative feedback theory
[AD-A266718] p 870 N94-15730
The design and analysis of robust feedback systems
[AD-A267152] p 1165 N94-15778
A new feedback system for instruments equipped with a capacitive transducer p 1037 N94-15802
Adaptive weld control for high-integrity welding applications
[TABES PAPER 93-604] p 1049 N94-16140
Pulse response based control for minimum time maneuver of flexible spacecraft
[AD-A266186] p 886 N94-16455
Contextually dependent control strategies for manipulation
[TR-416] p 1165 N94-16580
Active turbulence control in wall bounded flows using direct numerical simulation
[AD-A267261] p 1028 N94-17286
Optimal tuning of heavy equipment motion controllers
[AD-A267873] p 1167 N94-17392
Precise flux control for lattice matched superlattice materials
[AD-A268254] p 1215 N94-17417

FELDSPARS
Induced thermoluminescence study of experimentally shock-loaded oligoclase p 953 N94-16266
Heterogeneous plagioclase compositions in the Maralinga CK4 chondrite p 1243 N94-16308
Mixing model analysis of telescopic lunar spectra p 1284 N94-16371

FEMALES
Maximizing participation of women in collegiate aviation education
[NIAR-93-14] p 1222 N94-17261
FERMENTATION
Contribution to the elaboration of some adaptive control algorithms for fermentation processes monitoring
[LAAS-92513] p 1116 N94-15643
An advanced bioprocessing concept for the conversion of wastepaper to ethanol
[DE93-015209] p 975 N94-16807
FERROCENES
Synthesis, characterization, and polymerization of new ferrocene-fluorene complexes. A novel high-molecular weight conjugated polymer with pendant ferrocene groups
[AD-A267717] p 972 N94-17273
FERROELECTRICITY
Nanocomposites for electronic applications, volume 1
[AD-A267070] p 1009 N94-15669
Nanocomposites for electronic applications, volume 3
[AD-A267073] p 1009 N94-15672
Nanocomposites for electronic applications, volume 2
[AD-A267074] p 1009 N94-15673
Sputtered ferroelectric thin films of KTN for electro-optic devices
[AD-A266573] p 968 N94-16723
FERROFLUIDS
Benard convection of magnetic colloids under microgravity p 943 N94-15159
FERROMAGNETIC MATERIALS
A study of relaxation transitions in the polymers under the influence of magnetic fields
[AD-A263878] p 963 N94-15133
FIBER COMPOSITES
Dynamic behavior of fiber and particle reinforced composites
[AD-A266905] p 930 N94-15143
Production Technology for Components from Nonmetallic Fiber Reinforced Materials
[ETN-93-94607] p 931 N94-15254
Construction, testing, and representation of resin and fiber reinforced materials p 931 N94-15255
Construction and calculation p 931 N94-15256
High temperature advanced structural composites. Volume 2: Ceramic matrix composites, fiber processiing and properties, and interfaces
[AD-A267023] p 933 N94-15528
High temperature advanced structural composites. Volume 1: Executive summary and intermetallic compounds
[AD-A267022] p 933 N94-15835
Carbon-carbon grid for ion engines
[NASA-CASE-NPO-19174-1-CU] p 925 N94-15876
Method of producing a silicon carbide fiber reinforced strontium aluminosilicate glass-ceramic matrix composite
[NASA-CASE-LEW-15263-2] p 934 N94-15929
NEXTEL(trademark)/SiC composites using forced chemical vapor infiltration
[DE93-013532] p 934 N94-16008
Modeling the thermal conductivity of fiber-reinforced ceramic composites
[DE93-015340] p 934 N94-16017
Overview of chemical vapor infiltration
[DE93-015440] p 934 N94-16065
Evaluation of the interfacial mechanical properties in fiber-reinforced ceramic composites
[DE93-015494] p 935 N94-16461
The processing and mechanical properties of high temperature/high performance composites. Book 1: Coonstituent properties of composites
[AD-A266394] p 935 N94-16483
The processing and mechanical properties of high temperature/high performance composites. Book 2: Coonstituent properties and macroscopic performance
[AD-A266395] p 935 N94-16484
The processing and mechanical properties of high temperature/high performance composites. Book 3: Coonstituent properties and macroscopic performance
[AD-A266396] p 935 N94-16485
The processing and mechanical properties of high temperature/high performance composites. Book 4: Coonstitutive laws and design
[AD-A266397] p 935 N94-16528
The processing and mechanical properties of high temperature/high performance composites. Book 5: Processing and miscellaneous properties
[AD-A266398] p 935 N94-16529
Continuous fabrication of SiC fiber tows by chemical vapor deposition
[AD-A266460] p 936 N94-16569
FIBER-TEX 1992: The Sixth Conference on Advanced Engineering Fibers and Textile Structures for Composites
[NASA-CP-3211] p 936 N94-16845
Production and application of chemical fibers with special properties for manufacturing composite materials and goods of different usage p 938 N94-16854
Influence of fiber packing structure on permeability p 938 N94-16857
Interfacial shear behavior and its influence on fiber damage in sapphire-reinforced gamma titanium aluminide composites
[AD-A267943] p 1060 N94-17043
Evaluation of interfacial properties of fiber-reinforced ceramic composites using fiber push-in tests
[DE93-015427] p 972 N94-17253
Fiber strength utilization in carbon/carbon composites
[AD-A267713] p 940 N94-17271
Aspects of high temperature damage in fiber reinforced titanium metal matrix composites
[AD-A267907] p 941 N94-17379
Micromechanics modeling and analysis of Haversian compact bone tissues as a fiber reinforced composite material
[AD-A268250] p 1129 N94-17456
Interface chemistry in ceramic matrix composites
[AD-A268629] p 973 N94-17466
Thermo-mechanical analysis of oxidation protected carbon-carbon composites
[AD-A268191] p 941 N94-17597
FIBER OPTICS
Proceedings of the 1992 Antenna Applications Symposium, volume 2
[AD-A266916] p 986 N94-14998
Congestion control of high-speed networks
[AD-A267013] p 989 N94-15748
Evaluation of midband analog fiber optic telemetry links
[DE93-015128] p 883 N94-16056
A formal protocol test procedure for the Survivable Adaptable Fiber Optic Embedded Network (SAFENET)
[AD-A267410] p 1192 N94-16975
Investigation of the optical, electronic, and structural properties of fiber optic glasses
[AD-A267645] p 971 N94-17204
A 27 channels, 1 MHz fibre-optic measuring system
[AD-A266943] p 1003 N94-17307
Applications of advanced diffractive optical elements p 1197 N94-17356
FIBER ORIENTATION
Design and cost drivers in 2-D braiding p 937 N94-16849
Influence of fiber packing structure on permeability p 938 N94-16857
FIBER STRENGTH
Production and application of chemical fibers with special properties for manufacturing composite materials and goods of different usage p 938 N94-16854
Fiber strength utilization in carbon/carbon composites
[AD-A267713] p 940 N94-17271
Interface chemistry in ceramic matrix composites
[AD-A268629] p 973 N94-17466
FIBER VOLUME FRACTION
Influence of fiber packing structure on permeability p 938 N94-16857
FIBERS
Production process p 931 N94-15257
Electrostatic fiber spreader including a corona discharge device
[AD-D015793] p 936 N94-16537
FIBROBLASTS
Heat shock protein induction in human cells by CO2 laser irradiation
[AD-A266430] p 1117 N94-16545
FIELD ALIGNED CURRENTS
Formation of the stable auroral arc that intensifies at substorm onset
[NASA-CR-193637] p 1098 N94-15433
Linear and non-linear studies of Alfven waves in space. Stationary and dynamic processes in magnetospheric plasmas
[NASA-CR-193585] p 1239 N94-16647
FIELD COILS
ITER-HARD Toroidal Field coil structural analysis
[DE93-014834] p 1201 N94-15981
FIELD EFFECT TRANSISTORS
DLTS and dynamic transconductance analysis of deep-submicron fully-depleted SOI MOSFET's
[AD-A267291] p 1214 N94-17243
RF vacuum microelectronics
[AD-A268399] p 1014 N94-17423
FIELD EMISSION
Preparation and investigation of improved low voltage electron excitable phosphors
[AD-A266852] p 963 N94-14948
RF vacuum microelectronics
[AD-A268399] p 1014 N94-17423
Field-emitter arrays for RF vacuum microelectronics
[AD-A268397] p 1015 N94-17526
FIELD STRENGTH
A study of high field transport in wide band gap electronic materials using a picosecond transient charge technique
[AD-A267098] p 1008 N94-15636
FIELD THEORY (PHYSICS)
Relativistic mean-field caiculations of lambda and sigma hypernuclei
[DE93-015269] p 1181 N94-16013
Experimental study of weak interactions by precision measurement by rare kaon decay
[DE93-016864] p 1182 N94-16117
The universality of the shift of the Chern-Simons parameter for a general class of BRS invariant regularizations
[NIKHEF-H/93-03] p 1220 N94-17602
SUSY in the sky
[NIKHEF-H/93-04] p 1240 N94-17603
Derivation of the Verlinde formula from Chern-Simons theory and the G/G model
[DE93-628620] p 1221 N94-17632
FIGHTER AIRCRAFT
Technical evaluation report on the AGARD-PEP Specialists Meeting on Combat Aircraft Noise
[NLR-TP-91445-U] p 1177 N94-15506
FIGURE OF MERIT
Figures of merit for laser beam quality p 1043 N94-14994
Radome depolarization effects on monopulse receiver tracking performance
[AD-A267446] p 1001 N94-17031
FILE MAINTENANCE (COMPUTERS)
Experience with disconnected operation in a mobile computing environment
[AD-A267524] p 1141 N94-17115
FILLING
Ground testing for the no-vent fill of cryogenic tanks: Results of tests for a 71 cubic foot tank
[NASA-TM-106293] p 1030 N94-17486
FILM CONDENSATION
Theoretical study of laminar film condensation on horizontal ellipitical tubes under conditions of free and forced convection
[AD-A267161] p 1021 N94-15737
FILM COOLING
Turbine blade tip film cooling measurements
[AD-A267686] p 868 N94-14964
FILM THICKNESS
MeV ion-beam analysis of optical data storage films p 1226 N94-14984
Determination of average refractive index of spin coated DCG films for HOE fabrication p 1036 N94-14992
FILTERS
Multilayer thin film design for far ultraviolet polarizers using an induced transmission and absorption technique
[NASA-CR-194631] p 1190 N94-15869
FINANCIAL MANAGEMENT
NASA directives master list and index
[NHB-1410.13L] p 1229 N94-15414
NASA information resources management handbook
[NHB-2410.1E] p 1230 N94-15941
FINE STRUCTURE
Local environment about O atoms in Pr-Y-Ba-Cu-O films studied by O K-edge XAFS
[DE93-016218] p 1209 N94-16447
Convergence of the multiple scattering expansion in XAFS and XANES
[DE93-011001] p 948 N94-16772
Characterization of nanoscale oxide and oxyhydroxide powders using EXAFS spectroscopy
[DE93-015683] p 940 N94-17235
FINGERS
Temporal segmentation of tasks from human hand motion
[AD-A266596] p 1166 N94-16725
FINITE DIFFERENCE THEORY
Construction and calculation p 931 N94-15256
Full-wave simulation of the thumbtack laser
[DE93-015110] p 1039 N94-16054
Finite difference time domain analysis of chirped dielectric gratings p 1195 N94-17339
Application of the finite-difference time-domain method to scattering and radiation problems involving wires and plates
[AD-A268396] p 1005 N94-17496
Numerically solving a transient heat conduction problem with convection and radiation
[AD-A268521] p 1220 N94-17540
Currents induced in the human body for exposure to ultrawideband electromagnetic pulses
[AD-A268570] p 1130 N94-17621
FINITE ELEMENT METHOD
Static aeroelastic response of an aircraft with asymmetric wing planforms representative of combat damage
[AD-A266890] p 865 N94-14951

Parametric study of a finite element model of the Sidewinder missile
[AD-A267245] p 865 N94-14976
Inelastic deformation of metal matrix composites
[NASA-CR-191522] p 930 N94-15106
Construction and calculation p 931 N94-15256
An assessment of finite-element modeling techniques for thick-solid/thin-shell joints analysis
[NASA-TM-108426] p 1058 N94-15534
Verification of a two-dimensional infiltration model for the resin transfer molding process
[NASA-CR-194597] p 964 N94-15656
Prediction of stable tearing of 2024-T3 aluminum alloy using the crack-tip opening angle approach
[NASA-TM-109023] p 955 N94-15708
Preliminary analysis and design optimization of the short spacer truss of Space Station Freedom
[NASA-TM-4470] p 1058 N94-15709
Modal element method for potential flow in non-uniform ducts: Combining closed form analysis with CFD
[NASA-TM-106347] p 1169 N94-15799
Measurement and analysis of critical CTOA for an aluminum alloy sheet
[NASA-TM-109024] p 956 N94-15948
ITER-HARD Toroidal Field coil structural analysis
[DE93-014834] p 1201 N94-15981
Finite element analytical techniques for ceramic production in microgravity: A hypoelastic model
p 981 N94-16099
The design and analysis of a modular microgravity test platform for use aboard the NASA KC-135 aircraft
p 899 N94-16101
Design of a cruciform bend specimen for determination of out-of-plane biaxial tensile stress effects on fracture toughness for shallow cracks
[DE93-015455] p 1059 N94-16104
Aspects of modelling the tectonics of large volcanoes on the terrestrial planets p 1104 N94-16396
Modal ring method for the scattering of sound
[NASA-TM-106342] p 1177 N94-16497
ASTROS enhancements. Volume 1: ASTRO user's manual
[AD-A266818] p 1151 N94-16768
ASTROS enhancements. Volume 2: ASTRO programmer's manual
[AD-A266819] p 1151 N94-16769
Finite element analysis of structural engineering problems using a viscoplastic model incorporating two back stresses
[NASA-TM-106046] p 1060 N94-16881
Interfacial shear behavior and its influence on fiber damage in sapphire-reinforced gamma titanium aluminide composites
[AD-A267943] p 1060 N94-17043
Reliability analysis of Surface Mount Technology (SMT)
[AD-A267598] p 1055 N94-17194
Phased array antenna analysis using hybrid finite element methods
[AD-A267620] p 1002 N94-17196
Numerical solution of SUPG finite-element method for supersonic viscous flow
[AD-A267762] p 860 N94-17222
Mathmatical modeling for diffractive optics
p 1195 N94-17342
Solution of elastic-plastic stress analysis problems by the p-version of the finite element method
[NASA-CR-194267] p 1062 N94-17445
Nonlinear random response prediction using MSC/NASTRAN
[NASA-TM-109029] p 1179 N94-17650

FINS
Aerodynamic flight control to increase payload capability of future launch vehicles
[NASA-CR-193850] p 870 N94-15532
An experimental investigation of the effects of leading edge geometry on the dynamics of blunt fin-induced shock wave turbulent boundary layer interaction
[AD-A267656] p 860 N94-17221

FIRE (CLIMATOLOGY)
Preliminary analysis of University of North Dakota aircraft data from the FIRE Cirrus IFO-2
[NASA-CR-193357] p 866 N94-15429

FIRE CONTROL
Thermal Weapon Sight (TWS) AN/PAS-13 diffractive optics designed for producibility p 1197 N94-17354

FIRE FIGHTING
STS-27 crew fire training and glove molding
[NASA-TM-109554] p 1136 N94-15406
STS-31 crew training: firefighting, food tasting, EVA prep and post
[NASA-TM-109484] p 876 N94-15451
STS-38 crew training: Habitation equipment procedures, bailout in CCT, 70mm photo class, EVA prep and post, and firefighting
[NASA-TM-109494] p 1136 N94-15453

FIRE PREVENTION
Basic principles of helicopter crashworthiness
[AD-A267099] p 862 N94-15637

FIRES
STS-27 crew fire training and glove molding
[NASA-TM-109554] p 1136 N94-15406

FIRST AID
Illness/injury pattern complex 40 (Titan)
p 1125 N94-16625

FISHES
Finding fish from above --- remote sensing
[NASA-TM-109602] p 1081 N94-15310

FISHING
Finding fish from above --- remote sensing
[NASA-TM-109602] p 1081 N94-15310

FISSION PRODUCTS
GAM-HEAT: A computer code to compute heat transfer in complex enclosures
[DE93-014724] p 1023 N94-15980

FLAME PROPAGATION
Studies of premixed laminar and turbulent flames at microgravity
[NASA-CR-194656] p 951 N94-17125

FLAME STABILITY
Studies of premixed laminar and turbulent flames at microgravity
[NASA-CR-194656] p 951 N94-17125
Lifted turbulent jet flames
[AD-A267911] p 952 N94-17381

FLAME TEMPERATURE
Mechanisms of combustion limits in premixed gas flames at microgravity
[NASA-CR-194557] p 946 N94-15713

FLAMES
Modeling study to evaluate the ionic mechanism of soot formation in flames
[AD-A266242] p 950 N94-16930

FLAMMABLE GASES
Mechanisms of combustion limits in premixed gas flames at microgravity
[NASA-CR-194557] p 946 N94-15713

FLAPS (CONTROL SURFACES)
Effects of internal yaw-vectoring devices on the static performance of a pitch-vectoring nonaxisymmetric convergent-divergent nozzle
[NASA-TP-3369] p 858 N94-16572

FLASHING (VAPORIZING)
Explosive boiling at very low heat fluxes: A microgravity phenomenon
[NASA-TM-106325] p 1046 N94-15817

FLASHOVER
Surface flashover of semiconductors: A fundamental study
[AD-A267382] p 1012 N94-17023

FLAT PLATES
Tollmien-Schlichting/vortex interactions in compressible boundary layer flows
[NASA-CR-191515] p 1017 N94-15183
Boundary layer flow of air over water on a flat plate
[NASA-CR-191517] p 1019 N94-15479
Analysis of electromagnetic scattering from irregularly shaped, thin, metallic flat plates
[NASA-TP-3361] p 998 N94-16655
Transition induced by fixed and freely convecting spherical particles in laminar boundary layers
[AD-A267757] p 1028 N94-17276
On the stability of a time dependent boundary layer
[NASA-CR-191542] p 1030 N94-17450
Numerically solving a transient heat conduction problem with convection and radiation
[AD-A268521] p 1220 N94-17540

FLAVOR (PARTICLE PHYSICS)
Production of D-mesons in pp-collisions and quark-gluon string model
[DE93-626721] p 1185 N94-17312

FLEXIBILITY
Compounds containing meta-biphenylenedioxy moieties and polymers therefrom
[NASA-CASE-LAR-14517-1] p 965 N94-15879
NEXTEL(trademark)/SiC composites using forced chemical vapor infiltration
[DE93-013532] p 934 N94-16008

FLEXIBLE BODIES
Improved composite flexible blanket insulation
[NASA-CASE-ARC-11955-1-CU] p 934 N94-15926

FLEXIBLE SPACECRAFT
Pulse response based control for minimum time maneuver of flexible spacecraft
[AD-A266186] p 886 N94-16455

FLIGHT CHARACTERISTICS
Fidelity assessment of a UH-60A simulation on the NASA Ames vertical motion simulator
[NASA-TM-104016] p 870 N94-15793
Looking at science on board Eureca
[ESA-BR-80] p 874 N94-16584
NEXT launch system p 878 N94-17141

FLIGHT CONTROL
Better way to fly
[NASA-TM-109447] p 866 N94-15396
Research in robust control for hypersonic aircraft
[NASA-CR-194106] p 870 N94-15416
Aerodynamic flight control to increase payload capability of future launch vehicles
[NASA-CR-193850] p 870 N94-15532
Aerodynamic control of NASP-type vehicles through vortex manipulation, volume 4
[NASA-CR-177626-VOL-4] p 857 N94-15720
Flight instrument software for the F/A-18 research simulator
[AD-A267170] p 872 N94-15856
Embedded computer systems: Status of C-17 software
[AD-A267307] p 1160 N94-16993
System performance modeling and analysis of a fault-tolerant, real time parallel processor
[AD-A268070] p 1162 N94-17551

FLIGHT CREWS
Human factor studies
[NASA-TM-109665] p 875 N94-15236
Activity/rest patterns of instructor and rates student pilots during rapid transitions from daytime to nighttime duty hours at the Eastern Army Aviation Training site
[AD-A267038] p 1131 N94-15659
Mission management aircraft operations manual
[NHB-7900.3] p 1225 N94-16729
Theoretical implications and empirical findings on instructional control and part-whole-task training
[AD-A267826] p 872 N94-17403
An introduction to structural models
[AD-A268151] p 1155 N94-17429
Aircrew/groundcrew life support systems research. Volume 1: CLIN 0001 research requirements
[AD-A268229] p 1139 N94-17563
Aircrew/groundcrew life support systems research. Volume 2: CLIN 0002 task order requirements
[AD-A268230] p 1139 N94-17564

FLIGHT INSTRUMENTS
Testing and management of flight instruments and their data
[NASA-CR-194332] p 868 N94-15187
Better way to fly
[NASA-TM-109447] p 866 N94-15396
Flight instrument software for the F/A-18 research simulator
[AD-A267170] p 872 N94-15856
A virtual acoustic orientation instrument
[AD-A268181] p 1134 N94-17510

FLIGHT MECHANICS
Trajectory optimization for the National Aerospace Plane
[NASA-CR-194618] p 867 N94-16498

FLIGHT OPERATIONS
STS-26 crew participation in meetings
[NASA-TM-109519] p 873 N94-15469
Mission management aircraft operations manual
[NHB-7900.3] p 1225 N94-16729
Aircraft operations management manual
[NHB-7900.3(V1)] p 1225 N94-16730

FLIGHT PATHS
Non-lethal Unmanned Aerial Vehicles (UAVs)
[AD-A267139] p 866 N94-15692
Trajectory optimization for the National Aerospace Plane
[NASA-CR-194618] p 867 N94-16498
Strategic planning for aircraft noise route impact analysis: A three dimensional approach
[NASA-CR-191484] p 1178 N94-17278
Windshear database for forward-looking systems certification
[NASA-TM-109012] p 1108 N94-17283

FLIGHT PLANS
AIRSAR South American deployment: Operation plan, version 3.0 p 994 N94-15919

FLIGHT RULES
Aviation inspection prospects p 853 N94-15125
STS-26 crew participation in meetings
[NASA-TM-109519] p 873 N94-15469

FLIGHT SAFETY
Aviation inspection prospects p 853 N94-15125
The 1968 highlights --- NASA programs and research
[NASA-TM-109627] p 1302 N94-15413
Non-lethal Unmanned Aerial Vehicles (UAVs)
[AD-A267139] p 866 N94-15692
An analysis of tactical airlifter characteristics and their impact on theater airlift system performance
[AD-A266719] p 866 N94-15731
Aircraft operations management manual
[NHB-7900.3(V1)] p 1225 N94-16730

FLIGHT SIMULATION
Manned vehicle systems research facility
[NASA-TM-109650] p 875 N94-15318
Spacework 16 --- Simulated Space Shuttle Program
[NASA-TM-109436] p 1221 N94-15420

Aerodynamic control of NASP-type vehicles through vortex manipulation, volume 4
[NASA-CR-177626-VOL-4] p 857 N94-15720
Fidelity assessment of a UH-60A simulation on the NASA Ames vertical motion simulator
[NASA-TM-104016] p 870 N94-15793
Flight simulator-induced sickness and visual displays evaluation
[AD-A267019] p 1122 N94-15845
Theoretical implications and empirical findings on instructional control and part-whole-task training
[AD-A267826] p 872 N94-17403

FLIGHT SIMULATORS
Activity/rest patterns of instructor and rates student pilots during rapid transitions from daytime to nighttime duty hours at the Eastern Army Aviation Training site
[AD-A267038] p 1131 N94-15659
Flight simulator-induced sickness and visual displays evaluation
[AD-A267019] p 1122 N94-15845
Flight instrument software for the F/A-18 research simulator
[AD-A267170] p 872 N94-15856
An introduction to structural models
[AD-A268151] p 1155 N94-17429

FLIGHT TESTS
Flight-determined engine exhaust characteristics of an F404 engine in an F-18 airplane
[NASA-TM-4538] p 869 N94-15141
X-29: Experiment in flight
[NASA-TM-109454] p 865 N94-15327
Non-lethal Unmanned Aerial Vehicles (UAVs)
[AD-A267139] p 866 N94-15692
Flight testing of airbreathing hypersonic vehicles
[NASA-TM-4524] p 886 N94-15753
In-flight investigation of a rotating cylinder-based structural excitation system for flutter testing
[NASA-TM-4512] p 867 N94-15783
Lift-fan aircraft: Lessons learned-the pilot's perspective
[NASA-CR-177620] p 867 N94-15950
Test plan for the evaluation of the initial capability of the National Satellite Test Bed: Phase 1D
[DOT/FAA/RD-93/20] p 876 N94-16025
The vibro-acoustic mapping of low gravity trajectories on a Learjet aircraft p 978 N94-16078
Comparison of preliminary results from Airborne Aster Simulator (AAS) with TIMS data p 1064 N94-16600
Noise measurement flight test of five light helicopters
[AD-A268566] p 1179 N94-17599
Postflight hardware evaluation 360T026 (RSRM-26, STS-47)
[NASA-CR-192559] p 882 N94-17656

FLIGHT TRAINING
Theoretical implications and empirical findings on instructional control and part-whole-task training
[AD-A267826] p 872 N94-17403
An introduction to structural models
[AD-A268151] p 1155 N94-17429

FLIR DETECTORS
Thermal Weapon Sight (TWS) AN/PAS-13 diffractive optics designed for producibility p 1197 N94-17354
Atmospheric propagation analysis program
[AD-A268231] p 1006 N94-17565

FLOCCULATING
Efficacy of flocculating and other emergency water purification tablets
[AD-A266695] p 1148 N94-15840

FLOOD PLAINS
Strategies for detection of floodplain inundation with multi-frequency polarimetric SAR p 1076 N94-16739

FLOOD PREDICTIONS
On hydrologic similarity: A dimensionless flood frequency model using a generalized geomorphologic unit hydrograph and partial area runoff generation
[PAPER-89WR01579] p 1083 N94-16027
Similarity and scale in catchment storm response
[PAPER-89RG01615] p 1083 N94-16028

FLOODS
On hydrologic similarity: A dimensionless flood frequency model using a generalized geomorphologic unit hydrograph and partial area runoff generation
[PAPER-89WR01579] p 1083 N94-16027
Similarity and scale in catchment storm response
[PAPER-89RG01615] p 1083 N94-16028
Tessera terrain on Venus: Implications of tessera flooding models and boundary characteristics for global distribution and mode of formation p 1258 N94-16226

FLOW CHARACTERISTICS
Fractal geometry of some Martian lava flow margins: Alba Patera p 1270 N94-16298
Fundamental studies of rocket combustion chemistry and combustion instability
[AD-A266248] p 925 N94-16482

FLOW DISTORTION
An uncertainty analysis of inlet dynamic flow distortion using an analog/digital hybrid editing system
[AD-A266924] p 855 N94-15105
Numerical investigations in three-dimensional internal flows
[NASA-CR-194594] p 1020 N94-15551

FLOW DISTRIBUTION
The effect of the nose shape and wing location toward the wing vortex breakdown
[AD-A267724] p 855 N94-14942
Unsteady separated flows: Empirical model and control
[AD-A267282] p 855 N94-14959
Benard convection of magnetic colloids under microgravity p 943 N94-15159
Swept shock/boundary-layer interactions: Scaling laws, flowfield structure, and experimental methods p 1017 N94-15197
Swept shock wave/laminar boundary layer interactions, experimental, and numerical results p 1017 N94-15198
Numerical simulation of 3-D shock wave turbulent boundary layer interactions p 1017 N94-15199
Unsteady phenomena in shock wave/boundary layer interaction p 1017 N94-15200
Rocket motor plume flowfields: Phenomenology and simulation p 924 N94-15221
DSMC simulations of Mach 20 nitrogen flows about a 70 degree blunted cone and its wake
[NASA-TM-107762] p 1018 N94-15291
Development of the seeding system used for laser velocimeter surveys of the NASA Low-Speed Centrifugal Compressor flow field
[NASA-TM-4485] p 1032 N94-15445
On the interaction between the shock wave attached to a wedge and freestream disturbances
[NASA-CR-191528] p 1019 N94-15478
An experimental study of ASTOVL related jet flows to produce CFD code validation data. Phase 3: Results of experiments
[TT-9203] p 1020 N94-15645
Aerodynamic control of NASP-type vehicles through Vortex manipulation. Volume 2: Static wind tunnel tests
[NASA-CR-177626-VOL-2] p 856 N94-15677
Parametric resonant triad interactions in a free shear layer
[NASA-TM-106365] p 1021 N94-15751
Aerodynamic/dynamic/control interaction
[AD-A266187] p 871 N94-16107
Lava flow-field morphological classification and interpretation: Examples from Venus p 1259 N94-16230
Emplacement of multiple flow units on very shallow slopes, east Kawelu Planitia flow field, Venus p 1260 N94-16235
Sheet flow fields on Venus p 1278 N94-16338
Martian lavas: Three complementary remote sensing techniques to derive flow properties p 1283 N94-16366
Computation of a controlled store separation from a cavity p 858 N94-16513
Complex terrain wind model evaluation
[AD-A266467] p 1096 N94-16589
The use of TIMS for mapping different pahoehoe surfaces: Mauna Iki, Kilauea p 1065 N94-16606
Nonequilibrium radiation and chemistry models for aerocapture vehicle flowfields
[NASA-CR-194645] p 1027 N94-17095
Studies on nonequilibrium phenomena in supersonic chemically reacting flows
[NASA-CR-194662] p 1027 N94-17215
ASRM nozzle thermal analysis
[NASA-CR-194672] p 928 N94-17277
Experimental and computational investigation of the NASA low-speed centrifugal compressor flow field
[NASA-TM-4481] p 869 N94-17386
On the stability of a time dependent boundary layer
[NASA-CR-191542] p 1030 N94-17450
Laser velocimetry measurements of vortex flows on a delta wing at Mach 1.9
[AD-A268596] p 861 N94-17609

FLOW EQUATIONS
A domain-partition method for the advection-diffusion equation
[INRIA-RR-1740] p 1030 N94-17534

FLOW GEOMETRY
Design of round-to-square transition section; analysis and computer code
[AD-A267173] p 872 N94-15847

FLOW MEASUREMENT
Contribution of laser Doppler velocimetry to the physical description of shock wave/turbulent boundary layer interactions with incidence on turbulence modelling p 1018 N94-15201
NASA Lewis 9- by 15-foot low-speed wind tunnel user manual
[NASA-TM-106247] p 872 N94-15819

FLOW NETS
Numerical solution of a second order boundary problem for two dimensions using galerkin approximations
[AD-A268128] p 1171 N94-17521

FLOW REGULATORS
Geometrical vapor blocker for parallel condensation tubes requiring cooling
[NASA-CASE-MSC-22090-1] p 1022 N94-15962
Design of a fluid elastic actuator with application to structure control
[AD-A267649] p 897 N94-17246

FLOW RESISTANCE
Development of braided fiber seals for engine applications p 939 N94-16859

FLOW STABILITY
Inviscid instability of streamwise corner flow
[NASA-CR-191514] p 1021 N94-15834
Receptivity of boundary layers to convected gusts
[AD-A267206] p 1022 N94-15860
Experimental study of nonassociated flow and instability of frictional materials
[AD-A266421] p 1024 N94-16555
Stability of flows in fluidized beds
[DE93-000245] p 1024 N94-16763
The stability and dynamics of elastic structures and fluid flows
[AD-A267990] p 1029 N94-17414
On the stability of a time dependent boundary layer
[NASA-CR-191542] p 1030 N94-17450
Flow instability tests for a particle bed reactor nuclear thermal rocket fuel element
[AD-A268012] p 929 N94-17474

FLOW VELOCITY
The turbulent wall jet
[AD-A267675] p 855 N94-14963
Parametric resonant triad interactions in a free shear layer
[NASA-TM-106365] p 1021 N94-15751
Inviscid instability of streamwise corner flow
[NASA-CR-191514] p 1021 N94-15834
Martian lavas: Three complementary remote sensing techniques to derive flow properties p 1283 N94-16366
Flow instability tests for a particle bed reactor nuclear thermal rocket fuel element
[AD-A268012] p 929 N94-17474
Measurement of the velocity field and void fraction in a planar plunging jet
[AD-A268183] p 1030 N94-17511
Nonintrusive fast response oxygen monitoring system for high temperature flows
[NASA-CR-4553] p 1036 N94-17655

FLOW VISUALIZATION
Laser Doppler velocimetry measurements across a normal shock in transonic flow
[AD-A267240] p 855 N94-14973
Visualization of solidification front phenomena
[NASA-CR-193838] p 976 N94-15006
Swept shock/boundary-layer interactions: Scaling laws, flowfield structure, and experimental methods p 1017 N94-15197
A microprocessor controller for a towing tank drive and flow visualisation system
[AD-A267087] p 872 N94-15543
Aerodynamic control of NASP-type vehicles through Vortex manipulation. Volume 1: Static water tunnel tests
[NASA-CR-177626-VOL-1] p 855 N94-15655
Suppression of dynamic stall with a leading-edge slat on a VR-7 airfoil
[NASA-TP-3357] p 856 N94-15657
Aerodynamic control of NASP-type vehicles through vortex manipulation. Volume 3: Wing rock experiments
[NASA-CR-177626] p 857 N94-15780
Clouding tracing: Visualization of the mixing of fluid elements in convection-diffusion systems
[NASA-CR-191529] p 1148 N94-15965
Adaptive algorithm for aircraft configuration in turbulent flow
[AD-A266188] p 867 N94-16122
Wind tunnel investigations of forebody strakes for yaw control on F/A-18 model at subsonic and transonic speeds
[NASA-TP-3360] p 859 N94-16573
Textile composite processing science p 938 N94-16856
Adaptive Navier-Stokes calculations for vortical flow
[AD-A266236] p 1026 N94-16966
Natural convection above a horizontal heat source
[AD-A267212] p 1026 N94-16985
Structure of high Reynolds number turbulent boundary layer
[AD-A267476] p 860 N94-17099

Supersonic flow visualization of a nacelle in close proximity to a simulated wing
[NASA-CR-194675] p 860 N94-17260
Transition induced by fixed and freely convecting spherical particles in laminar boundary layers
[AD-A267757] p 1028 N94-17276
Experimental and computational investigation of the NASA low-speed centrifugal compressor flow field
[NASA-TM-4481] p 869 N94-17386
Laser velocimetry measurements of vortex flows on a delta wing at Mach 1.9
[AD-A268596] p 861 N94-17609
Nonintrusive fast response oxygen monitoring system for high temperature flows
[NASA-CR-4553] p 1036 N94-17655

FLUE GASES
Direct catalytic decomposition of nitric oxide
[DE93-016689] p 949 N94-16896

FLUID BOUNDARIES
Physical and chemical properties of some new perfluoropolyalkylether lubricants prepared by direct fluorination
[NASA-TM-106299] p 967 N94-16543
The stability and dynamics of elastic structures and fluid flows
[AD-A267990] p 1029 N94-17414

FLUID DYNAMICS
Special course on Shock-Wave/Boundary-Layer Interactions in Supersonic and Hypersonic Flows
[AGARD-R-792] p 1017 N94-15196
New findings and instrumentation from the NASA Lewis Microgravity Facility p 977 N94-16076
Lava crusts and flow dynamics p 1103 N94-16316
Looking at science on board Eureca
[ESA-BR-80] p 874 N94-16584
Nonlinear problems in fluid dynamics and inverse scattering
[AD-A266234] p 1026 N94-16927
The structure of turbulent boundary layers and shock wave boundary layer interactions
[AD-A266240] p 1026 N94-16929

FLUID FLOW
Particle simulations on massively parallel machines
[DE93-015644] p 1157 N94-14927
The 1988 computational fluid dynamics highlights
[NASA-TM-109645] p 1019 N94-15431
Lava flow-field morphological classification and interpretation: Examples from Venus
p 1259 N94-16230
Emplacement of multiple flow units on very shallow slopes, east Kawelu Planitia flow field, Venus
p 1260 N94-16235
Martian lavas: Three complementary remote sensing techniques to derive flow properties
p 1283 N94-16366
Operator overloading as an enabling technology for automatic differentiation
[DE93-012899] p 1170 N94-16778
High pressure pump for electro-rheological fluids
[AD-D015888] p 1048 N94-16915
Modeling, estimation and control of distributed parameter systems
[AD-A267325] p 1026 N94-17003
Design of a fluid elastic actuator with application to structure control
[AD-A267649] p 897 N94-17246
The stability and dynamics of elastic structures and fluid flows
[AD-A267990] p 1029 N94-17414

FLUID JETS
Mechanism of intermittent atomization
[AD-A266625] p 1021 N94-15770
Computation of confined coflow jets with three turbulence models
[NASA-TM-106378] p 1025 N94-16879
Two-dimensional, high flow, precisely controlled monodisperse drop source
[AD-A267660] p 1028 N94-17250
Cryogenic spray vaporization in high-velocity helium, argon and nitrogen gasflows
[NASA-TM-106363] p 1035 N94-17446
Measurement of the velocity field and void fraction in a planar plunging jet
[AD-A268183] p 1030 N94-17511

FLUID MANAGEMENT
Ground testing for the no-vent fill of cryogenic tanks: Results of tests for a 71 cubic foot tank
[NASA-TM-106293] p 1030 N94-17486

FLUID MECHANICS
The turbulent wall jet
[AD-A267675] p 855 N94-14963

FLUID POWER
Electrorheological (ER) fluids: A research needs assessment
[AD-A267588] p 951 N94-17210

FLUID PRESSURE
High pressure pump for electro-rheological fluids
[AD-D015888] p 1048 N94-16915

FLUID-SOLID INTERACTIONS
Modeling, estimation and control of distributed parameter systems
[AD-A267325] p 1026 N94-17003

FLUIDICS
Sounding Rocket Experiments in Fluid Science and Materials Sciences: TEXUS 25 to 27 and MASER 4, volume 3
[ESA-SP-1132-VOL-3] p 943 N94-15157

FLUORESCENCE
Theoretical prediction of the UV adsorption and fluorescence spectra of tyrosine and phenylalanine
[AD-A266970] p 943 N94-15111

FLUORINATION
Physical and chemical properties of some new perfluoropolyalkylether lubricants prepared by direct fluorination
[NASA-TM-106299] p 967 N94-16543

FLUORINE COMPOUNDS
Synthesis, characterization, and polymerization of new ferrocene-fluorene complexes. A novel high-molecular weight conjugated polymer with pendant ferrocene groups
[AD-A267717] p 972 N94-17273

FLUOROCARBONS
Synthesis and chemistry of novel cyclic fluorocarbons
[AD-A267148] p 929 N94-15734
Wide angle, single screen, gridded square-loop frequency selective surface for diplexing two closely separated frequency bands
[NASA-CASE-NPO-18664-1-CU] p 1237 N94-17438

FLUOROHYDROCARBONS
Synthesis and chemistry of novel cyclic fluorocarbons
[AD-A267148] p 929 N94-15734
Detection and dosimetry of chemical contaminants in polymeric materials
[AD-A266605] p 968 N94-16727
Cycle performance testing of nonazeotropic mixtures of HFC-142A/HCFC-124 and HFC-32/HCFC-124 with enhanced surface heat exchangers
[DE93-015215] p 1024 N94-16808

FLUOROPOLYMERS
Modification of fluoropolymer surfaces with electronically conductive polymers
[AD-A266294] p 967 N94-16475
Synthesis and evaluation of polymeric materials
[AD-A267809] p 973 N94-17408

FLUTTER
In-flight investigation of a rotating cylinder-based structural excitation system for flutter testing
[NASA-TM-4512] p 867 N94-15783
Dynamics, stability, and control of maglev systems
[DE93-015163] p 1047 N94-16806
The stability and dynamics of elastic structures and fluid flows
[AD-A267990] p 1029 N94-17414
Flutter analysis using transversality theory
[NASA-TM-106382] p 1062 N94-17481

FLUTTER ANALYSIS
Physical properties of the benchmark models program supercritical wing
[NASA-TM-4457] p 866 N94-15722
Flutter analysis using transversality theory
[NASA-TM-106382] p 1062 N94-17481

FLUX (RATE)
Effects of bulk composition on production rates of cosmogenic nuclides in meteorites p 1245 N94-16385
Precise flux control for lattice matched superlattice materials
[AD-A268254] p 1215 N94-17417

FLUX DENSITY
A comparison of solar wind parameters measured by IMP 8, Voyager 1 and Voyager 2
[AD-A266728] p 1298 N94-15821
Revisiting the BCS, a measurement system for characterizing the optics of solar collectors
[DE93-015030] p 1091 N94-15993
A decade's overview of Io's volcanic activity
p 1245 N94-16386

FLUX QUANTIZATION
Determination of momentum flux using a bivane and cup anemometer
[AD-A265414] p 1105 N94-15137

FLYBY MISSIONS
Galileo imaging results from the second Earth-Moon flyby: Lunar Maria and related units
p 1252 N94-16199
Earth imaging results from Galileo's second encounter
p 1252 N94-16201
Galileo photometry of Apollo landing sites
p 1259 N94-16234
Earth-based and Galileo SSI multispectral observations of eastern mare serenitatis and the Apollo 17 landing site p 1261 N94-16244
Mass of Saturn's A ring p 1263 N94-16252
Clementine: Anticipated scientific datasets from the Moon and Geographos p 1288 N94-16392
Lunar multispectral mosaics from Galileo's second Earth-Moon flyby p 1288 N94-16394
Chairmanship of the Neptune/Pluto outer planets science working group
[NASA-CR-194625] p 1297 N94-16832

FLYING PERSONNEL
Preliminary validation of the task analysis/workload methodology
[AD-A267514] p 1138 N94-17077

FOCAL PLANE DEVICES
Large scientific 2-D arrays for the 1-5 micron region
p 902 N94-15044
BIB photodetectors based on antimony doped silicon
p 902 N94-15047
Schottky barrier focal plane arrays for SWIR and MWIR p 903 N94-15050
Advanced high performance CdHgTe multiplexed arrays p 903 N94-15051
Characterization of detectors and calibration of the ISOPHOT experiment p 907 N94-15082
Cryogenic readout electronics for astronomical applications p 910 N94-15099
A monolithic PbTeCCD focal plane array for MWIR imaging p 910 N94-15100
Sensor modelling for the Cyclops focal plane detector array based technology demonstrator
[AD-A267172] p 1190 N94-15846
Development of ultra-low noise, high performance 3-V Quantum Well Infrared Photodectors (QWIP's) for focal plane array staring image sensor systems
[AD-A267715] p 1214 N94-17272

FOCI
Diffractive optical elements for generating arbitrary line foci p 1195 N94-17338

FOCUSING
Ring lens focusing and push-pull tracking scheme for optical disk systems p 1227 N94-14990
A complete study of differential wax-wane focus servo technique p 1199 N94-14996
Outlook for hard x ray and gamma ray astronomy
p 904 N94-15057
Experimental evaluation of an adaptive focusing algorithm for a microwave planar phased-array hyperthermia system at UCSF
[AD-A267004] p 1121 N94-15634
Advanced transport systems for electron beams in high brightness accelerators and FELs
[AD-A267322] p 1041 N94-17001
Study of brightness and current limitations in intense charged particle beams
[AD-A268283] p 1186 N94-17578

FOG
An assessment of acid fog
[DE93-009347] p 1095 N94-15940

FOKKER AIRCRAFT
Expectations for the future of Fokker
p 854 N94-15127

FOKKER-PLANCK EQUATION
Looking at Fokker-Planck dynamics with a noisy instrument
[AD-A267049] p 1117 N94-15662
Stochastic chaos: An analog of quantum chaos
[DE93-016619] p 1220 N94-16956

FOLIAGE
A surface energy budget model modifying heat flow by foliage effects
[AD-A268598] p 1085 N94-17610

FOOD
International food research project
[NASA-TM-109540] p 1135 N94-15371
STS-29 crew food tasting in building 45
[NASA-TM-109547] p 1136 N94-15382
Food for space
[NASA-TM-109668] p 1136 N94-15435

FOOD PRODUCTION (IN SPACE)
Supporting life in space
[NASA-TM-109593] p 1135 N94-15285

FOOTPRINTS
Radar properties of several fluidized ejecta blankets on Venus p 1267 N94-16278

FORCED CONVECTION
Theoretical study of laminar film condensation on horizontal elliptical tubes under conditions of free and forced convection
[AD-A267161] p 1021 N94-15737

FORCED VIBRATION
Forced harmonic vibration of the generally orthotropic cylindrical shell with inner and outer fluid loading
[AD-A266985] p 1057 N94-15150

FOREBODIES
Wind tunnel investigations of forebody strakes for yaw control on F/A-18 model at subsonic and transonic speeds
[NASA-TP-3360] p 859 N94-16573
FORECASTING
Forecasting the ducting of electromagnetic waves on the mesoscale
[AD-A268101] p 1109 N94-17571
FOREST FIRES
Saving Yellowstone
[NASA-TM-109596] p 1094 N94-15289
TOMS computer graphics
[NASA-TM-109597] p 1094 N94-15290
Forest fire study
[NASA-TM-109615] p 1095 N94-15425
FOREST MANAGEMENT
What's killing the trees? --- causes for forest decline
[NASA-TM-109621] p 1094 N94-15350
FORESTS
What's killing the trees? --- causes for forest decline
[NASA-TM-109621] p 1094 N94-15350
Recent advances in radar remote sensing of forest p 991 N94-15897
Radar response of vegetation: An overview p 991 N94-15898
A summary of microwave remote sensing investigations planned for BOREAS p 993 N94-15914
Exploring the remote sensing of foliar biochemical concentrations with AVIRIS data p 1069 N94-16683
Oregon transect: Comparison of leaf-level reflectance with canopy-level and modelled reflectance p 1073 N94-16702
Multitemporal diurnal AVIRIS images of a forested ecosystem p 1074 N94-16709
Comparison of modeled backscatter with SAR data at P-band p 1076 N94-16735
SAR backscatter from coniferous forest gaps p 1076 N94-16736
Retrieval of pine forest biomass using JPL AIRSAR data p 1076 N94-16737
Characterization of wetland, forest, and agricultural ecosystems in Belize with airborne radar (AIRSAR) p 1076 N94-16738
Supervised fully polarimetric classification of the Black Forest test site: From MAESTRO! to MAC Europe p 1076 N94-16740
Relating multifrequency radar backscattering to forest biomass: Modeling and AIRSAR measurement p 1077 N94-16741
FORGING
Production and evaluation of dense ceramic compounds by combustion synthesis and dynamic compaction
[AD-A266742] p 965 N94-15773
The effect of oxygen, grain size, and strain rate on the mechanical behavior of forged P/M tantalum
[DE93-011251] p 959 N94-16764
FORMALDEHYDE
Design of a formaldehyde photodissociation process for carbon and oxygen isotope separation
[DE93-016435] p 1039 N94-16450
Transient studies of low temperature catalysts for methane conversion
[DE93-017710] p 950 N94-16962
FORMALISM
VDM specification of the MD4 message digest algorithm
[NPL-DITC-204/92] p 1142 N94-14944
The use of formal methods in data security standards
[NPL-DITC-205/92] p 1142 N94-15008
RAISE specification of the MD4 message digest algorithm
[NPL-DITC-206/92] p 1142 N94-15010
The value of reference implementations and prototyping in a formal design and testing methodology
[NPL-DITC-208/92] p 1142 N94-15011
The application of programming languages to the production of reference implementations
[NPL-DITC-209/92] p 1143 N94-15012
Standards and conformance testing in data security: Results of initial programme of investigation
[NPL-DITC-218/92] p 1143 N94-15014
A formal language for the specification and verification of synchronous and asynchronous circuits
[NASA-CR-191509] p 1144 N94-15443
FORMING TECHNIQUES
Thermal spray forming of refractory sample ampoule cartridges for single crystal growth space furnaces
[TABES PAPER 93-605] p 1051 N94-16141
FORMS (PAPER)
Index of NASA prefixed forms
[NHB-1420.21] p 1230 N94-15936
FORSTERITE
Olivines in the Kaba carbonaceous chondrite and constraints on their formation p 1219 N94-16255
Evaporation kinetics of Mg2SiO4 crystals and melts from molecular dynamics simulations p 1219 N94-16331
FORTRAN
User manual and program description of the data acquisition system of PML-pulse physics
[AD-A266752] p 1147 N94-15776
Efficient compilation of array statements for private memory multicomputers
[AD-A266595] p 1160 N94-16724
FORWARD SCATTERING
Simulations of wave-particle interactions in stimulated Raman forward scattering in a magnetized plasma
[TKK-F-A704] p 1201 N94-15210
Magnetic effects in anomalous dispersion
[DE93-014291] p 1175 N94-15978
FOSSIL FUELS
Biomass energy: State of the technology present obstacles and future potential
[DE93-016295] p 1092 N94-16766
Publications of the Oak Ridge National Laboratory Fossil Energy Program, 1 October 1991 - 31 March 1993
[DE93-014643] p 1232 N94-16967
FOULING
Regulation of attached bacterial growth by adsorbed proteins
[AD-A267756] p 1118 N94-17275
Heating of lubricant with an electric resistance heater
[VTT-TIED-1359] p 974 N94-17547
FOUNDRIES
NASA Space Engineering Research Center for VLSI System Design
[NASA-CR-194587] p 1008 N94-15547
FOUR-WAVE MIXING
Theoretical studies relating to the interaction of radiation with matter
[AD-A266894] p 1179 N94-14949
Theoretical studies relating to the interaction of radiation with matter
[AD-A267134] p 1180 N94-15689
FOURIER ANALYSIS
Construction and calculation p 931 N94-15256
Effects of window size and shape on accuracy of subpixel centroid estimation of target images
[NASA-TP-3331] p 1034 N94-15990
Detection of subsurface defects in machined silicon nitride ceramics by optical scattering methods
[DE93-015554] p 968 N94-16658
Scattering from binary optics p 1195 N94-17341
FOURIER SERIES
Comparison of level-1 and level-2 buckling and postbuckling solutions
[NASA-CR-194611] p 1057 N94-15154
FOURIER TRANSFORMATION
Optical residue processing module
[AD-A267721] p 1188 N94-14940
Acousto-optical classifier
[AD-D015894] p 1000 N94-16921
FOVEA
The effects of luminance boundaries on color perception
[AD-A268398] p 1133 N94-17397
FRACTALS
Study of fractal aggregates p 979 N94-16086
Fractal geometry of some Martian lava flow margins: Alba Patera p 1270 N94-16298
Multi-resolution processing for fractal analysis of airborne remotely sensed data p 1065 N94-16604
FRACTIONATION
Petrologic models of 15388, a unique Apollo 15 mare basalt p 1264 N94-16258
Os isotopes in SNC meteorites and their implications to the early evolution of Mars and Earth p 1242 N94-16272
Searching for neuKREEP: An EMP study of Apollo 11 Group A basalts p 1266 N94-16275
On the composition of neuKREEP: QMD contamination at Apollo 11? p 1266 N94-16276
The monzonorite-anorthosite connection: The petrogenesis of terrestrial KREEP p 1104 N94-16365
Igneous fractionation and subsolidus equilibration of diogenite meteorites p 1245 N94-16413
Siderophile element fractionation in meteor crater impact glasses and metallic spherules p 1246 N94-16414
FRACTURE MECHANICS
Fracture toughness tests for particulate MMC UK COSI (IACFA) task group. Meeting report, October 1992
[NPL-DMM(A)-81] p 1057 N94-15021
Prediction of stable tearing of 2024-T3 aluminum alloy using the crack-tip opening angle approach
[NASA-TM-109023] p 955 N94-15708
Recent advances in ordered intermetallics
[DE93-015308] p 955 N94-15862
Measurement and analysis of critical CTOA for an aluminum alloy sheet
[NASA-TM-109024] p 956 N94-15948
Anisotropic damage mechanics modeling in metal matrix composites
[AD-A266328] p 934 N94-16440
The processing and mechanical properties of high temperature/high performance composites. Book 1: Coonstituent properties of composites
[AD-A266394] p 935 N94-16483
The processing and mechanical properties of high temperature/high performance composites. Book 3: Coonstituent properties and macroscopic performance
[AD-A266396] p 935 N94-16485
The processing and mechanical properties of high temperature/high performance composites. Book 4: Coonstitutive laws and design
[AD-A266397] p 935 N94-16528
The processing and mechanical properties of high temperature/high performance composites. Book 5: Processing and miscellaneous properties
[AD-A266398] p 935 N94-16529
Development of a constitutive model for creep and life prediction of advanced silicon nitride ceramics
[DE93-015894] p 968 N94-16813
Bulk and defect properties of ordered intermetallics: A first-principles total-energy investigation
[DE93-015492] p 959 N94-16873
Mean strain effects on the strain life fatigue curve
[AD-A267211] p 960 N94-16984
J-integral and HRR field associated with stable crack growth in thin aluminum SEN specimen
[AD-A267879] p 960 N94-17041
Direct observation of fracture of CAS-glass/SiC composites and processing of toughened alumina
[AD-A268275] p 941 N94-17457
The effect of electric discharge machined notches on the fracture toughness of several structural alloys
[AD-A268605] p 962 N94-17464
Environment enhanced fatigue crack propagation in metals: Inputs to fracture mechanics life prediction models
[NASA-CR-191538] p 942 N94-17638
FRACTURE STRENGTH
Fracture toughness tests for particulate MMC UK COSI (IACFA) task group. Meeting report, October 1992
[NPL-DMM(A)-81] p 1057 N94-15021
Environmental embrittlement in ordered intermetallic alloys
[DE93-015307] p 955 N94-15830
Recent advances in ordered intermetallics
[DE93-015308] p 955 N94-15862
The influence of microstructure on the mechanical behavior of silicon nitride ceramics
[DE93-015363] p 966 N94-16018
Mechanical properties of magnesium ammonium phosphate cements and their zeolite composites
[DE93-015155] p 934 N94-16057
Crystallization of grain boundary phases in silicon nitride with low additive contents by microwave annealing
[DE93-015801] p 1209 N94-16164
The effect of irradiation on the mechanical properties of 6061-T651 aluminum
[DE93-015825] p 958 N94-16168
The processing and mechanical properties of high temperature/high performance composites. Book 1: Coonstituent properties of composites
[AD-A266394] p 935 N94-16483
The processing and mechanical properties of high temperature/high performance composites. Book 3: Coonstituent properties and macroscopic performance
[AD-A266396] p 935 N94-16485
The Ceramic Technology Project: Ten years of progress
[DE93-015991] p 968 N94-16843
Bulk and defect properties of ordered intermetallics: A first-principles total-energy investigation
[DE93-015492] p 959 N94-16873
RSRM nozzle actuator bracket/lug fracture mechanics qualification test
[NASA-CR-193859] p 927 N94-17080
Micromechanisms of monotonic and cyclic subcritical crack growth in advanced high melting point low-ductility intermetallics
[AD-A267764] p 961 N94-17223
Prediction of thermal cycling induced cracking in polymer matrix composites
[NASA-CR-194677] p 941 N94-17295
The effect of electric discharge machined notches on the fracture toughness of several structural alloys
[AD-A268605] p 962 N94-17464
FRACTURES (MATERIALS)
A Monazite-bearing clast in Apollo 17 melt breccia p 1267 N94-16279
FRACTURING
Environmental embrittlement in ordered intermetallic alloys
[DE93-015307] p 955 N94-15830

Recent advances in ordered intermetallics
[DE93-015308] p 955 N94-15862
Weibull analysis applied to the pull adhesion test and fracture of a metal-ceramic interface
[DE93-012913] p 1059 N94-15997
Anisotropic damage mechanics modeling in metal matrix composites
[AD-A266328] p 934 N94-16440
The processing and mechanical properties of high temperature/high performance composites. Book 5: Processing and miscellaneous properties
[AD-A266398] p 935 N94-16529
Highly transient elastodynamic crack growth in a bimaterial interface: Higher order asymptotic analysis and optical experiments
[AD-A266465] p 1059 N94-16587
Direct observation of fracture of CAS-glass/SiC composites and processing of toughened alumina
[AD-A268275] p 941 N94-17457
The effect of electric discharge machined notches on the fracture toughness of several structural alloys
[AD-A268605] p 962 N94-17464

FRAGMENTATION
The fragmentation of Kosmos 2163
[NASA-CR-191643] p 887 N94-16503
The fragmentation of the Nimbus 6 rocket body
[NASA-CR-191645] p 926 N94-16504
Dynamic testing and characterization of pre-fractured ceramic
[DE93-016457] p 972 N94-17238

FRAGMENTS
Simulation of collisional fragmentation with explosives p 1063 N94-16254
A Monazite-bearing clast in Apollo 17 melt breccia p 1267 N94-16279
Identification of new meteorite, Mihonoseki (L), from broken fragments in Japan p 1246 N94-16415

FRAMES
Preliminary analysis and design optimization of the short spacer truss of Space Station Freedom
[NASA-TM-4470] p 1058 N94-15709

FRAMING CAMERAS
Multi-frame x ray imaging with a large area 40ps camera
[DE93-017179] p 1035 N94-16960

FREE CONVECTION
Benard convection of magnetic colloids under microgravity p 943 N94-15159
Theoretical study of laminar film condensation on horizontal elliptical tubes under conditions of free and forced convection
[AD-A267161] p 1021 N94-15737
Natural convection above a horizontal heat source
[AD-A267212] p 1026 N94-16985
The roles of fluid motion and other transport phenomena in the morphology of materials
[NASA-CR-194665] p 1028 N94-17298

FREE ELECTRON LASERS
High frequency Raman current drive p 1201 N94-15208
Current drive with free electron lasers in high and low temperature tokamaks p 1201 N94-15209
Thomson backscattered x rays from an intense laser beam
[AD-A267125] p 1038 N94-15686

FREE ENERGY
Structural effects in electron transfer reactions: Comparative interfacial electrochemical kinetics for cis- versus trans-dioxorhenium (V) (bi)pyridine oxidation
[AD-A266307] p 1182 N94-16466

FREE FLOW
Parametric resonant triad interactions in a free shear layer
[NASA-TM-106365] p 1021 N94-15751
Receptivity of boundary layers to convected gusts
[AD-A267206] p 1022 N94-15860
Turbulence and transition modeling for high-speed flows
[AD-A266748] p 1022 N94-15953
Computation of a controlled store separation from a cavity p 858 N94-16513
Complex terrain wind model evaluation
[AD-A266467] p 1096 N94-16589
Transition induced by fixed and freely convecting spherical particles in laminar boundary layers
[AD-A267757] p 1028 N94-17276

FREE VIBRATION
Development and comparison of advanced reduced-basis methods for the transient structural analysis of unconstrained structures
[NASA-TM-109015] p 1061 N94-17259

FREE-PISTON ENGINES
SPDE/SPRE final summary report
[NASA-CR-187086] p 924 N94-15482

FREEZE DRYING
Evaluation of dried storage of platelets for transfusion: Physiologic integrity and hemostatic functionality
[AD-A266958] p 1120 N94-15180

FREEZING
Mathematical model of frost heave and thaw settlement in pavements
[AD-A267037] p 983 N94-15676

FRENCH SPACE PROGRAM
ARIANE 5 light derivatives p 878 N94-17140

FREON
Explosive boiling at very low heat fluxes: A microgravity phenomenon
[NASA-TM-106325] p 1046 N94-15817

FREQUENCIES
Regulation of low Earth orbit satellites p 892 N94-17159
TAOS (S80): A (LEO-MSS) system for position reporting and telemanagement services p 893 N94-17162
Extracavity frequency doubling study of a pulsed photodissociation iodine laser
[AD-A267893] p 1042 N94-17394
Frequency resolution of an acousto-optical spectrometer
[AD-A267822] p 1035 N94-17401
Wide angle, single screen, gridded square-loop frequency selective surface for diplexing two closely separated frequency bands
[NASA-CASE-NPO-18664-1-CU] p 1237 N94-17438
Radar transmitter procedures
[AD-A268274] p 1005 N94-17523

FREQUENCY ANALYZERS
Remote tire pressure sensing technique
[NASA-CASE-LAR-14160-1] p 1033 N94-15884

FREQUENCY CONTROL
Regulation of low Earth orbit satellites p 892 N94-17159
Quartz crystal resonators and oscillators for frequency control and timing applications: A tutorial, revision 6.1
[AD-A268205] p 1216 N94-17480

FREQUENCY DISTRIBUTION
On hydrologic similarity: A dimensionless flood frequency model using a generalized geomorphologic unit hydrograph and partial area runoff generation
[PAPER-89WR01579] p 1083 N94-16027
Cortical adaptive filtering in bioacoustic signal classification
[AD-A266229] p 1177 N94-16939

FREQUENCY DIVIDERS
Synchronous sampling phase and amplitude detection method and apparatus
[NASA-CASE-LAR-14725-1] p 1050 N94-15870

FREQUENCY DIVISION MULTIPLE ACCESS
Regulation of low Earth orbit satellites p 892 N94-17159
The ELLIPSO (tm) system: Elliptical low orbits for mobile communications p 893 N94-17167

FREQUENCY HOPPING
Spaceborne Imaging Radar-C instrument p 990 N94-15890
Design of broadband wire antennas for frequency hopping applications
[AD-A267405] p 1001 N94-17025
True time delay optically controlled dual band transmitter
[AD-A267663] p 1003 N94-17228

FREQUENCY MEASUREMENT
Remote tire pressure sensing technique
[NASA-CASE-LAR-14160-1] p 1033 N94-15884

FREQUENCY RANGES
Method and apparatus for non-destructive evaluation of composite materials with cloth surface impressions
[NASA-CASE-LAR-14535-1] p 933 N94-15878

FREQUENCY SHIFT
Stress sensitivity of dielectric resonators
[AD-A266767] p 1009 N94-15825
Spatial and frequency diversity in lidar systems
[AD-A266192] p 1039 N94-16124
Performance of coded coherent FSK lightwave system with noncoherent detection
[AD-A267442] p 1193 N94-17028

FREQUENCY SHIFT KEYING
Four Frequency-Shift Keying (4-FSK) spread spectrum modulator and demodulator
[AD-A267433] p 1000 N94-16979
Performance of coded coherent FSK lightwave system with noncoherent detection
[AD-A267442] p 1193 N94-17028

FREQUENCY STANDARDS
Quartz crystal resonators and oscillators for frequency control and timing applications: A tutorial, revision 6.1
[AD-A268205] p 1216 N94-17480

FRESNEL INTEGRALS
Diffraction of microwaves at rectangular facades of buildings with and without ground reflections (Fresnel-Kirchhoff-Approximation)
[DLR-FB-92-35] p 987 N94-15155

FRESNEL LENSES
Phase holograms in PMMA with proximity effect correction p 1037 N94-17348

FRESNEL REGION
Analysis of an electromagnetic field in the vicinity of a caustic by asymptotic methods
[IFTR-12/1991] p 998 N94-16853

FRICTION
Bibliography on snow and ice friction
[AD-A266868] p 1045 N94-14920
The friction and wear of ceramic/ceramic and ceramic/metal combinations in sliding contact
[NASA-TM-106348] p 930 N94-15769
Solid lubricants for space structures, phase 2
[AD-A266653] p 968 N94-16767
Evaluation of interfacial properties of fiber-reinforced ceramic composites using fiber push-in tests
[DE93-015427] p 972 N94-17253
Atomic-scale friction measurements using friction force microscopy. Part 1: General principles and new measurement techniques
[AD-A268391] p 1048 N94-17533

FRICTION FACTOR
Experimental study of nonassociated flow and instability of frictional materials
[AD-A266421] p 1024 N94-16555

FRICTION MEASUREMENT
Atomic-scale friction measurements using friction force microscopy. Part 1: General principles and new measurement techniques
[AD-A268391] p 1048 N94-17533

FRICTION REDUCTION
The turbulent wall jet
[AD-A267675] p 855 N94-14963

FRIENDSHIP 7
Astronauts number 3 --- Friendship 7
[NASA-TM-109430] p 874 N94-15501

FRONTS (METEOROLOGY)
Mesoscale frontogenesis: An analysis of two cold front case studies
[AD-A267950] p 1107 N94-17054

FROST
Mathematical model of frost heave and thaw settlement in pavements
[AD-A267037] p 983 N94-15676
Far-infrared spectra of CO2 clathrate hydrate frosts p 954 N94-16340

FUEL CELL POWER PLANTS
Status of molten carbonate fuel cell technology development
[DE93-015666] p 1092 N94-16715

FUEL CELLS
Chemical interactions between interconnect and electrode materials during sintering in solid oxide fuel cells
[DE93-015696] p 1092 N94-16160
Status of molten carbonate fuel cell technology development
[DE93-015666] p 1092 N94-16715
Strategy for the reduction of total integrated fluid logistics to the Space Station Freedom
[NASA-TM-107744] p 1138 N94-17452

FUEL COMBUSTION
Scholarly research program in fuel analysis and combustion research
[AD-A266789] p 942 N94-14911
Supersonic Combustion Research Laboratory. Volume 1: Design and fabrication
[AD-A267667] p 943 N94-14962
Rotary engine performance computer program (RCEMAP and RCEMAPPC): User's guide
[NASA-CR-191192] p 869 N94-15192
Biomass energy: State of the technology present obstacles and future potential
[DE93-016295] p 1092 N94-16766
Modeling study to evaluate the ionic mechanism of soot formation in flames
[AD-A266242] p 950 N94-16930

FUEL CONSUMPTION
Assessment of trends in the development of residential buildings from the standpoint of the fuel and energy requirements
[IFTR-6/1991] p 1093 N94-17092

FUEL INJECTION
Coaxial airblast atomizers
[NASA-CR-193845] p 1016 N94-15109

FUEL PRODUCTION
Helium-3 inventory of lunar samples: A potential future energy resource for mankind? p 1295 N94-16428

FUEL PUMPS
Liquid hydrogen and liquid oxygen feedline passive recirculation analysis
[TABES PAPER 93-620] p 1031 N94-16145
Space Shuttle main engine. NASA has not evaluated the alternate fuel turbopump costs and benefits. Report to the Administrator of the National Aeronautics and Space Administration
[GAO/NSIAD-94-54] p 926 N94-16834
FUEL SPRAYS
Coaxial airblast atomizers
[NASA-CR-193845] p 1016 N94-15109
Mechanism of intermittent atomization
[AD-A266625] p 1021 N94-15770
Cryogenic spray vaporization in high-velocity helium, argon and nitrogen gasflows
[NASA-TM-106363] p 1035 N94-17446
FUEL TESTS
Effects of RVP, T(50), and oxygenates on hot-start and driveability performance at high and low altitude
[AD-A266382] p 869 N94-16516
FUELS
Scholarly research program in fuel analysis and combustion research
[AD-A266789] p 942 N94-14911
FULL SCALE TESTS
Liquid Oxygen (LO2) propellant conditioning concept testing
[TABES PAPER 93-621] p 976 N94-16146
FULLERENES
Fullerene superconductors
[AD-A266749] p 1010 N94-15954
In situ Raman spectroscopy of lithium electrode surface in ambient temperature lithium secondary battery
[DE93-015238] p 1010 N94-16061
FUNCTION SPACE
Sequential functions on indexed domains and full abstraction for a sub-language of PCF
[AD-A267838] p 1152 N94-17009
FUNCTIONAL DESIGN SPECIFICATIONS
Bench checkout equipment for spaceborne laser altimeter systems p 921 N94-15618
Feasibility study of a personal communications system IRIDIUM-like p 893 N94-17165
Diffractive optics in adverse environments p 1197 N94-17352
FUNCTIONS (MATHEMATICS)
Automatic differentiation of limit functions
[DE93-016376] p 1168 N94-14928
FURANS
Solar absorptance of optical surfaces contaminated with spacecraft material outgassing products
[AD-A267202] p 886 N94-15857
FURNACES
Automated directional solidification furnace
[NASA-TM-109662] p 1175 N94-15233
QUESTS: A microgravity research facility for materials science experiments p 978 N94-16082
Thermal spray forming of refractory sample ampoule cartridges for single crystal growth space furnaces
[TABES PAPER 93-605] p 1051 N94-16141
FUSION REACTORS
Nuclear fusion of protons with ions of boron
[DE93-015399] p 1202 N94-16019
High beta and confinement studies of TFTR
[DE93-016204] p 1202 N94-16446
FUZZY SETS
A fuzzy method for preliminary design random access memory failure rate prediction
[AD-A267948] p 1055 N94-17044
FUZZY SYSTEMS
Fuzzy control and fuzzy kinematic mapping for a redundant space robot
[AD-A266866] p 1163 N94-14950
Fuzzy inverse kinematic mapping: Rule generation, efficiency, and implementation
[AD-A266967] p 1163 N94-14954
Notes on the use of Dempster-Shafer and fuzzy reasoning to fuse identity attribute data
[AD-A267426] p 1004 N94-17309

G

GABBRO
Potassium isotope cosmochemistry, volatile depletion and the origin of the Earth p 953 N94-16259
The monzonorite-anorthosite connection: The petrogenesis of terrestrial KREEP p 1104 N94-16365
The thickness of eucritic crust in the HED parent body p 1104 N94-16416
GALACTIC CLUSTERS
Participation in the north ecliptic pole sky survey
[NASA-CR-191933] p 1059 N94-16815
Complex QSO absorbers: High-redshift clusters of galaxies?
[NASA-CR-194617] p 1237 N94-16833
GALACTIC COSMIC RAYS
Calculations of cosmic-ray helium transport in shielding materials
[NASA-TP-3354] p 1301 N94-17666
GALACTIC HALOS
The theory of QSO absorption line systems and their relationship to the galaxies
[NASA-CR-194596] p 1236 N94-15679
GALACTIC STRUCTURE
The theory of QSO absorption line systems and their relationship to the galaxies
[NASA-CR-194596] p 1236 N94-15679
Collisional dynamics of perturbed particle disks in the solar system
[NASA-CR-193584] p 1239 N94-16648
GALAXIES
The theory of QSO absorption line systems and their relationship to the galaxies
[NASA-CR-194596] p 1236 N94-15679
A typical pointed observation in IRAS designed to fit into a 15 minute window
[NASA-CR-194653] p 1199 N94-17443
GALERKIN METHOD
Numerical solution of a second order boundary problem for two dimensions using galerkin approximations
[AD-A268128] p 1171 N94-17521
GALILEO PROBE
Galileo probe ready to go
[NASA-TM-109648] p 1247 N94-15432
Galileo probe spacecraft mission to Jupiter
[NASA-TM-109646] p 1247 N94-16070
GALILEO PROJECT
Galileo probe spacecraft mission to Jupiter
[NASA-TM-109646] p 1247 N94-16070
Earth imaging results from Galileo's second encounter p 1252 N94-16201
Lunar scout missions: Galileo encounter results and application to scientific problems and exploration requirements p 1259 N94-16229
Galileo photometry of Apollo landing sites p 1259 N94-16234
GALILEO SPACECRAFT
STS-26 through STS-34, deploy activities
[NASA-TM-109566] p 1301 N94-15315
STS-34 Galileo integrated deploy sim
[NASA-TM-109463] p 880 N94-15358
The 1970 highlights --- NASA programs and research
[NASA-TM-109628] p 1302 N94-15415
Earth-based and Galileo SSI multispectral observations of eastern mare serenitatis and the Apollo 17 landing site p 1261 N94-16244
GALLIUM
Silicon gallium doped photoconductor development for the AROME balloon borne instrument p 908 N94-15087
Pseudomorphic semiconducting heterostructures from combinations of AlN, GaN and selected SiC polytypes: Theoretical advancement and its coordination with experimental studies of nucleation, growth, characterization and device deployment
[AD-A267561] p 1213 N94-17108
GALLIUM ARSENIDE LASERS
Curved grating fabrication techniques for concentric-circle grating, surface-emitting semiconductor lasers p 1045 N94-17349
GALLIUM ARSENIDES
Cryogenic measurements of aerojet GaAs n-JFETs
[NASA-TM-103972] p 1009 N94-15765
Method for doping GaAs with high vapor pressure elements
[AD-D015794] p 1210 N94-16538
Large signal characterization and modeling of heterojunction bipolar transistors
[AD-A266184] p 1012 N94-16935
Photo-assisted epitaxial growth for III-V semiconductors
[AD-A267889] p 1213 N94-17042
Curved grating fabrication techniques for concentric-circle grating, surface-emitting semiconductor lasers p 1045 N94-17349
Rare earth doped III-V semiconductors for optoelectronics
[AD-A268279] p 1216 N94-17577
GALLIUM COMPOUNDS
Interface properties of wide bandgap semiconductor structures
[AD-A268269] p 1215 N94-17377
GALLIUM NITRIDES
Laser assisted CVD growth of AlN and GaN
[AD-A267150] p 1206 N94-15764
An alternative approach to the growth of single crystal gallium nitride
[AD-A267876] p 1213 N94-17037
GAME THEORY
Congestion control of high-speed networks
[AD-A267013] p 989 N94-15748
GAMMA RAY ASTRONOMY
Background suppression techniques in germanium detectors p 899 N94-15026
Prospects for high pressure imaging gas scintillation drift chambers p 901 N94-15040
Outlook for hard x ray and gamma ray astronomy p 904 N94-15057
Gamma ray spectrometer for Lunar Scout 2 p 1037 N94-16426
GAMMA RAY BURSTS
ALEXIS and HETE: Two small, low cost, scientific satellite systems p 896 N94-17185
GAMMA RAY SPECTROMETERS
Background suppression techniques in germanium detectors p 899 N94-15026
Applications for large area silicon drift detectors on x ray and gamma ray astronomy p 909 N94-15090
Gamma ray spectrometer for Lunar Scout 2 p 1037 N94-16426
GAMMA RAY TELESCOPES
Gamma large area silicon telescope: Applying Si strip detector technology to the detection of gamma rays in space p 904 N94-15061
GAMMA RAYS
Silicon radiation sensor systems for gamma and x ray detection at SI p 909 N94-15095
GAM-HEAT: A computer code to compute heat transfer in complex enclosures
[DE93-014724] p 1023 N94-15980
Induced thermoluminescence study of experimentally shock-loaded oligoclase p 953 N94-16266
Astrophysics with MILAGRO
[DE93-012722] p 1240 N94-17657
GARNETS
Water in Earth's mantle: Hydrogen analysis of mantle olivine, pyroxenes and garnet using the SIMS p 1104 N94-16336
GAS ANALYSIS
Gas Analysis System
[DE93-014617] p 949 N94-16891
Electron reversal ionizer for detection of trace species using a spherical cathode
[NASA-CASE-NPO-18870-1-CU] p 1185 N94-17329
GAS ATOMIZATION
Solid lubricants for space structures, phase 2
[AD-A266653] p 968 N94-16767
GAS BEARINGS
A mechanical system damping measurement technique using a one-degree-of-freedom (1DOF) cylindrical gas bearing
[AD-A268402] p 1048 N94-17462
GAS CHROMATOGRAPHY
Scholarly research program in fuel analysis and combustion research
[AD-A266789] p 942 N94-14911
Space Shuttle solid rocket motor exposure monitoring p 976 N94-16624
On-line gas chromatographic studies of Rutherfordium (element 104), hahnium (element 105), and homologs
[DE93-013890] p 948 N94-16821
Gas Analysis System
[DE93-014617] p 949 N94-16891
Trace analysis of chemical warfare agents in air: Sampling in porous polymers followed with thermal desorption analysis
[FOA-C-40302-4.6] p 1097 N94-17625
GAS COMPOSITION
Evolution of Triton's volatile budget p 1284 N94-16373
Possible sources of H2 to H2O enrichment at evaporation of parent chondritic material p 1244 N94-16377
Solar noble gases revealed by closed system stepped etching of a metal separate from Fayetteville p 954 N94-16432
Gas Analysis System
[DE93-014617] p 949 N94-16891
Laser ignition of solid propellants: 1. Ignition delays
[AD-A268454] p 976 N94-17538
GAS DENSITY
Flow instability tests for a particle bed reactor nuclear thermal rocket fuel element
[AD-A268012] p 929 N94-17474
GAS DETECTORS
Gas Analysis System
[DE93-014617] p 949 N94-16891
GAS DISCHARGES
Cathode sheath charge transfer effects
[AD-A268393] p 1186 N94-17536
GAS DISSOCIATION
Dissociation rates of diatomic molecules
[AD-A266464] p 1182 N94-16586

GAS DYNAMICS
Accurate upwind methods for the Euler equations
[NASA-TM-106388] p 1170 N94-16882
GAS EXCHANGE
Driving terrestrial ecosystem models from space
p 991 N94-15896
The dynamics of hydroponic crops for simulation studies of the CELSS initial reference configurations
[NASA-CR-194654] p 1118 N94-17279
Oxygen diffusion in YBa2Cu3O(6+delta) ceramics on heating
[DE93-629161] p 974 N94-17633
Influence of the granular surface on the oxygen uptake in YBa2Cu3O(6+delta) ceramics
[DE93-629162] p 974 N94-17634
GAS FLOW
Turbine blade tip film cooling measurements
[AD-A267686] p 868 N94-14964
Coaxial airblast atomizers
[NASA-CR-193845] p 1016 N94-15109
Flight 20 (STS-45) polysulfide gas path investigation
[NASA-CR-193861] p 928 N94-17213
Nonintrusive fast response oxygen monitoring system for high temperature flows
[NASA-CR-4553] p 1036 N94-17655
GAS GIANT PLANETS
Chairmanship of the Neptune/Pluto outer planets science working group
[NASA-CR-194625] p 1297 N94-16832
GAS HEATING
Flow instability tests for a particle bed reactor nuclear thermal rocket fuel element
[AD-A268012] p 929 N94-17474
Some single-piston closed-cycle machines and Peter Tailer's thermal lag engine
[DE93-015983] p 1049 N94-17675
GAS IONIZATION
Absolute, Extreme-Ultraviolet Solar Spectral Irradiance Monitor (AESSIM)
[AD-A267045] p 1299 N94-15836
Observation of nonsequential ionization of helium and its impact on intensity monitoring
[DE93-017174] p 949 N94-16904
GAS JETS
Studies in turbulence and turbulence control
[AD-A266318] p 1026 N94-16950
GAS LASERS
Spectroscopic and computer modeling investigations of a laser-sustained plasma
[IFTR-30/1991] p 1204 N94-17066
GAS MIXTURES
Mechanisms of combustion limits in premixed gas flames at microgravity
[NASA-CR-194557] p 946 N94-15713
Cathode sheath charge transfer effects
[AD-A268393] p 1186 N94-17536
GAS PATH ANALYSIS
Flight 20 (STS-45) polysulfide gas path investigation
[NASA-CR-193861] p 928 N94-17213
GAS PRESSURE
Remote tire pressure sensing technique
[NASA-CASE-LAR-14160-1] p 1033 N94-15884
GAS TEMPERATURE
Nonintrusive fast response oxygen monitoring system for high temperature flows
[NASA-CR-4553] p 1036 N94-17655
GAS TUNGSTEN ARC WELDING
Determination of GTA welding efficiencies
[AD-A267163] p 1046 N94-15738
GAS TURBINE ENGINES
Turbine blade tip film cooling measurements
[AD-A267686] p 868 N94-14964
GAS TURBINES
Surface reactivity of combustion generated soot particles
[AD-A268017] p 952 N94-17532
GAS VISCOSITY
Flow instability tests for a particle bed reactor nuclear thermal rocket fuel element
[AD-A268012] p 929 N94-17474
GAS-LIQUID INTERACTIONS
Mechanism of intermittent atomization
[AD-A266625] p 1021 N94-15770
GAS-SOLID INTERACTIONS
Olivines in the Kaba carbonaceous chondrite and constraints on their formation p 1219 N94-16255
GAS-SOLID INTERFACES
Particle simulation of hypersonic flow
[AD-A267185] p 857 N94-15787
GASDYNAMIC LASERS
Experimental studies on a gas dynamic laser with narrow throat and high area-ratio grid nozzles
[AD-A267818] p 1042 N94-17400
Three short articles from Japanese laser journal
[AD-A268249] p 1042 N94-17415
GASEOUS DIFFUSION
Electronic and atomic structure of semiconductors and of high-temperature superconductors
[AD-A266805] p 1205 N94-14913
GASEOUS FUELS
Publications of the Oak Ridge National Laboratory Fossil Energy Program, 1 October 1991 - 31 March 1993
[DE93-014643] p 1232 N94-16967
GASOHOL (FUEL)
Effects of RVP, T(50), and oxygenates on hot-start and driveability performance at high and low altitude
[AD-A266382] p 869 N94-16516
GASOLINE
Effects of RVP, T(50), and oxygenates on hot-start and driveability performance at high and low altitude
[AD-A266382] p 869 N94-16516
GATES (CIRCUITS)
Improvements to pulsed phase locked loop strain monitor
[NASA-CASE-LAR-14887-1] p 1033 N94-15877
Computer-aided design package for designers of digital optical computers
[AD-A267866] p 1154 N94-17390
GAUGE INVARIANCE
Supersymmetry of gauge equations and geometric nonadiabatic phases
[DE93-626671] p 1219 N94-14935
Theoretical high energy physics research at the University of Chicago
[DE93-016863] p 1187 N94-16116
A high sensitivity search for CP violating rare K(sub L) decays and precision measurement of the direct CP violation parameter (epsilon)(prime)/(epsilon) via the four K (yields) 2(pi) decay modes
[DE93-016866] p 1184 N94-16899
Multipolar-like form of nonabelian gauge theories
[DE93-626690] p 1171 N94-17314
Derivation of the Verlinde formula from Chern-Simons theory and the G/G model
[DE93-628620] p 1221 N94-17632
GAUGE THEORY
Supersymmetry of gauge equations and geometric nonadiabatic phases
[DE93-626671] p 1219 N94-14935
Theoretical high energy physics
[DE93-015884] p 1187 N94-16170
Multipolar-like form of nonabelian gauge theories
[DE93-626690] p 1171 N94-17314
The universality of the shift of the Chern-Simons parameter for a general class of BRS invariant regularizations
[NIKHEF-H/93-03] p 1220 N94-17602
Derivation of the Verlinde formula from Chern-Simons theory and the G/G model
[DE93-628620] p 1221 N94-17632
GEARS
Solid lubricants for space structures, phase 2
[AD-A266653] p 968 N94-16767
Mechanical Systems Technology Branch research summary, 1985 - 1992
[NASA-TM-106329] p 1049 N94-17583
GELATINS
Determination of average refractive index of spin coated DCG films for HOE fabrication p 1036 N94-14992
GELATION
Preparation of homogeneous aluminosilicate gels by sol/gel techniques
[AD-A266823] p 962 N94-14914
Multinuclear NMR study of aluminosilicate sol-gel synthesis reasons for the homogeneous gelation using the prehydrolysis method
[AD-A266877] p 962 N94-14921
Intramolecular versus intermolecular condensation rates in the acidic polymerization of octaethoxytrisiloxane
[AD-A266982] p 963 N94-15490
Electrorheological (ER) fluids: A research needs assessment
[AD-A267588] p 951 N94-17210
Characterization of the lithium/pan-based polymer electrolytes interface
[AD-A268401] p 973 N94-17434
GELS
Multinuclear NMR study of aluminosilicate sol-gel synthesis reasons for the homogeneous gelation using the prehydrolysis method
[AD-A266877] p 962 N94-14921
Effects of aging time on V2O5 sol-gel coatings
[AD-A266824] p 965 N94-15843
Swelling equilibria for temperature-sensitive ampholytic hydrogels
[DE93-015264] p 966 N94-15996
Process of shaping an electrorheological solid
[AD-D015885] p 1012 N94-16914
The photochemistry of poly(methylphenylphosphazene)
[AD-A267320] p 970 N94-16948
Characterization of the lithium/pan-based polymer electrolytes interface
[AD-A268401] p 973 N94-17434
GENES
Isolation of thermostable enzyme mutants by cloning and selection in thermophilic bacteria
[AD-A266378] p 1117 N94-16514
GENETIC ALGORITHMS
Multiobjective functions optimization for task allocation mapping to multicomputer nodes
[AD-A267071] p 1146 N94-15670
GEOCHEMISTRY
Directory of research projects: Planetary materials and geochemistry
[NASA-TM-4484] p 1095 N94-15781
Twenty-Fourth Lunar and Planetary Science Conference. Part 2: G-M
[NASA-CR-193174] p 1247 N94-16173
Euromet Ureilite Consortium: A preliminary report on carbon and nitrogen geochemistry p 1241 N94-16192
Chemical differentiation, thermal evolution, and catastrophic overturn on Venus: Predictions and geologic observations p 1259 N94-16232
Geochemistry and cosmochemistry of fullerenes 3: Reaction of C60 and C70 with ozone
p 953 N94-16243
Os isotopes in SNC meteorites and their implications to the early evolution of Mars and Earth
p 1242 N94-16272
Experimental segregation of iron-nickel metal, iron-sulfide, and olivine in a thermal gradient: Preliminary results p 1243 N94-16288
Manson impact structure, Iowa: First geochemical results for drill core M-1 p 1103 N94-16322
Geochemical evidences for two chondritic-like cometary or asteroidal impacts before and at the K/T boundary
p 1244 N94-16359
GEOCHRONOLOGY
Age determinations and Earth-based multispectral observations of lunar light plains p 1275 N94-16323
Preliminary Ar-40/Ar-39 age spectrum and laser probe dating of the M1 core of the Manson Impact Structure, Iowa: A K-T boundary crater candidate
p 1104 N94-16334
GEODESY
New techniques for the combination of heterogenous data when determining the Earth's gravity field
[SER-C-395] p 1098 N94-15153
Applications of SLR p 911 N94-15556
Millimeter accuracy satellites for two color ranging
p 916 N94-15583
New perspectives for high accuracy SLR with second generation geodesic satellites p 916 N94-15585
State-of-the-art satellite laser range modeling for geodetic and oceanographic applications
p 916 N94-15586
LLR: Activities in Wettzell p 876 N94-15600
Airborne 2 color ranging experiment
p 920 N94-15614
Tectonic deformation in southern California
[NASA-CR-194621] p 1101 N94-16021
BRIDGE: A small scientific satellite for geodesy
p 890 N94-17146
GEODETIC ACCURACY
Analysis of the accuracy of strapdown inertial surveying systems
[SER-C-391] p 1081 N94-15156
Improved mapping system
[NASA-TM-109643] p 1082 N94-15428
GEODETIC SATELLITES
Laser ranging application to time transfer using geodetic satellite and to other Japanese space programs
p 911 N94-15555
The precision of today's satellite laser ranging systems p 912 N94-15559
Millimeter accuracy satellites for two color ranging
p 916 N94-15583
New perspectives for high accuracy SLR with second generation geodesic satellites p 916 N94-15585
GEODETIC SURVEYS
Applications of SLR p 911 N94-15556
GEODYNAMICS
Laser tracking for vertical control p 911 N94-15553
Nd:YLF laser for airborne/spaceborne laser ranging
p 913 N94-15563
Experience and results of the 1991 MTLRS-1 USSR campaign p 914 N94-15575
Test results from LAGEOS-2 optical characterization using pulsed lasers p 915 N94-15577
Historical MOBLAS system characterization
p 915 N94-15579
Upgrading NASA/DOSE laser ranging system control computers p 918 N94-15595
Lunar laser ranging data processing in a Unix/X windows environment p 918 N94-15599

Effects of turbulence on the geodynamic laser ranging system p 921 N94-15616
Report of the International Center for Earth Tides for the period 1985-1989 p 1099 N94-15801
Cooperative projects in geodynamical instrumentation between the State Seismological Bureau (China) and the Royal Observatory of Belgium p 1037 N94-15806
Tectonic deformation in southern California [NASA-CR-194621] p 1101 N94-16021
Ishtar deformed belts: Evidence for deformation from below? p 1256 N94-16218
Constraints on the differentiation of the Earth from the coupled Sm-146,147-Nd-142,143 systematics p 1103 N94-16271
Geophysical models of Western Aphrodite-Niobe region: Venus p 1286 N94-16382

GEOGRAPHIC INFORMATION SYSTEMS
Application of modified VICAR/IBIS GIS to analysis of July 1991 Flevoland AIRSAR data p 1080 N94-16757
Soil conservation applications with C-band SAR p 1080 N94-16760
A Geographic Information System approach to modeling nutrient and sediment transport [DE93-013747] p 1097 N94-17426

GEOIDS
Megaplumes on Venus p 1271 N94-16301
An inversion of geoid and topography for mantle and crustal structure on Mars p 1273 N94-16315
Spectral study of Venus global topography and geoid from Magellan and PVO data p 1276 N94-16332

GEOLOGICAL FAULTS
Composite refraction-reflection stack sections: Tracing faults in the Atlantic coastal plain sediments [DE93-013581] p 1112 N94-16009
Importance of expansion and contraction in the formation of tectonic features on the Moon p 1250 N94-16189
Ishtar deformed belts: Evidence for deformation from below? p 1256 N94-16218
Mode of emplacement of lunar mare volcanic deposits: Graben formation due to near surface deformation accompanying dike emplacement at Rima Parry 5 p 1258 N94-16227
Estimates of lithospheric thickness on Venus p 1267 N94-16277
Structural mapping of Maxwell Montes p 1271 N94-16304
Tectonic resurfacing of Venus p 1285 N94-16380

GEOLOGICAL SURVEYS
Geologic remote sensing with radar p 991 N94-15900
Pargo Chasma and its relationship to global tectonics p 1249 N94-16181
A discontinuous melt sheet in the Manson impact structure p 1103 N94-16269
Global Magellan-image map of Venus at full resolution p 1274 N94-16319
Tectonic resurfacing of Venus p 1285 N94-16380
Integrating remote sensing techniques at Cuprite, Nevada: AVIRIS, Thematic Mapper, and field spectroscopy p 1072 N94-16701
Expert system-based mineral mapping using AVIRIS p 1073 N94-16704
A comparison of LOWTRAN-7 corrected Airborne Visible/Infrared Imaging Spectrometer (AVIRIS) data with ground spectral measurements p 1074 N94-16710
Lithological and textural controls on radar and diurnal thermal signatures of weathered volcanic deposits, Lunar Crater region, Nevada p 1080 N94-16762
A geological and geophysical information system for Eurasia [AD-A267841] p 1232 N94-17036

GEOLOGY
LFASE report: Crustal study [AD-A266893] p 1111 N94-14947
Spaceborne radar for geoscientific applications in North China p 993 N94-15915
Ishtar deformed belts: Evidence for deformation from below? p 1256 N94-16218
Lunar scout missions: Galileo encounter results and application to scientific problems and exploration requirements p 1259 N94-16229
High-resolution seismic reflection survey at the Manson crater, Iowa p 1103 N94-16307
Summaries of the Third Annual JPL Airborne Geoscience Workshop. Volume 2: TIMS Workshop [NASA-CR-194541] p 1063 N94-16595
Summaries of the Third Annual JPL Airborne Geoscience Workshop. Volume 1: AVIRIS Workshop [NASA-CR-194540] p 1066 N94-16666

GEOMETRICAL OPTICS
Laboratory for x ray optics [AD-A267149] p 1189 N94-15735
Analysis of an electromagnetic field in the vicinity of a caustic by asymptotic methods [IFTR-12/1991] p 998 N94-16653
Optical system storage design with diffractive optical elements p 1198 N94-17360

GEOMETRICAL THEORY OF DIFFRACTION
Sound exposure level prediction for impulse sound sources above variable terrain [AD-A267535] p 1178 N94-17119

GEOMORPHOLOGY
Morphometric comparison of Icelandic lava shield volcanoes versus selected Venusian edifices p 1248 N94-16178
Pargo Chasma and its relationship to global tectonics p 1249 N94-16181
A calibration of the production rate ratio P-21/P-26 by low energy secondry neutrons: Identification of Ne spallation components at the 10(exp 6) atoms/g level in terrestrial samples p 1187 N94-16194
Collisional and dynamical history of Gaspra p 1241 N94-16202
Fluvial erosion on Mars: Implications for paleoclimatic change p 1241 N94-16210
The Acraman impact structure: Estimation of the diameter by the ejecta layer thickness p 1103 N94-16211
Morphology and models for the evolution of eastern Hecate Chasma, Venus p 1256 N94-16215
Lava flow-field morphological classification and interpretation: Examples from Venus p 1259 N94-16230
Modes of formation of lunar light plains and the detection of cryptomaria deposits p 1259 N94-16231
Estimates of lithospheric thickness on Venus p 1267 N94-16277
Geomorphic processes in the Argyre-Dorsa Argentea region of Mars p 1270 N94-16293
Tectonic resurfacing of Venus p 1285 N94-16380
Guide to Magellan image interpretation [NASA-CR-194340] p 1298 N94-17654

GEOPHYSICAL OBSERVATORIES
TLRS-3 system upgrades p 877 N94-15609

GEOPHYSICAL SATELLITES
On-board spatial scientific experiment project on small satellites p 896 N94-17184

GEOPHYSICS
Papers presented at the Eleventh International Symposium on Earth Tides [COMMUNICATIONS-SER-B-158] p 1098 N94-15800
Proceedings of the Third Spaceborne Imaging Radar Symposium [NASA-CR-194104] p 989 N94-15886
SIR-C/X-SAR free flyer concept p 898 N94-15903
EOS SAR: A new approach p 992 N94-15904
Calibration: Practical experience with ERS-1 p 992 N94-15907
Geophysical models of Western Aphrodite-Niobe region: Venus p 1286 N94-16382
Summaries of the Third Annual JPL Airborne Geoscience Workshop. Volume 2: TIMS Workshop [NASA-CR-194541] p 1063 N94-16595
Summaries of the Third Annual JPL Airborne Geoscience Workshop. Volume 1: AVIRIS Workshop [NASA-CR-194540] p 1066 N94-16666
Summaries of the Third Annual JPL Airborne Geoscience Workshop. Volume 3: AIRSAR Workshop [NASA-CR-194542] p 1075 N94-16731
A geological and geophysical information system for Eurasia [AD-A267841] p 1232 N94-17036
Workshop on early Mars: How warm and how wet, part 2? [NASA-CR-193503] p 1297 N94-17637

GEOPOTENTIAL
State-of-the-art satellite laser range modeling for geodetic and oceanographic applications p 916 N94-15586
Implementing a 50x50 gravity field model in an orbit determination system [AD-A267548] p 888 N94-17103

GEOSTROPHIC WIND
A two-layer quasi-geotrophic spherical model: Formulation and climatology [DM-63] p 1110 N94-17593

GEOSYNCHRONOUS ORBITS
TITUS: A micro-satellite for technology demonstration p 896 N94-17186

GEOTEMPERATURE
Pyroxene equilibration temperatures in metamorphosed ordinary chondrites p 1242 N94-16224

GEOTHERMAL ANOMALIES
Megaplumes on Venus p 1271 N94-16301

GERMANIUM
Background suppression techniques in germanium detectors p 899 N94-15026
Performance testing of doped-germanium photoconductors for the ISO long wavelength spectrometer p 905 N94-15066
Non-linear effects in doped-germanium photoconductors for the ISO long wavelength spectrometer p 905 N94-15067
Extrinsic photoconductor detectors for the wavelength range 2 microns to 240 microns p 906 N94-15073
Ionising radiation-induced effects in doped germanium FIR photoconductors p 907 N94-15077
Growth of new materials for solid state laser applications. The growth of ZnGeP2 by the vertical Bridgman method [NASA-CR-194571] p 1038 N94-15530
Structural characterization of epitaxial layers for infrared detectors [AD-A267875] p 940 N94-17013
Buried porous silicon-germanium layers in monocrystalline silicon lattices and method of producing [NASA-CASE-NPO-18836-1-CU] p 1215 N94-17327

GERMANIUM ALLOYS
Metastable phases in mechanically alloyed aluminum germanium powders [DE93-008727] p 958 N94-16463

GET AWAY SPECIALS (STS)
GAS highlights, 1988 --- Get Away Specials [NASA-TM-109600] p 873 N94-15308

GEYSERS
Tidal interaction: A possible explanation for geysers and other fluid phenomena in the Neptune-Triton system p 1272 N94-16311

GIANT STARS
The formation process of the He I lambda 10830 line in cool giant stars [NASA-CR-194648] p 1240 N94-17094

GIOTTO MISSION
Comet Halley returns [NASA-TM-109608] p 885 N94-15296
Giotto's second encounter: The mission to Comet Grigg-Skjellerup [ESA-BR-93] p 1239 N94-16524
Small satellite missions to long-period comets p 874 N94-17144

GLACIAL DRIFT
Geomorphic processes in the Argyre-Dorsa Argentea region of Mars p 1270 N94-16293

GLACIERS
Geomorphic processes in the Argyre-Dorsa Argentea region of Mars p 1270 N94-16293
Preliminary results of polarization signatures for glacial moraines in the Mono Basin, Eastern Sierra Nevada p 1078 N94-16746

GLACIOLOGY
A calibration of the production rate ratio P-21/P-26 by low energy secondry neutrons: Identification of Ne spallation components at the 10(exp 6) atoms/g level in terrestrial samples p 1187 N94-16194

GLASS
Analysis of leading edge and trailing edge cover glass samples before and after treatment with advanced satellite contamination removal techniques [AD-A267055] p 885 N94-15666
Search for far infrared radiation from optically pumped defect modes [AD-A266744] p 1206 N94-15822
Optical and infrared spectra of thermally annealed Pb implanted SiO2 glasses [DE93-015304] p 965 N94-15828
Method of producing a silicon carbide fiber reinforced strontium aluminosilicate glass-ceramic matrix composite [NASA-CASE-LEW-15263-2] p 934 N94-15929
Contained liquids in microgravity, part 2 p 979 N94-16085
High-performance nonlinear optical material developed in Japan [AD-A266194] p 1191 N94-16126
A test of the applicability of independent scattering to high albedo planetary regoliths p 1250 N94-16187
Why is the Moon dark? p 1256 N94-16219
The ilmenite liquidus and depths of segregation for high-Ti picrite glasses p 975 N94-16241
Trace-element composition of Chicxulub crater melt rock, K/T tektites and Yucatan basement p 1242 N94-16245
Siderophile elements in the upper mantle of the Earth: New clues from metal-silicate partition coefficients p 1103 N94-16250
Grain surface features of Apollo 17 orange and black glass p 1289 N94-16397
Siderophile element fractionation in meteor crater impact glasses and metallic spherules p 1246 N94-16414
An investigation of the hydrolytic resistance of sodium-calcium plate glass with a layer of silica deposited on its surface [IFTR-34/1991] p 971 N94-17120
Optical studies of glasses embedded with inorganic ions and organic dyes [AD-A268146] p 1199 N94-17455
Interface chemistry in ceramic matrix composites [AD-A268629] p 973 N94-17466

Design, development and characterization studies of a large aperture high power Nd: Glass rod amplifier stage
[DE93-624944] p 1042 N94-17630
Kinetics of silica-phase transitions
[DE93-016231] p 1217 N94-17659

GLASS FIBER REINFORCED PLASTICS
Effect of Impact Damage and Open Hole on Compressive Strength of Hybrid Composite Laminates
[NASA-CR-194603] p 936 N94-16836

GLASS FIBERS
Production process p 931 N94-15257
Characterization of voids formed during liquid impregnation of nonwoven multifilament glass networks as related to composite processing p 939 N94-16858
Investigation of the optical, electronic, and structural properties of fiber optic glasses
[AD-A267645] p 971 N94-17204

GLINT
What is the radar tracking Glint problem and can it be solved?
[AD-A266509] p 999 N94-16789

GLOBAL AIR POLLUTION
Statement on global climate change before the Subcommittee on Energy and Power, United States House of Representatives
[DE93-013163] p 1095 N94-16006

GLOBAL POSITIONING SYSTEM
Applications of SLR p 911 N94-15556
Tectonic deformation in southern California
[NASA-CR-194621] p 1101 N94-16021
Test plan for the evaluation of the initial capability of the National Satellite Test Bed: Phase 1D
[DOT/FAA/RD-93/20] p 876 N94-16025
Interferometric GPS attitude: A stochastic error model, DREO report
[AD-A266411] p 864 N94-16457
Category (CAT) 3B level 1 test plan for Global Positioning System (GPS)
[DOT/FAA/RD-93/21] p 864 N94-16835
Wide-area Differential Global Positioning System (WDGPS)/Wide-area Integrity Broadcast (WIB) alternatives analysis
[DOT/FAA/SE-93/3] p 864 N94-16906

GLOBAL TRACKING NETWORK
Laser tracking for vertical control p 911 N94-15553

GLOBAL WARMING
Global Greenhouse Expedition
[NASA-TM-109613] p 1095 N94-15364
EOS SAR: A new approach p 992 N94-15904
A summary of microwave remote sensing investigations planned for BOREAS p 993 N94-15914
Discrimination among semi-arid landscape endmembers using the Spectral Angle Mapper (SAM) algorithm p 1074 N94-16711
Incorporating global warming risks in power sector planning. Volume 1: A case study of the New England region
[DE93-015241] p 1096 N94-17289

GLOVES
STS-27 crew fire training and glove molding
[NASA-TM-109554] p 1136 N94-15406
Investigation of the effects of extravehicular activity (EVA) gloves on performance
[NASA-TM-3401] p 1137 N94-15717
Force-endurance capabilities of extravehicular activity (EVA) gloves at different pressure levels
[NASA-TP-3420] p 1139 N94-17653

GLOW DISCHARGES
Investigation of the energy distribution of ions, striking the cathode in an abnormal glow discharge
[DE93-623987] p 1013 N94-17316

GLUONS
PHENIX Conceptual Design Report
[DE93-015759] p 1182 N94-16161
Mesons at finite temperature in the NJL model with gluon condensate
[DE93-626697] p 1185 N94-17310
Quark-loop effects in high energy spin-flip processes
[DE93-626692] p 1188 N94-17313
The three-loop QCD beta-function and anomalous dimensions
[NIKHEF-H/92-17] p 1186 N94-17617

GLUTAMATES
Synaptic plasticity and memory formation
[AD-A267988] p 1133 N94-17453

GLYCEROLS
Contained liquids in microgravity, part 2 p 979 N94-16085

GLYCOLS
Contained liquids in microgravity, part 2 p 979 N94-16085

GODDARD TRAJECTORY DETERMINATION SYSTEM
Implementing a 50x50 gravity field model in an orbit determination system
[AD-A267548] p 888 N94-17103

GOERTLER INSTABILITY
On the receptivity problem for 0(1) wavelength Goertler vortices
[NASA-CR-191519] p 1016 N94-15005

GOES SATELLITES
The Central American cold surge: An observational analysis of the deep southward penetration of North American cold fronts
[AD-A268592] p 1110 N94-17607

GOES 4
The 1980 highlights
[NASA-TM-109672] p 1303 N94-15509

GOGGLES
Comparative night vision goggle visual acuity measurements performed in the A-10 aircraft in an operational setting
[AD-A266721] p 1137 N94-15820
Evaluation of Night Vision Goggles (NVG) for maritime search and rescue (HH-3/HH-60) comparison report
[AD-A266493] p 1138 N94-16793

GOLD
Low dielectric constant insulators and gold metallization for GHz multi-chip modules, part 2
[AD-A268590] p 1176 N94-17605

GOLD ALLOYS
Characterization of metallic multilayers using x ray diffraction analysis
[NIAR-93-13] p 961 N94-17282

GOODNESS OF FIT
Moments in statistics: Approximations to densities and goodness-of-fit
[AD-A266600] p 1173 N94-16726

GOVERNMENT PROCUREMENT
Equipment management user's handbook for property custodians
[NHB-4200.2A] p 1224 N94-15957
Equipment Management Manual
[NHB-4200.1D] p 1225 N94-16799

GOVERNMENT/INDUSTRY RELATIONS
Industrial labor relations manual
[NHB-5200.1B] p 1224 N94-15939
Government/contractor development teams
[TABES PAPER 93-460] p 1050 N94-16134
New health and safety initiatives at the Department of Energy (DOE) p 1124 N94-16610
Technology transfer. Determining industry needs: A guide for communities
[NASA-CR-194676] p 1235 N94-17293
Technology in action
[NASA-TM-109345] p 1235 N94-17294
Satellite communications systems and technology. Executive summary
[NASA-TM-109346] p 1006 N94-17661

GRAIN BOUNDARIES
STS-26 SSIP briefing --- Titanium Grain Formation Experiment and Crystal Membrane Experiment
[NASA-TM-109556] p 976 N94-15280
Diamond epitaxy and diamondlike coatings
[AD-A266657] p 1206 N94-15747
A reexamination of grain boundary fracture in Ni3Al: Environmental and alloying effects
[DE93-015431] p 1208 N94-16063
Crystallization of grain boundary phases in silicon nitride with low additive contents by microwave annealing
[DE93-015801] p 1209 N94-16164
Superconducting ceramics: Selected properties and methods of production
[IFTR-23/1991] p 969 N94-16924
UHV-stem studies on nucleation and growth of thin metal silicide films on silicon
[DE93-017604] p 1212 N94-16961
Influence of grain size on the energy storing ability during uniaxial stretching of austenite steel
[IFTR-22/1992] p 961 N94-17121
Advanced thin-film deposition and physical properties of high-temperature and other novel superconducting materials
[AD-A268199] p 1216 N94-17561

GRAIN SIZE
Synthesis of ceramic oxide powders in a microwave plasma device
[DE93-012741] p 965 N94-15920
Rheology of water and ammonia-water ices p 953 N94-16188
Densities of 5-15 micron interplanetary dust particles p 1244 N94-16367
Exsolved kirschsteinite in angrite LEW86010 olivine p 1245 N94-16410
The effect of oxygen, grain size, and strain rate on the mechanical behavior of forged P/M tantalum
[DE93-011251] p 959 N94-16764
Influence of grain size on the energy storing ability during uniaxial stretching of austenite steel
[IFTR-22/1992] p 961 N94-17121

GRAMMARS
Using multiple adaptively-weighted strategies for the resolution of demonstratives
[AD-A266463] p 1150 N94-16585
Visual parallel programming with determinacy: A language specification, an analysis technique, and a programming tool
[AD-A267560] p 1153 N94-17107

GRANITE
The Karakul depression in Pamirs: The first impact structure in Central Asia p 1241 N94-16212

GRANTS
Research grant handbook
[NHB-5800.1C] p 1225 N94-16907

GRANULAR MATERIALS
Experimental study of nonassociated flow and instability of frictional materials
[AD-A266421] p 1024 N94-16555
Stability analysis for the flow of granular materials down an inclined plane using kinetic model
[DE93-016852] p 1026 N94-16958
Influence of the granular surface on the oxygen uptake in YBa2Cu3O(6+delta) ceramics
[DE93-629162] p 974 N94-17634

GRAPH THEORY
Homogeneously traceable results in claw-free graphs
[AD-A266196] p 1169 N94-16127
Discovering sequence similarity by the algorithmic significance method
[DE93-015556] p 1150 N94-16659

GRAPHICAL USER INTERFACE
HP upgrade operational streamlining p 918 N94-15596
User's manual for the HYPGEN hyperbolic grid generator and the HGUI graphical user interface
[NASA-TM-108791] p 1148 N94-15784
Computing science and statistics. Volume 24: Graphics and visualization
[AD-A266571] p 1150 N94-16721
Design and implementation of an interface editor for the Amadeus multi-relational database front-end system
[AD-A267403] p 1233 N94-17114

GRAPHITE
Measurement of the specific heat capacity of the electron-beam graphite calorimeter
[NPL-RSA(EXT)-40] p 1031 N94-15018
Negative ion formation in small carbon clusters
[DE93-015436] p 1182 N94-16064
Corrosion kinetics and mechanisms for nuclear grade graphites
[DE93-015462] p 947 N94-16105

GRAPHITE-EPOXY COMPOSITES
Aeroelastic airfoil smart spar p 868 N94-16865

GRASSES
Radar response of vegetation: An overview p 991 N94-15898

GRASSLANDS
Evaluation of spatial productivity patterns in an annual grassland during an AVIRIS overflight
[CIW-PUBL-1134] p 1067 N94-16672
Measuring dry plant residues in grasslands: A case study using AVIRIS p 1072 N94-16697

GRATINGS (SPECTRA)
Gratings and waveguides p 1226 N94-14987
The development of back-illuminated CCD's for XMM p 900 N94-15035
Development of ultra-low noise, high performance 3-V Quantum Well Infrared Photodectors (QWIP's) for focal plane array staring image sensor systems
[AD-A267715] p 1214 N94-17272
Conference on Binary Optics: An Opportunity for Technical Exchange
[NASA-CP-3227] p 1194 N94-17331
Diffractive optics: Design, fabrication, and applications p 1194 N94-17334
Scalar limitations of diffractive optical elements p 1194 N94-17336
Subwavelength structured surfaces and their applications p 1194 N94-17337
Finite difference time domain analysis of chirped dielectric gratings p 1195 N94-17339
Asymmetric three-beam binary optic grating p 1195 N94-17340
Scattering from binary optics p 1195 N94-17341
Mathmatical modeling for diffractive optics p 1195 N94-17342
Binary optics at Hughes Danbury Optical Systems p 1195 N94-17344
Curved grating fabrication techniques for concentric-circle grating, surface-emitting semiconductor lasers p 1045 N94-17349
Optical system storage design with diffractive optical elements p 1198 N94-17360
Color separation gratings p 1198 N94-17362

GRAVIMETERS
A new feedback system for instruments equipped with a capacitive transducer p 1037 N94-15802
Calibration platforms for gravimeters p 1037 N94-15805
On tidal parameters at Brussels fundamental station p 1100 N94-15807
Nontidal gravity changes observed with a superconducting gravimeter p 1100 N94-15808
Earth tides results obtained with gravimeters, clinometers, and strainmeters in Belgium and in Grand Duchy of Luxembourg p 1100 N94-15809

GRAVITATION
Ishtar deformed belts: Evidence for deformation from below? p 1256 N94-16218

GRAVITATIONAL COLLAPSE
Numerical simulation of three-dimensional self-gravitating flow
[NASA-TM-109021] p 1021 N94-15768

GRAVITATIONAL CONSTANT
A simultaneous estimation of the mass of Mars and its natural satellites, Phobos and Deimos, from the orbital perturbations on the Mariner 9, Viking 1, and Viking 2 orbiters p 1279 N94-16347

GRAVITATIONAL EFFECTS
Measurements of Interfacial Tension: MITE p 943 N94-15158
Pool boiling: Single bubble experiment p 944 N94-15160
Pressures of supercritical salt solutions p 945 N94-15166
Finding stable orientations of assemblies with linear programming
[AD-A266990] p 1143 N94-15212
Proceedings of the Second Workshop on Microgravity Experimentation
[DSS-NR15-43-1990] p 977 N94-16071
Canadian microgravity experiments flown in 1989-1990 p 977 N94-16075
Development of the Laser-based R/D Test-bed System (LTS) p 978 N94-16080
Optical systems for the visualization of fluid and solid transparent media under microgravity conditions p 978 N94-16081
The size of complex craters p 1262 N94-16249
Growth of single crystals of mercuric iodide on the ground and in space
[DE93-015523] p 1209 N94-16442
The 1990-1991 NASA space biology accomplishments
[NASA-TM-4501] p 1118 N94-17257
Gravity dependent condensation pressure drop and heat transfer in ammonia two-phase heat transport systems
[NLR-TP-92121-U] p 1031 N94-17615
Ontogenesis of mammals in microgravity
[NASA-TM-103978] p 1139 N94-17636

GRAVITATIONAL FIELDS
New techniques for the combination of heterogenous data when determining the Earth's gravity field
[SER-C-395] p 1098 N94-15153
Impending motion direction of contacting rigid bodies
[AD-A266814] p 1164 N94-15756
Apparatus and method for producing an artificial gravitational field
[NASA-CASE-MSC-22021-1] p 886 N94-15935
Energy potential analysis of zero velocity curves in the restricted three-body problem
[AD-A267512] p 1170 N94-17076
Implementing a 50x50 gravity field model in an orbit determination system
[AD-A267548] p 888 N94-17103
Relativistic dynamics of spin in strong external fields
[NIKHEF-H/93-06] p 1240 N94-17604

GRAVITATIONAL PHYSIOLOGY
Living well in space: Ensuring crew capability
[NASA-TM-109538] p 1120 N94-15369
Ontogenesis of mammals in microgravity
[NASA-TM-103978] p 1139 N94-17636

GRAVITATIONAL WAVE ANTENNAS
Lunar LIGO: A new concept in gravitational wave astronomy p 1277 N94-16337

GRAVITATIONAL WAVES
Particle physics and cosmology, Task C
[DE93-016865] p 1239 N94-16118
Lunar LIGO: A new concept in gravitational wave astronomy p 1277 N94-16337

GRAVITY ANOMALIES
An inversion of geoid and topography for mantle and crustal structure on Mars p 1273 N94-16315

GRAVITY WAVES
Effective elastic thickness of the Venusian lithosphere with lateral viscosity variations in the mantle p 1293 N94-16421
Field observations of infragravity, sea and swell directional spectra
[AD-A266439] p 1113 N94-16561

GRAZING INCIDENCE
The grazing incidence detectors for the SOHO coronal diagnostic spectrometer p 905 N94-15063
Data processing system for flight spectrometer p 908 N94-15086

GREEN'S FUNCTIONS
Shielding from space radiations
[NASA-CR-194578] p 1180 N94-15715
Volume integral equations applied to circular and square cylinders
[AD-A266635] p 1169 N94-15785
Approximate Green's function methods for HZE transport in multilayered materials
[NASA-TM-4519] p 1300 N94-17084
Shielding from space radiations
[NASA-CR-194664] p 1301 N94-17255
Time dependent turbulence modeling and analytical theories of turbulence
[NASA-TM-106379] p 1029 N94-17385
The universality of the shift of the Chern-Simons parameter for a general class of BRS invariant regularizations
[NIKHEF-H/93-03] p 1220 N94-17602

GREENHOUSE EFFECT
Global Greenhouse Expedition
[NASA-TM-109613] p 1095 N94-15364
Forest fire study
[NASA-TM-109615] p 1095 N94-15425
Statement on global climate change before the Subcommittee on Energy and Power, United States House of Representatives
[DE93-013163] p 1095 N94-16006
The use of General Circulation Models in detecting climate change induced by greenhouse gases
[DE93-014369] p 1096 N94-16802
Incorporating global warming risks in power sector planning. Volume 1: A case study of the New England region
[DE93-015241] p 1096 N94-17289

GRID GENERATION (MATHEMATICS)
A parallel adaptive mesh refinement algorithm
[NASA-CR-191530] p 1168 N94-15724
User's manual for the HYPGEN hyperbolic grid generator and the HGUI graphical user interface
[NASA-TM-108791] p 1148 N94-15784
Modal element method for potential flow in non-uniform ducts: Combining closed form analysis with CFD
[NASA-TM-106347] p 1169 N94-15799
Adaptive algorithm for aircraft configuration in turbulent flow
[AD-A266188] p 867 N94-16122
Modal ring method for the scattering of sound
[NASA-TM-106342] p 1177 N94-16497
Adaptive Cartesian grid methods for representing geometry in inviscid compressible flow
[DE93-016430] p 1025 N94-16894
Three dimensional hydrodynamic calculations with adaptive mesh refinement of the evolution of Rayleigh Taylor and Richtmyer Meshkov instabilities in converging geometry: Multi-mode perturbations
[DE93-017155] p 1025 N94-16903
Single block three-dimensional volume grids about complex aerodynamic vehicles
[NASA-TM-108986] p 1030 N94-17476
Numerical solution of a second order boundary problem for two dimensions using galerkin approximations
[AD-A268128] p 1171 N94-17521
Compressible flow solvers using unstructured grids
[INRIA-RR-1732] p 1030 N94-17531
Multigrid direct numerical simulation of the whole process of flow transition in 3-D boundary layers
[NASA-TM-106369] p 1030 N94-17557

GRIGG-SKJELLERUP COMET
Giotto's second encounter: The mission to Comet Grigg-Skjellerup
[ESA-BR-93] p 1239 N94-16524

GROOVES
Fabrication techniques for very fast diffractive lenses p 1196 N94-17345

GROUND BASED CONTROL
STS-26 missions highlight resource tape
[NASA-TM-109559] p 881 N94-15407
The ELLIPSO (tm) system: Elliptical low orbits for mobile communications p 893 N94-17167

GROUND CREWS
USAF physiological studies of personal microclimate cooling: A review
[AD-A267203] p 1022 N94-15858
Aircrew/groundcrew life support systems research. Volume 2: CLIN 0002 task order requirements
[AD-A268230] p 1139 N94-17564

GROUND EFFECT (AERODYNAMICS)
An experimental study of ASTOVL related jet flows to produce CFD code validation data. Phase 3: Results of experiments
[TT-9203] p 1020 N94-15645

GROUND EFFECT (COMMUNICATIONS)
Diffraction of microwaves at rectangular facades of buildings with and without ground reflections (Fresnel-Kirchhoff-Approximation)
[DLR-FB-92-35] p 987 N94-15155
Designing clutter rejection filters with complex coefficients for airborne pulsed Doppler weather radar
[NASA-CR-4550] p 862 N94-15444

GROUND HANDLING
Mission management aircraft operations manual
[NHB-7900.3] p 1225 N94-16729

GROUND STATE
Theoretical prediction of the UV adsorption and fluorescence spectra of tyrosine and phenylalanine
[AD-A266970] p 943 N94-15111
Synthesis and chemistry of novel cyclic fluorocarbons
[AD-A267148] p 929 N94-15734
The fractional quantum Hall effect and the rotation group
[DE93-010348] p 1207 N94-15972
Dissociation rates of diatomic molecules
[AD-A266464] p 1182 N94-16586
Crystalline beam ground state
[DE93-014331] p 1211 N94-16827

GROUND STATIONS
New perspectives for high accuracy SLR with second generation geodesic satellites p 916 N94-15585
LLR: Activities in Wettzell p 876 N94-15600
Upgrading of the Borowiec laser station p 877 N94-15604
Ground based laser ranging for satellite location p 919 N94-15607
New progress of ranging technology at Wuhan Satellite Laser Ranging Station p 877 N94-15608
Satellite laser station Helwan status 1992 p 877 N94-15621
The third generation SLR station Potsdam no. 7836 p 877 N94-15623
Station report on the Goddard Space Flight Center (GSFC) 1.2 meter telescope facility p 922 N94-15625
Optical measurements of NASA/USAF CRRES high altitude rocket borne chemical release experiments in conjunction with the USAF airborne ionospheric observatory aircraft
[AD-A266404] p 1101 N94-16551
Small Satellites Systems and Services
[ISBN-2-85-428327-9] p 888 N94-17131
A proposed ground segment design for small satellites p 878 N94-17154
Ground segment definition for the Spanish small satellite program (MINISAT) p 878 N94-17155
OREMUS: Prototype of an orbit determination center dedicated to mini-satellite control p 878 N94-17156
Data processing system for ARSENE ground station: A tool for small satellite control and development p 878 N94-17157
Satellite control: A comprehensive approach p 878 N94-17158
S 80/T: A micro satellite system combining high performances and limited resources p 893 N94-17166
The ELLIPSO (tm) system: Elliptical low orbits for mobile communications p 893 N94-17167
ALEXIS and HETE: Two small, low cost, scientific satellite systems p 896 N94-17185

GROUND SUPPORT EQUIPMENT
Space Station Facility government estimating
[NASA-TM-109324] p 1223 N94-15545
Estimating and bidding for the Space Station Processing Facility
[NASA-TM-109323] p 1223 N94-15546

GROUND SUPPORT SYSTEMS
Development of a prototype kinestatic platform for application to space and ground servicing tasks. Phase 1: Concept Modeling
[NASA-CR-194036] p 887 N94-16905

GROUND TESTS
Flight testing of airbreathing hypersonic vehicles
[NASA-TM-4524] p 886 N94-15753
Comparative night vision goggle visual acuity measurements performed in the A-10 aircraft in an operational setting
[AD-A266721] p 1137 N94-15820
Overview of the solar dynamic ground test demonstration program
[NASA-TM-106296] p 928 N94-17256
Design of non-sled setup to measure head injury criteria
[NIAR-92-20] p 872 N94-17263
Ground testing for the no-vent fill of cryogenic tanks: Results of tests for a 71 cubic foot tank
[NASA-TM-106293] p 1030 N94-17486

GROUND TRUTH
Ground truth spectrometry and imagery of eruption clouds to maximize utility of satellite imagery
[NASA-CR-194358] p 1081 N94-15181

An algorithm for the estimation of bounds on the emissivity and temperatures from thermal multispectral airborne remotely sensed data p 1064 N94-16603
Ground-truthing AVIRIS mineral mapping at Cuprite, Nevada p 1069 N94-16682
Evaluation of the TOPSAR performance by using passive and active calibrators p 1078 N94-16750
GROUND WATER
Equatorial ground ice on Mars: Steady-state stability p 1290 N94-16403
AVIRIS study of Death Valley evaporite deposits using least-squares band-fitting methods p 1067 N94-16676
GROUND WAVE PROPAGATION
Environmental assessment for northwestern Indiana relay node site no. RN 8C902IN
[AD-A267849] p 1004 N94-17406
GROUND-AIR-GROUND COMMUNICATION
STS-35 mission highlights resource tape
[NASA-TM-109501] p 881 N94-15465
Johnson-Gierhart program predictions of excess propagation loss for super-high frequency air-to-ground paths. Volume 1: Theory and numerical results
[AD-A267105] p 986 N94-15649
GROUP THEORY
Application of group theory to integral-difference equations of plasma physics
[IFTR-23/1992] p 1204 N94-17067
Distributively generated matrix near rings
[DE93-626588] p 1175 N94-17641
Quantum Heisenberg groups and Sklyanin algebras
[DE93-626590] p 1175 N94-17643
GUIDE VANES
Heat transfer and aerodynamics of a 3D design nozzle guide vane tested in the Pyestock isentropic light piston facility
[RAE-TM-AERO/PROP-19] p 856 N94-15696
GULF OF MEXICO
On the application and evaluation of the relocatable diecast ocean circulation model in coastal and semi-enclosed seas
[AD-A266626] p 1112 N94-15771
SAR observations in the Gulf of Mexico p 1077 N94-16742
GULF STREAM
Investigation of AIRSAR signatures of the Gulf Stream p 1077 N94-16743
GULFS
On the application and evaluation of the relocatable diecast ocean circulation model in coastal and semi-enclosed seas
[AD-A266626] p 1112 N94-15771
GUSTS
Receptivity of boundary layers to convected gusts
[AD-A267206] p 1022 N94-15860
Radar diagnostic parameters as indicators of severe weather in central Florida
[PB93-183507] p 1106 N94-16465
GYRES
Meridional circulation in the tropical north atlantic
[AD-A268222] p 1114 N94-17555
GYROSCOPIC PENDULUMS
Analysis of the accuracy of strapdown inertial surveying systems
[SER-C-391] p 1081 N94-15156

H

H WAVES
The exact solution of the problem of diffraction of an electromagnetic plane wave by a conductive half-plane situated at an interface
[IFTR-3/91] p 1002 N94-17057
H-INFINITY CONTROL
The design and analysis of robust feedback systems
[AD-A267152] p 1165 N94-15778
H-60 HELICOPTER
Basic principles of helicopter crashworthiness
[AD-A267099] p 862 N94-15637
Evaluation of Night Vision Goggles (NVG) for maritime search and rescue (HH-3/HH-60) comparison report
[AD-A266493] p 1138 N94-16793
HADRONS
Astronomy and astrophysics p 1239 N94-15970
Evolution of hadron beams under intrabeam scattering
[DE93-014330] p 1184 N94-16826
Calorimeter based detectors for high energy hadron colliders
[DE93-017055] p 1188 N94-16900
Heavy ion physics research at Creighton University
[DE93-016809] p 1185 N94-16957
HAFNIUM CARBIDES
Tensile and stress-rupture behavior of hafnium carbide dispersed molybdenum and tungsten base alloy wires
[NASA-TM-106350] p 962 N94-17652
HAILSTORMS
Radar diagnostic parameters as indicators of severe weather in central Florida
[PB93-183507] p 1106 N94-16465
HALL EFFECT
The fractional quantum Hall effect and the rotation group
[DE93-010348] p 1207 N94-15972
Numerical studies of the photoluminescence spectrum of quantum Hall systems
[DE93-015822] p 1220 N94-16810
HALLEY'S COMET
Comet Halley returns
[NASA-TM-109608] p 885 N94-15296
HALOGENS
Basic optical studies of high T(c) oxide superconductors
[AD-A268148] p 1014 N94-17428
HAMILTONIAN FUNCTIONS
Supersymmetry of gauge equations and geometric nonadiabatic phases
[DE93-626671] p 1219 N94-14935
The fractional quantum Hall effect and the rotation group
[DE93-010348] p 1207 N94-15972
Homogeneously traceable results in claw-free graphs
[AD-A266196] p 1169 N94-16127
Stochastic chaos: An analog of quantum chaos
[DE93-016619] p 1220 N94-16956
Multipolar-like form of nonabelian gauge theories
[DE93-626690] p 1171 N94-17314
HAND (ANATOMY)
Carpal tunnel syndrome and other cumulative trauma disorders of the arm and hand and occupation in US Navy enlisted personnel
[AD-A267747] p 1129 N94-17374
HANDBOOKS
NASA directives master list and index
[NHB-1410.13L] p 1229 N94-15414
An overview of the text propagation effects for land-mobile-satellite systems: Experimental and modeling results p 996 N94-16048
Research grant handbook
[NHB-5800.1C] p 1225 N94-16907
A handbook of cost risk analysis methods
[AD-A267253] p 1235 N94-16988
Defense Logistics Information System (DLIS) procedures manual. Products and services end-user manual
[AD-A267766] p 1232 N94-17007
CALS test network handbook
[AD-A267587] p 1160 N94-17209
HARDNESS TESTS
Investigation of the origin of hot spots in deformed crystals: Ammonium perchlorate studies
[AD-A267692] p 1214 N94-17270
Mechanical properties and crystal growth studies of semiconductor alloys
[AD-A268144] p 1216 N94-17454
HARDWARE
Design of an experiment hardware for the ESA space facility BIOPAN
[DLR-FB-93-06] p 876 N94-17548
HARMONIC ANALYSIS
What we can learn about ocean tides from tide gauge and gravity loading measurements?
p 1100 N94-15811
HARMONIC CONTROL
Tilt mechanism
[AD-D015780] p 1047 N94-16548
HARMONIC EXCITATION
Nonlinear analysis of mechanical systems under combined harmonic and stochastic excitation
[AD-A266217] p 1173 N94-16937
HARMONIC GENERATIONS
Organic polymeric electro-optic materials: Synthesis, processing, and device applications
[AD-A267133] p 964 N94-15688
Rational design, construction, and processing of high-performance nonlinear optical materials
[AD-A266185] p 1191 N94-16454
In-situ electron and optical spectroscopies of translational and vibrational activated bond breaking and formation on semiconductors
[AD-A268192] p 1015 N94-17560
HARMONIC OSCILLATION
Forced harmonic vibration of the generally orthotropic cylindrical shell with inner and outer fluid loading
[AD-A266985] p 1057 N94-15150
HARMONIC OSCILLATORS
Breakdown of adiabatic invariance
[AD-A267246] p 1219 N94-14977
Design, synthesis and characterization of novel nonlinear optical polymers
[AD-A267035] p 964 N94-15675
Theoretical studies of nonlinear optical properties of conjugated polymers
[AD-A267390] p 1193 N94-17024
HARMONIC RADIATION
On the decay of a dipole pump wave to half-harmonics p 1201 N94-15211
HARMONICS
Emittance and beam size distortion due to linear coupling
[DE93-015402] p 1184 N94-16886
A search for evidence of nonlinear elasticity in the earth
[DE93-015279] p 1102 N94-17252
HARTMANN NUMBER
Clusterization of quantum states in the Hartmann model
[DE93-626624] p 1220 N94-17315
HATCHES
Crew escape certification test
[NASA-TM-109530] p 1136 N94-15392
HAZARDS
Emergency preparedness and planning p 1124 N94-16613
Education and training of professional industrial hygienists for 2020 p 1125 N94-16618
Efficient management of cardiovascular risk screening programs p 1125 N94-16622
HEAD (ANATOMY)
Reference frames in vision
[AD-A266174] p 1132 N94-16925
Design of non-sled setup to measure head injury criteria
[NIAR-92-20] p 872 N94-17263
HEAD MOVEMENT
Reference frames in vision
[AD-A266174] p 1132 N94-16925
HEAD-UP DISPLAYS
STS-26 STA training (Hauck)
[NASA-TM-109555] p 870 N94-15279
HEALTH
Living well in space: Monitoring environment
[NASA-TM-109537] p 1120 N94-15368
Living well in space: Clinical care challenge
[NASA-TM-109539] p 1120 N94-15370
Answering the space medicine challenge
[NASA-TM-109511] p 1120 N94-15457
Proceedings of the 1992 Annual Meeting NASA Occupational Health Program
[NASA-CR-193462] p 1123 N94-16609
New health and safety initiatives at the Department of Energy (DOE) p 1124 N94-16610
Americans with Disabilities Act considerations for the practice of occupational medicine p 1124 N94-16611
Medical surveillance and biological monitoring of lead exposed employees p 1124 N94-16615
Programs and resources for control of job stress in the Federal workplace p 1124 N94-16617
The Goddard Space Flight Center ergonomics program p 1125 N94-16621
Efficient management of cardiovascular risk screening programs p 1125 N94-16622
Industrial Hygiene Laboratory accreditation: The JSC experience p 1125 N94-16623
Illness/injury pattern complex 40 (Titan) p 1125 N94-16625
Physical fitness and health education program at NASA Headquarters p 1126 N94-16631
Johnson Space Center health related fitness program p 1126 N94-16633
Kennedy Space Center exercise program p 1126 N94-16634
The Langley Fitness Center p 1126 N94-16635
Physical Exercise Program p 1127 N94-16636
Bloodborne Pathogens Program p 1127 N94-16644
OSHA bloodborne pathogens standards exposure control plan p 1127 N94-16645
HEALTH PHYSICS
Efficient management of cardiovascular risk screening programs p 1125 N94-16622
HEAO
The 1979 highlights
[NASA-TM-109443] p 1247 N94-15342
The 1978 highlights
[NASA-TM-109625] p 1302 N94-15411
HEAO 1
The 1977 highlights
[NASA-TM-109626] p 1302 N94-15412
HEARING
Hearing Conservation Medical Program p 1127 N94-16639
Studies of aural acoustic emmissions with the use of an original apparatus and investigative methodology
[IFTR-20/1992] p 1177 N94-16650
HEART DISEASES
Laser artery repair
[NASA-TM-109604] p 1120 N94-15312

HEART RATE
Heart rate response to parabolic flight manoeuvres p 981 N94-16098
HEAT ENGINES
Chemical vapor deposition of Ta2O5 corrosion resistant coatings
[DE93-015488] p 969 N94-16889
HEAT EXCHANGERS
Advanced cooling for high power electric actuators
[AD-A266984] p 866 N94-15761
Liquid Oxygen (LO2) propellant conditioning concept testing
[TABES PAPER 93-621] p 976 N94-16146
Optimization of two-stage hot water exchange points p 1029 N94-17440
HEAT FLUX
Advanced cooling for high power electric actuators
[AD-A266984] p 866 N94-15761
Imaging radar studies of polar ice p 991 N94-15899
Dual active surface, miniature, plug-type heat flux gauge
[NASA-CASE-LEW-15643-1] p 1033 N94-15928
A comparison of one and two dimensional flame quenching: Heat transfer results
[DE93-015196] p 947 N94-16060
Implementation of an anisotropic turbulence model in the COMMIX-1C/ATM computer code
[DE93-015541] p 1023 N94-16444
An analysis of the radiation field beneath a bank of tubular quartz lamps
[NASA-CR-191551] p 1024 N94-16542
High heat flux engineering in solar energy applications
[DE93-016500] p 1093 N94-16954
Validation and analysis of microwave-derived rainfall over the tropics
[AD-A267785] p 1108 N94-17303
A surface energy budget model modifying heat flow by foliage effects
[AD-A268598] p 1085 N94-17610
Boundary layer structure over areas of heterogeneous heat fluxes
[DE93-010657] p 1110 N94-17673
HEAT MEASUREMENT
Turbine blade tip film cooling measurements
[AD-A267686] p 868 N94-14964
Description of cooling water calorimetry and wall thermometry diagnostic at tokamak ASDEX-Upgrade
[IPP-5/46] p 1200 N94-14966
Dual active surface, miniature, plug-type heat flux gauge
[NASA-CASE-LEW-15643-1] p 1033 N94-15928
The specific heat of titanium disilicide
[AD-A267543] p 960 N94-17100
HEAT OF FORMATION
Coefficients for calculating thermodynamic and transport properties of individual species
[NASA-TM-4513] p 1220 N94-17624
HEAT PIPES
Heat storage module p 946 N94-15172
SPDE/SPRE final summary report
[NASA-CR-187086] p 924 N94-15482
HEAT PUMPS
Cycle performance testing of nonazeotropic mixtures of HFC-142A/HCFC-124 and HFC-32/HCFC-124 with enhanced surface heat exchangers
[DE93-015215] p 1024 N94-16808
HEAT RESISTANT ALLOYS
A sulfur segregation study of PWA 1480, NiCrAl, and NiAl alloys
[NASA-TM-106289] p 956 N94-15992
Development and commercialization status of Fe3Al-based intermetallic alloys
[DE93-015802] p 957 N94-16165
HEAT SINKS
Translating wedge heat sink
[AD-D015814] p 1011 N94-16488
HEAT SOURCES
Natural convection above a horizontal heat source
[AD-A267212] p 1026 N94-16985
Variational principles of heat exchange and their applications in construction physics, part 2
[IFTR-19/1991] p 1061 N94-17069
HEAT STORAGE
Heat storage module p 946 N94-15172
Space Station thermal storage/refrigeration system research and development
[NASA-CR-193841] p 879 N94-15191
HEAT TOLERANCE
USAF physiological studies of personal microclimate cooling: A review
[AD-A267203] p 1022 N94-15858
Heat shock protein induction in human cells by CO2 laser irradiation
[AD-A266430] p 1117 N94-16545
HEAT TRANSFER
A posteriori error estimation for hierarchic models of elliptic boundary value problems on thin domains
[AD-A267714] p 1168 N94-14939
Turbine blade tip film cooling measurements
[AD-A267686] p 868 N94-14964
Pool boiling: Single bubble experiment p 944 N94-15160
Density and temperature relaxation near the critical point of carbon dioxide under reduced gravity p 944 N94-15164
Hypersonic shock wave boundary layer interactions over simplified deflected control surface configurations p 1018 N94-15203
Incorporation of boundary layer heating predictive methodology into NSWCDD aeroprediction code
[AD-A267000] p 1020 N94-15632
Heat transfer and aerodynamics of a 3D design nozzle guide vane tested in the Pyestock isentropic light piston facility
[RAE-TM-AERO/PROP-19] p 856 N94-15696
Determination of GTA welding efficiencies
[AD-A267163] p 1046 N94-15738
Effects of rotation on coolant passage heat transfer. Volume 2: Coolant passages with trips normal and skewed to the flow
[NASA-CR-4396-VOL-2] p 1023 N94-15991
A comparison of one and two dimensional flame quenching: Heat transfer results
[DE93-015196] p 947 N94-16060
Laser-liquid interactions under reduced gravity conditions p 977 N94-16077
Investigation of two-phase flow and boiling heat transfer during quenching of a tube under microgravity p 979 N94-16087
Translating wedge heat sink
[AD-D015814] p 1011 N94-16488
Biomass energy: State of the technology present obstacles and future potential
[DE93-016295] p 1092 N94-16766
Cycle performance testing of nonazeotropic mixtures of HFC-142A/HCFC-124 and HFC-32/HCFC-124 with enhanced surface heat exchangers
[DE93-015215] p 1024 N94-16808
Numerical study of compressible boundary-level transition between two concentric cylinders
[NASA-CR-194622] p 1025 N94-16842
Natural convection above a horizontal heat source
[AD-A267212] p 1026 N94-16985
Variational principles of heat exchange and their applications in construction physics, part 2
[IFTR-19/1991] p 1061 N94-17069
Convection effects on radial segregation and crystal melt interface in vertical Bridgman growth
[NASA-CR-191541] p 1029 N94-17387
Gravity dependent condensation pressure drop and heat transfer in ammonia two-phase heat transport systems
[NLR-TP-92121-U] p 1031 N94-17615
Some single-piston closed-cycle machines and Peter Tailer's thermal lag engine
[DE93-015983] p 1049 N94-17675
HEAT TRANSMISSION
Tidal gravity anomalies and tectonics p 1101 N94-15814
A decade's overview of Io's volcanic activity p 1245 N94-16386
The effects of orbital and climatic variations on Martian surface heat flow p 1290 N94-16402
A surface energy budget model modifying heat flow by foliage effects
[AD-A268598] p 1085 N94-17610
HEAT TREATMENT
NEXTEL(trademark)/SiC composites using forced chemical vapor infiltration
[DE93-013532] p 934 N94-16008
High-performance nonlinear optical material developed in Japan
[AD-A266194] p 1191 N94-16126
Structural studies of sol-gel glasses
[AD-A266277] p 967 N94-16472
Wear resistant titanium material development
[AD-A266474] p 959 N94-16780
Fiber strength utilization in carbon/carbon composites
[AD-A267713] p 940 N94-17271
HEATERS
Liquid hydrogen and liquid oxygen feedline passive recirculation analysis
[TABES PAPER 93-620] p 1031 N94-16145
Natural convection above a horizontal heat source
[AD-A267212] p 1026 N94-16985
HEATING
Was Martian mantle wet? A possible consequence of rapid core formation p 1277 N94-16335
Processing of complex sintered reaction bonded silicon nitride parts by microwave heating
[DE93-015811] p 969 N94-16877
Oxygen diffusion in YBa2Cu3O(6+delta) ceramics on heating
[DE93-629161] p 974 N94-17633
HEATING EQUIPMENT
Hollow cathode heater development for the Space Station plasma contactor
[NASA-CR-191131] p 926 N94-16880
HEAVING
Mathematical model of frost heave and thaw settlement in pavements
[AD-A267037] p 983 N94-15676
HEAVY IONS
Shielding from space radiations
[NASA-CR-194578] p 1180 N94-15715
Astronomy and astrophysics p 1239 N94-15970
Theoretical high energy physics
[DE93-015884] p 1187 N94-16170
Multispectral observations of the Jovian aurora
[NASA-CR-193628] p 1297 N94-16884
Heavy ion physics research at Creighton University
[DE93-016809] p 1185 N94-16957
Shielding from space radiations
[NASA-CR-194664] p 1301 N94-17255
Characterization of Ni on Si wafers: Comparison of surface analysis techniques
[DE93-016501] p 953 N94-17649
3D and r,z particle simulations of heavy ion fusion beams
[DE93-013417] p 1205 N94-17670
HEAVY LIFT LAUNCH VEHICLES
ALS engine propellant effector system
[NASA-CR-194650] p 926 N94-16590
HEAVY WATER
The pressure broadening of HDO by O2, N2, H2, and He between 100 K and 600 K
[AD-A267118] p 946 N94-15684
Neutral-current detection in the Sudbury Neutrino Observatory
[DE93-014481] p 1185 N94-16951
HEIGHT
The distribution of large volcanoes on Venus as a function of height and altitude p 1271 N94-16303
HEISENBERG THEORY
Quantum Heisenberg groups and Sklyanin algebras
[DE93-628590] p 1175 N94-17643
HELICOPTER CONTROL
Fidelity assessment of a UH-60A simulation on the NASA Ames vertical motion simulator
[NASA-TM-104016] p 870 N94-15793
HELICOPTER DESIGN
Helicopter structures: A review of loads, fatigue design techniques, and usage monitoring
[AD-A267115] p 866 N94-15651
Mechanical Systems Technology Branch research summary, 1985 - 1992
[NASA-TM-106329] p 1049 N94-17583
HELICOPTER PERFORMANCE
Fidelity assessment of a UH-60A simulation on the NASA Ames vertical motion simulator
[NASA-TM-104016] p 870 N94-15793
Noise measurement flight test of five light helicopters
[AD-A268566] p 1179 N94-17599
HELICOPTERS
On the use of the noncentral chi-square density function for the distribution of helicopter spectral estimates
[NASA-CR-191546] p 1176 N94-15487
Helicopter structures: A review of loads, fatigue design techniques, and usage monitoring
[AD-A267115] p 866 N94-15651
HELIOSPHERE
A comparison of solar wind parameters measured by IMP 8, Voyager 1 and Voyager 2
[AD-A266728] p 1298 N94-15821
Strategy for a small satellite program and a proposal for a first mission p 874 N94-17143
HELIOSTATS
Revisiting the BCS, a measurement system for characterizing the optics of solar collectors
[DE93-015030] p 1091 N94-15993
HELIUM
Electronic structure and enthalpy of hydrogen and helium mixtures
[DE93-014128] p 1208 N94-15976
Observation of nonsequential ionization of helium and its impact on intensity monitoring
[DE93-017174] p 949 N94-16904
Investigation of the energy distribution of ions, striking the cathode in an abnormal glow discharge
[DE93-623987] p 1013 N94-17316
HELIUM ISOTOPES
Helium-3 inventory of lunar samples: A potential future energy resource for mankind? p 1295 N94-16428
Solar noble gases revealed by closed system stepped etching of a metal separate from Fayetteville p 954 N94-16432

The formation process of the He I lambda 10830 line in cool giant stars
[NASA-CR-194648] p 1240 N94-17094
Calculations of cosmic-ray helium transport in shielding materials
[NASA-TP-3354] p 1301 N94-17666

HELIUM-NEON LASERS
Detection of subsurface defects in machined silicon nitride ceramics by optical scattering methods
[DE93-015554] p 968 N94-16658
Transmission of light through a turbulent mixing layer
[AD-A267266] p 1193 N94-17264
Three short articles from Japanese laser journal
[AD-A268249] p 1042 N94-17415

HELMET MOUNTED DISPLAYS
Optical displays: A tutorial on images and image formation
[AD-A266230] p 1192 N94-16926

HEMATITE
Terrestrial impact melts as analogues for the hematization of Martian surface materials
p 1104 N94-16424

HEMODYNAMIC RESPONSES
A review of the efficacy of 7.5 percent NaCl/6 percent Dextran-70 (HSD) in experimental animals and humans
[AD-A266633] p 1122 N94-15740

HEMODYNAMICS
Increased vascular resistance with hemoglobin-based oxygen carriers
[AD-A266454] p 1123 N94-16565

HEMOGLOBIN
Evaluation of hemoglobin-oxygen equilibrium binding by rapid-scanning spectrophotometry and singular-value decomposition
[AD-A266453] p 1123 N94-16564
Increased vascular resistance with hemoglobin-based oxygen carriers
[AD-A266454] p 1123 N94-16565
Hemoglobin
[AD-A266455] p 1123 N94-16566
Release of iron from hemoglobin
[AD-A266503] p 1128 N94-16784
Encapsulation of hemoglobin in non-phospholipid vesicles
[AD-A266505] p 1128 N94-16785
Neurotoxicity of hemoglobin in cortical cell culture
[AD-A266506] p 1128 N94-16786

HEMORRHAGES
A review of the efficacy of 7.5 percent NaCl/6 percent Dextran-70 (HSD) in experimental animals and humans
[AD-A266633] p 1122 N94-15740
A mathematical model for the study of hemorrhagic shock and fluid resuscitation: Transcapillary exchange
[AD-A266427] p 1123 N94-16544
A mathematical model for the study of hemorrhagic shock and fluid resuscitation: Exchange of fluid and solutes between vascular, interstitial, and tissue cell compartments
[AD-A266426] p 1123 N94-16558

HEMOSTATICS
Evaluation of dried storage of platelets for transfusion: Physiologic integrity and hemostatic functionality
[AD-A266958] p 1120 N94-15180

HEPATITIS
Bloodborne Pathogens Program p 1127 N94-16644
OSHA bloodborne pathogens standards exposure control plan p 1127 N94-16645

HERMITIAN POLYNOMIAL
Quantum phase fluctuations in the Jaynes-Cummings model: Effects of cavity damping
[DE93-627984] p 1186 N94-17612

HETEROCYCLIC COMPOUNDS
Electrical conductivity of ion implanted ladder and semi-ladder polymers
[AD-A267432] p 970 N94-16978
Laser photoionization time-of-flight mass spectrometry of nitrated polycyclic aromatic hydrocarbons and nitrated heterocyclic compounds
[AD-A268126] p 952 N94-17520

HETERODYNING
Heterodyne efficiency for a coherent laser radar with diffuse or aerosol targets
[NASA-CR-194563] p 1038 N94-15477

HETEROGENEITY
Heterogeneity and scaling land-atmospheric water and energy fluxes in climate systems p 1083 N94-16030

HETEROJUNCTION DEVICES
Large signal characterization and modeling of heterojunction bipolar transistors
[AD-A266184] p 1012 N94-16935

HETEROJUNCTIONS
Atomic layer epitaxy of boron nitride
[AD-A266260] p 1212 N94-16932
Large signal characterization and modeling of heterojunction bipolar transistors
[AD-A266184] p 1012 N94-16935
Structural characterization of epitaxial layers for infrared detectors
[AD-A267875] p 940 N94-17013

HEURISTIC METHODS
Fuzzy inverse kinematic mapping: Rule generation, efficiency, and implementation
[AD-A266967] p 1163 N94-14954
HSTS: Integrating planning and scheduling
[AD-A266991] p 1222 N94-15213
Using multiple adaptively-weighted strategies for the resolution of demonstratives
[AD-A266463] p 1150 N94-16585
Analysis of an electromagnetic field in the vicinity of a caustic by asymptotic methods
[IFTR-12/1991] p 998 N94-16653

HEWLETT-PACKARD COMPUTERS
HP upgrade operational streamlining
p 918 N94-15596

HEXADIENE
Synthetic and mechanistic investigation of olefin polymerization catalyzed by early transition metal compounds
[DE93-018301] p 970 N94-16963

HF LASERS
Pulsed hydrogen fluoride overtone chemical laser studies
[AD-A267597] p 1041 N94-17193

HIERARCHIES
Models for reactivity
[AD-A266419] p 1149 N94-16554

HIGH ALTITUDE
Optical measurements of NASA/USAF CRRES high altitude rocket borne chemical release experiments in conjunction with the USAF airborne ionospheric observatory aircraft
[AD-A266404] p 1101 N94-16551
Ground wave emergency network final operational capability: Environmental assessment for southern Nevada relay node site number RN 8W918NV
[AD-A267647] p 1002 N94-17205
Ground wave emergency network final operational capability: Environmental assessment for northwestern Nebraska relay node, site number RN 8C930NE
[AD-A267629] p 1003 N94-17212
Ground wave emergency network. Final operational capability. Environmental assessment for southeastern Idaho relay node, site no. RN8W927ID
[AD-A267796] p 1003 N94-17304

HIGH ASPECT RATIO
ITER-HARD Toroidal Field coil structural analysis
[DE93-014834] p 1201 N94-15981

HIGH DEFINITION TELEVISION
Video applications development platform
[AD-A266966] p 1163 N94-14953

HIGH ENERGY ELECTRONS
Pseudomorphic semiconducting heterostructures from combinations of AlN, GaN and selected SiC polytypes: Theoretical advancement and its coordination with experimental studies of nucleation, growth, characterization and device deployment
[AD-A267561] p 1213 N94-17108
Mechanical properties of interfaces and superlattices
[AD-A268591] p 1217 N94-17606

HIGH ENERGY FUELS
Synthesis of potential high-energy fuels
[AD-A267508] p 975 N94-17073

HIGH ENERGY INTERACTIONS
The TAUVEX experiment p 905 N94-15064
Study of the rare decays K(sub L)(sup 0) yields (mu)e, K(sub L)(sup 0) yields ee, and K(sub L)(sup 0) yields (mu)(mu) at KEK
[DE93-753247] p 1180 N94-15135
Theoretical high energy physics research at the University of Chicago
[DE93-016863] p 1187 N94-16116
Experimental study of weak interactions by precision measurement by rare kaon decay
[DE93-016864] p 1182 N94-16117
PHENIX Conceptual Design Report
[DE93-015759] p 1182 N94-16161
Theoretical high energy physics
[DE93-015884] p 1187 N94-16170
Heavy ion physics research at Creighton University
[DE93-016809] p 1185 N94-16957

HIGH FLUX ISOTOPE REACTORS
The effect of irradiation on the mechanical properties of 6061-T651 aluminum
[DE93-015825] p 958 N94-16168

HIGH FREQUENCIES
Evaluation of site effects on a high frequency direction finding single site location system
[AD-A267465] p 1001 N94-17035
Effect of powerful oblique HF waves on ionospheric D-layer absorption
[AD-A268443] p 1102 N94-17499

HIGH LEVEL LANGUAGES
Integration ToolKit and Methods (ITKM) manufacturing methods and prototype toolkit. A combined modeling method using IDEFO, IDEF1x and XSpec
[AD-A266176] p 984 N94-16981

HIGH PASS FILTERS
Designing clutter rejection filters with complex coefficients for airborne pulsed Doppler weather radar
[NASA-CR-4550] p 862 N94-15444

HIGH POWER LASERS
Matera Laser Ranging Observatory (MLRO): An overview p 877 N94-15601
A new method of designing multilayer optical thin film coatings
[DE93-624683] p 974 N94-17611
Design, development and characterization studies of a large aperture high power Nd: Glass rod amplifier stage
[DE93-624944] p 1042 N94-17630

HIGH PRESSURE
Liquidus equilibria of lunar analogs at high pressure
p 1283 N94-16364
Pulsed laser deposition of metastable Ca(1-x)Sr(x)CuO2 thin films
[DE93-015804] p 1040 N94-16663
High pressure pump for electro-rheological fluids
[AD-D015888] p 1048 N94-16915
Pulsed laser kinetic studies of liquids under high pressure
[DE93-017826] p 1041 N94-16998
Human central nervous system oxygen toxicity data from 1945 to 1986
[AD-A268225] p 1130 N94-17556

HIGH RESOLUTION
The MADONA experiments (Meteorology and Diffusion Over Non-uniform Areas): High-resolution in-plume concentration fluctuations measurements using lidar remote sensing technique
[AD-A267711] p 1105 N94-14938
High resolution SAR applications and instrument design p 993 N94-15913
Resolving topographic detail on Venus by modeling complex Magellan altimetry echoes
p 1283 N94-16368
Gamma ray spectrometer for Lunar Scout 2
p 1037 N94-16426
JPL activities on development of acousto-optic tunable filter imaging spectrometer p 1037 N94-16696
Insights into semiconducting materials and growth phenomena through Z-contrast STEM
[DE93-015964] p 1212 N94-16841
Moving target indicator using higher order statistics
[AD-D015890] p 1000 N94-16917
High resolution radar profiling using higher-order statistics
[AD-D015891] p 1000 N94-16918
An investigation of the Ground-Based High-Resolution Interferometer Sounder (GB-HIS) in a costal marine environment
[AD-A268052] p 1114 N94-17503

HIGH REYNOLDS NUMBER
Tollmien-Schlichting/vortex interactions in compressible boundary layer flows
[NASA-CR-191515] p 1017 N94-15183
Structure of high Reynolds number turbulent boundary layer
[AD-A267476] p 860 N94-17099

HIGH SPEED
VLSI for high-speed digital signal processing
[AD-A267709] p 1007 N94-14936
Performance comparison of high speed microchannel plate photomultiplier tubes p 922 N94-15624

HIGH SPEED PHOTOGRAPHY
Study of high speed interference photography with two-dimensional acousto-optical lattice deflection
[AD-A267823] p 1035 N94-17402

HIGH TEMPERATURE
Processing and protection of high temperature structural materials
[AD-A267292] p 954 N94-14961
High temperature advanced structural composites. Volume 3: Mechanics
[AD-A267024] p 933 N94-15626
Structures from low dielectric polyimides
[NASA-CASE-LAR-14988-1] p 965 N94-15880
Payloads for the processing of high temperature materials p 979 N94-16083
Trapping of water vapor from an atmosphere by condensed silicate matter formed by high-temperature pulse vaporization p 1248 N94-16180
Pulsed laser deposition of metastable Ca(1-x)Sr(x)CuO2 thin films
[DE93-015804] p 1040 N94-16663
Effects of processing and prolonged high temperature exposure on the microstructure of Nb-1Zr-C sheet
[NASA-TM-106370] p 959 N94-16883

Electrical conductivity of ion implanted ladder and semi-ladder polymers
[AD-A267432] p 970 N94-16978
Stress corrosion cracking of 316 SS and Incoloy-800 in high temperature aqueous containing sulfate and chloride
[DE93-623325] p 952 N94-17302
High temperature deformation behavior of YBa2Cu3O(6+x) superconducting ceramic materials
[AD-A268164] p 973 N94-17430
High temperature hydraulic seals
[AD-A268257] p 1048 N94-17433

HIGH TEMPERATURE ENVIRONMENTS
Environmental embrittlement in ordered intermetallic alloys
[DE93-015307] p 955 N94-15830
Recent advances in ordered intermetallics
[DE93-015308] p 955 N94-15862
Aspects of high temperature damage in fiber reinforced titanium metal matrix composites
[AD-A267907] p 941 N94-17379
Nonintrusive fast response oxygen monitoring system for high temperature flows
[NASA-CR-4553] p 1036 N94-17655

HIGH TEMPERATURE GASES
Gas separations using ceramic membranes
[DE93-000278] p 947 N94-15861
Plasma arc welding repair of space flight hardware
[TABES PAPER 93-603] p 1049 N94-16139

HIGH TEMPERATURE LUBRICANTS
Physical and chemical properties of some new perfluoropolyalkylether lubricants prepared by direct fluorination
[NASA-TM-106299] p 967 N94-16543

HIGH TEMPERATURE PLASMAS
High frequency Raman current drive
p 1201 N94-15208

HIGH TEMPERATURE SUPERCONDUCTORS
Electronic and atomic structure of semiconductors and of high-temperature superconductors
[AD-A266805] p 1205 N94-14913
Partial melting experiment of Y-Ba-Cu oxide
p 945 N94-15168
High temperature superconductivity
[AD-A267006] p 1008 N94-15635
Molten salt electrodeposition of high temperature superconductors
[AD-A266620] p 1009 N94-15726
Nonaqueous slip casting of high temperature ceramic superconductors using an investment casting technique
[NASA-CASE-LAR-14918-1] p 983 N94-15881
Roles of oxygen defects in copper-oxide superconductors
[DE93-014875] p 1208 N94-15982
Pulsed laser deposition of metastable Ca(1-x)Sr(x)CuO2 thin films
[DE93-015804] p 1040 N94-16663
Powder diffraction studies using anomalous dispersion
[DE93-012531] p 1210 N94-16775
Superconducting ceramics: Selected properties and methods of production
[IFTR-23/1991] p 969 N94-16924
Engineering design of a high-temperature superconductor current lead
[DE93-015156] p 1013 N94-17226

HIGH TEMPERATURE TESTS
Systematic study of effects of load misalignment in uniaxial low cycle fatigue testing at high temperatures
[NPL-DMM(A)-27] p 1057 N94-15015

HIGH VACUUM
Investigation of onset of plasma formation at anode of fast-pulsed high-voltage vacuum diode
[AD-A267214] p 1204 N94-16987

HIGH VOLTAGES
Investigation of onset of plasma formation at anode of fast-pulsed high-voltage vacuum diode
[AD-A267214] p 1204 N94-16987

HIGHLANDS
Fluvial erosion on Mars: Implications for paleoclimatic change p 1241 N94-16210
Assimilation of solids during ascent of magmas from the Bartoy Field of the Baikal Region, Siberia
p 1103 N94-16214
Apollo 17 materials viewed from 2 to 4 mm soil particles: Pre-serenitatis highlands components
p 1267 N94-16280
Preliminary analysis of Dione Regio, Venus: The final Magellan regional imaging gap p 1271 N94-16302

HIGHLY MANEUVERABLE AIRCRAFT
The 1979 highlights
[NASA-TM-109443] p 1247 N94-15342

HIGHWAYS
Mathematical model of frost heave and thaw settlement in pavements
[AD-A267037] p 983 N94-15676

HIPPOCAMPUS
Cortical adaptive filtering in bioacoustic signal classification
[AD-A266229] p 1177 N94-16939

HISTORIES
Symposium on the Future of Aeronautics in the Netherlands
[ETN-93-93780] p 853 N94-15120
Fifty years of the Netherlands Association of Aeronautical Engineers p 853 N94-15121
Aviation and the KLM: Past and future
p 853 N94-15126
NACA-NASA: 75 years of flight
[NASA-TM-109449] p 1302 N94-15322
Aircraft accident investigation at ARL: The first 50 years
[AD-A267086] p 862 N94-15542
Annual historical report, calendar year 1992
[AD-A267050] p 1121 N94-15663
On the 17-keV neutrino
[DE93-012638] p 1181 N94-15974
History of the manned space flight program
[NASA-TM-109529] p 1303 N94-16069
The definition of a scientific policy: ESRO's satellite programme in 1969-1973
[ESA-HSR-6] p 1303 N94-16500
History of on-orbit satellite fragmentations
[NASA-CR-191644] p 887 N94-16502
Choosing ESRO's first scientific satellites
[ESA-HSR-3] p 887 N94-16523
The early development of the Telecommunications Satellite Programme in ESRO (1965-1971)
[ESA-HSR-9] p 887 N94-16525
Europe in space: Edoardo Amaldi and the inception of ESRO
[ESA-HSR-5] p 1303 N94-16526
Europe into space: The Auger years (1959-1967)
[ESA-HSR-8] p 1303 N94-16592
Maximizing participation of women in collegiate aviation education
[NIAR-93-14] p 1222 N94-17261

HOLE BURNING
Search for far infrared radiation from optically pumped defect modes
[AD-A266744] p 1206 N94-15822

HOLE GEOMETRY (MECHANICS)
Effect of Impact Damage and Open Hole on Compressive Strength of Hybrid Composite Laminates
[NASA-CR-194603] p 936 N94-16836

HOLE MOBILITY
Optoelectronics based on SiGe/Si heterostructures
[AD-A267178] p 1190 N94-15848

HOLES (ELECTRON DEFICIENCIES)
A study of high field transport in wide band gap electronic materials using a picosecond transient charge technique
[AD-A267098] p 1008 N94-15636
Optoelectronics based on SiGe/Si heterostructures
[AD-A267178] p 1190 N94-15848
Numerical studies of the photoluminescence spectrum of quantum Hall systems
[DE93-015822] p 1220 N94-16810

HOLLOW CATHODES
Hollow cathode heater development for the Space Station plasma contactor
[NASA-CR-191131] p 926 N94-16880
Three short articles from Japanese laser journal
[AD-A268249] p 1042 N94-17415

HOLMIUM
Growth of new materials for solid state laser applications. The growth of ZnGeP2 by the vertical Bridgman method
[NASA-CR-194571] p 1038 N94-15530

HOLOGRAPHIC INTERFEROMETRY
Optical systems for the visualization of fluid and solid transparent media under microgravity conditions
p 978 N94-16081

HOLOGRAPHY
Optical residue processing module
[AD-A267721] p 1188 N94-14940
Application of holographic optical elements to magneto-optic read/write heads p 1226 N94-14985
Determination of average refractive index of spin coated DCG films for HOE fabrication p 1036 N94-14992
Display system employing acousto-optic tunable filter
[NASA-CASE-NPO-18736-1-CU] p 1190 N94-15933
Aberration correction of unstable resonators
[NASA-CASE-NPO-18791-1-CU] p 1034 N94-15987
Optical computing
[AD-A267881] p 1141 N94-17015
Display of dynamic, volume graphic images by holographic voxel projection: Initial investigation
[AD-A267622] p 1035 N94-17197
Conically scanned holographic lidar telescope
[NASA-CASE-GSC-13462-1] p 1194 N94-17321
Conference on Binary Optics: An Opportunity for Technical Exchange
[NASA-CP-3227] p 1194 N94-17331
Manufacturing the key to binary optics
p 1194 N94-17332
Subwavelength structured surfaces and their applications p 1194 N94-17337
Fabrication techniques for very fast diffractive lenses
p 1196 N94-17345
Phase holograms in PMMA with proximity effect correction p 1037 N94-17348
Applications of advanced diffractive optical elements
p 1197 N94-17356
SURPHEX (tm): New dry photopolymers for replication of surface relief diffractive optics p 1198 N94-17358
Predesign of diamond turned refractive/diffractive elements for IR objectives p 1198 N94-17359
3-D optical memory disk
[AD-A267908] p 1141 N94-17380

HOMOGENEITY
Multinuclear NMR study of aluminosilicate sol-gel synthesis reasons for the homogeneous gelation using the prehydrolysis method
[AD-A266877] p 962 N94-14921
Homogeneously traceable results in claw-free graphs
[AD-A266196] p 1169 N94-16127

HOMOGENEOUS TURBULENCE
A numerical investigation of energy transfer and subgrid-scale eddy-viscosity in homogeneous, isotropic, and shear turbulence
[AD-A267265] p 1029 N94-17363

HONEYCOMB STRUCTURES
Improved composite flexible blanket insulation
[NASA-CASE-ARC-11955-1-CU] p 934 N94-15926
Slidesurfaces with adaptive new definitions (SAND) for transient analysis
[DE93-014909] p 1059 N94-15983

HOOKS
Attachment device
[NASA-CASE-MSC-21885-1] p 1047 N94-15925

HOT CORROSION
Vanadium corrosion studies
[AD-A266489] p 959 N94-16781
Chemical vapor deposition of Ta2O5 corrosion resistant coatings
[DE93-015488] p 969 N94-16889

HOT ELECTRONS
Hot electron mixers, the potential competition
p 903 N94-15055

HOT ISOSTATIC PRESSING
Solid lubricants for space structures, phase 2
[AD-A266653] p 968 N94-16767

HOT PRESSING
Method of producing a silicon carbide fiber reinforced strontium aluminosilicate glass-ceramic matrix composite
[NASA-CASE-LEW-15263-2] p 934 N94-15929
Solid lubricants for space structures, phase 2
[AD-A266653] p 968 N94-16767

HOUSTON (TX)
Johnson Space Center and downtown Houston, Texas aerials
[NASA-TM-109522] p 1032 N94-15472

HUBBLE SPACE TELESCOPE
The STIS MAMA status: Current detector performance
p 905 N94-15069
HSTS: Integrating planning and scheduling
[AD-A266991] p 1222 N94-15213
The 1979 highlights
[NASA-TM-109443] p 1247 N94-15342
STS-31 Post-Flight Conference
[NASA-TM-109477] p 881 N94-15384
NASA's Hubble Space Telescope: The challenge and complexity of operations
[NASA-TM-109577] p 1236 N94-15422
STS-31 mission highlights resource tape
[NASA-TM-109479] p 881 N94-15440
STS-31 Hubble space telescope deploy: Training at MDF with Hawley
[NASA-TM-109481] p 876 N94-15442
STS-31 HST deploy sim in SMS and MOCR
[NASA-TM-109482] p 876 N94-15449
The 1982 highlights
[NASA-TM-109671] p 1303 N94-15508

HUGONIOT EQUATION OF STATE
The shock Hugoniot of 316 SS and sound velocity measurements
[DE93-016525] p 1178 N94-16955

HUMAN BEHAVIOR
Astro smile
[NASA-TM-109506] p 879 N94-15225

HUMAN BEINGS
Sleep management user's guide for special operations personnel
[AD-A267746] p 1119 N94-14943
USAF physiological studies of personal microclimate cooling: A review
[AD-A267203] p 1022 N94-15858
Screening for prostate cancer p 1126 N94-16630

HUMAN BODY
Currents induced in the human body for exposure to ultrawideband electromagnetic pulses
[AD-A268570] p 1130 N94-17621

HUMAN FACTORS ENGINEERING
Engineering Physics and Mathematics Division progress report, period ending 31 December 1992
[DE93-015118] p 1301 N94-14926
Human factor studies
[NASA-TM-109665] p 875 N94-15236
Investigation of the effects of extravehicular activity (EVA) gloves on performance
[NASA-TP-3401] p 1137 N94-15717
Ergonomics in the office environment
p 1124 N94-16612
The Goddard Space Flight Center ergonomics program p 1125 N94-16621
Efficient management of cardiovascular risk screening programs p 1125 N94-16622
Evaluation of Night Vision Goggles (NVG) for maritime search and rescue (HH-3/HH-60) comparison report
[AD-A266493] p 1138 N94-16793
Acquisition and production of skilled behavior in dynamic decision-making tasks
[NASA-CR-194658] p 1133 N94-17296
Human Transportation System (HTS) study, volume 2
[NASA-TM-104779-VOL-2] p 882 N94-17320
Computer-human interface issues: Theory and application
[AD-A268013] p 1138 N94-17475
Visual display principles for C3I system tasks
[AD-A267969] p 1005 N94-17498
Aircrew/groundcrew life support systems research. Volume 1: CLIN 0001 research requirements
[AD-A268229] p 1139 N94-17563
Force-endurance capabilities of extravehicular activity (EVA) gloves at different pressure levels
[NASA-TP-3420] p 1139 N94-17653

HUMAN IMMUNODEFICIENCY VIRUS
Tuberculosis: A case for increased screening
p 1126 N94-16627
OSHA bloodborne pathogens standards exposure control plan p 1127 N94-16645

HUMAN PERFORMANCE
Human factor studies
[NASA-TM-109665] p 875 N94-15236
Complex information coordination performance: Differential changes in working memory contributions following training
[AD-A267007] p 1132 N94-15762
Scuba-diving, anxiety and task performance
p 1132 N94-15938
Infrared spot tracker
[AD-D015778] p 1191 N94-16547
States of awareness 1: Subliminal perception relationship to situational awareness
[AD-A267249] p 1132 N94-16942
Acquisition and production of skilled behavior in dynamic decision-making tasks
[NASA-CR-194658] p 1133 N94-17296
Processes involved in the integration of pictures and discourse
[AD-A268150] p 1134 N94-17468

HUMAN TOLERANCES
Cumulative effect of repeated brief cerebral ischemia
[AD-A267155] p 1121 N94-15736

HUMIDITY
A comparison of cloud attenuation models using measured cloud data p 996 N94-16044
Empirical relationships among atmospheric variables from rawinsonde and field data as surrogates for AVIRIS measurements: Estimation of regional land surface evapotranspiration p 1074 N94-16712

HURRICANES
Radar diagnostic parameters as indicators of severe weather in central Florida
[PB93-183507] p 1106 N94-16465

HYBRID COMPOSITES
Effect of Impact Damage and Open Hole on Compressive Strength of Hybrid Composite Laminates
[NASA-CR-194603] p 936 N94-16836
Low and high velocity impact response of thick hybrid composites p 936 N94-16837

HYBRID COMPUTERS
An uncertainty analysis of inlet dynamic flow distortion using an analog/digital hybrid editing system
[AD-A266924] p 855 N94-15105

HYDRATION
Encapsulation of hemoglobin in non-phospholipid vesicles
[AD-A266505] p 1128 N94-16785

HYDRAULIC CONTROL
Optimal tuning of heavy equipment motion controllers
[AD-A267873] p 1167 N94-17392

HYDRAULIC EQUIPMENT
Hydraulic pump with integral electric motor
[AD-D015782] p 1011 N94-16549
A measurement station for study of Earth moving tools and ground cutting processes
[IFTR-10/1991] p 985 N94-17068
Optimal tuning of heavy equipment motion controllers
[AD-A267873] p 1167 N94-17392
The IOSDL SeaSoar hydraulic unit
[IOS-300-1992] p 1114 N94-17516

HYDRAULIC FLUIDS
High temperature hydraulic seals
[AD-A268257] p 1048 N94-17433

HYDRIDES
Hydride-containing molten salts and their technology implications
[AD-A266458] p 1092 N94-16567

HYDROCARBON FUELS
Effects of RVP, T(50), and oxygenates on hot-start and driveability performance at high and low altitude
[AD-A266382] p 869 N94-16516
Synthesis of potential high-energy fuels
[AD-A267508] p 975 N94-17073

HYDROCARBONS
Extraction and isotopic analysis of medium molecular weight hydrocarbons from Murchison using supercritical carbon dioxide p 1241 N94-16184

HYDROCYANIC ACID
The interaction of HCN(DCN) with Si(111)-7x7 studied with HREELS, UPS, and XPS
[AD-A266237] p 1182 N94-16111

HYDRODYNAMIC EQUATIONS
Three dimensional hydrodynamic calculations with adaptive mesh refinement of the evolution of Rayleigh Taylor and Richtmyer Meshkov instabilities in converging geometry: Multi-mode perturbations
[DE93-017155] p 1025 N94-16903

HYDRODYNAMICS
Riblets: New speed technology
[NASA-TM-109641] p 1018 N94-15252
Three dimensional hydrodynamic calculations with adaptive mesh refinement of the evolution of Rayleigh Taylor and Richtmyer Meshkov instabilities in converging geometry: Multi-mode perturbations
[DE93-017155] p 1025 N94-16903
Phillips Laboratory global spectral numerical weather prediction model
[AD-A267293] p 1107 N94-17244

HYDROGEN
Electronic and atomic structure of semiconductors and of high-temperature superconductors
[AD-A266805] p 1205 N94-14913
An apparatus for measuring the biological oxidation of hydrogen gas under hyperbaric conditions
[AD-A266834] p 1119 N94-14916
Molecular processes in comets
[NASA-CR-194148] p 1239 N94-15188
Boundary conditions for the paleoenvironment: Chemical and physical processes in the pre-solar nebula
[NASA-CR-194418] p 1298 N94-15421
Electronic structure and enthalpy of hydrogen and helium mixtures
[DE93-014128] p 1208 N94-15976
Evolutionary implications of a steady-state water abundance on Venus p 1254 N94-16206
Water in Earth's mantle: Hydrogen analysis of mantle olivine, pyroxenes and garnet using the SIMS
p 1104 N94-16336
Possible sources of H2 to H2O enrichment at evaporation of parent chondritic material
p 1244 N94-16377
Clusterization of quantum states in the Hartmann model
[DE93-626624] p 1220 N94-17315
Investigation of the energy distribution of ions, striking the cathode in an abnormal glow discharge
[DE93-623987] p 1013 N94-17316

HYDROGEN ATOMS
Merged beam studies of laser stimulated radiative recombination
[AD-A267186] p 1037 N94-15145

HYDROGEN BONDS
Electronic spectroscopy of the gas-phase OH-Kr van der Waals complex
[AD-A266891] p 942 N94-14946
Self-diffusion coefficients of sol-gel intermediates
[AD-A266957] p 963 N94-15179
Study of protein-H2O interactions by multidimensional NMR spectroscopy
[AD-A266955] p 946 N94-15760

HYDROGEN CHLORIDES
Second flight of the Spacelab grille spectrometer during the Atlas-1 mission
[AERONAUTICA-ACTA-A-367-199] p 923 N94-17592

HYDROGEN EMBRITTLEMENT
Environmental embrittlement in ordered intermetallic alloys
[DE93-015307] p 955 N94-15830
Development and commercialization status of Fe3Al-based intermetallic alloys
[DE93-015802] p 957 N94-16165

HYDROGEN IONS
Atomic processes in hydrogen and deuterium negative ion discharges
[DE93-013432] p 1183 N94-16817
Six dimensional tracking simulator for H(-) injection in AGS Booster
[DE93-015396] p 1184 N94-16885

HYDROGEN ISOTOPES
Evolutionary implications of a steady-state water abundance on Venus p 1254 N94-16206
A hydrogen isotope study of CO3 type carbonaceous chondrites; comparison with type 3 ordinary chondrites
p 1246 N94-16425

HYDROGEN METABOLISM
An apparatus for measuring the biological oxidation of hydrogen gas under hyperbaric conditions
[AD-A266834] p 1119 N94-14916

HYDROGEN OXYGEN ENGINES
Liquid hydrogen and liquid oxygen feedline passive recirculation analysis
[TABES PAPER 93-620] p 1031 N94-16145

HYDROGEN PLASMA
Modification of fluoropolymer surfaces with electronically conductive polymers
[AD-A266294] p 967 N94-16475

HYDROGEN PRODUCTION
Strategy for the reduction of total integrated fluid logistics to the Space Station Freedom
[NASA-TM-107744] p 1138 N94-17452

HYDROGEN SULFIDE
Application of non-thermal plasmas to pollution control
[DE93-016432] p 1096 N94-16449

HYDROGEN-BASED ENERGY
Hydride-containing molten salts and their technology implications
[AD-A266458] p 1092 N94-16567

HYDROGENATION
Boundary conditions for the paleoenvironment: Chemical and physical processes in the pre-solar nebula
[NASA-CR-194418] p 1298 N94-15421
Interface properties of wide bandgap semiconductor structures
[AD-A268269] p 1215 N94-17377

HYDROGEOLOGY
Sedimentation, volcanism, and ancestral lakes in the Valles Marineris: Clues from topography
p 1283 N94-16369

HYDROLOGICAL CYCLE
Recent scientific advances in the use of radar in scientific hydrology p 991 N94-15895
Some thoughts on future rain mapping missions (TRMM follow-on) p 992 N94-15906
Global Energy and Water Cycle Experiment (GEWEX) and the Continental-scale International Project (GCIP)
p 994 N94-15918
Research into the influence of spatial variability and scale on the parameterization of hydrological processes
[NASA-CR-194610] p 1082 N94-16026
Effects of spatial variability and scale on areal -average evapotranspiration p 1084 N94-16033

HYDROLOGY
Recent scientific advances in the use of radar in scientific hydrology p 991 N94-15895
Martian carbon dioxide: Clues from isotopes in SNC meteorites p 1270 N94-16295

HYDROLOGY MODELS
Global Energy and Water Cycle Experiment (GEWEX) and the Continental-scale International Project (GCIP)
p 994 N94-15918
Research into the influence of spatial variability and scale on the parameterization of hydrological processes
[NASA-CR-194610] p 1082 N94-16026
On hydrologic similarity: A dimensionless flood frequency model using a generalized geomorphologic unit hydrograph and partial area runoff generation
[PAPER-89WR01579] p 1083 N94-16027
A detailed model for simulation of catchment scale subsurface hydrologic processes
[PAPER-92WR02333] p 1084 N94-16032
Scaling, soil moisture and evapotranspiration in runoff models p 1084 N94-16034
A snow wetness retrieval algorithm for SAR
p 1075 N94-16732
Strategies for detection of floodplain inundation with multi-frequency polarimetric SAR p 1076 N94-16739

HYDROLYSIS
Multinuclear NMR study of aluminosilicate sol-gel synthesis reasons for the homogeneous gelation using the prehydrolysis method
[AD-A266877] p 962 N94-14921
Efficacy of flocculating and other emergency water purification tablets
[AD-A266695] p 1148 N94-15840
An advanced bioprocessing concept for the conversion of wastepaper to ethanol
[DE93-015209] p 975 N94-16807
HYDROPONICS
The dynamics of hydroponic crops for simulation studies of the CELSS initial reference configurations
[NASA-CR-194654] p 1118 N94-17279
HYDROSTATIC PRESSURE
A mathematical model for the study of hemorrhagic shock and fluid resuscitation: Exchange of fluid and solutes between vascular, interstitial, and tissue cell compartments
[AD-A266426] p 1123 N94-16558
HYDROTHERMAL SYSTEMS
Terrestrial impact melts as analogues for the hematization of Martian surface materials
p 1104 N94-16424
HYDROXIDES
Characterization of nanoscale oxide and oxyhydroxide powders using EXAFS spectroscopy
[DE93-015683] p 940 N94-17235
HYGIENE
Education and training of professional industrial hygienists for 2020 p 1125 N94-16618
Efficient management of cardiovascular risk screening programs p 1125 N94-16622
Industrial Hygiene Laboratory accreditation: The JSC experience p 1125 N94-16623
Space Shuttle solid rocket motor exposure monitoring
p 976 N94-16624
HYGROSCOPICITY
Optical studies of glasses embedded with inorganic ions and organic dyes
[AD-A268146] p 1199 N94-17455
HYPERCUBE MULTIPROCESSORS
Parallel spatial direct numerical simulations on the Intel iPSC/860 hypercube
[NASA-CR-191513] p 1144 N94-15483
Multiphase complete exchange: A theoretical analysis
[NASA-CR-191531] p 1145 N94-15489
Applications and development of communication models for the touchstone GAMMA and DELTA prototypes
[NASA-CR-193617] p 999 N94-16867
Construction of d-dimensional hyperoctrees on a hypercube multiprocessor
[INRIA-RR-1752] p 1162 N94-17539
HYPERNUCLEI
Relativistic mean-field calculations of lambda and sigma hypernuclei
[DE93-015269] p 1181 N94-16013
HYPERONS
Relativistic mean-field calculations of lambda and sigma hypernuclei
[DE93-015269] p 1181 N94-16013
HYPEROXIA
Human central nervous system oxygen toxicity data from 1945 to 1986
[AD-A268225] p 1130 N94-17556
HYPERSONIC AIRCRAFT
Research in robust control for hypersonic aircraft
[NASA-CR-194106] p 870 N94-15416
HYPERSONIC FLIGHT
Particle kinetic simulation of high altitude hypervelocity flight
[NASA-CR-194599] p 856 N94-15678
Flight testing of airbreathing hypersonic vehicles
[NASA-TM-4524] p 886 N94-15753
Trajectory optimization for the National Aerospace Plane
[NASA-CR-194618] p 867 N94-16498
An experimental study of fluctuating wall pressures in a highly swept, sharp fin-induced, Mach 5 shock wave/turbulent boundary layer interaction
[AD-A268394] p 861 N94-17461
HYPERSONIC FLOW
Special course on Shock-Wave/Boundary-Layer Interactions in Supersonic and Hypersonic Flows
[AGARD-R-792] p 1017 N94-15196
Swept shock wave/laminar boundary layer interactions, experimental, and numerical results
p 1017 N94-15198
Unsteady phenomena in shock wave/boundary layer interaction p 1017 N94-15200
Particle kinetic simulation of high altitude hypervelocity flight
[NASA-CR-194599] p 856 N94-15678
Particle simulation of hypersonic flow
[AD-A267185] p 857 N94-15787
Turbulence and transition modeling for high-speed flows
[AD-A266748] p 1022 N94-15953
To extend the thirteen-moment theory and its application to problems in rarefied hypersonic flow
[AD-A267384] p 859 N94-17021
Single block three-dimensional volume grids about complex aerodynamic vehicles
[NASA-TM-108986] p 1030 N94-17476
HYPERSONIC REENTRY
Particle kinetic simulation of high altitude hypervelocity flight
[NASA-CR-194599] p 856 N94-15678
HYPERSONIC SHOCK
Hypersonic shock wave boundary layer interactions over simplified deflected control surface configurations
p 1018 N94-15203
HYPERSONIC VEHICLES
Flight testing of airbreathing hypersonic vehicles
[NASA-TM-4524] p 886 N94-15753
Aerothermoelastic analysis of a NASP demonstrator model
[NASA-TM-109007] p 867 N94-17055
HYPERSONIC WAKES
DSMC simulations of Mach 20 nitrogen flows about a 70 degree blunted cone and its wake
[NASA-TM-107762] p 1018 N94-15291
HYPERSONIC WIND TUNNELS
Nonintrusive fast response oxygen monitoring system for high temperature flows
[NASA-CR-4553] p 1036 N94-17655
HYPERSONICS
Particle kinetic simulation of high altitude hypervelocity flight
[NASA-CR-194599] p 856 N94-15678
HYPERTHERMIA
Experimental evaluation of an adaptive focusing algorithm for a microwave planar phased-array hyperthermia system at UCSF
[AD-A267004] p 1121 N94-15634
HYPERVELOCITY IMPACT
An analysis of the dynamic response of the Space Station Freedom due to a module perforation by an orbital debris particle impact
[TABES PAPER 93-653] p 899 N94-16154
HYPERVELOCITY PROJECTILES
Impact penetration experiments in teflon targets of variable thickness p 1063 N94-16253
Simulation of collisional fragmentation with explosives
p 1063 N94-16254
HYPOBARIC ATMOSPHERES
Metabolic monitoring of hypobaric subjects
[AD-A268221] p 1130 N94-17554
HYPOTENSION
A review of the efficacy of 7.5 percent NaCl/6 percent Dextran-70 (HSD) in experimental animals and humans
[AD-A266633] p 1122 N94-15740
HYPOTHALAMUS
Diffusible driving and coupling signals of the biological clock
[AD-A267046] p 1121 N94-15660
Melatonin, the pineal gland, and circadian rhythms
[AD-A268200] p 1129 N94-17478
HYPOTHESES
The three ages of Venus: A hypothesis based on the cratering record p 1261 N94-16239
Geomorphic processes in the Argyre-Dorsa Argentea region of Mars p 1270 N94-16293
HYPOXIA
Aircrew/groundcrew life support systems research. Volume 1: CLIN 0001 research requirements
[AD-A268229] p 1139 N94-17563
HYSTERESIS
Adaptive Navier-Stokes calculations for vortical flow
[AD-A266236] p 1026 N94-16966

I

ICE
Bibliography on snow and ice friction
[AD-A266868] p 1045 N94-14920
Rheology of water and ammonia-water ices
p 953 N94-16188
Equatorial ground ice on Mars: Steady-state stability
p 1290 N94-16403
Catalytic crystallization of ices by small silicate smokes at temperatures less than 20K p 1219 N94-16420
Optical properties of water released in low Earth orbit
[AD-A266197] p 1192 N94-16936
Atmospheric ionization by solar particles detected by nitrate measurement in antarctic snow
[AD-A267583] p 1299 N94-17208
ICE ENVIRONMENTS
Arctic cyclones and Marginal Ice Zone (MIZ) variability
[AD-A268610] p 1108 N94-17465
ICE FORMATION
Arctic cyclones and Marginal Ice Zone (MIZ) variability
[AD-A268610] p 1108 N94-17465
An empirical study of tropical cloud clusters using special sensor microwave imager data
[AD-A268072] p 1110 N94-17595
ICE MAPPING
Sea ice motions in the central arctic ice central arctic pack ice as inferred from AVHRR imagery
[NASA-CR-194572] p 1112 N94-15701
Arctic and Antarctic sea ice, 1978-1987: Satellite passive-microwave observations and analysis
[NASA-SP-511] p 1114 N94-17439
ICELAND
Morphometric comparison of Icelandic lava shield volcanoes versus selected Venusian edifices
p 1248 N94-16178
ICY SATELLITES
Phase equilibria of the magnesium sulfate-water system to 4 kbars p 953 N94-16247
The rheology and composition of cryovolcanic flows on icy satellites p 1243 N94-16294
IDEAL FLUIDS
A priori inequalities for an ideal-incompressible liquid in an electromagnetic field
[IFTR-9/1992] p 998 N94-16652
IDENTIFYING
Nowcasting methods for satellite imagery
[AD-A267294] p 1108 N94-17267
IGNEOUS ROCKS
Explosive mafic volcanism on Earth and Mars
p 1253 N94-16204
Crustal structure and igneous processes in a chondritic Io p 1243 N94-16292
Liquidus equilibria of lunar analogs at high pressure
p 1283 N94-16364
Preliminary analysis of thermal-infrared multispectral scanner data of the Iron Hill, Colorado carbonatite-alkalic rock complex p 1065 N94-16605
ILLUMINATING
Comparative night vision goggle visual acuity measurements performed in the A-10 aircraft in an operational setting
[AD-A266721] p 1137 N94-15820
ILMENITE
First oxygen from lunar basalt p 1249 N94-16182
The ilmenite liquidus and depths of segregation for high-Ti picrite glasses p 975 N94-16241
Overturn of magma ocean ilmenite cumulate layer: Implications for lunar magmatic evolution and formation of a lunar core p 1261 N94-16242
Solar noble gases revealed by closed system stepped etching of a metal separate from Fayetteville
p 954 N94-16432
IMAGE ANALYSIS
Optical residue processing module
[AD-A267721] p 1188 N94-14940
RACCOON: A Real-Time Autonomous Car Chaser Operating Optimally at Night
[AD-A266963] p 863 N94-14971
Evaluation of the TOPSAR performance by using passive and active calibrators p 1078 N94-16750
Automated image analysis method for the detection of cracks on wood surface
[VTT-JULK-755] p 1056 N94-17542
A high-speed object recognition chip based on a biologically-realistic hybrid temporal processing
[AD-A268270] p 1134 N94-17576
Guide to Magellan image interpretation
[NASA-CR-194340] p 1298 N94-17654
IMAGE CLASSIFICATION
Visually guided touching and manual tracking
[TR-412] p 1166 N94-16581
Supervised fully polarimetric classification of the Black Forest test site: From MAESTRO! to MAC Europe
p 1076 N94-16740
Application of modified VICAR/IBIS GIS to analysis of July 1991 Flevoland AIRSAR data p 1080 N94-16757
IMAGE CONTRAST
Diffuse scattering and image contrast of tweed in superconducting oxides: A simulation and interpretation
[DE93-016131] p 1212 N94-16844
Method and apparatus to characterize ultrasonically reflective contrast agents
[NASA-CASE-LAR-14969-1] p 1129 N94-17085
IMAGE CORRELATORS
Spatial filters for optical correlation
[AD-A267199] p 1189 N94-15791
IMAGE ENHANCEMENT
Image accuracy and representational enhancement through low-level, multi-sensor integration techniques
[DE93-014888] p 1167 N94-17287
IMAGE INTENSIFIERS
Thinned, backside illuminated, area CCD imager for electron detection p 901 N94-15036

The MIC photon counting detector
p 901 N94-15039
Development of an ultra violet auroral imager for the Freja project p 904 N94-15060
The Rutherford Appleton Laboratory photon counting detector p 910 N94-15096
Comparative night vision goggle visual acuity measurements performed in the A-10 aircraft in an operational setting
[AD-A266721] p 1137 N94-15820
SYDONI: An intensified system for night observation
p 891 N94-17153

IMAGE PROCESSING
Video applications development platform
[AD-A266966] p 1163 N94-14953
Assessment of TDI operation of a frame transfer CCD for high resolution imaging from a fast spinning spacecraft p 910 N94-15097
Massively parallel, adaptive, color image processing for autonomous road following
[AD-A266988] p 864 N94-15498
Streak camera based SLR receiver for two color atmospheric measurements p 914 N94-15573
Characterization of spatial and temporal variability of phytoplankton blooms in coastal waters
[AD-A267102] p 1116 N94-15633
Cooperativity and 3-D representation
[AD-A267180] p 1131 N94-15694
Spatial filters for optical correlation
[AD-A267199] p 1189 N94-15791
An electronic imaging system for the Aeroballistic Research Facility
[AD-A267157] p 1033 N94-15826
A multilevel-multiresolution method for image processing. A Bayesian framework for reconstructing and representing shapes
[AD-A266772] p 1082 N94-15842
Primary studies of Chinese spaceborne SAR
p 993 N94-15916
Revisiting the BCS, a measurement system for characterizing the optics of solar collectors
[DE93-015030] p 1091 N94-15993
A task adaptive parallel graphics renderer
[DE93-017123] p 1149 N94-16119
Galileo imaging results from the second Earth-Moon flyby: Lunar Maria and related units
p 1252 N94-16199
Visually guided touching and manual tracking
[TR-412] p 1166 N94-16581
The Spectral Image Processing System (SIPS): Software for integrated analysis of AVIRIS data
p 1067 N94-16674
Comparison of JPL-AIRSAR and DLR E-SAR images from the MAC Europe 1991 campaign over testsite Oberpfaffenhofen: Frequency and polarization dependent backscatter variations from agricultural fields
p 1075 N94-16733
Application of modified VICAR/IBIS GIS to analysis of July 1991 Flevoland AIRSAR data p 1080 N94-16757
Optical displays: A tutorial on images and image formation
[AD-A266230] p 1192 N94-16926
Applications of the phi-transform
[AD-A266247] p 1170 N94-16940
Optical computing
[AD-A267881] p 1141 N94-17015
Neural basis of motion perception
[AD-A267267] p 1133 N94-17265
Image accuracy and representational enhancement through low-level, multi-sensor integration techniques
[DE93-014888] p 1167 N94-17287
Automated image analysis method for the detection of cracks on wood surface
[VTT-JULK-755] p 1056 N94-17542
Three dimensional visualization of GOES cloud data using OCTRESS
[AD-A268102] p 1109 N94-17572
A high-speed object recognition chip based on a biologically-realistic hybrid temporal processing
[AD-A268270] p 1134 N94-17576
Detecting small debris using a ground-based photon counting detector
[DE93-012623] p 898 N94-17669

IMAGE RECONSTRUCTION
Lossless compression of AVIRIS data: Comparison of methods and instrument constraints
p 1075 N94-16713

IMAGE RESOLUTION
Programmable Remapper project
[NASA-TM-109508] p 1164 N94-15515
Measurements of the radar cross section and Inverse Synthetic Aperture Radar (ISAR) images of a Piper Navajo at 9.5 GHz and 49 GHz
[AD-A267570] p 1002 N94-17110

IMAGERY
Multiple dataset water-quality analyses in the vicinity of an ocean wastewater plume p 1069 N94-16687
SYDONI: An intensified system for night observation
p 891 N94-17153

IMAGES
NASA images 12 --- Voyager encounters
[NASA-TM-109417] p 1247 N94-15511
NASA images 13
[NASA-TM-109418] p 1247 N94-15512
Display of dynamic, volume graphic images by holographic voxel projection: Initial investigation
[AD-A267622] p 1035 N94-17197

IMAGING RADAR
Fine scale measurements of microwave backscatter from the ocean surface
[AD-A264516] p 1111 N94-15134
Proceedings of the Third Spaceborne Imaging Radar Symposium
[NASA-CR-194104] p 989 N94-15886
Almaz p 898 N94-15889
Spaceborne Imaging Radar-C instrument
p 990 N94-15890
Imaging radar studies of polar ice p 991 N94-15899
Application of Cloude's target decomposition theorem to polarimetric imaging radar data p 991 N94-15901
SIR-C/X-SAR free flyer concept p 898 N94-15903
AIRSAR South American deployment: Operation plan, version 3.0 p 994 N94-15919
Characterization of wetland, forest, and agricultural ecosystems in Belize with airborne radar (AIRSAR)
p 1076 N94-16738
Sea bottom topography imaging with SAR
p 1077 N94-16745

IMAGING SPECTROMETERS
Advanced high performance CdHgTe multiplexed arrays p 903 N94-15051
CCD's on high resistivity bulk silicon for x ray spectroscopy on XMM p 907 N94-15080
Ground truth spectrometry and imagery of eruption clouds to maximize utility of satellite imagery
[NASA-CR-194358] p 1081 N94-15181
In-flight calibration of the spectral and radiometric characteristics of AVIRIS in 1991 p 1037 N94-16667
Using AVIRIS images to measure temporal trends in abundance of photosynthetic and nonphotosynthetic canopy components p 1066 N94-16668
Unmixing AVIRIS data to provide a method for vegetation fraction subtraction p 1066 N94-16669
The Spectral Image Processing System (SIPS): Software for integrated analysis of AVIRIS data
p 1067 N94-16674
AVIRIS study of Death Valley evaporite deposits using least-squares band-fitting methods p 1067 N94-16676
A field measure of the shade fraction
p 1068 N94-16677
Volcanic thermal features observed by AVIRIS
p 1068 N94-16680
Retrieval of biophysical parameters with AVIRIS and ISM: The Landes Forest, south west France
p 1068 N94-16681
Ground-truthing AVIRIS mineral mapping at Cuprite, Nevada p 1069 N94-16682
AVIRIS calibration and application in coastal oceanic environments p 1069 N94-16685
Mapping vegetation types with the multiple spectral feature mapping algorithm in both emission and absorption p 1069 N94-16686
MAC Europe 1991: Evaluation of AVIRIS, GER imaging spectrometry data for the land application testsite Oberpfaffenhofen p 1070 N94-16688
Using endmembers in AVIRIS images to estimate changes in vegetative biomass p 1070 N94-16689
The 1991 AVIRIS/POLDER experiment in Camargue, France p 1070 N94-16691
AVIRIS ground data processing system
p 1071 N94-16692
Use of AVIRIS data to the definition of optimised specifications for land applications with future spaceborne imaging spectrometers p 1071 N94-16694
Primary studies of trace quantities of green vegetation in Mono Lake area using 1990 AVIRIS data
p 1071 N94-16695
JPL activities on development of acousto-optic tunable filter imaging spectrometer p 1037 N94-16696
Measuring dry plant residues in grasslands: A case study using AVIRIS p 1072 N94-16697
Tracking photosynthetic efficiency with narrow-band spectroradiometry
[CIW-PUBL-1133] p 1072 N94-16698
Software for the derivation of scaled surface reflectances from AVIRIS data p 1072 N94-16700
Integrating remote sensing techniques at Cuprite, Nevada: AVIRIS, Thematic Mapper, and field spectroscopy p 1072 N94-16701
AVIRIS as a tool for carbonatite exploration: Comparison of SPAM and Mbandmap data analysis methods
p 1073 N94-16703
Expert system-based mineral mapping using AVIRIS
p 1073 N94-16704
AVIRIS data and neural networks applied to an urban ecosystem p 1073 N94-16705
Temporal variation in spectral detection thresholds of substrate and vegetation in AVIRIS images
p 1073 N94-16706
Discussion of band selection and methodologies for the estimation of precipitable water vapour from AVIRIS data p 1074 N94-16707
Abundance recovery error analysis using simulated AVIRIS data p 1074 N94-16708
A comparison of LOWTRAN-7 corrected Airborne Visible/Infrared Imaging Spectrometer (AVIRIS) data with ground spectral measurements p 1074 N94-16710
Simulation of AVHRR-K band ratios with AVIRIS
p 1075 N94-16714
Investigation of cloud properties and atmospheric stability with MODIS
[NASA-CR-193475] p 1107 N94-16717
Earth observational research using multistage EOS-like data
[NASA-CR-194626] p 1084 N94-16831

IMAGING TECHNIQUES
Visualization of solidification front phenomena
[NASA-CR-193838] p 976 N94-15006
Microchannel plate imaging detectors for the ultraviolet p 901 N94-15037
Requirements on CCD-detectors for ground-based auroral imaging p 909 N94-15093
Assessment of TDI operation of a frame transfer CCD for high resolution imaging from a fast spinning spacecraft p 910 N94-15097
Medical imaging
[NASA-TM-109675] p 1229 N94-15520
An electronic imaging system for the Aeroballistic Research Facility
[AD-A267157] p 1033 N94-15826
Sensor modelling for the Cyclops focal plane detector array based technology demonstrator
[AD-A267172] p 1190 N94-15846
Spaceborne Imaging Radar-C instrument
p 990 N94-15890
Spaceborne radar for geoscientific applications in North China p 993 N94-15915
Plasma arc welding weld imaging
[NASA-CASE-MFS-28797-1] p 1047 N94-15949
Revisiting the BCS, a measurement system for characterizing the optics of solar collectors
[DE93-015030] p 1091 N94-15993
Composite refraction-reflection stack sections: Tracing faults in the Atlantic coastal plain sediments
[DE93-013581] p 1112 N94-16009
Application of Z-contrast imaging to obtain column-by-column spectroscopic analysis of materials
[DE93-015333] p 947 N94-16014
Earth imaging results from Galileo's second encounter
p 1252 N94-16201
Global Magellan-image map of Venus at full resolution
p 1274 N94-16319
Vertical structure models of the 1990 equatorial disturbance on Saturn p 1277 N94-16333
Resolving topographic detail on Venus by modeling complex Magellan altimetry echoes
p 1283 N94-16368
From minerals to rocks: Toward modeling lithologies with remote sensing p 1086 N94-16437
MAC Europe 1991: Evaluation of AVIRIS, GER imaging spectrometry data for the land application testsite Oberpfaffenhofen p 1070 N94-16688
Separation of cirrus cloud from clear surface from AVIRIS data using the 1.38 micron water vapor band
p 1072 N94-16699
Earth observational research using multistage EOS-like data
[NASA-CR-194626] p 1084 N94-16831
Insights into semiconducting materials and growth phenomena through Z-contrast STEM
[DE93-015964] p 1212 N94-16841
High resolution radar profiling using higher-order statistics
[AD-D015891] p 1000 N94-16918
Multi-frame x ray imaging with a large area 40ps camera
[DE93-017179] p 1035 N94-16960
Speckles statistics and decorrelation effects in complex ABCD optical systems
[AD-A267843] p 1193 N94-17012
Method and apparatus to characterize ultrasonically reflective contrast agents
[NASA-CASE-LAR-14969-1] p 1129 N94-17085
Small imaging satellite for Earth observing system adjunct p 891 N94-17151

Applications of advanced diffractive optical elements
p 1197 N94-17356
Test methods for acceptance testing of telescopes
[AD-A268316] p 1237 N94-17568
Three dimensional visualization of GOES cloud data using OCTRESS
[AD-A268102] p 1109 N94-17572
X ray computed tomography for geometry acquisition
[AD-A268085] p 1157 N94-17590
Resist performance in soft x ray projection lithography
[DE93-016490] p 1036 N94-17647

IMIDES
Photodegradation of polyimides. V1: Effect of donor-acceptor groups on the photooxidative stability of polyimides and model compounds
[AD-A267319] p 970 N94-16947

IMP
The 1971 highlights --- NASA programs and research
[NASA-TM-109629] p 1302 N94-15417

IMPACT DAMAGE
An analysis of the dynamic response of the Space Station Freedom due to a module perforation by an orbital debris particle impact
[TABES PAPER 93-653] p 899 N94-16154
Collisional and dynamical history of Gaspra
p 1241 N94-16202
The Acraman impact structure: Estimation of the diameter by the ejecta layer thickness
p 1103 N94-16211
The physical mechanism of comet outbursts: An experiment p 1242 N94-16221
Impact penetration experiments in teflon targets of variable thickness p 1063 N94-16253
Simulation of collisional fragmentation with explosives
p 1063 N94-16254
A first-order model for impact crater degradation on Venus p 1265 N94-16268
National Transportation Safety Board annual review of aircraft accident data, US general aviation, calendar year 1989
[PB93-160687] p 863 N94-16464
Effect of Impact Damage and Open Hole on Compressive Strength of Hybrid Composite Laminates
[NASA-CR-194603] p 936 N94-16836
Low and high velocity impact response of thick hybrid composites p 936 N94-16837

IMPACT MELTS
A discontinuous melt sheet in the Manson impact structure p 1103 N94-16269
A Monazite-bearing clast in Apollo 17 melt breccia
p 1267 N94-16279
Apollo 17 materials viewed from 2 to 4 mm soil particles: Pre-serenitatis highlands components
p 1267 N94-16280
I-Xe structure of ILAFEGH 009 and shallowater: Evidence for early formation and rapid cooling of impact-derived enstatite meteorites
p 1243 N94-16305
Cat Mountain: A meteoritic sample of an impact-melted chondritic asteroid p 1244 N94-16328
Chromite-rich mafic silicate chondrules in ordinary chondrites: Formation by impact melting
p 1244 N94-16330
Siderophile element fractionation in meteor crater impact glasses and metallic spherules p 1246 N94-16414
Terrestrial impact melts as analogues for the hematization of Martian surface materials
p 1104 N94-16424

IMPACT RESISTANCE
An engineering approach for the application of textile composites to a structural component
p 938 N94-16852

IMPACT STRENGTH
The effect of long-term aging on the impact properties of modified 9Cr-1Mo steel
[DE93-015453] p 957 N94-16068

IMPACT TESTING MACHINES
Design of non-sled setup to measure head injury criteria
[NIAR-92-20] p 872 N94-17263

IMPACT TOLERANCES
Effect of Impact Damage and Open Hole on Compressive Strength of Hybrid Composite Laminates
[NASA-CR-194603] p 936 N94-16836
Low and high velocity impact response of thick hybrid composites p 936 N94-16837

IMPEDANCE
Operation of digital systems in severe electromagnetic environments
[AD-A267176] p 988 N94-15693
Assessment of chromate and non-chromate conversion coatings for Al alloys using electrochemical impedance spectroscopy
[AD-A267205] p 965 N94-15859
Design of broadband wire antennas for frequency hopping applications
[AD-A267405] p 1001 N94-17025

IMPEDANCE MEASUREMENT
Determination of equivalent circuit for PVDF shock-pressure gauges
[DE93-016492] p 1034 N94-16452

IMPEDANCE PROBES
Measurement of the velocity field and void fraction in a planar plunging jet
[AD-A268183] p 1030 N94-17511

IMPELLERS
ALS liquid hydrogen turbopump
[NASA-CR-194646] p 927 N94-17016
Experimental and computational investigation of the NASA low-speed centrifugal compressor flow field
[NASA-TM-4481] p 869 N94-17386

IMPLOSIONS
Direct drive foil implosion experiments on Pegasus 2
[DE93-012666] p 1202 N94-16776
Three dimensional hydrodynamic calculations with adaptive mesh refinement of the evolution of Rayleigh Taylor and Richtmyer Meshkov instabilities in converging geometry: Multi-mode perturbations
[DE93-017155] p 1025 N94-16903
Plasma flow switch and foil implosion experiments on Pegasus 2
[DE93-016464] p 1013 N94-17318

IMPREGNATING
A new NASA LaRC Multi-Purpose Prepregging Unit
p 932 N94-15276
Processing, properties and applications of composites using powder-coated epoxy towpreg technology
p 933 N94-15277
Characterization of voids formed during liquid impregnation of nonwoven multifilament glass networks as related to composite processing p 939 N94-16858

IMPULSES
Optical effects of regolith processes on S asteroids as simulated by laser impulse alteration of ordinary chondrite p 1246 N94-16422

IMPURITIES
BIB photodetectors based on antimony doped silicon
p 902 N94-15047
Optimisation of FIR photoconductors for atmospheric spectroscopy p 902 N94-15048
A study of relaxation transitions in the polymers under the influence of magnetic fields
[AD-A263878] p 963 N94-15133

IN SITU MEASUREMENT
Workshop on advanced technologies for planetary instruments
[NASA-CR-194585] p 1032 N94-15797

IN-FLIGHT MONITORING
SYNMOD: A low-resource, low-cost means of monitoring the near-Earth space debris environment
p 891 N94-17148

INCIDENCE
Measurements of the radar cross section and Inverse Synthetic Aperture Radar (ISAR) images of a Piper Navajo at 9.5 GHz and 49 GHz
[AD-A267570] p 1002 N94-17110
Review of rigorous coupled-wave analysis and of homogeneous effective medium approximations for high spatial-frequency surface-relief gratings
p 1194 N94-17335

INCLUSIONS
Grosnaja ABCs: Magnesium isotope compositions
p 1241 N94-16191
Petrography, mineralogy, and Mg isotope composition of VICTA: A vigarano CaAl4O7-bearing type A inclusion
p 1103 N94-16203
An iridium-rich iron micrometeorite with silicate inclusions from the Moon p 1242 N94-16281
Experimental segregation of iron-nickel metal, iron-sulfide, and olivine in a thermal gradient: Preliminary results p 1243 N94-16288
An experimental study of trace element partitioning between perovskite, hibonite and melt: Equilibrium values p 954 N94-16313
On origin of the olivine inclusions from the Kainsaz CO carbonaceous chondrite p 1244 N94-16345
Limited subsolidus diffusion in type B1 CAI: Evidence from Ti distribution in spinel p 954 N94-16401
Refractory precursor components in an Allende ferromagnesian chondrule p 1245 N94-16412

INCOHERENT SCATTERING
Insights into semiconducting materials and growth phenomena through Z-contrast STEM
[DE93-015964] p 1212 N94-16841
Speckles statistics and decorrelation effects in complex ABCD optical systems
[AD-A267843] p 1193 N94-17012

INCOMPRESSIBILITY
A priori inequalities for an ideal-incompressible liquid in an electromagnetic field
[IFTR-9/1992] p 998 N94-16652

INCOMPRESSIBLE FLOW
Large-Eddy Simulations (LES) of flows and turbulence distribution
[AD-A267182] p 1016 N94-15151
Surface and internal signatures of organized vortex motions in stratified fluid
[AD-A267015] p 1020 N94-15526
Inviscid instability of streamwise corner flow
[NASA-CR-191514] p 1021 N94-15834
A rapid computational model for estimating the performance of compliant airfoils in cascades
[AD-A266275] p 857 N94-16471
Hoph bifurcation in viscous, low speed flows about an airfoil with structural coupling
[AD-A266542] p 859 N94-16798

INCOMPRESSIBLE FLUIDS
Broken symmetry in ideal magnetohydrodynamic turbulence
[NASA-TM-109017] p 1023 N94-15964

INDENTATION
Laser weld repair of tantalum sheet
[DE93-016417] p 1041 N94-16871

INDEXES (DOCUMENTATION)
SeaWiFS technical report series. Volume 12, SeaWiFS technical report series cumulative index: Volumes 1-11
[NASA-TM-104566-VOL-12] p 1111 N94-15529
Aeronautical engineering: A continuing bibliography with indexes (supplement 295)
[NASA-SP-7037(295)] p 854 N94-16480
Commonwealth of Independent States aerospace science and technology, 1992: A bibliography with indexes
[NASA-SP-7106] p 854 N94-16481

INDIANA
Environmental assessment for northwestern Indiana relay node site no. RN 8C902IN
[AD-A267849] p 1004 N94-17406

INDIUM
Photo-assisted epitaxial growth for III-V semiconductors
[AD-A267889] p 1213 N94-17042

INDIUM ANTIMONIDES
The growth of InAs(1-x)Sb(x)/InAs strained-layer superlattices by metal-organic chemical vapor deposition
[DE93-015028] p 1208 N94-16012

INDIUM ARSENIDES
The growth of InAs(1-x)Sb(x)/InAs strained-layer superlattices by metal-organic chemical vapor deposition
[DE93-015028] p 1208 N94-16012
Photo-assisted epitaxial growth for III-V semiconductors
[AD-A267889] p 1213 N94-17042
Proceedings of the 6th International Conference on Narrow Gap Semiconductors
[AD-A268097] p 1015 N94-17570

INDIUM COMPOUNDS
Characterization of InTlSb grown by low pressure metalorganic chemical vapor deposition on GaAs substrate
[AD-A266878] p 1206 N94-14922

INDIUM GALLIUM ARSENIDES
Monolithic, two-terminal InP/Ga(0.47)In(0.53)As tandem solar cells
[DE93-014037] p 1093 N94-16824

INDIUM PHOSPHIDES
Monolithic, two-terminal InP/Ga(0.47)In(0.53)As tandem solar cells
[DE93-014037] p 1093 N94-16824
Lattice-mismatched In(0.40)Al(0.60)As window layers for indium phosphide solar cells
[NASA-TM-106255] p 1013 N94-17113

INDOLES
TransRapid TR-07 maglev-spectrum magnetic field effects on daily pineal indoleamine metabolic rhythms in rodents
[DE93-015143] p 1117 N94-16893

INDOOR AIR POLLUTION
Space Shuttle solid rocket motor exposure monitoring
p 976 N94-16624

INDUCTANCE
Forback DC-to-DC converter
[NASA-CASE-GSC-13404-1] p 1010 N94-15874

INDUCTORS
Forback DC-to-DC converter
[NASA-CASE-GSC-13404-1] p 1010 N94-15874

INDUSTRIAL MANAGEMENT
Environmental management lessons to be learned from the upcoming CFC phase out or how to insure that we survive the next environmentally mandated process change
[TABES PAPER 93-570] p 1050 N94-16136

Emergency preparedness and planning
p 1124 N94-16613
Efficient management of cardiovascular risk screening programs p 1125 N94-16622
INDUSTRIAL PLANTS
Status of molten carbonate fuel cell technology development
[DE93-015666] p 1092 N94-16715
INDUSTRIAL SAFETY
New health and safety initiatives at the Department of Energy (DOE) p 1124 N94-16610
Ergonomics in the office environment
p 1124 N94-16612
Emergency preparedness and planning
p 1124 N94-16613
Medical surveillance and biological monitoring of lead exposed employees p 1124 N94-16615
Programs and resources for control of job stress in the Federal workplace p 1124 N94-16617
Education and training of professional industrial hygienists for 2020 p 1125 N94-16618
Efficient management of cardiovascular risk screening programs p 1125 N94-16622
Industrial Hygiene Laboratory accreditation: The JSC experience p 1125 N94-16623
Space Shuttle solid rocket motor exposure monitoring
p 976 N94-16624
Illness/injury pattern complex 40 (Titan)
p 1125 N94-16625
INDUSTRIAL WASTES
Environmental use of a Laser Range Finder and the Advanced Visualization System
[DE93-016163] p 1043 N94-17677
INDUSTRIES
From space to Earth
[NASA-TM-109638] p 1235 N94-15249
Finding fish from above --- remote sensing
[NASA-TM-109602] p 1081 N94-15310
Space commerce in a global economy: Comparison of US and Australian approaches
[NASA-TM-109341] p 1235 N94-17290
Technology transfer. Determining industry needs: A guide for communities
[NASA-CR-194676] p 1235 N94-17293
Technology in action
[NASA-TM-109345] p 1235 N94-17294
The impact of industry/university consortia programs on space education
[NASA-TM-109340] p 1222 N94-17441
INEQUALITIES
A priori inequalities for an ideal-incompressible liquid in an electromagnetic field
[IFTR-9/1992] p 998 N94-16652
INERTIAL CONFINEMENT FUSION
A state-of-the-art plasma polymerization coater for ICF targets
[DE93-016452] p 1204 N94-17237
The effects of radiation transport on line ratios used as temperature and density diagnostic
[DE93-016424] p 1205 N94-17663
INERTIAL NAVIGATION
Analysis of the accuracy of strapdown inertial surveying systems
[SER-C-391] p 1081 N94-15156
INERTIAL UPPER STAGE
Inertial Upper Stage
[NASA-TM-109654] p 885 N94-15278
STS-26 generic integrated IUS deploy simulation
[NASA-TM-109562] p 875 N94-15332
INFECTIOUS DISEASES
Bloodborne Pathogens Program p 1127 N94-16644
INFERENCE
Combinatorial semantics
[TR-444] p 1149 N94-16575
INFILTRATION
Polymer Infiltration Studies
[NASA-CR-194494] p 932 N94-15275
Verification of a two-dimensional infiltration model for the resin transfer molding process
[NASA-CR-194597] p 964 N94-15656
Evaluation of a distributed catchment scale water balance model
[PAPER-93WR00398] p 1083 N94-16031
Textile composite processing science
p 938 N94-16856
INFLATABLE STRUCTURES
Inflatable rescue device
[NASA-CASE-MSC-22244-1] p 1137 N94-15883
INFLUENCE COEFFICIENT
Effect of wind tunnel acoustic modes on linear oscillating cascade aerodynamics
[NASA-TM-106367] p 869 N94-15866
INFORMATION DISSEMINATION
NASA/DOD Aerospace Knowledge Diffusion Research Project. Paper 32: A new era in international technical communication: American-Russian collaboration
[NASA-TM-109336] p 1230 N94-15838
NASA/DOD Aerospace Knowledge Diffusion Research Project. Paper 34: Technical communications practices and the use of information technologies as reported by Dutch and US aerospace engineers
[NASA-TM-109337] p 1230 N94-15839
NASA information resources management handbook
[NHB-2410.1E] p 1230 N94-15941
NASA/DOD Aerospace Knowledge Diffusion Research Project. Report 15: Technical uncertainty and project complexity as correlates of information use by US industry-affiliated aerospace engineers and scientists: Results of an exploratory investigation
[NASA-TM-107693] p 1233 N94-17291
NASA/DOD Aerospace Knowledge Diffusion Research Project. Report 15: Technical uncertainty and project complexity as correlates of information use by US industry-affiliated aerospace engineers and scientists: Results of an exploratory investigation
[NASA-TM-107693] p 1233 N94-17300
INFORMATION FLOW
Electronic messaging for the 1990's
[AD-A267143] p 1229 N94-15437
NASA/DOD Aerospace Knowledge Diffusion Research Project. Paper 32: A new era in international technical communication: American-Russian collaboration
[NASA-TM-109336] p 1230 N94-15838
NASA/DOD Aerospace Knowledge Diffusion Research Project. Paper 34: Technical communications practices and the use of information technologies as reported by Dutch and US aerospace engineers
[NASA-TM-109337] p 1230 N94-15839
Efficient scheduling of real-time compute-intensive periodic graphs on large grain data flow multiprocessor
[AD-A267444] p 1141 N94-17030
INFORMATION MANAGEMENT
Department of Defense technical architecture framework for information management. Volume 1: Overview, version 2.0
[AD-A267193] p 1228 N94-15152
SIMS: Single Interface to Multiple Systems
[AD-A266934] p 1143 N94-15175
NASA directives master list and index
[NHB-1410.13L] p 1229 N94-15414
Department of Defense technical architecture framework for information management. Volume 2: Technical reference model and standards profile, version 2.0
[AD-A267194] p 1229 N94-15788
Department of Defense technical architecture framework for information management. Volume 3: Architecture concepts and design guidance, version 2.0
[AD-A267195] p 1230 N94-15789
NASA/DOD Aerospace Knowledge Diffusion Research Project. Paper 32: A new era in international technical communication: American-Russian collaboration
[NASA-TM-109336] p 1230 N94-15838
NASA/DOD Aerospace Knowledge Diffusion Research Project. Paper 34: Technical communications practices and the use of information technologies as reported by Dutch and US aerospace engineers
[NASA-TM-109337] p 1230 N94-15839
Index of NASA prefixed forms
[NHB-1420.21] p 1230 N94-15936
NASA security handbook
[NHB-1620.3C] p 1224 N94-15937
NASA information resources management handbook
[NHB-2410.1E] p 1230 N94-15941
Information Technology Resources Assessment
[DE93-013899] p 1230 N94-16010
NASA Electronic Library System (NELS): The system impact of security
[NASA-CR-194614] p 1231 N94-16499
Managing information as a corporate asset: Key strategies for information professionals to remain competitive
[DE93-015515] p 1232 N94-16875
INFORMATION PROCESSING (BIOLOGY)
An information processing classification of beyond-visual-range air intercepts
[AD-A266927] p 1131 N94-15108
Altitude deviations: Breakdowns of an error-tolerant system
[NASA-TM-108788] p 862 N94-15550
Neural mechanisms of attention
[AD-A266315] p 1132 N94-16456
Localizing visual function in the brain
[AD-A267381] p 1133 N94-17020
Theoretical and experimental research into biological mechanisms underlying learning and memory
[AD-A267441] p 1133 N94-17022
INFORMATION RETRIEVAL
NASA's online machine aided indexing system
[NASA-CR-4518] p 1228 N94-15009
SIMS: Single Interface to Multiple Systems
[AD-A266934] p 1143 N94-15175
A TRALINET guide to the Internet
[AD-A266946] p 1229 N94-15178
A browsing tool for the Internet Logical Library of the HPCC Software Exchange
[NASA-CR-194545] p 1143 N94-15189
Monotone approximate query processing
[AD-A267153] p 1169 N94-15779
A proposed research program in strategic computing
[AD-A267516] p 1153 N94-17078
Defense RDT&E online system (DROLS) handbook
[AD-A267546] p 1232 N94-17101
Defense Logistics Information System (DLIS). Procedures manual: Logistics On-Line Access (LOLA) procedures manual
[AD-A267685] p 1233 N94-17229
INFORMATION SYSTEMS
Department of Defense technical architecture framework for information management. Volume 1: Overview, version 2.0
[AD-A267193] p 1228 N94-15152
NASA Spacelink computer
[NASA-TM-109657] p 1140 N94-15228
Electronic messaging for the 1990's
[AD-A267143] p 1229 N94-15437
NASA/DOD Aerospace Knowledge Diffusion Research Project. Paper 34: Technical communications practices and the use of information technologies as reported by Dutch and US aerospace engineers
[NASA-TM-109337] p 1230 N94-15839
Expert system for welding engineering
p 984 N94-16003
Information Technology Resources Assessment
[DE93-013899] p 1230 N94-16010
Materials, processes, and environmental engineering network
[TABES PAPER 93-610] p 1051 N94-16142
NASA Operational Environment Team (NOET): NASA's key to environmental technology
[TABES PAPER 93-611] p 1052 N94-16143
Computing and Information Sciences
[DE93-017149] p 1151 N94-16902
Information technology division technical paper abstracts
[AD-A266227] p 1166 N94-16938
Design and implementation of an object-oriented interface for the multi-model/multi-lingual database system
[AD-A267413] p 1232 N94-16977
Computer Science and Telecommunications Board activities
[DE93-018141] p 1000 N94-17000
Defense Logistics Information System (DLIS) procedures manual. Products and services end-user manual
[AD-A267766] p 1232 N94-17007
A geological and geophysical information system for Eurasia
[AD-A267841] p 1232 N94-17036
Defense Logistics Information System (DLIS). Procedures manual: Logistics On-Line Access (LOLA) procedures manual
[AD-A267685] p 1233 N94-17229
NASA/DOD Aerospace Knowledge Diffusion Research Project. Report 15: Technical uncertainty and project complexity as correlates of information use by US industry-affiliated aerospace engineers and scientists: Results of an exploratory investigation
[NASA-TM-107693] p 1233 N94-17300
Model designation of military aerospace vehicles
[AD-A267852] p 898 N94-17388
Integration of several computer systems within a heterogeneous environment
[AD-A267978] p 1155 N94-17500
INFORMATION THEORY
Low-Complexity, High-Performance Bandwidth Efficient Coding and Coded Modulation Techniques for Satellite and Space Communications
[NASA-CR-194623] p 997 N94-16506
Bandwidth efficient coding: Theoretical limits and real achievements. Error control techniques for satellite and space communications p 997 N94-16507
INFORMATION TRANSFER
NASA/DOD Aerospace Knowledge Diffusion Research Project. Paper 32: A new era in international technical communication: American-Russian collaboration
[NASA-TM-109336] p 1230 N94-15838

NASA/DOD Aerospace Knowledge Diffusion Research Project. Report 15: Technical uncertainty and project complexity as correlates of information use by US industry-affiliated aerospace engineers and scientists: Results of an exploratory investigation
[NASA-TM-107693] p 1233 N94-17291
Technology transfer. Determining industry needs: A guide for communities
[NASA-CR-194676] p 1235 N94-17293
Technology in action
[NASA-TM-109345] p 1235 N94-17294
Military space programs in the press: An analysis for change
[AD-A267799] p 874 N94-17306

INFRARED ASTRONOMY
Photoconductors and arrays for the far-infrared p 902 N94-15045
Infrared detectors and coolers for space instrumentation: Summary and concluding remarks p 904 N94-15059
Ionising radiation-induced effects in doped germanium FIR photoconductors p 907 N94-15077
Cryogenic readout electronics for astronomical applications p 910 N94-15099
New K type asteroids p 1241 N94-16195
A decade's overview of Io's volcanic activity p 1245 N94-16386
Critically evaluated/distributed database of IRAS LRS spectra
[NASA-CR-193611] p 1232 N94-17038

INFRARED ASTRONOMY SATELLITE
The chromosphere of VV cephei and the distribution of circumstellar dust around red giants and supergiants
[NASA-CR-193594] p 1297 N94-16866
Critically evaluated/distributed database of IRAS LRS spectra
[NASA-CR-193611] p 1232 N94-17038
A typical pointed observation in IRAS designed to fit into a 15 minute window
[NASA-CR-194653] p 1199 N94-17443

INFRARED DETECTORS
Large scientific 2-D arrays for the 1-5 micron region p 902 N94-15044
Impurity conduction photoconductor detectors p 902 N94-15046
Schottky barrier focal plane arrays for SWIR and MWIR p 903 N94-15050
Advanced high performance CdHgTe multiplexed arrays p 903 N94-15051
A 12.5 micron infrared detector for Earth observation p 903 N94-15052
Lead chalcogenides based IR photosensitive array detectors with coordinate addressing p 903 N94-15053
Infrared detectors and coolers for space instrumentation: Summary and concluding remarks p 904 N94-15059
Discrete CMT infrared detectors for space application, from ISSR to second generation Meteosat and MIPAS p 905 N94-15065
Extrinsic photoconductor detectors for the wavelength range 2 microns to 240 microns p 906 N94-15073
Characterization of detectors and calibration of the ISOPHOT experiment p 907 N94-15082
Characteristics of the ISO short wavelength spectrometer detectors p 908 N94-15084
IR detectors and subsystems for space applications p 909 N94-15091
Infrared detector annealing and calibration with IR-laser diodes p 909 N94-15092
A linear monolithic 4-6 on silicon IR detector array p 910 N94-15098
Cryogenic readout electronics for astronomical applications p 910 N94-15099
Sensor modelling for the Cyclops focal plane detector array based technology demonstrator
[AD-A267172] p 1190 N94-15846
Clementine: Anticipated scientific datasets from the Moon and Geographos p 1288 N94-16392
Structural characterization of epitaxial layers for infrared detectors
[AD-A267875] p 940 N94-17013
Development of ultra-low noise, high performance 3-V Quantum Well Infrared Photodectors (QWIP's) for focal plane array staring image sensor systems
[AD-A267715] p 1214 N94-17272

INFRARED IMAGERY
Schottky barrier focal plane arrays for SWIR and MWIR p 903 N94-15050
A linear monolithic 4-6 on silicon IR detector array p 910 N94-15098
A monolithic PbTeCCD focal plane array for MWIR imaging p 910 N94-15100
Environmental characterization for target acquisition. Report 1: Site descriptions and measurements
[AD-A267192] p 1106 N94-15851
Recent advances in outdoor performance evaluation of PV systems
[DE93-015031] p 1091 N94-15994
Earth imaging results from Galileo's second encounter p 1252 N94-16201
Thermogeologic mapping of the Moon from lunar orbit p 1290 N94-16405
Deucalionis Regio, Mars: Evidence for a unique mineralogic endmember and a crusted surface p 1291 N94-16406
Spatial resolution and cloud optical thickness retrievals p 1066 N94-16671
Seasonal and spatial variations in phytoplanktonic chlorophyll in eutrophic Mono Lake, California, measured with the Airborne Visible and Infrared Imaging Spectrometer (AVIRIS) p 1069 N94-16684
AVIRIS calibration and application in coastal oceanic environments p 1069 N94-16685
Atmospheric correction of AVIRIS data in ocean waters p 1070 N94-16690
Separation of cirrus cloud from clear surface from AVIRIS data using the 1.38 micron water vapor band p 1072 N94-16699
Developing automated analysis methods for sea ice imagery: A status report with recommendations
[AD-A267284] p 1113 N94-17241
Nowcasting methods for satellite imagery
[AD-A267294] p 1108 N94-17267
Three dimensional visualization of GOES cloud data using OCTRESS
[AD-A268102] p 1109 N94-17572
An empirical study of tropical cloud clusters using special sensor microwave imager data
[AD-A268072] p 1110 N94-17595

INFRARED LASERS
Photo-assisted epitaxial growth for III-V semiconductors
[AD-A267889] p 1213 N94-17042

INFRARED RADAR
Clementine: Anticipated scientific datasets from the Moon and Geographos p 1288 N94-16392

INFRARED RADIATION
Infrared remote activity transceiver universal model
[AD-A266965] p 1188 N94-15144
Ground truth spectrometry and imagery of eruption clouds to maximize utility of satellite imagery
[NASA-CR-194358] p 1081 N94-15181
A global traveling wave on Venus
[NASA-CR-194356] p 1246 N94-15182
Optoelectronics based on SiGe/Si heterostructures
[AD-A267178] p 1190 N94-15848
Environmental characterization for target acquisition. Report 1: Site descriptions and measurements
[AD-A267192] p 1106 N94-15851
Near-surface temperature gradients and their effects on thermal-infrared emission spectra of particulate planetary surfaces p 1260 N94-16236
Infrared spot tracker
[AD-D015778] p 1191 N94-16547
Ultrafast processes in tunneling microstructure devices
[AD-A266570] p 1210 N94-16720
The feasibility of tropospheric and total ozone determination using a Fabry-Perot interferometer as a satellite-based nadir-viewing atmospheric sensor
[NASA-TM-109342] p 1102 N94-17214
Development of ultra-low noise, high performance 3-V Quantum Well Infrared Photodectors (QWIP's) for focal plane array staring image sensor systems
[AD-A267715] p 1214 N94-17272
Fabricating binary optics: An overview of binary optics process technology p 1195 N94-17343
Predesign of diamond turned refractive/diffractive elements for IR objectives p 1198 N94-17359

INFRARED RADIOMETERS
Ground truth spectrometry and imagery of eruption clouds to maximize utility of satellite imagery
[NASA-CR-194358] p 1081 N94-15181
Testing the waters from space --- Thermal mapping
[NASA-TM-109623] p 1082 N94-15409
A conceptual design study for a two-dimensional, electronically scanned thinned array radiometer
[NASA-TM-109051] p 1085 N94-17665

INFRARED SCANNERS
Summaries of the Third Annual JPL Airborne Geoscience Workshop. Volume 2: TIMS Workshop
[NASA-CR-194541] p 1063 N94-16595
TIMS performance evaluation summary p 1063 N94-16596
A quantitative analysis of TIMS data obtained on the Learjet 23 at various altitudes p 1063 N94-16597
Analysis of TIMS performance subjected to simulated wind blast p 1063 N94-16598
Sensitivity of blackbody reference panels to wind blast p 1063 N94-16599
Comparison of preliminary results from Airborne Aster Simulator (AAS) with TIMS data p 1064 N94-16600
Application of split window technique to TIMS data p 1064 N94-16601
Atmospheric corrections for TIMS estimated emittance p 1064 N94-16602
An algorithm for the estimation of bounds on the emissivity and temperatures from thermal multispectral airborne remotely sensed data p 1064 N94-16603
Preliminary analysis of thermal-infrared multispectral scanner data of the Iron Hill, Colorado carbonatite-alkalic rock complex p 1065 N94-16605

INFRARED SPACE OBSERVATORY (ISO)
Photoconductors and arrays for the far-infrared p 902 N94-15045
The detector assemblies of ISOPHOT and the spectrometers ISO-SWS and ISO-LWS p 906 N94-15074
Characterization of detectors and calibration of the ISOPHOT experiment p 907 N94-15082
Characteristics of the ISO short wavelength spectrometer detectors p 908 N94-15084

INFRARED SPECTRA
Optical and infrared spectra of thermally annealed Pb implanted SiO2 glasses
[DE93-015304] p 965 N94-15828
New K type asteroids p 1241 N94-16195
Critically evaluated/distributed database of IRAS LRS spectra
[NASA-CR-193611] p 1232 N94-17038

INFRARED SPECTROMETERS
Performance testing of doped-germanium photoconductors for the ISO long wavelength spectrometer p 905 N94-15066
Non-linear effects in doped-germanium photoconductors for the ISO long wavelength spectrometer p 905 N94-15067
IR detectors and subsystems for space applications p 909 N94-15091
Summaries of the Third Annual JPL Airborne Geoscience Workshop. Volume 1: AVIRIS Workshop
[NASA-CR-194540] p 1066 N94-16666
In-flight calibration of the spectral and radiometric characteristics of AVIRIS in 1991 p 1037 N94-16667
Using AVIRIS images to measure temporal trends in abundance of photosynthetic and nonphotosynthetic canopy components p 1066 N94-16668
Unmixing AVIRIS data to provide a method for vegetation fraction subtraction p 1066 N94-16669
The Spectral Image Processing System (SIPS): Software for integrated analysis of AVIRIS data p 1067 N94-16674
AVIRIS study of Death Valley evaporite deposits using least-squares band-fitting methods p 1067 N94-16676
Retrieval of biophysical parameters with AVIRIS and ISM: The Landes Forest, south west France p 1068 N94-16681
Ground-truthing AVIRIS mineral mapping at Cuprite, Nevada p 1069 N94-16682
AVIRIS calibration and application in coastal oceanic environments p 1069 N94-16685
Mapping vegetation types with the multiple spectral feature mapping algorithm in both emission and absorption p 1069 N94-16686
MAC Europe 1991: Evaluation of AVIRIS, GER imaging spectrometry data for the land application testsite Oberpfaffenhofen p 1070 N94-16688
Using endmembers in AVIRIS images to estimate changes in vegetative biomass p 1070 N94-16689
The 1991 AVIRIS/POLDER experiment in Camargue, France p 1070 N94-16691
AVIRIS ground data processing system p 1071 N94-16692
Simulation of ASTER data using AVIRIS images p 1071 N94-16693
Use of AVIRIS data to the definition of optimised specifications for land applications with future spaceborne imaging spectrometers p 1071 N94-16694
Primary studies of trace quantities of green vegetation in Mono Lake area using 1990 AVIRIS data p 1071 N94-16695
Measuring dry plant residues in grasslands: A case study using AVIRIS p 1072 N94-16697
Tracking photosynthetic efficiency with narrow-band spectroradiometry
[CIW-PUBL-1133] p 1072 N94-16698
Software for the derivation of scaled surface reflectances from AVIRIS data p 1072 N94-16700
Integrating remote sensing techniques at Cuprite, Nevada: AVIRIS, Thematic Mapper, and field spectroscopy p 1072 N94-16701
AVIRIS as a tool for carbonatite exploration: Comparison of SPAM and Mbandmap data analysis methods p 1073 N94-16703
Expert system-based mineral mapping using AVIRIS p 1073 N94-16704
AVIRIS data and neural networks applied to an urban ecosystem p 1073 N94-16705

Temporal variation in spectral detection thresholds of substrate and vegetation in AVIRIS images p 1073 N94-16706
Discussion of band selection and methodologies for the estimation of precipitable water vapour from AVIRIS data p 1074 N94-16707
Abundance recovery error analysis using simulated AVIRIS data p 1074 N94-16708
A comparison of LOWTRAN-7 corrected Airborne Visible/Infrared Imaging Spectrometer (AVIRIS) data with ground spectral measurements p 1074 N94-16710
Simulation of AVHRR-K band ratios with AVIRIS p 1075 N94-16714
Investigation of cloud properties and atmospheric stability with MODIS
[NASA-CR-193475] p 1107 N94-16717
Second flight of the Spacelab grille spectrometer during the Atlas-1 mission
[AERONAUTICA-ACTA-A-367-199] p 923 N94-17592

INFRARED SPECTROPHOTOMETERS
The detector assemblies of ISOPHOT and the spectrometers ISO-SWS and ISO-LWS p 906 N94-15074

INFRARED SPECTROSCOPY
Characteristics of the ISO short wavelength spectrometer detectors p 908 N94-15084
New K type asteroids p 1241 N94-16195
Water adsorption on diamond (110) studied by multiple internal reflection infrared spectroscopy
[AD-A266415] p 948 N94-16553
Amide and tetrazene complexes of transition and main group elements as precursors for the low temperature synthesis of elemental nitrides
[AD-A266246] p 950 N94-16931
Photodegradation of MDI based polyurethane/urea elastomers
[AD-A267308] p 971 N94-16994

INFRARED TELESCOPES
Silicon gallium doped photoconductor development for the AROME balloon borne instrument p 908 N94-15087
New K type asteroids p 1241 N94-16195
A typical pointed observation in IRAS designed to fit into a 15 minute window
[NASA-CR-194653] p 1199 N94-17443

INGOTS
Aluminum-lithium technology
[TABES PAPER 93-601] p 962 N94-16137
Solid lubricants for space structures, phase 2
[AD-A266653] p 968 N94-16767
Techniques for preparation of ingot metallurgical discontinuous composites
[AD-D015748] p 940 N94-16933

INHIBITORS
Thermo-mechanical analysis of oxidation protected carbon-carbon composites
[AD-A268191] p 941 N94-17597

INJECTION MOLDING
Army P/M research and development overview
[AD-A266921] p 954 N94-15104
Fabrication of advanced design (grooved) cermet anodes
[DE93-014590] p 1012 N94-16765
Fabrication of piezoelectric ceramic/polymer composites by injection molding
[AD-A267302] p 972 N94-17227

INJECTORS
3D and r,z particle simulations of heavy ion fusion beams
[DE93-013417] p 1205 N94-17670

INJURIES
A review of the efficacy of 7.5 percent NaCl/6 percent Dextran-70 (HSD) in experimental animals and humans
[AD-A266633] p 1122 N94-15740
The relationship of metallothionein induction to the heat shock response
[AD-A266634] p 1122 N94-15741
General Medical Surveillance Program p 1127 N94-16643

INLET AIRFRAME CONFIGURATIONS
Cruise noise measurements of a scale model advanced ducted propulsor
[NASA-TM-105808] p 1176 N94-15115

INLET FLOW
An uncertainty analysis of inlet dynamic flow distortion using an analog/digital hybrid editing system
[AD-A266924] p 855 N94-15105
Numerical investigations in three-dimensional internal flows
[NASA-CR-194594] p 1020 N94-15551

INLET NOZZLES
Numerical investigations in three-dimensional internal flows
[NASA-CR-194594] p 1020 N94-15551

INLET PRESSURE
Mechanism of intermittent atomization
[AD-A266625] p 1021 N94-15770

INORGANIC COATINGS
Restoring Miss Liberty — inorganic coatings
[NASA-TM-109605] p 963 N94-15313

INORGANIC COMPOUNDS
Optical studies of glasses embedded with inorganic ions and organic dyes
[AD-A268146] p 1199 N94-17455

INPUT
Determination of GTA welding efficiencies
[AD-A267163] p 1046 N94-15738

INPUT/OUTPUT ROUTINES
A software interface for the ARL wind tunnel data acquisition system
[AD-A267114] p 1146 N94-15650
FSM test: A functional test generation system for sequential circuits
[REPT-93-017] p 1014 N94-17505

INSECTS
Combating malaria
[NASA-TM-109609] p 1081 N94-15297

INSPECTION
Geometric tolerance assessment
[NPL-DITC-210/92] p 1049 N94-15013
Effects of inspection error on optimal inspection policies and software fault detection models
[AD-A267511] p 1153 N94-17075
Automated image analysis method for the detection of cracks on wood surface
[VTT-JULK-755] p 1056 N94-17542

INSTALLING
Satellite communications installation plan
[AD-A266303] p 1000 N94-16965

INSTANTONS
Existence of a new instanton in constrained Yang-Mills-Higgs theory
[NIKHEF-H/93-02] p 1186 N94-17601

INSTRUCTORS
Teacher in space
[NASA-TM-109666] p 1131 N94-15237

INSTRUMENT COMPENSATION
Temperature and pressure effects on capacitance probe cryogenic liquid level measurement accuracy
[NASA-CR-190763] p 1034 N94-16521

INSTRUMENT ERRORS
Ring lens focusing and push-pull tracking scheme for optical disk systems p 1227 N94-14990
Temperature and pressure effects on capacitance probe cryogenic liquid level measurement accuracy
[NASA-CR-190763] p 1034 N94-16521
Sensitivity of blackbody reference panels to wind blast p 1063 N94-16599

INSTRUMENT ORIENTATION
Neural-network-directed alignment of optical systems using the laser-beam spatial filter as an example
[NASA-TP-3372] p 1034 N94-15961
Tilt mechanism
[AD-D015780] p 1047 N94-16548

INSULATION
XPS analysis of Al/EPDM bondlines from IUS SRM-1 polar bosses
[AD-A266851] p 1056 N94-14945
Ablation, surface activation, and electroless metallization of insulating materials by pulsed excimer laser irradiation
[DE93-015808] p 1040 N94-16664
Postflight hardware evaluation 360T026 (RSRM-26, STS-47)
[NASA-CR-192559] p 882 N94-17656

INSULATORS
A simple chemical procedure for extending the conductive state of polypyrrole to more negative potentials
[AD-A266235] p 969 N94-16928
Atomic layer epitaxy of boron nitride
[AD-A266260] p 1212 N94-16932
Low dielectric constant insulators and gold metallization for GHz multi-chip modules, part 2
[AD-A268590] p 1176 N94-17605

INSULIN
New insulin pump
[NASA-TM-109642] p 1120 N94-15253

INTEGRAL EQUATIONS
Volume integral equations applied to circular and square cylinders
[AD-A266635] p 1169 N94-15785
Application of group theory to integral-difference equations of plasma physics
[IFTR-23/1992] p 1204 N94-17067

INTEGRATED CIRCUITS
VLSI for high-speed digital signal processing
[AD-A267709] p 1007 N94-14936
Multichip module high speed testing
[AD-A266968] p 986 N94-14955
Reliability characterization of digital microcircuits: Investigation of an in-process oxide reliability screening method
[AD-A267053] p 1008 N94-15665
OETC optical backplane bus testbed. IBM tasks: Receiver OEIC and link simulation tools and analysis
[AD-A266198] p 1191 N94-16128
Measurements of the operation of the SINUS-6/BWO system
[AD-A266423] p 1011 N94-16556
Large signal characterization and modeling of heterojunction bipolar transistors
[AD-A266184] p 1012 N94-16935
Stray insensitive switched capacitor composite operational amplifiers
[AD-A267412] p 1012 N94-16976
Optically-switched submillimeter-wave oscillator and radiator
[NASA-CASE-NPO-18547-1-CU] p 1014 N94-17324
Isochronets: A high-speed network switching architecture
[AD-A267811] p 1161 N94-17409
Smart Power: New power integrated circuit technologies and their applications
[VTT-TIED-1358] p 1015 N94-17546

INTEGRATED LIBRARY SYSTEMS
NASA Electronic Library System (NELS): The system impact of security
[NASA-CR-194614] p 1231 N94-16499

INTEGRATED MISSION CONTROL CENTER
A proposed ground segment design for small satellites p 878 N94-17154

INTELLIGENCE
Classified information: Volume could be reduced by changing retention policy
[AD-A266938] p 1228 N94-15176

INTELSAT SATELLITES
The 1970 highlights --- NASA programs and research
[NASA-TM-109628] p 1302 N94-15415

INTERACTIONAL AERODYNAMICS
Parametric resonant triad interactions in a free shear layer
[NASA-TM-106365] p 1021 N94-15751

INTERATOMIC FORCES
A molecular dynamics simulator for optimal control of molecular motion
[AD-A266572] p 1183 N94-16722

INTERCALATION
Diamond p-n junction cold cathode
[AD-A266926] p 1206 N94-15107

INTERCONTINENTAL BALLISTIC MISSILES
Hypervelocity orbital intercept guidance using certainty control
[AD-A267297] p 1174 N94-17219

INTERFACES
Overview of chemical vapor infiltration
[DE93-015440] p 934 N94-16065
Soyuz/ACRV accommodation study
[NASA-TM-107733] p 888 N94-17072

INTERFACIAL TENSION
Measurements of Interfacial Tension: MITE p 943 N94-15158
Liquid phase sintering of tungsten composites under microgravity. Effect of matrix composition p 945 N94-15171
Theoretical study of laminar film condensation on horizontal ellipitical tubes under conditions of free and forced convection
[AD-A267161] p 1021 N94-15737
Laser-liquid interactions under reduced gravity conditions p 977 N94-16077
Experimental segregation of iron-nickel metal, iron-sulfide, and olivine in a thermal gradient: Preliminary results p 1243 N94-16288
Physical and chemical properties of some new perfluoropolyalkylether lubricants prepared by direct fluorination
[NASA-TM-106299] p 967 N94-16543

INTERFERENCE GRATING
Application of holographic optical elements to magneto-optic read/write heads p 1226 N94-14985

INTERFEROMETERS
Simultaneous compression of the passively mode-locked pulsewidth and pulse train p 913 N94-15566
An investigation of the Ground-Based High-Resolution Interferometer Sounder (GB-HIS) in a costal marine environment
[AD-A268052] p 1114 N94-17503

INTERFEROMETRY
Velocity matched millimeterwave electro-optic modulator
[AD-A267264] p 1188 N94-14957
Spaceborne Imaging Radar-C instrument p 990 N94-15890

TOPSAT: Global space topographic mission
p 992 N94-15905
Interferometric GPS attitude: A stochastic error model, DREO report
[AD-A266411] p 864 N94-16457
The TOPSAR interferometric radar topographic mapping instrument p 1078 N94-16749
Measuring ocean coherence time with dual-baseline interferometry p 1080 N94-16759
Speckles statistics and decorrelation effects in complex ABCD optical systems
[AD-A267843] p 1193 N94-17012
Photo-assisted epitaxial growth for III-V semiconductors
[AD-A267889] p 1213 N94-17042
Fabrication techniques for very fast diffractive lenses
p 1196 N94-17345
SURPHEX (tm): New dry photopolymers for replication of surface relief diffractive optics p 1198 N94-17358
Study of high speed interference photography with two-dimensional acousto-optical lattice deflection
[AD-A267823] p 1035 N94-17402
An investigation of the Ground-Based High-Resolution Interferometer Sounder (GB-HIS) in a costal marine environment
[AD-A268052] p 1114 N94-17503

INTERGALACTIC MEDIA
The theory of QSO absorption line systems and their relationship to the galaxies
[NASA-CR-194596] p 1236 N94-15679

INTERIOR BALLISTICS
TDNOVA interactive graphics
[AD-A268000] p 1156 N94-17530

INTERLAMINAR STRESS
Dynamic behavior of fiber and particle reinforced composites
[AD-A266905] p 930 N94-15143

INTERMETALLICS
Army P/M research and development overview
[AD-A266921] p 954 N94-15104
Environmental embrittlement in ordered intermetallic alloys
[DE93-015307] p 955 N94-15830
High temperature advanced structural composites. Volume 1: Executive summary and intermetallic compounds
[AD-A267022] p 933 N94-15835
Recent advances in ordered intermetallics
[DE93-015308] p 955 N94-15862
A reexamination of grain boundary fracture in Ni3Al: Environmental and alloying effects
[DE93-015431] p 1208 N94-16063
Development and commercialization status of Fe3Al-based intermetallic alloys
[DE93-015802] p 957 N94-16165
Microstructure of Zr3Al after 2 MeV proton bombardment
[DE93-015331] p 1211 N94-16814
Bulk and defect properties of ordered intermetallics: A first-principles total-energy investigation
[DE93-015492] p 959 N94-16873
Micromechanisms of monotonic and cyclic subcritical crack growth in advanced high melting point low-ductility intermetallics
[AD-A267764] p 961 N94-17223

INTERNAL COMBUSTION ENGINES
Mechanism of intermittent atomization
[AD-A266625] p 1021 N94-15770

INTERNAL ENERGY
Some thoughts on future rain mapping missions (TRMM follow-on) p 992 N94-15906

INTERNAL PRESSURE
Remote tire pressure sensing technique
[NASA-CASE-LAR-14160-1] p 1033 N94-15884
Design of a fluid elastic actuator with application to structure control
[AD-A267649] p 897 N94-17246

INTERNAL WAVES
Arctic internal waves (CEAREX)
[AD-A265822] p 1111 N94-15139

INTERNATIONAL COOPERATION
International food research project
[NASA-TM-109540] p 1135 N94-15371
NASA/DOD Aerospace Knowledge Diffusion Research Project. Paper 32: A new era in international technical communication: American-Russian collaboration
[NASA-TM-109336] p 1230 N94-15838
NASA/DOD Aerospace Knowledge Diffusion Research Project. Paper 34: Technical communications practices and the use of information technologies as reported by Dutch and US aerospace engineers
[NASA-TM-109337] p 1230 N94-15839
International collaboration in SAR ground data systems p 993 N94-15917
Global Energy and Water Cycle Experiment (GEWEX) and the Continental-scale International Project (GCIP)
p 994 N94-15918
The Japanese Space Station utilization plan
p 977 N94-16074
The Canadian Space Station user development program. Where do we go from here? p 898 N94-16084
The definition of a scientific policy: ESRO's satellite programme in 1969-1973
[ESA-HSR-6] p 1303 N94-16500
The launch of ELDO
[ESA-HSR-7] p 886 N94-16501
Europe in space: Edoardo Amaldi and the inception of ESRO
[ESA-HSR-5] p 1303 N94-16526
Radar transmitter procedures
[AD-A268274] p 1005 N94-17523
Surface energy balance modeling at mesoscale: The contribution of the future Earth observing system
[BCRS-91-04] p 1085 N94-17616
Ontogenesis of mammals in microgravity
[NASA-TM-103978] p 1139 N94-17636

INTERNATIONAL LAW
Aviation inspection prospects p 853 N94-15125
Environmental management lessons to be learned from the upcoming CFC phase out or how to insure that we survive the next environmentally mandated process change
[TABES PAPER 93-570] p 1050 N94-16136
NASA Operational Environment Team (NOET): NASA's key to environmental technology
[TABES PAPER 93-611] p 1052 N94-16143

INTERNATIONAL RELATIONS
The strategic environmental research and development program: A new paradigm for space, the environment, and national security
[AD-A266222] p 1174 N94-16109

INTERPLANETARY DUST
Orbital evolution of dust from comet Schwassmann-Wachmann 1: A case of one-to-one resonance trapping p 1242 N94-16270
Carbon abundances, major element chemistry, and mineralogy of hydrated interplanetary dust particles
p 1243 N94-16309
Densities of 5-15 micron interplanetary dust particles
p 1244 N94-16367
The effect of an on-orbit near encounter on the number flux density of micron sized particles
p 899 N94-16374
Dust grain resonant capture: A statistical study
p 1245 N94-16384
Size distribution of interplanetary iron and stony particles related with deep-sea spherules p 1245 N94-16388
SYNMOD: A low-resource, low-cost means of monitoring the near-Earth space debris environment
p 891 N94-17148

INTERPLANETARY FLIGHT
Small spacecraft for planetary exploration
p 874 N94-17145

INTERPLANETARY SPACECRAFT
Workshop on advanced technologies for planetary instruments
[NASA-CR-194585] p 1032 N94-15797
Space transfer concepts and analyses for exploration missions, phase 4
[NASA-CR-193849] p 882 N94-15831

INTERPLANETARY TRANSFER ORBITS
A mission concept of Phobos/Deimos exploration
p 1287 N94-16387

INTERPOLATION
The multivariate optimum interpolation analysis of meteorological data at the Fleet Numerical Oceanography Center
[AD-A266459] p 1106 N94-16568
Fast algorithms for polynomial interpolation, integration and differentiation
[AD-A267505] p 1154 N94-17370

INTERPROCESSOR COMMUNICATION
The alignment-distribution graph
[NASA-CR-194292] p 1168 N94-15112
Mobile and replicated alignment of arrays in data-parallel programs
[NASA-CR-194294] p 1158 N94-15113
Overview of Enhanced Data Stream Array Processor (EDSAP)
[AD-A266986] p 1158 N94-15492
Generating local addresses and communication sets for data-parallel programs
[NASA-CR-194605] p 1159 N94-15796
Asynchronous design for parallel processing architectures
[AD-A266523] p 1160 N94-16791
Applications and development of communication models for the touchstone GAMMA and DELTA prototypes
[NASA-CR-193617] p 999 N94-16867
The IMS software integration platform
[AD-A266285] p 1151 N94-16910

INTERSTELLAR CHEMISTRY
Nd-142/Nd-144 in bulk planetary reservoirs, the problem of incomplete mixing of interstellar components and significance of very high precision Nd-145/Nd-144 measurements p 1256 N94-16220
Carbon abundances, major element chemistry, and mineralogy of hydrated interplanetary dust particles
p 1243 N94-16309

INTERSTELLAR MATTER
Boundary conditions for the paleoenvironment: Chemical and physical processes in the pre-solar nebula
[NASA-CR-194418] p 1298 N94-15421
The astrophysical interpretation of isotope anomalies in graphite and SiC grains of chondrites
p 1244 N94-16343
Collisional dynamics of perturbed particle disks in the solar system
[NASA-CR-193584] p 1239 N94-16648

INTERSTITIALS
Roles of oxygen defects in copper-oxide superconductors
[DE93-014875] p 1208 N94-15982
Microstructure of Zr3Al after 2 MeV proton bombardment
[DE93-015331] p 1211 N94-16814

INTRAVEHICULAR ACTIVITY
STS-35 onboard photography quick release
[NASA-TM-109500] p 881 N94-15464
STS-35 mission highlights resource tape
[NASA-TM-109501] p 881 N94-15465
Science operation in space: Lessons
[NASA-TM-109502] p 881 N94-15466

INTRAVENOUS PROCEDURES
Methods to obtain blood samples periodically during exercise research studies while subjects are immersed in water or otherwise inaccessible
[AD-A268227] p 1130 N94-17562

INTRUSION
AVIRIS as a tool for carbonatite exploration: Comparison of SPAM and Mbandmap data analysis methods
p 1073 N94-16703

INVARIANCE
On the nature of mirror particles
[DE93-626670] p 1179 N94-14934
Breakdown of adiabatic invariance
[AD-A267246] p 1219 N94-14977
Invariance of slip movements with respect to the control matrix
[IFTR-43/1991] p 1170 N94-17045

INVENTORIES
Equipment Management Manual
[NHB-4200.1D] p 1225 N94-16799
Materials inventory management manual
[NHB-4100.1C] p 1225 N94-16830

INVENTORY CONTROLS
Equipment management user's handbook for property custodians
[NHB-4200.2A] p 1224 N94-15957

INVENTORY MANAGEMENT
Facilities maintenance handbook
[NHB-8831.2] p 1224 N94-15934
Equipment management user's handbook for property custodians
[NHB-4200.2A] p 1224 N94-15957
Equipment Management Manual
[NHB-4200.1D] p 1225 N94-16799
Materials inventory management manual
[NHB-4100.1C] p 1225 N94-16830
Applicability of computer spreadsheet simulation for solving resource allocation problems
[AD-A267436] p 1152 N94-17027

INVERSE KINEMATICS
Fuzzy control and fuzzy kinematic mapping for a redundant space robot
[AD-A266866] p 1163 N94-14950
Fuzzy inverse kinematic mapping: Rule generation, efficiency, and implementation
[AD-A266967] p 1163 N94-14954
Development of a prototype kinestatic platform for application to space and ground servicing tasks. Phase 1: Concept Modeling
[NASA-CR-194036] p 887 N94-16905

INVERSE SCATTERING
Nonlinear problems in fluid dynamics and inverse scattering
[AD-A266234] p 1026 N94-16927
Spectral inverse scattering theory for dielectric media: Application to optical devices
[AD-A268635] p 1199 N94-17427

INVERTED CONVERTERS (DC TO AC)
Circuits and control processes for combining direct converters and inverter motors
[ETN-93-94399] p 1008 N94-15448

INVERTERS
Circuits and control processes for combining direct converters and inverter motors
[ETN-93-94399] p 1008 N94-15448
INVESTMENT CASTING
Nonaqueous slip casting of high temperature ceramic superconductors using an investment casting technique
[NASA-CASE-LAR-14918-1] p 983 N94-15881
INVISCID FLOW
Incorporation of boundary layer heating predictive methodology into NSWCDD aeroprediction code
[AD-A267000] p 1020 N94-15632
Inviscid instability of streamwise corner flow
[NASA-CR-191514] p 1021 N94-15834
Broken symmetry in ideal magnetohydrodynamic turbulence
[NASA-TM-109017] p 1023 N94-15964
Adaptive algorithm for aircraft configuration in turbulent flow
[AD-A266188] p 867 N94-16122
Adaptive Cartesian grid methods for representing geometry in inviscid compressible flow
[DE93-016430] p 1025 N94-16894
IO
Crustal structure and igneous processes in a chondritic Io p 1243 N94-16292
A decade's overview of Io's volcanic activity p 1245 N94-16386
IODIDES
Optical properties and surface morphology studies of palladium contacts on mercuric iodide single crystals
[DE93-012510] p 1207 N94-15973
Elemental impurity analysis of mercuric iodide by ICP/MS
[DE93-015531] p 949 N94-16876
IODINE LASERS
Extracavity frequency doubling study of a pulsed photodissociation iodine laser
[AD-A267893] p 1042 N94-17394
ION ACCELERATORS
A microsecond-pulsewidth, intense, light-ion beam accelerator
[DE93-016455] p 1202 N94-16451
3D and r,z particle simulations of heavy ion fusion beams
[DE93-013417] p 1205 N94-17670
ION BEAMS
Ion mixing of thin ZrO2 films on sapphire
[DE93-015214] p 1206 N94-14925
MeV ion-beam analysis of optical data storage films p 1226 N94-14984
Testing and management of flight instruments and their data
[NASA-CR-194332] p 868 N94-15187
Analytical and experimental investigation of the feasibility of accelerated lifetime testing of materials exposed to an atomic oxygen beam
[NASA-CR-193851] p 946 N94-15766
Selective formation of porous silicon
[NASA-CASE-NPO-18735-1-CU] p 966 N94-15960
Nuclear fusion of protons with ions of boron
[DE93-015399] p 1202 N94-16019
A microsecond-pulsewidth, intense, light-ion beam accelerator
[DE93-016455] p 1202 N94-16451
Crystalline beam ground state
[DE93-014331] p 1211 N94-16827
The stability of ions in a storage ring in the presence of small gap insertion devices
[DE93-015387] p 1184 N94-16828
Approximate Green's function methods for HZE transport in multilayered materials
[NASA-TM-4519] p 1300 N94-17084
Atomic beam studies relevant to the space environment
[AD-A268628] p 1186 N94-17436
Study of brightness and current limitations in intense charged particle beams
[AD-A268283] p 1186 N94-17578
Optimal pulse modulator design criteria for plasma source ion implanters
[DE93-016465] p 1205 N94-17645
3D and r,z particle simulations of heavy ion fusion beams
[DE93-013417] p 1205 N94-17670
Emittance growth in displaced, space-charge-dominated beams with energy spread
[DE93-016514] p 1188 N94-17672
ION CURRENTS
Investigation of onset of plasma formation at anode of fast-pulsed high-voltage vacuum diode
[AD-A267214] p 1204 N94-16987
ION DENSITY (CONCENTRATION)
Microwave interaction with plasmas
[AD-A267048] p 1201 N94-15661
Optimal pulse modulator design criteria for plasma source ion implanters
[DE93-016465] p 1205 N94-17645
The effects of radiation transport on line ratios used as temperature and density diagnostic
[DE93-016424] p 1205 N94-17663
ION DISTRIBUTION
Kinetic plasma processes occurring in the outer plasmasphere
[NASA-CR-193452] p 1300 N94-17524
ION ENGINES
Carbon-carbon grid for ion engines
[NASA-CASE-NPO-19174-1-CU] p 925 N94-15876
Segmented ion thruster
[NASA-CASE-NPO-18192-1-CU] p 925 N94-15927
ION EXCHANGE MEMBRANE ELECTROLYTES
Characterization of the lithium/pan-based polymer electrolytes interface
[AD-A268401] p 973 N94-17434
ION EXCHANGING
Direct catalytic decomposition of nitric oxide
[DE93-016689] p 949 N94-16896
ION IMPLANTATION
Ion mixing of thin ZrO2 films on sapphire
[DE93-015214] p 1206 N94-14925
Optical and infrared spectra of thermally annealed Pb implanted SiO2 glasses
[DE93-015304] p 965 N94-15828
Thin Ni silicide formation by low temperature-induced metal atom reaction with ion implanted amorphous silicon
[DE93-015449] p 1209 N94-16066
Ion implantation effects on surface-mechanical properties of metals and polymers
[DE93-014661] p 958 N94-16453
Electrical conductivity of ion implanted ladder and semi-ladder polymers
[AD-A267432] p 970 N94-16978
Single crystal diamond thin films
[AD-A266457] p 1214 N94-17216
Continuing research on friction and wear of materials
[AD-A268291] p 1049 N94-17566
Optimal pulse modulator design criteria for plasma source ion implanters
[DE93-016465] p 1205 N94-17645
ION INJECTION
Six dimensional tracking simulator for H(-) injection in AGS Booster
[DE93-015396] p 1184 N94-16885
ION IRRADIATION
Investigation of onset of plasma formation at anode of fast-pulsed high-voltage vacuum diode
[AD-A267214] p 1204 N94-16987
ION PROPULSION
Segmented ion thruster
[NASA-CASE-NPO-18192-1-CU] p 925 N94-15927
ION RECOMBINATION
Merged beam studies of laser stimulated radiative recombination
[AD-A267186] p 1037 N94-15145
ION SOURCES
A microsecond-pulsewidth, intense, light-ion beam accelerator
[DE93-016455] p 1202 N94-16451
ION TEMPERATURE
ARIES tokamak reactor study
[DE93-017059] p 1203 N94-16901
The effects of radiation transport on line ratios used as temperature and density diagnostic
[DE93-016424] p 1205 N94-17663
ION TRAPS (INSTRUMENTATION)
The cooling of confined ions driven by laser beams
[DE93-016612] p 1039 N94-16114
IONIC COLLISIONS
Investigation of the interactions of radiation with matter
[AD-A266743] p 1181 N94-15774
PHENIX Conceptual Design Report
[DE93-015759] p 1182 N94-16161
Theoretical high energy physics
[DE93-015884] p 1187 N94-16170
IONIC REACTIONS
Modeling study to evaluate the ionic mechanism of soot formation in flames
[AD-A266242] p 950 N94-16930
Cathode sheath charge transfer effects
[AD-A268393] p 1186 N94-17536
IONIC WAVES
Double stimulated Brillouin scattering p 1200 N94-15205
Soliton-like structures in double stimulated Brillouin scattering p 1200 N94-15207
IONIZATION
Thermochemistry of silicate speciation in aqueous sodium silicate solutions: Ionization and polymerization of small silicate ion
[AD-A266825] p 964 N94-15683
Femtosecond growth dynamics of an underdense ionization front measured by spectral blueshifting
[DE93-013582] p 1183 N94-16818
Laser probing of the kinetics and dynamics of 3-5 semiconductor growth
[AD-A268388] p 1215 N94-17422
Properties of nuclei in astrophysical environments: Binding energies, weak-interaction rates
[MPA-706] p 1240 N94-17628
IONIZATION CHAMBERS
Segmented ion thruster
[NASA-CASE-NPO-18192-1-CU] p 925 N94-15927
IONIZATION CROSS SECTIONS
Studies of combustion reactions at the state-resolved differential cross section level
[DE93-017605] p 948 N94-16462
IONIZATION POTENTIALS
Monte Carlo simulation of the microstrip gas counter
[NIKHEF-H/93-07] p 1035 N94-17619
IONIZED GASES
Femtosecond growth dynamics of an underdense ionization front measured by spectral blueshifting
[DE93-013582] p 1183 N94-16818
IONIZERS
Electron reversal ionizer for detection of trace species using a spherical cathode
[NASA-CASE-NPO-18870-1-CU] p 1185 N94-17329
IONIZING RADIATION
Radiation hardening of a CCD technology through process and design modifications p 906 N94-15071
Fault handling schemes in electronic systems with specific application to radiation tolerance and VLSI design
[NASA-CR-194559] p 1008 N94-15640
Third LDEF Post-Retrieval Symposium Abstracts
[NASA-CP-10120] p 1303 N94-16495
AFRRI reports, first quarter 1993
[AD-A266380] p 1123 N94-16515
IONOGRAMS
Comparison of RADARC high-frequency radar performance prediction model and ROTHR Amchitka data
[AD-A267077] p 987 N94-15540
IONOSPHERIC CURRENTS
Formation of the stable auroral arc that intensifies at substorm onset
[NASA-CR-193637] p 1098 N94-15433
IONOSPHERIC DISTURBANCES
Optimization of satellite coverage in observing cause and effect changes in the ionosphere, magnetosphere, and solar wind
[AD-A267956] p 1102 N94-17493
IONOSPHERIC ELECTRON DENSITY
A physical model for one-dimension and time-dependent ionosphere. Part 2: Results and discussions
[DE93-627959] p 1103 N94-17631
IONOSPHERIC HEATING
An electromagnetic interference study of potential transmitter sites for the HF Active Auroral Research Program (HAARP)
[AD-A267743] p 1004 N94-17373
Effect of powerful oblique HF waves on ionospheric D-layer absorption
[AD-A268443] p 1102 N94-17499
IONOSPHERIC PROPAGATION
Evaluation of site effects on a high frequency direction finding single site location system
[AD-A267465] p 1001 N94-17035
On-board spatial scientific experiment project on small satellites p 896 N94-17184
Effect of powerful oblique HF waves on ionospheric D-layer absorption
[AD-A268443] p 1102 N94-17499
IONS
Nuclear fusion of protons with ions of boron
[DE93-015399] p 1202 N94-16019
The cooling of confined ions driven by laser beams
[DE93-016612] p 1039 N94-16114
Bioorganic models for protein ion channels
[AD-A266365] p 1117 N94-16441
Thermal disorder in adsorbed Cl on Si(100)
[AD-A266295] p 1210 N94-16476
Investigation of the energy distribution of ions, striking the cathode in an abnormal glow discharge
[DE93-623987] p 1013 N94-17316
IRIDIUM
Cretaceous-tertiary boundary spherules and Cenozoic microtektites: Similarities and differences p 1241 N94-16186

The Acraman impact structure: Estimation of the diameter by the ejecta layer thickness p 1103 N94-16211
An iridium-rich iron micrometeorite with silicate inclusions from the Moon p 1242 N94-16281
Geochemical evidences for two chondritic-like cometary or asteroidal impacts before and at the K/T boundary p 1244 N94-16359

IRON
Why is the Moon dark? p 1256 N94-16219
A Moessbauer spectrometer for the mineralogical analysis of the Mars surface: First temperature dependent tests of the detector and drive system p 1259 N94-16233
Release of iron from hemoglobin [AD-A266503] p 1128 N94-16784
Neurotoxicity of hemoglobin in cortical cell culture [AD-A266506] p 1128 N94-16786
Neutron and x ray scattering studies of (FeF2)(sub m)(CoF2)(sub n) multilayers [DE93-015809] p 1184 N94-16838
Creep ductility of iron at very low strain rates: The effects of sulfur [DE93-015490] p 959 N94-16890
Continuing research on friction and wear of materials [AD-A268291] p 1049 N94-17566
Epitaxial iron films [AD-A268286] p 1217 N94-17579
Comparison of computer predictions and magnetic field measurements for an iron spectrometer magnet [DE93-016164] p 1176 N94-17658

IRON ALLOYS
Remelting of Fe-C-Si-alloy in a ceramic mold skin p 945 N94-15169
In situ studies of passive film chemistry using x ray absorption spectroscopy [DE93-014023] p 947 N94-16011
Environmental effects on iron aluminides [DE93-015820] p 958 N94-16166
Robotic weld overlay coatings for erosion control [DE93-016938] p 970 N94-16959

IRON METEORITES
The Fe2(+)-Mg interdiffusion in orthopyroxene: Constraints from cation ordering and structural data and implications for cooling rates of meteorites p 1241 N94-16175
Systematic chemical variations in large 3AB iron meteorites: Clues to core crystallization p 1241 N94-16213
Al-26-Mg-26 ages of iron meteorites p 1242 N94-16240
An iridium-rich iron micrometeorite with silicate inclusions from the Moon p 1242 N94-16281
Experimental segregation of iron-nickel metal, iron-sulfide, and olivine in a thermal gradient: Preliminary results p 1243 N94-16288
Explosive volcanism and the compositions of the cores of differentiated asteroids p 1243 N94-16306
Size distribution of interplanetary iron and stony particles related with deep-sea spherules p 1245 N94-16388

IRON OXIDES
A mineralized zone in Western Candor Chasma, Mars p 1248 N94-16179
Iron oxide bands in the visible and near-infrared reflectance spectra of primitive asteroids p 1242 N94-16274
Complex zoning behavior in pyroxene in FeO-rich chondrules in the Semarkona ordinary chondrite p 1243 N94-16284
Characterization of nanoscale oxide and oxyhydroxide powders using EXAFS spectroscopy [DE93-015683] p 940 N94-17235

IRRADIATION
Induced thermoluminescence study of experimentally shock-loaded oligoclase p 953 N94-16266
Fast-ICCD photography and gated photon counting measurements of blackbody emission from particulates generated in the KrF-laser ablation of BN and YBC [DE93-015491] p 1210 N94-16460
Heat shock protein induction in human cells by CO2 laser irradiation [AD-A266430] p 1117 N94-16545
Evolution of microstructure in face centered cubic metals during irradiation: A review [DE93-015682] p 958 N94-16662
Ablation, surface activation, and electroless metallization of insulating materials by pulsed excimer laser irradiation [DE93-015808] p 1040 N94-16664
Bioeffects of radiofrequency radiation on cell growth and differentation. Volume 1: Engineering considerations [AD-A267754] p 1118 N94-17232
The behavioral toxicology of high-peak, low average power, pulsed microwave irradiation [AD-A268392] p 1134 N94-17535
Growth of dielectric thin films by irradiation of condensed molecular precursors with synchrotron radiation [DE93-016161] p 974 N94-17676

ISCHEMIA
Cumulative effect of repeated brief cerebral ischemia [AD-A267155] p 1121 N94-15736
Neurotoxicity of hemoglobin in cortical cell culture [AD-A266506] p 1128 N94-16786

ISING MODEL
Dynamical Ising model simulations of nucleation and growth in copper-cobalt alloys [DE93-015336] p 957 N94-16015

ISOMERIZATION
Mechanistic models of soot formation [AD-A267806] p 950 N94-17008

ISOSTATIC PRESSURE
Fabrication of advanced design (grooved) cermet anodes [DE93-014590] p 1012 N94-16765

ISOTHERMS
Structural and dynamical aspects of electrodeposition [AD-A266786] p 942 N94-14909
Pyroxene equilibration temperatures in metamorphosed ordinary chondrites p 1242 N94-16224

ISOTOPE SEPARATION
Design of a formaldehyde photodissociation process for carbon and oxygen isotope separation [DE93-016435] p 1039 N94-16450

ISOTOPES
Extraction and isotopic analysis of medium molecular weight hydrocarbons from Murchison using supercritical carbon dioxide p 1241 N94-16184
A search for noble-gas evidence for presolar oxide grains p 954 N94-16353
Shielding from space radiations [NASA-CR-194664] p 1301 N94-17255

ISOTOPIC ENRICHMENT
Effects of bulk composition on production rates of cosmogenic nuclides in meteorites p 1245 N94-16385
Design of a formaldehyde photodissociation process for carbon and oxygen isotope separation [DE93-016435] p 1039 N94-16450

ISOTOPIC LABELING
Chemical and isotopic compositions in acid residues from various meteorites p 1243 N94-16291
Isotopic signatures and distribution of nitrogen and trapped and radiogenic xenon in the Acapulco and FRO90011 meteorites p 1243 N94-16317
The astrophysical interpretation of isotope anomalies in graphite and SiC grains of chondrites p 1244 N94-16343

ISOTROPIC MEDIA
Surface waves in an inhomogeneous, isotropic, elastic half-space [IFTR-18/1991] p 1060 N94-17047

ISOTROPIC TURBULENCE
A numerical investigation of energy transfer and subgrid-scale eddy-viscosity in homogeneous, isotropic, and shear turbulence [AD-A267265] p 1029 N94-17363

ITERATION
Fixed point iterations for strictly hemi-contractive maps in uniformly smooth Banach spaces [DE93-628591] p 1175 N94-17644

ITERATIVE SOLUTION
Iteration scheme for the multiparameter nonlinear boundary value problem with the additional conditions and its application to some field models [DE93-626638] p 1168 N94-14933
A sequential quadratic programming algorithm using an incomplete solution of the subproblem [DE93-017439] p 1149 N94-16120
Development of iterative techniques for the solution of unsteady compressible viscous flows [NASA-CR-194657] p 1027 N94-17129
Steepest descent approximations for accretive operator equations [DE93-628586] p 1171 N94-17667

IUE
ROSAT-IUE observations of symbiotic stars. The x ray morphology of high latitude associations [NASA-CR-194616] p 1236 N94-16492
The chromosphere of VV cephei and the distribution of circumstellar dust around red giants and supergiants [NASA-CR-193594] p 1297 N94-16866

J

J INTEGRAL
Prediction of stable tearing of 2024-T3 aluminum alloy using the crack-tip opening angle approach [NASA-TM-109023] p 955 N94-15708
J-integral and HRR field associated with stable crack growth in thin aluminum SEN specimen [AD-A267879] p 960 N94-17041

JAMMING
Alternative optical architectures for multichannel adaptive optical processing [AD-A267052] p 1189 N94-15664
Signal processing in impulsive electromagnetic interference [AD-A266425] p 998 N94-16557

JAPANESE SPACE PROGRAM
Laser ranging application to time transfer using geodetic satellite and to other Japanese space programs p 911 N94-15555
The Japanese Space Station utilization plan p 977 N94-16074

JAPANESE SPACECRAFT
Pre-phase a study report of lunar polar orbiter [NASDA-TK-SS0440] p 873 N94-15000
TRMM radar p 990 N94-15894

JET AIRCRAFT NOISE
The 1968 highlights --- NASA programs and research [NASA-TM-109627] p 1302 N94-15413
The 1971 highlights --- NASA programs and research [NASA-TM-109629] p 1302 N94-15417
Technical evaluation report on the AGARD-PEP Specialists Meeting on Combat Aircraft Noise [NLR-TP-91445-U] p 1177 N94-15506

JET BOUNDARIES
The turbulent wall jet [AD-A267675] p 855 N94-14963

JET CONTROL
Heat transfer parametric system identification [AD-A268525] p 929 N94-17543

JET ENGINE FUELS
Advanced thermally stable jet fuels [DE93-017711] p 975 N94-16996
Lifted turbulent jet flames [AD-A267911] p 952 N94-17381

JET ENGINES
Jet engine performance enhancement through use of a wave-rotor topping cycle [NASA-TM-4486] p 870 N94-17470

JET FLOW
The turbulent wall jet [AD-A267675] p 855 N94-14963
An experimental study of ASTOVL related jet flows to produce CFD code validation data. Phase 3: Results of experiments [TT-9203] p 1020 N94-15645
Mechanistic models of soot formation [AD-A267806] p 950 N94-17008
Two-dimensional, high flow, precisely controlled monodisperse drop source [AD-A267660] p 1028 N94-17250
Lifted turbulent jet flames [AD-A267911] p 952 N94-17381

JET IMPINGEMENT
Fluid flow and heat convection studies for actively cooled airframes [NASA-CR-194624] p 1024 N94-16491

JET VANES
Heat transfer parametric system identification [AD-A268525] p 929 N94-17543

JETTISONING
Crew escape certification test [NASA-TM-109530] p 1136 N94-15392

JFET
Cryogenic measurements of aerojet GaAs n-JFETs [NASA-TM-103972] p 1009 N94-15765

JOINTS (JUNCTIONS)
End-effector: Joint conjugates for robotic assembly of large truss structures in space: Extended concepts [NASA-CR-193576] p 1048 N94-17088

JOSEPHSON JUNCTIONS
Nb-based SJTJ for nuclear detection: Preliminary results with alpha radiation p 905 N94-15068

JP-8 JET FUEL
Advanced thermally stable jet fuels [DE93-017711] p 975 N94-16996

JUNCTION DIODES
Submillimeterwave SIS mixer developments p 903 N94-15054
Substrate effects in superconducting tunnel junction detectors p 908 N94-15083
A multilayered approach to superconducting tunnel junction x ray detectors p 908 N94-15089
Quasiparticle trapping in distributed superconducting three-terminal tunnel junction devices p 910 N94-15101
Design of broadband wire antennas for frequency hopping applications [AD-A267405] p 1001 N94-17025

JUPITER (PLANET)
Voyager encounter highlights [NASA-TM-109420] p 1246 N94-15239
Orbital evolution of dust from comet Schwassmann-Wachmann 1: A case of one-to-one resonance trapping p 1242 N94-16270

JUPITER ATMOSPHERE
Galileo probe ready to go
[NASA-TM-109648] p 1247 N94-15432
Multispectral observations of the Jovian aurora
[NASA-CR-193628] p 1297 N94-16884
JUPITER RED SPOT
Voyager encounter highlights
[NASA-TM-109420] p 1246 N94-15239
JUPITER SATELLITES
Voyager encounter highlights
[NASA-TM-109420] p 1246 N94-15239

K

K-EPSILON TURBULENCE MODEL
Implementation of an anisotropic turbulence model in the COMMIX-1C/ATM computer code
[DE93-015541] p 1023 N94-16444
Computation of confined coflow jets with three turbulence models
[NASA-TM-106378] p 1025 N94-16879
KALMAN FILTERS
Target detection by way of Kalman filtering
[AD-A267314] p 1000 N94-16945
Hypervelocity orbital intercept guidance using certainty control
[AD-A267297] p 1174 N94-17219
High order nonlinear estimation with signal processing applications
[AD-A268407] p 1005 N94-17463
KAONS
On the nature of mirror particles
[DE93-626670] p 1179 N94-14934
Experimental study of weak interactions by precision measurement by rare kaon decay
[DE93-016864] p 1182 N94-16117
A high sensitivity search for CP violating rare K(sub L) decays and precision measurement of the direct CP violation parameter (epsilon)(prime)/(epsilon) via the four K (yields) 2(pi) decay modes
[DE93-016866] p 1184 N94-16899
KAPOETA ACHONDRITE
Shock-thermal history of Kapoeta howardite matter on data of thermoluminescence analysis of individual mineral grains p 953 N94-16267
KARHUNEN-LOEVE EXPANSION
A novel approach for structural mechanics problems with stochasticity
[AD-A266189] p 1059 N94-16123
KETONES
Soluble precursor route to polyanilines
[AD-A268015] p 973 N94-17494
KEVLAR (TRADEMARK)
The effect of plasma treatment on interfacial bond characteristics of Kevlar/epoxy laminates as measured by T-peel tests
[AD-A266920] p 930 N94-14999
SRB thermal curtain design support
[NASA-CR-193857] p 927 N94-17123
SRB thermal curtain design support
[NASA-CR-193858] p 928 N94-17124
KINEMATICS
An experimental comparison of CLOS and C(++) implementations of an object-oriented graphical simulation of walking robot kinematics
[AD-A267168] p 1165 N94-15855
A measurement station for study of Earth moving tools and ground cutting processes
[IFTR-10/1991] p 985 N94-17068
KINETIC THEORY
Stability analysis for the flow of granular materials down an inclined plane using kinetic model
[DE93-016852] p 1026 N94-16958
Discrete models of the Boltzmann equation: Structure of the collision operator of sound propagation
[IFTR-2/1992] p 1178 N94-17051
A basic principles description of liquid vapor phase transitions
[AD-A268331] p 1176 N94-17581
KINETICS
A measurement station for study of Earth moving tools and ground cutting processes
[IFTR-10/1991] p 985 N94-17068
KINOFORM
Fabrication techniques for very fast diffractive lenses p 1196 N94-17345
Laser figuring for the generation of analog micro-optics and kineform surfaces p 1196 N94-17346
KNOWLEDGE BASED SYSTEMS
KBSA concept demo
[AD-A267054] p 1166 N94-16770
Design and diagnosis problem solving with multifunctional technical knowledge bases
[AD-A268375] p 1234 N94-17419
Incremental rederivation of software artifacts: FY 1992
[AD-A267968] p 1155 N94-17491
KNOWLEDGE BASES (ARTIFICIAL INTELLIGENCE)
Development of a computer supported instrumentation for economic planning and evaluation of production facilities for fiber reinforced composites elements p 932 N94-15260
Design and diagnosis problem solving with multifunctional technical knowledge bases
[AD-A268375] p 1234 N94-17419
KNOWLEDGE REPRESENTATION
An automated approach for classifying generic terrain features using digital elevation data
[AD-A268385] p 1084 N94-17421
KNUDSEN FLOW
DSMC simulations of Mach 20 nitrogen flows about a 70 degree blunted cone and its wake
[NASA-TM-107762] p 1018 N94-15291
KOHOUTEK COMET
The 1973 highlights --- Pioneer and Mariner space probes and other advancements
[NASA-TM-109624] p 1302 N94-15410
KOLMOGOROV THEORY
Time dependent turbulence modeling and analytical theories of turbulence
[NASA-TM-106379] p 1029 N94-17385
KOLMOGOROV-SMIRNOV TEST
The distribution of a sum of binomial random variables
[AD-A266969] p 1172 N94-15002
KREEP
On the composition of neuKREEP: QMD contamination at Apollo 11? p 1266 N94-16276
The monzonorite-anorthosite connection: The petrogenesis of terrestrial KREEP p 1104 N94-16365
KUIPER AIRBORNE OBSERVATORY
C 141 KAO solar eclipse mission
[NASA-TM-109676] p 1298 N94-15522

L

LABOR
Industrial labor relations manual
[NHB-5200.1B] p 1224 N94-15939
The NASA competitive placement plan for positions GS-15 and below (including trades and labor positions)
[NHB-3335.1C] p 1224 N94-15944
LABORATORIES
Industrial Hygiene Laboratory accreditation: The JSC experience p 1125 N94-16623
A ten year review of performance of photovoltaic systems
[DE93-015649] p 1093 N94-17217
LACTATES
Increased vascular resistance with hemoglobin-based oxygen carriers
[AD-A266454] p 1123 N94-16565
LAGEOS (SATELLITE)
Prelaunch optical characterization of the Laser Geodynamic Satellite (LAGEOS 2)
[NASA-TP-3400] p 884 N94-15193
Laser tracking for vertical control p 911 N94-15553
Test results from LAGEOS-2 optical characterization using pulsed lasers p 915 N94-15577
Historical MOBLAS system characterization p 915 N94-15579
LAGRANGE MULTIPLIERS
A sequential quadratic programming algorithm using an incomplete solution of the subproblem
[DE93-017439] p 1149 N94-16120
LAGRANGIAN EQUILIBRIUM POINTS
Energy potential analysis of zero velocity curves in the restricted three-body problem
[AD-A267512] p 1170 N94-17076
LAGRANGIAN FUNCTION
A sequential quadratic programming algorithm using an incomplete solution of the subproblem
[DE93-017439] p 1149 N94-16120
Variational principles of heat exchange and their applications in construction physics, part 2
[IFTR-19/1991] p 1061 N94-17069
LAGUERRE FUNCTIONS
Expansions of cumulative distribution functions directly from characteristic functions
[AD-A267727] p 1173 N94-17372
LAKES
On the application and evaluation of the relocatable diecast ocean circulation model in coastal and semi-enclosed seas
[AD-A266626] p 1112 N94-15771
Sedimentation, volcanism, and ancestral lakes in the Valles Marineris: Clues from topography p 1283 N94-16369
Do it yourself remote sensing: Generating an inexpensive, high tech, real science lake mapping project for the classroom p 1086 N94-16407
Seasonal and spatial variations in phytoplanktonic chlorophyll in eutrophic Mono Lake, California, measured with the Airborne Visible and Infrared Imaging Spectrometer (AVIRIS) p 1069 N94-16684
A Geographic Information System approach to modeling nutrient and sediment transport
[DE93-013747] p 1097 N94-17426
LAMINAR BOUNDARY LAYER
Swept shock wave/laminar boundary layer interactions, experimental, and numerical results p 1017 N94-15198
Receptivity of boundary layers to convected gusts
[AD-A267206] p 1022 N94-15860
Transition induced by fixed and freely convecting spherical particles in laminar boundary layers
[AD-A267757] p 1028 N94-17276
LAMINAR FLOW
Electrophoresis visualisation p 944 N94-15163
Theoretical study of laminar film condensation on horizontal ellipitical tubes under conditions of free and forced convection
[AD-A267161] p 1021 N94-15737
Investigation of radiative interaction in laminar flows using Monte Carlo simulation
[NASA-CR-194604] p 1021 N94-15795
A comparison of one and two dimensional flame quenching: Heat transfer results
[DE93-015196] p 947 N94-16060
Natural convection above a horizontal heat source
[AD-A267212] p 1026 N94-16985
Mechanistic models of soot formation
[AD-A267806] p 950 N94-17008
Numerical solution of SUPG finite-element method for supersonic viscous flow
[AD-A267762] p 860 N94-17222
Flow instability tests for a particle bed reactor nuclear thermal rocket fuel element
[AD-A268012] p 929 N94-17474
Surface reactivity of combustion generated soot particles
[AD-A268017] p 952 N94-17532
LAMINATES
A posteriori error estimation for hierarchic models of elliptic boundary value problems on thin domains
[AD-A267714] p 1168 N94-14939
Thermal stresses of a trimaterial medium in a nonuniform temperature field
[AD-A267243] p 930 N94-14975
The effect of plasma treatment on interfacial bond characteristics of Kevlar/epoxy laminates as measured by T-peel tests
[AD-A266920] p 930 N94-14999
Dynamic behavior of fiber and particle reinforced composites
[AD-A266905] p 930 N94-15143
Physical interpretation and development of ultrasonic nondestructive evaluation techniques applied to the quantitative characterization of textile composite materials
[NASA-CR-194549] p 931 N94-15190
Sound radiation from infinite laminated composite shell with periodic rib stiffening
[DRA/TM(USGR)92326] p 933 N94-15699
Anisotropic damage mechanics modeling in metal matrix composites
[AD-A266328] p 934 N94-16440
The processing and mechanical properties of high temperature/high performance composites. Book 2: Coonstituent properties and macroscopic performance
[AD-A266395] p 935 N94-16484
Stress analysis of laminated composites with preformed holes. Part 1: Single plies with embedded material discontinuities
[AD-A266524] p 936 N94-16795
Effect of Impact Damage and Open Hole on Compressive Strength of Hybrid Composite Laminates
[NASA-CR-194603] p 936 N94-16836
Stochastic damage evolution in textile laminates p 939 N94-16861
Direct observation of fracture of CAS-glass/SiC composites and processing of toughened alumina
[AD-A268275] p 941 N94-17457
LAND MANAGEMENT
Louisiana delta study
[NASA-TM-109622] p 1095 N94-15408
Measuring dry plant residues in grasslands: A case study using AVIRIS p 1072 N94-16697
LAND MOBILE SATELLITE SERVICE
Planned LMSS propagation experiment using ACTS: Preliminary antenna pointing results during mobile operations p 995 N94-16041
An overview of the text propagation effects for land-mobile-satellite systems: Experimental and modeling results p 996 N94-16048
A study of land mobile satellite service multipath effects using SATLAB software p 997 N94-16051

Regulation of low Earth orbit satellites
p 892 N94-17159

LANDAU DAMPING
Structure and damping of toroidal drift waves (and their implications for anomalous transport)
[DE93-014005] p 1203 N94-16822
Nonlinear gyrofluid models of shear Alfven instabilities in ignited and beam heated toroidal plasmas
[DE93-016235] p 1203 N94-16869

LANDAU FACTOR
The fractional quantum Hall effect and the rotation group
[DE93-010348] p 1207 N94-15972

LANDAU-GINZBURG EQUATIONS
Thermally-sustained structure in convectively unstable systems
[NASA-TM-106375] p 1027 N94-17112

LANDFORMS
Magellan: Principal Venus science findings
p 989 N94-15887
Separation of topographic and intrinsic backscatter variations in biscopic radar images: A magic airbrush
p 1086 N94-16318
Relief of some small landforms on Venus
p 1293 N94-16418
An automated approach for classifying generic terrain features using digital elevation data
[AD-A268385] p 1084 N94-17421

LANDING AIDS
Wide-area Differential Global Positioning System (WDGPS)/Wide-area Integrity Broadcast (WIB) alternatives analysis
[DOT/FAA/SE-93/3] p 864 N94-16906

LANDING GEAR
Tetrahedral lander
[NASA-CASE-MSC-22082-1] p 886 N94-15951

LANDING LOADS
Tetrahedral lander
[NASA-CASE-MSC-22082-1] p 886 N94-15951

LANDING MODULES
Space transfer concepts and analyses for exploration missions, phase 4
[NASA-CR-193849] p 882 N94-15831

LANDING SITES
Mars Analog Site Study (MASS) p 1252 N94-16200
Fluvial erosion on Mars: Implications for paleoclimatic change p 1241 N94-16210
Galileo photometry of Apollo landing sites
p 1259 N94-16234
Earth-based and Galileo SSI multispectral observations of eastern mare serenitatis and the Apollo 17 landing site p 1261 N94-16244
Searching for neuKREEP: An EMP study of Apollo 11 Group A basalts p 1266 N94-16275
Mars exobiology landing sites for future exploration
p 1278 N94-16339

LANDMARKS
Unitary plan wind tunnel landmark dedication and revitalization
[NASA-TM-109649] p 1302 N94-15434

LANDSAT SATELLITES
The 1979 highlights
[NASA-TM-109443] p 1247 N94-15342
The 1977 highlights
[NASA-TM-109626] p 1302 N94-15412
EOS Laser Atmosphere Wind Sounder (LAWS) investigation
[NASA-CR-193445] p 1109 N94-17525

LANDSAT 4
The 1982 highlights
[NASA-TM-109671] p 1303 N94-15508

LANGMUIR-BLODGETT FILMS
Organic polymeric electro-optic materials: Synthesis, processing, and device applications
[AD-A267133] p 964 N94-15688
Synthesis of novel electrically conducting polymers: Potential conducting Langmuir-Blodgett films and conducting polymers on defined surfaces
[NASA-CR-194651] p 972 N94-17297

LANGUAGE PROGRAMMING
A CENTAUR tutorial
[INRIA-RT-140] p 1142 N94-14978
Visual parallel programming with determinacy: A language specification, an analysis technique, and a programming tool
[AD-A267560] p 1153 N94-17107

LANGUAGES
Design and implementation of an object-oriented interface for the multi-model/multi-lingual database system
[AD-A267413] p 1232 N94-16977

LANTHANUM OXIDES
Structural phase transition and superconductivity in La(2-x)Ba(x)CuO4
[DE93-015812] p 1212 N94-16868
Low-temperature sintering and phase changes in chromite interconnect materials
[DE93-015676] p 961 N94-17234

LAP JOINTS
Overview of the FAA/DCA/NLR programs related to ageing aircraft
[NLR-TR-92119-U] p 854 N94-17614

LAPLACE EQUATION
An upwind multigrid method for solving viscous flows on unstructured triangular meshes
[NASA-TM-109343] p 1027 N94-17061

LAPLACE TRANSFORMATION
Numerical solution of a second order boundary problem for two dimensions using galerkin approximations
[AD-A268128] p 1171 N94-17521

LARGE SCALE INTEGRATION
Full-wave simulation of the thumbtack laser
[DE93-015110] p 1039 N94-16054

LARGE SPACE STRUCTURES
Results of an electrical power system fault study (CDDF)
[NASA-TP-3413] p 884 N94-15007
End-effector: Joint conjugates for robotic assembly of large truss structures in space: Extended concepts
[NASA-CR-193576] p 1048 N94-17088
A mechanical system damping measurement technique using a one-degree-of-freedom (1DOF) cylindrical gas bearing
[AD-A268402] p 1048 N94-17462
Structural mechanics division research and technology accomplishments for CY 1992 and plans for CY 1993
[NASA-TM-107752] p 1062 N94-17479

LASER ABLATION
Laser assisted CVD growth of AlN and GaN
[AD-A267150] p 1206 N94-15764
Experimental investigations of superconductivity in quasi-two-dimensional epitaxial copper oxide superlattices and trilayers
[DE93-015306] p 1207 N94-15829
Negative ion formation in small carbon clusters
[DE93-015436] p 1182 N94-16064
Fast-ICCD photography and gated photon counting measurements of blackbody emission from particulates generated in the KrF-laser ablation of BN and YBC
[DE93-015491] p 1210 N94-16460

LASER ALTIMETERS
Development of the Mars Observer Laser Altimeter (MOLA) p 921 N94-15617
Bench checkout equipment for spaceborne laser altimeter systems p 921 N94-15618
Mars laser altimeter based on a single photon ranging technique p 921 N94-15619
Multi-beam laser altimeter p 921 N94-15620

LASER ANEMOMETERS
Experimental and computational investigation of the NASA low-speed centrifugal compressor flow field
[NASA-TM-4481] p 869 N94-17386

LASER ANNEALING
Activation and deactivation of high concentration arsenic with some evidence of precipitation
[DE93-016437] p 950 N94-16952

LASER APPLICATIONS
Design of pulse stretching cell for a sodium guide star optical system
[DE93-016436] p 1236 N94-14929
Supersonic Combustion Research Laboratory. Volume 1: Design and fabrication
[AD-A267667] p 943 N94-14962
Merged beam studies of laser stimulated radiative recombination
[AD-A267186] p 1037 N94-15145
Lunar ranging
[NASA-TM-109603] p 1236 N94-15311
Laser ranging application to time transfer using geodetic satellite and to other Japanese space programs
p 911 N94-15555
Applications of SLR p 911 N94-15556
SLR data screening; location of peak of data distribution p 912 N94-15560
Preliminary results from the portable standard satellite laser ranging intercomparison with MOBLAS-7
p 913 N94-15568
Tracking capabilities of SPADs for laser ranging
p 914 N94-15570
Test results from LAGEOS-2 optical characterization using pulsed lasers p 915 N94-15577
Analysis of TOPEX laser retroreflector array characteristics p 915 N94-15578
Optimum wavelengths for two color ranging
p 915 N94-15580
Two wavelength satellite laser ranging using SPAD
p 916 N94-15584
Geometric analysis of satellite laser ranging data
p 917 N94-15587
Compensation for the distortion in satellite laser range predictions due to varying pulse travel times
p 917 N94-15590
Timebias corrections to predictions
p 875 N94-15591
Poisson filtering of laser ranging data
p 917 N94-15593
Theoretical studies relating to the interaction of radiation with matter
[AD-A267134] p 1180 N94-15689
Determination of GTA welding efficiencies
[AD-A267163] p 1046 N94-15738
RELMA: On-line quality control in the rubber mixing room using laser analysis p 984 N94-16005
Development of the Laser-based R/D Test-bed System (LTS) p 978 N94-16080
Center of Excellence in Laser Medicine
[DE93-016541] p 1122 N94-16113
Ablation, surface activation, and electroless metallization of insulating materials by pulsed excimer laser irradiation
[DE93-015808] p 1040 N94-16664
Laser weld repair of tantalum sheet
[DE93-016417] p 1041 N94-16871
Tip-tilt compensation: Resolution limits for ground-based telescopes using laser guide star adaptive optics
[DE93-016426] p 1237 N94-16872
Acousto-optical classifier
[AD-D015894] p 1000 N94-16921
Performance of coded coherent FSK lightwave system with noncoherent detection
[AD-A267442] p 1193 N94-17028
The determination of the Young moduli of a material after exposure to laser light and delineation of the zone of laser alterations
[IFTR-37/1991] p 1061 N94-17058
Laser figuring for the generation of analog micro-optics and kineform surfaces p 1196 N94-17346
Low cost paths to binary optics p 1197 N94-17353
Atomic beam studies relevant to the space environment
[AD-A268628] p 1186 N94-17436
EOS Laser Atmosphere Wind Sounder (LAWS) investigation
[NASA-CR-193445] p 1109 N94-17525
Surface reactivity of combustion generated soot particles
[AD-A268017] p 952 N94-17532
A new method of designing multilayer optical thin film coatings
[DE93-624683] p 974 N94-17611

LASER ARRAYS
Analysis of TOPEX laser retroreflector array characteristics p 915 N94-15578

LASER BEAMS
Figures of merit for laser beam quality
p 1043 N94-14994
Merged beam studies of laser stimulated radiative recombination
[AD-A267186] p 1037 N94-15145
Multi-beam laser altimeter p 921 N94-15620
Thomson backscattered x rays from an intense laser beam
[AD-A267125] p 1038 N94-15686
Full-wave simulation of the thumbtack laser
[DE93-015110] p 1039 N94-16054
Development of the Laser-based R/D Test-bed System (LTS) p 978 N94-16080
Center of Excellence in Laser Medicine
[DE93-016541] p 1122 N94-16113
The cooling of confined ions driven by laser beams
[DE93-016612] p 1039 N94-16114
Femtosecond growth dynamics of an underdense ionization front measured by spectral blueshifting
[DE93-013582] p 1183 N94-16818
Proposal of a simple mathematical model for the action of a laser on a metal plate
[IFTR-36/1991] p 1041 N94-17065
Hazard calculations of diffuse reflected laser radiation for the SELENE program
[NASA-TM-4520] p 1042 N94-17285
Laser beam steering device p 1045 N94-17357
Basic studies of the liquid state of matter: Electrical properties and laser interactions
[AD-A268311] p 1042 N94-17567

LASER CAVITIES
Laser with optically driven Q-switch
[NASA-CASE-NPO-18470-1-CU] p 1038 N94-15932
Atomic beam studies relevant to the space environment
[AD-A268628] p 1186 N94-17436

LASER DAMAGE
Laser-shock damage of iron-based materials
[AD-A267196] p 1038 N94-15852

Wound healing after laser injury to skin: The effect of occlusion and vitamin E
[AD-A266473] p 1128 N94-16779
Hazard calculations of diffuse reflected laser radiation for the SELENE program
[NASA-TM-4520] p 1042 N94-17285

LASER DOPPLER VELOCIMETERS
Laser Doppler velocimetry measurements across a normal shock in transonic flow
[AD-A267240] p 855 N94-14973
Contribution of laser Doppler velocimetry to the physical description of shock wave/turbulent boundary layer interactions with incidence on turbulence modelling
p 1018 N94-15201
Development of the seeding system used for laser velocimeter surveys of the NASA Low-Speed Centrifugal Compressor flow field
[NASA-TM-4485] p 1032 N94-15445
Transition induced by fixed and freely convecting spherical particles in laminar boundary layers
[AD-A267757] p 1028 N94-17276

LASER GUIDANCE
Design of pulse stretching cell for a sodium guide star optical system
[DE93-016436] p 1236 N94-14929

LASER INDUCED FLUORESCENCE
Electronic spectroscopy of the gas-phase OH-Kr van der Waals complex
[AD-A266891] p 942 N94-14946
Sensitive detection of gas-phase nitro-containing energetic materials employing 226-nm radiation
[AD-A267633] p 951 N94-17203
Laser probing of the kinetics and dynamics of 3-5 semiconductor growth
[AD-A268388] p 1215 N94-17422

LASER MATERIALS
Growth of new materials for solid state laser applications. The growth of ZnGeP2 by the vertical Bridgman method
[NASA-CR-194571] p 1038 N94-15530
An improved light source for laser ranging
p 913 N94-15567

LASER MODE LOCKING
New methods of generation of ultrashort laser pulses for ranging p 913 N94-15565
Simultaneous compression of the passively mode-locked pulsewidth and pulse train
p 913 N94-15566
An improved light source for laser ranging
p 913 N94-15567

LASER MODES
Full-wave simulation of the thumbtack laser
[DE93-015110] p 1039 N94-16054
Pulsed hydrogen fluoride overtone chemical laser studies
[AD-A267597] p 1041 N94-17193

LASER OUTPUTS
Ion doped quantum well lasers
[AD-A267198] p 1038 N94-15853
Laser with optically driven Q-switch
[NASA-CASE-NPO-18470-1-CU] p 1038 N94-15932
Optical effects of regolith processes on S asteroids as simulated by laser impulse alteration of ordinary chondrite p 1246 N94-16422
Porous silicon for pumping solid-state lasers
[AD-A266293] p 1039 N94-16474
Controlling chaotic behavior in CO2 and other lasers
[AD-A266431] p 1040 N94-16546
Ablation, surface activation, and electroless metallization of insulating materials by pulsed excimer laser irradiation
[DE93-015808] p 1040 N94-16664
Performance of coded coherent FSK lightwave system with noncoherent detection
[AD-A267442] p 1193 N94-17028
The determination of the Young moduli of a material after exposure to laser light and delineation of the zone of laser alterations
[IFTR-37/1991] p 1061 N94-17058
Sodium-mercury excimer laser, phase 1
[AD-A267728] p 1042 N94-17230

LASER PLASMA INTERACTIONS
High frequency Raman current drive
p 1201 N94-15208
Current drive with free electron lasers in high and low temperature tokamaks p 1201 N94-15209
X ray laser program
[AD-A267075] p 1038 N94-15628
Multi-frame x ray imaging with a large area 40ps camera
[DE93-017179] p 1035 N94-16960
Design, development and characterization studies of a large aperture high power Nd: Glass rod amplifier stage
[DE93-624944] p 1042 N94-17630
The effects of radiation transport on line ratios used as temperature and density diagnostic
[DE93-016424] p 1205 N94-17663

LASER PLASMAS
Laser-shock damage of iron-based materials
[AD-A267196] p 1038 N94-15852
Spectroscopic and computer modeling investigations of a laser-sustained plasma
[IFTR-30/1991] p 1204 N94-17066
Design, development and characterization studies of a large aperture high power Nd: Glass rod amplifier stage
[DE93-624944] p 1042 N94-17630
Resist performance in soft x ray projection lithography
[DE93-016490] p 1036 N94-17647

LASER POWER BEAMING
Comparisons of selected laser beam power missions to conventionally powered missions
[NASA-TM-106110] p 1040 N94-16522

LASER PROPULSION
Comparisons of selected laser beam power missions to conventionally powered missions
[NASA-TM-106110] p 1040 N94-16522

LASER PUMPING
Development of the Mars Observer Laser Altimeter (MOLA) p 921 N94-15617
Porous silicon for pumping solid-state lasers
[AD-A266293] p 1039 N94-16474
Design, development and characterization studies of a large aperture high power Nd: Glass rod amplifier stage
[DE93-624944] p 1042 N94-17630

LASER RANGE FINDERS
Prelaunch optical characterization of the Laser Geodynamic Satellite (LAGEOS 2)
[NASA-TP-3400] p 884 N94-15193
Lunar ranging
[NASA-TM-109603] p 1236 N94-15311
Eighth International Workshop on Laser Ranging Instrumentation
[NASA-CP-3214] p 911 N94-15552
Laser tracking for vertical control p 911 N94-15553
Laser ranging network performance and routine orbit determination at D-PAF p 911 N94-15554
Laser ranging application to time transfer using geodetic satellite and to other Japanese space programs
p 911 N94-15555
Applications of SLR p 911 N94-15556
Satellite signatures in SLR observations
p 912 N94-15557
Work at Graz on satellite signatures
p 898 N94-15558
The precision of today's satellite laser ranging systems p 912 N94-15559
SLR data screening; location of peak of data distribution p 912 N94-15560
Adaptive median filtering for preprocessing of time series measurements p 912 N94-15561
SATCOP mission planning software package
p 912 N94-15562
Nd:YLF laser for airborne/spaceborne laser ranging
p 913 N94-15563
Alternative wavelengths for laser ranging
p 913 N94-15564
New methods of generation of ultrashort laser pulses for ranging p 913 N94-15565
Simultaneous compression of the passively mode-locked pulsewidth and pulse train
p 913 N94-15566
An improved light source for laser ranging
p 913 N94-15567
Preliminary results from the portable standard satellite laser ranging intercomparison with MOBLAS-7
p 913 N94-15568
Performance optimization of detector electronics for millimeter laser ranging p 913 N94-15569
Tracking capabilities of SPADs for laser ranging
p 914 N94-15570
How to squeeze high quantum efficiency and high time resolution out of a SPAD p 914 N94-15571
The solid state detector technology for picosecond laser ranging p 914 N94-15572
Streak camera based SLR receiver for two color atmospheric measurements p 914 N94-15573
The first satellite laser echoes recorded on the streak camera p 914 N94-15574
Experience and results of the 1991 MTLRS-1 USSR campaign p 914 N94-15575
ETALON-1,-2 center of mass correction and array reflectivity p 915 N94-15576
Test results from LAGEOS-2 optical characterization using pulsed lasers p 915 N94-15577
Analysis of TOPEX laser retroreflector array characteristics p 915 N94-15578
Historical MOBLAS system characterization
p 915 N94-15579
Optimum wavelengths for two color ranging
p 915 N94-15580
Two color satellite laser ranging upgrades at Goddard's 1.2m telescope facility p 915 N94-15581
Measuring atmospheric dispersion with WLRS in multiple wavelength mode p 916 N94-15582
Millimeter accuracy satellites for two color ranging
p 916 N94-15583
Two wavelength satellite laser ranging using SPAD
p 916 N94-15584
New perspectives for high accuracy SLR with second generation geodesic satellites p 916 N94-15585
State-of-the-art satellite laser range modeling for geodetic and oceanographic applications
p 916 N94-15586
Geometric analysis of satellite laser ranging data
p 917 N94-15587
Improvement of SLR accuracy, a possible new step
p 917 N94-15588
On the accuracy of ERS-1 orbit predictions
p 874 N94-15589
Compensation for the distortion in satellite laser range predictions due to varying pulse travel times
p 917 N94-15590
Timebias corrections to predictions
p 875 N94-15591
Formation of on-site normal points
p 917 N94-15592
Poisson filtering of laser ranging data
p 917 N94-15593
Computer networking at SLR stations
p 917 N94-15594
Upgrading NASA/DOSE laser ranging system control computers p 918 N94-15595
HP upgrade operational streamlining
p 918 N94-15596
Application of the robust estimate in SLR data preprocessing p 918 N94-15597
A computer-controlled x-y offset guiding stage for the MLRS p 918 N94-15598
Lunar laser ranging data processing in a Unix/X windows environment p 918 N94-15599
LLR: Activities in Wettzell p 876 N94-15600
Matera Laser Ranging Observatory (MLRO): An overview p 877 N94-15601
Performance of the upgraded Orroral laser ranging system p 877 N94-15602
Sub-cm ranging and other improvements in Graz
p 919 N94-15603
Upgrading of the Borowiec laser station
p 877 N94-15604
Development of Shanghai satellite laser ranging station p 877 N94-15605
WLRS --- Wettzell Laser Ranging System (WLRS)
p 877 N94-15606
Ground based laser ranging for satellite location
p 919 N94-15607
New progress of ranging technology at Wuhan Satellite Laser Ranging Station p 877 N94-15608
TLRS-3 system upgrades p 877 N94-15609
Results of the MTLRS-1 upgrade p 877 N94-15610
The new MTLRS-1 receiving system
p 877 N94-15611
The new MTLRS transmitting system
p 877 N94-15612
Transputer based control system for MTLRS
p 877 N94-15613
Airborne 2 color ranging experiment
p 920 N94-15614
GLRS-R 2-colour retroreflector target design and predicted performance p 921 N94-15615
Effects of turbulence on the geodynamic laser ranging system p 921 N94-15616
Satellite laser station Helwan status 1992
p 877 N94-15621
Optical attenuation mechanism upgrades, MOBLAS, and TLRS systems p 922 N94-15622
The third generation SLR station Potsdam no. 7836
p 877 N94-15623
Performance comparison of high speed microchannel plate photomultiplier tubes p 922 N94-15624
Station report on the Goddard Space Flight Center (GSFC) 1.2 meter telescope facility p 922 N94-15625
Tectonic deformation in southern California
[NASA-CR-194621] p 1101 N94-16021
Clementine: Anticipated scientific datasets from the Moon and Geographos p 1288 N94-16392
Digital laser range finder emulator
[AD-D015811] p 1040 N94-16540
Environmental use of a Laser Range Finder and the Advanced Visualization System
[DE93-016163] p 1043 N94-17677

LASER SPECTROSCOPY
Laser photoionization time-of-flight mass spectrometry of nitrated polycyclic aromatic hydrocarbons and nitrated heterocyclic compounds
[AD-A268126] p 952 N94-17520

LASER STABILITY
The stability and dynamics of elastic structures and fluid flows
[AD-A267990] p 1029 N94-17414
LASER TARGET INTERACTIONS
Theoretical studies relating to the interaction of radiation with matter
[AD-A267134] p 1180 N94-15689
Laser-liquid interactions under reduced gravity conditions p 977 N94-16077
Development of the Laser-based R/D Test-bed System (LTS) p 978 N94-16080
Soft x ray emission from Alexandrite laser-matter-interaction
[AD-A267905] p 1042 N94-17378
The effects of radiation transport on line ratios used as temperature and density diagnostic
[DE93-016424] p 1205 N94-17663
LASER TARGETS
Airborne 2 color ranging experiment p 920 N94-15614
GLRS-R 2-colour retroreflector target design and predicted performance p 921 N94-15615
A state-of-the-art plasma polymerization coater for ICF targets
[DE93-016452] p 1204 N94-17237
The effects of radiation transport on line ratios used as temperature and density diagnostic
[DE93-016424] p 1205 N94-17663
LASER WELDING
Determination of GTA welding efficiencies
[AD-A267163] p 1046 N94-15738
Laser weld repair of tantalum sheet
[DE93-016417] p 1041 N94-16871
LASERS
Reduction of parasitic lasing
[NASA-CASE-LAR-14645-1-SB] p 1039 N94-15942
LASING
Reduction of parasitic lasing
[NASA-CASE-LAR-14645-1-SB] p 1039 N94-15942
Lasing dye sensor for chemical vapors
[AD-D015786] p 1040 N94-16533
LATCHES
Attachment device
[NASA-CASE-MSC-21885-1] p 1047 N94-15925
LATENT HEAT
Some thoughts on future rain mapping missions (TRMM follow-on) p 992 N94-15906
Validation and analysis of microwave-derived rainfall over the tropics
[AD-A267785] p 1108 N94-17303
A surface energy budget model modifying heat flow by foliage effects
[AD-A268598] p 1085 N94-17610
Boundary layer structure over areas of heterogeneous heat fluxes
[DE93-010657] p 1110 N94-17673
LATTICE VIBRATIONS
Search for far infrared radiation from optically pumped defect modes
[AD-A266744] p 1206 N94-15822
LAUGHING
Astro smile
[NASA-TM-109506] p 879 N94-15225
LAUNCH DATES
RADARSAT program p 898 N94-15893
LAUNCH VEHICLE CONFIGURATIONS
Role and development of small satellite missions in space plasma physics p 891 N94-17149
LAUNCH VEHICLES
Aerodynamic flight control to increase payload capability of future launch vehicles
[NASA-CR-193850] p 870 N94-15532
Aluminum-lithium technology
[TABES PAPER 93-601] p 962 N94-16137
Liquid Oxygen (LO2) propellant conditioning concept testing
[TABES PAPER 93-621] p 976 N94-16146
The closing window of opportunity: Addressing the US space launch vehicle crisis
[TABES PAPER 93-640] p 878 N94-16148
Small launchers (current and future projects in the world) p 878 N94-17137
Small satellite constellation deployment strategies p 878 N94-17138
NEXT launch system p 878 N94-17141
LAUNCHING
Small satellite missions to long-period comets p 874 N94-17144
LAUNCHING SITES
Small launchers (current and future projects in the world) p 878 N94-17137
Small satellite constellation deployment strategies p 878 N94-17138
Delta launch vehicle: Accommodations for small satellites p 878 N94-17139
LAVA
Morphometric comparison of Icelandic lava shield volcanoes versus selected Venusian edifices p 1248 N94-16178
Mode of emplacement of lunar mare volcanic deposits: Graben formation due to near surface deformation accompanying dike emplacement at Rima Parry 5 p 1258 N94-16227
Lava flow-field morphological classification and interpretation: Examples from Venus p 1259 N94-16230
Emplacement of multiple flow units on very shallow slopes, east Kawelu Planitia flow field, Venus p 1260 N94-16235
The cooling rates of pahoehoe flows: The importance of lava porosity p 1103 N94-16282
The rheology and composition of cryovolcanic flows on icy satellites p 1243 N94-16294
Fractal geometry of some Martian lava flow margins: Alba Patera p 1270 N94-16298
The distribution of large volcanoes on Venus as a function of height and altitude p 1271 N94-16303
Lava crusts and flow dynamics p 1103 N94-16316
Meander properties of Venusian channels p 1275 N94-16324
Sheet flow fields on Venus p 1278 N94-16338
Martian lavas: Three complementary remote sensing techniques to derive flow properties p 1283 N94-16366
Venusian pancake domes: Insights from terrestrial voluminous silicic lavas and thermal modeling p 1286 N94-16381
Relief of some small landforms on Venus p 1293 N94-16418
The use of TIMS for mapping different pahoehoe surfaces: Mauna Iki, Kilauea p 1065 N94-16606
Volcanic thermal features observed by AVIRIS p 1068 N94-16680
LAW (JURISPRUDENCE)
Emerging technologies for the changing global market [TABES PAPER 93-612] p 930 N94-16144
Americans with Disabilities Act considerations for the practice of occupational medicine p 1124 N94-16611
LAWS
Quantitative assessment of the accuracy of constitutive laws for plasticity with an emphasis on cyclic deformation
[AD-A267562] p 961 N94-17109
LAY-UP
Anisotropic damage mechanics modeling in metal matrix composites
[AD-A266328] p 934 N94-16440
LEACHING
Stalking the LREE-enriched component in ureilites p 1241 N94-16190
LEAD (METAL)
Lead Surveillance Program p 1127 N94-16640
LEAD COMPOUNDS
Lead chalcogenides based IR photosensitive array detectors with coordinate addressing p 903 N94-15053
Densifying and stabilizing ingredient
[AD-D015751] p 975 N94-16934
LEAD POISONING
Lead poisoning: An overview p 1124 N94-16614
Medical surveillance and biological monitoring of lead exposed employees p 1124 N94-16615
Lead Surveillance Program p 1127 N94-16640
LEAD TELLURIDES
A monolithic PbTeCCD focal plane array for MWIR imaging p 910 N94-15100
LEADING EDGE SWEEP
An experimental investigation of the effects of leading edge geometry on the dynamics of blunt fin-induced shock wave turbulent boundary layer interaction
[AD-A267656] p 860 N94-17221
LEADING EDGES
Suppression of dynamic stall with a leading-edge slat on a VR-7 airfoil
[NASA-TP-3357] p 856 N94-15657
Fluid flow and heat convection studies for actively cooled airframes
[NASA-CR-194624] p 1024 N94-16491
An experimental investigation of the effects of leading edge geometry on the dynamics of blunt fin-induced shock wave turbulent boundary layer interaction
[AD-A267656] p 860 N94-17221
LEAKAGE
Development of braided fiber seals for engine applications p 939 N94-16859
Leak detection utilizing analog binaural (VLSI) techniques
[NASA-CASE-NPO-18399-1-CU] p 1014 N94-17323
Electrical properties of sol-gel PZT thin films for decoupling capacitor applications
[DE93-016491] p 1015 N94-17648
LEAR JET AIRCRAFT
The vibro-acoustic mapping of low gravity trajectories on a Learjet aircraft p 978 N94-16078
LEARNING
Complex information coordination performance: Differential changes in working memory contributions following training
[AD-A267007] p 1132 N94-15762
Theoretical and experimental research into biological mechanisms underlying learning and memory
[AD-A267441] p 1133 N94-17022
Processes involved in the integration of pictures and discourse
[AD-A268150] p 1134 N94-17468
LEARNING CURVES
Questioning mechanisms during tutoring, conversation, and human-computer interaction
[AD-A266199] p 1137 N94-16108
LEAST SQUARES METHOD
Ground-truthing AVIRIS mineral mapping at Cuprite, Nevada p 1069 N94-16682
LEAVES
Oregon transect: Comparison of leaf-level reflectance with canopy-level and modelled reflectance p 1073 N94-16702
LECTURES
Fundamental theory of light for applications: Notes for five informal lectures
[DE93-016463] p 1192 N94-16953
LEE WAVES
Orographic microbursts in a severe winter windstorm
[AD-A267651] p 1108 N94-17247
LENGTH
Wind tunnel investigation of three axisymmetric cowls of different lengths at Mach numbers from 0.60 to 0.92
[NASA-TM-4488] p 856 N94-15681
LENSES
Ring lens focusing and push-pull tracking scheme for optical disk systems p 1227 N94-14990
Optical displays: A tutorial on images and image formation
[AD-A266230] p 1192 N94-16926
Diffractive optical elements for generating arbitrary line foci p 1195 N94-17338
Fabricating binary optics: An overview of binary optics process technology p 1195 N94-17343
Binary optics at Hughes Danbury Optical Systems p 1195 N94-17344
Fabrication techniques for very fast diffractive lenses p 1196 N94-17345
Fabrication of micro-optical devices p 1197 N94-17351
Diffractive optics in adverse environments p 1197 N94-17352
Measurements of microlens performance p 1197 N94-17355
Predesign of diamond turned refractive/diffractive elements for IR objectives p 1198 N94-17359
Theory of dispersive microlenses p 1198 N94-17361
LEPTONS
On the nature of mirror particles
[DE93-626670] p 1179 N94-14934
LEVITATION
Superconductive material and magnetic field for damping and levitation support and damping of cryogenic instruments
[NASA-CASE-NPO-18458-1-CU] p 1033 N94-15875
Effects of levitated dust on astronomical observations from the lunar surface p 1239 N94-16433
LIBRARIES
A TRALINET guide to the Internet
[AD-A266946] p 1229 N94-15178
Managing information as a corporate asset: Key strategies for information professionals to remain competitive
[DE93-015515] p 1232 N94-16875
LICENSING
Industrial Hygiene Laboratory accreditation: The JSC experience p 1125 N94-16623
LIE GROUPS
Quantum Heisenberg groups and Sklyanin algebras
[DE93-628590] p 1175 N94-17643
LIFE (DURABILITY)
Multiaxial deformation and life prediction model and experimental data for advanced silicon nitride ceramics
[DE93-015450] p 967 N94-16067
Software Engineering Guidebook
[NASA-CR-177625] p 1150 N94-16656
Development of a constitutive model for creep and life prediction of advanced silicon nitride ceramics
[DE93-015894] p 968 N94-16813
The Ceramic Technology Project: Ten years of progress
[DE93-015991] p 968 N94-16843

Environment enhanced fatigue crack propagation in metals: Inputs to fracture mechanics life prediction models
[NASA-CR-191538] p 942 N94-17638

LIFE SCIENCES
STS-40 crew during spacelab Sim
[NASA-TM-109493] p 876 N94-15452
Canadian microgravity experiments flown in 1989-1990 p 977 N94-16075
Statistical techniques for study design of microgravity life sciences experiments p 980 N94-16094
Aerospace medicine and biology: A continuing bibliography with indexes (supplement 378)
[NASA-SP-7011(378)] p 1122 N94-16478
Aerospace medicine and biology: A continuing bibliography with indexes (supplement 380)
[NASA-SP-7011(380)] p 1122 N94-16479
Looking at science on board Eureca
[ESA-BR-80] p 874 N94-16584
Design of an experiment hardware for the ESA space facility BIOPAN
[DLR-FB-93-06] p 876 N94-17548

LIFE SUPPORT SYSTEMS
Aerospace medicine and biology: A continuing bibliography with indexes (supplement 378)
[NASA-SP-7011(378)] p 1122 N94-16478
Aerospace medicine and biology: A continuing bibliography with indexes (supplement 380)
[NASA-SP-7011(380)] p 1122 N94-16479
Illness/injury pattern complex 40 (Titan) p 1125 N94-16625
Aircrew/groundcrew life support systems research. Volume 1: CLIN 0001 research requirements
[AD-A268229] p 1139 N94-17563
Aircrew/groundcrew life support systems research. Volume 2: CLIN 0002 task order requirements
[AD-A268230] p 1139 N94-17564

LIFT FANS
The lift-fan powered-lift aircraft concept: Lessons learned
[NASA-CR-177616] p 866 N94-15718
Lift-fan aircraft: Lessons learned-the pilot's perspective
[NASA-CR-177620] p 867 N94-15950

LIFTING BODIES
The 1966 highlights — NASA research programs
[NASA-TM-109444] p 1302 N94-15343
The 1968 highlights — NASA programs and research
[NASA-TM-109627] p 1302 N94-15413
Subsonic aerodynamic characteristics of the HL-20 lifting-body configuration
[NASA-TM-4515] p 861 N94-17284

LIGAMENTS
Carpal tunnel syndrome and other cumulative trauma disorders of the arm and hand and occupation in US Navy enlisted personnel
[AD-A267747] p 1129 N94-17374
Direct observation of fracture of CAS-glass/SiC composites and processing of toughened alumina
[AD-A268275] p 941 N94-17457

LIGANDS
Binding of carbon dioxide to metal macrocycles: Toward a mechanistic understanding of electrochemical and photochemical carbon dioxide reduction
[DE93-016244] p 949 N94-16870
Pulsed laser kinetic studies of liquids under high pressure
[DE93-017826] p 1041 N94-16998
Synthesis, reactivity, and characterization of (-hexacarbocyclic) manganese dicarbonyl complexes with sulfur and phosphorus ligands
[AD-A267592] p 930 N94-17192

LIGHT (VISIBLE RADIATION)
Visible light photon counters for astronomy p 902 N94-15043
Method and apparatus for performing scanning tunneling optical absorption spectroscopy
[AD-D015796] p 948 N94-16539

LIGHT AMPLIFIERS
Design, development and characterization studies of a large aperture high power Nd: Glass rod amplifier stage
[DE93-624944] p 1042 N94-17630

LIGHT BEAMS
Plume primary smoke p 923 N94-15218
Linear encoding device
[NASA-CASE-GSC-13562-1] p 1147 N94-15703
Rotary encoding device
[NASA-CASE-GSC-13543-1] p 1189 N94-15705
Rotary encoding device
[NASA-CASE-GSC-13556-1] p 1148 N94-15943
Controlling chaotic behavior in CO2 and other lasers
[AD-A266431] p 1040 N94-16546
Frequency resolution of an acousto-optical spectrometer
[AD-A267822] p 1035 N94-17401
Study of high speed interference photography with two-dimensional acousto-optical lattice deflection
[AD-A267823] p 1035 N94-17402

LIGHT CURVE
X ray emission from Wolf-Rayet stars with recurrent dust formation
[NASA-CR-194567] p 1300 N94-15533
Variability of the Seyfert galaxy MKN 766 in the Rosat all sky survey
[MPE-PREPRINT-221] p 1240 N94-17591

LIGHT EMITTING DIODES
Laser with optically driven Q-switch
[NASA-CASE-NPO-18470-1-CU] p 1038 N94-15932
JSEP fellowship
[AD-A266568] p 1211 N94-16800

LIGHT HELICOPTERS
Noise measurement flight test of five light helicopters
[AD-A268566] p 1179 N94-17599

LIGHT IONS
Calculations of cosmic-ray helium transport in shielding materials
[NASA-TP-3354] p 1301 N94-17666

LIGHT MODULATION
Optical residue processing module
[AD-A267721] p 1188 N94-14940
Velocity matched millimeterwave electro-optic modulator
[AD-A267264] p 1188 N94-14957
An optically modulated scatterer for microwave antenna metrology
[NPL-DES-126] p 986 N94-15020
Two-dimensional acousto-optical interaction theory and experimental analysis
[AD-A267761] p 1193 N94-17254
Measurements of microlens performance p 1197 N94-17355

LIGHT SCATTERING
Secondary smoke p 924 N94-15220
Convective flow effects on protein crystal growth
[NASA-CR-194560] p 1206 N94-15476
Spatial and frequency diversity in lidar systems
[AD-A266192] p 1039 N94-16124
A test of the applicability of independent scattering to high albedo planetary regoliths p 1250 N94-16187
Effects of levitated dust on astronomical observations from the lunar surface p 1239 N94-16433
Maximum likelihood techniques applied to quasi-elastic light scattering
[NASA-CR-193550] p 1192 N94-16718
Speckles statistics and decorrelation effects in complex ABCD optical systems
[AD-A267843] p 1193 N94-17012
Scattering from binary optics p 1195 N94-17341

LIGHT SOURCES
Velocity matched millimeterwave electro-optic modulator
[AD-A267264] p 1188 N94-14957
An improved light source for laser ranging p 913 N94-15567
Linear encoding device
[NASA-CASE-GSC-13562-1] p 1147 N94-15703
Laser with optically driven Q-switch
[NASA-CASE-NPO-18470-1-CU] p 1038 N94-15932
Acousto-optical classifier
[AD-D015894] p 1000 N94-16921

LIGHT TRANSMISSION
A method of detecting and locating electrical current imbalances
[NASA-CASE-LEW-15407-1] p 1009 N94-15706
Optical properties and surface morphology studies of palladium contacts on mercuric iodide single crystals
[DE93-012510] p 1207 N94-15973
Method and apparatus for performing scanning tunneling optical absorption spectroscopy
[AD-D015796] p 948 N94-16539
Detection of subsurface defects in machined silicon nitride ceramics by optical scattering methods
[DE93-015554] p 968 N94-16658
Transmission of light through a turbulent mixing layer
[AD-A267266] p 1193 N94-17264

LIGHTNING
Mesoscale lightning
[NASA-TM-109655] p 1105 N94-15226
Venus lightning
[NASA-TM-109644] p 1105 N94-15430
Middle atmospheric electric fields over thunderstorms
[NASA-CR-194619] p 1106 N94-16493
Remote sensing of precipitation and electrification with a dual-polarization, coherent, wideband radar system
[AD-A267479] p 1004 N94-17364

LIGNIN
A linear spectral matching technique for retrieving equivalent water thickness and biochemical constituents of green vegetation p 1068 N94-16678

LIMB DARKENING
Atmospheric corrections for TIMS estimated emittance p 1064 N94-16602

LIMESTONE
Earth's partial pressure of CO2 over the past 100-500 Ma; evidence from Ce anomalies in mostly shallow seas (less than 200 m) as recorded in carbonate sediments, 2 p 1104 N94-16360
CO2 production by impact in carbonates? An ATEM and stable isotope (C,O) study p 954 N94-16383

LIMITS (MATHEMATICS)
Automatic differentiation of limit functions
[DE93-016376] p 1168 N94-14928

LINE OF SIGHT
Hypervelocity orbital intercept guidance using certainty control
[AD-A267297] p 1174 N94-17219

LINE SPECTRA
Background suppression techniques in germanium detectors p 899 N94-15026
CdTe array detectors for high energy astronomy p 899 N94-15029
Optical fiber spectroscopy: A study of the luminescent properties of the europium ion for thermal sensors
[NASA-CR-194576] p 1189 N94-15647
The pressure broadening of HDO by O2, N2, H2, and He between 100 K and 600 K
[AD-A267118] p 946 N94-15684
Spectroscopic and computer modeling investigations of a laser-sustained plasma
[IFTR-30/1991] p 1204 N94-17066
The formation process of the He I lambda 10830 line in cool giant stars
[NASA-CR-194648] p 1240 N94-17094

LINEAR ALTERNATORS
SPDE/SPRE final summary report
[NASA-CR-187086] p 924 N94-15482

LINEAR ARRAYS
A 12.5 micron infrared detector for Earth observation p 903 N94-15052
A linear monolithic 4-6 on silicon IR detector array p 910 N94-15098
Rotary encoding device
[NASA-CASE-GSC-13543-1] p 1189 N94-15705
Sensor modelling for the Cyclops focal plane detector array based technology demonstrator
[AD-A267172] p 1190 N94-15846

LINEAR ENERGY TRANSFER (LET)
Approximate Green's function methods for HZE transport in multilayered materials
[NASA-TM-4519] p 1300 N94-17084
Energy deposition fluctuations induced by ions in microvolumes and nanovolumes: An analytic approach. 1: Theory
[AD-A267959] p 1173 N94-17495

LINEAR POLARIZATION
A test of the applicability of independent scattering to high albedo planetary regoliths p 1250 N94-16187

LINEAR PROGRAMMING
Finding stable orientations of assemblies with linear programming
[AD-A266990] p 1143 N94-15212

LINEAR SYSTEMS
Efficiency effects of variation in controlled experimental variables
[DE93-014345] p 1169 N94-15979
Invariance of slip movements with respect to the control matrix
[IFTR-43/1991] p 1170 N94-17045

LINEAR TRANSFORMATIONS
The alignment-distribution graph
[NASA-CR-194292] p 1168 N94-15112
Reducing data dimension to lower signal processing computational requirements and maximize performance
[AD-A266606] p 999 N94-16728
Robust control of uncertain nonlinear systems
[AD-A268056] p 1167 N94-17506

LINEARIZATION
Nonlinear random response prediction using MSC/NASTRAN
[NASA-TM-109029] p 1179 N94-17650

LINGUISTICS
Using multiple adaptively-weighted strategies for the resolution of demonstratives
[AD-A266463] p 1150 N94-16585
Monads and comonads in intensional semantics
[AD-A266522] p 1151 N94-16790
Activities of the Research Laboratory of Electronics
[AD-A266730] p 1304 N94-17651

LIPIDS
Encapsulation of hemoglobin in non-phospholipid vesicles
[AD-A266505] p 1128 N94-16785

LIQUID ATOMIZATION
Mechanism of intermittent atomization
[AD-A266625] p 1021 N94-15770

LIQUID COOLING
Description of cooling water calorimetry and wall thermometry diagnostic at tokamak ASDEX-Upgrade
[IPP-5/46] p 1200 N94-14966
USAF physiological studies of personal microclimate cooling: A review
[AD-A267203] p 1022 N94-15858
LIQUID CRYSTALS
Unidirectional solidification of liquid-crystal material
p 945 N94-15167
LIQUID FLOW
Coaxial airblast atomizers
[NASA-CR-193845] p 1016 N94-15109
LIQUID FUELS
Publications of the Oak Ridge National Laboratory Fossil Energy Program, 1 October 1991 - 31 March 1993
[DE93-014643] p 1232 N94-16967
LIQUID HELIUM
Cryogenic measurements of aerojet GaAs n-JFETs
[NASA-TM-103972] p 1009 N94-15765
LIQUID HYDROGEN
Liquid hydrogen and liquid oxygen feedline passive recirculation analysis
[TABES PAPER 93-620] p 1031 N94-16145
Power Reactant Storage Assembly (PRSA) (Space Shuttle). PRSA hydrogen and oxygen DVT tank refurbishment
[NASA-CR-188262] p 926 N94-16922
ALS liquid hydrogen turbopump
[NASA-CR-194646] p 927 N94-17016
LIQUID INJECTION
Mechanism of intermittent atomization
[AD-A266625] p 1021 N94-15770
LIQUID LEVELS
Temperature and pressure effects on capacitance probe cryogenic liquid level measurement accuracy
[NASA-CR-190763] p 1034 N94-16521
LIQUID NITROGEN
Liquid Oxygen (LO2) propellant conditioning concept testing
[TABES PAPER 93-621] p 976 N94-16146
Cryogenic spray vaporization in high-velocity helium, argon and nitrogen gasflows
[NASA-TM-106363] p 1035 N94-17446
LIQUID OXYGEN
Liquid hydrogen and liquid oxygen feedline passive recirculation analysis
[TABES PAPER 93-620] p 1031 N94-16145
Liquid Oxygen (LO2) propellant conditioning concept testing
[TABES PAPER 93-621] p 976 N94-16146
Power Reactant Storage Assembly (PRSA) (Space Shuttle). PRSA hydrogen and oxygen DVT tank refurbishment
[NASA-CR-188262] p 926 N94-16922
LIQUID PHASE SINTERING
Army P/M research and development overview
[AD-A266921] p 954 N94-15104
Liquid phase sintering of tungsten composites under microgravity. Effect of matrix composition
p 945 N94-15171
LIQUID PHASES
The influence of microstructure on the mechanical behavior of silicon nitride ceramics
[DE93-015363] p 966 N94-16018
Process of shaping an electrorheological solid
[AD-D015885] p 1012 N94-16914
Ceramic fiber coatings development and demonstration
[AD-A267286] p 972 N94-17242
A basic principles description of liquid vapor phase transitions
[AD-A268331] p 1176 N94-17581
LIQUID PROPELLANT ROCKET ENGINES
Computational analysis of Variable Thrust Engine (VTE) performance
[NASA-CR-193852] p 928 N94-17442
CPIA/M5 liquid propellant engine manual
[AD-A268062] p 929 N94-17589
LIQUID ROCKET PROPELLANTS
Liquid Oxygen (LO2) propellant conditioning concept testing
[TABES PAPER 93-621] p 976 N94-16146
Lunar lander and return propulsion system trade study
[NASA-TP-3388] p 925 N94-16496
LIQUID-SOLID INTERFACES
Unidirectional solidification of liquid-crystal material
p 945 N94-15167
Liquidus equilibria of lunar analogs at high pressure
p 1283 N94-16364
Particle Engulfment and Pushing by Solidifying Interfaces (PEPSI)
[NASA-CR-193856] p 960 N94-17079
LIQUID-VAPOR EQUILIBRIUM
Explosive boiling at very low heat fluxes: A microgravity phenomenon
[NASA-TM-106325] p 1046 N94-15817
LIQUID-VAPOR INTERFACES
Space Station thermal storage/refrigeration system research and development
[NASA-CR-193841] p 879 N94-15191
Mechanism of intermittent atomization
[AD-A266625] p 1021 N94-15770
LIQUIDS
Contained liquids in microgravity, part 2
p 979 N94-16085
Partitioning of Nb, Mo, Ba, Ce, Pb, Th and U between immiscible carbonate and silicate liquids: Evaluating the effects of P2O5,F, and carbonate composition
p 953 N94-16283
A priori inequalities for an ideal-incompressible liquid in an electromagnetic field
[IFTR-9/1992] p 998 N94-16652
Pulsed laser kinetic studies of liquids under high pressure
[DE93-017826] p 1041 N94-16998
An automated system for ultrasound measurements of liquids by the resonance (Eggers) method
[IFTR-17/1992] p 1178 N94-17087
Basic studies of the liquid state of matter: Electrical properties and laser interactions
[AD-A268311] p 1042 N94-17567
LIQUIDUS
The ilmenite liquidus and depths of segregation for high-Ti picrite glasses p 975 N94-16241
Transition metals in superheat melts
p 962 N94-16273
The rheology and composition of cryovolcanic flows on icy satellites p 1243 N94-16294
Liquidus equilibria of lunar analogs at high pressure
p 1283 N94-16364
LISP (PROGRAMMING LANGUAGE)
An experimental comparison of CLOS and C(++) implementations of an object-oriented graphical simulation of walking robot kinematics
[AD-A267168] p 1165 N94-15855
LITHIUM
In situ Raman spectroscopy of lithium electrode surface in ambient temperature lithium secondary battery
[DE93-015238] p 1010 N94-16061
Lithium D-cell study
[NASA-CR-192705] p 1011 N94-16505
Thin composite solid electrolyte film for lithium batteries
[NASA-CASE-NPO-18694-1-CU] p 1014 N94-17325
Characterization of the lithium/pan-based polymer electrolytes interface
[AD-A268401] p 973 N94-17434
LITHIUM CHLORIDES
Hydride-containing molten salts and their technology implications
[AD-A266458] p 1092 N94-16567
LITHIUM COMPOUNDS
Tritium diffusion and desorption in single crystal LiAlO2
[DE93-015140] p 1211 N94-16805
LITHIUM FLUORIDES
Heat storage module p 946 N94-15172
An improved light source for laser ranging
p 913 N94-15567
LITHIUM NIOBATES
Development of the Mars Observer Laser Altimeter (MOLA) p 921 N94-15617
Extracavity frequency doubling study of a pulsed photodissociation iodine laser
[AD-A267893] p 1042 N94-17394
LITHIUM SULFUR BATTERIES
The 1987 Goddard Space Flight Center Battery Workshop
[NASA-CP-3236] p 1012 N94-17062
LITHOGRAPHY
Aberration correction of unstable resonators
[NASA-CASE-NPO-18791-1-CU] p 1034 N94-15987
Subwavelength structured surfaces and their applications p 1194 N94-17337
Soft x ray emission from Alexandrite laser-matter-interaction
[AD-A267905] p 1042 N94-17378
Low voltage electron beam lithography
[AD-A267865] p 1215 N94-17389
Resist performance in soft x ray projection lithography
[DE93-016490] p 1036 N94-17647
LITHOLOGY
Fluvial erosion on Mars: Implications for paleoclimatic change p 1241 N94-16210
Trace-element composition of Chicxulub crater melt rock, K/T tektites and Yucatan basement
p 1242 N94-16245
A Monazite-bearing clast in Apollo 17 melt breccia
p 1267 N94-16279
Apollo 17 materials viewed from 2 to 4 mm soil particles: Pre-serenitatis highlands components
p 1267 N94-16280
The dregs of crystallization in Zagami
p 1245 N94-16390
Bright soil units on Mars determined from ISM imaging spectrometer data p 1295 N94-16430
From minerals to rocks: Toward modeling lithologies with remote sensing p 1086 N94-16437
Mapping the mineralogy and lithology of Canyonlands, Utah with imaging spectrometer data and the multiple spectral feature mapping algorithm
p 1066 N94-16670
First results from analysis of coordinated AVIRIS, TIMS, and ISM (French) data for the Ronda (Spain) and Beni Bousera (Morocco) peridotites p 1067 N94-16675
LITHOSPHERE
LFASE report: Crustal study
[AD-A266893] p 1111 N94-14947
The formation and evolution of Alpha and Tellus tesserae on Venus p 1249 N94-16183
Ishtar deformed belts: Evidence for deformation from below? p 1256 N94-16218
Estimates of lithospheric thickness on Venus
p 1267 N94-16277
Effective elastic thickness of the Venusian lithosphere with lateral viscosity variations in the mantle
p 1293 N94-16421
LOAD CARRYING CAPACITY
Influence of the loading rate on the endurance and deformability of cement matrix composites
[IFTR-1/1992] p 1060 N94-17052
LOAD DISTRIBUTION (FORCES)
Systematic study of effects of load misalignment in uniaxial low cycle fatigue testing at high temperatures
[NPL-DMM(A)-27] p 1057 N94-15015
Static analysis of beams on an elastic base as stated by generalized functions
[IFTR-27/1991] p 1060 N94-16923
LOAD TESTS
Systematic study of effects of load misalignment in uniaxial low cycle fatigue testing at high temperatures
[NPL-DMM(A)-27] p 1057 N94-15015
Measurement and analysis of critical CTOA for an aluminum alloy sheet
[NASA-TM-109024] p 956 N94-15948
Mean strain effects on the strain life fatigue curve
[AD-A267211] p 960 N94-16984
The IOSDL SeaSoar hydraulic unit
[IOS-300-1992] p 1114 N94-17516
LOADING RATE
An analysis of ways of determining the material constants for viscoelastic materials
[IFTR-28/91] p 951 N94-17050
Influence of the loading rate on the endurance and deformability of cement matrix composites
[IFTR-1/1992] p 1060 N94-17052
LOADS (FORCES)
Helicopter structures: A review of loads, fatigue design techniques, and usage monitoring
[AD-A267115] p 866 N94-15651
Investigation of the origin of hot spots in deformed crystals: Ammonium perchlorate studies
[AD-A267692] p 1214 N94-17270
LOCAL AREA NETWORKS
Applying paperless technology to achieve excellence in manufacturing operations
[TABES PAPER 93-630] p 1052 N94-16147
LOCKING
Connector systems for structures
[NASA-CASE-MSC-21998-1] p 1046 N94-15707
LOGIC CIRCUITS
A formal language for the specification and verification of synchronous and asynchronous circuits
[NASA-CR-191509] p 1144 N94-15443
Digital laser range finder emulator
[AD-D015811] p 1040 N94-16540
Computer-aided design package for designers of digital optical computers
[AD-A267866] p 1154 N94-17390
Orpheus: A synthesis framework for regular architectures
[REPT-93-016] p 1156 N94-17504
LOGIC DESIGN
Models for reactivity
[AD-A266419] p 1149 N94-16554
LOGIC PROGRAMMING
Automatic translation of database integrity constraints into compensating production rules
[REPT-92-055] p 1234 N94-17502
LOGISTICS
Sleep management user's guide for special operations personnel
[AD-A267746] p 1119 N94-14943

Defense Logistics Information System (DLIS) procedures manual. Products and services end-user manual
[AD-A267766] p 1232 N94-17007
CALS test network handbook
[AD-A267587] p 1160 N94-17209

LOGISTICS MANAGEMENT
Facilities maintenance handbook
[NHB-8831.2] p 1224 N94-15934
Defense Logistics Information System (DLIS) procedures manual. Products and services end-user manual
[AD-A267766] p 1232 N94-17007
Defense Logistics Information System (DLIS). Procedures manual: Logistics On-Line Access (LOLA) procedures manual
[AD-A267685] p 1233 N94-17229

LONG DURATION EXPOSURE FACILITY
Long Duration Exposure Facility is coming home
[NASA-TM-109656] p 884 N94-15227
STS-32 onboard 16mm photography quick release
[NASA-TM-109472] p 880 N94-15376
STS-32 LDEF EVA training in WETF with Low and Dunbar
[NASA-TM-109473] p 1135 N94-15377
STS-32 LDEF approach in SES
[NASA-TM-109474] p 880 N94-15379
Long Duration Exposure Facility retrieval animation
[NASA-TM-109426] p 885 N94-15496
Long Duration Exposure Facility
[NASA-TM-109427] p 885 N94-15497
Analysis of leading edge and trailing edge cover glass samples before and after treatment with advanced satellite contamination removal techniques
[AD-A267055] p 885 N94-15666
Long Duration Exposure Facility experiment M0003 deintegration/findings and impacts
[AD-A267140] p 885 N94-15749
Impact penetration experiments in teflon targets of variable thickness p 1063 N94-16253
Resolving LDEF's flux distribution: Orbital (debris?) and natural meteoroid populations p 1245 N94-16391
Third LDEF Post-Retrieval Symposium Abstracts
[NASA-CP-10120] p 1303 N94-16495
Performance of silvered Teflon thermal control blankets on spacecraft
[AD-A266284] p 887 N94-16909
Long duration exposure facility experiment m0003 deintegration observation database
[AD-A267579] p 951 N94-17207

LONG DURATION SPACE FLIGHT
Supporting life in space
[NASA-TM-109593] p 1135 N94-15285
STS-26 long duration simulation: Crew entering SMS
[NASA-TM-109560] p 876 N94-15474

LONGITUDINAL CONTROL
Computation of a controlled store separation from a cavity p 858 N94-16513

LOOPS
The renormalization of the axial anomaly in dimensional regularization
[NIKHEF-H/92-18] p 1220 N94-17618

LOSS OF COOLANT
GAM-HEAT: A computer code to compute heat transfer in complex enclosures
[DE93-014724] p 1023 N94-15980

LOUDNESS
A virtual acoustic orientation instrument
[AD-A268181] p 1134 N94-17510

LOW ALTITUDE
Radiocommunication problems of a position reporting and bidirectional messagery system using VHF/UHF with low-Earth orbit satellites p 889 N94-17136
Delta launch vehicle: Accommodations for small satellites p 878 N94-17139
Small imaging satellite for Earth observing system adjunct p 891 N94-17151
Regulation of low Earth orbit satellites p 892 N94-17159
LEOCOM-SPES: Low cost message communications p 892 N94-17161
TAOS (S80): A (LEO-MSS) system for position reporting and telemanagement services p 893 N94-17162
Feasibility study of a personal communications system IRIDIUM-like p 893 N94-17165

LOW CARBON STEELS
Laser-shock damage of iron-based materials
[AD-A267196] p 1038 N94-15852

LOW COST
A proposed ground segment design for small satellites p 878 N94-17154
LEOCOM-SPES: Low cost message communications p 892 N94-17161
The ORBCOMM system p 893 N94-17163
S-80: A satellite for less than 50 MF p 894 N94-17172
A mini satellite called Arsene: The way to make it at a minimum cost p 895 N94-17179
TUBSAT: Low cost access to space technology p 895 N94-17180

LOW DENSITY MATERIALS
Removal of carbonaceous contaminants from silica aerogel p 953 N94-16256

LOW GRAVITY MANUFACTURING
Visualization of solidification front phenomena
[NASA-CR-193838] p 976 N94-15006

LOW NOISE
The (delta)f algorithm for beam dynamics
[DE93-015632] p 1187 N94-16660

LOW REYNOLDS NUMBER
Hoph bifurcation in viscous, low speed flows about an airfoil with structural coupling
[AD-A266542] p 859 N94-16798

LOW SPEED
Hoph bifurcation in viscous, low speed flows about an airfoil with structural coupling
[AD-A266542] p 859 N94-16798
Experimental and computational investigation of the NASA low-speed centrifugal compressor flow field
[NASA-TM-4481] p 869 N94-17386

LOW SPEED WIND TUNNELS
A software interface for the ARL wind tunnel data acquisition system
[AD-A267114] p 1146 N94-15650
NASA Lewis 9- by 15-foot low-speed wind tunnel user manual
[NASA-TM-106247] p 872 N94-15819

LOW TEMPERATURE
Spectroscopic investigations of nonambient systems with millimeter and submillimeter probes
[AD-A266537] p 968 N94-16796
Amide and tetrazene complexes of transition and main group elements as precursors for the low temperature synthesis of elemental nitrides
[AD-A266246] p 950 N94-16931
Transient studies of low temperature catalysts for methane conversion
[DE93-017710] p 950 N94-16962

LOW VOLTAGE
Preparation and investigation of improved low voltage electron excitable phosphors
[AD-A266852] p 963 N94-14948
Low voltage electron beam lithography
[AD-A267865] p 1215 N94-17389

LOWER ATMOSPHERE
A ray trace model for propagation loss
[AD-A266314] p 997 N94-16467

LOWER BODY NEGATIVE PRESSURE
STS-32 crew training for lower body negative pressure unit and AFE
[NASA-TM-109475] p 1120 N94-15381

LUBRICANTS
Scholarly research program in fuel analysis and combustion research
[AD-A266789] p 942 N94-14911
Heating of lubricant with an electric resistance heater
[VTT-TIED-1359] p 974 N94-17547

LUBRICATING OILS
Contained liquids in microgravity, part 2 p 979 N94-16085

LUBRICATION
Atomic-scale friction measurements using friction force microscopy. Part 1: General principles and new measurement techniques
[AD-A268391] p 1048 N94-17533

LUGS
RSRM nozzle actuator bracket/lug fracture mechanics qualification test
[NASA-CR-193859] p 927 N94-17080

LUMINANCE
The effects of luminance boundaries on color perception
[AD-A268398] p 1133 N94-17397
Perception of lightness and brightness in complex patterns
[AD-A268435] p 1134 N94-17513

LUMINOSITY
X ray emission from Wolf-Rayet stars with recurrent dust formation
[NASA-CR-194567] p 1300 N94-15533

LUNAR ALBEDO
Mixing model analysis of telescopic lunar spectra p 1284 N94-16371

LUNAR ATMOSPHERE
Effects of levitated dust on astronomical observations from the lunar surface p 1239 N94-16433

LUNAR BASES
Lunar base concepts
[NASA-TM-109607] p 1247 N94-15294
Building a lunar base
[NASA-TM-109674] p 983 N94-15519
The first lunar outpost: The design reference mission and a new era in lunar science p 874 N94-16362
Study of the National Science Foundation's South Pole Station as an analogous data base for the logistical support of a Moon laboratory
[NASA-TM-108429] p 1174 N94-17469

LUNAR COMPOSITION
Why is the Moon dark? p 1256 N94-16219
Lunar scout missions: Galileo encounter results and application to scientific problems and exploration requirements p 1259 N94-16229
Earth-based and Galileo SSI multispectral observations of eastern mare serenitatis and the Apollo 17 landing site p 1261 N94-16244
On the composition of neuKREEP: QMD contamination at Apollo 11? p 1266 N94-16276
Composition and maturity of the 60013/14 core p 1275 N94-16327
Grain surface features of Apollo 17 orange and black glass p 1289 N94-16397
Gamma ray spectrometer for Lunar Scout 2 p 1037 N94-16426

LUNAR CORE
Overturn of magma ocean ilmenite cumulate layer: Implications for lunar magmatic evolution and formation of a lunar core p 1261 N94-16242

LUNAR CRATERS
Twenty-Fourth Lunar and Planetary Science Conference. Part 2: G-M
[NASA-CR-193174] p 1247 N94-16173
Galileo imaging results from the second Earth-Moon flyby: Lunar Maria and related units p 1252 N94-16199
Remote sensing studies of the northeastern portion of the lunar nearside p 1258 N94-16225
Lunar impact basins: New data for the nearside northern high latitudes and eastern limb from the second Galileo flyby p 1258 N94-16228
Modes of formation of lunar light plains and the detection of cryptomaria deposits p 1259 N94-16231
The size of complex craters p 1262 N94-16249
The history of mare volcanism in the Orientale Basin: Mare deposit ages, compositions and morphologies p 1269 N94-16289
Galileo SSI lunar observations: Copernican craters and soils p 1288 N94-16395
Thermogeologic mapping of the Moon from lunar orbit p 1290 N94-16405

LUNAR CRUST
Remote sensing studies of the northeastern portion of the lunar nearside p 1258 N94-16225
Mode of emplacement of lunar mare volcanic deposits: Graben formation due to near surface deformation accompanying dike emplacement at Rima Parry 5 p 1258 N94-16227
The ilmenite liquidus and depths of segregation for high-Ti picrite glasses p 975 N94-16241
Overturn of magma ocean ilmenite cumulate layer: Implications for lunar magmatic evolution and formation of a lunar core p 1261 N94-16242

LUNAR DUST
Lunar Curatorial Facility resource
[NASA-TM-109531] p 875 N94-15393
Effects of levitated dust on astronomical observations from the lunar surface p 1239 N94-16433

LUNAR ECLIPSES
EUVE observations of the Moon p 1250 N94-16185

LUNAR EVOLUTION
Overturn of magma ocean ilmenite cumulate layer: Implications for lunar magmatic evolution and formation of a lunar core p 1261 N94-16242
Tidal regime of intact planetoid capture model for the Earth-Moon system: Does it relate to the archean sedimentary rock record? p 1245 N94-16378

LUNAR EXPLORATION
Pre-phase a study report of lunar polar orbiter
[NASDA-TK-SS0440] p 873 N94-15000
The 1966 highlights --- NASA research programs
[NASA-TM-109444] p 1302 N94-15343
Lunar scout missions: Galileo encounter results and application to scientific problems and exploration requirements p 1259 N94-16229
Clementine: Anticipated scientific datasets from the Moon and Geographos p 1288 N94-16392
Opportunity for early science return by the Artemis Program p 1291 N94-16408

LUNAR FAR SIDE
The history of mare volcanism in the Orientale Basin: Mare deposit ages, compositions and morphologies p 1269 N94-16289

LUNAR GEOLOGY
The SCR Ne-21 and Ar-38 in lunar rock 68815: The solar proton energy spectrum over the past 2 MYR p 1248 N94-16177
First oxygen from lunar basalt p 1249 N94-16182

Importance of expansion and contraction in the formation of tectonic features on the Moon
p 1250 N94-16189
Remote sensing studies of the northeastern portion of the lunar nearside p 1258 N94-16225
Mode of emplacement of lunar mare volcanic deposits: Graben formation due to near surface deformation accompanying dike emplacement at Rima Parry 5
p 1258 N94-16227
Lunar impact basins: New data for the nearside northern high latitudes and eastern limb from the second Galileo flyby p 1258 N94-16228
Modes of formation of lunar light plains and the detection of cryptomaria deposits p 1259 N94-16231
Galileo photometry of Apollo landing sites
p 1259 N94-16234
An iridium-rich iron micrometeorite with silicate inclusions from the Moon p 1242 N94-16281
Nitrogen isotopic signatures in agglutinates from breccia 79035 p 954 N94-16314
Age determinations and Earth-based multispectral observations of lunar light plains p 1275 N94-16323
Composition of Apollo 17 core 76001
p 1275 N94-16326
Composition and maturity of the 60013/14 core
p 1275 N94-16327
Lunar phase function effects on spectral ratios used for resource assessment p 1278 N94-16342

LUNAR LABORATORIES
The first lunar outpost: The design reference mission and a new era in lunar science p 874 N94-16362
Study of the National Science Foundation's South Pole Station as an analogous data base for the logistical support of a Moon laboratory
[NASA-TM-108429] p 1174 N94-17469

LUNAR LANDING
Galileo photometry of Apollo landing sites
p 1259 N94-16234
Lunar lander and return propulsion system trade study
[NASA-TP-3388] p 925 N94-16496
Comparisons of selected laser beam power missions to conventionally powered missions
[NASA-TM-106110] p 1040 N94-16522

LUNAR LANDING MODULES
Pre-phase a study report of lunar polar orbiter
[NASDA-TK-SS0440] p 873 N94-15000

LUNAR LAUNCH
Lunar lander and return propulsion system trade study
[NASA-TP-3388] p 925 N94-16496
Neighboring extremal guidance for systems with piecewise linear control using time as the reference variable
[AD-A267942] p 874 N94-17010

LUNAR LIMB
Total solar eclipse of 3 November 1994
[NASA-RP-1318] p 1236 N94-15481

LUNAR MANTLE
Mode of emplacement of lunar mare volcanic deposits: Graben formation due to near surface deformation accompanying dike emplacement at Rima Parry 5
p 1258 N94-16227
The ilmenite liquidus and depths of segregation for high-Ti picrite glasses p 975 N94-16241
Overturn of magma ocean ilmenite cumulate layer: Implications for lunar magmatic evolution and formation of a lunar core p 1261 N94-16242

LUNAR MAPS
Galileo imaging results from the second Earth-Moon flyby: Lunar Maria and related units
p 1252 N94-16199
Lunar impact basins: New data for the nearside northern high latitudes and eastern limb from the second Galileo flyby p 1258 N94-16228
Thermogeologic mapping of the Moon from lunar orbit
p 1290 N94-16405

LUNAR MARIA
Galileo imaging results from the second Earth-Moon flyby: Lunar Maria and related units
p 1252 N94-16199
Confirmation of saturation equilibrium conditions in crater populations p 1103 N94-16222
Remote sensing studies of the northeastern portion of the lunar nearside p 1258 N94-16225
Mode of emplacement of lunar mare volcanic deposits: Graben formation due to near surface deformation accompanying dike emplacement at Rima Parry 5
p 1258 N94-16227
Lunar impact basins: New data for the nearside northern high latitudes and eastern limb from the second Galileo flyby p 1258 N94-16228
Modes of formation of lunar light plains and the detection of cryptomaria deposits p 1259 N94-16231
Overturn of magma ocean ilmenite cumulate layer: Implications for lunar magmatic evolution and formation of a lunar core p 1261 N94-16242
Earth-based and Galileo SSI multispectral observations of eastern mare serenitatis and the Apollo 17 landing site p 1261 N94-16244
Petrologic models of 15388, a unique Apollo 15 mare basalt p 1264 N94-16258
Apollo 17 materials viewed from 2 to 4 mm soil particles: Pre-serenitatis highlands components
p 1267 N94-16280
The history of mare volcanism in the Orientale Basin: Mare deposit ages, compositions and morphologies
p 1269 N94-16289
Thermogeologic mapping of the Moon from lunar orbit
p 1290 N94-16405

LUNAR ORBITER
The 1966 highlights --- NASA research programs
[NASA-TM-109444] p 1302 N94-15343

LUNAR ORBITS
A guidance and navigation system for two spacecraft rendezvous in translunar halo orbit
[AD-A267498] p 898 N94-17368

LUNAR PHASES
Lunar phase function effects on spectral ratios used for resource assessment p 1278 N94-16342

LUNAR PHOTOGRAPHS
Lunar multispectral mosaics from Galileo's second Earth-Moon flyby p 1288 N94-16394

LUNAR PHOTOGRAPHY
Lunar phase function effects on spectral ratios used for resource assessment p 1278 N94-16342

LUNAR PROBES
Pre-phase a study report of lunar polar orbiter
[NASDA-TK-SS0440] p 873 N94-15000
The Clementine instrument complement
p 1086 N94-16370

LUNAR PROGRAMS
The first lunar outpost: The design reference mission and a new era in lunar science p 874 N94-16362
Opportunity for early science return by the Artemis Program p 1291 N94-16408

LUNAR RANGEFINDING
Lunar ranging
[NASA-TM-109603] p 1236 N94-15311
Eighth International Workshop on Laser Ranging Instrumentation
[NASA-CP-3214] p 911 N94-15552
Poisson filtering of laser ranging data
p 917 N94-15593
Lunar laser ranging data processing in a Unix/X windows environment p 918 N94-15599
LLR: Activities in Wettzell p 876 N94-15600
Performance of the upgraded Orroral laser ranging system p 877 N94-15602
WLRS --- Wettzell Laser Ranging System (WLRS)
p 877 N94-15606

LUNAR RESOURCES
Helium-3 inventory of lunar samples: A potential future energy resource for mankind? p 1295 N94-16428

LUNAR ROCKS
Lunar Curatorial Facility resource
[NASA-TM-109531] p 875 N94-15393
Building a lunar base
[NASA-TM-109674] p 983 N94-15519
The SCR Ne-21 and Ar-38 in lunar rock 68815: The solar proton energy spectrum over the past 2 MYR
p 1248 N94-16177
First oxygen from lunar basalt p 1249 N94-16182
A test of the applicability of independent scattering to high albedo planetary regoliths p 1250 N94-16187
Why is the Moon dark? p 1256 N94-16219
Lunar impact basins: New data for the nearside northern high latitudes and eastern limb from the second Galileo flyby p 1258 N94-16228
Galileo photometry of Apollo landing sites
p 1259 N94-16234
A Monazite-bearing clast in Apollo 17 melt breccia
p 1267 N94-16279
Apollo 17 materials viewed from 2 to 4 mm soil particles: Pre-serenitatis highlands components
p 1267 N94-16280
An iridium-rich iron micrometeorite with silicate inclusions from the Moon p 1242 N94-16281
Liquidus equilibria of lunar analogs at high pressure
p 1283 N94-16364

LUNAR ROVING VEHICLES
Space transfer concepts and analyses for exploration missions, phase 4
[NASA-CR-193849] p 882 N94-15831
Rover mounted ground penetrating radar as a tool for investigating the near-surface of Mars and beyond
p 1007 N94-16197
The first lunar outpost: The design reference mission and a new era in lunar science p 874 N94-16362

LUNAR SATELLITES
Pre-phase a study report of lunar polar orbiter
[NASDA-TK-SS0440] p 873 N94-15000

LUNAR SHADOW
Total solar eclipse of 3 November 1994
[NASA-RP-1318] p 1236 N94-15481

LUNAR SOIL
Lunar Curatorial Facility resource
[NASA-TM-109531] p 875 N94-15393
Building a lunar base
[NASA-TM-109674] p 983 N94-15519
First oxygen from lunar basalt p 1249 N94-16182
Galileo imaging results from the second Earth-Moon flyby: Lunar Maria and related units
p 1252 N94-16199
Lunar impact basins: New data for the nearside northern high latitudes and eastern limb from the second Galileo flyby p 1258 N94-16228
Galileo photometry of Apollo landing sites
p 1259 N94-16234
Apollo 17 materials viewed from 2 to 4 mm soil particles: Pre-serenitatis highlands components
p 1267 N94-16280
An iridium-rich iron micrometeorite with silicate inclusions from the Moon p 1242 N94-16281
Composition of Apollo 17 core 76001
p 1275 N94-16326
Composition and maturity of the 60013/14 core
p 1275 N94-16327
Lunar phase function effects on spectral ratios used for resource assessment p 1278 N94-16342
Mixing model analysis of telescopic lunar spectra
p 1284 N94-16371
Galileo SSI lunar observations: Copernican craters and soils p 1288 N94-16395
Grain surface features of Apollo 17 orange and black glass p 1289 N94-16397
JSC-1: A new lunar regolith simulant
p 1289 N94-16398

LUNAR SPACECRAFT
Space transfer concepts and analyses for exploration missions, phase 4
[NASA-CR-193849] p 882 N94-15831
Lunar scout missions: Galileo encounter results and application to scientific problems and exploration requirements p 1259 N94-16229
Lunar lander and return propulsion system trade study
[NASA-TP-3388] p 925 N94-16496
Neighboring extremal guidance for systems with piecewise linear control using time as the reference variable
[AD-A267942] p 874 N94-17010

LUNAR SURFACE
The SCR Ne-21 and Ar-38 in lunar rock 68815: The solar proton energy spectrum over the past 2 MYR
p 1248 N94-16177
Importance of expansion and contraction in the formation of tectonic features on the Moon
p 1250 N94-16189
Confirmation of saturation equilibrium conditions in crater populations p 1103 N94-16222
Galileo photometry of Apollo landing sites
p 1259 N94-16234
Earth-based and Galileo SSI multispectral observations of eastern mare serenitatis and the Apollo 17 landing site p 1261 N94-16244
Mixing model analysis of telescopic lunar spectra
p 1284 N94-16371
Lunar multispectral mosaics from Galileo's second Earth-Moon flyby p 1288 N94-16394
Galileo SSI lunar observations: Copernican craters and soils p 1288 N94-16395
Remote visual detection of impacts on the lunar surface p 1290 N94-16404
Thermogeologic mapping of the Moon from lunar orbit
p 1290 N94-16405
Opportunity for early science return by the Artemis Program p 1291 N94-16408
Gamma ray spectrometer for Lunar Scout 2
p 1037 N94-16426
Effects of levitated dust on astronomical observations from the lunar surface p 1239 N94-16433

LUNAR TEMPERATURE
Thermogeologic mapping of the Moon from lunar orbit
p 1290 N94-16405

LUNAR TOPOGRAPHY
Mode of emplacement of lunar mare volcanic deposits: Graben formation due to near surface deformation accompanying dike emplacement at Rima Parry 5
p 1258 N94-16227
Lunar scout missions: Galileo encounter results and application to scientific problems and exploration requirements p 1259 N94-16229

LUNGS
Asbestos Surveillance Program p 1127 N94-16638

LYMAN SPECTRA
The theory of QSO absorption line systems and their relationship to the galaxies
[NASA-CR-194596] p 1236 N94-15679

LYSOZYME
Convective flow effects on protein crystal growth
[NASA-CR-194560] p 1206 N94-15476

M

MACH NUMBER
Flight-determined engine exhaust characteristics of an F404 engine in an F-18 airplane
[NASA-TM-4538] p 869 N94-15141
Tollmien-Schlichting/vortex interactions in compressible boundary layer flows
[NASA-CR-191515] p 1017 N94-15183
Numerical investigations in three-dimensional internal flows
[NASA-CR-194594] p 1020 N94-15551
Wind tunnel investigation of three axisymmetric cowls of different lengths at Mach numbers from 0.60 to 0.92
[NASA-TM-4488] p 856 N94-15681
Wind tunnel investigation with an operational turbojet engine
[TABES PAPER 93-662] p 870 N94-16157
Aerothermoelastic analysis of a NASP demonstrator model
[NASA-TM-109007] p 867 N94-17055
Higher-order accurate Osher schemes with application to compressible boundary layer stability
[NASA-TM-106355] p 1026 N94-17056
Boundary conditions and the simulation of low Mach number flows
[NASA-TM-106374] p 1029 N94-17448
MACHINE LEARNING
Hidden Markov model approach to skill learning and its application to telerobotics
[AD-A266989] p 1164 N94-15502
Representation in incremental learning
[NASA-CR-194595] p 1221 N94-15719
Temporal segmentation of tasks from human hand motion
[AD-A266596] p 1166 N94-16725
Information technology division technical paper abstracts
[AD-A266227] p 1166 N94-16938
Integrating reactive and deliberative planning for agents
[AD-A267631] p 1166 N94-17201
MACHINE TRANSLATION
Using multiple adaptively-weighted strategies for the resolution of demonstratives
[AD-A266463] p 1150 N94-16585
Automatic generation of production rules for integrity maintenance
[REPT-92-054] p 1156 N94-17501
Automatic translation of database integrity constraints into compensating production rules
[REPT-92-055] p 1234 N94-17502
MACHINING
Detection of subsurface defects in machined silicon nitride ceramics by optical scattering methods
[DE93-015554] p 968 N94-16658
Predesign of diamond turned refractive/diffractive elements for IR objectives p 1198 N94-17359
MAGELLAN PROJECT (NASA)
Magellan: Principal Venus science findings
p 989 N94-15887
Guide to Magellan image interpretation
[NASA-CR-194340] p 1298 N94-17654
MAGELLAN SPACECRAFT (NASA)
STS-30 Magellan deploy Sim in SMS and MOCR
[NASA-TM-109571] p 875 N94-15301
STS-26 through STS-34, deploy activities
[NASA-TM-109566] p 1301 N94-15315
STS-30 onboard 16mm photography quick release
[NASA-TM-109579] p 861 N94-15423
The depths of the largest impact craters on Venus
p 1264 N94-16261
Tessera terrain on Venus: Global characterization from Magellan data p 1264 N94-16262
MAGMA
Assimilation of solids during ascent of magmas from the Bartoy Field of the Baikal Region, Siberia
p 1103 N94-16214
Bubble coalescence in magmas p 1103 N94-16237
Overturn of magma ocean ilmenite cumulate layer: Implications for lunar magmatic evolution and formation of a lunar core p 1261 N94-16242
Experimental constraints on CO2 and H2O in the Martian mantle and primary magmas p 1262 N94-16248
Petrologic models of 15388, a unique Apollo 15 mare basalt p 1264 N94-16258
Constraints on the differentiation of the Earth from the coupled Sm-146,147-Nd-142,143 systematics
p 1103 N94-16271
Explosive volcanism and the compositions of the cores of differentiated asteroids p 1243 N94-16306
Venusian pancake domes: Insights from terrestrial voluminous silicic lavas and thermal modeling
p 1286 N94-16381
MAGNESIUM
Mechanical properties of magnesium ammonium phosphate cements and their zeolite composites
[DE93-015155] p 934 N94-16057
The Fe2(+)-Mg interdiffusion in orthopyroxene: Constraints from cation ordering and structural data and implications for cooling rates of meteorites
p 1241 N94-16175
MAGNESIUM ALLOYS
Aircraft carrier exposure tests of cast magnesium alloys
[AD-A268260] p 962 N94-17418
MAGNESIUM ISOTOPES
Grosnaja ABCs: Magnesium isotope compositions
p 1241 N94-16191
Petrography, mineralogy, and Mg isotope composition of VICTA: A vigarano CaAl4O7-bearing type A inclusion
p 1103 N94-16203
MAGNESIUM SULFATES
Phase equilibria of the magnesium sulfate-water system to 4 kbars p 953 N94-16247
Crustal structure and igneous processes in a chondritic Io p 1243 N94-16292
MAGNET COILS
Electrodynamic forces of the cross-connected figure-eight null-flux coil suspension system
[DE93-015139] p 1048 N94-16969
MAGNETIC COOLING
Proceedings of the 7th International Cryocooler Conference, part 1
[AD-A268448] p 985 N94-17482
Proceedings of the 7th International Cryocooler Conference, part 2
[AD-A268449] p 985 N94-17484
Proceedings of the 7th International Cryocooler Conference, part 3
[AD-A268450] p 985 N94-17485
MAGNETIC EFFECTS
A study of relaxation transitions in the polymers under the influence of magnetic fields
[AD-A263878] p 963 N94-15133
Magnetic effects in anomalous dispersion
[DE93-014291] p 1175 N94-15978
Magnetic effects in Venus/solar wind interaction
[NASA-CR-194666] p 1299 N94-17281
MAGNETIC ENERGY STORAGE
Engineering design of a high-temperature superconductor current lead
[DE93-015156] p 1013 N94-17226
MAGNETIC FIELD CONFIGURATIONS
Method and apparatus for forming an agile plasma mirror effective as a microwave reflector
[AD-D015788] p 998 N94-16535
The inverse problem to the evaluation of magnetic fields
[DE93-015239] p 1175 N94-17288
MAGNETIC FIELDS
An adiabatic demagnetisation refrigerator with a mechanical pre-cooler for space applications
p 906 N94-15070
Benard convection of magnetic colloids under microgravity p 943 N94-15159
Formation of the stable auroral arc that intensifies at substorm onset
[NASA-CR-193637] p 1098 N94-15433
Superconductive material and magnetic field for damping and levitation support and damping of cryogenic instruments
[NASA-CASE-NPO-18458-1-CU] p 1033 N94-15875
The fractional quantum Hall effect and the rotation group
[DE93-010348] p 1207 N94-15972
Method and apparatus for forming an agile plasma mirror effective as a microwave reflector
[AD-D015788] p 998 N94-16535
TransRapid TR-07 maglev-spectrum magnetic field effects on daily pineal indoleamine metabolic rhythms in rodents
[DE93-015143] p 1117 N94-16893
The inverse problem to the evaluation of magnetic fields
[DE93-015239] p 1175 N94-17288
High power steady state MPD thrusters
[AD-A267277] p 928 N94-17308
Comparison of computer predictions and magnetic field measurements for an iron spectrometer magnet
[DE93-016164] p 1176 N94-17658
MAGNETIC FILMS
Epitaxial iron films
[AD-A268286] p 1217 N94-17579
MAGNETIC FLUX
Global auroral imaging: Dynamics of Explorer Miss ion
[NASA-CR-194284] p 1097 N94-15003
Effects of spin-orbit coupling on disordered mesoscopic systems
[ITN-93-85220] p 1180 N94-15288
Solar vector magnetic field research
[AD-A267367] p 1299 N94-17004
MAGNETIC LEVITATION VEHICLES
Controls of maglev suspension systems
[DE93-015540] p 1011 N94-16443
Dynamics, stability, and control of maglev systems
[DE93-015163] p 1047 N94-16806
TransRapid TR-07 maglev-spectrum magnetic field effects on daily pineal indoleamine metabolic rhythms in rodents
[DE93-015143] p 1117 N94-16893
Electrodynamic forces of the cross-connected figure-eight null-flux coil suspension system
[DE93-015139] p 1048 N94-16969
MAGNETIC MATERIALS
Thermal inertia and radar reflectivity of the Martian north polar ERG: Low-density aggregates
p 1260 N94-16238
MAGNETIC MEASUREMENT
Comparison of computer predictions and magnetic field measurements for an iron spectrometer magnet
[DE93-016164] p 1176 N94-17658
MAGNETIC PERMEABILITY
Comparative magnetic and thermoanalytical study of two enstatite chondrites: Adhi Kot and Atlanta
p 1244 N94-16329
Structural phase transition and superconductivity in La(2-x)Ba(x)CuO4
[DE93-015812] p 1212 N94-16868
Synthesis and characterization of new low-dimensional metal complex conductors
[AD-A268251] p 952 N94-17416
MAGNETIC PROBES
Suggestion for extended Viking magnetic properties experiment on future Mars missions
p 1285 N94-16375
MAGNETIC PROPERTIES
Magneto-optic superlattice thin films: Fabrication, structural and magnetic characterization
p 974 N94-14982
Fullerene superconductors
[AD-A266749] p 1010 N94-15954
Magnetic effects in anomalous dispersion
[DE93-014291] p 1175 N94-15978
Comparative magnetic and thermoanalytical study of two enstatite chondrites: Adhi Kot and Atlanta
p 1244 N94-16329
Suggestion for extended Viking magnetic properties experiment on future Mars missions
p 1285 N94-16375
Atomic-scale friction measurements using friction force microscopy. Part 1: General principles and new measurement techniques
[AD-A268391] p 1048 N94-17533
Epitaxial iron films
[AD-A268286] p 1217 N94-17579
MAGNETIC PUMPING
Studies on the parametric decay of waves in fusion plasmas
[VTT-PUBS-110] p 1200 N94-15204
High frequency Raman current drive
p 1201 N94-15208
On the decay of a dipole pump wave to half-harmonics p 1201 N94-15211
MAGNETIC RECORDING
Magnetic and magneto-optical properties and domain structure of Co/Pd multilayers p 1227 N94-14991
MAGNETIC SIGNATURES
Solar vector magnetic field research
[AD-A267367] p 1299 N94-17004
MAGNETIC STORAGE
Characterization facility for magneto-optic media and systems p 1226 N94-14983
Magnetic and magneto-optical properties and domain structure of Co/Pd multilayers p 1227 N94-14991
Atomic-scale friction measurements using friction force microscopy. Part 1: General principles and new measurement techniques
[AD-A268391] p 1048 N94-17533
MAGNETIC STORMS
Formation of the stable auroral arc that intensifies at substorm onset
[NASA-CR-193637] p 1098 N94-15433
The Solar Flare Myth in solar-terrestrial physics
[DE93-016487] p 1299 N94-16895
A correlative comparison of geomagnetic storms and auroral substorms using geomagnetic indeces
[AD-A268081] p 1102 N94-17512
MAGNETIC SUSPENSION
Controls of maglev suspension systems
[DE93-015540] p 1011 N94-16443
Dynamics, stability, and control of maglev systems
[DE93-015163] p 1047 N94-16806

Electrodynamic forces of the cross-connected figure-eight null-flux coil suspension system
[DE93-015139] p 1048 N94-16969

MAGNETICALLY TRAPPED PARTICLES
Investigations of YBaCuO materials with near-room-temperature resistivity transitions
[AD-A268016] p 1216 N94-17477

MAGNETIZATION
Magnetic and magneto-optical properties and domain structure of Co/Pd multilayers p 1227 N94-14991
Comparative magnetic and thermoanalytical study of two enstatite chondrites: Adhi Kot and Atlanta p 1244 N94-16329
Neutron and x ray scattering studies of (FeF2)(sub m)(CoF2)(sub n) multilayers
[DE93-015809] p 1184 N94-16838

MAGNETO-OPTICS
Research Studies on Advanced Optical Module/Head Designs for Optical Disk Recording Devices
[NASA-CR-194390] p 1226 N94-14981
Magneto-optic superlattice thin films: Fabrication, structural and magnetic characterization p 974 N94-14982
Characterization facility for magneto-optic media and systems p 1226 N94-14983
Application of holographic optical elements to magneto-optic read/write heads p 1226 N94-14985
Measurement of birefringence for optical recording disk substrates p 1227 N94-14989
Magnetic and magneto-optical properties and domain structure of Co/Pd multilayers p 1227 N94-14991
A near-field scanning optical microscope for analysis of magneto-optic media p 1199 N94-14995
Determining the locations of the various CIRC recording format information blocks (user data blocks, C2 and C1 words and EFM frames) on a recorded compact disc p 1228 N94-14997

MAGNETOACOUSTIC WAVES
Simulation of enhanced tokamak performance on D3-D using fast wave current drive
[DE93-014009] p 1203 N94-16823

MAGNETOHYDRODYNAMIC FLOW
High power steady state MPD thrusters
[AD-A267277] p 928 N94-17308
Plasma flow switch and foil implosion experiments on Pegasus 2
[DE93-016464] p 1013 N94-17318

MAGNETOHYDRODYNAMIC GENERATORS
Application of a NEPTUNE propulsion concept to a manned Mars excursion
[AD-A268053] p 929 N94-17587

MAGNETOHYDRODYNAMIC STABILITY
Studies on the parametric decay of waves in fusion plasmas
[VTT-PUBS-110] p 1200 N94-15204
High beta and confinement studies of TFTR
[DE93-016204] p 1202 N94-16446
Direct drive foil implosion experiments on Pegasus 2
[DE93-012666] p 1202 N94-16776
Fundamental-mode RF design in e(+)e(-) storage ring factories
[DE93-015249] p 1183 N94-16809
Structure and damping of toroidal drift waves (and their implications for anomalous transport)
[DE93-014005] p 1203 N94-16822
Nonlinear gyrofluid models of shear Alfven instabilities in ignited and beam heated toroidal plasmas
[DE93-016235] p 1203 N94-16869
High power steady state MPD thrusters
[AD-A267277] p 928 N94-17308
Plasma instabilities and transport in the MPD thruster
[AD-A268268] p 1204 N94-17575

MAGNETOHYDRODYNAMIC TURBULENCE
Broken symmetry in ideal magnetohydrodynamic turbulence
[NASA-TM-109017] p 1023 N94-15964

MAGNETOHYDRODYNAMIC WAVES
Linear and non-linear studies of Alfven waves in space. Stationary and dynamic processes in magnetospheric plasmas
[NASA-CR-193585] p 1239 N94-16647
Nonlinear gyrofluid models of shear Alfven instabilities in ignited and beam heated toroidal plasmas
[DE93-016235] p 1203 N94-16869

MAGNETOHYDRODYNAMICS
Magnetic effects in Venus/solar wind interaction
[NASA-CR-194666] p 1299 N94-17281

MAGNETOPLASMADYNAMICS
High power steady state MPD thrusters
[AD-A267277] p 928 N94-17308

MAGNETOSPHERIC INSTABILITY
Linear and non-linear studies of Alfven waves in space. Stationary and dynamic processes in magnetospheric plasmas
[NASA-CR-193585] p 1239 N94-16647

MAGNETOSTATIC FIELDS
A study of relaxation transitions in the polymers under the influence of magnetic fields
[AD-A263878] p 963 N94-15133

MAGNETRON SPUTTERING
Application of cylindrical distribution functions to anisotropic scattering from amorphous films
[DE93-015256] p 1183 N94-16811
Application of hard coatings to substrates at low temperatures
[NASA-CR-193867] p 971 N94-17122
Anisotropic phase separation in amorphous Fe-Ge alloys
[DE93-015255] p 961 N94-17251

MAGNETRONS
Anisotropic phase separation in amorphous Fe-Ge alloys
[DE93-015255] p 961 N94-17251

MAGNETS
Automated directional solidification furnace
[NASA-TM-109662] p 1175 N94-15233
Comparison of computer predictions and magnetic field measurements for an iron spectrometer magnet
[DE93-016164] p 1176 N94-17658

MAGNIFICATION
Optical displays: A tutorial on images and image formation
[AD-A266230] p 1192 N94-16926
Diffractive optical elements for generating arbitrary line foci p 1195 N94-17338

MAGNONS
Theoretical high energy physics
[DE93-015884] p 1187 N94-16170
Lattice relaxation theory of localized excitations in quasi-one-dimensional systems
[DE93-624947] p 1215 N94-17437

MAINTAINABILITY
RAMCAD design methodology
[AD-A267010] p 1145 N94-15525
Conflict Resolution (CORE) for software quality factors
[AD-A267248] p 1151 N94-16941
Reliability and maintainability of modular robot systems: A roadmap for design
[AD-A268104] p 1168 N94-17517

MAINTENANCE
Helicopter structures: A review of loads, fatigue design techniques, and usage monitoring
[AD-A267115] p 866 N94-15651
Facilities maintenance handbook
[NHB-8831.2] p 1224 N94-15934
Effects of inspection error on optimal inspection policies and software fault detection models
[AD-A267511] p 1153 N94-17075
Application of thermal spray and ceramic coatings and reinforced epoxy for cavitation damage repair of hydroelectric turbines and pumps
[AD-A267624] p 971 N94-17198

MAINTENANCE TRAINING
STS-31 crew training inflight maintenance and bailout exercises in CCT and WFTF
[NASA-TM-109483] p 876 N94-15450

MALES
Screening for prostate cancer p 1126 N94-16630

MAMMALS
An apparatus for measuring the biological oxidation of hydrogen gas under hyperbaric conditions
[AD-A266834] p 1119 N94-14916
Ontogenesis of mammals in microgravity
[NASA-TM-103978] p 1139 N94-17636

MAMMARY GLANDS
Bioeffects of radiofrequency radiation on cell growth and differentation. Volume 1: Engineering considerations
[AD-A267754] p 1118 N94-17232

MAN ENVIRONMENT INTERACTIONS
Recent advances in radar remote sensing of forest p 991 N94-15897
Statement on global climate change before the Subcommittee on Energy and Power, United States House of Representatives
[DE93-013163] p 1095 N94-16006
Global change research: Science and policy
[DE93-015675] p 1096 N94-16445

MAN MACHINE SYSTEMS
Manned vehicle systems research facility
[NASA-TM-109650] p 875 N94-15318
Aerospace medicine and biology: A continuing bibliography with indexes (supplement 378)
[NASA-SP-7011(378)] p 1122 N94-16478
Aerospace medicine and biology: A continuing bibliography with indexes (supplement 380)
[NASA-SP-7011(380)] p 1122 N94-16479
OREMUS: Prototype of an orbit determination center dedicated to mini-satellite control p 878 N94-17156
Acquisition and production of skilled behavior in dynamic decision-making tasks
[NASA-CR-194658] p 1133 N94-17296

MAN-COMPUTER INTERFACE
Serpentine manipulator planning and control for NASA Space-Shuttle payload servicing
[AD-A266961] p 879 N94-14969
A CENTAUR tutorial
[INRIA-RT-140] p 1142 N94-14978
Questioning mechanisms during tutoring, conversation, and human-computer interaction
[AD-A266199] p 1137 N94-16108
Information technology division technical paper abstracts
[AD-A266227] p 1166 N94-16938
A proposed research program in strategic computing
[AD-A267516] p 1153 N94-17078
Design and implementation of an interface editor for the Amadeus multi-relational database front-end system
[AD-A267403] p 1233 N94-17114
Defense Logistics Information System (DLIS). Procedures manual: Logistics On-Line Access (LOLA) procedures manual
[AD-A267685] p 1233 N94-17229
Computer-human interface issues: Theory and application
[AD-A268013] p 1138 N94-17475
Visual display principles for C3I system tasks
[AD-A267969] p 1005 N94-17498

MANAGEMENT INFORMATION SYSTEMS
Department of Defense technical architecture framework for information management. Volume 2: Technical reference model and standards profile, version 2.0
[AD-A267194] p 1229 N94-15788
Department of Defense technical architecture framework for information management. Volume 3: Architecture concepts and design guidance, version 2.0
[AD-A267195] p 1230 N94-15789
Performance Information Management System (PIMS) communication
[AD-A267040] p 1231 N94-16458
Managing information as a corporate asset: Key strategies for information professionals to remain competitive
[DE93-015515] p 1232 N94-16875
Defense Logistics Information System (DLIS) procedures manual. Products and services end-user manual
[AD-A267766] p 1232 N94-17007
A proposed research program in strategic computing
[AD-A267516] p 1153 N94-17078
Defense Logistics Information System (DLIS). Procedures manual: Logistics On-Line Access (LOLA) procedures manual
[AD-A267685] p 1233 N94-17229

MANAGEMENT METHODS
NASA directives master list and index
[NHB-1410.13L] p 1229 N94-15414
Facilities maintenance handbook
[NHB-8831.2] p 1224 N94-15934
NASA information resources management handbook
[NHB-2410.1E] p 1230 N94-15941
Creating and maintaining a visionary quality program
[DE93-015122] p 1050 N94-16055
Environmental management lessons to be learned from the upcoming CFC phase out or how to insure that we survive the next environmentally mandated process change
[TABES PAPER 93-570] p 1050 N94-16136
Development of a proposed international standard for certification of aircraft to High Intensity Radiated Fields (HIRF)
[NASA-TM-106357] p 863 N94-16520
Software Engineering Guidebook
[NASA-CR-177625] p 1150 N94-16656
Applicability of computer spreadsheet simulation for solving resource allocation problems
[AD-A267436] p 1152 N94-17027
Module interconnection frameworks for a real-time spreadsheet
[AD-A267317] p 1153 N94-17220
Software Capability Evaluation (SCE) version 1.5 method description. Software capability evaluation project
[AD-A267895] p 1154 N94-17395

MANAGEMENT PLANNING
Testing and management of flight instruments and their data
[NASA-CR-194332] p 868 N94-15187
Facilities maintenance handbook
[NHB-8831.2] p 1224 N94-15934
NASA information resources management handbook
[NHB-2410.1E] p 1230 N94-15941
Design Quality Task Force survey comments
[AD-A266283] p 1225 N94-16473
Emergency preparedness and planning p 1124 N94-16613

MANAGEMENT SYSTEMS
Fault management for data systems
[NASA-TM-103953] p 1116 N94-15548
Equipment management user's handbook for property custodians
[NHB-4200.2A] p 1224 N94-15957
Equipment Management Manual
[NHB-4200.1D] p 1225 N94-16799
A comparison of queueing, cluster and distributed computing systems
[NASA-TM-109025] p 1160 N94-16878
Visual display principles for C3I system tasks
[AD-A267969] p 1005 N94-17498
MANEUVERABLE SPACECRAFT
The fragmentation of Kosmos 2163
[NASA-CR-191643] p 887 N94-16503
MANGANESE
Synthesis, reactivity, and characterization of (-hexacarbocyclic) manganese dicarbonyl complexes with sulfur and phosphorus ligands
[AD-A267592] p 930 N94-17192
MANGANESE COMPOUNDS
Synthesis, reactivity, and characterization of (-hexacarbocyclic) manganese dicarbonyl complexes with sulfur and phosphorus ligands
[AD-A267592] p 930 N94-17192
MANGANESE ISOTOPES
On possible Mn-53 heterogeneity in the early solar system p 1244 N94-16344
MANIPULATORS
Tactile sensing and control in humans and robotic/teleoperated systems
[AD-A267710] p 1163 N94-14937
Fuzzy control and fuzzy kinematic mapping for a redundant space robot
[AD-A266866] p 1163 N94-14950
Fuzzy inverse kinematic mapping: Rule generation, efficiency, and implementation
[AD-A266967] p 1163 N94-14954
Serpentine manipulator planning and control for NASA Space-Shuttle payload servicing
[AD-A266961] p 879 N94-14969
Real-time implementation of neural network learning control of a flexible space manipulator
[AD-A266962] p 1045 N94-14970
Welding nozzle position manipulator
[NASA-CASE-MFS-29837-1] p 1047 N94-15882
Contextually dependent control strategies for manipulation
[TR-416] p 1165 N94-16580
A modular control architecture for real-time synchronous and asynchronous systems
[DE93-015439] p 1166 N94-16888
Development of a prototype kinestatic platform for application to space and ground servicing tasks. Phase 1: Concept Modeling
[NASA-CR-194036] p 887 N94-16905
Three axis force override rate control of a PUMA 560 manipulator
[AD-A267313] p 1048 N94-16944
MANNED MARS MISSIONS
Application of a NEPTUNE propulsion concept to a manned Mars excursion
[AD-A268053] p 929 N94-17587
MANNED SPACE FLIGHT
Cohen program management briefing
[NASA-TM-109536] p 1223 N94-15367
President Kennedy's speech at Rice University
[NASA-TM-109532] p 1302 N94-15394
History of the manned space flight program
[NASA-TM-109529] p 1303 N94-16069
Human Transportation System (HTS) study, volume 2
[NASA-TM-104779-VOL-2] p 882 N94-17320
MANNED SPACECRAFT
Human Transportation System (HTS) study, volume 2
[NASA-TM-104779-VOL-2] p 882 N94-17320
MANUAL CONTROL
Unistick vehicle controller
[NASA-TM-109618] p 1046 N94-15347
Visually guided touching and manual tracking
[TR-412] p 1166 N94-16581
MANUALS
User's guide: Hot-mix recycling of asphalt concrete pavements
[AD-A266939] p 983 N94-15177
Defense Logistics Information System (DLIS) procedures manual. Products and services end-user manual
[AD-A267766] p 1232 N94-17007
MANUFACTURING
Geometric tolerance assessment
[NPL-DITC-210/92] p 1049 N94-15013
Production Technology for Components from Nonmetallic Fiber Reinforced Materials
[ETN-93-94607] p 931 N94-15254
Galileo probe spacecraft mission to Jupiter
[NASA-TM-109646] p 1247 N94-16070
Lithium D-cell study
[NASA-CR-192705] p 1011 N94-16505
Status of molten carbonate fuel cell technology development
[DE93-015666] p 1092 N94-16715
Manufacturing tolerance requirements for frequency selective surfaces
[AD-A266541] p 999 N94-16797
Materials processing and manufacturing technologies for diamond substrate multichip modules (DSMCM)
[AD-A267316] p 969 N94-16946
Integration ToolKit and Methods (ITKM) manufacturing methods and prototype toolkit. A combined modeling method using IDEFO, IDEF1x and XSpec
[AD-A266176] p 984 N94-16981
Manufacturing the key to binary optics p 1194 N94-17332
Laser figuring for the generation of analog micro-optics and kineform surfaces p 1196 N94-17346
Applications of advanced diffractive optical elements p 1197 N94-17356
MANY BODY PROBLEM
Many-body quantum mechanical studies of molecular clusters
[AD-A266624] p 1180 N94-15727
Dust grain resonant capture: A statistical study p 1245 N94-16384
Numerical studies of the photoluminescence spectrum of quantum Hall systems
[DE93-015822] p 1220 N94-16810
MAPPING
Perception for outdoor navigation
[AD-A266867] p 863 N94-14919
Improved mapping system
[NASA-TM-109643] p 1082 N94-15428
Develop advanced nonlinear signal analysis topographical mapping system
[NASA-CR-194577] p 1082 N94-15646
The role of carbon and temperature in determining electrical conductivity of basins, crust and mantle
[DE93-015936] p 1101 N94-16840
MAPS
Pargo Chasma and its relationship to global tectonics p 1249 N94-16181
MARIA
Assimilation of solids during ascent of magmas from the Bartoy Field of the Baikal Region, Siberia p 1103 N94-16214
The ilmenite liquidus and depths of segregation for high-Ti picrite glasses p 975 N94-16241
MARINE BIOLOGY
Abstracts of manuscripts submitted in 1992 for publication
[AD-A267963] p 1113 N94-17383
MARINE ENVIRONMENTS
STS-29 crew bailout in WETF
[NASA-TM-109548] p 1136 N94-15385
Chondritic ratios of Fe/Cr/Ir in Kerguelen Plateau (Hole 738C) K/T carbonate-rich sediments support asteroid-cometary impact at K/T time p 1244 N94-16357
AVIRIS calibration and application in coastal oceanic environments p 1069 N94-16685
Atmospheric correction of AVIRIS data in ocean waters p 1070 N94-16690
MARINE METEOROLOGY
An investigation of the Ground-Based High-Resolution Interferometer Sounder (GB-HIS) in a costal marine environment
[AD-A268052] p 1114 N94-17503
MARINE RESOURCES
The 1970 highlights --- NASA programs and research
[NASA-TM-109628] p 1302 N94-15415
MARINE TECHNOLOGY
Abstracts of manuscripts submitted in 1992 for publication
[AD-A267963] p 1113 N94-17383
MARINER SPACECRAFT
The 1971 highlights --- NASA programs and research
[NASA-TM-109629] p 1302 N94-15417
MARINER-MERCURY 1973
The 1973 highlights --- Pioneer and Mariner space probes and other advancements
[NASA-TM-109624] p 1302 N94-15410
MARITIME SATELLITES
Propagation research in Japan p 996 N94-16043
MARKARIAN GALAXIES
Astrophysics with MILAGRO
[DE93-012722] p 1240 N94-17657
MARKET RESEARCH
The closing window of opportunity: Addressing the US space launch vehicle crisis
[TABES PAPER 93-640] p 878 N94-16148
Status of molten carbonate fuel cell technology development
[DE93-015666] p 1092 N94-16715
Satellite communications systems and technology. Executive summary
[NASA-TM-109346] p 1006 N94-17661
MARKOV CHAINS
Nonparametric statistics: Weighted rankings analysis
[AD-A266607] p 1173 N94-16657
An approximation for computing reduction in bandwidth requirements using intelligent multiplexers
[AD-A267434] p 1001 N94-17026
MARKOV PROCESSES
Hidden Markov model approach to skill learning and its application to telerobotics
[AD-A266989] p 1164 N94-15502
A multilevel-multiresolution method for image processing. A Bayesian framework for reconstructing and representing shapes
[AD-A266772] p 1082 N94-15842
Nonparametric statistics: Weighted rankings analysis
[AD-A266607] p 1173 N94-16657
Using Markov chains to model the error behavior of data communications channels
[AD-A266468] p 999 N94-16777
MARS (PLANET)
Mars laser altimeter based on a single photon ranging technique p 921 N94-15619
Space transfer concepts and analyses for exploration missions, phase 4
[NASA-CR-193849] p 882 N94-15831
A mineralized zone in Western Candor Chasma, Mars p 1248 N94-16179
Explosive mafic volcanism on Earth and Mars p 1253 N94 16204
A Moessbauer spectrometer for the mineralogical analysis of the Mars surface: First temperature dependent tests of the detector and drive system p 1259 N94-16233
Thermal inertia and radar reflectivity of the Martian north polar ERG: Low-density aggregates p 1260 N94-16238
Experimental constraints on CO2 and H2O in the Martian mantle and primary magmas p 1262 N94-16248
Geomorphic processes in the Argyre-Dorsa Argentea region of Mars p 1270 N94-16293
Was Martian mantle wet? A possible consequence of rapid core formation p 1277 N94-16335
MARS ATMOSPHERE
Mars laser altimeter based on a single photon ranging technique p 921 N94-15619
Nitrates in SNCs: Implications for the nitrogen cycle on Mars p 1251 N94-16193
Sand transport on Mars: Preliminary results from models p 1252 N94-16198
Martian carbon dioxide: Clues from isotopes in SNC meteorites p 1270 N94-16295
Altitude profile of aerosols on Mars from measurements of its thermal radiation on limb p 1294 N94-16423
Dust-dynamic feedbacks in the Martian atmosphere: Surface dust lifting p 1296 N94-16434
MARS CRATERS
Martian crater degradation by eolian processes: Analogy with the Rio Cuarto Crater Field, Argentina p 1251 N94-16196
The seismic response of an aquifer to the propagation of an impact generated shock wave: A possible trigger of the Martian outflow channels? p 1281 N94-16354
MARS ENVIRONMENT
Mars look-alike
[NASA-TM-109667] p 1094 N94-15238
Sand transport on Mars: Preliminary results from models p 1252 N94-16198
International testing of a Mars rover prototype p 1273 N94-16312
Workshop on early Mars: How warm and how wet, part 2?
[NASA-CR-193503] p 1297 N94-17637
MARS LANDING
First US Mars landing
[NASA-TM-109669] p 885 N94-15436
Mars exobiology landing sites for future exploration p 1278 N94-16339
MARS OBSERVER
Development of the Mars Observer Laser Altimeter (MOLA) p 921 N94-15617
Bench checkout equipment for spaceborne laser altimeter systems p 921 N94-15618
MARS PROBES
Mars Analog Site Study (MASS) p 1252 N94-16200
MARS SAMPLE RETURN MISSIONS
Mars rover sample return mission
[NASA-TM-109521] p 873 N94-15471
MARS SURFACE
A mineralized zone in Western Candor Chasma, Mars p 1248 N94-16179

Nitrates in SNCs: Implications for the nitrogen cycle on Mars p 1251 N94-16193
Martian crater degradation by eolian processes: Analogy with the Rio Cuarto Crater Field, Argentina p 1251 N94-16196
Rover mounted ground penetrating radar as a tool for investigating the near-surface of Mars and beyong p 1007 N94-16197
Sand transport on Mars: Preliminary results from models p 1252 N94-16198
Explosive mafic volcanism on Earth and Mars p 1253 N94-16204
Fluvial erosion on Mars: Implications for paleoclimatic change p 1241 N94-16210
Modeling the reflectance of CO2 frost with new optical constants: Application to Martian south polar cap spectra p 1256 N94-16217
Confirmation of saturation equilibrium conditions in crater populations p 1103 N94-16222
A Moessbauer spectrometer for the mineralogical analysis of the Mars surface: First temperature dependent tests of the detector and drive system p 1259 N94-16233
Thermal inertia and radar reflectivity of the Martian north polar ERG: Low-density aggregates p 1260 N94-16238
Geomorphic processes in the Argyre-Dorsa Argentea region of Mars p 1270 N94-16293
Martian carbon dioxide: Clues from isotopes in SNC meteorites p 1270 N94-16295
Was Martian mantle wet? A possible consequence of rapid core formation p 1277 N94-16335
Hellas basin, Mars: Formation by oblique impact p 1280 N94-16350
The seismic response of an aquifer to the propagation of an impact generated shock wave: A possible trigger of the Martian outflow channels? p 1281 N94-16354
Sedimentation, volcanism, and ancestral lakes in the Valles Marineris: Clues from topography p 1283 N94-16369
Suggestion for extended Viking magnetic properties experiment on future Mars missions p 1285 N94-16375
The dregs of crystallization in Zagami p 1245 N94-16390
Global and regional/seasonal color mosaics of Mars p 1288 N94-16393
The effects of orbital and climatic variations on Martian surface heat flow p 1290 N94-16402
Equatorial ground ice on Mars: Steady-state stability p 1290 N94-16403
Deucalionis Regio, Mars: Evidence for a unique mineralogic endmember and a crusted surface p 1291 N94-16406
Analysis of pyroxene absorptions observed in Martian dark regions p 1292 N94-16411
Mars brine formation experiment p 1293 N94-16419
Terrestrial impact melts as analogues for the hematization of Martian surface materials p 1104 N94-16424
The influence of oceans on Martian volcanism p 1295 N94-16427
Bright soil units on Mars determined from ISM imaging spectrometer data p 1295 N94-16430
Variations in the Fe mineralogy of bright Martian soil p 1295 N94-16431
Dust-dynamic feedbacks in the Martian atmosphere: Surface dust lifting p 1296 N94-16434
Composition of weakly altered Martian crust p 1296 N94-16436

MARS VOLCANOES
Explosive mafic volcanism on Earth and Mars p 1253 N94-16204
Fractal geometry of some Martian lava flow margins: Alba Patera p 1270 N94-16298
Martian lavas: Three complementary remote sensing techniques to derive flow properties p 1283 N94-16366
The influence of oceans on Martian volcanism p 1295 N94-16427

MARS 4 SPACECRAFT
The 1982 highlights
[NASA-TM-109671] p 1303 N94-15508

MARTENSITIC TRANSFORMATION
Transient phenomena following precipitation and re-solution anneals in a NiTi alloy
[AD-A267557] p 961 N94-17106

MASERS
Fundamental theory of light for applications: Notes for five informal lectures
[DE93-016463] p 1192 N94-16953

MASS DISTRIBUTION
Incorporation of boundary layer heating predictive methodology into NSWCDD aeroprediction code
[AD-A267000] p 1020 N94-15632

MASS FLOW
Flow instability tests for a particle bed reactor nuclear thermal rocket fuel element
[AD-A268012] p 929 N94-17474

MASS FLOW RATE
High power steady state MPD thrusters
[AD-A267277] p 928 N94-17308
Flow instability tests for a particle bed reactor nuclear thermal rocket fuel element
[AD-A268012] p 929 N94-17474

MASS RATIOS
Dissociation rates of diatomic molecules
[AD-A266464] p 1182 N94-16586

MASS SPECTRA
Negative ion formation in small carbon clusters
[DE93-015436] p 1182 N94-16064

MASS SPECTROMETERS
Precise flux control for lattice matched superlattice materials
[AD-A268254] p 1215 N94-17417

MASS SPECTROSCOPY
Osmium isotopes in Ivory Coast tektites: Confirmation of a meteoritic component and rhenium depletion p 1244 N94-16321
Space Shuttle solid rocket motor exposure monitoring p 976 N94-16624
Elemental impurity analysis of mercuric iodide by ICP/MS
[DE93-015531] p 949 N94-16876
Laser photoionization time-of-flight mass spectrometry of nitrated polycyclic aromatic hydrocarbons and nitrated heterocyclic compounds
[AD-A268126] p 952 N94-17520
Growth of dielectric thin films by irradiation of condensed molecular precursors with synchrotron radiation
[DE93-016161] p 974 N94-17676

MASS TRANSFER
Density and temperature relaxation near the critical point of carbon dioxide under reduced gravity p 944 N94-15164
Investigation of the influence of applied potential on erosion-corrosion of copper in alkaline chloride solutions
[AD-A266448] p 958 N94-16562

MASSIFS
Composition of Apollo 17 core 76001 p 1275 N94-16326

MASSIVE STARS
The astrophysical interpretation of isotope anomalies in graphite and SiC grains of chondrites p 1244 N94-16343

MASSIVELY PARALLEL PROCESSORS
Particle simulations on massively parallel machines
[DE93-015644] p 1157 N94-14927
Overview of Enhanced Data Stream Array Processor (EDSAP)
[AD-A266986] p 1158 N94-15492
Requirements for supercomputing in energy research: The transition to massively parallel computing
[DE93-012376] p 1160 N94-16774
Efficient scheduling of real-time compute-intensive periodic graphs on large grain data flow multiprocessor
[AD-A267444] p 1141 N94-17030
Benchmarking massively parallel architectures
[DE93-016486] p 1162 N94-17646

MATCHED FILTERS
Signal processing in impulsive electromagnetic interference
[AD-A266425] p 998 N94-16557
Expansions of cumulative distribution functions directly from characteristic functions
[AD-A267727] p 1173 N94-17372

MATERIALS HANDLING
Materials processing in space: Issues for the third decade
[TABES PAPER 93-260] p 983 N94-16133
Biomass energy: State of the technology present obstacles and future potential
[DE93-016295] p 1092 N94-16766
Materials inventory management manual
[NHB-4100.1C] p 1225 N94-16830

MATERIALS RECOVERY
Investigations into the recovery of waste sulfuric acid with concentrated solar radiation
[DLR-FB-93-11] p 952 N94-17594

MATERIALS SCIENCE
Sounding Rocket Experiments in Fluid Science and Materials Sciences: TEXUS 25 to 27 and MASER 4, volume 3
[ESA-SP-1132-VOL-3] p 943 N94-15157
QUESTS: A microgravity research facility for materials science experiments p 978 N94-16082

MATERIALS TESTS
Building a lunar base
[NASA-TM-109674] p 983 N94-15519
Long Duration Exposure Facility experiment M0003 deintegration/findings and impacts
[AD-A267140] p 885 N94-15749
Materials, processes, and environmental engineering network
[TABES PAPER 93-610] p 1051 N94-16142

MATHEMATICAL LOGIC
Combinatorial semantics
[TR-444] p 1149 N94-16575
Notes on the use of Dempster-Shafer and fuzzy reasoning to fuse identity attribute data
[AD-A267426] p 1004 N94-17309

MATHEMATICAL MODELS
A mathematical model for the study of hemorrhagic shock and fluid resuscitation: The systemic and pulmonary vasculature
[AD-A266835] p 1119 N94-14917
Engineering Physics and Mathematics Division progress report, period ending 31 December 1992
[DE93-015118] p 1301 N94-14926
Static aeroelastic response of an aircraft with asymmetric wing planforms representative of combat damage
[AD-A266890] p 865 N94-14951
Unsteady separated flows: Empirical model and control
[AD-A267282] p 855 N94-14959
Modelling of creep data for plastics
[NPL-DMM(A)-92] p 1057 N94-15017
Inelastic deformation of metal matrix composites
[NASA-CR-191522] p 930 N94-15106
Advanced methods for cascade testing
[AGARD-AG-328] p 1016 N94-15119
Predicted and real development in the aviation in the period 1961-1991 p 853 N94-15122
Rotary engine performance computer program (RCEMAP and RCEMAPPC): User's guide
[NASA-CR-191192] p 869 N94-15192
On the use of the noncentral chi-square density function for the distribution of helicopter spectral estimates
[NASA-CR-191546] p 1176 N94-15487
Hidden Markov model approach to skill learning and its application to telerobotics
[AD-A266989] p 1164 N94-15502
Comparison of RADARC high-frequency radar performance prediction model and ROTHR Amchitka data
[AD-A267077] p 987 N94-15540
Verification of a two-dimensional infiltration model for the resin transfer molding process
[NASA-CR-194597] p 964 N94-15656
Mathematical model of frost heave and thaw settlement in pavements
[AD-A267037] p 983 N94-15676
Nontidal gravity changes observed with a superconducting gravimeter p 1100 N94-15808
Report of the working group on theoretical tidal model p 1101 N94-15815
Fast simulation of steady-state availability in non-Markovian highly dependable systems
[AD-A266747] p 1174 N94-15823
Nuclear rocket plume studies
[AD-A267154] p 925 N94-15837
A feasibility study of a microgravity enhancement system for Space Station Freedom
[NASA-CR-191550] p 886 N94-15864
Effects of rotation on coolant passage heat transfer. Volume 2: Coolant passages with trips normal and skewed to the flow
[NASA-CR-4396-VOL-2] p 1023 N94-15991
A CCIR-based prediction model for Earth-Space propagation p 997 N94-16050
Aerodynamic/dynamic/control interaction
[AD-A266187] p 871 N94-16107
Cost-effective test methods for Shuttle payloads
[TABES PAPER 93-651] p 883 N94-16151
Modeling and simulation: A key to future defense technology
[TABES PAPER 93-654] p 1054 N94-16153
Sand transport on Mars: Preliminary results from models p 1252 N94-16198
Explosive mafic volcanism on Earth and Mars p 1253 N94-16204
Morphology and models for the evolution of eastern Hecate Chasma, Venus p 1256 N94-16215
Ishtar deformed belts: Evidence for deformation from below? p 1256 N94-16218
Why is the Moon dark? p 1256 N94-16219
An experimental study of trace element partitioning between perovskite, hibonite and melt: Equilibrium values p 954 N94-16313
Lava crusts and flow dynamics p 1103 N94-16316
On the relationship between tectonic plates and thermal mantle plume morphology p 1104 N94-16349
Aspects of modelling the tectonics of large volcanoes on the terrestrial planets p 1104 N94-16396

Controls of maglev suspension systems
[DE93-015540] p 1011 N94-16443
A mathematical model for the study of hemorrhagic shock and fluid resuscitation: Transcapillary exchange
[AD-A266427] p 1123 N94-16544
Numerical modeling of the temperature gradients and spectra of the plasma armature on Thunderbolt
[AD-A266414] p 878 N94-16552
A mathematical model for the study of hemorrhagic shock and fluid resuscitation: Exchange of fluid and solutes between vascular, interstitial, and tissue cell compartments
[AD-A266426] p 1123 N94-16558
Spatial resolution and cloud optical thickness retrievals p 1066 N94-16671
Lossless compression of AVIRIS data: Comparison of methods and instrument constraints
p 1075 N94-16713
Comparison of modeled backscatter with SAR data at P-band p 1076 N94-16735
SAR backscatter from coniferous forest gaps
p 1076 N94-16736
Retrieval of pine forest biomass using JPL AIRSAR data p 1076 N94-16737
Sea bottom topography imaging with SAR
p 1077 N94-16745
Development of a constitutive model for creep and life prediction of advanced silicon nitride ceramics
[DE93-015894] p 968 N94-16813
Emissions of volatile organic compounds from stationary combustion sources: Numerical modeling capabilities
[DE93-014123] p 1096 N94-16825
Textile composite processing science
p 938 N94-16856
Development of braided fiber seals for engine applications p 939 N94-16859
Quantification of processing artifacts in textile composites p 939 N94-16860
Stochastic damage evolution in textile laminates
p 939 N94-16861
Integration ToolKit and Methods (ITKM) manufacturing methods and prototype toolkit. A combined modeling method using IDEFO, IDEF1x and XSpec
[AD-A266176] p 984 N94-16981
Modeling, estimation and control of distributed parameter systems
[AD-A267325] p 1026 N94-17003
Ensemble forecasting techniques in medium-range forecasting
[AD-A267443] p 1107 N94-17029
Studies of changes in the energy stored in metals as a result of subjecting them to a surface type technological process
[IFTR-25/1991] p 960 N94-17063
Proposal of a simple mathematical model for the action of a laser on a metal plate
[IFTR-36/1991] p 1041 N94-17065
Nonequilibrium radiation and chemistry models for aerocapture vehicle flowfields
[NASA-CR-194645] p 1027 N94-17095
Phased array antenna analysis using hybrid finite element methods
[AD-A267620] p 1002 N94-17196
Shielding from space radiations
[NASA-CR-194664] p 1301 N94-17255
Characterization of metallic multilayers using x ray diffraction analysis
[NIAR-93-13] p 961 N94-17282
The roles of fluid motion and other transport phenomena in the morphology of materials
[NASA-CR-194665] p 1028 N94-17298
ONRASIA scientific information bulletin, volume 18, number 2
[AD-A267798] p 1304 N94-17305
Mathmatical modeling for diffractive optics
p 1195 N94-17342
A Geographic Information System approach to modeling nutrient and sediment transport
[DE93-013747] p 1097 N94-17426
Energy deposition fluctuations induced by ions in microvolumes and nanovolumes: An analytic approach. 1: Theory
[AD-A267959] p 1173 N94-17495
Application of the finite-difference time-domain method to scattering and radiation problems involving wires and plates
[AD-A268396] p 1005 N94-17496
Compressible flow solvers using unstructured grids
[INRIA-RR-1732] p 1030 N94-17531
Structured finite volume modeling of US Navy aircraft engine test cells. Task 2: Turboprop engine. Volume 2: Code documentation and listings
[AD-A268386] p 873 N94-17569
A basic principles description of liquid vapor phase transitions
[AD-A268331] p 1176 N94-17581
A two-layer quasi-geotrophic spherical model: Formulation and climatology
[DM-63] p 1110 N94-17593

MATHEMATICAL PROGRAMMING
Geometric tolerance assessment
[NPL-DITC-210/92] p 1049 N94-15013

MATRICES (MATHEMATICS)
Automatic differentiation of limit functions
[DE93-016376] p 1168 N94-14928
Decomposition of large sparse symmetric systems for parallel computation. Part 2: Parallelization tool roadmap
[AD-A267072] p 1158 N94-15671
Decomposition of large sparse symmetric systems for parallel computation. Part 1: Theoretical foundations
[AD-A267144] p 1159 N94-15750
Generating local addresses and communication sets for data-parallel programs
[NASA-CR-194605] p 1159 N94-15796
Maximum likelihood techniques applied to quasi-elastic light scattering
[NASA-CR-193550] p 1192 N94-16718
Invariance of slip movements with respect to the control matrix
[IFTR-43/1991] p 1170 N94-17045
The renormalization of the axial anomaly in dimensional regularization
[NIKHEF-H/92-18] p 1220 N94-17618

MATRIX MATERIALS
Construction, testing, and representation of resin and fiber reinforced materials p 931 N94-15255
Machine development p 932 N94-15258
Carbon-carbon grid for ion engines
[NASA-CASE-NPO-19174-1-CU] p 925 N94-15876
NEXTEL(trademark)/SiC composites using forced chemical vapor infiltration
[DE93-013532] p 934 N94-16008
Overview of chemical vapor infiltration
[DE93-015440] p 934 N94-16065
Wear resistant titanium material development
[AD-A266474] p 959 N94-16780
Influence of the loading rate on the endurance and deformability of cement matrix composites
[IFTR-1/1992] p 1060 N94-17052

MATRIX METHODS
Finding stable orientations of assemblies with linear programming
[AD-A266990] p 1143 N94-15212
Construction and calculation p 931 N94-15256
Decomposition of large sparse symmetric systems for parallel computation. Part 1: Theoretical foundations
[AD-A267144] p 1159 N94-15750
Eigenfunctions of the transfer matrix in the presence of linear coupling
[DE93-015020] p 1151 N94-16892
Speckles statistics and decorrelation effects in complex ABCD optical systems
[AD-A267843] p 1193 N94-17012

MATRIX THEORY
The quantum mass shift of the soliton in Skyrme model
[ITN-93-85219] p 1180 N94-15283

MATTER (PHYSICS)
Fast pulsars, compact stars, and the strange matter hypothesis
[DE93-015039] p 1239 N94-16052
Basic studies of the liquid state of matter: Electrical properties and laser interactions
[AD-A268311] p 1042 N94-17567

MAXIMUM LIKELIHOOD ESTIMATES
A new method for generating Bayes classifiers assuming mixtures of Gaussian densities
[FFI-91/4029] p 1172 N94-15298
Statistical analysis of trigonometric parallaxes
[NASA-CR-194558] p 1172 N94-15641
A multilevel-multiresolution method for image processing. A Bayesian framework for reconstructing and representing shapes
[AD-A266772] p 1082 N94-15842
Maximum likelihood techniques applied to quasi-elastic light scattering
[NASA-CR-193550] p 1192 N94-16718

MAXWELL EQUATION
Measurement of birefringence for optical recording disk substrates p 1227 N94-14989
Stress sensitivity of dielectric resonators
[AD-A266767] p 1009 N94-15825
An asymptotic expansion of an electromagnetic field in the velocity of a caustic in the form of simple waves
[IFTR-14/1991] p 1002 N94-17048
Mathmatical modeling for diffractive optics
p 1195 N94-17342

MEAN
Bounds on inconsistent inferences for sequences of trials with varying probabilities
[AD-A267146] p 1172 N94-15733

MEAN SQUARE VALUES
An investigation of the Ground-Based High-Resolution Interferometer Sounder (GB-HIS) in a costal marine environment
[AD-A268052] p 1114 N94-17503

MEANDERS
Meander properties of Venusian channels
p 1275 N94-16324

MEASURE AND INTEGRATION
Volume integral equations applied to circular and square cylinders
[AD-A266635] p 1169 N94-15785

MEASUREMENT
Lecture notes on engineering measurement for software engineers
[AD-A266959] p 1142 N94-14967

MEASURING INSTRUMENTS
Simultaneous measurement of temperature and strain using four connecting wires
[NASA-TM-104271] p 1032 N94-15754
Dual active surface, miniature, plug-type heat flux gauge
[NASA-CASE-LEW-15643-1] p 1033 N94-15928
Wind tunnel investigation with an operational turbojet engine
[TABES PAPER 93-662] p 870 N94-16157
Passive tracking of a target using an array of sensors
[DE93-015870] p 997 N94-16169
Cosmic dust and space debris measurements on board the small satellites HITEN and BREM-SAT
p 890 N94-17147
S 80/T: A micro satellite system combining high performances and limited resources
p 893 N94-17166

MECHANICAL DEVICES
Attachment device
[NASA-CASE-MSC-21885-1] p 1047 N94-15925
Nonlinear analysis of mechanical systems under combined harmonic and stochastic excitation
[AD-A266217] p 1173 N94-16937
Electrorheological (ER) fluids: A research needs assessment
[AD-A267588] p 951 N94-17210
Computer modeling and animation of mechanical systems
[NIAR-93-3] p 1153 N94-17299

MECHANICAL ENGINEERING
Krupp technical reports no. 2, English edition, October 1992
[ETN-93-94631] p 984 N94-16000
Expert system for welding engineering
p 984 N94-16003
Remote diagnosis as used for mechanized parking systems p 984 N94-16004

MECHANICAL MEASUREMENT
A mechanical system damping measurement technique using a one-degree-of-freedom (1DOF) cylindrical gas bearing
[AD-A268402] p 1048 N94-17462

MECHANICAL PROPERTIES
The effect of aging at 343 C on the mechanical properties and microstructure of type 308 stainless steel weldments
[DE93-015454] p 957 N94-16103
Evaluation of the interfacial mechanical properties in fiber-reinforced ceramic composites
[DE93-015494] p 935 N94-16461
Thermal stress effects in intermetallic matrix composites
[NASA-CR-191191] p 1054 N94-16518
Evolution of microstructure in face centered cubic metals during irradiation: A review
[DE93-015682] p 958 N94-16662
The effect of oxygen, grain size, and strain rate on the mechanical behavior of forged P/M tantalum
[DE93-011251] p 959 N94-16764
Processing of complex sintered reaction bonded silicon nitride parts by microwave heating
[DE93-015811] p 969 N94-16877
Electrical conductivity of ion implanted ladder and semi-ladder polymers
[AD-A267432] p 970 N94-16978
Mean strain effects on the strain life fatigue curve
[AD-A267211] p 960 N94-16984
Dynamic testing and characterization of pre-fractured ceramic
[DE93-016457] p 972 N94-17238
Micromechanics modeling and analysis of Haversian compact bone tissues as a fiber reinforced composite material
[AD-A268250] p 1129 N94-17456

MECHANICAL SHOCK
Shear wave measurements in shock-induced, high-pressure phases
[DE93-016461] p 1062 N94-17664

MECHANICAL TWINNING
Slip, twinning and transformation in Laves phases
[DE93-018164] p 960 N94-16972
MEDICAL EQUIPMENT
Cool suit
[NASA-TM-109639] p 1120 N94-15250
New insulin pump
[NASA-TM-109642] p 1120 N94-15253
Living well in space: Clinical care challenge
[NASA-TM-109539] p 1120 N94-15370
Medical imaging
[NASA-TM-109675] p 1229 N94-15520
Annual historical report, calendar year 1992
[AD-A267050] p 1121 N94-15663
Method and apparatus to characterize ultrasonically reflective contrast agents
[NASA-CASE-LAR-14969-1] p 1129 N94-17085
Automated data collection system for the TCM3 transcutaneous pO2/pCO2 monitoring system
[AD-A268400] p 1129 N94-17424
MEDICAL PERSONNEL
Illness/injury pattern complex 40 (Titan)
p 1125 N94-16625
Tuberculosis: A case for increased screening
p 1126 N94-16627
OSHA bloodborne pathogens standards exposure control plan p 1127 N94-16645
MEDICAL SCIENCE
New insulin pump
[NASA-TM-109642] p 1120 N94-15253
Annual historical report, calendar year 1992
[AD-A267050] p 1121 N94-15663
Localizing visual function in the brain
[AD-A267381] p 1133 N94-17020
MEDICAL SERVICES
Living well in space: Clinical care challenge
[NASA-TM-109539] p 1120 N94-15370
Annual historical report, calendar year 1992
[AD-A267050] p 1121 N94-15663
Proceedings of the 1992 Annual Meeting NASA Occupational Health Program
[NASA-CR-193462] p 1123 N94-16609
Americans with Disabilities Act considerations for the practice of occupational medicine p 1124 N94-16611
Emergency preparedness and planning
p 1124 N94-16613
Ongoing Recovery Basic Information Tool (ORBIT)
p 1124 N94-16616
Illness/injury pattern complex 40 (Titan)
p 1125 N94-16625
Identifying and responding to customer needs at the Kennedy Space Center p 1056 N94-16626
Tuberculosis: A case for increased screening
p 1126 N94-16627
Summary of follow-up results from potential tuberculosis exposures p 1126 N94-16628
Screening for prostate cancer p 1126 N94-16630
Physical fitness and health education program at NASA Headquarters p 1126 N94-16631
Ames Fitness Program p 1126 N94-16632
Asbestos Surveillance Program p 1127 N94-16638
Hearing Conservation Medical Program
p 1127 N94-16639
Lead Surveillance Program p 1127 N94-16640
Mercury Surveillance Program p 1127 N94-16641
Respiratory Protection Program medical clearance for respirator use p 1127 N94-16642
General Medical Surveillance Program
p 1127 N94-16643
Bloodborne Pathogens Program p 1127 N94-16644
MELTING
Partial melting experiment of Y-Ba-Cu oxide
p 945 N94-15168
Remelting of Fe-C-Si-alloy in a ceramic mold skin
p 945 N94-15169
Mathematical model of frost heave and thaw settlement in pavements
[AD-A267037] p 983 N94-15676
Partial melting of ordinary chondrites: Lost City (H) and St. Severin (LL) p 1243 N94-16286
On origin of the olivine inclusions from the Kainsaz CO carbonaceous chondrite p 1244 N94-16345
First results from analysis of coordinated AVIRIS, TIMS, and ISM (French) data for the Ronda (Spain) and Beni Bousera (Morocco) peridotites p 1067 N94-16675
MELTING POINTS
Micromechanisms of monotonic and cyclic subcritical crack growth in advanced high melting point low-ductility intermetallics
[AD-A267764] p 951 N94-17223
MELTS (CRYSTAL GROWTH)
Siderophile elements in the upper mantle of the Earth: New clues from metal-silicate partition coefficients
p 1103 N94-16250
Os isotopes in SNC meteorites and their implications to the early evolution of Mars and Earth
p 1242 N94-16272
Transition metals in superheat melts
p 962 N94-16273
Angrite LEW87051: Are the olivines pheno's or xeno's? A continuing story p 1103 N94-16285
Explosive volcanism and the compositions of the cores of differentiated asteroids p 1243 N94-16306
Evaporation kinetics of Mg2SiO4 crystals and melts from molecular dynamics simulations p 1219 N94-16331
Was Martian mantle wet? A possible consequence of rapid core formation p 1277 N94-16335
Hydride-containing molten salts and their technology implications
[AD-A266458] p 1092 N94-16567
Convection effects on radial segregation and crystal melt interface in vertical Bridgman growth
[NASA-CR-191541] p 1029 N94-17387
MEMBRANES
Gas separations using ceramic membranes
[DE93-000278] p 947 N94-15861
Modification of fluoropolymer surfaces with electronically conductive polymers
[AD-A266294] p 967 N94-16475
MEMORY
The 12th Annual Carmel Conference, distinctiveness and Memory: Cognitive Psychophysiological and Physiological Considerations
[AD-A267181] p 1131 N94-15148
Theoretical and experimental research into biological mechanisms underlying learning and memory
[AD-A267441] p 1133 N94-17022
Synaptic plasticity and memory formation
[AD-A267988] p 1133 N94-17453
MEMORY (COMPUTERS)
Relaxing consistency in recoverable distributed shared memory
[AD-A266931] p 1140 N94-15174
The design of self-checking reduced instruction set computers
[AD-A267012] p 1140 N94-15763
Generating local addresses and communication sets for data-parallel programs
[NASA-CR-194605] p 1159 N94-15796
The alignment-distribution graph
[NASA-CR-194609] p 1148 N94-15956
Unipolar terminal-attractor based neural associative memory with adaptive threshold
[NASA-CASE-NPO-18790-1-CU] p 1165 N94-15958
A decision criteria to select an associative-memory organization that minimizes the execution time of a mix of associative-search operations
[AD-A266438] p 1149 N94-16560
A trace-based comparison of shared memory multiprocessor architectures
[TR-432] p 1159 N94-16577
Shared-memory multiprocessor trends and the implications for parallel program performance
[TR-420] p 1159 N94-16578
SONOS technology for commercial and military nonvolatile memory applications
[DE93-015647] p 1011 N94-16661
Fault-tolerant architectures for multiprocessor and VLSI-based systems
[AD-A267370] p 1140 N94-17005
MENISCI
Evaporation from a meniscus within a capillary tube in microgravity
[NASA-CR-194593] p 976 N94-15654
MENTAL PERFORMANCE
Complex information coordination performance: Differential changes in working memory contributions following training
[AD-A267007] p 1132 N94-15762
Scuba-diving, anxiety and task performance
p 1132 N94-15938
Cognitive engineering models in space systems
[NASA-CR-193473] p 1140 N94-16716
The behavioral toxicology of high-peak, low average power, pulsed microwave irradiation
[AD-A268392] p 1134 N94-17535
MERCURY (METAL)
Mercury Surveillance Program p 1127 N94-16641
Sodium-mercury excimer laser, phase 1
[AD-A267728] p 1042 N94-17230
MERCURY CADMIUM TELLURIDES
Advanced high performance CdHgTe multiplexed arrays p 903 N94-15051
A 12.5 micron infrared detector for Earth observation
p 903 N94-15052
Proceedings of the 6th International Conference on Narrow Gap Semiconductors
[AD-A268097] p 1015 N94-17570
MERCURY COMPOUNDS
Optical properties and surface morphology studies of palladium contacts on mercuric iodide single crystals
[DE93-012510] p 1207 N94-15973
Elemental impurity analysis of mercuric iodide by ICP/MS
[DE93-015531] p 949 N94-16876
MERCURY MA-6 FLIGHT
Astronauts number 3 --- Friendship 7
[NASA-TM-109430] p 874 N94-15501
MERCURY PROJECT
Astronauts number 1 --- mercury project
[NASA-TM-109428] p 1131 N94-15499
MERCURY SPACECRAFT
Astronauts number 2
[NASA-TM-109429] p 873 N94-15500
MESOMETEOROLOGY
Sensitivity testing of a single-Doppler temperature retrieval and forecast system
[AD-A267278] p 1105 N94-14958
Mesoscale frontogenesis: An analysis of two cold front case studies
[AD-A267950] p 1107 N94-17054
Opposing mesoscale flows in a broken midlatitude squall line
[AD-A268011] p 1109 N94-17492
MESON-MESON INTERACTIONS
Theoretical high energy physics
[DE93-015884] p 1187 N94-16170
MESON-NUCLEON INTERACTIONS
The quantum mass shift of the soliton in Skyrme model
[ITN-93-85219] p 1180 N94-15283
Past, present and future ((pi),(eta)) experiments
[DE93-016631] p 1182 N94-16115
MESONS
Closed orbit distortion and the beam-beam interaction
[DE93-015284] p 1190 N94-15854
Status of (alpha)(sub s) measurements
[DE93-015179] p 1181 N94-16059
Mesons at finite temperature in the NJL model with gluon condensate
[DE93-626697] p 1185 N94-17310
Production of D-mesons in pp-collisions and quark-gluon string model
[DE93-626721] p 1185 N94-17312
MESOSCALE PHENOMENA
Sensitivity testing of a single-Doppler temperature retrieval and forecast system
[AD-A267278] p 1105 N94-14958
Mesoscale modeling of the atmosphere
[AD-A263236] p 1098 N94-15132
Short term weather forecasting in real time in a base weather station setting
[AD-A266872] p 1105 N94-15142
Mesoscale lightning
[NASA-TM-109655] p 1105 N94-15226
Mesoscale frontogenesis: An analysis of two cold front case studies
[AD-A267950] p 1107 N94-17054
Opposing mesoscale flows in a broken midlatitude squall line
[AD-A268011] p 1109 N94-17492
Propagation characteristics of mesoscale convective systems
[AD-A268130] p 1109 N94-17522
Forecasting the ducting of electromagnetic waves on the mesoscale
[AD-A268101] p 1109 N94-17571
Surface energy balance modeling at mesoscale: The contribution of the future Earth observing system
[BCRS-91-04] p 1085 N94-17616
MESOZOIC ERA
Earth's partial pressure of CO2 over the past 100-500 Ma; evidence from Ce anomalies in mostly shallow seas (less than 200 m) as recorded in carbonate sediments, 2
p 1104 N94-16360
MESSAGE PROCESSING
VDM specification of the MD4 message digest algorithm
[NPL-DITC-204/92] p 1142 N94-14944
RAISE specification of the MD4 message digest algorithm
[NPL-DITC-206/92] p 1142 N94-15010
Understanding partitions and the no partition assumption
[AD-A266296] p 1000 N94-16911
Ground wave emergency network final operational capability: Environmental assessment for central Wyoming relay node, site number RN 8C928WY
[AD-A267842] p 1001 N94-17011
Intel NX to PVM 3.2 message passing conversion library
[NASA-TM-109038] p 1152 N94-17060

Causality-preserving timestamps in distributed programs
[AD-A267534] p 1153 N94-17118
Radiocommunication problems of a position reporting and bidirectional messagery system using VHF/UHF with low-Earth orbit satellites p 889 N94-17136
LEOCOM-SPES: Low cost message communications p 892 N94-17161
STARSYS: A view after WARC-92 — satellite position and messaging system p 893 N94-17168

MESSAGES
Multiphase complete exchange: A theoretical analysis
[NASA-CR-191531] p 1145 N94-15489
A parallel adaptive mesh refinement algorithm
[NASA-CR-191530] p 1168 N94-15724

METABOLISM
TransRapid TR-07 maglev-spectrum magnetic field effects on daily pineal indoleamine metabolic rhythms in rodents
[DE93-015143] p 1117 N94-16893

METABOLITES
Cumulative effect of repeated brief cerebral ischemia
[AD-A267155] p 1121 N94-15736

METAL BONDING
The thermal dissociation of NH2CHO(ND2CHO) on Si(100)-2x1
[AD-A266903] p 942 N94-14956

METAL COATINGS
Restoring Miss Liberty — inorganic coatings
[NASA-TM-109605] p 963 N94-15313
Optical properties and surface morphology studies of palladium contacts on mercuric iodide single crystals
[DE93-012510] p 1207 N94-15973
Transparent conductive coatings in the far ultraviolet
[NASA-CR-194632] p 1191 N94-16024
The role of carbon and temperature in determining electrical conductivity of basins, crust and mantle
[DE93-015936] p 1101 N94-16840
Robotic weld overlay coatings for erosion control
[DE93-016938] p 970 N94-16959
Application of hard coatings to substrates at low temperatures
[NASA-CR-193867] p 971 N94-17122

METAL CRYSTALS
High temperature materials technology research for advanced thermionic systems
[DE93-018302] p 960 N94-16964

METAL FATIGUE
Laser-shock damage of iron-based materials
[AD-A267196] p 1038 N94-15852
Ion implantation effects on surface-mechanical properties of metals and polymers
[DE93-014661] p 958 N94-16453
Fatigue life program using strain-life methods
[AD-A267310] p 1060 N94-16943
Mean strain effects on the strain life fatigue curve
[AD-A267211] p 960 N94-16984

METAL FIBERS
Integrated fundamental research on current collection
[AD-A266987] p 1008 N94-15494

METAL FILMS
Ion mixing of thin ZrO2 films on sapphire
[DE93-015214] p 1206 N94-14925
Laboratory for x ray optics
[AD-A267149] p 1189 N94-15735
Cellulose triacetate, thin film dielectric capacitor
[NASA-CASE-NPO-18935-1-CU] p 1010 N94-15952
Aberration correction of unstable resonators
[NASA-CASE-NPO-18791-1-CU] p 1034 N94-15987
Weibull analysis applied to the pull adhesion test and fracture of a metal-ceramic interface
[DE93-012913] p 1059 N94-15997
Design and fabrication of a reflection far ultraviolet polarizer and retarder
[NASA-CR-194630] p 1191 N94-16023
Transparent conductive coatings in the far ultraviolet
[NASA-CR-194632] p 1191 N94-16024
UHV-stem studies on nucleation and growth of thin metal silicide films on silicon
[DE93-017604] p 1212 N94-16961
Characterization of metallic multilayers using x ray diffraction analysis
[NIAR-93-13] p 961 N94-17282
Epitaxial iron films
[AD-A268286] p 1217 N94-17579

METAL FINISHING
Dry stripping as a surface treatment method
[VTT-TIED-1348] p 965 N94-17544

METAL FLUORIDES
Neutron and x ray scattering studies of (FeF2)(sub m)(CoF2)(sub n) multilayers
[DE93-015809] p 1184 N94-16838

METAL FOILS
Direct drive foil implosion experiments on Pegasus 2
[DE93-012666] p 1202 N94-16776
Plasma flow switch and foil implosion experiments on Pegasus 2
[DE93-016464] p 1013 N94-17318

METAL HYDRIDES
Small satellite nickel-hydrogen and nickel-metal hydride power applications p 895 N94-17175

METAL IONS
Ion mixing of thin ZrO2 films on sapphire
[DE93-015214] p 1206 N94-14925
Optical and infrared spectra of thermally annealed Pb implanted SiO2 glasses
[DE93-015304] p 965 N94-15828
Application of in situ scanning x ray fluorescence to study the concentration of metal ions in simulated pits
[DE93-014054] p 956 N94-15921
Investigation of the effects of polyelectrolyte coatings on colloid transport in porous media
[DE93-018300] p 970 N94-16973
Single crystal diamond thin films
[AD-A266457] p 1214 N94-17216

METAL JOINTS
Physical interpretation and development of ultrasonic nondestructive evaluation techniques applied to the quantitative characterization of textile composite materials
[NASA-CR-194549] p 931 N94-15190

METAL MATRIX COMPOSITES
Fracture toughness tests for particulate MMC UK COSI (IACFA) task group. Meeting report, October 1992
[NPL-DMM(A)-81] p 1057 N94-15021
Inelastic deformation of metal matrix composites
[NASA-CR-191522] p 930 N94-15106
Liquid phase sintering of tungsten composites under microgravity. Effect of matrix composition p 945 N94-15171
Anisotropic damage mechanics modeling in metal matrix composites
[AD-A266328] p 934 N94-16440
The processing and mechanical properties of high temperature/high performance composites. Book 1: Coonstituent properties of composites
[AD-A266394] p 935 N94-16483
The processing and mechanical properties of high temperature/high performance composites. Book 3: Coonstituent properties and macroscopic performance
[AD-A266396] p 935 N94-16485
Thermal stress effects in intermetallic matrix composites
[NASA-CR-191191] p 1054 N94-16518
The processing and mechanical properties of high temperature/high performance composites. Book 4: Coonstitutive laws and design
[AD-A266397] p 935 N94-16528
The processing and mechanical properties of high temperature/high performance composites. Book 5: Processing and miscellaneous properties
[AD-A266398] p 935 N94-16529
Continuous fabrication of SiC fiber tows by chemical vapor deposition
[AD-A266460] p 936 N94-16569
Techniques for preparation of ingot metallurgical discontinuous composites
[AD-D015748] p 940 N94-16933
Interfacial shear behavior and its influence on fiber damage in sapphire-reinforced gamma titanium aluminide composites
[AD-A267943] p 1060 N94-17043
Ceramic fiber coatings development and demonstration
[AD-A267286] p 972 N94-17242
Elastic-plastic finite-difference analysis of unidirectional composites subjected to thermomechanical cyclic loading
[AD-A267666] p 1061 N94-17269
Aspects of high temperature damage in fiber reinforced titanium metal matrix composites
[AD-A267907] p 941 N94-17379

METAL NITRIDES
Amide and tetrazene complexes of transition and main group elements as precursors for the low temperature synthesis of elemental nitrides
[AD-A266246] p 950 N94-16931

METAL OXIDE SEMICONDUCTORS
DLTS and dynamic transconductance analysis of deep-submicron fully-depleted SOI MOSFET's
[AD-A267291] p 1214 N94-17243

METAL OXIDES
Ion mixing of thin ZrO2 films on sapphire
[DE93-015214] p 1206 N94-14925
Molten salt electrodeposition of high temperature superconductors
[AD-A266620] p 1009 N94-15726
The friction and wear of ceramic/ceramic and ceramic/metal combinations in sliding contact
[NASA-TM-106348] p 930 N94-15769

METAL PLATES
Microwave interaction with plasmas
[AD-A267048] p 1201 N94-15661
Analysis of electromagnetic scattering from irregularly shaped, thin, metallic flat plates
[NASA-TP-3361] p 998 N94-16655
Proposal of a simple mathematical model for the action of a laser on a metal plate
[IFTR-36/1991] p 1041 N94-17065

METAL POWDER
Solid lubricants for space structures, phase 2
[AD-A266653] p 968 N94-16767
Characterization of nanoscale oxide and oxyhydroxide powders using EXAFS spectroscopy
[DE93-015683] p 940 N94-17235

METAL SHEETS
Measurement and analysis of critical CTOA for an aluminum alloy sheet
[NASA-TM-109024] p 956 N94-15948
Laser weld repair of tantalum sheet
[DE93-016417] p 1041 N94-16871

METAL SURFACES
The friction and wear of ceramic/ceramic and ceramic/metal combinations in sliding contact
[NASA-TM-106348] p 930 N94-15769
Passive oxide films on well-defined nickel surfaces: An examination of film growth on Ni(100) with ex situ scanning tunneling microscopy
[DE93-014056] p 1207 N94-15923
A Moessbauer spectrometer for the mineralogical analysis of the Mars surface: First temperature dependent tests of the detector and drive system p 1259 N94-16233
Hydride-containing molten salts and their technology implications
[AD-A266458] p 1092 N94-16567
Vectorial electron transfer in spatially ordered arrays
[DE93-018150] p 1185 N94-16971

METALLIZING
Ablation, surface activation, and electroless metallization of insulating materials by pulsed excimer laser irradiation
[DE93-015808] p 1040 N94-16664
Robotic weld overlay coatings for erosion control
[DE93-016938] p 970 N94-16959
Low dielectric constant insulators and gold metallization for GHz multi-chip modules, part 2
[AD-A268590] p 1176 N94-17605

METALLOGRAPHY
Cation ordering in orthopyroxenes and cooling rates of meteorites: Low temperature cooling rates of Estherville, Bondoc and Shaw p 1241 N94-16176
Effects of processing and prolonged high temperature exposure on the microstructure of Nb-1Zr-C sheet
[NASA-TM-106370] p 959 N94-16883

METALLOIDS
Electronic and atomic structure of semiconductors and of high-temperature superconductors
[AD-A266805] p 1205 N94-14913

METALLURGY
Fabrication of advanced design (grooved) cermet anodes
[DE93-014590] p 1012 N94-16765

METALORGANIC CHEMICAL VAPOR DEPOSITION
Characterization of InTISb grown by low pressure metalorganic chemical vapor deposition on GaAs substrate
[AD-A266878] p 1206 N94-14922
Ion doped quantum well lasers
[AD-A267198] p 1038 N94-15853
The growth of InAs(1-x)Sb(x)/InAs strained-layer superlattices by metal-organic chemical vapor deposition
[DE93-015028] p 1208 N94-16012
Rare earth doped III-V semiconductors for optoelectronics
[AD-A268279] p 1216 N94-17577

METALS
Vacancy condensation as the precursor to passivity breakdown
[DE93-012925] p 956 N94-15998
Evolution of microstructure in face centered cubic metals during irradiation: A review
[DE93-015682] p 958 N94-16662
Studies of changes in the energy stored in metals as a result of subjecting them to a surface type technological process
[IFTR-25/1991] p 960 N94-17063

METAMORPHIC ROCKS
The role of carbon and temperature in determining electrical conductivity of basins, crust and mantle
[DE93-015936] p 1101 N94-16840

METAMORPHISM (GEOLOGY)
The Karakul depression in Pamirs: The first impact structure in Central Asia p 1241 N94-16212
Pyroxene equilibration temperatures in metamorphosed ordinary chondrites p 1242 N94-16224

Comparison of reflectance spectra of C asteroids and unique C chondrites Y86720, Y82162, and B7904
p 1242 N94-16246
The group A3 chondrules of Krymka: Further evidence for major evaporative loss during the formation of chondrules p 1242 N94-16257
Different radiation and metamorphic history of the Kainsaz CO 3.2 chondrules p 1243 N94-16296
Heterogeneous plagioclase compositions in the Maralinga CK4 chondrite p 1243 N94-16308
A hydrogen isotope study of CO3 type carbonaceous chondrites; comparison with type 3 ordinary chondrites
p 1246 N94-16425

METASTABLE STATE
Astronomy and astrophysics p 1239 N94-15970
Metastable phases in mechanically alloyed aluminum germanium powders
[DE93-008727] p 958 N94-16463
The processing and mechanical properties of high temperature/high performance composites. Book 5: Processing and miscellaneous properties
[AD-A266398] p 935 N94-16529
Pulsed laser deposition of metastable Ca(1-x)Sr(x)CuO2 thin films
[DE93-015804] p 1040 N94-16663
Kinetics of silica-phase transitions
[DE93-016231] p 1217 N94-17659

METEORITE COLLISIONS
Osmium isotopes in Ivory Coast tektites: Confirmation of a meteoritic component and rhenium depletion
p 1244 N94-16321
Geochemical evidences for two chondritic-like cometary or asteroidal impacts before and at the K/T boundary
p 1244 N94-16359
Possible sources of H2 to H2O enrichment at evaporation of parent chondritic material
p 1244 N94-16377
CO2 production by impact in carbonates? An ATEM and stable isotope (C,O) study p 954 N94-16383
Remote visual detection of impacts on the lunar surface p 1290 N94-16404

METEORITE CRATERS
Twenty-Fourth Lunar and Planetary Science Conference. Part 2: G-M
[NASA-CR-193174] p 1247 N94-16173
Martian crater degradation by eolian processes: Analogy with the Rio Cuarto Crater Field, Argentina
p 1251 N94-16196
Collisional and dynamical history of Gaspra
p 1241 N94-16202
The Acraman impact structure: Estimation of the diameter by the ejecta layer thickness
p 1103 N94-16211
The Karakul depression in Pamirs: The first impact structure in Central Asia p 1241 N94-16212
Confirmation of saturation equilibrium conditions in crater populations p 1103 N94-16222
Corvid meteoroids and a Giordano Bruno ray are genetically related p 1242 N94-16223
Lunar impact basins: New data for the nearside northern high latitudes and eastern limb from the second Galileo flyby p 1258 N94-16228
Trace-element composition of Chicxulub crater melt rock, K/T tektites and Yucatan basement
p 1242 N94-16245
The depths of the largest impact craters on Venus
p 1264 N94-16261
Density of impact craters on tessera, Venus
p 1264 N94-16263
A first-order model for impact crater degradation on Venus p 1265 N94-16268
A discontinuous melt sheet in the Manson impact structure p 1103 N94-16269
Al-26 production profile and model comparisons in Canyon Diablo p 1245 N94-16409
Siderophile element fractionation in meteor crater impact glasses and metallic spherules p 1246 N94-16414
Ejecta patterns of Meteor Crater, Arizona derived from the linear un-mixing of TIMS data and laboratory thermal emission spectra p 1065 N94-16607

METEORITES
Twenty-Fourth Lunar and Planetary Science Conference. Part 2: G-M
[NASA-CR-193174] p 1247 N94-16173
Cation ordering in orthopyroxenes and cooling rates of meteorites: Low temperature cooling rates of Estherville, Bondoc and Shaw p 1241 N94-16176
Petrography, mineralogy, and Mg isotope composition of VICTA: A vigarano CaAl4O7-bearing type A inclusion
p 1103 N94-16203
The group A3 chondrules of Krymka: Further evidence for major evaporative loss during the formation of chondrules p 1242 N94-16257
I-Xe structure of ILAFEGH 009 and shallowater: Evidence for early formation and rapid cooling of impact-derived enstatite meteorites
p 1243 N94-16305
Isotopic signatures and distribution of nitrogen and trapped and radiogenic xenon in the Acapulco and FRO90011 meteorites p 1243 N94-16317
Effects of bulk composition on production rates of cosmogenic nuclides in meteorites p 1245 N94-16385
Classificational parameters for acapulcoites and lodranites: The cases of FRO 90011, EET 84302 and ALH A81187/84190 p 1245 N94-16389
The dregs of crystallization in Zagami
p 1245 N94-16390
The Nakhla parent melt: REE partition coefficients and clues to major element composition
p 1245 N94-16399
More on the cooling history of angrite LEW 86010
p 1245 N94-16400
Limited subsolidus diffusion in type B1 CAI: Evidence from Ti distribution in spinel p 954 N94-16401
Remote visual detection of impacts on the lunar surface p 1290 N94-16404
Identification of new meteorite, Mihonoseki (L), from broken fragments in Japan p 1246 N94-16415
The thickness of eucritic crust in the HED parent body
p 1104 N94-16416

METEORITIC COMPOSITION
Twenty-Fourth Lunar and Planetary Science Conference. Part 2: G-M
[NASA-CR-193174] p 1247 N94-16173
The Fe2(+)-Mg interdiffusion in orthopyroxene: Constraints from cation ordering and structural data and implications for cooling rates of meteorites
p 1241 N94-16175
Cation ordering in orthopyroxenes and cooling rates of meteorites: Low temperature cooling rates of Estherville, Bondoc and Shaw p 1241 N94-16176
Extraction and isotopic analysis of medium molecular weight hydrocarbons from Murchison using supercritical carbon dioxide p 1241 N94-16184
Cretaceous-tertiary boundary spherules and Cenozoic microtektites: Similarities and differences
p 1241 N94-16186
Stalking the LREE-enriched component in ureilites
p 1241 N94-16190
Grosnaja ABCs: Magnesium isotope compositions
p 1241 N94-16191
Euromet Ureilite Consortium: A preliminary report on carbon and nitrogen geochemistry p 1241 N94-16192
Nitrates in SNCs: Implications for the nitrogen cycle on Mars p 1251 N94-16193
Martian crater degradation by eolian processes: Analogy with the Rio Cuarto Crater Field, Argentina
p 1251 N94-16196
Petrography, mineralogy, and Mg isotope composition of VICTA: A vigarano CaAl4O7-bearing type A inclusion
p 1103 N94-16203
Petrologic constraints on the surface processes on asteroid 4 Vesta and on excavation depths of diogenite fragments p 1241 N94-16208
Systematic chemical variations in large 3AB iron meteorites: Clues to core crystallization
p 1241 N94-16213
Nd-142/Nd-144 in bulk planetary reservoirs, the problem of incomplete mixing of interstellar components and significance of very high precision Nd-145/Nd-144 measurements p 1256 N94-16220
Comparison of reflectance spectra of C asteroids and unique C chondrites Y86720, Y82162, and B7904
p 1242 N94-16246
Gas-grain energy transfer in solar nebula shock waves: Implications for the origin of chondrules
p 1262 N94-16251
The group A3 chondrules of Krymka: Further evidence for major evaporative loss during the formation of chondrules p 1242 N94-16257
Potassium isotope cosmochemistry, volatile depletion and the origin of the Earth p 953 N94-16259
First investigation of noble gases in the Dengli H3,8 chondrite p 953 N94-16264
Shock-thermal history of Kapoeta howardite matter on data of thermoluminescence analysis of individual mineral grains p 953 N94-16267
Os isotopes in SNC meteorites and their implications to the early evolution of Mars and Earth
p 1242 N94-16272
Complex zoning behavior in pyroxene in FeO-rich chondrules in the Semarkona ordinary chondrite
p 1243 N94-16284
Partial melting of ordinary chondrites: Lost City (H) and St. Severin (LL) p 1243 N94-16286
Experimental partitioning of Zr, Ti, and Nb between silicate liquid and a complex noble metal alloy and the partitioning of Ti between perovskite and platinum metal
p 962 N94-16287
Experimental segregation of iron-nickel metal, iron-sulfide, and olivine in a thermal gradient: Preliminary results p 1243 N94-16288
The Al Rais meteorite: A CR chondrite or close relative? p 1243 N94-16290
Chemical and isotopic compositions in acid residues from various meteorites p 1243 N94-16291
Martian carbon dioxide: Clues from isotopes in SNC meteorites p 1270 N94-16295
Different radiation and metamorphic history of the Kainsaz CO 3.2 chondrules p 1243 N94-16296
Complex radiation-thermal history of Kaidun meteorite on data of track study of silicate minerals
p 1243 N94-16297
I-Xe structure of ILAFEGH 009 and shallowater: Evidence for early formation and rapid cooling of impact-derived enstatite meteorites
p 1243 N94-16305
Heterogeneous plagioclase compositions in the Maralinga CK4 chondrite p 1243 N94-16308
An experimental study of trace element partitioning between perovskite, hibonite and melt: Equilibrium values p 954 N94-16313
Isotopic signatures and distribution of nitrogen and trapped and radiogenic xenon in the Acapulco and FRO90011 meteorites p 1243 N94-16317
Osmium isotopes in Ivory Coast tektites: Confirmation of a meteoritic component and rhenium depletion
p 1244 N94-16321
Terrestrial bitumen analogue of orgueil organic material demonstrates high sensitivity to usual HF-HCl treatment
p 930 N94-16325
Chromite-rich mafic silicate chondrules in ordinary chondrites: Formation by impact melting
p 1244 N94-16330
The astrophysical interpretation of isotope anomalies in graphite and SiC grains of chondrites
p 1244 N94-16343
On possible Mn-53 heterogeneity in the early solar system p 1244 N94-16344
On origin of the olivine inclusions from the Kainsaz CO carbonaceous chondrite p 1244 N94-16345
A search for noble-gas evidence for presolar oxide grains p 954 N94-16353
INAA of CAIs from the Maralinga CK4 chondrite: Effects of parent body thermal metamorphism
p 1244 N94-16355
Chondritic ratios of Fe/Cr/Ir in Kerguelen Plateau (Hole 738C) K/T carbonate-rich sediments support asteroid-cometary impact at K/T time
p 1244 N94-16357
Noble gases in twenty Yamato H-chondrites: Comparison with Allan Hills chondrites and modern falls
p 1244 N94-16361
Experimentally reproduced relict enstatite in porphyritic chondrules of enstatite chondrite composition
p 1244 N94-16363
Possible sources of H2 to H2O enrichment at evaporation of parent chondritic material
p 1244 N94-16377
Effects of bulk composition on production rates of cosmogenic nuclides in meteorites p 1245 N94-16385
Classificational parameters for acapulcoites and lodranites: The cases of FRO 90011, EET 84302 and ALH A81187/84190 p 1245 N94-16389
The dregs of crystallization in Zagami
p 1245 N94-16390
The Nakhla parent melt: REE partition coefficients and clues to major element composition
p 1245 N94-16399
More on the cooling history of angrite LEW 86010
p 1245 N94-16400
Limited subsolidus diffusion in type B1 CAI: Evidence from Ti distribution in spinel p 954 N94-16401
Remote visual detection of impacts on the lunar surface p 1290 N94-16404
Al-26 production profile and model comparisons in Canyon Diablo p 1245 N94-16409
Exsolved kirschsteinite in angrite LEW86010 olivine
p 1245 N94-16410
Refractory precursor components in an Allende ferromagnesian chondrule p 1245 N94-16412
Igneous fractionation and subsolidus equilibration of diogenite meteorites p 1245 N94-16413
Siderophile element fractionation in meteor crater impact glasses and metallic spherules p 1246 N94-16414
Identification of new meteorite, Mihonoseki (L), from broken fragments in Japan p 1246 N94-16415
The thickness of eucritic crust in the HED parent body
p 1104 N94-16416
Zaoyang chondrite cooling history from pyroxene Fe(2+)-Mg intracrystalline ordering and exolutions
p 1246 N94-16417
A hydrogen isotope study of CO3 type carbonaceous chondrites; comparison with type 3 ordinary chondrites
p 1246 N94-16425

Solar noble gases revealed by closed system stepped etching of a metal separate from Fayetteville p 954 N94-16432
Nitrogen and light noble gases in Parsa enstatite chondrite p 1246 N94-16435

METEORITIC DAMAGE
Collisional and dynamical history of Gaspra p 1241 N94-16202
The depths of the largest impact craters on Venus p 1264 N94-16261

METEORITIC MICROSTRUCTURES
Experimentally reproduced relict enstatite in porphyritic chondrules of enstatite chondrite composition p 1244 N94-16363

METEOROID SHOWERS
Corvid meteoroids and a Giordano Bruno ray are genetically related p 1242 N94-16223

METEOROIDS
Corvid meteoroids and a Giordano Bruno ray are genetically related p 1242 N94-16223
Resolving LDEF's flux distribution: Orbital (debris?) and natural meteoroid populations p 1245 N94-16391
Remote visual detection of impacts on the lunar surface p 1290 N94-16404

METEOROLOGICAL INSTRUMENTS
A comparison of ceiling and visibility observation for NWS manned observation sites and ASOS sites [AD-A268356] p 1108 N94-17459

METEOROLOGICAL PARAMETERS
The MADONA experiments (Meteorology and Diffusion Over Non-uniform Areas): High-resolution in-plume concentration fluctuations measurements using lidar remote sensing technique [AD-A267711] p 1105 N94-14938
IAI topic: El Nino. Southern oscillation and interannual climate variability [INPE-5410-PRE/1757] p 1111 N94-15186
Determination of sunshine duration from radiation intensity pyranometric measurements of global and sky radiation [BER-181] p 1105 N94-15302
TAFVER 2 users manual [AD-A266850] p 1106 N94-15757
Environmental characterization for target acquisition. Report 1: Site descriptions and measurements [AD-A267192] p 1106 N94-15851
A comparison of cloud attenuation models using measured cloud data p 996 N94-16044
Spatial and frequency diversity in lidar systems [AD-A266192] p 1039 N94-16124
Earth imaging results from Galileo's second encounter p 1252 N94-16201
The multivariate optimum interpolation analysis of meteorological data at the Fleet Numerical Oceanography Center [AD-A266459] p 1106 N94-16568
Investigation of cloud properties and atmospheric stability with MODIS [NASA-CR-193475] p 1107 N94-16717
Mesoscale frontogenesis: An analysis of two cold front case studies [AD-A267950] p 1107 N94-17054
Phillips Laboratory global spectral numerical weather prediction model [AD-A267293] p 1107 N94-17244
Windshear database for forward-looking systems certification [NASA-TM-109012] p 1108 N94-17283
Arctic cyclones and Marginal Ice Zone (MIZ) variability [AD-A268610] p 1108 N94-17465
Atmospheric propagation analysis program [AD-A268231] p 1006 N94-17565
Forecasting the ducting of electromagnetic waves on the mesoscale [AD-A268101] p 1109 N94-17571
An empirical study of tropical cloud clusters using special sensor microwave imager data [AD-A268072] p 1110 N94-17595
The Central American cold surge: An observational analysis of the deep southward penetration of North American cold fronts [AD-A268592] p 1110 N94-17607

METEOROLOGICAL RADAR
Sensitivity testing of a single-Doppler temperature retrieval and forecast system [AD-A267278] p 1105 N94-14958
The Next Generation Weather Radar (NEXRAD)/Air Route Surveillance Radar (ARSR) operational comparison [REPT-93W0000145] p 987 N94-15439
Designing clutter rejection filters with complex coefficients for airborne pulsed Doppler weather radar [NASA-CR-4550] p 862 N94-15444
TRMM radar p 990 N94-15894
Windshear detection radar signal processing studies [NASA-CR-194615] p 994 N94-16022
Radar diagnostic parameters as indicators of severe weather in central Florida [PB93-183507] p 1106 N94-16465
Remote sensing of precipitation and electrification with a dual-polarization, coherent, wideband radar system [AD-A267479] p 1004 N94-17364
Automatic suppression of anomalous propagation clutter for noncoherent weather radars [KNMI-WR-92-06] p 1004 N94-17407

METEOROLOGICAL SATELLITES
The 1980 highlights [NASA-TM-109672] p 1303 N94-15509
Optical measurements of NASA/USAF CRRES high altitude rocket borne chemical release experiments in conjunction with the USAF airborne ionospheric observatory aircraft [AD-A266404] p 1101 N94-16551
The multivariate optimum interpolation analysis of meteorological data at the Fleet Numerical Oceanography Center [AD-A266459] p 1106 N94-16568
Nowcasting methods for satellite imagery [AD-A267294] p 1108 N94-17267

METEOROLOGICAL SERVICES
TAFVER 2 users manual [AD-A266850] p 1106 N94-15757
A comparison of ceiling and visibility observation for NWS manned observation sites and ASOS sites [AD-A268356] p 1108 N94-17459

METEOROLOGY
The MADONA experiments (Meteorology and Diffusion Over Non-uniform Areas): High-resolution in-plume concentration fluctuations measurements using lidar remote sensing technique [AD-A267711] p 1105 N94-14938
Mesoscale modeling of the atmosphere [AD-A263236] p 1098 N94-15132
Ensemble forecasting techniques in medium-range forecasting [AD-A267443] p 1107 N94-17029
Phillips Laboratory global spectral numerical weather prediction model [AD-A267293] p 1107 N94-17244

METHANE
Development of vanadium-phosphate catalysts for methanol production by selective oxidation of methane [DE93-016850] p 949 N94-16897
The photochemistry of poly(methylphenylphosphazene) [AD-A267320] p 970 N94-16948
Transient studies of low temperature catalysts for methane conversion [DE93-017710] p 950 N94-16962
Biofilm structure and diversity [AD-A267254] p 1118 N94-16989
Methyl chloride via oxyhydrochlorination of methane [DE93-017548] p 952 N94-17218
Strategy for the reduction of total integrated fluid logistics to the Space Station Freedom [NASA-TM-107744] p 1138 N94-17452

METHIONINE
The relationship of metallothionein induction to the heat shock response [AD-A266634] p 1122 N94-15741

METHOD OF CHARACTERISTICS
Shock-free supersonic elliptic nozzles and method of forming same [NASA-CASE-LAR-14054-1] p 925 N94-15947
General order characteristic methods for solving neutron transport problems [DE93-015824] p 1170 N94-16167
The (delta)f algorithm for beam dynamics [DE93-015632] p 1187 N94-16660

METHOD OF MOMENTS
Resonant frequencies of irregularly shaped microstrip antennas using method of moments [NASA-TP-3386] p 989 N94-15767
Analysis of electromagnetic scattering from irregularly shaped, thin, metallic flat plates [NASA-TP-3361] p 998 N94-16655
Application of the finite-difference time-domain method to scattering and radiation problems involving wires and plates [AD-A268396] p 1005 N94-17496

METHYL ALCOHOL
Contained liquids in microgravity, part 2 p 979 N94-16085
Development of vanadium-phosphate catalysts for methanol production by selective oxidation of methane [DE93-016850] p 949 N94-16897

METHYL CHLORIDE
Methyl chloride via oxyhydrochlorination of methane [DE93-017548] p 952 N94-17218

METHYL COMPOUNDS
High-valent oxo, methoxorhenium complexes: Models for intermediates and transition states in proton-coupled multi-electron transfer reactions [AD-A266492] p 1211 N94-16782
High octane ethers from synthesis gas-derived alcohols [DE93-016861] p 975 N94-16898
The photophysics of poly(methylphenylphosphazene) [AD-A267321] p 970 N94-16949

METROLOGY
An optically modulated scatterer for microwave antenna metrology [NPL-DES-126] p 986 N94-15020
Improved optical radiation detectors and their calibration: 200 nm - 30 microns p 906 N94-15075

MICA
The processing and mechanical properties of high temperature/high performance composites. Book 1: Coonstituent properties of composites [AD-A266394] p 935 N94-16483

MICROANALYSIS
Application of Z-contrast imaging to obtain column-by-column spectroscopic analysis of materials [DE93-015333] p 947 N94-16014
The role of carbon and temperature in determining electrical conductivity of basins, crust and mantle [DE93-015936] p 1101 N94-16840
Insights into semiconducting materials and growth phenomena through Z-contrast STEM [DE93-015964] p 1212 N94-16841
Electron spectroscopy analysis [NASA-CR-193591] p 951 N94-17039

MICROBURSTS (METEOROLOGY)
Windshear database for forward-looking systems certification [NASA-TM-109012] p 1108 N94-17283

MICROCHANNEL PLATES
Microchannel plate imaging detectors for the ultraviolet p 901 N94-15037
Microchannel plate detectors for space astronomy p 901 N94-15038
The MIC photon counting detector p 901 N94-15039
The STIS MAMA status: Current detector performance p 905 N94-15069
The Rutherford Appleton Laboratory photon counting detector p 910 N94-15096
Testing and management of flight instruments and their data [NASA-CR-194332] p 868 N94-15187
Performance optimization of detector electronics for millimeter laser ranging p 913 N94-15569
Performance comparison of high speed microchannel plate photomultiplier tubes p 922 N94-15624
Multi-frame x ray imaging with a large area 40ps camera [DE93-017179] p 1035 N94-16960
Detecting small debris using a ground-based photon counting detector [DE93-012623] p 898 N94-17669

MICROCLIMATOLOGY
USAF physiological studies of personal microclimate cooling: A review [AD-A267203] p 1022 N94-15858

MICROCOMPUTERS
Upgrading NASA/DOSE laser ranging system control computers p 918 N94-15595

MICROCRACKS
Thermo-mechanical analysis of oxidation protected carbon-carbon composites [AD-A268191] p 941 N94-17597

MICROCRYSTALS
A discontinuous melt sheet in the Manson impact structure p 1103 N94-16269

MICROELECTRONICS
Reliability characterization of digital microcircuits: Investigation of an in-process oxide reliability screening method [AD-A267053] p 1008 N94-15665
The specific heat of titanium disilicide [AD-A267543] p 960 N94-17100
Reliability analysis of Surface Mount Technology (SMT) [AD-A267598] p 1055 N94-17194
RF vacuum microelectronics [AD-A268399] p 1014 N94-17423
Field-emitter arrays for RF vacuum microelectronics [AD-A268397] p 1015 N94-17526
Smart Power: New power integrated circuit technologies and their applications [VTT-TIED-1358] p 1015 N94-17546
Field emitter arrays for RF vacuum microelectronics [AD-A268595] p 1015 N94-17608

MICROGRAVITY
Sounding Rocket Experiments in Fluid Science and Materials Sciences: TEXUS 25 to 27 and MASER 4, volume 3
[ESA-SP-1132-VOL-3] p 943 N94-15157
Measurements of Interfacial Tension: MITE p 943 N94-15158
Orientation of DNA during free-solution electrophoresis p 944 N94-15162
Density and temperature relaxation near the critical point of carbon dioxide under reduced gravity p 944 N94-15164
Temperature propagation in near-critical fluids prior to and during separation p 944 N94-15165
Pressures of supercritical salt solutions p 945 N94-15166
Unidirectional solidification of liquid-crystal material p 945 N94-15167
Partial melting experiment of Y-Ba-Cu oxide p 945 N94-15168
Liquid phase sintering of tungsten composites under microgravity. Effect of matrix composition p 945 N94-15171
Heat storage module p 946 N94-15172
Movement in microgravity
[NASA-TM-109526] p 881 N94-15389
Evaporation from a meniscus within a capillary tube in microgravity
[NASA-CR-194593] p 976 N94-15654
Mechanisms of combustion limits in premixed gas flames at microgravity
[NASA-CR-194557] p 946 N94-15713
Explosive boiling at very low heat fluxes: A microgravity phenomenon
[NASA-TM-106325] p 1046 N94-15817
A feasibility study of a microgravity enhancement system for Space Station Freedom
[NASA-CR-191550] p 886 N94-15864
Cultured normal mammalian tissue and process
[NASA-CASE-MSC-21984-1] p 1117 N94-15969
Proceedings of the Second Workshop on Microgravity Experimentation
[DSS-NR15-43-1990] p 977 N94-16071
Scientific use of Space Station Freedom p 977 N94-16072
The Japanese Space Station utilization plan p 977 N94-16074
Canadian microgravity experiments flown in 1989-1990 p 977 N94-16075
New findings and instrumentation from the NASA Lewis Microgravity Facility p 977 N94-16076
Laser-liquid interactions under reduced gravity conditions p 977 N94-16077
The vibro-acoustic mapping of low gravity trajectories on a Learjet aircraft p 978 N94-16078
MAXUS: The new sounding rocket program for long duration microgravity flight p 978 N94-16079
Optical systems for the visualization of fluid and solid transparent media under microgravity conditions p 978 N94-16081
QUESTS: A microgravity research facility for materials science experiments p 978 N94-16082
Payloads for the processing of high temperature materials p 979 N94-16083
The Canadian Space Station user development program. Where do we go from here? p 898 N94-16084
Contained liquids in microgravity, part 2 p 979 N94-16085
Study of fractal aggregates p 979 N94-16086
Investigation of two-phase flow and boiling heat transfer during quenching of a tube under microgravity p 979 N94-16087
Use of microgravity in the synthesis of ceramics using sol gel techniques p 979 N94-16088
Gas bubble generation and transport in microgravity p 980 N94-16089
Infra Link: A data transmission system for microgravity research p 980 N94-16091
Characteristics of aimed arm movements in humans under low gravity p 980 N94-16093
Statistical techniques for study design of microgravity life sciences experiments p 980 N94-16094
Transcranial Doppler ultrasound studies of cerebral blood-flow in microgravity p 981 N94-16095
Human ocular torsion during parabolic flight: An investigation using electromagnetic scleral search coil p 981 N94-16096
Heart rate response to parabolic flight manoeuvres p 981 N94-16098
Finite element analytical techniques for ceramic production in microgravity: A hypoelastic model p 981 N94-16099
Precise measurement and utilization of acceleration data p 923 N94-16100
The design and analysis of a modular microgravity test platform for use aboard the NASA KC-135 aircraft p 899 N94-16101
Solution behaviour in microgravity: Considerations for protein crystal growth p 982 N94-16102
Materials processing in space: Issues for the third decade
[TABES PAPER 93-260] p 983 N94-16133
Growth of single crystals of mercuric iodide on the ground and in space
[DE93-015523] p 1209 N94-16442
Looking at science on board Eureca
[ESA-BR-80] p 874 N94-16584
Studies of premixed laminar and turbulent flames at microgravity
[NASA-CR-194656] p 951 N94-17125
The 1990-1991 NASA space biology accomplishments
[NASA-TM-4501] p 1118 N94-17257
Ground testing for the no-vent fill of cryogenic tanks: Results of tests for a 71 cubic foot tank
[NASA-TM-106293] p 1030 N94-17486
Ontogenesis of mammals in microgravity
[NASA-TM-103978] p 1139 N94-17636

MICROGRAVITY APPLICATIONS
Scientific use of Space Station Freedom p 977 N94-16072
The ESA telescience program p 977 N94-16073
The Japanese Space Station utilization plan p 977 N94-16074
New findings and instrumentation from the NASA Lewis Microgravity Facility p 977 N94-16076
Laser-liquid interactions under reduced gravity conditions p 977 N94-16077
The vibro-acoustic mapping of low gravity trajectories on a Learjet aircraft p 978 N94-16078
MAXUS: The new sounding rocket program for long duration microgravity flight p 978 N94-16079
Development of the Laser-based R/D Test-bed System (LTS) p 978 N94-16080
Optical systems for the visualization of fluid and solid transparent media under microgravity conditions p 978 N94-16081
QUESTS: A microgravity research facility for materials science experiments p 978 N94-16082
Payloads for the processing of high temperature materials p 979 N94-16083
Materials processing in space: Issues for the third decade
[TABES PAPER 93-260] p 983 N94-16133

MICROHARDNESS
Laser-shock damage of iron-based materials
[AD-A267196] p 1038 N94-15852
Ion implantation effects on surface-mechanical properties of metals and polymers
[DE93-014661] p 958 N94-16453
Investigation of the origin of hot spots in deformed crystals: Ammonium perchlorate studies
[AD-A267692] p 1214 N94-17270
Mechanical properties and crystal growth studies of semiconductor alloys
[AD-A268144] p 1216 N94-17454

MICROMECHANICS
Inelastic deformation of metal matrix composites
[NASA-CR-191522] p 930 N94-15106
Environmental effects on elevated temperature subcritical crack growth of SiC/SiC composites
[DE93-015688] p 934 N94-16158
Micromechanisms of monotonic and cyclic subcritical crack growth in advanced high melting point low-ductility intermetallics
[AD-A267764] p 961 N94-17223
Micromechanics modeling and analysis of Haversian compact bone tissues as a fiber reinforced composite material
[AD-A268250] p 1129 N94-17456
Thermo-mechanical analysis of oxidation protected carbon-carbon composites
[AD-A268191] p 941 N94-17597

MICROMETEORITES
Removal of carbonaceous contaminants from silica aerogel p 953 N94-16256
An iridium-rich iron micrometeorite with silicate inclusions from the Moon p 1242 N94-16281
Size distribution of interplanetary iron and stony particles related with deep-sea spherules p 1245 N94-16388

MICROMETEOROIDS
Long Duration Exposure Facility experiment M0003 deintegration/findings and impacts
[AD-A267140] p 885 N94-15749
Impact penetration experiments in teflon targets of variable thickness p 1063 N94-16253
Densities of 5-15 micron interplanetary dust particles p 1244 N94-16367
The effect of an on-orbit near encounter on the number flux density of micron sized particles p 899 N94-16374
Dust grain resonant capture: A statistical study p 1245 N94-16384
Resolving LDEF's flux distribution: Orbital (debris?) and natural meteoroid populations p 1245 N94-16391

MICROORGANISMS
Regulation of attached bacterial growth by adsorbed proteins
[AD-A267756] p 1118 N94-17275

MICROPHONES
Free-field sensitivity calibration of laboratory standard microphones by the reciprocity technique: Measurements for the 1991 EEC intercomparison
[NPL-RSA(EXT)-0043] p 1176 N94-15019

MICROPHOTOGRAPHS
The effect of an on-orbit near encounter on the number flux density of micron sized particles p 899 N94-16374

MICROPOROSITY
Gas separations using ceramic membranes
[DE93-000278] p 947 N94-15861

MICROPROCESSORS
VLSI for high-speed digital signal processing
[AD-A267709] p 1007 N94-14936
A microprocessor controller for a towing tank drive and flow visualisation system
[AD-A267087] p 872 N94-15543
Embedded computer systems: Status of C-17 software
[AD-A267307] p 1160 N94-16993

MICROSCOPES
Optical displays: A tutorial on images and image formation
[AD-A266230] p 1192 N94-16926

MICROSCOPY
Atomic-scale friction measurements using friction force microscopy. Part 1: General principles and new measurement techniques
[AD-A268391] p 1048 N94-17533

MICROSTRIP ANTENNAS
Proceedings of the 1992 Antenna Applications Symposium, volume 2
[AD-A266916] p 986 N94-14998
Resonant frequencies of irregularly shaped microstrip antennas using method of moments
[NASA-TP-3386] p 989 N94-15767
Dual polarization microstrip array antenna
[CA-PATENT-1-307-842] p 994 N94-15986
Proceedings of the 1992 Antenna Applications Symposium, volume 1
[AD-A268167] p 1005 N94-17431

MICROSTRIP DEVICES
The imaging microstrip proportional counter: Features of a practical design p 900 N94-15030
Monte Carlo simulation of the microstrip gas counter
[NIKHEF-H/93-07] p 1035 N94-17619

MICROSTRUCTURE
Characterization of the cyclic plasticity of polycrystalline aluminum in the 90-300K domain: Use of the ultrasonic wave coupling technique - low frequency restraint
[ISAL-92-0083] p 954 N94-14930
Dynamic behavior of fiber and particle reinforced composites
[AD-A266905] p 930 N94-15143
Partial melting experiment of Y-Ba-Cu oxide p 945 N94-15168
Self-diffusion coefficients of sol-gel intermediates
[AD-A266957] p 963 N94-15179
Structural investigation of electrochemically etched silicon
[DE93-015300] p 1207 N94-15827
Laser-shock damage of iron-based materials
[AD-A267196] p 1038 N94-15852
Ternary alloying effects in polycrystalline (beta)-NiAl
[DE93-012675] p 955 N94-15885
Passive oxide films on well-defined nickel surfaces: An examination of film growth on Ni(100) with ex situ scanning tunneling microscopy
[DE93-014056] p 1207 N94-15923
Dynamical Ising model simulations of nucleation and growth in copper-cobalt alloys
[DE93-015336] p 957 N94-16015
Rheology and microstructure of concentrated zirconia-alumina suspensions for gelcasting composites
[DE93-015339] p 966 N94-16016
The influence of microstructure on the mechanical behavior of silicon nitride ceramics
[DE93-015363] p 966 N94-16018
The effect of long-term aging on the impact properties of modified 9Cr-1Mo steel
[DE93-015453] p 957 N94-16068
The influence of thermal aging on the microstructure and fatigue properties of modified 9Cr-1Mo steel
[DE93-015489] p 957 N94-16106
Cation ordering in orthopyroxenes and cooling rates of meteorites: Low temperature cooling rates of Estherville, Bondoc and Shaw p 1241 N94-16176

Classificational parameters for acapulcoites and lodranites: The cases of FRO 90011, EET 84302 and ALH A81187/84190 p 1245 N94-16389
Ion implantation effects on surface-mechanical properties of metals and polymers
[DE93-014661] p 958 N94-16453
Thermal stress effects in intermetallic matrix composites
[NASA-CR-191191] p 1054 N94-16518
Evolution of microstructure in face centered cubic metals during irradiation: A review
[DE93-015682] p 958 N94-16662
Ultrafast processes in tunneling microstructure devices
[AD-A266570] p 1210 N94-16720
Microstructure of Zr3Al after 2 MeV proton bombardment
[DE93-015331] p 1211 N94-16814
The Ceramic Technology Project: Ten years of progress
[DE93-015991] p 968 N94-16843
Effects of processing and prolonged high temperature exposure on the microstructure of Nb-1Zr-C sheet
[NASA-TM-106370] p 959 N94-16883
Slip, twinning and transformation in Laves phases
[DE93-018164] p 960 N94-16972
Transformation toughening of composite ceramics
[AD-A267304] p 971 N94-16980
Investigation of the origin of hot spots in deformed crystals: Ammonium perchlorate studies
[AD-A267692] p 1214 N94-17270
Micromechanics modeling and analysis of Haversian compact bone tissues as a fiber reinforced composite material
[AD-A268250] p 1129 N94-17456

MICROWAVE AMPLIFIERS
Field-emitter arrays for RF vacuum microelectronics
[AD-A268397] p 1015 N94-17526

MICROWAVE ANTENNAS
An optically modulated scatterer for microwave antenna metrology
[NPL-DES-126] p 986 N94-15020
Experimental evaluation of an adaptive focusing algorithm for a microwave planar phased-array hyperthermia system at UCSF
[AD-A267004] p 1121 N94-15634
Method and apparatus for forming an agile plasma mirror effective as a microwave reflector
[AD-D015788] p 998 N94-16535
The TOPSAR interferometric radar topographic mapping instrument p 1078 N94-16749
True time delay optically controlled dual band transmitter
[AD-A267663] p 1003 N94-17228

MICROWAVE EQUIPMENT
Synthesis of ceramic oxide powders in a microwave plasma device
[DE93-012741] p 965 N94-15920
A modified two-fluid model of conductivity for superconducting surface resistance calculation
[AD-A267549] p 1013 N94-17104

MICROWAVE FREQUENCIES
Recent scientific advances in the use of radar in scientific hydrology p 991 N94-15895

MICROWAVE IMAGERY
Fine scale measurements of microwave backscatter from the ocean surface
[AD-A264516] p 1111 N94-15134
A summary of microwave remote sensing investigations planned for BOREAS p 993 N94-15914
An analysis of simulated and actual DMSP SSM/T-2 brightness temperatures
[AD-A268103] p 1109 N94-17573
An empirical study of tropical cloud clusters using special sensor microwave imager data
[AD-A268072] p 1110 N94-17595

MICROWAVE OSCILLATORS
Measurements of the operation of the SINUS-6/BWO system
[AD-A266423] p 1011 N94-16556
Optically-switched submillimeter-wave oscillator and radiator
[NASA-CASE-NPO-18547-1-CU] p 1014 N94-17324

MICROWAVE PROBES
An optically modulated scatterer for microwave antenna metrology
[NPL-DES-126] p 986 N94-15020

MICROWAVE RADIOMETERS
Comparison of OLYMPUS beacon and radiometric attenuation measurements at Blacksburg, Virginia p 996 N94-16046
Earth observation from small satellites p 891 N94-17150
Validation and analysis of microwave-derived rainfall over the tropics
[AD-A267785] p 1108 N94-17303
Arctic and Antarctic sea ice, 1978-1987: Satellite passive-microwave observations and analysis
[NASA-SP-511] p 1114 N94-17439
A conceptual design study for a two-dimensional, electronically scanned thinned array radiometer
[NASA-TM-109051] p 1085 N94-17665

MICROWAVE REFLECTOMETERS
Microwave reflectometer ionization sensor
[NASA-CR-191464] p 922 N94-17083

MICROWAVE SCATTERING
Fine scale measurements of microwave backscatter from the ocean surface
[AD-A264516] p 1111 N94-15134

MICROWAVE SENSORS
Relating multifrequency radar backscattering to forest biomass: Modeling and AIRSAR measurement p 1077 N94-16741

MICROWAVE SIGNATURES
Microwave properties and systems overview p 924 N94-15222

MICROWAVE TRANSMISSION
True time delay optically controlled dual band transmitter
[AD-A267663] p 1003 N94-17228

MICROWAVES
Velocity matched millimeterwave electro-optic modulator
[AD-A267264] p 1188 N94-14957
Microwave interaction with plasmas
[AD-A267048] p 1201 N94-15661
The pressure broadening of HDO by O2, N2, H2, and He between 100 K and 600 K
[AD-A267118] p 946 N94-15684
Crystallization of grain boundary phases in silicon nitride with low additive contents by microwave annealing
[DE93-015801] p 1209 N94-16164
Efficient computational methods to study new and innovative signal detection techniques in SETI
[NASA-CR-193602] p 998 N94-16649
Processing of complex sintered reaction bonded silicon nitride parts by microwave heating
[DE93-015811] p 969 N94-16877
Large signal characterization and modeling of heterojunction bipolar transistors
[AD-A266184] p 1012 N94-16935
The behavioral toxicology of high-peak, low average power, pulsed microwave irradiation
[AD-A268392] p 1134 N94-17535

MID-OCEAN RIDGES
Assimilation of solids during ascent of magmas from the Bartoy Field of the Baikal Region, Siberia p 1103 N94-16214

MIDAIR COLLISIONS
National Transportation Safety Board annual review of aircraft accident data, US general aviation, calendar year 1989
[PB93-160687] p 863 N94-16464

MIDALTITUDE
MAGSS-14: Medium Altitude Global Mobile Satellite System with enhanced regional coverage p 893 N94-17164

MIDDLE ATMOSPHERE
Second flight of the Spacelab grille spectrometer during the Atlas-1 mission
[AERONAUTICA-ACTA-A-367-199] p 923 N94-17592

MIE SCATTERING
A test of the applicability of independent scattering to high albedo planetary regoliths p 1250 N94-16187

MILITARY AIR FACILITIES
The use of the Air Force Academy high wind alert system in forecasting moderate intensity wind events for military bases in the Colorado Springs area
[AD-A267648] p 1107 N94-17245

MILITARY AIRCRAFT
Naval aviation: The Navy is taking actions to improve the combat capabilities of its tactical aircraft. Report to Congressional Requesters
[AD-A268002] p 868 N94-17472

MILITARY AVIATION
Naval aviation: The Navy is taking actions to improve the combat capabilities of its tactical aircraft. Report to Congressional Requesters
[AD-A268002] p 868 N94-17472

MILITARY OPERATIONS
Sleep management user's guide for special operations personnel
[AD-A267746] p 1119 N94-14943
Space countersurveillance: A requisite for theater defense planning
[AD-A266871] p 884 N94-15147
Technical evaluation report on the AGARD-PEP Specialists Meeting on Combat Aircraft Noise
[NLR-TP-91445-U] p 1177 N94-15506
Annual historical report, calendar year 1992
[AD-A267050] p 1121 N94-15663
Technical urban search and rescue, System To Locate Survivors (STOLS) units: Operator's manual
[AD-A266317] p 862 N94-16438
Design Quality Task Force survey comments
[AD-A266283] p 1225 N94-16473
Not ready for the first space war. What about the second?
[AD-A266557] p 1174 N94-16665
Nonlinear methods for communications
[AD-A267376] p 1001 N94-17019
Military space programs in the press: An analysis for change
[AD-A267799] p 874 N94-17306

MILITARY SPACECRAFT
Military satellite communications: Opportunity to save billions of dollars. Report to the Chairman, Legislation, and National Security Subcommittee, Committee on Government Operations, House of Representatives
[AD-A267627] p 1002 N94-17199

MILITARY TECHNOLOGY
Symposium on the Future of Aeronautics in the Netherlands
[ETN-93-93780] p 853 N94-15120
Expectations for the future of military aviation p 854 N94-15128
Annual historical report, calendar year 1992
[AD-A267050] p 1121 N94-15663
Multiobjective functions optimization for task allocation mapping to multicomputer nodes
[AD-A267071] p 1146 N94-15670
TABES 1993: 9th Annual Technical and Business Exhibition and Symposium p 1050 N94-16129
Modeling and simulation: A key to future defense technology
[TABES PAPER 93-654] p 1054 N94-16153
SONOS technology for commercial and military nonvolatile memory applications
[DE93-015647] p 1011 N94-16661
Not ready for the first space war. What about the second?
[AD-A266557] p 1174 N94-16665
Diffractive optics in adverse environments p 1197 N94-17352
Radar transmitter procedures
[AD-A268274] p 1005 N94-17523

MILLIMETER WAVES
Velocity matched millimeterwave electro-optic modulator
[AD-A267264] p 1188 N94-14957
Applications of SLR p 911 N94-15556
New methods of generation of ultrashort laser pulses for ranging p 913 N94-15565
Millimeter accuracy satellites for two color ranging p 916 N94-15583
Improvement of SLR accuracy, a possible new step p 917 N94-15588

MILLING
Selective formation of porous silicon
[NASA-CASE-NPO-18735-1-CU] p 966 N94-15960

MIMD (COMPUTERS)
A trace-based comparison of shared memory multiprocessor architectures
[TR-432] p 1159 N94-16577

MINERAL DEPOSITS
A mineralized zone in Western Candor Chasma, Mars p 1248 N94-16179
Explosive mafic volcanism on Earth and Mars p 1253 N94-16204
A Moessbauer spectrometer for the mineralogical analysis of the Mars surface: First temperature dependent tests of the detector and drive system p 1259 N94-16233
A Monazite-bearing clast in Apollo 17 melt breccia p 1267 N94-16279
The influence of oceans on Martian volcanism p 1295 N94-16427
AVIRIS study of Death Valley evaporite deposits using least-squares band-fitting methods p 1067 N94-16676
Ground-truthing AVIRIS mineral mapping at Cuprite, Nevada p 1069 N94-16682
Expert system-based mineral mapping using AVIRIS p 1073 N94-16704

MINERALOGY
A mineralized zone in Western Candor Chasma, Mars p 1248 N94-16179
Grosnaja ABCs: Magnesium isotope compositions p 1241 N94-16191
Euromet Ureilite Consortium: A preliminary report on carbon and nitrogen geochemistry p 1241 N94-16192
Rover mounted ground penetrating radar as a tool for investigating the near-surface of Mars and beyong p 1007 N94-16197
Petrography, mineralogy, and Mg isotope composition of VICTA: A vigarano CaAl4O7-bearing type A inclusion p 1103 N94-16203

Explosive mafic volcanism on Earth and Mars p 1253 N94-16204
Pyroxene equilibration temperatures in metamorphosed ordinary chondrites p 1242 N94-16224
Lunar impact basins: New data for the nearside northern high latitudes and eastern limb from the second Galileo flyby p 1258 N94-16228
Lunar scout missions: Galileo encounter results and application to scientific problems and exploration requirements p 1259 N94-16229
A Moessbauer spectrometer for the mineralogical analysis of the Mars surface: First temperature dependent tests of the detector and drive system p 1259 N94-16233
The group A3 chondrules of Krymka: Further evidence for major evaporative loss during the formation of chondrules p 1242 N94-16257
Shock-thermal history of Kapoeta howardite matter on data of thermoluminescence analysis of individual mineral grains p 953 N94-16267
Searching for neuKREEP: An EMP study of Apollo 11 Group A basalts p 1266 N94-16275
A Monazite-bearing clast in Apollo 17 melt breccia p 1267 N94-16279
Carbon abundances, major element chemistry, and mineralogy of hydrated interplanetary dust particles p 1243 N94-16309
An initial perspective of S-asteroid subtypes within asteroid families p 1243 N94-16310
Isotopic signatures and distribution of nitrogen and trapped and radiogenic xenon in the Acapulco and FRO90011 meteorites p 1243 N94-16317
Chromite-rich mafic silicate chondrules in ordinary chondrites: Formation by impact melting p 1244 N94-16330
On possible Mn-53 heterogeneity in the early solar system p 1244 N94-16344
The Nakhla parent melt: REE partition coefficients and clues to major element composition p 1245 N94-16399
More on the cooling history of angrite LEW 86010 p 1245 N94-16400
Deucalionis Regio, Mars: Evidence for a unique mineralogic endmember and a crusted surface p 1291 N94-16406
Exsolved kirschsteinite in angrite LEW86010 olivine p 1245 N94-16410
Analysis of pyroxene absorptions observed in Martian dark regions p 1292 N94-16411
Igneous fractionation and subsolidus equilibration of diogenite meteorites p 1245 N94-16413
Siderophile element fractionation in meteor crater impact glasses and metallic spherules p 1246 N94-16414
Identification of new meteorite, Mihonoseki (L), from broken fragments in Japan p 1246 N94-16415
The thickness of eucritic crust in the HED parent body p 1104 N94-16416
Optical effects of regolith processes on S asteroids as simulated by laser impulse alteration of ordinary chondrite p 1246 N94-16422
Bright soil units on Mars determined from ISM imaging spectrometer data p 1295 N94-16430
Variations in the Fe mineralogy of bright Martian soil p 1295 N94-16431
Composition of weakly altered Martian crust p 1296 N94-16436
Mapping the mineralogy and lithology of Canyonlands, Utah with imaging spectrometer data and the multiple spectral feature mapping algorithm p 1066 N94-16670
First results from analysis of coordinated AVIRIS, TIMS, and ISM (French) data for the Ronda (Spain) and Beni Bousera (Morocco) peridotites p 1067 N94-16675
Integrating remote sensing techniques at Cuprite, Nevada: AVIRIS, Thematic Mapper, and field spectroscopy p 1072 N94-16701
Expert system-based mineral mapping using AVIRIS p 1073 N94-16704

MINERALS
The Fe2(+)-Mg interdiffusion in orthopyroxene: Constraints from cation ordering and structural data and implications for cooling rates of meteorites p 1241 N94-16175
Stalking the LREE-enriched component in ureilites p 1241 N94-16190
Euromet Ureilite Consortium: A preliminary report on carbon and nitrogen geochemistry p 1241 N94-16192
Lunar impact basins: New data for the nearside northern high latitudes and eastern limb from the second Galileo flyby p 1258 N94-16228
A Moessbauer spectrometer for the mineralogical analysis of the Mars surface: First temperature dependent tests of the detector and drive system p 1259 N94-16233
Complex radiation-thermal history of Kaidun meteorite on data of track study of silicate minerals p 1243 N94-16297
Refractory precursor components in an Allende ferromagnesian chondrule p 1245 N94-16412
From minerals to rocks: Toward modeling lithologies with remote sensing p 1086 N94-16437
Preliminary analysis of thermal-infrared multispectral scanner data of the Iron Hill, Colorado carbonatite-alkalic rock complex p 1065 N94-16605
Ejecta patterns of Meteor Crater, Arizona derived from the linear un-mixing of TIMS data and laboratory thermal emission spectra p 1065 N94-16607
Mapping the mineralogy and lithology of Canyonlands, Utah with imaging spectrometer data and the multiple spectral feature mapping algorithm p 1066 N94-16670
AVIRIS as a tool for carbonatite exploration: Comparison of SPAM and Mbandmap data analysis methods p 1073 N94-16703

MINICOMPUTERS
Upgrading NASA/DOSE laser ranging system control computers p 918 N94-15595

MINIMAX TECHNIQUE
Finding stable orientations of assemblies with linear programming [AD-A266990] p 1143 N94-15212

MIRANDA
Voyager encounters Uranus [NASA-TM-109619] p 1247 N94-15348
Spacework 16 — Simulated Space Shuttle Program [NASA-TM-109436] p 1221 N94-15420

MIRRORS
Rotary encoding device [NASA-CASE-GSC-13556-1] p 1148 N94-15943
Method and apparatus for forming an agile plasma mirror effective as a microwave reflector [AD-D015788] p 998 N94-16535

MIS (SEMICONDUCTORS)
Atomic layer epitaxy of boron nitride [AD-A266260] p 1212 N94-16932

MISALIGNMENT
Systematic study of effects of load misalignment in uniaxial low cycle fatigue testing at high temperatures [NPL-DMM(A)-27] p 1057 N94-15015

MISS DISTANCE
Hypervelocity orbital intercept guidance using certainty control [AD-A267297] p 1174 N94-17219

MISSILE CONFIGURATIONS
Missile datcom user's manual [AD-A267447] p 1152 N94-17032

MISSILE CONTROL
Wind tunnel investigation with an operational turbojet engine [TABES PAPER 93-662] p 870 N94-16157

MISSILE DEFENSE
Plume radiation p 924 N94-15223

MISSILE DESIGN
Missile datcom user's manual [AD-A267447] p 1152 N94-17032

MISSILE DETECTION
Rocket Motor Plume Technology [AGARD-LS-188] p 923 N94-15217
Plume primary smoke p 923 N94-15218
Microwave properties and systems overview p 924 N94-15222

MISSILE SIGNATURES
Propulsion p 924 N94-15219
Microwave properties and systems overview p 924 N94-15222

MISSILE SYSTEMS
Propulsion p 924 N94-15219
Dependable software technology exchange [AD-A267103] p 1146 N94-15638

MISSILE TRAJECTORIES
Hypervelocity orbital intercept guidance usirlg certainty control [AD-A267297] p 1174 N94-17219

MISSILES
The effect of the nose shape and wing location toward the wing vortex breakdown [AD-A267724] p 855 N94-14942
Wind tunnel investigation with an operational turbojet engine [TABES PAPER 93-662] p 870 N94-16157
Missile datcom user's manual [AD-A267447] p 1152 N94-17032

MISSION ADAPTIVE WINGS
Mission adaptive wing [NASA-TM-109448] p 865 N94-15321

MISSION PLANNING
Pre-phase a study report of lunar polar orbiter [NASDA-TK-SS0440] p 873 N94-15000
HSTS: Integrating planning and scheduling [AD-A266991] p 1222 N94-15213
Dare to dream — The Space Station Freedom development [NASA-TM-109512] p 885 N94-15458
STS-26 crew participation in meetings [NASA-TM-109519] p 873 N94-15469
Mars rover sample return mission [NASA-TM-109521] p 873 N94-15471
Commitment to challenge [NASA-TM-109523] p 876 N94-15473
Long Duration Exposure Facility [NASA-TM-109427] p 885 N94-15497
SATCOP mission planning software package p 912 N94-15562
AIRSAR South American deployment: Operation plan, version 3.0 p 994 N94-15919
Scientific use of Space Station Freedom p 977 N94-16072
Approaching the new reality [TABES PAPER 93-230] p 1050 N94-16131
A mission concept of Phobos/Deimos exploration p 1287 N94-16387
Chairmanship of the Neptune/Pluto outer planets science working group [NASA-CR-194625] p 1297 N94-16832
AMIGAU: A prototype tool aimed at mission analysis for satellites and satellite constellations p 888 N94-17133
Small missions for space science p 874 N94-17142
Strategy for a small satellite program and a proposal for a first mission p 874 N94-17143
Small satellite missions to long-period comets p 874 N94-17144
Big results with small space systems: What small systems are doing today p 896 N94-17187
Human Transportation System (HTS) study, volume 2 [NASA-TM-104779-VOL-2] p 882 N94-17320

MIXING
Hot electron mixers, the potential competition p 903 N94-15055

MIXING LAYERS (FLUIDS)
Large eddy simulation and direct numerical simulation of high speed turbulent reacting flows [NASA-CR-193131] p 1018 N94-15427
Parametric resonant triad interactions in a free shear layer [NASA-TM-106365] p 1021 N94-15751
Three dimensional hydrodynamic calculations with adaptive mesh refinement of the evolution of Rayleigh Taylor and Richtmyer Meshkov instabilities in converging geometry: Multi-mode perturbations [DE93-017155] p 1025 N94-16903
Transmission of light through a turbulent mixing layer [AD-A267266] p 1193 N94-17264

MOBILE COMMUNICATION SYSTEMS
Propagation-related AMT design aspects and supporting experiments p 995 N94-16042
Propagation research in Japan p 996 N94-16043
The ORBCOMM system p 893 N94-17163
MAGSS-14: Medium Altitude Global Mobile Satellite System with enhanced regional coverage p 893 N94-17164
The ELLIPSO (tm) system: Elliptical low orbits for mobile communications p 893 N94-17167

MODAL RESPONSE
A simplistic look at limit stresses from random loading [NASA-TM-108427] p 1058 N94-15710

MODELS
Infrared remote activity transceiver universal model [AD-A266965] p 1188 N94-15144
Geophysical models of Western Aphrodite-Niobe region: Venus p 1286 N94-16382
Multi-resolution processing for fractal analysis of airborne remotely sensed data p 1065 N94-16604
The dynamics of hydroponic crops for simulation studies of the CELSS initial reference configurations [NASA-CR-194654] p 1118 N94-17279

MODULATED CONTINUOUS RADIATION
Microwave reflectometer ionization sensor [NASA-CR-191464] p 922 N94-17083

MODULATION
Controlling chaotic behavior in CO2 and other lasers [AD-A266431] p 1040 N94-16546
Diffuse scattering and image contrast of tweed in superconducting oxides: A simulation and interpretation [DE93-016131] p 1212 N94-16844
Nonlinear methods for communications [AD-A267376] p 1001 N94-17019
Field-emitter arrays for RF vacuum microelectronics [AD-A268397] p 1015 N94-17526

MODULATORS
Optical residue processing module [AD-A267721] p 1188 N94-14940
Velocity matched millimeterwave electro-optic modulator [AD-A267264] p 1188 N94-14957

Controlling chaotic behavior in CO2 and other lasers
[AD-A266431] p 1040 N94-16546
Four Frequency-Shift Keying (4-FSK) spread spectrum modulator and demodulator
[AD-A267433] p 1000 N94-16979
High-speed nonlinear switching mechanisms and devices for multi-gigabit data processing
[AD-A267753] p 1014 N94-17375
Optimal pulse modulator design criteria for plasma source ion implanters
[DE93-016465] p 1205 N94-17645

MODULES
SAR sensor electronics: T/R modules
p 993 N94-15911

MODULUS OF ELASTICITY
Experimental study of nonassociated flow and instability of frictional materials
[AD-A266421] p 1024 N94-16555
The determination of the Young moduli of a material after exposure to laser light and delineation of the zone of laser alterations
[IFTR-37/1991] p 1061 N94-17058

MOIRE INTERFEROMETRY
Optical systems for the visualization of fluid and solid transparent media under microgravity conditions
p 978 N94-16081
J-integral and HRR field associated with stable crack growth in thin aluminum SEN specimen
[AD-A267879] p 960 N94-17041

MOISTURE CONTENT
An assessment of acid fog
[DE93-009347] p 1095 N94-15940
A detailed model for simulation of catchment scale subsurface hydrologic processes
[PAPER-92WR02333] p 1084 N94-16032
Water in Earth's mantle: Hydrogen analysis of mantle olivine, pyroxenes and garnet using the SIMS
p 1104 N94-16336
Bright soil units on Mars determined from ISM imaging spectrometer data p 1295 N94-16430
A snow wetness retrieval algorithm for SAR
p 1075 N94-16732

MOLDING MATERIALS
Fabrication of advanced design (grooved) cermet anodes
[DE93-014590] p 1012 N94-16765

MOLDS
Remelting of Fe-C-Si-alloy in a ceramic mold skin
p 945 N94-15169

MOLECULAR BEAM EPITAXY
Magneto-optic superlattice thin films: Fabrication, structural and magnetic characterization
p 974 N94-14982
High temperature superconductivity
[AD-A267006] p 1008 N94-15635
Laboratory for x ray optics
[AD-A267149] p 1189 N94-15735
A high flux radical beam diamond growth
[AD-A266754] p 1207 N94-15955
JSEP fellowship
[AD-A266568] p 1211 N94-16800
Growth and doping of Al(x)Ga(1-x)N films by electron cyclotron resonance assisted molecular beam epitaxy
[AD-A267305] p 1212 N94-16992
Nitride semiconductors for ultraviolet detection
[AD-A267877] p 1012 N94-17040
Photo-assisted epitaxial growth for III-V semiconductors
[AD-A267889] p 1213 N94-17042
Curved grating fabrication techniques for concentric-circle grating, surface-emitting semiconductor lasers p 1045 N94-17349
Interface properties of wide bandgap semiconductor structures
[AD-A268269] p 1215 N94-17377
Precise flux control for lattice matched superlattice materials
[AD-A268254] p 1215 N94-17417
Low temperature deposition and characterization of n- and p-type silicon carbide thin films and associated ohmic and Schottky contacts
[AD-A267966] p 973 N94-17490
Epitaxial iron films
[AD-A268286] p 1217 N94-17579
Mechanical properties of interfaces and superlattices
[AD-A268591] p 1217 N94-17606

MOLECULAR BEAMS
Molecular beam studies of reaction dynamics
[DE93-015035] p 1181 N94-15995

MOLECULAR CLOUDS
Boundary conditions for the paleoenvironment: Chemical and physical processes in the pre-solar nebula
[NASA-CR-194418] p 1298 N94-15421
ROSAT-IUE observations of symbiotic stars. The x ray morphology of high latitude associations
[NASA-CR-194616] p 1236 N94-16492
Collisional dynamics of perturbed particle disks in the solar system
[NASA-CR-193584] p 1239 N94-16648

MOLECULAR COLLISIONS
Single-collision studies of energy transfer and chemical reaction
[DE93-017603] p 1182 N94-16121
Atomic processes in hydrogen and deuterium negative ion discharges
[DE93-013432] p 1183 N94-16817

MOLECULAR DIFFUSION
Reaction and diffusion in turbulent combustion
[DE93-017085] p 943 N94-15146
The influence of an electric field on the kinetics of nucleation
[IFTR-2/91] p 1213 N94-17046

MOLECULAR EXCITATION
Theoretical prediction of the UV adsorption and fluorescence spectra of tyrosine and phenylalanine
[AD-A266970] p 943 N94-15111
Molecular processes in comets
[NASA-CR-194148] p 1239 N94-15188
Synthesis and chemistry of novel cyclic fluorocarbons
[AD-A267148] p 929 N94-15734
The photophysics of poly(methylphenylphosphazene)
[AD-A267321] p 970 N94-16949
Interface properties of wide bandgap semiconductor structures
[AD-A268269] p 1215 N94-17377
In-situ electron and optical spectroscopies of transiational and vibrational activated bond breaking and formation on semiconductors
[AD-A268192] p 1015 N94-17560

MOLECULAR GASES
Study of multi-dimensional radiative energy transfer in molecular gases
[NASA-CR-194613] p 1181 N94-15752
BACKSCAT lidar simulation version 3.0: Technical documentation and users guide
[AD-A267296] p 1003 N94-17268

MOLECULAR INTERACTIONS
Modeling study to evaluate the ionic mechanism of soot formation in flames
[AD-A266242] p 950 N94-16930
Supercritical thermodynamics of sulfur and nitrogen species
[DE93-017727] p 1220 N94-16997
Interface properties of wide bandgap semiconductor structures
[AD-A268269] p 1215 N94-17377
Cathode sheath charge transfer effects
[AD-A268393] p 1186 N94-17536

MOLECULAR IONS
Merged beam studies of laser stimulated radiative recombination
[AD-A267186] p 1037 N94-15145

MOLECULAR ORBITALS
Theoretical prediction of the UV adsorption and fluorescence spectra of tyrosine and phenylalanine
[AD-A266970] p 943 N94-15111
Thermochemistry of silicate speciation in aqueous sodium silicate solutions: Ionization and polymerization of small silicate ion
[AD-A266825] p 964 N94-15683

MOLECULAR OSCILLATIONS
A molecular dynamics simulator for optimal control of molecular motion
[AD-A266572] p 1183 N94-16722

MOLECULAR OSCILLATORS
Design, synthesis and characterization of novel nonlinear optical polymers
[AD-A267035] p 964 N94-15675
A molecular dynamics simulator for optimal control of molecular motion
[AD-A266572] p 1183 N94-16722

MOLECULAR PHYSICS
Particle simulations on massively parallel machines
[DE93-015644] p 1157 N94-14927

MOLECULAR ROTATION
The influence of an electric field on the kinetics of nucleation
[IFTR-2/91] p 1213 N94-17046

MOLECULAR STRUCTURE
Thermochemistry of silicate speciation in aqueous sodium silicate solutions: Ionization and polymerization of small silicate ion
[AD-A266825] p 964 N94-15683
Many-body quantum mechanical studies of molecular clusters
[AD-A266624] p 1180 N94-15727
Study of protein-H2O interactions by multidimensional NMR spectroscopy
[AD-A266955] p 946 N94-15760
Chemical and displacement atomic pair correlations in crystalline solid solutions recovered by anomalous x ray scattering in Fe-Ni alloys
[DE93-015906] p 1209 N94-16171
Structural effects in electron transfer reactions: Comparative interfacial electrochemical kinetics for cis- versus trans-dioxorhenium (V) (bi)pyridine oxidation
[AD-A266307] p 1182 N94-16466
Structural studies of sol-gel glasses
[AD-A266277] p 967 N94-16472
The photochemistry of poly(methylphenylphosphazene)
[AD-A267320] p 970 N94-16948
Responsive copolymers for enhanced petroleum recovery
[DE93-018030] p 971 N94-16999
Synthesis, characterization, and polymerization of new ferrocene-fluorene complexes. A novel high-molecular weight conjugated polymer with pendant ferrocene groups
[AD-A267717] p 972 N94-17273
Theoretical crystallography with the Advanced Visualization System
[DE93-015692] p 1215 N94-17319

MOLECULAR THEORY
A molecular dynamics simulator for optimal control of molecular motion
[AD-A266572] p 1183 N94-16722

MOLECULAR WEIGHT
Hemoglobin
[AD-A266455] p 1123 N94-16566
Photodegradation of MDI based polyurethane/urea elastomers
[AD-A267308] p 971 N94-16994

MOLECULES
Dissociation rates of diatomic molecules
[AD-A266464] p 1182 N94-16586
Optical properties of water released in low Earth orbit
[AD-A266197] p 1192 N94-16936

MOLTEN SALTS
Ultrasound absorption in molten salts
p 944 N94-15161
Molten salt electrodeposition of high temperature superconductors
[AD-A266620] p 1009 N94-15726
Hydride-containing molten salts and their technology implications
[AD-A266458] p 1092 N94-16567

MOLYBDENUM ALLOYS
Tensile and stress-rupture behavior of hafnium carbide dispersed molybdenum and tungsten base alloy wires
[NASA-TM-106350] p 962 N94-17652

MOLYBDENUM OXIDES
Siderophile elements in the upper mantle of the Earth: New clues from metal-silicate partition coefficients
p 1103 N94-16250

MOMENTUM
Determination of momentum flux using a bivane and cup anemometer
[AD-A265414] p 1105 N94-15137

MOMENTUM TRANSFER
A global traveling wave on Venus
[NASA-CR-194356] p 1246 N94-15182
Gas-grain energy transfer in solar nebula shock waves: Implications for the origin of chondrules
p 1262 N94-16251
The pp elastic scattering experiment at RHIC and polarization studies in the Coulomb Nuclear Interference region
[DE93-015391] p 1187 N94-16829
Production of D-mesons in pp-collisions and quark-gluon string model
[DE93-626721] p 1185 N94-17312

MONATOMIC GASES
To extend the thirteen-moment theory and its application to problems in rarefied hypersonic flow
[AD-A267384] p 859 N94-17021

MONITORS
Automated data collection system for the TCM3 transcutaneous pO2/pCO2 monitoring system
[AD-A268400] p 1129 N94-17424

MONOCHROMATIC RADIATION
A comparison of calculated and observed monochromatic type Ia supernova light curves
[MPA-709] p 1237 N94-17629

MONOMERS
Compounds containing meta-biphenylenedioxy moieties and polymers therefrom
[NASA-CASE-LAR-14517-1] p 965 N94-15879
Swelling equilibria for temperature-sensitive ampholytic hydrogels
[DE93-015264] p 966 N94-15996

MONOPOLE ANTENNAS
Design of broadband wire antennas for frequency hopping applications
[AD-A267405] p 1001 N94-17025

The analysis of low-profile, broadband, monopole, vehicle antennas and matching network synthesis
[AD-A268340] p 1006 N94-17582

MONOPULSE RADAR
Enhanced down-range profiles of complex targets using wideband radar echo returns
[AD-A266508] p 999 N94-16788
Radome depolarization effects on monopulse receiver tracking performance
[AD-A267446] p 1001 N94-17031

MONOTECTIC ALLOYS
Separation behaviour of monotectic alloys
p 945 N94-15170

MONOTONE FUNCTIONS
Monotone approximate query processing
[AD-A267153] p 1169 N94-15779

MONTE CARLO METHOD
Particle simulations on massively parallel machines
[DE93-015644] p 1157 N94-14927
DSMC simulations of Mach 20 nitrogen flows about a 70 degree blunted cone and its wake
[NASA-TM-107762] p 1018 N94-15291
Particle kinetic simulation of high altitude hypervelocity flight
[NASA-CR-194599] p 856 N94-15678
Study of multi-dimensional radiative energy transfer in molecular gases
[NASA-CR-194613] p 1181 N94-15752
Particle simulation of hypersonic flow
[AD-A267185] p 857 N94-15787
Investigation of radiative interaction in laminar flows using Monte Carlo simulation
[NASA-CR-194604] p 1021 N94-15795
General Monte Carlo reliability simulation code including common mode failures and HARP fault/error-handling
[NASA-CR-187587] p 1150 N94-16594
Abundance recovery error analysis using simulated AVIRIS data p 1074 N94-16708
Diffuse scattering and image contrast of tweed in superconducting oxides: A simulation and interpretation
[DE93-016131] p 1212 N94-16844
Simulation reduction using the Taguchi method
[NASA-CR-4542] p 1055 N94-17082

MOON
EUVE observations of the Moon p 1250 N94-16185

MORPHOLOGY
Effects of aging time on V205 sol-gel coatings
[AD-A266824] p 965 N94-15843
Micro- and meso-scale simulations of magnetospheric processes related to the aurora and substorm morphology
[NASA-CR-193437] p 1102 N94-17527

MOSAICS
Global Magellan-image map of Venus at full resolution
p 1274 N94-16319
Global and regional/seasonal color mosaics of Mars
p 1288 N94-16393
Lunar multispectral mosaics from Galileo's second Earth-Moon flyby p 1288 N94-16394

MOSSBAUER EFFECT
A Moessbauer spectrometer for the mineralogical analysis of the Mars surface: First temperature dependent tests of the detector and drive system
p 1259 N94-16233
Suppression of charge scattering in Moessbauer experiments using synchrotron radiation
[DE93-015406] p 1212 N94-16887

MOTION PERCEPTION
Neural basis of motion perception
[AD-A267267] p 1133 N94-17265

MOTION SICKNESS
Autogenic-Feedback Training (AFT) as a preventive method for space motion sickness: Background and experimental design
[NASA-TM-108780] p 1120 N94-15537
Reliability of autonomic responses and malaise across multiple motion sickness stimulation tests
[NASA-TM-108787] p 1121 N94-15711
Flight simulator-induced sickness and visual displays evaluation
[AD-A267019] p 1122 N94-15845
Evaluation of putative neurochemical intermediaries in space/motion sickness
[NASA-CR-193607] p 1118 N94-17090

MOTION SIMULATION
Temporal segmentation of tasks from human hand motion
[AD-A266596] p 1166 N94-16725

MOTOR VEHICLES
Effects of RVP, T(50), and oxygenates on hot-start and driveability performance at high and low altitude
[AD-A266382] p 869 N94-16516

MOUNTAINS
Ishtar deformed belts: Evidence for deformation from below? p 1256 N94-16218

MOVING TARGET INDICATORS
Moving target indicator using higher order statistics
[AD-D015890] p 1000 N94-16917

MULLITES
Interface chemistry in ceramic matrix composites
[AD-A268629] p 973 N94-17466

MULTIBEAM ANTENNAS
Proceedings of the 1992 Antenna Applications Symposium, volume 2
[AD-A266916] p 986 N94-14998
Proceedings of the 1992 Antenna Applications Symposium, volume 1
[AD-A268167] p 1005 N94-17431

MULTICHANNEL COMMUNICATION
Call sign intelligibility improvement using a spatial auditory display
[NASA-TM-104014] p 1177 N94-15549
On-board packet switch architectures for communication satellites
[NASA-TM-106328] p 883 N94-17488

MULTIGRID METHODS
A parallel adaptive mesh refinement algorithm
[NASA-CR-191530] p 1168 N94-15724
A multilevel-multiresolution method for image processing. A Bayesian framework for reconstructing and representing shapes
[AD-A266772] p 1082 N94-15842
An upwind multigrid method for solving viscous flows on unstructured triangular meshes
[NASA-TM-109343] p 1027 N94-17061
Multigrid time-accurate integration of Navier-Stokes equations
[NASA-TM-106373] p 1028 N94-17258
Multigrid direct numerical simulation of the whole process of flow transition in 3-D boundary layers
[NASA-TM-106369] p 1030 N94-17557
Thin-layer and full Navier-Stokes calculations for turbulent supersonic flow over a cone at an angle of attack
[NASA-CR-189103] p 861 N94-17558

MULTILAYER INSULATION
Approximate Green's function methods for HZE transport in multilayered materials
[NASA-TM-4519] p 1300 N94-17084
SRB thermal curtain design support
[NASA-CR-193858] p 928 N94-17124

MULTIMEDIA
Bandwidth characteristics of multimedia data traffic on a local area network
[NASA-TM-104026] p 883 N94-15648
Processor capacity reserves for multimedia operating systems
[AD-A266639] p 1158 N94-15745
A computer-based training system combining virtual reality and multimedia
[DE93-013768] p 1132 N94-16819

MULTIMISSION MODULAR SPACECRAFT
Earth observation from small satellites
p 891 N94-17150

MULTIPATH TRANSMISSION
Diffraction of microwaves at rectangular facades of buildings with and without ground reflections (Fresnel-Kirchhoff-Approximation)
[DLR-FB-92-35] p 987 N94-15155
Johnson-Gierhart program predictions of excess propagation loss for super-high frequency air-to-ground paths. Volume 2: Appendices
[AD-A267021] p 987 N94-15527
Broadband conventional beamforming incorporating adaptive equalization
[AD-A267090] p 987 N94-15544
Alternative optical architectures for multichannel adaptive optical processing
[AD-A267052] p 1189 N94-15664
Development and analysis of ARMA parameter estimation schemes in the presence of noise
[AD-A267184] p 989 N94-15786
Satellite sound broadcast propagation measurements
p 996 N94-16047
An overview of the text propagation effects for land-mobile-satellite systems: Experimental and modeling results p 996 N94-16048
A study of land mobile satellite service multipath effects using SATLAB software p 997 N94-16051
ATCRBS reply environment at Memphis International Airport
[AD-A266322] p 864 N94-16439

MULTIPHASE FLOW
Fundamental studies of rocket combustion chemistry and combustion instability
[AD-A266248] p 925 N94-16482

MULTIPHOTON ABSORPTION
Multiphoton ionization studies of WF6 and UF6
[DE93-016232] p 1181 N94-15863
Characterization of UV emissions resulting from electronic energy transfer in atmospheric molecules
[AD-A266244] p 1101 N94-16469
Sensitive detection of gas-phase nitro-containing energetic materials employing 226-nm radiation
[AD-A267633] p 951 N94-17203
Laser photoionization time-of-flight mass spectrometry of nitrated polycyclic aromatic hydrocarbons and nitrated heterocyclic compounds
[AD-A268126] p 952 N94-17520

MULTIPLE ACCESS
Signal processing in impulsive electromagnetic interference
[AD-A266425] p 998 N94-16557

MULTIPLEXING
Advanced high performance CdHgTe multiplexed arrays p 903 N94-15051
A linear monolithic 4-6 on silicon IR detector array
p 910 N94-15098
An approximation for computing reduction in bandwidth requirements using intelligent multiplexers
[AD-A267434] p 1001 N94-17026
Review of rigorous coupled-wave analysis and of homogeneous effective medium approximations for high spatial-frequency surface-relief gratings
p 1194 N94-17335
3-D optical memory disk
[AD-A267908] p 1141 N94-17380

MULTIPLIERS
Method and apparatus for spur-reduced digital sinusoid synthesis
[NASA-CASE-NPO-18789-1-CU] p 1154 N94-17326

MULTIPOLAR FIELDS
X-SAR: The X-band synthetic aperture radar on board the Space Shuttle p 990 N94-15891
Multipolar-like form of nonabelian gauge theories
[DE93-626690] p 1171 N94-17314

MULTIPROCESSING (COMPUTERS)
Relaxing consistency in recoverable distributed shared memory
[AD-A266931] p 1140 N94-15174
Multiobjective functions optimization for task allocation mapping to multicomputer nodes
[AD-A267071] p 1146 N94-15670
A trace-based comparison of shared memory multiprocessor architectures
[TR-432] p 1159 N94-16577
Shared-memory multiprocessor trends and the implications for parallel program performance
[TR-420] p 1159 N94-16578
Efficient compilation of array statements for private memory multicomputers
[AD-A266595] p 1160 N94-16724
Applications and development of communication models for the touchstone GAMMA and DELTA prototypes
[NASA-CR-193617] p 999 N94-16867
Fault-tolerant architectures for multiprocessor and VLSI-based systems
[AD-A267370] p 1140 N94-17005

MULTISENSOR APPLICATIONS
Comparison of JPL-AIRSAR and DLR E-SAR images from the MAC Europe 1991 campaign over testsite Oberpfaffenhofen: Frequency and polarization dependent backscatter variations from agricultural fields
p 1075 N94-16733
Image accuracy and representational enhancement through low-level, multi-sensor integration techniques
[DE93-014888] p 1167 N94-17287

MULTISPECTRAL BAND SCANNERS
Medical imaging
[NASA-TM-109675] p 1229 N94-15520
Summaries of the Third Annual JPL Airborne Geoscience Workshop. Volume 2: TIMS Workshop
[NASA-CR-194541] p 1063 N94-16595
TIMS performance evaluation summary
p 1063 N94-16596
A quantitative analysis of TIMS data obtained on the Learjet 23 at various altitudes p 1063 N94-16597
Analysis of TIMS performance subjected to simulated wind blast p 1063 N94-16598
Sensitivity of blackbody reference panels to wind blast
p 1063 N94-16599
Comparison of preliminary results from Airborne Aster Simulator (AAS) with TIMS data p 1064 N94-16600
Application of split window technique to TIMS data
p 1064 N94-16601
Atmospheric corrections for TIMS estimated emittance
p 1064 N94-16602
An algorithm for the estimation of bounds on the emissivity and temperatures from thermal multispectral airborne remotely sensed data p 1064 N94-16603
Preliminary analysis of thermal-infrared multispectral scanner data of the Iron Hill, Colorado carbonatite-alkalic rock complex p 1065 N94-16605

Summaries of the Third Annual JPL Airborne Geoscience Workshop. Volume 1: AVIRIS Workshop
[NASA-CR-194540] p 1066 N94-16666
MULTISPECTRAL PHOTOGRAPHY
Age determinations and Earth-based multispectral observations of lunar light plains p 1275 N94-16323
Lunar multispectral mosaics from Galileo's second Earth-Moon flyby p 1288 N94-16394
MULTISPECTRAL RESOURCE SAMPLER
Earth observational research using multistage EOS-like data
[NASA-CR-194626] p 1084 N94-16831
MULTISTAGE ROCKET VEHICLES
ARIANE 5 light derivatives p 878 N94-17140
NEXT launch system p 878 N94-17141
MULTIVARIATE STATISTICAL ANALYSIS
Development of pattern recognition techniques for the evaluation of toxicant impacts to multispecies systems
[AD-A267197] p 1095 N94-15790
The multivariate optimum interpolation analysis of meteorological data at the Fleet Numerical Oceanography Center
[AD-A266459] p 1106 N94-16568
Nonparametric statistics: Weighted rankings analysis
[AD-A266607] p 1173 N94-16657
Computing science and statistics. Volume 24: Graphics and visualization
[AD-A266571] p 1150 N94-16721
MUONS
Electroweak physics from D0
[DE93-015041] p 1181 N94-16053
PHENIX Conceptual Design Report
[DE93-015759] p 1182 N94-16161
The 3D-Flow processor for a programmable level-1 trigger (feasibility study)
[DE93-016045] p 1159 N94-16172
Calorimeter based detectors for high energy hadron colliders
[DE93-017055] p 1188 N94-16900
Electroweak results from D0
[DE93-014926] p 1185 N94-16968
MURCHISON METEORITE
Extraction and isotopic analysis of medium molecular weight hydrocarbons from Murchison using supercritical carbon dioxide p 1241 N94-16184
Do SiC grains in Orgueil differ from those in Murchison? p 1242 N94-16260
MUSCLES
Currents induced in the human body for exposure to ultrawideband electromagnetic pulses
[AD-A268570] p 1130 N94-17621
MUSIC
Sights and sounds of space
[NASA-TM-109610] p 1302 N94-15424
MUTATIONS
Isolation of thermostable enzyme mutants by cloning and selection in thermophilic bacteria
[AD-A266378] p 1117 N94-16514
MYSTERE 20 AIRCRAFT
Evaluation of Night Vision Goggles (NVG) for maritime search and rescue (HH-3/HH-60) comparison report
[AD-A266493] p 1138 N94-16793

N

N-TYPE SEMICONDUCTORS
Diamond p-n junction cold cathode
[AD-A266926] p 1206 N94-15107
NACELLES
Flow analysis for the nacelle of an advanced ducted propeller at high angle-of-attack and at cruise with boundary layer control
[NASA-TM-106371] p 858 N94-16571
Supersonic flow visualization of a nacelle in close proximity to a simulated wing
[NASA-CR-194675] p 860 N94-17260
NAKHLITES
Nitrates in SNCs: Implications for the nitrogen cycle on Mars p 1251 N94-16193
Os isotopes in SNC meteorites and their implications to the early evolution of Mars and Earth p 1242 N94-16272
Martian carbon dioxide: Clues from isotopes in SNC meteorites p 1270 N94-16295
NAMING
Model designation of military aerospace vehicles
[AD-A267852] p 898 N94-17388
NARROWBAND
Filters for the International Solar Terrestrial Physics (ISTP) mission far ultraviolet imager
[NASA-CR-194633] p 1190 N94-15868
Use of AVIRIS data to the definition of optimised specifications for land applications with future spaceborne imaging spectrometers p 1071 N94-16694
NASA PROGRAMS
SHARP
[NASA-TM-109659] p 1221 N94-15230
University Joint Venture: JOVE
[NASA-TM-109660] p 1229 N94-15231
Space classroom
[NASA-TM-109661] p 1221 N94-15232
Return to flight 1
[NASA-TM-109663] p 1223 N94-15234
Teacher in space
[NASA-TM-109666] p 1131 N94-15237
The 1969 highlights
[NASA-TM-109630] p 1301 N94-15241
The 1972 highlights
[NASA-TM-109631] p 1301 N94-15242
The 1965 highlights --- NASA programs
[NASA-TM-109632] p 1301 N94-15243
The 1967 highlights
[NASA-TM-109633] p 1301 N94-15244
From space to Earth
[NASA-TM-109638] p 1235 N94-15249
GAS highlights, 1988 --- Get Away Specials
[NASA-TM-109600] p 873 N94-15308
Space Shuttle highlights
[NASA-TM-109606] p 880 N94-15314
Return to flight 3, the journey continues
[NASA-TM-109651] p 1223 N94-15319
IG nuts and bolts
[NASA-TM-109652] p 1049 N94-15320
NACA-NASA: 75 years of flight
[NASA-TM-109449] p 1302 N94-15322
NASA images 6
[NASA-TM-109437] p 862 N94-15336
NASA images 7
[NASA-TM-109438] p 1235 N94-15337
NASA images 16
[NASA-TM-109440] p 1235 N94-15339
Back to propellers
[NASA-TM-109445] p 869 N94-15344
Better airplane wings
[NASA-TM-109446] p 933 N94-15345
Cohen program management briefing
[NASA-TM-109536] p 1223 N94-15367
CORE/TRC
[NASA-TM-109434] p 1221 N94-15418
Improved mapping system
[NASA-TM-109643] p 1082 N94-15428
Challenger Center: Orientation
[NASA-TM-109433] p 1221 N94-15505
Coast encounters: A space age adventure in science literacy
[NASA-TM-109334] p 1229 N94-15523
NASA Space Engineering Research Center for VLSI System Design
[NASA-CR-194587] p 1008 N94-15547
NASA trend analysis procedures
[NASA-RP-1290] p 1223 N94-15782
NAS technical summaries: Numerical aerodynamic simulation program, March 1991 - February 1992
[NASA-TM-109335] p 854 N94-15798
NASA/DOD Aerospace Knowledge Diffusion Research Project. Paper 34: Technical communications practices and the use of information technologies as reported by Dutch and US aerospace engineers
[NASA-TM-109337] p 1230 N94-15839
The strategic environmental research and development program: A new paradigm for space, the environment, and national security
[AD-A266222] p 1174 N94-16109
Proceedings of the 1992 Annual Meeting NASA Occupational Health Program
[NASA-CR-193462] p 1123 N94-16609
The Goddard Space Flight Center ergonomics program p 1125 N94-16621
Industrial Hygiene Laboratory accreditation: The JSC experience p 1125 N94-16623
Summary of follow-up results from potential tuberculosis exposures p 1126 N94-16628
Physical fitness and health education program at NASA Headquarters p 1126 N94-16631
Ames Fitness Program p 1126 N94-16632
Johnson Space Center health related fitness program p 1126 N94-16633
Kennedy Space Center exercise program p 1126 N94-16634
The Langley Fitness Center p 1126 N94-16635
Physical Exercise Program p 1127 N94-16636
Arsenic surveillance program p 1127 N94-16637
Asbestos Surveillance Program p 1127 N94-16638
Hearing Conservation Medical Program p 1127 N94-16639
Lead Surveillance Program p 1127 N94-16640
Mercury Surveillance Program p 1127 N94-16641
Respiratory Protection Program medical clearance for respirator use p 1127 N94-16642
General Medical Surveillance Program p 1127 N94-16643
Bloodborne Pathogens Program p 1127 N94-16644
Mission management aircraft operations manual
[NHB-7900.3] p 1225 N94-16729
Aircraft operations management manual
[NHB-7900.3(V1)] p 1225 N94-16730
Equipment Management Manual
[NHB-4200.1D] p 1225 N94-16799
NASA/DOD Aerospace Knowledge Diffusion Research Project. Report 15: Technical uncertainty and project complexity as correlates of information use by US industry-affiliated aerospace engineers and scientists: Results of an exploratory investigation
[NASA-TM-107693] p 1233 N94-17300
NASA SPACE PROGRAMS
The 1969 highlights
[NASA-TM-109630] p 1301 N94-15241
The 1972 highlights
[NASA-TM-109631] p 1301 N94-15242
The 1965 highlights --- NASA programs
[NASA-TM-109632] p 1301 N94-15243
The 1967 highlights
[NASA-TM-109633] p 1301 N94-15244
Stock footage of Goddard Space Flight Center and Headquarters
[NASA-TM-109589] p 875 N94-15273
Space Station: The link to America's future
[NASA-TM-109653] p 884 N94-15274
Lunar base concepts
[NASA-TM-109607] p 1247 N94-15294
NASA: The 25th year
[NASA-TM-109457] p 1302 N94-15352
NASA's Hubble Space Telescope: The challenge and complexity of operations
[NASA-TM-109577] p 1236 N94-15422
Mars rover sample return mission
[NASA-TM-109521] p 873 N94-15471
Commitment to challenge
[NASA-TM-109523] p 876 N94-15473
History of the manned space flight program
[NASA-TM-109529] p 1303 N94-16069
TABES 1993: 9th Annual Technical and Business Exhibition and Symposium p 1050 N94-16129
Approaching the new reality
[TABES PAPER 93-230] p 1050 N94-16131
Commercial space opportunities advanced concepts and technology overview
[TABES PAPER 93-240] p 1050 N94-16132
NATIONAL AEROSPACE PLANE PROGRAM
National Aero-Space Plane
[NASA-TM-109450] p 865 N94-15323
National Aero-Space Plane resource reel
[NASA-TM-109451] p 865 N94-15324
Fluid flow and heat convection studies for actively cooled airframes
[NASA-CR-194624] p 1024 N94-16491
Trajectory optimization for the National Aerospace Plane
[NASA-CR-194618] p 867 N94-16498
NATIONAL LAUNCH VEHICLE PROGRAM
Aerodynamic flight control to increase payload capability of future launch vehicles
[NASA-CR-193850] p 870 N94-15532
NATURAL GAS
Biomass energy: State of the technology present obstacles and future potential
[DE93-016295] p 1092 N94-16766
Methyl chloride via oxyhydrochlorination of methane
[DE93-017548] p 952 N94-17218
NATURAL LANGUAGE (COMPUTERS)
Using multiple adaptively-weighted strategies for the resolution of demonstratives
[AD-A266463] p 1150 N94-16585
Information technology division technical paper abstracts
[AD-A266227] p 1166 N94-16938
NATURAL SATELLITES
Rover mounted ground penetrating radar as a tool for investigating the near-surface of Mars and beyond p 1007 N94-16197
NAUSEA
Reliability of autonomic responses and malaise across multiple motion sickness stimulation tests
[NASA-TM-108787] p 1121 N94-15711
NAVIER-STOKES EQUATION
Rocket motor plume flowfields: Phenomenology and simulation p 924 N94-15221
Proteus two-dimensional Navier-Stokes computer code, version 2.0. Volume 2: User's guide
[NASA-TM-106338-VOL-2] p 1019 N94-15475
Proteus two-dimensional Navier-Stokes computer code, version 2.0. Volume 1: Analysis description
[NASA-TM-106336-VOL-1] p 1019 N94-15485

Proteus three-dimensional Navier-Stokes computer code, version 1.0. Volume 2: User's guide
[NASA-TM-106340-VOL-2] p 1020 N94-15488
On the stability analysis of approximate factorization methods for 3D Euler and Navier-Stokes equations
[NASA-TM-106314] p 1169 N94-15818
Proteus three-dimensional Navier-Stokes computer code, version 1.0. Volume 3: Programmer's reference
[NASA-TM-106341] p 1022 N94-15865
Proteus two-dimensional Navier-Stokes computer code, version 2.0. Volume 3: Programmer's reference
[NASA-TM-106339] p 1022 N94-15867
Computation of a controlled store separation from a cavity p 858 N94-16513
Proteus three-dimensional Navier-Stokes computer code, version 1.0. Volume 1: Analysis description
[NASA-TM-106337] p 1024 N94-16527
Flow analysis for the nacelle of an advanced ducted propeller at high angle-of-attack and at cruise with boundary layer control
[NASA-TM-106371] p 858 N94-16571
Hoph bifurcation in viscous, low speed flows about an airfoil with structural coupling
[AD-A266542] p 859 N94-16798
Adaptive Navier-Stokes calculations for vortical flow
[AD-A266236] p 1026 N94-16966
An upwind multigrid method for solving viscous flows on unstructured triangular meshes
[NASA-TM-109343] p 1027 N94-17061
Computational aerodynamics with icing effects
[AD-A267509] p 860 N94-17074
On solving the compressible Navier-Stokes equations for unsteady flows at very low Mach numbers
[NASA-TM-106380] p 1027 N94-17128
Multigrid time-accurate integration of Navier-Stokes equations
[NASA-TM-106373] p 1028 N94-17258
Convection effects on radial segregation and crystal melt interface in vertical Bridgman growth
[NASA-CR-191541] p 1029 N94-17387
Boundary conditions and the simulation of low Mach number flows
[NASA-TM-106374] p 1029 N94-17448
Thin-layer and full Navier-Stokes calculations for turbulent supersonic flow over a cone at an angle of attack
[NASA-CR-189103] p 861 N94-17558
Granular fluctuations in plasma turbulence and their role in transport
[DE93-013465] p 1187 N94-17674

NAVIGATION

Wide-area Differential Global Positioning System (WDGPS)/Wide-area Integrity Broadcast (WIB) alternatives analysis
[DOT/FAA/SE-93/3] p 864 N94-16906

NAVIGATION INSTRUMENTS

Perception for outdoor navigation
[AD-A266867] p 863 N94-14919

NAVIGATION SATELLITES

Not ready for the first space war. What about the second?
[AD-A266557] p 1174 N94-16665

NAVY

Structured finite volume modeling of US Navy aircraft engine test cells task 2: Turboprop engine, volume 1
[AD-A267833] p 872 N94-17405
Structured finite volume modeling of US Navy aircraft engine test cells. Task 1: Turboshaft engine, volume 1
[AD-A268176] p 873 N94-17432
Naval aviation: The Navy is taking actions to improve the combat capabilities of its tactical aircraft. Report to Congressional Requesters
[AD-A268002] p 868 N94-17472
Structured finite volume modeling of US Navy aircraft engine test cells. Task 1: Turboshaft engine-code documentation and listings, volume 2
[AD-A268177] p 873 N94-17508

NEAR FIELDS

A near-field scanning optical microscope for analysis of magneto-optic media p 1199 N94-14995
Phased array antenna analysis using hybrid finite element methods
[AD-A267620] p 1002 N94-17196
How to deduce the far field of an antenna from planar near-field measurements
[NPL-DES-123] p 1006 N94-17545

NEAR INFRARED RADIATION

New K type asteroids p 1241 N94-16195

NEBULAE

Boundary conditions for the paleoenvironment: Chemical and physical processes in the pre-solar nebula
[NASA-CR-194418] p 1298 N94-15421

NEGATIVE ELECTRON AFFINITY

Diamond p-n junction cold cathode
[AD-A266926] p 1206 N94-15107

NEGATIVE IONS

Swelling equilibria for temperature-sensitive ampholytic hydrogels
[DE93-015264] p 966 N94-15996
Negative ion formation in small carbon clusters
[DE93-015436] p 1182 N94-16064
Atomic processes in hydrogen and deuterium negative ion discharges
[DE93-013432] p 1183 N94-16817
Atomic beam studies relevant to the space environment
[AD-A268628] p 1186 N94-17436

NEODYMIUM ISOTOPES

Nd-142/Nd-144 in bulk planetary reservoirs, the problem of incomplete mixing of interstellar components and significance of very high precision Nd-145/Nd-144 measurements p 1256 N94-16220
Constraints on the differentiation of the Earth from the coupled Sm-146,147-Nd-142,143 systematics p 1103 N94-16271

NEODYMIUM LASERS

Nd:YLF laser for airborne/spaceborne laser ranging p 913 N94-15563
An improved light source for laser ranging p 913 N94-15567
Two color satellite laser ranging upgrades at Goddard's 1.2m telescope facility p 915 N94-15581
Measuring atmospheric dispersion with WLRS in multiple wavelength mode p 916 N94-15582
Upgrading of the Borowiec laser station p 877 N94-15604
Results of the MTLRS-1 upgrade p 877 N94-15610
The new MTLRS transmitting system p 877 N94-15612
Effects of turbulence on the geodynamic laser ranging system p 921 N94-15616
Development of the Mars Observer Laser Altimeter (MOLA) p 921 N94-15617
The third generation SLR station Potsdam no. 7836 p 877 N94-15623
Laser weld repair of tantalum sheet
[DE93-016417] p 1041 N94-16871
Design, development and characterization studies of a large aperture high power Nd: Glass rod amplifier stage
[DE93-624944] p 1042 N94-17630

NEON

Observation of nonsequential ionization of helium and its impact on intensity monitoring
[DE93-017174] p 949 N94-16904

NEON ISOTOPES

The SCR Ne-21 and Ar-38 in lunar rock 68815: The solar proton energy spectrum over the past 2 MYR p 1248 N94-16177
Effects of bulk composition on production rates of cosmogenic nuclides in meteorites p 1245 N94-16385
Solar noble gases revealed by closed system stepped etching of a metal separate from Fayetteville p 954 N94-16432

NEPTUNE (PLANET)

Neptune encounter highlights
[NASA-TM-109421] p 1246 N94-15240
NASA report to education, volume 7
[NASA-TM-109435] p 1247 N94-15419
Voyager 2: Neptune encounter
[NASA-TM-109423] p 1247 N94-15491
Tidal interaction: A possible explanation for geysers and other fluid phenomena in the Neptune-Triton system p 1272 N94-16311
Mapping the stability region of the 3:2 Neptune-Pluto resonance p 1280 N94-16351

NERVES

Cortical adaptive filtering in bioacoustic signal classification
[AD-A266229] p 1177 N94-16939

NERVOUS SYSTEM

Development of the OMPAT neuropsychological/psychomotor performance evaluation and OMPAT data and timing support programs
[AD-A266954] p 1122 N94-15759
Neural mechanisms of attention
[AD-A266315] p 1132 N94-16456

NETHERLANDS

Symposium on the Future of Aeronautics in the Netherlands
[ETN-93-93780] p 853 N94-15120
Aviation and the KLM: Past and future p 853 N94-15126
Developments in the Higher Technical Aerospace Education p 854 N94-15130

NETWORK ANALYSIS

Stochastic scheduling in in-forest networks
[INRIA-RR-1719] p 1164 N94-15695
Congestion control of high-speed networks
[AD-A267013] p 989 N94-15748
State space partitioning methods for solving a class of stochastic network problems
[AD-A267494] p 1173 N94-17585

NETWORK CONTROL

Real-time implementation of neural network learning control of a flexible space manipulator
[AD-A266962] p 1045 N94-14970
Panacea: An active sensor controller for the ALVINN autonomous driving system
[AD-A266964] p 864 N94-14972
The distributed database dynamic reconfiguration project
[AD-A267116] p 1229 N94-15652
The IMS software integration platform
[AD-A266285] p 1151 N94-16910

NEURAL NETS

Unsteady separated flows: Empirical model and control
[AD-A267282] p 855 N94-14959
Real-time implementation of neural network learning control of a flexible space manipulator
[AD-A266962] p 1045 N94-14970
Panacea: An active sensor controller for the ALVINN autonomous driving system
[AD-A266964] p 864 N94-14972
Multiobjective functions optimization for task allocation mapping to multicomputer nodes
[AD-A267071] p 1146 N94-15670
The bootstrapped algorithm: Fast algorithm for blind signal separation
[AD-A266671] p 1147 N94-15772
Unipolar terminal-attractor based neural associative memory with adaptive threshold
[NASA-CASE-NPO-18790-1-CU] p 1165 N94-15958
Neural-network-directed alignment of optical systems using the laser-beam spatial filter as an example
[NASA-TP-3372] p 1034 N94-15961
Real-time adaptive neural network data processing
[TABES PAPER 93-660] p 1054 N94-16155
Neural mechanisms of attention
[AD-A266315] p 1132 N94-16456
AVIRIS data and neural networks applied to an urban ecosystem p 1073 N94-16705
Information technology division technical paper abstracts
[AD-A266227] p 1166 N94-16938
ONRASIA scientific information bulletin, volume 18, number 2
[AD-A267798] p 1304 N94-17305

NEUROLOGY

Development of the OMPAT neuropsychological/psychomotor performance evaluation and OMPAT data and timing support programs
[AD-A266954] p 1122 N94-15759
Localizing visual function in the brain
[AD-A267381] p 1133 N94-17020

NEUROMUSCULAR TRANSMISSION

Synaptic plasticity and memory formation
[AD-A267988] p 1133 N94-17453

NEURONS

Neurotoxicity of hemoglobin in cortical cell culture
[AD-A266506] p 1128 N94-16786
Theoretical and experimental research into biological mechanisms underlying learning and memory
[AD-A267441] p 1133 N94-17022

NEUROPHYSIOLOGY

The 12th Annual Carmel Conference, distinctiveness and Memory: Cognitive Psychophysiological and Physiological Considerations
[AD-A267181] p 1131 N94-15148
Cumulative effect of repeated brief cerebral ischemia
[AD-A267155] p 1121 N94-15736
Unipolar terminal-attractor based neural associative memory with adaptive threshold
[NASA-CASE-NPO-18790-1-CU] p 1165 N94-15958
Neurotoxicity of hemoglobin in cortical cell culture
[AD-A266506] p 1128 N94-16786
Cortical adaptive filtering in bioacoustic signal classification
[AD-A266229] p 1177 N94-16939
Localizing visual function in the brain
[AD-A267381] p 1133 N94-17020
Evaluation of putative neurochemical intermediaries in space/motion sickness
[NASA-CR-193607] p 1118 N94-17090
Neural basis of motion perception
[AD-A267267] p 1133 N94-17265

NEUROTRANSMITTERS

Synaptic plasticity and memory formation
[AD-A267988] p 1133 N94-17453

NEUTRAL BEAMS

High beta and confinement studies of TFTR
[DE93-016204] p 1202 N94-16446

NEUTRAL CURRENTS
Neutral-current detection in the Sudbury Neutrino Observatory
[DE93-014481] p 1185 N94-16951
NEUTRAL PARTICLES
Linear characteristic spatial quadrature for discrete ordinates neutral particle transport on arbitrary triangles
[AD-A267485] p 1185 N94-17365
NEUTRINOS
On the 17-keV neutrino
[DE93-012638] p 1181 N94-15974
Possible dust contamination of the early solar system p 1244 N94-16352
Contained (nu) events observed in Soudan 2
[DE93-015548] p 1300 N94-17233
NEUTRON ACTIVATION ANALYSIS
INAA of CAIs from the Maralinga CK4 chondrite: Effects of parent body thermal metamorphism p 1244 N94-16355
NEUTRON COUNTERS
Preliminary results from bubble detector measurements aboard Biocosmos-2044 p 981 N94-16097
Neutral-current detection in the Sudbury Neutrino Observatory
[DE93-014481] p 1185 N94-16951
NEUTRON DIFFRACTION
Roles of oxygen defects in copper-oxide superconductors
[DE93-014875] p 1208 N94-15982
Thermal stress effects in intermetallic matrix composites
[NASA-CR-191191] p 1054 N94-16518
NEUTRON IRRADIATION
The effect of irradiation on the mechanical properties of 6061-T651 aluminum
[DE93-015825] p 958 N94-16168
NEUTRON SCATTERING
Multiple process simulations for correction factor calculations in experiments with neutrons. LUSMK program
[DE93-623957] p 1179 N94-14932
Structural investigation of electrochemically etched silicon
[DE93-015300] p 1207 N94-15827
Neutron and x ray scattering studies of (FeF2)(sub m)(CoF2)(sub n) multilayers
[DE93-015809] p 1184 N94-16838
NEUTRON SPECTRA
Preliminary results from bubble detector measurements aboard Biocosmos-2044 p 981 N94-16097
NEUTRON STARS
Astronomy and astrophysics p 1239 N94-15970
Relativistic mean-field calculations of lambda and sigma hypernuclei
[DE93-015269] p 1181 N94-16013
Fast pulsars, compact stars, and the strange matter hypothesis
[DE93-015039] p 1239 N94-16052
NEUTRONS
Multiple process simulations for correction factor calculations in experiments with neutrons. LUSMK program
[DE93-623957] p 1179 N94-14932
General order characteristic methods for solving neutron transport problems
[DE93-015824] p 1170 N94-16167
A calibration of the production rate ratio P-21/P-26 by low energy secondry neutrons: Identification of Ne spallation components at the 10(exp 6) atoms/g level in terrestrial samples p 1187 N94-16194
ARIES tokamak reactor study
[DE93-017059] p 1203 N94-16901
Energy-loss cross sections for inclusive charge-exchange reactions at intermediate energies
[NASA-TM-4522] p 1188 N94-17018
NEWS MEDIA
COBE video news
[NASA-TM-109598] p 987 N94-15292
NICKEL
Passive oxide films on well-defined nickel surfaces: An examination of film growth on Ni(100) with ex situ scanning tunneling microscopy
[DE93-014056] p 1207 N94-15923
Thin Ni silicide formation by low temperature-induced metal atom reaction with ion implanted amorphous silicon
[DE93-015449] p 1209 N94-16066
Characterization of Ni on Si wafers: Comparison of surface analysis techniques
[DE93-016501] p 953 N94-17649
NICKEL ALLOYS
The friction and wear of ceramic/ceramic and ceramic/metal combinations in sliding contact
[NASA-TM-106348] p 930 N94-15769
Ternary alloying effects in polycrystalline (beta)-NiAl
[DE93-012675] p 955 N94-15885
A sulfur segregation study of PWA 1480, NiCrAl, and NiAl alloys
[NASA-TM-106289] p 956 N94-15992
A reexamination of grain boundary fracture in Ni3Al: Environmental and alloying effects
[DE93-015431] p 1208 N94-16063
Robotic weld overlay coatings for erosion control
[DE93-016938] p 970 N94-16959
Transient phenomena following precipitation and re-solution anneals in a NiTi alloy
[AD-A267557] p 961 N94-17106
Characterization of metallic multilayers using x ray diffraction analysis
[NIAR-93-13] p 961 N94-17282
NICKEL CADMIUM BATTERIES
The 1987 Goddard Space Flight Center Battery Workshop
[NASA-CP-3236] p 1012 N94-17062
A power system for a microsatellite p 895 N94-17176
NICKEL HYDROGEN BATTERIES
The 1987 Goddard Space Flight Center Battery Workshop
[NASA-CP-3236] p 1012 N94-17062
Small satellite nickel-hydrogen and nickel-metal hydride power applications p 895 N94-17175
NICKEL OXIDES
Passive oxide films on well-defined nickel surfaces: An examination of film growth on Ni(100) with ex situ scanning tunneling microscopy
[DE93-014056] p 1207 N94-15923
Siderophile elements in the upper mantle of the Earth: New clues from metal-silicate partition coefficients p 1103 N94-16250
NICKEL STEELS
Stress corrosion cracking of 316 SS and Incoloy-800 in high temperature aqueous containing sulfate and chloride
[DE93-623325] p 952 N94-17302
NIGHT
Sleep management user's guide for special operations personnel
[AD-A267746] p 1119 N94-14943
NIGHT SKY
Tip-tilt compensation: Resolution limits for ground-based telescopes using laser guide star adaptive optics
[DE93-016426] p 1237 N94-16872
NIGHT VISION
Comparative night vision goggle visual acuity measurements performed in the A-10 aircraft in an operational setting
[AD-A266721] p 1137 N94-15820
Evaluation of Night Vision Goggles (NVG) for maritime search and rescue (HH-3/HH-60) comparison report
[AD-A266493] p 1138 N94-16793
SYDONI: An intensified system for night observation p 891 N94-17153
NIMBUS 6 SATELLITE
The fragmentation of the Nimbus 6 rocket body
[NASA-CR-191645] p 926 N94-16504
NIMBUS 7 SATELLITE
Coastal zone color scanner: Nimbus 7
[NASA-TM-109590] p 1111 N94-15281
Arctic and Antarctic sea ice, 1978-1987: Satellite passive-microwave observations and analysis
[NASA-SP-511] p 1114 N94-17439
NIOBIUM
Submillimeterwave SIS mixer developments p 903 N94-15054
Nb-based SJTJ for nuclear detection: Preliminary results with alpha radiation p 905 N94-15068
Preparation and properties of Nb/Al SIS and SIN junctions for millimeter and submillimeter radioastronomical receivers p 907 N94-15078
NIOBIUM ALLOYS
Processing and protection of high temperature structural materials
[AD-A267292] p 954 N94-14961
Effects of processing and prolonged high temperature exposure on the microstructure of Nb-1Zr-C sheet
[NASA-TM-106370] p 959 N94-16883
NIOBIUM CARBIDES
Effects of processing and prolonged high temperature exposure on the microstructure of Nb-1Zr-C sheet
[NASA-TM-106370] p 959 N94-16883
NITRAMINE PROPELLANTS
Spectral studies of solid propellant combustion 4: Absorption and burn rate results for M43, XM39, and M10 propellants
[AD-A267119] p 946 N94-15685
Laser ignition of solid propellants: 1. Ignition delays
[AD-A268454] p 976 N94-17538
NITRATE ESTERS
Laser ignition of solid propellants: 1. Ignition delays
[AD-A268454] p 976 N94-17538
NITRATES
Nitrates in SNCs: Implications for the nitrogen cycle on Mars p 1251 N94-16193
Atmospheric ionization by solar particles detected by nitrate measurement in antarctic snow
[AD-A267583] p 1299 N94-17208
Chemical tracer studies at IOSDL. 3: The measurement of silicate, nitrate and phosphate in seawater
[IOS-302-1992] p 1114 N94-17489
NITRIC ACID
An assessment of acid fog
[DE93-009347] p 1095 N94-15940
NITRIC OXIDE
Direct catalytic decomposition of nitric oxide
[DE93-016689] p 949 N94-16896
Factors determining the release of nitric oxide --- Calcium/cadmium transport by renal cortical collectin duct cells
[AD-A266232] p 1118 N94-17224
NITRIDES
SONOS technology for commercial and military nonvolatile memory applications
[DE93-015647] p 1011 N94-16661
Atomic layer epitaxy of boron nitride
[AD-A266260] p 1212 N94-16932
Nitride semiconductors for ultraviolet detection
[AD-A267877] p 1012 N94-17040
Interface chemistry in ceramic matrix composites
[AD-A268629] p 973 N94-17466
NITRO COMPOUNDS
Sensitive detection of gas-phase nitro-containing energetic materials employing 226-nm radiation
[AD-A267633] p 951 N94-17203
NITROGEN
Euromet Ureilite Consortium: A preliminary report on carbon and nitrogen geochemistry p 1241 N94-16192
Nitrates in SNCs: Implications for the nitrogen cycle on Mars p 1251 N94-16193
A Pluto thermal model p 1256 N94-16216
Nitrogen and light noble gases in Parsa enstatite chondrite p 1246 N94-16435
Static characteristics of a conduction and radiation dominated electric arc in nitrogen
[DE93-627106] p 1204 N94-17311
Laser ignition of solid propellants: 1. Ignition delays
[AD-A268454] p 976 N94-17538
NITROGEN COMPOUNDS
Supercritical thermodynamics of sulfur and nitrogen species
[DE93-017727] p 1220 N94-16997
NITROGEN ISOTOPES
Euromet Ureilite Consortium: A preliminary report on carbon and nitrogen geochemistry p 1241 N94-16192
Nitrogen isotopic signatures in agglutinates from breccia 79035 p 954 N94-16314
NITROGEN LASERS
Bibliography of short wavelength chemical laser research
[AD-A267619] p 1041 N94-17195
NITROGEN OXIDES
Application of non-thermal plasmas to pollution control
[DE93-016432] p 1096 N94-16449
SONOS technology for commercial and military nonvolatile memory applications
[DE93-015647] p 1011 N94-16661
Atomic beam studies relevant to the space environment
[AD-A268628] p 1186 N94-17436
NOBLE METALS
Experimental partitioning of Zr, Ti, and Nb between silicate liquid and a complex noble metal alloy and the partitioning of Ti between perovskite and platinum metal p 962 N94-16287
NOCTURNAL VARIATIONS
Formation of the stable auroral arc that intensifies at substorm onset
[NASA-CR-193637] p 1098 N94-15433
NOISE INTENSITY
Cruise noise measurements of a scale model advanced ducted propulsor
[NASA-TM-105808] p 1176 N94-15115
Technical evaluation report on the AGARD-PEP Specialists Meeting on Combat Aircraft Noise
[NLR-TP-91445-U] p 1177 N94-15506
NOISE MEASUREMENT
Cruise noise measurements of a scale model advanced ducted propulsor
[NASA-TM-105808] p 1176 N94-15115
Cryogenic measurements of aerojet GaAs n-JFETs
[NASA-TM-103972] p 1009 N94-15765
Noise measurement flight test of five light helicopters
[AD-A268566] p 1179 N94-17599
NOISE POLLUTION
Strategic planning for aircraft noise route impact analysis: A three dimensional approach
[NASA-CR-191484] p 1178 N94-17278

NOISE PREDICTION (AIRCRAFT)
Strategic planning for aircraft noise route impact analysis: A three dimensional approach
[NASA-CR-191484] p 1178 N94-17278
NOISE PROPAGATION
Sound exposure level prediction for impulse sound sources above variable terrain
[AD-A267535] p 1178 N94-17119
NOISE REDUCTION
The 1968 highlights --- NASA programs and research
[NASA-TM-109627] p 1302 N94-15413
The 1971 highlights --- NASA programs and research
[NASA-TM-109629] p 1302 N94-15417
Technical evaluation report on the AGARD-PEP Specialists Meeting on Combat Aircraft Noise
[NLR-TP-91445-U] p 1177 N94-15506
Hydraulic pump with integral electric motor
[AD-D015782] p 1011 N94-16549
NOISE SPECTRA
Maximum likelihood techniques applied to quasi-elastic light scattering
[NASA-CR-193550] p 1192 N94-16718
NONADIABATIC CONDITIONS
Supersymmetry of gauge equations and geometric nonadiabatic phases
[DE93-626671] p 1219 N94-14935
NONDESTRUCTIVE TESTS
Physical interpretation and development of ultrasonic nondestructive evaluation techniques applied to the quantitative characterization of textile composite materials
[NASA-CR-194549] p 931 N94-15190
Component testing and quality assurance
p 932 N94-15259
The Marshall Automated Weld System (MAWS)
[TABES PAPER 93-602] p 1049 N94-16138
Detection of subsurface defects in machined silicon nitride ceramics by optical scattering methods
[DE93-015554] p 968 N94-16658
Ultrasonic wave propagation model for nondestructive evaluation of solid rocker motor propellant
[AD-A267653] p 976 N94-17248
Synthesis and evaluation of polymeric materials
[AD-A267809] p 973 N94-17408
X ray computed tomography for failure analysis investigations
[AD-A268086] p 1055 N94-17515
X ray computed tomography for casting demonstration
[AD-A268084] p 1056 N94-17596
NONEQUILIBRIUM FLOW
Particle kinetic simulation of high altitude hypervelocity flight
[NASA-CR-194599] p 856 N94-15678
Studies on nonequilibrium phenomena in supersonic chemically reacting flows
[NASA-CR-194662] p 1027 N94-17215
NONEQUILIBRIUM PLASMAS
Synthesis of ceramic oxide powders in a microwave plasma device
[DE93-012741] p 965 N94-15920
NONEQUILIBRIUM RADIATION
Nonequilibrium radiation and chemistry models for aerocapture vehicle flowfields
[NASA-CR-194645] p 1027 N94-17095
NONGRAY GAS
Study of multi-dimensional radiative energy transfer in molecular gases
[NASA-CR-194613] p 1181 N94-15752
NONINTRUSIVE MEASUREMENT
Nonintrusive fast response oxygen monitoring system for high temperature flows
[NASA-CR-4553] p 1036 N94-17655
NONLINEAR EQUATIONS
Adaptive wavelet collocation methods for initial value boundary problems of nonlinear PDE's
[NASA-CR-191507] p 1169 N94-15833
Nonlinear problems in fluid dynamics and inverse scattering
[AD-A266234] p 1026 N94-16927
Applications of the phi-transform
[AD-A266247] p 1170 N94-16940
Numerically solving a transient heat conduction problem with convection and radiation
[AD-A268521] p 1220 N94-17540
NONLINEAR FILTERS
Development and analysis of ARMA parameter estimation schemes in the presence of noise
[AD-A267184] p 989 N94-15786
High order nonlinear estimation with signal processing applications
[AD-A268407] p 1005 N94-17463
NONLINEAR OPTICS
Optimum wavelengths for two color ranging
p 915 N94-15580
Design, synthesis and characterization of novel nonlinear optical polymers
[AD-A267035] p 964 N94-15675
Organic polymeric electro-optic materials: Synthesis, processing, and device applications
[AD-A267133] p 964 N94-15688
High-performance nonlinear optical material developed in Japan
[AD-A266194] p 1191 N94-16126
Rational design, construction, and processing of high-performance nonlinear optical materials
[AD-A266185] p 1191 N94-16454
New organic materials for nonlinear optics applications
[AD-A266451] p 1192 N94-16563
Main chain chromophoric polymers with second order nonlinear optical properties
[AD-D015893] p 969 N94-16920
Theoretical studies of nonlinear optical properties of conjugated polymers
[AD-A267390] p 1193 N94-17024
Two-dimensional acousto-optical interaction theory and experimental analysis
[AD-A267761] p 1193 N94-17254
High-speed nonlinear switching mechanisms and devices for multi-gigabit data processing
[AD-A267753] p 1014 N94-17375
Spectral inverse scattering theory for dielectric media: Application to optical devices
[AD-A268635] p 1199 N94-17427
Optical studies of glasses embedded with inorganic ions and organic dyes
[AD-A268146] p 1199 N94-17455
NONLINEAR PROGRAMMING
A sequential quadratic programming algorithm using an incomplete solution of the subproblem
[DE93-017439] p 1149 N94-16120
NONLINEAR SYSTEMS
Iteration scheme for the multiparameter nonlinear boundary value problem with the additional conditions and its application to some field models
[DE93-626638] p 1168 N94-14933
Controlling chaotic behavior in CO2 and other lasers
[AD-A266431] p 1040 N94-16546
Operator overloading as an enabling technology for automatic differentiation
[DE93-012899] p 1170 N94-16778
Nonlinear problems in fluid dynamics and inverse scattering
[AD-A266234] p 1026 N94-16927
Nonlinear analysis of mechanical systems under combined harmonic and stochastic excitation
[AD-A266217] p 1173 N94-16937
Stochastic chaos: An analog of quantum chaos
[DE93-016619] p 1220 N94-16956
Nonlinear methods for communications
[AD-A267376] p 1001 N94-17019
Discrete sliding mode control for nonlinear sampled data systems
[AD-A267500] p 1167 N94-17369
Extracavity frequency doubling study of a pulsed photodissociation iodine laser
[AD-A267893] p 1042 N94-17394
Robust control of uncertain nonlinear systems
[AD-A268056] p 1167 N94-17506
Nonlinear random response prediction using MSC/NASTRAN
[NASA-TM-109029] p 1179 N94-17650
NONLINEARITY
High-performance nonlinear optical material developed in Japan
[AD-A266194] p 1191 N94-16126
Nonlinear gyrofluid models of shear Alfven instabilities in ignited and beam heated toroidal plasmas
[DE93-016235] p 1203 N94-16869
Processing of resonance parameter covariance files
[DE93-015506] p 1231 N94-16874
Acoustic waves in complicated geometries and their interactions with liquid-propellant droplet combustion
[AD-A267260] p 1178 N94-16991
Nonlinear methods for communications
[AD-A267376] p 1001 N94-17019
Theoretical studies of nonlinear optical properties of conjugated polymers
[AD-A267390] p 1193 N94-17024
A search for evidence of nonlinear elasticity in the earth
[DE93-015279] p 1102 N94-17252
High order nonlinear estimation with signal processing applications
[AD-A268407] p 1005 N94-17463
NONPARAMETRIC STATISTICS
Nonparametric statistics: Weighted rankings analysis
[AD-A266607] p 1173 N94-16657
Computing science and statistics. Volume 24: Graphics and visualization
[AD-A266571] p 1150 N94-16721
NONPOINT SOURCES
A Geographic Information System approach to modeling nutrient and sediment transport
[DE93-013747] p 1097 N94-17426
NONRELATIVISTIC MECHANICS
Effects of spin-orbit coupling on disordered mesoscopic systems
[ITN-93-85220] p 1180 N94-15288
NONUNIFORMITY
The MADONA experiments (Meteorology and Diffusion Over Non-uniform Areas): High-resolution in-plume concentration fluctuations measurements using lidar remote sensing technique
[AD-A267711] p 1105 N94-14938
NOREPINEPHRINE
Neuropeptide-Y (NPY) increases total blood flow in the tail, and reduces cutaneous microvascular blood flow in the tail and foot of the rat
[AD-A266839] p 1115 N94-14918
NORMAL DENSITY FUNCTIONS
High order nonlinear estimation with signal processing applications
[AD-A268407] p 1005 N94-17463
NORMAL SHOCK WAVES
Laser Doppler velocimetry measurements across a normal shock in transonic flow
[AD-A267240] p 855 N94-14973
NORMS
A posteriori error estimation for hierarchic models of elliptic boundary value problems on thin domains
[AD-A267714] p 1168 N94-14939
NORTHERN HEMISPHERE
Southern and Northern Hemisphere total ozone as seen by TOMS
[NASA-TM-109591] p 1098 N94-15282
NOSE CONES
The effect of the nose shape and wing location toward the wing vortex breakdown
[AD-A267724] p 855 N94-14942
NOTCH SENSITIVITY
The processing and mechanical properties of high temperature/high performance composites. Book 2: Coonstituent properties and macroscopic performance
[AD-A266395] p 935 N94-16484
The processing and mechanical properties of high temperature/high performance composites. Book 4: Coonstitutive laws and design
[AD-A266397] p 935 N94-16528
NOTCH STRENGTH
The effect of electric discharge machined notches on the fracture toughness of several structural alloys
[AD-A268605] p 962 N94-17464
NOTCHES
The effect of electric discharge machined notches on the fracture toughness of several structural alloys
[AD-A268605] p 962 N94-17464
NOWCASTING
Nowcasting methods for satellite imagery
[AD-A267294] p 1108 N94-17267
NOZZLE DESIGN
Heat transfer and aerodynamics of a 3D design nozzle guide vane tested in the Pyestock isentropic light piston facility
[RAE-TM-AERO/PROP-19] p 856 N94-15696
Welding nozzle position manipulator
[NASA-CASE-MFS-29837-1] p 1047 N94-15882
Shock-free supersonic elliptic nozzles and method of forming same
[NASA-CASE-LAR-14054-1] p 925 N94-15947
Flight 20 (STS-45) polysulfide gas path investigation
[NASA-CR-193861] p 928 N94-17213
NOZZLE FLOW
Numerical investigations in three-dimensional internal flows
[NASA-CR-194594] p 1020 N94-15551
Design of round-to-square transition section; analysis and computer code
[AD-A267173] p 872 N94-15847
Effects of internal yaw-vectoring devices on the static performance of a pitch-vectoring nonaxisymmetric convergent-divergent nozzle
[NASA-TP-3369] p 858 N94-16572
Flight 20 (STS-45) polysulfide gas path investigation
[NASA-CR-193861] p 928 N94-17213
Two-dimensional, high flow, precisely controlled monodisperse drop source
[AD-A267660] p 1028 N94-17250
Experimental studies on a gas dynamic laser with narrow throat and high area-ratio grid nozzles
[AD-A267818] p 1042 N94-17400

NOZZLE GEOMETRY
Shock-free supersonic elliptic nozzles and method of forming same
[NASA-CASE-LAR-14054-1] p 925 N94-15947
Experimental studies on a gas dynamic laser with narrow throat and high area-ratio grid nozzles
[AD-A267818] p 1042 N94-17400
NOZZLE INSERTS
SRB thermal curtain design support
[NASA-CR-193857] p 927 N94-17123
NOZZLE WALLS
Numerical investigations in three-dimensional internal flows
[NASA-CR-194594] p 1020 N94-15551
NOZZLES
Welding nozzle position manipulator
[NASA-CASE-MFS-29837-1] p 1047 N94-15882
NUCLEAR ASTROPHYSICS
Fast pulsars, compact stars, and the strange matter hypothesis
[DE93-015039] p 1239 N94-16052
Properties of nuclei in astrophysical environments: Binding energies, weak-interaction rates
[MPA-706] p 1240 N94-17628
NUCLEAR BINDING ENERGY
Electronic spectroscopy of the gas-phase OH-Kr van der Waals complex
[AD-A266891] p 942 N94-14946
Simulation studies for surfaces and materials strength
[NASA-CR-193387] p 1056 N94-15004
Photoemission study of diamond (100) surface
[DE93-015251] p 1208 N94-16062
NUCLEAR ELECTRIC PROPULSION
Space exploration initiative fuels, materials and related nuclear propulsion technologies panel
[NASA-TM-105706] p 923 N94-15118
Application of a NEPTUNE propulsion concept to a manned Mars excursion
[AD-A268053] p 929 N94-17587
NUCLEAR EXPLOSIONS
Ground wave emergency network environmental assessment for northwestern Colorado relay node site number RN 8C924CO
[AD-A267654] p 1003 N94-17249
Ground wave emergency network final operational capability. Environmental assessment for southern Arkansas relay node site no. RN 8C912AR
[AD-A268001] p 1004 N94-17376
Environmental assessment for northwestern Indiana relay node site no. RN 8C902IN
[AD-A267849] p 1004 N94-17406
NUCLEAR FISSION
Engineering Physics and Mathematics Division progress report, period ending 31 December 1992
[DE93-015118] p 1301 N94-14926
NUCLEAR FUEL ELEMENTS
Flow instability tests for a particle bed reactor nuclear thermal rocket fuel element
[AD-A268012] p 929 N94-17474
NUCLEAR FUELS
Space exploration initiative fuels, materials and related nuclear propulsion technologies panel
[NASA-TM-105706] p 923 N94-15118
Space Nuclear Facility test capability at the Baikal-1 and IGR sites Semipalatinsk-21, Kazakhstan
[DE93-011662] p 926 N94-16773
NUCLEAR FUSION
Nuclear fusion of protons with ions of boron
[DE93-015399] p 1202 N94-16019
Chemical and isotopic compositions in acid residues from various meteorites p 1243 N94-16291
The astrophysical interpretation of isotope anomalies in graphite and SiC grains of chondrites p 1244 N94-16343
NUCLEAR INTERACTIONS
Calculations of cosmic-ray helium transport in shielding materials
[NASA-TP-3354] p 1301 N94-17666
NUCLEAR MAGNETIC RESONANCE
Multinuclear NMR study of aluminosilicate sol-gel synthesis reasons for the homogeneous gelation using the prehydrolysis method
[AD-A266877] p 962 N94-14921
NMR and theoretical investigation of cation binding with sol-gel silicates
[AD-A266999] p 963 N94-15631
Study of protein-H2O interactions by multidimensional NMR spectroscopy
[AD-A266955] p 946 N94-15760
Detection and dosimetry of chemical contaminants in polymeric materials
[AD-A266605] p 968 N94-16727
Suppression of charge scattering in Moessbauer experiments using synchrotron radiation
[DE93-015406] p 1212 N94-16887
NUCLEAR MODELS
Engineering Physics and Mathematics Division progress report, period ending 31 December 1992
[DE93-015118] p 1301 N94-14926
NUCLEAR PHYSICS
Engineering Physics and Mathematics Division progress report, period ending 31 December 1992
[DE93-015118] p 1301 N94-14926
NUCLEAR PROPULSION
Space exploration initiative fuels, materials and related nuclear propulsion technologies panel
[NASA-TM-105706] p 923 N94-15118
Space Nuclear Facility test capability at the Baikal-1 and IGR sites Semipalatinsk-21, Kazakhstan
[DE93-011662] p 926 N94-16773
Development and analysis of startup strategies for particle bed nuclear rocket engine
[AD-A267949] p 927 N94-17053
NUCLEAR RADIATION
AFRRI reports, first quarter 1993
[AD-A266380] p 1123 N94-16515
NUCLEAR REACTIONS
Multiple process simulations for correction factor calculations in experiments with neutrons. LUSMK program
[DE93-623957] p 1179 N94-14932
Al-26-Mg-26 ages of iron meteorites p 1242 N94-16240
Possible dust contamination of the early solar system p 1244 N94-16352
NUCLEAR REACTOR CONTROL
System performance modeling and analysis of a fault-tolerant, real time parallel processor
[AD-A268070] p 1162 N94-17551
NUCLEAR REACTORS
GAM-HEAT: A computer code to compute heat transfer in complex enclosures
[DE93-014724] p 1023 N94-15980
System performance modeling and analysis of a fault-tolerant, real time parallel processor
[AD-A268070] p 1162 N94-17551
NUCLEAR ROCKET ENGINES
Nuclear rocket plume studies
[AD-A267154] p 925 N94-15837
Space Nuclear Facility test capability at the Baikal-1 and IGR sites Semipalatinsk-21, Kazakhstan
[DE93-011662] p 926 N94-16773
Development and analysis of startup strategies for particle bed nuclear rocket engine
[AD-A267949] p 927 N94-17053
Flow instability tests for a particle bed reactor nuclear thermal rocket fuel element
[AD-A268012] p 929 N94-17474
NUCLEAR SCATTERING
Suppression of charge scattering in Moessbauer experiments using synchrotron radiation
[DE93-015406] p 1212 N94-16887
NUCLEATION
Diamond epitaxy and diamondlike coatings
[AD-A266657] p 1206 N94-15747
Dynamical Ising model simulations of nucleation and growth in copper-cobalt alloys
[DE93-015336] p 957 N94-16015
The role of interfacial chemistry in surface nucleation and growth of calcium oxalate
[DE93-015689] p 1209 N94-16159
Creep ductility of iron at very low strain rates: The effects of sulfur
[DE93-015490] p 959 N94-16890
UHV-stem studies on nucleation and growth of thin metal silicide films on silicon
[DE93-017604] p 1212 N94-16961
The influence of an electric field on the kinetics of nucleation
[IFTR-2/91] p 1213 N94-17046
Pseudomorphic semiconducting heterostructures from combinations of AlN, GaN and selected SiC polytypes: Theoretical advancement and its coordination with experimental studies of nucleation, growth, characterization and device deployment
[AD-A267561] p 1213 N94-17108
Atomic layer epitaxy group IV materials: Surface processes, thin films, devices and their characterization
[AD-A267527] p 1213 N94-17116
Diamond growth on carbide surfaces using a selective etching technique
[AD-A267989] p 973 N94-17413
Growth, characterization and device development in monocrystalline diamond films
[AD-A268206] p 1216 N94-17553
NUCLEI (NUCLEAR PHYSICS)
Properties of nuclei in astrophysical environments: Binding energies, weak-interaction rates
[MPA-706] p 1240 N94-17628
NUCLEIC ACIDS
Release of iron from hemoglobin
[AD-A266503] p 1128 N94-16784
NUCLEON-NUCLEON INTERACTIONS
Energy-loss cross sections for inclusive charge-exchange reactions at intermediate energies
[NASA-TM-4522] p 1188 N94-17018
NUCLEON-NUCLEON SCATTERING
Energy-loss cross sections for inclusive charge-exchange reactions at intermediate energies
[NASA-TM-4522] p 1188 N94-17018
NUCLEOPHILES
Amide and tetrazene complexes of transition and main group elements as precursors for the low temperature synthesis of elemental nitrides
[AD-A266246] p 950 N94-16931
NUCLIDES
Effects of bulk composition on production rates of cosmogenic nuclides in meteorites p 1245 N94-16385
NUMERICAL ANALYSIS
Engineering Physics and Mathematics Division progress report, period ending 31 December 1992
[DE93-015118] p 1301 N94-14926
Prediction of stable tearing of 2024-T3 aluminum alloy using the crack-tip opening angle approach
[NASA-TM-109023] p 955 N94-15708
C++ as a language for object-oriented numerics
[DE93-015027] p 1148 N94-15985
Analysis of electromagnetic scattering from irregularly shaped, thin, metallic flat plates
[NASA-TP-3361] p 998 N94-16655
Numerical studies of the photoluminescence spectrum of quantum Hall systems
[DE93-015822] p 1220 N94-16810
Applications of the phi-transform
[AD-A266247] p 1170 N94-16940
Elastic waves in discretely continuous mechanical systems
[IFTR-21/1992] p 1061 N94-17091
Phillips Laboratory global spectral numerical weather prediction model
[AD-A267293] p 1107 N94-17244
Mathematical Sciences Division 1992 programs
[AD-A268586] p 1140 N94-17623
NUMERICAL CONTROL
A microprocessor controller for a towing tank drive and flow visualisation system
[AD-A267087] p 872 N94-15543
A computer-controlled x-y offset guiding stage for the MLRS p 918 N94-15598
A modular control architecture for real-time synchronous and asynchronous systems
[DE93-015439] p 1166 N94-16888
Automated strain gauge plethysmograph
[AD-A267323] p 1035 N94-17002
A measurement station for study of Earth moving tools and ground cutting processes
[IFTR-10/1991] p 985 N94-17068
A state-of-the-art plasma polymerization coater for ICF targets
[DE93-016452] p 1204 N94-17237
NUMERICAL FLOW VISUALIZATION
The 1989 computational fluid dynamics highlights
[NASA-TM-109635] p 1018 N94-15246
Large eddy simulation and direct numerical simulation of high speed turbulent reacting flows
[NASA-CR-193131] p 1018 N94-15427
The 1988 computational fluid dynamics highlights
[NASA-TM-109645] p 1019 N94-15431
NAS technical summaries: Numerical aerodynamic simulation program, March 1991 - February 1992
[NASA-TM-109335] p 854 N94-15798
NUMERICAL INTEGRATION
Comparison of level-1 and level-2 buckling and postbuckling solutions
[NASA-CR-194611] p 1057 N94-15154
Volume integral equations applied to circular and square cylinders
[AD-A266635] p 1169 N94-15785
Fast algorithms for polynomial interpolation, integration and differentiation
[AD-A267505] p 1154 N94-17370
NUMERICAL STABILITY
Linear stability of stationary solutions of the Vlasov-Poisson system in three dimensions
[DE93-013873] p 1174 N94-16820
NUMERICAL WEATHER FORECASTING
Sensitivity testing of a single-Doppler temperature retrieval and forecast system
[AD-A267278] p 1105 N94-14958
TAFVER 2 users manual
[AD-A266850] p 1106 N94-15757
Ensemble forecasting techniques in medium-range forecasting
[AD-A267443] p 1107 N94-17029

Phillips Laboratory global spectral numerical weather prediction model
[AD-A267293] p 1107 N94-17244

NUTATION
State-of-the-art satellite laser range modeling for geodetic and oceanographic applications
p 916 N94-15586

NUTRITION
International food research project
[NASA-TM-109540] p 1135 N94-15371

NUTS (FASTENERS)
Tilt mechanism
[AD-D015780] p 1047 N94-16548

NYLON (TRADEMARK)
Soluble precursor route to polyanilines
[AD-A268015] p 973 N94-17494

O

O RING SEALS
Flight 20 (STS-45) polysulfide gas path investigation
[NASA-CR-193861] p 928 N94-17213

OAO
The 1968 highlights --- NASA programs and research
[NASA-TM-109627] p 1302 N94-15413

OBJECT-ORIENTED PROGRAMMING
Development of a computer supported instrumentation for economic planning and evaluation of production facilities for fiber reinforced composites elements
p 932 N94-15260
The distributed database dynamic reconfiguration project
[AD-A267116] p 1229 N94-15652
An experimental comparison of CLOS and C(++) implementations of an object-oriented graphical simulation of walking robot kinematics
[AD-A267168] p 1165 N94-15855
Integration ToolKit and Methods (ITKM) manufacturing methods and prototype toolkit. A combined modeling method using IDEFO, IDEF1x and XSpec
[AD-A266176] p 984 N94-16981
An object-oriented program specification for a mobile robot motion control language
[AD-A267213] p 1166 N94-16986
Design and implementation of an interface editor for the Amadeus multi-relational database front-end system
[AD-A267403] p 1233 N94-17114
An object-oriented dynamic software process model
[AD-A267726] p 1154 N94-17371
Research in presistent simulation: Development of the persistent ModSim object-oriented programming language
[AD-A268568] p 1157 N94-17620

OBLIQUE SHOCK WAVES
On the interaction between the shock wave attached to a wedge and freestream disturbances
[NASA-CR-191528] p 1019 N94-15478
An investigation of oblique shock/boundary layer interaction control
[AD-A268106] p 861 N94-17574

OBLIQUE WINGS
The 1980 highlights
[NASA-TM-109672] p 1303 N94-15509

OBSERVATORIES
Unmasking the Sun
[NASA-TM-109595] p 1298 N94-15287
Lunar ranging
[NASA-TM-109603] p 1236 N94-15311
A computer-controlled x-y offset guiding stage for the MLRS p 918 N94-15598
Neutral-current detection in the Sudbury Neutrino Observatory
[DE93-014481] p 1185 N94-16951

OBSTACLE AVOIDANCE
Perception for outdoor navigation
[AD-A266867] p 863 N94-14919
Environmental use of a Laser Range Finder and the Advanced Visualization System
[DE93-016163] p 1043 N94-17677

OCCUPATION
Carpal tunnel syndrome and other cumulative trauma disorders of the arm and hand and occupation in US Navy enlisted personnel
[AD-A267747] p 1129 N94-17374

OCCUPATIONAL DISEASES
Proceedings of the 1992 Annual Meeting NASA Occupational Health Program
[NASA-CR-193462] p 1123 N94-16609
New health and safety initiatives at the Department of Energy (DOE) p 1124 N94-16610
Americans with Disabilities Act considerations for the practice of occupational medicine p 1124 N94-16611
Programs and resources for control of job stress in the Federal workplace p 1124 N94-16617
Tuberculosis: A case for increased screening
p 1126 N94-16627
Summary of follow-up results from potential tuberculosis exposures p 1126 N94-16628
Legionella: An overview p 1126 N94-16629
Asbestos Surveillance Program p 1127 N94-16638
Lead Surveillance Program p 1127 N94-16640
Mercury Surveillance Program p 1127 N94-16641
General Medical Surveillance Program
p 1127 N94-16643
OSHA bloodborne pathogens standards exposure control plan p 1127 N94-16645
Carpal tunnel syndrome and other cumulative trauma disorders of the arm and hand and occupation in US Navy enlisted personnel
[AD-A267747] p 1129 N94-17374

OCEAN BOTTOM
LFASE report: Crustal study
[AD-A266893] p 1111 N94-14947
Composite refraction-reflection stack sections: Tracing faults in the Atlantic coastal plain sediments
[DE93-013581] p 1112 N94-16009
Mapping of sea bottom topography
p 1077 N94-16744
Sea bottom topography imaging with SAR
p 1077 N94-16745
The Megascience Forum
[DE93-014445] p 1303 N94-16804
Real time system for practical acoustic monitoring of global ocean temperature
[AD-A267868] p 1113 N94-17391
Fabrication of a NAVMAP, a deep-sea mapping system
[AD-A268630] p 1085 N94-17467
Report detailing modifications to the 1/8 degree global bathymetry
[AD-A268178] p 1114 N94-17509

OCEAN COLOR SCANNER
SeaWiFS technical report series. Volume 12, SeaWiFS technical report series cumulative index: Volumes 1-11
[NASA-TM-104566-VOL-12] p 1111 N94-15529

OCEAN CURRENTS
IAI topic: El Nino. Southern oscillation and interannual climate variability
[INPE-5410-PRE/1757] p 1111 N94-15186
Optical properties of the Red Sea
[AD-A266466] p 1113 N94-16588
SAR observations in the Gulf of Mexico
p 1077 N94-16742
Real time system for practical acoustic monitoring of global ocean temperature
[AD-A267868] p 1113 N94-17391
Meridional circulation in the tropical north atlantic
[AD-A268222] p 1114 N94-17555

OCEAN DATA ACQUISITIONS SYSTEMS
The IOSDL SeaSoar hydraulic unit
[IOS-300-1992] p 1114 N94-17516

OCEAN DYNAMICS
On the application and evaluation of the relocatable diecast ocean circulation model in coastal and semi-enclosed seas
[AD-A266626] p 1112 N94-15771
Observations and modelling of winds and waves during the Surface Wave Dynamics Experiment. Report 1: Intensive observation period IOP-1, 20-31 October 1990
[AD-A266384] p 1113 N94-16517
Earth system dynamics: The interrelation of atmospheric, ocean and solid earth dynamics
[NASA-CR-193487] p 1081 N94-17444
Statistics and physical oceanography
[AD-A268565] p 1115 N94-17598

OCEAN MODELS
Exploring the southern ocean response to climate change
[NASA-CR-194601] p 1112 N94-15680
On the application and evaluation of the relocatable diecast ocean circulation model in coastal and semi-enclosed seas
[AD-A266626] p 1112 N94-15771
Observations and modelling of winds and waves during the Surface Wave Dynamics Experiment. Report 1: Intensive observation period IOP-1, 20-31 October 1990
[AD-A266384] p 1113 N94-16517
The use of General Circulation Models in detecting climate change induced by greenhouse gases
[DE93-014369] p 1096 N94-16802
Real time system for practical acoustic monitoring of global ocean temperature
[AD-A267868] p 1113 N94-17391
Report detailing modifications to the 1/8 degree global bathymetry
[AD-A268178] p 1114 N94-17509
Statistics and physical oceanography
[AD-A268565] p 1115 N94-17598

OCEAN SURFACE
Fine scale measurements of microwave backscatter from the ocean surface
[AD-A264516] p 1111 N94-15134
Arctic internal waves (CEAREX)
[AD-A265822] p 1111 N94-15139
Testing the waters from space --- Thermal mapping
[NASA-TM-109623] p 1082 N94-15409
Exploring the southern ocean response to climate change
[NASA-CR-194601] p 1112 N94-15680
Observations and modelling of winds and waves during the Surface Wave Dynamics Experiment. Report 1: Intensive observation period IOP-1, 20-31 October 1990
[AD-A266384] p 1113 N94-16517
Field observations of infragravity, sea and swell directional spectra
[AD-A266439] p 1113 N94-16561
Investigation of AIRSAR signatures of the Gulf Stream
p 1077 N94-16743
Preliminary estimates of frequency-direction spectra derived from the SAMSON pressure gage array, November 1990 to May 1991
[AD-A267960] p 1114 N94-17497

OCEAN TEMPERATURE
Real time system for practical acoustic monitoring of global ocean temperature
[AD-A267868] p 1113 N94-17391

OCEANOGRAPHIC PARAMETERS
Preliminary estimates of frequency-direction spectra derived from the SAMSON pressure gage array, November 1990 to May 1991
[AD-A267960] p 1114 N94-17497

OCEANOGRAPHY
Short walk to everywhere --- Space, Earth, Ocean Center
[NASA-TM-109541] p 1221 N94-15372
State-of-the-art satellite laser range modeling for geodetic and oceanographic applications
p 916 N94-15586
On the application and evaluation of the relocatable diecast ocean circulation model in coastal and semi-enclosed seas
[AD-A266626] p 1112 N94-15771
Proceedings of the Third Spaceborne Imaging Radar Symposium
[NASA-CR-194104] p 989 N94-15886
The multivariate optimum interpolation analysis of meteorological data at the Fleet Numerical Oceanography Center
[AD-A266459] p 1106 N94-16568
SAR observations in the Gulf of Mexico
p 1077 N94-16742
The Megascience Forum
[DE93-014445] p 1303 N94-16804
Adequation of mini satellites to oceanic altimetry missions p 891 N94-17152
Abstracts of manuscripts submitted in 1992 for publication
[AD-A267963] p 1113 N94-17383
Arctic cyclones and Marginal Ice Zone (MIZ) variability
[AD-A268610] p 1108 N94-17485
Fabrication of a NAVMAP, a deep-sea mapping system
[AD-A268630] p 1085 N94-17467
Report detailing modifications to the 1/8 degree global bathymetry
[AD-A268178] p 1114 N94-17509
List of the scientific and personal papers of Sir George Deacon, FRS
[IOS-301-1992] p 1114 N94-17518
Statistics and physical oceanography
[AD-A268565] p 1115 N94-17598

OCEANS
Coastal zone color scanner: Nimbus 7
[NASA-TM-109590] p 1111 N94-15281
What we can learn about ocean tides from tide gauge and gravity loading measurements?
p 1100 N94-15811
A study of the observed tidal residue vectors B versus oceanic tidal load vectors L p 1100 N94-15813
The influence of oceans on Martian volcanism
p 1295 N94-16427
AVIRIS calibration and application in coastal oceanic environments p 1069 N94-16685
Fabrication of a NAVMAP, a deep-sea mapping system
[AD-A268630] p 1085 N94-17467
Statistics and physical oceanography
[AD-A268565] p 1115 N94-17598

OFFGASSING
Space Shuttle solid rocket motor exposure monitoring
p 976 N94-16624

OGO
The 1966 highlights --- NASA research programs
[NASA-TM-109444] p 1302 N94-15343

The 1968 highlights --- NASA programs and research
[NASA-TM-109627] p 1302 N94-15413

OHMS LAW
Nonlinear gyrofluid models of shear Alfven instabilities in ignited and beam heated toroidal plasmas
[DE93-016235] p 1203 N94-16869

OIL RECOVERY
Responsive copolymers for enhanced petroleum recovery
[DE93-018030] p 971 N94-16999

OLEIC ACID
Contained liquids in microgravity, part 2
p 979 N94-16085

OLIGOMERS
New organic materials for nonlinear optics applications
[AD-A266451] p 1192 N94-16563
Photodegradation of MDI based polyurethane/urea elastomers
[AD-A267308] p 971 N94-16994

OLIVINE
The Fe2(+)-Mg interdiffusion in orthopyroxene: Constraints from cation ordering and structural data and implications for cooling rates of meteorites
p 1241 N94-16175
Stalking the LREE-enriched component in ureilites
p 1241 N94-16190
Angrite LEW87051: Are the olivines pheno's or xeno's? A continuing story p 1103 N94-16285
Experimental segregation of iron-nickel metal, iron-sulfide, and olivine in a thermal gradient: Preliminary results p 1243 N94-16288
Water in Earth's mantle: Hydrogen analysis of mantle olivine, pyroxenes and garnet using the SIMS
p 1104 N94-16336
On origin of the olivine inclusions from the Kainsaz CO carbonaceous chondrite p 1244 N94-16345
Liquidus equilibria of lunar analogs at high pressure
p 1283 N94-16364
Mixing model analysis of telescopic lunar spectra
p 1284 N94-16371
Possible sources of H2 to H2O enrichment at evaporation of parent chondritic material
p 1244 N94-16377
More on the cooling history of angrite LEW 86010
p 1245 N94-16400
The thickness of eucritic crust in the HED parent body
p 1104 N94-16416

ON-LINE SYSTEMS
Complexity analysis of real-time reinforcement learning applied to finding shortest paths in deterministic domains
[AD-A266636] p 1131 N94-15742
RELMA: On-line quality control in the rubber mixing room using laser analysis p 984 N94-16005
NASA Electronic Library System (NELS): The system impact of security
[NASA-CR-194614] p 1231 N94-16499
Development of dynamic, contex-driven help systems
[AD-A267409] p 1152 N94-16974
Critically evaluated/distributed database of IRAS LRS spectra
[NASA-CR-193611] p 1232 N94-17038
Defense RDT&E online system (DROLS) handbook
[AD-A267546] p 1232 N94-17101
Defense Logistics Information System (DLIS). Procedures manual: Logistics On-Line Access (LOLA) procedures manual
[AD-A267685] p 1233 N94-17229
Processes involved in the integration of pictures and discourse
[AD-A268150] p 1134 N94-17468

ONBOARD DATA PROCESSING
NASA Lewis Meshed VSAT Workshop meeting summary
[NASA-TM-106332] p 883 N94-17487

ONBOARD EQUIPMENT
STS-29 crew IMAX camera training
[NASA-TM-109546] p 1031 N94-15380
Regulated emergency oxygen system
[AD-A266228] p 1138 N94-16983
The STRV On Board Data Handling (OBDH) system: An introduction p 895 N94-17178
MINISAT programme p 896 N94-17182
The space technology research vehicle: Development status p 896 N94-17183
TITUS: A micro-satellite for technology demonstration
p 896 N94-17186
Key trends of the small satellite market
p 897 N94-17191

ONTOGENY
Ontogenesis of mammals in microgravity
[NASA-TM-103978] p 1139 N94-17636

OPEN CIRCUIT VOLTAGE
Potential transients, transmission and electrochemical corrosion detection
[DE93-014055] p 956 N94-15922

OPERATING SYSTEMS (COMPUTERS)
Integrated trusted systems development environment
[AD-A267029] p 1146 N94-15674
Fast interrupt priority management in operating system kernels
[AD-A266638] p 1140 N94-15744
Processor capacity reserves for multimedia operating systems
[AD-A266639] p 1158 N94-15745
Disconnected operation in a distributed file system
[AD-A266461] p 1231 N94-16570
An internetwork authentication architecture
[AD-A268579] p 1162 N94-17622

OPERATING TEMPERATURE
Cryogenic measurements of aerojet GaAs n-JFETs
[NASA-TM-103972] p 1009 N94-15765

OPERATIONAL AMPLIFIERS
Stray insensitive switched capacitor composite operational amplifiers
[AD-A267412] p 1012 N94-16976

OPERATIONAL PROBLEMS
The airline quality report 1993
[NIAR-93-11] p 863 N94-17262

OPERATIONS RESEARCH
Logarithmic asymptotics for steady-state tail probabilities in a single-server queue
[AD-A266746] p 1165 N94-15775
Fast simulation of steady-state availability in non-Markovian highly dependable systems
[AD-A266747] p 1174 N94-15823
Research and development: Engine of innovation at Krupp p 984 N94-16001
Kennedy Space Center exercise program
p 1126 N94-16634
An object-oriented dynamic software process model
[AD-A267726] p 1154 N94-17371
Mathematical Sciences Division 1992 programs
[AD-A268586] p 1140 N94-17623

OPERATOR PERFORMANCE
Cognitive engineering models in space systems
[NASA-CR-193473] p 1140 N94-16716
Preliminary validation of the task analysis/workload methodology
[AD-A267514] p 1138 N94-17077

OPERATORS (MATHEMATICS)
Steepest descent approximations for accretive operator equations
[DE93-628586] p 1171 N94-17667

OPTICAL COMMUNICATION
Congestion control of high-speed networks
[AD-A267013] p 989 N94-15748
A formal protocol test procedure for the Survivable Adaptable Fiber Optic Embedded Network (SAFENET)
[AD-A267410] p 1192 N94-16975
Performance of coded coherent FSK lightwave system with noncoherent detection
[AD-A267442] p 1193 N94-17028
Non-blocking crossbar permutation engine with constant routing latency
[NASA-CASE-NPO-18864-1-CU] p 1161 N94-17328
A scalable wrap-around shuffle exchange network with deflection routing
[NASA-CASE-NPO-18983-1-CU] p 1161 N94-17330
Laser beam steering device p 1045 N94-17357
Activities of the Research Laboratory of Electronics
[AD-A266730] p 1304 N94-17651

OPTICAL COMPUTERS
Optical residue processing module
[AD-A267721] p 1188 N94-14940
Database system studies in fine grain optoelectronic computing
[AD-A267026] p 1145 N94-15627
Alternative optical architectures for multichannel adaptive optical processing
[AD-A267052] p 1189 N94-15664
Wideband acousto-optic correlator for an ESM receiver upgrade
[TABES PAPER 93-661] p 1054 N94-16156
Optical computing
[AD-A267881] p 1141 N94-17015
Low cost paths to binary optics p 1197 N94-17353
Computer-aided design package for designers of digital optical computers
[AD-A267866] p 1154 N94-17390

OPTICAL CONTROL
True time delay optically controlled dual band transmitter
[AD-A267663] p 1003 N94-17228

OPTICAL CORRECTION PROCEDURE
Emittance and beam size distortion due to linear coupling
[DE93-015402] p 1184 N94-16886

OPTICAL CORRELATORS
Alternative optical architectures for multichannel adaptive optical processing
[AD-A267052] p 1189 N94-15664
Spatial filters for optical correlation
[AD-A267199] p 1189 N94-15791

OPTICAL COUPLING
Optical coupling elements for coherent optical multiport receivers
[ETN-93-94398] p 1188 N94-15447

OPTICAL DATA PROCESSING
Optical residue processing module
[AD-A267721] p 1188 N94-14940
Research Studies on Advanced Optical Module/Head Designs for Optical Disk Recording Devices
[NASA-CR-194390] p 1226 N94-14981
Spatial filters for optical correlation
[AD-A267199] p 1189 N94-15791
Optical computing
[AD-A267881] p 1141 N94-17015
A scalable wrap-around shuffle exchange network with deflection routing
[NASA-CASE-NPO-18983-1-CU] p 1161 N94-17330
Asymmetric three-beam binary optic grating
p 1195 N94-17340
Low cost paths to binary optics p 1197 N94-17353
Color separation gratings p 1198 N94-17362
The photonical, pure grid method
[NLR-TP-91478-U] p 1062 N94-17600

OPTICAL DATA STORAGE MATERIALS
MeV ion-beam analysis of optical data storage films
p 1226 N94-14984
Application of holographic optical elements to magneto-optic read/write heads p 1226 N94-14985
Dynamic testbed laboratory and micro-optics
p 1199 N94-14986
Magnetic and magneto-optical properties and domain structure of Co/Pd multilayers p 1227 N94-14991
Effects of a shading band in the data path of an optical drive p 1199 N94-14993

OPTICAL DISKS
Characterization facility for magneto-optic media and systems p 1226 N94-14983
Compact disk error measurements
p 1227 N94-14988
Measurement of birefringence for optical recording disk substrates p 1227 N94-14989
Ring lens focusing and push-pull tracking scheme for optical disk systems p 1227 N94-14990
Determining the locations of the various CIRC recording format information blocks (user data blocks, C2 and C1 words and EFM frames) on a recorded compact disc
p 1228 N94-14997
3-D optical memory disk
[AD-A267908] p 1141 N94-17380

OPTICAL EMISSION SPECTROSCOPY
Optical fiber spectroscopy: A study of the luminescent properties of the europium ion for thermal sensors
[NASA-CR-194576] p 1189 N94-15647
Growth and doping of Al(x)Ga(1-x)N films by electron cyclotron resonance assisted molecular beam epitaxy
[AD-A267305] p 1212 N94-16992

OPTICAL EQUIPMENT
A novel solid-state optical temporal analyzer with picosecond resolution and picowatt sensitivity
[AD-A266804] p 986 N94-14912
Design of pulse stretching cell for a sodium guide star optical system
[DE93-016436] p 1236 N94-14929
Velocity matched millimeterwave electro-optic modulator
[AD-A267264] p 1188 N94-14957
Visualization of solidification front phenomena
[NASA-CR-193838] p 976 N94-15006
Polished substrate surface and cleaning study for coated optic quality
[DE93-014116] p 1190 N94-15975
Optical ionospheric instrumentation and research
[AD-A266403] p 1192 N94-16550
Conference on Binary Optics: An Opportunity for Technical Exchange
[NASA-CP-3227] p 1194 N94-17331
Manufacturing the key to binary optics
p 1194 N94-17332
Binary optics: Trends and limitations
p 1194 N94-17333
Diffractive optics: Design, fabrication, and applications
p 1194 N94-17334
Scalar limitations of diffractive optical elements
p 1194 N94-17336
Diffractive optical elements for generating arbitrary line foci p 1195 N94-17338
Asymmetric three-beam binary optic grating
p 1195 N94-17340
Scattering from binary optics p 1195 N94-17341

Mathmatical modeling for diffractive optics
p 1195 N94-17342
Binary optics at Hughes Danbury Optical Systems
p 1195 N94-17344
Diffractive optics fabricated by direct write methods with an electron beam p 1196 N94-17347
Applications of advanced diffractive optical elements
p 1197 N94-17356
SURPHEX (tm): New dry photopolymers for replication of surface relief diffractive optics p 1198 N94-17358
Predesign of diamond turned refractive/diffractive elements for IR objectives p 1198 N94-17359
Optical system storage design with diffractive optical elements p 1198 N94-17360
Spectral inverse scattering theory for dielectric media: Application to optical devices
[AD-A268635] p 1199 N94-17427
Test methods for acceptance testing of telescopes
[AD-A268316] p 1237 N94-17568
Comparison of computer predictions and magnetic field measurements for an iron spectrometer magnet
[DE93-016164] p 1176 N94-17658

OPTICAL FIBERS
Optical residue processing module
[AD-A267721] p 1188 N94-14940
Prospects for high pressure imaging gas scintillation drift chambers p 901 N94-15040
Optical coupling elements for coherent optical multiport receivers
[ETN-93-94398] p 1188 N94-15447
Optical fiber spectroscopy: A study of the luminescent properties of the europium ion for thermal sensors
[NASA-CR-194576] p 1189 N94-15647
The three-dimensional ray trajectories of the WKB optical fiber modes
[AD-A267167] p 1189 N94-15739
Plasma arc welding weld imaging
[NASA-CASE-MFS-28797-1] p 1047 N94-15949
Pulse propagation in inhomogeneous optical waveguides
[DE93-013378] p 1191 N94-16007
Fundamental theory of light for applications: Notes for five informal lectures
[DE93-016463] p 1192 N94-16953
Investigation of the optical, electronic, and structural properties of fiber optic glasses
[AD-A267645] p 971 N94-17204
The stability and dynamics of elastic structures and fluid flows
[AD-A267990] p 1029 N94-17414

OPTICAL FILTERS
Display system employing acousto-optic tunable filter
[NASA-CASE-NPO-18736-1-CU] p 1190 N94-15933

OPTICAL HETERODYNING
Optical coupling elements for coherent optical multiport receivers
[ETN-93-94398] p 1188 N94-15447

OPTICAL MATERIALS
Design, synthesis and characterization of novel nonlinear optical polymers
[AD-A267035] p 964 N94-15675
Organic polymeric electro-optic materials: Synthesis, processing, and device applications
[AD-A267133] p 964 N94-15688
High-performance nonlinear optical material developed in Japan
[AD-A266194] p 1191 N94-16126
Rational design, construction, and processing of high-performance nonlinear optical materials
[AD-A266185] p 1191 N94-16454
Main chain chromophoric polymers with second order nonlinear optical properties
[AD-D015893] p 969 N94-16920
Static and dynamic investigations of brittle elasto-optical material
[IFTR-3/1992] p 1061 N94-17086

OPTICAL MEASUREMENT
Measurement of birefringence for optical recording disk substrates p 1227 N94-14989
Sensor modelling for the Cyclops focal plane detector array based technology demonstrator
[AD-A267172] p 1190 N94-15846
Optical measurements of NASA/USAF CRRES high altitude rocket borne chemical release experiments in conjunction with the USAF airborne ionospheric observatory aircraft
[AD-A266404] p 1101 N94-16551
A 27 channels, 1 MHz fibre-optic measuring system
[AD-A266943] p 1003 N94-17307
High power steady state MPD thrusters
[AD-A267277] p 928 N94-17308

OPTICAL MEASURING INSTRUMENTS
Neural-network-directed alignment of optical systems using the laser-beam spatial filter as an example
[NASA-TP-3372] p 1034 N94-15961
Revisiting the BCS, a measurement system for characterizing the optics of solar collectors
[DE93-015030] p 1091 N94-15993
Earth observation from small satellites
p 891 N94-17150

OPTICAL MEMORY (DATA STORAGE)
Database system studies in fine grain optoelectronic computing
[AD-A267026] p 1145 N94-15627
Optical system storage design with diffractive optical elements p 1198 N94-17360
3-D optical memory disk
[AD-A267908] p 1141 N94-17380

OPTICAL MICROSCOPES
A near-field scanning optical microscope for analysis of magneto-optic media p 1199 N94-14995

OPTICAL PATHS
A method of detecting and locating electrical current imbalances
[NASA-CASE-LEW-15407-1] p 1009 N94-15706
Fabrication and phase tuning of an optical waveguide device
[AD-D015815] p 1191 N94-16489

OPTICAL POLARIZATION
Application of holographic optical elements to magneto-optic read/write heads p 1226 N94-14985

OPTICAL PROPERTIES
Plume primary smoke p 923 N94-15218
Design, synthesis and characterization of novel nonlinear optical polymers
[AD-A267035] p 964 N94-15675
Why is the Moon dark? p 1256 N94-16219
Optical effects of regolith processes on S asteroids as simulated by laser impulse alteration of ordinary chondrite p 1246 N94-16422
Variations in the Fe mineralogy of bright Martian soil
p 1295 N94-16431
Optical properties of the Red Sea
[AD-A266466] p 1113 N94-16588
Elastooptical brittle materials in experimental studies of the state of stress and deformation
[IFTR-22/1991] p 1059 N94-16651
Detection of subsurface defects in machined silicon nitride ceramics by optical scattering methods
[DE93-015554] p 968 N94-16658
Main chain chromophoric polymers with second order nonlinear optical properties
[AD-D015893] p 969 N94-16920
Optical properties of water released in low Earth orbit
[AD-A266197] p 1192 N94-16936
Speckles statistics and decorrelation effects in complex ABCD optical systems
[AD-A267843] p 1193 N94-17012
Theoretical studies of nonlinear optical properties of conjugated polymers
[AD-A267390] p 1193 N94-17024
Transmission of light through a turbulent mixing layer
[AD-A267266] p 1193 N94-17264
Laser ignition of solid propellants: 1. Ignition delays
[AD-A268454] p 976 N94-17538
A new method of designing multilayer optical thin film coatings
[DE93-624683] p 974 N94-17611

OPTICAL PUMPING
Theoretical studies relating to the interaction of radiation with matter
[AD-A267134] p 1180 N94-15689

OPTICAL RADAR
The MADONA experiments (Meteorology and Diffusion Over Non-uniform Areas): High-resolution in-plume concentration fluctuations measurements using lidar remote sensing technique
[AD-A267711] p 1105 N94-14938
IR detectors and subsystems for space applications
p 909 N94-15091
Prelaunch optical characterization of the Laser Geodynamic Satellite (LAGEOS 2)
[NASA-TP-3400] p 884 N94-15193
Heterodyne efficiency for a coherent laser radar with diffuse or aerosol targets
[NASA-CR-194563] p 1038 N94-15477
System architecture of optically controlled phased array radar
[AD-A267056] p 988 N94-15667
Spatial filters for optical correlation
[AD-A267199] p 1189 N94-15791
Spatial and frequency diversity in lidar systems
[AD-A266192] p 1039 N94-16124
Clementine: Anticipated scientific datasets from the Moon and Geographos p 1288 N94-16392
BACKSCAT lidar simulation version 3.0: Technical documentation and users guide
[AD-A267296] p 1003 N94-17268
Conically scanned holographic lidar telescope
[NASA-CASE-GSC-13462-1] p 1194 N94-17321
Micro pulse laser radar
[NASA-CASE-GSC-13493-1] p 1004 N94-17322
Laser beam steering device p 1045 N94-17357

OPTICAL REFLECTION
Engineering design of sub-micron topographies for simultaneously adherent and reflective metal-polymer interfaces
[NASA-CR-194573] p 964 N94-15700
Fullerene superconductors
[AD-A266749] p 1010 N94-15954
Optical properties and surface morphology studies of palladium contacts on mercuric iodide single crystals
[DE93-012510] p 1207 N94-15973

OPTICAL RESONATORS
Pulsed hydrogen fluoride overtone chemical laser studies
[AD-A267597] p 1041 N94-17193

OPTICAL SCANNERS
A near-field scanning optical microscope for analysis of magneto-optic media p 1199 N94-14995
Conically scanned holographic lidar telescope
[NASA-CASE-GSC-13462-1] p 1194 N94-17321

OPTICAL SWITCHING
Infrared remote activity transceiver universal model
[AD-A266965] p 1188 N94-15144
Optical coupling elements for coherent optical multiport receivers
[ETN-93-94398] p 1188 N94-15447
Optically-switched submillimeter-wave oscillator and radiator
[NASA-CASE-NPO-18547-1-CU] p 1014 N94-17324
A scalable wrap-around shuffle exchange network with deflection routing
[NASA-CASE-NPO-18983-1-CU] p 1161 N94-17330
High-speed nonlinear switching mechanisms and devices for multi-gigabit data processing
[AD-A267753] p 1014 N94-17375

OPTICAL THICKNESS
Altitude profile of aerosols on Mars from measurements of its thermal radiation on limb p 1294 N94-16423
Spatial resolution and cloud optical thickness retrievals p 1066 N94-16671

OPTICAL TRACKING
RACCOON: A Real-Time Autonomous Car Chaser Operating Optimally at Night
[AD-A266963] p 863 N94-14971
Laser tracking for vertical control p 911 N94-15553
Historical MOBLAS system characterization
p 915 N94-15579
Two color satellite laser ranging upgrades at Goddard's 1.2m telescope facility p 915 N94-15581
Millimeter accuracy satellites for two color ranging
p 916 N94-15583
Two wavelength satellite laser ranging using SPAD
p 916 N94-15584
State-of-the-art satellite laser range modeling for geodetic and oceanographic applications
p 916 N94-15586
On the accuracy of ERS-1 orbit predictions
p 874 N94-15589
HP upgrade operational streamlining
p 918 N94-15596
A computer-controlled x-y offset guiding stage for the MLRS p 918 N94-15598
Ground based laser ranging for satellite location
p 919 N94-15607
Station report on the Goddard Space Flight Center (GSFC) 1.2 meter telescope facility p 922 N94-15625

OPTICAL TRANSITION
Evaluation of hemoglobin-oxygen equilibrium binding by rapid-scanning spectrophotometry and singular-value decomposition
[AD-A266453] p 1123 N94-16564

OPTICAL WAVEGUIDES
Pulse propagation in inhomogeneous optical waveguides
[DE93-013378] p 1191 N94-16007
OETC optical backplane bus testbed. IBM tasks: Receiver OEIC and link simulation tools and analysis
[AD-A266198] p 1191 N94-16128
Fabrication and phase tuning of an optical waveguide device
[AD-D015815] p 1191 N94-16489
Performance of coded coherent FSK lightwave system with noncoherent detection
[AD-A267442] p 1193 N94-17028
Spectral inverse scattering theory for dielectric media: Application to optical devices
[AD-A268635] p 1199 N94-17427

OPTICS
VUV thin films, chapter 7
[NASA-CR-194634] p 967 N94-16494
Conference on Binary Optics: An Opportunity for Technical Exchange
[NASA-CP-3227] p 1194 N94-17331

Manufacturing the key to binary optics p 1194 N94-17332
Binary optics: Trends and limitations p 1194 N94-17333
Diffractive optics: Design, fabrication, and applications p 1194 N94-17334
Scattering from binary optics p 1195 N94-17341

OPTIMAL CONTROL
A molecular dynamics simulator for optimal control of molecular motion
[AD-A266572] p 1183 N94-16722
Neighboring extremal guidance for systems with piecewise linear control using time as the reference variable
[AD-A267942] p 874 N94-17010
A comparative study of analog and digital control laws for the UMCSL truss
[AD-A267980] p 871 N94-17412
Robust control of uncertain nonlinear systems
[AD-A268056] p 1167 N94-17506

OPTIMIZATION
Development of x ray CCDs p 900 N94-15033
Optimisation of FIR photoconductors for atmospheric spectroscopy p 902 N94-15048
Preliminary analysis and design optimization of the short spacer truss of Space Station Freedom
[NASA-TM-4470] p 1058 N94-15709
Stochastic scheduling in a multiclass G/G/1 queue
[INRIA-RR-1746] p 1162 N94-17537
Optimisation and specification of Auger electron spectrometers for signal-to-noise ratio performance
[NPL-DMM(A)-101] p 1006 N94-17549
State space partitioning methods for solving a class of stochastic network problems
[AD-A267494] p 1173 N94-17585

OPTOELECTRONIC DEVICES
Optical coupling elements for coherent optical multiport receivers
[ETN-93-94398] p 1188 N94-15447
System architecture of optically controlled phased array radar
[AD-A267056] p 988 N94-15667
Organic polymeric electro-optic materials: Synthesis, processing, and device applications
[AD-A267133] p 964 N94-15688
Almaz p 898 N94-15889
Sputtered ferroelectric thin films of KTN for electro-optic devices
[AD-A266573] p 968 N94-16723
JSEP fellowship
[AD-A266568] p 1211 N94-16800
Laser figuring for the generation of analog micro-optics and kineform surfaces p 1196 N94-17346
Diffractive optics fabricated by direct write methods with an electron beam p 1196 N94-17347
Micro-optics technology and sensor systems applications p 1197 N94-17350
Fabrication of micro-optical devices p 1197 N94-17351
Diffractive optics in adverse environments p 1197 N94-17352
Thermal Weapon Sight (TWS) AN/PAS-13 diffractive optics designed for producibility p 1197 N94-17354
Measurements of microlens performance p 1197 N94-17355
Laser beam steering device p 1045 N94-17357
Theory of dispersive microlenses p 1198 N94-17361
Color separation gratings p 1198 N94-17362
OSA proceedings on Ultrafast Electronics and Optoelectronics, volume 14
[AD-A267972] p 1014 N94-17410
Mechanical properties and crystal growth studies of semiconductor alloys
[AD-A268144] p 1216 N94-17454

OPTOMETRY
Enhancing sight
[NASA-TM-109637] p 1221 N94-15248

ORBIT CALCULATION
Laser ranging network performance and routine orbit determination at D-PAF p 911 N94-15554
State-of-the-art satellite laser range modeling for geodetic and oceanographic applications p 916 N94-15586
Closed orbit distortion and the beam-beam interaction
[DE93-015284] p 1190 N94-15854
Implementing a 50x50 gravity field model in an orbit determination system
[AD-A267548] p 888 N94-17103
BRIDGE: A small scientific satellite for geodesy p 890 N94-17146
Adequation of mini satellites to oceanic altimetry missions p 891 N94-17152
OREMUS: Prototype of an orbit determination center dedicated to mini-satellite control p 878 N94-17156

ORBIT DECAY
On the delivery of planetesimals to a protoplanet in the solar nebula p 1245 N94-16379

ORBIT INSERTION
Inertial Upper Stage
[NASA-TM-109654] p 885 N94-15278
Tidal regime of intact planetoid capture model for the Earth-Moon system: Does it relate to the archean sedimentary rock record? p 1245 N94-16378
Small launchers (current and future projects in the world) p 878 N94-17137
NEXT launch system p 878 N94-17141
TITUS: A micro-satellite for technology demonstration p 896 N94-17186

ORBIT PERTURBATION
A simultaneous estimation of the mass of Mars and its natural satellites, Phobos and Deimos, from the orbital perturbations on the Mariner 9, Viking 1, and Viking 2 orbiters p 1279 N94-16347
On the delivery of planetesimals to a protoplanet in the solar nebula p 1245 N94-16379
Dust grain resonant capture: A statistical study p 1245 N94-16384

ORBIT TRANSFER VEHICLES
Minimum accommodation for aerobrake assembly. Phase 2: Structural concepts for a lunar transfer vehicle aerobrake which can be assembled on orbit
[NASA-TM-107610] p 885 N94-15446
Space transfer concepts and analyses for exploration missions, phase 4
[NASA-CR-193849] p 882 N94-15831
Comparisons of selected laser beam power missions to conventionally powered missions
[NASA-TM-106110] p 1040 N94-16522

ORBITAL ASSEMBLY
Minimum accommodation for aerobrake assembly. Phase 2: Structural concepts for a lunar transfer vehicle aerobrake which can be assembled on orbit
[NASA-TM-107610] p 885 N94-15446
Ground integrated ET-derived space platforms for onorbit applications
[TABES PAPER 93-652] p 899 N94-16152
End-effector: Joint conjugates for robotic assembly of large truss structures in space: Extended concepts
[NASA-CR-193576] p 1048 N94-17088
Space Station/Orbiter berthing dynamics during an assembly flight
[NASA-TM-109049] p 1062 N94-17451

ORBITAL ELEMENTS
On the accuracy of ERS-1 orbit predictions p 874 N94-15589
Formation of on-site normal points p 917 N94-15592
The effects of orbital and climatic variations on Martian surface heat flow p 1290 N94-16402

ORBITAL LAUNCHING
STS-26 through STS-34, deploy activities
[NASA-TM-109566] p 1301 N94-15315

ORBITAL MANEUVERING VEHICLES
Computational analysis of Variable Thrust Engine (VTE) performance
[NASA-CR-193852] p 928 N94-17442

ORBITAL MECHANICS
Space flight: The application of orbital mechanics
[NASA-TM-109424] p 874 N94-15493
Tidal regime of intact planetoid capture model for the Earth-Moon system: Does it relate to the archean sedimentary rock record? p 1245 N94-16378

ORBITAL POSITION ESTIMATION
On the accuracy of ERS-1 orbit predictions p 874 N94-15589
Laser ranging data analysis
[NASA-CR-193547] p 1041 N94-16719

ORBITAL RESONANCES (CELESTIAL MECHANICS)
Mapping the stability region of the 3:2 Neptune-Pluto resonance p 1280 N94-16351
On the delivery of planetesimals to a protoplanet in the solar nebula p 1245 N94-16379
Dust grain resonant capture: A statistical study p 1245 N94-16384

ORBITAL SERVICING
STS-37 CETA evaluation with Ross
[NASA-TM-109495] p 1135 N94-15330
Spline screw payload fastening system
[NASA-CASE-GSC-13454-1] p 1046 N94-15871

ORBITAL SPACE TESTS
Third LDEF Post-Retrieval Symposium Abstracts
[NASA-CP-10120] p 1303 N94-16495

ORBITAL VELOCITY
Optical properties of water released in low Earth orbit
[AD-A266197] p 1192 N94-16936

ORDER-DISORDER TRANSFORMATIONS
Electron-microscopy study of antiphase boundaries in Cu3Pd and Fe3Al alloys near the order-disorder transition
[ONERA-NT-1993-1] p 1206 N94-15295
Structural studies of sol-gel glasses
[AD-A266277] p 967 N94-16472
Thermal disorder in adsorbed Cl on Si(100)
[AD-A266295] p 1210 N94-16476
Microstructure of Zr3Al after 2 MeV proton bombardment
[DE93-015331] p 1211 N94-16814
Kinetics of silica-phase transitions
[DE93-016231] p 1217 N94-17659

ORGANIC COMPOUNDS
Emissions of volatile organic compounds from stationary combustion sources: Numerical modeling capabilities
[DE93-014123] p 1096 N94-16825
Optical studies of glasses embedded with inorganic ions and organic dyes
[AD-A268146] p 1199 N94-17455

ORGANIC MATERIALS
Organic polymeric electro-optic materials: Synthesis, processing, and device applications
[AD-A267133] p 964 N94-15688
Terrestrial bitumen analogue of orgueil organic material demonstrates high sensitivity to usual HF-HCl treatment p 930 N94-16325
Bioorganic models for protein ion channels
[AD-A266365] p 1117 N94-16441
New organic materials for nonlinear optics applications
[AD-A266451] p 1192 N94-16563

ORGANIC SULFUR COMPOUNDS
Supercritical thermodynamics of sulfur and nitrogen species
[DE93-017727] p 1220 N94-16997

ORGANIC WASTES (FUEL CONVERSION)
Statement on global climate change before the Subcommittee on Energy and Power, United States House of Representatives
[DE93-013163] p 1095 N94-16006

ORGANIZATIONS
Fifty years of the Netherlands Association of Aeronautical Engineers p 853 N94-15121
PET team
[NASA-TM-109599] p 1223 N94-15293
Managing information as a corporate asset: Key strategies for information professionals to remain competitive
[DE93-015515] p 1232 N94-16875
Research grant handbook
[NHB-5800.1C] p 1225 N94-16907
Plasma Science Committee (PLSC) and the Panel on Opportunities in Plasma Science and Technology (OPST)
[DE93-018142] p 1204 N94-16995
Establishing a software measurement process
[AD-A267896] p 1154 N94-17396

ORGANOMETALLIC COMPOUNDS
Amide and tetrazene complexes of transition and main group elements as precursors for the low temperature synthesis of elemental nitrides
[AD-A266246] p 950 N94-16931

ORGUEIL METEORITE
Do SiC grains in Orgueil differ from those in Murchison? p 1242 N94-16260
Terrestrial bitumen analogue of orgueil organic material demonstrates high sensitivity to usual HF-HCl treatment p 930 N94-16325

ORIENTATION
Challenger Center: Orientation
[NASA-TM-109433] p 1221 N94-15505

OROGRAPHY
Orographic microbursts in a severe winter windstorm
[AD-A267651] p 1108 N94-17247

ORR-SOMMERFELD EQUATIONS
On the stability of a time dependent boundary layer
[NASA-CR-191542] p 1030 N94-17450

ORTHOGONAL FUNCTIONS
Simulation reduction using the Taguchi method
[NASA-CR-4542] p 1055 N94-17082

ORTHOTROPIC SHELLS
Forced harmonic vibration of the generally orthotropic cylindrical shell with inner and outer fluid loading
[AD-A266985] p 1057 N94-15150

OSCILLATIONS
Breakdown of adiabatic invariance
[AD-A267246] p 1219 N94-14977
Effect of wind tunnel acoustic modes on linear oscillating cascade aerodynamics
[NASA-TM-106367] p 869 N94-15866
Ventilated oscillatory boundary layers
[AD-A266226] p 1023 N94-16110
Search for chaos in free shear flows
[AD-A266245] p 1023 N94-16470
The (delta)f algorithm for beam dynamics
[DE93-015632] p 1187 N94-16660

OSCILLATOR STRENGTHS
Optical and infrared spectra of thermally annealed Pb implanted SiO2 glasses
[DE93-015304] p 965 N94-15828
OSCILLATORS
Melatonin, the pineal gland, and circadian rhythms
[AD-A268200] p 1129 N94-17478
OSMIUM ISOTOPES
Os isotopes in SNC meteorites and their implications to the early evolution of Mars and Earth
p 1242 N94-16272
Osmium isotopes in Ivory Coast tektites: Confirmation of a meteoritic component and rhenium depletion
p 1244 N94-16321
OSO
The 1971 highlights --- NASA programs and research
[NASA-TM-109629] p 1302 N94-15417
OUTGASSING
Solar absorptance of optical surfaces contaminated with spacecraft material outgassing products
[AD-A267202] p 886 N94-15857
Evolutionary implications of a steady-state water abundance on Venus p 1254 N94-16206
CO2 production by impact in carbonates? An ATEM and stable isotope (C,O) study p 954 N94-16383
OVER-THE-HORIZON RADAR
Comparison of RADARC high-frequency radar performance prediction model and ROTHR Amchitka data
[AD-A267077] p 987 N94-15540
OXALATES
The role of interfacial chemistry in surface nucleation and growth of calcium oxalate
[DE93-015689] p 1209 N94-16159
OXIDATION
An apparatus for measuring the biological oxidation of hydrogen gas under hyperbaric conditions
[AD-A266834] p 1119 N94-14916
Processing and protection of high temperature structural materials
[AD-A267292] p 954 N94-14961
Effects of alloying and temperature on the high-temperature oxidation of Cr-Cr2Nb
[DE93-015800] p 957 N94-16163
Powder diffraction studies using anomalous dispersion
[DE93-012531] p 1210 N94-16775
Development of vanadium-phosphate catalysts for methanol production by selective oxidation of methane
[DE93-016850] p 949 N94-16897
Transient studies of low temperature catalysts for methane conversion
[DE93-017710] p 950 N94-16962
Mechanistic models of soot formation
[AD-A267806] p 950 N94-17008
Synthesis, characterization, and polymerization of new ferrocene-fluorene complexes. A novel high-molecular weight conjugated polymer with pendant ferrocene groups
[AD-A267717] p 972 N94-17273
Thermo-mechanical analysis of oxidation protected carbon-carbon composites
[AD-A268191] p 941 N94-17597
OXIDATION RESISTANCE
A sulfur segregation study of PWA 1480, NiCrAl, and NiAl alloys
[NASA-TM-106289] p 956 N94-15992
Overview of chemical vapor infiltration
[DE93-015440] p 934 N94-16065
Effects of alloying and temperature on the high-temperature oxidation of Cr-Cr2Nb
[DE93-015800] p 957 N94-16163
Development and commercialization status of Fe3Al-based intermetallic alloys
[DE93-015802] p 957 N94-16165
Environmental effects on iron aluminides
[DE93-015820] p 958 N94-16166
Thermo-mechanical analysis of oxidation protected carbon-carbon composites
[AD-A268191] p 941 N94-17597
OXIDATION-REDUCTION REACTIONS
In situ Raman spectroscopy of lithium electrode surface in ambient temperature lithium secondary battery
[DE93-015238] p 1010 N94-16061
Earth's partial pressure of CO2 over the past 120 Ma; evidence from Ce anomalies in the deep (greater than 600 m) Pacific Ocean, 1 p 1104 N94-16358
High-valent oxo, methoxorhenium complexes: Models for intermediates and transition states in proton-coupled multi-electron transfer reactions
[AD-A266492] p 1211 N94-16782
Release of iron from hemoglobin
[AD-A266503] p 1128 N94-16784
A simple chemical procedure for extending the conductive state of polypyrrole to more negative potentials
[AD-A266235] p 969 N94-16928
Solvational barriers to interfacial electron transfer: Minimization by way of valence delocalization
[AD-A267371] p 950 N94-17006
OXIDE FILMS
Ion mixing of thin ZrO2 films on sapphire
[DE93-015214] p 1206 N94-14925
Passive oxide films on well-defined nickel surfaces: An examination of film growth on Ni(100) with ex situ scanning tunneling microscopy
[DE93-014056] p 1207 N94-15923
Vacancy condensation as the precursor to passivity breakdown
[DE93-012925] p 956 N94-15998
OXIDES
A search for noble-gas evidence for presolar oxide grains p 954 N94-16353
Thin composite solid electrolyte film for lithium batteries
[NASA-CASE-NPO-18694-1-CU] p 1014 N94-17325
OXYGEN
Roles of oxygen defects in copper-oxide superconductors
[DE93-014875] p 1208 N94-15982
First oxygen from lunar basalt p 1249 N94-16182
The effect of oxygen, grain size, and strain rate on the mechanical behavior of forged P/M tantalum
[DE93-011251] p 959 N94-16764
Regulated emergency oxygen system
[AD-A266228] p 1138 N94-16983
Automated data collection system for the TCM3 transcutaneous pO2/pCO2 monitoring system
[AD-A268400] p 1129 N94-17424
Oxygen diffusion in YBa2Cu3O(6+delta) ceramics on heating
[DE93-629161] p 974 N94-17633
Influence of the granular surface on the oxygen uptake in YBa2Cu3O(6+delta) ceramics
[DE93-629162] p 974 N94-17634
OXYGEN ATOMS
Analysis of leading edge and trailing edge cover glass samples before and after treatment with advanced satellite contamination removal techniques
[AD-A267055] p 885 N94-15666
Long Duration Exposure Facility experiment M0003 deintegration/findings and impacts
[AD-A267140] p 885 N94-15749
Analytical and experimental investigation of the feasibility of accelerated lifetime testing of materials exposed to an atomic oxygen beam
[NASA-CR-193851] p 946 N94-15766
Local environment about O atoms in Pr-Y-Ba-Cu-O films studied by O K-edge XAFS
[DE93-016218] p 1209 N94-16447
Atomic beam studies relevant to the space environment
[AD-A268628] p 1186 N94-17436
OXYGEN CONSUMPTION
Increased vascular resistance with hemoglobin-based oxygen carriers
[AD-A266454] p 1123 N94-16565
Metabolic monitoring of hypobaric subjects
[AD-A268221] p 1130 N94-17554
OXYGEN IONS
Analytical and experimental investigation of the feasibility of accelerated lifetime testing of materials exposed to an atomic oxygen beam
[NASA-CR-193851] p 946 N94-15766
Atomic beam studies relevant to the space environment
[AD-A268628] p 1186 N94-17436
OXYGEN ISOTOPES
CO2 production by impact in carbonates? An ATEM and stable isotope (C,O) study p 954 N94-16383
OXYGEN PRODUCTION
First oxygen from lunar basalt p 1249 N94-16182
Strategy for the reduction of total integrated fluid logistics to the Space Station Freedom
[NASA-TM-107744] p 1138 N94-17452
OXYGEN SUPPLY EQUIPMENT
Liquid hydrogen and liquid oxygen feedline passive recirculation analysis
[TABES PAPER 93-620] p 1031 N94-16145
Regulated emergency oxygen system
[AD-A266228] p 1138 N94-16983
OXYGEN 17
Design of a formaldehyde photodissociation process for carbon and oxygen isotope separation
[DE93-016435] p 1039 N94-16450
OXYGEN 18
Design of a formaldehyde photodissociation process for carbon and oxygen isotope separation
[DE93-016435] p 1039 N94-16450
OZONE
Southern and Northern Hemisphere total ozone as seen by TOMS
[NASA-TM-109591] p 1098 N94-15282
Atlas of TOMS ozone, 1978-1988
[NASA-TM-109456] p 1094 N94-15329
Emerging technologies for the changing global market
[TABES PAPER 93-612] p 930 N94-16144
Geochemistry and cosmochemistry of fullerenes 3: Reaction of C60 and C70 with ozone
p 953 N94-16243
The feasibility of tropospheric and total ozone determination using a Fabry-Perot interferometer as a satellite-based nadir-viewing atmospheric sensor
[NASA-TM-109342] p 1102 N94-17214
OZONE DEPLETION
Atlas of TOMS ozone, 1978-1988
[NASA-TM-109456] p 1094 N94-15329
Arctic ozone
[NASA-TM-109614] p 1095 N94-15365
Prioritization methodology for chemical replacement
[NASA-TP-3421] p 976 N94-15723
Environmental management lessons to be learned from the upcoming CFC phase out or how to insure that we survive the next environmentally mandated process change
[TABES PAPER 93-570] p 1050 N94-16136
NASA Operational Environment Team (NOET): NASA's key to environmental technology
[TABES PAPER 93-611] p 1052 N94-16143
Emerging technologies for the changing global market
[TABES PAPER 93-612] p 930 N94-16144
OZONOSPHERE
Atlas of TOMS ozone, 1978-1988
[NASA-TM-109456] p 1094 N94-15329
NASA Operational Environment Team (NOET): NASA's key to environmental technology
[TABES PAPER 93-611] p 1052 N94-16143

P

P WAVES
NORSAR basic seismological research
[AD-A266193] p 1101 N94-16125
P-I-N JUNCTIONS
Design of broadband wire antennas for frequency hopping applications
[AD-A267405] p 1001 N94-17025
P-N JUNCTIONS
The XMM pn-CCD detector system: First results
p 900 N94-15034
PACIFIC OCEAN
IAI topic: El Nino. Southern oscillation and interannual climate variability
[INPE-5410-PRE/1757] p 1111 N94-15186
PACKET SWITCHING
Overview of Enhanced Data Stream Array Processor (EDSAP)
[AD-A266986] p 1158 N94-15492
On-board B-ISDN fast packet switching architectures. Phase 1: Study
[NASA-CR-191143] p 883 N94-17111
Non-blocking crossbar permutation engine with constant routing latency
[NASA-CASE-NPO-18864-1-CU] p 1161 N94-17328
A scalable wrap-around shuffle exchange network with deflection routing
[NASA-CASE-NPO-18983-1-CU] p 1161 N94-17330
Isochronets: A high-speed network switching architecture
[AD-A267811] p 1161 N94-17409
NASA Lewis Meshed VSAT Workshop meeting summary
[NASA-TM-106332] p 883 N94-17487
On-board packet switch architectures for communication satellites
[NASA-TM-106328] p 883 N94-17488
PACKET TRANSMISSION
Bandwidth characteristics of multimedia data traffic on a local area network
[NASA-TM-104026] p 883 N94-15648
Non-blocking crossbar permutation engine with constant routing latency
[NASA-CASE-NPO-18864-1-CU] p 1161 N94-17328
PACKETS (COMMUNICATION)
An approximation for computing reduction in bandwidth requirements using intelligent multiplexers
[AD-A267434] p 1001 N94-17026
Non-blocking crossbar permutation engine with constant routing latency
[NASA-CASE-NPO-18864-1-CU] p 1161 N94-17328
PAINTS
XPS analysis of Al/EPDM bondlines from IUS SRM-1 polar bosses
[AD-A266851] p 1056 N94-14945
An improved patch for radiative coolers
[NASA-CASE-GSC-13503-1] p 1046 N94-15873

Automated image analysis method for the detection of cracks on wood surface
[VTT-JULK-755] p 1056 N94-17542
Dry stripping as a surface treatment method
[VTT-TIED-1348] p 985 N94-17544

PALEOCLIMATOLOGY
Earth's partial pressure of CO2 over the past 100-500 Ma; evidence from Ce anomalies in mostly shallow seas (less than 200 m) as recorded in carbonate sediments, 2
p 1104 N94-16360

PALEONTOLOGY
Fluvial erosion on Mars: Implications for paleoclimatic change p 1241 N94-16210

PALEOZOIC ERA
Earth's partial pressure of CO2 over the past 100-500 Ma; evidence from Ce anomalies in mostly shallow seas (less than 200 m) as recorded in carbonate sediments, 2
p 1104 N94-16360

PALLADIUM
Optical properties and surface morphology studies of palladium contacts on mercuric iodide single crystals
[DE93-012510] p 1207 N94-15973

PANEL METHOD (FLUID DYNAMICS)
Flow analysis for the nacelle of an advanced ducted propeller at high angle-of-attack and at cruise with boundary layer control
[NASA-TM-106371] p 858 N94-16571
Computational aerodynamics with icing effects
[AD-A267509] p 860 N94-17074

PARABOLIC DIFFERENTIAL EQUATIONS
Higher-order accurate Osher schemes with application to compressible boundary layer stability
[NASA-TM-106355] p 1026 N94-17056

PARABOLIC FLIGHT
The vibro-acoustic mapping of low gravity trajectories on a Learjet aircraft p 978 N94-16078
Heart rate response to parabolic flight manoeuvres
p 981 N94-16098

PARACHUTE DESCENT
1990 ASCAN ground egress/parasail
[NASA-TM-109528] p 1136 N94-15391
Galileo probe ready to go
[NASA-TM-109648] p 1247 N94-15432

PARACHUTES
Galileo probe ready to go
[NASA-TM-109648] p 1247 N94-15432
Adamson, Jim — ASCAN training programs
[NASA-TM-109507] p 1137 N94-15454

PARALLEL COMPUTERS
A task adaptive parallel graphics renderer
[DE93-017123] p 1149 N94-16119
Computation of the Fluid and Optical Fields About the Stratospheric Observatory for Infrared Astronomy (SOFIA) and the Coupling of Fluids, Dynamics, and Control Laws on Parallel Computers
[NASA-CR-193168] p 858 N94-16510
Requirements for supercomputing in energy research: The transition to massively parallel computing
[DE93-012376] p 1160 N94-16774
Asynchronous design for parallel processing architectures
[AD-A266523] p 1160 N94-16791
Testing string superprimitivity in parallel
[AD-A267814] p 1155 N94-17399

PARALLEL PLATES
Investigation of radiative interaction in laminar flows using Monte Carlo simulation
[NASA-CR-194604] p 1021 N94-15795
On the stability of a time dependent boundary layer
[NASA-CR-191542] p 1030 N94-17450

PARALLEL PROCESSING (COMPUTERS)
Engineering Physics and Mathematics Division progress report, period ending 31 December 1992
[DE93-015118] p 1301 N94-14926
Particle simulations on massively parallel machines
[DE93-015644] p 1157 N94-14927
The alignment-distribution graph
[NASA-CR-194292] p 1168 N94-15112
Mobile and replicated alignment of arrays in data-parallel programs
[NASA-CR-194294] p 1158 N94-15113
The application of compiler-assisted multiple instruction retry to VLIW architectures
[AD-A266930] p 1158 N94-15173
Parallel spatial direct numerical simulations on the Intel iPSC/860 hypercube
[NASA-CR-191513] p 1144 N94-15483
Multiphase complete exchange: A theoretical analysis
[NASA-CR-191531] p 1145 N94-15489
Overview of Enhanced Data Stream Array Processor (EDSAP)
[AD-A266986] p 1158 N94-15492
Massively parallel, adaptive, color image processing for autonomous road following
[AD-A266988] p 864 N94-15498
Decomposition of large sparse symmetric systems for parallel computation. Part 2: Parallelization tool roadmap
[AD-A267072] p 1158 N94-15671
A parallel adaptive mesh refinement algorithm
[NASA-CR-191530] p 1168 N94-15724
Decomposition of large sparse symmetric systems for parallel computation. Part 1: Theoretical foundations
[AD-A267144] p 1159 N94-15750
Particle simulation of hypersonic flow
[AD-A267185] p 857 N94-15787
Generating local addresses and communication sets for data-parallel programs
[NASA-CR-194605] p 1159 N94-15796
Parallel processing and scientific applications
[AD-A267179] p 1159 N94-15849
Distributed computing feasibility in a non-dedicated homogeneous distributed system
[NASA-CR-191532] p 1149 N94-15989
Information Technology Resources Assessment
[DE93-013899] p 1230 N94-16010
A task adaptive parallel graphics renderer
[DE93-017123] p 1149 N94-16119
The 3D-Flow processor for a programmable level-1 trigger (feasibility study)
[DE93-016045] p 1159 N94-16172
A decision criteria to select an associative-memory organization that minimizes the execution time of a mix of associative-search operations
[AD-A266438] p 1149 N94-16560
Requirements for supercomputing in energy research: The transition to massively parallel computing
[DE93-012376] p 1160 N94-16774
Asynchronous design for parallel processing architectures
[AD-A266523] p 1160 N94-16791
Information technology division technical paper abstracts
[AD-A266227] p 1166 N94-16938
Optical computing
[AD-A267881] p 1141 N94-17015
Efficient scheduling of real-time compute-intensive periodic graphs on large grain data flow multiprocessor
[AD-A267444] p 1141 N94-17030
Networked workstations and parallel processing utilizing functional languages
[AD-A267464] p 1160 N94-17034
Intel NX to PVM 3.2 message passing conversion library
[NASA-TM-109038] p 1152 N94-17060
Visual parallel programming with determinacy: A language specification, an analysis technique, and a programming tool
[AD-A267560] p 1153 N94-17107
Development of iterative techniques for the solution of unsteady compressible viscous flows
[NASA-CR-194657] p 1027 N94-17129
ONRASIA scientific information bulletin, volume 18, number 2
[AD-A267798] p 1304 N94-17305
Estimating task execution delay in a real-time system via static source code analysis
[AD-A267496] p 1161 N94-17367
Accurate analysis of array references
[AD-A268069] p 1162 N94-17550
System performance modeling and analysis of a fault-tolerant, real time parallel processor
[AD-A268070] p 1162 N94-17551
Benchmarking massively parallel architectures
[DE93-016486] p 1162 N94-17646

PARALLEL PROGRAMMING
Reactive system verification case study: Fault-tolerant transputer communication
[NASA-TM-108784] p 1145 N94-15538
Decomposition of large sparse symmetric systems for parallel computation. Part 1: Theoretical foundations
[AD-A267144] p 1159 N94-15750
The alignment-distribution graph
[NASA-CR-194609] p 1148 N94-15956
Shared-memory multiprocessor trends and the implications for parallel program performance
[TR-420] p 1159 N94-16578
Networked workstations and parallel processing utilizing functional languages
[AD-A267464] p 1160 N94-17034
Visual parallel programming with determinacy: A language specification, an analysis technique, and a programming tool
[AD-A267560] p 1153 N94-17107
Testing string superprimitivity in parallel
[AD-A267814] p 1155 N94-17399
Construction of d-dimensional hyperoctrees on a hypercube multiprocessor
[INRIA-RR-1752] p 1162 N94-17539

PARAMETER IDENTIFICATION
Exploitation of cyclostationarity for signal-parameter estimation and system identification
[AD-A267137] p 988 N94-15690
Development and analysis of ARMA parameter estimation schemes in the presence of noise
[AD-A267184] p 989 N94-15786
Operator overloading as an enabling technology for automatic differentiation
[DE93-012899] p 1170 N94-16778
Small satellite constellation system: Optimization criteria p 888 N94-17132

PARASITIC DISEASES
Combating malaria
[NASA-TM-109609] p 1081 N94-15297

PARTIAL DIFFERENTIAL EQUATIONS
Adaptive wavelet collocation methods for initial value boundary problems of nonlinear PDE's
[NASA-CR-191507] p 1169 N94-15833
C++ as a language for object-oriented numerics
[DE93-015027] p 1148 N94-15985
Operator overloading as an enabling technology for automatic differentiation
[DE93-012899] p 1170 N94-16778
Applications of the phi-transform
[AD-A266247] p 1170 N94-16940

PARTIAL PRESSURE
Earth's partial pressure of CO2 over the past 120 Ma; evidence from Ce anomalies in the deep (greater than 600 m) Pacific Ocean, 1 p 1104 N94-16358
Earth's partial pressure of CO2 over the past 100-500 Ma; evidence from Ce anomalies in mostly shallow seas (less than 200 m) as recorded in carbonate sediments, 2
p 1104 N94-16360

PARTICLE ACCELERATOR TARGETS
Past, present and future ((pi),(eta)) experiments
[DE93-016631] p 1182 N94-16115
3D and r,z particle simulations of heavy ion fusion beams
[DE93-013417] p 1205 N94-17670

PARTICLE ACCELERATORS
Calorimeter based detectors for high energy hadron colliders
[DE93-017055] p 1188 N94-16900
Search for the top quark from (e(mu)) and (e,e) events in the D0 detector in p(bar-p) collisions at the square root of s = 1.8 TeV
[DE93-016350] p 1186 N94-17662

PARTICLE BEAMS
Channel of the system for pulse charged particle beam diagnostics
[DE93-623867] p 1179 N94-14931
Confinement and stability of a Crystal Beam
[DE93-015400] p 1181 N94-16020
The (delta)f algorithm for beam dynamics
[DE93-015632] p 1187 N94-16660
Evolution of hadron beams under intrabeam scattering
[DE93-014330] p 1184 N94-16826
A review of some dynamics models in six-dimensional phase space and their suitable conditions of motion equation
[DE93-623741] p 1175 N94-17317

PARTICLE COLLISIONS
The pressure broadening of HDO by O2, N2, H2, and He between 100 K and 600 K
[AD-A267118] p 946 N94-15684
Theoretical studies relating to the interaction of radiation with matter
[AD-A267134] p 1180 N94-15689
The cooling of confined ions driven by laser beams
[DE93-016612] p 1039 N94-16114
Fundamental-mode RF design in e(+)e(-) storage ring factories
[DE93-015249] p 1183 N94-16809
Energy-loss cross sections for inclusive charge-exchange reactions at intermediate energies
[NASA-TM-4522] p 1188 N94-17018
Production of D-mesons in pp-collisions and quark-gluon string model
[DE93-626721] p 1185 N94-17312
Search for the top quark from (e(mu)) and (e,e) events in the D0 detector in p(bar-p) collisions at the square root of s = 1.8 TeV
[DE93-016350] p 1186 N94-17662

PARTICLE DIFFUSION
The (delta)f algorithm for beam dynamics
[DE93-015632] p 1187 N94-16660

PARTICLE FLUX DENSITY
The effect of an on-orbit near encounter on the number flux density of micron sized particles
p 899 N94-16374

PARTICLE IMAGE VELOCIMETRY
Evaporation from a meniscus within a capillary tube in microgravity
[NASA-CR-194593] p 976 N94-15654

PARTICLE IN CELL TECHNIQUE
Emittance growth in displaced, space-charge-dominated beams with energy spread
[DE93-016514] p 1188 N94-17672
PARTICLE INTERACTIONS
Analytical and experimental investigation of the feasibility of accelerated lifetime testing of materials exposed to an atomic oxygen beam
[NASA-CR-193851] p 946 N94-15766
The three-loop QCD beta-function and anomalous dimensions
[NIKHEF-H/92-17] p 1186 N94-17617
PARTICLE MASS
Densities of 5-15 micron interplanetary dust particles
p 1244 N94-16367
PARTICLE MOTION
Granular fluctuations in plasma turbulence and their role in transport
[DE93-013465] p 1187 N94-17674
PARTICLE PRODUCTION
Electroweak physics from D0
[DE93-015041] p 1181 N94-16053
Status of (alpha)(sub s) measurements
[DE93-015179] p 1181 N94-16059
Past, present and future ((pi),(eta)) experiments
[DE93-016631] p 1182 N94-16115
A calibration of the production rate ratio P-21/P-26 by low energy secondry neutrons: Identification of Ne spallation components at the 10(exp 6) atoms/g level in terrestrial samples p 1187 N94-16194
Electroweak results from D0
[DE93-014926] p 1185 N94-16968
Energy-loss cross sections for inclusive charge-exchange reactions at intermediate energies
[NASA-TM-4522] p 1188 N94-17018
Production of D-mesons in pp-collisions and quark-gluon string model
[DE93-626721] p 1185 N94-17312
Search for the top quark from (e(mu)) and (e,e) events in the D0 detector in p(bar-p) collisions at the square root of s = 1.8 TeV
[DE93-016350] p 1186 N94-17662
PARTICLE SIZE DISTRIBUTION
Size distribution of interplanetary iron and stony particles related with deep-sea spherules p 1245 N94-16388
From minerals to rocks: Toward modeling lithologies with remote sensing p 1086 N94-16437
PARTICLE SPIN
Quark-loop effects in high energy spin-flip processes
[DE93-626692] p 1188 N94-17313
PARTICLE THEORY
On the nature of mirror particles
[DE93-626670] p 1179 N94-14934
On the 17-keV neutrino
[DE93-012638] p 1181 N94-15974
Particle physics and cosmology, Task C
[DE93-016865] p 1239 N94-16118
Multipolar-like form of nonabelian gauge theories
[DE93-626690] p 1171 N94-17314
PARTICLE TRAJECTORIES
Molecular processes in comets
[NASA-CR-194148] p 1239 N94-15188
PARTICLES
An assessment of acid fog
[DE93-009347] p 1095 N94-15940
Particle Engulfment and Pushing by Solidifying Interfaces (PEPSI)
[NASA-CR-193856] p 960 N94-17079
PARTICULATE REINFORCED COMPOSITES
Fracture toughness tests for particulate MMC UK COSI (IACFA) task group. Meeting report, October 1992
[NPL-DMM(A)-81] p 1057 N94-15021
PARTICULATE SAMPLING
Suggestion for extended Viking magnetic properties experiment on future Mars missions
p 1285 N94-16375
PARTICULATES
Analysis of leading edge and trailing edge cover glass samples before and after treatment with advanced satellite contamination removal techniques
[AD-A267055] p 885 N94-15666
Near-surface temperature gradients and their effects on thermal-infrared emission spectra of particulate planetary surfaces p 1260 N94-16236
PARTITIONS (MATHEMATICS)
Understanding partitions and the no partition assumption
[AD-A266296] p 1000 N94-16911
A domain-partition method for the advection-diffusion equation
[INRIA-RR-1740] p 1030 N94-17534
PASSIVITY
Vacancy condensation as the precursor to passivity breakdown
[DE93-012925] p 956 N94-15998
In situ studies of passive film chemistry using x ray absorption spectroscopy
[DE93-014023] p 947 N94-16011
PATHOGENS
Bloodborne Pathogens Program p 1127 N94-16644
OSHA bloodborne pathogens standards exposure control plan p 1127 N94-16645
PATTERN RECOGNITION
Segmenting textured 3D surfaces using the space/frequency representation
[AD-A266960] p 1163 N94-14968
A new method for generating Bayes classifiers assuming mixtures of Gaussian densities
[FFI-91/4029] p 1172 N94-15298
Cooperativity and 3-D representation
[AD-A267180] p 1131 N94-15694
The bootstrapped algorithm: Fast algorithm for blind signal separation
[AD-A266671] p 1147 N94-15772
Efficient algorithmic techniques for combinatorial problems
[AD-A267151] p 1172 N94-15777
Development of pattern recognition techniques for the evaluation of toxicant impacts to multispecies systems
[AD-A267197] p 1095 N94-15790
Spatial filters for optical correlation
[AD-A267199] p 1189 N94-15791
Exploiting world structure to efficiently search for objects
[TR-434] p 1231 N94-16576
Discovering sequence similarity by the algorithmic significance method
[DE93-015556] p 1150 N94-16659
Image accuracy and representational enhancement through low-level, multi-sensor integration techniques
[DE93-014888] p 1167 N94-17287
A high-speed object recognition chip based on a biologically-realistic hybrid temporal processing
[AD-A268270] p 1134 N94-17576
PAVEMENTS
Mathematical model of frost heave and thaw settlement in pavements
[AD-A267037] p 983 N94-15676
PAYLOAD DELIVERY (STS)
Inertial Upper Stage
[NASA-TM-109654] p 885 N94-15278
PAYLOAD DEPLOYMENT & RETRIEVAL SYSTEM
Cognitive engineering models in space systems
[NASA-CR-193473] p 1140 N94-16716
PAYLOAD INTEGRATION
Serpentine manipulator planning and control for NASA Space-Shuttle payload servicing
[AD-A266961] p 879 N94-14969
PAYLOAD RETRIEVAL (STS)
STS-32 onboard 16mm photography quick release
[NASA-TM-109472] p 880 N94-15376
STS-32 LDEF EVA training in WETF with Low and Dunbar
[NASA-TM-109473] p 1135 N94-15377
STS-32 LDEF approach in SES
[NASA-TM-109474] p 880 N94-15379
PAYLOAD STATIONS
STS-30 onboard 16mm photography quick release
[NASA-TM-109579] p 881 N94-15423
PAYLOADS
Non-lethal Unmanned Aerial Vehicles (UAVs)
[AD-A267139] p 866 N94-15692
MAXUS: The new sounding rocket program for long duration microgravity flight p 978 N94-16079
QUESTS: A microgravity research facility for materials science experiments p 978 N94-16082
Choosing ESRO's first scientific satellites
[ESA-HSR-3] p 887 N94-16523
ARIANE 5 light derivatives p 878 N94-17140
PEARSON DISTRIBUTIONS
The distribution of a sum of binomial random variables
[AD-A266969] p 1172 N94-15002
PEEK
Progress in the modeling of the shock response and mitigation of thick composite shells
[AD-A267009] p 1057 N94-15524
PEELING
The effect of plasma treatment on interfacial bond characteristics of Kevlar/epoxy laminates as measured by T-peel tests
[AD-A266920] p 930 N94-14999
PEGASUS AIR-LAUNCHED BOOSTER
NASA report to education, volume 7
[NASA-TM-109435] p 1247 N94-15419
PENDULUMS
Results of tidal gravity observations with a conical pendulum p 1100 N94-15810
Design of non-sled setup to measure head injury criteria
[NIAR-92-20] p 872 N94-17263
PENETRANTS
Detection and dosimetry of chemical contaminants in polymeric materials
[AD-A266605] p 968 N94-16727
PENETRATION
X-SAR: The X-band synthetic aperture radar on board the Space Shuttle p 990 N94-15891
Slidesurfaces with adaptive new definitions (SAND) for transient analysis
[DE93-014909] p 1059 N94-15983
PENTABORANES
A proposed mechanism for the pyrolysis of diborane
[DE93-014275] p 947 N94-15977
PENTANES
Synthesis of potential high-energy fuels
[AD-A267508] p 975 N94-17073
PEPTIDES
Neuropeptide-Y (NPY) increases total blood flow in the tail, and reduces cutaneous microvascular blood flow in the tail and foot of the rat
[AD-A266839] p 1115 N94-14918
Bioorganic models for protein ion channels
[AD-A266365] p 1117 N94-16441
Vectorial electron transfer in spatially ordered arrays
[DE93-018150] p 1185 N94-16971
PERCEPTION
Perception for outdoor navigation
[AD-A266867] p 863 N94-14919
PERCEPTUAL ERRORS
Perception of lightness and brightness in complex patterns
[AD-A268435] p 1134 N94-17513
PERCOLATION
Ventilated oscillatory boundary layers
[AD-A266226] p 1023 N94-16110
PERFORATING
An analysis of the dynamic response of the Space Station Freedom due to a module perforation by an orbital debris particle impact
[TABES PAPER 93-653] p 899 N94-16154
PERFORMANCE
Performance of the upgraded Orroral laser ranging system p 877 N94-15602
PERFORMANCE PREDICTION
Development of Japanese Earth Resources Satellite-1 (JERS-1; FUYO-1) and it's operational results
[NASDA-SPP-930001] p 884 N94-15001
Rotary engine performance computer program (RCEMAP and RCEMAPPC): User's guide
[NASA-CR-191192] p 869 N94-15192
Concepts on measuring the benefits of software process improvements
[AD-A266994] p 1144 N94-15215
Comparison of RADARC high-frequency radar performance prediction model and ROTHR Amchitka data
[AD-A267077] p 987 N94-15540
GLRS-R 2-colour retroreflector target design and predicted performance p 921 N94-15615
A rapid computational model for estimating the performance of compliant airfoils in cascades
[AD-A266275] p 857 N94-16471
Predicting radiation induced performance decrements of AH-1 helicopter crews. Volume 1: Predicted veersus actual performance of AH-1 crews induced with symptoms simulating radiation sickness
[AD-A268376] p 1138 N94-17460
Space Station Freedom electrical performance model
[NASA-TM-106395] p 929 N94-17483
System performance modeling and analysis of a fault-tolerant, real time parallel processor
[AD-A268070] p 1162 N94-17551
PERFORMANCE TESTS
Performance comparison of high speed microchannel plate photomultiplier tubes p 922 N94-15624
Development of the OMPAT neuropsychological/psychomotor performance evaluation and OMPAT data and timing support programs
[AD-A266954] p 1122 N94-15759
Recent advances in outdoor performance evaluation of PV systems
[DE93-015031] p 1091 N94-15994
Test plan for the evaluation of the initial capability of the National Satellite Test Bed: Phase 1D
[DOT/FAA/RD-93/20] p 876 N94-16025
Cost-effective test methods for Shuttle payloads
[TABES PAPER 93-651] p 883 N94-16151
Lithium D-cell study
[NASA-CR-192705] p 1011 N94-16505
ALS engine propellant effector system
[NASA-CR-194650] p 926 N94-16590
TIMS performance evaluation summary
p 1063 N94-16596

Cycle performance testing of nonazeotropic mixtures of HFC-142A/HCFC-124 and HFC-32/HCFC-124 with enhanced surface heat exchangers
[DE93-015215] p 1024 N94-16808
Category (CAT) 3B level 1 test plan for Global Positioning System (GPS)
[DOT/FAA/RD-93/21] p 864 N94-16835
CALS test network handbook
[AD-A267587] p 1160 N94-17209
A ten year review of performance of photovoltaic systems
[DE93-015649] p 1093 N94-17217
Measurements of microlens performance
p 1197 N94-17355
Radar transmitter procedures
[AD-A268274] p 1005 N94-17523
Optimisation and specification of Auger electron spectrometers for signal-to-noise ratio performance
[NPL-DMM(A)-101] p 1006 N94-17549
Test methods for acceptance testing of telescopes
[AD-A268316] p 1237 N94-17568

PERIDOTITE
First results from analysis of coordinated AVIRIS, TIMS, and ISM (French) data for the Ronda (Spain) and Beni Bousera (Morocco) peridotites p 1067 N94-16675

PERIHELIONS
Dust grain resonant capture: A statistical study
p 1245 N94-16384

PERIOD DOUBLING
Transition induced by fixed and freely convecting spherical particles in laminar boundary layers
[AD-A267757] p 1028 N94-17276
Extracavity frequency doubling study of a pulsed photodissociation iodine laser
[AD-A267893] p 1042 N94-17394

PERIODIC VARIATIONS
Nonlinear acoustics: Periodic waveguide, scattering of sound by sound, three-layer fluid, finite amplitude sound in a medium having a distribution of relaxation processes, and production of an isolated negative pulse in water
[AD-A267145] p 1177 N94-15732
Research into the influence of spatial variability and scale on the parameterization of hydrological processes
[NASA-CR-194610] p 1082 N94-16026
Similarity and scale in catchment storm response
[PAPER-89RG01615] p 1083 N94-16028

PERIPHERAL CIRCULATION
Automated strain gauge plethysmograph
[AD-A267323] p 1035 N94-17002

PERIPHERAL VISION
The effects of luminance boundaries on color perception
[AD-A268398] p 1133 N94-17397

PERISCOPES
Atmospheric propagation analysis program
[AD-A268231] p 1006 N94-17565

PERMANENT MAGNETS
Suggestion for extended Viking magnetic properties experiment on future Mars missions
p 1285 N94-16375
Electrodynamic forces of the cross-connected figure-eight null-flux coil suspension system
[DE93-015139] p 1048 N94-16969

PERMEABILITY
HyperVentilate: Decision-support software for soil vapor extraction technology application
[PB93-134880] p 1094 N94-15136
Verification of a two-dimensional infiltration model for the resin transfer molding process
[NASA-CR-194597] p 964 N94-15656
Influence of fiber packing structure on permeability
p 938 N94-16857
Flight 20 (STS-45) polysulfide gas path investigation
[NASA-CR-193861] p 928 N94-17213
Factors determining the release of nitric oxide --- Calcium/cadmium transport by renal cortical collectin duct cells
[AD-A266232] p 1118 N94-17224

PERMITTIVITY
Stress sensitivity of dielectric resonators
[AD-A266767] p 1009 N94-15825
Cyanoresin, cyanoresin/cellulose triacetate blends for thin film, dielectric capacitors
[NASA-CASE-NPO-18913-1-CU] p 966 N94-15930
Temperature and pressure effects on capacitance probe cryogenic liquid level measurement accuracy
[NASA-CR-190763] p 1034 N94-16521
Low dielectric constant insulators and gold metallization for GHz multi-chip modules, part 2
[AD-A268590] p 1176 N94-17605

PERMUTATIONS
Nonparametric statistics: Weighted rankings analysis
[AD-A266607] p 1173 N94-16657
Non-blocking crossbar permutation engine with constant routing latency
[NASA-CASE-NPO-18864-1-CU] p 1161 N94-17328

PEROVSKITES
Experimental partitioning of Zr, Ti, and Nb between silicate liquid and a complex noble metal alloy and the partitioning of Ti between perovskite and platinum metal
p 982 N94-16287
An experimental study of trace element partitioning between perovskite, hibonite and melt: Equilibrium values p 954 N94-16313

PERSONAL COMPUTERS
Applying paperless technology to achieve excellence in manufacturing operations
[TABES PAPER 93-630] p 1052 N94-16147

PERSONNEL
Sleep management user's guide for special operations personnel
[AD-A267746] p 1119 N94-14943
Return to flight 3, the journey continues
[NASA-TM-109651] p 1223 N94-15319
Permanent change of station: The NASA employee's guide to an easier move
[NHB-9760.1A] p 1223 N94-15931
The Senior Executive Service
[NHB-3100.6] p 1224 N94-15945
Proceedings of the 1992 Annual Meeting NASA Occupational Health Program
[NASA-CR-193462] p 1123 N94-16609
New health and safety initiatives at the Department of Energy (DOE) p 1124 N94-16610
The Langley Fitness Center p 1126 N94-16635
Carpal tunnel syndrome and other cumulative trauma disorders of the arm and hand and occupation in US Navy enlisted personnel
[AD-A267747] p 1129 N94-17374

PERSONNEL DEVELOPMENT
PET team
[NASA-TM-109599] p 1223 N94-15293
The Senior Executive Service
[NHB-3100.6] p 1224 N94-15945

PERSONNEL MANAGEMENT
NASA directives master list and index
[NHB-1410.13L] p 1229 N94-15414
Permanent change of station: The NASA employee's guide to an easier move
[NHB-9760.1A] p 1223 N94-15931
NASA security handbook
[NHB-1620.3C] p 1224 N94-15937
Industrial labor relations manual
[NHB-5200.1B] p 1224 N94-15939
The NASA competitive placement plan for positions GS-15 and below (including trades and labor positions)
[NHB-3335.1C] p 1224 N94-15944
The Senior Executive Service
[NHB-3100.6] p 1224 N94-15945
Medical surveillance and biological monitoring of lead exposed employees p 1124 N94-16615
Ongoing Recovery Basic Information Tool (ORBIT)
p 1124 N94-16616
Programs and resources for control of job stress in the Federal workplace p 1124 N94-16617
The Goddard Space Flight Center ergonomics program p 1125 N94-16621
Efficient management of cardiovascular risk screening programs p 1125 N94-16622
Industrial Hygiene Laboratory accreditation: The JSC experience p 1125 N94-16623

PERSONNEL SELECTION
Astronauts number 1 --- mercury project
[NASA-TM-109428] p 1131 N94-15499
The NASA competitive placement plan for positions GS-15 and below (including trades and labor positions)
[NHB-3335.1C] p 1224 N94-15944
The Senior Executive Service
[NHB-3100.6] p 1224 N94-15945

PERTURBATION THEORY
Shielding from space radiations
[NASA-CR-194578] p 1180 N94-15715
Many-body quantum mechanical studies of molecular clusters
[AD-A266624] p 1180 N94-15727
Implementing a 50x50 gravity field model in an orbit determination system
[AD-A267548] p 888 N94-17103
The renormalization of the axial anomaly in dimensional regularization
[NIKHEF-H/92-18] p 1220 N94-17618

PETROGRAPHY
Stalking the LREE-enriched component in ureilites
p 1241 N94-16190
Grosnaja ABCs: Magnesium isotope compositions
p 1241 N94-16191
Euromet Ureilite Consortium: A preliminary report on carbon and nitrogen geochemistry p 1241 N94-16192
Petrography, mineralogy, and Mg isotope composition of VICTA: A vigarano CaAl4O7-bearing type A inclusion
p 1103 N94-16203
Pyroxene equilibration temperatures in metamorphosed ordinary chondrites p 1242 N94-16224
Angrite LEW87051: Are the olivines pheno's or xeno's? A continuing story p 1103 N94-16285
Cat Mountain: A meteoritic sample of an impact-melted chondritic asteroid p 1244 N94-16328
Classificational parameters for acapulcoites and lodranites: The cases of FRO 90011, EET 84302 and ALH A81187/84190 p 1245 N94-16389
A hydrogen isotope study of CO3 type carbonaceous chondrites; comparison with type 3 ordinary chondrites
p 1246 N94-16425

PETROLOGY
Stalking the LREE-enriched component in ureilites
p 1241 N94-16190
Euromet Ureilite Consortium: A preliminary report on carbon and nitrogen geochemistry p 1241 N94-16192
Petrologic constraints on the surface processes on asteroid 4 Vesta and on excavation depths of diogenite fragments p 1241 N94-16208
Petrologic models of 15388, a unique Apollo 15 mare basalt p 1264 N94-16258
Complex zoning behavior in pyroxene in FeO-rich chondrules in the Semarkona ordinary chondrite
p 1243 N94-16284
Angrite LEW87051: Are the olivines pheno's or xeno's? A continuing story p 1103 N94-16285
Experimental segregation of iron-nickel metal, iron-sulfide, and olivine in a thermal gradient: Preliminary results p 1243 N94-16288
An initial perspective of S-asteroid subtypes within asteroid families p 1243 N94-16310
Manson impact structure, Iowa: First geochemical results for drill core M-1 p 1103 N94-16322
The monzonorite-anorthosite connection: The petrogenesis of terrestrial KREEP p 1104 N94-16365
The dregs of crystallization in Zagami
p 1245 N94-16390
The Nakhla parent melt: REE partition coefficients and clues to major element composition
p 1245 N94-16399
Igneous fractionation and subsolidus equilibration of diogenite meteorites p 1245 N94-16413
The role of carbon and temperature in determining electrical conductivity of basins, crust and mantle
[DE93-015936] p 1101 N94-16840

PH
Factors determining the release of nitric oxide --- Calcium/cadmium transport by renal cortical collectin duct cells
[AD-A266232] p 1118 N94-17224

PHARMACOLOGY
Evaluation of putative neurochemical intermediaries in space/motion sickness
[NASA-CR-193607] p 1118 N94-17090

PHASE CHANGE MATERIALS
Advanced cooling for high power electric actuators
[AD-A266984] p 866 N94-15761

PHASE CONTROL
Ceramic fiber coatings development and demonstration
[AD-A267286] p 972 N94-17242

PHASE DETECTORS
Synchronous sampling phase and amplitude detection method and apparatus
[NASA-CASE-LAR-14725-1] p 1050 N94-15870

PHASE DIAGRAMS
Silica-bearing objects in the Dengli H3.8 and Gorlovka H3-4 chondrites p 1242 N94-16265

PHASE LOCKED SYSTEMS
Improvements to pulsed phase locked loop strain monitor
[NASA-CASE-LAR-14887-1] p 1033 N94-15877

PHASE SEPARATION (MATERIALS)
Sounding Rocket Experiments in Fluid Science and Materials Sciences: TEXUS 25 to 27 and MASER 4, volume 3
[ESA-SP-1132-VOL-3] p 943 N94-15157
Temperature propagation in near-critical fluids prior to and during separation p 944 N94-15165

PHASE SHIFT
Adaptive beamforming with imperfect arrays: Pattern effects and their partial correction
[AD-A267079] p 987 N94-15541
A study of the observed tidal residue vectors B versus oceanic tidal load vectors L p 1100 N94-15813
Interaction types and their like-polarization phase-angle difference signatures p 1079 N94-16756
Fundamental-mode RF design in e(+)e(-) storage ring factories
[DE93-015249] p 1183 N94-16809
Speckles statistics and decorrelation effects in complex ABCD optical systems
[AD-A267843] p 1193 N94-17012
Optical system storage design with diffractive optical elements p 1198 N94-17360

PHASE STABILITY (MATERIALS)
Mesons at finite temperature in the NJL model with gluon condensate
[DE93-626697] p 1185 N94-17310
Kinetics of silica-phase transitions
[DE93-016231] p 1217 N94-17659
PHASE TRANSFORMATIONS
Pressures of supercritical salt solutions
p 945 N94-15166
Unidirectional solidification of liquid-crystal material
p 945 N94-15167
Ternary alloying effects in polycrystalline (beta)-NiAl
[DE93-012675] p 955 N94-15885
Dynamical Ising model simulations of nucleation and growth in copper-cobalt alloys
[DE93-015336] p 957 N94-16015
Scaling, soil moisture and evapotranspiration in runoff models p 1084 N94-16034
Phase equilibria of the magnesium sulfate-water system to 4 kbars p 953 N94-16247
Electrorheological fluid chemical processing
[AD-D015785] p 948 N94-16532
Process for shaping articles from electrosetting compositions
[AD-D015787] p 935 N94-16534
Encapsulation of hemoglobin in non-phospholipid vesicles
[AD-A266505] p 1128 N94-16785
Structural phase transition and superconductivity in La(2-x)Ba(x)CuO4
[DE93-015812] p 1212 N94-16868
Process of shaping an electrorheological solid
[AD-D015885] p 1012 N94-16914
Slip, twinning and transformation in Laves phases
[DE93-018164] p 960 N94-16972
An investigation of the hydrolytic resistance of sodium-calcium plate glass with a layer of silica deposited on its surface
[IFTR-34/1991] p 971 N94-17120
Anisotropic phase separation in amorphous Fe-Ge alloys
[DE93-015255] p 961 N94-17251
A basic principles description of liquid vapor phase transitions
[AD-A268331] p 1176 N94-17581
Kinetics of silica-phase transitions
[DE93-016231] p 1217 N94-17659
Shear wave measurements in shock-induced, high-pressure phases
[DE93-016461] p 1062 N94-17664
PHASED ARRAYS
Overview of Enhanced Data Stream Array Processor (EDSAP)
[AD-A266986] p 1158 N94-15492
Experimental evaluation of an adaptive focusing algorithm for a microwave planar phased-array hyperthermia system at UCSF
[AD-A267004] p 1121 N94-15634
System architecture of optically controlled phased array radar
[AD-A267056] p 988 N94-15667
Phased array antenna analysis using hybrid finite element methods
[AD-A267620] p 1002 N94-17196
True time delay optically controlled dual band transmitter
[AD-A267663] p 1003 N94-17228
Proceedings of the 1992 Antenna Applications Symposium, volume 1
[AD-A268167] p 1005 N94-17431
PHENOLOGY
Recent advances in radar remote sensing of forest
p 991 N94-15897
PHENOLS
Preconversion catalytic deoxygenation of phenolic functional groups
[DE93-017034] p 950 N94-16912
Interpenetrating polymer network acoustic damping material
[AD-D015889] p 969 N94-16916
PHENYLALANINE
Theoretical prediction of the UV adsorption and fluorescence spectra of tyrosine and phenylalanine
[AD-A266970] p 943 N94-15111
PHENYLS
The photophysics of poly(methylphenylphosphazene)
[AD-A267321] p 970 N94-16949
PHOBOS
A simultaneous estimation of the mass of Mars and its natural satellites, Phobos and Deimos, from the orbital perturbations on the Mariner 9, Viking 1, and Viking 2 orbiters p 1279 N94-16347
A mission concept of Phobos/Deimos exploration
p 1287 N94-16387
The spectrum of Phobos from Phobos 2 observations at 0.3-2.6 microns: Comparison to previous data and meteorite analogs p 1295 N94-16429
PHONONS
Basic optical studies of high T(c) oxide superconductors
[AD-A268148] p 1014 N94-17428
PHOSPHATES
Development of vanadium-phosphate catalysts for methanol production by selective oxidation of methane
[DE93-016850] p 949 N94-16897
PHOSPHAZENE
The photochemistry of poly(methylphenylphosphazene)
[AD-A267320] p 970 N94-16948
The photophysics of poly(methylphenylphosphazene)
[AD-A267321] p 970 N94-16949
PHOSPHIDES
Growth of new materials for solid state laser applications. The growth of ZnGeP2 by the vertical Bridgman method
[NASA-CR-194571] p 1038 N94-15530
PHOSPHINES
Synthesis, reactivity, and characterization of (-hexacarbocyclic) manganese dicarbonyl complexes with sulfur and phosphorus ligands
[AD-A267592] p 930 N94-17192
PHOSPHORESCENCE
The photophysics of poly(methylphenylphosphazene)
[AD-A267321] p 970 N94-16949
PHOSPHORS
Preparation and investigation of improved low voltage electron excitable phosphors
[AD-A266852] p 963 N94-14948
PHOSPHORUS
Synthesis, reactivity, and characterization of (-hexacarbocyclic) manganese dicarbonyl complexes with sulfur and phosphorus ligands
[AD-A267592] p 930 N94-17192
PHOSPHORUS ISOTOPES
A calibration of the production rate ratio P-21/P-26 by low energy secondry neutrons: Identification of Ne spallation components at the 10(exp 6) atoms/g level in terrestrial samples p 1187 N94-16194
PHOTOACOUSTIC SPECTROSCOPY
An electroacoustic transducer for purposes of photoacoustic spectroscopy
[IFTR-7/1992] p 1013 N94-17071
PHOTOCATHODES
Microchannel plate imaging detectors for the ultraviolet p 901 N94-15037
PHOTOCHEMICAL REACTIONS
Design, synthesis and characterization of novel nonlinear optical polymers
[AD-A267035] p 964 N94-15675
Organic polymeric electro-optic materials: Synthesis, processing, and device applications
[AD-A267133] p 964 N94-15688
Photochemistry in thin polymeric films
[AD-A266716] p 964 N94-15729
Molecular beam studies of reaction dynamics
[DE93-015035] p 1181 N94-15995
Binding of carbon dioxide to metal macrocycles: Toward a mechanistic understanding of electrochemical and photochemical carbon dioxide reduction
[DE93-016244] p 949 N94-16870
The photochemistry of poly(methylphenylphosphazene)
[AD-A267320] p 970 N94-16948
The photophysics of poly(methylphenylphosphazene)
[AD-A267321] p 970 N94-16949
Optical studies of glasses embedded with inorganic ions and organic dyes
[AD-A268146] p 1199 N94-17455
PHOTOCONDUCTIVITY
Characterization of InTISb grown by low pressure metalorganic chemical vapor deposition on GaAs substrate
[AD-A266878] p 1206 N94-14922
Impurity conduction photoconductor detectors
p 902 N94-15046
Lead chalcogenides based IR photosensitive array detectors with coordinate addressing
p 903 N94-15053
Electrical conductivity of ion implanted ladder and semi-ladder polymers
[AD-A267432] p 970 N94-16978
Surface flashover of semiconductors: A fundamental study
[AD-A267382] p 1012 N94-17023
OSA proceedings on Ultrafast Electronics and Optoelectronics, volume 14
[AD-A267972] p 1014 N94-17410
PHOTOCONDUCTORS
Nonstationary behaviour of low background photon detectors p 902 N94-15049
Performance testing of doped-germanium photoconductors for the ISO long wavelength spectrometer p 905 N94-15066
Non-linear effects in doped-germanium photoconductors for the ISO long wavelength spectrometer p 905 N94-15067
Extrinsic photoconductor detectors for the wavelength range 2 microns to 240 microns p 906 N94-15073
Ionising radiation-induced effects in doped germanium FIR photoconductors p 907 N94-15077
Silicon gallium doped photoconductor development for the AROME balloon borne instrument
p 908 N94-15087
A monolithic PbTeCCD focal plane array for MWIR imaging p 910 N94-15100
PHOTODETACHMENT
Atomic beam studies relevant to the space environment
[AD-A268628] p 1186 N94-17436
PHOTODIODES
Advanced high performance CdHgTe multiplexed arrays p 903 N94-15051
X-ray spectroscopy with silicon pin and avalanche photo diodes p 906 N94-15072
Improved optical radiation detectors and their calibration: 200 nm - 30 microns p 906 N94-15075
Applications for large area silicon drift detectors on x ray and gamma ray astronomy p 909 N94-15090
Measuring atmospheric dispersion with WLRS in multiple wavelength mode p 916 N94-15582
Two wavelength satellite laser ranging using SPAD
p 916 N94-15584
Micro pulse laser radar
[NASA-CASE-GSC-13493-1] p 1004 N94-17322
Frequency resolution of an acousto-optical spectrometer
[AD-A267822] p 1035 N94-17401
PHOTODISSOCIATION
Molecular processes in comets
[NASA-CR-194148] p 1239 N94-15188
Molecular beam studies of reaction dynamics
[DE93-015035] p 1181 N94-15995
Design of a formaldehyde photodissociation process for carbon and oxygen isotope separation
[DE93-016435] p 1039 N94-16450
Studies of combustion reactions at the state-resolved differential cross section level
[DE93-017605] p 948 N94-16462
Extracavity frequency doubling study of a pulsed photodissociation iodine laser
[AD-A267893] p 1042 N94-17394
PHOTOELASTIC ANALYSIS
Use of photostress and strain gages to analyze behavior of weldments and use of photostress and strain gages to analyze behavior of an aft skirt test specimen
[NASA-CR-194575] p 1058 N94-15716
PHOTOELASTIC MATERIALS
Use of photostress and strain gages to analyze behavior of weldments and use of photostress and strain gages to analyze behavior of an aft skirt test specimen
[NASA-CR-194575] p 1058 N94-15716
PHOTOELECTRIC EMISSION
Photoemission study of diamond (100) surface
[DE93-015251] p 1208 N94-16062
Structural characterization of epitaxial layers for infrared detectors
[AD-A267875] p 940 N94-17013
Low temperature deposition and characterization of n- and p-type silicon carbide thin films and associated ohmic and Schottky contacts
[AD-A267966] p 973 N94-17490
In-situ electron and optical spectroscopies of translational and vibrational activated bond breaking and formation on semiconductors
[AD-A268192] p 1015 N94-17560
PHOTOELECTRON SPECTROSCOPY
A sulfur segregation study of PWA 1480, NiCrAl, and NiAl alloys
[NASA-TM-106289] p 956 N94-15992
Design and fabrication of a reflection far ultraviolet polarizer and retarder
[NASA-CR-194630] p 1191 N94-16023
Photoemission study of diamond (100) surface
[DE93-015251] p 1208 N94-16062
The interaction of HCN(DCN) with Si(111)-7x7 studied with HREELS, UPS, and XPS
[AD-A266237] p 1182 N94-16111
Electron spectroscopy analysis
[NASA-CR-193591] p 951 N94-17039
Growth of dielectric thin films by irradiation of condensed molecular precursors with synchrotron radiation
[DE93-016161] p 974 N94-17676
PHOTOEXCITATION
X ray laser program
[AD-A267075] p 1038 N94-15628

PHOTOGEOLOGY
Geomorphic processes in the Argyre-Dorsa Argentea region of Mars p 1270 N94-16293
PHOTOGRAPHIC EQUIPMENT
STS-30 crew photo in building 4
[NASA-TM-109573] p 1031 N94-15304
STS-27 crew photo training and habitation procedures
[NASA-TM-109553] p 1032 N94-15405
STS-35 payload specialists Durrance and Parise: 70mm photo training and cabin familiarization
[NASA-TM-109499] p 1032 N94-15463
PHOTOGRAPHIC FILM
Optical computing
[AD-A267881] p 1141 N94-17015
PHOTOGRAPHS
Characterization of spatial and temporal variability of phytoplankton blooms in coastal waters
[AD-A267102] p 1116 N94-15633
A mineralized zone in Western Candor Chasma, Mars p 1248 N94-16179
PHOTOGRAPHY
National Aero-Space Plane
[NASA-TM-109450] p 865 N94-15323
National Aero-Space Plane resource reel
[NASA-TM-109451] p 865 N94-15324
STS-34 onboard 16mm photography quick release
[NASA-TM-109460] p 880 N94-15355
STS-27 crew photo training and habitation procedures
[NASA-TM-109553] p 1032 N94-15405
STS-41 crew training bailout in CCT, 16mm camera class EVA prep, habitation equipment procedures, and food tasting
[NASA-TM-109517] p 876 N94-15517
Fast-ICCD photography and gated photon counting measurements of blackbody emission from particulates generated in the KrF-laser ablation of BN and YBC
[DE93-015491] p 1210 N94-16460
Optical computing
[AD-A267881] p 1141 N94-17015
PHOTOIONIZATION
Investigation of the interactions of radiation with matter
[AD-A266743] p 1181 N94-15774
Multiphoton ionization studies of WF6 and UF6
[DE93-016232] p 1181 N94-15863
Characterization of UV emissions resulting from electronic energy transfer in atmospheric molecules
[AD-A266244] p 1101 N94-16469
Femtosecond growth dynamics of an underdense ionization front measured by spectral blueshifting
[DE93-013582] p 1183 N94-16818
Sensitive detection of gas-phase nitro-containing energetic materials employing 226-nm radiation
[AD-A267633] p 951 N94-17203
Laser photoionization time-of-flight mass spectrometry of nitrated polycyclic aromatic hydrocarbons and nitrated heterocyclic compounds
[AD-A268126] p 952 N94-17520
A physical model for one-dimension and time-dependent ionosphere. Part 2: Results and discussions
[DE93-627959] p 1103 N94-17631
PHOTOLITHOGRAPHY
Scalar limitations of diffractive optical elements p 1194 N94-17336
Fabricating binary optics: An overview of binary optics process technology p 1195 N94-17343
Laser figuring for the generation of analog micro-optics and kineform surfaces p 1196 N94-17346
Diffractive optics fabricated by direct write methods with an electron beam p 1196 N94-17347
Phase holograms in PMMA with proximity effect correction p 1037 N94-17348
Curved grating fabrication techniques for concentric-circle grating, surface-emitting semiconductor lasers p 1045 N94-17349
Fabrication of micro-optical devices p 1197 N94-17351
SURPHEX (tm): New dry photopolymers for replication of surface relief diffractive optics p 1198 N94-17358
Predesign of diamond turned refractive/diffractive elements for IR objectives p 1198 N94-17359
PHOTOLUMINESCENCE
Structural investigation of electrochemically etched silicon
[DE93-015300] p 1207 N94-15827
Numerical studies of the photoluminescence spectrum of quantum Hall systems
[DE93-015822] p 1220 N94-16810
Electrical conductivity of ion implanted ladder and semi-ladder polymers
[AD-A267432] p 970 N94-16978
Growth and doping of Al(x)Ga(1-x)N films by electron cyclotron resonance assisted molecular beam epitaxy
[AD-A267305] p 1212 N94-16992
Nitride semiconductors for ultraviolet detection
[AD-A267877] p 1012 N94-17040
Investigation of the optical, electronic, and structural properties of fiber optic glasses
[AD-A267645] p 971 N94-17204
Lattice relaxation theory of localized excitations in quasi-one-dimensional systems
[DE93-624947] p 1215 N94-17437
PHOTOLYSIS
Photodegradation of polyimides. V1: Effect of donor-acceptor groups on the photooxidative stability of polyimides and model compounds
[AD-A267319] p 970 N94-16947
The photophysics of poly(methylphenylphosphazene)
[AD-A267321] p 970 N94-16949
Pulsed laser kinetic studies of liquids under high pressure
[DE93-017826] p 1041 N94-16998
PHOTOMAPPING
Galileo imaging results from the second Earth-Moon flyby: Lunar Maria and related units p 1252 N94-16199
Lunar impact basins: New data for the nearside northern high latitudes and eastern limb from the second Galileo flyby p 1258 N94-16228
PHOTOMASKS
Fabrication of micro-optical devices p 1197 N94-17351
Low cost paths to binary optics p 1197 N94-17353
PHOTOMETERS
A novel solid-state optical temporal analyzer with picosecond resolution and picowatt sensitivity
[AD-A266804] p 986 N94-14912
Visible light photon counters for astronomy p 902 N94-15043
Photoconductors and arrays for the far-infrared p 902 N94-15045
Impurity conduction photoconductor detectors p 902 N94-15046
BIB photodetectors based on antimony doped silicon p 902 N94-15047
Optimisation of FIR photoconductors for atmospheric spectroscopy p 902 N94-15048
Nonstationary behaviour of low background photon detectors p 902 N94-15049
A 12.5 micron infrared detector for Earth observation p 903 N94-15052
Lead chalcogenides based IR photosensitive array detectors with coordinate addressing p 903 N94-15053
Performance optimization of detector electronics for millimeter laser ranging p 913 N94-15569
Tracking capabilities of SPADs for laser ranging p 914 N94-15570
How to squeeze high quantum efficiency and high time resolution out of a SPAD p 914 N94-15571
Streak camera based SLR receiver for two color atmospheric measurements p 914 N94-15573
Two wavelength satellite laser ranging using SPAD p 916 N94-15584
The new MTLRS-1 receiving system p 877 N94-15611
Linear encoding device
[NASA-CASE-GSC-13562-1] p 1147 N94-15703
Mass of Saturn's A ring p 1263 N94-16252
Optical ionospheric instrumentation and research
[AD-A266403] p 1192 N94-16550
Acousto-optical classifier
[AD-D015894] p 1000 N94-16921
Fundamental theory of light for applications: Notes for five informal lectures
[DE93-016463] p 1192 N94-16953
Development of ultra-low noise, high performance 3-V Quantum Well Infrared Photodectors (QWIP's) for focal plane array staring image sensor systems
[AD-A267715] p 1214 N94-17272
PHOTOMICROGRAPHS
Grain surface features of Apollo 17 orange and black glass p 1289 N94-16397
Long duration exposure facility experiment m0003 deintegration observation database
[AD-A267579] p 951 N94-17207
PHOTOMULTIPLIER TUBES
A new detector concept for energetic auroral x ray imaging p 907 N94-15081
Performance optimization of detector electronics for millimeter laser ranging p 913 N94-15569
Two color satellite laser ranging upgrades at Goddard's 1.2m telescope facility p 915 N94-15581
Two wavelength satellite laser ranging using SPAD p 916 N94-15584
Performance comparison of high speed microchannel plate photomultiplier tubes p 922 N94-15624
PHOTON-ELECTRON INTERACTION
Ultrafast processes in tunneling microstructure devices
[AD-A266570] p 1210 N94-16720
PHOTONICS
Alternative optical architectures for multichannel adaptive optical processing
[AD-A267052] p 1189 N94-15664
Fabricating binary optics: An overview of binary optics process technology p 1195 N94-17343
The photonical, pure grid method
[NLR-TP-91478-U] p 1062 N94-17600
PHOTONS
Proceedings of an ESA Symposium on Photon Detectors for Space Instrumentation
[ESA-SP-356] p 899 N94-15025
A new approach to optical photon detection p 899 N94-15028
Superconductive x ray photon detectors p 900 N94-15031
Metastable superconductors as photon detectors p 900 N94-15032
The MIC photon counting detector p 901 N94-15039
CCDs and photon counting devices: Applications in space and from the ground p 901 N94-15041
Visible light photon counters for astronomy p 902 N94-15043
Outlook for hard x ray and gamma ray astronomy p 904 N94-15057
Developments in extreme ultraviolet and x ray instrumentation p 904 N94-15058
The TAUVEX experiment p 905 N94-15064
The Rutherford Appleton Laboratory photon counting detector p 910 N94-15096
Work at Graz on satellite signatures p 898 N94-15558
Sensor modelling for the Cyclops focal plane detector array based technology demonstrator
[AD-A267172] p 1190 N94-15846
The cooling of confined ions driven by laser beams
[DE93-016612] p 1039 N94-16114
Ablation, surface activation, and electroless metallization of insulating materials by pulsed excimer laser irradiation
[DE93-015808] p 1040 N94-16664
Scintillation mechanism in stoichiometric cerium compounds
[DE93-015499] p 948 N94-16771
Optical properties of water released in low Earth orbit
[AD-A266197] p 1192 N94-16936
Detecting small debris using a ground-based photon counting detector
[DE93-012623] p 898 N94-17669
PHOTORECEPTORS
Melatonin, the pineal gland, and circadian rhythms
[AD-A268200] p 1129 N94-17478
PHOTOSENSITIVITY
A novel solid-state optical temporal analyzer with picosecond resolution and picowatt sensitivity
[AD-A266804] p 986 N94-14912
PHOTOSTRESSES
Use of photostress and strain gages to analyze behavior of weldments and use of photostress and strain gages to analyze behavior of an aft skirt test specimen
[NASA-CR-194575] p 1058 N94-15716
PHOTOSYNTHESIS
Using AVIRIS images to measure temporal trends in abundance of photosynthetic and nonphotosynthetic canopy components p 1066 N94-16668
Multiple dataset water-quality analyses in the vicinity of an ocean wastewater plume p 1069 N94-16687
Atmospheric correction of AVIRIS data in ocean waters p 1070 N94-16690
Tracking photosynthetic efficiency with narrow-band spectroradiometry
[CIW-PUBL-1133] p 1072 N94-16698
The dynamics of hydroponic crops for simulation studies of the CELSS initial reference configurations
[NASA-CR-194654] p 1118 N94-17279
PHOTOVOLTAIC CELLS
Recent advances in outdoor performance evaluation of PV systems
[DE93-015031] p 1091 N94-15994
Space systems environmental interaction studies
[AD-A267280] p 897 N94-17240
Field investigation of the relationship between battery size and PV system performance
[DE93-016503] p 1016 N94-17671
PHOTOVOLTAIC CONVERSION
Futurepath 1 --- power systems
[NASA-TM-109431] p 925 N94-15503
A ten year review of performance of photovoltaic systems
[DE93-015649] p 1093 N94-17217
PHYSICAL CHEMISTRY
Dissociation rates of diatomic molecules
[AD-A266464] p 1182 N94-16586

PHYSICAL EXAMINATIONS
Monograph of the aviation epidemiology data register for FY 1991
[AD-A266896] p 1119 N94-14952
Ames Fitness Program p 1126 N94-16632
PHYSICAL EXERCISE
GSFC Fun Run
[NASA-TM-109587] p 1120 N94-15271
Living well in space: Ensuring crew capability
[NASA-TM-109538] p 1120 N94-15369
STS-27 crew presentation clip
[NASA-TM-109551] p 881 N94-15403
Ames Fitness Program p 1126 N94-16632
Johnson Space Center health related fitness program p 1126 N94-16633
Kennedy Space Center exercise program p 1126 N94-16634
The Langley Fitness Center p 1126 N94-16635
Physical Exercise Program p 1127 N94-16636
Metabolic monitoring of hypobaric subjects
[AD-A268221] p 1130 N94-17554
PHYSICAL FACTORS
Particle simulations on massively parallel machines
[DE93-015644] p 1157 N94-14927
PHYSICAL FITNESS
Monograph of the aviation epidemiology data register for FY 1991
[AD-A266896] p 1119 N94-14952
Living well in space: Ensuring crew capability
[NASA-TM-109538] p 1120 N94-15369
Proceedings of the 1992 Annual Meeting NASA Occupational Health Program
[NASA-CR-193462] p 1123 N94-16609
Physical fitness and the Healthy People 2000 goals p 1125 N94-16619
Physical fitness and health education program at NASA Headquarters p 1126 N94-16631
Physical Exercise Program p 1127 N94-16636
The behavioral toxicology of high-peak, low average power, pulsed microwave irradiation
[AD-A268392] p 1134 N94-17535
PHYSICAL OPTICS
Detection of subsurface defects in machined silicon nitride ceramics by optical scattering methods
[DE93-015554] p 968 N94-16658
Investigation of the optical, electronic, and structural properties of fiber optic glasses
[AD-A267645] p 971 N94-17204
PHYSICAL WORK
Complex terrain wind model evaluation
[AD-A266467] p 1096 N94-16589
PHYSICIANS
Tuberculosis: A case for increased screening p 1126 N94-16627
PHYSIOLOGICAL EFFECTS
Evaluation of dried storage of platelets for transfusion: Physiologic integrity and hemostatic functionality
[AD-A266958] p 1120 N94-15180
Living well in space: Ensuring crew capability
[NASA-TM-109538] p 1120 N94-15369
Transcranial Doppler ultrasound studies of cerebral blood-flow in microgravity p 981 N94-16095
Synaptic plasticity and memory formation
[AD-A267988] p 1133 N94-17453
Ontogenesis of mammals in microgravity
[NASA-TM-103978] p 1139 N94-17636
PHYSIOLOGICAL RESPONSES
Neuropeptide-Y (NPY) increases total blood flow in the tail, and reduces cutaneous microvascular blood flow in the tail and foot of the rat
[AD-A266839] p 1115 N94-14918
Autogenic-Feedback Training (AFT) as a preventive method for space motion sickness: Background and experimental design
[NASA-TM-108780] p 1120 N94-15537
Activity/rest patterns of instructor and rates student pilots during rapid transitions from daytime to nighttime duty hours at the Eastern Army Aviation Training site
[AD-A267038] p 1131 N94-15659
Reliability of autonomic responses and malaise across multiple motion sickness stimulation tests
[NASA-TM-108787] p 1121 N94-15711
Heart rate response to parabolic flight manoeuvres p 981 N94-16098
AFRRI reports, first quarter 1993
[AD-A266380] p 1123 N94-16515
The nature of dynamic arteriolar vasoreactivity: A mini-review and A classification scheme
[AD-A266499] p 1128 N94-16783
Neurotoxicity of hemoglobin in cortical cell culture
[AD-A266506] p 1128 N94-16786
TransRapid TR-07 maglev-spectrum magnetic field effects on daily pineal indoleamine metabolic rhythms in rodents
[DE93-015143] p 1117 N94-16893
Synaptic plasticity and memory formation
[AD-A267988] p 1133 N94-17453
PHYSIOLOGICAL TESTS
STS-32 crew training for lower body negative pressure unit and AFE
[NASA-TM-109475] p 1120 N94-15381
Reliability of autonomic responses and malaise across multiple motion sickness stimulation tests
[NASA-TM-108787] p 1121 N94-15711
PHYSIOLOGY
USAF physiological studies of personal microclimate cooling: A review
[AD-A267203] p 1022 N94-15858
Studies of aural acoustic emmissions with the use of an original apparatus and investigative methodology
[IFTR-20/1992] p 1177 N94-16650
Evaluation of spatial productivity patterns in an annual grassland during an AVIRIS overflight
[CIW-PUBL-1134] p 1067 N94-16672
Multitemporal diurnal AVIRIS images of a forested ecosystem p 1074 N94-16709
PHYTOPLANKTON
Characterization of spatial and temporal variability of phytoplankton blooms in coastal waters
[AD-A267102] p 1116 N94-15633
Seasonal and spatial variations in phytoplanktonic chlorophyll in eutrophic Mono Lake, California, measured with the Airborne Visible and Infrared Imaging Spectrometer (AVIRIS) p 1069 N94-16684
PICOSECOND PULSES
Nd:YLF laser for airborne/spaceborne laser ranging p 913 N94-15563
A study of high field transport in wide band gap electronic materials using a picosecond transient charge technique
[AD-A267098] p 1008 N94-15636
PIEZOELECTRIC TRANSDUCERS
Nanocomposites for electronic applications, volume 1
[AD-A267070] p 1009 N94-15669
Nanocomposites for electronic applications, volume 3
[AD-A267073] p 1009 N94-15672
Nanocomposites for electronic applications, volume 2
[AD-A267074] p 1009 N94-15673
Mechanical and surface force nanoprobe
[AD-D015792] p 1034 N94-16536
Fabrication of piezoelectric ceramic/polymer composites by injection molding
[AD-A267302] p 972 N94-17227
PIEZOELECTRICITY
Nanocomposites for electronic applications, volume 1
[AD-A267070] p 1009 N94-15669
Nanocomposites for electronic applications, volume 3
[AD-A267073] p 1009 N94-15672
Nanocomposites for electronic applications, volume 2
[AD-A267074] p 1009 N94-15673
Fabrication of piezoelectric ceramic/polymer composites by injection molding
[AD-A267302] p 972 N94-17227
Two-dimensional, high flow, precisely controlled monodisperse drop source
[AD-A267660] p 1028 N94-17250
PIGMENTS
Materials Research Society Symposium Proceedings, Volume 292: Biomolecular Materials
[AD-A265776] p 1116 N94-15138
PILOT ERROR
Altitude deviations: Breakdowns of an error-tolerant system
[NASA-TM-108788] p 862 N94-15550
PILOT PERFORMANCE
An information processing classification of beyond-visual-range air intercepts
[AD-A266927] p 1131 N94-15108
Predicting radiation induced performance decrements of AH-1 helicopter crews. Volume 1: Predicted veersus actual performance of AH-1 crews induced with symptoms simulating radiation sickness
[AD-A268376] p 1138 N94-17460
PILOT TRAINING
Activity/rest patterns of instructor and rates student pilots during rapid transitions from daytime to nighttime duty hours at the Eastern Army Aviation Training site
[AD-A267038] p 1131 N94-15659
PINEAL GLAND
TransRapid TR-07 maglev-spectrum magnetic field effects on daily pineal indoleamine metabolic rhythms in rodents
[DE93-015143] p 1117 N94-16893
Melatonin, the pineal gland, and circadian rhythms
[AD-A268200] p 1129 N94-17478
PIONEER SPACE PROBES
The 1978 highlights
[NASA-TM-109625] p 1302 N94-15411
The 1968 highlights --- NASA programs and research
[NASA-TM-109627] p 1302 N94-15413
The 1982 highlights
[NASA-TM-109671] p 1303 N94-15508
PIONEER VENUS SPACECRAFT
Pioneer-Venus press clip --- Solar System formation and extraterrestrial life
[NASA-TM-109425] p 1239 N94-15495
PIONEER VENUS 1 SPACECRAFT
Pioneer Venus data analysis for the retarding potential analyzer
[NASA-CR-194673] p 1297 N94-17292
PIONS
Experimental study of weak interactions by precision measurement by rare kaon decay
[DE93-016864] p 1182 N94-16117
A high sensitivity search for CP violating rare K(sub L) decays and precision measurement of the direct CP violation parameter (epsilon)(prime)/(epsilon) via the four K (yields) 2(pi) decay modes
[DE93-016866] p 1184 N94-16899
PIPE FLOW
On solving the compressible Navier-Stokes equations for unsteady flows at very low Mach numbers
[NASA-TM-106380] p 1027 N94-17128
PIPES (TUBES)
Long baseline watertubes p 1037 N94-15803
Potential transients, transmission and electrochemical corrosion detection
[DE93-014055] p 956 N94-15922
Investigation of two-phase flow and boiling heat transfer during quenching of a tube under microgravity p 979 N94-16087
PISTON ENGINES
Some single-piston closed-cycle machines and Peter Tailer's thermal lag engine
[DE93-015983] p 1049 N94-17675
PISTONS
Hydraulic pump with integral electric motor
[AD-D015782] p 1011 N94-16549
Design of non-sled setup to measure head injury criteria
[NIAR-92-20] p 872 N94-17263
High temperature hydraulic seals
[AD-A268257] p 1048 N94-17433
Some single-piston closed-cycle machines and Peter Tailer's thermal lag engine
[DE93-015983] p 1049 N94-17675
PITCH (INCLINATION)
The free decay of coupled heave and pitch motions of a model frigate
[DRA/TM(AWMH)92340] p 1146 N94-15702
Effects of internal yaw-vectoring devices on the static performance of a pitch-vectoring nonaxisymmetric convergent-divergent nozzle
[NASA-TP-3369] p 858 N94-16572
PITCHING MOMENTS
Suppression of dynamic stall with a leading-edge slat on a VR-7 airfoil
[NASA-TP-3357] p 856 N94-15657
PITS
Application of in situ scanning x ray fluorescence to study the concentration of metal ions in simulated pits
[DE93-014054] p 956 N94-15921
PIVOTS
Tilt mechanism
[AD-D015780] p 1047 N94-16548
PIXELS
A monolithic PbTeCCD focal plane array for MWIR imaging p 910 N94-15100
Massively parallel, adaptive, color image processing for autonomous road following
[AD-A266988] p 864 N94-15498
Pixel-level fusion using interest images
[AD-A266640] p 1164 N94-15746
A task adaptive parallel graphics renderer
[DE93-017123] p 1149 N94-16119
PLAINS
Modes of formation of lunar light plains and the detection of cryptomaria deposits p 1259 N94-16231
PLANAR STRUCTURES
Orientation of Planar Deformation Features (PDFs) in quartz p 1219 N94-16341
PLANE STRAIN
Solution of elastic-plastic stress analysis problems by the p-version of the finite element method
[NASA-CR-194267] p 1062 N94-17445
PLANE STRESS
Analysis of the strengthening of aluminum alloy undergoing plastic deformation under conditions of a compound state of stress
[IFTR-21/1991] p 960 N94-17093
Solution of elastic-plastic stress analysis problems by the p-version of the finite element method
[NASA-CR-194267] p 1062 N94-17445
PLANE WAVES
Parametric resonant triad interactions in a free shear layer
[NASA-TM-106365] p 1021 N94-15751

Regular and irregular reflection of a wave from a slanting flat wall
[IFTR-13/1991] p 1193 N94-17049
The exact solution of the problem of diffraction of an electromagnetic plane wave by a conductive half-plane situated at an interface
[IFTR-3/91] p 1002 N94-17057

PLANETARY ATMOSPHERES
Twenty-Fourth Lunar and Planetary Science Conference. Part 2: G-M
[NASA-CR-193174] p 1247 N94-16173
Trapping of water vapor from an atmosphere by condensed silicate matter formed by high-temperature pulse vaporization p 1248 N94-16180

PLANETARY BOUNDARY LAYER
Phillips Laboratory global spectral numerical weather prediction model
[AD-A267293] p 1107 N94-17244
Further development and testing of a second-order bulk boundary layer model
[AD-A268071] p 1109 N94-17552

PLANETARY COMPOSITION
Twenty-Fourth Lunar and Planetary Science Conference. Part 2: G-M
[NASA-CR-193174] p 1247 N94-16173
A mineralized zone in Western Candor Chasma, Mars p 1248 N94-16179
Evolutionary implications of a steady-state water abundance on Venus p 1254 N94-16206
A Pluto thermal model p 1256 N94-16216
Modeling the reflectance of CO2 frost with new optical constants: Application to Martian south polar cap spectra p 1256 N94-16217
Nd-142/Nd-144 in bulk planetary reservoirs, the problem of incomplete mixing of interstellar components and significance of very high precision Nd-145/Nd-144 measurements p 1256 N94-16220
A Moessbauer spectrometer for the mineralogical analysis of the Mars surface: First temperature dependent tests of the detector and drive system p 1259 N94-16233
Explosive volcanism and the compositions of the cores of differentiated asteroids p 1243 N94-16306
Evolution of Triton's volatile budget p 1284 N94-16373
Mars brine formation experiment p 1293 N94-16419

PLANETARY CORES
Was Martian mantle wet? A possible consequence of rapid core formation p 1277 N94-16335

PLANETARY CRATERS
Magellan: Principal Venus science findings p 989 N94-15887
Twenty-Fourth Lunar and Planetary Science Conference. Part 2: G-M
[NASA-CR-193174] p 1247 N94-16173
Fluvial erosion on Mars: Implications for paleoclimatic change p 1241 N94-16210
Confirmation of saturation equilibrium conditions in crater populations p 1103 N94-16222
Chemical differentiation, thermal evolution, and catastrophic overturn on Venus: Predictions and geologic observations p 1259 N94-16232
The three ages of Venus: A hypothesis based on the cratering record p 1261 N94-16239
Trace-element composition of Chicxulub crater melt rock, K/T tektites and Yucatan basement p 1242 N94-16245
The size of complex craters p 1262 N94-16249
The depths of the largest impact craters on Venus p 1264 N94-16261
A first-order model for impact crater degradation on Venus p 1265 N94-16268
Radar properties of several fluidized ejecta blankets on Venus p 1267 N94-16278
Implications of crater distributions on Venus p 1270 N94-16300
Manson impact structure, Iowa: First geochemical results for drill core M-1 p 1103 N94-16322
Preliminary Ar-40/Ar-39 age spectrum and laser probe dating of the M1 core of the Manson Impact Structure, Iowa: A K-T boundary crater candidate p 1104 N94-16334
Tectonic resurfacing of Venus p 1285 N94-16380
Relief of some small landforms on Venus p 1293 N94-16418
Guide to Magellan image interpretation
[NASA-CR-194340] p 1298 N94-17654

PLANETARY CRUSTS
Spatially extensive uniform stress fields on Venus inferred from radial dike swarm geometries: The Aphrodite Terra example p 1254 N94-16207
Chemical differentiation, thermal evolution, and catastrophic overturn on Venus: Predictions and geologic observations p 1259 N94-16232
The depths of the largest impact craters on Venus p 1264 N94-16261
Tessera terrain on Venus: Global characterization from Magellan data p 1264 N94-16262
Density of impact craters on tessera, Venus p 1264 N94-16263
An inversion of geoid and topography for mantle and crustal structure on Mars p 1273 N94-16315
Models of thermal/chemical boundary layer convection: Potential application to Venus p 1279 N94-16348
Large-scale volcanism associated with coronae on Venus p 1285 N94-16376
Geophysical models of Western Aphrodite-Niobe region: Venus p 1286 N94-16382
Variations in the Fe mineralogy of bright Martian soil p 1295 N94-16431
Composition of weakly altered Martian crust p 1296 N94-16436
A geological and geophysical information system for Eurasia
[AD-A267841] p 1232 N94-17036

PLANETARY ENVIRONMENTS
Directory of research projects: Planetary materials and geochemistry
[NASA-TM-4484] p 1095 N94-15781
First results from a laboratory facility for measurement of emission spectra under simulated planetary conditions p 954 N94-16372

PLANETARY EVOLUTION
Pioneer-Venus press clip --- Solar System formation and extraterrestrial life
[NASA-TM-109425] p 1239 N94-15495
Trapping of water vapor from an atmosphere by condensed silicate matter formed by high-temperature pulse vaporization p 1248 N94-16180
The formation and evolution of Alpha and Tellus tesserae on Venus p 1249 N94-16183
Tessera terrain on Venus: Implications of tessera flooding models and boundary characteristics for global distribution and mode of formation p 1258 N94-16226
Chemical differentiation, thermal evolution, and catastrophic overturn on Venus: Predictions and geologic observations p 1259 N94-16232
Potassium isotope cosmochemistry, volatile depletion and the origin of the Earth p 953 N94-16259
Was Martian mantle wet? A possible consequence of rapid core formation p 1277 N94-16335
Evolution of Triton's volatile budget p 1284 N94-16373
Workshop on early Mars: How warm and how wet, part 2?
[NASA-CR-193503] p 1297 N94-17637

PLANETARY GEOLOGY
Magellan: Principal Venus science findings p 989 N94-15887
Twenty-Fourth Lunar and Planetary Science Conference. Part 2: G-M
[NASA-CR-193174] p 1247 N94-16173
Morphometric comparison of Icelandic lava shield volcanoes versus selected Venusian edifices p 1248 N94-16178
A mineralized zone in Western Candor Chasma, Mars p 1248 N94-16179
Pargo Chasma and its relationship to global tectonics p 1249 N94-16181
The formation and evolution of Alpha and Tellus tesserae on Venus p 1249 N94-16183
Cretaceous-tertiary boundary spherules and Cenozoic microtektites: Similarities and differences p 1241 N94-16186
Rheology of water and ammonia-water ices p 953 N94-16188
Sand transport on Mars: Preliminary results from models p 1252 N94-16198
Mars Analog Site Study (MASS) p 1252 N94-16200
Earth imaging results from Galileo's second encounter p 1252 N94-16201
Collisional and dynamical history of Gaspra p 1241 N94-16202
Explosive mafic volcanism on Earth and Mars p 1253 N94-16204
Evolutionary implications of a steady-state water abundance on Venus p 1254 N94-16206
Spatially extensive uniform stress fields on Venus inferred from radial dike swarm geometries: The Aphrodite Terra example p 1254 N94-16207
The Acraman impact structure: Estimation of the diameter by the ejecta layer thickness p 1103 N94-16211
The Karakul depression in Pamirs: The first impact structure in Central Asia p 1241 N94-16212
Ishtar deformed belts: Evidence for deformation from below? p 1256 N94-16218
Confirmation of saturation equilibrium conditions in crater populations p 1103 N94-16222
Lava flow-field morphological classification and interpretation: Examples from Venus p 1259 N94-16230
Chemical differentiation, thermal evolution, and catastrophic overturn on Venus: Predictions and geologic observations p 1259 N94-16232
Emplacement of multiple flow units on very shallow slopes, east Kawelu Planitia flow field, Venus p 1260 N94-16235
Thermal inertia and radar reflectivity of the Martian north polar ERG: Low-density aggregates p 1260 N94-16238
Tessera terrain on Venus: Global characterization from Magellan data p 1264 N94-16262
A first-order model for impact crater degradation on Venus p 1265 N94-16268
Fractal geometry of some Martian lava flow margins: Alba Patera p 1270 N94-16298
Tectonics of Neyterkob corona on Venus p 1270 N94-16299
Implications of crater distributions on Venus p 1270 N94-16300
Megaplumes on Venus p 1271 N94-16301
Preliminary analysis of Dione Regio, Venus: The final Magellan regional imaging gap p 1271 N94-16302
The distribution of large volcanoes on Venus as a function of height and altitude p 1271 N94-16303
Tidal interaction: A possible explanation for geysers and other fluid phenomena in the Neptune-Triton system p 1272 N94-16311
An inversion of geoid and topography for mantle and crustal structure on Mars p 1273 N94-16315
Global Magellan-image map of Venus at full resolution p 1274 N94-16319
Meander properties of Venusian channels p 1275 N94-16324
Cat Mountain: A meteoritic sample of an impact-melted chondritic asteroid p 1244 N94-16328
Spectral study of Venus global topography and geoid from Magellan and PVO data p 1276 N94-16332
Vertical structure models of the 1990 equatorial disturbance on Saturn p 1277 N94-16333
Sheet flow fields on Venus p 1278 N94-16338
Hellas basin, Mars: Formation by oblique impact p 1280 N94-16350
Sedimentation, volcanism, and ancestral lakes in the Valles Marineris: Clues from topography p 1283 N94-16369
Evolution of Triton's volatile budget p 1284 N94-16373
Suggestion for extended Viking magnetic properties experiment on future Mars missions p 1285 N94-16375
Large-scale volcanism associated with coronae on Venus p 1285 N94-16376
Tectonic resurfacing of Venus p 1285 N94-16380
Geophysical models of Western Aphrodite-Niobe region: Venus p 1286 N94-16382
The dregs of crystallization in Zagami p 1245 N94-16390
Aspects of modelling the tectonics of large volcanoes on the terrestrial planets p 1104 N94-16396
Deucalionis Regio, Mars: Evidence for a unique mineralogic endmember and a crusted surface p 1291 N94-16406
Analysis of pyroxene absorptions observed in Martian dark regions p 1292 N94-16411
Relief of some small landforms on Venus p 1293 N94-16418
Mars brine formation experiment p 1293 N94-16419
Bright soil units on Mars determined from ISM imaging spectrometer data p 1295 N94-16430
A geological and geophysical information system for Eurasia
[AD-A267841] p 1232 N94-17036
Guide to Magellan image interpretation
[NASA-CR-194340] p 1298 N94-17654

PLANETARY IONOSPHERES
Pioneer Venus data analysis for the retarding potential analyzer
[NASA-CR-194673] p 1297 N94-17292

PLANETARY LIMB
Altitude profile of aerosols on Mars from measurements of its thermal radiation on limb p 1294 N94-16423

PLANETARY MAGNETIC FIELDS
Magnetic effects in Venus/solar wind interaction
[NASA-CR-194666] p 1299 N94-17281

PLANETARY MAGNETOSPHERES
Multispectral observations of the Jovian aurora
[NASA-CR-193628] p 1297 N94-16884

PLANETARY MAGNETOTAILS
Linear and non-linear studies of Alfven waves in space. Stationary and dynamic processes in magnetospheric plasmas
[NASA-CR-193585] p 1239 N94-16647

PLANETARY MANTLES
Experimental constraints on CO2 and H2O in the Martian mantle and primary magmas p 1262 N94-16248
Estimates of lithospheric thickness on Venus p 1267 N94-16277
An inversion of geoid and topography for mantle and crustal structure on Mars p 1273 N94-16315
Models of thermal/chemical boundary layer convection: Potential application to Venus p 1279 N94-16348
Geophysical models of Western Aphrodite-Niobe region: Venus p 1286 N94-16382
Effective elastic thickness of the Venusian lithosphere with lateral viscosity variations in the mantle p 1293 N94-16421

PLANETARY MAPPING
Pargo Chasma and its relationship to global tectonics p 1249 N94-16181
Earth imaging results from Galileo's second encounter p 1252 N94-16201
Separation of topographic and intrinsic backscatter variations in biscopic radar images: A magic airbrush p 1086 N94-16318
Global Magellan-image map of Venus at full resolution p 1274 N94-16319
The cartography of Venus with Magellan data p 1274 N94-16320
Hellas basin, Mars: Formation by oblique impact p 1280 N94-16350
Tectonic resurfacing of Venus p 1285 N94-16380
The use of TIMS for mapping different pahoehoe surfaces: Mauna Iki, Kilauea p 1065 N94-16606
Unmixing AVIRIS data to provide a method for vegetation fraction subtraction p 1066 N94-16669
Mapping the mineralogy and lithology of Canyonlands, Utah with imaging spectrometer data and the multiple spectral feature mapping algorithm p 1066 N94-16670

PLANETARY MASS
A simultaneous estimation of the mass of Mars and its natural satellites, Phobos and Deimos, from the orbital perturbations on the Mariner 9, Viking 1, and Viking 2 orbiters p 1279 N94-16347

PLANETARY NEBULAE
Gas-grain energy transfer in solar nebula shock waves: Implications for the origin of chondrules p 1262 N94-16251
Evolution of Triton's volatile budget p 1284 N94-16373
On the delivery of planetesimals to a protoplanet in the solar nebula p 1245 N94-16379

PLANETARY ORBITS
The effects of orbital and climatic variations on Martian surface heat flow p 1290 N94-16402

PLANETARY QUAKES
The seismic response of an aquifer to the propagation of an impact generated shock wave: A possible trigger of the Martian outflow channels? p 1281 N94-16354

PLANETARY RADIATION
Altitude profile of aerosols on Mars from measurements of its thermal radiation on limb p 1294 N94-16423

PLANETARY ROTATION
Neptune encounter highlights [NASA-TM-109421] p 1246 N94-15240

PLANETARY STRUCTURE
Experimental constraints on CO2 and H2O in the Martian mantle and primary magmas p 1262 N94-16248
Geophysical models of Western Aphrodite-Niobe region: Venus p 1286 N94-16382

PLANETARY SURFACES
Twenty-Fourth Lunar and Planetary Science Conference. Part 2: G-M [NASA-CR-193174] p 1247 N94-16173
Rover mounted ground penetrating radar as a tool for investigating the near-surface of Mars and beyong p 1007 N94-16197
Lava flow-field morphological classification and interpretation: Examples from Venus p 1259 N94-16230
Near-surface temperature gradients and their effects on thermal-infrared emission spectra of particulate planetary surfaces p 1260 N94-16236
Guide to Magellan image interpretation [NASA-CR-194340] p 1298 N94-17654

PLANETARY SYSTEMS
Teaching planetary sciences to elementary school teachers: Programs that work p 1222 N94-16346

PLANETARY TEMPERATURE
The effects of orbital and climatic variations on Martian surface heat flow p 1290 N94-16402
Equatorial ground ice on Mars: Steady-state stability p 1290 N94-16403

PLANETARY WAVES
A global traveling wave on Venus [NASA-CR-194356] p 1246 N94-15182
Ray tracing on topographic Rossby waves [AD-A267014] p 1112 N94-15844
Real time system for practical acoustic monitoring of global ocean temperature [AD-A267868] p 1113 N94-17391

PLANETS
The planetary data system educational CD-ROM p 1234 N94-16209

PLANFORMS
Wind-tunnel investigation of aerodynamic efficiency of three planar elliptical wings with curvature of quarter-chord line [NASA-TP-3359] p 859 N94-16574

PLANTS (BOTANY)
Plant research [NASA-TM-109664] p 1116 N94-15235
The 1990-1991 NASA space biology accomplishments [NASA-TM-4501] p 1118 N94-17257

PLASMA ACCELERATION
Numerical modeling of the temperature gradients and spectra of the plasma armature on Thunderbolt [AD-A266414] p 878 N94-16552

PLASMA ARC WELDING
Plasma arc welding weld imaging [NASA-CASE-MFS-28797-1] p 1047 N94-15949
The Marshall Automated Weld System (MAWS) [TABES PAPER 93-602] p 1049 N94-16138
Plasma arc welding repair of space flight hardware [TABES PAPER 93-603] p 1049 N94-16139
Robotic weld overlay coatings for erosion control [DE93-016938] p 970 N94-16959

PLASMA CONTROL
ITER-HARD Toroidal Field coil structural analysis [DE93-014834] p 1201 N94-15981
Active probing of plasma edge turbulence and feedback studies on the Texas experimental tokamak (TEXT) [DE93-015799] p 1202 N94-16162
High beta and confinement studies of TFTR [DE93-016204] p 1202 N94-16446
Method and apparatus for forming an agile plasma mirror effective as a microwave reflector [AD-D015788] p 998 N94-16535
3D and r,z particle simulations of heavy ion fusion beams [DE93-013417] p 1205 N94-17670

PLASMA CURRENTS
Inductive effects during second harmonic current drive experiments on T-10 [DE93-014411] p 1202 N94-16803
Simulation of enhanced tokamak performance on D3-D using fast wave current drive [DE93-014009] p 1203 N94-16823

PLASMA DECAY
Studies on the parametric decay of waves in fusion plasmas [VTT-PUBS-110] p 1200 N94-15204
On the decay of a dipole pump wave to half-harmonics p 1201 N94-15211

PLASMA DIAGNOSTICS
Active probing of plasma edge turbulence and feedback studies on the Texas experimental tokamak (TEXT) [DE93-015799] p 1202 N94-16162
Numerical modeling of the temperature gradients and spectra of the plasma armature on Thunderbolt [AD-A266414] p 878 N94-16552
Femtosecond growth dynamics of an underdense ionization front measured by spectral blueshifting [DE93-013582] p 1183 N94-16818
The effects of radiation transport on line ratios used as temperature and density diagnostic [DE93-016424] p 1205 N94-17663

PLASMA DRIFT
Structure and damping of toroidal drift waves (and their implications for anomalous transport) [DE93-014005] p 1203 N94-16822

PLASMA DYNAMICS
Analysis of leading edge and trailing edge cover glass samples before and after treatment with advanced satellite contamination removal techniques [AD-A267055] p 885 N94-15666
Spectroscopic and computer modeling investigations of a laser-sustained plasma [IFTR-30/1991] p 1204 N94-17066
Granular fluctuations in plasma turbulence and their role in transport [DE93-013465] p 1187 N94-17674

PLASMA ENGINES
Plasma instabilities and transport in the MPD thruster [AD-A268268] p 1204 N94-17575

PLASMA EQUILIBRIUM
Active probing of plasma edge turbulence and feedback studies on the Texas experimental tokamak (TEXT) [DE93-015799] p 1202 N94-16162

PLASMA FREQUENCIES
Double stimulated Brillouin scattering p 1200 N94-15205

PLASMA GENERATORS
Investigation of onset of plasma formation at anode of fast-pulsed high-voltage vacuum diode [AD-A267214] p 1204 N94-16987

PLASMA HEATING
High frequency Raman current drive p 1201 N94-15208
Current drive with free electron lasers in high and low temperature tokamaks p 1201 N94-15209
Simulations of wave-particle interactions in stimulated Raman forward scattering in a magnetized plasma [TKK-F-A704] p 1201 N94-15210
Synthesis of ceramic oxide powders in a microwave plasma device [DE93-012741] p 965 N94-15920
Inductive effects during second harmonic current drive experiments on T-10 [DE93-014411] p 1202 N94-16803
Recent results from the 60 GHz inside launch ECH system on the D3-D tokamak [DE93-013027] p 1203 N94-16816
Simulation of enhanced tokamak performance on D3-D using fast wave current drive [DE93-014009] p 1203 N94-16823

PLASMA INTERACTIONS
Synthesis of ceramic oxide powders in a microwave plasma device [DE93-012741] p 965 N94-15920

PLASMA LAYERS
The effect of process parameters on the surface finish of plasma polymers [DE93-014112] p 966 N94-15924
Method and apparatus for forming an agile plasma mirror effective as a microwave reflector [AD-D015788] p 998 N94-16535

PLASMA OSCILLATIONS
Double stimulated Brillouin scattering p 1200 N94-15205

PLASMA PHYSICS
Direct drive foil implosion experiments on Pegasus 2 [DE93-012666] p 1202 N94-16776
Linear stability of stationary solutions of the Vlasov-Poisson system in three dimensions [DE93-013873] p 1174 N94-16820
Nonlinear problems in fluid dynamics and inverse scattering [AD-A266234] p 1026 N94-16927
Investigation of onset of plasma formation at anode of fast-pulsed high-voltage vacuum diode [AD-A267214] p 1204 N94-16987
Plasma Science Committee (PLSC) and the Panel on Opportunities in Plasma Science and Technology (OPST) [DE93-018142] p 1204 N94-16995
Application of group theory to integral-difference equations of plasma physics [IFTR-23/1992] p 1204 N94-17067
Role and development of small satellite missions in space plasma physics p 891 N94-17149
Granular fluctuations in plasma turbulence and their role in transport [DE93-013465] p 1187 N94-17674

PLASMA PRESSURE
Formation of the stable auroral arc that intensifies at substorm onset [NASA-CR-193637] p 1098 N94-15433

PLASMA PROPULSION
Plasma instabilities and transport in the MPD thruster [AD-A268268] p 1204 N94-17575
Application of a NEPTUNE propulsion concept to a manned Mars excursion [AD-A268053] p 929 N94-17587

PLASMA SPECTRA
Active probing of plasma edge turbulence and feedback studies on the Texas experimental tokamak (TEXT) [DE93-015799] p 1202 N94-16162

PLASMA SPRAYING
Krupp technical reports no. 2, English edition, October 1992 [ETN-93-94631] p 984 N94-16000
Vacuum plasma spraying p 975 N94-16002

PLASMA TEMPERATURE
ARIES tokamak reactor study [DE93-017059] p 1203 N94-16901

PLASMA TURBULENCE
Active probing of plasma edge turbulence and feedback studies on the Texas experimental tokamak (TEXT) [DE93-015799] p 1202 N94-16162
Plasma instabilities and transport in the MPD thruster [AD-A268268] p 1204 N94-17575
Granular fluctuations in plasma turbulence and their role in transport [DE93-013465] p 1187 N94-17674

PLASMA WAVES
Studies on the parametric decay of waves in fusion plasmas
[VTT-PUBS-110] p 1200 N94-15204
Double stimulated Brillouin scattering
p 1200 N94-15205
Dynamics of douple stimulated Brillouin scattering
p 1200 N94-15206
Soliton-like structures in double stimulated Brillouin scattering p 1200 N94-15207
High frequency Raman current drive
p 1201 N94-15208
Current drive with free electron lasers in high and low temperature tokamaks p 1201 N94-15209
Simulations of wave-particle interactions in stimulated Raman forward scattering in a magnetized plasma
[TKK-F-A704] p 1201 N94-15210
On the decay of a dipole pump wave to half-harmonics p 1201 N94-15211
Structure and damping of toroidal drift waves (and their implications for anomalous transport)
[DE93-014005] p 1203 N94-16822
PLASMA-ELECTROMAGNETIC INTERACTION
Femtosecond growth dynamics of an underdense ionization front measured by spectral blueshifting
[DE93-013582] p 1183 N94-16818
PLASMA-PARTICLE INTERACTIONS
Simulations of wave-particle interactions in stimulated Raman forward scattering in a magnetized plasma
[TKK-F-A704] p 1201 N94-15210
PLASMAS (PHYSICS)
PHENIX Conceptual Design Report
[DE93-015759] p 1182 N94-16161
Application of non-thermal plasmas to pollution control
[DE93-016432] p 1096 N94-16449
Numerical modeling of the temperature gradients and spectra of the plasma armature on Thunderbolt
[AD-A266414] p 878 N94-16552
Linear and non-linear studies of Alfven waves in space. Stationary and dynamic processes in magnetospheric plasmas
[NASA-CR-193585] p 1239 N94-16647
Elemental impurity analysis of mercuric iodide by ICP/MS
[DE93-015531] p 949 N94-16876
Hollow cathode heater development for the Space Station plasma contactor
[NASA-CR-191131] p 926 N94-16880
ARIES tokamak reactor study
[DE93-017059] p 1203 N94-16901
Plasma Science Committee (PLSC) and the Panel on Opportunities in Plasma Science and Technology (OPST)
[DE93-018142] p 1204 N94-16995
A state-of-the-art plasma polymerization coater for ICF targets
[DE93-016452] p 1204 N94-17237
High power steady state MPD thrusters
[AD-A267277] p 928 N94-17308
Plasma flow switch and foil implosion experiments on Pegasus 2
[DE93-016464] p 1013 N94-17318
Kinetic plasma processes occurring in the outer plasmasphere
[NASA-CR-193452] p 1300 N94-17524
Optimal pulse modulator design criteria for plasma source ion implanters
[DE93-016465] p 1205 N94-17645
3D and r,z particle simulations of heavy ion fusion beams
[DE93-013417] p 1205 N94-17670
PLASMASPHERE
Kinetic plasma processes occurring in the outer plasmasphere
[NASA-CR-193452] p 1300 N94-17524
PLASTIC DEFORMATION
Systematology for elastic-plastic material equations by large deformations on the basis of the Cosserat-continuum model
[SCHRIFTENR-PHYSIKAL-ING-BD] p 1058 N94-15642
Anisotropic damage mechanics modeling in metal matrix composites
[AD-A266328] p 934 N94-16440
Slip, twinning and transformation in Laves phases
[DE93-018164] p 960 N94-16972
Studies of changes in the energy stored in metals as a result of subjecting them to a surface type technological process
[IFTR-25/1991] p 960 N94-17063
Analysis of the strengthening of aluminum alloy undergoing plastic deformation under conditions of a compound state of stress
[IFTR-21/1991] p 960 N94-17093
PLASTIC PROPERTIES
Characterization of the cyclic plasticity of polycrystalline aluminum in the 90-300K domain: Use of the ultrasonic wave coupling technique - low frequency restraint
[ISAL-92-0083] p 954 N94-14930
Anisotropic damage mechanics modeling in metal matrix composites
[AD-A266328] p 934 N94-16440
Quantitative assessment of the accuracy of constitutive laws for plasticity with an emphasis on cyclic deformation
[AD-A267562] p 961 N94-17109
Solution of elastic-plastic stress analysis problems by the p-version of the finite element method
[NASA-CR-194267] p 1062 N94-17445
PLASTICS
Modelling of creep data for plastics
[NPL-DMM(A)-92] p 1057 N94-15017
Dry stripping as a surface treatment method
[VTT-TIED-1348] p 985 N94-17544
PLATEAUS
A mineralized zone in Western Candor Chasma, Mars
p 1248 N94-16179
PLATELETS
Evaluation of dried storage of platelets for transfusion: Physiologic integrity and hemostatic functionality
[AD-A266958] p 1120 N94-15180
PLATES (STRUCTURAL MEMBERS)
A posteriori error estimation for hierarchic models of elliptic boundary value problems on thin domains
[AD-A267714] p 1168 N94-14939
Stress analysis of laminated composites with preformed holes. Part 1: Single plies with embedded material discontinuities
[AD-A266524] p 936 N94-16795
PLATES (TECTONICS)
Tectonic deformation in southern California
[NASA-CR-194621] p 1101 N94-16021
Chemical differentiation, thermal evolution, and catastrophic overturn on Venus: Predictions and geologic observations p 1259 N94-16232
On the relationship between tectonic plates and thermal mantle plume morphology p 1104 N94-16349
PLATINUM
Experimental partitioning of Zr, Ti, and Nb between silicate liquid and a complex noble metal alloy and the partitioning of Ti between perovskite and platinum metal
p 962 N94-16287
PLETHYSMOGRAPHY
Validation of respiratory inductive plethysmography for measuring exercise tidal volumes
[AD-A266883] p 1119 N94-14923
Automated strain gauge plethysmograph
[AD-A267323] p 1035 N94-17002
PLUMES
The MADONA experiments (Meteorology and Diffusion Over Non-uniform Areas): High-resolution in-plume concentration fluctuations measurements using lidar remote sensing technique
[AD-A267711] p 1105 N94-14938
Rocket Motor Plume Technology
[AGARD-LS-188] p 923 N94-15217
Propulsion p 924 N94-15219
Nuclear rocket plume studies
[AD-A267154] p 925 N94-15837
Megaplumes on Venus p 1271 N94-16301
On the relationship between tectonic plates and thermal mantle plume morphology p 1104 N94-16349
Venusian pancake domes: Insights from terrestrial voluminous silicic lavas and thermal modeling
p 1286 N94-16381
The use of TIMS data to estimate the SO2 concentrations of volcanic plumes: A case study at Mount Etna, Sicily p 1065 N94-16608
High power steady state MPD thrusters
[AD-A267277] p 928 N94-17308
PLUTO (PLANET)
A Pluto thermal model p 1256 N94-16216
Mapping the stability region of the 3:2 Neptune-Pluto resonance p 1280 N94-16351
PLUTO ATMOSPHERE
A Pluto thermal model p 1256 N94-16216
POINT DEFECTS
Bulk and defect properties of ordered intermetallics: A first-principles total-energy investigation
[DE93-015492] p 959 N94-16873
POINT SPREAD FUNCTIONS
Measurements of microlens performance
p 1197 N94-17355
POINTING CONTROL SYSTEMS
Performance of the upgraded Orroral laser ranging system p 877 N94-15602
POISSON DENSITY FUNCTIONS
Poisson filtering of laser ranging data
p 917 N94-15593
POISSON EQUATION
Linear stability of stationary solutions of the Vlasov-Poisson system in three dimensions
[DE93-013873] p 1174 N94-16820
POLAR CAPS
Global auroral imaging: Dynamics of Explorer Miss ion
[NASA-CR-194284] p 1097 N94-15003
A Pluto thermal model p 1256 N94-16216
POLAR ORBITS
Small launchers (current and future projects in the world) p 878 N94-17137
POLAR REGIONS
Imaging radar studies of polar ice p 991 N94-15899
TOPSAT: Global space topographic mission
p 992 N94-15905
POLAR SUBSTORMS
A correlative comparison of geomagnetic storms and auroral substorms using geomagnetic indeces
[AD-A268081] p 1102 N94-17512
POLAR WANDERING (GEOLOGY)
Nontidal gravity changes observed with a superconducting gravimeter p 1100 N94-15808
POLARIMETERS
Ultraviolet spectrometer and polarimeter (UVSP) catalog of observations. Volume 1: Experiments 1-30719, February 1980 - April 1985
[NASA-CR-4529-VOL-1] p 1298 N94-15023
Ultraviolet spectrometer and polarimeter (UVSP) catalog of observations. Volume 2: Experiments 30720-63057, April 1985 - February 1988
[NASA-CR-4529-VOL-2] p 1298 N94-15024
Mass of Saturn's A ring p 1263 N94-16252
POLARIMETRY
Application of Cloude's target decomposition theorem to polarimetric imaging radar data p 991 N94-15901
Comparison of JPL-AIRSAR and DLR E-SAR images from the MAC Europe 1991 campaign over testsite Oberpfaffenhofen: Frequency and polarization dependent backscatter variations from agricultural fields
p 1075 N94-16733
Characterization of wetland, forest, and agricultural ecosystems in Belize with airborne radar (AIRSAR)
p 1076 N94-16738
Supervised fully polarimetric classification of the Black Forest test site: From MAESTROI to MAC Europe
p 1076 N94-16740
Processing of polarimetric SAR data for soil moisture estimation over Mahantango watershed area
p 1079 N94-16754
POLARIZATION (WAVES)
Multilayer thin film design for far ultraviolet polarizers using an induced transmission and absorption technique
[NASA-CR-194631] p 1190 N94-15869
POLARIZATION CHARACTERISTICS
Interaction types and their like-polarization phase-angle difference signatures p 1079 N94-16756
The influence of an electric field on the kinetics of nucleation
[IFTR-2/91] p 1213 N94-17046
POLARIZED LIGHT
Display system employing acousto-optic tunable filter
[NASA-CASE-NPO-18736-1-CU] p 1190 N94-15933
A test of the applicability of independent scattering to high albedo planetary regoliths p 1250 N94-16187
POLARIZED RADIATION
Current drive with free electron lasers in high and low temperature tokamaks p 1201 N94-15209
POLARIZERS
Multilayer thin film design for far ultraviolet polarizers using an induced transmission and absorption technique
[NASA-CR-194631] p 1190 N94-15869
Design and fabrication of a reflection far ultraviolet polarizer and retarder
[NASA-CR-194630] p 1191 N94-16023
POLARONS
New organic materials for nonlinear optics applications
[AD-A266451] p 1192 N94-16563
Lattice relaxation theory of localized excitations in quasi-one-dimensional systems
[DE93-624947] p 1215 N94-17437
POLICIES
Mission management aircraft operations manual
[NHB-7900.3] p 1225 N94-16729
Aircraft operations management manual
[NHB-7900.3(V1)] p 1225 N94-16730
Equipment Management Manual
[NHB-4200.1D] p 1225 N94-16799
The Megascience Forum
[DE93-014445] p 1303 N94-16804
Computer Science and Telecommunications Board activities
[DE93-018141] p 1000 N94-17000
Abstracts of manuscripts submitted in 1992 for publication
[AD-A267963] p 1113 N94-17383

POLISHING
Polished substrate surface and cleaning study for coated optic quality
[DE93-014116] p 1190 N94-15975
POLITICS
The strategic environmental research and development program: A new paradigm for space, the environment, and national security
[AD-A266222] p 1174 N94-16109
POLLUTION CONTROL
TABES 1993: 9th Annual Technical and Business Exhibition and Symposium p 1050 N94-16129
Emerging technologies for the changing global market
[TABES PAPER 93-612] p 930 N94-16144
Application of non-thermal plasmas to pollution control
[DE93-016432] p 1096 N94-16449
Biomass energy: State of the technology present obstacles and future potential
[DE93-016295] p 1092 N94-16766
The 11th annual report of accomplishments under the airport improvement program: Fiscal year 1992
[AD-A268328] p 865 N94-17458
POLLUTION MONITORING
New York MARKAL: An evaluation of carbon dioxide emission control strategies in New York State
[DE93-013149] p 1095 N94-15999
Statement on global climate change before the Subcommittee on Energy and Power, United States House of Representatives
[DE93-013163] p 1095 N94-16006
Utility emissions associated with electric and hybrid vehicle (EHV) charging
[DE93-013734] p 1011 N94-16459
POLYACRYLONITRILE
Characterization of the lithium/pan-based polymer electrolytes interface
[AD-A268401] p 973 N94-17434
POLYATOMIC MOLECULES
Geochemistry and cosmochemistry of fullerenes 3: Reaction of C60 and C70 with ozone
p 953 N94-16243
Spectroscopic investigations of nonambient systems with millimeter and submillimeter probes
[AD-A266537] p 968 N94-16796
POLYCARBONATES
Optical studies of glasses embedded with inorganic ions and organic dyes
[AD-A268146] p 1199 N94-17455
POLYCRYSTALS
Ternary alloying effects in polycrystalline (beta)-NiAl
[DE93-012675] p 955 N94-15885
Powder diffraction studies using anomalous dispersion
[DE93-012531] p 1210 N94-16775
POLYETHYLENES
Thin composite solid electrolyte film for lithium batteries
[NASA-CASE-NPO-18694-1-CU] p 1014 N94-17325
POLYIMIDES
Structures from low dielectric polyimides
[NASA-CASE-LAR-14988-1] p 965 N94-15880
Improved composite flexible blanket insulation
[NASA-CASE-ARC-11955-1-CU] p 934 N94-15926
Photodegradation of polyimides. V1: Effect of donor-acceptor groups on the photooxidative stability of polyimides and model compounds
[AD-A267319] p 970 N94-16947
Low dielectric polyimides
[NASA-CASE-LAR-14987-2] p 974 N94-17559
POLYMER BLENDS
Polymer Infiltration Studies
[NASA-CR-194494] p 932 N94-15275
Cyanoresin, cyanoresin/cellulose triacetate blends for thin film, dielectric capacitors
[NASA-CASE-NPO-18913-1-CU] p 966 N94-15930
POLYMER CHEMISTRY
Intramolecular versus intermolecular condensation rates in the acidic polymerization of octaethoxytrisiloxane
[AD-A266982] p 963 N94-15490
Electrical conductivity of ion implanted ladder and semi-ladder polymers
[AD-A267432] p 970 N94-16978
Soluble precursor route to polyanilines
[AD-A268015] p 973 N94-17494
POLYMER MATRIX COMPOSITES
Prediction of thermal cycling induced cracking in polymer matrix composites
[NASA-CR-194677] p 941 N94-17295
POLYMERIC FILMS
Organic polymeric electro-optic materials: Synthesis, processing, and device applications
[AD-A267133] p 964 N94-15688
Photochemistry in thin polymeric films
[AD-A266716] p 964 N94-15729
The effect of process parameters on the surface finish of plasma polymers
[DE93-014112] p 966 N94-15924
Improved composite flexible blanket insulation
[NASA-CASE-ARC-11955-1-CU] p 934 N94-15926
Cyanoresin, cyanoresin/cellulose triacetate blends for thin film, dielectric capacitors
[NASA-CASE-NPO-18913-1-CU] p 966 N94-15930
Synthesis of novel electrically conducting polymers: Potential conducting Langmuir-Blodgett films and conducting polymers on defined surfaces
[NASA-CR-194651] p 972 N94-17297
POLYMERIZATION
Intramolecular versus intermolecular condensation rates in the acidic polymerization of octaethoxytrisiloxane
[AD-A266982] p 963 N94-15490
Analysis of leading edge and trailing edge cover glass samples before and after treatment with advanced satellite contamination removal techniques
[AD-A267055] p 885 N94-15666
Thermochemistry of silicate speciation in aqueous sodium silicate solutions: Ionization and polymerization of small silicate ion
[AD-A266825] p 964 N94-15683
Photochemistry in thin polymeric films
[AD-A266716] p 964 N94-15729
Effects of aging time on V205 sol-gel coatings
[AD-A266824] p 965 N94-15843
Structures from low dielectric polyimides
[NASA-CASE-LAR-14988-1] p 965 N94-15880
Use of microgravity in the synthesis of ceramics using sol gel techniques p 979 N94-16088
Interpenetrating polymer network acoustic damping material
[AD-D015889] p 969 N94-16916
Synthetic and mechanistic investigation of olefin polymerization catalyzed by early transition metal compounds
[DE93-018301] p 970 N94-16963
A state-of-the-art plasma polymerization coater for ICF targets
[DE93-016452] p 1204 N94-17237
Synthesis, characterization, and polymerization of new ferrocene-fluorene complexes. A novel high-molecular weight conjugated polymer with pendant ferrocene groups
[AD-A267717] p 972 N94-17273
Soluble precursor route to polyanilines
[AD-A268015] p 973 N94-17494
POLYMERS
Detection and dosimetry of chemical contaminants in polymeric materials
[AD-A266605] p 968 N94-16727
Main chain chromophoric polymers with second order nonlinear optical properties
[AD-D015893] p 969 N94-16920
Electrical conductivity of ion implanted ladder and semi-ladder polymers
[AD-A267432] p 970 N94-16978
SURPHEX (tm): New dry photopolymers for replication of surface relief diffractive optics p 1198 N94-17358
POLYMETHYL METHACRYLATE
Progress in the modeling of the shock response and mitigation of thick composite shells
[AD-A267009] p 1057 N94-15524
Contained liquids in microgravity, part 2
p 979 N94-16085
Phase holograms in PMMA with proximity effect correction p 1037 N94-17348
POLYMORPHISM
C++ as a language for object-oriented numerics
[DE93-015027] p 1148 N94-15985
POLYNOMIALS
Adaptive wavelet collocation methods for initial value boundary problems of nonlinear PDE's
[NASA-CR-191507] p 1169 N94-15833
Reductions to sets of low information content
[TR-417] p 1150 N94-16579
Fast algorithms for polynomial interpolation, integration and differentiation
[AD-A267505] p 1154 N94-17370
POLYPHENYLS
The photochemistry of poly(methylphenylphosphazene)
[AD-A267320] p 970 N94-16948
POLYSTYRENE
Soluble precursor route to polyanilines
[AD-A268015] p 973 N94-17494
POLYSULFIDES
Flight 20 (STS-45) polysulfide gas path investigation
[NASA-CR-193861] p 928 N94-17213
POLYTETRAFLUOROETHYLENE
Wide angle, single screen, gridded square-loop frequency selective surface for diplexing two closely separated frequency bands
[NASA-CASE-NPO-18664-1-CU] p 1237 N94-17438
POLYURETHANE RESINS
Photodegradation of MDI based polyurethane/urea elastomers
[AD-A267308] p 971 N94-16994
POLYVINYL CHLORIDE
A model for non-linear creep and physical ageing in PVC
[NPL-DMM(A)-91] p 1057 N94-15016
A study of relaxation transitions in the polymers under the influence of magnetic fields
[AD-A263878] p 963 N94-15133
POPULATION INVERSION
X ray laser program
[AD-A267075] p 1038 N94-15628
POPULATIONS
Development of pattern recognition techniques for the evaluation of toxicant impacts to multispecies systems
[AD-A267197] p 1095 N94-15790
Confirmation of saturation equilibrium conditions in crater populations p 1103 N94-16222
Resolving LDEF's flux distribution: Orbital (debris?) and natural meteoroid populations p 1245 N94-16391
Biofilm structure and diversity
[AD-A267254] p 1118 N94-16989
POROSITY
Structural investigation of electrochemically etched silicon
[DE93-015300] p 1207 N94-15827
Gas separations using ceramic membranes
[DE93-000278] p 947 N94-15861
Selective formation of porous silicon
[NASA-CASE-NPO-18735-1-CU] p 966 N94-15960
Mechanical properties of magnesium ammonium phosphate cements and their zeolite composites
[DE93-015155] p 934 N94-16057
The cooling rates of pahoehoe flows: The importance of lava porosity p 1103 N94-16282
Superconducting ceramics: Selected properties and methods of production
[IFTR-23/1991] p 969 N94-16924
Investigation of the effects of polyelectrolyte coatings on colloid transport in porous media
[DE93-018300] p 970 N94-16973
Influence of the loading rate on the endurance and deformability of cement matrix composites
[IFTR-1/1992] p 1060 N94-17052
Micromechanics modeling and analysis of Haversian compact bone tissues as a fiber reinforced composite material
[AD-A268250] p 1129 N94-17456
X ray computed tomography for casting demonstration
[AD-A268084] p 1056 N94-17596
POROUS MATERIALS
Structural investigation of electrochemically etched silicon
[DE93-015300] p 1207 N94-15827
Structural studies of sol-gel glasses
[AD-A266277] p 967 N94-16472
Porous silicon for pumping solid-state lasers
[AD-A266293] p 1039 N94-16474
Operator overloading as an enabling technology for automatic differentiation
[DE93-012899] p 1170 N94-16778
Investigation of the effects of polyelectrolyte coatings on colloid transport in porous media
[DE93-018300] p 970 N94-16973
Buried porous silicon-germanium layers in monocrystalline silicon lattices and method of producing
[NASA-CASE-NPO-18836-1-CU] p 1215 N94-17327
PORTABLE EQUIPMENT
Experience and results of the 1991 MTLRS-1 USSR campaign p 914 N94-15575
Experience with disconnected operation in a mobile computing environment
[AD-A267524] p 1141 N94-17115
MAGSS-14: Medium Altitude Global Mobile Satellite System with enhanced regional coverage
p 893 N94-17164
POSEIDON SATELLITE
Analysis of TOPEX laser retroreflector array characteristics p 915 N94-15578
POSITION (LOCATION)
Satellite sound broadcast propagation measurements
p 996 N94-16047
POSITION (TITLE)
The Senior Executive Service
[NHB-3100.6] p 1224 N94-15945
POSITION ERRORS
Laser ranging data analysis
[NASA-CR-193547] p 1041 N94-16719
Category (CAT) 3B level 1 test plan for Global Positioning System (GPS)
[DOT/FAA/RD-93/21] p 864 N94-16835
POSITION INDICATORS
Double-driven shield capacitive type proximity sensor
[NASA-CASE-GSC-13541-1] p 1165 N94-15946

Evaluation of site effects on a high frequency direction finding single site location system
[AD-A267465] p 1001 N94-17035

POSITION SENSING
Rotary encoding device
[NASA-CASE-GSC-13543-1] p 1189 N94-15705
Capacifiector camera
[NASA-CASE-GSC-13564-1] p 1033 N94-15872
Double-driven shield capacitive type proximity sensor
[NASA-CASE-GSC-13541-1] p 1165 N94-15946

POSITIONING
Wide-area Differential Global Positioning System (WDGPS)/Wide-area Integrity Broadcast (WIB) alternatives analysis
[DOT/FAA/SE-93/3] p 864 N94-16906
Radiocommunication problems of a position reporting and bidirectional messagery system using VHF/UHF with low-Earth orbit satellites p 889 N94-17136
Adequation of mini satellites to oceanic altimetry missions p 891 N94-17152
The ORBCOMM system p 893 N94-17163

POSITIVE IONS
Investigation of the effects of polyelectrolyte coatings on colloid transport in porous media
[DE93-018300] p 970 N94-16973

POSITRONS
Experimental study of weak interactions by precision measurement by rare kaon decay
[DE93-016864] p 1182 N94-16117

POSTFLIGHT ANALYSIS
Long duration exposure facility experiment m0003 deintegration observation database
[AD-A267579] p 951 N94-17207
Postflight hardware evaluation 360T026 (RSRM-26, STS-47)
[NASA-CR-192559] p 882 N94-17656

POTASSIUM ISOTOPES
Potassium isotope cosmochemistry, volatile depletion and the origin of the Earth p 953 N94-16259

POTENTIAL ENERGY
Molecular processes in comets
[NASA-CR-194148] p 1239 N94-15188
Impending motion direction of contacting rigid bodies
[AD-A266814] p 1164 N94-15756
A molecular dynamics simulator for optimal control of molecular motion
[AD-A266572] p 1183 N94-16722

POTENTIAL FIELDS
Energy potential analysis of zero velocity curves in the restricted three-body problem
[AD-A267512] p 1170 N94-17076
Path planning for robotic truss assembly
[NASA-CR-194652] p 897 N94-17280

POTENTIAL FLOW
Modal element method for potential flow in non-uniform ducts: Combining closed form analysis with CFD
[NASA-TM-106347] p 1169 N94-15799

POWDER (PARTICLES)
Polymer Infiltration Studies
[NASA-CR-194494] p 932 N94-15275
Synthesis of ceramic oxide powders in a microwave plasma device
[DE93-012741] p 965 N94-15920
The physical mechanism of comet outbursts: An experiment p 1242 N94-16221
Comparison of reflectance spectra of C asteroids and unique C chondrites Y86720, Y82162, and B7904 p 1242 N94-16246
Powder diffraction studies using anomalous dispersion
[DE93-012531] p 1210 N94-16775
Characterization of nanoscale oxide and oxyhydroxide powders using EXAFS spectroscopy
[DE93-015683] p 940 N94-17235

POWDER METALLURGY
Army P/M research and development overview
[AD-A266921] p 954 N94-15104
The effect of oxygen, grain size, and strain rate on the mechanical behavior of forged P/M tantalum
[DE93-011251] p 959 N94-16764

POWER CONDITIONING
Overview of the solar dynamic ground test demonstration program
[NASA-TM-106296] p 928 N94-17256

POWER CONVERTERS
SPDE/SPRE final summary report
[NASA-CR-187066] p 924 N94-15482
Forback DC-to-DC converter
[NASA-CASE-GSC-13404-1] p 1010 N94-15874
Overview of the solar dynamic ground test demonstration program
[NASA-TM-106296] p 928 N94-17256

POWER GAIN
Windshear radar calibration, 1992 flights: Transmitter power and receiver gain stability
[NASA-TM-108997] p 986 N94-15140
Sodium-mercury excimer laser, phase 1
[AD-A267728] p 1042 N94-17230

POWER LINES
Operation of digital systems in severe electromagnetic environments
[AD-A267176] p 988 N94-15693

POWER SERIES
Confirmation of saturation equilibrium conditions in crater populations p 1103 N94-16222

POWER SPECTRA
Segmenting textured 3D surfaces using the space/frequency representation
[AD-A266960] p 1163 N94-14968

POWER SUPPLY CIRCUITS
Circle diagram approach for self excited induction generators
[DE93-010031] p 1010 N94-15971
A power system for a microsatellite p 895 N94-17176
Smart Power: New power integrated circuit technologies and their applications
[VTT-TIED-1358] p 1015 N94-17546

POWERED LIFT AIRCRAFT
The lift-fan powered-lift aircraft concept: Lessons learned
[NASA-CR-177616] p 866 N94-15718

PRASEODYMIUM
Local environment about O atoms in Pr-Y-Ba-Cu-O films studied by O K-edge XAFS
[DE93-016218] p 1209 N94-16447

PREAMPLIFIERS
Discrete CMT infrared detectors for space application, from ISSR to second generation Meteosat and MIPAS p 905 N94-15065

PRECAMBRIAN PERIOD
Assimilation of solids during ascent of magmas from the Bartoy Field of the Baikal Region, Siberia p 1103 N94-16214
Tidal regime of intact planetoid capture model for the Earth-Moon system: Does it relate to the archean sedimentary rock record? p 1245 N94-16378

PRECESSION
State-of-the-art satellite laser range modeling for geodetic and oceanographic applications p 916 N94-15586

PRECIPITATES
Effects of processing and prolonged high temperature exposure on the microstructure of Nb-1Zr-C sheet
[NASA-TM-106370] p 959 N94-16883

PRECIPITATION (METEOROLOGY)
The standardized precipitation index and its use in the western contiguous United States
[AD-A267547] p 1107 N94-17102
Phillips Laboratory global spectral numerical weather prediction model
[AD-A267293] p 1107 N94-17244

PRECIPITATION HARDENING
Ternary alloying effects in polycrystalline (beta)-NiAl
[DE93-012675] p 955 N94-15885

PRECISION
The precision of today's satellite laser ranging systems p 912 N94-15559

PRECONDITIONING
On solving the compressible Navier-Stokes equations for unsteady flows at very low Mach numbers
[NASA-TM-106380] p 1027 N94-17128

PREDICTION ANALYSIS TECHNIQUES
On the accuracy of ERS-1 orbit predictions p 874 N94-15589
Compensation for the distortion in satellite laser range predictions due to varying pulse travel times p 917 N94-15590
Incorporation of boundary layer heating predictive methodology into NSWCDD aeroprediction code
[AD-A267000] p 1020 N94-15632
Multiaxial deformation and life prediction model and experimental data for advanced silicon nitride ceramics
[DE93-015450] p 967 N94-16067
A fuzzy method for preliminary design random access memory failure rate prediction
[AD-A267948] p 1055 N94-17044

PREDICTIONS
Predicted and real development in the aviation in the period 1961-1991 p 853 N94-15122
On predicting the person-in-water drift for search and rescue
[AD-A268083] p 1055 N94-17514

PREFORMS
Verification of a two-dimensional infiltration model for the resin transfer molding process
[NASA-CR-194597] p 964 N94-15656
An overview of the NASA textile composites program p 937 N94-16846
Design and cost drivers in 2-D braiding p 937 N94-16849
Weaving multi-layer fabrics for reinforcement of engineering components p 937 N94-16850
Textile composite processing science p 938 N94-16856

PRELAUNCH SUMMARIES
Galileo probe spacecraft mission to Jupiter
[NASA-TM-109646] p 1247 N94-16070

PREMIXED FLAMES
Mechanisms of combustion limits in premixed gas flames at microgravity
[NASA-CR-194557] p 946 N94-15713
A comparison of one and two dimensional flame quenching: Heat transfer results
[DE93-015196] p 947 N94-16060
Studies of premixed laminar and turbulent flames at microgravity
[NASA-CR-194656] p 951 N94-17125

PREMIXING
Mechanisms of combustion limits in premixed gas flames at microgravity
[NASA-CR-194557] p 946 N94-15713

PREPARATION
Food for space
[NASA-TM-109668] p 1136 N94-15435

PREPOLYMERS
Preparation of homogeneous aluminosilicate gels by sol/gel techniques
[AD-A266823] p 962 N94-14914

PREPREGS
Machine development p 932 N94-15258
Polymer Infiltration Studies
[NASA-CR-194494] p 932 N94-15275
A new NASA LaRC Multi-Purpose Prepregging Unit p 932 N94-15276

PREPROCESSING
Adaptive median filtering for preprocessing of time series measurements p 912 N94-15561
Application of the robust estimate in SLR data preprocessing p 918 N94-15597
Data acquisition, preprocessing and analysis for the Virginia Tech OLYMPUS experiment p 995 N94-16038

PRESSURE
Hypersonic shock wave boundary layer interactions over simplified deflected control surface configurations p 1018 N94-15203
First results from a laboratory facility for measurement of emission spectra under simulated planetary conditions p 954 N94-16372

PRESSURE BROADENING
The pressure broadening of HDO by O2, N2, H2, and He between 100 K and 600 K
[AD-A267118] p 946 N94-15684

PRESSURE CHAMBERS
Simulation of collisional fragmentation with explosives p 1063 N94-16254

PRESSURE DEPENDENCE
Orientation of Planar Deformation Features (PDFs) in quartz p 1219 N94-16341

PRESSURE DISTRIBUTION
Laser Doppler velocimetry measurements across a normal shock in transonic flow
[AD-A267240] p 855 N94-14973
Wind tunnel investigation of three axisymmetric cowls of different lengths at Mach numbers from 0.60 to 0.92
[NASA-TM-4488] p 856 N94-15681

PRESSURE EFFECTS
Temperature and pressure effects on capacitance probe cryogenic liquid level measurement accuracy
[NASA-CR-190763] p 1034 N94-16521
Structural phase transition and superconductivity in La(2-x)Ba(x)CuO4
[DE93-015812] p 1212 N94-16868

PRESSURE GAGES
Determination of equivalent circuit for PVDF shock-pressure gauges
[DE93-016492] p 1034 N94-16452

PRESSURE GRADIENTS
Orographic microbursts in a severe winter windstorm
[AD-A267651] p 1108 N94-17247

PRESSURE HEADS
Evaluation of a distributed catchment scale water balance model
[PAPER-93WR00398] p 1083 N94-16031

PRESSURE MEASUREMENT
Measurements of Interfacial Tension: MITE p 943 N94-15158
Pressures of supercritical salt solutions p 945 N94-15166
Mechanical and surface force nanoprobe
[AD-D015792] p 1034 N94-16536
An experimental investigation of the effects of leading edge geometry on the dynamics of blunt fin-induced shock wave turbulent boundary layer interaction
[AD-A267656] p 860 N94-17221

Experimental study of vortex and aerodynamic characteristics of stack wings with sideslip
[AD-A267722] p 860 N94-17274
An experimental study of fluctuating wall pressures in a highly swept, sharp fin-induced, Mach 5 shock wave/turbulent boundary layer interaction
[AD-A268394] p 861 N94-17461

PRESSURE PULSES
Acousto-optical confirmation of the localized wave phenomena
[DE93-016425] p 1177 N94-16448

PRESSURE REDUCTION
Effects of rotation on coolant passage heat transfer. Volume 2: Coolant passages with trips normal and skewed to the flow
[NASA-CR-4396-VOL-2] p 1023 N94-15991

PRESSURE SUITS
Aircrew/groundcrew life support systems research. Volume 1: CLIN 0001 research requirements
[AD-A268229] p 1139 N94-17563
Aircrew/groundcrew life support systems research. Volume 2: CLIN 0002 task order requirements
[AD-A268230] p 1139 N94-17564

PRESSURE VESSELS
Design of a cruciform bend specimen for determination of out-of-plane biaxial tensile stress effects on fracture toughness for shallow cracks
[DE93-015455] p 1059 N94-16104
Design of a fluid elastic actuator with application to structure control
[AD-A267649] p 897 N94-17246

PRETREATMENT
Assessment of chromate and non-chromate conversion coatings for Al alloys using electrochemical impedance spectroscopy
[AD-A267205] p 965 N94-15859
Wound healing after laser injury to skin: The effect of occlusion and vitamin E
[AD-A266473] p 1128 N94-16779

PREVENTION
Legionella: An overview p 1126 N94-16629

PRIMITIVE EARTH ATMOSPHERE
Earth's partial pressure of CO2 over the past 100-500 Ma; evidence from Ce anomalies in mostly shallow seas (less than 200 m) as recorded in carbonate sediments, 2 p 1104 N94-16360

PRIORITIES
Chairmanship of the Neptune/Pluto outer planets science working group
[NASA-CR-194625] p 1297 N94-16832

PRISMS
Three short articles from Japanese laser journal
[AD-A268249] p 1042 N94-17415

PRIVACY
NASA security handbook
[NHB-1620.3C] p 1224 N94-15937

PROBABILITY DENSITY FUNCTIONS
A new method for generating Bayes classifiers assuming mixtures of Gaussian densities
[FFI-91/4029] p 1172 N94-15298
On the use of the noncentral chi-square density function for the distribution of helicopter spectral estimates
[NASA-CR-191546] p 1176 N94-15487
Expansions of cumulative distribution functions directly from characteristic functions
[AD-A267727] p 1173 N94-17372

PROBABILITY DISTRIBUTION FUNCTIONS
The distribution of a sum of binomial random variables
[AD-A266969] p 1172 N94-15002
Expansions of cumulative distribution functions directly from characteristic functions
[AD-A267727] p 1173 N94-17372

PROBABILITY THEORY
Statistical computation of tolerance limits
[NASA-TM-108424] p 1172 N94-15535
Logarithmic asymptotics for steady-state tail probabilities in a single-server queue
[AD-A266746] p 1165 N94-15775
The cooling of confined ions driven by laser beams
[DE93-016612] p 1039 N94-16114
Combinatorial semantics
[TR-444] p 1149 N94-16575
Set-based Bayesianism
[TR-407] p 1170 N94-16582
Discovering sequence similarity by the algorithmic significance method
[DE93-015556] p 1150 N94-16659
Nonlinear methods for communications
[AD-A267376] p 1001 N94-17019
Statistics of the half-integer stopband
[DE93-016101] p 1173 N94-17236
High order nonlinear estimation with signal processing applications
[AD-A268407] p 1005 N94-17463
Mathematical Sciences Division 1992 programs
[AD-A268586] p 1140 N94-17623

PROBLEM SOLVING
HSTS: Integrating planning and scheduling
[AD-A266991] p 1222 N94-15213
Representation in incremental learning
[NASA-CR-194595] p 1221 N94-15719
Module interconnection frameworks for a real-time spreadsheet
[AD-A267317] p 1153 N94-17220
Design and diagnosis problem solving with multifunctional technical knowledge bases
[AD-A268375] p 1234 N94-17419

PROCEDURES
A TRALINET guide to the Internet
[AD-A266946] p 1229 N94-15178

PROCESS CONTROL (INDUSTRY)
Contribution to the elaboration of some adaptive control algorithms for fermentation processes monitoring
[LAAS-92513] p 1116 N94-15643
A software process framework for the SEI capability maturity model: Repeatable level
[AD-A268059] p 1157 N94-17588

PROCUREMENT
Software reliability management through metrics
[AD-A267129] p 1146 N94-15687
CALS test network handbook
[AD-A267587] p 1160 N94-17209

PROCUREMENT MANAGEMENT
Facilities maintenance handbook
[NHB-8831.2] p 1224 N94-15934
NASA information resources management handbook
[NHB-2410.1E] p 1230 N94-15941
Equipment Management Manual
[NHB-4200.1D] p 1225 N94-16799
Materials inventory management manual
[NHB-4100.1C] p 1225 N94-16830

PROCUREMENT POLICY
Equipment management user's handbook for property custodians
[NHB-4200.2A] p 1224 N94-15957

PRODUCT DEVELOPMENT
Production Technology for Components from Nonmetallic Fiber Reinforced Materials
[ETN-93-94607] p 931 N94-15254
Production process p 931 N94-15257
Prioritization methodology for chemical replacement
[NASA-TP-3421] p 976 N94-15723
Research and development: Engine of innovation at Krupp p 984 N94-16001
Government/contractor development teams
[TABES PAPER 93-460] p 1050 N94-16134
Status of molten carbonate fuel cell technology development
[DE93-015666] p 1092 N94-16715
Small satellite product assurance p 896 N94-17188
Key trends of the small satellite market p 897 N94-17191
X ray computed tomography for failure analysis investigations
[AD-A268086] p 1055 N94-17515
The development of flexible software for the Italian/Dutch satellite SAX: Advantages and disadvantages of the use of CASE tools
[NLR-TP-91288-U] p 1157 N94-17626

PRODUCTION COSTS
Production process p 931 N94-15257
Development of a computer supported instrumentation for economic planning and evaluation of production facilities for fiber reinforced composites elements p 932 N94-15260
Conflict Resolution (CORE) for software quality factors
[AD-A267248] p 1151 N94-16941

PRODUCTION ENGINEERING
Government/contractor development teams
[TABES PAPER 93-460] p 1050 N94-16134
Design of a formaldehyde photodissociation process for carbon and oxygen isotope separation
[DE93-016435] p 1039 N94-16450

PRODUCTION PLANNING
Production Technology for Components from Nonmetallic Fiber Reinforced Materials
[ETN-93-94607] p 931 N94-15254
Development of a computer supported instrumentation for economic planning and evaluation of production facilities for fiber reinforced composites elements p 932 N94-15260

PRODUCTIVITY
PET team
[NASA-TM-109599] p 1223 N94-15293
The Langley Fitness Center p 1126 N94-16635
Evaluation of spatial productivity patterns in an annual grassland during an AVIRIS overflight
[CIW-PUBL-1134] p 1067 N94-16672

PROGRAM VERIFICATION (COMPUTERS)
Army Software Test and Evaluation Panel (STEP) software metrics initiatives report
[AD-A266889] p 1142 N94-14924
Lecture notes on engineering measurement for software engineers
[AD-A266959] p 1142 N94-14967
Evaluation of ALSYS 037 Ada Compiler
[AD-A266972] p 1143 N94-15110
Safety-critical software: Status report and annotated bibliography
[AD-A266993] p 1144 N94-15214
Concepts on measuring the benefits of software process improvements
[AD-A266994] p 1144 N94-15215
An expert system shell for inferring vegetation characteristics: Atmospheric techniques (Task G)
[NASA-CR-194570] p 1082 N94-15531
An elementary tutorial on formal specification and verification using PVS
[NASA-TM-108991] p 1158 N94-15536
Process-centered development environments: An exploration of issues
[AD-A266997] p 1145 N94-15630
Integrated trusted systems development environment
[AD-A267029] p 1146 N94-15674
Mechanistic models of soot formation
[AD-A267806] p 950 N94-17008
Effects of inspection error on optimal inspection policies and software fault detection models
[AD-A267511] p 1153 N94-17075
Progress in computational unsteady aerodynamics
[NASA-CR-177630] p 860 N94-17081
Causality-preserving timestamps in distributed programs
[AD-A267534] p 1153 N94-17118
Establishing a software measurement process
[AD-A267896] p 1154 N94-17396
A protocol validator for the SCM and CFSM models
[AD-A268523] p 1156 N94-17541

PROGRAMMERS
Process-centered development environments: An exploration of issues
[AD-A266997] p 1145 N94-15630
ACE: Lessons learned, volume 1
[AD-A267979] p 1155 N94-17411

PROGRAMMING ENVIRONMENTS
Open environments to support systems engineering tool integration: A study using the Portable Common Tool Environment (PCTE)
[NASA-TM-4489] p 1144 N94-15486
Visual parallel programming with determinacy: A language specification, an analysis technique, and a programming tool
[AD-A267560] p 1153 N94-17107
Process evolution for the MARVEL environment
[AD-A267813] p 1155 N94-17398
Concurrency control in rule-based software development environments
[AD-A267829] p 1155 N94-17404
Language-based document processing
[INRIA-RR-1731] p 1234 N94-17529

PROGRAMMING LANGUAGES
VDM specification of the MD4 message digest algorithm
[NPL-DITC-204/92] p 1142 N94-14944
A CENTAUR tutorial
[INRIA-RT-140] p 1142 N94-14978
The CAML numbers reference manual
[INRIA-RT-141] p 1142 N94-14979
Applicability of the session and the presentation layers for the support of high speed applications
[INRIA-RT-144] p 1158 N94-14980
The use of formal methods in data security standards
[NPL-DITC-205/92] p 1142 N94-15008
RAISE specification of the MD4 message digest algorithm
[NPL-DITC-206/92] p 1142 N94-15010
The application of programming languages to the production of reference implementations
[NPL-DITC-209/92] p 1143 N94-15012
Testability of data security standards
[NPL-DITC-217/93] p 1143 N94-15022
ACM SIGPLAN Workshop on ML and Its Applications
[AD-A266617] p 1147 N94-15725
Models for reactivity
[AD-A266419] p 1149 N94-16554
Monads and comonads in intensional semantics
[AD-A266522] p 1151 N94-16790
Design and implementation of an object-oriented interface for the multi-model/multi-lingual database system
[AD-A267413] p 1232 N94-16977
Sequential functions on indexed domains and full abstraction for a sub-language of PCF
[AD-A267838] p 1152 N94-17009
Networked workstations and parallel processing utilizing functional languages
[AD-A267464] p 1160 N94-17034

Visual parallel programming with determinacy: A language specification, an analysis technique, and a programming tool
[AD-A267560] p 1153 N94-17107
Automatic translation of database integrity constraints into compensating production rules
[REPT-92-055] p 1234 N94-17502
Language-based document processing
[INRIA-RR-1731] p 1234 N94-17529

PROJECT MANAGEMENT
Cohen program management briefing
[NASA-TM-109536] p 1223 N94-15367
An analysis of SEI software process assessment results: 1987-1991
[AD-A266996] p 1145 N94-15629
Creating and maintaining a visionary quality program
[DE93-015122] p 1050 N94-16055
Scientific use of Space Station Freedom
p 977 N94-16072
Design Quality Task Force survey comments
[AD-A266283] p 1225 N94-16473
Physical fitness and health education program at NASA Headquarters p 1126 N94-16631
Chairmanship of the Neptune/Pluto outer planets science working group
[NASA-CR-194625] p 1297 N94-16832
Cost drivers: Why do conventional satellites cost so much? p 897 N94-17190
An object-oriented dynamic software process model
[AD-A267726] p 1154 N94-17371
Software Capability Evaluation (SCE) version 1.5 method description. Software capability evaluation project
[AD-A267895] p 1154 N94-17395
Establishing a software measurement process
[AD-A267896] p 1154 N94-17396

PROJECT PLANNING
Information Technology Resources Assessment
[DE93-013899] p 1230 N94-16010
Creating and maintaining a visionary quality program
[DE93-015122] p 1050 N94-16055

PROJECT SETI
Search for Extraterrestrial Intelligence (SETI)
p 1125 N94-16620
Efficient computational methods to study new and innovative signal detection techniques in SETI
[NASA-CR-193602] p 998 N94-16649

PROJECTILES
An electronic imaging system for the Aeroballistic Research Facility
[AD-A267157] p 1033 N94-15826
The physical mechanism of comet outbursts: An experiment p 1242 N94-16221

PROJECTORS
Display of dynamic, volume graphic images by holographic voxel projection: Initial investigation
[AD-A267622] p 1035 N94-17197

PROLATENESS
Anisotropic phase separation in amorphous Fe-Ge alloys
[DE93-015255] p 961 N94-17251

PROP-FAN TECHNOLOGY
Back to propellers
[NASA-TM-109445] p 869 N94-15344
The 1982 highlights
[NASA-TM-109671] p 1303 N94-15508

PROPELLANT ADDITIVES
Damage evolution in filled elastomers
[AD-A268067] p 1062 N94-17507

PROPELLANT CHEMISTRY
Spectral studies of solid propellant combustion 4: Absorption and burn rate results for M43, XM39, and M10 propellants
[AD-A267119] p 946 N94-15685
Space Shuttle solid rocket motor exposure monitoring
p 976 N94-16624

PROPELLANT SENSITIVITY
Densifying and stabilizing ingredient
[AD-D015751] p 975 N94-16934

PROPELLANT SPRAYS
Computational analysis of Variable Thrust Engine (VTE) performance
[NASA-CR-193852] p 928 N94-17442

PROPELLANT TANKS
Power Reactant Storage Assembly (PRSA) (Space Shuttle). PRSA hydrogen and oxygen OVT tank refurbishment
[NASA-CR-188262] p 926 N94-16922

PROPELLANT TESTS
Supersonic Combustion Research Laboratory. Volume 1: Design and fabrication
[AD-A267667] p 943 N94-14962

PROPELLANTS
Densifying and stabilizing ingredient
[AD-D015751] p 975 N94-16934

PROPELLER BLADES
Cruise noise measurements of a scale model advanced ducted propulsor
[NASA-TM-105808] p 1176 N94-15115

PROPELLER FANS
Back to propellers
[NASA-TM-109445] p 869 N94-15344
The 1982 highlights
[NASA-TM-109671] p 1303 N94-15508

PROPELLER NOISE
Cruise noise measurements of a scale model advanced ducted propulsor
[NASA-TM-105808] p 1176 N94-15115

PROPELLERS
Cruise noise measurements of a scale model advanced ducted propulsor
[NASA-TM-105808] p 1176 N94-15115

PROPORTIONAL CONTROL
Real-time implementation of neural network learning control of a flexible space manipulator
[AD-A266962] p 1045 N94-14970
Optimal tuning of heavy equipment motion controllers
[AD-A267873] p 1167 N94-17392

PROPORTIONAL COUNTERS
The imaging microstrip proportional counter: Features of a practical design p 900 N94-15030
The high pressure gas scintillation proportional counter for SAX p 906 N94-15076
Performance of the position-sensitive proportional counters of the Yohkoh Bragg crystal spectrometer
p 909 N94-15094
The formation process of the He I lambda 10830 line in cool giant stars
[NASA-CR-194648] p 1240 N94-17094
Monte Carlo simulation of the microstrip gas counter
[NIKHEF-H/93-07] p 1035 N94-17619

PROPULSION
Propulsion p 924 N94-15219

PROPULSION SYSTEM CONFIGURATIONS
NASA Operational Environment Team (NOET): NASA's key to environmental technology
[TABES PAPER 93-611] p 1052 N94-16143
Emerging technologies for the changing global market
[TABES PAPER 93-612] p 930 N94-16144
Space Propulsion Synergy Group ETO technology assessments
[TABES PAPER 93-641] p 929 N94-16149
Lunar lander and return propulsion system trade study
[NASA-TP-3388] p 925 N94-16496
Advanced transportation system studies technical area 3: Alternate propulsion subsystem concepts, volume 2
[NASA-CR-193863] p 927 N94-17096
Advanced transportation system studies technical area 3: Alternate propulsion subsystem concepts, volume 3
[NASA-CR-193864] p 927 N94-17097
Advanced transportation system studies technical area 3: Alternate propulsion system concepts. SSME upper stage use
[NASA-CR-193865] p 927 N94-17098

PROPULSION SYSTEM PERFORMANCE
Development of Japanese Earth Resources Satellite-1 (JERS-1; FUYO-1) and it's operational results
[NASDA-SPP-930001] p 884 N94-15001
Research in robust control for hypersonic aircraft
[NASA-CR-194106] p 870 N94-15416
NASA Operational Environment Team (NOET): NASA's key to environmental technology
[TABES PAPER 93-611] p 1052 N94-16143
Emerging technologies for the changing global market
[TABES PAPER 93-612] p 930 N94-16144
Space Propulsion Synergy Group ETO technology assessments
[TABES PAPER 93-641] p 929 N94-16149
Lunar lander and return propulsion system trade study
[NASA-TP-3388] p 925 N94-16496
Comparisons of selected laser beam power missions to conventionally powered missions
[NASA-TM-106110] p 1040 N94-16522
Effects of internal yaw-vectoring devices on the static performance of a pitch-vectoring nonaxisymmetric convergent-divergent nozzle
[NASA-TP-3369] p 858 N94-16572
ALS engine propellant effector system
[NASA-CR-194650] p 926 N94-16590
Space Shuttle main engine. NASA has not evaluated the alternate fuel turbopump costs and benefits. Report to the Administrator of the National Aeronautics and Space Administration
[GAO/NSIAD-94-54] p 926 N94-16834

PROPULSIVE EFFICIENCY
Plasma instabilities and transport in the MPD thruster
[AD-A268268] p 1204 N94-17575

PROPYLENE
Synthesis of potential high-energy fuels
[AD-A267508] p 975 N94-17073

PROSTATE GLAND
Screening for prostate cancer p 1126 N94-16630

PROTEASE
Regulation of attached bacterial growth by adsorbed proteins
[AD-A267756] p 1118 N94-17275

PROTECTION
NASA security handbook
[NHB-1620.3C] p 1224 N94-15937

PROTECTIVE CLOTHING
Firefighters breathing system
[NASA-TM-109611] p 1135 N94-15362
STS-29 crew bailout in WETF
[NASA-TM-109548] p 1136 N94-15385
Investigation of the effects of extravehicular activity (EVA) gloves on performance
[NASA-TP-3401] p 1137 N94-15717
USAF physiological studies of personal microclimate cooling: A review
[AD-A267203] p 1022 N94-15858
Aerospace medicine and biology: A continuing bibliography with indexes (supplement 378)
[NASA-SP-7011(378)] p 1122 N94-16478
Aerospace medicine and biology: A continuing bibliography with indexes (supplement 380)
[NASA-SP-7011(380)] p 1122 N94-16479

PROTECTIVE COATINGS
Restoring Miss Liberty --- inorganic coatings
[NASA-TM-109605] p 963 N94-15313
Assessment of chromate and non-chromate conversion coatings for Al alloys using electrochemical impedance spectroscopy
[AD-A267205] p 965 N94-15859
Krupp technical reports no. 2, English edition, October 1992
[ETN-93-94631] p 984 N94-16000
Vacuum plasma spraying p 975 N94-16002
Chemical vapor deposition of Ta2O5 corrosion resistant coatings
[DE93-015488] p 969 N94-16889
Robotic weld overlay coatings for erosion control
[DE93-016938] p 970 N94-16959
Evaluation of hybrid reinforcement (fiber-reinforced-plastic rod with steel core)
[AD-A268009] p 941 N94-17473

PROTEIN CRYSTAL GROWTH
STS-26 protein growth (PCG) experiment
[NASA-TM-109533] p 976 N94-15395
Convective flow effects on protein crystal growth
[NASA-CR-194560] p 1206 N94-15476
Solution behaviour in microgravity: Considerations for protein crystal growth p 982 N94-16102
The roles of fluid motion and other transport phenomena in the morphology of materials
[NASA-CR-194665] p 1028 N94-17298

PROTEINS
Materials Research Society Symposium Proceedings, Volume 292: Biomolecular Materials
[AD-A265776] p 1116 N94-15138
The relationship of metallothionein induction to the heat shock response
[AD-A266634] p 1122 N94-15741
Study of protein-H2O interactions by multidimensional NMR spectroscopy
[AD-A266955] p 946 N94-15760
Bioorganic models for protein ion channels
[AD-A266365] p 1117 N94-16441
Heat shock protein induction in human cells by CO2 laser irradiation
[AD-A266430] p 1117 N94-16545
Hemoglobin
[AD-A266455] p 1123 N94-16566
Release of iron from hemoglobin
[AD-A266503] p 1128 N94-16784
Regulation of attached bacterial growth by adsorbed proteins
[AD-A267756] p 1118 N94-17275

PROTOCOL (COMPUTERS)
Applicability of the session and the presentation layers for the support of high speed applications
[INRIA-RT-144] p 1158 N94-14980
The Third Annual NASA Science Internet User Working Group Conference
[NASA-CP-3170] p 1228 N94-15116
A formal protocol test procedure for the Survivable Adaptable Fiber Optic Embedded Network (SAFENET)
[AD-A267410] p 1192 N94-16975
Isochronets: A high-speed network switching architecture
[AD-A267811] p 1161 N94-17409
NASA Lewis Meshed VSAT Workshop meeting summary
[NASA-TM-106332] p 883 N94-17487
A protocol validator for the SCM and CFSM models
[AD-A268523] p 1156 N94-17541

An internetwork authentication architecture
[AD-A268579] p 1162 N94-17622
PROTON BEAMS
Microstructure of Zr3Al after 2 MeV proton bombardment
[DE93-015331] p 1211 N94-16814
PROTON FLUX DENSITY
The SCR Ne-21 and Ar-38 in lunar rock 68815: The solar proton energy spectrum over the past 2 MYR
p 1248 N94-16177
PROTON SCATTERING
The pp elastic scattering experiment at RHIC and polarization studies in the Coulomb Nuclear Interference region
[DE93-015391] p 1187 N94-16829
PROTONS
Study of the rare decays K(sub L)(sup 0) yields (mu)e, K(sub L)(sup 0) yields ee, and K(sub L)(sup 0) yields (mu)(mu) at KEK
[DE93-753247] p 1180 N94-15135
Nuclear fusion of protons with ions of boron
[DE93-015399] p 1202 N94-16019
Energy-loss cross sections for inclusive charge-exchange reactions at intermediate energies
[NASA-TM-4522] p 1188 N94-17018
Search for the top quark from (e(mu)) and (e,e) events in the D0 detector in p(bar-p) collisions at the square root of s = 1.8 TeV
[DE93-016350] p 1186 N94-17662
PROTOPLANETS
Petrologic constraints on the surface processes on asteroid 4 Vesta and on excavation depths of diogenite fragments p 1241 N94-16208
I-Xe structure of ILAFEGH 009 and shallowater: Evidence for early formation and rapid cooling of impact-derived enstatite meteorites
p 1243 N94-16305
An initial perspective of S-asteroid subtypes within asteroid families p 1243 N94-16310
On the delivery of planetesimals to a protoplanet in the solar nebula p 1245 N94-16379
PROTOTYPES
Progress in the concentrator initiative program
[DE93-015006] p 1091 N94-15984
Center of Excellence in Laser Medicine
[DE93-016541] p 1122 N94-16113
Prototype instrumentation and design studies
[AD-A266402] p 882 N94-16530
ACE: Lessons learned, volume 1
[AD-A267979] p 1155 N94-17411
PROXIMITY
Steering capacifiector sensor
[NASA-CASE-GSC-13489-1] p 1164 N94-15704
PSYCHOLOGICAL EFFECTS
Scuba-diving, anxiety and task performance
p 1132 N94-15938
PSYCHOLOGY
Development of the OMPAT neuropsychological/psychomotor performance evaluation and OMPAT data and timing support programs
[AD-A266954] p 1122 N94-15759
PSYCHOMOTOR PERFORMANCE
Development of the OMPAT neuropsychological/psychomotor performance evaluation and OMPAT data and timing support programs
[AD-A266954] p 1122 N94-15759
PSYCHOPHYSICS
The 12th Annual Carmel Conference, distinctiveness and Memory: Cognitive Psychophysiological and Physiological Considerations
[AD-A267181] p 1131 N94-15148
PSYCHOPHYSIOLOGY
The 12th Annual Carmel Conference, distinctiveness and Memory: Cognitive Psychophysiological and Physiological Considerations
[AD-A267181] p 1131 N94-15148
Activity/rest patterns of instructor and rates student pilots during rapid transitions from daytime to nighttime duty hours at the Eastern Army Aviation Training site
[AD-A267038] p 1131 N94-15659
Perception of lightness and brightness in complex patterns
[AD-A268435] p 1134 N94-17513
PUBLIC HEALTH
An assessment of acid fog
[DE93-009347] p 1095 N94-15940
Physical fitness and the Healthy People 2000 goals
p 1125 N94-16619
PUBLIC RELATIONS
Military space programs in the press: An analysis for change
[AD-A267799] p 874 N94-17306
PULSARS
Fast pulsars, compact stars, and the strange matter hypothesis
[DE93-015039] p 1239 N94-16052
PULSE COMMUNICATION
Operation of digital systems in severe electromagnetic environments
[AD-A267176] p 988 N94-15693
Signal processing in impulsive electromagnetic interference
[AD-A266425] p 998 N94-16557
Four Frequency-Shift Keying (4-FSK) spread spectrum modulator and demodulator
[AD-A267433] p 1000 N94-16979
A study on an experimental communication system using microsatellites p 892 N94-17160
PULSE COMPRESSION
Simultaneous compression of the passively mode-locked pulsewidth and pulse train
p 913 N94-15566
PULSE DOPPLER RADAR
Designing clutter rejection filters with complex coefficients for airborne pulsed Doppler weather radar
[NASA-CR-4550] p 862 N94-15444
PULSE DURATION
Dynamics of douple stimulated Brillouin scattering
p 1200 N94-15206
Simultaneous compression of the passively mode-locked pulsewidth and pulse train
p 913 N94-15566
Optimum wavelengths for two color ranging
p 915 N94-15580
Pulse response based control for minimum time maneuver of flexible spacecraft
[AD-A266186] p 886 N94-16455
PULSE GENERATORS
User manual and program description of the data acquisition system of PML-pulse physics
[AD-A266752] p 1147 N94-15776
A microsecond-pulsewidth, intense, light-ion beam accelerator
[DE93-016455] p 1202 N94-16451
Digital laser range finder emulator
[AD-D015811] p 1040 N94-16540
Multi-frame x ray imaging with a large area 40ps camera
[DE93-017179] p 1035 N94-16960
PULSE MODULATION
A 27 channels, 1 MHz fibre-optic measuring system
[AD-A266943] p 1003 N94-17307
PULSE RADAR
Target detection by way of Kalman filtering
[AD-A267314] p 1000 N94-16945
PULSED LASER DEPOSITION
Laser assisted CVD growth of AlN and GaN
[AD-A267150] p 1206 N94-15764
Pulsed laser deposition of metastable Ca(1-x)Sr(x)CuO2 thin films
[DE93-015804] p 1040 N94-16663
PULSED LASERS
Channel of the system for pulse charged particle beam diagnostics
[DE93-623867] p 1179 N94-14931
Prelaunch optical characterization of the Laser Geodynamic Satellite (LAGEOS 2)
[NASA-TP-3400] p 884 N94-15193
Nd:YLF laser for airborne/spaceborne laser ranging
p 913 N94-15563
New methods of generation of ultrashort laser pulses for ranging p 913 N94-15565
An improved light source for laser ranging
p 913 N94-15567
The solid state detector technology for picosecond laser ranging p 914 N94-15572
Streak camera based SLR receiver for two color atmospheric measurements p 914 N94-15573
Test results from LAGEOS-2 optical characterization using pulsed lasers p 915 N94-15577
Bench checkout equipment for spaceborne laser altimeter systems p 921 N94-15618
Multi-beam laser altimeter p 921 N94-15620
X ray laser program
[AD-A267075] p 1038 N94-15628
Experimental investigations of superconductivity in quasi-two-dimensional epitaxial copper oxide superlattices and trilayers
[DE93-015306] p 1207 N94-15829
Laser-shock damage of iron-based materials
[AD-A267196] p 1038 N94-15852
Laser with optically driven Q-switch
[NASA-CASE-NPO-18470-1-CU] p 1038 N94-15932
Ablation, surface activation, and electroless metallization of insulating materials by pulsed excimer laser irradiation
[DE93-015808] p 1040 N94-16664
Observation of nonsequential ionization of helium and its impact on intensity monitoring
[DE93-017174] p 949 N94-16904
Pulsed laser kinetic studies of liquids under high pressure
[DE93-017826] p 1041 N94-16998
Pulsed hydrogen fluoride overtone chemical laser studies
[AD-A267597] p 1041 N94-17193
Sensitive detection of gas-phase nitro-containing energetic materials employing 226-nm radiation
[AD-A267633] p 951 N94-17203
Micro pulse laser radar
[NASA-CASE-GSC-13493-1] p 1004 N94-17322
Extracavity frequency doubling study of a pulsed photodissociation iodine laser
[AD-A267893] p 1042 N94-17394
Basic studies of the liquid state of matter: Electrical properties and laser interactions
[AD-A268311] p 1042 N94-17567
PULSED RADIATION
A review of some dynamics models in six-dimensional phase space and their suitable conditions of motion equation
[DE93-623741] p 1175 N94-17317
The behavioral toxicology of high-peak, low average power, pulsed microwave irradiation
[AD-A268392] p 1134 N94-17535
PUMPS
New insulin pump
[NASA-TM-109642] p 1120 N94-15253
Electro-rheological disk pump
[AD-D015783] p 1047 N94-16531
Hydraulic pump with integral electric motor
[AD-D015782] p 1011 N94-16549
High pressure pump for electro-rheological fluids
[AD-D015888] p 1048 N94-16915
Application of thermal spray and ceramic coatings and reinforced epoxy for cavitation damage repair of hydroelectric turbines and pumps
[AD-A267624] p 971 N94-17198
PUSHING
Particle Engulfment and Pushing by Solidifying Interfaces (PEPSI)
[NASA-CR-193856] p 960 N94-17079
PYRANOMETERS
Determination of sunshine duration from radiation intensity pyranometric measurements of global and sky radiation
[BER-181] p 1105 N94-15302
PYRIDINES
Pulsed laser kinetic studies of liquids under high pressure
[DE93-017826] p 1041 N94-16998
PYROLYSIS
Synthesis of ceramic oxide powders in a microwave plasma device
[DE93-012741] p 965 N94-15920
A proposed mechanism for the pyrolysis of diborane
[DE93-014275] p 947 N94-15977
Nitrogen isotopic signatures in agglutinates from breccia 79035 p 954 N94-16314
Advanced thermally stable jet fuels
[DE93-017711] p 975 N94-16996
PYROLYTIC GRAPHITE
Solvational barriers to interfacial electron transfer: Minimization by way of valence delocalization
[AD-A267371] p 950 N94-17006
PYROTECHNICS
Densifying and stabilizing ingredient
[AD-D015751] p 975 N94-16934
PYROXENES
The Fe2(+)-Mg interdiffusion in orthopyroxene: Constraints from cation ordering and structural data and implications for cooling rates of meteorites
p 1241 N94-16175
Stalking the LREE-enriched component in ureilites
p 1241 N94-16190
Pyroxene equilibration temperatures in metamorphosed ordinary chondrites p 1242 N94-16224
Complex zoning behavior in pyroxene in FeO-rich chondrules in the Semarkona ordinary chondrite
p 1243 N94-16284
Water in Earth's mantle: Hydrogen analysis of mantle olivine, pyroxenes and garnet using the SIMS
p 1104 N94-16336
Mixing model analysis of telescopic lunar spectra
p 1284 N94-16371
Analysis of pyroxene absorptions observed in Martian dark regions p 1292 N94-16411
Zaoyang chondrite cooling history from pyroxene Fe(2+)-Mg intracrystalline ordering and exolutions
p 1246 N94-16417
Composition of weakly altered Martian crust
p 1296 N94-16436

PYRROLES
A simple chemical procedure for extending the conductive state of polypyrrole to more negative potentials
[AD-A266235] p 969 N94-16928

Q

Q FACTORS
Structural investigation of electrochemically etched silicon
[DE93-015300] p 1207 N94-15827
Q SWITCHED LASERS
Development of the Mars Observer Laser Altimeter (MOLA) p 921 N94-15617
Laser with optically driven Q-switch
[NASA-CASE-NPO-18470-1-CU] p 1038 N94-15932
Pulsed laser kinetic studies of liquids under high pressure
[DE93-017826] p 1041 N94-16998
QUADRATIC PROGRAMMING
Impending motion direction of contacting rigid bodies
[AD-A266814] p 1164 N94-15756
A sequential quadratic programming algorithm using an incomplete solution of the subproblem
[DE93-017439] p 1149 N94-16120
QUADRATURE AMPLITUDE MODULATION
Exploitation of cyclostationarity for signal-parameter estimation and system identification
[AD-A267137] p 988 N94-15690
QUADRATURES
High resolution radar profiling using higher-order statistics
[AD-D015891] p 1000 N94-16918
Linear characteristic spatial quadrature for discrete ordinates neutral particle transport on arbitrary triangles
[AD-A267485] p 1185 N94-17365
QUADRUPOLES
Magnetic effects in anomalous dispersion
[DE93-014291] p 1175 N94-15978
Emittance and beam size distortion due to linear coupling
[DE93-015402] p 1184 N94-16886
Statistics of the half-integer stopband
[DE93-016101] p 1173 N94-17236
QUALIFICATIONS
The Senior Executive Service
[NHB-3100.6] p 1224 N94-15945
QUALITY
The airline quality report 1993
[NIAR-93-11] p 863 N94-17262
QUALITY CONTROL
Geometric tolerance assessment
[NPL-DITC-210/92] p 1049 N94-15013
Component testing and quality assurance p 932 N94-15259
IG nuts and bolts
[NASA-TM-109652] p 1049 N94-15320
Statistical computation of tolerance limits
[NASA-TM-108424] p 1172 N94-15535
An analysis of SEI software process assessment results: 1987-1991
[AD-A266996] p 1145 N94-15629
Prioritization methodology for chemical replacement
[NASA-TP-3421] p 976 N94-15723
TAFVER 2 users manual
[AD-A266850] p 1106 N94-15757
Krupp technical reports no. 2, English edition, October 1992
[ETN-93-94631] p 984 N94-16000
RELMA: On-line quality control in the rubber mixing room using laser analysis p 984 N94-16005
Design Quality Task Force survey comments
[AD-A266283] p 1225 N94-16473
Mission management aircraft operations manual
[NHB-7900.3] p 1225 N94-16729
Conflict Resolution (CORE) for software quality factors
[AD-A267248] p 1151 N94-16941
Simulation reduction using the Taguchi method
[NASA-CR-4542] p 1055 N94-17082
Small satellite product assurance p 896 N94-17188
Software Capability Evaluation (SCE) version 1.5 method description. Software capability evaluation project
[AD-A267895] p 1154 N94-17395
Establishing a software measurement process
[AD-A267896] p 1154 N94-17396
QUANTITATIVE ANALYSIS
A quantitative analysis of TIMS data obtained on the Learjet 23 at various altitudes p 1063 N94-16597
Elemental impurity analysis of mercuric iodide by ICP/MS
[DE93-015531] p 949 N94-16876
QUANTUM CHROMODYNAMICS
Iteration scheme for the multiparameter nonlinear boundary value problem with the additional conditions and its application to some field models
[DE93-626638] p 1168 N94-14933
The quantum mass shift of the soliton in Skyrme model
[ITN-93-85219] p 1180 N94-15283
PHENIX Conceptual Design Report
[DE93-015759] p 1182 N94-16161
Theoretical high energy physics
[DE93-015884] p 1187 N94-16170
Quark-loop effects in high energy spin-flip processes
[DE93-626692] p 1188 N94-17313
The three-loop QCD beta-function and anomalous dimensions
[NIKHEF-H/92-17] p 1186 N94-17617
The renormalization of the axial anomaly in dimensional regularization
[NIKHEF-H/92-18] p 1220 N94-17618
QUANTUM EFFICIENCY
CCDs and photon counting devices: Applications in space and from the ground p 901 N94-15041
Visible light photon counters for astronomy p 902 N94-15043
How to squeeze high quantum efficiency and high time resolution out of a SPAD p 914 N94-15571
Porous silicon for pumping solid-state lasers
[AD-A266293] p 1039 N94-16474
Development of ultra-low noise, high performance 3-V Quantum Well Infrared Photodectors (QWIP's) for focal plane array staring image sensor systems
[AD-A267715] p 1214 N94-17272
QUANTUM ELECTRODYNAMICS
Fundamental theory of light for applications: Notes for five informal lectures
[DE93-016463] p 1192 N94-16953
Multipolar-like form of nonabelian gauge theories
[DE93-626690] p 1171 N94-17314
QUANTUM ELECTRONICS
Electronic and atomic structure of semiconductors and of high-temperature superconductors
[AD-A266805] p 1205 N94-14913
Spectroscopic investigations of nonambient systems with millimeter and submillimeter probes
[AD-A266537] p 968 N94-16796
Activities of the Research Laboratory of Electronics
[AD-A266730] p 1304 N94-17651
QUANTUM MECHANICS
Molecular processes in comets
[NASA-CR-194148] p 1239 N94-15188
Electronic structure and enthalpy of hydrogen and helium mixtures
[DE93-014128] p 1208 N94-15976
Theoretical high energy physics research at the University of Chicago
[DE93-016863] p 1187 N94-16116
Bulk and defect properties of ordered intermetallics: A first-principles total-energy investigation
[DE93-015492] p 959 N94-16873
Stochastic chaos: An analog of quantum chaos
[DE93-016619] p 1220 N94-16956
SUSY in the sky
[NIKHEF-H/93-04] p 1240 N94-17603
Quantum phase fluctuations in the Jaynes-Cummings model: Effects of cavity damping
[DE93-627984] p 1186 N94-17612
The renormalization of the axial anomaly in dimensional regularization
[NIKHEF-H/92-18] p 1220 N94-17618
QUANTUM NUMBERS
Clusterization of quantum states in the Hartmann model
[DE93-626624] p 1220 N94-17315
QUANTUM OPTICS
Quantum phase fluctuations in the Jaynes-Cummings model: Effects of cavity damping
[DE93-627984] p 1186 N94-17612
QUANTUM THEORY
Fundamental theory of light for applications: Notes for five informal lectures
[DE93-016463] p 1192 N94-16953
The universality of the shift of the Chern-Simons parameter for a general class of BRS invariant regularizations
[NIKHEF-H/93-03] p 1220 N94-17602
Quantum Heisenberg groups and Sklyanin algebras
[DE93-628590] p 1175 N94-17643
QUANTUM WELL LASERS
Ion doped quantum well lasers
[AD-A267198] p 1038 N94-15853
QUANTUM WELLS
Optoelectronics based on SiGe/Si heterostructures
[AD-A267178] p 1190 N94-15848
JSEP fellowship
[AD-A266568] p 1211 N94-16800
Structural characterization of epitaxial layers for infrared detectors
[AD-A267875] p 940 N94-17013
Development of ultra-low noise, high performance 3-V Quantum Well Infrared Photodectors (QWIP's) for focal plane array staring image sensor systems
[AD-A267715] p 1214 N94-17272
High-speed nonlinear switching mechanisms and devices for multi-gigabit data processing
[AD-A267753] p 1014 N94-17375
QUARK MODELS
Production of D-mesons in pp-collisions and quark-gluon string model
[DE93-626721] p 1185 N94-17312
The three-loop QCD beta-function and anomalous dimensions
[NIKHEF-H/92-17] p 1186 N94-17617
The renormalization of the axial anomaly in dimensional regularization
[NIKHEF-H/92-18] p 1220 N94-17618
QUARKS
On the nature of mirror particles
[DE93-626670] p 1179 N94-14934
Astronomy and astrophysics p 1239 N94-15970
PHENIX Conceptual Design Report
[DE93-015759] p 1182 N94-16161
Calorimeter based detectors for high energy hadron colliders
[DE93-017055] p 1188 N94-16900
Heavy ion physics research at Creighton University
[DE93-016809] p 1185 N94-16957
Mesons at finite temperature in the NJL model with gluon condensate
[DE93-626697] p 1185 N94-17310
Quark-loop effects in high energy spin-flip processes
[DE93-626692] p 1188 N94-17313
Search for the top quark from (e(mu)) and (e,e) events in the D0 detector in p(bar-p) collisions at the square root of s = 1.8 TeV
[DE93-016350] p 1186 N94-17662
QUARTZ
A calibration of the production rate ratio P-21/P-26 by low energy secondry neutrons: Identification of Ne spallation components at the 10(exp 6) atoms/g level in terrestrial samples p 1187 N94-16194
Orientation of Planar Deformation Features (PDFs) in quartz p 1219 N94-16341
Investigation of the effects of polyelectrolyte coatings on colloid transport in porous media
[DE93-018300] p 970 N94-16973
SRB thermal curtain design support
[NASA-CR-193857] p 927 N94-17123
SRB thermal curtain design support
[NASA-CR-193858] p 928 N94-17124
Quartz crystal resonators and oscillators for frequency control and timing applications: A tutorial, revision 6.1
[AD-A268205] p 1216 N94-17480
Kinetics of silica-phase transitions
[DE93-016231] p 1217 N94-17659
QUARTZ CRYSTALS
Quartz crystal resonators and oscillators for frequency control and timing applications: A tutorial, revision 6.1
[AD-A268205] p 1216 N94-17480
QUARTZ LAMPS
An analysis of the radiation field beneath a bank of tubular quartz lamps
[NASA-CR-191551] p 1024 N94-16542
QUASARS
The theory of QSO absorption line systems and their relationship to the galaxies
[NASA-CR-194596] p 1236 N94-15679
Complex QSO absorbers: High-redshift clusters of galaxies?
[NASA-CR-194617] p 1237 N94-16833
QUENCHING (COOLING)
A comparison of one and two dimensional flame quenching: Heat transfer results
[DE93-015196] p 947 N94-16060
Investigation of two-phase flow and boiling heat transfer during quenching of a tube under microgravity p 979 N94-16087
QUEUEING THEORY
Stochastic scheduling in in-forest networks
[INRIA-RR-1719] p 1164 N94-15695
Logarithmic asymptotics for steady-state tail probabilities in a single-server queue
[AD-A266746] p 1165 N94-15775
A comparison of queueing, cluster and distributed computing systems
[NASA-TM-109025] p 1160 N94-16878
Stochastic scheduling in a multiclass G/G/1 queue
[INRIA-RR-1746] p 1162 N94-17537

R

RADAR
Notes on the use of Dempster-Shafer and fuzzy reasoning to fuse identity attribute data
[AD-A267426] p 1004 N94-17309
RADAR ANTENNAS
System architecture of optically controlled phased array radar
[AD-A267056] p 988 N94-15667
Advanced antennas for SAR spacecraft
p 993 N94-15912
Manufacturing tolerance requirements for frequency selective surfaces
[AD-A266541] p 999 N94-16797
RADAR BEACONS
ATCRBS reply environment at Memphis International Airport
[AD-A266322] p 864 N94-16439
RADAR BEAMS
System architecture of optically controlled phased array radar
[AD-A267056] p 988 N94-15667
RADAR CORNER REFLECTORS
Prelaunch optical characterization of the Laser Geodynamic Satellite (LAGEOS 2)
[NASA-TP-3400] p 884 N94-15193
Laser ranging application to time transfer using geodetic satellite and to other Japanese space programs
p 911 N94-15555
Evaluation of the TOPSAR performance by using passive and active calibrators p 1078 N94-16750
External calibration of polarimetric radar images using distributed targets p 1079 N94-16753
RADAR CROSS SECTIONS
Analysis of electromagnetic scattering from irregularly shaped, thin, metallic flat plates
[NASA-TP-3361] p 998 N94-16655
Measurements of the radar cross section and Inverse Synthetic Aperture Radar (ISAR) images of a Piper Navajo at 9.5 GHz and 49 GHz
[AD-A267570] p 1002 N94-17110
RADAR DATA
Sensitivity testing of a single-Doppler temperature retrieval and forecast system
[AD-A267278] p 1105 N94-14958
Proceedings of the Third Spaceborne Imaging Radar Symposium
[NASA-CR-194104] p 989 N94-15886
Recent advances in radar remote sensing of forest
p 991 N94-15897
Imaging radar studies of polar ice p 991 N94-15899
Application of Cloude's target decomposition theorem to polarimetric imaging radar data p 991 N94-15901
Recent advances and plans in processing and geocoding of SAR data at the DFD p 992 N94-15909
Data distribution p 993 N94-15910
International collaboration in SAR ground data systems p 993 N94-15917
Morphology and models for the evolution of eastern Hecate Chasma, Venus p 1256 N94-16215
Separation of topographic and intrinsic backscatter variations in biscopic radar images: A magic airbrush
p 1086 N94-16318
SAR backscatter from coniferous forest gaps
p 1076 N94-16736
Characterization of wetland, forest, and agricultural ecosystems in Belize with airborne radar (AIRSAR)
p 1076 N94-16738
Supervised fully polarimetric classification of the Black Forest test site: From MAESTROI to MAC Europe
p 1076 N94-16740
Extraction of quantitative surface characteristics from AIRSAR data for Death Valley, California
p 1078 N94-16748
Opposing mesoscale flows in a broken midlatitude squall line
[AD-A268011] p 1109 N94-17492
RADAR DETECTION
Adaptive interference canceller
[CA-PATENT-1-310-709] p 988 N94-15698
Windshear detection radar signal processing studies
[NASA-CR-194615] p 994 N94-16022
Enhanced down-range profiles of complex targets using wideband radar echo returns
[AD-A266508] p 999 N94-16788
Target detection by way of Kalman filtering
[AD-A267314] p 1000 N94-16945
Signal detection in correlated Gaussian and non-Gaussian radar clutter
[AD-A267453] p 1001 N94-17033
Intelligent use of CFAR algorithms
[AD-A267755] p 1003 N94-17206
Remote sensing of precipitation and electrification with a dual-polarization, coherent, wideband radar system
[AD-A267479] p 1004 N94-17364
RADAR ECHOES
Enhanced down-range profiles of complex targets using wideband radar echo returns
[AD-A266508] p 999 N94-16788
RADAR EQUIPMENT
High resolution SAR applications and instrument design p 993 N94-15913
RADAR FILTERS
Adaptive interference canceller
[CA-PATENT-1-310-709] p 988 N94-15698
RADAR GEOLOGY
Geologic remote sensing with radar
p 991 N94-15900
Summaries of the Third Annual JPL Airborne Geoscience Workshop. Volume 3: AIRSAR Workshop
[NASA-CR-194542] p 1075 N94-16731
A snow wetness retrieval algorithm for SAR
p 1075 N94-16732
RADAR HOMING MISSILES
Enhanced down-range profiles of complex targets using wideband radar echo returns
[AD-A266508] p 999 N94-16788
RADAR IMAGERY
Proceedings of the Third Spaceborne Imaging Radar Symposium
[NASA-CR-194104] p 989 N94-15886
Almaz p 898 N94-15889
Recent advances in radar remote sensing of forest
p 991 N94-15897
Imaging radar studies of polar ice p 991 N94-15899
Geologic remote sensing with radar
p 991 N94-15900
Multifrequency observations p 992 N94-15902
Spaceborne radar for geoscientific applications in North China p 993 N94-15915
Primary studies of Chinese spaceborne SAR
p 993 N94-15916
Rover mounted ground penetrating radar as a tool for investigating the near-surface of Mars and beyong
p 1007 N94-16197
Radar properties of several fluidized ejecta blankets on Venus p 1267 N94-16278
Separation of topographic and intrinsic backscatter variations in biscopic radar images: A magic airbrush
p 1086 N94-16318
The cartography of Venus with Magellan data
p 1274 N94-16320
Resolving topographic detail on Venus by modeling complex Magellan altimetry echoes
p 1283 N94-16368
Relief of some small landforms on Venus
p 1293 N94-16418
Comparison of JPL-AIRSAR and DLR E-SAR images from the MAC Europe 1991 campaign over testsite Oberpfaffenhofen: Frequency and polarization dependent backscatter variations from agricultural fields
p 1075 N94-16733
Monitoring environmental state of Alaskan forests with AIRSAR p 1075 N94-16734
Comparison of modeled backscatter with SAR data at P-band p 1076 N94-16735
Characterization of wetland, forest, and agricultural ecosystems in Belize with airborne radar (AIRSAR)
p 1076 N94-16738
SAR observations in the Gulf of Mexico
p 1077 N94-16742
Investigation of AIRSAR signatures of the Gulf Stream
p 1077 N94-16743
Mapping of sea bottom topography
p 1077 N94-16744
Sea bottom topography imaging with SAR
p 1077 N94-16745
Preliminary results of polarization signatures for glacial moraines in the Mono Basin, Eastern Sierra Nevada
p 1078 N94-16746
Fitting a three-component scattering model to polarimetric SAR data p 1079 N94-16751
External calibration of polarimetric radar images using distributed targets p 1079 N94-16753
Processing of polarimetric SAR data for soil moisture estimation over Mahantango watershed area
p 1079 N94-16754
Evaluation of polarimetric SAR parameters for soil moisture retrieval p 1079 N94-16755
Interaction types and their like-polarization phase-angle difference signatures p 1079 N94-16756
Radar Analysis and Visualization Environment (RAVEN): Software for polarimetric radar analysis
p 1080 N94-16758
Measuring ocean coherence time with dual-baseline interferometry p 1080 N94-16759
Comparison of edges detected at different polarisations in MAESTRO data p 1080 N94-16761
Moving target indicator using higher order statistics
[AD-D015890] p 1000 N94-16917
High resolution radar profiling using higher-order statistics
[AD-D015891] p 1000 N94-16918
Measurements of the radar cross section and Inverse Synthetic Aperture Radar (ISAR) images of a Piper Navajo at 9.5 GHz and 49 GHz
[AD-A267570] p 1002 N94-17110
Developing automated analysis methods for sea ice imagery: A status report with recommendations
[AD-A267284] p 1113 N94-17241
Arctic cyclones and Marginal Ice Zone (MIZ) variability
[AD-A268610] p 1108 N94-17465
Guide to Magellan image interpretation
[NASA-CR-194340] p 1298 N94-17654
RADAR MAPS
The TOPSAR interferometric radar topographic mapping instrument p 1078 N94-16749
RADAR MEASUREMENT
TRMM radar p 990 N94-15894
Application of Cloude's target decomposition theorem to polarimetric imaging radar data p 991 N94-15901
Calibration: Practical experience with ERS-1
p 992 N94-15907
Spatial and frequency diversity in lidar systems
[AD-A266192] p 1039 N94-16124
A snow wetness retrieval algorithm for SAR
p 1075 N94-16732
Fitting a three-component scattering model to polarimetric SAR data p 1079 N94-16751
RADAR RECEIVERS
Radome depolarization effects on monopulse receiver tracking performance
[AD-A267446] p 1001 N94-17031
Signal detection in correlated Gaussian and non-Gaussian radar clutter
[AD-A267453] p 1001 N94-17033
RADAR REFLECTORS
Method and apparatus for forming an agile plasma mirror effective as a microwave reflector
[AD-D015788] p 998 N94-16535
RADAR SCATTERING
Radar response of vegetation: An overview
p 991 N94-15898
Relating multifrequency radar backscattering to forest biomass: Modeling and AIRSAR measurement
p 1077 N94-16741
Evaluation of polarimetric SAR parameters for soil moisture retrieval p 1079 N94-16755
What is the radar tracking Glint problem and can it be solved?
[AD-A266509] p 999 N94-16789
RADAR SIGNATURES
Investigation of AIRSAR signatures of the Gulf Stream
p 1077 N94-16743
Lithological and textural controls on radar and diurnal thermal signatures of weathered volcanic deposits, Lunar Crater region, Nevada p 1080 N94-16762
RADAR TARGETS
Enhanced down-range profiles of complex targets using wideband radar echo returns
[AD-A266508] p 999 N94-16788
Moving target indicator using higher order statistics
[AD-D015890] p 1000 N94-16917
High resolution radar profiling using higher-order statistics
[AD-D015891] p 1000 N94-16918
Target detection by way of Kalman filtering
[AD-A267314] p 1000 N94-16945
Radome depolarization effects on monopulse receiver tracking performance
[AD-A267446] p 1001 N94-17031
Measurements of the radar cross section and Inverse Synthetic Aperture Radar (ISAR) images of a Piper Navajo at 9.5 GHz and 49 GHz
[AD-A267570] p 1002 N94-17110
RADAR TRACKING
Sea ice motions in the central arctic ice central arctic pack ice as inferred from AVHRR imagery
[NASA-CR-194572] p 1112 N94-15701
Radar diagnostic parameters as indicators of severe weather in central Florida
[PB93-183507] p 1106 N94-16465
What is the radar tracking Glint problem and can it be solved?
[AD-A266509] p 999 N94-16789
RADAR TRANSMISSION
Comparison of RADARC high-frequency radar performance prediction model and ROTHR Amchitka data
[AD-A267077] p 987 N94-15540
Forecasting the ducting of electromagnetic waves on the mesoscale
[AD-A268101] p 1109 N94-17571

RADAR TRANSMITTERS
Radar transmitter procedures
[AD-A268274] p 1005 N94-17523
RADARSAT
RADARSAT program p 898 N94-15893
RADIAL DISTRIBUTION
Effects of levitated dust on astronomical observations from the lunar surface p 1239 N94-16433
RADIANCE
Unmixing AVIRIS data to provide a method for vegetation fraction subtraction p 1066 N94-16669
Hyperspectral modeling for extracting aerosols from aircraft/satellite data p 1067 N94-16673
A field measure of the shade fraction p 1068 N94-16677
Seasonal and spatial variations in phytoplanktonic chlorophyll in eutrophic Mono Lake, California, measured with the Airborne Visible and Infrared Imaging Spectrometer (AVIRIS) p 1069 N94-16684
Multiple dataset water-quality analyses in the vicinity of an ocean wastewater plume p 1069 N94-16687
Atmospheric correction of AVIRIS data in ocean waters p 1070 N94-16690
Simulation of AVHRR-K band ratios with AVIRIS p 1075 N94-16714
RADIANT COOLING
Investigate wave-mean flow interaction and transport in the extratropical winter stratosphere
[NASA-CR-194555] p 1098 N94-15639
An improved patch for radiative coolers
[NASA-CASE-GSC-13503-1] p 1046 N94-15873
RADIANT FLUX DENSITY
Observation of nonsequential ionization of helium and its impact on intensity monitoring
[DE93-017174] p 949 N94-16904
Spectroscopic and computer modeling investigations of a laser-sustained plasma
[IFTR-30/1991] p 1204 N94-17066
RADIANT HEATING
Investigation of radiative interaction in laminar flows using Monte Carlo simulation
[NASA-CR-194604] p 1021 N94-15795
An analysis of the radiation field beneath a bank of tubular quartz lamps
[NASA-CR-191551] p 1024 N94-16542
RADIATION
Global climate study
[NASA-TM-109612] p 1098 N94-15363
RADIATION ABSORPTION
Spectroscopic and computer modeling investigations of a laser-sustained plasma
[IFTR-30/1991] p 1204 N94-17066
RADIATION COUNTERS
The MIC photon counting detector p 901 N94-15039
CCDs and photon counting devices: Applications in space and from the ground p 901 N94-15041
Visible light photon counters for astronomy p 902 N94-15043
The TAUVEX experiment p 905 N94-15064
The Rutherford Appleton Laboratory photon counting detector p 910 N94-15096
The 3D-Flow processor for a programmable level-1 trigger (feasibility study)
[DE93-016045] p 1159 N94-16172
Calorimeter based detectors for high energy hadron colliders
[DE93-017055] p 1188 N94-16900
Electroweak results from D0
[DE93-014926] p 1185 N94-16968
Astrophysics with MILAGRO
[DE93-012722] p 1240 N94-17657
Detecting small debris using a ground-based photon counting detector
[DE93-012623] p 898 N94-17669
RADIATION DAMAGE
Radiation hardening of a CCD technology through process and design modifications p 906 N94-15071
RADIATION DETECTORS
Metastable superconductors as photon detectors p 900 N94-15032
Thinned, backside illuminated, area CCD imager for electron detection p 901 N94-15036
Outlook for hard x ray and gamma ray astronomy p 904 N94-15057
Work at Graz on satellite signatures p 898 N94-15558
The solid state detector technology for picosecond laser ranging p 914 N94-15572
Electroweak physics from D0
[DE93-015041] p 1181 N94-16053
ALEXIS and HETE: Two small, low cost, scientific satellite systems p 896 N94-17185
Contained (nu) events observed in Soudan 2
[DE93-015548] p 1300 N94-17233
Detecting small debris using a ground-based photon counting detector
[DE93-012623] p 898 N94-17669
RADIATION DISTRIBUTION
An analysis of the radiation field beneath a bank of tubular quartz lamps
[NASA-CR-191551] p 1024 N94-16542
RADIATION DOSAGE
Exposure fluctuations of astronauts due to orientation
[NASA-TP-3364] p 1300 N94-15816
Aberration correction of unstable resonators
[NASA-CASE-NPO-18791-1-CU] p 1034 N94-15987
Quantifying lifetime exposure to ultraviolet radiation in the epidemiology of cutaneous malignant melanoma: A pilot study
[DE93-015274] p 1128 N94-16812
The determination of the Young moduli of a material after exposure to laser light and delineation of the zone of laser alterations
[IFTR-37/1991] p 1061 N94-17058
Bioeffects of radiofrequency radiation on cell growth and differentation. Volume 1: Engineering considerations
[AD-A267754] p 1118 N94-17232
Predicting radiation induced performance decrements of AH-1 helicopter crews. Volume 1: Predicted veersus actual performance of AH-1 crews induced with symptoms simulating radiation sickness
[AD-A268376] p 1138 N94-17460
Energy deposition fluctuations induced by ions in microvolumes and nanovolumes: An analytic approach. 1: Theory
[AD-A267959] p 1173 N94-17495
RADIATION EFFECTS
Theoretical studies relating to the interaction of radiation with matter
[AD-A266894] p 1179 N94-14949
Merged beam studies of laser stimulated radiative recombination
[AD-A267186] p 1037 N94-15145
Plume radiation p 924 N94-15223
Fault handling schemes in electronic systems with specific application to radiation tolerance and VLSI design
[NASA-CR-194559] p 1008 N94-15640
Long Duration Exposure Facility experiment M0003 deintegration/findings and impacts
[AD-A267140] p 885 N94-15749
Investigation of radiative interaction in laminar flows using Monte Carlo simulation
[NASA-CR-194604] p 1021 N94-15795
Exposure fluctuations of astronauts due to orientation
[NASA-TP-3364] p 1300 N94-15816
PHENIX Conceptual Design Report
[DE93-015759] p 1182 N94-16161
The effect of irradiation on the mechanical properties of 6061-T651 aluminum
[DE93-015825] p 958 N94-16168
AFRRI reports, first quarter 1993
[AD-A266380] p 1123 N94-16515
Ergonomics in the office environment p 1124 N94-16612
Evolution of microstructure in face centered cubic metals during irradiation: A review
[DE93-015682] p 958 N94-16662
The role of constitutive and inducible processes in the response of human squamous cell carcinoma cell lines to ionizing radiation
[DE93-015150] p 1129 N94-16970
L-shell binning and display of sensor data from the CRRES spacecraft
[AD-A267256] p 888 N94-16990
The determination of the Young moduli of a material after exposure to laser light and delineation of the zone of laser alterations
[IFTR-37/1991] p 1061 N94-17058
Studies of premixed laminar and turbulent flames at microgravity
[NASA-CR-194656] p 951 N94-17125
Bioeffects of radiofrequency radiation on cell growth and differentation. Volume 1: Engineering considerations
[AD-A267754] p 1118 N94-17232
Predicting radiation induced performance decrements of AH-1 helicopter crews. Volume 1: Predicted veersus actual performance of AH-1 crews induced with symptoms simulating radiation sickness
[AD-A268376] p 1138 N94-17460
Quartz crystal resonators and oscillators for frequency control and timing applications: A tutorial, revision 6.1
[AD-A268205] p 1216 N94-17480
Energy deposition fluctuations induced by ions in microvolumes and nanovolumes: An analytic approach. 1: Theory
[AD-A267959] p 1173 N94-17495
The behavioral toxicology of high-peak, low average power, pulsed microwave irradiation
[AD-A268392] p 1134 N94-17535
Basic studies of the liquid state of matter: Electrical properties and laser interactions
[AD-A268311] p 1042 N94-17567
Growth of dielectric thin films by irradiation of condensed molecular precursors with synchrotron radiation
[DE93-016161] p 974 N94-17676
RADIATION HARDENING
Impurity conduction photoconductor detectors p 902 N94-15046
Radiation hardening of a CCD technology through process and design modifications p 906 N94-15071
SONOS technology for commercial and military nonvolatile memory applications
[DE93-015647] p 1011 N94-16661
RADIATION HAZARDS
Hazard calculations of diffuse reflected laser radiation for the SELENE program
[NASA-TM-4520] p 1042 N94-17285
RADIATION INJURIES
Wound healing after laser injury to skin: The effect of occlusion and vitamin E
[AD-A266473] p 1128 N94-16779
RADIATION MEASUREMENT
Real time radiation measurements in space p 980 N94-16092
RADIATION MEASURING INSTRUMENTS
Proceedings of an ESA Symposium on Photon Detectors for Space Instrumentation
[ESA-SP-356] p 899 N94-15025
Outlook for hard x ray and gamma ray astronomy p 904 N94-15057
Nb-based SJTJ for nuclear detection: Preliminary results with alpha radiation p 905 N94-15068
Improved optical radiation detectors and their calibration: 200 nm - 30 microns p 906 N94-15075
In orbit adiabatic demagnetization refrigeration for bolometric and microcalorimetric detectors p 907 N94-15079
Silicon radiation sensor systems for gamma and x ray detection at SI p 909 N94-15095
The space technology research vehicle: Development status p 896 N94-17183
RADIATION PROTECTION
Exposure fluctuations of astronauts due to orientation
[NASA-TP-3364] p 1300 N94-15816
RADIATION SHIELDING
Engineering Physics and Mathematics Division progress report, period ending 31 December 1992
[DE93-015118] p 1301 N94-14926
Shielding from space radiations
[NASA-CR-194578] p 1180 N94-15715
Exposure fluctuations of astronauts due to orientation
[NASA-TP-3364] p 1300 N94-15816
Approximate Green's function methods for HZE transport in multilayered materials
[NASA-TM-4519] p 1300 N94-17084
Shielding from space radiations
[NASA-CR-194664] p 1301 N94-17255
Calculations of cosmic-ray helium transport in shielding materials
[NASA-TP-3354] p 1301 N94-17666
RADIATION SICKNESS
Predicting radiation induced performance decrements of AH-1 helicopter crews. Volume 1: Predicted veersus actual performance of AH-1 crews induced with symptoms simulating radiation sickness
[AD-A268376] p 1138 N94-17460
RADIATION SOURCES
Powder diffraction studies using anomalous dispersion
[DE93-012531] p 1210 N94-16775
RADIATION SPECTRA
Earth observational research using multistage EOS-like data
[NASA-CR-194626] p 1084 N94-16831
RADIATION THERAPY
The role of constitutive and inducible processes in the response of human squamous cell carcinoma cell lines to ionizing radiation
[DE93-015150] p 1129 N94-16970
RADIATION TOLERANCE
Fault handling schemes in electronic systems with specific application to radiation tolerance and VLSI design
[NASA-CR-194559] p 1008 N94-15640
The role of constitutive and inducible processes in the response of human squamous cell carcinoma cell lines to ionizing radiation
[DE93-015150] p 1129 N94-16970
RADIATION TRANSPORT
Engineering Physics and Mathematics Division progress report, period ending 31 December 1992
[DE93-015118] p 1301 N94-14926
The effects of radiation transport on line ratios used as temperature and density diagnostic
[DE93-016424] p 1205 N94-17663

RADIATIVE HEAT TRANSFER
Study of multi-dimensional radiative energy transfer in molecular gases
[NASA-CR-194613] p 1181 N94-15752
The cooling rates of pahoehoe flows: The importance of lava porosity p 1103 N94-16282
Studies on nonequilibrium phenomena in supersonic chemically reacting flows
[NASA-CR-194662] p 1027 N94-17215

RADIATIVE LIFETIME
Scintillation mechanism in stoichiometric cerium compounds
[DE93-015499] p 948 N94-16771

RADIATIVE RECOMBINATION
Merged beam studies of laser stimulated radiative recombination
[AD-A267186] p 1037 N94-15145

RADIATIVE TRANSFER
Ground truth spectrometry and imagery of eruption clouds to maximize utility of satellite imagery
[NASA-CR-194358] p 1081 N94-15181
Study of multi-dimensional radiative energy transfer in molecular gases
[NASA-CR-194613] p 1181 N94-15752

RADIATORS
Optically-switched submillimeter-wave oscillator and radiator
[NASA-CASE-NPO-18547-1-CU] p 1014 N94-17324

RADICALS
Synthesis, characterization, and polymerization of new ferrocene-fluorene complexes. A novel high-molecular weight conjugated polymer with pendant ferrocene groups
[AD-A267717] p 972 N94-17273

RADIO ALTIMETERS
The cartography of Venus with Magellan data
p 1274 N94-16320
Resolving topographic detail on Venus by modeling complex Magellan altimetry echoes
p 1283 N94-16368

RADIO ANTENNAS
A review of OPEX activities and measurement results
p 994 N94-16036
The analysis of low-profile, broadband, monopole, vehicle antennas and matching network synthesis
[AD-A268340] p 1006 N94-17582

RADIO ASTRONOMY
Preparation and properties of Nb/Al SIS and SIN junctions for millimeter and submillimeter radioastronomical receivers p 907 N94-15078
Activities of the Research Laboratory of Electronics
[AD-A266730] p 1304 N94-17651

RADIO BEACONS
Olympus propagation measurement results at Virginia Tech p 995 N94-16037
Data acquisition, preprocessing and analysis for the Virginia Tech OLYMPUS experiment
p 995 N94-16038
Propagation measurements in Alaska using ACTS beacons p 995 N94-16040
Comparison of OLYMPUS beacon and radiometric attenuation measurements at Blacksburg, Virginia
p 996 N94-16046

RADIO COMMUNICATION
The ACTS propagation program p 995 N94-16039
Four Frequency-Shift Keying (4-FSK) spread spectrum modulator and demodulator
[AD-A267433] p 1000 N94-16979
Ground wave emergency network final operational capability: Environmental assessment for central Wyoming relay node, site number RN 8C928WY
[AD-A267842] p 1001 N94-17011
Small Satellites Systems and Services
[ISBN-2-85-428327-9] p 888 N94-17131
Radiocommunication problems of a position reporting and bidirectional messagery system using VHF/UHF with low-Earth orbit satellites p 889 N94-17136
Ground wave emergency network final operational capability: Environmental assessment for central Nevada relay node, site number RN 8W917NV
[AD-A267630] p 1002 N94-17200
Ground wave emergency network environmental assessment for northwestern Colorado relay node site number RN 8C924CO
[AD-A267654] p 1003 N94-17249
Ground wave emergency network final operational capability. Environmental assessment for southern Arkansas relay node site no. RN 8C912AR
[AD-A268001] p 1004 N94-17376

RADIO ELECTRONICS
Spaceborne Imaging Radar-C instrument
p 990 N94-15890

RADIO EQUIPMENT
Ground wave emergency network final operational capability: Environmental assessment for central Nevada relay node, site number RN 8W917NV
[AD-A267630] p 1002 N94-17200
Ground wave emergency network final operational capability: Environmental assessment for southern Nevada relay node site number RN 8W918NV
[AD-A267647] p 1002 N94-17205
Ground wave emergency network final operational capability: Environmental assessment for central Utah relay node, site number RN 8C920UT
[AD-A267628] p 1003 N94-17211
Ground wave emergency network final operational capability: Environmental assessment for northwestern Nebraska relay node, site number RN 8C930NE
[AD-A267629] p 1003 N94-17212
Environmental assessment for northwestern Indiana relay node site no. RN 8C902IN
[AD-A267849] p 1004 N94-17406

RADIO FREQUENCIES
Velocity matched millimeterwave electro-optic modulator
[AD-A267264] p 1188 N94-14957
Display system employing acousto-optic tunable filter
[NASA-CASE-NPO-18736-1-CU] p 1190 N94-15933
Satellite sound broadcast propagation measurements
p 996 N94-16047
Measurements of the operation of the SINUS-6/BWO system
[AD-A266423] p 1011 N94-16556
Fundamental-mode RF design in e(+)e(-) storage ring factories
[DE93-015249] p 1183 N94-16809
Cortical adaptive filtering in bioacoustic signal classification
[AD-A266229] p 1177 N94-16939
Radiocommunication problems of a position reporting and bidirectional messagery system using VHF/UHF with low-Earth orbit satellites p 889 N94-17136
RF vacuum microelectronics
[AD-A268399] p 1014 N94-17423
Field-emitter arrays for RF vacuum microelectronics
[AD-A268397] p 1015 N94-17526
Field emitter arrays for RF vacuum microelectronics
[AD-A268595] p 1015 N94-17608

RADIO FREQUENCY INTERFERENCE
A simulation study of the performance of the NASA (2,1,6) convolutional code on RFI/burst channels
p 997 N94-16508

RADIO HORIZONS
Johnson-Gierhart program predictions of excess propagation loss for super-high frequency air-to-ground paths. Volume 2: Appendices
[AD-A267021] p 987 N94-15527

RADIO RECEIVERS
On-board spatial scientific experiment project on small satellites p 896 N94-17184

RADIO RELAY SYSTEMS
Ground wave emergency network final operational capability: Environmental assessment for central Wyoming relay node, site number RN 8C928WY
[AD-A267842] p 1001 N94-17011
Ground wave emergency network final operational capability: Environmental assessment for central Nevada relay node, site number RN 8W917NV
[AD-A267630] p 1002 N94-17200
Ground wave emergency network final operational capability: Environmental assessment for southern Nevada relay node site number RN 8W918NV
[AD-A267647] p 1002 N94-17205
Ground wave emergency network final operational capability: Environmental assessment for central Utah relay node, site number RN 8C920UT
[AD-A267628] p 1003 N94-17211
Ground wave emergency network final operational capability: Environmental assessment for northwestern Nebraska relay node, site number RN 8C930NE
[AD-A267629] p 1003 N94-17212
Ground wave emergency network. Final operational capability. Environmental assessment for southeastern Idaho relay node, site no. RN8W927ID
[AD-A267796] p 1003 N94-17304
Ground wave emergency network final operational capability. Environmental assessment for southern Arkansas relay node site no. RN 8C912AR
[AD-A268001] p 1004 N94-17376
Environmental assessment for northwestern Indiana relay node site no. RN 8C902IN
[AD-A267849] p 1004 N94-17406

RADIO TELESCOPES
Search for Extraterrestrial Intelligence (SETI)
p 1125 N94-16620
Solar Electro-Optical Network (SEON) upgrade/replacement program. Phase 1: Qualification operational test and evaluation plan
[AD-A266364] p 1237 N94-17225

RADIO TRANSMISSION
Johnson-Gierhart program predictions of excess propagation loss for super-high frequency air-to-ground paths. Volume 2: Appendices
[AD-A267021] p 987 N94-15527
Proceedings of the Fifteenth NASA Propagation Experimenters Meeting (NAPEX 15) and the Advanced Communications Technology Satellite (ACTS) Propagation Studies Miniworkshop
[NASA-CR-194539] p 994 N94-16035
A review of OPEX activities and measurement results
p 994 N94-16036
An overview of the text propagation effects for land-mobile-satellite systems: Experimental and modeling results p 996 N94-16048
Database for propagation models p 996 N94-16049
A CCIR-based prediction model for Earth-Space propagation p 997 N94-16050

RADIO TRANSMITTERS
Ground wave emergency network environmental assessment for northwestern Colorado relay node site number RN 8C924CO
[AD-A267654] p 1003 N94-17249
An electromagnetic interference study of potential transmitter sites for the HF Active Auroral Research Program (HAARP)
[AD-A267743] p 1004 N94-17373

RADIO WAVES
Proceedings of the Fifteenth NASA Propagation Experimenters Meeting (NAPEX 15) and the Advanced Communications Technology Satellite (ACTS) Propagation Studies Miniworkshop
[NASA-CR-194539] p 994 N94-16035
A review of OPEX activities and measurement results
p 994 N94-16036
Propagation measurements in Alaska using ACTS beacons p 995 N94-16040
Planned LMSS propagation experiment using ACTS: Preliminary antenna pointing results during mobile operations p 995 N94-16041
A comparison of cloud attenuation models using measured cloud data p 996 N94-16044
Comparison of OLYMPUS beacon and radiometric attenuation measurements at Blacksburg, Virginia
p 996 N94-16046
Satellite sound broadcast propagation measurements
p 996 N94-16047
An overview of the text propagation effects for land-mobile-satellite systems: Experimental and modeling results p 996 N94-16048
Database for propagation models p 996 N94-16049
A CCIR-based prediction model for Earth-Space propagation p 997 N94-16050
A study of land mobile satellite service multipath effects using SATLAB software p 997 N94-16051
Ground wave emergency network final operational capability: Environmental assessment for central Utah relay node, site number RN 8C920UT
[AD-A267628] p 1003 N94-17211
Effect of powerful oblique HF waves on ionospheric D-layer absorption
[AD-A268443] p 1102 N94-17499

RADIOACTIVE DECAY
On the 17-keV neutrino
[DE93-012638] p 1181 N94-15974
Electroweak physics from D0
[DE93-015041] p 1181 N94-16053
Experimental study of weak interactions by precision measurement by rare kaon decay
[DE93-016864] p 1182 N94-16117
Neutrino mass and mixing: Summary of the neutrino sessions
[DE93-014342] p 1183 N94-16801
A high sensitivity search for CP violating rare K(sub L) decays and precision measurement of the direct CP violation parameter (epsilon)(prime)/(epsilon) via the four K (yields) 2(pi) decay modes
[DE93-016866] p 1184 N94-16899
Neutral-current detection in the Sudbury Neutrino Observatory
[DE93-014481] p 1185 N94-16951
Search for the top quark from (e(mu)) and (e,e) events in the D0 detector in p(bar-p) collisions at the square root of s = 1.8 TeV
[DE93-016350] p 1186 N94-17662

RADIOACTIVE MATERIALS
Nuclear rocket plume studies
[AD-A267154] p 925 N94-15837

RADIOACTIVITY
Al-26-Mg-26 ages of iron meteorites
p 1242 N94-16240

Operator overloading as an enabling technology for automatic differentiation
[DE93-012699] p 1170 N94-16778

RADIOBIOLOGY
AFRRI reports, first quarter 1993
[AD-A266380] p 1123 N94-16515

RADIOGENIC MATERIALS
Isotopic signatures and distribution of nitrogen and trapped and radiogenic xenon in the Acapulco and FRO90011 meteorites p 1243 N94-16317

RADIOGRAPHY
Laser weld repair of tantalum sheet
[DE93-016417] p 1041 N94-16871

RADIOMETERS
Absolute Radiometric Measurements in Space: ARMS p 908 N94-15085
The laboratory performance of the short wavelength instrument for the Along Track Scanning Radiometer ATSR-2 (initial results) p 908 N94-15088
Absolute, Extreme-Ultraviolet Solar Spectral Irradiance Monitor (AESSIM)
[AD-A267045] p 1299 N94-15836
ERS-1: 18 months in orbit p 990 N94-15888
Olympus propagation measurement results at Virginia Tech p 995 N94-16037
Data acquisition, preprocessing and analysis for the Virginia Tech OLYMPUS experiment p 995 N94-16038
Brightness temperature and attenuation statistics at 20.6 and 31.65 GHz p 996 N94-16045
Comparison of preliminary results from Airborne Aster Simulator (AAS) with TIMS data p 1064 N94-16600
In-flight calibration of the spectral and radiometric characteristics of AVIRIS in 1991 p 1037 N94-16667
Simulation of ASTER data using AVIRIS images p 1071 N94-16693

RADIOMETRIC RESOLUTION
Improved optical radiation detectors and their calibration: 200 nm - 30 microns p 906 N94-15075

RADOMES
Antenna gain loss and pattern degradation due to transmission through dielectric radomes
[AD-A267242] p 986 N94-14974
Manufacturing tolerance requirements for frequency selective surfaces
[AD-A266541] p 999 N94-16797
Radome depolarization effects on monopulse receiver tracking performance
[AD-A267446] p 1001 N94-17031

RAILGUN ACCELERATORS
Numerical modeling of the temperature gradients and spectra of the plasma armature on Thunderbolt
[AD-A266414] p 878 N94-16552

RAIN
Wind shear and heavy rain --- effects on flight stability
[NASA-TM-109453] p 1105 N94-15326
TRMM radar p 990 N94-15894
Recent scientific advances in the use of radar in scientific hydrology p 991 N94-15895
Some thoughts on future rain mapping missions (TRMM follow-on) p 992 N94-15906
Similarity and scale in catchment storm response
[PAPER-89RG01615] p 1083 N94-16028
Olympus propagation measurement results at Virginia Tech p 995 N94-16037
A CCIR-based prediction model for Earth-Space propagation p 997 N94-16050
Validation and analysis of microwave-derived rainfall over the tropics
[AD-A267785] p 1108 N94-17303

RAIN FORESTS
Application of symmetry properties to polarimetric remote sensing with JPL AIRSAR data p 1079 N94-16752

RAINSTORMS
Wind shear and heavy rain --- effects on flight stability
[NASA-TM-109453] p 1105 N94-15326

RAMAN SPECTRA
Studies on the parametric decay of waves in fusion plasmas
[VTT-PUBS-110] p 1200 N94-15204
High frequency Raman current drive p 1201 N94-15208
Current drive with free electron lasers in high and low temperature tokamaks p 1201 N94-15209
Simulations of wave-particle interactions in stimulated Raman forward scattering in a magnetized plasma
[TKK-F-A704] p 1201 N94-15210
New methods of generation of ultrashort laser pulses for ranging p 913 N94-15565
Investigation of the optical, electronic, and structural properties of fiber optic glasses
[AD-A267645] p 971 N94-17204
BACKSCAT lidar simulation version 3.0: Technical documentation and users guide
[AD-A267296] p 1003 N94-17268

RAMAN SPECTROSCOPY
In situ Raman spectroscopy of lithium electrode surface in ambient temperature lithium secondary battery
[DE93-015238] p 1010 N94-16061

RAMJET ENGINES
Equations of motion of a hinged body over a spherical earth
[AD-A268408] p 868 N94-17435

RANDOM ACCESS MEMORY
A fuzzy method for preliminary design random access memory failure rate prediction
[AD-A267948] p 1055 N94-17044

RANDOM LOADS
A simplistic look at limit stresses from random loading
[NASA-TM-108427] p 1058 N94-15710

RANDOM NOISE
A simulation study of the performance of the NASA (2,1,6) convolutional code on RFI/burst channels p 997 N94-16508
Analysis of temporal symmetry in non-gaussian random fields
[AD-A266496] p 999 N94-16794
High resolution radar profiling using higher-order statistics
[AD-D015891] p 1000 N94-16918
High order nonlinear estimation with signal processing applications
[AD-A268407] p 1005 N94-17463

RANDOM PROCESSES
Implications of crater distributions on Venus p 1270 N94-16300
Towards dynamic randomized algorithms in computational geometry
[INRIA-RR-1727] p 1156 N94-17528

RANDOM SAMPLING
Fast simulation of steady-state availability in non-Markovian highly dependable systems
[AD-A266747] p 1174 N94-15823

RANDOM VARIABLES
The distribution of a sum of binomial random variables
[AD-A266969] p 1172 N94-15002
Bounds on inconsistent inferences for sequences of trials with varying probabilities
[AD-A267146] p 1172 N94-15733
Performance of coded coherent FSK lightwave system with noncoherent detection
[AD-A267442] p 1193 N94-17028
Closed form characteristic function for general complex second-order form in correlated complex Gaussian random variables
[AD-A267883] p 1171 N94-17393

RANGEFINDING
Eighth International Workshop on Laser Ranging Instrumentation
[NASA-CP-3214] p 911 N94-15552
Laser tracking for vertical control p 911 N94-15553
Laser ranging network performance and routine orbit determination at D-PAF p 911 N94-15554
Laser ranging application to time transfer using geodetic satellite and to other Japanese space programs p 911 N94-15555
Satellite signatures in SLR observations p 912 N94-15557
Work at Graz on satellite signatures p 898 N94-15558
The precision of today's satellite laser ranging systems p 912 N94-15559
SLR data screening; location of peak of data distribution p 912 N94-15560
Adaptive median filtering for preprocessing of time series measurements p 912 N94-15561
SATCOP mission planning software package p 912 N94-15562
Nd:YLF laser for airborne/spaceborne laser ranging p 913 N94-15563
Alternative wavelengths for laser ranging p 913 N94-15564
New methods of generation of ultrashort laser pulses for ranging p 913 N94-15565
An improved light source for laser ranging p 913 N94-15567
Preliminary results from the portable standard satellite laser ranging intercomparison with MOBLAS-7 p 913 N94-15568
Performance optimization of detector electronics for millimeter laser ranging p 913 N94-15569
Tracking capabilities of SPADs for laser ranging p 914 N94-15570
The solid state detector technology for picosecond laser ranging p 914 N94-15572
Streak camera based SLR receiver for two color atmospheric measurements p 914 N94-15573
The first satellite laser echoes recorded on the streak camera p 914 N94-15574
Experience and results of the 1991 MTLRS-1 USSR campaign p 914 N94-15575
Test results from LAGEOS-2 optical characterization using pulsed lasers p 915 N94-15577
Historical MOBLAS system characterization p 915 N94-15579
Optimum wavelengths for two color ranging p 915 N94-15580
Two color satellite laser ranging upgrades at Goddard's 1.2m telescope facility p 915 N94-15581
Measuring atmospheric dispersion with WLRS in multiple wavelength mode p 916 N94-15582
Millimeter accuracy satellites for two color ranging p 916 N94-15583
Two wavelength satellite laser ranging using SPAD p 916 N94-15584
New perspectives for high accuracy SLR with second generation geodesic satellites p 916 N94-15585
State-of-the-art satellite laser range modeling for geodetic and oceanographic applications p 916 N94-15586
Geometric analysis of satellite laser ranging data p 917 N94-15587
Improvement of SLR accuracy, a possible new step p 917 N94-15588
Compensation for the distortion in satellite laser range predictions due to varying pulse travel times p 917 N94-15590
Timebias corrections to predictions p 875 N94-15591
Formation of on-site normal points p 917 N94-15592
Poisson filtering of laser ranging data p 917 N94-15593
Computer networking at SLR stations p 917 N94-15594
Upgrading NASA/DOSE laser ranging system control computers p 918 N94-15595
HP upgrade operational streamlining p 918 N94-15596
Application of the robust estimate in SLR data preprocessing p 918 N94-15597
A computer-controlled x-y offset guiding stage for the MLRS p 918 N94-15598
LLR: Activities in Wettzell p 876 N94-15600
Matera Laser Ranging Observatory (MLRO): An overview p 877 N94-15601
Sub-cm ranging and other improvements in Graz p 919 N94-15603
Upgrading of the Borowiec laser station p 877 N94-15604
Development of Shanghai satellite laser ranging station p 877 N94-15605
WLRS --- Wettzell Laser Ranging System (WLRS) p 877 N94-15606
New progress of ranging technology at Wuhan Satellite Laser Ranging Station p 877 N94-15608
TLRS-3 system upgrades p 877 N94-15609
Results of the MTLRS-1 upgrade p 877 N94-15610
The new MTLRS-1 receiving system p 877 N94-15611
The new MTLRS transmitting system p 877 N94-15612
Airborne 2 color ranging experiment p 920 N94-15614
GLRS-R 2-colour retroreflector target design and predicted performance p 921 N94-15615
Effects of turbulence on the geodynamic laser ranging system p 921 N94-15616
Mars laser altimeter based on a single photon ranging technique p 921 N94-15619
Satellite laser station Helwan status 1992 p 877 N94-15621
Optical attenuation mechanism upgrades, MOBLAS, and TLRS systems p 922 N94-15622
The third generation SLR station Potsdam no. 7836 p 877 N94-15623
Performance comparison of high speed microchannel plate photomultiplier tubes p 922 N94-15624
Station report on the Goddard Space Flight Center (GSFC) 1.2 meter telescope facility p 922 N94-15625
Clementine: Anticipated scientific datasets from the Moon and Geographos p 1288 N94-16392
Digital laser range finder emulator
[AD-D015811] p 1040 N94-16540
Atomic beam studies relevant to the space environment
[AD-A268628] p 1186 N94-17436

RANGELANDS
Using AVIRIS images to measure temporal trends in abundance of photosynthetic and nonphotosynthetic canopy components p 1066 N94-16668

RANKING
Nonparametric statistics: Weighted rankings analysis
[AD-A266607] p 1173 N94-16657

RARE EARTH ELEMENTS
An experimental study of trace element partitioning between perovskite, hibonite and melt: Equilibrium values p 954 N94-16313
AVIRIS as a tool for carbonatite exploration: Comparison of SPAM and Mbandmap data analysis methods p 1073 N94-16703
Theoretical studies of the crystal structure of rare earths and actinides at zero temperature
[DE93-016488] p 1214 N94-17301
RARE GASES
Al-26-Mg-26 ages of iron meteorites p 1242 N94-16240
First investigation of noble gases in the Dengli H3,8 chondrite p 953 N94-16264
Transition metals in superheat melts p 962 N94-16273
A search for noble-gas evidence for presolar oxide grains p 954 N94-16353
Noble gases in twenty Yamato H-chondrites: Comparison with Allan Hills chondrites and modern falls p 1244 N94-16361
Nitrogen and light noble gases in Parsa enstatite chondrite p 1246 N94-16435
RAREFACTION
DSMC simulations of Mach 20 nitrogen flows about a 70 degree blunted cone and its wake
[NASA-TM-107762] p 1018 N94-15291
RAREFIED GAS DYNAMICS
Particle kinetic simulation of high altitude hypervelocity flight
[NASA-CR-194599] p 856 N94-15678
Particle simulation of hypersonic flow
[AD-A267185] p 857 N94-15787
To extend the thirteen-moment theory and its application to problems in rarefied hypersonic flow
[AD-A267384] p 859 N94-17021
RAREFIED GASES
Electronic spectroscopy of the gas-phase OH-Kr van der Waals complex
[AD-A266891] p 942 N94-14946
RASTER SCANNING
Krupp technical reports no. 2, English edition, October 1992
[ETN-93-94631] p 984 N94-16000
RELMA: On-line quality control in the rubber mixing room using laser analysis p 984 N94-16005
RATINGS
The airline quality report 1993
[NIAR-93-11] p 863 N94-17262
RATIOS
A calibration of the production rate ratio P-21/P-26 by low energy secondry neutrons: Identification of Ne spallation components at the 10(exp 6) atoms/g level in terrestrial samples p 1187 N94-16194
Encapsulation of hemoglobin in non-phospholipid vesicles
[AD-A266505] p 1128 N94-16785
RATS
Neuropeptide-Y (NPY) increases total blood flow in the tail, and reduces cutaneous microvascular blood flow in the tail and foot of the rat
[AD-A266839] p 1115 N94-14918
TransRapid TR-07 maglev-spectrum magnetic field effects on daily pineal indoleamine metabolic rhythms in rodents
[DE93-015143] p 1117 N94-16893
The behavioral toxicology of high-peak, low average power, pulsed microwave irradiation
[AD-A268392] p 1134 N94-17535
RAWINSONDES
Empirical relationships among atmospheric variables from rawinsonde and field data as surrogates for AVIRIS measurements: Estimation of regional land surface evapotranspiration p 1074 N94-16712
RAY TRACING
The three-dimensional ray trajectories of the WKB optical fiber modes
[AD-A267167] p 1189 N94-15739
Ray tracing on topographic Rossby waves
[AD-A267014] p 1112 N94-15844
A ray trace model for propagation loss
[AD-A266314] p 997 N94-16467
RAYLEIGH SCATTERING
The structure of turbulent boundary layers and shock wave boundary layer interactions
[AD-A266240] p 1026 N94-16929
RDX
Laser ignition of solid propellants: 1. Ignition delays
[AD-A268454] p 976 N94-17538
REACTING FLOW
Reaction and diffusion in turbulent combustion
[DE93-017085] p 943 N94-15146
Large eddy simulation and direct numerical simulation of high speed turbulent reacting flows
[NASA-CR-193131] p 1018 N94-15427
Fundamental studies of rocket combustion chemistry and combustion instability
[AD-A266248] p 925 N94-16482
Studies in turbulence and turbulence control
[AD-A266318] p 1026 N94-16950
Studies on nonequilibrium phenomena in supersonic chemically reacting flows
[NASA-CR-194662] p 1027 N94-17215
Chemical reactions in turbulent mixing flows
[AD-A268287] p 881 N94-17580
REACTION BONDING
NMR and theoretical investigation of cation binding with sol-gel silicates
[AD-A266999] p 963 N94-15631
REACTION KINETICS
Reactions of chemiluminescence induced by singlet oxygen with metals
[ONERA-NT-1992-13] p 955 N94-15149
Intramolecular versus intermolecular condensation rates in the acidic polymerization of octaethoxytrisiloxane
[AD-A266982] p 963 N94-15490
Particle simulation of hypersonic flow
[AD-A267185] p 857 N94-15787
A proposed mechanism for the pyrolysis of diborane
[DE93-014275] p 947 N94-15977
Molecular beam studies of reaction dynamics
[DE93-015035] p 1181 N94-15995
A comparison of one and two dimensional flame quenching: Heat transfer results
[DE93-015196] p 947 N94-16060
Corrosion kinetics and mechanisms for nuclear grade graphites
[DE93-015462] p 947 N94-16105
Single-collision studies of energy transfer and chemical reaction
[DE93-017603] p 1182 N94-16121
Evaporation kinetics of Mg2SiO4 crystals and melts from molecular dynamics simulations p 1219 N94-16331
Studies of combustion reactions at the state-resolved differential cross section level
[DE93-017605] p 948 N94-16462
Structural effects in electron transfer reactions: Comparative interfacial electrochemical kinetics for cis- versus trans-dioxorhenium (V) (bi)pyridine oxidation
[AD-A266307] p 1182 N94-16466
Tritium diffusion and desorption in single crystal LiAlO2
[DE93-015140] p 1211 N94-16805
Emissions of volatile organic compounds from stationary combustion sources: Numerical modeling capabilities
[DE93-014123] p 1096 N94-16825
Modeling study to evaluate the ionic mechanism of soot formation in flames
[AD-A266242] p 950 N94-16930
Materials processing and manufacturing technologies for diamond substrate multichip modules (DSMCM)
[AD-A267316] p 969 N94-16946
Advanced thermally stable jet fuels
[DE93-017711] p 975 N94-16996
Pulsed laser kinetic studies of liquids under high pressure
[DE93-017826] p 1041 N94-16998
Solvational barriers to interfacial electron transfer: Minimization by way of valence delocalization
[AD-A267371] p 950 N94-17006
The influence of an electric field on the kinetics of nucleation
[IFTR-2/91] p 1213 N94-17046
Surface reactivity of combustion generated soot particles
[AD-A268017] p 952 N94-17532
Cathode sheath charge transfer effects
[AD-A268393] p 1186 N94-17536
Laser ignition of solid propellants: 1. Ignition delays
[AD-A268454] p 976 N94-17538
Coefficients for calculating thermodynamic and transport properties of individual species
[NASA-TM-4513] p 1220 N94-17624
Kinetics of silica-phase transitions
[DE93-016231] p 1217 N94-17659
REACTION PRODUCTS
Geochemistry and cosmochemistry of fullerenes 3: Reaction of C60 and C70 with ozone p 953 N94-16243
Studies of combustion reactions at the state-resolved differential cross section level
[DE93-017605] p 948 N94-16462
REACTION TIME
A novel solid-state optical temporal analyzer with picosecond resolution and picowatt sensitivity
[AD-A266804] p 986 N94-14912
Apparatus for and a method of growing thin films of elemental semiconductors
[AD-D015813] p 1210 N94-16487
REACTIVITY
Models for reactivity
[AD-A266419] p 1149 N94-16554
Synthesis, reactivity, and characterization of (-hexacarbocyclic) manganese dicarbonyl complexes with sulfur and phosphorus ligands
[AD-A267592] p 930 N94-17192
Surface reactivity of combustion generated soot particles
[AD-A268017] p 952 N94-17532
REACTOR MATERIALS
Space exploration initiative fuels, materials and related nuclear propulsion technologies panel
[NASA-TM-105706] p 923 N94-15118
The effect of irradiation on the mechanical properties of 6061-T651 aluminum
[DE93-015825] p 958 N94-16168
REACTOR SAFETY
System performance modeling and analysis of a fault-tolerant, real time parallel processor
[AD-A268070] p 1162 N94-17551
REACTOR TECHNOLOGY
Space exploration initiative fuels, materials and related nuclear propulsion technologies panel
[NASA-TM-105706] p 923 N94-15118
READERS
The impact of report of investigation writing style on the assessment times, impressions, perceptions and preferences of adjudicators
[AD-A265748] p 1223 N94-15682
READING
Enhancing sight
[NASA-TM-109637] p 1221 N94-15248
The impact of report of investigation writing style on the assessment times, impressions, perceptions and preferences of adjudicators
[AD-A265748] p 1223 N94-15682
READOUT
Cryogenic readout electronics for astronomical applications p 910 N94-15099
REAL TIME OPERATION
The MADONA experiments (Meteorology and Diffusion Over Non-uniform Areas): High-resolution in-plume concentration fluctuations measurements using lidar remote sensing technique
[AD-A267711] p 1105 N94-14938
Fuzzy inverse kinematic mapping: Rule generation, efficiency, and implementation
[AD-A266967] p 1163 N94-14954
Visualization of solidification front phenomena
[NASA-CR-193838] p 976 N94-15006
Evaluation of ALSYS 037 Ada Compiler
[AD-A266972] p 1143 N94-15110
Short term weather forecasting in real time in a base weather station setting
[AD-A266872] p 1105 N94-15142
Overview of Enhanced Data Stream Array Processor (EDSAP)
[AD-A266986] p 1158 N94-15492
Hidden Markov model approach to skill learning and its application to telerobotics
[AD-A266989] p 1164 N94-15502
Upgrading NASA/DOSE laser ranging system control computers p 918 N94-15595
HP upgrade operational streamlining p 918 N94-15596
Complexity analysis of real-time reinforcement learning applied to finding shortest paths in deterministic domains
[AD-A266636] p 1131 N94-15742
Adaptive weld control for high-integrity welding applications
[TABES PAPER 93-604] p 1049 N94-16140
Real-time adaptive neural network data processing
[TABES PAPER 93-660] p 1054 N94-16155
Visually guided touching and manual tracking
[TR-412] p 1166 N94-16581
Efficient scheduling of real-time compute-intensive periodic graphs on large grain data flow multiprocessor
[AD-A267444] p 1141 N94-17030
Causality-preserving timestamps in distributed programs
[AD-A267534] p 1153 N94-17118
ARPA unmanned ground vehicle stereo vision program at Teleos Research
[AD-A267632] p 1167 N94-17202
Module interconnection frameworks for a real-time spreadsheet
[AD-A267317] p 1153 N94-17220
Module interconnection frameworks for a real-time spreadsheet
[AD-A267752] p 1153 N94-17231
Image accuracy and representational enhancement through low-level, multi-sensor integration techniques
[DE93-014888] p 1167 N94-17287

Estimating task execution delay in a real-time system via static source code analysis
[AD-A267496] p 1161 N94-17367
Real time system for practical acoustic monitoring of global ocean temperature
[AD-A267868] p 1113 N94-17391
Femtosecond carrier processes in compound semiconductors and real time signal processing
[AD-A268122] p 1005 N94-17519
System performance modeling and analysis of a fault-tolerant, real time parallel processor
[AD-A268070] p 1162 N94-17551

RECEIVERS
Preparation and properties of Nb/Al SIS and SIN junctions for millimeter and submillimeter radioastronomical receivers p 907 N94-15078
Streak camera based SLR receiver for two color atmospheric measurements p 914 N94-15573
The new MTLRS-1 receiving system p 877 N94-15611
Optical attenuation mechanism upgrades, MOBLAS, and TLRS systems p 922 N94-15622
The third generation SLR station Potsdam no. 7836 p 877 N94-15623
Planned LMSS propagation experiment using ACTS: Preliminary antenna pointing results during mobile operations p 995 N94-16041
OETC optical backplane bus testbed. IBM tasks: Receiver OEIC and link simulation tools and analysis
[AD-A266198] p 1191 N94-16128
Notes on the use of Dempster-Shafer and fuzzy reasoning to fuse identity attribute data
[AD-A267426] p 1004 N94-17309

RECEPTION DIVERSITY
Spatial and frequency diversity in lidar systems
[AD-A266192] p 1039 N94-16124

RECOMBINATION REACTIONS
Merged beam studies of laser stimulated radiative recombination
[AD-A267186] p 1037 N94-15145
OSA proceedings on Ultrafast Electronics and Optoelectronics, volume 14
[AD-A267972] p 1014 N94-17410

RECONNAISSANCE
Space countersurveillance: A requisite for theater defense planning
[AD-A266871] p 884 N94-15147

RECONNAISSANCE SPACECRAFT
Space countersurveillance: A requisite for theater defense planning
[AD-A266871] p 884 N94-15147

RECONSTRUCTION
Unitary plan wind tunnel landmark dedication and revitalization
[NASA-TM-109649] p 1302 N94-15434

RECORDS
Monitoring history
[NASA-TM-109640] p 1229 N94-15251

RECORDS MANAGEMENT
Monitoring history
[NASA-TM-109640] p 1229 N94-15251
NASA security handbook
[NHB-1620.3C] p 1224 N94-15937
Managing information as a corporate asset: Key strategies for information professionals to remain competitive
[DE93-015515] p 1232 N94-16875

RECREATION
GSFC Fun Run
[NASA-TM-109587] p 1120 N94-15271

RECRYSTALLIZATION
Thin Ni silicide formation by low temperature-induced metal atom reaction with ion implanted amorphous silicon
[DE93-015449] p 1209 N94-16066
Isotopic signatures and distribution of nitrogen and trapped and radiogenic xenon in the Acapulco and FRO90011 meteorites p 1243 N94-16317
Tensile and stress-rupture behavior of hafnium carbide dispersed molybdenum and tungsten base alloy wires
[NASA-TM-106350] p 962 N94-17652

RECTANGULAR BEAMS
A simplistic look at limit stresses from random loading
[NASA-TM-108427] p 1058 N94-15710

RECTENNAS
Dual polarization microstrip array antenna
[CA-PATENT-1-307-842] p 994 N94-15986

RECYCLING
User's guide: Hot-mix recycling of asphalt concrete pavements
[AD-A266939] p 983 N94-15177
Investigations into the recovery of waste sulfuric acid with concentrated solar radiation
[DLR-FB-93-11] p 952 N94-17594

RED SEA
Optical properties of the Red Sea
[AD-A266466] p 1113 N94-16588

RED SHIFT
Complex QSO absorbers: High-redshift clusters of galaxies?
[NASA-CR-194617] p 1237 N94-16833

REDOX CELLS
Solvational barriers to interfacial electron transfer: Minimization by way of valence delocalization
[AD-A267371] p 950 N94-17006

REDUCTION (CHEMISTRY)
In situ studies of passive film chemistry using x ray absorption spectroscopy
[DE93-014023] p 947 N94-16011

REDUNDANCY ENCODING
System performance modeling and analysis of a fault-tolerant, real time parallel processor
[AD-A268070] p 1162 N94-17551

REED-SOLOMON CODES
Compact disk error measurements p 1227 N94-14988

REENTRY VEHICLES
Tetrahedral lander
[NASA-CASE-MSC-22082-1] p 886 N94-15951

REFERENCE STARS
Design of pulse stretching cell for a sodium guide star optical system
[DE93-016436] p 1236 N94-14929
Tip-tilt compensation: Resolution limits for ground-based telescopes using laser guide star adaptive optics
[DE93-016426] p 1237 N94-16872

REFILLING
Kinetic plasma processes occurring in the outer plasmasphere
[NASA-CR-193452] p 1300 N94-17524

REFLECTANCE
An expert system shell for inferring vegetation characteristics: Atmospheric techniques (Task G)
[NASA-CR-194570] p 1082 N94-15531
ETALON-1,-2 center of mass correction and array reflectivity p 915 N94-15576
Engineering design of sub-micron topographies for simultaneously adherent and reflective metal-polymer interfaces
[NASA-CR-194573] p 964 N94-15700
Laboratory for x ray optics
[AD-A267149] p 1189 N94-15735
Multilayer thin film design for far ultraviolet polarizers using an induced transmission and absorption technique
[NASA-CR-194631] p 1190 N94-15869
Modeling the reflectance of CO2 frost with new optical constants: Application to Martian south polar cap spectra p 1256 N94-16217
Thermal inertia and radar reflectivity of the Martian north polar ERG: Low-density aggregates p 1260 N94-16238
Iron oxide bands in the visible and near-infrared reflectance spectra of primitive asteroids p 1242 N94-16274
Radar properties of several fluidized ejecta blankets on Venus p 1267 N94-16278
VUV thin films, chapter 7
[NASA-CR-194634] p 967 N94-16494
Unmixing AVIRIS data to provide a method for vegetation fraction subtraction p 1066 N94-16669
Ground-truthing AVIRIS mineral mapping at Cuprite, Nevada p 1069 N94-16682
MAC Europe 1991: Evaluation of AVIRIS, GER imaging spectrometry data for the land application testsite Oberpfaffenhofen p 1070 N94-16688
Simulation of ASTER data using AVIRIS images p 1071 N94-16693
Investigation of the optical, electronic, and structural properties of fiber optic glasses
[AD-A267645] p 971 N94-17204

REFLECTED WAVES
Regular and irregular reflection of a wave from a slanting flat wall
[IFTR-13/1991] p 1193 N94-17049

REFLECTION
Composite refraction-reflection stack sections: Tracing faults in the Atlantic coastal plain sediments
[DE93-013581] p 1112 N94-16009
High-resolution seismic reflection survey at the Manson crater, Iowa p 1103 N94-16307
ATCRBS reply environment at Memphis International Airport
[AD-A266322] p 864 N94-16439

REFLECTOR ANTENNAS
Proceedings of the 1992 Antenna Applications Symposium, volume 2
[AD-A266916] p 986 N94-14998
Proceedings of the 1992 Antenna Applications Symposium, volume 1
[AD-A268167] p 1005 N94-17431

REFLECTORS
An improved patch for radiative coolers
[NASA-CASE-GSC-13503-1] p 1046 N94-15873

REFRACTION
Composite refraction-reflection stack sections: Tracing faults in the Atlantic coastal plain sediments
[DE93-013581] p 1112 N94-16009

REFRACTIVITY
Determination of average refractive index of spin coated DCG films for HOE fabrication p 1036 N94-14992
A test of the applicability of independent scattering to high albedo planetary regoliths p 1250 N94-16187
A ray trace model for propagation loss
[AD-A266314] p 997 N94-16467
Characterization of voids formed during liquid impregnation of nonwoven multifilament glass networks as related to composite processing p 939 N94-16858
BACKSCAT lidar simulation version 3.0: Technical documentation and users guide
[AD-A267296] p 1003 N94-17268
Review of rigorous coupled-wave analysis and of homogeneous effective medium approximations for high spatial-frequency surface-relief gratings p 1194 N94-17335
Diffractive optical elements for generating arbitrary line foci p 1195 N94-17338
Applications of advanced diffractive optical elements p 1197 N94-17356
Predesign of diamond turned refractive/diffractive elements for IR objectives p 1198 N94-17359

REFRACTORIES
Refractory precursor components in an Allende ferromagnesian chondrule p 1245 N94-16412

REFRACTORY MATERIALS
Processing and protection of high temperature structural materials
[AD-A267292] p 954 N94-14961
High temperature advanced structural composites. Volume 2: Ceramic matrix composites, fiber processiing and properties, and interfaces
[AD-A267023] p 933 N94-15528
High temperature advanced structural composites. Volume 1: Executive summary and intermetallic compounds
[AD-A267022] p 933 N94-15835
Techniques for preparation of ingot metallurgical discontinuous composites
[AD-D015748] p 940 N94-16933

REFRACTORY METAL ALLOYS
High temperature materials technology research for advanced thermionic systems
[DE93-018302] p 960 N94-16964

REFRACTORY METALS
Thermal spray forming of refractory sample ampoule cartridges for single crystal growth space furnaces
[TABES PAPER 93-605] p 1051 N94-16141
Experimental partitioning of Zr, Ti, and Nb between silicate liquid and a complex noble metal alloy and the partitioning of Ti between perovskite and platinum metal p 962 N94-16287
Properties of thin films for high temperature flow sensors
[NASA-CR-191526] p 967 N94-16541

REFRIGERANTS
Cycle performance testing of nonazeotropic mixtures of HFC-142A/HCFC-124 and HFC-32/HCFC-124 with enhanced surface heat exchangers
[DE93-015215] p 1024 N94-16808

REFRIGERATING
Space Station thermal storage/refrigeration system research and development
[NASA-CR-193841] p 879 N94-15191
Proceedings of the 7th International Cryocooler Conference, part 1
[AD-A268448] p 985 N94-17482
Proceedings of the 7th International Cryocooler Conference, part 2
[AD-A268449] p 985 N94-17484
Proceedings of the 7th International Cryocooler Conference, part 3
[AD-A268450] p 985 N94-17485

REFRIGERATORS
An adiabatic demagnetisation refrigerator with a mechanical pre-cooler for space applications p 906 N94-15070
In orbit adiabatic demagnetization refrigeration for bolometric and microcalorimetric detectors p 907 N94-15079
Proceedings of the 7th International Cryocooler Conference, part 1
[AD-A268448] p 985 N94-17482
Proceedings of the 7th International Cryocooler Conference, part 2
[AD-A268449] p 985 N94-17484

Proceedings of the 7th International Cryocooler Conference, part 3
[AD-A268450] p 985 N94-17485

REGENERATIVE COOLING
Proceedings of the 7th International Cryocooler Conference, part 1
[AD-A268448] p 985 N94-17482
Proceedings of the 7th International Cryocooler Conference, part 2
[AD-A268449] p 985 N94-17484
Proceedings of the 7th International Cryocooler Conference, part 3
[AD-A268450] p 985 N94-17485

REGOLITH
A test of the applicability of independent scattering to high albedo planetary regoliths p 1250 N94-16187
Nitrates in SNCs: Implications for the nitrogen cycle on Mars p 1251 N94-16193
Why is the Moon dark? p 1256 N94-16219
The physical mechanism of comet outbursts: An experiment p 1242 N94-16221
JSC-1: A new lunar regolith simulant p 1289 N94-16398
Equatorial ground ice on Mars: Steady-state stability p 1290 N94-16403
Mars brine formation experiment p 1293 N94-16419
Helium-3 inventory of lunar samples: A potential future energy resource for mankind? p 1295 N94-16428

REGRESSION ANALYSIS
Efficiency effects of variation in controlled experimental variables
[DE93-014345] p 1169 N94-15979
A linear spectral matching technique for retrieving equivalent water thickness and biochemical constituents of green vegetation p 1068 N94-16678
Computing science and statistics. Volume 24: Graphics and visualization
[AD-A266571] p 1150 N94-16721
Ensemble forecasting techniques in medium-range forecasting
[AD-A267443] p 1107 N94-17029

REGULARITY
On a class of singular quasilinear elliptic equations with general structure and distribution data
[DE93-628585] p 1171 N94-17613

REGULATIONS
Permanent change of station: The NASA employee's guide to an easier move
[NHB-9760.1A] p 1223 N94-15931
Incorporating global warming risks in power sector planning. Volume 1: A case study of the New England region
[DE93-015241] p 1096 N94-17289

REGULATORS
Regulated emergency oxygen system
[AD-A266228] p 1138 N94-16983

REINFORCED PLASTICS
Evaluation of hybrid reinforcement (fiber-reinforced-plastic rod with steel core)
[AD-A268009] p 941 N94-17473

REINFORCED PLATES
Dynamic behavior of fiber and particle reinforced composites
[AD-A266905] p 930 N94-15143

REINFORCEMENT (STRUCTURES)
Evaluation of hybrid reinforcement (fiber-reinforced-plastic rod with steel core)
[AD-A268009] p 941 N94-17473

REINFORCING FIBERS
Construction, testing, and representation of resin and fiber reinforced materials p 931 N94-15255
Production process p 931 N94-15257
Sound radiation from infinite laminated composite shell with periodic rib stiffening
[DRA/TM(USGR)92326] p 933 N94-15699
NEXTEL(trademark)/SiC composites using forced chemical vapor infiltration
[DE93-013532] p 934 N94-16008
Overview of chemical vapor infiltration
[DE93-015440] p 934 N94-16065
Environmental effects on elevated temperature subcritical crack growth of SiC/SiC composites
[DE93-015688] p 934 N94-16158
Continuous fabrication of SiC fiber tows by chemical vapor deposition
[AD-A266460] p 936 N94-16569
Interfacial shear behavior and its influence on fiber damage in sapphire-reinforced gamma titanium aluminide composites
[AD-A267943] p 1060 N94-17043
Fiber strength utilization in carbon/carbon composites
[AD-A267713] p 940 N94-17271
Direct observation of fracture of CAS-glass/SiC composites and processing of toughened alumina
[AD-A268275] p 941 N94-17457

REINFORCING MATERIALS
Continuous fabrication of SiC fiber tows by chemical vapor deposition
[AD-A266460] p 936 N94-16569

RELATIVISTIC EFFECTS
Investigation of the interactions of radiation with matter
[AD-A266743] p 1181 N94-15774

RELATIVISTIC THEORY
Relativistic mean-field calculations of lambda and sigma hypernuclei
[DE93-015269] p 1181 N94-16013
Lunar LIGO: A new concept in gravitational wave astronomy p 1277 N94-16337
Relativistic dynamics of spin in strong external fields
[NIKHEF-H/93-06] p 1240 N94-17604

RELAXATION OSCILLATORS
The stability and dynamics of elastic structures and fluid flows
[AD-A267990] p 1029 N94-17414

RELIABILITY
Statistical computation of tolerance limits
[NASA-TM-108424] p 1172 N94-15535
Reliability characterization of digital microcircuits: Investigation of an in-process oxide reliability screening method
[AD-A267053] p 1008 N94-15665
Reliability of autonomic responses and malaise across multiple motion sickness stimulation tests
[NASA-TM-108787] p 1121 N94-15711
Fast simulation of steady-state availability in non-Markovian highly dependable systems
[AD-A266747] p 1174 N94-15823
General Monte Carlo reliability simulation code including common mode failures and HARP fault/error-handling
[NASA-CR-187587] p 1150 N94-16594
The 1987 Goddard Space Flight Center Battery Workshop
[NASA-CP-3236] p 1012 N94-17062
A ten year review of performance of photovoltaic systems
[DE93-015649] p 1093 N94-17217
X ray computed tomography for failure analysis investigations
[AD-A268086] p 1055 N94-17515
Reliability and maintainability of modular robot systems: A roadmap for design
[AD-A268104] p 1168 N94-17517

RELIABILITY ANALYSIS
Software reliability through fault-avoidance and fault-tolerance
[NASA-CR-194353] p 1143 N94-15114
Safety-critical software: Status report and annotated bibliography
[AD-A266993] p 1144 N94-15214
Concepts on measuring the benefits of software process improvements
[AD-A266994] p 1144 N94-15215
Technology transfers and reliable oxides
[AD-A266948] p 1175 N94-15758
NASA trend analysis procedures
[NASA-RP-1290] p 1223 N94-15782
General Monte Carlo reliability simulation code including common mode failures and HARP fault/error-handling
[NASA-CR-187587] p 1150 N94-16594
Reducing data dimension to lower signal processing computational requirements and maximize performance
[AD-A266606] p 999 N94-16728
Reliability analysis of Surface Mount Technology (SMT)
[AD-A267598] p 1055 N94-17194
Tutorial: Advanced fault tree applications using HARP
[NASA-TM-102747] p 1155 N94-17447

RELIABILITY ENGINEERING
Concepts on measuring the benefits of software process improvements
[AD-A266994] p 1144 N94-15215
Small satellite product assurance p 896 N94-17188

RELIEF MAPS
Separation of topographic and intrinsic backscatter variations in biscopic radar images: A magic airbrush p 1086 N94-16318

RELOCATION
Permanent change of station: The NASA employee's guide to an easier move
[NHB-9760.1A] p 1223 N94-15931

REMOTE CONTROL
Infrared remote activity transceiver universal model
[AD-A266965] p 1188 N94-15144
Remote tire pressure sensing technique
[NASA-CASE-LAR-14160-1] p 1033 N94-15884
Krupp technical reports no. 2, English edition, October 1992
[ETN-93-94631] p 984 N94-16000
Remote diagnosis as used for mechanized parking systems p 984 N94-16004
The ESA telescience program p 977 N94-16073
MAXUS: The new sounding rocket program for long duration microgravity flight p 978 N94-16079

REMOTE HANDLING
STS-41 VCS training with mission specialist Bruce Melnick and Bill Shepard
[NASA-TM-109513] p 1046 N94-15459

REMOTE MANIPULATOR SYSTEM
STS-26 EVA rescue training
[NASA-TM-109563] p 875 N94-15333
Space Station/Orbiter berthing dynamics during an assembly flight
[NASA-TM-109049] p 1062 N94-17451

REMOTE SENSING
The MADONA experiments (Meteorology and Diffusion Over Non-uniform Areas): High-resolution in-plume concentration fluctuations measurements using lidar remote sensing technique
[AD-A267711] p 1105 N94-14938
Views from space
[NASA-TM-109634] p 1081 N94-15245
Combating malaria
[NASA-TM-109609] p 1081 N94-15297
Heterodyne efficiency for a coherent laser radar with diffuse or aerosol targets
[NASA-CR-194563] p 1038 N94-15477
SeaWiFS technical report series. Volume 12, SeaWiFS technical report series cumulative index: Volumes 1-11
[NASA-TM-104566-VOL-12] p 1111 N94-15529
An expert system shell for inferring vegetation characteristics: Atmospheric techniques (Task G)
[NASA-CR-194570] p 1082 N94-15531
Steering capaciflector sensor
[NASA-CASE-GSC-13489-1] p 1164 N94-15704
Workshop on advanced technologies for planetary instruments
[NASA-CR-194585] p 1032 N94-15797
Environmental characterization for target acquisition. Report 1: Site descriptions and measurements
[AD-A267192] p 1106 N94-15851
Proceedings of the Third Spaceborne Imaging Radar Symposium
[NASA-CR-194104] p 989 N94-15886
ERS-1: 18 months in orbit p 990 N94-15888
X-SAR: The X-band synthetic aperture radar on board the Space Shuttle p 990 N94-15891
ENVISAT ASAR p 898 N94-15892
TRMM radar p 990 N94-15894
Driving terrestrial ecosystem models from space p 991 N94-15896
Recent advances in radar remote sensing of forest p 991 N94-15897
Radar response of vegetation: An overview p 991 N94-15898
Geologic remote sensing with radar p 991 N94-15900
SIR-C/X-SAR free flyer concept p 898 N94-15903
EOS SAR: A new approach p 992 N94-15904
A summary of microwave remote sensing investigations planned for BOREAS p 993 N94-15914
Primary studies of Chinese spaceborne SAR p 993 N94-15916
AIRSAR South American deployment: Operation plan, version 3.0 p 994 N94-15919
Spatial and frequency diversity in lidar systems
[AD-A266192] p 1039 N94-16124
Earth imaging results from Galileo's second encounter p 1252 N94-16201
Remote sensing studies of the northeastern portion of the lunar nearside p 1258 N94-16225
Far-infrared spectra of CO2 clathrate hydrate frosts p 954 N94-16340
Martian lavas: Three complementary remote sensing techniques to derive flow properties p 1283 N94-16366
The Clementine instrument complement p 1086 N94-16370
A mission concept of Phobos/Deimos exploration p 1287 N94-16387
Remote visual detection of impacts on the lunar surface p 1290 N94-16404
Do it yourself remote sensing: Generating an inexpensive, high tech, real science lake mapping project for the classroom p 1086 N94-16407
A quantitative analysis of TIMS data obtained on the Learjet 23 at various altitudes p 1063 N94-16597
Comparison of preliminary results from Airborne Aster Simulator (AAS) with TIMS data p 1064 N94-16600
An algorithm for the estimation of bounds on the emissivity and temperatures from thermal multispectral airborne remotely sensed data p 1064 N94-16603
Multi-resolution processing for fractal analysis of airborne remotely sensed data p 1065 N94-16604
Ejecta patterns of Meteor Crater, Arizona derived from the linear un-mixing of TIMS data and laboratory thermal emission spectra p 1065 N94-16607

Using AVIRIS images to measure temporal trends in abundance of photosynthetic and nonphotosynthetic canopy components p 1066 N94-16668
Mapping the mineralogy and lithology of Canyonlands, Utah with imaging spectrometer data and the multiple spectral feature mapping algorithm p 1066 N94-16670
Hyperspectral modeling for extracting aerosols from aircraft/satellite data p 1067 N94-16673
AVIRIS study of Death Valley evaporite deposits using least-squares band-fitting methods p 1067 N94-16676
A field measure of the shade fraction p 1068 N94-16677
A linear spectral matching technique for retrieving equivalent water thickness and biochemical constituents of green vegetation p 1068 N94-16678
Mapping the spectral variability in photosynthetic and non-photosynthetic vegetation, soils, and shade using AVIRIS p 1068 N94-16679
Exploring the remote sensing of foliar biochemical concentrations with AVIRIS data p 1069 N94-16683
AVIRIS calibration and application in coastal oceanic environments p 1069 N94-16685
Mapping vegetation types with the multiple spectral feature mapping algorithm in both emission and absorption p 1069 N94-16686
Multiple dataset water-quality analyses in the vicinity of an ocean wastewater plume p 1069 N94-16687
Using endmembers in AVIRIS images to estimate changes in vegetative biomass p 1070 N94-16689
The 1991 AVIRIS/POLDER experiment in Camargue, France p 1070 N94-16691
JPL activities on development of acousto-optic tunable filter imaging spectrometer p 1037 N94-16696
Measuring dry plant residues in grasslands: A case study using AVIRIS p 1072 N94-16697
Tracking photosynthetic efficiency with narrow-band spectroradiometry
| CIW-PUBL-1133 | p 1072 N94-16698
Integrating remote sensing techniques at Cuprite, Nevada: AVIRIS, Thematic Mapper, and field spectroscopy p 1072 N94-16701
Oregon transect: Comparison of leaf-level reflectance with canopy-level and modelled reflectance p 1073 N94-16702
Expert system-based mineral mapping using AVIRIS p 1073 N94-16704
AVIRIS data and neural networks applied to an urban ecosystem p 1073 N94-16705
Temporal variation in spectral detection thresholds of substrate and vegetation in AVIRIS images p 1073 N94-16706
A comparison of LOWTRAN-7 corrected Airborne Visible/Infrared Imaging Spectrometer (AVIRIS) data with ground spectral measurements p 1074 N94-16710
Discrimination among semi-arid landscape endmembers using the Spectral Angle Mapper (SAM) algorithm p 1074 N94-16711
Empirical relationships among atmospheric variables from rawinsonde and field data as surrogates for AVIRIS measurements: Estimation of regional land surface evapotranspiration p 1074 N94-16712
Retrieval of pine forest biomass using JPL AIRSAR data p 1076 N94-16737
Characterization of wetland, forest, and agricultural ecosystems in Belize with airborne radar (AIRSAR) p 1076 N94-16738
Strategies for detection of floodplain inundation with multi-frequency polarimetric SAR p 1076 N94-16739
Supervised fully polarimetric classification of the Black Forest test site: From MAESTRO1 to MAC Europe p 1076 N94-16740
Relating multifrequency radar backscattering to forest biomass: Modeling and AIRSAR measurement p 1077 N94-16741
Mapping of sea bottom topography p 1077 N94-16744
Preliminary results of polarization signatures for glacial moraines in the Mono Basin, Eastern Sierra Nevada p 1078 N94-16746
Extraction of quantitative surface characteristics from AIRSAR data for Death Valley, California p 1078 N94-16748
Application of symmetry properties to polarimetric remote sensing with JPL AIRSAR data p 1079 N94-16752
Processing of polarimetric SAR data for soil moisture estimation over Mahantango watershed area p 1079 N94-16754
Soil conservation applications with C-band SAR p 1080 N94-16760
Earth observational research using multistage EOS-like data
| NASA-CR-194626 | p 1084 N94-16831
Remote sensing of precipitation and electrification with a dual-polarization, coherent, wideband radar system
| AD-A267479 | p 1004 N94-17364
Arctic cyclones and Marginal Ice Zone (MIZ) variability
| AD-A268610 | p 1108 N94-17465
An investigation of the Ground-Based High-Resolution Interferometer Sounder (GB-HIS) in a costal marine environment
| AD-A268052 | p 1114 N94-17503
An analysis of simulated and actual DMSP SSM/T-2 brightness temperatures
| AD-A268103 | p 1109 N94-17573

REMOTE SENSORS
The laboratory performance of the short wavelength instrument for the Along Track Scanning Radiometer ATSR-2 (initial results) p 908 N94-15088
IR detectors and subsystems for space applications p 909 N94-15091
ENVISAT ASAR p 898 N94-15892

REMOTELY PILOTED VEHICLES
Non-lethal Unmanned Aerial Vehicles (UAVs)
| AD-A267139 | p 866 N94-15692

REMOVAL
Dry stripping as a surface treatment method
| VTT-TIED-1348 | p 985 N94-17544

RENDEZVOUS GUIDANCE
A guidance and navigation system for two spacecraft rendezvous in translunar halo orbit
| AD-A267498 | p 898 N94-17368

RENDEZVOUS TRAJECTORIES
A mission concept of Phobos/Deimos exploration p 1287 N94-16387

RENORMALIZATION GROUP METHODS
Large-Eddy Simulations (LES) of flows and turbulence distribution
| AD-A267182 | p 1016 N94-15151
Computation of confined coflow jets with three turbulence models
| NASA-TM-106378 | p 1025 N94-16879

REPORTS
AFOSR technical report summaries, January - March 1993
| AD-A267187 | p 1230 N94-15850
List of the scientific and personal papers of Sir George Deacon, FRS
| IOS-301-1992 | p 1114 N94-17518

REPRODUCTION (COPYING)
Design and implementation of an object-oriented interface for the multi-model/multi-lingual database system
| AD-A267413 | p 1232 N94-16977
Theory of dispersive microlenses p 1198 N94-17361

RESCUE OPERATIONS
STS-26 EVA rescue training
| NASA-TM-109563 | p 875 N94-15333
Life saving satellites
| NASA-TM-109616 | p 862 N94-15426
Inflatable rescue device
| NASA-CASE-MSC-22244-1 | p 1137 N94-15883
Technical urban search and rescue, System To Locate Survivors (STOLS) units: Operator's manual
| AD-A266317 | p 862 N94-16438
Evaluation of Night Vision Goggles (NVG) for maritime search and rescue (HH-3/HH-60) comparison report
| AD-A266493 | p 1138 N94-16793
On predicting the person-in-water drift for search and rescue
| AD-A268083 | p 1055 N94-17514

RESEARCH
NASA Space Engineering Research Center for VLSI System Design
| NASA-CR-194587 | p 1008 N94-15547

RESEARCH AIRCRAFT
Canadian microgravity experiments flown in 1989-1990 p 977 N94-16075
The vibro-acoustic mapping of low gravity trajectories on a Learjet aircraft p 978 N94-16078

RESEARCH AND DEVELOPMENT
Infrared detectors and coolers for space instrumentation: Summary and concluding remarks p 904 N94-15059
Expectations for the future of military aviation p 854 N94-15128
Expectations for the future of the National Aerospace Laboratory p 854 N94-15129
Expectations for the future of the Faculty of Aeronautics and Astronautics of the Technical University of Delft p 854 N94-15131
Return to flight 1
| NASA-TM-109663 | p 1223 N94-15234
The 1969 highlights
| NASA-TM-109630 | p 1301 N94-15241
The 1972 highlights
| NASA-TM-109631 | p 1301 N94-15242
The 1965 highlights --- NASA programs
| NASA-TM-109632 | p 1301 N94-15243
NASA images 6
| NASA-TM-109437 | p 862 N94-15336
Student researchers
| NASA-TM-109441 | p 1221 N94-15340
Back to propellers
| NASA-TM-109445 | p 869 N94-15344
Annual historical report, calendar year 1992
| AD-A267050 | p 1121 N94-15663
Report on computing and networking in the Space Science Laboratory by the SSL Computer Committee
| NASA-TM-108422 | p 1147 N94-15721
AFOSR technical report summaries, January - March 1993
| AD-A267187 | p 1230 N94-15850
Research and development: Engine of innovation at Krupp p 984 N94-16001
Modeling and simulation: A key to future defense technology
| TABES PAPER 93-654 | p 1054 N94-16153
Looking at science on board Eureca
| ESA-BR-80 | p 874 N94-16584
The early activities of the COPERS and the drafting of the ESRO Convention (1961/62)
| ESA-HSR-4 | p 1225 N94-16593
Resources and activities of the European Space Agency p 1303 N94-16792
The Megascience Forum
| DE93-014445 | p 1303 N94-16804
Research grant handbook
| NHB-5800.1C | p 1225 N94-16907
Plasma Science Committee (PLSC) and the Panel on Opportunities in Plasma Science and Technology (OPST)
| DE93-018142 | p 1204 N94-16995
Computer Science and Telecommunications Board activities
| DE93-018141 | p 1000 N94-17000
Technology in action
| NASA-TM-109345 | p 1235 N94-17294
ONRASIA scientific information bulletin, volume 18, number 2
| AD-A267798 | p 1304 N94-17305
Mechanical Systems Technology Branch research summary, 1985 - 1992
| NASA-TM-106329 | p 1049 N94-17583
Satellite communications systems and technology. Executive summary
| NASA-TM-109346 | p 1006 N94-17661

RESEARCH FACILITIES
Supersonic Combustion Research Laboratory. Volume 1: Design and fabrication
| AD-A267667 | p 943 N94-14962
Expectations for the future of the National Aerospace Laboratory p 854 N94-15129
GFSC-TV demo tape
| NASA-TM-109586 | p 875 N94-15270
Stock footage of Goddard Space Flight Center and Headquarters
| NASA-TM-109589 | p 875 N94-15273
Manned vehicle systems research facility
| NASA-TM-109650 | p 875 N94-15318
NASA images 6
| NASA-TM-109437 | p 862 N94-15336
Building 46 grand opening
| NASA-TM-109524 | p 875 N94-15386
Lunar Curatorial Facility resource
| NASA-TM-109531 | p 875 N94-15393
Johnson Space Center and downtown Houston, Texas aerials
| NASA-TM-109522 | p 1032 N94-15472
Commitment to challenge
| NASA-TM-109523 | p 876 N94-15473
Heat transfer and aerodynamics of a 3D design nozzle guide vane tested in the Pyestock isentropic light piston facility
| RAE-TM-AERO/PROP-19 | p 856 N94-15696
Facilities maintenance handbook
| NHB-8831.2 | p 1224 N94-15934
Scientific use of Space Station Freedom p 977 N94-16072
New findings and instrumentation from the NASA Lewis Microgravity Facility p 977 N94-16076
QUESTS: A microgravity research facility for materials science experiments p 978 N94-16082
First results from a laboratory facility for measurement of emission spectra under simulated planetary conditions p 954 N94-16372
An electromagnetic interference study of potential transmitter sites for the HF Active Auroral Research Program (HAARP)
| AD-A267743 | p 1004 N94-17373
Design of an experiment hardware for the ESA space facility BIOPAN
| DLR-FB-93-06 | p 876 N94-17548

RESEARCH MANAGEMENT
Army Software Test and Evaluation Panel (STEP) software metrics initiatives report
[AD-A266889] p 1142 N94-14924
NASA information resources management handbook
[NHB-2410.1E] p 1230 N94-15941
Krupp technical reports no. 2, English edition, October 1992
[ETN-93-94631] p 984 N94-16000
Research and development: Engine of innovation at Krupp p 984 N94-16001
Mathematical Sciences Division 1992 programs
[AD-A268586] p 1140 N94-17623
RESEARCH PROJECTS
Earth system dynamics: The interrelation of atmospheric, ocean and solid earth dynamics
[NASA-CR-193487] p 1081 N94-17444
RESERVOIRS
Numerical modelling of an active direct nonpotable hot water heating system making use of the energy of solar radiation
[IFTR-38/1991] p 1093 N94-17070
RESIDUAL STRENGTH
Low and high velocity impact response of thick hybrid composites p 936 N94-16837
RESIDUAL STRESS
Finite element analytical techniques for ceramic production in microgravity: A hypoelastic model p 981 N94-16099
Evaluation of the interfacial mechanical properties in fiber-reinforced ceramic composites
[DE93-015494] p 935 N94-16461
Thermal stress effects in intermetallic matrix composites
[NASA-CR-191191] p 1054 N94-16518
The processing and mechanical properties of high temperature/high performance composites. Book 5: Processing and miscellaneous properties
[AD-A266398] p 935 N94-16529
Interfacial shear behavior and its influence on fiber damage in sapphire-reinforced gamma titanium aluminide composites
[AD-A267943] p 1060 N94-17043
Measurement and theory of the dependence of hardness on residual stress
[AD-A267553] p 1061 N94-17105
Evaluation of interfacial properties of fiber-reinforced ceramic composites using fiber push-in tests
[DE93-015427] p 972 N94-17253
Aspects of high temperature damage in fiber reinforced titanium metal matrix composites
[AD-A267907] p 941 N94-17379
Low dielectric constant insulators and gold metallization for GHz multi-chip modules, part 2
[AD-A268590] p 1176 N94-17605
RESIN MATRIX COMPOSITES
Construction, testing, and representation of resin and fiber reinforced materials p 931 N94-15255
Polymer Infiltration Studies
[NASA-CR-194494] p 932 N94-15275
RESIN TRANSFER MOLDING
An overview of the NASA textile composites program p 937 N94-16846
Textile composite processing science p 938 N94-16856
RESINS
Construction, testing, and representation of resin and fiber reinforced materials p 931 N94-15255
Cyanoresin, cyanoresin/cellulose triacetate blends for thin film, dielectric capacitors
[NASA-CASE-NPO-18913-1-CU] p 966 N94-15930
RESISTANCE HEATING
Heating of lubricant with an electric resistance heater
[VTT-TIED-1359] p 974 N94-17547
RESISTOJET ENGINES
Strategy for the reduction of total integrated fluid logistics to the Space Station Freedom
[NASA-TM-107744] p 1138 N94-17452
RESISTORS
Stray insensitive switched capacitor composite operational amplifiers
[AD-A267412] p 1012 N94-16976
RESONANCE
Magnetic effects in anomalous dispersion
[DE93-014291] p 1175 N94-15978
Orbital evolution of dust from comet Schwassmann-Wachmann 1: A case of one-to-one resonance trapping p 1242 N94-16270
Processing of resonance parameter covariance files
[DE93-015506] p 1231 N94-16874
An automated system for ultrasound measurements of liquids by the resonance (Eggers) method
[IFTR-17/1992] p 1178 N94-17087
RESONANCE SCATTERING
Suppression of charge scattering in Moessbauer experiments using synchrotron radiation
[DE93-015406] p 1212 N94-16887
RESONANT FREQUENCIES
Parametric study of a finite element model of the Sidewinder missile
[AD-A267245] p 865 N94-14976
Resonant frequencies of irregularly shaped microstrip antennas using method of moments
[NASA-TP-3386] p 989 N94-15767
Digital reverberation time measurement system
[AD-D015892] p 1177 N94-16919
Wide angle, single screen, gridded square-loop frequency selective surface for diplexing two closely separated frequency bands
[NASA-CASE-NPO-18664-1-CU] p 1237 N94-17438
RESONATORS
Stress sensitivity of dielectric resonators
[AD-A266767] p 1009 N94-15825
Aberration correction of unstable resonators
[NASA-CASE-NPO-18791-1-CU] p 1034 N94-15987
Quartz crystal resonators and oscillators for frequency control and timing applications: A tutorial, revision 6.1
[AD-A268205] p 1216 N94-17480
RESOURCE ALLOCATION
Applicability of computer spreadsheet simulation for solving resource allocation problems
[AD-A267436] p 1152 N94-17027
Satellite communications systems and technology. Executive summary
[NASA-TM-109346] p 1006 N94-17661
RESOURCES MANAGEMENT
Applicability of computer spreadsheet simulation for solving resource allocation problems
[AD-A267436] p 1152 N94-17027
RESPIRATION
Validation of respiratory inductive plethysmography for measuring exercise tidal volumes
[AD-A266883] p 1119 N94-14923
RESPIRATORS
Respiratory Protection Program medical clearance for respirator use p 1127 N94-16642
RESPIRATORY DISEASES
Respiratory Protection Program medical clearance for respirator use p 1127 N94-16642
RESPIRATORY PHYSIOLOGY
Validation of respiratory inductive plethysmography for measuring exercise tidal volumes
[AD-A266883] p 1119 N94-14923
RESPIRATORY SYSTEM
Respiratory Protection Program medical clearance for respirator use p 1127 N94-16642
RESPIROMETERS
Validation of respiratory inductive plethysmography for measuring exercise tidal volumes
[AD-A266883] p 1119 N94-14923
RESTARTABLE ROCKET ENGINES
Advanced transportation system studies technical area 3: Alternate propulsion system concepts. SSME upper stage use
[NASA-CR-193865] p 927 N94-17098
RESTORATION
Restoring Miss Liberty --- inorganic coatings
[NASA-TM-109605] p 963 N94-15313
Computing and Information Sciences
[DE93-017149] p 1151 N94-16902
RESUSCITATION
A mathematical model for the study of hemorrhagic shock and fluid resuscitation: Transcapillary exchange
[AD-A266427] p 1123 N94-16544
A mathematical model for the study of hemorrhagic shock and fluid resuscitation: Exchange of fluid and solutes between vascular, interstitial, and tissue cell compartments
[AD-A266426] p 1123 N94-16558
Increased vascular resistance with hemoglobin-based oxygen carriers
[AD-A266454] p 1123 N94-16565
The nature of dynamic arteriolar vasoreactivity: A mini-review and A classification scheme
[AD-A266499] p 1128 N94-16783
RETENTION (PSYCHOLOGY)
SONOS technology for commercial and military nonvolatile memory applications
[DE93-015647] p 1011 N94-16661
RETICLES
Test methods for acceptance testing of telescopes
[AD-A268316] p 1237 N94-17568
RETINA
Reference frames in vision
[AD-A266174] p 1132 N94-16925
RETRIEVAL
EVA retriever demonstration
[NASA-TM-109510] p 1046 N94-15456
RETROREFLECTION
Reduction of parasitic lasing
[NASA-CASE-LAR-14645-1-SB] p 1039 N94-15942
RETROREFLECTORS
Work at Graz on satellite signatures p 898 N94-15558
Alternative wavelengths for laser ranging p 913 N94-15564
ETALON-1,-2 center of mass correction and array reflectivity p 915 N94-15576
Analysis of TOPEX laser retroreflector array characteristics p 915 N94-15578
Millimeter accuracy satellites for two color ranging p 916 N94-15583
New perspectives for high accuracy SLR with second generation geodesic satellites p 916 N94-15585
A computer-controlled x-y offset guiding stage for the MLRS p 918 N94-15598
GLRS-R 2-colour retroreflector target design and predicted performance p 921 N94-15615
Effects of turbulence on the geodynamic laser ranging system p 921 N94-15616
Reduction of parasitic lasing
[NASA-CASE-LAR-14645-1-SB] p 1039 N94-15942
REVERBERATION
Digital reverberation time measurement system
[AD-D015892] p 1177 N94-16919
REYNOLDS EQUATION
Proteus three-dimensional Navier-Stokes computer code, version 1.0. Volume 3: Programmer's reference
[NASA-TM-106341] p 1022 N94-15865
Unsteady fluid and optical simulation of transonic aero-windows
[AIAA PAPER 93-3017] p 858 N94-16512
Computation of a controlled store separation from a cavity p 858 N94-16513
REYNOLDS NUMBER
Transmission of light through a turbulent mixing layer
[AD-A267266] p 1193 N94-17264
Lifted turbulent jet flames
[AD-A267911] p 952 N94-17381
REYNOLDS STRESS
Computation of confined coflow jets with three turbulence models
[NASA-TM-106378] p 1025 N94-16879
Three-dimensional turbulent boundary layer
[AD-A266261] p 1025 N94-16908
Structure of high Reynolds number turbulent boundary layer
[AD-A267476] p 860 N94-17099
Investigation of high-speed free shear flows using improved pressure-strain correlated Reynolds stress turbulence model
[NASA-CR-194661] p 1027 N94-17127
Structure of turbulence in three-dimensional boundary layers
[NASA-CR-194655] p 1027 N94-17130
RHENIUM
Osmium isotopes in Ivory Coast tektites: Confirmation of a meteoritic component and rhenium depletion p 1244 N94-16321
Structural effects in electron transfer reactions: Comparative interfacial electrochemical kinetics for cis- versus trans-dioxorhenium (V) (bi)pyridine oxidation
[AD-A266307] p 1182 N94-16466
RHENIUM COMPOUNDS
High-valent oxo, methoxorhenium complexes: Models for intermediates and transition states in proton-coupled multi-electron transfer reactions
[AD-A266492] p 1211 N94-16782
RHEOLOGY
Rheology and microstructure of concentrated zirconia-alumina suspensions for gelcasting composites
[DE93-015339] p 966 N94-16016
Rheology of water and ammonia-water ices p 953 N94-16188
The rheology and composition of cryovolcanic flows on icy satellites p 1243 N94-16294
Geophysical models of Western Aphrodite-Niobe region: Venus p 1286 N94-16382
Electro-rheological disk pump
[AD-D015783] p 1047 N94-16531
RHYOLITE
Venusian pancake domes: Insights from terrestrial voluminous silicic lavas and thermal modeling p 1286 N94-16381
RIBBONS
Polymer Infiltration Studies
[NASA-CR-194494] p 932 N94-15275
RIBLETS
Riblets: New speed technology
[NASA-TM-109641] p 1018 N94-15252
Active turbulence control in wall bounded flows using direct numerical simulation
[AD-A267261] p 1028 N94-17286

RIBONUCLEIC ACIDS
Biofilm structure and diversity
[AD-A267254] p 1118 N94-16989
RIBS (SUPPORTS)
Sound radiation from infinite laminated composite shell with periodic rib stiffening
[DRA/TM(USGR)92326] p 933 N94-15699
RICHARDSON NUMBER
Lifted turbulent jet flames
[AD-A267911] p 952 N94-17381
RIFLES
Thermal Weapon Sight (TWS) AN/PAS-13 diffractive optics designed for producibility p 1197 N94-17354
RIGID STRUCTURES
Impending motion direction of contacting rigid bodies
[AD-A266814] p 1164 N94-15756
Computation of a controlled store separation from a cavity p 858 N94-16513
Equations of motion of a hinged body over a spherical earth
[AD-A268408] p 868 N94-17435
RINGS (MATHEMATICS)
Modal ring method for the scattering of sound
[NASA-TM-106342] p 1177 N94-16497
Distributively generated matrix near rings
[DE93-628588] p 1175 N94-17641
RISK
Efficient management of cardiovascular risk screening programs p 1125 N94-16622
A handbook of cost risk analysis methods
[AD-A267253] p 1235 N94-16988
X ray computed tomography for failure analysis investigations
[AD-A268086] p 1055 N94-17515
ROADS
YARF: An open-ended framework for robot road following
[AD-A266788] p 1163 N94-14910
Massively parallel, adaptive, color image processing for autonomous road following
[AD-A266988] p 864 N94-15498
ROBOT ARMS
Fuzzy inverse kinematic mapping: Rule generation, efficiency, and implementation
[AD-A266967] p 1163 N94-14954
Contextually dependent control strategies for manipulation
[TR-416] p 1165 N94-16580
Visually guided touching and manual tracking
[TR-412] p 1166 N94-16581
Three axis force override rate control of a PUMA 560 manipulator
[AD-A267313] p 1048 N94-16944
ROBOT CONTROL
Tactile sensing and control in humans and robotic/teleoperated systems
[AD-A267710] p 1163 N94-14937
Fuzzy inverse kinematic mapping: Rule generation, efficiency, and implementation
[AD-A266967] p 1163 N94-14954
Real-time implementation of neural network learning control of a flexible space manipulator
[AD-A266962] p 1045 N94-14970
Infrared remote activity transceiver universal model
[AD-A266965] p 1188 N94-15144
Contextually dependent control strategies for manipulation
[TR-416] p 1165 N94-16580
Visually guided touching and manual tracking
[TR-412] p 1166 N94-16581
A modular control architecture for real-time synchronous and asynchronous systems
[DE93-015439] p 1166 N94-16888
Development of a prototype kinestatic platform for application to space and ground servicing tasks. Phase 1: Concept Modeling
[NASA-CR-194036] p 887 N94-16905
Three axis force override rate control of a PUMA 560 manipulator
[AD-A267313] p 1048 N94-16944
An object-oriented program specification for a mobile robot motion control language
[AD-A267213] p 1166 N94-16986
End-effector: Joint conjugates for robotic assembly of large truss structures in space: Extended concepts
[NASA-CR-193576] p 1048 N94-17088
Path planning for robotic truss assembly
[NASA-CR-194652] p 897 N94-17280
ROBOT DYNAMICS
An experimental comparison of CLOS and C(++) implementations of an object-oriented graphical simulation of walking robot kinematics
[AD-A267168] p 1165 N94-15855
Temporal segmentation of tasks from human hand motion
[AD-A266596] p 1166 N94-16725
Development of a prototype kinestatic platform for application to space and ground servicing tasks. Phase 1: Concept Modeling
[NASA-CR-194036] p 887 N94-16905
Reference frames in vision
[AD-A266174] p 1132 N94-16925
An object-oriented program specification for a mobile robot motion control language
[AD-A267213] p 1166 N94-16986
ROBOT SENSORS
Panacea: An active sensor controller for the ALVINN autonomous driving system
[AD-A266964] p 864 N94-14972
Programmable Remapper project
[NASA-TM-109508] p 1164 N94-15515
ROBOTICS
Tactile sensing and control in humans and robotic/teleoperated systems
[AD-A267710] p 1163 N94-14937
Fuzzy control and fuzzy kinematic mapping for a redundant space robot
[AD-A266866] p 1163 N94-14950
Infrared remote activity transceiver universal model
[AD-A266965] p 1188 N94-15144
Robotics for Space Station tape 2
[NASA-TM-109578] p 1045 N94-15263
Robotics in space
[NASA-TM-109584] p 1045 N94-15268
Robotics for Space Station, tape 1
[NASA-TM-109588] p 1045 N94-15272
Future of robotics
[NASA-TM-109592] p 1045 N94-15284
Plasma arc welding repair of space flight hardware
[TABES PAPER 93-603] p 1049 N94-16139
Contextually dependent control strategies for manipulation
[TR-416] p 1165 N94-16580
Visually guided touching and manual tracking
[TR-412] p 1166 N94-16581
Temporal segmentation of tasks from human hand motion
[AD-A266596] p 1166 N94-16725
A modular control architecture for real-time synchronous and asynchronous systems
[DE93-015439] p 1166 N94-16888
End-effector: Joint conjugates for robotic assembly of large truss structures in space: Extended concepts
[NASA-CR-193576] p 1048 N94-17088
Path planning for robotic truss assembly
[NASA-CR-194652] p 897 N94-17280
Reliability and maintainability of modular robot systems: A roadmap for design
[AD-A268104] p 1168 N94-17517
Environmental use of a Laser Range Finder and the Advanced Visualization System
[DE93-016163] p 1043 N94-17677
ROBOTS
Perception for outdoor navigation
[AD-A266867] p 863 N94-14919
Engineering Physics and Mathematics Division progress report, period ending 31 December 1992
[DE93-015118] p 1301 N94-14926
Hidden Markov model approach to skill learning and its application to telerobotics
[AD-A266989] p 1164 N94-15502
Opportunity for early science return by the Artemis Program p 1291 N94-16408
Exploiting world structure to efficiently search for objects
[TR-434] p 1231 N94-16576
Integrating reactive and deliberative planning for agents
[AD-A267631] p 1166 N94-17201
Reliability and maintainability of modular robot systems: A roadmap for design
[AD-A268104] p 1168 N94-17517
ROBUSTNESS (MATHEMATICS)
Research in robust control for hypersonic aircraft
[NASA-CR-194106] p 870 N94-15416
Application of the robust estimate in SLR data preprocessing p 918 N94-15597
The design and analysis of robust feedback systems
[AD-A267152] p 1165 N94-15778
ROCK INTRUSIONS
Spatially extensive uniform stress fields on Venus inferred from radial dike swarm geometries: The Aphrodite Terra example p 1254 N94-16207
Mode of emplacement of lunar mare volcanic deposits: Graben formation due to near surface deformation accompanying dike emplacement at Rima Parry 5 p 1258 N94-16227
Geomorphic processes in the Argyre-Dorsa Argentea region of Mars p 1270 N94-16293
The monzonorite-anorthosite connection: The petrogenesis of terrestrial KREEP p 1104 N94-16365
Preliminary analysis of thermal-infrared multispectral scanner data of the Iron Hill, Colorado carbonatite-alkalic rock complex p 1065 N94-16605
ROCKET ENGINE DESIGN
ALS engine controller system
[NASA-CR-194647] p 926 N94-16654
Development and analysis of startup strategies for particle bed nuclear rocket engine
[AD-A267949] p 927 N94-17053
Advanced transportation system studies technical area 3: Alternate propulsion system concepts. SSME upper stage use
[NASA-CR-193865] p 927 N94-17098
Computational analysis of Variable Thrust Engine (VTE) performance
[NASA-CR-193852] p 928 N94-17442
CPIA/M5 liquid propellant engine manual
[AD-A268062] p 929 N94-17589
ROCKET ENGINES
Coaxial airblast atomizers
[NASA-CR-193845] p 1016 N94-15109
TABES 1993: 9th Annual Technical and Business Exhibition and Symposium p 1050 N94-16129
ALS engine controller system
[NASA-CR-194647] p 926 N94-16654
Heat transfer parametric system identification
[AD-A268525] p 929 N94-17543
ROCKET EXHAUST
Rocket Motor Plume Technology
[AGARD-LS-188] p 923 N94-15217
Plume primary smoke p 923 N94-15218
Propulsion p 924 N94-15219
Secondary smoke p 924 N94-15220
Rocket motor plume flowfields: Phenomenology and simulation p 924 N94-15221
Microwave properties and systems overview p 924 N94-15222
Plume radiation p 924 N94-15223
Fundamental studies of rocket combustion chemistry and combustion instability
[AD-A266248] p 925 N94-16482
ROCKET LAUNCHERS
The launch of ELDO
[ESA-HSR-7] p 886 N94-16501
ROCKET LAUNCHING
The launch of ELDO
[ESA-HSR-7] p 886 N94-16501
ROCKET NOZZLES
ASRM nozzle thermal analysis
[NASA-CR-194672] p 928 N94-17277
Postflight hardware evaluation 360T026 (RSRM-26, STS-47)
[NASA-CR-192559] p 882 N94-17656
ROCKET SOUNDING
The 1980 highlights
[NASA-TM-109672] p 1303 N94-15509
Principal investigators data package for Project Initiation Conference (PIC): EUVS sounding rocket no. 36.117CL. Target: Venus
[NASA-CR-194663] p 923 N94-17126
ROCKS
Temperature measurements p 1037 N94-15804
Stalking the LREE-enriched component in ureilites p 1241 N94-16190
Mars Analog Site Study (MASS) p 1252 N94-16200
Near-surface temperature gradients and their effects on thermal-infrared emission spectra of particulate planetary surfaces p 1260 N94-16236
Trace-element composition of Chicxulub crater melt rock, K/T tektites and Yucatan basement p 1242 N94-16245
From minerals to rocks: Toward modeling lithologies with remote sensing p 1086 N94-16437
AVIRIS as a tool for carbonatite exploration: Comparison of SPAM and Mbandmap data analysis methods p 1073 N94-16703
ROCKWELL HARDNESS
Measurement and theory of the dependence of hardness on residual stress
[AD-A267553] p 1061 N94-17105
RODS
Attachment device
[NASA-CASE-MSC-21885-1] p 1047 N94-15925
Evaluation of hybrid reinforcement (fiber-reinforced-plastic rod with steel core)
[AD-A268009] p 941 N94-17473
ROLL
Equations of motion of a hinged body over a spherical earth
[AD-A268408] p 868 N94-17435
ROLLER BEARINGS
Mechanical Systems Technology Branch research summary, 1985 - 1992
[NASA-TM-106329] p 1049 N94-17583

ROLLERS
Electrostatic fiber spreader including a corona discharge device
[AD-D015793] p 936 N94-16537
ROLLING MOMENTS
A mechanical system damping measurement technique using a one-degree-of-freedom (1DOF) cylindrical gas bearing
[AD-A268402] p 1048 N94-17462
ROOM TEMPERATURE
Technology transfers and reliable oxides
[AD-A266948] p 1175 N94-15758
ROOT-MEAN-SQUARE ERRORS
Sub-cm ranging and other improvements in Graz
p 919 N94-15603
ROSAT MISSION
ROSAT-IUE observations of symbiotic stars. The x ray morphology of high latitude associations
[NASA-CR-194616] p 1236 N94-16492
Participation in the north ecliptic pole sky survey
[NASA-CR-191933] p 1059 N94-16815
The formation process of the He I lambda 10830 line in cool giant stars
[NASA-CR-194648] p 1240 N94-17094
Variability of the Seyfert galaxy MKN 766 in the Rosat all sky survey
[MPE-PREPRINT-221] p 1240 N94-17591
ROTARY ENGINES
Rotary engine performance computer program (RCEMAP and RCEMAPPC): User's guide
[NASA-CR-191192] p 869 N94-15192
ROTARY WING AIRCRAFT
Rotorcraft research
[NASA-TM-109452] p 871 N94-15325
Center for Rotorcraft Education and Research progress report, 1987 - 1992
[AD-A266760] p 857 N94-15824
ROTATING CYLINDERS
In-flight investigation of a rotating cylinder-based structural excitation system for flutter testing
[NASA-TM-4512] p 867 N94-15783
Numerical study of compressible boundary-level transition between two concentric cylinders
[NASA-CR-194622] p 1025 N94-16842
ROTATING ENVIRONMENTS
Apparatus and method for producing an artificial gravitational field
[NASA-CASE-MSC-22021-1] p 886 N94-15935
ROTATING SHAFTS
Rotary encoding device
[NASA-CASE-GSC-13543-1] p 1189 N94-15705
Rotary encoding device
[NASA-CASE-GSC-13556-1] p 1148 N94-15943
ROTATIONAL SPECTRA
Molecular processes in comets
[NASA-CR-194148] p 1239 N94-15188
ROTOR AERODYNAMICS
Center for Rotorcraft Education and Research progress report, 1987 - 1992
[AD-A266760] p 857 N94-15824
Jet engine performance enhancement through use of a wave-rotor topping cycle
[NASA-TM-4486] p 870 N94-17470
ROTOR BLADES (TURBOMACHINERY)
A rapid computational model for estimating the performance of compliant airfoils in cascades
[AD-A266275] p 857 N94-16471
Experimental and computational investigation of the NASA low-speed centrifugal compressor flow field
[NASA-TM-4481] p 869 N94-17386
ROTOR DYNAMICS
Center for Rotorcraft Education and Research progress report, 1987 - 1992
[AD-A266760] p 857 N94-15824
ROTOR SYSTEMS RESEARCH AIRCRAFT
The 1982 highlights
[NASA-TM-109671] p 1303 N94-15508
The 1980 highlights
[NASA-TM-109672] p 1303 N94-15509
ROTORCRAFT AIRCRAFT
Rotorcraft research
[NASA-TM-109452] p 871 N94-15325
Center for Rotorcraft Education and Research progress report, 1987 - 1992
[AD-A266760] p 857 N94-15824
ROTORS
Helicopter structures: A review of loads, fatigue design techniques, and usage monitoring
[AD-A267115] p 866 N94-15651
Jet engine performance enhancement through use of a wave-rotor topping cycle
[NASA-TM-4486] p 870 N94-17470
ROUTES
Strategic planning for aircraft noise route impact analysis: A three dimensional approach
[NASA-CR-191484] p 1178 N94-17278
ROVING VEHICLES
Rover mounted ground penetrating radar as a tool for investigating the near-surface of Mars and beyong
p 1007 N94-16197
International testing of a Mars rover prototype
p 1273 N94-16312
RUBBER
XPS analysis of Al/EPDM bondlines from IUS SRM-1 polar bosses
[AD-A266851] p 1056 N94-14945
RELMA: On-line quality control in the rubber mixing room using laser analysis p 984 N94-16005
Synthesis and evaluation of polymeric materials
[AD-A267809] p 973 N94-17408
Damage evolution in filled elastomers
[AD-A268067] p 1062 N94-17507
RULES
Automatic generation of production rules for integrity maintenance
[REPT-92-054] p 1156 N94-17501
RUNGE-KUTTA METHOD
Multigrid time-accurate integration of Navier-Stokes equations
[NASA-TM-106373] p 1028 N94-17258
Numerically solving a transient heat conduction problem with convection and radiation
[AD-A268521] p 1220 N94-17540
RUNWAYS
The 1971 highlights --- NASA programs and research
[NASA-TM-109629] p 1302 N94-15417
RUSSIAN FEDERATION
Commonwealth of Independent States aerospace science and technology, 1992: A bibliography with indexes
[NASA-SP-7106] p 854 N94-16481

S

S GLASS
SRB thermal curtain design support
[NASA-CR-193857] p 927 N94-17123
SRB thermal curtain design support
[NASA-CR-193858] p 928 N94-17124
S MATRIX THEORY
Convergence of the multiple scattering expansion in XAFS and XANES
[DE93-011001] p 948 N94-16772
S WAVES
Shear wave measurements in shock-induced, high-pressure phases
[DE93-016461] p 1062 N94-17664
SAFETY
Americans with Disabilities Act considerations for the practice of occupational medicine p 1124 N94-16611
Programs and resources for control of job stress in the Federal workplace p 1124 N94-16617
Industrial Hygiene Laboratory accreditation: The JSC experience p 1125 N94-16623
Space Shuttle main engine. NASA has not evaluated the alternate fuel turbopump costs and benefits. Report to the Administrator of the National Aeronautics and Space Administration
[GAO/NSIAD-94-54] p 926 N94-16834
The 1987 Goddard Space Flight Center Battery Workshop
[NASA-CP-3236] p 1012 N94-17062
SAFETY DEVICES
Respiratory Protection Program medical clearance for respirator use p 1127 N94-16642
Regulated emergency oxygen system
[AD-A266228] p 1138 N94-16983
SAFETY FACTORS
Safety-critical software: Status report and annotated bibliography
[AD-A266993] p 1144 N94-15214
ASRM nozzle thermal analysis
[NASA-CR-194672] p 928 N94-17277
SAFETY MANAGEMENT
NASA directives master list and index
[NHB-1410.13L] p 1229 N94-15414
New health and safety initiatives at the Department of Energy (DOE) p 1124 N94-16610
SAMARIUM ISOTOPES
Nd-142/Nd-144 in bulk planetary reservoirs, the problem of incomplete mixing of interstellar components and significance of very high precision Nd-145/Nd-144 measurements p 1256 N94-16220
Constraints on the differentiation of the Earth from the coupled Sm-146,147-Nd-142,143 systematics
p 1103 N94-16271
SAMPLED DATA SYSTEMS
The design and analysis of robust feedback systems
[AD-A267152] p 1165 N94-15778
Discrete sliding mode control for nonlinear sampled data systems
[AD-A267500] p 1167 N94-17369
SAMPLERS
Methods to obtain blood samples periodically during exercise research studies while subjects are immersed in water or otherwise inaccessible
[AD-A268227] p 1130 N94-17562
SAMPLING
A mission concept of Phobos/Deimos exploration
p 1287 N94-16387
Exploring the remote sensing of foliar biochemical concentrations with AVIRIS data p 1069 N94-16683
Gas Analysis System
[DE93-014617] p 949 N94-16891
SAN MARCO SATELLITES
Mission San Marco
[NASA-TM-109442] p 878 N94-15341
SANDS
Sand transport on Mars: Preliminary results from models p 1252 N94-16198
Experimental study of nonassociated flow and instability of frictional materials
[AD-A266421] p 1024 N94-16555
SANDWICH STRUCTURES
Multilayer thin film design for far ultraviolet polarizers using an induced transmission and absorption technique
[NASA-CR-194631] p 1190 N94-15869
Effect of Impact Damage and Open Hole on Compressive Strength of Hybrid Composite Laminates
[NASA-CR-194603] p 936 N94-16836
Research in textile composites at KU, Leuven
p 937 N94-16848
SAPPHIRE
Ion mixing of thin ZrO2 films on sapphire
[DE93-015214] p 1206 N94-14925
The processing and mechanical properties of high temperature/high performance composites. Book 5: Processing and miscellaneous properties
[AD-A266398] p 935 N94-16529
Growth and doping of Al(x)Ga(1-x)N films by electron cyclotron resonance assisted molecular beam epitaxy
[AD-A267305] p 1212 N94-16992
Nitride semiconductors for ultraviolet detection
[AD-A267877] p 1012 N94-17040
Interfacial shear behavior and its influence on fiber damage in sapphire-reinforced gamma titanium aluminide composites
[AD-A267943] p 1060 N94-17043
SARSAT
Life saving satellites
[NASA-TM-109616] p 862 N94-15426
SATELLITE ALTIMETRY
The depths of the largest impact craters on Venus
p 1264 N94-16261
Resolving topographic detail on Venus by modeling complex Magellan altimetry echoes
p 1283 N94-16368
TAOS (S80): A (LEO-MSS) system for position reporting and telemanagement services p 893 N94-17162
Developing automated analysis methods for sea ice imagery: A status report with recommendations
[AD-A267284] p 1113 N94-17241
SATELLITE ANTENNAS
Proceedings of the 1992 Antenna Applications Symposium, volume 2
[AD-A266916] p 986 N94-14998
Small satellite constellation system: Optimization criteria p 888 N94-17132
Proceedings of the 1992 Antenna Applications Symposium, volume 1
[AD-A268167] p 1005 N94-17431
SATELLITE ATTITUDE CONTROL
MINISAT programme p 896 N94-17182
The development of flexible software for the Italian/Dutch satellite SAX: Advantages and disadvantages of the use of CASE tools
[NLR-TP-91288-U] p 1157 N94-17626
SATELLITE COMMUNICATION
Development of Japanese Earth Resources Satellite-1 (JERS-1; FUYO-1) and it's operational results
[NASDA-SPP-930001] p 884 N94-15001
TDRS video clip
[NASA-TM-109585] p 884 N94-15269
Activities of Canadian Satellite Communications, Inc.
[CTN-93-60864] p 994 N94-15959
Data acquisition, preprocessing and analysis for the Virginia Tech OLYMPUS experiment
p 995 N94-16038
The ACTS propagation program p 995 N94-16039
Propagation measurements in Alaska using ACTS beacons p 995 N94-16040
Planned LMSS propagation experiment using ACTS: Preliminary antenna pointing results during mobile operations p 995 N94-16041

Propagation-related AMT design aspects and supporting experiments p 995 N94-16042
Propagation research in Japan p 996 N94-16043
Low-Complexity, High-Performance Bandwidth Efficient Coding and Coded Modulation Techniques for Satellite and Space Communications
[NASA-CR-194623] p 997 N94-16506
Satellite communications installation plan
[AD-A266303] p 1000 N94-16965
Four Frequency-Shift Keying (4-FSK) spread spectrum modulator and demodulator
[AD-A267433] p 1000 N94-16979
On-board B-ISDN fast packet switching architectures. Phase 1: Study
[NASA-CR-191143] p 883 N94-17111
Small Satellites Systems and Services
[ISBN-2-85-428327-9] p 888 N94-17131
Low Earth orbit constellations: Orbit control or not p 875 N94-17134
Data processing system for ARSENE ground station: A tool for small satellite control and development p 878 N94-17157
A study on an experimental communication system using microsatellites p 892 N94-17160
LEOCOM-SPES: Low cost message communications p 892 N94-17161
TAOS (S80): A (LEO-MSS) system for position reporting and telemanagement services p 893 N94-17162
S 80/T: A micro satellite system combining high performances and limited resources p 893 N94-17166
The ELLIPSO (tm) system: Elliptical low orbits for mobile communications p 893 N94-17167
Solar Electro-Optical Network (SEON) upgrade/replacement program. Phase 1: Qualification operational test and evaluation plan
[AD-A266364] p 1237 N94-17225
NASA Lewis Meshed VSAT Workshop meeting summary
[NASA-TM-106332] p 883 N94-17487
Satellite communications systems and technology. Executive summary
[NASA-TM-109346] p 1006 N94-17661

SATELLITE CONFIGURATIONS
Development of Japanese Earth Resources Satellite-1 (JERS-1; FUYO-1) and it's operational results
[NASDA-SPP-930001] p 884 N94-15001

SATELLITE CONTROL
Development of Japanese Earth Resources Satellite-1 (JERS-1; FUYO-1) and it's operational results
[NASDA-SPP-930001] p 884 N94-15001
Low Earth orbit constellations: Orbit control or not p 875 N94-17134
Impact of launching uncertainties on the visibility of communication satellite constellations without orbit control p 889 N94-17135
Data processing system for ARSENE ground station: A tool for small satellite control and development p 878 N94-17157
Satellite control: A comprehensive approach p 878 N94-17158
TAOS (S80): A (LEO-MSS) system for position reporting and telemanagement services p 893 N94-17162
S 80/T: A micro satellite system combining high performances and limited resources p 893 N94-17166

SATELLITE DESIGN
Pre-phase a study report of lunar polar orbiter
[NASDA-TK-SS0440] p 873 N94-15000
Development of Japanese Earth Resources Satellite-1 (JERS-1; FUYO-1) and it's operational results
[NASDA-SPP-930001] p 884 N94-15001
Small Satellites Systems and Services
[ISBN-2-85-428327-9] p 888 N94-17131
Small missions for space science p 874 N94-17142
UoSAT: A decade of experience pioneering microsatellites p 894 N94-17169
A mini satellite called Arsene: The way to make it at a minimum cost p 895 N94-17179
The space technology research vehicle: Development status p 896 N94-17183
On-board spatial scientific experiment project on small satellites p 896 N94-17184
Big results with small space systems: What small systems are doing today p 896 N94-17187
Environment tests for mini satellites p 896 N94-17189
Cost drivers: Why do conventional satellites cost so much? p 897 N94-17190
A conceptual design study for a two-dimensional, electronically scanned thinned array radiometer
[NASA-TM-109051] p 1085 N94-17665

SATELLITE DOPPLER POSITIONING
STARSYS: A view after WARC-92 --- satellite position and messaging system p 893 N94-17168

SATELLITE GUIDANCE
Development of Japanese Earth Resources Satellite-1 (JERS-1; FUYO-1) and it's operational results
[NASDA-SPP-930001] p 884 N94-15001

SATELLITE IMAGERY
Assessment of TDI operation of a frame transfer CCD for high resolution imaging from a fast spinning spacecraft p 910 N94-15097
Ground truth spectrometry and imagery of eruption clouds to maximize utility of satellite imagery
[NASA-CR-194358] p 1081 N94-15181
Sea ice motions in the central arctic ice central arctic pack ice as inferred from AVHRR imagery
[NASA-CR-194572] p 1112 N94-15701
ERS-1: 18 months in orbit p 990 N94-15888
Almaz p 898 N94-15889
EUVE observations of the Moon p 1250 N94-16185
Remote sensing studies of the northeastern portion of the lunar nearside p 1258 N94-16225
A geological and geophysical information system for Eurasia
[AD-A267841] p 1232 N94-17036
Developing automated analysis methods for sea ice imagery: A status report with recommendations
[AD-A267284] p 1113 N94-17241
Nowcasting methods for satellite imagery
[AD-A267294] p 1108 N94-17267
Three dimensional visualization of GOES cloud data using OCTRESS
[AD-A268102] p 1109 N94-17572
An empirical study of tropical cloud clusters using special sensor microwave imager data
[AD-A268072] p 1110 N94-17595
The Central American cold surge: An observational analysis of the deep southward penetration of North American cold fronts
[AD-A268592] p 1110 N94-17607

SATELLITE INSTRUMENTS
Development of Japanese Earth Resources Satellite-1 (JERS-1; FUYO-1) and it's operational results
[NASDA-SPP-930001] p 884 N94-15001
Eighth International Workshop on Laser Ranging Instrumentation
[NASA-CP-3214] p 911 N94-15552
Laser ranging application to time transfer using geodetic satellite and to other Japanese space programs p 911 N94-15555
Applications of SLR p 911 N94-15556
The precision of today's satellite laser ranging systems p 912 N94-15559
New methods of generation of ultrashort laser pulses for ranging p 913 N94-15565
Preliminary results from the portable standard satellite laser ranging intercomparison with MOBLAS-7 p 913 N94-15568
Test results from LAGEOS-2 optical characterization using pulsed lasers p 915 N94-15577
Two wavelength satellite laser ranging using SPAD p 916 N94-15584
State-of-the-art satellite laser range modeling for geodetic and oceanographic applications p 916 N94-15586
Improvement of SLR accuracy, a possible new step p 917 N94-15588
Poisson filtering of laser ranging data p 917 N94-15593
Results of the MTLRS-1 upgrade p 877 N94-15610
Satellite laser station Helwan status 1992 p 877 N94-15621
Optical attenuation mechanism upgrades, MOBLAS, and TLRS systems p 922 N94-15622
The third generation SLR station Potsdam no. 7836 p 877 N94-15623
Station report on the Goddard Space Flight Center (GSFC) 1.2 meter telescope facility p 922 N94-15625
ENVISAT ASAR p 898 N94-15892
Tectonic deformation in southern California
[NASA-CR-194621] p 1101 N94-16021
L-shell binning and display of sensor data from the CRRES spacecraft
[AD-A267256] p 888 N94-16990
Big results with small space systems: What small systems are doing today p 896 N94-17187

SATELLITE LIFETIME
Satellite situation report, volume 33, no. 3
[NASA-TM-109278] p 885 N94-15712
Satellite control: A comprehensive approach p 878 N94-17158

SATELLITE NAVIGATION SYSTEMS
BRIDGE: A small scientific satellite for geodesy p 890 N94-17146

SATELLITE NETWORKS
Laser ranging network performance and routine orbit determination at D-PAF p 911 N94-15554
SATCOP mission planning software package p 912 N94-15562
ECS: Ninth year in orbit
[ESA-BR-91] p 987 N94-15644
On-board B-ISDN fast packet switching architectures. Phase 1: Study
[NASA-CR-191143] p 883 N94-17111
Small Satellites Systems and Services
[ISBN-2-85-428327-9] p 888 N94-17131
Small satellite constellation system: Optimization criteria p 888 N94-17132
AMIGAU: A prototype tool aimed at mission analysis for satellites and satellite constellations p 888 N94-17133
Low Earth orbit constellations: Orbit control or not p 875 N94-17134
Impact of launching uncertainties on the visibility of communication satellite constellations without orbit control p 889 N94-17135
Small satellite constellation deployment strategies p 878 N94-17138
Delta launch vehicle: Accommodations for small satellites p 878 N94-17139
Adequation of mini satellites to oceanic altimetry missions p 891 N94-17152
Regulation of low Earth orbit satellites p 892 N94-17159
LEOCOM-SPES: Low cost message communications p 892 N94-17161
TAOS (S80): A (LEO-MSS) system for position reporting and telemanagement services p 893 N94-17162
The ORBCOMM system p 893 N94-17163
MAGSS-14: Medium Altitude Global Mobile Satellite System with enhanced regional coverage p 893 N94-17164
Feasibility study of a personal communications system IRIDIUM-like p 893 N94-17165
The ELLIPSO (tm) system: Elliptical low orbits for mobile communications p 893 N94-17167
STARSYS: A view after WARC-92 --- satellite position and messaging system p 893 N94-17168
S-80: A satellite for less than 50 MF p 894 N94-17172
Key trends of the small satellite market p 897 N94-17191
Solar Electro-Optical Network (SEON) upgrade/replacement program. Phase 1: Qualification operational test and evaluation plan
[AD-A266364] p 1237 N94-17225

SATELLITE OBSERVATION
Finding fish from above --- remote sensing
[NASA-TM-109602] p 1081 N94-15310
ATLAS-2 and UARS correlative measurement opportunities during Space Shuttle mission on April 8-17, 1993
[NASA-TM-109020] p 1105 N94-15480
SeaWiFS technical report series. Volume 12, SeaWiFS technical report series cumulative index: Volumes 1-11
[NASA-TM-104566-VOL-12] p 1111 N94-15529
ERS-1: 18 months in orbit p 990 N94-15888
ENVISAT ASAR p 898 N94-15892
Some thoughts on future rain mapping missions (TRMM follow-on) p 992 N94-15906
EUVE observations of the Moon p 1250 N94-16185
Galileo photometry of Apollo landing sites p 1259 N94-16234
Big results with small space systems: What small systems are doing today p 896 N94-17187
Developing automated analysis methods for sea ice imagery: A status report with recommendations
[AD-A267284] p 1113 N94-17241
Arctic and Antarctic sea ice, 1978-1987: Satellite passive-microwave observations and analysis
[NASA-SP-511] p 1114 N94-17439
Optimization of satellite coverage in observing cause and effect changes in the ionosphere, magnetosphere, and solar wind
[AD-A267956] p 1102 N94-17493
An analysis of simulated and actual DMSP SSM/T-2 brightness temperatures
[AD-A268103] p 1109 N94-17573

SATELLITE ORBITS
Development of Japanese Earth Resources Satellite-1 (JERS-1; FUYO-1) and it's operational results
[NASDA-SPP-930001] p 884 N94-15001
Satellite situation report, volume 33, no. 3
[NASA-TM-109278] p 885 N94-15712
ERS-1: 18 months in orbit p 990 N94-15888
On the delivery of planetesimals to a protoplanet in the solar nebula p 1245 N94-16379
Low Earth orbit constellations: Orbit control or not p 875 N94-17134
Impact of launching uncertainties on the visibility of communication satellite constellations without orbit control p 889 N94-17135
Delta launch vehicle: Accommodations for small satellites p 878 N94-17139
CERISE microsatellite system p 894 N94-17170

SATELLITE ORIENTATION
ETALON-1,-2 center of mass correction and array reflectivity p 915 N94-15576
SATELLITE SOUNDING
EOS Laser Atmosphere Wind Sounder (LAWS) investigation
[NASA-CR-193445] p 1109 N94-17525
SATELLITE SURFACES
Crustal structure and igneous processes in a chondritic Io p 1243 N94-16292
The rheology and composition of cryovolcanic flows on icy satellites p 1243 N94-16294
The spectrum of Phobos from Phobos 2 observations at 0.3-2.6 microns: Comparison to previous data and meteorite analogs p 1295 N94-16429
SATELLITE TRACKING
Development of Japanese Earth Resources Satellite-1 (JERS-1; FUYO-1) and it's operational results
[NASDA-SPP-930001] p 884 N94-15001
Eighth International Workshop on Laser Ranging Instrumentation
[NASA-CP-3214] p 911 N94-15552
Laser ranging network performance and routine orbit determination at D-PAF p 911 N94-15554
Satellite signatures in SLR observations p 912 N94-15557
Work at Graz on satellite signatures p 898 N94-15558
The precision of today's satellite laser ranging systems p 912 N94-15559
SLR data screening; location of peak of data distribution p 912 N94-15560
Adaptive median filtering for preprocessing of time series measurements p 912 N94-15561
SATCOP mission planning software package p 912 N94-15562
Preliminary results from the portable standard satellite laser ranging intercomparison with MOBLAS-7 p 913 N94-15568
Tracking capabilities of SPADs for laser ranging p 914 N94-15570
Streak camera based SLR receiver for two color atmospheric measurements p 914 N94-15573
The first satellite laser echoes recorded on the streak camera p 914 N94-15574
ETALON-1,-2 center of mass correction and array reflectivity p 915 N94-15576
Test results from LAGEOS-2 optical characterization using pulsed lasers p 915 N94-15577
Analysis of TOPEX laser retroreflector array characteristics p 915 N94-15578
Two color satellite laser ranging upgrades at Goddard's 1.2m telescope facility p 915 N94-15581
Measuring atmospheric dispersion with WLRS in multiple wavelength mode p 916 N94-15582
Two wavelength satellite laser ranging using SPAD p 916 N94-15584
New perspectives for high accuracy SLR with second generation geodesic satellites p 916 N94-15585
State-of-the-art satellite laser range modeling for geodetic and oceanographic applications p 916 N94-15586
Geometric analysis of satellite laser ranging data p 917 N94-15587
Improvement of SLR accuracy, a possible new step p 917 N94-15588
On the accuracy of ERS-1 orbit predictions p 874 N94-15589
Compensation for the distortion in satellite laser range predictions due to varying pulse travel times p 917 N94-15590
Timebias corrections to predictions p 875 N94-15591
Formation of on-site normal points p 917 N94-15592
Poisson filtering of laser ranging data p 917 N94-15593
Computer networking at SLR stations p 917 N94-15594
HP upgrade operational streamlining p 918 N94-15596
Application of the robust estimate in SLR data preprocessing p 918 N94-15597
A computer-controlled x-y offset guiding stage for the MLRS p 918 N94-15598
Lunar laser ranging data processing in a Unix/X windows environment p 918 N94-15599
LLR: Activities in Wettzell p 876 N94-15600
Upgrading of the Borowiec laser station p 877 N94-15604
Development of Shanghai satellite laser ranging station p 877 N94-15605
WLRS --- Wettzell Laser Ranging System (WLRS) p 877 N94-15606
Ground based laser ranging for satellite location p 919 N94-15607
New progress of ranging technology at Wuhan Satellite Laser Ranging Station p 877 N94-15608
Results of the MTLRS-1 upgrade p 877 N94-15610
The new MTLRS-1 receiving system p 877 N94-15611
The new MTLRS transmitting system p 877 N94-15612
Transputer based control system for MTLRS p 877 N94-15613
Optical attenuation mechanism upgrades, MOBLAS, and TLRS systems p 922 N94-15622
Station report on the Goddard Space Flight Center (GSFC) 1.2 meter telescope facility p 922 N94-15625
Satellite control: A comprehensive approach p 878 N94-17158
SATELLITE TRANSMISSION
Almaz p 898 N94-15889
BRIDGE: A small scientific satellite for geodesy p 890 N94-17146
SATELLITE-BORNE INSTRUMENTS
The XMM pn-CCD detector system: First results p 900 N94-15034
Prospects for high pressure imaging gas scintillation drift chambers p 901 N94-15040
Development of an ultra violet auroral imager for the Freja project p 904 N94-15060
The high pressure gas scintillation proportional counter for SAX p 906 N94-15076
A new detector concept for energetic auroral x ray imaging p 907 N94-15081
The laboratory performance of the short wavelength instrument for the Along Track Scanning Radiometer ATSR-2 (initial results) p 908 N94-15088
ENVISAT ASAR p 898 N94-15892
Transparent conductive coatings in the far ultraviolet
[NASA-CR-194632] p 1191 N94-16024
Strategy for a small satellite program and a proposal for a first mission p 874 N94-17143
Cosmic dust and space debris measurements on board the small satellites HITEN and BREM-SAT p 890 N94-17147
Environment tests for mini satellites p 896 N94-17189
SATELLITE-BORNE RADAR
Almaz p 898 N94-15889
SATURATION
Evaluation of a distributed catchment scale water balance model
[PAPER-93WR00398] p 1083 N94-16031
SATURN (PLANET)
NASA images 12 --- Voyager encounters
[NASA-TM-109417] p 1247 N94-15511
Life and the solar system: The CRAF and Cassini missions
[NASA-TM-109422] p 1247 N94-15513
SATURN ATMOSPHERE
Vertical structure models of the 1990 equatorial disturbance on Saturn p 1277 N94-16333
SATURN RINGS
Voyager encounter highlights
[NASA-TM-109420] p 1246 N94-15239
Mass of Saturn's A ring p 1263 N94-16252
SAUDI ARABIA
Martian crater degradation by eolian processes: Analogy with the Rio Cuarto Crater Field, Argentina p 1251 N94-16196
SCALARS
Scalar limitations of diffractive optical elements p 1194 N94-17336
SCALE (CORROSION)
Effects of alloying and temperature on the high-temperature oxidation of Cr-Cr2Nb
[DE93-015800] p 957 N94-16163
SCALE MODELS
Cruise noise measurements of a scale model advanced ducted propulsor
[NASA-TM-105808] p 1176 N94-15115
Evaluation of a distributed catchment scale water balance model
[PAPER-93WR00398] p 1083 N94-16031
A detailed model for simulation of catchment scale subsurface hydrologic processes
[PAPER-92WR02333] p 1084 N94-16032
Scaling, soil moisture and evapotranspiration in runoff models p 1084 N94-16034
SCALING LAWS
Swept shock/boundary-layer interactions: Scaling laws, flowfield structure, and experimental methods p 1017 N94-15197
The size of complex craters p 1262 N94-16249
Evolution of hadron beams under intrabeam scattering
[DE93-014330] p 1184 N94-16826
SCANNERS
Display system employing acousto-optic tunable filter
[NASA-CASE-NPO-18736-1-CU] p 1190 N94-15933
Laser beam steering device p 1045 N94-17357
Environmental use of a Laser Range Finder and the Advanced Visualization System
[DE93-016163] p 1043 N94-17677
SCANNING
Medical imaging
[NASA-TM-109675] p 1229 N94-15520
SCANNING ELECTRON MICROSCOPY
Application of Z-contrast imaging to obtain column-by-column spectroscopic analysis of materials
[DE93-015333] p 947 N94-16014
Insights into semiconducting materials and growth phenomena through Z-contrast STEM
[DE93-015964] p 1212 N94-16841
UHV-stem studies on nucleation and growth of thin metal silicide films on silicon
[DE93-017604] p 1212 N94-16961
SCANNING TUNNELING MICROSCOPY
Method and apparatus for performing scanning tunneling optical absorption spectroscopy
[AD-D015796] p 948 N94-16539
Methods of tunneling spectroscopy with the STM
[AD-A266507] p 948 N94-16787
SCATTERING
Effects of spin-orbit coupling on disordered mesoscopic systems
[ITN-93-85220] p 1180 N94-15288
Interfacial structure of lattice mismatched bcc(110)/bcc(110) transition metal superlattices
[DE93-015162] p 1208 N94-16058
Application of symmetry properties to polarimetric remote sensing with JPL AIRSAR data p 1079 N94-16752
External calibration of polarimetric radar images using distributed targets p 1079 N94-16753
Convergence of the multiple scattering expansion in XAFS and XANES
[DE93-011001] p 948 N94-16772
Evolution of hadron beams under intrabeam scattering
[DE93-014330] p 1184 N94-16826
Diffuse scattering and image contrast of tweed in superconducting oxides: A simulation and interpretation
[DE93-016131] p 1212 N94-16844
SCATTERING AMPLITUDE
Convergence of the multiple scattering expansion in XAFS and XANES
[DE93-011001] p 948 N94-16772
Quark-loop effects in high energy spin-flip processes
[DE93-626692] p 1188 N94-17313
SCATTERING COEFFICIENTS
Radar response of vegetation: An overview p 991 N94-15898
Multifrequency observations p 992 N94-15902
Application of symmetry properties to polarimetric remote sensing with JPL AIRSAR data p 1079 N94-16752
SCATTERING CROSS SECTIONS
The quantum mass shift of the soliton in Skyrme model
[ITN-93-85219] p 1180 N94-15283
SCHEDULES
Sleep management user's guide for special operations personnel
[AD-A267746] p 1119 N94-14943
HSTS: Integrating planning and scheduling
[AD-A266991] p 1222 N94-15213
Activity/rest patterns of instructor and rates student pilots during rapid transitions from daytime to nighttime duty hours at the Eastern Army Aviation Training site
[AD-A267038] p 1131 N94-15659
AIRSAR South American deployment: Operation plan, version 3.0 p 994 N94-15919
Establishing a software measurement process
[AD-A267896] p 1154 N94-17396
SCHEDULING
HSTS: Integrating planning and scheduling
[AD-A266991] p 1222 N94-15213
Stochastic scheduling in in-forest networks
[INRIA-RR-1719] p 1164 N94-15695
Fast interrupt priority management in operating system kernels
[AD-A266638] p 1140 N94-15744
Processor capacity reserves for multimedia operating systems
[AD-A266639] p 1158 N94-15745
Efficient scheduling of real-time compute-intensive periodic graphs on large grain data flow multiprocessor
[AD-A267444] p 1141 N94-17030
Stochastic scheduling in a multiclass G/G/1 queue
[INRIA-RR-1746] p 1162 N94-17537
SCHLIEREN PHOTOGRAPHY
Supersonic flow visualization of a nacelle in close proximity to a simulated wing
[NASA-CR-194675] p 860 N94-17260
SCHOOLS
Developments in the Higher Technical Aerospace Education p 854 N94-15130

From the Moons of Jupiter to the Milky Way
[NASA-CR-194649] p 1240 N94-17059
SCHOTTKY DIODES
Schottky barrier focal plane arrays for SWIR and MWIR p 903 N94-15050
SCHROEDINGER EQUATION
Many-body quantum mechanical studies of molecular clusters
[AD-A266624] p 1180 N94-15727
SCHWASSMANN-WACHMANN COMET
Orbital evolution of dust from comet Schwassmann-Wachmann 1: A case of one-to-one resonance trapping p 1242 N94-16270
SCIENCE
From the Moons of Jupiter to the Milky Way
[NASA-CR-194649] p 1240 N94-17059
SCIENTIFIC SATELLITES
The definition of a scientific policy: ESRO's satellite programme in 1969-1973
[ESA-HSR-6] p 1303 N94-16500
Choosing ESRO's first scientific satellites
[ESA-HSR-3] p 887 N94-16523
Optical measurements of NASA/USAF CRRES high altitude rocket borne chemical release experiments in conjunction with the USAF airborne ionospheric observatory aircraft
[AD-A266404] p 1101 N94-16551
SCIENTIFIC VISUALIZATION
The 1989 computational fluid dynamics highlights
[NASA-TM-109635] p 1018 N94-15246
The 1986 computational fluid dynamics highlights
[NASA-TM-109645] p 1019 N94-15431
Computing science and statistics. Volume 24: Graphics and visualization
[AD-A266571] p 1150 N94-16721
Theoretical crystallography with the Advanced Visualization System
[DE93-015692] p 1215 N94-17319
TDNOVA interactive graphics
[AD-A268000] p 1156 N94-17530
SCIENTISTS
NASA/DOD Aerospace Knowledge Diffusion Research Project. Report 15: Technical uncertainty and project complexity as correlates of information use by US industry-affiliated aerospace engineers and scientists: Results of an exploratory investigation
[NASA-TM-107693] p 1233 N94-17291
SCINTILLATION
Optical ionospheric instrumentation and research
[AD-A266403] p 1192 N94-16550
Scintillation mechanism in stoichiometric cerium compounds
[DE93-015499] p 948 N94-16771
SCINTILLATION COUNTERS
Prospects for high pressure imaging gas scintillation drift chambers p 901 N94-15040
The high pressure gas scintillation proportional counter for SAX p 906 N94-15076
A new detector concept for energetic auroral x ray imaging p 907 N94-15081
Applications for large area silicon drift detectors on x ray and gamma ray astronomy p 909 N94-15090
Scintillation mechanism in stoichiometric cerium compounds
[DE93-015499] p 948 N94-16771
SCORPIUS CONSTELLATION
Mass of Saturn's A ring p 1263 N94-16252
SEA ICE
Exploring the southern ocean response to climate change
[NASA-CR-194601] p 1112 N94-15680
Sea ice motions in the central arctic ice central arctic pack ice as inferred from AVHRR imagery
[NASA-CR-194572] p 1112 N94-15701
Imaging radar studies of polar ice p 991 N94-15899
Developing automated analysis methods for sea ice imagery: A status report with recommendations
[AD-A267284] p 1113 N94-17241
Arctic and Antarctic sea ice, 1978-1987: Satellite passive-microwave observations and analysis
[NASA-SP-511] p 1114 N94-17439
Arctic cyclones and Marginal Ice Zone (MIZ) variability
[AD-A268610] p 1109 N94-17465
SEA LEVEL
Atmospheric transmittance between 1.0 and 2.0 micrometers
[AD-A267076] p 1098 N94-15539
The Central American cold surge: An observational analysis of the deep southward penetration of North American cold fronts
[AD-A268592] p 1110 N94-17607
SEA SURFACE TEMPERATURE
The laboratory performance of the short wavelength instrument for the Along Track Scanning Radiometer ATSR-2 (initial results) p 908 N94-15088
SEA WATER
Earth's partial pressure of CO2 over the past 120 Ma: evidence from Ce anomalies in the deep (greater than 600 m) Pacific Ocean, 1 p 1104 N94-16358
Regulation of attached bacterial growth by adsorbed proteins
[AD-A267756] p 1118 N94-17275
Chemical tracer studies at IOSDL. 3: The measurement of silicate, nitrate and phosphate in seawater
[IOS-302-1992] p 1114 N94-17489
SEALING
High temperature hydraulic seals
[AD-A268257] p 1048 N94-17433
SEALS (STOPPERS)
Development of braided fiber seals for engine applications p 939 N94-16859
ASRM nozzle thermal analysis
[NASA-CR-194672] p 928 N94-17277
High temperature hydraulic seals
[AD-A268257] p 1048 N94-17433
SEAMS (JOINTS)
Flight 20 (STS-45) polysulfide gas path investigation
[NASA-CR-193861] p 928 N94-17213
SEARCH RADAR
Alternative optical architectures for multichannel adaptive optical processing
[AD-A267052] p 1189 N94-15664
SEARCHING
A browsing tool for the Internet Logical Library of the HPCC Software Exchange
[NASA-CR-194545] p 1143 N94-15189
SEAS
On the application and evaluation of the relocatable diecast ocean circulation model in coastal and semi-enclosed seas
[AD-A266626] p 1112 N94-15771
Field observations of infragravity, sea and swell directional spectra
[AD-A266439] p 1113 N94-16561
SEASONS
Global and regional/seasonal color mosaics of Mars p 1288 N94-16393
SEATS
Basic principles of helicopter crashworthiness
[AD-A267099] p 862 N94-15637
Ergonomics in the office environment p 1124 N94-16612
SECONDARY FLOW
Turbine blade tip film cooling measurements
[AD-A267686] p 868 N94-14964
SECONDARY RADAR
Diffraction of microwaves at rectangular facades of buildings with and without ground reflections (Fresnel-Kirchhoff-Approximation)
[DLR-FB-92-35] p 987 N94-15155
SECURITY
Classified information: Volume could be reduced by changing retention policy
[AD-A266938] p 1228 N94-15176
NASA security handbook
[NHB-1620.3C] p 1224 N94-15937
Military space programs in the press: An analysis for change
[AD-A267799] p 874 N94-17306
SEDIMENT TRANSPORT
Louisiana delta study
[NASA-TM-109622] p 1095 N94-15408
Ventilated oscillatory boundary layers
[AD-A266226] p 1023 N94-16110
A Geographic Information System approach to modeling nutrient and sediment transport
[DE93-013747] p 1097 N94-17426
SEDIMENTARY ROCKS
The Karakul depression in Pamirs: The first impact structure in Central Asia p 1241 N94-16212
Geomorphic processes in the Argyre-Dorsa Argentea region of Mars p 1270 N94-16293
Tidal regime of intact planetoid capture model for the Earth-Moon system: Does it relate to the archean sedimentary rock record? p 1245 N94-16378
SEDIMENTS
Efficacy of flocculating and other emergency water purification tablets
[AD-A266695] p 1148 N94-15840
Ventilated oscillatory boundary layers
[AD-A266226] p 1023 N94-16110
Martian crater degradation by eolian processes: Analogy with the Rio Cuarto Crater Field, Argentina p 1251 N94-16196
Sedimentation, volcanism, and ancestral lakes in the Valles Marineris: Clues from topography p 1283 N94-16369
Multiple dataset water-quality analyses in the vicinity of an ocean wastewater plume p 1069 N94-16687
A Geographic Information System approach to modeling nutrient and sediment transport
[DE93-013747] p 1097 N94-17426
SEGMENTS
Segmenting textured 3D surfaces using the space/frequency representation
[AD-A266960] p 1163 N94-14968
Segmented ion thruster
[NASA-CASE-NPO-18192-1-CU] p 925 N94-15927
SEISMIC ENERGY
NORSAR basic seismological research
[AD-A266193] p 1101 N94-16125
SEISMIC WAVES
Broadband teleseismic array recording in the Adirondack Mountains, New York State
[AD-A267290] p 1097 N94-14960
Generation of artificial helioseismic time-series
[NASA-CR-194612] p 1299 N94-15968
Composite refraction-reflection stack sections: Tracing faults in the Atlantic coastal plain sediments
[DE93-013581] p 1112 N94-16009
NORSAR basic seismological research
[AD-A266193] p 1101 N94-16125
A search for evidence of nonlinear elasticity in the earth
[DE93-015279] p 1102 N94-17252
Preliminary estimates of frequency-direction spectra derived from the SAMSON pressure gage array, November 1990 to May 1991
[AD-A267960] p 1114 N94-17497
SEISMOGRAMS
NORSAR basic seismological research
[AD-A266193] p 1101 N94-16125
SEISMOGRAPHS
Broadband teleseismic array recording in the Adirondack Mountains, New York State
[AD-A267290] p 1097 N94-14960
SEISMOLOGY
Papers presented at the Eleventh International Symposium on Earth Tides
[COMMUNICATIONS-SER-B-158] p 1098 N94-15800
NORSAR basic seismological research
[AD-A266193] p 1101 N94-16125
High-resolution seismic reflection survey at the Manson crater, Iowa p 1103 N94-16307
The seismic response of an aquifer to the propagation of an impact generated shock wave: A possible trigger of the Martian outflow channels? p 1281 N94-16354
A geological and geophysical information system for Eurasia
[AD-A267841] p 1232 N94-17036
SELECTIVE DISSEMINATION OF INFORMATION
Classified information: Volume could be reduced by changing retention policy
[AD-A266938] p 1228 N94-15176
NASA security handbook
[NHB-1620.3C] p 1224 N94-15937
NASA Electronic Library System (NELS): The system impact of security
[NASA-CR-194614] p 1231 N94-16499
Military space programs in the press: An analysis for change
[AD-A267799] p 874 N94-17306
SELECTIVE SURFACES
Manufacturing tolerance requirements for frequency selective surfaces
[AD-A266541] p 999 N94-16797
SELENOLOGY
Mixing model analysis of telescopic lunar spectra p 1284 N94-16371
Tidal regime of intact planetoid capture model for the Earth-Moon system: Does it relate to the archean sedimentary rock record? p 1245 N94-16378
SELF ALIGNMENT
Neural-network-directed alignment of optical systems using the laser-beam spatial filter as an example
[NASA-TP-3372] p 1034 N94-15961
SELF CONSISTENT FIELDS
Continuum solvent models for computational chemistry
[DE93-016329] p 953 N94-17660
3D and r,z particle simulations of heavy ion fusion beams
[DE93-013417] p 1205 N94-17670
Granular fluctuations in plasma turbulence and their role in transport
[DE93-013465] p 1187 N94-17674
SEMANTICS
Combinatorial semantics
[TR-444] p 1149 N94-16575
Monads and comonads in intensional semantics
[AD-A266522] p 1151 N94-16790
SEMICONDUCTING FILMS
Growth, characterization and device development in monocrystalline diamond films
[AD-A268206] p 1216 N94-17553

SEMICONDUCTOR DEVICES
Interface properties of wide bandgap semiconductor structures
[AD-A268269] p 1215 N94-17377
Smart Power: New power integrated circuit technologies and their applications
[VTT-TIED-1358] p 1015 N94-17546
Proceedings of the 6th International Conference on Narrow Gap Semiconductors
[AD-A268097] p 1015 N94-17570
SEMICONDUCTOR DIODES
Infrared detector annealing and calibration with IR-laser diodes p 909 N94-15092
SEMICONDUCTOR JUNCTIONS
A new approach to optical photon detection p 899 N94-15028
Superconductive x ray photon detectors p 900 N94-15031
Atomic layer epitaxy of boron nitride
[AD-A266260] p 1212 N94-16932
SEMICONDUCTOR LASERS
Infrared detector annealing and calibration with IR-laser diodes p 909 N94-15092
Nd:YLF laser for airborne/spaceborne laser ranging p 913 N94-15563
Development of the Mars Observer Laser Altimeter (MOLA) p 921 N94-15617
Laser with optically driven Q-switch
[NASA-CASE-NPO-18470-1-CU] p 1038 N94-15932
Fundamental theory of light for applications: Notes for five informal lectures
[DE93-016463] p 1192 N94-16953
Curved grating fabrication techniques for concentric-circle grating, surface-emitting semiconductor lasers p 1045 N94-17349
Nonintrusive fast response oxygen monitoring system for high temperature flows
[NASA-CR-4553] p 1036 N94-17655
SEMICONDUCTORS (MATERIALS)
Electronic and atomic structure of semiconductors and of high-temperature superconductors
[AD-A266805] p 1205 N94-14913
Transparent conductive coatings in the far ultraviolet
[NASA-CR-194632] p 1191 N94-16024
Thermal spray forming of refractory sample ampoule cartridges for single crystal growth space furnaces
[TABES PAPER 93-605] p 1051 N94-16141
Apparatus for and a method of growing thin films of elemental semiconductors
[AD-D015813] p 1210 N94-16487
Properties of thin films for high temperature flow sensors
[NASA-CR-191526] p 967 N94-16541
SONOS technology for commercial and military nonvolatile memory applications
[DE93-015647] p 1011 N94-16661
Ultrafast processes in tunneling microstructure devices
[AD-A266570] p 1210 N94-16720
Methods of tunneling spectroscopy with the STM
[AD-A266507] p 948 N94-16787
JSEP fellowship
[AD-A266568] p 1211 N94-16800
Insights into semiconducting materials and growth phenomena through Z-contrast STEM
[DE93-015964] p 1212 N94-16841
Activation and deactivation of high concentration arsenic with some evidence of precipitation
[DE93-016437] p 950 N94-16952
Vectorial electron transfer in spatially ordered arrays
[DE93-018150] p 1185 N94-16971
Surface flashover of semiconductors: A fundamental study
[AD-A267382] p 1012 N94-17023
Nitride semiconductors for ultraviolet detection
[AD-A267877] p 1012 N94-17040
Photo-assisted epitaxial growth for III-V semiconductors
[AD-A267889] p 1213 N94-17042
Investigation of the optical, electronic, and structural properties of fiber optic glasses
[AD-A267645] p 971 N94-17204
A state-of-the-art plasma polymerization coater for ICF targets
[DE93-016452] p 1204 N94-17237
A 27 channels, 1 MHz fibre-optic measuring system
[AD-A266943] p 1003 N94-17307
Subwavelength structured surfaces and their applications p 1194 N94-17337
Curved grating fabrication techniques for concentric-circle grating, surface-emitting semiconductor lasers p 1045 N94-17349
OSA proceedings on Ultrafast Electronics and Optoelectronics, volume 14
[AD-A267972] p 1014 N94-17410
Laser probing of the kinetics and dynamics of 3-5 semiconductor growth
[AD-A268388] p 1215 N94-17422
Mechanical properties and crystal growth studies of semiconductor alloys
[AD-A268144] p 1216 N94-17454
Femtosecond carrier processes in compound semiconductors and real time signal processing
[AD-A268122] p 1005 N94-17519
In-situ electron and optical spectroscopies of translational and vibrational activated bond breaking and formation on semiconductors
[AD-A268192] p 1015 N94-17560
Proceedings of the 6th International Conference on Narrow Gap Semiconductors
[AD-A268097] p 1015 N94-17570
Rare earth doped III-V semiconductors for optoelectronics
[AD-A268279] p 1216 N94-17577
Activities of the Research Laboratory of Electronics
[AD-A266730] p 1304 N94-17651
SENSITIVITY
The role of constitutive and inducible processes in the response of human squamous cell carcinoma cell lines to ionizing radiation
[DE93-015150] p 1129 N94-16970
SENSORIMOTOR PERFORMANCE
Characteristics of aimed arm movements in humans under low gravity p 980 N94-16093
SENSORS
Passive tracking of a target using an array of sensors
[DE93-015870] p 997 N94-16169
Micro-optics technology and sensor systems applications p 1197 N94-17350
SENSORY STIMULATION
States of awareness 1: Subliminal perception relationship to situational awareness
[AD-A267249] p 1132 N94-16942
SENTENCES
The impact of report of investigation writing style on the assessment times, impressions, perceptions and preferences of adjudicators
[AD-A265748] p 1223 N94-15682
Segment-based acoustic models for continuous speech recognition
[AD-A267138] p 988 N94-15691
SEPARATED FLOW
Unsteady separated flows: Empirical model and control
[AD-A267282] p 855 N94-14959
Unsteady phenomena in shock wave/boundary layer interaction p 1017 N94-15200
Hypersonic shock wave boundary layer interactions over simplified deflected control surface configurations p 1018 N94-15203
Study into the limits of an Euler equation method applied to leading-edge vortex flow
[NLR-TP-91350-U] p 1031 N94-17627
SEPARATION
Electrophoresis visualisation p 944 N94-15163
SEPARATORS
The bootstrapped algorithm: Fast algorithm for blind signal separation
[AD-A266671] p 1147 N94-15772
SEQUENCING
Temporal segmentation of tasks from human hand motion
[AD-A266596] p 1166 N94-16725
FSM test: A functional test generation system for sequential circuits
[REPT-93-017] p 1014 N94-17505
SEQUENTIAL CONTROL
Digital laser range finder emulator
[AD-D015811] p 1040 N94-16540
Temporal segmentation of tasks from human hand motion
[AD-A266596] p 1166 N94-16725
SERIES EXPANSION
Analysis of an electromagnetic field in the vicinity of a caustic by asymptotic methods
[IFTR-12/1991] p 998 N94-16653
Convergence of the multiple scattering expansion in XAFS and XANES
[DE93-011001] p 948 N94-16772
Expansions of cumulative distribution functions directly from characteristic functions
[AD-A267727] p 1173 N94-17372
Convection effects on radial segregation and crystal melt interface in vertical Bridgman growth
[NASA-CR-191541] p 1029 N94-17387
SERVICE LIFE
Field investigation of the relationship between battery size and PV system performance
[DE93-016503] p 1016 N94-17671
SERVOMECHANISMS
Dynamic testbed laboratory and micro-optics p 1199 N94-14986
A complete study of differential wax-wane focus servo technique p 1199 N94-14996
Optimal tuning of heavy equipment motion controllers
[AD-A267873] p 1167 N94-17392
SET THEORY
Reductions to sets of low information content
[TR-417] p 1150 N94-16579
A fuzzy method for preliminary design random access memory failure rate prediction
[AD-A267948] p 1055 N94-17044
SEYFERT GALAXIES
Variability of the Seyfert galaxy MKN 766 in the Rosat all sky survey
[MPE-PREPRINT-221] p 1240 N94-17591
SH-3 HELICOPTER
Evaluation of Night Vision Goggles (NVG) for maritime search and rescue (HH-3/HH-60) comparison report
[AD-A266493] p 1138 N94-16793
SHADOWS
Cooperativity and 3-D representation
[AD-A267180] p 1131 N94-15694
A field measure of the shade fraction p 1068 N94-16677
Mapping the spectral variability in photosynthetic and non-photosynthetic vegetation, soils, and shade using AVIRIS p 1068 N94-16679
Multitemporal diurnal AVIRIS images of a forested ecosystem p 1074 N94-16709
SHAPE FUNCTIONS
Analysis of electromagnetic scattering from irregularly shaped, thin, metallic flat plates
[NASA-TP-3361] p 998 N94-16655
SHAPES
Segmenting textured 3D surfaces using the space/frequency representation
[AD-A266960] p 1163 N94-14968
Process for shaping articles from electrosetting compositions
[AD-D015787] p 935 N94-16534
SHARP LEADING EDGES
Study into the limits of an Euler equation method applied to leading-edge vortex flow
[NLR-TP-91350-U] p 1031 N94-17627
SHEAR FLOW
The turbulent wall jet
[AD-A267675] p 855 N94-14963
Parametric resonant triad interactions in a free shear layer
[NASA-TM-106365] p 1021 N94-15751
Turbulence and transition modeling for high-speed flows
[AD-A266748] p 1022 N94-15953
Implementation of an anisotropic turbulence model in the COMMIX-1C/ATM computer code
[DE93-015541] p 1023 N94-16444
Search for chaos in free shear flows
[AD-A266245] p 1023 N94-16470
Investigation of high-speed free shear flows using improved pressure-strain correlated Reynolds stress turbulence model
[NASA-CR-194661] p 1027 N94-17127
A numerical investigation of energy transfer and subgrid-scale eddy-viscosity in homogeneous, isotropic, and shear turbulence
[AD-A267265] p 1029 N94-17363
Time dependent turbulence modeling and analytical theories of turbulence
[NASA-TM-106379] p 1029 N94-17385
SHEAR LAYERS
Parametric resonant triad interactions in a free shear layer
[NASA-TM-106365] p 1021 N94-15751
Search for chaos in free shear flows
[AD-A266245] p 1023 N94-16470
Selected computations of transonic cavity flows p 858 N94-16511
Unsteady fluid and optical simulation of transonic aero-windows
[AIAA PAPER 93-3017] p 858 N94-16512
The structure of turbulent boundary layers and shock wave boundary layer interactions
[AD-A266240] p 1026 N94-16929
Investigation of high-speed free shear flows using improved pressure-strain correlated Reynolds stress turbulence model
[NASA-CR-194661] p 1027 N94-17127
Structure of turbulence in three-dimensional boundary layers
[NASA-CR-194655] p 1027 N94-17130
Chemical reactions in turbulent mixing flows
[AD-A268287] p 861 N94-17580

SHEAR PROPERTIES
The processing and mechanical properties of high temperature/high performance composites. Book 4: Coonstitutive laws and design
[AD-A266397] p 935 N94-16528
Interfacial shear behavior and its influence on fiber damage in sapphire-reinforced gamma titanium aluminide composites
[AD-A267943] p 1060 N94-17043
Shear wave measurements in shock-induced, high-pressure phases
[DE93-016461] p 1062 N94-17664
SHEAR STRESS
Thermal stresses of a trimaterial medium in a nonuniform temperature field
[AD-A267243] p 930 N94-14975
Forced harmonic vibration of the generally orthotropic cylindrical shell with inner and outer fluid loading
[AD-A266985] p 1057 N94-15150
Theoretical study of laminar film condensation on horizontal elliptical tubes under conditions of free and forced convection
[AD-A267161] p 1021 N94-15737
Adaptive algorithm for aircraft configuration in turbulent flow
[AD-A266188] p 867 N94-16122
Evaluation of the interfacial mechanical properties in fiber-reinforced ceramic composites
[DE93-015494] p 935 N94-16461
Structure of high Reynolds number turbulent boundary layer
[AD-A267476] p 860 N94-17099
Convection effects on radial segregation and crystal melt interface in vertical Bridgman growth
[NASA-CR-191541] p 1029 N94-17387
SHEATHS
Cathode sheath charge transfer effects
[AD-A268393] p 1186 N94-17536
SHELL STABILITY
Comparison of level-1 and level-2 buckling and postbuckling solutions
[NASA-CR-194611] p 1057 N94-15154
SHELL THEORY
Sound radiation from infinite laminated composite shell with periodic rib stiffening
[DRA/TM(USGR)92326] p 933 N94-15699
SHELLS (STRUCTURAL FORMS)
Dynamic behavior of fiber and particle reinforced composites
[AD-A266905] p 930 N94-15143
Comparison of level-1 and level-2 buckling and postbuckling solutions
[NASA-CR-194611] p 1057 N94-15154
Progress in the modeling of the shock response and mitigation of thick composite shells
[AD-A267009] p 1057 N94-15524
SHERGOTTITES
Nitrates in SNCs: Implications for the nitrogen cycle on Mars p 1251 N94-16193
Potassium isotope cosmochemistry, volatile depletion and the origin of the Earth p 953 N94-16259
Os isotopes in SNC meteorites and their implications to the early evolution of Mars and Earth p 1242 N94-16272
Martian carbon dioxide: Clues from isotopes in SNC meteorites p 1270 N94-16295
The dregs of crystallization in Zagami p 1245 N94-16390
SHIPS
The free decay of coupled heave and pitch motions of a model frigate
[DRA/TM(AWMH)92340] p 1146 N94-15702
SHOCK (PHYSIOLOGY)
A review of the efficacy of 7.5 percent NaCl/6 percent Dextran-70 (HSD) in experimental animals and humans
[AD-A266633] p 1122 N94-15740
A mathematical model for the study of hemorrhagic shock and fluid resuscitation: Transcapillary exchange
[AD-A266427] p 1123 N94-16544
A mathematical model for the study of hemorrhagic shock and fluid resuscitation: Exchange of fluid and solutes between vascular, interstitial, and tissue cell compartments
[AD-A266426] p 1123 N94-16558
Increased vascular resistance with hemoglobin-based oxygen carriers
[AD-A266454] p 1123 N94-16565
SHOCK ABSORBERS
Mechanical energy absorber
[NASA-CASE-MSC-22111-1] p 1047 N94-15966
SHOCK FRONTS
Dynamic testing and characterization of pre-fractured ceramic
[DE93-016457] p 972 N94-17238
SHOCK LOADS
Progress in the modeling of the shock response and mitigation of thick composite shells
[AD-A267009] p 1057 N94-15524
Design of a cruciform bend specimen for determination of out-of-plane biaxial tensile stress effects on fracture toughness for shallow cracks
[DE93-015455] p 1059 N94-16104
Orientation of Planar Deformation Features (PDFs) in quartz p 1219 N94-16341
SHOCK MEASURING INSTRUMENTS
Determination of equivalent circuit for PVDF shock-pressure gauges
[DE93-016492] p 1034 N94-16452
SHOCK TESTS
CO2 production by impact in carbonates? An ATEM and stable isotope (C,O) study p 954 N94-16383
SHOCK TUBES
Mechanistic models of soot formation
[AD-A267806] p 950 N94-17008
SHOCK WAVE INTERACTION
Laser Doppler velocimetry measurements across a normal shock in transonic flow
[AD-A267240] p 855 N94-14973
Special course on Shock-Wave/Boundary-Layer Interactions in Supersonic and Hypersonic Flows
[AGARD-R-792] p 1017 N94-15196
Swept shock/boundary-layer interactions: Scaling laws, flowfield structure, and experimental methods p 1017 N94-15197
Swept shock wave/laminar boundary layer interactions, experimental, and numerical results p 1017 N94-15198
Numerical simulation of 3-D shock wave turbulent boundary layer interactions p 1017 N94-15199
Unsteady phenomena in shock wave/boundary layer interaction p 1017 N94-15200
Contribution of laser Doppler velocimetry to the physical description of shock wave/turbulent boundary layer interactions with incidence on turbulence modelling p 1018 N94-15201
Turbulence modelling for shock wave/boundary layer interactions specific issues and examples of applications p 1018 N94-15202
Hypersonic shock wave boundary layer interactions over simplified deflected control surface configurations p 1018 N94-15203
On the interaction between the shock wave attached to a wedge and freestream disturbances
[NASA-CR-191528] p 1019 N94-15478
The structure of turbulent boundary layers and shock wave boundary layer interactions
[AD-A266240] p 1026 N94-16929
An investigation of oblique shock/boundary layer interaction control
[AD-A268106] p 861 N94-17574
SHOCK WAVE PROPAGATION
Laser-shock damage of iron-based materials
[AD-A267196] p 1038 N94-15852
On possible Mn-53 heterogeneity in the early solar system p 1244 N94-16344
SHOCK WAVES
Adaptive algorithm for aircraft configuration in turbulent flow
[AD-A266188] p 867 N94-16122
Gas-grain energy transfer in solar nebula shock waves: Implications for the origin of chondrules p 1262 N94-16251
Orientation of Planar Deformation Features (PDFs) in quartz p 1219 N94-16341
The seismic response of an aquifer to the propagation of an impact generated shock wave: A possible trigger of the Martian outflow channels? p 1281 N94-16354
The structure of turbulent boundary layers and shock wave boundary layer interactions
[AD-A266240] p 1026 N94-16929
The shock Hugoniot of 316 SS and sound velocity measurements
[DE93-016525] p 1178 N94-16955
An experimental investigation of the effects of leading edge geometry on the dynamics of blunt fin-induced shock wave turbulent boundary layer interaction
[AD-A267656] p 860 N94-17221
Numerical solution of SUPG finite-element method for supersonic viscous flow
[AD-A267762] p 860 N94-17222
Dynamic testing and characterization of pre-fractured ceramic
[DE93-016457] p 972 N94-17238
Supersonic flow visualization of a nacelle in close proximity to a simulated wing
[NASA-CR-194675] p 860 N94-17260
Experimental studies on a gas dynamic laser with narrow throat and high area-ratio grid nozzles
[AD-A267818] p 1042 N94-17400
An experimental study of fluctuating wall pressures in a highly swept, sharp fin-induced, Mach 5 shock wave/turbulent boundary layer interaction
[AD-A268394] p 861 N94-17461
Design, development and characterization studies of a large aperture high power Nd: Glass rod amplifier stage
[DE93-624944] p 1042 N94-17630
Shear wave measurements in shock-induced, high-pressure phases
[DE93-016461] p 1062 N94-17664
SHORT CIRCUITS
A device for testing cables
[NASA-CASE-LAR-14093-1] p 1010 N94-15988
SHORT TAKEOFF AIRCRAFT
An experimental study of ASTOVL related jet flows to produce CFD code validation data. Phase 3: Results of experiments
[TT-9203] p 1020 N94-15645
SHROUDED PROPELLERS
Flow analysis for the nacelle of an advanced ducted propeller at high angle-of-attack and at cruise with boundary layer control
[NASA-TM-106371] p 858 N94-16571
SHUTTLE ENGINEERING SIMULATOR
STS-32 LDEF approach in SES
[NASA-TM-109474] p 880 N94-15379
SHUTTLE IMAGING RADAR
Spaceborne Imaging Radar-C instrument p 990 N94-15890
X-SAR: The X-band synthetic aperture radar on board the Space Shuttle p 990 N94-15891
Spaceborne radar for geoscientific applications in North China p 993 N94-15915
SIBERIA
Assimilation of solids during ascent of magmas from the Bartoy Field of the Baikal Region, Siberia p 1103 N94-16214
SIDELOBES
Adaptive beamforming with imperfect arrays: Pattern effects and their partial correction
[AD-A267079] p 987 N94-15541
Frequency resolution of an acousto-optical spectrometer
[AD-A267822] p 1035 N94-17401
SIDESLIP
Experimental study of vortex and aerodynamic characteristics of stack wings with sideslip
[AD-A267722] p 860 N94-17274
SIDEWINDER MISSILES
Parametric study of a finite element model of the Sidewinder missile
[AD-A267245] p 865 N94-14976
SIGNAL ANALYSIS
Develop advanced nonlinear signal analysis topographical mapping system
[NASA-CR-194577] p 1082 N94-15646
Automatic suppression of anomalous propagation clutter for noncoherent weather radars
[KNMI-WR-92-06] p 1004 N94-17407
SIGNAL DETECTION
New methods of generation of ultrashort laser pulses for ranging p 913 N94-15565
Develop advanced nonlinear signal analysis topographical mapping system
[NASA-CR-194577] p 1082 N94-15646
Signal processing in impulsive electromagnetic interference
[AD-A266425] p 998 N94-16557
Search for Extraterrestrial Intelligence (SETI) p 1125 N94-16620
Efficient computational methods to study new and innovative signal detection techniques in SETI
[NASA-CR-193602] p 998 N94-16649
States of awareness 1: Subliminal perception relationship to situational awareness
[AD-A267249] p 1132 N94-16942
Signal detection in correlated Gaussian and non-Gaussian radar clutter
[AD-A267453] p 1001 N94-17033
SIGNAL DETECTORS
Two wavelength satellite laser ranging using SPAD p 916 N94-15584
Development and analysis of ARMA parameter estimation schemes in the presence of noise
[AD-A267184] p 989 N94-15786
High resolution radar profiling using higher-order statistics
[AD-D015891] p 1000 N94-16918
Signal detection in correlated Gaussian and non-Gaussian radar clutter
[AD-A267453] p 1001 N94-17033
SIGNAL FADING
Expansions of cumulative distribution functions directly from characteristic functions
[AD-A267727] p 1173 N94-17372

SIGNAL GENERATORS
Synchronous sampling phase and amplitude detection method and apparatus
[NASA-CASE-LAR-14725-1] p 1050 N94-15870
Improvements to pulsed phase locked loop strain monitor
[NASA-CASE-LAR-14887-1] p 1033 N94-15877
SIGNAL PROCESSING
VLSI for high-speed digital signal processing
[AD-A267709] p 1007 N94-14936
Optical residue processing module
[AD-A267721] p 1188 N94-14940
Compact disk error measurements
p 1227 N94-14988
Broadband conventional beamforming incorporating adaptive equalization
[AD-A267090] p 987 N94-15544
New methods of generation of ultrashort laser pulses for ranging p 913 N94-15565
Test results from LAGEOS-2 optical characterization using pulsed lasers p 915 N94-15577
Exploitation of cyclostationarity for signal-parameter estimation and system identification
[AD-A267137] p 988 N94-15690
Higher order statistics in signal processing
[FFI-92/2008] p 989 N94-15714
Simultaneous measurement of temperature and strain using four connecting wires
[NASA-TM-104271] p 1032 N94-15754
The bootstrapped algorithm: Fast algorithm for blind signal separation
[AD-A266671] p 1147 N94-15772
Development and analysis of ARMA parameter estimation schemes in the presence of noise
[AD-A267184] p 989 N94-15786
Synthetic aperture radar signal processing: Trends and technologies p 992 N94-15908
Windshear detection radar signal processing studies
[NASA-CR-194615] p 994 N94-16022
Passive tracking of a target using an array of sensors
[DE93-015870] p 997 N94-16169
Signal processing in impulsive electromagnetic interference
[AD-A266425] p 998 N94-16557
Search for Extraterrestrial Intelligence (SETI)
p 1125 N94-16620
Efficient computational methods to study new and innovative signal detection techniques in SETI
[NASA-CR-193602] p 998 N94-16649
Reducing data dimension to lower signal processing computational requirements and maximize performance
[AD-A266606] p 999 N94-16728
Analysis of temporal symmetry in non-gaussian random fields
[AD-A266496] p 999 N94-16794
High resolution radar profiling using higher-order statistics
[AD-D015891] p 1000 N94-16918
Digital reverberation time measurement system
[AD-D015892] p 1177 N94-16919
Reference frames in vision
[AD-A266174] p 1132 N94-16925
Natural convection above a horizontal heat source
[AD-A267212] p 1026 N94-16985
Intelligent use of CFAR algorithms
[AD-A267755] p 1003 N94-17206
Method and apparatus for spur-reduced digital sinusoid synthesis
[NASA-CASE-NPO-18789-1-CU] p 1154 N94-17326
Asymmetric three-beam binary optic grating
p 1195 N94-17340
Theory of dispersive microlenses
p 1198 N94-17361
Expansions of cumulative distribution functions directly from characteristic functions
[AD-A267727] p 1173 N94-17372
High order nonlinear estimation with signal processing applications
[AD-A268407] p 1005 N94-17463
Fabrication of a NAVMAP, a deep-sea mapping system
[AD-A268630] p 1085 N94-17467
Femtosecond carrier processes in compound semiconductors and real time signal processing
[AD-A268122] p 1005 N94-17519
Activities of the Research Laboratory of Electronics
[AD-A266730] p 1304 N94-17651
SIGNAL TO NOISE RATIOS
Effects of window size and shape on accuracy of subpixel centroid estimation of target images
[NASA-TP-3331] p 1034 N94-15990
Spatial and frequency diversity in lidar systems
[AD-A266192] p 1039 N94-16124
The Clementine instrument complement
p 1086 N94-16370
Simulation of ASTER data using AVIRIS images
p 1071 N94-16693
Moving target indicator using higher order statistics
[AD-D015890] p 1000 N94-16917
High resolution radar profiling using higher-order statistics
[AD-D015891] p 1000 N94-16918
Performance of coded coherent FSK lightwave system with noncoherent detection
[AD-A267442] p 1193 N94-17028
SYDONI: An intensified system for night observation
p 891 N94-17153
The feasibility of tropospheric and total ozone determination using a Fabry-Perot interferometer as a satellite-based nadir-viewing atmospheric sensor
[NASA-TM-109342] p 1102 N94-17214
Optimisation and specification of Auger electron spectrometers for signal-to-noise ratio performance
[NPL-DMM(A)-101] p 1006 N94-17549
SIGNAL TRANSMISSION
VDM specification of the MD4 message digest algorithm
[NPL-DITC-204/92] p 1142 N94-14944
RAISE specification of the MD4 message digest algorithm
[NPL-DITC-206/92] p 1142 N94-15010
Improvements to pulsed phase locked loop strain monitor
[NASA-CASE-LAR-14887-1] p 1033 N94-15877
An electroacoustic transducer for purposes of photoacoustic spectroscopy
[IFTR-7/1992] p 1013 N94-17071
Wide angle, single screen, gridded square-loop frequency selective surface for diplexing two closely separated frequency bands
[NASA-CASE-NPO-18664-1-CU] p 1237 N94-17438
A virtual acoustic orientation instrument
[AD-A268181] p 1134 N94-17510
Optimisation and specification of Auger electron spectrometers for signal-to-noise ratio performance
[NPL-DMM(A)-101] p 1006 N94-17549
SIGNATURE ANALYSIS
Satellite signatures in SLR observations
p 912 N94-15557
SIGNATURES
Surface and internal signatures of organized vortex motions in stratified fluid
[AD-A267015] p 1020 N94-15526
Satellite signatures in SLR observations
p 912 N94-15557
Work at Graz on satellite signatures
p 898 N94-15558
New perspectives for high accuracy SLR with second generation geodesic satellites p 916 N94-15585
SIGNS AND SYMPTOMS
Flight simulator-induced sickness and visual displays evaluation
[AD-A267019] p 1122 N94-15845
Arsenic surveillance program p 1127 N94-16637
Predicting radiation induced performance decrements of AH-1 helicopter crews. Volume 1: Predicted veersus actual performance of AH-1 crews induced with symptoms simulating radiation sickness
[AD-A268376] p 1138 N94-17460
SILANES
Cathode sheath charge transfer effects
[AD-A268393] p 1186 N94-17536
SILICA GLASS
Structural studies of sol-gel glasses
[AD-A266277] p 967 N94-16472
Fabricating binary optics: An overview of binary optics process technology p 1195 N94-17343
SILICATES
NMR and theoretical investigation of cation binding with sol-gel silicates
[AD-A266999] p 963 N94-15631
Trapping of water vapor from an atmosphere by condensed silicate matter formed by high-temperature pulse vaporization p 1248 N94-16180
Iron oxide bands in the visible and near-infrared reflectance spectra of primitive asteroids
p 1242 N94-16274
An iridium-rich iron micrometeorite with silicate inclusions from the Moon p 1242 N94-16281
Partitioning of Nb, Mo, Ba, Ce, Pb, Th and U between immiscible carbonate and silicate liquids: Evaluating the effects of P2O5,F, and carbonate composition
p 953 N94-16283
Experimental partitioning of Zr, Ti, and Nb between silicate liquid and a complex noble metal alloy and the partitioning of Ti between perovskite and platinum metal
p 962 N94-16287
Complex radiation-thermal history of Kaidun meteorite on data of track study of silicate minerals
p 1243 N94-16297
Catalytic crystallization of ices by small silicate smokes at temperatures less than 20K p 1219 N94-16420
Transformation toughening of composite ceramics
[AD-A267304] p 971 N94-16980
Chemical tracer studies at IOSDL. 3: The measurement of silicate, nitrate and phosphate in seawater
[IOS-302-1992] p 1114 N94-17489
SILICIDES
Schottky barrier focal plane arrays for SWIR and MWIR p 903 N94-15050
Environmental embrittlement in ordered intermetallic alloys
[DE93-015307] p 955 N94-15830
Recent advances in ordered intermetallics
[DE93-015308] p 955 N94-15862
Thin Ni silicide formation by low temperature-induced metal atom reaction with ion implanted amorphous silicon
[DE93-015449] p 1209 N94-16066
UHV-stem studies on nucleation and growth of thin metal silicide films on silicon
[DE93-017604] p 1212 N94-16961
SILICON
BIB photodetectors based on antimony doped silicon
p 902 N94-15047
Gamma large area silicon telescope: Applying Si strip detector technology to the detection of gamma rays in space p 904 N94-15061
CCD's on high resistivity bulk silicon for x ray spectroscopy on XMM p 907 N94-15080
Silicon gallium doped photoconductor development for the AROME balloon borne instrument
p 908 N94-15087
Applications for large area silicon drift detectors on x ray and gamma ray astronomy p 909 N94-15090
Silicon radiation sensor systems for gamma and x ray detection at SI p 909 N94-15095
The epitaxial Si x ray bolometer an alternative to ion implanted devices p 911 N94-15103
Structural investigation of electrochemically etched silicon
[DE93-015300] p 1207 N94-15827
Selective formation of porous silicon
[NASA-CASE-NPO-18735-1-CU] p 966 N94-15960
Porous silicon for pumping solid-state lasers
[AD-A266293] p 1039 N94-16474
Thermal disorder in adsorbed Cl on Si(100)
[AD-A266295] p 1210 N94-16476
UHV-stem studies on nucleation and growth of thin metal silicide films on silicon
[DE93-017604] p 1212 N94-16961
Structural characterization of epitaxial layers for infrared detectors
[AD-A267875] p 940 N94-17013
Buried porous silicon-germanium layers in monocrystalline silicon lattices and method of producing
[NASA-CASE-NPO-18836-1-CU] p 1215 N94-17327
Low voltage electron beam lithography
[AD-A267865] p 1215 N94-17389
Laser probing of the kinetics and dynamics of 3-5 semiconductor growth
[AD-A268388] p 1215 N94-17422
Characterization of Ni on Si wafers: Comparison of surface analysis techniques
[DE93-016501] p 953 N94-17649
SILICON CARBIDES
Improved composite flexible blanket insulation
[NASA-CASE-ARC-11955-1-CU] p 934 N94-15926
Method of producing a silicon carbide fiber reinforced strontium aluminosilicate glass-ceramic matrix composite
[NASA-CASE-LEW-15263-2] p 934 N94-15929
NEXTEL(trademark)/SiC composites using forced chemical vapor infiltration
[DE93-013532] p 934 N94-16008
Environmental effects on elevated temperature subcritical crack growth of SiC/SiC composites
[DE93-015688] p 934 N94-16158
Do SiC grains in Orgueil differ from those in Murchison? p 1242 N94-16260
The astrophysical interpretation of isotope anomalies in graphite and SiC grains of chondrites
p 1244 N94-16343
Properties of thin films for high temperature flow sensors
[NASA-CR-191526] p 967 N94-16541
Pseudomorphic semiconducting heterostructures from combinations of AlN, GaN and selected SiC polytypes: Theoretical advancement and its coordination with experimental studies of nucleation, growth, characterization and device deployment
[AD-A267561] p 1213 N94-17108
Diamond growth on carbide surfaces using a selective etching technique
[AD-A267989] p 973 N94-17413
Interface chemistry in ceramic matrix composites
[AD-A268629] p 973 N94-17466

Low temperature deposition and characterization of n- and p-type silicon carbide thin films and associated ohmic and Schottky contacts
[AD-A267966] p 973 N94-17490

SILICON DIOXIDE

NMR and theoretical investigation of cation binding with sol-gel silicates
[AD-A266999] p 963 N94-15631
Optical and infrared spectra of thermally annealed Pb implanted SiO2 glasses
[DE93-015304] p 965 N94-15828
Gas separations using ceramic membranes
[DE93-000278] p 947 N94-15861
Removal of carbonaceous contaminants from silica aerogel p 953 N94-16256
Silica-bearing objects in the Dengli H3.8 and Gorlovka H3-4 chondrites p 1242 N94-16265
An investigation of the hydrolytic resistance of sodium-calcium plate glass with a layer of silica deposited on its surface
[IFTR-34/1991] p 971 N94-17120
Kinetics of silica-phase transitions
[DE93-016231] p 1217 N94-17659

SILICON FILMS

Thin Ni silicide formation by low temperature-induced metal atom reaction with ion implanted amorphous silicon
[DE93-015449] p 1209 N94-16066

SILICON ISOTOPES

Simulation studies for surfaces and materials strength
[NASA-CR-193387] p 1056 N94-15004
Do SiC grains in Orgueil differ from those in Murchison? p 1242 N94-16260

SILICON NITRIDES

Laser assisted CVD growth of AlN and GaN
[AD-A267150] p 1206 N94-15764
The influence of microstructure on the mechanical behavior of silicon nitride ceramics
[DE93-015363] p 966 N94-16018
Multiaxial deformation and life prediction model and experimental data for advanced silicon nitride ceramics
[DE93-015450] p 967 N94-16067
Crystallization of grain boundary phases in silicon nitride with low additive contents by microwave annealing
[DE93-015801] p 1209 N94-16164
Detection of subsurface defects in machined silicon nitride ceramics by optical scattering methods
[DE93-015554] p 968 N94-16658
Development of a constitutive model for creep and life prediction of advanced silicon nitride ceramics
[DE93-015894] p 968 N94-16813
The Ceramic Technology Project: Ten years of progress
[DE93-015991] p 968 N94-16843
Processing of complex sintered reaction bonded silicon nitride parts by microwave heating
[DE93-015811] p 969 N94-16877

SILICON OXIDES

SONOS technology for commercial and military nonvolatile memory applications
[DE93-015647] p 1011 N94-16661
Kinetics of silica-phase transitions
[DE93-016231] p 1217 N94-17659

SILICON RADIATION DETECTORS

Gamma large area silicon telescope: Applying Si strip detector technology to the detection of gamma rays in space p 904 N94-15061

SILICON TRANSISTORS

Technology transfers and reliable oxides
[AD-A266948] p 1175 N94-15758

SILX

Materials Research Society Symposium Proceedings, Volume 292: Biomolecular Materials
[AD-A265776] p 1116 N94-15138

SILOXANES

Intramolecular versus intermolecular condensation rates in the acidic polymerization of octaethoxytrisiloxane
[AD-A266982] p 963 N94-15490

SILVER

Performance of silvered Teflon thermal control blankets on spacecraft
[AD-A266284] p 887 N94-16909
Growth of dielectric thin films by irradiation of condensed molecular precursors with synchrotron radiation
[DE93-016161] p 974 N94-17676

SIM

STS-40 crew during spacelab Sim
[NASA-TM-109493] p 876 N94-15452

SIMPLE HARMONIC MOTION

An asymptotic expansion of an electromagnetic field in the velocity of a caustic in the form of simple waves
[IFTR-14/1991] p 1002 N94-17048

SIMPLIFICATION

Time dependent turbulence modeling and analytical theories of turbulence
[NASA-TM-106379] p 1029 N94-17385

SIMULATION

Fuzzy control and fuzzy kinematic mapping for a redundant space robot
[AD-A266866] p 1163 N94-14950
STS-26 generic integrated IUS deploy simulation
[NASA-TM-109562] p 875 N94-15332
STS-32 LDEF approach in SES
[NASA-TM-109474] p 880 N94-15379
STS-31 HST deploy sim in SMS and MOCR
[NASA-TM-109482] p 876 N94-15449
STS-26 long duration simulation: Crew entering SMS
[NASA-TM-109560] p 876 N94-15474
A measurement station for study of Earth moving tools and ground cutting processes
[IFTR-10/1991] p 985 N94-17068

SIMULATORS

STS-40 crew during spacelab Sim
[NASA-TM-109493] p 876 N94-15452
Liquid hydrogen and liquid oxygen feedline passive recirculation analysis
[TABES PAPER 93-620] p 1031 N94-16145
The Spacelab IPS Star Simulator
[TABES PAPER 93-650] p 877 N94-16150

SINE WAVES

Method and apparatus for spur-reduced digital sinusoid synthesis
[NASA-CASE-NPO-18789-1-CU] p 1154 N94-17326

SINGLE CRYSTALS

Magneto-optic superlattice thin films: Fabrication, structural and magnetic characterization p 974 N94-14982
Growth of new materials for solid state laser applications. The growth of ZnGeP2 by the vertical Bridgman method
[NASA-CR-194571] p 1038 N94-15530
Laboratory for x ray optics
[AD-A267149] p 1189 N94-15735
Study of protein-H2O interactions by multidimensional NMR spectroscopy
[AD-A266955] p 946 N94-15760
Passive oxide films on well-defined nickel surfaces: An examination of film growth on Ni(100) with ex situ scanning tunneling microscopy
[DE93-014056] p 1207 N94-15923
Optical properties and surface morphology studies of palladium contacts on mercuric iodide single crystals
[DE93-012510] p 1207 N94-15973
Thermal spray forming of refractory sample ampoule cartridges for single crystal growth space furnaces
[TABES PAPER 93-605] p 1051 N94-16141
Orientation of Planar Deformation Features (PDFs) in quartz p 1219 N94-16341
Growth of single crystals of mercuric iodide on the ground and in space
[DE93-015523] p 1209 N94-16442
Porous silicon for pumping solid-state lasers
[AD-A266293] p 1039 N94-16474
Thermal disorder in adsorbed Cl on Si(100)
[AD-A266295] p 1210 N94-16476
Tritium diffusion and desorption in single crystal LiAlO2
[DE93-015140] p 1211 N94-16805
High temperature materials technology research for advanced thermionic systems
[DE93-018302] p 960 N94-16964
Growth and doping of Al(x)Ga(1-x)N films by electron cyclotron resonance assisted molecular beam epitaxy
[AD-A267305] p 1212 N94-16992
An alternative approach to the growth of single crystal gallium nitride
[AD-A267876] p 1213 N94-17037
Nitride semiconductors for ultraviolet detection
[AD-A267877] p 1012 N94-17040
Pseudomorphic semiconducting heterostructures from combinations of AlN, GaN and selected SiC polytypes: Theoretical advancement and its coordination with experimental studies of nucleation, growth, characterization and device deployment
[AD-A267561] p 1213 N94-17108
Single crystal diamond thin films
[AD-A266457] p 1214 N94-17216
Investigation of the origin of hot spots in deformed crystals: Ammonium perchlorate studies
[AD-A267692] p 1214 N94-17270
Synthesis, characterization, and polymerization of new ferrocene-fluorene complexes. A novel high-molecular weight conjugated polymer with pendant ferrocene groups
[AD-A267717] p 972 N94-17273
Buried porous silicon-germanium layers in monocrystalline silicon lattices and method of producing
[NASA-CASE-NPO-18836-1-CU] p 1215 N94-17327
Low voltage electron beam lithography
[AD-A267865] p 1215 N94-17389
Laser probing of the kinetics and dynamics of 3-5 semiconductor growth
[AD-A268388] p 1215 N94-17422
Investigations of YBaCuO materials with near-room-temperature resistivity transitions
[AD-A268016] p 1216 N94-17477
Low temperature deposition and characterization of n- and p-type silicon carbide thin films and associated ohmic and Schottky contacts
[AD-A267966] p 973 N94-17490
Growth, characterization and device development in monocrystalline diamond films
[AD-A268206] p 1216 N94-17553
Advanced thin-film deposition and physical properties of high-temperature and other novel superconducting materials
[AD-A268199] p 1216 N94-17561

SINGLE STAGE TO ORBIT VEHICLES

Space Propulsion Synergy Group ETO technology assessments
[TABES PAPER 93-641] p 929 N94-16149

SINGULAR INTEGRAL EQUATIONS

Numerically solving a transient heat conduction problem with convection and radiation
[AD-A268521] p 1220 N94-17540

SINTERING

Finite element analytical techniques for ceramic production in microgravity: A hypoelastic model p 981 N94-16099
Chemical interactions between interconnect and electrode materials during sintering in solid oxide fuel cells
[DE93-015696] p 1092 N94-16160
Processing of complex sintered reaction bonded silicon nitride parts by microwave heating
[DE93-015811] p 969 N94-16877
Low-temperature sintering and phase changes in chromite interconnect materials
[DE93-015676] p 961 N94-17234

SIS (SUPERCONDUCTORS)

Submillimeterwave SIS mixer developments p 903 N94-15054
Preparation and properties of Nb/Al SIS and SIN junctions for millimeter and submillimeter radioastronomical receivers p 907 N94-15078

SITE SELECTION

Mars Analog Site Study (MASS) p 1252 N94-16200
Mars exobiology landing sites for future exploration p 1278 N94-16339
An electromagnetic interference study of potential transmitter sites for the HF Active Auroral Research Program (HAARP)
[AD-A267743] p 1004 N94-17373

SITES

Facilities maintenance handbook
[NHB-8831.2] p 1224 N94-15934

SIZE DETERMINATION

Maximum likelihood techniques applied to quasi-elastic light scattering
[NASA-CR-193550] p 1192 N94-16718

SKIN (ANATOMY)

Wound healing after laser injury to skin: The effect of occlusion and vitamin E
[AD-A266473] p 1128 N94-16779

SKIN (STRUCTURAL MEMBER)

Remelting of Fe-C-Si-alloy in a ceramic mold skin p 945 N94-15169

SKIN FRICTION

The turbulent wall jet
[AD-A267675] p 855 N94-14963
Active turbulence control in wall bounded flows using direct numerical simulation
[AD-A267261] p 1028 N94-17286

SKIRTS

SRB thermal curtain design support
[NASA-CR-193857] p 927 N94-17123
SRB thermal curtain design support
[NASA-CR-193858] p 928 N94-17124

SKY RADIATION

Determination of sunshine duration from radiation intensity pyranometric measurements of global and sky radiation
[BER-181] p 1105 N94-15302

SKY SURVEYS (ASTRONOMY)

EUVE observations of the Moon p 1250 N94-16185
Search for Extraterrestrial Intelligence (SETI) p 1125 N94-16620
Participation in the north ecliptic pole sky survey
[NASA-CR-191933] p 1059 N94-16815

SLEEP

Sleep management user's guide for special operations personnel
[AD-A267746] p 1119 N94-14943

SLEEP DEPRIVATION

Sleep management user's guide for special operations personnel
[AD-A267746] p 1119 N94-14943

Activity/rest patterns of instructor and rates student pilots during rapid transitions from daytime to nighttime duty hours at the Eastern Army Aviation Training site
[AD-A267038] p 1131 N94-15659

SLIDING
The processing and mechanical properties of high temperature/high performance composites. Book 1: Coonstituent properties of composites
[AD-A266394] p 935 N94-16483

SLIDING FRICTION
Integrated fundamental research on current collection
[AD-A266987] p 1008 N94-15494
The friction and wear of ceramic/ceramic and ceramic/metal combinations in sliding contact
[NASA-TM-106348] p 930 N94-15769
Continuing research on friction and wear of materials
[AD-A268291] p 1049 N94-17566

SLIP CASTING
Nonaqueous slip casting of high temperature ceramic superconductors using an investment casting technique
[NASA-CASE-LAR-14918-1] p 983 N94-15881
Finite element analytical techniques for ceramic production in microgravity: A hypoelastic model
p 981 N94-16099
Fabrication of advanced design (grooved) cermet anodes
[DE93-014590] p 1012 N94-16765

SLOPES
Emplacement of multiple flow units on very shallow slopes, east Kawelu Planitia flow field, Venus
p 1260 N94-16235

SLOTS
Wall interference and boundary simulation in a transonic wind tunnel with a discretely slotted test section
[NASA-TP-3334] p 872 N94-15794
Manufacturing tolerance requirements for frequency selective surfaces
[AD-A266541] p 999 N94-16797

SLURRIES
Method of producing a silicon carbide fiber reinforced strontium aluminosilicate glass-ceramic matrix composite
[NASA-CASE-LEW-15263-2] p 934 N94-15929

SMALL SCIENTIFIC SATELLITES
The 1971 highlights --- NASA programs and research
[NASA-TM-109629] p 1302 N94-15417
Small Satellites Systems and Services
[ISBN-2-85-428327-9] p 888 N94-17131
Small satellite constellation system: Optimization criteria p 888 N94-17132
AMIGAU: A prototype tool aimed at mission analysis for satellites and satellite constellations
p 888 N94-17133
Small launchers (current and future projects in the world) p 878 N94-17137
Small satellite constellation deployment strategies
p 878 N94-17138
Delta launch vehicle: Accommodations for small satellites p 878 N94-17139
ARIANE 5 light derivatives p 878 N94-17140
NEXT launch system p 878 N94-17141
Small missions for space science p 874 N94-17142
Strategy for a small satellite program and a proposal for a first mission p 874 N94-17143
Small satellite missions to long-period comets
p 874 N94-17144
BRIDGE: A small scientific satellite for geodesy
p 890 N94-17146
Cosmic dust and space debris measurements on board the small satellites HITEN and BREM-SAT
p 890 N94-17147
SYNMOD: A low-resource, low-cost means of monitoring the near-Earth space debris environment
p 891 N94-17148
Role and development of small satellite missions in space plasma physics p 891 N94-17149
Earth observation from small satellites
p 891 N94-17150
Small imaging satellite for Earth observing system adjunct p 891 N94-17151
Adequation of mini satellites to oceanic altimetry missions p 891 N94-17152
SYDONI: An intensified system for night observation
p 891 N94-17153
A proposed ground segment design for small satellites
p 878 N94-17154
Ground segment definition for the Spanish small satellite program (MINISAT) p 878 N94-17155
OREMUS: Prototype of an orbit determination center dedicated to mini-satellite control p 878 N94-17156
Data processing system for ARSENE ground station: A tool for small satellite control and development
p 878 N94-17157
Satellite control: A comprehensive approach
p 878 N94-17158
Regulation of low Earth orbit satellites
p 892 N94-17159
A study on an experimental communication system using microsatellites p 892 N94-17160
LEOCOM-SPES: Low cost message communications
p 892 N94-17161
TAOS (S80): A (LEO-MSS) system for position reporting and telemanagement services p 893 N94-17162
The ORBCOMM system p 893 N94-17163
MAGSS-14: Medium Altitude Global Mobile Satellite System with enhanced regional coverage
p 893 N94-17164
S 80/T: A micro satellite system combining high performances and limited resources
p 893 N94-17166
The ELLIPSO (tm) system: Elliptical low orbits for mobile communications p 893 N94-17167
UoSAT: A decade of experience pioneering microsatellites p 894 N94-17169
CERISE microsatellite system p 894 N94-17170
Impact of advances in technology on future spacecraft design p 894 N94-17171
S-80: A satellite for less than 50 MF
p 894 N94-17172
Small satellite modular design and application prospect p 894 N94-17173
Arsene GaAs solar array p 894 N94-17174
Small satellite nickel-hydrogen and nickel-metal hydride power applications p 895 N94-17175
A power system for a microsatellite
p 895 N94-17176
Data handling strategy for the Spanish small satellite program (MINISAT) p 895 N94-17177
The STRV On Board Data Handling (OBDH) system: An introduction p 895 N94-17178
A mini satellite called Arsene: The way to make it at a minimum cost p 895 N94-17179
TUBSAT: Low cost access to space technology
p 895 N94-17180
Standard platforms for small satellites
p 895 N94-17181
MINISAT programme p 896 N94-17182
The space technology research vehicle: Development status p 896 N94-17183
On-board spatial scientific experiment project on small satellites p 896 N94-17184
ALEXIS and HETE: Two small, low cost, scientific satellite systems p 896 N94-17185
TITUS: A micro-satellite for technology demonstration
p 896 N94-17186
Big results with small space systems: What small systems are doing today p 896 N94-17187
Small satellite product assurance p 896 N94-17188
Environment tests for mini satellites
p 896 N94-17189
Cost drivers: Why do conventional satellites cost so much? p 897 N94-17190
Key trends of the small satellite market
p 897 N94-17191

SMART STRUCTURES
Aeroelastic airfoil smart spar p 868 N94-16865

SMELTING
Fabrication of advanced design (grooved) cermet anodes
[DE93-014590] p 1012 N94-16765

SMOKE
The MADONA experiments (Meteorology and Diffusion Over Non-uniform Areas): High-resolution in-plume concentration fluctuations measurements using lidar remote sensing technique
[AD-A267711] p 1105 N94-14938
Secondary smoke p 924 N94-15220

SNOW
Bibliography on snow and ice friction
[AD-A266868] p 1045 N94-14920
Atmospheric ionization by solar particles detected by nitrate measurement in antarctic snow
[AD-A267583] p 1299 N94-17208

SNOW COVER
A snow wetness retrieval algorithm for SAR
p 1075 N94-16732
Monitoring environmental state of Alaskan forests with AIRSAR p 1075 N94-16734

SOBOLEV SPACE
Adaptive wavelet collocation methods for initial value boundary problems of nonlinear PDE's
[NASA-CR-191507] p 1169 N94-15833

SOCIAL FACTORS
Predicted and real development in the aviation in the period 1961-1991 p 853 N94-15122

SODIUM
Design of pulse stretching cell for a sodium guide star optical system
[DE93-016436] p 1236 N94-14929
Contained liquids in microgravity, part 2
p 979 N94-16085
Sodium-mercury excimer laser, phase 1
[AD-A267728] p 1042 N94-17230

SODIUM CHLORIDES
Pressures of supercritical salt solutions
p 945 N94-15166

SODIUM HYDROXIDES
A simple chemical procedure for extending the conductive state of polypyrrole to more negative potentials
[AD-A266235] p 969 N94-16928

SODIUM SILICATES
Thermochemistry of silicate speciation in aqueous sodium silicate solutions: Ionization and polymerization of small silicate ion
[AD-A266825] p 964 N94-15683

SOFIA (AIRBORNE OBSERVATORY)
Computation of the Fluid and Optical Fields About the Stratospheric Observatory for Infrared Astronomy (SOFIA) and the Coupling of Fluids, Dynamics, and Control Laws on Parallel Computers
[NASA-CR-193168] p 858 N94-16510
Selected computations of transonic cavity flows
p 858 N94-16511
Unsteady fluid and optical simulation of transonic aero-windows
[AIAA PAPER 93-3017] p 858 N94-16512

SOFTWARE ENGINEERING
Army Software Test and Evaluation Panel (STEP) software metrics initiatives report
[AD-A266889] p 1142 N94-14924
Lecture notes on engineering measurement for software engineers
[AD-A266959] p 1142 N94-14967
The value of reference implementations and prototyping in a formal design and testing methodology
[NPL-DITC-208/92] p 1142 N94-15011
The application of programming languages to the production of reference implementations
[NPL-DITC-209/92] p 1143 N94-15012
Testability of data security standards
[NPL-DITC-217/93] p 1143 N94-15022
SIMS: Single Interface to Multiple Systems
[AD-A266934] p 1143 N94-15175
Safety-critical software: Status report and annotated bibliography
[AD-A266993] p 1144 N94-15214
Concepts on measuring the benefits of software process improvements
[AD-A266994] p 1144 N94-15215
Software architecture for shared information systems
[AD-A266995] p 1144 N94-15216
Open environments to support systems engineering tool integration: A study using the Portable Common Tool Environment (PCTE)
[NASA-TM-4489] p 1144 N94-15486
An analysis of SEI software process assessment results: 1987-1991
[AD-A266996] p 1145 N94-15629
Process-centered development environments: An exploration of issues
[AD-A266997] p 1145 N94-15630
Dependable software technology exchange
[AD-A267103] p 1146 N94-15638
Reengineering: An engineering problem
[AD-A267117] p 1146 N94-15653
Flight instrument software for the F/A-18 research simulator
[AD-A267170] p 872 N94-15856
Database for propagation models p 996 N94-16049
Software Engineering Guidebook
[NASA-CR-177625] p 1150 N94-16656
Software for the derivation of scaled surface reflectances from AVIRIS data p 1072 N94-16700
KBSA concept demo
[AD-A267054] p 1166 N94-16770
Conflict Resolution (CORE) for software quality factors
[AD-A267248] p 1151 N94-16941
Development of dynamic, contex-driven help systems
[AD-A267409] p 1152 N94-16974
Design and implementation of an object-oriented interface for the multi-model/multi-lingual database system
[AD-A267413] p 1232 N94-16977
Sequential functions on indexed domains and full abstraction for a sub-language of PCF
[AD-A267838] p 1152 N94-17009
A proposed research program in strategic computing
[AD-A267516] p 1153 N94-17078
CALS test network handbook
[AD-A267587] p 1160 N94-17209
An object-oriented dynamic software process model
[AD-A267726] p 1154 N94-17371
Establishing a software measurement process
[AD-A267896] p 1154 N94-17396
An introduction to structural models
[AD-A268151] p 1155 N94-17429

A software process framework for the SEI capability maturity model: Repeatable level
[AD-A268059] p 1157 N94-17588
The development of flexible software for the Italian/Dutch satellite SAX: Advantages and disadvantages of the use of CASE tools
[NLR-TP-91288-U] p 1157 N94-17626

SOFTWARE RELIABILITY
Army Software Test and Evaluation Panel (STEP) software metrics initiatives report
[AD-A266889] p 1142 N94-14924
Software reliability through fault-avoidance and fault-tolerance
[NASA-CR-194353] p 1143 N94-15114
Safety-critical software: Status report and annotated bibliography
[AD-A266993] p 1144 N94-15214
Concepts on measuring the benefits of software process improvements
[AD-A266994] p 1144 N94-15215
RAMCAD design methodology
[AD-A267010] p 1145 N94-15525
Process-centered development environments: An exploration of issues
[AD-A266997] p 1145 N94-15630
Dependable software technology exchange
[AD-A267103] p 1146 N94-15638
Software reliability management through metrics
[AD-A267129] p 1146 N94-15687
The design of self-checking reduced instruction set computers
[AD-A267012] p 1140 N94-15763
NASA trend analysis procedures
[NASA-RP-1290] p 1223 N94-15782
Performance Information Management System (PIMS) communication
[AD-A267040] p 1231 N94-16458
Consistent failure reporting in reliable communication systems
[AD-A266298] p 997 N94-16477
Software Engineering Guidebook
[NASA-CR-177625] p 1150 N94-16656
Conflict Resolution (CORE) for software quality factors
[AD-A267248] p 1151 N94-16941
Fault-tolerant architectures for multiprocessor and VLSI-based systems
[AD-A267370] p 1140 N94-17005
Effects of inspection error on optimal inspection policies and software fault detection models
[AD-A267511] p 1153 N94-17075
The development of flexible software for the Italian/Dutch satellite SAX: Advantages and disadvantages of the use of CASE tools
[NLR-TP-91288-U] p 1157 N94-17626

SOFTWARE REUSE
Open environments to support systems engineering tool integration: A study using the Portable Common Tool Environment (PCTE)
[NASA-TM-4489] p 1144 N94-15486
Intel NX to PVM 3.2 message passing conversion library
[NASA-TM-109038] p 1152 N94-17060

SOFTWARE TOOLS
Safety-critical software: Status report and annotated bibliography
[AD-A266993] p 1144 N94-15214
Open environments to support systems engineering tool integration: A study using the Portable Common Tool Environment (PCTE)
[NASA-TM-4489] p 1144 N94-15486
A software interface for the ARL wind tunnel data acquisition system
[AD-A267114] p 1146 N94-15650
Software Engineering Guidebook
[NASA-CR-177625] p 1150 N94-16656
The Spectral Image Processing System (SIPS): Software for integrated analysis of AVIRIS data
p 1067 N94-16674
Detailed example of using ACEC release 3.0 with the DEC VAX Ada compiler
[AD-A267880] p 1152 N94-17014
Theoretical crystallography with the Advanced Visualization System
[DE93-015692] p 1215 N94-17319
ACE: Lessons learned, volume 1
[AD-A267979] p 1155 N94-17411
Orpheus: A synthesis framework for regular architectures
[REPT-93-016] p 1156 N94-17504
Language-based document processing
[INRIA-RR-1731] p 1234 N94-17529
A protocol validator for the SCM and CFSM models
[AD-A268523] p 1156 N94-17541
The development of flexible software for the Italian/Dutch satellite SAX: Advantages and disadvantages of the use of CASE tools
[NLR-TP-91288-U] p 1157 N94-17626

SOHO MISSION
The grazing incidence detectors for the SOHO coronal diagnostic spectrometer p 905 N94-15063
Data processing system for flight spectrometer
p 908 N94-15086

SOI (SEMICONDUCTORS)
Technology transfers and reliable oxides
[AD-A266948] p 1175 N94-15758
DLTS and dynamic transconductance analysis of deep-submicron fully-depleted SOI MOSFET's
[AD-A267291] p 1214 N94-17243

SOIL MECHANICS
A measurement station for study of Earth moving tools and ground cutting processes
[IFTR-10/1991] p 985 N94-17068

SOIL MOISTURE
Mathematical model of frost heave and thaw settlement in pavements
[AD-A267037] p 983 N94-15676
On hydrologic similarity: A dimensionless flood frequency model using a generalized geomorphologic unit hydrograph and partial area runoff generation
[PAPER-89WR01579] p 1083 N94-16027
Evapotranspiration and runoff from large land areas: Land surface hydrology for atmospheric general circulation models p 1083 N94-16029
Heterogeneity and scaling land-atmospheric water and energy fluxes in climate systems p 1083 N94-16030
Evaluation of a distributed catchment scale water balance model
[PAPER-93WR00398] p 1083 N94-16031
A detailed model for simulation of catchment scale subsurface hydrologic processes
[PAPER-92WR02333] p 1084 N94-16032
Scaling, soil moisture and evapotranspiration in runoff models p 1084 N94-16034
Bright soil units on Mars determined from ISM imaging spectrometer data p 1295 N94-16430
Processing of polarimetric SAR data for soil moisture estimation over Mahantango watershed area
p 1079 N94-16754
Evaluation of polarimetric SAR parameters for soil moisture retrieval p 1079 N94-16755

SOILS
HyperVentilate: Decision-support software for soil vapor extraction technology application
[PB93-134880] p 1094 N94-15136
X-SAR: The X-band synthetic aperture radar on board the Space Shuttle p 990 N94-15891
Radar response of vegetation: An overview
p 991 N94-15898
Mars Analog Site Study (MASS) p 1252 N94-16200
A Moessbauer spectrometer for the mineralogical analysis of the Mars surface: First temperature dependent tests of the detector and drive system
p 1259 N94-16233
Suggestion for extended Viking magnetic properties experiment on future Mars missions
p 1285 N94-16375
Deucalionis Regio, Mars: Evidence for a unique mineralogic endmember and a crusted surface
p 1291 N94-16406
Bright soil units on Mars determined from ISM imaging spectrometer data p 1295 N94-16430
Variations in the Fe mineralogy of bright Martian soil
p 1295 N94-16431
Experimental study of nonassociated flow and instability of frictional materials
[AD-A266421] p 1024 N94-16555
Mapping the spectral variability in photosynthetic and non-photosynthetic vegetation, soils, and shade using AVIRIS p 1068 N94-16679
Soil conservation applications with C-band SAR
p 1080 N94-16760

SOL-GEL PROCESSES
Preparation of homogeneous aluminosilicate gels by sol/gel techniques
[AD-A266823] p 962 N94-14914
Multinuclear NMR study of aluminosilicate sol-gel synthesis reasons for the homogeneous gelation using the prehydrolysis method
[AD-A266877] p 962 N94-14921
Self-diffusion coefficients of sol-gel intermediates
[AD-A266957] p 963 N94-15179
Intramolecular versus intermolecular condensation rates in the acidic polymerization of octaethoxytrisiloxane
[AD-A266982] p 963 N94-15490
NMR and theoretical investigation of cation binding with sol-gel silicates
[AD-A266999] p 963 N94-15631
Design, synthesis and characterization of novel nonlinear optical polymers
[AD-A267035] p 964 N94-15675
Effects of aging time on V205 sol-gel coatings
[AD-A266824] p 965 N94-15843
Use of microgravity in the synthesis of ceramics using sol gel techniques p 979 N94-16088
Structural studies of sol-gel glasses
[AD-A266277] p 967 N94-16472
Ceramic fiber coatings development and demonstration
[AD-A267286] p 972 N94-17242
Electrical properties of sol-gel PZT thin films for decoupling capacitor applications
[DE93-016491] p 1015 N94-17648

SOLAR ACTIVITY
Orbiting solar operations
[NASA-TM-109583] p 884 N94-15267
FNAS/solar flare energetics
[NASA-CR-193574] p 1299 N94-17089
Solar Electro-Optical Network (SEON) upgrade/replacement program. Phase 1: Qualification operational test and evaluation plan
[AD-A266364] p 1237 N94-17225

SOLAR ARRAYS
ERS-1: 18 months in orbit p 990 N94-15888
Recent advances in outdoor performance evaluation of PV systems
[DE93-015031] p 1091 N94-15994
Arsene GaAs solar array p 894 N94-17174
A power system for a microsatellite
p 895 N94-17176
Space systems environmental interaction studies
[AD-A267280] p 897 N94-17240
High voltage conductors in spacecraft
[AD-A267268] p 897 N94-17266

SOLAR ATMOSPHERE
ATLAS-2 and UARS correlative measurement opportunities during Space Shuttle mission on April 8-17, 1993
[NASA-TM-109020] p 1105 N94-15480

SOLAR CELLS
Solar absorptance of optical surfaces contaminated with spacecraft material outgassing products
[AD-A267202] p 886 N94-15857
Progress in the concentrator initiative program
[DE93-015006] p 1091 N94-15984
Monolithic, two-terminal InP/Ga(0.47)In(0.53)As tandem solar cells
[DE93-014037] p 1093 N94-16824
Lattice-mismatched In(0.40)Al(0.60)As window layers for indium phosphide solar cells
[NASA-TM-106255] p 1013 N94-17113
A ten year review of performance of photovoltaic systems
[DE93-015649] p 1093 N94-17217
High voltage conductors in spacecraft
[AD-A267268] p 897 N94-17266

SOLAR COLLECTORS
Progress in the concentrator initiative program
[DE93-015006] p 1091 N94-15984
Revisiting the BCS, a measurement system for characterizing the optics of solar collectors
[DE93-015030] p 1091 N94-15993
Recent advances in outdoor performance evaluation of PV systems
[DE93-015031] p 1091 N94-15994
Proposed guidelines for reporting performance of a solar dish/Stirling electric generation system
[DE93-016493] p 1092 N94-16112
High heat flux engineering in solar energy applications
[DE93-016500] p 1093 N94-16954
Overview of the solar dynamic ground test demonstration program
[NASA-TM-106296] p 928 N94-17256

SOLAR CORONA
The grazing incidence detectors for the SOHO coronal diagnostic spectrometer p 905 N94-15063
The Solar Flare Myth in solar-terrestrial physics
[DE93-016487] p 1299 N94-16895

SOLAR COSMIC RAYS
The SCR Ne-21 and Ar-38 in lunar rock 68815: The solar proton energy spectrum over the past 2 MYR
p 1248 N94-16177

SOLAR CYCLES
A correlative comparison of geomagnetic storms and auroral substorms using geomagnetic indeces
[AD-A268081] p 1102 N94-17512

SOLAR DYNAMIC POWER SYSTEMS
Futurepath 1 --- power systems
[NASA-TM-109431] p 925 N94-15503
Proposed guidelines for reporting performance of a solar dish/Stirling electric generation system
[DE93-016493] p 1092 N94-16112

Overview of the solar dynamic ground test demonstration program
[NASA-TM-106296] p 928 N94-17256

SOLAR ECLIPSES
The 1970 highlights --- NASA programs and research
[NASA-TM-109628] p 1302 N94-15415
Total solar eclipse of 3 November 1994
[NASA-RP-1318] p 1236 N94-15481
C 141 KAO solar eclipse mission
[NASA-TM-109676] p 1298 N94-15522

SOLAR ENERGY
High heat flux engineering in solar energy applications
[DE93-016500] p 1093 N94-16954
Numerical modelling of an active direct nonpotable hot water heating system making use of the energy of solar radiation
[IFTR-38/1991] p 1093 N94-17070
Energy from the sun: Evolution of federal support for solar energy
[AD-A267944] p 1093 N94-17382

SOLAR ENERGY ABSORBERS
Solar absorptance of optical surfaces contaminated with spacecraft material outgassing products
[AD-A267202] p 886 N94-15857

SOLAR ENERGY CONVERSION
Space Station thermal storage/refrigeration system research and development
[NASA-CR-193841] p 879 N94-15191
Proposed guidelines for reporting performance of a solar dish/Stirling electric generation system
[DE93-016493] p 1092 N94-16112
High heat flux engineering in solar energy applications
[DE93-016500] p 1093 N94-16954
Numerical modelling of an active direct nonpotable hot water heating system making use of the energy of solar radiation
[IFTR-38/1991] p 1093 N94-17070
Energy from the sun: Evolution of federal support for solar energy
[AD-A267944] p 1093 N94-17382

SOLAR FLARES
The Solar Flare Myth in solar-terrestrial physics
[DE93-016487] p 1299 N94-16895
Solar vector magnetic field research
[AD-A267367] p 1299 N94-17004
FNAS/solar flare energetics
[NASA-CR-193574] p 1299 N94-17089

SOLAR FLUX
Revisiting the BCS, a measurement system for characterizing the optics of solar collectors
[DE93-015030] p 1091 N94-15993

SOLAR GENERATORS
High heat flux engineering in solar energy applications
[DE93-016500] p 1093 N94-16954

SOLAR HEATING
Heliocentric zoning of the asteroid belt by aluminum-26 heating p 1241 N94-16205

SOLAR INSTRUMENTS
Solar vector magnetic field research
[AD-A267367] p 1299 N94-17004

SOLAR INTERIOR
Possible dust contamination of the early solar system p 1244 N94-16352

SOLAR MAGNETIC FIELD
Solar vector magnetic field research
[AD-A267367] p 1299 N94-17004

SOLAR MAXIMUM MISSION
Ultraviolet spectrometer and polarimeter (UVSP) catalog of observations. Volume 1: Experiments 1-30719, February 1980 - April 1985
[NASA-CR-4529-VOL-1] p 1298 N94-15023
Ultraviolet spectrometer and polarimeter (UVSP) catalog of observations. Volume 2: Experiments 30720-63057, April 1985 - February 1988
[NASA-CR-4529-VOL-2] p 1298 N94-15024
The 1980 highlights
[NASA-TM-109672] p 1303 N94-15509

SOLAR NEUTRINOS
Neutrino mass and mixing: Summary of the neutrino sessions
[DE93-014342] p 1183 N94-16801
Neutral-current detection in the Sudbury Neutrino Observatory
[DE93-014481] p 1185 N94-16951

SOLAR OBSERVATORIES
Orbiting solar operations
[NASA-TM-109583] p 884 N94-15267
Solar Electro-Optical Network (SEON) upgrade/replacement program. Phase 1: Qualification operational test and evaluation plan
[AD-A266364] p 1237 N94-17225

SOLAR OSCILLATIONS
Generation of artificial helioseismic time-series
[NASA-CR-194612] p 1299 N94-15968

SOLAR PHYSICS
Unmasking the Sun
[NASA-TM-109595] p 1298 N94-15287
Possible dust contamination of the early solar system p 1244 N94-16352

SOLAR PLANETARY INTERACTIONS
Magnetic effects in Venus/solar wind interaction
[NASA-CR-194666] p 1299 N94-17281

SOLAR POSITION
Iron oxide bands in the visible and near-infrared reflectance spectra of primitive asteroids p 1242 N94-16274

SOLAR PROTONS
A comparison of solar wind parameters measured by IMP 8, Voyager 1 and Voyager 2
[AD-A266728] p 1298 N94-15821
The SCR Ne-21 and Ar-38 in lunar rock 68815: The solar proton energy spectrum over the past 2 MYR p 1248 N94-16177
Atmospheric ionization by solar particles detected by nitrate measurement in antarctic snow
[AD-A267583] p 1299 N94-17208

SOLAR RADIATION
Absolute Radiometric Measurements in Space: ARMS p 908 N94-15085
Determination of sunshine duration from radiation intensity pyranometric measurements of global and sky radiation
[BER-181] p 1105 N94-15302
Analysis of leading edge and trailing edge cover glass samples before and after treatment with advanced satellite contamination removal techniques
[AD-A267055] p 885 N94-15666
Absolute, Extreme-Ultraviolet Solar Spectral Irradiance Monitor (AESSIM)
[AD-A267045] p 1299 N94-15836
Dust grain resonant capture: A statistical study p 1245 N94-16384
Numerical modelling of an active direct nonpotable hot water heating system making use of the energy of solar radiation
[IFTR-38/1991] p 1093 N94-17070
Investigations into the recovery of waste sulfuric acid with concentrated solar radiation
[DLR-FB-93-11] p 952 N94-17594

SOLAR SENSORS
Space systems environmental interaction studies
[AD-A267280] p 897 N94-17240

SOLAR SIMULATORS
Solar absorptance of optical surfaces contaminated with spacecraft material outgassing products
[AD-A267202] p 886 N94-15857

SOLAR SPECTROMETERS
The grazing incidence detectors for the SOHO coronal diagnostic spectrometer p 905 N94-15063
Data processing system for flight spectrometer p 908 N94-15086

SOLAR SYSTEM
Do SiC grains in Orgueil differ from those in Murchison? p 1242 N94-16260
Chemical and isotopic compositions in acid residues from various meteorites p 1243 N94-16291

SOLAR SYSTEM EVOLUTION
Pioneer-Venus press clip --- Solar System formation and extraterrestrial life
[NASA-TM-109425] p 1239 N94-15495

SOLAR TERRESTRIAL INTERACTIONS
The Solar Flare Myth in solar-terrestrial physics
[DE93-016487] p 1299 N94-16895
FNAS/solar flare energetics
[NASA-CR-193574] p 1299 N94-17089
Optimization of satellite coverage in observing cause and effect changes in the ionosphere, magnetosphere, and solar wind
[AD-A267956] p 1102 N94-17493

SOLAR WIND
A comparison of solar wind parameters measured by IMP 8, Voyager 1 and Voyager 2
[AD-A266728] p 1298 N94-15821
Helium-3 inventory of lunar samples: A potential future energy resource for mankind? p 1295 N94-16428
Solar noble gases revealed by closed system stepped etching of a metal separate from Fayetteville p 954 N94-16432
Nitrogen and light noble gases in Parsa enstatite chondrite p 1246 N94-16435
Magnetic effects in Venus/solar wind interaction
[NASA-CR-194666] p 1299 N94-17281

SOLAR WIND VELOCITY
A comparison of solar wind parameters measured by IMP 8, Voyager 1 and Voyager 2
[AD-A266728] p 1298 N94-15821

SOLAR X-RAYS
FNAS/solar flare energetics
[NASA-CR-193574] p 1299 N94-17089

SOLDERED JOINTS
Reliability analysis of Surface Mount Technology (SMT)
[AD-A267598] p 1055 N94-17194

SOLID ELECTROLYTES
Chemical interactions between interconnect and electrode materials during sintering in solid oxide fuel cells
[DE93-015696] p 1092 N94-16160
Thin composite solid electrolyte film for lithium batteries
[NASA-CASE-NPO-18694-1-CU] p 1014 N94-17325

SOLID LUBRICANTS
Solid lubricants for space structures, phase 2
[AD-A266653] p 968 N94-16767

SOLID NITROGEN
A Pluto thermal model p 1256 N94-16216

SOLID PHASES
Process of shaping an electrorheological solid
[AD-D015885] p 1012 N94-16914
Slip, twinning and transformation in Laves phases
[DE93-018164] p 960 N94-16972

SOLID PROPELLANT COMBUSTION
Spectral studies of solid propellant combustion 4: Absorption and burn rate results for M43, XM39, and M10 propellants
[AD-A267119] p 946 N94-15685

SOLID PROPELLANT IGNITION
Laser ignition of solid propellants: 1. Ignition delays
[AD-A268454] p 976 N94-17538

SOLID PROPELLANT ROCKET ENGINES
Advanced Solid Rocket Motor
[NASA-TM-109658] p 924 N94-15229
Ultrasonic wave propagation model for nondestructive evaluation of solid rocker motor propellant
[AD-A267653] p 976 N94-17248
Postflight hardware evaluation 360T026 (RSRM-26, STS-47)
[NASA-CR-192559] p 882 N94-17656

SOLID PROPELLANTS
Ultrasonic wave propagation model for nondestructive evaluation of solid rocker motor propellant
[AD-A267653] p 976 N94-17248
Damage evolution in filled elastomers
[AD-A268067] p 1062 N94-17507
Laser ignition of solid propellants: 1. Ignition delays
[AD-A268454] p 976 N94-17538

SOLID ROCKET PROPELLANTS
Fundamental studies of rocket combustion chemistry and combustion instability
[AD-A266248] p 925 N94-16482
Space Shuttle solid rocket motor exposure monitoring p 976 N94-16624

SOLID SOLUTIONS
Ternary alloying effects in polycrystalline (beta)-NiAl
[DE93-012675] p 955 N94-15885
Roles of oxygen defects in copper-oxide superconductors
[DE93-014875] p 1208 N94-15982
Chemical interactions between interconnect and electrode materials during sintering in solid oxide fuel cells
[DE93-015696] p 1092 N94-16160
Chemical and displacement atomic pair correlations in crystalline solid solutions recovered by anomalous x ray scattering in Fe-Ni alloys
[DE93-015906] p 1209 N94-16171
Rheology of water and ammonia-water ices p 953 N94-16188
Pulsed laser deposition of metastable Ca(1-x)Sr(x)CuO2 thin films
[DE93-015804] p 1040 N94-16663
Pseudomorphic semiconducting heterostructures from combinations of AlN, GaN and selected SiC polytypes: Theoretical advancement and its coordination with experimental studies of nucleation, growth, characterization and device deployment
[AD-A267561] p 1213 N94-17108

SOLID STATE
Design, synthesis and characterization of novel nonlinear optical polymers
[AD-A267035] p 964 N94-15675
Detection and dosimetry of chemical contaminants in polymeric materials
[AD-A266605] p 968 N94-16727

SOLID STATE DEVICES
CdTe array detectors for high energy astronomy p 899 N94-15029
The solid state detector technology for picosecond laser ranging p 914 N94-15572

SOLID STATE LASERS
The solid state detector technology for picosecond laser ranging p 914 N94-15572
Bench checkout equipment for spaceborne laser altimeter systems p 921 N94-15618
Multi-beam laser altimeter p 921 N94-15620

Full-wave simulation of the thumbtack laser
[DE93-015110] p 1039 N94-16054
Porous silicon for pumping solid-state lasers
[AD-A266293] p 1039 N94-16474
Micro pulse laser radar
[NASA-CASE-GSC-13493-1] p 1004 N94-17322

SOLID-SOLID INTERFACES
Laboratory for x ray optics
[AD-A267149] p 1189 N94-15735
Weibull analysis applied to the pull adhesion test and fracture of a metal-ceramic interface
[DE93-012913] p 1059 N94-15997
Low temperature deposition and characterization of n- and p-type silicon carbide thin films and associated ohmic and Schottky contacts
[AD-A267966] p 973 N94-17490

SOLIDIFICATION
Partial melting experiment of Y-Ba-Cu oxide
p 945 N94-15168
Remelting of Fe-C-Si-alloy in a ceramic mold skin
p 945 N94-15169
Separation behaviour of monotectic alloys
p 945 N94-15170
Mechanical properties of magnesium ammonium phosphate cements and their zeolite composites
[DE93-015155] p 934 N94-16057
Particle Engulfment and Pushing by Solidifying Interfaces (PEPSI)
[NASA-CR-193856] p 960 N94-17079

SOLIDIFIED GASES
Modeling the reflectance of CO2 frost with new optical constants: Application to Martian south polar cap spectra p 1256 N94-16217

SOLIDS
Assimilation of solids during ascent of magmas from the Bartoy Field of the Baikal Region, Siberia
p 1103 N94-16214
Process of shaping an electrorheological solid
[AD-D015885] p 1012 N94-16914

SOLIDS FLOW
Stability analysis for the flow of granular materials down an inclined plane using kinetic model
[DE93-016852] p 1026 N94-16958

SOLITARY WAVES
Dynamics of douple stimulated Brillouin scattering
p 1200 N94-15206
Soliton-like structures in double stimulated Brillouin scattering p 1200 N94-15207
The quantum mass shift of the soliton in Skyrme model
[ITN-93-85219] p 1180 N94-15283
Search for far infrared radiation from optically pumped defect modes
[AD-A266744] p 1206 N94-15822
Pulse propagation in inhomogeneous optical waveguides
[DE93-013378] p 1191 N94-16007
Lattice relaxation theory of localized excitations in quasi-one-dimensional systems
[DE93-624947] p 1215 N94-17437

SOLUBILITY
Efficacy of flocculating and other emergency water purification tablets
[AD-A266695] p 1148 N94-15840
Siderophile elements in the upper mantle of the Earth: New clues from metal-silicate partition coefficients
p 1103 N94-16250
Partitioning of Nb, Mo, Ba, Ce, Pb, Th and U between immiscible carbonate and silicate liquids: Evaluating the effects of P2O5,F, and carbonate composition
p 953 N94-16283
Soluble precursor route to polyanilines
[AD-A268015] p 973 N94-17494

SOLVATION
Removal of carbonaceous contaminants from silica aerogel p 953 N94-16256
Supercritical thermodynamics of sulfur and nitrogen species
[DE93-017727] p 1220 N94-16997
Solvational barriers to interfacial electron transfer: Minimization by way of valence delocalization
[AD-A267371] p 950 N94-17006
Continuum solvent models for computational chemistry
[DE93-016329] p 953 N94-17660

SOLVENTS
The photophysics of poly(methylphenylphosphazene)
[AD-A267321] p 970 N94-16949
Supercritical thermodynamics of sulfur and nitrogen species
[DE93-017727] p 1220 N94-16997
Pulsed laser kinetic studies of liquids under high pressure
[DE93-017826] p 1041 N94-16998
Continuum solvent models for computational chemistry
[DE93-016329] p 953 N94-17660

SONAR
Signal processing in impulsive electromagnetic interference
[AD-A266425] p 998 N94-16557
Synthesis and evaluation of polymeric materials
[AD-A267809] p 973 N94-17408
Fabrication of a NAVMAP, a deep-sea mapping system
[AD-A268630] p 1085 N94-17467

SONIC ANEMOMETERS
Determination of momentum flux using a bivane and cup anemometer
[AD-A265414] p 1105 N94-15137

SOOT
Modeling study to evaluate the ionic mechanism of soot formation in flames
[AD-A266242] p 950 N94-16930
Mechanistic models of soot formation
[AD-A267806] p 950 N94-17008
Surface reactivity of combustion generated soot particles
[AD-A268017] p 952 N94-17532

SORPTION
Fibers and materials of medical application
p 938 N94-16855

SOS (SEMICONDUCTORS)
Porous silicon for pumping solid-state lasers
[AD-A266293] p 1039 N94-16474

SOUND PRESSURE
Vibro-acoustic analysis of an aircraft maintenance dock
[AD-A266778] p 871 N94-14908
Free-field sensitivity calibration of laboratory standard microphones by the reciprocity technique: Measurements for the 1991 EEC intercomparison
[NPL-RSA(EXT)-0043] p 1176 N94-15019
Cruise noise measurements of a scale model advanced ducted propulsor
[NASA-TM-105808] p 1176 N94-15115

SOUND PROPAGATION
Discrete models of the Boltzmann equation: Structure of the collision operator of sound propagation
[IFTR-2/1992] p 1178 N94-17051
Sound exposure level prediction for impulse sound sources above variable terrain
[AD-A267535] p 1178 N94-17119

SOUND TRANSMISSION
Ultrasound absorption in molten salts
p 944 N94-15161
Nonlinear acoustics: Periodic waveguide, scattering of sound by sound, three-layer fluid, finite amplitude sound in a medium having a distribution of relaxation processes, and production of an isolated negative pulse in water
[AD-A267145] p 1177 N94-15732

SOUND WAVES
Ultrasound absorption in molten salts
p 944 N94-15161
Dynamics of douple stimulated Brillouin scattering
p 1200 N94-15206
On the use of the noncentral chi-square density function for the distribution of helicopter spectral estimates
[NASA-CR-191546] p 1176 N94-15487
Sound radiation from infinite laminated composite shell with periodic rib stiffening
[DRA/TM(USGR)92326] p 933 N94-15699
Acousto-optical confirmation of the localized wave phenomena
[DE93-016425] p 1177 N94-16448
Cortical adaptive filtering in bioacoustic signal classification
[AD-A266229] p 1177 N94-16939
The shock Hugoniot of 316 SS and sound velocity measurements
[DE93-016525] p 1178 N94-16955
Acoustic waves in complicated geometries and their interactions with liquid-propellant droplet combustion
[AD-A267260] p 1178 N94-16991
An electroacoustic transducer for purposes of photoacoustic spectroscopy
[IFTR-7/1992] p 1013 N94-17071
Sound exposure level prediction for impulse sound sources above variable terrain
[AD-A267535] p 1178 N94-17119
Two-dimensional, high flow, precisely controlled monodisperse drop source
[AD-A267660] p 1028 N94-17250
Boundary conditions and the simulation of low Mach number flows
[NASA-TM-106374] p 1029 N94-17448
A virtual acoustic orientation instrument
[AD-A268181] p 1134 N94-17510

SOUND-SOUND INTERACTIONS
Nonlinear acoustics: Periodic waveguide, scattering of sound by sound, three-layer fluid, finite amplitude sound in a medium having a distribution of relaxation processes, and production of an isolated negative pulse in water
[AD-A267145] p 1177 N94-15732

SOUNDING ROCKETS
Sounding Rocket Experiments in Fluid Science and Materials Sciences: TEXUS 25 to 27 and MASER 4, volume 3
[ESA-SP-1132-VOL-3] p 943 N94-15157
Measurements of Interfacial Tension: MITE
p 943 N94-15158
Benard convection of magnetic colloids under microgravity p 943 N94-15159
Pool boiling: Single bubble experiment
p 944 N94-15160
Ultrasound absorption in molten salts
p 944 N94-15161
Orientation of DNA during free-solution electrophoresis p 944 N94-15162
Electrophoresis visualisation p 944 N94-15163
Temperature propagation in near-critical fluids prior to and during separation p 944 N94-15165
Separation behaviour of monotectic alloys
p 945 N94-15170
Heat storage module p 946 N94-15172
The 1973 highlights --- Pioneer and Mariner space probes and other advancements
[NASA-TM-109624] p 1302 N94-15410
The 1968 highlights --- NASA programs and research
[NASA-TM-109627] p 1302 N94-15413
The 1971 highlights --- NASA programs and research
[NASA-TM-109629] p 1302 N94-15417
MAXUS: The new sounding rocket program for long duration microgravity flight p 978 N94-16079

SOUNDS (TOPOGRAPHIC FEATURES)
Orographic microbursts in a severe winter windstorm
[AD-A267651] p 1108 N94-17247

SOURCE PROGRAMS
Reductions to sets of low information content
[TR-417] p 1150 N94-16579
Estimating task execution delay in a real-time system via static source code analysis
[AD-A267496] p 1161 N94-17367

SOUTHERN HEMISPHERE
Southern and Northern Hemisphere total ozone as seen by TOMS
[NASA-TM-109591] p 1098 N94-15282

SOUTHERN OSCILLATION
IAI topic: El Nino. Southern oscillation and interannual climate variability
[INPE-5410-PRE/1757] p 1111 N94-15186

SOVIET SATELLITES
Almaz p 898 N94-15889

SOVIET SPACECRAFT
The fragmentation of Kosmos 2163
[NASA-CR-191643] p 887 N94-16503

SOYUZ SPACECRAFT
Soyuz/ACRV accommodation study
[NASA-TM-107733] p 888 N94-17072

SPACE ADAPTATION SYNDROME
Space adaptation
[NASA-TM-109601] p 1120 N94-15309

SPACE BASED RADAR
Proceedings of the Third Spaceborne Imaging Radar Symposium
[NASA-CR-194104] p 989 N94-15886
SIR-C/X-SAR free flyer concept p 898 N94-15903
EOS SAR: A new approach p 992 N94-15904

SPACE CHARGE
Nuclear fusion of protons with ions of boron
[DE93-015399] p 1202 N94-16019
Polar 2 model of the wake shield experiment
[AD-A266243] p 882 N94-16468
Prototype instrumentation and design studies
[AD-A266402] p 882 N94-16530
A review of some dynamics models in six-dimensional phase space and their suitable conditions of motion equation
[DE93-623741] p 1175 N94-17317
Emittance growth in displaced, space-charge-dominated beams with energy spread
[DE93-016514] p 1188 N94-17672

SPACE COMMERCIALIZATION
TABES 1993: 9th Annual Technical and Business Exhibition and Symposium p 1050 N94-16129
Commercial space opportunities advanced concepts and technology overview
[TABES PAPER 93-240] p 1050 N94-16132
The closing window of opportunity: Addressing the US space launch vehicle crisis
[TABES PAPER 93-640] p 878 N94-16148
Space commerce in a global economy: Comparison of US and Australian approaches
[NASA-TM-109341] p 1235 N94-17290

The impact of industry/university consortia programs on space education
[NASA-TM-109340] p 1222 N94-17441

SPACE COMMUNICATION
STS-29 mission highlights resource tape
[NASA-TM-109542] p 880 N94-15373
STS-26 missions highlight resource tape
[NASA-TM-109559] p 881 N94-15407
Low-Complexity, High-Performance Bandwidth Efficient Coding and Coded Modulation Techniques for Satellite and Space Communications
[NASA-CR-194623] p 997 N94-16506
Search for optimal distance spectrum convolutional codes p 998 N94-16509

SPACE DEBRIS
Satellite situation report, volume 33, no. 3
[NASA-TM-109278] p 885 N94-15712
Long Duration Exposure Facility experiment M0003 deintegration/findings and impacts
[AD-A267140] p 885 N94-15749
An analysis of the dynamic response of the Space Station Freedom due to a module perforation by an orbital debris particle impact
[TABES PAPER 93-653] p 899 N94-16154
Impact penetration experiments in teflon targets of variable thickness p 1063 N94-16253
The effect of an on-orbit near encounter on the number flux density of micron sized particles p 899 N94-16374
Resolving LDEF's flux distribution: Orbital (debris?) and natural meteoroid populations p 1245 N94-16391
History of on-orbit satellite fragmentations
[NASA-CR-191644] p 887 N94-16502
Cosmic dust and space debris measurements on board the small satellites HITEN and BREM-SAT p 890 N94-17147
SYNMOD: A low-resource, low-cost means of monitoring the near-Earth space debris environment p 891 N94-17148
Detecting small debris using a ground-based photon counting detector
[DE93-012623] p 898 N94-17669

SPACE ENVIRONMENT SIMULATION
The 61-M long duration sim video highlights resource tape
[NASA-TM-109569] p 875 N94-15299
Richards, Dick: Training clip
[NASA-TM-109503] p 876 N94-15467

SPACE EXPLORATION
Robotics in space
[NASA-TM-109584] p 1045 N94-15268
NASA: The 25th year
[NASA-TM-109457] p 1302 N94-15352
First US Mars landing
[NASA-TM-109669] p 885 N94-15436
Mars laser altimeter based on a single photon ranging technique p 921 N94-15619
Workshop on advanced technologies for planetary instruments
[NASA-CR-194585] p 1032 N94-15797
Space transfer concepts and analyses for exploration missions, phase 4
[NASA-CR-193849] p 882 N94-15831
Twenty-Fourth Lunar and Planetary Science Conference. Part 2: G-M
[NASA-CR-193174] p 1247 N94-16173
Rover mounted ground penetrating radar as a tool for investigating the near-surface of Mars and beyong p 1007 N94-16197
Mars Analog Site Study (MASS) p 1252 N94-16200
Gamma ray spectrometer for Lunar Scout 2 p 1037 N94-16426
Chairmanship of the Neptune/Pluto outer planets science working group
[NASA-CR-194625] p 1297 N94-16832
Small spacecraft for planetary exploration p 874 N94-17145

SPACE FLIGHT TRAINING
STS-33 Carter and Thorton during WETF activities
[NASA-TM-109471] p 1136 N94-15402
STS-36 crew EVA prep and post-training, bailout exercises, final bench review
[NASA-TM-109498] p 1137 N94-15462
STS-35 payload specialists Durrance and Parise: 70mm photo training and cabin familiarization
[NASA-TM-109499] p 1032 N94-15463

SPACE HABITATS
Living well in space: Monitoring environment
[NASA-TM-109537] p 1120 N94-15368
STS-38 crew training: Habitation equipment procedures, bailout in CCT, 70mm photo class, EVA prep and post, and firefighting
[NASA-TM-109494] p 1136 N94-15453
An analysis of the dynamic response of the Space Station Freedom due to a module perforation by an orbital debris particle impact
[TABES PAPER 93-653] p 899 N94-16154

SPACE LABORATORIES
Commitment to challenge
[NASA-TM-109523] p 876 N94-15473
Scientific use of Space Station Freedom p 977 N94-16072

SPACE LOGISTICS
Strategy for the reduction of total integrated fluid logistics to the Space Station Freedom
[NASA-TM-107744] p 1138 N94-17452

SPACE MANUFACTURING
TABES 1993: 9th Annual Technical and Business Exhibition and Symposium p 1050 N94-16129
Study of the National Science Foundation's South Pole Station as an analogous data base for the logistical support of a Moon laboratory
[NASA-TM-108429] p 1174 N94-17469

SPACE MISSIONS
The 1969 highlights
[NASA-TM-109630] p 1301 N94-15241
The 1972 highlights
[NASA-TM-109631] p 1301 N94-15242
The 1965 highlights --- NASA programs
[NASA-TM-109632] p 1301 N94-15243
The 1967 highlights
[NASA-TM-109633] p 1301 N94-15244
Return to Space Mission: The STS-26 crew report
[NASA-TM-109568] p 880 N94-15317
Apollo presentation for Astrodome
[NASA-TM-109535] p 1302 N94-15366
Mars laser altimeter based on a single photon ranging technique p 921 N94-15619
Approaching the new reality
[TABES PAPER 93-230] p 1050 N94-16131
Commercial space opportunities advanced concepts and technology overview
[TABES PAPER 93-240] p 1050 N94-16132
Role and development of small satellite missions in space plasma physics p 891 N94-17149
MINISAT programme p 896 N94-17182

SPACE NAVIGATION
Space flight: The application of orbital mechanics
[NASA-TM-109424] p 874 N94-15493
A guidance and navigation system for two spacecraft rendezvous in translunar halo orbit
[AD-A267498] p 898 N94-17368

SPACE PERCEPTION
Characteristics of aimed arm movements in humans under low gravity p 980 N94-16093
Neural basis of motion perception
[AD-A267267] p 1133 N94-17265
A virtual acoustic orientation instrument
[AD-A268181] p 1134 N94-17510

SPACE PLASMAS
Global auroral imaging: Dynamics of Explorer Miss ion
[NASA-CR-194284] p 1097 N94-15003
Polar 2 model of the wake shield experiment
[AD-A266243] p 882 N94-16468
Prototype instrumentation and design studies
[AD-A266402] p 882 N94-16530
Role and development of small satellite missions in space plasma physics p 891 N94-17149
Space systems environmental interaction studies
[AD-A267280] p 897 N94-17240
High voltage conductors in spacecraft
[AD-A267268] p 897 N94-17266

SPACE PLATFORMS
ERS-1: 18 months in orbit p 990 N94-15888
Ground integrated ET-derived space platforms for onorbit applications
[TABES PAPER 93-652] p 899 N94-16152
Ground segment definition for the Spanish small satellite program (MINISAT) p 878 N94-17155
TAOS (S80): A (LEO-MSS) system for position reporting and telemanagement services p 893 N94-17162
TUBSAT: Low cost access to space technology p 895 N94-17180
Standard platforms for small satellites p 895 N94-17181
MINISAT programme p 896 N94-17182
ALEXIS and HETE: Two small, low cost, scientific satellite systems p 896 N94-17185
Military satellite communications: Opportunity to save billions of dollars. Report to the Chairman, Legislation, and National Security Subcommittee, Committee on Government Operations, House of Representatives
[AD-A267627] p 1002 N94-17199

SPACE PROBES
Search for optimal distance spectrum convolutional codes p 998 N94-16509

SPACE PROCESSING
Visualization of solidification front phenomena
[NASA-CR-193838] p 976 N94-15006
STS-26 protein growth (PCG) experiment
[NASA-TM-109533] p 976 N94-15395
Payloads for the processing of high temperature materials p 979 N94-16083
Materials processing in space: Issues for the third decade
[TABES PAPER 93-260] p 983 N94-16133
Growth of single crystals of mercuric iodide on the ground and in space
[DE93-015523] p 1209 N94-16442

SPACE PROGRAMS
Military space programs in the press: An analysis for change
[AD-A267799] p 874 N94-17306
The impact of industry/university consortia programs on space education
[NASA-TM-109340] p 1222 N94-17441

SPACE RENDEZVOUS
A guidance and navigation system for two spacecraft rendezvous in translunar halo orbit
[AD-A267498] p 898 N94-17368

SPACE SHUTTLE BOOSTERS
Space Shuttle solid rocket motor exposure monitoring p 976 N94-16624
RSRM nozzle actuator bracket/lug fracture mechanics qualification test
[NASA-CR-193859] p 927 N94-17080
SRB thermal curtain design support
[NASA-CR-193857] p 927 N94-17123
SRB thermal curtain design support
[NASA-CR-193858] p 928 N94-17124

SPACE SHUTTLE MAIN ENGINE
An assessment of finite-element modeling techniques for thick-solid/thin-shell joints analysis
[NASA-TM-108426] p 1058 N94-15534
Develop advanced nonlinear signal analysis topographical mapping system
[NASA-CR-194577] p 1082 N94-15646
Plasma arc welding repair of space flight hardware
[TABES PAPER 93-603] p 1049 N94-16139
Space Shuttle main engine. NASA has not evaluated the alternate fuel turbopump costs and benefits. Report to the Administrator of the National Aeronautics and Space Administration
[GAO/NSIAD-94-54] p 926 N94-16834
Advanced transportation system studies technical area 3: Alternate propulsion subsystem concepts, volume 3
[NASA-CR-193864] p 927 N94-17097
Advanced transportation system studies technical area 3: Alternate propulsion system concepts. SSME upper stage use
[NASA-CR-193865] p 927 N94-17098

SPACE SHUTTLE MISSION 51-F
Gearing up for 1988
[NASA-TM-109617] p 880 N94-15346
Sights and sounds of space
[NASA-TM-109610] p 1302 N94-15424

SPACE SHUTTLE MISSIONS
STS-26 Post-Flight Press Conference
[NASA-TM-109557] p 879 N94-15261
STS-26 onboard 16mm photography quick release
[NASA-TM-109558] p 879 N94-15262
STS-30 Post-Flight Press Conference --- Space Shuttle Launch, Magellan/IUS deploy, Crew Activites, and Landing
[NASA-TM-109580] p 879 N94-15264
STS-30 suited ascent training in fixed base SMS
[NASA-TM-109581] p 875 N94-15265
STS-30 mission tape --- Space Shuttle Launch, Crew Activities, Landing, and Air-to-Ground Transmission
[NASA-TM-109582] p 879 N94-15266
STS-26 SSIP briefing --- Titanium Grain Formation Experiment and Crystal Membrane Experiment
[NASA-TM-109556] p 976 N94-15280
The 61-M long duration sim video highlights resource tape
[NASA-TM-109569] p 875 N94-15299
Text and graphics systems
[NASA-TM-109570] p 1229 N94-15300
STS-30 Magellan deploy Sim in SMS and MOCR
[NASA-TM-109571] p 875 N94-15301
STS-30 EVA prep in CCT: Grabe, Lee, and Thagard
[NASA-TM-109572] p 1135 N94-15303
STS-29 Post-Flight Press Conference --- Shuttle Launch, TDRS-D/IUS Deployment, Crew Activites, and Shuttle Landing
[NASA-TM-109575] p 880 N94-15306
STS-29 onboard 16mm photography quick release
[NASA-TM-109576] p 880 N94-15307
STS-26 through STS-34, deploy activities
[NASA-TM-109566] p 1301 N94-15315
STS-32 IMAX camera training
[NASA-TM-109567] p 1031 N94-15316
STS-26 generic integrated IUS deploy simulation
[NASA-TM-109562] p 875 N94-15332

STS-26 EVA rescue training
[NASA-TM-109563] p 875 N94-15333
STS-26 Shuttle Earth views, April 1990, part 1
[NASA-TM-109564] p 1082 N94-15334
STS-26 Shuttle Earth views, April 1990, part 2
[NASA-TM-109565] p 1082 N94-15335
STS-34 post-flight press conference
[NASA-TM-109459] p 880 N94-15354
STS-34 onboard 16mm photography quick release
[NASA-TM-109460] p 880 N94-15355
STS-34 mission highlights resource tape, part 1
[NASA-TM-109461] p 880 N94-15356
STS-34 Galileo integrated deploy sim
[NASA-TM-109463] p 880 N94-15358
STS-34 crew bailout exercise in CCT
[NASA-TM-109465] p 1135 N94-15360
STS-29 mission highlights resource tape
[NASA-TM-109542] p 880 N94-15373
STS-29 IMAX camera audio class FFT
[NASA-TM-109543] p 1031 N94-15374
STS-29 EVA prep in FFT
[NASA-TM-109544] p 1135 N94-15375
STS-32 onboard 16mm photography quick release
[NASA-TM-109472] p 880 N94-15376
STS-31 Post-Flight Conference
[NASA-TM-109477] p 881 N94-15384
STS-33 crew post flight film
[NASA-TM-109470] p 881 N94-15400
STS-27 crew presentation clip
[NASA-TM-109551] p 881 N94-15403
STS-27 crew post-insertion deorbit-prep in CCT
[NASA-TM-109552] p 1136 N94-15404
STS-26 missions highlight resource tape
[NASA-TM-109559] p 881 N94-15407
NASA report to education, volume 7
[NASA-TM-109435] p 1247 N94-15419
STS-31 onboard 16mm photography quick release --- Onboard Activities
[NASA-TM-109478] p 881 N94-15438
STS-31 mission highlights resource tape
[NASA-TM-109479] p 881 N94-15440
STS-31 Hubble space telescope deploy: Training at MDF with Hawley
[NASA-TM-109481] p 876 N94-15442
STS-31 crew training inflight maintenance and bailout exercises in CCT and WFTF
[NASA-TM-109483] p 876 N94-15450
STS-40 crew during spacelab Sim
[NASA-TM-109493] p 876 N94-15452
STS-36 crew presentation clip
[NASA-TM-109497] p 881 N94-15461
STS-36 crew EVA prep and post-training, bailout exercises, final bench review
[NASA-TM-109498] p 1137 N94-15462
STS-35 payload specialists Durrance and Parise: 70mm photo training and cabin familiarization
[NASA-TM-109499] p 1032 N94-15463
STS-35 onboard photography quick release
[NASA-TM-109500] p 881 N94-15464
STS-35 mission highlights resource tape
[NASA-TM-109501] p 881 N94-15465

SPACE SHUTTLE ORBITERS
Vertical-tail aerodynamic configuration of space shuttle orbiter
[AD-A267723] p 879 N94-14941
Views from space
[NASA-TM-109634] p 1081 N94-15245
STS-30 Post-Flight Press Conference --- Space Shuttle Launch, Magellan/IUS deploy, Crew Activites, and Landing
[NASA-TM-109580] p 879 N94-15264
STS-30 crew photo in building 4
[NASA-TM-109573] p 1031 N94-15304
STS-29 Post-Flight Press Conference --- Shuttle Launch, TDRS-D/IUS Deployment, Crew Activites, and Shuttle Landing
[NASA-TM-109575] p 880 N94-15306
STS-34 Space Shuttle Portable Onboard Computer (SPOC) briefing
[NASA-TM-109458] p 880 N94-15353
STS-34 final bench review
[NASA-TM-109464] p 1135 N94-15359
Crew escape certification test
[NASA-TM-109530] p 1136 N94-15392
STS-30 onboard 16mm photography quick release
[NASA-TM-109579] p 881 N94-15423
Space Station/Orbiter berthing dynamics during an assembly flight
[NASA-TM-109049] p 1062 N94-17451

SPACE SHUTTLE PAYLOADS
Serpentine manipulator planning and control for NASA Space-Shuttle payload servicing
[AD-A266961] p 879 N94-14969
STS-29 mission highlights resource tape
[NASA-TM-109542] p 880 N94-15373
STS-32 onboard 16mm photography quick release
[NASA-TM-109472] p 880 N94-15376
STS-35 onboard photography quick release
[NASA-TM-109500] p 881 N94-15464
Science operation in space: Lessons
[NASA-TM-109502] p 881 N94-15466
Long Duration Exposure Facility
[NASA-TM-109427] p 885 N94-15497
The Canadian Space Station user development program. Where do we go from here? p 898 N94-16084
Cost-effective test methods for Shuttle payloads
[TABES PAPER 93-651] p 883 N94-16151
Looking at science on board Eureca
[ESA-BR-80] p 874 N94-16584

SPACE SHUTTLES
Vertical-tail aerodynamic configuration of space shuttle orbiter
[AD-A267723] p 879 N94-14941
STS-29 pre-launch and post-landing egress
[NASA-TM-109574] p 1135 N94-15305
GAS highlights, 1988 --- Get Away Specials
[NASA-TM-109600] p 873 N94-15308
Space Shuttle highlights
[NASA-TM-109606] p 880 N94-15314
The 1979 highlights
[NASA-TM-109443] p 1247 N94-15342
STS-34 Space Shuttle Portable Onboard Computer (SPOC) briefing
[NASA-TM-109458] p 880 N94-15353
STS-34 McCully and Baker during IFM training
[NASA-TM-109462] p 880 N94-15357
STS-29 crew IMAX camera training
[NASA-TM-109546] p 1031 N94-15380
The 1978 highlights
[NASA-TM-109625] p 1302 N94-15411
The 1977 highlights
[NASA-TM-109626] p 1302 N94-15412
Spacework 16 --- Simulated Space Shuttle Program
[NASA-TM-109436] p 1221 N94-15420
The 1980 highlights
[NASA-TM-109672] p 1303 N94-15509
The Marshall Automated Weld System (MAWS)
[TABES PAPER 93-602] p 1049 N94-16138
Plasma arc welding repair of space flight hardware
[TABES PAPER 93-603] p 1049 N94-16139
Ground integrated ET-derived space platforms for onorbit applications
[TABES PAPER 93-652] p 899 N94-16152
Power Reactant Storage Assembly (PRSA) (Space Shuttle). PRSA hydrogen and oxygen DVT tank refurbishment
[NASA-CR-188262] p 926 N94-16922
Optical properties of water released in low Earth orbit
[AD-A266197] p 1192 N94-16936

SPACE STATION FREEDOM
Space Station Freedom
[NASA-TM-109636] p 1031 N94-15247
Robotics for Space Station, tape 1
[NASA-TM-109588] p 1045 N94-15272
Space Station: The link to America's future
[NASA-TM-109653] p 884 N94-15274
Futurepath 1
[NASA-TM-109439] p 869 N94-15338
Dare to dream --- The Space Station Freedom development
[NASA-TM-109512] p 885 N94-15458
Space Station Facility government estimating
[NASA-TM-109324] p 1223 N94-15545
Estimating and bidding for the Space Station Processing Facility
[NASA-TM-109323] p 1223 N94-15546
Preliminary analysis and design optimization of the short spacer truss of Space Station Freedom
[NASA-TM-4470] p 1058 N94-15709
A feasibility study of a microgravity enhancement system for Space Station Freedom
[NASA-CR-191550] p 886 N94-15864
Scientific use of Space Station Freedom p 977 N94-16072
The Canadian Space Station user development program. Where do we go from here? p 898 N94-16084
An analysis of the dynamic response of the Space Station Freedom due to a module perforation by an orbital debris particle impact
[TABES PAPER 93-653] p 899 N94-16154
Soyuz/ACRV accommodation study
[NASA-TM-107733] p 888 N94-17072
Space Station/Orbiter berthing dynamics during an assembly flight
[NASA-TM-109049] p 1062 N94-17451
Strategy for the reduction of total integrated fluid logistics to the Space Station Freedom
[NASA-TM-107744] p 1138 N94-17452
Space Station Freedom electrical performance model
[NASA-TM-106395] p 929 N94-17483

SPACE STATION POWER SUPPLIES
Futurepath 1
[NASA-TM-109439] p 869 N94-15338
Futurepath 1 --- power systems
[NASA-TM-109431] p 925 N94-15503
Space Station Freedom electrical performance model
[NASA-TM-106395] p 929 N94-17483

SPACE STATION STRUCTURES
STS-37 CETA evaluation with Ross
[NASA-TM-109495] p 1135 N94-15330
STS-37 astronauts Ross and Apt during CETA hardware checkout
[NASA-TM-109496] p 1137 N94-15460
Preliminary analysis and design optimization of the short spacer truss of Space Station Freedom
[NASA-TM-4470] p 1058 N94-15709
Spline screw payload fastening system
[NASA-CASE-GSC-13454-1] p 1046 N94-15871

SPACE STATIONS
Space Station thermal storage/refrigeration system research and development
[NASA-CR-193841] p 879 N94-15191
Robotics for Space Station tape 2
[NASA-TM-109578] p 1045 N94-15263
Living well in space: Clinical care challenge
[NASA-TM-109539] p 1120 N94-15370
Answering the space medicine challenge
[NASA-TM-109511] p 1120 N94-15457
Space Station resource reel
[NASA-TM-109673] p 885 N94-15510
The Japanese Space Station utilization plan p 977 N94-16074
ALEXIS and HETE: Two small, low cost, scientific satellite systems p 896 N94-17185

SPACE SUITS
Ancient skills: Modern use
[NASA-TM-109594] p 1135 N94-15286
STS-30 EVA prep in CCT: Grabe, Lee, and Thagard
[NASA-TM-109572] p 1135 N94-15303
STS-27 crew fire training and glove molding
[NASA-TM-109554] p 1136 N94-15406
STS-31 Hubble space telescope contingency training in WETF with McCandless and Sullivan
[NASA-TM-109480] p 1136 N94-15441
STS-36 crew EVA prep and post-training, bailout exercises, final bench review
[NASA-TM-109498] p 1137 N94-15462
STS-26 crew clothing, glove molding, and personal hygiene
[NASA-TM-109520] p 1137 N94-15470
Space suit design
[NASA-TM-109670] p 1137 N94-15507
Mark 111 suit test evaluation in WETF with Jerry Ross
[NASA-TM-109504] p 1137 N94-15514

SPACE SURVEILLANCE (SPACEBORNE)
Space countersurveillance: A requisite for theater defense planning
[AD-A266871] p 884 N94-15147

SPACE TECHNOLOGY EXPERIMENTS
STS-37 CETA evaluation with Ross
[NASA-TM-109495] p 1135 N94-15330
STS-37 astronauts Ross and Apt during CETA hardware checkout
[NASA-TM-109496] p 1137 N94-15460
The Clementine instrument complement p 1086 N94-16370
The space technology research vehicle: Development status p 896 N94-17183

SPACE TOOLS
STS-37 CETA evaluation with Ross
[NASA-TM-109495] p 1135 N94-15330
STS-37 astronauts Ross and Apt during CETA hardware checkout
[NASA-TM-109496] p 1137 N94-15460

SPACE TRANSPORTATION
Space transfer concepts and analyses for exploration missions, phase 4
[NASA-CR-193849] p 882 N94-15831
Comparisons of selected laser beam power missions to conventionally powered missions
[NASA-TM-106110] p 1040 N94-16522
Advanced transportation system studies technical area 3: Alternate propulsion subsystem concepts, volume 2
[NASA-CR-193863] p 927 N94-17096
Advanced transportation system studies technical area 3: Alternate propulsion subsystem concepts, volume 3
[NASA-CR-193864] p 927 N94-17097
Human Transportation System (HTS) study, volume 2
[NASA-TM-104779-VOL-2] p 882 N94-17320

SPACE TRANSPORTATION SYSTEM
The 1982 highlights
[NASA-TM-109671] p 1303 N94-15508
Advanced transportation system studies technical area 3: Alternate propulsion system concepts. SSME upper stage use
[NASA-CR-193865] p 927 N94-17098

Flight 20 (STS-45) polysulfide gas path investigation
[NASA-CR-193861] p 928 N94-17213
SPACE TRANSPORTATION SYSTEM FLIGHTS
Space Shuttle highlights
[NASA-TM-109606] p 880 N94-15314
Return to Space Mission: The STS-26 crew report
[NASA-TM-109568] p 880 N94-15317
STS-29 mission highlights resource tape
[NASA-TM-109542] p 880 N94-15373
STS-29 EVA prep in FFT
[NASA-TM-109544] p 1135 N94-15375
STS-27 crew presentation clip
[NASA-TM-109551] p 881 N94-15403
STS-27 crew post-insertion deorbit-prep in CCT
[NASA-TM-109552] p 1136 N94-15404
STS-40 crew during spacelab Sim
[NASA-TM-109493] p 876 N94-15452
STS-36 crew presentation clip
[NASA-TM-109497] p 881 N94-15461
STS-36 crew EVA prep and post-training, bailout exercises, final bench review
[NASA-TM-109498] p 1137 N94-15462
STS-35 payload specialists Durrance and Parise: 70mm photo training and cabin familiarization
[NASA-TM-109499] p 1032 N94-15463
STS-35 mission highlights resource tape
[NASA-TM-109501] p 881 N94-15465
Science operation in space: Lessons
[NASA-TM-109502] p 881 N94-15466
STS-27 crew deorbit prep in SMS with Gibson, Shepard, Mullane, Ross, and G. Gardner
[NASA-TM-109518] p 882 N94-15468
STS-26 crew participation in meetings
[NASA-TM-109519] p 873 N94-15469
STS-26 crew clothing, glove molding, and personal hygiene
[NASA-TM-109520] p 1137 N94-15470
STS-41 post-flight press presentation
[NASA-TM-109514] p 882 N94-15516
STS-41 crew training bailout in CCT, 16mm camera class EVA prep, habitation equipment procedures, and food tasting
[NASA-TM-109517] p 876 N94-15517
STS-41 onboard 16mm photography quick release
[NASA-TM-109515] p 882 N94-15518
STS-41 mission highlights resource tape
[NASA-TM-109516] p 882 N94-15521
SPACE TRANSPORTATION SYSTEM 3 FLIGHT
The 1982 highlights
[NASA-TM-109671] p 1303 N94-15508
SPACE TRANSPORTATION SYSTEM 4 FLIGHT
The 1982 highlights
[NASA-TM-109671] p 1303 N94-15508
SPACE VEHICLE CHECKOUT PROGRAM
STS-31 crew training: firefighting, food tasting, EVA prep and post
[NASA-TM-109484] p 876 N94-15451
Galileo probe spacecraft mission to Jupiter
[NASA-TM-109646] p 1247 N94-16070
SPACE WEAPONS
Not ready for the first space war. What about the second?
[AD-A266557] p 1174 N94-16665
SPACEBORNE ASTRONOMY
Proceedings of an ESA Symposium on Photon Detectors for Space Instrumentation
[ESA-SP-356] p 899 N94-15025
Background suppression techniques in germanium detectors p 899 N94-15026
X ray microcalorimeters: Principles and performance p 899 N94-15027
A new approach to optical photon detection p 899 N94-15028
Development of x ray CCDs p 900 N94-15033
The development of back-illuminated CCD's for XMM p 900 N94-15035
Microchannel plate detectors for space astronomy p 901 N94-15038
Infrared detectors and coolers for space instrumentation: Summary and concluding remarks p 904 N94-15059
SPACEBORNE EXPERIMENTS
Sounding Rocket Experiments in Fluid Science and Materials Sciences: TEXUS 25 to 27 and MASER 4, volume 3
[ESA-SP-1132-VOL-3] p 943 N94-15157
Electrophoresis visualisation p 944 N94-15163
Remelting of Fe-C-Si-alloy in a ceramic mold skin p 945 N94-15169
Heat storage module p 946 N94-15172
Long Duration Exposure Facility is coming home
[NASA-TM-109656] p 884 N94-15227
STS-26 SSIP briefing --- Titanium Grain Formation Experiment and Crystal Membrane Experiment
[NASA-TM-109556] p 976 N94-15280
GAS highlights, 1988 --- Get Away Specials
[NASA-TM-109600] p 873 N94-15308
STS-29 crew with student experiment
[NASA-TM-109545] p 1116 N94-15378
STS-26 protein growth (PCG) experiment
[NASA-TM-109533] p 976 N94-15395
STS-31 onboard 16mm photography quick release --- Onboard Activities
[NASA-TM-109478] p 881 N94-15438
STS-40 crew during spacelab Sim
[NASA-TM-109493] p 876 N94-15452
Science operation in space: Lessons
[NASA-TM-109502] p 881 N94-15466
Long Duration Exposure Facility experiment M0003 deintegration/findings and impacts
[AD-A267140] p 885 N94-15749
Explosive boiling at very low heat fluxes: A microgravity phenomenon
[NASA-TM-106325] p 1046 N94-15817
Proceedings of the Second Workshop on Microgravity Experimentation
[DSS-NR15-43-1990] p 977 N94-16071
Scientific use of Space Station Freedom p 977 N94-16072
The ESA telescience program p 977 N94-16073
Canadian microgravity experiments flown in 1989-1990 p 977 N94-16075
MAXUS: The new sounding rocket program for long duration microgravity flight p 978 N94-16079
QUESTS: A microgravity research facility for materials science experiments p 978 N94-16082
The Canadian Space Station user development program. Where do we go from here? p 898 N94-16084
Study of fractal aggregates p 979 N94-16086
Polar 2 model of the wake shield experiment
[AD-A266243] p 882 N94-16468
Third LDEF Post-Retrieval Symposium Abstracts
[NASA-CP-10120] p 1303 N94-16495
Looking at science on board Eureca
[ESA-BR-80] p 874 N94-16584
Design of an experiment hardware for the ESA space facility BIOPAN
[DLR-FB-93-06] p 876 N94-17548
SPACEBORNE LASERS
Nd:YLF laser for airborne/spaceborne laser ranging p 913 N94-15563
GLRS-R 2-colour retroreflector target design and predicted performance p 921 N94-15615
Bench checkout equipment for spaceborne laser altimeter systems p 921 N94-15618
Multi-beam laser altimeter p 921 N94-15620
Satellite laser station Helwan status 1992 p 877 N94-15621
SPACEBORNE PHOTOGRAPHY
STS-30 crew photo in building 4
[NASA-TM-109573] p 1031 N94-15304
STS-34 Arriflex and IMAX camera training
[NASA-TM-109467] p 1031 N94-15397
STS-35 onboard photography quick release
[NASA-TM-109500] p 881 N94-15464
SPACEBORNE TELESCOPES
Gamma large area silicon telescope: Applying Si strip detector technology to the detection of gamma rays in space p 904 N94-15061
The STIS MAMA status: Current detector performance p 905 N94-15069
SPACECRAFT
The 1972 highlights
[NASA-TM-109631] p 1301 N94-15242
The 1965 highlights --- NASA programs
[NASA-TM-109632] p 1301 N94-15243
The 1967 highlights
[NASA-TM-109633] p 1301 N94-15244
SPACECRAFT BREAKUP
History of on-orbit satellite fragmentations
[NASA-CR-191644] p 887 N94-16502
The fragmentation of Kosmos 2163
[NASA-CR-191643] p 887 N94-16503
The fragmentation of the Nimbus 6 rocket body
[NASA-CR-191645] p 926 N94-16504
SPACECRAFT CHARGING
Polar 2 model of the wake shield experiment
[AD-A266243] p 882 N94-16468
Prototype instrumentation and design studies
[AD-A266402] p 882 N94-16530
SPACECRAFT COMMUNICATION
STS-35 mission highlights resource tape
[NASA-TM-109501] p 881 N94-15465
Computer networking at SLR stations p 917 N94-15594
Bandwidth characteristics of multimedia data traffic on a local area network
[NASA-TM-104026] p 883 N94-15648
SPACECRAFT COMPONENTS
Development of Japanese Earth Resources Satellite-1 (JERS-1; FUYO-1) and it's operational results
[NASDA-SPP-930001] p 884 N94-15001
Galileo probe ready to go
[NASA-TM-109648] p 1247 N94-15432
High voltage conductors in spacecraft
[AD-A267268] p 897 N94-17266
SPACECRAFT CONFIGURATIONS
Small spacecraft for planetary exploration p 874 N94-17145
A conceptual design study for a two-dimensional, electronically scanned thinned array radiometer
[NASA-TM-109051] p 1085 N94-17665
SPACECRAFT CONSTRUCTION MATERIALS
Processing and protection of high temperature structural materials
[AD-A267292] p 954 N94-14961
Aluminum-lithium technology
[TABES PAPER 93-601] p 962 N94-16137
Third LDEF Post-Retrieval Symposium Abstracts
[NASA-CP-10120] p 1303 N94-16495
Performance of silvered Teflon thermal control blankets on spacecraft
[AD-A266284] p 887 N94-16909
SPACECRAFT CONTAMINATION
Analysis of leading edge and trailing edge cover glass samples before and after treatment with advanced satellite contamination removal techniques
[AD-A267055] p 885 N94-15666
Solar absorptance of optical surfaces contaminated with spacecraft material outgassing products
[AD-A267202] p 886 N94-15857
Long duration exposure facility experiment m0003 deintegration observation database
[AD-A267579] p 951 N94-17207
SPACECRAFT CONTROL
Pulse response based control for minimum time maneuver of flexible spacecraft
[AD-A266186] p 886 N94-16455
Neighboring extremal guidance for systems with piecewise linear control using time as the reference variable
[AD-A267942] p 874 N94-17010
A guidance and navigation system for two spacecraft rendezvous in translunar halo orbit
[AD-A267498] p 898 N94-17368
SPACECRAFT DESIGN
Vertical-tail aerodynamic configuration of space shuttle orbiter
[AD-A267723] p 879 N94-14941
Space Station resource reel
[NASA-TM-109673] p 885 N94-15510
New perspectives for high accuracy SLR with second generation geodesic satellites p 916 N94-15585
Flight testing of airbreathing hypersonic vehicles
[NASA-TM-4524] p 886 N94-15753
Space transfer concepts and analyses for exploration missions, phase 4
[NASA-CR-193849] p 882 N94-15831
Apparatus and method for producing an artificial gravitational field
[NASA-CASE-MSC-22021-1] p 886 N94-15935
Lunar lander and return propulsion system trade study
[NASA-TP-3388] p 925 N94-16496
ALS engine propellant effector system
[NASA-CR-194650] p 926 N94-16590
Small spacecraft for planetary exploration p 874 N94-17145
Feasibility study of a personal communications system IRIDIUM-like p 893 N94-17165
Impact of advances in technology on future spacecraft design p 894 N94-17171
Small satellite modular design and application prospect p 894 N94-17173
SPACECRAFT DOCKING
A mission concept of Phobos/Deimos exploration p 1287 N94-16387
Space Station/Orbiter berthing dynamics during an assembly flight
[NASA-TM-109049] p 1062 N94-17451
SPACECRAFT ENVIRONMENTS
Living well in space: Monitoring environment
[NASA-TM-109537] p 1120 N94-15368
Precise measurement and utilization of acceleration data p 923 N94-16100
SPACECRAFT EQUIPMENT
Pre-phase a study report of lunar polar orbiter
[NASDA-TK-SS0440] p 873 N94-15000
Development of Japanese Earth Resources Satellite-1 (JERS-1; FUYO-1) and it's operational results
[NASDA-SPP-930001] p 884 N94-15001
STS-36 crew EVA prep and post-training, bailout exercises, final bench review
[NASA-TM-109498] p 1137 N94-15462
SPACECRAFT GUIDANCE
Neighboring extremal guidance for systems with piecewise linear control using time as the reference variable
[AD-A267942] p 874 N94-17010

A guidance and navigation system for two spacecraft rendezvous in translunar halo orbit
[AD-A267498] p 898 N94-17368
SPACECRAFT INSTRUMENTS
Pre-phase a study report of lunar polar orbiter
[NASDA-TK-SS0440] p 873 N94-15000
Proceedings of an ESA Symposium on Photon Detectors for Space Instrumentation
[ESA-SP-356] p 899 N94-15025
Background suppression techniques in germanium detectors p 899 N94-15026
Discrete CMT infrared detectors for space application, from ISSR to second generation Meteosat and MIPAS p 905 N94-15065
An adiabatic demagnetisation refrigerator with a mechanical pre-cooler for space applications p 906 N94-15070
Extrinsic photoconductor detectors for the wavelength range 2 microns to 240 microns p 906 N94-15073
The detector assemblies of ISOPHOT and the spectrometers ISO-SWS and ISO-LWS p 906 N94-15074
Ionising radiation-induced effects in doped germanium FIR photoconductors p 907 N94-15077
In orbit adiabatic demagnetization refrigeration for bolometric and microcalorimetric detectors p 907 N94-15079
CCD's on high resistivity bulk silicon for x ray spectroscopy on XMM p 907 N94-15080
Characterization of detectors and calibration of the ISOPHOT experiment p 907 N94-15082
Characteristics of the ISO short wavelength spectrometer detectors p 908 N94-15084
Absolute Radiometric Measurements in Space: ARMS p 908 N94-15085
IR detectors and subsystems for space applications p 909 N94-15091
Infrared detector annealing and calibration with IR-laser diodes p 909 N94-15092
Performance of the position-sensitive proportional counters of the Yohkoh Bragg crystal spectrometer p 909 N94-15094
Workshop on advanced technologies for planetary instruments
[NASA-CR-194585] p 1032 N94-15797
Precise measurement and utilization of acceleration data p 923 N94-16100
The Clementine instrument complement p 1086 N94-16370
Principal investigators data package for Project Initiation Conference (PIC): EUVS sounding rocket no. 36.117CL. Target: Venus
[NASA-CR-194663] p 923 N94-17126
Pioneer Venus data analysis for the retarding potential analyzer
[NASA-CR-194673] p 1297 N94-17292
SPACECRAFT LANDING
Return to Space Mission: The STS-26 crew report
[NASA-TM-109568] p 880 N94-15317
STS-27 crew presentation clip
[NASA-TM-109551] p 881 N94-15403
STS-26 missions highlight resource tape
[NASA-TM-109559] p 881 N94-15407
STS-35 mission highlights resource tape
[NASA-TM-109501] p 881 N94-15465
Tetrahedral lander
[NASA-CASE-MSC-22082-1] p 886 N94-15951
A mission concept of Phobos/Deimos exploration p 1287 N94-16387
SPACECRAFT LAUNCHING
COBE video news
[NASA-TM-109598] p 987 N94-15292
Return to Space Mission: The STS-26 crew report
[NASA-TM-109568] p 880 N94-15317
Mission San Marco
[NASA-TM-109442] p 878 N94-15341
STS-29 mission highlights resource tape
[NASA-TM-109542] p 880 N94-15373
STS-27 crew presentation clip
[NASA-TM-109551] p 881 N94-15403
STS-26 missions highlight resource tape
[NASA-TM-109559] p 881 N94-15407
Long Duration Exposure Facility
[NASA-TM-109427] p 885 N94-15497
RADARSAT program p 898 N94-15893
Liquid hydrogen and liquid oxygen feedline passive recirculation analysis
[TABES PAPER 93-620] p 1031 N94-16145
The closing window of opportunity: Addressing the US space launch vehicle crisis
[TABES PAPER 93-640] p 878 N94-16148
Space Propulsion Synergy Group ETO technology assessments
[TABES PAPER 93-641] p 929 N94-16149
Prototype instrumentation and design studies
[AD-A266402] p 882 N94-16530
Small Satellites Systems and Services
[ISBN-2-85-428327-9] p 888 N94-17131
Impact of launching uncertainties on the visibility of communication satellite constellations without orbit control p 889 N94-17135
Small launchers (current and future projects in the world) p 878 N94-17137
Small satellite constellation deployment strategies p 878 N94-17138
NEXT launch system p 878 N94-17141
Role and development of small satellite missions in space plasma physics p 891 N94-17149
Satellite situation report, volume 31, number 1
[NASA-TM-105088] p 898 N94-17584
SPACECRAFT MAINTENANCE
STS-31 crew training: firefighting, food tasting, EVA prep and post
[NASA-TM-109484] p 876 N94-15451
Plasma arc welding repair of space flight hardware
[TABES PAPER 93-603] p 1049 N94-16139
SPACECRAFT MODELS
Space Station Freedom
[NASA-TM-109636] p 1031 N94-15247
Cost-effective test methods for Shuttle payloads
[TABES PAPER 93-651] p 883 N94-16151
SPACECRAFT MODULES
The Japanese Space Station utilization plan p 977 N94-16074
An analysis of the dynamic response of the Space Station Freedom due to a module perforation by an orbital debris particle impact
[TABES PAPER 93-653] p 899 N94-16154
Small satellite modular design and application prospect p 894 N94-17173
SPACECRAFT PERFORMANCE
International testing of a Mars rover prototype p 1273 N94-16312
SPACECRAFT POWER SUPPLIES
Results of an electrical power system fault study (CDDF)
[NASA-TP-3413] p 884 N94-15007
SPDE/SPRE final summary report
[NASA-CR-187086] p 924 N94-15482
The 1987 Goddard Space Flight Center Battery Workshop
[NASA-CP-3236] p 1012 N94-17062
Lattice-mismatched In(0.40)Al(0.60)As window layers for indium phosphide solar cells
[NASA-TM-106255] p 1013 N94-17113
Arsene GaAs solar array p 894 N94-17174
Small satellite nickel-hydrogen and nickel-metal hydride power applications p 895 N94-17175
A power system for a microsatellite p 895 N94-17176
The space technology research vehicle: Development status p 896 N94-17183
Overview of the solar dynamic ground test demonstration program
[NASA-TM-106296] p 928 N94-17256
High voltage conductors in spacecraft
[AD-A267268] p 897 N94-17266
SPACECRAFT PROPULSION
Space transfer concepts and analyses for exploration missions, phase 4
[NASA-CR-193849] p 882 N94-15831
Proteus three-dimensional Navier-Stokes computer code, version 1.0. Volume 3: Programmer's reference
[NASA-TM-106341] p 1022 N94-15865
Proteus two-dimensional Navier-Stokes computer code, version 2.0. Volume 3: Programmer's reference
[NASA-TM-106339] p 1022 N94-15867
Liquid hydrogen and liquid oxygen feedline passive recirculation analysis
[TABES PAPER 93-620] p 1031 N94-16145
Liquid Oxygen (LO2) propellant conditioning concept testing
[TABES PAPER 93-621] p 976 N94-16146
Space Propulsion Synergy Group ETO technology assessments
[TABES PAPER 93-641] p 929 N94-16149
Comparisons of selected laser beam power missions to conventionally powered missions
[NASA-TM-106110] p 1040 N94-16522
Power Reactant Storage Assembly (PRSA) (Space Shuttle). PRSA hydrogen and oxygen DVT tank refurbishment
[NASA-CR-188262] p 926 N94-16922
Advanced transportation system studies technical area 3: Alternate propulsion subsystem concepts, volume 2
[NASA-CR-193863] p 927 N94-17096
Advanced transportation system studies technical area 3: Alternate propulsion subsystem concepts, volume 3
[NASA-CR-193864] p 927 N94-17097
Application of a NEPTUNE propulsion concept to a manned Mars excursion
[AD-A268053] p 929 N94-17587
SPACECRAFT RADIATORS
Geometrical vapor blocker for parallel condensation tubes requiring cooling
[NASA-CASE-MSC-22090-1] p 1022 N94-15962
SPACECRAFT RECOVERY
Long Duration Exposure Facility retrieval animation
[NASA-TM-109426] p 885 N94-15496
Long Duration Exposure Facility
[NASA-TM-109427] p 885 N94-15497
SPACECRAFT RELIABILITY
Gearing up for 1988
[NASA-TM-109617] p 880 N94-15346
Lunar lander and return propulsion system trade study
[NASA-TP-3388] p 925 N94-16496
SPACECRAFT SHIELDING
Exposure fluctuations of astronauts due to orientation
[NASA-TP-3364] p 1300 N94-15816
Calculations of cosmic-ray helium transport in shielding materials
[NASA-TP-3354] p 1301 N94-17666
SPACECRAFT STRUCTURES
An analysis of the dynamic response of the Space Station Freedom due to a module perforation by an orbital debris particle impact
[TABES PAPER 93-653] p 899 N94-16154
Solid lubricants for space structures, phase 2
[AD-A266653] p 968 N94-16767
Principal investigators data package for Project Initiation Conference (PIC): EUVS sounding rocket no. 36.117CL. Target: Venus
[NASA-CR-194663] p 923 N94-17126
A mechanical system damping measurement technique using a one-degree-of-freedom (1DOF) cylindrical gas bearing
[AD-A268402] p 1048 N94-17462
Structural mechanics division research and technology accomplishments for CY 1992 and plans for CY 1993
[NASA-TM-107752] p 1062 N94-17479
SPACECRAFT TEMPERATURE
Gravity dependent condensation pressure drop and heat transfer in ammonia two-phase heat transport systems
[NLR-TP-92121-U] p 1031 N94-17615
SPACECRAFT TRAJECTORIES
Neptune encounter highlights
[NASA-TM-109421] p 1246 N94-15240
Neighboring extremal guidance for systems with piecewise linear control using time as the reference variable
[AD-A267942] p 874 N94-17010
Soyuz/ACRV accommodation study
[NASA-TM-107733] p 888 N94-17072
SPACECREWS
Astro smile
[NASA-TM-109506] p 879 N94-15225
STS-29 Post-Flight Press Conference — Shuttle Launch, TDRS-D/IUS Deployment, Crew Activites, and Shuttle Landing
[NASA-TM-109575] p 880 N94-15306
STS-26 IUS and latch contingency training
[NASA-TM-109561] p 875 N94-15331
STS-26 generic integrated IUS deploy simulation
[NASA-TM-109562] p 875 N94-15332
STS-34 post-flight press conference
[NASA-TM-109459] p 880 N94-15354
STS-34 mission highlights resource tape, part 1
[NASA-TM-109461] p 880 N94-15356
STS-34 McCully and Baker during IFM training
[NASA-TM-109462] p 880 N94-15357
STS-34 final bench review
[NASA-TM-109464] p 1135 N94-15359
STS-29 mission highlights resource tape
[NASA-TM-109542] p 880 N94-15373
STS-32 LDEF EVA training in WETF with Low and Dunbar
[NASA-TM-109473] p 1135 N94-15377
STS-29 crew IMAX camera training
[NASA-TM-109546] p 1031 N94-15380
STS-32 crew training for lower body negative pressure unit and AFE
[NASA-TM-109475] p 1120 N94-15381
STS-29 crew food tasting in building 45
[NASA-TM-109547] p 1136 N94-15382
STS-29 crew bailout in WETF
[NASA-TM-109548] p 1136 N94-15385
STS-28 Adamson and Brown EMU walk through
[NASA-TM-109549] p 1136 N94-15387
STS-34 Arriflex and IMAX camera training
[NASA-TM-109467] p 1031 N94-15397
STS-33 EVA prep and post with Gregory, Blaha, Carter, Thorton, and Musgrave in FFT
[NASA-TM-109469] p 881 N94-15398
ASTP 15th anniversary clip-media release
[NASA-TM-109534] p 1302 N94-15399
STS-33 crew post flight film
[NASA-TM-109470] p 881 N94-15400

STS-27 EMU and RMS contingency training
[NASA-TM-109550] p 1136 N94-15401
STS-33 Carter and Thorton during WETF activities
[NASA-TM-109471] p 1136 N94-15402
STS-27 crew post-insertion deorbit-prep in CCT
[NASA-TM-109552] p 1136 N94-15404
STS-27 crew fire training and glove molding
[NASA-TM-109554] p 1136 N94-15406
STS-26 missions highlight resource tape
[NASA-TM-109559] p 881 N94-15407
STS-38 crew training: Habitation equipment procedures, bailout in CCT, 70mm photo class, EVA prep and post, and firefighting
[NASA-TM-109494] p 1136 N94-15453
Answering the space medicine challenge
[NASA-TM-109511] p 1120 N94-15457
STS-36 crew presentation clip
[NASA-TM-109497] p 881 N94-15461
STS-36 crew EVA prep and post-training, bailout exercises, final bench review
[NASA-TM-109498] p 1137 N94-15462
STS-27 crew deorbit prep in SMS with Gibson, Shepard, Mullane, Ross, and G. Gardner
[NASA-TM-109518] p 882 N94-15468
STS-26 crew participation in meetings
[NASA-TM-109519] p 873 N94-15469
STS-26 crew clothing, glove molding, and personal hygiene
[NASA-TM-109520] p 1137 N94-15470
STS-41 onboard 16mm photography quick release
[NASA-TM-109515] p 882 N94-15518
STS-41 mission highlights resource tape
[NASA-TM-109516] p 882 N94-15521

SPACELAB
The 1977 highlights
[NASA-TM-109626] p 1302 N94-15412
STS-40 crew during spacelab Sim
[NASA-TM-109493] p 876 N94-15452
The Japanese Space Station utilization plan
p 977 N94-16074
The Spacelab IPS Star Simulator
[TABES PAPER 93-650] p 877 N94-16150

SPACELAB PAYLOADS
STS-40 crew during spacelab Sim
[NASA-TM-109493] p 876 N94-15452

SPACERS
Preliminary analysis and design optimization of the short spacer truss of Space Station Freedom
[NASA-TM-4470] p 1058 N94-15709

SPALLATION
A calibration of the production rate ratio P-21/P-26 by low energy secondry neutrons: Identification of Ne spallation components at the 10(exp 6) atoms/g level in terrestrial samples p 1187 N94-16194

SPANISH SPACE PROGRAM
Ground segment definition for the Spanish small satellite program (MINISAT) p 878 N94-17155
Data handling strategy for the Spanish small satellite program (MINISAT) p 895 N94-17177

SPARK IGNITION
Dynamic behavior of an electric arc gas discharge
[DE93-630197] p 1205 N94-17635

SPARKS
An electronic imaging system for the Aeroballistic Research Facility
[AD-A267157] p 1033 N94-15826

SPATIAL DISTRIBUTION
Broadband conventional beamforming incorporating adaptive equalization
[AD-A267090] p 987 N94-15544
Characterization of spatial and temporal variability of phytoplankton blooms in coastal waters
[AD-A267102] p 1116 N94-15633
Tessera terrain on Venus: Implications of tessera flooding models and boundary characteristics for global distribution and mode of formation p 1258 N94-16226
Reference frames in vision
[AD-A266174] p 1132 N94-16925
Biofilm structure and diversity
[AD-A267254] p 1118 N94-16989
Arctic and Antarctic sea ice, 1978-1987: Satellite passive-microwave observations and analysis
[NASA-SP-511] p 1114 N94-17439
Measurement of the velocity field and void fraction in a planar plunging jet
[AD-A268183] p 1030 N94-17511

SPATIAL FILTERING
Exploitation of cyclostationarity for signal-parameter estimation and system identification
[AD-A267137] p 988 N94-15690
Spatial filters for optical correlation
[AD-A267199] p 1189 N94-15791
Neural-network-directed alignment of optical systems using the laser-beam spatial filter as an example
[NASA-TP-3372] p 1034 N94-15961

SPATIAL RESOLUTION
Streak camera based SLR receiver for two color atmospheric measurements p 914 N94-15573
High resolution SAR applications and instrument design p 993 N94-15913
Morphometric comparison of Icelandic lava shield volcanoes versus selected Venusian edifices
p 1248 N94-16178
Multi-resolution processing for fractal analysis of airborne remotely sensed data p 1065 N94-16604
Spatial resolution and cloud optical thickness retrievals p 1066 N94-16671
Tip-tilt compensation: Resolution limits for ground-based telescopes using laser guide star adaptive optics
[DE93-016426] p 1237 N94-16872

SPECIFIC HEAT
Measurement of the specific heat capacity of the electron-beam graphite calorimeter
[NPL-RSA(EXT)-40] p 1031 N94-15018
The specific heat of titanium disilicide
[AD-A267543] p 960 N94-17100
Convection effects on radial segregation and crystal melt interface in vertical Bridgman growth
[NASA-CR-191541] p 1029 N94-17387

SPECIFICATIONS
VDM specification of the MD4 message digest algorithm
[NPL-DITC-204/92] p 1142 N94-14944
RAISE specification of the MD4 message digest algorithm
[NPL-DITC-206/92] p 1142 N94-15010
TITUS: A micro-satellite for technology demonstration
p 896 N94-17186
CALS test network handbook
[AD-A267587] p 1160 N94-17209

SPECKLE INTERFEROMETRY
Speckles statistics and decorrelation effects in complex ABCD optical systems
[AD-A267843] p 1193 N94-17012

SPECKLE PATTERNS
Spatial and frequency diversity in lidar systems
[AD-A266192] p 1039 N94-16124

SPECTRA
A posteriori error estimation for hierarchic models of elliptic boundary value problems on thin domains
[AD-A267714] p 1168 N94-14939
Why is the Moon dark? p 1256 N94-16219
Field observations of infragravity, sea and swell directional spectra
[AD-A266439] p 1113 N94-16561
Efficient computational methods to study new and innovative signal detection techniques in SETI
[NASA-CR-193602] p 998 N94-16649
In-flight calibration of the spectral and radiometric characteristics of AVIRIS in 1991 p 1037 N94-16667

SPECTRAL BANDS
BIB photodetectors based on antimony doped silicon
p 902 N94-15047
Atmospheric transmittance between 1.0 and 2.0 micrometers
[AD-A267076] p 1098 N94-15539
Seasonal and spatial variations in phytoplanktonic chlorophyll in eutrophic Mono Lake, California, measured with the Airborne Visible and Infrared Imaging Spectrometer (AVIRIS) p 1069 N94-16684
Use of AVIRIS data to the definition of optimised specifications for land applications with future spaceborne imaging spectrometers p 1071 N94-16694
Spectroscopic investigations of nonambient systems with millimeter and submillimeter probes
[AD-A266537] p 968 N94-16796
Earth observational research using multistage EOS-like data
[NASA-CR-194626] p 1084 N94-16831
The feasibility of tropospheric and total ozone determination using a Fabry-Perot interferometer as a satellite-based nadir-viewing atmospheric sensor
[NASA-TM-109342] p 1102 N94-17214

SPECTRAL EMISSION
Plume radiation p 924 N94-15223
Preliminary analysis of thermal-infrared multispectral scanner data of the Iron Hill, Colorado carbonatite-alkalic rock complex p 1065 N94-16605

SPECTRAL METHODS
Numerical simulation of three-dimensional self-gravitating flow
[NASA-TM-109021] p 1021 N94-15768

SPECTRAL REFLECTANCE
Fullerene superconductors
[AD-A266749] p 1010 N94-15954
Spectral evidence of size dependent space weathering processes on asteroid surfaces p 1241 N94-16174
Comparison of reflectance spectra of C asteroids and unique C chondrites Y86720, Y82162, and B7904
p 1242 N94-16246
Iron oxide bands in the visible and near-infrared reflectance spectra of primitive asteroids
p 1242 N94-16274
Mixing model analysis of telescopic lunar spectra
p 1284 N94-16371
Galileo SSI lunar observations: Copernican craters and soils p 1288 N94-16395
Analysis of pyroxene absorptions observed in Martian dark regions p 1292 N94-16411
Optical effects of regolith processes on S asteroids as simulated by laser impulse alteration of ordinary chondrite p 1246 N94-16422
Terrestrial impact melts as analogues for the hematization of Martian surface materials
p 1104 N94-16424
The spectrum of Phobos from Phobos 2 observations at 0.3-2.6 microns: Comparison to previous data and meteorite analogs p 1295 N94-16429
Variations in the Fe mineralogy of bright Martian soil
p 1295 N94-16431
Composition of weakly altered Martian crust
p 1296 N94-16436
From minerals to rocks: Toward modeling lithologies with remote sensing p 1086 N94-16437
The 1991 AVIRIS/POLDER experiment in Camargue, France p 1070 N94-16691
Tracking photosynthetic efficiency with narrow-band spectroradiometry
[CIW-PUBL-1133] p 1072 N94-16698
Oregon transect: Comparison of leaf-level reflectance with canopy-level and modelled reflectance
p 1073 N94-16702
Discussion of band selection and methodologies for the estimation of precipitable water vapour from AVIRIS data p 1074 N94-16707

SPECTRAL RESOLUTION
Spatial resolution and cloud optical thickness retrievals p 1066 N94-16671
Primary studies of trace quantities of green vegetation in Mono Lake area using 1990 AVIRIS data
p 1071 N94-16695
AVIRIS as a tool for carbonatite exploration: Comparison of SPAM and Mbandmap data analysis methods
p 1073 N94-16703
Earth observational research using multistage EOS-like data
[NASA-CR-194626] p 1084 N94-16831
The feasibility of tropospheric and total ozone determination using a Fabry-Perot interferometer as a satellite-based nadir-viewing atmospheric sensor
[NASA-TM-109342] p 1102 N94-17214

SPECTRAL SIGNATURES
Spectral evidence of size dependent space weathering processes on asteroid surfaces p 1241 N94-16174
Terrestrial impact melts as analogues for the hematization of Martian surface materials
p 1104 N94-16424
Mapping vegetation types with the multiple spectral feature mapping algorithm in both emission and absorption p 1069 N94-16686
Atmospheric correction of AVIRIS data in ocean waters p 1070 N94-16690
Use of AVIRIS data to the definition of optimised specifications for land applications with future spaceborne imaging spectrometers p 1071 N94-16694

SPECTRAL THEORY
Phillips Laboratory global spectral numerical weather prediction model
[AD-A267293] p 1107 N94-17244

SPECTROMETERS
CdTe array detectors for high energy astronomy
p 899 N94-15029
The development of back-illuminated CCD's for XMM
p 900 N94-15035
Optimisation of FIR photoconductors for atmospheric spectroscopy p 902 N94-15048
Applications for large area silicon drift detectors on x ray and gamma ray astronomy p 909 N94-15090
Performance of the position-sensitive proportional counters of the Yohkoh Bragg crystal spectrometer
p 909 N94-15094
Preliminary results from bubble detector measurements aboard Biocosmos-2044 p 981 N94-16097
A Moessbauer spectrometer for the mineralogical analysis of the Mars surface: First temperature dependent tests of the detector and drive system
p 1259 N94-16233
Frequency resolution of an acousto-optical spectrometer
[AD-A267822] p 1035 N94-17401
Optimisation and specification of Auger electron spectrometers for signal-to-noise ratio performance
[NPL-DMM(A)-101] p 1006 N94-17549
Comparison of computer predictions and magnetic field measurements for an iron spectrometer magnet
[DE93-016164] p 1176 N94-17658

SPECTROPHOTOMETRY
Heliocentric zoning of the asteroid belt by aluminum-26 heating p 1241 N94-16205
Evaluation of hemoglobin-oxygen equilibrium binding by rapid-scanning spectrophotometry and singular-value decomposition
[AD-A266453] p 1123 N94-16564
SPECTRORADIOMETERS
Almaz p 898 N94-15889
SPECTROSCOPIC ANALYSIS
Effects of aging time on V205 sol-gel coatings
[AD-A266824] p 965 N94-15843
A high flux radical beam diamond growth
[AD-A266754] p 1207 N94-15955
Application of Z-contrast imaging to obtain column-by-column spectroscopic analysis of materials
[DE93-015333] p 947 N94-16014
Space Shuttle solid rocket motor exposure monitoring p 976 N94-16624
Electron spectroscopy analysis
[NASA-CR-193591] p 951 N94-17039
DLTS and dynamic transconductance analysis of deep-submicron fully-depleted SOI MOSFET's
[AD-A267291] p 1214 N94-17243
SPECTROSCOPY
Theoretical studies relating to the interaction of radiation with matter
[AD-A266894] p 1179 N94-14949
BIB photodetectors based on antimony doped silicon p 902 N94-15047
Study of protein-H2O interactions by multidimensional NMR spectroscopy
[AD-A266955] p 946 N94-15760
First results from a laboratory facility for measurement of emission spectra under simulated planetary conditions p 954 N94-16372
Methods of tunneling spectroscopy with the STM
[AD-A266507] p 948 N94-16787
Spectroscopic investigations of nonambient systems with millimeter and submillimeter probes
[AD-A266537] p 968 N94-16796
Suppression of charge scattering in Moessbauer experiments using synchrotron radiation
[DE93-015406] p 1212 N94-16887
DLTS and dynamic transconductance analysis of deep-submicron fully-depleted SOI MOSFET's
[AD-A267291] p 1214 N94-17243
SPECTRUM ANALYSIS
On the use of the noncentral chi-square density function for the distribution of helicopter spectral estimates
[NASA-CR-191546] p 1176 N94-15487
Spectral studies of solid propellant combustion 4: Absorption and burn rate results for M43, XM39, and M10 propellants
[AD-A267119] p 946 N94-15685
Higher order statistics in signal processing
[FFI-92/2008] p 989 N94-15714
Why is the Moon dark? p 1256 N94-16219
Remote sensing studies of the northeastern portion of the lunar nearside p 1258 N94-16225
Spectral study of Venus global topography and geoid from Magellan and PVO data p 1276 N94-16332
Lunar phase function effects on spectral ratios used for resource assessment p 1278 N94-16342
Mixing model analysis of telescopic lunar spectra p 1284 N94-16371
Optical effects of regolith processes on S asteroids as simulated by laser impulse alteration of ordinary chondrite p 1246 N94-16422
Search for Extraterrestrial Intelligence (SETI) p 1125 N94-16620
A field measure of the shade fraction p 1068 N94-16677
Mapping the spectral variability in photosynthetic and non-photosynthetic vegetation, soils, and shade using AVIRIS p 1068 N94-16679
Using endmembers in AVIRIS images to estimate changes in vegetative biomass p 1070 N94-16689
Separation of cirrus cloud from clear surface from AVIRIS data using the 1.38 micron water vapor band p 1072 N94-16699
Expert system-based mineral mapping using AVIRIS p 1073 N94-16704
Multitemporal diurnal AVIRIS images of a forested ecosystem p 1074 N94-16709
A comparison of LOWTRAN-7 corrected Airborne Visible/Infrared Imaging Spectrometer (AVIRIS) data with ground spectral measurements p 1074 N94-16710
Femtosecond growth dynamics of an underdense ionization front measured by spectral blueshifting
[DE93-013582] p 1183 N94-16818
Evaluation of site effects on a high frequency direction finding single site location system
[AD-A267465] p 1001 N94-17035
Chemical tracer studies at IOSDL. 3: The measurement of silicate, nitrate and phosphate in seawater
[IOS-302-1992] p 1114 N94-17489
Optimisation and specification of Auger electron spectrometers for signal-to-noise ratio performance
[NPL-DMM(A)-101] p 1006 N94-17549
SPECULAR REFLECTION
Radome depolarization effects on monopulse receiver tracking performance
[AD-A267446] p 1001 N94-17031
Hazard calculations of diffuse reflected laser radiation for the SELENE program
[NASA-TM-4520] p 1042 N94-17285
SPEECH RECOGNITION
Call sign intelligibility improvement using a spatial auditory display
[NASA-TM-104014] p 1177 N94-15549
Segment-based acoustic models for continuous speech recognition
[AD-A267138] p 988 N94-15691
A multilevel-multiresolution method for image processing. A Bayesian framework for reconstructing and representing shapes
[AD-A266772] p 1082 N94-15842
The influence of the level formants on the perception of synthetic vowel sounds
[IFTR-41/1991] p 1002 N94-17064
SPHERES
Metastable superconductors as photon detectors p 900 N94-15032
Use of microgravity in the synthesis of ceramics using sol gel techniques p 979 N94-16088
Three dimensional hydrodynamic calculations with adaptive mesh refinement of the evolution of Rayleigh Taylor and Richtmyer Meshkov instabilities in converging geometry: Multi-mode perturbations
[DE93-017155] p 1025 N94-16903
Stability analysis for the flow of granular materials down an inclined plane using kinetic model
[DE93-016852] p 1026 N94-16958
SPHERICAL COORDINATES
A review of some dynamics models in six-dimensional phase space and their suitable conditions of motion equation
[DE93-623741] p 1175 N94-17317
SPHERULES
Cretaceous-tertiary boundary spherules and Cenozoic microtektites: Similarities and differences p 1241 N94-16186
Size distribution of interplanetary iron and stony particles related with deep-sea spherules p 1245 N94-16388
Siderophile element fractionation in meteor crater impact glasses and metallic spherules p 1246 N94-16414
Optical properties of water released in low Earth orbit
[AD-A266197] p 1192 N94-16936
SPIN
Systematology for elastic-plastic material equations by large deformations on the basis of the Cosserat-continuum model
[SCHRIFTENR-PHYSIKAL-ING-BD] p 1058 N94-15642
SPIN DYNAMICS
Relativistic dynamics of spin in strong external fields
[NIKHEF-H/93-06] p 1240 N94-17604
SPIN TESTS
Reliability of autonomic responses and malaise across multiple motion sickness stimulation tests
[NASA-TM-108787] p 1121 N94-15711
SPIN-ORBIT INTERACTIONS
Effects of spin-orbit coupling on disordered mesoscopic systems
[ITN-93-85220] p 1180 N94-15288
SPINEL
Limited subsolidus diffusion in type B1 CAI: Evidence from Ti distribution in spinel p 954 N94-16401
SPLINE FUNCTIONS
Adaptive wavelet collocation methods for initial value boundary problems of nonlinear PDE's
[NASA-CR-191507] p 1169 N94-15833
Three-dimensional analysis of anisotropic spatially reinforced structures p 939 N94-16863
Aeroelastic airfoil smart spar p 868 N94-16865
SPLINES
Spline screw payload fastening system
[NASA-CASE-GSC-13454-1] p 1046 N94-15871
SPOOLS
Electrostatic fiber spreader including a corona discharge device
[AD-D015793] p 936 N94-16537
SPRAY CHARACTERISTICS
Cryogenic spray vaporization in high-velocity helium, argon and nitrogen gasflows
[NASA-TM-106363] p 1035 N94-17446
SPRAY NOZZLES
Coaxial airblast atomizers
[NASA-CR-193845] p 1016 N94-15109
Two-dimensional, high flow, precisely controlled monodisperse drop source
[AD-A267660] p 1028 N94-17250
SPRAYED COATINGS
Application of thermal spray and ceramic coatings and reinforced epoxy for cavitation damage repair of hydroelectric turbines and pumps
[AD-A267624] p 971 N94-17198
SPRAYERS
Thermal spray forming of refractory sample ampoule cartridges for single crystal growth space furnaces
[TABES PAPER 93-605] p 1051 N94-16141
SPREAD SPECTRUM TRANSMISSION
Four Frequency-Shift Keying (4-FSK) spread spectrum modulator and demodulator
[AD-A267433] p 1000 N94-16979
SPREADING
Electrostatic fiber spreader including a corona discharge device
[AD-D015793] p 936 N94-16537
SPRINGS (ELASTIC)
Mechanical energy absorber
[NASA-CASE-MSC-22111-1] p 1047 N94-15966
SPUTTERING
Laboratory for x ray optics
[AD-A267149] p 1189 N94-15735
Interfacial structure of lattice mismatched bcc(110)/bcc(110) transition metal superlattices
[DE93-015162] p 1208 N94-16058
Sputtered ferroelectric thin films of KTN for electro-optic devices
[AD-A266573] p 968 N94-16723
Epitaxial iron films
[AD-A268286] p 1217 N94-17579
Mechanical properties of interfaces and superlattices
[AD-A268591] p 1217 N94-17606
SQUALLS
Opposing mesoscale flows in a broken midlatitude squall line
[AD-A268011] p 1109 N94-17492
SQUID (DETECTORS)
Future development in cryogenic techniques for space p 901 N94-15042
STABILITY
Finding stable orientations of assemblies with linear programming
[AD-A266990] p 1143 N94-15212
Reliability of autonomic responses and malaise across multiple motion sickness stimulation tests
[NASA-TM-108787] p 1121 N94-15711
On the stability analysis of approximate factorization methods for 3D Euler and Navier-Stokes equations
[NASA-TM-106314] p 1169 N94-15818
Confinement and stability of a Crystal Beam
[DE93-015400] p 1181 N94-16020
Dynamics, stability, and control of maglev systems
[DE93-015163] p 1047 N94-16806
The stability of ions in a storage ring in the presence of small gap insertion devices
[DE93-015387] p 1184 N94-16828
Reference frames in vision
[AD-A266174] p 1132 N94-16925
Advanced transport systems for electron beams in high brightness accelerators and FELs
[AD-A267322] p 1041 N94-17001
STABILITY TESTS
Stability of flows in fluidized beds
[DE93-000245] p 1024 N94-16763
Stability analysis for the flow of granular materials down an inclined plane using kinetic model
[DE93-016852] p 1026 N94-16958
STABILIZATION
Densifying and stabilizing ingredient
[AD-D015751] p 975 N94-16934
TITUS: A micro-satellite for technology demonstration p 896 N94-17186
STABILIZERS (FLUID DYNAMICS)
Vertical-tail aerodynamic configuration of space shuttle orbiter
[AD-A267723] p 879 N94-14941
STAINLESS STEELS
The effect of aging at 343 C on the mechanical properties and microstructure of type 308 stainless steel weldments
[DE93-015454] p 957 N94-16103
Application of hard coatings to substrates at low temperatures
[NASA-CR-193867] p 971 N94-17122
Stress corrosion cracking of 316 SS and Incoloy-800 in high temperature aqueous containing sulfate and chloride
[DE93-623325] p 952 N94-17302

STANDARDIZATION
The development of flexible software for the Italian/Dutch satellite SAX: Advantages and disadvantages of the use of CASE tools
[NLR-TP-91288-U] p 1157 N94-17626
STANDARDS
The use of formal methods in data security standards
[NPL-DITC-205/92] p 1142 N94-15008
The value of reference implementations and prototyping in a formal design and testing methodology
[NPL-DITC-208/92] p 1142 N94-15011
The application of programming languages to the production of reference implementations
[NPL-DITC-209/92] p 1143 N94-15012
Standards and conformance testing in data security: Results of initial programme of investigation
[NPL-DITC-218/92] p 1143 N94-15014
Testability of data security standards
[NPL-DITC-217/93] p 1143 N94-15022
Development of a proposed international standard for certification of aircraft to High Intensity Radiated Fields (HIRF)
[NASA-TM-106357] p 863 N94-16520
CALS test network handbook
[AD-A267587] p 1160 N94-17209
Radar transmitter procedures
[AD-A268274] p 1005 N94-17523
STAR CLUSTERS
Statistical analysis of trigonometric parallaxes
[NASA-CR-194558] p 1172 N94-15641
STAR FORMATION
ROSAT-IUE observations of symbiotic stars. The x ray morphology of high latitude associations
[NASA-CR-194616] p 1236 N94-16492
Collisional dynamics of perturbed particle disks in the solar system
[NASA-CR-193584] p 1239 N94-16648
STAR TRACKERS
The Spacelab IPS Star Simulator
[TABES PAPER 93-650] p 877 N94-16150
Clementine: Anticipated scientific datasets from the Moon and Geographos p 1288 N94-16392
STATIC CHARACTERISTICS
Static and dynamic investigations of brittle elasto-optical material
[IFTR-3/1992] p 1061 N94-17086
Static characteristics of a conduction and radiation dominated electric arc in nitrogen
[DE93-627106] p 1204 N94-17311
STATIC PRESSURE
Wind tunnel investigation of three axisymmetric cowls of different lengths at Mach numbers from 0.60 to 0.92
[NASA-TM-4488] p 856 N94-15681
STATIC STABILITY
Development of a prototype kinestatic platform for application to space and ground servicing tasks. Phase 1: Concept Modeling
[NASA-CR-194036] p 887 N94-16905
STATIC TESTS
Aerodynamic control of NASP-type vehicles through Vortex manipulation. Volume 2: Static wind tunnel tests
[NASA-CR-177626-VOL-2] p 856 N94-15677
Effects of internal yaw-vectoring devices on the static performance of a pitch-vectoring nonaxisymmetric convergent-divergent nozzle
[NASA-TP-3369] p 858 N94-16572
STATISTICAL ANALYSIS
A posteriori error estimation for hierarchic models of elliptic boundary value problems on thin domains
[AD-A267714] p 1168 N94-14939
US civil airmen statistics: Calendar year 1992
[AD-A267708] p 853 N94-14965
Statistical computation of tolerance limits
[NASA-TM-108424] p 1172 N94-15535
Poisson filtering of laser ranging data
p 917 N94-15593
Statistical analysis of trigonometric parallaxes
[NASA-CR-194558] p 1172 N94-15641
A simplistic look at limit stresses from random loading
[NASA-TM-108427] p 1058 N94-15710
Higher order statistics in signal processing
[FFI-92/2008] p 989 N94-15714
Brightness temperature and attenuation statistics at 20.6 and 31.65 GHz p 996 N94-16045
Statistical techniques for study design of microgravity life sciences experiments p 980 N94-16094
Dust grain resonant capture: A statistical study
p 1245 N94-16384
Moving target indicator using higher order statistics
[AD-D015890] p 1000 N94-16917
The use of the Air Force Academy high wind alert system in forecasting moderate intensity wind events for military bases in the Colorado Springs area
[AD-A267648] p 1107 N94-17245
A Geographic Information System approach to modeling nutrient and sediment transport
[DE93-013747] p 1097 N94-17426
Statistics and physical oceanography
[AD-A268565] p 1115 N94-17598
STATISTICAL CORRELATION
Speckles statistics and decorrelation effects in complex ABCD optical systems
[AD-A267843] p 1193 N94-17012
STATISTICAL DISTRIBUTIONS
The MADONA experiments (Meteorology and Diffusion Over Non-uniform Areas): High-resolution in-plume concentration fluctuations measurements using lidar remote sensing technique
[AD-A267711] p 1105 N94-14938
Moments in statistics: Approximations to densities and goodness-of-fit
[AD-A266600] p 1173 N94-16726
Mean strain effects on the strain life fatigue curve
[AD-A267211] p 960 N94-16984
STATISTICAL TESTS
Formation of on-site normal points
p 917 N94-15592
Bounds on inconsistent inferences for sequences of trials with varying probabilities
[AD-A267146] p 1172 N94-15733
Moments in statistics: Approximations to densities and goodness-of-fit
[AD-A266600] p 1173 N94-16726
STATORS
Circle diagram approach for self excited induction generators
[DE93-010031] p 1010 N94-15971
STEADY FLOW
Study into the limits of an Euler equation method applied to leading-edge vortex flow
[NLR-TP-91350-U] p 1031 N94-17627
STEADY STATE
Logarithmic asymptotics for steady-state tail probabilities in a single-server queue
[AD-A266746] p 1165 N94-15775
Fast simulation of steady-state availability in non-Markovian highly dependable systems
[AD-A266747] p 1174 N94-15823
Evolutionary implications of a steady-state water abundance on Venus p 1254 N94-16206
High power steady state MPD thrusters
[AD-A267277] p 928 N94-17308
Static characteristics of a conduction and radiation dominated electric arc in nitrogen
[DE93-627106] p 1204 N94-17311
STEELS
The corrosion protection of metals by ion vapor deposited aluminum
[NASA-TM-108425] p 955 N94-15832
Measurement and theory of the dependence of hardness on residual stress
[AD-A267553] p 1061 N94-17105
Influence of grain size on the energy storing ability during uniaxial stretching of austenite steel
[IFTR-22/1992] p 961 N94-17121
The effect of electric discharge machined notches on the fracture toughness of several structural alloys
[AD-A268605] p 962 N94-17464
Evaluation of hybrid reinforcement (fiber-reinforced-plastic rod with steel core)
[AD-A268009] p 941 N94-17473
Environment enhanced fatigue crack propagation in metals: Inputs to fracture mechanics life prediction models
[NASA-CR-191538] p 942 N94-17638
STEEPEST DESCENT METHOD
Steepest descent approximations for accretive operator equations
[DE93-628586] p 1171 N94-17667
STEERING
Laser beam steering device p 1045 N94-17357
STELLAR ENVELOPES
X ray emission from Wolf-Rayet stars with recurrent dust formation
[NASA-CR-194567] p 1300 N94-15533
The chromosphere of VV cephei and the distribution of circumstellar dust around red giants and supergiants
[NASA-CR-193594] p 1297 N94-16866
STELLAR EVOLUTION
ROSAT-IUE observations of symbiotic stars. The x ray morphology of high latitude associations
[NASA-CR-194616] p 1236 N94-16492
STELLAR MASS ACCRETION
ROSAT-IUE observations of symbiotic stars. The x ray morphology of high latitude associations
[NASA-CR-194616] p 1236 N94-16492
Variability of the Seyfert galaxy MKN 766 in the Rosat all sky survey
[MPE-PREPRINT-221] p 1240 N94-17591
STELLAR PARALLAX
Statistical analysis of trigonometric parallaxes
[NASA-CR-194558] p 1172 N94-15641
STELLAR RADIATION
A comparison of calculated and observed monochromatic type Ia supernova light curves
[MPA-709] p 1237 N94-17629
STELLAR SYSTEMS
ROSAT-IUE observations of symbiotic stars. The x ray morphology of high latitude associations
[NASA-CR-194616] p 1236 N94-16492
STELLAR WINDS
The astrophysical interpretation of isotope anomalies in graphite and SiC grains of chondrites
p 1244 N94-16343
STELLARATORS
Nonlinear gyrofluid models of shear Alfven instabilities in ignited and beam heated toroidal plasmas
[DE93-016235] p 1203 N94-16869
STEPPING MOTORS
Tilt mechanism
[AD-D015780] p 1047 N94-16548
STEREOSCOPIC VISION
ARPA unmanned ground vehicle stereo vision program at Teleos Research
[AD-A267632] p 1167 N94-17202
Neural basis of motion perception
[AD-A267267] p 1133 N94-17265
STIRLING CYCLE
Proposed guidelines for reporting performance of a solar dish/Stirling electric generation system
[DE93-016493] p 1092 N94-16112
STIRLING ENGINES
SPDE/SPRE final summary report
[NASA-CR-187086] p 924 N94-15482
Proposed guidelines for reporting performance of a solar dish/Stirling electric generation system
[DE93-016493] p 1092 N94-16112
STOCHASTIC PROCESSES
Looking at Fokker-Planck dynamics with a noisy instrument
[AD-A267049] p 1117 N94-15662
Theoretical studies relating to the interaction of radiation with matter
[AD-A267134] p 1180 N94-15689
Segment-based acoustic models for continuous speech recognition
[AD-A267138] p 988 N94-15691
Stochastic scheduling in in-forest networks
[INRIA-RR-1719] p 1164 N94-15695
Efficient algorithmic techniques for combinatorial problems
[AD-A267151] p 1172 N94-15777
Generation of artificial helioseismic time-series
[NASA-CR-194612] p 1299 N94-15968
A novel approach for structural mechanics problems with stochasticity
[AD-A266189] p 1059 N94-16123
Interferometric GPS attitude: A stochastic error model, DREO report
[AD-A266411] p 864 N94-16457
Stochastic damage evolution in textile laminates
p 939 N94-16861
Nonlinear analysis of mechanical systems under combined harmonic and stochastic excitation
[AD-A266217] p 1173 N94-16937
Stochastic chaos: An analog of quantum chaos
[DE93-016619] p 1220 N94-16956
A handbook of cost risk analysis methods
[AD-A267253] p 1235 N94-16988
An approximation for computing reduction in bandwidth requirements using intelligent multiplexers
[AD-A267434] p 1001 N94-17026
Energy deposition fluctuations induced by ions in microvolumes and nanovolumes: An analytic approach. 1: Theory
[AD-A267959] p 1173 N94-17495
Stochastic scheduling in a multiclass G/G/1 queue
[INRIA-RR-1746] p 1162 N94-17537
State space partitioning methods for solving a class of stochastic network problems
[AD-A267494] p 1173 N94-17585
STOICHIOMETRY
MeV ion-beam analysis of optical data storage films
p 1226 N94-14984
Scintillation mechanism in stoichiometric cerium compounds
[DE93-015499] p 948 N94-16771
Transient phenomena following precipitation and re-solution anneals in a NiTi alloy
[AD-A267557] p 961 N94-17106
STONY METEORITES
Size distribution of interplanetary iron and stony particles related with deep-sea spherules p 1245 N94-16388

STONY-IRON METEORITES
Experimental segregation of iron-nickel metal, iron-sulfide, and olivine in a thermal gradient: Preliminary results p 1243 N94-16288
STORAGE BATTERIES
In situ Raman spectroscopy of lithium electrode surface in ambient temperature lithium secondary battery [DE93-015238] p 1010 N94-16061
Field investigation of the relationship between battery size and PV system performance [DE93-016503] p 1016 N94-17671
STORAGE RINGS (PARTICLE ACCELERATORS)
Fundamental-mode RF design in e(+)e(-) storage ring factories [DE93-015249] p 1183 N94-16809
The stability of ions in a storage ring in the presence of small gap insertion devices [DE93-015387] p 1184 N94-16828
STORAGE STABILITY
Efficacy of flocculating and other emergency water purification tablets [AD-A266695] p 1148 N94-15840
Lithium D-cell study [NASA-CR-192705] p 1011 N94-16505
STORAGE TANKS
Ground testing for the no-vent fill of cryogenic tanks: Results of tests for a 71 cubic foot tank [NASA-TM-106293] p 1030 N94-17486
Environmental use of a Laser Range Finder and the Advanced Visualization System [DE93-016163] p 1043 N94-17677
STORMS
Orographic microbursts in a severe winter windstorm [AD-A267651] p 1108 N94-17247
Propagation characteristics of mesoscale convective systems [AD-A268130] p 1109 N94-17522
STOVL AIRCRAFT
The lift-fan powered-lift aircraft concept: Lessons learned [NASA-CR-177616] p 866 N94-15718
Lift-fan aircraft: Lessons learned-the pilot's perspective [NASA-CR-177620] p 867 N94-15950
STRAIN DISTRIBUTION
J-integral and HRR field associated with stable crack growth in thin aluminum SEN specimen [AD-A267879] p 960 N94-17041
Damage evolution in filled elastomers [AD-A268067] p 1062 N94-17507
STRAIN ENERGY RELEASE RATE
J-integral and HRR field associated with stable crack growth in thin aluminum SEN specimen [AD-A267879] p 960 N94-17041
STRAIN GAGE BALANCES
Monopiece strain gauge sting mounted wind tunnel balance [CA-PATENT-1-311-626] p 1032 N94-15697
STRAIN GAGES
Use of photostress and strain gages to analyze behavior of weldments and use of photostress and strain gages to analyze behavior of an aft skirt test specimen [NASA-CR-194575] p 1058 N94-15716
Simultaneous measurement of temperature and strain using four connecting wires [NASA-TM-104271] p 1032 N94-15754
Automated strain gauge plethysmograph [AD-A267323] p 1035 N94-17002
STRAIN HARDENING
The effect of oxygen, grain size, and strain rate on the mechanical behavior of forged P/M tantalum [DE93-011251] p 959 N94-16764
Fatigue life program using strain-life methods [AD-A267310] p 1060 N94-16943
STRAIN MEASUREMENT
Report of the International Center for Earth Tides for the period 1985-1989 p 1099 N94-15801
Cooperative projects in geodynamical instrumentation between the State Seismological Bureau (China) and the Royal Observatory of Belgium p 1037 N94-15806
Earth tides results obtained with gravimeters, clinometers, and strainmeters in Belgium and in Grand Duchy of Luxembourg p 1100 N94-15809
Damage evolution in filled elastomers [AD-A268067] p 1062 N94-17507
The photonical, pure grid method [NLR-TP-91478-U] p 1062 N94-17600
STRAIN RATE
Rheology of water and ammonia-water ices p 953 N94-16188
Experimental study of nonassociated flow and instability of frictional materials [AD-A266421] p 1024 N94-16555
The effect of oxygen, grain size, and strain rate on the mechanical behavior of forged P/M tantalum [DE93-011251] p 959 N94-16764
Creep ductility of iron at very low strain rates: The effects of sulfur [DE93-015490] p 959 N94-16890
Time dependent turbulence modeling and analytical theories of turbulence [NASA-TM-106379] p 1029 N94-17385
Tensiie and stress-rupture behavior of hafnium carbide dispersed molybdenum and tungsten base alloy wires [NASA-TM-106350] p 962 N94-17652
Shear wave measurements in shock-induced, high-pressure phases [DE93-016461] p 1062 N94-17664
STRAKES
Wind tunnel investigations of forebody strakes for yaw control on F/A-18 model at subsonic and transonic speeds [NASA-TP-3360] p 859 N94-16573
STRANGENESS
Fast pulsars, compact stars, and the strange matter hypothesis [DE93-015039] p 1239 N94-16052
STRAPDOWN INERTIAL GUIDANCE
Analysis of the accuracy of strapdown inertial surveying systems [SER-C-391] p 1081 N94-15156
STRATIFICATION
Subwavelength structured surfaces and their applications p 1194 N94-17337
STRATIFIED FLOW
Surface and internal signatures of organized vortex motions in stratified fluid [AD-A267015] p 1020 N94-15526
STRATIGRAPHY
Rover mounted ground penetrating radar as a tool for investigating the near-surface of Mars and beyong p 1007 N94-16197
Remote sensing studies of the northeastern portion of the lunar nearside p 1258 N94-16225
Geochemical evidences for two chondritic-like cometary or asteroidal impacts before and at the K/T boundary p 1244 N94-16359
STRATOSPHERE
Middle atmospheric electric fields over thunderstorms [NASA-CR-194619] p 1106 N94-16493
STRATOSPHERIC WARMING
Investigate wave-mean flow interaction and transport in the extratropical winter stratosphere [NASA-CR-194555] p 1098 N94-15639
STREAK CAMERAS
Streak camera based SLR receiver for two color atmospheric measurements p 914 N94-15573
The first satellite laser echoes recorded on the streak camera p 914 N94-15574
Test results from LAGEOS-2 optical characterization using pulsed lasers p 915 N94-15577
Two color satellite laser ranging upgrades at Goddard's 1.2m telescope facility p 915 N94-15581
Two wavelength satellite laser ranging using SPAD p 916 N94-15584
New perspectives for high accuracy SLR with second generation geodesic satellites p 916 N94-15585
Station report on the Goddard Space Flight Center (GSFC) 1.2 meter telescope facility p 922 N94-15625
STRESS (BIOLOGY)
Programs and resources for control of job stress in the Federal workplace p 1124 N94-16617
STRESS (PHYSIOLOGY)
Sleep management user's guide for special operations personnel [AD-A267746] p 1119 N94-14943
Activity/rest patterns of instructor and rates student pilots during rapid transitions from daytime to nighttime duty hours at the Eastern Army Aviation Training site [AD-A267038] p 1131 N94-15659
Programs and resources for control of job stress in the Federal workplace p 1124 N94-16617
STRESS (PSYCHOLOGY)
Scuba-diving, anxiety and task performance p 1132 N94-15938
Programs and resources for control of job stress in the Federal workplace p 1124 N94-16617
STRESS ANALYSIS
Construction and calculation p 931 N94-15256
High temperature advanced structural composites. Volume 3: Mechanics [AD-A267024] p 933 N94-15626
A simplistic look at limit stresses from random loading [NASA-TM-108427] p 1058 N94-15710
Continuous fabrication of SiC fiber tows by chemical vapor deposition [AD-A266460] p 936 N94-16569
Programs and resources for control of job stress in the Federal workplace p 1124 N94-16617
Elastooptical brittle materials in experimental studies of the state of stress and deformation [IFTR-22/1991] p 1059 N94-16651
Stress analysis of laminated composites with preformed holes. Part 1: Single plies with embedded material discontinuities [AD-A266524] p 936 N94-16795
Creep ductility of iron at very low strain rates: The effects of sulfur [DE93-015490] p 959 N94-16890
Static analysis of beams on an elastic base as stated by generalized functions [IFTR-27/1991] p 1060 N94-16923
Mean strain effects on the strain life fatigue curve [AD-A267211] p 960 N94-16984
Surface waves in an inhomogeneous, isotropic, elastic half-space [IFTR-18/1991] p 1060 N94-17047
Analysis of the strengthening of aluminum alloy undergoing plastic deformation under conditions of a compound state of stress [IFTR-21/1991] p 960 N94-17093
A review of Australian and New Zealand investigations on aeronautical fatigue during the period April 1991 to March 1993 [AD-A267532] p 868 N94-17117
Elastic-plastic finite-difference analysis of unidirectional composites subjected to thermomechanical cyclic loading [AD-A267666] p 1061 N94-17269
Solution of elastic-plastic stress analysis problems by the p-version of the finite element method [NASA-CR-194267] p 1062 N94-17445
STRESS CONCENTRATION
ITER-HARD Toroidal Field coil structural analysis [DE93-014834] p 1201 N94-15981
Fatigue life program using strain-life methods [AD-A267310] p 1060 N94-16943
STRESS CORROSION CRACKING
Environmental effects on elevated temperature subcritical crack growth of SiC/SiC composites [DE93-015688] p 934 N94-16158
Stress corrosion cracking of 316 SS and Incoloy-800 in high temperature aqueous containing sulfate and chloride [DE93-623325] p 952 N94-17302
Environment enhanced fatigue crack propagation in metals: Inputs to fracture mechanics life prediction models [NASA-CR-191538] p 942 N94-17638
STRESS DISTRIBUTION
Thermal stresses of a trimaterial medium in a nonuniform temperature field [AD-A267243] p 930 N94-14975
Spatially extensive uniform stress fields on Venus inferred from radial dike swarm geometries: The Aphrodite Terra example p 1254 N94-16207
Highly transient elastodynamic crack growth in a bimaterial interface: Higher order asymptotic analysis and optical experiments [AD-A266465] p 1059 N94-16587
Static analysis of beams on an elastic base as stated by generalized functions [IFTR-27/1991] p 1060 N94-16923
High temperature materials technology research for advanced thermionic systems [DE93-018302] p 960 N94-16964
Measurement and theory of the dependence of hardness on residual stress [AD-A267553] p 1061 N94-17105
Elastic-plastic finite-difference analysis of unidirectional composites subjected to thermomechanical cyclic loading [AD-A267666] p 1061 N94-17269
STRESS INTENSITY FACTORS
Environmental effects on elevated temperature subcritical crack growth of SiC/SiC composites [DE93-015688] p 934 N94-16158
Environment enhanced fatigue crack propagation in metals: Inputs to fracture mechanics life prediction models [NASA-CR-191538] p 942 N94-17638
STRESS MEASUREMENT
Thermal stress effects in intermetallic matrix composites [NASA-CR-191191] p 1054 N94-16518
The processing and mechanical properties of high temperature/high performance composites. Book 5: Processing and miscellaneous properties [AD-A266398] p 935 N94-16529
Shear wave measurements in shock-induced, high-pressure phases [DE93-016461] p 1062 N94-17664
STRESS RELAXATION
On the design of structural components using materials with time-dependent properties [NASA-TM-108428] p 1059 N94-16519

STRESS TENSORS
Systematology for elastic-plastic material equations by large deformations on the basis of the Cosserat-continuum model
[SCHRIFTENR-PHYSIKAL-ING-BD] p 1058 N94-15642

STRESS-STRAIN RELATIONSHIPS
Forced harmonic vibration of the generally orthotropic cylindrical shell with inner and outer fluid loading
[AD-A266985] p 1057 N94-15150
Systematology for elastic-plastic material equations by large deformations on the basis of the Cosserat-continuum model
[SCHRIFTENR-PHYSIKAL-ING-BD] p 1058 N94-15642
Experimental study of nonassociated flow and instability of frictional materials
[AD-A266421] p 1024 N94-16555
Effect of tow alignment on the mechanical performance of 3D woven textile composites p 937 N94-16851
Fatigue life program using strain-life methods
[AD-A267310] p 1060 N94-16943
Mean strain effects on the strain life fatigue curve
[AD-A267211] p 960 N94-16984
Quantitative assessment of the accuracy of constitutive laws for plasticity with an emphasis on cyclic deformation
[AD-A267562] p 961 N94-17109
Aspects of high temperature damage in fiber reinforced titanium metal matrix composites
[AD-A267907] p 941 N94-17379
The effect of electric discharge machined notches on the fracture toughness of several structural alloys
[AD-A268605] p 962 N94-17464
Damage evolution in filled elastomers
[AD-A268067] p 1062 N94-17507

STRESSES
A model for non-linear creep and physical ageing in PVC
[NPL-DMM(A)-91] p 1057 N94-15016
Stress sensitivity of dielectric resonators
[AD-A266767] p 1009 N94-15825

STRETCHING
Influence of grain size on the energy storing ability during uniaxial stretching of austenite steel
[IFTR-22/1992] p 961 N94-17121

STRING THEORY
Theoretical high energy physics research at the University of Chicago
[DE93-016863] p 1187 N94-16116
Particle physics and cosmology, Task C
[DE93-016865] p 1239 N94-16118

STRINGS
Testing string superprimitivity in parallel
[AD-A267814] p 1155 N94-17399

STRIP TRANSMISSION LINES
Determination of equivalent circuit for PVDF shock-pressure gauges
[DE93-016492] p 1034 N94-16452

STROBOSCOPES
Channel of the system for pulse charged particle beam diagnostics
[DE93-623867] p 1179 N94-14931

STRONG INTERACTIONS (FIELD THEORY)
The quantum mass shift of the soliton in Skyrme model
[ITN-93-85219] p 1180 N94-15283

STRONTIUM COMPOUNDS
An improved light source for laser ranging p 913 N94-15567

STRONTIUM OXIDES
Method of producing a silicon carbide fiber reinforced strontium aluminosilicate glass-ceramic matrix composite
[NASA-CASE-LEW-15263-2] p 934 N94-15929

STRUCTURAL ANALYSIS
An assessment of finite-element modeling techniques for thick-solid/thin-shell joints analysis
[NASA-TM-108426] p 1058 N94-15534
Structural investigation of electrochemically etched silicon
[DE93-015300] p 1207 N94-15827
Parallel processing and scientific applications
[AD-A267179] p 1159 N94-15849
ITER-HARD Toroidal Field coil structural analysis
[DE93-014834] p 1201 N94-15981
The design and analysis of a modular microgravity test platform for use aboard the NASA KC-135 aircraft p 899 N94-16101
A novel approach for structural mechanics problems with stochasticity
[AD-A266189] p 1059 N94-16123
On the design of structural components using materials with time-dependent properties
[NASA-TM-108428] p 1059 N94-16519
Evaluation of hemoglobin-oxygen equilibrium binding by rapid-scanning spectrophotometry and singular-value decomposition
[AD-A266453] p 1123 N94-16564
ASTROS enhancements. Volume 1: ASTRO user's manual
[AD-A266818] p 1151 N94-16768
ASTROS enhancements. Volume 2: ASTRO programmer's manual
[AD-A266819] p 1151 N94-16769
Quantification of processing artifacts in textile composites p 939 N94-16860
Three-dimensional analysis of anisotropic spatially reinforced structures p 939 N94-16863
Finite element analysis of structural engineering problems using a viscoplastic model incorporating two back stresses
[NASA-TM-106046] p 1060 N94-16881
Static analysis of beams on an elastic base as stated by generalized functions
[IFTR-27/1991] p 1060 N94-16923
Superconducting ceramics: Selected properties and methods of production
[IFTR-23/1991] p 969 N94-16924
Modeling, estimation and control of distributed parameter systems
[AD-A267325] p 1026 N94-17003
Structure of high Reynolds number turbulent boundary layer
[AD-A267476] p 860 N94-17099
Design of a fluid elastic actuator with application to structure control
[AD-A267649] p 897 N94-17246
Structural mechanics division research and technology accomplishments for CY 1992 and plans for CY 1993
[NASA-TM-107752] p 1062 N94-17479

STRUCTURAL BASINS
Similarity and scale in catchment storm response
[PAPER-89RG01615] p 1083 N94-16028
Evaluation of a distributed catchment scale water balance model
[PAPER-93WR00398] p 1083 N94-16031
Martian crater degradation by eolian processes: Analogy with the Rio Cuarto Crater Field, Argentina p 1251 N94-16196
Lunar impact basins: New data for the nearside northern high latitudes and eastern limb from the second Galileo flyby p 1258 N94-16228
Modes of formation of lunar light plains and the detection of cryptomaria deposits p 1259 N94-16231
Hellas basin, Mars: Formation by oblique impact p 1280 N94-16350

STRUCTURAL DESIGN
Processing and protection of high temperature structural materials
[AD-A267292] p 954 N94-14961
Minimum accommodation for aerobrake assembly. Phase 2: Structural concepts for a lunar transfer vehicle aerobrake which can be assembled on orbit
[NASA-TM-107610] p 885 N94-15446
Helicopter structures: A review of loads, fatigue design techniques, and usage monitoring
[AD-A267115] p 866 N94-15651
Recent advances in ordered intermetallics
[DE93-015308] p 955 N94-15862
Hoph bifurcation in viscous, low speed flows about an airfoil with structural coupling
[AD-A266542] p 859 N94-16798
Optimal tuning of heavy equipment motion controllers
[AD-A267873] p 1167 N94-17392
The effect of electric discharge machined notches on the fracture toughness of several structural alloys
[AD-A268605] p 962 N94-17464
Structural mechanics division research and technology accomplishments for CY 1992 and plans for CY 1993
[NASA-TM-107752] p 1062 N94-17479
X ray computed tomography for casting demonstration
[AD-A268084] p 1056 N94-17596
Nonlinear random response prediction using MSC/NASTRAN
[NASA-TM-109029] p 1179 N94-17650

STRUCTURAL ENGINEERING
Design Quality Task Force survey comments
[AD-A266283] p 1225 N94-16473
Finite element analysis of structural engineering problems using a viscoplastic model incorporating two back stresses
[NASA-TM-106046] p 1060 N94-16881

STRUCTURAL FAILURE
Influence of the loading rate on the endurance and deformability of cement matrix composites
[IFTR-1/1992] p 1060 N94-17052

STRUCTURAL PROPERTIES (GEOLOGY)
Importance of expansion and contraction in the formation of tectonic features on the Moon p 1250 N94-16189
Structural mapping of Maxwell Montes p 1271 N94-16304
Was Martian mantle wet? A possible consequence of rapid core formation p 1277 N94-16335

STRUCTURAL RELIABILITY
The Ceramic Technology Project: Ten years of progress
[DE93-015991] p 968 N94-16843
Overview of the FAA/DCA/NLR programs related to ageing aircraft
[NLR-TR-92119-U] p 854 N94-17614

STRUCTURAL STABILITY
The stability and dynamics of elastic structures and fluid flows
[AD-A267990] p 1029 N94-17414

STRUCTURAL STRAIN
A review of Australian and New Zealand investigations on aeronautical fatigue during the period April 1991 to March 1993
[AD-A267532] p 868 N94-17117

STRUCTURAL VIBRATION
Vibro-acoustic analysis of an aircraft maintenance dock
[AD-A266778] p 871 N94-14908
Forced harmonic vibration of the generally orthotropic cylindrical shell with inner and outer fluid loading
[AD-A266985] p 1057 N94-15150
In-flight investigation of a rotating cylinder-based structural excitation system for flutter testing
[NASA-TM-4512] p 867 N94-15783
Hoph bifurcation in viscous, low speed flows about an airfoil with structural coupling
[AD-A266542] p 859 N94-16798
A comparative study of analog and digital control laws for the UMCSL truss
[AD-A267980] p 871 N94-17412
A mechanical system damping measurement technique using a one-degree-of-freedom (1DOF) cylindrical gas bearing
[AD-A268402] p 1048 N94-17462

STUDENTS
US civil airmen statistics: Calendar year 1992
[AD-A267708] p 853 N94-14965
Developments in the Higher Technical Aerospace Education p 854 N94-15130
Student researchers
[NASA-TM-109441] p 1221 N94-15340
STS-29 crew with student experiment
[NASA-TM-109545] p 1116 N94-15378
Questioning mechanisms during tutoring, conversation, and human-computer interaction
[AD-A266199] p 1137 N94-16108
Spaceship Earth: A partnership in curriculum writing p 1222 N94-16356
From the Moons of Jupiter to the Milky Way
[NASA-CR-194649] p 1240 N94-17059

SUBDUCTION (GEOLOGY)
Chemical differentiation, thermal evolution, and catastrophic overturn on Venus: Predictions and geologic observations p 1259 N94-16232
Estimates of lithospheric thickness on Venus p 1267 N94-16277
Models of thermal/chemical boundary layer convection: Potential application to Venus p 1279 N94-16348

SUBLETHAL DOSAGE
The relationship of metallothionein induction to the heat shock response
[AD-A266634] p 1122 N94-15741

SUBLIMATION
Thermal inertia and radar reflectivity of the Martian north polar ERG: Low-density aggregates p 1260 N94-16238
Equatorial ground ice on Mars: Steady-state stability p 1290 N94-16403

SUBLIMINAL STIMULI
States of awareness 1: Subliminal perception relationship to situational awareness
[AD-A267249] p 1132 N94-16942

SUBMERGED BODIES
Surface and internal signatures of organized vortex motions in stratified fluid
[AD-A267015] p 1020 N94-15526

SUBMILLIMETER WAVES
Submillimeterwave SIS mixer developments p 903 N94-15054
Hot electron mixers, the potential competition p 903 N94-15055
Submm/FIR bolometers p 904 N94-15056
Optically-switched submillimeter-wave oscillator and radiator
[NASA-CASE-NPO-18547-1-CU] p 1014 N94-17324

SUBORBITAL FLIGHT
Astronauts number 2
[NASA-TM-109429] p 873 N94-15500

SUBROUTINE LIBRARIES (COMPUTERS)
Intel NX to PVM 3.2 message passing conversion library
[NASA-TM-109038] p 1152 N94-17060
SUBROUTINES
Mobile and replicated alignment of arrays in data-parallel programs
[NASA-CR-194294] p 1158 N94-15113
Mechanistic models of soot formation
[AD-A267806] p 950 N94-17008
Intel NX to PVM 3.2 message passing conversion library
[NASA-TM-109038] p 1152 N94-17060
SUBSONIC AIRCRAFT
Subsonic aerodynamic characteristics of the HL-20 lifting-body configuration
[NASA-TM-4515] p 861 N94-17284
SUBSONIC FLOW
Effect of wind tunnel acoustic modes on linear oscillating cascade aerodynamics
[NASA-TM-106367] p 869 N94-15866
On solving the compressible Navier-Stokes equations for unsteady flows at very low Mach numbers
[NASA-TM-106380] p 1027 N94-17128
Study into the limits of an Euler equation method applied to leading-edge vortex flow
[NLR-TP-91350-U] p 1031 N94-17627
SUBSONIC SPEED
Wind tunnel investigation of three axisymmetric cowls of different lengths at Mach numbers from 0.60 to 0.92
[NASA-TM-4488] p 856 N94-15681
Flow analysis for the nacelle of an advanced ducted propeller at high angle-of-attack and at cruise with boundary layer control
[NASA-TM-106371] p 858 N94-16571
Wind tunnel investigations of forebody strakes for yaw control on F/A-18 model at subsonic and transonic speeds
[NASA-TP-3360] p 859 N94-16573
Wind-tunnel investigation of aerodynamic efficiency of three planar elliptical wings with curvature of quarter-chord line
[NASA-TP-3359] p 859 N94-16574
SUBSONIC WIND TUNNELS
Determining the effect of endwall boundary layer suction in a large scale subsonic compressor cascade
[AD-A267208] p 859 N94-16913
User's manual for the Langley Research Center 14- by 22- foot subsonic tunnel static data acquisition system
[NASA-TM-109027] p 861 N94-17639
SUBSTITUTES
Prioritization methodology for chemical replacement
[NASA-TP-3421] p 976 N94-15723
SUBSTRATES
Substrate effects in superconducting tunnel junction detectors p 908 N94-15083
Selective formation of porous silicon
[NASA-CASE-NPO-18735-1-CU] p 966 N94-15960
Polished substrate surface and cleaning study for coated optic quality
[DE93-014116] p 1190 N94-15975
Ablation, surface activation, and electroless metallization of insulating materials by pulsed excimer laser irradiation
[DE93-015808] p 1040 N94-16664
Materials processing and manufacturing technologies for diamond substrate multichip modules (DSMCM)
[AD-A267316] p 969 N94-16946
Single crystal diamond thin films
[AD-A266457] p 1214 N94-17216
Growth, characterization and device development in monocrystalline diamond films
[AD-A268206] p 1216 N94-17553
SUCROSE
Contained liquids in microgravity, part 2
p 979 N94-16085
SUCTION
Determining the effect of endwall boundary layer suction in a large scale subsonic compressor cascade
[AD-A267208] p 859 N94-16913
SUITS
Cool suit
[NASA-TM-109639] p 1120 N94-15250
SULFATES
Stress corrosion cracking of 316 SS and Incoloy-800 in high temperature aqueous containing sulfate and chloride
[DE93-623325] p 952 N94-17302
SULFIDATION
Development and commercialization status of Fe3Al-based intermetallic alloys
[DE93-015802] p 957 N94-16165
Vanadium corrosion studies
[AD-A266489] p 959 N94-16781
SULFUR
Creep ductility of iron at very low strain rates: The effects of sulfur
[DE93-015490] p 959 N94-16890
Synthesis, reactivity, and characterization of (-hexacarbocyclic) manganese dicarbonyl complexes with sulfur and phosphorus ligands
[AD-A267592] p 930 N94-17192
SULFUR DIOXIDES
The use of TIMS data to estimate the SO2 concentrations of volcanic plumes: A case study at Mount Etna, Sicily p 1065 N94-16608
SULFUR HEXAFLUORIDE
Field-emitter arrays for RF vacuum microelectronics
[AD-A268397] p 1015 N94-17526
SULFURIC ACID
Investigations into the recovery of waste sulfuric acid with concentrated solar radiation
[DLR-FB-93-11] p 952 N94-17594
SUN
Unmasking the Sun
[NASA-TM-109595] p 1298 N94-15287
SUNLIGHT
Effects of levitated dust on astronomical observations from the lunar surface p 1239 N94-16433
SUPERCOMPUTERS
Parallel processing and scientific applications
[AD-A267179] p 1159 N94-15849
Requirements for supercomputing in energy research: The transition to massively parallel computing
[DE93-012376] p 1160 N94-16774
ONRASIA scientific information bulletin, volume 18, number 2
[AD-A267798] p 1304 N94-17305
Benchmarking massively parallel architectures
[DE93-016486] p 1162 N94-17646
SUPERCONDUCTING DEVICES
Substrate effects in superconducting tunnel junction detectors p 908 N94-15083
A multilayered approach to superconducting tunnel junction x ray detectors p 908 N94-15089
Nontidal gravity changes observed with a superconducting gravimeter p 1100 N94-15808
SUPERCONDUCTING FILMS
High temperature superconductivity
[AD-A267006] p 1008 N94-15635
Local environment about O atoms in Pr-Y-Ba-Cu-O films studied by O K-edge XAFS
[DE93-016218] p 1209 N94-16447
Advanced thin-film deposition and physical properties of high-temperature and other novel superconducting materials
[AD-A268199] p 1216 N94-17561
SUPERCONDUCTING MAGNETS
Superconductive material and magnetic field for damping and levitation support and damping of cryogenic instruments
[NASA-CASE-NPO-18458-1-CU] p 1033 N94-15875
Engineering design of a high-temperature superconductor current lead
[DE93-015156] p 1013 N94-17226
The inverse problem to the evaluation of magnetic fields
[DE93-015239] p 1175 N94-17288
SUPERCONDUCTING SUPER COLLIDER
The (delta)f algorithm for beam dynamics
[DE93-015632] p 1187 N94-16660
Statistics of the half-integer stopband
[DE93-016101] p 1173 N94-17236
SUPERCONDUCTIVITY
Experimental investigations of superconductivity in quasi-two-dimensional epitaxial copper oxide superlattices and trilayers
[DE93-015306] p 1207 N94-15829
Superconductive material and magnetic field for damping and levitation support and damping of cryogenic instruments
[NASA-CASE-NPO-18458-1-CU] p 1033 N94-15875
Fullerene superconductors
[AD-A266749] p 1010 N94-15954
Theoretical high energy physics
[DE93-015884] p 1187 N94-16170
Structural phase transition and superconductivity in La(2-x)Ba(x)CuO4
[DE93-015812] p 1212 N94-16868
Superconducting ceramics: Selected properties and methods of production
[IFTR-23/1991] p 969 N94-16924
A modified two-fluid model of conductivity for superconducting surface resistance calculation
[AD-A267549] p 1013 N94-17104
Basic optical studies of high T(c) oxide superconductors
[AD-A268148] p 1014 N94-17428
High temperature deformation behavior of YBa2Cu3O(6+x) superconducting ceramic materials
[AD-A268164] p 973 N94-17430
SUPERCONDUCTORS
A new approach to optical photon detection
p 899 N94-15028
Superconductive x ray photon detectors
p 900 N94-15031
Metastable superconductors as photon detectors
p 900 N94-15032
Hot electron mixers, the potential competition
p 903 N94-15055
Quasiparticle trapping in distributed superconducting three-terminal tunnel junction devices
p 910 N94-15101
Fullerene superconductors
[AD-A266749] p 1010 N94-15954
Density of states and tunneling characteristics of layered superconductors
[DE93-015898] p 1211 N94-16839
SUPERCRITICAL FLUIDS
Extraction and isotopic analysis of medium molecular weight hydrocarbons from Murchison using supercritical carbon dioxide p 1241 N94-16184
Removal of carbonaceous contaminants from silica aerogel p 953 N94-16256
Supercritical thermodynamics of sulfur and nitrogen species
[DE93-017727] p 1220 N94-16997
SUPERCRITICAL PRESSURES
Removal of carbonaceous contaminants from silica aerogel p 953 N94-16256
SUPERCRITICAL WINGS
Physical properties of the benchmark models program supercritical wing
[NASA-TM-4457] p 866 N94-15722
SUPERGIANT STARS
The chromosphere of VV cephei and the distribution of circumstellar dust around red giants and supergiants
[NASA-CR-193594] p 1297 N94-16866
SUPERHEATING
Explosive boiling at very low heat fluxes: A microgravity phenomenon
[NASA-TM-106325] p 1046 N94-15817
SUPERHIGH FREQUENCIES
Johnson-Gierhart program predictions of excess propagation loss for super-high frequency air-to-ground paths. Volume 1: Theory and numerical results
[AD-A267105] p 988 N94-15649
X-SAR: The X-band synthetic aperture radar on board the Space Shuttle p 990 N94-15891
High resolution SAR applications and instrument design p 993 N94-15913
Data acquisition, preprocessing and analysis for the Virginia Tech OLYMPUS experiment
p 995 N94-16038
The ACTS propagation program p 995 N94-16039
SUPERLATTICES
Magneto-optic superlattice thin films: Fabrication, structural and magnetic characterization
p 974 N94-14982
A multilayered approach to superconducting tunnel junction x ray detectors p 908 N94-15089
Design, synthesis and characterization of novel nonlinear optical polymers
[AD-A267035] p 964 N94-15675
Experimental investigations of superconductivity in quasi-two-dimensional epitaxial copper oxide superlattices and trilayers
[DE93-015306] p 1207 N94-15829
The growth of InAs(1-x)Sb(x)/InAs strained-layer superlattices by metal-organic chemical vapor deposition
[DE93-015028] p 1208 N94-16012
Interfacial structure of lattice mismatched bcc(110)/bcc(110) transition metal superlattices
[DE93-015162] p 1208 N94-16058
Rational design, construction, and processing of high-performance nonlinear optical materials
[AD-A266185] p 1191 N94-16454
Microstructure of Zr3Al after 2 MeV proton bombardment
[DE93-015331] p 1211 N94-16814
Neutron and x ray scattering studies of (FeF2)(sub m)(CoF2)(sub n) multilayers
[DE93-015809] p 1184 N94-16838
Pseudomorphic semiconducting heterostructures from combinations of AlN, GaN and selected SiC polytypes: Theoretical advancement and its coordination with experimental studies of nucleation, growth, characterization and device deployment
[AD-A267561] p 1213 N94-17108
Characterization of metallic multilayers using x ray diffraction analysis
[NIAR-93-13] p 961 N94-17282

Precise flux control for lattice matched superlattice materials
[AD-A268254] p 1215 N94-17417
Mechanical properties of interfaces and superlattices
[AD-A268591] p 1217 N94-17606

SUPERNOVA REMNANTS
A comparison of calculated and observed monochromatic type Ia supernova light curves
[MPA-709] p 1237 N94-17629

SUPERNOVAE
A comparison of calculated and observed monochromatic type Ia supernova light curves
[MPA-709] p 1237 N94-17629

SUPERPLASTICITY
High temperature deformation behavior of YBa2Cu3O(6+x) superconducting ceramic materials
[AD-A268164] p 973 N94-17430

SUPERSONIC BOUNDARY LAYERS
Incorporation of boundary layer heating predictive methodology into NSWCDD aeroprediction code
[AD-A267000] p 1020 N94-15632
The structure of turbulent boundary layers and shock wave boundary layer interactions
[AD-A268240] p 1026 N94-16929

SUPERSONIC COMBUSTION
Supersonic Combustion Research Laboratory. Volume 1: Design and fabrication
[AD-A267667] p 943 N94-14962
Studies on nonequilibrium phenomena in supersonic chemically reacting flows
[NASA-CR-194662] p 1027 N94-17215
Chemical reactions in turbulent mixing flows
[AD-A268287] p 861 N94-17580

SUPERSONIC COMBUSTION RAMJET ENGINES
Flight testing of airbreathing hypersonic vehicles
[NASA-TM-4524] p 886 N94-15753

SUPERSONIC FLOW
Advanced methods for cascade testing
[AGARD-AG-328] p 1016 N94-15119
Special course on Shock-Wave/Boundary-Layer Interactions in Supersonic and Hypersonic Flows
[AGARD-R-792] p 1017 N94-15196
Swept shock wave/laminar boundary layer interactions, experimental, and numerical results
p 1017 N94-15198
Unsteady phenomena in shock wave/boundary layer interaction p 1017 N94-15200
Contribution of laser Doppler velocimetry to the physical description of shock wave/turbulent boundary layer interactions with incidence on turbulence modelling
p 1018 N94-15201
On the interaction between the shock wave attached to a wedge and freestream disturbances
[NASA-CR-191528] p 1019 N94-15478
Numerical investigations in three-dimensional internal flows
[NASA-CR-194594] p 1020 N94-15551
Numerical solution of SUPG finite-element method for supersonic viscous flow
[AD-A267762] p 860 N94-17222
Supersonic flow visualization of a nacelle in close proximity to a simulated wing
[NASA-CR-194675] p 860 N94-17260
Single block three-dimensional volume grids about complex aerodynamic vehicles
[NASA-TM-108986] p 1030 N94-17476
Thin-layer and full Navier-Stokes calculations for turbulent supersonic flow over a cone at an angle of attack
[NASA-CR-189103] p 861 N94-17558
An investigation of oblique shock/boundary layer interaction control
[AD-A268106] p 861 N94-17574
Laser velocimetry measurements of vortex flows on a delta wing at Mach 1.9
[AD-A268596] p 861 N94-17609

SUPERSONIC FLUTTER
Aerothermoelastic analysis of a NASP demonstrator model
[NASA-TM-109007] p 867 N94-17055

SUPERSONIC INLETS
Numerical investigations in three-dimensional internal flows
[NASA-CR-194594] p 1020 N94-15551

SUPERSONIC NOZZLES
Shock-free supersonic elliptic nozzles and method of forming same
[NASA-CASE-LAR-14054-1] p 925 N94-15947
Studies on nonequilibrium phenomena in supersonic chemically reacting flows
[NASA-CR-194662] p 1027 N94-17215

SUPERSONIC SPEED
Development of a quiet supersonic wind tunnel with a cryogenic adaptive nozzle
[NASA-CR-194548] p 871 N94-15117

SUPERSONIC WIND TUNNELS
Supersonic Combustion Research Laboratory. Volume 1: Design and fabrication
[AD-A267667] p 943 N94-14962
Development of a quiet supersonic wind tunnel with a cryogenic adaptive nozzle
[NASA-CR-194548] p 871 N94-15117

SUPERSYMMETRY
Supersymmetry of gauge equations and geometric nonadiabatic phases
[DE93-626671] p 1219 N94-14935
Theoretical high energy physics research at the University of Chicago
[DE93-016863] p 1187 N94-16116
Existence of a new instanton in constrained Yang-Mills-Higgs theory
[NIKHEF-H/93-02] p 1186 N94-17601
The universality of the shift of the Chern-Simons parameter for a general class of BRS invariant regularizations
[NIKHEF-H/93-03] p 1220 N94-17602
SUSY in the sky
[NIKHEF-H/93-04] p 1240 N94-17603
Derivation of the Verlinde formula from Chern-Simons theory and the G/G model
[DE93-628620] p 1221 N94-17632

SUPPORT SYSTEMS
NASA Lewis 9- by 15-foot low-speed wind tunnel user manual
[NASA-TM-106247] p 872 N94-15819

SUPPORTS
Reliability analysis of Surface Mount Technology (SMT)
[AD-A267598] p 1055 N94-17194

SURFACE DEFECTS
Optical properties and surface morphology studies of palladium contacts on mercuric iodide single crystals
[DE93-012510] p 1207 N94-15973

SURFACE DIFFUSION
Surface reactivity of combustion generated soot particles
[AD-A268017] p 952 N94-17532

SURFACE EMITTING LASERS
JSEP fellowship
[AD-A266568] p 1211 N94-16800
Curved grating fabrication techniques for concentric-circle grating, surface-emitting semiconductor lasers p 1045 N94-17349

SURFACE ENERGY
Simulation studies for surfaces and materials strength
[NASA-CR-193387] p 1056 N94-15004
Two-dimensional, high flow, precisely controlled monodisperse drop source
[AD-A267660] p 1028 N94-17250
Regulation of attached bacterial growth by adsorbed proteins
[AD-A267756] p 1118 N94-17275
A surface energy budget model modifying heat flow by foliage effects
[AD-A268598] p 1085 N94-17610
Surface energy balance modeling at mesoscale: The contribution of the future Earth observing system
[BCRS-91-04] p 1085 N94-17616

SURFACE FINISHING
Assessment of chromate and non-chromate conversion coatings for Al alloys using electrochemical impedance spectroscopy
[AD-A267205] p 965 N94-15859
The effect of process parameters on the surface finish of plasma polymers
[DE93-014112] p 966 N94-15924
The role of carbon and temperature in determining electrical conductivity of basins, crust and mantle
[DE93-015936] p 1101 N94-16840
Application of hard coatings to substrates at low temperatures
[NASA-CR-193867] p 971 N94-17122

SURFACE IONIZATION
Characterization of Ni on Si wafers: Comparison of surface analysis techniques
[DE93-016501] p 953 N94-17649

SURFACE LAYERS
In situ Raman spectroscopy of lithium electrode surface in ambient temperature lithium secondary battery
[DE93-015238] p 1010 N94-16061
Spectral evidence of size dependent space weathering processes on asteroid surfaces p 1241 N94-16174
Kinetics of silica-phase transitions
[DE93-016231] p 1217 N94-17659

SURFACE NAVIGATION
Perception for outdoor navigation
[AD-A266867] p 863 N94-14919

SURFACE PROPERTIES
Engineering design of sub-micron topographies for simultaneously adherent and reflective metal-polymer interfaces
[NASA-CR-194573] p 964 N94-15700
Analytical and experimental investigation of the feasibility of accelerated lifetime testing of materials exposed to an atomic oxygen beam
[NASA-CR-193851] p 946 N94-15766
Passive oxide films on well-defined nickel surfaces: An examination of film growth on Ni(100) with ex situ scanning tunneling microscopy
[DE93-014056] p 1207 N94-15923
Spectral evidence of size dependent space weathering processes on asteroid surfaces p 1241 N94-16174
Discussion of band selection and methodologies for the estimation of precipitable water vapour from AVIRIS data p 1074 N94-16707
Electron spectroscopy analysis
[NASA-CR-193591] p 951 N94-17039
A modified two-fluid model of conductivity for superconducting surface resistance calculation
[AD-A267549] p 1013 N94-17104
Automated image analysis method for the detection of cracks on wood surface
[VTT-JULK-755] p 1056 N94-17542
Guide to Magellan image interpretation
[NASA-CR-194340] p 1298 N94-17654

SURFACE REACTIONS
The thermal dissociation of NH2CHO(ND2CHO) on Si(100)-2x1
[AD-A266903] p 942 N94-14956
The role of interfacial chemistry in surface nucleation and growth of calcium oxalate
[DE93-015689] p 1209 N94-16159
An investigation of the hydrolytic resistance of sodium-calcium plate glass with a layer of silica deposited on its surface
[IFTR-34/1991] p 971 N94-17120
Laser probing of the kinetics and dynamics of 3-5 semiconductor growth
[AD-A268388] p 1215 N94-17422
Surface reactivity of combustion generated soot particles
[AD-A268017] p 952 N94-17532

SURFACE ROUGHNESS
On the receptivity problem for O(1) wavelength Goertler vortices
[NASA-CR-191519] p 1016 N94-15005
Johnson-Gierhart program predictions of excess propagation loss for super-high frequency air-to-ground paths. Volume 1: Theory and numerical results
[AD-A267105] p 988 N94-15649
Method and apparatus for non-destructive evaluation of composite materials with cloth surface impressions
[NASA-CASE-LAR-14535-1] p 933 N94-15878
The effect of process parameters on the surface finish of plasma polymers
[DE93-014112] p 966 N94-15924
Polished substrate surface and cleaning study for coated optic quality
[DE93-014116] p 1190 N94-15975
The processing and mechanical properties of high temperature/high performance composites. Book 1: Coonstituent properties of composites
[AD-A266394] p 935 N94-16483
Scattering from binary optics p 1195 N94-17341
Guide to Magellan image interpretation
[NASA-CR-194340] p 1298 N94-17654

SURFACE ROUGHNESS EFFECTS
Preliminary results of polarization signatures for glacial moraines in the Mono Basin, Eastern Sierra Nevada
p 1078 N94-16746
Detecting surface roughness effects on the atmospheric boundary layer via AIRSAR data: A field experiment in Death Valley, California p 1078 N94-16747

SURFACE TEMPERATURE
Testing the waters from space --- Thermal mapping
[NASA-TM-109623] p 1082 N94-15409
Particle kinetic simulation of high altitude hypervelocity flight
[NASA-CR-194599] p 856 N94-15678
In situ Raman spectroscopy of lithium electrode surface in ambient temperature lithium secondary battery
[DE93-015238] p 1010 N94-16061
Effective elastic thickness of the Venusian lithosphere with lateral viscosity variations in the mantle
p 1293 N94-16421
Numerically solving a transient heat conduction problem with convection and radiation
[AD-A268521] p 1220 N94-17540

SURFACE TREATMENT
Studies of changes in the energy stored in metals as a result of subjecting them to a surface type technological process
[IFTR-25/1991] p 960 N94-17063

Atomic layer epitaxy group IV materials: Surface processes, thin films, devices and their characterization [AD-A267527] p 1213 N94-17116
Dry stripping as a surface treatment method [VTT-TIED-1348] p 985 N94-17544
Influence of the granular surface on the oxygen uptake in YBa2Cu3O(6+delta) ceramics [DE93-629162] p 974 N94-17634

SURFACE WATER
Heterogeneity and scaling land-atmospheric water and energy fluxes in climate systems p 1083 N94-16030

SURFACE WAVES
Fine scale measurements of microwave backscatter from the ocean surface [AD-A264516] p 1111 N94-15134
Determination of the electromagnetic fields radiated from the ARES EMP simulator [AD-A267069] p 988 N94-15668
Observations and modelling of winds and waves during the Surface Wave Dynamics Experiment. Report 1: Intensive observation period IOP-1, 20-31 October 1990 [AD-A266384] p 1113 N94-16517
Surface waves in an inhomogeneous, isotropic, elastic half-space [IFTR-18/1991] p 1060 N94-17047

SURGERY
Laser artery repair [NASA-TM-109604] p 1120 N94-15312

SURGES
Potential transients, transmission and electrochemical corrosion detection [DE93-014055] p 956 N94-15922
OSA proceedings on Ultrafast Electronics and Optoelectronics, volume 14 [AD-A267972] p 1014 N94-17410
The Central American cold surge: An observational analysis of the deep southward penetration of North American cold fronts [AD-A268592] p 1110 N94-17607

SURVEILLANCE
Alternative optical architectures for multichannel adaptive optical processing [AD-A267052] p 1189 N94-15664
Decomposition of large sparse symmetric systems for parallel computation. Part 1: Theoretical foundations [AD-A267144] p 1159 N94-15750

SURVEYOR PROJECT
The 1968 highlights --- NASA programs and research [NASA-TM-109627] p 1302 N94-15413

SURVEYS
Design Quality Task Force survey comments [AD-A266283] p 1225 N94-16473
Identifying and responding to customer needs at the Kennedy Space Center p 1056 N94-16626
What is the radar tracking Glint problem and can it be solved? [AD-A266509] p 999 N94-16789
Maximizing participation of women in collegiate aviation education [NIAR-93-14] p 1222 N94-17261

SURVIVAL
STS-29 crew bailout in WETF [NASA-TM-109548] p 1136 N94-15385
1990 ASCAN land survival training [NASA-TM-109527] p 1136 N94-15390
On predicting the person-in-water drift for search and rescue [AD-A268083] p 1055 N94-17514

SUSPENSION SYSTEMS (VEHICLES)
Electrodynamic forces of the cross-connected figure-eight null-flux coil suspension system [DE93-015139] p 1048 N94-16969

SWEAT
Cool suit [NASA-TM-109639] p 1120 N94-15250

SWELLING
Swelling equilibria for temperature-sensitive ampholytic hydrogels [DE93-015264] p 966 N94-15996

SWEPT FORWARD WINGS
X-29: Experiment in flight [NASA-TM-109454] p 865 N94-15327

SWEPT WINGS
Special course on Shock-Wave/Boundary-Layer Interactions in Supersonic and Hypersonic Flows [AGARD-R-792] p 1017 N94-15196
Aerodynamic control of NASP-type vehicles through vortex manipulation. Volume 3: Wing rock experiments [NASA-CR-177626] p 857 N94-15780

SWINE
Increased vascular resistance with hemoglobin-based oxygen carriers [AD-A266454] p 1123 N94-16565

SWITCHES
Plasma flow switch and foil implosion experiments on Pegasus 2 [DE93-016464] p 1013 N94-17318
Isochronets: A high-speed network switching architecture [AD-A267811] p 1161 N94-17409

SWITCHING CIRCUITS
Stray insensitive switched capacitor composite operational amplifiers [AD-A267412] p 1012 N94-16976
Design of broadband wire antennas for frequency hopping applications [AD-A267405] p 1001 N94-17025
Non-blocking crossbar permutation engine with constant routing latency [NASA-CASE-NPO-18864-1-CU] p 1161 N94-17328
A scalable wrap-around shuffle exchange network with deflection routing [NASA-CASE-NPO-18983-1-CU] p 1161 N94-17330

SYMBIOSIS
Biofilm structure and diversity [AD-A267254] p 1118 N94-16989

SYMBIOTIC STARS
ROSAT-IUE observations of symbiotic stars. The x ray morphology of high latitude associations [NASA-CR-194616] p 1236 N94-16492

SYMBOLIC PROGRAMMING
Visual parallel programming with determinacy: A language specification, an analysis technique, and a programming tool [AD-A267560] p 1153 N94-17107

SYMBOLS
SeaWiFS technical report series. Volume 12, SeaWiFS technical report series cumulative index: Volumes 1-11 [NASA-TM-104566-VOL-12] p 1111 N94-15529
Testing string superprimitivity in parallel [AD-A267814] p 1155 N94-17399

SYMMETRY
Application of symmetry properties to polarimetric remote sensing with JPL AIRSAR data p 1079 N94-16752
Analysis of temporal symmetry in non-gaussian random fields [AD-A266496] p 999 N94-16794

SYMPATHETIC NERVOUS SYSTEM
Melatonin, the pineal gland, and circadian rhythms [AD-A268200] p 1129 N94-17478

SYMPTOMOLOGY
Flight simulator-induced sickness and visual displays evaluation [AD-A267019] p 1122 N94-15845

SYNAPSES
Theoretical and experimental research into biological mechanisms underlying learning and memory [AD-A267441] p 1133 N94-17022
Synaptic plasticity and memory formation [AD-A267988] p 1133 N94-17453

SYNCHRONISM
Complexity analysis of real-time reinforcement learning applied to finding shortest paths in deterministic domains [AD-A266636] p 1131 N94-15742
Digital laser range finder emulator [AD-D015811] p 1040 N94-16540
Hydraulic pump with integral electric motor [AD-D015782] p 1011 N94-16549
Asynchronous design for parallel processing architectures [AD-A266523] p 1160 N94-16791
Verification of fault-tolerant clock synchronization systems [NASA-TP-3349] p 1161 N94-17449

SYNCHRONOUS MOTORS
Circuits and control processes for combining direct converters and inverter motors [ETN-93-94399] p 1008 N94-15448

SYNCHRONOUS SATELLITES
AMIGAU: A prototype tool aimed at mission analysis for satellites and satellite constellations p 888 N94-17133
ARIANE 5 light derivatives p 878 N94-17140
Small imaging satellite for Earth observing system adjunct p 891 N94-17151
Adequation of mini satellites to oceanic altimetry missions p 891 N94-17152
A study on an experimental communication system using microsatellites p 892 N94-17160

SYNCHROTRON RADIATION
Powder diffraction studies using anomalous dispersion [DE93-012531] p 1210 N94-16775
Application of cylindrical distribution functions to anisotropic scattering from amorphous films [DE93-015256] p 1183 N94-16811
Suppression of charge scattering in Moessbauer experiments using synchrotron radiation [DE93-015406] p 1212 N94-16887
Growth of dielectric thin films by irradiation of condensed molecular precursors with synchrotron radiation [DE93-016161] p 974 N94-17676

SYNCHROTRONS
Study of the rare decays K(sub L)(sup 0) yields (mu)e, K(sub L)(sup 0) yields ee, and K(sub L)(sup 0) yields (mu)(mu) at KEK [DE93-753247] p 1180 N94-15135
The (delta)f algorithm for beam dynamics [DE93-015632] p 1187 N94-16660
Fundamental-mode RF design in e(+)e(-) storage ring factories [DE93-015249] p 1183 N94-16809
ARIES tokamak reactor study [DE93-017059] p 1203 N94-16901

SYNCOM 4 SATELLITE
STS-32 onboard 16mm photography quick release [NASA-TM-109472] p 880 N94-15376

SYNTHESIS (CHEMISTRY)
Synthesis and chemistry of novel cyclic fluorocarbons [AD-A267148] p 929 N94-15734
High temperature advanced structural composites. Volume 1: Executive summary and intermetallic compounds [AD-A267022] p 933 N94-15835
Ion doped quantum well lasers [AD-A267198] p 1038 N94-15853
Synthesis of ceramic oxide powders in a microwave plasma device [DE93-012741] p 965 N94-15920
Use of microgravity in the synthesis of ceramics using sol gel techniques p 979 N94-16088
High octane ethers from synthesis gas-derived alcohols [DE93-016861] p 975 N94-16898
Amide and tetrazene complexes of transition and main group elements as precursors for the low temperature synthesis of elemental nitrides [AD-A266246] p 950 N94-16931
Photodegradation of MDI based polyurethane/urea elastomers [AD-A267308] p 971 N94-16994
Theoretical studies of nonlinear optical properties of conjugated polymers [AD-A267390] p 1193 N94-17024
Synthesis of potential high-energy fuels [AD-A267508] p 975 N94-17073
Synthesis, reactivity, and characterization of (-hexacarbocyclic) manganese dicarbonyl complexes with sulfur and phosphorus ligands [AD-A267592] p 930 N94-17192
Synthesis, characterization, and polymerization of new ferrocene-fluorene complexes. A novel high-molecular weight conjugated polymer with pendant ferrocene groups [AD-A267717] p 972 N94-17273
Synthesis and characterization of new low-dimensional metal complex conductors [AD-A268251] p 952 N94-17416

SYNTHETIC APERTURE RADAR
Overview of Enhanced Data Stream Array Processor (EDSAP) [AD-A266986] p 1158 N94-15492
Proceedings of the Third Spaceborne Imaging Radar Symposium [NASA-CR-194104] p 989 N94-15886
Almaz p 898 N94-15889
X-SAR: The X-band synthetic aperture radar on board the Space Shuttle p 990 N94-15891
ENVISAT ASAR p 898 N94-15892
RADARSAT program p 898 N94-15893
Recent scientific advances in the use of radar in scientific hydrology p 991 N94-15895
Recent advances in radar remote sensing of forest p 991 N94-15897
Multifrequency observations p 992 N94-15902
SIR-C/X-SAR free flyer concept p 898 N94-15903
EOS SAR: A new approach p 992 N94-15904
TOPSAT: Global space topographic mission p 992 N94-15905
Calibration: Practical experience with ERS-1 p 992 N94-15907
Synthetic aperture radar signal processing: Trends and technologies p 992 N94-15908
Recent advances and plans in processing and geocoding of SAR data at the DFD p 992 N94-15909
Data distribution p 993 N94-15910
SAR sensor electronics: T/R modules p 993 N94-15911
Advanced antennas for SAR spacecraft p 993 N94-15912
High resolution SAR applications and instrument design p 993 N94-15913

Primary studies of Chinese spaceborne SAR p 993 N94-15916
International collaboration in SAR ground data systems p 993 N94-15917
AIRSAR South American deployment: Operation plan, version 3.0 p 994 N94-15919
Summaries of the Third Annual JPL Airborne Geoscience Workshop. Volume 1: AVIRIS Workshop [NASA-CR-194540] p 1066 N94-16666
MAC Europe 1991: Evaluation of AVIRIS, GER imaging spectrometry data for the land application testsite Oberpfaffenhofen p 1070 N94-16688
Summaries of the Third Annual JPL Airborne Geoscience Workshop. Volume 3: AIRSAR Workshop [NASA-CR-194542] p 1075 N94-16731
A snow wetness retrieval algorithm for SAR p 1075 N94-16732
Comparison of JPL-AIRSAR and DLR E-SAR images from the MAC Europe 1991 campaign over testsite Oberpfaffenhofen: Frequency and polarization dependent backscatter variations from agricultural fields p 1075 N94-16733
Monitoring environmental state of Alaskan forests with AIRSAR p 1075 N94-16734
Comparison of modeled backscatter with SAR data at P-band p 1076 N94-16735
SAR backscatter from coniferous forest gaps p 1076 N94-16736
Retrieval of pine forest biomass using JPL AIRSAR data p 1076 N94-16737
Characterization of wetland, forest, and agricultural ecosystems in Belize with airborne radar (AIRSAR) p 1076 N94-16738
Strategies for detection of floodplain inundation with multi-frequency polarimetric SAR p 1076 N94-16739
Supervised fully polarimetric classification of the Black Forest test site: From MAESTROI to MAC Europe p 1076 N94-16740
Relating multifrequency radar backscattering to forest biomass: Modeling and AIRSAR measurement p 1077 N94-16741
SAR observations in the Gulf of Mexico p 1077 N94-16742
Investigation of AIRSAR signatures of the Gulf Stream p 1077 N94-16743
Mapping of sea bottom topography p 1077 N94-16744
Sea bottom topography imaging with SAR p 1077 N94-16745
Preliminary results of polarization signatures for glacial moraines in the Mono Basin, Eastern Sierra Nevada p 1078 N94-16746
Extraction of quantitative surface characteristics from AIRSAR data for Death Valley, California p 1078 N94-16748
The TOPSAR interferometric radar topographic mapping instrument p 1078 N94-16749
Evaluation of the TOPSAR performance by using passive and active calibrators p 1078 N94-16750
Fitting a three-component scattering model to polarimetric SAR data p 1079 N94-16751
Application of symmetry properties to polarimetric remote sensing with JPL AIRSAR data p 1079 N94-16752
External calibration of polarimetric radar images using distributed targets p 1079 N94-16753
Processing of polarimetric SAR data for soil moisture estimation over Mahantango watershed area p 1079 N94-16754
Evaluation of polarimetric SAR parameters for soil moisture retrieval p 1079 N94-16755
Interaction types and their like-polarization phase-angle difference signatures p 1079 N94-16756
Application of modified ViCAR/IBIS GIS to analysis of July 1991 Flevoland AIRSAR data p 1080 N94-16757
Radar Analysis and Visualization Environment (RAVEN): Software for polarimetric radar analysis p 1080 N94-16758
Measuring ocean coherence time with dual-baseline interferometry p 1080 N94-16759
Soil conservation applications with C-band SAR p 1080 N94-16760
Comparison of edges detected at different polarisations in MAESTRO data p 1080 N94-16761
Lithological and textural controls on radar and diurnal thermal signatures of weathered volcanic deposits, Lunar Crater region, Nevada p 1080 N94-16762
Measurements of the radar cross section and Inverse Synthetic Aperture Radar (ISAR) images of a Piper Navajo at 9.5 GHz and 49 GHz [AD-A267570] p 1002 N94-17110
Arctic cyclones and Marginal Ice Zone (MIZ) variability [AD-A268610] p 1108 N94-17465

SYNTHETIC APERTURES
Spaceborne Imaging Radar-C instrument p 990 N94-15890
A conceptual design study for a two-dimensional, electronically scanned thinned array radiometer [NASA-TM-109051] p 1085 N94-17665

SYSTEM FAILURES
Concurrent garbage collection of persistent heaps [AD-A266831] p 1141 N94-14915
The distributed database dynamic reconfiguration project [AD-A267116] p 1229 N94-15652
Reliability characterization of digital microcircuits: Investigation of an in-process oxide reliability screening method [AD-A267053] p 1008 N94-15665
Fast simulation of steady-state availability in non-Markovian highly dependable systems [AD-A266747] p 1174 N94-15823
Consistent failure reporting in reliable communication systems [AD-A266298] p 997 N94-16477
Disconnected operation in a distributed file system [AD-A266461] p 1231 N94-16570
Understanding partitions and the no partition assumption [AD-A266296] p 1000 N94-16911

SYSTEM IDENTIFICATION
Exploitation of cyclostationarity for signal-parameter estimation and system identification [AD-A267137] p 988 N94-15690
The design and analysis of robust feedback systems [AD-A267152] p 1165 N94-15778
Development and analysis of ARMA parameter estimation schemes in the presence of noise [AD-A267184] p 989 N94-15786
Heat transfer parametric system identification [AD-A268525] p 929 N94-17543

SYSTEMS ANALYSIS
Integrated trusted systems development environment [AD-A267029] p 1146 N94-15674
A handbook of cost risk analysis methods [AD-A267253] p 1235 N94-16988
Soyuz/ACRV accommodation study [NASA-TM-107733] p 888 N94-17072
Small Satellites Systems and Services [ISBN-2-85-428327-9] p 888 N94-17131

SYSTEMS ENGINEERING
The detector assemblies of ISOPHOT and the spectrometers ISO-SWS and ISO-LWS p 906 N94-15074
RAMCAD design methodology [AD-A267010] p 1145 N94-15525
ECS: Ninth year in orbit [ESA-BR-91] p 987 N94-15644
Integrated trusted systems development environment [AD-A267029] p 1146 N94-15674
Department of Defense technical architecture framework for information management. Volume 3: Architecture concepts and design guidance, version 2.0 [AD-A267195] p 1230 N94-15789
Remote diagnosis as used for mechanized parking systems p 984 N94-16004
Center of Excellence in Laser Medicine [DE93-016541] p 1122 N94-16113
Microwave reflectometer ionization sensor [NASA-CR-191464] p 922 N94-17083
Human Transportation System (HTS) study, volume 2 [NASA-TM-104779-VOL-2] p 882 N94-17320
Design and diagnosis problem solving with multifunctional technical knowledge bases [AD-A268375] p 1234 N94-17419
Gravity dependent condensation pressure drop and heat transfer in ammonia two-phase heat transport systems [NLR-TP-92121-U] p 1031 N94-17615

SYSTEMS INTEGRATION
SIMS: Single Interface to Multiple Systems [AD-A266934] p 1143 N94-15175
Software architecture for shared information systems [AD-A266995] p 1144 N94-15216
Integration ToolKit and Methods (ITKM) manufacturing methods and prototype toolkit. A combined modeling method using IDEFO, IDEF1x and XSpec [AD-A266176] p 984 N94-16981
Soyuz/ACRV accommodation study [NASA-TM-107733] p 888 N94-17072
Integration of several computer systems within a heterogeneous environment [AD-A267978] p 1155 N94-17500

SYSTEMS SIMULATION
Fast simulation of steady-state availability in non-Markovian highly dependable systems [AD-A266747] p 1174 N94-15823
Space Station Freedom electrical performance model [NASA-TM-106395] p 929 N94-17483

SYSTEMS STABILITY
Nonlinear analysis of mechanical systems under combined harmonic and stochastic excitation [AD-A266217] p 1173 N94-16937

T

T-38 AIRCRAFT
Static aeroelastic response of an aircraft with asymmetric wing planforms representative of combat damage [AD-A266890] p 865 N94-14951
Adamson, Jim --- ASCAN training programs [NASA-TM-109507] p 1137 N94-15454

TABLES (DATA)
Module interconnection frameworks for a real-time spreadsheet [AD-A267317] p 1153 N94-17220
Human central nervous system oxygen toxicity data from 1945 to 1986 [AD-A268225] p 1130 N94-17556
Satellite situation report, volume 31, number 1 [NASA-TM-105088] p 898 N94-17584

TABLETS
Efficacy of flocculating and other emergency water purification tablets [AD-A266695] p 1148 N94-15840

TACTILE SENSORS (ROBOTICS)
Tactile sensing and control in humans and robotic/teleoperated systems [AD-A267710] p 1163 N94-14937

TAIL ASSEMBLIES
Vertical-tail aerodynamic configuration of space shuttle orbiter [AD-A267723] p 879 N94-14941

TANTALUM
The effect of oxygen, grain size, and strain rate on the mechanical behavior of forged P/M tantalum [DE93-011251] p 959 N94-16764
Laser weld repair of tantalum sheet [DE93-016417] p 1041 N94-16871

TANTALUM ALLOYS
Processing and protection of high temperature structural materials [AD-A267292] p 954 N94-14961

TANTALUM OXIDES
The effect of oxygen, grain size, and strain rate on the mechanical behavior of forged P/M tantalum [DE93-011251] p 959 N94-16764

TAPE RECORDERS
Laser weld repair of tantalum sheet [DE93-016417] p 1041 N94-16871

TARGET ACQUISITION
EVA retriever demonstration [NASA-TM-109510] p 1046 N94-15456
Airborne 2 color ranging experiment p 920 N94-15614
Pixel-level fusion using interest images [AD-A266640] p 1164 N94-15746
Environmental characterization for target acquisition. Report 1: Site descriptions and measurements [AD-A267192] p 1106 N94-15851
Exploiting world structure to efficiently search for objects [TR-434] p 1231 N94-16576
Enhanced down-range profiles of complex targets using wideband radar echo returns [AD-A266508] p 999 N94-16788
Target detection by way of Kalman filtering [AD-A267314] p 1000 N94-16945
Signal detection in correlated Gaussian and non-Gaussian radar clutter [AD-A267453] p 1001 N94-17033
A virtual acoustic orientation instrument [AD-A268181] p 1134 N94-17510

TARGET RECOGNITION
Pixel-level fusion using interest images [AD-A266640] p 1164 N94-15746
Development and analysis of ARMA parameter estimation schemes in the presence of noise [AD-A267184] p 989 N94-15786
Environmental characterization for target acquisition. Report 1: Site descriptions and measurements [AD-A267192] p 1106 N94-15851
Enhanced down-range profiles of complex targets using wideband radar echo returns [AD-A266508] p 999 N94-16788

TARGETS
Effects of window size and shape on accuracy of subpixel centroid estimation of target images [NASA-TP-3331] p 1034 N94-15990
Passive tracking of a target using an array of sensors [DE93-015870] p 997 N94-16169
An algorithm for the estimation of bounds on the emissivity and temperatures from thermal multispectral airborne remotely sensed data p 1064 N94-16603

TASK COMPLEXITY
NASA/DOD Aerospace Knowledge Diffusion Research Project. Report 15: Technical uncertainty and project complexity as correlates of information use by US industry-affiliated aerospace engineers and scientists: Results of an exploratory investigation
[NASA-TM-107693] p 1233 N94-17291
Theoretical implications and empirical findings on instructional control and part-whole-task training
[AD-A267826] p 872 N94-17403
TASKS
Preliminary validation of the task analysis/workload methodology
[AD-A267514] p 1138 N94-17077
TASTE
STS-29 crew food tasting in building 45
[NASA-TM-109547] p 1136 N94-15382
TAYLOR INSTABILITY
Mechanism of intermittent atomization
[AD-A266625] p 1021 N94-15770
TAYLOR SERIES
Automatic differentiation of limit functions
[DE93-016376] p 1168 N94-14928
A handbook of cost risk analysis methods
[AD-A267253] p 1235 N94-16988
TDR SATELLITES
STS-26 Post-Flight Press Conference
[NASA-TM-109557] p 879 N94-15261
STS-26 onboard 16mm photography quick release
[NASA-TM-109558] p 879 N94-15262
TDRS video clip
[NASA-TM-109585] p 884 N94-15269
STS-26 through STS-34, deploy activities
[NASA-TM-109566] p 1301 N94-15315
STS-26 generic integrated IUS deploy simulation
[NASA-TM-109562] p 875 N94-15332
STS-29 mission highlights resource tape
[NASA-TM-109542] p 880 N94-15373
STS-26 missions highlight resource tape
[NASA-TM-109559] p 881 N94-15407
TEARING
Crack-tip-opening angle measurements and crack tunneling under stable tearing in thin sheet 2024-T3 aluminum alloy
[NASA-CR-191523] p 931 N94-15184
Prediction of stable tearing of 2024-T3 aluminum alloy using the crack-tip opening angle approach
[NASA-TM-109023] p 955 N94-15708
Measurement and analysis of critical CTOA for an aluminum alloy sheet
[NASA-TM-109024] p 956 N94-15948
TECHNICAL WRITING
The impact of report of investigation writing style on the assessment times, impressions, perceptions and preferences of adjudicators
[AD-A265748] p 1223 N94-15682
TECHNOLOGICAL FORECASTING
Aviation and the KLM: Past and future
p 853 N94-15126
Expectations for the future of Fokker
p 854 N94-15127
Expectations for the future of military aviation
p 854 N94-15128
Expectations for the future of the National Aerospace Laboratory p 854 N94-15129
Expectations for the future of the Faculty of Aeronautics and Astronautics of the Technical University of Delft
p 854 N94-15131
TECHNOLOGY ASSESSMENT
X ray microcalorimeters: Principles and performance
p 899 N94-15027
Superconductive x ray photon detectors
p 900 N94-15031
Metastable superconductors as photon detectors
p 900 N94-15032
Development of x ray CCDs p 900 N94-15033
Large scientific 2-D arrays for the 1-5 micron region
p 902 N94-15044
Submm/FIR bolometers p 904 N94-15056
NASA's Ultraviolet Astrophysics Branch: Present and future detector program p 910 N94-15102
Expectations for the future of the National Aerospace Laboratory p 854 N94-15129
Information Technology Resources Assessment
[DE93-013899] p 1230 N94-16010
Space Propulsion Synergy Group ETO technology assessments
[TABES PAPER 93-641] p 929 N94-16149
Space Nuclear Facility test capability at the Baikal-1 and IGR sites Semipalatinsk-21, Kazakhstan
[DE93-011662] p 926 N94-16773
An overview of the NASA textile composites program
p 937 N94-16846
Plasma Science Committee (PLSC) and the Panel on Opportunities in Plasma Science and Technology (OPST)
[DE93-018142] p 1204 N94-16995
Key trends of the small satellite market
p 897 N94-17191
Binary optics: Trends and limitations
p 1194 N94-17333
Satellite communications systems and technology. Executive summary
[NASA-TM-109346] p 1006 N94-17661
TECHNOLOGY TRANSFER
From space to Earth
[NASA-TM-109638] p 1235 N94-15249
Medical imaging
[NASA-TM-109675] p 1229 N94-15520
NASA Space Engineering Research Center for VLSI System Design
[NASA-CR-194587] p 1008 N94-15547
Dependable software technology exchange
[AD-A267103] p 1146 N94-15638
Technology transfers and reliable oxides
[AD-A266948] p 1175 N94-15758
KBSA concept demo
[AD-A267054] p 1166 N94-16770
Earth observational research using multistage EOS-like data
[NASA-CR-194626] p 1084 N94-16831
Technology transfer. Determining industry needs: A guide for communities
[NASA-CR-194676] p 1235 N94-17293
Technology in action
[NASA-TM-109345] p 1235 N94-17294
TECHNOLOGY UTILIZATION
From space to Earth
[NASA-TM-109638] p 1235 N94-15249
Monitoring history
[NASA-TM-109640] p 1229 N94-15251
Saving Yellowstone
[NASA-TM-109596] p 1094 N94-15289
Finding fish from above --- remote sensing
[NASA-TM-109602] p 1081 N94-15310
NASA images 7
[NASA-TM-109438] p 1235 N94-15337
NASA images 16
[NASA-TM-109440] p 1235 N94-15339
Unistick vehicle controller
[NASA-TM-109618] p 1046 N94-15347
Improved mapping system
[NASA-TM-109643] p 1082 N94-15428
Workshop on advanced technologies for planetary instruments
[NASA-CR-194585] p 1032 N94-15797
The strategic environmental research and development program: A new paradigm for space, the environment, and national security
[AD-A266222] p 1174 N94-16109
Commercial space opportunities advanced concepts and technology overview
[TABES PAPER 93-240] p 1050 N94-16132
A Moessbauer spectrometer for the mineralogical analysis of the Mars surface: First temperature dependent tests of the detector and drive system
p 1259 N94-16233
Techno-economic requirements for automotive composites p 937 N94-16847
Technology in action
[NASA-TM-109345] p 1235 N94-17294
Micro-optics technology and sensor systems applications p 1197 N94-17350
Reliability and maintainability of modular robot systems: A roadmap for design
[AD-A268104] p 1168 N94-17517
Smart Power: New power integrated circuit technologies and their applications
[VTT-TIED-1358] p 1015 N94-17546
TECTONICS
Laser tracking for vertical control p 911 N94-15553
Experience and results of the 1991 MTLRS-1 USSR campaign p 914 N94-15575
Papers presented at the Eleventh International Symposium on Earth Tides
[COMMUNICATIONS-SER-B-158] p 1098 N94-15800
Tidal gravity anomalies and tectonics
p 1101 N94-15814
Magellan: Principal Venus science findings
p 989 N94-15887
Tectonic deformation in southern California
[NASA-CR-194621] p 1101 N94-16021
Pargo Chasma and its relationship to global tectonics
p 1249 N94-16181
The formation and evolution of Alpha and Tellus tesserae on Venus p 1249 N94-16183
Rheology of water and ammonia-water ices
p 953 N94-16188
Importance of expansion and contraction in the formation of tectonic features on the Moon
p 1250 N94-16189
The Karakul depression in Pamirs: The first impact structure in Central Asia p 1241 N94-16212
Morphology and models for the evolution of eastern Hecate Chasma, Venus p 1256 N94-16215
The three ages of Venus: A hypothesis based on the cratering record p 1261 N94-16239
Tessera terrain on Venus: Global characterization from Magellan data p 1264 N94-16262
Density of impact craters on tessera, Venus
p 1264 N94-16263
Estimates of lithospheric thickness on Venus
p 1267 N94-16277
Tectonics of Neyterkob corona on Venus
p 1270 N94-16299
On the relationship between tectonic plates and thermal mantle plume morphology p 1104 N94-16349
Tectonic resurfacing of Venus p 1285 N94-16380
Aspects of modelling the tectonics of large volcanoes on the terrestrial planets p 1104 N94-16396
Guide to Magellan image interpretation
[NASA-CR-194340] p 1298 N94-17654
TEFLON (TRADEMARK)
Impact penetration experiments in teflon targets of variable thickness p 1063 N94-16253
Performance of silvered Teflon thermal control blankets on spacecraft
[AD-A266284] p 887 N94-16909
TEKTITES
Cretaceous-tertiary boundary spherules and Cenozoic microtektites: Similarities and differences
p 1241 N94-16186
Trace-element composition of Chicxulub crater melt rock, K/T tektites and Yucatan basement
p 1242 N94-16245
Osmium isotopes in Ivory Coast tektites: Confirmation of a meteoritic component and rhenium depletion
p 1244 N94-16321
TELECOMMUNICATION
Computer Science and Telecommunications Board activities
[DE93-018141] p 1000 N94-17000
Nonlinear methods for communications
[AD-A267376] p 1001 N94-17019
An approximation for computing reduction in bandwidth requirements using intelligent multiplexers
[AD-A267434] p 1001 N94-17026
Feasibility study of a personal communications system IRIDIUM-like p 893 N94-17165
TUBSAT: Low cost access to space technology
p 895 N94-17180
Big results with small space systems: What small systems are doing today p 896 N94-17187
Ground wave emergency network final operational capability: Environmental assessment for central Utah relay node, site number RN 8C920UT
[AD-A267628] p 1003 N94-17211
Activities of the Research Laboratory of Electronics
[AD-A266730] p 1304 N94-17651
TELEMETRY
Evaluation of midband analog fiber optic telemetry links
[DE93-015128] p 883 N94-16056
MAXUS: The new sounding rocket program for long duration microgravity flight p 978 N94-16079
Principal investigators data package for Project Initiation Conference (PIC): EUVS sounding rocket no. 36.117CL. Target: Venus
[NASA-CR-194663] p 923 N94-17126
Satellite control: A comprehensive approach
p 878 N94-17158
TELEOPERATORS
Tactile sensing and control in humans and robotic/teleoperated systems
[AD-A267710] p 1163 N94-14937
The ESA telescience program p 977 N94-16073
MAXUS: The new sounding rocket program for long duration microgravity flight p 978 N94-16079
Contextually dependent control strategies for manipulation
[TR-416] p 1165 N94-16580
TELEROBOTICS
Tactile sensing and control in humans and robotic/teleoperated systems
[AD-A267710] p 1163 N94-14937
Hidden Markov model approach to skill learning and its application to telerobotics
[AD-A266989] p 1164 N94-15502
Ground integrated ET-derived space platforms for onorbit applications
[TABES PAPER 93-652] p 899 N94-16152
A computer-based training system combining virtual reality and multimedia
[DE93-013768] p 1132 N94-16819

TELESCOPES
Design of pulse stretching cell for a sodium guide star optical system
[DE93-016436] p 1236 N94-14929
Fault management for data systems
[NASA-TM-103953] p 1116 N94-15548
Two color satellite laser ranging upgrades at Goddard's 1.2m telescope facility p 915 N94-15581
A computer-controlled x-y offset guiding stage for the MLRS p 918 N94-15598
Matera Laser Ranging Observatory (MLRO): An overview p 877 N94-15601
Performance of the upgraded Orroral laser ranging system p 877 N94-15602
Transputer based control system for MTLRS p 877 N94-15613
Station report on the Goddard Space Flight Center (GSFC) 1.2 meter telescope facility p 922 N94-15625
Tip-tilt compensation: Resolution limits for ground-based telescopes using laser guide star adaptive optics
[DE93-016426] p 1237 N94-16872
Optical displays: A tutorial on images and image formation
[AD-A266230] p 1192 N94-16926
Conically scanned holographic lidar telescope
[NASA-CASE-GSC-13462-1] p 1194 N94-17321
Diffractive optical elements for generating arbitrary line foci p 1195 N94-17338
Test methods for acceptance testing of telescopes
[AD-A268316] p 1237 N94-17568

TELEVISION SYSTEMS
International testing of a Mars rover prototype p 1273 N94-16312

TEMPERATURE COMPENSATION
Precise flux control for lattice matched superlattice materials
[AD-A268254] p 1215 N94-17417

TEMPERATURE CONTROL
Development of Japanese Earth Resources Satellite-1 (JERS-1; FUYO-1) and it's operational results
[NASDA-SPP-930001] p 884 N94-15001
Cool suit
[NASA-TM-109639] p 1120 N94-15250
Advanced cooling for high power electric actuators
[AD-A266984] p 866 N94-15761
Solar absorptance of optical surfaces contaminated with spacecraft material outgassing products
[AD-A267202] p 886 N94-15857
Performance of silvered Teflon thermal control blankets on spacecraft
[AD-A266284] p 887 N94-16909
Variational principles of heat exchange and their applications in construction physics, part 2
[IFTR-19/1991] p 1061 N94-17069
Overview of the solar dynamic ground test demonstration program
[NASA-TM-106296] p 928 N94-17256

TEMPERATURE DEPENDENCE
The pressure broadening of HDO by O2, N2, H2, and He between 100 K and 600 K
[AD-A267118] p 946 N94-15684
Experimental investigations of superconductivity in quasi-two-dimensional epitaxial copper oxide superlattices and trilayers
[DE93-015306] p 1207 N94-15829
Density of states and tunneling characteristics of layered superconductors
[DE93-015898] p 1211 N94-16839
Chemical vapor deposition of Ta2O5 corrosion resistant coatings
[DE93-015488] p 969 N94-16889
Transient studies of low temperature catalysts for methane conversion
[DE93-017710] p 950 N94-16962
Mechanical properties of interfaces and superlattices
[AD-A268591] p 1217 N94-17606

TEMPERATURE DISTRIBUTION
Thermal stresses of a trimaterial medium in a nonuniform temperature field
[AD-A267243] p 930 N94-14975
Near-surface temperature gradients and their effects on thermal-infrared emission spectra of particulate planetary surfaces p 1260 N94-16236
Volcanic thermal features observed by AVIRIS p 1068 N94-16680
Aerothermoelastic analysis of a NASP demonstrator model
[NASA-TM-109007] p 867 N94-17055
Numerically solving a transient heat conduction problem with convection and radiation
[AD-A268521] p 1220 N94-17540

TEMPERATURE EFFECTS
Thermal stresses of a trimaterial medium in a nonuniform temperature field
[AD-A267243] p 930 N94-14975
The influence of thermal aging on the microstructure and fatigue properties of modified 9Cr-1Mo steel
[DE93-015489] p 957 N94-16106
Effects of alloying and temperature on the high-temperature oxidation of Cr-Cr2Nb
[DE93-015800] p 957 N94-16163
Rheology of water and ammonia-water ices p 953 N94-16188
Effective elastic thickness of the Venusian lithosphere with lateral viscosity variations in the mantle p 1293 N94-16421
A hydrogen isotope study of CO3 type carbonaceous chondrites; comparison with type 3 ordinary chondrites p 1246 N94-16425
Temperature and pressure effects on capacitance probe cryogenic liquid level measurement accuracy
[NASA-CR-190763] p 1034 N94-16521
Chemical vapor deposition of Ta2O5 corrosion resistant coatings
[DE93-015488] p 969 N94-16889
Creep ductility of iron at very low strain rates: The effects of sulfur
[DE93-015490] p 959 N94-16890
Studies on nonequilibrium phenomena in supersonic chemically reacting flows
[NASA-CR-194662] p 1027 N94-17215
Prediction of thermal cycling induced cracking in polymer matrix composites
[NASA-CR-194677] p 941 N94-17295
Mesons at finite temperature in the NJL model with gluon condensate
[DE93-626697] p 1185 N94-17310
Precise flux control for lattice matched superlattice materials
[AD-A268254] p 1215 N94-17417
High temperature deformation behavior of YBa2Cu3O(6+x) superconducting ceramic materials
[AD-A268164] p 973 N94-17430
Heat transfer parametric system identification
[AD-A268525] p 929 N94-17543
Design, development and characterization studies of a large aperture high power Nd: Glass rod amplifier stage
[DE93-624944] p 1042 N94-17630

TEMPERATURE GRADIENTS
Near-surface temperature gradients and their effects on thermal-infrared emission spectra of particulate planetary surfaces p 1260 N94-16236
Experimental segregation of iron-nickel metal, iron-sulfide, and olivine in a thermal gradient: Preliminary results p 1243 N94-16288
Implementation of an anisotropic turbulence model in the COMMIX-1C/ATM computer code
[DE93-015541] p 1023 N94-16444
Numerical modeling of the temperature gradients and spectra of the plasma armature on Thunderbolt
[AD-A266414] p 878 N94-16552
A surface energy budget model modifying heat flow by foliage effects
[AD-A268598] p 1085 N94-17610

TEMPERATURE MEASUREMENT
Description of cooling water calorimetry and wall thermometry diagnostic at tokamak ASDEX-Upgrade
[IPP-5/46] p 1200 N94-14966
Measurement of the specific heat capacity of the electron-beam graphite calorimeter
[NPL-RSA(EXT)-40] p 1031 N94-15018
Temperature propagation in near-critical fluids prior to and during separation p 944 N94-15165
Optical fiber spectroscopy: A study of the luminescent properties of the europium ion for thermal sensors
[NASA-CR-194576] p 1189 N94-15647
Simultaneous measurement of temperature and strain using four connecting wires
[NASA-TM-104271] p 1032 N94-15754
Temperature measurements p 1037 N94-15804
Pyroxene equilibration temperatures in metamorphosed ordinary chondrites p 1242 N94-16224
The cooling rates of pahoehoe flows: The importance of lava porosity p 1103 N94-16282
Analysis of TIMS performance subjected to simulated wind blast p 1063 N94-16598
Sensitivity of blackbody reference panels to wind blast p 1063 N94-16599
An algorithm for the estimation of bounds on the emissivity and temperatures from thermal multispectral airborne remotely sensed data p 1064 N94-16603

TEMPERATURE PROFILES
Pool boiling: Single bubble experiment p 944 N94-15160
Static characteristics of a conduction and radiation dominated electric arc in nitrogen
[DE93-627106] p 1204 N94-17311
An investigation of the Ground-Based High-Resolution Interferometer Sounder (GB-HIS) in a costal marine environment
[AD-A268052] p 1114 N94-17503
A surface energy budget model modifying heat flow by foliage effects
[AD-A268598] p 1085 N94-17610
Dynamic behavior of an electric arc gas discharge
[DE93-630197] p 1205 N94-17635

TEMPERATURE RATIO
The effects of radiation transport on line ratios used as temperature and density diagnostic
[DE93-016424] p 1205 N94-17663

TEMPERATURE SENSORS
Arctic internal waves (CEAREX)
[AD-A265822] p 1111 N94-15139
Optical fiber spectroscopy: A study of the luminescent properties of the europium ion for thermal sensors
[NASA-CR-194576] p 1189 N94-15647
Properties of thin films for high temperature flow sensors
[NASA-CR-191526] p 967 N94-16541

TEMPORAL DISTRIBUTION
Characterization of spatial and temporal variability of phytoplankton blooms in coastal waters
[AD-A267102] p 1116 N94-15633
A decade's overview of Io's volcanic activity p 1245 N94-16386
Temporal variation in spectral detection thresholds of substrate and vegetation in AVIRIS images p 1073 N94-16706
Arctic and Antarctic sea ice, 1978-1987: Satellite passive-microwave observations and analysis
[NASA-SP-511] p 1114 N94-17439

TEMPORAL RESOLUTION
How to squeeze high quantum efficiency and high time resolution out of a SPAD p 914 N94-15571

TENSILE PROPERTIES
A reexamination of grain boundary fracture in Ni3Al: Environmental and alloying effects
[DE93-015431] p 1208 N94-16063
The effect of long-term aging on the impact properties of modified 9Cr-1Mo steel
[DE93-015453] p 957 N94-16068
The effect of irradiation on the mechanical properties of 6061-T651 aluminum
[DE93-015825] p 958 N94-16168
The processing and mechanical properties of high temperature/high performance composites. Book 2: Coonstituent properties and macroscopic performance
[AD-A266395] p 935 N94-16484

TENSILE STRENGTH
The processing and mechanical properties of high temperature/high performance composites. Book 3: Coonstituent properties and macroscopic performance
[AD-A266396] p 935 N94-16485
The processing and mechanical properties of high temperature/high performance composites. Book 4: Coonstitutive laws and design
[AD-A266397] p 935 N94-16528
Weaving multi-layer fabrics for reinforcement of engineering components p 937 N94-16850
Effect of tow alignment on the mechanical performance of 3D woven textile composites p 937 N94-16851
New textile composite materials development, production, application p 938 N94-16853
Influence of the loading rate on the endurance and deformability of cement matrix composites
[IFTR-1/1992] p 1060 N94-17052
Fiber strength utilization in carbon/carbon composites
[AD-A267713] p 940 N94-17271
Tensile and stress-rupture behavior of hafnium carbide dispersed molybdenum and tungsten base alloy wires
[NASA-TM-106350] p 962 N94-17652

TENSILE STRESS
Simulation studies for surfaces and materials strength
[NASA-CR-193387] p 1056 N94-15004
A model for non-linear creep and physical ageing in PVC
[NPL-DMM(A)-91] p 1057 N94-15016
J-integral and HRR field associated with stable crack growth in thin aluminum SEN specimen
[AD-A267879] p 960 N94-17041
Interfacial shear behavior and its influence on fiber damage in sapphire-reinforced gamma titanium aluminide composites
[AD-A267943] p 1060 N94-17043
Influence of the loading rate on the endurance and deformability of cement matrix composites
[IFTR-1/1992] p 1060 N94-17052

TENSILE TESTS
The effect of aging at 343 C on the mechanical properties and microstructure of type 308 stainless steel weldments
[DE93-015454] p 957 N94-16103
Development of test methods for textile composites p 939 N94-16862
RSRM nozzle actuator bracket/lug fracture mechanics qualification test
[NASA-CR-193859] p 927 N94-17080

Evaluation of hybrid reinforcement (fiber-reinforced-plastic rod with steel core)
[AD-A268009] p 941 N94-17473
TERMINAL FACILITIES
MAGSS-14: Medium Altitude Global Mobile Satellite System with enhanced regional coverage
p 893 N94-17164
TERMINAL GUIDANCE
Hypervelocity orbital intercept guidance using certainty control
[AD-A267297] p 1174 N94-17219
TERMINOLOGY
NASA's online machine aided indexing system
[NASA-CR-4518] p 1228 N94-15009
Illustrated glossary of textile terms for composites
[NASA-CR-191539] p 933 N94-15484
Definitions of terms relating to aircraft windscreens, canopies, and transparencies
[AD-A268403] p 868 N94-17425
TERMS
Definitions of terms relating to aircraft windscreens, canopies, and transparencies
[AD-A268403] p 868 N94-17425
TERNARY ALLOYS
Ternary alloying effects in polycrystalline (beta)-NiAl
[DE93-012675] p 955 N94-15885
Powder diffraction studies using anomalous dispersion
[DE93-012531] p 1210 N94-16775
Slip, twinning and transformation in Laves phases
[DE93-018164] p 960 N94-16972
TERRAIN
Improved mapping system
[NASA-TM-109643] p 1082 N94-15428
Johnson-Gierhart program predictions of excess propagation loss for super-high frequency air-to-ground paths. Volume 1: Theory and numerical results
[AD-A267105] p 988 N94-15649
Environmental characterization for target acquisition. Report 1: Site descriptions and measurements
[AD-A267192] p 1106 N94-15851
Multifrequency observations p 992 N94-15902
Fluvial erosion on Mars: Implications for paleoclimatic change p 1241 N94-16210
Tessera terrain on Venus: Global characterization from Magellan data p 1264 N94-16262
Density of impact craters on tessera, Venus
p 1264 N94-16263
Complex terrain wind model evaluation
[AD-A266467] p 1096 N94-16589
Fitting a three-component scattering model to polarimetric SAR data p 1079 N94-16751
Sound exposure level prediction for impulse sound sources above variable terrain
[AD-A267535] p 1178 N94-17119
An automated approach for classifying generic terrain features using digital elevation data
[AD-A268385] p 1084 N94-17421
TERRESTRIAL DUST BELT
The effect of an on-orbit near encounter on the number flux density of micron sized particles
p 899 N94-16374
TERRESTRIAL PLANETS
Rover mounted ground penetrating radar as a tool for investigating the near-surface of Mars and beyong
p 1007 N94-16197
Aspects of modelling the tectonics of large volcanoes on the terrestrial planets p 1104 N94-16396
TESSERAL HARMONICS
Implementing a 50x50 gravity field model in an orbit determination system
[AD-A267548] p 888 N94-17103
TEST CHAMBERS
Unitary plan wind tunnel landmark dedication and revitalization
[NASA-TM-109649] p 1302 N94-15434
First results from a laboratory facility for measurement of emission spectra under simulated planetary conditions
p 954 N94-16372
TEST EQUIPMENT
Bench checkout equipment for spaceborne laser altimeter systems p 921 N94-15618
The Spacelab IPS Star Simulator
[TABES PAPER 93-650] p 877 N94-16150
TEST FACILITIES
Supersonic Combustion Research Laboratory. Volume 1: Design and fabrication
[AD-A267667] p 943 N94-14962
A test facility to calibrate EUV detectors
p 873 N94-15062
GFSC-TV demo tape
[NASA-TM-109586] p 875 N94-15270
Facilities maintenance handbook
[NHB-8831.2] p 1224 N94-15934
The ESA telescience program p 977 N94-16073
Payloads for the processing of high temperature materials p 979 N94-16083
The design and analysis of a modular microgravity test platform for use aboard the NASA KC-135 aircraft
p 899 N94-16101
Structured finite volume modeling of US Navy aircraft engine test cells task 2: Turboprop engine, volume 1
[AD-A267833] p 872 N94-17405
Structured finite volume modeling of US Navy aircraft engine test cells. Task 2: Turboprop engine. Volume 2: Code documentation and listings
[AD-A268386] p 873 N94-17569
TEST STANDS
Test plan for the evaluation of the initial capability of the National Satellite Test Bed: Phase 1D
[DOT/FAA/RD-93/20] p 876 N94-16025
TETHERED BALLOONS
Middle atmospheric electric fields over thunderstorms
[NASA-CR-194619] p 1106 N94-16493
TETHERED SATELLITES
Prototype instrumentation and design studies
[AD-A266402] p 882 N94-16530
TETHERLINES
Prototype instrumentation and design studies
[AD-A266402] p 882 N94-16530
TETRAHEDRONS
Tetrahedral lander
[NASA-CASE-MSC-22082-1] p 886 N94-15951
Structural studies of sol-gel glasses
[AD-A266277] p 967 N94-16472
TEXTBOOKS
Processes involved in the integration of pictures and discourse
[AD-A268150] p 1134 N94-17468
TEXTILES
Processing, properties and applications of composites using powder-coated epoxy towpreg technology
p 933 N94-15277
Illustrated glossary of textile terms for composites
[NASA-CR-191539] p 933 N94-15484
Verification of a two-dimensional infiltration model for the resin transfer molding process
[NASA-CR-194597] p 964 N94-15656
FIBER-TEX 1992: The Sixth Conference on Advanced Engineering Fibers and Textile Structures for Composites
[NASA-CP-3211] p 936 N94-16845
An overview of the NASA textile composites program
p 937 N94-16846
Research in textile composites at KU, Leuven
p 937 N94-16848
Effect of tow alignment on the mechanical performance of 3D woven textile composites p 937 N94-16851
An engineering approach for the application of textile composites to a structural component
p 938 N94-16852
New textile composite materials development, production, application p 938 N94-16853
Production and application of chemical fibers with special properties for manufacturing composite materials and goods of different usage p 938 N94-16854
Textile composite processing science
p 938 N94-16856
Development of braided fiber seals for engine applications p 939 N94-16859
Quantification of processing artifacts in textile composites p 939 N94-16860
Stochastic damage evolution in textile laminates
p 939 N94-16861
Development of test methods for textile composites
p 939 N94-16862
TEXTURES
Segmenting textured 3D surfaces using the space/frequency representation
[AD-A266960] p 1163 N94-14968
THALLIUM
Characterization of InTISb grown by low pressure metalorganic chemical vapor deposition on GaAs substrate
[AD-A266878] p 1206 N94-14922
THALLIUM COMPOUNDS
Characterization of InTISb grown by low pressure metalorganic chemical vapor deposition on GaAs substrate
[AD-A266878] p 1206 N94-14922
THEMATIC MAPPERS (LANDSAT)
Volcanic thermal features observed by AVIRIS
p 1068 N94-16680
Integrating remote sensing techniques at Cuprite, Nevada: AVIRIS, Thematic Mapper, and field spectroscopy p 1072 N94-16701
THEMATIC MAPPING
Do it yourself remote sensing: Generating an inexpensive, high tech, real science lake mapping project for the classroom p 1086 N94-16407
Mapping vegetation types with the multiple spectral feature mapping algorithm in both emission and absorption p 1069 N94-16686
THEOREM PROVING
An elementary tutorial on formal specification and verification using PVS
[NASA-TM-108991] p 1158 N94-15536
Global solutions to a system of strongly coupled reaction-diffusion equations
[DE93-628587] p 1171 N94-17640
Distributively generated matrix near rings
[DE93-628588] p 1175 N94-17641
THEOREMS
Fixed point iterations for strictly hemi-contractive maps in uniformly smooth Banach spaces
[DE93-628591] p 1175 N94-17644
THEORETICAL PHYSICS
Theoretical high energy physics research at the University of Chicago
[DE93-016863] p 1187 N94-16116
Experimental study of weak interactions by precision measurement by rare kaon decay
[DE93-016864] p 1182 N94-16117
Theoretical high energy physics
[DE93-015884] p 1187 N94-16170
Neutrino mass and mixing: Summary of the neutrino sessions
[DE93-014342] p 1183 N94-16801
Heavy ion physics research at Creighton University
[DE93-016809] p 1185 N94-16957
Derivation of the Verlinde formula from Chern-Simons theory and the G/G model
[DE93-628620] p 1221 N94-17632
THERAPY
Center of Excellence in Laser Medicine
[DE93-016541] p 1122 N94-16113
THERMAL ANALYSIS
A novel solid-state optical temporal analyzer with picosecond resolution and picowatt sensitivity
[AD-A266804] p 986 N94-14912
High temperature advanced structural composites. Volume 2: Ceramic matrix composites, fiber processiing and properties, and interfaces
[AD-A267023] p 933 N94-15528
A Pluto thermal model p 1256 N94-16216
Comparative magnetic and thermoanalytical study of two enstatite chondrites: Adhi Kot and Atlanta
p 1244 N94-16329
SRB thermal curtain design support
[NASA-CR-193857] p 927 N94-17123
SRB thermal curtain design support
[NASA-CR-193858] p 928 N94-17124
Overview of the solar dynamic ground test demonstration program
[NASA-TM-106296] p 928 N94-17256
ASRM nozzle thermal analysis
[NASA-CR-194672] p 928 N94-17277
Structural mechanics division research and technology accomplishments for CY 1992 and plans for CY 1993
[NASA-TM-107752] p 1062 N94-17479
THERMAL BOUNDARY LAYER
Models of thermal/chemical boundary layer convection: Potential application to Venus p 1279 N94-16348
On the relationship between tectonic plates and thermal mantle plume morphology p 1104 N94-16349
THERMAL CONDUCTIVITY
A posteriori error estimation for hierarchic models of elliptic boundary value problems on thin domains
[AD-A267714] p 1168 N94-14939
Modeling the thermal conductivity of fiber-reinforced ceramic composites
[DE93-015340] p 934 N94-16017
SRB thermal curtain design support
[NASA-CR-193858] p 928 N94-17124
Low dielectric constant insulators and gold metallization for GHz multi-chip modules, part 2
[AD-A268590] p 1176 N94-17605
Coefficients for calculating thermodynamic and transport properties of individual species
[NASA-TM-4513] p 1220 N94-17624
THERMAL CYCLING TESTS
Density and temperature relaxation near the critical point of carbon dioxide under reduced gravity
p 944 N94-15164
Hollow cathode heater development for the Space Station plasma contactor
[NASA-CR-191131] p 926 N94-16880
Reliability analysis of Surface Mount Technology (SMT)
[AD-A267598] p 1055 N94-17194
Elastic-plastic finite-difference analysis of unidirectional composites subjected to thermomechanical cyclic loading
[AD-A267666] p 1061 N94-17269
Prediction of thermal cycling induced cracking in polymer matrix composites
[NASA-CR-194677] p 941 N94-17295

THERMAL DEGRADATION
Advanced thermally stable jet fuels
[DE93-017711] p 975 N94-16996
THERMAL DIFFUSIVITY
Investigation of radiative interaction in laminar flows using Monte Carlo simulation
[NASA-CR-194604] p 1021 N94-15795
THERMAL DISSOCIATION
The thermal dissociation of NH2CHO(ND2CHO) on Si(100)-2x1
[AD-A266903] p 942 N94-14956
THERMAL EMISSION
Thermal inertia and radar reflectivity of the Martian north polar ERG: Low-density aggregates
p 1260 N94-16238
A decade's overview of Io's volcanic activity
p 1245 N94-16386
Comparison of preliminary results from Airborne Aster Simulator (AAS) with TIMS data p 1064 N94-16600
Ejecta patterns of Meteor Crater, Arizona derived from the linear un-mixing of TIMS data and laboratory thermal emission spectra p 1065 N94-16607
Simulation of ASTER data using AVIRIS images
p 1071 N94-16693
THERMAL ENERGY
Optical and infrared spectra of thermally annealed Pb implanted SiO2 glasses
[DE93-015304] p 965 N94-15828
Synthesis of ceramic oxide powders in a microwave plasma device
[DE93-012741] p 965 N94-15920
GAM-HEAT: A computer code to compute heat transfer in complex enclosures
[DE93-014724] p 1023 N94-15980
High heat flux engineering in solar energy applications
[DE93-016500] p 1093 N94-16954
Emittance growth in displaced, space-charge-dominated beams with energy spread
[DE93-016514] p 1188 N94-17672
THERMAL ENVIRONMENTS
First results from a laboratory facility for measurement of emission spectra under simulated planetary conditions
p 954 N94-16372
Diffractive optics in adverse environments
p 1197 N94-17352
THERMAL EXPANSION
Thermal stresses of a trimaterial medium in a nonuniform temperature field
[AD-A267243] p 930 N94-14975
High temperature advanced structural composites. Volume 3: Mechanics
[AD-A267024] p 933 N94-15626
Carbon-carbon grid for ion engines
[NASA-CASE-NPO-19174-1-CU] p 925 N94-15876
THERMAL FATIGUE
Crystallization of grain boundary phases in silicon nitride with low additive contents by microwave annealing
[DE93-015801] p 1209 N94-16164
Hollow cathode heater development for the Space Station plasma contactor
[NASA-CR-191131] p 926 N94-16880
Prediction of thermal cycling induced cracking in polymer matrix composites
[NASA-CR-194677] p 941 N94-17295
Aspects of high temperature damage in fiber reinforced titanium metal matrix composites
[AD-A267907] p 941 N94-17379
THERMAL INSULATION
Improved composite flexible blanket insulation
[NASA-CASE-ARC-11955-1-CU] p 934 N94-15926
Impact penetration experiments in teflon targets of variable thickness p 1063 N94-16253
SRB thermal curtain design support
[NASA-CR-193857] p 927 N94-17123
SRB thermal curtain design support
[NASA-CR-193858] p 928 N94-17124
THERMAL MAPPING
Ground truth spectrometry and imagery of eruption clouds to maximize utility of satellite imagery
[NASA-CR-194358] p 1081 N94-15181
Testing the waters from space — Thermal mapping
[NASA-TM-109623] p 1082 N94-15409
Sand transport on Mars: Preliminary results from models p 1252 N94-16198
Clementine: Anticipated scientific datasets from the Moon and Geographos p 1288 N94-16392
Thermogeologic mapping of the Moon from lunar orbit
p 1290 N94-16405
TIMS performance evaluation summary
p 1063 N94-16596
Atmospheric propagation analysis program
[AD-A268231] p 1006 N94-17565
THERMAL NOISE
Cryogenic measurements of aerojet GaAs n-JFETs
[NASA-TM-103972] p 1009 N94-15765
Thermally-sustained structure in convectively unstable systems
[NASA-TM-106375] p 1027 N94-17112
THERMAL PROTECTION
Processing and protection of high temperature structural materials
[AD-A267292] p 954 N94-14961
THERMAL RADIATION
Near-surface temperature gradients and their effects on thermal-infrared emission spectra of particulate planetary surfaces p 1260 N94-16236
A decade's overview of Io's volcanic activity
p 1245 N94-16386
Altitude profile of aerosols on Mars from measurements of its thermal radiation on limb p 1294 N94-16423
THERMAL RESISTANCE
Crystallization of grain boundary phases in silicon nitride with low additive contents by microwave annealing
[DE93-015801] p 1209 N94-16164
Development and commercialization status of Fe3Al-based intermetallic alloys
[DE93-015802] p 957 N94-16165
THERMAL SHOCK
The relationship of metallothionein induction to the heat shock response
[AD-A266634] p 1122 N94-15741
Design of a cruciform bend specimen for determination of out-of-plane biaxial tensile stress effects on fracture toughness for shallow cracks
[DE93-015455] p 1059 N94-16104
Heat shock protein induction in human cells by CO2 laser irradiation
[AD-A266430] p 1117 N94-16545
THERMAL SIMULATION
Venusian pancake domes: Insights from terrestrial voluminous silicic lavas and thermal modeling
p 1286 N94-16381
THERMAL STABILITY
Scholarly research program in fuel analysis and combustion research
[AD-A266789] p 942 N94-14911
Compounds containing meta-biphenylenedioxy moieties and polymers therefrom
[NASA-CASE-LAR-14517-1] p 965 N94-15879
Isolation of thermostable enzyme mutants by cloning and selection in thermophilic bacteria
[AD-A266378] p 1117 N94-16514
Electrical conductivity of ion implanted ladder and semi-ladder polymers
[AD-A267432] p 970 N94-16978
Advanced thermally stable jet fuels
[DE93-017711] p 975 N94-16996
Diffractive optics in adverse environments
p 1197 N94-17352
THERMAL STRESSES
Scholarly research program in fuel analysis and combustion research
[AD-A266789] p 942 N94-14911
XPS analysis of Al/EPDM bondlines from IUS SRM-1 polar bosses
[AD-A266851] p 1056 N94-14945
Thermal stresses of a trimaterial medium in a nonuniform temperature field
[AD-A267243] p 930 N94-14975
High temperature advanced structural composites. Volume 3: Mechanics
[AD-A267024] p 933 N94-15626
Thermal stress effects in intermetallic matrix composites
[NASA-CR-191191] p 1054 N94-16518
Elastic-plastic finite-difference analysis of unidirectional composites subjected to thermomechanical cyclic loading
[AD-A267666] p 1061 N94-17269
Fiber strength utilization in carbon/carbon composites
[AD-A267713] p 940 N94-17271
Aspects of high temperature damage in fiber reinforced titanium metal matrix composites
[AD-A267907] p 941 N94-17379
THERMIONIC CONVERTERS
High temperature materials technology research for advanced thermionic systems
[DE93-018302] p 960 N94-16964
THERMIONIC EMITTERS
High temperature materials technology research for advanced thermionic systems
[DE93-018302] p 960 N94-16964
THERMISTORS
Analysis of TIMS performance subjected to simulated wind blast p 1063 N94-16598
THERMOCHEMICAL PROPERTIES
Laser ignition of solid propellants: 1. Ignition delays
[AD-A268454] p 976 N94-17536
THERMOCHEMISTRY
Processing and protection of high temperature structural materials
[AD-A267292] p 954 N94-14961
Rocket motor plume flowfields: Phenomenology and simulation p 924 N94-15221
Thermochemistry of silicate speciation in aqueous sodium silicate solutions: Ionization and polymerization of small silicate ion
[AD-A266825] p 964 N94-15683
Particle simulation of hypersonic flow
[AD-A267185] p 857 N94-15787
Ceramic fiber coatings development and demonstration
[AD-A267286] p 972 N94-17242
Interface chemistry in ceramic matrix composites
[AD-A268629] p 973 N94-17466
THERMOCOUPLES
Simultaneous measurement of temperature and strain using four connecting wires
[NASA-TM-104271] p 1032 N94-15754
Dual active surface, miniature, plug-type heat flux gauge
[NASA-CASE-LEW-15643-1] p 1033 N94-15928
Wind tunnel investigation with an operational turbojet engine
[TABES PAPER 93-662] p 870 N94-16157
THERMODYNAMIC CYCLES
Some single-piston closed-cycle machines and Peter Tailer's thermal lag engine
[DE93-015983] p 1049 N94-17675
THERMODYNAMIC EFFICIENCY
Jet engine performance enhancement through use of a wave-rotor topping cycle
[NASA-TM-4486] p 870 N94-17470
THERMODYNAMIC EQUILIBRIUM
Modeling study to evaluate the ionic mechanism of soot formation in flames
[AD-A266242] p 950 N94-16930
THERMODYNAMIC PROPERTIES
Processing and protection of high temperature structural materials
[AD-A267292] p 954 N94-14961
PHENIX Conceptual Design Report
[DE93-015759] p 1182 N94-16161
The effect of irradiation on the mechanical properties of 6061-T651 aluminum
[DE93-015825] p 958 N94-16168
Cation ordering in orthopyroxenes and cooling rates of meteorites: Low temperature cooling rates of Estherville, Bondoc and Shaw p 1241 N94-16176
Thermal disorder in adsorbed Cl on Si(100)
[AD-A266295] p 1210 N94-16476
On-line gas chromatographic studies of Rutherfordium (element 104), hahnium (element 105), and homologs
[DE93-013890] p 948 N94-16821
Modeling study to evaluate the ionic mechanism of soot formation in flames
[AD-A266242] p 950 N94-16930
Mechanistic models of soot formation
[AD-A267806] p 950 N94-17008
Convection effects on radial segregation and crystal melt interface in vertical Bridgman growth
[NASA-CR-191541] p 1029 N94-17387
Flow instability tests for a particle bed reactor nuclear thermal rocket fuel element
[AD-A268012] p 929 N94-17474
Soluble precursor route to polyanilines
[AD-A268015] p 973 N94-17494
Numerically solving a transient heat conduction problem with convection and radiation
[AD-A268521] p 1220 N94-17540
THERMODYNAMICS
Inelastic deformation of metal matrix composites
[NASA-CR-191522] p 930 N94-15106
High temperature advanced structural composites. Volume 1: Executive summary and intermetallic compounds
[AD-A267022] p 933 N94-15835
Implementation of an anisotropic turbulence model in the COMMIX-1C/ATM computer code
[DE93-015541] p 1023 N94-16444
Supercritical thermodynamics of sulfur and nitrogen species
[DE93-017727] p 1220 N94-16997
Thermo-mechanical analysis of oxidation protected carbon-carbon composites
[AD-A268191] p 941 N94-17597
THERMOELASTICITY
Thermal stresses of a trimaterial medium in a nonuniform temperature field
[AD-A267243] p 930 N94-14975
THERMOELECTRICITY
Simultaneous measurement of temperature and strain using four connecting wires
[NASA-TM-104271] p 1032 N94-15754

THERMOGRAVIMETRY
Direct catalytic decomposition of nitric oxide
[DE93-016689] p 949 N94-16896
THERMOLUMINESCENCE
Optical fiber spectroscopy: A study of the luminescent properties of the europium ion for thermal sensors
[NASA-CR-194576] p 1189 N94-15647
Induced thermoluminescence study of experimentally shock-loaded oligoclase p 953 N94-16266
Shock-thermal history of Kapoeta howardite matter on data of thermoluminescence analysis of individual mineral grains p 953 N94-16267
THERMOMECHANICAL TREATMENT
Development and commercialization status of Fe3Al-based intermetallic alloys
[DE93-015802] p 957 N94-16165
Elastic-plastic finite-difference analysis of unidirectional composites subjected to thermomechanical cyclic loading
[AD-A267666] p 1061 N94-17269
THERMOMETERS
Temperature measurements p 1037 N94-15804
THERMONUCLEAR REACTIONS
Nuclear fusion of protons with ions of boron
[DE93-015399] p 1202 N94-16019
THERMOPHILES
Isolation of thermostable enzyme mutants by cloning and selection in thermophilic bacteria
[AD-A266378] p 1117 N94-16514
THERMOPHYSICAL PROPERTIES
The specific heat of titanium disilicide
[AD-A267543] p 960 N94-17100
THERMOPLASTIC RESINS
A new NASA LaRC Multi-Purpose Prepregging Unit p 932 N94-15276
Process of shaping an electrorheological solid
[AD-D015885] p 1012 N94-16914
THERMOPLASTICITY
Machine development p 932 N94-15258
THERMOREGULATION
Melatonin, the pineal gland, and circadian rhythms
[AD-A268200] p 1129 N94-17478
THERMOSETTING RESINS
A new NASA LaRC Multi-Purpose Prepregging Unit p 932 N94-15276
THESAURI
A browsing tool for the Internet Logical Library of the HPCC Software Exchange
[NASA-CR-194545] p 1143 N94-15189
THICK FILMS
Mechanical properties and crystal growth studies of semiconductor alloys
[AD-A268144] p 1216 N94-17454
THICKNESS
Experimental investigations into the deflagration to detonation transition at TNO/PML
[AD-A266753] p 1021 N94-15755
The Acraman impact structure: Estimation of the diameter by the ejecta layer thickness p 1103 N94-16211
Estimates of lithospheric thickness on Venus p 1267 N94-16277
On the a-posteriori estimation of the modelling error for the heat conduction in a plate and its use for adaptive hierarchic modelling
[AD-A267965] p 1029 N94-17384
THIN FILMS
Ion mixing of thin ZrO2 films on sapphire
[DE93-015214] p 1206 N94-14925
Preparation and investigation of improved low voltage electron excitable phosphors
[AD-A266852] p 963 N94-14948
Magneto-optic superlattice thin films: Fabrication, structural and magnetic characterization p 974 N94-14982
A new NASA LaRC Multi-Purpose Prepregging Unit p 932 N94-15276
Photochemistry in thin polymeric films
[AD-A266716] p 964 N94-15729
Diamond epitaxy and diamondlike coatings
[AD-A266657] p 1206 N94-15747
Laser assisted CVD growth of AlN and GaN
[AD-A267150] p 1206 N94-15764
Experimental investigations of superconductivity in quasi-two-dimensional epitaxial copper oxide superlattices and trilayers
[DE93-015306] p 1207 N94-15829
Absolute, Extreme-Ultraviolet Solar Spectral Irradiance Monitor (AESSIM)
[AD-A267045] p 1299 N94-15836
Multilayer thin film design for far ultraviolet polarizers using an induced transmission and absorption technique
[NASA-CR-194631] p 1190 N94-15869
Cyanoresin, cyanoresin/cellulose triacetate blends for thin film, dielectric capacitors
[NASA-CASE-NPO-18913-1-CU] p 966 N94-15930
Cellulose triacetate, thin film dielectric capacitor
[NASA-CASE-NPO-18935-1-CU] p 1010 N94-15952
Modification of fluoropolymer surfaces with electronically conductive polymers
[AD-A266294] p 967 N94-16475
Apparatus for and a method of growing thin films of elemental semiconductors
[AD-D015813] p 1210 N94-16487
VUV thin films, chapter 7
[NASA-CR-194634] p 967 N94-16494
Properties of thin films for high temperature flow sensors
[NASA-CR-191526] p 967 N94-16541
Pulsed laser deposition of metastable Ca(1-x)Sr(x)CuO2 thin films
[DE93-015804] p 1040 N94-16663
Sputtered ferroelectric thin films of KTN for electro-optic devices
[AD-A266573] p 968 N94-16723
Neutron and x ray scattering studies of (FeF2)(sub m)(CoF2)(sub n) multilayers
[DE93-015809] p 1184 N94-16838
Performance of silvered Teflon thermal control blankets on spacecraft
[AD-A266284] p 887 N94-16909
A simple chemical procedure for extending the conductive state of polypyrrole to more negative potentials
[AD-A266235] p 969 N94-16928
UHV-stem studies on nucleation and growth of thin metal silicide films on silicon
[DE93-017604] p 1212 N94-16961
Nitride semiconductors for ultraviolet detection
[AD-A267877] p 1012 N94-17040
Atomic layer epitaxy group IV materials: Surface processes, thin films, devices and their characterization
[AD-A267527] p 1213 N94-17116
Single crystal diamond thin films
[AD-A266457] p 1214 N94-17216
Characterization of metallic multilayers using x ray diffraction analysis
[NIAR-93-13] p 961 N94-17282
Thin composite solid electrolyte film for lithium batteries
[NASA-CASE-NPO-18694-1-CU] p 1014 N94-17325
Low temperature deposition and characterization of n- and p-type silicon carbide thin films and associated ohmic and Schottky contacts
[AD-A267966] p 973 N94-17490
Advanced thin-film deposition and physical properties of high-temperature and other novel superconducting materials
[AD-A268199] p 1216 N94-17561
Epitaxial iron films
[AD-A268286] p 1217 N94-17579
Mechanical properties of interfaces and superlattices
[AD-A268591] p 1217 N94-17606
A new method of designing multilayer optical thin film coatings
[DE93-624683] p 974 N94-17611
Electrical properties of sol-gel PZT thin films for decoupling capacitor applications
[DE93-016491] p 1015 N94-17648
Growth of dielectric thin films by irradiation of condensed molecular precursors with synchrotron radiation
[DE93-016161] p 974 N94-17676
THIN PLATES
Analysis of electromagnetic scattering from irregularly shaped, thin, metallic flat plates
[NASA-TP-3361] p 998 N94-16655
THREAT EVALUATION
NASA security handbook
[NHB-1620.3C] p 1224 N94-15937
THREE AXIS STABILIZATION
Standard platforms for small satellites p 895 N94-17181
THREE BODY PROBLEM
Energy potential analysis of zero velocity curves in the restricted three-body problem
[AD-A267512] p 1170 N94-17076
A guidance and navigation system for two spacecraft rendezvous in translunar halo orbit
[AD-A267498] p 898 N94-17368
THREE DIMENSIONAL BOUNDARY LAYER
Three-dimensional turbulent boundary layer
[AD-A266261] p 1025 N94-16908
Structure of turbulence in three-dimensional boundary layers
[NASA-CR-194655] p 1027 N94-17130
Multigrid direct numerical simulation of the whole process of flow transition in 3-D boundary layers
[NASA-TM-106369] p 1030 N94-17557
THREE DIMENSIONAL FLOW
Numerical simulation of 3-D shock wave turbulent boundary layer interactions p 1017 N94-15199
Numerical investigations in three-dimensional internal flows
[NASA-CR-194594] p 1020 N94-15551
Numerical simulation of three-dimensional self-gravitating flow
[NASA-TM-109021] p 1021 N94-15768
On the stability analysis of approximate factorization methods for 3D Euler and Navier-Stokes equations
[NASA-TM-106314] p 1169 N94-15818
Inviscid instability of streamwise corner flow
[NASA-CR-191514] p 1021 N94-15834
Proteus three-dimensional Navier-Stokes computer code, version 1.0. Volume 1: Analysis description
[NASA-TM-106337] p 1024 N94-16527
Adaptive Cartesian grid methods for representing geometry in inviscid compressible flow
[DE93-016430] p 1025 N94-16894
Computational aerodynamics with icing effects
[AD-A267509] p 860 N94-17074
THREE DIMENSIONAL MODELS
Surface and internal signatures of organized vortex motions in stratified fluid
[AD-A267015] p 1020 N94-15526
Cooperativity and 3-D representation
[AD-A267180] p 1131 N94-15694
Display of dynamic, volume graphic images by holographic voxel projection: Initial investigation
[AD-A267622] p 1035 N94-17197
Strategic planning for aircraft noise route impact analysis: A three dimensional approach
[NASA-CR-191484] p 1178 N94-17278
Single block three-dimensional volume grids about complex aerodynamic vehicles
[NASA-TM-108986] p 1030 N94-17476
Three dimensional visualization of GOES cloud data using OCTRESS
[AD-A268102] p 1109 N94-17572
THROATS
Experimental studies on a gas dynamic laser with narrow throat and high area-ratio grid nozzles
[AD-A267818] p 1042 N94-17400
THRUST VECTOR CONTROL
Effects of internal yaw-vectoring devices on the static performance of a pitch-vectoring nonaxisymmetric convergent-divergent nozzle
[NASA-TP-3369] p 858 N94-16572
Equations of motion of a hinged body over a spherical earth
[AD-A268408] p 868 N94-17435
Heat transfer parametric system identification
[AD-A268525] p 929 N94-17543
THRUSTORS
Segmented ion thruster
[NASA-CASE-NPO-18192-1-CU] p 925 N94-15927
THULIUM
Growth of new materials for solid state laser applications. The growth of ZnGeP2 by the vertical Bridgman method
[NASA-CR-194571] p 1038 N94-15530
THUNDERSTORMS
Sensitivity testing of a single-Doppler temperature retrieval and forecast system
[AD-A267278] p 1105 N94-14958
Venus lightning
[NASA-TM-109644] p 1105 N94-15430
Radar diagnostic parameters as indicators of severe weather in central Florida
[PB93-183507] p 1106 N94-16465
Middle atmospheric electric fields over thunderstorms
[NASA-CR-194619] p 1106 N94-16493
Remote sensing of precipitation and electrification with a dual-polarization, coherent, wideband radar system
[AD-A267479] p 1004 N94-17364
TIDES
Characterization of spatial and temporal variability of phytoplankton blooms in coastal waters
[AD-A267102] p 1116 N94-15633
Tidal interaction: A possible explanation for geysers and other fluid phenomena in the Neptune-Triton system p 1272 N94-16311
TILT ROTOR AIRCRAFT
XV-15: Tiltrotor
[NASA-TM-109455] p 865 N94-15328
TILT ROTOR RESEARCH AIRCRAFT PROGRAM
XV-15: Tiltrotor
[NASA-TM-109455] p 865 N94-15328
TILTING ROTORS
XV-15: Tiltrotor
[NASA-TM-109455] p 865 N94-15328
TILTMETERS
Long baseline watertubes p 1037 N94-15803
Cooperative projects in geodynamical instrumentation between the State Seismological Bureau (China) and the Royal Observatory of Belgium p 1037 N94-15806
Earth tides results obtained with gravimeters, clinometers, and strainmeters in Belgium and in Grand Duchy of Luxembourg p 1100 N94-15809

TIME DEPENDENCE
Timebias corrections to predictions p 875 N94-15591
Formation of on-site normal points p 917 N94-15592
Reliability characterization of digital microcircuits: Investigation of an in-process oxide reliability screening method
[AD-A267053] p 1008 N94-15665
On the design of structural components using materials with time-dependent properties
[NASA-TM-108428] p 1059 N94-16519
The use of General Circulation Models in detecting climate change induced by greenhouse gases
[DE93-014369] p 1096 N94-16802
Finite difference time domain analysis of chirped dielectric gratings p 1195 N94-17339
Time dependent turbulence modeling and analytical theories of turbulence
[NASA-TM-106379] p 1029 N94-17385
On the stability of a time dependent boundary layer
[NASA-CR-191542] p 1030 N94-17450
A physical model for one-dimension and time-dependent ionosphere. Part 2: Results and discussions
[DE93-627959] p 1103 N94-17631

TIME LAG
Assessment of TDI operation of a frame transfer CCD for high resolution imaging from a fast spinning spacecraft p 910 N94-15097
System architecture of optically controlled phased array radar
[AD-A267056] p 988 N94-15667
Passive tracking of a target using an array of sensors
[DE93-015870] p 997 N94-16169
Pulse response based control for minimum time maneuver of flexible spacecraft
[AD-A266186] p 886 N94-16455
Measuring ocean coherence time with dual-baseline interferometry p 1080 N94-16759
True time delay optically controlled dual band transmitter
[AD-A267663] p 1003 N94-17228

TIME MARCHING
Multigrid time-accurate integration of Navier-Stokes equations
[NASA-TM-106373] p 1028 N94-17258

TIME MEASUREMENT
Adaptive median filtering for preprocessing of time series measurements p 912 N94-15561
Measuring ocean coherence time with dual-baseline interferometry p 1080 N94-16759
Digital reverberation time measurement system
[AD-D015892] p 1177 N94-16919
Target detection by way of Kalman filtering
[AD-A267314] p 1000 N94-16945
Quartz crystal resonators and oscillators for frequency control and timing applications: A tutorial, revision 6.1
[AD-A268205] p 1216 N94-17480

TIME OF FLIGHT SPECTROMETERS
Laser photoionization time-of-flight mass spectrometry of nitrated polycyclic aromatic hydrocarbons and nitrated heterocyclic compounds
[AD-A268126] p 952 N94-17520

TIME RESPONSE
Target detection by way of Kalman filtering
[AD-A267314] p 1000 N94-16945

TIME SERIES ANALYSIS
Arctic internal waves (CEAREX)
[AD-A265822] p 1111 N94-15139
Adaptive median filtering for preprocessing of time series measurements p 912 N94-15561
Generation of artificial helioseismic time-series
[NASA-CR-194612] p 1299 N94-15968

TIME SHARING
Processor capacity reserves for multimedia operating systems
[AD-A266639] p 1158 N94-15745

TIME SIGNALS
Neighboring extremal guidance for systems with piecewise linear control using time as the reference variable
[AD-A267942] p 874 N94-17010
Femtosecond carrier processes in compound semiconductors and real time signal processing
[AD-A268122] p 1005 N94-17519

TIMING DEVICES
Development of the OMPAT neuropsychological/psychomotor performance evaluation and OMPAT data and timing support programs
[AD-A266954] p 1122 N94-15759

TIRES
Remote tire pressure sensing technique
[NASA-CASE-LAR-14160-1] p 1033 N94-15884

TISSUES (BIOLOGY)
An apparatus for measuring the biological oxidation of hydrogen gas under hyperbaric conditions
[AD-A266834] p 1119 N94-14916
Cultured normal mammalian tissue and process
[NASA-CASE-MSC-21984-1] p 1117 N94-15969

TITANIUM
STS-26 SSIP briefing --- Titanium Grain Formation Experiment and Crystal Membrane Experiment
[NASA-TM-109556] p 976 N94-15280
Limited subsolidus diffusion in type B1 CAI: Evidence from Ti distribution in spinel p 954 N94-16401
Interfacial shear behavior and its influence on fiber damage in sapphire-reinforced gamma titanium aluminide composites
[AD-A267943] p 1060 N94-17043
The specific heat of titanium disilicide
[AD-A267543] p 960 N94-17100
Aspects of high temperature damage in fiber reinforced titanium metal matrix composites
[AD-A267907] p 941 N94-17379

TITANIUM ALLOYS
The corrosion protection of metals by ion vapor deposited aluminum
[NASA-TM-108425] p 955 N94-15832
Bulk and defect properties of ordered intermetallics: A first-principles total-energy investigation
[DE93-015492] p 959 N94-16873
Transient phenomena following precipitation and re-solution anneals in a NiTi alloy
[AD-A267557] p 961 N94-17106
Characterization of metallic multilayers using x ray diffraction analysis
[NIAR-93-13] p 961 N94-17282

TITANIUM BORIDES
Production and evaluation of dense ceramic compounds by combustion synthesis and dynamic compaction
[AD-A266742] p 965 N94-15773
Dynamic testing and characterization of pre-fractured ceramic
[DE93-016457] p 972 N94-17238

TITANIUM CARBIDES
Wear resistant titanium material development
[AD-A266474] p 959 N94-16780

TITANIUM COMPOUNDS
Structural studies of sol-gel glasses
[AD-A266277] p 967 N94-16472

TITANIUM OXIDES
Searching for neuKREEP: An EMP study of Apollo 11 Group A basalts p 1266 N94-16275
Lunar phase function effects on spectral ratios used for resource assessment p 1278 N94-16342

TOCOPHEROL
Wound healing after laser injury to skin: The effect of occlusion and vitamin E
[AD-A266473] p 1128 N94-16779

TOKAMAK DEVICES
Description of cooling water calorimetry and wall thermometry diagnostic at tokamak ASDEX-Upgrade
[IPP-5/46] p 1200 N94-14966
Studies on the parametric decay of waves in fusion plasmas
[VTT-PUBS-110] p 1200 N94-15204
Current drive with free electron lasers in high and low temperature tokamaks p 1201 N94-15209
ITER-HARD Toroidal Field coil structural analysis
[DE93-014834] p 1201 N94-15981
High beta and confinement studies of TFTR
[DE93-016204] p 1202 N94-16446
Inductive effects during second harmonic current drive experiments on T-10
[DE93-014411] p 1202 N94-16803
Recent results from the 60 GHz inside launch ECH system on the D3-D tokamak
[DE93-013027] p 1203 N94-16816
Simulation of enhanced tokamak performance on D3-D using fast wave current drive
[DE93-014009] p 1203 N94-16823
Nonlinear gyrofluid models of shear Alfven instabilities in ignited and beam heated toroidal plasmas
[DE93-016235] p 1203 N94-16869
ARIES tokamak reactor study
[DE93-017059] p 1203 N94-16901

TOLERANCES (MECHANICS)
Geometric tolerance assessment
[NPL-DITC-210/92] p 1049 N94-15013
A review of Australian and New Zealand investigations on aeronautical fatigue during the period April 1991 to March 1993
[AD-A267532] p 868 N94-17117

TOLLMIEN-SCHLICHTING WAVES
Tollmien-Schlichting/vortex interactions in compressible boundary layer flows
[NASA-CR-191515] p 1017 N94-15183
Receptivity of boundary layers to convected gusts
[AD-A267206] p 1022 N94-15860
Higher-order accurate Osher schemes with application to compressible boundary layer stability
[NASA-TM-106355] p 1026 N94-17056
On the stability of a time dependent boundary layer
[NASA-CR-191542] p 1030 N94-17450

TOMOGRAPHY
Requirements on CCD-detectors for ground-based auroral imaging p 909 N94-15093

TOPEX
Analysis of TOPEX laser retroreflector array characteristics p 915 N94-15578

TOPOGRAPHY
Improved mapping system
[NASA-TM-109643] p 1082 N94-15428
Multi-beam laser altimeter p 921 N94-15620
Engineering design of sub-micron topographies for simultaneously adherent and reflective metal-polymer interfaces
[NASA-CR-194573] p 964 N94-15700
A multilevel-multiresolution method for image processing. A Bayesian framework for reconstructing and representing shapes
[AD-A266772] p 1082 N94-15842
Ray tracing on topographic Rossby waves
[AD-A267014] p 1112 N94-15844
Magellan: Principal Venus science findings p 989 N94-15887
TOPSAT: Global space topographic mission p 992 N94-15905
Research into the influence of spatial variability and scale on the parameterization of hydrological processes
[NASA-CR-194610] p 1082 N94-16026
Similarity and scale in catchment storm response
[PAPER-89RG01615] p 1083 N94-16028
Evapotranspiration and runoff from large land areas: Land surface hydrology for atmospheric general circulation models p 1083 N94-16029
Heterogeneity and scaling land-atmospheric water and energy fluxes in climate systems p 1083 N94-16030
A detailed model for simulation of catchment scale subsurface hydrologic processes
[PAPER-92WR02333] p 1084 N94-16032
Morphology and models for the evolution of eastern Hecate Chasma, Venus p 1256 N94-16215
Ishtar deformed belts: Evidence for deformation from below? p 1256 N94-16218
Confirmation of saturation equilibrium conditions in crater populations p 1103 N94-16222
Megaplumes on Venus p 1271 N94-16301
An inversion of geoid and topography for mantle and crustal structure on Mars p 1273 N94-16315
Separation of topographic and intrinsic backscatter variations in biscopic radar images: A magic airbrush p 1086 N94-16318
The cartography of Venus with Magellan data p 1274 N94-16320
Meander properties of Venusian channels p 1275 N94-16324
Spectral study of Venus global topography and geoid from Magellan and PVO data p 1276 N94-16332
Resolving topographic detail on Venus by modeling complex Magellan altimetry echoes p 1283 N94-16368
Sedimentation, volcanism, and ancestral lakes in the Valles Marineris: Clues from topography p 1283 N94-16369
Effective elastic thickness of the Venusian lithosphere with lateral viscosity variations in the mantle p 1293 N94-16421
Dust-dynamic feedbacks in the Martian atmosphere: Surface dust lifting p 1296 N94-16434
Mapping of sea bottom topography p 1077 N94-16744
Sea bottom topography imaging with SAR p 1077 N94-16745
Detecting surface roughness effects on the atmospheric boundary layer via AIRSAR data: A field experiment in Death Valley, California p 1078 N94-16747
The TOPSAR interferometric radar topographic mapping instrument p 1078 N94-16749
A geological and geophysical information system for Eurasia
[AD-A267841] p 1232 N94-17036

TORNADOES
Radar diagnostic parameters as indicators of severe weather in central Florida
[PB93-183507] p 1106 N94-16465

TOROIDAL PLASMAS
ITER-HARD Toroidal Field coil structural analysis
[DE93-014834] p 1201 N94-15981
Structure and damping of toroidal drift waves (and their implications for anomalous transport)
[DE93-014005] p 1203 N94-16822
Nonlinear gyrofluid models of shear Alfven instabilities in ignited and beam heated toroidal plasmas
[DE93-016235] p 1203 N94-16869

TOTAL OZONE MAPPING SPECTROMETER
Southern and Northern Hemisphere total ozone as seen by TOMS
[NASA-TM-109591] p 1098 N94-15282
TOMS computer graphics
[NASA-TM-109597] p 1094 N94-15290
Atlas of TOMS ozone, 1978-1988
[NASA-TM-109456] p 1094 N94-15329
TOTAL QUALITY MANAGEMENT
Army Software Test and Evaluation Panel (STEP) software metrics initiatives report
[AD-A266889] p 1142 N94-14924
Creating and maintaining a visionary quality program
[DE93-015122] p 1050 N94-16055
Impact of TQM concepts on inspection of aerospace systems
[TABES PAPER 93-350] p 1050 N94-16130
Total quality environmental management leadership through quality
[TABES PAPER 93-540] p 1050 N94-16135
Identifying and responding to customer needs at the Kennedy Space Center p 1056 N94-16626
TOUGHNESS
Transformation toughening of composite ceramics
[AD-A267304] p 971 N94-16980
Micromechanisms of monotonic and cyclic subcritical crack growth in advanced high melting point low-ductility intermetallics
[AD-A267764] p 961 N94-17223
TOWED BODIES
A microprocessor controller for a towing tank drive and flow visualisation system
[AD-A267087] p 872 N94-15543
TOWING
A microprocessor controller for a towing tank drive and flow visualisation system
[AD-A267087] p 872 N94-15543
TOXIC DISEASES
Fibers and materials of medical application p 938 N94-16855
TOXIC HAZARDS
Toxic substances registry system: Index of material safety data sheets
[NASA-TM-109332] p 1121 N94-15658
Proceedings of the 1992 Annual Meeting NASA Occupational Health Program
[NASA-CR-193462] p 1123 N94-16609
Emergency preparedness and planning p 1124 N94-16613
Lead poisoning: An overview p 1124 N94-16614
Medical surveillance and biological monitoring of lead exposed employees p 1124 N94-16615
Education and training of professional industrial hygienists for 2020 p 1125 N94-16618
Arsenic surveillance program p 1127 N94-16637
Lead Surveillance Program p 1127 N94-16640
Respiratory Protection Program medical clearance for respirator use p 1127 N94-16642
General Medical Surveillance Program p 1127 N94-16643
Environmental use of a Laser Range Finder and the Advanced Visualization System
[DE93-016163] p 1043 N94-17677
TOXICITY
Toxic substances registry system: Index of material safety data sheets
[NASA-TM-109332] p 1121 N94-15658
Neurotoxicity of hemoglobin in cortical cell culture
[AD-A266506] p 1128 N94-16786
TOXICITY AND SAFETY HAZARD
Emergency preparedness and planning p 1124 N94-16613
Medical surveillance and biological monitoring of lead exposed employees p 1124 N94-16615
TOXICOLOGY
Development of pattern recognition techniques for the evaluation of toxicant impacts to multispecies systems
[AD-A267197] p 1095 N94-15790
The behavioral toxicology of high-peak, low average power, pulsed microwave irradiation
[AD-A268392] p 1134 N94-17535
TRACE CONTAMINANTS
Gas separations using ceramic membranes
[DE93-000278] p 947 N94-15861
Application of non-thermal plasmas to pollution control
[DE93-016432] p 1096 N94-16449
Trace analysis of chemical warfare agents in air: Sampling in porous polymers followed with thermal desorption analysis
[FOA-C-40302-4.6] p 1097 N94-17625
Characterization of Ni on Si wafers: Comparison of surface analysis techniques
[DE93-016501] p 953 N94-17649
TRACE ELEMENTS
A proposed mechanism for the pyrolysis of diborane
[DE93-014275] p 947 N94-15977
Assimilation of solids during ascent of magmas from the Bartoy Field of the Baikal Region, Siberia p 1103 N94-16214
Trace-element composition of Chicxulub crater melt rock, K/T tektites and Yucatan basement p 1242 N94-16245
Searching for neuKREEP: An EMP study of Apollo 11 Group A basalts p 1266 N94-16275
On the composition of neuKREEP: QMD contamination at Apollo 11? p 1266 N94-16276
Partitioning of Nb, Mo, Ba, Ce, Pb, Th and U between immiscible carbonate and silicate liquids: Evaluating the effects of P2O5,F, and carbonate composition p 953 N94-16283
Explosive volcanism and the compositions of the cores of differentiated asteroids p 1243 N94-16306
An experimental study of trace element partitioning between perovskite, hibonite and melt: Equilibrium values p 954 N94-16313
Noble gases in twenty Yamato H-chondrites: Comparison with Allan Hills chondrites and modern falls p 1244 N94-16361
Sensitive detection of gas-phase nitro-containing energetic materials employing 226-nm radiation
[AD-A267633] p 951 N94-17203
Electron reversal ionizer for detection of trace species using a spherical cathode
[NASA-CASE-NPO-18870-1-CU] p 1185 N94-17329
Chemical tracer studies at IOSDL. 3: The measurement of silicate, nitrate and phosphate in seawater
[IOS-302-1992] p 1114 N94-17489
TRACKING (POSITION)
Programmable Remapper project
[NASA-TM-109508] p 1164 N94-15515
Effects of window size and shape on accuracy of subpixel centroid estimation of target images
[NASA-TP-3331] p 1034 N94-15990
Visually guided touching and manual tracking
[TR-412] p 1166 N94-16581
TRACKING NETWORKS
On the accuracy of ERS-1 orbit predictions p 874 N94-15589
TRACKING PROBLEM
What is the radar tracking Glint problem and can it be solved?
[AD-A266509] p 999 N94-16789
TRACKING RADAR
Infrared spot tracker
[AD-D015778] p 1191 N94-16547
TRACKING STATIONS
New perspectives for high accuracy SLR with second generation geodesic satellites p 916 N94-15585
Computer networking at SLR stations p 917 N94-15594
LLR: Activities in Wettzell p 876 N94-15600
Upgrading of the Borowiec laser station p 877 N94-15604
WLRS --- Wettzell Laser Ranging System (WLRS) p 877 N94-15606
Ground based laser ranging for satellite location p 919 N94-15607
The third generation SLR station Potsdam no. 7836 p 877 N94-15623
Station report on the Goddard Space Flight Center (GSFC) 1.2 meter telescope facility p 922 N94-15625
TRADEOFFS
Lunar lander and return propulsion system trade study
[NASA-TP-3388] p 925 N94-16496
TRAILING EDGES
The effect of the nose shape and wing location toward the wing vortex breakdown
[AD-A267724] p 855 N94-14942
TRAINING AIRCRAFT
STS-26 STA training (Hauck)
[NASA-TM-109555] p 870 N94-15279
TRAINING ANALYSIS
An information processing classification of beyond-visual-range air intercepts
[AD-A266927] p 1131 N94-15108
TRAINING DEVICES
Defense RDT&E online system (DROLS) handbook
[AD-A267546] p 1232 N94-17101
TRAINING SIMULATORS
Space adaptation
[NASA-TM-109601] p 1120 N94-15309
Richards, Dick: Training clip
[NASA-TM-109503] p 876 N94-15467
Infrared spot tracker
[AD-D015778] p 1191 N94-16547
An introduction to structural models
[AD-A268151] p 1155 N94-17429
TRAJECTORY ANALYSIS
Simulation reduction using the Taguchi method
[NASA-CR-4542] p 1055 N94-17082
TRAJECTORY CONTROL
Neighboring extremal guidance for systems with piecewise linear control using time as the reference variable
[AD-A267942] p 874 N94-17010
TRAJECTORY OPTIMIZATION
Trajectory optimization for the National Aerospace Plane
[NASA-CR-194618] p 867 N94-16498
TRAJECTORY PLANNING
An object-oriented program specification for a mobile robot motion control language
[AD-A267213] p 1166 N94-16986
Path planning for robotic truss assembly
[NASA-CR-194652] p 897 N94-17280
Environmental use of a Laser Range Finder and the Advanced Visualization System
[DE93-016163] p 1043 N94-17677
TRANSCONDUCTANCE
DLTS and dynamic transconductance analysis of deep-submicron fully-depleted SOI MOSFET's
[AD-A267291] p 1214 N94-17243
TRANSDUCERS
Long baseline watertubes p 1037 N94-15803
Cooperative projects in geodynamical instrumentation between the State Seismological Bureau (China) and the Royal Observatory of Belgium p 1037 N94-15806
TRANSFER FUNCTIONS
Report of the working group on theoretical tidal model p 1101 N94-15815
TRANSFORMATIONS (MATHEMATICS)
On the nature of mirror particles
[DE93-626670] p 1179 N94-14934
TRANSFORMERS
Forback DC-to-DC converter
[NASA-CASE-GSC-13404-1] p 1010 N94-15874
A 27 channels, 1 MHz fibre-optic measuring system
[AD-A266943] p 1003 N94-17307
TRANSGRANULAR CORROSION
Stress corrosion cracking of 316 SS and Incoloy-800 in high temperature aqueous containing sulfate and chloride
[DE93-623325] p 952 N94-17302
TRANSIENT HEATING
Gas-grain energy transfer in solar nebula shock waves: Implications for the origin of chondrules p 1262 N94-16251
TRANSIENT LOADS
Development and comparison of advanced reduced-basis methods for the transient structural analysis of unconstrained structures
[NASA-TM-109015] p 1061 N94-17259
TRANSIENT RESPONSE
Nonstationary behaviour of low background photon detectors p 902 N94-15049
Dynamic behavior of fiber and particle reinforced composites
[AD-A266905] p 930 N94-15143
Pulse response based control for minimum time maneuver of flexible spacecraft
[AD-A266186] p 886 N94-16455
Development and comparison of advanced reduced-basis methods for the transient structural analysis of unconstrained structures
[NASA-TM-109015] p 1061 N94-17259
Precise flux control for lattice matched superlattice materials
[AD-A268254] p 1215 N94-17417
Heat transfer parametric system identification
[AD-A268525] p 929 N94-17543
TRANSISTORS
Large signal characterization and modeling of heterojunction bipolar transistors
[AD-A266184] p 1012 N94-16935
TRANSITION FLOW
Parallel spatial direct numerical simulations on the Intel iPSC/860 hypercube
[NASA-CR-191513] p 1144 N94-15483
Inviscid instability of streamwise corner flow
[NASA-CR-191514] p 1021 N94-15834
Turbulence and transition modeling for high-speed flows
[AD-A266748] p 1022 N94-15953
TRANSITION METALS
Magneto-optic superlattice thin films: Fabrication, structural and magnetic characterization p 974 N94-14982
Photochemistry in thin polymeric films
[AD-A266716] p 964 N94-15729
Interfacial structure of lattice mismatched bcc(110)/bcc(110) transition metal superlattices
[DE93-015162] p 1208 N94-16058
Transition metals in superheat melts p 962 N94-16273

Heat shock protein induction in human cells by CO2 laser irradiation
[AD-A266430] p 1117 N94-16545
Synthetic and mechanistic investigation of olefin polymerization catalyzed by early transition metal compounds
[DE93-018301] p 970 N94-16963
Synthesis and characterization of new low-dimensional metal complex conductors
[AD-A268251] p 952 N94-17416

TRANSITION TEMPERATURE
High temperature superconductivity
[AD-A267006] p 1008 N94-15635
Roles of oxygen defects in copper-oxide superconductors
[DE93-014875] p 1208 N94-15982
The effect of long-term aging on the impact properties of modified 9Cr-1Mo steel
[DE93-015453] p 957 N94-16068
Density of states and tunneling characteristics of layered superconductors
[DE93-015898] p 1211 N94-16839
Structural phase transition and superconductivity in La(2-x)Ba(x)CuO4
[DE93-015812] p 1212 N94-16868

TRANSLATIONAL MOTION
Linear encoding device
[NASA-CASE-GSC-13562-1] p 1147 N94-15703

TRANSMISSION EFFICIENCY
Optimisation and specification of Auger electron spectrometers for signal-to-noise ratio performance
[NPL-DMM(A)-101] p 1006 N94-17549

TRANSMISSION ELECTRON MICROSCOPY
Application of Z-contrast imaging to obtain column-by-column spectroscopic analysis of materials
[DE93-015333] p 947 N94-16014
Insights into semiconducting materials and growth phenomena through Z-contrast STEM
[DE93-015964] p 1212 N94-16841
UHV-stem studies on nucleation and growth of thin metal silicide films on silicon
[DE93-017604] p 1212 N94-16961

TRANSMISSION LINES
Determination of the electromagnetic fields radiated from the ARES EMP simulator
[AD-A267069] p 988 N94-15668

TRANSMISSION LOSS
Antenna gain loss and pattern degradation due to transmission through dielectric radomes
[AD-A267242] p 986 N94-14974
Johnson-Gierhart program predictions of excess propagation loss for super-high frequency air-to-ground paths. Volume 2: Appendices
[AD-A267021] p 987 N94-15527
Johnson-Gierhart program predictions of excess propagation loss for super-high frequency air-to-ground paths. Volume 1: Theory and numerical results
[AD-A267105] p 988 N94-15649
OETC optical backplane bus testbed. IBM tasks: Receiver OEIC and link simulation tools and analysis
[AD-A266198] p 1191 N94-16128

TRANSMISSION RATE (COMMUNICATIONS)
Causality-preserving timestamps in distributed programs
[AD-A267534] p 1153 N94-17118

TRANSMISSIONS (MACHINE ELEMENTS)
Mechanical Systems Technology Branch research summary, 1985 - 1992
[NASA-TM-106329] p 1049 N94-17583

TRANSMITTANCE
Characterization of InTISb grown by low pressure metalorganic chemical vapor deposition on GaAs substrate
[AD-A266878] p 1206 N94-14922
Atmospheric transmittance between 1.0 and 2.0 micrometers
[AD-A267076] p 1098 N94-15539
Filters for the International Solar Terrestrial Physics (ISTP) mission far ultraviolet imager
[NASA-CR-194633] p 1190 N94-15868
Multilayer thin film design for far ultraviolet polarizers using an induced transmission and absorption technique
[NASA-CR-194631] p 1190 N94-15869
VUV thin films, chapter 7
[NASA-CR-194634] p 967 N94-16494
A comparison of LOWTRAN-7 corrected Airborne Visible/Infrared Imaging Spectrometer (AVIRIS) data with ground spectral measurements p 1074 N94-16710
Atmospheric propagation analysis program
[AD-A268231] p 1006 N94-17565

TRANSMITTER RECEIVERS
Infrared remote activity transceiver universal model
[AD-A266965] p 1188 N94-15144
SAR sensor electronics: T/R modules
p 993 N94-15911
Microwave reflectometer ionization sensor
[NASA-CR-191464] p 922 N94-17083

TRANSMITTERS
Infrared remote activity transceiver universal model
[AD-A266965] p 1188 N94-15144
The new MTLRS transmitting system
p 877 N94-15612
Development of the Mars Observer Laser Altimeter (MOLA) p 921 N94-15617
Multi-beam laser altimeter p 921 N94-15620
OETC optical backplane bus testbed. IBM tasks: Receiver OEIC and link simulation tools and analysis
[AD-A266198] p 1191 N94-16128
Evaluation of site effects on a high frequency direction finding single site location system
[AD-A267465] p 1001 N94-17035
True time delay optically controlled dual band transmitter
[AD-A267663] p 1003 N94-17228

TRANSONIC FLOW
Laser Doppler velocimetry measurements across a normal shock in transonic flow
[AD-A267240] p 855 N94-14973
Advanced methods for cascade testing
[AGARD-AG-328] p 1016 N94-15119
Contribution of laser Doppler velocimetry to the physical description of shock wave/turbulent boundary layer interactions with incidence on turbulence modelling
p 1018 N94-15201
Computation of the Fluid and Optical Fields About the Stratospheric Observatory for Infrared Astronomy (SOFIA) and the Coupling of Fluids, Dynamics, and Control Laws on Parallel Computers
[NASA-CR-193168] p 858 N94-16510
Selected computations of transonic cavity flows
p 858 N94-16511
Unsteady fluid and optical simulation of transonic aero-windows
[AIAA PAPER 93-3017] p 858 N94-16512

TRANSONIC SPEED
Wind tunnel investigations of forebody strakes for yaw control on F/A-18 model at subsonic and transonic speeds
[NASA-TP-3360] p 859 N94-16573
Highly transient elastodynamic crack growth in a bimaterial interface: Higher order asymptotic analysis and optical experiments
[AD-A266465] p 1059 N94-16587

TRANSONIC WIND TUNNELS
A software interface for the ARL wind tunnel data acquisition system
[AD-A267114] p 1146 N94-15650
Physical properties of the benchmark models program supercritical wing
[NASA-TM-4457] p 866 N94-15722
Wall interference and boundary simulation in a transonic wind tunnel with a discretely slotted test section
[NASA-TP-3334] p 872 N94-15794
Wind tunnel investigation with an operational turbojet engine
[TABES PAPER 93-662] p 870 N94-16157

TRANSPARENCE
Aberration correction of unstable resonators
[NASA-CASE-NPO-18791-1-CU] p 1034 N94-15987

TRANSPIRATION
Evapotranspiration and runoff from large land areas: Land surface hydrology for atmospheric general circulation models p 1083 N94-16029

TRANSPONDERS
Calibration: Practical experience with ERS-1
p 992 N94-15907
Planned LMSS propagation experiment using ACTS: Preliminary antenna pointing results during mobile operations p 995 N94-16041

TRANSPORT AIRCRAFT
Embedded computer systems: Status of C-17 software
[AD-A267307] p 1160 N94-16993

TRANSPORT PROPERTIES
Effects of spin-orbit coupling on disordered mesoscopic systems
[ITN-93-85220] p 1180 N94-15288
X ray laser program
[AD-A267075] p 1038 N94-15628
High temperature superconductivity
[AD-A267006] p 1008 N94-15635
Optoelectronics based on SiGe/Si heterostructures
[AD-A267178] p 1190 N94-15848
Gas bubble generation and transport in microgravity
p 980 N94-16089
General order characteristic methods for solving neutron transport problems
[DE93-015824] p 1170 N94-16167
Sand transport on Mars: Preliminary results from models p 1252 N94-16198
Pulsed laser deposition of metastable Ca(1-x)Sr(x)CuO2 thin films
[DE93-015804] p 1040 N94-16663
Factors determining the release of nitric oxide --- Calcium/cadmium transport by renal cortical collectin duct cells
[AD-A266232] p 1118 N94-17224
Plasma instabilities and transport in the MPD thruster
[AD-A268268] p 1204 N94-17575
Coefficients for calculating thermodynamic and transport properties of individual species
[NASA-TM-4513] p 1220 N94-17624
Granular fluctuations in plasma turbulence and their role in transport
[DE93-013465] p 1187 N94-17674

TRANSPORT THEORY
Turbulence modelling for shock wave/boundary layer interactions specific issues and examples of applications
p 1018 N94-15202
Shielding from space radiations
[NASA-CR-194578] p 1180 N94-15715
General order characteristic methods for solving neutron transport problems
[DE93-015824] p 1170 N94-16167
Shielding from space radiations
[NASA-CR-194664] p 1301 N94-17255
Linear characteristic spatial quadrature for discrete ordinates neutral particle transport on arbitrary triangles
[AD-A267485] p 1185 N94-17365

TRANSPUTERS
Data processing system for flight spectrometer
p 908 N94-15086
Reactive system verification case study: Fault-tolerant transputer communication
[NASA-TM-108784] p 1145 N94-15538
Transputer based control system for MTLRS
p 877 N94-15613

TRANSVERSE WAVES
Acoustic waves in complicated geometries and their interactions with liquid-propellant droplet combustion
[AD-A267260] p 1178 N94-16991

TRAPPED PARTICLES
Quasiparticle trapping in distributed superconducting three-terminal tunnel junction devices
p 910 N94-15101
Nitrogen and light noble gases in Parsa enstatite chondrite p 1246 N94-16435
Kinetic plasma processes occurring in the outer plasmasphere
[NASA-CR-193452] p 1300 N94-17524

TRAPPING
Trapping of water vapor from an atmosphere by condensed silicate matter formed by high-temperature pulse vaporization p 1248 N94-16180
Orbital evolution of dust from comet Schwassmann-Wachmann 1: A case of one-to-one resonance trapping p 1242 N94-16270

TRAVELING WAVES
Velocity matched millimeterwave electro-optic modulator
[AD-A267264] p 1188 N94-14957

TRAYS
Long duration exposure facility experiment m0003 deintegration observation database
[AD-A267579] p 951 N94-17207

TREES (MATHEMATICS)
Construction of d-dimensional hyperoctrees on a hypercube multiprocessor
[INRIA-RR-1752] p 1162 N94-17539

TRELLIS CODING
Low-Complexity, High-Performance Bandwidth Efficient Coding and Coded Modulation Techniques for Satellite and Space Communications
[NASA-CR-194623] p 997 N94-16506

TREND ANALYSIS
NASA trend analysis procedures
[NASA-RP-1290] p 1223 N94-15782

TRIANGLES
Linear characteristic spatial quadrature for discrete ordinates neutral particle transport on arbitrary triangles
[AD-A267485] p 1185 N94-17365

TRIANGULATION
The cartography of Venus with Magellan data
p 1274 N94-16320

TRIAXIAL STRESSES
J-integral and HRR field associated with stable crack growth in thin aluminum SEN specimen
[AD-A267879] p 960 N94-17041

TRIBOLOGY
The friction and wear of ceramic/ceramic and ceramic/metal combinations in sliding contact
[NASA-TM-106348] p 930 N94-15769
Atomic-scale friction measurements using friction force microscopy. Part 1: General principles and new measurement techniques
[AD-A268391] p 1048 N94-17533

Continuing research on friction and wear of materials
[AD-A268291] p 1049 N94-17566

TRIGGER CIRCUITS
The 3D-Flow processor for a programmable level-1 trigger (feasibility study)
[DE93-016045] p 1159 N94-16172

TRIGONOMETRIC FUNCTIONS
Statistical analysis of trigonometric parallaxes
[NASA-CR-194558] p 1172 N94-15641

TRIMERS
Intramolecular versus intermolecular condensation rates in the acrilic polymerization of octaethoxytrisiloxane
[AD-A266982] p 963 N94-15490

TRIODES
RF vacuum microelectronics
[AD-A268399] p 1014 N94-17423

TRITIUM
An apparatus for measuring the biological oxidation of hydrogen gas under hyperbaric conditions
[AD-A266834] p 1119 N94-14916
Tritium diffusion and desorption in single crystal LiAlO2
[DE93-015140] p 1211 N94-16805

TRITON
Neptune encounter highlights
[NASA-TM-109421] p 1246 N94-15240
Tidal interaction: A possible explanation for geysers and other fluid phenomena in the Neptune-Triton system
p 1272 N94-16311
Evolution of Triton's volatile budget
p 1284 N94-16373

TROPICAL METEOROLOGY
TRMM radar p 990 N94-15894

TROPICAL REGIONS
IAI topic: El Nino. Southern oscillation and interannual climate variability
[INPE-5410-PRE/1757] p 1111 N94-15186
Validation and analysis of microwave-derived rainfall over the tropics
[AD-A267785] p 1108 N94-17303
Meridional circulation in the tropical north atlantic
[AD-A268222] p 1114 N94-17555
An empirical study of tropical cloud clusters using special sensor microwave imager data
[AD-A268072] p 1110 N94-17595

TROPOSPHERE
Hyperspectral modeling for extracting aerosols from aircraft/satellite data p 1067 N94-16673
The feasibility of tropospheric and total ozone determination using a Fabry-Perot interferometer as a satellite-based nadir-viewing atmospheric sensor
[NASA-TM-109342] p 1102 N94-17214
An investigation of the Ground-Based High-Resolution Interferometer Sounder (GB-HIS) in a costal marine environment
[AD-A268052] p 1114 N94-17503

TROPOSPHERIC SCATTERING
Johnson-Gierhart program predictions of excess propagation loss for super-high frequency air-to-ground paths. Volume 1: Theory and numerical results
[AD-A267105] p 988 N94-15649

TROUGHS
Ventilated oscillatory boundary layers
[AD-A266226] p 1023 N94-16110
Morphology and models for the evolution of eastern Hecate Chasma, Venus p 1256 N94-16215
Sedimentation, volcanism, and ancestral lakes in the Valles Marineris: Clues from topography
p 1283 N94-16369

TRUSSES
Preliminary analysis and design optimization of the short spacer truss of Space Station Freedom
[NASA-TM-4470] p 1058 N94-15709
End-effector: Joint conjugates for robotic assembly of large truss structures in space: Extended concepts
[NASA-CR-193576] p 1048 N94-17088
A comparative study of analog and digital control laws for the UMCSL truss
[AD-A267980] p 871 N94-17412

TUBERCULOSIS
Tuberculosis: A case for increased screening
p 1126 N94-16627
Summary of follow-up results from potential tuberculosis exposures p 1126 N94-16628

TUMORS
Quantitative method of measuring cancer cell urokinase and metastatic potential
[NASA-CASE-MSC-21715-1] p 1117 N94-15967
The role of constitutive and inducible processes in the response of human squamous cell carcinoma cell lines to ionizing radiation
[DE93-015150] p 1129 N94-16970

TUNERS
Display system employing acousto-optic tunable filter
[NASA-CASE-NPO-18736-1-CU] p 1190 N94-15933

TUNGSTEN
Liquid phase sintering of tungsten composites under microgravity. Effect of matrix composition
p 945 N94-15171

TUNGSTEN ALLOYS
Tensile and stress-rupture behavior of hafnium carbide dispersed molybdenum and tungsten base alloy wires
[NASA-TM-106350] p 962 N94-17652

TUNGSTEN CARBIDES
Diamond growth on carbide surfaces using a selective etching technique
[AD-A267989] p 973 N94-17413

TUNGSTEN FLUORIDES
Multiphoton ionization studies of WF6 and UF6
[DE93-016232] p 1181 N94-15863

TUNING
Fabrication and phase tuning of an optical waveguide device
[AD-D015815] p 1191 N94-16489
Design of broadband wire antennas for frequency hopping applications
[AD-A267405] p 1001 N94-17025
Optimal tuning of heavy equipment motion controllers
[AD-A267873] p 1167 N94-17392

TUNNEL DIODES
Submillimeterwave SIS mixer developments
p 903 N94-15054
Substrate effects in superconducting tunnel junction detectors p 908 N94-15083
A multilayered approach to superconducting tunnel junction x ray detectors p 908 N94-15089
Quasiparticle trapping in distributed superconducting three-terminal tunnel junction devices
p 910 N94-15101

TUNNEL JUNCTIONS
Monolithic, two-terminal InP/Ga(0.47)In(0.53)As tandem solar cells
[DE93-014037] p 1093 N94-16824

TURBINE BLADES
Turbine blade tip film cooling measurements
[AD-A267686] p 868 N94-14964
Slidesurfaces with adaptive new definitions (SAND) for transient analysis
[DE93-014909] p 1059 N94-15983
Effects of rotation on coolant passage heat transfer. Volume 2: Coolant passages with trips normal and skewed to the flow
[NASA-CR-4396-VOL-2] p 1023 N94-15991

TURBINE PUMPS
Liquid Oxygen (LO2) propellant conditioning concept testing
[TABES PAPER 93-621] p 976 N94-16146
Space Shuttle main engine. NASA has not evaluated the alternate fuel turbopump costs and benefits. Report to the Administrator of the National Aeronautics and Space Administration
[GAO/NSIAD-94-54] p 926 N94-16834
ALS liquid hydrogen turbopump
[NASA-CR-194646] p 927 N94-17016

TURBINES
Heat transfer and aerodynamics of a 3D design nozzle guide vane tested in the Pyestock isentropic light piston facility
[RAE-TM-AERO/PROP-19] p 856 N94-15696
ALS liquid hydrogen turbopump
[NASA-CR-194646] p 927 N94-17016
Application of thermal spray and ceramic coatings and reinforced epoxy for cavitation damage repair of hydroelectric turbines and pumps
[AD-A267624] p 971 N94-17198

TURBOJET ENGINES
Wind tunnel investigation with an operational turbojet engine
[TABES PAPER 93-662] p 870 N94-16157

TURBOMACHINERY
A mechanical system damping measurement technique using a one-degree-of-freedom (1DOF) cylindrical gas bearing
[AD-A268402] p 1048 N94-17462

TURBOPROP AIRCRAFT
Futurepath 1 --- power systems
[NASA-TM-109431] p 925 N94-15503

TURBOPROP ENGINES
Futurepath 1
[NASA-TM-109439] p 869 N94-15338
Structured finite volume modeling of US Navy aircraft engine test cells task 2: Turboprop engine, volume 1
[AD-A267833] p 872 N94-17405
Structured finite volume modeling of US Navy aircraft engine test cells. Task 2: Turboprop engine. Volume 2: Code documentation and listings
[AD-A268386] p 873 N94-17569

TURBOSHAFTS
Structured finite volume modeling of US Navy aircraft engine test cells. Task 1: Turboshaft engine, volume 1
[AD-A268176] p 873 N94-17432
Structured finite volume modeling of US Navy aircraft engine test cells. Task 1: Turboshaft engine-code documentation and listings, volume 2
[AD-A268177] p 873 N94-17508

TURBULENCE
Large eddy simulation and direct numerical simulation of high speed turbulent reacting flows
[NASA-CR-193131] p 1018 N94-15427
An experimental study of ASTOVL related jet flows to produce CFD code validation data. Phase 3: Results of experiments
[TT-9203] p 1020 N94-15645
Inviscid instability of streamwise corner flow
[NASA-CR-191514] p 1021 N94-15834
Detecting surface roughness effects on the atmospheric boundary layer via AIRSAR data: A field experiment in Death Valley, California p 1078 N94-16747
Three dimensional hydrodynamic calculations with adaptive mesh refinement of the evolution of Rayleigh Taylor and Richtmyer Meshkov instabilities in converging geometry: Multi-mode perturbations
[DE93-017155] p 1025 N94-16903
The structure of turbulent boundary layers and shock wave boundary layer interactions
[AD-A266240] p 1026 N94-16929
Studies in turbulence and turbulence control
[AD-A266318] p 1026 N94-16950
Structure of turbulence in three-dimensional boundary layers
[NASA-CR-194655] p 1027 N94-17130
Transition induced by fixed and freely convecting spherical particles in laminar boundary layers
[AD-A267757] p 1028 N94-17276
Active turbulence control in wall bounded flows using direct numerical simulation
[AD-A267261] p 1028 N94-17286
Lifted turbulent jet flames
[AD-A267911] p 952 N94-17381
Measurement of the velocity field and void fraction in a planar plunging jet
[AD-A268183] p 1030 N94-17511

TURBULENCE EFFECTS
Effects of turbulence on the geodynamic laser ranging system p 921 N94-15616
Plasma instabilities and transport in the MPD thruster
[AD-A268268] p 1204 N94-17575

TURBULENCE MODELS
Mesoscale modeling of the atmosphere
[AD-A263236] p 1098 N94-15132
Numerical simulation of 3-D shock wave turbulent boundary layer interactions p 1017 N94-15199
Contribution of laser Doppler velocimetry to the physical description of shock wave/turbulent boundary layer interactions with incidence on turbulence modelling
p 1018 N94-15201
Turbulence modelling for shock wave/boundary layer interactions specific issues and examples of applications
p 1018 N94-15202
Proteus two-dimensional Navier-Stokes computer code, version 2.0. Volume 2: User's guide
[NASA-TM-106338-VOL-2] p 1019 N94-15475
Proteus two-dimensional Navier-Stokes computer code, version 2.0. Volume 1: Analysis description
[NASA-TM-106336-VOL-1] p 1019 N94-15485
Proteus three-dimensional Navier-Stokes computer code, version 1.0. Volume 2: User's guide
[NASA-TM-106340-VOL-2] p 1020 N94-15488
Turbulence and transition modeling for high-speed flows
[AD-A266748] p 1022 N94-15953
Selected computations of transonic cavity flows
p 858 N94-16511
Computation of confined coflow jets with three turbulence models
[NASA-TM-106378] p 1025 N94-16879
The structure of turbulent boundary layers and shock wave boundary layer interactions
[AD-A266240] p 1026 N94-16929
Investigation of high-speed free shear flows using improved pressure-strain correlated Reynolds stress turbulence model
[NASA-CR-194661] p 1027 N94-17127
Structure of turbulence in three-dimensional boundary layers
[NASA-CR-194655] p 1027 N94-17130
Time dependent turbulence modeling and analytical theories of turbulence
[NASA-TM-106379] p 1029 N94-17385

TURBULENT BOUNDARY LAYER
Numerical simulation of 3-D shock wave turbulent boundary layer interactions p 1017 N94-15199
Contribution of laser Doppler velocimetry to the physical description of shock wave/turbulent boundary layer interactions with incidence on turbulence modelling
p 1018 N94-15201

Turbulence and transition modeling for high-speed flows
[AD-A266748] p 1022 N94-15953
Ventilated oscillatory boundary layers
[AD-A266226] p 1023 N94-16110
Three-dimensional turbulent boundary layer
[AD-A266261] p 1025 N94-16908
The structure of turbulent boundary layers and shock wave boundary layer interactions
[AD-A266240] p 1026 N94-16929
Studies in turbulence and turbulence control
[AD-A266318] p 1026 N94-16950
Structure of high Reynolds number turbulent boundary layer
[AD-A267476] p 860 N94-17099
Structure of turbulence in three-dimensional boundary layers
[NASA-CR-194655] p 1027 N94-17130
An experimental investigation of the effects of leading edge geometry on the dynamics of blunt fin-induced shock wave turbulent boundary layer interaction
[AD-A267656] p 860 N94-17221
Transmission of light through a turbulent mixing layer
[AD-A267266] p 1193 N94-17264
Transition induced by fixed and freely convecting spherical particles in laminar boundary layers
[AD-A267757] p 1028 N94-17276
Active turbulence control in wall bounded flows using direct numerical simulation
[AD-A267261] p 1028 N94-17286
An experimental study of fluctuating wall pressures in a highly swept, sharp fin-induced, Mach 5 shock wave/turbulent boundary layer interaction
[AD-A268394] p 861 N94-17461
An investigation of oblique shock/boundary layer interaction control
[AD-A268106] p 861 N94-17574

TURBULENT COMBUSTION
Reaction and diffusion in turbulent combustion
[DE93-017085] p 943 N94-15146

TURBULENT FLOW
Large-Eddy Simulations (LES) of flows and turbulence distribution
[AD-A267182] p 1016 N94-15151
Turbulence modelling for shock wave/boundary layer interactions specific issues and examples of applications
p 1018 N94-15202
Large eddy simulation and direct numerical simulation of high speed turbulent reacting flows
[NASA-CR-193131] p 1018 N94-15427
Inviscid instability of streamwise corner flow
[NASA-CR-191514] p 1021 N94-15834
Turbulence and transition modeling for high-speed flows
[AD-A266748] p 1022 N94-15953
Implementation of an anisotropic turbulence model in the COMMIX-1C/ATM computer code
[DE93-015541] p 1023 N94-16444
Search for chaos in free shear flows
[AD-A266245] p 1023 N94-16470
Selected computations of transonic cavity flows
p 858 N94-16511
Computation of confined coflow jets with three turbulence models
[NASA-TM-106378] p 1025 N94-16879
Three-dimensional turbulent boundary layer
[AD-A266261] p 1025 N94-16908
Studies in turbulence and turbulence control
[AD-A266318] p 1026 N94-16950
Adaptive Navier-Stokes calculations for vortical flow
[AD-A266236] p 1026 N94-16966
Natural convection above a horizontal heat source
[AD-A267212] p 1026 N94-16985
Structure of high Reynolds number turbulent boundary layer
[AD-A267476] p 860 N94-17099
Active turbulence control in wall bounded flows using direct numerical simulation
[AD-A267261] p 1028 N94-17286
Lifted turbulent jet flames
[AD-A267911] p 952 N94-17381
Time dependent turbulence modeling and analytical theories of turbulence
[NASA-TM-106379] p 1029 N94-17385
Thin-layer and full Navier-Stokes calculations for turbulent supersonic flow over a cone at an angle of attack
[NASA-CR-189103] p 861 N94-17558
Laser velocimetry measurements of vortex flows on a delta wing at Mach 1.9
[AD-A268596] p 861 N94-17609

TURBULENT HEAT TRANSFER
Investigation of two-phase flow and boiling heat transfer during quenching of a tube under microgravity
p 979 N94-16087

TURBULENT JETS
The turbulent wall jet
[AD-A267675] p 855 N94-14963
Lifted turbulent jet flames
[AD-A267911] p 952 N94-17381

TURBULENT MIXING
Surface and internal signatures of organized vortex motions in stratified fluid
[AD-A267015] p 1020 N94-15526
Three dimensional hydrodynamic calculations with adaptive mesh refinement of the evolution of Rayleigh Taylor and Richtmyer Meshkov instabilities in converging geometry: Multi-mode perturbations
[DE93-017155] p 1025 N94-16903
Transmission of light through a turbulent mixing layer
[AD-A267266] p 1193 N94-17264
Chemical reactions in turbulent mixing flows
[AD-A268287] p 861 N94-17580

TURBULENT WAKES
The 1970 highlights --- NASA programs and research
[NASA-TM-109628] p 1302 N94-15415

TURING MACHINES
FSM test: A functional test generation system for sequential circuits
[REPT-93-017] p 1014 N94-17505

TWO BODY PROBLEM
Tidal regime of intact planetoid capture model for the Earth-Moon system: Does it relate to the archean sedimentary rock record? p 1245 N94-16378

TWO DIMENSIONAL FLOW
Modal element method for potential flow in non-uniform ducts: Combining closed form analysis with CFD
[NASA-TM-106347] p 1169 N94-15799
Inviscid instability of streamwise corner flow
[NASA-CR-191514] p 1021 N94-15834
A rapid computational model for estimating the performance of compliant airfoils in cascades
[AD-A266275] p 857 N94-16471
Determining the effect of endwall boundary layer suction in a large scale subsonic compressor cascade
[AD-A267208] p 859 N94-16913
An upwind multigrid method for solving viscous flows on unstructured triangular meshes
[NASA-TM-109343] p 1027 N94-17061
Investigation of high-speed free shear flows using improved pressure-strain correlated Reynolds stress turbulence model
[NASA-CR-194661] p 1027 N94-17127
Development of iterative techniques for the solution of unsteady compressible viscous flows
[NASA-CR-194657] p 1027 N94-17129
Two-dimensional, high flow, precisely controlled monodisperse drop source
[AD-A267660] p 1028 N94-17250

TWO DIMENSIONAL MODELS
A posteriori error estimation for hierarchic models of elliptic boundary value problems on thin domains
[AD-A267714] p 1168 N94-14939
Crack-tip-opening angle measurements and crack tunneling under stable tearing in thin sheet 2024-T3 aluminum alloy
[NASA-CR-191523] p 931 N94-15184

TWO FLUID MODELS
Boundary layer flow of air over water on a flat plate
[NASA-CR-191517] p 1019 N94-15479
A modified two-fluid model of conductivity for superconducting surface resistance calculation
[AD-A267549] p 1013 N94-17104

TWO PHASE FLOW
Investigation of two-phase flow and boiling heat transfer during quenching of a tube under microgravity
p 979 N94-16087
Cryogenic spray vaporization in high-velocity helium, argon and nitrogen gasflows
[NASA-TM-106363] p 1035 N94-17446
Gravity dependent condensation pressure drop and heat transfer in ammonia two-phase heat transport systems
[NLR-TP-92121-U] p 1031 N94-17615

TWO-WAVELENGTH LASERS
An improved light source for laser ranging
p 913 N94-15567

TYROSINE
Theoretical prediction of the UV adsorption and fluorescence spectra of tyrosine and phenylalanine
[AD-A266970] p 943 N94-15111

U

U.S.S.R.
NASA/DOD Aerospace Knowledge Diffusion Research Project. Paper 32: A new era in international technical communication: American-Russian collaboration
[NASA-TM-109336] p 1230 N94-15838

UH-60A HELICOPTER
Fidelity assessment of a UH-60A simulation on the NASA Ames vertical motion simulator
[NASA-TM-104016] p 870 N94-15793

ULTRAHIGH FREQUENCIES
An overview of the text propagation effects for land-mobile-satellite systems: Experimental and modeling results p 996 N94-16048

ULTRAHIGH VACUUM
UHV-stem studies on nucleation and growth of thin metal silicide films on silicon
[DE93-017604] p 1212 N94-16961

ULTRASONIC FLAW DETECTION
Physical interpretation and development of ultrasonic nondestructive evaluation techniques applied to the quantitative characterization of textile composite materials
[NASA-CR-194549] p 931 N94-15190
Component testing and quality assurance
p 932 N94-15259

ULTRASONIC RADIATION
Method and apparatus to characterize ultrasonically reflective contrast agents
[NASA-CASE-LAR-14969-1] p 1129 N94-17085
An automated system for ultrasound measurements of liquids by the resonance (Eggers) method
[IFTR-17/1992] p 1178 N94-17087
Ultrasonic wave propagation model for nondestructive evaluation of solid rocker motor propellant
[AD-A267653] p 976 N94-17248

ULTRASONIC SCANNERS
Method and apparatus to characterize ultrasonically reflective contrast agents
[NASA-CASE-LAR-14969-1] p 1129 N94-17085

ULTRASONIC TESTS
Characterization of the cyclic plasticity of polycrystalline aluminum in the 90-300K domain: Use of the ultrasonic wave coupling technique - low frequency restraint
[ISAL-92-0083] p 954 N94-14930
Physical interpretation and development of ultrasonic nondestructive evaluation techniques applied to the quantitative characterization of textile composite materials
[NASA-CR-194549] p 931 N94-15190
Transcranial Doppler ultrasound studies of cerebral blood-flow in microgravity p 981 N94-16095

ULTRASONICS
Thermal stress effects in intermetallic matrix composites
[NASA-CR-191191] p 1054 N94-16518
Ultrasonic wave propagation model for nondestructive evaluation of solid rocker motor propellant
[AD-A267653] p 976 N94-17248

ULTRAVIOLET ASTRONOMY
NASA's Ultraviolet Astrophysics Branch: Present and future detector program p 910 N94-15102
The spectrum of Phobos from Phobos 2 observations at 0.3-2.6 microns: Comparison to previous data and meteorite analogs p 1295 N94-16429

ULTRAVIOLET DETECTORS
A new approach to optical photon detection
p 899 N94-15028
Microchannel plate imaging detectors for the ultraviolet p 901 N94-15037
Microchannel plate detectors for space astronomy
p 901 N94-15038
Development of an ultra violet auroral imager for the Freja project p 904 N94-15060
A test facility to calibrate EUV detectors
p 873 N94-15062
The grazing incidence detectors for the SOHO coronal diagnostic spectrometer p 905 N94-15063
The TAUVEX experiment p 905 N94-15064
The Rutherford Appleton Laboratory photon counting detector p 910 N94-15096
NASA's Ultraviolet Astrophysics Branch: Present and future detector program p 910 N94-15102

ULTRAVIOLET FILTERS
Filters for the International Solar Terrestrial Physics (ISTP) mission far ultraviolet imager
[NASA-CR-194633] p 1190 N94-15868

ULTRAVIOLET LASERS
Modification of fluoropolymer surfaces with electronically conductive polymers
[AD-A266294] p 967 N94-16475

ULTRAVIOLET RADIATION
Quantifying lifetime exposure to ultraviolet radiation in the epidemiology of cutaneous malignant melanoma: A pilot study
[DE93-015274] p 1128 N94-16812
The feasibility of tropospheric and total ozone determination using a Fabry-Perot interferometer as a satellite-based nadir-viewing atmospheric sensor
[NASA-TM-109342] p 1102 N94-17214

ULTRAVIOLET REFLECTION
Design and fabrication of a reflection far ultraviolet polarizer and retarder
[NASA-CR-194630] p 1191 N94-16023
ULTRAVIOLET SPECTRA
Theoretical prediction of the UV adsorption and fluorescence spectra of tyrosine and phenylalanine
[AD-A266970] p 943 N94-15111
ULTRAVIOLET SPECTROMETERS
Ultraviolet spectrometer and polarimeter (UVSP) catalog of observations. Volume 1: Experiments 1-30719, February 1980 - April 1985
[NASA-CR-4529-VOL-1] p 1298 N94-15023
Ultraviolet spectrometer and polarimeter (UVSP) catalog of observations. Volume 2: Experiments 30720-63057, April 1985 - February 1988
[NASA-CR-4529-VOL-2] p 1298 N94-15024
The spectrum of Phobos from Phobos 2 observations at 0.3-2.6 microns: Comparison to previous data and meteorite analogs p 1295 N94-16429
ULTRAVIOLET SPECTROSCOPY
The STIS MAMA status: Current detector performance p 905 N94-15069
Photodegradation of MDI based polyurethane/urea elastomers
[AD-A267308] p 971 N94-16994
Principal investigators data package for Project Initiation Conference (PIC): EUVS sounding rocket no. 36.117CL. Target: Venus
[NASA-CR-194663] p 923 N94-17126
ULTRAVIOLET TELESCOPES
The TAUVEX experiment p 905 N94-15064
ULYSSES MISSION
STS-41 post-flight press presentation
[NASA-TM-109514] p 882 N94-15516
STS-41 onboard 16mm photography quick release
[NASA-TM-109515] p 882 N94-15518
STS-41 mission highlights resource tape
[NASA-TM-109516] p 882 N94-15521
Strategy for a small satellite program and a proposal for a first mission p 874 N94-17143
UNDAMPED OSCILLATIONS
Flutter analysis using transversality theory
[NASA-TM-106382] p 1062 N94-17481
UNDERGROUND STORAGE
Environmental use of a Laser Range Finder and the Advanced Visualization System
[DE93-016163] p 1043 N94-17677
UNITED STATES
The closing window of opportunity: Addressing the US space launch vehicle crisis
[TABES PAPER 93-640] p 878 N94-16148
The standardized precipitation index and its use in the western contiguous United States
[AD-A267547] p 1107 N94-17102
Space commerce in a global economy: Comparison of US and Australian approaches
[NASA-TM-109341] p 1235 N94-17290
UNIVERSITIES
Maximizing participation of women in collegiate aviation education
[NIAR-93-14] p 1222 N94-17261
The impact of industry/university consortia programs on space education
[NASA-TM-109340] p 1222 N94-17441
UNIVERSITY PROGRAM
Symposium on the Future of Aeronautics in the Netherlands
[ETN-93-93780] p 853 N94-15120
University Joint Venture: JOVE
[NASA-TM-109660] p 1229 N94-15231
The impact of industry/university consortia programs on space education
[NASA-TM-109340] p 1222 N94-17441
UNIX (OPERATING SYSTEM)
Upgrading NASA/DOSE laser ranging system control computers p 918 N94-15595
HP upgrade operational streamlining p 918 N94-15596
Lunar laser ranging data processing in a Unix/X windows environment p 918 N94-15599
User manual and program description of the data acquisition system of PML-pulse physics
[AD-A266752] p 1147 N94-15776
Department of Defense technical architecture framework for information management. Volume 2: Technical reference model and standards profile, version 2.0
[AD-A267194] p 1229 N94-15788
UNSTEADY AERODYNAMICS
Effect of wind tunnel acoustic modes on linear oscillating cascade aerodynamics
[NASA-TM-106367] p 869 N94-15866
Aerodynamic/dynamic/control interaction
[AD-A266187] p 871 N94-16107
Aeroelastic airfoil smart spar p 866 N94-16865
Progress in computational unsteady aerodynamics
[NASA-CR-177630] p 860 N94-17081
UNSTEADY FLOW
Unsteady separated flows: Empirical model and control
[AD-A267282] p 855 N94-14959
Computation of the Fluid and Optical Fields About the Stratospheric Observatory for Infrared Astronomy (SOFIA) and the Coupling of Fluids, Dynamics, and Control Laws on Parallel Computers
[NASA-CR-193168] p 858 N94-16510
Proteus three-dimensional Navier-Stokes computer code, version 1.0. Volume 1: Analysis description
[NASA-TM-106337] p 1024 N94-16527
The structure of turbulent boundary layers and shock wave boundary layer interactions
[AD-A266240] p 1026 N94-16929
On solving the compressible Navier-Stokes equations for unsteady flows at very low Mach numbers
[NASA-TM-106380] p 1027 N94-17128
Development of iterative techniques for the solution of unsteady compressible viscous flows
[NASA-CR-194657] p 1027 N94-17129
Multigrid time-accurate integration of Navier-Stokes equations
[NASA-TM-106373] p 1028 N94-17258
On the stability of a time dependent boundary layer
[NASA-CR-191542] p 1030 N94-17450
An investigation of oblique shock/boundary layer interaction control
[AD-A268106] p 861 N94-17574
UPPER ATMOSPHERE
Southern and Northern Hemisphere total ozone as seen by TOMS
[NASA-TM-109591] p 1098 N94-15282
Optical measurements of NASA/USAF CRRES high altitude rocket borne chemical release experiments in conjunction with the USAF airborne ionospheric observatory aircraft
[AD-A266404] p 1101 N94-16551
Opposing mesoscale flows in a broken midlatitude squall line
[AD-A268011] p 1109 N94-17492
Second flight of the Spacelab grille spectrometer during the Atlas-1 mission
[AERONAUTICA-ACTA-A-367-199] p 923 N94-17592
The Central American cold surge: An observational analysis of the deep southward penetration of North American cold fronts
[AD-A268592] p 1110 N94-17607
UPPER ATMOSPHERE RESEARCH SATELLITE (UARS)
ATLAS-2 and UARS correlative measurement opportunities during Space Shuttle mission on April 8-17, 1993
[NASA-TM-109020] p 1105 N94-15480
UPSTREAM
An experimental investigation of the effects of leading edge geometry on the dynamics of blunt fin-induced shock wave turbulent boundary layer interaction
[AD-A267656] p 860 N94-17221
UPWIND SCHEMES (MATHEMATICS)
Accurate upwind methods for the Euler equations
[NASA-TM-106388] p 1170 N94-16882
An upwind multigrid method for solving viscous flows on unstructured triangular meshes
[NASA-TM-109343] p 1027 N94-17061
URANIUM FLUORIDES
Multiphoton ionization studies of WF6 and UF6
[DE93-016232] p 1181 N94-15863
URANUS (PLANET)
Voyager encounters Uranus
[NASA-TM-109619] p 1247 N94-15348
NASA images 12 --- Voyager encounters
[NASA-TM-109417] p 1247 N94-15511
NASA images 13
[NASA-TM-109418] p 1247 N94-15512
Mapping the stability region of the 3:2 Neptune-Pluto resonance p 1280 N94-16351
URBAN DEVELOPMENT
AVIRIS data and neural networks applied to an urban ecosystem p 1073 N94-16705
UREAS
Photodegradation of MDI based polyurethane/urea elastomers
[AD-A267308] p 971 N94-16994
UREILITES
Stalking the LREE-enriched component in ureilites p 1241 N94-16190
Euromet Ureilite Consortium: A preliminary report on carbon and nitrogen geochemistry p 1241 N94-16192
URINE
Strategy for the reduction of total integrated fluid logistics to the Space Station Freedom
[NASA-TM-107744] p 1138 N94-17452
USER MANUALS (COMPUTER PROGRAMS)
The CAML numbers reference manual
[INRIA-RT-141] p 1142 N94-14979
Proteus two-dimensional Navier-Stokes computer code, version 2.0. Volume 2: User's guide
[NASA-TM-106338-VOL-2] p 1019 N94-15475
Proteus three-dimensional Navier-Stokes computer code, version 1.0. Volume 2: User's guide
[NASA-TM-106340-VOL-2] p 1020 N94-15488
TAFVER 2 users manual
[AD-A266850] p 1106 N94-15757
User manual and program description of the data acquisition system of PML-pulse physics
[AD-A266752] p 1147 N94-15776
User's manual for the HYPGEN hyperbolic grid generator and the HGUI graphical user interface
[NASA-TM-108791] p 1148 N94-15784
ASTROS enhancements. Volume 1: ASTRO user's manual
[AD-A266818] p 1151 N94-16768
ASTROS enhancements. Volume 2: ASTRO programmer's manual
[AD-A266819] p 1151 N94-16769
Missile datcom user's manual
[AD-A267447] p 1152 N94-17032
Defense RDT&E online system (DROLS) handbook
[AD-A267546] p 1232 N94-17101
BACKSCAT lidar simulation version 3.0: Technical documentation and users guide
[AD-A267296] p 1003 N94-17268
User's manual for the Langley Research Center 14- by 22- foot subsonic tunnel static data acquisition system
[NASA-TM-109027] p 861 N94-17639
USER REQUIREMENTS
Computer-human interface issues: Theory and application
[AD-A268013] p 1138 N94-17475
UTILITIES
Utility emissions associated with electric and hybrid vehicle (EHV) charging
[DE93-013734] p 1011 N94-16459

V

V/STOL AIRCRAFT
Lift-fan aircraft: Lessons learned-the pilot's perspective
[NASA-CR-177620] p 867 N94-15950
VACANCIES (CRYSTAL DEFECTS)
Vacancy condensation as the precursor to passivity breakdown
[DE93-012925] p 956 N94-15998
VACUUM APPARATUS
Investigation of onset of plasma formation at anode of fast-pulsed high-voltage vacuum diode
[AD-A267214] p 1204 N94-16987
Field-emitter arrays for RF vacuum microelectronics
[AD-A268397] p 1015 N94-17526
VACUUM SPECTROSCOPY
Structural and dynamical aspects of electrodeposition
[AD-A266786] p 942 N94-14909
VACUUM TUBES
RF vacuum microelectronics
[AD-A268399] p 1014 N94-17423
VALLEYS
Fluvial erosion on Mars: Implications for paleoclimatic change p 1241 N94-16210
VAN DER WAALS FORCES
Electronic spectroscopy of the gas-phase OH-Kr van der Waals complex
[AD-A266891] p 942 N94-14946
The roles of fluid motion and other transport phenomena in the morphology of materials
[NASA-CR-194665] p 1028 N94-17298
VANADIUM
The corrosion protection of metals by ion vapor deposited aluminum
[NASA-TM-108425] p 955 N94-15832
Effects of aging time on V205 sol-gel coatings
[AD-A266824] p 965 N94-15843
Development of vanadium-phosphate catalysts for methanol production by selective oxidation of methane
[DE93-016850] p 949 N94-16897
VANADIUM ALLOYS
The corrosion protection of metals by ion vapor deposited aluminum
[NASA-TM-108425] p 955 N94-15832
VANADIUM OXIDES
Vanadium corrosion studies
[AD-A266489] p 959 N94-16781
VANELESS DIFFUSERS
Experimental and computational investigation of the NASA low-speed centrifugal compressor flow field
[NASA-TM-4481] p 869 N94-17386

VANES
In-flight investigation of a rotating cylinder-based structural excitation system for flutter testing
[NASA-TM-4512] p 867 N94-15783
VAPOR DEPOSITION
Diamond epitaxy and diamondlike coatings
[AD-A266657] p 1206 N94-15747
Laser assisted CVD growth of AlN and GaN
[AD-A267150] p 1206 N94-15764
The corrosion protection of metals by ion vapor deposited aluminum
[NASA-TM-108425] p 955 N94-15832
Method of producing a silicon carbide fiber reinforced strontium aluminosilicate glass-ceramic matrix composite
[NASA-CASE-LEW-15263-2] p 934 N94-15929
A high flux radical beam diamond growth
[AD-A266754] p 1207 N94-15955
Continuous fabrication of SiC fiber tows by chemical vapor deposition
[AD-A266460] p 936 N94-16569
Chemical vapor deposition of Ta2O5 corrosion resistant coatings
[DE93-015488] p 969 N94-16889
Single crystal diamond thin films
[AD-A266457] p 1214 N94-17216
Anisotropic phase separation in amorphous Fe-Ge alloys
[DE93-015255] p 961 N94-17251
Diamond growth on carbide surfaces using a selective etching technique
[AD-A267989] p 973 N94-17413
Growth, characterization and device development in monocrystalline diamond films
[AD-A268206] p 1216 N94-17553
VAPOR PHASE EPITAXY
Mechanical properties and crystal growth studies of semiconductor alloys
[AD-A268144] p 1216 N94-17454
Femtosecond carrier processes in compound semiconductors and real time signal processing
[AD-A268122] p 1005 N94-17519
VAPOR PHASES
Electronic spectroscopy of the gas-phase OH-Kr van der Waals complex
[AD-A266891] p 942 N94-14946
Fundamental studies of rocket combustion chemistry and combustion instability
[AD-A266248] p 925 N94-16482
Sensitive detection of gas-phase nitro-containing energetic materials employing 226-nm radiation
[AD-A267633] p 951 N94-17203
Ceramic fiber coatings development and demonstration
[AD-A267286] p 972 N94-17242
Laser probing of the kinetics and dynamics of 3-5 semiconductor growth
[AD-A268388] p 1215 N94-17422
A basic principles description of liquid vapor phase transitions
[AD-A268331] p 1176 N94-17581
VAPOR PRESSURE
The pressure broadening of HDO by O2, N2, H2, and He between 100 K and 600 K
[AD-A267118] p 946 N94-15684
Effects of RVP, T(50), and oxygenates on hot-start and driveability performance at high and low altitude
[AD-A266382] p 869 N94-16516
Method for doping GaAs with high vapor pressure elements
[AD-D015794] p 1210 N94-16538
Sodium-mercury excimer laser, phase 1
[AD-A267728] p 1042 N94-17230
VAPORIZING
Trapping of water vapor from an atmosphere by condensed silicate matter formed by high-temperature pulse vaporization p 1248 N94-16180
Cryogenic spray vaporization in high-velocity helium, argon and nitrogen gasflows
[NASA-TM-106363] p 1035 N94-17446
VAPORS
HyperVentilate: Decision-support software for soil vapor extraction technology application
[PB93-134880] p 1094 N94-15136
Geometrical vapor blocker for parallel condensation tubes requiring cooling
[NASA-CASE-MSC-22090-1] p 1022 N94-15962
Lasing dye sensor for chemical vapors
[AD-D015786] p 1040 N94-16533
VARIABILITY
X ray emission from Wolf-Rayet stars with recurrent dust formation
[NASA-CR-194567] p 1300 N94-15533
Reliability of autonomic responses and malaise across multiple motion sickness stimulation tests
[NASA-TM-108787] p 1121 N94-15711
The use of General Circulation Models in detecting climate change induced by greenhouse gases
[DE93-014369] p 1096 N94-16802
Variability of the Seyfert galaxy MKN 766 in the Rosat all sky survey
[MPE-PREPRINT-221] p 1240 N94-17591
VARIABLE AMPLITUDE LOADING
A simplistic look at limit stresses from random loading
[NASA-TM-108427] p 1058 N94-15710
VARIABLE THRUST
Computational analysis of Variable Thrust Engine (VTE) performance
[NASA-CR-193852] p 928 N94-17442
VARIANCE (STATISTICS)
Bounds on inconsistent inferences for sequences of trials with varying probabilities
[AD-A267146] p 1172 N94-15733
Speckles statistics and decorrelation effects in complex ABCD optical systems
[AD-A267843] p 1193 N94-17012
An investigation of the Ground-Based High-Resolution Interferometer Sounder (GB-HIS) in a costal marine environment
[AD-A268052] p 1114 N94-17503
VARIATIONAL PRINCIPLES
Three-dimensional analysis of anisotropic spatially reinforced structures p 939 N94-16863
VARIATIONS
Water-levels fluctuations in a borehole at the Royal Observatory of Belgium: Effects on local gravity, Earth tidal, and barometric responses p 1100 N94-15812
VAX COMPUTERS
Detailed example of using ACEC release 3.0 with the DEC VAX Ada compiler
[AD-A267880] p 1152 N94-17014
VECTOR MESONS
PHENIX Conceptual Design Report
[DE93-015759] p 1182 N94-16161
VECTOR SPACES
Development and comparison of advanced reduced-basis methods for the transient structural analysis of unconstrained structures
[NASA-TM-109015] p 1061 N94-17259
VEGA PROJECT
Comet Halley returns
[NASA-TM-109608] p 885 N94-15296
VEGETATION
An expert system shell for inferring vegetation characteristics: Atmospheric techniques (Task G)
[NASA-CR-194570] p 1082 N94-15531
X-SAR: The X-band synthetic aperture radar on board the Space Shuttle p 990 N94-15891
Radar response of vegetation: An overview p 991 N94-15898
Application of Cloude's target decomposition theorem to polarimetric imaging radar data p 991 N94-15901
Multifrequency observations p 992 N94-15902
Heterogeneity and scaling land-atmospheric water and energy fluxes in climate systems p 1083 N94-16030
Unmixing AVIRIS data to provide a method for vegetation fraction subtraction p 1066 N94-16669
Mapping the spectral variability in photosynthetic and non-photosynthetic vegetation, soils, and shade using AVIRIS p 1068 N94-16679
Retrieval of biophysical parameters with AVIRIS and ISM: The Landes Forest, south west France p 1068 N94-16681
Mapping vegetation types with the multiple spectral feature mapping algorithm in both emission and absorption p 1069 N94-16686
MAC Europe 1991: Evaluation of AVIRIS, GER imaging spectrometry data for the land application testsite Oberpfaffenhofen p 1070 N94-16688
Using endmembers in AVIRIS images to estimate changes in vegetative biomass p 1070 N94-16689
Primary studies of trace quantities of green vegetation in Mono Lake area using 1990 AVIRIS data p 1071 N94-16695
Temporal variation in spectral detection thresholds of substrate and vegetation in AVIRIS images p 1073 N94-16706
The dynamics of hydroponic crops for simulation studies of the CELSS initial reference configurations
[NASA-CR-194654] p 1118 N94-17279
VEGETATION GROWTH
Driving terrestrial ecosystem models from space p 991 N94-15896
VELOCITY DISTRIBUTION
Parametric resonant triad interactions in a free shear layer
[NASA-TM-106365] p 1021 N94-15751
Studies of combustion reactions at the state-resolved differential cross section level
[DE93-017605] p 948 N94-16462
The structure of turbulent boundary layers and shock wave boundary layer interactions
[AD-A266240] p 1026 N94-16929
To extend the thirteen-moment theory and its application to problems in rarefied hypersonic flow
[AD-A267384] p 859 N94-17021
Experimental and computational investigation of the NASA low-speed centrifugal compressor flow field
[NASA-TM-4481] p 869 N94-17386
Measurement of the velocity field and void fraction in a planar plunging jet
[AD-A268183] p 1030 N94-17511
Kinetic plasma processes occurring in the outer plasmasphere
[NASA-CR-193452] p 1300 N94-17524
VELOCITY MEASUREMENT
An experimental study of ASTOVL related jet flows to produce CFD code validation data. Phase 3: Results of experiments
[TT-9203] p 1020 N94-15645
Evaporation from a meniscus within a capillary tube in microgravity
[NASA-CR-194593] p 976 N94-15654
The shock Hugoniot of 316 SS and sound velocity measurements
[DE93-016525] p 1178 N94-16955
Measurement of the velocity field and void fraction in a planar plunging jet
[AD-A268183] p 1030 N94-17511
Laser velocimetry measurements of vortex flows on a delta wing at Mach 1.9
[AD-A268596] p 861 N94-17609
VENTILATION
Ventilated oscillatory boundary layers
[AD-A266226] p 1023 N94-16110
VENTING
Optical properties of water released in low Earth orbit
[AD-A266197] p 1192 N94-16936
VENUS (PLANET)
Venus lightning
[NASA-TM-109644] p 1105 N94-15430
NASA images 13
[NASA-TM-109418] p 1247 N94-15512
Magellan: Principal Venus science findings p 989 N94-15887
Morphometric comparison of Icelandic lava shield volcanoes versus selected Venusian edifices p 1248 N94-16178
Pargo Chasma and its relationship to global tectonics p 1249 N94-16181
The formation and evolution of Alpha and Tellus tesserae on Venus p 1249 N94-16183
Evolutionary implications of a steady-state water abundance on Venus p 1254 N94-16206
Spatially extensive uniform stress fields on Venus inferred from radial dike swarm geometries: The Aphrodite Terra example p 1254 N94-16207
Morphology and models for the evolution of eastern Hecate Chasma, Venus p 1256 N94-16215
Ishtar deformed belts: Evidence for deformation from below? p 1256 N94-16218
Tessera terrain on Venus: Implications of tessera flooding models and boundary characteristics for global distribution and mode of formation p 1258 N94-16226
Lava flow-field morphological classification and interpretation: Examples from Venus p 1259 N94-16230
Chemical differentiation, thermal evolution, and catastrophic overturn on Venus: Predictions and geologic observations p 1259 N94-16232
The three ages of Venus: A hypothesis based on the cratering record p 1261 N94-16239
Tessera terrain on Venus: Global characterization from Magellan data p 1264 N94-16262
Density of impact craters on tessera, Venus p 1264 N94-16263
Radar properties of several fluidized ejecta blankets on Venus p 1267 N94-16278
Venusian pancake domes: Insights from terrestrial voluminous silicic lavas and thermal modeling p 1286 N94-16381
Geophysical models of Western Aphrodite-Niobe region: Venus p 1286 N94-16382
Effective elastic thickness of the Venusian lithosphere with lateral viscosity variations in the mantle p 1293 N94-16421
VENUS ATMOSPHERE
A global traveling wave on Venus
[NASA-CR-194356] p 1246 N94-15182
Evolutionary implications of a steady-state water abundance on Venus p 1254 N94-16206
Principal investigators data package for Project Initiation Conference (PIC): EUVS sounding rocket no. 36.117CL. Target: Venus
[NASA-CR-194663] p 923 N94-17125

Magnetic effects in Venus/solar wind interaction
[NASA-CR-194666] p 1299 N94-17281
Pioneer Venus data analysis for the retarding potential analyzer
[NASA-CR-194673] p 1297 N94-17292

VENUS CLOUDS
A global traveling wave on Venus
[NASA-CR-194356] p 1246 N94-15182
Venus lightning
[NASA-TM-109644] p 1105 N94-15430

VENUS RADAR ECHOES
Resolving topographic detail on Venus by modeling complex Magellan altimetry echoes
p 1283 N94-16368

VENUS SURFACE
Magellan: Principal Venus science findings
p 989 N94-15887
Pargo Chasma and its relationship to global tectonics
p 1249 N94-16181
The formation and evolution of Alpha and Tellus tesserae on Venus p 1249 N94-16183
Spatially extensive uniform stress fields on Venus inferred from radial dike swarm geometries: The Aphrodite Terra example p 1254 N94-16207
Morphology and models for the evolution of eastern Hecate Chasma, Venus p 1256 N94-16215
Ishtar deformed belts: Evidence for deformation from below? p 1256 N94-16218
Tessera terrain on Venus: Implications of tessera flooding models and boundary characteristics for global distribution and mode of formation p 1258 N94-16226
Lava flow-field morphological classification and interpretation: Examples from Venus
p 1259 N94-16230
Chemical differentiation, thermal evolution, and catastrophic overturn on Venus: Predictions and geologic observations p 1259 N94-16232
Emplacement of multiple flow units on very shallow slopes, east Kawelu Planitia flow field, Venus
p 1260 N94-16235
The three ages of Venus: A hypothesis based on the cratering record p 1261 N94-16239
The depths of the largest impact craters on Venus
p 1264 N94-16261
Tessera terrain on Venus: Global characterization from Magellan data p 1264 N94-16262
Density of impact craters on tessera, Venus
p 1264 N94-16263
A first-order model for impact crater degradation on Venus p 1265 N94-16268
Estimates of lithospheric thickness on Venus
p 1267 N94-16277
Radar properties of several fluidized ejecta blankets on Venus p 1267 N94-16278
Tectonics of Neyterkob corona on Venus
p 1270 N94-16299
Implications of crater distributions on Venus
p 1270 N94-16300
Megaplumes on Venus p 1271 N94-16301
Preliminary analysis of Dione Regio, Venus: The final Magellan regional imaging gap p 1271 N94-16302
The distribution of large volcanoes on Venus as a function of height and altitude p 1271 N94-16303
Structural mapping of Maxwell Montes
p 1271 N94-16304
Global Magellan-image map of Venus at full resolution
p 1274 N94-16319
The cartography of Venus with Magellan data
p 1274 N94-16320
Meander properties of Venusian channels
p 1275 N94-16324
Spectral study of Venus global topography and geoid from Magellan and PVO data p 1276 N94-16332
Sheet flow fields on Venus p 1278 N94-16338
Models of thermal/chemical boundary layer convection: Potential application to Venus p 1279 N94-16348
Resolving topographic detail on Venus by modeling complex Magellan altimetry echoes
p 1283 N94-16368
Large-scale volcanism associated with coronae on Venus p 1285 N94-16376
Tectonic resurfacing of Venus p 1285 N94-16380
Relief of some small landforms on Venus
p 1293 N94-16418

VERBAL COMMUNICATION
Complex information coordination performance: Differential changes in working memory contributions following training
[AD-A267007] p 1132 N94-15762

VERTICAL DISTRIBUTION
Vertical structure models of the 1990 equatorial disturbance on Saturn p 1277 N94-16333
Altitude profile of aerosols on Mars from measurements of its thermal radiation on limb p 1294 N94-16423
Second flight of the Spacelab grille spectrometer during the Atlas-1 mission
[AERONAUTICA-ACTA-A-367-199] p 923 N94-17592
A surface energy budget model modifying heat flow by foliage effects
[AD-A266598] p 1085 N94-17610

VERTICAL MOTION
The free decay of coupled heave and pitch motions of a model frigate
[DRA/TM(AWMH)92340] p 1146 N94-15702

VERTICAL MOTION SIMULATORS
Fidelity assessment of a UH-60A simulation on the NASA Ames vertical motion simulator
[NASA-TM-104016] p 870 N94-15793

VERY LARGE SCALE INTEGRATION
VLSI for high-speed digital signal processing
[AD-A267709] p 1007 N94-14936
NASA Space Engineering Research Center for VLSI System Design
[NASA-CR-194587] p 1008 N94-15547
Fault handling schemes in electronic systems with specific application to radiation tolerance and VLSI design
[NASA-CR-194559] p 1008 N94-15640
Technology transfers and reliable oxides
[AD-A266948] p 1175 N94-15758
Leak detection utilizing analog binaural (VLSI) techniques
[NASA-CASE-NPO-18399-1-CU] p 1014 N94-17323
Fabricating binary optics: An overview of binary optics process technology p 1195 N94-17343
Applications of advanced diffractive optical elements
p 1197 N94-17356
Femtosecond carrier processes in compound semiconductors and real time signal processing
[AD-A268122] p 1005 N94-17519

VERY LONG BASE INTERFEROMETRY
Applications of SLR p 911 N94-15556
Tectonic deformation in southern California
[NASA-CR-194621] p 1101 N94-16021

VESTA ASTEROID
Petrologic constraints on the surface processes on asteroid 4 Vesta and on excavation depths of diogenite fragments p 1241 N94-16208

VESTS
STS-29 crew bailout in WETF
[NASA-TM-109548] p 1136 N94-15385

VIBRATION
Dynamics, stability, and control of maglev systems
[DE93-015163] p 1047 N94-16806
In-situ electron and optical spectroscopies of translational and vibrational activated bond breaking and formation on semiconductors
[AD-A268192] p 1015 N94-17560
Mechanical properties of interfaces and superlattices
[AD-A268591] p 1217 N94-17606

VIBRATION DAMPING
Superconductive material and magnetic field for damping and levitation support and damping of cryogenic instruments
[NASA-CASE-NPO-18458-1-CU] p 1033 N94-15875
Hoph bifurcation in viscous, low speed flows about an airfoil with structural coupling
[AD-A266542] p 859 N94-16798
Digital reverberation time measurement system
[AD-D015892] p 1177 N94-16919
A mechanical system damping measurement technique using a one-degree-of-freedom (1DOF) cylindrical gas bearing
[AD-A268402] p 1048 N94-17462

VIBRATION EFFECTS
Parametric study of a finite element model of the Sidewinder missile
[AD-A267245] p 865 N94-14976

VIBRATION ISOLATORS
A feasibility study of a microgravity enhancement system for Space Station Freedom
[NASA-CR-191550] p 886 N94-15864

VIBRATION MEASUREMENT
Remote tire pressure sensing technique
[NASA-CASE-LAR-14160-1] p 1033 N94-15884

VIBRATION MODE
Parametric study of a finite element model of the Sidewinder missile
[AD-A267245] p 865 N94-14976
A simplistic look at limit stresses from random loading
[NASA-TM-108427] p 1058 N94-15710
Development and comparison of advanced reduced-basis methods for the transient structural analysis of unconstrained structures
[NASA-TM-109015] p 1061 N94-17259

VIBRATION TESTS
Parametric study of a finite element model of the Sidewinder missile
[AD-A267245] p 865 N94-14976

VIBRATIONAL SPECTRA
Molecular processes in comets
[NASA-CR-194148] p 1239 N94-15188
The quantum mass shift of the soliton in Skyrme model
[ITN-93-85219] p 1180 N94-15283

VIBRATORY LOADS
Vibro-acoustic analysis of an aircraft maintenance dock
[AD-A266778] p 871 N94-14908

VIDEO COMMUNICATION
Application of modified VICAR/IBIS GIS to analysis of July 1991 Flevoland AIRSAR data p 1080 N94-16757

VIDEO COMPRESSION
Bandwidth characteristics of multimedia data traffic on a local area network
[NASA-TM-104026] p 883 N94-15648

VIDEO DATA
Massively parallel, adaptive, color image processing for autonomous road following
[AD-A266988] p 864 N94-15498

VIDEO EQUIPMENT
Video applications development platform
[AD-A266966] p 1163 N94-14953

VIDEO SIGNALS
Display system employing acousto-optic tunable filter
[NASA-CASE-NPO-18736-1-CU] p 1190 N94-15933

VIKING MARS PROGRAM
First US Mars landing
[NASA-TM-109669] p 885 N94-15436

VIKING SPACECRAFT
A mineralized zone in Western Candor Chasma, Mars
p 1248 N94-16179

VINYL POLYMERS
A study of relaxation transitions in the polymers under the influence of magnetic fields
[AD-A263878] p 963 N94-15133
Interpenetrating polymer network acoustic damping material
[AD-D015889] p 969 N94-16916

VIOLENCE
Criminal acts against civil aviation, fiscal year 1992
[AD-A268014] p 863 N94-17586

VIRTUAL REALITY
Future of robotics
[NASA-TM-109592] p 1045 N94-15284
A computer-based training system combining virtual reality and multimedia
[DE93-013768] p 1132 N94-16819

VISCOELASTICITY
On the design of structural components using materials with time-dependent properties
[NASA-TM-108428] p 1059 N94-16519
An analysis of ways of determining the material constants for viscoelastic materials
[IFTR-28/91] p 951 N94-17050
Electrorheological (ER) fluids: A research needs assessment
[AD-A267588] p 951 N94-17210
Damage evolution in filled elastomers
[AD-A268067] p 1062 N94-17507

VISCOPLASTICITY
Finite element analysis of structural engineering problems using a viscoplastic model incorporating two back stresses
[NASA-TM-106046] p 1060 N94-16881

VISCOSITY
Effects of aging time on V205 sol-gel coatings
[AD-A266824] p 965 N94-15843
Physical and chemical properties of some new perfluoropolyalkylether lubricants prepared by direct fluorination
[NASA-TM-106299] p 967 N94-16543
Coefficients for calculating thermodynamic and transport properties of individual species
[NASA-TM-4513] p 1220 N94-17624

VISCOUS DAMPING
Time dependent turbulence modeling and analytical theories of turbulence
[NASA-TM-106379] p 1029 N94-17385
A mechanical system damping measurement technique using a one-degree-of-freedom (1DOF) cylindrical gas bearing
[AD-A268402] p 1048 N94-17462

VISCOUS FLOW
Proteus two-dimensional Navier-Stokes computer code, version 2.0. Volume 2: User's guide
[NASA-TM-106338-VOL-2] p 1019 N94-15475
Proteus two-dimensional Navier-Stokes computer code, version 2.0. Volume 1: Analysis description
[NASA-TM-106336-VOL-1] p 1019 N94-15485
Proteus three-dimensional Navier-Stokes computer code, version 1.0. Volume 2: User's guide
[NASA-TM-106340-VOL-2] p 1020 N94-15488

Proteus three-dimensional Navier-Stokes computer code, version 1.0. Volume 3: Programmer's reference
[NASA-TM-106341] p 1022 N94-15865
Proteus two-dimensional Navier-Stokes computer code, version 2.0. Volume 3: Programmer's reference
[NASA-TM-106339] p 1022 N94-15867
Effective elastic thickness of the Venusian lithosphere with lateral viscosity variations in the mantle
p 1293 N94-16421
Proteus three-dimensional Navier-Stokes computer code, version 1.0. Volume 1: Analysis description
[NASA-TM-106337] p 1024 N94-16527
Hoph bifurcation in viscous, low speed flows about an airfoil with structural coupling
[AD-A266542] p 859 N94-16798
Process of shaping an electrorheological solid
[AD-D015885] p 1012 N94-16914
An upwind multigrid method for solving viscous flows on unstructured triangular meshes
[NASA-TM-109343] p 1027 N94-17061
Computational aerodynamics with icing effects
[AD-A267509] p 860 N94-17074
Development of iterative techniques for the solution of unsteady compressible viscous flows
[NASA-CR-194657] p 1027 N94-17129
Numerical solution of SUPG finite-element method for supersonic viscous flow
[AD-A267762] p 860 N94-17222
Multigrid time-accurate integration of Navier-Stokes equations
[NASA-TM-106373] p 1028 N94-17258
Experimental and computational investigation of the NASA low-speed centrifugal compressor flow field
[NASA-TM-4481] p 869 N94-17386

VISCOUS FLUIDS
Stability of flows in fluidized beds
[DE93-000245] p 1024 N94-16763

VISIBILITY
Low Earth orbit constellations: Orbit control or not
p 875 N94-17134
Impact of launching uncertainties on the visibility of communication satellite constellations without orbit control p 889 N94-17135
A comparison of ceiling and visibility observation for NWS manned observation sites and ASOS sites
[AD-A268356] p 1108 N94-17459

VISIBLE SPECTRUM
New K type asteroids p 1241 N94-16195

VISION
Enhancing sight
[NASA-TM-109637] p 1221 N94-15248

VISUAL ACUITY
Comparative night vision goggle visual acuity measurements performed in the A-10 aircraft in an operational setting
[AD-A266721] p 1137 N94-15820

VISUAL AIDS
Processes involved in the integration of pictures and discourse
[AD-A268150] p 1134 N94-17468

VISUAL CONTROL
Visually guided touching and manual tracking
[TR-412] p 1166 N94-16581

VISUAL PERCEPTION
YARF: An open-ended framework for robot road following
[AD-A266788] p 1163 N94-14910
Enhancing sight
[NASA-TM-109637] p 1221 N94-15248
Cooperativity and 3-D representation
[AD-A267180] p 1131 N94-15694
Reference frames in vision
[AD-A266174] p 1132 N94-16925
Localizing visual function in the brain
[AD-A267381] p 1133 N94-17020
ARPA unmanned ground vehicle stereo vision program at Teleos Research
[AD-A267632] p 1167 N94-17202
Neural basis of motion perception
[AD-A267267] p 1133 N94-17265
The effects of luminance boundaries on color perception
[AD-A268398] p 1133 N94-17397
A virtual acoustic orientation instrument
[AD-A268181] p 1134 N94-17510
Perception of lightness and brightness in complex patterns
[AD-A268435] p 1134 N94-17513

VISUAL STIMULI
Perception of lightness and brightness in complex patterns
[AD-A268435] p 1134 N94-17513

VISUAL TASKS
Enhancing sight
[NASA-TM-109637] p 1221 N94-15248
Perception of lightness and brightness in complex patterns
[AD-A268435] p 1134 N94-17513

VLASOV EQUATIONS
Linear stability of stationary solutions of the Vlasov-Poisson system in three dimensions
[DE93-013873] p 1174 N94-16820

VOICE COMMUNICATION
Call sign intelligibility improvement using a spatial auditory display
[NASA-TM-104014] p 1177 N94-15549
A study on an experimental communication system using microsatellites p 892 N94-17160
MAGSS-14: Medium Altitude Global Mobile Satellite System with enhanced regional coverage
p 893 N94-17164

VOICE CONTROL
STS-41 VCS training with mission specialist Bruce Melnick and Bill Shepard
[NASA-TM-109513] p 1046 N94-15459

VOID RATIO
Characterization of voids formed during liquid impregnation of nonwoven multifilament glass networks as related to composite processing p 939 N94-16858

VOIDS
Characterization of voids formed during liquid impregnation of nonwoven multifilament glass networks as related to composite processing p 939 N94-16858
Ultrasonic wave propagation model for nondestructive evaluation of solid rocker motor propellant
[AD-A267653] p 976 N94-17248
Measurement of the velocity field and void fraction in a planar plunging jet
[AD-A268183] p 1030 N94-17511

VOLATILITY
On-line gas chromatographic studies of Rutherfordium (element 104), hahnium (element 105), and homologs
[DE93-013890] p 948 N94-16821

VOLCANOES
Ground truth spectrometry and imagery of eruption clouds to maximize utility of satellite imagery
[NASA-CR-194358] p 1081 N94-15181
Magellan: Principal Venus science findings
p 989 N94-15887
Morphometric comparison of Icelandic lava shield volcanoes versus selected Venusian edifices
p 1248 N94-16178
Pargo Chasma and its relationship to global tectonics
p 1249 N94-16181
Explosive mafic volcanism on Earth and Mars
p 1253 N94-16204
Morphology and models for the evolution of eastern Hecate Chasma, Venus p 1256 N94-16215
Tessera terrain on Venus: Implications of tessera flooding models and boundary characteristics for global distribution and mode of formation p 1258 N94-16226
Mode of emplacement of lunar mare volcanic deposits: Graben formation due to near surface deformation accompanying dike emplacement at Rima Parry 5
p 1258 N94-16227
Modes of formation of lunar light plains and the detection of cryptomaria deposits p 1259 N94-16231
Chemical differentiation, thermal evolution, and catastrophic overturn on Venus: Predictions and geologic observations p 1259 N94-16232
Tessera terrain on Venus: Global characterization from Magellan data p 1264 N94-16262
Preliminary analysis of Dione Regio, Venus: The final Magellan regional imaging gap p 1271 N94-16302
The distribution of large volcanoes on Venus as a function of height and altitude p 1271 N94-16303
Large-scale volcanism associated with coronae on Venus p 1285 N94-16376
A decade's overview of Io's volcanic activity
p 1245 N94-16386
Aspects of modelling the tectonics of large volcanoes on the terrestrial planets p 1104 N94-16396
Relief of some small landforms on Venus
p 1293 N94-16418
The use of TIMS data to estimate the SO2 concentrations of volcanic plumes: A case study at Mount Etna, Sicily p 1065 N94-16608
Volcanic thermal features observed by AVIRIS
p 1068 N94-16680

VOLCANOLOGY
Morphometric comparison of Icelandic lava shield volcanoes versus selected Venusian edifices
p 1248 N94-16178
Pargo Chasma and its relationship to global tectonics
p 1249 N94-16181
The formation and evolution of Alpha and Tellus tesserae on Venus p 1249 N94-16183
Explosive mafic volcanism on Earth and Mars
p 1253 N94-16204
Remote sensing studies of the northeastern portion of the lunar nearside p 1258 N94-16225
Mode of emplacement of lunar mare volcanic deposits: Graben formation due to near surface deformation accompanying dike emplacement at Rima Parry 5
p 1258 N94-16227
Bubble coalescence in magmas p 1103 N94-16237
The history of mare volcanism in the Orientale Basin: Mare deposit ages, compositions and morphologies
p 1269 N94-16289
The rheology and composition of cryovolcanic flows on icy satellites p 1243 N94-16294
Explosive volcanism and the compositions of the cores of differentiated asteroids p 1243 N94-16306
Martian lavas: Three complementary remote sensing techniques to derive flow properties
p 1283 N94-16366
Venusian pancake domes: Insights from terrestrial voluminous silicic lavas and thermal modeling
p 1286 N94-16381
Grain surface features of Apollo 17 orange and black glass p 1289 N94-16397

VOLT-AMPERE CHARACTERISTICS
Polar 2 model of the wake shield experiment
[AD-A266243] p 882 N94-16468

VOLTAGE CONVERTERS (DC TO DC)
Forback DC-to-DC converter
[NASA-CASE-GSC-13404-1] p 1010 N94-15874

VOLTERRA EQUATIONS
Numerically solving a transient heat conduction problem with convection and radiation
[AD-A268521] p 1220 N94-17540

VOMITING
Evaluation of putative neurochemical intermediaries in space/motion sickness
[NASA-CR-193607] p 1118 N94-17090

VORTEX BREAKDOWN
The effect of the nose shape and wing location toward the wing vortex breakdown
[AD-A267724] p 855 N94-14942
Adaptive Navier-Stokes calculations for vortical flow
[AD-A266236] p 1026 N94-16966
Experimental study of vortex and aerodynamic characteristics of stack wings with sideslip
[AD-A267722] p 860 N94-17274

VORTEX SHEDDING
Unsteady separated flows: Empirical model and control
[AD-A267282] p 855 N94-14959

VORTICES
Unsteady separated flows: Empirical model and control
[AD-A267282] p 855 N94-14959
The turbulent wall jet
[AD-A267675] p 855 N94-14963
On the receptivity problem for O(1) wavelength Goertler vortices
[NASA-CR-191519] p 1016 N94-15005
Large-Eddy Simulations (LES) of flows and turbulence distribution
[AD-A267182] p 1016 N94-15151
Tollmien-Schlichting/vortex interactions in compressible boundary layer flows
[NASA-CR-191515] p 1017 N94-15183
Large eddy simulation and direct numerical simulation of high speed turbulent reacting flows
[NASA-CR-193131] p 1018 N94-15427
Surface and internal signatures of organized vortex motions in stratified fluid
[AD-A267015] p 1020 N94-15526
Aerodynamic control of NASP-type vehicles through Vortex manipulation. Volume 1: Static water tunnel tests
[NASA-CR-177626-VOL-1] p 855 N94-15655
Aerodynamic control of NASP-type vehicles through Vortex manipulation. Volume 2: Static wind tunnel tests
[NASA-CR-177626-VOL-2] p 856 N94-15677
Aerodynamic control of NASP-type vehicles through vortex manipulation, volume 4
[NASA-CR-177626-VOL-4] p 857 N94-15720
Parametric resonant triad interactions in a free shear layer
[NASA-TM-106365] p 1021 N94-15751
Aerodynamic control of NASP-type vehicles through vortex manipulation. Volume 3: Wing rock experiments
[NASA-CR-177626] p 857 N94-15780
Nuclear rocket plume studies
[AD-A267154] p 925 N94-15837
Receptivity of boundary layers to convected gusts
[AD-A267206] p 1022 N94-15860
Adaptive algorithm for aircraft configuration in turbulent flow
[AD-A266188] p 867 N94-16122
Search for chaos in free shear flows
[AD-A266245] p 1023 N94-16470
Wind tunnel investigations of forebody strakes for yaw control on F/A-18 model at subsonic and transonic speeds
[NASA-TP-3360] p 859 N94-16573

Complex terrain wind model evaluation
[AD-A266467] p 1096 N94-16589
Adaptive Navier-Stokes calculations for vortical flow
[AD-A266236] p 1026 N94-16966
Structure of turbulence in three-dimensional boundary layers
[NASA-CR-194655] p 1027 N94-17130
Transmission of light through a turbulent mixing layer
[AD-A267266] p 1193 N94-17264
Experimental study of vortex and aerodynamic characteristics of stack wings with sideslip
[AD-A267722] p 860 N94-17274
Time dependent turbulence modeling and analytical theories of turbulence
[NASA-TM-106379] p 1029 N94-17385
Laser velocimetry measurements of vortex flows on a delta wing at Mach 1.9
[AD-A268596] p 861 N94-17609
Study into the limits of an Euler equation method applied to leading-edge vortex flow
[NLR-TP-91350-U] p 1031 N94-17627
Granular fluctuations in plasma turbulence and their role in transport
[DE93-013465] p 1187 N94-17674

VORTICITY
Mesoscale frontogenesis: An analysis of two cold front case studies
[AD-A267950] p 1107 N94-17054
Granular fluctuations in plasma turbulence and their role in transport
[DE93-013465] p 1187 N94-17674

VORTICITY EQUATIONS
Nonlinear gyrofluid models of shear Alfven instabilities in ignited and beam heated toroidal plasmas
[DE93-016235] p 1203 N94-16869

VOYAGER PROJECT
NASA report to education, volume 7
[NASA-TM-109435] p 1247 N94-15419
NASA images 12 --- Voyager encounters
[NASA-TM-109417] p 1247 N94-15511

VOYAGER 1 SPACECRAFT
Voyager encounter highlights
[NASA-TM-109420] p 1246 N94-15239
The 1980 highlights
[NASA-TM-109672] p 1303 N94-15509

VOYAGER 2 SPACECRAFT
Voyager encounter highlights
[NASA-TM-109420] p 1246 N94-15239
Neptune encounter highlights
[NASA-TM-109421] p 1246 N94-15240
Voyager encounters Uranus
[NASA-TM-109619] p 1247 N94-15348
Voyager 2: Neptune encounter
[NASA-TM-109423] p 1247 N94-15491
Mass of Saturn's A ring p 1263 N94-16252

VSAT (NETWORK)
The ACTS propagation program p 995 N94-16039
NASA Lewis Meshed VSAT Workshop meeting summary
[NASA-TM-106332] p 883 N94-17487
On-board packet switch architectures for communication satellites
[NASA-TM-106326] p 883 N94-17488

W

WAFERS
Pseudomorphic semiconducting heterostructures from combinations of AlN, GaN and selected SiC polytypes: Theoretical advancement and its coordination with experimental studies of nucleation, growth, characterization and device deployment
[AD-A267561] p 1213 N94-17108

WAKES
Receptivity of boundary layers to convected gusts
[AD-A267206] p 1022 N94-15860
Search for chaos in free shear flows
[AD-A266245] p 1023 N94-16470

WALL FLOW
On the receptivity problem for 0(1) wavelength Goertler vortices
[NASA-CR-191519] p 1016 N94-15005
Wall interference and boundary simulation in a transonic wind tunnel with a discretely slotted test section
[NASA-TP-3334] p 872 N94-15794
Determination of the effect of the walls of a wind-tunnel from the parameters of flow near them
[RAE-UB-TRANS-2201] p 859 N94-16583
Transition induced by fixed and freely convecting spherical particles in laminar boundary layers
[AD-A267757] p 1028 N94-17276
Active turbulence control in wall bounded flows using direct numerical simulation
[AD-A267261] p 1028 N94-17286

WALL JETS
The turbulent wall jet
[AD-A267675] p 855 N94-14963

WALL PRESSURE
Wall interference and boundary simulation in a transonic wind tunnel with a discretely slotted test section
[NASA-TP-3334] p 872 N94-15794
An experimental investigation of the effects of leading edge geometry on the dynamics of blunt fin-induced shock wave turbulent boundary layer interaction
[AD-A267656] p 860 N94-17221
An experimental study of fluctuating wall pressures in a highly swept, sharp fin-induced, Mach 5 shock wave/turbulent boundary layer interaction
[AD-A268394] p 861 N94-17461

WALL TEMPERATURE
Description of cooling water calorimetry and wall thermometry diagnostic at tokamak ASDEX-Upgrade
[IPP-5/46] p 1200 N94-14966

WALLS
Experimental investigations into the deflagration to detonation transition at TNO/PML
[AD-A266753] p 1021 N94-15755

WARFARE
Sleep management user's guide for special operations personnel
[AD-A267746] p 1119 N94-14943
An information processing classification of beyond-visual-range air intercepts
[AD-A266927] p 1131 N94-15108
Not ready for the first space war. What about the second?
[AD-A266557] p 1174 N94-16665

WARNING SYSTEMS
Test plan for the evaluation of the initial capability of the National Satellite Test Bed: Phase 1D
[DOT/FAA/RD-93/20] p 876 N94-16025
The use of the Air Force Academy high wind alert system in forecasting moderate intensity wind events for military bases in the Colorado Springs area
[AD-A267648] p 1107 N94-17245

WASTE DISPOSAL
Nuclear rocket plume studies
[AD-A267154] p 925 N94-15837
Biomass energy: State of the technology present obstacles and future potential
[DE93-016295] p 1092 N94-16766

WASTE WATER
Multiple dataset water-quality analyses in the vicinity of an ocean wastewater plume p 1069 N94-16687

WATER
STS-29 crew bailout in WETF
[NASA-TM-109548] p 1136 N94-15385
Study of protein-H2O interactions by multidimensional NMR spectroscopy
[AD-A266955] p 946 N94-15760
Global Energy and Water Cycle Experiment (GEWEX) and the Continental-scale International Project (GCIP) p 994 N94-15918
Laser-liquid interactions under reduced gravity conditions p 977 N94-16077
Contained liquids in microgravity, part 2 p 979 N94-16085
A mineralized zone in Western Candor Chasma, Mars p 1248 N94-16179
Evolutionary implications of a steady-state water abundance on Venus p 1254 N94-16206
Experimental constraints on CO2 and H2O in the Martian mantle and primary magmas p 1262 N94-16248
Catalytic crystallization of ices by small silicate smokes at temperatures less than 20K p 1219 N94-16420
Water adsorption on diamond (110) studied by multiple internal reflection infrared spectroscopy
[AD-A266415] p 948 N94-16553
Optical properties of water released in low Earth orbit
[AD-A266197] p 1192 N94-16936
Natural convection above a horizontal heat source
[AD-A267212] p 1026 N94-16985
Numerical modelling of an active direct nonpotable hot water heating system making use of the energy of solar radiation
[IFTR-38/1991] p 1093 N94-17070
The standardized precipitation index and its use in the western contiguous United States
[AD-A267547] p 1107 N94-17102
Strategy for the reduction of total integrated fluid logistics to the Space Station Freedom
[NASA-TM-107744] p 1138 N94-17452
Continuum solvent models for computational chemistry
[DE93-016329] p 953 N94-17660

WATER BALANCE
Research into the influence of spatial variability and scale on the parameterization of hydrological processes
[NASA-CR-194610] p 1082 N94-16026
Evapotranspiration and runoff from large land areas: Land surface hydrology for atmospheric general circulation models p 1083 N94-16029
Heterogeneity and scaling land-atmospheric water and energy fluxes in climate systems p 1083 N94-16030
Evaluation of a distributed catchment scale water balance model
[PAPER-93WR00398] p 1083 N94-16031
A detailed model for simulation of catchment scale subsurface hydrologic processes
[PAPER-92WR02333] p 1084 N94-16032
Effects of spatial variability and scale on areal -average evapotranspiration p 1084 N94-16033
Scaling, soil moisture and evapotranspiration in runoff models p 1084 N94-16034

WATER CIRCULATION
Meridional circulation in the tropical north atlantic
[AD-A268222] p 1114 N94-17555

WATER COLOR
Coastal zone color scanner: Nimbus 7
[NASA-TM-109590] p 1111 N94-15281
SeaWiFS technical report series. Volume 12, SeaWiFS technical report series cumulative index: Volumes 1-11
[NASA-TM-104566-VOL-12] p 1111 N94-15529
Optical properties of the Red Sea
[AD-A266466] p 1113 N94-16588

WATER CONSUMPTION
Optimization of two-stage hot water exchange points p 1029 N94-17440

WATER DEPTH
Water-levels fluctuations in a borehole at the Royal Observatory of Belgium: Effects on local gravity, Earth tidal, and barometric responses p 1100 N94-15812

WATER EROSION
Sedimentation, volcanism, and ancestral lakes in the Valles Marineris: Clues from topography p 1283 N94-16369

WATER FLOW
Boundary layer flow of air over water on a flat plate
[NASA-CR-191517] p 1019 N94-15479
A detailed model for simulation of catchment scale subsurface hydrologic processes
[PAPER-92WR02333] p 1084 N94-16032

WATER HEATING
Numerical modelling of an active direct nonpotable hot water heating system making use of the energy of solar radiation
[IFTR-38/1991] p 1093 N94-17070
Optimization of two-stage hot water exchange points p 1029 N94-17440

WATER LANDING
STS-32 bailout training in WETF
[NASA-TM-109476] p 1136 N94-15383

WATER QUALITY
Multiple dataset water-quality analyses in the vicinity of an ocean wastewater plume p 1069 N94-16687
A Geographic Information System approach to modeling nutrient and sediment transport
[DE93-013747] p 1097 N94-17426

WATER RUNOFF
On hydrologic similarity: A dimensionless flood frequency model using a generalized geomorphologic unit hydrograph and partial area runoff generation
[PAPER-89WR01579] p 1083 N94-16027
Similarity and scale in catchment storm response
[PAPER-89RG01615] p 1083 N94-16028
Evapotranspiration and runoff from large land areas: Land surface hydrology for atmospheric general circulation models p 1083 N94-16029
Scaling, soil moisture and evapotranspiration in runoff models p 1084 N94-16034

WATER TABLES
Water-levels fluctuations in a borehole at the Royal Observatory of Belgium: Effects on local gravity, Earth tidal, and barometric responses p 1100 N94-15812
Evaluation of a distributed catchment scale water balance model
[PAPER-93WR00398] p 1083 N94-16031

WATER TEMPERATURE
Temperature measurements p 1037 N94-15804
Efficacy of flocculating and other emergency water purification tablets
[AD-A266695] p 1148 N94-15840
Optimization of two-stage hot water exchange points p 1029 N94-17440

WATER TREATMENT
Plant research
[NASA-TM-109664] p 1116 N94-15235
Efficacy of flocculating and other emergency water purification tablets
[AD-A266695] p 1148 N94-15840

WATER TUNNEL TESTS
Aerodynamic control of NASP-type vehicles through Vortex manipulation. Volume 1: Static water tunnel tests
[NASA-CR-177626-VOL-1] p 855 N94-15655

Aerodynamic control of NASP-type vehicles through vortex manipulation. Volume 3: Wing rock experiments
[NASA-CR-177626] p 857 N94-15780

WATER VAPOR

Corrosion kinetics and mechanisms for nuclear grade graphites
[DE93-015462] p 947 N94-16105

Trapping of water vapor from an atmosphere by condensed silicate matter formed by high-temperature pulse vaporization p 1248 N94-16180

Possible sources of H2 to H2O enrichment at evaporation of parent chondritic material
p 1244 N94-16377

A linear spectral matching technique for retrieving equivalent water thickness and biochemical constituents of green vegetation p 1068 N94-16678

Separation of cirrus cloud from clear surface from AVIRIS data using the 1.38 micron water vapor band
p 1072 N94-16699

Discussion of band selection and methodologies for the estimation of precipitable water vapour from AVIRIS data p 1074 N94-16707

Empirical relationships among atmospheric variables from rawinsonde and field data as surrogates for AVIRIS measurements: Estimation of regional land surface evapotranspiration p 1074 N94-16712

Optical properties of water released in low Earth orbit
[AD-A266197] p 1192 N94-16936

Atmospheric propagation analysis program
[AD-A268231] p 1006 N94-17565

An analysis of simulated and actual DMSP SSM/T-2 brightness temperatures
[AD-A268103] p 1109 N94-17573

An empirical study of tropical cloud clusters using special sensor microwave imager data
[AD-A268072] p 1110 N94-17595

WATER WAVES

Arctic internal waves (CEAREX)
[AD-A265822] p 1111 N94-15139

Ocean wave study
[NASA-TM-109620] p 1111 N94-15349

Ventilated oscillatory boundary layers
[AD-A266226] p 1023 N94-16110

Observations and modelling of winds and waves during the Surface Wave Dynamics Experiment. Report 1: Intensive observation period IOP-1, 20-31 October 1990
[AD-A266384] p 1113 N94-16517

Field observations of infragravity, sea and swell directional spectra
[AD-A266439] p 1113 N94-16561

Preliminary estimates of frequency-direction spectra derived from the SAMSON pressure gage array, November 1990 to May 1991
[AD-A267960] p 1114 N94-17497

Measurement of the velocity field and void fraction in a planar plunging jet
[AD-A268183] p 1030 N94-17511

WATERSHEDS

On hydrologic similarity: A dimensionless flood frequency model using a generalized geomorphologic unit hydrograph and partial area runoff generation
[PAPER-89WR01579] p 1083 N94-16027

Effects of spatial variability and scale on areal -average evapotranspiration p 1084 N94-16033

A Geographic Information System approach to modeling nutrient and sediment transport
[DE93-013747] p 1097 N94-17426

WAVE ATTENUATION

Optical attenuation mechanism upgrades, MOBLAS, and TLRS systems p 922 N94-15622

WAVE DIFFRACTION

Diffraction of microwaves at rectangular facades of buildings with and without ground reflections (Fresnel-Kirchhoff-Approximation)
[DLR-FB-92-35] p 987 N94-15155

The exact solution of the problem of diffraction of an electromagnetic plane wave by a conductive half-plane situated at an interface
[IFTR-3/91] p 1002 N94-17057

Two-dimensional acousto-optical interaction theory and experimental analysis
[AD-A267761] p 1193 N94-17254

Review of rigorous coupled-wave analysis and of homogeneous effective medium approximations for high spatial-frequency surface-relief gratings
p 1194 N94-17335

WAVE DISPERSION

Nonlinear acoustics: Periodic waveguide, scattering of sound by sound, three-layer fluid, finite amplitude sound in a medium having a distribution of relaxation processes, and production of an isolated negative pulse in water
[AD-A267145] p 1177 N94-15732

Magnetic effects in anomalous dispersion
[DE93-014291] p 1175 N94-15978

WAVE EQUATIONS

Soliton-like structures in double stimulated Brillouin scattering p 1200 N94-15207

Nonlinear problems in fluid dynamics and inverse scattering
[AD-A266234] p 1026 N94-16927

Elastic waves in discretely continuous mechanical systems
[IFTR-21/1992] p 1061 N94-17091

Two-dimensional acousto-optical interaction theory and experimental analysis
[AD-A267761] p 1193 N94-17254

WAVE FRONTS

Fabrication techniques for very fast diffractive lenses
p 1196 N94-17345

Test methods for acceptance testing of telescopes
[AD-A268316] p 1237 N94-17568

WAVE FUNCTIONS

Supersymmetry of gauge equations and geometric nonadiabatic phases
[DE93-626671] p 1219 N94-14935

The fractional quantum Hall effect and the rotation group
[DE93-010348] p 1207 N94-15972

Quark-loop effects in high energy spin-flip processes
[DE93-626692] p 1188 N94-17313

Continuum solvent models for computational chemistry
[DE93-016329] p 953 N94-17660

WAVE GENERATION

Field observations of infragravity, sea and swell directional spectra
[AD-A266439] p 1113 N94-16561

WAVE INTERACTION

Current drive with free electron lasers in high and low temperature tokamaks p 1201 N94-15209

On the decay of a dipole pump wave to half-harmonics p 1201 N94-15211

Investigate wave-mean flow interaction and transport in the extratropical winter stratosphere
[NASA-CR-194555] p 1098 N94-15639

The exact solution of the problem of diffraction of an electromagnetic plane wave by a conductive half-plane situated at an interface
[IFTR-3/91] p 1002 N94-17057

An experimental investigation of the effects of leading edge geometry on the dynamics of blunt fin-induced shock wave turbulent boundary layer interaction
[AD-A267656] p 860 N94-17221

WAVE PROPAGATION

Dynamic behavior of fiber and particle reinforced composites
[AD-A266905] p 930 N94-15143

Improvement of SLR accuracy, a possible new step
p 917 N94-15588

Pulse propagation in inhomogeneous optical waveguides
[DE93-013378] p 1191 N94-16007

Proceedings of the Fifteenth NASA Propagation Experimenters Meeting (NAPEX 15) and the Advanced Communications Technology Satellite (ACTS) Propagation Studies Miniworkshop
[NASA-CR-194539] p 994 N94-16035

A review of OPEX activities and measurement results
p 994 N94-16036

Propagation measurements in Alaska using ACTS beacons p 995 N94-16040

Planned LMSS propagation experiment using ACTS: Preliminary antenna pointing results during mobile operations p 995 N94-16041

Propagation-related AMT design aspects and supporting experiments p 995 N94-16042

A comparison of cloud attenuation models using measured cloud data p 996 N94-16044

Comparison of OLYMPUS beacon and radiometric attenuation measurements at Blacksburg, Virginia
p 996 N94-16046

Satellite sound broadcast propagation measurements
p 996 N94-16047

An overview of the text propagation effects for land-mobile-satellite systems: Experimental and modeling results p 996 N94-16048

Database for propagation models p 996 N94-16049

A CCIR-based prediction model for Earth-Space propagation p 997 N94-16050

A study of land mobile satellite service multipath effects using SATLAB software p 997 N94-16051

NORSAR basic seismological research
[AD-A266193] p 1101 N94-16125

Acousto-optical confirmation of the localized wave phenomena
[DE93-016425] p 1177 N94-16448

A ray trace model for propagation loss
[AD-A266314] p 997 N94-16467

Surface waves in an inhomogeneous, isotropic, elastic half-space
[IFTR-18/1991] p 1060 N94-17047

Ultrasonic wave propagation model for nondestructive evaluation of solid rocker motor propellant
[AD-A267653] p 976 N94-17248

A search for evidence of nonlinear elasticity in the earth
[DE93-015279] p 1102 N94-17252

WAVE REFLECTION

Diffraction of microwaves at rectangular facades of buildings with and without ground reflections (Fresnel-Kirchhoff-Approximation)
[DLR-FB-92-35] p 987 N94-15155

Nonlinear acoustics: Periodic waveguide, scattering of sound by sound, three-layer fluid, finite amplitude sound in a medium having a distribution of relaxation processes, and production of an isolated negative pulse in water
[AD-A267145] p 1177 N94-15732

Regular and irregular reflection of a wave from a slanting flat wall
[IFTR-13/1991] p 1193 N94-17049

Numerical solution of SUPG finite-element method for supersonic viscous flow
[AD-A267762] p 860 N94-17222

WAVE SCATTERING

Double stimulated Brillouin scattering
p 1200 N94-15205

Dynamics of douple stimulated Brillouin scattering
p 1200 N94-15206

Soliton-like structures in double stimulated Brillouin scattering p 1200 N94-15207

Convergence of the multiple scattering expansion in XAFS and XANES
[DE93-011001] p 948 N94-16772

Spectral inverse scattering theory for dielectric media: Application to optical devices
[AD-A268635] p 1199 N94-17427

WAVE-PARTICLE INTERACTIONS

Simulations of wave-particle interactions in stimulated Raman forward scattering in a magnetized plasma
[TKK-F-A704] p 1201 N94-15210

WAVEFORMS

High resolution radar profiling using higher-order statistics
[AD-D015891] p 1000 N94-16918

An asymptotic expansion of an electromagnetic field in the velocity of a caustic in the form of simple waves
[IFTR-14/1991] p 1002 N94-17048

WAVEGUIDE ANTENNAS

Experimental evaluation of an adaptive focusing algorithm for a microwave planar phased-array hyperthermia system at UCSF
[AD-A267004] p 1121 N94-15634

WAVEGUIDES

Gratings and waveguides p 1226 N94-14987

Nonlinear acoustics: Periodic waveguide, scattering of sound by sound, three-layer fluid, finite amplitude sound in a medium having a distribution of relaxation processes, and production of an isolated negative pulse in water
[AD-A267145] p 1177 N94-15732

Stress sensitivity of dielectric resonators
[AD-A266767] p 1009 N94-15825

WAVELENGTHS

Alternative wavelengths for laser ranging
p 913 N94-15564

Optimum wavelengths for two color ranging
p 915 N94-15580

WAVELET ANALYSIS

Adaptive wavelet collocation methods for initial value boundary problems of nonlinear PDE's
[NASA-CR-191507] p 1169 N94-15833

Nonlinear problems in fluid dynamics and inverse scattering
[AD-A266234] p 1026 N94-16927

Applications of the phi-transform
[AD-A266247] p 1170 N94-16940

Studies in turbulence and turbulence control
[AD-A266318] p 1026 N94-16950

Diffractive optical elements for generating arbitrary line foci p 1195 N94-17338

WEAK ENERGY INTERACTIONS

A high sensitivity search for CP violating rare K(sub L) decays and precision measurement of the direct CP violation parameter (epsilon)(prime)/(epsilon) via the four K (yields) 2(pi) decay modes
[DE93-016866] p 1184 N94-16899

Existence of a new instanton in constrained Yang-Mills-Higgs theory
[NIKHEF-H/93-02] p 1186 N94-17601

Properties of nuclei in astrophysical environments: Binding energies, weak-interaction rates
[MPA-706] p 1240 N94-17628

WEAK INTERACTIONS (FIELD THEORY)

Electroweak physics from D0
[DE93-015041] p 1181 N94-16053

Theoretical high energy physics research at the University of Chicago
[DE93-016863] p 1187 N94-16116
Electroweak results from D0
[DE93-014926] p 1185 N94-16968

WEAPON SYSTEMS
Army P/M research and development overview
[AD-A266921] p 954 N94-15104
RAMCAD design methodology
[AD-A267010] p 1145 N94-15525
Infrared spot tracker
[AD-D015778] p 1191 N94-16547
Preliminary validation of the task analysis/workload methodology
[AD-A267514] p 1138 N94-17077

WEAR
The friction and wear of ceramic/ceramic and ceramic/metal combinations in sliding contact
[NASA-TM-106348] p 930 N94-15769
Ion implantation effects on surface-mechanical properties of metals and polymers
[DE93-014661] p 958 N94-16453
Atomic-scale friction measurements using friction force microscopy. Part 1: General principles and new measurement techniques
[AD-A268391] p 1048 N94-17533
Continuing research on friction and wear of materials
[AD-A268291] p 1049 N94-17566

WEAR RESISTANCE
Vacuum plasma spraying p 975 N94-16002
Wear resistant titanium material development
[AD-A266474] p 959 N94-16780
Application of hard coatings to substrates at low temperatures
[NASA-CR-193867] p 971 N94-17122

WEAR TESTS
Wear resistant titanium material development
[AD-A266474] p 959 N94-16780

WEATHER
Venus lightning
[NASA-TM-109644] p 1105 N94-15430
Boundary layer structure over areas of heterogeneous heat fluxes
[DE93-010657] p 1110 N94-17673

WEATHER FORECASTING
Mesoscale modeling of the atmosphere
[AD-A263236] p 1098 N94-15132
Short term weather forecasting in real time in a base weather station setting
[AD-A266872] p 1105 N94-15142
The Next Generation Weather Radar (NEXRAD)/Air Route Surveillance Radar (ARSR) operational comparison
[REPT-93W0000145] p 987 N94-15439
Radar diagnostic parameters as indicators of severe weather in central Florida
[PB93-183507] p 1106 N94-16465
The multivariate optimum interpolation analysis of meteorological data at the Fleet Numerical Oceanography Center
[AD-A266459] p 1106 N94-16568
A snow wetness retrieval algorithm for SAR
p 1075 N94-16732
The standardized precipitation index and its use in the western contiguous United States
[AD-A267547] p 1107 N94-17102
Solar Electro-Optical Network (SEON) upgrade/replacement program. Phase 1: Qualification operational test and evaluation plan
[AD-A266364] p 1237 N94-17225
Developing automated analysis methods for sea ice imagery: A status report with recommendations
[AD-A267284] p 1113 N94-17241
The use of the Air Force Academy high wind alert system in forecasting moderate intensity wind events for military bases in the Colorado Springs area
[AD-A267648] p 1107 N94-17245
Nowcasting methods for satellite imagery
[AD-A267294] p 1108 N94-17267
Propagation characteristics of mesoscale convective systems
[AD-A268130] p 1109 N94-17522
Micro- and meso-scale simulations of magnetospheric processes related to the aurora and substorm morphology
[NASA-CR-193437] p 1102 N94-17527

WEATHER STATIONS
Short term weather forecasting in real time in a base weather station setting
[AD-A266872] p 1105 N94-15142
TAFVER 2 users manual
[AD-A266850] p 1106 N94-15757
The multivariate optimum interpolation analysis of meteorological data at the Fleet Numerical Oceanography Center
[AD-A266459] p 1106 N94-16568

WEATHERING
Spectral evidence of size dependent space weathering processes on asteroid surfaces p 1241 N94-16174
Variations in the Fe mineralogy of bright Martian soil
p 1295 N94-16431
Lithological and textural controls on radar and diurnal thermal signatures of weathered volcanic deposits, Lunar Crater region, Nevada p 1080 N94-16762

WEAVING
Processing, properties and applications of composites using powder-coated epoxy towpreg technology
p 933 N94-15277
Research in textile composites at KU, Leuven
p 937 N94-16848
Weaving multi-layer fabrics for reinforcement of engineering components p 937 N94-16850

WEDGE FLOW
On the interaction between the shock wave attached to a wedge and freestream disturbances
[NASA-CR-191528] p 1019 N94-15478

WEDGES
Translating wedge heat sink
[AD-D015814] p 1011 N94-16488

WEIBULL DENSITY FUNCTIONS
Weibull analysis applied to the pull adhesion test and fracture of a metal-ceramic interface
[DE93-012913] p 1059 N94-15997

WEIGHTING FUNCTIONS
Adaptive beamforming with imperfect arrays: Pattern effects and their partial correction
[AD-A267079] p 987 N94-15541
Nonparametric statistics: Weighted rankings analysis
[AD-A266607] p 1173 N94-16657

WEIGHTLESSNESS
Movement in microgravity
[NASA-TM-109526] p 881 N94-15389

WEIGHTLESSNESS SIMULATION
STS-35 Crew training: Bailout in CCT, firefighting, TAGS class and bailout in WFTF
[NASA-TM-109489] p 1135 N94-15195
STS-26 IUS and latch contingency training
[NASA-TM-109561] p 875 N94-15331
STS-34 Chang-Diaz and E. Baker during Galileo contingency training in WFTF
[NASA-TM-109466] p 1135 N94-15361
STS-32 LDEF EVA training in WETF with Low and Dunbar
[NASA-TM-109473] p 1135 N94-15377
STS-32 crew training for lower body negative pressure unit and AFE
[NASA-TM-109475] p 1120 N94-15381
STS-33 Carter and Thorton during WETF activities
[NASA-TM-109471] p 1136 N94-15402
STS-31 Hubble space telescope contingency training in WETF with McCandless and Sullivan
[NASA-TM-109480] p 1136 N94-15441
STS-31 crew training inflight maintenance and bailout exercises in CCT and WFTF
[NASA-TM-109483] p 876 N94-15450
Richards, Dick: Training clip
[NASA-TM-109503] p 876 N94-15467

WELD STRENGTH
The Marshall Automated Weld System (MAWS)
[TABES PAPER 93-602] p 1049 N94-16138

WELD TESTS
The Marshall Automated Weld System (MAWS)
[TABES PAPER 93-602] p 1049 N94-16138

WELDED JOINTS
Use of photostress and strain gages to analyze behavior of weldments and use of photostress and strain gages to analyze behavior of an aft skirt test specimen
[NASA-CR-194575] p 1058 N94-15716
The effect of aging at 343 C on the mechanical properties and microstructure of type 308 stainless steel weldments
[DE93-015454] p 957 N94-16103
The Marshall Automated Weld System (MAWS)
[TABES PAPER 93-602] p 1049 N94-16138
Adaptive weld control for high-integrity welding applications
[TABES PAPER 93-604] p 1049 N94-16140

WELDING
Krupp technical reports no. 2, English edition, October 1992
[ETN-93-94631] p 984 N94-16000
Expert system for welding engineering
p 984 N94-16003

WELDING MACHINES
Welding nozzle position manipulator
[NASA-CASE-MFS-29837-1] p 1047 N94-15882

WENTZEL-KRAMER-BRILLOUIN METHOD
The three-dimensional ray trajectories of the WKB optical fiber modes
[AD-A267167] p 1189 N94-15739

WETLANDS
Characterization of wetland, forest, and agricultural ecosystems in Belize with airborne radar (AIRSAR)
p 1076 N94-16738

WETTING
Separation behaviour of monotectic alloys
p 945 N94-15170

WHISKER COMPOSITES
The influence of microstructure on the mechanical behavior of silicon nitride ceramics
[DE93-015363] p 966 N94-16018
Interface chemistry in ceramic matrix composites
[AD-A268629] p 973 N94-17466

WHISPERING GALLERY MODES
Full-wave simulation of the thumbtack laser
[DE93-015110] p 1039 N94-16054

WHITE NOISE
Analysis of temporal symmetry in non-gaussian random fields
[AD-A266496] p 999 N94-16794
High order nonlinear estimation with signal processing applications
[AD-A268407] p 1005 N94-17463

WIND (METEOROLOGY)
The use of the Air Force Academy high wind alert system in forecasting moderate intensity wind events for military bases in the Colorado Springs area
[AD-A267648] p 1107 N94-17245
Boundary layer structure over areas of heterogeneous heat fluxes
[DE93-010657] p 1110 N94-17673

WIND DIRECTION
Determination of momentum flux using a bivane and cup anemometer
[AD-A265414] p 1105 N94-15137
Complex terrain wind model evaluation
[AD-A266467] p 1096 N94-16589
Analysis of TIMS performance subjected to simulated wind blast p 1063 N94-16598

WIND EFFECTS
Sand transport on Mars: Preliminary results from models p 1252 N94-16198
Dust-dynamic feedbacks in the Martian atmosphere: Surface dust lifting p 1296 N94-16434
Detecting surface roughness effects on the atmospheric boundary layer via AIRSAR data: A field experiment in Death Valley, California p 1078 N94-16747

WIND MEASUREMENT
Observations and modelling of winds and waves during the Surface Wave Dynamics Experiment. Report 1: Intensive observation period IOP-1, 20-31 October 1990
[AD-A266384] p 1113 N94-16517
EOS Laser Atmosphere Wind Sounder (LAWS) investigation
[NASA-CR-193445] p 1109 N94-17525

WIND PROFILES
Investigate wave-mean flow interaction and transport in the extratropical winter stratosphere
[NASA-CR-194555] p 1098 N94-15639

WIND SHEAR
Windshear radar calibration, 1992 flights: Transmitter power and receiver gain stability
[NASA-TM-108997] p 986 N94-15140
Wind shear and heavy rain --- effects on flight stability
[NASA-TM-109453] p 1105 N94-15326
Windshear detection radar signal processing studies
[NASA-CR-194615] p 994 N94-16022
Windshear database for forward-looking systems certification
[NASA-TM-109012] p 1108 N94-17283

WIND TUNNEL APPARATUS
Monopiece strain gauge sting mounted wind tunnel balance
[CA-PATENT-1-311-626] p 1032 N94-15697
NASA Lewis 9- by 15-foot low-speed wind tunnel user manual
[NASA-TM-106247] p 872 N94-15819

WIND TUNNEL MODELS
NASA Lewis 9- by 15-foot low-speed wind tunnel user manual
[NASA-TM-106247] p 872 N94-15819
Design of round-to-square transition section; analysis and computer code
[AD-A267173] p 872 N94-15847

WIND TUNNEL NOZZLES
Design of round-to-square transition section; analysis and computer code
[AD-A267173] p 872 N94-15847

WIND TUNNEL TESTS
An uncertainty analysis of inlet dynamic flow distortion using an analog/digital hybrid editing system
[AD-A266924] p 855 N94-15105
Rotorcraft research
[NASA-TM-109452] p 871 N94-15325
Spacework 16 --- Simulated Space Shuttle Program
[NASA-TM-109436] p 1221 N94-15420

A software interface for the ARL wind tunnel data acquisition system
[AD-A267114] p 1146 N94-15650
Aerodynamic control of NASP-type vehicles through Vortex manipulation. Volume 2: Static wind tunnel tests
[NASA-CR-177626-VOL-2] p 856 N94-15677
Wind tunnel investigation of three axisymmetric cowls of different lengths at Mach numbers from 0.60 to 0.92
[NASA-TM-4488] p 856 N94-15681
Physical properties of the benchmark models program supercritical wing
[NASA-TM-4457] p 866 N94-15722
Aerodynamic control of NASP-type vehicles through vortex manipulation. Volume 3: Wing rock experiments
[NASA-CR-177626] p 857 N94-15780
Wall interference and boundary simulation in a transonic wind tunnel with a discretely slotted test section
[NASA-TP-3334] p 872 N94-15794
NASA Lewis 9- by 15-foot low-speed wind tunnel user manual
[NASA-TM-106247] p 872 N94-15819
Wind tunnel investigation with an operational turbojet engine
[TABES PAPER 93-662] p 870 N94-16157
Effects of internal yaw-vectoring devices on the static performance of a pitch-vectoring nonaxisymmetric convergent-divergent nozzle
[NASA-TP-3369] p 858 N94-16572
Wind tunnel investigations of forebody strakes for yaw control on F/A-18 model at subsonic and transonic speeds
[NASA-TP-3360] p 859 N94-16573
Wind-tunnel investigation of aerodynamic efficiency of three planar elliptical wings with curvature of quarter-chord line
[NASA-TP-3359] p 859 N94-16574
Determining the effect of endwall boundary layer suction in a large scale subsonic compressor cascade
[AD-A267208] p 859 N94-16913
An experimental investigation of the effects of leading edge geometry on the dynamics of blunt fin-induced shock wave turbulent boundary layer interaction
[AD-A267656] p 860 N94-17221
Supersonic flow visualization of a nacelle in close proximity to a simulated wing
[NASA-CR-194675] p 860 N94-17260
Subsonic aerodynamic characteristics of the HL-20 lifting-body configuration
[NASA-TM-4515] p 861 N94-17284
User's manual for the Langley Research Center 14- by 22- foot subsonic tunnel static data acquisition system
[NASA-TM-109027] p 861 N94-17639

WIND TUNNEL WALLS
Wall interference and boundary simulation in a transonic wind tunnel with a discretely slotted test section
[NASA-TP-3334] p 872 N94-15794
Determination of the effect of the walls of a wind-tunnel from the parameters of flow near them
[RAE-LIB-TRANS-2201] p 859 N94-16583

WIND TUNNELS
Spacework 16 --- Simulated Space Shuttle Program
[NASA-TM-109436] p 1221 N94-15420
Unitary plan wind tunnel landmark dedication and revitalization
[NASA-TM-109649] p 1302 N94-15434
Determination of the effect of the walls of a wind-tunnel from the parameters of flow near them
[RAE-LIB-TRANS-2201] p 859 N94-16583

WIND TURBINES
DOE/NREL Advanced Wind Turbine Development Program
[DE93-010028] p 1093 N94-17668

WIND VELOCITY
Determination of momentum flux using a bivane and cup anemometer
[AD-A265414] p 1105 N94-15137
Complex terrain wind model evaluation
[AD-A266467] p 1096 N94-16589
Analysis of TIMS performance subjected to simulated wind blast p 1063 N94-16598
The use of the Air Force Academy high wind alert system in forecasting moderate intensity wind events for military bases in the Colorado Springs area
[AD-A267648] p 1107 N94-17245
Orographic microbursts in a severe winter windstorm
[AD-A267651] p 1108 N94-17247
On predicting the person-in-water drift for search and rescue
[AD-A268083] p 1055 N94-17514

WINDOWS (COMPUTER PROGRAMS)
Upgrading NASA/DOSE laser ranging system control computers p 918 N94-15595
Lunar laser ranging data processing in a Unix/X windows environment p 918 N94-15599
Radar Analysis and Visualization Environment (RAVEN): Software for polarimetric radar analysis p 1080 N94-16758

WINDPOWER UTILIZATION
The 1982 highlights
[NASA-TM-109671] p 1303 N94-15508
DOE/NREL Advanced Wind Turbine Development Program
[DE93-010028] p 1093 N94-17668

WINDSHIELDS
Comparative night vision goggle visual acuity measurements performed in the A-10 aircraft in an operational setting
[AD-A266721] p 1137 N94-15820
Definitions of terms relating to aircraft windscreens, canopies, and transparencies
[AD-A268403] p 868 N94-17425

WING CAMBER
Mission adaptive wing
[NASA-TM-109448] p 865 N94-15321

WING NACELLE CONFIGURATIONS
Supersonic flow visualization of a nacelle in close proximity to a simulated wing
[NASA-CR-194675] p 860 N94-17260

WING PLANFORMS
Static aeroelastic response of an aircraft with asymmetric wing planforms representative of combat damage
[AD-A266890] p 865 N94-14951
Experimental study of vortex and aerodynamic characteristics of stack wings with sideslip
[AD-A267722] p 860 N94-17274

WING PROFILES
Mission adaptive wing
[NASA-TM-109448] p 865 N94-15321

WING SLOTS
Fluid flow and heat convection studies for actively cooled airframes
[NASA-CR-194624] p 1024 N94-16491

WINGS
Better airplane wings
[NASA-TM-109446] p 933 N94-15345
Wind-tunnel investigation of aerodynamic efficiency of three planar elliptical wings with curvature of quarter-chord line
[NASA-TP-3359] p 859 N94-16574
Adaptive Navier-Stokes calculations for vortical flow
[AD-A266236] p 1026 N94-16966
Supersonic flow visualization of a nacelle in close proximity to a simulated wing
[NASA-CR-194675] p 860 N94-17260
Experimental study of vortex and aerodynamic characteristics of stack wings with sideslip
[AD-A267722] p 860 N94-17274

WINTER
Orographic microbursts in a severe winter windstorm
[AD-A267651] p 1108 N94-17247

WIRELESS COMMUNICATION
Infra Link: A data transmission system for microgravity research p 980 N94-16091

WIRING
Operation of digital systems in severe electromagnetic environments
[AD-A267176] p 988 N94-15693

WOLF-RAYET STARS
X ray emission from Wolf-Rayet stars with recurrent dust formation
[NASA-CR-194567] p 1300 N94-15533

WOOD
Biomass energy: State of the technology present obstacles and future potential
[DE93-016295] p 1092 N94-16766
Automated image analysis method for the detection of cracks on wood surface
[VTT-JULK-755] p 1056 N94-17542

WORDS (LANGUAGE)
Discovering sequence similarity by the algorithmic significance method
[DE93-015556] p 1150 N94-16659

WORK FUNCTIONS
High voltage conductors in spacecraft
[AD-A267268] p 897 N94-17266

WORK HARDENING
The effect of oxygen, grain size, and strain rate on the mechanical behavior of forged P/M tantalum
[DE93-011251] p 959 N94-16764

WORKING FLUIDS
Geometrical vapor blocker for parallel condensation tubes requiring cooling
[NASA-CASE-MSC-22090-1] p 1022 N94-15962

WORKLOADS (PSYCHOPHYSIOLOGY)
Preliminary validation of the task analysis/workload methodology
[AD-A267514] p 1138 N94-17077
System performance modeling and analysis of a fault-tolerant, real time parallel processor
[AD-A268070] p 1162 N94-17551

WORKSTATIONS
HP upgrade operational streamlining p 918 N94-15596
Lunar laser ranging data processing in a Unix/X windows environment p 918 N94-15599
Distributed computing feasibility in a non-dedicated homogeneous distributed system
[NASA-CR-191532] p 1149 N94-15989
Ergonomics in the office environment p 1124 N94-16612
Networked workstations and parallel processing utilizing functional languages
[AD-A267464] p 1160 N94-17034

WOUND HEALING
Wound healing after laser injury to skin: The effect of occlusion and vitamin E
[AD-A266473] p 1128 N94-16779

WOVEN COMPOSITES
Physical interpretation and development of ultrasonic nondestructive evaluation techniques applied to the quantitative characterization of textile composite materials
[NASA-CR-194549] p 931 N94-15190
Processing, properties and applications of composites using powder-coated epoxy towpreg technology p 933 N94-15277
Carbon-carbon grid for ion engines
[NASA-CASE-NPO-19174-1-CU] p 925 N94-15876
FIBER-TEX 1992: The Sixth Conference on Advanced Engineering Fibers and Textile Structures for Composites
[NASA-CP-3211] p 936 N94-16845
Research in textile composites at KU, Leuven p 937 N94-16848
Weaving multi-layer fabrics for reinforcement of engineering components p 937 N94-16850
Effect of tow alignment on the mechanical performance of 3D woven textile composites p 937 N94-16851
An engineering approach for the application of textile composites to a structural component p 938 N94-16852
New textile composite materials development, production, application p 938 N94-16853
Quantification of processing artifacts in textile composites p 939 N94-16860
Stochastic damage evolution in textile laminates p 939 N94-16861
Three-dimensional analysis of anisotropic spatially reinforced structures p 939 N94-16863

WROUGHT ALLOYS
The effect of oxygen, grain size, and strain rate on the mechanical behavior of forged P/M tantalum
[DE93-011251] p 959 N94-16764

X

X RAY ABSORPTION
In situ studies of passive film chemistry using x ray absorption spectroscopy
[DE93-014023] p 947 N94-16011

X RAY ANALYSIS
Solution behaviour in microgravity: Considerations for protein crystal growth p 982 N94-16102
X ray computed tomography for failure analysis investigations
[AD-A268086] p 1055 N94-17515
X ray computed tomography for geometry acquisition
[AD-A268085] p 1157 N94-17590
X ray computed tomography for casting demonstration
[AD-A268084] p 1056 N94-17596

X RAY ASTRONOMY
X ray microcalorimeters: Principles and performance p 899 N94-15027
A new approach to optical photon detection p 899 N94-15028
The imaging microstrip proportional counter: Features of a practical design p 900 N94-15030
Development of x ray CCDs p 900 N94-15033
The XMM pn-CCD detector system: First results p 900 N94-15034
The development of back-illuminated CCD's for XMM p 900 N94-15035
Microchannel plate detectors for space astronomy p 901 N94-15038
Prospects for high pressure imaging gas scintillation drift chambers p 901 N94-15040
Outlook for hard x ray and gamma ray astronomy p 904 N94-15057
The high pressure gas scintillation proportional counter for SAX p 906 N94-15076

X ray emission from Wolf-Rayet stars with recurrent dust formation
[NASA-CR-194567] p 1300 N94-15533
ROSAT-IUE observations of symbiotic stars. The x ray morphology of high latitude associations
[NASA-CR-194616] p 1236 N94-16492
Participation in the north ecliptic pole sky survey
[NASA-CR-191933] p 1059 N94-16815
The formation process of the He I lambda 10830 line in cool giant stars
[NASA-CR-194648] p 1240 N94-17094

X RAY DETECTORS
Outlook for hard x ray and gamma ray astronomy p 904 N94-15057
Developments in extreme ultraviolet and x ray instrumentation p 904 N94-15058
A new detector concept for energetic auroral x ray imaging p 907 N94-15081
A multilayered approach to superconducting tunnel junction x ray detectors p 908 N94-15089
Applications for large area silicon drift detectors on x ray and gamma ray astronomy p 909 N94-15090
Silicon radiation sensor systems for gamma and x ray detection at SI p 909 N94-15095
The epitaxial Si x ray bolometer an alternative to ion implanted devices p 911 N94-15103

X RAY DIFFRACTION
Laboratory for x ray optics
[AD-A267149] p 1189 N94-15735
Interfacial structure of lattice mismatched bcc(110)/bcc(110) transition metal superlattices
[DE93-015162] p 1208 N94-16058
Thermal stress effects in intermetallic matrix composites
[NASA-CR-191191] p 1054 N94-16518
Characterization of metallic multilayers using x ray diffraction analysis
[NIAR-93-13] p 961 N94-17282

X RAY FLUORESCENCE
X ray emission from Wolf-Rayet stars with recurrent dust formation
[NASA-CR-194567] p 1300 N94-15533
Application of in situ scanning x ray fluorescence to study the concentration of metal ions in simulated pits
[DE93-014054] p 956 N94-15921
Complex QSO absorbers: High-redshift clusters of galaxies?
[NASA-CR-194617] p 1237 N94-16833
Characterization of Ni on Si wafers: Comparison of surface analysis techniques
[DE93-016501] p 953 N94-17649

X RAY IMAGERY
The XMM pn-CCD detector system: First results p 900 N94-15034
The Rutherford Appleton Laboratory photon counting detector p 910 N94-15096

X RAY INSPECTION
Component testing and quality assurance p 932 N94-15259

X RAY LASERS
X ray laser program
[AD-A267075] p 1038 N94-15628

X RAY SCATTERING
Thomson backscattered x rays from an intense laser beam
[AD-A267125] p 1038 N94-15686
Laboratory for x ray optics
[AD-A267149] p 1189 N94-15735
Magnetic effects in anomalous dispersion
[DE93-014291] p 1175 N94-15978
Chemical and displacement atomic pair correlations in crystalline solid solutions recovered by anomalous x ray scattering in Fe-Ni alloys
[DE93-015906] p 1209 N94-16171
Application of cylindrical distribution functions to anisotropic scattering from amorphous films
[DE93-015256] p 1183 N94-16811
Neutron and x ray scattering studies of (FeF2)(sub m)(CoF2)(sub n) multilayers
[DE93-015809] p 1184 N94-16838
Anisotropic phase separation in amorphous Fe-Ge alloys
[DE93-015255] p 961 N94-17251

X RAY SOURCES
Direct drive foil implosion experiments on Pegasus 2
[DE93-012666] p 1202 N94-16776
Participation in the north ecliptic pole sky survey
[NASA-CR-191933] p 1059 N94-16815
Resist performance in soft x ray projection lithography
[DE93-016490] p 1036 N94-17647

X RAY SPECTRA
X ray emission from Wolf-Rayet stars with recurrent dust formation
[NASA-CR-194567] p 1300 N94-15533
Variability of the Seyfert galaxy MKN 766 in the Rosat all sky survey
[MPE-PREPRINT-221] p 1240 N94-17591

X RAY SPECTROSCOPY
Structural and dynamical aspects of electrodeposition
[AD-A266786] p 942 N94-14909
X ray microcalorimeters: Principles and performance p 899 N94-15027
The imaging microstrip proportional counter: Features of a practical design p 900 N94-15030
Development of x ray CCDs p 900 N94-15033
The XMM pn-CCD detector system: First results p 900 N94-15034
The development of back-illuminated CCD's for XMM p 900 N94-15035
X-ray spectroscopy with silicon pin and avalanche photo diodes p 906 N94-15072
CCD's on high resistivity bulk silicon for x ray spectroscopy on XMM p 907 N94-15080
Substrate effects in superconducting tunnel junction detectors p 908 N94-15083
Performance of the position-sensitive proportional counters of the Yohkoh Bragg crystal spectrometer p 909 N94-15094
Application of in situ scanning x ray fluorescence to study the concentration of metal ions in simulated pits
[DE93-014054] p 956 N94-15921
A sulfur segregation study of PWA 1480, NiCrAl, and NiAl alloys
[NASA-TM-106289] p 956 N94-15992
In situ studies of passive film chemistry using x ray absorption spectroscopy
[DE93-014023] p 947 N94-16011
Design and fabrication of a reflection far ultraviolet polarizer and retarder
[NASA-CR-194630] p 1191 N94-16023
The interaction of HCN(DCN) with Si(111)-7x7 studied with HREELS, UPS, and XPS
[AD-A266237] p 1182 N94-16111
Electron spectroscopy analysis
[NASA-CR-193591] p 951 N94-17039
Characterization of nanoscale oxide and oxyhydroxide powders using EXAFS spectroscopy
[DE93-015683] p 940 N94-17235
Soft x ray emission from Alexandrite laser-matter-interaction
[AD-A267905] p 1042 N94-17378

X RAYS
Thomson backscattered x rays from an intense laser beam
[AD-A267125] p 1038 N94-15686
Direct drive foil implosion experiments on Pegasus 2
[DE93-012666] p 1202 N94-16776
Multi-frame x ray imaging with a large area 40ps camera
[DE93-017179] p 1035 N94-16960
Ultrasonic wave propagation model for nondestructive evaluation of solid rocker motor propellant
[AD-A267653] p 976 N94-17248
Review of rigorous coupled-wave analysis and of homogeneous effective medium approximations for high spatial-frequency surface-relief gratings p 1194 N94-17335
Soft x ray emission from Alexandrite laser-matter-interaction
[AD-A267905] p 1042 N94-17378
Resist performance in soft x ray projection lithography
[DE93-016490] p 1036 N94-17647

X-14 AIRCRAFT
Lift-fan aircraft: Lessons learned-the pilot's perspective
[NASA-CR-177620] p 867 N94-15950

X-15 AIRCRAFT
The 1966 highlights --- NASA research programs
[NASA-TM-109444] p 1302 N94-15343

X-29 AIRCRAFT
X-29: Experiment in flight
[NASA-TM-109454] p 865 N94-15327

XENON
Prospects for high pressure imaging gas scintillation drift chambers p 901 N94-15040

XV-15 AIRCRAFT
XV-15: Tiltrotor
[NASA-TM-109455] p 865 N94-15328
The 1979 highlights
[NASA-TM-109443] p 1247 N94-15342
The 1982 highlights
[NASA-TM-109671] p 1303 N94-15508

XV-5 AIRCRAFT
Lift-fan aircraft: Lessons learned-the pilot's perspective
[NASA-CR-177620] p 867 N94-15950

Y

YAG LASERS
Growth of new materials for solid state laser applications. The growth of ZnGeP2 by the vertical Bridgman method
[NASA-CR-194571] p 1038 N94-15530
An improved light source for laser ranging p 913 N94-15567
Two color satellite laser ranging upgrades at Goddard's 1.2m telescope facility p 915 N94-15581
Measuring atmospheric dispersion with WLRS in multiple wavelength mode p 916 N94-15582
Upgrading of the Borowiec laser station p 877 N94-15604
Results of the MTLRS-1 upgrade p 877 N94-15610
Effects of turbulence on the geodynamic laser ranging system p 921 N94-15616
Development of the Mars Observer Laser Altimeter (MOLA) p 921 N94-15617
The third generation SLR station Potsdam no. 7836 p 877 N94-15623

YANG-MILLS THEORY
Existence of a new instanton in constrained Yang-Mills-Higgs theory
[NIKHEF-H/93-02] p 1186 N94-17601
Derivation of the Verlinde formula from Chern-Simons theory and the G/G model
[DE93-628620] p 1221 N94-17632

YAW
Effects of internal yaw-vectoring devices on the static performance of a pitch-vectoring nonaxisymmetric convergent-divergent nozzle
[NASA-TP-3369] p 858 N94-16572
Wind tunnel investigations of forebody strakes for yaw control on F/A-18 model at subsonic and transonic speeds
[NASA-TP-3360] p 859 N94-16573

YBCO SUPERCONDUCTORS
Experimental investigations of superconductivity in quasi-two-dimensional epitaxial copper oxide superlattices and trilayers
[DE93-015306] p 1207 N94-15829
Application of Z-contrast imaging to obtain column-by-column spectroscopic analysis of materials
[DE93-015333] p 947 N94-16014
Local environment about O atoms in Pr-Y-Ba-Cu-O films studied by O K-edge XAFS
[DE93-016218] p 1209 N94-16447
Fast-ICCD photography and gated photon counting measurements of blackbody emission from particulates generated in the KrF-laser ablation of BN and YBC
[DE93-015491] p 1210 N94-16460
Powder diffraction studies using anomalous dispersion
[DE93-012531] p 1210 N94-16775
Diffuse scattering and image contrast of tweed in superconducting oxides: A simulation and interpretation
[DE93-016131] p 1212 N94-16844
Structural phase transition and superconductivity in La(2-x)Ba(x)CuO4
[DE93-015812] p 1212 N94-16868
A modified two-fluid model of conductivity for superconducting surface resistance calculation
[AD-A267549] p 1013 N94-17104
Basic optical studies of high T(c) oxide superconductors
[AD-A268148] p 1014 N94-17428
High temperature deformation behavior of YBa2Cu3O(6+x) superconducting ceramic materials
[AD-A268164] p 973 N94-17430
Advanced thin-film deposition and physical properties of high-temperature and other novel superconducting materials
[AD-A268199] p 1216 N94-17561
Oxygen diffusion in YBa2Cu3O(6+delta) ceramics on heating
[DE93-629161] p 974 N94-17633
Influence of the granular surface on the oxygen uptake in YBa2Cu3O(6+delta) ceramics
[DE93-629162] p 974 N94-17634

YELLOWSTONE NATIONAL PARK (ID-MT-WY)
Saving Yellowstone
[NASA-TM-109596] p 1094 N94-15289
TOMS computer graphics
[NASA-TM-109597] p 1094 N94-15290

YIELD STRENGTH
The effect of irradiation on the mechanical properties of 6061-T651 aluminum
[DE93-015825] p 958 N94-16168
Bulk and defect properties of ordered intermetallics: A first-principles total-energy investigation
[DE93-015492] p 959 N94-16873

YTTRIUM OXIDES
Vanadium corrosion studies
[AD-A266489] p 959 N94-16781

Z

ZEOLITES
Mechanical properties of magnesium ammonium phosphate cements and their zeolite composites
[DE93-015155] p 934 N94-16057
ZETA PINCH
Direct drive foil implosion experiments on Pegasus 2
[DE93-012666] p 1202 N94-16776
ZINC
Growth of new materials for solid state laser applications. The growth of ZnGeP2 by the vertical Bridgman method
[NASA-CR-194571] p 1038 N94-15530
ZINC TELLURIDES
Laser figuring for the generation of analog micro-optics and kineform surfaces p 1196 N94-17346
ZIRCONIUM ALLOYS
Microstructure of Zr3Al after 2 MeV proton bombardment
[DE93-015331] p 1211 N94-16814
Effects of processing and prolonged high temperature exposure on the microstructure of Nb-1Zr-C sheet
[NASA-TM-106370] p 959 N94-16883
ZIRCONIUM CARBIDES
Effects of processing and prolonged high temperature exposure on the microstructure of Nb-1Zr-C sheet
[NASA-TM-106370] p 959 N94-16883
ZIRCONIUM OXIDES
Ion mixing of thin ZrO2 films on sapphire
[DE93-015214] p 1206 N94-14925
Synthesis of ceramic oxide powders in a microwave plasma device
[DE93-012741] p 965 N94-15920
Rheology and microstructure of concentrated zirconia-alumina suspensions for gelcasting composites
[DE93-015339] p 966 N94-16016
Transformation toughening of composite ceramics
[AD-A267304] p 971 N94-16980
Characterization of nanoscale oxide and oxyhydroxide powders using EXAFS spectroscopy
[DE93-015683] p 940 N94-17235
ZONAL FLOW (METEOROLOGY)
Investigate wave-mean flow interaction and transport in the extratropical winter stratosphere
[NASA-CR-194555] p 1098 N94-15639
ZONAL HARMONICS
Implementing a 50x50 gravity field model in an orbit determination system
[AD-A267548] p 888 N94-17103

Typical Personal Author Index Listing

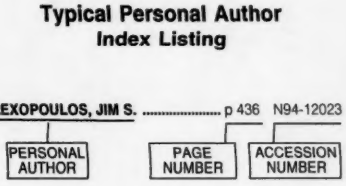

Listings in this index are arranged alphabetically by personal author. The page number helps you locate the citation in the abstract section. The accession number denotes the number by which the citation is identified.

A

AANSTOOS, J. V. ..... p 1108 N94-17283
AARTS, H. J. M. ..... p 900 N94-15035
ABBASI, S. J. ..... p 1175 N94-17641
ABBATE, A. ..... p 1061 N94-17105
ABBOTT, ARNOLD ..... p 922 N94-15625
ABDULLAH, Z. ..... p 980 N94-16089
ABDULLAYEV, N. A. ..... p 963 N94-15133
ABEYOUNIS, WILLIAM K. ..... p 856 N94-15681
ABLOWITZ, MARK J. ..... p 1026 N94-16927
ABRAHAM, J. ..... p 905 N94-15069
ABRAMS, MICHAEL ..... p 1068 N94-16680
p 1071 N94-16693
ABRUNA, HECTOR D. ..... p 942 N94-14909
ABSHIRE, JAMES B. ..... p 920 N94-15614
ACHARD, V. ..... p 923 N94-17592
ACTIS, RICARDO L. ..... p 1062 N94-17445
ADAMS, D. ..... p 1011 N94-16661
ADAMS, JOHN B. ..... p 1068 N94-16679
p 1070 N94-16689
p 1073 N94-16706
p 1074 N94-16709
ADAMS, N. P. ..... p 1091 N94-15994
ADAMS, PHYLIS ..... p 1075 N94-16734
ADAMS, VANCE H. ..... p 1021 N94-15737
ADAMSKI, MARIUSZ ..... p 1029 N94-17440
ADE, P. ..... p 906 N94-15073
ADE, P. A. R. ..... p 902 N94-15048
p 905 N94-15066
p 905 N94-15067
p 906 N94-15070
p 907 N94-15077
p 907 N94-15079
p 911 N94-15103
ADEMA, J. ..... p 901 N94-15036
p 904 N94-15060
ADET, P. ..... p 902 N94-15047
ADLER, E. ..... p 1054 N94-16156
ADUMITROAIE, V. ..... p 1018 N94-15427
AFFELDER, LINDA O. ..... p 1233 N94-17291
p 1233 N94-17300
AFOLABI, D. ..... p 1062 N94-17481
AGER, CATHY ..... p 1069 N94-16686
AGRANOV, G. A. ..... p 903 N94-15053
AGRINIER, P. ..... p 954 N94-16383
AGUTTES, J. P. ..... p 891 N94-17152
AHEARN, JOHN S., JR. ..... p 958 N94-16486
AHLBORN, H. ..... p 945 N94-15170
AHUJA, K. K. ..... p 1178 N94-17278
AIDUN, J. B. ..... p 1062 N94-17664
AILEY, K. S. ..... p 1213 N94-17108
AKCHURIN, N. ..... p 1187 N94-16829
AKIN, CEM ..... p 1141 N94-17030
AKOH, H. ..... p 905 N94-15068
AKYEL, Y. ..... p 1134 N94-17535
AL-SAADI, JASSIM A. ..... p 872 N94-15794
ALAERTS, A. ..... p 906 N94-15071
ALBERT, DAVID J. ..... p 1220 N94-17540
ALBERTI, G. ..... p 1078 N94-16750
ALBERTI, GIOVANNI ..... p 1078 N94-16749
ALBIN, SACHARIA ..... p 967 N94-16541
ALBRIDGE, ROYAL ..... p 946 N94-15766
ALDEN, ADRIAN W. ..... p 994 N94-15986
ALEXANDER, D. J. ..... p 957 N94-16068
p 957 N94-16103
p 958 N94-16168
ALEXANDER, K. B. ..... p 957 N94-16103
ALEXANDER, W. MERLE ..... p 899 N94-16374
ALEXEFF, IGOR ..... p 1201 N94-15661
ALFANO, R. R. ..... p 1210 N94-16720
ALFANO, SALVATORE ..... p 1174 N94-17219
ALLEN, C. C. ..... p 1249 N94-16182
ALLEN, CARLTON C. ..... p 1289 N94-16398
ALLEN, JANET K. ..... p 1055 N94-17082
ALLEN, JONATHAN ..... p 1304 N94-17651
ALLEN, S. M. ..... p 960 N94-16972
ALLEY, RON ..... p 1074 N94-16712
ALLISON, PATTI ..... p 937 N94-16851
ALLTON, JUDITH H. ..... p 1289 N94-16398
ALTER, STEPHEN J. ..... p 1030 N94-17476
ALVING, AMY E. ..... p 1019 N94-15479
ALYAN, SAAD MOHAMED HARB ..... p 961 N94-17282
AMBATS, I. ..... p 1300 N94-17233
AMBERG, L. ..... p 877 N94-15610
AMENDE, W. ..... p 945 N94-15169
AMIDEI, DAVID ..... p 925 N94-16496
AMIRKHANOV, I. V. ..... p 1168 N94-14933
AMME, ROBERT C. ..... p 1186 N94-17436
ANDERSON, C. ..... p 1054 N94-16156
ANDERSON, DREW ..... p 1188 N94-15144
ANDERSON, ERIK H. ..... p 1045 N94-17349
ANDERSON, F. S. ..... p 1252 N94-16198
p 1252 N94-16200
ANDERSON, J. ..... p 1063 N94-16596
ANDERSON, J. STEVEN ..... p 1197 N94-17354
ANDERSON, JAY ..... p 1236 N94-15481
ANDERSON, L. W. ..... p 1207 N94-15955
ANDERSON, LOY A. ..... p 1005 N94-17498
ANDERSON, M. U. ..... p 1034 N94-16452
ANDERSON, MICHAEL W. ..... p 1145 N94-15525
ANDERSON, R. R. ..... p 1103 N94-16307
ANDERSON, RAYMOND R. ..... p 1103 N94-16322
ANDERSON, RONALD D. ..... p 1156 N94-17530
ANDERSON, T. S. ..... p 965 N94-15828
ANDERSON, W. ..... p 1197 N94-17350
ANDERSON, W. W. ..... p 1197 N94-17351
ANDREWS, A. P. ..... p 1045 N94-17357
ANDREWS, H. G. ..... p 895 N94-17178
ANDROLAKE, S. G. ..... p 1058 N94-15534
ANDRUSKIEWITSCH, NICOLAS ..... p 1175 N94-17643
ANGEBAULT, L. P. ..... p 903 N94-15052
ANGOTTI, CATHY ..... p 1126 N94-16631
ANTAR, B. N. ..... p 979 N94-16087
ANTONENKO, IRENE ..... p 1259 N94-16231
ANTONIK, P. ..... p 1003 N94-17206
ANTONIO, JOSEPH C. ..... p 1137 N94-15820
APOSTOLICO, A. ..... p 1172 N94-15777
APPARAO, K. V. S. R. ..... p 974 N94-17611
APPLEBY, G. M. ..... p 912 N94-15557
p 917 N94-15592
APPLEBY, J. ..... p 1032 N94-15797
APRIGLIANO, L. F. ..... p 973 N94-17430
APRUZESE, JOHN P. ..... p 1038 N94-15628
ARAI, Y. ..... p 945 N94-15167
ARAVINTHAN, SANJEEV ..... p 872 N94-17263
ARBESSER-RASTBURG, B. ..... p 994 N94-16036
ARBOCZ, J. ..... p 1057 N94-15154
ARDELL, A. J. ..... p 1211 N94-16814
AREND, LAWRENCE E., JR. ..... p 1134 N94-17513
ARENS, YIGAL ..... p 1143 N94-15175
p 1153 N94-17078
ARFORS, K. E. ..... p 1128 N94-16783
ARGEBRIGHT, V. ..... p 905 N94-15069
ARMANDILLO, E. ..... p 903 N94-15054
ARMANTE, R. ..... p 923 N94-17592
ARMSTRONG, D. P. ..... p 1181 N94-15863
ARMSTRONG, T. P. ..... p 1299 N94-17208
ARMSTRONG, T. R. ..... p 1092 N94-16160
p 961 N94-17234
ARNOLD, CRAIG L. ..... p 1171 N94-17521
ARNOLD, J. F. ..... p 1075 N94-16713
ARNOLD, K. ..... p 980 N94-16093
ARNOLD, SCOT ..... p 937 N94-16847
ARNON, DENNIS S. ..... p 1234 N94-17529
ARNONE, ANDREA ..... p 1028 N94-17258
ARNONE, ROBERT ..... p 1070 N94-16690
ARNONE, ROBERT A. ..... p 1113 N94-16588
ARORA, O. P. ..... p 973 N94-17430
ARTEMJEVA, N. A. ..... p 1290 N94-16404
ARTHUR, TREY ..... p 1152 N94-17060
ARTHURS, C. ..... p 903 N94-15051
ARVIDSON, R. E. ..... p 1234 N94-16209
ARVIDSON, RAYMOND E. ..... p 1265 N94-16268
ARVIND, V. ..... p 1150 N94-16579
ARYA, VINOD K. ..... p 1060 N94-16881
ASBURY, SCOTT C. ..... p 858 N94-16572
ASH, ROBERT L. ..... p 1024 N94-16542
ASHBAUGH, NOEL E. ..... p 1061 N94-17269
ASHBY, M. F. ..... p 941 N94-17457
ASHDOWN, B. G. ..... p 1232 N94-16875
ASHTON, C. J. ..... p 878 N94-17154
ASKARI, F. ..... p 1077 N94-16743
ASRAR, GHASSEM ..... p 1081 N94-17444
ASSONOV, S. S. ..... p 953 N94-16264
ASTORG, JEAN-MARC ..... p 878 N94-17140
ATALLAH, M. J. ..... p 1172 N94-15777
ATENCIO, ADOLPH, JR. ..... p 870 N94-15793
ATHALE, RAVINDRA A. ..... p 1188 N94-14940
ATKINSON, RANDALL J. ..... p 1162 N94-17622
ATTALI, ISABELLE ..... p 1234 N94-17529
ATTIA, ALAN I. ..... p 1014 N94-17325
ATTIA, JOHN OKYERE ..... p 1008 N94-15640
ATTREP, M., JR. ..... p 1242 N94-16245
ATWELL, WILLIAM ..... p 1300 N94-15816
ATWOOD, CHRISTOPHER A. ..... p 858 N94-16510
p 858 N94-16511
p 858 N94-16512
p 858 N94-16513
ATWOOD, W. B. ..... p 904 N94-15061
AUBERT, PIERRE ..... p 1030 N94-17534
AUDEBERT, P. ..... p 903 N94-15052
AUDET, L. ..... p 978 N94-16080
AUMAN, LAMAR M. ..... p 870 N94-16157
AUSTON, DAVID H. ..... p 986 N94-14955
AUWERA, J. VANDER ..... p 1104 N94-16365
AUWETER-KURTZ, MONIKA ..... p 928 N94-17308
AVILA, M. ..... p 857 N94-16471
AYAZ, D. M. ..... p 968 N94-16658
AYRES, D. S. ..... p 1300 N94-17233
AZMY, Y. Y. ..... p 1170 N94-16167
AZOULAY, M. ..... p 1207 N94-15973

B

BABB, PHILLIP D. ..... p 1042 N94-17285
BABUSKA, I. ..... p 961 N94-17109
p 1029 N94-17384
BABUSKA, IVO ..... p 1168 N94-14939
BACHE, T. C. ..... p 1151 N94-16910
BACHOR, E. ..... p 874 N94-17143
BADAVI, FOROOZ F. ..... p 1180 N94-15715
p 1301 N94-17255
BADAVI, FRANCIS F. ..... p 1300 N94-17084
BADER, S. D. ..... p 1208 N94-16058
BADJUKOV, D. D. ..... p 953 N94-16266
BADO, P. ..... p 1042 N94-17378
BAEUMER, T. ..... p 932 N94-15258
BAGANOFF, DONALD ..... p 857 N94-15787
BAGHOS, B. B. ..... p 877 N94-15621
BAHNSEN, A. ..... p 900 N94-15030
BAHR, BEHNAM ..... p 1153 N94-17299
BAITY, F. W. ..... p 1203 N94-16823
BAJWA, A. R. ..... p 1028 N94-17276
BAKER, C. P. ..... p 1043 N94-17677
BAKER, I. M. ..... p 903 N94-15051
BAKER, J. E. ..... p 1167 N94-17287
BAKER, J. P. ..... p 966 N94-15996
BAKER, V. R. ..... p 1267 N94-16278
p 1275 N94-16324
BAKER, VICTOR R. ..... p 1241 N94-16210
BAKUCKAS, J. G., JR. ..... p 955 N94-15708
BALACHANDAR, S. ..... p 1021 N94-15834

BALAGUROV, A. M. p 974 N94-17633
BALAZS, L. p 1129 N94-17374
BALCERZAK, ANDRZEJ p 1178 N94-17087
BALDAZZI, G. p 899 N94-15029
BALDWIN, JACK W. p 937 N94-16851
p 938 N94-16852
BALKA, L. p 1300 N94-17233
BALKUS, NANCY J. p 1138 N94-16983
BALLARD, DANA H. p 1165 N94-16580
BALMINO, GEORGES p 890 N94-17146
BALUJA, SHUMEET p 864 N94-15498
BANAS, GRZEGORZ p 1038 N94-15852
BANERDT, W. B. p 1250 N94-16189
p 1286 N94-16382
BANISH, MICHAEL p 1210 N94-16646
BANKS, DAVID L. p 1118 N94-17232
BANKS, H. T. p 1026 N94-17003
BANKS, J. C. p 953 N94-17649
BANSAL, NAROTTAM P. p 934 N94-15929
BANTON, DAVID W. p 1149 N94-16560
BAPNA, R. C. p 1042 N94-17630
BAR-NESS, YEHESKEL p 1147 N94-15772
BARAFF, DAVID p 1143 N94-15212
p 1164 N94-15756
BARAZANGI, MUAWIA p 1232 N94-17036
BARBATO, MARYANN H. p 868 N94-17425
BARBEE, T. W., III p 1208 N94-15976
BARCLAY, REBECCA O. p 1230 N94-15838
p 1230 N94-15839
p 1233 N94-17291
p 1233 N94-17300
BARDSLEY, J. N. p 1096 N94-16449
BARDWELL, J. A. p 947 N94-16011
BARET, F. p 1070 N94-16691
BARET, FREDERIC p 1073 N94-16702
BARGHOUTI, NASER S. p 1155 N94-17404
BARHAM, R. G. p 1176 N94-15019
BARHEN, JACOB p 1165 N94-15958
BARL, L. p 908 N94-15084
BARLIER, FRANCOIS p 890 N94-17146
BARLOON, P. J. p 1067 N94-16674
BARNARD, J. J. p 1188 N94-17672
BARNES, ALAN p 946 N94-15766
BARNES, F. J. p 1110 N94-17673
BARNET, CHRISTOPHER DWIGHT
p 1277 N94-16333
BARON, M. H. p 898 N94-17669
BARONE, A. p 905 N94-15068
BARRESI, G. p 892 N94-17161
BARRETT, TERENCE W. p 1040 N94-16533
BARRETT, W. L. p 1300 N94-17233
BARTLETT, RODNEY J. p 1180 N94-15727
BARTRAND, TIMOTHY A. p 869 N94-15192
BARTSCH, R. R. p 1202 N94-16451
p 1202 N94-16776
BASILEVSKY, A. T. p 1013 N94-17318
BASKIN, R. p 1264 N94-16263
BASS, B. R. p 1064 N94-16603
BASSOM, ANDREW P. p 1059 N94-16104
BASTON, D. W. p 1016 N94-15005
BATES, F. p 987 N94-15644
BATES, J. L. p 1134 N94-17535
p 1092 N94-16160
p 961 N94-17234
BATES, K. A. p 1226 N94-14987
BATES, RICHARD p 1191 N94-16128
BATMAN, JOE p 1155 N94-17429
BATSON, EILEEN p 1125 N94-16621
BATT, J. p 1174 N94-16820
BATTRICK, B. p 1239 N94-16524
BATY, ROY S. p 925 N94-15947
BAUCOM, K. C. p 1208 N94-16012
BAUER, WENDY HAGEN p 1297 N94-16866
BAUMANN, P. K. p 1216 N94-17553
BAUMEISTER, JOSEPH F. p 1169 N94-15799
BAUMEISTER, KENNETH J. p 1169 N94-15799
p 1177 N94-16497
BAUR, H. p 954 N94-16432
BAVUSO, SALVATORE J. p 1155 N94-17447
BAXA, ERNEST G., JR. p 994 N94-16022
BAYHA, T. D. p 933 N94-15277
BAZIOR, ZBIGNIEW p 1178 N94-17087
BEARD, B. C. p 1214 N94-17270
BEASLEY, M. R. p 1216 N94-17561
BEAUCHAMP, JOHN J. p 1097 N94-17426
BEAUDOIN, A. p 1068 N94-16681
p 1076 N94-16737
BEAUMONT, P. W. p 941 N94-17457
BECHER, P. F. p 966 N94-16018
BECK, FRED B. p 998 N94-16655
BECKER, T. p 1258 N94-16228
BECKER, T. L. p 1252 N94-16199
p 1288 N94-16394
BECKLOFF, B. N. p 936 N94-16569
BEDAIR, SALAH p 1213 N94-17116
BEDARD, D. p 1080 N94-16760
BEEBE, R. F. p 1277 N94-16333
BEECHER, S. C. p 934 N94-16017
BEEK, WIARD p 877 N94-15612
p 877 N94-15613
BEEKHUIS, J. H. p 1004 N94-17407
BEELER, R. H. p 996 N94-16046
BEGAULT, DURAND R. p 1177 N94-15549
BEGUELIN, ADAM p 1153 N94-17107
p 1153 N94-17118
BEHRENS, KLAUS p 1105 N94-15302
BEHRMANN, GREGORY P. p 1197 N94-17352
BEHROUZI, P. p 1020 N94-15645
BEINTEMA, D. p 908 N94-15084
BEKER, B. p 1005 N94-17496
BELANGER, D. P. p 1184 N94-16838
BELL, J. p 1025 N94-16903
BELL, J. B. p 1025 N94-16894
BELL, J. F. p 1241 N94-16174
p 1258 N94-16225
BELL, J. F., III p 1258 N94-16225
BELL, JEFFREY F. p 1241 N94-16195
BELL, LEROY p 1229 N94-15178
BELL, P. M. p 1035 N94-16960
BELLAIECHE, G. p 891 N94-17152
BELLE, J. P. p 903 N94-15052
BELLIS, J. G. p 901 N94-15039
BELTON, M. p 1252 N94-16201
p 1258 N94-16228
p 1259 N94-16229
BELTON, M. J. S. p 1252 N94-16199
BEN-SHAUL, ISRAEL Z. p 1155 N94-17398
BENAGE, J. F. p 1202 N94-16776
BENAGE, J. R. p 1013 N94-17318
BENECKE, W. p 908 N94-15083
BENEDICTO, J. p 893 N94-17164
BENGTSON, ROGER D. p 1202 N94-16162
BENNETT, M. L. p 1242 N94-16224
BENNETT, ROBERT p 1071 N94-16692
BENNETT, ROBERT M. p 866 N94-15722
BENNIGHOF, JEFFREY K. p 886 N94-16455
BENOIT, P. H. p 1242 N94-16257
BENSON, LESLIE J. p 1178 N94-17119
BENTZ, M. D. p 1046 N94-15817
BERCAW, J. E. p 970 N94-16963
BERDICHEVSKY, ALEXANDER L. p 938 N94-16857
BERG, RICHARD L. p 983 N94-15676
BERGER, DAVID p 1154 N94-17390
BERGER, ROBERT p 1163 N94-14953
BERGERS, DIETHARD p 984 N94-16001
BERGMANN, U. p 1212 N94-16887
BERINATO, R. J. p 1189 N94-15664
BERKE, L. p 1058 N94-15709
BERMAN, E. p 948 N94-16771
BERMAN, P. R. p 1179 N94-14949
p 1180 N94-15689
BERNHARD, R. P. p 1063 N94-16253
BERROCAL, JULIO p 1158 N94-14980
BERRY, P. p 971 N94-16994
BERRY, TOMMY p 1106 N94-15851
BERSHAD, BRIAN N. p 1140 N94-15744
BERTRAND, P. p 1201 N94-15210
BERTRAND, R. p 896 N94-17186
BERTRAND, REINHOLD p 890 N94-17146
BERTRAND, W. T. p 886 N94-15857
BESMANN, T. M. p 934 N94-16008
p 934 N94-16065
BESSON, J. p 923 N94-17592
BETTERTON, WILLIAM J. p 1241 N94-16186
BETZ, HENRY P. p 1142 N94-14924
BEVEN, KEITH p 1083 N94-16028
BEVEN, KEITH J. p 1083 N94-16027
BEYER, L. p 877 N94-15610
BEYER, RICHARD A. p 976 N94-17538
BEYLKIN, GREGORY p 1026 N94-16927
BEYSENS, D. p 944 N94-15164
BHARAT, R. p 902 N94-15043
BHAT, SUDIN p 1166 N94-16770
BHATTACHARJEE, A. p 1202 N94-16446
p 1239 N94-16647
BHATTACHARYYA, S. K. p 923 N94-15118
BHUSHAN, BHARAT p 1048 N94-17533
BIANCO, GIUSEPPE p 877 N94-15601
BIAO, Y. p 1207 N94-15973
BIBBO, GREG p 973 N94-17466
BIBER, KASIM p 860 N94-17260
BIBRING, JEAN-PIERRE p 899 N94-16374
BIDSTRUP, SUE A. p 1176 N94-17605
BIEFELD, R. M. p 1208 N94-16012
BIENENSTOCK, A. p 1183 N94-16811
p 961 N94-17251
BIERSCHENK, T. R. p 967 N94-16543
BIGAN, E. p 1206 N94-14922
BIGELOW, C. A. p 956 N94-15948
BIGELOW, SCOTT p 870 N94-15532
BILLINGHAM, JOHN p 1125 N94-16620
BILLON-PIERRON, D. p 907 N94-15078
BILLS, BRUCE p 1273 N94-16315
BINGHAM, ELDON W. p 1012 N94-16976
BIRMAN, KENNETH p 1000 N94-16911
p 1152 N94-16982
BIRMAN, KENNETH P. p 997 N94-16477
p 1161 N94-17239
BIRO, ROSS p 1143 N94-15189
BISCHOFF, I. p 903 N94-15052
BISHOP, KAYLYNN M. p 1267 N94-16280
p 1275 N94-16326
BISHU, RAM R. p 1137 N94-15717
p 1139 N94-17653
BJORKMAN, REY C. p 928 N94-17213
BJORN, LENNART p 978 N94-16079
BLACK, R. p 1103 N94-16307
BLACKABY, NICHOLAS D. p 1017 N94-15183
BLACKSTOCK, DAVID T. p 1177 N94-15732
BLAKE, W. B. p 1152 N94-17032
BLAMIRE, M. G. p 910 N94-15101
BLANCH, H. W. p 966 N94-15996
BLAND, TIMOTHY J. p 866 N94-15761
BLANEY, D. L. p 1245 N94-16386
BLASDELL, SHARON p 1125 N94-16625
p 1127 N94-16644
BLAU, M. p 1221 N94-17632
BLEEKER, J. A. M. p 904 N94-15058
BLEIER, A. p 966 N94-16016
BLENSKI, G. p 877 N94-15610
BLEWETT, D. T. p 1258 N94-16225
BLOOM, E. D. p 904 N94-15061
BLOOM, R. M. p 1102 N94-17499
BLOUKE, M. M. p 901 N94-15041
BLUMBERG, D. p 1252 N94-16198
BLUMBERG, DAN G. p 1078 N94-16747
BLUME, M. p 1175 N94-15978
BLUMENTHAL, M. S. p 1000 N94-17000
BLY, VINCENT T. p 1046 N94-15873
BLYTHE, JIM p 1166 N94-17201
BOARDMAN, J. W. p 1067 N94-16674
BOARDMAN, JOE W. p 1074 N94-16711
BOCHENEK, WANDA p 1177 N94-16650
BOCK, LAWRENCE A. p 1176 N94-15115
BOCK, O. p 980 N94-16093
BODE, ARTHUR P. p 1120 N94-15180
BODECHTEL, J. p 1071 N94-16694
BOEHM, F. p 1150 N94-16594
BOGARD, D. D. p 1248 N94-16177
BOGDANOVICH, ALEXANDER E. p 939 N94-16861
p 939 N94-16863
BOHN, S. p 1043 N94-17677
BOHOR, BRUCE F. p 1241 N94-16186
BOKHARI, SHAHID H. p 1145 N94-15489
BOLDMAN, D. R. p 858 N94-16571
BOLES, WALTER W. p 1289 N94-16398
BOLLANI, B. p 894 N94-17174
BOLOSKY, WILLIAM J. p 1159 N94-16577
BOLTON, P. R. p 949 N94-16904
BOMMANNAVAR, A. S. p 1208 N94-16058
BONANNO, GIOVANNI p 873 N94-15062
BONCEK, R. p 1014 N94-17375
BONDAR, R. L. p 981 N94-16095
BONE, D. A. p 901 N94-15039
BONETTO, F. p 1030 N94-17511
BONHAUS, DARYL LAWRENCE p 1027 N94-17061
BONURA, A. p 906 N94-15076
BOQUIST, W. P. p 1101 N94-16551
BORDEN, BRETT p 999 N94-16788
p 999 N94-16789
BORDERIES, N. J. p 1276 N94-16332
BORG, JANET p 899 N94-16374
BORGSTROM, P. p 1128 N94-16783
BORISOV, A. p 1103 N94-16250
BORN, I. p 901 N94-15036
BORNSTEIN, NORMAN p 959 N94-16781
BORTIATYNSKI, J. p 975 N94-16996
BOSCH, L. p 901 N94-15036
BOSSI, RICHARD H. p 1055 N94-17515
p 1157 N94-17590
p 1056 N94-17596
BOSTIAN, CHARLES W. p 1006 N94-17661
BOSTIC, SUSAN W. p 1061 N94-17259
BOTTKE, W. F., JR. p 1241 N94-16202
BOTTONI, M. p 1023 N94-16444
BOUMSELLEK, SAID p 1185 N94-17329
BOURES, GERARD p 896 N94-17189
BOUSQUET, MICHEL p 890 N94-17146
BOUVIER, KENNETH p 1124 N94-16613
BOWDEN, C. M. p 1054 N94-16155
BOWEN, BRENT D. p 863 N94-17262
BOWLES, B. p 1003 N94-17206
BOWLES, T. J. p 1183 N94-16801
p 1185 N94-16951
BOWMAN, P. D. p 1122 N94-15741
BOWMAN, PHILLIP D. p 1117 N94-16545
BOWN, CHARLES W. p 928 N94-17213
BOYD, MARK A. p 1116 N94-15548
p 1155 N94-17447

BOYD, W. T. ..... p 1250 N94-16185
BOYLE, ROBERT V. ..... p 928 N94-17256
BOYNTON, W. V. ..... p 1242 N94-16245
BOYSON, W. E. ..... p 1091 N94-15994
BOZEK, JOHN M. ..... p 1040 N94-16522
BOZOKI, E. ..... p 1184 N94-16828
BRADA, M. P. ..... p 968 N94-16658
BRADBURN, J. C. ..... p 1146 N94-15702
BRADLEY, D. K. ..... p 1035 N94-16960
BRADY, V. ..... p 1175 N94-17288
BRAENDSTROEM, U. ..... p 909 N94-15093
BRAEUNINGER, H. ..... p 900 N94-15034
BRAFF, R. ..... p 864 N94-16835
BRAGDON, C. R. ..... p 1178 N94-17278
BRAKE, M. L. ..... p 1041 N94-17001
BRAMBILLA, L. ..... p 894 N94-17174
BRANCH, MELVYN C. ..... p 925 N94-16482
BRANDL, N. ..... p 876 N94-15600
BRANDON, WILLIAM T. ..... p 1006 N94-17661
BRASE, J. M. ..... p 1237 N94-16872
BRAUN, OFER ..... p 905 N94-15064
BRAY, JAMES ..... p 929 N94-16149
BREEVELD, A. A. ..... p 905 N94-15063
BREKKE, D. W. ..... p 1249 N94-16182
BRENNAN, MARTIN J. ..... p 864 N94-16439
BRESLAUER, DANY ..... p 1155 N94-17399
BREWER, W. V. ..... p 1048 N94-17088
BRIDENBAUGH, JOHN C. ..... p 868 N94-17425
BRIDGES, WILLIAM B. ..... p 1188 N94-14957
BRINKMAN, A. C. ..... p 900 N94-15035
BRINKMAN, C. R. ..... p 967 N94-16067
p 957 N94-16068
p 957 N94-16106
p 968 N94-16813
BRINSON, H. F. ..... p 936 N94-16836
BRISCO, B. ..... p 1080 N94-16760
BRIZI, E. ..... p 1246 N94-16417
BROADHEAD, B. L. ..... p 1231 N94-16874
BROADWELL, JAMES E. ..... p 861 N94-17580
BROCK, B. C. ..... p 1034 N94-16452
BROCKETT, ROGER ..... p 1163 N94-14937
BROEK, B. ..... p 1080 N94-16757
BROOKES, STEPHEN ..... p 1151 N94-16790
p 1152 N94-17009
BROOKS, DAVID S. ..... p 1129 N94-17478
BROOKS, R. R. ..... p 1241 N94-16213
BROPHY, JOHN R. ..... p 925 N94-15927
BROSCH, NOAH ..... p 905 N94-15064
BROWN, A. J. ..... p 1024 N94-16808
BROWN, CHRISTOPHER A. ..... p 964 N94-15700
BROWN, JOSEPH A. ..... p 1223 N94-15545
p 1223 N94-15546
BROWN, R. H. ..... p 1241 N94-16174
BROWN, R. J. ..... p 1080 N94-16760
BROWN, RALF D. ..... p 1150 N94-16585
BROWN, S. W. ..... p 976 N94-16624
BROWN, T. M. ..... p 1299 N94-15968
BROWNING, N. D. ..... p 947 N94-16014
p 1212 N94-16841
BROWNLEE, D. E. ..... p 1244 N94-16367
BRUEGGE, CAROL J. ..... p 1037 N94-16667
BRUENEMAN, D. J. ..... p 1249 N94-16182
BRUGER, STEVEN J. ..... p 1174 N94-16665
BRUMLIK, CHARLES J. ..... p 967 N94-16475
BRUNDRETT, DAVID L. ..... p 1194 N94-17335
BRUNO, B. C. ..... p 1283 N94-16366
BRUSASCO, R. ..... p 1204 N94-17237
BRUTTIG, S. P. ..... p 1128 N94-16783
BRYANT, NEVIN A. ..... p 1073 N94-16705
BRYSON, J. W. ..... p 1059 N94-16104
BU, Y. ..... p 942 N94-14956
p 1182 N94-16111
BUCEY, STEVE ..... p 912 N94-15562
BUCEY, STEVEN ..... p 917 N94-15587
BUCK, GREGORY M. ..... p 983 N94-15881
BUCKLES, W. E. ..... p 1013 N94-17226
BUCKLEY, JOHN D. ..... p 983 N94-15881
p 936 N94-16845
BUDAI, J. D. ..... p 1040 N94-16663
BUDGE, K. G. ..... p 1148 N94-15985
BUDGE, M. C., JR. ..... p 1189 N94-15664
BUDTZ-JORGENSEN, C. ..... p 900 N94-15030
BUFFLER, P. A. ..... p 1128 N94-16812
BUFFUM, DANIEL H. ..... p 869 N94-15866
BUFTON, JACK L. ..... p 921 N94-15620
BUHL, M. ..... p 997 N94-16169
BUHL, R. A. ..... p 1211 N94-16814
BUI, TRONG T. ..... p 1019 N94-15475
p 1019 N94-15485
p 1020 N94-15488
p 1022 N94-15865
p 1022 N94-15867
p 1024 N94-16527
BULBUL, ZEKI B. ..... p 1156 N94-17541
BULLOCK, MARK A. ..... p 1293 N94-16419
BULMER, CATHERINE H. ..... p 1191 N94-16489
BULSARA, ADI ..... p 1117 N94-15662
BUNING, PIETER G. ..... p 1148 N94-15784
BUNKER, B. C. ..... p 1209 N94-16159
BUONCRISTIANI, A. MARTIN ..... p 1189 N94-15647
BURBINE, T. H. ..... p 1241 N94-16174
BURCHAM, FRANK W., JR. ..... p 869 N94-15141
BURGER, A. ..... p 1207 N94-15973
BURGER, ROBERT H. ..... p 1230 N94-15838
BURGESS, C. ..... p 975 N94-16996
BURGESS, ED ..... p 1229 N94-15178
BURKE, EDWARD A. ..... p 1173 N94-17495
BURKE, J. J. ..... p 1226 N94-14987
BURKE, JAMES J. ..... p 1226 N94-14981
BURKHALTER, P. G. ..... p 1042 N94-17378
BURNHAM, NANCY A. ..... p 1034 N94-16536
BURNS, D. T. ..... p 1031 N94-15018
BURNS, K. A. ..... p 1152 N94-17032
BURNS, KAREN D. ..... p 999 N94-16777
BURNS, WILLIAM K. ..... p 1191 N94-16489
BURT, D. ..... p 900 N94-15035
BURT, D. J. ..... p 900 N94-15033
p 907 N94-15080
BURT, W. W. ..... p 1037 N94-16426
BURTON, DOUGLAS R. ..... p 1146 N94-15687
BUSCH, J. ..... p 1096 N94-17289
BUSECK, P. R. ..... p 1219 N94-16255
BUTKIEWICZ, E. ..... p 877 N94-15604
BUTLER, J. E. ..... p 948 N94-16553
BUTLER, KEN ..... p 1172 N94-15002
BUTLER, P. L. ..... p 1166 N94-16888
BUTLER, RICKY W. ..... p 1158 N94-15536
BUTTERFIELD, C. P. ..... p 1093 N94-17668
BUTTON, P. ..... p 987 N94-15644
BUTZ, P. ..... p 895 N94-17180
BYBEE, R. ..... p 905 N94-15069

C

CABANSKA, KATARZYNA ..... p 1060 N94-16923
CADE, WILLIAM B., III ..... p 1102 N94-17512
CADELEC, JACQUES ..... p 896 N94-17188
CAI, L. ..... p 1001 N94-17033
CAI, QING-FU ..... p 877 N94-15608
CAI, WEI ..... p 1169 N94-15833
CAI, WEI-LIN ..... p 1037 N94-15806
CAI, Y. ..... p 1011 N94-16443
p 1047 N94-16806
CAI, ZHI-XIONG ..... p 1212 N94-16844
CAI, ZHONG ..... p 938 N94-16857
p 939 N94-16859
CALAWAY, W. F. ..... p 953 N94-17649
CALCOTE, H. F. ..... p 950 N94-16930
CALISE, A. J. ..... p 870 N94-15416
CALKOEN, C. J. ..... p 1077 N94-16744
CALLAHAN, D. A. ..... p 1205 N94-17670
CAMARDA, CHARLES J. ..... p 1061 N94-17259
CAMERON, C. P. ..... p 1093 N94-16954
CAMPAN, GENEVIEVE ..... p 878 N94-17156
CAMPBELL, A. A. ..... p 1209 N94-16159
CAMPBELL, E. ..... p 1226 N94-14985
CAMPBELL, EUGENE W. ..... p 1036 N94-14992
CAMPBELL, GLEN S. ..... p 977 N94-16075
CAMPBELL, RICHARD L. ..... p 997 N94-16051
CAMPBELL, WILLIAM J. ..... p 1114 N94-17439
CAMY-PEYRET, C. ..... p 923 N94-17592
CANCILLO, F. ..... p 878 N94-17155
CANNON, J. E. ..... p 1091 N94-15994
CAO, QINGXI ..... p 1175 N94-17317
CAO, R. ..... p 1208 N94-16062
CAO, XIAONING ..... p 952 N94-17302
CAON, A. ..... p 894 N94-17174
CAPORICCI, L. ..... p 892 N94-17161
p 893 N94-17165
CAPRARO, G. ..... p 1003 N94-17206
CAR, R. ..... p 1205 N94-14913
CARANDE, RICHARD E. ..... p 1080 N94-16759
CARDER, KENDALL L. ..... p 1069 N94-16685
CARETTI, DAVID M. ..... p 1119 N94-14923
CAREY, P. G. ..... p 950 N94-16952
CARLIN, P. W. ..... p 1010 N94-15971
CARLSON, LELAND A. ..... p 1027 N94-17095
CARLSON, P. T. ..... p 1232 N94-16967
CARMAN, H. S., JR. ..... p 1182 N94-16064
CAROLI, E. ..... p 899 N94-15029
CARRERAS, B. A. ..... p 1202 N94-16162
p 1203 N94-16869
CARRERE, V. ..... p 1070 N94-16691
CARRERE, VERONIQUE ..... p 1037 N94-16667
p 1068 N94-16680
CARSEY, FRANK ..... p 991 N94-15899
CARSON, L. J. ..... p 957 N94-16163
CARTER, JAMES L. ..... p 1289 N94-16398
CARTER, M. K. ..... p 910 N94-15096
CARUSO, MICHAEL J. ..... p 1113 N94-16517
CASE, STEVEN T. ..... p 1116 N94-15138
CASERTANO, STEFANO ..... p 1172 N94-15641
CASPI, S. ..... p 1175 N94-17288
CASSEDY, JOAN WALSH ..... p 1118 N94-17224
CASSIN, THOMAS ..... p 941 N94-17597
CASSONE, VINCENT M. ..... p 1129 N94-17478
CASTIEL, DAVID ..... p 893 N94-17167
CAVALIERI, DONALD J. ..... p 1114 N94-17439
CAVANAGH, PATRICK ..... p 1131 N94-15694
CAVANAUGH, JOHN F. ..... p 921 N94-15618
CAVENOR, M. C. ..... p 1075 N94-16713
CAVES, RONALD G. ..... p 1080 N94-16761
CECH, M. ..... p 877 N94-15821
CELESTIAN, JOHN P. ..... p 899 N94-16154
CELI, F. ..... p 906 N94-15076
CENDROWICZ, JULIAN ..... p 985 N94-17068
CEREZO, A. ..... p 957 N94-16015
CERI, STEFANO ..... p 1156 N94-17501
CHA, Y. S. ..... p 1013 N94-17226
CHABOT, RICHARD S. ..... p 922 N94-15625
CHADHA, S. S. ..... p 963 N94-14948
CHAKOUMAKOS, B. C. ..... p 1040 N94-16663
CHAKRABARTI, KALYAN K. ..... p 1055 N94-17194
CHAKRABORTY, DAYAMOY ..... p 995 N94-16039
CHAKRAVARTHI, P. ..... p 1001 N94-17033
CHAKY, D. A. ..... p 1241 N94-16174
CHAMONAL, J. P. ..... p 903 N94-15052
CHAN, V. S. ..... p 1203 N94-16823
CHAN, VINCENT W. S. ..... p 1006 N94-17661
CHAN, WILLIAM M. ..... p 1148 N94-15784
CHANA, K. S. ..... p 856 N94-15696
CHANDRASEKARAN, B. ..... p 1234 N94-17419
CHANDRASEKHAR, RAJNISH ..... p 1027 N94-17215
CHANG, B. ..... p 949 N94-16904
CHANG, C. KEN ..... p 1180 N94-15715
p 1301 N94-17255
CHANG, F. ..... p 965 N94-15859
CHANG, F. C. ..... p 1023 N94-16444
CHANG, R. P. ..... p 973 N94-17413
CHANG, S. W. ..... p 1020 N94-15526
CHANG, SAM ..... p 1107 N94-17244
CHANG, SHENG-HUEI ..... p 1064 N94-16600
CHAO, TIEN-HSIN ..... p 1037 N94-16696
CHAPARRO, ALEX ..... p 1133 N94-17397
CHARLTON, D. E. ..... p 903 N94-15051
p 905 N94-15065
CHARLTON, JANE ..... p 1236 N94-15679
CHARVIEUX, FRANCK ..... p 954 N94-14930
CHASE, MELISSA ..... p 1155 N94-17491
CHASTENET, J. C. ..... p 923 N94-15218
CHATO, DAVID J. ..... p 1030 N94-17486
CHATTERJEE, SIDDHARTHA ..... p 1168 N94-15112
p 1158 N94-15113
p 1159 N94-15796
p 1148 N94-15956
CHATTERJEE, TAPAN ..... p 959 N94-16764
CHATTERTON, P. ..... p 970 N94-16948
p 970 N94-16949
CHAUDHURI, JHARNA ..... p 961 N94-17282
CHAUTARD, F. ..... p 1173 N94-17236
CHAVEZ, EDWIN V. ..... p 999 N94-16797
CHAWLA, K. K. ..... p 935 N94-16461
CHAWLA, N. ..... p 934 N94-16057
CHEEK, JACK ..... p 918 N94-15595
CHEEK, JACK W. ..... p 922 N94-15625
CHEIDA, M. A. ..... p 908 N94-15089
CHEN, C. S. ..... p 1164 N94-15502
CHEN, CHUNGTE W. ..... p 1197 N94-17354
CHEN, F. C. ..... p 1211 N94-16814
CHEN, I.-WEI ..... p 966 N94-16018
CHEN, J. B. ..... p 1140 N94-15744
CHEN, J. T. ..... p 1216 N94-17477
CHEN, J.-P. ..... p 877 N94-15605
CHEN, JIN-JUN ..... p 894 N94-17173
CHEN, K.-H. ..... p 1027 N94-17128
CHEN, S. S. ..... p 1011 N94-16443
p 1047 N94-16806
CHEN, SHYH-KWEI ..... p 1158 N94-15173
CHEN, TZONG H. ..... p 872 N94-15847
CHEN, WAN-ZHEN ..... p 913 N94-15566
p 877 N94-15605
CHEN, X. M. ..... p 1220 N94-16810
CHEN, ZHI-KANG ..... p 1071 N94-16695
CHENARD, STEPHANE ..... p 897 N94-17191
CHENG, C. C. ..... p 1210 N94-16476
CHENG, GRACE ..... p 877 N94-15609
CHENG, H. K. ..... p 859 N94-17021
CHENG, LI-JEN ..... p 1037 N94-16696
CHENG, Y.-M. ..... p 870 N94-15532
CHERNEY, M. ..... p 1185 N94-16957
CHERNOFF, HERMAN ..... p 1172 N94-15733
CHEUNG, B. ..... p 981 N94-16096
CHEUNG, CYNTHIA ..... p 899 N94-15026
CHIANG, ANDREW H. ..... p 1177 N94-16919
CHIANG, C. K. ..... p 1179 N94-17650
CHIARAMONTE, JAMES A. ..... p 1131 N94-15659
CHIBANTE, L. P. F. ..... p 953 N94-16243

CHICK, L. A. p 1092 N94-16160
p 961 N94-17234
CHIDUME, C. E. p 1175 N94-17644
p 1171 N94-17667
CHIEU, F. K. p 974 N94-17633
p 974 N94-17634
CHIH-MING, HO p 1023 N94-16470
CHIN, Y. H. p 1190 N94-15854
CHISHOLM, M. F. p 1212 N94-16841
CHIU, ING-TSAU p 1148 N94-15784
CHO, JEONG-HWAN p 956 N94-15922
CHOI, Y. H. p 1206 N94-14922
CHOMA, CHRISTIN T. p 982 N94-16102
CHOPRA, INDERJIT p 857 N94-15824
CHOUEIRI, EDGAR Y. p 1204 N94-17575
CHOW, CHUEN-YEN p 1025 N94-16842
CHOW, PETER P. p 1215 N94-17417
CHOW, W. W. p 1036 N94-17647
CHOYKY, W. J. p 1210 N94-16476
CHRISS, RANDALL M. p 869 N94-17386
CHRISTENSEN, PHILIP R. p 1065 N94-16607
CHRISTIAN, KENT D. p 921 N94-15618
CHRISTIE, ALAN M. p 1145 N94-15630
CHRISTOPHER, SUNDAR A. p 1066 N94-16671
CHRISTOPHOROU, L. G. p 1042 N94-17567
CHROMIK, CHRISTOPHER C. p 1085 N94-17665
CHU, JINN P. p 1038 N94-15852
CHUANG, SHERY L. p 883 N94-15648
CHURCH, S. p 906 N94-15073
CHURCH, S. E. p 905 N94-15066
p 905 N94-15067
p 907 N94-15077
CHURNSIDE, JAMES H. p 921 N94-15616
CHUTJIAN, ARA p 1185 N94-17329
CHYRCZAKOWSKI, STANISLAW p 1093 N94-17092
CIARKOWSKI, ADAM p 1002 N94-17057
CICCOLI, MARIE-CLAUDE p 1030 N94-17534
CIERO, MARK K. p 897 N94-17246
CINTALA, M. J. p 1063 N94-16253
CLAEYS, C. p 901 N94-15036
p 906 N94-15071
CLAEYS, P. p 1242 N94-16245
CLARK, BETH C. p 1284 N94-16371
CLARK, DOUGLAS S. p 1107 N94-17245
CLARK, PAUL C. p 1093 N94-17382
CLARK, R. N. p 1067 N94-16676
CLARK, RICHARD p 1153 N94-17231
CLARK, ROBERT W. p 878 N94-16552
CLARK, ROGER N. p 1066 N94-16670
p 1069 N94-16682
p 1069 N94-16686
CLARK, STEVEN R. p 938 N94-16852
CLARKE, CHRISTOPHER p 914 N94-15573
p 915 N94-15577
CLARKE, RICHARD p 1153 N94-17220
CLASEN, ROBERT J. p 1162 N94-17551
CLAYTON, R. N. p 953 N94-16259
p 1270 N94-16295
p 1245 N94-16389
CLEARY, NICOLE L. p 1031 N94-16145
CLIFFORD, STEPHEN M. p 1281 N94-16354
COATES, DWAINE p 895 N94-17175
COBBOLD, R. S. C. p 981 N94-16095
COCHEO, PETER A. p 1262 N94-16248
COCHRAN, BROOKS B. p 972 N94-17273
COCHRAN, JOHN E., JR. p 870 N94-15532
COCHRANE, J. C. p 1202 N94-16776
p 1013 N94-17318
COCKRELL, C. R. p 989 N94-15767
p 998 N94-16655
COFFEY, G. W. p 961 N94-17234
COFFEY, H. T. p 1047 N94-16806
p 1048 N94-16969
COGGI, J. M. p 951 N94-17207
COHEN, ARTHUR p 976 N94-17538
COHEN, MARTIN p 1240 N94-17059
COKER, DEMIRKAN p 1061 N94-17269
COLBECK, SAMUEL C. p 1045 N94-14920
COLBY, FRANK P., JR. p 1105 N94-15142
COLE, HELEN J. p 1194 N94-17331
COLELLA, P. p 1025 N94-16894
COLEMAN, M. M. p 975 N94-16996
COLKET, M. B. p 947 N94-15977
COLKET, MEREDITH B., III p 950 N94-17008
COLLINS, EDWARD A. p 951 N94-17210
COLLINS, J. p 1278 N94-16342
COLMON, A. p 891 N94-17153
COLTON, RICHARD J. p 1034 N94-16536
COLVIN, M. p 953 N94-17660
COMFORT, RICHARD H. p 868 N94-15187
COMISO, JOSEFINO C. p 1114 N94-17439
COMPERATORE, CARLOS A. p 1131 N94-15659
COMPTON, R. N. p 1181 N94-15863
p 1182 N94-16064
CONEL, JAMES E. p 1037 N94-16667
p 1074 N94-16712
CONESSA, HUGUETTE p 878 N94-17156
CONKLIN, BRION p 917 N94-15587
CONKLIN, J. C. p 1024 N94-16808
CONLEY, DANIEL C. p 1023 N94-16110
CONNELL, JOHN p 1150 N94-16656
CONNOR, J. p 1203 N94-16822
CONNOR, MATTHEW C. p 998 N94-16509
CONSTABE, ROXANNE p 1129 N94-17424
CONSTABLE, STEFAN H. p 1022 N94-15858
CONTINI, R. p 894 N94-17174
COOK, BETH p 1052 N94-16143
COOK, R. p 1204 N94-17237
COOK, R. C. p 966 N94-15924
COOK, ROGER V. p 928 N94-17213
COOK, WILLIAM DEAN p 895 N94-17175
COOMBS, C. R. p 1258 N94-16225
COON, S. R. p 953 N94-17649
COON, VICTORIA T. p 1216 N94-17577
COOPER, PAUL A. p 1062 N94-17451
COOPER, R. p 923 N94-15118
COOPER, R. E. p 1023 N94-15980
COOPER, ROBERT C. p 1161 N94-17239
COPPER, V. p 1123 N94-16565
CORLISS, G. F. p 1170 N94-16778
CORNICK, JON C. p 1108 N94-17459
CORNWELL, JOHN p 1022 N94-15962
CORUH, C. p 1112 N94-16009
COS, S. p 910 N94-15099
COSBY, PHILIP C. p 1182 N94-16586
COSTAIN, J. K. p 1112 N94-16009
COSTARD, F. p 1252 N94-16200
COSTELLO, DANIEL J., JR. p 997 N94-16506
p 997 N94-16507
p 997 N94-16508
p 998 N94-16509
COSTEN, ROBERT C. p 1300 N94-17084
COTE, P. J. p 961 N94-17106
COTTON, J. D. p 955 N94-15885
COULTER, R. L. p 1110 N94-17673
COURTNEY, THEODORE K. p 1124 N94-16612
COURTURIER, SERVANNE p 997 N94-16507
COUTTS, T. J. p 1093 N94-16824
COVA, SERGIO p 913 N94-15569
p 914 N94-15570
COVINGTON, H. p 914 N94-15571
COWINGS, PATRICIA S. p 898 N94-17388
p 1120 N94-15537
COX, D. E. p 1121 N94-15711
COX, J. ALLEN p 1210 N94-16775
CRAMPTON, GEORGE H. p 1195 N94-17342
CRANE, C. p 1118 N94-17090
CRANE, D. FRANCIS p 887 N94-16905
CRAVENS, T. p 1145 N94-15538
CRAWFORD, T. L. p 1299 N94-17208
CRAWFORD, WILLIAM p 1110 N94-17673
CREED, D. p 877 N94-15609
p 970 N94-16947
p 970 N94-16948
p 970 N94-16949
p 877 N94-15609
CRESSWELL, DON p 1157 N94-17590
CREWS, ALAN R. p 903 N94-15051
CRISTIANO, R. p 905 N94-15068
CROCKETT, D. B. p 1202 N94-16162
CROOKS, HENRY A. p 877 N94-15601
p 877 N94-15609
CROSETTO, D. p 1159 N94-16172
CROSS, E. S. p 949 N94-16876
CROSS, KENNETH D. p 1138 N94-17077
CROSS, L. E. p 1009 N94-15669
p 1009 N94-15672
p 1009 N94-15673
CROSSLAND, P. p 1146 N94-15702
CROW, JOHN p 1191 N94-16128
CROWLEY, J. K. p 1067 N94-16676
CROWLEY, JAMES K. p 1073 N94-16703
CROWSON, ANDREW p 954 N94-15104
CRUIT, W. p 976 N94-15723
CRUIT, WENDY p 930 N94-16144
CRUTCHFIELD, W. Y. p 1025 N94-16894
CRUZ, CHRISTOPHER I. p 861 N94-17284
CRUZ, JONATHAN p 888 N94-17072
CUBASCH, U. p 1096 N94-16802
CUCCI, ALESSANDRO p 1078 N94-16749
CUCINOTTA, FRANCIS A. p 1188 N94-17018
p 1301 N94-17666
CUPP, CHRISTIAN M. p 1232 N94-17101
CURLANDER, JOHN C. p 992 N94-15908
p 993 N94-15917
CURRAN, PAUL J. p 1069 N94-16683
CURRERI, PETER A. p 960 N94-17079
CUTKOSKY, MARK R. p 1163 N94-14937

D

DABBOUS, WALID p 1158 N94-14980
DACCOLTI, G. p 894 N94-17174
DAHLBERT, E. D. p 1217 N94-17579
DAHLSTROM, ERIC p 888 N94-17072
DAILEY, WILLIAM P. p 975 N94-17073
DAILY, JOHN W. p 925 N94-16482
DALEY, P. L. p 872 N94-17405
p 873 N94-17569
DALEY, P.L. p 873 N94-17432
p 873 N94-17508
DALEY, T. M. p 1102 N94-17252
DALGARNO, A. p 1239 N94-15188
DALLAS, JOSEPH L. p 913 N94-15563
DANBY, G. T. p 1176 N94-17658
DANDY, DAVID S. p 969 N94-16946
DANFORD, M. D. p 955 N94-15832
DANKS, A. C. p 905 N94-15069
DANNER, R. p 900 N94-15034
DANSBERRY, BRYAN E. p 866 N94-15722
DANTONI, M. p 910 N94-15100
DANZER, GERALD D. p 1182 N94-16466
DAPP, TIMOTHY L. p 969 N94-16916
DARAB, J. G. p 940 N94-17235
DASCH, E. J. p 1264 N94-16258
DASCHNER, WALTER p 1196 N94-17347
DASH, SANFORD M. p 924 N94-15221
DASSING, REINER p 916 N94-15582
p 876 N94-15600
p 877 N94-15606
DATTA, SUBHENDU K. p 930 N94-15143
DAUGHERTY, M. A. p 1013 N94-17226
DAUGHERTY, ROBERT H. p 1033 N94-15884
DAVARIAN, FARAMAZ p 994 N94-16035
p 995 N94-16039
DAVENPORT, A. J. p 956 N94-15921
p 1207 N94-15923
p 947 N94-16011
DAVENPORT, I. p 907 N94-15079
DAVENPORT, I. J. p 906 N94-15070
DAVIDSON, SANDRA L. p 1165 N94-15855
DAVIDSON, STEVEN A. p 1152 N94-17014
DAVIS, CURTISS O. p 1069 N94-16687
DAVIS, FRANK W. p 1076 N94-16735
p 1076 N94-16736
DAVIS, GUY D. p 958 N94-16486
DAVIS, H. A. p 1202 N94-16451
DAVIS, K. p 1190 N94-15975
DAVIS, PAUL R. p 1206 N94-15107
DAVIS, ROBERT F. p 1012 N94-17040
p 1213 N94-17108
p 1213 N94-17116
p 1215 N94-17377
p 973 N94-17490
p 1216 N94-17553
DAVIS, ROBERT J. p 986 N94-14955
DAVISON, B. H. p 975 N94-16807
DAWICKE, D. S. p 931 N94-15184
p 956 N94-15948
DAWSON, J. p 1300 N94-17233
DAY, JOHN L. p 1076 N94-16736
DEACON, M. B. p 1114 N94-17518
DEAN, G. D. p 1057 N94-15016
p 1057 N94-15017
DEAN, W. G. p 879 N94-15191
DEANS, STANLEY R. p 998 N94-16649
DEATON, M. A. p 1122 N94-15741
DEBACKKER, K. p 901 N94-15036
DEBELLIS, MICHAEL p 1166 N94-16770
DEBUSSCHERE, I. p 901 N94-15036
p 906 N94-15071
DECKER, ARTHUR J. p 1034 N94-15961
DECKER, WINFIELD M. p 917 N94-15587
p 877 N94-15601
DECKERT, WALLACE H. p 866 N94-15718
DECKETT, MARTIN p 893 N94-17163
DEES, C. p 975 N94-16807
DEFORD, J. F. p 1039 N94-16054
DEFRESE, RAYMOND J. p 1129 N94-17456
DEGNAN, JOHN J. p 911 N94-15552
p 915 N94-15580
p 915 N94-15581
p 916 N94-15583
p 917 N94-15587
p 922 N94-15625
DEGRAAUW, T. p 903 N94-15054
p 908 N94-15084
DEGRADO, WILLIAM F. p 1117 N94-16441
DEGRANDI, G. p 1076 N94-16740
DEGRASSIE, J. S. p 1203 N94-16823
DEGREZ, G. p 1017 N94-15198
DEGROOF, H. p 1076 N94-16740
DEHANT, V. p 1101 N94-15815
DEHART, JOHN M. p 1244 N94-16363

DEHNE, FRANK ..... p 1162 N94-17539
DEISSLER, ROBERT J. ..... p 1027 N94-17112
DEJONG, E. ..... p 1252 N94-16201
DEJONG, E. G. ..... p 1021 N94-15755
DEJONG, T. ..... p 854 N94-15131
DEJONGE, J. BEN ..... p 854 N94-17614
DEKKER, G. J. ..... p 1157 N94-17626
DEKONING, J. P. F. ..... p 853 N94-15124
DEKORTE, P. A. J. ..... p 900 N94-15031
p 900 N94-15035
DELAMERE, W. A. ..... p 901 N94-15041
DELANGE, G. ..... p 903 N94-15054
DELANOY, RICHARD L. ..... p 1164 N94-15746
DELCOURT-HONOREZ, M. ..... p 1100 N94-15812
DELERY, J. M. ..... p 1018 N94-15201
DELIL, A. A. M. ..... p 1031 N94-17615
DELLACORTE, CHRISTOPHER ..... p 930 N94-15769
DELONGE, RENE ..... p 876 N94-17548
DELOREY, DENNIS E. ..... p 888 N94-16990
DELRICCO, R. ..... p 892 N94-17161
p 893 N94-17165
DELUCIA, FRANK C. ..... p 946 N94-15684
p 968 N94-16796
DEMARIA, MICHELANGELO ..... p 1303 N94-16526
DEMARTEAU, M. ..... p 1185 N94-16968
DEMAYER, F. ..... p 1100 N94-15808
p 1100 N94-15809
DEMAZIERE, M. ..... p 923 N94-17592
DEMELENNE, B. ..... p 987 N94-15644
DEMONTLIVAULT, J. ..... p 896 N94-17188
DEMUREN, A. O. ..... p 1169 N94-15818
DENBESTEN, R. ..... p 853 N94-15123
DENBOGGENDE, A. J. F. ..... p 900 N94-15035
DENDOR, PAUL F. ..... p 975 N94-16934
DENHARTOG, C. ..... p 853 N94-15126
DENN, FRED M. ..... p 1105 N94-15480
DENSON, MICHAEL ..... p 1052 N94-16147
DENTAMARO, ANTHONY V. ..... p 1101 N94-16469
DENYAK, V. M. ..... p 1179 N94-14931
DEPIERO, NANETTE L. ..... p 1003 N94-17268
DERBYSHIRE, K. R. ..... p 987 N94-15644
DERIDDER, JEAN JACQUES ..... p 889 N94-17135
DERVIEUX, ALAIN ..... p 1030 N94-17531
DESAI, U. D. ..... p 906 N94-15072
DESHPANDE, MANOHAR D. ..... p 989 N94-15767
p 998 N94-16655
DESIDERI, JEAN-ANTOINE ..... p 1030 N94-17531
p 1030 N94-17534
DESMARAIS, DAVID ..... p 1278 N94-16339
DESSOUKY, KHALED ..... p 995 N94-16042
DETERS, K. J. ..... p 1152 N94-17032
DEUERLER, FRIEDERIKE ..... p 975 N94-16002
DEUTSCH, A. ..... p 1219 N94-16341
p 954 N94-16383
DEVAN, J. H. ..... p 957 N94-16163
p 958 N94-16166
DEVILBISS, CARITA A. ..... p 1137 N94-15820
DEVILLERS, G. ..... p 1201 N94-15211
DEVINE, G. ..... p 1204 N94-17237
DEVORE, RONALD ..... p 1170 N94-16940
DEVOTO, JORGE ..... p 1175 N94-17643
DEWOLF, W. B. ..... p 1177 N94-15506
DEXTER, H. BENSON ..... p 964 N94-15656
p 937 N94-16846
DHARESHWAR, L. J. ..... p 1042 N94-17630
DIAMOND, PRESTON S. ..... p 886 N94-15864
DIAZ, AL V. ..... p 1050 N94-16131
DICERA, ENRICO ..... p 1117 N94-15662
DICKINSON, TAMARA ..... p 1095 N94-15781
DICKINSON, TAMMY L. ..... p 1244 N94-16363
DICOCCO, G. ..... p 899 N94-15029
DIEBOLD, A. C. ..... p 953 N94-17649
DIEDERICH, CHRIS J. ..... p 1121 N94-15634
DIEFENDORF, R. J. ..... p 933 N94-15528
p 933 N94-15626
p 933 N94-15835
DIERICHS, M. M. T. M. ..... p 903 N94-15054
DIERICKX, B. ..... p 910 N94-15099
DIETRICH, DAVID E. ..... p 1112 N94-15771
DIETRICH, LECH ..... p 951 N94-17050
DIETZ, J. B. ..... p 1073 N94-16704
DIGIROLAMO, S. ..... p 892 N94-17161
p 893 N94-17165
DIKOV, YU. P. ..... p 1248 N94-16180
DIMOS, D. ..... p 1015 N94-17648
DIMOTAKIS, PAUL E. ..... p 861 N94-17580
DINC, A. ..... p 1147 N94-15772
DING, DAJUN ..... p 1181 N94-15863
DING, J. L. ..... p 967 N94-16067
p 968 N94-16813
DINGER, R. ..... p 1002 N94-17110
DINWIDDIE, R. B. ..... p 934 N94-16017
DIONISIO, C. ..... p 993 N94-15913
DIRAFFAELE, R. ..... p 906 N94-15076
DIRSCHERL, R. ..... p 924 N94-15223
DITTMAR, JAMES H. ..... p 1176 N94-15115
DIVECHA, AMARNATH P. ..... p 940 N94-16933
DIXON, CARL A. ..... p 927 N94-17123
p 928 N94-17124
DIXON, D. ..... p 932 N94-15276
DIXON, IAIN ..... p 1085 N94-17665
DIZIO, PAUL A. ..... p 981 N94-16096
DOBSON, DAVID ..... p 1195 N94-17342
DOBSON, LARRY ..... p 1092 N94-16766
DOBSON, M. CRAIG ..... p 991 N94-15898
DOCHAT, GEORGE ..... p 924 N94-15482
DOE, P. J. ..... p 1185 N94-16951
DOGRA, VIRENDRA K. ..... p 1018 N94-15291
DOHERTY, TAMMY J. ..... p 1119 N94-14917
p 1123 N94-16544
p 1123 N94-16558
p 1035 N94-17002
DOHNALEK, Z. ..... p 1210 N94-16476
DOLGIN, BENJAMIN P. ..... p 1033 N94-15875
DOLLING, D. S. ..... p 1017 N94-15200
DOMANIK, KENNETH J. ..... p 1262 N94-16248
DOMARADZKI, J. A. ..... p 1029 N94-17363
DOMASH, LAWRENCE ..... p 1197 N94-17353
DOMERGUE-SCHMIDT, NATALIE ..... p 954 N94-16372
DONAGHY, KEVIN H. ..... p 1151 N94-16941
DONAHUE, CHRISTOPHER A. ..... p 1106 N94-15757
DONATI, A. ..... p 899 N94-15029
DONCHIN, EMANUEL ..... p 1131 N94-15148
DONELAN, MARK A. ..... p 1113 N94-16517
DONG, XIAOYI ..... p 1193 N94-17254
DONOVAN, HOWARD ..... p 877 N94-15609
DOON, A. Z. ..... p 903 N94-15053
DORADO, JOSE M. ..... p 896 N94-17182
DORAN, J. C. ..... p 1110 N94-17673
DOREYE, N. ..... p 1037 N94-15803
DOROFEYEVA, V. A. ..... p 1244 N94-16377
DORSETT, A. ..... p 1054 N94-16156
DORSEY, JOHN T. ..... p 885 N94-15446
DOUBEK, SHARON ..... p 883 N94-15648
DOUBT, T. J. ..... p 1130 N94-17562
DOWDING, ROBERT J. ..... p 954 N94-15104
DOWNER, M. C. ..... p 1183 N94-16818
DOYLE, E. J., JR. ..... p 1129 N94-17374
DOZIER, JEFF ..... p 1075 N94-16732
DRESCHHOFF, G. ..... p 1299 N94-17208
DRESSELHAUS, G. ..... p 1014 N94-17428
DRESSELHAUS, M. S. ..... p 1014 N94-17428
DRESSLER, JOHN L. ..... p 1028 N94-17250
DU, GUANG-WU ..... p 939 N94-16859
DU, WEI-MIN ..... p 1037 N94-15806
DUBBELDAY, W. B. ..... p 1039 N94-16474
DUBEY, RAJENDRA R. ..... p 1188 N94-17018
DUBICK, M. A. ..... p 1122 N94-15740
DUCARME, B ..... p 1101 N94-15814
DUCARME, B. ..... p 1037 N94-15806
p 1100 N94-15807
p 1100 N94-15808
p 1100 N94-15809
p 1100 N94-15813
p 1101 N94-15815
DUCK, PETER W. ..... p 1019 N94-15478
DUDGEON, DAN E. ..... p 1164 N94-15746
DUECK, S. ..... p 1234 N94-16209
DUFFY, C. J. ..... p 1217 N94-17659
DUFFY, J. ..... p 887 N94-16905
DUGAL-WHITEHEAD, N. R. ..... p 884 N94-15007
DUGAN, JOANNE BECHTA ..... p 1155 N94-17447
DUGGIN, MICHAEL J. ..... p 1067 N94-16673
DULEY, W. W. ..... p 977 N94-16077
DUMONT, P. ..... p 893 N94-17162
DUNBAR, BRIAN ..... p 987 N94-15439
DUNG, LE ..... p 1171 N94-17613
DUNKIN, V. E. ..... p 981 N94-16097
DUNN, PETER ..... p 911 N94-15553
DUNN, PETER J. ..... p 912 N94-15559
DUNNING, T. H., JR. ..... p 1151 N94-16902
DUNPHY, P. ..... p 981 N94-16095
DUPONT, J. N. ..... p 970 N94-16959
DURAND, ALAIN ..... p 899 N94-16101
DURAND, S. J. ..... p 1093 N94-17217
DURDEN, S. ..... p 1079 N94-16751
DURHAM, MICHAEL H. ..... p 866 N94-15722
DURHAM, W. B. ..... p 953 N94-16188
DUSI, W. ..... p 899 N94-15029
DUTT, A. ..... p 1154 N94-17370
p 1171 N94-17420
DUTT, S. ..... p 1173 N94-17236
DUTTA, JYOTSNA M. ..... p 946 N94-15684
DUTTA, R. ..... p 975 N94-16996
DVORAK, GEORGE J. ..... p 933 N94-15528
p 933 N94-15626
p 933 N94-15835
DYKA, C. T. ..... p 1057 N94-15524
DYSON, BRIAN F. ..... p 1057 N94-15015
DZENIS, YURIS A. ..... p 939 N94-16861

E

EATHER, ROBERT H. ..... p 1192 N94-16550
EBEL, J. ..... p 1097 N94-14960
EBEL, PHIL ..... p 1072 N94-16701
EBERT, D. ..... p 1185 N94-17310
EBLING, MARIA R. ..... p 1141 N94-17115
ECKERT, C. A. ..... p 1220 N94-16997
ECKHARDT, DAVE E., JR. ..... p 1144 N94-15486
ECKSTEIN, JAMES N. ..... p 1008 N94-15635
EDBERG, T. K. ..... p 901 N94-15040
EDELSON, BURTON I. ..... p 1006 N94-17661
EDELSTEIN, ALAN ..... p 936 N94-16537
EDEN, J. ..... p 1190 N94-15854
EDGE, DAVID R. ..... p 918 N94-15596
p 877 N94-15609
EDGETT, K. S. ..... p 1291 N94-16406
EDMONDS, J. A. ..... p 1095 N94-16006
EDWARDS, B. C. ..... p 1037 N94-16426
EDWARDS, BERNELL J. ..... p 872 N94-17403
EDWARDS, G. D. ..... p 1006 N94-17565
EDWARDS, K. B. ..... p 1274 N94-16319
EDWARDS, LAWRENCE G. ..... p 1034 N94-16521
EDWARDS, ROBERT V. ..... p 1192 N94-16718
EFSTRATIOU, VASSILIOS ..... p 937 N94-16848
EGETH, HOWARD ..... p 1132 N94-16456
EHRLICH, S. N. ..... p 1208 N94-16058
EICHINGER, RICHARD ..... p 877 N94-15609
p 922 N94-15622
EICKELBERG, W. ..... p 1190 N94-15975
EIKEN, STEVEN D. ..... p 1006 N94-17582
EKBOM, L. B. ..... p 945 N94-15171
EL-MASRY, NADIA ..... p 1213 N94-17116
ELBAN, W. L. ..... p 1214 N94-17270
ELEY, ADRIAN S. ..... p 1004 N94-17373
ELIASSON, A. ..... p 945 N94-15171
ELLIBEE, D. E. ..... p 1091 N94-15994
ELLINGSON, W. A. ..... p 968 N94-16658
ELLIOTT, CHRIS ..... p 897 N94-17190
ELLIS, DAVID R. ..... p 860 N94-17260
ELMAN, GREGORY C. ..... p 921 N94-15618
ELMORE, D. ..... p 1245 N94-16409
ELSAYED-ALI, HANI E. ..... p 1038 N94-15852
ELSON, E. C. ..... p 1134 N94-17535
ELVIDGE, CHRIS D. ..... p 1071 N94-16695
EMENHEISER, KENNETH S. ..... p 918 N94-15595
p 918 N94-15596
p 877 N94-15609
EMERY, K. A. ..... p 1093 N94-16824
EMERY, R. J. ..... p 905 N94-15066
p 905 N94-15067
EMERY, WILLIAM ..... p 1112 N94-15701
EMETZ, A. I. ..... p 915 N94-15576
EMMITT, GEORGE D. ..... p 1109 N94-17525
ENGEL, B. N. ..... p 974 N94-14982
ENGELMANN, B. E. ..... p 1059 N94-15983
ENGELUND, WALTER C. ..... p 867 N94-17055
ENGEMANN, D. ..... p 902 N94-15046
p 906 N94-15073
p 906 N94-15074
ENGLAND, A. W. ..... p 954 N94-16340
ENGMAN, EDWIN T. ..... p 991 N94-15895
p 1079 N94-16755
ENNIX, KIMBERLY A. ..... p 869 N94-15141
ENRIGHT, E. M. ..... p 899 N94-16152
ENSELL, G. ..... p 911 N94-15103
ENTING, I. G. ..... p 1094 N94-15185
EPSTEIN, ARTHUR J. ..... p 970 N94-16978
ERARD, S. ..... p 1296 N94-16436
ERARD, STEPHANE ..... p 1295 N94-16429
p 1295 N94-16431
ERCK, R. A. ..... p 1059 N94-15997
ERICKSON, GARY E. ..... p 859 N94-16573
ERIKSSON, O. ..... p 1214 N94-17301
ERIKSSON, TORE ..... p 944 N94-15162
ERIKSTAD, STEIN OWE ..... p 1055 N94-17082
EROKHIN, Y. N. ..... p 1209 N94-16056
ERWIN, J. K. ..... p 1226 N94-14983
p 1226 N94-14987
p 1227 N94-14989
p 1227 N94-14990
ERWIN, K. ..... p 1199 N94-14986
ESCUDIER, BENEDICTE ..... p 890 N94-17146
ESENER, SADIK C. ..... p 1145 N94-15627
ESER, S. ..... p 975 N94-16996
ESIPCHUK, Y. ..... p 1202 N94-16803
ESPENAK, FRED ..... p 1236 N94-15481
ESPOSITO, E. ..... p 905 N94-15068
ESTABROOK, POLLY ..... p 995 N94-16042
ETIEVE, P. ..... p 902 N94-15047
ETLING, W. ..... p 877 N94-15610
EULISS, GARY W. ..... p 1188 N94-14940
EVANS, ANTHONY G. ..... p 935 N94-16483
p 935 N94-16484
p 935 N94-16485
p 935 N94-16528

	p 935	N94-16529
EVANS, N. D.	p 1206	N94-14925
EVANS, R. L.	p 1058	N94-15963
EVENSEN, LARS	p 909	N94-15095
EVENSON, ERIK	p 1046	N94-15707
EVEREST, A. W.	p 882	N94-16530
EVERETT, RICHARD	p 936	N94-16537
EVERHART, K.	p 976	N94-15723
EVERHART, KURT	p 930	N94-16144
EYRING, E. M.	p 1041	N94-16998
EZAKA, TERUYA	p 1064	N94-16600
EZEKOYE, O. A.	p 947	N94-16060

F

FABBRICOTTI, M.	p 903	N94-15050
	p 910	N94-15098
	p 910	N94-15100
FABRE, N.	p 902	N94-15047
FABRI, ANDREAS	p 1162	N94-17539
FADNER, DAWN E.	p 1125	N94-16623
FAIDAS, H.	p 1042	N94-17567
FAIRLIE, B. D.	p 1146	N94-15650
FALCO, C. M.	p 974	N94-14982
FALCO, CHARLES M.	p 1189	N94-15735
FALLS, M. J.	p 996	N94-16045
FAMIGLIETTI, J. S.	p 1083	N94-16029
	p 1084	N94-16033
FARHAT, CHARBEL	p 1159	N94-15849
FARHAT, NABIL H.	p 1165	N94-15958
FARIS, FARIS	p 883	N94-17111
FARMER, JACK D.	p 1278	N94-16339
FARN, MICHAEL W.	p 1194	N94-17333
	p 1198	N94-17362
FARR, THOMAS G.	p 991	N94-15900
FARR, TOM G.	p 1298	N94-17654
FARRAND, WILLIAM H.	p 1074	N94-16708
FARRELL, P.	p 1011	N94-16661
FATHAUER, JONES	p 966	N94-15960
FATHAUER, ROBERT W.	p 1215	N94-17327
FAUCHER, GILLES	p 1032	N94-15697
FAULKNER, COLIN	p 926	N94-16590
FAYMONVILLE, R.	p 902	N94-15046
	p 906	N94-15073
	p 906	N94-15074
	p 910	N94-15099
FAZIO, G.	p 906	N94-15076
FEARON, E.	p 966	N94-15924
FEDRO, MARK J.	p 939	N94-16862
FEELEY, O. C.	p 975	N94-16898
FEHSENFELD, BERND	p 984	N94-16003
FEIGELSON, R. S.	p 1038	N94-15530
FEILER, PETER H.	p 1146	N94-15653
FEIND, RAND E.	p 1066	N94-16671
FEIT, M. D.	p 1039	N94-16054
FELDMAN, MICHAEL R.	p 1197	N94-17356
FELTEN, R.	p 902	N94-15046
	p 906	N94-15073
	p 906	N94-15074
FENN, ALAN J.	p 1121	N94-15634
FERBER, M. K.	p 935	N94-16461
FERGUSON, DAVID W.	p 946	N94-15684
FERGUSON, E. B.	p 1124	N94-16615
	p 1056	N94-16626
FERNAND, JEAN M.	p 1167	N94-17369
FERNANDEZ-BACA, J. A.	p 1212	N94-16868
FERNANDEZ, J.	p 1037	N94-15804
FERRANDO, RONALD E.	p 1117	N94-16545
FERRANDO, WILLIAM A.	p 940	N94-16933
FERRANTE, R.	p 1219	N94-16420
FETTERER, FLORENCE M.	p 1113	N94-17241
FIECHTNER, GREGORY J.	p 925	N94-16482
FIELD, CHRISTOPHER B.	p 1066	N94-16668
	p 1067	N94-16672
	p 1072	N94-16698
FIELD, D.	p 908	N94-15088
FIELDING, ERIC J.	p 1232	N94-17036
FIELDS, ERIK	p 1112	N94-15844
FIELDS, T.	p 1300	N94-17233
FILIPOV, A.	p 1054	N94-16156
FINDEIS, N.	p 900	N94-15034
FINLEY, CHARLES J.	p 929	N94-17587
FIRESTONE, ELAINE R.	p 1111	N94-15529
FISCHER, E.	p 1258	N94-16228
FISCHER, E. M.	p 1252	N94-16199
	p 1288	N94-16395
FISCHER, H.	p 877	N94-15623
FISCHER, JOHN	p 969	N94-16920
FISENKO, A. V.	p 1246	N94-16422
FITTINGHOFF, D. N.	p 949	N94-16904
FITTS, STEPHEN D.	p 1237	N94-17225
FITZGERALD, JIM D.	p 922	N94-15625
FITZGERALD, MICHAEL	p 1072	N94-16697
FLAMMIA, MADELYN	p 1230	N94-15838
FLANAGAN, MICHAEL J.	p 1154	N94-17326
FLANNERY, DAVID L.	p 1189	N94-15791
FLAUX, BRUNO	p 909	N94-15091
FLEETER, RICK	p 896	N94-17185
FLEETER, SANFORD	p 869	N94-15866
FLEISHAUER, ROBERT P.	p 1108	N94-17303
FLEMING, GREGG G.	p 1179	N94-17599
FLICK, J. A.	p 1037	N94-15806
	p 1100	N94-15809
FLOOD, DENNIS J.	p 1013	N94-17113
FLORES, C.	p 894	N94-17174
FLORES, J. S.	p 901	N94-15041
FLORISSI, DANILO	p 1161	N94-17409
FLOWERS, D. L.	p 947	N94-15861
FLYTZANI-STEPHANOPOULOS, M.	p 949	N94-16896
FODEN, C. L.	p 899	N94-15028
FOH, J.	p 1259	N94-16233
FOLIARD, JACQUES	p 888	N94-17133
FONTE, DANIEL J., JR.	p 888	N94-17103
FONTEYN, D.	p 923	N94-17592
FORBES, A. B.	p 1049	N94-15013
FORD, GARY	p 1142	N94-14967
FORD, JOHN P.	p 1298	N94-17654
FORD, P. G.	p 1264	N94-16261
FORDHAM, J. L. A.	p 901	N94-15039
FORDHAM, JEFFREY A.	p 922	N94-17083
FOREST, C. B.	p 1202	N94-16803
FORMAN, KEITH	p 1107	N94-17102
FORMAN, P. R.	p 1202	N94-16776
	p 1013	N94-17318
FORSTER, RICHARD R.	p 1078	N94-16746
FORTUNY, J.	p 893	N94-17164
FOSHA, CHARLES E., JR.	p 1174	N94-17219
FOUKS, B. I.	p 902	N94-15049
FOWLER, A. M.	p 902	N94-15044
FOWLER, CHARLES	p 1112	N94-15701
FOWLER, M. M.	p 1185	N94-16951
FOX, ANDREW N.	p 1078	N94-16746
FOX, M. A.	p 1185	N94-16971
FOX, N. P.	p 908	N94-15085
FOX, NIGEL	p 906	N94-15075
FOX, STANLEY L., II	p 1160	N94-17034
FOX, W. K.	p 1151	N94-16910
FRAME, W. W.	p 901	N94-15041
FRANCHE, CANDONINO P.	p 1046	N94-15738
FRANCHI-ZANNETTACCI, PAUL	p 1234	N94-17529
FRANCHI, I. A.	p 1251	N94-16193
FRANCIS, O.	p 1100	N94-15811
FRANCIS, PETER	p 1068	N94-16680
FRANK, L. A.	p 1097	N94-15003
FRANKEL, J.	p 1061	N94-17105
FRANKEL, S. H.	p 1018	N94-15427
FRASER, G. W.	p 901	N94-15038
FRATERNALI, PIERO	p 1156	N94-17501
	p 1234	N94-17502
FREEMAN, A.	p 1079	N94-16751
	p 1080	N94-16757
FREEMAN, G. B.	p 936	N94-16569
FREHLICH, R. G.	p 1038	N94-15477
FRENCH, B. M.	p 1104	N94-16334
FRENZL, O.	p 902	N94-15046
	p 906	N94-15073
	p 906	N94-15074
FREY, HERB	p 1273	N94-16315
FRICKE, S. K.	p 1279	N94-16347
FRIDMAN, L. I.	p 938	N94-16855
FRIEDMAN, A.	p 1205	N94-17670
FRIEDMAN, H. W.	p 1236	N94-14929
FRIEDMAN, L.	p 1273	N94-16312
FRIEDRICHS, MARJORIE A.	p 1114	N94-17555
FRIETAS, J. A., JR.	p 971	N94-17204
FRISCH, H. L.	p 968	N94-16727
FRITZ, J. N.	p 1178	N94-16955
FROEHLICH, F.	p 1199	N94-14986
FROEHLICH, FRED F.	p 1199	N94-14995
FROGGATT, MARK E.	p 1050	N94-15870
	p 1033	N94-15877
FRUNZIO, L.	p 905	N94-15068
FRYE, JOAN M.	p 1206	N94-15764
FU, C. L.	p 959	N94-16873
FU, H.	p 1226	N94-14983
FU, HONG	p 1227	N94-14989
FUCHS, W. K.	p 1158	N94-15173
	p 1140	N94-15174
FUJITA, E.	p 949	N94-16870
FUJITA, TAKASHI	p 1245	N94-16412
FULLER, L. E., JR.	p 947	N94-16105
FULLERTON, E. E.	p 1208	N94-16058
FULTON, D.	p 1298	N94-17654
FUMMI, FRANCO	p 1156	N94-17504
	p 1014	N94-17505
FUNAHASHI, S.	p 1212	N94-16868
FUNG, Y. T.	p 1020	N94-15526
FURMAN, M.	p 1190	N94-15854
FURSE, CYNTHIA M.	p 1130	N94-17621

G

GABL, E. F.	p 1042	N94-17378
GADAJ, STEFAN P.	p 960	N94-17063
GADETSKY, S.	p 1226	N94-14983
	p 1227	N94-14991
GAFFEY, M. J.	p 1241	N94-16174
	p 1243	N94-16310
GAFFEY, MICHAEL J.	p 1242	N94-16274
GAGNON, F. A.	p 980	N94-16094
GAIL, WILLIAM B.	p 993	N94-15912
GAL, GEORGE	p 1197	N94-17350
	p 1197	N94-17351
	p 1197	N94-17355
	p 1198	N94-17361
GALBRAITH, JAY M.	p 1060	N94-17043
GALLAGHER, ANDREA	p 1066	N94-16670
	p 1069	N94-16682
GALLAGHER, D. L.	p 1147	N94-15721
GALLAHER, G. R.	p 947	N94-15861
GAMBRELL, S. C.	p 1058	N94-15716
GAMON, JOHN A.	p 1066	N94-16668
	p 1067	N94-16672
	p 1072	N94-16698
GAMPE, F.	p 894	N94-17171
GANASAN, J. P.	p 953	N94-16247
GANDHI, OM P.	p 1130	N94-17621
GANGLOFF, RICHARD P.	p 942	N94-17638
GANGULY, J.	p 1241	N94-16175
	p 1241	N94-16176
GAO, BO-CAI	p 1068	N94-16678
	p 1072	N94-16699
	p 1072	N94-16700
GAO, FENGQIN	p 952	N94-17302
GAO, Q.	p 1210	N94-16476
GARBER, DONALD P.	p 1176	N94-15487
GARDNER, JAMES A., II	p 1192	N94-16936
GARDNER, WILLIAM A.	p 988	N94-15690
GARFINKLE, MOISHE	p 868	N94-16865
GARLAN, DAVID	p 1147	N94-15728
GARLAND, C. F.	p 1129	N94-17374
GARLAND, F. C.	p 1129	N94-17374
GARN, PAUL A.	p 1085	N94-17665
GARNER, CHARLES E.	p 925	N94-15876
GARNER, F. A.	p 958	N94-16662
GARNER, J. T.	p 878	N94-17158
GARRABOS, Y.	p 944	N94-15164
GARRISON, D. H.	p 1248	N94-16177
GARVIN, JAMES B.	p 1248	N94-16178
GARY, J. PATRICK	p 1228	N94-15116
GASKELL, ROBERT W.	p 1103	N94-16222
GASTELLU-ETCHEGORRY, J. P.	p 1068	N94-16681
GASTIL, MARY	p 1069	N94-16684
GATES, D.	p 978	N94-16082
GATES, L. P.	p 1157	N94-17588
GAUNCE, M. T.	p 882	N94-17320
GAUTIER, A.	p 893	N94-17162
GAVEL, D. T.	p 1237	N94-16872
GAYLORD, THOMAS K.	p 1194	N94-17335
GAZENKO, O. G.	p 1139	N94-17636
GEBALLE, T. H.	p 1216	N94-17561
GEHRELS, NEIL	p 899	N94-15026
GEISSLER, P.	p 1252	N94-16201
GEISSLER, P. E.	p 1248	N94-16179
GEISSLER, PAUL	p 1295	N94-16431
GEKTIN, YU. M.	p 1294	N94-16423
GENDEL, NEIL	p 1124	N94-16614
GENDY, A. S.	p 1058	N94-15709
GENTLE, K. W.	p 1202	N94-16162
GENUARDI, MICHAEL T.	p 1228	N94-15009
GEOHEGAN, D. B.	p 1210	N94-16460
GEORGE, E. P.	p 1208	N94-16063
	p 959	N94-16890
GEORGE, M. A.	p 1207	N94-15973
GEORGE, T. J.	p 1092	N94-16715
GEORGE, THOMAS	p 1215	N94-17327
GEORGESON, GARY E.	p 1157	N94-17590
	p 1056	N94-17596
GERACE, GERALD C.	p 996	N94-16044
GERASIMOV, M. V.	p 1248	N94-16180
GERASOULIS, APOSTOLOS	p 1154	N94-17390
GERBER, R.	p 1226	N94-14983
	p 1227	N94-14990
GERDES, RONALD M.	p 867	N94-15950
GERDES, T. E.	p 947	N94-15861
GERGOVA, K.	p 975	N94-16996
GERIG, R.	p 1173	N94-17236
GERINGER, M. A.	p 1252	N94-16200
GERR, NEIL L.	p 1140	N94-17623
GERSHENZON, E.	p 903	N94-15055
GEVA, SHAI	p 1152	N94-17009
GEYER, M. S.	p 882	N94-17320
GHAIL, R. C.	p 1249	N94-16181
GHIZZO, A.	p 1201	N94-15210
GHONEM, H.	p 941	N94-17379

GHOSE, S. p 1241 N94-16176
GIARD, M. p 908 N94-15087
GIARRUSSO, S. p 906 N94-15076
GIAVARINI, G. p 1220 N94-17602
GIBBONS, G. W. p 1240 N94-17603
GIBBS, PHILIP p 875 N94-15591
GIBSON, E. K., JR. p 1270 N94-16295
GIBSON, GARY G. p 1105 N94-15480
GIBSON, M. A. p 1249 N94-16182
GIBSON, W. M. p 968 N94-16727
GIDAS, BASILIS p 1082 N94-15842
GIERASCH, PETER J. p 1246 N94-15182
GIESEKE, B. G. p 957 N94-16106
GIFFORD, DAVID p 1141 N94-14915
GILBERT, JEFFREY L. p 1047 N94-15882
GILBERT, JOHN R. p 1168 N94-15112
p 1158 N94-15113
p 1159 N94-15796
p 1148 N94-15956
GILBREATH, G. C. p 919 N94-15607
GILGENBACH, R. M. p 1041 N94-17001
GILL, R. J. p 950 N94-16930
GILLESPIE, ALAN R. p 1068 N94-16677
GILMORE, M. S. p 1249 N94-16183
GILMOUR, I. p 953 N94-16256
GILMOUR, IAIN p 1241 N94-16184
GINOCCHIO, J. N. p 1207 N94-15972
GIORDANO, G. p 1068 N94-16681
GIRARD, BERTRAND p 1032 N94-15697
GIRARD, T. p 900 N94-15032
GIRIDHARAN, M. G. p 928 N94-17442
GIULIANI, JOHN F. p 1040 N94-16533
GIVEN, J. W. p 1151 N94-16910
GIVI, P. p 1018 N94-15427
GLADE, BRADFORD B. p 997 N94-16477
p 1161 N94-17239
GLADSTONE, G. R. p 1250 N94-16185
GLANCY, B. C. p 1214 N94-17270
GLASKOV, S. A. p 859 N94-16583
GLASS, B. P. p 1241 N94-16186
GLASS, J. T. p 1216 N94-17553
GLASS, JEFFREY T. p 1213 N94-17116
GLASSMAN, NANCI A. p 1233 N94-17291
p 1233 N94-17300
GLEMBOCKI, OREST J. p 948 N94-16539
GLENBERG, ARTHUR p 1134 N94-17468
GLENDENNING, N. K. p 1181 N94-16013
p 1239 N94-16052
GLICK, F. p 980 N94-16094
GLINICKI, MICHAL A. p 1060 N94-17052
GLINKA, C. J. p 1207 N94-15827
GLITZ, R. p 992 N94-15902
GLOERSEN, PER p 1114 N94-17439
GLYNN, PETER W. p 1165 N94-15775
p 1174 N94-15823
GLYTSIS, ELIAS N. p 1194 N94-17335
GODBOLE, M. J. p 1040 N94-16664
GODFREY, G. L. p 904 N94-15061
GOEBEL, JOHN H. p 1009 N94-15765
GOEDEL, M. p 931 N94-15257
GOEHRING, G. S. p 1119 N94-14916
GOERSS, JAMES S. p 1106 N94-16568
GOETZ, A. F. H. p 1067 N94-16674
GOETZ, ALEXANDER F. H. p 1068 N94-16678
p 1072 N94-16699
p 1072 N94-16700
p 1074 N94-16711
GOGUEN, J. D. p 1250 N94-16187
p 1245 N94-16386
GOLDBERG, B. p 976 N94-15723
GOLDBERG, BEN p 930 N94-16144
GOLDBERG, MATTHEW S. p 1235 N94-16988
GOLDEN, D. C. p 1104 N94-16424
GOLDHIRSH, JULIUS p 995 N94-16041
p 996 N94-16048
GOLDMAN, P. p 1093 N94-17668
GOLDSBY, D. L. p 953 N94-16188
GOLDSTEIN, JOSEPH A. p 1004 N94-17373
GOLOMBEK, M. P. p 1250 N94-16189
GOLOSKOKOV, S. V. p 1188 N94-17313
GOLTSMAN, G. p 903 N94-15055
GOLUB, A. P. p 1290 N94-16404
GOMEZ, C. S. p 1123 N94-16565
GOMEZ, J. p 1034 N94-16452
GONDOIN, P. p 910 N94-15097
GONZALEZ, RICHARD R. p 1035 N94-17002
GOODMAN, ALVIN M. p 1211 N94-16800
GOODMAN, M. C. p 1300 N94-17233
GOODMAN, S. p 978 N94-16082
GOODMAN, T. p 1226 N94-14983
p 1227 N94-14989
GOODRICH, CYRENA ANNE p 1241 N94-16190
GOODWIN, THOMAS J. p 1117 N94-15969
GOPI, N. p 1042 N94-17630
GORDON, M. p 953 N94-17649
GORDON, SANFORD p 1220 N94-17624
GOSLING, J. T. p 1299 N94-16895
GOSWAMI, J. N. p 1241 N94-16191
GOULD, MARSTON J. p 888 N94-17072
p 1138 N94-17452
GOULDING, R. H. p 1203 N94-16823
GOYETTE, THOMAS M. p 946 N94-15684
GRABER, HANS C. p 1113 N94-16517
GRABSKI, MACIEJ W. p 961 N94-17121
GRACIAS, BRIAN K. p 937 N94-16851
p 938 N94-16852
GRADY, MONICA M. p 1241 N94-16192
p 1251 N94-16193
GRAESSER, ARTHUR C. p 1137 N94-16108
GRAF, TH. p 1187 N94-16194
GRAFF, LINDA H. p 1084 N94-17421
GRAHAM, D. W. p 969 N94-16889
GRAHAM, R. A. p 1034 N94-16452
GRANAHAN, JAMES C. p 1241 N94-16195
GRANDAGE, J. M. p 868 N94-17117
GRANDJEAN, ALICE p 1239 N94-15970
GRANNEN, K. J. p 973 N94-17413
GRANT, J. A. p 1251 N94-16196
p 1007 N94-16197
GRASSO, ROBERT J. p 1003 N94-17268
GRATRIX, EDWARD J. p 1196 N94-17346
GRAY, GEORGE T., III p 959 N94-16764
GRAY, GRANT p 1004 N94-17364
GREELEY, R. p 1252 N94-16198
p 1252 N94-16199
p 1252 N94-16200
p 1258 N94-16228
p 1259 N94-16229
p 1269 N94-16289
p 1288 N94-16395
GREELEY, RONALD p 1278 N94-16339
p 1074 N94-16710
p 1078 N94-16747
GREEN, BILL p 1050 N94-16136
GREEN, R. A. p 949 N94-16891
GREEN, ROBERT D. p 929 N94-17483
GREEN, ROBERT O. p 1066 N94-16666
p 1037 N94-16667
p 1073 N94-16705
GREENBERG, PAUL S. p 977 N94-16076
GREENBERG, R. p 1252 N94-16201
p 1241 N94-16202
GREENBLATT, ARTHUR S. p 1191 N94-16489
GREENHALGH, SKOTT p 868 N94-15865
GREENLY, J. B. p 1202 N94-16451
GREENWALD, ANTON C. p 1038 N94-15853
GREENWALD, E. p 973 N94-17408
GREENWOOD, R. C. p 1103 N94-16203
GREGG, TRACY K. P. p 1253 N94-16204
GREGOIRE, D. C. p 1242 N94-16245
GREGORICH, D. p 1199 N94-17443
GREGORY, JOHN C. p 951 N94-17039
GREIF, R. p 947 N94-16060
GREVE, D. W. p 940 N94-17013
GRIBBLE, R. F. p 1202 N94-16776
p 1013 N94-17318
GRIEWANK, A. p 1170 N94-16778
GRIFFIN, M. p 902 N94-15047
p 906 N94-15073
GRIFFIN, M. J. p 902 N94-15048
p 905 N94-15066
p 905 N94-15067
p 907 N94-15077
GRIFFIN, P. B. p 950 N94-16952
GRIM, CARL J. p 1166 N94-16986
GRIMM, R. E. p 1241 N94-16205
GRIMM, ROBERT E. p 1285 N94-16380
GRINSPOON, DAVID H. p 1254 N94-16206
GRITTNER, J. p 931 N94-15256
GRODSINSKY, C. M. p 978 N94-16078
GROENEVELD, DAVID P. p 1071 N94-16695
GROEZINGER, U. p 907 N94-15082
GROH, K. R. p 1117 N94-16893
GROHMANN, D. p 1114 N94-17516
GROLEMUND, DAVID A. p 922 N94-15625
GROSFILS, ERIC B. p 1254 N94-16207
GROSS, R. p 908 N94-15083
GROTE, D. P. p 1205 N94-17670
GROVE, T. L. p 1241 N94-16208
GRUBER, MARK R. p 943 N94-14962
GRUEN, D. M. p 953 N94-17649
GRUM, T. P. p 1193 N94-17012
GRUNWALDT, LUDWIG p 877 N94-15623
GU, M. p 1154 N94-17370
GU, X. F. p 1070 N94-16691
GUENOUN, P. p 944 N94-15164
GUENTHER, BOB D. p 1194 N94-17332
GUEST, J. E. p 1278 N94-16338
GUETHER, H.-M. p 877 N94-15611
GUHARAY, S. p 1186 N94-17578
GUI, TIE-JI p 1042 N94-17394
GUINNESS, E. A. p 1234 N94-16209
GULICK, VIRGINIA C. p 1241 N94-16210
GUMMIN, M. A. p 901 N94-15037
GUNDLACH, K. H. p 907 N94-15078
GUNNING, W. J. p 1045 N94-17357
GUO, HUA-DONG p 993 N94-15915
p 993 N94-15916
GUO, X. p 1241 N94-16213
GUOHUA, BAO p 860 N94-17274
GUPTA, VIPUL p 1154 N94-17390
GURIN, A. A. p 1013 N94-17316
GUROV, E. P. p 1103 N94-16211
p 1241 N94-16212
GUROVA, H. P. p 1241 N94-16212
GURYN, W. p 1187 N94-16829
GUTIERREZ, D. F. p 1241 N94-16213
GUTOW, DAVID A. p 1047 N94-15882
GUYENNE, T. D. p 899 N94-15025
p 1303 N94-16792
GUYMON, GARY L. p 983 N94-15876
GUYOT, F. p 954 N94-16383
GUZMAN, L. p 878 N94-17155
GWILLIAM, T. J. P. p 1114 N94-17516
GYETVAY, S. R. p 885 N94-15749
p 951 N94-17207

H

HA, K. p 1062 N94-17507
HAACK, H. p 1241 N94-16213
HAAS, BRIAN L. p 856 N94-15678
HAAS, JOHNSON R. p 1103 N94-16214
HABER, I. p 1205 N94-17670
p 1188 N94-17672
HABERBUSCH, MARK p 1034 N94-16521
HABIGER, HARALD p 928 N94-17308
HADDOCK, M. REED p 928 N94-17213
HADE, EDWARD W. p 1138 N94-16983
HAEDER, WALTER p 984 N94-16005
HAFIZI, B. p 1038 N94-15686
HAFT, M. p 1181 N94-16013
HAGER, E. PAUL p 1006 N94-17661
HAGGANS, CHARLES W. p 1198 N94-17360
HAGSTROM, THOMAS p 1029 N94-17448
HAHN, DOUGLAS C. p 1107 N94-17244
HAINES, RICHARD F. p 883 N94-15548
HALFORD, GARY R. p 1060 N94-16881
HALICIOGLU, TIMUR p 1056 N94-15004
HALL, DAVID G. p 1176 N94-15115
HALL, DENNIS G. p 1045 N94-17349
HALL, G. p 909 N94-15090
HALL, PHILIP p 1016 N94-15005
HALL, ROBERT J. p 950 N94-17008
HALLINAN, K. P. p 976 N94-15654
HALPERN, JOSHUA B. p 1206 N94-15764
HALPERT, GERALD p 1014 N94-17325
HALSTEAD, THORA W. p 1118 N94-17257
HALTER, MEGAERA C. p 868 N94-17435
HAMAL, KAREL p 913 N94-15564
p 913 N94-15565
p 913 N94-15567
p 914 N94-15574
p 916 N94-15584
p 921 N94-15619
p 877 N94-15621
HAMANO, N. p 945 N94-15168
HAMED, A. p 861 N94-17574
HAMEETMAN, G. J. p 1157 N94-17626
HAMEKA, HENDRIK F. p 943 N94-15111
HAMERS, R. J. p 948 N94-16787
HAMILL, THOMAS C. p 1108 N94-17267
HAMILL, THOMAS M. p 1105 N94-14958
HAMILTON, DAVID B. p 1138 N94-17077
HAMILTON, L. D. p 1095 N94-15999
HAMILTON, MICHAEL p 1069 N94-16687
HAMILTON, VICTORIA E. p 1256 N94-16215
HAMMER, JAY A. p 952 N94-17381
HAMMOND, VINCENT H. p 964 N94-15656
p 938 N94-16856
HAMORY, PHILIP J. p 1145 N94-15538
HAMPEL, G. p 874 N94-17143
HAN, H. C. p 1076 N94-16737
HAN, S. J. p 1184 N94-16838
HAN, Y. p 1150 N94-16579
HANEBUTTE, ULF R. p 1168 N94-15724
HANEY, MICHAEL W. p 1188 N94-14940
HANIGOFSKY, J. A. p 936 N94-16569
HANKS, R. L. p 1035 N94-16960
HANOCQ, J. F. p 1070 N94-16691
HANRAHAN, WILLIAM P., III p 918 N94-15595
p 918 N94-15596
p 877 N94-15609
HANSEN, C. J. p 1256 N94-16216
HANSEN, EARL G. p 1071 N94-16692
HANSEN, G. J. p 883 N94-16056
HANSEN, GARY B. p 1256 N94-16217

HANSEN, V. L.	p 1256	N94-16218
HANSEN, VICKI L.	p 1271	N94-16304
HANSON, S. G.	p 1193	N94-17012
HAPKE, B.	p 1256	N94-16219
HARABIN, A. L.	p 1119	N94-14916
HARABIN, ANDREA L.	p 1130	N94-17556
HARDALUPAS, Y.	p 1016	N94-15109
HARDIE, A. L.	p 908	N94-15088
HARDIN, R. D.	p 936	N94-16569
HARDING, DAVID J.	p 921	N94-15620
HARGRAVES, R. B.	p 1285	N94-16375
HARGROVE, JAMES P.	p 1233	N94-17114
HARKINS, D. A.	p 1181	N94-15863
HARLAN, S. S.	p 1104	N94-16334
HARLEY, PETER J.	p 1080	N94-16761
HARMATHY, P.	p 945	N94-15169
HARPER, C. L., JR.	p 1256	N94-16220
	p 1103	N94-16271
HARRIMAN, K.	p 1227	N94-14988
HARRINGTON, S.	p 1016	N94-17671
HARRISON, EDWIN F.	p 1105	N94-15480
HARRISON, P. ANN	p 1082	N94-15531
HARRISON, PATRICK R.	p 1082	N94-15531
HARRY, A.	p 1142	N94-14944
HARRY, ANDREW	p 1142	N94-15008
	p 1142	N94-15010
	p 1142	N94-15011
	p 1143	N94-15012
	p 1143	N94-15022
HARSANYI, JOSEPH C.	p 1074	N94-16708
HARTER, D. J.	p 1042	N94-17378
HARTLEY, FRANK T.	p 1014	N94-17323
HARTLEY, P.	p 962	N94-16137
HARTMAN, BRYCE O.	p 1132	N94-16942
HARTMANN, WILLIAM K.	p 1242	N94-16221
	p 1103	N94-16222
HARTNESS, J. T.	p 933	N94-15277
HARTUNG, JACK B.	p 1242	N94-16223
	p 1103	N94-16322
HARVEY, E.	p 978	N94-16081
HARVEY, R. P.	p 1242	N94-16224
HARVEY, R. W.	p 1202	N94-16803
	p 1203	N94-16816
HARWELL, WILLIAM	p 1022	N94-15962
HASAN, M. M.	p 1046	N94-15817
HASAN, MOHD A.	p 993	N94-15911
HASBROOK, WILLIAM	p 870	N94-15532
HASCHBERGER, D.	p 902	N94-15046
HASEGAWA, A.	p 1239	N94-16647
HASHIMOTO, Y.	p 892	N94-17160
HASHIN, ZVI	p 941	N94-17597
HASKIN, LARRY A.	p 1103	N94-16214
	p 1242	N94-16281
HASKO, GREGORY H.	p 964	N94-15656
	p 938	N94-16856
HASTINGS, DANIEL	p 925	N94-15837
	p 897	N94-17266
HASTINGS, J. B.	p 1212	N94-16887
HATCHER, P. G.	p 975	N94-16996
HATFIELD, WILLIAM E.	p 952	N94-17416
HATHAWAY, MICHAEL D.	p 1032	N94-15445
	p 869	N94-17386
HATTAN, C. P.	p 997	N94-16467
HAUCK, H.	p 914	N94-15575
HAUFE, K. H.	p 916	N94-15582
	p 876	N94-15600
HAUFF, D.	p 900	N94-15034
HAUFF, PHOEBE L.	p 1072	N94-16701
HAUSKNECHT, P.	p 1070	N94-16688
HAUSMANN, MARTHA A.	p 868	N94-17425
HAWKE, B. R.	p 1258	N94-16225
HAWKE, B. RAY	p 1259	N94-16231
	p 1284	N94-16371
HAWKINS, R. J.	p 1039	N94-16054
HAXTON, W. C.	p 1207	N94-15972
HAYHOE, MARY M.	p 1132	N94-16925
HAYHURST, ARTHUR RAY	p 1010	N94-15988
HAYKIN, S.	p 988	N94-15698
HAZEN, D. A.	p 996	N94-16046
HAZLEBECK, D.	p 972	N94-17242
HE, ANZHI	p 1035	N94-17402
HE, J. L.	p 1048	N94-16969
HEAD, J. W.	p 1249	N94-16183
	p 1252	N94-16199
	p 1258	N94-16227
	p 1258	N94-16228
	p 1259	N94-16229
	p 1259	N94-16230
	p 1271	N94-16303
HEAD, JAMES W.	p 1254	N94-16207
	p 1258	N94-16226
	p 1259	N94-16231
	p 1259	N94-16232
	p 1259	N94-16234
	p 1264	N94-16262
	p 1285	N94-16376
	p 1288	N94-16395
HEADLY, DEAN E.	p 863	N94-17262
HEADRICK, JAMES M.	p 987	N94-15540
HEATH, M. E.	p 1115	N94-14918
HEBERT, MARTIAL	p 863	N94-14919
HEBRANK, F.	p 908	N94-15083
HECHT, LAURA M.	p 1233	N94-17291
	p 1233	N94-17300
HEDRICK, C. L.	p 1203	N94-16869
HEEG, JENNIFER	p 867	N94-17055
HEEL, F.	p 992	N94-15902
HEERD, STEFAN	p 874	N94-16584
HEFFERNAN, C.	p 1288	N94-16394
HEGARTY, CHRIS	p 864	N94-16906
HEGERL, G.	p 1096	N94-16802
HEIDEBRECHT, K. B.	p 1067	N94-16674
HEIDEBRECHT, KATHLEEN	p 1072	N94-16700
HEIDELBERGER, PHILIP	p 1174	N94-15823
HEIKKINEN, J. A.	p 1201	N94-15211
HEINEMAN, GEORGE T.	p 1155	N94-17398
HEINICK, J. MICHAEL	p 877	N94-15609
HEINICK, MICHAEL	p 913	N94-15568
HELALI, Y.	p 877	N94-15621
HELD, P.	p 1259	N94-16233
HELFENSTEIN, P.	p 1259	N94-16234
HELGERUD, MICHAEL B.	p 1260	N94-16235
HELM, HANSPETER	p 1182	N94-16586
HELM, M.	p 1175	N94-17288
HELM, NEIL R.	p 1006	N94-17661
HEMACHANDRA, L.	p 1150	N94-16579
HEMMATI, HAMID	p 1038	N94-15932
HEMMINGER, C. S.	p 887	N94-16909
HEMMINGER, CAROL S.	p 1056	N94-14945
HENAGER, C. H., JR.	p 934	N94-16158
HENDERSON, B. G.	p 1260	N94-16236
HENDERSON, BRADLEY G.	p 954	N94-16372
HENDERSON, D. O.	p 965	N94-15828
HENDRICKS, KYLE J.	p 1011	N94-16556
HENNAUX, S.	p 1037	N94-15803
HENNEKE, MARKUS J.	p 941	N94-17473
HENNINGTON, L.	p 1003	N94-17206
HENRY, J. PATRICK	p 1059	N94-16815
HENRY, RONALD	p 969	N94-16920
HENSON, LESLEY J.	p 1001	N94-17026
HENZE, WILLIAM, JR.	p 1298	N94-15023
	p 1298	N94-15024
HEPBURN, I.	p 906	N94-15070
HEPBURN, I. D.	p 907	N94-15079
	p 911	N94-15103
HERAKOVICH, C. T.	p 930	N94-15106
HERD, RICHARD A.	p 1103	N94-16237
HERENDEEN, D. L.	p 1151	N94-16768
	p 1151	N94-16769
HERGE, DONNA C.	p 1153	N94-17075
HERKENHOFF, K. E.	p 1260	N94-16238
HERMAN, B.	p 1197	N94-17350
	p 1197	N94-17355
	p 1198	N94-17361
HERMAN, HERMAN	p 879	N94-14969
HERMAN, R. G.	p 975	N94-16898
HEROLD, G.	p 876	N94-15600
HERRICK, R. R.	p 1261	N94-16239
HERRICK, ROBERT R.	p 1285	N94-16380
HERRING, CHARLES	p 1157	N94-17620
HERTHER, J. C.	p 988	N94-15649
HERTHER, JOHN C.	p 987	N94-15527
HERTLING, DAVID	p 1176	N94-17605
HERTZ, P. L.	p 904	N94-15061
HERTZ, ROGER	p 899	N94-16101
HERZOG, G. F.	p 1242	N94-16240
HESS, A. C.	p 1215	N94-17319
HESS, GERALD L.	p 1131	N94-15659
HESS, J. R.	p 1123	N94-16565
HESS, LAURA L.	p 1076	N94-16739
HESS, P. C.	p 1259	N94-16232
	p 975	N94-16241
	p 1261	N94-16242
HESSELMANS, G. H. F. M.	p 1077	N94-16744
HESSELS, U.	p 877	N94-15610
	p 877	N94-15611
	p 877	N94-15612
HESTER, R.	p 971	N94-16999
HETHERINGTON, HOBY	p 1121	N94-15736
HEUSER, B. J.	p 1207	N94-15827
HEYMANN, D.	p 953	N94-16243
HICKAM, H. H., JR.	p 1174	N94-17469
HICKMAN, G. DANIEL	p 1067	N94-16673
HICKS, DIXON K.	p 1152	N94-17027
HICKS, JOHN W.	p 886	N94-15753
HICKS, LANA P.	p 983	N94-15881
HIEL, CLEMENT	p 936	N94-16836
	p 936	N94-16837
HIESINGER, H.	p 1261	N94-16244
HIGH, WAYNE	p 1192	N94-16975
HILANDS, T. W.	p 1005	N94-17463
HILDEBRAND, A. R.	p 1242	N94-16245
HILL, B. J.	p 937	N94-16850
HILL, BRADLEY	p 1072	N94-16701
HILL, N.	p 1300	N94-17233
HILL, T. J.	p 926	N94-16773
HILLAND, J. E.	p 993	N94-15910
HILLEBRANDT, W.	p 1240	N94-17628
HIME, A.	p 1181	N94-15974
	p 1185	N94-16951
HIMEL, M. D.	p 1036	N94-17647
HINCHLIFFE, I.	p 1181	N94-16059
HINKS, D. G.	p 1208	N94-15982
HINSDALE, JOHN K.	p 1155	N94-17398
HINTON, D. A.	p 1108	N94-17283
HINTZ, T. M.	p 1006	N94-17565
HIROI, T.	p 1242	N94-16246
HIRSCH, CHARLES	p 1016	N94-15119
HiSKES, J. R.	p 1183	N94-16817
HIXON, DUANE	p 1027	N94-17129
HIXSON, R. S.	p 1178	N94-16955
HO, C.	p 898	N94-17669
HO, TRUNG DUNG	p 1186	N94-17612
HO, WILSON	p 1015	N94-17560
HOBBS, R. H.	p 1186	N94-17536
HOCHMUTH, DIANE	p 1194	N94-17336
HOCHMUTH, DIANE H.	p 1195	N94-17339
HOCKADAY, M. Y. P.	p 1202	N94-16776
HOCKADAY, R. G.	p 1202	N94-16776
HOEFLICH, P.	p 1237	N94-17629
HOEIJMAKERS, H. W. M.	p 1031	N94-17627
HOERZ, F.	p 1063	N94-16253
HOESLY, R. L.	p 1151	N94-16769
HOFFMAN, CRISTY	p 1126	N94-16634
HOFFMAN, D. J.	p 1203	N94-16823
HOFFMAN, DAVID S.	p 1049	N94-16139
HOFFMANN, H.	p 1259	N94-16234
HOFFMANN, M. J.	p 966	N94-16018
HOFTIEZER, J. H.	p 1300	N94-17233
HOGAN, HARRY A.	p 1129	N94-17456
HOGENBOOM, D. L.	p 953	N94-16247
HOHENBERG, C. M.	p 1243	N94-16305
HOJNICKI, JEFFREY S.	p 929	N94-17483
HOKE, D.	p 965	N94-15773
HOLCOMBE, C. E.	p 969	N94-16877
HOLDEN, KRITINA L.	p 1005	N94-17498
HOLL, P.	p 900	N94-15034
HOLLAND, A. D.	p 907	N94-15080
HOLLAND, ORGAL T.	p 1040	N94-16540
HOLLEY, S. E.	p 1114	N94-17489
HOLLINGSHEAD, MIKE	p 980	N94-16091
HOLLISTER, KATHERINE M.	p 864	N94-16439
HOLLOWAY, JOHN R.	p 1262	N94-16248
HOLMES, RICHARD	p 1051	N94-16141
HOLSAPPLE, K. A.	p 1262	N94-16249
HOLT, KIMBERLY ANN	p 1031	N94-16145
HOLZBECHER, J.	p 1241	N94-16213
HOLZER, STEFAN M.	p 1062	N94-17445
HOLZHEID, A.	p 1103	N94-16250
HOLZWORTH, ROBERT H.	p 1106	N94-16493
HONG, F.	p 1209	N94-16066
HONINGH, C. E.	p 903	N94-15054
HOOD, L. L.	p 1262	N94-16251
HOOKER, MATTHEW W.	p 983	N94-15881
HOOKER, STANFORD B.	p 1111	N94-15529
HOOVER, GORDON	p 1063	N94-16599
	p 1037	N94-16667
	p 1074	N94-16712
HOOVER, JAMES	p 969	N94-16920
HOOVER, SCOTT M.	p 940	N94-16933
HOPF, DAN E.	p 921	N94-15618
HOPKINS, D. A.	p 1058	N94-15709
HOPPEL, K.	p 1077	N94-16743
HOPPIN, ANDREW	p 1086	N94-16437
HORANYI, M.	p 1262	N94-16251
HORN, L. J.	p 1263	N94-16252
HORNEMANN, U.	p 954	N94-16383
HORTON, J. A.	p 1236	N94-14929
HOSOKAWA, S.	p 945	N94-15167
HOTALING, S. P.	p 885	N94-15666
HOUCK, MICHAEL R.	p 1131	N94-15108
HOUGHTON, R. A.	p 1094	N94-15185
HOURIGAN, D. T.	p 872	N94-15543
HOUSEN, KEVIN	p 1063	N94-16254
HOUSTON, P. L.	p 948	N94-16462
HOWARD, I.	p 980	N94-16093
	p 981	N94-16096
HOWARD, LARRY	p 1155	N94-17429
HOWE, D.	p 1227	N94-14988
HOWE, DENNIS G.	p 1228	N94-14997
HOWE, ROBERT D.	p 1163	N94-14937
HOWELL, WILLIAM C.	p 1005	N94-17498
HOWINGTON-KRAUS, A.	p 1283	N94-16369
HOYLE, C. E.	p 970	N94-16947
	p 970	N94-16948
	p 970	N94-16949
	p 971	N94-16994
HROMADKA, THEODORE V.	p 983	N94-15676
HSU, C. C.	p 1076	N94-16737

HSUEH, C. H. p 972 N94-17253
HU, CHEN-MING p 1175 N94-15758
HU, H. p 973 N94-17408
HU, Z.-Q. p 877 N94-15605
HUA, X. p 1219 N94-16255
HUANG, HUI-PING p 953 N94-16256
HUANG, S. p 1242 N94-16257
p 1209 N94-16447
HUBER, ALAN C. p 882 N94-16530
p 897 N94-17240
HUDSON, R. p 1219 N94-16420
HUEBENER, R. P. p 908 N94-15083
HUEBER, WERNER G. p 1000 N94-16921
HUERRE, PATRICK p 1023 N94-16470
HUETTIG, F. R. p 1012 N94-16765
HUGH, M. K. p 933 N94-15277
HUGHES, C. E. p 858 N94-16571
HUGHES, CHRISTOPHER E. p 1176 N94-15115
HUGHES, S. S. p 1264 N94-16258
HUIE, R. p 965 N94-15859
HUITEMA, CHRISTIAN p 1158 N94-14980
HULL, J. R. p 1013 N94-17226
HUMAYUN, M. p 953 N94-16259
HUMBERG, HEINZ p 984 N94-16004
HUMMEL, JOHN R. p 1003 N94-17268
HUMPHREYS, T. P. p 1216 N94-17553
HUNEYCUTT, BRYAN L. p 990 N94-15890
HUNSAKER, CAROLYN T. p 1097 N94-17426
HUNT, C. P. p 1006 N94-17549
HUNT, J. J. p 899 N94-15025
HUNTER, B. A. p 1208 N94-15982
HUNTER, D. A. p 972 N94-17238
HUPP, JOSEPH T. p 1182 N94-16466
p 1211 N94-16782
p 950 N94-17006
HURLBERT, ERIC A. p 925 N94-16496
HURTREZ, S. p 1067 N94-16675
HURWITZ, P. D. p 1202 N94-16162
HUSS, GARY R. p 1242 N94-16260
HUSSAINI, M. Y. p 1019 N94-15478
HUSSEN, VAN S. p 912 N94-15559
HUSSON, VAN S. p 915 N94-15579
p 917 N94-15587
HUTCHEON, IAN D. p 1242 N94-16260
HUTCHIN, P. p 911 N94-15103
HUTCHINS, EDWIN L. p 862 N94-15550
HUYNH, HUNG T. p 1170 N94-16882
HWANG, D. P. p 858 N94-16571
HWANG, J. C. p 1012 N94-16935
HWANG, S. L. p 966 N94-16018
HWU, WEN-MEI W. p 1158 N94-15173
HYDE, J. M. p 957 N94-16015
HYGATE, GRAHAM p 986 N94-15020
p 1006 N94-17545

I

IACONO, R. p 1202 N94-16446
IARVE, ENDEL V. p 936 N94-16795
IBRAHEEM, S. O. p 1169 N94-15818
ICE, G. E. p 1209 N94-16171
IFARRAGUERRI, AGUSTIN p 1143 N94-15110
IFJU, PETER G. p 939 N94-16862
IGLSEDER, H. p 890 N94-17147
IGNATENKO, K. I. p 1244 N94-16345
IKEUCHI, KATSUSHI p 1166 N94-16725
ILDEFONSE, PH. p 954 N94-16383
ING, H. p 981 N94-16097
INGEBO, ROBERT D. p 1035 N94-17446
INGERSOLL, A. p 1252 N94-16201
INMAN, DOUGLAS L. p 1023 N94-16110
INMAN, VAUGHN W. p 1138 N94-17460
INNOCENTI, LOUISA p 874 N94-16584
INTAGLIETTA, M. p 1128 N94-16783
INUKAI, THOMAS p 883 N94-17111
IOANNOU, DIMITRIS E. p 1214 N94-17243
IORIO, VINCENT M. p 1047 N94-16531
IRVINE, WILLIAM M. p 1298 N94-15421
ISAACS, H. S. p 956 N94-15921
p 956 N94-15922
p 947 N94-16011
ISACKS, BRYAN p 1078 N94-16746
ISACKS, BRYAN L. p 1232 N94-17036
ISBELL, N. K. p 1283 N94-16369
ISHAI, ORI p 936 N94-16837
ISHII, YOSHINORI p 1064 N94-16601
ISHIKAWA, M. p 945 N94-15167
ITABE, TOSHIKAZU p 911 N94-15555
IVANCIC, WILLIAM p 883 N94-17487
IVANOV, A. I. p 903 N94-15053
IVANOV, B. A. p 1264 N94-16261
IVANOV, M. A. p 1264 N94-16263
IVANOV, MIKHAIL p 1258 N94-16226
p 1264 N94-16262
IVANOVA, M. A. p 953 N94-16264
p 1242 N94-16265
IVENS, JAN p 937 N94-16848
IVERSON, DAVID L. p 1116 N94-15548
IVLIEV, A. I. p 953 N94-16266
p 953 N94-16267
IWASAKI, A. p 945 N94-15167
IZENBERG, NOAM R. p 1265 N94-16268
IZETT, G. A. p 1103 N94-16269

J

JACKSON, A. A. p 1242 N94-16270
JACKSON, DAVID D. p 1101 N94-16021
JACKSON, J. W. p 1176 N94-17658
JACOBS, IAN p 1142 N94-14978
JACOBSEN, S. B. p 1256 N94-16220
p 1103 N94-16271
JACOBSON, JAY A. p 1173 N94-17585
JACOBSON, M. D. p 996 N94-16046
JACOBSSON, ULF p 944 N94-15162
JACQUEMOUD, S. p 1070 N94-16691
JACUNSKI, M. p 1011 N94-16661
JAEGER, H. p 1259 N94-16233
JAGGERS, C. H. p 885 N94-15749
JAGGI, S. p 1063 N94-16596
p 1063 N94-16597
p 1063 N94-16598
p 1064 N94-16603
p 1065 N94-16604
JAGOUTZ, E. p 1242 N94-16272
JAHN, ROBERT G. p 1204 N94-17575
JAIN, RAJ K. p 1013 N94-17113
JAKES, PETR p 962 N94-16273
JAKOSKY, B. M. p 1260 N94-16236
JAKOSKY, BRUCE p 954 N94-16372
JAKOSKY, BRUCE M. p 1290 N94-16402
p 1290 N94-16403
JAKUBCZAK, J. p 1011 N94-16661
JAMES, J. H. p 933 N94-15699
JAMES, R. A. p 1203 N94-16816
JAMORA, DENNIS A. p 862 N94-15444
JAMROZ, W. p 978 N94-16080
JANKOWSKI, D. J. p 1300 N94-17233
JANSEN, ADRIAN J. p 1026 N94-16985
JANSEN, F. A. p 900 N94-15035
JANSSENS, BOB p 1140 N94-15174
JARECKI, LESZEK p 1213 N94-17046
JARVIS, D. R. p 1176 N94-15019
JARVIS, KANDY S. p 1242 N94-16274
JAUMANN, R. p 1258 N94-16225
p 1259 N94-16234
p 1261 N94-16244
p 1275 N94-16323
JAVOY, M. p 954 N94-16383
JAWERTH, B. p 1170 N94-16940
JAYASURIYA, DON p 892 N94-17159
JAYNE, D. T. p 956 N94-15992
JEANJAQUET, S. p 1009 N94-15726
JELINKOVA, HELENA p 913 N94-15565
p 916 N94-15584
p 877 N94-15621
JELLISON, G. E., JR. p 1040 N94-16664
JENISTA, J. p 1204 N94-17311
p 1205 N94-17635
JENNINGS, RAYMOND D. p 1006 N94-17661
JENSEN, JAMES O. p 943 N94-15111
JENSEN, ROBERT E. p 1113 N94-16517
JENSERUD, TROND p 989 N94-15714
JENSTROM, DEL T. p 1164 N94-15704
JENTZSCH, G. p 1101 N94-15815
JEONG-HWAN, CHO p 956 N94-15921
JERDE, ERIC A. p 1266 N94-16275
p 1266 N94-16276
JERINA, K. p 961 N94-17109
JERNIGAN, JAMES L. p 1000 N94-16921
JESSON, D. E. p 1212 N94-16841
JEUDY, V. p 900 N94-15032
JHA, M. C. p 949 N94-16897
JIA, PEIZ-HANG p 918 N94-15597
JIN, YU-QI p 1042 N94-17394
JIPPING, MICHAEL J. p 1144 N94-15486
JOCHEM, TODD p 864 N94-15498
JOERGENSEN, HANS E. p 1105 N94-14938
JOHANNSEN, C. J. p 1084 N94-16831
JOHANSEN, G. A. p 907 N94-15081
JOHANSSON, M. A. p 975 N94-16898
JOHANSSON, ROLAND p 1163 N94-14937
JOHNS, JANET F. p 1165 N94-16559
JOHNS, S. p 1014 N94-17375
JOHNSON, B. V. p 1023 N94-15991
JOHNSON, BERTRAND L., JR p 921 N94-15617
JOHNSON, C. E. p 1211 N94-16805
JOHNSON, C. L. p 1267 N94-16277
JOHNSON, CHRISTOPHER S. p 1211 N94-16782
JOHNSON, CRAIG E. p 975 N94-16934
JOHNSON, D. R. p 968 N94-16843
JOHNSON, DON H. p 999 N94-16794
JOHNSON, ERIC G. p 1194 N94-17336
p 1195 N94-17339
p 1195 N94-17340
JOHNSON, J. R. p 1267 N94-16278
p 1278 N94-16342
JOHNSON, LEE F. p 1073 N94-16702
JOHNSON, NICHOLAS L. p 926 N94-16504
JOHNSON, T. V. p 1245 N94-16386
p 1288 N94-16395
JOHNSON, TONI p 922 N94-15622
JOHNSON, W. p 981 N94-16096
JOHNSON, Y. B. p 884 N94-15007
JOHNSTON, K. W. p 981 N94-16095
JOHNSTON, N. J. p 932 N94-15276
p 933 N94-15277
JOICE, WENDELL p 1124 N94-16617
JOLLIFF, BRADLEY L. p 1267 N94-16279
p 1267 N94-16280
p 1242 N94-16281
JONATHAN, NEVILLE p 1213 N94-17037
JONES, ALUN C. p 1103 N94-16282
JONES, BRIAN L. p 898 N94-17368
JONES, CHARLES R. p 946 N94-15684
JONES, D. R. p 1215 N94-17319
p 1043 N94-17677
JONES, J. H. p 953 N94-16283
p 1243 N94-16288
JONES, J. P. p 1166 N94-16888
JONES, JOHN H. p 1243 N94-16286
p 962 N94-16287
JONES, KENNETH E. p 1179 N94-17599
JONES, MARK p 941 N94-17597
JONES, R. H. p 934 N94-16158
JONES, RHIAN H. p 1243 N94-16284
JONES, ROSS M. p 874 N94-17145
JONES, S. p 1002 N94-17110
JONES, W. R., JR. p 967 N94-16543
JONG, JEN-YI p 1082 N94-15646
JONSSON, MATS p 944 N94-15162
JORDAN, J. L. p 1295 N94-16428
JORDAN, REBECCA H. p 1045 N94-17349
JORGENSEN, J. D. p 1208 N94-15982
JOSEPH, C. p 905 N94-15069
JOSEPH, DANIEL D. p 1019 N94-15479
JOSEPH, MICHAEL p 1138 N94-17475
JOSEPHSON, JOHN p 1234 N94-17419
JOSLIN, D. L. p 1206 N94-14925
JOSLIN, RONALD D. p 1144 N94-15483
JOSWIAK, D. J. p 1244 N94-16367
JOW, T. RICHARD p 966 N94-15930
p 1010 N94-15952
JOYCE, J. A. p 962 N94-17464
JUDA, M. p 899 N94-15027
JUENEMANN, D. p 1242 N94-16240
JUHLKE, T. J. p 967 N94-16543
JULL, A. J. T. p 1270 N94-16295
JURETSKO, F. p 960 N94-17079
JUREWICZ, A. J. G. p 1103 N94-16285
JUREWICZ, AMY J. G. p 1243 N94-16286
JUREWICZ, STEPHEN R. p 962 N94-16287
p 1243 N94-16288

K

KAANDERS, M. A. p 1003 N94-17307
KACED, J. p 894 N94-17170
KADEL, S. D. p 1252 N94-16199
p 1269 N94-16289
KADKHODAYAN, B. p 948 N94-16821
KAEAERIAEINEN, J. p 1037 N94-15803
p 1101 N94-15815
KAHN, R. p 876 N94-15600
KAHN, STEPHEN p 1150 N94-16591
KAISER, GAIL E. p 1155 N94-17398
KAISER, J. A. C. p 1077 N94-16743
KAKKURI, J. p 1098 N94-15800
KALATHIL, BIJU p 1157 N94-17620
KALDEICH, BRIGITTE p 943 N94-15157
KALDENHOFF, R. p 931 N94-15255
KALININA, G. V. p 1243 N94-16296
KALINOVSKIJ, YU. L. p 1185 N94-17310
KALLEMEYN, G. W. p 1243 N94-16290
KALLINDERIS, JOHN p 867 N94-16122
KALLMAN, J. S. p 1039 N94-16054
KAMA, WILLIAM N. p 868 N94-17425
KAMEI, S. p 945 N94-15167
KAMINSKY, ARNOLD D. p 864 N94-16439
KAMMASH, T. p 1041 N94-17001
KANADE, TAKEO p 883 N94-14919
KANAMORI, H. p 1249 N94-16182
KANDIL, FATHY A. p 1057 N94-15015
KANER, RICHARD B. p 1010 N94-15954
KANG, KYO C. p 1144 N94-15214
KANG, SING B. p 1166 N94-16725

KANKELEIT, E. p 1259 N94-16233
KANN, J. p 1199 N94-14986
KANNARI, YOSHIAKI p 1064 N94-16600
KANO, N. p 1243 N94-16291
KANTAK, ANIL V. p 996 N94-16049
KAO, Y. H. p 1209 N94-16447
KAPITULNIK, A. p 1216 N94-17561
KAPLAN, JOSEPH A. p 1160 N94-16878
KARGEL, J. S. p 953 N94-16247
p 1243 N94-16292
p 1270 N94-16293
KARGEL, JEFFREY S. p 1243 N94-16294
KARLIDERE, TURGAY p 1232 N94-16977
KARLSSON, H. R. p 1270 N94-16295
KARMARKAR, SUBHASH D. p 940 N94-16933
KARR, GERALD R. p 1058 N94-15716
KARTTUNEN, S. J. p 1201 N94-15208
p 1201 N94-15209
p 1201 N94-15210
KARU, Z. S. p 879 N94-15191
KASHKAROV, L. L. p 953 N94-16266
p 953 N94-16267
p 1243 N94-16296
p 1243 N94-16297
KASSAM, M. S. p 981 N94-16095
KASSER, MICHEL p 917 N94-15588
KASTING, J. p 1297 N94-17637
KATANO, S. p 1212 N94-16868
KATHMAN, ALAN D. p 1195 N94-17340
KATTAN, PETER I. p 934 N94-16440
KATTERLOHER, R. p 908 N94-15084
KAUFFMANN, S. p 1173 N94-17236
KAUFMAN, M. J. p 955 N94-15885
KAUHANEN, K. p 1270 N94-16298
p 1270 N94-16299
KAULA, W. M. p 1270 N94-16300
p 1271 N94-16301
p 1279 N94-16348
p 1104 N94-16349
KAVEESHWAR, ASHOK p 893 N94-17168
KAWA, H. p 967 N94-16543
KAWAI, S. p 945 N94-15167
KAWAJI, M. p 979 N94-16087
KAYAR, S. R. p 1119 N94-14916
KEANE, C. J. p 1205 N94-17663
KEANE, JOHN p 1228 N94-15152
p 1229 N94-15788
p 1230 N94-15789
KEDDIE, S. T. p 1271 N94-16302
p 1271 N94-16303
KEE, R. J. p 1096 N94-16825
KEENE, MICHAEL L. p 1230 N94-15838
KEEP, MYRA p 1271 N94-16304
KEFFER, CHARLES E. p 1191 N94-16024
KEHM, K. p 1243 N94-16305
KEIL, D. G. p 950 N94-16930
KEIL, K. p 1243 N94-16305
p 1245 N94-16389
p 1245 N94-16390
KEIL, KLAUS p 1243 N94-16306
KEISWETTER, D. A. p 1103 N94-16307
KELLEHER, T. p 1025 N94-16903
KELLER, AMANDA S. p 1179 N94-17599
KELLER, L. P. p 1249 N94-16182
p 1243 N94-16309
p 1244 N94-16355
KELLER, LINDSAY P. p 1243 N94-16308
KELLER, W. C. p 1077 N94-16743
KELLEY, M. S. p 1243 N94-16310
KELLEY, PEGGY p 927 N94-17080
KELLEY, R. L. p 899 N94-15027
KELLY, ARNOLD J. p 1204 N94-17575
KELLY, SHAWN L. p 1035 N94-17197
KELLY, TAMSIN p 1119 N94-14943
KELLY, W. D. p 1272 N94-16311
KEMMER, J. p 900 N94-15034
KEMURJIAN, ALEXSANDR LEONOVICH p 1273 N94-16312
KENDALL, ROBERT R. p 1131 N94-15108
KENDIG, M. W. p 1009 N94-15726
KENDZIORRA, E. p 900 N94-15034
KENNEDY, A. K. p 954 N94-16313
KENNEDY, EDWARD J. p 1004 N94-17373
KENNEDY, JOHN p 874 N94-17306
KENNEDY, JOHN M. p 1230 N94-15838
p 1230 N94-15839
p 1233 N94-17291
p 1233 N94-17300
KENNEL, ELLIOT B. p 1206 N94-15107
KEPERT, J. L. p 862 N94-15542
KEPPLE, PAUL C. p 878 N94-16552
KERN, R. S. p 1213 N94-17108
KEROUB, I. H. p 896 N94-17184
KERR, JAMES M. p 940 N94-16933
KERRIDGE, JOHN F. p 954 N94-16314
KERSLAKE, THOMAS W. p 929 N94-17483
KESNER, J. p 1202 N94-16446
KESSEL, P. A. p 924 N94-15220
KETTERSON, J. B. p 908 N94-15089
KEVORKIAN, A. K. p 1158 N94-15671
p 1159 N94-15750
KEWLEY, D. J. p 1004 N94-17309
KHALIL, B. p 944 N94-15164
KHAN, M. A. p 1212 N94-16932
KHARGONEKAR, PRAMOD P. p 1165 N94-15778
KHOSLA, PRADEEP p 1143 N94-15212
KICIAK, JAN p 1177 N94-16650
KIEFER, WALTER p 1273 N94-16315
KIEREIN-YOUNG, K. S. p 1078 N94-16748
p 1080 N94-16758
KIETZMANN, H. p 992 N94-15902
KIGGANS, J. O. p 1209 N94-16164
p 969 N94-16877
KILBURN, C. R. J. p 1103 N94-16316
p 1283 N94-16366
p 1035 N94-16960
KILKENNY, J. D. p 891 N94-17151
KILSTON, STEVEN p 891 N94-17151
KILSTON, VERA p 954 N94-16314
KIM, JIN S. p 1190 N94-15868
KIM, JONGMIN p 1190 N94-15869
p 1191 N94-16023
p 1191 N94-16024
KIM, SANG-SHIK p 942 N94-17638
KIM, T. p 1226 N94-14985
KIM, T. J. p 1036 N94-14992
KIM, Y. p 1243 N94-16317
KIM, YOOSOOK p 954 N94-16314
KIMBLE, R. p 905 N94-15069
KIMREY, H. D. p 969 N94-16877
KING, BELINDA p 928 N94-17277
KING, D. L. p 1091 N94-15994
KING, OLIVER p 1045 N94-17349
KING, R. A. p 904 N94-15060
KINGSTON, MARGUERITE J. p 1073 N94-16703
KINZEL, G. p 1002 N94-17110
KIPPLE, BLAIR M. p 1177 N94-16919
KIRANE, MOKHTAR p 1171 N94-17640
KIRBY, CHRISTINE M. p 1113 N94-16588
KIRCHES, S. p 907 N94-15082
KIRCHMAN, DAVID L. p 1118 N94-17275
KIRCHNER, GEORG p 898 N94-15558
p 914 N94-15574
p 916 N94-15584
p 919 N94-15603
KIRIENKO, N. p 981 N94-16096
KIRK, R. L. p 1086 N94-16318
p 1274 N94-16319
p 1274 N94-16320
KIRKLAND, E. J. p 1212 N94-16961
KIRKPATRICK, ALLEN p 1214 N94-17216
KIRLIK, ALEX p 1133 N94-17296
KISTLER, JAMES J. p 1231 N94-16570
p 1141 N94-17115
KITAMURA, MASAO p 1245 N94-16412
KITSON, DAVID H. p 1145 N94-15629
KITZMILLER, CHARLES T. p 1145 N94-15525
KJENSMO, ARNE p 909 N94-15095
KLAASEN, K. p 1252 N94-16201
p 1258 N94-16228
p 1259 N94-16234
KLAASEN, K. P. p 1288 N94-16394
KLAPWIJK, T. M. p 903 N94-15054
KLAVETTER, FLOYD L. p 973 N94-17494
KLECHA, TADEUSZ p 1060 N94-17047
KLEIFGES, KELLY p 860 N94-17221
KLEIN, H. p 944 N94-15165
KLEIN, HAROLD p 1278 N94-16339
KLEIN, J. p 1242 N94-16240
KLEIN, R. I. p 1025 N94-16903
KLEINTZ, MICHAEL p 987 N94-15155
KLEMAS, V. p 1116 N94-15633
KLEMM, R. A. p 1211 N94-16839
KLEPEIS, J. E. p 1208 N94-15976
KLEPPNER, DANIEL p 1304 N94-17651
KLEVIT, RACHEL E. p 946 N94-15760
KLIER, K. p 975 N94-16898
KLINGBIEL, PAUL H. p 1228 N94-15009
KLINGELHOEFER, G. p 1259 N94-16233
KLINKHAMER, F. R. p 1186 N94-17601
KLOPP, KARL A. p 986 N94-14974
KLOSKO, STEVE M. p 916 N94-15586
KLUGE, KARL p 1163 N94-14910
KLUTE, GLENN p 1137 N94-15717
KLUTE, GLENN K. p 1139 N94-17653
KNAP, W. p 902 N94-15047
KNAPP, J. A. p 953 N94-17649
KNIGHT, DOYLE D. p 1017 N94-15199
KNOLL, M. p 1011 N94-16661
KNOLL, R. H. p 1046 N94-15817
KNOW, K. R. p 878 N94-17139
KNOWLDEN, ROBERT E. p 1198 N94-17362
KNOWLTON, LAWRENCE W. p 1108 N94-17267
KNUDSEN, C. W. p 1249 N94-16182
KNUDSEN, HELGE p 1239 N94-15970
KNUDSEN, J. M. p 1285 N94-16375
KNUDSEN, WILLIAM C. p 1297 N94-17292
KO, DONG-SHAN p 1112 N94-15771
KO, FRANK K. p 939 N94-16859
KOBAYASHI, A. S. p 960 N94-17041
KOBRICK, M. p 994 N94-15919
KOCH, CHRISTOPHER p 1069 N94-16686
KOCH, JOHN, JR. p 1033 N94-15928
KOCH, MELISSA B. p 998 N94-16655
KODAMA, H. p 945 N94-15168
KOEBERL, CHRISTIAN p 1244 N94-16321
p 1103 N94-16322
KOEBLER, J. p 1150 N94-16579
KOEHLER, U. p 1275 N94-16323
KOENIG, JOHN R. p 928 N94-17124
KOENIG, ROLF p 911 N94-15554
p 874 N94-15589
KOENIG, SVEN p 1131 N94-15742
KOFSKY, IRVING L. p 1192 N94-16936
KOGA, J. p 1187 N94-16660
KOGER, JOHN J. p 866 N94-15731
KOHL, PAUL p 1176 N94-17605
KOHLSTEDT, D. L. p 953 N94-16188
KOIDL, F. p 914 N94-15574
p 916 N94-15584
KOIDL, FRANZ p 898 N94-15558
p 919 N94-15603
KOLENKIEWICZ, RON p 911 N94-15553
KOLKA, MARGARET A. p 1035 N94-17002
KOLLBERG, ERIK L. p 903 N94-15055
KOLVOORD, R. A. p 1241 N94-16202
KOMATSU, G. p 1249 N94-16179
p 1275 N94-16324
KOMATSUBARA, TAKESHI K. p 1180 N94-15135
KONG, J. A. p 1076 N94-16737
KONITZER, D. G. p 959 N94-16780
KONONKOVA, N. N. p 1242 N94-16265
KOOMEY, J. p 1096 N94-17289
KOONS, K. p 1190 N94-15975
KOPASZ, J. P. p 1211 N94-16805
KOPP, O. C. p 947 N94-16105
KORELSKY, TANYA p 1146 N94-15674
KOROCHANTSEV, A. V. p 930 N94-16325
KOROTEV, RANDY L. p 1242 N94-16281
p 1275 N94-16326
p 1275 N94-16327
KOROTKOVA, N. N. p 1243 N94-16297
KOROTKOVA, YU. YU. p 953 N94-16267
KOSCIELNY, A. p 1003 N94-17206
KOSHIISHI, H. p 1287 N94-16387
KOSTUK, R. K. p 1226 N94-14985
KOSTUK, RAYMOND K. p 1036 N94-14992
p 1198 N94-17360
KOTOWSKI, STEFAN p 1170 N94-17045
KOTULSKI, J. D. p 1034 N94-16452
KOUACHI, SAID p 1171 N94-17640
KOURTIDES, DEMETRIUS A. p 934 N94-15926
KOUSKY, VERNON EDGARD p 1111 N94-15186
KOVACS, GREGORY T. p 1163 N94-14937
KOVALEV, E. E. p 981 N94-16097
KOWALCZYK, K. R. p 988 N94-15693
KOZANECKI, W. p 1190 N94-15854
KOZLOWSKI, ZDZISLAW p 1178 N94-17087
KOZOL, JOSEPH p 962 N94-17418
KRAEMER, J. p 900 N94-15034
KRAMER, BRIAN R. p 856 N94-15677
p 857 N94-15780
KRANBUEHL, DAVID E. p 938 N94-16856
KRANTZ, TIMOTHY L. p 1049 N94-17583
KRASNER, RICHARD D. p 1109 N94-17552
KRASOWSKI, MICHAEL J. p 1034 N94-15961
KRATOCHVIL, J. p 1016 N94-17671
KRAUSE, F. p 1096 N94-17289
KREHBIEL, PAUL p 1004 N94-17364
KREIDER, KEVIN L. p 1177 N94-16497
KRESS, BERNARD p 1196 N94-17347
KREYSA, E. p 904 N94-15056
KRIEGER, IRVIN M. p 951 N94-17210
KRIGE, JOHN p 886 N94-16501
p 1303 N94-16592
p 1225 N94-16593
KRING, DAVID A. p 1244 N94-16328
KRISHNAN, A. p 928 N94-17442
KRIVEN, WALTRAUD M. p 971 N94-16980
KROL, A. p 1209 N94-16447
KROL, ELIZABETH p 1244 N94-16329
KROL, M. p 1014 N94-17375
KRONAUER, RICHARD E. p 1133 N94-17397
KROT, ALEXANDER N. p 1244 N94-16330
KROTZ, PHIL p 1051 N94-16141
KRUGER, C. A. p 1094 N94-15136
KRUGLIKOV, K. L. p 1013 N94-17316
KRUMM, JOHN p 1163 N94-14968

KRUSE, F. A. ..... p 1067 N94-16674
p 1078 N94-16748
p 1080 N94-16758
KRUSE, FRED ..... p 1069 N94-16682
KRUSE, FRED A. ..... p 1073 N94-16704
KRUSIUS, J. P. ..... p 1005 N94-17519
KRUSZKA, LEOPOLD ..... p 1059 N94-16651
p 1061 N94-17086
KRUTZ, ROBERT W., JR. ..... p 1139 N94-17563
p 1139 N94-17564
KUAN, CH. A. ..... p 974 N94-17633
KUBECEK, V. ..... p 913 N94-15565
KUBIAK, C. P. ..... p 950 N94-16912
KUBIAK, G. D. ..... p 1036 N94-17647
KUBICKI, J. D. ..... p 1219 N94-16331
KUBZDELA, HENRYK ..... p 1002 N94-17064
KUCHEROV, RAFAIL Y. ..... p 1206 N94-15107
KUCHTA, DAN ..... p 1191 N94-16128
KUCINSKAS, A. B. ..... p 1276 N94-16332
KUDO, I. ..... p 945 N94-15167
KUEHN, D. M. ..... p 1277 N94-16333
KUHLMANN-WILSDORF, DORIS ..... p 1008 N94-15494
KUHLMANN, WADE D. ..... p 1119 N94-14923
KUI, L. K. ..... p 974 N94-17633
p 974 N94-17634
KUIVALAINEN, PEKKA ..... p 1015 N94-17546
KUKLO, T. J. ..... p 1236 N94-14929
KUKWA, ANDRZEJ ..... p 1177 N94-16650
KULANDER, K. C. ..... p 949 N94-16904
KULKARNI, SURESH B. ..... p 928 N94-17213
KUMAR, ASHOK ..... p 971 N94-17198
KUMAR, JAYANT ..... p 964 N94-15688
KUMAR, PARVEZ ..... p 898 N94-16084
KUMAR, PUNEET ..... p 1141 N94-17115
KUNIMORI, HIROO ..... p 911 N94-15555
KUNK, M. J. ..... p 1104 N94-16334
KUNOW, H. ..... p 874 N94-17143
KUO, S. ..... p 1063 N94-16596
p 1063 N94-16598
KUPPERMAN, D. S. ..... p 1054 N94-16518
KURAMOTO, KIYOSHI ..... p 1277 N94-16335
KUROSAWA, MASANORI ..... p 1104 N94-16336
KURTZ, HELMUT ..... p 928 N94-17308
KURTZ, S. R. ..... p 1208 N94-16012
KUWABATA, SUSUMU ..... p 969 N94-16928
KUZMIN, R. ..... p 1252 N94-16200
KWAN, ROBERT ..... p 1006 N94-17661
KWARK, YOUNG ..... p 1191 N94-16128
KWOK, R. ..... p 1079 N94-16752
p 1079 N94-16753
KYBURG, HENRY E., JR. ..... p 1149 N94-16575
p 1170 N94-16582
KYTOE, MATTI ..... p 974 N94-17547

L

LACAITA, A. ..... p 913 N94-15569
p 914 N94-15570
p 914 N94-15571
LACKEY, W. J. ..... p 936 N94-16569
LACKNER, L. ..... p 981 N94-16096
LADE, POUL V. ..... p 1024 N94-16555
LADISH, J. S. ..... p 1202 N94-16776
p 1013 N94-17318
LAFAVE, NORMAN ..... p 1277 N94-16337
LAFERRIERE, A. ..... p 978 N94-16080
LAGOW, R. J. ..... p 967 N94-16543
LAHEY, R. T., JR. ..... p 1030 N94-17511
LAKSHMANAN, B. ..... p 1027 N94-17127
LAKSO, HANS-AAKE ..... p 1097 N94-17625
LAM, N. ..... p 1065 N94-16604
LAM, W. ..... p 1002 N94-17110
LAMAISON, JACQUES ..... p 878 N94-17157
LAMARRE, JEAN ..... p 955 N94-15149
LAMBERT, JAMES L. ..... p 1190 N94-15933
LAMBROS, JOHN ..... p 1059 N94-16587
LAMOTHE, A. ..... p 894 N94-17172
LAMY, ALAIN ..... p 888 N94-17133
LANCASTER, M. G. ..... p 1278 N94-16338
LANCE, N. ..... p 882 N94-17320
LANDEN, O. L. ..... p 1035 N94-16960
LANDGREBE, D. A. ..... p 1084 N94-16831
LANDHEIM, R. ..... p 1252 N94-16200
LANDHEIM, RAGNHILD ..... p 1278 N94-16339
LANDIS, GEOFFREY A. ..... p 1040 N94-16522
p 1013 N94-17113
LANDIS, WAYNE G. ..... p 1095 N94-15790
LANDRY, J. C. ..... p 954 N94-16340
LANE, DAVID M. ..... p 1005 N94-17498
LANG, BRUNO ..... p 1244 N94-16329
LANG, LARRY ..... p 1225 N94-16473
LANGDON, A. B. ..... p 1205 N94-17670
LANGENHORST, F. ..... p 1219 N94-16341
LANGENHORST, RALF ..... p 1188 N94-15447
LANGER, S. H. ..... p 1205 N94-17663
LANGLOIS, P. ..... p 978 N94-16081
LANKARANI, HAMID M. ..... p 872 N94-17263
LAPORTE, FRANCOIS ..... p 878 N94-17156
LAPPALAINEN, TIMO ..... p 1056 N94-17542
LAPRUS, WLODZIMIERZ ..... p 998 N94-16653
p 1002 N94-17048
LARAR, ALLEN MAURICE ..... p 1102 N94-17214
LARIN, S. A. ..... p 1186 N94-17617
p 1220 N94-17618
LAROSA, G. ..... p 906 N94-15076
LARSON, S. M. ..... p 1278 N94-16342
LARSON, STEVE ..... p 1071 N94-16692
LASALVIA, J. C. ..... p 965 N94-15773
LASKY, JEFFREY A. ..... p 1151 N94-16941
LASLETT, L. J. ..... p 1175 N94-17288
LASSEIGNE, D. GLENN ..... p 1019 N94-15478
LASSEY, K. R. ..... p 1094 N94-15185
LATTANZI, MARIO G. ..... p 1172 N94-15641
LAU, K. Y. ..... p 988 N94-15667
LAU, Y. Y. ..... p 1041 N94-17001
LAUER, H. V., JR. ..... p 1104 N94-16424
LAUER, HOWARD V., JR. ..... p 1275 N94-16327
LAURENT, J. Y. ..... p 903 N94-15052
LAUTENSCHLAGER, UME ..... p 1055 N94-17082
LAUX, LILA F. ..... p 1005 N94-17498
LAVALLE, C. ..... p 1076 N94-16740
LAVE, P. ..... p 979 N94-16083
LAVIOLETTE, MARK ..... p 1223 N94-15682
LAVRENTJEVA, Z. A. ..... p 1244 N94-16345
LAVRUKHINA, A. K. ..... p 1244 N94-16343
p 1244 N94-16344
p 1244 N94-16345
LAW, D. B. ..... p 1006 N94-17565
LAW, DAVID J. ..... p 1132 N94-15762
LAWLER, J. E. ..... p 1207 N94-15955
LAWLESS, KIRBY G. ..... p 1049 N94-16138
LAWRENCE, FREDERICK V. ..... p 1038 N94-15852
LAWRENCE, RONALD ..... p 924 N94-15222
LAWRENCE, TIMOTHY J. ..... p 929 N94-17474
LAXSON, A. ..... p 1093 N94-17668
LE, L. ..... p 1245 N94-16399
LEA, C. S. ..... p 1128 N94-16812
LEAVITT, J. A. ..... p 1226 N94-14984
LEBLANC, THOMAS J. ..... p 1159 N94-16578
LEBOFSKY, LARRY A. ..... p 1222 N94-16346
LEBOFSKY, NANCY R. ..... p 1222 N94-16346
LECHNER, P. ..... p 900 N94-15034
LECKIE, FREDERICK A. ..... p 935 N94-16483
p 935 N94-16484
p 935 N94-16485
p 935 N94-16528
p 935 N94-16529
LEDERMAN, D. ..... p 1184 N94-16838
LEDLEY, B. G. ..... p 1101 N94-16551
LEE, FRED ..... p 883 N94-17111
LEE, H. M. ..... p 1058 N94-15710
LEE, I. ..... p 1029 N94-17384
LEE, J. S. ..... p 1077 N94-16743
LEE, L. ..... p 953 N94-16247
LEE, MARTIN E. ..... p 1096 N94-16589
LEE, PETER ..... p 1147 N94-15725
LEE, PETER C. ..... p 1009 N94-15825
LEE, S. Y. ..... p 1184 N94-16885
LEE, SING H. ..... p 1196 N94-17347
LEE, T. D. ..... p 1187 N94-16170
LEE, YUAN T. ..... p 1181 N94-15995
LEFKOFF, A. B. ..... p 1067 N94-16674
p 1073 N94-16704
p 1080 N94-16758
LEGGETT, P. J. ..... p 987 N94-15644
LEHMANN, F. ..... p 1070 N94-16688
LEHNERT, T. ..... p 907 N94-15078
LEI, JUNTING ..... p 967 N94-16475
LEIGH, CHAROLETTE V. ..... p 1219 N94-14977
LEISKI, DARYL ..... p 981 N94-16098
LELEUX, TODD ..... p 870 N94-15532
LEMAL, DAVID M. ..... p 929 N94-15734
LEMIEUX, HENRY F. ..... p 896 N94-17187
LEMIRE, GEORGE W. ..... p 942 N94-14946
p 951 N94-17203
LEMKE, D. ..... p 904 N94-15059
p 907 N94-15082
p 909 N94-15092
p 910 N94-15099
LEMKE, S. ..... p 908 N94-15083
LEMOINE, F. G. ..... p 1279 N94-16347
LEMPICKI, A. ..... p 948 N94-16771
LENARDIC, A. ..... p 1279 N94-16348
p 1104 N94-16349
LENEINDRE, B. ..... p 944 N94-15164
LENKKERI, JAAKKO ..... p 1015 N94-17546
LENSKE, H. ..... p 1181 N94-16013
LEONARD, ANTHONY ..... p 861 N94-17580
LEONARD, GREGORY J. ..... p 1280 N94-16350
LEONE, STEPHEN R. ..... p 1215 N94-17422
LEOTIN, J. ..... p 902 N94-15047
p 902 N94-15048
p 908 N94-15087
LEPRIEUR, C. ..... p 1070 N94-16691
LESAUTER, JOSEPH ..... p 1121 N94-15660
LESSER, BARBARA ..... p 1232 N94-17101
LESTHIEVENT, G. ..... p 889 N94-17136
LETOAN, T. ..... p 1068 N94-16681
p 1076 N94-16737
LETOAN, THUY ..... p 991 N94-15897
LETTS, S. ..... p 1204 N94-17237
LETTS, S. A. ..... p 966 N94-15924
LEUTE, FRANK A., IV ..... p 1109 N94-17573
LEUTENEGGER, SCOTT T. ..... p 1149 N94-15989
LEV, BRIAN S. ..... p 1228 N94-15116
LEVAK, DANIEL ..... p 927 N94-17096
p 927 N94-17097
p 927 N94-17098
LEVANDOWSKI, D. W. ..... p 1064 N94-16602
LEVENBERRY, L. ..... p 973 N94-17408
LEVIN, B. F. ..... p 970 N94-16959
LEVINE, ARLENE S. ..... p 1303 N94-16495
LEVINE, DANIEL A. ..... p 1097 N94-17426
LEVINE, MURRAY ..... p 1111 N94-15139
LEVINE, R. ..... p 1129 N94-17374
LEVISON, H. F. ..... p 1280 N94-16351
LEVIT, R. ..... p 938 N94-16854
LEVITON, DOUGLAS B. ..... p 1147 N94-15703
p 1189 N94-15705
p 1148 N94-15943
LEVY, E. H. ..... p 1244 N94-16352
LEVY, JAMES J. ..... p 1188 N94-14940
LEVY, M. ..... p 965 N94-15859
LEVY, SAUL ..... p 1154 N94-17390
LEVY, YANNICK ..... p 997 N94-16507
LEWIS, C. F. ..... p 1241 N94-16213
LEWIS, D. K. ..... p 1177 N94-16448
LEWIS, E. E. ..... p 1150 N94-16594
LEWIS, J. R. ..... p 1151 N94-16902
LEWIS, ROY S. ..... p 954 N94-16353
LEYVA, IVETT A. ..... p 1281 N94-16354
LI, F. K. ..... p 1079 N94-16752
LI, G. X. ..... p 1202 N94-16162
LI, G. Y. ..... p 1101 N94-15815
LI, H. ..... p 911 N94-15554
p 874 N94-15589
LI, L. ..... p 1226 N94-14987
LI, SHENG ..... p 1191 N94-16126
LI, SHENG S. ..... p 1214 N94-17272
LI, W. ..... p 1199 N94-14986
LI, WEIQUAN ..... p 1199 N94-14993
LI, XIAO-PING ..... p 1211 N94-16827
LI, Y. ..... p 961 N94-17109
LIANG, WENBIN ..... p 967 N94-16475
LIAO, HANS H. ..... p 1117 N94-16514
LIAW, BOR Y. ..... p 1092 N94-16567
LIAW, YOON ..... p 1051 N94-16141
LIBBY, WILLIAM A. ..... p 874 N94-17010
LIBRANT, ZDZISLAW ..... p 969 N94-16924
LIDIARD, K. A. ..... p 908 N94-15088
LIEBERT, CURT H. ..... p 1033 N94-15928
LIGGIERI, L. ..... p 943 N94-15158
LIMAGNE, D. ..... p 900 N94-15032
LIN-LIU, Y. R. ..... p 1203 N94-16816
p 1203 N94-16823
LIN, C. L. ..... p 947 N94-15861
LIN, C. S. ..... p 1046 N94-15817
LIN, FANGLIANG ..... p 952 N94-17302
LIN, H. T. ..... p 966 N94-16018
LIN, M. C. ..... p 942 N94-14956
p 1182 N94-16111
LIN, S. P. ..... p 1021 N94-15770
LIN, YING-CHI ..... p 904 N94-15061
LIN, Z. ..... p 1226 N94-14984
LINDAU, I. ..... p 1208 N94-16062
LINDEN, DEREK S. ..... p 1013 N94-17104
LINDNER, F. ..... p 946 N94-15172
LINDSAY, DON ..... p 1163 N94-14953
LINDSAY, GEOFFREY ..... p 969 N94-16920
LINDSTROM, D. J. ..... p 1244 N94-16355
LINDSTROM, MARILYN M. ..... p 1222 N94-16356
LINDSTROM, ROBERT E. ..... p 928 N94-17213
LINEHAN, J. C. ..... p 940 N94-17235
LINK, R. E. ..... p 962 N94-17464
LINK, Y. Y. ..... p 872 N94-15856
LINKIN, V. ..... p 1273 N94-16312
LINLIU, Y. R. ..... p 1202 N94-16803
LINTON, P. D. ..... p 1158 N94-15492
LINTON, RICHARD W. ..... p 964 N94-15729
LIOU, MENG-SING ..... p 1028 N94-17258
LIPFERT, F. W. ..... p 1095 N94-15940
LIPPENS, C. ..... p 923 N94-17592
LIPPNER, G. ..... p 874 N94-17143
p 894 N94-17171
LIPSCHUTZ, M. ..... p 1245 N94-16409
LISSENDEN, C. J. ..... p 930 N94-15106
LITTERMAN, R. L. ..... p 1208 N94-15982
LITVINSKIJ, L. L. ..... p 1179 N94-14932

LIU, C. T. ..... p 955 N94-15830
p 955 N94-15862
p 1208 N94-16063
LIU, CHAOQUN ..... p 1030 N94-17557
LIU, CHENG ..... p 1059 N94-16587
LIU, HUA-KUANG ..... p 1165 N94-15958
LIU, JANE ..... p 1169 N94-15779
LIU, JIWEN ..... p 1181 N94-15752
p 1021 N94-15795
LIU, K. C. ..... p 967 N94-16067
p 968 N94-16813
LIU, P. K. T. ..... p 947 N94-15861
LIU, S. H. ..... p 1211 N94-16839
LIU, Y. G. ..... p 1244 N94-16357
LIU, Y.-G ..... p 1104 N94-16358
LIU, Y.-G. ..... p 1244 N94-16359
p 1104 N94-16360
LIU, ZHEN ..... p 1164 N94-15695
LIU, ZHINING ..... p 1030 N94-17557
LIVINGSTON, J. D. ..... p 960 N94-16972
LIVNE, HILLEL ..... p 1180 N94-15283
LJUL, A. YU. ..... p 1244 N94-16345
LLAREUS, JEAN-HENRI ..... p 878 N94-17157
LLORENS, JEAN-CLAUDE ..... p 893 N94-17166
LO, E. ..... p 1252 N94-16198
LOBAO, X. ..... p 895 N94-17177
LOCKWOOD, S. J. ..... p 1015 N94-17648
LOEHBERG, K. ..... p 945 N94-15170
LOEKEN, TH. ..... p 1244 N94-16361
LOFGREN, G. E. ..... p 954 N94-16313
LOFGREN, GARY E. ..... p 874 N94-16362
p 1244 N94-16363
LOFTIN, HERMAN E. ..... p 1237 N94-17225
LOGUE, JAMES ..... p 1195 N94-17344
LOHR, J. ..... p 1202 N94-16803
p 1203 N94-16816
LOMATCH, S. ..... p 908 N94-15089
LOMBARDO, D. C. ..... p 866 N94-15651
LOMBARDO, L. ..... p 906 N94-15076
LONG, CHARLES E. ..... p 1114 N94-17497
LONG, FRED J. E. ..... p 1159 N94-15796
LONG, J. V. P. ..... p 1103 N94-16203
LONG, W. E., JR. ..... p 1119 N94-14916
LONGDON, N. ..... p 1303 N94-16792
LONGDON, NORMAN ..... p 987 N94-15644
p 1150 N94-16591
LONGHI, J. ..... p 1283 N94-16364
p 1104 N94-16365
LONGTIN, DAVID R. ..... p 1003 N94-17268
LOOS, ALFRED C. ..... p 964 N94-15656
p 938 N94-16856
LOPES-GAUTIER, R. ..... p 1283 N94-16366
LORANS, DOMINIQUE ..... p 909 N94-15091
LORD, J. D. ..... p 1057 N94-15021
LORENZ, JENS ..... p 1029 N94-17448
LORENZEN, CLAUS-JUERGEN ..... p 984 N94-16005
LOUET, JACQUES ..... p 990 N94-15888
p 898 N94-15892
p 992 N94-15907
LOVE, S. G. ..... p 1244 N94-16367
LOVELESS, MARTIN J. ..... p 1102 N94-17493
LOVELL, AMY J. ..... p 1283 N94-16368
LOWDEN, R. A. ..... p 934 N94-16008
p 934 N94-16065
p 935 N94-16461
LOWE, DAVID M. ..... p 934 N94-15926
LOWNDES, D. H. ..... p 1207 N94-15829
p 1040 N94-16663
p 1040 N94-16664
LOY, LUKE W. ..... p 1047 N94-16531
p 1048 N94-16915
LOZANO, A. ..... p 1150 N94-16579
LU, JUN ..... p 1129 N94-17478
LU, PING ..... p 867 N94-16498
LU, S.-T. ..... p 1134 N94-17535
LU, WEN-HU ..... p 913 N94-15566
p 877 N94-15605
LU, YU ..... p 1215 N94-17437
LUBECK, O. ..... p 1162 N94-17646
LUCAS, G. ..... p 908 N94-15087
LUCCHITTA, B. K. ..... p 1283 N94-16369
LUCE, T. C. ..... p 1202 N94-16803
p 1203 N94-16816
LUCEY, P. G. ..... p 1258 N94-16225
LUCEY, PAUL G. ..... p 1086 N94-16370
p 1284 N94-16371
p 954 N94-16372
LUCK, J. M. ..... p 1242 N94-16272
LUCK, JOHN M. ..... p 877 N94-15602
LUCKEVICH, L. M. ..... p 979 N94-16088
LUCOT, JAMES B. ..... p 1118 N94-17090
LUEBKE-OSSENBECK, B. ..... p 895 N94-17180
LUEDTKE, JACQUELINE R. ..... p 1222 N94-17261
LUGMAIR, GUENTER W. ..... p 1241 N94-16190
LUHR, JAMES ..... p 1103 N94-16214
LUHRS, CARO ELISE ..... p 1127 N94-16645
LUINGE, W. ..... p 908 N94-15084
LUKEMIRE, ALAN T. ..... p 1010 N94-15874
LUND, GLENN ..... p 916 N94-15585
p 921 N94-15615
LUND, NIELS ..... p 904 N94-15057
LUND, SOERN W. ..... p 1105 N94-14938
LUNDBLAD, WAYNE E. ..... p 928 N94-17124
LUNINE, J. I. ..... p 1284 N94-16373
LUPO, CHRISTIAN ..... p 1046 N94-15707
LURIE, PHILIP M. ..... p 1235 N94-16988
LUTSENKO, I. V. ..... p 1220 N94-17315
LUTTERMOSER, DONALD G. ..... p 1240 N94-17094
LUTTGES, MARVIN ..... p 855 N94-14959
LUTTON, MARK J. ..... p 859 N94-16798
LUTZ, A. J. ..... p 1096 N94-16825
LUTZ, G. ..... p 900 N94-15034
LYKASOV, G. I. ..... p 1185 N94-17312
LYKINS, CRAIG ..... p 1052 N94-16147
LYNCH, GARY ..... p 1133 N94-17453
LYONS, L. R. ..... p 1098 N94-15433

M

MA, KWAN-LIU ..... p 1148 N94-15965
MA, L. ..... p 1182 N94-16111
MA, Y. ..... p 940 N94-17235
MAAG, ANDREW J. ..... p 899 N94-16374
MAAG, CARL R. ..... p 899 N94-16374
MACCACARO, TOMMASO ..... p 1240 N94-17591
MACDONALD, D. D. ..... p 956 N94-15998
MACDONALD, V. W. ..... p 1123 N94-16565
MACDOUGALL, B. ..... p 947 N94-16011
MACHADO, M. E. ..... p 1299 N94-17089
MACKAY, G. ..... p 980 N94-16092
MACKE, H. C. ..... p 1033 N94-15826
MACKENZIE, ANNE I. ..... p 986 N94-15140
MACKENZIE, JAMES C. ..... p 1050 N94-16135
MACKIE, WILLIAM A. ..... p 1206 N94-15107
MADARAS, ERIC IRVINE ..... p 933 N94-15878
MADDEN, DANIEL ..... p 888 N94-16990
MADNIA, C. K. ..... p 1018 N94-15427
MADSEN, M. B. ..... p 1285 N94-16375
MADSEN, N. K. ..... p 1039 N94-16054
MADSEN, SOREN N. ..... p 1078 N94-16749
MAEDER, HANS FRIEDRICH ..... p 984 N94-16004
MAGAKYAN, A. D. ..... p 1220 N94-17315
MAGLIC, S. R. ..... p 908 N94-15089
MAGRAW, J. E. ..... p 908 N94-15088
MAGRUDER, R. H., III ..... p 965 N94-15828
MAGUIRE, H. ..... p 948 N94-16553
MAHAFFEY, W. A. ..... p 872 N94-17405
p 873 N94-17569
MAHAFFEY, W.A. ..... p 873 N94-17432
p 873 N94-17508
MAHALE, ANANT D. ..... p 939 N94-16858
MAHALINGAM, SHANKAR ..... p 925 N94-16482
MAHLE, CHRISTOPH E. ..... p 1006 N94-17661
MAILLOT, P. ..... p 953 N94-17649
MAISH, A. B. ..... p 1091 N94-15984
MAIT, JOSEPH N. ..... p 1195 N94-17338
MAKALKIN, A. B. ..... p 1244 N94-16377
MAKER, PAUL D. ..... p 1034 N94-15987
p 1037 N94-17348
MAKJAVIC, IGOR ..... p 981 N94-16098
MAKOWSKI, HENRYK ..... p 1013 N94-17071
MALAGUTI, G. ..... p 899 N94-15029
MALCOLM, GERALD N. ..... p 855 N94-15655
p 856 N94-15677
p 857 N94-15720
p 857 N94-15780
MALCUIT, ROBERT J. ..... p 1245 N94-16378
MALHOTRA, RENU ..... p 1245 N94-16379
MALIK, M. R. ..... p 1021 N94-15834
MALIN, MICHAEL C. ..... p 1285 N94-16380
MALITSON, PAUL ..... p 922 N94-15622
MALLIER, R. ..... p 1021 N94-15751
MALONE, JOHN B. ..... p 1062 N94-17479
MANCINI, MARCO ..... p 1083 N94-16031
MANGINO, S. ..... p 1097 N94-14960
MANHEIMER, WALLACE M. ..... p 998 N94-16535
MANLEY, CURTIS R. ..... p 1286 N94-16381
MANNA, ZOHAR ..... p 1149 N94-16554
MANNING, ROGER ..... p 1143 N94-15022
MANSON, STEVEN T. ..... p 1181 N94-15774
MANSURIPUR, M. ..... p 1226 N94-14983
p 1227 N94-14989
p 1227 N94-14990
p 1227 N94-14991
MANZO, G. ..... p 906 N94-15076
MARAL, GERARD ..... p 875 N94-17134
p 889 N94-17135
MARANGONI, G. ..... p 903 N94-15050
p 910 N94-15100
MARCAULT, J. ..... p 923 N94-17592
MARCHELLO, J. M. ..... p 932 N94-15276
p 933 N94-15277
MARCHELLO, JOSEPH M. ..... p 932 N94-15275
MARCHENKOV, K. I. ..... p 1286 N94-16382
MARDER, A. R. ..... p 970 N94-16959
MARGERY, M. ..... p 889 N94-17136
MARGOLIS, JACK ..... p 1074 N94-16712
MARGOLIS, JACK S. ..... p 1037 N94-16667
MARION, F. ..... p 903 N94-15052
MARKATOS, EVANGELOS P. ..... p 1159 N94-16578
MARKIN, KELLY ..... p 864 N94-16906
MARKS, T. J. ..... p 1191 N94-16454
MARKUS, LISA R. ..... p 1169 N94-16127
MARLEY, J. ..... p 1197 N94-17351
MARMORINO, G. O. ..... p 1077 N94-16743
MARQUART, E. J. ..... p 1048 N94-17462
MARQUEZ, NICHOLAS ..... p 1056 N94-14945
MARRERO, WILFREDO ..... p 1155 N94-17398
MARRON, JOSEPH C. ..... p 1196 N94-17345
MARSH, D. ..... p 901 N94-15037
MARSHALL, ALBERT H. ..... p 1191 N94-16547
MARTEL, FRANCOIS ..... p 896 N94-17185
MARTI, K. ..... p 1187 N94-16194
p 1243 N94-16317
MARTI, KURT ..... p 954 N94-16314
MARTIN, C. P. ..... p 1220 N94-17602
MARTIN, CHARLES R. ..... p 967 N94-16475
p 969 N94-16928
MARTIN, J. E. ..... p 908 N94-15085
MARTIN, JAN ..... p 1078 N94-16749
MARTIN, M. ..... p 1234 N94-16209
MARTIN, R. A. ..... p 1037 N94-16426
MARTIN, TERRY Z. ..... p 1256 N94-16217
MARTINEC, E. J. ..... p 1187 N94-16116
MARTINELL, J. S. ..... p 926 N94-16773
MARTINEZ, I. ..... p 954 N94-16383
MARTINEZ, R. R. ..... p 1244 N94-16355
MARTINSON, DOUGLAS G. ..... p 1112 N94-15680
MARTY, G. ..... p 1068 N94-16681
MARZARI, F. ..... p 1245 N94-16384
MASARIK, J. ..... p 1245 N94-16409
MASARIK, JOZEF ..... p 1245 N94-16385
MASCI, ENRICO ..... p 878 N94-17138
MASEK, J. ..... p 910 N94-15098
MASERJIAN, JOSEPH ..... p 1014 N94-17324
MASLANIK, JAMES ..... p 1112 N94-15701
MASLOWE, S. A. ..... p 1021 N94-15751
MASSMANN, FRANZ-HEINRICH ..... p 911 N94-15554
p 874 N94-15589
MASTERS, JOHN E. ..... p 939 N94-16862
MASTERS, STEPHEN ..... p 1145 N94-15629
MATHEZ, E. ..... p 1101 N94-16840
MATHIAS, KARL S. ..... p 1154 N94-17366
MATSON, D. L. ..... p 1245 N94-16386
MATSON, D. W. ..... p 940 N94-17235
MATSUDA, K. ..... p 1203 N94-16816
MATSUI, M. ..... p 892 N94-17160
MATSUI, TAKAFUMI ..... p 1277 N94-16335
MATSUNAGA, TSUNEO ..... p 1064 N94-16601
MATSUSHIMA, K. ..... p 1287 N94-16387
MATSUZAKI, H. ..... p 1243 N94-16291
p 1245 N94-16388
MATTHEWS, R. B. ..... p 923 N94-15118
MATTHEWS, ROBIN A. ..... p 1095 N94-15790
MATTIKALI, RAJU ..... p 1164 N94-15756
MATTIKALLI, RAJU ..... p 1143 N94-15212
MATTOON, JOSEPH S. ..... p 872 N94-17403
MAUEL, M. E. ..... p 1202 N94-16446
MAUPIN, G. D. ..... p 961 N94-17234
MAURER, N. O. ..... p 959 N94-16780
MAURICE, MARK S. ..... p 861 N94-17609
MAX, C. E. ..... p 1237 N94-16872
MAY, G. B. ..... p 960 N94-17041
MAYDAN, DROR E. ..... p 1162 N94-17550
MAYEDA, T. K. ..... p 1270 N94-16295
p 1245 N94-16389
MAYER, CHARLES E. ..... p 995 N94-16040
MAYES, PAUL ..... p 986 N94-14998
p 1005 N94-17431
MAZIASZ, P. J. ..... p 957 N94-16068
p 957 N94-16106
MAZZEGA, P. ..... p 1100 N94-15811
MCAFEE, W. J. ..... p 1059 N94-16104
MCALISTER, K. W. ..... p 856 N94-15657
MCALLISTER, DAVID F. ..... p 1143 N94-15114
MCANDREWS, DONALD R. ..... p 1154 N94-17396
MCBRIDE, BONNIE J. ..... p 1220 N94-17624
MCBRYAN, OLIVER A. ..... p 1159 N94-15849
MCCALDEN, A. J. ..... p 908 N94-15086
MCCAMMON, D. ..... p 899 N94-15027
MCCANNA, JASON ..... p 886 N94-15935
MCCARTHY, J. J. ..... p 1279 N94-16347
MCCLELLAN, NANCY J. ..... p 1152 N94-16974
MCCOLLUMS, D. ..... p 918 N94-15596
MCCONNELL, ROBERT L. ..... p 1164 N94-15704
MCCORD, T. ..... p 1259 N94-16229
MCCORMACK, ROBERT T. ..... p 1191 N94-16547
MCCORMICK, A. V. ..... p 962 N94-14914
p 962 N94-14921

	p 963	N94-15179
	p 963	N94-15490
	p 963	N94-15631
	p 964	N94-15683
	p 965	N94-15843
MCCORMICK, C.	p 971	N94-16999
MCCORMICK, R. L.	p 949	N94-16897
MCCOY, T. J.	p 1243	N94-16305
	p 1245	N94-16389
	p 1245	N94-16390
MCCOYD, GERALD	p 1155	N94-17411
MCCREADY, D. E.	p 961	N94-17234
MCDONALD, J. S.	p 1250	N94-16185
MCDONALD, KYLE C.	p 993	N94-15914
	p 1075	N94-16734
MCDONNELL, J. A. M.	p 1245	N94-16391
MCDOWELL, VAUGHN P.	p 1040	N94-16540
MCEACHERN, R.	p 966	N94-15924
MCEVILLY, T. V.	p 1102	N94-17252
MCEWEN, A.	p 1258	N94-16228
	p 1259	N94-16229
MCEWEN, A. S.	p 1252	N94-16199
	p 1288	N94-16392
	p 1288	N94-16394
	p 1288	N94-16395
MCEWEN, ALFRED S.	p 1288	N94-16393
MCEWEN, M. R.	p 1031	N94-15018
MCGARITY, JOHN O.	p 882	N94-16530
	p 897	N94-17240
MCGARRY, JAN F.	p 915	N94-15581
	p 918	N94-15595
	p 920	N94-15614
	p 922	N94-15625
MCGEE, J. J.	p 1104	N94-16334
MCGEE, WILLIAM F.	p 1047	N94-15949
MCGEOCH, MALCOLM W.	p 1042	N94-17230
MCGILL, GEORGE E.	p 1283	N94-16368
MCGINNIS, TIMOTHY A.	p 1033	N94-15884
MCGONIGAL, M.	p 948	N94-16553
MCGOVERN, PATRICK J.	p 1104	N94-16396
MCGOWAN, DAVID M.	p 1061	N94-17259
MCGRATH, DANIEL T.	p 1002	N94-17196
MCGREGOR, TERRY L.	p 1231	N94-16499
MCGUIRK, J. J.	p 1020	N94-15645
MCHARGUE, C. J.	p 1206	N94-14925
MCILHAGGER, R.	p 937	N94-16850
MCINTYRE, L. C., JR.	p 1226	N94-14984
MCINVILLE, ROY M.	p 1020	N94-15632
MCKAMEY, C. G.	p 957	N94-16165
MCKAY, D. S.	p 1243	N94-16309
MCKAY, DAVID S.	p 1289	N94-16397
	p 1289	N94-16398
MCKAY, G.	p 1245	N94-16399
	p 1245	N94-16400
MCKAY, G. A.	p 1103	N94-16285
MCKAY, GORDON	p 1245	N94-16410
MCKECHNIE, TIMOTHY	p 1051	N94-16141
MCKISSOCK, DAVID B.	p 929	N94-17483
MCLAUGHLIN, J. C.	p 934	N94-16008
MCLAUGHLIN, P.	p 937	N94-16850
MCLEAN, SEAN A.	p 1130	N94-17554
MCMANUS, HUGH L.	p 941	N94-17295
MCMILLAN, J. C.	p 864	N94-16457
MCMILLAN, W. I.	p 905	N94-15065
MCNALLY, J.	p 898	N94-15893
MCQUEEN, R. G.	p 1178	N94-16955
MCSWEEN, H. Y., JR.	p 1241	N94-16205
	p 1242	N94-16224
MEAD, JAMES B.	p 1111	N94-15134
MEAD, JOEY L.	p 930	N94-14999
MEEKER, G. P.	p 954	N94-16401
MEEKS, G.	p 1063	N94-16596
MEEKS, HOWARD	p 1000	N94-16965
MEGER, ROBERT A.	p 998	N94-16535
MEHNE, MICHAEL	p 1008	N94-15448
MEHTA, GOPAL K.	p 976	N94-16146
MEIER, H.	p 987	N94-15644
MEINEN, CHRISTOPHER	p 1112	N94-15844
MEISEL, L. V.	p 961	N94-17106
MELACK, JOHN M.	p 1069	N94-16684
	p 1076	N94-16735
	p 1076	N94-16739
MELCHIOR, P.	p 1099	N94-15801
	p 1100	N94-15809
	p 1100	N94-15813
	p 1101	N94-15814
MELENDREZ, D. E.	p 1278	N94-16342
MELIUS, C.	p 953	N94-17660
MELLON, MICHAEL T.	p 1290	N94-16402
	p 1290	N94-16403
MELOSH, H. JAY	p 1290	N94-16404
MELSHEIMER, FRANK M.	p 918	N94-15598
MENDELL, W. W.	p 1290	N94-16405
MENENTI, M.	p 1085	N94-17616
MENG, TERESA H.-Y.	p 1160	N94-16791
MENG, W.	p 1176	N94-17658
MENISSIER-MORAIN, VALERIE	p 1142	N94-14979
MENY, C.	p 902	N94-15047
	p 902	N94-15048
	p 908	N94-15087
MENYUK, C. R.	p 1191	N94-16007
MENZEL, PAUL	p 1107	N94-16717
MERCER, CLIFFORD W.	p 1158	N94-15745
MERENYI, E.	p 1291	N94-16406
MERIGAN, WILLIAM H.	p 1133	N94-17020
MERISON, RUDOLF J. W.	p 854	N94-15128
MERLET, JOSEPH	p 896	N94-17189
MERLINO, DONALD H.	p 1055	N94-17194
MESHISHNEK, M. J.	p 885	N94-15749
	p 951	N94-17207
MESLAND, DICK	p 874	N94-16584
MESSER-YARON, H.	p 1147	N94-15772
METZGER, STEPHEN M.	p 1086	N94-16407
MEYER, CHARLES	p 1291	N94-16408
MEYER, DAVID M.	p 1237	N94-16833
MEYER, DONALD A.	p 884	N94-15147
MEYER, THOMAS J.	p 964	N94-15729
MEYERS, M. A.	p 965	N94-15773
MICHAELS, GREGORY	p 1298	N94-17654
MICHAELSON, DENNIS	p 980	N94-16091
MICHALUK, CHRISTOPHER A.	p 959	N94-16764
MICHAUD, RACHEL A.	p 930	N94-14999
MICHELOTTI, L.	p 1168	N94-14928
MICHELS, H. H.	p 1186	N94-17536
MICHELSON, P. F.	p 904	N94-15061
MICHLOVICH, E.	p 1245	N94-16409
MIDDEL, BURKHARD	p 1098	N94-15153
MIDDLETON, R.	p 1242	N94-16240
MIKHAILOV, PETR Y.	p 938	N94-16853
MIKKELSEN, TORBEN	p 1105	N94-14938
MIKOLAJEWICZ, U.	p 1096	N94-16802
MIKOUCHI, TAKASHI	p 1245	N94-16410
MILATOS, GERASIMOS D.	p 1001	N94-17035
MILLAR, PAMELA S.	p 920	N94-15614
MILLER, C. D.	p 861	N94-17609
MILLER, DENNIS J.	p 1185	N94-17365
MILLER, J.	p 1188	N94-17672
MILLER, J. S.	p 1292	N94-16411
MILLER, JAMES G.	p 931	N94-15190
MILLER, M. K.	p 957	N94-16015
	p 957	N94-16103
MILLER, SUSANNE H.	p 1065	N94-16605
MILLER, WILLIAM V.	p 1167	N94-17392
MILLONAS, M. M.	p 1220	N94-16956
MILLS, A. F.	p 1024	N94-16491
MILLS, DIANE G.	p 997	N94-16507
MILLS, FRANKLIN	p 1064	N94-16600
MILONNI, P. W.	p 1192	N94-16953
MILOSAVLJEVIC, A.	p 1150	N94-16659
MILSTER, T.	p 1199	N94-14986
MILSTER, T. D.	p 1199	N94-14993
	p 1043	N94-14994
MILSTER, TOM D.	p 1199	N94-14995
	p 1199	N94-14996
MIN, J. B.	p 1058	N94-15534
MINECK, RAYMOND E.	p 859	N94-16574
MINER, BARBARA D.	p 1109	N94-17492
MINER, GILDA A.	p 1042	N94-17285
MINER, PAUL S.	p 1161	N94-17449
MING, Z. H.	p 1209	N94-16447
MINI, S.	p 1208	N94-16058
MINOTT, PETER O.	p 884	N94-15193
MINSTER, OLIVIER	p 943	N94-15157
	p 874	N94-16584
MIRIYALA, KANTH	p 1166	N94-16770
MIRONOV, N. T.	p 915	N94-15576
MISAWA, KEIJI	p 1245	N94-16412
MISHRA, UMESH	p 1014	N94-17410
MISTREE, FARROKH	p 1055	N94-17082
MITCHELL, ANTHONY M.	p 871	N94-17412
MITCHELL, CHRISTINE M.	p 1140	N94-16716
MITCHELL, DARREN	p 899	N94-16101
MITCHELL, J. B.	p 1037	N94-15145
MITCHELL, J. F.	p 1208	N94-15982
MITTELMAN, JEFF	p 987	N94-15439
MITTLEFEHLDT, DAVID W.	p 1243	N94-16286
	p 1245	N94-16413
	p 1246	N94-16414
MIURA, R.	p 892	N94-17160
MIURA, Y.	p 1246	N94-16415
MIYAMOTO, M.	p 1245	N94-16400
	p 1104	N94-16416
MIYAMOTO, MASAMICHI	p 1245	N94-16410
MIYAZAKI, K.	p 892	N94-17160
MO, CHARLES T.	p 988	N94-15668
MOCCIA, A.	p 1078	N94-16750
MOELLER, C. P.	p 1203	N94-16816
MOERSCH, J.	p 1252	N94-16201
MOHARAM, M. G.	p 1194	N94-17336
MOHLMADSEN, M.	p 900	N94-15030
MOIN, PARVIZ	p 1025	N94-16908
	p 1028	N94-17286
MOLENDI, SILVANO	p 1240	N94-17591
MOLER, JEFFREY L.	p 930	N94-17192
MOLIN, G. M.	p 1246	N94-16417
MOLODENSKY, S. M.	p 1101	N94-15815
MONACO, LISA A.	p 1206	N94-15476
MONACOS, STEVE P.	p 1161	N94-17328
	p 1161	N94-17330
MONEY, K.	p 980	N94-16093
	p 981	N94-16096
MONSON, R.	p 898	N94-15903
MONTGOMERY, F.	p 972	N94-17242
MONTGOMERY, J. A., JR.	p 947	N94-15977
MOOK, DEAN T.	p 871	N94-16107
MOORE, FRANK G.	p 1020	N94-15632
MOORE, H. J.	p 1293	N94-16418
MOORE, J.	p 1162	N94-17646
MOORE, J. F.	p 974	N94-17676
MOORE, JEFFREY M.	p 1293	N94-16419
MOORE, JOHN W.	p 1232	N94-16977
MOORE, L. G.	p 905	N94-15065
MOORE, M.	p 1219	N94-16420
MOORHEAD, JANE N.	p 999	N94-16777
MORALES, ALBERTO	p 937	N94-16849
MORAN, SCOTT J.	p 897	N94-17240
MORELAND, ROBERT	p 925	N94-16496
MORELIERE, M.	p 896	N94-17186
MORESI, LOUIS	p 1293	N94-16421
MORGAN, H. F.	p 1274	N94-16319
	p 1274	N94-16320
MORGAN, M. A.	p 897	N94-17240
MORGAN, S. H.	p 965	N94-15828
MORI, HIROSHI	p 1245	N94-16410
MORI, N.	p 1212	N94-16868
MOROZ, L. V.	p 1246	N94-16422
MOROZ, V. I.	p 1294	N94-16423
MORRIN, KEVIN A.	p 1132	N94-15762
MORRIS, G. MICHAEL	p 1194	N94-17334
	p 1194	N94-17337
MORRIS, JAMES E.	p 1197	N94-17356
MORRIS, P. J.	p 1028	N94-17276
MORRIS, R. V.	p 1249	N94-16182
	p 1104	N94-16424
MORRIS, RICHARD V.	p 1275	N94-16327
MORRISON, DENNIS R.	p 1117	N94-15967
MORRISON, P. J.	p 1174	N94-16820
MORROW, GEORGE	p 1012	N94-17062
MORROW, H.	p 1197	N94-17350
MORSE, A.	p 1103	N94-16203
MORSE, A. D.	p 1246	N94-16425
MORSE, J. G.	p 1094	N94-15136
MORTIMER, A.	p 981	N94-16097
MOSELEY, S. H.	p 899	N94-15027
MOSHER, TODD	p 878	N94-16148
MOSHIER, WILLIAM C.	p 958	N94-16486
MOSS, C. E.	p 1037	N94-16426
MOSS, FRANK	p 1117	N94-15662
MOSS, JAMES N.	p 1018	N94-15291
MOTAMEDI, M. E.	p 1045	N94-17357
MOTZ, R.	p 877	N94-15610
	p 877	N94-15611
	p 877	N94-15612
MOUCH, THOMAS N.	p 860	N94-17074
MOUGIN, E.	p 1068	N94-16681
MOUGINIS-MARK, PETER	p 1295	N94-16427
MOURA, ANTONIO DIVINO	p 1111	N94-15186
MOURAIN, JEAN	p 1229	N94-15437
MOUSSA, K.	p 971	N94-16994
MOUSTAKAS, THEODORE D.	p 1212	N94-16992
MROZ, E.	p 949	N94-16876
MU, R.	p 965	N94-15828
MUCCIO, ANTHONY B.	p 1054	N94-16153
MUELLER, A.	p 1070	N94-16688
MUELLER, E.	p 1237	N94-17629
MUELLER, J.	p 876	N94-15600
MUELLER, R. E.	p 977	N94-16077
MULHOLLAND, J. DERRAL	p 891	N94-17148
MULHOLLAND, JOHN	p 925	N94-16496
MULJADI, E.	p 1010	N94-15971
MULLANEY, J. L.	p 1157	N94-17588
MULLER, C.	p 923	N94-17592
MULLER, R. E.	p 1037	N94-17348
MULLER, RICHARD E.	p 1034	N94-15987
MULLIN, J. B.	p 1015	N94-17570
MUMMERT, LILY B.	p 1141	N94-17115
MUNDHENK, M.	p 1150	N94-16579
MURALI, A. V.	p 1295	N94-16428
MURALI, C. G.	p 1042	N94-17630
MURANAKA, N.	p 892	N94-17160
MURAYAMA, C.	p 1212	N94-16868
MURCHIE, S. L.	p 1296	N94-16436
MURCHIE, SCOTT	p 1295	N94-16429
	p 1295	N94-16430
	p 1295	N94-16431
MURDOCCA, MILES	p 1154	N94-17390
MURER, CH.	p 954	N94-16432
MURLEY, I.	p 979	N94-16083

MURMAN, EARLL M. ..... p 1026 N94-16966
MURPHY, D. L. ..... p 1239 N94-16433
MURPHY, J. G. ..... p 981 N94-16099
MURPHY, JAMES R. ..... p 1296 N94-16434
MURRAY, A. ..... p 902 N94-15047
p 906 N94-15073
MURRAY, A. G. ..... p 902 N94-15048
p 907 N94-15077
MURRAY, J. ..... p 1011 N94-16661
MURRAY, TERRENCE J. ..... p 1000 N94-16979
MURRAY, W. ..... p 1149 N94-16120
MURRI, DANIEL G. ..... p 859 N94-16573
MURTY, S. V. S. ..... p 1246 N94-16435
MURUGESH, L. ..... p 961 N94-17223
MUSCETTOLA, NICOLA ..... p 1222 N94-15213
MUSTARD, J. ..... p 1259 N94-16234
MUSTARD, J. F. ..... p 1296 N94-16436
p 1067 N94-16675
MUSTARD, JOHN ..... p 1259 N94-16231
p 1295 N94-16430
p 1295 N94-16431
MUSTARD, JOHN F. ..... p 1086 N94-16437
MUTHARASAN, RAJAKKANNU ..... p 939 N94-16859
MUTTON, PHILIP ..... p 1085 N94-17665
MYERS, CHRIS A. ..... p 1055 N94-17194
MYKKELTVEIT, SVEIN ..... p 1101 N94-16125

N

NAASZ, B. ..... p 952 N94-17218
NAGARAJAN, R. ..... p 970 N94-16947
NAGASUBRAMANIAN, GANESAN ..... p 1014 N94-17325
NAGODE, J. ..... p 973 N94-17408
NAIN, PHILIPPE ..... p 1162 N94-17537
NAITOH, PAUL ..... p 1119 N94-14943
NAJA, G. ..... p 977 N94-16073
NAKAGAWA, H. ..... p 905 N94-15068
NAKAGAWA, O. ..... p 892 N94-17160
NAKAMURA, NOBORU ..... p 1245 N94-16412
NAKANO, GEORGE H. ..... p 1037 N94-16426
NALETTO, GIAMPIERO ..... p 873 N94-15062
NAMACHCHIVAYA, N. S. ..... p 1173 N94-16937
NANSTAD, R. K. ..... p 957 N94-16103
NARAEVA, M. K. ..... p 1294 N94-16423
NARAYAN, B. S. ..... p 1042 N94-17630
NARAYAN, J. ..... p 1206 N94-15747
NARITA, TATSUHIKO ..... p 1064 N94-16600
NASH, GREG ..... p 1072 N94-16701
NASON, D. ..... p 1207 N94-15973
NASSAR, MOSTAFA ..... p 1162 N94-17539
NASSOPOULOS, ATHANASIOS ..... p 1189 N94-15739
NAUER, DAVID J. ..... p 887 N94-16502
p 926 N94-16504
NAUMANN, ROBERT J. ..... p 983 N94-16133
NAUMANN, W. G. ..... p 878 N94-17137
NAUNHEIMER, J. ..... p 1080 N94-16760
NAVRATIL, G. A. ..... p 1202 N94-16446
NAYFEH, ALI H. ..... p 871 N94-16107
NEALY, JOHN E. ..... p 1300 N94-15816
NECHYBA, MICHAEL C. ..... p 1163 N94-14954
NEELY, THOMAS E. ..... p 1193 N94-17028
NEHORAI, ARYE ..... p 989 N94-15786
NEHRKORN, THOMAS ..... p 1105 N94-14958
p 1108 N94-17267
NEIBERT, MICHAEL J. ..... p 930 N94-14975
NEILL, D. J. ..... p 1151 N94-16768
p 1151 N94-16769
NEJAD, ABDOLLAH S. ..... p 943 N94-14962
p 872 N94-15847
NELSON, ARTHUR ..... p 1197 N94-17353
NELSON, JOHN ..... p 1019 N94-15479
NELSON, MICHAEL L. ..... p 1160 N94-16878
p 1152 N94-17060
NEMANICH, R. J. ..... p 1215 N94-17377
p 1216 N94-17553
NEMCHINOV, I. V. ..... p 1290 N94-16404
NEMCHUK, I. K. ..... p 903 N94-15053
NEPHEDOV, N. A. ..... p 981 N94-16097
NEREM, STEVE ..... p 1273 N94-16315
NESS, R. O. ..... p 1249 N94-16182
NESTEROV, V. K. ..... p 903 N94-15053
NETTLES, SCOTT ..... p 1141 N94-14915
NEUBERT, REINHART ..... p 877 N94-15623
NEUGEBAUER, G. ..... p 1199 N94-17443
NEUKUM, G. ..... p 1252 N94-16199
p 1258 N94-16228
p 1259 N94-16229
p 1259 N94-16234
p 1261 N94-16244
p 1269 N94-16289
p 1275 N94-16323
p 1288 N94-16395
NEUMANN, W. E. ..... p 987 N94-15644
NEUSCHAEFER, ROBERT W. ..... p 1050 N94-16130
NEVO, BARUCH ..... p 1132 N94-15938
NEWBEGIN, R. ..... p 973 N94-17408
NEWBY, HAROLD D. ..... p 919 N94-15607
NEWMAN, D. A. ..... p 1042 N94-17378
NEWMAN, J. C., JR. ..... p 955 N94-15708
p 956 N94-15948
NEWTON, H. J. ..... p 1150 N94-16721
NEWTON, J. ..... p 1246 N94-16425
NEWTON, R. T. ..... p 1045 N94-14970
NG, L. ..... p 963 N94-15179
NG, T. TERRY ..... p 855 N94-15655
p 857 N94-15780
NGHIEM, S. V. ..... p 1079 N94-16752
p 1079 N94-16753
NI, XIAO-WU ..... p 1035 N94-17402
NICHOLAS, J. B. ..... p 1215 N94-17319
NICHOLS, ANDREW J. ..... p 1031 N94-16145
NICHOLS, F. A. ..... p 1059 N94-15997
NICHOLS, R. H., JR. ..... p 1243 N94-16305
NICI, ROSARIO ..... p 976 N94-17248
NICOLA, VICTOR F. ..... p 1174 N94-15823
NIEDERMANN, S. ..... p 1187 N94-16194
NIELSON, GREG ..... p 882 N94-17656
NIEMANN, R. C. ..... p 1013 N94-17226
NIEMEYER, J. ..... p 908 N94-15083
NIEMINEN, ILKKA ..... p 985 N94-17544
NIKOLAEVA, O. V. ..... p 930 N94-16325
NING, PETER A. ..... p 1192 N94-16550
NISHI, J. M. ..... p 1103 N94-16269
NISHIHARA, H. K. ..... p 1167 N94-17202
NITHACK, J. ..... p 1075 N94-16733
NOACK, W. ..... p 992 N94-15909
NOBLITT, JAMES P. ..... p 1050 N94-16134
NOEBE, R. D. ..... p 955 N94-15885
NOGAMI, K. ..... p 1243 N94-16291
NOLAN, M. C. ..... p 1241 N94-16202
NOLAN, P. L. ..... p 904 N94-15061
NOLIN, ANNE ..... p 1074 N94-16712
NOLL, DOUGLAS A. ..... p 1177 N94-16919
NOMA, Y. ..... p 1246 N94-16415
NOONAN, J. K. ..... p 1158 N94-15492
NORDEN, BENGT ..... p 944 N94-15162
NORIKANE, L. ..... p 1080 N94-16757
NORMAN, TIMOTHY L. ..... p 937 N94-16851
NORQUIST, DONALD C. ..... p 1107 N94-17244
NORTH, RICHARD C. ..... p 987 N94-15544
NORTON, D. P. ..... p 1207 N94-15829
p 1040 N94-16663
NORTON, K. ..... p 972 N94-17242
NORTON, T. J. ..... p 901 N94-15039
NOTKIN, G. ..... p 1202 N94-16803
NOVACK, H. IAN ..... p 1071 N94-16692
NOVOSELOV, S. K. ..... p 903 N94-15053
NOVOTNY, ANTONIN ..... p 917 N94-15594
p 877 N94-15621
NOWACKI, WOJCIECH K. ..... p 1061 N94-17086
NOYES, RAE A. ..... p 952 N94-17520
NUNES, A. C. ..... p 1049 N94-16138
NUNNALLY, W. C. ..... p 1012 N94-17023
NUTH, J. ..... p 1219 N94-16420
NUTT, GARY ..... p 1153 N94-17107
NUTTALL, ALBERT H. ..... p 1173 N94-17372
p 1171 N94-17393
NYBERG, KAREN L. ..... p 886 N94-15951
NYGAARD, EINAR ..... p 909 N94-15095
NYQUIST, L. E. ..... p 1264 N94-16258

O

OBAYASHI, SHIGERU ..... p 860 N94-17081
OBERG, DONALD ..... p 1124 N94-16616
OBORNE, M. W. ..... p 1303 N94-16804
OBUCHI, T. ..... p 892 N94-17160
OCONNELL, W. ..... p 968 N94-16658
ODEA, DAMIAN ..... p 1229 N94-15652
ODENBACH, S. ..... p 943 N94-15159
ODONNELL, P. A. ..... p 864 N94-16835
OETTL, H. ..... p 992 N94-15902
OFFIERSKI, JACEK W. ..... p 877 N94-15612
p 877 N94-15613
OGAWA, T. ..... p 1245 N94-16400
OGIWARA, M. ..... p 1150 N94-16579
OH, DANIEL B. ..... p 1036 N94-17655
OHLCKERS, PER ..... p 909 N94-15095
OHLHAUSEN, JOHN H. ..... p 1138 N94-16983
OHNO, TOM T. ..... p 994 N94-15986
OIKNINE, C. ..... p 878 N94-17141
OKAMOTO, KENICHI ..... p 990 N94-15894
OKAYAMA, AKIRA ..... p 945 N94-15168
OKUBO, S. ..... p 1101 N94-15815
OLAUGHLIN, DAN ..... p 864 N94-16906
OLAUGHLIN, DANIEL G. ..... p 876 N94-16025
OLDANI, J. J. ..... p 1041 N94-16871
OLDFIELD, M. K. ..... p 901 N94-15039
OLDHAM, THOMAS ..... p 913 N94-15568
p 914 N94-15573
p 915 N94-15577
p 922 N94-15622
p 922 N94-15624
OLESON, STEVEN R. ..... p 1040 N94-16522
OLIFERUK, WIERA ..... p 961 N94-17121
OLIVARES, J. A. ..... p 949 N94-16876
OLIVIER, M. ..... p 978 N94-16080
OLIVIER, S. S. ..... p 1237 N94-16872
OLSEN, C. ..... p 923 N94-15118
OLSON, ROBERT W. ..... p 1130 N94-17554
OLSON, T. M. ..... p 970 N94-16973
OLSON, TIMOTHY G. ..... p 1157 N94-17588
OLSSON, DAN ..... p 895 N94-17176
OLTHOF, G. H. ..... p 1147 N94-15776
OLTHOF, H. ..... p 874 N94-17142
OLTMAN-SHAY, JOAN ..... p 1113 N94-16561
OLTMAN-SHAY, JOAN M. ..... p 1114 N94-17497
OLTON, DAVID S. ..... p 1132 N94-16456
OMATETE, O. O. ..... p 966 N94-16016
ONDREY, LARRY P. ..... p 1048 N94-16944
ONEILL, PATRICK J. ..... p 1142 N94-14924
ONG, LIH-YENN ..... p 855 N94-15655
p 857 N94-15780
OONA, H. ..... p 1202 N94-16776
p 1013 N94-17318
OOSTDAM, R. ..... p 1021 N94-15755
OPPENHEIMER, CLIVE ..... p 1068 N94-16680
OPYDO, WLADYSLAW ..... p 1013 N94-17071
ORAZEM, MARK E. ..... p 958 N94-16562
ORCUTT, JOHN A. ..... p 1111 N94-14947
OREG, YUVAL ..... p 1180 N94-15288
ORIE, NETTIE M. ..... p 861 N94-17639
ORIOL, R. A. ..... p 1113 N94-16588
ORSZAG, STEVEN A. ..... p 1016 N94-15151
ORTH, MICHAEL S. ..... p 976 N94-16146
OSBORNE, P. P. ..... p 933 N94-15277
OSGOOD, R. M. ..... p 1010 N94-15971
OSILIKE, M. O. ..... p 1175 N94-17644
OSTENDORF, MARI ..... p 988 N94-15691
OTHMAN, D. BEN ..... p 1242 N94-16272
OTOOLE, JAMES ..... p 1141 N94-14915
OTTEN, KLAUS H. ..... p 877 N94-15613
OTTENS, HAROLD H. ..... p 854 N94-17614
OTTO, S. R. ..... p 1030 N94-17450
OVER, J. W. ..... p 1157 N94-17588
OVERHAMM, M. ..... p 906 N94-15073
p 906 N94-15074
OWSIANNY, MARIUZ ..... p 1002 N94-17064

P

PACINI, LINDA K. ..... p 920 N94-15614
PAGANO, A. R., JR. ..... p 899 N94-16152
PAGANO, S. ..... p 905 N94-15068
PAGE, JOHN R. ..... p 1235 N94-17290
p 1222 N94-17441
PAGESY, A. ..... p 900 N94-15032
PAGESY, V. ..... p 900 N94-15032
PAIGE, D. A. ..... p 1256 N94-16216
PAILER, N. ..... p 874 N94-17143
PALETTA, F. ..... p 894 N94-17174
PALEVSKY, ALAN ..... p 1014 N94-17423
PALM, HANS CHRISTIAN ..... p 1172 N94-15298
PALME, H. ..... p 1103 N94-16250
PALMER, EDWARD G. ..... p 1055 N94-17194
PALMER, EVERETT A. ..... p 862 N94-15550
PALMER, RAY ..... p 940 N94-16864
PALMUCCI, P. ..... p 888 N94-17132
PALYS, JOHN ..... p 888 N94-16990
PANDEY, C. ..... p 970 N94-16947
PANG, H. ..... p 960 N94-17079
PANG, KEVIN ..... p 1132 N94-16456
PANHUYZEN, R. A. ..... p 903 N94-15054
PANICONI, CLAUDIO ..... p 1083 N94-16031
p 1084 N94-16032
PANKIN, A. YU. ..... p 1013 N94-17316
PANTANO, CARLO G. ..... p 973 N94-17466
PANTAZIS, JOHN A. ..... p 882 N94-16530
PANTER, S. S. ..... p 1128 N94-16784
p 1128 N94-16786
PAPIKE, J. J. ..... p 1243 N94-16284
PAPPAS, CHARLES H. ..... p 1109 N94-17522
PAQUE, JULIE M. ..... p 954 N94-16401
PARABOSCHI, STEFANO ..... p 1156 N94-17501
PARADIS, MARC-ANDRE ..... p 1032 N94-15697
PARASHAR, S. ..... p 898 N94-15893
PAREKH, D. E. ..... p 1022 N94-15860
PARIS, JACK F. ..... p 1076 N94-16738
p 1079 N94-16756
PARK, JUNG HO ..... p 1191 N94-16024
PARK, S. ..... p 1062 N94-17507
PARK, TAEHYO ..... p 934 N94-16440
PARKER, ALLEN R., JR. ..... p 1032 N94-15754
PARKER, GREGORY K. ..... p 929 N94-17543
PARKER, J. V. ..... p 1202 N94-16776
p 1013 N94-17318

PARKER, T. J. p 1293 N94-16418
PARKER, TIMOTHY J. p 1298 N94-17654
PARKINSON, CLAIRE p 1112 N94-15680
PARKINSON, CLAIRE L. p 1114 N94-17439
PARKINSON, W. H. p 1299 N94-15836
PARKS, ALLEN D. p 1231 N94-16490
PARMENTIER, E. M. p 1259 N94-16232
p 1261 N94-16242
PARMETER, MICHELLE M. p 1113 N94-16588
PARRISH, J. A. p 1122 N94-16113
PARSONS, A. p 901 N94-15040
PARSONS, E. L., JR. p 1092 N94-16715
PARZEN, G. p 1184 N94-16886
p 1151 N94-16892
PASCAL, STEPHANE p 888 N94-17133
PASHKEVICH, A. V. p 903 N94-15053
PASQUIER, S. p 902 N94-15047
PASSERONE, A. p 943 N94-15158
PASSONI, D. p 894 N94-17174
PASTORE, CHRISTOPHER M. p 933 N94-15484
p 939 N94-16860
p 939 N94-16861
p 868 N94-16865
PASTUREL, P. p 907 N94-15078
PATCHETT, B. E. p 910 N94-15096
PATNAIK, B. K. p 1209 N94-16066
PATNAIK, S. N. p 1058 N94-15709
PATTERSON-HINE, F. ANN p 1116 N94-15548
PATTERSON, R. p 1213 N94-17108
PATTERSON, RICHARD L. p 1009 N94-15706
PATTIKANGAS, T. J. H. p 1200 N94-15205
p 1200 N94-15206
p 1200 N94-15207
p 1201 N94-15208
p 1201 N94-15209
p 1201 N94-15210
p 1201 N94-15211
PATTIKANGAS, TIMO p 1200 N94-15204
PAUL, ALORA p 1113 N94-17383
PAUL, DILIP p 883 N94-17111
PAULEY, ROBERT G. p 922 N94-17083
PAULSON, CLAYTON p 1111 N94-15139
PAUNONEN, MATTI p 912 N94-15561
p 917 N94-15590
PAVESI, B. p 888 N94-17132
p 892 N94-17161
PAVLIS, ERRICOS p 911 N94-15553
PAXSON, DANIEL E. p 870 N94-17470
PAXTON, C. H. p 1106 N94-16465
PAYLOR, R. p 1114 N94-17489
PAYNE, ROGER p 926 N94-16590
p 926 N94-16654
PEACOCK, A. p 899 N94-15028
p 904 N94-15058
PEARCE, R. P. p 1098 N94-15132
PEARLMAN, MICHAEL R. p 912 N94-15559
PEARSON, JACQUELYN Y. p 1131 N94-15659
PEDRAZA, A. J. p 1040 N94-16664
PEDRAZA, D. F. p 1211 N94-16814
PEERY, J. S. p 1148 N94-15985
PEHRSSON, P. E. p 948 N94-16553
PELED, EMMANUEL p 1014 N94-17325
PELLEGRINO, J. p 1054 N94-16156
PELLEGRINO, JAMES W. p 1132 N94-15762
PELLIN, M. J. p 953 N94-17649
PELLO, EDWARD F. p 1055 N94-17194
PELOQUIN, MARK S. p 1057 N94-15150
PELTON, JOSEPH N. p 1006 N94-17661
PELUSO, G. p 905 N94-15068
PEMBER, R. p 1025 N94-16903
PEMBER, R. B. p 1025 N94-16894
PENETRANTE, B. M. p 1096 N94-16449
PENG, J. C. p 1182 N94-16115
PENNELL, W. E. p 1059 N94-16104
PENNYCOOK, S. J. p 947 N94-16014
p 1212 N94-16841
PEPE, G. p 905 N94-15068
PEREZ, LANCE C. p 997 N94-16507
p 997 N94-16508
p 998 N94-16509
PEREZ, WILLIAM A. p 1138 N94-17460
PERITT, JONATHAN M. p 936 N94-16537
PEROZZI, ETTORE p 874 N94-17144
PERRAM, GLEN P. p 1041 N94-17195
PERRETTA, DAVID A. p 855 N94-14973
PERRY, CAROLE C. p 967 N94-16472
PERRY, GRETCHEN L. E. p 1031 N94-16145
p 976 N94-16146
PERRYMAN, M. A. C. p 899 N94-15028
PERSHIN, S. p 921 N94-15619
PERUN, N. V. p 1179 N94-14931
PETAEV, M. I. p 1242 N94-16265
PETERS, JOSEPH I. p 1138 N94-17460
PETERSEIM, JUERGEN p 975 N94-16002
PETERSON, C. A. p 1258 N94-16225
PETERSON, DAVID L. p 1073 N94-16702
PETERSON, J. E., JR. p 1102 N94-17252
PETHEL, S. D. p 1054 N94-16155
PETRIE, H. L. p 1028 N94-17276
PETROFF, M. D. p 902 N94-15043
PETTERSSON, LARS E. p 987 N94-15541
PETTY, C. C. p 1203 N94-16816
p 1203 N94-16823
PEYGHAMBARIAN, N. p 1014 N94-17375
PHALNIKAR, R. p 960 N94-17079
PHILLIPS, R. J. p 1256 N94-16218
PHILLIPS, ROGER J. p 1265 N94-16268
PHOEBUS, PATRICIA A. p 1106 N94-16568
PIANETTA, P. p 1208 N94-16062
PIATEK, J. L. p 1241 N94-16174
PICAULT, ROBERT p 909 N94-15091
PICKART, ROBERT p 1112 N94-15844
PIDGEON, A. N. p 878 N94-17154
PIECHOR, KAZIMIERZ p 1178 N94-17051
PIELORZ, AMALIA p 1061 N94-17091
PIERCE, ROBERT D. p 1000 N94-16917
p 1000 N94-16918
PIERI, DAVID p 1068 N94-16680
PIERSON, DAVID p 1117 N94-15662
PIETERS, C. p 1258 N94-16228
p 1259 N94-16229
p 1259 N94-16234
PIETERS, C. M. p 1252 N94-16199
p 1242 N94-16246
p 1288 N94-16395
p 1246 N94-16422
PIETERS, CARLE M. p 1086 N94-16437
PIKE, ROSCOE p 959 N94-16781
PILLINGER, C. T. p 1241 N94-16192
p 1251 N94-16193
p 953 N94-16256
p 1246 N94-16425
PILLINGER, COLIN p 1241 N94-16184
PILMANIS, ANDREW A. p 1130 N94-17554
PINA, L. p 895 N94-17177
PINDERA, M-J. p 930 N94-15106
PINELLI, THOMAS E. p 1230 N94-15838
p 1230 N94-15839
p 1233 N94-17291
p 1233 N94-17300
PINET, P. p 1067 N94-16675
PINKERTON, H. p 1259 N94-16230
PINKERTON, HARRY p 1103 N94-16237
PINSKER, R. I. p 1203 N94-16823
PIONECKI, LESZEK p 985 N94-17068
PIPPIN, G. p 887 N94-16909
PITTARELLI, MICHAEL p 1170 N94-16582
PITTICH, EDUARD M. p 874 N94-17144
PITTMAN, WILLIAM C. p 1194 N94-17331
PITZ, W. J. p 1096 N94-16825
PLACE, PATRICK R. p 1144 N94-15214
PLATT, M. E. p 1150 N94-16594
PLATZ, W. p 903 N94-15050
p 910 N94-15100
PLAUT, J. J. p 1293 N94-16418
PLAUT, JEFFREY J. p 1080 N94-16762
p 1298 N94-17654
PLETCHER, R. H. p 1027 N94-17128
PLIMPTON, S. p 1157 N94-14927
PLISHKA, RICHARD M. p 1143 N94-15110
PLOETZ, K. L. p 1209 N94-16164
PLOURDE, J. V. p 1138 N94-16793
PLUMMER, J. D. p 950 N94-16952
PNUELI, AMIR p 1149 N94-16554
PODLESKI, STEVE D. p 861 N94-17558
POELLOT, MICHAEL R. p 866 N94-15429
POEPEL, R. p 908 N94-15083
POHJONEN, HELENA p 1015 N94-17546
POLLACK, J. p 1252 N94-16198
POLLACK, JAMES B. p 1296 N94-16434
POMERLEAU, DEAN p 863 N94-14919
p 864 N94-14972
POMMET, DREW p 1194 N94-17336
PONTE, S. p 1078 N94-16750
POOK, POLLY K. p 1165 N94-16580
POOL, P. p 900 N94-15035
POORMAN, RICHARD p 1051 N94-16141
POPE, D. P. p 1208 N94-16063
p 959 N94-16890
POPE, KEVIN O. p 1076 N94-16738
POPE, S. B. p 943 N94-15146
PORADA, WILLIAM M. p 857 N94-15720
POROPAT, G. V. p 1190 N94-15846
POSIOLOVA, LILIYA V. p 1111 N94-14947
POSTAWKO, SUSAN E. p 1290 N94-16403
POTOTZKY, ANTHONY S. p 867 N94-17055
POTVIN, L. p 979 N94-16086
p 923 N94-16100
POVINELLI, LOUIS A. p 1028 N94-17258
POWELL, BRADLEY W. p 1049 N94-16140
POWELL, M. A. p 1092 N94-16112
POWER, MICHAEL p 1195 N94-17344
POWERS, E. p 962 N94-16137
POWERS, EDMUND M. p 1148 N94-15840
POWERS, EDWARD J. p 1211 N94-16800
POZARNSKY, G. A. p 962 N94-14921
p 965 N94-15843
PRADHAN, DHIRAJ K. p 1140 N94-17005
PRAMANICK, S. p 1209 N94-16066
PRASAD, S. E. p 979 N94-16083
PRATER, R. p 1203 N94-16816
p 1203 N94-16823
PRATHER, DENNIS W. p 1195 N94-17338
PRATT, JOHN RICHARD p 965 N94-15879
PRATT, RANDY p 1126 N94-16632
PRATT, S. p 1259 N94-16234
PRATT, STEPHAN F. p 1086 N94-16437
PRAUSNITZ, J. M. p 966 N94-15996
PREMO, LESLIE A. p 1119 N94-14923
PRETLOW, ROBERT A., III p 1129 N94-17085
PREWETT, TACEY L. p 1117 N94-15969
PREYSS, ALBERT E. p 993 N94-15911
PRICE, M. C. p 905 N94-15066
p 905 N94-15067
p 907 N94-15077
PRIDGEON, CHARLES p 1150 N94-16591
PRIEDHORSKY, W. C. p 898 N94-17669
PRIESTLEY, K. p 1097 N94-14960
PRIETO, F. J. p 1149 N94-16120
PROCHAZKA, IVAN p 913 N94-15565
p 914 N94-15572
p 914 N94-15574
p 916 N94-15584
p 921 N94-15619
p 877 N94-15621
PROCTOR, F. H. p 1108 N94-17283
PRUDHOMME, ROBERT K. p 939 N94-16858
PRUNEAU, PAUL N. p 888 N94-16990
PRZEKWAS, A. J. p 928 N94-17442
PSALTIS, DEMETRI p 1141 N94-17380
PUGH, DAVID p 1147 N94-15743
PULLEN, PAUL V. p 1119 N94-14923
PUMPHREY, SHELLEY L. p 977 N94-16072
PURDY, DON p 1197 N94-17351
PURVIS, EDWARD J. p 1191 N94-16547
PUTNAM, WILLIAM O. p 1155 N94-17500
PUZYNIN, I. V. p 1168 N94-14933

Q

QUALLS, GARY p 1300 N94-15816
QUATTROCHI, D. p 1064 N94-16603
p 1065 N94-16604
QUEGAN, SHAUN p 1080 N94-16761
QUICK, J. E. p 954 N94-16401
QUINN, J. J. p 1220 N94-16810
QUINTANA, JORGE A. p 883 N94-17488
QUINTANA, M. A. p 1091 N94-15994
QUINTO, P. FRANK p 861 N94-17639
QUIRK, JAMES J. p 1168 N94-15724
QUONG, JULIE A. p 1117 N94-16545

R

RAABE, JERZY p 969 N94-16924
RABITZ, HERSCHEL p 1183 N94-16722
RADAELLI, P. G. p 1208 N94-15982
RADAR, MARK p 1201 N94-15661
RADBONE, J. M. p 894 N94-17169
RADICELLA, S. M. p 1103 N94-17631
RADZIK, JOSE p 875 N94-17134
RAGLIN, ADRIENNE p 1155 N94-17411
RAGUIN, DANIEL H. p 1194 N94-17337
RAIMONDO, J. C. p 911 N94-15554
p 874 N94-15589
RAJA, R. p 1186 N94-17662
RAJAGOPAL, K. R. p 1026 N94-16958
RAJASENAN, C. p 911 N94-15554
p 874 N94-15589
RAKITSKAYA, R. B. p 1241 N94-16212
RALL, DAVID L. p 1192 N94-16936
RAM, M. S. p 1211 N94-16782
RAMACHANDRAN, V. S. p 1133 N94-17265
RAMANUJAM, N. p 1226 N94-14987
RAMBOW, OWEN p 1166 N94-16770
RAMOS-IZQUIERDO, LUIS p 921 N94-15618
p 921 N94-15620
RAMSEY, MICHAEL S. p 1065 N94-16607
RANACHOWSKI, JERZY p 969 N94-16924
p 1013 N94-17071
RANACHOWSKI, ZBIGNIEW p 1177 N94-16650
RANC, MARYLINE p 890 N94-17146
RANDLES, P. W. p 1057 N94-15524
RANGASWAMY, M. p 1001 N94-17033
RANSON, K. JON p 1077 N94-16741
RAO, A. S. p 973 N94-17430

RAO, G. R. ..... p 958 N94-16453
RAO, K. S. ..... p 1079 N94-16754
RAO, M. N. ..... p 1248 N94-16177
RAO, T. R. ..... p 1140 N94-15763
RASIS, E. P. ..... p 1048 N94-17088
RASLEAR, T. G. ..... p 1134 N94-17535
RASSKAZOV, SERGEI ..... p 1103 N94-16214
RASSON, J. ..... p 1100 N94-15809
p 1100 N94-15810
RASTRILLA, P. ..... p 893 N94-17164
RATLIFF, C. L. ..... p 1048 N94-17462
RATNATUNGA, KAVAN U. ..... p 1172 N94-15641
RATNER, M. A. ..... p 1191 N94-16454
RAU-CHAPLIN, ANDREW ..... p 1162 N94-17539
RAVERA, F. ..... p 943 N94-15158
RAWLEY, GAYLE L. ..... p 1300 N94-15533
RAYNER, S. ..... p 1096 N94-16445
RAZEGHI, M. ..... p 1206 N94-14922
RAZUMOVA, K. ..... p 1202 N94-16803
RE, RICHARD J. ..... p 856 N94-15681
RE, S. ..... p 906 N94-15076
READ, B. E. ..... p 1057 N94-15016
p 1057 N94-15017
READ, P. D. ..... p 908 N94-15088
p 910 N94-15096
REALMUTO, VINCENT J. ..... p 1063 N94-16595
p 1065 N94-16608
REASS, W. ..... p 1205 N94-17645
REBENFELD, LUDWIG ..... p 939 N94-16858
RECK, GREGORY M. ..... p 1050 N94-16132
REDDY, B. R. ..... p 1199 N94-17455
REDEKOPP, LARRY G. ..... p 1023 N94-16470
REDING, PHILIP J. ..... p 1110 N94-17607
REDON, JEAN-PIERRE ..... p 895 N94-17179
REED, K. L. ..... p 1241 N94-16174
REEDY, R. C. ..... p 1245 N94-16409
p 1037 N94-16426
REEDY, ROBERT C. ..... p 1245 N94-16385
REESE, M. ..... p 962 N94-14914
REEVES, DENNIS L. ..... p 1122 N94-15759
REGAN, M. J. ..... p 1183 N94-16811
p 961 N94-17251
REGAN, RAYMOND F. ..... p 1128 N94-16786
REHR, J. J. ..... p 948 N94-16772
REIFENRATH, WILLIAM G. ..... p 1128 N94-16779
REIGBER, C. ..... p 911 N94-15554
p 874 N94-15589
REILLY, W. S. ..... p 1166 N94-17201
REIMOLD, WOLF UWE ..... p 1103 N94-16322
REIN, G. ..... p 1174 N94-16820
REINHARDT, J. W. ..... p 1104 N94-16360
REISER, M. ..... p 1186 N94-17578
REISS, EDWARD ..... p 1029 N94-17414
REITER, MICHAEL ..... p 1152 N94-16982
REITZ, RONALD P. ..... p 948 N94-16532
p 935 N94-16534
p 1012 N94-16914
REIZER, N. R. ..... p 1157 N94-17588
REJ, D. J. ..... p 1202 N94-16451
REJEK, E. P. ..... p 944 N94-15161
RELINGHAUS, ROBERT ..... p 984 N94-16003
RELLICK, GERRY S. ..... p 940 N94-17271
REMAKLUS, P. WILL ..... p 995 N94-16038
REMPT, RAYMOND D. ..... p 1056 N94-17596
REN, ZHAN-XIANG ..... p 1193 N94-17254
RENNER, U. ..... p 895 N94-17180
RENO, MARTIN A. ..... p 1220 N94-17624
REPETTO, BRUNO ..... p 1143 N94-15212
REUBENSTEIN, HOWARD ..... p 1155 N94-17491
REY-BENAYAS, JOSE MARIA ..... p 1076 N94-16738
REYES, GEORGE ..... p 1037 N94-16696
REYNA, L. G. ..... p 1039 N94-16114
REYNOLDS, R. L. ..... p 1103 N94-16269
REZKALLAH, KAMIEL S. ..... p 899 N94-16101
RHEA, W. JOSEPH ..... p 1069 N94-16687
RICCI, E. ..... p 943 N94-15158
RICCIARDI, ALETA ..... p 1000 N94-16911
RICHARDS, B. ..... p 1202 N94-16162
RICHARDS, J. A. ..... p 1075 N94-16713
RICHARDSON, MARTIN ..... p 913 N94-15567
RICHTER, J. ..... p 944 N94-15161
RICHTER, R. ..... p 1070 N94-16688
RICHTER, TH. ..... p 1200 N94-14966
RICKLEFS, RANDALL L. ..... p 917 N94-15593
p 918 N94-15595
p 918 N94-15596
p 918 N94-15598
p 918 N94-15599
RICKLEY, EDWARD J. ..... p 1179 N94-17599
RICKMAN, DEBORAH K. ..... p 927 N94-17016
RICKS, DOUGLAS W. ..... p 1195 N94-17341
RICOLLEAU, CHRISTIAN ..... p 1206 N94-15295
RIDD, MERRILL ..... p 1072 N94-16701
RIDD, MERRILL K. ..... p 1073 N94-16705
RIDE, SALLY K. ..... p 1038 N94-15686
RIDEAU-GALLOT, LAURENCE ... p 1142 N94-14978
RIEDL, MAX J. ..... p 1198 N94-17359
RIES, JUDIT G. ..... p 918 N94-15599
RIESTER, L. ..... p 935 N94-16461
RIETDIJK, R. H. ..... p 1240 N94-17603
RIGNEY, D. A. ..... p 1049 N94-17566
RIGNOT, ERIC ..... p 1075 N94-16734
RIGSBEE, JAMES M. ..... p 1038 N94-15852
RIHET, JEAN-PAUL ..... p 895 N94-17179
RIND, DAVID ..... p 1112 N94-15680
RIOUX, C. ..... p 979 N94-16086
p 923 N94-16100
RIPAMONTI, GIANCARLO ..... p 913 N94-15569
p 914 N94-15570
p 914 N94-15571
RIPPERT, E. D. ..... p 908 N94-15089
RISTORCELLI, I. ..... p 908 N94-15087
RITCHIE, R. O. ..... p 961 N94-17223
RITTER, NILES D. ..... p 1073 N94-16705
RITTER, RICHARD D. ..... p 862 N94-15550
RIVARD, BENOIT ..... p 1080 N94-16762
RIVERA, JOSE A., JR. ..... p 866 N94-15722
RIVERA, SALVADOR, JR. ..... p 1106 N94-15851
RIVERS, M. L. ..... p 956 N94-15921
RIZHI, LIU ..... p 855 N94-14942
RIZZI, S. A. ..... p 1179 N94-17650
ROARK, JIM ..... p 1273 N94-16315
ROBE, R. Q. ..... p 1138 N94-16793
ROBERTS, CATHY C. ..... p 1144 N94-15486
ROBERTS, DAR ..... p 1066 N94-16668
ROBERTS, DAR A. ..... p 1068 N94-16679
p 1070 N94-16689
p 1073 N94-16706
ROBERTS, J. R. ..... p 1130 N94-17562
ROBERTS, K. M. ..... p 1278 N94-16338
ROBERTS, K. MAGEE ..... p 1259 N94-16230
p 1285 N94-16376
ROBERTS, WILLIAM W., JR. ..... p 1239 N94-16648
ROBERTSON, EDWARD A. ..... p 925 N94-16496
ROBERTSON, R. G. H. ..... p 1185 N94-16951
ROBINSON, A. C. ..... p 1148 N94-15985
ROBINSON, CHARLES T. ..... p 1035 N94-17197
ROBINSON, HOWARD H. ..... p 1033 N94-15884
ROBINSON, J. H. ..... p 1179 N94-17650
ROBINSON, M. S. ..... p 1252 N94-16199
p 1258 N94-16225
p 1288 N94-16394
ROBINSON, MICHAEL ..... p 855 N94-14959
ROBINSON, MITCHELL S. ..... p 1235 N94-16988
ROBSON, ANTHONY E. ..... p 998 N94-16535
ROCA, E. ..... p 903 N94-15050
ROCCO, A. G. ..... p 1158 N94-15492
ROCHESTER, G. K. ..... p 909 N94-15090
RODRIGUEZ, PEDRO I. ..... p 1059 N94-16519
RODRIGUEZ, RAUL ..... p 893 N94-17168
ROE, N. A. ..... p 1181 N94-16053
ROEBUCK, B. ..... p 1057 N94-15021
ROETTCHER, K. ..... p 876 N94-15600
ROGER, R. E. ..... p 1075 N94-16713
ROGERS, DENNIS ..... p 1191 N94-16128
ROHLICEK, J. R. ..... p 988 N94-15691
ROKHLIN, V. ..... p 1154 N94-17370
p 1171 N94-17420
ROKUGAWA, SHUICHI ..... p 1064 N94-16601
RONDEAUX, G. ..... p 1070 N94-16691
RONDINELLI, G. ..... p 892 N94-17161
p 893 N94-17165
RONDINELLI, GIUSEPPE ..... p 878 N94-17138
RONNEY, PAUL D. ..... p 946 N94-15713
p 951 N94-17125
ROOKS, MICHAEL J. ..... p 1045 N94-17349
ROORDA, A. ..... p 979 N94-16083
ROOT, BENJAMIN T. ..... p 987 N94-15540
ROSAKIS, ARES J. ..... p 1059 N94-16587
ROSE, M. F. ..... p 960 N94-16964
ROSE, WILLIAM C. ..... p 1020 N94-15551
ROSE, WILLIAM I. ..... p 1081 N94-15181
ROSENBAUM, J. G. ..... p 1103 N94-16269
ROSENBERGER, FRANZ ..... p 1206 N94-15476
p 1210 N94-16646
ROSENGREEN, A. ..... p 1015 N94-17526
p 1015 N94-17608
ROSENTHAL, A. L. ..... p 1093 N94-17217
ROSENTHAL, DAVID ..... p 1146 N94-15674
ROSHKO, ANATOL ..... p 1193 N94-17264
ROSNER, J. L. ..... p 1187 N94-16116
ROSS, HOWARD D. ..... p 977 N94-16076
ROSS, M. ..... p 1208 N94-15976
ROSSI, E. ..... p 894 N94-17174
ROTE, D. M. ..... p 1011 N94-16443
p 1047 N94-16806
p 1048 N94-16969
ROTH, CAROL ..... p 1125 N94-16622
ROTH, HILTON ..... p 959 N94-16781
ROTH, MARK A. ..... p 1154 N94-17366
ROTHERY, DAVID ..... p 1068 N94-16680
ROTHFUSS, H. ..... p 1070 N94-16688
ROTHROCK, D. S. ..... p 975 N94-16807
ROUHANI, B. D. ..... p 1171 N94-17642
ROUSSEAU, P. M. ..... p 950 N94-16952
ROUX-DEBALMANN, HELENE ..... p 944 N94-15163
ROUX, GILLES ..... p 1116 N94-15643
ROWAN, LAWRENCE C. ..... p 1065 N94-16605
ROWAN, M. J. ..... p 1178 N94-17278
ROWAN, W. L. ..... p 1202 N94-16162
ROWE, W. J. ..... p 1033 N94-15826
ROWLAND, JOHN R. ..... p 995 N94-16041
ROWLAND, S. ..... p 1283 N94-16366
ROWLAND, SCOTT K. ..... p 1065 N94-16606
ROYER, MICHEL ..... p 909 N94-15091
ROZGONYI, G. A. ..... p 1209 N94-16066
ROZUM, JAMES A. ..... p 1144 N94-15215
RUAN, JU-AI ..... p 1048 N94-17533
RUBIN, ALAN E. ..... p 1244 N94-16330
RUBINSTEIN, R. ..... p 1029 N94-17385
RUBIO, G. S. ..... p 1241 N94-16213
RUCKMAN, M. W. ..... p 974 N94-17676
RUEMENAPP, S. ..... p 932 N94-15259
RUFUS, I. B. ..... p 970 N94-16948
p 970 N94-16949
p 971 N94-16994
RUGG, STEVEN A. ..... p 1114 N94-17503
RUGGIERO, A. G. ..... p 1202 N94-16019
p 1181 N94-16020
RUIZRUIZ, F. ..... p 1220 N94-17602
RUPAR, MICHAEL A. ..... p 1004 N94-17373
RUSSELL, C. T. ..... p 1263 N94-16252
RUSSELL, CAROLYN K. ..... p 1049 N94-16138
RUSSELL, J. F. ..... p 1274 N94-16320
RUSSELL, J. N., JR. ..... p 948 N94-16553
RUSSELL, S. D. ..... p 1039 N94-16474
RUSSINOFF, DAVID M. ..... p 1144 N94-15443
RUSSO, ARTURO ..... p 1303 N94-16500
p 887 N94-16523
p 887 N94-16525
RUST, DAVID M. ..... p 1299 N94-17004
RUTHERFORD, JOHN ..... p 1108 N94-17465
RUZGA, RICHARD ..... p 971 N94-17198
RUZMAIKINA, T. V. ..... p 1244 N94-16352
RYAN, D. E. ..... p 1241 N94-16213
RYBICKI, DANIEL J. ..... p 1047 N94-15949
RYDEN, K. A. ..... p 896 N94-17183
RYE, GILBERT D. ..... p 896 N94-17187
RYON, L. B. ..... p 1059 N94-16123
RZESZOTARSKA, JADWIGA ..... p 1013 N94-17071

S

SABBAGH, S. A. ..... p 1202 N94-16446
SABOL, BRUCE ..... p 1106 N94-15851
SABOL, DONALD E. ..... p 1068 N94-16677
p 1068 N94-16679
SABOL, DONALD E., JR. ..... p 1073 N94-16706
SACHS, R. G. ..... p 1187 N94-16116
SADOULET, B. ..... p 901 N94-15040
SAITO, J. ..... p 1287 N94-16387
SAKURAI, H. ..... p 945 N94-15167
SALAMA, IBRAHIM A. ..... p 1173 N94-16657
SALCUDEAN, M. ..... p 980 N94-16089
SALOMAA, R. R. E. ..... p 1200 N94-15205
p 1200 N94-15206
p 1200 N94-15207
p 1201 N94-15208
p 1201 N94-15209
p 1201 N94-15210
SAM, S. S. ..... p 1146 N94-15650
SAMORI, C. ..... p 914 N94-15570
SAMSON, J. C. ..... p 1098 N94-15433
SANCHEZ, J. ..... p 962 N94-14914
p 963 N94-15490
p 963 N94-15631
SANCHEZ, ROBERT R. ..... p 1138 N94-17460
SANCHEZ, VICTOR ..... p 944 N94-15163
SANDERS, GERALD B. ..... p 925 N94-16496
SANDERSON, ARTHUR C. ..... p 897 N94-17280
SANDON, PETER A. ..... p 1166 N94-16581
SANDS, WILLIAM ..... p 1188 N94-15144
SANDUSKY, H. W. ..... p 1214 N94-17270
SANDWELL, D. T. ..... p 1267 N94-16277
SANJOSE, L. A. ..... p 878 N94-17155
SANKAR, LAKSHMI ..... p 1027 N94-17129
SANTABARBARA, JOSEP M. ..... p 1105 N94-14938
SANTER, B. D. ..... p 1096 N94-16802
SANTORO, ROBERT J. ..... p 952 N94-17532
SARGENT, NOEL B. ..... p 863 N94-16520
SAROFIM, A. F. ..... p 949 N94-16896
SASAMOTO, WASHITO A. ..... p 1085 N94-17665
SASHITAL, SANAT ..... p 968 N94-16723
SASSO, WILLIAM C. ..... p 1166 N94-16770
SATHER, DUANE P. ..... p 1026 N94-16927
SATYANARAYANAN, M. ..... p 1141 N94-17115
SAUNDERS, R. S. ..... p 1286 N94-16382

SAUNDERS, R. STEPHEN ..... p 989 N94-15887
SAUSA, ROSARIO C. ..... p 942 N94-14946
p 951 N94-17203
SAVAGE, STEFAN ..... p 1158 N94-15745
SAVILLE, D. A. ..... p 1028 N94-17298
SCHACHERBAUER, ALOIS ..... p 1163 N94-14950
SCHAEFER, MARC ..... p 895 N94-17181
SCHAEFFER, H. H. A. ..... p 903 N94-15054
SCHAEIDT, STEFAN ..... p 1240 N94-17591
SCHAERER, U. ..... p 954 N94-16383
SCHAFER, K. J. ..... p 1208 N94-15976
SCHANZER, DENA ..... p 1074 N94-16707
SCHAPERY, R. A. ..... p 1062 N94-17507
SCHEIBNER, K. F. ..... p 1039 N94-16450
SCHELKER, BILL ..... p 1155 N94-17429
SCHEMPF, HAGEN ..... p 879 N94-14969
SCHENEIDER, FRED B. ..... p 1146 N94-15638
SCHERER, P. ..... p 1244 N94-16361
SCHIANO, THOMAS L. ..... p 1105 N94-15137
SCHIESSL, U. ..... p 909 N94-15092
SCHILLAK, STANISLAW ..... p 877 N94-15604
SCHINDER, PAUL J. ..... p 1246 N94-15182
SCHIPER, ANDRE ..... p 1000 N94-16911
SCHLICHTING, W. ..... p 1199 N94-14986
SCHLOERB, F. PETER ..... p 1298 N94-15421
p 1283 N94-16368
SCHLUETER, W. ..... p 877 N94-15606
SCHLUMP, WOLFGANG ..... p 975 N94-16002
SCHMERA, GABOR ..... p 1117 N94-15662
SCHMID, PETER ..... p 1128 N94-16779
SCHMIDT, J. A. ..... p 1128 N94-16783
SCHMISSEUR, J. D. ..... p 861 N94-17461
SCHMITT, R. A. ..... p 1244 N94-16357
p 1104 N94-16358
p 1244 N94-16359
p 1104 N94-16360
SCHMITZ, G. ..... p 944 N94-15165
SCHMITZ, J. ..... p 1035 N94-17619
SCHMULLIUS, C. ..... p 992 N94-15902
p 1075 N94-16733
SCHNAKENBERG, U. ..... p 908 N94-15083
SCHNEIDER, DEAN L. ..... p 1168 N94-17517
SCHNEIDER, LEO E. ..... p 1041 N94-17193
SCHNEIDER, MICHAEL G. ..... p 866 N94-15761
SCHNEIDER, WILLIAM E. ..... p 1011 N94-16549
SCHNEIR, I. ..... p 972 N94-17242
SCHNOPPER, H. W. ..... p 900 N94-15030
SCHOBERT, H. H. ..... p 975 N94-16996
SCHOENING, U. ..... p 1150 N94-16579
SCHOESTER, L. ..... p 944 N94-15161
SCHOLZ, W. ..... p 1061 N94-17105
SCHONBERG, WILLIAM P. ..... p 899 N94-16154
SCHOU, J. ..... p 1299 N94-15968
SCHRADE, HERBERT ..... p 928 N94-17308
SCHREIBER, ROBERT ..... p 1168 N94-15112
p 1158 N94-15113
p 1159 N94-15796
p 1148 N94-15956
SCHREIBER, ULRICH ..... p 916 N94-15582
p 876 N94-15600
p 877 N94-15606
SCHRIMSHER, ROBERT H. ..... p 1119 N94-14952
SCHROEDER, DIETRICH ..... p 1081 N94-15156
SCHUBERT, J. ..... p 907 N94-15082
SCHULER, D. L. ..... p 1077 N94-16743
SCHULLER, IVAN K. ..... p 1217 N94-17606
SCHULT, D. L. ..... p 1059 N94-15997
SCHULTZ, L. ..... p 1244 N94-16361
SCHULTZ, P. H. ..... p 1251 N94-16196
p 1007 N94-16197
SCHULZ, B. ..... p 907 N94-15082
SCHULZ, R. B. ..... p 968 N94-16843
SCHUSCHEREBA, S. T. ..... p 1122 N94-15741
SCHUSCHEREBA, STEVEN T. ..... p 1117 N94-16545
SCHUTZ, BOB E. ..... p 911 N94-15556
SCHUTZENHOFER, S. ..... p 976 N94-15723
SCHUTZENHOFER, SCOTT ..... p 930 N94-16144
SCHWAB, C. ..... p 1168 N94-14939
p 1029 N94-17384
SCHWAB, JOHN R. ..... p 1019 N94-15475
p 1019 N94-15485
p 1020 N94-15488
p 1022 N94-15865
p 1022 N94-15867
p 1024 N94-16527
SCHWARTZ, J. L. ..... p 1129 N94-16970
SCHWARTZ, R. W. ..... p 1015 N94-17648
SCHWARZ, O. J. ..... p 934 N94-16008
SCHWARZ, R. B. ..... p 958 N94-16463
SCHWEMMER, GEARY ..... p 1194 N94-17321
SCHWOEBEL, P. R. ..... p 1015 N94-17526
p 1015 N94-17608
SCOTT, C. D. ..... p 975 N94-16807
SCOTT, CRAIG J. ..... p 1008 N94-15636
SCOTT, E. R. D. ..... p 1241 N94-16213
p 1246 N94-16414
SCOTT, MICHAEL L. ..... p 1159 N94-16577
SCOTT, MILES L. ..... p 1195 N94-17340
SCOTT, T. C. ..... p 975 N94-16807
SCROSATI, BRUNO ..... p 973 N94-17434
SCUDDER, D. W. ..... p 1013 N94-17318
SEAH, M. P. ..... p 1006 N94-17549
SEALS, JOSEPH ..... p 922 N94-17083
SEARS, D. W. G. ..... p 1242 N94-16257
SEBAHAR, DAVID A. ..... p 928 N94-17213
SECRIST, GRANT E. ..... p 1132 N94-16942
SEE, T. H. ..... p 1063 N94-16253
p 1246 N94-16414
SEEBOLD, J. G. ..... p 1096 N94-16825
SEERY, BERNARD D. ..... p 1226 N94-14981
SEERY, PAUL J. ..... p 918 N94-15595
p 918 N94-15596
SEESDORF, DAVE ..... p 937 N94-16851
SEIBERT, GEORGE L. ..... p 861 N94-17609
SEIDEL, STEVEN R. ..... p 999 N94-16867
SEILS, C. A. ..... p 1211 N94-16805
SEINER, JOHN M. ..... p 925 N94-15947
SEITTER, KEITH L. ..... p 1105 N94-15142
SELDEN, MICHAEL ..... p 913 N94-15568
p 914 N94-15573
p 915 N94-15577
p 922 N94-15624
SELDON, MICHAEL ..... p 884 N94-15193
SELF, HERSCHEL C. ..... p 1192 N94-16926
SELIGMAN, ERIK ..... p 1153 N94-17118
SELIVANOV, A. S. ..... p 1294 N94-16423
SELKER, MARK D. ..... p 913 N94-15563
SELLARS, B. G. ..... p 979 N94-16088
SELLER, P. ..... p 909 N94-15090
SELVIN, S. ..... p 1128 N94-16812
SEMJONOVA, L. F. ..... p 1246 N94-16422
SENSKE, DAVID A. ..... p 1298 N94-17654
SENSMEIER, M. D. ..... p 1054 N94-16518
SEOANE, JOAQUIN ..... p 1158 N94-14980
SERCK-HANSSEN, FIN ..... p 909 N94-15095
SERGEENKO, M. N. ..... p 1185 N94-17312
SERGIENKO, V. P. ..... p 1179 N94-14931
SERRA, G. ..... p 908 N94-15087
SESSLER, A. M. ..... p 1211 N94-16827
SETNA, R. P. ..... p 957 N94-16015
SETTLES, GARY S. ..... p 1017 N94-15197
SEVENHUIJSEN, PIETER J. ..... p 1062 N94-17600
SEWELL, MARK W. ..... p 1011 N94-16488
SEXTON, GARY N. ..... p 1035 N94-17002
SHAFER, STEVEN A. ..... p 1163 N94-14968
SHAFFER, L. B. ..... p 1209 N94-16171
SHAH, H. ..... p 971 N94-16994
SHAH, JAGDEEP ..... p 1014 N94-17410
SHAHABUDDIN, PERWEZ ..... p 1174 N94-15823
SHAKED, H. ..... p 1208 N94-15982
SHALKHAUSER, MARY JO ..... p 883 N94-17488
SHALTENS, RICHARD K. ..... p 928 N94-17256
SHANAHAN, DENNIS F. ..... p 862 N94-15637
SHANG, C. C. ..... p 1039 N94-16054
SHANNON, DAVID T., JR. ..... p 1138 N94-17452
SHANNON, S. G. ..... p 1119 N94-14952
SHAPIRO, A. T. ..... p 1067 N94-16674
SHARP, L. L. ..... p 1249 N94-16182
SHAW, MARY ..... p 1144 N94-15216
p 1147 N94-15728
SHEBALIN, JOHN V. ..... p 1021 N94-15768
p 1023 N94-15964
SHEEHY, FINBAR T. ..... p 1188 N94-14957
SHELTON, WESLEY W. ..... p 1118 N94-17232
SHELUS, PETER J. ..... p 917 N94-15593
p 918 N94-15598
SHEMI, AMOTZ ..... p 905 N94-15064
SHEN, JIAN-JUN ..... p 1035 N94-17401
SHENG, QUI-QIN ..... p 1193 N94-17254
SHEPHERD, J. M. ..... p 1106 N94-16465
SHEPHERD, WILLIAM ..... p 1055 N94-17515
SHERCLIFF, H. R. ..... p 941 N94-17457
SHERES, DAVID ..... p 1077 N94-16742
SHERWOOD, R. J. ..... p 1125 N94-16618
SHETTY, R. ..... p 1199 N94-14986
SHI, JIAN-CHENG ..... p 1075 N94-16732
p 1079 N94-16755
SHIFFLER, MARK E. ..... p 1048 N94-16915
SHIH, H. R. ..... p 1048 N94-17088
SHIH, T. H. ..... p 1025 N94-16879
SHIMABUKURO, R. L. ..... p 1039 N94-16474
SHINN, JUDY L. ..... p 1300 N94-15816
p 1300 N94-17084
SHIREY, STEVEN B. ..... p 1244 N94-16321
SHIRLEY, K. W. ..... p 1050 N94-16055
SHIROKOV, M. I. ..... p 1171 N94-17314
SHIVELY, C. A. ..... p 864 N94-16835
SHIVELY, DAVID G. ..... p 989 N94-15767
SHLACHTER, J. S. ..... p 1013 N94-17318
SHOENBERGER, JAMES E. ..... p 983 N94-15177
SHOR, ALEXANDER ..... p 1085 N94-17467
SHORE, B. W. ..... p 1039 N94-16054
SHOUCRI, M. ..... p 1201 N94-15210
SHOUGH, D. ..... p 1197 N94-17355
SHRAGER, RICHARD I. ..... p 1123 N94-16564
SHUKOLYUKOV, YU. A. ..... p 953 N94-16264
SHULTS, THEODORE ..... p 1124 N94-16611
SHUM, KAI ..... p 1210 N94-16720
SHUMOVSKIJ, A. S. ..... p 1186 N94-17612
SHUVALOV, V. V. ..... p 1290 N94-16404
SHVARTSMAN, FELIX P. ..... p 1198 N94-17358
SHYY, DONG-JYE ..... p 883 N94-17111
SICKAFUS, K. E. ..... p 965 N94-15920
SIDDONS, D. P. ..... p 1212 N94-16887
SIDERS, C. W. ..... p 1183 N94-16818
SIEBER, A. ..... p 1076 N94-16740
SIEGMUND, O. H. W. ..... p 901 N94-15037
SIEVERS, A. J. ..... p 1206 N94-15822
SIEVERT, RAINER ..... p 1058 N94-15642
SIGNER, P. ..... p 954 N94-16432
SIKKA, V. K. ..... p 957 N94-16165
SILBERMAN, E. ..... p 1207 N94-15973
SILBEY, ROBERT J. ..... p 1193 N94-17024
SILCOX, J. ..... p 1212 N94-16961
SILVA, WALTER A. ..... p 886 N94-15722
SILVER, RAE ..... p 1121 N94-15660
SILVESTER, JUNE P. ..... p 1228 N94-15009
SILVESTRI, R. ..... p 1150 N94-16579
SIMARD, S. ..... p 978 N94-16080
SIMCOX, SCOTT P. ..... p 1109 N94-17571
SIMEONIDES, G. ..... p 1018 N94-15203
SIMEONSSON, JOSEF B. ..... p 951 N94-17203
SIMMERER, STEPHEN J. ..... p 1298 N94-15821
SIMMONS, M. ..... p 1162 N94-17646
SIMMONS, REID G. ..... p 1131 N94-15742
SIMON, GAD A. ..... p 1128 N94-16779
SIMONE, A. ..... p 906 N94-15071
SIMONSEN, LISA C. ..... p 1300 N94-15816
SIMONUTTI, MARIO D. ..... p 922 N94-17083
SINCLAIR, ANDREW T. ..... p 912 N94-15560
p 917 N94-15592
SINGER, R. B. ..... p 1248 N94-16179
p 1278 N94-16342
p 1291 N94-16406
p 1292 N94-16411
SINGER, ROBERT ..... p 1295 N94-16431
SINGH, ANANT ..... p 973 N94-17466
SINGH, D. ..... p 934 N94-16057
SINGH, GURBAX ..... p 946 N94-15685
SIPE, GARY A. ..... p 1000 N94-16945
SIPILA, S. K. ..... p 1201 N94-15208
SIRMAIN, G. ..... p 902 N94-15047
p 902 N94-15048
p 908 N94-15087
SISAKYAN, A. N. ..... p 1220 N94-17315
SISTO, F. ..... p 857 N94-16471
SIVAPALAN, MURUGESU ..... p 1083 N94-16027
p 1083 N94-16028
SIZE, P. ..... p 1011 N94-16505
SKALARE, A. ..... p 903 N94-15054
SKEENS-JONES, LISA M. ..... p 1211 N94-16782
SKELLY, MICHAEL V. ..... p 1060 N94-16943
SKLENICKA, V. ..... p 959 N94-16890
SKORIUKIN, V. E. ..... p 903 N94-15053
SKRIPNIK, A. YA. ..... p 1243 N94-16297
SLAUGHTER, K. ..... p 979 N94-16083
SLEZIONA, CRISTIAN ..... p 928 N94-17308
SLINEY, HAROLD E. ..... p 930 N94-15769
SLOBODRIAN, R. J. ..... p 979 N94-16086
p 923 N94-16100
SLOBODYAN, V. M. ..... p 1013 N94-17316
SMIALEK, J. L. ..... p 958 N94-15992
SMITH, A. ..... p 906 N94-15070
p 907 N94-15079
SMITH, ANNE K. ..... p 1098 N94-15639
SMITH, B. ..... p 1093 N94-17668
SMITH, BRADLEY J. ..... p 1154 N94-17371
SMITH, BROOKE C. ..... p 856 N94-15677
p 857 N94-15720
p 857 N94-15780
SMITH, BYRON L. ..... p 960 N94-16984
SMITH, CRAWFORD F. ..... p 861 N94-17558
SMITH, D. E. ..... p 1279 N94-16347
SMITH, D. W. ..... p 963 N94-14948
SMITH, DAVID ..... p 911 N94-15553
SMITH, DAVID E. ..... p 916 N94-15586
SMITH, ERNEST K. ..... p 996 N94-16044
p 997 N94-16050
SMITH, G. ..... p 901 N94-15040
SMITH, G. C. ..... p 1209 N94-16447
SMITH, G. D. W. ..... p 957 N94-16015
SMITH, G. W. ..... p 947 N94-15861
SMITH, GEOFFREY M. ..... p 1069 N94-16683
SMITH, GREG ..... p 1241 N94-16195
SMITH, GUY A. ..... p 976 N94-15006
SMITH, IAN E. ..... p 1155 N94-17500
SMITH, JAMES C. ..... p 921 N94-15618
SMITH, LINDA G. ..... p 861 N94-17609

SMITH, MICHAEL D. ..... p 1246 N94-15182
SMITH, MILTON O. ..... p 1066 N94-16668
p 1068 N94-16677
p 1068 N94-16679
p 1070 N94-16689
p 1073 N94-16706
p 1074 N94-16709
SMITH, P. ..... p 961 N94-17109
SMITH, P. K. ..... p 924 N94-15219
SMITH, PHILIP J. ..... p 1148 N94-15965
SMITH, R. W. ..... p 978 N94-16082
SMITH, SCOTT D. ..... p 928 N94-17213
SMITH, WAYNE D. ..... p 999 N94-16777
SMITS, ALEXANDER J. ..... p 1026 N94-16929
SMOOKE, MITCH D. ..... p 950 N94-17008
SMYTHE-WRIGHT, D. ..... p 1114 N94-17489
SNEE, L. W. ..... p 1104 N94-16334
SNIDER, J. B. ..... p 996 N94-16046
SNOW, ERIC S. ..... p 948 N94-16539
SNYDER, A. E. ..... p 904 N94-15061
SNYDER, D. B. ..... p 1033 N94-15826
SNYDER, GREGORY A. ..... p 1266 N94-16276
SOBEHART, J. R. ..... p 1039 N94-16114
SODDU, C. ..... p 893 N94-17165
SODERBLOM, L. A. ..... p 1274 N94-16319
SODERBLOM, LAURENCE A. ..... p 1288 N94-16393
SOEDER, RONALD H. ..... p 872 N94-15819
SOLOMON, SEAN C. ..... p 1104 N94-16396
SONG, C. ..... p 975 N94-16996
SONG, L. ..... p 1209 N94-16159
SONG, L. W. ..... p 1209 N94-16447
SONG, S. N. ..... p 908 N94-15089
SONNTAG, DIETRICH ..... p 1105 N94-15302
SOO, Y. L. ..... p 1209 N94-16447
SOPKO, B. ..... p 921 N94-15619
SORATHIA, USMAN A. ..... p 969 N94-16916
SOTIN, C. ..... p 1067 N94-16675
SOULAS, GEORGE C. ..... p 926 N94-16880
SOUZIS, A. E. ..... p 1242 N94-16240
SOWERS, C. H. ..... p 1208 N94-16058
SPAIN, CHARLES V. ..... p 867 N94-17055
SPANDE, ROBERT A. ..... p 1197 N94-17354
SPANGLER, CHARLES W. ..... p 1192 N94-16563
SPANN, JAMES F. ..... p 1190 N94-15868
SPANOS, POL D. ..... p 1059 N94-16123
SPARKS, C. J. ..... p 1209 N94-16171
SPATARO, C. ..... p 1176 N94-17658
SPAULDING, GLENN F. ..... p 1117 N94-15969
SPEAR, KARL ..... p 973 N94-17466
SPEE, B. M. ..... p 854 N94-15129
SPENCER, A. C. ..... p 1050 N94-16055
SPENCER, MICHAEL G. ..... p 1014 N94-17324
SPENCER, THOMAS A. ..... p 1011 N94-16556
SPENDLEY, WILLIAM J., JR. ..... p 1107 N94-17054
SPERBER, PETER ..... p 914 N94-15575
p 877 N94-15610
p 877 N94-15611
p 877 N94-15612
p 877 N94-15613
SPERRY, DAVID J. ..... p 882 N94-16530
p 897 N94-17240
SPIERING, BRUCE ..... p 1063 N94-16596
SPINDT, C. A. ..... p 1015 N94-17526
p 1015 N94-17608
SPINELLI, A. ..... p 914 N94-15571
SPINHIRNE, JAMES ..... p 1004 N94-17322
SPONG, D. A. ..... p 1203 N94-16869
SPOONER, S. ..... p 1207 N94-15827
SPROUL, WILLIAM D. ..... p 971 N94-17122
SQUYRES, S. ..... p 1297 N94-17637
SREENIVASAN, K. R. ..... p 1026 N94-16950
p 860 N94-17099
SRINIVASAN, B. ..... p 954 N94-16353
SRINIVASAN, G. ..... p 1241 N94-16191
ST.CLAIR, ANNE K. ..... p 965 N94-15880
p 974 N94-17559
ST.CLAIR, STEVEN ..... p 1124 N94-16611
ST.CLAIR, TERRY L. ..... p 965 N94-15879
p 965 N94-15880
p 974 N94-17559
ST.JOHN, H. ..... p 1203 N94-16823
STACY, J. ..... p 1014 N94-17375
STADSNES, J. ..... p 907 N94-15081
STAEHLE, H. J. ..... p 946 N94-15172
STAENZ, KARL ..... p 1074 N94-16707
STAHL, DAVID A. ..... p 1118 N94-16989
STAHLE, C. K. ..... p 899 N94-15027
STANLEY, M. L. ..... p 926 N94-16773
STANSFIELD, S. A. ..... p 1132 N94-16819
STANTON, ALAN C. ..... p 1036 N94-17655
STAPELBROEK, M. G. ..... p 902 N94-15043
STARK, KENNETH W. ..... p 1047 N94-16548
STATHAM, RICHARD B. ..... p 1085 N94-17665
STAUFFER, PAUL R. ..... p 1121 N94-15634
STAVETEIG, P. T. ..... p 1206 N94-14922
STAVNES, MARK W. ..... p 1040 N94-16522
STEEN, A. ..... p 909 N94-15093
STEEPLES, D. W. ..... p 1103 N94-16307
STEFANESCU, DORU MICHAEL ..... p 960 N94-17079
STEIN, F. ..... p 981 N94-16095
STEIN, ROBERT ..... p 1196 N94-17347
STEINER, D. ..... p 1203 N94-16901
STEINETZ, BRUCE M. ..... p 939 N94-16859
STEINOLFSON, RICHARD S. ..... p 1299 N94-17281
STENCEL, R. E. ..... p 1232 N94-17038
STENCEL, ROBERT E. ..... p 1236 N94-16492
STENGER-SMITH, JOHN ..... p 969 N94-16920
STEPANOV, R. M. ..... p 903 N94-15053
STEPHEN, J. B. ..... p 899 N94-15029
STEPHENS, D. R. ..... p 966 N94-15996
STEPHENS, MICHAEL ..... p 1172 N94-15002
STEPHENS, MICHAEL A. ..... p 1173 N94-16726
STEPHENSON, D. E. ..... p 1112 N94-16009
STEPHENSON, LOU A. ..... p 1035 N94-17002
STERK, F. J. ..... p 853 N94-15121
STERN, MARGARET B. ..... p 1195 N94-17343
STERN, P. ..... p 979 N94-16083
STERN, R. C. ..... p 1039 N94-16450
STERN, S. A. ..... p 1280 N94-16351
STERN, S. ALAN ..... p 1297 N94-16832
p 923 N94-17126
STEUBER, G. D. ..... p 1023 N94-15991
STEVEN, M. ..... p 1070 N94-16691
STEVENS, J. ..... p 1016 N94-17671
STEVENSON, DAVID A. ..... p 1216 N94-17454
STEVENSON, TIM J. ..... p 899 N94-16374
STEWART, BILL ..... p 980 N94-16091
STEWART, LOYAL ..... p 922 N94-15622
STICHNOTH, JAMES M. ..... p 1160 N94-16724
STILLWAGEN, FREDERIC H. ..... p 1085 N94-17665
STINE, W. B. ..... p 1092 N94-16112
STINN, JENNIFER ..... p 980 N94-16091
STINTON, D. P. ..... p 934 N94-16008
p 934 N94-16065
p 969 N94-16889
STOCK, J. ..... p 901 N94-15037
STOCKWELL, ALAN E. ..... p 1062 N94-17451
STODOLSKY, DANIEL ..... p 1140 N94-15744
STOEGER, R. ..... p 876 N94-15600
STOEWE, T. L. ..... p 1274 N94-16319
STOFAN, ELLEN R. ..... p 1256 N94-16215
p 1298 N94-17654
STOKER, CAROL R. ..... p 1293 N94-16419
STOLOFF, N. S. ..... p 955 N94-15830
STOLPER, E. M. ..... p 1219 N94-16331
STONE, BARBARA A. ..... p 1235 N94-17290
p 1222 N94-17441
STONE, LEWIS W. ..... p 1131 N94-15659
STONER, WILLIAM W. ..... p 1074 N94-16708
STORM, MARK E. ..... p 1039 N94-15942
STOUT, CYNTHIA S. ..... p 1121 N94-15711
STOY, S. L. ..... p 1152 N94-17032
STRACHAN, J. W. ..... p 1091 N94-15993
STRADLING, R. A. ..... p 1015 N94-17570
STRANGELAND, ERIC ..... p 927 N94-17098
STRAUB, J. ..... p 944 N94-15160
STRAZISAR, ANTHONY J. ..... p 869 N94-17386
STRECKERT, H. ..... p 972 N94-17242
STRIEBICH, R. C. ..... p 942 N94-14911
STRIZH, T. A. ..... p 1168 N94-14933
STROBEL, FORREST ..... p 928 N94-17277
STROBL, P. ..... p 1070 N94-16688
STROMEYER, CHARLES F., III ..... p 1133 N94-17397
STRONGIN, D. R. ..... p 974 N94-17676
STRONGIN, M. ..... p 974 N94-17676
STROPE, L. A. ..... p 1043 N94-17677
STUCK, B. E. ..... p 1122 N94-15741
STUCK, BRUCE E. ..... p 1128 N94-16779
STUCKEY, W. K. ..... p 887 N94-16909
STUTZMAN, WARREN ..... p 995 N94-16037
SU, TSUNG-CHOW ..... p 1055 N94-17514
SU, ZHAO-BIN ..... p 1215 N94-17437
SUAREZ, CARLOS J. ..... p 855 N94-15655
p 856 N94-15677
p 857 N94-15720
p 857 N94-15780
SUBHAN, W. ..... p 934 N94-16057
SUBRAMANIAN, CHELAKARA S. ..... p 1027 N94-17130
SUBRAMANIAN, P. ..... p 970 N94-16947
p 970 N94-16948
p 970 N94-16949
SUCHAN, JAMES E. ..... p 1223 N94-15682
SUDARSHAN, T. S. ..... p 968 N94-16767
SUENO, SHIGEHO ..... p 1104 N94-16336
SUERMANN, THOMAS C. ..... p 1174 N94-16109
SUGAYA, S. ..... p 1226 N94-14983
p 1227 N94-14989
SUKTHANKAR, RAHUL ..... p 863 N94-14971
p 864 N94-14972
SULLIVAN, PATRICK J. ..... p 868 N94-16090
SUMMERS, GEOFFREY P. ..... p 1173 N94-17495
SUMNER, T. J. ..... p 906 N94-15070
p 907 N94-15079
p 909 N94-15090
p 911 N94-15103
SUN, GUO-QING ..... p 1077 N94-16741
SUN, XIAN-HE ..... p 1149 N94-15989
SUN, YI-ZHU ..... p 1042 N94-17394
SUN, ZHAN-AO ..... p 913 N94-15566
SUNG, C. C. ..... p 1054 N94-16155
SUNSHINE, J. ..... p 1258 N94-16228
SUNSHINE, J. M. ..... p 1288 N94-16394
SUNSHINE, JESSICA M. ..... p 1086 N94-16437
SUSAK, L. E. ..... p 980 N94-16094
SUTHERLAND, LOUIS ..... p 871 N94-14908
SUTLEY, STEVE ..... p 1069 N94-16682
SUTLIFF, T. J. ..... p 978 N94-16078
SUTTON, C. W. ..... p 872 N94-15543
SUTTON, M. A. ..... p 931 N94-15184
p 956 N94-15948
SUTTON, S. R. ..... p 956 N94-15921
SUZKO, A. A. ..... p 1219 N94-14935
SUZUKI, DAVID E. ..... p 927 N94-17053
SUZUKI, R. ..... p 892 N94-17160
SUZUKI, T. ..... p 1227 N94-14991
SVENSSON, C. ROBERT ..... p 1206 N94-15107
SWAN, SCOTT A. ..... p 1137 N94-15883
SWAYZE, GREGG ..... p 1069 N94-16682
SWAYZE, GREGG A. ..... p 1066 N94-16670
p 1069 N94-16686
SWEATT, W. C. ..... p 1036 N94-17647
SWEETING, M. N. ..... p 894 N94-17169
SWIATNICKI, WIESLAW ..... p 961 N94-17121
SWIFT, DANIEL W. ..... p 1102 N94-17527
SWINYARD, B. ..... p 909 N94-15090
SWINYARD, B. M. ..... p 905 N94-15066
p 905 N94-15067
SWITZER, G. F. ..... p 1108 N94-17283
SYLLA, WILLIAM K. ..... p 960 N94-17100
SYTSMA, H. A. ..... p 1031 N94-17627
SZABO, BARNA A. ..... p 1062 N94-17445
SZCZEBOIT, RYSZARD ..... p 960 N94-17093
SZCZYGIEL, BRONIA ..... p 1143 N94-15022
SZPANKOWSKI, W. ..... p 1172 N94-15777
SZWEDOWSKA-KOTLINSKA, JOANNA
p 971 N94-17120
SZYBA, DIONIZY ..... p 985 N94-17068
SZYMANSKI, ZYGMUNT ..... p 1204 N94-17066
SZYMKOWIAK, A. E. ..... p 899 N94-15027

T

TACHIKAWA, HIROYASU ..... p 1010 N94-16061
TACKE, M. ..... p 909 N94-15092
TADAYON, BIJAN ..... p 1210 N94-16538
TADAYON, SAIED ..... p 1210 N94-16538
TAHERI, F. ..... p 981 N94-16099
TAI, ANTHONY M. ..... p 1196 N94-17345
TAJIMA, T. ..... p 1187 N94-16660
TAKADA, S. ..... p 905 N94-15088
TAKAHASHI, FUJINOBU ..... p 911 N94-15555
TAKAHASHI, K. ..... p 1240 N94-17628
TAKEDA, H. ..... p 1245 N94-16400
p 1104 N94-16416
TAKEDA, HIROSHI ..... p 1245 N94-16410
TAKEUCHI, ESTHER S. ..... p 1011 N94-16505
TAKHTAMYSHEV, G. G. ..... p 1179 N94-14934
TAMIL, LAKSHMAN S. ..... p 1199 N94-17427
TAMIN, M. ..... p 941 N94-17379
TAMISE, CHANTAL ..... p 889 N94-17135
TAN, AXEL S. T. ..... p 1230 N94-15839
TAN, DE-TONG ..... p 913 N94-15566
p 918 N94-15597
p 877 N94-15605
TANABE, T. ..... p 1219 N94-16420
TANAKA, KENNETH L. ..... p 1280 N94-16350
TANAKA, M. ..... p 892 N94-17160
TANAKA, S. ..... p 1213 N94-17108
TANCA, LETIZIA ..... p 1156 N94-17501
TANDON, K. N. ..... p 978 N94-16082
TANG, CHA-MEI ..... p 1038 N94-15686
TANG, SHI-LIN ..... p 1037 N94-15806
TANG, W. J. ..... p 1227 N94-14989
TANG, W.-F. ..... p 877 N94-15605
TANIMOTO, M. ..... p 945 N94-15167
TANKINS, EDWIN ..... p 962 N94-17418
TANNER, WILLIAM G. ..... p 899 N94-16374
TANVEER, S. ..... p 1029 N94-17387
TAPLEY, BYRON D. ..... p 1081 N94-17444
TASK, HARRY L. ..... p 868 N94-17425
TAUTZ, M. F. ..... p 882 N94-16468
TAWADROS, M. J. ..... p 877 N94-15621
TAYAG, TRISTAN J. ..... p 1195 N94-17338
TAYLOR, G. J. ..... p 1258 N94-16225
p 1283 N94-16366
p 1245 N94-16390
TAYLOR, H. S. ..... p 908 N94-15088
TAYLOR, J. B. ..... p 1203 N94-16822

TAYLOR, J. R. p 1023 N94-15980
TAYLOR, K. P. p 959 N94-16780
TAYLOR, LAWRENCE A. p 1266 N94-16275
p 1266 N94-16276
TAYLOR, R. E. p 904 N94-15061
TAYLOR, THEODORE D. p 983 N94-15881
TAZZOLI, V. p 1241 N94-16175
TCHEBOTAREV, V. E. p 915 N94-15576
TEAGUE, M. W. p 946 N94-15685
TEAS, DON C. p 1134 N94-17510
TEHRANCHI, B. p 1227 N94-14988
TEILLAUD, MONIQUE p 1156 N94-17528
TEITELBAUM, RITA p 1127 N94-16645
TEMPLE, MICHAEL A. p 1001 N94-17031
TENCH, D. M. p 1009 N94-15726
TENG, SHANG-HUA p 1159 N94-15796
TENG, W. L. p 1079 N94-16754
TENNYSON, J p 1190 N94-15854
TEO, JOSEPH p 1157 N94-17620
TEPIKIAN, S. p 1184 N94-16885
TEPPER, S. p 1054 N94-16156
TER-ANTONYAN, V. M. p 1220 N94-17315
TERPENING, L. p 1006 N94-17565
TERRIE, GREGORY p 1070 N94-16690
TERRY, P. W. p 1187 N94-17674
TESAR, A. p 1190 N94-15975
TESCHE, FRED M. p 988 N94-15668
TEUCHER, R. p 1259 N94-16233
THAI, SEREY p 1003 N94-17228
THEISS, T. J. p 1059 N94-16104
THEON, JOHN S. p 992 N94-15906
THIBADEAU, ROBERT p 1163 N94-14953
p 1188 N94-15144
THIEM, KEEM B. p 1001 N94-17025
THIERAUF, T. p 1150 N94-16579
THOMAS, C. p 908 N94-15089
THOMAS, J. R. p 1115 N94-14918
THOMAS, JOSEPH M. p 1101 N94-16469
THOMAS, K. L. p 1243 N94-16309
THOMAS, M. G. p 1093 N94-17217
THOMAS, P. D. p 905 N94-15063
THOMPSON, C. M. p 1242 N94-16245
THOMPSON, G. p 1221 N94-17632
THOMPSON, KEITH L. p 1232 N94-17101
THOMPSON, M. p 941 N94-17379
THOMPSON, R. S. p 878 N94-17154
THOMPSON, W. R. p 1252 N94-16201
THOMSON, I. p 980 N94-16092
THORNEWELL, P. M. p 1185 N94-16951
THORNTON, E. N. p 1215 N94-17319
p 1043 N94-17677
THORP, J. W. p 1130 N94-17562
THORPE, CHARLES p 863 N94-14919
p 864 N94-14972
THRASHER, T. P. p 933 N94-15277
THRESHER, B. p 1093 N94-17668
THYKIER-NIELSEN, SOEREN p 1105 N94-14938
TICHENOR, D. A. p 1036 N94-17647
TIEGS, T. N. p 1209 N94-16164
p 969 N94-16877
TILMANS, E. p 987 N94-15644
TIMMINS, SIDEY P. p 1097 N94-17426
TINKER, MICHAEL L. p 883 N94-16151
TIRABOSCHI, ALEJANDRO p 1175 N94-17643
TISSOT, M. p 891 N94-17153
TITOV, D. V. p 1294 N94-16423
TITRAN, R. H. p 959 N94-16883
TITRAN, R. J. p 923 N94-15118
TITRAN, ROBERT H. p 962 N94-17652
TIWARI, S. N. p 1181 N94-15752
p 1021 N94-15795
p 1027 N94-17127
p 1027 N94-17215
TOFSTED, DAVID H. p 1085 N94-17610
TOKUDA, HIDEYUKI p 1158 N94-15745
TOLER, JAMES C. p 1118 N94-17232
TOLK, NORMAN p 946 N94-15766
TOLSON, ROBERT H. p 886 N94-15864
TOMLINS, P. E. p 1057 N94-15016
p 1057 N94-15017
TONDELLO, GIUSEPPE p 873 N94-15062
TONG, R. p 1006 N94-17565
TOPAZ, JEREMY p 905 N94-15064
TORR, DOUGLAS G. p 1190 N94-15868
p 1190 N94-15869
p 1191 N94-16023
p 1191 N94-16024
p 967 N94-16494
TORR, MARSHA R. p 1190 N94-15868
TORRE, A. p 993 N94-15913
TORRENCE, GEOFFREY W. p 995 N94-16041
p 996 N94-16047
TORRENCE, MARK p 911 N94-15553
TORRENCE, MARK H. p 912 N94-15559
TORRES, V. M. p 1015 N94-17648
TORTORELLI, P. F. p 957 N94-16163
p 958 N94-16166
TOSATTI, E. p 1205 N94-14913
TOSCANO, P. J. p 968 N94-16727
TOSCANO, WILLIAM B. p 1120 N94-15537
p 1121 N94-15711
TOSH, I. A. J. p 908 N94-15088
TOURETZKY, DAVID p 1163 N94-14953
TOWNE, CHARLES E. p 1019 N94-15475
p 1019 N94-15485
p 1020 N94-15488
p 1022 N94-15865
p 1022 N94-15867
p 1024 N94-16527
TOWNSEND, LAWRENCE W. p 1188 N94-17018
TOWSLEY, DON p 1164 N94-15695
p 1162 N94-17537
TRACY, MATTHEW C., II p 1145 N94-15525
TRAMPCZYNSKI, WIESLW p 985 N94-17068
TRAN, LEO p 1008 N94-15494
TREADWELL, STEVE B. p 1161 N94-17367
TREMBLAY, K. p 981 N94-16097
TRIBAUDINO, M. p 1246 N94-16417
TRIFEL, B. YU. p 963 N94-15133
TRIFOGLIO, M. p 899 N94-15029
TRIMBLE, V. R. p 979 N94-16088
TRIPATHI, RAM K. p 1180 N94-15715
p 1301 N94-17255
TRIPATHY, SUKANT p 964 N94-15675
p 964 N94-15688
TROCH, PETER A. p 1083 N94-16031
TROESKEN, FRIEDHELM p 984 N94-16003
TROGLER, WILLIAM C. p 950 N94-16931
TROSEN, DENNIS W. p 870 N94-15730
TROW, M. W. p 909 N94-15094
TROWBRIDGE, CHRISTIAN A. p 1192 N94-16936
TROWER, M. A. p 908 N94-15088
TRUBETSKAYA, I. A. p 1290 N94-16404
TRUDELL, JEFFREY J. p 929 N94-17483
TRUSTY, G. L. p 1098 N94-15539
TRYGGVASON, B. V. p 981 N94-16098
TRYGGVASON, BJARNI p 980 N94-16091
TRYGGVASON, BJARNI V. p 868 N94-16090
TSANG, I. K. Y. p 980 N94-16094
TSUI, H. Y. W. p 1202 N94-16162
TU, C. W. p 1213 N94-17042
TUASON, CHRISTOPHER M. p 1170 N94-17076
TUCKER, ZENA A. p 1108 N94-17247
TUNG, C. p 856 N94-15657
TUNHEIM, SVEIN p 909 N94-15095
TUONG, V. KH. p 974 N94-17634
TURCOTTE, D. L. p 1276 N94-16332
TUREK, ZBIGNIEW p 1061 N94-17058
p 1041 N94-17065
TURNER, D. J. p 945 N94-15166
TURNER, M. J. L. p 907 N94-15080
TURNER, M. S. p 1239 N94-16118
TURNOCK, DAVID L. p 866 N94-15722
TURON, P. p 891 N94-17153
TURSKI, KAROL p 951 N94-17050
TUSZYNSKI, WACLAW p 971 N94-17120
TUTTEROW, ROBIN D. p 885 N94-15446
TYC, G. p 978 N94-16082
TYLER, CHARLES p 861 N94-17609
TYSON, RICHARD W. p 977 N94-16072

U

UCKAN, T. p 1202 N94-16162
UEDA, Y. p 1212 N94-16868
UKRAINEC, A. p 988 N94-15698
ULABY, FAWWAZ T. p 991 N94-15898
ULLMANN, C. p 932 N94-15260
ULMER, M. P. p 908 N94-15089
ULYANOV, A. A. p 1241 N94-16191
UNDERWOOD, A. D. p 947 N94-16105
UNGAR, EUGENE p 1022 N94-15962
UNITE, THEODORE p 1125 N94-16621
URQUHART, KRIS p 1196 N94-17347
USTIN, SUSAN L. p 1066 N94-16668
p 1067 N94-16672
p 1068 N94-16679
p 1070 N94-16689
p 1070 N94-16691
p 1072 N94-16697
p 1074 N94-16709
USTINOVA, G. K. p 1244 N94-16344
UTASHIMA, M. p 1287 N94-16387
UTSCH, THOMAS F. p 891 N94-17151
UZ, MEHMET p 959 N94-16883

V

VAEL, G. p 945 N94-15169
VAITKUS, P. J. p 981 N94-16095
VALDES-PEREZ, RAUL E. p 1148 N94-15841
VALENTIJN, E. A. p 908 N94-15084
VALENTINI, J. J. p 1182 N94-16121
VALENTINO, M. A. p 1033 N94-15826
VALENZUELA, A. p 891 N94-17149
VALENZUELA, G. R. p 1077 N94-16743
VALIVETI, RADA p 1162 N94-17539
VANAARTSEN, BRUCE H. p 1109 N94-17572
VANBREDA, I. G. p 910 N94-15096
VANCLEEMPUT, INGE p 862 N94-15550
VANDAMME, J. p 910 N94-15098
p 910 N94-15100
VANDEGRIFF, K. D. p 1128 N94-16785
VANDEGRIFF, KIM D. p 1123 N94-16564
p 1123 N94-16566
VANDENBERG, J. I. p 1031 N94-17627
VANDENBERG, L. p 1209 N94-16442
VANDENBOSCH, JEANNETTE p 1069 N94-16687
VANDERBILT, V. p 1070 N94-16691
VANDERGRACHT, JOSEPH p 1195 N94-17338
VANDERHOFF, JOHN A. p 946 N94-15685
VANDERKOOIJ, M. W. A. p 1077 N94-16745
VANDERVEEN, M. p 854 N94-15127
VANDERVEGT, J. J. W. p 1026 N94-17056
VANDERZANDEN, P. J. L. M. p 854 N94-15130
VANDESTADT, H. p 903 N94-15054
VANDROMME, D. p 1018 N94-15202
VANDYKE, GREGORY G. p 865 N94-14976
VANDYKE, LEON S. p 967 N94-16475
p 969 N94-16928
VANE, DEBORAH p 994 N94-15918
VANE, GREGG p 1037 N94-16667
VANES, C. p 877 N94-15612
p 877 N94-15613
VANHOLTEN, J. W. p 1240 N94-17603
p 1240 N94-17604
VANLEEUWEN, R. A. p 974 N94-14982
VANRAVENSWAAY, THEODORE p 1128 N94-16779
VANRENESSE, ROBBERT p 1152 N94-16982
p 1161 N94-17239
VANRUYMBEKE, M. p 1037 N94-15802
p 1037 N94-15803
p 1037 N94-15804
p 1037 N94-15805
p 1037 N94-15806
p 1100 N94-15807
p 1100 N94-15809
VANSTONE, KATHRYN p 1151 N94-16790
VANVEEN, BARRY D. p 999 N94-16728
VANWALLEGEM, L. p 1037 N94-15803
VANZANI, V. p 1245 N94-16384
VANZYL, JAKOB p 1075 N94-16731
VANZYL, JAKOB J. p 991 N94-15901
p 1079 N94-16755
VARGHESE, THOMAS p 884 N94-15193
p 922 N94-15624
VARGHESE, THOMAS K. p 913 N94-15568
p 914 N94-15573
p 915 N94-15577
p 915 N94-15578
p 915 N94-15581
p 877 N94-15601
VARNAVA, WILLIAM N. p 1167 N94-17392
VASQUEZ, PETER p 983 N94-15881
VECHT, A. p 963 N94-14948
VEDELER, ERIK p 998 N94-16655
VEEDER, G. J. p 1245 N94-16386
VEI, M. p 911 N94-15554
VEKINIS, G. p 941 N94-17457
VELDKAMP, WILFRID B. p 1194 N94-17333
VENKATESWARARAO, K. T. p 961 N94-17223
VENSON, ANTHONY R. p 934 N94-16440
VERBEEK, H. J. p 1021 N94-15755
VERBIST, A. p 901 N94-15036
VERCHEVAL, J. p 923 N94-17592
VERGHESE, M. p 979 N94-16083
VERHOEFF, PETER p 910 N94-15097
VERHOEVE, P. W. A. M. p 900 N94-15035
VERINK, ELLIS D., JR. p 954 N94-14961
VERLY, JACQUES G. p 1164 N94-15746
VERMAAT, ERIK p 877 N94-15613
VERMASEREN, J. A. M. p 1186 N94-17617
VERMEIREN, J. p 903 N94-15050
p 910 N94-15098
p 910 N94-15099
p 910 N94-15100
VERNICKEL, H. p 1200 N94-14966
VERNON, LURA p 867 N94-15783
VERPOEST, IGNAAS p 937 N94-16848
VERZENI, G. p 894 N94-17174
VETRELLA, S. p 1078 N94-16750
VETRELLA, SERGIO p 992 N94-15905
p 1078 N94-16749
VEVERKA, J. p 1259 N94-16234
VIALET, C. p 891 N94-17150
VIDALLERSISO, LEON p 1158 N94-14980
VIDDELEER, R. p 987 N94-15644

VIERECK, LES ..... p 1075 N94-16734
VIERECK, RODNEY A. ..... p 1192 N94-16936
VIG, JOHN R. ..... p 1216 N94-17480
VIJGEN, PAUL M. H. W. ..... p 859 N94-16574
VILAS, FAITH ..... p 1242 N94-16274
VINCENT, D. C. ..... p 1028 N94-17276
VINEY, CHRISTOPHER ..... p 1116 N94-15138
VINEYARD, E. A. ..... p 1024 N94-16808
VISTISEN, L. ..... p 1285 N94-16375
VISWANATHAN, S. ..... p 957 N94-16165
VITELLO, P. A. ..... p 1096 N94-16449
VITER, V. ..... p 898 N94-15889
VITT, F. ..... p 1299 N94-17208
VITTITOE, C. N. ..... p 1034 N94-16452
VITUS, C. M. ..... p 1207 N94-15923
VITYAZEV, A. V. ..... p 1244 N94-16377
VLADIMIROV, YU. V. ..... p 1179 N94-14931
VOGEL, B. ..... p 944 N94-15160
VOGEL, WOLFHARD J. ..... p 995 N94-16041
p 996 N94-16047
p 996 N94-16048
VOGELZANG, J. ..... p 1077 N94-16745
VOGT, M. ..... p 944 N94-15161
VOGT, S. ..... p 1245 N94-16409
VOGTLIN, G. E. ..... p 1096 N94-16449
VOLK, TYLER ..... p 1118 N94-17279
VOLKOV, M. K. ..... p 1185 N94-17310
VOLLATH, D. ..... p 965 N94-15920
VONDRAK, R. R. ..... p 1239 N94-16433
VONEIFF, D. ..... p 1181 N94-16013
VONTHEUMER, ALFRED E. ..... p 1085 N94-17665
VOSS, M. ..... p 907 N94-15078
VOUK, MLADEN A. ..... p 1143 N94-15114
VOYIADJIS, GEORGE Z. ..... p 934 N94-16440
VRANISH, JOHN M. ..... p 1046 N94-15871
p 1033 N94-15872
p 1165 N94-15946
VUKELICH, S. R. ..... p 1152 N94-17032
VUONG, N. V. ..... p 974 N94-17633
p 974 N94-17634

W

WADE, C. E. ..... p 1122 N94-15740
WADLEY, H. N. G. ..... p 1054 N94-16518
WAGANAAR, W. J. ..... p 1202 N94-16451
WAGH, A. S. ..... p 934 N94-16057
WAGNER, J. H. ..... p 1023 N94-15991
WAGNER, J. L. ..... p 1208 N94-15982
WAGNER, R. ..... p 1269 N94-16289
WAGSTAFF, J. ..... p 1245 N94-16399
WAH, YAU W. ..... p 1184 N94-16899
WAHR, J. M. ..... p 1101 N94-15815
WAITE, J. H. ..... p 1116 N94-15138
WAKANA, HIROMITSU ..... p 996 N94-16043
WALCK, JIM ..... p 973 N94-17466
WALENTA, ZBIGNIEW A. ..... p 1193 N94-17049
WALKER, CRAIG S. ..... p 928 N94-17213
WALKER, D. ..... p 953 N94-16283
WALKER, E. ..... p 1199 N94-14986
WALKER, E. P. ..... p 1043 N94-14994
WALLACE, R. F. ..... p 1114 N94-17516
WALLACH, D. F. ..... p 1128 N94-16785
WALLMAN, P. H. ..... p 1096 N94-16449
WALSH, P. M. ..... p 975 N94-16996
WALTER, C. ..... p 923 N94-15118
WALTERS, JERRY L. ..... p 928 N94-17213
WANG, CHUI-LIN ..... p 1215 N94-17437
WANG, F. X. ..... p 960 N94-17041
WANG, FU-QUAN ..... p 997 N94-16507
WANG, H. ..... p 1001 N94-17033
WANG, J. ..... p 1184 N94-16838
p 1151 N94-16910
WANG, J. R. ..... p 1079 N94-16754
WANG, JIAN-ZHONG ..... p 1169 N94-15833
WANG, JING-SHENG ..... p 1035 N94-17401
WANG, KANG L. ..... p 1190 N94-15848
WANG, M. ..... p 1199 N94-14986
WANG, M. S. ..... p 1199 N94-14993
WANG, MARK S. ..... p 1199 N94-14996
WANG, ROSE W. ..... p 1169 N94-15785
WANG, YONG ..... p 1076 N94-16735
WANG, ZHEN-SONG ..... p 993 N94-15915
p 993 N94-15916
WANKE, H. ..... p 1242 N94-16272
WANLASS, M. W. ..... p 1093 N94-16824
WANNER, M. ..... p 901 N94-15042
WARBURTON, P. A. ..... p 910 N94-15101
WARD, DEAN A. ..... p 868 N94-14964
WARD, J. S. ..... p 1093 N94-16824
WARD, JOHN F. ..... p 1039 N94-16124
WARD, R. C. ..... p 1301 N94-14926
WARE, GEORGE M. ..... p 861 N94-17284
WARING, R. H. ..... p 991 N94-15896
WARNER, HAROLD D. ..... p 1122 N94-15845
WARNER, T. A. ..... p 1064 N94-16602
WARREN, STEVEN W. ..... p 1107 N94-17029
WARREN, W. R., JR. ..... p 1041 N94-17193
WARREN, WADE S. ..... p 1129 N94-17478
WASSERBAUER, CHARLES A. ..... p 1032 N94-15445
WASSERBURG, G. J. ..... p 1242 N94-16260
p 954 N94-16313
WASSERMAN, H. ..... p 1162 N94-17646
WASSON, J. T. ..... p 1241 N94-16213
WATANABE, HIROSHI ..... p 1064 N94-16600
WATANABE, T. ..... p 945 N94-15167
WATSON, JUDITH J. ..... p 885 N94-15446
WATSON, KENNETH ..... p 1065 N94-16605
WATTS, D. R. ..... p 1112 N94-15844
WAY, JOBEA ..... p 992 N94-15904
p 1075 N94-16734
WAYMAN, RICHARD J. ..... p 1232 N94-17101
WAYSAND, G. ..... p 900 N94-15032
WAZOE, TAKESHI ..... p 873 N94-15000
WEADON, MARK P. ..... p 1110 N94-17595
WEAVER, B. L. ..... p 934 N94-16008
WEBB, JAMES T. ..... p 1139 N94-17563
p 1139 N94-17564
WEBB, LANNIE D. ..... p 869 N94-15141
WEBBER, MATTHEW A. ..... p 859 N94-16913
WEBER, EGON T. ..... p 1243 N94-16286
WEBER, F. ..... p 1239 N94-16052
WEBER, THEODORE T. ..... p 1009 N94-15765
WEI, C. J. ..... p 1012 N94-16935
WEI, JIE ..... p 1184 N94-16826
p 1211 N94-16827
WEI, ZHONG-QUAN ..... p 993 N94-15916
WEIDENSCHILLING, S. J. ..... p 1245 N94-16384
WEIGEL, M. K. ..... p 1181 N94-16013
WEILAND, KENNETH E. ..... p 1034 N94-15961
WEILMUENSTER, K. JAMES ..... p 1030 N94-17476
WEIMANN, T. ..... p 908 N94-15083
WEINBERGER, NORMAN M. ..... p 1177 N94-16939
WEINER, D. ..... p 1001 N94-17033
WEINER, M. M. ..... p 988 N94-15649
WEINER, MELVIN M. ..... p 987 N94-15527
WEINMANN, OLIVER ..... p 952 N94-17594
WEINSTOCK, CHARLES B. ..... p 1146 N94-15638
WEIRICH, STEPHEN A. ..... p 1126 N94-16627
p 1126 N94-16628
p 1126 N94-16629
p 1126 N94-16630
WEISS, S. ..... p 901 N94-15040
WEITZ, CATHERINE M. ..... p 1298 N94-17654
WELCH, J. A. ..... p 1098 N94-15539
WELCH, J. T. ..... p 968 N94-16727
WELCH, P. ..... p 966 N94-15924
WELCH, RONALD M. ..... p 1066 N94-16671
p 1075 N94-16714
WELCH, SHARON S. ..... p 1034 N94-15990
WELCH, W. HUDSON ..... p 1197 N94-17356
WELCOME, M. L. ..... p 1025 N94-16894
WELLS, A. A. ..... p 907 N94-15080
WELLS, MARTIN G. ..... p 954 N94-15104
WELSH, BARRY Y. ..... p 910 N94-15102
WEN, LI ..... p 1153 N94-17299
WENDELBEGER, J. R. ..... p 1169 N94-15979
WENGER, LOWELL E. ..... p 1216 N94-17477
WENNESON, GREG ..... p 1150 N94-16656
WENRICH, M. L. ..... p 1252 N94-16200
WENSINK, G. J. ..... p 1077 N94-16744
p 1077 N94-16745
WENSINK, J. W. ..... p 908 N94-15084
WENTWORTH, SUE J. ..... p 1289 N94-16397
WERESZCZAK, A. A. ..... p 935 N94-16461
WERNER, K. ..... p 1070 N94-16688
WERNER, MARIAN U. ..... p 990 N94-15891
WESSELS, H. R. A. ..... p 1004 N94-17407
WESSELSKI, CLARENCE ..... p 1046 N94-15707
WESSELSKI, CLARENCE J. ..... p 1047 N94-15966
WESSLING, FRANCIS C., III ..... p 877 N94-16150
WEST, C. D. ..... p 1049 N94-17675
WESTBROOK, C. K. ..... p 1096 N94-16825
WESTBYE, C. J. ..... p 979 N94-16087
WESTERHAUS, H. ..... p 1037 N94-15804
WESTRICH, C. N. ..... p 1041 N94-16871
WESTWATER, EDGEWORTH R. ..... p 996 N94-16044
p 996 N94-16045
WETZEL, MELANIE A. ..... p 1075 N94-16714
WEYENBERG, KEITH R. ..... p 1055 N94-17044
WHEADON, R. J. ..... p 909 N94-15090
WHEELER, J. T. ..... p 1172 N94-15535
WHIPPLE, A. L. ..... p 918 N94-15598
WHIRLEY, R. G. ..... p 1059 N94-15983
WHITAKER, LESLIE A. ..... p 1131 N94-15108
WHITE, C. W. ..... p 1209 N94-16066
WHITE, D. J. ..... p 908 N94-15088
WHITE, MARGO M. ..... p 1051 N94-16142
WHITE, MICHAEL J. ..... p 1178 N94-17119
WHITEFIELD, D. S. ..... p 1012 N94-16935
WHITELAW, J. H. ..... p 1016 N94-15109
WHITMAN, S. ..... p 1149 N94-16119
WHITNEY, R. ..... p 1197 N94-17350
WHITT, WARD ..... p 1165 N94-15775
WIANT, J. R. ..... p 918 N94-15598
WICKER, J. M. ..... p 1178 N94-16991
WICKS, GARY W. ..... p 1045 N94-17349
WIECZOREK, M. A. ..... p 1290 N94-16405
WIEDWALD, J. D. ..... p 1035 N94-16960
WIEGMAN, JANET F. ..... p 1130 N94-17554
WIELER, R. ..... p 954 N94-16432
WIER, LARRY T. ..... p 1125 N94-16619
p 1126 N94-16633
WIKTOROWSKI, J. ..... p 877 N94-15604
WILCOSKI, JAMES ..... p 871 N94-14908
WILCOX, DAVID C. ..... p 1022 N94-15953
WILD, CHRIS J. ..... p 1144 N94-15486
WILEY, CATHY J. ..... p 1166 N94-16938
WILHELMY, J. B. ..... p 1185 N94-16951
WILKERSON, CHRISTINA G. ..... p 1040 N94-16540
WILKERSON, J. ..... p 901 N94-15040
WILKERSON, J. F. ..... p 1185 N94-16951
WILKINSON, A. P. ..... p 1210 N94-16775
WILKINSON, RON ..... p 977 N94-16075
WILKINSON, S. P. ..... p 932 N94-15276
WILL, FRANK ..... p 984 N94-16004
WILLBRAND, JUERGEN ..... p 975 N94-16002
WILLEMVANVUURE, AART ..... p 937 N94-16848
WILLIAMS, A. J. ..... p 1031 N94-15018
WILLIAMS, CINDY ..... p 1075 N94-16734
WILLIAMS, D. ..... p 1011 N94-16661
WILLIAMS, JESSE ..... p 1146 N94-15670
WILLIAMS, K. R. ..... p 1048 N94-17433
WILLIAMS, M. C. ..... p 1092 N94-16715
WILLIAMS, P. F. ..... p 1012 N94-17023
WILLIAMS, RICHARD S., JR. ..... p 1248 N94-16178
WILLIAMS, STANLEY N. ..... p 1253 N94-16204
WILLIAMSON, STEVEN ..... p 986 N94-14912
WILLIS, EDWARD A. ..... p 869 N94-15192
WILLIS, GREGORY ..... p 1204 N94-16987
WILLIS, PAUL ..... p 971 N94-17198
WILLS, J. M. ..... p 1214 N94-17301
WILLSON, ALAN N., JR. ..... p 1007 N94-14936
WILMOTH, RICHARD G. ..... p 1018 N94-15291
WILSON, GORDON R. ..... p 1300 N94-17524
WILSON, H. R. ..... p 1203 N94-16822
WILSON, HOLLY J. ..... p 1232 N94-17101
WILSON, JACK ..... p 870 N94-17470
WILSON, JOHN W. ..... p 1300 N94-15816
p 1300 N94-17084
WILSON, L. ..... p 1258 N94-16227
p 1259 N94-16230
WILSON, LIONEL ..... p 1243 N94-16306
WILSON, MICHELE M. ..... p 1191 N94-16023
p 1191 N94-16024
WILSON, P. A. ..... p 1146 N94-15702
WILSON, P. B. ..... p 1183 N94-16809
WILSON, THOMAS L. ..... p 1277 N94-16337
WILT, DAVID M. ..... p 1013 N94-17113
WIN, Y. ..... p 941 N94-17379
WINCHENBACH, G. L. ..... p 1033 N94-15826
WINDISCH, C. F., JR. ..... p 1012 N94-16765
WINEMAN, S. J. ..... p 1201 N94-15981
WINFREE, WILLIAM P. ..... p 965 N94-15880
p 974 N94-17559
WING, P. C. ..... p 980 N94-16094
WINKLER-DREWS, TADEUSZ ..... p 998 N94-16652
WINSLOW, R. M. ..... p 1128 N94-16785
WINSTON, R. ..... p 1182 N94-16117
WINTER, KATHRYN P. ..... p 1122 N94-15759
p 1231 N94-16458
WINTERS, RONALD R. ..... p 1245 N94-16378
WISE, STEPHANIE A. ..... p 983 N94-15881
WISSLER, JOHN ..... p 1193 N94-17264
WITTENBERG, H. ..... p 853 N94-15122
WITTIG, J. E. ..... p 965 N94-15828
WIXSON, LAMBERT E. ..... p 1231 N94-16576
WLOCHOWICZ, R. ..... p 904 N94-15060
WLOTZKA, F. ..... p 1248 N94-16180
WNUK, RYSZARD ..... p 1093 N94-17070
WOERMANN, D. ..... p 944 N94-15165
WOJTOWICZ, A. J. ..... p 948 N94-16771
WOLF, DAVID A. ..... p 1117 N94-15969
WOLF, E. E. ..... p 950 N94-16962
WOLF, J. ..... p 902 N94-15045
p 907 N94-15082
WOLF, STEPHEN W. D. ..... p 871 N94-15117
WOLFBAUER, MICHAEL-PATRICK ..... p 962 N94-16273
WOLFF, RONALD S. ..... p 1191 N94-16547
WOLLESWINKEL, H. N. ..... p 853 N94-15125
WOLNA, MALGORZATA ..... p 1059 N94-16651
p 1061 N94-17086
p 971 N94-17120
WONG, G. K. ..... p 1191 N94-16454
WONG, JENNIFER A. ..... p 1074 N94-16708
WONG, M. K. ..... p 1148 N94-15985
WONG, N. J. ..... p 1236 N94-14929

WOO, JONG-HO p 865 N94-14951
WOOD, B. E. p 886 N94-15857
WOOD, C. L. p 1272 N94-16311
WOOD, ERIC F. p 1082 N94-16026
p 1083 N94-16027
p 1083 N94-16028
p 1083 N94-16029
p 1083 N94-16030
p 1083 N94-16031
p 1084 N94-16032
p 1084 N94-16033
p 1084 N94-16034
WOOD, JAMES S. p 1300 N94-15816
WOOD, JERRY R. p 869 N94-17386
WOOD, K. S. p 904 N94-15061
WOOD, ROGER p 875 N94-15591
WOOD, W. M. p 1183 N94-16818
WOODCOCK, GORDON R. p 882 N94-15831
WOODGATE, B. p 905 N94-15069
WOODS, P. S. p 872 N94-15543
WOODWARD, J. p 975 N94-16807
WOODWORTH, J. R. p 1091 N94-15994
WORKMAN, GARY L. p 976 N94-15006
WOUTERS, J. M. p 1185 N94-16951
WOZNIAK, JAN p 1061 N94-17069
WRIGHT, I. P. p 1251 N94-16193
WRIGHT, L. p 965 N94-15843
WRIGHT, MICHAEL E. p 972 N94-17273
WRIGHT, P. K. p 1054 N94-16518
WU, CHUNG P. p 1008 N94-15665
WU, CHWAN-HWA p 1165 N94-15958
WU, GUO-XIANG p 993 N94-15915
p 993 N94-15916
WU, J. p 1208 N94-16062
WU, J. C. S. p 947 N94-15861
WU, SHIH-CHIN p 1062 N94-17451
WU, T. H. p 1226 N94-14983
WU, TE-KAO p 1237 N94-17438
WU, TEHO p 1227 N94-14991
WU, YING-NIAN p 1172 N94-15733
WU, ZHAO-QING p 913 N94-15566
WYGNANSKI, I. p 855 N94-14963

X

XAPSOS, MICHAEL A. p 1173 N94-17495
XI, QIN-WEN p 1101 N94-15815
XIA, ZHIZ-HONG p 877 N94-15608
XIALING, GUAN p 1175 N94-17317
XIAO, CHI-KUN p 913 N94-15566
p 877 N94-15605
XU, GUO-QUN p 860 N94-17222
XU, HUA-GUAN p 918 N94-15597
XU, P. p 1252 N94-16198
XU, PENG-YANG p 1074 N94-16710
XU, YANGSHENG p 1163 N94-14950
p 1163 N94-14954
p 1045 N94-14970
p 1164 N94-15502
XUE, S. p 1242 N94-16240
XUEJIAN, XIA p 855 N94-14942

Y

YAJIMA, HIROYOSHI p 1141 N94-17015
YAKOVLEV, O. I. p 1248 N94-16180
YAMAKOSHI, K. p 1243 N94-16291
p 1245 N94-16388
YAMAMOTO, ATSUSHI p 911 N94-15555
YAMAMURO, JERRY A. p 1024 N94-16555
YAMNICHENKO, A. YU. p 1241 N94-16212
YAN, DA-PENG p 1035 N94-17402
YAN, Z. p 1227 N94-14989
YANAN, FENG p 855 N94-14942
YANG, CHIEN-HSIUNG p 1107 N94-17244
YANG, FU-MIN p 913 N94-15566
p 877 N94-15605
YANG, H. p 1241 N94-16176
YANG, J. p 964 N94-15683
YANG, J. M. p 1122 N94-15741
p 940 N94-17271
YANG, JANET M. p 1117 N94-16545
YANG, JIE p 1164 N94-15502
YANG, SHUTING p 1110 N94-17593
YANG, VIGOR p 1178 N94-16991
YANG, X. p 1208 N94-16062
YANG, XIANG-CHUN p 913 N94-15566
YATES, J. T., JR. p 1210 N94-16476
YE, WEN-WEI p 877 N94-15608
YE, Y. Y. p 959 N94-16873
YEAGER, WILLIAM L. p 969 N94-16916
YECKLEY, R. L. p 1209 N94-16164
YEH, ALEXANDER p 1155 N94-17491
YEMINI, YECHIAM p 1161 N94-17409
YEN, SHIAO-PING p 966 N94-15930
YEN, SHIAO-PING S. p 1010 N94-15952
YESKE, LANNY A. p 1112 N94-15771
YI, THOMAS Y. p 1012 N94-17062
YIKUN, ZHU p 879 N94-14941
YLI-PIETILAE, TIMO p 1015 N94-17546
YNGVESSON, K. S. p 903 N94-15055
YODA, S. p 977 N94-16074
YODER, MAX N. p 1210 N94-16487
YOO, M. H. p 959 N94-16873
YOON, M. W. p 1178 N94-16991
YOSHINARI, AKIRA p 945 N94-15168
YOUNG, E. T. p 908 N94-15084
YOUNG, ROBERT W. p 1138 N94-17460
YOUNKIN, C. R. p 1215 N94-17319
YOUTSEY, WESLEY J. p 1114 N94-17509
YU, J. p 974 N94-14982
YUAN, JIE p 894 N94-17173
YUEH, SIMON H. p 1079 N94-16752
p 1079 N94-16753
YUHAS, ROBERTA H. p 1074 N94-16711
YUN, HEE MANN p 962 N94-17652
YURA, H. T. p 1193 N94-17012
YURIMOTO, HISAYOSHI p 1104 N94-16336
YVON, P. J. p 958 N94-16463

Z

ZABIN, SERENA M. p 998 N94-16557
ZAGOLSKI, F. p 1068 N94-16681
p 1076 N94-16737
ZAGULI, RONALD J. p 1047 N94-15925
ZAGWODZKI, THOMAS p 915 N94-15577
ZAGWODZKI, THOMAS W. p 884 N94-15193
p 915 N94-15581
p 920 N94-15614
p 922 N94-15625
ZAHAROV, A. N. p 915 N94-15576
ZAIBYSHEV, VLADIMIR Z. p 1206 N94-15107
ZALDIVAR, R. J. p 940 N94-17271
ZALETA, DAVID p 1196 N94-17347
ZAMBUTO, J. p 1226 N94-14983
p 1227 N94-14990
ZAMMIT, C. C. p 911 N94-15103
ZAMUDIO, J. A. p 1066 N94-16669
ZAPPA, F. p 914 N94-15570
p 914 N94-15571
ZARI, M. p 1054 N94-16156
ZARI, M. C. p 1189 N94-15664
ZAWISTOWSKI, JACEK p 1204 N94-17067
ZEBKER, HOWARD A. p 1078 N94-16749
ZEE, R. H. p 960 N94-16964
ZEIDNER, MOSHE p 1132 N94-15938
ZEIL, STEVEN J. p 1144 N94-15486
ZEILER, THOMAS A. p 867 N94-17055
ZELENAK, MARYANN p 855 N94-15105
ZHANG, GUO-FU p 860 N94-17222
ZHANG, J. p 899 N94-15027
ZHANG, J.-H. p 877 N94-15605
ZHANG, JIAN-ZHONG p 1193 N94-17254
ZHANG, SHUNRONG p 1103 N94-17631
ZHANG, WEIGUO p 952 N94-17302
ZHANG, XIAO L. p 1182 N94-16466
p 1211 N94-16782
p 950 N94-17006
ZHANG, YANPING p 949 N94-16896
ZHANG, Z.-P. p 877 N94-15605
ZHANG, ZENGJUN p 997 N94-16050
ZHANG, ZHONG-PING p 918 N94-15597
ZHAO, QIDA p 1193 N94-17254
ZHENG, D. p 941 N94-17379
ZHOU, HONGYI p 952 N94-17302
ZHOU, M. D. p 855 N94-14963
ZHU, J. p 1025 N94-16879
ZHU, MIN-HUI p 993 N94-15916
ZHU, S. p 1011 N94-16443
ZHU, XIAO-LEI p 913 N94-15566
ZHU, YIMEI p 1212 N94-16844
ZHUANG, HONG C. p 1178 N94-17119
ZIEMER, PAUL L. p 1124 N94-16610
ZIMBELMAN, JAMES R. p 1260 N94-16235
ZIMMER, HANS p 972 N94-17297
ZIMMERMAN, FRANK p 1051 N94-16141
ZIMMERMAN, GEORGE A. p 1154 N94-17326
ZOGG, H. p 910 N94-15098
ZOLENSKY, M. E. p 1242 N94-16246
p 953 N94-16256
ZOOK, H. A. p 1242 N94-16270
ZSCHAU, J. p 1101 N94-15815
ZUBAIR, MOHAMMAD p 1144 N94-15483
ZUBER, MARIA p 1273 N94-16315
ZUHR, R. A. p 965 N94-15828
ZUKIC, MUAMER p 1190 N94-15868
p 1190 N94-15869
p 1191 N94-16023
p 1191 N94-16024
ZUREK, A. K. p 967 N94-16494
p 972 N94-17238
ZWALLY, H. JAY p 1114 N94-17439

Typical Corporate Source Index Listing

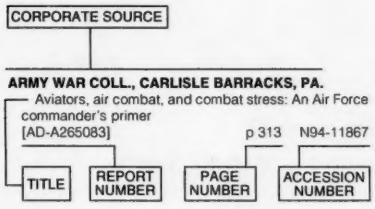

Listings in this index are arranged alphabetically by corporate source. The title of the document provides the user with a brief description of the subject matter. The report number helps to indicate the type of document cited (e.g., NASA report, translation, NASA contractor report). The accession number denotes the number by which the citation is identified. The page number helps you locate the citation in the abstract section. The titles are arranged under each corporate source in ascending accession number order.

A

AARHUS UNIV. (DENMARK).
Generation of artificial helioseismic time-series
[NASA-CR-194612] p 1299 N94-15968
Astronomy and astrophysics p 1239 N94-15970

ACADEMIA SINICA, BEIJING (CHINA).
Spaceborne radar for geoscientific applications in North China p 993 N94-15915
Primary studies of Chinese spaceborne SAR p 993 N94-15916

ACADEMIA SINICA, SHANGHAI (CHINA).
Simultaneous compression of the passively mode-locked pulsewidth and pulse train p 913 N94-15566

ACADEMY OF SCIENCES, POTSDAM (GERMAN D.R.).
The third generation SLR station Potsdam no. 7836 p 877 N94-15623

ACADEMY OF SCIENCES OF THE UKRAINE, KHARKOV.
Channel of the system for pulse charged particle beam diagnostics
[DE93-623867] p 1179 N94-14931

ACADEMY OF SCIENCES OF THE UKRAINE, KIEV.
Multiple process simulations for correction factor calculations in experiments with neutrons. LUSMK program
[DE93-623957] p 1179 N94-14932
The Acraman impact structure: Estimation of the diameter by the ejecta layer thickness p 1103 N94-16211
The Karakul depression in Pamirs: The first impact structure in Central Asia p 1241 N94-16212
Investigation of the energy distribution of ions, striking the cathode in an abnormal glow discharge
[DE93-623987] p 1013 N94-17316

ACADEMY OF SCIENCES (USSR), MOSCOW.
Nonstationary behaviour of low background photon detectors p 902 N94-15049
Trapping of water vapor from an atmosphere by condensed silicate matter formed by high-temperature pulse vaporization p 1248 N94-16180
The depths of the largest impact craters on Venus p 1264 N94-16261
Tessera terrain on Venus: Global characterization from Magellan data p 1264 N94-16262
Density of impact craters on tessera, Venus p 1264 N94-16263
First investigation of noble gases in the Dengli H3,8 chondrite p 953 N94-16264
Silica-bearing objects in the Dengli H3.8 and Gorlovka H3-4 chondrites p 1242 N94-16265
Induced thermoluminescence study of experimentally shock-loaded oligoclase p 953 N94-16266
Shock-thermal history of Kapoeta howardite matter on data of thermoluminescence analysis of individual mineral grains p 953 N94-16267
Different radiation and metamorphic history of the Kainsaz CO 3.2 chondrules p 1243 N94-16296
Complex radiation-thermal history of Kaidun meteorite on data of track study of silicate minerals p 1243 N94-16297
Terrestrial bitumen analogue of orgueil organic material demonstrates high sensitivity to usual HF-HCl treatment p 930 N94-16325
The astrophysical interpretation of isotope anomalies in graphite and SiC grains of chondrites p 1244 N94-16343
On possible Mn-53 heterogeneity in the early solar system p 1244 N94-16344
On origin of the olivine inclusions from the Kainsaz CO carbonaceous chondrite p 1244 N94-16345
Possible sources of H2 to H2O enrichment at evaporation of parent chondritic material p 1244 N94-16377
Geophysical models of Western Aphrodite-Niobe region: Venus p 1286 N94-16382
Optical effects of regolith processes on S asteroids as simulated by laser impulse alteration of ordinary chondrite p 1246 N94-16422
Altitude profile of aerosols on Mars from measurements of its thermal radiation on limb p 1294 N94-16423

ACADEMY OF SCIENCES (USSR), SAINT PETERSBURG.
Lead chalcogenides based IR photosensitive array detectors with coordinate addressing p 903 N94-15053
International testing of a Mars rover prototype p 1273 N94-16312

ADAPTIVE RESEARCH CORP., HUNTSVILLE, AL.
Structured finite volume modeling of US Navy aircraft engine test cells. Task 1: Turboshaft engine, volume 1
[AD-A268176] p 873 N94-17432
Structured finite volume modeling of US Navy aircraft engine test cells. Task 1: Turboshaft engine-code documentation and listings, volume 2
[AD-A268177] p 873 N94-17508
Structured finite volume modeling of US Navy aircraft engine test cells. Task 2: Turboprop engine. Volume 2: Code documentation and listings
[AD-A268386] p 873 N94-17569

ADMIRALTY RESEARCH ESTABLISHMENT, GOSPORT (ENGLAND).
Sound radiation from infinite laminated composite shell with periodic rib stiffening
[DRA/TM(USGR)92326] p 933 N94-15699
The free decay of coupled heave and pitch motions of a model frigate
[DRA/TM(AWMH)92340] p 1146 N94-15702

ADVISORY GROUP FOR AEROSPACE RESEARCH AND DEVELOPMENT, NEUILLY-SUR-SEINE (FRANCE).
Advanced methods for cascade testing
[AGARD-AG-328] p 1016 N94-15119
Special course on Shock-Wave/Boundary-Layer Interactions in Supersonic and Hypersonic Flows
[AGARD-R-792] p 1017 N94-15196
Rocket Motor Plume Technology
[AGARD-LS-188] p 923 N94-15217
Electronic messaging for the 1990's
[AD-A267143] p 1229 N94-15437

AEROASTRO, INC., HERNDON, VA.
ALEXIS and HETE: Two small, low cost, scientific satellite systems p 896 N94-17185

AEROCHEM RESEARCH LABS., INC., PRINCETON, NJ.
Modeling study to evaluate the ionic mechanism of soot formation in flames
[AD-A266242] p 950 N94-16930

AEROJET-GENERAL CORP., SACRAMENTO, CA.
ALS engine propellant effector system
[NASA-CR-194650] p 926 N94-16590
ALS engine controller system
[NASA-CR-194647] p 926 N94-16654
ALS liquid hydrogen turbopump
[NASA-CR-194646] p 927 N94-17016

AERONAUTICAL RESEARCH LABS., MELBOURNE (AUSTRALIA).
Aircraft accident investigation at ARL: The first 50 years
[AD-A267086] p 862 N94-15542
A microprocessor controller for a towing tank drive and flow visualisation system
[AD-A267087] p 872 N94-15543
A software interface for the ARL wind tunnel data acquisition system
[AD-A267114] p 1146 N94-15650
Helicopter structures: A review of loads, fatigue design techniques, and usage monitoring
[AD-A267115] p 866 N94-15651
Flight instrument software for the F/A-18 research simulator
[AD-A267170] p 872 N94-15856
The influence of secondary bending on fatigue life improvement in bolted joints
[ARL-RR-14] p 1058 N94-15963
A review of Australian and New Zealand investigations on aeronautical fatigue during the period April 1991 to March 1993
[AD-A267532] p 868 N94-17117

AERONAUTICAL SYSTEMS DIV., WRIGHT-PATTERSON AFB, OH.
An uncertainty analysis of inlet dynamic flow distortion using an analog/digital hybrid editing system
[AD-A266924] p 855 N94-15105

AEROSPACE CORP., EL SEGUNDO, CA.
XPS analysis of Al/EPDM bondlines from IUS SRM-1 polar bosses
[AD-A266851] p 1056 N94-14945
Formation of the stable auroral arc that intensifies at substorm onset
[NASA-CR-193637] p 1098 N94-15433
Long Duration Exposure Facility experiment M0003 deintegration/findings and impacts
[AD-A267140] p 885 N94-15749
Performance of silvered Teflon thermal control blankets on spacecraft
[AD-A266284] p 887 N94-16909
Speckles statistics and decorrelation effects in complex ABCD optical systems
[AD-A267843] p 1193 N94-17012
Long duration exposure facility experiment m0003 deintegration observation database
[AD-A267579] p 951 N94-17207
Fiber strength utilization in carbon/carbon composites
[AD-A267713] p 940 N94-17271

AEROSPACE MEDICAL RESEARCH LABS., BROOKS AFB, TX.
USAF physiological studies of personal microclimate cooling: A review
[AD-A267203] p 1022 N94-15858
Theoretical implications and empirical findings on instructional control and part-whole-task training
[AD-A267826] p 872 N94-17403

AEROSPACE MEDICAL RESEARCH LABS., WRIGHT-PATTERSON AFB, OH.
Optical displays: A tutorial on images and image formation
[AD-A266230] p 1192 N94-16926

AEROSPATIALE, CANNES (FRANCE).
New perspectives for high accuracy SLR with second generation geodesic satellites p 916 N94-15585
GLRS-R 2-colour retroreflector target design and predicted performance p 921 N94-15615

S-80: A satellite for less than 50 MF
p 894 N94-17172
A mini satellite called Arsene: The way to make it at a minimum cost
p 895 N94-17179

AEROTHERM CORP., HUNTSVILLE, AL.
ASRM nozzle thermal analysis
[NASA-CR-194672] p 928 N94-17277

AI SIGNAL RESEARCH, INC., HUNTSVILLE, AL.
Develop advanced nonlinear signal analysis topographical mapping system
[NASA-CR-194577] p 1082 N94-15646

AIR FORCE ACADEMY, CO.
Hypervelocity orbital intercept guidance using certainty control
[AD-A267297] p 1174 N94-17219

AIR FORCE ENVIRONMENTAL TECHNICAL APPLICATIONS CENTER, SCOTT AFB, IL.
TAFVER 2 users manual
[AD-A266850] p 1106 N94-15757

AIR FORCE INST. OF TECH., WRIGHT-PATTERSON AFB, OH.
Turbine blade tip film cooling measurements
[AD-A267686] p 868 N94-14964
A study of relaxation transitions in the polymers under the influence of magnetic fields
[AD-A263878] p 963 N94-15133
Determination of momentum flux using a bivane and cup anemometer
[AD-A265414] p 1105 N94-15137
Development of an air-to-air refueling automatic flight control system using quantitative feedback theory
[AD-A266718] p 870 N94-15730
An analysis of tactical airlifter characteristics and their impact on theater airlift system performance
[AD-A266719] p 866 N94-15731
A decision criteria to select an associative-memory organization that minimizes the execution time of a mix of associative-search operations
[AD-A266438] p 1149 N94-16560
Manufacturing tolerance requirements for frequency selective surfaces
[AD-A266541] p 999 N94-16797
Hoph bifurcation in viscous, low speed flows about an airfoil with structural coupling
[AD-A266542] p 859 N94-16798
Neighboring extremal guidance for systems with piecewise linear control using time as the reference variable
[AD-A267942] p 874 N94-17010
Optical computing
[AD-A267881] p 1141 N94-17015
Radome depolarization effects on monopulse receiver tracking performance
[AD-A267446] p 1001 N94-17031
Interfacial shear behavior and its influence on fiber damage in sapphire-reinforced gamma titanium aluminide composites
[AD-A267943] p 1060 N94-17043
A fuzzy method for preliminary design random access memory failure rate prediction
[AD-A267948] p 1055 N94-17044
Development and analysis of startup strategies for particle bed nuclear rocket engine
[AD-A267949] p 927 N94-17053
Mesoscale frontogenesis: An analysis of two cold front case studies
[AD-A267950] p 1107 N94-17054
Computational aerodynamics with icing effects
[AD-A267509] p 860 N94-17074
Effects of inspection error on optimal inspection policies and software fault detection models
[AD-A267511] p 1153 N94-17075
Energy potential analysis of zero velocity curves in the restricted three-body problem
[AD-A267512] p 1170 N94-17076
The specific heat of titanium disilicide
[AD-A267543] p 960 N94-17100
The standardized precipitation index and its use in the western contiguous United States
[AD-A267547] p 1107 N94-17102
Implementing a 50x50 gravity field model in an orbit determination system
[AD-A267548] p 888 N94-17103
A modified two-fluid model of conductivity for superconducting surface resistance calculation
[AD-A267549] p 1013 N94-17104
Synthesis, reactivity, and characterization of (-hexacarbocyclic) manganese dicarbonyl complexes with sulfur and phosphorus ligands
[AD-A267592] p 930 N94-17192
Bibliography of short wavelength chemical laser research
[AD-A267619] p 1041 N94-17195
Phased array antenna analysis using hybrid finite element methods
[AD-A267620] p 1002 N94-17196
An experimental investigation of the effects of leading edge geometry on the dynamics of blunt fin-induced shock wave turbulent boundary layer interaction
[AD-A267656] p 860 N94-17221
Numerical solution of SUPG finite-element method for supersonic viscous flow
[AD-A267762] p 860 N94-17222
Design of a fluid elastic actuator with application to structure control
[AD-A267649] p 897 N94-17246
Orographic microbursts in a severe winter windstorm
[AD-A267651] p 1108 N94-17247
Ultrasonic wave propagation model for nondestructive evaluation of solid rocker motor propellant
[AD-A267653] p 976 N94-17248
Two-dimensional acousto-optical interaction theory and experimental analysis
[AD-A267761] p 1193 N94-17254
Validation and analysis of microwave-derived rainfall over the tropics
[AD-A267785] p 1108 N94-17303
Military space programs in the press: An analysis for change
[AD-A267799] p 874 N94-17306
Linear characteristic spatial quadrature for discrete ordinates neutral particle transport on arbitrary triangles
[AD-A267485] p 1185 N94-17365
An examination of two Ada language object-oriented databases
[AD-A267486] p 1154 N94-17366
Estimating task execution delay in a real-time system via static source code analysis
[AD-A267496] p 1161 N94-17367
A guidance and navigation system for two spacecraft rendezvous in translunar halo orbit
[AD-A267498] p 898 N94-17368
Discrete sliding mode control for nonlinear sampled data systems
[AD-A267500] p 1167 N94-17369
An object-oriented dynamic software process model
[AD-A267726] p 1154 N94-17371
Energy from the sun: Evolution of federal support for solar energy
[AD-A267944] p 1093 N94-17382
Extracavity frequency doubling study of a pulsed photodissociation iodine laser
[AD-A267893] p 1042 N94-17394
Experimental studies on a gas dynamic laser with narrow throat and high area-ratio grid nozzles
[AD-A267818] p 1042 N94-17400
Frequency resolution of an acousto-optical spectrometer
[AD-A267822] p 1035 N94-17401
Study of high speed interference photography with two-dimensional acousto-optical lattice deflection
[AD-A267823] p 1035 N94-17402
A comparative study of analog and digital control laws for the UMCSL truss
[AD-A267980] p 871 N94-17412
A comparison of ceiling and visibility observation for NWS manned observation sites and ASOS sites
[AD-A268356] p 1108 N94-17459
Evaluation of hybrid reinforcement (fiber-reinforced-plastic rod with steel core)
[AD-A268009] p 941 N94-17473
Flow instability tests for a particle bed reactor nuclear thermal rocket fuel element
[AD-A268012] p 929 N94-17474
Computer-human interface issues: Theory and application
[AD-A268013] p 1138 N94-17475
Opposing mesoscale flows in a broken midlatitude squall line
[AD-A268011] p 1109 N94-17492
Optimization of satellite coverage in observing cause and effect changes in the ionosphere, magnetosphere, and solar wind
[AD-A267956] p 1102 N94-17493
An investigation of the Ground-Based High-Resolution Interferometer Sounder (GB-HIS) in a costal marine environment
[AD-A268052] p 1114 N94-17503
A correlative comparison of geomagnetic storms and auroral substorms using geomagnetic indeces
[AD-A268081] p 1102 N94-17512
Reliability and maintainability of modular robot systems: A roadmap for design
[AD-A268104] p 1168 N94-17517
Laser photoionization time-of-flight mass spectrometry of nitrated polycyclic aromatic hydrocarbons and nitrated heterocyclic compounds
[AD-A268126] p 952 N94-17520
Numerical solution of a second order boundary problem for two dimensions using galerkin approximations
[AD-A268128] p 1171 N94-17521
Propagation characteristics of mesoscale convective systems
[AD-A268130] p 1109 N94-17522
System performance modeling and analysis of a fault-tolerant, real time parallel processor
[AD-A268070] p 1162 N94-17551
Further development and testing of a second-order bulk boundary layer model
[AD-A268071] p 1109 N94-17552
Forecasting the ducting of electromagnetic waves on the mesoscale
[AD-A268101] p 1109 N94-17571
Three dimensional visualization of GOES cloud data using OCTRESS
[AD-A268102] p 1109 N94-17572
An analysis of simulated and actual DMSP SSM/T-2 brightness temperatures
[AD-A268103] p 1109 N94-17573
The analysis of low-profile, broadband, monopole, vehicle antennas and matching network synthesis
[AD-A268340] p 1006 N94-17582
State space partitioning methods for solving a class of stochastic network problems
[AD-A267494] p 1173 N94-17585
Application of a NEPTUNE propulsion concept to a manned Mars excursion
[AD-A268053] p 929 N94-17587
An empirical study of tropical cloud clusters using special sensor microwave imager data
[AD-A268072] p 1110 N94-17595

AIR FORCE OFFICE OF SCIENTIFIC RESEARCH, BOLLING AFB, WASHINGTON, DC.
AFOSR technical report summaries, January - March 1993
[AD-A267187] p 1230 N94-15850

AIR FORCE OPERATIONAL TEST AND EVALUATION CENTER, SCOTT AFB, IL.
Solar Electro-Optical Network (SEON) upgrade/replacement program. Phase 1: Qualification operational test and evaluation plan
[AD-A266364] p 1237 N94-17225

AIR FORCE SYSTEMS COMMAND, BROOKS AFB, TX.
Automated data collection system for the TCM3 transcutaneous pO2/pCO2 monitoring system
[AD-A268400] p 1129 N94-17424

AIR FORCE SYSTEMS COMMAND, WRIGHT-PATTERSON AFB, OH.
Vertical-tail aerodynamic configuration of space shuttle orbiter
[AD-A267723] p 879 N94-14941
The effect of the nose shape and wing location toward the wing vortex breakdown
[AD-A267724] p 855 N94-14942
High-performance nonlinear optical material developed in Japan
[AD-A266194] p 1191 N94-16126
CALS test network handbook
[AD-A267587] p 1160 N94-17209
Experimental study of vortex and aerodynamic characteristics of stack wings with sideslip
[AD-A267722] p 860 N94-17274
Three short articles from Japanese laser journal
[AD-A268249] p 1042 N94-17415

ALABAMA A & M UNIV., NORMAL.
Optical studies of glasses embedded with inorganic ions and organic dyes
[AD-A268146] p 1199 N94-17455

ALABAMA UNIV., BIRMINGHAM.
Cumulative effect of repeated brief cerebral ischemia
[AD-A267155] p 1121 N94-15736

ALABAMA UNIV., HUNTSVILLE.
Visualization of solidification front phenomena
[NASA-CR-193838] p 976 N94-15006
Testing and management of flight instruments and their data
[NASA-CR-194332] p 868 N94-15187
Convective flow effects on protein crystal growth
[NASA-CR-194560] p 1206 N94-15476
Use of photostress and strain gages to analyze behavior of weldments and use of photostress and strain gages to analyze behavior of an aft skirt test specimen
[NASA-CR-194575] p 1058 N94-15716
Filters for the International Solar Terrestrial Physics (ISTP) mission far ultraviolet imager
[NASA-CR-194633] p 1190 N94-15868
Multilayer thin film design for far ultraviolet polarizers using an induced transmission and absorption technique
[NASA-CR-194631] p 1190 N94-15869
Design and fabrication of a reflection far ultraviolet polarizer and retarder
[NASA-CR-194630] p 1191 N94-16023
Transparent conductive coatings in the far ultraviolet
[NASA-CR-194632] p 1191 N94-16024
Materials processing in space: Issues for the third decade
[TABES PAPER 93-260] p 983 N94-16133

An analysis of the dynamic response of the Space Station Freedom due to a module perforation by an orbital debris particle impact
[TABES PAPER 93-653] p 899 N94-16154
VUV thin films, chapter 7
[NASA-CR-194634] p 967 N94-16494
Research support for cadmium telluride crystal growth
[NASA-CR-193557] p 1210 N94-16646
Electron spectroscopy analysis
[NASA-CR-193591] p 951 N94-17039
FNAS/solar flare energetics
[NASA-CR-193574] p 1299 N94-17089
Kinetic plasma processes occurring in the outer plasmasphere
[NASA-CR-193452] p 1300 N94-17524

ALABAMA UNIV., TUSCALOOSA.
Particle Engulfment and Pushing by Solidifying Interfaces (PEPSI)
[NASA-CR-193856] p 960 N94-17079

ALASKA UNIV., FAIRBANKS.
Propagation measurements in Alaska using ACTS beacons p 995 N94-16040
Micro- and meso-scale simulations of magnetospheric processes related to the aurora and substorm morphology
[NASA-CR-193437] p 1102 N94-17527

ALCATEL ESPACE, TOULOUSE (FRANCE).
CERISE microsatellite system p 894 N94-17170

ALEM ASSOCIATES, BOSTON, MA.
Scintillation mechanism in stoichiometric cerium compounds
[DE93-015499] p 948 N94-16771

ALENIA SPAZIO S.P.A., ROME (ITALY).
High resolution SAR applications and instrument design p 993 N94-15913

ALUMINUM CO. OF AMERICA, ALCOA CENTER, PA.
Gas separations using ceramic membranes
[DE93-000278] p 947 N94-15861

AMAX RESEARCH AND DEVELOPMENT CENTER, GOLDEN, CO.
Development of vanadium-phosphate catalysts for methanol production by selective oxidation of methane
[DE93-016850] p 949 N94-16897

AMERICAN MUSEUM OF NATURAL HISTORY, NEW YORK, NY.
The role of carbon and temperature in determining electrical conductivity of basins, crust and mantle
[DE93-015936] p 1101 N94-16840

AMPTEK, INC., BEDFORD, MA.
Prototype instrumentation and design studies
[AD-A266402] p 882 N94-16530
Space systems environmental interaction studies
[AD-A267280] p 897 N94-17240

ANACAPA SCIENCES, INC., FORT RUCKER, AL.
Preliminary validation of the task analysis/workload methodology
[AD-A267514] p 1138 N94-17077

ANALEX CORP., BROOK PARK, OH.
Temperature and pressure effects on capacitance probe cryogenic liquid level measurement accuracy
[NASA-CR-190763] p 1034 N94-16521

ANALYSIS AND TECHNOLOGY, INC., NEW LONDON, CT.
Evaluation of Night Vision Goggles (NVG) for maritime search and rescue (HH-3/HH-60) comparison report
[AD-A266493] p 1138 N94-16793

ANALYTICAL SERVICES AND MATERIALS, INC., HAMPTON, VA.
Crack-tip-opening angle measurements and crack tunneling under stable tearing in thin sheet 2024-T3 aluminum alloy
[NASA-CR-191523] p 931 N94-15184

ANALYTICAL TECHNOLOGY APPLICATIONS CORP., MOFFETT FIELD, CA.
Measuring dry plant residues in grasslands: A case study using AVIRIS p 1072 N94-16697

ANDERSEN (ARTHUR) AND CO., CHICAGO, IL.
KBSA concept demo
[AD-A267054] p 1166 N94-16770

APA OPTICS, INC., BLAINE, MN.
Atomic layer epitaxy of boron nitride
[AD-A266260] p 1212 N94-16932

APPLIED RESEARCH, INC., HUNTSVILLE, AL.
Adaptive weld control for high-integrity welding applications
[TABES PAPER 93-604] p 1049 N94-16140

APPLIED RESEARCH CORP., LANDOVER, MD.
X ray emission from Wolf-Rayet stars with recurrent dust formation
[NASA-CR-194567] p 1300 N94-15533

ARGONNE NATIONAL LAB., IDAHO FALLS, ID.
Roles of oxygen defects in copper-oxide superconductors
[DE93-014875] p 1208 N94-15982
Weibull analysis applied to the pull adhesion test and fracture of a metal-ceramic interface
[DE93-012913] p 1059 N94-15997

ARGONNE NATIONAL LAB., IL.
Mechanical properties of magnesium ammonium phosphate cements and their zeolite composites
[DE93-015155] p 934 N94-16057
Interfacial structure of lattice mismatched bcc(110)/bcc(110) transition metal superlattices
[DE93-015162] p 1208 N94-16058
Controls of maglev suspension systems
[DE93-015540] p 1011 N94-16443
Implementation of an anisotropic turbulence model in the COMMIX-1C/ATM computer code
[DE93-015541] p 1023 N94-16444
Detection of subsurface defects in machined silicon nitride ceramics by optical scattering methods
[DE93-015554] p 968 N94-16658
Discovering sequence similarity by the algorithmic significance method
[DE93-015556] p 1150 N94-16659
Operator overloading as an enabling technology for automatic differentiation
[DE93-012899] p 1170 N94-16778
Tritium diffusion and desorption in single crystal LiAlO2
[DE93-015140] p 1211 N94-16805
Dynamics, stability, and control of maglev systems
[DE93-015163] p 1047 N94-16806
TransRapid TR-07 maglev-spectrum magnetic field effects on daily pineal indoleamine metabolic rhythms in rodents
[DE93-015143] p 1117 N94-16893
Electrodynamic forces of the cross-connected figure-eight null-flux coil suspension system
[DE93-015139] p 1048 N94-16969
The role of constitutive and inducible processes in the response of human squamous cell carcinoma cell lines to ionizing radiation
[DE93-015150] p 1129 N94-16970
Engineering design of a high-temperature superconductor current lead
[DE93-015156] p 1013 N94-17226
Contained (nu) events observed in Soudan 2
[DE93-015548] p 1300 N94-17233
Boundary layer structure over areas of heterogeneous heat fluxes
[DE93-010657] p 1110 N94-17673

ARIZONA STATE UNIV., TEMPE.
Sand transport on Mars: Preliminary results from models p 1252 N94-16198
Galileo imaging results from the second Earth-Moon flyby: Lunar Maria and related units p 1252 N94-16199
Mars Analog Site Study (MASS) p 1252 N94-16200
Explosive mafic volcanism on Earth and Mars p 1253 N94-16204
Heliocentric zoning of the asteroid belt by aluminum-26 heating p 1241 N94-16205
Experimental constraints on CO2 and H2O in the Martian mantle and primary magmas p 1262 N94-16248
Olivines in the Kaba carbonaceous chondrite and constraints on their formation p 1219 N94-16255
The history of mare volcanism in the Orientale Basin: Mare deposit ages, compositions and morphologies p 1269 N94-16289
Mars exobiology landing sites for future exploration p 1278 N94-16339
Venusian pancake domes: Insights from terrestrial voluminous silicic lavas and thermal modeling p 1286 N94-16381
Ejecta patterns of Meteor Crater, Arizona derived from the linear un-mixing of TIMS data and laboratory thermal emission spectra p 1065 N94-16607
A comparison of LOWTRAN-7 corrected Airborne Visible/Infrared Imaging Spectrometer (AVIRIS) data with ground spectral measurements p 1074 N94-16710
Detecting surface roughness effects on the atmospheric boundary layer via AIRSAR data: A field experiment in Death Valley, California p 1078 N94-16747

ARIZONA UNIV., PHOENIX.
Collisional and dynamical history of Gaspra p 1241 N94-16202

ARIZONA UNIV., TUCSON.
The turbulent wall jet
[AD-A267675] p 855 N94-14963
Research Studies on Advanced Optical Module/Head Designs for Optical Disk Recording Devices
[NASA-CR-194390] p 1226 N94-14981
Magneto-optic superlattice thin films: Fabrication, structural and magnetic characterization p 974 N94-14982
Characterization facility for magneto-optic media and systems p 1226 N94-14983
MeV ion-beam analysis of optical data storage films p 1226 N94-14984

ARMY AEROMEDICAL RESEARCH LAB.
Application of holographic optical elements to magneto-optic read/write heads p 1226 N94-14985
Dynamic testbed laboratory and micro-optics p 1199 N94-14986
Gratings and waveguides p 1226 N94-14987
Compact disk error measurements p 1227 N94-14988
Measurement of birefringence for optical recording disk substrates p 1227 N94-14989
Ring lens focusing and push-pull tracking scheme for optical disk systems p 1227 N94-14990
Magnetic and magneto-optical properties and domain structure of Co/Pd multilayers p 1227 N94-14991
Determination of average refractive index of spin coated DCG films for HOE fabrication p 1036 N94-14992
Effects of a shading band in the data path of an optical drive p 1199 N94-14993
Figures of merit for laser beam quality p 1043 N94-14994
A near-field scanning optical microscope for analysis of magneto-optic media p 1199 N94-14995
A complete study of differential wax-wane focus servo technique p 1199 N94-14996
Determining the locations of the various CIRC recording format information blocks (user data blocks, C2 and C1 words and EFM frames) on a recorded compact disc p 1228 N94-14997
Laboratory for x ray optics
[AD-A267149] p 1189 N94-15735
The Fe2(+)-Mg interdiffusion in orthopyroxene: Constraints from cation ordering and structural data and implications for cooling rates of meteorites p 1241 N94-16175
Cation ordering in orthopyroxenes and cooling rates of meteorites: Low temperature cooling rates of Estherville, Bondoc and Shaw p 1241 N94-16176
A mineralized zone in Western Candor Chasma, Mars p 1248 N94-16179
Stalking the LREE-enriched component in ureilites p 1241 N94-16190
Earth imaging results from Galileo's second encounter p 1252 N94-16201
Fluvial erosion on Mars: Implications for paleoclimatic change p 1241 N94-16210
Gas-grain energy transfer in solar nebula shock waves: Implications for the origin of chondrules p 1262 N94-16251
Radar properties of several fluidized ejecta blankets on Venus p 1267 N94-16278
Meander properties of Venusian channels p 1275 N94-16324
Cat Mountain: A meteoritic sample of an impact-melted chondritic asteroid p 1244 N94-16328
Lunar phase function effects on spectral ratios used for resource assessment p 1278 N94-16342
Teaching planetary sciences to elementary school teachers: Programs that work p 1222 N94-16346
Possible dust contamination of the early solar system p 1244 N94-16352
Evolution of Triton's volatile budget p 1284 N94-16373
Remote visual detection of impacts on the lunar surface p 1290 N94-16404
Deucalionis Regio, Mars: Evidence for a unique mineralogic endmember and a crusted surface p 1291 N94-16406
Analysis of pyroxene absorptions observed in Martian dark regions p 1292 N94-16411
Optical system storage design with diffractive optical elements p 1198 N94-17360
High-speed nonlinear switching mechanisms and devices for multi-gigabit data processing
[AD-A267753] p 1014 N94-17375

ARKANSAS UNIV., FAYETTEVILLE.
The group A3 chondrules of Krymka: Further evidence for major evaporative loss during the formation of chondrules p 1242 N94-16257

ARMED FORCES RADIOBIOLOGY RESEARCH INST., BETHESDA, MD.
AFRRI reports, first quarter 1993
[AD-A266380] p 1123 N94-16515

ARMY AEROMEDICAL RESEARCH LAB., FORT RUCKER, AL.
Monograph of the aviation epidemiology data register for FY 1991
[AD-A266896] p 1119 N94-14952
Basic principles of helicopter crashworthiness
[AD-A267099] p 862 N94-15637
Activity/rest patterns of instructor and rates student pilots during rapid transitions from daytime to nighttime duty hours at the Eastern Army Aviation Training site
[AD-A267038] p 1131 N94-15659

ARMY ARMAMENT RESEARCH, DEVELOPMENT AND ENGINEERING CENTER, WATERVLIET, NY.
Measurement and theory of the dependence of hardness on residual stress
[AD-A267553] p 1061 N94-17105
Transient phenomena following precipitation and re-solution anneals in a NiTi alloy
[AD-A267557] p 961 N94-17106
ARMY COLD REGIONS RESEARCH AND ENGINEERING LAB., HANOVER, NH.
Bibliography on snow and ice friction
[AD-A266868] p 1045 N94-14920
Mathematical model of frost heave and thaw settlement in pavements
[AD-A267037] p 983 N94-15676
ARMY CONSTRUCTION ENGINEERING RESEARCH LAB., CHAMPAIGN, IL.
Vibro-acoustic analysis of an aircraft maintenance dock
[AD-A266778] p 871 N94-14908
Sound exposure level prediction for impulse sound sources above variable terrain
[AD-A267535] p 1178 N94-17119
Application of thermal spray and ceramic coatings and reinforced epoxy for cavitation damage repair of hydroelectric turbines and pumps
[AD-A267624] p 971 N94-17198
Research in presistent simulation: Development of the persistent ModSim object-oriented programming language
[AD-A268568] p 1157 N94-17620
ARMY ENGINEER STUDIES CENTER, FORT BELVOIR, VA.
Design Quality Task Force survey comments
[AD-A266283] p 1225 N94-16473
ARMY ENGINEER WATERWAYS EXPERIMENT STATION, VICKSBURG, MS.
User's guide: Hot-mix recycling of asphalt concrete pavements
[AD-A266939] p 983 N94-15177
Environmental characterization for target acquisition. Report 1: Site descriptions and measurements
[AD-A267192] p 1106 N94-15851
Technical urban search and rescue, System To Locate Survivors (STOLS) units: Operator's manual
[AD-A266317] p 862 N94-16438
ARMY INST. FOR RESEARCH IN MANAGEMENT INFORMATION AND COMPUTER SCIENCES, ATLANTA, GA.
ACE: Lessons learned, volume 1
[AD-A267979] p 1155 N94-17411
Integration of several computer systems within a heterogeneous environment
[AD-A267978] p 1155 N94-17500
ARMY LAB. COMMAND, FORT MONMOUTH, NJ.
Quartz crystal resonators and oscillators for frequency control and timing applications: A tutorial, revision 6.1
[AD-A268205] p 1216 N94-17480
ARMY MATERIEL SYSTEMS ANALYSIS ACTIVITY, ABERDEEN PROVING GROUND, MD.
Army Software Test and Evaluation Panel (STEP) software metrics initiatives report
[AD-A266889] p 1142 N94-14924
ARMY MISSILE COMMAND, REDSTONE ARSENAL, AL.
Wind tunnel investigation with an operational turbojet engine
[TABES PAPER 93-662] p 870 N94-16157
ARMY MISSILE RESEARCH, DEVELOPMENT AND ENGINEERING LAB., REDSTONE ARSENAL, AL.
Real-time adaptive neural network data processing
[TABES PAPER 93-660] p 1054 N94-16155
ARMY NATICK RESEARCH AND DEVELOPMENT COMMAND, MA.
Efficacy of flocculating and other emergency water purification tablets
[AD-A266695] p 1148 N94-15840
ARMY RESEARCH DEVELOPMENT AND STANDARDIZATION GROUP (UNITED KINGDOM), FPO NEW YORK, NY.
Preparation and investigation of improved low voltage electron excitable phosphors
[AD-A266852] p 963 N94-14948
ARMY RESEARCH INST. OF ENVIRONMENTAL MEDICINE, NATICK, MA.
Annual historical report, calendar year 1992
[AD-A267050] p 1121 N94-15663
Automated strain gauge plethysmograph
[AD-A267323] p 1035 N94-17002
ARMY RESEARCH LAB., ABERDEEN PROVING GROUND, MD.
Electronic spectroscopy of the gas-phase OH-Kr van der Waals complex
[AD-A266891] p 942 N94-14946
Static aeroelastic response of an aircraft with asymmetric wing planforms representative of combat damage
[AD-A266890] p 865 N94-14951
Spectral studies of solid propellant combustion 4: Absorption and burn rate results for M43, XM39, and M10 propellants
[AD-A267119] p 946 N94-15685
Sensitive detection of gas-phase nitro-containing energetic materials employing 226-nm radiation
[AD-A267633] p 951 N94-17203
TDNOVA interactive graphics
[AD-A268000] p 1156 N94-17530
Laser ignition of solid propellants: 1. Ignition delays
[AD-A268454] p 976 N94-17538
ARMY RESEARCH LAB., ADELPHI, MD.
Diffractive optical elements for generating arbitrary line foci p 1195 N94-17338
Diffractive optics in adverse environments p 1197 N94-17352
ARMY RESEARCH LAB., CLEVELAND, OH.
Experimental and computational investigation of the NASA low-speed centrifugal compressor flow field
[NASA-TM-4481] p 869 N94-17386
ARMY RESEARCH LAB., WATERTOWN, MA.
The effect of plasma treatment on interfacial bond characteristics of Kevlar/epoxy laminates as measured by T-peel tests
[AD-A266920] p 930 N94-14999
Army P/M research and development overview
[AD-A266921] p 954 N94-15104
Assessment of chromate and non-chromate conversion coatings for Al alloys using electrochemical impedance spectroscopy
[AD-A267205] p 965 N94-15859
ARMY RESEARCH LAB., WHITE SANDS MISSLE RANGE, NM.
Complex terrain wind model evaluation
[AD-A266467] p 1096 N94-16589
A surface energy budget model modifying heat flow by foliage effects
[AD-A268598] p 1085 N94-17610
ARMY RESEARCH OFFICE, RESEARCH TRIANGLE PARK, NC.
Manufacturing the key to binary optics p 1194 N94-17332
ARMY TEST AND EVALUATION COMMAND, ABERDEEN PROVING GROUND, MD.
Non-lethal Unmanned Aerial Vehicles (UAVs)
[AD-A267139] p 866 N94-15692
Radar transmitter procedures
[AD-A268274] p 1005 N94-17523
ARMY TOPOGRAPHIC ENGINEERING CENTER, FORT BELVOIR, VA.
An automated approach for classifying generic terrain features using digital elevation data
[AD-A268385] p 1084 N94-17421
ARMY TRAINING AND DOCTRINE COMMAND, FORT MONROE, VA.
A TRALINET guide to the Internet
[AD-A266946] p 1229 N94-15178
ARMY WAR COLL., CARLISLE BARRACKS, PA.
The strategic environmental research and development program: A new paradigm for space, the environment, and national security
[AD-A266222] p 1174 N94-16109
ARNOLD ENGINEERING DEVELOPMENT CENTER, ARNOLD AFS, TN.
Solar absorptance of optical surfaces contaminated with spacecraft material outgassing products
[AD-A267202] p 886 N94-15857
A mechanical system damping measurement technique using a one-degree-of-freedom (1DOF) cylindrical gas bearing
[AD-A268402] p 1048 N94-17462
ASSISTANT SECRETARY OF DEFENSE (PRODUCTION AND LOGISTICS), WASHINGTON, DC.
Model designation of military aerospace vehicles
[AD-A267852] p 898 N94-17388
ATMOSPHERIC AND ENVIRONMENTAL RESEARCH, INC., CAMBRIDGE, MA.
Sensitivity testing of a single-Doppler temperature retrieval and forecast system
[AD-A267278] p 1105 N94-14958
Nowcasting methods for satellite imagery
[AD-A267294] p 1108 N94-17267
AUBURN UNIV., AL.
Aerodynamic flight control to increase payload capability of future launch vehicles
[NASA-CR-193850] p 870 N94-15532
High temperature materials technology research for advanced thermionic systems
[DE93-018302] p 960 N94-16964
AUSTRALIAN DEFENCE FORCE ACADEMY, CANBERRA.
Lossless compression of AVIRIS data: Comparison of methods and instrument constraints
p 1075 N94-16713

B

BALL AEROSPACE SYSTEMS DIV., BOULDER, CO.
CCDs and photon counting devices: Applications in space and from the ground p 901 N94-15041
Power Reactant Storage Assembly (PRSA) (Space Shuttle). PRSA hydrogen and oxygen DVT tank refurbishment
[NASA-CR-188262] p 926 N94-16922
BALL COMMUNICATION SYSTEMS DIV., BROOMFIELD, CO.
Advanced antennas for SAR spacecraft
p 993 N94-15912
BATTELLE INST., FRANKFURT AM MAIN (GERMANY).
Impurity conduction photoconductor detectors
p 902 N94-15046
Extrinsic photoconductor detectors for the wavelength range 2 microns to 240 microns p 906 N94-15073
The detector assemblies of ISOPHOT and the spectrometers ISO-SWS and ISO-LWS
p 906 N94-15074
BDM INTERNATIONAL, INC., MCLEAN, VA.
Optical residue processing module
[AD-A267721] p 1188 N94-14940
BELEIDSCOMMISSIE REMOTE SENSING, DELFT (NETHERLANDS).
Surface energy balance modeling at mesoscale: The contribution of the future Earth observing system
[BCRS-91-04] p 1085 N94-17616
BELGIAN ROYAL OBSERVATORY, BRUSSELS.
Papers presented at the Eleventh International Symposium on Earth Tides
[COMMUNICATIONS-SER-B-158] p 1098 N94-15800
Report of the International Center for Earth Tides for the period 1985-1989 p 1099 N94-15801
A new feedback system for instruments equipped with a capacitive transducer p 1037 N94-15802
Long baseline watertubes p 1037 N94-15803
Temperature measurements p 1037 N94-15804
Calibration platforms for gravimeters
p 1037 N94-15805
On tidal parameters at Brussels fundamental station
p 1100 N94-15807
Earth tides results obtained with gravimeters, clinometers, and strainmeters in Belgium and in Grand Duchy of Luxembourg p 1100 N94-15809
What we can learn about ocean tides from tide gauge and gravity loading measurements?
p 1100 N94-15811
Water-levels fluctuations in a borehole at the Royal Observatory of Belgium: Effects on local gravity, Earth tidal, and barometric responses p 1100 N94-15812
A study of the observed tidal residue vectors B versus oceanic tidal load vectors L p 1100 N94-15813
Tidal gravity anomalies and tectonics
p 1101 N94-15814
Report of the working group on theoretical tidal model
p 1101 N94-15815
BENDIX FIELD ENGINEERING CORP., SEABROOK, MD.
SATCOP mission planning software package
p 912 N94-15562
Preliminary results from the portable standard satellite laser ranging intercomparison with MOBLAS-7
p 913 N94-15568
Streak camera based SLR receiver for two color atmospheric measurements p 914 N94-15573
Analysis of TOPEX laser retroreflector array characteristics p 915 N94-15578
Historical MOBLAS system characterization
p 915 N94-15579
HP upgrade operational streamlining
p 918 N94-15596
Matera Laser Ranging Observatory (MLRO): An overview p 877 N94-15601
TLRS-3 system upgrades p 877 N94-15609
Optical attenuation mechanism upgrades, MOBLAS, and TLRS systems p 922 N94-15622
Performance comparison of high speed microchannel plate photomultiplier tubes p 922 N94-15624
BERGEN UNIV. (NORWAY).
A new detector concept for energetic auroral x ray imaging p 907 N94-15081
BHABHA ATOMIC RESEARCH CENTRE, BOMBAY (INDIA).
A new method of designing multilayer optical thin film coatings
[DE93-624683] p 974 N94-17611

Design, development and characterization studies of a large aperture high power Nd: Glass rod amplifier stage
[DE93-624944] p 1042 N94-17630

BIONETICS CORP., COCOA BEACH, FL.
Kennedy Space Center exercise program
p 1126 N94-16634

BIOTECHNOLOGY, INC., FALLS CHURCH, VA.
Proceedings of the 1992 Annual Meeting NASA Occupational Health Program
[NASA-CR-193462] p 1123 N94-16609

BM HI-TECH, INC., COLLINGWOOD (ONTARIO).
Payloads for the processing of high temperature materials p 979 N94-16083

BOEING CO., HUNTSVILLE, AL.
Government/contractor development teams
[TABES PAPER 93-460] p 1050 N94-16134

BOEING CO., SEATTLE, WA.
Simulation of collisional fragmentation with explosives
p 1063 N94-16254

BOEING COMPUTER SERVICES CO., SEATTLE, WA.
RAMCAD design methodology
[AD-A267010] p 1145 N94-15525

BOEING DEFENSE AND SPACE GROUP, HUNTSVILLE, AL.
Space transfer concepts and analyses for exploration missions, phase 4
[NASA-CR-193849] p 882 N94-15831

BOEING DEFENSE AND SPACE GROUP, SEATTLE, WA.
X ray computed tomography for failure analysis investigations
[AD-A268086] p 1055 N94-17515
X ray computed tomography for geometry acquisition
[AD-A268085] p 1157 N94-17590
X ray computed tomography for casting demonstration
[AD-A268084] p 1056 N94-17596

BOSTON COLL., CHESTNUT HILL, MA.
L-shell binning and display of sensor data from the CRRES spacecraft
[AD-A267256] p 888 N94-16990

BOSTON UNIV., MA.
Segment-based acoustic models for continuous speech recognition
[AD-A267138] p 988 N94-15691
Scintillation mechanism in stoichiometric cerium compounds
[DE93-015499] p 948 N94-16771
Growth and doping of Al(x)Ga(1-x)N films by electron cyclotron resonance assisted molecular beam epitaxy
[AD-A267305] p 1212 N94-16992

BREMEN UNIV. (GERMANY).
Cosmic dust and space debris measurements on board the small satellites HITEN and BREM-SAT
p 890 N94-17147

BRISTOL AEROSPACE LTD., WINNIPEG (MANITOBA).
QUESTS: A microgravity research facility for materials science experiments p 978 N94-16082

BRISTOL UNIV. (ENGLAND).
Pressures of supercritical salt solutions
p 945 N94-15166

BRITISH COLUMBIA UNIV., VANCOUVER.
Gas bubble generation and transport in microgravity
p 980 N94-16089
Statistical techniques for study design of microgravity life sciences experiments p 980 N94-16094

BROOKHAVEN NATIONAL LAB., UPTON, NY.
Application of in situ scanning x ray fluorescence to study the concentration of metal ions in simulated pits
[DE93-014054] p 956 N94-15921
Potential transients, transmission and electrochemical corrosion detection
[DE93-014055] p 956 N94-15922
Passive oxide films on well-defined nickel surfaces: An examination of film growth on Ni(100) with ex situ scanning tunneling microscopy
[DE93-014056] p 1207 N94-15923
An assessment of acid fog
[DE93-009347] p 1095 N94-15940
Magnetic effects in anomalous dispersion
[DE93-014291] p 1175 N94-15978
New York MARKAL: An evaluation of carbon dioxide emission control strategies in New York State
[DE93-013149] p 1095 N94-15999
In situ studies of passive film chemistry using x ray absorption spectroscopy
[DE93-014023] p 947 N94-16011
Nuclear fusion of protons with ions of boron
[DE93-015399] p 1202 N94-16019
Confinement and stability of a Crystal Beam
[DE93-015400] p 1181 N94-16020
PHENIX Conceptual Design Report
[DE93-015759] p 1182 N94-16161
Local environment about O atoms in Pr-Y-Ba-Cu-O films studied by O K-edge XAFS
[DE93-016218] p 1209 N94-16447
Powder diffraction studies using anomalous dispersion
[DE93-012531] p 1210 N94-16775
Evolution of hadron beams under intrabeam scattering
[DE93-014330] p 1184 N94-16826
Crystalline beam ground state
[DE93-014331] p 1211 N94-16827
The stability of ions in a storage ring in the presence of small gap insertion devices
[DE93-015387] p 1184 N94-16828
The pp elastic scattering experiment at RHIC and polarization studies in the Coulomb Nuclear Interference region
[DE93-015391] p 1187 N94-16829
Diffuse scattering and image contrast of tweed in superconducting oxides: A simulation and interpretation
[DE93-016131] p 1212 N94-16844
Binding of carbon dioxide to metal macrocycles: Toward a mechanistic understanding of electrochemical and photochemical carbon dioxide reduction
[DE93-016244] p 949 N94-16870
Six dimensional tracking simulator for H(-) injection in AGS Booster
[DE93-015396] p 1184 N94-16885
Emittance and beam size distortion due to linear coupling
[DE93-015402] p 1184 N94-16886
Suppression of charge scattering in Moessbauer experiments using synchrotron radiation
[DE93-015406] p 1212 N94-16887
Eigenfunctions of the transfer matrix in the presence of linear coupling
[DE93-015020] p 1151 N94-16892
Comparison of computer predictions and magnetic field measurements for an iron spectrometer magnet
[DE93-016164] p 1176 N94-17658
Growth of dielectric thin films by irradiation of condensed molecular precursors with synchrotron radiation
[DE93-016161] p 974 N94-17676

BROWN UNIV., PROVIDENCE, RI.
A multilevel-multiresolution method for image processing. A Bayesian framework for reconstructing and representing shapes
[AD-A266772] p 1082 N94-15842
The formation and evolution of Alpha and Tellus tesserae on Venus p 1249 N94-16183
Martian crater degradation by eolian processes: Analogy with the Rio Cuarto Crater Field, Argentina
p 1251 N94-16196
Rover mounted ground penetrating radar as a tool for investigating the near-surface of Mars and beyong
p 1007 N94-16197
Spatially extensive uniform stress fields on Venus inferred from radial dike swarm geometries: The Aphrodite Terra example p 1254 N94-16207
Tessera terrain on Venus: Implications of tessera flooding models and boundary characteristics for global distribution and mode of formation p 1258 N94-16226
Mode of emplacement of lunar mare volcanic deposits: Graben formation due to near surface deformation accompanying dike emplacement at Rima Parry 5
p 1258 N94-16227
Lunar impact basins: New data for the nearside northern high latitudes and eastern limb from the second Galileo flyby p 1258 N94-16228
Lunar scout missions: Galileo encounter results and application to scientific problems and exploration requirements p 1259 N94-16229
Lava flow-field morphological classification and interpretation: Examples from Venus
p 1259 N94-16230
Modes of formation of lunar light plains and the detection of cryptomaria deposits p 1259 N94-16231
Chemical differentiation, thermal evolution, and catastrophic overturn on Venus: Predictions and geologic observations p 1259 N94-16232
The ilmenite liquidus and depths of segregation for high-Ti picrite glasses p 975 N94-16241
Overturn of magma ocean ilmenite cumulate layer: Implications for lunar magmatic evolution and formation of a lunar core p 1261 N94-16242
Preliminary analysis of Dione Regio, Venus: The final Magellan regional imaging gap p 1271 N94-16302
The distribution of large volcanoes on Venus as a function of height and altitude p 1271 N94-16303
Large-scale volcanism associated with coronae on Venus p 1285 N94-16376
Composition of weakly altered Martian crust
p 1296 N94-16436
From minerals to rocks: Toward modeling lithologies with remote sensing p 1086 N94-16437
First results from analysis of coordinated AVIRIS, TIMS, and ISM (French) data for the Ronda (Spain) and Beni Bousera (Morocco) peridotites p 1067 N94-16675
Theoretical and experimental research into biological mechanisms underlying learning and memory
[AD-A267441] p 1133 N94-17022

BRUNEL UNIV., UXBRIDGE (ENGLAND).
Structural studies of sol-gel glasses
[AD-A266277] p 967 N94-16472

BUBBLE TECHNOLOGY INDUSTRIES, INC., CHALK RIVER (ONTARIO).
Preliminary results from bubble detector measurements aboard Biocosmos-2044 p 981 N94-16097

BUREAU VERITAS, COURBEVOIE (FRANCE).
Small satellite product assurance p 896 N94-17188

C

CALIFORNIA INST. OF TECH., PASADENA.
Velocity matched millimeterwave electro-optic modulator
[AD-A267264] p 1188 N94-14957
Do SiC grains in Orgueil differ from those in Murchison? p 1242 N94-16260
An experimental study of trace element partitioning between perovskite, hibonite and melt: Equilibrium values p 954 N94-16313
Evaporation kinetics of Mg2SiO4 crystals and melts from molecular dynamics simulations p 1219 N94-16331
The seismic response of an aquifer to the propagation of an impact generated shock wave: A possible trigger of the Martian outflow channels? p 1281 N94-16354
Effective elastic thickness of the Venusian lithosphere with lateral viscosity variations in the mantle
p 1293 N94-16421
Highly transient elastodynamic crack growth in a bimaterial interface: Higher order asymptotic analysis and optical experiments
[AD-A266465] p 1059 N94-16587
Synthetic and mechanistic investigation of olefin polymerization catalyzed by early transition metal compounds
[DE93-018301] p 970 N94-16963
Transmission of light through a turbulent mixing layer
[AD-A267266] p 1193 N94-17264
3-D optical memory disk
[AD-A267908] p 1141 N94-17380
Lifted turbulent jet flames
[AD-A267911] p 952 N94-17381
A typical pointed observation in IRAS designed to fit into a 15 minute window
[NASA-CR-194653] p 1199 N94-17443
Robust control of uncertain nonlinear systems
[AD-A268056] p 1167 N94-17506
Chemical reactions in turbulent mixing flows
[AD-A268287] p 861 N94-17580

CALIFORNIA STATE UNIV., FRESNO.
Interaction types and their like-polarization phase-angle difference signatures p 1079 N94-16756

CALIFORNIA STATE UNIV., LOS ANGELES.
Evaluation of spatial productivity patterns in an annual grassland during an AVIRIS overflight
[CIW-PUBL-1134] p 1067 N94-16672
Tracking photosynthetic efficiency with narrow-band spectroradiometry
[CIW-PUBL-1133] p 1072 N94-16698

CALIFORNIA UNIV., BERKELEY.
Microchannel plate imaging detectors for the ultraviolet p 901 N94-15037
Prospects for high pressure imaging gas scintillation drift chambers p 901 N94-15040
Technology transfers and reliable oxides
[AD-A266948] p 1175 N94-15758
EUVE observations of the Moon p 1250 N94-16185
From the Moons of Jupiter to the Milky Way
[NASA-CR-194649] p 1240 N94-17059
Micromechanisms of monotonic and cyclic subcritical crack growth in advanced high melting point low-ductility intermetallics
[AD-A267764] p 961 N94-17223

CALIFORNIA UNIV., BERKELEY. LAWRENCE BERKELEY LAB.
Closed orbit distortion and the beam-beam interaction
[DE93-015284] p 1190 N94-15854
Molecular beam studies of reaction dynamics
[DE93-015035] p 1181 N94-15995
Swelling equilibria for temperature-sensitive ampholytic hydrogels
[DE93-015264] p 966 N94-15996
Relativistic mean-field calculations of lambda and sigma hypernuclei
[DE93-015269] p 1181 N94-16013
Fast pulsars, compact stars, and the strange matter hypothesis
[DE93-015039] p 1239 N94-16052
Electroweak physics from D0
[DE93-015041] p 1181 N94-16053
Status of (alpha)(sub s) measurements
[DE93-015179] p 1181 N94-16059

A comparison of one and two dimensional flame quenching: Heat transfer results
[DE93-015196] p 947 N94-16060
In situ Raman spectroscopy of lithium electrode surface in ambient temperature lithium secondary battery
[DE93-015238] p 1010 N94-16061
Quantifying lifetime exposure to ultraviolet radiation in the epidemiology of cutaneous malignant melanoma: A pilot study
[DE93-015274] p 1128 N94-16812
On-line gas chromatographic studies of Rutherfordium (element 104), hahnium (element 105), and homologs
[DE93-013890] p 948 N94-16821
A search for evidence of nonlinear elasticity in the earth
[DE93-015279] p 1102 N94-17252
The inverse problem to the evaluation of magnetic fields
[DE93-015239] p 1175 N94-17288
Incorporating global warming risks in power sector planning. Volume 1: A case study of the New England region
[DE93-015241] p 1096 N94-17289

CALIFORNIA UNIV., DAVIS.
Exploitation of cyclostationarity for signal-parameter estimation and system identification
[AD-A267137] p 988 N94-15690
Using AVIRIS images to measure temporal trends in abundance of photosynthetic and nonphotosynthetic canopy components p 1066 N94-16668
Multitemporal diurnal AVIRIS images of a forested ecosystem p 1074 N94-16709

CALIFORNIA UNIV., IRVINE.
Cortical adaptive filtering in bioacoustic signal classification
[AD-A266229] p 1177 N94-16939
Investigation of the effects of polyelectrolyte coatings on colloid transport in porous media
[DE93-018300] p 970 N94-16973
Synaptic plasticity and memory formation
[AD-A267988] p 1133 N94-17453

CALIFORNIA UNIV., LOS ANGELES.
VLSI for high-speed digital signal processing
[AD-A267709] p 1007 N94-14936
Optoelectronics based on SiGe/Si heterostructures
[AD-A267178] p 1190 N94-15848
Fullerene superconductors
[AD-A266749] p 1010 N94-15954
Tectonic deformation in southern California
[NASA-CR-194621] p 1101 N94-16021
The Al Rais meteorite: A CR chondrite or close relative? p 1243 N94-16290
Implications of crater distributions on Venus p 1270 N94-16300
Megaplumes on Venus p 1271 N94-16301
Chromite-rich mafic silicate chondrules in ordinary chondrites: Formation by impact melting p 1244 N94-16330
Models of thermal/chemical boundary layer convection: Potential application to Venus p 1279 N94-16348
On the relationship between tectonic plates and thermal mantle plume morphology p 1104 N94-16349
Fluid flow and heat convection studies for actively cooled airframes
[NASA-CR-194624] p 1024 N94-16491
Experimental study of nonassociated flow and instability of frictional materials
[AD-A266421] p 1024 N94-16555

CALIFORNIA UNIV., SAN DIEGO, LA JOLLA.
Database system studies in fine grain optoelectronic computing
[AD-A267026] p 1145 N94-15627
Production and evaluation of dense ceramic compounds by combustion synthesis and dynamic compaction
[AD-A266742] p 965 N94-15773
A calibration of the production rate ratio P-21/P-26 by low energy secondry neutrons: Identification of Ne spallation components at the 10(exp 6) atoms/g level in terrestrial samples p 1187 N94-16194
Nitrogen isotopic signatures in agglutinates from breccia 79035 p 954 N94-16314
Isotopic signatures and distribution of nitrogen and trapped and radiogenic xenon in the Acapulco and FRO90011 meteorites p 1243 N94-16317
Amide and tetrazene complexes of transition and main group elements as precursors for the low temperature synthesis of elemental nitrides
[AD-A266246] p 950 N94-16931
Photo-assisted epitaxial growth for III-V semiconductors
[AD-A267889] p 1213 N94-17042
Neural basis of motion perception
[AD-A267267] p 1133 N94-17265
Diffractive optics fabricated by direct write methods with an electron beam p 1196 N94-17347
Mechanical properties of interfaces and superlattices
[AD-A268591] p 1217 N94-17606

CALIFORNIA UNIV., SANTA BARBARA.
The processing and mechanical properties of high temperature/high performance composites. Book 1: Coonstituent properties of composites
[AD-A266394] p 935 N94-16483
The processing and mechanical properties of high temperature/high performance composites. Book 2: Coonstituent properties and macroscopic performance
[AD-A266395] p 935 N94-16484
The processing and mechanical properties of high temperature/high performance composites. Book 3: Coonstituent properties and macroscopic performance
[AD-A266396] p 935 N94-16485
The processing and mechanical properties of high temperature/high performance composites. Book 4: Coonstitutive laws and design
[AD-A266397] p 935 N94-16528
The processing and mechanical properties of high temperature/high performance composites. Book 5: Processing and miscellaneous properties
[AD-A266398] p 935 N94-16529
Seasonal and spatial variations in phytoplanktonic chlorophyll in eutrophic Mono Lake, California, measured with the Airborne Visible and Infrared Imaging Spectrometer (AVIRIS) p 1069 N94-16684
Comparison of modeled backscatter with SAR data at P-band p 1076 N94-16735
SAR backscatter from coniferous forest gaps p 1076 N94-16736
Strategies for detection of floodplain inundation with multi-frequency polarimetric SAR p 1076 N94-16739

CAMBRIDGE UNIV. (ENGLAND).
Quasiparticle trapping in distributed superconducting three-terminal tunnel junction devices p 910 N94-15101
Direct observation of fracture of CAS-glass/SiC composites and processing of toughened alumina
[AD-A268275] p 941 N94-17457

CANADIAN SATELLITE COMMUNICATIONS, INC., MISSISSAUGA (ONTARIO).
Activities of Canadian Satellite Communications, Inc.
[CTN-93-60864] p 994 N94-15959

CANADIAN SPACE AGENCY, OTTAWA (ONTARIO).
RADARSAT program p 898 N94-15893
The Canadian Space Station user development program. Where do we go from here? p 898 N94-16084

CARBOTEK, INC., HOUSTON, TX.
First oxygen from lunar basalt p 1249 N94-16182

CARLETON COLL., NORTHFIELD, MN.
Emplacement of multiple flow units on very shallow slopes, east Kawelu Planitia flow field, Venus p 1260 N94-16235

CARNEGIE-MELLON UNIV., PITTSBURGH, PA.
YARF: An open-ended framework for robot road following
[AD-A266788] p 1163 N94-14910
Concurrent garbage collection of persistent heaps
[AD-A266831] p 1141 N94-14915
Perception for outdoor navigation
[AD-A266867] p 863 N94-14919
Fuzzy control and fuzzy kinematic mapping for a redundant space robot
[AD-A266866] p 1163 N94-14950
Video applications development platform
[AD-A266966] p 1163 N94-14953
Fuzzy inverse kinematic mapping: Rule generation, efficiency, and implementation
[AD-A266967] p 1163 N94-14954
Lecture notes on engineering measurement for software engineers
[AD-A266959] p 1142 N94-14967
Segmenting textured 3D surfaces using the space/frequency representation
[AD-A266960] p 1163 N94-14968
Serpentine manipulator planning and control for NASA Space-Shuttle payload servicing
[AD-A266961] p 879 N94-14969
Real-time implementation of neural network learning control of a flexible space manipulator
[AD-A266962] p 1045 N94-14970
RACCOON: A Real-Time Autonomous Car Chaser Operating Optimally at Night
[AD-A266963] p 863 N94-14971
Panacea: An active sensor controller for the ALVINN autonomous driving system
[AD-A266964] p 864 N94-14972
Infrared remote activity transceiver universal model
[AD-A266965] p 1188 N94-15144
Finding stable orientations of assemblies with linear programming
[AD-A266990] p 1143 N94-15212
HSTS: Integrating planning and scheduling
[AD-A266991] p 1222 N94-15213
Safety-critical software: Status report and annotated bibliography
[AD-A266993] p 1144 N94-15214
Concepts on measuring the benefits of software process improvements
[AD-A266994] p 1144 N94-15215
Software architecture for shared information systems
[AD-A266995] p 1144 N94-15216
Massively parallel, adaptive, color image processing for autonomous road following
[AD-A266988] p 864 N94-15498
Hidden Markov model approach to skill learning and its application to telerobotics
[AD-A266989] p 1164 N94-15502
An analysis of SEI software process assessment results: 1987-1991
[AD-A266996] p 1145 N94-15629
Process-centered development environments: An exploration of issues
[AD-A266997] p 1145 N94-15630
Dependable software technology exchange
[AD-A267103] p 1146 N94-15638
Reengineering: An engineering problem
[AD-A267117] p 1146 N94-15653
ACM SIGPLAN Workshop on ML and Its Applications
[AD-A266617] p 1147 N94-15725
Architectures for software systems: A curriculum development proposal in undergraduate software engineering
[AD-A266703] p 1147 N94-15728
Complexity analysis of real-time reinforcement learning applied to finding shortest paths in deterministic domains
[AD-A266636] p 1131 N94-15742
Using interactive sketch interpretation to design solid objects
[AD-A266637] p 1147 N94-15743
Fast interrupt priority management in operating system kernels
[AD-A266638] p 1140 N94-15744
Processor capacity reserves for multimedia operating systems
[AD-A266639] p 1158 N94-15745
Impending motion direction of contacting rigid bodies
[AD-A266814] p 1164 N94-15756
A scientific basis for computational science
[AD-A266697] p 1148 N94-15841
Disconnected operation in a distributed file system
[AD-A266461] p 1231 N94-16570
Using multiple adaptively-weighted strategies for the resolution of demonstratives
[AD-A266463] p 1150 N94-16585
Efficient compilation of array statements for private memory multicomputers
[AD-A266595] p 1160 N94-16724
Temporal segmentation of tasks from human hand motion
[AD-A266596] p 1166 N94-16725
Monads and comonads in intensional semantics
[AD-A266522] p 1151 N94-16790
Sequential functions on indexed domains and full abstraction for a sub-language of PCF
[AD-A267838] p 1152 N94-17009
Structural characterization of epitaxial layers for infrared detectors
[AD-A267875] p 940 N94-17013
Visual parallel programming with determinacy: A language specification, an analysis technique, and a programming tool
[AD-A267560] p 1153 N94-17107
Experience with disconnected operation in a mobile computing environment
[AD-A267524] p 1141 N94-17115
Causality-preserving timestamps in distributed programs
[AD-A267534] p 1153 N94-17118
Integrating reactive and deliberative planning for agents
[AD-A267631] p 1166 N94-17201
Software Capability Evaluation (SCE) version 1.5 method description. Software capability evaluation project
[AD-A267895] p 1154 N94-17395
Establishing a software measurement process
[AD-A267896] p 1154 N94-17396
An introduction to structural models
[AD-A268151] p 1155 N94-17429
A software process framework for the SEI capability maturity model: Repeatable level
[AD-A268059] p 1157 N94-17588

CASE WESTERN RESERVE UNIV., CLEVELAND, OH.
Maximum likelihood techniques applied to quasi-elastic light scattering
[NASA-CR-193550] p 1192 N94-16718

CATANIA ASTROPHYSICAL OBSERVATORY (ITALY).
A test facility to calibrate EUV detectors p 873 N94-15062

CENTER FOR INDUSTRIAL RESEARCH, OSLO (NORWAY).
Silicon radiation sensor systems for gamma and x ray detection at SI p 909 N94-15095
CENTER FOR OCCUPATIONAL PROGRAMS FOR EMPLOYEES, INC., WASHINGTON, DC.
Ongoing Recovery Basic Information Tool (ORBIT) p 1124 N94-16616
CENTRE D'ETUDE SPATIALE DES RAYONNEMENTS, TOULOUSE (FRANCE).
Recent advances in radar remote sensing of forest p 991 N94-15897
Retrieval of biophysical parameters with AVIRIS and ISM: The Landes Forest, south west France p 1068 N94-16681
Retrieval of pine forest biomass using JPL AIRSAR data p 1076 N94-16737
CENTRE NATIONAL D'ETUDES SPATIALES, PARIS (FRANCE).
ARIANE 5 light derivatives p 878 N94-17140
CENTRE NATIONAL D'ETUDES SPATIALES, TOULOUSE (FRANCE).
Small Satellites Systems and Services [ISBN-2-85-428327-9] p 888 N94-17131
AMIGAU: A prototype tool aimed at mission analysis for satellites and satellite constellations p 888 N94-17133
Radiocommunication problems of a position reporting and bidirectional messagery system using VHF/UHF with low-Earth orbit satellites p 889 N94-17136
Adequation of mini satellites to oceanic altimetry missions p 891 N94-17152
OREMUS: Prototype of an orbit determination center dedicated to mini-satellite control p 878 N94-17156
TAOS (S80): A (LEO-MSS) system for position reporting and telemanagement services p 893 N94-17162
S 80/T: A micro satellite system combining high performances and limited resources p 893 N94-17166
The STRV On Board Data Handling (OBDH) system: An introduction p 895 N94-17178
CESKOSLOVENSKA AKADEMIE VED, PRAGUE.
Static characteristics of a conduction and radiation dominated electric arc in nitrogen [DE93-627106] p 1204 N94-17311
Dynamic behavior of an electric arc gas discharge [DE93-630197] p 1205 N94-17635
CHALMERS UNIV. OF TECHNOLOGY, GOETEBORG (SWEDEN).
Hot electron mixers, the potential competition p 903 N94-15055
Orientation of DNA during free-solution electrophoresis p 944 N94-15162
CHICAGO UNIV., IL.
Theoretical high energy physics research at the University of Chicago [DE93-016863] p 1187 N94-16116
Experimental study of weak interactions by precision measurement by rare kaon decay [DE93-016864] p 1182 N94-16117
Particle physics and cosmology, Task C [DE93-016865] p 1239 N94-16118
Potassium isotope cosmochemistry, volatile depletion and the origin of the Earth p 953 N94-16259
A search for noble-gas evidence for presolar oxide grains p 954 N94-16353
A high sensitivity search for CP violating rare K(sub L) decays and precision measurement of the direct CP violation parameter (epsilon)(prime)/(epsilon) via the four K (yields) 2(pi) decay modes [DE93-016866] p 1184 N94-16899
CHINA NUCLEAR INFORMATION CENTRE, BEIJING.
Stress corrosion cracking of 316 SS and Incoloy-800 in high temperature aqueous containing sulfate and chloride [DE93-623325] p 952 N94-17302
A review of some dynamics models in six-dimensional phase space and their suitable conditions of motion equation [DE93-623741] p 1175 N94-17317
CHRISTOPHER NEWPORT COLL., NEWPORT NEWS, VA.
Optical fiber spectroscopy: A study of the luminescent properties of the europium ion for thermal sensors [NASA-CR-194576] p 1189 N94-15647
Shielding from space radiations [NASA-CR-194578] p 1180 N94-15715
Shielding from space radiations [NASA-CR-194664] p 1301 N94-17255
CINCINNATI UNIV., OH.
Synthesis of novel electrically conducting polymers: Potential conducting Langmuir-Blodgett films and conducting polymers on defined surfaces [NASA-CR-194651] p 972 N94-17297
An investigation of oblique shock/boundary layer interaction control [AD-A268106] p 861 N94-17574
CITY COLL. OF THE CITY UNIV. OF NEW YORK, NY.
Ultrafast processes in tunneling microstructure devices [AD-A266570] p 1210 N94-16720
CLARKSON UNIV., POTSDAM, NY.
Mechanism of intermittent atomization [AD-A266625] p 1021 N94-15770
CLEMSON UNIV., SC.
Designing clutter rejection filters with complex coefficients for airborne pulsed Doppler weather radar [NASA-CR-4550] p 862 N94-15444
Windshear detection radar signal processing studies [NASA-CR-194615] p 994 N94-16022
COALITION TO PREVENT LEAD POISONING, SAN FRANCISCO, CA.
Lead poisoning: An overview p 1124 N94-16614
COASTAL ENGINEERING RESEARCH CENTER, VICKSBURG, MS.
Observations and modelling of winds and waves during the Surface Wave Dynamics Experiment. Report 1: Intensive observation period IOP-1, 20-31 October 1990 [AD-A266384] p 1113 N94-16517
Preliminary estimates of frequency-direction spectra derived from the SAMSON pressure gage array, November 1990 to May 1991 [AD-A267960] p 1114 N94-17497
COLORADO STATE UNIV., FORT COLLINS.
Modification of fluoropolymer surfaces with electronically conductive polymers [AD-A266294] p 967 N94-16475
A simple chemical procedure for extending the conductive state of polypyrrole to more negative potentials [AD-A266235] p 969 N94-16928
Materials processing and manufacturing technologies for diamond substrate multichip modules (DSMCM) [AD-A267316] p 969 N94-16946
COLORADO UNIV., BOULDER.
Unsteady separated flows: Empirical model and control [AD-A267282] p 855 N94-14959
Dynamic behavior of fiber and particle reinforced composites [AD-A266905] p 930 N94-15143
Heterodyne efficiency for a coherent laser radar with diffuse or aerosol targets [NASA-CR-194563] p 1038 N94-15477
Sea ice motions in the central arctic ice central arctic pack ice as inferred from AVHRR imagery [NASA-CR-194572] p 1112 N94-15701
Parallel processing and scientific applications [AD-A267179] p 1159 N94-15849
A comparison of cloud attenuation models using measured cloud data p 996 N94-16044
A CCIR-based prediction model for Earth-Space propagation p 997 N94-16050
Evolutionary implications of a steady-state water abundance on Venus p 1254 N94-16206
Near-surface temperature gradients and their effects on thermal-infrared emission spectra of particulate planetary surfaces p 1260 N94-16236
The effects of orbital and climatic variations on Martian surface heat flow p 1290 N94-16402
Equatorial ground ice on Mars: Steady-state stability p 1290 N94-16403
Fundamental studies of rocket combustion chemistry and combustion instability [AD-A266248] p 925 N94-16482
ROSAT-IUE observations of symbiotic stars. The x ray morphology of high latitude associations [NASA-CR-194616] p 1236 N94-16492
Unmixing AVIRIS data to provide a method for vegetation fraction subtraction p 1066 N94-16669
The Spectral Image Processing System (SIPS): Software for integrated analysis of AVIRIS data p 1067 N94-16674
A linear spectral matching technique for retrieving equivalent water thickness and biochemical constituents of green vegetation p 1068 N94-16678
Separation of cirrus cloud from clear surface from AVIRIS data using the 1.38 micron water vapor band p 1072 N94-16699
Software for the derivation of scaled surface reflectances from AVIRIS data p 1072 N94-16700
Expert system-based mineral mapping using AVIRIS p 1073 N94-16704
Discrimination among semi-arid landscape endmembers using the Spectral Angle Mapper (SAM) algorithm p 1074 N94-16711
Extraction of quantitative surface characteristics from AIRSAR data for Death Valley, California p 1078 N94-16748
Radar Analysis and Visualization Environment (RAVEN): Software for polarimetric radar analysis p 1080 N94-16758
Numerical study of compressible boundary-level transition between two concentric cylinders [NASA-CR-194622] p 1025 N94-16842
Nonlinear problems in fluid dynamics and inverse scattering [AD-A266234] p 1026 N94-16927
Critically evaluated/distributed database of IRAS LRS spectra [NASA-CR-193611] p 1232 N94-17038
Laser probing of the kinetics and dynamics of 3-5 semiconductor growth [AD-A268388] p 1215 N94-17422
COLUMBIA UNIV., NEW YORK, NY.
Multichip module high speed testing [AD-A266968] p 986 N94-14955
Diffusible driving and coupling signals of the biological clock [AD-A267046] p 1121 N94-15660
Exploring the southern ocean response to climate change [NASA-CR-194601] p 1112 N94-15680
Congestion control of high-speed networks [AD-A267013] p 989 N94-15748
Single-collision studies of energy transfer and chemical reaction [DE93-017603] p 1182 N94-16121
Theoretical high energy physics [DE93-015884] p 1187 N94-16170
High beta and confinement studies of TFTR [DE93-016204] p 1202 N94-16446
Linear and non-linear studies of Alfven waves in space. Stationary and dynamic processes in magnetospheric plasmas [NASA-CR-193585] p 1239 N94-16647
Process evolution for the MARVEL environment [AD-A267813] p 1155 N94-17398
Testing string superprimitivity in parallel [AD-A267814] p 1155 N94-17399
Concurrency control in rule-based software development environments [AD-A267829] p 1155 N94-17404
Isochronets: A high-speed network switching architecture [AD-A267811] p 1161 N94-17409
COMITATO NAZIONALE PER L'ENERGIA NUCLEARE, NAPLES (ITALY).
Evaluation of the TOPSAR performance by using passive and active calibrators p 1078 N94-16750
COMMISSARIAT A L'ENERGIE ATOMIQUE, GIF-SUR-YVETTE (FRANCE).
Density and temperature relaxation near the critical point of carbon dioxide under reduced gravity p 944 N94-15164
COMMISSARIAT A L'ENERGIE ATOMIQUE, GRENOBLE (FRANCE).
A 12.5 micron infrared detector for Earth observation p 903 N94-15052
COMMISSION OF THE EUROPEAN COMMUNITIES, ISPRA (ITALY).
Supervised fully polarimetric classification of the Black Forest test site: From MAESTRO1 to MAC Europe p 1076 N94-16740
COMMUNICATIONS RESEARCH CENTRE, OTTAWA (ONTARIO).
Dual polarization microstrip array antenna [CA-PATENT-1-307-842] p 994 N94-15986
COMMUNICATIONS SATELLITE CORP., CLARKSBURG, MD.
On-board B-ISDN fast packet switching architectures. Phase 1: Study [NASA-CR-191143] p 883 N94-17111
COMPUTATIONAL FLUID DYNAMICS RESEARCH CORP., HUNTSVILLE, AL.
Computational analysis of Variable Thrust Engine (VTE) performance [NASA-CR-193852] p 928 N94-17442
COMPUTATIONAL LOGIC, INC., AUSTIN, TX.
A formal language for the specification and verification of synchronous and asynchronous circuits [NASA-CR-191509] p 1144 N94-15443
CONSIGLIO NAZIONALE DELLE RICERCHE, BOLOGNA (ITALY).
CdTe array detectors for high energy astronomy p 899 N94-15029
CONSIGLIO NAZIONALE DELLE RICERCHE, GENOA (ITALY).
Measurements of Interfacial Tension: MITE p 943 N94-15158
CONSIGLIO NAZIONALE DELLE RICERCHE, NAPLES (ITALY).
Nb-based SJTJ for nuclear detection: Preliminary results with alpha radiation p 905 N94-15068

CONSIGLIO NAZIONALE DELLE RICERCHE, PALERMO (ITALY).
The high pressure gas scintillation proportional counter for SAX p 906 N94-15076
CONSULTEC SCIENTIFIC, INC., KNOXVILLE, TN.
Electrorheological (ER) fluids: A research needs assessment
[AD-A267588] p 951 N94-17210
COORDINATING RESEARCH COUNCIL, INC., ATLANTA, GA.
Effects of RVP, T(50), and oxygenates on hot-start and driveability performance at high and low altitude
[AD-A266382] p 869 N94-16516
CORNELL UNIV., ITHACA, NY.
Structural and dynamical aspects of electrodeposition
[AD-A266786] p 942 N94-14909
Reaction and diffusion in turbulent combustion
[DE93-017085] p 943 N94-15146
A global traveling wave on Venus
[NASA-CR-194356] p 1246 N94-15182
Galileo photometry of Apollo landing sites p 1259 N94-16234
Studies of combustion reactions at the state-resolved differential cross section level
[DE93-017605] p 948 N94-16462
Consistent failure reporting in reliable communication systems
[AD-A266298] p 997 N94-16477
Preliminary results of polarization signatures for glacial moraines in the Mono Basin, Eastern Sierra Nevada p 1078 N94-16746
Understanding partitions and the no partition assumption
[AD-A266296] p 1000 N94-16911
UHV-stem studies on nucleation and growth of thin metal silicide films on silicon
[DE93-017604] p 1212 N94-16961
A security architecture for fault-tolerant systems
[AD-A266178] p 1152 N94-16982
A geological and geophysical information system for Eurasia
[AD-A267841] p 1232 N94-17036
Light-weight process groups in the ISIS system
[NASA-CR-194544] p 1161 N94-17239
Femtosecond carrier processes in compound semiconductors and real time signal processing
[AD-A268122] p 1005 N94-17519
In-situ electron and optical spectroscopies of translational and vibrational activated bond breaking and formation on semiconductors
[AD-A268192] p 1015 N94-17560
CREIGHTON UNIV., OMAHA, NE.
Heavy ion physics research at Creighton University
[DE93-016809] p 1185 N94-16957
CZECH TECHNICAL UNIV., PRAGUE.
Alternative wavelengths for laser ranging p 913 N94-15564
New methods of generation of ultrashort laser pulses for ranging p 913 N94-15565
An improved light source for laser ranging p 913 N94-15567
The solid state detector technology for picosecond laser ranging p 914 N94-15572
The first satellite laser echoes recorded on the streak camera p 914 N94-15574
Two wavelength satellite laser ranging using SPAD p 916 N94-15584
Computer networking at SLR stations p 917 N94-15594
Mars laser altimeter based on a single photon ranging technique p 921 N94-15619
Satellite laser station Helwan status 1992 p 877 N94-15621

D

DANISH SPACE RESEARCH INST., LYNGBY.
The imaging microstrip proportional counter: Features of a practical design p 900 N94-15030
Outlook for hard x ray and gamma ray astronomy p 904 N94-15057
DARTMOUTH COLL., HANOVER, NH.
Synthesis and chemistry of novel cyclic fluorocarbons
[AD-A267148] p 929 N94-15734
DASSAULT AVIATION, ISTRES (FRANCE).
Low Earth orbit constellations: Orbit control or not p 875 N94-17134
DAYTON UNIV., OH.
Scholarly research program in fuel analysis and combustion research
[AD-A266789] p 942 N94-14911
An information processing classification of beyond-visual-range air intercepts
[AD-A266927] p 1131 N94-15108
Evaporation from a meniscus within a capillary tube in microgravity
[NASA-CR-194593] p 976 N94-15654
System architecture of optically controlled phased array radar
[AD-A267056] p 988 N94-15667
Comparative night vision goggle visual acuity measurements performed in the A-10 aircraft in an operational setting
[AD-A266721] p 1137 N94-15820
Center for Rotorcraft Education and Research progress report, 1987 - 1992
[AD-A266760] p 857 N94-15824
Elastic-plastic finite-difference analysis of unidirectional composites subjected to thermomechanical cyclic loading
[AD-A267666] p 1061 N94-17269
DAYTON UNIV. RESEARCH INST., OH.
Spatial filters for optical correlation
[AD-A267199] p 1189 N94-15791
Flight simulator-induced sickness and visual displays evaluation
[AD-A267019] p 1122 N94-15845
DCW INDUSTRIES, LA CANADA, CA.
Turbulence and transition modeling for high-speed flows
[AD-A266748] p 1022 N94-15953
DEFENCE RESEARCH AGENCY, FARNBOROUGH (ENGLAND).
The space technology research vehicle: Development status p 896 N94-17183
DEFENCE RESEARCH ESTABLISHMENT, OTTAWA (ONTARIO).
Interferometric GPS attitude: A stochastic error model, DREO report
[AD-A266411] p 864 N94-16457
DEFENSE INFORMATION SYSTEMS AGENCY, ARLINGTON, VA.
Department of Defense technical architecture framework for information management. Volume 1: Overview, version 2.0
[AD-A267193] p 1228 N94-15152
Department of Defense technical architecture framework for information management. Volume 2: Technical reference model and standards profile, version 2.0
[AD-A267194] p 1229 N94-15788
Department of Defense technical architecture framework for information management. Volume 3: Architecture concepts and design guidance, version 2.0
[AD-A267195] p 1230 N94-15789
DEFENSE LOGISTICS SERVICES CENTER, BATTLE CREEK, MI.
Defense Logistics Information System (DLIS) procedures manual. Products and services end-user manual
[AD-A267766] p 1232 N94-17007
Defense Logistics Information System (DLIS). Procedures manual: Logistics On-Line Access (LOLA) procedures manual
[AD-A267685] p 1233 N94-17229
DEFENSE PERSONNEL SECURITY RESEARCH CENTRE, MONTEREY, CA.
The impact of report of investigation writing style on the assessment times, impressions, perceptions and preferences of adjudicators
[AD-A265748] p 1223 N94-15682
DEFENSE TECHNICAL INFORMATION CENTER, ALEXANDRIA, VA.
Defense RDT&E online system (DROLS) handbook
[AD-A267546] p 1232 N94-17101
DELAWARE UNIV., LEWES.
Regulation of attached bacterial growth by adsorbed proteins
[AD-A267756] p 1118 N94-17275
DELAWARE UNIV., NEWARK.
Characterization of spatial and temporal variability of phytoplankton blooms in coastal waters
[AD-A267102] p 1116 N94-15633
Cretaceous-tertiary boundary spherules and Cenozoic microtektites: Similarities and differences p 1241 N94-16186
DELFT ELECTRONIC PRODUCTS, RODEN (NETHERLANDS).
Development of an ultra violet auroral imager for the Freja project p 904 N94-15060
DELFT HYDRAULICS LAB., EMMELOORD (NETHERLANDS).
Mapping of sea bottom topography p 1077 N94-16744
DENISON UNIV., GRANVILLE, OH.
Tidal regime of intact planetoid capture model for the Earth-Moon system: Does it relate to the archean sedimentary rock record? p 1245 N94-16378
DENVER UNIV., CO.
Atomic beam studies relevant to the space environment
[AD-A268628] p 1186 N94-17436
DEPARTMENT OF ADMINISTRATIVE SERVICES, CANBERRA (AUSTRALIA).
Performance of the upgraded Orroral laser ranging system p 877 N94-15602
DEPARTMENT OF ENERGY, IDAHO FALLS, ID.
Space Nuclear Facility test capability at the Baikal-1 and IGR sites Semipalatinsk-21, Kazakhstan
[DE93-011662] p 926 N94-16773
DEPARTMENT OF ENERGY, MORGANTOWN, WV.
Status of molten carbonate fuel cell technology development
[DE93-015666] p 1092 N94-16715
DEPARTMENT OF ENERGY, WASHINGTON, DC.
The friction and wear of ceramic/ceramic and ceramic/metal combinations in sliding contact
[NASA-TM-106348] p 930 N94-15769
Information Technology Resources Assessment
[DE93-013899] p 1230 N94-16010
Utility emissions associated with electric and hybrid vehicle (EHV) charging
[DE93-013734] p 1011 N94-16459
New health and safety initiatives at the Department of Energy (DOE) p 1124 N94-16610
Requirements for supercomputing in energy research: The transition to massively parallel computing
[DE93-012376] p 1160 N94-16774
DEPARTMENT OF NATURAL RESOURCES, SALT LAKE CITY, UT.
Integrating remote sensing techniques at Cuprite, Nevada: AVIRIS, Thematic Mapper, and field spectroscopy p 1072 N94-16701
DEPARTMENT OF THE NAVY, WASHINGTON, DC.
Formation of pitting resistant anodized films on aluminum
[AD-D015812] p 958 N94-16486
Apparatus for and a method of growing thin films of elemental semiconductors
[AD-D015813] p 1210 N94-16487
Translating wedge heat sink
[AD-D015814] p 1011 N94-16488
Fabrication and phase tuning of an optical waveguide device
[AD-D015815] p 1191 N94-16489
Method for restructuring a database using a relational database scheme derived by selecting subscheme joins to avoid cycles
[AD-D015816] p 1231 N94-16490
Electro-rheological disk pump
[AD-D015783] p 1047 N94-16531
Electrorheological fluid chemical processing
[AD-D015785] p 948 N94-16532
Lasing dye sensor for chemical vapors
[AD-D015786] p 1040 N94-16533
Process for shaping articles from electrosetting compositions
[AD-D015787] p 935 N94-16534
Method and apparatus for forming an agile plasma mirror effective as a microwave reflector
[AD-D015788] p 998 N94-16535
Mechanical and surface force nanoprobe
[AD-D015792] p 1034 N94-16536
Electrostatic fiber spreader including a corona discharge device
[AD-D015793] p 936 N94-16537
Method for doping GaAs with high vapor pressure elements
[AD-D015794] p 1210 N94-16538
Method and apparatus for performing scanning tunneling optical absorption spectroscopy
[AD-D015796] p 948 N94-16539
Digital laser range finder emulator
[AD-D015811] p 1040 N94-16540
Infrared spot tracker
[AD-D015778] p 1191 N94-16547
Tilt mechanism
[AD-D015780] p 1047 N94-16548
Hydraulic pump with integral electric motor
[AD-D015782] p 1011 N94-16549
Process of shaping an electrorheological solid
[AD-D015885] p 1012 N94-16914
High pressure pump for electro-rheological fluids
[AD-D015888] p 1048 N94-16915
Interpenetrating polymer network acoustic damping material
[AD-D015889] p 969 N94-16916
Moving target indicator using higher order statistics
[AD-D015890] p 1000 N94-16917
High resolution radar profiling using higher-order statistics
[AD-D015891] p 1000 N94-16918
Digital reverberation time measurement system
[AD-D015892] p 1177 N94-16919

Main chain chromophoric polymers with second order nonlinear optical properties
[AD-D015893] p 969 N94-16920
Acousto-optical classifier
[AD-D015894] p 1000 N94-16921
Techniques for preparation of ingot metallurgical discontinuous composites
[AD-D015748] p 940 N94-16933
Densifying and stabilizing ingredient
[AD-D015751] p 975 N94-16934

DEPARTMENT OF TRADE AND INDUSTRY, STEVENAGE (ENGLAND).
Regulation of low Earth orbit satellites
p 892 N94-17159

DESERET TEST CENTER, FORT DOUGLAS, UT.
Reliability characterization of digital microcircuits: Investigation of an in-process oxide reliability screening method
[AD-A267053] p 1008 N94-15665

DESERT RESEARCH INST., RENO, NV.
Primary studies of trace quantities of green vegetation in Mono Lake area using 1990 AVIRIS data
p 1071 N94-16695
Simulation of AVHRR-K band ratios with AVIRIS
p 1075 N94-16714

DEUTSCHE AEROSPACE A.G., MUNICH (GERMANY).
Plume radiation p 924 N94-15223

DEUTSCHE FORSCHUNGS- UND VERSUCHSANSTALT FUER LUFT- UND RAUMFAHRT, OBERPFAFFENHOFEN (GERMANY).
X-SAR: The X-band synthetic aperture radar on board the Space Shuttle p 990 N94-15891
Multifrequency observations p 992 N94-15902
Recent advances and plans in processing and geocoding of SAR data at the DFD p 992 N94-15909

DEUTSCHE FORSCHUNGSANSTALT FUER LUFT- UND RAUMFAHRT, COLOGNE (GERMANY).
Temperature propagation in near-critical fluids prior to and during separation p 944 N94-15165
Design of an experiment hardware for the ESA space facility BIOPAN
[DLR-FB-93-06] p 876 N94-17548
Investigations into the recovery of waste sulfuric acid with concentrated solar radiation
[DLR-FB-93-11] p 952 N94-17594

DEUTSCHE FORSCHUNGSANSTALT FUER LUFT- UND RAUMFAHRT, OBERPFAFFENHOFEN (GERMANY).
Diffraction of microwaves at rectangular facades of buildings with and without ground reflections (Fresnel-Kirchhoff-Approximation)
[DLR-FB-92-35] p 987 N94-15155
Earth-based and Galileo SSI multispectral observations of eastern mare serenitatis and the Apollo 17 landing site p 1261 N94-16244
Age determinations and Earth-based multispectral observations of lunar light plains p 1275 N94-16323
MAC Europe 1991: Evaluation of AVIRIS, GER imaging spectrometry data for the land application testsite Oberpfaffenhofen p 1070 N94-16688
Comparison of JPL-AIRSAR and DLR E-SAR images from the MAC Europe 1991 campaign over testsite Oberpfaffenhofen: Frequency and polarization dependent backscatter variations from agricultural fields
p 1075 N94-16733

DEUTSCHE FORSCHUNGSANSTALT FUER LUFT- UND RAUMFAHRT, STUTTGART (GERMANY).
Heat storage module p 946 N94-15172

DEUTSCHE GEODAETISCHE KOMMISSION, MUNICH (GERMANY).
New techniques for the combination of heterogenous data when determining the Earth's gravity field
[SER-C-395] p 1098 N94-15153
Analysis of the accuracy of strapdown inertial surveying systems
[SER-C-391] p 1081 N94-15156
Laser ranging network performance and routine orbit determination at D-PAF p 911 N94-15554
On the accuracy of ERS-1 orbit predictions
p 874 N94-15589

DEUTSCHER WETTERDIENST, OFFENBACH AM MAIN (GERMANY).
Determination of sunshine duration from radiation intensity pyranometric measurements of global and sky radiation
[BER-181] p 1105 N94-15302

DEUTSCHES GEODAETISCHES FORSCHUNGSINST., MUNICH (GERMANY).
Laser ranging network performance and routine orbit determination at D-PAF p 911 N94-15554
On the accuracy of ERS-1 orbit predictions
p 874 N94-15589

DIGITAL OPTICS CORP., CHARLOTTE, NC.
Applications of advanced diffractive optical elements
p 1197 N94-17356

DORNIER SYSTEM G.M.B.H., FRIEDRICHSHAFEN (GERMANY).
Strategy for a small satellite program and a proposal for a first mission p 874 N94-17143

DOUGLAS AIRCRAFT CO., INC., LONG BEACH, CA.
Techno-economic requirements for composite aircraft components p 940 N94-16864

DOW CORNING CORP., CARROLLTON, KY.
Methyl chloride via oxyhydrochlorination of methane
[DE93-017548] p 952 N94-17218

DREXEL UNIV., PHILADELPHIA, PA.
Influence of fiber packing structure on permeability
p 938 N94-16857

DU PONT DE NEMOURS (E. I.) AND CO., WILMINGTON, DE.
Bioorganic models for protein ion channels
[AD-A266365] p 1117 N94-16441
SURPHEX (tm): New dry photopolymers for replication of surface relief diffractive optics p 1198 N94-17358

DUKE UNIV., DURHAM, NC.
Spectroscopic investigations of nonambient systems with millimeter and submillimeter probes
[AD-A266537] p 968 N94-16796

DUNSINK OBSERVATORY, DUBLIN (IRELAND).
The Rutherford Appleton Laboratory photon counting detector p 910 N94-15096

DYNETICS, INC., HUNTSVILLE, AL.
Alternative optical architectures for multichannel adaptive optical processing
[AD-A267052] p 1189 N94-15664
Wideband acousto-optic correlator for an ESM receiver upgrade
[TABES PAPER 93-661] p 1054 N94-16156

E

EAGLE-PICHER INDUSTRIES, INC., JOPLIN, MO.
Small satellite nickel-hydrogen and nickel-metal hydride power applications p 895 N94-17175

EAST CAROLINA UNIV., GREENVILLE, NC.
Evaluation of dried storage of platelets for transfusion: Physiologic integrity and hemostatic functionality
[AD-A266958] p 1120 N94-15180

ECOLE NATIONALE SUPERIEURE DE L'AERONAUTIQUE ET DE L'ESPACE, TOULOUSE (FRANCE).
BRIDGE: A small scientific satellite for geodesy
p 890 N94-17146
Data processing system for ARSENE ground station: A tool for small satellite control and development
p 878 N94-17157

ECOLE NATIONALE SUPERIEURE DES TELECOMMUNICATIONS, TOULOUSE (FRANCE).
Impact of launching uncertainties on the visibility of communication satellite constellations without orbit control p 889 N94-17135

ECOLE SUPERIEURE DES GEOMETRES ET TOPOGRAPHES, EVRY (FRANCE).
Improvement of SLR accuracy, a possible new step
p 917 N94-15588

ECOLINK, INC., ATLANTA, GA.
Environmental management lessons to be learned from the upcoming CFC phase out or how to insure that we survive the next environmentally mandated process change
[TABES PAPER 93-570] p 1050 N94-16136

EDGERTON, GERMESHAUSEN AND GRIER, INC., COCOA BEACH, FL.
Medical surveillance and biological monitoring of lead exposed employees p 1124 N94-16615
Efficient management of cardiovascular risk screening programs p 1125 N94-16622
Space Shuttle solid rocket motor exposure monitoring
p 976 N94-16624
Illness/injury pattern complex 40 (Titan)
p 1125 N94-16625
Identifying and responding to customer needs at the Kennedy Space Center p 1056 N94-16626
Bloodborne Pathogens Program p 1127 N94-16644

EDGERTON, GERMESHAUSEN AND GRIER, INC., GOLETA, CA.
Elemental impurity analysis of mercuric iodide by ICP/MS
[DE93-015531] p 949 N94-16876

EG AND G ENERGY MEASUREMENTS, INC., GOLETA, CA.
Optical properties and surface morphology studies of palladium contacts on mercuric iodide single crystals
[DE93-012510] p 1207 N94-15973
Growth of single crystals of mercuric iodide on the ground and in space
[DE93-015523] p 1209 N94-16442

EIDETICS INTERNATIONAL, INC., TORRANCE, CA.
Aerodynamic control of NASP-type vehicles through Vortex manipulation. Volume 1: Static water tunnel tests
[NASA-CR-177626-VOL-1] p 855 N94-15655
Aerodynamic control of NASP-type vehicles through Vortex manipulation. Volume 2: Static wind tunnel tests
[NASA-CR-177626-VOL-2] p 856 N94-15677
Aerodynamic control of NASP-type vehicles through vortex manipulation, volume 4
[NASA-CR-177626-VOL-4] p 857 N94-15720
Aerodynamic control of NASP-type vehicles through vortex manipulation. Volume 3: Wing rock experiments
[NASA-CR-177626] p 857 N94-15780

EIDGENOESSISCHE TECHNISCHE HOCHSCHULE, ZURICH (SWITZERLAND).
Solar noble gases revealed by closed system stepped etching of a metal separate from Fayetteville
p 954 N94-16432

ELECTROMAGNETIC SCIENCES, INC., NORCROSS, GA.
Microwave reflectometer ionization sensor
[NASA-CR-191464] p 922 N94-17083

ELECTRONIC SYSTEMS DIV., HANSCOM AFB, MA.
Ground wave emergency network final operational capability: Environmental assessment for central Wyoming relay node, site number RN 8C928WY
[AD-A267842] p 1001 N94-17011
Ground wave emergency network final operational capability: Environmental assessment for central Nevada relay node, site number RN 8W917NV
[AD-A267630] p 1002 N94-17200
Ground wave emergency network final operational capability: Environmental assessment for southern Nevada relay node site number RN 8W918NV
[AD-A267647] p 1002 N94-17205
Ground wave emergency network final operational capability: Environmental assessment for central Utah relay node, site number RN 8C920UT
[AD-A267628] p 1003 N94-17211
Ground wave emergency network final operational capability: Environmental assessment for northwestern Nebraska relay node, site number RN 8C930NE
[AD-A267629] p 1003 N94-17212
Ground wave emergency network environmental assessment for northwestern Colorado relay node site number RN 8C924CO
[AD-A267654] p 1003 N94-17249
Ground wave emergency network. Final operational capability. Environmental assessment for southeastern Idaho relay node, site no. RN8W927ID
[AD-A267796] p 1003 N94-17304
Ground wave emergency network final operational capability. Environmental assessment for southern Arkansas relay node site no. RN 8C912AR
[AD-A268001] p 1004 N94-17376
Environmental assessment for northwestern Indiana relay node site no. RN 8C902IN
[AD-A267849] p 1004 N94-17406

ELECTRONICS RESEARCH LAB., SALISBURY (AUSTRALIA).
The distributed database dynamic reconfiguration project
[AD-A267116] p 1229 N94-15652

ELECTROTECHNICAL LAB., TSUKUBA (JAPAN).
Unidirectional solidification of liquid-crystal material
p 945 N94-15167

ELLIPSAT CORP., WASHINGTON, DC.
The ELLIPSO (tm) system: Elliptical low orbits for mobile communications p 893 N94-17167

ELORET CORP., SUNNYVALE, CA.
Simulation studies for surfaces and materials strength
[NASA-CR-193387] p 1056 N94-15004
Particle kinetic simulation of high altitude hypervelocity flight
[NASA-CR-194599] p 856 N94-15678

EMORY UNIV., ATLANTA, GA.
The thermal dissociation of NH2CHO(ND2CHO) on Si(100)-2x1
[AD-A266903] p 942 N94-14956
The interaction of HCN(DCN) with Si(111)-7x7 studied with HREELS, UPS, and XPS
[AD-A266237] p 1182 N94-16111

ENGLISH ELECTRIC VALVE CO. LTD., CHELMSFORD (ENGLAND).
Development of x ray CCDs p 900 N94-15033

ENVIRONMENTAL RESEARCH INST. OF MICHIGAN, ANN ARBOR.
Fabrication techniques for very fast diffractive lenses
p 1196 N94-17345

EPION CORP., BEDFORD, MA.
Single crystal diamond thin films
[AD-A266457] p 1214 N94-17216

ETUDE ET REALISATION DE MICRO-SATELLITES, PARIS (FRANCE).
Standard platforms for small satellites
p 895 N94-17181

EUROCONSULT, PARIS (FRANCE).
Key trends of the small satellite market
p 897 N94-17191
EUROPEAN SPACE AGENCY, PARIS (FRANCE).
Proceedings of an ESA Symposium on Photon Detectors for Space Instrumentation
[ESA-SP-356] p 899 N94-15025
Sounding Rocket Experiments in Fluid Science and Materials Sciences: TEXUS 25 to 27 and MASER 4, volume 3
[ESA-SP-1132-VOL-3] p 943 N94-15157
ECS: Ninth year in orbit
[ESA-BR-91] p 987 N94-15644
The ESA telescience program p 977 N94-16073
Small launchers (current and future projects in the world) p 878 N94-17137
EUROPEAN SPACE AGENCY. EUROPEAN SPACE RESEARCH AND TECHNOLOGY CENTER, ESTEC, NOORDWIJK (NETHERLANDS).
A new approach to optical photon detection
p 899 N94-15028
Developments in extreme ultraviolet and x ray instrumentation p 904 N94-15058
Hypersonic shock wave boundary layer interactions over simplified deflected control surface configurations
p 1018 N94-15203
The definition of a scientific policy: ESRO's satellite programme in 1969-1973
[ESA-HSR-6] p 1303 N94-16500
The launch of ELDO
[ESA-HSR-7] p 886 N94-16501
Choosing ESRO's first scientific satellites
[ESA-HSR-3] p 887 N94-16523
Giotto's second encounter: The mission to Comet Grigg-Skjellerup
[ESA-BR-93] p 1239 N94-16524
The early development of the Telecommunications Satellite Programme in ESRO (1965-1971)
[ESA-HSR-9] p 887 N94-16525
Europe in space: Edoardo Amaldi and the inception of ESRO
[ESA-HSR-5] p 1303 N94-16526
Looking at science on board Eureca
[ESA-BR-80] p 874 N94-16584
The ESA Tele-Invoicing System (ETIS)
[ESA-INT-6] p 1150 N94-16591
Europe into space: The Auger years (1959-1967)
[ESA-HSR-8] p 1303 N94-16592
The early activities of the COPERS and the drafting of the ESRO Convention (1961/62)
[ESA-HSR-4] p 1225 N94-16593
Resources and activities of the European Space Agency p 1303 N94-16792
Small missions for space science p 874 N94-17142
Satellite control: A comprehensive approach
p 878 N94-17158
MAGSS-14: Medium Altitude Global Mobile Satellite System with enhanced regional coverage
p 893 N94-17164
Impact of advances in technology on future spacecraft design p 894 N94-17171
A power system for a microsatellite
p 895 N94-17176
EUROPEAN SPACE RESEARCH LAB., NOORDWIJK (NETHERLANDS).
ERS-1: 18 months in orbit p 990 N94-15888
ENVISAT ASAR p 898 N94-15892
Calibration: Practical experience with ERS-1
p 992 N94-15907
EUROPEAN SPACE RESEARCH ORGANIZATION, NOORDWIKJ (NETHERLANDS).
A review of OPEX activities and measurement results
p 994 N94-16036

F

FABRICA ITALIANA APPARECCHIATURE RADIOELETTRICHE S.P.A., MILAN.
Arsene GaAs solar array p 894 N94-17174
FEDERAL AVIATION ADMINISTRATION, ATLANTIC CITY, NJ.
Satellite communications installation plan
[AD-A266303] p 1000 N94-16965
FEDERAL AVIATION ADMINISTRATION, CAMBRIDGE, MA.
Noise measurement flight test of five light helicopters
[AD-A268566] p 1179 N94-17599
FEDERAL AVIATION ADMINISTRATION, WASHINGTON, DC.
US civil airmen statistics: Calendar year 1992
[AD-A267708] p 853 N94-14965
The 11th annual report of accomplishments under the airport improvement program: Fiscal year 1992
[AD-A268328] p 865 N94-17458
Criminal acts against civil aviation, fiscal year 1992
[AD-A268014] p 863 N94-17586
FERMI NATIONAL ACCELERATOR LAB., BATAVIA, IL.
Automatic differentiation of limit functions
[DE93-016376] p 1168 N94-14928
Electroweak results from D0
[DE93-014926] p 1185 N94-16968
Search for the top quark from (e(mu)) and (e,e) events in the D0 detector in p(bar-p) collisions at the square root of s = 1.8 TeV
[DE93-016350] p 1186 N94-17662
FLORIDA ATLANTIC UNIV., BOCA RATON.
On predicting the person-in-water drift for search and rescue
[AD-A268083] p 1055 N94-17514
FLORIDA INST. OF TECH., MELBOURNE.
Structure of turbulence in three-dimensional boundary layers
[NASA-CR-194655] p 1027 N94-17130
FLORIDA STATE UNIV., TALLAHASSEE.
Radar diagnostic parameters as indicators of severe weather in central Florida
[PB93-183507] p 1106 N94-16465
FLORIDA UNIV., GAINESVILLE.
Processing and protection of high temperature structural materials
[AD-A267292] p 954 N94-14961
Many-body quantum mechanical studies of molecular clusters
[AD-A266624] p 1180 N94-15727
Investigation of the influence of applied potential on erosion-corrosion of copper in alkaline chloride solutions
[AD-A266448] p 958 N94-16562
Development of a prototype kinestatic platform for application to space and ground servicing tasks. Phase 1: Concept Modeling
[NASA-CR-194036] p 887 N94-16905
Development of ultra-low noise, high performance 3-V Quantum Well Infrared Photodectors (QWIP's) for focal plane array staring image sensor systems
[AD-A267715] p 1214 N94-17272
FLUID JET ASSOCIATES, SPRING VALLEY, OH.
Two-dimensional, high flow, precisely controlled monodisperse drop source
[AD-A267660] p 1028 N94-17250
FOKKER B.V., AMSTERDAM (NETHERLANDS).
Expectations for the future of Fokker
p 854 N94-15127
FORD MOTOR CO., DEARBORN, MI.
Techno-economic requirements for automotive composites p 937 N94-16847
FORSS, INC., NAPERVILLE, IL.
Validation of respiratory inductive plethysmography for measuring exercise tidal volumes
[AD-A266883] p 1119 N94-14923
FOSTER-MILLER ASSOCIATES, INC., WALTHAM, MA.
Low cost paths to binary optics p 1197 N94-17353
FRAUNHOFER INST. FUER PHYSIKALISCHE MESSTECHNIK, FREIBURG (GERMANY).
Infrared detector annealing and calibration with IR-laser diodes p 909 N94-15092

G

GARNEAU (MARC) COLLEGIATE INST., DON MILLS (ONTARIO).
Contained liquids in microgravity, part 2
p 979 N94-16085
GEC HIRST RESEARCH CENTRE, WEMBLEY (ENGLAND).
Development of x ray CCDs p 900 N94-15033
GENERAL ACCOUNTING OFFICE, WASHINGTON, DC.
Classified information: Volume could be reduced by changing retention policy
[AD-A266938] p 1228 N94-15176
Space Shuttle main engine. NASA has not evaluated the alternate fuel turbopump costs and benefits. Report to the Administrator of the National Aeronautics and Space Administration
[GAO/NSIAD-94-54] p 926 N94-16834
Embedded computer systems: Status of C-17 software
[AD-A267307] p 1160 N94-16993
Military satellite communications: Opportunity to save billions of dollars. Report to the Chairman, Legislation, and National Security Subcommittee, Committee on Government Operations, House of Representatives
[AD-A267627] p 1002 N94-17199
Naval aviation: The Navy is taking actions to improve the combat capabilities of its tactical aircraft. Report to Congressional Requesters
[AD-A268002] p 868 N94-17472
GENERAL ATOMIC CO., SAN DIEGO, CA.
Inductive effects during second harmonic current drive experiments on T-10
[DE93-014411] p 1202 N94-16803
Recent results from the 60 GHz inside launch ECH system on the D3-D tokamak
[DE93-013027] p 1203 N94-16816
Simulation of enhanced tokamak performance on D3-D using fast wave current drive
[DE93-014009] p 1203 N94-16823
Ceramic fiber coatings development and demonstration
[AD-A267286] p 972 N94-17242
GENERAL DYNAMICS CORP., HUNTSVILLE, AL.
The closing window of opportunity: Addressing the US space launch vehicle crisis
[TABES PAPER 93-640] p 878 N94-16148
GENERAL ELECTRIC CO., CINCINNATI, OH.
Thermal stress effects in intermetallic matrix composites
[NASA-CR-191191] p 1054 N94-16518
Wear resistant titanium material development
[AD-A266474] p 959 N94-16780
An engineering approach for the application of textile composites to a structural component
p 938 N94-16852
GENERAL ELECTRIC CO., MOORESTOWN, NJ.
SAR sensor electronics: T/R modules
p 993 N94-15911
GEO-CENTERS, INC., NEWTON, MA.
Synthesis and evaluation of polymeric materials
[AD-A267809] p 973 N94-17408
GEO ECO ARC RESEARCH, LA CANADA, CA.
Characterization of wetland, forest, and agricultural ecosystems in Belize with airborne radar (AIRSAR)
p 1076 N94-16738
GEODETIC INST., HELSINKI (FINLAND).
Adaptive median filtering for preprocessing of time series measurements p 912 N94-15561
Compensation for the distortion in satellite laser range predictions due to varying pulse travel times
p 917 N94-15590
GEOLOGICAL SURVEY, DENVER, CO.
A discontinuous melt sheet in the Manson impact structure p 1103 N94-16269
Limited subsolidus diffusion in type B1 CAI: Evidence from Ti distribution in spinel p 954 N94-16401
Mapping the mineralogy and lithology of Canyonlands, Utah with imaging spectrometer data and the multiple spectral feature mapping algorithm
p 1066 N94-16670
Ground-truthing AVIRIS mineral mapping at Cuprite, Nevada p 1069 N94-16682
Mapping vegetation types with the multiple spectral feature mapping algorithm in both emission and absorption p 1069 N94-16686
GEOLOGICAL SURVEY, FLAGSTAFF, AZ.
Crustal structure and igneous processes in a chondritic Io p 1243 N94-16292
Geomorphic processes in the Argyre-Dorsa Argentea region of Mars p 1270 N94-16293
The rheology and composition of cryovolcanic flows on icy satellites p 1243 N94-16294
Separation of topographic and intrinsic backscatter variations in biscopic radar images: A magic airbrush
p 1086 N94-16318
Global Magellan-image map of Venus at full resolution
p 1274 N94-16319
The cartography of Venus with Magellan data
p 1274 N94-16320
Hellas basin, Mars: Formation by oblique impact
p 1280 N94-16350
Sedimentation, volcanism, and ancestral lakes in the Valles Marineris: Clues from topography
p 1283 N94-16369
Clementine: Anticipated scientific datasets from the Moon and Geographos p 1288 N94-16392
Global and regional/seasonal color mosaics of Mars
p 1288 N94-16393
Lunar multispectral mosaics from Galileo's second Earth-Moon flyby p 1288 N94-16394
Galileo SSI lunar observations: Copernican craters and soils p 1288 N94-16395
GEOLOGICAL SURVEY, MENLO PARK, CA.
Relief of some small landforms on Venus
p 1293 N94-16418
GEOLOGICAL SURVEY, RESTON, VA.
Preliminary Ar-40/Ar-39 age spectrum and laser probe dating of the M1 core of the Manson Impact Structure, Iowa: A K-T boundary crater candidate
p 1104 N94-16334
Preliminary analysis of thermal-infrared multispectral scanner data of the Iron Hill, Colorado carbonatite-alkalic rock complex p 1065 N94-16605
AVIRIS study of Death Valley evaporite deposits using least-squares band-fitting methods p 1067 N94-16676
AVIRIS as a tool for carbonatite exploration: Comparison of SPAM and Mbandmap data analysis methods
p 1073 N94-16703

GEOLOGICAL SURVEY OF CANADA, OTTAWA (ONTARIO).
Trace-element composition of Chicxulub crater melt rock, K/T tektites and Yucatan basement
p 1242 N94-16245
GEORGE MASON UNIV., FAIRFAX, VA.
DLTS and dynamic transconductance analysis of deep-submicron fully-depleted SOI MOSFET's
[AD-A267291] p 1214 N94-17243
GEORGE WASHINGTON UNIV., HAMPTON, VA.
A feasibility study of a microgravity enhancement system for Space Station Freedom
[NASA-CR-191550] p 886 N94-15864
GEORGE WASHINGTON UNIV., WASHINGTON, DC.
Publications of the Exobiology Program for 1991: A special bibliography
[NASA-TM-4483] p 1139 N94-17017
GEORGIA INST. OF TECH., ATLANTA.
Research in robust control for hypersonic aircraft
[NASA-CR-194106] p 870 N94-15416
Signal processing in impulsive electromagnetic interference
[AD-A266425] p 998 N94-16557
Continuous fabrication of SiC fiber tows by chemical vapor deposition
[AD-A266460] p 936 N94-16569
Ergonomics in the office environment
p 1124 N94-16612
Cognitive engineering models in space systems
[NASA-CR-193473] p 1140 N94-16716
Supercritical thermodynamics of sulfur and nitrogen species
[DE93-017727] p 1220 N94-16997
Development of iterative techniques for the solution of unsteady compressible viscous flows
[NASA-CR-194657] p 1027 N94-17129
Bioeffects of radiofrequency radiation on cell growth and differentation. Volume 1: Engineering considerations
[AD-A267754] p 1118 N94-17232
Strategic planning for aircraft noise route impact analysis: A three dimensional approach
[NASA-CR-191484] p 1178 N94-17278
Acquisition and production of skilled behavior in dynamic decision-making tasks
[NASA-CR-194658] p 1133 N94-17296
Review of rigorous coupled-wave analysis and of homogeneous effective medium approximations for high spatial-frequency surface-relief gratings
p 1194 N94-17335
Low dielectric constant insulators and gold metallization for GHz multi-chip modules, part 2
[AD-A268590] p 1176 N94-17605
GEORGIA STATE UNIV., ATLANTA.
Investigation of the interactions of radiation with matter
[AD-A266743] p 1181 N94-15774
GHENT UNIV. (BELGIUM).
Evaluation of a distributed catchment scale water balance model
[PAPER-93WR00398] p 1083 N94-16031

H

HAARLEM UNIV. (NETHERLANDS).
Developments in the Higher Technical Aerospace Education p 854 N94-15130
HAIFA UNIV. (ISRAEL).
Scuba-diving, anxiety and task performance
p 1132 N94-15938
HAMBURG UNIV. (GERMANY).
Separation behaviour of monotectic alloys
p 945 N94-15170
HARRIS CORP., MELBOURNE, FL.
Reliability analysis of Surface Mount Technology (SMT)
[AD-A267598] p 1055 N94-17194
HARTUNG (JACK B.), GREAT FALLS, VA.
Corvid meteoroids and a Giordano Bruno ray are genetically related p 1242 N94-16223
HARVARD COLL. OBSERVATORY, CAMBRIDGE, MA.
Absolute, Extreme-Ultraviolet Solar Spectral Irradiance Monitor (AESSIM)
[AD-A267045] p 1299 N94-15836
HARVARD SCHOOL OF PUBLIC HEALTH, BOSTON, MA.
Education and training of professional industrial hygienists for 2020 p 1125 N94-16618
HARVARD UNIV., CAMBRIDGE, MA.
Cooperativity and 3-D representation
[AD-A267180] p 1131 N94-15694
Bounds on inconsistent inferences for sequences of trials with varying probabilities
[AD-A267146] p 1172 N94-15733
Nd-142/Nd-144 in bulk planetary reservoirs, the problem of incomplete mixing of interstellar components and significance of very high precision Nd-145/Nd-144 measurements p 1256 N94-16220
Constraints on the differentiation of the Earth from the coupled Sm-146,147-Nd-142,143 systematics
p 1103 N94-16271
The effects of luminance boundaries on color perception
[AD-A268398] p 1133 N94-17397
HAWAII NATURAL ENERGY INST., HONOLULU.
Hydride-containing molten salts and their technology implications
[AD-A266458] p 1092 N94-16567
HAWAII UNIV., HONOLULU.
New K type asteroids p 1241 N94-16195
Systematic chemical variations in large 3AB iron meteorites: Clues to core crystallization
p 1241 N94-16213
Remote sensing studies of the northeastern portion of the lunar nearside p 1258 N94-16225
Explosive volcanism and the compositions of the cores of differentiated asteroids p 1243 N94-16306
The Clementine instrument complement
p 1086 N94-16370
Mixing model analysis of telescopic lunar spectra
p 1284 N94-16371
First results from a laboratory facility for measurement of emission spectra under simulated planetary conditions
p 954 N94-16372
Classificational parameters for acapulcoites and lodranites: The cases of FRO 90011, EET 84302 and ALH A81187/84190 p 1245 N94-16389
The dregs of crystallization in Zagami
p 1245 N94-16390
The influence of oceans on Martian volcanism
p 1295 N94-16427
The use of TIMS for mapping different pahoehoe surfaces: Mauna Iki, Kilauea p 1065 N94-16606
Participation in the north ecliptic pole sky survey
[NASA-CR-191933] p 1059 N94-16815
HAWAII UNIV., MANOA.
Fabrication of a NAVMAP, a deep-sea mapping system
[AD-A268630] p 1085 N94-17467
HELSINKI UNIV. OF TECHNOLOGY, ESPOO (FINLAND).
Double stimulated Brillouin scattering
p 1200 N94-15205
Dynamics of douple stimulated Brillouin scattering
p 1200 N94-15206
Soliton-like structures in double stimulated Brillouin scattering p 1200 N94-15207
HITACHI LTD., TOKYO (JAPAN).
Partial melting experiment of Y-Ba-Cu oxide
p 945 N94-15168
HOUSTON UNIV., TX.
Simulation reduction using the Taguchi method
[NASA-CR-4542] p 1055 N94-17082
HOWARD UNIV., WASHINGTON, DC.
Laser assisted CVD growth of AlN and GaN
[AD-A267150] p 1206 N94-15764
HUGHES AIRCRAFT CO., EL SEGUNDO, CA.
Thermal Weapon Sight (TWS) AN/PAS-13 diffractive optics designed for producibility p 1197 N94-17354
HUGHES DANBURY OPTICAL SYSTEMS, INC., CT.
Binary optics at Hughes Danbury Optical Systems
p 1195 N94-17344
Laser figuring for the generation of analog micro-optics and kineform surfaces p 1196 N94-17346
HUGHES STX, INC., LANHAM, MD.
The precision of today's satellite laser ranging systems p 912 N94-15559
HUMMER ASSOCIATES, WASHINGTON, DC.
OSHA bloodborne pathogens standards exposure control plan p 1127 N94-16645
HUNTSVILLE ASSOCIATION OF TECHNICAL SOCIETIES, AL.
TABES 1993: 9th Annual Technical and Business Exhibition and Symposium p 1050 N94-16129

I

ICI FIBERITE, GREENVILLE, TX.
Design and cost drivers in 2-D braiding
p 937 N94-16849
IDAHO STATE UNIV., POCATELLO.
Petrologic models of 15388, a unique Apollo 15 mare basalt p 1264 N94-16258
IDAHO UNIV., MOSCOW.
NASA Space Engineering Research Center for VLSI System Design
[NASA-CR-194587] p 1008 N94-15547
ILLINOIS UNIV., CHAMPAIGN.
The 12th Annual Carmel Conference, distinctiveness and Memory: Cognitive Psychophysiological and Physiological Considerations
[AD-A267181] p 1131 N94-15148
ILLINOIS UNIV., URBANA.
Monotone approximate query processing
[AD-A267153] p 1169 N94-15779
Laser-shock damage of iron-based materials
[AD-A267196] p 1038 N94-15852
Nonlinear analysis of mechanical systems under combined harmonic and stochastic excitation
[AD-A266217] p 1173 N94-16937
Transformation toughening of composite ceramics
[AD-A267304] p 971 N94-16980
Biofilm structure and diversity
[AD-A267254] p 1118 N94-16989
ILLINOIS UNIV., URBANA-CHAMPAIGN.
The application of compiler-assisted multiple instruction retry to VLIW architectures
[AD-A266930] p 1158 N94-15173
Relaxing consistency in recoverable distributed shared memory
[AD-A266931] p 1140 N94-15174
Statistical analysis of trigonometric parallaxes
[NASA-CR-194558] p 1172 N94-15641
IMPERIAL COLL. OF SCIENCE AND TECHNOLOGY, LONDON (ENGLAND).
Applications for large area silicon drift detectors on x ray and gamma ray astronomy p 909 N94-15090
The epitaxial Si x ray bolometer an alternative to ion implanted devices p 911 N94-15103
Coaxial airblast atomizers
[NASA-CR-193845] p 1016 N94-15109
Proceedings of the 6th International Conference on Narrow Gap Semiconductors
[AD-A268097] p 1015 N94-17570
INDUSTRIAL TECHNOLOGY INST., ANN ARBOR, MI.
Integration ToolKit and Methods (ITKM) manufacturing methods and prototype toolkit. A combined modeling method using IDEFO, IDEF1x and XSpec
[AD-A266176] p 984 N94-16981
INISEL, TORREJON DE ARDOZ (SPAIN).
Ground segment definition for the Spanish small satellite program (MINISAT) p 878 N94-17155
Data handling strategy for the Spanish small satellite program (MINISAT) p 895 N94-17177
INSTITUT D'AERONOMIE SPATIALE DE BELGIQUE, BRUSSELS.
Second flight of the Spacelab grille spectrometer during the Atlas-1 mission
[AERONAUTICA-ACTA-A-367-199] p 923 N94-17592
INSTITUT DE RADIO ASTRONOMIE MILLIMETRIQUE, GRENOBLE (FRANCE).
Preparation and properties of Nb/Al SIS and SIN junctions for millimeter and submillimeter radioastronomical receivers p 907 N94-15078
INSTITUT FUER ALLGEMEINE UND ANGEWANDTE GEOPHYSIK, MUNICH (GERMANY).
Use of AVIRIS data to the definition of optimised specifications for land applications with future spaceborne imaging spectrometers p 1071 N94-16694
INSTITUT FUER ANGEWANDTE GEODAESIE, KOETZING (GERMANY).
Experience and results of the 1991 MTLRS-1 USSR campaign p 914 N94-15575
Measuring atmospheric dispersion with WLRS in multiple wavelength mode p 916 N94-15582
LLR: Activities in Wettzell p 876 N94-15600
WLRS p 877 N94-15606
Results of the MTLRS-1 upgrade p 877 N94-15610
The new MTLRS-1 receiving system
p 877 N94-15611
The new MTLRS transmitting system
p 877 N94-15612
INSTITUT NATIONAL DE RECHERCHE D'INFORMATIQUE ET D'AUTOMATIQUE, VALBONNE (FRANCE).
A CENTAUR tutorial
[INRIA-RT-140] p 1142 N94-14978
The CAML numbers reference manual
[INRIA-RT-141] p 1142 N94-14979
Applicability of the session and the presentation layers for the support of high speed applications
[INRIA-RT-144] p 1158 N94-14980
Stochastic scheduling in in-forest networks
[INRIA-RR-1719] p 1164 N94-15695
Towards dynamic randomized algorithms in computational geometry
[INRIA-RR-1727] p 1156 N94-17528
Language-based document processing
[INRIA-RR-1731] p 1234 N94-17529
Compressible flow solvers using unstructured grids
[INRIA-RR-1732] p 1030 N94-17531

A domain-partition method for the advection-diffusion equation
[INRIA-RR-1740] p 1030 N94-17534
Stochastic scheduling in a multiclass G/G/1 queue
[INRIA-RR-1746] p 1162 N94-17537
Construction of d-dimensional hyperoctrees on a hypercube multiprocessor
[INRIA-RR-1752] p 1162 N94-17539

INSTITUT NATIONAL DES SCIENCES APPLIQUEES, ROUTEN (FRANCE).
Turbulence modelling for shock wave/boundary layer interactions specific issues and examples of applications p 1018 N94-15202

INSTITUT NATIONAL DES SCIENCES APPLIQUEES, TOULOUSE (FRANCE).
BIB photodetectors based on antimony doped silicon p 902 N94-15047
Silicon gallium doped photoconductor development for the AROME balloon borne instrument p 908 N94-15087

INSTITUT NATIONAL DES SCIENCES APPLIQUEES DE LYON, VILLEURBANNE (FRANCE).
Characterization of the cyclic plasticity of polycrystalline aluminum in the 90-300K domain: Use of the ultrasonic wave coupling technique - low frequency restraint
[ISAL-92-0083] p 954 N94-14930

INSTITUT ROYAL METEOROLOGIQUE DE BELGIQUE, BRUSSELS.
Nontidal gravity changes observed with a superconducting gravimeter p 1100 N94-15808

INSTITUT ROYAL METEOROLOGIQUE DE BELGIQUE, DOURBES.
Results of tidal gravity observations with a conical pendulum p 1100 N94-15810

INSTITUTE FOR COMPUTER APPLICATIONS IN SCIENCE AND ENGINEERING, HAMPTON, VA.
On the receptivity problem for 0(1) wavelength Goertler vortices
[NASA-CR-191519] p 1016 N94-15005
Tollmien-Schlichting/vortex interactions in compressible boundary layer flows
[NASA-CR-191515] p 1017 N94-15183
On the interaction between the shock wave attached to a wedge and freestream disturbances
[NASA-CR-191526] p 1019 N94-15478
Boundary layer flow of air over water on a flat plate
[NASA-CR-191517] p 1019 N94-15479
Parallel spatial direct numerical simulations on the Intel iPSC/860 hypercube
[NASA-CR-191513] p 1144 N94-15483
Multiphase complete exchange: A theoretical analysis
[NASA-CR-191531] p 1145 N94-15489
A parallel adaptive mesh refinement algorithm
[NASA-CR-191530] p 1168 N94-15724
Numerical simulation of three-dimensional self-gravitating flow
[NASA-TM-109021] p 1021 N94-15768
Adaptive wavelet collocation methods for initial value boundary problems of nonlinear PDE's
[NASA-CR-191507] p 1169 N94-15833
Inviscid instability of streamwise corner flow
[NASA-CR-191514] p 1021 N94-15834
Broken symmetry in ideal magnetohydrodynamic turbulence
[NASA-TM-109017] p 1023 N94-15964
Clouding tracing: Visualization of the mixing of fluid elements in convection-diffusion systems
[NASA-CR-191529] p 1148 N94-15965
Distributed computing feasibility in a non-dedicated homogeneous distributed system
[NASA-CR-191532] p 1149 N94-15989
Convection effects on radial segregation and crystal melt interface in vertical Bridgman growth
[NASA-CR-191541] p 1029 N94-17387
On the stability of a time dependent boundary layer
[NASA-CR-191542] p 1030 N94-17450

INSTITUTE FOR DEFENSE ANALYSES, ALEXANDRIA, VA.
A handbook of cost risk analysis methods
[AD-A267253] p 1235 N94-16988

INSTITUTE FOR SPACE AND TERRESTRIAL SCIENCE, YORK (ONTARIO).
Human ocular torsion during parabolic flight: An investigation using electromagnetic scleral search coil p 981 N94-16096

INSTITUTE FOR SPACE SCIENCE AND TECHNOLOGY, INC., GAINESVILLE, FL.
SYNMOD: A low-resource, low-cost means of monitoring the near-Earth space debris environment p 891 N94-17148

INSTITUTE FOR SPACE SCIENCE AND TECHNOLOGY, INC., MAGAGNOSE (FRANCE).
SYNMOD: A low-resource, low-cost means of monitoring the near-Earth space debris environment p 891 N94-17148

INSTITUTE OF OCEANOGRAPHIC SCIENCES, WORMLEY (ENGLAND).
Chemical tracer studies at IOSDL. 3: The measurement of silicate, nitrate and phosphate in seawater
[IOS-302-1992] p 1114 N94-17489
The IOSDL SeaSoar hydraulic unit
[IOS-300-1992] p 1114 N94-17516
List of the scientific and personal papers of Sir George Deacon, FRS
[IOS-301-1992] p 1114 N94-17518

INSTITUTO DE PESQUISAS ESPACIAIS, SAO JOSE DOS CAMPOS (BRAZIL).
IAI topic: El Nino. Southern oscillation and interannual climate variability
[INPE-5410-PRE/1757] p 1111 N94-15186

INSTITUTO NACIONAL DE TECNICA AEROESPACIAL, MADRID (SPAIN).
MINISAT programme p 896 N94-17182

INTELLIGENT REASONING SYSTEMS, INC., LAS CRUCES, NM.
A high-speed object recognition chip based on a biologically-realistic hybrid temporal processing
[AD-A268270] p 1134 N94-17576

INTERA TECHNOLOGIES LTD., NEPEAN (ONTARIO).
Soil conservation applications with C-band SAR p 1080 N94-16760

INTERA TECHNOLOGIES LTD., OTTAWA (ONTARIO).
Discussion of band selection and methodologies for the estimation of precipitable water vapour from AVIRIS data p 1074 N94-16707

INTERFACE FOUNDATION OF NORTH AMERICA, INC., FAIRFAX STATION, VA.
Computing science and statistics. Volume 24: Graphics and visualization
[AD-A266571] p 1150 N94-16721

INTERNATIONAL BUSINESS MACHINES CORP., YORKTOWN HEIGHTS, NY.
OETC optical backplane bus testbed. IBM tasks: Receiver OEIC and link simulation tools and analysis
[AD-A266198] p 1191 N94-16128

INTERNATIONAL CENTRE FOR THEORETICAL PHYSICS, TRIESTE (ITALY).
Lattice relaxation theory of localized excitations in quasi-one-dimensional systems
[DE93-624947] p 1215 N94-17437
On a class of singular quasilinear elliptic equations with general structure and distribution data
[DE93-628585] p 1171 N94-17613
A physical model for one-dimension and time-dependent ionosphere. Part 2: Results and discussions
[DE93-627959] p 1103 N94-17631
Derivation of the Verlinde formula from Chern-Simons theory and the G/G model
[DE93-628620] p 1221 N94-17632
Global solutions to a system of strongly coupled reaction-diffusion equations
[DE93-628587] p 1171 N94-17640
Distributively generated matrix near rings
[DE93-628588] p 1175 N94-17641
Asymptotic behavior of firmly non expansive sequences
[DE93-628589] p 1171 N94-17642
Quantum Heisenberg groups and Sklyanin algebras
[DE93-628590] p 1175 N94-17643
Fixed point iterations for strictly hemi-contractive maps in uniformly smooth Banach spaces
[DE93-628591] p 1175 N94-17644
Steepest descent approximations for accretive operator equations
[DE93-628586] p 1171 N94-17667

INTERNATIONAL METEOROLOGICAL INST., STOCKHOLM (SWEDEN).
A two-layer quasi-geotrophic spherical model: Formulation and climatology
[DM-63] p 1110 N94-17593

INTERUNIVERSITY MICRO-ELECTRONICS CENTER, LEUVEN (BELGIUM).
Thinned, backside illuminated, area CCD imager for electron detection p 901 N94-15036
Radiation hardening of a CCD technology through process and design modifications p 906 N94-15071
A linear monolithic 4-6 on silicon IR detector array p 910 N94-15098
Cryogenic readout electronics for astronomical applications p 910 N94-15099
A monolithic PbTeCCD focal plane array for MWIR imaging p 910 N94-15100

INTESPACE, TOULOUSE (FRANCE).
Environment tests for mini satellites p 896 N94-17189

IOWA STATE UNIV. OF SCIENCE AND TECHNOLOGY, AMES.
Trajectory optimization for the National Aerospace Plane
[NASA-CR-194618] p 867 N94-16498
The formation process of the He I lambda 10830 line in cool giant stars
[NASA-CR-194648] p 1240 N94-17094

IOWA UNIV., IOWA CITY.
Global auroral imaging: Dynamics of Explorer Miss ion
[NASA-CR-194284] p 1097 N94-15003

ISRAEL AIRCRAFT INDUSTRIES LTD., TEL-AVIV.
NEXT launch system p 878 N94-17141

IT CORP., KNOXVILLE, TN.
HyperVentilate: Decision-support software for soil vapor extraction technology application
[PB93-134880] p 1094 N94-15136

ITALSPAZIO, ROME (ITALY).
LEOCOM-SPES: Low cost message communications p 892 N94-17161
Feasibility study of a personal communications system IRIDIUM-like p 893 N94-17165

J

JACKSON STATE UNIV., MS.
End-effector: Joint conjugates for robotic assembly of large truss structures in space: Extended concepts
[NASA-CR-193576] p 1048 N94-17088

JAPEX GEOSCIENCE INST., TOKYO (JAPAN).
Comparison of preliminary results from Airborne Aster Simulator (AAS) with TIMS data p 1064 N94-16600

JET PROPULSION LAB., CALIFORNIA INST. OF TECH., PASADENA.
Voyager encounter highlights
[NASA-TM-109420] p 1246 N94-15239
Neptune encounter highlights
[NASA-TM-109421] p 1246 N94-15240
Voyager 2: Neptune encounter
[NASA-TM-109423] p 1247 N94-15491
Life and the solar system: The CRAF and Cassini missions
[NASA-TM-109422] p 1247 N94-15513
Superconductive material and magnetic field for damping and levitation support and damping of cryogenic instruments
[NASA-CASE-NPO-18458-1-CU] p 1033 N94-15875
Carbon-carbon grid for ion engines
[NASA-CASE-NPO-19174-1-CU] p 925 N94-15876
Proceedings of the Third Spaceborne Imaging Radar Symposium
[NASA-CR-194104] p 989 N94-15886
Magellan: Principal Venus science findings p 989 N94-15887
Spaceborne Imaging Radar-C instrument p 990 N94-15890
Imaging radar studies of polar ice p 991 N94-15899
Geologic remote sensing with radar p 991 N94-15900
Application of Cloude's target decomposition theorem to polarimetric imaging radar data p 991 N94-15901
EOS SAR: A new approach p 992 N94-15904
Data distribution p 993 N94-15910
A summary of microwave remote sensing investigations planned for BOREAS p 993 N94-15914
Global Energy and Water Cycle Experiment (GEWEX) and the Continental-scale International Project (GCIP) p 994 N94-15918
AIRSAR South American deployment: Operation plan, version 3.0 p 994 N94-15919
Segmented ion thruster
[NASA-CASE-NPO-18192-1-CU] p 925 N94-15927
Cyanoresin, cyanoresin/cellulose triacetate blends for thin film, dielectric capacitors
[NASA-CASE-NPO-18913-1-CU] p 966 N94-15930
Laser with optically driven Q-switch
[NASA-CASE-NPO-18470-1-CU] p 1038 N94-15932
Display system employing acousto-optic tunable filter
[NASA-CASE-NPO-18736-1-CU] p 1190 N94-15933
Cellulose triacetate, thin film dielectric capacitor
[NASA-CASE-NPO-18935-1-CU] p 1010 N94-15952
Unipolar terminal-attractor based neural associative memory with adaptive threshold
[NASA-CASE-NPO-18790-1-CU] p 1165 N94-15958
Selective formation of porous silicon
[NASA-CASE-NPO-18735-1-CU] p 966 N94-15960
Aberration correction of unstable resonators
[NASA-CASE-NPO-18791-1-CU] p 1034 N94-15987
Proceedings of the Fifteenth NASA Propagation Experimenters Meeting (NAPEX 15) and the Advanced Communications Technology Satellite (ACTS) Propagation Studies Miniworkshop
[NASA-CR-194539] p 994 N94-16035
The ACTS propagation program p 995 N94-16039
Propagation-related AMT design aspects and supporting experiments p 995 N94-16042
Database for propagation models p 996 N94-16049
Spectral evidence of size dependent space weathering processes on asteroid surfaces p 1241 N94-16174

A test of the applicability of independent scattering to high albedo planetary regoliths p 1250 N94-16187
Importance of expansion and contraction in the formation of tectonic features on the Moon p 1250 N94-16189
A Pluto thermal model p 1256 N94-16216
Thermal inertia and radar reflectivity of the Martian north polar ERG: Low-density aggregates p 1260 N94-16238
Mass of Saturn's A ring p 1263 N94-16252
Spectral study of Venus global topography and geoid from Magellan and PVO data p 1276 N94-16332
Martian lavas: Three complementary remote sensing techniques to derive flow properties p 1283 N94-16366
A decade's overview of Io's volcanic activity p 1245 N94-16386
Summaries of the Third Annual JPL Airborne Geoscience Workshop. Volume 2: TIMS Workshop [NASA-CR-194541] p 1063 N94-16595
Sensitivity of blackbody reference panels to wind blast p 1063 N94-16599
The use of TIMS data to estimate the SO2 concentrations of volcanic plumes: A case study at Mount Etna, Sicily p 1065 N94-16608
Summaries of the Third Annual JPL Airborne Geoscience Workshop. Volume 1: AVIRIS Workshop [NASA-CR-194540] p 1066 N94-16666
In-flight calibration of the spectral and radiometric characteristics of AVIRIS in 1991 p 1037 N94-16667
Volcanic thermal features observed by AVIRIS p 1068 N94-16680
Multiple dataset water-quality analyses in the vicinity of an ocean wastewater plume p 1069 N94-16687
AVIRIS ground data processing system p 1071 N94-16692
Simulation of ASTER data using AVIRIS images p 1071 N94-16693
JPL activities on development of acousto-optic tunable filter imaging spectrometer p 1037 N94-16696
AVIRIS data and neural networks applied to an urban ecosystem p 1073 N94-16705
Empirical relationships among atmospheric variables from rawinsonde and field data as surrogates for AVIRIS measurements: Estimation of regional land surface evapotranspiration p 1074 N94-16712
Summaries of the Third Annual JPL Airborne Geoscience Workshop. Volume 3: AIRSAR Workshop [NASA-CR-194542] p 1075 N94-16731
Monitoring environmental state of Alaskan forests with AIRSAR p 1075 N94-16734
The TOPSAR interferometric radar topographic mapping instrument p 1078 N94-16749
Fitting a three-component scattering model to polarimetric SAR data p 1079 N94-16751
Application of symmetry properties to polarimetric remote sensing with JPL AIRSAR data p 1079 N94-16752
External calibration of polarimetric radar images using distributed targets p 1079 N94-16753
Application of modified VICAR/IBIS GIS to analysis of July 1991 Flevoland AIRSAR data p 1080 N94-16757
Measuring ocean coherence time with dual-baseline interferometry p 1080 N94-16759
Lithological and textural controls on radar and diurnal thermal signatures of weathered volcanic deposits, Lunar Crater region, Nevada p 1080 N94-16762
Small spacecraft for planetary exploration p 874 N94-17145
Leak detection utilizing analog binaural (VLSI) techniques [NASA-CASE-NPO-18399-1-CU] p 1014 N94-17323
Optically-switched submillimeter-wave oscillator and radiator [NASA-CASE-NPO-18547-1-CU] p 1014 N94-17324
Thin composite solid electrolyte film for lithium batteries [NASA-CASE-NPO-18694-1-CU] p 1014 N94-17325
Method and apparatus for spur-reduced digital sinusoid synthesis [NASA-CASE-NPO-18789-1-CU] p 1154 N94-17326
Buried porous silicon-germanium layers in monocrystalline silicon lattices and method of producing [NASA-CASE-NPO-18836-1-CU] p 1215 N94-17327
Non-blocking crossbar permutation engine with constant routing latency [NASA-CASE-NPO-18864-1-CU] p 1161 N94-17328
Electron reversal ionizer for detection of trace species using a spherical cathode [NASA-CASE-NPO-18870-1-CU] p 1185 N94-17329
A scalable wrap-around shuffle exchange network with deflection routing [NASA-CASE-NPO-18983-1-CU] p 1161 N94-17330
Phase holograms in PMMA with proximity effect correction p 1037 N94-17348
Wide angle, single screen, gridded square-loop frequency selective surface for diplexing two closely separated frequency bands [NASA-CASE-NPO-18664-1-CU] p 1237 N94-17438
Guide to Magellan image interpretation [NASA-CR-194340] p 1298 N94-17654

JJM SYSTEMS, INC., IVYLAND, PA.
An expert system shell for inferring vegetation characteristics: Atmospheric techniques (Task G) [NASA-CR-194570] p 1082 N94-15531

JOHNS HOPKINS UNIV., BALTIMORE, MD.
Neural mechanisms of attention [AD-A266315] p 1132 N94-16456

JOHNS HOPKINS UNIV., COLUMBIA, MD.
CPIA/M5 liquid propellant engine manual [AD-A268062] p 929 N94-17589

JOHNS HOPKINS UNIV., LAUREL, MD.
Planned LMSS propagation experiment using ACTS: Preliminary antenna pointing results during mobile operations p 995 N94-16041
An overview of the text propagation effects for land-mobile-satellite systems: Experimental and modeling results p 996 N94-16048
Solar vector magnetic field research [AD-A267367] p 1299 N94-17004

JOINT INST. FOR NUCLEAR RESEARCH, DUBNA (USSR).
Iteration scheme for the multiparameter nonlinear boundary value problem with the additional conditions and its application to some field models [DE93-626638] p 1168 N94-14933
On the nature of mirror particles [DE93-626670] p 1179 N94-14934
Supersymmetry of gauge equations and geometric nonadiabatic phases [DE93-626671] p 1219 N94-14935
Mesons at finite temperature in the NJL model with gluon condensate [DE93-626697] p 1185 N94-17310
Production of D-mesons in pp-collisions and quark-gluon string model [DE93-626721] p 1185 N94-17312
Quark-loop effects in high energy spin-flip processes [DE93-626692] p 1188 N94-17313
Multipolar-like form of nonabelian gauge theories [DE93-626690] p 1171 N94-17314
Clusterization of quantum states in the Hartmann model [DE93-626624] p 1220 N94-17315
Quantum phase fluctuations in the Jaynes-Cummings model: Effects of cavity damping [DE93-627984] p 1186 N94-17612
Oxygen diffusion in YBa2Cu3O(6+delta) ceramics on heating [DE93-629161] p 974 N94-17633
Influence of the granular surface on the oxygen uptake in YBa2Cu3O(6+delta) ceramics [DE93-629162] p 974 N94-17634

K

KAMAN SCIENCES CORP., UTICA, NY.
Signal detection in correlated Gaussian and non-Gaussian radar clutter [AD-A267453] p 1001 N94-17033
Intelligent use of CFAR algorithms [AD-A267755] p 1003 N94-17206

KANSAS UNIV., LAWRENCE.
High-resolution seismic reflection survey at the Manson crater, Iowa p 1103 N94-16307

KANSAS UNIV. CENTER FOR RESEARCH, INC., LAWRENCE.
Atmospheric ionization by solar particles detected by nitrate measurement in antarctic snow [AD-A267583] p 1299 N94-17208

KARLOVA UNIV., PRAGUE (CZECHOSLOVAKIA).
Transition metals in superheat melts p 962 N94-16273

KATHOLIEKE UNIV. TE LEUVEN (BELGIUM).
Research in textile composites at KU, Leuven p 937 N94-16848

KELSEY SEYBOLD CLINIC, P.A., HOUSTON, TX.
Industrial Hygiene Laboratory accreditation: The JSC experience p 1125 N94-16623

KENT UNIV., CANTERBURY (ENGLAND).
Resolving LDEF's flux distribution: Orbital (debris?) and natural meteoroid populations p 1245 N94-16391

KEO CONSULTANTS, BROOKLINE, MA.
Optical ionospheric instrumentation and research [AD-A266403] p 1192 N94-16550

KLM AEROCARTO, SCHIPHOL (NETHERLANDS).
Aviation and the KLM: Past and future p 853 N94-15126

KNUDSEN GEOPHYSICAL BRANCH, MONTE SERENO, CA.
Pioneer Venus data analysis for the retarding potential analyzer [NASA-CR-194673] p 1297 N94-17292

KRUG INTERNATIONAL, SAN ANTONIO, TX.
Aircrew/groundcrew life support systems research. Volume 1: CLIN 0001 research requirements [AD-A268229] p 1139 N94-17563

KRUG LIFE SCIENCES, INC., SAN ANTONIO, TX.
Regulated emergency oxygen system [AD-A266228] p 1138 N94-16983
A virtual acoustic orientation instrument [AD-A268181] p 1134 N94-17510
Metabolic monitoring of hypobaric subjects [AD-A268221] p 1130 N94-17554
Aircrew/groundcrew life support systems research. Volume 2: CLIN 0002 task order requirements [AD-A268230] p 1139 N94-17564

KRUPP (FRIED.) G.M.B.H., ESSEN (GERMANY).
Krupp technical reports no. 2, English edition, October 1992 [ETN-93-94631] p 984 N94-16000
Research and development: Engine of innovation at Krupp p 984 N94-16001
Vacuum plasma spraying p 975 N94-16002
Expert system for welding engineering p 984 N94-16003
Remote diagnosis as used for mechanized parking systems p 984 N94-16004
RELMA: On-line quality control in the rubber mixing room using laser analysis p 984 N94-16005

L

LABORATOIRE D'AUTOMATIQUE ET D'ANALYSE DES SYSTEMES, TOULOUSE (FRANCE).
Contribution to the elaboration of some adaptive control algorithms for fermentation processes monitoring [LAAS-92513] p 1116 N94-15643

LAFAYETTE COLL., EASTON, PA.
Phase equilibria of the magnesium sulfate-water system to 4 kbars p 953 N94-16247

LAMAR UNIV., BEAUMONT, TX.
Helium-3 inventory of lunar samples: A potential future energy resource for mankind? p 1295 N94-16428

LAMONT-DOHERTY GEOLOGICAL OBSERVATORY, PALISADES, NY.
Liquidus equilibria of lunar analogs at high pressure p 1283 N94-16364
The monzonorite-anorthosite connection: The petrogenesis of terrestrial KREEP p 1104 N94-16365

LANCASTER UNIV. (ENGLAND).
Pargo Chasma and its relationship to global tectonics p 1249 N94-16181
Bubble coalescence in magmas p 1103 N94-16237
The cooling rates of pahoehoe flows: The importance of lava porosity p 1103 N94-16282
Lava crusts and flow dynamics p 1103 N94-16316

LAVAL UNIV. (QUEBEC).
Study of fractal aggregates p 979 N94-16086
Precise measurement and utilization of acceleration data p 923 N94-16100

LAWRENCE LIVERMORE NATIONAL LAB., CA.
Design of pulse stretching cell for a sodium guide star optical system [DE93-016436] p 1236 N94-14929
The effect of process parameters on the surface finish of plasma polymers [DE93-014112] p 966 N94-15924
Polished substrate surface and cleaning study for coated optic quality [DE93-014116] p 1190 N94-15975
Electronic structure and enthalpy of hydrogen and helium mixtures [DE93-014128] p 1208 N94-15976
ITER-HARD Toroidal Field coil structural analysis [DE93-014834] p 1201 N94-15981
Slidesurfaces with adaptive new definitions (SAND) for transient analysis [DE93-014909] p 1059 N94-15983
Full-wave simulation of the thumbtack laser [DE93-015110] p 1039 N94-16054
A task adaptive parallel graphics renderer [DE93-017123] p 1149 N94-16119
Passive tracking of a target using an array of sensors [DE93-015870] p 997 N94-16169
Acousto-optical confirmation of the localized wave phenomena [DE93-016425] p 1177 N94-16448
Application of non-thermal plasmas to pollution control [DE93-016432] p 1096 N94-16449
Design of a formaldehyde photodissociation process for carbon and oxygen isotope separation [DE93-016435] p 1039 N94-16450

The effect of oxygen, grain size, and strain rate on the mechanical behavior of forged P/M tantalum
[DE93-011251] p 959 N94-16764
The use of General Circulation Models in detecting climate change induced by greenhouse gases
[DE93-014369] p 1096 N94-16802
Atomic processes in hydrogen and deuterium negative ion discharges
[DE93-013432] p 1183 N94-16817
Emissions of volatile organic compounds from stationary combustion sources: Numerical modeling capabilities
[DE93-014123] p 1096 N94-16825
Laser weld repair of tantalum sheet
[DE93-016417] p 1041 N94-16871
Tip-tilt compensation: Resolution limits for ground-based telescopes using laser guide star adaptive optics
[DE93-016426] p 1237 N94-16872
Adaptive Cartesian grid methods for representing geometry in inviscid compressible flow
[DE93-016430] p 1025 N94-16894
Three dimensional hydrodynamic calculations with adaptive mesh refinement of the evolution of Rayleigh Taylor and Richtmyer Meshkov instabilities in converging geometry: Multi-mode perturbations
[DE93-017155] p 1025 N94-16903
Observation of nonsequential ionization of helium and its impact on intensity monitoring
[DE93-017174] p 949 N94-16904
Activation and deactivation of high concentration arsenic with some evidence of precipitation
[DE93-016437] p 950 N94-16952
Multi-frame x ray imaging with a large area 40ps camera
[DE93-017179] p 1035 N94-16960
A state-of-the-art plasma polymerization coater for ICF targets
[DE93-016452] p 1204 N94-17237
The effects of radiation transport on line ratios used as temperature and density diagnostic
[DE93-016424] p 1205 N94-17663
3D and r,z particle simulations of heavy ion fusion beams
[DE93-013417] p 1205 N94-17670
Emittance growth in displaced, space-charge-dominated beams with energy spread
[DE93-016514] p 1188 N94-17672

LEHIGH UNIV., BETHLEHEM, PA.
High octane ethers from synthesis gas-derived alcohols
[DE93-016861] p 975 N94-16898
Large signal characterization and modeling of heterojunction bipolar transistors
[AD-A266184] p 1012 N94-16935
Robotic weld overlay coatings for erosion control
[DE93-016938] p 970 N94-16959

LEICESTER UNIV. (ENGLAND).
Microchannel plate detectors for space astronomy p 901 N94-15038
CCD's on high resistivity bulk silicon for x ray spectroscopy on XMM p 907 N94-15080

LETTERMAN ARMY INST. OF RESEARCH, SAN FRANCISCO, CA.
A mathematical model for the study of hemorrhagic shock and fluid resuscitation: The systemic and pulmonary vasculature
[AD-A266835] p 1119 N94-14917
A review of the efficacy of 7.5 percent NaCl/6 percent Dextran-70 (HSD) in experimental animals and humans
[AD-A266633] p 1122 N94-15740
The relationship of metallothionein induction to the heat shock response
[AD-A266634] p 1122 N94-15741
A mathematical model for the study of hemorrhagic shock and fluid resuscitation: Transcapillary exchange
[AD-A266427] p 1123 N94-16544
Heat shock protein induction in human cells by CO2 laser irradiation
[AD-A266430] p 1117 N94-16545
A mathematical model for the study of hemorrhagic shock and fluid resuscitation: Exchange of fluid and solutes between vascular, interstitial, and tissue cell compartments
[AD-A266426] p 1123 N94-16558
Evaluation of hemoglobin-oxygen equilibrium binding by rapid-scanning spectrophotometry and singular-value decomposition
[AD-A266453] p 1123 N94-16564
Increased vascular resistance with hemoglobin-based oxygen carriers
[AD-A266454] p 1123 N94-16565
Hemoglobin
[AD-A266455] p 1123 N94-16566
Wound healing after laser injury to skin: The effect of occlusion and vitamin E
[AD-A266473] p 1128 N94-16779
The nature of dynamic arteriolar vasoreactivity: A mini-review and A classification scheme
[AD-A266499] p 1128 N94-16783
Release of iron from hemoglobin
[AD-A266503] p 1128 N94-16784
Encapsulation of hemoglobin in non-phospholipid vesicles
[AD-A266505] p 1128 N94-16785
Neurotoxicity of hemoglobin in cortical cell culture
[AD-A266506] p 1128 N94-16786

LINDE A.G., MUNICH (GERMANY).
Future development in cryogenic techniques for space p 901 N94-15042

LOCKHEED AIRCRAFT CORP., PALO ALTO, CA.
Effects of levitated dust on astronomical observations from the lunar surface p 1239 N94-16433
Small imaging satellite for Earth observing system adjunct p 891 N94-17151

LOCKHEED ENGINEERING AND SCIENCES CO., BAY SAINT LOUIS, MS.
A quantitative analysis of TIMS data obtained on the Learjet 23 at various altitudes p 1063 N94-16597
Analysis of TIMS performance subjected to simulated wind blast p 1063 N94-16598

LOCKHEED ENGINEERING AND SCIENCES CO., HAMPTON, VA.
On the use of the noncentral chi-square density function for the distribution of helicopter spectral estimates
[NASA-CR-191546] p 1176 N94-15487
Development of test methods for textile composites p 939 N94-16862

LOCKHEED ENGINEERING AND SCIENCES CO., HOUSTON, TX.
Orbital evolution of dust from comet Schwassmann-Wachmann 1: A case of one-to-one resonance trapping p 1242 N94-16270
Angrite LEW87051: Are the olivines pheno's or xeno's? A continuing story p 1103 N94-16285
Partial melting of ordinary chondrites: Lost City (H) and St. Severin (LL) p 1243 N94-16286
Tidal interaction: A possible explanation for geysers and other fluid phenomena in the Neptune-Triton system p 1272 N94-16311
Lunar LIGO: A new concept in gravitational wave astronomy p 1277 N94-16337
Igneous fractionation and subsolidus equilibration of diogenite meteorites p 1245 N94-16413
Siderophile element fractionation in meteor crater impact glasses and metallic spherules p 1246 N94-16414

LOCKHEED MISSILES AND SPACE CO., HUNTSVILLE, AL.
Space Station thermal storage/refrigeration system research and development
[NASA-CR-193841] p 879 N94-15191

LOCKHEED MISSILES AND SPACE CO., PALO ALTO, CA.
Micro-optics technology and sensor systems applications p 1197 N94-17350
Fabrication of micro-optical devices p 1197 N94-17351
Measurements of microlens performance p 1197 N94-17355
Theory of dispersive microlenses p 1198 N94-17361

LOGICON R AND D ASSOCIATES, LOS ANGELES, CA.
Determination of the electromagnetic fields radiated from the ARES EMP simulator
[AD-A267069] p 988 N94-15668

LOGICON TECHNICAL SERVICES, INC., DAYTON, OH.
Definitions of terms relating to aircraft windscreens, canopies, and transparencies
[AD-A268403] p 868 N94-17425

LONDON UNIV. (ENGLAND).
Optimisation of FIR photoconductors for atmospheric spectroscopy p 902 N94-15048
Performance testing of doped-germanium photoconductors for the ISO long wavelength spectrometer p 905 N94-15066
Non-linear effects in doped-germanium photoconductors for the ISO long wavelength spectrometer p 905 N94-15067
Ionising radiation-induced effects in doped germanium FIR photoconductors p 907 N94-15077
In orbit adiabatic demagnetization refrigeration for bolometric and microcalorimetric detectors p 907 N94-15079

LONDON UNIV. OBSERVATORY (ENGLAND).
Sheet flow fields on Venus p 1278 N94-16338

LORAL WESTERN DEVELOPMENT LABS., SAN JOSE, CA.
Nonlinear methods for communications
[AD-A267376] p 1001 N94-17019

LOS ALAMOS NATIONAL LAB., NM.
Ternary alloying effects in polycrystalline (beta)-NiAl
[DE93-012675] p 955 N94-15885
Synthesis of ceramic oxide powders in a microwave plasma device
[DE93-012741] p 965 N94-15920
The fractional quantum Hall effect and the rotation group
[DE93-010348] p 1207 N94-15972
On the 17-keV neutrino
[DE93-012638] p 1181 N94-15974
Efficiency effects of variation in controlled experimental variables
[DE93-014345] p 1169 N94-15979
The cooling of confined ions driven by laser beams
[DE93-016612] p 1039 N94-16114
Past, present and future ((pi),(eta)) experiments
[DE93-016631] p 1182 N94-16115
Effects of bulk composition on production rates of cosmogenic nuclides in meteorites p 1245 N94-16385
Gamma ray spectrometer for Lunar Scout 2 p 1037 N94-16426
A microsecond-pulsewidth, intense, light-ion beam accelerator
[DE93-016455] p 1202 N94-16451
Metastable phases in mechanically alloyed aluminum germanium powders
[DE93-008727] p 958 N94-16463
Direct drive foil implosion experiments on Pegasus 2
[DE93-012666] p 1202 N94-16776
Neutrino mass and mixing: Summary of the neutrino sessions
[DE93-014342] p 1183 N94-16801
The Solar Flare Myth in solar-terrestrial physics
[DE93-016487] p 1299 N94-16895
Neutral-current detection in the Sudbury Neutrino Observatory
[DE93-014481] p 1185 N94-16951
Fundamental theory of light for applications: Notes for five informal lectures
[DE93-016463] p 1192 N94-16953
The shock Hugoniot of 316 SS and sound velocity measurements
[DE93-016525] p 1178 N94-16955
Stochastic chaos: An analog of quantum chaos
[DE93-016619] p 1220 N94-16956
Dynamic testing and characterization of pre-fractured ceramic
[DE93-016457] p 972 N94-17238
Theoretical studies of the crystal structure of rare earths and actinides at zero temperature
[DE93-016488] p 1214 N94-17301
Plasma flow switch and foil implosion experiments on Pegasus 2
[DE93-016464] p 1013 N94-17318
Optimal pulse modulator design criteria for plasma source ion implanters
[DE93-016465] p 1205 N94-17645
Benchmarking massively parallel architectures
[DE93-016486] p 1162 N94-17646
Astrophysics with MILAGRO
[DE93-012722] p 1240 N94-17657
Kinetics of silica-phase transitions
[DE93-016231] p 1217 N94-17659
Shear wave measurements in shock-induced, high-pressure phases
[DE93-016461] p 1062 N94-17664
Detecting small debris using a ground-based photon counting detector
[DE93-012623] p 898 N94-17669

LOUGHBOROUGH UNIV. OF TECHNOLOGY (ENGLAND).
An experimental study of ASTOVL related jet flows to produce CFD code validation data. Phase 3: Results of experiments
[TT-9203] p 1020 N94-15645

LOUISIANA STATE UNIV., BATON ROUGE.
Anisotropic damage mechanics modeling in metal matrix composites
[AD-A266328] p 934 N94-16440

LOWELL UNIV., MA.
Volume integral equations applied to circular and square cylinders
[AD-A266635] p 1169 N94-15785

LOYOLA COLL., BALTIMORE, MD.
Satellite communications systems and technology. Executive summary
[NASA-TM-109346] p 1006 N94-17661

LUNAR AND PLANETARY INST., HOUSTON, TX.
Workshop on advanced technologies for planetary instruments
[NASA-CR-194585] p 1032 N94-15797
Twenty-Fourth Lunar and Planetary Science Conference. Part 2: G-M
[NASA-CR-193174] p 1247 N94-16173
The three ages of Venus: A hypothesis based on the cratering record p 1261 N94-16239
On the delivery of planetesimals to a protoplanet in the solar nebula p 1245 N94-16379

The spectrum of Phobos from Phobos 2 observations at 0.3-2.6 microns: Comparison to previous data and meteorite analogs p 1295 N94-16429
Bright soil units on Mars determined from ISM imaging spectrometer data p 1295 N94-16430
Variations in the Fe mineralogy of bright Martian soil p 1295 N94-16431
Workshop on early Mars: How warm and how wet, part 2?
[NASA-CR-193503] p 1297 N94-17637

M

MAIN ASTRONOMICAL OBSERVATORY, KIEV (UKRAINE).
ETALON-1,-2 center of mass correction and array reflectivity p 915 N94-15576
MALIN SPACE SCIENCE SYSTEMS, SAN DIEGO, CA.
Tectonic resurfacing of Venus p 1285 N94-16380
MARTIN MARIETTA CORP., NEW ORLEANS, LA.
Aluminum-lithium technology
[TABES PAPER 93-601] p 962 N94-16137
Space Propulsion Synergy Group ETO technology assessments
[TABES PAPER 93-641] p 929 N94-16149
MARTIN MARIETTA ENERGY SYSTEMS, INC., OAK RIDGE, TN.
Managing information as a corporate asset: Key strategies for information professionals to remain competitive
[DE93-015515] p 1232 N94-16875
MARYLAND UNIV., COLLEGE PARK.
A posteriori error estimation for hierarchic models of elliptic boundary value problems on thin domains
[AD-A267714] p 1168 N94-14939
Quantitative assessment of the accuracy of constitutive laws for plasticity with an emphasis on cyclic deformation
[AD-A267562] p 961 N94-17109
On the a-posteriori estimation of the modelling error for the heat conduction in a plate and its use for adaptive hierarchic modelling
[AD-A267965] p 1029 N94-17384
Study of brightness and current limitations in intense charged particle beams
[AD-A268283] p 1186 N94-17578
MARYLAND UNIV. BALTIMORE COUNTY, CATONSVILLE.
Pulse propagation in inhomogeneous optical waveguides
[DE93-013378] p 1191 N94-16007
MASCHINENFABRIK AUGSBURG-NUERNBERG A.G., MUNICH (GERMANY).
Remelting of Fe-C-Si-alloy in a ceramic mold skin p 945 N94-15169
MASSACHUSETTS GENERAL HOSPITAL, BOSTON.
Center of Excellence in Laser Medicine
[DE93-016541] p 1122 N94-16113
MASSACHUSETTS INST. OF TECH., CAMBRIDGE.
Nuclear rocket plume studies
[AD-A267154] p 925 N94-15837
Petrologic constraints on the surface processes on asteroid 4 Vesta and on excavation depths of diogenite fragments p 1241 N94-16208
Aspects of modelling the tectonics of large volcanoes on the terrestrial planets p 1104 N94-16396
Direct catalytic decomposition of nitric oxide
[DE93-016689] p 949 N94-16896
Adaptive Navier-Stokes calculations for vortical flow
[AD-A266236] p 1026 N94-16966
Slip, twinning and transformation in Laves phases
[DE93-018164] p 960 N94-16972
Theoretical studies of nonlinear optical properties of conjugated polymers
[AD-A267390] p 1193 N94-17024
High voltage conductors in spacecraft
[AD-A267268] p 897 N94-17266
Prediction of thermal cycling induced cracking in polymer matrix composites
[NASA-CR-194677] p 941 N94-17295
Basic optical studies of high T(c) oxide superconductors
[AD-A268148] p 1014 N94-17428
Activities of the Research Laboratory of Electronics
[AD-A266730] p 1304 N94-17651
MASSACHUSETTS INST. OF TECH., LEXINGTON.
Overview of Enhanced Data Stream Array Processor (EDSAP)
[AD-A266986] p 1158 N94-15492
Experimental evaluation of an adaptive focusing algorithm for a microwave planar phased-array hyperthermia system at UCSF
[AD-A267004] p 1121 N94-15634
Pixel-level fusion using interest images
[AD-A266640] p 1164 N94-15746
ATCRBS reply environment at Memphis International Airport
[AD-A266322] p 864 N94-16439
Binary optics: Trends and limitations p 1194 N94-17333
Fabricating binary optics: An overview of binary optics process technology p 1195 N94-17343
Color separation gratings p 1198 N94-17362
MASSACHUSETTS UNIV., AMHERST.
Boundary conditions for the paleoenvironment: Chemical and physical processes in the pre-solar nebula
[NASA-CR-194418] p 1298 N94-15421
Representation in incremental learning
[NASA-CR-194595] p 1221 N94-15719
Resolving topographic detail on Venus by modeling complex Magellan altimetry echoes p 1283 N94-16368
Fault-tolerant architectures for multiprocessor and VLSI-based systems
[AD-A267370] p 1140 N94-17005
MASSACHUSETTS UNIV., LOWELL.
Short term weather forecasting in real time in a base weather station setting
[AD-A266872] p 1105 N94-15142
Design, synthesis and characterization of novel nonlinear optical polymers
[AD-A267035] p 964 N94-15675
Organic polymeric electro-optic materials: Synthesis, processing, and device applications
[AD-A267133] p 964 N94-15688
MATERIALS MODIFICATION, INC., FAIRFAX, VA.
Solid lubricants for space structures, phase 2
[AD-A266653] p 968 N94-16767
MATERIALS RESEARCH SOCIETY, PITTSBURG, PA.
Materials Research Society Symposium Proceedings, Volume 292: Biomolecular Materials
[AD-A265776] p 1116 N94-15138
MATERIALS SCIENCES CORP., BLUE BELL, PA.
Thermo-mechanical analysis of oxidation protected carbon-carbon composites
[AD-A268191] p 941 N94-17597
MATERIALS SYSTEMS, INC., CONCORD, MA.
Fabrication of piezoelectric ceramic/polymer composites by injection molding
[AD-A267302] p 972 N94-17227
MATRA MARCONI SPACE, TOULOUSE (FRANCE).
Earth observation from small satellites p 891 N94-17150
MAX-PLANCK-INST. FUER ASTRONOMIE, HEIDELBERG (GERMANY).
Photoconductors and arrays for the far-infrared p 902 N94-15045
Infrared detectors and coolers for space instrumentation: Summary and concluding remarks p 904 N94-15059
Characterization of detectors and calibration of the ISOPHOT experiment p 907 N94-15082
MAX-PLANCK-INST. FUER CHEMIE, MAINZ (GERMANY).
Siderophile elements in the upper mantle of the Earth: New clues from metal-silicate partition coefficients p 1103 N94-16250
Os isotopes in SNC meteorites and their implications to the early evolution of Mars and Earth p 1242 N94-16272
Noble gases in twenty Yamato H-chondrites: Comparison with Allan Hills chondrites and modern falls p 1244 N94-16361
MAX-PLANCK-INST. FUER EXTRATERRESTRISCHE PHYSIK, GARCHING (GERMANY).
The XMM pn-CCD detector system: First results p 900 N94-15034
Role and development of small satellite missions in space plasma physics p 891 N94-17149
MAX-PLANCK-INST. FUER PHYSIK UND ASTROPHYSIK, GARCHING (GERMANY).
Variability of the Seyfert galaxy MKN 766 in the Rosat all sky survey
[MPE-PREPRINT-221] p 1240 N94-17591
Properties of nuclei in astrophysical environments: Binding energies, weak-interaction rates
[MPA-706] p 1240 N94-17628
A comparison of calculated and observed monochromatic type Ia supernova light curves
[MPA-709] p 1237 N94-17629
MAX-PLANCK-INST. FUER PLASMAPHYSIK, MUNICH (GERMANY).
Description of cooling water calorimetry and wall thermometry diagnostic at tokamak ASDEX-Upgrade
[IPP-5/46] p 1200 N94-14966
MAX-PLANCK-INST. FUER RADIOASTRONOMIE, BONN (GERMANY).
Submm/FIR bolometers p 904 N94-15056
MCAT INST., SAN JOSE, CA.
Development of a quiet supersonic wind tunnel with a cryogenic adaptive nozzle
[NASA-CR-194548] p 871 N94-15117
Computation of the Fluid and Optical Fields About the Stratospheric Observatory for Infrared Astronomy (SOFIA) and the Coupling of Fluids, Dynamics, and Control Laws on Parallel Computers
[NASA-CR-193168] p 858 N94-16510
Selected computations of transonic cavity flows p 858 N94-16511
Unsteady fluid and optical simulation of transonic aero-windows
[AIAA PAPER 93-3017] p 858 N94-16512
Computation of a controlled store separation from a cavity p 858 N94-16513
Progress in computational unsteady aerodynamics
[NASA-CR-177630] p 860 N94-17081
MCDONALD OBSERVATORY, AUSTIN, TX.
Poisson filtering of laser ranging data p 917 N94-15593
A computer-controlled x-y offset guiding stage for the MLRS p 918 N94-15598
Lunar laser ranging data processing in a Unix/X windows environment p 918 N94-15599
MCDONNELL-DOUGLAS AEROSPACE, LONG BEACH, CA.
High temperature hydraulic seals
[AD-A268257] p 1048 N94-17433
MCDONNELL-DOUGLAS AEROSPACE INFORMATION SERVICES CO., SAINT LOUIS, MO.
Receptivity of boundary layers to convected gusts
[AD-A267206] p 1022 N94-15860
MCDONNELL-DOUGLAS CORP., HUNTSVILLE, AL.
The Spacelab IPS Star Simulator
[TABES PAPER 93-650] p 877 N94-16150
Ground integrated ET-derived space platforms for onorbit applications
[TABES PAPER 93-652] p 899 N94-16152
MCDONNELL-DOUGLAS CORP., SAINT LOUIS, MO.
Missile datcom user's manual
[AD-A267447] p 1152 N94-17032
MCDONNELL-DOUGLAS SPACE SYSTEMS CO., HUNTINGTON BEACH, CA.
Delta launch vehicle: Accommodations for small satellites p 878 N94-17139
MCMASTER UNIV., HAMILTON (ONTARIO).
Adaptive interference canceller
[CA-PATENT-1-310-709] p 988 N94-15698
MECHANICAL TECHNOLOGY, INC., LATHAM, NY.
SPDE/SPRE final summary report
[NASA-CR-187086] p 924 N94-15482
MEDICAL ASSOCIATES, INC., CHARLOTTE, NC.
Americans with Disabilities Act considerations for the practice of occupational medicine p 1124 N94-16611
MEMPHIS STATE UNIV., TN.
Questioning mechanisms during tutoring, conversation, and human-computer interaction
[AD-A266199] p 1137 N94-16108
MICHIGAN TECHNOLOGICAL UNIV., HOUGHTON.
Ground truth spectrometry and imagery of eruption clouds to maximize utility of satellite imagery
[NASA-CR-194358] p 1081 N94-15181
A study of land mobile satellite service multipath effects using SATLAB software p 997 N94-16051
Applications and development of communication models for the touchstone GAMMA and DELTA prototypes
[NASA-CR-193617] p 999 N94-16867
MICHIGAN UNIV., ANN ARBOR.
Investigate wave-mean flow interaction and transport in the extratropical winter stratosphere
[NASA-CR-194555] p 1098 N94-15639
The design and analysis of robust feedback systems
[AD-A267152] p 1165 N94-15778
Radar response of vegetation: An overview p 991 N94-15898
Spatial and frequency diversity in lidar systems
[AD-A266192] p 1039 N94-16124
Far-infrared spectra of CO2 clathrate hydrate frosts p 954 N94-16340
Advanced transport systems for electron beams in high brightness accelerators and FELs
[AD-A267322] p 1041 N94-17001
The feasibility of tropospheric and total ozone determination using a Fabry-Perot interferometer as a satellite-based nadir-viewing atmospheric sensor
[NASA-TM-109342] p 1102 N94-17214
MICROTRONICS ASSOCIATES, PITTSBURGH, PA.
Rare earth doped III-V semiconductors for optoelectronics
[AD-A268279] p 1216 N94-17577
MIDWEST RESEARCH INST., FALLS CHURCH, VA.
HyperVentilate: Decision-support software for soil vapor extraction technology application
[PB93-134880] p 1094 N94-15136
MIDWEST RESEARCH INST., GOLDEN, CO.
Circle diagram approach for self excited induction generators
[DE93-010031] p 1010 N94-15971

Monolithic, two-terminal InP/Ga(0.47)In(0.53)As tandem solar cells
[DE93-014037] p 1093 N94-16824
DOE/NREL Advanced Wind Turbine Development Program
[DE93-010028] p 1093 N94-17668
MINISTRY OF AERONAUTICS AND ASTRONAUTICS, SHANGHAI (CHINA).
Small satellite modular design and application prospect p 894 N94-17173
MINISTRY OF DEFENCE, THE HAGUE (NETHERLANDS).
Expectations for the future of military aviation p 854 N94-15128
MINISTRY OF POSTS AND TELECOMMUNICATIONS, IBARAKI (JAPAN).
Propagation research in Japan p 996 N94-16043
MINISTRY OF POSTS AND TELECOMMUNICATIONS, TOKYO (JAPAN).
Laser ranging application to time transfer using geodetic satellite and to other Japanese space programs p 911 N94-15555
TRMM radar p 990 N94-15894
A study on an experimental communication system using microsatellites p 892 N94-17160
MINNESOTA UNIV., MINNEAPOLIS.
Preparation of homogeneous aluminosilicate gels by sol/gel techniques
[AD-A266823] p 962 N94-14914
Multinuclear NMR study of aluminosilicate sol-gel synthesis reasons for the homogeneous gelation using the prehydrolysis method
[AD-A266877] p 962 N94-14921
Self-diffusion coefficients of sol-gel intermediates
[AD-A266957] p 963 N94-15179
Intramolecular versus intermolecular condensation rates in the acidic polymerization of octaethoxytrisiloxane
[AD-A266982] p 963 N94-15490
NMR and theoretical investigation of cation binding with sol-gel silicates
[AD-A266999] p 963 N94-15631
Thermochemistry of silicate speciation in aqueous sodium silicate solutions: Ionization and polymerization of small silicate ion
[AD-A266825] p 964 N94-15683
Search for far infrared radiation from optically pumped defect modes
[AD-A266744] p 1206 N94-15822
Effects of aging time on V205 sol-gel coatings
[AD-A266824] p 965 N94-15843
Rheology of water and ammonia-water ices p 953 N94-16188
Mathmatical modeling for diffractive optics p 1195 N94-17342
Epitaxial iron films
[AD-A268286] p 1217 N94-17579
MISSISSIPPI STATE UNIV., MISSISSIPPI STATE.
On the application and evaluation of the relocatable diecast ocean circulation model in coastal and semi-enclosed seas
[AD-A266626] p 1112 N94-15771
Using Markov chains to model the error behavior of data communications channels
[AD-A266468] p 999 N94-16777
Gas Analysis System
[DE93-014617] p 949 N94-16891
MITRE CORP., BEDFORD, MA.
Johnson-Gierhart program predictions of excess propagation loss for super-high frequency air-to-ground paths. Volume 2: Appendices
[AD-A267021] p 987 N94-15527
Johnson-Gierhart program predictions of excess propagation loss for super-high frequency air-to-ground paths. Volume 1: Theory and numerical results
[AD-A267105] p 988 N94-15649
Proceedings of the Association for Computing Machinery Special Interest Group for Ada Artificial Intelligence Working Group
[AD-A266422] p 1165 N94-16559
Incremental rederivation of software artifacts: FY 1992
[AD-A267968] p 1155 N94-17491
MITRE CORP., MCLEAN, VA.
The Next Generation Weather Radar (NEXRAD)/Air Route Surveillance Radar (ARSR) operational comparison
[REPT-93W0000145] p 987 N94-15439
Test plan for the evaluation of the initial capability of the National Satellite Test Bed: Phase 1D
[DOT/FAA/RD-93/20] p 876 N94-16025
Category (CAT) 3B level 1 test plan for Global Positioning System (GPS)
[DOT/FAA/RD-93/21] p 864 N94-16835
Wide-area Differential Global Positioning System (WDGPS)/Wide-area Integrity Broadcast (WIB) alternatives analysis
[DOT/FAA/SE-93/3] p 864 N94-16906
MONSANTO CO., LULING, LA.
Emergency preparedness and planning p 1124 N94-16613
MORGAN STATE UNIV., BALTIMORE, MD.
A study of high field transport in wide band gap electronic materials using a picosecond transient charge technique
[AD-A267098] p 1008 N94-15636
MPB TECHNOLOGIES, INC., POINTE CLAIRE (QUEBEC).
Development of the Laser-based R/D Test-bed System (LTS) p 978 N94-16080
MUENSTER UNIV. (GERMANY).
Orientation of Planar Deformation Features (PDFs) in quartz p 1219 N94-16341
MULLARD SPACE SCIENCE LAB., DORKING (ENGLAND).
The grazing incidence detectors for the SOHO coronal diagnostic spectrometer p 905 N94-15063
An adiabatic demagnetisation refrigerator with a mechanical pre-cooler for space applications p 906 N94-15070
Data processing system for flight spectrometer p 908 N94-15086
Performance of the position-sensitive proportional counters of the Yohkoh Bragg crystal spectrometer p 909 N94-15094
MUSEUM OF NATURAL HISTORY, LONDON (ENGLAND).
Euromet Ureilite Consortium: A preliminary report on carbon and nitrogen geochemistry p 1241 N94-16192
Nitrates in SNCs: Implications for the nitrogen cycle on Mars p 1251 N94-16193
Petrography, mineralogy, and Mg isotope composition of VICTA: A vigarano CaAl4O7-bearing type A inclusion p 1103 N94-16203

N

NANCY UNIV. (FRANCE).
Simulations of wave-particle interactions in stimulated Raman forward scattering in a magnetized plasma
[TKK-F-A704] p 1201 N94-15210
NAPLES UNIV. (ITALY).
TOPSAT: Global space topographic mission p 992 N94-15905
NASA CENTER FOR AEROSPACE INFORMATION, BALTIMORE-WASHINGTON INTERNATIONAL AIRPORT, MD.
NASA's online machine aided indexing system
[NASA-CR-4518] p 1228 N94-15009
NATIONAAL INST. VOOR KERNFYSICA EN HOGE ENERGIEFYSICA, AMSTERDAM (NETHERLANDS).
Existence of a new instanton in constrained Yang-Mills-Higgs theory
[NIKHEF-H/93-02] p 1186 N94-17601
The universality of the shift of the Chern-Simons parameter for a general class of BRS invariant regularizations
[NIKHEF-H/93-03] p 1220 N94-17602
SUSY in the sky
[NIKHEF-H/93-04] p 1240 N94-17603
Relativistic dynamics of spin in strong external fields
[NIKHEF-H/93-06] p 1240 N94-17604
The three-loop QCD beta-function and anomalous dimensions
[NIKHEF-H/92-17] p 1186 N94-17617
The renormalization of the axial anomaly in dimensional regularization
[NIKHEF-H/92-18] p 1220 N94-17618
Monte Carlo simulation of the microstrip gas counter
[NIKHEF-H/93-07] p 1035 N94-17619
NATIONAL ACADEMY OF SCIENCES - NATIONAL RESEARCH COUNCIL, WASHINGTON, DC.
Plasma Science Committee (PLSC) and the Panel on Opportunities in Plasma Science and Technology (OPST)
[DE93-018142] p 1204 N94-16995
Computer Science and Telecommunications Board activities
[DE93-018141] p 1000 N94-17000
Statistics and physical oceanography
[AD-A268565] p 1115 N94-17598
NATIONAL AERONAUTICS AND SPACE ADMINISTRATION, WASHINGTON, DC.
NASA's Ultraviolet Astrophysics Branch: Present and future detector program p 910 N94-15102
Plant research
[NASA-TM-109664] p 1116 N94-15235
Human factor studies
[NASA-TM-109665] p 875 N94-15236
Teacher in space
[NASA-TM-109666] p 1131 N94-15237
Mars look-alike
[NASA-TM-109667] p 1094 N94-15238
The 1969 highlights
[NASA-TM-109630] p 1301 N94-15241
The 1972 highlights
[NASA-TM-109631] p 1301 N94-15242
The 1965 highlights
[NASA-TM-109632] p 1301 N94-15243
The 1967 highlights
[NASA-TM-109633] p 1301 N94-15244
Views from space
[NASA-TM-109634] p 1081 N94-15245
Space Station Freedom
[NASA-TM-109636] p 1031 N94-15247
Enhancing sight
[NASA-TM-109637] p 1221 N94-15248
From space to Earth
[NASA-TM-109638] p 1235 N94-15249
Cool suit
[NASA-TM-109639] p 1120 N94-15250
Monitoring history
[NASA-TM-109640] p 1229 N94-15251
Riblets: New speed technology
[NASA-TM-109641] p 1018 N94-15252
New insulin pump
[NASA-TM-109642] p 1120 N94-15253
Future of robotics
[NASA-TM-109592] p 1045 N94-15284
Supporting life in space
[NASA-TM-109593] p 1135 N94-15285
Ancient skills: Modern use
[NASA-TM-109594] p 1135 N94-15286
Unmasking the Sun
[NASA-TM-109595] p 1298 N94-15287
Saving Yellowstone
[NASA-TM-109596] p 1094 N94-15289
Lunar base concepts
[NASA-TM-109607] p 1247 N94-15294
Comet Halley returns
[NASA-TM-109608] p 885 N94-15296
Combating malaria
[NASA-TM-109609] p 1081 N94-15297
Space adaptation
[NASA-TM-109601] p 1120 N94-15309
Finding fish from above
[NASA-TM-109602] p 1081 N94-15310
Lunar ranging
[NASA-TM-109603] p 1236 N94-15311
Laser artery repair
[NASA-TM-109604] p 1120 N94-15312
Restoring Miss Liberty
[NASA-TM-109605] p 963 N94-15313
Space Shuttle highlights
[NASA-TM-109606] p 880 N94-15314
Mission adaptive wing
[NASA-TM-109448] p 865 N94-15321
NACA-NASA: 75 years of flight
[NASA-TM-109449] p 1302 N94-15322
National Aero-Space Plane
[NASA-TM-109450] p 865 N94-15323
National Aero-Space Plane resource reel
[NASA-TM-109451] p 865 N94-15324
Rotorcraft research
[NASA-TM-109452] p 871 N94-15325
Wind shear and heavy rain
[NASA-TM-109453] p 1105 N94-15326
X-29: Experiment in flight
[NASA-TM-109454] p 865 N94-15327
XV-15: Tiltrotor
[NASA-TM-109455] p 865 N94-15328
Student researchers
[NASA-TM-109441] p 1221 N94-15340
Mission San Marco
[NASA-TM-109442] p 878 N94-15341
The 1979 highlights
[NASA-TM-109443] p 1247 N94-15342
The 1966 highlights
[NASA-TM-109444] p 1302 N94-15343
Back to propellers
[NASA-TM-109445] p 869 N94-15344
Better airplane wings
[NASA-TM-109446] p 933 N94-15345
Gearing up for 1988
[NASA-TM-109617] p 880 N94-15346
Unistick vehicle controller
[NASA-TM-109618] p 1046 N94-15347
Voyager encounters Uranus
[NASA-TM-109619] p 1247 N94-15348
Ocean wave study
[NASA-TM-109620] p 1111 N94-15349
What's killing the trees?
[NASA-TM-109621] p 1094 N94-15350
NASA: The 25th year
[NASA-TM-109457] p 1302 N94-15352
Firefighters breathing system
[NASA-TM-109611] p 1135 N94-15362
Global climate study
[NASA-TM-109612] p 1098 N94-15363

Global Greenhouse Expedition
[NASA-TM-109613] p 1095 N94-15364
Arctic ozone
[NASA-TM-109614] p 1095 N94-15365
Better way to fly
[NASA-TM-109447] p 866 N94-15396
Louisiana delta study
[NASA-TM-109622] p 1095 N94-15408
Testing the waters from space
[NASA-TM-109623] p 1082 N94-15409
The 1973 highlights
[NASA-TM-109624] p 1302 N94-15410
The 1978 highlights
[NASA-TM-109625] p 1302 N94-15411
The 1977 highlights
[NASA-TM-109626] p 1302 N94-15412
The 1968 highlights
[NASA-TM-109627] p 1302 N94-15413
NASA directives master list and index
[NHB-1410.13L] p 1229 N94-15414
The 1970 highlights
[NASA-TM-109628] p 1302 N94-15415
The 1971 highlights
[NASA-TM-109629] p 1302 N94-15417
Sights and sounds of space
[NASA-TM-109610] p 1302 N94-15424
Forest fire study
[NASA-TM-109615] p 1095 N94-15425
Life saving satellites
[NASA-TM-109616] p 862 N94-15426
Improved mapping system
[NASA-TM-109643] p 1082 N94-15428
Food for space
[NASA-TM-109668] p 1136 N94-15435
First US Mars landing
[NASA-TM-109669] p 885 N94-15436
Space flight: The application of orbital mechanics
[NASA-TM-109424] p 874 N94-15493
Space suit design
[NASA-TM-109670] p 1137 N94-15507
The 1982 highlights
[NASA-TM-109671] p 1303 N94-15508
The 1980 highlights
[NASA-TM-109672] p 1303 N94-15509
Space Station resource reel
[NASA-TM-109673] p 885 N94-15510
Building a lunar base
[NASA-TM-109674] p 983 N94-15519
Medical imaging
[NASA-TM-109675] p 1229 N94-15520
Directory of research projects: Planetary materials and geochemistry
[NASA-TM-4484] p 1095 N94-15781
NASA trend analysis procedures
[NASA-RP-1290] p 1223 N94-15782
SIR-C/X-SAR free flyer concept p 898 N94-15903
Some thoughts on future rain mapping missions (TRMM follow-on) p 992 N94-15906
Permanent change of station: The NASA employee's guide to an easier move
[NHB-9760.1A] p 1223 N94-15931
Facilities maintenance handbook
[NHB-8831.2] p 1224 N94-15934
Index of NASA prefixed forms
[NHB-1420.21] p 1230 N94-15936
NASA security handbook
[NHB-1620.3C] p 1224 N94-15937
Industrial labor relations manual
[NHB-5200.1B] p 1224 N94-15939
NASA information resources management handbook
[NHB-2410.1E] p 1230 N94-15941
The NASA competitive placement plan for positions GS-15 and below (including trades and labor positions)
[NHB-3335.1C] p 1224 N94-15944
The Senior Executive Service
[NHB-3100.6] p 1224 N94-15945
Equipment management user's handbook for property custodians
[NHB-4200.2A] p 1224 N94-15957
Approaching the new reality
[TABES PAPER 93-230] p 1050 N94-16131
Commercial space opportunities advanced concepts and technology overview
[TABES PAPER 93-240] p 1050 N94-16132
Aerospace medicine and biology: A continuing bibliography with indexes (supplement 378)
[NASA-SP-7011(378)] p 1122 N94-16478
Aerospace medicine and biology: A continuing bibliography with indexes (supplement 380)
[NASA-SP-7011(380)] p 1122 N94-16479
Aeronautical engineering: A continuing bibliography with indexes (supplement 295)
[NASA-SP-7037(295)] p 854 N94-16480
Commonwealth of Independent States aerospace science and technology, 1992: A bibliography with indexes
[NASA-SP-7106] p 854 N94-16481
Physical fitness and health education program at NASA Headquarters p 1126 N94-16631
Mission management aircraft operations manual
[NHB-7900.3] p 1225 N94-16729
Aircraft operations management manual
[NHB-7900.3(V1)] p 1225 N94-16730
Equipment Management Manual
[NHB-4200.1D] p 1225 N94-16799
Materials inventory management manual
[NHB-4100.1C] p 1225 N94-16830
Research grant handbook
[NHB-5800.1C] p 1225 N94-16907
Publications of the Exobiology Program for 1991: A special bibliography
[NASA-TM-4483] p 1139 N94-17017
The 1990-1991 NASA space biology accomplishments
[NASA-TM-4501] p 1118 N94-17257
Space commerce in a global economy: Comparison of US and Australian approaches
[NASA-TM-109341] p 1235 N94-17290
Arctic and Antarctic sea ice, 1978-1987: Satellite passive-microwave observations and analysis
[NASA-SP-511] p 1114 N94-17439
The impact of industry/university consortia programs on space education
[NASA-TM-109340] p 1222 N94-17441
Earth system dynamics: The interrelation of atmospheric, ocean and solid earth dynamics
[NASA-CR-193487] p 1081 N94-17444

NATIONAL AERONAUTICS AND SPACE ADMINISTRATION. AMES RESEARCH CENTER, MOFFETT FIELD, CA.

The 1989 computational fluid dynamics highlights
[NASA-TM-109635] p 1018 N94-15246
Manned vehicle systems research facility
[NASA-TM-109650] p 875 N94-15318
Venus lightning
[NASA-TM-109644] p 1105 N94-15430
The 1988 computational fluid dynamics highlights
[NASA-TM-109645] p 1019 N94-15431
Galileo probe ready to go
[NASA-TM-109648] p 1247 N94-15432
Unitary plan wind tunnel landmark dedication and revitalization
[NASA-TM-109649] p 1302 N94-15434
Pioneer-Venus press clip
[NASA-TM-109425] p 1239 N94-15495
C 141 KAO solar eclipse mission
[NASA-TM-109676] p 1298 N94-15522
Autogenic-Feedback Training (AFT) as a preventive method for space motion sickness: Background and experimental design
[NASA-TM-108780] p 1120 N94-15537
Reactive system verification case study: Fault-tolerant transputer communication
[NASA-TM-108784] p 1145 N94-15538
Fault management for data systems
[NASA-TM-103953] p 1116 N94-15548
Call sign intelligibility improvement using a spatial auditory display
[NASA-TM-104014] p 1177 N94-15549
Altitude deviations: Breakdowns of an error-tolerant system
[NASA-TM-108788] p 862 N94-15550
Bandwidth characteristics of multimedia data traffic on a local area network
[NASA-TM-104026] p 883 N94-15648
Suppression of dynamic stall with a leading-edge slat on a VR-7 airfoil
[NASA-TP-3357] p 856 N94-15657
Reliability of autonomic responses and malaise across multiple motion sickness stimulation tests
[NASA-TM-108787] p 1121 N94-15711
The lift-fan powered-lift aircraft concept: Lessons learned
[NASA-CR-177616] p 866 N94-15718
Cryogenic measurements of aerojet GaAs n-JFETs
[NASA-TM-103972] p 1009 N94-15765
User's manual for the HYPGEN hyperbolic grid generator and the HGUI graphical user interface
[NASA-TM-108791] p 1148 N94-15784
Fidelity assessment of a UH-60A simulation on the NASA Ames vertical motion simulator
[NASA-TM-104016] p 870 N94-15793
NAS technical summaries: Numerical aerodynamic simulation program, March 1991 - February 1992
[NASA-TM-109335] p 854 N94-15798
Improved composite flexible blanket insulation
[NASA-CASE-ARC-11955-1-CU] p 934 N94-15926
Lift-fan aircraft: Lessons learned-the pilot's perspective
[NASA-CR-177620] p 867 N94-15950
Galileo probe spacecraft mission to Jupiter
[NASA-TM-109646] p 1247 N94-16070
Mars brine formation experiment
p 1293 N94-16419
Dust-dynamic feedbacks in the Martian atmosphere: Surface dust lifting p 1296 N94-16434
Search for Extraterrestrial Intelligence (SETI)
p 1125 N94-16620
Ames Fitness Program p 1126 N94-16632
Oregon transect: Comparison of leaf-level reflectance with canopy-level and modelled reflectance
p 1073 N94-16702
Low and high velocity impact response of thick hybrid composites p 936 N94-16837
Ontogenesis of mammals in microgravity
[NASA-TM-103978] p 1139 N94-17636

NATIONAL AERONAUTICS AND SPACE ADMINISTRATION. GODDARD SPACE FLIGHT CENTER, GREENBELT, MD.

Background suppression techniques in germanium detectors p 899 N94-15026
X ray microcalorimeters: Principles and performance
p 899 N94-15027
The STIS MAMA status: Current detector performance
p 905 N94-15069
X-ray spectroscopy with silicon pin and avalanche photo diodes p 906 N94-15072
The Third Annual NASA Science Internet User Working Group Conference
[NASA-CP-3170] p 1228 N94-15116
Prelaunch optical characterization of the Laser Geodynamic Satellite (LAGEOS 2)
[NASA-TP-3400] p 884 N94-15193
Robotics for Space Station tape 2
[NASA-TM-109578] p 1045 N94-15263
Orbiting solar operations
[NASA-TM-109583] p 884 N94-15267
Robotics in space
[NASA-TM-109584] p 1045 N94-15268
TDRS video clip
[NASA-TM-109585] p 884 N94-15269
GFSC-TV demo tape
[NASA-TM-109586] p 875 N94-15270
GSFC Fun Run
[NASA-TM-109587] p 1120 N94-15271
Robotics for Space Station, tape 1
[NASA-TM-109588] p 1045 N94-15272
Stock footage of Goddard Space Flight Center and Headquarters
[NASA-TM-109589] p 875 N94-15273
Coastal zone color scanner: Nimbus 7
[NASA-TM-109590] p 1111 N94-15281
Southern and Northern Hemisphere total ozone as seen by TOMS
[NASA-TM-109591] p 1098 N94-15282
TOMS computer graphics
[NASA-TM-109597] p 1094 N94-15290
COBE video news
[NASA-TM-109598] p 987 N94-15292
PET team
[NASA-TM-109599] p 1223 N94-15293
GAS highlights, 1988
[NASA-TM-109600] p 873 N94-15308
Atlas of TOMS ozone, 1978-1988
[NASA-TM-109456] p 1094 N94-15329
NASA's Hubble Space Telescope: The challenge and complexity of operations
[NASA-TM-109577] p 1236 N94-15422
Total solar eclipse of 3 November 1994
[NASA-RP-1318] p 1236 N94-15481
SeaWiFS technical report series. Volume 12, SeaWiFS technical report series cumulative index: Volumes 1-11
[NASA-TM-104566-VOL-12] p 1111 N94-15529
Eighth International Workshop on Laser Ranging Instrumentation
[NASA-CP-3214] p 911 N94-15552
Laser tracking for vertical control p 911 N94-15553
Nd:YLF laser for airborne/spaceborne laser ranging
p 913 N94-15563
Test results from LAGEOS-2 optical characterization using pulsed lasers p 915 N94-15577
Optimum wavelengths for two color ranging
p 915 N94-15580
Two color satellite laser ranging upgrades at Goddard's 1.2m telescope facility p 915 N94-15581
Millimeter accuracy satellites for two color ranging
p 916 N94-15583
State-of-the-art satellite laser range modeling for geodetic and oceanographic applications
p 916 N94-15586
Geometric analysis of satellite laser ranging data
p 917 N94-15587
Upgrading NASA/DOSE laser ranging system control computers p 918 N94-15595
Airborne 2 color ranging experiment
p 920 N94-15614

Development of the Mars Observer Laser Altimeter (MOLA) p 921 N94-15617
Bench checkout equipment for spaceborne laser altimeter systems p 921 N94-15618
Multi-beam laser altimeter p 921 N94-15620
Station report on the Goddard Space Flight Center (GSFC) 1.2 meter telescope facility p 922 N94-15625
Linear encoding device
[NASA-CASE-GSC-13562-1] p 1147 N94-15703
Steering capacifiector sensor
[NASA-CASE-GSC-13489-1] p 1164 N94-15704
Rotary encoding device
[NASA-CASE-GSC-13543-1] p 1189 N94-15705
Satellite situation report, volume 33, no. 3
[NASA-TM-109278] p 885 N94-15712
Spline screw payload fastening system
[NASA-CASE-GSC-13454-1] p 1046 N94-15871
Capacifiector camera
[NASA-CASE-GSC-13564-1] p 1033 N94-15872
An improved patch for radiative coolers
[NASA-CASE-GSC-13503-1] p 1046 N94-15873
Forback DC-to-DC converter
[NASA-CASE-GSC-13404-1] p 1010 N94-15874
Recent scientific advances in the use of radar in scientific hydrology p 991 N94-15895
Rotary encoding device
[NASA-CASE-GSC-13556-1] p 1148 N94-15943
Double-driven shield capacitive type proximity sensor
[NASA-CASE-GSC-13541-1] p 1165 N94-15946
Morphometric comparison of Icelandic lava shield volcanoes versus selected Venusian edifices p 1248 N94-16178
An inversion of geoid and topography for mantle and crustal structure on Mars p 1273 N94-16315
A simultaneous estimation of the mass of Mars and its natural satellites, Phobos and Deimos, from the orbital perturbations on the Mariner 9, Viking 1, and Viking 2 orbiters p 1279 N94-16347
Catalytic crystallization of ices by small silicate smokes at temperatures less than 20K p 1219 N94-16420
A snow wetness retrieval algorithm for SAR p 1075 N94-16732
Relating multifrequency radar backscattering to forest biomass: Modeling and AIRSAR measurement p 1077 N94-16741
Processing of polarimetric SAR data for soil moisture estimation over Mahantango watershed area p 1079 N94-16754
Evaluation of polarimetric SAR parameters for soil moisture retrieval p 1079 N94-16755
The 1987 Goddard Space Flight Center Battery Workshop
[NASA-CP-3236] p 1012 N94-17062
Conically scanned holographic lidar telescope
[NASA-CASE-GSC-13462-1] p 1194 N94-17321
Micro pulse laser radar
[NASA-CASE-GSC-13493-1] p 1004 N94-17322
Satellite situation report, volume 31, number 1
[NASA-TM-105088] p 898 N94-17584

NATIONAL AERONAUTICS AND SPACE ADMINISTRATION. HUGH L. DRYDEN FLIGHT RESEARCH FACILITY, EDWARDS, CA.

Flight-determined engine exhaust characteristics of an F404 engine in an F-18 airplane
[NASA-TM-4536] p 869 N94-15141
Flight testing of airbreathing hypersonic vehicles
[NASA-TM-4524] p 886 N94-15753
Simultaneous measurement of temperature and strain using four connecting wires
[NASA-TM-104271] p 1032 N94-15754
In-flight investigation of a rotating cylinder-based structural excitation system for flutter testing
[NASA-TM-4512] p 867 N94-15783

NATIONAL AERONAUTICS AND SPACE ADMINISTRATION. JOHN C. STENNIS SPACE CENTER, BAY SAINT LOUIS, MS.

Coast encounters: A space age adventure in science literacy
[NASA-TM-109334] p 1229 N94-15523
TIMS performance evaluation summary p 1063 N94-16596
An algorithm for the estimation of bounds on the emissivity and temperatures from thermal multispectral airborne remotely sensed data p 1064 N94-16603
Multi-resolution processing for fractal analysis of airborne remotely sensed data p 1065 N94-16604

NATIONAL AERONAUTICS AND SPACE ADMINISTRATION. JOHN F. KENNEDY SPACE CENTER, COCOA BEACH, FL.

Space Station Facility government estimating
[NASA-TM-109324] p 1223 N94-15545
Toxic substances registry system: Index of material safety data sheets
[NASA-TM-109332] p 1121 N94-15658

NATIONAL AERONAUTICS AND SPACE ADMINISTRATION. LYNDON B. JOHNSON SPACE CENTER, HOUSTON, TX.

STS-35 crew training: EMU walk through and EVA prep and post
[NASA-TM-109488] p 1134 N94-15194
STS-35 Crew training: Bailout in CCT, firefighting, TAGS class and bailout in WFTF
[NASA-TM-109489] p 1135 N94-15195
Brown, Mark
[NASA-TM-109505] p 1135 N94-15224
Astro smile
[NASA-TM-109506] p 879 N94-15225
STS-26 Post-Flight Press Conference
[NASA-TM-109557] p 879 N94-15261
STS-26 onboard 16mm photography quick release
[NASA-TM-109558] p 879 N94-15262
STS-30 Post-Flight Press Conference
[NASA-TM-109580] p 879 N94-15264
STS-30 suited ascent training in fixed base SMS
[NASA-TM-109581] p 875 N94-15265
STS-30 mission tape
[NASA-TM-109582] p 879 N94-15266
STS-26 STA training (Hauck)
[NASA-TM-109555] p 870 N94-15279
STS-26 SSIP briefing
[NASA-TM-109556] p 976 N94-15280
The 61-M long duration sim video highlights resource tape
[NASA-TM-109569] p 875 N94-15299
Text and graphics systems
[NASA-TM-109570] p 1229 N94-15300
STS-30 Magellan deploy Sim in SMS and MOCR
[NASA-TM-109571] p 875 N94-15301
STS-30 EVA prep in CCT: Grabe, Lee, and Thagard
[NASA-TM-109572] p 1135 N94-15303
STS-30 crew photo in building 4
[NASA-TM-109573] p 1031 N94-15304
STS-29 pre-launch and post-landing egress
[NASA-TM-109574] p 1135 N94-15305
STS-29 Post-Flight Press Conference
[NASA-TM-109575] p 880 N94-15306
STS-29 onboard 16mm photography quick release
[NASA-TM-109576] p 880 N94-15307
STS-26 through STS-34, deploy activities
[NASA-TM-109566] p 1301 N94-15315
STS-32 IMAX camera training
[NASA-TM-109567] p 1031 N94-15316
Return to Space Mission: The STS-26 crew report
[NASA-TM-109568] p 880 N94-15317
STS-37 CETA evaluation with Ross
[NASA-TM-109495] p 1135 N94-15330
STS-26 IUS and latch contingency training
[NASA-TM-109561] p 875 N94-15331
STS-26 generic integrated IUS deploy simulation
[NASA-TM-109562] p 875 N94-15332
STS-26 EVA rescue training
[NASA-TM-109563] p 875 N94-15333
STS-26 Shuttle Earth views, April 1990, part 1
[NASA-TM-109564] p 1082 N94-15334
STS-26 Shuttle Earth views, April 1990, part 2
[NASA-TM-109565] p 1082 N94-15335
STS-34 Space Shuttle Portable Onboard Computer (SPOC) briefing
[NASA-TM-109458] p 880 N94-15353
STS-34 post-flight press conference
[NASA-TM-109459] p 880 N94-15354
STS-34 onboard 16mm photography quick release
[NASA-TM-109460] p 880 N94-15355
STS-34 mission highlights resource tape, part 1
[NASA-TM-109461] p 880 N94-15356
STS-34 McCully and Baker during IFM training
[NASA-TM-109462] p 880 N94-15357
STS-34 Galileo integrated deploy sim
[NASA-TM-109463] p 880 N94-15358
STS-34 final bench review
[NASA-TM-109464] p 1135 N94-15359
STS-34 crew bailout exercise in CCT
[NASA-TM-109465] p 1135 N94-15360
STS-34 Chang-Diaz and E. Baker during Galileo contingency training in WFTF
[NASA-TM-109466] p 1135 N94-15361
Apollo presentation for Astrodome
[NASA-TM-109535] p 1302 N94-15366
Cohen program management briefing
[NASA-TM-109536] p 1223 N94-15367
Living well in space: Monitoring environment
[NASA-TM-109537] p 1120 N94-15368
Living well in space: Ensuring crew capability
[NASA-TM-109538] p 1120 N94-15369
Living well in space: Clinical care challenge
[NASA-TM-109539] p 1120 N94-15370
International food research project
[NASA-TM-109540] p 1135 N94-15371
Short walk to everywhere
[NASA-TM-109541] p 1221 N94-15372
STS-29 mission highlights resource tape
[NASA-TM-109542] p 880 N94-15373
STS-29 IMAX camera audio class FFT
[NASA-TM-109543] p 1031 N94-15374
STS-29 EVA prep in FFT
[NASA-TM-109544] p 1135 N94-15375
STS-32 onboard 16mm photography quick release
[NASA-TM-109472] p 880 N94-15376
STS-32 LDEF EVA training in WETF with Low and Dunbar
[NASA-TM-109473] p 1135 N94-15377
STS-29 crew with student experiment
[NASA-TM-109545] p 1116 N94-15378
STS-32 LDEF approach in SES
[NASA-TM-109474] p 880 N94-15379
STS-29 crew IMAX camera training
[NASA-TM-109546] p 1031 N94-15380
STS-32 crew training for lower body negative pressure unit and AFE
[NASA-TM-109475] p 1120 N94-15381
STS-29 crew food tasting in building 45
[NASA-TM-109547] p 1136 N94-15382
STS-32 bailout training in WETF
[NASA-TM-109476] p 1136 N94-15383
STS-31 Post-Flight Conference
[NASA-TM-109477] p 881 N94-15384
STS-29 crew bailout in WETF
[NASA-TM-109548] p 1136 N94-15385
Building 46 grand opening
[NASA-TM-109524] p 875 N94-15386
STS-28 Adamson and Brown EMU walk through
[NASA-TM-109549] p 1136 N94-15387
STS-33 emergency egress training
[NASA-TM-109525] p 1136 N94-15388
Movement in microgravity
[NASA-TM-109526] p 881 N94-15389
1990 ASCAN land survival training
[NASA-TM-109527] p 1136 N94-15390
1990 ASCAN ground egress/parasail
[NASA-TM-109528] p 1136 N94-15391
Crew escape certification test
[NASA-TM-109530] p 1136 N94-15392
Lunar Curatorial Facility resource
[NASA-TM-109531] p 875 N94-15393
President Kennedy's speech at Rice University
[NASA-TM-109532] p 1302 N94-15394
STS-26 protein growth (PCG) experiment
[NASA-TM-109533] p 976 N94-15395
STS-34 Arriflex and IMAX camera training
[NASA-TM-109467] p 1031 N94-15397
STS-33 EVA prep and post with Gregory, Blaha, Carter, Thorton, and Musgrave in FFT
[NASA-TM-109469] p 881 N94-15398
ASTP 15th anniversary clip-media release
[NASA-TM-109534] p 1302 N94-15399
STS-33 crew post flight film
[NASA-TM-109470] p 881 N94-15400
STS-27 EMU and RMS contingency training
[NASA-TM-109550] p 1136 N94-15401
STS-33 Carter and Thorton during WETF activities
[NASA-TM-109471] p 1136 N94-15402
STS-27 crew presentation clip
[NASA-TM-109551] p 881 N94-15403
STS-27 crew post-insertion deorbit-prep in CCT
[NASA-TM-109552] p 1136 N94-15404
STS-27 crew photo training and habitation procedures
[NASA-TM-109553] p 1032 N94-15405
STS-27 crew fire training and glove molding
[NASA-TM-109554] p 1136 N94-15406
STS-26 missions highlight resource tape
[NASA-TM-109559] p 881 N94-15407
STS-30 onboard 16mm photography quick release
[NASA-TM-109579] p 881 N94-15423
STS-31 onboard 16mm photography quick release
[NASA-TM-109478] p 881 N94-15438
STS-31 mission highlights resource tape
[NASA-TM-109479] p 881 N94-15440
STS-31 Hubble space telescope contingency training in WETF with McCandless and Sullivan
[NASA-TM-109480] p 1136 N94-15441
STS-31 Hubble space telescope deploy: Training at MDF with Hawley
[NASA-TM-109481] p 876 N94-15442
STS-31 HST deploy sim in SMS and MOCR
[NASA-TM-109482] p 876 N94-15449
STS-31 crew training inflight maintenance and bailout exercises in CCT and WFTF
[NASA-TM-109483] p 876 N94-15450
STS-31 crew training: firefighting, food tasting, EVA prep and post
[NASA-TM-109484] p 876 N94-15451
STS-40 crew during spacelab Sim
[NASA-TM-109493] p 876 N94-15452

STS-38 crew training: Habitation equipment procedures, bailout in CCT, 70mm photo class, EVA prep and post, and firefighting
[NASA-TM-109494] p 1136 N94-15453
Adamson, Jim
[NASA-TM-109507] p 1137 N94-15454
Freedom system Text and Graphics Systems (TAGS)
[NASA-TM-109509] p 1140 N94-15455
EVA retriever demonstration
[NASA-TM-109510] p 1046 N94-15456
Answering the space medicine challenge
[NASA-TM-109511] p 1120 N94-15457
Dare to dream
[NASA-TM-109512] p 885 N94-15458
STS-41 VCS training with mission specialist Bruce Melnick and Bill Shepard
[NASA-TM-109513] p 1046 N94-15459
STS-37 astronauts Ross and Apt during CETA hardware checkout
[NASA-TM-109496] p 1137 N94-15460
STS-36 crew presentation clip
[NASA-TM-109497] p 881 N94-15461
STS-36 crew EVA prep and post-training, bailout exercises, final bench review
[NASA-TM-109498] p 1137 N94-15462
STS-35 payload specialists Durrance and Parise: 70mm photo training and cabin familiarization
[NASA-TM-109499] p 1032 N94-15463
STS-35 onboard photography quick release
[NASA-TM-109500] p 881 N94-15464
STS-35 mission highlights resource tape
[NASA-TM-109501] p 881 N94-15465
Science operation in space: Lessons
[NASA-TM-109502] p 881 N94-15466
Richards, Dick: Training clip
[NASA-TM-109503] p 876 N94-15467
STS-27 crew deorbit prep in SMS with Gibson, Shepard, Mullane, Ross, and G. Gardner
[NASA-TM-109518] p 882 N94-15468
STS-26 crew participation in meetings
[NASA-TM-109519] p 873 N94-15469
STS-26 crew clothing, glove molding, and personal hygiene
[NASA-TM-109520] p 1137 N94-15470
Mars rover sample return mission
[NASA-TM-109521] p 873 N94-15471
Johnson Space Center and downtown Houston, Texas aerials
[NASA-TM-109522] p 1032 N94-15472
Commitment to challenge
[NASA-TM-109523] p 876 N94-15473
STS-26 long duration simulation: Crew entering SMS
[NASA-TM-109560] p 876 N94-15474
Mark 111 suit test evaluation in WETF with Jerry Ross
[NASA-TM-109504] p 1137 N94-15514
Programmable Remapper project
[NASA-TM-109508] p 1164 N94-15515
STS-41 post-flight press presentation
[NASA-TM-109514] p 882 N94-15516
STS-41 crew training bailout in CCT, 16mm camera class EVA prep, habitation equipment procedures, and food tasting
[NASA-TM-109517] p 876 N94-15517
STS-41 onboard 16mm photography quick release
[NASA-TM-109515] p 882 N94-15518
STS-41 mission highlights resource tape
[NASA-TM-109516] p 882 N94-15521
Estimating and bidding for the Space Station Processing Facility
[NASA-TM-109323] p 1223 N94-15546
Connector systems for structures
[NASA-CASE-MSC-21998-1] p 1046 N94-15707
Investigation of the effects of extravehicular activity (EVA) gloves on performance
[NASA-TP-3401] p 1137 N94-15717
STS-31 crew Linof, Arriflex, and IMAX camera training
[NASA-TM-109485] p 1032 N94-15792
Inflatable rescue device
[NASA-CASE-MSC-22244-1] p 1137 N94-15883
Attachment device
[NASA-CASE-MSC-21885-1] p 1047 N94-15925
Apparatus and method for producing an artificial gravitational field
[NASA-CASE-MSC-22021-1] p 886 N94-15935
Tetrahedral lander
[NASA-CASE-MSC-22082-1] p 886 N94-15951
Geometrical vapor blocker for parallel condensation tubes requiring cooling
[NASA-CASE-MSC-22090-1] p 1022 N94-15962
Mechanical energy absorber
[NASA-CASE-MSC-22111-1] p 1047 N94-15966
Quantitative method of measuring cancer cell urokinase and metastatic potential
[NASA-CASE-MSC-21715-1] p 1117 N94-15967
Cultured normal mammalian tissue and process
[NASA-CASE-MSC-21984-1] p 1117 N94-15969
History of the manned space flight program
[NASA-TM-109529] p 1303 N94-16069
The SCR Ne-21 and Ar-38 in lunar rock 68815: The solar proton energy spectrum over the past 2 MYR
p 1248 N94-16177
Comparison of reflectance spectra of C asteroids and unique C chondrites Y86720, Y82162, and B7904
p 1242 N94-16246
Impact penetration experiments in teflon targets of variable thickness p 1063 N94-16253
Partitioning of Nb, Mo, Ba, Ce, Pb, Th and U between immiscible carbonate and silicate liquids: Evaluating the effects of P2O5,F, and carbonate composition
p 953 N94-16283
Experimental partitioning of Zr, Ti, and Nb between silicate liquid and a complex noble metal alloy and the partitioning of Ti between perovskite and platinum metal
p 962 N94-16287
Experimental segregation of iron-nickel metal, iron-sulfide, and olivine in a thermal gradient: Preliminary results p 1243 N94-16288
Heterogeneous plagioclase compositions in the Maralinga CK4 chondrite p 1243 N94-16308
Carbon abundances, major element chemistry, and mineralogy of hydrated interplanetary dust particles
p 1243 N94-16309
INAA of CAIs from the Maralinga CK4 chondrite: Effects of parent body thermal metamorphism
p 1244 N94-16355
Spaceship Earth: A partnership in curriculum writing
p 1222 N94-16356
The first lunar outpost: The design reference mission and a new era in lunar science p 874 N94-16362
Experimentally reproduced relict enstatite in porphyritic chondrules of enstatite chondrite composition
p 1244 N94-16363
Grain surface features of Apollo 17 orange and black glass p 1289 N94-16397
JSC-1: A new lunar regolith simulant
p 1289 N94-16398
The Nakhla parent melt: REE partition coefficients and clues to major element composition
p 1245 N94-16399
More on the cooling history of angrite LEW 86010
p 1245 N94-16400
Thermogeologic mapping of the Moon from lunar orbit
p 1290 N94-16405
Opportunity for early science return by the Artemis Program p 1291 N94-16408
Terrestrial impact melts as analogues for the hematization of Martian surface materials
p 1104 N94-16424
Lunar lander and return propulsion system trade study
[NASA-TP-3388] p 925 N94-16496
Physical fitness and the Healthy People 2000 goals
p 1125 N94-16619
Johnson Space Center health related fitness program
p 1126 N94-16633
Human Transportation System (HTS) study, volume 2
[NASA-TM-104779-VOL-2] p 882 N94-17320
Force-endurance capabilities of extravehicular activity (EVA) gloves at different pressure levels
[NASA-TP-3420] p 1139 N94-17653

NATIONAL AERONAUTICS AND SPACE ADMINISTRATION. LANGLEY RESEARCH CENTER, HAMPTON, VA.

Windshear radar calibration, 1992 flights: Transmitter power and receiver gain stability
[NASA-TM-108997] p 986 N94-15140
A new NASA LaRC Multi-Purpose Prepregging Unit
p 932 N94-15276
Processing, properties and applications of composites using powder-coated epoxy towpreg technology
p 933 N94-15277
DSMC simulations of Mach 20 nitrogen flows about a 70 degree blunted cone and its wake
[NASA-TM-107762] p 1018 N94-15291
Minimum accommodation for aerobrake assembly. Phase 2: Structural concepts for a lunar transfer vehicle aerobrake which can be assembled on orbit
[NASA-TM-107610] p 885 N94-15446
ATLAS-2 and UARS correlative measurement opportunities during Space Shuttle mission on April 8-17, 1993
[NASA-TM-109020] p 1105 N94-15480
Open environments to support systems engineering tool integration: A study using the Portable Common Tool Environment (PCTE)
[NASA-TM-4489] p 1144 N94-15486
Long Duration Exposure Facility retrieval animation
[NASA-TM-109426] p 885 N94-15496
Long Duration Exposure Facility
[NASA-TM-109427] p 885 N94-15497
An elementary tutorial on formal specification and verification using PVS
[NASA-TM-108991] p 1158 N94-15536
Wind tunnel investigation of three axisymmetric cowls of different lengths at Mach numbers from 0.60 to 0.92
[NASA-TM-4488] p 856 N94-15681
Prediction of stable tearing of 2024-T3 aluminum alloy using the crack-tip opening angle approach
[NASA-TM-109023] p 955 N94-15708
Physical properties of the benchmark models program supercritical wing
[NASA-TM-4457] p 866 N94-15722
Resonant frequencies of irregularly shaped microstrip antennas using method of moments
[NASA-TP-3386] p 989 N94-15767
Wall interference and boundary simulation in a transonic wind tunnel with a discretely slotted test section
[NASA-TP-3334] p 872 N94-15794
Exposure fluctuations of astronauts due to orientation
[NASA-TP-3364] p 1300 N94-15816
NASA/DOD Aerospace Knowledge Diffusion Research Project. Paper 32: A new era in international technical communication: American-Russian collaboration
[NASA-TM-109336] p 1230 N94-15838
NASA/DOD Aerospace Knowledge Diffusion Research Project. Paper 34: Technical communications practices and the use of information technologies as reported by Dutch and US aerospace engineers
[NASA-TM-109337] p 1230 N94-15839
Synchronous sampling phase and amplitude detection method and apparatus
[NASA-CASE-LAR-14725-1] p 1050 N94-15870
Improvements to pulsed phase locked loop strain monitor
[NASA-CASE-LAR-14887-1] p 1033 N94-15877
Method and apparatus for non-destructive evaluation of composite materials with cloth surface impressions
[NASA-CASE-LAR-14535-1] p 933 N94-15878
Compounds containing meta-biphenylenedioxy moieties and polymers therefrom
[NASA-CASE-LAR-14517-1] p 965 N94-15879
Structures from low dielectric polyimides
[NASA-CASE-LAR-14988-1] p 965 N94-15880
Nonaqueous slip casting of high temperature ceramic superconductors using an investment casting technique
[NASA-CASE-LAR-14918-1] p 983 N94-15881
Remote tire pressure sensing technique
[NASA-CASE-LAR-14160-1] p 1033 N94-15884
Reduction of parasitic lasing
[NASA-CASE-LAR-14645-1-SB] p 1039 N94-15942
Shock-free supersonic elliptic nozzles and method of forming same
[NASA-CASE-LAR-14054-1] p 925 N94-15947
Measurement and analysis of critical CTOA for an aluminum alloy sheet
[NASA-TM-109024] p 956 N94-15948
A device for testing cables
[NASA-CASE-LAR-14093-1] p 1010 N94-15988
Effects of window size and shape on accuracy of subpixel centroid estimation of target images
[NASA-TP-3331] p 1034 N94-15990
Third LDEF Post-Retrieval Symposium Abstracts
[NASA-CP-10120] p 1303 N94-16495
Effects of internal yaw-vectoring devices on the static performance of a pitch-vectoring nonaxisymmetric convergent-divergent nozzle
[NASA-TP-3369] p 858 N94-16572
Wind tunnel investigations of forebody strakes for yaw control on F/A-18 model at subsonic and transonic speeds
[NASA-TP-3360] p 859 N94-16573
Wind-tunnel investigation of aerodynamic efficiency of three planar elliptical wings with curvature of quarter-chord line
[NASA-TP-3359] p 859 N94-16574
The Langley Fitness Center p 1126 N94-16635
Analysis of electromagnetic scattering from irregularly shaped, thin, metallic flat plates
[NASA-TP-3361] p 998 N94-16655
The 1991 AVIRIS/POLDER experiment in Camargue, France p 1070 N94-16691
FIBER-TEX 1992: The Sixth Conference on Advanced Engineering Fibers and Textile Structures for Composites
[NASA-CP-3211] p 936 N94-16845
An overview of the NASA textile composites program
p 937 N94-16846
A comparison of queueing, cluster and distributed computing systems
[NASA-TM-109025] p 1160 N94-16878
Energy-loss cross sections for inclusive charge-exchange reactions at intermediate energies
[NASA-TM-4522] p 1188 N94-17018
Aerothermoelastic analysis of a NASP demonstrator model
[NASA-TM-109007] p 867 N94-17055
Intel NX to PVM 3.2 message passing conversion library
[NASA-TM-109038] p 1152 N94-17060

An upwind multigrid method for solving viscous flows on unstructured triangular meshes
[NASA-TM-109343] p 1027 N94-17061
Soyuz/ACRV accommodation study
[NASA-TM-107733] p 888 N94-17072
Approximate Green's function methods for HZE transport in multilayered materials
[NASA-TM-4519] p 1300 N94-17084
Method and apparatus to characterize ultrasonically reflective contrast agents
[NASA-CASE-LAR-14969-1] p 1129 N94-17085
Development and comparison of advanced reduced-basis methods for the transient structural analysis of unconstrained structures
[NASA-TM-109015] p 1061 N94-17259
Windshear database for forward-looking systems certification
[NASA-TM-109012] p 1108 N94-17283
Subsonic aerodynamic characteristics of the HL-20 lifting-body configuration
[NASA-TM-4515] p 861 N94-17284
Hazard calculations of diffuse reflected laser radiation for the SELENE program
[NASA-TM-4520] p 1042 N94-17285
NASA/DOD Aerospace Knowledge Diffusion Research Project. Report 15: Technical uncertainty and project complexity as correlates of information use by US industry-affiliated aerospace engineers and scientists: Results of an exploratory investigation
[NASA-TM-107693] p 1233 N94-17291
NASA/DOD Aerospace Knowledge Diffusion Research Project. Report 15: Technical uncertainty and project complexity as correlates of information use by US industry-affiliated aerospace engineers and scientists: Results of an exploratory investigation
[NASA-TM-107693] p 1233 N94-17300
Tutorial: Advanced fault tree applications using HARP
[NASA-TM-102747] p 1155 N94-17447
Verification of fault-tolerant clock synchronization systems
[NASA-TP-3349] p 1161 N94-17449
Space Station/Orbiter berthing dynamics during an assembly flight
[NASA-TM-109049] p 1062 N94-17451
Strategy for the reduction of total integrated fluid logistics to the Space Station Freedom
[NASA-TM-107744] p 1138 N94-17452
Single block three-dimensional volume grids about complex aerodynamic vehicles
[NASA-TM-108986] p 1030 N94-17476
Structural mechanics division research and technology accomplishments for CY 1992 and plans for CY 1993
[NASA-TM-107752] p 1062 N94-17479
Low dielectric polyimides
[NASA-CASE-LAR-14987-2] p 974 N94-17559
User's manual for the Langley Research Center 14- by 22- foot subsonic tunnel static data acquisition system
[NASA-TM-109027] p 861 N94-17639
Nonlinear random response prediction using MSC/NASTRAN
[NASA-TM-109029] p 1179 N94-17650
A conceptual design study for a two-dimensional, electronically scanned thinned array radiometer
[NASA-TM-109051] p 1085 N94-17665
Calculations of cosmic-ray helium transport in shielding materials
[NASA-TP-3354] p 1301 N94-17666

NATIONAL AERONAUTICS AND SPACE ADMINISTRATION. LEWIS RESEARCH CENTER, CLEVELAND, OH.

Cruise noise measurements of a scale model advanced ducted propulsor
[NASA-TM-105808] p 1176 N94-15115
Space exploration initiative fuels, materials and related nuclear propulsion technologies panel
[NASA-TM-105706] p 923 N94-15118
NASA images 6
[NASA-TM-109437] p 862 N94-15336
NASA images 7
[NASA-TM-109438] p 1235 N94-15337
Futurepath 1
[NASA-TM-109439] p 869 N94-15338
NASA images 16
[NASA-TM-109440] p 1235 N94-15339
NASA images 10
[NASA-TM-109419] p 924 N94-15351
CORE/TRC
[NASA-TM-109434] p 1221 N94-15418
NASA report to education, volume 7
[NASA-TM-109435] p 1247 N94-15419
Spacework 16
[NASA-TM-109436] p 1221 N94-15420
Development of the seeding system used for laser velocimeter surveys of the NASA Low-Speed Centrifugal Compressor flow field
[NASA-TM-4485] p 1032 N94-15445
Proteus two-dimensional Navier-Stokes computer code, version 2.0. Volume 2: User's guide
[NASA-TM-106338-VOL-2] p 1019 N94-15475
Proteus two-dimensional Navier-Stokes computer code, version 2.0. Volume 1: Analysis description
[NASA-TM-106336-VOL-1] p 1019 N94-15485
Proteus three-dimensional Navier-Stokes computer code, version 1.0. Volume 2: User's guide
[NASA-TM-106340-VOL-2] p 1020 N94-15488
Astronauts number 1
[NASA-TM-109428] p 1131 N94-15499
Astronauts number 2
[NASA-TM-109429] p 873 N94-15500
Astronauts number 3
[NASA-TM-109430] p 874 N94-15501
Futurepath 1
[NASA-TM-109431] p 925 N94-15503
Challenger Center
[NASA-TM-109432] p 1221 N94-15504
Challenger Center: Orientation
[NASA-TM-109433] p 1221 N94-15505
NASA images 12
[NASA-TM-109417] p 1247 N94-15511
NASA images 13
[NASA-TM-109418] p 1247 N94-15512
A method of detecting and locating electrical current imbalances
[NASA-CASE-LEW-15407-1] p 1009 N94-15706
Preliminary analysis and design optimization of the short spacer truss of Space Station Freedom
[NASA-TM-4470] p 1058 N94-15709
Parametric resonant triad interactions in a free shear layer
[NASA-TM-106365] p 1021 N94-15751
The friction and wear of ceramic/ceramic and ceramic/metal combinations in sliding contact
[NASA-TM-106348] p 930 N94-15769
Modal element method for potential flow in non-uniform ducts: Combining closed form analysis with CFD
[NASA-TM-106347] p 1169 N94-15799
Explosive boiling at very low heat fluxes: A microgravity phenomenon
[NASA-TM-106325] p 1046 N94-15817
On the stability analysis of approximate factorization methods for 3D Euler and Navier-Stokes equations
[NASA-TM-106314] p 1169 N94-15818
NASA Lewis 9- by 15-foot low-speed wind tunnel user manual
[NASA-TM-106247] p 872 N94-15819
Proteus three-dimensional Navier-Stokes computer code, version 1.0. Volume 3: Programmer's reference
[NASA-TM-106341] p 1022 N94-15865
Effect of wind tunnel acoustic modes on linear oscillating cascade aerodynamics
[NASA-TM-106367] p 869 N94-15866
Proteus two-dimensional Navier-Stokes computer code, version 2.0. Volume 3: Programmer's reference
[NASA-TM-106339] p 1022 N94-15867
Dual active surface, miniature, plug-type heat flux gauge
[NASA-CASE-LEW-15643-1] p 1033 N94-15928
Method of producing a silicon carbide fiber reinforced strontium aluminosilicate glass-ceramic matrix composite
[NASA-CASE-LEW-15263-2] p 934 N94-15929
Neural-network-directed alignment of optical systems using the laser-beam spatial filter as an example
[NASA-TP-3372] p 1034 N94-15961
A sulfur segregation study of PWA 1480, NiCrAl, and NiAl alloys
[NASA-TM-106289] p 956 N94-15992
New findings and instrumentation from the NASA Lewis Microgravity Facility p 977 N94-16076
The vibro-acoustic mapping of low gravity trajectories on a Learjet aircraft p 978 N94-16078
Modal ring method for the scattering of sound
[NASA-TM-106342] p 1177 N94-16497
Development of a proposed international standard for certification of aircraft to High Intensity Radiated Fields (HIRF)
[NASA-TM-106357] p 863 N94-16520
Comparisons of selected laser beam power missions to conventionally powered missions
[NASA-TM-106110] p 1040 N94-16522
Proteus three-dimensional Navier-Stokes computer code, version 1.0. Volume 1: Analysis description
[NASA-TM-106337] p 1024 N94-16527
Physical and chemical properties of some new perfluoropolyalkylether lubricants prepared by direct fluorination
[NASA-TM-106299] p 967 N94-16543
Flow analysis for the nacelle of an advanced ducted propeller at high angle-of-attack and at cruise with boundary layer control
[NASA-TM-106371] p 858 N94-16571
Tuberculosis: A case for increased screening p 1126 N94-16627
Summary of follow-up results from potential tuberculosis exposures p 1126 N94-16628
Legionella: An overview p 1126 N94-16629
Screening for prostate cancer p 1126 N94-16630
Arsenic surveillance program p 1127 N94-16637
Asbestos Surveillance Program p 1127 N94-16638
Hearing Conservation Medical Program p 1127 N94-16639
Lead Surveillance Program p 1127 N94-16640
Mercury Surveillance Program p 1127 N94-16641
Respiratory Protection Program medical clearance for respirator use p 1127 N94-16642
General Medical Surveillance Program p 1127 N94-16643
Development of braided fiber seals for engine applications p 939 N94-16859
Computation of confined coflow jets with three turbulence models
[NASA-TM-106378] p 1025 N94-16879
Finite element analysis of structural engineering problems using a viscoplastic model incorporating two back stresses
[NASA-TM-106046] p 1060 N94-16881
Accurate upwind methods for the Euler equations
[NASA-TM-106388] p 1170 N94-16882
Effects of processing and prolonged high temperature exposure on the microstructure of Nb-1Zr-C sheet
[NASA-TM-106370] p 959 N94-16883
Higher-order accurate Osher schemes with application to compressible boundary layer stability
[NASA-TM-106355] p 1026 N94-17056
Thermally-sustained structure in convectively unstable systems
[NASA-TM-106375] p 1027 N94-17112
Lattice-mismatched In(0.40)Al(0.60)As window layers for indium phosphide solar cells
[NASA-TM-106255] p 1013 N94-17113
On solving the compressible Navier-Stokes equations for unsteady flows at very low Mach numbers
[NASA-TM-106380] p 1027 N94-17128
Overview of the solar dynamic ground test demonstration program
[NASA-TM-106296] p 928 N94-17256
Multigrid time-accurate integration of Navier-Stokes equations
[NASA-TM-106373] p 1028 N94-17258
Time dependent turbulence modeling and analytical theories of turbulence
[NASA-TM-106379] p 1029 N94-17385
Experimental and computational investigation of the NASA low-speed centrifugal compressor flow field
[NASA-TM-4481] p 869 N94-17386
Cryogenic spray vaporization in high-velocity helium, argon and nitrogen gasflows
[NASA-TM-106363] p 1035 N94-17446
Boundary conditions and the simulation of low Mach number flows
[NASA-TM-106374] p 1029 N94-17448
Jet engine performance enhancement through use of a wave-rotor topping cycle
[NASA-TM-4486] p 870 N94-17470
Flutter analysis using transversality theory
[NASA-TM-106382] p 1062 N94-17481
Space Station Freedom electrical performance model
[NASA-TM-106395] p 929 N94-17483
Ground testing for the no-vent fill of cryogenic tanks: Results of tests for a 71 cubic foot tank
[NASA-TM-106293] p 1030 N94-17486
NASA Lewis Meshed VSAT Workshop meeting summary
[NASA-TM-106332] p 883 N94-17487
On-board packet switch architectures for communication satellites
[NASA-TM-106328] p 883 N94-17488
Multigrid direct numerical simulation of the whole process of flow transition in 3-D boundary layers
[NASA-TM-106369] p 1030 N94-17557
Mechanical Systems Technology Branch research summary, 1985 - 1992
[NASA-TM-106329] p 1049 N94-17583
Coefficients for calculating thermodynamic and transport properties of individual species
[NASA-TM-4513] p 1220 N94-17624
Tensile and stress-rupture behavior of hafnium carbide dispersed molybdenum and tungsten base alloy wires
[NASA-TM-106350] p 962 N94-17652

NATIONAL AERONAUTICS AND SPACE ADMINISTRATION. MARSHALL SPACE FLIGHT CENTER, HUNTSVILLE, AL.

Results of an electrical power system fault study (CDDF)
[NASA-TP-3413] p 884 N94-15007
Mesoscale lightning
[NASA-TM-109655] p 1105 N94-15226
Long Duration Exposure Facility is coming home
[NASA-TM-109656] p 884 N94-15227

NASA Spacelink computer
[NASA-TM-109657] p 1140 N94-15228
Advanced Solid Rocket Motor
[NASA-TM-109658] p 924 N94-15229
SHARP
[NASA-TM-109659] p 1221 N94-15230
University Joint Venture: JOVE
[NASA-TM-109660] p 1229 N94-15231
Space classroom
[NASA-TM-109661] p 1221 N94-15232
Automated directional solidification furnace
[NASA-TM-109662] p 1175 N94-15233
Return to flight 1
[NASA-TM-109663] p 1223 N94-15234
Space Station: The link to America's future
[NASA-TM-109653] p 884 N94-15274
Inertial Upper Stage
[NASA-TM-109654] p 885 N94-15278
Return to flight 3, the journey continues
[NASA-TM-109651] p 1223 N94-15319
IG nuts and bolts
[NASA-TM-109652] p 1049 N94-15320
An assessment of finite-element modeling techniques for thick-solid/thin-shell joints analysis
[NASA-TM-108426] p 1058 N94-15534
Statistical computation of tolerance limits
[NASA-TM-108424] p 1172 N94-15535
A simplistic look at limit stresses from random loading
[NASA-TM-108427] p 1058 N94-15710
Report on computing and networking in the Space Science Laboratory by the SSL Computer Committee
[NASA-TM-108422] p 1147 N94-15721
Prioritization methodology for chemical replacement
[NASA-TP-3421] p 976 N94-15723
The corrosion protection of metals by ion vapor deposited aluminum
[NASA-TM-108425] p 955 N94-15832
Welding nozzle position manipulator
[NASA-CASE-MFS-29837-1] p 1047 N94-15882
Plasma arc welding weld imaging
[NASA-CASE-MFS-28797-1] p 1047 N94-15949
Impact of TQM concepts on inspection of aerospace systems
[TABES PAPER 93-350] p 1050 N94-16130
The Marshall Automated Weld System (MAWS)
[TABES PAPER 93-602] p 1049 N94-16138
Plasma arc welding repair of space flight hardware
[TABES PAPER 93-603] p 1049 N94-16139
Thermal spray forming of refractory sample ampoule cartridges for single crystal growth space furnaces
[TABES PAPER 93-605] p 1051 N94-16141
Materials, processes, and environmental engineering network
[TABES PAPER 93-610] p 1051 N94-16142
NASA Operational Environment Team (NOET): NASA's key to environmental technology
[TABES PAPER 93-611] p 1052 N94-16143
Emerging technologies for the changing global market
[TABES PAPER 93-612] p 930 N94-16144
Liquid hydrogen and liquid oxygen feedline passive recirculation analysis
[TABES PAPER 93-620] p 1031 N94-16145
Liquid Oxygen (LO2) propellant conditioning concept testing
[TABES PAPER 93-621] p 976 N94-16146
Cost-effective test methods for Shuttle payloads
[TABES PAPER 93-651] p 883 N94-16151
Modeling and simulation: A key to future defense technology
[TABES PAPER 93-654] p 1054 N94-16153
On the design of structural components using materials with time-dependent properties
[NASA-TM-108428] p 1059 N94-16519
Physical Exercise Program p 1127 N94-16636
Technology in action
[NASA-TM-109345] p 1235 N94-17294
Conference on Binary Optics: An Opportunity for Technical Exchange
[NASA-CP-3227] p 1194 N94-17331
Study of the National Science Foundation's South Pole Station as an analogous data base for the logistical support of a Moon laboratory
[NASA-TM-108429] p 1174 N94-17469

NATIONAL AERONAUTICS AND SPACE ADMINISTRATION. PASADENA OFFICE, CA.

Superconductive material and magnetic field for damping and levitation support and damping of cryogenic instruments
[NASA-CASE-NPO-18458-1-CU] p 1033 N94-15875
Carbon-carbon grid for ion engines
[NASA-CASE-NPO-19174-1-CU] p 925 N94-15876
Segmented ion thruster
[NASA-CASE-NPO-18192-1-CU] p 925 N94-15927
Cyanoresin, cyanoresin/cellulose triacetate blends for thin film, dielectric capacitors
[NASA-CASE-NPO-18913-1-CU] p 966 N94-15930
Laser with optically driven Q-switch
[NASA-CASE-NPO-18470-1-CU] p 1038 N94-15932
Display system employing acousto-optic tunable filter
[NASA-CASE-NPO-18736-1-CU] p 1190 N94-15933
Cellulose triacetate, thin film dielectric capacitor
[NASA-CASE-NPO-18935-1-CU] p 1010 N94-15952
Unipolar terminal-attractor based neural associative memory with adaptive threshold
[NASA-CASE-NPO-18790-1-CU] p 1165 N94-15958
Selective formation of porous silicon
[NASA-CASE-NPO-18735-1-CU] p 966 N94-15960
Aberration correction of unstable resonators
[NASA-CASE-NPO-18791-1-CU] p 1034 N94-15987
Leak detection utilizing analog binaural (VLSI) techniques
[NASA-CASE-NPO-18399-1-CU] p 1014 N94-17323
Optically-switched submillimeter-wave oscillator and radiator
[NASA-CASE-NPO-18547-1-CU] p 1014 N94-17324
Thin composite solid electrolyte film for lithium batteries
[NASA-CASE-NPO-18694-1-CU] p 1014 N94-17325
Method and apparatus for spur-reduced digital sinusoid synthesis
[NASA-CASE-NPO-18789-1-CU] p 1154 N94-17326
Buried porous silicon-germanium layers in monocrystalline silicon lattices and method of producing
[NASA-CASE-NPO-18836-1-CU] p 1215 N94-17327
Non-blocking crossbar permutation engine with constant routing latency
[NASA-CASE-NPO-18864-1-CU] p 1161 N94-17328
Electron reversal ionizer for detection of trace species using a spherical cathode
[NASA-CASE-NPO-18870-1-CU] p 1185 N94-17329
A scalable wrap-around shuffle exchange network with deflection routing
[NASA-CASE-NPO-18983-1-CU] p 1161 N94-17330
Wide angle, single screen, gridded square-loop frequency selective surface for diplexing two closely separated frequency bands
[NASA-CASE-NPO-18664-1-CU] p 1237 N94-17438

NATIONAL AEROSPACE LAB., AMSTERDAM (NETHERLANDS).

Symposium on the Future of Aeronautics in the Netherlands
[ETN-93-93780] p 853 N94-15120
Expectations for the future of the National Aerospace Laboratory p 854 N94-15129
Technical evaluation report on the AGARD-PEP Specialists Meeting on Combat Aircraft Noise
[NLR-TP-91445-U] p 1177 N94-15506
The photonical, pure grid method
[NLR-TP-91478-U] p 1062 N94-17600
The development of flexible software for the Italian/Dutch satellite SAX: Advantages and disadvantages of the use of CASE tools
[NLR-TP-91288-U] p 1157 N94-17626
Study into the limits of an Euler equation method applied to leading-edge vortex flow
[NLR-TP-91350-U] p 1031 N94-17627

NATIONAL AEROSPACE LAB., EMMELOORD (NETHERLANDS).

Overview of the FAA/DCA/NLR programs related to ageing aircraft
[NLR-TR-92119-U] p 854 N94-17614
Gravity dependent condensation pressure drop and heat transfer in ammonia two-phase heat transport systems
[NLR-TP-92121-U] p 1031 N94-17615

NATIONAL AEROSPACE LAB., TOKYO (JAPAN).

A mission concept of Phobos/Deimos exploration p 1287 N94-16387

NATIONAL DEFENCE HEADQUARTERS, OTTAWA (ONTARIO).

Monopiece strain gauge sting mounted wind tunnel balance
[CA-PATENT-1-311-626] p 1032 N94-15697

NATIONAL DEFENCE RESEARCH ESTABLISHMENT, UMEA (SWEDEN).

Trace analysis of chemical warfare agents in air: Sampling in porous polymers followed with thermal desorption analysis
[FOA-C-40302-4.6] p 1097 N94-17625

NATIONAL HEALTH SERVICES, INC., NEW YORK, NY.

The Goddard Space Flight Center ergonomics program p 1125 N94-16621

NATIONAL INST. OF POLAR RESEARCH, TOKYO (JAPAN).

Refractory precursor components in an Allende ferromagnesian chondrule p 1245 N94-16412

NATIONAL INST. OF WATER AND ATMOSPHERIC RESEARCH, LOWER HUTT (NEW ZEALAND).

Projections of future CO2
[NIWA/ATMOS/R/93-001] p 1094 N94-15185

NATIONAL OCEANIC AND ATMOSPHERIC ADMINISTRATION, BOULDER, CO.

Effects of turbulence on the geodynamic laser ranging system p 921 N94-15616
Brightness temperature and attenuation statistics at 20.6 and 31.65 GHz p 996 N94-16045
Comparison of OLYMPUS beacon and radiometric attenuation measurements at Blacksburg, Virginia p 996 N94-16046

NATIONAL OPTICAL ASTRONOMY LAB. TUCSON, AZ.

Large scientific 2-D arrays for the 1-5 micron region p 902 N94-15044

NATIONAL OPTICS INST., STE-FOY (QUEBEC).

Optical systems for the visualization of fluid and solid transparent media under microgravity conditions p 978 N94-16081

NATIONAL PHYSICAL LAB., TEDDINGTON (ENGLAND).

VDM specification of the MD4 message digest algorithm
[NPL-DITC-204/92] p 1142 N94-14944
The use of formal methods in data security standards
[NPL-DITC-205/92] p 1142 N94-15008
RAISE specification of the MD4 message digest algorithm
[NPL-DITC-206/92] p 1142 N94-15010
The value of reference implementations and prototyping in a formal design and testing methodology
[NPL-DITC-208/92] p 1142 N94-15011
The application of programming languages to the production of reference implementations
[NPL-DITC-209/92] p 1143 N94-15012
Geometric tolerance assessment
[NPL-DITC-210/92] p 1049 N94-15013
Standards and conformance testing in data security: Results of initial programme of investigation
[NPL-DITC-218/92] p 1143 N94-15014
Systematic study of effects of load misalignment in uniaxial low cycle fatigue testing at high temperatures
[NPL-DMM(A)-27] p 1057 N94-15015
A model for non-linear creep and physical ageing in PVC
[NPL-DMM(A)-91] p 1057 N94-15016
Modelling of creep data for plastics
[NPL-DMM(A)-92] p 1057 N94-15017
Measurement of the specific heat capacity of the electron-beam graphite calorimeter
[NPL-RSA(EXT)-40] p 1031 N94-15018
Free-field sensitivity calibration of laboratory standard microphones by the reciprocity technique: Measurements for the 1991 EEC intercomparison
[NPL-RSA(EXT)-0043] p 1176 N94-15019
An optically modulated scatterer for microwave antenna metrology
[NPL-DES-126] p 986 N94-15020
Fracture toughness tests for particulate MMC UK COSI (IACFA) task group. Meeting report, October 1992
[NPL-DMM(A)-81] p 1057 N94-15021
Testability of data security standards
[NPL-DITC-217/93] p 1143 N94-15022
Improved optical radiation detectors and their calibration: 200 nm - 30 microns p 906 N94-15075
Absolute Radiometric Measurements in Space: ARMS p 908 N94-15085
How to deduce the far field of an antenna from planar near-field measurements
[NPL-DES-123] p 1006 N94-17545
Optimisation and specification of Auger electron spectrometers for signal-to-noise ratio performance
[NPL-DMM(A)-101] p 1006 N94-17549

NATIONAL RESEARCH COUNCIL OF CANADA, OTTAWA (ONTARIO).

Proceedings of the Second Workshop on Microgravity Experimentation
[DSS-NR15-43-1990] p 977 N94-16071
Scientific use of Space Station Freedom p 977 N94-16072
Canadian microgravity experiments flown in 1989-1990 p 977 N94-16075
KC-135 acceleration monitoring and data acquisition system p 868 N94-16090
Finite element analytical techniques for ceramic production in microgravity: A hypoelastic model p 981 N94-16099

NATIONAL SPACE DEVELOPMENT AGENCY, IBARAKI (JAPAN).

Pre-phase a study report of lunar polar orbiter
[NASDA-TK-SS0440] p 873 N94-15000

NATIONAL SPACE DEVELOPMENT AGENCY, TOKYO (JAPAN).

Development of Japanese Earth Resources Satellite-1 (JERS-1; FUYO-1) and it's operational results
[NASDA-SPP-930001] p 884 N94-15001
The Japanese Space Station utilization plan p 977 N94-16074

NATIONAL TRANSPORTATION SAFETY BOARD, WASHINGTON, DC.
National Transportation Safety Board annual review of aircraft accident data, US general aviation, calendar year 1989
[PB93-160687] p 863 N94-16464
Annual review of aircraft accident data. US air carrier operations, calendar year 1990
[PB94-102787] p 863 N94-17471
NATIONAL WEATHER SERVICE, FORT WORTH, TX.
Radar diagnostic parameters as indicators of severe weather in central Florida
[PB93-183507] p 1106 N94-16465
NAUCHNO-PROIZVODSTVENNOE OBEDINENIE RADIO, MOSCOW (USSR).
Almaz p 898 N94-15889
NAVAL AIR STATION, PENSACOLA, FL.
Development of the OMPAT neuropsychological/psychomotor performance evaluation and OMPAT data and timing support programs
[AD-A266954] p 1122 N94-15759
Performance Information Management System (PIMS) communication
[AD-A267040] p 1231 N94-16458
NAVAL AIR WARFARE CENTER, CHINA LAKE, CA.
Enhanced down-range profiles of complex targets using wideband radar echo returns
[AD-A266508] p 999 N94-16786
What is the radar tracking Glint problem and can it be solved?
[AD-A266509] p 999 N94-16789
Scattering from binary optics p 1195 N94-17341
Equations of motion of a hinged body over a spherical earth
[AD-A268408] p 868 N94-17435
NAVAL AIR WARFARE CENTER, WARMINSTER, PA.
Multiobjective functions optimization for task allocation mapping to multicomputer nodes
[AD-A267071] p 1146 N94-15670
Aircraft carrier exposure tests of cast magnesium alloys
[AD-A268260] p 962 N94-17418
NAVAL CIVIL ENGINEERING LAB., PORT HUENEME, CA.
Optimal tuning of heavy equipment motion controllers
[AD-A267873] p 1167 N94-17392
Structured finite volume modeling of US Navy aircraft engine test cells task 2: Turboprop engine, volume 1
[AD-A267833] p 872 N94-17405
NAVAL COMMAND, CONTROL AND OCEAN SURVEILLANCE CENTER, SAN DIEGO, CA.
Broadband conventional beamforming incorporating adaptive equalization
[AD-A267090] p 987 N94-15544
Looking at Fokker-Planck dynamics with a noisy instrument
[AD-A267049] p 1117 N94-15662
Decomposition of large sparse symmetric systems for parallel computation. Part 2: Parallelization tool roadmap
[AD-A267072] p 1158 N94-15671
Decomposition of large sparse symmetric systems for parallel computation. Part 1: Theoretical foundations
[AD-A267144] p 1159 N94-15750
A ray trace model for propagation loss
[AD-A266314] p 997 N94-16467
Porous silicon for pumping solid-state lasers
[AD-A266293] p 1039 N94-16474
Measurements of the radar cross section and Inverse Synthetic Aperture Radar (ISAR) images of a Piper Navajo at 9.5 GHz and 49 GHz
[AD-A267570] p 1002 N94-17110
Application of the finite-difference time-domain method to scattering and radiation problems involving wires and plates
[AD-A268396] p 1005 N94-17496
Atmospheric propagation analysis program
[AD-A268231] p 1006 N94-17565
NAVAL HEALTH RESEARCH CENTER, SAN DIEGO, CA.
Sleep management user's guide for special operations personnel
[AD-A267746] p 1119 N94-14943
Carpal tunnel syndrome and other cumulative trauma disorders of the arm and hand and occupation in US Navy enlisted personnel
[AD-A267747] p 1129 N94-17374
NAVAL MEDICAL RESEARCH INST., BETHESDA, MD.
An apparatus for measuring the biological oxidation of hydrogen gas under hyperbaric conditions
[AD-A266834] p 1119 N94-14916
Neuropeptide-Y (NPY) increases total blood flow in the tail, and reduces cutaneous microvascular blood flow in the tail and foot of the rat
[AD-A266839] p 1115 N94-14918
Human central nervous system oxygen toxicity data from 1945 to 1986
[AD-A268225] p 1130 N94-17556
Methods to obtain blood samples periodically during exercise research studies while subjects are immersed in water or otherwise inaccessible
[AD-A268227] p 1130 N94-17562
NAVAL OCEANOGRAPHIC OFFICE, BAY SAINT LOUIS, MS.
Optical properties of the Red Sea
[AD-A266466] p 1113 N94-16588
NAVAL POSTGRADUATE SCHOOL, MONTEREY, CA.
Laser Doppler velocimetry measurements across a normal shock in transonic flow
[AD-A267240] p 855 N94-14973
Antenna gain loss and pattern degradation due to transmission through dielectric radomes
[AD-A267242] p 986 N94-14974
Thermal stresses of a trimaterial medium in a nonuniform temperature field
[AD-A267243] p 930 N94-14975
Parametric study of a finite element model of the Sidewinder missile
[AD-A267245] p 865 N94-14976
Breakdown of adiabatic invariance
[AD-A267246] p 1219 N94-14977
Software reliability management through metrics
[AD-A267129] p 1146 N94-15687
Theoretical study of laminar film condensation on horizontal elliptical tubes under conditions of free and forced convection
[AD-A267161] p 1021 N94-15737
Determination of GTA welding efficiencies
[AD-A267163] p 1046 N94-15738
The three-dimensional ray trajectories of the WKB optical fiber modes
[AD-A267167] p 1189 N94-15739
An experimental comparison of CLOS and C(++) implementations of an object-oriented graphical simulation of walking robot kinematics
[AD-A267168] p 1165 N94-15855
A rapid computational model for estimating the performance of compliant airfoils in cascades
[AD-A266275] p 857 N94-16471
Determining the effect of endwall boundary layer suction in a large scale subsonic compressor cascade
[AD-A267208] p 859 N94-16913
Fatigue life program using strain-life methods
[AD-A267310] p 1060 N94-16943
Three axis force override rate control of a PUMA 560 manipulator
[AD-A267313] p 1048 N94-16944
Target detection by way of Kalman filtering
[AD-A267314] p 1000 N94-16945
Development of dynamic, contex-driven help systems
[AD-A267409] p 1152 N94-16974
A formal protocol test procedure for the Survivable Adaptable Fiber Optic Embedded Network (SAFENET)
[AD-A267410] p 1192 N94-16975
Stray insensitive switched capacitor composite operational amplifiers
[AD-A267412] p 1012 N94-16976
Design and implementation of an object-oriented interface for the multi-model/multi-lingual database system
[AD-A267413] p 1232 N94-16977
Four Frequency-Shift Keying (4-FSK) spread spectrum modulator and demodulator
[AD-A267433] p 1000 N94-16979
Mean strain effects on the strain life fatigue curve
[AD-A267211] p 960 N94-16984
Natural convection above a horizontal heat source
[AD-A267212] p 1026 N94-16985
An object-oriented program specification for a mobile robot motion control language
[AD-A267213] p 1166 N94-16986
Investigation of onset of plasma formation at anode of fast-pulsed high-voltage vacuum diode
[AD-A267214] p 1204 N94-16987
Design of broadband wire antennas for frequency hopping applications
[AD-A267405] p 1001 N94-17025
An approximation for computing reduction in bandwidth requirements using intelligent multiplexers
[AD-A267434] p 1001 N94-17026
Applicability of computer spreadsheet simulation for solving resource allocation problems
[AD-A267436] p 1152 N94-17027
Performance of coded coherent FSK lightwave system with noncoherent detection
[AD-A267442] p 1193 N94-17028
Ensemble forecasting techniques in medium-range forecasting
[AD-A267443] p 1107 N94-17029
Efficient scheduling of real-time compute-intensive periodic graphs on large grain data flow multiprocessor
[AD-A267444] p 1141 N94-17030
Networked workstations and parallel processing utilizing functional languages
[AD-A267464] p 1160 N94-17034
Evaluation of site effects on a high frequency direction finding single site location system
[AD-A267465] p 1001 N94-17035
Design and implementation of an interface editor for the Amadeus multi-relational database front-end system
[AD-A267403] p 1233 N94-17114
Arctic cyclones and Marginal Ice Zone (MIZ) variability
[AD-A268610] p 1108 N94-17465
Numerically solving a transient heat conduction problem with convection and radiation
[AD-A268521] p 1220 N94-17540
A protocol validator for the SCM and CFSM models
[AD-A268523] p 1156 N94-17541
Heat transfer parametric system identification
[AD-A268525] p 929 N94-17543
NAVAL RESEARCH LAB., BAY SAINT LOUIS, MS.
Hyperspectral modeling for extracting aerosols from aircraft/satellite data p 1067 N94-16673
Atmospheric correction of AVIRIS data in ocean waters p 1070 N94-16690
Developing automated analysis methods for sea ice imagery: A status report with recommendations
[AD-A267284] p 1113 N94-17241
Report detailing modifications to the 1/8 degree global bathymetry
[AD-A268178] p 1114 N94-17509
NAVAL RESEARCH LAB., MONTEREY, CA.
The multivariate optimum interpolation analysis of meteorological data at the Fleet Numerical Oceanography Center
[AD-A266459] p 1106 N94-16568
NAVAL RESEARCH LAB., WASHINGTON, DC.
Progress in the modeling of the shock response and mitigation of thick composite shells
[AD-A267009] p 1057 N94-15524
Surface and internal signatures of organized vortex motions in stratified fluid
[AD-A267015] p 1020 N94-15526
Atmospheric transmittance between 1.0 and 2.0 micrometers
[AD-A267076] p 1098 N94-15539
Comparison of RADARC high-frequency radar performance prediction model and ROTHR Amchitka data
[AD-A267077] p 987 N94-15540
Ground based laser ranging for satellite location p 919 N94-15607
X ray laser program
[AD-A267075] p 1038 N94-15628
Thomson backscattered x rays from an intense laser beam
[AD-A267125] p 1038 N94-15686
Numerical modeling of the temperature gradients and spectra of the plasma armature on Thunderbolt
[AD-A266414] p 878 N94-16552
Water adsorption on diamond (110) studied by multiple internal reflection infrared spectroscopy
[AD-A266415] p 948 N94-16553
Investigation of AIRSAR signatures of the Gulf Stream p 1077 N94-16743
Information technology division technical paper abstracts
[AD-A266227] p 1166 N94-16938
An electromagnetic interference study of potential transmitter sites for the HF Active Auroral Research Program (HAARP)
[AD-A267743] p 1004 N94-17373
Soft x ray emission from Alexandrite laser-matter-interaction
[AD-A267905] p 1042 N94-17378
Energy deposition fluctuations induced by ions in microvolumes and nanovolumes: An analytic approach. 1: Theory
[AD-A267959] p 1173 N94-17495
An internetwork authentication architecture
[AD-A268579] p 1162 N94-17622
NAVAL SURFACE WARFARE CENTER, BETHESDA, MD.
High temperature deformation behavior of YBa2Cu3O(6+x) superconducting ceramic materials
[AD-A268164] p 973 N94-17430
The effect of electric discharge machined notches on the fracture toughness of several structural alloys
[AD-A268605] p 962 N94-17464
NAVAL SURFACE WARFARE CENTER, DAHLGREN, VA.
Incorporation of boundary layer heating predictive methodology into NSWCDD aeroprediction code
[AD-A267000] p 1020 N94-15632
Investigation of the origin of hot spots in deformed crystals: Ammonium perchlorate studies
[AD-A267692] p 1214 N94-17270

NAVAL UNDERSEA WARFARE CENTER, NEW LONDON, CT.
Operation of digital systems in severe electromagnetic environments
[AD-A267176] p 988 N94-15693
Expansions of cumulative distribution functions directly from characteristic functions
[AD-A267727] p 1173 N94-17372
NAVAL UNDERSEA WARFARE CENTER, NEWPORT, RI.
Forced harmonic vibration of the generally orthotropic cylindrical shell with inner and outer fluid loading
[AD-A266985] p 1057 N94-15150
Closed form characteristic function for general complex second-order form in correlated complex Gaussian random variables
[AD-A267883] p 1171 N94-17393
NAVAL WAR COLL., NEWPORT, RI.
Space countersurveillance: A requisite for theater defense planning
[AD-A266871] p 884 N94-15147
Not ready for the first space war. What about the second?
[AD-A266557] p 1174 N94-16665
NEBRASKA UNIV., LINCOLN.
Surface flashover of semiconductors: A fundamental study
[AD-A267382] p 1012 N94-17023
NETHERLANDS ASSOCIATION OF AERONAUTICAL ENGINEERS, AMSTERDAM.
Fifty years of the Netherlands Association of Aeronautical Engineers p 853 N94-15121
The future of Schiphol: Growth within boundaries p 853 N94-15123
NEVADA UNIV., RENO.
Numerical investigations in three-dimensional internal flows
[NASA-CR-194594] p 1020 N94-15551
NEW JERSEY INST. OF TECH., NEWARK.
The bootstrapped algorithm: Fast algorithm for blind signal separation
[AD-A266671] p 1147 N94-15772
NEW MEXICO INST. OF MINING AND TECHNOLOGY, SOCORRO.
Remote sensing of precipitation and electrification with a dual-polarization, coherent, wideband radar system
[AD-A267479] p 1004 N94-17364
NEW MEXICO UNIV., ALBUQUERQUE.
NASA Space Engineering Research Center for VLSI System Design
[NASA-CR-194587] p 1008 N94-15547
Complex zoning behavior in pyroxene in FeO-rich chondrules in the Semarkona ordinary chondrite p 1243 N94-16284
NEW YORK UNIV., NEW YORK.
Theoretical studies relating to the interaction of radiation with matter
[AD-A266894] p 1179 N94-14949
Theoretical studies relating to the interaction of radiation with matter
[AD-A267134] p 1180 N94-15689
The dynamics of hydroponic crops for simulation studies of the CELSS initial reference configurations
[NASA-CR-194654] p 1118 N94-17279
NORTH CAROLINA CENTRAL UNIV., DURHAM.
The pressure broadening of HDO by O2, N2, H2, and He between 100 K and 600 K
[AD-A267118] p 946 N94-15684
Nonparametric statistics: Weighted rankings analysis
[AD-A266607] p 1173 N94-16657
NORTH CAROLINA STATE UNIV., RALEIGH.
Software reliability through fault-avoidance and fault-tolerance
[NASA-CR-194353] p 1143 N94-15114
Illustrated glossary of textile terms for composites
[NASA-CR-191539] p 933 N94-15484
Diamond epitaxy and diamondlike coatings
[AD-A266657] p 1206 N94-15747
Quantification of processing artifacts in textile composites p 939 N94-16860
Three-dimensional analysis of anisotropic spatially reinforced structures p 939 N94-16863
Aeroelastic airfoil smart spar p 868 N94-16865
Nitride semiconductors for ultraviolet detection
[AD-A267877] p 1012 N94-17040
Pseudomorphic semiconducting heterostructures from combinations of AlN, GaN and selected SiC polytypes: Theoretical advancement and its coordination with experimental studies of nucleation, growth, characterization and device deployment
[AD-A267561] p 1213 N94-17108
Atomic layer epitaxy group IV materials: Surface processes, thin films, devices and their characterization
[AD-A267527] p 1213 N94-17116
Interface properties of wide bandgap semiconductor structures
[AD-A268269] p 1215 N94-17377
Low temperature deposition and characterization of n- and p-type silicon carbide thin films and associated ohmic and Schottky contacts
[AD-A267966] p 973 N94-17490
Growth, characterization and device development in monocrystalline diamond films
[AD-A268206] p 1216 N94-17553
NORTH CAROLINA UNIV., CHAPEL HILL.
Photochemistry in thin polymeric films
[AD-A266716] p 964 N94-15729
Synthesis and characterization of new low-dimensional metal complex conductors
[AD-A268251] p 952 N94-17416
NORTH CAROLINA UNIV., CHARLOTTE.
Applications of advanced diffractive optical elements p 1197 N94-17356
NORTH DAKOTA UNIV., GRAND FORKS.
Preliminary analysis of University of North Dakota aircraft data from the FIRE Cirrus IFO-2
[NASA-CR-193357] p 866 N94-15429
NORTH TEXAS RESEARCH AND DEVELOPMENT INST., DENTON.
Controlling chaotic behavior in CO2 and other lasers
[AD-A266431] p 1040 N94-16546
NORTHERN LIGHT RESEARCH AND DEVELOPMENT, SEATTLE, WA.
Biomass energy: State of the technology present obstacles and future potential
[DE93-016295] p 1092 N94-16766
NORTHWESTERN UNIV., CHICAGO, IL.
Complex QSO absorbers: High-redshift clusters of galaxies?
[NASA-CR-194617] p 1237 N94-16833
NORTHWESTERN UNIV., EVANSTON, IL.
Characterization of InTlSb grown by low pressure metalorganic chemical vapor deposition on GaAs substrate
[AD-A266878] p 1206 N94-14922
A multilayered approach to superconducting tunnel junction x ray detectors p 908 N94-15089
Rational design, construction, and processing of high-performance nonlinear optical materials
[AD-A266185] p 1191 N94-16454
Structural effects in electron transfer reactions: Comparative interfacial electrochemical kinetics for cis- versus trans-dioxorhenium (V) (bi)pyridine oxidation
[AD-A266307] p 1182 N94-16466
General Monte Carlo reliability simulation code including common mode failures and HARP fault/error-handling
[NASA-CR-187587] p 1150 N94-16594
High-valent oxo, methoxorhenium complexes: Models for intermediates and transition states in proton-coupled multi-electron transfer reactions
[AD-A266492] p 1211 N94-16782
Solvational barriers to interfacial electron transfer: Minimization by way of valence delocalization
[AD-A267371] p 950 N94-17006
Application of hard coatings to substrates at low temperatures
[NASA-CR-193867] p 971 N94-17122
Diamond growth on carbide surfaces using a selective etching technique
[AD-A267989] p 973 N94-17413
The stability and dynamics of elastic structures and fluid flows
[AD-A267990] p 1029 N94-17414
NORWEGIAN DEFENCE RESEARCH ESTABLISHMENT, KJELLER.
A new method for generating Bayes classifiers assuming mixtures of Gaussian densities
[FFI-91/4029] p 1172 N94-15298
Higher order statistics in signal processing
[FFI-92/2008] p 989 N94-15714
NOTRE DAME UNIV., IN.
Low-Complexity, High-Performance Bandwidth Efficient Coding and Coded Modulation Techniques for Satellite and Space Communications
[NASA-CR-194623] p 997 N94-16506
Bandwidth efficient coding: Theoretical limits and real achievements. Error control techniques for satellite and space communications p 997 N94-16507
A simulation study of the performance of the NASA (2,1,6) convolutional code on RFI/burst channels p 997 N94-16508
Search for optimal distance spectrum convolutional codes p 998 N94-16509
Transient studies of low temperature catalysts for methane conversion
[DE93-017710] p 950 N94-16962

O

OAK RIDGE INST. FOR SCIENCE AND EDUCATION, TN.
Ion mixing of thin ZrO2 films on sapphire
[DE93-015214] p 1206 N94-14925
OAK RIDGE K-25 SITE, TN.
Multiphoton ionization studies of WF6 and UF6
[DE93-016232] p 1181 N94-15863
OAK RIDGE NATIONAL LAB., TN.
Engineering Physics and Mathematics Division progress report, period ending 31 December 1992
[DE93-015118] p 1301 N94-14926
Structural investigation of electrochemically etched silicon
[DE93-015300] p 1207 N94-15827
Optical and infrared spectra of thermally annealed Pb implanted SiO2 glasses
[DE93-015304] p 965 N94-15828
Experimental investigations of superconductivity in quasi-two-dimensional epitaxial copper oxide superlattices and trilayers
[DE93-015306] p 1207 N94-15829
Environmental embrittlement in ordered intermetallic alloys
[DE93-015307] p 955 N94-15830
Recent advances in ordered intermetallics
[DE93-015308] p 955 N94-15862
NEXTEL(trademark)/SiC composites using forced chemical vapor infiltration
[DE93-013532] p 934 N94-16008
Application of Z-contrast imaging to obtain column-by-column spectroscopic analysis of materials
[DE93-015333] p 947 N94-16014
Dynamical Ising model simulations of nucleation and growth in copper-cobalt alloys
[DE93-015336] p 957 N94-16015
Rheology and microstructure of concentrated zirconia-alumina suspensions for gelcasting composites
[DE93-015339] p 966 N94-16016
Modeling the thermal conductivity of fiber-reinforced ceramic composites
[DE93-015340] p 934 N94-16017
The influence of microstructure on the mechanical behavior of silicon nitride ceramics
[DE93-015363] p 966 N94-16018
A reexamination of grain boundary fracture in Ni3Al: Environmental and alloying effects
[DE93-015431] p 1208 N94-16063
Negative ion formation in small carbon clusters
[DE93-015436] p 1182 N94-16064
Overview of chemical vapor infiltration
[DE93-015440] p 934 N94-16065
Thin Ni silicide formation by low temperature-induced metal atom reaction with ion implanted amorphous silicon
[DE93-015449] p 1209 N94-16066
Multiaxial deformation and life prediction model and experimental data for advanced silicon nitride ceramics
[DE93-015450] p 967 N94-16067
The effect of long-term aging on the impact properties of modified 9Cr-1Mo steel
[DE93-015453] p 957 N94-16068
The effect of aging at 343 C on the mechanical properties and microstructure of type 308 stainless steel weldments
[DE93-015454] p 957 N94-16103
Design of a cruciform bend specimen for determination of out-of-plane biaxial tensile stress effects on fracture toughness for shallow cracks
[DE93-015455] p 1059 N94-16104
Corrosion kinetics and mechanisms for nuclear grade graphites
[DE93-015462] p 947 N94-16105
The influence of thermal aging on the microstructure and fatigue properties of modified 9Cr-1Mo steel
[DE93-015489] p 957 N94-16106
Proposed guidelines for reporting performance of a solar dish/Stirling electric generation system
[DE93-016493] p 1092 N94-16112
Active probing of plasma edge turbulence and feedback studies on the Texas experimental tokamak (TEXT)
[DE93-015799] p 1202 N94-16162
Effects of alloying and temperature on the high-temperature oxidation of Cr-Cr2Nb
[DE93-015800] p 957 N94-16163
Crystallization of grain boundary phases in silicon nitride with low additive contents by microwave annealing
[DE93-015801] p 1209 N94-16164
Development and commercialization status of Fe3Al-based intermetallic alloys
[DE93-015802] p 957 N94-16165
Environmental effects on iron aluminides
[DE93-015820] p 958 N94-16166

General order characteristic methods for solving neutron transport problems
[DE93-015824] p 1170 N94-16167
The effect of irradiation on the mechanical properties of 6061-T651 aluminum
[DE93-015825] p 958 N94-16168
Chemical and displacement atomic pair correlations in crystalline solid solutions recovered by anomalous x ray scattering in Fe-Ni alloys
[DE93-015906] p 1209 N94-16171
Ion implantation effects on surface-mechanical properties of metals and polymers
[DE93-014661] p 958 N94-16453
Fast-ICCD photography and gated photon counting measurements of blackbody emission from particulates generated in the KrF-laser ablation of BN and YBC
[DE93-015491] p 1210 N94-16460
Evaluation of the interfacial mechanical properties in fiber-reinforced ceramic composites
[DE93-015494] p 935 N94-16461
Pulsed laser deposition of metastable Ca(1-x)Sr(x)CuO2 thin films
[DE93-015804] p 1040 N94-16663
Ablation, surface activation, and electroless metallization of insulating materials by pulsed excimer laser irradiation
[DE93-015808] p 1040 N94-16664
An advanced bioprocessing concept for the conversion of wastepaper to ethanol
[DE93-015209] p 975 N94-16807
Cycle performance testing of nonazeotropic mixtures of HFC-142A/HCFC-124 and HFC-32/HCFC-124 with enhanced surface heat exchangers
[DE93-015215] p 1024 N94-16808
Numerical studies of the photoluminescence spectrum of quantum Hall systems
[DE93-015822] p 1220 N94-16810
Development of a constitutive model for creep and life prediction of advanced silicon nitride ceramics
[DE93-015894] p 968 N94-16813
Microstructure of Zr3Al after 2 MeV proton bombardment
[DE93-015331] p 1211 N94-16814
Neutron and x ray scattering studies of (FeF2)(sub m)(CoF2)(sub n) multilayers
[DE93-015809] p 1184 N94-16838
Density of states and tunneling characteristics of layered superconductors
[DE93-015898] p 1211 N94-16839
Insights into semiconducting materials and growth phenomena through Z-contrast STEM
[DE93-015964] p 1212 N94-16841
The Ceramic Technology Project: Ten years of progress
[DE93-015991] p 968 N94-16843
Structural phase transition and superconductivity in La(2-x)Ba(x)CuO4
[DE93-015812] p 1212 N94-16868
Nonlinear gyrofluid models of shear Alfven instabilities in ignited and beam heated toroidal plasmas
[DE93-016235] p 1203 N94-16869
Bulk and defect properties of ordered intermetallics: A first-principles total-energy investigation
[DE93-015492] p 959 N94-16873
Processing of resonance parameter covariance files
[DE93-015506] p 1231 N94-16874
Processing of complex sintered reaction bonded silicon nitride parts by microwave heating
[DE93-015811] p 969 N94-16877
A modular control architecture for real-time synchronous and asynchronous systems
[DE93-015439] p 1166 N94-16888
Chemical vapor deposition of Ta2O5 corrosion resistant coatings
[DE93-015488] p 969 N94-16889
Creep ductility of iron at very low strain rates: The effects of sulfur
[DE93-015490] p 959 N94-16890
Publications of the Oak Ridge National Laboratory Fossil Energy Program, 1 October 1991 - 31 March 1993
[DE93-014643] p 1232 N94-16967
Evaluation of interfacial properties of fiber-reinforced ceramic composites using fiber push-in tests
[DE93-015427] p 972 N94-17253
Image accuracy and representational enhancement through low-level, multi-sensor integration techniques
[DE93-014888] p 1167 N94-17287
A Geographic Information System approach to modeling nutrient and sediment transport
[DE93-013747] p 1097 N94-17426
Some single-piston closed-cycle machines and Peter Tailer's thermal lag engine
[DE93-015983] p 1049 N94-17675

OCCIDENTAL COLL., LOS ANGELES, CA.
Morphology and models for the evolution of eastern Hecate Chasma, Venus p 1256 N94-16215

OFC CORP., KEENE, NH.
Predesign of diamond turned refractive/diffractive elements for IR objectives p 1198 N94-17359

OFFICE NATIONAL D'ETUDES ET DE RECHERCHES AEROSPATIALES, PARIS (FRANCE).
Reactions of chemiluminescence induced by singlet oxygen with metals
[ONERA-NT-1992-13] p 955 N94-15149
Contribution of laser Doppler velocimetry to the physical description of shock wave/turbulent boundary layer interactions with incidence on turbulence modelling p 1018 N94-15201
Electron-microscopy study of antiphase boundaries in Cu3Pd and Fe3Al alloys near the order-disorder transition
[ONERA-NT-1993-1] p 1206 N94-15295

OFFICE OF NAVAL RESEARCH, ARLINGTON, VA.
Mathematical Sciences Division 1992 programs
[AD-A268586] p 1140 N94-17623

OFFICE OF NAVAL RESEARCH LIAISON OFFICE, FAR EAST, APO SAN FRANCISCO, CA.
ONRASIA scientific information bulletin, volume 18, number 2
[AD-A267798] p 1304 N94-17305

OFFICE OF PERSONNEL MANAGEMENT, WASHINGTON, DC.
Programs and resources for control of job stress in the Federal workplace p 1124 N94-16617

OHIO STATE UNIV., COLUMBUS.
Electrical conductivity of ion implanted ladder and semi-ladder polymers
[AD-A267432] p 970 N94-16978
Design and diagnosis problem solving with multifunctional technical knowledge bases
[AD-A268375] p 1234 N94-17419
Atomic-scale friction measurements using friction force microscopy. Part 1: General principles and new measurement techniques
[AD-A268391] p 1048 N94-17533
Continuing research on friction and wear of materials
[AD-A268291] p 1049 N94-17566

OLD DOMINION UNIV., NORFOLK, VA.
Polymer Infiltration Studies
[NASA-CR-194494] p 932 N94-15275
Study of multi-dimensional radiative energy transfer in molecular gases
[NASA-CR-194613] p 1181 N94-15752
Investigation of radiative interaction in laminar flows using Monte Carlo simulation
[NASA-CR-194604] p 1021 N94-15795
Properties of thin films for high temperature flow sensors
[NASA-CR-191526] p 967 N94-16541
An analysis of the radiation field beneath a bank of tubular quartz lamps
[NASA-CR-191551] p 1024 N94-16542
Investigation of high-speed free shear flows using improved pressure-strain correlated Reynolds stress turbulence model
[NASA-CR-194661] p 1027 N94-17127
Studies on nonequilibrium phenomena in supersonic chemically reacting flows
[NASA-CR-194662] p 1027 N94-17215

OPEN UNIV., MILTON (ENGLAND).
Extraction and isotopic analysis of medium molecular weight hydrocarbons from Murchison using supercritical carbon dioxide p 1241 N94-16184
Removal of carbonaceous contaminants from silica aerogel p 953 N94-16256
A hydrogen isotope study of CO3 type carbonaceous chondrites; comparison with type 3 ordinary chondrites p 1246 N94-16425

OPTICAL SOCIETY OF AMERICA, WASHINGTON, DC.
OSA proceedings on Ultrafast Electronics and Optoelectronics, volume 14
[AD-A267972] p 1014 N94-17410

ORA CORP., ITHACA, NY.
Integrated trusted systems development environment
[AD-A267029] p 1146 N94-15674

ORBITAL SCIENCES CORP., FAIRFAX, VA.
The ORBCOMM system p 893 N94-17163
Big results with small space systems: What small systems are doing today p 896 N94-17187

OREGON STATE UNIV., CORVALLIS.
Arctic internal waves (CEAREX)
[AD-A265822] p 1111 N94-15139
Driving terrestrial ecosystem models from space p 991 N94-15896
Chondritic ratios of Fe/Cr/Ir in Kerguelen Plateau (Hole 738C) K/T carbonate-rich sediments support asteroid-cometary impact at K/T time p 1244 N94-16357
Earth's partial pressure of CO2 over the past 120 Ma; evidence from Ce anomalies in the deep (greater than 600 m) Pacific Ocean, 1 p 1104 N94-16358
Geochemical evidences for two chondritic-like cometary or asteroidal impacts before and at the K/T boundary p 1244 N94-16359
Earth's partial pressure of CO2 over the past 100-500 Ma; evidence from Ce anomalies in mostly shallow seas (less than 200 m) as recorded in carbonate sediments, 2 p 1104 N94-16360

ORGANISATIE VOOR TOEGEPAST NATUURWETENSCHAPPELIJK ONDERZOEK, DELFT (NETHERLANDS).
Sea bottom topography imaging with SAR p 1077 N94-16745

ORGANIZATION FOR ECONOMIC CO-OPERATION AND DEVELOPMENT, PARIS (FRANCE).
The Megascience Forum
[DE93-014445] p 1303 N94-16804

ORION INTERNATIONAL TECHNOLOGIES, ALBUQUERQUE, NM.
Characterization of UV emissions resulting from electronic energy transfer in atmospheric molecules
[AD-A266244] p 1101 N94-16469

ORSTED INST., COPENHAGEN (DENMARK).
Suggestion for extended Viking magnetic properties experiment on future Mars missions p 1285 N94-16375

ORTECH INTERNATIONAL, MISSISSAUGA (ONTARIO).
Use of microgravity in the synthesis of ceramics using sol gel techniques p 979 N94-16088

OTTAWA UNIV. (ONTARIO).
Solution behaviour in microgravity: Considerations for protein crystal growth p 982 N94-16102

OULU UNIV. (FINLAND).
Fractal geometry of some Martian lava flow margins: Alba Patera p 1270 N94-16298
Tectonics of Neyterkob corona on Venus p 1270 N94-16299

P

PACIFIC APPLIED RESEARCH, RANCHO PALOS VERDES, CA.
Pulsed hydrogen fluoride overtone chemical laser studies
[AD-A267597] p 1041 N94-17193

PACIFIC NORTHWEST LAB., RICHLAND, WA.
Statement on global climate change before the Subcommittee on Energy and Power, United States House of Representatives
[DE93-013163] p 1095 N94-16006
Environmental effects on elevated temperature subcritical crack growth of SiC/SiC composites
[DE93-015688] p 934 N94-16158
The role of interfacial chemistry in surface nucleation and growth of calcium oxalate
[DE93-015689] p 1209 N94-16159
Chemical interactions between interconnect and electrode materials during sintering in solid oxide fuel cells
[DE93-015696] p 1092 N94-16160
Global change research: Science and policy
[DE93-015675] p 1096 N94-16445
Evolution of microstructure in face centered cubic metals during irradiation: A review
[DE93-015682] p 958 N94-16662
Fabrication of advanced design (grooved) cermet anodes
[DE93-014590] p 1012 N94-16765
Computing and Information Sciences
[DE93-017149] p 1151 N94-16902
Low-temperature sintering and phase changes in chromite interconnect materials
[DE93-015676] p 961 N94-17234
Characterization of nanoscale oxide and oxyhydroxide powders using EXAFS spectroscopy
[DE93-015683] p 940 N94-17235
Theoretical crystallography with the Advanced Visualization System
[DE93-015692] p 1215 N94-17319
Environmental use of a Laser Range Finder and the Advanced Visualization System
[DE93-016163] p 1043 N94-17677

PACIFIC-SIERRA RESEARCH CORP., LOS ANGELES, CA.
Effect of powerful oblique HF waves on ionospheric D-layer absorption
[AD-A268443] p 1102 N94-17499

PADUA UNIV. (ITALY).
Dust grain resonant capture: A statistical study p 1245 N94-16384
Zaoyang chondrite cooling history from pyroxene Fe(2+)-Mg intracrystalline ordering and exolutions p 1246 N94-16417

PARAMAX SYSTEMS CORP., HUNTSVILLE, AL.
Applying paperless technology to achieve excellence in manufacturing operations
[TABES PAPER 93-630] p 1052 N94-16147
PARIS UNIV. (FRANCE).
CO2 production by impact in carbonates? An ATEM and stable isotope (C,O) study p 954 N94-16383
PARIS VI UNIV. (FRANCE).
Metastable superconductors as photon detectors p 900 N94-15032
PARIS VII UNIV. (FRANCE).
Metastable superconductors as photon detectors p 900 N94-15032
PENNSYLVANIA STATE UNIV., UNIVERSITY PARK.
Swept shock/boundary-layer interactions: Scaling laws, flowfield structure, and experimental methods p 1017 N94-15197
Nanocomposites for electronic applications, volume 1
[AD-A267070] p 1009 N94-15669
Nanocomposites for electronic applications, volume 3
[AD-A267073] p 1009 N94-15672
Nanocomposites for electronic applications, volume 2
[AD-A267074] p 1009 N94-15673
The theory of QSO absorption line systems and their relationship to the galaxies
[NASA-CR-194596] p 1236 N94-15679
Vacancy condensation as the precursor to passivity breakdown
[DE93-012925] p 956 N94-15998
Acoustic waves in complicated geometries and their interactions with liquid-propellant droplet combustion
[AD-A267260] p 1178 N94-16991
Advanced thermally stable jet fuels
[DE93-017711] p 975 N94-16996
The use of the Air Force Academy high wind alert system in forecasting moderate intensity wind events for military bases in the Colorado Springs area
[AD-A267648] p 1107 N94-17245
Transition induced by fixed and freely convecting spherical particles in laminar boundary layers
[AD-A267757] p 1028 N94-17276
High order nonlinear estimation with signal processing applications
[AD-A268407] p 1005 N94-17463
Interface chemistry in ceramic matrix composites
[AD-A268629] p 973 N94-17466
Surface reactivity of combustion generated soot particles
[AD-A268017] p 952 N94-17532
PENNSYLVANIA UNIV., PHILADELPHIA.
Theoretical prediction of the UV adsorption and fluorescence spectra of tyrosine and phenylalanine
[AD-A266970] p 943 N94-15111
Synthesis of potential high-energy fuels
[AD-A267508] p 975 N94-17073
PHILIPS COMPONENTS LTD., SOUTHAMPTON (ENGLAND).
Advanced high performance CdHgTe multiplexed arrays p 903 N94-15051
Discrete CMT infrared detectors for space application, from ISSR to second generation Meteosat and MIPAS p 905 N94-15065
PHILLIPS LAB., EDWARDS AFB, CA.
Secondary smoke p 924 N94-15220
PHILLIPS LAB., HANSCOM AFB, MA.
Phillips Laboratory global spectral numerical weather prediction model
[AD-A267293] p 1107 N94-17244
PHILLIPS LAB., KIRTLAND AFB, NM.
Measurements of the operation of the SINUS-6/BWO system
[AD-A266423] p 1011 N94-16556
Proceedings of the 7th International Cryocooler Conference, part 1
[AD-A268448] p 985 N94-17482
Proceedings of the 7th International Cryocooler Conference, part 2
[AD-A268449] p 985 N94-17484
Proceedings of the 7th International Cryocooler Conference, part 3
[AD-A268450] p 985 N94-17485
PHOTOMETRICS, INC., WOBURN, MA.
Optical properties of water released in low Earth orbit
[AD-A266197] p 1192 N94-16936
PHYSICAL RESEARCH LAB., AHMEDABAD (INDIA).
Grosnaja ABCs: Magnesium isotope compositions p 1241 N94-16191
Nitrogen and light noble gases in Parsa enstatite chondrite p 1246 N94-16435
PICOTRONIX, INC., ANN ARBOR, MI.
A novel solid-state optical temporal analyzer with picosecond resolution and picowatt sensitivity
[AD-A266804] p 986 N94-14912
PITTSBURGH STATE UNIV., KS.
Vertical structure models of the 1990 equatorial disturbance on Saturn p 1277 N94-16333
PITTSBURGH UNIV., PA.
Why is the Moon dark? p 1256 N94-16219
Thermal disorder in adsorbed Cl on Si(100)
[AD-A266295] p 1210 N94-16476
Stability analysis for the flow of granular materials down an inclined plane using kinetic model
[DE93-016852] p 1026 N94-16958
PLANETARY SCIENCE INST., TUCSON, AZ.
The physical mechanism of comet outbursts: An experiment p 1242 N94-16221
Confirmation of saturation equilibrium conditions in crater populations p 1103 N94-16222
PLEX CORP., BROOKLINE, MA.
Sodium-mercury excimer laser, phase 1
[AD-A267728] p 1042 N94-17230
POLISH ACADEMY OF SCIENCES, KORNIK.
Upgrading of the Borowiec laser station p 877 N94-15604
POLISH ACADEMY OF SCIENCES, WARSAW.
Comparative magnetic and thermoanalytical study of two enstatite chondrites: Adhi Kot and Atlanta p 1244 N94-16329
Studies of aural acoustic emmissions with the use of an original apparatus and investigative methodology
[IFTR-20/1992] p 1177 N94-16650
Elastooptical brittle materials in experimental studies of the state of stress and deformation
[IFTR-22/1991] p 1059 N94-16651
A priori inequalities for an ideal-incompressible liquid in an electromagnetic field
[IFTR-9/1992] p 998 N94-16652
Analysis of an electromagnetic field in the vicinity of a caustic by asymptotic methods
[IFTR-12/1991] p 998 N94-16653
Static analysis of beams on an elastic base as stated by generalized functions
[IFTR-27/1991] p 1060 N94-16923
Superconducting ceramics: Selected properties and methods of production
[IFTR-23/1991] p 969 N94-16924
Invariance of slip movements with respect to the control matrix
[IFTR-43/1991] p 1170 N94-17045
The influence of an electric field on the kinetics of nucleation
[IFTR-2/91] p 1213 N94-17046
Surface waves in an inhomogeneous, isotropic, elastic half-space
[IFTR-18/1991] p 1060 N94-17047
An asymptotic expansion of an electromagnetic field in the velocity of a caustic in the form of simple waves
[IFTR-14/1991] p 1002 N94-17048
Regular and irregular reflection of a wave from a slanting flat wall
[IFTR-13/1991] p 1193 N94-17049
An analysis of ways of determining the material constants for viscoelastic materials
[IFTR-28/91] p 951 N94-17050
Discrete models of the Boltzmann equation: Structure of the collision operator of sound propagation
[IFTR-2/1992] p 1178 N94-17051
Influence of the loading rate on the endurance and deformability of cement matrix composites
[IFTR-1/1992] p 1060 N94-17052
The exact solution of the problem of diffraction of an electromagnetic plane wave by a conductive half-plane situated at an interface
[IFTR-3/91] p 1002 N94-17057
The determination of the Young moduli of a material after exposure to laser light and delineation of the zone of laser alterations
[IFTR-37/1991] p 1061 N94-17058
Studies of changes in the energy stored in metals as a result of subjecting them to a surface type technological process
[IFTR-25/1991] p 960 N94-17063
The influence of the level formants on the perception of synthetic vowel sounds
[IFTR-41/1991] p 1002 N94-17064
Proposal of a simple mathematical model for the action of a laser on a metal plate
[IFTR-36/1991] p 1041 N94-17065
Spectroscopic and computer modeling investigations of a laser-sustained plasma
[IFTR-30/1991] p 1204 N94-17066
Application of group theory to integral-difference equations of plasma physics
[IFTR-23/1992] p 1204 N94-17067
A measurement station for study of Earth moving tools and ground cutting processes
[IFTR-10/1991] p 985 N94-17068
Variational principles of heat exchange and their applications in construction physics, part 2
[IFTR-19/1991] p 1061 N94-17069
Numerical modelling of an active direct nonpotable hot water heating system making use of the energy of solar radiation
[IFTR-38/1991] p 1093 N94-17070
An electroacoustic transducer for purposes of photoacoustic spectroscopy
[IFTR-7/1992] p 1013 N94-17071
Static and dynamic investigations of brittle elasto-optical material
[IFTR-3/1992] p 1061 N94-17086
An automated system for ultrasound measurements of liquids by the resonance (Eggers) method
[IFTR-17/1992] p 1178 N94-17087
Elastic waves in discretely continuous mechanical systems
[IFTR-21/1992] p 1061 N94-17091
Assessment of trends in the development of residential buildings from the standpoint of the fuel and energy requirements
[IFTR-6/1991] p 1093 N94-17092
Analysis of the strengthening of aluminum alloy undergoing plastic deformation under conditions of a compound state of stress
[IFTR-21/1991] p 960 N94-17093
An investigation of the hydrolytic resistance of sodium-calcium plate glass with a layer of silica deposited on its surface
[IFTR-34/1991] p 971 N94-17120
Influence of grain size on the energy storing ability during uniaxial stretching of austenite steel
[IFTR-22/1992] p 961 N94-17121
Optimization of two-stage hot water exchange points p 1029 N94-17440
POLITECNICO DI MILANO (ITALY).
Performance optimization of detector electronics for millimeter laser ranging p 913 N94-15569
Tracking capabilities of SPADs for laser ranging p 914 N94-15570
How to squeeze high quantum efficiency and high time resolution out of a SPAD p 914 N94-15571
Automatic generation of production rules for integrity maintenance
[REPT-92-054] p 1156 N94-17501
Automatic translation of database integrity constraints into compensating production rules
[REPT-92-055] p 1234 N94-17502
Orpheus: A synthesis framework for regular architectures
[REPT-93-016] p 1156 N94-17504
FSM test: A functional test generation system for sequential circuits
[REPT-93-017] p 1014 N94-17505
PRAIRIE OBSERVATORY, URBANA, IL.
Fault handling schemes in electronic systems with specific application to radiation tolerance and VLSI design
[NASA-CR-194559] p 1008 N94-15640
PRATT AND WHITNEY AIRCRAFT, EAST HARTFORD, CT.
Effects of rotation on coolant passage heat transfer. Volume 2: Coolant passages with trips normal and skewed to the flow
[NASA-CR-4396-VOL-2] p 1023 N94-15991
PRINCETON UNIV., NJ.
Large-Eddy Simulations (LES) of flows and turbulence distribution
[AD-A267182] p 1016 N94-15151
Mechanisms of combustion limits in premixed gas flames at microgravity
[NASA-CR-194557] p 946 N94-15713
Stress sensitivity of dielectric resonators
[AD-A266767] p 1009 N94-15825
Research into the influence of spatial variability and scale on the parameterization of hydrological processes
[NASA-CR-194610] p 1082 N94-16026
On hydrologic similarity: A dimensionless flood frequency model using a generalized geomorphologic unit hydrograph and partial area runoff generation
[PAPER-89WR01579] p 1083 N94-16027
Similarity and scale in catchment storm response
[PAPER-89RG01615] p 1083 N94-16028
Evapotranspiration and runoff from large land areas: Land surface hydrology for atmospheric general circulation models p 1083 N94-16029
Heterogeneity and scaling land-atmospheric water and energy fluxes in climate systems p 1083 N94-16030
A detailed model for simulation of catchment scale subsurface hydrologic processes
[PAPER-92WR02333] p 1084 N94-16032
Effects of spatial variability and scale on areal -average evapotranspiration p 1084 N94-16033
Scaling, soil moisture and evapotranspiration in runoff models p 1084 N94-16034
A molecular dynamics simulator for optimal control of molecular motion
[AD-A266572] p 1183 N94-16722

Characterization of voids formed during liquid impregnation of nonwoven multifilament glass networks as related to composite processing p 939 N94-16858
The structure of turbulent boundary layers and shock wave boundary layer interactions
[AD-A266240] p 1026 N94-16929
Studies of premixed laminar and turbulent flames at microgravity
[NASA-CR-194656] p 951 N94-17125
The roles of fluid motion and other transport phenomena in the morphology of materials
[NASA-CR-194665] p 1028 N94-17298
Plasma instabilities and transport in the MPD thruster
[AD-A268268] p 1204 N94-17575

PRINS MAURITS LAB. TNO, RIJSWIJK (NETHERLANDS).
Experimental investigations into the deflagration to detonation transition at TNO/PML
[AD-A266753] p 1021 N94-15755
User manual and program description of the data acquisition system of PML-pulse physics
[AD-A266752] p 1147 N94-15776
A 27 channels, 1 MHz fibre-optic measuring system
[AD-A266943] p 1003 N94-17307

PURDUE UNIV., WEST LAFAYETTE, IN.
Efficient algorithmic techniques for combinatorial problems
[AD-A267151] p 1172 N94-15777
Al-26 production profile and model comparisons in Canyon Diablo p 1245 N94-16409
Atmospheric corrections for TIMS estimated emittance p 1064 N94-16602
Earth observational research using multistage EOS-like data
[NASA-CR-194626] p 1084 N94-16831
Preconversion catalytic deoxygenation of phenolic functional groups
[DE93-017034] p 950 N94-16912

Q

QUADRANT ENGINEERING, INC., AMHERST, MA.
Fine scale measurements of microwave backscatter from the ocean surface
[AD-A264516] p 1111 N94-15134

QUEST INTEGRATED, INC., KENT, WA.
Field observations of infragravity, sea and swell directional spectra
[AD-A266439] p 1113 N94-16561

R

RADEX, INC., BEDFORD, MA.
Polar 2 model of the wake shield experiment
[AD-A266243] p 882 N94-16468

RANGE COMMANDERS COUNCIL, WHITE SANDS MISSILE RANGE, NM.
Test methods for acceptance testing of telescopes
[AD-A268316] p 1237 N94-17568

RAYTHEON CO., LEXINGTON, MA.
RF vacuum microelectronics
[AD-A268399] p 1014 N94-17423

READING UNIV. (ENGLAND).
Mesoscale modeling of the atmosphere
[AD-A263236] p 1098 N94-15132

RENSSELAER POLYTECHNIC INST., TROY, NY.
High temperature advanced structural composites. Volume 2: Ceramic matrix composites, fiber processiing and properties, and interfaces
[AD-A267023] p 933 N94-15528
High temperature advanced structural composites. Volume 3: Mechanics
[AD-A267024] p 933 N94-15626
High temperature advanced structural composites. Volume 1: Executive summary and intermetallic compounds
[AD-A267022] p 933 N94-15835
An initial perspective of S-asteroid subtypes within asteroid families p 1243 N94-16310
ARIES tokamak reactor study
[DE93-017059] p 1203 N94-16901
Path planning for robotic truss assembly
[NASA-CR-194652] p 897 N94-17280
Measurement of the velocity field and void fraction in a planar plunging jet
[AD-A268183] p 1030 N94-17511

RESEARCH INST. FOR ADVANCED COMPUTER SCIENCE, MOFFETT FIELD, CA.
The alignment-distribution graph
[NASA-CR-194292] p 1168 N94-15112
Mobile and replicated alignment of arrays in data-parallel programs
[NASA-CR-194294] p 1158 N94-15113
A browsing tool for the Internet Logical Library of the HPCC Software Exchange
[NASA-CR-194545] p 1143 N94-15189
Generating local addresses and communication sets for data-parallel programs
[NASA-CR-194605] p 1159 N94-15796
The alignment-distribution graph
[NASA-CR-194609] p 1148 N94-15956

RESEARCH INST. FOR COMPUTING AND INFORMATION SYSTEMS, HOUSTON, TX.
NASA Electronic Library System (NELS): The system impact of security
[NASA-CR-194614] p 1231 N94-16499

RETINA FOUNDATION, BOSTON, MA.
Perception of lightness and brightness in complex patterns
[AD-A268435] p 1134 N94-17513

RHODE ISLAND UNIV., KINGSTON.
Aspects of high temperature damage in fiber reinforced titanium metal matrix composites
[AD-A267907] p 941 N94-17379

RHODE ISLAND UNIV., NARRAGANSETT.
Ray tracing on topographic Rossby waves
[AD-A267014] p 1112 N94-15844

RICE UNIV., HOUSTON, TX.
A novel approach for structural mechanics problems with stochasticity
[AD-A266189] p 1059 N94-16123
Geochemistry and cosmochemistry of fullerenes 3: Reaction of C60 and C70 with ozone p 953 N94-16243
Analysis of temporal symmetry in non-gaussian random fields
[AD-A266496] p 999 N94-16794
Visual display principles for C3I system tasks
[AD-A267969] p 1005 N94-17498

RIJKSLUCHTVAARTDIENST, SCHIPHOL (NETHERLANDS).
Aviation inspection prospects p 853 N94-15125

RIJKSLUCHTVAARTDIENST, THE HAGUE (NETHERLANDS).
Developments in the European air traffic control p 853 N94-15124

RISOE NATIONAL LAB., ROSKILDE (DENMARK).
The MADONA experiments (Meteorology and Diffusion Over Non-uniform Areas): High-resolution in-plume concentration fluctuations measurements using lidar remote sensing technique
[AD-A267711] p 1105 N94-14938

ROCHESTER INST. OF TECH., NY.
Conflict Resolution (CORE) for software quality factors
[AD-A267248] p 1151 N94-16941

ROCHESTER PHOTONICS CORP., NY.
Diffractive optics: Design, fabrication, and applications p 1194 N94-17334

ROCHESTER UNIV., NY.
Combinatorial semantics
[TR-444] p 1149 N94-16575
Exploiting world structure to efficiently search for objects
[TR-434] p 1231 N94-16576
A trace-based comparison of shared memory multiprocessor architectures
[TR-432] p 1159 N94-16577
Shared-memory multiprocessor trends and the implications for parallel program performance
[TR-420] p 1159 N94-16578
Reductions to sets of low information content
[TR-417] p 1150 N94-16579
Contextually dependent control strategies for manipulation
[TR-416] p 1165 N94-16580
Visually guided touching and manual tracking
[TR-412] p 1166 N94-16581
Set-based Bayesianism
[TR-407] p 1170 N94-16582
Reference frames in vision
[AD-A266174] p 1132 N94-16925
Localizing visual function in the brain
[AD-A267381] p 1133 N94-17020
Diffractive optics: Design, fabrication, and applications p 1194 N94-17334
Subwavelength structured surfaces and their applications p 1194 N94-17337
Curved grating fabrication techniques for concentric-circle grating, surface-emitting semiconductor lasers p 1045 N94-17349

ROCKWELL INTERNATIONAL CORP., CANOGA PARK, CA.
Advanced transportation system studies technical area 3: Alternate propulsion subsystem concepts, volume 2
[NASA-CR-193863] p 927 N94-17096
Advanced transportation system studies technical area 3: Alternate propulsion subsystem concepts, volume 3
[NASA-CR-193864] p 927 N94-17097
Advanced transportation system studies technical area 3: Alternate propulsion system concepts. SSME upper stage use
[NASA-CR-193865] p 927 N94-17098

ROCKWELL INTERNATIONAL CORP., THOUSAND OAKS, CA.
Molten salt electrodeposition of high temperature superconductors
[AD-A266620] p 1009 N94-15726

ROCKWELL INTERNATIONAL SCIENCE CENTER, ANAHEIM, CA.
Visible light photon counters for astronomy p 902 N94-15043

ROCKWELL INTERNATIONAL SCIENCE CENTER, THOUSAND OAKS, CA.
Laser beam steering device p 1045 N94-17357

ROME LAB., GRIFFISS AFB, NY.
Analysis of leading edge and trailing edge cover glass samples before and after treatment with advanced satellite contamination removal techniques
[AD-A267055] p 885 N94-15666
True time delay optically controlled dual band transmitter
[AD-A267663] p 1003 N94-17228
Proceedings of the 1992 Antenna Applications Symposium, volume 1
[AD-A268167] p 1005 N94-17431

ROME LAB., HANSCOM AFB, MA.
Proceedings of the 1992 Antenna Applications Symposium, volume 2
[AD-A266916] p 986 N94-14998
Adaptive beamforming with imperfect arrays: Pattern effects and their partial correction
[AD-A267079] p 987 N94-15541

ROME UNIV. (ITALY).
Characterization of the lithium/pan-based polymer electrolytes interface
[AD-A268401] p 973 N94-17434

ROYAL AEROSPACE ESTABLISHMENT, FARNBOROUGH (ENGLAND).
Heat transfer and aerodynamics of a 3D design nozzle guide vane tested in the Pyestock isentropic light piston facility
[RAE-TM-AERO/PROP-19] p 856 N94-15696

ROYAL AIRCRAFT ESTABLISHMENT, FARNBOROUGH (ENGLAND).
Determination of the effect of the walls of a wind-tunnel from the parameters of flow near them
[RAE-LIB-TRANS-2201] p 859 N94-16583

ROYAL GREENWICH OBSERVATORY, CAMBRIDGE (ENGLAND).
Satellite signatures in SLR observations p 912 N94-15557
SLR data screening; location of peak of data distribution p 912 N94-15560
Formation of on-site normal points p 917 N94-15592

ROYAL INST. OF TECH., STOCKHOLM (SWEDEN).
Liquid phase sintering of tungsten composites under microgravity. Effect of matrix composition p 945 N94-15171

ROYAL NETHERLANDS METEOROLOGICAL INST., DE BILT.
Automatic suppression of anomalous propagation clutter for noncoherent weather radars
[KNMI-WR-92-06] p 1004 N94-17407

ROYAL NORWEGIAN COUNCIL FOR SCIENTIFIC AND INDUSTRIAL RESEARCH, KJELLER.
NORSAR basic seismological research
[AD-A266193] p 1101 N94-16125

ROYAL ORDNANCE PLC, AYLESBURY (ENGLAND).
Microwave properties and systems overview p 924 N94-15222

ROYAL ORDNANCE PLC, KIDDERMINSTER (ENGLAND).
Propulsion p 924 N94-15219

RTWARE, INC., DURHAM, NC.
Module interconnection frameworks for a real-time spreadsheet
[AD-A267317] p 1153 N94-17220
Module interconnection frameworks for a real-time spreadsheet
[AD-A267752] p 1153 N94-17231

RUTGERS - THE STATE UNIV., NEW BRUNSWICK, NJ.
Computer-aided design package for designers of digital optical computers
[AD-A267866] p 1154 N94-17390

RUTGERS - THE STATE UNIV., PISCATAWAY, NJ.
Numerical simulation of 3-D shock wave turbulent boundary layer interactions p 1017 N94-15199

RUTGERS UNIV., NEW BRUNSWICK, NJ.
Al-26-Mg-26 ages of iron meteorites p 1242 N94-16240

RUTHERFORD APPLETON LAB., CHILTON (ENGLAND).
The laboratory performance of the short wavelength instrument for the Along Track Scanning Radiometer ATSR-2 (initial results) p 908 N94-15088
RYERSON POLYTECHNICAL INST., TORONTO (ONTARIO).
Transcranial Doppler ultrasound studies of cerebral *blood-flow in microgravity* p 981 N94-16095

S

SAINT LAWRENCE UNIV., CANTON, NY.
Do it yourself remote sensing: Generating an inexpensive, high tech, real science lake mapping project for the classroom p 1086 N94-16407
SAINT PETERSBURG SCIENTIFIC RESEARCH INST. OF CHEMICAL FIBERS AND COMPOSITE MATERIALS (RUSSIA).
New textile composite materials development, production, application p 938 N94-16853
Production and application of chemical fibers with special properties for manufacturing composite materials and goods of different usage p 938 N94-16854
Fibers and materials of medical application p 938 N94-16855
SANDIA NATIONAL LABS., ALBUQUERQUE, NM.
Particle simulations on massively parallel machines [DE93-015644] p 1157 N94-14927
Progress in the concentrator initiative program [DE93-015006] p 1091 N94-15984
C++ as a language for object-oriented numerics [DE93-015027] p 1148 N94-15985
Revisiting the BCS, a measurement system for characterizing the optics of solar collectors [DE93-015030] p 1091 N94-15993
Recent advances in outdoor performance evaluation of PV systems [DE93-015031] p 1091 N94-15994
The growth of InAs(1-x)Sb(x)/InAs strained-layer superlattices by metal-organic chemical vapor deposition [DE93-015028] p 1208 N94-16012
Creating and maintaining a visionary quality program [DE93-015122] p 1050 N94-16055
Evaluation of midband analog fiber optic telemetry links [DE93-015128] p 883 N94-16056
Determination of equivalent circuit for PVDF shock-pressure gauges [DE93-016492] p 1034 N94-16452
A computer-based training system combining virtual reality and multimedia [DE93-013768] p 1132 N94-16819
High heat flux engineering in solar energy applications [DE93-016500] p 1093 N94-16954
A ten year review of performance of photovoltaic systems [DE93-015649] p 1093 N94-17217
Resist performance in soft x ray projection lithography [DE93-016490] p 1036 N94-17647
Electrical properties of sol-gel PZT thin films for decoupling capacitor applications [DE93-016491] p 1015 N94-17648
Characterization of Ni on Si wafers: Comparison of surface analysis techniques [DE93-016501] p 953 N94-17649
Field investigation of the relationship between battery size and PV system performance [DE93-016503] p 1016 N94-17671
SANDIA NATIONAL LABS., LIVERMORE, CA.
Continuum solvent models for computational chemistry [DE93-016329] p 953 N94-17660
SASKATCHEWAN UNIV., SASKATOON.
The design and analysis of a modular microgravity test platform for use aboard the NASA KC-135 aircraft p 899 N94-16101
SATELLITE LASER RANGER GROUP, HAILSHAM (ENGLAND).
Timebias corrections to predictions p 875 N94-15591
SCIENCE APPLICATIONS INTERNATIONAL CORP., FALLS CHURCH, VA.
Abundance recovery error analysis using simulated AVIRIS data p 1074 N94-16708
SCIENCE APPLICATIONS INTERNATIONAL CORP., FORT WASHINGTON, PA.
Rocket motor plume flowfields: Phenomenology and simulation p 924 N94-15221
SCIENCE APPLICATIONS INTERNATIONAL CORP., GLENDORA, CA.
The effect of an on-orbit near encounter on the number flux density of micron sized particles p 899 N94-16374
SCIENCE APPLICATIONS INTERNATIONAL CORP., MCLEAN, VA.
Predicting radiation induced performance decrements of AH-1 helicopter crews. Volume 1: Predicted veersus *actual performance of AH-1 crews induced with symptoms* simulating radiation sickness [AD-A268376] p 1138 N94-17460
SCIENCE APPLICATIONS INTERNATIONAL CORP., SAN DIEGO, CA.
The IMS software integration platform [AD-A266285] p 1151 N94-16910
SCIENTIFIC RESEARCH ASSOCIATES, INC., GLASTONBURY, CT.
Coaxial airblast atomizers [NASA-CR-193845] p 1016 N94-15109
SCRANTON UNIV., PA.
Evaluation of ALSYS 037 Ada Compiler [AD-A266972] p 1143 N94-15110
SCRIPPS INSTITUTION OF OCEANOGRAPHY, LA JOLLA, CA.
LFASE report: Crustal study [AD-A266893] p 1111 N94-14947
Ventilated oscillatory boundary layers [AD-A266226] p 1023 N94-16110
Estimates of lithospheric thickness on Venus p 1267 N94-16277
SFA, INC., LANDOVER, MD.
Investigation of the optical, electronic, and structural *properties of fiber optic glasses* [AD-A267645] p 971 N94-17204
SHANGHAI OBSERVATORY (CHINA).
Application of the robust estimate in SLR data preprocessing p 918 N94-15597
Development of Shanghai satellite laser ranging station p 877 N94-15605
SHEFFIELD UNIV. (ENGLAND).
Comparison of edges detected at different polarisations in MAESTRO data p 1080 N94-16761
SIMON FRASER UNIV., BURNABY (BRITISH COLUMBIA).
Infra Link: A data transmission system for microgravity research p 980 N94-16091
Heart rate response to parabolic flight manoeuvres p 981 N94-16098
SIMPSON WEATHER ASSOCIATES, INC., CHARLOTTESVILLE, VA.
EOS Laser Atmosphere Wind Sounder (LAWS) investigation [NASA-CR-193445] p 1109 N94-17525
SMITH SYSTEM ENGINEERING LTD., GUILDFORD (ENGLAND).
Cost drivers: Why do conventional satellites cost so much? p 897 N94-17190
SMITHSONIAN ASTROPHYSICAL OBSERVATORY, CAMBRIDGE, MA.
Molecular processes in comets [NASA-CR-194148] p 1239 N94-15188
SOCIETE ANONYME D'ETUDES ET REALISATIONS NUCLEAIRES, LIMEIL-BREVANNES (FRANCE).
SYDONI: An intensified system for night observation p 891 N94-17153
SOCIETE ANONYME DE TELECOMMUNICATIONS, PARIS (FRANCE).
IR detectors and subsystems for space applications p 909 N94-15091
SOCIETE NATIONALE DES POUDRES ET EXPLOSIFS, VERT-LE-PETIT (FRANCE).
Plume primary smoke p 923 N94-15218
SOCIETY OF TOXICOLOGY, WASHINGTON, DC.
Factors determining the release of nitric oxide [AD-A266232] p 1118 N94-17224
SOUTH CAROLINA UNIV., COLUMBIA.
Applications of the phi-transform [AD-A266247] p 1170 N94-16940
SOUTH DAKOTA SCHOOL OF MINES AND TECHNOLOGY, RAPID CITY.
Spatial resolution and cloud optical thickness retrievals p 1066 N94-16671
SOUTHAMPTON UNIV. (ENGLAND).
An alternative approach to the growth of single crystal gallium nitride [AD-A267876] p 1213 N94-17037
SOUTHEASTERN CENTER FOR ELECTRICAL ENGINEERING EDUCATION, INC., SAINT CLOUD, FL.
States of awareness 1: Subliminal perception relationship to situational awareness [AD-A267249] p 1132 N94-16942
SOUTHERN METHODIST UNIV., DALLAS, TX.
Ishtar deformed belts: Evidence for deformation from below? p 1256 N94-16218
Structural mapping of Maxwell Montes p 1271 N94-16304
SOUTHERN RESEARCH INST., BIRMINGHAM, AL.
SRB thermal curtain design support [NASA-CR-193857] p 927 N94-17123
SRB thermal curtain design support [NASA-CR-193858] p 928 N94-17124
SOUTHWEST RESEARCH INST., HOUSTON, TX.
Principal investigators data package for Project Initiation Conference (PIC): EUVS sounding rocket no. 36.117CL. Target: Venus [NASA-CR-194663] p 923 N94-17126
SOUTHWEST RESEARCH INST., SAN ANTONIO, TX.
Mapping the stability region of the 3:2 Neptune-Pluto resonance p 1280 N94-16351
Chairmanship of the Neptune/Pluto outer planets science working group [NASA-CR-194625] p 1297 N94-16832
Multispectral observations of the Jovian aurora [NASA-CR-193628] p 1297 N94-16884
Magnetic effects in Venus/solar wind interaction [NASA-CR-194666] p 1299 N94-17281
SOUTHWEST SCIENCES, INC., SANTA FE, NM.
Nonintrusive fast response oxygen monitoring system for high temperature flows [NASA-CR-4553] p 1036 N94-17655
SPACE EXPLORATION ASSOCIATION, CEDARVILLE, OH.
Diamond p-n junction cold cathode [AD-A266926] p 1206 N94-15107
SPACE RESEARCH ORGANIZATION NETHERLANDS, GRONINGEN.
Submillimeterwave SIS mixer developments p 903 N94-15054
Characteristics of the ISO short wavelength spectrometer detectors p 908 N94-15084
SPACE RESEARCH ORGANIZATION NETHERLANDS, UTRECHT.
Superconductive x ray photon detectors p 900 N94-15031
The development of back-illuminated CCD's for XMM p 900 N94-15035
SPARTA, INC., LEXINGTON, MA.
BACKSCAT lidar simulation version 3.0: Technical documentation and users guide [AD-A267296] p 1003 N94-17268
SPIRE CORP., BEDFORD, MA.
Ion doped quantum well lasers [AD-A267198] p 1038 N94-15853
SRI INTERNATIONAL CORP., MENLO PARK, CA.
Dissociation rates of diatomic molecules [AD-A266464] p 1182 N94-16586
Field-emitter arrays for RF vacuum microelectronics [AD-A268397] p 1015 N94-17526
Field emitter arrays for RF vacuum microelectronics [AD-A268595] p 1015 N94-17608
STANFORD LINEAR ACCELERATOR CENTER, CA.
Gamma large area silicon telescope: Applying Si strip detector technology to the detection of gamma rays in space p 904 N94-15061
Photoemission study of diamond (100) surface [DE93-015251] p 1208 N94-16062
Fundamental-mode RF design in e(+)e(-) storage ring factories [DE93-015249] p 1183 N94-16809
Application of cylindrical distribution functions to anisotropic scattering from amorphous films [DE93-015256] p 1183 N94-16811
Anisotropic phase separation in amorphous Fe-Ge alloys [DE93-015255] p 961 N94-17251
STANFORD UNIV., CA.
Tactile sensing and control in humans and robotic/teleoperated systems [AD-A267710] p 1163 N94-14937
The distribution of a sum of binomial random variables [AD-A266969] p 1172 N94-15002
Growth of new materials for solid state laser applications. The growth of ZnGeP2 by the vertical Bridgman method [NASA-CR-194571] p 1038 N94-15530
Logarithmic asymptotics for steady-state tail probabilities in a single-server queue [AD-A266746] p 1165 N94-15775
Particle simulation of hypersonic flow [AD-A267185] p 857 N94-15787
Fast simulation of steady-state availability in non-Markovian highly dependable systems [AD-A266747] p 1174 N94-15823
A sequential quadratic programming algorithm using an incomplete solution of the subproblem [DE93-017439] p 1149 N94-16120
Models for reactivity [AD-A266419] p 1149 N94-16554
Moments in statistics: Approximations to densities and goodness-of-fit [AD-A266600] p 1173 N94-16726
Asynchronous design for parallel processing architectures [AD-A266523] p 1160 N94-16791
Three-dimensional turbulent boundary layer [AD-A266261] p 1025 N94-16908

Active turbulence control in wall bounded flows using direct numerical simulation
| AD-A267261 | p 1028 N94-17286
Low voltage electron beam lithography
| AD-A267865 | p 1215 N94-17389
Mechanical properties and crystal growth studies of semiconductor alloys
| AD-A268144 | p 1216 N94-17454
Accurate analysis of array references
| AD-A268069 | p 1162 N94-17550
Advanced thin-film deposition and physical properties of high-temperature and other novel superconducting materials
| AD-A268199 | p 1216 N94-17561

STARSYS RESEARCH CORP., BOULDER, CO.
STARSYS: A view after WARC-92
p 893 N94-17168

STATE SEISMOLOGICAL BUREAU OF CHINA, BEIJING.
New progress of ranging technology at Wuhan Satellite Laser Ranging Station p 877 N94-15608

STATE SEISMOLOGICAL BUREAU OF CHINA, WUHAN.
Cooperative projects in geodynamical instrumentation between the State Seismological Bureau (China) and the Royal Observatory of Belgium p 1037 N94-15806

STATE UNIV. OF NEW YORK, ALBANY.
Detection and dosimetry of chemical contaminants in polymeric materials
| AD-A266605 | p 968 N94-16727
Calorimeter based detectors for high energy hadron colliders
| DE93-017055 | p 1188 N94-16900

STATE UNIV. OF NEW YORK, BUFFALO.
Large eddy simulation and direct numerical simulation of high speed turbulent reacting flows
| NASA-CR-193131 | p 1018 N94-15427

STERLING SOFTWARE, INC., PALO ALTO, CA.
Software Engineering Guidebook
| NASA-CR-177625 | p 1150 N94-16656

STOCKHOLM UNIV. (SWEDEN).
A two-layer quasi-geotrophic spherical model: Formulation and climatology
| DM-63 | p 1110 N94-17593

STUTTGART UNIV. (GERMANY).
High power steady state MPD thrusters
| AD-A267277 | p 928 N94-17308

SUNDSTRAND CORP., ROCKFORD, IL.
Advanced cooling for high power electric actuators
| AD-A266984 | p 866 N94-15761

SUPERCONDUCTING SUPER COLLIDER LAB., DALLAS, TX.
The 3D-Flow processor for a programmable level-1 trigger (feasibility study)
| DE93-016045 | p 1159 N94-16172
Statistics of the half-integer stopband
| DE93-016101 | p 1173 N94-17236

SUPERIOR VACUUM TECHNOLOGY, EDEN PRAIRIE, NM.
Precise flux control for lattice matched superlattice materials
| AD-A268254 | p 1215 N94-17417

SURREY SATELLITE TECHNOLOGY LTD., GUILDFORD (ENGLAND).
UoSAT: A decade of experience pioneering microsatellites p 894 N94-17169

SURREY UNIV., GUILDFORD (ENGLAND).
UoSAT: A decade of experience pioneering microsatellites p 894 N94-17169

SURVEILLANCE RESEARCH LAB., SALISBURY (AUSTRALIA).
Sensor modelling for the Cyclops focal plane detector array based technology demonstrator
| AD-A267172 | p 1190 N94-15846
Notes on the use of Dempster-Shafer and fuzzy reasoning to fuse identity attribute data
| AD-A267426 | p 1004 N94-17309

SVERDRUP TECHNOLOGY, INC., BROOK PARK, OH.
Rotary engine performance computer program (RCEMAP and RCEMAPPC): User's guide
| NASA-CR-191192 | p 869 N94-15192
Hollow cathode heater development for the Space Station plasma contactor
| NASA-CR-191131 | p 926 N94-16880
Thin-layer and full Navier-Stokes calculations for turbulent supersonic flow over a cone at an angle of attack
| NASA-CR-189103 | p 861 N94-17558

SWEDISH INST. OF SPACE PHYSICS, KIRUNA.
Requirements on CCD-detectors for ground-based auroral imaging p 909 N94-15093

SWEDISH SPACE CORP., SOLNA.
MAXUS: The new sounding rocket program for long duration microgravity flight p 978 N94-16079

T

TECHNICAL RESEARCH CENTRE OF FINLAND, ESPOO.
Studies on the parametric decay of waves in fusion plasmas
| VTT-PUBS-110 | p 1200 N94-15204
High frequency Raman current drive
p 1201 N94-15208
Current drive with free electron lasers in high and low temperature tokamaks p 1201 N94-15209
On the decay of a dipole pump wave to half-harmonics p 1201 N94-15211
Automated image analysis method for the detection of cracks on wood surface
| VTT-JULK-755 | p 1056 N94-17542
Dry stripping as a surface treatment method
| VTT-TIED-1348 | p 985 N94-17544
Smart Power: New power integrated circuit technologies and their applications
| VTT-TIED-1358 | p 1015 N94-17546
Heating of lubricant with an electric resistance heater
| VTT-TIED-1359 | p 974 N94-17547

TECHNION - ISRAEL INST. OF TECH., HAIFA.
On-board spatial scientific experiment project on small satellites p 896 N94-17184

TECHNISCHE HOCHSCHULE, AACHEN (GERMANY).
Ultrasound absorption in molten salts
p 944 N94-15161
Production Technology for Components from Nonmetallic Fiber Reinforced Materials
| ETN-93-94607 | p 931 N94-15254
Construction, testing, and representation of resin and fiber reinforced materials p 931 N94-15255
Construction and calculation p 931 N94-15256
Production process p 931 N94-15257
Machine development p 932 N94-15258
Component testing and quality assurance
p 932 N94-15259
Development of a computer supported instrumentation for economic planning and evaluation of production facilities for fiber reinforced composites elements
p 932 N94-15260

TECHNISCHE HOGESCHOOL, DELFT (NETHERLANDS).
Transputer based control system for MTLRS
p 877 N94-15613

TECHNISCHE PHYSISCHE DIENST TNO-TH, DELFT (NETHERLANDS).
Assessment of TDI operation of a frame transfer CCD for high resolution imaging from a fast spinning spacecraft p 910 N94-15097

TECHNISCHE UNIV., BERLIN (GERMANY).
Optical coupling elements for coherent optical multiport receivers
| ETN-93-94398 | p 1188 N94-15447
Circuits and control processes for combining direct converters and inverter motors
| ETN-93-94399 | p 1008 N94-15448
Systematology for elastic-plastic material equations by large deformations on the basis of the Cosserat-continuum model
| SCHRIFTENR-PHYSIKAL-ING-BD |
p 1058 N94-15642
TUBSAT: Low cost access to space technology
p 895 N94-17180

TECHNISCHE UNIV., DARMSTADT (GERMANY).
A Moessbauer spectrometer for the mineralogical analysis of the Mars surface: First temperature dependent tests of the detector and drive system
p 1259 N94-16233

TECHNISCHE UNIV., DELFT (NETHERLANDS).
Predicted and real development in the aviation in the period 1961-1991 p 853 N94-15122
Expectations for the future of the Faculty of Aeronautics and Astronautics of the Technical University of Delft
p 854 N94-15131
Comparison of level-1 and level-2 buckling and postbuckling solutions
| NASA-CR-194611 | p 1057 N94-15154

TECHNISCHE UNIV., GRAZ (AUSTRIA).
Work at Graz on satellite signatures
p 898 N94-15558
Sub-cm ranging and other improvements in Graz
p 919 N94-15603

TECHNISCHE UNIV., MUNICH (GERMANY).
Benard convection of magnetic colloids under microgravity p 943 N94-15159
Pool boiling: Single bubble experiment
p 944 N94-15160

TECHNOLOGY INTERNATIONAL CORP., BEDFORD, MA.
Optical measurements of NASA/USAF CRRES high altitude rocket borne chemical release experiments in conjunction with the USAF airborne ionospheric observatory aircraft
| AD-A266404 | p 1101 N94-16551

TEL-AVIV UNIV. (ISRAEL).
The quantum mass shift of the soliton in Skyrme model
| ITN-93-85219 | p 1180 N94-15283
Effects of spin-orbit coupling on disordered mesoscopic systems
| ITN-93-85220 | p 1180 N94-15288

TELEDYNE BROWN ENGINEERING, COLORADO SPRINGS, CO.
History of on-orbit satellite fragmentations
| NASA-CR-191644 | p 887 N94-16502
The fragmentation of Kosmos 2163
| NASA-CR-191643 | p 887 N94-16503
The fragmentation of the Nimbus 6 rocket body
| NASA-CR-191645 | p 926 N94-16504

TELEDYNE BROWN ENGINEERING, HUNTSVILLE, AL.
Ultraviolet spectrometer and polarimeter (UVSP) catalog of observations. Volume 1: Experiments 1-30719, February 1980 - April 1985
| NASA-CR-4529-VOL-1 | p 1298 N94-15023
Ultraviolet spectrometer and polarimeter (UVSP) catalog of observations. Volume 2: Experiments 30720-63057, April 1985 - February 1988
| NASA-CR-4529-VOL-2 | p 1298 N94-15024
Scalar limitations of diffractive optical elements
p 1194 N94-17336
Finite difference time domain analysis of chirped dielectric gratings p 1195 N94-17339
Asymmetric three-beam binary optic grating
p 1195 N94-17340

TELEOS RESEARCH, PALO ALTO, CA.
ARPA unmanned ground vehicle stereo vision program at Teleos Research
| AD-A267632 | p 1167 N94-17202

TELESPAZIO S.P.A., ROME (ITALY).
Small satellite constellation system: Optimization criteria p 888 N94-17132
Small satellite constellation deployment strategies
p 878 N94-17138
Small satellite missions to long-period comets
p 874 N94-17144

TENNESSEE UNIV., KNOXVILLE.
Microwave interaction with plasmas
| AD-A267048 | p 1201 N94-15661
Pyroxene equilibration temperatures in metamorphosed ordinary chondrites p 1242 N94-16224
Searching for neuKREEP: An EMP study of Apollo 11 Group A basalts p 1266 N94-16275
On the composition of neuKREEP: OMD contamination at Apollo 11? p 1266 N94-16276
Basic studies of the liquid state of matter: Electrical properties and laser interactions
| AD-A268311 | p 1042 N94-17567

TENNESSEE UNIV. SPACE INST., TULLAHOMA.
Technology transfer. Determining industry needs: A guide for communities
| NASA-CR-194676 | p 1235 N94-17293

TEXAS A&M UNIV., COLLEGE STATION.
Nonequilibrium radiation and chemistry models for aerocapture vehicle flowfields
| NASA-CR-194645 | p 1027 N94-17095
Micromechanics modeling and analysis of Haversian compact bone tissues as a fiber reinforced composite material
| AD-A268250 | p 1129 N94-17456
Melatonin, the pineal gland, and circadian rhythms
| AD-A268200 | p 1129 N94-17478
The Central American cold surge: An observational analysis of the deep southward penetration of North American cold fronts
| AD-A268592 | p 1110 N94-17607

TEXAS TECHNOLOGICAL UNIV., LUBBOCK.
Martian carbon dioxide: Clues from isotopes in SNC meteorites p 1270 N94-16295

TEXAS UNIV., ARLINGTON.
Stochastic damage evolution in textile laminates
p 939 N94-16861

TEXAS UNIV., AUSTIN.
Unsteady phenomena in shock wave/boundary layer interaction p 1017 N94-15200
Applications of SLR p 911 N94-15556
Nonlinear acoustics: Periodic waveguide, scattering of sound by sound, three-layer fluid, finite amplitude sound in a medium having a distribution of relaxation processes, and production of an isolated negative pulse in water
| AD-A267145 | p 1177 N94-15732
Satellite sound broadcast propagation measurements
p 996 N94-16047

Adaptive algorithm for aircraft configuration in turbulent flow
[AD-A266188] p 867 N94-16122
Pulse response based control for minimum time maneuver of flexible spacecraft
[AD-A266186] p 886 N94-16455
The (delta)f algorithm for beam dynamics
[DE93-015632] p 1187 N94-16660
Laser ranging data analysis
[NASA-CR-193547] p 1041 N94-16719
JSEP fellowship
[AD-A266568] p 1211 N94-16800
Femtosecond growth dynamics of an underdense ionization front measured by spectral blueshifting
[DE93-013582] p 1183 N94-16818
Linear stability of stationary solutions of the Vlasov-Poisson system in three dimensions
[DE93-013873] p 1174 N94-16820
Structure and damping of toroidal drift waves (and their implications for anomalous transport)
[DE93-014005] p 1203 N94-16822
Vectorial electron transfer in spatially ordered arrays
[DE93-018150] p 1185 N94-16971
Damage evolution in filled elastomers
[AD-A268067] p 1062 N94-17507

TEXAS UNIV., SAN ANTONIO.
Effect of Impact Damage and Open Hole on Compressive Strength of Hybrid Composite Laminates
[NASA-CR-194603] p 936 N94-16836

TEXAS UNIV. AT DALLAS, RICHARDSON.
Spectral inverse scattering theory for dielectric media: Application to optical devices
[AD-A268635] p 1199 N94-17427

TEXTILE RESEARCH INST., PRINCETON, NJ.
Characterization of voids formed during liquid impregnation of nonwoven multifilament glass networks as related to composite processing p 939 N94-16858

THARSYS (FRANCE).
TITUS: A micro-satellite for technology demonstration p 896 N94-17186

THIOKOL CORP., BRIGHAM CITY, UT.
RSRM nozzle actuator bracket/lug fracture mechanics qualification test
[NASA-CR-193859] p 927 N94-17080
Flight 20 (STS-45) polysulfide gas path investigation
[NASA-CR-193861] p 928 N94-17213
Postflight hardware evaluation 360T026 (RSRM-26, STS-47)
[NASA-CR-192559] p 882 N94-17656

THOMSON AND NIELSEN ELECTRONICS, OTTAWA (ONTARIO).
Real time radiation measurements in space p 980 N94-16092

TOKYO UNIV. (JAPAN).
Study of the rare decays K(sub L)(sup 0) yields (mu)e, K(sub L)(sup 0) yields ee, and K(sub L)(sup 0) yields (mu)(mu) at KEK
[DE93-753247] p 1180 N94-15135
Chemical and isotopic compositions in acid residues from various meteorites p 1243 N94-16291
Was Martian mantle wet? A possible consequence of rapid core formation p 1277 N94-16335
Size distribution of interplanetary iron and stony particles related with deep-sea spherules p 1245 N94-16388
Exsolved kirschsteinite in angrite LEW86010 olivine p 1245 N94-16410
The thickness of eucritic crust in the HED parent body p 1104 N94-16416
Application of split window technique to TIMS data p 1064 N94-16601

TORONTO UNIV. (ONTARIO).
Investigation of two-phase flow and boiling heat transfer during quenching of a tube under microgravity p 979 N94-16087

TOTAL ARMY PERSONNEL AGENCY (PROVISIONAL), ALEXANDRIA, VA.
A comparison of solar wind parameters measured by IMP 8, Voyager 1 and Voyager 2
[AD-A266728] p 1298 N94-15821

TOULOUSE UNIV. (FRANCE).
Electrophoresis visualisation p 944 N94-15163

TRIESTE UNIV. (ITALY).
Electronic and atomic structure of semiconductors and of high-temperature superconductors
[AD-A266805] p 1205 N94-14913

TRW, INC., REDONDO BEACH, CA.
Sputtered ferroelectric thin films of KTN for electro-optic devices
[AD-A266573] p 968 N94-16723

TSUKUBA UNIV. (JAPAN).
Water in Earth's mantle: Hydrogen analysis of mantle olivine, pyroxenes and garnet using the SIMS p 1104 N94-16336

TUEBINGEN UNIV. (GERMANY).
Substrate effects in superconducting tunnel junction detectors p 908 N94-15083

U

ULSTER COLL., NEWTOWNABBEY (NORTH IRELAND).
Weaving multi-layer fabrics for reinforcement of engineering components p 937 N94-16850

UNIAX CORP., SANTA BARBARA, CA.
Soluble precursor route to polyanilines
[AD-A268015] p 973 N94-17494

UNITED TECHNOLOGIES RESEARCH CENTER, EAST HARTFORD, CT.
A proposed mechanism for the pyrolysis of diborane
[DE93-014275] p 947 N94-15977
Vanadium corrosion studies
[AD-A266489] p 959 N94-16781
Mechanistic models of soot formation
[AD-A267806] p 950 N94-17008
Cathode sheath charge transfer effects
[AD-A268393] p 1186 N94-17536

UNIVERSAL ANALYTICS, INC., TORRANCE, CA.
ASTROS enhancements. Volume 1: ASTRO user's manual
[AD-A266818] p 1151 N94-16768
ASTROS enhancements. Volume 2: ASTRO programmer's manual
[AD-A266819] p 1151 N94-16769

UNIVERSAL TECHNOLOGY CORP., DAYTON, OH.
Stress analysis of laminated composites with preformed holes. Part 1: Single plies with embedded material discontinuities
[AD-A266524] p 936 N94-16795

UNIVERSIDAD POLITECNICA DE BARCELONA (SPAIN).
Schottky barrier focal plane arrays for SWIR and MWIR p 903 N94-15050

UNIVERSITY COLL., LONDON (ENGLAND).
The MIC photon counting detector p 901 N94-15039

UNIVERSITY COLL. OF SWANSEA (WALES).
Exploring the remote sensing of foliar biochemical concentrations with AVIRIS data p 1069 N94-16683

UNIVERSITY OF NORTHERN ILLINOIS, DE KALB.
New organic materials for nonlinear optics applications
[AD-A266451] p 1192 N94-16563

UNIVERSITY OF SOUTH FLORIDA, SAINT PETERSBURG.
AVIRIS calibration and application in coastal oceanic environments p 1069 N94-16685

UNIVERSITY OF SOUTH FLORIDA, TAMPA.
Efficient computational methods to study new and innovative signal detection techniques in SETI
[NASA-CR-193602] p 998 N94-16649

UNIVERSITY OF SOUTHERN CALIFORNIA, LOS ANGELES.
Search for chaos in free shear flows
[AD-A266245] p 1023 N94-16470
Modeling, estimation and control of distributed parameter systems
[AD-A267325] p 1026 N94-17003
To extend the thirteen-moment theory and its application to problems in rarefied hypersonic flow
[AD-A267384] p 859 N94-17021
A numerical investigation of energy transfer and subgrid-scale eddy-viscosity in homogeneous, isotropic, and shear turbulence
[AD-A267265] p 1029 N94-17363

UNIVERSITY OF SOUTHERN CALIFORNIA, MARINA DEL REY.
SIMS: Single Interface to Multiple Systems
[AD-A266934] p 1143 N94-15175
A proposed research program in strategic computing
[AD-A267516] p 1153 N94-17078

UNIVERSITY OF SOUTHERN MISSISSIPPI, BAY SAINT LOUIS.
SAR observations in the Gulf of Mexico p 1077 N94-16742

UNIVERSITY OF SOUTHERN MISSISSIPPI, HATTIESBURG.
Photodegradation of polyimides. V1: Effect of donor-acceptor groups on the photooxidative stability of polyimides and model compounds
[AD-A267319] p 970 N94-16947
The photochemistry of poly(methylphenylphosphazene)
[AD-A267320] p 970 N94-16948
The photophysics of poly(methylphenylphosphazene)
[AD-A267321] p 970 N94-16949
Photodegradation of MDI based polyurethane/urea elastomers
[AD-A267308] p 971 N94-16994
Responsive copolymers for enhanced petroleum recovery
[DE93-018030] p 971 N94-16999

UNIVERSITY OF SOUTHWESTERN LOUISIANA, LAFAYETTE.
The design of self-checking reduced instruction set computers
[AD-A267012] p 1140 N94-15763

UNIVERSITY OF WESTERN ONTARIO, LONDON.
Merged beam studies of laser stimulated radiative recombination
[AD-A267186] p 1037 N94-15145

UNIVERSITY OF WESTERN WASHINGTON, BELLINGHAM.
Development of pattern recognition techniques for the evaluation of toxicant impacts to multispecies systems
[AD-A267197] p 1095 N94-15790

UTAH STATE UNIV., LOGAN.
Synthesis, characterization, and polymerization of new ferrocene-fluorene complexes. A novel high-molecular weight conjugated polymer with pendant ferrocene groups
[AD-A267717] p 972 N94-17273

UTAH UNIV., SALT LAKE CITY.
Pulsed laser kinetic studies of liquids under high pressure
[DE93-017826] p 1041 N94-16998
Currents induced in the human body for exposure to ultrawideband electromagnetic pulses
[AD-A268570] p 1130 N94-17621

V

VANDERBILT UNIV., NASHVILLE, TN.
Complex information coordination performance: Differential changes in working memory contributions following training
[AD-A267007] p 1132 N94-15762
Analytical and experimental investigation of the feasibility of accelerated lifetime testing of materials exposed to an atomic oxygen beam
[NASA-CR-193851] p 946 N94-15766
Homogeneously traceable results in claw-free graphs
[AD-A266196] p 1169 N94-16127

VARIAN ASSOCIATES, PALO ALTO, CA.
High temperature superconductivity
[AD-A267006] p 1008 N94-15635

VEGA SPACE SYSTEMS ENGINEERING LTD., HARPENDEN (ENGLAND).
A proposed ground segment design for small satellites p 878 N94-17154

VEXCEL CORP., BOULDER, CO.
Synthetic aperture radar signal processing: Trends and technologies p 992 N94-15908
International collaboration in SAR ground data systems p 993 N94-15917

VIRGINIA POLYTECHNIC INST. AND STATE UNIV., BLACKSBURG.
Verification of a two-dimensional infiltration model for the resin transfer molding process
[NASA-CR-194597] p 964 N94-15656
Olympus propagation measurement results at Virginia Tech p 995 N94-16037
Data acquisition, preprocessing and analysis for the Virginia Tech OLYMPUS experiment p 995 N94-16038
Aerodynamic/dynamic/control interaction
[AD-A266187] p 871 N94-16107
Textile composite processing science p 938 N94-16856

VIRGINIA UNIV., CHARLOTTESVILLE.
Inelastic deformation of metal matrix composites
[NASA-CR-191522] p 930 N94-15106
Integrated fundamental research on current collection
[AD-A266987] p 1008 N94-15494
Collisional dynamics of perturbed particle disks in the solar system
[NASA-CR-193584] p 1239 N94-16648
Environment enhanced fatigue crack propagation in metals: Inputs to fracture mechanics life prediction models
[NASA-CR-191538] p 942 N94-17638

VISCOUSTECH, ALLISON PARK, PA.
Stability of flows in fluidized beds
[DE93-000245] p 1024 N94-16763

VON KARMAN INST. FOR FLUID DYNAMICS, RHODE-SAINT-GENESE (BELGIUM).
Swept shock wave/laminar boundary layer interactions, experimental, and numerical results p 1017 N94-15198

W

WALTER REED ARMY INST. OF RESEARCH, WASHINGTON, DC.
The behavioral toxicology of high-peak, low average power, pulsed microwave irradiation
[AD-A268392] p 1134 N94-17535
WASHINGTON UNIV., SAINT LOUIS, MO.
Physical interpretation and development of ultrasonic nondestructive evaluation techniques applied to the quantitative characterization of textile composite materials
[NASA-CR-194549] p 931 N94-15190
The planetary data system educational CD-ROM p 1234 N94-16209
Assimilation of solids during ascent of magmas from the Bartoy Field of the Baikal Region, Siberia p 1103 N94-16214
A first-order model for impact crater degradation on Venus p 1265 N94-16268
A Monazite-bearing clast in Apollo 17 melt breccia p 1267 N94-16279
Apollo 17 materials viewed from 2 to 4 mm soil particles: Pre-serenitatis highlands components p 1267 N94-16280
An iridium-rich iron micrometeorite with silicate inclusions from the Moon p 1242 N94-16281
I-Xe structure of ILAFEGH 009 and shallowater: Evidence for early formation and rapid cooling of impact-derived enstatite meteorites p 1243 N94-16305
Composition of Apollo 17 core 76001 p 1275 N94-16326
Composition and maturity of the 60013/14 core p 1275 N94-16327
Solution of elastic-plastic stress analysis problems by the p-version of the finite element method
[NASA-CR-194267] p 1062 N94-17445
WASHINGTON UNIV., SEATTLE.
Study of protein-H2O interactions by multidimensional NMR spectroscopy
[AD-A266955] p 946 N94-15760
Modeling the reflectance of CO2 frost with new optical constants: Application to Martian south polar cap spectra p 1256 N94-16217
The size of complex craters p 1262 N94-16249
Densities of 5-15 micron interplanetary dust particles p 1244 N94-16367
Middle atmospheric electric fields over thunderstorms
[NASA-CR-194619] p 1106 N94-16493
A field measure of the shade fraction p 1068 N94-16677
Mapping the spectral variability in photosynthetic and non-photosynthetic vegetation, soils, and shade using AVIRIS p 1068 N94-16679
Using endmembers in AVIRIS images to estimate changes in vegetative biomass p 1070 N94-16689
Temporal variation in spectral detection thresholds of substrate and vegetation in AVIRIS images p 1073 N94-16706
Convergence of the multiple scattering expansion in XAFS and XANES
[DE93-011001] p 948 N94-16772
J-integral and HRR field associated with stable crack growth in thin aluminum SEN specimen
[AD-A267879] p 960 N94-17041
WAYNE STATE UNIV., DETROIT, MI.
Investigations of YBaCuO materials with near-room-temperature resistivity transitions
[AD-A268016] p 1216 N94-17477
WELLESLEY COLL., MA.
The chromosphere of VV cephei and the distribution of circumstellar dust around red giants and supergiants
[NASA-CR-193594] p 1297 N94-16866
WEST VIRGINIA UNIV., MORGANTOWN.
Effect of tow alignment on the mechanical performance of 3D woven textile composites p 937 N94-16851
WESTINGHOUSE ELECTRIC CORP., BALTIMORE, MD.
SONOS technology for commercial and military nonvolatile memory applications
[DE93-015647] p 1011 N94-16661
WESTINGHOUSE SAVANNAH RIVER CO., AIKEN, SC.
GAM-HEAT: A computer code to compute heat transfer in complex enclosures
[DE93-014724] p 1023 N94-15980
Composite refraction-reflection stack sections: Tracing faults in the Atlantic coastal plain sediments
[DE93-013581] p 1112 N94-16009
WESTON OBSERVATORY, MA.
Broadband teleseismic array recording in the Adirondack Mountains, New York State
[AD-A267290] p 1097 N94-14980
WICHITA STATE UNIV., KS.
Supersonic flow visualization of a nacelle in close proximity to a simulated wing
[NASA-CR-194675] p 860 N94-17260
Maximizing participation of women in collegiate aviation education
[NIAR-93-14] p 1222 N94-17261
The airline quality report 1993
[NIAR-93-11] p 863 N94-17262
Design of non-sled setup to measure head injury criteria
[NIAR-92-20] p 872 N94-17263
Characterization of metallic multilayers using x ray diffraction analysis
[NIAR-93-13] p 961 N94-17282
Computer modeling and animation of mechanical systems
[NIAR-93-3] p 1153 N94-17299
WIEN UNIV. (AUSTRIA).
Osmium isotopes in Ivory Coast tektites: Confirmation of a meteoritic component and rhenium depletion p 1244 N94-16321
Manson impact structure, Iowa: First geochemical results for drill core M-1 p 1103 N94-16322
WILSON GREATBATCH LTD., CLARENCE, NY.
Lithium D-cell study
[NASA-CR-192705] p 1011 N94-16505
WISCONSIN UNIV., MADISON.
A high flux radical beam diamond growth
[AD-A266754] p 1207 N94-15955
Isolation of thermostable enzyme mutants by cloning and selection in thermophilic bacteria
[AD-A266378] p 1117 N94-16514
Investigation of cloud properties and atmospheric stability with MODIS
[NASA-CR-193475] p 1107 N94-16717
Reducing data dimension to lower signal processing computational requirements and maximize performance
[AD-A266606] p 999 N94-16728
Methods of tunneling spectroscopy with the STM
[AD-A266507] p 948 N94-16787
Processes involved in the integration of pictures and discourse
[AD-A268150] p 1134 N94-17468
A basic principles description of liquid vapor phase transitions
[AD-A268331] p 1176 N94-17581
Granular fluctuations in plasma turbulence and their role in transport
[DE93-013465] p 1187 N94-17674
WISE OBSERVATORY, TEL AVIV (ISRAEL).
The TAUVEX experiment p 905 N94-15064
WOODS HOLE OCEANOGRAPHIC INST., MA.
Abstracts of manuscripts submitted in 1992 for publication
[AD-A267963] p 1113 N94-17383
Real time system for practical acoustic monitoring of global ocean temperature
[AD-A267868] p 1113 N94-17391
Meridional circulation in the tropical north atlantic
[AD-A268222] p 1114 N94-17555
WORCESTER POLYTECHNIC INST., MA.
Engineering design of sub-micron topographies for simultaneously adherent and reflective metal-polymer interfaces
[NASA-CR-194573] p 964 N94-15700
WRIGHT LAB., EGLIN AFB, FL.
An electronic imaging system for the Aeroballistic Research Facility
[AD-A267157] p 1033 N94-15826
WRIGHT LAB., WRIGHT-PATTERSON AFB, OH.
Supersonic Combustion Research Laboratory. Volume 1: Design and fabrication
[AD-A267667] p 943 N94-14962
Design of round-to-square transition section; analysis and computer code
[AD-A267173] p 872 N94-15847
Detailed example of using ACEC release 3.0 with the DEC VAX Ada compiler
[AD-A267880] p 1152 N94-17014
Display of dynamic, volume graphic images by holographic voxel projection: Initial investigation
[AD-A267622] p 1035 N94-17197
An experimental study of fluctuating wall pressures in a highly swept, sharp fin-induced, Mach 5 shock wave/turbulent boundary layer interaction
[AD-A268394] p 861 N94-17461
Laser velocimetry measurements of vortex flows on a delta wing at Mach 1.9
[AD-A268596] p 861 N94-17609
WRIGHT STATE UNIV., DAYTON, OH.
Iron oxide bands in the visible and near-infrared reflectance spectra of primitive asteroids p 1242 N94-16274
Evaluation of putative neurochemical intermediaries in space/motion sickness
[NASA-CR-193607] p 1118 N94-17090

X

XEROX CORP., WEBSTER, NY.
Total quality environmental management leadership through quality
[TABES PAPER 93-540] p 1050 N94-16135

Y

YALE UNIV., NEW HAVEN, CT.
Development and analysis of ARMA parameter estimation schemes in the presence of noise
[AD-A267184] p 989 N94-15786
Studies in turbulence and turbulence control
[AD-A266318] p 1026 N94-16950
Structure of high Reynolds number turbulent boundary layer
[AD-A267476] p 860 N94-17099
Fast algorithms for polynomial interpolation, integration and differentiation
[AD-A267505] p 1154 N94-17370
Fast Fourier Transforms for nonequispaced data 2
[AD-A268383] p 1171 N94-17420
YAMAGUCHI UNIV. (JAPAN).
Identification of new meteorite, Mihonoseki (L), from broken fragments in Japan p 1246 N94-16415
YORK UNIV. (ONTARIO).
Characteristics of aimed arm movements in humans under low gravity p 980 N94-16093
YORK UNIV., TORONTO (ONTARIO).
Laser-liquid interactions under reduced gravity conditions p 977 N94-16077

Typical Contract Number Index Listing

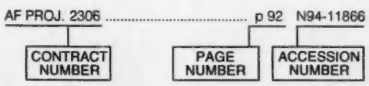

Listings in this index are arranged alphanumerically by contract number. Under each contract number the accession numbers denoting documents that have been produced as a result of research done under that contract are arranged in ascending order. The page number helps to locate the citation in the abstract section. The accession number denotes the number by which the citation is identified.

AERO-0027-C ..... p 1017 N94-15198
AF PROJ. 1105 ..... p 985 N94-17482
p 985 N94-17484
p 985 N94-17485
AF PROJ. 1123 ..... p 872 N94-17403
AF PROJ. 2308 ..... p 943 N94-14962
p 872 N94-15847
AF PROJ. 2404 ..... p 861 N94-17461
p 861 N94-17609
AF PROJ. 4600 ..... p 1005 N94-17431
AF PROJ. 7755 ..... p 1132 N94-16942
AF PROJ. 9993 ..... p 1174 N94-17219
AF-AFOSR-0004-91 ..... p 1059 N94-16123
AF-AFOSR-0015-90 ..... p 929 N94-15734
AF-AFOSR-0022-91 ..... p 867 N94-16122
AF-AFOSR-0032-90 ..... p 871 N94-16107
AF-AFOSR-0041-91 ..... p 1173 N94-16937
AF-AFOSR-0053-90 ..... p 1165 N94-15778
AF-AFOSR-0057-90 ..... p 1149 N94-16554
AF-AFOSR-0060-90 ..... p 1192 N94-16563
AF-AFOSR-0063-90 ..... p 1299 N94-15836
AF-AFOSR-0071-90 ..... p 1191 N94-16454
AF-AFOSR-0077-90 ..... p 1193 N94-17024
AF-AFOSR-0091-90 ..... p 1026 N94-17003
AF-AFOSR-0101-91 ..... p 861 N94-17574
AF-AFOSR-0102-90 ..... p 1299 N94-17004
AF-AFOSR-0104-91 ..... p 859 N94-17021
AF-AFOSR-0107-90 ..... p 1172 N94-15777
AF-AFOSR-0110-91 ..... p 1132 N94-16456
AF-AFOSR-0117-91 ..... p 1024 N94-16555
AF-AFOSR-0119-90 ..... p 1186 N94-17436
AF-AFOSR-0120-90 ..... p 860 N94-17099
AF-AFOSR-0121-90 ..... p 925 N94-16482
AF-AFOSR-0123-90 ..... p 1014 N94-17428
AF-AFOSR-0124-90 ..... p 1016 N94-15151
AF-AFOSR-0139-90 ..... p 1029 N94-17414
AF-AFOSR-0139-91 ..... p 1026 N94-16950
AF-AFOSR-0140-90 ..... p 1189 N94-15735
AF-AFOSR-0160-90 ..... p 1199 N94-17455
AF-AFOSR-0162-91 ..... p 1204 N94-17575
AF-AFOSR-0164-90 ..... p 989 N94-15786
AF-AFOSR-0166-90 ..... p 1215 N94-17422
AF-AFOSR-0167-90 ..... p 961 N94-17223
AF-AFOSR-0169-91 ..... p 1131 N94-15694
AF-AFOSR-0171-91 ..... p 1178 N94-16991
AF-AFOSR-0174-91 ..... p 1025 N94-16908
AF-AFOSR-0176-88 ..... p 855 N94-14963
AF-AFOSR-0185-90 ..... p 1038 N94-15852
AF-AFOSR-0187-89 ..... p 1118 N94-17224
AF-AFOSR-0193-90 ..... p 1169 N94-15779
AF-AFOSR-0221-91 ..... p 941 N94-17457
AF-AFOSR-0227-90 ..... p 934 N94-16440
AF-AFOSR-0232-90 ..... p 857 N94-15787
AF-AFOSR-0253-89 ..... p 1012 N94-17023
AF-AFOSR-0272-88 ..... p 855 N94-14959
AF-AFOSR-0291-91 ..... p 1095 N94-15790
AF-AFOSR-0297-90 ..... p 886 N94-16455
AF-AFOSR-0299-90 ..... p 1023 N94-16470
AF-AFOSR-0300-89 ..... p 971 N94-16980
AF-AFOSR-0300-90 ..... p 1029 N94-17363
AF-AFOSR-0302-90 ..... p 1012 N94-16935
AF-AFOSR-0304-89 ..... p 1133 N94-17397
AF-AFOSR-0304-90 ..... p 861 N94-17580
AF-AFOSR-0313-91 ..... p 1190 N94-15848
AF-AFOSR-0319-91 ..... p 1216 N94-17477
AF-AFOSR-0332-91 ..... p 1132 N94-16925
AF-AFOSR-0337-90 ..... p 1213 N94-17037
AF-AFOSR-0340-87 ..... p 897 N94-17266
AF-AFOSR-0377-89 ..... p 1134 N94-17513
AF-AFOSR-0395-89 ..... p 1026 N94-16966
AF-AFOSR-0403-91 ..... p 1140 N94-17005
AF-AFOSR-0408-89 ..... p 950 N94-16931
AF-AFOSR-0411-89 ..... p 1028 N94-17286
AF-AFOSR-0414-89 ..... p 1133 N94-17265
AF-AFOSR-0415-91 ..... p 925 N94-15837
AF-AFOSR-0420-89 ..... p 1026 N94-16929
AF-AFOSR-0422-89 ..... p 1159 N94-15849
AF-AFOSR-0450-89 ..... p 1004 N94-17364
AF-AFOSR-0455-89 ..... p 1170 N94-16940
AF-AFOSR-0489-89 ..... p 967 N94-16472
AF-AFOSR-0535-89 ..... p 928 N94-17308
AF-AFOSR-0537-89 ..... p 1216 N94-17454
AF-AFOSR-0552-89 ..... p 1193 N94-17264
ARPA ORDER 6873 ..... p 1188 N94-15144
ARPA ORDER 7330 ..... p 1140 N94-15744
p 1160 N94-16724
p 1153 N94-17118
ARPA ORDER 7597 ..... p 1231 N94-16570
p 1166 N94-16725
p 1141 N94-17115
p 1166 N94-17201
ARPA ORDER 8162 ..... p 1015 N94-17526
p 1015 N94-17608
BMFT-0328823A ..... p 952 N94-17594
BMFT-50-OX-90020/XMM-EPIC ..... p 900 N94-15034
BMFT-511/DARA-01-RS-89376 ..... p 909 N94-15092
CS-86-90 ..... p 1076 N94-16736
DA PROJ. BR0-5202 ..... p 999 N94-16788
p 999 N94-16789
DA PROJ. MR0-4101 ..... p 1119 N94-14916
DA PROJ. MR0-4120 ..... p 1115 N94-14918
DA PROJ. NWE-DQAX ..... p 1123 N94-16515
DA PROJ. SO2-53 ..... p 1006 N94-17565
DA PROJ. S40-030 ..... p 1214 N94-17216
DA PROJ. 1L1-61102-AH-43 ..... p 942 N94-14946
p 946 N94-15685
p 1156 N94-17530
DA PROJ. 1L1-62211-A-47-A ..... p 1049 N94-17583
DA PROJ. 1L1-62618-AH-80 ..... p 865 N94-14951
p 976 N94-17538
DA PROJ. 1L1-72605-AH-94 ..... p 1216 N94-17480
DA PROJ. 3M1-62787-A-878 ..... p 862 N94-15637
DA PROJ. 3M1-62787-A-879 ..... p 1119 N94-14952
p 1131 N94-15659
DA PROJ. 302-63002-D-995 ..... p 1122 N94-15759
DA PROJ. 4A1-62720-A-896 ..... p 1178 N94-17119
DA PROJ. 4A1-62784-AT-41 ..... p 1157 N94-17620
DA PROJ. 4A7-62784-AT-42 ..... p 1045 N94-14920
DAAA21-89-C-0027 ..... p 1008 N94-15494
DAAB07-91-C-K254 ..... p 1197 N94-17354
DAAE07-90-C-R059 ..... p 863 N94-14971
p 864 N94-14972
p 864 N94-15498
DAAH01-93-C-R031 ..... p 1206 N94-15107
DAAL03-86-G-0084 ..... p 1173 N94-16657
DAAL03-88-C-0002 ..... p 857 N94-15824
DAAL03-88-K-0194 ..... p 965 N94-15773
DAAL03-88-K-0198 ..... p 968 N94-16727
DAAL03-89-G-0110 ..... p 1210 N94-16720
DAAL03-89-K-0098 ..... p 1181 N94-15774
DAAL03-89-K-0118 ..... p 1206 N94-15747
DAAL03-89-K-0141 ..... p 999 N94-16728
DAAL03-89-K-0179 ..... p 1021 N94-15770
DAAL03-89-K-0181 ..... p 968 N94-16796
DAAL03-90-G-0033 ..... p 1082 N94-15842
DAAL03-90-G-0040 ..... p 1206 N94-15822
DAAL03-90-G-0048 ..... p 942 N94-14909
DAAL03-90-G-0062 ..... p 964 N94-15729
DAAL03-90-G-0079 ..... p 1009 N94-15825
DAAL03-90-G-0115 ..... p 1207 N94-15955
DAAL03-90-G-0204 ..... p 965 N94-15773
DAAL03-91-C-0034 ..... p 1143 N94-15110
p 943 N94-15111
DAAL03-91-C-0048 ..... p 968 N94-16723
DAAL03-91-G-0012 ..... p 1183 N94-16722
DAAL03-91-G-0101 ..... p 1165 N94-15775
p 1174 N94-15823
DAAL03-91-G-0165 ..... p 1083 N94-16031
DAAL03-92-C-0001 ..... p 1304 N94-17651
DAAL03-92-C-0035 ..... p 986 N94-14912
DAAL03-92-G-0035 ..... p 1150 N94-16721
DAAL03-92-G-0188 ..... p 1022 N94-15953
p 1010 N94-15954
DAAL04-91-C-0036 ..... p 959 N94-16780
DACA76-89-C-0014 ..... p 863 N94-14919
p 863 N94-14971
p 864 N94-14972
p 864 N94-15498
DACA76-92-C-0005 ..... p 1167 N94-17202
DAJA45-89-C-0025 ..... p 1205 N94-14913
DAJA45-90-C-0009 ..... p 1098 N94-15132
DAJA45-92-C-0007 ..... p 963 N94-14948
DAJA45-92-M-0334 ..... p 1015 N94-17570
DAJA45-92-M-0344 ..... p 1105 N94-14938
DARPA ORDER 6096 ..... p 1143 N94-15175
DARPA ORDER 6873 ..... p 1163 N94-14953
DARPA ORDER 6919 ..... p 1234 N94-17419
DASG60-90-C-0114 ..... p 968 N94-16767
DASG60-92-C-0140 ..... p 1042 N94-17230
DE-AC02-76CH-00016 ..... p 956 N94-15921
p 956 N94-15922
p 1207 N94-15923
p 1095 N94-15940
p 1175 N94-15978
p 1095 N94-15999
p 947 N94-16011
p 1202 N94-16019
p 1181 N94-16020
p 1182 N94-16161
p 1209 N94-16447
p 1210 N94-16775
p 1184 N94-16826
p 1211 N94-16827
p 1184 N94-16828
p 1187 N94-16829
p 1212 N94-16844
p 949 N94-16870
p 1184 N94-16885
p 1184 N94-16886
p 1212 N94-16887
p 1151 N94-16892
p 1176 N94-17658
p 974 N94-17676
DE-AC02-76CH-03000 ..... p 1168 N94-14928
p 1185 N94-16968
p 1186 N94-17662
DE-AC02-80ET-15601 ..... p 949 N94-16891
DE-AC02-83CH-10093 ..... p 1010 N94-15971
p 1093 N94-16824
p 1093 N94-17668
DE-AC03-76SF-00098 ..... p 1190 N94-15854
p 1181 N94-15995
p 966 N94-15996
p 1181 N94-16013
p 1239 N94-16052
p 1181 N94-16053
p 1181 N94-16059
p 947 N94-16060
p 1010 N94-16061
p 1128 N94-16812
p 948 N94-16821
p 1211 N94-16827
p 1102 N94-17252
p 1175 N94-17288
p 1096 N94-17289
p 1045 N94-17349
p 1205 N94-17670
DE-AC03-76SF-00515 ..... p 1208 N94-16062
p 1183 N94-16809
p 1183 N94-16811
p 961 N94-17251
DE-AC03-89ER-51114 ..... p 1202 N94-16803
p 1203 N94-16816
p 1203 N94-16823
DE-AC04-76DP-00789 ..... p 1157 N94-14927
p 1091 N94-15984
p 1148 N94-15985

	p 1091	N94-15993
	p 1091	N94-15994
	p 1208	N94-16012
	p 1050	N94-16055
	p 883	N94-16056
	p 1092	N94-16112
	p 1034	N94-16452
	p 1011	N94-16661
	p 1132	N94-16819
	p 1096	N94-16825
	p 1093	N94-16954
	p 1093	N94-17217
	p 1036	N94-17647
	p 1015	N94-17648
	p 953	N94-17649
	p 1016	N94-17671
DE-AC04-76DR-00789	p 953	N94-17660
DE-AC04-91ER-30172	p 951	N94-17210
DE-AC05-76OR-00001	p 1181	N94-15863
DE-AC05-76OR-00033	p 1206	N94-14925
DE-AC05-84OR-21400	p 1206	N94-14925
	p 1301	N94-14926
	p 1207	N94-15827
	p 965	N94-15828
	p 1207	N94-15829
	p 955	N94-15830
	p 955	N94-15862
	p 934	N94-16008
	p 947	N94-16014
	p 957	N94-16015
	p 966	N94-16016
	p 934	N94-16017
	p 966	N94-16018
	p 1208	N94-16063
	p 1182	N94-16064
	p 934	N94-16065
	p 1209	N94-16066
	p 967	N94-16067
	p 957	N94-16068
	p 957	N94-16103
	p 1059	N94-16104
	p 947	N94-16105
	p 957	N94-16106
	p 1202	N94-16162
	p 957	N94-16163
	p 1209	N94-16164
	p 957	N94-16165
	p 958	N94-16166
	p 1170	N94-16167
	p 958	N94-16168
	p 1209	N94-16171
	p 958	N94-16453
	p 1210	N94-16460
	p 935	N94-16461
	p 1040	N94-16663
	p 1040	N94-16664
	p 975	N94-16807
	p 1024	N94-16808
	p 1220	N94-16810
	p 968	N94-16813
	p 1211	N94-16814
	p 1203	N94-16823
	p 1184	N94-16838
	p 1211	N94-16839
	p 1212	N94-16841
	p 968	N94-16843
	p 1212	N94-16868
	p 1203	N94-16869
	p 959	N94-16873
	p 1231	N94-16874
	p 1232	N94-16875
	p 969	N94-16877
	p 1166	N94-16888
	p 969	N94-16889
	p 959	N94-16890
	p 1232	N94-16967
	p 972	N94-17253
	p 1167	N94-17287
	p 1097	N94-17426
	p 1049	N94-17675
DE-AC05-84OT-21400	p 1181	N94-15863
DE-AC06-76RL-01830	p 1095	N94-16006
	p 934	N94-16158
	p 1209	N94-16159
	p 1092	N94-16160
	p 1096	N94-16445
	p 958	N94-16662
	p 1012	N94-16765
	p 1151	N94-16902
	p 961	N94-17234
	p 940	N94-17235
	p 1215	N94-17319
	p 1110	N94-17673
	p 1043	N94-17677
DE-AC07-76ID-01570	p 926	N94-16773
DE-AC08-88NV-10617	p 1207	N94-15973

DE-AC09-89SR-18035	p 1023	N94-15980
	p 1112	N94-16009
DE-AC21-88MC-25135	p 947	N94-15861
DE-AC21-89MC-26302	p 1024	N94-16763
DE-AC22-90PC-90044	p 975	N94-16898
DE-AC22-91PC-90180	p 1026	N94-16958
DE-AC22-91PC-91030	p 952	N94-17218
DE-AC22-92BC-14882	p 971	N94-16999
DE-AC22-92PC-92110	p 949	N94-16897
DE-AC35-89ER-40486	p 1159	N94-16172
	p 1173	N94-17236
DE-AI03-86SF-16310	p 959	N94-16883
	p 962	N94-17652
DE-FG01-89CE-15425	p 1092	N94-16766
DE-FG02-84ER-13227	p 1041	N94-16998
DE-FG02-85ER-52118	p 1203	N94-16901
DE-FG02-86ER-13560	p 947	N94-15977
DE-FG02-87ER-45283	p 1209	N94-16447
DE-FG02-87ER-45322	p 1212	N94-16961
DE-FG02-88ER-13934	p 948	N94-16462
DE-FG02-89ER-53291	p 1187	N94-17674
DE-FG02-89ER-53297	p 1202	N94-16446
DE-FG02-90ER-14128	p 943	N94-15146
DE-FG02-90ER-40560	p 1187	N94-16116
	p 1182	N94-16117
	p 1239	N94-16118
	p 1184	N94-16899
DE-FG02-90ER-45426	p 960	N94-16972
DE-FG02-90ER-61033	p 948	N94-16771
DE-FG02-91ER-14225	p 1182	N94-16121
DE-FG02-91ER-40652	p 1185	N94-16957
DE-FG02-91ER-45461	p 956	N94-15998
DE-FG02-91ER-61228	p 1122	N94-16113
DE-FG02-92ER-14265	p 1101	N94-16840
DE-FG02-92ER-35166	p 1303	N94-16804
DE-FG02-92ER-40697	p 1188	N94-16900
DE-FG02-92ER-40699	p 1187	N94-16170
DE-FG02-92ER-81360	p 948	N94-16771
DE-FG03-85ER-13431	p 970	N94-16963
DE-FG03-87ER-45324	p 1184	N94-16838
DE-FG03-89ER-60849	p 970	N94-16973
DE-FG03-91ER-61152	p 1150	N94-16659
DE-FG03-92ER-25117	p 1149	N94-16120
DE-FG03-92ER-25128	p 1029	N94-17448
DE-FG03-92ER-25140	p 1025	N94-16894
DE-FG03-93SF-19645	p 960	N94-16964
DE-FG05-80ET-53088	p 1187	N94-16660
	p 1174	N94-16820
	p 1203	N94-16822
DE-FG05-85ER-13387	p 1185	N94-16971
DE-FG05-87ER-25029	p 1000	N94-17000
DE-FG05-88ER-53267	p 1202	N94-16162
DE-FG05-88ER-53279	p 1204	N94-16995
DE-FG05-89ER-14090	p 1191	N94-16007
DE-FG05-92ER-40739	p 1183	N94-16818
DE-FG06-88ER-40427	p 1207	N94-15972
DE-FG06-89ER-75522	p 1209	N94-16159
DE-FG06-90ER-40561	p 1207	N94-15972
DE-FG06-90ER-45415	p 948	N94-16772
DE-FG22-89PC-89770	p 950	N94-16912
DE-FG22-91PC-91287	p 1220	N94-16997
DE-FG22-91PC-91293	p 949	N94-16896
DE-FG22-92PC-92104	p 975	N94-16996
DE-FG22-92PC-92529	p 950	N94-16962
DE-FG22-92PC-92542	p 970	N94-16959
DI-BM-G1114118	p 1064	N94-16602
DNA001-86-C-0308	p 1138	N94-17460
DNA001-88-C-0046	p 988	N94-15668
DTCG39-89-C-E10G56	p 1138	N94-16793
DTFA01-93-C-00001	p 987	N94-15439
	p 876	N94-16025
	p 864	N94-16835
	p 864	N94-16906
DTFA01-93-Z-02012	p 864	N94-16439
EPA-68-C2-0108	p 1094	N94-15136
ERS-1/7831/91	p 877	N94-15621
ERS-1/7831/92	p 877	N94-15621
ESA-6044/84/NL/PB	p 903	N94-15050
	p 910	N94-15100
ESA-7085/87/NL/PB	p 910	N94-15098
ESA-7898/88/NL/PB(SC)	p 903	N94-15054
ESA-8819/90/NL/US(SC)	p 901	N94-15039
ESA-9180/90/NL/PR	p 910	N94-15097
ESTEC-8615/90/NL/PM(SC)	p 906	N94-15071
FSS-SAX-90/005-NL/TS	p 1157	N94-17626
FWF PROJ. P8794-GEO	p 1103	N94-16322
FWF PROJ. P9026-GEO	p 1244	N94-16321
F04701-88-C-0089	p 1056	N94-14945
	p 885	N94-15749
	p 887	N94-16909
	p 1193	N94-17012
	p 951	N94-17207
	p 940	N94-17271
F19628-87-C-0094	p 882	N94-16530

F19628-88-K-0048	p 964	N94-15688
F19628-89-C-0001	p 987	N94-15527
	p 988	N94-15649
	p 1155	N94-17491
F19628-89-C-0068	p 882	N94-16468
F19628-89-C-0187	p 1192	N94-16550
F19628-90-C-0002	p 1158	N94-15492
	p 1121	N94-15634
	p 1164	N94-15746
	p 864	N94-16439
F19628-90-C-0003	p 1142	N94-14967
	p 1144	N94-15214
	p 1144	N94-15215
	p 1144	N94-15216
	p 1145	N94-15629
	p 1145	N94-15630
	p 1146	N94-15638
	p 1146	N94-15653
	p 1155	N94-17429
	p 1157	N94-17588
F19628-90-C-0030	p 1101	N94-16469
F19628-90-C-0100	p 1102	N94-17499
F19628-91-C-0010	p 1101	N94-16551
F19628-91-C-0011	p 1105	N94-14958
F19628-91-C-0061	p 1192	N94-16936
F19628-91-C-0093	p 1003	N94-17268
F19628-91-C-0112	p 897	N94-17240
F19628-91-C-0168	p 1141	N94-14915
F19628-91-K-0009	p 1097	N94-14960
F19628-91-K-0040	p 1105	N94-15142
F19628-92-C-0014	p 1108	N94-17267
F19628-92-K-0003	p 888	N94-16990
F29601-91-K-DB08	p 1232	N94-17036
F30602-88-D-0025	p 1147	N94-15772
F30602-88-D-0026	p 1188	N94-14957
	p 1151	N94-16941
F30602-88-D-0028	p 1189	N94-15791
F30602-89-C-0057	p 1055	N94-17194
F30602-89-C-0082	p 1001	N94-17033
F30602-89-C-0160	p 1166	N94-16770
F30602-90-C-0063	p 1008	N94-15665
F30602-91-C-0017	p 1003	N94-17206
F30602-91-C-0052	p 1188	N94-14940
F30602-91-C-0057	p 988	N94-15667
F30602-91-C-0058	p 1146	N94-15674
F30602-91-D-0001	p 1169	N94-15785
F30602-91-F-0016	p 1222	N94-15213
F30602-92-C-0020	p 1014	N94-17375
F30602-92-C-0023	p 999	N94-16777
F30602-92-C-0026	p 1189	N94-15664
F33615-83-K-0600	p 1118	N94-17232
F33615-85-C-2560	p 1182	N94-16586
F33615-87-C-0001	p 1145	N94-15525
F33615-87-C-1507	p 1014	N94-17423
F33615-87-C-2710	p 1048	N94-17433
F33615-87-C-2714	p 942	N94-14911
F33615-87-C-2718	p 1186	N94-17536
F33615-87-C-3216	p 1151	N94-16768
	p 1151	N94-16769
F33615-88-C-5404	p 1055	N94-17515
	p 1157	N94-17590
	p 1056	N94-17596
F33615-89-C-0532	p 868	N94-17425
F33615-89-C-0603	p 1138	N94-16983
	p 1134	N94-17510
	p 1130	N94-17554
	p 1139	N94-17563
	p 1139	N94-17564
F33615-89-C-2973	p 1028	N94-17250
F33615-89-C-5609	p 936	N94-16795
F33615-89-D-2198	p 1152	N94-17032
F33615-90-C-0005	p 1131	N94-15108
	p 1137	N94-15820
	p 1122	N94-15845
F33615-90-C-1465	p 1141	N94-14915
	p 1231	N94-16570
	p 1166	N94-16725
	p 1141	N94-17115
	p 1166	N94-17201
F33615-90-C-5946	p 1213	N94-17042
F33615-91-C-0600	p 1130	N94-17621
F33615-91-C-2139	p 866	N94-15761
F33615-91-C-5606	p 1061	N94-17269
F33615-91-C-5725	p 984	N94-16981
F33615-92-C-5937	p 1215	N94-17417
F49620-89-C-0038	p 1101	N94-16125
F49620-89-C-0078	p 972	N94-17242
F49620-89-C-0080	p 946	N94-15684
F49620-89-C-0108	p 1206	N94-15764
F49620-89-C-0110	p 1234	N94-17419
F49620-90-C-0008	p 1041	N94-17193
F49620-90-C-0031	p 1022	N94-15860
F49620-90-C-0039	p 1005	N94-17519
F49620-90-C-0065	p 1001	N94-17019
F49620-91-C-0021	p 950	N94-16930
F49620-91-C-0056	p 950	N94-17008

F49620-91-C-0092 p 973 N94-17494
F49620-92-C-0002 p 970 N94-16978
F49620-92-C-0004 p 1216 N94-17561
F49620-92-C-0024 p 941 N94-17597
F49620-92-C-0037 p 1212 N94-16932
F49620-92-C-0038 p 1216 N94-17577
F49620-92-C-0060 p 1038 N94-15853
F49620-92-J-0102 p 1131 N94-15148
F49620-92-J-0185 p 1217 N94-17579
F49620-92-J-0195 p 1121 N94-15660
F49620-92-J-0208 p 1129 N94-17456
F49620-92-J-0235 p 1299 N94-17208
F49620-92-J-0238 p 1129 N94-17478
F49620-92-J-0251 p 1037 N94-15145
F49620-92-J-0266 p 1201 N94-15661
F49620-92-J-0273 p 975 N94-17073
F49620-92-J-0285 p 940 N94-17013
F49620-92-J-0291 p 941 N94-17379
F49620-92-J-0307 p 1133 N94-17453
F49620-92-J-0309 p 1015 N94-17560
F49620-92-J-0310 p 1134 N94-17468
F49620-92-J-0314 p 952 N94-17532
F49620-92-J-0362 p 1121 N94-15736
F49620-92-J-0369 p 1133 N94-17020
F49620-92-J-0400 p 1141 N94-17380
F49620-93-1-0005 p 1017 N94-15199
HV-CCD-N88/20/21/22 p 901 N94-15036
JPL-956520 p 995 N94-16041
p 996 N94-16048
JPL-958456 p 1078 N94-16748
p 1080 N94-16758
JPL-958468 p 1076 N94-16736
JPL-958469 p 1076 N94-16739
MDA903-85-C-0347 p 1005 N94-17498
MDA903-87-C-0641 p 1143 N94-15175
p 1153 N94-17078
MDA971-91-C-0032 p 1014 N94-17423
MDA972-90-C-0035 p 1140 N94-15744
p 1160 N94-16724
p 1153 N94-17118
MDA972-91-C-0029 p 1015 N94-17526
p 1015 N94-17608
MDA972-92-C-0026 p 1151 N94-16910
MDA972-92-C-0075 p 1191 N94-16128
MDA972-92-J-1002 p 1147 N94-15728
MDA972-92-J-1010 p 1163 N94-14953
p 1188 N94-15144
MDA972-93-1-0004 p 1113 N94-17391
MIPR-ENM9486 p 871 N94-14908
MIPR-9MM2501 p 1231 N94-16458
MIPR-91MM1504 p 1122 N94-15759
MRT-89553 p 1142 N94-14979
NAGW-1143 p 1073 N94-16704
NAGW-1290 p 901 N94-15037
NAGW-1334 p 954 N94-16340
NAGW-1392 p 1082 N94-16026
NAGW-1561 p 1239 N94-15188
NAGW-1601 p 1067 N94-16674
p 1073 N94-16704
NAGW-1610 p 1239 N94-16647
NAGW-1657 p 1297 N94-16884
NAGW-1744 p 1098 N94-15639
NAGW-1787 p 1102 N94-17527
NAGW-1844 p 1112 N94-15680
NAGW-1879 p 901 N94-15037
NAGW-2032 p 901 N94-15037
NAGW-2115 p 901 N94-15040
NAGW-2615 p 1081 N94-17444
NAGW-2640 p 901 N94-15037
NAGW-270 p 1074 N94-16711
NAGW-2736 p 1057 N94-15154
NAGW-2859 p 908 N94-15089
NAGW-2898 p 1190 N94-15868
p 1190 N94-15869
p 1191 N94-16023
p 1191 N94-16024
p 967 N94-16494
NAGW-2914 p 1297 N94-16832
NAGW-2945 p 1172 N94-15641
NAGW-2948 p 1112 N94-15701
NAGW-3154 p 1240 N94-17059
NAGW-3281 p 1241 N94-16213
NAGW-3293 p 1008 N94-15547
NAGW-3571 p 1236 N94-15679
NAGW-436 p 1298 N94-15421
NAGW-642 p 1241 N94-16174
p 1242 N94-16274
p 1243 N94-16310
NAGW-748 p 1242 N94-16246
NAGW-894 p 1239 N94-16647
NAGW-925 p 1084 N94-16831
NAGW-929 p 1239 N94-16648
NAG1-1003 p 1027 N94-17095
NAG1-1031 p 1150 N94-16594
NAG1-1067 p 932 N94-15275
NAG1-1122 p 1018 N94-15427
NAG1-1125 p 1048 N94-17088
NAG1-1217 p 1027 N94-17129
NAG1-1255 p 867 N94-16498
NAG1-1286 p 1301 N94-17255
NAG1-1351 p 866 N94-15429
NAG1-1413 p 897 N94-17280
NAG1-1443 p 1189 N94-15647
NAG1-1451 p 870 N94-15416
NAG1-1476 p 964 N94-15700
NAG1-1489 p 931 N94-15184
NAG1-1493 p 941 N94-17295
NAG1-1541 p 1027 N94-17130
NAG1-237 p 938 N94-16856
NAG1-343 p 964 N94-15656
p 938 N94-16856
NAG1-363 p 1181 N94-15752
p 1021 N94-15795
NAG1-423 p 1027 N94-17127
p 1027 N94-17215
NAG1-698 p 1038 N94-15530
NAG1-745 p 930 N94-15106
p 942 N94-17638
NAG1-928 p 862 N94-15444
p 994 N94-16022
NAG1-983 p 1143 N94-15114
NAG10-0109 p 887 N94-16905
NAG2-593 p 1161 N94-17239
NAG2-656 p 1133 N94-17296
NAG2-680 p 1246 N94-15182
NAG2-692 p 1299 N94-17281
NAG2-703 p 1149 N94-16554
NAG2-757 p 999 N94-16867
NAG3-1242 p 951 N94-17125
NAG3-1391 p 976 N94-15654
NAG3-1415 p 1029 N94-17387
NAG3-965 p 946 N94-15713
NAG3-995 p 972 N94-17297
NAG5-1021 p 1041 N94-16719
NAG5-1213 p 1297 N94-16866
NAG5-1214 p 1232 N94-17038
NAG5-1249 p 1084 N94-16032
NAG5-1346 p 1226 N94-14981
NAG5-1446 p 1059 N94-16815
NAG5-1541 p 1098 N94-15433
NAG5-1555 p 1300 N94-17524
NAG5-1628 p 1083 N94-16031
NAG5-1655 p 1240 N94-17094
NAG5-1710 p 1199 N94-17443
NAG5-1779 p 1237 N94-16833
NAG5-1798 p 1236 N94-16492
NAG5-1838 p 1081 N94-15181
NAG5-447 p 1101 N94-16021
NAG5-483 p 1097 N94-15003
NAG5-491 p 1083 N94-16027
p 1083 N94-16028
NAG5-5006 p 923 N94-17126
NAG5-557 p 997 N94-16506
p 997 N94-16507
p 997 N94-16508
p 998 N94-16509
NAG5-604 p 1106 N94-16493
NAG5-899 p 1083 N94-16030
p 1084 N94-16032
p 1084 N94-16034
NAG8-122 p 868 N94-15187
NAG8-253 p 1038 N94-15477
NAG8-293 p 1058 N94-15716
NAG8-749 p 1028 N94-17298
NAG8-842 p 1210 N94-16646
NAG8-872 p 1299 N94-17089
NAG8-950 p 1206 N94-15476
NAG9-337 p 1008 N94-15640
NAG9-422 p 1140 N94-16716
NAG9-454 p 1241 N94-16213
p 1245 N94-16390
NAG9-497 p 1243 N94-16284
NAG9-56 p 1267 N94-16279
p 1267 N94-16280
p 1242 N94-16281
p 1275 N94-16326
NAG9-616 p 1055 N94-17082
NAG9-622 p 1062 N94-17445
NAG9-81 p 1242 N94-16257
NASA ORDER A-24364-D p 867 N94-15950
NASA ORDER A-24888-D p 860 N94-17260
NASA ORDER A-25364-D p 866 N94-15718
NASA ORDER H-01099-D p 951 N94-17039
NASA ORDER L-18543-D p 933 N94-15484
NASA ORDER S-93065-E p 1300 N94-15533
NASA ORDER W-17678 p 1299 N94-15968
NASW-4176 p 1123 N94-16609
NASW-4528 p 883 N94-17111
NASW-4574 p 1032 N94-15797
p 1247 N94-16173
p 1297 N94-17637
NASW-4584 p 1228 N94-15009
NAS1-10312 p 1030 N94-17557
NAS1-1286 p 1180 N94-15715
NAS1-18584 p 967 N94-16541
NAS1-18605 p 1019 N94-15478
p 1145 N94-15489
p 1029 N94-17387
NAS1-18862 p 940 N94-16864
NAS1-18878 p 1144 N94-15443
NAS1-19000 p 1176 N94-15487
NAS1-19061 p 1178 N94-17278
NAS1-19063 p 922 N94-17083
NAS1-19097 p 1036 N94-17655
NAS1-19299 p 1021 N94-15834
NAS1-19399 p 931 N94-15184
NAS1-19480 p 1016 N94-15005
p 1017 N94-15183
p 1019 N94-15478
p 1019 N94-15479
p 1144 N94-15483
p 1145 N94-15489
p 1168 N94-15724
p 1169 N94-15833
p 1021 N94-15834
p 1148 N94-15965
p 1149 N94-15989
p 1029 N94-17387
p 1030 N94-17450
NAS1-9434 p 1024 N94-16542
NAS2-12902 p 1297 N94-17292
NAS2-13196 p 855 N94-15655
p 856 N94-15677
p 857 N94-15720
p 857 N94-15780
NAS2-13210 p 1150 N94-16656
NAS2-13721 p 1168 N94-15112
p 1158 N94-15113
p 1143 N94-15189
p 1148 N94-15956
NAS3-23691 p 1023 N94-15991
NAS3-23883 p 924 N94-15482
NAS3-25266 p 869 N94-15192
p 1040 N94-16522
p 926 N94-16880
p 1013 N94-17113
p 861 N94-17558
NAS3-25776 p 1034 N94-16521
NAS3-25790 p 1054 N94-16518
NAS5-30127 p 1082 N94-15531
NAS5-30386 p 1299 N94-15968
NAS5-30552 p 1067 N94-16674
p 1068 N94-16678
p 1072 N94-16699
p 1072 N94-16700
NAS5-30751 p 1109 N94-17525
NAS5-30768 p 1066 N94-16671
NAS5-30958 p 1066 N94-16671
NAS5-31367 p 1107 N94-16717
NAS5-31718 p 1066 N94-16671
NAS7-918 p 1033 N94-15875
p 925 N94-15876
p 989 N94-15886
p 925 N94-15927
p 966 N94-15930
p 1038 N94-15932
p 1190 N94-15933
p 1010 N94-15952
p 1165 N94-15958
p 966 N94-15960
p 1034 N94-15987
p 994 N94-16035
p 1014 N94-17323
p 1014 N94-17324
p 1014 N94-17325
p 1154 N94-17326
p 1215 N94-17327
p 1161 N94-17328
p 1185 N94-17329
p 1161 N94-17330
p 1237 N94-17438
NAS8-30490 p 927 N94-17080
NAS8-35921 p 1298 N94-15023
p 1298 N94-15024
NAS8-36401 p 879 N94-15191
NAS8-37196 p 928 N94-17442
NAS8-37593 p 927 N94-17016
NAS8-37686 p 971 N94-17122
NAS8-37744 p 946 N94-15766
NAS8-37857 p 882 N94-15831
NAS8-38073 p 926 N94-16590
NAS8-38074 p 926 N94-16654
NAS8-38100 p 928 N94-17213
p 882 N94-17656
NAS8-38145 p 1190 N94-15868
p 1190 N94-15869
p 1191 N94-16023
p 1191 N94-16024

NAS8-38261 ..... p 927 N94-17123
p 928 N94-17124
NAS8-38609 ..... p 976 N94-15006
NAS8-38872 ..... p 1016 N94-15109
NAS8-39131 ..... p 870 N94-15532
NAS8-39210 ..... p 927 N94-17096
p 927 N94-17097
p 927 N94-17098
NAS8-39393 ..... p 1082 N94-15646
NAS8-39400 ..... p 877 N94-16150
NAS8-39611 ..... p 928 N94-17277
NAS8-39715 ..... p 960 N94-17079
NAS9-17900 ..... p 1295 N94-16428
NAS9-18209 ..... p 887 N94-16502
p 887 N94-16503
p 926 N94-16504
NAS9-18395 ..... p 1011 N94-16505
NAS9-18398 ..... p 926 N94-16922
NCC1-104 ..... p 886 N94-15864
NCC2-229 ..... p 1118 N94-17090
NCC2-233 ..... p 1025 N94-16879
NCC2-297 ..... p 1056 N94-15004
NCC2-374 ..... p 1024 N94-16491
NCC2-387 ..... p 1158 N94-15113
p 1159 N94-15796
NCC2-507 ..... p 1020 N94-15551
NCC2-580 ..... p 998 N94-16649
NCC2-582 ..... p 856 N94-15678
NCC2-604 ..... p 871 N94-15117
NCC2-605 ..... p 860 N94-17081
NCC2-608 ..... p 1118 N94-17279
NCC2-658 ..... p 1221 N94-15719
NCC2-677 ..... p 858 N94-16510
NCC2-724 ..... p 936 N94-16836
NCC3-115 ..... p 1192 N94-16718
NCC3-168 ..... p 1025 N94-16842
NCC3-233 ..... p 1169 N94-15818
p 1026 N94-17056
p 1027 N94-17112
p 1028 N94-17258
p 1029 N94-17385
p 1029 N94-17448
p 1062 N94-17481
p 1030 N94-17557
NCC9-16 ..... p 1231 N94-16499
NERC-GR3/6264 ..... p 1083 N94-16028
NGT-50462 ..... p 901 N94-15040
NGT-50728 ..... p 1078 N94-16748
p 1080 N94-16758
NGT-60153 ..... p 1083 N94-16029
p 1084 N94-16033
NGT-70109 ..... p 997 N94-16508
NIVR-07701N ..... p 1031 N94-17627
NR PROJ. RS3-4-P-11 ..... p 1146 N94-15670
NR PROJ. S11-42-CS ..... p 1132 N94-15762
NRC-91-02615-PF42 ..... p 1083 N94-16031
NSF ASC-88-02764 ..... p 1164 N94-15695
p 1162 N94-17537
NSF ASC-91-13895 ..... p 1169 N94-15833
NSF AST-90-12180 ..... p 1241 N94-16174
p 1243 N94-16310
NSF ATM-90-17637 ..... p 1098 N94-15433
NSF CCR-88-02283 ..... p 1153 N94-17107
NSF CCR-88-58029 ..... p 1155 N94-17398
NSF CCR-89-57604 ..... p 1150 N94-16579
NSF CCR-90-02292 ..... p 1150 N94-16579
NSF CCR-90-05633 ..... p 1159 N94-16578
NSF CCR-90-06064 ..... p 1151 N94-16790
p 1152 N94-17009
NSF CCR-91-06368 ..... p 1155 N94-17398
NSF CDA-88-22724 ..... p 1159 N94-16577
p 1159 N94-16578
NSF CTS-92-53488 ..... p 1018 N94-15427
NSF DMR-88-09864 ..... p 908 N94-15089
NSF DMS-91-07608 ..... p 1029 N94-17387
NSF DMS-91-07612 ..... p 1029 N94-17448
NSF DMS-91-08072 ..... p 1029 N94-17448
NSF EAR-92-18847 ..... p 1244 N94-16321
NSF ECS-86-19049 ..... p 1045 N94-17349
NSF ECS-91-12973 ..... p 1045 N94-17349
NSF IRI-89-03582 ..... p 1231 N94-16576
p 1165 N94-16580
NSF IRI-90-02659 ..... p 1149 N94-16575
NSF IRI-90-10692 ..... p 1165 N94-16580
NSF IRI-90-108999 ..... p 1166 N94-16581
NSF MDS-90-12751 ..... p 1154 N94-17370
NSF NCR-89-03429 ..... p 998 N94-16509
NSF NCR-91-01627 ..... p 1161 N94-17409
NSF NCR-91-16183 ..... p 1162 N94-17537
NSF OCE-87-16314 ..... p 1114 N94-17555
NSF OCE-87-17144 ..... p 1112 N94-15844
NSF OCE-91-01636 ..... p 1114 N94-17555
NSG-1601 ..... p 931 N94-15190
N000014-86-K-0770 ..... p 933 N94-15626
N00014-82-K-0280 ..... p 1210 N94-16476
N00014-82-K-0612 ..... p 967 N94-16475
N00014-86-K-0770 ..... p 969 N94-16928
p 933 N94-15528
p 933 N94-15835
N00014-87-K-0429 ..... p 961 N94-17109
N00014-88-C-0760 ..... p 1008 N94-15635
N00014-88-J-1028 ..... p 1113 N94-16517
N00014-88-J-1046 ..... p 1180 N94-15727
N00014-88-J-1100 ..... p 954 N94-14961
N00014-89-C-0053 ..... p 959 N94-16781
N00014-89-C-0064 ..... p 1111 N94-14947
N00014-89-J-1028 ..... p 970 N94-16948
N00014-89-J-1060 ..... p 1023 N94-16110
N00014-89-J-1109 ..... p 1177 N94-15732
N00014-89-J-1235 ..... p 942 N94-14956
p 1182 N94-16111
N00014-89-J-1276 ..... p 960 N94-17041
N00014-89-J-1527 ..... p 1154 N94-17370
p 1171 N94-17420
N00014-89-J-1619 ..... p 958 N94-16562
N00014-89-J-1848 ..... p 973 N94-17413
N00014-89-J-1990 ..... p 1042 N94-17567
N00014-89-J-1991 ..... p 952 N94-17381
N00014-89-J-3036 ..... p 1160 N94-16791
N00014-89-J-3134 ..... p 1117 N94-16514
N00014-89-J-3152 ..... p 999 N94-16794
N00014-89-J-3213 ..... p 1039 N94-16124
N00014-90-C-0083 ..... p 1117 N94-16441
N00014-90-C-0225 ..... p 1009 N94-15726
N00014-90-C-2020 ..... p 971 N94-17204
N00014-90-C-2269 ..... p 973 N94-17408
N00014-90-J-1030 ..... p 1168 N94-14939
p 1029 N94-17384
N00014-90-J-1036 ..... p 1111 N94-15139
N00014-90-J-1148 ..... p 964 N94-15675
N00014-90-J-1289 ..... p 989 N94-15748
N00014-90-J-1392 ..... p 973 N94-17466
N00014-90-J-1403 ..... p 1018 N94-15427
N00014-90-J-1427 ..... p 1213 N94-17108
N00014-90-J-1464 ..... p 1113 N94-16517
N00014-90-J-1558 ..... p 1009 N94-15669
p 1009 N94-15672
p 1009 N94-15673
N00014-90-J-1568 ..... p 1112 N94-15844
N00014-90-J-1887 ..... p 1163 N94-14937
N00014-90-J-1913 ..... p 1186 N94-17578
N00014-90-J-1973 ..... p 1118 N94-17275
N00014-90-J-4009 ..... p 1085 N94-17467
N00014-90-J-4018 ..... p 1154 N94-17390
N00014-91-C-0004 ..... p 1113 N94-16561
N00014-91-C-0138 ..... p 1111 N94-15134
N00014-91-J-1028 ..... p 970 N94-16947
p 970 N94-16949
p 971 N94-16994
N00014-91-J-1035 ..... p 1182 N94-16466
p 1211 N94-16782
p 950 N94-17006
N00014-91-J-1067 ..... p 1140 N94-15763
N00014-91-J-1128 ..... p 1158 N94-15173
N00014-91-J-1142 ..... p 1169 N94-16127
N00014-91-J-1146 ..... p 1179 N94-14949
p 1180 N94-15689
N00014-91-J-1177 ..... p 1217 N94-17606
N00014-91-J-1193 ..... p 1177 N94-16939
N00014-91-J-1271 ..... p 1030 N94-17511
N00014-91-J-1282 ..... p 1180 N94-15727
N00014-91-J-1283 ..... p 1140 N94-15174
N00014-91-J-1297 ..... p 930 N94-15143
N00014-91-J-1316 ..... p 1133 N94-17022
N00014-91-J-1334 ..... p 998 N94-16557
N00014-91-J-1416 ..... p 1213 N94-17116
N00014-91-J-1420 ..... p 1055 N94-17514
N00014-91-J-1441 ..... p 1214 N94-17243
N00014-91-J-1629 ..... p 948 N94-16787
N00014-91-J-1636 ..... p 1211 N94-16800
N00014-91-J-1646 ..... p 1028 N94-17276
N00014-91-J-1709 ..... p 1132 N94-15762
N00014-91-J-1737 ..... p 1116 N94-15633
N00014-91-J-1738 ..... p 1062 N94-17507
N00014-91-J-1766 ..... p 946 N94-15760
N00014-91-J-1852 ..... p 1007 N94-14936
N00014-91-J-1893 ..... p 962 N94-14914
p 962 N94-14921
p 963 N94-15179
p 963 N94-15490
p 963 N94-15631
p 964 N94-15683
p 965 N94-15843
N00014-91-J-1941 ..... p 1041 N94-17001
N00014-91-J-1976 ..... p 1214 N94-17272
N00014-91-J-4008 ..... p 1176 N94-17605
N00014-91-J-4037 ..... p 1026 N94-16927
N00014-91-J-4045 ..... p 986 N94-14955
N00014-91-J-4061 ..... p 1158 N94-15745
N00014-92-C-0010 ..... p 972 N94-17227
N00014-92-C-0172 ..... p 1214 N94-17216
N00014-92-J-1030 ..... p 1199 N94-17427
N00014-92-J-1218 ..... p 988 N94-15690
N00014-92-J-1244 ..... p 1120 N94-15180
N00014-92-J-1264 ..... p 1172 N94-15002
N00014-92-J-1436 ..... p 1212 N94-16992
N00014-92-J-1477 ..... p 1215 N94-17377
N00014-92-J-1500 ..... p 973 N94-17490
N00014-92-J-1546 ..... p 1113 N94-16517
N00014-92-J-1608 ..... p 1049 N94-17566
N00014-92-J-1637 ..... p 952 N94-17416
N00014-92-J-1673 ..... p 1092 N94-16567
N00014-92-J-1710 ..... p 1118 N94-16989
N00014-92-J-1720 ..... p 1012 N94-17040
N00014-92-J-1757 ..... p 1175 N94-15758
N00014-92-J-1778 ..... p 988 N94-15691
N00014-92-J-1808 ..... p 935 N94-16483
p 935 N94-16484
p 935 N94-16485
p 935 N94-16528
p 935 N94-16529
N00014-92-J-1826 ..... p 1137 N94-16108
N00014-92-J-1866 ..... p 997 N94-16477
p 1000 N94-16911
p 1152 N94-16982
p 1161 N94-17239
N00014-92-J-4013 ..... p 1112 N94-15844
N00014-92-J-4109 ..... p 1112 N94-15771
N00014-92-3-1606 ..... p 1042 N94-17567
N00014-93-C-0051 ..... p 1040 N94-16546
N00014-93-C-0118 ..... p 1134 N94-17576
N00014-93-I-0414 ..... p 1145 N94-15627
N00014-93-I-0437 ..... p 1216 N94-17553
N00014-93-1-0015 ..... p 1176 N94-17581
N00014-93-1-0067 ..... p 1048 N94-17533
N00014-93-1-0120 ..... p 1116 N94-15138
N00014-93-1-0128 ..... p 1008 N94-15636
N00014-93-1-2002 ..... p 969 N94-16946
N00039-89-C-0001 ..... p 995 N94-16041
p 996 N94-16048
N00039-91-C-0138 ..... p 1162 N94-17550
N47408-91-C-1228 ..... p 872 N94-17405
p 873 N94-17432
p 873 N94-17508
p 873 N94-17569
PROJ. ZW6-2 ..... p 1158 N94-15671
RICIS PROJ. RB-08 ..... p 1231 N94-16499
RTOP 106-10-04 ..... p 1139 N94-17636
RTOP 199-45-16-11 ..... p 1300 N94-15816
p 1188 N94-17018
p 1300 N94-17084
p 1301 N94-17666
RTOP 199-70-12-14 ..... p 1120 N94-15537
p 1121 N94-15711
RTOP 307-52-00 ..... p 1174 N94-17469
RTOP 324-02-01 ..... p 1036 N94-17655
RTOP 370-24-11 ..... p 1297 N94-17292
RTOP 419-09-01 ..... p 1085 N94-17665
RTOP 462-61-14 ..... p 1082 N94-15531
RTOP 474-12-10 ..... p 929 N94-17483
RTOP 474-46-10 ..... p 1058 N94-15709
p 926 N94-16880
RTOP 476-14-03 ..... p 1116 N94-15548
p 883 N94-15648
RTOP 476-14-06-01 ..... p 886 N94-15864
RTOP 476-14-06 ..... p 888 N94-17072
p 1138 N94-17452
RTOP 505-40-61-01 ..... p 861 N94-17284
RTOP 505-59-00 ..... p 1148 N94-15784
RTOP 505-59-10-03 ..... p 859 N94-16574
RTOP 505-59-52 ..... p 870 N94-15793
RTOP 505-59-54-01 ..... p 872 N94-15794
RTOP 505-61-01-05 ..... p 967 N94-16541
RTOP 505-61-51 ..... p 856 N94-15657
RTOP 505-62-10 ..... p 869 N94-15866
p 870 N94-17470
p 1049 N94-17583
RTOP 505-62-11 ..... p 869 N94-15192
RTOP 505-62-52 ..... p 1032 N94-15445
p 1019 N94-15475
p 1019 N94-15485
p 1020 N94-15488
p 1169 N94-15799
p 1022 N94-15865
p 1022 N94-15867
p 1177 N94-16497
p 1024 N94-16527
p 1170 N94-16882
p 869 N94-17386
p 1035 N94-17446
p 1220 N94-17624
RTOP 505-62-61 ..... p 1023 N94-15991
RTOP 505-62-84 ..... p 872 N94-15819
RTOP 505-63-5A ..... p 930 N94-15769
p 956 N94-15992
p 967 N94-16543
RTOP 505-63-5B ..... p 1060 N94-16881
RTOP 505-63-50-05 ..... p 936 N94-16845

RTOP 505-63-50-07 ..... p 1062 N94-17479
RTOP 505-63-50-10 ..... p 1024 N94-16542
p 1179 N94-17650
RTOP 505-63-50-15 ..... p 867 N94-17055
RTOP 505-63-50-16 ..... p 866 N94-15722
RTOP 505-63-50 ..... p 867 N94-15783
RTOP 505-63-70-02 ..... p 1176 N94-15487
RTOP 505-64-10-13 ..... p 1144 N94-15443
p 1158 N94-15536
RTOP 505-64-12-01 ..... p 1108 N94-17283
RTOP 505-64-12-02 ..... p 986 N94-15140
p 862 N94-15444
RTOP 505-64-12-04 ..... p 922 N94-17083
RTOP 505-64-13 ..... p 862 N94-15550
RTOP 505-64-50-03 ..... p 1161 N94-17449
RTOP 505-64-50-05 ..... p 1144 N94-15486
RTOP 505-64-52 ..... p 1145 N94-15538
RTOP 505-64-70-01 ..... p 989 N94-15767
p 998 N94-16655
RTOP 505-66-21 ..... p 1150 N94-16594
p 1155 N94-17447
RTOP 505-67-01 ..... p 1177 N94-15549
RTOP 505-68-30-03 ..... p 859 N94-16573
RTOP 505-68-70-06 ..... p 858 N94-16572
RTOP 505-70-00 ..... p 886 N94-15753
RTOP 505-70-63 ..... p 1032 N94-15754
RTOP 505-90-00 ..... p 1233 N94-17291
p 1233 N94-17300
RTOP 505-90-5K ..... p 1021 N94-15751
p 1169 N94-15818
p 1025 N94-16879
p 1026 N94-17056
p 1027 N94-17112
p 1027 N94-17128
p 1028 N94-17258
p 1029 N94-17385
p 1062 N94-17481
p 1030 N94-17557
RTOP 505-90-52-01 ..... p 1016 N94-15005
p 1017 N94-15183
p 1019 N94-15478
p 1019 N94-15479
p 1144 N94-15483
p 1145 N94-15489
p 1168 N94-15724
p 1021 N94-15768
p 1169 N94-15833
p 1023 N94-15964
p 1148 N94-15965
p 1149 N94-15989
p 1029 N94-17387
p 1030 N94-17450
RTOP 505-90-53-02 ..... p 1160 N94-16878
p 1152 N94-17060
RTOP 506-40-91-02 ..... p 1030 N94-17476
RTOP 506-40-91-03 ..... p 1018 N94-15291
RTOP 506-41-11 ..... p 1013 N94-17113
RTOP 506-41-41-01 ..... p 1042 N94-17285
RTOP 506-42-00 ..... p 1034 N94-16521
RTOP 506-42-73 ..... p 1046 N94-15817
p 1030 N94-17486
RTOP 506-43-41-02 ..... p 885 N94-15446
RTOP 506-72-21 ..... p 883 N94-17111
p 883 N94-17487
p 883 N94-17488
RTOP 506-73-43-03 ..... p 930 N94-15106
RTOP 510-01-50 ..... p 1054 N94-16518
RTOP 510-02-11-08 ..... p 933 N94-15484
RTOP 510-02-12-10 ..... p 942 N94-17638
RTOP 533-02-35 ..... p 861 N94-17558
RTOP 535-03-10-01 ..... p 856 N94-15681
RTOP 535-03-10-02 ..... p 861 N94-17639
RTOP 535-03-10 ..... p 1176 N94-15115
p 858 N94-16571
RTOP 537-03-20 ..... p 869 N94-15141
RTOP 537-03-21-03 ..... p 1178 N94-17278
RTOP 537-06-21-09 ..... p 1061 N94-17259
RTOP 538-02-10-01 ..... p 931 N94-15184
p 955 N94-15708
p 956 N94-15948
RTOP 583-02-21 ..... p 959 N94-16883
RTOP 585-03-11-02 ..... p 1062 N94-17451
RTOP 585-03-21 ..... p 928 N94-17256
RTOP 590-13-11 ..... p 924 N94-15482
p 962 N94-17652
RTOP 590-21-11 ..... p 1034 N94-15961
RTOP 590-31-11 ..... p 1009 N94-15765
RTOP 593-32-41 ..... p 1040 N94-16522
RTOP 593-71-00 ..... p 923 N94-15118
RTOP 618-22-31-03 ..... p 1105 N94-15480
RTOP 656-63-00 ..... p 1228 N94-15116
RTOP 693-00-00 ..... p 1236 N94-15481
RTOP 906-11-01-01 ..... p 882 N94-17320
RTOP 940-30-09-21 ..... p 863 N94-16520
RTOP-590-14-11-02 ..... p 1034 N94-15990
SBIR-02.11-1322 ..... p 1036 N94-17655
SC-900376 ..... p 1220 N94-17602
SRI PROJ. 2743 ..... p 1015 N94-17526
SWRI PROJ. 15-4170 ..... p 1299 N94-17281
SWRI PROJ. 15-4945 ..... p 1297 N94-16832
USDA-58-3K47-0-039 ..... p 1083 N94-16031
USGS-14-08-0001-G1138 ..... p 1083 N94-16027
p 1083 N94-16028
USGS-14-08-0001-G1753 ..... p 1083 N94-16029
W-31-109-ENG-38 ..... p 1208 N94-15982
p 1059 N94-15997
p 934 N94-16057
p 1208 N94-16058
p 1011 N94-16443
p 1023 N94-16444
p 968 N94-16658
p 1150 N94-16659
p 1170 N94-16778
p 1211 N94-16805
p 1047 N94-16806
p 1211 N94-16839
p 1117 N94-16893
p 1048 N94-16969
p 1129 N94-16970
p 1013 N94-17226
p 1300 N94-17233
p 953 N94-17649
p 1110 N94-17673
W-7405-ENG-36 ..... p 955 N94-15885
p 965 N94-15920
p 1181 N94-15974
p 1169 N94-15979
p 1039 N94-16114
p 1182 N94-16115
p 958 N94-16463
p 959 N94-16764
p 1202 N94-16776
p 1183 N94-16801
p 1299 N94-16895
p 1185 N94-16951
p 1192 N94-16953
p 1178 N94-16955
p 1220 N94-16956
p 1214 N94-17301
p 1013 N94-17318
p 1205 N94-17645
p 1162 N94-17646
p 1240 N94-17657
p 1217 N94-17659
p 1062 N94-17664
p 898 N94-17669
p 1110 N94-17673
W-7405-ENG-48 ..... p 1236 N94-14929
p 966 N94-15924
p 1190 N94-15975
p 1208 N94-15976
p 1201 N94-15981
p 1059 N94-15983
p 1039 N94-16054
p 1149 N94-16119
p 997 N94-16169
p 1177 N94-16448
p 1096 N94-16449
p 1039 N94-16450
p 1202 N94-16451
p 1096 N94-16802
p 1203 N94-16816
p 1183 N94-16817
p 1096 N94-16825
p 1041 N94-16871
p 1237 N94-16872
p 1025 N94-16894
p 1025 N94-16903
p 949 N94-16904
p 950 N94-16952
p 1035 N94-16960
p 1204 N94-17237
p 972 N94-17238
p 1205 N94-17663
p 1205 N94-17670
p 1188 N94-17672

Typical Report Number Index Listing

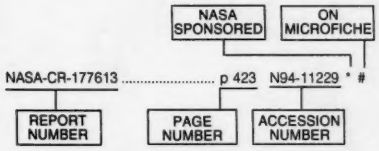

Listings in this index are arranged alphanumerically by report number. The accession number denotes the number by which the citation is identified. The page number helps to locate the citation in the abstract section. An asterisk (*) indicates that the item is a NASA report. A pound sign (#) indicates that the item is available on microfiche.

A-92147 ..... p 1116 N94-15548 * #
A-92177 ..... p 1009 N94-15765 * #
A-92192 ..... p 1139 N94-17636 * #
A-93006 ..... p 856 N94-15657 * #
A-93067 ..... p 1177 N94-15549 * #
A-93071 ..... p 870 N94-15793 * #
A-93088 ..... p 883 N94-15648 * #
A-93095 ..... p 1120 N94-15537 * #
A-93103 ..... p 1145 N94-15538 * #
A-93107 ..... p 866 N94-15718 * #
A-93114 ..... p 867 N94-15950 * #
A-93118 ..... p 1121 N94-15711 * #
A-93119 ..... p 862 N94-15550 * #
A-93133 ..... p 1148 N94-15784 * #
A-93135 ..... p 1150 N94-16656 * #
A-93138-VOL-1 ..... p 855 N94-15655 * #
A-93138-VOL-2 ..... p 856 N94-15677 * #
A-93138 ..... p 857 N94-15720 * #
A-93138 ..... p 857 N94-15780 * #
A-94021 ..... p 860 N94-17081 * #

AARHUS-ASTRO-93-12 ..... p 1299 N94-15968 * #

AD-A261911 ..... p 1228 N94-15152 #
AD-A263236 ..... p 1098 N94-15132
AD-A263878 ..... p 963 N94-15133 #
AD-A264516 ..... p 1111 N94-15134 #
AD-A265414 ..... p 1105 N94-15137 #
AD-A265748 ..... p 1223 N94-15682 #
AD-A265776 ..... p 1116 N94-15138
AD-A265822 ..... p 1111 N94-15139 #
AD-A266174 ..... p 1132 N94-16925 #
AD-A266176 ..... p 984 N94-16981 #
AD-A266178 ..... p 1152 N94-16982 #
AD-A266184 ..... p 1012 N94-16935 #
AD-A266185 ..... p 1191 N94-16454 #
AD-A266186 ..... p 886 N94-16455 #
AD-A266187 ..... p 871 N94-16107 #
AD-A266188 ..... p 867 N94-16122 #
AD-A266189 ..... p 1059 N94-16123 #
AD-A266192 ..... p 1039 N94-16124 #
AD-A266193 ..... p 1101 N94-16125 #
AD-A266194 ..... p 1191 N94-16126 #
AD-A266196 ..... p 1169 N94-16127 #
AD-A266197 ..... p 1192 N94-16936 #
AD-A266198 ..... p 1191 N94-16128 #
AD-A266199 ..... p 1137 N94-16108 #
AD-A266217 ..... p 1173 N94-16937 #
AD-A266222 ..... p 1174 N94-16109 #
AD-A266226 ..... p 1023 N94-16110 #
AD-A266227 ..... p 1166 N94-16938 #
AD-A266228 ..... p 1138 N94-16983 #
AD-A266229 ..... p 1177 N94-16939 #
AD-A266230 ..... p 1192 N94-16926 #
AD-A266232 ..... p 1118 N94-17224 #
AD-A266234 ..... p 1026 N94-16927 #
AD-A266235 ..... p 969 N94-16928 #
AD-A266236 ..... p 1026 N94-16966 #
AD-A266237 ..... p 1182 N94-16111 #
AD-A266240 ..... p 1026 N94-16929 #
AD-A266242 ..... p 950 N94-16930 #
AD-A266243 ..... p 882 N94-16468 #
AD-A266244 ..... p 1101 N94-16469 #
AD-A266245 ..... p 1023 N94-16470 #
AD-A266246 ..... p 950 N94-16931 #
AD-A266247 ..... p 1170 N94-16940 #
AD-A266248 ..... p 925 N94-16482 #
AD-A266260 ..... p 1212 N94-16932 #
AD-A266261 ..... p 1025 N94-16908 #
AD-A266275 ..... p 857 N94-16471*
AD-A266277 ..... p 967 N94-16472 #
AD-A266283 ..... p 1225 N94-16473
AD-A266284 ..... p 887 N94-16909 #
AD-A266285 ..... p 1151 N94-16910 #
AD-A266293 ..... p 1039 N94-16474
AD-A266294 ..... p 967 N94-16475 #
AD-A266295 ..... p 1210 N94-16476 #
AD-A266296 ..... p 1000 N94-16911 #
AD-A266298 ..... p 997 N94-16477 #
AD-A266303 ..... p 1000 N94-16965 #
AD-A266307 ..... p 1182 N94-16466 #
AD-A266314 ..... p 997 N94-16467 #
AD-A266315 ..... p 1132 N94-16456 #
AD-A266317 ..... p 862 N94-16438 #
AD-A266318 ..... p 1026 N94-16950 #
AD-A266322 ..... p 864 N94-16439 #
AD-A266328 ..... p 934 N94-16440 #
AD-A266364 ..... p 1237 N94-17225 #
AD-A266365 ..... p 1117 N94-16441 #
AD-A266378 ..... p 1117 N94-16514
AD-A266380 ..... p 1123 N94-16515 #
AD-A266382 ..... p 869 N94-16516 #
AD-A266384 ..... p 1113 N94-16517 #
AD-A266394 ..... p 935 N94-16483 #
AD-A266395 ..... p 935 N94-16484 #
AD-A266396 ..... p 935 N94-16485 #
AD-A266397 ..... p 935 N94-16528 #
AD-A266398 ..... p 935 N94-16529 #
AD-A266402 ..... p 882 N94-16530 #
AD-A266403 ..... p 1192 N94-16550 #
AD-A266404 ..... p 1101 N94-16551 #
AD-A266411 ..... p 864 N94-16457
AD-A266414 ..... p 878 N94-16552 #
AD-A266415 ..... p 948 N94-16553 #
AD-A266419 ..... p 1149 N94-16554 * #
AD-A266421 ..... p 1024 N94-16555 #
AD-A266422 ..... p 1165 N94-16559 #
AD-A266423 ..... p 1011 N94-16556 #
AD-A266425 ..... p 998 N94-16557 #
AD-A266426 ..... p 1123 N94-16558 #
AD-A266427 ..... p 1123 N94-16544 #
AD-A266430 ..... p 1117 N94-16545 #
AD-A266431 ..... p 1040 N94-16546 #
AD-A266438 ..... p 1149 N94-16560 #
AD-A266439 ..... p 1113 N94-16561 #
AD-A266448 ..... p 958 N94-16562 #
AD-A266451 ..... p 1192 N94-16563 #
AD-A266453 ..... p 1123 N94-16564 #
AD-A266454 ..... p 1123 N94-16565 #
AD-A266455 ..... p 1123 N94-16566 #
AD-A266457 ..... p 1214 N94-17216 #
AD-A266458 ..... p 1092 N94-16567
AD-A266459 ..... p 1106 N94-16568
AD-A266460 ..... p 936 N94-16569 #
AD-A266461 ..... p 1231 N94-16570 #
AD-A266463 ..... p 1150 N94-16585 #
AD-A266464 ..... p 1182 N94-16586 #
AD-A266465 ..... p 1059 N94-16587 #
AD-A266466 ..... p 1113 N94-16588 #
AD-A266467 ..... p 1096 N94-16589 #
AD-A266468 ..... p 999 N94-16777
AD-A266473 ..... p 1128 N94-16779
AD-A266474 ..... p 959 N94-16780
AD-A266489 ..... p 959 N94-16781 #
AD-A266492 ..... p 1211 N94-16782
AD-A266493 ..... p 1138 N94-16793
AD-A266496 ..... p 999 N94-16794 #
AD-A266499 ..... p 1128 N94-16783 #
AD-A266503 ..... p 1128 N94-16784
AD-A266505 ..... p 1128 N94-16785
AD-A266506 ..... p 1128 N94-16786
AD-A266507 ..... p 948 N94-16787 #
AD-A266508 ..... p 999 N94-16788
AD-A266509 ..... p 999 N94-16789
AD-A266522 ..... p 1151 N94-16790
AD-A266523 ..... p 1160 N94-16791 #
AD-A266524 ..... p 936 N94-16795
AD-A266537 ..... p 968 N94-16796 #
AD-A266541 ..... p 999 N94-16797 #
AD-A266542 ..... p 859 N94-16798 #
AD-A266557 ..... p 1174 N94-16665 #
AD-A266568 ..... p 1211 N94-16800 #
AD-A266570 ..... p 1210 N94-16720 #
AD-A266571 ..... p 1150 N94-16721 #
AD-A266572 ..... p 1183 N94-16722 #
AD-A266573 ..... p 968 N94-16723 #
AD-A266595 ..... p 1160 N94-16724 #
AD-A266596 ..... p 1166 N94-16725 #
AD-A266600 ..... p 1173 N94-16726 #
AD-A266605 ..... p 968 N94-16727 #
AD-A266606 ..... p 999 N94-16728 #
AD-A266607 ..... p 1173 N94-16657 #
AD-A266617 ..... p 1147 N94-15725 #
AD-A266620 ..... p 1009 N94-15726 #
AD-A266624 ..... p 1180 N94-15727 #
AD-A266625 ..... p 1021 N94-15770 #
AD-A266626 ..... p 1112 N94-15771 #
AD-A266633 ..... p 1122 N94-15740 #
AD-A266634 ..... p 1122 N94-15741 #
AD-A266635 ..... p 1169 N94-15785
AD-A266636 ..... p 1131 N94-15742 #
AD-A266637 ..... p 1147 N94-15743 #
AD-A266638 ..... p 1140 N94-15744 #
AD-A266639 ..... p 1158 N94-15745 #
AD-A266640 ..... p 1164 N94-15746 #
AD-A266653 ..... p 968 N94-16767 #
AD-A266657 ..... p 1206 N94-15747 #
AD-A266671 ..... p 1147 N94-15772
AD-A266695 ..... p 1148 N94-15840 #
AD-A266697 ..... p 1148 N94-15841 #
AD-A266703 ..... p 1147 N94-15728 #
AD-A266716 ..... p 964 N94-15729 #
AD-A266718 ..... p 870 N94-15730 #
AD-A266719 ..... p 866 N94-15731 #
AD-A266721 ..... p 1137 N94-15820 #
AD-A266728 ..... p 1298 N94-15821 #
AD-A266730 ..... p 1304 N94-17651 #
AD-A266742 ..... p 965 N94-15773
AD-A266743 ..... p 1181 N94-15774
AD-A266744 ..... p 1206 N94-15822 #
AD-A266746 ..... p 1165 N94-15775
AD-A266747 ..... p 1174 N94-15823 #
AD-A266748 ..... p 1022 N94-15953 #
AD-A266749 ..... p 1010 N94-15954 #
AD-A266752 ..... p 1147 N94-15776
AD-A266753 ..... p 1021 N94-15755
AD-A266754 ..... p 1207 N94-15955 #
AD-A266760 ..... p 857 N94-15824 #
AD-A266767 ..... p 1009 N94-15825 #
AD-A266772 ..... p 1082 N94-15842 #
AD-A266778 ..... p 871 N94-14908 #
AD-A266786 ..... p 942 N94-14909 #
AD-A266788 ..... p 1163 N94-14910 #
AD-A266789 ..... p 942 N94-14911 #
AD-A266804 ..... p 986 N94-14912 #
AD-A266805 ..... p 1205 N94-14913 #
AD-A266814 ..... p 1164 N94-15756
AD-A266818 ..... p 1151 N94-16768 #
AD-A266819 ..... p 1151 N94-16769
AD-A266823 ..... p 962 N94-14914 #
AD-A266824 ..... p 965 N94-15843 #
AD-A266825 ..... p 964 N94-15683 #
AD-A266831 ..... p 1141 N94-14915 #
AD-A266834 ..... p 1119 N94-14916 #
AD-A266835 ..... p 1119 N94-14917 #
AD-A266839 ..... p 1115 N94-14918 #
AD-A266850 ..... p 1106 N94-15757
AD-A266851 ..... p 1056 N94-14945 #
AD-A266852 ..... p 963 N94-14948 #
AD-A266866 ..... p 1163 N94-14950 #
AD-A266867 ..... p 863 N94-14919 #

AD-A266868 ..... p 1045 N94-14920 #
AD-A266871 ..... p 884 N94-15147 #
AD-A266872 ..... p 1105 N94-15142 #
AD-A266877 ..... p 962 N94-14921 #
AD-A266878 ..... p 1206 N94-14922 #
AD-A266883 ..... p 1119 N94-14923 #
AD-A266889 ..... p 1142 N94-14924 #
AD-A266890 ..... p 865 N94-14951 #
AD-A266891 ..... p 942 N94-14946 #
AD-A266893 ..... p 1111 N94-14947 #
AD-A266894 ..... p 1179 N94-14949 #
AD-A266896 ..... p 1119 N94-14952 #
AD-A266903 ..... p 942 N94-14956 #
AD-A266905 ..... p 930 N94-15143 #
AD-A266916 ..... p 986 N94-14998 #
AD-A266920 ..... p 930 N94-14999 #
AD-A266921 ..... p 954 N94-15104 #
AD-A266924 ..... p 855 N94-15105 #
AD-A266926 ..... p 1206 N94-15107 #
AD-A266927 ..... p 1131 N94-15108 #
AD-A266930 ..... p 1158 N94-15173 #
AD-A266931 ..... p 1140 N94-15174 #
AD-A266934 ..... p 1143 N94-15175 #
AD-A266938 ..... p 1228 N94-15176 #
AD-A266939 ..... p 983 N94-15177 #
AD-A266943 ..... p 1003 N94-17307 #
AD-A266946 ..... p 1229 N94-15178 #
AD-A266948 ..... p 1175 N94-15758
AD-A266954 ..... p 1122 N94-15759
AD-A266955 ..... p 946 N94-15760
AD-A266957 ..... p 963 N94-15179 #
AD-A266958 ..... p 1120 N94-15180 #
AD-A266959 ..... p 1142 N94-14967 #
AD-A266960 ..... p 1163 N94-14968 #
AD-A266961 ..... p 879 N94-14969 #
AD-A266962 ..... p 1045 N94-14970 #
AD-A266963 ..... p 863 N94-14971 #
AD-A266964 ..... p 864 N94-14972 #
AD-A266965 ..... p 1188 N94-15144 #
AD-A266966 ..... p 1163 N94-14953 #
AD-A266967 ..... p 1163 N94-14954 #
AD-A266968 ..... p 986 N94-14955 #
AD-A266969 ..... p 1172 N94-15002 #
AD-A266970 ..... p 943 N94-15111 #
AD-A266972 ..... p 1143 N94-15110 #
AD-A266982 ..... p 963 N94-15490 #
AD-A266984 ..... p 866 N94-15761
AD-A266985 ..... p 1057 N94-15150 #
AD-A266986 ..... p 1158 N94-15492 #
AD-A266987 ..... p 1008 N94-15494 #
AD-A266988 ..... p 864 N94-15498 #
AD-A266989 ..... p 1164 N94-15502 #
AD-A266990 ..... p 1143 N94-15212 #
AD-A266991 ..... p 1222 N94-15213 #
AD-A266993 ..... p 1144 N94-15214 #
AD-A266994 ..... p 1144 N94-15215 #
AD-A266995 ..... p 1144 N94-15216 #
AD-A266996 ..... p 1145 N94-15629 #
AD-A266997 ..... p 1145 N94-15630 #
AD-A266999 ..... p 963 N94-15631 #
AD-A267000 ..... p 1020 N94-15632 #
AD-A267004 ..... p 1121 N94-15634 #
AD-A267006 ..... p 1008 N94-15635 #
AD-A267007 ..... p 1132 N94-15762
AD-A267009 ..... p 1057 N94-15524 #
AD-A267010 ..... p 1145 N94-15525 #
AD-A267012 ..... p 1140 N94-15763
AD-A267013 ..... p 989 N94-15748
AD-A267014 ..... p 1112 N94-15844
AD-A267015 ..... p 1020 N94-15526 #
AD-A267019 ..... p 1122 N94-15845
AD-A267021 ..... p 987 N94-15527 #
AD-A267022 ..... p 933 N94-15835
AD-A267023 ..... p 933 N94-15528 #
AD-A267024 ..... p 933 N94-15626 #
AD-A267026 ..... p 1145 N94-15627 #
AD-A267029 ..... p 1146 N94-15674 #
AD-A267035 ..... p 964 N94-15675 #
AD-A267037 ..... p 983 N94-15676 #
AD-A267038 ..... p 1131 N94-15659 #
AD-A267040 ..... p 1231 N94-16458 #
AD-A267045 ..... p 1299 N94-15836
AD-A267046 ..... p 1121 N94-15660 #
AD-A267048 ..... p 1201 N94-15661 #
AD-A267049 ..... p 1117 N94-15662 #
AD-A267050 ..... p 1121 N94-15663 #
AD-A267052 ..... p 1189 N94-15664 #
AD-A267053 ..... p 1008 N94-15665 #
AD-A267054 ..... p 1166 N94-16770 #
AD-A267055 ..... p 885 N94-15666 #
AD-A267056 ..... p 988 N94-15667 #
AD-A267069 ..... p 988 N94-15668 #
AD-A267070 ..... p 1009 N94-15669 #
AD-A267071 ..... p 1146 N94-15670 #
AD-A267072 ..... p 1158 N94-15671 #
AD-A267073 ..... p 1009 N94-15672 #
AD-A267074 ..... p 1009 N94-15673 #
AD-A267075 ..... p 1038 N94-15628 #
AD-A267076 ..... p 1098 N94-15539 #
AD-A267077 ..... p 987 N94-15540 #
AD-A267079 ..... p 987 N94-15541 #
AD-A267086 ..... p 862 N94-15542 #
AD-A267087 ..... p 872 N94-15543 #
AD-A267090 ..... p 987 N94-15544 #
AD-A267098 ..... p 1008 N94-15636 #
AD-A267099 ..... p 862 N94-15637 #
AD-A267102 ..... p 1116 N94-15633 #
AD-A267103 ..... p 1146 N94-15638 #
AD-A267105 ..... p 988 N94-15649 #
AD-A267114 ..... p 1146 N94-15650 #
AD-A267115 ..... p 866 N94-15651 #
AD-A267116 ..... p 1229 N94-15652 #
AD-A267117 ..... p 1146 N94-15653 #
AD-A267118 ..... p 946 N94-15684 #
AD-A267119 ..... p 946 N94-15685 #
AD-A267125 ..... p 1038 N94-15686 #
AD-A267129 ..... p 1146 N94-15687 #
AD-A267133 ..... p 964 N94-15688 #
AD-A267134 ..... p 1180 N94-15689 #
AD-A267137 ..... p 988 N94-15690 #
AD-A267138 ..... p 988 N94-15691 #
AD-A267139 ..... p 866 N94-15692 #
AD-A267140 ..... p 885 N94-15749 #
AD-A267143 ..... p 1229 N94-15437 #
AD-A267144 ..... p 1159 N94-15750 #
AD-A267145 ..... p 1177 N94-15732 #
AD-A267146 ..... p 1172 N94-15733 #
AD-A267148 ..... p 929 N94-15734 #
AD-A267149 ..... p 1189 N94-15735 #
AD-A267150 ..... p 1206 N94-15764 #
AD-A267151 ..... p 1172 N94-15777 #
AD-A267152 ..... p 1165 N94-15778 #
AD-A267153 ..... p 1169 N94-15779 #
AD-A267154 ..... p 925 N94-15837
AD-A267155 ..... p 1121 N94-15736 #
AD-A267157 ..... p 1033 N94-15826
AD-A267161 ..... p 1021 N94-15737 #
AD-A267163 ..... p 1046 N94-15738 #
AD-A267167 ..... p 1189 N94-15739 #
AD-A267168 ..... p 1165 N94-15855
AD-A267170 ..... p 872 N94-15856
AD-A267172 ..... p 1190 N94-15846
AD-A267173 ..... p 872 N94-15847
AD-A267176 ..... p 988 N94-15693 #
AD-A267178 ..... p 1190 N94-15848
AD-A267179 ..... p 1159 N94-15849
AD-A267180 ..... p 1131 N94-15694 #
AD-A267181 ..... p 1131 N94-15148 #
AD-A267182 ..... p 1016 N94-15151 #
AD-A267184 ..... p 989 N94-15786 #
AD-A267185 ..... p 857 N94-15787 #
AD-A267186 ..... p 1037 N94-15145 #
AD-A267187 ..... p 1230 N94-15850
AD-A267192 ..... p 1106 N94-15851
AD-A267193 ..... p 1228 N94-15152 #
AD-A267194 ..... p 1229 N94-15788 #
AD-A267195 ..... p 1230 N94-15789 #
AD-A267196 ..... p 1038 N94-15852
AD-A267197 ..... p 1095 N94-15790 #
AD-A267198 ..... p 1038 N94-15853
AD-A267199 ..... p 1189 N94-15791 #
AD-A267202 ..... p 886 N94-15857 #
AD-A267203 ..... p 1022 N94-15858 #
AD-A267205 ..... p 965 N94-15859 #
AD-A267206 ..... p 1022 N94-15860 #
AD-A267208 ..... p 859 N94-16913 #
AD-A267211 ..... p 960 N94-16984 #
AD-A267212 ..... p 1026 N94-16985 #
AD-A267213 ..... p 1166 N94-16986 #
AD-A267214 ..... p 1204 N94-16987 #
AD-A267216 ..... p 1149 N94-16120 #
AD-A267240 ..... p 855 N94-14973 #
AD-A267242 ..... p 986 N94-14974
AD-A267243 ..... p 930 N94-14975 #
AD-A267245 ..... p 865 N94-14976 #
AD-A267246 ..... p 1219 N94-14977 #
AD-A267248 ..... p 1151 N94-16941 #
AD-A267249 ..... p 1132 N94-16942 #
AD-A267253 ..... p 1235 N94-16988 #
AD-A267254 ..... p 1118 N94-16989 #
AD-A267256 ..... p 888 N94-16990 #
AD-A267260 ..... p 1178 N94-16991 #
AD-A267261 ..... p 1028 N94-17286 #
AD-A267264 ..... p 1188 N94-14957 #
AD-A267265 ..... p 1029 N94-17363 #
AD-A267266 ..... p 1193 N94-17264 #
AD-A267267 ..... p 1133 N94-17265 #
AD-A267268 ..... p 897 N94-17266 #
AD-A267270 ..... p 1161 N94-17239 * #
AD-A267277 ..... p 928 N94-17308
AD-A267278 ..... p 1105 N94-14958 #
AD-A267280 ..... p 897 N94-17240 #
AD-A267282 ..... p 855 N94-14959 #
AD-A267284 ..... p 1113 N94-17241 #
AD-A267286 ..... p 972 N94-17242 #
AD-A267290 ..... p 1097 N94-14960 #
AD-A267291 ..... p 1214 N94-17243 #
AD-A267292 ..... p 954 N94-14961 #
AD-A267293 ..... p 1107 N94-17244 #
AD-A267294 ..... p 1108 N94-17267 #
AD-A267296 ..... p 1003 N94-17268 #
AD-A267297 ..... p 1174 N94-17219 #
AD-A267302 ..... p 972 N94-17227 #
AD-A267304 ..... p 971 N94-16980 #
AD-A267305 ..... p 1212 N94-16992 #
AD-A267307 ..... p 1160 N94-16993 #
AD-A267308 ..... p 971 N94-16994 #
AD-A267310 ..... p 1060 N94-16943 #
AD-A267313 ..... p 1048 N94-16944 #
AD-A267314 ..... p 1000 N94-16945 #
AD-A267316 ..... p 969 N94-16946 #
AD-A267317 ..... p 1153 N94-17220 #
AD-A267319 ..... p 970 N94-16947 #
AD-A267320 ..... p 970 N94-16948 #
AD-A267321 ..... p 970 N94-16949 #
AD-A267322 ..... p 1041 N94-17001 #
AD-A267323 ..... p 1035 N94-17002 #
AD-A267325 ..... p 1026 N94-17003 #
AD-A267367 ..... p 1299 N94-17004 #
AD-A267370 ..... p 1140 N94-17005 #
AD-A267371 ..... p 950 N94-17006 #
AD-A267376 ..... p 1001 N94-17019 #
AD-A267381 ..... p 1133 N94-17020 #
AD-A267382 ..... p 1012 N94-17023 #
AD-A267384 ..... p 859 N94-17021 #
AD-A267390 ..... p 1193 N94-17024 #
AD-A267403 ..... p 1233 N94-17114 #
AD-A267405 ..... p 1001 N94-17025 #
AD-A267409 ..... p 1152 N94-16974 #
AD-A267410 ..... p 1192 N94-16975 #
AD-A267412 ..... p 1012 N94-16976 #
AD-A267413 ..... p 1232 N94-16977 #
AD-A267426 ..... p 1004 N94-17309
AD-A267432 ..... p 970 N94-16978 #
AD-A267433 ..... p 1000 N94-16979 #
AD-A267434 ..... p 1001 N94-17026
AD-A267436 ..... p 1152 N94-17027 #
AD-A267441 ..... p 1133 N94-17022 #
AD-A267442 ..... p 1193 N94-17028 #
AD-A267443 ..... p 1107 N94-17029 #
AD-A267444 ..... p 1141 N94-17030 #
AD-A267446 ..... p 1001 N94-17031 #
AD-A267447 ..... p 1152 N94-17032 #
AD-A267453 ..... p 1001 N94-17033 #
AD-A267464 ..... p 1160 N94-17034 #
AD-A267465 ..... p 1001 N94-17035 #
AD-A267476 ..... p 860 N94-17099 #
AD-A267479 ..... p 1004 N94-17364 #
AD-A267485 ..... p 1185 N94-17365 #
AD-A267486 ..... p 1154 N94-17366 #
AD-A267494 ..... p 1173 N94-17585
AD-A267496 ..... p 1161 N94-17367
AD-A267498 ..... p 898 N94-17368 #
AD-A267500 ..... p 1167 N94-17369 #
AD-A267505 ..... p 1154 N94-17370 #
AD-A267508 ..... p 975 N94-17073
AD-A267509 ..... p 860 N94-17074 #
AD-A267511 ..... p 1153 N94-17075 #
AD-A267512 ..... p 1170 N94-17076 #
AD-A267514 ..... p 1138 N94-17077 #
AD-A267516 ..... p 1153 N94-17078
AD-A267524 ..... p 1141 N94-17115 #
AD-A267527 ..... p 1213 N94-17116 #
AD-A267532 ..... p 868 N94-17117
AD-A267534 ..... p 1153 N94-17118 #
AD-A267535 ..... p 1178 N94-17119
AD-A267543 ..... p 960 N94-17100
AD-A267546 ..... p 1232 N94-17101
AD-A267547 ..... p 1107 N94-17102 #
AD-A267548 ..... p 888 N94-17103 #
AD-A267549 ..... p 1013 N94-17104 #
AD-A267553 ..... p 1061 N94-17105 #
AD-A267557 ..... p 961 N94-17106 #
AD-A267560 ..... p 1153 N94-17107 #
AD-A267561 ..... p 1213 N94-17108 #
AD-A267562 ..... p 961 N94-17109 #
AD-A267570 ..... p 1002 N94-17110 #
AD-A267579 ..... p 951 N94-17207 #
AD-A267583 ..... p 1299 N94-17208 #
AD-A267587 ..... p 1160 N94-17209 #
AD-A267588 ..... p 951 N94-17210 #
AD-A267592 ..... p 930 N94-17192
AD-A267597 ..... p 1041 N94-17193 #
AD-A267598 ..... p 1055 N94-17194 #
AD-A267619 ..... p 1041 N94-17195 #
AD-A267620 ..... p 1002 N94-17196 #
AD-A267622 ..... p 1035 N94-17197 #
AD-A267624 ..... p 971 N94-17198 #

AD-A267627 ..... p 1002 N94-17199 #
AD-A267628 ..... p 1003 N94-17211 #
AD-A267629 ..... p 1003 N94-17212 #
AD-A267630 ..... p 1002 N94-17200 #
AD-A267631 ..... p 1166 N94-17201
AD-A267632 ..... p 1167 N94-17202
AD-A267633 ..... p 951 N94-17203
AD-A267645 ..... p 971 N94-17204
AD-A267647 ..... p 1002 N94-17205 #
AD-A267648 ..... p 1107 N94-17245
AD-A267649 ..... p 897 N94-17246 #
AD-A267651 ..... p 1108 N94-17247 #
AD-A267653 ..... p 976 N94-17248 #
AD-A267654 ..... p 1003 N94-17249 #
AD-A267656 ..... p 860 N94-17221 #
AD-A267660 ..... p 1028 N94-17250 #
AD-A267663 ..... p 1003 N94-17228 #
AD-A267666 ..... p 1061 N94-17269
AD-A267667 ..... p 943 N94-14962
AD-A267675 ..... p 855 N94-14963
AD-A267685 ..... p 1233 N94-17229 #
AD-A267686 ..... p 868 N94-14964
AD-A267692 ..... p 1214 N94-17270 #
AD-A267708 ..... p 853 N94-14965 #
AD-A267709 ..... p 1007 N94-14936 #
AD-A267710 ..... p 1163 N94-14937 #
AD-A267711 ..... p 1105 N94-14938 #
AD-A267713 ..... p 940 N94-17271
AD-A267714 ..... p 1168 N94-14939
AD-A267715 ..... p 1214 N94-17272
AD-A267717 ..... p 972 N94-17273
AD-A267721 ..... p 1188 N94-14940
AD-A267722 ..... p 860 N94-17274 #
AD-A267723 ..... p 879 N94-14941 #
AD-A267724 ..... p 855 N94-14942 #
AD-A267726 ..... p 1154 N94-17371
AD-A267727 ..... p 1173 N94-17372 #
AD-A267728 ..... p 1042 N94-17230 #
AD-A267743 ..... p 1004 N94-17373 #
AD-A267746 ..... p 1119 N94-14943
AD-A267747 ..... p 1129 N94-17374
AD-A267752 ..... p 1153 N94-17231 #
AD-A267753 ..... p 1014 N94-17375 #
AD-A267754 ..... p 1118 N94-17232 #
AD-A267755 ..... p 1003 N94-17206 #
AD-A267756 ..... p 1118 N94-17275 #
AD-A267757 ..... p 1028 N94-17276 #
AD-A267761 ..... p 1193 N94-17254 #
AD-A267762 ..... p 860 N94-17222 #
AD-A267764 ..... p 961 N94-17223 #
AD-A267766 ..... p 1232 N94-17007
AD-A267785 ..... p 1108 N94-17303 #
AD-A267796 ..... p 1003 N94-17304 #
AD-A267798 ..... p 1304 N94-17305 #
AD-A267799 ..... p 874 N94-17306 #
AD-A267806 ..... p 950 N94-17008
AD-A267809 ..... p 973 N94-17408 #
AD-A267811 ..... p 1161 N94-17409 #
AD-A267813 ..... p 1155 N94-17398 #
AD-A267814 ..... p 1155 N94-17399 #
AD-A267818 ..... p 1042 N94-17400 #
AD-A267822 ..... p 1035 N94-17401 #
AD-A267823 ..... p 1035 N94-17402 #
AD-A267826 ..... p 872 N94-17403 #
AD-A267829 ..... p 1155 N94-17404 #
AD-A267833 ..... p 872 N94-17405 #
AD-A267838 ..... p 1152 N94-17009 #
AD-A267841 ..... p 1232 N94-17036 #
AD-A267842 ..... p 1001 N94-17011 #
AD-A267843 ..... p 1193 N94-17012 #
AD-A267849 ..... p 1004 N94-17406 #
AD-A267852 ..... p 898 N94-17388 #
AD-A267865 ..... p 1215 N94-17389 #
AD-A267866 ..... p 1154 N94-17390 #
AD-A267868 ..... p 1113 N94-17391 #
AD-A267873 ..... p 1167 N94-17392 #
AD-A267875 ..... p 940 N94-17013 #
AD-A267876 ..... p 1213 N94-17037
AD-A267877 ..... p 1012 N94-17040
AD-A267879 ..... p 960 N94-17041 #
AD-A267880 ..... p 1152 N94-17014
AD-A267881 ..... p 1141 N94-17015
AD-A267883 ..... p 1171 N94-17393 #
AD-A267889 ..... p 1213 N94-17042
AD-A267893 ..... p 1042 N94-17394 #
AD-A267895 ..... p 1154 N94-17395 #
AD-A267896 ..... p 1154 N94-17396 #
AD-A267905 ..... p 1042 N94-17378 #
AD-A267907 ..... p 941 N94-17379 #
AD-A267908 ..... p 1141 N94-17380 #
AD-A267911 ..... p 952 N94-17381 #
AD-A267942 ..... p 874 N94-17010
AD-A267943 ..... p 1060 N94-17043
AD-A267944 ..... p 1093 N94-17382 #
AD-A267948 ..... p 1055 N94-17044
AD-A267949 ..... p 927 N94-17053
AD-A267950 ..... p 1107 N94-17054
AD-A267956 ..... p 1102 N94-17493
AD-A267959 ..... p 1173 N94-17495
AD-A267960 ..... p 1114 N94-17497
AD-A267963 ..... p 1113 N94-17383 #
AD-A267965 ..... p 1029 N94-17384 #
AD-A267966 ..... p 973 N94-17490 #
AD-A267968 ..... p 1155 N94-17491 #
AD-A267969 ..... p 1005 N94-17498
AD-A267972 ..... p 1014 N94-17410 #
AD-A267978 ..... p 1155 N94-17500
AD-A267979 ..... p 1155 N94-17411 #
AD-A267980 ..... p 871 N94-17412 #
AD-A267988 ..... p 1133 N94-17453 #
AD-A267989 ..... p 973 N94-17413 #
AD-A267990 ..... p 1029 N94-17414 #
AD-A268000 ..... p 1156 N94-17530
AD-A268001 ..... p 1004 N94-17376 #
AD-A268002 ..... p 868 N94-17472
AD-A268009 ..... p 941 N94-17473
AD-A268011 ..... p 1109 N94-17492 #
AD-A268012 ..... p 929 N94-17474 #
AD-A268013 ..... p 1138 N94-17475
AD-A268014 ..... p 863 N94-17586
AD-A268015 ..... p 973 N94-17494 #
AD-A268016 ..... p 1216 N94-17477 #
AD-A268017 ..... p 952 N94-17532 #
AD-A268052 ..... p 1114 N94-17503 #
AD-A268053 ..... p 929 N94-17587
AD-A268056 ..... p 1167 N94-17506 #
AD-A268059 ..... p 1157 N94-17588
AD-A268062 ..... p 929 N94-17589
AD-A268067 ..... p 1062 N94-17507 #
AD-A268069 ..... p 1162 N94-17550 #
AD-A268070 ..... p 1162 N94-17551 #
AD-A268071 ..... p 1109 N94-17552 #
AD-A268072 ..... p 1110 N94-17595 #
AD-A268081 ..... p 1102 N94-17512
AD-A268083 ..... p 1055 N94-17514
AD-A268084 ..... p 1056 N94-17596 #
AD-A268085 ..... p 1157 N94-17590 #
AD-A268086 ..... p 1055 N94-17515
AD-A268097 ..... p 1015 N94-17570 #
AD-A268101 ..... p 1109 N94-17571 #
AD-A268102 ..... p 1109 N94-17572 #
AD-A268103 ..... p 1109 N94-17573 #
AD-A268104 ..... p 1168 N94-17517
AD-A268106 ..... p 861 N94-17574 #
AD-A268122 ..... p 1005 N94-17519 #
AD-A268126 ..... p 952 N94-17520
AD-A268128 ..... p 1171 N94-17521
AD-A268130 ..... p 1109 N94-17522 #
AD-A268144 ..... p 1216 N94-17454
AD-A268146 ..... p 1199 N94-17455
AD-A268148 ..... p 1014 N94-17428 #
AD-A268150 ..... p 1134 N94-17468 #
AD-A268151 ..... p 1155 N94-17429
AD-A268164 ..... p 973 N94-17430 #
AD-A268167 ..... p 1005 N94-17431 #
AD-A268176 ..... p 873 N94-17432 #
AD-A268177 ..... p 873 N94-17508 #
AD-A268178 ..... p 1114 N94-17509 #
AD-A268181 ..... p 1134 N94-17510 #
AD-A268183 ..... p 1030 N94-17511 #
AD-A268191 ..... p 941 N94-17597
AD-A268192 ..... p 1015 N94-17560
AD-A268199 ..... p 1216 N94-17561
AD-A268200 ..... p 1129 N94-17478
AD-A268205 ..... p 1216 N94-17480
AD-A268206 ..... p 1216 N94-17553
AD-A268221 ..... p 1130 N94-17554
AD-A268222 ..... p 1114 N94-17555 #
AD-A268225 ..... p 1130 N94-17556 #
AD-A268227 ..... p 1130 N94-17562 #
AD-A268229 ..... p 1139 N94-17563
AD-A268230 ..... p 1139 N94-17564
AD-A268231 ..... p 1006 N94-17565
AD-A268249 ..... p 1042 N94-17415
AD-A268250 ..... p 1129 N94-17456
AD-A268251 ..... p 952 N94-17416
AD-A268254 ..... p 1215 N94-17417
AD-A268257 ..... p 1048 N94-17433
AD-A268260 ..... p 962 N94-17418
AD-A268268 ..... p 1204 N94-17575 #
AD-A268269 ..... p 1215 N94-17377
AD-A268270 ..... p 1134 N94-17576 #
AD-A268274 ..... p 1005 N94-17523 #
AD-A268275 ..... p 941 N94-17457
AD-A268279 ..... p 1216 N94-17577 #
AD-A268283 ..... p 1186 N94-17578 #
AD-A268286 ..... p 1217 N94-17579 #
AD-A268287 ..... p 861 N94-17580 #
AD-A268291 ..... p 1049 N94-17566 #
AD-A268311 ..... p 1042 N94-17567 #
AD-A268316 ..... p 1237 N94-17568 #
AD-A268328 ..... p 865 N94-17458
AD-A268331 ..... p 1176 N94-17581 #
AD-A268340 ..... p 1006 N94-17582 #
AD-A268356 ..... p 1108 N94-17459
AD-A268375 ..... p 1234 N94-17419
AD-A268376 ..... p 1138 N94-17460
AD-A268383 ..... p 1171 N94-17420
AD-A268385 ..... p 1084 N94-17421
AD-A268386 ..... p 873 N94-17569 #
AD-A268388 ..... p 1215 N94-17422
AD-A268391 ..... p 1048 N94-17533 #
AD-A268392 ..... p 1134 N94-17535 #
AD-A268393 ..... p 1186 N94-17536 #
AD-A268394 ..... p 861 N94-17461
AD-A268396 ..... p 1005 N94-17496
AD-A268397 ..... p 1015 N94-17526
AD-A268398 ..... p 1133 N94-17397
AD-A268399 ..... p 1014 N94-17423
AD-A268400 ..... p 1129 N94-17424
AD-A268401 ..... p 973 N94-17434
AD-A268402 ..... p 1048 N94-17462
AD-A268403 ..... p 868 N94-17425
AD-A268407 ..... p 1005 N94-17463
AD-A268408 ..... p 868 N94-17435
AD-A268435 ..... p 1134 N94-17513
AD-A268443 ..... p 1102 N94-17499
AD-A268448 ..... p 985 N94-17482
AD-A268449 ..... p 985 N94-17484
AD-A268450 ..... p 985 N94-17485
AD-A268454 ..... p 976 N94-17538 #
AD-A268521 ..... p 1220 N94-17540 #
AD-A268523 ..... p 1156 N94-17541 #
AD-A268525 ..... p 929 N94-17543 #
AD-A268565 ..... p 1115 N94-17598 #
AD-A268566 ..... p 1179 N94-17599 #
AD-A268568 ..... p 1157 N94-17620 #
AD-A268570 ..... p 1130 N94-17621 #
AD-A268579 ..... p 1162 N94-17622 #
AD-A268586 ..... p 1140 N94-17623 #
AD-A268590 ..... p 1176 N94-17605 #
AD-A268591 ..... p 1217 N94-17606 #
AD-A268592 ..... p 1110 N94-17607 #
AD-A268595 ..... p 1015 N94-17608 #
AD-A268596 ..... p 861 N94-17609 #
AD-A268598 ..... p 1085 N94-17610 #
AD-A268605 ..... p 962 N94-17464
AD-A268610 ..... p 1108 N94-17465
AD-A268628 ..... p 1186 N94-17436
AD-A268629 ..... p 973 N94-17466
AD-A268630 ..... p 1085 N94-17467
AD-A268635 ..... p 1199 N94-17427

AD-B169653L ..... p 1177 N94-15506

AD-D015748 ..... p 940 N94-16933
AD-D015751 ..... p 975 N94-16934
AD-D015778 ..... p 1191 N94-16547
AD-D015780 ..... p 1047 N94-16548
AD-D015782 ..... p 1011 N94-16549
AD-D015783 ..... p 1047 N94-16531
AD-D015785 ..... p 948 N94-16532
AD-D015786 ..... p 1040 N94-16533
AD-D015787 ..... p 935 N94-16534
AD-D015788 ..... p 998 N94-16535
AD-D015792 ..... p 1034 N94-16536
AD-D015793 ..... p 936 N94-16537
AD-D015794 ..... p 1210 N94-16538
AD-D015796 ..... p 948 N94-16539
AD-D015811 ..... p 1040 N94-16540
AD-D015812 ..... p 958 N94-16486
AD-D015813 ..... p 1210 N94-16487
AD-D015814 ..... p 1011 N94-16488
AD-D015815 ..... p 1191 N94-16489
AD-D015816 ..... p 1231 N94-16490
AD-D015885 ..... p 1012 N94-16914
AD-D015888 ..... p 1048 N94-16915
AD-D015889 ..... p 969 N94-16916
AD-D015890 ..... p 1000 N94-16917
AD-D015891 ..... p 1000 N94-16918
AD-D015892 ..... p 1177 N94-16919
AD-D015893 ..... p 969 N94-16920
AD-D015894 ..... p 1000 N94-16921

AD-E201472 ..... p 1105 N94-15142 #
AD-E201480 ..... p 1101 N94-16551 #
AD-E201487 ..... p 1011 N94-16556 #
AD-E201500 ..... p 1107 N94-17244 #
AD-E201501 ..... p 1003 N94-17268 #
AD-E201508 ..... p 1174 N94-17219 #
AD-E201515 ..... p 985 N94-17482
AD-E201517 ..... p 985 N94-17484
AD-E201518 ..... p 985 N94-17485
AD-E201548 ..... p 1097 N94-14960 #
AD-E501670 ..... p 1235 N94-16988 #

AD-871331 ..... p 866 N94-15692 #

AEDC-TR-93-10 ..... p 1048 N94-17462
AEDC-TR-93-7 ..... p 886 N94-15857 #

AEPA/SW/DK-A93/033A ..... p 1094 N94-15136 #

AERONAUTICA-ACTA-A-367-1992 p 923 N94-17592

AEROTHERM-FR-7186-93-15 ..... p 928 N94-17277 * #

AFGAN-2 ..... p 1213 N94-17037

AFIT/CI/CIA-92-119 ..... p 1105 N94-15137 #
AFIT/CI/CIA-93-001D ..... p 1060 N94-17043
AFIT/CI/CIA-93-004D ..... p 1168 N94-17517
AFIT/CI/CIA-93-006D ..... p 1173 N94-17585
AFIT/CI/CIA-93-007D ..... p 860 N94-17074 #
AFIT/CI/CIA-93-008D ..... p 1167 N94-17369 #
AFIT/CI/CIA-93-008 ..... p 871 N94-17412 #
AFIT/CI/CIA-93-011D ..... p 898 N94-17368 #
AFIT/CI/CIA-93-011 ..... p 868 N94-14964
AFIT/CI/CIA-93-012D ..... p 930 N94-17192
AFIT/CI/CIA-93-012 ..... p 1109 N94-17492 #
AFIT/CI/CIA-93-014D ..... p 1153 N94-17075 #
AFIT/CI/CIA-93-014 ..... p 1055 N94-17044
AFIT/CI/CIA-93-016 ..... p 1109 N94-17573 #
AFIT/CI/CIA-93-018 ..... p 1109 N94-17552 #
AFIT/CI/CIA-93-019 ..... p 1108 N94-17247 #
AFIT/CI/CIA-93-020 ..... p 1108 N94-17303 #
AFIT/CI/CIA-93-021 ..... p 1109 N94-17522 #
AFIT/CI/CIA-93-022 ..... p 1108 N94-17459
AFIT/CI/CIA-93-030 ..... p 1093 N94-17382 #
AFIT/CI/CIA-93-037 ..... p 1107 N94-17054
AFIT/CI/CIA-93-051 ..... p 1006 N94-17582 #
AFIT/CI/CIA-93-054 ..... p 1114 N94-17503 #
AFIT/CI/CIA-93-058 ..... p 1171 N94-17521
AFIT/CI/CIA-93-070 ..... p 952 N94-17520
AFIT/CI/CIA-93-072 ..... p 1161 N94-17367
AFIT/CI/CIA-93-077 ..... p 1013 N94-17104 #
AFIT/CI/CIA-93-079 ..... p 929 N94-17474 #
AFIT/CI/CIA-93-068 ..... p 927 N94-17053
AFIT/CI/CIA-93-089 ..... p 888 N94-17103 #
AFIT/CI/CIA-93-092 ..... p 1154 N94-17371
AFIT/CI/CIA-93-093 ..... p 860 N94-17221 #
AFIT/CI/CIA-93-094 ..... p 960 N94-17100
AFIT/CI/CIA-93-096 ..... p 1170 N94-17076 #
AFIT/CI/CIA-93-097 ..... p 1107 N94-17102 #
AFIT/CI/CIA-93-111 ..... p 929 N94-17587
AFIT/CI/CIA-93-112 ..... p 1162 N94-17551 #
AFIT/CI/CIA-93-113 ..... p 874 N94-17010
AFIT/CI/CIA-93-114 ..... p 941 N94-17473
AFIT/CI/CIA-93-116 ..... p 1102 N94-17512
AFIT/CI/CIA-93-117 ..... p 1138 N94-17475
AFIT/CI/CIA-93-118 ..... p 1102 N94-17493
AFIT/CI/CIA-93-119 ..... p 1109 N94-17572 #
AFIT/CI/CIA-93-120 ..... p 1110 N94-17595 #
AFIT/CI/CIA-93-122 ..... p 1109 N94-17571 #
AFIT/CI/CIA-93-17D ..... p 976 N94-17248 #

AFIT/DS/AA/93-1 ..... p 859 N94-16798 #

AFIT/DS/ENG/93-02 ..... p 1149 N94-16560 #
AFIT/DS/ENG/93-03 ..... p 1001 N94-17031 #
AFIT/DS/ENG/93-4 ..... p 1002 N94-17196 #

AFIT/DS/ENP/93-02 ..... p 1185 N94-17365 #

AFIT/EN/TR-93-6 ..... p 1154 N94-17366 #

AFIT/EN/TR/93-03 ..... p 1041 N94-17195 #

AFIT/GE/ENG/93J-01 ..... p 999 N94-16797 #
AFIT/GE/ENG/93J-03 ..... p 870 N94-15730 #

AFIT/GST/ENS/93M-05 ..... p 866 N94-15731 #

AFOSR-0574TR ..... p 1005 N94-17519 #
AFOSR-93-0195TR ..... p 1192 N94-16563 #
AFOSR-93-0388TR ..... p 1212 N94-16932 #
AFOSR-93-0422TR ..... p 1132 N94-16925 #
AFOSR-93-0424TR ..... p 967 N94-16472 #
AFOSR-93-0425TR ..... p 950 N94-16931 #
AFOSR-93-0429TR ..... p 886 N94-16455 #
AFOSR-93-0430TR ..... p 1059 N94-16123 #
AFOSR-93-0431TR ..... p 934 N94-16440 #
AFOSR-93-0432TR ..... p 925 N94-16482 #
AFOSR-93-0433TR ..... p 867 N94-16122 #
AFOSR-93-0438TR ..... p 1012 N94-16935 #
AFOSR-93-0439TR ..... p 1026 N94-16966 #
AFOSR-93-0440TR ..... p 1191 N94-16454 #
AFOSR-93-0442TR ..... p 1170 N94-16940 #
AFOSR-93-0443TR ..... p 871 N94-16107 #
AFOSR-93-0444TR ..... p 1173 N94-16937 #
AFOSR-93-0448TR ..... p 1118 N94-17224 #
AFOSR-93-0449TR ..... p 1026 N94-16950 #
AFOSR-93-0451TR ..... p 1026 N94-16929 #
AFOSR-93-0453TR ..... p 1023 N94-16470 #
AFOSR-93-0454TR ..... p 1132 N94-16456 #
AFOSR-93-0456TR ..... p 1038 N94-15852
AFOSR-93-0457TR ..... p 857 N94-15787 #
AFOSR-93-0458TR ..... p 1022 N94-15860 #
AFOSR-93-0459TR ..... p 1121 N94-15736 #
AFOSR-93-0459TR ..... p 1025 N94-16908 #
AFOSR-93-0460TR ..... p 1095 N94-15790 #
AFOSR-93-0461TR ..... p 925 N94-15837
AFOSR-93-0462TR ..... p 897 N94-17266 #
AFOSR-93-0463TR ..... p 1178 N94-16991 #
AFOSR-93-0464TR ..... p 1133 N94-17265 #
AFOSR-93-0466TR ..... p 855 N94-14959 #
AFOSR-93-0467TR ..... p 1028 N94-17286 #
AFOSR-93-0468TR ..... p 1193 N94-17264 #
AFOSR-93-0469TR ..... p 929 N94-15734 #
AFOSR-93-0470TR ..... p 1159 N94-15849
AFOSR-93-0471TR ..... p 860 N94-17099 #
AFOSR-93-0472TR ..... p 1016 N94-15151 #
AFOSR-93-0474TR ..... p 1172 N94-15777 #
AFOSR-93-0475TR ..... p 1165 N94-15778 #
AFOSR-93-0476TR ..... p 1026 N94-17003 #
AFOSR-93-0477TR ..... p 859 N94-17021 #
AFOSR-93-0478TR ..... p 1169 N94-15779 #
AFOSR-93-0479TR ..... p 1029 N94-17363 #
AFOSR-93-0480TR ..... p 1189 N94-15735 #
AFOSR-93-0481TR ..... p 1012 N94-17023 #
AFOSR-93-0482TR ..... p 971 N94-16980 #
AFOSR-93-0484TR ..... p 1001 N94-17019 #
AFOSR-93-0485TR ..... p 855 N94-14963
AFOSR-93-0497TR ..... p 1038 N94-15853
AFOSR-93-0498TR ..... p 1206 N94-15764 #
AFOSR-93-0499TR ..... p 972 N94-17242 #
AFOSR-93-0514TR ..... p 989 N94-15786 #
AFOSR-93-0525TR ..... p 1131 N94-15148 #
AFOSR-93-0526TR ..... p 1201 N94-15661 #
AFOSR-93-0527TR ..... p 1133 N94-17020 #
AFOSR-93-0540TR ..... p 946 N94-15684 #
AFOSR-93-0545TR ..... p 1190 N94-15848
AFOSR-93-0546TR ..... p 1299 N94-15836
AFOSR-93-0547TR ..... p 1131 N94-15694 #
AFOSR-93-0548TR ..... p 1121 N94-15660 #
AFOSR-93-0549TR ..... p 1037 N94-15145 #
AFOSR-93-0556TR ..... p 1299 N94-17208 #
AFOSR-93-0558TR ..... p 1299 N94-17004 #
AFOSR-93-0560TR ..... p 1193 N94-17024 #
AFOSR-93-0561TR ..... p 1140 N94-17005 #
AFOSR-93-0563TR ..... p 1029 N94-17414 #
AFOSR-93-0564TR ..... p 1004 N94-17364 #
AFOSR-93-0565TR ..... p 1133 N94-17453 #
AFOSR-93-0566TR ..... p 975 N94-17073
AFOSR-93-0567TR ..... p 970 N94-16978 #
AFOSR-93-0568TR ..... p 861 N94-17580 #
AFOSR-93-0569TR ..... p 1204 N94-17575 #
AFOSR-93-0572TR ..... p 973 N94-17494 #
AFOSR-93-0573TR ..... p 1216 N94-17577 #
AFOSR-93-0575TR ..... p 1234 N94-17419
AFOSR-93-0579TR ..... p 1199 N94-17455
AFOSR-93-0582TR ..... p 941 N94-17457
AFOSR-93-0583TR ..... p 1215 N94-17422
AFOSR-93-0584TR ..... p 1014 N94-17428 #
AFOSR-93-0585TR ..... p 1216 N94-17454
AFOSR-93-0587TR ..... p 1216 N94-17477 #
AFOSR-93-0591TR ..... p 941 N94-17597
AFOSR-93-0592TR ..... p 950 N94-17008
AFOSR-93-0593TR ..... p 1216 N94-17561
AFOSR-93-0594TR ..... p 1141 N94-17380 #
AFOSR-93-0595TR ..... p 1015 N94-17560
AFOSR-93-0596TR ..... p 1217 N94-17579 #
AFOSR-93-0597TR ..... p 940 N94-17013 #
AFOSR-93-0598TR ..... p 1129 N94-17456
AFOSR-93-0599TR ..... p 941 N94-17379 #
AFOSR-93-0601TR ..... p 952 N94-17532 #
AFOSR-93-0602TR ..... p 1129 N94-17478
AFOSR-93-0613TR ..... p 861 N94-17574 #
AFOSR-93-0615TR ..... p 1134 N94-17468 #
AFOSR-93-0617TR ..... p 1134 N94-17513
AFOSR-93-0621TR ..... p 1186 N94-17436
AFOSR-93-0639TR-VOL-14 ..... p 1014 N94-17410 #
AFOSR-93-103TR ..... p 1041 N94-17193 #

AFOTEC-DET1/TP-92-007 ..... p 1237 N94-17225 #

AFRRI-SR93-1 ..... p 1123 N94-16515 #
AFRRI-SR93-2 ..... p 1123 N94-16515 #

AGARD-AG-328 ..... p 1016 N94-15119 #

AGARD-AR-309 ..... p 1229 N94-15437 #

AGARD-LS-188 ..... p 923 N94-15217 #

AGARD-R-792 ..... p 1017 N94-15196 #

AGS/AD-93-7 ..... p 1184 N94-16885 #

AIAA PAPER 92-4057 ..... p 1031 N94-17615 #
AIAA PAPER 93-0813 ..... p 1169 N94-15799 * #
AIAA PAPER 93-1967 ..... p 1030 N94-17486 * #
AIAA PAPER 93-2543 ..... p 869 N94-15141 * #
AIAA PAPER 93-3017 ..... p 858 N94-16512 * #
AIAA PAPER 93-3051 ..... p 1026 N94-17056 * #
AIAA PAPER 93-3120 ..... p 1025 N94-16879 * #
AIAA PAPER 93-3368 ..... p 1027 N94-17128 * #
AIAA PAPER 93-4400 ..... p 1176 N94-15115 * #
AIAA PAPER 94-0391 ..... p 858 N94-16571 * #
AIAA PAPER 94-0687 ..... p 1035 N94-17446 * #
AIAA PAPER 94-0993 ..... p 883 N94-17487 * #

AL-TP-1992-0041 ..... p 1138 N94-16983 #

AL-TR-1991-0057 ..... p 1130 N94-17554
AL-TR-1992-0085 ..... p 1132 N94-16942 #
AL-TR-1992-0106-VOL-1 ..... p 1116 N94-17232 #
AL-TR-1992-0156 ..... p 1130 N94-17621 #
AL-TR-1992-0157 ..... p 1134 N94-17510 #
AL-TR-1992-0178 ..... p 1192 N94-16926 #
AL-TR-1993-0012-VOL-1 ..... p 1139 N94-17563
AL-TR-1993-0012-VOL-2 ..... p 1139 N94-17564
AL-TR-1993-0030 ..... p 1022 N94-15858 #
AL-TR-1993-0036 ..... p 868 N94-17425

AL/DO-TP-1993-0025 ..... p 1129 N94-17424

AL/HR-TP-1993-0017 ..... p 1145 N94-15525 #

AL/HR-TR-1993-0056 ..... p 1122 N94-15845
AL/HR-TR-1993-0061 ..... p 1131 N94-15108 #
AL/HR-TR-1993-0066 ..... p 1137 N94-15820 #
AL/HR-TR-1993-0089 ..... p 872 N94-17403 #

AM-93-03 ..... p 930 N94-15106 * #

ANL-HEP-CP-93-34 ..... p 1300 N94-17233 #

ANL/BIM/CP-78918 ..... p 1150 N94-16659 #
ANL/BIM/CP-79650 ..... p 1117 N94-16893 #
ANL/BIM/CP-79672 ..... p 1129 N94-16970 #

ANL/CMT/CP-79667 ..... p 1211 N94-16805 #

ANL/ER/CP-79191 ..... p 1110 N94-17673 #

ANL/ES/CP-79716 ..... p 1048 N94-16969 #

ANL/MCS/CP-79481 ..... p 1170 N94-16778 #

ANL/MCT/CP-77641 ..... p 1013 N94-17226 #
ANL/MCT/CP-77789 ..... p 1059 N94-15997 #
ANL/MCT/CP-78063 ..... p 934 N94-16057 #
ANL/MCT/CP-78162 ..... p 1011 N94-16443 #
ANL/MCT/CP-78185 ..... p 1023 N94-16444 #
ANL/MCT/CP-79253 ..... p 968 N94-16658 #
ANL/MCT/CP-79590 ..... p 1047 N94-16806 #

ANL/MSD/CP-79578 ..... p 1208 N94-15982 #

ANL/XFD/CP-79634 ..... p 1208 N94-16058 #

AR-008-384 ..... p 1058 N94-15963 #

ARCCB-TR-93021 ..... p 961 N94-17106 #
ARCCB-TR-93022 ..... p 1061 N94-17105 #

ARFSD-CR-93004 ..... p 1008 N94-15494 #

ARI-RN-93-19 ..... p 1005 N94-17498

ARI-93-18 ..... p 1138 N94-17077 #

ARL-CR-51 ..... p 959 N94-16780

ARL-GD-37 ..... p 862 N94-15542 #

ARL-RR-14 ..... p 1058 N94-15963 #

ARL-TN-17 ..... p 872 N94-15856
ARL-TN-24 ..... p 872 N94-15543 #
ARL-TN-32 ..... p 868 N94-17117

ARL-TR-140 ..... p 954 N94-15104 #
ARL-TR-141 ..... p 930 N94-14999 #
ARL-TR-142 ..... p 965 N94-15859 #
ARL-TR-14 ..... p 1146 N94-15650 #
ARL-TR-153 ..... p 865 N94-14951 #
ARL-TR-157 ..... p 951 N94-17203
ARL-TR-15 ..... p 866 N94-15651 #
ARL-TR-161 ..... p 942 N94-14946 #
ARL-TR-162 ..... p 976 N94-17538 #
ARL-TR-165 ..... p 1156 N94-17530
ARL-TR-180 ..... p 946 N94-15685 #
ARL-TR-237 ..... p 1049 N94-17583 * #
ARL-TR-54 ..... p 1096 N94-16589 #

ARL-TR-60 ..... p 1085 N94-17610 #
ARL-TR-93-11 ..... p 1177 N94-15732 #

ARO-23369.6-MA ..... p 1173 N94-16657 #
ARO-25467.74-EG-RW ..... p 857 N94-15824 #
ARO-26072.25-CH-A ..... p 968 N94-16727 #
ARO-26460.22-EL ..... p 999 N94-16728 #
ARO-26601.2-MS ..... p 1206 N94-15747 #
ARO-26709.13-PH ..... p 1181 N94-15774
ARO-26797.10-EG ..... p 1021 N94-15770 #
ARO-26811.7-MA-SDI ..... p 1082 N94-15842 #
ARO-26863.8-EG-S ..... p 1174 N94-15823 #
ARO-26863.8-EG-S ..... p 1022 N94-15953 #
ARO-26909.6-MA ..... p 1009 N94-15825 #
ARO-26996.8-PH ..... p 1206 N94-15822 #
ARO-27154-8-PH-SAH ..... p 1210 N94-16720 #
ARO-27431.3-PH ..... p 968 N94-16796 #
ARO-27502.4-CH ..... p 942 N94-14909 #
ARO-27646.9-PH ..... p 1207 N94-15955 #
ARO-27664.7-CH-SM ..... p 964 N94-15729 #
ARO-28368.1-MS ..... p 965 N94-15773
ARO-28555.1-CH ..... p 1183 N94-16722 #
ARO-28809.13-MA-SDI ..... p 1165 N94-15775
ARO-28925.58-EL ..... p 1304 N94-17651 #
ARO-28979.2-PH ..... p 968 N94-16723 #
ARO-29708.7-CH ..... p 1010 N94-15954 #
ARO-29748.1-MA-CF-VOL-24 ..... p 1150 N94-16721 #
ARO-30499.1-EL-SBI ..... p 986 N94-14912 #

ASC-TR-93-5005 ..... p 855 N94-15105 #
ASC-TR-93-5008 ..... p 1155 N94-17429

ASQB-GC-92-023-VOL-1 ..... p 1155 N94-17411 #

ASQB-GM-92-024 ..... p 1155 N94-17500

AS1690-353-92 ..... p 1138 N94-17077 #

ATCOM-TR-92-A-013 ..... p 856 N94-15657 * #

ATR-92(7248)-2 ..... p 1098 N94-15433 * #

AVSCOM-TR-91-C-052 ..... p 869 N94-17386 * #

AWS-TN-93/003 ..... p 1106 N94-15757

A8612-009/1 ..... p 1178 N94-17278 * #

B-255456 ..... p 926 N94-16834 #

BARC-1992/E/029 ..... p 1042 N94-17630
BARC-1992/E/031 ..... p 974 N94-17611

BC-ISR-93-02 ..... p 888 N94-16990 #

BCRS-91-04 ..... p 1085 N94-17616 #

BER-181 ..... p 1105 N94-15302

BN-1145 ..... p 1029 N94-17384 #
BN-1146 ..... p 961 N94-17109 #

BNL-48268 ..... p 1151 N94-16892 #
BNL-48269 ..... p 1184 N94-16886 #
BNL-48306 ..... p 1176 N94-17658 #
BNL-48361 ..... p 1209 N94-16447 #
BNL-48373 ..... p 1181 N94-16020 #
BNL-48384 ..... p 1184 N94-16826 #
BNL-48385 ..... p 1211 N94-16827 #
BNL-48420 ..... p 974 N94-17676 #
BNL-48498 ..... p 1212 N94-16844 #
BNL-48499 ..... p 1095 N94-15940 #
BNL-48626 ..... p 1210 N94-16775 #
BNL-48642 ..... p 1202 N94-16019 #
BNL-48655 ..... p 1207 N94-15923 #
BNL-48665 ..... p 947 N94-16011 #
BNL-48706 ..... p 956 N94-15921 #
BNL-48707 ..... p 956 N94-15922 #
BNL-48755 ..... p 1095 N94-15999 #
BNL-48895 ..... p 1175 N94-15978 #
BNL-48922 ..... p 1182 N94-16161 #
BNL-48932 ..... p 1187 N94-16829 #
BNL-48950 ..... p 1184 N94-16885 #
BNL-48963 ..... p 1212 N94-16887 #
BNL-48965 ..... p 1184 N94-16828 #
BNL-49082 ..... p 949 N94-16870 #

BR315173 ..... p 1146 N94-15702 #
BR315174 ..... p 933 N94-15699 #
BR316026 ..... p 856 N94-15696 #

CA-PATENT-1-307-842 ..... p 994 N94-15986
CA-PATENT-1-310-709 ..... p 988 N94-15698
CA-PATENT-1-311-626 ..... p 1032 N94-15697

CAR-92-8 ..... p 867 N94-16122 #

CAST-TR-93-1 ..... p 1112 N94-15771 #

CCMS-93-15 ..... p 964 N94-15656 * #

CCR-93-01 ..... p 925 N94-16482 #

CDNSWC/SSM-61-93/18 ..... p 973 N94-17430 #

CECOM-TR-93-E-1 ..... p 989 N94-15767 * #

CERC-MP-93-3 ..... p 1114 N94-17497

CERC-93-6 ..... p 1113 N94-16517 #

CERL-IR-FF-93/07 ..... p 1157 N94-17620 #

CERL-TR-EC-93/02 ..... p 1178 N94-17119

CERL-TR-FM-92/03 ..... p 871 N94-14908 #
CERL-TR-FM-93/01 ..... p 971 N94-17198 #

CETEC-ES-P-93-7 ..... p 1225 N94-16473

CFDRC-4075/3 ..... p 928 N94-17442 * #

CIW-PUBL-1133 ..... p 1072 N94-16698 * #
CIW-PUBL-1134 ..... p 1067 N94-16672 * #

CMOTT-93-12 ..... p 1026 N94-17056 * #
CMOTT-93-13 ..... p 1030 N94-17557 * #
CMOTT-93-14 ..... p 1025 N94-16879 * #
CMOTT-93-15 ..... p 1029 N94-17385 * #

CMR-93-3 ..... p 1038 N94-15530 * #

CMU-CS-93-104 ..... p 1163 N94-14910 #
CMU-CS-93-105 ..... p 1147 N94-15725 #
CMU-CS-93-106 ..... p 1131 N94-15742 #
CMU-CS-93-109 ..... p 1160 N94-16724 #
CMU-CS-93-137 ..... p 1141 N94-14915 #
CMU-CS-93-140 ..... p 1151 N94-16790
CMU-CS-93-147 ..... p 1147 N94-15743 #
CMU-CS-93-148 ..... p 1150 N94-16585 #
CMU-CS-93-150 ..... p 1166 N94-16725 #
CMU-CS-93-152 ..... p 1140 N94-15744 #
CMU-CS-93-155 ..... p 1166 N94-17201
CMU-CS-93-156 ..... p 1231 N94-16570 #
CMU-CS-93-157 ..... p 1158 N94-15745 #
CMU-CS-93-162 ..... p 1148 N94-15841 #
CMU-CS-93-163 ..... p 1152 N94-17009 #
CMU-CS-93-166 ..... p 1153 N94-17107 #
CMU-CS-93-167 ..... p 1153 N94-17118 #
CMU-CS-93-168 ..... p 1141 N94-17115 #

CMU-RI-TR-92-10 ..... p 879 N94-14969 #
CMU-RI-TR-92-11 ..... p 1045 N94-14970 #
CMU-RI-TR-92-12 ..... p 1163 N94-14950 #
CMU-RI-TR-92-13 ..... p 863 N94-14971 #
CMU-RI-TR-92-16 ..... p 863 N94-14919 #
CMU-RI-TR-93-02 ..... p 1163 N94-14954 #
CMU-RI-TR-93-04 ..... p 1163 N94-14953 #
CMU-RI-TR-93-09 ..... p 864 N94-14972 #
CMU-RI-TR-93-10 ..... p 864 N94-15498 #
CMU-RI-TR-93-12 ..... p 1188 N94-15144 #
CMU-RI-TR-93-14 ..... p 1163 N94-14968 #
CMU-RI-TR-93-15 ..... p 1164 N94-15756

CMU/RI-TR-93-01 ..... p 1164 N94-15502 #
CMU/RI-TR-93-05 ..... p 1222 N94-15213 #
CMU/RI-TR-93-13 ..... p 1143 N94-15212 #

CMU/SEI-92-TR-24 ..... p 1145 N94-15629 #
CMU/SEI-93-SR-04 ..... p 1146 N94-15638 #
CMU/SEI-93-SR-5 ..... p 1146 N94-15653 #
CMU/SEI-93-TR-04 ..... p 1145 N94-15630 #
CMU/SEI-93-TR-05 ..... p 1144 N94-15214 #
CMU/SEI-93-TR-09 ..... p 1144 N94-15215 #
CMU/SEI-93-TR-16 ..... p 1154 N94-17396 #
CMU/SEI-93-TR-17 ..... p 1154 N94-17395 #
CMU/SEI-93-TR-3 ..... p 1144 N94-15216 #

CMY/SEI-93-EM-9 ..... p 1142 N94-14967 #

CNIC-00537 ..... p 1175 N94-17317
CNIC-00598 ..... p 952 N94-17302

COMMUNICATIONS-SER-B-158 . p 1098 N94-15800 #

CONF-9201150-1 ..... p 1095 N94-15999 #
CONF-9203139-5-REV-2 ..... p 1237 N94-16872 #
CONF-9205173-1-VUGRAPHS ..... p 1170 N94-16167 #
CONF-9205354-1 ..... p 1177 N94-16448 #
CONF-920556-1 ..... p 1095 N94-15940 #
CONF-920673-19 ..... p 958 N94-16168 #
CONF-9207204-1 ..... p 1205 N94-17663 #
CONF-920792-61 ..... p 965 N94-15828 #
CONF-920792-65 ..... p 1035 N94-16960 #
CONF-9208109-84 ..... p 1205 N94-17670 #
CONF-9208135-7 ..... p 1208 N94-15976 #
CONF-9208164-3 ..... p 1207 N94-15972 #
CONF-9208184-2 ..... p 1209 N94-16171 #
CONF-9208186-2 ..... p 1175 N94-15978 #
CONF-9208186-4 ..... p 1212 N94-16887 #
CONF-9208207-2 ..... p 969 N94-16889 #
CONF-9208221-1 ..... p 948 N94-16772 #
CONF-9209177-SUMM ..... p 926 N94-16773 #
CONF-9209253-5 ..... p 948 N94-16771 #
CONF-920944-7 ..... p 1209 N94-16447 #
CONF-920970-8 ..... p 958 N94-16662 #
CONF-9210173-5 ..... p 1231 N94-16874 #
CONF-9210255-2 ..... p 1211 N94-16805 #
CONF-9210300-3 ..... p 1203 N94-16816 #
CONF-9210313-3 ..... p 1183 N94-16809 #
CONF-9210359-1 ..... p 1096 N94-16825 #
CONF-921101-123 ..... p 1210 N94-16460 #
CONF-921101-124 ..... p 959 N94-16873 #
CONF-921101-125 ..... p 947 N94-16014 #
CONF-921101-126 ..... p 1209 N94-16066 #
CONF-921101-127 ..... p 1211 N94-16814 #
CONF-921101-131 ..... p 966 N94-16018 #
CONF-921101-132 ..... p 957 N94-16015 #
CONF-921101-133 ..... p 966 N94-16016 #
CONF-921101-135 ..... p 974 N94-17676 #
CONF-921109-6 ..... p 957 N94-16068 #
CONF-921109-7 ..... p 957 N94-16103 #
CONF-9211110-50 ..... p 1059 N94-15983 #
CONF-9211101-11 ..... p 968 N94-16813 #
CONF-9211104-10 ..... p 1236 N94-14929 #
CONF-9211104-9 ..... p 1190 N94-15975 #
CONF-9211110-2 ..... p 957 N94-16106 #
CONF-9211117-8 ..... p 959 N94-16890 #
CONF-9211117-9 ..... p 955 N94-15830 #
CONF-9211205-2 ..... p 955 N94-15862 #
CONF-921129-10 ..... p 1208 N94-16062 #
CONF-921145-7 ..... p 1183 N94-16817 #
CONF-921206-13 ..... p 1207 N94-15827 #
CONF-921256-4 ..... p 1041 N94-16871 #
CONF-9301109-3 ..... p 1239 N94-16052 #
CONF-9301114-1 ..... p 1212 N94-16844 #
CONF-930133-11 ..... p 1110 N94-17673 #
CONF-930159-40 ..... p 1039 N94-16450 #
CONF-930159-45 ..... p 949 N94-16904 #
CONF-930164-10 ..... p 935 N94-16461 #
CONF-930164-11 ..... p 967 N94-16067 #
CONF-930164-12 ..... p 934 N94-16017 #
CONF-930187-3 ..... p 1183 N94-16801 #
CONF-930187-4 ..... p 1185 N94-16951 #
CONF-930202-10 ..... p 1207 N94-15829 #
CONF-9302111-1 ..... p 959 N94-16764 #
CONF-9302115-4 ..... p 1299 N94-16895 #
CONF-9302117-1 ..... p 1187 N94-17674 #
CONF-9302130-1 ..... p 1036 N94-17647 #
CONF-930256-1-REV-1 ..... p 1096 N94-16449 #
CONF-930304-22 ..... p 966 N94-15924 #
CONF-930304-29 ..... p 1204 N94-17237
CONF-9303126-4 ..... p 1025 N94-16903 #
CONF-930315-1 ..... p 1093 N94-17668 #
CONF-9303160-1 ..... p 1181 N94-15974 #
CONF-930317-1 ..... p 934 N94-16158 #
CONF-9303171-2 ..... p 1181 N94-16059 #
CONF-9303172-1 ..... p 1181 N94-16053 #
CONF-9303172-2 ..... p 1186 N94-17662 #
CONF-930318-10 ..... p 947 N94-16105 #
CONF-9303190-1 ..... p 1212 N94-16868 #
CONF-930332-1 ..... p 1039 N94-16054 #
CONF-930363-2 ..... p 1185 N94-16968 #
CONF-930389-18 ..... p 1187 N94-16829 #
CONF-930389-21 ..... p 1182 N94-16115 #
CONF-930392-2 ..... p 947 N94-15977 #
CONF-930405-17 ..... p 961 N94-17251 #
CONF-930405-18 ..... p 1208 N94-16058 #
CONF-930405-20 ..... p 1209 N94-16159 #
CONF-930405-21 ..... p 1209 N94-16442 #
CONF-930405-23 ..... p 940 N94-17235 #
CONF-930405-24 ..... p 1184 N94-16838 #
CONF-930405-28 ..... p 1015 N94-17648 #
CONF-9304112-15 ..... p 1202 N94-16803 #
CONF-9304114-5 ..... p 1170 N94-16778 #
CONF-9304126-4 ..... p 1202 N94-16776 #
CONF-9304133-1 ..... p 1059 N94-15997 #
CONF-9304144-3 ..... p 1182 N94-16064 #
CONF-9304144-5 ..... p 1040 N94-16664 #
CONF-9304144-6 ..... p 1040 N94-16663 #
CONF-9304151-1 ..... p 1093 N94-16824 #
CONF-9304155-1 ..... p 1183 N94-16811 #
CONF-9304159-1 ..... p 1157 N94-14927 #
CONF-930419-2 ..... p 1207 N94-15973 #
CONF-930438-21 ..... p 934 N94-16057 #
CONF-930438-24 ..... p 1209 N94-16164 #
CONF-930438-25 ..... p 972 N94-17253 #
CONF-930438-26 ..... p 969 N94-16877 #
CONF-930445-10 ..... p 898 N94-17669 #

CONF-930445-15 ..... p 1166 N94-16888 #
CONF-9305100-1 ..... p 961 N94-17234 #
CONF-9305100-2 ..... p 1092 N94-16160 #
CONF-9305101-2 ..... p 1092 N94-16715 #
CONF-930511-152 ..... p 1181 N94-16020 #
CONF-930511-153 ..... p 1184 N94-16828 #
CONF-930511-154 ..... p 1184 N94-16886 #
CONF-930511-161 ..... p 1151 N94-16892 #
CONF-930511-185 ..... p 1173 N94-17236 #
CONF-930511-196 ..... p 1176 N94-17658 #
CONF-930511-209 ..... p 1168 N94-14928 #
CONF-930511-212 ..... p 1188 N94-17672 #
CONF-930511-63 ..... p 1211 N94-16827 #
CONF-930511-71 ..... p 1184 N94-16826 #
CONF-9305135-4 ..... p 957 N94-16163 #
CONF-9305135-5 ..... p 958 N94-16166 #
CONF-9305136-1 ..... p 1202 N94-16019 #
CONF-9305168-4 ..... p 1215 N94-17319 #
CONF-9305168-5 ..... p 1043 N94-17677 #
CONF-9305194-1 ..... p 1132 N94-16819 #
CONF-9305202-2 ..... p 1129 N94-16970 #
CONF-9305219-1 ..... p 1096 N94-16445 #
CONF-9305222-1 ..... p 949 N94-16876 #
CONF-9305225-1 ..... p 1220 N94-16810 #
CONF-9305226-1 ..... p 968 N94-16843 #
CONF-9305231-1 ..... p 1203 N94-16869 #
CONF-930537-53 ..... p 1013 N94-17226 #
CONF-930540-10 ..... p 1016 N94-17671 #
CONF-930540-2 ..... p 1091 N94-15994 #
CONF-930540-8 ..... p 1091 N94-15984 #
CONF-930540-9 ..... p 1093 N94-17217 #
CONF-930550-1 ..... p 1117 N94-16893 #
CONF-930550-2 ..... p 1048 N94-16969 #
CONF-930550-5 ..... p 1047 N94-16806 #
CONF-930552-2 ..... p 975 N94-16807 #
CONF-930561-6 ..... p 1091 N94-15993 #
CONF-930571-21 ..... p 950 N94-16952 #
CONF-9306125-2 ..... p 1181 N94-15863 #
CONF-930616-5 ..... p 1202 N94-16451 #
CONF-930616-6 ..... p 1205 N94-17645 #
CONF-930616-7 ..... p 1013 N94-17318 #
CONF-9306167-12 ..... p 1178 N94-16955 #
CONF-9306167-6 ..... p 972 N94-17238 #
CONF-9306167-7 ..... p 1214 N94-17301 #
CONF-9306167-8 ..... p 1034 N94-16452 #
CONF-9306167-9 ..... p 1062 N94-17664 #
CONF-9306172-1 ..... p 1181 N94-15995 #
CONF-9306177-1 ..... p 1232 N94-16875 #
CONF-9306181-1 ..... p 1011 N94-16661 #
CONF-9306183-1 ..... p 1212 N94-16841 #
CONF-9306186-1 ..... p 1192 N94-16953 #
CONF-930675-4 ..... p 1024 N94-16808 #
CONF-930682-1 ..... p 1208 N94-15982 #
CONF-930686-1 ..... p 953 N94-17649 #
CONF-930702-38 ..... p 1023 N94-16444 #
CONF-930702-41 ..... p 1011 N94-16443 #
CONF-9307100-1 ..... p 1162 N94-17646 #
CONF-930714-1 ..... p 1025 N94-16894 #
CONF-930720-11 ..... p 1202 N94-16162 #
CONF-930720-2 ..... p 1203 N94-16823 #
CONF-930722-4 ..... p 1093 N94-16954 #
CONF-930745-2 ..... p 1150 N94-16659 #
CONF-930779-15 ..... p 1300 N94-17233 #
CONF-930779-1 ..... p 1240 N94-17657 #
CONF-930783-2 ..... p 1206 N94-14925 #
CONF-930791-1 ..... p 1148 N94-15985 #
CONF-930793-1 ..... p 968 N94-16658 #
CONF-930801-5 ..... p 1211 N94-16839 #
CONF-930803-13 ..... p 1059 N94-16104 #
CONF-930804-8 ..... p 1049 N94-17675 #
CONF-930804-9 ..... p 1092 N94-16112 #
CONF-9308107-1 ..... p 1169 N94-15979 #
CONF-930830-22 ..... p 947 N94-16060 #
CONF-930851-1 ..... p 1208 N94-16012 #
CONF-930866-2 ..... p 1220 N94-16956 #
CONF-930881-3 ..... p 1149 N94-16119 #
CONF-930899-1 ..... p 1210 N94-16775 #
CONF-930901-4 ..... p 1112 N94-16009 #
CONF-9309104-1 ..... p 958 N94-16463 #
CONF-9309149-1 ..... p 934 N94-16008 #
CONF-9309150-1 ..... p 947 N94-16011 #
CONF-9309150-2 ..... p 1207 N94-15923 #
CONF-9309150-3 ..... p 956 N94-15921 #
CONF-9309150-4 ..... p 956 N94-15922 #
CONF-9309168-1 ..... p 1050 N94-16055 #
CONF-9309182-1 ..... p 949 N94-16870 #
CONF-9309185-1 ..... p 1039 N94-16114 #
CONF-930927-1 ..... p 965 N94-15920 #
CONF-930961-2 ..... p 934 N94-16065 #
CONF-930997-1 ..... p 955 N94-15885 #
CONF-930997-2 ..... p 1208 N94-16063 #
CONF-930997-3 ..... p 957 N94-16165 #
CONF-930998-1 ..... p 956 N94-15998 #

CPIA-LBP/MJP-06-93 ..... p 929 N94-17589

CRC-584 ..... p 869 N94-16516 #

CRDKNSWC-SSM-61-93-01 ..... p 962 N94-17464

CREEL-93-2 ..... p 983 N94-15676 #

CRREL-SR-93-6 ..... p 1045 N94-14920 #

CR0009-1039 ..... p 926 N94-16922 * #

CSL-TR-92-547 ..... p 1162 N94-17550 #

CS91-TR-JSC-017 ..... p 926 N94-16504 * #
CS92-TR-JSC-002 ..... p 887 N94-16503 * #
CS92-TR-JSC-007 ..... p 887 N94-16502 * #

CTN-93-60777 ..... p 1032 N94-15697
CTN-93-60778 ..... p 988 N94-15698
CTN-93-60779 ..... p 994 N94-15986
CTN-93-60782 ..... p 977 N94-16071
CTN-93-60864 ..... p 994 N94-15959 #

CU-CSD-TR-93-1349 ..... p 997 N94-16477 #

CUCS-047-92 ..... p 1155 N94-17398 #
CUCS-050-92 ..... p 1161 N94-17409 #
CUCS-053-92 ..... p 1155 N94-17399 #

CUED/C-MATS/TR203 ..... p 941 N94-17457

C931031-U-2R06 ..... p 1082 N94-15531 * #

DAMTP-R92/43 ..... p 1240 N94-17603

DE93-000245 ..... p 1024 N94-16763 #
DE93-000278 ..... p 947 N94-15861 #
DE93-008727 ..... p 958 N94-16463 #
DE93-009347 ..... p 1095 N94-15940 #
DE93-010028 ..... p 1093 N94-17668 #
DE93-010031 ..... p 1010 N94-15971 #
DE93-010348 ..... p 1207 N94-15972 #
DE93-010657 ..... p 1110 N94-17673 #
DE93-011001 ..... p 948 N94-16772 #
DE93-011251 ..... p 959 N94-16764 #
DE93-011662 ..... p 926 N94-16773 #
DE93-012376 ..... p 1160 N94-16774 #
DE93-012510 ..... p 1207 N94-15973 #
DE93-012531 ..... p 1210 N94-16775 #
DE93-012623 ..... p 898 N94-17669 #
DE93-012638 ..... p 1181 N94-15974 #
DE93-012666 ..... p 1202 N94-16776 #
DE93-012675 ..... p 955 N94-15885 #
DE93-012722 ..... p 1240 N94-17657 #
DE93-012741 ..... p 965 N94-15920 #
DE93-012899 ..... p 1170 N94-16778 #
DE93-012913 ..... p 1059 N94-15997 #
DE93-012925 ..... p 956 N94-15998 #
DE93-013027 ..... p 1203 N94-16816 #
DE93-013149 ..... p 1095 N94-15999 #
DE93-013163 ..... p 1095 N94-16006 #
DE93-013378 ..... p 1191 N94-16007 #
DE93-013417 ..... p 1205 N94-17670 #
DE93-013432 ..... p 1183 N94-16817 #
DE93-013465 ..... p 1187 N94-17674 #
DE93-013532 ..... p 934 N94-16008 #
DE93-013581 ..... p 1112 N94-16009 #
DE93-013582 ..... p 1183 N94-16818 #
DE93-013734 ..... p 1011 N94-16459 #
DE93-013747 ..... p 1097 N94-17426 #
DE93-013768 ..... p 1132 N94-16819 #
DE93-013873 ..... p 1174 N94-16820 #
DE93-013890 ..... p 948 N94-16821 #
DE93-013899 ..... p 1230 N94-16010 #
DE93-014005 ..... p 1203 N94-16822 #
DE93-014009 ..... p 1203 N94-16823 #
DE93-014023 ..... p 947 N94-16011 #
DE93-014037 ..... p 1093 N94-16824 #
DE93-014054 ..... p 956 N94-15921 #
DE93-014055 ..... p 956 N94-15922 #
DE93-014056 ..... p 1207 N94-15923 #
DE93-014112 ..... p 966 N94-15924 #
DE93-014116 ..... p 1190 N94-15975 #
DE93-014123 ..... p 1096 N94-16825 #
DE93-014128 ..... p 1208 N94-15976 #
DE93-014275 ..... p 947 N94-15977 #
DE93-014291 ..... p 1175 N94-15978 #
DE93-014330 ..... p 1184 N94-16826 #
DE93-014331 ..... p 1211 N94-16827 #
DE93-014342 ..... p 1183 N94-16801 #
DE93-014345 ..... p 1169 N94-15979 #
DE93-014369 ..... p 1096 N94-16802 #
DE93-014411 ..... p 1202 N94-16803 #
DE93-014445 ..... p 1303 N94-16804 #
DE93-014481 ..... p 1185 N94-16951 #
DE93-014590 ..... p 1012 N94-16765 #
DE93-014617 ..... p 949 N94-16891 #
DE93-014643 ..... p 1232 N94-16967 #
DE93-014661 ..... p 958 N94-16453 #
DE93-014724 ..... p 1023 N94-15980 #
DE93-014834 ..... p 1201 N94-15981 #
DE93-014875 ..... p 1208 N94-15982 #
DE93-014888 ..... p 1167 N94-17287
DE93-014909 ..... p 1059 N94-15983 #
DE93-014926 ..... p 1185 N94-16968 #
DE93-015006 ..... p 1091 N94-15984 #
DE93-015020 ..... p 1151 N94-16892 #
DE93-015027 ..... p 1148 N94-15985 #
DE93-015028 ..... p 1208 N94-16012 #
DE93-015030 ..... p 1091 N94-15993 #
DE93-015031 ..... p 1091 N94-15994 #
DE93-015035 ..... p 1181 N94-15995 #
DE93-015039 ..... p 1239 N94-16052 #
DE93-015041 ..... p 1181 N94-16053 #
DE93-015110 ..... p 1039 N94-16054 #
DE93-015118 ..... p 1301 N94-14926
DE93-015122 ..... p 1050 N94-16055 #
DE93-015128 ..... p 883 N94-16056 #
DE93-015139 ..... p 1048 N94-16969 #
DE93-015140 ..... p 1211 N94-16805 #
DE93-015143 ..... p 1117 N94-16893 #
DE93-015150 ..... p 1129 N94-16970 #
DE93-015155 ..... p 934 N94-16057 #
DE93-015156 ..... p 1013 N94-17226 #
DE93-015162 ..... p 1208 N94-16058 #
DE93-015163 ..... p 1047 N94-16806 #
DE93-015179 ..... p 1181 N94-16059 #
DE93-015196 ..... p 947 N94-16060 #
DE93-015209 ..... p 975 N94-16807 #
DE93-015214 ..... p 1206 N94-14925 #
DE93-015215 ..... p 1024 N94-16808 #
DE93-015238 ..... p 1010 N94-16061 #
DE93-015239 ..... p 1175 N94-17288 #
DE93-015241 ..... p 1096 N94-17289 #
DE93-015249 ..... p 1183 N94-16809 #
DE93-015251 ..... p 1208 N94-16062 #
DE93-015255 ..... p 961 N94-17251 #
DE93-015256 ..... p 1183 N94-16811 #
DE93-015264 ..... p 966 N94-15996 #
DE93-015269 ..... p 1181 N94-16013 #
DE93-015274 ..... p 1128 N94-16812 #
DE93-015279 ..... p 1102 N94-17252 #
DE93-015284 ..... p 1190 N94-15854 #
DE93-015300 ..... p 1207 N94-15827 #
DE93-015304 ..... p 965 N94-15828 #
DE93-015306 ..... p 1207 N94-15829 #
DE93-015307 ..... p 955 N94-15830 #
DE93-015308 ..... p 955 N94-15862 #
DE93-015331 ..... p 1211 N94-16814 #
DE93-015333 ..... p 947 N94-16014 #
DE93-015336 ..... p 957 N94-16015 #
DE93-015339 ..... p 966 N94-16016 #
DE93-015340 ..... p 934 N94-16017 #
DE93-015363 ..... p 966 N94-16018 #
DE93-015387 ..... p 1184 N94-16828 #
DE93-015391 ..... p 1187 N94-16829 #
DE93-015396 ..... p 1184 N94-16885 #
DE93-015399 ..... p 1202 N94-16019 #
DE93-015400 ..... p 1181 N94-16020 #
DE93-015402 ..... p 1184 N94-16886 #
DE93-015406 ..... p 1212 N94-16887 #
DE93-015427 ..... p 972 N94-17253 #
DE93-015431 ..... p 1208 N94-16063 #
DE93-015436 ..... p 1182 N94-16064 #
DE93-015439 ..... p 1166 N94-16888 #
DE93-015440 ..... p 934 N94-16065 #
DE93-015449 ..... p 1209 N94-16066 #
DE93-015450 ..... p 967 N94-16067 #
DE93-015453 ..... p 957 N94-16068 #
DE93-015454 ..... p 957 N94-16103 #
DE93-015455 ..... p 1059 N94-16104 #
DE93-015462 ..... p 947 N94-16105 #
DE93-015488 ..... p 969 N94-16889 #
DE93-015489 ..... p 957 N94-16106 #
DE93-015490 ..... p 959 N94-16890 #
DE93-015491 ..... p 1210 N94-16460 #
DE93-015492 ..... p 959 N94-16873 #
DE93-015494 ..... p 935 N94-16461 #
DE93-015499 ..... p 948 N94-16771 #
DE93-015506 ..... p 1231 N94-16874 #
DE93-015515 ..... p 1232 N94-16875 #
DE93-015523 ..... p 1209 N94-16442 #
DE93-015531 ..... p 949 N94-16876 #
DE93-015540 ..... p 1011 N94-16443 #
DE93-015541 ..... p 1023 N94-16444 #
DE93-015548 ..... p 1300 N94-17233 #
DE93-015554 ..... p 968 N94-16658 #
DE93-015556 ..... p 1150 N94-16659 #
DE93-015632 ..... p 1187 N94-16660 #
DE93-015644 ..... p 1157 N94-14927 #
DE93-015647 ..... p 1011 N94-16661 #
DE93-015649 ..... p 1093 N94-17217 #
DE93-015666 ..... p 1092 N94-16715 #

DE93-015675 ..... p 1096 N94-16445 #
DE93-015676 ..... p 961 N94-17234 #
DE93-015682 ..... p 958 N94-16662 #
DE93-015683 ..... p 940 N94-17235 #
DE93-015688 ..... p 934 N94-16158 #
DE93-015689 ..... p 1209 N94-16159 #
DE93-015692 ..... p 1215 N94-17319 #
DE93-015696 ..... p 1092 N94-16160 #
DE93-015759 ..... p 1182 N94-16161 #
DE93-015799 ..... p 1202 N94-16162 #
DE93-015800 ..... p 957 N94-16163 #
DE93-015801 ..... p 1209 N94-16164 #
DE93-015802 ..... p 957 N94-16165 #
DE93-015804 ..... p 1040 N94-16663 #
DE93-015808 ..... p 1040 N94-16664 #
DE93-015809 ..... p 1184 N94-16838 #
DE93-015811 ..... p 969 N94-16877 #
DE93-015812 ..... p 1212 N94-16868 #
DE93-015820 ..... p 958 N94-16166 #
DE93-015822 ..... p 1220 N94-16810 #
DE93-015824 ..... p 1170 N94-16167 #
DE93-015825 ..... p 958 N94-16168 #
DE93-015870 ..... p 997 N94-16169 #
DE93-015884 ..... p 1187 N94-16170 #
DE93-015894 ..... p 968 N94-16813 #
DE93-015898 ..... p 1211 N94-16839 #
DE93-015906 ..... p 1209 N94-16171 #
DE93-015936 ..... p 1101 N94-16840 #
DE93-015964 ..... p 1212 N94-16841 #
DE93-015983 ..... p 1049 N94-17675 #
DE93-015991 ..... p 968 N94-16843 #
DE93-016045 ..... p 1159 N94-16172 #
DE93-016101 ..... p 1173 N94-17236 #
DE93-016131 ..... p 1212 N94-16844 #
DE93-016161 ..... p 974 N94-17676 #
DE93-016163 ..... p 1043 N94-17677 #
DE93-016164 ..... p 1176 N94-17658 #
DE93-016204 ..... p 1202 N94-16446 #
DE93-016218 ..... p 1209 N94-16447 #
DE93-016231 ..... p 1217 N94-17659 #
DE93-016232 ..... p 1181 N94-15863 #
DE93-016235 ..... p 1203 N94-16869 #
DE93-016244 ..... p 949 N94-16870 #
DE93-016295 ..... p 1092 N94-16766 #
DE93-016329 ..... p 953 N94-17660 #
DE93-016350 ..... p 1186 N94-17662 #
DE93-016376 ..... p 1168 N94-14928 #
DE93-016417 ..... p 1041 N94-16871 #
DE93-016424 ..... p 1205 N94-17663 #
DE93-016425 ..... p 1177 N94-16448 #
DE93-016426 ..... p 1237 N94-16872 #
DE93-016430 ..... p 1025 N94-16894 #
DE93-016432 ..... p 1096 N94-16449 #
DE93-016435 ..... p 1039 N94-16450 #
DE93-016436 ..... p 1236 N94-14929 #
DE93-016437 ..... p 950 N94-16952 #
DE93-016452 ..... p 1204 N94-17237
DE93-016455 ..... p 1202 N94-16451 #
DE93-016457 ..... p 972 N94-17238 #
DE93-016461 ..... p 1062 N94-17664 #
DE93-016463 ..... p 1192 N94-16953 #
DE93-016464 ..... p 1013 N94-17318 #
DE93-016465 ..... p 1205 N94-17645 #
DE93-016486 ..... p 1162 N94-17646 #
DE93-016487 ..... p 1299 N94-16895 #
DE93-016488 ..... p 1214 N94-17301 #
DE93-016490 ..... p 1036 N94-17647 #
DE93-016491 ..... p 1015 N94-17648 #
DE93-016492 ..... p 1034 N94-16452 #
DE93-016493 ..... p 1092 N94-16112 #
DE93-016500 ..... p 1093 N94-16954 #
DE93-016501 ..... p 953 N94-17649 #
DE93-016503 ..... p 1016 N94-17671 #
DE93-016514 ..... p 1188 N94-17672 #
DE93-016525 ..... p 1178 N94-16955 #
DE93-016541 ..... p 1122 N94-16113 #
DE93-016612 ..... p 1039 N94-16114 #
DE93-016619 ..... p 1220 N94-16956 #
DE93-016631 ..... p 1182 N94-16115 #
DE93-016689 ..... p 949 N94-16896 #
DE93-016809 ..... p 1185 N94-16957 #
DE93-016850 ..... p 949 N94-16897 #
DE93-016852 ..... p 1026 N94-16958 #
DE93-016861 ..... p 975 N94-16898 #
DE93-016863 ..... p 1187 N94-16116 #
DE93-016864 ..... p 1182 N94-16117 #
DE93-016865 ..... p 1239 N94-16118 #
DE93-016866 ..... p 1184 N94-16899 #
DE93-016938 ..... p 970 N94-16959 #
DE93-017034 ..... p 950 N94-16912 #
DE93-017055 ..... p 1188 N94-16900 #
DE93-017059 ..... p 1203 N94-16901 #
DE93-017085 ..... p 943 N94-15146 #
DE93-017123 ..... p 1149 N94-16119 #
DE93-017149 ..... p 1151 N94-16902 #
DE93-017155 ..... p 1025 N94-16903 #
DE93-017174 ..... p 949 N94-16904 #
DE93-017179 ..... p 1035 N94-16960 #
DE93-017439 ..... p 1149 N94-16120 #
DE93-017548 ..... p 952 N94-17218 #
DE93-017603 ..... p 1182 N94-16121 #
DE93-017604 ..... p 1212 N94-16961 #
DE93-017605 ..... p 948 N94-16462 #
DE93-017710 ..... p 950 N94-16962 #
DE93-017711 ..... p 975 N94-16996 #
DE93-017727 ..... p 1220 N94-16997 #
DE93-017826 ..... p 1041 N94-16998 #
DE93-018030 ..... p 971 N94-16999 #
DE93-018141 ..... p 1000 N94-17000 #
DE93-018142 ..... p 1204 N94-16995 #
DE93-018150 ..... p 1185 N94-16971 #
DE93-018164 ..... p 960 N94-16972 #
DE93-018300 ..... p 970 N94-16973 #
DE93-018301 ..... p 970 N94-16963 #
DE93-018302 ..... p 960 N94-16964 #
DE93-623325 ..... p 952 N94-17302
DE93-623741 ..... p 1175 N94-17317
DE93-623867 ..... p 1179 N94-14931
DE93-623957 ..... p 1179 N94-14932
DE93-623987 ..... p 1013 N94-17316
DE93-624683 ..... p 974 N94-17611
DE93-624944 ..... p 1042 N94-17630
DE93-624947 ..... p 1215 N94-17437
DE93-626624 ..... p 1220 N94-17315
DE93-626638 ..... p 1168 N94-14933
DE93-626670 ..... p 1179 N94-14934
DE93-626671 ..... p 1219 N94-14935
DE93-626690 ..... p 1171 N94-17314
DE93-626692 ..... p 1188 N94-17313
DE93-626697 ..... p 1185 N94-17310
DE93-626721 ..... p 1185 N94-17312 #
DE93-627106 ..... p 1204 N94-17311
DE93-627959 ..... p 1103 N94-17631
DE93-627984 ..... p 1186 N94-17612
DE93-628585 ..... p 1171 N94-17613
DE93-628586 ..... p 1171 N94-17667
DE93-628587 ..... p 1171 N94-17640
DE93-628588 ..... p 1175 N94-17641
DE93-628589 ..... p 1171 N94-17642
DE93-628590 ..... p 1175 N94-17643
DE93-628591 ..... p 1175 N94-17644
DE93-628620 ..... p 1221 N94-17632 #
DE93-629161 ..... p 974 N94-17633 #
DE93-629162 ..... p 974 N94-17634 #
DE93-630197 ..... p 1205 N94-17635 #
DE93-753247 ..... p 1180 N94-15135 #

DLAM 4185.4 ..... p 1232 N94-17101

DLR-FB-92-35 ..... p 987 N94-15155 #
DLR-FB-93-06 ..... p 876 N94-17548 #
DLR-FB-93-11 ..... p 952 N94-17594 #

DM-63 ..... p 1110 N94-17593

DNA-TR-92-153 ..... p 988 N94-15668 #
DNA-TR-92-54-VOL-1 ..... p 1138 N94-17460

DOD-4100.39-M ..... p 1232 N94-17007
DOD-4100.39-M ..... p 1233 N94-17229 #
DOD-4120.15-L ..... p 898 N94-17388 #

DODA-AR-006-680 ..... p 872 N94-15856
DODA-AR-007-012 ..... p 1004 N94-17309
DODA-AR-007-015 ..... p 1229 N94-15652 #
DODA-AR-007-087 ..... p 872 N94-15543 #
DODA-AR-007-134 ..... p 862 N94-15542 #
DODA-AR-007-135 ..... p 1146 N94-15650 #
DODA-AR-007-137 ..... p 866 N94-15651 #
DODA-AR-008-151 ..... p 1190 N94-15846
DODA-AR-008-351 ..... p 868 N94-17117

DOE/AD-0044 ..... p 1230 N94-16010 #

DOE/BC-14882/3 ..... p 971 N94-16999 #

DOE/CE-0395 ..... p 1011 N94-16459 #
DOE/CE-15425/T11 ..... p 1092 N94-16766 #

DOE/ER-0587 ..... p 1160 N94-16774 #
DOE/ER-13227/7 ..... p 1041 N94-16998 #
DOE/ER-13387/T1 ..... p 1185 N94-16971 #
DOE/ER-13431/T1 ..... p 970 N94-16963 #
DOE/ER-13934/T1 ..... p 948 N94-16462 #
DOE/ER-14090/4 ..... p 1191 N94-16007 #
DOE/ER-14128/T1 ..... p 943 N94-15146 #
DOE/ER-14225/2 ..... p 1182 N94-16121 #
DOE/ER-14265/1 ..... p 1101 N94-16840 #
DOE/ER-25029/4 ..... p 1000 N94-17000 #
DOE/ER-35166/1 ..... p 1303 N94-16804 #
DOE/ER-40560/4A ..... p 1187 N94-16116 #
DOE/ER-40560/4B ..... p 1182 N94-16117 #
DOE/ER-40560/4C ..... p 1239 N94-16118 #
DOE/ER-40560/4J ..... p 1184 N94-16899 #
DOE/ER-40561/084 ..... p 1207 N94-15972 #
DOE/ER-40652/2 ..... p 1185 N94-16957 #
DOE/ER-40697/2 ..... p 1188 N94-16900 #
DOE/ER-40699/2 ..... p 1187 N94-16170 #
DOE/ER-40739/T1 ..... p 1183 N94-16818 #
DOE/ER-45322/6 ..... p 1212 N94-16961 #
DOE/ER-45415/8 ..... p 948 N94-16772 #
DOE/ER-45426/2 ..... p 960 N94-16972 #
DOE/ER-45461/10 ..... p 956 N94-15998 #
DOE/ER-52118/8 ..... p 1203 N94-16901 #
DOE/ER-53279/3 ..... p 1204 N94-16995 #
DOE/ER-53291/217 ..... p 1187 N94-17674 #
DOE/ER-53297/5 ..... p 1202 N94-16446 #
DOE/ER-60849/T1 ..... p 970 N94-16973 #
DOE/ER-61228/T1 ..... p 1122 N94-16113 #

DOE/ET-15601/T56 ..... p 949 N94-16891 #
DOE/ET-53088-601 ..... p 1187 N94-16660 #
DOE/ET-53088/597 ..... p 1174 N94-16820 #
DOE/ET-53088/605 ..... p 1203 N94-16822 #

DOE/FTR-93011662 ..... p 926 N94-16773 #

DOE/MC-25135/3341 ..... p 947 N94-15861 #
DOE/MC-26302/3269 ..... p 1024 N94-16763 #

DOE/METC-C/93/7082 ..... p 1092 N94-16715 #

DOE/NASA/16310-18 ..... p 962 N94-17652 * #
DOE/NASA/16310-20 ..... p 959 N94-16883 * #
DOE/NASA/50306-3 ..... p 930 N94-15769 * #

DOE/PC-89770/T14 ..... p 950 N94-16912 #
DOE/PC-90044/9-REV-1 ..... p 975 N94-16898 #
DOE/PC-90180/T7 ..... p 1026 N94-16958 #
DOE/PC-91030/T4 ..... p 952 N94-17218 #
DOE/PC-91287/8 ..... p 1220 N94-16997 #
DOE/PC-91293/T2 ..... p 949 N94-16896 #
DOE/PC-92104/T1 ..... p 975 N94-16996 #
DOE/PC-92110/T2 ..... p 949 N94-16897 #
DOE/PC-92529/T1 ..... p 950 N94-16962 #
DOE/PC-92542/T2 ..... p 970 N94-16959 #

DOE/SF-19645/T1 ..... p 960 N94-16964 #

DOT/FAA/CT-TN93/1 ..... p 1000 N94-16965 #

DOT/FAA/EE-93-01 ..... p 1179 N94-17599 #

DOT/FAA/NR-93/3 ..... p 864 N94-16439 #

DOT/FAA/PP-93-2 ..... p 865 N94-17458

DOT/FAA/RD-93/20 ..... p 876 N94-16025 #
DOT/FAA/RD-93/21 ..... p 864 N94-16835 #
DOT/FAA/RD-93/24 ..... p 862 N94-15444 * #

DOT/FAA/SE-93/3 ..... p 864 N94-16906 #
DOT/FAA/SE-93/4 ..... p 987 N94-15439 #

DOTVNTSC-FAA-93-5 ..... p 1179 N94-17599 #

DRA/TM(AWMH)92340 ..... p 1146 N94-15702 #

DRA/TM(USGR)92326 ..... p 933 N94-15699 #

DREO-1168 ..... p 864 N94-16457

DSS-NR15-43-1990 ..... p 977 N94-16071

DTIC/TR/93-20 ..... p 1232 N94-17101

D615-10070 ..... p 882 N94-15831 * #

E-6470-1 ..... p 1023 N94-15991 * #
E-6886 ..... p 1049 N94-17583 * #
E-7524 ..... p 1034 N94-15961 * #
E-7651 ..... p 869 N94-17386 * #
E-7653 ..... p 1058 N94-15709 * #
E-7760 ..... p 1040 N94-16522 * #
E-7810 ..... p 1032 N94-15445 * #
E-7836 ..... p 870 N94-17470 * #
E-7846 ..... p 926 N94-16880 * #
E-7879 ..... p 1013 N94-17113 * #
E-7922 ..... p 1060 N94-16881 * #
E-7968 ..... p 872 N94-15819 * #
E-7981 ..... p 1220 N94-17624 * #
E-8001 ..... p 956 N94-15992 * #
E-8030 ..... p 1030 N94-17486 * #
E-8034 ..... p 928 N94-17256 * #
E-8038 ..... p 967 N94-16543 * #
E-8042 ..... p 1176 N94-15115 * #
E-8054 ..... p 1169 N94-15818 * #
E-8078 ..... p 1046 N94-15817 * #

E-8087 ..... p 883 N94-17488 * #
E-8093 ..... p 883 N94-17487 * #
E-8100 ..... p 923 N94-15118 * #
E-8105 ..... p 1019 N94-15485 * #
E-8106 ..... p 1024 N94-16527 * #
E-8107 ..... p 1019 N94-15475 * #
E-8108 ..... p 1022 N94-15867 * #
E-8109 ..... p 1020 N94-15488 * #
E-8110 ..... p 1022 N94-15865 * #
E-8111 ..... p 1177 N94-16497 * #
E-8118 ..... p 1169 N94-15799 * #
E-8121 ..... p 930 N94-15769 * #
E-8122 ..... p 1034 N94-16521 * #
E-8126 ..... p 924 N94-15482 * #
E-8127 ..... p 1054 N94-16518 * #
E-8128 ..... p 962 N94-17652 * #
E-8133 ..... p 869 N94-15192 * #
E-8137 ..... p 883 N94-17111 * #
E-8139 ..... p 1026 N94-17056 * #
E-8141 ..... p 863 N94-16520 * #
E-8161 ..... p 1035 N94-17446 * #
E-8166 ..... p 1021 N94-15751 * #
E-8171 ..... p 869 N94-15866 * #
E-8175 ..... p 1030 N94-17557 * #
E-8176 ..... p 959 N94-16883 * #
E-8181 ..... p 858 N94-16571 * #
E-8183 ..... p 1028 N94-17258 * #
E-8184 ..... p 1029 N94-17448 * #
E-8185 ..... p 1027 N94-17112 * #
E-8191 ..... p 1025 N94-16879 * #
E-8192 ..... p 1029 N94-17385 * #
E-8193 ..... p 1027 N94-17128 * #
E-8197 ..... p 861 N94-17558 * #
E-8200 ..... p 1062 N94-17481 * #
E-8210 ..... p 1170 N94-16882 * #
E-8220 ..... p 929 N94-17483 * #

EGG-10617-2168 ..... p 1207 N94-15973 #
EGG-10617-2186 ..... p 1209 N94-16442 #
EGG-10617-2197 ..... p 949 N94-16876 #

EOARD-TR-93-08 ..... p 1213 N94-17037

EPA/600/R-93/028 ..... p 1094 N94-15136 #

ERDEC-CR-040 ..... p 1143 N94-15110 #

ERDEC-TR-059 ..... p 943 N94-15111 #
ERDEC-TR-078 ..... p 1119 N94-14923 #

ERL-0663-RN ..... p 1229 N94-15652 #

ERP-1108 ..... p 1107 N94-17244 #

ESA-BR-80 ..... p 874 N94-16584 #
ESA-BR-91 ..... p 987 N94-15644 #
ESA-BR-93 ..... p 1239 N94-16524 #

ESA-HSR-3 ..... p 887 N94-16523 #
ESA-HSR-4 ..... p 1225 N94-16593 #
ESA-HSR-5 ..... p 1303 N94-16526 #
ESA-HSR-6 ..... p 1303 N94-16500 #
ESA-HSR-7 ..... p 886 N94-16501 #
ESA-HSR-8 ..... p 1303 N94-16592 #
ESA-HSR-9 ..... p 887 N94-16525 #

ESA-INT-6 ..... p 1150 N94-16591 #

ESA-SP-1132-VOL-3 ..... p 943 N94-15157 #
ESA-SP-356 ..... p 899 N94-15025 #

ESC-TR-92-203 ..... p 1121 N94-15634 #
ESC-TR-92-206 ..... p 1164 N94-15746 #
ESC-TR-92-24 ..... p 1145 N94-15629 #
ESC-TR-93-161-VOL-1 ..... p 988 N94-15649 #
ESC-TR-93-161-VOL-2 ..... p 987 N94-15527 #
ESC-TR-93-180 ..... p 1144 N94-15216 #
ESC-TR-93-181 ..... p 1145 N94-15630 #
ESC-TR-93-182 ..... p 1144 N94-15214 #
ESC-TR-93-186 ..... p 1144 N94-15215 #
ESC-TR-93-193 ..... p 1154 N94-17396 #
ESC-TR-93-194 ..... p 1154 N94-17395 #

ESG-193 ..... p 1190 N94-15854 #

ETN-93-93780 ..... p 853 N94-15120 #
ETN-93-93952 ..... p 899 N94-15025 #
ETN-93-94342 ..... p 1177 N94-15506
ETN-93-94358 ..... p 954 N94-14930 #
ETN-93-94398 ..... p 1188 N94-15447 #
ETN-93-94399 ..... p 1008 N94-15448 #
ETN-93-94400 ..... p 1058 N94-15642 #
ETN-93-94405 ..... p 1116 N94-15643 #
ETN-93-94408 ..... p 967 N94-15644 #
ETN-93-94413 ..... p 955 N94-15149 #
ETN-93-94414 ..... p 1206 N94-15295 #
ETN-93-94418 ..... p 1057 N94-15154 * #
ETN-93-94426 ..... p 943 N94-15157 #
ETN-93-94427 ..... p 1142 N94-14978 #
ETN-93-94428 ..... p 1142 N94-14979 #
ETN-93-94429 ..... p 1158 N94-14980 #
ETN-93-94430 ..... p 1164 N94-15695 #
ETN-93-94432 ..... p 1156 N94-17528 #
ETN-93-94433 ..... p 1234 N94-17529 #
ETN-93-94434 ..... p 1030 N94-17531 #
ETN-93-94436 ..... p 1030 N94-17534 #
ETN-93-94437 ..... p 1162 N94-17537 #
ETN-93-94438 ..... p 1162 N94-17539 #
ETN-93-94440 ..... p 888 N94-17131
ETN-93-94449 ..... p 1172 N94-15298 #
ETN-93-94450 ..... p 989 N94-15714 #
ETN-93-94467 ..... p 1056 N94-17542 #
ETN-93-94476 ..... p 1015 N94-17546 #
ETN-93-94477 ..... p 974 N94-17547 #
ETN-93-94484 ..... p 1200 N94-15204 #
ETN-93-94492 ..... p 1020 N94-15645 #
ETN-93-94495 ..... p 856 N94-15696 #
ETN-93-94502 ..... p 933 N94-15699 #
ETN-93-94503 ..... p 1146 N94-15702 #
ETN-93-94538 ..... p 1004 N94-17407
ETN-93-94539 ..... p 1142 N94-14944
ETN-93-94540 ..... p 1142 N94-15008
ETN-93-94541 ..... p 1142 N94-15010
ETN-93-94543 ..... p 1142 N94-15011
ETN-93-94544 ..... p 1143 N94-15012
ETN-93-94545 ..... p 1049 N94-15013
ETN-93-94547 ..... p 1143 N94-15014
ETN-93-94548 ..... p 1057 N94-15015
ETN-93-94549 ..... p 1057 N94-15016
ETN-93-94550 ..... p 1057 N94-15017
ETN-93-94551 ..... p 1031 N94-15018
ETN-93-94552 ..... p 1176 N94-15019
ETN-93-94553 ..... p 986 N94-15020
ETN-93-94554 ..... p 1057 N94-15021
ETN-93-94563 ..... p 1114 N94-17516 #
ETN-93-94564 ..... p 1114 N94-17518 #
ETN-93-94565 ..... p 1114 N94-17489 #
ETN-93-94566 ..... p 1156 N94-17501
ETN-93-94567 ..... p 1234 N94-17502
ETN-93-94568 ..... p 1156 N94-17504
ETN-93-94569 ..... p 1014 N94-17505
ETN-93-94605 ..... p 1143 N94-15022
ETN-93-94607 ..... p 931 N94-15254 #
ETN-93-94611 ..... p 1200 N94-14966
ETN-93-94613 ..... p 1240 N94-17591
ETN-93-94617 ..... p 1105 N94-15302
ETN-93-94618 ..... p 1081 N94-15156
ETN-93-94619 ..... p 1098 N94-15153
ETN-93-94620 ..... p 987 N94-15155 #
ETN-93-94621 ..... p 876 N94-17548 #
ETN-93-94625 ..... p 1098 N94-15800 #
ETN-93-94627 ..... p 923 N94-17592
ETN-93-94629 ..... p 1110 N94-17593
ETN-93-94630 ..... p 1097 N94-17625 #
ETN-93-94631 ..... p 984 N94-16000 #
ETN-93-94780 ..... p 1157 N94-17626
ETN-93-94781 ..... p 1031 N94-17627
ETN-93-94785 ..... p 1062 N94-17600
ETN-93-94786 ..... p 854 N94-17614
ETN-93-94787 ..... p 1031 N94-17615 #
ETN-93-94819 ..... p 1085 N94-17616 #
ETN-93-94822 ..... p 1186 N94-17617
ETN-93-94823 ..... p 1220 N94-17618 #
ETN-93-94824 ..... p 1186 N94-17601
ETN-93-94825 ..... p 1220 N94-17602
ETN-93-94826 ..... p 1240 N94-17603
ETN-93-94827 ..... p 1240 N94-17604
ETN-93-94828 ..... p 1035 N94-17619
ETN-93-94878 ..... p 952 N94-17594 #
ETN-93-94885 ..... p 1006 N94-17549
ETN-93-94913 ..... p 1240 N94-17628
ETN-93-94916 ..... p 1237 N94-17629
ETN-93-94959 ..... p 1006 N94-17545
ETN-94474 ..... p 985 N94-17544 #

FAA-APO-93-6 ..... p 853 N94-14965 #

FASTC-ID(RS)T-0034-93 ..... p 860 N94-17274 #
FASTC-ID(RS)T-0121-93 ..... p 1042 N94-17394 #
FASTC-ID(RS)T-0219-93 ..... p 1035 N94-17401 #
FASTC-ID(RS)T-0220-93 ..... p 1193 N94-17254 #
FASTC-ID(RS)T-0221-93 ..... p 1035 N94-17402 #
FASTC-ID(RS)T-0234-93 ..... p 963 N94-15133 #
FASTC-ID(RS)T-0729-92 ..... p 1042 N94-17415
FASTC-ID(RS)T-0731-92 ..... p 879 N94-14941 #
FASTC-ID(RS)T-0735-92 ..... p 855 N94-14942 #
FASTC-ID(RS)T-0868-91 ..... p 1042 N94-17400 #
FASTC-ID(RS)T-0890-92 ..... p 1141 N94-17015
FASTC-ID(RS)T-0932-92 ..... p 860 N94-17222 #

FASTC-IR(RS)T-0959-92 ..... p 1191 N94-16126 #

FEAP-UG-92/12 ..... p 983 N94-15177 #

FFI-91/4029 ..... p 1172 N94-15298 #
FFI-92/2008 ..... p 989 N94-15714 #

FNAL/C-93/127 ..... p 1185 N94-16968 #
FNAL/C-93/135 ..... p 1168 N94-14928 #
FNAL/C-93/143-E ..... p 1186 N94-17662 #

FOA-C-40302-4.6 ..... p 1097 N94-17625 #

FTUAM-93/03 ..... p 1220 N94-17602

GA-A-21134 ..... p 1203 N94-16816 #
GA-A-21293 ..... p 1202 N94-16803 #
GA-A-21312 ..... p 1203 N94-16823 #

GA-C21284 ..... p 972 N94-17242 #

GAO/NSIAD-93-127 ..... p 1228 N94-15176 #
GAO/NSIAD-93-204 ..... p 868 N94-17472
GAO/NSIAD-93-216 ..... p 1002 N94-17199 #
GAO/NSIAD-94-54 ..... p 926 N94-16834 #

GAO/T-IMTEC-93-2 ..... p 1160 N94-16993 #

GC-TR-93-2303 ..... p 973 N94-17408 #

GIT-A-9056 ..... p 936 N94-16569 #

GP-23-1 ..... p 1121 N94-15658 * #

GSO-TR-93-1 ..... p 1112 N94-15844

H-1883 ..... p 867 N94-15783 * #
H-1910 ..... p 869 N94-15141 * #
H-1934 ..... p 886 N94-15753 * #
H-1945 ..... p 1032 N94-15754 * #

IAA.1.2-93-651 ..... p 1235 N94-17290 *

IAE-0094 ..... p 1175 N94-17317
IAE-0102 ..... p 952 N94-17302

IAF-93-P.2.365 ..... p 1222 N94-17441 *

IC-93/108 ..... p 1171 N94-17613
IC-93/43 ..... p 1171 N94-17667
IC-93/46-PT-2 ..... p 1103 N94-17631
IC-93/71 ..... p 1215 N94-17437
IC-93/72 ..... p 1171 N94-17640
IC-93/79 ..... p 1175 N94-17641
IC-93/82 ..... p 1171 N94-17642
IC-93/83 ..... p 1221 N94-17632 #
IC-93/93 ..... p 1175 N94-17643
IC-93/96 ..... p 1175 N94-17644

ICASE-93-48 ..... p 1169 N94-15833 * #
ICASE-93-49 ..... p 1023 N94-15964 * #
ICASE-93-53 ..... p 1144 N94-15483 * #
ICASE-93-54 ..... p 1021 N94-15834 * #
ICASE-93-55 ..... p 1017 N94-15183 * #
ICASE-93-57 ..... p 1019 N94-15479 * #
ICASE-93-58 ..... p 1016 N94-15005 * #
ICASE-93-60 ..... p 1021 N94-15768 * #
ICASE-93-61 ..... p 1019 N94-15478 * #
ICASE-93-62 ..... p 1148 N94-15965 * #
ICASE-93-63 ..... p 1168 N94-15724 * #
ICASE-93-64 ..... p 1145 N94-15489 * #
ICASE-93-65 ..... p 1149 N94-15989 * #
ICASE-93-72 ..... p 1029 N94-17387 * #
ICASE-93-73 ..... p 1030 N94-17450 * #

ICOMP-93-29 ..... p 1169 N94-15818 * #
ICOMP-93-33 ..... p 1026 N94-17056 * #
ICOMP-93-35 ..... p 1021 N94-15751 * #
ICOMP-93-36 ..... p 1030 N94-17557 * #
ICOMP-93-37 ..... p 1028 N94-17258 * #
ICOMP-93-38 ..... p 1029 N94-17448 * #
ICOMP-93-39 ..... p 1027 N94-17112 * #
ICOMP-93-40 ..... p 1025 N94-16879 * #
ICOMP-93-41 ..... p 1029 N94-17385 * #
ICOMP-93-42 ..... p 1027 N94-17128 * #
ICOMP-93-43 ..... p 1062 N94-17481 * #

IDA-P-2734 ..... p 1235 N94-16988 #

IDA/HQ-92-41686 ..... p 1235 N94-16988 #

IFA-93/40 ..... p 1299 N94-15968 * #

IFSR-597 ..... p 1174 N94-16820 #
IFSR-601 ..... p 1187 N94-16660 #
IFSR-605 ..... p 1203 N94-16822 #

IFTR-1/1992 ..... p 1060 N94-17052 #

IFTR-10/1991 ..... p 985 N94-17068 #
IFTR-12/1991 ..... p 998 N94-16653 #
IFTR-13/1991 ..... p 1193 N94-17049 #
IFTR-14/1991 ..... p 1002 N94-17048 #
IFTR-17/1992 ..... p 1178 N94-17087 #
IFTR-18/1991 ..... p 1060 N94-17047 #
IFTR-19/1991 ..... p 1061 N94-17069 #
IFTR-2/1992 ..... p 1178 N94-17051 #
IFTR-2/91 ..... p 1213 N94-17046 #
IFTR-20/1992 ..... p 1177 N94-16650 #
IFTR-21/1991 ..... p 960 N94-17093 #
IFTR-21/1992 ..... p 1061 N94-17091 #
IFTR-22/1991 ..... p 1059 N94-16651 #
IFTR-22/1992 ..... p 961 N94-17121 #
IFTR-23/1991 ..... p 969 N94-16924 #
IFTR-23/1992 ..... p 1204 N94-17067 #
IFTR-25/1991 ..... p 960 N94-17063 #
IFTR-27/1991 ..... p 1060 N94-16923 #
IFTR-28/91 ..... p 951 N94-17050 #
IFTR-3/1992 ..... p 1061 N94-17086 #
IFTR-3/91 ..... p 1002 N94-17057 #
IFTR-30/1991 ..... p 1204 N94-17066 #
IFTR-34/1991 ..... p 971 N94-17120 #
IFTR-36/1991 ..... p 1041 N94-17065 #
IFTR-37/1991 ..... p 1061 N94-17058 #
IFTR-38/1991 ..... p 1093 N94-17070 #
IFTR-41/1991 ..... p 1002 N94-17064 #
IFTR-43/1991 ..... p 1170 N94-17045 #
IFTR-6/1991 ..... p 1093 N94-17092 #
IFTR-7/1992 ..... p 1013 N94-17071 #
IFTR-9/1992 ..... p 998 N94-16652 #

INPE-5410-PRE/1757 ..... p 1111 N94-15186 #

INRIA-RR-1719 ..... p 1164 N94-15695 #
INRIA-RR-1727 ..... p 1156 N94-17528 #
INRIA-RR-1731 ..... p 1234 N94-17529 #
INRIA-RR-1732 ..... p 1030 N94-17531 #
INRIA-RR-1740 ..... p 1030 N94-17534 #
INRIA-RR-1746 ..... p 1162 N94-17537 #
INRIA-RR-1752 ..... p 1162 N94-17539 #

INRIA-RT-140 ..... p 1142 N94-14978 #
INRIA-RT-141 ..... p 1142 N94-14979 #
INRIA-RT-144 ..... p 1158 N94-14980 #

INS-934 ..... p 1180 N94-15135 #

INT-PATENT-CLASS-G01M-9/00 p 1032 N94-15697

INT-PATENT-CLASS-H01R-13/08 p 994 N94-15986
INT-PATENT-CLASS-H01R-21/26 p 994 N94-15986
INT-PATENT-CLASS-H03H-17/04 p 988 N94-15698

IOS-300-1992 ..... p 1114 N94-17516 #
IOS-301-1992 ..... p 1114 N94-17518 #
IOS-302-1992 ..... p 1114 N94-17489 #

IPP-5/46 ..... p 1200 N94-14966

IPPCZ-323 ..... p 1204 N94-17311
IPPCZ-324 ..... p 1205 N94-17635 #

ISAL-92-0083 ..... p 954 N94-14930 #

ISBN-0-643-05252-6 ..... p 1094 N94-15185
ISBN-0-660-55771-1 ..... p 977 N94-16071
ISBN-0-904947-38-6 ..... p 1020 N94-15645 #
ISBN-2-85-428327-9 ..... p 888 N94-17131
ISBN-3-7696-9437-6 ..... p 1081 N94-15156
ISBN-3-7696-9441-4 ..... p 1098 N94-15153
ISBN-3-79-831517-5 ..... p 1058 N94-15642 #
ISBN-3-88-148273-3 ..... p 1105 N94-15302
ISBN-9-05-411054-6 ..... p 1085 N94-17616 #
ISBN-9-29-092104-8 ..... p 943 N94-15157 #
ISBN-9-29-092266-4 ..... p 899 N94-15025 #
ISBN-9-51-384102-2 ..... p 1056 N94-17542 #
ISBN-9-51-384161-8 ..... p 985 N94-17544 #
ISBN-9-51-384171-5 ..... p 1015 N94-17546 #
ISBN-9-51-384172-3 ..... p 974 N94-17547 #
ISBN-90-369-2028-0 ..... p 1004 N94-17407
ISBN-90-6275-839-8 ..... p 1057 N94-15154 * #
ISBN-92-835-0713-4 ..... p 923 N94-15217 #
ISBN-92-835-0717-7 ..... p 1016 N94-15119 #
ISBN-92-835-0718-5 ..... p 1017 N94-15196 #
ISBN-92-835-2117-X ..... p 1229 N94-15437 #
ISBN-92-9092-099-8 ..... p 874 N94-16584 #
ISBN-92-9092-143-9 ..... p 987 N94-15644 #
ISBN-92-9092-151-X ..... p 1239 N94-16524 #
ISBN-951-22-1091-6 ..... p 1201 N94-15210 #
ISBN-951-38-4228-2 ..... p 1200 N94-15204 #

ITI-CR-92-57A ..... p 984 N94-16981 #

ITN-93-85219 ..... p 1180 N94-15283
ITN-93-85220 ..... p 1180 N94-15288

ITOP-6-2-517 ..... p 1005 N94-17523 #
ITOP-6-2-530 ..... p 1005 N94-17523 #

JINR-D-2-92-44 ..... p 1179 N94-14934

JINR-E-11-92-236 ..... p 1168 N94-14933
JINR-E-17-92-201 ..... p 1186 N94-17612
JINR-E-2-92-103 ..... p 1188 N94-17313
JINR-E-2-92-268 ..... p 1185 N94-17310
JINR-E-2-92-269 ..... p 1171 N94-17314
JINR-E-2-92-51 ..... p 1185 N94-17312 #
JINR-E-4-92-282 ..... p 1219 N94-14935

JINR-R-17-91-340 ..... p 974 N94-17633 #
JINR-R-17-91-342 ..... p 974 N94-17634 #
JINR-R-2-92-48 ..... p 1220 N94-17315

JPL-PUBL-91-31 ..... p 994 N94-16035 * #
JPL-PUBL-92-14-VOL-1 ..... p 1066 N94-16666 * #
JPL-PUBL-92-14-VOL-2 ..... p 1063 N94-16595 * #
JPL-PUBL-92-14-VOL-3 ..... p 1075 N94-16731 * #
JPL-PUBL-93-16 ..... p 989 N94-15886 * #
JPL-PUBL-93-24 ..... p 1298 N94-17654 * #

JTN-93-80450 ..... p 873 N94-15000 #
JTN-93-80476 ..... p 884 N94-15001 #

K/ETO-127 ..... p 1181 N94-15863 #

KFTI-92-3 ..... p 1179 N94-14931

KIYAI-92-17 ..... p 1013 N94-17316
KIYAI-92-19 ..... p 1179 N94-14932

KNMI-WR-92-06 ..... p 1004 N94-17407

L-16973 ..... p 872 N94-15794 * #
L-17008 ..... p 1042 N94-17285 * #
L-17113 ..... p 1034 N94-15990 * #
L-17160 ..... p 989 N94-15767 * #
L-17177 ..... p 866 N94-15722 * #
L-17185 ..... p 859 N94-16574 * #
L-17191 ..... p 856 N94-15681 * #
L-17197 ..... p 859 N94-16573 * #
L-17202 ..... p 1144 N94-15486 * #
L-17209 ..... p 1161 N94-17449 * #
L-17218 ..... p 998 N94-16655 * #
L-17225 ..... p 1301 N94-17666 * #
L-17229 ..... p 858 N94-16572 * #
L-17254 ..... p 1300 N94-15816 * #
L-17261 ..... p 861 N94-17284 * #
L-17266 ..... p 936 N94-16845 * #
L-17277 ..... p 1188 N94-17018 * #
L-17302 ..... p 1300 N94-17084 * #

LA-UR-93-1199 ..... p 898 N94-17669 #
LA-UR-93-1348 ..... p 1181 N94-15974 #
LA-UR-93-1395 ..... p 955 N94-15885 #
LA-UR-93-1448 ..... p 1202 N94-16776 #
LA-UR-93-1518 ..... p 965 N94-15920 #
LA-UR-93-1603 ..... p 1240 N94-17657 #
LA-UR-93-1855 ..... p 1185 N94-16951 #
LA-UR-93-1981 ..... p 1169 N94-15979 #
LA-UR-93-2006 ..... p 1183 N94-16801 #
LA-UR-93-2021 ..... p 1182 N94-16115 #
LA-UR-93-2133 ..... p 1220 N94-16956 #
LA-UR-93-2155 ..... p 1039 N94-16114 #
LA-UR-93-2303 ..... p 1205 N94-17645 #
LA-UR-93-2304 ..... p 1013 N94-17318 #
LA-UR-93-2307 ..... p 1192 N94-16953 #
LA-UR-93-2319 ..... p 1062 N94-17664 #
LA-UR-93-2334 ..... p 972 N94-17238 #
LA-UR-93-2354 ..... p 1202 N94-16451 #
LA-UR-93-2368 ..... p 1214 N94-17301 #
LA-UR-93-2371 ..... p 1299 N94-16895 #
LA-UR-93-2373 ..... p 1162 N94-17646 #
LA-UR-93-2386 ..... p 1178 N94-16955 #
LA-UR-93-669 ..... p 958 N94-16463 #
LA-UR-93-712 ..... p 959 N94-16764 #

LA-12564-MS ..... p 1217 N94-17659 #

LAAS-92513 ..... p 1116 N94-15643 #

LAIR-IR-480 ..... p 1122 N94-15741 #
LAIR-IR-481 ..... p 1122 N94-15740 #
LAIR-IR-482 ..... p 1128 N94-16783 #

LAIR-477 ..... p 1123 N94-16544 #
LAIR-478 ..... p 1123 N94-16558 #
LAIR-486 ..... p 1117 N94-16545 #

LBL-30797-VOL-1 ..... p 1096 N94-17289 #
LBL-32435-DRAFT ..... p 1190 N94-15854 #
LBL-32745 ..... p 1128 N94-16812 #
LBL-32956 ..... p 966 N94-15996 #

LBL-33031 ..... p 1181 N94-16013 #
LBL-33046 ..... p 1010 N94-16061 #
LBL-33313 ..... p 1102 N94-17252 #
LBL-33316 ..... p 1175 N94-17288 #
LBL-33771 ..... p 1239 N94-16052 #
LBL-33817 ..... p 947 N94-16060 #
LBL-33919-ABS ..... p 1181 N94-15995 #
LBL-33952 ..... p 1181 N94-16059 #
LBL-33961 ..... p 948 N94-16821 #
LBL-34077 ..... p 1181 N94-16053 #

LC-93-22329 ..... p 1114 N94-17439 *

LMSC-HSV-TR-P037989 ..... p 879 N94-15191 * #

LPI-TR-93-02-PT-2 ..... p 1032 N94-15797 * #
LPI-TR-93-03-PT-2 ..... p 1297 N94-17637 * #

LPTHE-93/06 ..... p 1220 N94-17602

LR-700 ..... p 1057 N94-15154 * #

LTR92-017 ..... p 1003 N94-17268 #

M-724-VOL-1 ..... p 1298 N94-15023 * #
M-724-VOL-2 ..... p 1298 N94-15024 * #
M-728 ..... p 1194 N94-17331 * #
M-731 ..... p 884 N94-15007 * #
M-732 ..... p 976 N94-15723 * #

MCAT-93-09 ..... p 858 N94-16510 * #
MCAT-93-19 ..... p 871 N94-15117 * #

MDC-92K0395 ..... p 1048 N94-17433

MIT-LCS-TR-569 ..... p 1141 N94-14915 #

MPA-706 ..... p 1240 N94-17628
MPA-709 ..... p 1237 N94-17629

MPE-PREPRINT-221 ..... p 1240 N94-17591

MSC-TPR-3318/1507 ..... p 941 N94-17597

MTR-92B0000027V1 ..... p 988 N94-15649 #
MTR-92B0000027V2 ..... p 987 N94-15527 #
MTR-93W0000059 ..... p 864 N94-16906 #
MTR-93W0000075 ..... p 876 N94-16025 #
MTR-93W0000102 ..... p 864 N94-16835 #

M93B0000072 ..... p 1165 N94-16559 #

NAS 1.15:102747 ..... p 1155 N94-17447 * #
NAS 1.15:103953 ..... p 1116 N94-15548 * #
NAS 1.15:103972 ..... p 1009 N94-15765 * #
NAS 1.15:103978 ..... p 1139 N94-17636 * #
NAS 1.15:104014 ..... p 1177 N94-15549 * #
NAS 1.15:104016 ..... p 870 N94-15793 * #
NAS 1.15:104026 ..... p 883 N94-15648 * #
NAS 1.15:104271 ..... p 1032 N94-15754 * #
NAS 1.15:104566-VOL-12 ..... p 1111 N94-15529 * #
NAS 1.15:104779-VOL-2 ..... p 882 N94-17320 * #
NAS 1.15:105088 ..... p 898 N94-17584 * #
NAS 1.15:105706 ..... p 923 N94-15118 * #
NAS 1.15:105808 ..... p 1176 N94-15115 * #
NAS 1.15:106046 ..... p 1060 N94-16881 * #
NAS 1.15:106110 ..... p 1040 N94-16522 * #
NAS 1.15:106247 ..... p 872 N94-15819 * #
NAS 1.15:106255 ..... p 1013 N94-17113 * #
NAS 1.15:106289 ..... p 956 N94-15992 * #
NAS 1.15:106293 ..... p 1030 N94-17486 * #
NAS 1.15:106296 ..... p 928 N94-17256 * #
NAS 1.15:106299 ..... p 967 N94-16543 * #
NAS 1.15:106314 ..... p 1169 N94-15818 * #
NAS 1.15:106325 ..... p 1046 N94-15817 * #
NAS 1.15:106328 ..... p 883 N94-17488 * #
NAS 1.15:106329 ..... p 1049 N94-17583 * #
NAS 1.15:106332 ..... p 883 N94-17487 * #
NAS 1.15:106336-VOL-1 ..... p 1019 N94-15485 * #
NAS 1.15:106337 ..... p 1024 N94-16527 * #
NAS 1.15:106338-VOL-2 ..... p 1019 N94-15475 * #
NAS 1.15:106339 ..... p 1022 N94-15867 * #
NAS 1.15:106340-VOL-2 ..... p 1020 N94-15488 * #
NAS 1.15:106341 ..... p 1022 N94-15865 * #
NAS 1.15:106342 ..... p 1177 N94-16497 * #
NAS 1.15:106347 ..... p 1169 N94-15799 * #
NAS 1.15:106348 ..... p 930 N94-15769 * #
NAS 1.15:106350 ..... p 962 N94-17652 * #
NAS 1.15:106355 ..... p 1026 N94-17056 * #
NAS 1.15:106357 ..... p 863 N94-16520 * #
NAS 1.15:106363 ..... p 1035 N94-17446 * #
NAS 1.15:106365 ..... p 1021 N94-15751 * #
NAS 1.15:106367 ..... p 869 N94-15866 * #
NAS 1.15:106369 ..... p 1030 N94-17557 * #
NAS 1.15:106370 ..... p 959 N94-16883 * #
NAS 1.15:106371 ..... p 858 N94-16571 * #

NAS 1.15:106373 ..... p 1028 N94-17258 * #
NAS 1.15:106374 ..... p 1029 N94-17448 * #
NAS 1.15:106375 ..... p 1027 N94-17112 * #
NAS 1.15:106378 ..... p 1025 N94-16879 * #
NAS 1.15:106379 ..... p 1029 N94-17385 * #
NAS 1.15:106380 ..... p 1027 N94-17128 * #
NAS 1.15:106382 ..... p 1062 N94-17481 * #
NAS 1.15:106388 ..... p 1170 N94-16882 * #
NAS 1.15:106395 ..... p 929 N94-17483 * #
NAS 1.15:107610 ..... p 885 N94-15446 * #
NAS 1.15:107693 ..... p 1233 N94-17291 * #
NAS 1.15:107693 ..... p 1233 N94-17300 * #
NAS 1.15:107733 ..... p 888 N94-17072 * #
NAS 1.15:107744 ..... p 1138 N94-17452 * #
NAS 1.15:107752 ..... p 1062 N94-17479 * #
NAS 1.15:107762 ..... p 1018 N94-15291 * #
NAS 1.15:108422 ..... p 1147 N94-15721 * #
NAS 1.15:108424 ..... p 1172 N94-15535 * #
NAS 1.15:108425 ..... p 955 N94-15832 * #
NAS 1.15:108426 ..... p 1058 N94-15534 * #
NAS 1.15:108427 ..... p 1058 N94-15710 * #
NAS 1.15:108428 ..... p 1059 N94-16519 * #
NAS 1.15:108429 ..... p 1174 N94-17469 * #
NAS 1.15:108780 ..... p 1120 N94-15537 * #
NAS 1.15:108784 ..... p 1145 N94-15538 * #
NAS 1.15:108787 ..... p 1121 N94-15711 * #
NAS 1.15:108788 ..... p 862 N94-15550 * #
NAS 1.15:108791 ..... p 1148 N94-15784 * #
NAS 1.15:108986 ..... p 1030 N94-17476 * #
NAS 1.15:108991 ..... p 1158 N94-15536 * #
NAS 1.15:108997 ..... p 986 N94-15140 * #
NAS 1.15:109007 ..... p 867 N94-17055 * #
NAS 1.15:109012 ..... p 1108 N94-17283 * #
NAS 1.15:109015 ..... p 1061 N94-17259 * #
NAS 1.15:109017 ..... p 1023 N94-15964 * #
NAS 1.15:109020 ..... p 1105 N94-15480 * #
NAS 1.15:109021 ..... p 1021 N94-15768 * #
NAS 1.15:109023 ..... p 955 N94-15708 * #
NAS 1.15:109024 ..... p 956 N94-15948 * #
NAS 1.15:109025 ..... p 1160 N94-16878 * #
NAS 1.15:109027 ..... p 861 N94-17639 * #
NAS 1.15:109029 ..... p 1179 N94-17650 * #
NAS 1.15:109038 ..... p 1152 N94-17060 * #
NAS 1.15:109049 ..... p 1062 N94-17451 * #
NAS 1.15:109051 ..... p 1085 N94-17665 * #
NAS 1.15:109278 ..... p 885 N94-15712 * #
NAS 1.15:109323 ..... p 1223 N94-15546 * #
NAS 1.15:109324 ..... p 1223 N94-15545 * #
NAS 1.15:109332 ..... p 1121 N94-15658 * #
NAS 1.15:109335 ..... p 854 N94-15798 * #
NAS 1.15:109336 ..... p 1230 N94-15838 * #
NAS 1.15:109337 ..... p 1230 N94-15839 * #
NAS 1.15:109340 ..... p 1222 N94-17441 *
NAS 1.15:109341 ..... p 1235 N94-17290 *
NAS 1.15:109342 ..... p 1102 N94-17214 * #
NAS 1.15:109343 ..... p 1027 N94-17061 * #
NAS 1.15:109345 ..... p 1235 N94-17294 * #
NAS 1.15:109346 ..... p 1006 N94-17661 * #
NAS 1.15:4457 ..... p 866 N94-15722 * #
NAS 1.15:4470 ..... p 1058 N94-15709 * #
NAS 1.15:4481 ..... p 869 N94-17386 * #
NAS 1.15:4483 ..... p 1139 N94-17017 * #
NAS 1.15:4484 ..... p 1095 N94-15781 * #
NAS 1.15:4485 ..... p 1032 N94-15445 * #
NAS 1.15:4486 ..... p 870 N94-17470 * #
NAS 1.15:4488 ..... p 856 N94-15681 * #
NAS 1.15:4489 ..... p 1144 N94-15486 * #
NAS 1.15:4501 ..... p 1118 N94-17257 * #
NAS 1.15:4512 ..... p 867 N94-15783 * #
NAS 1.15:4513 ..... p 1220 N94-17624 * #
NAS 1.15:4515 ..... p 861 N94-17284 * #
NAS 1.15:4519 ..... p 1300 N94-17084 * #
NAS 1.15:4520 ..... p 1042 N94-17285 * #
NAS 1.15:4522 ..... p 1188 N94-17018 * #
NAS 1.15:4524 ..... p 886 N94-15753 * #
NAS 1.15:4538 ..... p 869 N94-15141 * #
NAS 1.18:1420.21 ..... p 1230 N94-15936 * #
NAS 1.18:1620.3C ..... p 1224 N94-15937 * #
NAS 1.18:2410.1E ..... p 1230 N94-15941 * #
NAS 1.18:3100.6 ..... p 1224 N94-15945 * #
NAS 1.18:3335.1C ..... p 1224 N94-15944 * #
NAS 1.18:4100.1C ..... p 1225 N94-16830 * #
NAS 1.18:4200.1D ..... p 1225 N94-16799 * #
NAS 1.18:4200.2A ..... p 1224 N94-15957 * #
NAS 1.18:5200.1B ..... p 1224 N94-15939 * #
NAS 1.18:5800.1C ..... p 1225 N94-16907 * #
NAS 1.18:7900.3(V1) ..... p 1225 N94-16730 * #
NAS 1.18:7900.3 ..... p 1225 N94-16729 * #
NAS 1.18:8831.2 ..... p 1224 N94-15934 * #
NAS 1.18:9760.1A ..... p 1223 N94-15931 * #
NAS 1.21:511 ..... p 1114 N94-17439 *
NAS 1.21:7011(378) ..... p 1122 N94-16478 *
NAS 1.21:7011(380) ..... p 1122 N94-16479 *
NAS 1.21:7037(295) ..... p 854 N94-16480 *
NAS 1.21:7106 ..... p 854 N94-16481 *
NAS 1.26:177616 ..... p 866 N94-15718 * #
NAS 1.26:177620 ..... p 867 N94-15950 * #
NAS 1.26:177625 ..... p 1150 N94-16656 * #
NAS 1.26:177626-VOL-1 ..... p 855 N94-15655 * #
NAS 1.26:177626-VOL-2 ..... p 856 N94-15677 * #
NAS 1.26:177626-VOL-4 ..... p 857 N94-15720 * #
NAS 1.26:177626 ..... p 857 N94-15780 * #
NAS 1.26:177630 ..... p 860 N94-17081 * #
NAS 1.26:187086 ..... p 924 N94-15482 * #
NAS 1.26:187587 ..... p 1150 N94-16594 * #
NAS 1.26:188262 ..... p 926 N94-16922 * #
NAS 1.26:189103 ..... p 861 N94-17558 * #
NAS 1.26:190763 ..... p 1034 N94-16521 * #
NAS 1.26:191131 ..... p 926 N94-16880 * #
NAS 1.26:191143 ..... p 883 N94-17111 * #
NAS 1.26:191191 ..... p 1054 N94-16518 * #
NAS 1.26:191192 ..... p 869 N94-15192 * #
NAS 1.26:191464 ..... p 922 N94-17083 * #
NAS 1.26:191484 ..... p 1178 N94-17278 * #
NAS 1.26:191507 ..... p 1169 N94-15833 * #
NAS 1.26:191509 ..... p 1144 N94-15443 * #
NAS 1.26:191513 ..... p 1144 N94-15483 * #
NAS 1.26:191514 ..... p 1021 N94-15834 * #
NAS 1.26:191515 ..... p 1017 N94-15183 * #
NAS 1.26:191517 ..... p 1019 N94-15479 * #
NAS 1.26:191519 ..... p 1016 N94-15005 * #
NAS 1.26:191522 ..... p 930 N94-15106 * #
NAS 1.26:191523 ..... p 931 N94-15184 * #
NAS 1.26:191526 ..... p 967 N94-16541 * #
NAS 1.26:191528 ..... p 1019 N94-15478 * #
NAS 1.26:191529 ..... p 1148 N94-15965 * #
NAS 1.26:191530 ..... p 1168 N94-15724 * #
NAS 1.26:191531 ..... p 1145 N94-15489 * #
NAS 1.26:191532 ..... p 1149 N94-15989 * #
NAS 1.26:191538 ..... p 942 N94-17638 * #
NAS 1.26:191539 ..... p 933 N94-15484 * #
NAS 1.26:191541 ..... p 1029 N94-17387 * #
NAS 1.26:191542 ..... p 1030 N94-17450 * #
NAS 1.26:191546 ..... p 1176 N94-15487 * #
NAS 1.26:191550 ..... p 886 N94-15864 * #
NAS 1.26:191551 ..... p 1024 N94-16542 * #
NAS 1.26:191643 ..... p 887 N94-16503 * #
NAS 1.26:191644 ..... p 887 N94-16502 * #
NAS 1.26:191645 ..... p 926 N94-16504 * #
NAS 1.26:191933 ..... p 1059 N94-16815 * #
NAS 1.26:192559 ..... p 882 N94-17656 * #
NAS 1.26:192705 ..... p 1011 N94-16505 * #
NAS 1.26:193131 ..... p 1018 N94-15427 * #
NAS 1.26:193168 ..... p 858 N94-16510 * #
NAS 1.26:193174 ..... p 1247 N94-16173 * #
NAS 1.26:193357 ..... p 866 N94-15429 * #
NAS 1.26:193387 ..... p 1056 N94-15004 * #
NAS 1.26:193437 ..... p 1102 N94-17527 * #
NAS 1.26:193445 ..... p 1109 N94-17525 * #
NAS 1.26:193452 ..... p 1300 N94-17524 * #
NAS 1.26:193462 ..... p 1123 N94-16609 * #
NAS 1.26:193473 ..... p 1140 N94-16716 * #
NAS 1.26:193475 ..... p 1107 N94-16717 * #
NAS 1.26:193487 ..... p 1081 N94-17444 * #
NAS 1.26:193503 ..... p 1297 N94-17637 * #
NAS 1.26:193547 ..... p 1041 N94-16719 * #
NAS 1.26:193550 ..... p 1192 N94-16718 * #
NAS 1.26:193557 ..... p 1210 N94-16646 * #
NAS 1.26:193574 ..... p 1299 N94-17089 * #
NAS 1.26:193576 ..... p 1048 N94-17088 * #
NAS 1.26:193584 ..... p 1239 N94-16648 * #
NAS 1.26:193585 ..... p 1239 N94-16647 * #
NAS 1.26:193591 ..... p 951 N94-17039 * #
NAS 1.26:193594 ..... p 1297 N94-16866 * #
NAS 1.26:193602 ..... p 998 N94-16649 * #
NAS 1.26:193607 ..... p 1118 N94-17090 * #
NAS 1.26:193611 ..... p 1232 N94-17038 * #
NAS 1.26:193617 ..... p 999 N94-16867 * #
NAS 1.26:193628 ..... p 1297 N94-16884 * #
NAS 1.26:193637 ..... p 1098 N94-15433 * #
NAS 1.26:193838 ..... p 976 N94-15006 * #
NAS 1.26:193841 ..... p 879 N94-15191 * #
NAS 1.26:193845 ..... p 1016 N94-15109 * #
NAS 1.26:193849 ..... p 882 N94-15831 * #
NAS 1.26:193850 ..... p 870 N94-15532 * #
NAS 1.26:193851 ..... p 946 N94-15766 * #
NAS 1.26:193852 ..... p 928 N94-17442 * #
NAS 1.26:193856 ..... p 960 N94-17079 * #
NAS 1.26:193857 ..... p 927 N94-17123 * #
NAS 1.26:193858 ..... p 928 N94-17124 * #
NAS 1.26:193859 ..... p 927 N94-17080 * #
NAS 1.26:193861 ..... p 928 N94-17213 * #
NAS 1.26:193863 ..... p 927 N94-17096 * #
NAS 1.26:193864 ..... p 927 N94-17097 * #
NAS 1.26:193865 ..... p 927 N94-17098 * #
NAS 1.26:193867 ..... p 971 N94-17122 * #
NAS 1.26:194036 ..... p 887 N94-16905 * #
NAS 1.26:194104 ..... p 989 N94-15886 * #
NAS 1.26:194106 ..... p 870 N94-15416 * #
NAS 1.26:194148 ..... p 1239 N94-15188 * #
NAS 1.26:194267 ..... p 1062 N94-17445 * #
NAS 1.26:194284 ..... p 1097 N94-15003 * #
NAS 1.26:194292 ..... p 1168 N94-15112 * #
NAS 1.26:194294 ..... p 1158 N94-15113 * #
NAS 1.26:194332 ..... p 868 N94-15187 * #
NAS 1.26:194340 ..... p 1298 N94-17654 * #
NAS 1.26:194353 ..... p 1143 N94-15114 * #
NAS 1.26:194356 ..... p 1246 N94-15182 * #
NAS 1.26:194358 ..... p 1081 N94-15181 * #
NAS 1.26:194390 ..... p 1226 N94-14981 * #
NAS 1.26:194418 ..... p 1298 N94-15421 * #
NAS 1.26:194494 ..... p 932 N94-15275 * #
NAS 1.26:194539 ..... p 994 N94-16035 * #
NAS 1.26:194540 ..... p 1066 N94-16666 * #
NAS 1.26:194541 ..... p 1063 N94-16595 * #
NAS 1.26:194542 ..... p 1075 N94-16731 * #
NAS 1.26:194544 ..... p 1161 N94-17239 * #
NAS 1.26:194545 ..... p 1143 N94-15189 * #
NAS 1.26:194548 ..... p 871 N94-15117 * #
NAS 1.26:194549 ..... p 931 N94-15190 * #
NAS 1.26:194555 ..... p 1098 N94-15639 * #
NAS 1.26:194557 ..... p 946 N94-15713 * #
NAS 1.26:194558 ..... p 1172 N94-15641 * #
NAS 1.26:194559 ..... p 1008 N94-15640 * #
NAS 1.26:194560 ..... p 1206 N94-15476 * #
NAS 1.26:194563 ..... p 1038 N94-15477 * #
NAS 1.26:194567 ..... p 1300 N94-15533 * #
NAS 1.26:194570 ..... p 1082 N94-15531 * #
NAS 1.26:194571 ..... p 1038 N94-15530 * #
NAS 1.26:194572 ..... p 1112 N94-15701 * #
NAS 1.26:194573 ..... p 964 N94-15700 * #
NAS 1.26:194575 ..... p 1058 N94-15716 * #
NAS 1.26:194576 ..... p 1189 N94-15647 * #
NAS 1.26:194577 ..... p 1082 N94-15646 * #
NAS 1.26:194578 ..... p 1180 N94-15715 * #
NAS 1.26:194585 ..... p 1032 N94-15797 * #
NAS 1.26:194587 ..... p 1008 N94-15347 * #
NAS 1.26:194593 ..... p 976 N94-15654 * #
NAS 1.26:194594 ..... p 1020 N94-15551 * #
NAS 1.26:194595 ..... p 1221 N94-15719 * #
NAS 1.26:194596 ..... p 1236 N94-15679 * #
NAS 1.26:194597 ..... p 964 N94-15656 * #
NAS 1.26:194599 ..... p 856 N94-15678 * #
NAS 1.26:194601 ..... p 1112 N94-15680 * #
NAS 1.26:194603 ..... p 936 N94-16836 * #
NAS 1.26:194604 ..... p 1021 N94-15795 * #
NAS 1.26:194605 ..... p 1159 N94-15796 * #
NAS 1.26:194609 ..... p 1148 N94-15956 * #
NAS 1.26:194610 ..... p 1082 N94-16026 * #
NAS 1.26:194611 ..... p 1057 N94-15154 * #
NAS 1.26:194612 ..... p 1299 N94-15968 * #
NAS 1.26:194613 ..... p 1181 N94-15752 * #
NAS 1.26:194614 ..... p 1231 N94-16499 * #
NAS 1.26:194615 ..... p 994 N94-16022 * #
NAS 1.26:194616 ..... p 1236 N94-16492 * #
NAS 1.26:194617 ..... p 1237 N94-16833 * #
NAS 1.26:194618 ..... p 867 N94-16498 * #
NAS 1.26:194619 ..... p 1106 N94-16493 * #
NAS 1.26:194621 ..... p 1101 N94-16021 * #
NAS 1.26:194622 ..... p 1025 N94-16842 * #
NAS 1.26:194623 ..... p 997 N94-16506 * #
NAS 1.26:194624 ..... p 1024 N94-16491 * #
NAS 1.26:194625 ..... p 1297 N94-16832 * #
NAS 1.26:194626 ..... p 1084 N94-16831 * #
NAS 1.26:194630 ..... p 1191 N94-16023 * #
NAS 1.26:194631 ..... p 1190 N94-15869 * #
NAS 1.26:194632 ..... p 1191 N94-16024 * #
NAS 1.26:194633 ..... p 1190 N94-15868 * #
NAS 1.26:194634 ..... p 967 N94-16494 * #
NAS 1.26:194645 ..... p 1027 N94-17095 * #
NAS 1.26:194646 ..... p 927 N94-17016 * #
NAS 1.26:194647 ..... p 926 N94-16654 * #
NAS 1.26:194648 ..... p 1240 N94-17094 * #
NAS 1.26:194649 ..... p 1240 N94-17059 * #
NAS 1.26:194650 ..... p 926 N94-16590 * #
NAS 1.26:194651 ..... p 972 N94-17297 * #
NAS 1.26:194652 ..... p 897 N94-17280 * #
NAS 1.26:194653 ..... p 1199 N94-17443 * #
NAS 1.26:194654 ..... p 1118 N94-17279 * #
NAS 1.26:194655 ..... p 1027 N94-17130 * #
NAS 1.26:194656 ..... p 951 N94-17125 * #
NAS 1.26:194657 ..... p 1027 N94-17129 * #
NAS 1.26:194658 ..... p 1133 N94-17296 * #
NAS 1.26:194661 ..... p 1027 N94-17127 * #
NAS 1.26:194662 ..... p 1027 N94-17215 * #
NAS 1.26:194663 ..... p 923 N94-17126 * #
NAS 1.26:194664 ..... p 1301 N94-17255 * #
NAS 1.26:194665 ..... p 1028 N94-17298 * #
NAS 1.26:194666 ..... p 1299 N94-17281 * #
NAS 1.26:194672 ..... p 928 N94-17277 * #
NAS 1.26:194673 ..... p 1297 N94-17292 * #
NAS 1.26:194675 ..... p 860 N94-17260 * #
NAS 1.26:194676 ..... p 1235 N94-17293 * #
NAS 1.26:194677 ..... p 941 N94-17295 * #
NAS 1.26:4396-VOL-2 ..... p 1023 N94-15991 * #
NAS 1.26:4518 ..... p 1228 N94-15009 * #
NAS 1.26:4529-VOL-1 ..... p 1298 N94-15023 * #
NAS 1.26:4529-VOL-2 ..... p 1298 N94-15024 * #

NAS 1.26:4542 ..... p 1055 N94-17082 * #
NAS 1.26:4550 ..... p 862 N94-15444 * #
NAS 1.26:4553 ..... p 1036 N94-17655 * #
NAS 1.55:10120 ..... p 1303 N94-16495 * #
NAS 1.55:3170 ..... p 1228 N94-15116 * #
NAS 1.55:3211 ..... p 936 N94-16845 * #
NAS 1.55:3214 ..... p 911 N94-15552 * #
NAS 1.55:3227 ..... p 1194 N94-17331 * #
NAS 1.55:3236 ..... p 1012 N94-17062 * #
NAS 1.60:3331 ..... p 1034 N94-15990 * #
NAS 1.60:3334 ..... p 872 N94-15794 * #
NAS 1.60:3349 ..... p 1161 N94-17449 * #
NAS 1.60:3354 ..... p 1301 N94-17666 * #
NAS 1.60:3357 ..... p 856 N94-15657 * #
NAS 1.60:3359 ..... p 859 N94-16574 * #
NAS 1.60:3360 ..... p 859 N94-16573 * #
NAS 1.60:3361 ..... p 998 N94-16655 * #
NAS 1.60:3364 ..... p 1300 N94-15816 * #
NAS 1.60:3369 ..... p 858 N94-16572 * #
NAS 1.60:3372 ..... p 1034 N94-15961 * #
NAS 1.60:3386 ..... p 989 N94-15767 * #
NAS 1.60:3388 ..... p 925 N94-16496 * #
NAS 1.60:3400 ..... p 864 N94-15193 * #
NAS 1.60:3401 ..... p 1137 N94-15717 * #
NAS 1.60:3413 ..... p 884 N94-15007 * #
NAS 1.60:3420 ..... p 1139 N94-17653 * #
NAS 1.60:3421 ..... p 976 N94-15723 * #
NAS 1.61:1290 ..... p 1223 N94-15782 * #
NAS 1.61:1318 ..... p 1236 N94-15481 * #
NAS 1.71:ARC-11955-1-CU ..... p 934 N94-15926 * #
NAS 1.71:GSC-13404-1 ..... p 1010 N94-15874 * #
NAS 1.71:GSC-13454-1 ..... p 1046 N94-15871 * #
NAS 1.71:GSC-13462-1 ..... p 1194 N94-17321 * #
NAS 1.71:GSC-13489-1 ..... p 1164 N94-15704 * #
NAS 1.71:GSC-13493-1 ..... p 1004 N94-17322 * #
NAS 1.71:GSC-13503-1 ..... p 1046 N94-15873 * #
NAS 1.71:GSC-13541-1 ..... p 1165 N94-15946 * #
NAS 1.71:GSC-13543-1 ..... p 1189 N94-15705 * #
NAS 1.71:GSC-13556-1 ..... p 1148 N94-15943 * #
NAS 1.71:GSC-13562-1 ..... p 1147 N94-15703 * #
NAS 1.71:GSC-13564-1 ..... p 1033 N94-15872 * #
NAS 1.71:LAR-14054-1 ..... p 925 N94-15947 * #
NAS 1.71:LAR-14093-1 ..... p 1010 N94-15988 * #
NAS 1.71:LAR-14160-1 ..... p 1033 N94-15884 * #
NAS 1.71:LAR-14517-1 ..... p 965 N94-15879 * #
NAS 1.71:LAR-14535-1 ..... p 933 N94-15878 * #
NAS 1.71:LAR-14645-1-SB ..... p 1039 N94-15942 * #
NAS 1.71:LAR-14725-1 ..... p 1050 N94-15870 * #
NAS 1.71:LAR-14887-1 ..... p 1033 N94-15877 * #
NAS 1.71:LAR-14918-1 ..... p 983 N94-15881 * #
NAS 1.71:LAR-14969-1 ..... p 1129 N94-17085 * #
NAS 1.71:LAR-14987-2 ..... p 974 N94-17559 * #
NAS 1.71:LAR-14988-1 ..... p 965 N94-15880 * #
NAS 1.71:LEW-15263-2 ..... p 934 N94-15929 * #
NAS 1.71:LEW-15407-1 ..... p 1009 N94-15706 * #
NAS 1.71:LEW-15643-1 ..... p 1033 N94-15928 * #
NAS 1.71:MFS-28797-1 ..... p 1047 N94-15949 * #
NAS 1.71:MFS-29837-1 ..... p 1047 N94-15882 * #
NAS 1.71:MSC-21715-1 ..... p 1117 N94-15967 * #
NAS 1.71:MSC-21885-1 ..... p 1047 N94-15925 * #
NAS 1.71:MSC-21984-1 ..... p 1117 N94-15969 * #
NAS 1.71:MSC-21998-1 ..... p 1046 N94-15707 * #
NAS 1.71:MSC-22021-1 ..... p 886 N94-15935 * #
NAS 1.71:MSC-22082-1 ..... p 886 N94-15951 * #
NAS 1.71:MSC-22090-1 ..... p 1022 N94-15962 * #
NAS 1.71:MSC-22111-1 ..... p 1047 N94-15966 * #
NAS 1.71:MSC-22244-1 ..... p 1137 N94-15883 * #
NAS 1.71:NPO-18192-1-CU ..... p 925 N94-15927 * #
NAS 1.71:NPO-18399-1-CU ..... p 1014 N94-17323 * #
NAS 1.71:NPO-18458-1-CU ..... p 1033 N94-15875 * #
NAS 1.71:NPO-18470-1-CU ..... p 1038 N94-15932 * #
NAS 1.71:NPO-18547-1-CU ..... p 1014 N94-17324 * #
NAS 1.71:NPO-18664-1-CU ..... p 1237 N94-17438 * #
NAS 1.71:NPO-18694-1-CU ..... p 1014 N94-17325 * #
NAS 1.71:NPO-18735-1-CU ..... p 966 N94-15960 * #
NAS 1.71:NPO-18736-1-CU ..... p 1190 N94-15933 * #
NAS 1.71:NPO-18789-1-CU ..... p 1154 N94-17326 * #
NAS 1.71:NPO-18790-1-CU ..... p 1165 N94-15958 * #
NAS 1.71:NPO-18791-1-CU ..... p 1034 N94-15987 * #
NAS 1.71:NPO-18836-1-CU ..... p 1215 N94-17327 * #
NAS 1.71:NPO-18864-1-CU ..... p 1161 N94-17328 * #
NAS 1.71:NPO-18870-1-CU ..... p 1185 N94-17329 * #
NAS 1.71:NPO-18913-1-CU ..... p 966 N94-15930 * #
NAS 1.71:NPO-18935-1-CU ..... p 1010 N94-15952 * #
NAS 1.71:NPO-18983-1-CU ..... p 1161 N94-17330 * #
NAS 1.71:NPO-19174-1-CU ..... p 925 N94-15876 * #

NASA-CASE-ARC-11955-1-CU .... p 934 N94-15926 * #

NASA-CASE-GSC-13404-1 ..... p 1010 N94-15874 * #
NASA-CASE-GSC-13454-1 ..... p 1046 N94-15871 * #
NASA-CASE-GSC-13462-1 ..... p 1194 N94-17321 * #
NASA-CASE-GSC-13489-1 ..... p 1164 N94-15704 * #
NASA-CASE-GSC-13493-1 ..... p 1004 N94-17322 * #
NASA-CASE-GSC-13503-1 ..... p 1046 N94-15873 * #
NASA-CASE-GSC-13541-1 ..... p 1165 N94-15946 * #
NASA-CASE-GSC-13543-1 ..... p 1189 N94-15705 * #
NASA-CASE-GSC-13556-1 ..... p 1148 N94-15943 * #
NASA-CASE-GSC-13562-1 ..... p 1147 N94-15703 * #
NASA-CASE-GSC-13564-1 ..... p 1033 N94-15872 * #

NASA-CASE-LAR-14054-1 ..... p 925 N94-15947 * #
NASA-CASE-LAR-14093-1 ..... p 1010 N94-15988 * #
NASA-CASE-LAR-14160-1 ..... p 1033 N94-15884 * #
NASA-CASE-LAR-14517-1 ..... p 965 N94-15879 * #
NASA-CASE-LAR-14535-1 ..... p 933 N94-15878 * #
NASA-CASE-LAR-14645-1-SB .... p 1039 N94-15942 * #
NASA-CASE-LAR-14725-1 ..... p 1050 N94-15870 * #
NASA-CASE-LAR-14887-1 ..... p 1033 N94-15877 * #
NASA-CASE-LAR-14918-1 ..... p 983 N94-15881 * #
NASA-CASE-LAR-14969-1 ..... p 1129 N94-17085 * #
NASA-CASE-LAR-14987-2 ..... p 974 N94-17559 * #
NASA-CASE-LAR-14988-1 ..... p 965 N94-15880 * #

NASA-CASE-LEW-15263-2 ..... p 934 N94-15929 * #
NASA-CASE-LEW-15407-1 ..... p 1009 N94-15706 * #
NASA-CASE-LEW-15643-1 ..... p 1033 N94-15928 * #

NASA-CASE-MFS-28797-1 ..... p 1047 N94-15949 * #
NASA-CASE-MFS-29837-1 ..... p 1047 N94-15882 * #

NASA-CASE-MSC-21715-1 ..... p 1117 N94-15967 * #
NASA-CASE-MSC-21885-1 ..... p 1047 N94-15925 * #
NASA-CASE-MSC-21984-1 ..... p 1117 N94-15969 * #
NASA-CASE-MSC-21998-1 ..... p 1046 N94-15707 * #
NASA-CASE-MSC-22021-1 ..... p 886 N94-15935 * #
NASA-CASE-MSC-22082-1 ..... p 886 N94-15951 * #
NASA-CASE-MSC-22090-1 ..... p 1022 N94-15962 * #
NASA-CASE-MSC-22111-1 ..... p 1047 N94-15966 * #
NASA-CASE-MSC-22244-1 ..... p 1137 N94-15883 * #

NASA-CASE-NPO-18192-1-CU .... p 925 N94-15927 * #
NASA-CASE-NPO-18399-1-CU .... p 1014 N94-17323 * #
NASA-CASE-NPO-18458-1-CU .... p 1033 N94-15875 * #
NASA-CASE-NPO-18470-1-CU .... p 1038 N94-15932 * #
NASA-CASE-NPO-18547-1-CU .... p 1014 N94-17324 * #
NASA-CASE-NPO-18664-1-CU .... p 1237 N94-17438 * #
NASA-CASE-NPO-18694-1-CU .... p 1014 N94-17325 * #
NASA-CASE-NPO-18735-1-CU .... p 966 N94-15960 * #
NASA-CASE-NPO-18736-1-CU .... p 1190 N94-15933 * #
NASA-CASE-NPO-18789-1-CU .... p 1154 N94-17326 * #
NASA-CASE-NPO-18790-1-CU .... p 1165 N94-15958 * #
NASA-CASE-NPO-18791-1-CU .... p 1034 N94-15987 * #
NASA-CASE-NPO-18836-1-CU .... p 1215 N94-17327 * #
NASA-CASE-NPO-18864-1-CU .... p 1161 N94-17328 * #
NASA-CASE-NPO-18870-1-CU .... p 1185 N94-17329 * #
NASA-CASE-NPO-18913-1-CU .... p 966 N94-15930 * #
NASA-CASE-NPO-18935-1-CU .... p 1010 N94-15952 * #
NASA-CASE-NPO-18983-1-CU .... p 1161 N94-17330 * #
NASA-CASE-NPO-19174-1-CU .... p 925 N94-15876 * #

NASA-CP-10120 ..... p 1303 N94-16495 * #
NASA-CP-3170 ..... p 1228 N94-15116 * #
NASA-CP-3211 ..... p 936 N94-16845 * #
NASA-CP-3214 ..... p 911 N94-15552 * #
NASA-CP-3227 ..... p 1194 N94-17331 * #
NASA-CP-3236 ..... p 1012 N94-17062 * #

NASA-CR-177616 ..... p 866 N94-15718 * #
NASA-CR-177620 ..... p 867 N94-15950 * #
NASA-CR-177625 ..... p 1150 N94-16656 * #
NASA-CR-177626-VOL-1 ..... p 855 N94-15655 * #
NASA-CR-177626-VOL-2 ..... p 856 N94-15677 * #
NASA-CR-177626-VOL-4 ..... p 857 N94-15720 * #
NASA-CR-177626 ..... p 857 N94-15780 * #
NASA-CR-177630 ..... p 860 N94-17081 * #
NASA-CR-187086 ..... p 924 N94-15482 * #
NASA-CR-187587 ..... p 1150 N94-16594 * #
NASA-CR-188262 ..... p 926 N94-16922 * #
NASA-CR-189103 ..... p 861 N94-17558 * #
NASA-CR-190763 ..... p 1034 N94-16521 * #
NASA-CR-191131 ..... p 926 N94-16880 * #
NASA-CR-191143 ..... p 883 N94-17111 * #
NASA-CR-191191 ..... p 1054 N94-16518 * #
NASA-CR-191192 ..... p 869 N94-15192 * #
NASA-CR-191464 ..... p 922 N94-17083 * #
NASA-CR-191484 ..... p 1178 N94-17278 * #
NASA-CR-191507 ..... p 1169 N94-15833 * #
NASA-CR-191509 ..... p 1144 N94-15443 * #
NASA-CR-191513 ..... p 1144 N94-15483 * #
NASA-CR-191514 ..... p 1021 N94-15834 * #
NASA-CR-191515 ..... p 1017 N94-15183 * #
NASA-CR-191517 ..... p 1019 N94-15479 * #
NASA-CR-191519 ..... p 1016 N94-15005 * #
NASA-CR-191522 ..... p 930 N94-15106 * #
NASA-CR-191523 ..... p 931 N94-15184 * #
NASA-CR-191526 ..... p 967 N94-16541 * #
NASA-CR-191528 ..... p 1019 N94-15478 * #
NASA-CR-191529 ..... p 1148 N94-15965 * #
NASA-CR-191530 ..... p 1168 N94-15724 * #
NASA-CR-191531 ..... p 1145 N94-15489 * #
NASA-CR-191532 ..... p 1149 N94-15989 * #

NASA-CR-191538 ..... p 942 N94-17638 * #
NASA-CR-191539 ..... p 933 N94-15484 * #
NASA-CR-191541 ..... p 1029 N94-17387 * #
NASA-CR-191542 ..... p 1030 N94-17450 * #
NASA-CR-191546 ..... p 1176 N94-15487 * #
NASA-CR-191550 ..... p 886 N94-15864 * #
NASA-CR-191551 ..... p 1024 N94-16542 * #
NASA-CR-191643 ..... p 887 N94-16503 * #
NASA-CR-191644 ..... p 887 N94-16502 * #
NASA-CR-191645 ..... p 926 N94-16504 * #
NASA-CR-191933 ..... p 1059 N94-16815 * #
NASA-CR-192559 ..... p 882 N94-17656 * #
NASA-CR-192705 ..... p 1011 N94-16505 * #
NASA-CR-193131 ..... p 1018 N94-15427 * #
NASA-CR-193168 ..... p 858 N94-16510 * #
NASA-CR-193174 ..... p 1247 N94-16173 * #
NASA-CR-193357 ..... p 866 N94-15429 * #
NASA-CR-193387 ..... p 1056 N94-15004 * #
NASA-CR-193437 ..... p 1102 N94-17527 * #
NASA-CR-193445 ..... p 1109 N94-17525 * #
NASA-CR-193452 ..... p 1300 N94-17524 * #
NASA-CR-193462 ..... p 1123 N94-16609 * #
NASA-CR-193473 ..... p 1140 N94-16716 * #
NASA-CR-193475 ..... p 1107 N94-16717 * #
NASA-CR-193487 ..... p 1081 N94-17444 * #
NASA-CR-193503 ..... p 1297 N94-17637 * #
NASA-CR-193547 ..... p 1041 N94-16719 * #
NASA-CR-193550 ..... p 1192 N94-16718 * #
NASA-CR-193557 ..... p 1210 N94-16646 * #
NASA-CR-193574 ..... p 1299 N94-17089 * #
NASA-CR-193576 ..... p 1048 N94-17088 * #
NASA-CR-193584 ..... p 1239 N94-16648 * #
NASA-CR-193585 ..... p 1239 N94-16647 * #
NASA-CR-193591 ..... p 951 N94-17039 * #
NASA-CR-193594 ..... p 1297 N94-16866 * #
NASA-CR-193602 ..... p 998 N94-16649 * #
NASA-CR-193607 ..... p 1118 N94-17090 * #
NASA-CR-193611 ..... p 1232 N94-17038 * #
NASA-CR-193617 ..... p 999 N94-16867 * #
NASA-CR-193628 ..... p 1297 N94-16884 * #
NASA-CR-193637 ..... p 1098 N94-15433 * #
NASA-CR-193838 ..... p 976 N94-15006 * #
NASA-CR-193841 ..... p 879 N94-15191 * #
NASA-CR-193845 ..... p 1016 N94-15109 * #
NASA-CR-193849 ..... p 882 N94-15831 * #
NASA-CR-193850 ..... p 870 N94-15532 * #
NASA-CR-193851 ..... p 946 N94-15766 * #
NASA-CR-193852 ..... p 928 N94-17442 * #
NASA-CR-193856 ..... p 960 N94-17079 * #
NASA-CR-193857 ..... p 927 N94-17123 * #
NASA-CR-193858 ..... p 928 N94-17124 * #
NASA-CR-193859 ..... p 927 N94-17080 * #
NASA-CR-193861 ..... p 928 N94-17213 * #
NASA-CR-193863 ..... p 927 N94-17096 * #
NASA-CR-193864 ..... p 927 N94-17097 * #
NASA-CR-193865 ..... p 927 N94-17098 * #
NASA-CR-193867 ..... p 971 N94-17122 * #
NASA-CR-194036 ..... p 887 N94-16905 * #
NASA-CR-194104 ..... p 989 N94-15886 * #
NASA-CR-194106 ..... p 870 N94-15416 * #
NASA-CR-194148 ..... p 1239 N94-15188 * #
NASA-CR-194267 ..... p 1062 N94-17445 * #
NASA-CR-194284 ..... p 1097 N94-15003 * #
NASA-CR-194292 ..... p 1168 N94-15112 * #
NASA-CR-194294 ..... p 1158 N94-15113 * #
NASA-CR-194332 ..... p 868 N94-15187 * #
NASA-CR-194340 ..... p 1298 N94-17654 * #
NASA-CR-194353 ..... p 1143 N94-15114 * #
NASA-CR-194356 ..... p 1246 N94-15182 * #
NASA-CR-194358 ..... p 1081 N94-15181 * #
NASA-CR-194390 ..... p 1226 N94-14981 * #
NASA-CR-194418 ..... p 1298 N94-15421 * #
NASA-CR-194494 ..... p 932 N94-15275 * #
NASA-CR-194539 ..... p 994 N94-16035 * #
NASA-CR-194540 ..... p 1066 N94-16666 * #
NASA-CR-194541 ..... p 1063 N94-16595 * #
NASA-CR-194542 ..... p 1075 N94-16731 * #
NASA-CR-194544 ..... p 1161 N94-17239 * #
NASA-CR-194545 ..... p 1143 N94-15189 * #
NASA-CR-194548 ..... p 871 N94-15117 * #
NASA-CR-194549 ..... p 931 N94-15190 * #
NASA-CR-194555 ..... p 1098 N94-15639 * #
NASA-CR-194557 ..... p 946 N94-15713 * #
NASA-CR-194558 ..... p 1172 N94-15841 * #
NASA-CR-194559 ..... p 1008 N94-15640 * #
NASA-CR-194560 ..... p 1206 N94-15476 * #
NASA-CR-194563 ..... p 1038 N94-15477 * #
NASA-CR-194567 ..... p 1300 N94-15533 * #
NASA-CR-194570 ..... p 1062 N94-15531 * #
NASA-CR-194571 ..... p 1038 N94-15530 * #
NASA-CR-194572 ..... p 1112 N94-15701 * #
NASA-CR-194573 ..... p 964 N94-15700 * #
NASA-CR-194575 ..... p 1058 N94-15716 * #
NASA-CR-194576 ..... p 1189 N94-15647 * #
NASA-CR-194577 ..... p 1082 N94-15646 * #
NASA-CR-194578 ..... p 1180 N94-15715 * #

NASA-CR-194585 ..... p 1032 N94-15797 * #
NASA-CR-194587 ..... p 1008 N94-15547 * #
NASA-CR-194593 ..... p 976 N94-15654 * #
NASA-CR-194594 ..... p 1020 N94-15551 * #
NASA-CR-194595 ..... p 1221 N94-15719 * #
NASA-CR-194596 ..... p 1236 N94-15679 * #
NASA-CR-194597 ..... p 964 N94-15656 * #
NASA-CR-194599 ..... p 856 N94-15678 * #
NASA-CR-194601 ..... p 1112 N94-15680 * #
NASA-CR-194603 ..... p 936 N94-16836 * #
NASA-CR-194604 ..... p 1021 N94-15795 * #
NASA-CR-194605 ..... p 1159 N94-15796 * #
NASA-CR-194609 ..... p 1148 N94-15956 * #
NASA-CR-194610 ..... p 1082 N94-16026 * #
NASA-CR-194611 ..... p 1057 N94-15154 * #
NASA-CR-194612 ..... p 1299 N94-15968 * #
NASA-CR-194613 ..... p 1181 N94-15752 * #
NASA-CR-194614 ..... p 1231 N94-16499 * #
NASA-CR-194615 ..... p 994 N94-16022 * #
NASA-CR-194616 ..... p 1236 N94-16492 * #
NASA-CR-194617 ..... p 1237 N94-16833 * #
NASA-CR-194618 ..... p 867 N94-16498 * #
NASA-CR-194619 ..... p 1106 N94-16493 * #
NASA-CR-194621 ..... p 1101 N94-16021 * #
NASA-CR-194622 ..... p 1025 N94-16842 * #
NASA-CR-194623 ..... p 997 N94-16506 * #
NASA-CR-194624 ..... p 1024 N94-16491 * #
NASA-CR-194625 ..... p 1297 N94-16832 * #
NASA-CR-194626 ..... p 1084 N94-16831 * #
NASA-CR-194630 ..... p 1191 N94-16023 * #
NASA-CR-194631 ..... p 1190 N94-15869 * #
NASA-CR-194632 ..... p 1191 N94-16024 * #
NASA-CR-194633 ..... p 1190 N94-15868 * #
NASA-CR-194634 ..... p 967 N94-16494 * #
NASA-CR-194645 ..... p 1027 N94-17095 * #
NASA-CR-194646 ..... p 927 N94-17016 * #
NASA-CR-194647 ..... p 926 N94-16654 * #
NASA-CR-194648 ..... p 1240 N94-17094 * #
NASA-CR-194649 ..... p 1240 N94-17059 * #
NASA-CR-194650 ..... p 926 N94-16590 * #
NASA-CR-194651 ..... p 972 N94-17297 * #
NASA-CR-194652 ..... p 897 N94-17280 * #
NASA-CR-194653 ..... p 1199 N94-17443 * #
NASA-CR-194654 ..... p 1118 N94-17279 * #
NASA-CR-194655 ..... p 1027 N94-17130 * #
NASA-CR-194656 ..... p 951 N94-17125 * #
NASA-CR-194657 ..... p 1027 N94-17129 * #
NASA-CR-194658 ..... p 1133 N94-17296 * #
NASA-CR-194661 ..... p 1027 N94-17127 * #
NASA-CR-194662 ..... p 1027 N94-17215 * #
NASA-CR-194663 ..... p 923 N94-17126 * #
NASA-CR-194664 ..... p 1301 N94-17255 * #
NASA-CR-194665 ..... p 1028 N94-17298 * #
NASA-CR-194666 ..... p 1299 N94-17281 * #
NASA-CR-194672 ..... p 928 N94-17277 * #
NASA-CR-194673 ..... p 1297 N94-17292 * #
NASA-CR-194675 ..... p 860 N94-17260 * #
NASA-CR-194676 ..... p 1235 N94-17293 * #
NASA-CR-194677 ..... p 941 N94-17295 * #
NASA-CR-4396-VOL-2 ..... p 1023 N94-15991 * #
NASA-CR-4518 ..... p 1228 N94-15009 * #
NASA-CR-4529-VOL-1 ..... p 1298 N94-15023 * #
NASA-CR-4529-VOL-2 ..... p 1298 N94-15024 * #
NASA-CR-4542 ..... p 1055 N94-17082 * #
NASA-CR-4550 ..... p 862 N94-15444 * #
NASA-CR-4553 ..... p 1036 N94-17655 * #

NASA-RP-1290 ..... p 1223 N94-15782 * #
NASA-RP-1318 ..... p 1236 N94-15481 * #

NASA-SP-511 ..... p 1114 N94-17439 *
NASA-SP-7011(378) ..... p 1122 N94-16478 *
NASA-SP-7011(380) ..... p 1122 N94-16479 *
NASA-SP-7037(295) ..... p 854 N94-16480 *
NASA-SP-7106 ..... p 854 N94-16481 *

NASA-TM-102747 ..... p 1155 N94-17447 * #
NASA-TM-103953 ..... p 1116 N94-15548 * #
NASA-TM-103972 ..... p 1009 N94-15765 * #
NASA-TM-103978 ..... p 1139 N94-17636 * #
NASA-TM-104014 ..... p 1177 N94-15549 * #
NASA-TM-104016 ..... p 870 N94-15793 * #
NASA-TM-104026 ..... p 883 N94-15648 * #
NASA-TM-104271 ..... p 1032 N94-15754 * #
NASA-TM-104566-VOL-12 ..... p 1111 N94-15529 * #
NASA-TM-104779-VOL-2 ..... p 882 N94-17320 * #
NASA-TM-105088 ..... p 898 N94-17584 * #
NASA-TM-105706 ..... p 923 N94-15118 * #
NASA-TM-105808 ..... p 1176 N94-15115 * #
NASA-TM-106046 ..... p 1060 N94-16881 * #
NASA-TM-106110 ..... p 1040 N94-16522 * #
NASA-TM-106247 ..... p 872 N94-15819 * #
NASA-TM-106255 ..... p 1013 N94-17113 * #
NASA-TM-106289 ..... p 956 N94-15992 * #
NASA-TM-106293 ..... p 1030 N94-17486 * #
NASA-TM-106296 ..... p 928 N94-17256 * #
NASA-TM-106299 ..... p 967 N94-16543 * #
NASA-TM-106314 ..... p 1169 N94-15818 * #
NASA-TM-106325 ..... p 1046 N94-15817 * #
NASA-TM-106328 ..... p 883 N94-17488 * #
NASA-TM-106329 ..... p 1049 N94-17583 * #
NASA-TM-106332 ..... p 883 N94-17487 * #
NASA-TM-106336-VOL-1 ..... p 1019 N94-15485 * #
NASA-TM-106337 ..... p 1024 N94-16527 * #
NASA-TM-106338-VOL-2 ..... p 1019 N94-15475 * #
NASA-TM-106339 ..... p 1022 N94-15867 * #
NASA-TM-106340-VOL-2 ..... p 1020 N94-15488 * #
NASA-TM-106341 ..... p 1022 N94-15865 * #
NASA-TM-106342 ..... p 1177 N94-16497 * #
NASA-TM-106347 ..... p 1169 N94-15799 * #
NASA-TM-106348 ..... p 930 N94-15769 * #
NASA-TM-106350 ..... p 962 N94-17652 * #
NASA-TM-106355 ..... p 1026 N94-17056 * #
NASA-TM-106357 ..... p 863 N94-16520 * #
NASA-TM-106363 ..... p 1035 N94-17446 * #
NASA-TM-106365 ..... p 1021 N94-15751 * #
NASA-TM-106367 ..... p 869 N94-15866 * #
NASA-TM-106369 ..... p 1030 N94-17557 * #
NASA-TM-106370 ..... p 959 N94-16883 * #
NASA-TM-106371 ..... p 858 N94-16571 * #
NASA-TM-106373 ..... p 1028 N94-17258 * #
NASA-TM-106374 ..... p 1029 N94-17448 * #
NASA-TM-106375 ..... p 1027 N94-17112 * #
NASA-TM-106378 ..... p 1025 N94-16879 * #
NASA-TM-106379 ..... p 1029 N94-17385 * #
NASA-TM-106380 ..... p 1027 N94-17128 * #
NASA-TM-106382 ..... p 1062 N94-17481 * #
NASA-TM-106388 ..... p 1170 N94-16882 * #
NASA-TM-106395 ..... p 929 N94-17483 * #
NASA-TM-107610 ..... p 885 N94-15446 * #
NASA-TM-107693 ..... p 1233 N94-17291 * #
NASA-TM-107693 ..... p 1233 N94-17300 * #
NASA-TM-107733 ..... p 888 N94-17072 * #
NASA-TM-107744 ..... p 1138 N94-17452 * #
NASA-TM-107752 ..... p 1062 N94-17479 * #
NASA-TM-107762 ..... p 1018 N94-15291 * #
NASA-TM-108422 ..... p 1147 N94-15721 * #
NASA-TM-108424 ..... p 1172 N94-15535 * #
NASA-TM-108425 ..... p 955 N94-15832 * #
NASA-TM-108426 ..... p 1058 N94-15534 * #
NASA-TM-108427 ..... p 1058 N94-15710 * #
NASA-TM-108428 ..... p 1059 N94-16519 * #
NASA-TM-108429 ..... p 1174 N94-17469 * #
NASA-TM-108780 ..... p 1120 N94-15537 * #
NASA-TM-108784 ..... p 1145 N94-15538 * #
NASA-TM-108787 ..... p 1121 N94-15711 * #
NASA-TM-108788 ..... p 862 N94-15550 * #
NASA-TM-108791 ..... p 1148 N94-15784 * #
NASA-TM-108986 ..... p 1030 N94-17476 * #
NASA-TM-108991 ..... p 1158 N94-15536 * #
NASA-TM-108997 ..... p 986 N94-15140 * #
NASA-TM-109007 ..... p 867 N94-17055 * #
NASA-TM-109012 ..... p 1108 N94-17283 * #
NASA-TM-109015 ..... p 1061 N94-17259 * #
NASA-TM-109017 ..... p 1023 N94-15964 * #
NASA-TM-109020 ..... p 1105 N94-15480 * #
NASA-TM-109021 ..... p 1021 N94-15768 * #
NASA-TM-109023 ..... p 955 N94-15708 * #
NASA-TM-109024 ..... p 956 N94-15948 * #
NASA-TM-109025 ..... p 1160 N94-16878 * #
NASA-TM-109027 ..... p 861 N94-17639 * #
NASA-TM-109029 ..... p 1179 N94-17650 * #
NASA-TM-109038 ..... p 1152 N94-17060 * #
NASA-TM-109049 ..... p 1062 N94-17451 * #
NASA-TM-109051 ..... p 1085 N94-17665 * #
NASA-TM-109278 ..... p 885 N94-15712 * #
NASA-TM-109323 ..... p 1223 N94-15546 * #
NASA-TM-109324 ..... p 1223 N94-15545 * #
NASA-TM-109332 ..... p 1121 N94-15658 * #
NASA-TM-109334 ..... p 1229 N94-15523 *
NASA-TM-109335 ..... p 854 N94-15798 * #
NASA-TM-109336 ..... p 1230 N94-15838 * #
NASA-TM-109337 ..... p 1230 N94-15839 * #
NASA-TM-109340 ..... p 1222 N94-17441 *
NASA-TM-109341 ..... p 1235 N94-17290 *
NASA-TM-109342 ..... p 1102 N94-17214 * #
NASA-TM-109343 ..... p 1027 N94-17061 * #
NASA-TM-109345 ..... p 1235 N94-17294 * #
NASA-TM-109346 ..... p 1006 N94-17661 * #
NASA-TM-109417 ..... p 1247 N94-15511 *
NASA-TM-109418 ..... p 1247 N94-15512 *
NASA-TM-109419 ..... p 924 N94-15351 *
NASA-TM-109420 ..... p 1246 N94-15239 *
NASA-TM-109421 ..... p 1246 N94-15240 *
NASA-TM-109422 ..... p 1247 N94-15513 *
NASA-TM-109423 ..... p 1247 N94-15491 *
NASA-TM-109424 ..... p 874 N94-15493 *
NASA-TM-109425 ..... p 1239 N94-15495 *
NASA-TM-109426 ..... p 885 N94-15496 *
NASA-TM-109427 ..... p 885 N94-15497 *
NASA-TM-109428 ..... p 1131 N94-15499 *
NASA-TM-109429 ..... p 873 N94-15500 *
NASA-TM-109430 ..... p 874 N94-15501 *
NASA-TM-109431 ..... p 925 N94-15503 *
NASA-TM-109432 ..... p 1221 N94-15504 *
NASA-TM-109433 ..... p 1221 N94-15505 *
NASA-TM-109434 ..... p 1221 N94-15418 *
NASA-TM-109435 ..... p 1247 N94-15419 *
NASA-TM-109436 ..... p 1221 N94-15420 *
NASA-TM-109437 ..... p 862 N94-15336 *
NASA-TM-109438 ..... p 1235 N94-15337 *
NASA-TM-109439 ..... p 869 N94-15338 *
NASA-TM-109440 ..... p 1235 N94-15339 *
NASA-TM-109441 ..... p 1221 N94-15340 *
NASA-TM-109442 ..... p 878 N94-15341 *
NASA-TM-109443 ..... p 1247 N94-15342 *
NASA-TM-109444 ..... p 1302 N94-15343 *
NASA-TM-109445 ..... p 869 N94-15344 *
NASA-TM-109446 ..... p 933 N94-15345 *
NASA-TM-109447 ..... p 866 N94-15396 *
NASA-TM-109448 ..... p 865 N94-15321 *
NASA-TM-109449 ..... p 1302 N94-15322 *
NASA-TM-109450 ..... p 865 N94-15323 *
NASA-TM-109451 ..... p 865 N94-15324 *
NASA-TM-109452 ..... p 871 N94-15325 *
NASA-TM-109453 ..... p 1105 N94-15326 *
NASA-TM-109454 ..... p 865 N94-15327 *
NASA-TM-109455 ..... p 865 N94-15328 *
NASA-TM-109456 ..... p 1094 N94-15329 *
NASA-TM-109457 ..... p 1302 N94-15352 *
NASA-TM-109458 ..... p 880 N94-15353 *
NASA-TM-109459 ..... p 880 N94-15354 *
NASA-TM-109460 ..... p 880 N94-15355 *
NASA-TM-109461 ..... p 880 N94-15356 *
NASA-TM-109462 ..... p 880 N94-15357 *
NASA-TM-109463 ..... p 880 N94-15358 *
NASA-TM-109464 ..... p 1135 N94-15359 *
NASA-TM-109465 ..... p 1135 N94-15360 *
NASA-TM-109466 ..... p 1135 N94-15361 *
NASA-TM-109467 ..... p 1031 N94-15397 *
NASA-TM-109469 ..... p 881 N94-15398 *
NASA-TM-109470 ..... p 881 N94-15400 *
NASA-TM-109471 ..... p 1136 N94-15402 *
NASA-TM-109472 ..... p 880 N94-15376 *
NASA-TM-109473 ..... p 1135 N94-15377 *
NASA-TM-109474 ..... p 880 N94-15379 *
NASA-TM-109475 ..... p 1120 N94-15381 *
NASA-TM-109476 ..... p 1136 N94-15383 *
NASA-TM-109477 ..... p 881 N94-15384 *
NASA-TM-109478 ..... p 881 N94-15438 *
NASA-TM-109479 ..... p 881 N94-15440 *
NASA-TM-109480 ..... p 1136 N94-15441 *
NASA-TM-109481 ..... p 876 N94-15442 *
NASA-TM-109482 ..... p 876 N94-15449 *
NASA-TM-109483 ..... p 876 N94-15450 *
NASA-TM-109484 ..... p 876 N94-15451 *
NASA-TM-109485 ..... p 1032 N94-15792 *
NASA-TM-109488 ..... p 1134 N94-15194 *
NASA-TM-109489 ..... p 1135 N94-15195 *
NASA-TM-109493 ..... p 876 N94-15452 *
NASA-TM-109494 ..... p 1136 N94-15453 *
NASA-TM-109495 ..... p 1135 N94-15330 *
NASA-TM-109496 ..... p 1137 N94-15460 *
NASA-TM-109497 ..... p 881 N94-15461 *
NASA-TM-109498 ..... p 1137 N94-15462 *
NASA-TM-109499 ..... p 1032 N94-15463 *
NASA-TM-109500 ..... p 881 N94-15464 *
NASA-TM-109501 ..... p 881 N94-15465 *
NASA-TM-109502 ..... p 881 N94-15466 *
NASA-TM-109503 ..... p 876 N94-15467 *
NASA-TM-109504 ..... p 1137 N94-15514 *
NASA-TM-109505 ..... p 1135 N94-15224 *
NASA-TM-109506 ..... p 879 N94-15225 *
NASA-TM-109507 ..... p 1137 N94-15454 *
NASA-TM-109508 ..... p 1164 N94-15515 *
NASA-TM-109509 ..... p 1140 N94-15455 *
NASA-TM-109510 ..... p 1046 N94-15456 *
NASA-TM-109511 ..... p 1120 N94-15457 *
NASA-TM-109512 ..... p 885 N94-15458 *
NASA-TM-109513 ..... p 1046 N94-15459 *
NASA-TM-109514 ..... p 882 N94-15516 *
NASA-TM-109515 ..... p 882 N94-15518 *
NASA-TM-109516 ..... p 882 N94-15521 *
NASA-TM-109517 ..... p 876 N94-15517 *
NASA-TM-109518 ..... p 882 N94-15468 *
NASA-TM-109519 ..... p 873 N94-15469 *
NASA-TM-109520 ..... p 1137 N94-15470 *
NASA-TM-109521 ..... p 873 N94-15471 *
NASA-TM-109522 ..... p 1032 N94-15472 *
NASA-TM-109523 ..... p 876 N94-15473 *
NASA-TM-109524 ..... p 875 N94-15386 *
NASA-TM-109525 ..... p 1136 N94-15388 *
NASA-TM-109526 ..... p 881 N94-15389 *
NASA-TM-109527 ..... p 1136 N94-15390 *
NASA-TM-109528 ..... p 1136 N94-15391 *
NASA-TM-109529 ..... p 1303 N94-16069 *
NASA-TM-109530 ..... p 1136 N94-15392 *
NASA-TM-109531 ..... p 875 N94-15393 *

NASA-TM-109532 ..... p 1302 N94-15394 *
NASA-TM-109533 ..... p 976 N94-15395 *
NASA-TM-109534 ..... p 1302 N94-15399 *
NASA-TM-109535 ..... p 1302 N94-15366 *
NASA-TM-109536 ..... p 1223 N94-15367 *
NASA-TM-109537 ..... p 1120 N94-15368 *
NASA-TM-109538 ..... p 1120 N94-15369 *
NASA-TM-109539 ..... p 1120 N94-15370 *
NASA-TM-109540 ..... p 1135 N94-15371 *
NASA-TM-109541 ..... p 1221 N94-15372 *
NASA-TM-109542 ..... p 880 N94-15373 *
NASA-TM-109543 ..... p 1031 N94-15374 *
NASA-TM-109544 ..... p 1135 N94-15375 *
NASA-TM-109545 ..... p 1116 N94-15378 *
NASA-TM-109546 ..... p 1031 N94-15380 *
NASA-TM-109547 ..... p 1136 N94-15382 *
NASA-TM-109548 ..... p 1136 N94-15385 *
NASA-TM-109549 ..... p 1136 N94-15387 *
NASA-TM-109550 ..... p 1136 N94-15401 *
NASA-TM-109551 ..... p 881 N94-15403 *
NASA-TM-109552 ..... p 1136 N94-15404 *
NASA-TM-109553 ..... p 1032 N94-15405 *
NASA-TM-109554 ..... p 1136 N94-15406 *
NASA-TM-109555 ..... p 870 N94-15279 *
NASA-TM-109556 ..... p 976 N94-15280 *
NASA-TM-109557 ..... p 879 N94-15261 *
NASA-TM-109558 ..... p 879 N94-15262 *
NASA-TM-109559 ..... p 881 N94-15407 *
NASA-TM-109560 ..... p 876 N94-15474 *
NASA-TM-109561 ..... p 875 N94-15331 *
NASA-TM-109562 ..... p 875 N94-15332 *
NASA-TM-109563 ..... p 875 N94-15333 *
NASA-TM-109564 ..... p 1082 N94-15334 *
NASA-TM-109565 ..... p 1082 N94-15335 *
NASA-TM-109566 ..... p 1301 N94-15315 *
NASA-TM-109567 ..... p 1031 N94-15316 *
NASA-TM-109568 ..... p 880 N94-15317 *
NASA-TM-109569 ..... p 875 N94-15299 *
NASA-TM-109570 ..... p 1229 N94-15300 *
NASA-TM-109571 ..... p 875 N94-15301 *
NASA-TM-109572 ..... p 1135 N94-15303 *
NASA-TM-109573 ..... p 1031 N94-15304 *
NASA-TM-109574 ..... p 1135 N94-15305 *
NASA-TM-109575 ..... p 880 N94-15306 *
NASA-TM-109576 ..... p 880 N94-15307 *
NASA-TM-109577 ..... p 1236 N94-15422 *
NASA-TM-109578 ..... p 1045 N94-15263 *
NASA-TM-109579 ..... p 881 N94-15423 *
NASA-TM-109580 ..... p 879 N94-15264 *
NASA-TM-109581 ..... p 875 N94-15265 *
NASA-TM-109582 ..... p 879 N94-15266 *
NASA-TM-109583 ..... p 884 N94-15267 *
NASA-TM-109584 ..... p 1045 N94-15268 *
NASA-TM-109585 ..... p 884 N94-15269 *
NASA-TM-109586 ..... p 875 N94-15270 *
NASA-TM-109587 ..... p 1120 N94-15271 *
NASA-TM-109588 ..... p 1045 N94-15272 *
NASA-TM-109589 ..... p 875 N94-15273 *
NASA-TM-109590 ..... p 1111 N94-15281 *
NASA-TM-109591 ..... p 1098 N94-15282 *
NASA-TM-109592 ..... p 1045 N94-15284 *
NASA-TM-109593 ..... p 1135 N94-15285 *
NASA-TM-109594 ..... p 1135 N94-15286 *
NASA-TM-109595 ..... p 1298 N94-15287 *
NASA-TM-109596 ..... p 1094 N94-15289 *
NASA-TM-109597 ..... p 1094 N94-15290 *
NASA-TM-109598 ..... p 987 N94-15292 *
NASA-TM-109599 ..... p 1223 N94-15293 *
NASA-TM-109600 ..... p 873 N94-15308 *
NASA-TM-109601 ..... p 1120 N94-15309 *
NASA-TM-109602 ..... p 1081 N94-15310 *
NASA-TM-109603 ..... p 1236 N94-15311 *
NASA-TM-109604 ..... p 1120 N94-15312 *
NASA-TM-109605 ..... p 963 N94-15313 *
NASA-TM-109606 ..... p 880 N94-15314 *
NASA-TM-109607 ..... p 1247 N94-15294 *
NASA-TM-109608 ..... p 885 N94-15296 *
NASA-TM-109609 ..... p 1081 N94-15297 *
NASA-TM-109610 ..... p 1302 N94-15424 *
NASA-TM-109611 ..... p 1135 N94-15362 *
NASA-TM-109612 ..... p 1098 N94-15363 *
NASA-TM-109613 ..... p 1095 N94-15364 *
NASA-TM-109614 ..... p 1095 N94-15365 *
NASA-TM-109615 ..... p 1095 N94-15425 *
NASA-TM-109616 ..... p 862 N94-15426 *
NASA-TM-109617 ..... p 880 N94-15346 *
NASA-TM-109618 ..... p 1046 N94-15347 *
NASA-TM-109619 ..... p 1247 N94-15348 *
NASA-TM-109620 ..... p 1111 N94-15349 *
NASA-TM-109621 ..... p 1094 N94-15350 *
NASA-TM-109622 ..... p 1095 N94-15408 *
NASA-TM-109623 ..... p 1082 N94-15409 *
NASA-TM-109624 ..... p 1302 N94-15410 *
NASA-TM-109625 ..... p 1302 N94-15411 *
NASA-TM-109626 ..... p 1302 N94-15412 *
NASA-TM-109627 ..... p 1302 N94-15413 *
NASA-TM-109628 ..... p 1302 N94-15415 *
NASA-TM-109629 ..... p 1302 N94-15417 *
NASA-TM-109630 ..... p 1301 N94-15241 *
NASA-TM-109631 ..... p 1301 N94-15242 *
NASA-TM-109632 ..... p 1301 N94-15243 *
NASA-TM-109633 ..... p 1301 N94-15244 *
NASA-TM-109634 ..... p 1081 N94-15245 *
NASA-TM-109635 ..... p 1018 N94-15246 *
NASA-TM-109636 ..... p 1031 N94-15247 *
NASA-TM-109637 ..... p 1221 N94-15248 *
NASA-TM-109638 ..... p 1235 N94-15249 *
NASA-TM-109639 ..... p 1120 N94-15250 *
NASA-TM-109640 ..... p 1229 N94-15251 *
NASA-TM-109641 ..... p 1018 N94-15252 *
NASA-TM-109642 ..... p 1120 N94-15253 *
NASA-TM-109643 ..... p 1082 N94-15428 *
NASA-TM-109644 ..... p 1105 N94-15430 *
NASA-TM-109645 ..... p 1019 N94-15431 *
NASA-TM-109646 ..... p 1247 N94-16070 *
NASA-TM-109648 ..... p 1247 N94-15432 *
NASA-TM-109649 ..... p 1302 N94-15434 *
NASA-TM-109650 ..... p 875 N94-15318 *
NASA-TM-109651 ..... p 1223 N94-15319 *
NASA-TM-109652 ..... p 1049 N94-15320 *
NASA-TM-109653 ..... p 884 N94-15274 *
NASA-TM-109654 ..... p 885 N94-15278 *
NASA-TM-109655 ..... p 1105 N94-15226 *
NASA-TM-109656 ..... p 884 N94-15227 *
NASA-TM-109657 ..... p 1140 N94-15228 *
NASA-TM-109658 ..... p 924 N94-15229 *
NASA-TM-109659 ..... p 1221 N94-15230 *
NASA-TM-109660 ..... p 1229 N94-15231 *
NASA-TM-109661 ..... p 1221 N94-15232 *
NASA-TM-109662 ..... p 1175 N94-15233 *
NASA-TM-109663 ..... p 1223 N94-15234 *
NASA-TM-109664 ..... p 1116 N94-15235 *
NASA-TM-109665 ..... p 875 N94-15236 *
NASA-TM-109666 ..... p 1131 N94-15237 *
NASA-TM-109667 ..... p 1094 N94-15238 *
NASA-TM-109668 ..... p 1136 N94-15435 *
NASA-TM-109669 ..... p 885 N94-15436 *
NASA-TM-109670 ..... p 1137 N94-15507 *
NASA-TM-109671 ..... p 1303 N94-15508 *
NASA-TM-109672 ..... p 1303 N94-15509 *
NASA-TM-109673 ..... p 885 N94-15510 *
NASA-TM-109674 ..... p 983 N94-15519 *
NASA-TM-109675 ..... p 1229 N94-15520 *
NASA-TM-109676 ..... p 1298 N94-15522 *
NASA-TM-4457 ..... p 866 N94-15722 * #
NASA-TM-4470 ..... p 1058 N94-15709 * #
NASA-TM-4481 ..... p 869 N94-17386 * #
NASA-TM-4483 ..... p 1139 N94-17017 * #
NASA-TM-4484 ..... p 1095 N94-15781 * #
NASA-TM-4485 ..... p 1032 N94-15445 * #
NASA-TM-4486 ..... p 870 N94-17470 * #
NASA-TM-4488 ..... p 856 N94-15681 * #
NASA-TM-4489 ..... p 1144 N94-15486 * #
NASA-TM-4501 ..... p 1118 N94-17257 * #
NASA-TM-4512 ..... p 867 N94-15783 * #
NASA-TM-4513 ..... p 1220 N94-17624 * #
NASA-TM-4515 ..... p 861 N94-17284 * #
NASA-TM-4519 ..... p 1300 N94-17084 * #
NASA-TM-4520 ..... p 1042 N94-17285 * #
NASA-TM-4522 ..... p 1188 N94-17018 * #
NASA-TM-4524 ..... p 886 N94-15753 * #
NASA-TM-4538 ..... p 869 N94-15141 * #

NASA-TP-3331 ..... p 1034 N94-15990 * #
NASA-TP-3334 ..... p 872 N94-15794 * #
NASA-TP-3349 ..... p 1161 N94-17449 * #
NASA-TP-3354 ..... p 1301 N94-17666 * #
NASA-TP-3357 ..... p 856 N94-15657 * #
NASA-TP-3359 ..... p 859 N94-16574 * #
NASA-TP-3360 ..... p 859 N94-16573 * #
NASA-TP-3361 ..... p 998 N94-16655 * #
NASA-TP-3364 ..... p 1300 N94-15816 * #
NASA-TP-3369 ..... p 858 N94-16572 * #
NASA-TP-3372 ..... p 1034 N94-15961 * #
NASA-TP-3386 ..... p 989 N94-15767 * #
NASA-TP-3388 ..... p 925 N94-16496 * #
NASA-TP-3400 ..... p 884 N94-15193 * #
NASA-TP-3401 ..... p 1137 N94-15717 * #
NASA-TP-3413 ..... p 884 N94-15007 * #
NASA-TP-3420 ..... p 1139 N94-17653 * #
NASA-TP-3421 ..... p 976 N94-15723 * #

NASDA-SPP-930001 ..... p 884 N94-15001 #

NASDA-TK-SS0440 ..... p 873 N94-15000 #

NAWC-WPNS-TP-8124 ..... p 999 N94-16788
NAWC-WPNS-TP-8125 ..... p 999 N94-16789

NAWCADWAR-92103-70 ..... p 1146 N94-15670 #
NAWCADWAR-93015-60 ..... p 962 N94-17418

NAWCWPNS-TP-8134 ..... p 868 N94-17435

NCCOSC/RDT/E-TD-2461 ..... p 1039 N94-16474

NCCOSC/RDT/E-TR-1576 ..... p 997 N94-16467 #
NCCOSC/RDT/E-TR-1577 ..... p 1006 N94-17565
NCCOSC/RDT/E-TR-1601-PT-2 . p 1158 N94-15671 #

NCCOSD/RDT/E-TD-2516 ..... p 1005 N94-17496

NCEL-CR-93-002-VOL-1 ..... p 873 N94-17432 #
NCEL-CR-93-002-VOL-2 ..... p 873 N94-17508 #
NCEL-CR-93-003-VOL-1 ..... p 872 N94-17405 #
NCEL-CR-93-003-VOL-2 ..... p 873 N94-17569 #

NCEL-TR-940 ..... p 1167 N94-17392 #

NHB-1410.13L ..... p 1229 N94-15414 * #
NHB-1420.21 ..... p 1230 N94-15936 * #
NHB-1620.3C ..... p 1224 N94-15937 * #
NHB-2410.1E ..... p 1230 N94-15941 * #
NHB-3100.6 ..... p 1224 N94-15945 * #
NHB-3335.1C ..... p 1224 N94-15944 * #
NHB-4100.1C ..... p 1225 N94-16830 * #
NHB-4200.1D ..... p 1225 N94-16799 * #
NHB-4200.2A ..... p 1224 N94-15957 * #
NHB-5200.1B ..... p 1224 N94-15939 * #
NHB-5800.1C ..... p 1225 N94-16907 * #
NHB-7900.3(V1) ..... p 1225 N94-16730 * #
NHB-7900.3 ..... p 1225 N94-16729 * #
NHB-8831.2 ..... p 1224 N94-15934 * #
NHB-9760.1A ..... p 1223 N94-15931 * #

NHRC-92-28 ..... p 1119 N94-14943
NHRC-93-7 ..... p 1129 N94-17374

NIAR-92-20 ..... p 872 N94-17263 #
NIAR-93-11 ..... p 863 N94-17262 #
NIAR-93-13 ..... p 961 N94-17282 #
NIAR-93-14 ..... p 1222 N94-17261 #
NIAR-93-18 ..... p 860 N94-17260 * #
NIAR-93-3 ..... p 1153 N94-17299 #

NIKHEF-H/92-17 ..... p 1186 N94-17617
NIKHEF-H/92-18 ..... p 1220 N94-17618 #
NIKHEF-H/93-02 ..... p 1186 N94-17601
NIKHEF-H/93-03 ..... p 1220 N94-17602
NIKHEF-H/93-04 ..... p 1240 N94-17603
NIKHEF-H/93-06 ..... p 1240 N94-17604
NIKHEF-H/93-07 ..... p 1035 N94-17619

NIWA/ATMOS/R/93-001 ..... p 1094 N94-15185

NLR-TP-91288-U ..... p 1157 N94-17626
NLR-TP-91350-U ..... p 1031 N94-17627
NLR-TP-91445-U ..... p 1177 N94-15506
NLR-TP-91478-U ..... p 1062 N94-17600
NLR-TP-92121-U ..... p 1031 N94-17615 #

NLR-TR-92119-U ..... p 854 N94-17614

NMRI-93-02 ..... p 1130 N94-17562 #
NMRI-93-03 ..... p 1130 N94-17556 #
NMRI-93-34 ..... p 1115 N94-14918 #
NMRI-93-38 ..... p 1119 N94-14916 #

NOAA-TM-NWS-SR-149 ..... p 1106 N94-16465 #

NOARL-31 ..... p 1106 N94-16568

NONP-VT-93-190214 ..... p 1247 N94-15511 *
NONP-VT-93-190215 ..... p 1247 N94-15512 *
NONP-VT-93-190216 ..... p 924 N94-15351 *
NONP-VT-93-190217 ..... p 1246 N94-15239 *
NONP-VT-93-190218 ..... p 1246 N94-15240 *
NONP-VT-93-190219 ..... p 1247 N94-15513 *
NONP-VT-93-190220 ..... p 1247 N94-15491 *
NONP-VT-93-190221 ..... p 874 N94-15493 *
NONP-VT-93-190222 ..... p 1239 N94-15495 *
NONP-VT-93-190223 ..... p 885 N94-15496 *
NONP-VT-93-190224 ..... p 885 N94-15497 *
NONP-VT-93-190225 ..... p 1131 N94-15499 *
NONP-VT-93-190226 ..... p 873 N94-15500 *
NONP-VT-93-190227 ..... p 874 N94-15501 *
NONP-VT-93-190228 ..... p 925 N94-15503 *
NONP-VT-93-190229 ..... p 1221 N94-15504 *
NONP-VT-93-190230 ..... p 1221 N94-15505 *
NONP-VT-93-190231 ..... p 1221 N94-15418 *
NONP-VT-93-190232 ..... p 1247 N94-15419 *
NONP-VT-93-190233 ..... p 1221 N94-15420 *
NONP-VT-93-190234 ..... p 862 N94-15336 *
NONP-VT-93-190235 ..... p 1235 N94-15337 *
NONP-VT-93-190236 ..... p 869 N94-15338 *
NONP-VT-93-190237 ..... p 1235 N94-15339 *
NONP-VT-93-190238 ..... p 1221 N94-15340 *
NONP-VT-93-190239 ..... p 878 N94-15341 *

NONP-VT-93-190240 ..... p 1247 N94-15342 *
NONP-VT-93-190241 ..... p 1302 N94-15343 *
NONP-VT-93-190242 ..... p 869 N94-15344 *
NONP-VT-93-190243 ..... p 933 N94-15345 *
NONP-VT-93-190244 ..... p 866 N94-15396 *
NONP-VT-93-190245 ..... p 865 N94-15321 *
NONP-VT-93-190246 ..... p 1302 N94-15322 *
NONP-VT-93-190247 ..... p 865 N94-15323 *
NONP-VT-93-190248 ..... p 865 N94-15324 *
NONP-VT-93-190249 ..... p 871 N94-15325 *
NONP-VT-93-190250 ..... p 1105 N94-15326 *
NONP-VT-93-190251 ..... p 865 N94-15327 *
NONP-VT-93-190252 ..... p 865 N94-15328 *
NONP-VT-93-190253 ..... p 1094 N94-15329 *
NONP-VT-93-190254 ..... p 1302 N94-15352 *
NONP-VT-93-190255 ..... p 880 N94-15353 *
NONP-VT-93-190256 ..... p 880 N94-15354 *
NONP-VT-93-190257 ..... p 880 N94-15355 *
NONP-VT-93-190258 ..... p 880 N94-15356 *
NONP-VT-93-190259 ..... p 880 N94-15357 *
NONP-VT-93-190260 ..... p 880 N94-15358 *
NONP-VT-93-190261 ..... p 1135 N94-15359 *
NONP-VT-93-190262 ..... p 1135 N94-15360 *
NONP-VT-93-190263 ..... p 1135 N94-15361 *
NONP-VT-93-190264 ..... p 1031 N94-15397 *
NONP-VT-93-190266 ..... p 881 N94-15398 *
NONP-VT-93-190267 ..... p 881 N94-15400 *
NONP-VT-93-190268 ..... p 1136 N94-15402 *
NONP-VT-93-190269 ..... p 880 N94-15376 *
NONP-VT-93-190270 ..... p 1135 N94-15377 *
NONP-VT-93-190271 ..... p 880 N94-15379 *
NONP-VT-93-190272 ..... p 1120 N94-15381 *
NONP-VT-93-190273 ..... p 1136 N94-15383 *
NONP-VT-93-190274 ..... p 881 N94-15384 *
NONP-VT-93-190275 ..... p 881 N94-15438 *
NONP-VT-93-190276 ..... p 881 N94-15440 *
NONP-VT-93-190277 ..... p 1136 N94-15441 *
NONP-VT-93-190278 ..... p 876 N94-15442 *
NONP-VT-93-190279 ..... p 876 N94-15449 *
NONP-VT-93-190280 ..... p 876 N94-15450 *
NONP-VT-93-190281 ..... p 876 N94-15451 *
NONP-VT-93-190282 ..... p 1032 N94-15792 *
NONP-VT-93-190285 ..... p 1134 N94-15194 *
NONP-VT-93-190286 ..... p 1135 N94-15195 *
NONP-VT-93-190290 ..... p 876 N94-15452 *
NONP-VT-93-190291 ..... p 1136 N94-15453 *
NONP-VT-93-190292 ..... p 1135 N94-15330 *
NONP-VT-93-190293 ..... p 1137 N94-15460 *
NONP-VT-93-190294 ..... p 881 N94-15461 *
NONP-VT-93-190295 ..... p 1137 N94-15462 *
NONP-VT-93-190296 ..... p 1032 N94-15463 *
NONP-VT-93-190297 ..... p 881 N94-15464 *
NONP-VT-93-190298 ..... p 881 N94-15465 *
NONP-VT-93-190299 ..... p 881 N94-15466 *
NONP-VT-93-190300 ..... p 876 N94-15467 *
NONP-VT-93-190301 ..... p 1137 N94-15514 *
NONP-VT-93-190302 ..... p 1135 N94-15224 *
NONP-VT-93-190303 ..... p 879 N94-15225 *
NONP-VT-93-190304 ..... p 1137 N94-15454 *
NONP-VT-93-190305 ..... p 1164 N94-15515 *
NONP-VT-93-190306 ..... p 1140 N94-15455 *
NONP-VT-93-190307 ..... p 1046 N94-15456 *
NONP-VT-93-190308 ..... p 1120 N94-15457 *
NONP-VT-93-190309 ..... p 885 N94-15458 *
NONP-VT-93-190310 ..... p 1046 N94-15459 *
NONP-VT-93-190311 ..... p 882 N94-15516 *
NONP-VT-93-190312 ..... p 882 N94-15518 *
NONP-VT-93-190313 ..... p 882 N94-15521 *
NONP-VT-93-190314 ..... p 876 N94-15517 *
NONP-VT-93-190315 ..... p 882 N94-15468 *
NONP-VT-93-190316 ..... p 873 N94-15469 *
NONP-VT-93-190317 ..... p 1137 N94-15470 *
NONP-VT-93-190318 ..... p 873 N94-15471 *
NONP-VT-93-190319 ..... p 1032 N94-15472 *
NONP-VT-93-190320 ..... p 876 N94-15473 *
NONP-VT-93-190321 ..... p 875 N94-15386 *
NONP-VT-93-190322 ..... p 1136 N94-15388 *
NONP-VT-93-190323 ..... p 881 N94-15389 *
NONP-VT-93-190324 ..... p 1136 N94-15390 *
NONP-VT-93-190325 ..... p 1136 N94-15391 *
NONP-VT-93-190326 ..... p 1303 N94-16069 *
NONP-VT-93-190327 ..... p 1136 N94-15392 *
NONP-VT-93-190328 ..... p 875 N94-15393 *
NONP-VT-93-190329 ..... p 1302 N94-15394 *
NONP-VT-93-190330 ..... p 976 N94-15395 *
NONP-VT-93-190331 ..... p 1302 N94-15399 *
NONP-VT-93-190332 ..... p 1302 N94-15366 *
NONP-VT-93-190333 ..... p 1223 N94-15367 *
NONP-VT-93-190334 ..... p 1120 N94-15368 *
NONP-VT-93-190335 ..... p 1120 N94-15369 *
NONP-VT-93-190336 ..... p 1120 N94-15370 *
NONP-VT-93-190337 ..... p 1135 N94-15371 *
NONP-VT-93-190338 ..... p 1221 N94-15372 *
NONP-VT-93-190339 ..... p 880 N94-15373 *
NONP-VT-93-190340 ..... p 1031 N94-15374 *
NONP-VT-93-190341 ..... p 1135 N94-15375 *
NONP-VT-93-190342 ..... p 1116 N94-15378 *
NONP-VT-93-190343 ..... p 1031 N94-15380 *
NONP-VT-93-190345 ..... p 1136 N94-15382 *
NONP-VT-93-190346 ..... p 1136 N94-15385 *
NONP-VT-93-190347 ..... p 1136 N94-15387 *
NONP-VT-93-190348 ..... p 1136 N94-15401 *
NONP-VT-93-190349 ..... p 881 N94-15403 *
NONP-VT-93-190350 ..... p 1136 N94-15404 *
NONP-VT-93-190351 ..... p 1032 N94-15405 *
NONP-VT-93-190352 ..... p 1136 N94-15406 *
NONP-VT-93-190353 ..... p 870 N94-15279 *
NONP-VT-93-190354 ..... p 976 N94-15280 *
NONP-VT-93-190355 ..... p 879 N94-15261 *
NONP-VT-93-190356 ..... p 879 N94-15262 *
NONP-VT-93-190357 ..... p 881 N94-15407 *
NONP-VT-93-190358 ..... p 876 N94-15474 *
NONP-VT-93-190359 ..... p 875 N94-15331 *
NONP-VT-93-190360 ..... p 875 N94-15332 *
NONP-VT-93-190361 ..... p 875 N94-15333 *
NONP-VT-93-190362 ..... p 1082 N94-15334 *
NONP-VT-93-190363 ..... p 1082 N94-15335 *
NONP-VT-93-190364 ..... p 1301 N94-15315 *
NONP-VT-93-190365 ..... p 1031 N94-15316 *
NONP-VT-93-190366 ..... p 880 N94-15317 *
NONP-VT-93-190367 ..... p 875 N94-15299 *
NONP-VT-93-190368 ..... p 1229 N94-15300 *
NONP-VT-93-190369 ..... p 875 N94-15301 *
NONP-VT-93-190370 ..... p 1135 N94-15303 *
NONP-VT-93-190371 ..... p 1031 N94-15304 *
NONP-VT-93-190372 ..... p 1135 N94-15305 *
NONP-VT-93-190373 ..... p 880 N94-15306 *
NONP-VT-93-190374 ..... p 880 N94-15307 *
NONP-VT-93-190375 ..... p 1236 N94-15422 *
NONP-VT-93-190376 ..... p 1045 N94-15263 *
NONP-VT-93-190377 ..... p 881 N94-15423 *
NONP-VT-93-190378 ..... p 879 N94-15264 *
NONP-VT-93-190379 ..... p 875 N94-15265 *
NONP-VT-93-190380 ..... p 879 N94-15266 *
NONP-VT-93-190381 ..... p 884 N94-15267 *
NONP-VT-93-190382 ..... p 1045 N94-15268 *
NONP-VT-93-190383 ..... p 884 N94-15269 *
NONP-VT-93-190384 ..... p 875 N94-15270 *
NONP-VT-93-190385 ..... p 1120 N94-15271 *
NONP-VT-93-190386 ..... p 1045 N94-15272 *
NONP-VT-93-190387 ..... p 875 N94-15273 *
NONP-VT-93-190388 ..... p 1111 N94-15281 *
NONP-VT-93-190389 ..... p 1098 N94-15282 *
NONP-VT-93-190390 ..... p 1045 N94-15284 *
NONP-VT-93-190391 ..... p 1135 N94-15285 *
NONP-VT-93-190392 ..... p 1135 N94-15286 *
NONP-VT-93-190393 ..... p 1298 N94-15287 *
NONP-VT-93-190394 ..... p 1094 N94-15289 *
NONP-VT-93-190395 ..... p 1094 N94-15290 *
NONP-VT-93-190396 ..... p 987 N94-15292 *
NONP-VT-93-190397 ..... p 1223 N94-15293 *
NONP-VT-93-190398 ..... p 873 N94-15308 *
NONP-VT-93-190399 ..... p 1120 N94-15309 *
NONP-VT-93-190400 ..... p 1081 N94-15310 *
NONP-VT-93-190401 ..... p 1236 N94-15311 *
NONP-VT-93-190402 ..... p 1120 N94-15312 *
NONP-VT-93-190403 ..... p 963 N94-15313 *
NONP-VT-93-190404 ..... p 880 N94-15314 *
NONP-VT-93-190405 ..... p 1247 N94-15294 *
NONP-VT-93-190406 ..... p 885 N94-15296 *
NONP-VT-93-190407 ..... p 1081 N94-15297 *
NONP-VT-93-190408 ..... p 1302 N94-15424 *
NONP-VT-93-190409 ..... p 1135 N94-15362 *
NONP-VT-93-190410 ..... p 1098 N94-15363 *
NONP-VT-93-190411 ..... p 1095 N94-15364 *
NONP-VT-93-190412 ..... p 1095 N94-15365 *
NONP-VT-93-190413 ..... p 1095 N94-15425 *
NONP-VT-93-190414 ..... p 862 N94-15426 *
NONP-VT-93-190415 ..... p 880 N94-15346 *
NONP-VT-93-190416 ..... p 1046 N94-15347 *
NONP-VT-93-190417 ..... p 1247 N94-15348 *
NONP-VT-93-190418 ..... p 1111 N94-15349 *
NONP-VT-93-190419 ..... p 1094 N94-15350 *
NONP-VT-93-190420 ..... p 1095 N94-15408 *
NONP-VT-93-190421 ..... p 1082 N94-15409 *
NONP-VT-93-190422 ..... p 1302 N94-15410 *
NONP-VT-93-190423 ..... p 1302 N94-15411 *
NONP-VT-93-190424 ..... p 1302 N94-15412 *
NONP-VT-93-190425 ..... p 1302 N94-15413 *
NONP-VT-93-190426 ..... p 1302 N94-15415 *
NONP-VT-93-190427 ..... p 1302 N94-15417 *
NONP-VT-93-190428 ..... p 1301 N94-15241 *
NONP-VT-93-190429 ..... p 1301 N94-15242 *
NONP-VT-93-190430 ..... p 1301 N94-15243 *
NONP-VT-93-190431 ..... p 1301 N94-15244 *
NONP-VT-93-190432 ..... p 1081 N94-15245 *
NONP-VT-93-190433 ..... p 1018 N94-15246 *
NONP-VT-93-190434 ..... p 1031 N94-15247 *
NONP-VT-93-190435 ..... p 1221 N94-15248 *
NONP-VT-93-190436 ..... p 1235 N94-15249 *
NONP-VT-93-190437 ..... p 1120 N94-15250 *
NONP-VT-93-190438 ..... p 1229 N94-15251 *
NONP-VT-93-190439 ..... p 1018 N94-15252 *
NONP-VT-93-190440 ..... p 1120 N94-15253 *
NONP-VT-93-190441 ..... p 1082 N94-15428 *
NONP-VT-93-190442 ..... p 1105 N94-15430 *
NONP-VT-93-190443 ..... p 1019 N94-15431 *
NONP-VT-93-190444 ..... p 1247 N94-16070 *
NONP-VT-93-190446 ..... p 1247 N94-15432 *
NONP-VT-93-190447 ..... p 1302 N94-15434 *
NONP-VT-93-190448 ..... p 875 N94-15318 *
NONP-VT-93-190449 ..... p 1223 N94-15319 *
NONP-VT-93-190450 ..... p 1049 N94-15320 *
NONP-VT-93-190451 ..... p 884 N94-15274 *
NONP-VT-93-190452 ..... p 885 N94-15278 *
NONP-VT-93-190453 ..... p 1105 N94-15226 *
NONP-VT-93-190454 ..... p 884 N94-15227 *
NONP-VT-93-190455 ..... p 1140 N94-15228 *
NONP-VT-93-190456 ..... p 924 N94-15229 *
NONP-VT-93-190457 ..... p 1221 N94-15230 *
NONP-VT-93-190458 ..... p 1229 N94-15231 *
NONP-VT-93-190459 ..... p 1221 N94-15232 *
NONP-VT-93-190460 ..... p 1175 N94-15233 *
NONP-VT-93-190461 ..... p 1223 N94-15234 *
NONP-VT-93-190462 ..... p 1116 N94-15235 *
NONP-VT-93-190463 ..... p 875 N94-15236 *
NONP-VT-93-190464 ..... p 1131 N94-15237 *
NONP-VT-93-190465 ..... p 1094 N94-15238 *
NONP-VT-93-190466 ..... p 1136 N94-15435 *
NONP-VT-93-190467 ..... p 885 N94-15436 *
NONP-VT-93-190468 ..... p 1137 N94-15507 *
NONP-VT-93-190469 ..... p 1303 N94-15508 *
NONP-VT-93-190470 ..... p 1303 N94-15509 *
NONP-VT-93-190471 ..... p 885 N94-15510 *
NONP-VT-93-190472 ..... p 983 N94-15519 *
NONP-VT-93-190473 ..... p 1229 N94-15520 *
NONP-VT-93-190474 ..... p 1298 N94-15522 *
NONP-VT-93-190475 ..... p 1229 N94-15523 *

NOO-TN-03-93 ..... p 1113 N94-16588 #

NPL-DES-123 ..... p 1006 N94-17545
NPL-DES-126 ..... p 986 N94-15020

NPL-DITC-204/92 ..... p 1142 N94-14944
NPL-DITC-205/92 ..... p 1142 N94-15008
NPL-DITC-206/92 ..... p 1142 N94-15010
NPL-DITC-208/92 ..... p 1142 N94-15011
NPL-DITC-209/92 ..... p 1143 N94-15012
NPL-DITC-210/92 ..... p 1049 N94-15013
NPL-DITC-217/93 ..... p 1143 N94-15022
NPL-DITC-218/92 ..... p 1143 N94-15014

NPL-DMM(A)-101 ..... p 1006 N94-17549
NPL-DMM(A)-27 ..... p 1057 N94-15015
NPL-DMM(A)-81 ..... p 1057 N94-15021
NPL-DMM(A)-91 ..... p 1057 N94-15016
NPL-DMM(A)-92 ..... p 1057 N94-15017

NPL-RSA(EXT)-0043 ..... p 1176 N94-15019
NPL-RSA(EXT)-40 ..... p 1031 N94-15018

NPS-AA-93-001 ..... p 857 N94-16471

NRAD-TR-1569 ..... p 1002 N94-17110 #
NRAD-TR-1572-PT-1 ..... p 1159 N94-15750 #
NRAD-TR-1575 ..... p 987 N94-15544 #

NRC-31485 ..... p 977 N94-16071

NREL/TP-422-5415 ..... p 1093 N94-17668 #
NREL/TP-441-5611 ..... p 1010 N94-15971 #

NRL/FR/5544-93-9561 ..... p 1162 N94-17622 #
NRL/FR/7240-93-9422 ..... p 1113 N94-17241 #
NRL/FR/7531-92-9413 ..... p 1106 N94-16568

NRL/MR/5320-93-7181 ..... p 987 N94-15540 #
NRL/MR/5510-93-7350 ..... p 1166 N94-16938 #
NRL/MR/5554-93-7375 ..... p 1004 N94-17373 #
NRL/MR/5632-93-7336 ..... p 1098 N94-15539 #
NRL/MR/6174-93-7351 ..... p 948 N94-16553 #
NRL/MR/6386-93-7369 ..... p 1057 N94-15524 #
NRL/MR/6615-93-6948 ..... p 1173 N94-17495
NRL/MR/6721-93-7312 ..... p 1038 N94-15628 #
NRL/MR/6721-93-7317 ..... p 878 N94-16552 #
NRL/MR/7225-93-7346 ..... p 1020 N94-15526 #
NRL/MR/7323-93-7023 ..... p 1114 N94-17509 #

NSWCDD/TR-92/206 ..... p 1214 N94-17270 #
NSWCDD/TR-93/29 ..... p 1020 N94-15632 #

NTSB/ARC-93/02 ..... p 863 N94-17471 #

NTSB/ARG-93/01 ..... p 863 N94-16464 #

NUREG-CR-5981 ..... p 962 N94-17464

NUWC-NL-TD-10345 ..... p 988 N94-15693 #

NUWC-NPT-TR-10199 ..... p 1057 N94-15150 #
NUWC-NPT-TR-10371 ..... p 1173 N94-17372 #
NUWC-NPT-TR-10403 ..... p 1171 N94-17393 #

OCNR-111192-12 ..... p 1140 N94-17623 #

ODU/ICAM-93-101 ..... p 1021 N94-15795 * #
ODU/ICAM-93-102 ..... p 1181 N94-15752 * #

ONERA-NT-1992-13 ..... p 955 N94-15149 #
ONERA-NT-1993-1 ..... p 1206 N94-15295 #

ONR-C-13 ..... p 1172 N94-15733 #

ONR-TR-93-1 ..... p 1137 N94-16108 #

ORNL-6736 ..... p 1097 N94-17426 #
ORNL-6753 ..... p 1301 N94-14926
ORNL-6755 ..... p 1232 N94-16967 #

ORNL/M-2711 ..... p 958 N94-16453 #

ORNL/TM-12218 ..... p 1167 N94-17287

PAPER-37 ..... p 886 N94-15753 * #
PAPER-89RG01615 ..... p 1083 N94-16028 * #
PAPER-89WR01579 ..... p 1083 N94-16027 * #
PAPER-92WR02333 ..... p 1084 N94-16032 * #
PAPER-93WR00398 ..... p 1083 N94-16031 * #

PAR-TM-93-103 ..... p 1041 N94-17193 #

PB93-134880 ..... p 1094 N94-15136 #
PB93-160687 ..... p 863 N94-16464 #
PB93-183507 ..... p 1106 N94-16465 #
PB94-102787 ..... p 863 N94-17471 #

PCMDI-10 ..... p 1096 N94-16802 #

PERS-TR-93-003 ..... p 1223 N94-15682 #

PL-CP-93-1001-PT-1 ..... p 985 N94-17482
PL-CP-93-1001-PT-2 ..... p 985 N94-17484
PL-CP-93-1001-PT-3 ..... p 985 N94-17485

PL-TR-92-2225 ..... p 1107 N94-17244 #
PL-TR-92-2326 ..... p 1101 N94-16551 #
PL-TR-92-2328 ..... p 1003 N94-17268 #
PL-TR-92-2342 ..... p 1192 N94-16550 #
PL-TR-92-2343 ..... p 882 N94-16468 #
PL-TR-92-3054 ..... p 928 N94-17308
PL-TR-93-1003 ..... p 1011 N94-16556 #
PL-TR-93-1020 ..... p 1174 N94-17219 #
PL-TR-93-2006 ..... p 897 N94-17240 #
PL-TR-93-2021 ..... p 1108 N94-17267 #
PL-TR-93-2042 ..... p 1101 N94-16469 #
PL-TR-93-2071 ..... p 1105 N94-14958 #
PL-TR-93-2074 ..... p 888 N94-16990 #
PL-TR-93-2080 ..... p 882 N94-16530 #
PL-TR-93-2085 ..... p 1101 N94-16125 #
PL-TR-93-2098 ..... p 1102 N94-17499
PL-TR-93-2108 ..... p 1097 N94-14960 #
PL-TR-93-2134 ..... p 1192 N94-16936 #

PLEX-003 ..... p 1042 N94-17230 #

PML-1992-114 ..... p 1003 N94-17307 #
PML-1992-72 ..... p 1147 N94-15776
PML-1992-77 ..... p 1021 N94-15755

PNL-SA-21234 ..... p 958 N94-16662 #
PNL-SA-21621 ..... p 1092 N94-16160 #
PNL-SA-21622 ..... p 961 N94-17234 #
PNL-SA-21667 ..... p 940 N94-17235 #
PNL-SA-21693 ..... p 934 N94-16158 #
PNL-SA-22038 ..... p 1209 N94-16159 #
PNL-SA-22080 ..... p 1095 N94-16006 #
PNL-SA-22209 ..... p 1215 N94-17319 #
PNL-SA-22213 ..... p 1043 N94-17677 #
PNL-SA-22390 ..... p 1096 N94-16445 #
PNL-SA-22693 ..... p 1151 N94-16902 #

PNL-8622 ..... p 1012 N94-16765 #

PSU/ARL/TR-93-08 ..... p 1005 N94-17463

PUBL-922023 ..... p 928 N94-17213 * #

R/D-6812-EE-01 ..... p 963 N94-14948 #
R/D-6858-EN-09 ..... p 1105 N94-14938 #
R/D-6971-EE-02 ..... p 1015 N94-17570 #

RAE-LIB-TRANS-2201 ..... p 859 N94-16583 #

RAE-TM-AERO/PROP-19 ..... p 856 N94-15696 #

RAY/RD/S-4921 ..... p 1014 N94-17423

RCC-457-93 ..... p 1237 N94-17568 #

RDA-TR-2-2240-1704-0001 ..... p 988 N94-15668 #

REPT-153-4645 ..... p 1026 N94-16927 #
REPT-15 ..... p 1233 N94-17291 * #
REPT-92-054 ..... p 1156 N94-17501
REPT-92-055 ..... p 1234 N94-17502
REPT-93-016 ..... p 1156 N94-17504
REPT-93-017 ..... p 1014 N94-17505
REPT-93B00034 ..... p 1111 N94-15529 * #
REPT-93B00048 ..... p 1228 N94-15116 * #
REPT-93B00079 ..... p 911 N94-15552 * #
REPT-93B00102 ..... p 884 N94-15193 * #
REPT-93B00120 ..... p 1236 N94-15481 * #
REPT-93W0000145 ..... p 987 N94-15439 #

RI/RD93-123-2 ..... p 927 N94-17096 * #
RI/RD93-123-3 ..... p 927 N94-17097 * #

RIACS-TR-93.03 ..... p 1159 N94-15796 * #
RIACS-TR-93.06 ..... p 1148 N94-15956 * #
RIACS-TR-93.09 ..... p 1143 N94-15189 * #
RIACS-TR-93-06 ..... p 1168 N94-15112 * #
RIACS-TR-93-08 ..... p 1158 N94-15113 * #

RL-TR-92-300 ..... p 1169 N94-15785
RL-TR-92-341 ..... p 987 N94-15541 #
RL-TR-93-119-VOL-1 ..... p 1005 N94-17431 #
RL-TR-93-119-VOL-2 ..... p 986 N94-14998 #
RL-TR-93-24 ..... p 1147 N94-15772
RL-TR-93-34 ..... p 1189 N94-15664 #
RL-TR-93-36 ..... p 964 N94-15688 #
RL-TR-93-38 ..... p 1166 N94-16770 #
RL-TR-93-41 ..... p 1008 N94-15665 #
RL-TR-93-49 ..... p 1146 N94-15674 #
RL-TR-93-51 ..... p 885 N94-15666 #
RL-TR-93-56 ..... p 988 N94-15667 #
RL-TR-93-57 ..... p 1188 N94-14957 #
RL-TR-93-58 ..... p 1188 N94-14940
RL-TR-93-60 ..... p 1155 N94-17491 #
RL-TR-93-65 ..... p 1189 N94-15791 #
RL-TR-93-6 ..... p 1055 N94-17194 #
RL-TR-93-75 ..... p 1003 N94-17206 #
RL-TR-93-79 ..... p 1001 N94-17033 #
RL-TR-93-80 ..... p 1151 N94-16941 #
RL-TR-93-84 ..... p 1003 N94-17228 #
RL-TR-93-87 ..... p 999 N94-16777
RL-TR-93-92 ..... p 1014 N94-17375 #

RXR-92121 ..... p 882 N94-16468 #

R93-213 ..... p 1300 N94-15533 * #

S-728 ..... p 925 N94-16496 * #
S-732 ..... p 1137 N94-15717 * #
S-734 ..... p 1055 N94-17082 * #
S-739 ..... p 882 N94-17320 * #
S-746 ..... p 1139 N94-17653 * #

SAIC-93/1069 ..... p 1151 N94-16910 #

SAND-92-2789C ..... p 1091 N94-15993 #
SAND-92-2829C ..... p 1091 N94-15994 #
SAND-92-2831C ..... p 1091 N94-15984 #
SAND-92-2870C ..... p 1092 N94-16112 #
SAND-92-2907C ..... p 1015 N94-17648 #
SAND-93-0229C ..... p 1093 N94-16954 #
SAND-93-0300C ..... p 1208 N94-16012 #
SAND-93-0370C ..... p 1034 N94-16452 #
SAND-93-0480C ..... p 1050 N94-16055 #
SAND-93-0507C ..... p 1157 N94-14927 #
SAND-93-0651C ..... p 953 N94-17649 #
SAND-93-0910 ..... p 883 N94-16056 #
SAND-93-0967C ..... p 1132 N94-16819 #
SAND-93-1252C ..... p 1093 N94-17217 #
SAND-93-1255C ..... p 1016 N94-17671 #
SAND-93-1300C ..... p 1011 N94-16661 #
SAND-93-1353C ..... p 1148 N94-15985 #
SAND-93-8239 ..... p 953 N94-17660 #
SAND-93-8541C ..... p 1036 N94-17647 #

SC-MAG-412 ..... p 1175 N94-17288 #

SCHRIFTENR-PHYSIKAL-ING-BD-23 ..... p 1058 N94-15642 #

SC71033.FR ..... p 1009 N94-15726 #

SER-C-391 ..... p 1081 N94-15156
SER-C-395 ..... p 1098 N94-15153

SER-GEOPHYS-177 ..... p 1098 N94-15800 #

SFA-93/002 ..... p 971 N94-17204

SLAC-ABC-49 ..... p 1190 N94-15854 #

SLAC/SSRL-0010 ..... p 961 N94-17251 #
SLAC/SSRL-0011 ..... p 1183 N94-16811 #
SLAC/SSRL-0015 ..... p 1208 N94-16062 #

SLCET-TR-88-1-REV-6.1 ..... p 1216 N94-17480

SM-92-37 ..... p 1059 N94-16587 #

SMC-TR-93-21 ..... p 885 N94-15749 #
SMC-TR-93-28 ..... p 1056 N94-14945 #
SMC-TR-93-33 ..... p 940 N94-17271
SMC-TR-93-35 ..... p 1193 N94-17012 #
SMC-TR-93-38 ..... p 951 N94-17207 #

SPO-3952 ..... p 1038 N94-15530 * #

SR-12 ..... p 882 N94-16468 #
SR-1 ..... p 1105 N94-15142 #
SR-1 ..... p 897 N94-17240 #
SR-1 ..... p 1108 N94-17267 #
SR-4 ..... p 1105 N94-14958 #

SRA-R93-9083-F ..... p 1016 N94-15109 * #

SRI-MME-92-564-7079 ..... p 927 N94-17123 * #
SRI-MME-92-564-7079 ..... p 928 N94-17124 * #

SRI-PYU-1147/MP-92-280 ..... p 1182 N94-16586 #

SRI-2743 ..... p 1015 N94-17608 #

SRL-0094-TM ..... p 1004 N94-17309
SRL-0112-RN ..... p 1190 N94-15846

SSCL-PREPRINT-442 ..... p 1173 N94-17236 #

SSCL-601 ..... p 1159 N94-16172 #

STAN-CS-92-1449 ..... p 1162 N94-17550 #
STAN-CS-92-1461 ..... p 1149 N94-16554 * #

SU-SLAC-PUB-6062 ..... p 1183 N94-16809 #
SU-SLAC-PUB-6078 ..... p 1208 N94-16062 #
SU-SLAC-PUB-6139 ..... p 961 N94-17251 #
SU-SLAC-PUB-6140 ..... p 1183 N94-16811 #

SU-SOL-93-3 ..... p 1149 N94-16120 #

SU-TR-57 ..... p 1025 N94-16908 #

TABES PAPER 93-230 ..... p 1050 N94-16131 * #
TABES PAPER 93-240 ..... p 1050 N94-16132 * #
TABES PAPER 93-260 ..... p 983 N94-16133 #
TABES PAPER 93-350 ..... p 1050 N94-16130 * #
TABES PAPER 93-460 ..... p 1050 N94-16134 #
TABES PAPER 93-540 ..... p 1050 N94-16135 #
TABES PAPER 93-570 ..... p 1050 N94-16136 #
TABES PAPER 93-601 ..... p 962 N94-16137 #
TABES PAPER 93-602 ..... p 1049 N94-16138 * #
TABES PAPER 93-603 ..... p 1049 N94-16139 * #
TABES PAPER 93-604 ..... p 1049 N94-16140 #
TABES PAPER 93-605 ..... p 1051 N94-16141 * #
TABES PAPER 93-610 ..... p 1051 N94-16142 * #
TABES PAPER 93-611 ..... p 1052 N94-16143 * #
TABES PAPER 93-612 ..... p 930 N94-16144 * #
TABES PAPER 93-620 ..... p 1031 N94-16145 * #
TABES PAPER 93-621 ..... p 976 N94-16146 * #
TABES PAPER 93-630 ..... p 1052 N94-16147 #
TABES PAPER 93-640 ..... p 878 N94-16148 #
TABES PAPER 93-641 ..... p 929 N94-16149 #
TABES PAPER 93-650 ..... p 877 N94-16150 * #
TABES PAPER 93-651 ..... p 883 N94-16151 * #
TABES PAPER 93-652 ..... p 899 N94-16152 #
TABES PAPER 93-653 ..... p 899 N94-16154 #
TABES PAPER 93-654 ..... p 1054 N94-16153 * #
TABES PAPER 93-660 ..... p 1054 N94-16155 #
TABES PAPER 93-661 ..... p 1054 N94-16156 #
TABES PAPER 93-662 ..... p 870 N94-16157 #

TAMRF-6382-93-02 ..... p 1027 N94-17095 * #

TDCK-92-2416 ..... p 1147 N94-15776
TDCK-92-2743 ..... p 1021 N94-15755
TDCK-92-2752 ..... p 1003 N94-17307 #

TEC-R-197 ..... p 1084 N94-17421

TEC-0034 ..... p 1167 N94-17202

TKK-F-A704 ..... p 1201 N94-15210 #

TOP-6-2-040 ..... p 866 N94-15692 #

TP-518 ..... p 950 N94-16930 #

TR-01-ONR ..... p 1092 N94-16567
TR-10-ONR ..... p 962 N94-14914 #
TR-110193-3570F ..... p 994 N94-16022 * #
TR-14 ..... p 1182 N94-16466 #
TR-14 ..... p 948 N94-16787 #
TR-14 ..... p 973 N94-17413 #
TR-15 ..... p 1211 N94-16782
TR-19 ..... p 1182 N94-16111 #
TR-1 ..... p 962 N94-14921 #
TR-2 ..... p 963 N94-15179 #
TR-3 ..... p 963 N94-15631 #
TR-4002-93-10 ..... p 1082 N94-15646 * #
TR-407 ..... p 1170 N94-16582 #
TR-412 ..... p 1166 N94-16581 #
TR-416 ..... p 1165 N94-16580 #
TR-417 ..... p 1150 N94-16579 #
TR-420 ..... p 1159 N94-16578 #
TR-432 ..... p 1159 N94-16577 #
TR-434 ..... p 1231 N94-16576 #
TR-444 ..... p 1149 N94-16575 #
TR-469 ..... p 1173 N94-16726 #
TR-56 ..... p 1210 N94-16476 #
TR-5 ..... p 963 N94-15490 #
TR-6-ONR ..... p 965 N94-15843 #
TR-72-T3 ..... p 1024 N94-16542 * #
TR-8-ONR ..... p 964 N94-15683 #
TR-85 ..... p 969 N94-16928 #
TR-86 ..... p 967 N94-16475 #
TR-92(2409)-3 ..... p 1193 N94-17012 #
TR-92(2935)-17 ..... p 885 N94-15749 #
TR-92(2935)-1 ..... p 940 N94-17271
TR-92(2935)-9 ..... p 951 N94-17207 #
TR-92-159 ..... p 1158 N94-15492 #
TR-92-2341 ..... p 1105 N94-15142 #
TR-93(3464)-1 ..... p 1056 N94-14945 #
TR-93(3935)-9 ..... p 887 N94-16909 #
TR-93-07 ..... p 1028 N94-17276 #
TR-93-1354 ..... p 1152 N94-16982 #
TR-93-1355 ..... p 1000 N94-16911 #
TR-974 ..... p 1158 N94-15492 #
TR-977 ..... p 1121 N94-15634 #
TR-979 ..... p 1164 N94-15746 #

TR/CUCS-001-92 ..... p 1155 N94-17404 #

TRW-18168 ..... p 927 N94-17080 * #
TRW-63941 ..... p 928 N94-17213 * #

TT-9203 ..... p 1020 N94-15645 #

TWR-64204 ..... p 882 N94-17656 * #

UAH-5-32465 ..... p 951 N94-17039 * #

UCB/R/93/A1091 ..... p 961 N94-17223 #

UCRL-ID-111954 ..... p 1201 N94-15981 #
UCRL-ID-113627 ..... p 1096 N94-16802 #
UCRL-ID-114251 ..... p 997 N94-16169 #

UCRL-JC-108924 ..... p 1059 N94-15983 #
UCRL-JC-109219-REV-2 ..... p 1237 N94-16872 #
UCRL-JC-110201 ..... p 1205 N94-17670 #
UCRL-JC-110669 ..... p 1041 N94-16871 #
UCRL-JC-110695 ..... p 1205 N94-17663 #
UCRL-JC-110714 ..... p 1236 N94-14929 #
UCRL-JC-110875 ..... p 1039 N94-16450 #
UCRL-JC-111213 ..... p 1035 N94-16960 #
UCRL-JC-111397 ..... p 1190 N94-15975 #
UCRL-JC-111829 ..... p 1096 N94-16825 #
UCRL-JC-111951 ..... p 1177 N94-16448 #
UCRL-JC-112217 ..... p 1039 N94-16054 #
UCRL-JC-112220 ..... p 1183 N94-16817 #
UCRL-JC-112340 ..... p 1188 N94-17672 #
UCRL-JC-112346 ..... p 1208 N94-15976 #
UCRL-JC-112360 ..... p 1204 N94-17237
UCRL-JC-112379 ..... p 966 N94-15924 #
UCRL-JC-112521 ..... p 950 N94-16952 #
UCRL-JC-112572 ..... p 1149 N94-16119 #
UCRL-JC-112689-REV-1 ..... p 1096 N94-16449 #
UCRL-JC-113277 ..... p 949 N94-16904 #
UCRL-JC-113851 ..... p 1025 N94-16894 #
UCRL-JC-114505 ..... p 1025 N94-16903 #

UCSD-CWT-93-R1 ..... p 1213 N94-17042

UILU-ENG-93-5100 ..... p 971 N94-16980 #

URI-MSL-93-10 ..... p 941 N94-17379 #

US-PATENT-APPL-SN-006413 ..... p 1009 N94-15706 * #
US-PATENT-APPL-SN-008426 ..... p 1165 N94-15946 * #
US-PATENT-APPL-SN-008427 ..... p 1046 N94-15873 * #
US-PATENT-APPL-SN-012893 ..... p 886 N94-15951 * #
US-PATENT-APPL-SN-022219 ..... p 1148 N94-15943 * #
US-PATENT-APPL-SN-037876 ..... p 1147 N94-15703 * #
US-PATENT-APPL-SN-038746 ..... p 1010 N94-15874 * #
US-PATENT-APPL-SN-047120 ..... p 1033 N94-15928 * #
US-PATENT-APPL-SN-048041 ..... p 1047 N94-15925 * #
US-PATENT-APPL-SN-062861 ..... p 965 N94-15879 * #
US-PATENT-APPL-SN-066271 ..... p 1046 N94-15707 * #
US-PATENT-APPL-SN-066274 ..... p 1137 N94-15883 * #
US-PATENT-APPL-SN-066292 ..... p 1117 N94-15969 * #
US-PATENT-APPL-SN-071131 ..... p 1034 N94-15987 * #
US-PATENT-APPL-SN-071416 ..... p 1010 N94-15952 * #
US-PATENT-APPL-SN-073015 ..... p 966 N94-15930 * #
US-PATENT-APPL-SN-073018 ..... p 1165 N94-15958 * #
US-PATENT-APPL-SN-073019 ..... p 966 N94-15960 * #
US-PATENT-APPL-SN-073235 ..... p 1190 N94-15933 * #
US-PATENT-APPL-SN-073845 ..... p 1010 N94-15988 * #
US-PATENT-APPL-SN-073847 ..... p 886 N94-15935 * #
US-PATENT-APPL-SN-077166 ..... p 974 N94-17559 * #
US-PATENT-APPL-SN-077470 ..... p 1033 N94-15875 * #
US-PATENT-APPL-SN-089064 ..... p 925 N94-15876 * #
US-PATENT-APPL-SN-090230 ..... p 1033 N94-15872 * #
US-PATENT-APPL-SN-094331 ..... p 1237 N94-17438 * #
US-PATENT-APPL-SN-094332 ..... p 1038 N94-15932 * #
US-PATENT-APPL-SN-095563 ..... p 925 N94-15947 * #
US-PATENT-APPL-SN-096498 ..... p 983 N94-15881 * #
US-PATENT-APPL-SN-097186 ..... p 1117 N94-15967 * #
US-PATENT-APPL-SN-098911 ..... p 1047 N94-15966 * #
US-PATENT-APPL-SN-098918 ..... p 1047 N94-15949 * #
US-PATENT-APPL-SN-105161 ..... p 1033 N94-15877 * #
US-PATENT-APPL-SN-105528 ..... p 1039 N94-15942 * #
US-PATENT-APPL-SN-105728 ..... p 1215 N94-17327 * #
US-PATENT-APPL-SN-110255 ..... p 1050 N94-15870 * #
US-PATENT-APPL-SN-110278 ..... p 933 N94-15878 * #
US-PATENT-APPL-SN-111317 ..... p 1014 N94-17323 * #
US-PATENT-APPL-SN-111318 ..... p 1161 N94-17328 * #
US-PATENT-APPL-SN-111321 ..... p 1033 N94-15884 * #
US-PATENT-APPL-SN-112483 ..... p 1014 N94-17325 * #
US-PATENT-APPL-SN-112497 ..... p 1161 N94-17330 * #
US-PATENT-APPL-SN-114043 ..... p 1047 N94-15882 * #
US-PATENT-APPL-SN-115832 ..... p 1022 N94-15962 * #
US-PATENT-APPL-SN-125966 ..... p 1014 N94-17324 * #
US-PATENT-APPL-SN-127653 ..... p 1185 N94-17329 * #
US-PATENT-APPL-SN-128007 ..... p 934 N94-15929 * #
US-PATENT-APPL-SN-141295 ..... p 1154 N94-17326 * #
US-PATENT-APPL-SN-153930 ..... p 1129 N94-17085 * #
US-PATENT-APPL-SN-405178 ..... p 935 N94-16534
US-PATENT-APPL-SN-521977 ..... p 975 N94-16934
US-PATENT-APPL-SN-541990 ..... p 1210 N94-16487
US-PATENT-APPL-SN-551104 ..... p 1231 N94-16490
US-PATENT-APPL-SN-560391 ..... p 1034 N94-16536
US-PATENT-APPL-SN-617317 ..... p 948 N94-16532
US-PATENT-APPL-SN-618190 ..... p 958 N94-16486
US-PATENT-APPL-SN-661932 ..... p 1177 N94-16919
US-PATENT-APPL-SN-672986 ..... p 1012 N94-16914
US-PATENT-APPL-SN-679904 ..... p 1047 N94-16548
US-PATENT-APPL-SN-680717 ..... p 969 N94-16920
US-PATENT-APPL-SN-695018 ..... p 1210 N94-16538
US-PATENT-APPL-SN-739026 ..... p 934 N94-15926 * #
US-PATENT-APPL-SN-750992 ..... p 969 N94-16916
US-PATENT-APPL-SN-752713 ..... p 1000 N94-16921
US-PATENT-APPL-SN-766939 ..... p 1191 N94-16489
US-PATENT-APPL-SN-787807 ..... p 940 N94-16933
US-PATENT-APPL-SN-788018 ..... p 936 N94-16537
US-PATENT-APPL-SN-788073 ..... p 1191 N94-16547
US-PATENT-APPL-SN-802926 ..... p 1040 N94-16533
US-PATENT-APPL-SN-811378 ..... p 948 N94-16539
US-PATENT-APPL-SN-812477 ..... p 1047 N94-16531
US-PATENT-APPL-SN-848885 ..... p 1194 N94-17321 * #
US-PATENT-APPL-SN-855827 ..... p 1011 N94-16549
US-PATENT-APPL-SN-867862 ..... p 998 N94-16535
US-PATENT-APPL-SN-884976 ..... p 1011 N94-16488
US-PATENT-APPL-SN-904927 ..... p 1000 N94-16918
US-PATENT-APPL-SN-925217 ..... p 1040 N94-16540
US-PATENT-APPL-SN-929216 ..... p 1004 N94-17322 * #
US-PATENT-APPL-SN-934988 ..... p 925 N94-15927 * #
US-PATENT-APPL-SN-947612 ..... p 1046 N94-15871 * #
US-PATENT-APPL-SN-953338 ..... p 1048 N94-16915
US-PATENT-APPL-SN-953622 ..... p 1000 N94-16917
US-PATENT-APPL-SN-954108 ..... p 965 N94-15880 * #
US-PATENT-APPL-SN-971035 ..... p 1189 N94-15705 * #
US-PATENT-APPL-SN-979987 ..... p 1164 N94-15704 * #

US-PATENT-CLASS-204-59R ..... p 948 N94-16532
US-PATENT-CLASS-205-332 ..... p 958 N94-16486
US-PATENT-CLASS-250-306 ..... p 948 N94-16539
US-PATENT-CLASS-250-324 ..... p 936 N94-16537
US-PATENT-CLASS-252-500 ..... p 935 N94-16534
US-PATENT-CLASS-252-500 ..... p 1012 N94-16914
US-PATENT-CLASS-315-111 ..... p 998 N94-16535
US-PATENT-CLASS-342-192 ..... p 1000 N94-16921
US-PATENT-CLASS-356-5 ..... p 1040 N94-16540
US-PATENT-CLASS-359-896 ..... p 1047 N94-16548
US-PATENT-CLASS-361-288 ..... p 1011 N94-16488
US-PATENT-CLASS-364-506 ..... p 1177 N94-16919
US-PATENT-CLASS-385-132 ..... p 1191 N94-16489
US-PATENT-CLASS-395-600 ..... p 1231 N94-16490
US-PATENT-CLASS-415-90 ..... p 1047 N94-16531
US-PATENT-CLASS-417-356 ..... p 1011 N94-16549
US-PATENT-CLASS-417-48 ..... p 1048 N94-16915
US-PATENT-CLASS-422-91 ..... p 1040 N94-16533
US-PATENT-CLASS-434-22 ..... p 1191 N94-16547
US-PATENT-CLASS-437-108 ..... p 1210 N94-16487
US-PATENT-CLASS-437-165 ..... p 1210 N94-16538
US-PATENT-CLASS-73-105 ..... p 1034 N94-16536

US-PATENT-5,153,597 ..... p 1000 N94-16921
US-PATENT-5,177,644 ..... p 1047 N94-16548
US-PATENT-5,182,496 ..... p 998 N94-16535
US-PATENT-5,183,779 ..... p 1210 N94-16538
US-PATENT-5,185,131 ..... p 1040 N94-16533
US-PATENT-5,186,604 ..... p 1047 N94-16531
US-PATENT-5,190,447 ..... p 1011 N94-16549
US-PATENT-5,190,624 ..... p 948 N94-16532
US-PATENT-5,192,379 ..... p 975 N94-16934
US-PATENT-5,193,383 ..... p 1034 N94-16536
US-PATENT-5,193,605 ..... p 940 N94-16933
US-PATENT-5,194,181 ..... p 935 N94-16534
US-PATENT-5,195,163 ..... p 1191 N94-16489
US-PATENT-5,198,667 ..... p 948 N94-16539
US-PATENT-5,200,620 ..... p 936 N94-16537
US-PATENT-5,205,922 ..... p 958 N94-16486
US-PATENT-5,212,269 ..... p 969 N94-16920
US-PATENT-5,213,713 ..... p 1012 N94-16914
US-PATENT-5,214,483 ..... p 1040 N94-16540
US-PATENT-5,215,465 ..... p 1191 N94-16547
US-PATENT-5,218,517 ..... p 1011 N94-16488
US-PATENT-5,222,233 ..... p 1231 N94-16490
US-PATENT-5,225,366 ..... p 1210 N94-16487
US-PATENT-5,225,498 ..... p 969 N94-16915
US-PATENT-5,227,801 ..... p 1000 N94-16918
US-PATENT-5,227,982 ..... p 1177 N94-16919
US-PATENT-5,228,837 ..... p 1048 N94-16915
US-PATENT-5,231,403 ..... p 1000 N94-16917

USAARL-93-12 ..... p 1119 N94-14952 #
USAARL-93-15 ..... p 862 N94-15637 #
USAARL-93-16 ..... p 1131 N94-15659 #

USAATC-TR-93-A-005 ..... p 870 N94-15793 * #

USAFETAC/TN-93/003 ..... p 1106 N94-15757

USARIEM-T13-93 ..... p 1035 N94-17002 #

USCG-D-09-93 ..... p 1138 N94-16793

UTD/CAO/26 ..... p 1199 N94-17427

UTRC-R93-918120-2 ..... p 959 N94-16781 #

UTRC-927703-1 ..... p 1186 N94-17536 #

UTRC93-28 ..... p 950 N94-17008

UVA/525234/MSE93/101 ..... p 1008 N94-15494 #

UWA/DME/TR-93/72 ..... p 960 N94-17041 #

VPI-E-93-09 ..... p 964 N94-15656 * #

VTT-JULK-755 ..... p 1056 N94-17542 #

VTT-PUBS-110 ..... p 1200 N94-15204 #

VTT-TIED-1348 ..... p 985 N94-17544 #
VTT-TIED-1358 ..... p 1015 N94-17546 #
VTT-TIED-1359 ..... p 974 N94-17547 #

WES/IR/GL-93-1 ..... p 862 N94-16438 #

WES/MP/GL-93-5 ..... p 983 N94-15177 #

WES/TR/EL-93-9-REPT-1 ..... p 1106 N94-15851

WHOI-93-06 ..... p 1114 N94-17555 #
WHOI-93-11 ..... p 1113 N94-17383 #

WL-TP-93-002 ..... p 1033 N94-15826

WL-TR-93-1046 ..... p 1152 N94-17014
WL-TR-93-1059 ..... p 1035 N94-17197 #
WL-TR-93-2004 ..... p 1182 N94-16586 #
WL-TR-93-2033 ..... p 942 N94-14911 #
WL-TR-93-2036 ..... p 1048 N94-17433
WL-TR-93-2047 ..... p 866 N94-15761
WL-TR-93-2049 ..... p 1028 N94-17250 #
WL-TR-93-2052-VOL-1 ..... p 943 N94-14962
WL-TR-93-2054 ..... p 872 N94-15847
WL-TR-93-2068 ..... p 973 N94-17434
WL-TR-93-2071 ..... p 1186 N94-17536 #

WL-TR-93-3025-VOL-1 ..... p 1151 N94-16768 #
WL-TR-93-3025-VOL-2 ..... p 1151 N94-16769
WL-TR-93-3043 ..... p 1152 N94-17032 #
WL-TR-93-3058 ..... p 861 N94-17461
WL-TR-93-3059 ..... p 861 N94-17609 #
WL-TR-93-4013 ..... p 936 N94-16569 #
WL-TR-93-4029 ..... p 1213 N94-17042
WL-TR-93-4036 ..... p 1157 N94-17590 #
WL-TR-93-4043 ..... p 1061 N94-17269
WL-TR-93-4047 ..... p 1055 N94-17515
WL-TR-93-4048 ..... p 1056 N94-17596 #
WL-TR-93-4063-PT-1 ..... p 936 N94-16795
WL-TR-93-4072 ..... p 1215 N94-17417
WL-TR-93-8019 ..... p 984 N94-16981 #

WSRC-MS-93-179 ..... p 1112 N94-16009 #

WSRC-TR-91-372-REV-2 ..... p 1023 N94-15980 #

WU/CCM-93/3 ..... p 1062 N94-17445 * #

YALEU/DCS/RR-977 ..... p 1154 N94-17370 #
YALEU/DCS/RR-980 ..... p 1171 N94-17420

APPENDIX

NASA SCIENTIFIC AND TECHNICAL INFORMATION PROGRAM PRODUCTS AND SERVICES

The NASA Scientific and Technical Information (STI) Program provides for the collection and announcement of aerospace-related reports and literature obtained worldwide through agreements and exchanges. The result of the collection is the comprehensive NASA STI Database that covers aeronautics, space, and supporting disciplines.

The STI Database, documents generated or obtained by NASA, and products and services derived from or supporting the database are made available to the NASA research community and to the public. Descriptions and sources of these items are presented in the following pages.

Scientific and Technical Aerospace Reports (STAR) is an abstract journal, listing citations with abstracts for aerospace-related reports obtained from worldwide sources. *STAR* is issued on the first of each month, and announces current documents that have been entered into the NASA STI Database during the previous month. The reports are of the following types:

- NASA, NASA contractor, and NASA grantee reports;
- Reports issued by other U.S. Government agencies, domestic and foreign institutions, universities, and private firms;
- Translations in report form;
- NASA-owned patents and patent applications
- Other U.S. Government agency and foreign patents and patent applications
- Domestic and foreign dissertations and theses.

Journal, book, and conference literature, journal translations, and certain foreign dissertations having the same subject scope as *STAR* are announced in a companion journal, *International Aerospace Abstracts (IAA). IAA* is issued on the 1st and 15th of each month and is available from the American Institute of Aeronautics and Astronautics, Technical Information Service, 555 West 57th Street, 12th Floor, New York, NY 10019.

ELIGIBILITY AND REGISTRATION FOR NASA STI PRODUCTS AND SERVICES

Organizations of the type listed below that have registered with NASA can receive products and services.

- NASA offices and installations, contractors, subcontractors, grantees, and consultants;
- Other U.S. Government agencies and their contractors;
- Libraries in the United States that have arrangements with NASA to maintain collections of NASA documents for public reference;
- Other organizations in the United States having a need for NASA documents in work related to aeronautics and space research;
- Organizations abroad that have established reciprocal documents exchange arrangements with NASA.

The central service points—central points of document acquisition and control within qualified organizations—or individuals are eligible to register for NASA STI products and services. Domestic organizations or individuals may be eligible to receive various classes of NASA publications and services and should address their requests for registration or further information to:

ATTN: Registration Services
NASA Center for AeroSpace Information
800 Elkridge Landing Road
Linthicum Heights, MD 21090-2934
301-621-0390

Organizations abroad should direct requests to:

National Aeronautics and Space Administration
Scientific and Technical Information Program (JTT)
International STI Program
Washington, DC 20546-0001
USA
703-271-5640

SUBJECT SCOPE

The subject scope of *STAR* and *IAA* includes all aspects of aeronautics and space research and development, supporting basic and applied research, and applications. Aerospace aspects of Earth resources, energy development, conservation, oceanography, environmental protection, urban transportation, and other topics of high national priority are also covered.

HOW TO USE *STAR* SUBJECT CATEGORIES

Abstracts in *STAR* are categorized by 10 major subject divisions that are divided further into 76 specific subject categories. The subject divisions and categories are listed in the Table of Contents together with a note for each that defines its scope and provides any cross-references. For example:

16 SPACE TRANSPORTATION

Includes passenger and cargo space transportation, e.g., shuttle operations; and space rescue techniques. For related information see also *03 Air Transportation and Safety* and *18 Spacecraft Design, Testing and Performance*. For space suits see *54 Man/System Technology and Life Support*.

CROSS-REFERENCES

Individual *STAR* abstracts are not ordinarily cross-referenced, except for certain conference reports or book translations that have had separate abstracts written for their component papers or chapters. Citations and abstracts of the components follow immediately after those of the parent document. When the subject content of a component differs sufficiently from the general content of the parent, a cross-reference citation also is printed at the end of the category to which it normally would have been assigned if it were independent.

DOCUMENTS ON MICROFICHE

Documents available on microfiche are designated by a pound sign (#) following the accession number.

LIMITED REPRODUCIBILITY

A note of limited reproducibility appears in the citation, if there are factors affecting the reproducibility of more than 20% of the document. These factors include faint or broken type, color photographs, black and white photographs, foldouts, dot matrix print, or some other factor that limits the reproducibility of the document. This notation also appears on the microfiche header.

COLOR COPIES

An increasing number of NASA scientific and technical reports are being produced with color graphs, charts, illustrations, and photographs. An indication that a document has color pages follows the source and pricing (SAP) information in the *STAR* citation.

Registered users of the NASA Scientific and Technical Information Program will receive ordered documents with color at no additional cost, as long as stock copies of the document are available. Otherwise, an additional fee of $2.00 per color page will be charged. The NASA Center for AeroSpace Information staff will contact registered users to determine individual user's needs.

NASA PATENTS AND PATENT APPLICATIONS

Patents and patent applications owned by NASA are announced in *STAR* under appropriate subject categories and are referenced in the *STAR* indexes. In the Report Number Index, patents are indexed by the NASA Case Number, and the U.S. Patent Class. Patent applications are indexed by the NASA Case Number and the U.S. Patent Application Serial Number.

Printed copies of patents (which are not microfiched) are available for purchase from the U.S. Patent and Trademark Office.

When ordering patents, the U.S. Patent Number should be used, and payment must be remitted in advance, by money order or check payable to the Commissioner of Patents and Trademarks. Prepaid purchase coupons for ordering are also available from the U.S. Patent and Trademark Office.

NASA patent application specifications are sold in both paper copy and microfiche by the NASA Center for AeroSpace Information (CASI). The N accession number should be used in ordering either paper copy or microfiche from CASI.

The patents and patent applications announced in *STAR* are owned by NASA and are available for royalty-free licensing. Requests for licensing terms and further information should be addressed to:

National Aeronautics and Space Administration
Associate General Counsel for Intellectual Property
Code GP
Washington, DC 20546-0001

SOURCES FOR DOCUMENTS

One or more sources from which a document announced in *STAR* is available to the public is ordinarily given on the last line of the citation. The most commonly indicated sources and their acronyms or abbreviations are listed below, and their addresses are listed on page A-6. If the publication is available from a source other than those listed, the publisher and his address will be displayed on the availability line or in combination with the corporate source line.

Avail: CASI. Sold by the NASA Center for AeroSpace Information. Prices for hard copy (HC) and microfiche (MF) are indicated by a price code following the letters HC or MF in the *STAR* citation. Current values for the price codes are given in the tables on page A-7.

NOTE ON ORDERING DOCUMENTS: When ordering publications from CASI, use the N accession number or other report number. It is also advisable to cite the title and other bibliographic identification.

Avail: SOD (or GPO). Sold by the Superintendent of Documents, U.S. Government Printing Office, in hard copy.

Avail: BLL (formerly NLL): British Library Lending Division, Boston Spa, Wetherby, Yorkshire, England. Photocopies available from this organization at the price shown. (If none is given, inquiry should be addressed to the BLL.)

Avail: DOE Depository Libraries. Organizations in U.S. cities and abroad that maintain collections of Department of Energy reports, usually in microfiche form, are listed in *Energy Research Abstracts*. Services available from the DOE and its depositories are described in a booklet, *DOE Technical Information Center - Its Functions and Services* (TID-4660), which may be obtained without charge from the DOE Technical Information Center.

Avail: ESDU. Pricing information on specific data, computer programs, and details on Engineering Sciences Data Unit (ESDU) topic categories can be obtained from ESDU International Ltd. Requesters in North America should use the Virginia address while all other requesters should use the London address, both of which are on page A-6.

Avail: Fachinformationszentrum, Karlsruhe. Gesellschaft für wissenschaftlich-technische Information mbH 7514 Eggenstein-Leopoldshafen 2, Germany.

Avail: HMSO. Publications of Her Majesty's Stationery Office are sold in the U.S. by Pendragon House, Inc. (PHI), Redwood City, CA. The U.S. price (including a service and mailing charge) is given, or a conversion table may be obtained from PHI.

Avail: Issuing Activity, or Corporate Author, or no indication of availability. Inquiries as to the availability of these documents should be addressed to the organization shown in the citation as the corporate author of the document.

Avail: NASA Public Document Rooms. Documents so indicated may be examined at or purchased from the National Aeronautics and Space Administration (JBD-4), Public Documents Room (Room 1H23), Washington, DC 20546-0001, or public document rooms located at NASA installations, and the NASA Pasadena Office at the Jet Propulsion Laboratory.

Avail: NTIS. Sold by the National Technical Information Service. Initially distributed microfiche under the NTIS SRIM (Selected Research in Microfiche) are available. For information concerning this service, consult the NTIS Subscription Section, Springfield, VA 22161.

Avail: Univ. Microfilms. Documents so indicated are dissertations selected from *Dissertation Abstracts* and are sold by University Microfilms as xerographic copy (HC) and microfilm. All requests should cite the author and the Order Number as they appear in the citation.

Avail: US Patent and Trademark Office. Sold by Commissioner of Patents and Trademarks, U.S. Patent and Trademark Office, at the standard price of $1.50 each, postage free. (See discussion of NASA patents and patent applications on page A-3.)

Avail: (US Sales Only). These foreign documents are available to users within the United States from the National Technical Information Service (NTIS). They are available to users outside the United States through the International Nuclear Information Service (INIS) representative in their country, or by applying directly to the issuing organization.

Avail: USGS. Originals of many reports from the U.S. Geological Survey, which may contain color illustrations, or otherwise may not have the quality of illustrations preserved in the microfiche or facsimile reproduction, may be examined by the public at the libraries of the USGS field offices whose addresses are listed on page A-6. The libraries may be queried concerning the availability of specific documents and the possible utilization of local copying services, such as color reproduction.

FEDERAL DEPOSITORY LIBRARY PROGRAM

In order to provide the general public with greater access to U.S. Government publications, Congress established the Federal Depository Library Program under the Government Printing Office (GPO), with 53 regional depositories responsible for permanent retention of material, inter-library loan, and reference services. At least one copy of nearly every NASA and NASA-sponsored publication, either in printed or microfiche format, is received and retained by the 53 regional depositories. A list of the regional GPO libraries, arranged alphabetically by state, appears on page A-8. These libraries are *not* sales outlets. A local library can contact a regional depository to help locate specific reports, or direct contact may be made by an individual.

PUBLIC COLLECTION OF NASA DOCUMENTS

An extensive collection of NASA and NASA-sponsored publications is maintained by the British Library Lending Division, Boston Spa, Wetherby, Yorkshire, England for public access. The British Library Lending Division also has available many of the non-NASA publications cited in *STAR*. European requesters may purchase facsimile copy or microfiche of NASA and NASA-sponsored documents, those identified by both the symbols # and * from ESA — Information Retrieval Service European Space Agency, 8-10 rue Mario-Nikis, 75738 CEDEX 15, France.

SUBMITTING DOCUMENTS

All users of this abstract service are urged to forward reports to be considered for announcement in *STAR*. This will aid NASA in its efforts to provide the fullest possible coverage of all scientific and technical publications that might support aeronautics and space research and development. If you have prepared relevant reports (other than those you will transmit to NASA, DOD, or DOE through the usual contract- or grant-reporting channels), please send them for consideration to the NASA Center for AeroSpace Information, 800 Elkridge Landing Road, Linthicum Heights, MD 21090-2934.

Reprints of journal articles, book chapters, and conference papers are also welcome. These will be considered for announcement in *STAR's* companion journal, *IAA*.

You may specify a particular source to be included in a report announcement if you wish; otherwise the report will be placed on a public sale at the NASA Center for AeroSpace Information. Copyrighted publications will be announced but not distributed or sold.

PURCHASE OF *STAR*

STAR is publicly available on annual subscription from the NASA Center for AeroSpace Information (CASI) at $94.00/domestic, $117.00/foreign. Single copy prices: $33.00/domestic, $41.00/foreign.

An annual, cumulative *STAR Index* is also available at $54.00/domestic, $65.00/foreign.

STAR is available to registered users on annual subscription from the NASA Center for AeroSpace Information, ATTN: Registration Services, 800 Elkridge Landing Road, Linthicum Heights, MD 21090-2934.

ADDRESSES OF ORGANIZATIONS

American Institute of Aeonautics
and Astronautics
Technical Information Service
555 West 57th Street, 12th Floor
New York, NY 10019

British Library Lending Division
Boston Spa, Wetherby, Yorkshire
England

Commissioner of Patents and Trademarks
U.S. Patent and Trademark Office
Washington, DC 20231

Department of Energy
Technical Information Center
P.O. Box 62
Oak Ridge, TN 37830

European Space Agency-
Information Retrieval Service ESRIN
Via Galileo Galilei
00044 Frascati (Rome) Italy

Engineering Sciences Data Unit International
P.O. Box 1633
Manassas, VA 22110

Engineering Sciences Data Unit
International, Ltd.
251-259 Regent Street
London, W1R 7AD, England

Fachinformationszentrum Karlsruhe
Gesellschaft für wissenschaftlich-technische
Information mbH
7514 Eggenstein-Leopoldshafen 2, Germany

Her Majesty's Stationery Office
P.O. Box 569, S.E. 1
London, England

NASA Center for AeroSpace Information
800 Elkridge Landing Road
Linthicum Heights, MD 21090-2934

National Aeronautics and Space Administration
Scientific and Technical Information Program
(JTT)
Washington, DC 20546-0001

National Technical Information Service
5285 Port Royal Road
Springfield, VA 22161

Pendragon House, Inc.
899 Broadway Avenue
Redwood City, CA 94063

Superintendent of Documents
U.S. Government Printing Office
Washington, DC 20402

University Microfilms
A Xerox Company
300 North Zeeb Road
Ann Arbor, MI 48106

University Microfilms, Ltd.
Tylers Green
London, England

U.S. Geological Survey Library National Center
MS 950
12201 Sunrise Valley Drive
Reston, VA 22092

U.S. Geological Survey Library
2255 North Gemini Drive
Flagstaff, AZ 86001

U.S. Geological Survey
345 Middlefield Road
Menlo Park, CA 94025

U.S. Geological Survey Library
Box 25046
Denver Federal Center, MS914
Denver, CO 80225

CASI PRICE TABLES

(Effective August 1, 1993)

STANDARD PRICE DOCUMENTS

PRICE CODE	NORTH AMERICAN PRICE	FOREIGN PRICE
A01	$ 9.00	$ 18.00
A02	12.50	25.00
A03	17.50	35.00
A04-A05	19.50	39.00
A06-A09	27.00	54.00
A10-A13	36.50	73.00
A14-A17	44.50	89.00
A18-A21	52.00	104.00
A22-A25	61.00	122.00
A99	Call For Price	Call For Price

MICROFICHE

PRICE CODE	NORTH AMERICAN PRICE	FOREIGN PRICE
A01	$ 9.00	$ 18.00
A02	12.50	25.00
A03	17.50	35.00
A04	19.50	39.00
A06	27.00	54.00
A10	36.50	73.00

IMPORTANT NOTICE

CASI Shipping and Handling Charges
U.S.—ADD $3.00 per TOTAL ORDER
Canada and Mexico—ADD $3.50 per TOTAL ORDER
All Other Countries—ADD $7.50 per TOTAL ORDER
Does NOT apply to orders
requesting CASI RUSH HANDLING.
CASI accepts charges to American Express, Diners Club, MasterCard and VISA.

FEDERAL REGIONAL DEPOSITORY LIBRARIES

ALABAMA

AUBURN UNIV. AT MONTGOMERY LIBRARY
Documents Dept.
7300 University Dr.
Montgomery, AL 36117-3596
(205) 244-3650 Fax: (205) 244-0678

UNIV. OF ALABAMA
Amelia Gayle Gorgas Library
Govt. Documents
Box 870266
Tuscaloosa, AL 35487-0266
(205) 348-6046 Fax: (205) 348-8833

ARIZONA

DEPT. OF LIBRARY, ARCHIVES, AND PUBLIC RECORDS
Federal Documents
Third Floor State Capitol
1700 West Washington
Phoenix, AZ 85007
(602) 542-4121 Fax: (602) 542-4400, 542-4500

ARKANSAS

ARKANSAS STATE LIBRARY
State Library Services
One Capitol Mall
Little Rock, AR 72201
(501) 682-2869

CALIFORNIA

CALIFORNIA STATE LIBRARY
Govt. Publications Section
914 Capitol Mall - P.O. Box 942837
Sacramento, CA 94237-0001
(916) 322-4572 Fax: (916) 324-8120

COLORADO

UNIV. OF COLORADO - BOULDER
Norlin Library
Govt. Publications
Campus Box 184
Boulder, CO 80309-0184
(303) 492-8834 Fax: (303) 492-2185

DENVER PUBLIC LIBRARY
Govt. Publications Dept. BS/GPD
1357 Broadway
Denver, CO 80203
(303) 571-2135

CONNECTICUT

CONNECTICUT STATE LIBRARY
231 Capitol Avenue
Hartford, CT 06106
(203) 566-4971 Fax: (203) 566-3322

FLORIDA

UNIV. OF FLORIDA LIBRARIES
Documents Dept.
Library West
Gainesville, FL 32611-2048
(904) 392-0366 Fax: (904) 392-7251

GEORGIA

UNIV. OF GEORGIA LIBRARIES
Govt. Documents Dept.
Jackson Street
Athens, GA 30602
(404) 542-8949 Fax: (404) 542-6522

HAWAII

UNIV. OF HAWAII
Hamilton Library
Govt. Documents Collection
2550 The Mall
Honolulu, HI 96822
(808) 948-8230 Fax: (808) 956-5968

IDAHO

UNIV. OF IDAHO LIBRARY
Documents Section
Moscow, ID 83843
(208) 885-6344 Fax: (208) 885-6817

ILLINOIS

ILLINOIS STATE LIBRARY
Reference Dept.
300 South Second
Springfield, IL 62701-1796
(217) 782-7596 Fax: (217) 524-0041

INDIANA

INDIANA STATE LIBRARY
Serials/Documents Section
140 North Senate Avenue
Indianapolis, IN 46204
(317) 232-3678 Fax: (317) 232-3728

IOWA

UNIV. OF IOWA LIBRARIES
Govt. Publications Dept.
Washington & Madison Streets
Iowa City, IA 52242
(319) 335-5926 Fax: (319) 335-5830

KANSAS

UNIV. OF KANSAS
Govt. Documents & Map Library
6001 Malatt Hall
Lawrence, KS 66045-2800
(913) 864-4660 Fax: (913) 864-5380

KENTUCKY

UNIV. OF KENTUCKY LIBRARIES
Govt. Publications/Maps Dept.
Lexington, KY 40506-0039
(606) 257-3139 Fax: (606) 257-1563, 257-8379

LOUISIANA

LOUISIANA STATE UNIV.
Middleton Library
Govt. Documents Dept.
Baton Rouge, LA 70803
(504) 388-2570 Fax: (504) 388-6992

LOUISIANA TECHNICAL UNIV.
Prescott Memorial Library
Govt. Documents Dept.
305 Wisteria Street
Ruston, LA 71270-9985
(318) 257-4962 Fax: (318) 257-2447

MAINE

TRI-STATE DOCUMENTS DEPOS.
Raymond H. Fogler Library
Govt. Documents & Microforms Dept.
Univ. of Maine
Orono, ME 04469
(207) 581-1680

MARYLAND

UNIV. OF MARYLAND
Hornbake Library
Govt. Documents/Maps Unit
College Park, MD 20742
(301) 454-3034 Fax: (301) 454-4985

MASSACHUSETTS

BOSTON PUBLIC LIBRARY
Govt. Documents Dept.
666 Boylston Street
Boston, MA 02117
(617) 536-5400 ext. 226
Fax: (617) 267-8273, 267-8248

MICHIGAN

DETROIT PUBLIC LIBRARY
5201 Woodward Avenue
Detroit, MI 48202-4093
(313) 833-1440, 833-1409
Fax: (313) 833-5039

LIBRARY OF MICHIGAN
Govt. Documents Unit
P.O. Box 30007
Lansing, MI 48909
(517) 373-0640 Fax: (517) 373-3381

MINNESOTA

UNIV. OF MINNESOTA
Wilson Library
Govt. Publications Library
309 19th Avenue South
Minneapolis, MN 55455
(612) 624-5073 Fax: (612) 626-9353

MISSISSIPPI

UNIV. OF MISSISSIPPI
J.D. Williams Library
Federal Documents Dept.
106 Old Gym Bldg.
University, MS 38677
(601) 232-5857 Fax: (601) 232-5453

MISSOURI

UNIV. OF MISSOURI - COLUMBIA
Ellis Library
Govt. Documents
Columbia, MO 65201
(314) 882-6733 Fax: (314) 882-8044

MONTANA

UNIV. OF MONTANA
Maureen & Mike Mansfield Library
Documents Div.
Missoula, MT 59812-1195
(406)243-6700 Fax: (406) 243-2060

NEBRASKA

UNIV. OF NEBRASKA - LINCOLN
D.L. Love Memorial Library
Documents Dept.
Lincoln, NE 68588
(402) 472-2562

NEVADA

UNIV. OF NEVADA
Reno Library
Govt. Publications Dept.
Reno, NV 89557
(702) 784-6579 Fax: (702) 784-1751

NEW JERSEY

NEWARK PUBLIC LIBRARY
U.S. Documents Div.
5 Washington Street -
P.O. Box 630
Newark, NJ 07101-0630
(201) 733-7812 Fax: (201) 733-5648

NEW MEXICO

UNIV. OF NEW MEXICO
General Library
Govt. Publications Dept.
Albuquerque, NM 87131-1466
(505) 277-5441 Fax: (505) 277-6019

NEW MEXICO STATE LIBRARY
325 Don Gaspar Avenue
Santa Fe, NM 87503
(505) 827-3826 Fax: (505) 827-3820

NEW YORK

NEW YORK STATE LIBRARY
Documents/Gift & Exchange Section
Federal Depository Program
Cultural Education Center
Albany, NY 12230
(518) 474-5563 Fax: (518) 474-5786

NORTH CAROLINA

UNIV. OF NORTH CAROLINA - CHAPEL HILL
CB#3912, Davis Library
BA/SS Dept. - Documents
Chapel Hill, NC 27599
(919) 962-1151 Fax: (919) 962-0484

NORTH DAKOTA

NORTH DAKOTA STATE UNIV. LIB.
Documents Office
Fargo, ND 58105
(701) 237-8886 Fax: (701) 237-7138
In cooperation with Univ. of North Dakota, Chester Fritz Library
Grand Forks

OHIO

STATE LIBRARY OF OHIO
Documents Dept.
65 South Front Street
Columbus, OH 43266
(614) 644-7051 Fax: (614) 752-9178

OKLAHOMA

OKLAHOMA DEPT. OF LIBRARIES
U.S. Govt. Information Div.
200 NE 18th Street
Oklahoma City, OK 73105-3298
(405) 521-2502, ext. 252, 253
Fax: (405) 525-7804

OKLAHOMA STATE UNIV.
Edmon Low Library
Documents Dept.
Stillwater, OK 74078
(405) 744-6546 Fax: (405) 744-5183

OREGON

PORTLAND STATE UNIV.
Millar Library
934 SW Harrison - P.O. Box 1151
Portland, OR 97207
(503) 725-3673 Fax: (503) 725-4527

PENNSYLVANIA

STATE LIBRARY OF PENN.
Govt. Publications Section
Walnut St. & Commonwealth Ave. -
P.O. Box 1601
Harrisburg, PA 17105
(717) 787-3752

SOUTH CAROLINA

CLEMSON UNIV.
Cooper Library
Public Documents Unit
Clemson, SC 29634-3001
(803) 656-5174 Fax: (803) 656-3025
In cooperation with Univ. of South Carolina, Thomas Cooper Library, Columbia

TENNESSEE

MEMPHIS STATE UNIV. LIBRARIES
Govt. Documents
Memphis, TN 38152
(901) 678-2586 Fax: (901) 678-2511

TEXAS

TEXAS STATE LIBRARY
United States Documents
P.O. Box 12927 - 1201 Brazos
Austin, TX 78711
(512) 463-5455 Fax: (512) 463-5436

TEXAS TECH. UNIV. LIBRARY
Documents Dept.
Lubbock, TX 79409
(806) 742-2268 Fax: (806) 742-1920

UTAH

UTAH STATE UNIV.
Merrill Library & Learning Resources Center, UMC-3000
Documents Dept.
Logan, UT 84322-3000
(801) 750-2684 Fax: (801) 750-2677

VIRGINIA

UNIV. OF VIRGINIA
Aldermman Library
Govt. Documents
Charlottesville, VA 22903-2498
(804) 824-3133 Fax: (804) 924-4337

WASHINGTON

WASHINGTON STATE LIBRARY
Document Section
MS AJ-11
Olympia, WA 98504-0111
(206) 753-4027 Fax: (206) 753-3546

WEST VIRGINIA

WEST VIRGINIA UNIV. LIBRARY
Govt. Documents Section
P.O. Box 6069
Morgantown, WV 26506
(304) 293-3640

WISCONSIN

ST. HIST. SOC. OF WISCONSIN LIBRARY
Govt. Publications Section
816 State Street
Madison, WI 53706
(608) 262-2781 Fax: (608) 262-4711
In cooperation with Univ. of Wisconsin - Madison, Memorial Library

MILWAUKEE PUBLIC LIBRARY
Documents Div.
814 West Wisconsin Avenue
Milwaukee, WI 53233
(414) 278-2167 Fax: (414) 278-2137

*U.S. GOVERNMENT PRINTING OFFICE:1994-301-249/00002

POSTMASTER
Address Correction Requested
(Sections 137 and 159 Post Manual)

National Aeronautics and
Space Administration
Code JTT
Washington, DC 20546-0001

Official Business
Penalty for Private Use, $300

BULK RATE
POSTAGE & FEES PAID
NASA
PERMIT No. G-27

NASA

POSTMASTER: If Undeliverable (Section 158 Postal Manual) Do Not Return

Please circulate this publication to other colleagues within your organization.

NASA STI PROGRAM
SCIENTIFIC &
TECHNICAL
INFORMATION